Virchows Arch (2012) 461:1–2
DOI 10.1007/s00428-012-1278-z

INVITED EDITORIAL

A compulsory examination in pathology: redundant or necessary?

Jan G. van den Tweel · Claude Cuvelier · Anthony J. Freemont

Received: 24 June 2012 / Accepted: 25 June 2012 / Published online: 8 July 2012
© The Author(s) 2012. This article is published with open access at Springerlink.com

In this issue Lehr et al. describe the compulsory examination used by the Swiss Society of Pathology to assess senior residents, and thereby assure the professional competence of its future qualified members [1]. With this examination, Switzerland is, with Britain, one of the few European countries with a comprehensive examination (lasting several days) that tests the full range of theoretical and practical competencies required of a medical specialist-pathologist.

There is considerable variation across Europe in the way that the final competencies of pathology trainees are assessed [2]. The reason for this variation is the fact that European countries are all entirely autonomous with regard to training, licensing and the issuing of specialty diplomas in postgraduate medical education. For example, in pathology six countries do not require any form of testing at all at the end of specialty training. In the remaining 26 there is considerable heterogeneity of testing [2], with autopsy competency tested in 11, gross specimen examination and sampling in 9 and cytology in 18. No exact data about the duration of these examinations are known.

Harmonization of training and the assessment of its effectiveness in producing competent specialists has proven to be very difficult because very few countries are willing to give up their autonomy to decide on the competencies of their medical specialists, to be acquired during residency training. This is in stark contrast to many countries where obligatory specialty examinations, sometimes with considerable failure rates, are the norm. Examples include the North American specialty boards and the examinations of the British Royal Colleges [3, 4]. For the Royal College of Pathologists, examinations are one of the principal benchmarks by which trainees are judged to have reached professional competence. The British examinations are still copied in one form or another by their old colonies (e.g. Australia, Canada, many African countries). When one of us (JGvdT) was an external examiner in Zimbabwe in the 90's it was much more difficult to become a pathologist there (or indeed a specialist in any medical discipline) than in the Netherlands and many other European countries. The same applies e.g. to Tanzania where, to progress further in the specialty, residents have to pass a general pathology examination already after 6 months of training.

To tackle this diversity in training and testing in 1997 the European Board of Pathology (EBP) of the European Union of Medical Specialists (UEMS), introduced an annual voluntary examination for senior pathology residents, based upon a similar examination successfully introduced by the European Board of Urology. Although introduction of the examination was supported by a large majority of the members of EBP, due to the lack of any consequence of failing, and poor support by senior pathologists, the test never really got off the ground and is currently taken by only a handful of people, mainly those from outside the EU hoping to

J. G. van den Tweel (✉)
Department of Pathology, University Medical Center,
Heidelberglaan 100,
3508 GA Utrecht, The Netherlands
e-mail: j.vandentweel@umcutrecht.nl

C. Cuvelier
Department of Pathology, Ghent University,
9000, Ghent, Belgium
e-mail: Claude.Cuvelier@ugent.be

A. J. Freemont
Manchester Medical School, The University of Manchester,
Manchester, UK
e-mail: tony.freemont@manchester.ac.uk

increase their prospect of finding work as pathologist in Europe. The only exception is Malta where since 2011 the UEMS examinations are officially recognized for all medical specialisms.

With support of a grant from the EU, the European Association of Pathology Chairs and Program Directors (EAPCP) developed a voluntary progress test (EUROPALS) [5], comparable to the American RISE (Resident In Service Examination). The latter test is given for all medical specialties in the USA and is for pathology a good outcome predictor for the American Board Examination [6]. This EUROPALS test had a high participation rate and is now, thanks to the support of the European Society of Pathology being developed as an official progress test, not only for residents but also for specialised pathologists and subspecialists.

The relevant question here of course is why trainee medical specialists, including in pathology, in so many countries in Europe are not thoroughly tested at the end of their training. This is relevant in view of the results of the American and British examinations, showing that a proportion of advanced residents do not have the core competencies, as defined by senior members of the profession, considered necessary for practicing safely. As there is no suggestion that the training in the UK or USA is substandard, the question is relevant whether introduction of similar assessments across Europe would demonstrate lacunar competencies in some of the examined residents. That is not to suggest that trainees across Europe might be less competent than their North American or UK homologues, merely that as the experience in the e.g. USA and UK indicates, assessment stimulates learning. Creating a knowledgeable, thoughtful and competent pool of specialists is surely the fundamental goal of any postgraduate medical training programme.

Open Access This article is distributed under the terms of the Creative Commons Attribution License which permits any use, distribution, and reproduction in any medium, provided the original author(s) and the source are credited.

References

1. Lehr H-A, Moch H, Christen B, Safret A, Gugger M, Rössle M, von Gunten M, Lemoine R, Kurt AM, Caduff R, Arnold W, Singer G, Luscieti P, Bannwart F, Genton CY (2012) Board examination for anatomical pathology in Switzerland: two intense days to verify professional competence. doi:10.1007/s00428-012-1262-7
2. Bosman FT, van den Tweel JG (2009) Unison or cacophony: postgraduate training in pathology in Europe. Virchows Arch 454:497–503
3. Picarsic J, Raval JS, Macpherson T (2010) United States Medical Licensing Examination step 1 two-digit score: a correlation with the American Board of Pathology first-time test taker pass/fail rate at the University of Pittsburgh Medical Center. Arch Pathol Lab Med 135:1349–1352
4. Gray TA (2009) The Royal College of Pathologists Annual Report of Examinations and Assessments undertaken in 2009 Dr. T.A. Gray. Director of Examinations and Assessment. http://www.rcpath.org/Resources/RCPath/Migrated%20Resources/Documents/A/annual_report_2009.pdf
5. European Pathology Training Curriculum (2009) http://www.eapcp.org/Europals/training.htm
6. Rinder HM, Grimes MM, Wagner J, Bennett BD, RISE Committee, American Society for Clinical Pathology and the American Board of Pathology (2011) Senior pathology resident in-service examination scores correlate with outcomes of the American Board of Pathology certifying examinations. Am J Clin Pathol 136:499–506

Virchows Arch (2012) 461:3–11
DOI 10.1007/s00428-012-1254-7

INVITED EDITORIAL

Historical milestones in renal pathology

Jan J. Weening · J. Charles Jennette

Received: 11 April 2012 / Revised: 10 May 2012 / Accepted: 11 May 2012 / Published online: 3 June 2012
© The Author(s) 2012. This article is published with open access at Springerlink.com

Introduction

The history of renal pathology can be divided into two eras: one starting with the invention of the microscope and its application to renal tissue; the second with the introduction of the renal biopsy, which coincided with the development of electron microscopy and immunofluorescence microscopy that allowed the analysis of pathological changes in great detail with an eye for pathogenesis and pathophysiology. These two eras started in 1650 and 1950, respectively; an interval of no less than three centuries during which clinicians and pathologists struggled with a lack of clear understanding of the causes and evolution of renal disease. In concordance with the design of this series on the history of pathology, we focus primarily on the history of renal pathology before 1970.

The early phase

Renal histology

The origins of renal pathology can be traced back to the earliest descriptions of the microanatomy of the kidney by Marcello Malpighi in the year 1666 [1]. Based on his observations with the newly developed microscope, Malpighi (1628–1694; Fig. 1) hypothesized that the formation of urine took place in the kidneys through a filtering mechanism between blood and renal tubules [1]. Malpighi had studied medicine in Bologna and was professor in medicine first in Pisa and then at his alma mater and at the academy of Messina where he published his microscopic observations of various organs including the kidney. Before his illuminating studies, the relation between the kidney and the excretion of urine had been unclear and a subject of wild speculation as was true for renal function and disease in general.

The microscope was a new device at that time used by only a handful of researchers including Malpighi, Antoni van Leeuwenhoek, and Robert Hooke. Hooke had made an improved version of the instrument that was used by his Italian colleague. In combination with a talent for drawing and a sharp inventive mind, Malpighi was able to make giant strides forward, notwithstanding opposition from many colleagues at the time.

In spite of the seminal contributions of Malpighi based on the use of the microscope, his findings were completely overlooked by Giovanni Battista Morgagni who is regarded as the father of pathological anatomy. Morgagni was born in 1682 and lived and worked immediately after Malpighi, who had died in 1694. Morgagni was an anatomist and clinician and related postmortem findings to his clinical observations. He performed over 600 autopsies that form the basis for his major work *De Sedibus et causis morborum per anatomem indagatis* that was published in 1761 (Fig. 2) and had many reprints throughout Europe [2]. However, a complete understanding of the various diseases described in this book including those of the kidneys failed because of a lack of microscopic analysis, which Morgagni refused to rely on as an important tool.

J. J. Weening
Department of Pathology,
Erasmus MC University Medical Center,
Rotterdam, The Netherlands

J. J. Weening (✉)
Department of Pathology, Tergooiziekenhuizen,
Hilversum, The Netherlands
e-mail: jweening@tergooiziekenhuizen.nl

J. C. Jennette
Department of Pathology and Laboratory Medicine,
University of North Carolina at Chapel Hill,
Chapel Hill, NC, USA

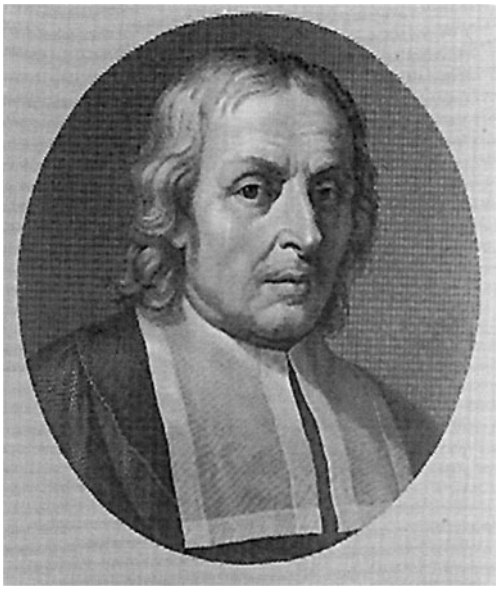

Fig. 1 Marcello Malpighi, approx 1660. From the Istituto e Museo di Storia della Scienza, Museo Galileo, Firenze, Italy

Malpighi's work was taken to a higher level by William Bowman, an English physician (1816–1892) who would later become a renowned ophthalmologist but devoted his early scientific life to the study of anatomy and physiology of the human body. One of his major contributions was the description of the components of the proximal part of the nephron with the periglomerular capsule (later named after him) as it is connected to the proximal tubule allowing the escape of filtrate produced by the glomerular capillary network (Figs. 3 and 4) [3].

Clinical nephrology

During the time of Bowman's early work, Richard Bright (1789–1858) together with John Bostock in England, Pierre Francois Rayer in France, and Friedrich Theodor von Frerichs in Germany studied patients with kidney diseases in great detail by correlating clinical symptoms and chemical derangements in blood and urine [4–7]. Pathology was limited to macroscopy and its contribution to diagnosis was therefore limited. Edema (dropsy as it was termed by Bright), hypertension, hematuria, oliguria, albuminuria, and uremia were quite well described but the underlying processes remained obscure. We now know that these symptoms can be caused by primary or secondary renal disease, affecting the glomeruli, the tubules, or the interstitium based on many different underlying events, which can only be recognized by microscopic analysis. The philosophy held at that time, however, was that in disease, functional alterations led to visible changes, and the latter, being secondary, were considered of less importance.

Richard Bright described three main macroscopic appearances of the diseased kidneys and tried to classify renal diseases accordingly [4] but admitted that he did not know whether these were mere stages of one disease or the faces of many different diseases from acute inflammatory to degenerative to sclerotic. Carl von Rokitansky, the famous pathologist from Vienna (1809–1878), took this to an extreme and used no less than eight classes of renal disease in albuminuric patients, one of which was renal amyloidosis [8]. Clearly, until microscopic analysis was applied to the pathological diagnosis of patients with various clinical syndromes, a rational classification of renal diseases was impossible.

Renal pathology (1850–1900)

The contribution of pathology was on its way, but it took many steps to achieve a level of refinement necessary to understand what is really going on in diseased renal tissues allowing a precise diagnosis of renal disease. Microscopic evaluation of renal tissue was facilitated by a number of technical advances in the mid nineteenth century. In 1837, Gabriel Valentin, a Swiss–German professor of physiology at Bern University, developed the technique of making thin tissue slides. Valentin described renal histology in patients who had died from massive proteinuria [9]. He observed no changes in the corpora Malpighia, but extensive accumulation of a grayish substance in the tubules soon to be recognized as fat, which subsequently led to the term lipoid nephrosis. In 1854 as a result of the invention of aniline dyes, more stains became available in addition to carmine, the only tissue stain that could be used until that year. Edwin Klebs, a pathologist who had worked with Virchow in Berlin, but had moved on to Switzerland and later to the US, introduced paraffin embedding in 1869 and used his improved histologic preparations to study renal

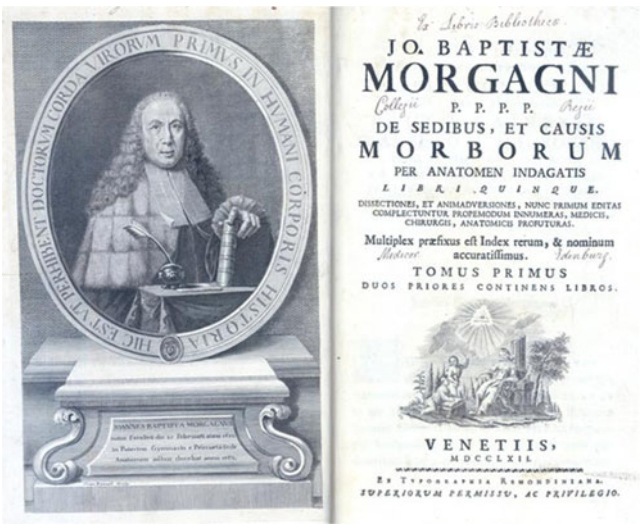

Fig. 2 Giovanni Baptista Morgagni's major work "DE SEDIBUS ET CAUSIS MORBORUM" (Ed. Venice, 1762). From the Bibliotheca Accademia Pugliese, Italy

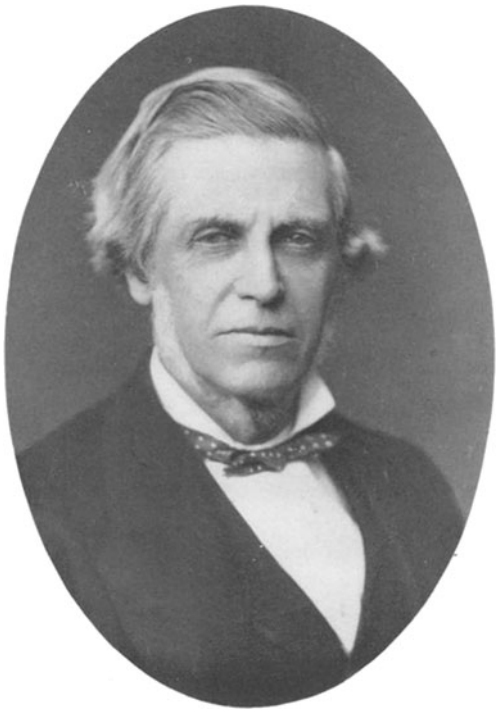

Fig. 3 Sir William Bowman, approx 1875, From the Science Photolibrary

disease. He coined the term glomerulonephritis in his pathology textbook [10].

The field then expanded quickly and from different sources evidence accumulated that pathological changes varied considerably between patients with similar "classes" of kidney disease. Based on microscopic analysis, several renal diseases were specifically identified including post-scarlatina glomerulonephritis, renal amyloidosis, and nephrosclerosis.

Cellular pathology

Important for the unraveling of tissue injury was the concept of cellular injury. The view of the cell as the basic unit of structure and function in the human body was first reported by Robert Remak [11], a Polish Jewish scientist, based on his observations that cell division led to cell renewal. In 1858 after first opposing this view, Rudolph Virchow applied it to his concept of cellular pathology [12], although he did not acknowledge the seminal work of Remak. The concept of cellular pathology was as valid for the kidney as for any other organ, but it took over a hundred years to unravel the characteristics of the variously differentiated cells of the nephron and their role in renal pathology.

Cellular physiology

Friedrich Henle (1809–1885) carefully dissected the microanatomy of the kidney (and many other organs) and discovered the tubular segment named after him as the loop of Henle [13]. He studied medicine at Heidelberg and Bonn, worked in anatomy in Berlin, and then became professor of anatomy in Zürich, Switzerland (Fig. 5). From there he went to Heidelberg to teach pathology, anatomy, and physiology. From Heidelberg, he published the *Handbuch der systematischen Anatomie des Menschen* [14], based on his concept that pathology and physiology were branches of one science. The cellular diversity of the tubular compartment became evident, ready to be unraveled by physiologists over the next century, starting with Carl Ludwig (1816–1895) and Claude Bernard (1813–1878), followed by Homer Smith (1895–1962), A. Newton Richards (1876–1966), Carl Gottschalk (1922–1997), and many others. Crucial for their studies were the contributions of chemists, among whom we can mention Donald van Slyke (1883–1971) and Lawrence Henderson (1878–1942), who developed techniques to allow microanalysis of plasma and urine.

Friedrich Theodor von Frerichs (professor of medicine at Berlin, 1819–1885) was perhaps the first to try to integrate clinical findings with microscopic analysis. This was taken further by his successor Friedrich von Mueller (Marburg, 1858–1941), and then by Volhard and Fahr [15].

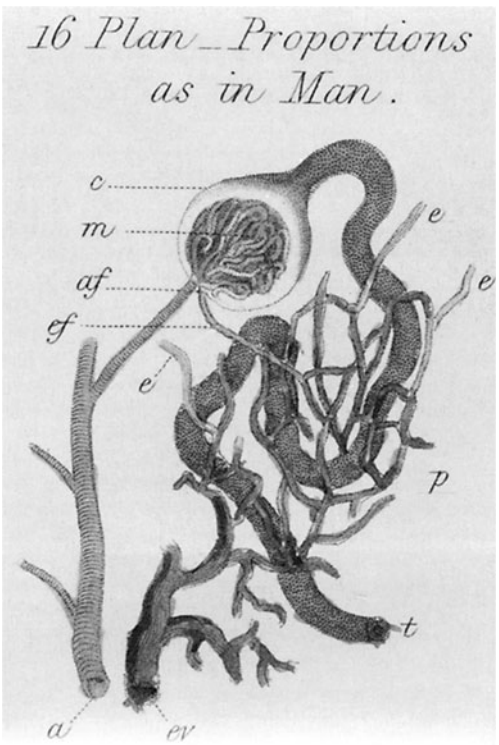

Fig. 4 Bowman's schematic drawing of the nephron. From The Science Photolibrary

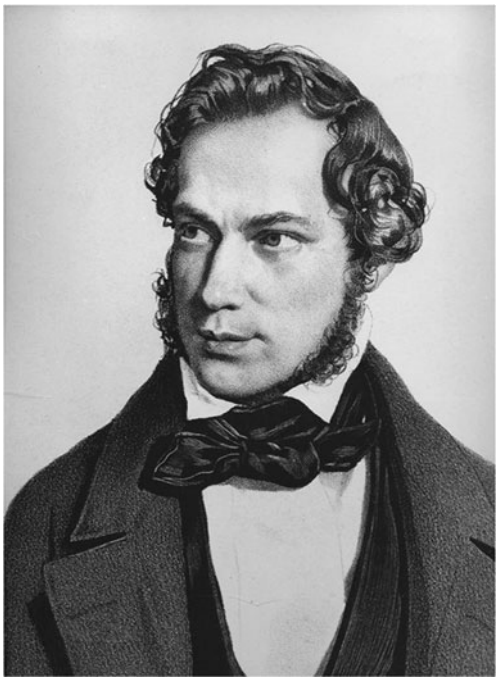

Fig. 5 Friedrich Gustav Jakob Henle (1809–1885). Henle worked in Berlin, Zürich, Heidelberg, and Göttingen. Robert Koch was his student and together they established the Henle–Koch postulates concerning the definition of disease-causing microbes. From Images from the History of Medicine

Renal pathology (1900–1950)

Theodor Fahr (1877–1945) was the first modern renal pathologist, documenting pathological changes in renal tissue with an exact eye for detail and relating these with the internist Franz Volhard to clinical expression of renal disease [15]. Fahr had trained in Giessen and received further training in Hamburg and Paris, where he worked with Ilya Metchnikoff, who in 1908 received the Nobel Prize for his work on phagocytosis. Fahr was made chairman of the institute of pathology at Hamburg University-Eppendorf in 1924 (Fig. 6).

The fruitful collaboration with Franz Volhard who worked at the university of Frankfurt-am-Main resulted in many publications, including the seminal *Die Bright'sche Nierenkrankenheit, Klinik, Pathologie und Atlas* (1914) [15] and his volume on the kidney in the series on pathological anatomy by Henke and Lubarsch [16].

In their classification of Bright'sche Nierenkrankenheiten, Fahr and Volhard classified renal disease into three major syndromes: the degenerative diseases (nephrosis), inflammatory diseases (nephritides), and chronic nephrosclerosis. Because of a lack of ultrastructural detail (the electron microscopy was not invented until 50 years later) and limited by only a superficial insight in renal inflammatory processes, the authors failed to recognize the glomerulus as the origin of proteinuria in patients with the nephrotic syndrome and placed too much emphasis on tubular reabsorption patterns coined lipoid nephrosis. However, by removing much of the confusion and controversies created by the publications of Bright and Morgagni, this new classification based on the combination of pathology and clinical expression of disease was a major improvement and became widely accepted.

Sir Arthur Ellis (1883–1966) published one of the earliest clinicopathologic studies of glomerular disease based on observations of the clinical courses of 600 patients with Bright's disease in the London Hospital including *postmortem* histological observations in 200 patients [17]. Ellis began his career in Toronto as a clinical chemist, trained in pathology at Western Reserve University in Cleveland, and eventually became a renowned professor of medicine at the University of London and Oxford before being knighted in 1953 for his contributions to the study of kidney disease. His multidisciplinary background in clinical chemistry, pathology, and internal medicine provided a unique perspective for making clinicopathologic correlations. He correlated clinical features, associated conditions (e.g., pharyngitis), blood and urine laboratory results, and histologic findings to propose two types of nephritis. Type I nephritis had an abrupt acute onset, often following an infection, with many but not all patients recovering. Type II nephritis had a more insidious onset characterized by edema and severe proteinuria. He described and illustrated with photomicrographs distinct patterns of glomerular injury that correlated with the clinical course, including glomerular hypercellularity with numerous neutrophils in

Fig. 6 Theodor Fahr as the director of the Institute of Pathology at the University of Hamburg. From Historical Archives of the University Hospital Hamburg-Eppendorf, Institute of Medical History, University Hamburg, Germany

acute type I nephritis, fibrinoid necrosis, and crescents in severe type I nephritis and focal and nodular sclerosis in type II nephritis.

Further insight in the etiology and pathogenesis of renal disease was hampered by the fact that only autopsy material was available for analysis, mostly revealing no more than the endpoint of diseases, obscuring their kinetics and evolution. In addition, more knowledge was required in the field of genetics, cell biology, and immunology before renal diseases could be understood by pathologists and nephrologists as they are today. An important step forward was the introduction of experimental pathology. In a similar way as animal autopsies had preceded the precise study of the human body, laboratory animal experimentation allowed the early twentieth century scientist to induce renal disease and study its evolution over time. It permitted modulation of disease and the study of clinical symptoms. Several experimental models of renal disease were thus developed, preparing the field for a rational interpretation of renal biopsies in man.

Experimental renal pathology

Experimental renal pathology has contributed immensely to the understanding of renal disease for over a hundred years. In 1888, Theodor Tuffier (Paris, 1857–1929) studied the effects of partial renal ablation on renal structure and function [18]. This model would be explored in detail by many investigators in the last quarter of the twentieth century, documenting the role of intracapillary hypertension, glomerular cellular injury, and accelerating loss of nephrons, as a model for progressive renal disease [19–21].

A major impetus for the understanding of renal disease was derived from studies on infection and immunity. Infectious diseases had been by far the most important threat to health and society for ages and still were around the turn of the nineteenth to twentieth century. As of the nineteenth century, clinical and experimental works successfully started to reveal the basis of infection and immunity. Around 1900, the immune response was recognized as having a dark side causing disease by inflammation, anaphylaxis, allergy, and autoimmune reactions.

These early advances in immunology received much attention, were honored with Nobel prizes, and had their immediate impact on the renal field as on every other part of medicine. The Institut Pasteur in Paris was one of the centers of research in this field. It was there that Theodor Fahr worked with Metchnikoff and where kidney disease was studied in laboratory animals exposed to anaphylactic substances [22–24].

Also at Pasteur's Institute, W. Lindemann in 1900 developed a model of autoimmune glomerulonephritis by injecting rabbits with heterologous antiserum raised in guinea pigs against rabbit kidney [25]. This model was studied in depth by M. Masugi in 1933 [26] and was important in the new era that started in 1950. Between 1950 and 1960, *serum sickness-like glomerulonephritis* was identified as the first immune-mediated disease of the kidney caused by deposition of circulating immune complexes, a characteristic phenomenon in chronic infectious diseases and autoimmune diseases [27, 28].

The modern era

Renal pathology (1950–1970)

Three centuries had passed since Malpighi first observed the complex microanatomy of the renal glomerulus. Three centuries later, the almost simultaneous development of techniques to safely obtain renal tissue from a patient by means of a percutaneous needle biopsy and to analyze the tissue not only by light microscopy but also by electron microscopy and immunofluorescence microscopy suddenly provided the structural basis for diagnosis of the many different inflammatory and non-inflammatory, acute and chronic, relapsing and remitting, proteinuric and hematuric, hypertensive and non-hypertensive, and all other renal diseases that had been impossible to classify in an orderly fashion thus far. Within five decades, many questions were going to be answered, although several enigmas still remain today.

The renal needle biopsy was first used for clinical diagnosis of patients by Nils Alwall from Lund, Sweden in 1944. Alwall was successful in obtaining renal tissue by an aspiration technique from his first 13 patients but when 1 of them died from complications, he decided to no longer pursue the technique and did not publish his work until 1952 [29]. His efforts were continued by Paul Iversen and Claus Brun from Copenhagen who published their first series of renal biopsies in 1951 [30] and by Robert Kark from Chicago.

Robert M. Kark (Fig. 7), originally from Cape Town, a renowned rugby player while a medical student at Guy's Hospital, London, had developed an interest in nutrition during a fellowship at Harvard. In World War II, he used this expertise in nutrition to help develop K-rations and foiled a sabotage attempt on a plane to be used by Winston Churchill. Following the war, he became an expert on kidney disease at Rush-Presbyterian-St Luke's Medical Center in Chicago. Kark, who had met Iversen at a congress in Copenhagen in 1950, developed together with Muehrcke and Franklin a technique using the Vim Silverman needle (a cutting needle instead of an aspiration needle) in prone patients which proved to be much more successful than Alwall's procedure [31]. In collaboration with one of the first modern pathologists to specialize in renal pathology, Conrad Pirani, the Chicago group exploited the new development effectively, published widely, and established the Chicago unit as a teaching center for this new technique [31, 32]. The pathology world was at first skeptical, or should we

Fig. 7 Robert M. Kark who with Robert Muehrcke and renal pathologist Conrad Pirani pioneered the use of the renal biopsy in patient care. From Images from the History of Medicine

say hostile, to the idea of a tiny renal biopsy on which a full diagnosis was supposed to be made ("the smaller the biopsy, the more they want to know" is a frequently heard complaint in the practice of pathology). But several pathologists took up the challenge and successfully collaborated with nephrologists to advance the field of nephropathology.

Immunofluorescence microscopy as a technique to detect tissue-bound immune deposits had been developed by Coons and Kaplan in 1950 [33]. In 1955, Mellors first applied the technique to renal tissue [34]. Many renal diseases, particularly the various forms of glomerulonephritis, are antibody- and immune complex-mediated and the newly developed technique allowed for the first time observation of immune reactants that were contributing to the pathogenesis of many different forms of glomerulonephritis [35]. During the 1960s, Frank Dixon, Fred Germuth, and Robert McCluskey integrated the new knowledge about the pathogenesis of immune complex-mediated glomerulonephritis into concepts of diagnostic renal pathology.

Electron microscopy was new in the field as well and the first observations of ultrastructural changes in glomerular disease were published in 1957 [36].

The fenestrated endothelium, the multiple-layered glomerular basement membrane, the mesangium, and the intricate structure of the arborizing and interdigitating podocytes were discovered by thrilled pathologists staring through the binoculars of the first generation of electron microscopes [36, 37] (Fig. 8). Conrad Pirani in Chicago, Ramzi Cotran from Boston and Jacob Churg and Edith Grishman in New York were early pioneers in applying electron microscopy to renal biopsy diagnosis.

With the advent of the renal biopsy, and the application of better histology methods and electron microscopy, the understanding of the histopathology of renal disease developed rapidly at many centers around the world. During the 1950s, the Renal Association in London had monthly meetings at the Ciba Foundation where frequent discussions of renal biopsy findings and clinical correlations were discussed. This presaged the 1961 CIBA Foundation Symposium on Renal Biopsy in London, which was a landmark event in the maturation of the field of renal pathology. The session was chaired by Arnold Rich and pioneering renal pathologists who attended included A. Bergstrand (Sweden), R. Habib (France), R.H. Heptinstall (UK), R.B. Jennings (USA), H.Z. Movat (Canada), and C.L. Pirani (USA) [38]. Knowledge of renal pathology advanced to the stage that comprehensive textbooks became available to provide guidance to nephrologists and pathologists involved in the care of patients with kidney disease. Preeminent among these was Robert H. Heptinstall's (Fig. 9) *Pathology of the Kidney*, first published in 1966 [39], which has cataloged the progression of knowledge in nephropathology through seven editions [40]. Robert H. Heptinstall began his medical career in London as a surgeon, but after World War II he trained as a pathologist. As a young pathologist at St. Mary's in London he collaborated with the renowned internist George Pickering on clinicopathologic studies of hypertensive

Fig. 8 Early generation electron microscope. From Siemens, 1955; Science Museum London, UK

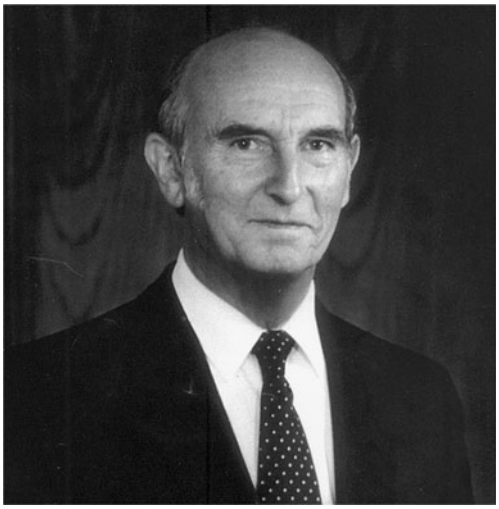

Fig. 9 Robert Heptinstall whose ground-breaking textbook *Pathology of the Kidney* influenced generations of nephropathologists and nephrologists. From Johns Hopkins University, Baltimore MD, USA

nephropathy, which was the beginning of a lifelong focus on renal pathology. With radiologist John Hodson, he worked on the pathogenesis of reflux nephropathy. In 1954 he did a fellowship at Johns Hopkins with Arnold Rich and Fred Germuth studying immune complex glomerulonephritis and in 1959 with Harry Goldblatt in Cleveland. He moved permanently to USA in 1960, briefly at Washington University in St. Louis and then at Johns Hopkins for the remainder of his illustrious career. At Hopkins he continued his research on hypertensive nephropathy and also studied pyelonephritis. His lasting legacy to renal pathology is the textbook that he first published in 1966 [39]. Several valuable books on renal pathology had been published already but his was the first to emphasize observations in renal biopsies rather than autopsies. The first edition primarily covered findings by light microscopy and electron microscopy, but the second edition in 1974 included immunofluorescence microscopy observations as well as a chapter by Robert McCluskey specifically devoted to immunologic mechanisms of renal disease [41]. These books by Heptinstall heralded the current era in renal pathology.

Renal pathology (1970 onward)

In the 1970s, the relatively few pioneers of renal pathology passed the baton to eager younger renal pathologists too numerous to name. Between 1970 and 2010, etiology, pathogenesis, clinicopathological correlations, and classification were established for renal diseases as diverse as lupus nephritis [42, 43], post-infectious glomerulonephritis [44], multiple forms of membranoproliferative glomerulonephritis [45], anti-GBM disease [46, 47], membranous glomerulopathy [48–50], IgA nephropathy [51–53], ANCA-associated vasculitis and glomerulonephritis [54–56], focal segmental glomerulosclerosis and other podocytopathies [57–59], hereditary renal diseases [47], hemolytic uremic syndrome [60], tubulointerstitial disease [61], renal injury in the kidney transplant patient [62], and many others (Table 1). Today's renal pathologists continue to build on the strong foundation laid by the pioneers of renal pathology to advance our knowledge of the pathology and pathogenesis of kidney diseases and to use this to improve the management of patients.

Perspective

In the almost 100 years since the pioneering clinicopathologic studies of Volhard the internist and Fahr the pathologist, tremendous advances have been made in our understanding

Table 1 Time table of seminal discoveries in renal pathology

1666	The glomerulus	[1]
1842	The nephron	[3]
1827	Clinical renal syndromes	[4]
1914	First renal histopathology classification	[15]
1900–1950	Experimental autoimmune glomerulonephritis	[25, 26]
1950–1960	Renal biopsy	[29–32]
1950–1970	Immunofluorescence microscopy, electron microscopy	[33–37]
1960–present	Immune complex diseases, anti-GBM, lupus nephritis, post-infectious GN, IgAN	[27, 28, 42–47, 51]
1975–present	Focal segmental glomerulosclerosis	[19–21, 58, 59]
1980–present	ANCA disease	[54–56]
1980–present	Membranous glomerulopathy pathogenesis	[48–50]
1990–2009	Hemolytic uremic syndrome	[60]
1990–present	Podocyte pathobiology	[57, 59]
1990–present	Classification of diseases of the transplanted kidney	[62]

of the pathology and pathophysiology of kidney disease and the care of patients with kidney disease. These advances have come as a result of intense collaboration between nephrologists and nephropathologists and have been facilitated by sharing new knowledge disseminated through national and international scientific societies, journals, and annual congresses in the field of pathology and nephrology. Advances in renal pathology also have been fostered in particular by the vitality of the Renal Pathology Society, which is international, and the Nephropathology Working Group of the European Society of Pathology. International collaborative efforts to benefit from advances in nephropathology have not been confined to economically well-off countries but also have been extended to the developing countries through the International Society of Nephrology [63]. Reviewing the history of renal pathology reveals how an entire field can only advance by the contributions of many, through implementing new technical developments, and fostered by the fortune of economic prosperity.

Acknowledgments The authors thank Dr. Joris Grond for the helpful comments.

Conflict of interest We declare that we have no conflict of interest.

Open Access This article is distributed under the terms of the Creative Commons Attribution License which permits any use, distribution, and reproduction in any medium, provided the original author(s) and the source are credited.

References

1. Malpighi M (1666) De Viscerum Structura execitatio anatomica. Bologna
2. Morgagni GB (1761) De Sedibus et causis morborum per anatomem indagatis. Venice
3. Bowman W (1842) On the structure and use of the Malpighian bodies of the kidney, with observations on the circulation through that gland. Philos Trans R Soc 132:57–80
4. Bright R (1827) Reports of medical cases selected with a view of illustrating the symptoms and cure of disease by a reference to morbid anatomy. Longman, Rees, Orme and Green, London
5. Bostock J (1803) Observations on the urine. London Med Phys J 9:349–355
6. Rayer PFO (1840) Traite des maladies des reins, vol II. Balliere, Paris
7. Frerichs FT (1851) Die Bright'sche Nierenkrankheitund deren Behandlung; eine Monographie. F Vieweg und Sohn, Braunschweig
8. Rokitansky KF (1846) Handbuch der allgemeinen pathologischen anatomie. Braumiller & Seidel, Wien
9. Valentin G (1837) Repertorium fuer anatomie und physiologie. Huber, Bern
10. Klebs TAE (1870) Handbuch der pathologischen anatomie. August Hirschwald, Berlin, pp 644–648
11. Remak R (1855) Untersuchungen uber die Entwickelung der Wirbelthiere. G Reimer, Berlin
12. Virchow R (1858) Die Cellular-Pathologie in ihrer Begründung auf physiologische und pathologische Gewebelehre. A Hirschwald, Berlin
13. Henle J (1862) Zur Anatomie der Niere. Dieterichschen Buchhandl, Goettingen
14. Henle J (1876) Handbuch der Systematischen Anatomie des Menschen. Druck und Verlag von Friedrich Vieweg und Sohn, Braunschweig
15. Volhard F, Fahr T (1914) Die Brightsche Nierenkrankheit. Klinik, Pathologie und Atlas. Julius Springer, Berlin
16. Fahr T (1925) Die Pathologische Anatomie des Morbus Brightii. In: Henke F, Lubarsch O (eds). Handbuch der speziellen pathologischen anatomie und histology, Vol VI/1. Julius Springer, Berlin, p. 177-178, 368-405
17. Ellis A (1942) Natural history of Bright's disease. Clinical, histological and experimental observations. Lancet 1:1–7
18. Tuffier T (1889) Etudes experimentales sur la Chirurgie des Reins. G. Steinhill, Paris
19. Elema JD, Arends A (1975) Focal and segmental glomerular hyalinosis and sclerosis in the rat. Lab Invest 33:554–561
20. Hostetter TH, Olson J, Rennke HG, Venkatachalam MA, Brenner BM (1981) Hyperfiltration in remnant nephrons: a potentially adverse response to renal ablation. Am J Physiol 241:F85–F93
21. Olson J, Hostetter TH, Rennke HG, Brenner BM, Venkatachalam MA (1981) Altered glomerular permselectivity and progressive sclerosis following extreme ablation of renal mass. Kidney Int 22:112–126
22. von Pirquet CE, Schick B (1905) Die serumkrankheit. Deuticke, Vienna
23. Schick B (1907) Die nachkrankheiten der Scharlachs. Jahrb Kinderheilk 65:132–172
24. Richet C (1902) Des effets anaphylactiques de l'actinotoxine sur la pression arteriolle. Compt Rendu Soc Biol 54:837
25. Lindemann W (1900) Sur le mode d'action de certain poisons renaux. Ann Inst Pasteur 14:49–59
26. Masugi M, Tomizuka Y (1931) Ueber die spezifischen zytotoxischen veraenderungen der niere und der leber durch das spezifische antiserum zugleich ein beitrag zur pathogenese die glomerulonephritis. Trans Jpn Pathol Soc 21:329–341
27. Germuth FG Jr (1953) A comparative histologic and immunologic study in rabbits of induced hypersensitivity of the serum sickness type. J Exp Med 97:257–282
28. Dixon FJ, Feldman JD, Vasquez JJ (1961) Experimental glomerulonephritis. The pathogenesis of a laboratory model resembling the spectrum of human glomerulonephritis. J Exp Med 113:899–920
29. Alwall N (1952) Aspiration biopsy of the kidney, including a report of a case of amyloidosis diagnosed in 1944 and investigated at autopsy in 1950. Acta Med Scandinavica 143:430–435
30. Iversen P, Brun C (1951) Aspiration biopsy of the kidney. Am J Med 11:324–330
31. Kark RM, Muehrcke RC (1954) Biopsy of the kidney in prone position. Lancet 266:1047–1049
32. Muehrcke RC, Kark RM, Pirani CL (1955) Biopsy of the kidney in the diagnosis and management of renal disease. N Engl J Med 253:537–546
33. Coons AH, Kaplan MH (1950) Localization of antigen in tissue cells; improvements in a method for the detection of antigen by means of fluorescent antibody. J Exp Med 91:1–13
34. Mellors RC (1955) Histochemical demonstration of the in vivo localization of antibodies: antigenic components and the pathogenesis of glomerulonephritis. J Histochem Cytochem 3:284–289
35. Freedman P, Peters JH (1959) Immunologic aspects of renal disease. N Engl J Med 261:1275–81
36. Farquhar MG, Vernier RL, Good RA (1957) An electron microscope study of the glomerulus in nephrosis, glomerulonephritis and lupus erythematosus. J Exp Med 106:649–660

37. Karnovsky MJ (1979) The ultrastructure of glomerular filtration. Ann Rev Med 30:213–224
38. Cameron JS and Hicks J. The introduction of renal biopsy into nephrology from 1901 to 1961: a paradigm of the forming of nephrology by technology. Am J Nephrol 17:347-358
39. Heptinstall RH Pathology of the kidney (1966) Little, Brown and Company, Boston
40. Jennette JC, Olson JL, Schwartz MM, Silva FG (2007) Heptinstall's pathology of the kidney. Lippincott Williams and Wilkins, Philadelphia
41. Heptinstall RH Pathology of the kidney (1974) Little, Brown and Company, Boston
42. Churg J, Sobin LH (1982) Lupus nephritis. Renal disease, classification and atlas of glomerular diseases Igaku-Shoin, New York pp 127-149
43. Weening JJ, D'Agati VD, Schwartz MM et al (2004) The classification of glomerulonephritis in systemic lupus erythematosus revisited. Kidney Int 65:521–530
44. Nasr SH, Markowitz GS, Stokes MB et al (2008) Acute postinfectious glomerulonephritis in the modern era: experience with 86 adults and review of the literature. Medicine 87:21–32
45. Sethi S, Fervenza FC (2012) Membranoproliferative glomerulonephritis, a new look at an old entity. N Engl J Med 366:1119–1131
46. Lerner RA, Glassock RJ, Dixon FJ (1967) The role of antiglomerular basement membrane antibody in pathogenesis of human glomerulonephritis. J Exp Med 126:989–1004
47. Hudson GB, Tryggvason K, Sundaramoorthy M, Neilson EG (2003) Alport's syndrome, Goodpasture's syndrome, and type IV collagen. N Engl J Med 348:2543–2556
48. van Damme BJC, Fleuren GJ, Bakker WW et al (1978) Experimental glomerulonephritis n the rat induced by antibodies to tubular antigens. V. Fixed glomerular antigens in the pathogenesis of heterologous immune complex glomerulonephritis. Lab Invest 38:502–510
49. Debiec H, Guignonis V, Mougenot B et al (2002) Antenatal membranous glomerulonephritis due to anti-neutral endopeptidase antibodies. N Engl J Med 346:2053–2060
50. Beck LH, Bonegio RGB, Lambeau G et al (2009) M-type phospholipase A2 receptor as target antigen in idiopathic membranous nephropathy. N Engl J Med 361:11–21
51. Berger J, Hinglais (1968) Les depots intracapillaires d'IgA–IgG. J Urol Nephrol 74:694–695
52. Cattran DC et al (2009) The Oxford classification of IgA nephropathy: rationale, clinicopathological correlations and classification. Kidney Int 76:536–546
53. Roberts IS et al (2009) The Oxford classification of IgA nephropathy: pathology definitions, correlations and classification. Kidney Int 76:546–556
54. Davies DJ, Moran JE, Niall JF, Ryan GB (1982) Segmental necrotising glomerulonephritis with antineutrophil antibody: possible arbovirus aetiology? Br Med J (Clin Res Ed) 285:606
55. van der Woude FJ, Rasmussen N, Lobatto S et al (1985) Autoantibodies against neutrophils and monocytes: tool for diagnosis and marker of disease activity in Wegener's granulomatosis. Lancet I:425–529
56. Falk RJ, Jennette JC (1988) Anti-neutrophil cytoplasmic autoantibodies with specificity for myeloperoxidase in patients with systemic vasculitis and idiopathic necrotizing and crescentic glomerulonephritis. N Engl J Med 318(25):1651–1657
57. Pavenstaedt H, Kriz W, Kretzler M (2003) Cell biology of the podocyte. Physiol Rev 83:253–307
58. Churg J, Habib R, White RHR (1970) Pathology of the nephrotic syndrome in children. A report of the international study of kidney disease in children. Lancet 1:1299–1302
59. D' Agati VD, Kaskel FJ, Falk RJ (2011) Focal segmental glomerulosclerosis. N Engl J Med 365:2398–2411
60. Noris M, Remuzzi G (2009) Atypical haemolytic-uremic syndrome. N Engl J Med 361:1676–1687
61. Zeisberg M, Neilson EG (2010) Mechanisms of tubulointerstitial fibrosis. J Am Soc Nephrol 21:1819–1834
62. Solez K (2010) History of the Banff classification of allograft pathology as it approaches its 20th year. Curr Opin Organ Transplant 15:49–51
63. Weening JJ, Brenner BM, Dirks JH, Schrier RW (1998) Toward global advancement of medicine: the International Society of Nephrology experience. Kidney Int 54:1017–1021

Virchows Arch (2012) 461:13–26
DOI 10.1007/s00428-012-1255-6

REVIEW AND PERSPECTIVES

Interpretation of needle biopsies of the kidney for investigation of renal masses

Benoît Lhermitte · Laurence de Leval

Received: 1 February 2012 / Revised: 17 April 2012 / Accepted: 18 May 2012 / Published online: 8 June 2012
© Springer-Verlag 2012

Abstract The development of new therapeutic options for renal tumors has lead to the need of a pretherapeutic diagnosis for an increasing proportion of patients presenting with a renal mass. This need is particularly important for a small, incidentally discovered renal mass (less than 4 cm) as it can be a benign lesion in a significant percentage of cases. Recent studies have shown that needle biopsy is an accurate and safe method allowing for a precise histopathological diagnosis of the mass in most cases. The aims of the biopsy are (1) to assess the benign or malignant nature of the lesion, (2) to assess the primary or secondary nature of the lesion, and (3), in case of a primary malignancy, to determine histological prognostic factors, such as the tumor type. This review, based on the most recent literature and our own experience, is intended to provide a practical approach to the diagnosis, relying on appropriate morphologic assessment and the use of immunohistochemistry.

Keywords Kidney · Tumor · Core biopsy · Renal cell carcinoma · Immunohistochemistry

Introduction

In the past, complete surgical resection (radical nephrectomy) without preoperative histological assessment has long been considered the gold standard for the management of renal masses, as indeed the majority of solid renal tumors are malignant primaries for which surgical management allows optimal staging and treatment. In that context, core needle biopsies were mostly restricted to situations where the indication of surgery was questionable, i.e., in cases of high suspicion of a benign tumor, metastasis, lymphoma, or abscess [1]. Other factors reported to compound preoperative biopsies included an overestimated risk of noncontributive samples, tumor dissemination along the needle track, and hemorrhagic complications [2].

For the past few years, the number of biopsies for renal masses has virtually exploded. The increased use of cross-sectional imaging for other pathologies has lead to the discovery of renal masses, especially of small size, without radiological criteria allowing to determine the nature of the tumor. Nowadays, more than half of all renal tumors are incidentally detected [3]. Moreover, a significant minority (between 15 and 35 %) of these small renal masses, by definition less than 4 cm, consist of benign lesions which do not require surgical removal [4–7]. At the same time, new therapeutic options including partial nephrectomy, imaging-guided ablative therapy (using radiofrequency ablation, high intensity focused ultrasound, or cryotherapy), active surveillance, or systemic neoadjuvant therapy have emerged for the treatment of renal cell carcinoma [8, 9]. In these cases (with the exception of partial nephrectomy), these new therapeutic options require pretherapeutic pathological diagnosis. Moreover, the diagnostic accuracy of the biopsy has increased in the last decade [10], as a result of both the improvement in biopsy techniques and the development of immunohistochemistry panels allowing the identification of almost all tumor subtypes and the newly described entities.

There are currently numerous conditions for which the indication of a biopsy can be discussed: (1) the discovery of a small renal mass because it can correspond to a benign lesion for which a partial or radical nephrectomy would not

B. Lhermitte (✉) · L. de Leval
University Institute of Pathology,
Centre Hospitalier Universitaire Vaudois (CHUV),
25 rue du Bugnon,
1011, Lausanne, Switzerland
e-mail: benoit.lhermitte@chuv.ch

be required; (2) in metastatic patients eligible for a systemic therapy with no previous pathology documentation, in order to select therapy by classifying the tumor; (3) a previous history of extrarenal malignancy raising the differential diagnosis of a metastasis or when suspecting lymphoma; (4) a mass associated with a febrile urinary tract infection, in this situation the differential diagnosis includes renal abscess or an inflammatory pseudotumor such as xanthogranulomatous pyelonephritis

Therefore, the aim of a pretherapeutic biopsy is to determine (1) the benign or malignant nature of the lesion, (2) the primary or secondary nature of a malignant lesion, and (3) the tumor type. Lesions that are mostly cystic are currently not an indication for pretherapeutic biopsy because of the difficulty to obtain representative samples of the lesion. The prognosis of cystic lesions can be determined to some extent by appropriate imaging modalities (mainly ultrasound, CT scan, and MRI) using Bosniak's classification [11].

This review is intended to provide a practical approach to the diagnosis of renal core biopsies performed for investigating kidney masses. It is based on the most recent literature concerning the subject and on our own experience.

Technical considerations and diagnostic accuracy

Biopsies are generally performed by the radiologist under US or helical CT guidance, with the patient in prone position under local anesthesia. CT is performed immediately after needle removal to exclude postbiopsy complications. The recommendation is to use 18-gauge (G) needles (yielding 1.7×0.1-cm cores) and to obtain at least two cores in the periphery of the tumor and in nonnecrotic areas [12]. In a prospective ex vivo study conducted on nephrectomy specimens, aimed to compare the yield of 14-, 18-, and 20-G core needle biopsies, Breda et al. [13] found that three biopsies with 14- and 18-G needles allowed to obtain an adequate diagnosis of solid renal masses in 94 and 97 % of the cases, respectively, while the yield of 20-G needles was significantly inferior (81 %). Although fine needle aspiration is not the topic of this review, it is worth mentioning that in some centers, smear preparations are examined extemporaneously to verify the adequacy of the sample. Others use it as a diagnostic tool, with an accuracy close to that of needle biopsies, especially in conjunction with immunocytology [16].

The samples are fixed in formalin and submitted as one core per cassette for standard processing and paraffin embedding. In our institution, sections from three levels are stained with hematoxylin and eosin for histopathological evaluation, and four additional sections per level are kept unstained for special stains and/or immunohistochemistry.

When an adequate sample is obtained, the ability to distinguish benign from malignant lesions is excellent and almost reaches 100 % of the cases. Indeed, in an in vivo study, all oncocytomas were well identified [14]. The ability to determine the histological subtype of renal cell carcinoma (RCC) is excellent, especially when adding adequate immunostain with an accuracy of 90 % overall and 99 % among the four most common subtypes [15].

Interpretation

Renal cell tumors are currently classified according to the World Health Organization (WHO) system which defines tumor entities based on their pathological features, clinical behavior, and genetic alterations (Table 1) [17]. The histopathological diagnosis primarily relies on the examination of routinely stained sections, by taking into account (1) the cytologic features of the tumor cells (i.e., clear, eosinophilic, chromophobic, oncocytic, spindle cells), and (2) the tumor architecture (i.e., solid, acinar, papillary). Assessment of the growth pattern and associated stroma may be of interest for the identification of some renal cell tumor entities and also in the differential diagnosis with non-renal cell tumors.

Clear cell tumors

Clear cell renal cell carcinoma

Clear cell renal cell carcinoma (CCRCC), by far the commonest malignant renal epithelial neoplasm, represents approximately 60 % of renal cortical tumors. Importantly, however, all clear cell lesions are not clear cell renal cell carcinomas, and clear cell renal cell carcinoma is not in fact always composed of clear cells, a reason why some authors advocate the designation "conventional" renal cell carcinoma. Nevertheless, the recommended nomenclature according to the WHO classification remains "clear cell" renal cell carcinoma [17].

In typical cases, the biopsy shows a proliferation of clear cells, possibly admixed with an eosinophilic granular cell component, with a solid or acinar architecture. A prominent delicate and branching vascularization network is characteristic and almost always observed. Secondary changes such as focal fibrosis or hyalinization, geographic necrosis, and focal hemorrhage are frequent. When typical features are observed, the diagnosis is straightforward by morphology and additional ancillary techniques are usually not necessary (Fig. 1). When facing unusual morphology (predominantly granular eosinophilic component or predominantly papillary architecture), immunohistochemistry is helpful to confirm the diagnosis.

Table 1 Classification of renal cell tumors (adapted from the WHO histological classification of tumors of the kidney, 2004)

Renal cell tumors
Clear cell renal cell carcinoma
Multilocular clear cell renal cell carcinoma
Papillary renal cell carcinoma
Type I
Type II
Chromophobe renal cell carcinoma
Carcinoma of the collecting ducts of Bellini
Renal medullary carcinoma
Xp11 translocation carcinomas
Carcinoma associated with neuroblastoma
Mucinous tubular and spindle cell carcinoma
Renal cell carcinoma, unclassified
Papillary adenoma[a]
Oncocytoma[a]
Tumors recently described, not yet listed in the WHO classification
Clear cell papillary renal cell carcinoma
Clear cell carcinoma with leiomyomatous stroma
Oncocytic type papillary carcinoma
Metanephric tumors
Nephroblastic tumors
Mesenchymal tumors
Mixed mesenchymal and epithelial tumors
Neuroendocrine tumors
Hematopoietic and lymphoid tumors
Germ cell tumors
Metastatic tumors

[a] Benign lesions

CCRCC expresses pan-cytokeratins (for example those recognized by the AE1/AE3 cocktail), epithelial membrane antigen (EMA), vimentin, and CD10 in a membranous distribution. Alpha-methyl CoA racemase (AMACR) expression is detected in up to 68 % but usually more focally than in papillary carcinoma. Cytokeratin 7 (CK7) expression is weak and focal. Less than 10 % of the cases show focal positivity for CD117 while the majority of cases are negative. HMB-45 is negative. Antibodies raised against carbonic anhydrase IX (CA-IX), a membranous enzyme acting to regulate both intracellular and extracellular pH and whose expression is induced by hypoxie, have been recently characterized and found of interest for diagnostic purposes. The majority (>85 %) of CCRCC strongly express CA-IX [18, 19]. Importantly, only a membranous pattern is characteristic for clear cell RCC, while cytoplasmic staining is not specific and often observed focally with preferential distribution around necrotic areas in other nonclear cell renal cell neoplasms.

Nuclear grading as per the Fuhrman grading system should be assigned because it is one of the most important prognostic factors in organ-confined carcinoma [20] and because some authors advocate that in elderly and unfit patients, low-grade carcinoma can be initially observed or ablated rather than operated on, while the former treatments are not appropriate for high-grade RCC [7]. However, the concordance is low (less than 50 %) between the grades assessed on paired biopsies and surgical specimens, reflecting intratumor heterogeneity [21]. Alternatively, several authors have advocated to combine lower grades (1 and 2) and higher grades (3 and 4) into a two-tier grading system, which has been shown to reduce the discrepancies between pre- and postsurgical grade assessments [21].

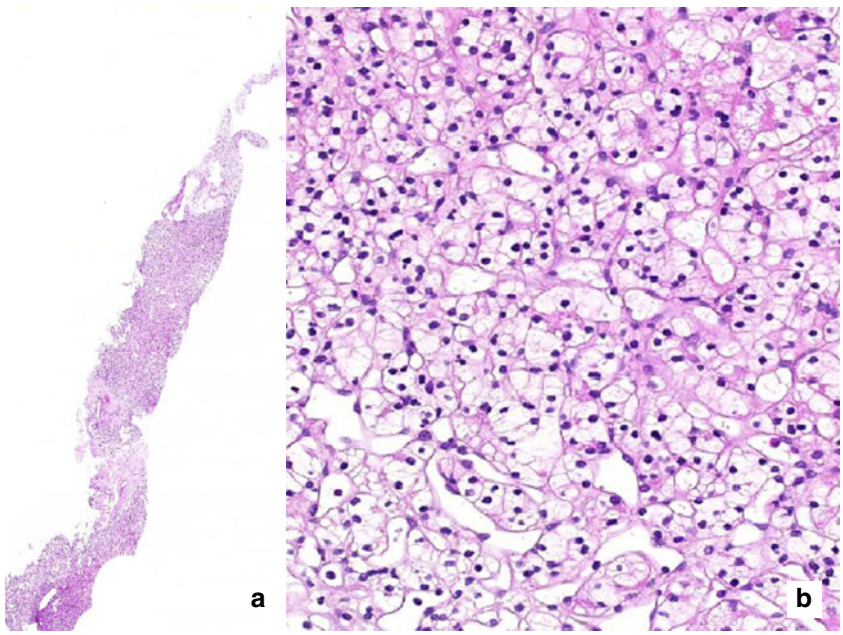

Fig. 1 Core biopsy of a clear cell RCC. Low magnification shows a solid epithelial proliferation (**a**, hematoxylin and eosin, ×2). Higher magnification shows a proliferation of large polygonal cells with clear or finely granular cytoplasm, with round hyperchromatic nuclei (**b**, hematoxylin and eosin, original magnification ×12). In such a case, no ancillary techniques are necessary to confirm the diagnosis

Differential diagnosis

Clear cell RCC can be confused with a variety of other benign or malignant lesions composed of clear cells (Table 2) [22]. In case of diagnostic problems, immunohistochemistry is a helpful adjunct to careful morphologic evaluation to distinguish between the several diagnostic possibilities (Table 3).

Chromophobe renal cell carcinoma Chromophobe carcinoma is generally composed of an admixture of clear and eosinophilic cells. The cellular contours are sharply delineated with thick membranes accounting for a pseudovegetal aspect. In the clear cells, the nuclei are characteristically wrinkled. Vascularization is less prominent than in CCRCC. The immunohistochemical profile differs from that of CCRCC since chromophobe carcinoma usually does not diffusely express vimentin, CD10, or CA-IX, while conversely CK7 and CD117 are both diffusely expressed.

Clear cell papillary renal cell carcinoma Clear cell papillary renal cell carcinoma, first described in the setting of end-stage kidney diseases, may also occur in the absence of impaired renal function. The few cases with documented clinical follow-up suggest an indolent course. These tumors are usually well circumscribed, encapsulated, and unilateral and measure less than 5 cm. In typical cases, there is a delicate papillary architecture with thin fibrovascular septa lined by a single layer of clear cell. The nuclei, generally relatively bland, are arranged in a linear fashion, centrally, or in the upper pole of the cytoplasm. Purely solid forms do exist as well, with a cord-like or trabeculated pattern, reminiscent of that of sex-cord neoplasms. The immunohistochemical profile is quite characteristic, and the distinguishing features from CCRCC are a strong and diffuse CK7 expression and usual negativity for CD10 [23, 24].

Leiomyomatous renal cell carcinoma Recently, a few cases of renal cell carcinoma with angioleiomyoma-like stroma have been described [24, 25]. These tumors which appear to run an indolent clinical course are composed of nests, cords, and sheets of epithelial clear cells, with low nuclear grade. This epithelial proliferation is dissociated by a stroma featuring mature smooth muscle appearance. The differential diagnosis includes not only CCRCC with fibrohyalinized stroma but also angiomyolipoma and sarcomatoid CCRCC with sarcomatoid component. Unlike CCRCC, the epithelial component of leiomyomatous RCC expresses CK7 and high molecular weight CK, and the stroma shows smooth muscle cell differentiation evidenced by positivity for smooth muscle actin and desmin. Leiomyomatous RCC is negative for melanocytic markers, at variance with angiomyolipoma, and the absence of significant atypia in the stromal component distinguishes it from sarcomatoid carcinoma (Fig. 2).

Table 2 Differential diagnosis of clear cell renal cell carcinoma

Malignant neoplasms
Chromophobe renal cell carcinoma
Clear cell papillary renal cell carcinoma
Clear cell carcinoma with leiomyomatous component
Translocation renal cell carcinoma
Benign lesions
Angiomyolipoma
Histiocytic infiltrates
Adrenocortical tissue

Translocation-associated renal carcinomas The presence of a mixed alveolar/papillary architecture, an admixture of large clear and eosinophilic cells, and calcifications, especially in a young patient, are features suggestive for a translocation carcinoma. Translocation carcinomas are commonly negative for all epithelial markers, although focal positivity may be observed, especially for EMA. CA-IX, CD10, and vimentin can be expressed, like AMACR, Melan-A, and human melanoma black-45 (HMB45). As discussed below, the diagnosis can be immunohistochemically proven by the nuclear positivity of transcription factor E3 (TFE3) or transcription factor EB (TFEB) or by fluorescence in situ hybridization (FISH) assays [26].

Angiomyolipoma with epithelioid component Angiomyolipomas are composed of variable combinations of spindle or epithelioid smooth muscle cells sometimes with clear cytoplasm, adipose tissue, and abnormal thick-walled blood vessels. In the presence of abnormal vessels or fat, the diagnosis is usually straightforward but in the presence of a fat-poor lesion with prominent epithelioid clear cell component; it can be confused with clear cell RCC. Immunohistochemistry is useful in this setting since the epithelioid cells of angiomyolipoma do not express any epithelial markers, CA-IX, CD10, or AMACR, while smooth muscle actin, desmin, HMB45, and Melan-A will be at least focally positive.

Histiocytic infiltrates Inflammatory lesions or pseudotumors with a high macrophage content can be present on biopsies as clear cell-rich lesions, which may be mistaken as CCRCC. Careful evaluation of the cytologic features will show xanthomatous rather than granular cytoplasm and consistently low-grade nuclear features. Another hint is the frequent admixture of other inflammatory cells and the presence of preserved normal or atrophic renal structures, while conversely carcinoma infiltrates in a pushing and destructive manner. In

Table 3 Immunohistochemistry for the differential diagnosis of RCC with clear cell features

	VIM	PanCK	CK7	CA-IX	CD10	AMACR	CD117
Clear cell RCC	++	+	−/+	++	++	+/− or −	−
Chromophobe RCC	−	++	++ or −	−	−	−	++
Translocation RCC	++	−	−	−	−/+	+/− or −	−
Leiomyomatous RCC	++	++	++	ND	ND	ND	ND
Clear cell papillary RCC	++	++	++	ND	−	ND	−

ND not determined, *RCC* renal cell carcinoma, *VIM* vimentin, ++ strong positivity in >75 % of tumor cells, + moderate positivity in >75 % of tumor cells, +/− positivity in 50–75 % of tumor cells, −/+ positivity in <50 % of tumor cells, − absence of significant expression

cases of doubt, a limited immunohistochemistry panel with antibodies directed against CD68 and cytokeratins can solve the differential diagnosis (Fig. 3).

Adrenocortical tissue Adrenocortical tissue—either normal or neoplastic and benign or malignant—may be misinterpreted as CCRCC. Biopsy sampling of adrenocortical tissue is more likely to occur when dealing with an upper pole lesion, but one has to be aware of the possibility of renal–adrenal fusion or ectopic adrenal tissue as well. Compared to CCRCC, adrenocortical cells have a more granular cytoplasm and are arranged in a trabecular or nested rather than acinar pattern. Upon immunostaining, adrenocortical tissue lacks expression of EMA or CA-IX and conversely is positive for inhibin, calretinin, synaptophysin, and Melan-A. In a minority of cases, CKAE1-AE3 and CD10 may be positive [22, 27].

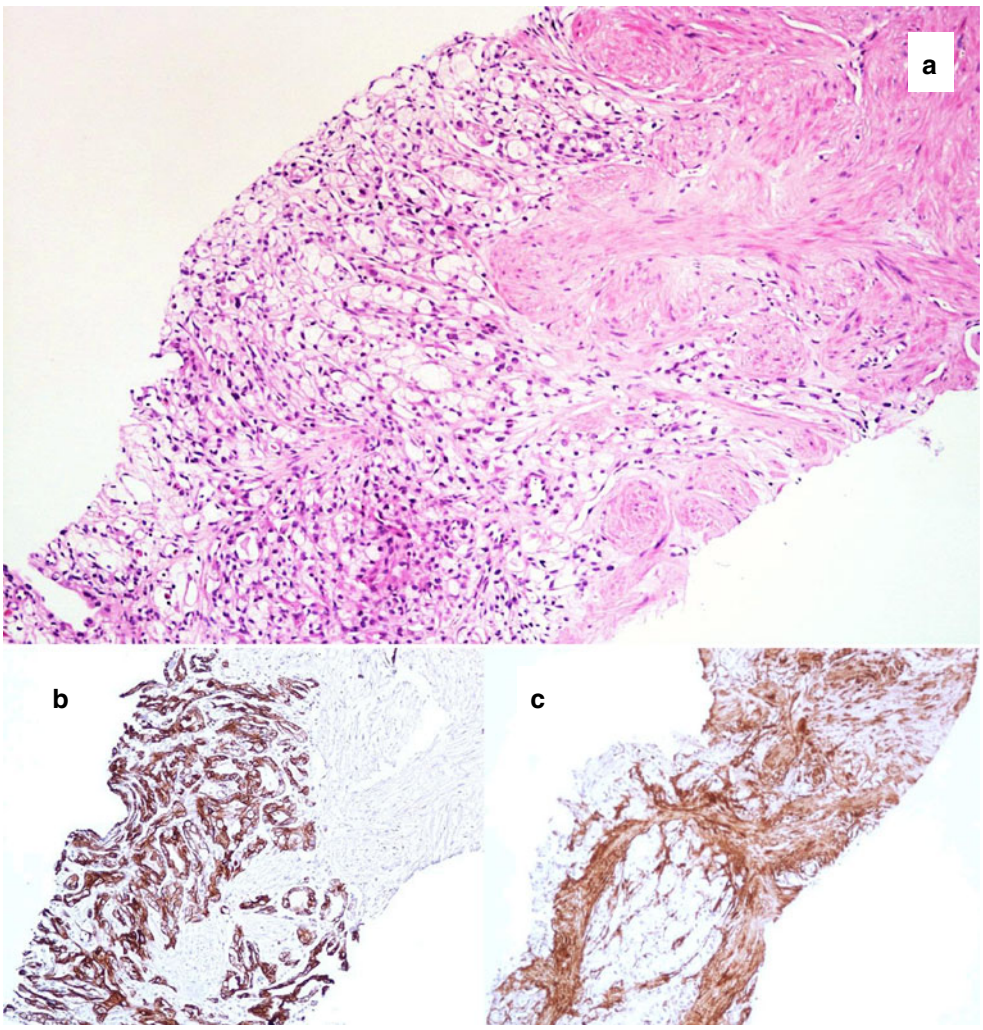

Fig. 2 Core biopsy of a leiomyomatous RCC showing a tubuloacinar clear cell epithelial component admixed with a leiomyomatous component (**a**, hematoxylin and eosin, original magnification ×20). Intense and diffuse expression of CK7 in the epithelial component (**b**, immunoperoxidase, ×10). Intense expression of actin in the leiomyomatous component (**c**, immunoperoxidase, ×10)

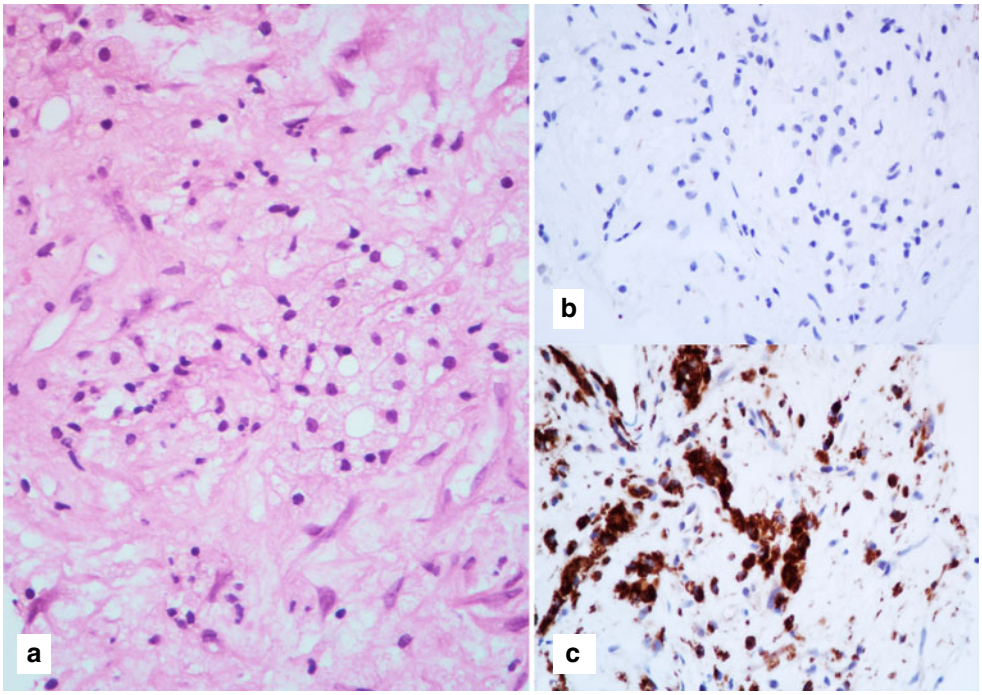

Fig. 3 Xanthogranulomatous pyelonephritis with pseudoglandular architecture of the foamy histiocytic infiltrate (**a**, hematoxylin and eosin, original magnification ×20). Negativity of the pan-keratine AE1/AE3 (**b**, immunoperoxidase, ×20) and expression of CD68 (**c**, immunoperoxidase, ×20)

Eosinophilic cell tumors

Chromophobe cell carcinoma and oncocytoma

Chromophobe renal cell carcinoma and oncocytoma account for the majority of eosinophilic renal cell tumors. The distinction is clinically of paramount importance, given distinct managerial consequences. The differential diagnosis which may be difficult due to overlap in morphological features is greatly aided by the use of ancillary techniques.

Chromophobe RCC (Fig. 4a–d) is composed of clear, eosinophilic, or an admixture of clear and eosinophilic territories. Compared to the classical clear cell variant, in the eosinophilic variant, the cells are generally smaller, with regular and small nuclei, sometimes binucleated, often with a perinuclear halo. The stroma can be focally abundant and fibroedematous. Oncocytomas (Fig. 4e–h) are composed of cells with abundant eosinophilic cytoplasm without sharp delineation of the cell borders. The nuclei are round or with smooth contours and may show atypias, in the form of large irregular hyperchromatic bizarre nuclei. Another characteristic feature of the oncocytoma is the presence of a focally abundant fibroedematous stroma, but this finding is not specific [28].

The expression of CK7 (Fig. 4c, g) is the most discriminant available marker for the differential diagnosis (Table 4), usually intense and diffuse in chromophobe renal cell carcinoma while negative or very focal—in single cells or small clusters of cells—in 95 % of oncocytomas. However, up to 20 % of chromophobe carcinomas lack CK7 expression; hence, negativity of CK7 does not exclude this diagnosis. CD117 (Fig. 4d, h) is another useful marker showing a diffuse cytoplasmic expression with peripheral accentuation in chromophobe renal cell carcinoma while being more often only focally expressed in oncocytoma (essentially in the cytoplasm without membrane reinforcement) [29, 30]. CD10 and AMACR are usually negative in both entities, and expression of vimentin is variable, negative in chromophobe RCC, and possibly focally positive in a large proportion of oncocytomas [31]. CA-IX can be positive in perinecrotic areas of a chromophobe RCC and is consistently negative in oncocytoma. Hale's colloidal iron staining, traditionally recommended as a marker for chromophobe carcinoma, is now obsolete because of technical and interpretation issues.

Clinicians may be doubtful when a diagnosis of oncocytoma is rendered on a biopsy because of the possibility of a hybrid oncocytic/chromophobe tumor of which the potentially malignant component would not have been sampled. However, except in Birt–Hogg–Dubé syndrome or in the setting of renal oncocytomatosis, hybrid tumors appear exceedingly rare, less than 2 % of oncocytoma and chromophobe RCC and do not justify a surgical management for all oncocytoma diagnosed on needles. Moreover, the behavior of these mixed neoplasms seems to be indolent [32].

Differential diagnosis

Other renal cell neoplasms less commonly presenting as eosinophilic cell lesions include a subset of CCRCC (discussed above) and papillary renal cell carcinomas (type II and oncocytic) which may comprise solid areas mimicking oncocytoma [33, 34]. In our institution, when dealing with

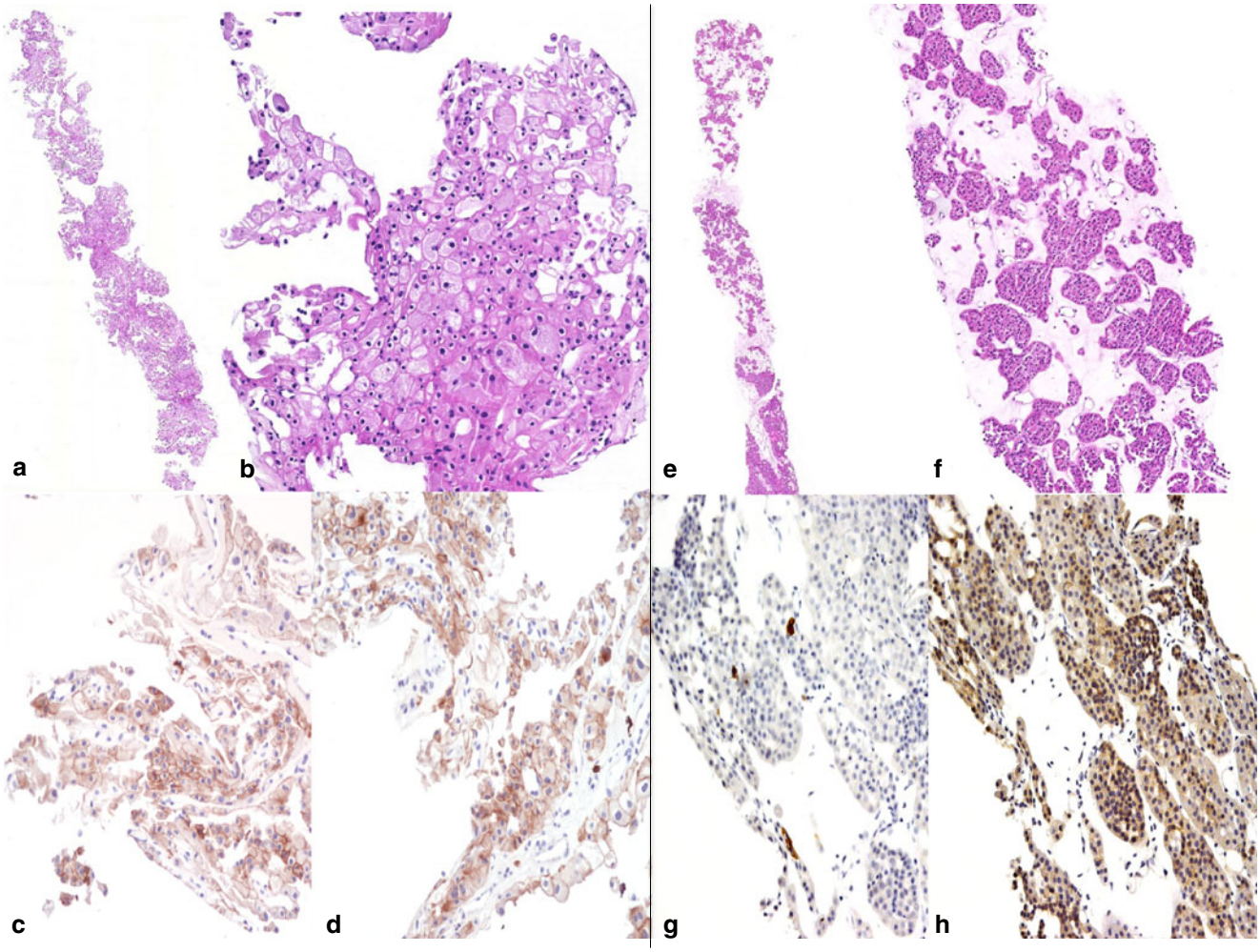

Fig. 4 Chromophobe RCC, mixed clear cell, and eosinophilic type (**a**–**d**). The tumor is composed of large cells with abundant cytoplasm, sharp delineation of the cell borders, and wrinkled nuclei or perinuclear halo. (**a**, **b**, hematoxylin and eosin, original magnification ×2 and ×10). Diffuse expression of CK7 (**c**, immunoperoxidase ×20) and diffuse and intense membranous and cytoplasmic expression of CD117 (**d**, immunoperoxidase ×20). Oncocytoma (**e**–**h**). Core biopsy comprising nests of eosinophilic cells with regular nuclei disposed in an abundant fibroedematous stroma (**e**, **f**, hematoxylin and eosin, original magnifications ×2 and ×20). Positivity of isolated or small cluster of cells for CK7 (**g**, immunoperoxidase ×20). Cytoplasmic expression of CD117 without membranous enhancement (**h**, immunoperoxidase ×20)

small specimen, eosinophilic cell tumors are systematically immunostained for vimentin, CD10, AMACR, CD117, and CK7 (Table 4). In addition, PS100 may be added to the panel as the possibility of metastatic melanoma should also always be borne in mind. If angiomyolipoma is suspected, expression of actin, desmin, HMB45, and Melan-A is also assessed. Exceptional examples of sarcomatoid carcinoma may exhibit rhabdoid features and present as an eosinophilic cell tumor (Fig. 5).

Papillary tumors

A variety of primary renal neoplasms or metastases may show a focal or extensive papillary pattern (Table 5). Once

Table 4 Immunohistochemistry for the differential diagnosis renal tumors with eosinophilic cells

	Vim	CK7	CA-IX	CD10	AMACR	CD117
Chromophobe RCC	−	++ or −	−	−/+	−	++
Oncocytoma	−/+ or −	− or −/+	−	−/+	−	+/−
Clear cell RCC	++	−/+	++	++	+/− or −	−
Papillary type II RCC	++	+ or +/−	−	+	++	−
Papillary oncocytic RCC	++	+ or +/−	−	ND	++	−

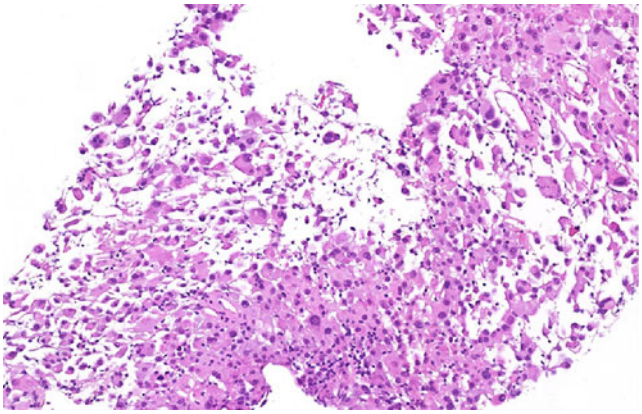

Fig. 5 Rhabdoid RCC. Sarcomatoid component presenting as rhabdoid tumor (hematoxylin and eosin ×20). Expression of CK and INI1 (not shown)

papillary pattern is recognized, morphological analysis should assess the cytoplasmic features (eosinophilic, basophilic, or clear cell), the nuclear grade, the number of layer of cells lining the papilla, and the presence of foamy histiocytes (Fig. 6). In case of a carcinoma featuring a papillary architecture, immunohistochemistry may suggest the renal cell derivation by the positivity of AMACR and CK7. Vimentin and CD10 are generally at least focally positive. If these markers are lacking, metastatic, urothelial, or collecting duct carcinoma should be considered (discussed later). Even in the absence of a clear papillary architecture, the presence of foamy histiocytes is suggestive for papillary RCC. This diagnosis should also be entertained when dealing with an eosinophilic cell lesion, even of solid architecture (see above). Metanephric adenoma, a rare benign entity, must also be considered in the differential diagnosis of papillary neoplasms.

Papillary renal cell carcinoma

Papillary RCC comprises type I, type II, and the oncocytic variant. It is of interest to determine the subgroup of the papillary carcinoma because their prognoses are different. The type I and oncocytic variants are considered low-grade malignant neoplasm while type II is overall more aggressive with a prognosis similar to or worse than that of a clear cell RCC.

Papillary carcinoma, type I This entity features a typical and homogeneous morphology characterized by a delicate papillary architecture lined by a single layer of basophilic cells, with low nuclear grade (Fuhrman 1 or 2). Accumulation of foamy histiocytes in the vascular cores is virtually constant. Necrosis and cholesterol clefts may be abundant. AMACR, CK7, vimentin, and CD10 are almost always expressed (Table 4). Some tumors show a prominent tubular architecture with only minimal papillary pattern, which may be the only component sampled on biopsy. The presence of foamy macrophages is helpful to distinguish this tumor type from the others of tubular architecture (Fig. 7).

Papillary carcinoma, type II Papillary carcinoma type II is a heterogeneous group of tumors with respect to their morphology, immunophenotype, molecular features, and prognosis. Expression of CK7 is not as systematic as in type I but AMACR is usually expressed. In general, the papillae are lined by one or several layers of eosinophilic cells. Fuhrman nuclear grade is higher than in type I (generally 3 or 4), and macrophages are less numerous. Necrosis and cholesterol deposits are frequent.

Oncocytic papillary renal cell carcinoma Oncocytic papillary renal cell carcinoma, formerly included in the group of type II carcinomas, was recently individualized because of its more indolent behavior. It consists of a proliferation of oncocytic cell with round nuclei and large nucleoli. At variance with papillary carcinoma type II, the papillae are mostly lined by a single layer of tumor cells. Foamy macrophages are more frequent than in papillary type II RCC. In all, the oncocytic type of papillary RCC is best described as a tumor resembling papillary type I with oncocytic cells [33].

Microphthalmia-associated transcription factor family–TFE3 translocation-associated renal carcinomas Translocation renal cell carcinoma comprises a group of neoplasms characterized by translocation involving genes encoding transcription factors of the microphthalmia-associated transcription factor family, TFE3, or less frequently TFEB, with various gene partners. The most frequent translocations

Table 5 Renal tumors with possibly focal or extensive papillary architecture

Renal tumors of papillary architecture
Papillary RCC type I and II, papillary oncocytic RCC
Translocation RCC
Clear cell papillary RCC
Hereditary leiomyomatosis and renal cell cancer syndrome related RCC
Other renal tumors possibly comprising a papillary component
Clear cell RCC
Collecting duct carcinoma
Metanephric adenoma
Mucinous tubular and spindle cell carcinoma
Urothelial carcinoma
Chromophobe RCC
Oncocytoma
Metastasis

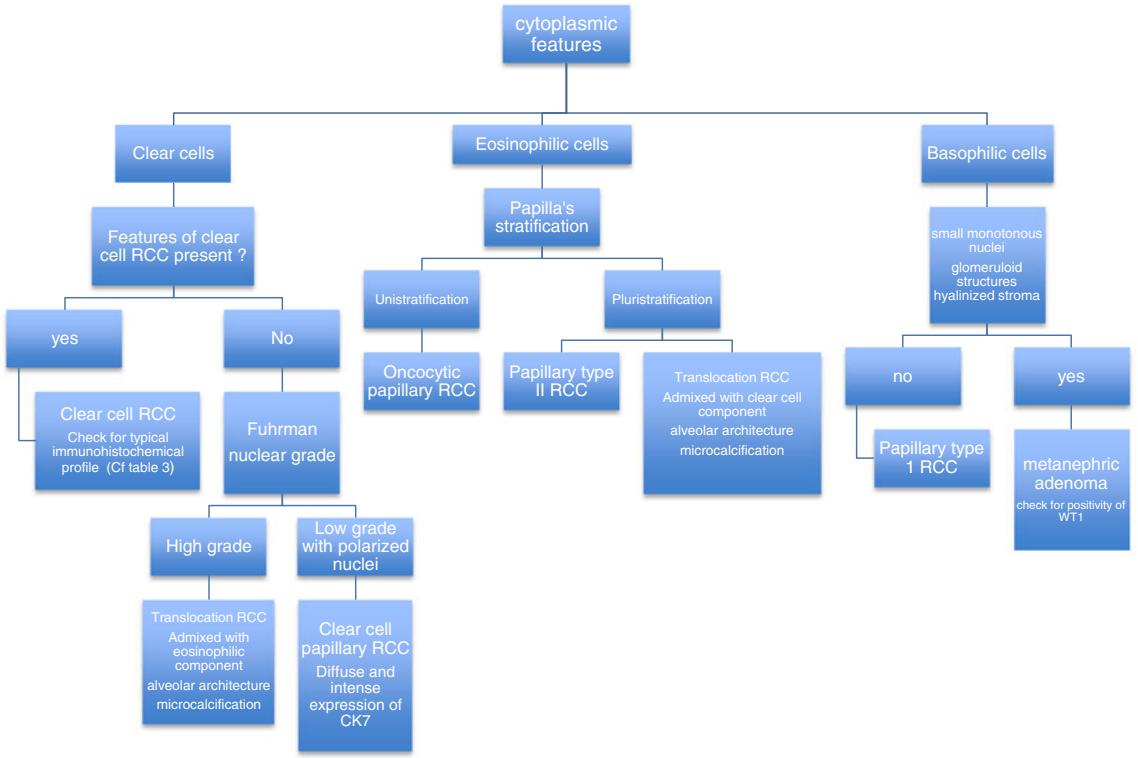

Fig. 6 Algorithm for assessment of papillary tumors on core renal biopsies (metastases are not listed but also enter in the differential diagnosis)

involve *TFE3* with *alveolar soft part sarcoma locus* or *papillary renal cell carcinoma*. First described in pediatric population, translocation RCC also occurs in adults accounting for 1 to 4 % of RCCs. Translocation RCC is often

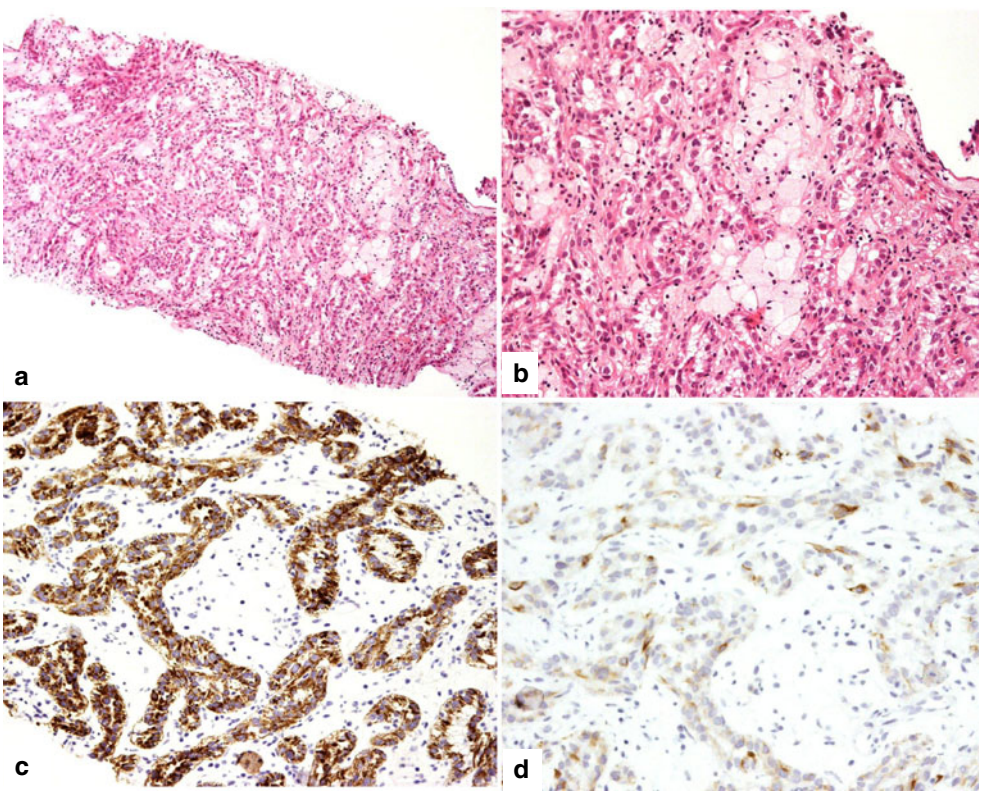

Fig. 7 Papillary RCC probably of type I with prominent tubular architecture (**a**, hematoxylin and eosin ×4). The presence of foamy histiocytes is a useful hint to the diagnosis (**b**, hematoxylin and eosin ×20). The typical immunohistochemical profile includes diffuse and strong expression of AMACR (**c**, immunoperoxidase ×20) and expression of CK7, which was focal in this case (**d**, immunoperoxidase ×20)

present with advanced disease and distant metastasis and carries a dismal prognosis.

Characteristic features of translocation carcinomas include the presence of a mixed alveolar/papillary architecture with an admixture of large clear and eosinophilic cells, the presence of calcifications, and high nuclear grade. Upon immunohistochemistry, translocation carcinomas are usually negative for keratin expression, and hence the diagnosis should always be entertained in front of a keratin-negative renal tumor. EMA can be focally positive, and there is a variable expression of vimentin, AMACR, Melan-A, and HMB45. The diagnosis is definitely proven by the demonstration of TFE3 or TFEB expression [26] and/or by evidencing the gene rearrangement by FISH assay [35].

Metanephric adenoma Metanephric adenoma is a rare benign neoplasm composed of small primitive cells resembling early metanephric tubular differentiation. Histologic features encompass small acini, papillary, and glomeruloid structures composed of monotonous cells with small nuclei and minimal blue cytoplasm. The stroma is often hyalinized and may be abundant. Mitoses are rare or absent. The papillary component may resemble type 1 papillary RCC but the nuclei are smaller, the cytoplasm is less abundant, and CK7 is usually less diffusely positive than in papillary carcinoma type 1. AMACR is positive in both entities. WT1 is helpful, showing often diffuse nuclear positivity in metanephric adenoma [36].

Tumors comprising a spindle cell component

High-grade spindle cell component

When facing a cytologically high-grade spindle cell component, the first diagnosis to consider is a sarcomatoid carcinoma. The probability of finding a sarcomatoid component in small renal masses is low and increases with the tumor size. The identification of sarcomatoid carcinoma is often supported by the presence of an admixed cytologically high-grade epithelial component. In case of proliferations composed exclusively of spindle cells, immunohistochemistry for demonstration of keratin and/or EMA expression is usually useful.

A large variety of primary or secondary sarcomas may involve the kidney. One of the most frequently encountered is synovial sarcoma. Kidney synovial sarcoma is a highly cellular tumor in which tumor cells form short, intersecting fascicles dissecting the native renal parenchyma. This spindle cell solid component is often admixed with cysts of different size lined by hobnail cells. EMA and cytokeratins can be focally positive in the spindle cells and in the cells lining the cyst. The diagnosis is definitely established by the demonstration of *SYT-SSX* fusion at the genetic level or demonstration of the fusion transcript by molecular studies [37].

Low-grade spindle cell lesions

Angiomyolipoma is the most common primary renal tumor with a low-grade spindle cell component. Expression of HMB45 and Melan-A in addition to smooth muscle actin and desmin is characteristic. Other entities in the differential diagnosis include clear cell carcinoma with leiomyomatous stroma (discussed above) and mucinous tubular and spindle cell carcinoma. The latter consists of low-grade epithelial cells in the form of elongated tubules and spindle cells, separated by variable amounts of mucinous stroma. CK7 and AMACR are usually positive. CD10 is negative [38].

Tumors with an infiltrative pattern and desmoplasia

Desmoplasia is not a feature of most renal cell carcinomas, which tend to grow in a pushing manner. An infiltrative pattern of growth between residual glomeruli or tubules brings up the differential diagnoses of collecting duct carcinoma, the very rare renal medullary carcinoma, urothelial carcinoma, and metastasis. In this setting, PAX2 and PAX8 transcription factors represent two potentially useful markers for the demonstration of renal cell derivation.

Collecting duct carcinoma and renal medullary carcinoma

Collecting duct carcinoma is extremely rare (less than 1 % of renal malignancies). It comprises a tubular or tubulopapillary infiltrative growth with a desmoplastic and often inflammatory stroma. Solid, cord-like features may be encountered. In case of prominent papillary architecture, papillary renal cell carcinoma may be suspected but the latter usually lacks desmoplasia.

Renal medullary carcinoma is a very rare entity occurring almost exclusively in young patients with sickled cell trait, viewed by some authors as an aggressive form of collecting duct carcinoma. Intratumoral inflammatory infiltrates, mostly neutrophils, are a constant finding and sickle red blood cell may be recognized. Recent data suggest consistent loss of INI-1 expression in these tumors [39].

Urothelial carcinoma

Invasive urothelial carcinoma in the kidney usually manifests as high-grade carcinoma, poorly differentiated, or with glandular differentiation. Immunohistochemistry is helpful to demonstrate the expression of CK7, CK20, CK5/6, and p63. The latter is very useful for distinguishing from collecting duct carcinoma [40]. Conversely, urothelial carcinoma lacks CD10 and other renal cell markers [30] (Fig. 8).

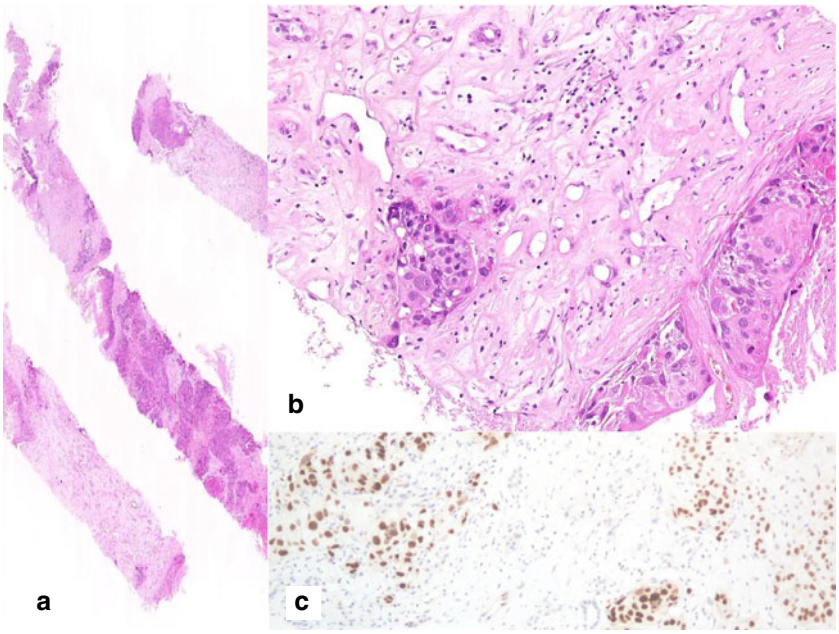

Fig. 8 Invasive high-grade urothelial carcinoma (**a**, hematoxylin and eosin ×2). This field illustrates nests of atypical cells, desmoplastic fibrous stroma, and residual atrophic renal tubules (**b**, hematoxylin and eosin ×10). Immunohistochemical profile includes nuclear expression of P63 (**c**, immunoperoxidase ×10)

Metastatic carcinoma

The possibility of metastasis should be considered whenever a renal neoplasm appears unclassifiable as a primary lesion, i.e., any lesion not showing the classical morphologic features of a renal carcinoma (glandular architecture, desmoplasia, absence of clear cell, etc.) and immunohistochemical expression of classic renal markers (Table 6). It is of importance to stress that AMACR has no specificity for renal primaries and it is expressed in many adenocarcinomas of other origins, for example prostatic, gastric, or colorectal [41, 42]. The most common primary sites are lung, breast, skin

Table 6 Commonly used markers for diagnostic immunohistochemistry: expression in normal kidney and in primary renal and extrarenal tumors

	Normal kidney	Primary renal tumors	Extrarenal tumors
Vimentin	Vessels	Clear cell RCC Papillary RCC	Carcinoma of endometrium, thyroid, and adrenal cortex
Pan-CK	Tubules and glomeruli	All types of RCC except translocation carcinoma	Carcinoma
CK7	Tubules and glomeruli	Papillary RCC Chromophobe RCC Leiomyomatous RCC Clear Cell papillary RCC may be focal in clear cell RCC	Variety of (adeno)carcinoma (breast, lung…)
AMACR	Epithelial cells of the renal tubules	Papillary RCC Clear cell and translocation RCC	Prostate, lung, colon, stomach, ovary, breast, endometrium, gallbladder, neuroendocrine carcinomas
CA IX	Not expressed	Clear cell RCC Collecting duct carcinoma	Endometrium, stomach, cervix, breast, lung, liver, brain tumors, neuroendocrine carcinomas, mesothelioma
CD10	Podocytes, proximal tubular cell brush borders	Typical in clear cell, papillary, and translocation RCC; can be expressed in other renal epithelial neoplasm	Various neoplasms of epithelial, stromal, or hematopoietic derivation
CD117	ND	Chromophobe RCC Oncocytoma	Gastrointestinal stromal tumor, seminoma
PAX2 and PAX8	Podocytes Distal tubular cells Lymphoid cells	All types of primary RCC, decreased in high grade, negative in sarcomatoid carcinoma	Lymphoma, nephrogenic adenoma, thyroid follicular cell neoplasm
RCC	Proximal tubular cell brush borders	Clear cell RCC Papillary RCC	Adrenocortical tumors, breast and colon carcinoma, embryonal carcinoma, parathyroid tumors,

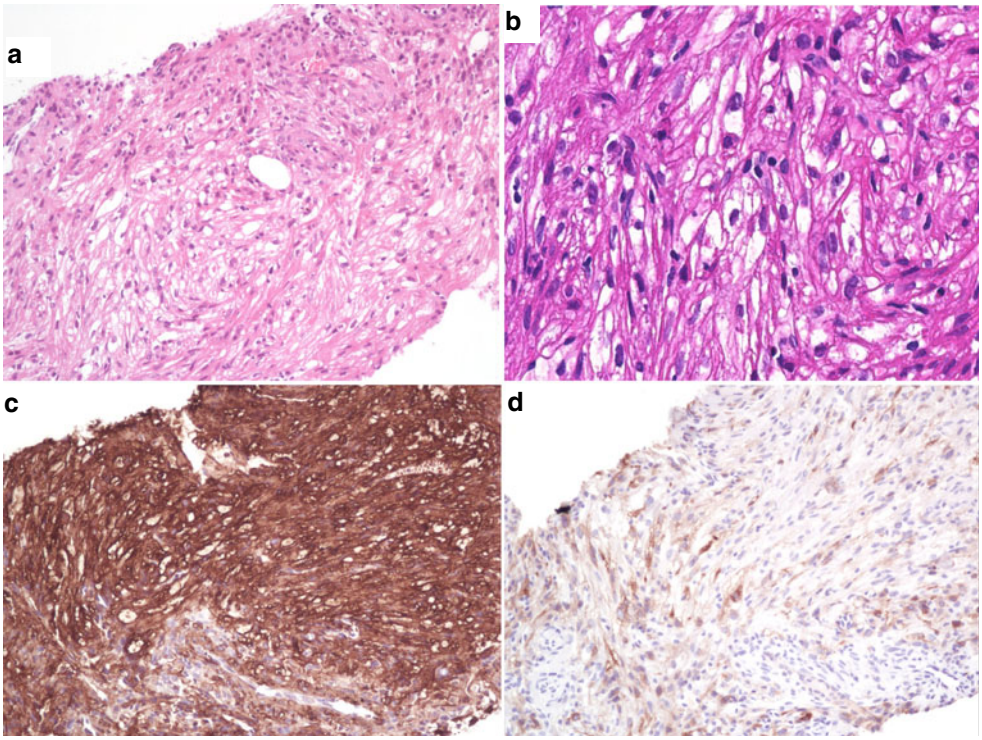

Fig. 9 Epithelioid angiomyolipoma. Proliferation of plump and spindle clear cells arranged in fascicle (**a**, hematoxylin and eosin ×20 and **b**, hematoxylin and eosin ×40). Immunohistochemical profile includes intense expression of actin (**c**, immunoperoxidase ×20) and partial expression of Melan-A (**d**, immunoperoxidase ×20)

(malignant melanoma), contralateral kidney, gastrointestinal tract, ovary, and testis [43]. Renal metastases appear commonly in the late stages of evolution whereas renal metastasis as the initial manifestation of the primary is highly unusual.

Angiomyolipoma

Angiomyolipoma is a benign neoplasm that belongs to the perivascular epithelioid cell (PEC)-oma family of tumors. Its classical triphasic pattern associating variable amounts of adipose tissue, spindle or epithelioid smooth muscle cells, and abnormal thick-walled blood vessels is usually easily recognized histologically and often largely suspected radiologically because of the presence of adipose tissue. When the triphasic pattern is well represented, ancillary techniques are not necessary, but in case of diagnostic doubt, the immunohistochemical pattern is characteristic, with the epithelioid or spindle cells expressing muscular marker (alpha-actin and less frequently desmin) and some melanocytic markers as HMB45 and Melan-A [44]. PEComas are benign, and a simple surveillance can be recommended if the lesion is asymptomatic and small. Large tumors have to be removed because of the rare but real hemorrhagic risk.

Epithelioid angiomyolipoma of the kidney is a rare disease, closely related to classic, triphasic angiomyolipoma and considered as a potentially malignant neoplasm [45]. The epithelioid component is composed of large globulous or plump spindle cells with clear or eosinophilic cytoplasm and voluminous nuclei, similar to those of soft tissue PEComas (Fig. 9). Epithelioid angiomyolipoma can be confused with clear cell RCC or with melanoma, but negativity of cytokeratin and PS100 and positivity of smooth muscle markers (actin and desmin) and HMB45 and/or Melan-A are diagnostic. The minimal amount of epithelioid component required to define angiomyolipoma as epithelioid, and so to suspect the lesion as potentially malignant, however, is not well defined. In our practice, epithelioid features in angiomyolipomas, when present, are systematically mentioned in the pathology report with a note suggesting that surgical removal would be performed.

The nondiagnostic biopsy

Normal renal tissue and fibrous or fibroinflammatory tissue

The proportion of biopsies composed of normal renal tissue or sampling only fibrous or fibroinflammatory tissue varies between 5 and 10 % in published series. Importantly, a diagnosis of malignancy is eventually rendered in more than half of the patients who undergo nephrectomy or repeat biopsies, advocating the need for a second biopsy in case of a nonconclusive biopsy [21]. A final diagnosis of scar or pyelonephritis should strictly correlate with clinical and radiological settings.

Necrotic tissue

Although biopsies are performed under imaging guidance in order to be directed to viable areas, in rare cases, biopsies

may exclusively sample necrotic tissue, raising the differential diagnosis of the underlying process as neoplastic versus inflammatory. Immunohistochemistry can be helpful, as the immunoreactivity of carcinomatous cells for CK or EMA is usually conserved, even when necrotic.

Concluding remarks

A good morphological analysis in conjunction with the appropriate use of an immunohistochemical panel can lead to a precise diagnosis for a vast majority of the renal masses sampled by core biopsy. This is now of importance because of the need of pretherapeutic diagnosis in an increasing number of situations. Nevertheless, definitive tumor typing is not always possible, for example in the case of cytologically low-grade neoplasms with clear cell features or in the case of eosinophilic cell proliferations. In those situations, it is important to state whether the renal cell origin of the lesion can be confirmed and to mention the nuclear grade. Deferring the definitive diagnosis to the examination of the surgical material appears as a reasonable option without impending appropriate management of the patient.

Cytogenetic studies, like FISH or comparative genomic hybridization (CGH) array, can determine changes known to be specifically or preferentially associated with each tumor type. For example, deletion of 3p is characteristic of CCRCC, hyperploidy is characteristic for papillary RCC, and hypoploidy for chromophobe RCC. This kind of ancillary techniques is currently not routinely performed, with the exception of *TFE3* break-apart FISH assays for the identification of translocation RCC. Nevertheless, FISH and CGH array have been proven to be feasible on biopsy samples and could be considered as an option in the future to improve the accuracy of biopsy diagnosis [46, 47].

Acknowledgments The authors thank Prof. L. Guillou and Dr. V. Lindner for critically reading the article and Dr. L. Dix and Dr. A. Nobile for the technical support.

Conflict of interest We declare that we have no conflict of interest.

References

1. Ljungberg B, Cowan NC, Hanbury DC et al (2010) EAU guidelines on renal cell carcinoma: the 2010 update. Eur Urol 58 (3):398–406
2. Leveridge MJ, Finelli A, Kachura JR et al (2011) Outcomes of small renal mass needle core biopsy, nondiagnostic percutaneous biopsy, and the role of repeat biopsy. Eur Urol 60(3):578–584
3. Jayson M, Sanders H (1998) Increased incidence of serendipitously discovered renal cell carcinoma. Urology 51(2):203–205
4. Remzi M, Marberger M (2009) Renal tumor biopsies for evaluation of small renal tumors: why, in whom, and how? Eur Urol 55 (2):359–367
5. Shah RB, Bakshi N, Hafez KS et al (2005) Image-guided biopsy in the evaluation of renal mass lesions in contemporary urological practice: indications, adequacy, clinical impact, and limitations of the pathological diagnosis. Hum Pathol 36(12):1309–1315
6. Wang R, Wolf JS Jr, Wood DP Jr et al (2009) Accuracy of percutaneous core biopsy in management of small renal masses. Urology 73(3):586–590, discussion 590-1
7. Volpe A, Mattar K, Finelli A et al (2008) Contemporary results of percutaneous biopsy of 100 small renal masses: a single center experience. J Urol 180(6):2333–2337
8. Breen DJ, Railton NJ (2010) Minimally invasive treatment of small renal tumors: trends in renal cancer diagnosis and management. Cardiovasc Intervent Radiol 33(5):896–908
9. Boorjian SA, Uzzo RG (2009) The evolving management of small renal masses. Curr Oncol Rep 11(3):211–217
10. Laguna MP, Kümmerlin I, Rioja J et al (2009) Biopsy of a renal mass: where are we now? Curr Opin Urol 19(5):447–453
11. Bosniak MA (1986) The current radiological approach to renal cysts. Radiology 158(1):1–10
12. Neuzillet Y, Lechevallier E, Andre M et al (2004) Accuracy and clinical role of fine needle percutaneous biopsy with computerized tomography guidance of small (less than 4.0 cm) renal masses. J Urol 171(5):1802–1805
13. Breda A, Treat EG, Haft-Candell L et al (2010) Comparison of accuracy of 14-, 18- and 20-G needles in ex-vivo renal mass biopsy: a prospective, blinded study. BJU 105(7):940–945
14. Ficarra V, Brunelli M, Novara G et al (2011) Accuracy of on-bench biopsies in the evaluation of the histological subtype, grade, and necrosis of renal tumours. Pathology 43(2):149–155
15. Al-Ahmadie HA, Alden D, Fine SW et al (2011) Role of immunohistochemistry in the evaluation of needle core biopsies in adult renal cortical tumors: an ex vivo study. Am J Surg Pathol 35 (7):949–961
16. Strojan Flezar M, Gutnik H, Jeruc J et al (2011) Typing of renal tumors by morphological and immunocytochemical evaluation of fine needle aspirates. Virchows Arch 459(6):607–614
17. Eble JN, Sauter G, Epstein JI et al (2004) World Health Organization classification of tumours, pathology and genetic of tumours of the urinary system and male genital organs. IARC Press, Lyon
18. Al-Ahmadie HA, Alden D, Qin LX et al (2008) Carbonic anhydrase IX expression in clear cell renal cell carcinoma: an immunohistochemical study comparing 2 antibodies. Am J Surg Pathol 32(3):377–382
19. Leppert JT, Lam JS, Pantuck AJ et al (2005) Carbonic anhydrase IX and the future of molecular markers in renal cell carcinoma. BJU Int 96(3):281–285
20. Zubac DP, Bostad L, Kihl B et al (2008) Organ-confined clear cell renal cell carcinoma: the prognostic impact of microvascular invasion, nuclear grade and tumour size. APMIS 116(12):1027–1033
21. Lebret T, Poulain JE, Molinie V et al (2007) Percutaneous core biopsy for renal masses: indications, accuracy and results. J Urol 178(4 Pt 1):1184–1188, discussion 1188
22. Reuter VE, Tickoo SK (2010) Differential diagnosis of renal tumours with clear cell histology. Pathology 42(4):374–383
23. Adam J, Couturier J, Molinie V et al (2011) Clear-cell papillary renal cell carcinoma: 24 cases of a distinct low-grade renal tumour and a comparative genomic hybridization array study of seven cases. Histopathology 58(7):1064–1071
24. Srigley JR, Delahunt B (2009) Uncommon and recently described renal carcinomas. Mod Pathol 22(Suppl 2):S2–S23
25. Kuhn E, De Anda J, Manoni S et al (2006) Renal cell carcinoma associated with prominent angioleiomyoma-like proliferation: report of 5 cases and review of the literature. Am J Surg Pathol 30 (11):1372–1381
26. Ross H, Argani P (2010) Xp11 translocation renal cell carcinoma. Pathology 42(4):369–373

27. Sangoi AR, Fujiwara M, West RB et al (2011) Immunohistochemical distinction of primary adrenal cortical lesions from metastatic clear cell renal cell carcinoma: a study of 248 cases. Am J Surg Pathol 35(5):678–686
28. Amin MB, McKenney JK, Tickoo SK et al (2010) Diagnostic pathology. Genitourinary. Amirsys, Inc, Canada
29. Carvalho JC, Wasco MJ, Kunju LP et al (2011) Cluster analysis of immunohistochemical profiles delineates CK7, vimentin, S100A1 and C-kit (CD117) as an optimal panel in the differential diagnosis of renal oncocytoma from its mimics. Histopathology 58(2):169–179
30. Truong LD, Shen SS (2011) Immunohistochemical diagnosis of renal neoplasms. Arch Pathol Lab Med 135(1):92–109
31. Hes O, Michal M, Kuroda N et al (2007) Vimentin reactivity in renal oncocytoma: immunohistochemical study of 234 cases. Arch Pathol Lab Med 131(12):1782–1788
32. Petersson F, Gatalica Z, Grossmann P et al (2010) Sporadic hybrid oncocytic/chromophobe tumor of the kidney: a clinicopathologic, histomorphologic, immunohistochemical, ultrastructural, and molecular cytogenetic study of 14 cases. Virchows Arch 456(4):355–365
33. Hes O, Brunelli M, Michal M et al (2006) Oncocytic papillary renal cell carcinoma: a clinicopathologic, immunohistochemical, ultrastructural, and interphase cytogenetic study of 12 cases. Ann Diagn Pathol 10(3):133–139
34. Mai KT, Kohler DM, Robertson SJ et al (2008) Oncocytic papillary renal cell carcinoma with solid architecture: mimic of renal oncocytoma. Pathol Int 58(3):164–168
35. Kim SH, Choi Y, Jeong HY et al (2011) Usefulness of a break-apart FISH assay in the diagnosis of Xp11.2 translocation renal cell carcinoma. Virchows Arch 459(3):299–306
36. Davis CJ Jr, Braton JH, Sesterhenn IA et al (1995) Metanephric adenoma. Clinicopathological study of fifty patients. Am J Surg Pathol 19(10):1101–1114
37. Argani P, Faria PA, Epstein JI et al (2000) Primary renal synovial sarcoma: molecular and morphologic delineation of an entity previously included among embryonal sarcomas of the kidney. Am J Surg Pathol 24(8):1087–1096
38. Ferlicot S, Allory Y, Comperat E et al (2005) Mucinous tubular and spindle cell carcinoma: a report of 15 cases and a review of the literature. Virchows Arch 447(6):978–983
39. Cheng JX, Tretiakova M, Gong C et al (2008) Renal medullary carcinoma: rhabdoid features and the absence of INI1 expression as markers of aggressive behavior. Mod Pathol 21(6):647–652
40. Kobayashi N, Matsuzaki O, Shirai S et al (2008) Collecting duct carcinoma of the kidney: an immunohistochemical evaluation of the use of antibodies for differential diagnosis. Hum Pathol 39 (9):1350–1359
41. Truong CD, Li W, Feng W et al (2008) Alpha-methylacyl-CoA racemase expression is upregulated in gastric adenocarcinoma: a study of 249 cases. Int J Clin Exp Pathol 1(6):518–523
42. Shi X, Gong E, Wu X (2007) Alpha-methylacyl-CoA racemase/P504S overexpression in colorectal carcinoma is correlated with tumor differentiation. Appl Immunohistochem Mol Morphol 15 (2):175–180
43. Murphy WM et al (2004) AFIP Atlas of Tumor Pathology series 4, tumors of the kidney, bladder and related urinary structures. American Registry of Pathology, Washington DC
44. Martignoni G, Pea M, Reghellin D et al (2008) PEComas: the past, the present and the future. Virchows Arch 452(2):119–132
45. Faraji H, Nguyen BN, Mai KT (2009) Renal epithelioid angiomyolipoma: a study of six cases and a meta-analytic study. Development of criteria for screening the entity with prognostic significance. Histopathology 55(5):525–534
46. Barocas DA, Mathew S, delPizzo JJ et al (2007) Renal cell carcinoma sub-typing by histopathology and fluorescence in situ hybridization on a needle-biopsy specimen. BJU Int 99 (2):290–295
47. Vieira J et al (2010) Feasibility of differential diagnosis of kidney tumors by comparative genomic hybridization of fine needle aspiration biopsies. Genes Chromosomes Cancer 49(10):935–947

Virchows Arch (2012) 461:27–32
DOI 10.1007/s00428-012-1251-x

REVIEW AND PERSPECTIVES

Teratoma with somatic-type malignant components of the testis. A review and an update

Gregor Mikuz · Maurizio Colecchia

Received: 3 March 2012 / Revised: 26 April 2012 / Accepted: 10 May 2012 / Published online: 24 May 2012
© Springer-Verlag 2012

Abstract Malignant transformation of germ cell tumors into somatic malignancy is uncommon. Its presentation differs from series to series, with 43 % of adult cases identified within the primary tumors and the remainder at the time of relapse or in the metastasis. Patients with stage I disease enjoy an excellent prognosis; whereas in metastatic sites when not completely resectable, the somatic type malignancies suffer a dismal prognosis. Radical surgery is significant for the prospects of cure and is standard chemotherapy for germ cell tumors; a transformation-oriented treatment can be effective for these patients. A deeper understanding of the biology of this phenomenon is essential for clinicians involved in such malignancies in order to permit a better control of the disease.

Keywords Germ cell · Teratoma · Somatic-type malignancy · Sarcoma

Introduction and historical review

Testicular tumors are of great interest to the pathologist because nearly all of them are of germ cell origin, with a potential for differentiation in many directions. Moreover, these potentially deadly tumors are highly responsive to therapy and more than 90 % can be completely cured. Among this great morphological variety of different subtypes of germ cell malignancies, teratomas can show a partial transformation into a malignant somatic-type tumor component (MSC) [1–3]. However, due to the small number of published clinic pathological studies, our knowledge about these tumors is very limited [4–10].

According to Ewing [11], it was St. Donat who in 1696, for the first time, identified a testicular tumor with the morphological features of teratomas, consisting of a rudimentary skull and embryonic eyes. As reported by Kaufmann [12], Wilms recognized the tendency of single tissue elements in teratomas to predominate over others, and described carcinomatous and sarcomatous tissue in so called "embrioid tumors".

Friedman and Moore [13] reviewed 922 testicular tumors observed at the Armed Forces Institute of Pathology and noted a few teratomas in which carcinoma, rhabdomyosarcoma, or neuroblastoma developed; but they did not report detailed pathological findings and left out certain clinical details of these cases. Finally, Mostofi and Price in the fascicle 8 of the second series of the AFIP Atlas of Tumor Pathology recognized the existence of teratomas with malignant transformation. The clinical information concerning the behavior of the disease was, however, extremely scarce [14].

In the 2004 edition of the WHO Classification of Tumors, this entity was classified as "teratoma with somatic-type malignancy," which was defined as "a teratoma containing a malignant component of a type typically encountered in other organs and tissues, e.g. sarcomas and carcinomas" [15]. It occurs in 3–6 % of patients with metastatic germ cell tumor (GCT). Further analyses have subsequently been

G. Mikuz
Department of Pathology, Medical University Innsbruck, Innsbruck, Austria

M. Colecchia
Department of Pathology, Fondazione IRCCS Istituto Nazionale dei Tumori, Milan, Italy

M. Colecchia (✉)
Department of Pathology, Istituto Nazionale dei Tumori di Milano, via Venezian, 20133 Milan, Italy
e-mail: maurizio.colecchia@istitutotumori.mi.it

reported, however, each one covering a small number of patients [5, 7, 10].

Teratoma with a malignant somatic component (TMSC) affects mainly young males (aged 20–40), but sporadic cases in the pediatric population have been reported with clinical–pathological features similar to those occurring in adults [16]. Clinical follow ups have shown that compared with teratomas without somatic type malignancies, these tumors in metastatic sites have poor prognosis if not completely resectable. The extent of the disease at onset and consequently, the feasibility of a radical surgical extirpation have been identified as the strongest prognostic parameters for durable remissions [3, 8–10].

Histopathology

For an accurate diagnosis of TMSC located in the testis as well as in the metastases, the pathologist has to assess the degree of atypia in the somatic components and whether the tumor is growing in an expansive way. Davey and Ulbright [17] found cellular atypia of epithelial and mesenchymal elements in teromatous metastases of patients treated with cisplatin-based chemotherapy for nonseminomatous GCTs. The follow-up, however, did not show significant differences compared to patients without significant atypia. The authors thus concluded that only the expansive growth of the somatic malignant proliferation is a significant feature for the diagnosis of a TMSC.

The amount of malignant somatic tissue required for the diagnosis of TSMC is still a controversial issue. Ulbright and Roth [18] suggested that the somatic malignancy is clinically important only if it fills a field of view at low magnification (4× lens). More clinicopathological study including adequate follow-ups is needed to find out whether or not this threshold is reliable.

A variety of somatic malignancies in GCT can occur in neoplasms of gonads, as well as in germinal extragonadal tumors of the mediastinum [19] and intracranial cavity [20]. The somatic neoplasia may be sarcomas of any type [2, 3, 5, 7, 8, 10, 21–26]. The most common were the rhabdomyosarcoma, followed by leiomyosarcoma, myxoid liposarcoma, chondrosarcoma, glioblastoma multiforme, epithelioid hemangioendothelioma, malignant peripheral nerve sheath tumor [5, 7, 10], but also adenocarcinoma or squamous cell carcinoma [27]. Other frequently reported somatic malignancies are nephroblastoma [10, 28, 29], carcinoids [30], and hematologic malignancies. In a series of 40 TMSC observed by one of the authors (MC), rhabdomyosarcoma was observed in 11 cases (27.5 %) [10]. Angiosarcoma has also been described as a primary tumor in the testis as well as in the metastases from testicular GCT [31].

Primitive neuroectodermal tumors (PNETs) are also likely to be a very frequent somatic malignancy arising in teratoma [9, 10, 32–37]. PNETs are sometimes incorrectly reported as immature teratoma [38], an inappropriate diagnosis that can be a source of confusion for clinicians. In the WHO 2004 classification (15), the terms “immature” and “mature” teratoma were abolished because they are clinically irrelevant. Moreover, the *epitheton ornans* “immature” was often mistaken for “malignant” or for a somatic-type malignancy.

Neuroectodermal components may resemble neuroblastoma, medulloepithelioma, peripheral neuroepithelioma, or ependymoblastoma sometimes with mixed differentiation and different immunophenotype. Most are cytokeratin positive [15] and variably stain with synaptophysin, S100 protein, GFAP, Hu, Nb 84, HBA.71, and SOX-2 (personal observation). PNETs occurring in metastatic sites are probably associated with worse prognosis (see below).

Nephroblastoma (Wilms tumor), like teratomas, are an uncommon finding in the testis (Fig. 1), while the occurrence in retroperitoneal teratoma [39] or in distant metastases is far more frequent [40]. A case has been reported arising inside an undescended testis [41]. The nephroblastoma is generally composed of mixture of tubules, blastema, and stromal elements (Fig. 2) and the immunohistochemical finding of a diffuse WT1 stain is sometimes absent. The myogenin and desmin expressions detected rhabdomyomatous differentiation inside the tumor: the skeletal muscle differentiation is apparently due to loss of function of WT1 gene [28].

Carcinomas are less often associated with GCTs of the testis, which is not really surprising, since the number of soft tissue components in teratoma usually exceeds that of the

Fig. 1 Nephroblastoma in teratoma of the testis: macroscopic features of huge enlargement of the right testis with a scrotal cutaneous fistula: at the gross inspection the testis showed a gr. 860 *gray–tan* partially cystic mass with necrosis and hemorragia; the largest diameter of the tumor was 8 cm

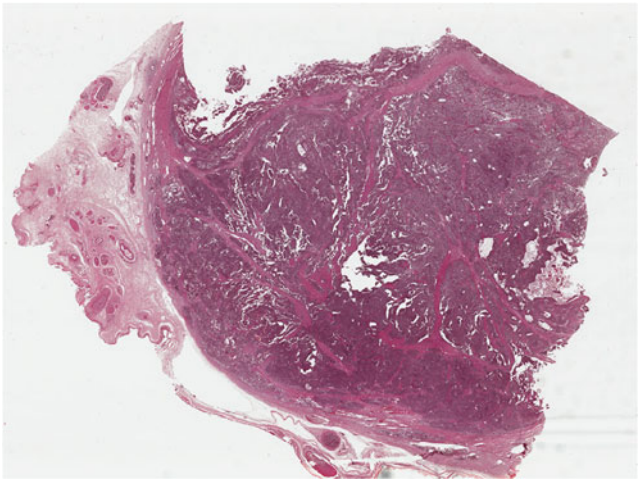

Fig. 2 Nephroblastoma in teratoma of the testis: microscopically, the nephroblastoma appearance of this tumor is easily detectable at low magnification and it is composed of mixtures of tubules, blastema and stromal elements (EE, 4×)

epithelial one. Adenocarcinomas, squamous carcinomas, and neuroendocrine carcinomas are the most frequently reported histological types [2, 3, 8, 9, 42]. These tumors stain for cytokeratins, EMA and sometimes CEA. Stains for PLAP, AFP, and HCG and OCT 3/4 are negative. Recently, a papillary renal cell-like carcinoma has been described in a retroperitoneal metastasis [43]. As in the kidney, the tumor cells positively stained with cytokeratin 7 and alpha-methyl acyl CoA racemase.

Organoid structures mimicking intestine or bronchus are commonly encountered in teratomas. As is the case for normal organs, neuroendocrine cells producing all kinds of hormones (gastrin, bombesin, somatostatin, etc.) are also scattered among the columnar epithelia [44, 45] in these organoid structures. Obviously, testicular carcinoids can arise from these cells and must be classified as MTSC. In case remnants of a germ cell tumor cannot be detected, carcinoids should be diagnosed as a distinct entity. Of the 80 well-documented cases of testicular carcinoid observed, 19 (24 %) were associated with teratoma [45]. They account for 0.2–1 % of all tumors of the testis in various statistics. Tumor cells are immunoreactive for the classical neuroendocrine markers (neuron-specific enolase, chromogranin A, synaptophysin) as well as for the specific peptide hormones produced by carcinoids (gastrin, serotonin, etc.). A small number of patients developed a typical "flash syndrome" [45].

Comparison of testicular and ovarian teratomas

Teratomas arise in the ovaries far more frequently than in the testis. Cystic teratomas account for 10–20 % of all ovarian neoplasms [46]. They are the most common ovarian germ cell tumor and also the most common ovarian neoplasm in patients younger than 20 years. They are bilateral in 8–14 % of cases. In its pure form, the cystic teratoma of the ovary is always benign, but in approximately 0.2–2 % of cases, it can undergo malignant transformation. That means this phenomenon occurs less often than in testicular teratomas. The female patients are mostly menopausal with a median age of 52.5 years (range, 29–77), thus are consistently older than diseased men. Since the single tissue components of ovarian and testicular teratomas differ slightly (Fig. 3) [47] the histology of the MTSC also differs. The dermoid cyst, extremely rare in the testis, is the most frequent ovarian teratoma. Consequently, the squamous carcinoma accounts for more than half of all somatic malignancies reported [48, 49]. Thyroid tissue is a frequent finding in benign teratoma of the ovaries but not existing in the testis, thus also thyroid cancer, generally called "struma maligna ovarii", has been described many times in the ovaries [50]. Carcinoid seems to be described as frequently as in the testis [51]. Extremely rare in the ovaries and never observed in the testis are one amelanotic malignant melanoma [52], a chordoma [53], and two glioblastomas [54].

Genetics and histogenesis

Chromosomal abnormalities typically associated with germ cell tumors, the isochromosome i(12p), were identified in the majority of the cases of TMSC [9] (Fig. 4). Such aberrations were described in the germ cell component as well in

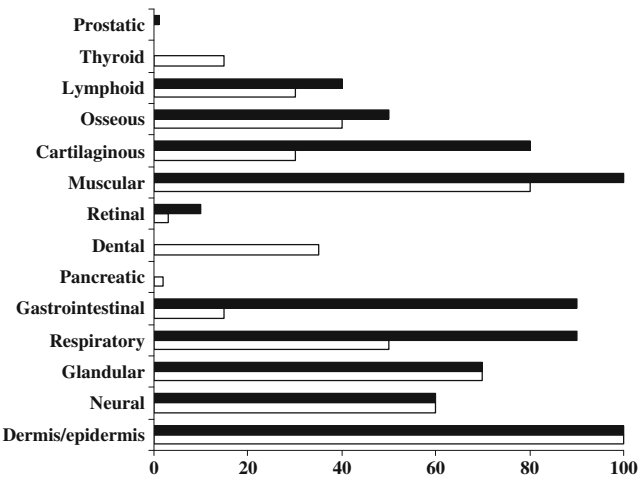

Fig. 3 Frequency of differentiated tissue in teratomas of the testis (*black bars*) and ovary (*white bars*). Respiratory, gastrointestinal, and soft tissue (muscular, osseous, cartilaginous) is more frequent in the testicular than in ovarian teratomas. Thyroid and pancreatic tissue, rather common in teratoma of the ovaries, is not encountered in testicular teratomas (modified after Damjanov [47])

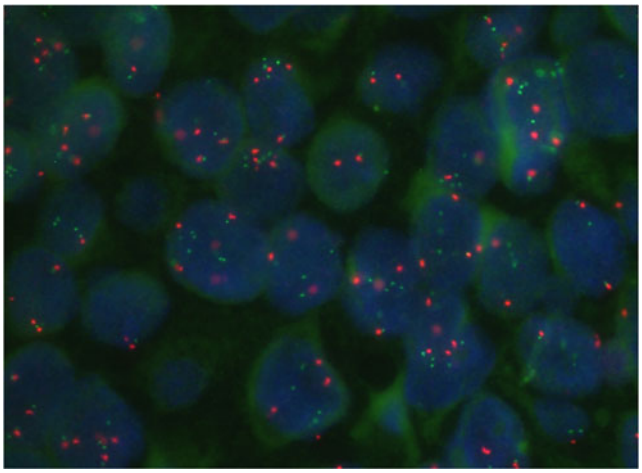

Fig. 4 Two-color FISH performed on teratoma with somatic malignant component occurring in a retroperitoneal lymph node. Overrepresentation of the peritelomeric region (12p13) of the short arm of chromosome 12 (*green*) relative to centromeric region of chromosome 12 (*red*)

the somatic malignancies [9]. Moreover, the typical aberration can also be found in the metastases of such tumors [55].

In a case of teratoma with angiosarcomatous component, the isochromosome 12p overrepresentations were consistently found in the primary germ cell tumor components, metastatic teratoma, and angiosarcoma. The results indicated a clonal origin of the tumors, which supports the conclusion that angiosarcoma, as well as the teratomas, arose from the testicular germ cell tumors sharing epithelioid features and a clonal origin with the other components of the germ cell tumor [42].

In some cases, additionally, chromosomal rearrangements or translocations characteristic of the somatic tumors in their conventional locations were detected [9]. Loss of heterozygosity was observed by Emerson et al. [28] at 11p13, the locus of WT1 inactivation in patients genetically predisposed to nephroblastoma, and may be an important genetic mechanism in nephroblastematous differentiation of GCTs. Loss of heterozygosity was found in four loci, and the same pattern of allelic loss was demonstrated at all four loci in all of the different components (nephroblastoma, mature and immature teratoma, and rhabdomyosarcoma) of the primary tumor and in the metastasis of teratomas, which strongly support the germ cell tumor origin of the nephroblastoma component.

What are actually the original mechanisms of the development of TMSC is still a matter of debate. Two possible explanations have been postulated by Ulbright et al. [3]: a partial differentiation of totipotential germ cells with concomitant malignant transformation or a new tumor arising from differentiated teratomatous elements [6, 8, 10, 29]. The atypical cells of the intratubular germ cell neoplasia (IGCN) cells seem to have a striking phenotypic similarity to embryonic stem cells [56]. Many cancers have been proposed as having originated from tissue-specific stem cells [so-called "cancer stem cells"]. Testicular IGCN may be a very good example of a cancer stem cell with exceptional features due to the retention of embryonic pluripotency. These cells possess a high resistance to exogenous and endogenous agents and are usually not targeted by cytotoxic chemotherapy [57].

Prognosis

Provided the malignant tumor is limited to the testis, the prognosis is not negatively affected [2, 9, 10]. In metastatic sites, the somatic type malignancies have a dismal prognosis if not completely resectable [9, 10, 58]. The presence of MSC in postchemotherapy retroperitoneal lymph node dissection specimens, reported by Little [6], showed a disease-specific survival of 68 % for various sarcomas at a mean follow-up of 2.5 years. Malagon et al. [7] reported only a 20 % survival at a mean of 1.5 years in either testicular TMSC or in their metastases. Comiter et al. [8] described a survival rate of 52 % with a median follow-up of 4 years for TMSC and a much poorer prognosis with a survival of 25 % after 3.5 years mean follow-up in patients showing rhabdomiosarcomatous tumor. Colecchia et al. [10] reported a stage-specific survival of 100 % for stage I, 87.5 % for stage II tumors, and 53 % for stage III patients and the overall survival after a long follow-up (mean 37 months) of 12 stage I patients compared to 28 stages II–III patients showed significant difference (p value<0.0139) [10] (Fig. 5).

GCT-oriented therapy combined with timely surgery seemed to be adequately effective both in first line (64 % of major responses in our series) and in salvage therapy [45]. Therapy designed for the specific type of somatic neoplasm may also be helpful [58].

The histological features of the somatic component do not have any impact on the prognosis. The occurrence of PNET in a stage I tumor seems not to be an unfavorable

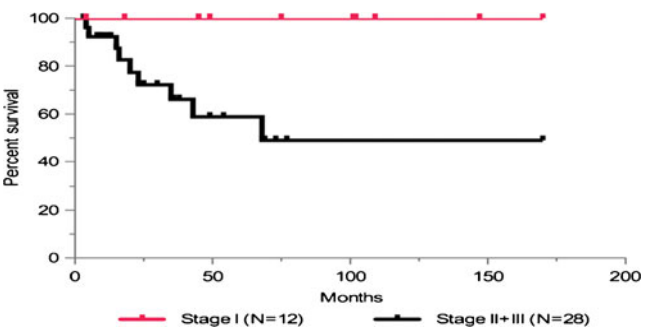

Fig. 5 Stage-specific survival in 40 TMSC followed at the Istituto Nazionale dei Tumori di Milano: the difference among 12 stage I and 28 stages II–III was statistically significant (p value 0.0139)

prognostic factor: these stage I tumors had similar long survival as tumors with other histologies [10], while PNETs occurring in metastatic sites are probably associated with a worse prognosis [34]. In a study from Indiana University, the authors claim that all patients with clinical stage I disease and primitive neuroectodermal tumor in the orchiectomy specimen should initially undergo retroperitoneal lymph node dissection. Of the patients who initially underwent a lymphadenectomy, 89 % had no evidence of disease, whereas the number of disease-free patients without surgery is significantly lower (50 %) [32].

In conclusion, patients who could undergo a radical excision of metastases had a better outcome compared with patients who did not receive a radical extirpation and the strongest prognosticator of a long survival remains tumor burden and the consequent feasibility to perform radical disease removal.

Conclusions and perspectives

Malignant transformation of germ cell tumors into somatic malignancy is uncommon [2, 3, 8, 15, 46]. To establish the therapy based on a wide surgical approach, the correct diagnosis is very important in primary testicular tumors as well as in the metastases. The incidence of intratesticular vs. metastatic occurrence differs in different series, with 43 % of adult cases identified within the primary tumors and the remaining ones at the time of relapse or in the metastasis [29]. The morphology of the teratoma (mature vs. immature teratomas) does not have any impact on the risk of TMSC development [59]. Conventional cytogenetics has been used to demonstrate germ cell origin of these somatic malignancies arising in germ cell tumors [60], but to clarify the biology of TMSC; further studies at molecular level are needed. In addition, new chemotherapies with integration of somatic malignancy tailored therapies and GCT-oriented regimens are necessary to provide a higher rate of cure.

Conflict of interest statement We declare that we have no conflict of interest.

References

1. Ulbright TM, Amin MB, Young RH (1997) Tumors of the testis, adnexa, spermatic cord, and scrotum. In: Rosai J, Sobin LH (eds) Atlas of Tumor Pathology, third series fascicle 25. Armed Force Institute of Pathology, Washington, DC
2. Ahmed T, Bosl GJ, Hajdu SI (1985) Teratoma with malignant transformation in germ cell tumors in men. Cancer 56:860–863
3. Ulbright TM, Loehrer PJ, Roth LM et al (1984) The development of non-germ cell malignancies within germ cell tumors. A clinicopathologic study of 11 cases. Cancer 54:1824–1833
4. Donadio AC, Motzer RJ, Bajorin DF et al (2003) Chemotherapy for teratoma with malignant transformation. J Clin Oncol 21:4285–4291
5. Guo CC, Punar M, Contreras AL et al (2009) Testicular germ cell tumors with sarcomatous components: an analysis of 33 cases. Am J Surg Pathol 33:1173–1788
6. Little JS Jr, Foster RS, Ulbright TM et al (1994) Unusual neoplasms detected in testis cancer patients undergoing post-chemotherapy retroperitoneal lymphadenectomy. J Urol 152:1144–1149
7. Malagón HD, Valdez AM, Moran CA et al (2007) Germ cell tumors with sarcomatous components: a clinicopathologic and immunohistochemical study of 46 cases. Am J Surg Pathol 31:1356–1362
8. Comiter CV, Kibel AS, Richie JP et al (1998) Prognostic features of teratomas with malignant transformation: a clinicopathological study of 21 cases. J Urol 159:859–863
9. Motzer RJ, Amsterdam A, Prieto V et al (1998) Teratoma with malignant transformation: diverse malignant histologies arising in men with germ cell tumors. J Urol 159(1):133–138
10. Colecchia M, Necchi A, Paolini B et al (2011) Teratoma with somatic-type malignant components in germ cell tumors of the testis: a clinicopathologic analysis of 40 cases with outcome correlation. Int J Surg Pathol 19:321–327
11. Ewing J (1911) Teratoma testis and its derivates. Surg Gynecol Obstet 12:230–261
12. Kaufmann E. (1903) Malattie degli organi genitali maschili. In: Trattato di anatomia patologica speciale per medici e studenti (2nd German edition), Vallardi, Milano, pp 782–783
13. Friedman NB, Moore RA (1946) Tumors of the testis: a report of 922 cases. Mil Surg 99:573–593
14. Mostofi FK, Price EP (1973) Tumors of the genital system. In: Atlas of Tumor Pathology, fascicle 8. Washington, DC, Armed Forces Institute of Pathology, pp 59–65
15. Eble JN, Sauter G, Epstein JI et al (eds) (2004) World Health Organization classification of tumors. Pathology and genetics tumors of the urinary system and male genital organs. IARC Press, Lyon
16. Terenziani M, D'Angelo P, Bisogno G et al (2010) Teratoma with a malignant somatic component in pediatric patients: the Associazione Italiana Ematologia Oncologia Pediatrica (AIEOP) experience. Pediatr Blood Cancer 54:532–537
17. Davey DD, Ulbright TM, Loehrer PJ et al (1987) The significance of atypia within teratomatous metastases after chemotherapy for malignant germ cell tumors. Cancer 59:533–539
18. Ulbright TM, Roth LM (1999) Testicular and paratesticular tumors. In: Sternberg SS (ed) Diagnostic surgical pathology, 3rd edn. Lippincott, Philadelphia, p 2000
19. Moran CA, Suster S (1997) Primary germ cell tumors of the mediastinum. Cancer 80:681–690
20. Pressing J, Smith H (1979) Rhabdomyosarcoma arising in pineal teratoma. Cancer 44:281–284
21. Ahlgren AD, Simrell CR, Triche TJ et al (1984) Sarcoma arising in a residual testicular teratoma after cytoreductive chemotherapy. Cancer 54:2015–2018
22. Klein FA, Herr HW, Vugrin D (1983) Fibrosarcoma associated with intensive chemotherapy for advanced germ cell testicular tumor. J Surg Oncol 23:5–7
23. Michael H (1998) Nongerm cell tumors arising in patients with testicular germ cell tumors. J Urol Pathol 9:39–60
24. Ritchey ML, Bagnall JW, McDonald EC et al (1985) Development of nongerm cell malignancies in nonseminomatous germ cell tumors. J Urol 134:146–149

25. Terrier-Lacombe MJ, Martinez-Madrigal F et al (1990) Embryonal rhabdomyosarcoma arising in a mature teratoma of the testis: a case report. J Urol 143:1232–1234
26. Ulbright TM, Michael H, Loehrer PJ et al (1990) Spindle cell tumors resected from male patients with germ cell tumors. A clinicopathologic study of 14 cases. Cancer 65:148–156
27. Kasai T, Moriyama K, Tsuji M et al (2003) Adenocarcinoma arising from a mature cystic teratoma of the testis. Int J Urol 10:505–509
28. Emerson RE, Ulbright TM, Zhang S et al (2004) Nephroblastoma arising in a germ cell tumor of testicular origin. Am J Surg Pathol 28:687–692
29. El Mesbahi O, Terrier-Lacombe MJ, Rebischung C et al (2007) Chemotherapy in patients with teratoma with malignant transformation. Eur Urol 51:1306–1311
30. Reyes A, Moran CA, Suster S et al (2003) Neuroendocrine carcinomas (carcinoid tumor) of the testis. A clinicopathologic and immunohistochemical study of ten cases. Am J Clin Pathol 120:182–187
31. Ulbright TM, Clark SA, Einhorn LH (1985) Angiosarcoma associated with germ cell tumors. Hum Pathol 16:268–272
32. Ganjoo KN, Foster RS, Michael H et al (2001) Germ cell tumor associated primitive neuroectodermal tumors. J Urol 165:1514–1516
33. Kato K, Ijiri R, Tanaka Y et al (2000) Testicular immature teratoma with primitive neuroectodermal tumor in early childhood. J Urol 164:2068–2069
34. Michael H, Hull MT, Ulbright TM et al (1997) Primitive neuroectodermal tumors arising in testicular germ cell neoplasms. Am J Surg Pathol 21:896–904
35. Aguirre P, Scully RE (1983) Primitiveneuroectodermal tumor of the testis. Report of a case. Arch Pathol Lab Med 107:643–645
36. Molenaar WM, Oosterhuis JW, Meiring A et al (1986) Histology and DNA contents of a secondary malignancy arising in a mature residual lesion six years after chemotherapy for a disseminated nonseminomatous testicular tumor. Cancer 58:264–268
37. Serrano-Olmo J, Tang CK, Seidmon EJ et al (1993) Neuroblastoma as a prominent component of a mixed germ cell tumor of testis. Cancer 72:3271–3276
38. Nocks BN, Dann JA (1983) Primitive neuroectodermal tumor (immature teratoma) of testis. Urology 22:543–544
39. Carney JA (1975) Wilms' tumor and renal cell carcinoma in retroperitoneal teratoma. Cancer 35:1179–1183
40. Michael H, Hull MT, Foster RS et al (1998) Nephroblastoma-like tumors in patients with testicular germ cell tumors. Am J Surg Pathol 22:1107–1114
41. Ho J, Ma L, Wong KC (1981) An extrarenal Wilms' tumor arising from an undescended testis. Pathology (Phila) 13:619–624
42. Idrees MT, Kuhar M, Ulbright TM et al (2010) Clonal evidence for the progression of a testicular germ cell tumor to angiosarcoma. Hum Pathol 41:139–144
43. Marusić Z, Zovak M, Hagenkord JM et al (2010) Papillary renal cell-like carcinoma in a retroperitoneal teratoma. Pathol Int 60:581–586
44. Pichman S, Mikuz G, Schmid KW (1993) Chromogranins A and B in non-seminomatous testicular tumors. J Urol Pathol 1:43–45
45. Mikuz G, Colecchia M (2007) Miscellaneous tumors of the testis. In: Mikuz G (ed) Clinical pathology of urologic tumor. Informa Healthcare, London, p 198
46. Comerci JT Jr, Licciardi F, Bergh PA et al (1994) Mature cystic teratoma: a clinicopathologic evaluation of 517 cases and review of the literature. Obstet Gynecol 84:22–28
47. Damjanov I (1997) Tumors of the testis and epididymis. In: Murphy WM (ed) Urological pathology, 2nd edn. Saunders, London, pp 271–341
48. Sakuma M, Otsuki T, Yoshinaga K et al (2010) Malignant transformation arising from mature cystic teratoma of the ovary: a retrospective study of 20 cases. Int J Gynecol Cancer 20:766–771
49. Dos Santos L, Mok E, Iasonos A et al (2007) Squamous cell carcinoma arising in mature cystic teratoma of the ovary: a case series and review of the literature. Gynecol Oncol 105:321–324
50. Marcy PY, Thariat J, Benisvy D et al (2010) Lethal, malignant, metastatic struma ovarii. Thyroid 20:1037–1340
51. Robboy SY, Scully RE (1980) Strumal carcinoid of the ovary: an analysis of 50 cases of a distinctive tumor composed of thyroid tissue and carcinoid. Cancer 46:2019–2034
52. Borup K, Leisgård Rasmussen K, Schierup L et al (1992) Amelanotic melanoma arising in an ovarian dermoid cyst. Acta Obstet Gynecol Scand 71:242–244
53. La Heras F, Pritzke KP, Colgan TJ (2007) Chordoma arising in a mature cystic teratoma of the ovary: acase report. Pathol Res Pract 203:467–471
54. Den Boon J, van Djik CM, Helfferich et al (1999) Glioblastoma multiforme in a dermoid cyst of the ovary. A case report. Eur J Gynaecol Oncol 20:187–188
55. Korski K, Breborowicz D, Filas V et al (2007) A case of primary testicular germ cell tumor with rhabdomyosarcoma metastases as an example of applying the FISH method to diagnostic pathology. APMIS 115:1296–1301
56. Almstrup K, Sonne SB, Hoei-Hansen CE et al (2006) From embryonic stem cells to testicular germ cell cancer—should we be concerned? Int J Androl 29:211–218
57. Mego M (2006) Cancer stem cell in relapsed testicular germ cell cancer: embryonic or somatic? Int J Androl 29:627
58. Necchi A, Colecchia M, Nicolai N et al (2010) Towards the definition of the best management and prognostic factors of teratoma with malignant transformation: a single-institution case series and new proposal. BJU Int 107:1088–1094
59. Biskup W, Calaminus G, Schneider DT et al (2006) Teratoma with malignant transformation: experiences of the cooperative GPOH protocols MAKEI 83/86/89/96. Klin Padiatr 218:303–308
60. Kernel KM, Ulbright TM, Zhang S et al (2003) Identical allelic losses in mature teratoma and other histologic components of malignant mixed germ cell tumors of the testis. Am J Pathol 163:2477–2484

Virchows Arch (2012) 461:33–39
DOI 10.1007/s00428-012-1252-9

ORIGINAL ARTICLE

Co-expression of VEGF and CA9 in ovarian high-grade serous carcinoma and relationship to survival

Emma Williams · Stewart Martin · Robert Moss · Lindy Durrant · Suha Deen

Received: 2 March 2012 / Revised: 4 May 2012 / Accepted: 11 May 2012 / Published online: 15 June 2012
© Springer-Verlag 2012

Abstract Poor prognosis in ovarian high-grade serous carcinoma (HGSC) is largely related to resistance to chemotherapy. Tumour hypoxia is known to be associated with chemotherapy resistance. Stabilisation of hypoxia-inducible factor-1α upregulates the expression of downstream genes such as carbonic anhydrase 9 (CA9) and vascular endothelial growth factor (VEGF). This study was undertaken to analyse the hypoxia profile as indicated by the co-expression of VEGF and CA9 and its correlation with survival. VEGF and CA9 expressions were examined in tissue microarray of 97 cases of ovarian high-grade serous carcinoma using immunohistochemistry. High expression of either VEGF or CA9, individually, was associated with decreased overall survival (p=0.006 and p=0.05 respectively). Combined high expression of both markers, to give a 'hypoxia profile', was associated with chemotherapy resistance (p=0.036) and showed worse overall survival with a significant p value (p=0.001). Using multivariate analysis, hypoxia profile was an independent prognostic factor for overall survival (p=0.028). The combined high expression CA9 and VEGF phenotype, described as high hypoxia profile group, was significantly associated with increased resistance to chemotherapy and poor overall survival. This group may benefit from combined targeted therapy for effective response in ovarian HGSC.

E. Williams · S. Deen (✉)
Department of Histopathology, Nottingham University Hospitals NHS Trust, Queen's Medical Centre Campus,
Derby Road,
Nottingham NG7 2UH, UK
e-mail: sdeen@doctors.org.uk

S. Martin · R. Moss · L. Durrant
Division of Clinical Oncology, School of Molecular Medical Sciences, University of Nottingham, City Hospital Campus,
Nottingham NG5 1PB, UK

Keywords Ovarian cancer · Serous carcinoma · Carbonic anhydrase · VEGF

Introduction

Ovarian high-grade serous carcinomas (HGSC) are the most common type of ovarian epithelial carcinomas and have the worst prognosis [1]. The 5-year survival rate is only 30 %, mainly due to chemotherapy resistance [2]. Tumour cells that manage to survive within a cluster of over 1 mm^3 undergo a state of hypoxia that necessitates activation of alternative survival pathways. One of the significant alternative pathways is a bypass of the mitochondrial oxidative phosphorylation, using glycolysis instead. On the other hand, the growth of solid tumours depends, at least partly, on establishing new blood supply to facilitate oxygen delivery through the process of angiogenesis; the latter involving production of vascular endothelial growth factor (VEGF), a potent angiogenic factor [3]. However, angiogenesis results in the development of an irregular, chaotic and fragile vascular network leading to further tumour hypoxia and necrosis [4]. Genes that facilitate anaerobic metabolism of glucose and genes that regulate vascularity such as VEGF are described as hypoxia-inducible genes and are regulated by the hypoxia inducible factor-1-α (HIF-1α) [4, 5]. Hypoxia-induced transcription is mediated through promoters of VEGF and carbonic anhydrase 9 (CA9) and controlled by HIF-1 pathway [6].

This state of hypoxia creates an acidic tumour microenvironment which is mainly due to accumulations of lactic acid, a by-product of glycolysis. The reversible hydration of carbon dioxide to carbonic acid, catalysed by carbonic anhydrases [7, 8] contributes further to the acidity of the tumour microenvironment. Tumour cells that succeed in

establishing themselves in an acidic hypoxic environment tend to be aggressive and capable of metastasis. Moreover, tumour hypoxia has been linked with chemotherapy and radiotherapy resistance as well as metastasis and poor clinical outcome [9, 10]. Some chemotherapy agents, such as mitoxantrone, doxorubicin and daunorubicin are weak alkalis and as such are inhibited by the acidic tumour microenvironment. On the other hand, cyclophosphamide, 5-fluorouracil and chlorambucil are weak acids and therefore they are enhanced by the tumour acidity. Hence, tumour microenvironment acidity may act as a significant barrier to tumour response to chemotherapy. The interruption of the previously described pathway of oxygen homeostasis and the reversal of an acidotic microenvironment seems to be a promising therapeutic target to enhance the efficacy of existing chemotherapies [11].

CA9 is a stable transmembrane zinc metalloenzyme. Overexpression of CA9, as a potential marker of hypoxia, has been reported in solid tumours with significant association between high levels of CA9 and unfavourable clinical outcome of several epithelial cancers such as breast, cervical and non-small cell [12–14]. Recently, a significant correlation between high level of co-expression of VEGF and CA9 and poor prognosis was reported in nasopharyngeal carcinoma and upper gastrointestinal adenocarcinoma [15, 16]. A treatment approach that targets hypoxic cells may indeed be important. Data concerning hypoxia in ovarian cancer are limited and mainly performed on cell lines. Effect of hypoxia in ovarian cancer and specifically in high-grade serous carcinoma has not been studied in depth except for the occasional report [17]. The current study was undertaken with the aim to assess the co-expression of CA9 and VEGF and its correlation with clinicopathological variables and survival, in ovarian high-grade serous carcinoma. We hypothesise that the combined increased expression of VEGF and CA9 is significantly correlated with disease outcome.

Materials and methods

Patient cohort and clinicopathological variables

Archival paraffin-embedded tissue blocks from 97 patients (range 36–85, mean 62 years) and with HGSC diagnosed between January 1, 1991 and December 31, 2007, were used. HGSC was defined as ovarian serous carcinomas with high nuclear grade (grades 2 and 3) showing complex branching papillary pattern, highly pleomorphic nuclei and brisk mitotic activity. Only cases treated initially with surgery with available follow-up data were included in this study. Sixteen percent of patients presented with International Federation of Gynaecology and Obstetrics (FIGO) stage 1, 18 % stage 2, 57 % stage 3 and 9 % stage 4. All patients were treated with surgery in an attempt to achieve optimal debulking (where residual tumour was either absent or less than 2 cm) with or without chemotherapy. The reporting of this study adheres to the RECIST guidelines [18]. Information on disease FIGO stage and presence or absence of residual macroscopic disease after surgery, date of recurrence and tumour-related death was collected from records when available (Table 1). According to the Gynaecological Oncology Group criteria, data on response to chemotherapy were categorised as resistant if recurred within 6 months of starting treatment or otherwise classified as responsive to chemotherapy [19].

Overall survival and progression-free survival

Five-year overall survival (OS) and progression-free survival (PFS) were available for calculation. OS was calculated from the date of surgery to August 2009 when any remaining survivors were censored. OS data were available for 97 patients (mean 37 months) with 65 % died within 5 years of diagnosis. Post-operative deaths were excluded. PFS was defined from the date of commencing surgical treatment until the date when recurrence was confirmed clinically; 70 % of cases recurred within 5 years of starting treatment (mean 30 months)

Table 1 Patient and tumour characteristics

Age (n=97) mean (range, year)	62 (36–85)
FIGO stage (n=97)	
Stage 1	16 (16 %)
Stage 2	17 (18 %)
Stage 3	55 (57 %)
Stage 4	9 (9 %)
Residual disease (n=94)	
More than 2 cm	35 (37 %)
Less than 2 cm or none	59 (63 %)
Recurrence within 5 years (n=82), mean 30 months	
Recurrence within 5 years	57 (70 %)
No recurrence within 5 years	25 (30 %)
Overall survival within 5 years (n=97), mean 37 months	
Dead within 5 years	63 (65 %)
Alive after 5 years	33 (35 %)
Type of chemotherapy (n=96)	
Platinum based chemotherapy	88 %
Response to chemotherapy (n=84)*	
Resistant	15 (18 %)
Responsive	69 (82 %)

*As defined by the Gynaecological Oncology Group

All cases were subsequently reviewed by a specialist gynaecological pathologist (SD) to ensure accuracy of histologic type and grade. To build tissue microarray (TMA) blocks, for each of the 97 patients, one 0.6 mm core was used. The validity of this technique has been repeatedly enforced by publications, especially in ovarian tumours where analysis of immunohistochemical markers in one core matched the staining pattern of a whole section in more than 90 % of the time [20, 21]. TMAs were constructed first as outlined by Kononen et al. [22] using Beecher Instruments' microarrayer.

Immunohistochemisty

A prediluted rabbit anti-human VEGF antibody was used (SP28, Abcam, Cambridge, UK) and A rabbit polyclonal antibody to CA9 (Abcam 15086, Cambridge, UK). Renal tissue was used as positive control as recommended by the manufacturer. Fresh 4-μm sections were prepared from each TMA block and placed on poly-L-lysine-coated glass slides for VEGF and CA9 immunohistochemistry to be performed, bearing in mind that it has been demonstrated that many proteins retain their antigenicity for more than 60 years [23]. Optimization of the staining was done on ovarian cancer spare using a range of dilutions and incubation times. For each of the antibodies, the dilution and incubation time that produced the best results with minimal background staining were chosen. Briefly, slides were dewaxed in xylene (2× 10 min) and rehydrated in three grades of ethanol (99, 90 and then 70 %) for 1 min each. Endogenous peroxidase activity was blocked by immersing the slides in a 0.03 % solution of H_2O_2 in methanol for 25 min. Heat-induced epitope retrieval was done using an 800-W rotary microwave oven. Slides were cooled and rinsed with Tris-buffered saline (TBS; Dako, Ely, Cambridgeshire, UK) for10 min. To reduce nonspecific adsorption of antibodies to tissue, the slides were incubated with normal swine serum (Dako) diluted 1:20 in TBS for 10 min. The test sections were then left to incubate with the prediluted rabbit anti-VEGF antibody (SP28, Abcam) and CA9 (1:1,000 dilution) accordingly for 1 h at room temperature. Negative control slides in which the primary antibody was omitted were included in all the assays.

Evaluation of the staining

High-resolution digital images at ×20 magnification of the immunohistochemically stained TMA were obtained (Nanozoomer, Hamamatsu Photonics) and assessed. Only tumour cells in individual cores were assessed using *H* scoring [24]. The *H* score value, for each marker, ranged from 0–300, calculated as the sum of the products of percentage of positive cells multiplied by staining intensity graded from 1+ to 3+. All cores were assessed by two of the authors (EW, SD) independently, both of whom were blind to the clinical and pathologic variables of the case. When there was non-concordance in assessment, cases were discussed using a double-headed microscope and a consensus was reached. Determination of the optimal cut-off points for the markers, based on OS, was assessed using X-tile Bioinformatics Software, version 3.6.1, 2003–2005 (Yale University, USA) [25]. X-tile is a bioinformatics tool that allows users to find out population cut-off points based on marker expression. The *H* score cut-off points between high and low expression groups were 100 and 80 for VEGF and CA9, respectively.

Statistical analysis

The statistical software package SPSS Version 16, (SPSS Inc., Chicago, IL, USA) was used to analyse for correlations between CA9 and VEGF expression and clinicopathological parameters, using Pearson's χ^2 test. Survival analysis, comparing protein expression and OS, was calculated using the Kaplan–Meier method and the statistical significance of the difference between the survival curves of evaluated groups was assessed using the log rank test. Multivariate analysis was performed using Cox regression. In all cases, a p value of <0.05 was taken as indicator of statistical significance.

Results

A significant association between the expression of each of the studied markers (VEGF and CA9) and survival was identified in isolation and when combined together as hypoxia profile which correlated significantly with response to chemotherapy. Moreover, the combined high expressions of high CA9 and VEGF were significantly associated with OS and this remained significant in multivariate analysis.

Marker expression

Granular cytoplasmic staining for VEGF and CA9 (Fig. 1a, b, c and d) was seen in tumour cells. Both markers showed weak occasional staining of the inflammatory cells. Unlike CA9, VEGF also stained endothelial cells; 94 and 86 cases were available for VEGF and CA9 assessment respectively. A total of 39 cases (41 %) and 55 cases (59 %) showed low expression (≤100) and high expression (>100) of VEGF expression, respectively. Nineteen cases (22 %) and 67 cases (78 %) showed low expression (≤80) and high expression (>80) of CA9 expression, respectively. Using Spearman's rank correlation coefficient, there was a significant correlation between CA9 and VEGF ($p=0.007$), albeit with a weak positive correlation coefficient of 0.287.

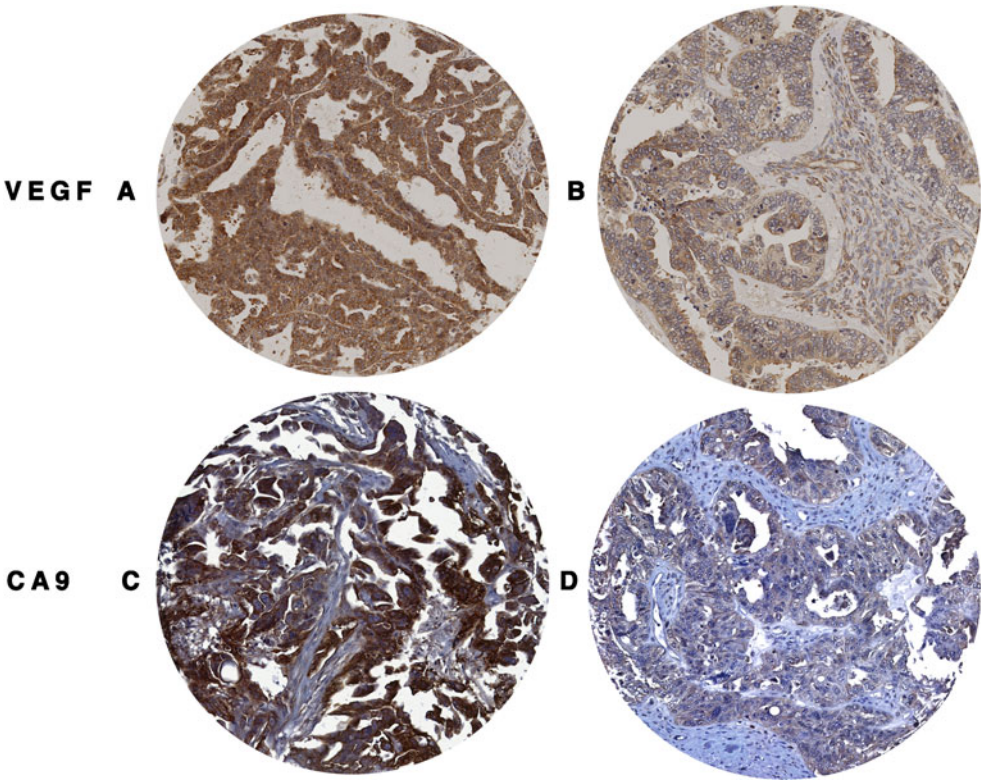

Fig. 1 Photomicrograph showing cytoplasmic staining with high (**a**) and low (**b**) expression of VEGF and high (**c**) and low (**d**) expression of CA9 (×20)

Correlation with clinicopathological variables

All tumours were of the same morphological type of HGSC and by definition they were all of high grade. The correlation between the expression of each marker, VEGF and CA9, with tumour FIGO stage and response to chemotherapy was analysed using Pearson χ^2 statistical test.

High expression of VEGF and tumour FIGO stage (p=0.05) was associated with advanced stage. An average of 66 % of cases in FIGO stages 3 and 4 disease and 45 % cases in FIGO stages 1 and 2 disease showed high expression of VEGF. On the other hand, there was no significant correlation between CA9 and tumour FIGO stage.

VEGF expression was inversely correlated with response to chemotherapy (p=0.039) with 27 % and 6 % of cases in the high and low VEGF expression groups, respectively, being resistant to chemotherapy. On the other hand, there was no significant correlation between CA9 and response to chemotherapy.

Correlation overall survival and progression-free survival

Ninety-four cases stained for VEGF and 86 cases stained for CA9 had follow-up data for survival and were available for assessment. High expressions of VEGF and CA9 were significantly associated with poor OS. In contrast, there was no significant correlation between any of the markers and PFS. Patients with a high VEGF expression had a mean OS of 34 months, in contrast to 46 months for those with a low expression (log rank 7.5, p=0.006, 95 %CI 31.7=54.3; Fig. 2a).

CA9 expression was also significantly associated with OS (Log Rank test 3.8, p=0.051, 95 %CI 29-60.9) with a mean survival of 37 months in the high expression group and 47 months in the low expression group (Fig. 2b).

Combined expressions of VEGF and CA9

The co-expression of VEGF and CA9 was incorporated into a single prognostic marker (hypoxia profile). A total of 86 cases with OS data and available expressions of both VEGF and CA9 were available for assessment and were categorised into 4 possible combinations; low VEGF, low CA9 (LL; n=14, 16 %), low VEGF, high CA9 (LH; n=23, 27 %), high VEGF, low CA9 (HL; n=5, 6 %) and high VEGF, high CA9 (HH; n=44, 51 %). When all four combination groups were analysed, there was a significant correlation with OS (logrank 10.02, p=0.018, 95 %CI 29–60.9), but not with PFS (Table 2, Fig. 2c).

In order to further interrogate the effect of co-expression of high VEGF and high CA9, the cases were re-categorised as high hypoxia profile group (HH group) and low hypoxia profile group showing other combination of co-expression of VEGF and CA9 (LH, HL and LL). The correlations of both groups with OS and PFS were analysed. The analysis demonstrated that the high hypoxia profile group had

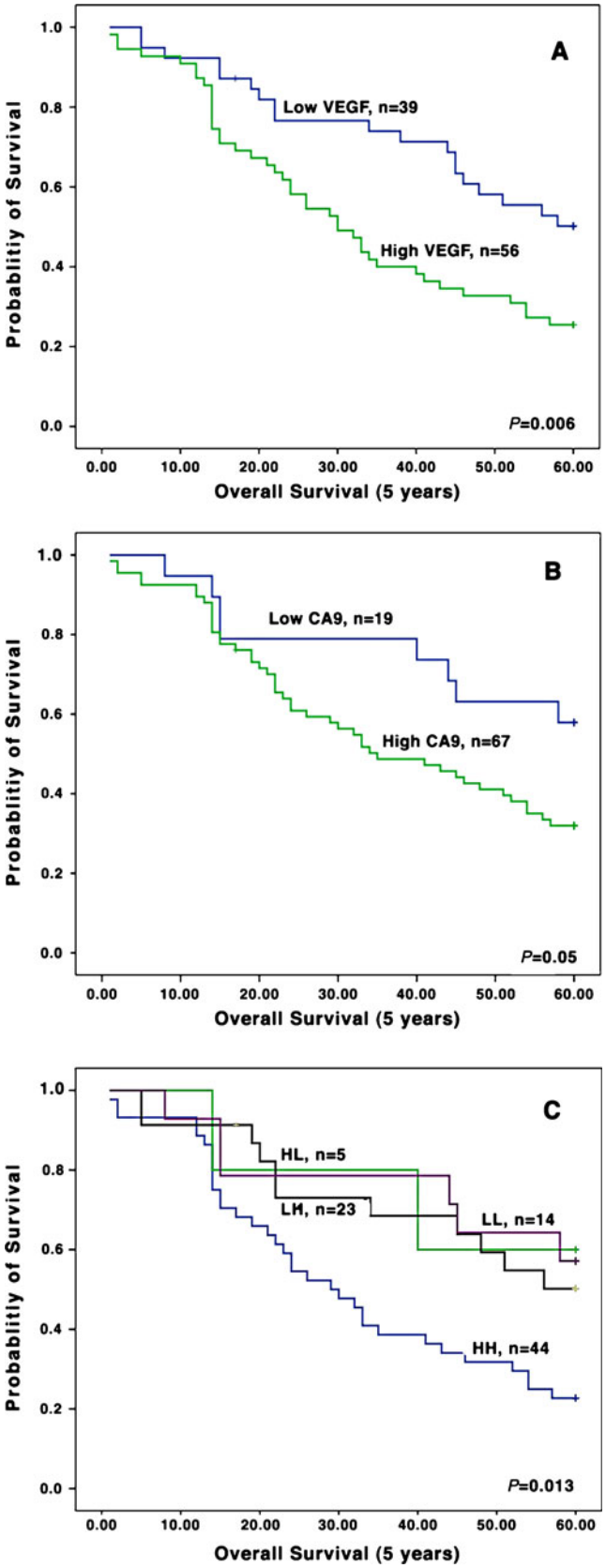

Fig. 2 Kaplan–Meier survival stratified for VEGF (**a**), CA9 (**b**) and co-expression of VEGF and CA9 (**c**) (*blue line* HH, *black line* LH, *green line* HL and *purple line* LL) in cases of ovarian HGSC

Table 2 Univariate analysis of various combinations of CA9 and VEGF expressions in association with OS and PFS

	LL (n=14)	LH (n=23)	HL (n=5)	HH (n=44)	Logrank	p value
OS	48	45	47	33	10.02	0.018
PFS	43	36	37	24	6.6	0.085

LL low VEGF/low CA9); *LH* low VEGF/high CA9; *HL* high VEGF/low CA9; *HH* high VEGF/high CA9

significantly shorter period of OS (logrank 11.2; p=0.001, 95 %CI 29–60.9) when compared with the low hypoxia profile group, with mean survival of 33 and 47, respectively. There was no significant correlation between the two groups and PFS.

When the analysis of each marker, individually, was extended to include tumour FIGO stage and residual disease, the two most important independent prognostic markers in ovarian cancer, using Cox regression multivariate analysis, VEGF, but not CA9, appeared to be an independent prognostic factor (p=0.05, 95 % CI 1.01–3.08). Interestingly, using multivariate analysis revealed that categorising tumours as high and low hypoxia profile groups is an independent prognostic factor with a high significant correlation with survival (p=0.028, 95 % 0.28–0.93; Table 3). Moreover, using Pearson χ^2, the hypoxia profile was significantly correlated with response to chemotherapy (p=0.036) with 28 % and 9 % of the high and low hypoxia profile groups respectively, being resistant to chemotherapy.

Discussion

Cancer growth, spread and chemotherapy resistance are promoted by hypoxic microenvironment which affects several genes through stabilisation of HIF-1α. The latter triggers the promoters of CA9 and VEGF, contributing to the extracellular acidity and neovascular formation [4, 5]. A small number of reports have examined the combined

Table 3 Cox Regression Multivariate model for tumour FIGO stage, residual disease and the co-expression of VEGF and CA9 into high risk and low risk groups

	p value	Exp(B)	95 % CI EXP(B)	
			Lower	Upper
FIGO stage	0.000	2.4	1.5	3.8
Residual disease	0.332	0.833	0.6	1.2
High vs low hypoxia profile groups of VEGF and CA9 co-expression	0.028	0.513	0.3	0.9

expression of CA9 and VEGF in various tumours [15, 16, 26], but this has not, to our knowledge, been conducted in ovarian cancer. In the current study, the combined high expression CA9 and VEGF phenotype, described as high hypoxia profile group, showed significant positive correlation with resistance to chemotherapy and poor OS using multivariate analysis, suggesting that this phenotype may have a useful role in stratifying ovarian cancer for prognostic and therapeutic purposes.

High expression of VEGF is associated with poor disease outcome in various tumours such as breast and ovarian epithelial cancer [27, 28]. In the present study, and consistent with our previous work [20], VEGF expression inversely correlated with OS of ovarian HGSC and that VEGF is an independent prognostic factor for overall survival. However, there was no significant correlation between VEGF expression and PFS.

Hypoxia may lead to enhanced tumour progression potential and resistance to chemotherapy [6]. However, ovarian tumours may reach a significantly large size with expected hypoxic environment albeit the tumour is still confined to the ovary as FIGO stage 1. Therefore, it would be naive to assume that hypoxia is directly correlated with mere tumour growth and spread. This may explain the lack of significant correlation between the expression of CA9 and tumour FIGO stage in the current study. There are no published reports on the correlation between CA9 and ovarian HGSC for comparison; whereas, in agreement with other publications [27], VEGF showed a significant correlation with FIGO stage.

To date, the reports on the correlation between the expression of CA9 and survival in cancer are controversial. Studies on cervical, endometrial and nasopharyngeal carcinomas showed that increased CA9 expression correlated with poor outcome [16, 29]. Conversely, studies on renal clear cell carcinoma [26] and colorectal cancer [30] have suggested that low expression of CA9 was associated with poor prognosis. Few studies on the role of hypoxia in ovarian cancer have been published. In a study by Birner et al. of 102 ovarian cancers, 50 borderline ovarian tumours and 20 benign ovarian tumours with follow-up period ranging between 1 and 130 months showed no correlation between the expression of HIF-1 and overall survival [31]. In the current study, high expression of CA9 was associated with poor overall survival. The main differences between the Birner et al. study and the current one is that they used HIF-1 rather than CA9 and also had a different study design to the current work, where the authors used a variety of ovarian tumour types of variable cell of origin and prognosis.

Under hypoxic conditions, upregulation of HIF-1α results in increased expression of VEGF and CA9, leading to increased angiogenesis and enhanced survival of tumour cells facilitated by a switch to anaerobic metabolism [32]. Few studies have examined the combined effect of CA9 and VEGF. The co-expression of these two markers as being more accurate in predicting prognosis than each marker individually has been reported in nasopharyngeal carcinoma [15] but in intestinal-type adenocarcinoma of upper gastrointestinal tract, only CA9 was an independent prognostic factor for survival [16]. In contrast, Phuoc et al. reported inverse correlation between CA9 and VEGF in clear cell renal cell carcinoma [26]. Moreover, Jubb et al. reported on a diverse cohort of human tumours exhibited VEGF expression in the absence of markers of hypoxia such as CA9 except in renal tumours where correlation between the expressions of both markers was demonstrated [33]. To our knowledge, the combined effect of CA9 and VEGF has not been studied in ovarian HGSC tissue samples. Our results showed significant correlation between the co-expression of VEGF and CA9 and survival in other tumours. To study the combined expression of VEGF and CA9, initially we classified cases into four possible combinations of high and low expression of both markers. These categories are significantly associated with OS and the correlation remained significant when the assessment extended to multivariate analysis. This finding was confirmed with significant results when cases re-classified into two groups of high hypoxia profile (showing high expression of VEGF and CA9) and low hypoxia profile showing other variable combination of both markers' expression. In this study, we propose to define a model of combined expression of VEGF and CA9 to stratify disease outcome as high and low hypoxia profile groups. The high hypoxia profile group showed a positive correlation with chemotherapy resistance and inverse correlation with disease outcome. Whilst the literature varies in the published data on the combined effect of VEGF and CA9, it seems that there is an agreement that studying both makers together is more meaningful than each marker separately. Our study has several limitations. First, whilst we tested 97 cases, this is still considered as a limited sample size and some of the associations were marginally significant. Validation of the results on a larger series would be favourable. Second, it would be beneficial to include other markers of hypoxia. Further, in vitro analysis and tissue molecular testing would be more informative to explain the role VEGF and CA9.

The data presented here indicate that CA9 and VEGF are expressed in epithelial ovarian cancer and the combined effect of the two markers should be evaluated as potential clinically useful markers and target molecules. Targeting both CA9 and VEGF may be more effective than inhibiting either of these proteins in isolation. It may be used in combination with chemotherapy or as a maintenance therapy.

In conclusion, HGSC has a poor prognosis, in part due to limited treatment options. In this study, we analysed the co-expression of VEGF and CA9 in HGSC and demonstrated that cases showing a high expression of VEGF combined with a high expression of CA9 had poor overall survival and were resistant to chemotherapy. This finding stayed significant with multivariate analysis and showed that combined high expression of VEGF and CA9 is an independent prognostic factor of overall survival. Although requiring validation, the findings of this study open the field for further development of targeted therapy in the form of a combined anti-CA9 and anti-VEGF approach that may improve survival of patients with this disease.

Conflict of interest The authors declare they have no conflict of interest.

References

1. Westfall D, Roma AA, Silva EG (2009) High-grade serous carcinoma of the ovary. Ann Diagn Pathol 13(4):285–290
2. Burger RA (2011) Overview of anti-angiogenic agents in development for ovarian cancer. Gynecol Oncol 121:230–238
3. Semenza GL (2001) Regulation of hypoxia-induced angiogenesis: a chaperone escorts VEGF to the dance. J Clin Invest 108:39–40
4. Ziello JE, Jovin IS, Huang Y (2007) Hypoxia-inducible factor (HIF)-1 regulatory pathway and its potential for therapeutic intervention in malignancy and ischemia. Yale J Biol Med 80(2):51–60
5. Ruan K, Song G, Ouyang G (2009) Role of hypoxia in the hallmarks of human cancer. J Cell Biochem 107:1053–1062
6. Wykoff CC, Beasley NJ, Watson PH et al (2000) Hypoxia-inducible expression of tumour-associated carbonic anhydrases. Cancer Res 60:7075–7083
7. Shannon AM, Bouchier-Hayes DJ, Condron CM et al (2003) Tumour hypoxia, chemotherapeutic resistance and hypoxia-related therapies. Cancer Treat Rev 29(4):297–307
8. Potter CPS, Harris AL (2003) Diagnostic, prognostic and therapeutic implications of carbonic anhydrases in cancer. Br J Cancer 89:2–7
9. Hockel M, Schlenger K, Aral B et al (1996) Association between tumor hypoxia and malignant progression in advanced cancer of the uterine cervix. Cancer Res 56:4509–4515
10. Brizel DM, Scully SP, Harrelson JM et al (1996) Tumor oxygenation predicts for the likelihood of distant metastases in human soft tissue sarcoma. Cancer Res 56:941–943
11. Mahoney BP, Raghunand N, Baggett B et al (2003) Tumor acidity, ion trapping and chemotherapeutics I. Acid pH affects the distribution of chemotherapeutic agents in vitro. Biochem Pharmacol 66:1207–1218
12. Hussain SA, Ganesan R, Reynolds G et al (2007) Hypoxia-regulated carbonic anhydrase IX expression is associated with poor survival in patients with invasive breast cancer. Br J Cancer 96(1):104–109
13. Loncaster JA, Harris AL, Davidson SE et al (2001) Carbonic anhydrase (CA IX) expression, a potential new intrinsic marker of hypoxia: correlations with tumour oxygen measurements and prognosis in locally advanced carcinoma of the cervix. Cancer Res 61(17):6394–6399
14. Kim SJ, Rabbani ZN, Dewhirst MW et al (2005) Expression of HIF-1α, CA IX, VEGF and MMP-9 in surgically resected non-small cell lung cancer. Lung Cancer 49(3):325–335
15. Driessen A, Landuyt W, Pastorekova S et al (2006) Expression of carbonic anhydrase IX (CA IX), a hypoxia-related protein, rather than vascular-endothelial growth factor (VEGF), a pro-angiogenic factor, correlates with an extremely poor prognosis in esophageal and gastric adenocarcinomas. Ann Surg 243:334–340
16. Hui EP, Chan ATC, Pezzella F et al (2002) Coexpression of hypoxia-inducible factors 1α and 2α, carbonic anhydrase IX, and vascular endothelial growth factor in nasopharyngeal carcinoma and relationship to survival. Clin Cancer Res 8:2595–2604
17. Hynninen P, Vaskivuo L, Saarnio J et al (2006) Expression of transmembrane carbonic anhydrases IX and XII in ovarian tumours. Histopathology 49:594–602
18. Eisenhauer EA, Therasse P, Bagaerts J et al (2009) New response evaluation criteria in solid tumors: revised RECIT guideline (Version 1.1). Eur J Cancer 45:228–247
19. Markman M, Hoskins W (1992) Responses to salvage chemotherapy in ovarian cancer: a critical need for precise definitions of the treated population. J Clin Oncol 10(4):513–514
20. Rosen DG, Huang X, Deavers MT et al (2004) Validation of tissue microarray technology in ovarian carcinoma. Mod Pathol 17:790–797
21. Camp RL, Charette LA, Rimm DL (2000) Validation of tissue microarray technology in breast carcinoma. Lab Invest 80(12):1943–1949
22. Kononen J, Bubendorf L, Kallioniemi A et al (1998) Tissue microarrays for high-throughput molecular profiling of tumour specimens. Nat Med 4:844–847
23. Shibata D, Martin WJ, Arnheim N (1988) Analysis of DNA sequences in forty-year-old paraffin-embedded thin-tissue sections: a bridge between molecular biology and classical histology. Cancer Res 48:4564–4566
24. McCarty KS Jr, Miller LS, Cox EB et al (1985) Estrogen receptor analyses. Correlation of biochemical and immuno-histochemical methods using monoclonal antireceptor antibodies. Arch Pathol Lab Med 109:716–721
25. Camp RL, Dolled-Filhart M, Rimm DL (2004) X-tile: a new bio-informatics tool for biomarker assessment and outcome-based cut-point optimization. Clin Cancer Res 10:7252–7259
26. Phuoc NB, Ehara H, Gotoh T et al (2008) Prognostic value of the co-expression of carbonic anhydrase IX and vascular endothelial growth factor in patients with clear cell renal cell carcinoma. Oncol Rep 20:525–530
27. Duncan TJ, Al-Attar A, Rolland P et al (2008) Vascular endothelial growth factor expression in ovarian cancer: a model for targeted use of novel therapies? Clin Cancer Res 14(10):3030–3035
28. Greenberg S, Rugo HS (2010) Triple-negative breast cancer: role of antiangiogenic agents. Cancer J 16(1):33–38
29. Sivridis E, Giatromanolaki A, Gatter KC et al (2002) Association of hypoxia-inducible factors 1α and 2α with activated angiogenic pathways and prognosis in patients with endometrial carcinoma. Cancer 95(5):1055–63
30. Saarnio J, Parkkila S, Parkkila A et al (1998) Immunohistochemical study of colorectal tumour for expression of a novel transmembrane carbonic anhydrase MN/CA IX, with potential value as a marker of cell proliferation. Am J Pathol 153(1):279–285
31. Birner P, Schindl M, Obermair A et al (2001) Expression of hypoxia-inducible factor 1a in epithelial ovarian tumors: its impact on prognosis and on response to chemotherapy. Clin Cancer Res 7:1661–1668
32. Wouters BG, Weppler SA, Koritzinsky M et al (2002) Hypoxia as a target for combined modality treatments. Eur J Cancer 38:240–257
33. Jubb AM, Pham TQ, Hanby AM et al (2004) Expression of vascular endothelial growth factor, hypoxia inducible factor 1alpha, and carbonic anhydrase IX in human tumours. J Clin Pathol 57:504–512

Virchows Arch (2012) 461:41–48
DOI 10.1007/s00428-012-1245-8

ORIGINAL ARTICLE

Histological examination and evaluation of donor bile ducts received during orthotopic liver transplantation—a morphological clue to ischemic-type biliary lesion?

Torsten Hansen · David Hollemann · Michael B. Pitton · Michael Heise · Maria Hoppe-Lotichius · Marcus Schuchmann · C. James Kirkpatrick · Gerd Otto

Received: 31 January 2012 / Revised: 11 April 2012 / Accepted: 2 May 2012 / Published online: 17 May 2012
© Springer-Verlag 2012

Abstract Ischemic-type biliary lesions (ITBL) belong to a group of biliary disorders that are regarded as the major complication in patients with orthotopic liver transplantation (OLT). We performed histological evaluation of donor common bile ducts received during OLT to find morphological clues to the pathomechanisms of ITBL. We investigated 93 grafts of 92 patients (recipients: mean age, 56.5 years; underlying disease: hepatocellular carcinoma (n=45), alcoholic cirrhosis (n=16), viral hepatitis with cirrhosis (n=9), retransplantations (n=9), others (n=14); donors: mean age, 53.2 years). Donor common bile ducts were received after recirculation of the hepatic artery prior to biliary end-to-end anastomosis and routinely processed. Statistical evaluation was performed by chi-square analysis and multivariate analysis using a logistic regression model. With regard to ITBL (observed in 19.4 %), the following phenomena were found to be statistically relevant: necrosis of the bile duct wall, arteriolonecrosis, vascular lesions (such as subintimal edema), and intramural bleeding (P<0.001, P<0.001, P=0.029, and P=0.031, respectively). In logistic regression analysis, arteriolonecrosis was the only parameter with significance (P=0.001). Based on these results on the morphology of the donor common bile duct, we conclude that these phenomena of vascular damage, reflecting microangiopathy, play a major role in the pathogenesis of ITBL.

Keywords Liver transplantation · Ischemic-type biliary lesion · Donor common bile duct · Histology · Arteriolonecrosis

T. Hansen (✉) · D. Hollemann · C. J. Kirkpatrick
Institute of Pathology, University of Mainz,
Langenbeckstr. 1,
55131 Mainz, Germany
e-mail: Torsten.Hansen@unimedizin-mainz.de

M. B. Pitton
Department of Radiology, University of Mainz,
Mainz, Germany

M. Heise · M. Hoppe-Lotichius · G. Otto
Department of Transplantation and Hepatobiliary Surgery,
University of Mainz,
Mainz, Germany

M. Schuchmann
First Medical Department, University of Mainz,
Mainz, Germany

Introduction

Ischemic-type biliary lesions (ITBL) belong to a large group of different biliary disorders that generally are regarded to be the major complication in patients with orthotopic liver transplantation (OLT). Of all liver transplant recipients, 10 to 40 % develop biliary complications which are associated with mortality rates of up to 15 %. There is a variety of disorders that can occur after OLT, the most common being bile leakage and bile duct strictures. Bile duct strictures are grouped into anastomotic biliary stricture and non-anastomotic biliary strictures. Anastomotic biliary strictures are isolated strictures at the site of the bile duct anastomosis. They result mainly from surgical technique and local ischemia, leading to fibrotic scarring of the anastomosis [1, 2]. Non-anastomotic biliary strictures are heterogeneous in origin. They were first described in OLT associated with hepatic artery thrombosis (HAT) causing ischemia. As a result, typical cholangiographic features such as biliary strictures, dilations, and intraductal cast formations could be observed. Therefore, this complication has been

designated as ischemic cholangitis or ischemic biliary lesion (IBL) [3, 4]. About 20 years ago, several authors described non-anastomotic biliary strictures in patients not fulfilling all the aforementioned criteria [5–7]. They suggested this complication to be related to preservation injury and to occur due to ischemia. Thus, the term ischemic-type biliary complication and later "ITBL" was established [1, 5, 8]. The reported incidence of ITBL differs greatly between respective series, ranging up to 26 %. Mortality rates also differ markedly between studies. In many cases, sequelae (cholestasis and cholangitis) require repeated interventional (that is endoscopic or surgical) treatment. It is generally estimated that up to 50 % of patients either die or need retransplantation (re-LTX) [1, 9, 10]. This underlines the need for comprising knowledge on causes and mechanisms of the disease.

The exact pathogenesis of ITBL is not known. It has been shown by various authors that ischemic injury as well as damage of the peribiliary vascular plexus could play a major role [1, 3, 4, 11]. Besides, several immunological factors such as chemokine motif C-C receptors are suggested to be relevant parameters [1, 2, 12]. Finally, bile salt toxicity has been considered to be a potential factor in the pathogenesis of bile duct injury [2, 13]. Based on the idea that morphological evaluation of the bile ducts might contribute to insight into the pathomechanisms of ITBL, we systematically investigated the donor bile ducts of patients with OLT. Histological changes were studied and evaluated by applying several scores. Statistical analysis was subsequently performed with regard to features associated with ITBL.

Table 1 Summary of patient data

Characteristics	Number
Grafts	93
Total number of patients	92
Mean recipient age (range, years)	56.5 (25–73)
Recipient male/female ratio	75:18 (~4:1)
Indication, *n* (%)	
HCC, total number	45 (48.4 %)
HCC combined with viral hepatitis	25 (26.9 %)
HCC combined with C2 toxic cirrhosis	13 (14 %)
Alcoholic cirrhosis without HCC	16 (17.2 %)
Viral-induced cirrhosis	9 (9.7 %)
PSC	4 (4.3 %)
PBC	3 (3.2 %)
Others	7 (7.5 %)
Re-LTX, total number	9 (9.7 %)
PNF	5 (5.4 %)
ITBL	3 (3.2 %)
HAT	1 (1.1 %)
Mean donor age (range, years)	53.2 (18–87)
Donor male/female ratio	45:47 (~1:1)
Cause of brain death, *n* (%)	
Intracerebral bleeding	25 (26.9 %)
Subarachnoid bleeding	22 (23.7 %)
Trauma	16 (17.2 %)
Hypoxia	10 (10.7 %)
Infarction	7 (7.5 %)
Others	13 (14 %)

Materials and methods

Patient data

We included 93 grafts of 92 patients who underwent OLT between November 2006 and September 2011 at our center. Patient characteristics are summarized in Table 1. Inclusion criteria for evaluation were (a) recipients ABO-compatible according to the donor; (b) survival of the recipients for more than 3 months; (c) graft survival for more than 3 months, except occurrence of ITBL in the first 3 months; and (d) tissue specimens of the donor bile ducts for histological evaluation available. Re-LTX was not a criterion of exclusion. Thus, we have included nine grafts of eight patients with re-LTX. In this cohort, four re-LTXs were performed due to primary nonfunction (PNF) of the graft; furthermore, there were three patients who underwent re-LTX because of ITBL in the first graft.

Cold ischemia time was 639±152 min. The tissue specimens were taken during the transplantation. Organ retrieval was performed according to the protocol of the Deutsche Stiftung für Organtransplantation. The liver was generally removed without dissecting the supplying vessels. Aortic flush perfusion was performed used histidine–tryptophan–ketoglutarate (HTK) solution. After retrieval, the cystic duct was ligated and the bile ducts were rinsed with HTK solution. Then, the dissected graft was shipped and prepared for transplantation in ice water. Transplantation was performed using the piggyback technique. Following caval anastomosis, blood supply to the graft was reestablished by the portal vein first in 79 cases and by synchronous—arterial and portal—recirculation in 14 cases. After portal and arterial recirculation of the graft, the biliary anastomosis was performed. Abundant donor bile duct was dissected in order to avoid kinking and submitted for routine assessment (see below). The length of the duct being excised ranged between 2 and 58 mm (median value, 12.8±3.9 mm).

In order to avoid additional surgical injuries and ischemia after recirculation, clamping of the bile duct was omitted at all times. Biliary end-to-end anastomosis was performed in all instances using 6×0 resorbable monofile running suture. A drain (diameter, 1.5 mm) was placed through the cystic

duct of the recipient into the duct and guided cephalad over the anastomosis in order to visualize the biliary system routinely after 3 weeks and in case of complications. The drain was removed after the third week following transplantation. Before the removal of the drain, the biliary tree was visualized by a contrast X-ray.

Histological evaluation

The tissue specimens were paraffin-embedded and further processed for routine diagnosis. For morphological analysis, the bile duct segments were cut in sections which measured between 2 and 4 mm; furthermore, the sections were completely embedded and prepared for histology. The 4-μm sectioned slides were routinely stained by hematoxylin and eosin and by Elastica–van Gieson reaction and Goldner's trichrome staining as special stains. All slides were evaluated by an Olympus microscope [type CX21, Olympus, Hamburg, Germany] by one investigator (TH) who was blinded to the clinical data with special regard to ITBL. Photographs were taken by a Zeiss microscope [type Axiophot, Zeiss, Jena, Germany; Olympus digital camera].

Analysis of the histomorphology of the bile ducts revealed several typical features. For the evaluation of the ducts, we then determined the details of the respective features as follows:

1. Mucosal loss, which was defined by the absence of the epithelial lining, leading to denuded subepithelial stroma (Fig. 1). This feature was subdivided into three categories depending on the severity of the lesion (0, no epithelial loss; 1, ≤50 % of the bile duct with absent epithelial lining; 2, epithelial loss in >50 % of the bile duct).
2. Bleeding: Mural bleeding was characterized by erythrocyte extravasation into the bile duct wall (Fig. 2). Three categories were determined for evaluation (0, no bleeding; 1, ≤50 % of the bile duct wall with bleeding; 2, hemorrhage in >50 % of the bile duct).
3. Thrombi: In several cases, we found hyaline thrombi in small intramural vessels (Fig. 3). This feature was scored in two categories (0, no thrombi; 1, occurrence of thrombi).
4. Vascular lesions: In this heterogeneous group, we summarized all pathological alterations of the small arteries and arterioles of the bile duct wall except necrosis. The most common finding was subendothelial edema (Fig. 4); in addition, loss of endothelial cells occurred as well. Moreover, initial necrotic change of the vessels was subsumed under this feature (e.g., loss of some vital cells either in the intima). The scoring was performed

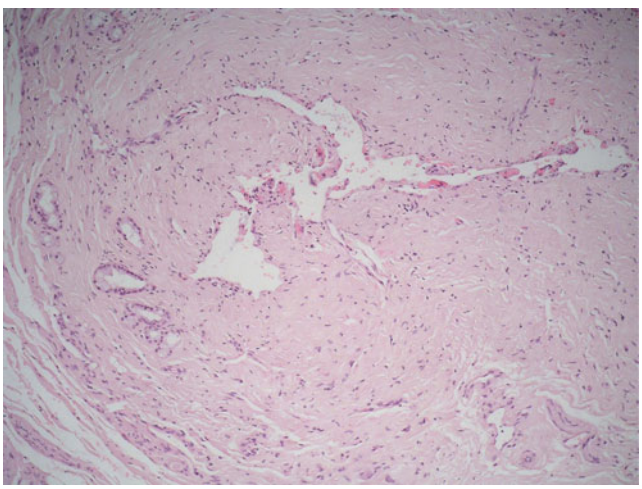

Fig. 1 Bile duct demonstrating mucosal loss >50 %; there is no necrosis and only mild inflammation (HE, original magnification × 100)

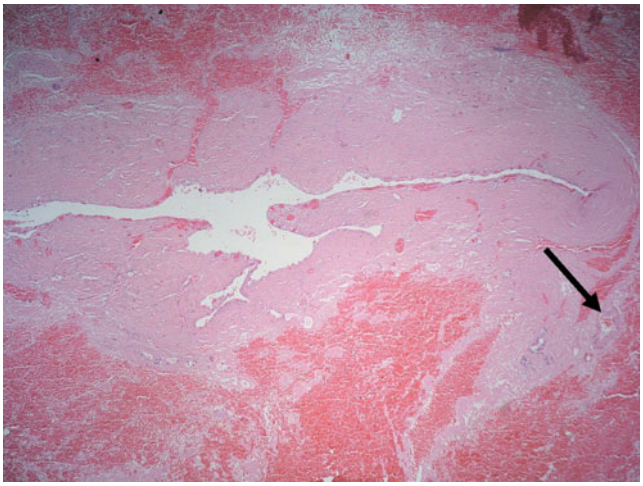

Fig. 2 Overview of a bile duct with massive intramural bleeding (score 2); furthermore, there is complete mucosal loss and necrosis of the bile duct wall, but no significant inflammation; *arrow* shows a necrotic arteriole (HE, magnification × 50)

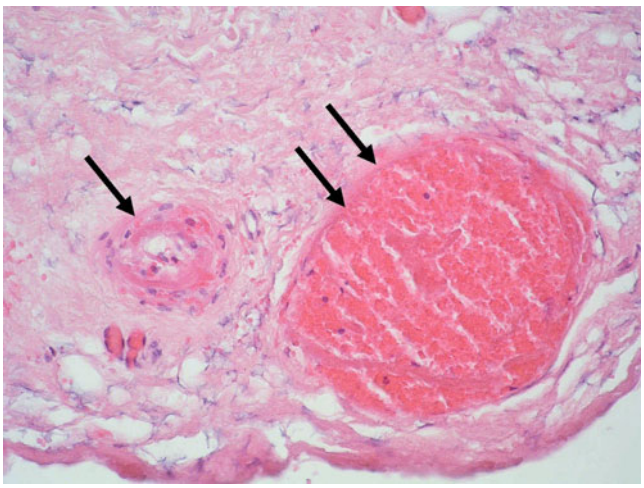

Fig. 3 Detailed view shows two vessels with hyaline thrombi (*two arrows*), on the left side (*one arrow*) also revealing vessel damage (HE, magnification × 250)

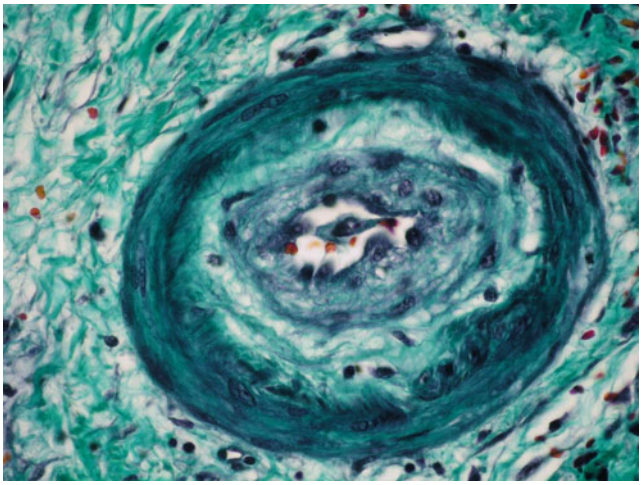

Fig. 4 Detailed view of an arteriole reveals prominent subintimal edema (Goldner reaction, magnification × 800)

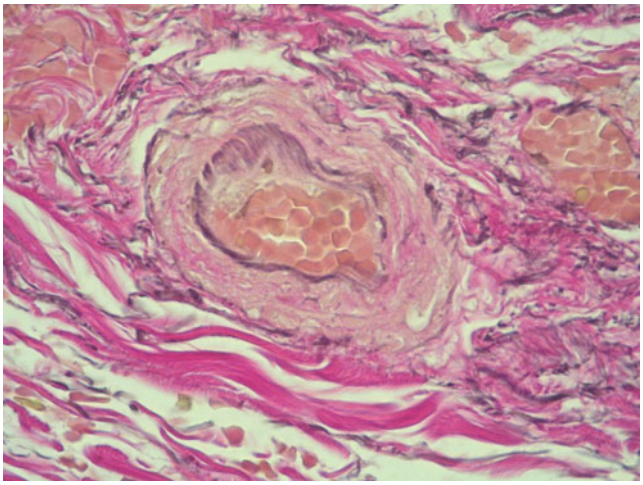

Fig. 6 Detailed view from the same patient as in Fig. 5 demonstrating an arteriole without viable cells. This patient developed ITBL (EVG reaction, magnification × 800)

according to the number of damaged vessels (0, no vascular lesion; 1, ≤50 % of vessels changed; 2, >50 % of vessels damaged).

5. Arteriolonecrosis was defined by complete loss of vital cells in the wall of arterioles and small arteries which commonly were arranged around the bile duct wall (Figs. 5, 6, and 7). One characteristic finding was degeneration of the collagen in the vessels leading to fibrinoid necrosis (Fig. 7). Arteriolonecrosis was scored in the same way as described under no. 4.
6. Duct necrosis: Bile duct necrosis exhibited loss of vital cells in the mural stroma. Although it was commonly accompanied by mucosal loss, the loss of epithelial lining alone was not interpreted as bile duct necrosis. Typically, bile duct necrosis was more pronounced at the inner mural layer and the avital areas showed scattered cells with karyolysis or no cellular remnant at all (Fig. 8). Bile duct necrosis was evaluated with respect to the damaged circumference of the duct as follows: 0, no necrosis; 1, ≤25 % of the bile duct wall necrotic; 2, >25 and ≤50 % of the bile duct wall necrotic; 3, >50 and ≤75 % of the bile duct wall necrotic; 4, >75 % of the bile duct wall necrotic).
7. Inflammation: Occurrence of leukocytes in the bile duct wall was evaluated as inflammation independent of the predominant cell type (lymphocytes or granulocytes; Fig. 9). Inflammation was scored according to the number of leukocytes in high-power field (HPF; 0.159 mm^2): 0, no inflammation; 1, at least one HPF with more than 10 leukocytes; 2, at least one HPF with more than 50 leukocytes.

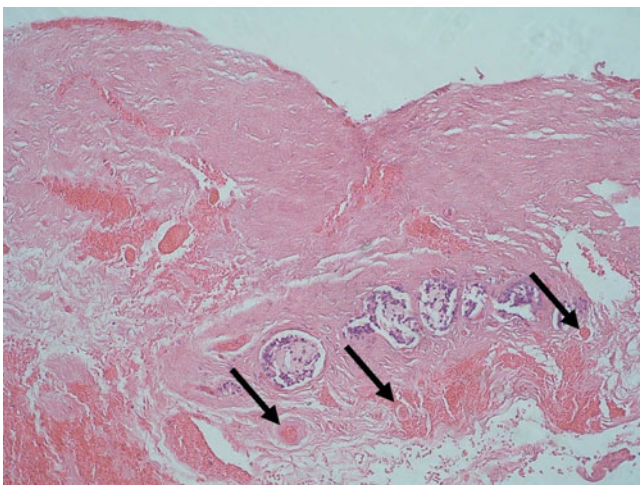

Fig. 5 Bile duct with mural necrosis and small necrotic arterioles (*arrows*, magnification × 100)

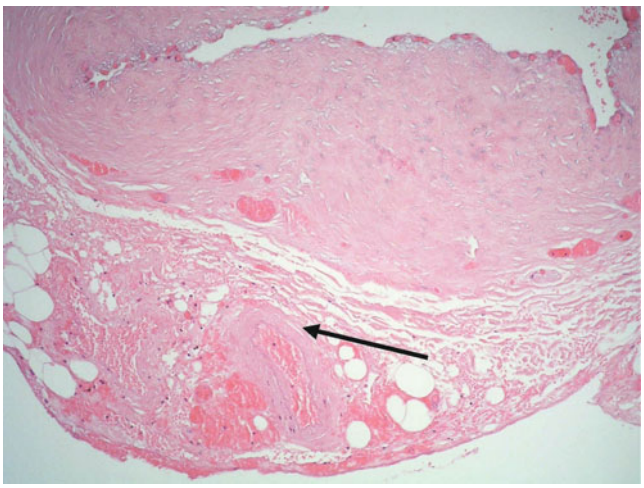

Fig. 7 Bile duct with mural necrosis and an arteriole showing necrosis (*arrow*). In this patient, ITBL was observed as well (HE, magnification × 100)

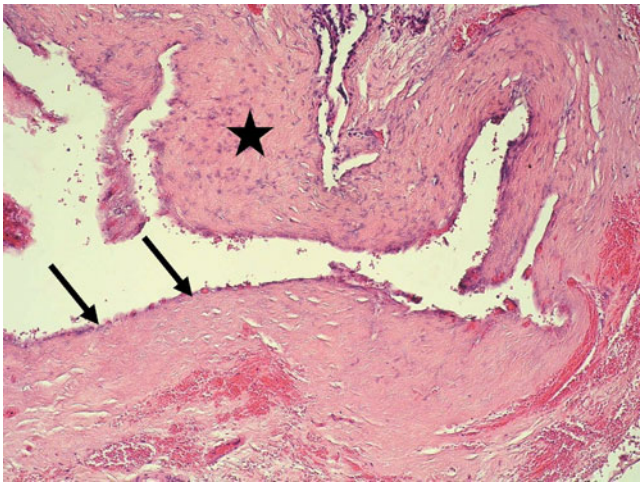

Fig. 8 View of a necrotic bile duct (ITBL patient): *arrows* show complete loss of viable stromal cells, while in the neighbourhood (*asterisk*) some intact tissue is visible (HE, magnification × 100)

Diagnosis of ITBL

Clinical symptoms of biliary obstruction including increased levels of bilirubin, alkaline phosphatase, and γ-glutamyl transferase led to the diagnostic procedure. Diagnosis of ITBL was confirmed by either endoscopic retrograde cholangiography or percutaneous transhepatic cholangiography showing typical signs of segmental or diffuse intrahepatic or extrahepatic strictures or destructive lesions of the biliary tree. HAT, ABO incompatibility, biliary anastomotic stricture, and/or chronic ductopenic rejection were always excluded prior to establishing the diagnosis of ITBL.

Statistical analysis

Chi-square analysis was performed to compare the association between the above-mentioned morphological features and the occurrence of ITBL. All statistical calculations were performed in IBM SPSS Statistics 19 [SPSS Inc., Chicago, IL, USA]. Multivariate analysis was carried out using a logistic regression model. *P* values of <0.05 were considered to be statistically significant.

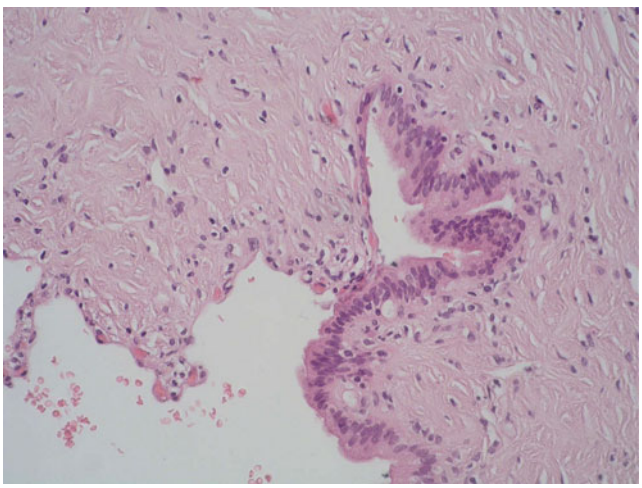

Fig. 9 Typical mild inflammation of a bile duct is presented, most of the cells comprising lymphocytes (HE, magnification × 250)

Results

In the present cohort, 18 patients (19.4 % of all cases examined) developed ITBL (mean age, 55.3 years; 15 male patients, 3 female patients). Underlying diseases were as follows: HCC combined with viral hepatitis (n=5), HCC combined with alcoholic cirrhosis (n=3), cryptogenic cirrhosis (n=3), one of them combined with HCC, combined HBV/HDV hepatitis with cirrhosis (n=2), C2 toxic cirrhosis (n=2), and others (n=3). It needs to be stressed that patients with re-LTX were not demonstrable in this specific group. In particular, none of the three patients who were retransplanted due to ITBL could be found in this cohort (i.e., they did not develop ITBL for a second time). The length of the bile duct segments was not significantly different between ITBL and non-ITBL patients (*P* value=0.202, respectively).

The results of the histological evaluation are summarized in Table 2. Mucosal loss was found in the vast majority of the tissue specimens investigated; only one case revealed a complete epithelial lining. Interestingly, only a very few cases showed bile extravasation into the mural stroma. Bile incrustations were not found. In 16.1 %, we found mucosal loss <50 %, while in 82.8 %, we observed severe damage with >50 % of epithelial lining being lost. Statistical analysis revealed no significant association between mucosal loss and later development of ITBL (*P* value=0.341).

Like mucosal loss, bleeding of the duct wall was a very common finding with 93.5 % of cases being affected. While minor bleeding (score 1) was often encountered (73.1 %), severe mural hemorrhage was observed in 19 recipients. Interestingly, comparison between all patients with bleeding (score 1 or 2) and without bleeding led to no statistically relevant result, while score 2 hemorrhage compared to score 1 and 0 showed a significant association with respect to the development of ITBL (*P* value=0.031).

Hyaline thrombi were found in 26.3 % of cases examined. Mostly, they were found in small capillaries in the mural wall. Larger vessels did not demonstrate relevant amounts of thrombi. There was no statistically significant difference for the patients with thrombosis or without thrombosis concerning establishment of ITBL (*P* value=0.061).

Vascular lesions could be demonstrated in 74.2 % of all grafts. The majority showed lesions in <50 % of vessels (n=60; 64.5 %). Applying chi-square analysis, we did not find relevant association with ITBL (*P* value=0.071). However, by comparison of the group without any vessel damage (score 0)

Table 2 Influence of histological parameters on occurrence of ITBL

	Without ITBL (n=75)	With ITBL (n=18)	P value
Mucosal loss			
Score 0	1	0	0.341
Score 1	14	1	
Score 2	60	17	
Bleeding			
Score 0	5	1	0.096
Score 1	58	10	
Score 2	12	7	
Score 0+1	63	11	0.031
Score 2	12	7	
Vascular lesion			
Score 0	23	1	0.071
Score 1	46	14	
Score 2	6	3	
Score 0	23	1	0.029
Score 1+2	52	17	
Arteriolonecrosis			
Score 0	51	3	<0.001
Score 1	19	12	
Score 2	5	3	
Score 0	51	3	<0.001
Score 1+2	24	15	
Mural necrosis			
Score 0	47	3	<0.001
Score 1	19	6	
Score 2	7	3	
Score 3	1	5	
Score 4	1	1	
Score 0	47	3	<0.001
Score 1+2+3+4	28	15	
Thrombosis			
Score 0	58	10	0.061
Score 1	17	8	
Inflammation			
Score 0	8	6	0.053
Score 1	60	11	
Score 2	7	1	
Score 0	8	6	0.016
Score 1+2	67	12	

with the combined group of score 1 and score 2 cases, we found statistical relevance (P value=0.029).

One of the most conspicuous results was the detection of necrotic arterioles and small arteries. A total percentage of 42.9 % of cases revealed this feature, which was prominent in 8.6 %. Statistical analysis established a highly significant correlation between the detection of arteriolonecrosis and the development of ITBL (P value<0.001).

Bile duct necrosis was a further common observation. Forty-three cases demonstrated a necrosis of the stromal layer. Approximately half of this cohort (n=25) revealed <25 % of the circumference damaged, while lesions were more pronounced (with lesion of more than 50 %) in about one fifth (n=8). Statistical evaluation of this score revealed a very close association with ITBL (P value<0.001).

Finally, inflammation was observed in 84.9 % of evaluated subjects. Most commonly, inflammation was only mild (score 1; 76.3 %). In eight cases, inflammation was pronounced, especially in the non-ITBL group. Inflammation in general was found in 89 % of the non-ITBL patients, but in a less percentage of ITBL patients (approximately 67 %). Further analysis demonstrated a statistically significant association (P value=0.016).

Based on these findings, we performed stepwise logistic regression analysis with regard to ITBL as endpoint. Arteriolonecrosis (independent on score 1 or 2) was the only parameter predictive for the development of ITBL (P value=0.001; odds ratio, 0.09; confidence interval, 0.03–0.36).

Discussion

ITBL comprises one of the most troublesome complications after OLT. Several risk factors are discussed to be major parameters for the development of ITBL. Among them, ischemic injury, immunological abnormalities, and bile salt toxicity appear to have the most important influence [1, 2]. We investigated the morphology of the donor bile ducts received during OLT in order to give some insights in the pathomechanism of this important disorder. Among the variety of abnormalities, we evaluated damage to the vasculature, first of all arteriolonecrosis, in combination with mural necrosis to be relevant for further development of ITBL. This confirms the previous concept of microangiopathy as the leading phenomenon in the pathogenesis of ITBL.

Evidence for a critical role of bile salt toxicity in the pathogenesis of ischemia/reperfusion injury of liver grafts has gradually emerged in the last years [2]. Bile salts have potent detergent properties towards biliary epithelial cells. Normally, the toxic effects of bile salts are prevented by complex formation (mixed micelles) with phospholipids. However, the formation of mixed micelles is impaired after OLT, since restoration of biliary secretion of phospholipids may recover more slowly compared to secretion of toxic bile salts [1, 2, 13]. It has been generally recommended to carefully rinse the bile ducts with preservation solution in order to remove residual bile salts [1, 13]. In our study, we observed mucosal loss in nearly all patients tested. There was no statistically significant difference between ITBL and non-ITBL patients. Based on these morphological findings, conclusions concerning a possible influence of bile salts cannot be made.

We found inflammatory infiltrates in about 85 % of evaluated cases. Most interestingly, inflammation in general was

found in 89 % of the non-ITBL patients, but in a less percentage of ITBL patients (approximately 67 %). This difference was statistically significant. Further investigation is needed to elucidate whether inflammation might serve as a protective factor in the pathogenesis of ITBL.

Injury of the peribiliary vascular plexus is believed to play a central role in the pathogenesis of ITBL. Preservation injury has been suggested to result in increased arterial resistance and may cause circulatory disturbances in small capillaries [6]. The crucial role of the vasculature has also been elucidated by clinical studies of Heidenhain et al. [10] and Moench et al. [4]. These authors demonstrated that use of high-pressure aortal perfusion resulted in a significantly lower number of ITBL cases. Since in IBL thrombosis is described as a central factor leading to vessel damage [1], we firstly analyzed the vasculature of the donor bile ducts for the occurrence of thrombi. However, on the basis of histological evaluation, we did not find a statistically significant difference between ITBL and non-ITBL patients. Thus, clotting of the peribiliary vascular plexus probably does not play a role in the pathogenesis of ITBL.

In one of the very early studies of ITBL, Sanchez-Urdazpal [5] and colleagues considered that bile duct strictures could represent injury of the microvasculature and mentioned arteriolar necrosis as one possible cause. In fact, arteriolonecrosis was the most conspicuous finding of our morphological study. We detected this feature in 42.9 % of all cases. Moreover, by statistical analysis, we could establish a significant association with ITBL: while about 83 % of the ITBL patients revealed arteriolonecrosis, we detected this phenomenon in only 32 % of the non-ITBL group (P value<0.001). The central role of arteriolonecrosis for the development of ITBL is additionally confirmed by our further statistical approach revealing that, in logistic regression analysis, only arteriolonecrosis could serve as a predictive factor. There were further lesions of the vasculature in the bile duct wall, with subendothelial or subintimal edema being the most common form. These were collected in the group of vascular lesions, which were observed in about 74 % of all cases. Interestingly, we also found statistical significance between ITBL and non-ITBL patients for this feature. Finally, we suggest strong intramural bleeding or hemorrhage to be further parameters that may be interpreted in this context of a multifactorial vascular damage, since we have found this phenomenon as a statistically significant parameter with regard to ITBL.

We believe that the vascular lesions can be attributed to hypoxic damage on the endothelial cells leading to subintimal edema and subsequently causing arteriolonecrosis. Following erythrocyte extravasation through damaged vessels, intramural hemorrhage might also reflect this pathway. In summary, these histological data of human donor bile duct contribute to the view that (hypoxic) injury of the microvasculature is crucial for the development of ITBL. We suggest that this type of microangiopathy plays a central role in the pathogenesis of ITBL.

Due to the close similarities with IBL, bile duct necrosis has also been supposed to be of major importance for ITBL [1, 5, 6]. In accordance, we demonstrated in this study a statistically relevant association between mural necrosis and ITBL. Since we found a close relationship between patients with arteriolonecrosis and patients with mural necrosis (P<0.001; data not shown in the "Results" section), both features might be closely associated according to the pathomechanism. Therefore, the necrosis of the bile duct wall is most likely caused by microangiopathy. In previous studies, it has been proposed to reclassify diffuse bile duct damage after OLT. Especially, it was considered that IBL and ITBL belong to the same group of ischemic biliary injuries, on one hand with IBL reflecting a macroangiopathic form due to thrombosis and/or stenosis of large vessels (first of all, the hepatic artery) and on the other hand with ITBL representing the microangiopathic variant of ischemic disease [12]. The results of our morphological study are in line with this pathogenetic model. We have summarized our results in a flowchart model for the possible pathogenetic steps leading to ITBL (Fig. 10). In previous studies, it became clear that several donor parameters such as donor age and cold ischemia time are significant risk factors for the development of ITBL [4, 10]. In our morphological study, the length of the bile duct segments did not have any significant influence for the development of ITBL. Based on the presented results, a thorough analysis of the clinical data

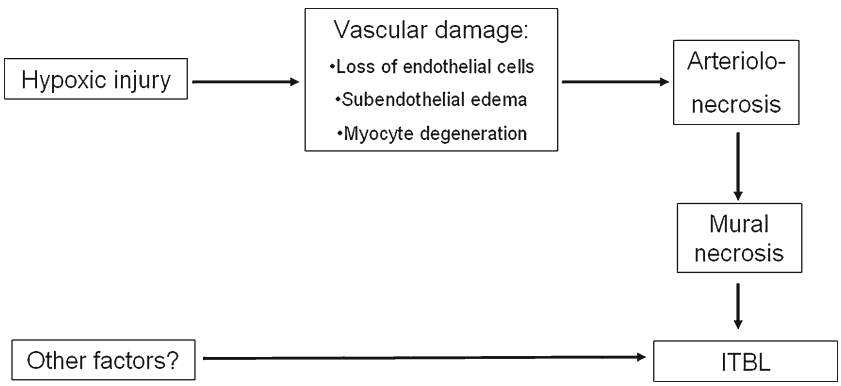

Fig. 10 Flowchart summarizes the pathogenetic model of ITBL as revealed by previous data and results of the present study

with respect to the histological features (arteriolonecrosis in particular) and ITBL will be performed.

Considering our data, it remains unresolved why a distinct percentage of ITBL patients (17 %) did not show arteriolonecrosis and/or mural necrosis (in particular with two patients missing both features). Two possible reasons might explain this discrepancy. First, as reflected by multifocal and discontinuous affection of the biliary tree, the angiopathy could be variably pronounced depending on the specific site of bile duct. In other words, the missing detection of the above-named features could be due to a "sampling error," since the ischemic damage might occur in more peripherally localized (i.e., intrahepatic) bile duct segments. Second, as already considered in previous studies, there might be forms of ITBL which are influenced by as yet unknown immunological factors [2, 12]. In those forms, vessel damage might be less well developed, thus leading to a rather bland morphology. Possibly, innate alloimmunity such as toll-like receptor-triggered signaling pathways could be involved in these pathomechanisms [14].

In summary, this is the first morphological study on bile ducts received during LTX. Our findings confirm the previous view that damage to the microvasculature is associated with an increased risk for the development of ITBL. In order to elucidate the possible causes of hypoxic injury, further analysis of the clinical data of the donor (such as the donor age, cause of death, and cold ischemia time) should be performed and correlated with the respective histopathological findings.

Conflict of interest We declare that we have no conflict of interest.

References

1. Buis CI, Hoekstra H, Verdonk RC, Porte RJ (2006) Causes and consequences of ischemic-type biliary lesions after liver transplantation. J Hepatobiliary Pancreat Surg 13:517–524
2. op den Dries S, Sutton ME, Lisman T, Porte RJ (2011) Protection of bile ducts in liver transplantation: looking beyond ischemia. Trasnplant 92:373–379
3. Batts KP (1998) Ischemic cholangitis. Mayo Clin Proc 73:380–385
4. Moench C, Moench K, Lohse AW, Thies J, Otto G (2003) Prevention of ischemic-type biliary lesions by arterial back-table pressure perfusion. Liver Transpl 9:285–289
5. Sanchez-Urdazpal L, Gores GJ, Ward EM, Maus TP, Wahlstrom HE, Moore SB, Wiesner RH, Krom RAF (1992) Ischemic-type biliary complications after orthotopic liver transplantation. Hepatol 16:49–53
6. Li S, Stratta RJ, Langnas AN, Wood P, Marujo W, Shaw BW Jr (1992) Diffuse biliary tract injury after orthotopic liver transplantation. Am J Surg 164:536–540
7. Kadmon M, Bleyl J, Küppers B, Otto G, Herfarth C (1993) Biliary complications after prolonged University of Wisconsin preservation of liver allografts. Transpl Proc 25:1651–1652
8. Hintze RE, Adler A, Veitzke W, Abou-Rebyeh H, Felix R, Neuhaus P (1997) Endoscopic management of biliary complications after orthotopic liver transplantation. Hepatogastroenterology 44:258–262
9. Verdonk RC, Buis CI, Porte RJ, Haagsma EB (2006) Biliary complications after liver transplantation: a review. Scand J Gastroenterol Suppl 243:89–101
10. Heidenhain C, Pratschke J, Puhl G, Neumann U, Pascher A, Vetzke-Schlieker W, Neuhaus P (2010) Incidence of and risk factors for ischemic-type biliary lesions following orthotopic liver transplantation. Transpl Int 23:14–22
11. Pirenne J, van Gelder F, Coosemans W, Aerts R, Gunson B, Koshiha T, Fourneau I, Mirza D, van Steenbergen W, Fevery J, Nevens F, McMaster P (2001) Type of donor aortic preservation solution and not cold ischemia time is a major determinant of biliary strictures after liver transplantation. Liver Transpl 7:540–545
12. Moench C, Uhrig A, Lohse AW, Otto G (2004) CC chemokine receptor 5Δ32 polymorphism—a risk factor for ischemic-type biliary lesions following orthotopic liver transplantation. Liver Transpl 10:434–439
13. Geuken E, Visser D, Kuipers F, Blokzijl H, Leuvenink HGD, de Jong KP, Peeters PMJG, Jansen PLM, Slooff MJH, Gouw ASH, Porte RJ (2004) Rapid increase of bile salt secretion is associated with bile duct injury after human liver transplantation. J Hepatol 41:1017–1025
14. Land GW (2007) Innate alloimmunity: history and current knowledge. Exp Clin Transpl 1:575–584

Virchows Arch (2012) 461:49–57
DOI 10.1007/s00428-012-1250-y

ORIGINAL ARTICLE

FGFR1 expression and gene copy numbers in human lung cancer

Lukas H. Kohler · Masoud Mireskandari · Thomas Knösel · Annelore Altendorf-Hofmann · Almut Kunze · Andreas Schmidt · Norbert Presselt · Yuan Chen · Iver Petersen

Received: 3 March 2012 / Revised: 5 April 2012 / Accepted: 10 May 2012 / Published online: 31 May 2012
© Springer-Verlag 2012

Abstract FGFR1 is a receptor tyrosine kinase of which the ligands belong to the fibroblast growth factor family. To evaluate the significance of FGFR1 in lung cancer, we analysed tumours by immunohistochemistry (IHC) and fluorescence in situ hybridization (FISH). Tissue microarrays were constructed containing 380 lung cancer samples including squamous cell carcinomas (SCC), adenocarcinomas (ADC), non-small cell lung cancer not otherwise specified, metastases, neuroendocrine tumours, large cell lung cancer and small cell lung cancer. FGFR1 expression was analysed by IHC and scored semi-quantitatively by a four-tier approach (0, 1, 2, 3). Using dual-colour interphase FISH with probes specific for the locus on 8p12 and the centromere of chromosome 8 (CEN8), copy numbers of FGFR1 were determined. High expression of FGFR1 was associated with increased FGFR1 gene copy numbers in squamous cell carcinoma ($p<0.001$). The FGFR1 locus was equally affected by copy number losses and gains. The higher FGFR1 gene copy numbers in SCC compared to ADC did not reach statistical significance. High copy number amplification of FGFR1 was a very rare event, the FGFR1/CEN8 signal ratio reaching a maximum value of 2.75. There were no significant associations between FGFR1 and clinicopathological parameters. Fibroblast growth factor signalling represents an interesting therapeutic target in lung cancer. However, the pathways are complex with potential oncogenic and anti-oncogenic activities. Our data may help to define criteria for selecting patients that may benefit from these new therapeutic options.

Keywords FGFR1 · Lung cancer · FGFR1 amplification · FGFR1 expression

L. H. Kohler · M. Mireskandari · T. Knösel · Y. Chen · I. Petersen (✉)
Institute of Pathology, Jena University Hospital,
Friedrich-Schiller-University,
Ziegelmuehlenweg 1,
07740 Jena, Germany
e-mail: Iver.Petersen@med.uni-jena.de

A. Altendorf-Hofmann
Department of General and Visceral and Vascular Surgery,
Jena University Hospital, Friedrich-Schiller-University,
Erlanger Allee 101,
07740 Jena, Germany

A. Kunze · A. Schmidt
Department of Pathology, Central Clinic Bad Berka,
Robert-Koch-Allee 9,
99438 Bad Berka, Germany

N. Presselt
Department of Thoracic and Vascular Surgery,
Central Clinic Bad Berka,
Robert-Koch-Allee 9,
99437 Bad Berka, Germany

Present Address:
T. Knösel
Institute of Pathology, Ludwig-Maximilian-University,
Thalkirchner Strasse 36,
80337 Munich, Germany

Introduction

Lung cancer is the leading cause for cancer-associated mortality in the USA and Germany [1, 2] and ranks first in worldwide cancer incidence (16.5 %) and mortality (22.5 %) in males [3]. Fibroblast growth factors and their receptors have diverse and important physiological roles in the mammalian organism including the regulation of angiogenesis, wound repair, as well as phosphate homeostasis [4, 5]. Specifically, the FGFR family consists of four members in which

mutations have been described not only in developmental disorders like achondroplasia and thanatophoric dysplasias but also several cancer types. For instance, nucleotide exchange mutations have been reported for FGFR2 in endometrial carcinomas and for FGFR3 in urothelial carcinomas. In contrast, FGFR1 seems to be preferentially affected by focal amplifications [6].

In lung cancer, FGFR1 was found to be amplified using large-scale single nucleotide polymorphism arrays [7]. We were involved in a recent publication demonstrating FGFR1 amplification and overexpression as a frequent event in lung squamous cell carcinoma [8]. This non-small-cell lung cancer (NSCLC) subtype thus far has not been subjected to targeted therapy, which, however, is probably going to change in the near future [9, 10].

In this study, we aimed to further evaluate FGFR1 gene copy numbers and protein expression in lung cancer and their potential association with clinicopathological parameters.

Material and methods

Tumour collective

The materials of this study originated from resections from the lung of 380 patients who underwent a surgical intervention at the thoracic surgery department at the Central Clinic Bad Berka between January 1999 and December 2002. The case series consisted of squamous cell carcinomas (n=194), adenocarcinomas (n=83), non-small cell lung carcinomas not otherwise specified (NOS) (n=47), large cell lung cancer (n=7), small cell lung cancer (n=10), metastases (n=29) and other neuroendocrine tumours consisting of carcinoids of the lung (n=10) (Table 1).

TMA construction

We constructed two tissue microarrays (TMAs) by using 1-mm punches from formalin-fixed, paraffin-embedded tumour specimens using standard procedure [11] and instrumentation (Beecher Instruments, Microarray Technology, Sun Prairie, WI, USA).

Immunohistochemistry

We analysed FGFR1 expression by performing immunohistochemistry using a FGFR1 antibody (Abcam ab71928) and standard procedures (antibody dilution, 1:250) with antigen retrieval (30-min steamer using a citrate buffer of pH 6,1) and a commercially available detection system [11].

High expression was defined as strong FGFR1 staining of the cell membrane or the cytoplasm. Expression levels were first scored semi-quantitatively by a four-tier approach (Fig. 1a). Later, it was reduced to the three subgroups no expression (immunohistochemistry (IHC)-score 0), low expression (IHC score 1+) and high expression (IHC score 2+ and 3+) (Table 1). For statistical analysis, the subgroups were finally dichotomized into IHC negative (IHC scores 0 or 1+) and IHC positive (IHC scores 2+ and 3+).

Fluorescence in situ hybridization

To determine the gene copy number of FGFR1, dual-colour fluorescence in situ hybridization (FISH) was performed on the lung cancer TMAs. Therefore, a Zytolight SPEC FGFR1/CEN8 Dual Color Probe (ZytoVision GmbH, Bremerhaven, Germany) was used to detect the FGFR1 gene on chromosome 8p12 as green signal and the centromeric region/alpha-satellite of chromosome 8 as a red signal. FISH was performed according to the manufacturer's instructions. Examples of representative FISH results are shown in Fig. 1b. For the analysis, 20 nuclei per case were analysed. Since there are as yet no standard criteria for the definition of FISH positivity, different cut-off values, i.e. FGFR1 signals≥ 2/3/3.5/4 per cell, were defined and submitted to the statistical analysis.

Statistical analysis

Fisher's exact test, Pearson correlation coefficient or Kruskal–Wallis test were used to test the correlation between the parameters as indicated. The p values <0.05 were considered significant. All calculations were performed on a PC using SPSS (version 18, Munich, Germany). For overall survival, all deaths were counted as events; patients who were alive in 2010 were censored at time of last observation. Differences in survival were tested for statistical significance with the log rank test.

Clinicopathological parameters were available for 324 cases (289 for the nodal stage, 323 for primary tumour (pT) category and 324 for grading); follow-up data could be obtained for 256 patients. Because of the small sample size, we excluded small cell lung cancer (SCLC), metastases (MTS) and neuroendocrine tumours (NET) from the statistical analysis while LCLC samples were combined with NSCLC-NOS (n=54)

Results

Immunohistochemistry

FGFR1 expression was scored semi-quantitatively by using a four-tier approach (Fig. 1a). In total, 320 samples were successfully analysed by immunohistochemistry (Table 1). In general, the IHC scores were similar for adenocarcinoma

Table 1 Tumour collective—clinicopathological and experimental data

	Parameter	SCC	ADC	NSCLC-NOS	LCLC	SCLC	MET	NET
Clinicopathological data	In total	195	83	46	7	10	29	10
	Median age	67	64	67	66	69	61	53
	Male	173	59	31	7	7	20	2
	Female	22	24	15	0	3	9	8
	Clinical data							
	T1/T2	150	68	36	4	8	0	3
	T3/T4	45	10	8	2	1	0	0
	N0	99	38	22	3	3	0	3
	N1/N2/N3	80	27	18	2	6	0	0
	G1/G2	128	42	27	1	0	3	3
	G3/G4	64	40	17	5	9	1	0
Expetrimental data	Immunohistochemistry							
	In total	n=180	n=80	n=40	n=6	n=9	n=3	n=2
	IHC0	102 (57 %)	41 (51 %)	23 (58 %)	4 (67 %)	3 (33 %)	2 (67 %)	0 (0 %)
	IHC1+	60 (33 %)	29 (36 %)	8 (21 %)	2 (33 %)	5 (56 %)	1 (33 %)	2 (100 %)
	IHC2+/IHC3+	18 (10 %)	10 (13 %)	9 (22 %)	0 (0 %)	1 (11 %)	0 (0 %)	0 (0 %)
	FISH							
	In total	n=133	n=64	n=29	n=4	n=9	n=15	n=6
	FGFR1 signals 0–2	57	28	9	2	2	10	2
	FGFR1 signals ≥2	76	36	20	2	7	5	4
	FGFR1 signals 0–4	119	61	27	4	9	15	5
	FGFR1 signals≥4 (ampl.)	14	3	2	0	0	0	1
	FGFR1 signals (median)	2.1	2.1	2.3	1.6	2.5	1.8	2.2

(ADC) and squamous cell carcinomas (SCC) while the higher score in NSCLC-NOS was not statistically significant (Fig. 2). Similarly, high expression of FGFR1 (scores 2+3) were not correlated to the clinicopathological parameters sex (p=0.689), age (p=0.206), pT stage (p=0.557), nodal stage (p=0.450) or grading (p=0.187). Overall, increased FGFR1 expression levels correlated with FGFR1 gene copy number, notably in lung squamous cell carcinomas, but there were also discordant cases (Fig. 3).

Fluorescence in situ hybridization

FISH data could be analysed for 260 tumour samples (Table 1). Significant differences in FGFR1 signal numbers between squamous cell carcinomas and adenocarcinomas were not found (Fig. 4). However, the analysis suggested that FGFR1 gene copy number increases are more frequent in lung SCC cases. Therefore, we specifically analysed those cases with gene copy number equal or above 4, a threshold that has been previously used to define FGFR1 amplifications [8]. We found that 14 out of 133 SCC cases (10.5 %) showed ≥4 copies of the FGFR1 gene on chromosome 8p12 while the frequency was considerably lower for lung ADC (3 out of 64 cases, 4.7 %). This difference, however, failed to reach statistical significance (Fig. 5). Similarly, there was no significant association between increased FGFR1 gene copy number (≥4) and any clinicopathological parameter (sex, p=0.57; age, p=0.247; pT stage, p=0.685; pathological nodal (pN) stage, p=0.602; grading, p=0.947).

In addition to the analysis of FGFR1 alone, we also evaluated the ratio between the signals of the locus-specific probe and centromere 8. Within the subgroup of cases with FGFR1 gene copies ≥4, all tumours showed a locus-specific gene copy number increase with ratio values above 1 (range, 1.14 to 2.75). We found almost equal numbers of cases with ratio values below 1 (n=117) suggesting a FGFR1 deletion and those with ratio values above 1 (n=143) indicative of a regional FGFR1 gene copy number gain. Within the subgroup of cases with reduced FGFR1 gene copies, there were also no significant associations with clinicopathological parameters or survival.

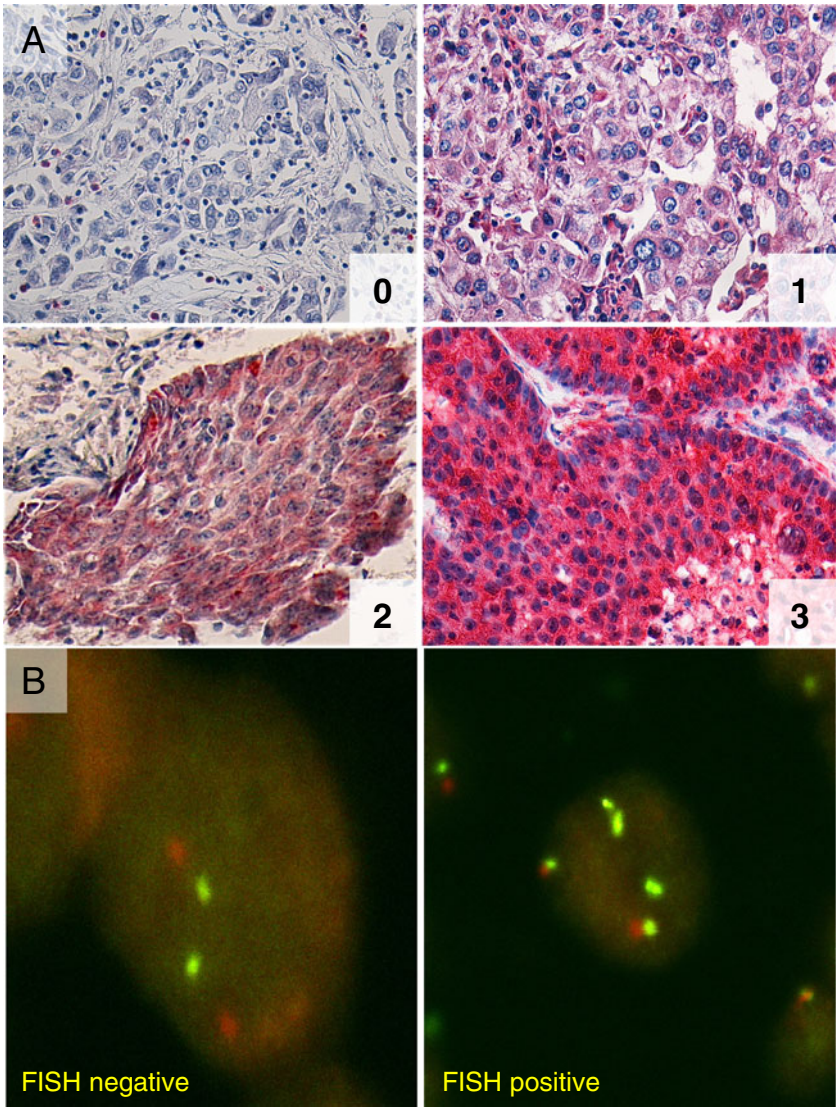

Fig. 1 **a** Immunohistochemical detection of FGFR1 and scoring of protein expression by a four-tier system: *0* no expression, *1* low, *2* moderate, *3* strong expression (magnification, ×630). **b** Representative examples of the dual-colour FISH analysis for FGFR1 (*green signals*) and CEN8 (*red signals*)

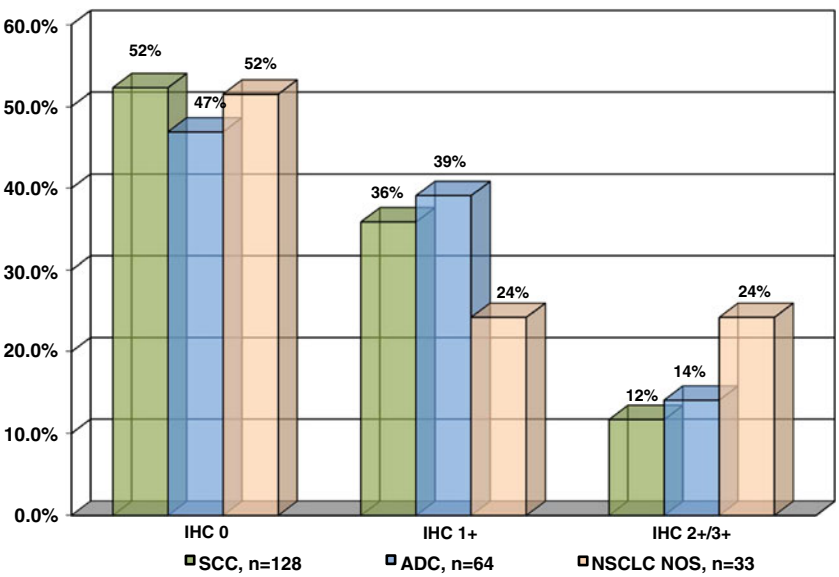

Fig. 2 FGFR1 protein expression in different lung cancer subtypes revealed no significant differences

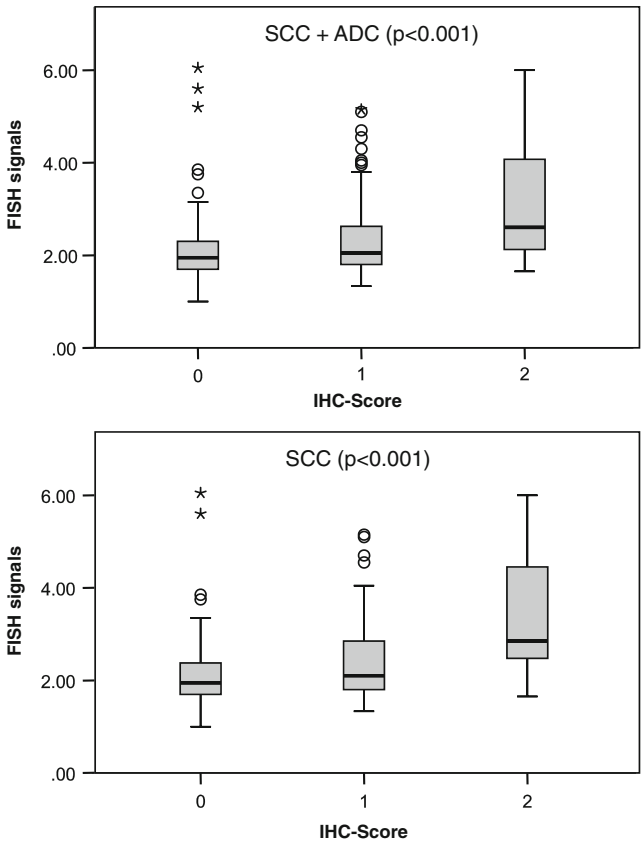

Fig. 3 Boxplot analysis for the correlation between FGFR1 gene copy numbers and protein expression indicated significant associations for lung SCC and ADC which was mainly due to the subgroup of SCC

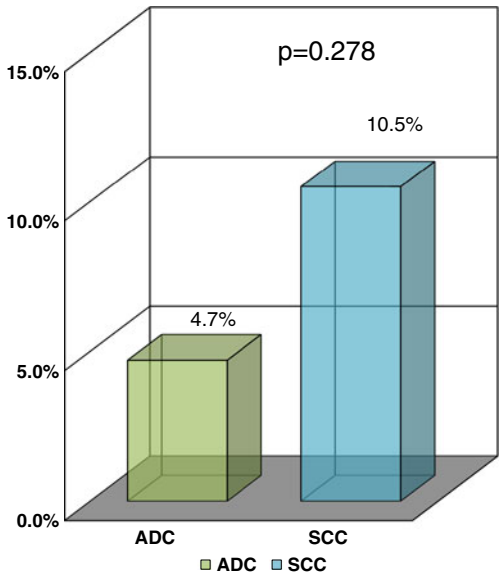

Fig. 5 FGFR1 amplification (≥4 FISH signals) was more frequent in lung SCC than ADC, however without reaching statistical significance

Survival analysis

In our case series, we observed significant correlations between clinicopathological parameters and patient survival. In the 5-year-survival analysis, ADC patients with grade 2 or 3 tumours showed a significantly shorter survival than patients with a grade 1 lung ADC ($p<0.05$). Similarly, ADC patients without lymph node metastasis ($n=39$) had a significantly higher 5-year survival than patients with lymph node metastases ($p<0.0001$); only about 15 % of the patients with pN1, pN2 or pN3 stages survived 60 months while more than 60 % of the patients with pN0 were alive after 5 years. For patients with SCC, we did not observe significant differences in 5-year survival according to the lymph node status or tumour grade. After 30 months of follow-up, 65 % of the patients with ADC and 45 % of SCC patients were still alive. After 5 years, the survival rates for ADC and SCC patients were 35 and 30 %, respectively. The pT stage did not correlate significantly with survival (SCC, $p=0.178$; ADC, $p=0.145$), but there was a trend towards a better survival of patients with T1/T2 tumours compared to those with a T3/T4 tumour stage.

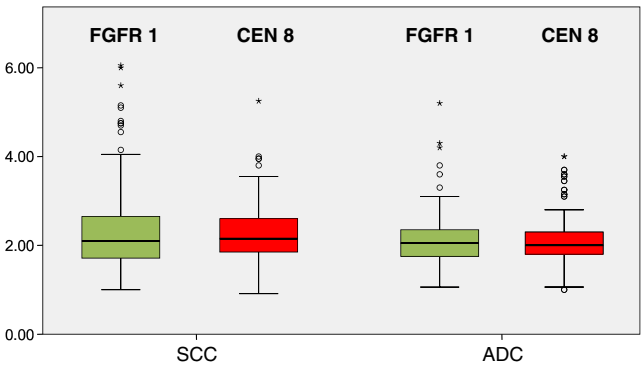

Fig. 4 Comparison of FISH signals indicated more SCC cases with higher FGFR1 copy numbers than ADC, however without reaching a statistical significant difference

FGFR1 expression or gene copy number alterations, in general, did not show any significant association with survival. However, there are some interesting trends when analysing overall survival in relation to different signal frequencies of the FGFR1 gene (Fig. 6). Specifically, with FGFR1 signal numbers above 3, the curves for lung SCC start to split. Patients with FGFR1 copy number increases carried a worse prognosis with survival curves being almost identical when comparing absolute FGFR1 signals (≥4 signals, Fig. 6d) and FGFR1/CEN8 ratio values (≥1.5, data not shown). In contrast, the few lung ADC with FGFR1 signals ≥4 ($n=3$) showed a better survival than the amplified squamous cell carcinoma patients. Due to the small number of cases, these differences did not reach statistical significance.

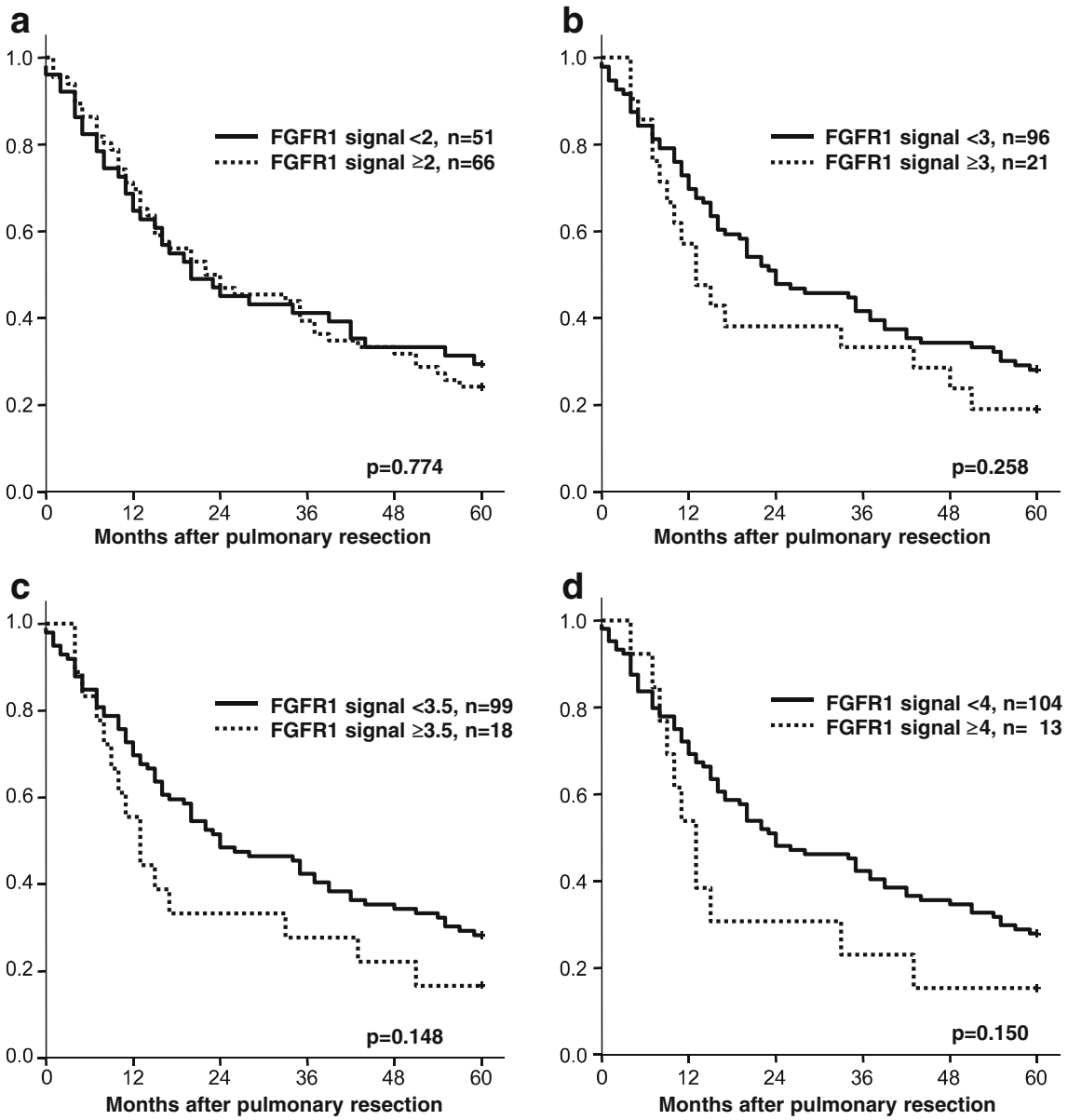

Fig. 6 Survival analysis of lung SCC according to different FGFR1 gene copy number cut-off values suggested a worse prognosis of cases with increased gene copy numbers, however without reaching statistical significance

Discussion

FGFR1 and its signalling pathway seem to be of key importance in tumour progression and survival [12, 13]. The genomic region of FGFR1 is located on chromosome 8p12, and frequent and focal amplifications at this region are described in several publications for different tumours. Breast cancer showed an amplification frequency of 10 % [14]. With lower frequency, bladder cancer [15], ovarian carcinoma [16] and rhabdomyosarcoma [17] also showed amplifications at chromosome 8p12. Alterations in the FGFR gene family have also been found for different tumour subgroups like bladder cancer, breast cancer, endometrium cancer and gastric cancer [4, 18–20].

To evaluate the amplification frequency of FGFR1 in human lung cancer specimens, we performed FISH on tissue microarrays to compare in particular lung SCC and ADC. Earlier publications suggested a significant difference in the amplification frequency in these two tumour subgroups [8, 21]. In principle, our analysis showed a similar percentage of 10 % of SCC cases with increased FGFR1 gene copies (≥4 signals) as shown by Weiss et al. [8]. The same study also reported on an independent case series of SCC harbouring ≥4 FGFR1 gene copies in 22 % of cases. This

number seems to be exaggerated; at least, it was not consistent with our data. In addition, we could also not confirm the statistical significant difference between lung SCC and ADC which may be due to the slightly lower number of cases that were analysed in our study.

Another possibility may be the lack of standardized criteria for defining FGFR1 amplification. In this regard, the study of Weiss et al. is helpful because it introduced a new threshold for defining FGFR1 amplifications. However, considerable heterogeneity exists in the assessment and terminology of gene amplifications. For HER2, it was traditionally defined as a gene to reference ratio above 2.0, and this cut-off value has achieved major practical relevance in selecting patients for targeted therapy. However, there are also other parameters like clusters of gene signals in 10 % of tumour cells or signal copy numbers >6 [22]. Other cut-off values may need to be defined for distinct genes. For FGFR1, Weiss et al. not only introduced the ≥4 threshold but also used the term low-level amplification for cases with ≥2 but <4 signals and high-level amplification for those with ≥9 signals. We did not find cases with high-level amplification. The maximum number of FGFR1 signals in our study was 6.05 (mean of signals per tumour cell). In fact, most carcinomas showed only a modest increase of the FGFR1 gene copies. However, a limitation of our study is that we analysed only one core punch biopsy per tumour resection specimen. Thus, we cannot make any statements on the heterogeneity of FGFR1 gene copy numbers within a single tumour.

A first follow-up study after the report of Weiss et al. reported that increased copy number status of FGFR1 in lung SCC correlated significantly with the parameters gender (females, 13.8 %, vs. males, 39.4 %), smoking status (never smoker, 4.2 %, vs. smokers, 40.8 %) and pathological subtypes (squamous cell carcinoma, 41.5 %, vs. non-squamous cell carcinoma, 40.8 %), but not with age, grade and lymph node status [21]. Significance for the smoking status was also reported earlier by Behrens et al. using FGFR1 IHC expression analysis [23].

It is interesting to analyse whether the FGFR1 gene copy number increase is due to chromosome 8 polysomy or a regional FGFR1 amplification. In the cases with a FGFR1 gene copy number increase ≥4, the ratio values FGFR1/CEN8 were all greater than 1 suggesting a regional copy number increase. However, the ratio values varied only between 1.14 and 2.75 indicating that local, high copy number amplifications with the generation of double minutes or homogenously staining region as reported for the myc oncogenes do not affect the FGFR1 locus or at least represent a very rare event that was not detectable in our collective. This view is supported by our conventional comparative genomic hybridization (CGH) data (Fig. 7, [24–30]). The FISH-positive case of Fig. 1b seems to be representative for the few lung carcinomas with FGFR1 amplifications. SCC is the lung cancer subtype with the highest DNA content [24]. Thus, polyploidy leading to chromosome 8 polysomy probably also contributes to the increase of FGFR1 gene copy numbers in SCC compared to lung ADC.

It is important to take note of the difference between absolute and relative gene copy numbers. CGH detects relative copy number changes. In case of triploid carcinomas, two copies of the FGFR1 gene would be interpreted as a deletion. In contrast, FISH detects absolute gene copy numbers which may be transformed into relative copy numbers by calculating ratio values between two distinct chromosomal probes. Our FISH ratio analysis confirmed the previous CGH findings that chromosome 8p is affected not only by DNA gains but also DNA losses. CGH as well as LOH data actually suggested that 8p deletions may be a marker for tumour progression and metastasis in lung cancer [28, 29]. Interestingly, one metastasis suppressor gene for hepatocellular carcinoma has been identified on chromosome 8p12 [31]. Furthermore, mutations of the Werner syndrome gene WRN at 8p12 may cause premature ageing and is associated with a predisposition to cancer [32].

Thus, it is not surprising that we could not find any association between FGFR1 protein expression or copy number gains and clinicopathological parameters indicative for tumour progression. Similar observations were made in a recent study using FISH and IHC [21] as well as an earlier protein expression study [23]. However, this statement may

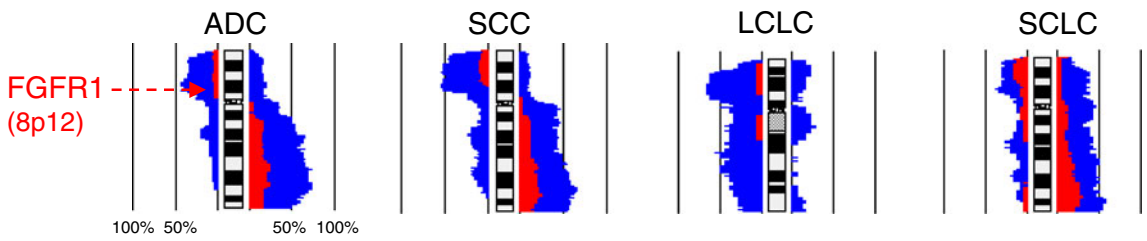

Fig. 7 DNA imbalances of lung cancer subtypes according to conventional comparative genomic hybridization/CGH (compiled from data of Petersen I in Travis et al. 2004, [30]). Cases with DNA gains were represented by the histogram on the *right side* of the chromosome ideogram, cases with DNA loss on the *left side*. The data indicated that 8p deletions are at least as frequent as DNA gains with pronounced gains (indicated by the *red colour*) as putative correlates of an amplification being undetectable in the NSCLC subtypes

need to be reassessed after the analysis of larger tumour collectives. At least, our survival analysis using different cut-off values for FGFR1 copy number gains suggested a trend towards worse prognosis in case of gene copy number increase (Fig. 6). A similar trend was observed by Sasaki et al. [21]; however, the authors also failed to confirm a significant difference in their case series of 100 lung SCC. Furthermore, it is noteworthy that increased FGFR1 expression has been associated with cancer cell survival and chemotherapy resistance [33, 34]. Several studies reported elevated levels of FGFR1 protein in NSCLC [35, 36]. The highest FGFR1 expression was found in lung SCC [37].

Following the study of Weiss et al., FGFR1 analysis of lung SCC has achieved considerable interest because of its potential use as a drug target [6, 8, 10]. The results of the clinical trials are eagerly awaited, and it is far too early to make final judgements on the importance of FGFR1 targeting in lung cancer. However, it must be stated that the fibroblast growth factor (FGF) signalling is quite complex with a high number of ligands and receptors. Furthermore, FGF and their receptors may not only have oncogenic functions but may also act as tumour suppressors in a tissue-dependent manner which has specifically been reported for FGFR2 [4]. Thus, it is fair to assume that targeting of FGFR1 alone will not bring a major breakthrough in the treatment of the majority of lung cancer patients.

Acknowledgments We thank Barbara Bergholz, Christiane Geier and other colleagues from the institute of pathology for technical assistance. In addition, we are indebted to Piere Rogalla and Sven Hauke from ZytoVision GmbH for providing the FGFR1/CEN8 dual-colour FISH probes in the context of the BMBF project for molecular sarcoma diagnosis (FKZ 0315509).

Conflict of interest All authors declare no conflict of competing interests.

References

1. Jemal A, Siegel R, Ward E, Murray T, Xu J, Smigal C, Thun MJ (2006) Cancer statistics, 2006. CancerJClin 56:106–130
2. GEKID/RKI (2012) Krebs in Deutschland 2007/2008. 8. Ausgabe. Robert Koch-Institut (Hrsg) und die Gesellschaft der epidemiologischen Krebsregister in Deutschland e.V. (Hrsg). Berlin, 2012
3. Ferlay J, Shin HR, Bray F, Forman D, Mathers C, Parkin DM (2008) GLOBOCAN 2008 v1.2, Cancer incidence and mortality worldwide: IARC CancerBase no. 10 [Internet]. Lyon, France: International Agency for Research on Cancer; 2010
4. Turner N, Grose R (2010) Fibroblast growth factor signalling: from development to cancer. Nat Rev Cancer 10(2):116–129
5. Prié D, Reciprocal FG (2010) Control of 1,25-dihydroxyvitamin D and FGF23 formation involving the FGF23/Klotho system. Clin J Am Soc Nephrol 5:1717–1722
6. Greulich H, Pollock MP (2011) Targeting mutant fibroblast growth factor receptors in cancer. Trends Mol Med 17(5):283–292
7. Bass AJ, Watanabe H, Mermel CH, Yu S, Perner S, Verhaak RG, Kim SY, Wardwell L, Tamayo P, Gat-Viks I, Ramos AH, Woo MS, Weir BA, Getz G, Beroukhim R, O'Kelly M, Dutt A, Rozenblatt-Rosen O, Dziunycz P, Komisarof J, Chirieac LR, Lafargue CJ, Scheble V, Wilbertz T, Ma C, Rao S, Nakagawa H, Stairs DB, Lin L, Giordano TJ, Wagner P, Minna JD, Gazdar AF, Zhu CQ, Brose MS, Cecconello I, Ribeiro U Jr, Marie SK, Dahl O, Shivdasani RA, Tsao MS, Rubin MA, Wong KK, Regev A, Hahn WC, Beer DG, Rustgi AK, Meyerson M (2009) SOX2 is an amplified lineage-survival oncogene in lung and esophageal squamous cell carcinomas. Nat Genet 41:1238–1242
8. Weiss J, Sos ML, Seidel D, Peifer M, Zander T, Heuckmann JM, Ullrich RT, Menon R, Maier S, Soltermann A, Moch H, Wagener P, Fischer F, Heynck S, Koker M, Schöttle J, Leenders F, Gabler F, Dabow I, Querings S, Heukamp LC, Balke-Want H, Ansén S, Rauh D, Baessmann I, Altmüller J, Wainer Z, Conron M, Wright G, Russell P, Solomon B, Brambilla E, Brambilla C, Lorimier P, Sollberg S, Brustugun OT, Engel-Riedel W, Ludwig C, Petersen I, Sänger J, Clement J, Groen H, Timens W, Sietsma H, Thunnissen E, Smit E, Heideman D, Cappuzzo F, Ligorio C, Damiani S, Hallek M, Beroukhim R, Pao W, Klebl B, Baumann M, Buettner R, Ernestus K, Stoelben E, Wolf J, Nürnberg P, Perner S, Thomas RK (2011) Frequent and focal FGFR1 amplification associates with therapeutically tractable FGFR1 dependency in squamous cell lung cancer. Sci Transl Med 2:62–93
9. Hammerman PS, Sos ML, Ramos AH, Xu C, Dutt A, Zhou W, Brace LE, Woods BA, Lin W, Zhang J, Deng X, Lim SM, Heynck S, Peifer M, Simard JR, Lawrence MS, Onofrio RC, Salvesen HB, Seidel D, Zander T, Heuckmann JM, Soltermann A, Moch H, Koker M, Leenders F, Gabler F, Querings S, Ansén S, Brambilla E, Brambilla C, Lorimier P, Brustugun OT, Helland A, Petersen I, Clement JH, Groen H, Timens W, Sietsma H, Stoelben E, Wolf J, Beer DG, Tsao MS, Hanna M, Hatton C, Eck MJ, Janne PA, Johnson BE, Winckler W, Greulich H, Bass AJ, Cho J, Rauh D, Gray NS, Wong KK, Haura EB, Thomas RK, Meyerson M (2011) Mutations in the DDR2 kinase gene identify a novel therapeutic target in squamous cell lung cancer. Cancer Discov 1(1):78–89
10. Thomas R, Wolf J (2012) Personalized therapy of lung cancer. Onkologie 35(Suppl 1):14–19
11. Hamidov Z, Altendorf-Hofmann A, Chen Y, Settmacher U, Petersen I, Knösel T (2011) Reduced expression of desmocollin 2 is an independent prognostic biomarker for shorter patients survival in pancreatic ductal adenocarcinoma. J Clin Pathol 64 (11):990–994
12. Dailey L, Ambrosetti D, Mansukhani A, Basilico C (2005) Mechanisms underlyingd differential responses to FGF signaling. Cytokine Growth Factor Rev 16:233–247
13. Ribatti D, Vacca A, Rusnati M, Presta M (2007) The discovery of basic fibroblast growth factor/fibroblast growth factor-2 and its role in haematological malignancies. Cytokine Growth Factor Rev 18:327–334
14. Courjal F, Cuny M, Simony-Lafontaine J, Louason G, Speiser P, Zeillinger R, Rodriguez C, Theillet C (1997) Mapping of DNA amplifications at 15 chromosomal localizations in 1875 breast tumors: definition of phenotypic groups. Cancer Res 57 (19):4360–4367
15. Simon R, Richter J, Wagner U, Fijan A, Bruderer J, Schmid U, Ackermann D, Maurer R, Alund G, Knönagel H, Rist M, Wilber K, Anabitarte M, Hering F, Hardmeier T, Schönenberger A, Flury R, Jäger P, Fehr JL, Schraml P, Moch H, Mihatsch MJ, Gasser T, Sauter G (2001) High-throughput tissue microarray analysis of 3p25 (RAF1) and 8p12 (FGFR1) copy number alterations in urinary bladder cancer. Cancer Res 61(11):4514–4519
16. Gorringe KL, Jacobs S, Thompson ER, Sridhar A, Qiu W, Choong DY, Campbell IG (2007) High-resolution single nucleotide polymorphism array analysis of epithelial ovarian cancer reveals

numerous microdeletions and amplifications. Clin Cancer Res 13 (16):4731–4739
17. Missiaglia E, Selfe J, Hamdi M, Williamson D, Schaaf G, Fang C, Koster J, Summersgill B, Messahel B, Versteeg R, Pritchard-Jones K, Kool M, Shipley J (2009) Genomic imbalances in rhabdomyosarcoma cell lines affect expression of genes frequently altered in primary tumors: an approach to identify candidate genes involved in tumor development. Genes Chromosomes Cancer 48(6):455–467
18. Cappellen D, De Oliveira C, Ricol D, de Medina S, Bourdin J, Sastre-Garau X, Chopin D, Thiery JP, Radvanyi F (1999) Frequent activating mutations of FGFR3 in human bladder and cervix carcinomas. Nat Genet 23:18–20
19. Dutt A, Salvesen HB, Chen TH, Ramos AH, Onofrio RC, Hatton C, Nicoletti R, Winckler W, Grewal R, Hanna M, Wyhs N, Ziaugra L, Richter DJ, Trovik J, Engelsen IB, Stefansson IM, Fennell T, Cibulskis K, Zody MC, Akslen LA, Gabriel S, Wong KK, Sellers WR, Meyerson M, Greulich H (2008) Drug sensitive FGFR2 mutations in endometrial carcinoma. Proc Natl Acad Sci 105:8713–8717
20. Kunii K, Davis L, Gorenstein J, Hatch H, Yashiro M, Di Bacco A, Elbi C, Lutterbach B (2008) FGFR2-amplified gastric cancer cell lines require FGFR2 and Erbb3 signaling for growth and survival. Cancer Res 68:2340–2348
21. Sasaki H, Shitara M, Yokota K, Hikosaka Y, Moriyama S, Yano M, Fujii Y (2012) Increased FGFR1 copy number in lung squamous cell carcinomas. Mol Med Report 5(3):725–728
22. Allison KH, Dintzis SM, Schmidt RA (2011) Frequency of HER2 heterogeneity by fluorescence in situ hybridization according to CAP expert panel recommendations: time for a new look at how to report heterogeneity. Am J Clin Pathol 136(6):864–871
23. Behrens C, Lin HY, Lee JJ, Raso MG, Hong WK, Wistuba II, Lotan R (2008) Immunohistochemical expression of basic fibroblast growth factor and fibroblast growth factor receptors 1 and 2 in the pathogenesis of lung cancer. Clin Cancer Res 14:6014–6022
24. Petersen I, Amin Kotb WFM, Friedrich KH, Schlüns K, Böcking A, Dietel M (2009) Core classification of lung cancer: correlating nuclear size and mitoses with ploidy and clinicopathological parameters. Lung Cancer 65:312–318
25. Ried T, Petersen I, Holtgreve-Grez H, Speicher MR, Schröck E, du Manoir S, Cremer T (1994) Mapping of multiple DNA gains and losses in primary small cell lung carcinomas by comparative genomic hybridization. Cancer Res 54(7):1801–1806
26. Petersen I, Langreck H, Wolf G, Schwendel A, Psille R, Vogt P, Reichel MB, Ried T, Dietel M (1997) Small-cell lung cancer is characterized by a high incidence of deletions on chromosomes 3p, 4q, 5q, 10q, 13q and 17p. Br J Cancer 75(1):79–86
27. Petersen I, Bujard M, Petersen S, Wolf G, Goeze A, Schwendel A, Langreck H, Gellert K, Reichel M, Just K, du Manoir S, Cremer T, Dietel M, Ried T (1997) Patterns of chromosomal imbalances in adenocarcinoma and squamous cell carcinoma of the lung. Cancer Res 57(12):2331–2335
28. Petersen S, Aninat-Meyer M, Schlüns K, Gellert K, Dietel M, Petersen I (2000) Chromosomal alterations in the clonal evolution to the metastatic stage of squamous cell carcinomas of the lung. Br J Cancer 82(1):65–73
29. Goeze A, Schlüns K, Wolf G, Thäsler Z, Petersen S, Petersen I (2002) Chromosomal imbalances of primary and metastatic lung adenocarcinomas. J Pathol 196(1):8–16
30. Travis WD, Brambilla E, Muller-Hermelink HK, Harris CC (2002) World Health Organization Classification of Tumours, Pathology and genetics of tumours of the lung, pleura, thymus and heart. IARC Press, Lyon, 2004
31. Ren N, Wu JC, Dong QZ, Sun HJ, Jia HL, Li GC, Sun BS, Dai C, Shi J, Wei JW, Sheng YY, Zhou HJ, Ye QH, Qin LX (2011) Association of specific genotypes in metastatic suppressor HTPAP with tumor metastasis and clinical prognosis in hepatocellular carcinoma. Cancer Res 71(9):3278–3286
32. Monnat RJ Jr (2010) Human RECQ helicases: roles in DNA metabolism, mutagenesis and cancer biology. Semin Cancer Biol 20(5):329–339
33. Pardo OE, Wellbrock C, Khanzada UK, Aubert M, Arozarena I, Davidson S, Bowen F, Parker PJ, Filonenko VV, Gout IT, Sebire N, Marais R, Downward J, Seckl MJ (2006) FGF-2 protects small cell lung cancer cells from apoptosis through a complex involving PKCepsilon, B-Raf and S6K2. EMBO J 25 (13):3078–3088
34. Pardo OE, Latigo J, Jeffery RE, Nye E, Poulsom R, Spencer-Dene B, Lemoine NR, Stamp GW, Aboagye EO, Seckl MJ (2009) The fibroblast growth factor receptor inhibitor PD173074 blocks small cell lung cancer growth in vitro and in vivo. Cancer Res 69 (22):8645–8651
35. Kuhn H, Kopff C, Konrad J, Riedel A, Gessner C, Wirtz H (2004) Influence of basic fibroblast growth factor on the proliferation of non-small cell lung cancer cell lines. Lung Cancer 44:167–174
36. Berger W, Setinek U, Mohr T, Kindas-Mügge I, Vetterlein M, Dekan G, Eckersberger F, Caldas C, Micksche M (1999) Evidence for a role of FGF-2 and FGF receptors in the proliferation of non-small cell lung cancer cells. Int J Cancer 83:415–423
37. Guddo F, Fontanini G, Reina C, Vignola AM, Angeletti A, Bonsignore G (1999) The expression of basic fibroblast growth factor (bFGF) in tumor-associated stromal cells and vessels is inversely correlated with non-small cell lung cancer progression. Hum Pathol 30:788–794

Virchows Arch (2012) 461:59–65
DOI 10.1007/s00428-012-1247-6

ORIGINAL ARTICLE

In pulmonary sclerosing hemangioma expression of β-catenin, Axin, and C-myc differs between the two cell types

Xu-Yong Lin · Di Zhang · Yong Zhang · Chui-Feng Fan · Shun-Dong Dai · En-Hua Wang

Received: 21 December 2011 / Revised: 3 April 2012 / Accepted: 2 May 2012 / Published online: 22 May 2012
© Springer-Verlag 2012

Abstract Previous studies have shown that pulmonary sclerosing hemangioma is a tumor derived from primitive respiratory epithelium, but its character and the differentiation status of the two cell types (polygonal and cuboidal) composing the lesion are still controversial. We hypothesize that the polygonal cells are immature compared with cuboidal cells and have higher proliferative activity. To further study this question, we examined the expression of β-catenin, Axin, and C-myc by immunostaining in 45 primary sclerosing hemangioma (PSH) specimens. The two cell types were captured by laser capture microdissection from 28 PSH specimens, and total RNA was extracted. Messenger RNA (mRNA) expression of Axin and C-myc was examined by reverse transcription polymerase chain reaction (RT-PCR). By immunostaining, β-catenin was predominantly strongly expressed on the cell membrane of cuboidal cells, while in polygonal cells, β-catenin was predominantly expressed in the cytoplasm and significantly decreased on cell membranes. Axin was expressed in cuboidal cells in 93 % of our 45 cases, but only expressed in 18 % of these in polygonal cells. C-myc expression in polygonal cells was significantly stronger than in cuboidal cells ($P<0.05$). RT-PCR showed that the expression level of Axin mRNA in cuboidal cells was significantly higher than in polygonal cells ($P<0.05$), and expression level of C-myc mRNA in polygonal cells was significantly higher than in cuboidal cells ($P<0.05$).The two PHS cell types have distinct expression of β-catenin, Axin, and C-myc, suggesting that their differentiation status may be different. The higher expression of C-myc in polygonal cells suggests that these cells might have higher proliferative activity.

Keywords Pulmonary sclerosing hemangioma · Laser capture microdissection (LCM) · Wnt signaling pathway

X.-Y. Lin · D. Zhang · Y. Zhang · C.-F. Fan · S.-D. Dai · E.-H. Wang (✉)
Department of Pathology, The First Affiliated Hospital and College of Basic Medical Sciences, China Medical University, Shenyang 110001, China
e-mail: wangeh@hotmail.com

X.-Y. Lin · D. Zhang · Y. Zhang · C.-F. Fan · S.-D. Dai · E.-H. Wang
Institute of pathology and pathophysiology, China Medical University, Shenyang 110001, China

Introduction

Pulmonary sclerosing hemangioma (PSH) is a rare pulmonary tumor first described by Liebow and Hubbel [1]. Its histogenesis and nature have been controversial for decades, and the pathogenesis of PSH remains unclear [2–7]. In the 1981 WHO classification of lung tumors, PSH was accepted as tumor-like lesion. However, recent studies have revealed that PSH is a true tumor rather than a hamartoma [8, 9]. Therefore, in the 1999 and 2004 WHO classifications of lung tumors, PSH was categorized as a miscellaneous tumor. It consists mainly of two types of cells: polygonal cells in the solid areas and the interstitium of papillary areas and cuboidal cells on the surface of papillary areas or in various lacunar spaces. The two cell types are significantly different in histological pattern, cellular morphology, and immunophenotype. Histologically, the cuboidal cells look like type II pneumocytes, but the polygonal cells are significantly different from pneumocytes. Literature reports and our previous study indicate that they have the same cellular origin [8, 9], and both originate from primitive respiratory epithelium [10–12]. Therefore, the use of the term pneumocytoma was recommended. The question arises as to what might be

the nature of the difference between the two types of cells. Our working hypothesis is that they are in a different differentiation status, the cuboidal cells being more mature than the polygonal cells. If the polygonal cells are in an immature status, they might be in an active state of proliferation. Although most scholars believe that the tumor is benign, there are reports of lymph node metastasis [13, 14], pleural dissemination [15], and metastatic spread to the stomach [16]. These findings have prompted us to study the differentiation status of the two types of cells and the clinical behavior of PSH.

The Wnt signaling pathway is a conserved signaling pathway, which plays a key role in embryonic development, and is involved in the regulation of cell growth, migration, and differentiation. Activation of Wnt signaling has been proven to be involved in the development of many tumors [17]. β-Catenin, Axin, and C-myc are major factors of Wnt signaling pathway, their abnormal expression having been detected in many tumors [17–19]. In nonsmall cell lung cancer, the activation of Wnt signaling has been found, as well as aberrant expression of β-catenin, Axin, and C-myc. In contrast, in mature epithelial cells, the Wnt signaling pathway is not activated. Dacic et al. found in PSH genetic changes similar to those in bronchioloalveolar carcinoma (BAC) [20]. This supports the notion that PSH may have mechanisms of tumorigenesis in common with BAC. Therefore, to further analyze the character of PSH and differentiation status of two types of cells, the above factors were chosen, and the expression was examined in PSH by immunochemical staining and reverse transcription polymerase chain reaction (RT-PCR).

Materials and methods

Patients and specimens

We collected 45 cases of PSH from The First Affiliated Hospital of China Medical University from 1990 to 2009. The patients with PSH included 11 men and 34 women. The age of the patients ranged from 26–66 years (average, 45 years). Most of the 45 patients exhibited no symptoms before operation and were diagnosed during routine examinations; a few patients had clinical symptoms including chest pain, blood-tinged sputum, and persistent coughing. In all cases, a peripheral round, solitary, well-circumscribed, and highly dense nodule was found by chest radiographs and computed tomography scans. The tumor mass diameters ranged from 0.6 to 5.0 cm. Of the 45 patients, 31 underwent wedge resection; the other 14 underwent lobectomy. In six cases, intraoperative frozen biopsy failed to exclude bronchioloalveolar carcinoma or acinar adenocarcinoma; as a consequence, the patients underwent lymph node dissection, but no lymph node metastases were found. Postoperative follow-up was obtained for 24 patients and ranged from 6 to 64 months (mean follow up, 25 months).

Immunohistochemical staining

All the resected specimens were fixed with 10 % neutral-buffered formalin and embedded in paraffin. Tissue blocks were cut into 4-μm sections, which were deparaffinized in xylene, rehydrated with graded alcohols, and immunostained with anti-Axin (rabbit polyclonal antibody, Santa, USA), anti-β-catenin, and anti-C-myc (mouse monoclonal antibody, Santa, USA).

Sections were stained with a streptavidin-peroxidase system (KIT-9720, ultrasensitive TM S-P, MaiXin, China). The chromogen used was diaminobenzidine tetrahydrochloride substrate (DAB kit, MaiXin, China), and the sections were slightly counterstained with hematoxylin, dehydrated, and mounted. As negative control, the primary antibody was replaced with phosphate-buffered saline. In each section, five random high power fields were observed, and 100 cells were counted in each field. The proportion of immunopositive cells was categorized as follows: 0, <5 %; 1, ≥5 to <25 %; 2, ≥25 to <50 %; and 3, ≥50 %. The staining intensity was categorized by relative intensity as follows: 0, no positivity; 1, weak; 2, moderate; and 3, strong. A final immunoreactivity score of each section was obtained by multiplying the two individual scores: (−), <2; (+), ≥2 to <4; (++), ≥4 to <7; (+++), ≥7. To obtain final statistical results, (−) was considered as negative, and (+)–(+++) were considered as positive. The location of β-catenin staining was on the membrane and/or cytoplasm and even nuclear. When more than 90 % of the tumor cells stained for β-catenin on the cell membrane, the case was defined as normal membranous expression. When fewer than 90 % of the tumor cells stained for membranous expression, and/or more than 10 % of the tumor cells stained for β-catenin in the cytoplasm or nuclear, the case was defined as abnormal expression. The location of Axin and C-myc staining was in the cytoplasm.

Laser capture target cells

The 28 specimens were cut into 6-μm serial sections, laid on a thin polyethylene foil slide, deparaffinized, and stained with laser capture microdissection (LCM) Staining Kit (AM1935, Ambion, USA). Then, the cuboidal and polygonal cells were separately captured by LCM (LEICA LMD6000, Leica, Germany). More than 10,000 cells were captured from each specimen.

Reverse transcription polymerase chain reaction

The total RNA of the captured cells was extracted with RNAqueous-Micro Kit (AM1931, Ambion, USA); RNA

quantity and quality was determined by OD at 260 and 280 nm on a NanoDrop® ND-1000 spectrophotometer (NanoDrop Technologies, Wilmington, DE, USA).The RNA concentration ranged from 60 to 120 ng/μl, the value of A_{260}/A_{280} ranged from 1.8 to 2.0. RT-PCR was performed using an EasyRT-PCR kit (TransGen Biotech, China), according to the manufacturer's instruction. The sequences of the primers and PCR conditions are listed in Table 1. After electrophoresis on 1.5 % agar gel, the bands of PCR products were visualized using BioImaging Systems (UVP, CA, USA). The grayscale of PCR products was measured. The relative messenger RNA (mRNA) expression levels were normalized relative to the amount of β-actin mRNA.

Statistical analysis

All statistical calculations were performed by SPSS version 13.0 for Windows software (SPSS Inc, Chicago, IL, USA). The chi-square test was used to analyze the results of immunohistochemical staining. The *t* test was used to compare data from the RT-PCR. $P<0.05$ were considered statistically significant

Results

Histological features and follow-up

Histologically, all cases exhibited the following features: solid (Fig. 1a), papillary (Fig. 1b), hemorrhagic (Fig. 1c), and sclerotic (Fig. 1d) areas were noted, and the lesions were composed entirely of polygonal and cuboidal cells. The two types of cells were significantly different in histological pattern and morphological phenotype (Fig. 1) .The cuboidal cells were arranged in a tight monolayer, had dense chromatin, and looked like type II pneumocytes, while polygonal cells were distributed in interstitial locations and displayed abundant clear to eosinophilic cytoplasm with centrally located nuclei. In addition, the polygonal cells occasionally demonstrated moderate to severe cellular atypia, notably nuclear pleomorphism, but typically with rare mitotic activity.

In the period of follow-up, no patient died from the tumor, but one patent developed acinar adenocarcinoma in the same lung lobe 56 months after the wedge resection, while another patient developed a recurrence 26 months after the wedge resection.

Imunohistochemical staining of β-catenin, Axin, and C-myc in PSH

By imunohistochemical staining β-catenin was found in cuboidal cells in all 45 PSH specimens, and clear and consistent expression on the membrane and weak expression in the cytoplasm was seen. In polygonal cells, β-catenin was predominantly expressed in cytoplasm; the expression levels on the membrane were significantly decreased, with even a lack of expression in some cases (Fig. 2). In 8.9 % (4/45) of PSH specimens, β-catenin expression was not detected in polygonal cells; in the remaining cases, expression could be detected in cytoplasm of polygonal cells, within 24.4 % (11/45) of PSH specimens strong expression (+++) in cytoplasm and expression in the nuclei of few cells (Table 2).

In 93.3 % (42/45) of PSH specimens, Axin was expressed in cuboidal cells, while in only 17.8 % (8/45) of PSH specimens, Axin expression was detected in polygonal cells. Axin expression was much stronger in cuboidal cells than in polygonal cells ($P<0.05$).

In 84.4 % (38/45) of PSH specimens, C-myc was expressed in polygonal cells, while in 20 %(9/45) of PSH specimens, C-myc was expressed in cuboidal cells. The expression level in polygonal cells was significantly higher than that in cuboidal cells ($P<0.05$; Fig. 3 and Table 2).

The mRNA expression of Axin and C-myc in two types of cells of PSH

By RT-PCR, the mean relative expression level of Axin mRNA in cuboidal cells was 0.26±0.05 and in polygonal cells was 0.85±0.09.The expression level of Axin in cuboidal cells was significantly higher than that in polygonal cells ($P<0.05$). The mean relative expression level of C-myc was 0.23±0.04 in cuboidal cells and 0.91±0.08 in polygonal cells, and the expression level in polygonal cells was significantly higher than in cuboidal cells ($P<0.05$, Fig. 4).

Table 1 Sequences of primers used and PCR conditions

Gene	Primer (5→3)	Annealing Temperature (°C)	Cycles	Fragment Size(bp)
Axin	Forward: ACCGAAAGTACATTCTTGATAAC Reverse: TCCATACCTGAACTCTCTGC	52.0	40	452
C-myc	Forward: CCTACCCTCAACGACAGC Reverse: CTCTGACCTTTTTGCCAGGAG	55.1	40	248
β-Actin	Forward: AGAGCTACGAGCTGCCTGAC Reverse: AGTACTTGCGCTCAGGAGGA	55.0	40	308

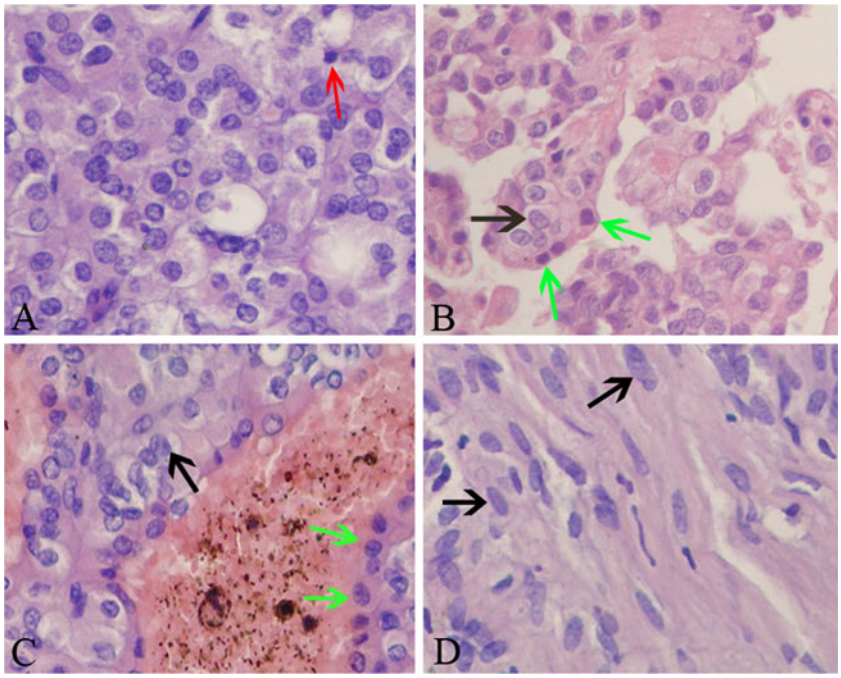

Fig. 1 Morphological changes of PSH. **a** Solid pattern with polygonal cells diffusely infiltrated with lymphocytes (*red arrow*). **b** Papillary pattern, surface covered with cuboidal cells (*green arrow*), and polygonal cells (*black arrow*)in the stroma. **c**The cuboidal cells (*green arrow*) cover the internal cavity of the hemorrhagic patterned polygonal cells (*black*) in the stroma. **d** Numerous collagen fibers and few polygonal cells (*black arrow*) in a sclerotic pattern

Discussion

Pulmonary sclerosing hemangioma (PSH) is an uncommon lung tumor, considered to be a particular type of epithelial tumor [10–12]. Histologically, PSH consists mainly of two types of cells: polygonal cells and cuboidal cells. The polygonal cells are located in the solid areas and interstitium of papillary areas, while the cuboidal cells are located on the surface of papillary areas and in various lacunar spaces or in the solid region with cells in clusters or in an adenoidal pattern. PSH has been considered as a hamartoma for several years. In a previous study, we performed clonality analysis using the X-linked androgen receptor and phosphoglycerate kinase gene polymorphisms, and the results revealed that this tumor is a true neoplasm rather than a tumor-like lesion [9]. However, the biological behavior of this tumor and differentiation status of the two types of cells is still controversial [10, 11, 13–16]. The cuboidal and polygonal cells significantly differ in histological pattern, cellular morphology, and even immunophenotype, but our

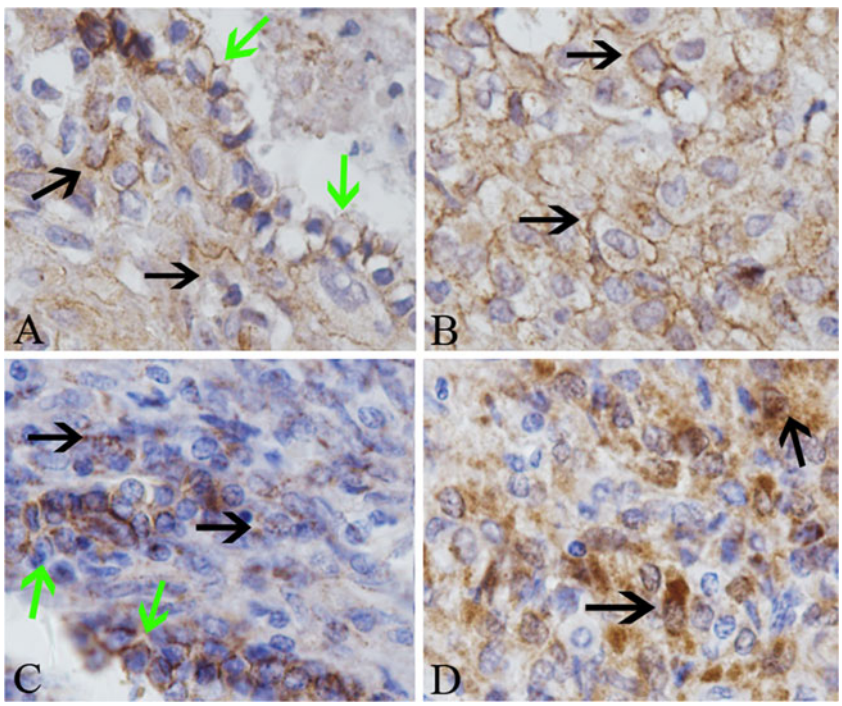

Fig. 2 Imunohistochemical staining of β-catenin in PSH. β-Catenin is strongly expressed on the membrane of cuboidal cells (**a**, **c**, *green arrow*); **a** in polygonal cells, weak staining of the cytoplasm and in few cells on the membrane (*black arrow*); **b** positive staining in both cytoplasm and on the membrane of polygonal cells (*black arrow*),while membrane expression was decreased in some cells; **c** absence of expression on the membrane of polygonal cells, spotty positive perinuclear staining (*black arrow*); **d** strong cytoplasmic expression within few cells nuclear stiaining (*black arrow*)

Table 2 Expression of β-catenin, Axin, and C-myc in two types of cells of PSH (*cyto*cytoplasm positive; *mem* membrane positive)

Antibodies	*n*	Cuboidal cells				Polygonal cells			
		−	+	++	+++	−	+	++	+++
β-Catenin	45	0	0	0	45 (mem)	4	16 (Cyto)	14 (Cyto)	11 (Cyto)
Axin	45	3	5	10	27	37	8	0	0
C-myc	45	36	9	0	0	7	10	13	15

previous study indicated that they have the same origin [9–11]. So far, there are several reports of lymph node metastases, and in cases of lymph node metastasis, the lymph node metastases consisted mainly of polygonal cells [13, 14]. This suggested that the two cell types might have different differentiation status and proliferative activity. We also had performed P53 mutation analysis in the two types of cells, and a sense mutation of the P53 gene was detected in polygonal cells [21]. Therefore, we deemed it necessary to further characterize this tumor and determine the differentiation of the two cell types.

The Wnt signaling pathway is involved in the regulation of cell growth, migration, and differentiation of lung tissue and other tissues, and many papers have reported abnormal activation of the Wnt signaling pathway in nonsmall cell lung cancer [17, 18]. Therefore, in order to further analyze the biological nature of PSH, we examined the expression of β-catenin, Axin, and C-myc in these lesions.

β-Catenin is a central factor in the Wnt signaling pathway. In normal tissue, Wnt signaling is not activated, β-catenin acting mainly as epithelial adhesion molecule localized in the epithelial cell membrane. Upon activation of Wnt signaling, β-catenin accumulates in the cytoplasm, releasing β-catenin, which might reach the nucleus as transcription factor, causing transcription of C-myc and other genes that promotes cell proliferation [17, 18]. Naoki et al. [22] reported a case of familial adenomatous polyposis patient who also developed PSH; aberrant nuclear and cytoplasmic expression of β-catenin was detected in the PSH. Therefore, abnormal Wnt signaling may be involved in this tumor. By immunohistochemical staining, we found strong β-catenin expression on cell membranes of cuboidal cells, but in polygonal cells, membrane expression was significantly decreased or even lacking, while aberrant cytoplasmic and even nuclear expression was detected. Anani et al. [23] found in invasive mesotheliomas more frequent cytoplasmic and nuclear staining and reduced membranous staining with β-catenin than in normal or reactive mesothelium, which showed distinct membranous β-catenin staining. The expression of β-catenin in both cell types supports that they both display epithelial differentiation, but at different levels of maturity. In this concept, cuboidal cells are mature as normal epithelium, but polygonal cells are poorly differentiated with an activated state of the Wnt signaling pathway. Some PSHs are located peripherally adjacent to the pleura even with pleural dissemination, which could cause pleural thickening or pleural fibrosis, which might lead to confusion with primary pleural tumors such as solitary fibrous tumor (SFT) [24]. SFT also expresses β-catenin in the cytoplasm and even in nuclei [25]. However, in tumor cells of SFT, membranous expression was never seen, and CD34 and TTF-1 staining are useful to distinguish between the two tumors.

As a negative regulator of Wnt pathway in normal tissue, Axin can form a complex with β-catenin, causing β-catenin degradation, thus avoiding activation of the Wnt signaling pathway. Axin is expressed in normal bronchial epithelium,

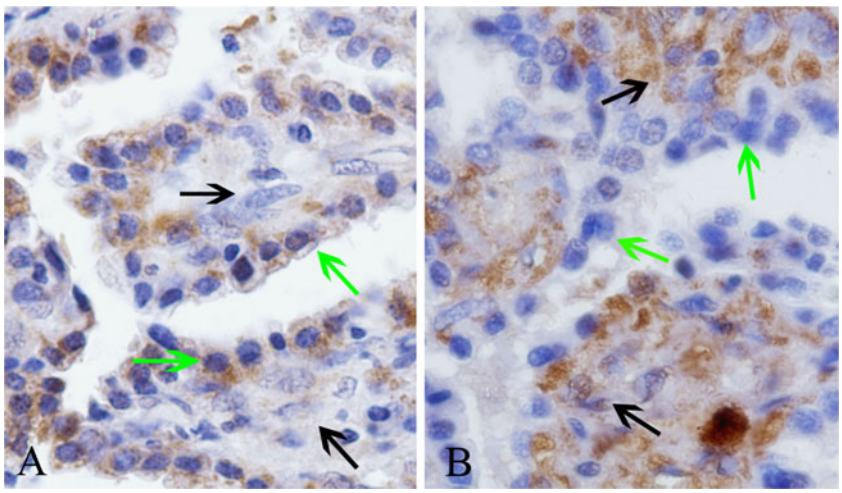

Fig. 3 Imunohistochemical staining of Axin and C-myc in PSH. **a** Axin strongly stains the cytoplasm in cuboidal cells (*green arrow*), but weakly stains few polygonal cells (*black arrow*); **b** expression of C-myc in polygonal cells (*black arrow*) is significantly higher than in cuboidal cells (*green arrow*)

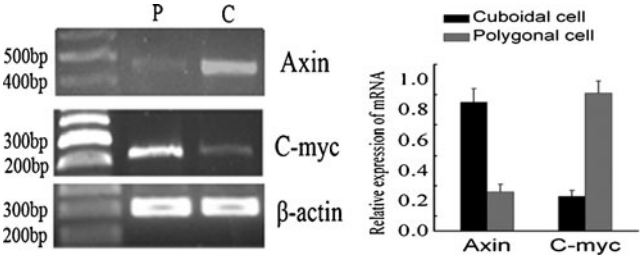

Fig. 4 The mRNA expression of Axin and C-myc in two types of cells (*P* polygonal cells; *C* cuboidal cells). The expression level of Axin in cuboidal cells is significantly higher in polygonal cells ($P<0.05$), while the expression level of C-myc in polygonal cells is significantly higher than in cuboidal cells ($P<0.05$)

but in lung cancer, expression of Axin was significantly decreased [18, 26]. By immunohistochemistry and RT-PCR, we found that expression of Axin is strong in cuboidal cells of PSH, but significantly reduced in polygonal cells, suggesting that compared with the cuboidal cells, polygonal cells might be in a poorly differentiated status. C-myc is an effector of the Wnt signaling pathway and can regulate cell growth and differentiation [17, 19]. Chiba et al [27] found in two cases of PSH that C-myc expression is significantly higher in the tumor cells than in the surrounding lymphocytes using flow cytometry, and C-myc protein and mRNA expression are significantly higher in polygonal cells than in cuboidal cells. The higher C-myc expression prompted us to consider polygonal cells to be immature and in a relatively active proliferative state.

The prevailing opinion was that PSH is a benign tumor, but because of more reports of lymph node metastasis, the notion has emerged that PSH might be a tumor with low malignant potential. Dacic et al. [20] proposed that PSH has the same origin and a similar molecular pathogenesis as bronchioloalveolar carcinoma, with PSH having a biological behavior similar to BAC. Liu et al. [28] recently reported a case of coexistence of PSH and primary adenocarcinoma in the same nodule of lung. This result also suggested that the two tumor types maybe closely related. In our follow-up studies, we found no tumor-related death, but one case with postoperative recurrence, and another case in which a lung adenocarcinoma had developed. The tumor recurrence demonstrated that PSH might be a tumor with low malignant potential and should be further followed up. For the case that developed adenocarcinoma, it was not clear whether the adenocarcinoma was related to the PSH. Bae et al. [16] recently reported a case with metastatic spread to stomach. This finding suggested that PSH has a capacity for distant metastasis. Therefore, to further elucidate the clinical behavior of this tumor, we need to collect more information and carry out longer follow-up.

In conclusion, we found higher β-catenin membrane expression, Axin expression, and lower level C-myc expression in cuboidal cells, suggesting that cuboidal cells are relatively mature. In polygonal cells, membranous expression of β-catenin was significantly reduced with aberrant expression in cytoplasm, and even in nuclei, Axin expression was reduced and C-myc expression level was significantly higher. These results suggest that polygonal cells are poorly differentiated and have high proliferative activity.

Acknowledgments All lung tissue samples were obtained from The First Affiliated Hospital of China Medical University. The study was conducted according to the regulations of the institutional review boards at China Medical University

Conflict of interest The authors declare that they have no competing financial interests. No part of this article has been published or submitted elsewhere, and there are no financial or other relationships that might lead to a conflict of interest of this article. The manuscript has been read and approved by all the authors, that the requirements for authorship have been met, and that each author believes that the manuscript represents honest work.

References

1. Liebow A, Hubbell DS (1956) Sclerosing hemangioma (histiocytoma, Xanthoma) of the lung. Cancer 9(1):53–75
2. Chan AC, Chan JK (2001) Pulmonary sclerosing hemangioma consistently expresses thyroid transcription facter-1: a new clue to its histogenesis. Arch Pathol Lab Med 125(10):1335–1339
3. Wang E, Lin D, Wang Y et al (2004) Immunohistochemical and ultrastructural markers suggest different origins for cuboidal and polygonal cells in pulmonary sclerosing hemangioma. Hum Pathol 35(4):503–508
4. Xu HM, Li WH, Hou N et al (1997) Neuroendocrine differentiation in 32 cases of so-called sclerosing hemangioma of the lung: identified by immunohistochemical and ultrastructural study. Am J Surg Pathol 21(9):1013–1022
5. Hill GS, Eggleston JC (1972) Electron microscopic study of so-called "pulmonary sclerosing hemangioma". Report of a case suggesting epithelial origin. Cancer 30(4):1092–1096
6. Kay S, Still WJ, Borochovitz D (1977) Sclerosing hemangioma of the lung: an endothelial or epithelial neoplasm? Hum Pathol 8 (4):468–474
7. Katzenstein AL, Weise DL, Fulling K, Battifora H (1983) Neuroendocrine differentiation in 32 cases of so-called sclerosing hemangioma of the lung: identified by immunohistochemical and ultrastructural study. Am J Surg Pathol 7(1):3–14
8. Niho S, Suzuki K, Yokose T et al (1998) Monoclonality of both pale cells and cuboidal cells of sclerosing hemangioma of the lung. Am J Pathol 152(4):1065–1069
9. Wang EH, Dai SD, Qi FJ et al (2007) Gene expression and clonality analysis of the androgen receptor and phosphoglycerate kinase genes in polygonal cells and cuboidal cells in so-called pulmonary sclerosing hemangioma. Mod Pathol 20(11):1208–1215
10. Nagata N, Dairaku M, Sueishi K, Tanaka K et al (1987) Sclerosing hemangioma of the lung. An epithelial tumor composed of immunohistochemically heterogenous cells. Am J Clin Pathol 88 (5):552–559
11. Devouassoux-Shisheboran M, Hayashi T, Linnoila RI et al (2000) A clinicopathologic study of 100 cases of pulmonary sclerosing hemangioma with immunohistochemical studies: TTF-1 is expressed in both round and surface cells, suggesting an origin from primitive respiratory epithelium. Am J Surg Pathol 24(7):906–916

12. Yamazaki K (2004) Type-II pneumocyte differentiation in pulmonary sclerosing hemangioma: ultrastructural differentiation and immunohistochemical distribution of lineage-specific transcription factors (TTF-1, HNF-3 alpha, and HNF-3 beta) and surfactant proteins. Virchows Arch 445:45–53
13. Miyagawa-Hayashino A, Tazelaar HD, Langel DJ, Colby TV (2003) Pulmonary sclerosing hemangioma with lymph node metastases: report of 4 cases. Arch Pathol Lab Med 127:321–325
14. Tanaka I, Inoue M, Matsui Y et al (1986) A case of pneumocytoma (so-called sclerosing hemangioma) with lymph node metastasis. Jpn J Clin Oncol 16:77–86
15. Suzuki H, Saitoh Y, Koh E et al (2011) Pulmonary sclerosing hemangioma with pleural dissemination: report of a case. Surg Today 41(2):258–261
16. Bae YS, Ro JY, Shim HS et al (2012) Pulmonary sclerosing haemangioma with metastatic spread to stomach. Histopathology. doi:10.1111/j.1365-2559.2012.04213.x
17. Mazieres J, He B, You L et al (2005) Wnt signaling in lung cancer. Cancer Lett 222(1):110
18. Hong-Tao Xu, Wang L, Wang En-Hua et al (2006) Abnormal β-catenin and Reduced Axin Expression Are Associated With Poor Differentiation and Progression in Non–Small Cell Lung Cancer. Am J Clin Pathol 125:534–541
19. Jaiswal AS, Kennedy CH, Narayan S (1999) A correlation of APC and c-myc mRNA levels in lung cancer cell lines. Oncol Rep 6 (6):1253–1256
20. Dacic S, Sasatomi E, Swalsky PA et al (2004) Loss of heterozygosity patterns of sclerosing hemangioma of the lung and bronchioloalveolarcarcinoma indicate a similar molecular pathogenesis. Arch Pathol Lab Med 128(8):880–884
21. Wang Y, Dai SD, Qi FJ et al (2008) p53 protein expression and genetic mutation in two primary cell types in pulmonary sclerosing haemangioma. J Clin Pathol 61(2):192–196
22. Hosaka N, Sasaki T, Adatoshi K et al (2004) Pulmonary sclerosing hemangioma associated with familial adenomatous polyposis. Hum Pathol 35(6):764–768
23. Kayser K, Trott J, Böhm G et al (2005) Localized fibrous tumors (LFTs) of the pleura: clinical data, asbestos burden, and syntactic structure analysis applied to newly defined angiogenic/growth-regulatory effectors. Pathol Res Pract 201 (12):791–801
24. Anani W, Bruggeman R, Zander DS (2011) β-catenin expression in benign and malignant pleural disorders. Int J Clin Exp Pathol 4 (8):742–747
25. Andino L, Cagle PT, Murer B et al (2006) Pleuropulmonary desmoid tumors immunohistochemical comparison with solitary fibrous tumors and assessment of β-Catenin and cyclin D1 expression. Arch Pathol Lab Med 130:1503–1509
26. Yang LH, Xu HT, Han Y et al (2010) Axin downregulates TCF-4 transcription via beta-catenin, but not p53, and inhibits the proliferation and invasion of lung cancer cells. Mol Cancer 2(9):25
27. Chiba W, Sawai S, Yasuda Y et al (1995) Positive expression of c-myc and p53 products in two cases of pulmonary sclerosing hemangioma. Nihon Kyobu Shikkan Gakkai Zasshi 33 (12):1348–1354
28. Liu W, Tian X-Y, Li Y, et al (2011) Coexistence of pulmonary sclerosing hemangioma and primary adenocarcinoma in the same nodule of lung. Diagn Pathol 6:41

Virchows Arch (2012) 461:67–78
DOI 10.1007/s00428-012-1256-5

ORIGINAL ARTICLE

A newly characterized human well-differentiated liposarcoma cell line contains amplifications of the 12q12-21 and 10p11-14 regions

Florence Pedeutour · Georges Maire · Anne Pierron · David M. Thomas · Dale W. Garsed · Laurence Bianchini · Valérie Duranton-Tanneur · Annabelle Cortes-Maurel · Antoine Italiano · Jeremy A. Squire · Jean-Michel Coindre

Received: 7 February 2012 / Revised: 16 May 2012 / Accepted: 21 May 2012 / Published online: 8 June 2012
© Springer-Verlag 2012

Abstract While surgery is the usual treatment for localized well-differentiated and dedifferentiated liposarcomas (WDLPS/DDLPS), the therapeutic options for patients with advanced disease are limited. The classical antimitotic treatments are most often inefficient. The establishment of genetically characterized cell lines is therefore crucial for providing in vitro models for novel targeted therapies. We have used spectral karyotyping, fluorescence in situ hybridization with whole chromosome painting and locus-specific probes, and array-comparative genomic hybridization to identify the chromosomal and molecular alterations of a novel cell line established from a recurring sclerosing WDLPS. The karyotype was hypertriploid and showed multiple structural anomalies. All cells retained the presence of a giant marker chromosome that had been previously identified in the primary cell cultures. This giant chromosome contained high-level amplification of chromosomal regions 12q13-21 and lacked the alpha-satellite centromeric sequences associated with WDLPS/DDLPS. The 12q amplicon was large, containing 370 amplified genes. The DNA copy

Florence Pedeutour and Georges Maire contributed equally to the work.

Electronic supplementary material The online version of this article (doi:10.1007/s00428-012-1256-5) contains supplementary material, which is available to authorized users.

F. Pedeutour · A. Pierron · L. Bianchini
Institute for Research on Cancer and Aging, University of Nice-Sophia-Antipolis,
Nice, France

F. Pedeutour (✉) · V. Duranton-Tanneur · A. Cortes-Maurel
Laboratory of Solid Tumors Genetics, Nice University Hospital, Faculty of Medicine,
28 avenue de Valombrose,
06107, Nice cedex 2, France
e-mail: florence.pedeutour@unice.fr

G. Maire · J. A. Squire
Department of Pathology and Molecular Medicine,
Queen's University,
Kingston, Ontario, Canada

D. M. Thomas · D. W. Garsed
Sarcoma Genomics and Genetics, Peter McCallum Cancer Centre,
East Melbourne, Victoria, Australia

D. W. Garsed
Department of Pathology, University of Melbourne,
Parkville, Victoria, Australia

A. Italiano
Department of Medical Oncology, Bergonié Institute,
Bordeaux, France

J. A. Squire
Clinical Trials Group of the National Cancer Institute of Canada,
Kingston, Ontario, Canada

J.-M. Coindre
Department of Pathology, Bergonié Institute,
Bordeaux, France

number ranged from 3 to 57. The highest levels of amplification were observed at 12q14.3 for *GNS*, *WIF1*, and *HMGA2*. We analyzed the mRNA expression status by real-time reverse transcription polymerase chain reaction for six genes from this amplicon: *MDM2*, *HMGA2*, *CDK4*, *TSPAN31*, *WIF1*, and *YEATS4*. mRNA overexpression was correlated with genomic amplification. A second amplicon originating from 10p11-14 was also present in the giant marker chromosome. The 10p amplicon contained 62 genes, including oncogenes such as *MLLT10*, previously described in chimeric fusion with *MLL* in leukemias, *NEBL*, and *BMI1*.

Keywords Liposarcoma · Cell line · Amplification · MDM2 · HMGA2 · MLLT10

Introduction

Well-differentiated and dedifferentiated liposarcomas (WDLPS/DDLPS) are the most frequent sarcomas in adults [1–3]. Histologically, WDLPS are made up of mature adipocytes, atypical cells, and lipoblasts. They are considered as tumors of intermediate malignancy because they demonstrate a high rate of recurrence but rarely metastasize. When mature adipocytes are prominent within a WDLPS, the main differential diagnosis is deep-seated lipoma or intramuscular lipoma. In approximately 10 % of cases, a poorly differentiated component is present and the tumor is classified as DDLPS [3, 4]. Most often, the transition between well-differentiated and non-lipogenic areas is abrupt. Difficulties for diagnosing DDLPS arise when the poorly differentiated component predominates. The distinction between DDLPS and poorly differentiated tumors can be hard in such cases.

Molecular cytogenetic analyses are valuable ancillary tools for correct recognition of WDLPS and DDLPS. Indeed, both are characterized by the presence of giant marker or ring chromosomes, containing amplification of the 12q14-15 chromosomal region [5]. The amplified 12q14-15 region consistently contains the *MDM2* gene, located at 12q15, and co-amplification may involve several other genes, including *HMGA2* (12q14.3), *CDK4*, *SAS/TSPAN31* (12q14.1), *YEATS4* [6–8], *CPM* [9], and *FRS2* [10] (12q15).

During the last decade, genomic studies have consistently improved the characterization of WDLPS/DDLPS. However, many points still need to be clarified concerning the biology, pathogenesis, and clinical management of these tumors. First, the mechanism of generation of the large marker chromosomes containing the amplified regions remains obscure. Numerous chromosomal regions have been described to be variably co-amplified with the 12q14-15 amplicon [5, 6, 8, 9, 11–22]. Moreover, the marker chromosomes present unusual centromere alterations that suggest a peculiar way of formation [15, 23]. Second, while surgery with or without radiotherapy is the usual treatment for localized WDLPS/DDLPS, the therapeutic options for patients with advanced disease are very limited. The classical antimitotic treatments such as doxorubicin or ifosfamide show low response rates [24]. Therefore, there is an urgent need for novel targeted therapies against WDLPS/DDLPS. Several strategies such as those targeting P53 or the JUN/JUNK pathways are currently studied [20, 25]. However, the lack of model systems impairs the development of new treatments. Indeed, WDLPS/DDLPS are difficult to grow in vitro. Most primary cultures do not provide enough material for extensive genomic and pharmacological studies. To our knowledge, only a few human cell lines, such as LS141, DDLS [26], FU-DDLS-1 [27], LS14 [28], LPS695, LP6 [29], GOT3 [30], 93449, and 94778 [6, 15], have been described as arising from WDLPS/DDLPS. We report here the molecular and cytogenetic characterization of a novel WDLPS cell line designated 95T1000.

Materials and methods

Clinical information and histological analysis

A 43-year-old man without significant medical history presented in 1990 with a swollen thigh. The tumor was located within the adductor muscles. Histologically, the surgical specimen showed two components: a sclerosing WDLPS zone without any necrotic area or mitotic activity and a cellular dedifferentiated area containing short spindle cells organized in a cartwheel pattern. Tumor cells of the dedifferentiated area presented hyperchromatic irregular nuclei, with low mitotic activity. Zones of tumor necrosis were present. Transition between WDLPS and poorly differentiated zones was abrupt. The diagnosis was sclerosing WDLPS with dedifferentiated zones of grade II malignancy. The metastatic workup, including a chest computed tomography scan, was negative. Surgery was considered as R0 [31] and adjuvant radiotherapy (50 Gy) was delivered.

A local recurrence presented in October 1995. The tumor measured 14×7.5 cm and was macroscopically well-delineated. Histologically, the tumor presented the features of a sclerosing WDLPS without any necrotic area or mitotic activity (Fig. 1a). Preoperative radiotherapy (45 Gy) was delivered. Immunohistochemistry showed strong expression of MDM2 protein (Fig. 1b). A second grade I sclerosing WDLPS recurrence presented in October 1997. The diagnosis of sclerosing WDLPS was established according to the World Health Organization Classification of Tumors [1, 32].

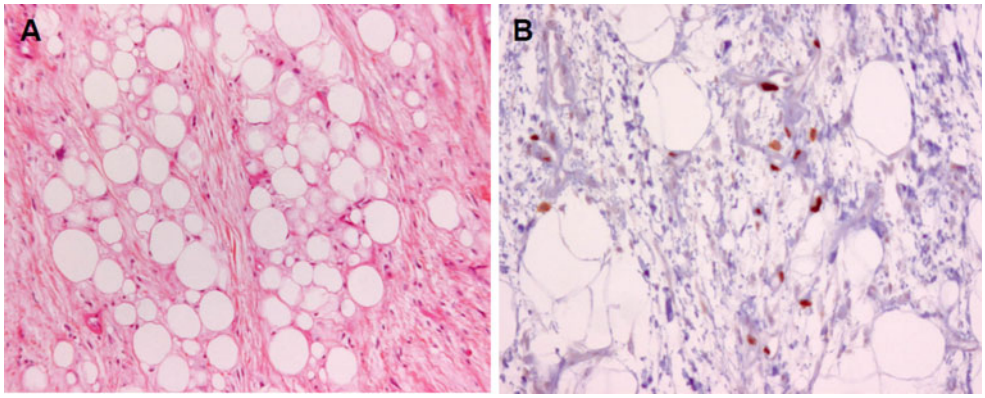

Fig. 1 Histological features and anti-MDM2 immunohistochemical staining of the 95T1000 well-differentiated liposarcoma. **a** Histological features of well-differentiated liposarcoma of the sclerosing subtype, characterized by adipocytic cells admixed with thick fibrous septa containing spindle cells with nuclear atypia (haematoxylin–eosin, magnification ×100). **b** Strong nuclear imunohistochemical staining of spindle cells with anti-MDM2 antibody (magnification ×200)

Establishment of the cell line and molecular cytogenetic analysis

Fresh tumor material from the first recurrence in 1995 was reserved for cell culture and cytogenetic analysis following surgical excision. Tumor tissue was disaggregated and cells from short-term cultures (10 days) were used for metaphase chromosome preparations according to established procedures [33]. Meanwhile, tumor cells were maintained in culture in RPMI 1640 medium (Gibco BRL, Life Technologies, Grand Island, NY, USA) supplemented with 10 % fetal calf serum (Gibco). Karyotype analyses of the 95T1000 cells were performed at passages 4, 10, 12, 31, 34, 54, 59, 60, 61, 69, and 80 (P80). Metaphase cells were analyzed by reverse banding using heat and Giemsa (RHG).

Spectral karyotyping (SKY) was performed on metaphases from P80 according to the manufacturer's instructions (Applied Spectral Imaging, Carlsbad, CA, USA) and as previously published [34, 35]. Fluorescence in situ hybridization (FISH) analyses were performed on metaphase and interphase cells. The FISH probes used for our study are listed in Table 1. Bacterial artificial chromosomes (BAC) clones from the Roswell Park Cancer Institute library were selected according to their location in the University of California Santa Cruz genome browser (http://genome.ucsc.edu/) and obtained from the Children's Hospital Oakland Research Institute (http://bacpac.chori.org/). Microscopic analysis was performed using a DM6000B microscope (Leica Microsystems, Wetzlar, Germany). FISH images were processed using the ISIS software (MetaSystems, Altussheim, Germany). Whole chromosome painting (WCP) probes and pan-alpha satellite probes were used according to supplier's recommendations (MetaSystems, Altussheim, Germany and QBIOgene, Illkirch, France, respectively). Preliminary FISH data using 12q probes have been published in Italiano et al. (case #16) [6].

Array-comparative genomic hybridization analyses

DNA was extracted using Qiagen Blood and Tissue DNeasy Kit (Doncaster, Victoria, Australia) following the manufacturer's instructions. Array-comparative genomic hybridization (aCGH) analysis was performed on 95T1000 and normal female reference DNA (Promega, Madison, WI, USA) using Affymetrix 250K *Nsp1* SNP microarrays (nominal average resolution, 1–5 kb), according to manufacturer's instructions (Affimetrix, Santa Clara, CA, USA). Copy number analysis of the 250K *Nsp* data was initially processed using Affymetrix Genotyping Console (GTC3.0.1) and subsequently analyzed using the Partek suite of software (St. Louis, MO, USA) as previously described [36]. Copy number information was derived after normalizing to the control reference DNA, and chromosome gains and losses were expressed as estimated relative copy number (ECN). The Partek segmentation algorithm used a minimum of one feature per region, a P value threshold of <0.00001, a signal-to-noise ratio of 0.3, and an expected range of 0.3 (Table S1).

Real-time quantitative RT-PCR

Real-time quantitative RT-PCR (qRT-PCR) was used to determine the expression levels of *GLI1*, *DDIT3*, *CDK4*, *TSPAN31*, *MDM2*, *YEATS4*, *WIF1*, *HMGA2*, *CDKN2A (p16INK4a* and *p14ARF)*, *CCND1*, and *RB1*. Total RNA was extracted from the 95T1000 cells (P57) and from short-term cultures of normal adipose tissue using

Table 1 Fluorescence in situ hybridization (FISH) probes used in this study

Probe name	Locus/gene or marker (alias)	Genome coordinates[a]
TelVysion™[b] 12p/12q	12pter/8M16-SP6, 12qter/ VIJ2yRM2196	
CTD-3109K12[c]	12q13.3/5′ *R3HDM2(INHC)*	chr12:56,048,383-56,074,880
RP11-16M7[d]	12q14.2-12q14.3/*GNS*	chr12:63,300,098-63,460,890
RP11-20P1[d]	12q14.3/3′*WIF1*	chr12:63,571,935-63,727,652
RP11-109N1[d]	12q14.3/5′*WIF1*	chr12:63,852,375-64,025,207
RP11-30I11[d]	12q14.3/5′*HMGA2*	chr12:64,178,505-64,349,708
RP11-118B13[d]	12q14.3/3′*HMGA2*	chr12:64,644,968-64,789,255
ZytoLight®[e] SPEC MDM2, CEN 12	12q14.3-12q15/*MDM2*, 12cen/D12Z3	chr12:67,488,247-67,520,481
TelVysion™[b]10p/10q	10pter/GenBank Z96139, 10qter/D10S2290	
RP11-150J3[d]	10p13/*FRMD4A*	chr10:14,125,465-14,277,321
RP11-269B1[d]	10p12.31/*NEBL*	chr10:21,093,656-21,254,619
RP11-34I5[d]	10p12.31/*NEBL*	chr10:21,413,645-21,559,356
RP11-177H22[d]	10p12.31/*MLLT10*	chr10:21,886,025-22,026,020
RP11-573G6[d]	10p12.31/*COMMD3,BMI1,SPAG6*	chr10:22,573,927-22,712,022
RP11-63G10[d]	1p32.1/*JUN*	chr1:58,951,678-59,094,341
RP3-325F22[d]	6q23.3/*MAP3K5(ASK1)*	chr6:136,892,189-137,046,976
AneuVysion®[b] LSI 13, LSI 21	13q14.2/*RB1*, 21q22.13-21q22.2/ D21S259-D21S341-D21S342	
RP11-313L9[d]	13q33.3-13q34	chr13:109,059,438-109,253,923
CTD-2328A22[c]	13q34	chr13:109,925,937-110,037,953
LSI CCND1[b], CEP11	11q13/*CCND1*, 11cen/D11Z1	
CDKN2A/CEP9[b]	9p21/CDKN2A, 9p11-q11	
UroVysion®[b]	3cen/D3Z1, 7cen/D7Z1, *CDKN2A*/9p21, 17cen/D16Z1	

chr chromosome

[a]Genome browser (www.genome.ucsc.edu) version March 2006

[b]Abbott Molecular, Des Plaines, IL, USA

[c]Invitrogen, Carlsbad, CA, USA

[d]Children's Hospital Oakland Research Institute (http://bacpac.chori.org/)

[e]Zytovision GmbH, Bremerhaven, Germany

Trizol™ (Invitrogen, Carlsbad, CA) according to the manufacturer's protocol. The RNA samples were treated with DNA-free™ (Applied Biosystems, Foster City, CA). The quality of RNA was evaluated using the 2100 BioAnalyser and RNA 6000 Nano Kit (Agilent Technologies, Santa Clara, CA). One microgram of total RNA was reverse-transcribed into cDNA using the High Capacity cDNA Reverse Transcription Kit (Applied Biosystems). Each quantitative PCR (Q-PCR) experiment was performed twice using either fluorescein amidite dye for *MDM2*, *CDK4*, *DDIT3*, *YEATS4*, *HMGA2* (exons 1–2), *HMGA2* (exons 3–4), *HMGA2* (exons 4–5), *TSPAN31*, *GLI1*, *WIF1*, *p14ARF*, *CCND1*, *RB1*, or SYBRGreen dye for *p16INK4a* according to the manufacturer's protocols (ABI PRISM 7500 Detection System, Applied Biosystems). *RPLP0* was used as endogenous control for normalization [37]. qRT-PCR was performed using the TaqMan gene expression assays (Applied Biosystems) (Table S2) as described in Italiano et al. [6]. The primers used for SYBRGreen experiments are described in Supplementary Table S3. The comparative threshold cycle method was used to achieve relative quantification of gene expression [6].

Results

Conventional and spectral karyotype: hypertriploid genome containing giant marker chromosomes

Cytogenetic analysis of the primary culture of the 95T1000 WDLPS showed a near-diploid karyotype. The number of chromosomes ranged from 45 to 49 after 10 days of culture. One or two giant marker chromosomes were observed in metaphase cells (Fig. 2a). Several structural abnormalities that were not identifiable by conventional banding techniques were also observed. At P80, the karyotype was hypertriploid; the number of chromosomes ranged from 62 to 89, with a modal number of 79. We observed one or two giant marker chromosomes apparently similar to those observed in the primary culture. In addition, several structural and numerical abnormalities were observed (Fig. 2b). These anomalies were too complex to be correctly interpreted by means of conventional cytogenetics and were characterized by SKY analysis that showed a variety of clonal and non-clonal aberrations (Fig. 2c). Both intra- and inter-chromosomal anomalies were observed. The extremities of

the giant markers had variable origins: they were most frequently composed of sequences from chromosome 14 and intermittently from chromosomes 1, 5, 6, and 11 (Fig. 2d and Table S4). The SKY method was not appropriate to identify the central region of the giant markers because the dyes were too closely intermixed for providing an interpretable pattern. The co-amplification of sequences from chromosomes 10 and 12 that constitutes the core of these giant markers was eventually identified by aCGH and complementary FISH analyses (see below).

Among abnormally sized chromosomes apparently composed of unique chromosome material, aberrant chromosomes 1, 2, 3, 4, 7, 10, 11, 12, 13, 16, 18, 20, 21, and 22 were frequently observed. In addition to the marker chromosomes with 10p-12q amplification mentioned above, 15 recurrent derivative chromosomes showing inter-chromosomal rearrangements were identified (Table 2 and Fig. S1). The derivative chromosomes A, F, H, J, and O were sometimes duplicated. Most derivative chromosomes were made up of two to three different chromosomes while the derivative B and C resulted from more complex rearrangements. Evidence for chromosomal instability was suggested by the heterogeneous presence of various derivative chromosomes within the different metaphase cells analyzed (Table 2), as well as variation in the number of giant markers (Table S4).

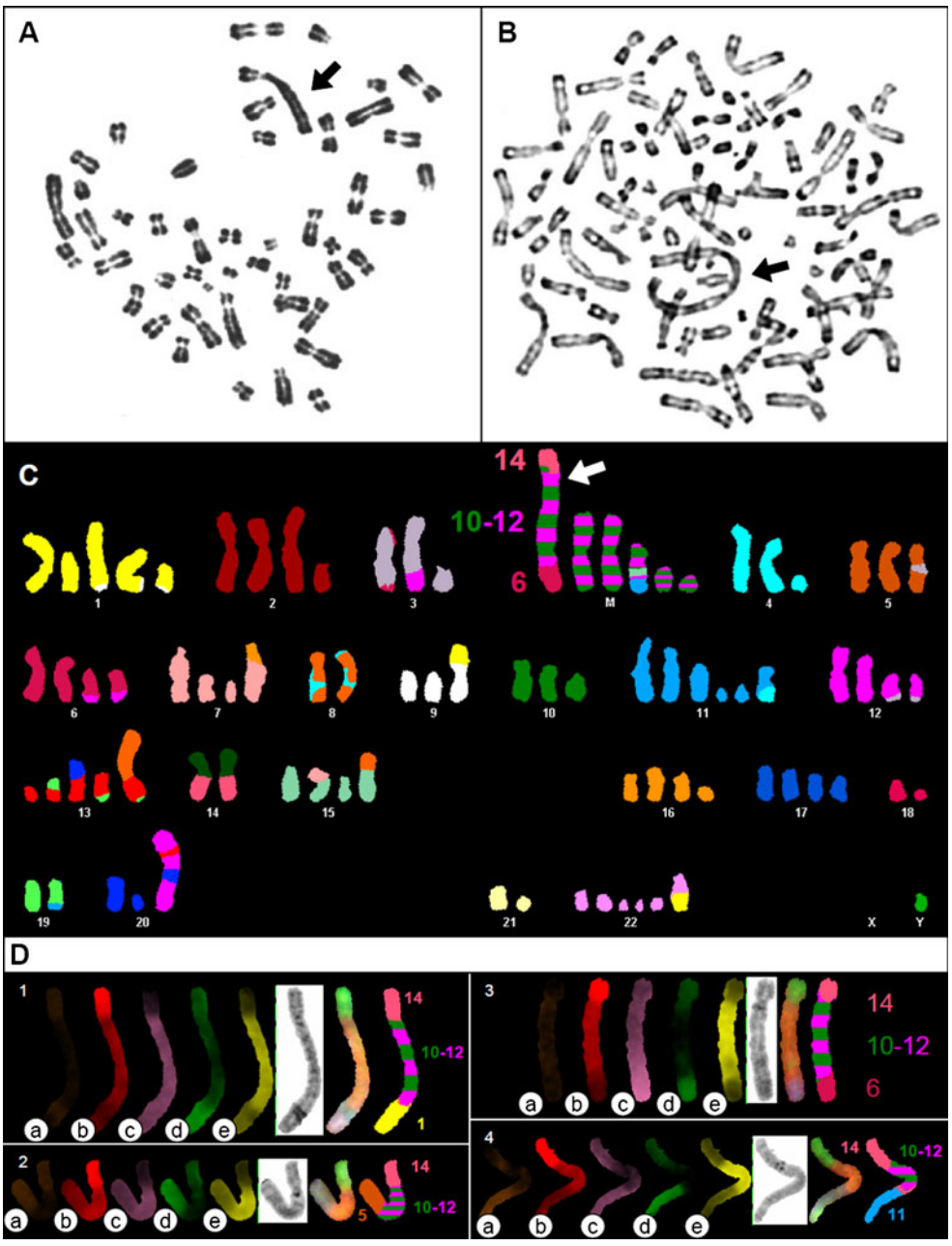

Fig. 2 Chromosomal analysis. **a** Representative RHG-banded near-diploid metaphase cell of the primary culture containing 47 chromosomes. The *arrow* indicates the supernumerary giant marker. **b** Representative RHG-banded metaphase cell at passage 80 (P80) containing 83 chromosomes including the giant marker chromosome (*arrow*). **c** False-colored SKY of a hypertriploid metaphase cell at P80. Complex numerical and structural abnormalities are observed. The *arrow* indicates the giant marker. The zebra pattern is deduced from complementary FISH analysis with whole chromosome painting and locus-specific probes and corresponds to co-amplified sequences from chromosomes 10 and 12. This co-amplification was also observed on additional marker chromosomes (*M*). **d** Individual dye spectra, inverted DAPI, SKY spectrum, and SKY false color of representative large markers selected from four metaphase cells (D1 to D4) (out of the ten metaphase cells analyzed). Each dye spectrum is identified by a lower case letter: *a*, *b*, *c*, *d*, and *e*

Amplification of 10p and 12q detected by array-comparative genomic hybridization

The detailed aCGH profile of losses, gains, and amplifications was identified across the genome (Fig. 3a and Supplementary Table S1). The most significant imbalances were represented by high-level amplification of chromosomes 10 and 12 (ECN higher than 10). The 10p-amplified regions spanned approximately 27 Mb from 10p14 to 10p11.21 and were composed of four distinct amplicons: a large one of 5.4 Mb from 10p14 to 10p12.2, two small ones (10p12.1/0.8 and 10p11.22/1 Mb), and an isolated focal amplification (31 ECN) of 0.2 Mb at 10p11.21 (Fig. 3b). A total of 45 segments showing various levels of gain and amplification (from 6 to 55 ECN) and sizes (from 30 kb to 0.7 Mb; average, 0.5 Mb) were identified (Table 3). Overall, these segments included 62 amplified genes.

The amplified regions from the long arm of chromosome 12 spanned 82 Mb from 12q12 to 12q24.21 (Fig. 3c) and consisted of 67 independent amplified segments; the size of which ranged from 70 kb to 2.4 Mb (average, 0.4 Mb; total size, 27.8 Mb). The ECN ranged from 3 to 57 (average, 18) (Table 3). Overall, these segments contained 370 amplified genes including *CDK4*, *TSPAN31* (12q14.1), *GNS*, *WIF1*, *HMGA2* (12q14.3), *MDM2*, *CPM YEATS4*, and *FRS2* (12q15). In contrast, *GLI1* and *DDIT3* (12q13.3) were not amplified (Fig. 3c).

No losses were observed except for a 1.3-Mb segment at 20p13 and a 3.4-Mb segment at 20q13.32-q13.33. On the proximal side of the 20q13-deleted segment, a moderate gain (4 ECN) of 16 Mb was observed. Chromosomes 4, 13, and 17 showed similar profiles characterized by moderate gain of long segments (from 3 to 7 ECN) across the full chromosome length (Table 3, S1).

Comprehensive structural analysis of amplified 10p and 12q segments within the giant marker chromosomes

The 10p- and 12q-amplified sequences were colocated and intermixed in the central region of the giant marker chromosome as well as in a few other marker chromosomes (B, C, G, J, and O) as shown by FISH analysis with WCP 10 and 12 probes as well as several locus-specific probes, such as RP11-150J3 (*FRMD4A*; 10p13), RP11-177H22 (*MLLT10*; 10p12.31), RP11-269B1 (*NEBL*; 10p12.31), and *MDM2* (12q15) (Fig. 4). Discontinuities in the 10p- and 12q-amplified regions were detected by shifts of amplification levels nearby or within several genes: for instance, BAC clone RP11-34I5 (10p12.31) that contained the 3′ region of *NEBL* did not show an amplified signal in contrast to the high amplification detected for clone RP11-269B1 that contained most part of the *NEBL* gene. A structural rearrangement was also detected in the vicinity of

Table 2 Clonal structural rearrangements other than the large marker detected by SKY analysis

Abnormal chromosome designation	Cell (modal number)										Composition
	1 (79)	2 (79)	3 (79)	4 (84)	5 (83)	6 (62)	7 (66)	8(89)	9 (84)	10 (82)	
A	++	+	++	++	+	+	+	++	+	++	der(8)(8;4;8)x2
B	+	+	+	+	+	None	None	+	+	+	der(20)(12;13;12;20;12)
C	+	+	+	+	+	None	None	+	+	+	der(12)(12;15;12;11)
D	None	None	+	+	+	+	+	+	+	+	der(5)(5;3;16)
E	+	+	+	+	+	None	+	None	+	None	der(22)(22;1)
F	None	+	++	++	+	None	+	+	+	++	der(3)(3;6)x2
G	+	+	+	+	+	None	+	None	+	+	der(3)(3;12;18)
H	+	++	++	+	+	++	None	++	++	++	der(14)(X;14)x2
I	+	+	+	None	+	+	None	+	+	+	der(9)(9;1)
J	++	+	++	+	+	+	++	++	++	++	der(6)(6;12)x2
K	None	None	None	None	+	+	None	+	+	None	der(13)(19;13;8)
L	+	+	+	None	None	+	+	+	+	+	der(15)(8;15)
M	None	None	None	None	None	None	+	+	None	+	der(4)(4;13)
N	None	+	+	+	+	+	None	+	+	None	der(11)(11;4)
O	+	None	+	+	++	+	++	+	++	+	der(12)(12;3)

+ and ++ : one (+) or two (++) derivative chromosome/cell

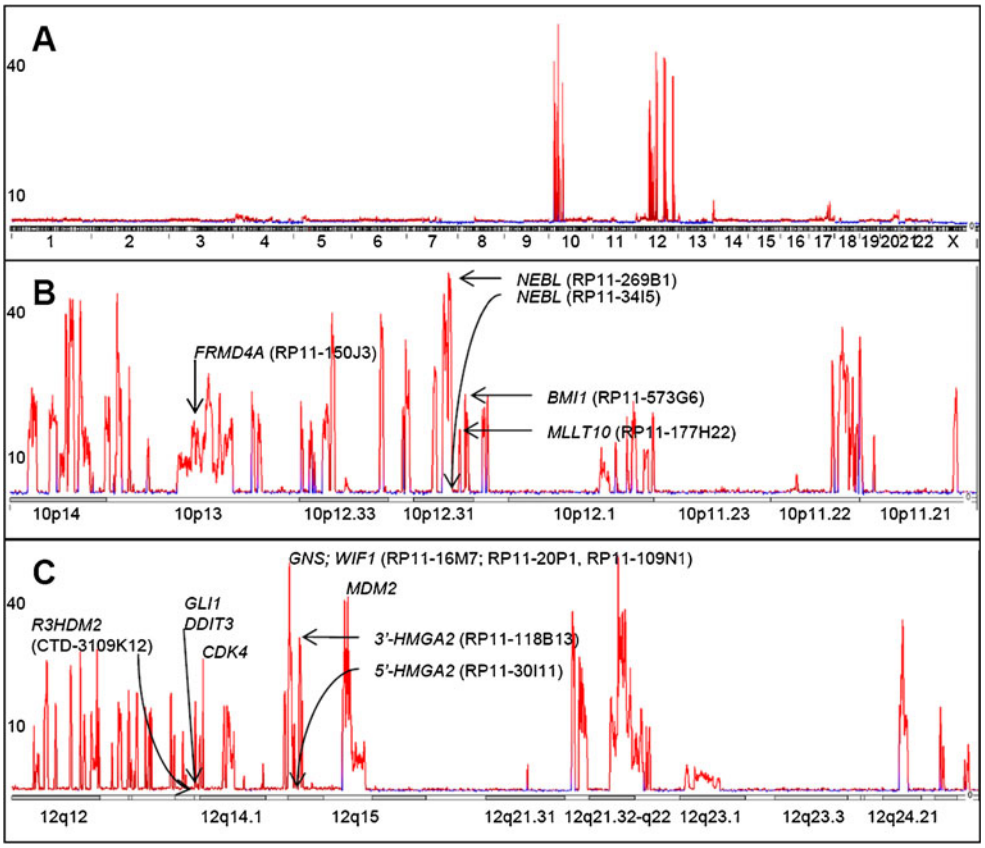

Fig. 3 aCGH profile. **a** Genome-wide copy number alterations in 95T1000 cells. The *x*-axis represents chromosome 1 to chromosome X and from pter to qter. The ECN is on the *y*-axis. The color gradient from *blue* to *red* corresponds to an ECN of 2 (*blue*) to high level of amplification (*red*). Discreet regions of gain are observed on chromosomes 4, 13, 17, and 20 and loss on chromosome 20. Large amplicons and multiple focal amplifications are observed on chromosome 10 p (**b**) and 12 q (**c**). Key genes and loci for which FISH had been performed are noted

HMGA2: while probes containing exons 1 to 5 (RP11-299L9, RP11-23C9, and CTC-782I9) and the telomeric side of the 3′ extremity of *HMGA2* (RP11-118B13) showed highly amplified signals, only a few gained copies were observed with RP11-30I11 probe, located on the centromeric side of the 5′ extremity of *HMGA2* (Fig. 4f). In addition, it is noteworthy that the giant marker did not contain any alpha-satellite sequences, suggesting the presence of an analphoid neocentromere (not shown).

Secondary chromosomal anomalies: complementary FISH analyses

The centromeric probes for chromosomes 3, 7, 9, and 17 showed a signal pattern consistent with the hypertriploid karyotype (Table 1). Four copies of each were identified on normal and abnormal chromosomes, respectively. The probes for chromosome 9 showed not only a pattern consistent with hypertriploidy, but also the presence of structural rearrangements. The *CDKN2A* locus (9p21) was disomic,

Table 3 Characteristics of the chromosome segmental gains/amplifications identified by array-comparative genomic hybridization

Chromosomes	Number of segment(s)	Minimum SL/ECN	Maximum SL/ECN	Average SL/ECN	Amplicon's total length (Mb)	Total size (Mb)
Gains						
4p16.3-q27	8	0.4 Mb/3	20.7 Mb/3	6.2 Mb/3	50	139
13q12.11-q34	4	0.1 Mb/3	3.2 Mb/7	1.6 Mb/6	6.6	96
17q11.1-q25.3	10	0.2 Mb/3	5.5 Mb/8	1.1 Mb/5	11.8	56
High-level amplifications						
10p14-p11.21	45	30 kb/3	0.7 Mb/56	0.5 Mb/22	7.6	27
12q12-24.31	67	70 kb/3	2.4 Mb/57	0.4 Mb/18	27.8	82

SL segment length, *ECN* estimated relative copy number

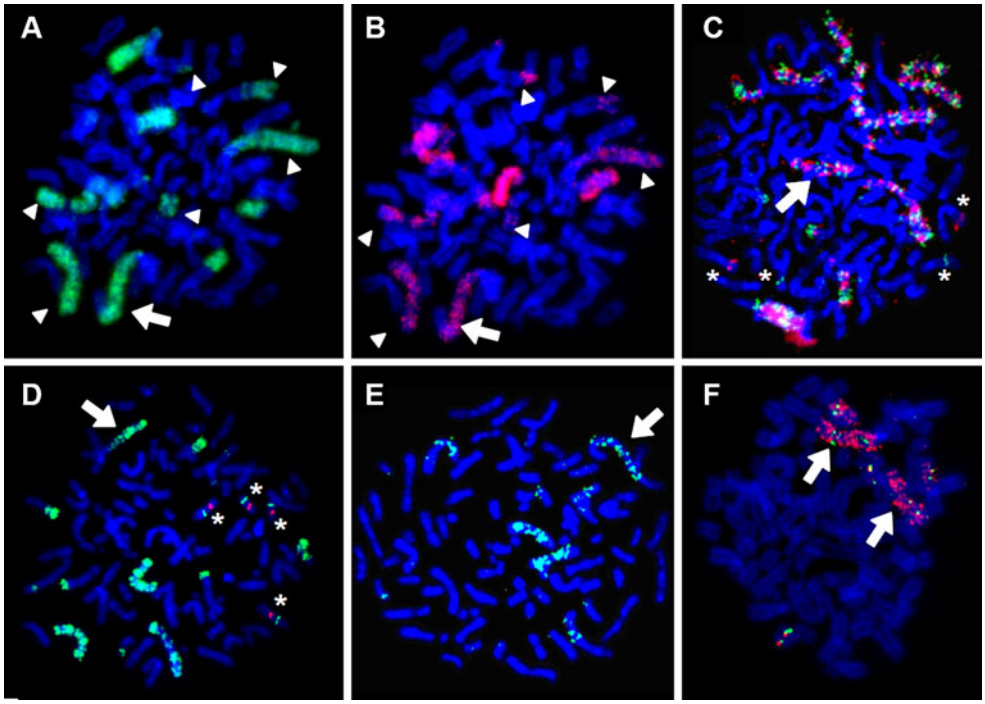

Fig. 4 Characterization of chromosomal imbalances and structural rearrangements by FISH on 95T1000 metaphase cells at passage P80. **a**–**c** Co-amplification of chromosome 10 and 12 regions. Co-localization of both *green* and *red* signals on the central region of the giant marker (*arrow*), as well as several other marker chromosomes (*arrowheads*), using WCP probes for chromosome 10 (**a**) and 12 (**b**). Co-amplification of the *MDM2* (*green*) and RP11-269B1 (*NEBL* 10p12.31) probes (*red*) on the giant marker (*arrow*) and on several other marker chromosomes (**c**). Apparently normal chromosomes 12 and 10 were also identified (*asterisk*). **d** High amplification of *MDM2* (*green signals*) located on one giant marker (*arrow*) and several marker chromosomes. Four apparently normal chromosomes 12 (*asterisk*) identified by centromere 12 (*red signals*) and *MDM2* at their expected position were also observed. **e** Hybridization with the RP11-177H22 probe containing *MLLT10* (10p12.31) shows a high level of amplification on the giant marker (*arrow*) and several marker chromosomes. **f** Hybridization with the dual-colored probes that flanks the 5′ (RP11-30I11-green) and 3′ (RP11-118B13-red) regions of *HMGA2*. High-level amplification of the 3′ region of *HMGA2* on the giant marker and marker chromosomes is observed. In contrast, the 5′ region is not amplified

indicating a relative loss of the 9p21 region since four chromosome 9 centromeres were observed. This loss was not detected by aCGH analysis, presumably because of a low statistical significance value related with the polyploidy of the specimen (Table S1). *MAP3K5* (*ASK1*) (6q23.3) and *JUN* (1p32.1) loci showed no imbalance, in concordance with the aCGH results (Table 1, S1). The *CCND1* gene was duplicated on abnormal derivative chromosomes 11. The interstitial gains of chromosome 13 long arm detected by aCGH were confirmed by FISH analysis, which showed two to six signals per cell for the CTD-2328A22 probe (13q34), while more than ten signals were observed with the RP11-313L9 probe (13q33.3-13q34) (not shown).

qRT-PCR

We have detected strong overexpression of the following genes: *MDM2*, *CDK4*, *YEATS4*, *HMGA2*, *TSPAN31*, and *WIF1* and no overexpression of *GLI1* and *DDIT3* (Table 4). Among the overexpressed genes from 12q region, *WIF1* showed the highest fold change (1,733, in comparison to normal adipose tissue). All the five exons of *HMGA2* showed overexpression (fold change values, 317 for exons 1 and 2 and 65 for exons 3 to 5, respectively). Genes of the RB1 pathway, such as *CCND1*, *CDK4*, *CDKN2A* (*p14ARF* and *p16INK4a*), were overexpressed, whereas *RB1* was not.

Discussion

We describe a novel WDLPS cell line designated 95T1000. This cell line was established spontaneously from primary cultures of a recurring sclerosing WDLPS and contained high-level amplification of the 12q14-15 region located on supernumerary giant marker chromosomes. The patient had received adjuvant radiotherapy following the excision of the primary liposarcoma and also a preoperative dose of 45 Gy prior to the excision of the first recurrent tumor that was used for establishing the cell line. This first recurrence did not present the features of a radiation-induced liposarcoma, since it was histologically similar to the primary tumor and with a near diploid karyotype, including the characteristic

Table 4 Real-time quantitative RT-PCR

Gene (exon)	Genomic locus	Fold change[a]
p14ARF	9p21.3	5.5
p16INK4a	9p21.3	22
TSPAN31	11p15.5	42
CCND1	11q13.2	5
DDIT3	12q13.3	2.5
GLI-1	12q13.3	0.6
CDK4	12q14.1	39
HMGA2 (1–2)	12q14.3	317
HMGA2 (3–4)	12q14.3	64
HMGA2 (4–5)	12q14.3	66
WIF1	12q14.3	1,733
MDM2	12q15	48
YEATS4	12q15	83
RB1	13q14.2	1.2

[a] Values from normal adipose tissue are used as reference

giant markers containing 12q14-15 amplification. It is possible that radiation contributed to the occurrence of several clonal and non-clonal chromosomal alterations seen in addition to the large markers. The giant marker chromosomes were retained along the subcultures and were still present after more than 80 passages.

The 12q14-15 amplification is fully characteristic of WDLPS/DDLPS. It constitutes the genetic hallmark of this group of tumors [5, 9, 10, 13–16, 21, 22, 26, 29, 30, 38–41]. Consequently, detection of 12q amplified genes is widely used for distinguishing WDLPS/DDLPS from other tumors. This detection can be done by FISH [15], Q-PCR [42], or aCGH [4] and indirectly by immunohistochemistry [43, 44]. *MDM2* has early been identified as the main driver gene of the WDLPS/DDLPS amplicon since it is consistently amplified in all cases of WDLPS and DDLPS [10, 43, 45, 46]. The overexpression of MDM2 protein generated by the genomic amplification inactivates TP53. Indeed, MDM2 targets TP53 degradation toward the proteasome and inhibits its P53-mediated transactivation [47]. Pharmaceutical compounds, such as nutlin, are currently being tested for the purpose of blocking the P53 inactivation mediated by MDM2 [48].

Despite its obvious major contribution, the amplification of *MDM2* does not seem to be sufficient by itself to account for the pathogenesis of WDLPS/DDLPS. Other genes from the 12q14-15 region are co-amplified and co-expressed with *MDM2* [7, 10, 49–51]. Similarly, a number of previously described WDLPS/DDLPS cases have identified giant marker chromosomes of comparable size to that in the 95T1000 cell line that also contained amplification of *CDK4* and *HMGA2*. *CDK4* is not consistently amplified in WDLPS/DDLPS. It is amplified only in approximately 85 % of cases [1, 6, 7, 10, 30]. The absence of *CDK4* amplification in WDLPS has been correlated to low-grade lipoma-like tumors of peripheral location and a better outcome [7]. In the present case, although the primary tumor was located peripherally, it had a high potential of recurrence that might be related to *CDK4* amplification and overexpression.

We observed amplification of the 5 exons as well as the 3′ region of *HMGA2* and this amplification resulted in the overexpression of the whole gene. It is noteworthy that the region immediately proximal to the 5′ part of *HMGA2* was not amplified (Fig. 4f). Structural rearrangements of *HMGA2* have initially been described in lipomas where they often consist in breakage within the third intron followed by fusion with various partner genes [52–54]. It was later shown that anomalies of *HMGA2* were not confined to benign adipose tumors since *HMGA2* was recurrently amplified, rearranged, and overexpressed in WDLPS/DDLPS [6, 55–59]. Although various ectopic sequences can be fused to *HMGA2* in WDLPS [56], it does not appear that bona fide fusion genes are present in WDLPS as they often are in lipomas. However, it has been shown that in lipomas as well as in other tumors, overexpression of *HMGA2* is not always generated by fusion genes [60–63]. The overexpression of *HMGA2* is a feature shared by both lipomas and WDLPS, though resulting from distinct events. The exact underlying mechanisms of dysregulation that makes *HMGA2* a central gene in differentiated adipose tumors still remain to be elucidated.

Overall, the size of the 95T1000 12q amplicon was large, comprising 370 genes. This is more than twice the number of amplified 12q genes found in the WDLPS cell line described by Persson et al. [30], but similar to the number observed in 93T449 and 94T778 WDLPS cell lines [23; D.M. Thomas, personal communication]. Among these amplified genes, we have found amplification of *TSPAN31*, *GNS*, *WIF1*, *CPM*, *YEATS4*, and *FRS2* as recurrently described in WDLPS/DDLPS [6, 7, 10, 30].

In addition to the amplification of 12q genes, we have found a high-level amplification of the 10p chromosomal region. The finding of co-amplification of at least one chromosomal region other than 12q14-15 [5, 6, 8, 9, 12–14, 16–22] is a recurrent feature of WDLPS/DDLPS. These "extra-12q14-15" co-amplified regions are variable among patients. The most frequent and most studied are 6q23, 1p32, and 1q23-24. While the amplification of *MAP3K5* at 6q23 and *JUN* at 1p32 has been correlated to the presence of a poorly differentiated component [17, 22, 29, 40, 41], the significance and role of other genomic regions that are co-amplified with 12q14-15 are not elucidated. We have emitted the hypothesis these co-amplified regions might provide

neocentromeric sequences to the giant markers that lack alpha-satellite sequences [15, 23]. The 1q23-24 amplicon [30, 56] has been recently suggested to be associated more frequently with WDLPS/DDLPS lacking *CDK4* amplification [7, 64]. The 10p11-14 region is rarely co-amplified with 12q in WDLPS/DDLPS, only a handful of cases have been described [22, 65]. In the 95T1000 cells, the 10p amplicon contained 62 genes. It was smaller than the 12q amplicon (27 Mb) but reached similar ECN. It also displayed a discontinuous pattern. Among the amplified genes, several of them are of interest because of their oncogenic functions. In particular, we found amplification of the oncogene *MLLT10*. This gene, previously called *AF10* encodes a transcription factor and is a fusion partner of *MLL* in acute leukemias with t(10;11)(p12;q23) [66, 67]. It has also been described to fuse with *PICALM* (11q14.2) in various hematologic malignancies, including acute lymphoblastic and myeloblastic leukemias and diffuse histiocytic lymphomas. In addition, *MLLT10* is a susceptibility locus for meningioma [68]. The *NEBL* gene that codes for nebulette protein highly expressed in cardiac muscle [69] is also amplified in 95T1000 cells. This gene is located closely nearby *MLLT10* and has also been described to be a fusion partner of *MLL* in a case of infant leukemia [70].

Another interesting oncogene contained in the 10p amplicon was *BMI1*. It encodes a polycomb-group protein involved in a multiprotein complex that represses the transcription of developmental genes, such as *Hox* genes. *BMI1* is required for proliferation of both normal and leukemic stem cells [71]. It is expressed in a variety of malignancies such as lymphoma, leukemia, carcinoma, medulloblastoma, as well as glioblastoma and has been shown to be moderately amplified in some cases of mantle cell lymphoma and gained in gliomas [72].

In conclusion, we describe here the genetic features of a novel WDLPS cell line characterized by typical 12q amplification. We provide a comprehensive description of the chromosomal anomalies present in these cells by using a panel of molecular cytogenetics methods. Notably, this cell line harbors an original amplification of the 10p11-14 region. Future studies on genes contained within this region will hopefully shed light on the pathogenesis of WDLPS.

Acknowledgments The authors are grateful to Association pour la Recherche sur le Cancer (ARC 4080 to FP), Institut National du Cancer (projet libre (GENOSTT), and Cancéropôle Provence Alpes Côte d'Azur and Conseil Régional Provence Alpes Côte d'Azur. DMT is the recipient of a Victorian Cancer Agency Clinician Researcher Fellowship.

Conflict of interest We declare that we have no conflict of interest.

References

1. Fletcher C, Unni K, Mertens F (2002) World Health Organization classification of tumours pathology and genetics of tumours of soft tissue and bone. Lyon
2. Pedeutour F, Maire G, Sirvent N (2004) From cytogenetics to cytogenomics of adipose tissue tumors: 2. Malignant adipose tissue tumors. Bull Cancer 91(4):317–323
3. Enzinger, Weiss SW, Goldblum JR (2008) Liposarcoma. In: Elsevier M (ed) Soft tissue tumors (5th ed). St. Louis, pp. 477–516
4. Coindre JM, Pedeutour F, Aurias A (2009) Well-differentiated and dedifferentiated liposarcomas. Virchows Arch 456(2):167–179
5. Pedeutour F, Forus A, Coindre JM, Berner JM, Nicolo G, Michiels JF, Terrier P, Ranchere-Vince D, Collin F, Myklebost O, Turc-Carel C (1999) Structure of the supernumerary ring and giant rod chromosomes in adipose tissue tumors. Genes Chromosomes Cancer 24 (1):30–41
6. Italiano A, Bianchini L, Keslair F, Bonnafous S, Cardot-Leccia N, Coindre JM, Dumollard JM, Hofman P, Leroux A, Mainguene C, Peyrottes I, Ranchere-Vince D, Terrier P, Tran A, Gual P, Pedeutour F (2008) HMGA2 is the partner of MDM2 in well-differentiated and dedifferentiated liposarcomas whereas CDK4 belongs to a distinct inconsistent amplicon. Int J Cancer 122(10):2233–2241
7. Italiano A, Bianchini L, Gjernes E, Keslair F, Ranchere-Vince D, Dumollard JM, Haudebourg J, Leroux A, Mainguene C, Terrier P, Chibon F, Coindre JM, Pedeutour F (2009) Clinical and biological significance of CDK4 amplification in well-differentiated and dedifferentiated liposarcomas. Clin Cancer Res 15(18):5696–5703
8. Barretina J, Taylor BS, Banerji S, Ramos AH, Lagos-Quintana M, Decarolis PL, Shah K, Socci ND, Weir BA, Ho A, Chiang DY, Reva B, Mermel CH, Getz G, Antipin Y, Beroukhim R, Major JE, Hatton C, Nicoletti R, Hanna M, Sharpe T, Fennell TJ, Cibulskis K, Onofrio RC, Saito T, Shukla N, Lau C, Nelander S, Silver SJ, Sougnez C, Viale A, Winckler W, Maki RG, Garraway LA, Lash A, Greulich H, Root DE, Sellers WR, Schwartz GK, Antonescu CR, Lander ES, Varmus HE, Ladanyi M, Sander C, Meyerson M, Singer S (2010) Subtype-specific genomic alterations define new targets for soft-tissue sarcoma therapy. Nat Genet 42(8):715–721
9. Erickson-Johnson MR, Seys AR, Roth CW, King AA, Hulshizer RL, Wang X, Asmann YW, Lloyd RV, Jacob EK, Oliveira AM (2009) Carboxypeptidase M: a biomarker for the discrimination of well-differentiated liposarcoma from lipoma. Mod Pathol 22 (12):1541–1547
10. Wang X, Asmann YW, Erickson-Johnson MR, Oliveira JL, Zhang H, Moura RD, Lazar AJ, Lev D, Bill K, Lloyd RV, Yaszemski MJ, Maran A, Oliveira AM (2011) High-resolution genomic mapping reveals consistent amplification of the fibroblast growth factor receptor substrate 2 gene in well-differentiated and dedifferentiated liposarcoma. Genes Chromosomes Cancer 50(11):849–858
11. Scheinin I, Myllykangas S, Borze I, Bohling T, Knuutila S, Saharinen J (2008) CanGEM: mining gene copy number changes in cancer. Nucleic Acids Res 36:D830–D835, Database issue
12. Baudis M (2007) Genomic imbalances in 5918 malignant epithelial tumors: an explorative meta-analysis of chromosomal CGH data. BMC Cancer 7:226
13. Pedeutour F, Suijkerbuijk RF, Forus A, Van Gaal J, Van de Klundert W, Coindre JM, Nicolo G, Collin F, Van Haelst U, Huffermann K et al (1994) Complex composition and co-amplification of SAS and MDM2 in ring and giant rod marker chromosomes in well-differentiated liposarcoma. Genes Chromosomes Cancer 10(2):85–94

14. Gisselsson D, Hoglund M, Mertens F, Mitelman F, Mandahl N (1998) Chromosomal organization of amplified chromosome 12 sequences in mesenchymal tumors detected by fluorescence in situ hybridization. Genes Chromosomes Cancer 23(3):203–212
15. Sirvent N, Forus A, Lescaut W, Burel F, Benzaken S, Chazal M, Bourgeon A, Vermeesch JR, Myklebost O, Turc-Carel C, Ayraud N, Coindre JM, Pedeutour F (2000) Characterization of centromere alterations in liposarcomas. Genes Chromosomes Cancer 29 (2):117–129
16. Dei Tos AP, Doglioni C, Piccinin S, Sciot R, Furlanetto A, Boiocchi M, Dal Cin P, Maestro R, Fletcher CD, Tallini G (2000) Coordinated expression and amplification of the MDM2, CDK4, and HMGI-C genes in atypical lipomatous tumours. J Pathol 190(5):531–536
17. Chibon F, Mariani O, Derre J, Malinge S, Coindre JM, Guillou L, Lagace R, Aurias A (2002) A subgroup of malignant fibrous histiocytomas is associated with genetic changes similar to those of well-differentiated liposarcomas. Cancer Genet Cytogenet 139(1):24–29
18. Micci F, Teixeira MR, Bjerkehagen B, Heim S (2002) Characterization of supernumerary rings and giant marker chromosomes in well-differentiated lipomatous tumors by a combination of G-banding, CGH, M-FISH, and chromosome- and locus-specific FISH. Cytogenet Genome Res 97(1–2):13–19
19. Kresse SH, Berner JM, Meza-Zepeda LA, Gregory SG, Kuo WL, Gray JW, Forus A, Myklebost O (2005) Mapping and characterization of the amplicon near APOA2 in 1q23 in human sarcomas by FISH and array CGH. Mol Cancer 4:39
20. Mariani O, Brennetot C, Coindre JM, Gruel N, Ganem C, Delattre O, Stern MH, Aurias A (2007) JUN oncogene amplification and overexpression block adipocytic differentiation in highly aggressive sarcomas. Cancer Cell 11(4):361–374
21. Johnson JE, Gettings EJ, Schwalm J, Pei J, Testa JR, Litwin S, von Mehren M, Broccoli D (2007) Whole-genome profiling in liposarcomas reveals genetic alterations common to specific telomere maintenance mechanisms. Cancer Res 67(19):9221–9228
22. Tap WD, Eilber FC, Ginther C, Dry SM, Reese N, Barzan-Smith K, Chen HW, Wu H, Eilber FR, Slamon DJ, Anderson L (2011) Evaluation of well-differentiated/de-differentiated liposarcomas by high-resolution oligonucleotide array-based comparative genomic hybridization. Genes Chromosomes Cancer 50(2):95–112
23. Italiano A, Maire G, Sirvent N, Nuin PA, Keslair F, Foa C, Louis C, Aurias A, Pedeutour F (2009) Variability of origin for the neocentromeric sequences in analphoid supernumerary marker chromosomes of well-differentiated liposarcomas. Cancer Lett 273(2):323–330
24. Italiano A, Toulmonde M, Cioffi A, Penel N, Isambert N, Bompas E, Duffaud F, Patrikidou A, Lortal B, Le Cesne A, Blay JY, Maki RG, Schwartz GK, Antonescu CR, Singer S, Coindre JM, Bui B (2012) Advanced well-differentiated/dedifferentiated liposarcomas: role of chemotherapy and survival. J Ann Oncol 23(6):1601–1607
25. Muller CR, Paulsen EB, Noordhuis P, Pedeutour F, Saeter G, Myklebost O (2007) Potential for treatment of liposarcomas with the MDM2 antagonist Nutlin-3A. Int J Cancer 121(1):199–205
26. Singer S, Socci ND, Ambrosini G, Sambol E, Decarolis P, Wu Y, O'Connor R, Maki R, Viale A, Sander C, Schwartz GK, Antonescu CR (2007) Gene expression profiling of liposarcoma identifies distinct biological types/subtypes and potential therapeutic targets in well-differentiated and dedifferentiated liposarcoma. Cancer Res 67(14):6626–6636
27. Nishio J, Iwasaki H, Ishiguro M, Ohjimi Y, Fujita C, Ikegami H, Ariyoshi A, Naito M, Kaneko Y, Kikuchi M (2003) Establishment of a novel human dedifferentiated liposarcoma cell line, FU-DDLS-1: conventional and molecular cytogenetic characterization. Int J Oncol 22(3):535–542
28. Hugo ER, Brandebourg TD, Comstock CE, Gersin KS, Sussman JJ, Ben-Jonathan N (2006) LS14: a novel human adipocyte cell line that produces prolactin. Endocrinology 147(1):306–313
29. Snyder EL, Sandstrom DJ, Law K, Fiore C, Sicinska E, Brito J, Bailey D, Fletcher JA, Loda M, Rodig SJ, Dal Cin P, Fletcher CD (2009) c-Jun amplification and overexpression are oncogenic in liposarcoma but not always sufficient to inhibit the adipocytic differentiation programme. J Pathol 218(3):292–300
30. Persson F, Olofsson A, Sjogren H, Chebbo N, Nilsson B, Stenman G, Aman P (2008) Characterization of the 12q amplicons by high-resolution, oligonucleotide array CGH and expression analyses of a novel liposarcoma cell line. Cancer Lett 260(1–2):37–47
31. Wittekind C, Compton CC, Greene FL, Sobin LH (2002) TNM residual tumor classification revisited. Cancer 94(9):2511–2516
32. Fletcher CD (2006) The evolving classification of soft tissue tumours: an update based on the new WHO classification. Histopathology 48(1):3–12
33. Limon J, Dal Cin P, Sandberg AA (1986) Application of long-term collagenase disaggregation for the cytogenetic analysis of human solid tumors. Cancer Genet Cytogenet 23(4):305–313
34. Bayani J, Zielenska M, Marrano P, Kwan Ng Y, Taylor MD, Jay V, Rutka JT, Squire JA (2000) Molecular cytogenetic analysis of medulloblastomas and supratentorial primitive neuroectodermal tumors by using conventional banding, comparative genomic hybridization, and spectral karyotyping. J Neurosurg 93(3):437–448
35. Schrock E, du Manoir S, Veldman T, Schoell B, Wienberg J, Ferguson-Smith MA, Ning Y, Ledbetter DH, Bar-Am I, Soenksen D, Garini Y, Ried T (1996) Multicolor spectral karyotyping of human chromosomes. Science 273(5274):494–497
36. Jacobs S, Thompson ER, Nannya Y, Yamamoto G, Pillai R, Ogawa S, Bailey DK, Campbell IG (2007) Genome-wide, high-resolution detection of copy number, loss of heterozygosity, and genotypes from formalin-fixed, paraffin-embedded tumor tissue using microarrays. Cancer Res 67(6):2544–2551
37. Gabrielsson BG, Olofsson LE, Sjogren A, Jernas M, Elander A, Lonn M, Rudemo M, Carlsson LM (2005) Evaluation of reference genes for studies of gene expression in human adipose tissue. Obes Res 13(4):649–652
38. Nilbert M, Rydholm A, Mitelman F, Meltzer PS, Mandahl N (1995) Characterization of the 12q13-15 amplicon in soft tissue tumors. Cancer Genet Cytogenet 83(1):32–36
39. Berner JM, Forus A, Elkahloun A, Meltzer PS, Fodstad O, Myklebost O (1996) Separate amplified regions encompassing CDK4 and MDM2 in human sarcomas. Genes Chromosomes Cancer 17(4):254–259
40. Fritz B, Schubert F, Wrobel G, Schwaenen C, Wessendorf S, Nessling M, Korz C, Rieker RJ, Montgomery K, Kucherlapati R, Mechtersheimer G, Eils R, Joos S, Lichter P (2002) Microarray-based copy number and expression profiling in dedifferentiated and pleomorphic liposarcoma. Cancer Res 62(11):2993–2998
41. Horvai AE, DeVries S, Roy R, O'Donnell RJ, Waldman F (2009) Similarity in genetic alterations between paired well-differentiated and dedifferentiated components of dedifferentiated liposarcoma. Mod Pathol 22(11):1477–1488
42. Hostein I, Pelmus M, Aurias A, Pedeutour F, Mathoulin-Pelissier S, Coindre JM (2004) Evaluation of MDM2 and CDK4 amplification by real-time PCR on paraffin wax-embedded material: a potential tool for the diagnosis of atypical lipomatous tumours/well-differentiated liposarcomas. J Pathol 202(1):95–102
43. Sirvent N, Coindre JM, Maire G, Hostein I, Keslair F, Guillou L, Ranchere-Vince D, Terrier P, Pedeutour F (2007) Detection of MDM2-CDK4 amplification by fluorescence in situ hybridization in 200 paraffin-embedded tumor samples: utility in diagnosing adipocytic lesions and comparison with immunohistochemistry and real-time PCR. Am J Surg Pathol 31(10):1476–1489
44. Aleixo PB, Hartmann AA, Menezes IC, Meurer RT, Oliveira AM (2009) Can MDM2 and CDK4 make the diagnosis of well differentiated/dedifferentiated liposarcoma? An immunohistochemical study on 129 soft tissue tumours. J Clin Pathol 62(12):1127–1135

45. Nishio J (2011) Contributions of cytogenetics and molecular cytogenetics to the diagnosis of adipocytic tumors. J Biomed Biotechnol 2011:524067
46. Tanas MR, Rubin BP, Tubbs RR, Billings SD, Downs-Kelly E, Goldblum JR (2010) Utilization of fluorescence in situ hybridization in the diagnosis of 230 mesenchymal neoplasms: an institutional experience. Arch Pathol Lab Med 134(12):1797–1803
47. Manfredi JJ (2010) The Mdm2-p53 relationship evolves: Mdm2 swings both ways as an oncogene and a tumor suppressor. Genes Dev 24(15):1580–1589
48. Muller KM, Tveteraas IH, Aasrum M, Odegard J, Dawood M, Dajani O, Christoffersen T, Sandnes DL (2011) Role of protein kinase C and epidermal growth factor receptor signalling in growth stimulation by neurotensin in colon carcinoma cells. BMC Cancer 11(1):421
49. Szymanska J, Virolainen M, Tarkkanen M, Wiklund T, Asko-Seljavaara S, Tukiainen E, Elomaa I, Blomqvist C, Knuutila S (1997) Overrepresentation of 1q21-23 and 12q13-21 in lipoma-like liposarcomas but not in benign lipomas: a comparative genomic hybridization study. Cancer Genet Cytogenet 99(1):14–18
50. Szymanska J, Tarkkanen M, Wiklund T, Virolainen M, Blomqvist C, Asko-Seljavaara S, Tukiainen E, Elomaa I, Knuutila S (1996) Gains and losses of DNA sequences in liposarcomas evaluated by comparative genomic hybridization. Genes Chromosomes Cancer 15(2):89–94
51. Suijkerbuijk RF, Olde Weghuis DE, Van den Berg M, Pedeutour F, Forus A, Myklebost O, Glier C, Turc-Carel C, Geurts van Kessel A (1994) Comparative genomic hybridization as a tool to define two distinct chromosome 12-derived amplification units in well-differentiated liposarcomas. Genes Chromosomes Cancer 9 (4):292–295
52. Ashar HR, Fejzo MS, Tkachenko A, Zhou X, Fletcher JA, Weremowicz S, Morton CC, Chada K (1995) Disruption of the architectural factor HMGI-C: DNA-binding AT hook motifs fused in lipomas to distinct transcriptional regulatory domains. Cell 82 (1):57–65
53. Petit MM, Mols R, Schoenmakers EF, Mandahl N, Van de Ven WJ (1996) LPP, the preferred fusion partner gene of HMGIC in lipomas, is a novel member of the LIM protein gene family. Genomics 36(1):118–129
54. Petit MM, Schoenmakers EF, Huysmans C, Geurts JM, Mandahl N, Van de Ven WJ (1999) LHFP, a novel translocation partner gene of HMGIC in a lipoma, is a member of a new family of LHFP-like genes. Genomics 57(3):438–441
55. Berner JM, Meza-Zepeda LA, Kools PF, Forus A, Schoenmakers EF, Van de Ven WJ, Fodstad O, Myklebost O (1997) HMGIC, the gene for an architectural transcription factor, is amplified and rearranged in a subset of human sarcomas. Oncogene 14(24):2935–2941
56. Meza-Zepeda LA, Berner JM, Henriksen J, South AP, Pedeutour F, Dahlberg AB, Godager LH, Nizetic D, Forus A, Myklebost O (2001) Ectopic sequences from truncated HMGIC in liposarcomas are derived from various amplified chromosomal regions. Genes Chromosomes Cancer 31(3):264–273
57. Bartuma H, Hallor KH, Panagopoulos I, Collin A, Rydholm A, Gustafson P, Bauer HC, Brosjo O, Domanski HA, Mandahl N, Mertens F (2007) Assessment of the clinical and molecular impact of different cytogenetic subgroups in a series of 272 lipomas with abnormal karyotype. Genes Chromosomes Cancer 46(6):594–606
58. Persson F, Andren Y, Winnes M, Wedell B, Nordkvist A, Gudnadottir G, Dahlenfors R, Sjogren H, Mark J, Stenman G (2009) High-resolution genomic profiling of adenomas and carcinomas of the salivary glands reveals amplification, rearrangement, and fusion of HMGA2. Genes Chromosomes Cancer 48(1):69–82
59. Dreux N, Marty M, Chibon F, Velasco V, Hostein I, Ranchere-Vince D, Terrier P, Coindre JM (2010) Value and limitation of immunohistochemical expression of HMGA2 in mesenchymal tumors: about a series of 1052 cases. Mod Pathol 23(12):1657–1666
60. Tallini G, Vanni R, Manfioletti G, Kazmierczak B, Faa G, Pauwels P, Bullerdiek J, Giancotti V, Van Den Berghe H, Dal Cin P (2000) HMGI-C and HMGI(Y) immunoreactivity correlates with cytogenetic abnormalities in lipomas, pulmonary chondroid hamartomas, endometrial polyps, and uterine leiomyomas and is compatible with rearrangement of the HMGI-C and HMGI(Y) genes. Lab Invest 80(3):359–369
61. Bartuma H, Panagopoulos I, Collin A, Trombetta D, Domanski HA, Mandahl N, Mertens F (2009) Expression levels of HMGA2 in adipocytic tumors correlate with morphologic and cytogenetic subgroups. Mol Cancer 8:36
62. Craver RD, Fonseca P, Carr R (2010) Pediatric epithelial salivary gland tumors: spectrum of histologies and cytogenetics at a children's hospital. Pediatr Dev Pathol 13(5):348–353
63. Bianchini L, Saada E, Gjernes E, Marty M, Haudebourg J, Birtwisle-Peyrottes I, Keslair F, Chignon-Sicard B, Chamorey E, Pedeutour F (2011) Let-7 microRNA and HMGA2 levels of expression are not inversely linked in adipocytic tumors: analysis of 56 lipomas and liposarcomas with molecular cytogenetic data. Genes Chromosomes Cancer 50(6):442–455
64. Louis-Brennetot C, Coindre JM, Ferreira C, Perot G, Terrier P, Aurias A (2011) The CDKN2A/CDKN2B/CDK4/CCND1 pathway is pivotal in well-differentiated and dedifferentiated liposarcoma oncogenesis. An analysis of 104 tumors. Genes Chromosomes Cancer 50(11):896–907
65. Rieker RJ, Joos S, Bartsch C, Willeke F, Schwarzbach M, Otano-Joos M, Ohl S, Hogel J, Lehnert T, Lichter P, Otto HF, Mechtersheimer G (2002) Distinct chromosomal imbalances in pleomorphic and in high-grade dedifferentiated liposarcomas. Int J Cancer 99(1):68–73
66. Chaplin T, Bernard O, Beverloo HB, Saha V, Hagemeijer A, Berger R, Young BD (1995) The t(10;11) translocation in acute myeloid leukemia (M5) consistently fuses the leucine zipper motif of AF10 onto the HRX gene. Blood 86(6):2073–2076
67. Tanabe S, Bohlander SK, Vignon CV, Espinosa R 3rd, Zhao N, Strissel PL, Zeleznik-Le NJ, Rowley JD (1996) AF10 is split by MLL and HEAB, a human homolog to a putative *Caenorhabditis elegans* ATP/GTP-binding protein in an invins(10;11)(p12;q23q12). Blood 88(9):3535–3545
68. Dobbins SE, Broderick P, Melin B, Feychting M, Johansen C, Andersson U, Brannstrom T, Schramm J, Olver B, Lloyd A, Ma YP, Hosking FJ, Lonn S, Ahlbom A, Henriksson R, Schoemaker MJ, Hepworth SJ, Hoffmann P, Muhleisen TW, Nothen MM, Moebus S, Eisele L, Kosteljanetz M, Muir K, Swerdlow A, Simon M, Houlston RS (2011) Common variation at 10p12.31 near MLLT10 influences meningioma risk. Nat Genet 43(9):825–827
69. Millevoi S, Trombitas K, Kolmerer B, Kostin S, Schaper J, Pelin K, Granzier H, Labeit S (1998) Characterization of nebulette and nebulin and emerging concepts of their roles for vertebrate Z-discs. J Mol Biol 282(1):111–123
70. Coser VM, Meyer C, Basegio R, Menezes J, Marschalek R, Pombo-de-Oliveira MS (2010) Nebulette is the second member of the nebulin family fused to the MLL gene in infant leukemia. Cancer Genet Cytogenet 198(2):151–154
71. Lessard J, Sauvageau G (2003) Bmi-1 determines the proliferative capacity of normal and leukaemic stem cells. Nature 423 (6937):255–260
72. Cao L, Bombard J, Cintron K, Sheedy J, Weetall ML, Davis TW (2011) BMI1 as a novel target for drug discovery in cancer. J Cell Biochem 112(10):2729–2741

Virchows Arch (2012) 461:79–86
DOI 10.1007/s00428-012-1258-3

ORIGINAL ARTICLE

Structural requirements of research tissue banks derived from standardized project surveillance

E. Herpel · N. Koleganova · B. Schreiber · B. Walter · C. v. Kalle · P. Schirmacher

Received: 2 February 2012 / Revised: 17 April 2012 / Accepted: 21 May 2012 / Published online: 1 June 2012
© Springer-Verlag 2012

Abstract Tissue banks constitute decisive and rate-limiting resource and technology platforms for basic and translational biomedical research, notably in the area of cancer. Thus, it is essential to plan and structure tissue banking and allocate resources according to research needs, but essential requirements are still incompletely defined. The tissue bank of the National Center of Tumor Diseases Heidelberg (NCT) was founded with the intention to provide tissues of optimal quality and to prioritize the realization of research projects. We analysed its structure and prospective project management registration as well as tracking records for all projects of the NCT tissue bank as of its start in 2005 in order to obtain information that may be relevant for tissue bank planning. All project proposals submitted to the NCT tissue bank (n=681) were included in the study. For a detailed evaluation of provided services, only projects that were completed until July 2011 (n=605) were analysed. For these 605 projects, NCT tissue bank provided 769 specific services. In all projects/services, we recorded project leader, type and amount of material provided, type of research (basic/translational), work load of project and project completion. Furthermore, all completed projects were tracked after 90 days according to a standard protocol to determine principal investigators' (PI) satisfaction and quality of the provided material. Until July 2011, 605 projects had been successfully completed as documented by material transfer agreement. Of the projects, 72.7 % addressed basic research, 22.3 % were translational research projects and 3 % concerned epidemiological research; 91 % (n=546) concerned a single PI and the NTC tissue bank. For these projects, 769 specific services were provided. Of these services, 288 concerned providing formalin-fixed and paraffin-embedded (FFPE) tissue (extracts, full size sections), 126 providing fresh frozen materials (including fresh frozen sections), 137 providing tissue microarray (TMA)-based sections and 199 providing immunohistochemical services. Project tracking demonstrated that all projects had started within 90 days after reception of the material by the PIs, and PI satisfaction with provided material exceeded 97 %. Standardized registration and tracking provides valuable structural information for planning and financing of tissue banks and allocation of resources. The high number of completed projects as well as high user satisfaction demonstrates that structuring of tissue banks should be preferably research-oriented and highly efficient. The comparable number of requests for FFPE and fresh frozen tissue as well as TMA-based services underpins the need for a broad approach in terms of methods and material types in order to fulfil research needs.

Keywords Tissue bank · Structural requirements · Biomedical and translational research · Resource allocation

E. Herpel · N. Koleganova · P. Schirmacher
Institute of Pathology, University of Heidelberg Medical School, Heidelberg, Germany

E. Herpel · N. Koleganova · B. Schreiber · B. Walter
Tissue Bank of the National Center for Tumor Disease, University of Heidelberg Medical School, Heidelberg, Germany

C. v. Kalle
National Center of Tumor Diseases (NCT), University of Heidelberg Medical School, Heidelberg, Germany

E. Herpel (✉)
Im Neuenheimer Feld 220,
69120 Heidelberg, Germany
e-mail: esther.herpel@med.uni-heidelberg.de

Introduction

Access to quality-assured and comprehensive biomaterial, especially human tissue samples, represents an essential resource for basic and translational biomedical research and its translation into clinical application [1–4]. Structured tissue banks fulfil essential tasks in guaranteeing good scientific practice in handling and evaluation of human tissues. Therefore, they are a decisive but also limiting resource. Thus, it is essential to plan and structure tissue banking and allocate resources according to research needs, but to date little is known about the actual requirements research tissue banks [5] are facing.

Many recommendations exist about organizational aspects of research biobanks or regarding ethical and legal aspects [6, 7]. Little is known about the necessary resource allocation for research biobanks, the infrastructural and/or organizational requirements including workflow and time lines in tissue bank procedures. Reported information and experience has been derived from biobanks with a low number of projects or refer to single projects [5, 8–10], and therefore useful information about large size respective research tissue biobanks are missing.

The tissue bank of the National Centre for Tumor Diseases (NCT) in Heidelberg, Germany, was founded in 2005 by the University of Heidelberg Medical School and the German Cancer Research Centre (DKFZ) as a section of the NCT [2]. It is a non-profit research tissue bank with a completely evaluated legal, ethical and data protection framework and represents an integral part of the Comprehensive Cancer Centre concept [2]. The NCT tissue bank has installed comprehensive quality management with all procedures documented in a complete quality management handbook and is the first fully accredited (DAkkS, DIN/ISO 17020) research tissue bank [11]. Its main aims are the acquisition, characterization and handling of fresh-frozen and paraffin-embedded human tissues (FFPE) solely for research purposes, the preparation of tissue specimen derivatives, while respecting and promoting good scientific practice and interdisciplinary tumor research of the Heidelberg research community/NCT and its cooperating partners. Since May 2005, the NCT tissue bank has stored fresh frozen tissue samples of more than 20,000 patients and provided access to more than one million FFPE tissue samples. Furthermore, the NCT tissue bank has produced 67 different entity-specific or epidemiological trial-related tissue micro-arrays (TMAs) covering a broad spectrum of neoplastic diseases and corresponding tumor-free tissues. As yet, the NCT tissue bank has supported more than 680 different research projects. In the context of these research projects, more than 769 specific services were provided.

Because of the high number and non-selected type of projects, the standardized project management and the clear separation from clinical diagnostic issues, the NCT tissue bank represents an ideal model of a comprehensive, single-location research tissue bank. In order to generate relevant basic structural information that may support tissue bank planning, implementation, operation and long-term sustainability/financing, we analysed the comprehensive prospective standardized registration and tracking records from all projects that the NCT tissue bank has supported.

We show that structured tissue bank project assessment is a necessary and relevant tool for tissue bank planning and allocation of resources. Our results demonstrate that research-oriented structures and regulation of a tissue bank can be highly efficient and are thus preferable. This is supported by the high project number and the high completion rates as well as the high user satisfaction rates. Furthermore, the important number of FFPE and fresh frozen tissue as well as TMA-based projects argues in favour of a broad spectrum platform approach of a tissue bank in order to fulfil research needs and to achieve maximum efficiency.

Materials and methods

All projects of the NCT tissue bank from its start in Spring 2005 until July 2011 were included in the analyses. The analyses were structured into two different aspects: (a) administrative aspects and (b) practical and scientific aspects.

The following administrative aspects were evaluated:

- Number of project requests to the NCT tissue bank, approved and rejected projects and number of complex projects that required detailed and specific evaluation by the scientific advisory board. A project was defined as a documented singular request for tissue, derivatives or specific analyses, or combinations of these, submitted by a named PI to the NCT tissue bank.
- Affiliation of applying PI.
- Types of research supported. Categories were: clinical and translational research, basic biomedical research and epidemiological research. Categorization of research type followed the mandatory and standardized project description that was provided by every researcher along with the project application. Research projects which were, e.g., biomarker or trial-associated projects were summarized in the category "clinical/translational research" and all research projects dealing, e.g., with functional or animal model-associated human research projects were summarized in the subgroup "basic research". The tissue bank also supports large-scale epidemiological trials; these associated projects were summarized in the subgroup "epidemiological research".
- Partners involved in application. Categories defined were: single applicant, more than one applicant, defined research networks and epidemiological trials.

- Number of projects completed by NCT tissue bank. Completion was defined as transfer of material to applicant and its documentation by countersigning of the material transfer agreement by the PI.

Regarding the practical and scientific aspects, all 769 services that were provided within the 605 projects were analysed. Because some projects generated different services, statistical analyses of the practical and scientific aspects were performed on all services. For example, some projects required FFPE slides and in a second step TMA sections, and in this case two different services were provided for one project and therefore separately evaluated.

The following services were provided by the NCT tissue bank: preparation of FFPE slides, fresh frozen tissue slides or TMA slides. Additionally, preparation of FFPE and fresh frozen tissue samples for extraction methods (e.g. DNA and RNA extraction) and immunohistochemical stains were provided as services. Last but not least, preparation of large scale tissue micro arrays was performed.

The following aspects of the services were evaluated:

- Type of tissue provided. Categories were: fresh frozen tissue, formalin-fixed and paraffin-embedded tissue, tissue-micro-array-slides.
- Type of service provided. Categories were: serial sections, immunohistochemistry, composition of TMAs and itemization of platform services (staff training, cooperations with, e.g., virtual microscopy).
- Project size categorized by number of samples employed: small [<10 samples/slides], medium [11–30 samples/slides] and large [>30 samples/ slides].
- Duration of projects. Categories were long term (>6 months) and short term (<6 months).
- Quality of provided service and satisfaction rate of PI as evaluated from standardized project tracking. To this end, the date of delivery was entered into the electronic calendar of the tissue bank on the day of material transfer. After 90 days, through an automatic reminder, the NCT tissue bank office sent a standard email to the respective PI or contacted him/her directly.

All presented data were submitted to continuous internal and external validation: Internal audits took place three times a year, and all project data were controlled twice annually by the board of the NCT tissue bank. Furthermore, all NCT tissue bank data were externally validated by DAkkS (Deutsche Akkreditierungsstelle) in the successful accreditation review in April 2009 and the external audit in February 2011. Additionally, the NCT tissue bank was twice successfully reviewed internationally as part of the review of the translational research area of the DKFZ in 2008 and 2011.

Results

Administrative aspects

In all, 697 project requests were submitted to the NCT tissue bank from May 2005 until July 2011 (Fig. 1).

Some requests (n=49) could not be decided upon directly by the NCT tissue bank according to its standing orders and therefore had to be reviewed by the advisory board of the NCT tissue bank, which is composed of representatives of all participating institutions of the NCT tissue bank. Of these requests, three were rejected after review by the advisory board for reasons of interference with clinical diagnostic necessities, incomplete project planning/incomplete preliminary work or lack of compliance to NCT tissue bank regulations by the PI. Overall, 13 project requests were withdrawn by the PIs after discussion of the project with the representatives of the NCT tissue bank.

Thus, 681 project requests were accepted and supported by the NCT tissue bank. From Spring 2005 until July 2011, 605 of the 681 supported projects were completed (Fig. 3). For some of the 605 projects, more than one specific service was provided. In total, 769 services emerged from the 605 projects. All 769 services were therefore considered for the evaluation of the practical and scientific aspects.

Regarding the type of research performed, of the 605 projects finished during the observation period, 440 projects (72.7 %) addressed basic biomedical research, 135 (22.3 %) were categorized as clinical and translational research, 21 (3 %) were associated with epidemiological trials (Fig. 2a) and nine (2 %) were others (e.g. re-evaluation of external tissue samples, staff training or virtual microscopy).

Affiliation of the researchers was as follows: In 456 (75 %) projects, researchers held working contracts with the Academic Hospital of the University Heidelberg. In 125 (21 %) projects, researchers were staff members of the DKFZ, a national research institution and 14 (2 %) projects were performed by researchers of the Thoracic Hospital

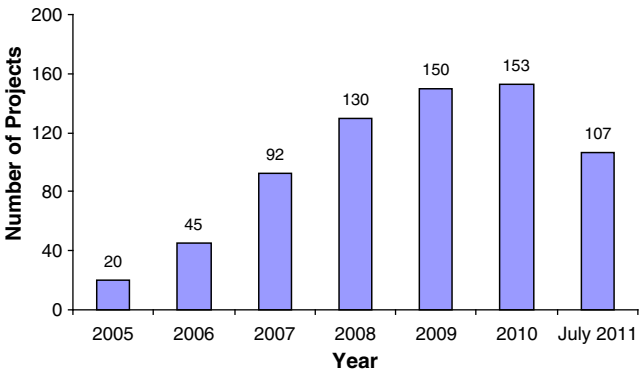

Fig. 1 Since May 2005 and July 2010 in total 697 project requests were sent to the NCT tissue bank

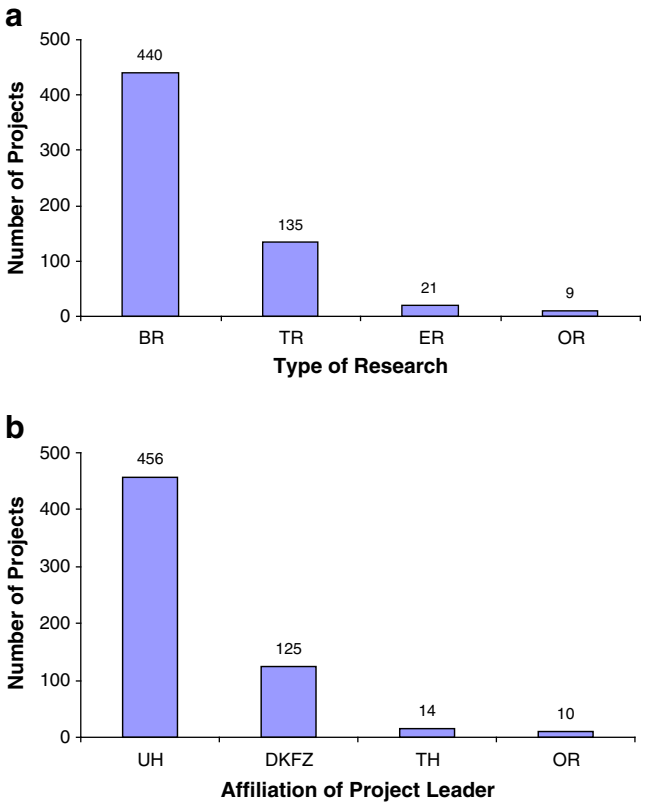

Fig. 2 **a** Type of supported research projects (n=605). TR = Translational and clinical research; BR = Basic biomedical research; ER = Epidemiological studies; OR = Others. **b** Affiliation of project leader (n=605). UH = University Hospital Heidelberg; DKFZ = German Cancer Research Center; TH = Thoracic Hospital Heidelberg; OR = Epidemiological studies

Heidelberg, a closely affiliated hospital. In ten (2 %) projects, the applicants were associated with large-scale epidemiological trials (e.g. ColoCare, DACHS, EPIC) (Fig. 2b).

Regarding the number of applying partners in a given project, 546 (90.2 %) of 605 research projects were single-applicant projects. These projects always consisted of a team of complementary histological and/or clinical partners (according to the standing order of the NCT tissue bank). For the other 9 % (n=56) of the projects, two or more applying cooperation partners were involved.

Practical and scientific aspects

A complete analysis of all 769 provided services that emerged from the 605 projects was performed for evaluation of the practical and scientific aspects.

In 414 services, either tissue samples of paraffin-embedded or fresh frozen tissue samples were requested. Samples of FFPE tissues were requested in 288 services; fresh frozen samples were requested in 126 services. In 137 services, slides of TMAs were requested. In 199 services, immunohistochemical staining was performed by the NCT tissue bank (Fig. 3). Other types of services, like re-evaluation of external tissue samples, staff training or virtual microscopy, were performed additionally in 19 of the 769 services.

Of the services using formalin-fixed and paraffin-embedded tissue samples (n=288), 238 services provided FFPE slides and 50 services provided whole samples or sections for RNA or DNA extraction procedures (Table 1). For all services using FFPE tissues, overall 8,268 blocks were used and 26,862 sections were prepared. On average, 112 sections were provided for each of the 238 FFPE slide projects. Grouping of the projects by effort resulted in the following numbers (Table 2): in 22 FFPE slide services (9.2 %) less than ten slides were provided, in 64 FFPE slide services (26.9 %) 11–30 slides were provided and in 152 services (63.9 %) more than 30 slides per service were provided.

By the 50 services which used FFPE tissue sections for extraction methods (RNA/DNA), in total 1,482 FFPE samples were provided and 2,350 tubes containing ten sections of 10 μm were prepared. The average number of tubes per service was 47.0 (for details, see Table 2).

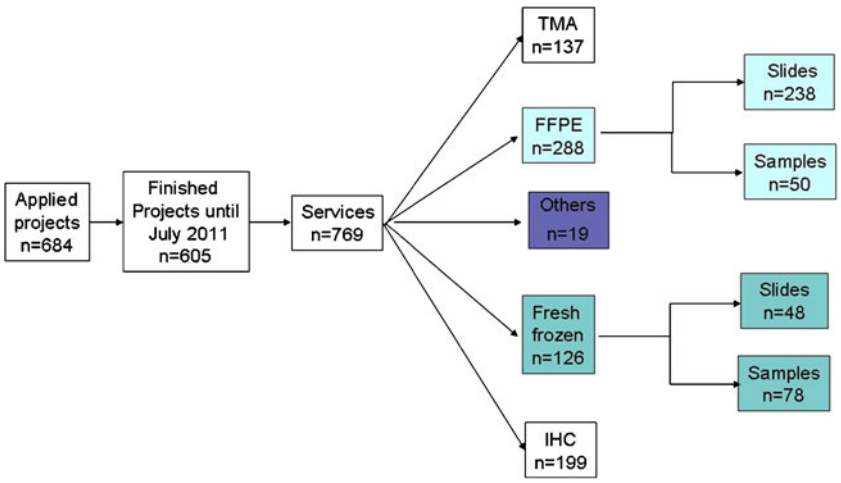

Fig. 3 In total since 2005 till July 2011 the tissue bank has supported 605 projects that generated 769 services. FFPE = Formalin fixed and paraffin embedded tissue; TMA = Tissue-Micro-Array; IHC = Immunohistochemistry

Table 1 Distribution of FFPE tissue and fresh frozen tissue services according to size

	Services (*n*)	Number/count, *n*	< 10	11 to 30	> 30
FFPE (*n*=288)	Samples	50	25	10	15
	Slides	238	22	64	152
Fresh frozen (*n*=126)	Samples	78	39	28	11
	Slides	48	5	18	25

Regarding the fresh frozen tissue sample services (*n*=126), 48 services provided fresh frozen tissue slides for histochemical and/or immunohistochemical analyses. A total of 78 services provided fresh frozen tissue sections for extraction methods (RNA/DNA) (Table 1). For the 48 fresh frozen tissue slide services, in total 264 different tissue probes were used and 2,407 sections were prepared. Thus, on average, 50 fresh frozen slides were provided per service. In detail (Table 3), for five fresh frozen slide services, less than ten slides were provided. For 18 services, 11–30 slides were provided and more than 30 slides per service were provided for 25 services. Looking at the 78 services where whole samples or sections were provided for extraction methods (RNA/DNA), in total 1,822 samples of fresh frozen samples were used. For 39 (50.0 %) services less than ten different fresh frozen samples were used, for 28 (35.9 %) services 11–30 were provided and for 11 (14.1 %) services more than 30 fresh frozen samples per service were provided (Table 3).

About one out of four project applications required TMA sections (*n*=137). In total, 3,056 TMA slides were handed out to researchers, resulting in an average of 22 TMA slides per service.

Furthermore, the NCT tissue bank also represents a technology platform that also provides specific biobanking-related technologies (e.g. virtual microscopy) for research purposes and under specific and limiting conditions operators in registered projects may also be trained in practical aspects of tissue processing (e.g. preparation of a TMA or cryo-sectioning). Therefore, for 19 services specific training of the researcher on tissue bank-based technologies concerning virtual microscopy were performed by the NCT tissue bank.

To qualify the duration of services provided by the NCT tissue bank, we defined long- and short-term services. Services exceeding 6 months in duration, e.g. TMAs for large-scale epidemiological trials or projects requiring large amounts of samples, were defined as long-term services. Services that were finished in less than 6 months were defined as short-term services. In total, 4.7 % services were rated as long-term and 95.3 % as short-term service.

Additionally, all projects supported by the NCT tissue bank were submitted to a standardized project tracking 90 days after the material was transferred to the PI to evaluate the quality of provided service and satisfaction of PI. Until July 2011, from the 605 projects, 412 projects had received their material more than 90 days earlier and therefore the query was sent to the responsible PI. Participation was voluntary and 382 PIs (92.7 %) replied, while 30 researchers (7.3 %) did not respond. A total of 374 responses revealed a positive feedback, six responses were negative, and in two projects the PIs stated that the material had quality limitations but was still useful for the specific analyses of the project**.** Thus, the satisfaction rate exceeded 97.9 % (Fig. 4).

Discussion

Access to quality-assured and comprehensive human tissue samples is essential for basic and translational molecular

Table 2 Description of FFPE slide services (*n*=238) subdivided upon the amount of provided slides and used samples and FFPE sample services (*n*=50) subdivided upon the amount of provided tubes and used samples

Size of FFPE slide service subdivided on slides performed/tubes provided	Services (*n*)	Total number performed slides/tubes	Mean performed slides/tubes	Total number used samples	Mean used samples
FFPE slide services (*n*=238) subdivided upon the amount of provided slides and used samples					
<10	22	170	7.73	100	4.55
11 bis 30	64	1,327	20.73	487	7.61
>30	152	25,365	166.88	7,681	50.53
Total	238	26,862	112.87	8,268	34.74
FFPE sample services (*n*=50) subdivided upon the amount of provided tubes and used samples					
<10	25	109	4.3	101	4.0
11 bis 30	10	186	18.6	154	15.4
>30	15	2,055	137.0	1,227	81.8
Total	50	2,350	47.0	1,482	29.64

Table 3 Description of fresh frozen slide services (n=48) subdivided upon the amount of provided slides and used samples and fresh frozen tissue services (n=78) subdivided upon the amount of provided samples

	Services (n)	Total number performed slides	Mean performed slides	Total number used samples	Mean used samples	Total number performed tissue	Mean performed tissue
Size of fresh frozen slide service subdivided on slides performed							
<10	5	44	8.8	9	1.8		
11 bis 30	18	385	21.4	61	3.4		
>30	25	1,978	79.0	194	7.7		
Total	48	2,407	50.2	264	5.5		
Size of fresh tissue service subdivided on samples provided							
<10	39					182	4.6
11 bis 30	28					556	19.8
>30	11					1,084	98.5
Total	78					1,822	50.2

Description of fresh frozen tissue services (n=78) subdivided upon amount of provided samples

cancer research and its translation into clinical application [2–4, 12, 13]. Therefore, structured information about tissue banks, the requests they are facing and their performance is mandatory in order to base tissue bank planning, financing, organization and sustainability on rational data. This can be obtained only from comprehensive, long-standing and structured tissue banks that provide standardized project management and tracking. All these prerequisites are fulfilled from its start for more than 6 years by the NCT tissue bank; thus, we undertook the task to subject these information to a structured and comprehensive analysis. These analyses provided several relevant and, in part, surprising conclusions.

Human tissue for research, especially fresh frozen tissue, is a sparse and rate-limiting resource [14], and therefore adequate use of tissue should and can be enforced via structured project management [12, 15, 16]. Consequently, most of the effort in general focuses on the acquisition, handling and storage of frozen tissue. From its start onwards, the NCT tissue bank included FFPE tissues, their handling and derivatives (including the fabrication of TMAs) into its portfolio and project management. Interestingly, our analyses showed that, for about half of services, FFPE tissues sufficed and for one out of four services TMA sections were sufficient. Only the remaining quarter of projects needed fresh frozen tissue. Consequently, it is necessary to check projects/service applications in a qualitative manner by the tissue bank, whether services may be performed with, e.g., FFPE tissue or even TMAs instead of frozen tissue. Furthermore, this implies that tissue banks should have a broad base of resources and technologies to achieve the highest possible efficiency. As a consequence, tissues with different types of fixation method (e.g. FFPE and cryopreserved) should be accessible, and different types of tissue preparation methods, like sectioning, TMAs and extraction procedures, should be provided [9, 17]. Consequently, tissue banks should not only be managed as tissue resources but also as technology and even training platforms which offer state-of-the-art technology to generate, e.g., derivatives (TMAs, extracts) or analyse tissue data (e.g. digital image analysis) in order to assure qualified and rational use of the sparse human tissue resource [2]. These resources can be increased, for example, by cooperation with large-scale epidemiological studies, which sometimes offer the potential to collect large and well-annotated collectives in a less biased and prospective manner compared to hospital-based approaches. Finally, it points to another relevant role of tissue banks: they can play a central role even as project brokers: for example, human tissues can be further processed by tissue banks, e.g., by preparing TMAs; these TMAs may enable a broad research community to work with a comparably low amount of well-annotated tissues that are of identical quality and even allow correlative analyses between different projects.

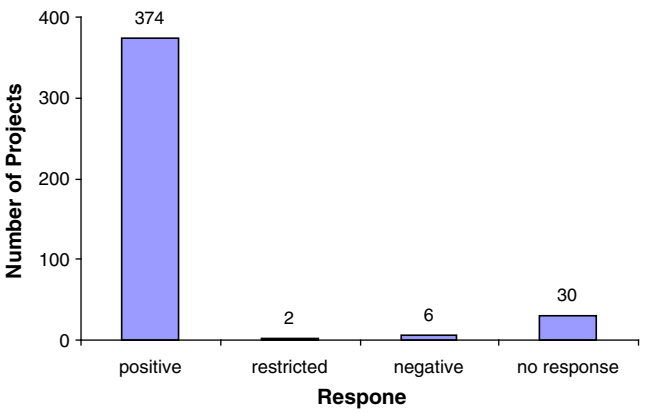

Fig. 4 Tracking request results after 90 days. In total the requests were sent to n=425 service projects

Quality aspects are central for all tissue banks as the quality of research results absolutely depends on the quality of the material used for analyses [16, 18]. To guarantee a consistent level of quality and good scientific practice, it is mandatory for research tissue banks to provide a quality management system [11, 14]. According to this, evaluation of tissue specimens by competent pathologists and a competent performance of tissue entry and exit controls and the reporting of the results is mandatory [3, 11, 19, 20]. In addition, a project-specific evaluation of tissue samples is necessary [14]. This is supported by the NCT tissue bank tracking results which revealed a high user satisfaction (>97 %) and indicated that structured entry and exit controls as well as project-specific processing are highly relevant for maximal efficiency. However, 7 % of project leaders did not respond to the tracking request. This is in part due to the fact that some of the researchers had participated in several projects but did not answer separately for every project or to the researcher having left the Heidelberg research community within the tracking period. Considering these aspects, we feel that the low non-responder rate does not pose a significant bias and does not invalidate our claim of a high satisfaction rate. These analyses are also evidence supporting that research-oriented structuring of tissue banks is highly efficient and superior to primary collection-oriented biobanking.

A regular standardized feedback or monitoring system has several other implications: as mentioned above, it can be used in a continuous manner to improve standard operating procedures that influence tissue/biomaterial quality. It is a valuable tool to discipline PI because it may be used to control whether the provided material has actually been used for the applied research project. Furthermore, data on standardized project tracking are important for the resource allocation of the individual tissue bank, e.g. regarding time efforts, finances and personnel. The NCT tissue bank data show that it takes more than 1–2 years for a tissue bank until it is well accepted within the local research community. Even after 6 years, project numbers of the NCT tissue bank are steadily increasing (see Fig. 1).

Networking of biobanks is a central topic in science politics as well as funding efforts especially when research projects involve many different locations or even different countries [5, 6, 21]. Reflecting the statistical analyses of the NCT tissue bank, however, it can be shown that the majority of projects (90 %) were performed between a single PI and the NCT tissue bank. This does not invalidate the notion of biobank networking and harmonization, but it should be kept in mind that local research projects are the predominant activity of a comprehensive research tissue bank.

The applicability of our analyses has several limitations; first of all, many different types of tissue banks exist worldwide. The NCT tissue bank is a good model for comprehensive, single-location biobanks for research purposes, which certainly represent a significant percentage of all tissue banks. The results of our analysis can be transferred in a modified manner to other academic and non-academic local tissue banks. Some aspects of NCT tissue bank analyses are helpful for constructing (meta-)tissue banks for research networks. For commercial/industry-driven tissue banks, comparable analyses should be performed.

In conclusion, standardized registration and tracking provides valuable structural information for planning and resources allocation (including financing) at the level of the individual tissue bank and for tissue banking in general. High project numbers and completion rates as well as a high user satisfaction rate demonstrate that research-oriented structuring of tissue banks is highly efficient and, in principle, preferable; significant numbers of paraffin and fresh frozen tissue as well as TMA-based projects argue in favour of a broad spectrum platform approach in order to fulfil research needs.

Conflict of interest We declare that we have no conflict of interest.

References

1. Riegman PH, Morente MM, Betsou F, de Blasio P, Geary P (2008) Biobanking for better healthcare. Mol Oncol 2(3):213–222
2. Herpel E, Koleganova N, Schirmacher P (2008) Tissue bank of the National Centre for Tumour Disease. An innovative platform for translational tumour. Pathologe 29(Suppl 2):204–209. doi:10.1007/s00292-008-1067-2
3. Riegman PH, Dinjens WN, Oosterhuis JW (2007) Biobanking for interdisciplinary clinical research. Pathobiology 74(4):239–244
4. Bates S (2010) Progress towards personalized medicine. Drug Discov Today 15(3–4):115–120
5. Zika E, Paci D, Braun A, Rijkers-Defrasne S, Deschenes M, Fortier I, Laage-Hellman J, Scerri CA, Ibarreta D (2011) A European survey on biobanks: trends and issues. Public Health Genomics 14(2):96–103
6. Cambon-Thomsen A, Rial-Sebbag E, Knoppers BM (2007) Trends in ethical and legal frameworks for the use of human biobanks. Eur Respir J 30(2):373–382
7. Hansson MG, Dillner J, Bartram CR, Carlson JA, Helgesson G (2006) Should donors be allowed to give broad consent to future biobank research? Lancet Oncol 7(3):266–269
8. Stege A, Hummel M (2008) Experience with establishment and operation of a biobank. Pathologe 29(Suppl 2):214–217. doi:10.1007/s00292-008-1043-x
9. Giannini C, Oelkers MM, Edwards WD, Aubry MC, Muncil MM, Mohamud KH, Sandleback SG, Nowak JM, Bridgeman A, Brown ME, Cheville JC (2011) Maintaining clinical tissue archives and supporting human research: challenges and solutions. Arch Pathol Lab Med 135(3):347–353. doi:10.1043/2010-0044-SA.1
10. Shickle D, Griffin M, El-Arifi K (2010) Inter- and intra-biobank networks: classification of biobanks. Pathobiology 77(4):181–190
11. Herpel E, Rocken C, Manke H, Schirmacher P, Flechtenmacher C (2010) Quality management and accreditation of research tissue banks: experience of the National Center for Tumor Diseases

(NCT) Heidelberg. Virchows Arch 457(6):741–747. doi:10.1007/s00428-010-0998-1
12. Villena C, Pozo F, Barbera JA, Vaquer P, Agusti A (2011) The CIBERES Pulmonary Biobank Consortium: an opportunity for cooperative international respiratory research. Eur Respir J 37 (1):204–206
13. Diamandis M, White NM, Yousef GM (2010) Personalized medicine: marking a new epoch in cancer patient management. Mol Cancer Res 8(9):1175–1187
14. Qualman SJ, France M, Grizzle WE, LiVolsi VA, Moskaluk CA, Ramirez NC, Washington MK (2004) Establishing a tumour bank: banking, informatics and ethics. Br J Cancer 90(6):1115–1119. doi:10.1038/sj.bjc.66016786601678
15. Ruiz-Godoy L, Meneses-Garcia A, Suarez-Roa L, Enriquez V, Lechuga-Rojas R, Reyes-Lira E (2010) Organization of a tumor bank: the experience of the National Cancer Institute of Mexico. Pathobiology 77(3):147–154
16. Hallmans G, Vaught JB (2011) Best practices for establishing a biobank. Methods Mol Biol 675:241–260. doi:10.1007/978-1-59745-423-0_13
17. Ennis DP, Pidgeon GP, Millar N, Ravi N, Reynolds JV (2010) Building a bioresource for esophageal research: lessons from the early experience of an academic medical center. Dis Esophagus 23(1):1–7
18. Riegman PH, van Veen EB (2011) Biobanking residual tissues. Hum Genet 130(3):357–368. doi:10.1007/s00439-011-1074-x
19. Bevilacqua G, Bosman F, Dassesse T, Hofler H, Janin A, Langer R, Larsimont D, Morente MM, Riegman P, Schirmacher P, Stanta G, Zatloukal K, Caboux E, Hainaut P (2010) The role of the pathologist in tissue banking: European Consensus Expert Group Report. Virchows Arch 456(4):449–454. doi:10.1007/s00428-010-0887-7
20. Riegman PH, Bosch AL (2008) OECI TuBaFrost tumor biobanking. Tumori 94(2):160–163
21. Asslaber M, Zatloukal K (2007) Biobanks: transnational, European and global networks. Brief Funct Genomic Proteomic 6(3):193–201

Virchows Arch (2012) 461:87–92
DOI 10.1007/s00428-012-1262-7

ORIGINAL ARTICLE

Board examination for anatomical pathology in Switzerland: two intense days to verify professional competence

Hans-Anton Lehr · Holger Moch · Brigitte Christen · Alexandra Safret · Mathias Gugger · Matthias Rössle · Michael von Gunten · Robert Lemoine · Ann-Marie Kurt · Rosmarie Caduff · Arnold Walter · Gad Singer · Peter Luscieti · Fridolin Bannwart · Claude Y. Genton

Received: 4 May 2012 / Revised: 4 June 2012 / Accepted: 5 June 2012 / Published online: 21 June 2012
© Springer-Verlag 2012

Abstract About 15 years ago, the Swiss Society of Pathology has developed and implemented a board examination in anatomical pathology. We describe herein the contents covered by this 2-day exam (autopsy pathology, cytology, histopathology, molecular pathology, and basic knowledge about mechanisms of disease) and its exact modalities, sketch a brief history of the exam, and finish with a concise discussion about the possible objectives and

H.-A. Lehr · C. Y. Genton
Institute of Pathology, University of Lausanne,
Lausanne, Switzerland

C. Y. Genton
e-mail: claude.genton@bluewin.ch

H. Moch · M. Rössle · R. Caduff
Institute of Pathology, University of Zurich,
Zurich, Switzerland

H. Moch
e-mail: holger.moch@usz.ch

M. Rössle
e-mail: Matthias.Roessle@usz.ch

R. Caduff
e-mail: rosmarie.caduff@usz.ch

B. Christen · A. Safret
Institute of Pathology ADMED,
Neuchâtel, Switzerland

B. Christen
e-mail: brigitte.christen@ne.ch

A. Safret
e-mail: alexandra.safret@ne.ch

M. Gugger
Institute of Pathology, University of Bern,
Bern, Switzerland
e-mail: mathias.gugger@pathology.unibe.ch

M. von Gunten
Institute of Pathology Länggasse,
Bern, Switzerland
e-mail: mvongunten@patholaenggasse.ch

R. Lemoine · A.-M. Kurt
Institute of Pathology Viollier,
Geneva, Switzerland

R. Lemoine
e-mail: robert.lemoine@viollier.ch

A.-M. Kurt
e-mail: anne-marie.kurt@viollier.ch

A. Walter
Cantonal Hospital of Lucerne,
Lucerne, Switzerland
e-mail: walter.arnold@luks.ch

G. Singer
Cantonal Hospital of Baden,
Baden, Switzerland
e-mail: Gad.Singer@ksb.ch

P. Luscieti
Cantonal Hospital of Locarno,
Locarno, Switzerland

F. Bannwart
Institute of Pathology Medica,
Zürich, Switzerland
e-mai: bannwart@medica-labor.ch

H.-A. Lehr (✉)
Institut Universitaire de Pathologie, Centre Hospitalier
Universitaire Vaudois (CHUV),
Rue du Bugnon 25,
1011 Lausanne, Switzerland
e-mail: hansanton.lehr@yahoo.de

putative benefits weighed against the hardship that it imposes on the candidates.

Keywords Board examination · Training · Anatomical pathology · Quality control

In 1996, the Swiss Society of Pathology (Schweizerische Gesellschaft für Pathologie, SGPath) definitely implemented a national examination to ensure the professional competence of its board members. This exam consists of a 2-day "tour de force" that covers all aspects of the professional activity of an anatomical pathologist. Only senior residents can apply for the exam by writing to the secretary of the president of the board committee, usually 6–12 months in advance, and usually dedicate most of their time to its preparation during their last year of residency. The examination takes place twice a year, sometimes even three times if the number of applicants largely exceeds the capacity of two sessions. Indeed, a maximum of six candidates can be accepted for each exam (seven in rare exceptional situations). The venue of the exam changes each time, according to a rotating system between academic pathology institutions (Basel, Bern, Geneva, Lausanne, and Zürich) and pathology departments in larger cantonal or city hospitals (Baden, Liestal, Lucerne, St. Gall, and Triemli Hospital, Zurich).

The main venue consists of a conference room with six tables on which the candidates find a diagnostic microscope as well as a collection of standard textbooks of diagnostic pathology which can be consulted freely during the slide sessions (Fig. 1). In addition, candidates are free to bring and use their own selection of textbooks for the diagnostic part of the exam, but on-line consultation of web sites is not allowed. In addition, a room with a multihead (three heads minimum) microscope has to be made available by the hosting institution for the discussion of slides between candidates and members of the exam committee. Finally, the institution that hosts the exam must assure that the candidates can examine the unfixed organs of a recent autopsy, usually in the autopsy suite (Fig. 2).

As a rule, the examination begins on a Thursday afternoon at one o'clock and ends the following day around four o'clock. Knowledge in cytopathology is first examined. For 1 hour, ten cases of gynecological and non-gynecological exfoliative and aspiration cytology are rotated between the candidates in such a way that each candidate has at least 4 minutes to examine each slide, with the possible option of reviewing selected slides once again if so wished. The best diagnosis must be chosen among five possible diagnoses in a multiple choice modus. The candidates are free to consult textbooks, just as they would do during their daily diagnostic activity. In addition, two free text questions about cytopathology have to be answered by the candidates, without the help of textbooks.

The second part of the examination covers autopsy pathology. For 3 hours, the candidates have to analyze and describe the pathological findings of three autopsy cases and formulate a final diagnostic conclusion that also integrates the pertinent clinical information. Two of the three autopsy cases are based on collections of slides (10–16 slides of the major organs), accompanied by a description of the macroscopic findings and relevant clinical information, including specific questions raised by the clinicians. For that purpose, all candidates receive one of six identical

Fig. 1 Candidates dispose of high-quality diagnostic microscopes and their proper sets of slides. The use of standard textbooks is permitted during the parts where slides are examined, but prohibited during the theoretical part with multiple choice and open questions (photo taken at the occasion of the exam in September 2011 in Lucerne, in the rooms of the Academy for Medical Training and Simulation)

Fig. 2 Autopsy exam: Candidates are asked to examine the fresh organs of a recent autopsy usually in the autopsy suite of the hosting institute and describe their macroscopic impressions, which are being transcribed by one of the examiners (photo taken at the occasion of the exam in September 2011 in Lucerne, autopsy suite of the Cantonal Institute of Pathology)

sets of slides. The third autopsy case is based on the examination of the fresh organs of a recent autopsy which are to be viewed in the local autopsy suite—along with a copy of the available clinical information and a list of specific questions to be addressed by the autopsy. For practical purposes, each of the six candidates is individually taken to the autopsy suite by two members of the exam committee. The candidate has 20 minutes to examine the organs and dictate his/her observations to one of the committee members (preferentially the one with the most readable handwriting!; Fig. 2) The candidate then returns to the examination room and writes up his/her observations, diagnoses, and final conclusions. For this part of the exam, textbooks can be freely used by the candidates. The autopsy exam terminates the first day of the examination.

The next morning starts at 8 o'clock with a 1 hour exam dedicated to macroscopic pathology. The candidates find a stack of 12 letter size high-quality color photos of "typical" macroscopic presentations of lesions in either surgical resection specimens or organs from autopsies. They have to identify the lesion, either by naming the pathological process/diagnosis (free text) or by selecting their best solution from a list of five possibilities (multiple choice). In addition, the candidates are asked to (a) draw on the illustration of the specimen in which regions they would select tissue blocks for the subsequent histological analysis and (b) indicate which auxiliary tests (i.e., special stains, immunohistochemistry, molecular pathology, other) they would like to perform in order to confirm, and/or to complement their diagnosis.

After a short pause follows a 3-hour period, during which candidates have to examine 24 histological slides and name the correct diagnosis. In the case that they are unable to come to a definite diagnosis, they have to list their differential diagnoses and state the approach they would choose to arrive at a final diagnosis (i.e., special stains, immunohistochemistry, molecular pathology, etc.). As for the cytopathology and the autopsy parts, candidates are free to use textbooks for this period, just as they would do during their daily diagnostic practice.

After the lunch break comes the theoretical part, in which 12 multiple choice and three of four free text questions have to be answered. This part of the exam is primarily intended to test the knowledge of the candidates in terms of pathophysiological concepts and novel techniques as they pertain to diagnostic anatomical pathology, but also in terms of scientific (for example: what do you have to consider when planning a biomarker study) and legal/ethical concepts (i.e., professional secret in clin–path conferences and research projects, use of human tissues for research and teaching, autopsy regulations, certification/accreditation of a diagnostic service, etc.). The candidates are asked to respond to at least three of the four free text questions, the fourth may be ignored. For this part of the examination, the use of textbooks is no longer permitted. This part of the exam also integrates an increasing number of questions related to concepts and techniques of molecular pathology.

The board examination comes to its end with a 15–30 minutes interview of each candidate separately with two members of the exam committee, around a multihead microscope. During this interview, the candidate gets a chance to review some of the cytology and histology slides that he/she had failed to correctly identify during the test, explain his/her initial line of reasoning, and propose a better solution. The members of the committee find this interview particularly helpful in getting a reliable feeling of the background knowledge of the candidates. As the distribution of points from the different parts of the exam shows (Table 1), it becomes apparent that this interview may be particularly helpful in all cases of "shaky" candidates, who have not been able, up to this point, to secure enough points in the preceding parts of the exam for a clear pass. It also gives the members of the committee quite a good idea of where the candidate stands in his/her formation, whether he/she has had so far missed out on certain aspects of his/her training (i.e., the cytology rotation), notions that will eventually help to arrive at a final

Table 1 Algorithm for point assignment for final "pass" score

Time	Test	Consisting of	Points per correct answer	Maximum
1 h	Cytology	10 slides, 2 questions	2 points per case/question	24 points
3 h[a]	Autopsy I	Autopsy, fresh organs	Case-specific distribution	16 points
	Autopsy II	Autopsy, slides	Case-specific distribution	16 points
	Autopsy III	Autopsy, slides	Case-specific distribution	16 points
1 h	Macro	12 specimen images	2 points per case	24 points
3 h	Histology	24 slides[b]	4 points per case	96 points
1 h[a]	Theory I	12 MC questions	2 points per case	24 points
	Theory II	3 free questions[c]	4 points per question	12 points
15–30 min	Interview	Multihead microscope	Individual	12 points
Total				240 points
Points needed to pass (75 %)				180 points

[a]For autopsies I–III combined

[b]The candidates are given 25 slides, of which one may be ignored

[c]The candidates are given four questions, of which one may be ignored

decision, and to council the candidate. Based on the results of the candidates in the different parts of the test, scores are assigned according to a pre-defined algorithm which is presented in Table 1.

Compared to similar tests in the USA and various European countries, the Swiss exam lasts certainly longer (2 days) and covers a wider field (cytology + autopsy + histology + macroscopy + theory). While this may be considered as a disadvantage, adding stress and hardship on the candidates who have to organize their lives (leave of absence, babysitter for children, etc.) and stay overnight in a foreign town, it does make sure that no one fails the exam simply because of bad chance with too few and over-focused questions. In that respect, the exam is designed to prevent false-negative results, i.e., failing a candidate who is competent, and to prevent false-positive results, i.e., allowing an unprepared candidate to pass unnoticed [1].

The questions and cases selected for the exam reflect the constant effort to recreate as closely as possible the real-world situation of the pathologists during their daily work dealing with a wide spectrum of simple, more challenging, and also some quite difficult cases, i.e., when they have to council clinicians about rare diagnoses and novel diagnostic techniques, and not to forget that they should be able to contribute also to academic activities. It is hence not surprising that the last few years have seen a gradual increase of questions that pertain to molecular pathology and its role in predicting the response of novel targeted treatments in an increasing number of malignant tumors. In this respect, the contents of the examination constantly adapt to changes in the postgraduate curriculum in medicine and anatomical pathology, respond for instance to a dwindling number of autopsies on one side, and an increased focus on molecular pathology on the other side. These modifications of the curriculum are currently being discussed and prepared in detail at the level of the respective professional societies and legal instances, and the exam will be modified accordingly.

History The initiative to create a professional exam in anatomical pathology goes back to the decision of the Swiss Society of Pathology (SSPath/SGPath) in the early 1990s. The scheme of the examination was first tested in 1993 with six candidates who participated on a purely voluntary basis (one of the candidates became father on the day of the exam, which was considered a positive omen for the project). In the first few years, unofficial diplomas were handed out to the candidates, stating that the candidates had passed the board examination in anatomical pathology. From 1994 on, the participation at the examination but not its passing became compulsory and only since 1996 did the successful outcome of the exam become compulsory for board certification. This was also the time when the exam was accredited by the Swiss Medical Association, Federatio Medicorum Helveticorum (FMH, the national institution that certifies medical specialties). It was only after intense discussions between members of the SSPath/SGPath and the FMH that this official institution acknowledged and accredited the board examination in anatomical pathology—and at the same time saluted the quality of the exam, its broad spectrum and the initiative of SSPath/SGPath members for mounting this exam. Today, FMH and SSPath/SGPath collaborate harmoniously in the certification of anatomical pathologists. The FMH verifies whether the candidates can document the necessary prerequisites for the board certification (i.e., a rotation through different diagnostic services, log book documenting the required minimum numbers of autopsies, histology and cytology cases, as well as frozen sections, participation in conferences and slide seminars, authorship in scientific publications, etc.). The SSPath/SGPath administers the board examination and issues a certificate of successful participation, without which no board certification will be ultimately issued by the FMH.

During the first years, the candidates also had to realize a frozen section (cutting, staining, and interpreting). In 1999, the cytology part was added to the exam and a few years later the discussion between candidates and examiners at a multi-head microscope. Over the years, failure rates have been low (5–10 %). Candidates who had failed had the chance to take the exam again, usually 6 months or 1 year after the initial exam, and so far everyone who had failed once eventually passed in the next exam for which he/she sat. Even though this has never happened in the history of the exam, the candidates are free to take the exam yet again in case they failed a second time. During the first years of the exam, a large collection of slides had been put together, and even though the collection was quite extensive, covering all aspects of anatomical pathology, candidates eventually realized that some of the cases/questions recurred and started to generate memory protocols that were then passed on to the "next generation" of candidates. This in turn did not escape the members of the exam committee who noticed that many of the more difficult cases were easily answered—if the cases had been used in an exam before. A graphic rendition of points reached in the different parts of the exam underlines this fact, where between 1999 and 2009 there was a steady and statistically significant increment of the points obtained on histological slides, while at the same time results in the autopsy and the cytology parts (which were renewed in every exam) remained at a rather constant level (Fig. 3). When in 2009 the decision was made to no longer reuse slides from the collection, the results obtained on histological slides fell to levels similar to those before the widespread distribution of "exam diagnoses." The simultaneous drop in the results obtained in the theory part of the exam reflects a change in the orientation of theoretical questions, with an increasing emphasis being placed on practical aspects of diagnostic molecular pathology—in agreement with the new spirit of the boards of anatomical pathology set

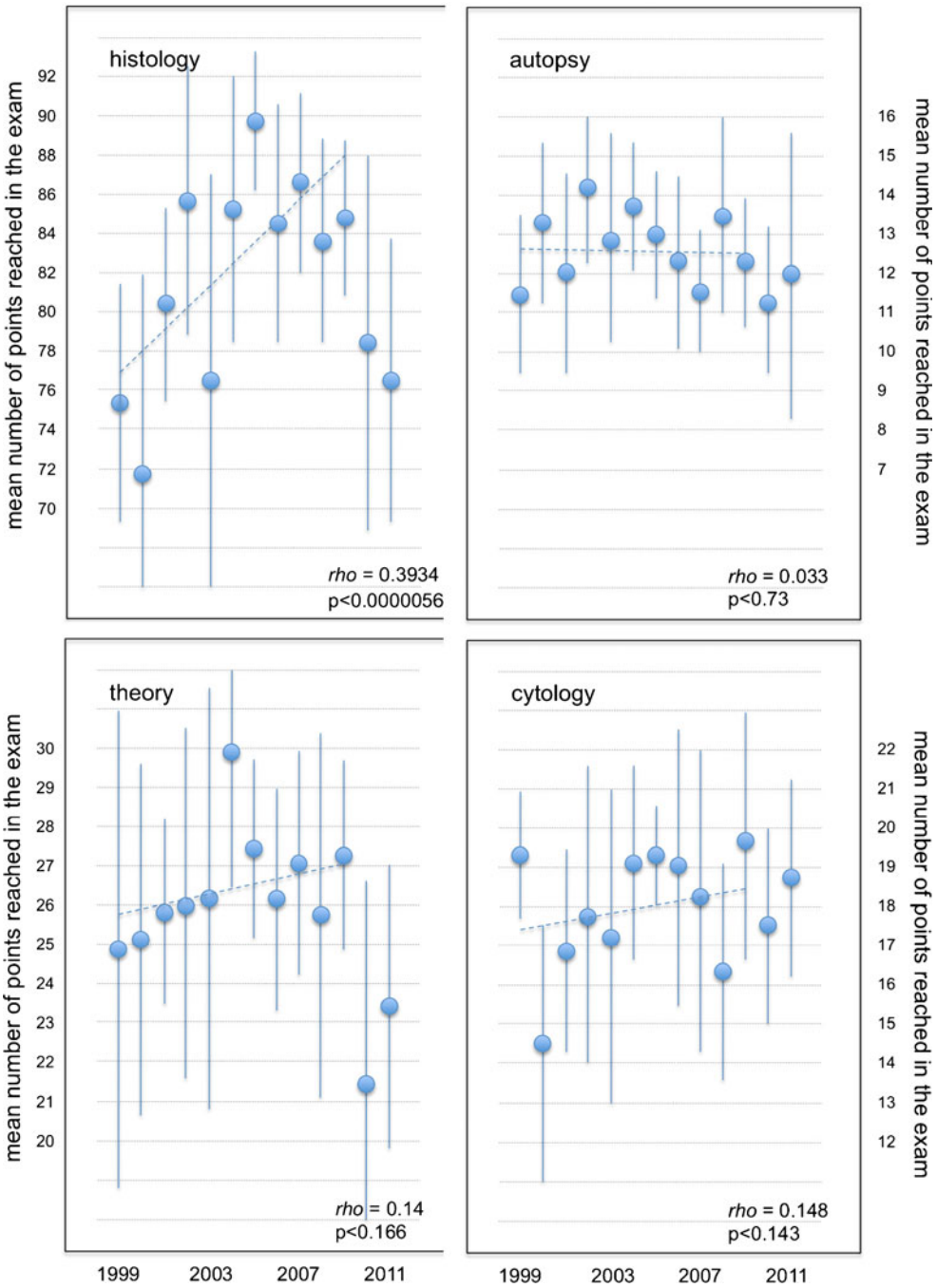

Fig. 3 Graphic rendition of points obtained by the candidates in the different parts of the exam over the past 12 years. Note that there was a significant increase from 1999 to 2009 of the results obtained in the histology part (*upper left panel*), likely due to the "tradition" of diagnoses of exam slides from one generation of candidates to the next. No such trend was observed for those parts where no "old cases" (cytology and autopsy) were being used. Note also that the results returned to "baseline" when the decision was made in 2009 to not reuse slides and theoretical questions from the exam collection that had been used in prior exams

forth by the educational committee of the SSPath/SGPath. Once the revised version of the board prerequisites, in particular the (reduced) number of autopsies, as well as surgical, and cytological cases, and the (increased) number of exams in molecular pathology (FISH and PCR), is accepted by the various instances, an increasing emphasis will be placed on the examination of molecular pathology, no longer limited to questions in the theory part of the exam (knowledge), but also in the practical part of the exam (skills).

Can a 2-day exam predict and verify if the candidates who pass the exam will be good anatomical pathologists? Certainly, it is not possible for such an exam to fully cover all aspects of the multi-faceted and complex nature of our profession. Communication skills, professional attitudes related to patient management, quality control, and error culture, as well as laboratory management, can certainly not be thoroughly tested, to name only a few examples. However, no board examination can claim to reliably test the future performance of medical professionals. In fact, Hamdy and coworkers have concluded from a thorough review of professional exams in various fields of medicine that evidence on predictors of performance in practice beyond residency training is rare

and weak [2]. Consistent with this notion, Cox has rightly stated that testing skills in an exam can at best test the prerequisites for professional performance rather than the performance itself, which includes processes and outputs in one of many practice settings [3]. The SGPath board examination in anatomical pathology tries its best to evaluate the skills and the knowledge of our future professionals. Whether or not the exam in its present design responds to this effort remains speculative. Even though we regularly ask candidates after the exam about their opinions, their mostly positive answers are likely biased by the particular situation in which they find themselves at that very moment, having just been told that the hard work of many months has been rewarded by a piece of paper with the magic word "passed."

End of service exams of professional proficiency are not mandatory in all member countries of the European Union. Based on a survey among members of countries represented in the European Section/Board of Pathology [4], all but six countries offer similar, albeit usually shorter (usually 1 day or less) and less extensive exams (often without autopsy or cytology parts). In six countries, in particular from southern Europe and Scandinavia, no end of service exams are offered. In these countries, the responsibility to verify the proficiency of former residents resides within the program director or the peer group of past and future colleagues.

Other than fulfilling a certain moral obligation towards society to verify the capacity of future professionals in anatomical pathology, the question may indeed be asked whether there is any gain to be derived from taking the exam. Since candidates are very well aware of the fact that the examination tests their knowledge and skills related to the diagnostic routine, they typically prepare for it by going over collections of slides, either alone or in study groups with one or several colleagues, and by reviewing quite a bit more than usual the existing diagnostic literature (i.e., pathology journals and recent textbooks). This preparation may in itself be considered as a clear advantage, and some former candidates have stated that they have never been more "fit" in pathology than during the preparation for the exam.

Acknowledgments The authors of this manuscript have either functioned as presidents and/or elected members of the standing exam committee for periods of usually 4–5 years and/or contributed in a substantial way to the exam and to this manuscript. They would like to acknowledge the excellent assistance and support by the secretaries of the presidents of the exam committee, Ghislaine Perriard and Murielle Barman in Lausanne, Doris Manca in Neuchâtel, as well as Brigitte Terrier in Zürich.

Conflict of interest Neither the presidents nor the elected members of the examination committee are paid for their activities, except for their travel costs to the exam venues, which are reimbursed by the SGPath. The price paid by the candidates for the examination is currently CHF 450.00 (reduced fee of CHF 300.00 for members of the SGPath), which is being used for travel expenses for the examiners, the rental of microscopes, and other expenses linked to the exam.

References

1. Van der Vleuten C (2000) Validity of final examinations in undergraduate medical training. BMJ 321:1217–1219
2. Hamdy H, Prasad K, Anderson MB, Scherpbier A, Williams R, Zwierstra R, Cuddihy H (2006) BEME systematic review: predictive values of measurements obtained in medical schools and future performance in medical practice. Med Teach 28:103–116
3. Cox K (2000) Examining and recording clinical performance: a critique and some recommendations. Educ Heal 13:45–52
4. Bosman FT, van den Tweel JG (2009) Unison or cacophony: postgraduate training in pathology in Europe. Virchow's Arch 454:497–503

Virchows Arch (2012) 461:93–98
DOI 10.1007/s00428-012-1261-8

CASE REPORT

Polymorphic lymphoid proliferations occurring in HIV-positive patients: report of a case responding to HAART

Jenny Buxton · Clifford Leen · John R. Goodlad

Received: 27 March 2012 / Revised: 1 June 2012 / Accepted: 4 June 2012 / Published online: 17 June 2012
© Springer-Verlag 2012

Abstract Epstein–Barr virus (EBV)-associated polymorphic lymphoid proliferations resembling polymorphic post-transplant lymphoproliferative disorders are a rare but recognised complication of the human immunodeficiency virus (HIV). These account for fewer than 5 % of HIV-associated lymphomas, and little information has been published regarding their treatment and outcome. Of the reported cases, many have presented with extranodal disease, not typical of lymphoma. We report the case of a patient presenting with lung infiltrates shown to be the result of an EBV-associated polymorphic lymphoproliferation resembling a polymorphic post-transplant lymphoproliferative disorder. The patient was simultaneously found to be HIV positive and commenced on highly active antiretroviral therapy. Without any specific antineoplastic treatment, the patient recovered completely and within 20 months had no symptoms or radiological evidence of a lymphoproliferative disorder. This illustrates the importance of recognising this uncommon condition in HIV-positive patients and avoiding potentially unnecessary chemotherapy.

J. Buxton (✉)
Department of Haematology, Western General Hospital,
Crewe Road South,
Edinburgh EH4 2XU, UK
e-mail: j.buxton@nhs.net

C. Leen
Regional Infectious Diseases Unit, Western General Hospital,
Edinburgh, UK

J. R. Goodlad
Department of Pathology, Western General Hospital,
Edinburgh, UK

Keywords Immunodeficiency-associated lymphoproliferative disorder · Post-transplant lymphoproliferative disorder · Human immunodeficiency virus (HIV) · Epstein–Barr virus (EBV) · Antiretroviral therapy

Introduction

The risk of developing a lymphoproliferative disorder is increased with immunosuppression of any cause, whether congenital, acquired through infection with the human immunodeficiency virus (HIV) or iatrogenic following solid organ transplant, stem cell transplant or immunosuppression for autoimmune disorders [1]. Although the relative risks vary between subtypes and have altered since the introduction of highly active antiretroviral therapy (HAART), the incidence of lymphoma in HIV-positive patients is increased by between 60 and 200 times [2, 3]. In the most recent World Health Organisation classification, HIV associated lymphoproliferations are separated into three groups: (1) lymphomas also occurring in immunocompetent patients such as Burkitt lymphoma, diffuse large B-cell lymphoma, primary central nervous system (CNS) lymphoma and Hodgkin lymphoma; (2) lymphomas more specifically seen in HIV-positive patients, including primary effusion lymphoma, plasmablastic lymphoma and lymphoma arising in human herpes virus 8 (HHV8)-associated multicentric Castleman's disease and (3) lymphoproliferations occurring in HIV but also seen in other immunodeficient states [2]. Clinically aggressive B-cell neoplasms, indistinguishable from those seen in immunocompetent patients, are by far the most common HIV-associated lymphomas [1, 3]. The current case is an example of the third group of much less frequently encountered and rarely reported polymorphic lymphoid proliferations associated with HIV infection.

Clinical history

A 42-year-old Zimbabwean lady presented with a short history of weight loss and general malaise. Two years previously, she had been successfully treated for pulmonary tuberculosis with a standard 6 month course of quadruple therapy resulting in complete resolution of all chest X-ray abnormalities and symptoms. On this occasion, her chest X-ray showed new bilateral nodular interstitial shadowing (Fig. 1), and a high-resolution CT confirmed widespread pulmonary parenchymal nodules. A presumptive diagnosis of miliary TB was made, but the patient's condition continued to deteriorate despite 4 weeks of quadruple anti-tuberculous therapy. It was at this stage she was found to be HIV positive [HIV ribonucleic acid (RNA) 278 481 copies/ml, CD4 count 57 cells/mm^3]. An initial transbronchial lung biopsy proved nondiagnostic, but a subsequent video-assisted thoracoscopic lung biopsy provided the diagnosis of an Epstein–Barr virus (EBV)-associated polymorphic lymphoid proliferation resembling a polymorphic post-transplant lymphoproliferative disorder (PTLD). Staging studies, including repeat CT and bone marrow, showed no other evidence of lymphoma. Serum EBV polymerase chain reaction (PCR) was positive at log 5.68 copies/ml. HAART was commenced with good effect. Within 1 month the $CD4^+$ count had risen to 388 cells/mm^3; the serum EBV PCR titre was undetectable, and the HIV viral load was falling, reaching <40 copies/ml 8 months later. By 20 months the chest X-ray was reported as normal and 4 years after diagnosis the patient remains well with no evidence of a lymphoproliferative disorder. $CD4^+$ count is 472 cells/mm^3, and HIV viral load is <40 copies/ml.

Materials and methods

The lung biopsy consisted of a wedge of tissue measuring 40×20×15 mm. This was fixed in 10 % buffered formalin, paraffin-embedded and 4-μm sections cut for routine haematoxylin and eosin staining in addition to sections for immunohistochemical (IHC) analysis.

Immunohistochemistry

IHC labelling was performed using the automated 'Bondmax' system (Leica Microsystems, Wetzlar, Germany), and the following antibodies were applied to sections: CD20, CD79a, Bcl-2, Epstein–Barr virus nuclear antigen 2 (EBNA 2), latent membrane protein 1 (LMP-1), CD138, kappa and lambda light chains (all DAKO, Cambridgeshire, UK); CD5, CD10, CD23, Bcl-6, HHV8 (Leica Biosystems, Newcastle upon Tyne, UK) and cyclin D1 (Thermo Scientific, Waltham, USA). Antigen retrieval for all antibodies was achieved using ethylenediaminetetraacetic acid with the exception of CD20 for which sodium citrate was used. The presence of Epstein–Barr virus-encoded RNAs (EBERs) was investigated using in situ hybridisation (ISH) on formalin-fixed paraffin-embedded sections with EBERs which were supplied in a kit complete with anti-fluoroscein antibody, RNA negative control probe and EBER probe (Leica Biosystems).

Polymerase chain reaction

DNA was extracted from 10-μm sections of formalin-fixed paraffin-embedded tissue, by incubating overnight with Qiagen lysis buffer (Qiagen, Crawley, UK) and proteinase K. DNA was then purified using the automated 12GC magtration system (Precision System Science, California, USA) and amplified using MasterMix with HotStar Taq polymerase (Qiagen) on a Peltier Thermal Cycler (Genetic Technologies, Miami, USA). The following Identiclone primers were applied: IGH, tubes A-E targeting framework 1, 2 and 3 regions and the diversity and joining regions of the

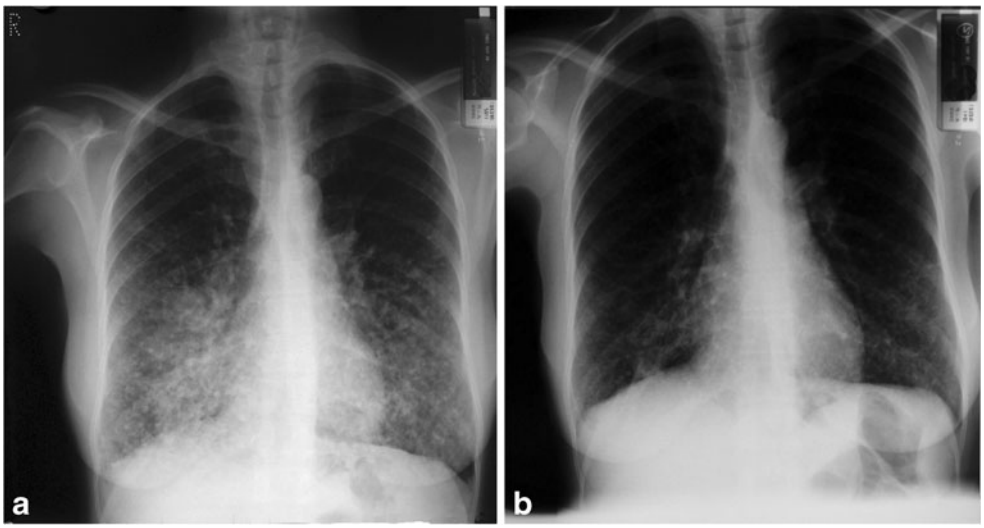

Fig. 1 Chest X-ray appearances before and after treatment with HAART. **a** Nodular interstitial infiltrate seen at presentation. **b** Clearing of lung fields at 12 months

immunoglobulin heavy chain gene; IGK, tubes A and B targeting the variable and joining regions, JK-CK intron and Kde regions of the immunoglobulin Kappa light chain gene and IGL targeting the V lambda and J lambda region of the immunoglobulin lambda light chain gene (Invivoscribe, San Diego, USA). Samples were then processed through a capillary electrophoresis system with laser detection of fluorescently labelled nucleic acids (3130 Genetic Analyser) and results analysed using GeneMapper software (both Applied Biosystems, California, USA).

Results

Haematoxylin and eosin-stained sections showed a dense lymphoid infiltrate forming large interstitial nodules and in places replacing the adjacent lung parenchyma (Fig. 2a). The infiltrate consisted of plasma cells, lymphoplasmacytoid cells, small lymphocytes, scattered immunoblasts, histiocytes and occasional eosinophils (Fig. 2b). In places, the polymorphic infiltrate was seen to surround ill-defined residual germinal centres. Most of the blasts and many of the lymphocytes and lymphoplasmacytoid cells were positive with the B-cell markers CD20 and CD79a (Fig. 2c). They also expressed Bcl-2 but were negative for CD5, CD10, CD23, Bcl-6 and cyclin D1. Immunohistochemistry for LMP-1 and EBNA 2 were negative, but ISH for EBER was positive in a moderate number of small and large lymphocytes (Fig. 2d). Immunohistochemistry for HHV8 was negative. Plasma cells expressed CD79a and CD138. Light chain expression was polytypic (Fig. 2e, f), but a small B-cell clone was demonstrable by PCR (Fig. 3). A diagnosis of EBV-associated polymorphic lymphoid proliferation resembling a polymorphic post-transplant lymphoproliferative disorder was made.

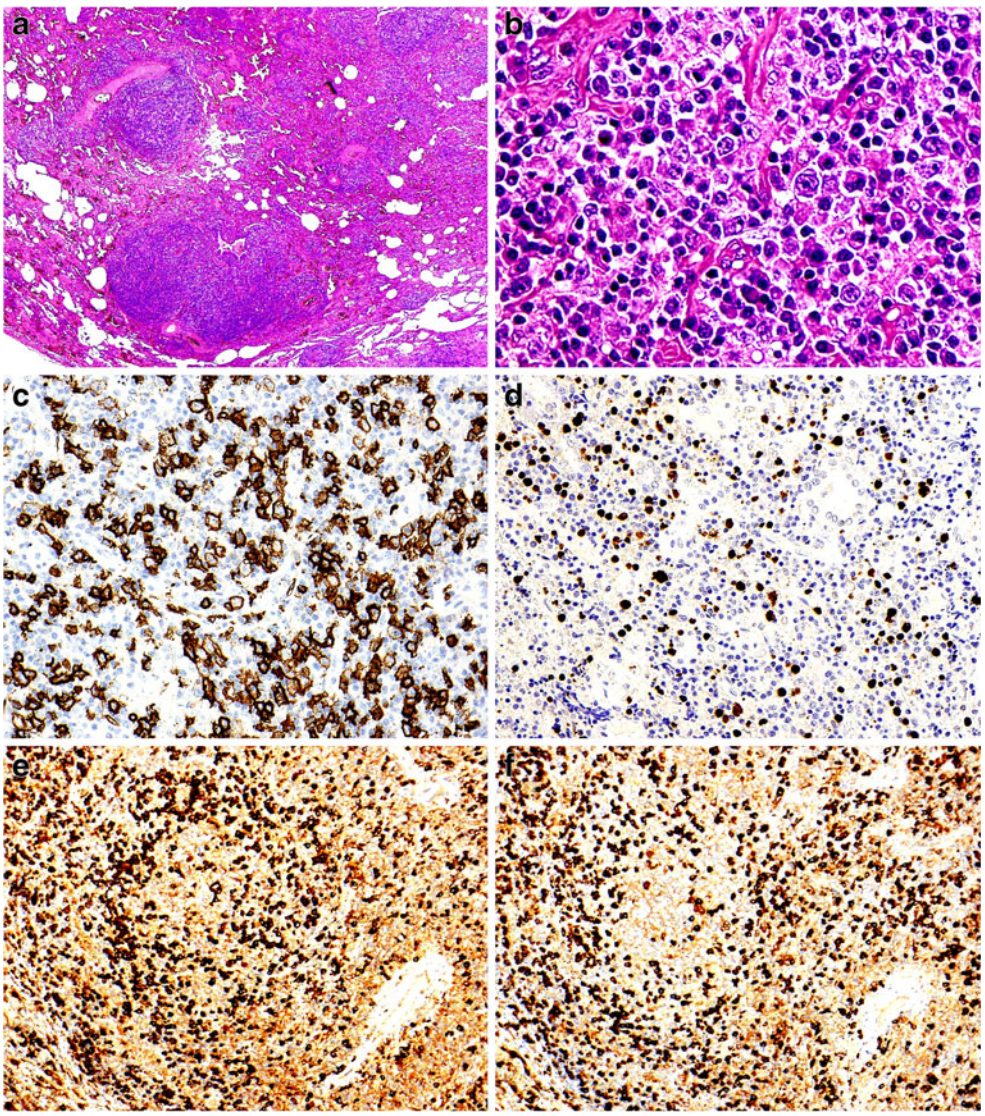

Fig. 2 Pathological features of pulmonary infiltrate. **a** Low-power view showing nodular interstitial lymphoid infiltrate. **b** Higher power view showing polymorphic nature of infiltrate with blasts, small lymphocytes and plasma cells. **c** Anti-CD20 immunostain. **d** In situ hybridization for EBER. **e** Light chain immunohistochemistry; kappa. **f** Light chain immunohistochemistry; lambda

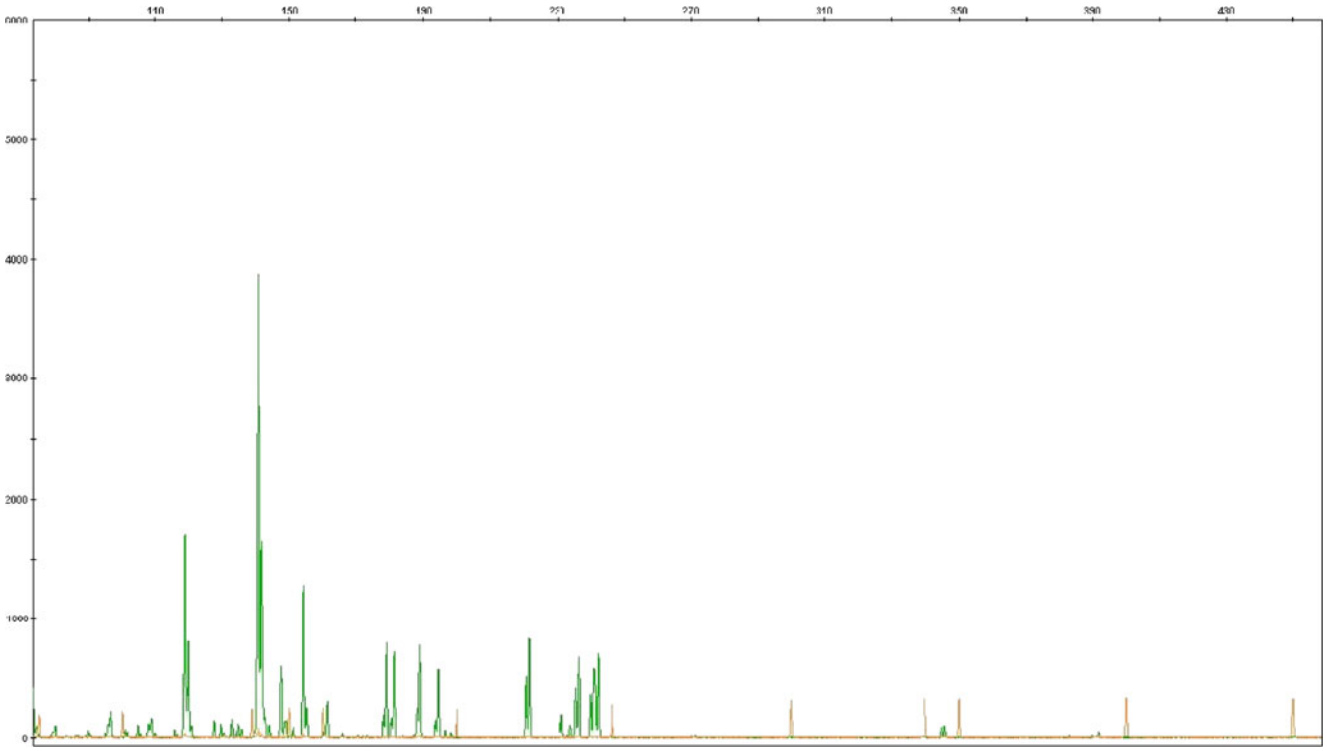

Fig. 3 BIOMED 2 PCR Genescan showing minor peak of 141 base pairs with DH-JH primers. PCR with primers for framework 1 and framework 2 regions could not be analysed due to poor DNA quality

Discussion

Most HIV-associated lymphoproliferations are clinically aggressive monoclonal B-cell lymphomas. These include primary effusion lymphoma, plasmablastic lymphoma and lymphoma arising in HHV8-associated multicentric Castleman's disease, as well as lymphomas similar to those occurring in immunocompetent patients, e.g. Burkitt lymphoma, diffuse large B-cell lymphoma and Hodgkin lymphoma [1, 3]. This case represents an EBV-associated polymorphic lymphoid proliferation resembling those more often encountered in transplant recipients [1, 4–8]. Such lymphoproliferations include early infectious mononucleosis (IM)-like PTLDs and polymorphic PTLDs, entities that show overlapping pathological features and represent closely related points on a continuous spectrum of disease. Effacement of underlying architecture and the presence of clonally rearranged immunoglobulin genes are the two main distinguishing criteria for polymorphic PTLD-like lymphoproliferations [2] and hence this designation was favoured. However, we accept that the architectural effacement was relatively minor and that small clones can rarely be encountered in early IM-like PTLDs [2]. Although polymorphic PTLDs constitute a relatively high proportion of the lymphoid proliferations in transplant patients, they have only rarely been reported in association with HIV infection and there is relatively little information on the response to treatment and prognosis [1, 2, 4–8].

Including the current patient, a total of 17 cases of HIV-associated polymorphic lymphoproliferations have been reported, including both adult and paediatric examples, with an excess of male patients (11 male to 6 female) [1, 4–8]. The majority of cases (11 out of 17) have presented at extranodal sites, including the lung (n=5), parotid gland (n=1), perineum (n=1), skin (n=1), stomach (n=1), terminal ileum (n=1) and CNS (n=1) [1, 4–8]. The histological features described in this case are similar to those described in previous reports, lesions being characterized by a polymorphic infiltrate of B cells showing all stages of maturation from immunoblasts to plasma cells, admixed with relatively numerous T cells. Cytological atypia may also be present, including immunoblasts reminiscent of Reed–Sternberg cells, and areas of necrosis have been reported [1, 4–8]. EBV is usually, but not always, present (13 out of 17 cases), and HHV8 has been identified in 1 of the 12 cases tested to date [1, 4–8].

Although the current case was polyclonal by light chain immunohistochemistry, a small B cell clone was demonstrable, by PCR, against a polyclonal background. Ten of the other 14 cases assessed by PCR and/or Southern blot analysis also showed evidence of a dominant B-cell clone, usually manifesting small peaks or faint positive bands, with only 4 cases being reported as polyclonal or oligoclonal [1, 4–8]. These findings suggest HIV-associated polymorphic lymphoproliferations represent the 'earliest' end of a spectrum

of lymphomas arising in HIV-positive patients. As a consequence of immunosuppression, a dominant clone evidently emerges from a polyclonal, usually EBV-stimulated, chronic lymphoproliferation. They appear to lack oncogene and tumour suppressor gene mutations, unlike most other AIDS-related systemic non-Hodgkin lymphoma, but can evolve into high-grade lymphoma, when they may be seen to have acquired such mutations [1].

Information regarding treatment and outcome for polymorphic HIV-associated lymphoproliferations is very limited. Follow-up details were only available for three of the patients described by Nador and colleagues. One received no treatment and died of disease at 5 months. Two received chemotherapy: one patient dying at 28 months with no evidence of disease and the other remaining alive but with disease recurrence at 7 months. The nature of chemotherapy was not stated in either case [1]. The case of Wang et al. died at 4 months but appeared to receive no treatment and had a concomitant high-grade B-cell lymphoma [7]. The two paediatric cases of Tao et al. had differing outcomes. One responded to a combination of zidovudine (nucleoside analogue reverse transcriptase inhibitor), nelfinavir (protease inhibitor) and intravenous immunoglobulin, and was stable 8 months after presentation, whilst the other received pentamidine, ceftriaxone and nelfinavir, but died of multiorgan failure just 7 weeks after presentation [4]. Kingma et al. also reported a paediatric HIV-associated polymorphic lymphoproliferation this time affecting the CNS. The patient was treated with steroids and antiretroviral therapy (zidovudine and didanosine, reverse transcriptase inhibitor) but subsequently developed cytomegalovirus retinitis and progressive HIV-associated encephalopathy, dying 10 months after diagnosis [6]. Our case, and that described by Fujito and colleagues, provides more encouraging observations. Both patients achieved complete remission following initiation of HAART [albeit the latter also received one course of CHOP-like chemotherapy (cyclophosphamide, doxorubicin, vincristine, prednisolone)] and remained in complete remission at 48 and 20 months, respectively [5]. Although fewer details are given, the case reported by Martin et al. also suggests at least partial resolution with antiretrovirals [8].

The widespread introduction of HAART in the mid-1990s resulted in fewer HIV-positive patients developing lymphoma, although this was not universal for all subtypes [3, 9]. More recently, HAART has also been recognised as a key component of treatment for established cancers in HIV-positive patients. For example, in primary CNS lymphoma, patients treated with HAART plus whole brain irradiation and chemotherapy do significantly better than those given chemo-radiotherapy alone [3, 10]. This certainly holds true for those patients who have a good response to antiretrovirals, with increases in $CD4^+$ counts and reductions in HIV viral load [11], but there is increasing evidence that HAART itself may have a direct antitumour effect independent of its immunomodulatory functions. For instance, in Kaposi's sarcoma, a high rate of complete tumour regression is seen in patients treated either with HAART alone or with HAART in combination with chemotherapy, but complete remission does not consistently correlate with a reduction in HIV viral load or increase in $CD4^+$ count [12].

Conclusion

Although uncommon, polymorphic lymphoproliferations are an important differential diagnosis to consider in HIV-positive patients who present with unusual signs and symptoms, especially those not responsive to antimicrobial treatment. It is imperative to appreciate that, even when dominant clonal B-cell populations are present, there is the potential for complete resolution with antiretroviral treatment alone, and anti-neoplastic chemotherapy may not be appropriate. Our patient achieved a good response to HAART with restoration of $CD4^+$ counts and a reduction in HIV viral load to undetectable levels. Improving immune surveillance certainly appears to be key in reversing EBV-driven lymphoproliferative disorders such as described here, but whether HAART may have additional, more direct antiproliferative effects is also of interest and merits further study.

Conflicts of interest The authors declare that they have no conflict of interest.

Funding sources None.

References

1. Nador RG, Chadburn A, Gundappa G et al (2003) Human immunodeficiency virus (HIV)-associated polymorphic lymphoproliferative disorders. Am J Surg Pathol 27(3):293–302
2. Raphael M, Said J, Borisch B et al (2008) Immunodeficiency-associated lymphoproliferative disorders. In: Swerdlow SH, Campo E, Harris NL et al (eds) WHO classification of tumours of haematopoietic and lymphoid tissues, 4th edn. International Agency for Research on Cancer, Lyon, pp 335–352
3. Grogg KL, Miller RF, Dogan A (2007) HIV infection and lymphoma. J Clin Pathol 60:1365–1372
4. Tao J, Valderrama E (1999) Epstein–Barr virus-associated polymorphic B-cell lymphoproliferative disorder in the lungs of children with AIDS: a report of two cases. Am J Surg Pathol 23(5):560–566
5. Fujita H, Nishikori M, Takaori-Kondo A et al (2010) A case of HIV-associated lymphoproliferative disease that was successfully treated with highly active antiretroviral therapy. Int J Hematol 91:692–698
6. Kingma DW, Mueller BU, Frekko K et al (1999) Low-grade monoclonal Epstein–Barr virus associated lymphoproliferative disorder of the brain presenting as human immunodeficiency virus-associated encephalopathy in a child with acquired immunodeficiency syndrome. Arch Pathol Lab Med 123:83–87

7. Wang X, Nathan S, Catchatourian R, Richter H III, Kovarik P (2007) Polymorphic lymphoid proliferation presenting as ileocecal intussusception. Ann Hematol 86:453–454
8. Martin SI, Zukerberg L, Robbins G (2005) Reactive Epstein–Barr virus-related polyclonal lymphoproliferative disorder in a patient with AIDS. Clin Infect Dis 41:e76–e79
9. Gucalp A, Noy A (2009) Spectrum of HIV lymphoma. Curr Opin Hematol 17:362–367
10. Hoffmann C, Wolf E, Fatkenheuer G et al (2003) Response to highly active antiretroviral therapy strongly predicts outcome in patients with AIDS-related lymphoma. AIDS 17:1521–1529
11. Oppenheim S (2009) Prognosis in HIV-associated malignancies #214. J Palliat Med 12(9):835–836
12. Monini P, Sgadari C, Toschi E et al (2004) Antitumour effects of antiretroviral therapy. Cancer 4:861–875

Virchows Arch (2012) 461:99–101
DOI 10.1007/s00428-012-1253-8

LETTER TO THE EDITOR

Urothelial carcinoma with abundant myxoid stroma: evidence for mucus production by cancer cells

Magdalena M. Gilg · Birgitta Wimmer · Arthur Ott · Cord Langner

Received: 14 March 2012 / Accepted: 11 May 2012 / Published online: 26 May 2012
© Springer-Verlag 2012

Dear Editor,

Urothelial carcinoma has a propensity for aberrant differentiation, with squamous and glandular being the most common histological variants [1]. Notably, divergent differentiation occurs more frequently in high-grade and high-stage tumours [2]. Recently, urothelial carcinoma with abundant myxoid stroma has been identified as a new histological variant [3]. The origin of stromal mucin, however, is currently unclear.

A 66-year-old male with history of gastric signet ring cell carcinoma presented with haematuria and unspecific lower abdominal pain. Cystoscopy disclosed a polypoid lesion, measuring 3 cm in largest diameter, which extended from the bladder wall into the lumen and was removed by transurethral resection.

Histology revealed non-invasive papillary urothelial low-grade carcinoma with mild architectural and cytologic atypia. Parts of the lesion showed infiltration of the lamina propria by high-grade cancer cells. The most striking morphological feature was an abundant myxoid stroma which covered approximately 30 % of the lesion. Notably, mucin production was evident also in non-invasive cancer areas, as documented by the presence of intercellular mucin leading to a cord-like and ultimately microcystic pattern (Fig. 1a–c). Neoplastic glandular epithelium was not observed. Histochemical stains for Alcian blue and PAS showed positivity of extracellular mucinous material, but reactivity was also observed within the cytoplasm of cancer cells (Fig. 1d–e). Upon immunohistochemistry, the tumour cells were positive for p63, keratin 7 and 20, E-cadherin, MUC1, MUC2 and MUC5AC (Fig. 1f–h). Electron microscopy performed on formalin-fixed, paraffin-embedded material disclosed non-membrane-bound cytoplasmatic globules, consistent with mucus droplets (Fig. 2).

Prominent myxoid stroma has been described as pseudosarcomatous stroma reaction associated with urothelial carcinoma and as sarcomatoid urothelial carcinoma. Recently, Tavora et al. [3] introduced the term "urothelial carcinoma with abundant myxoid stroma" for otherwise typical urothelial tumours showing marked extracellular mucin deposition which should not be confused with primary or secondary adenocarcinoma of the bladder as well as benign lesions, such as cystitis glandularis with intestinal metaplasia, endocervicosis and villous adenomas [3, 4]. Although their series was small and follow-up limited, the authors suggested that this new variant might be less aggressive compared to conventional urothelial carcinoma. Most probably, Cox et al. [5] described the same tumour variant under the name "invasive urothelial carcinoma with chordoid features". Their tumours were similarly characterized by prominent myxoid stroma and intercellular mucin deposition, leading to cord-like epithelial architecture and microcystic pattern, as was also shown for our case.

According to Tavora et al. [3], the origin of mucin is unclear, particularly in the absence of overt glandular epithelium. Our case, however, clearly shows mucin production by otherwise typical urothelial cancer cells in both invasive and non-invasive tumour areas. This finding illustrates the capacity of urothelial cancer cells to show divergent, i.e. aberrant mucinous differentiation. In our opinion,

M. M. Gilg · B. Wimmer · A. Ott · C. Langner (✉)
Institute of Pathology, Medical University of Graz,
Auenbruggerplatz 25,
8036 Graz, Austria
e-mail: cord.langner@medunigraz.at

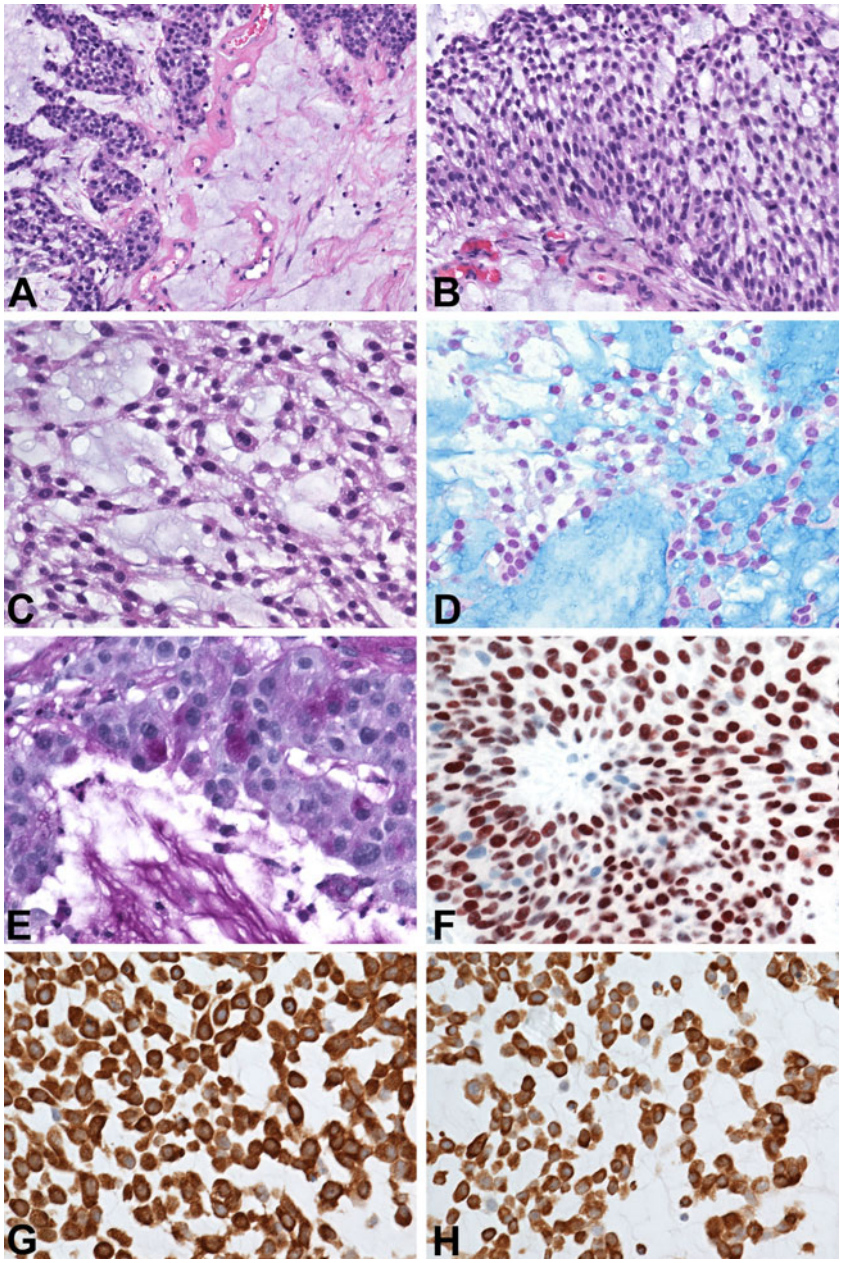

Fig. 1 Urothelial carcinoma with abundant myxoid stroma (**a**); note intercellular mucin deposition in non-invasive tumour areas (**b**), ultimately leading to cord-like epithelial architecture with microcystic pattern (**c**). The mucinous material is Alcian blue positive (**d**). PAS stain shows positivity of mucin but also decorates the cytoplasm of adjacent cancer cells (**e**). The neoplastic cells are positive for p63 (**f**), MUC1 (**g**), and MUC 2 (**h**)

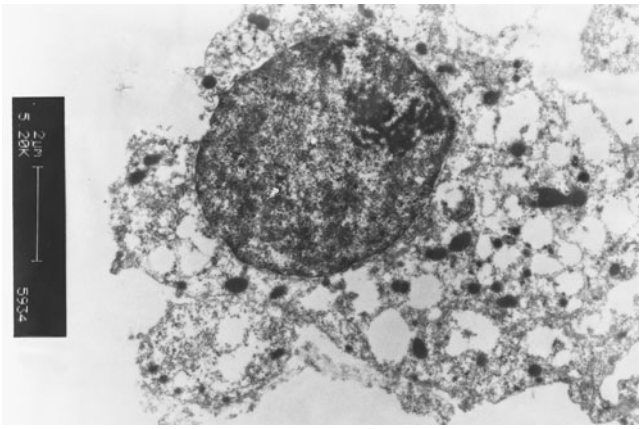

Fig. 2 Electron microscopy performed on formalin-fixed, paraffin-embedded material shows tumour cells with non-membrane-bound cytoplasmatic globules, consistent with mucus droplets (original ×5,200)

the term "mucinous urothelial carcinoma" would better characterize the lesion.

In conclusion, we present a new case of urothelial carcinoma with abundant myxoid stroma and prove the urothelial cancer cells to be the source of mucin. The term "mucinous urothelial carcinoma" might therefore better characterize this peculiar tumour variant.

Conflict of interest We declare that we have no conflict of interest.

References

1. Amin MB (2009) Histological variants of urothelial carcinoma: diagnostic, therapeutic and prognostic implications. Mod Pathol 22:S96–S118
2. Langner C, Hutterer G, Chromecki T, Rehak P, Zigeuner R (2006) Patterns of invasion and histological growth as prognostic indicators in urothelial carcinoma of the upper urinary tract. Virchows Arch 448:604–611
3. Tavora F, Epstein JI (2009) Urothelial carcinoma with abundant myxoid stroma. Hum Pathol 40:1391–1398
4. Molavi D, Argani P (2008) Distinguishing benign dissecting mucin (stromal mucin pools) from invasive mucinous carcinoma. Adv Anat Pathol 15:1–17
5. Cox RM, Schneider AG, Sangoni AR, Clingan WJ, Gokden N, McKenney JK (2009) Invasive urothelial carcinoma with chordoid features: a report of 12 distinct cases characterized by prominent myxoid stroma and cordlike epithelial architecture. Am J Surg Pathol 33:1213–1219

Virchows Arch (2012) 461:103–107
DOI 10.1007/s00428-012-1259-2

ORIGINAL ARTICLE

Neuroendocrine differentiation does not have independent prognostic value in conservatively treated prostate cancer

S. S. Jeetle · G. Fisher · Z. H. Yang · E. Stankiewicz · H. Møller · C. S. Cooper · J. Cuzick · D. M. Berney · on behalf of The Trans-Atlantic Prostate Group

Received: 24 January 2012 / Revised: 10 May 2012 / Accepted: 28 May 2012 / Published online: 6 July 2012
© Springer-Verlag 2012

Abstract In vitro studies have implicated neuroendocrine differentiation in the development of hormone resistant prostate cancer following administration of androgen blockers. Studies on clinical material are equivocal. We wished to understand the significance of neuroendocrine differentiation in our large and well-characterised cohort of clinically localised prostate cancer, treated conservatively. Immunohistochemical expression of chromogranin-A was assessed semi-quantitatively on tissue samples of 806 patients in a tissue microarray approach. The correlation of expression with 10-year prostate cancer survival was examined. Multivariate analysis including contemporary Gleason score was performed and sub-group analysis of early hormone treated patients was also undertaken. Chromogranin-A expression correlated with high Gleason score (χ^2=28.35, p<0.001) and early prostate cancer death (HR=1.61, 95 %CI=1.15–2.27, p<0.001). In univariate analysis, NE differentiation correlated significantly with outcome (HR=1.61, 95 % CI 1.15-2.27, p<0.001) However in multivariate analysis including Gleason score, chromogranin-A expression was not an independent predictor of survival (HR=0.97, 95 %CI=0.89–1.37, p=0.87). Although chromogranin-A expression was higher in patients with early hormone therapy (χ^2=7.25, p=0.007), there was no association with prostate cancer survival in this sub-group (p=0.083). Determination of neuroendocrine differentiation does not appear to have any bearing on the outcome of prostatic carcinoma and does not add to the established prognostic model.

Keywords Chromogranin · Biomarker · Outcome · Gleason

S. S. Jeetle · E. Stankiewicz · D. M. Berney (✉)
Department of Molecular Oncology, Barts Cancer Institute,
Charterhouse Square,
London EC1M 6BQ, UK
e-mail: d.berney@bartshealth.nhs.uk

G. Fisher · Z. H. Yang · J. Cuzick
Centre for Cancer Prevention, Wolfson Institute of Preventive Medicine, Queen Mary University of London,
Charterhouse Square,
London, UK

H. Møller
Thames Cancer Registry, Kings College London,
London, UK

C. S. Cooper
Male Urological Cancer Research Centre,
Institute of Cancer Research,
Surrey, UK

Introduction

A particular characteristic of carcinoma of the prostate is the inevitable development of an androgen-resistant phenotype in what is, in its initial stages, an exquisitely hormone-sensitive tumour. A mechanism to explain this phenomenon has been proposed which involves up-regulation of the signalling via neuroendocrine cells. Neuroendocrine (NE) cells, which are interspersed among basal cells and luminal epithelial cells, do not possess androgen receptors [1, 2]. Instead, signal transduction is performed with the release of various non-androgenic chemical messengers including chromogranins, bombesin, neuron-specific enolase and synaptophysin. Chromogranin-A, in particular, has been demonstrated to be the best marker of neuroendocrine differentiation [3, 4]. In the normal prostate gland, the cells are thought to be important in normal prostate development and control of secretory functions through autocrine and paracrine signalling mechanisms [5].

Gleason score [6, 7], tumour stage [7] and serum PSA [7] remain the best contemporary markers for prediction of outcome in prostatic carcinoma. However, this is suboptimal

[8, 9] and additional parameters which can improve on projections of mortality would greatly facilitate management of the disease, especially before treatment decisions are made.

Various molecular in vitro studies [10–18] have been able to implicate neuroendocrine signalling mechanisms in the development of hormone resistant prostate cancer but extrapolation to resection specimens and translational material has not yielded conclusive results.

It has been proposed in previous studies [19–24] that quantification of neuroendocrine differentiation in prostatic pre-treatment material might be useful in: (1) identifying aggressive disease which might be less sensitive to androgen deprivation therapy, (2) identifying those tumours that may develop androgen insensitivity more quickly and (3) understanding local signalling mechanisms mediated by neuroendocrine cells.

The Trans-Atlantic Prostate Group was formed to retrospectively investigate the behaviour of clinically localised prostate cancer in patients who had been conservatively treated, together with contemporary Gleason score and baseline PSA. Translational material from this resource remains the largest series of prostate cancers, treated conservatively and with all contemporaneous prognostic information available.

We hypothesised that increasing NE differentiation implies poor prognosis and its assessment could be helpful in deciding on treatment options in localised prostate cancer.

Patients and methods

The details of cohort assembly have been described previously [8]. In brief, patients diagnosed with histologically proven, localised prostate cancer between 1990 and 1996 were identified, by searching through six UK cancer registries. Exclusion criteria were: age older than 76 years; no baseline PSA or baseline PSA>100 ng/ml; invasive carcinoma within 5 years before diagnosis, or hormone treatment before biopsy. Patients were also excluded when they had undergone radical treatment within 6 months of diagnosis (hormonal treament was acceptable), when there was evidence of metastasis or they had died within 6 months of diagnosis. This was a pragmatic method to ensure that patients truly had localised disease. The patients were managed conservatively: approximately a third of patients were managed with early hormone manipulation and the rest were observed until clinically symptomatic. The primary endpoint was defined as death from prostate cancer. Where available, death certificates were reviewed to verify cause of the death and survival outcomes were determined from medical records and cancer registry data. In all, details on 1,656 patients were retrieved and prognostic tables were constructed after 10 years of follow up. Tissue from these cases was also obtained and Gleason scores were re-assessed [25] to modern criteria [26].

Carcinoma which was diagnosed on trans-urethral resection of the prostate (TURP) tissue was microarrayed into 24 wax blocks. Generally, one to three tissue cores of 0.6 mm diameter were taken from each formalin-fixed donor block and were transferred into a new recipient wax block. Sections cut from the tissue microarray (TMA) blocks were immunohistochemically stained for chromogranin-A (BioGenex-clone LK2H10, San Ramon, California) at a dilution of 1/3,000 and then counterstained with haematoxylin. Antigen retrieval was performed by pressure cooking in citrate buffer at pH 6.0 for 30 min. Colon and appendix mucosa served as positive controls, highlighting neuroendocrine cells. The tissue microarray without primary antibody incubation was used as negative control. Chromogranin-A was chosen as a marker of neuroendocrine differentiation as it has been shown to be the most reliable of available immunohistochemical markers [27], it is used extensively in routine histopathology practice, the staining protocol is reliable and it is been used extensively in other studies investigating neuroendocrine differentiation in prostate cancer.

Chromogranin-A expression was analysed in a semi-quantitative manner using a Leica DM2500 microscope (Leica, Germany) at ×200 power. The percentage of epithelial cells expressing chromogranin-A throughout the core was assessed between 0 and 100 % and the intensity of the staining was assessed as follows: 0, no staining; 1, weak; 2, medium; and 3, strong staining. The product of percentage expression and intensity gave a final composite score (CS) between 0 and 300. Staining was restricted to the cytoplasm of epithelial cells only. Scoring was performed by a single pathologist (S.J.) and supervised by a senior pathologist (D.M.B.)

The maximum CS was considered as representative of the tumour. The correlation of CS with demographics and tumour characteristics, including Gleason score, was examined (using the χ^2 test and Fisher's exact test for categorical variables and analysis of variance for numerical variables). The main end points were time to death from prostate cancer. Univariate and multivariate analysis including Gleason score was performed by proportional hazard (Cox) regression analysis. All p values were two sided and 95 % confidence intervals (95 %CIs) were based on normal distribution.

Results

Chromogranin-A expression was analysed in 2483 cores representing 806 patients. Around 60 % of cases were represented by one or two cores. Up to seven cores were taken in three individuals (Fig. 1).

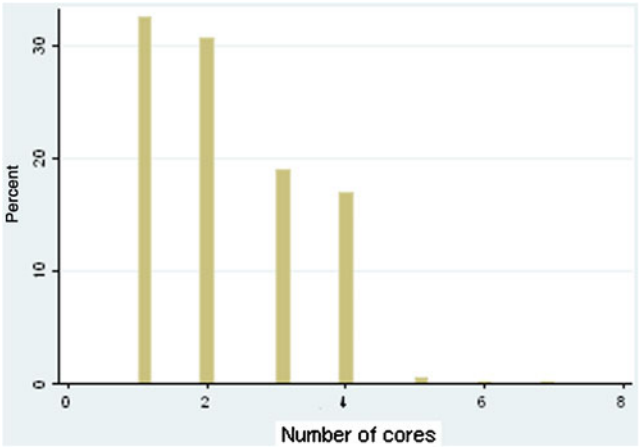

Fig. 1 Histogram showing number of cores per individual

Seventeen percent (133 out of 806) of assessable patient cores demonstrated chromogranin-A expression. On univariate analysis, NE expression significantly correlated with poor outcome (HR=1.61, 95 % CI 1.15-2.27, $p<0.001$; Fig. 2). Furthermore, chromogranin-A expression significantly correlated with higher Gleason score ($p<0.001$; Table 1). However, in multivariate analysis including Gleason score, neuroendocrine differentiation did not have independent prognostic value (HR=0.97, 95 %CI 0.89–0.37, $p=0.87$; Table 2).

Further sub-group analysis was performed on 147 patients who had been given early hormone manipulation therapy (within 6 months of diagnosis). These patients more frequently showed chromogranin-A expression ($\chi^2=7.25$, $p=0.007$) but there was no significant association with prostate cancer deaths ($p=0.083$).

Discussion

NE differentiation in prostatic carcinoma has attracted attention because it may represent an androgen-independent pathway along which tumour cells may progress. Neuroendocrine cells do not possess androgen receptors and are thought to be anti-apoptotic [28, 29]. It is hypothesised that the inevitable development of hormone resistant prostate cancer following the failure of androgen blockade may be due to selection of a neuroendocrine phenotype [30] or the ability for neuroendocrine messengers to bind and activate androgen receptors.

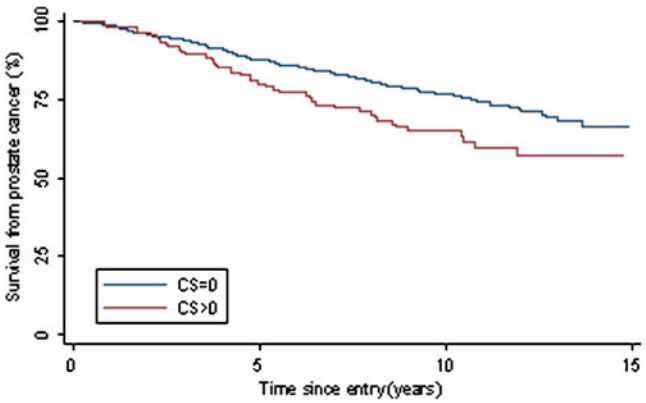

Fig. 2 Kaplan–Meier curves showing composite score (*CS*) with zero cut-off

Table 1 Univariate analysis of composite score according to Gleason grade

Gleason score	0	>0
≤6	377(90)	41(10)
7	156(78)	43(22)
8-10	139(74)	49(26)

$p<0.001$, $\chi^2=29.80$

Recent translational studies by other groups show divergent findings [19, 31–34]. Cindolo et al. [34] also performed chromogranin-A immunohistochemistry (as well as Ki-67, NeuroD and androgen receptor) on clinically localised prostate cancers using TMAs. Their cohort of 732 patients differed from our study group in that the tissue was derived from radical prostatectomies. Nevertheless the conclusions were broadly similar to ours in that chromogranin-A expression correlated with Gleason score but was not independently predictive of progression. Abrahamsson et al. [19] also studied NE differentiation in a conservatively treated cohort, albeit in smaller numbers (87 patients). In this study, there was no correlation of chromogranin-A either with Gleason score or survival. Allen et al. [31], Tan et al. [32] and Cerovic et al. [33] have also not been able to show association with mortality independent of other variables. Correlation with Gleason score is a consistent feature in all of these studies. There are two notable studies, published in the early 1990s, that have implicated NE differentiation with tumour progression [35, 36]. These studies included small cohorts of patients but the results were sufficient to generate further interest in this field.

The results from our study on conservatively treated, localised prostate cancer does not support this theory. Although univariate analysis of neuroendocrine differentiation correlated

Table 2 Comparison of univariate analysis and multivariate analysis including Gleason score

Variable	Prostate cancer	
	Hazard ratio (95 % CI)	
	Univariate analysis ($N=806$)	Gleason + CG-A ($N=806$)
0 (674)	1 (ref)	1 (ref)
>0 (132)	1.58 (1.15,2.18)	0.97 (0.70, 1.34)

with mortality, multivariate analysis failed to demonstrate significance. We therefore conclude that chromogranin-A as a marker for neuroendocrine differentiation fails to add anything to the prognostic model. Less than 20 % of our cohort had been exposed to hormone manipulation. Although there was correlation with chromogranin-A expression, there was no effect on survival from prostate cancer.

Pure small cell carcinoma was not diagnosed in any of the cores as these cases would have been referred for primary chemotherapy and would not have been included in this conservatively managed cohort.

Despite disappointing clinical data, there is good evidence from basic research to implicate NE mechanisms in the progression of prostate cancer. For example, vasoactive intestinal peptide, a NE transmitter, has been implicated in up-regulation of pro-angiogenic vascular endothelial growth factor [37]. Mechanisms that have been proposed as inducers of NE phenotype include ionising radiation [11], cytokines [12], Epidermal Growth Factor [38] and β-adrenergic agonists [10]. It might be too naive to assume that there is a simple relationship between the degree of NE differentiation and tumour behaviour. It has been described that NE cells secreting chromogranin can be stimulated further with dibutryl cyclic-AMP. This does not result in raised secretion of chromogranin but does cause the production of other NE-specific molecules (bombesin, neuron-specific enolase) [10, 39]. It could be that paracrine stimulation via these messengers is responsible for tumour proliferation independent of chromogranin immuno-expression.

NE differentiation may be more significant in patients that have been subjected to hormone manipulation. In vivo studies on prostate cancer cell lines have shown that NE phenotype is selected for in androgen deprived conditions [14, 30]. Assessment of NE differentiation may still be important in this cohort and numbers of groups have sought to explore whether NE differentiation can be predictive of relapse following hormonal manipulation [40, 41]. Even in this situation, the answer is not clear-cut: Krijnen and colleagues [20] concluded that NE differentiation was a predictor of progressive disease following hormone manipulation. Their work was conducted on localised prostate cancer and TURP chippings. Ahlgren et al. [40] showed an increase in neuroendocrine differentiation following the administration of androgen blockade but this did not translate into increased mortality. Hirano et al. [41] did show higher incidence of NE differentiation in autopsy specimens who had died from hormone refractory prostate cancer compared to living prostate cancer patients currently on hormone manipulation for a shorter duration. They were unable to conclude, however, whether this correlation was secondary to long term hormone manipulation or hormone refractoriness.

Conclusion

In this large series of conservatively treated prostate cancers in which NE differentiation has been assessed, we show that although NE differentiation correlates with higher Gleason score in univariate analysis it has no independent prognostic value in multivariate analysis and therefore does not add to the well-established prognostic models.

We therefore suggest that these tumours are treated by standard methodologies in the absence of small cell differentiation.

Disclosure of conflict of interest We declare that we have no conflict of interest.

References

1. Bonkhoff H, Stein U, Remberger K (1993) Androgen receptor status in endocrine-paracrine cell types of the normal, hyperplastic, and neoplastic human prostate. Virchows Arch A Pathol Anat Histopathol 423:291–294
2. Krijnen JL, Janssen PJ, Ruizeveld de Winter JA, van Krimpen H, Schroder FH, van der Kwast TH (1993) Do neuroendocrine cells in human prostate cancer express androgen receptor? Histochemistry 100:393–398
3. Ather MH, Abbas F, Faruqui N, Israr M, Pervez S (2008) Correlation of three immunohistochemically detected markers of neuroendocrine differentiation with clinical predictors of disease progression in prostate cancer. BMC Urol 8:21
4. Isshiki S, Akakura K, Komiya A, Suzuki H, Kamiya N, Ito H (2002) Chromogranin a concentration as a serum marker to predict prognosis after endocrine therapy for prostate cancer. J Urol 167:512–515
5. Di Sant' Agnese PA (1992) Neuroendocr Differ Carcinoma Prostate Cancer 70:254–268
6. Albertsen PC, Hanley JA, Fine J (2005) 20-year outcomes following conservative management of clinically localized prostate cancer. JAMA 293:2095–2101
7. Yokomizo A, Murai M, Baba S, Ogawa O, Tsukamoto T, Niwakawa M, Tobisu K, Kinukawa N, Naito S (2006) Percentage of positive biopsy cores, preoperative prostate-specific antigen (PSA) level, pT and Gleason score as predictors of PSA recurrence after radical prostatectomy: a multi-institutional outcome study in Japan. BJU Int 98:549–553
8. Cuzick J, Fisher G, Kattan MW, Berney D, Oliver T, Foster CS, Moller H, Reuter V, Fearn P, Eastham J, Scardino P (2006) Long-term outcome among men with conservatively treated localised prostate cancer. Br J Cancer 95:1186–1194
9. Tewari A, Johnson CC, Divine G, Crawford ED, Gamito EJ, Demers R, Menon M (2004) Long-term survival probability in men with clinically localized prostate cancer: a case-control, propensity modeling study stratified by race, age, treatment and comorbidities. J Urol 171:1513–1519
10. Cox ME, Deeble PD, Lakhani S, Parsons SJ (1999) Acquisition of neuroendocrine characteristics by prostate tumor cells is reversible: implications for prostate cancer progression. Cancer Res 59:3821–3830
11. Deng X, Liu H, Huang J, Cheng L, Keller ET, Parsons SJ, Hu CD (2008) Ionizing radiation induces prostate cancer neuroendocrine

differentiation through interplay of CREB and ATF2: implications for disease progression. Cancer Res 68:9663–9670
12. Diaz M, Abdul M, Hoosein N (1998) Modulation of neuroendocrine differentiation in prostate cancer by interleukin-1 and -2. Prostate Suppl 8:32–36
13. Huss WJ, Gregory CW, Smith GJ (2004) Neuroendocrine cell differentiation in the CWR22 human prostate cancer xenograft: association with tumor cell proliferation prior to recurrence. Prostate 60:91–97
14. Jongsma J, Oomen MH, Noordzij MA, Van Weerden WM, Martens GJ, van der Kwast TH, Schroder FH, van Steenbrugge GJ (2002) Different profiles of neuroendocrine cell differentiation evolve in the PC-310 human prostate cancer model during long-term androgen deprivation. Prostate 50:203–215
15. Nelson EC, Cambio AJ, Yang JC, Ok JH, Lara PN Jr, Evans CP (2007) Clinical implications of neuroendocrine differentiation in prostate cancer. Prostate Cancer Prostatic Dis 10:6–14
16. Quiros-Gonzalez I, Sainz RM, Hevia D, Mayo JC MnSOD drives neuroendocrine differentiation, androgen independence, and cell survival in prostate cancer cells. Free Radic Biol Med 50:525–536
17. Wu C, Huang J (2007) Phosphatidylinositol 3-kinase-AKT-mammalian target of rapamycin pathway is essential for neuroendocrine differentiation of prostate cancer. J Biol Chem 282:3571–3583
18. Zhang XQ, Kondrikov D, Yuan TC, Lin FF, Hansen J, Lin MF (2003) Receptor protein tyrosine phosphatase alpha signaling is involved in androgen depletion-induced neuroendocrine differentiation of androgen-sensitive LNCaP human prostate cancer cells. Oncogene 22:6704–6716
19. Abrahamsson PA, Cockett AT, di Sant'Agnese PA (1998) Prognostic significance of neuroendocrine differentiation in clinically localized prostatic carcinoma. Prostate Suppl 8:37–42
20. Krijnen JL, Bogdanowicz JF, Seldenrijk CA, Mulder PG, van der Kwast TH (1997) The prognostic value of neuroendocrine differentiation in adenocarcinoma of the prostate in relation to progression of disease after endocrine therapy. J Urol 158:171–174
21. Autorino R, Di Lorenzo G, D'Armiento FP, Mignogna C, Cindolo L, De Sio M, Perdona S, De Fortuna E, Salzano L, De Placido S, D'Armiento M (2005) Neuroendocrine differentiation after neoadjuvant hormonal treatment in prostate cancer. Minerva Urol Nefrol 57:319–324
22. Sciarra A, Mariotti G, Gentile V, Voria G, Pastore A, Monti S, Di Silverio F (2003) Neuroendocrine differentiation in human prostate tissue: is it detectable and treatable? BJU Int 91:438–445
23. Kadmon D, Thompson TC, Lynch GR, Scardino PT (1991) Elevated plasma chromogranin-A concentrations in prostatic carcinoma. J Urol 146:358–361
24. Gunia S, Albrecht K, Koch S, Herrmann T, Ecke T, Loy V, Linke J, Siegsmund M, May M (2008) Ki67 staining index and neuroendocrine differentiation aggravate adverse prognostic parameters in prostate cancer and are characterized by negligible inter-observer variability. World J Urol 26:243–250
25. Berney DM, Fisher G, Kattan MW, Oliver RT, Moller H, Fearn P, Eastham J, Scardino P, Cuzick J, Reuter VE, Foster CS (2007) Major shifts in the treatment and prognosis of prostate cancer due to changes in pathological diagnosis and grading. BJU Int 100:1240–1244
26. Epstein JI, Allsbrook WC Jr, Amin MB, Egevad LL (2005) The 2005 International Society of Urological Pathology (ISUP) consensus conference on Gleason grading of prostatic carcinoma. Am J Surg Pathol 29:1228–1242
27. Turbat-Herrera EA, Herrera GA, Gore I, Lott RL, Grizzle WE, Bonnin JM (1988) Neuroendocrine differentiation in prostatic carcinomas. A retrospective autopsy study. Arch Pathol Lab Med 112:1100–1105
28. Bonkhoff H (2001) Neuroendocrine differentiation in human prostate cancer. Morphogenesis, proliferation and androgen receptor status. Ann Oncol 12(Suppl 2):S141–S144
29. Xing N, Qian J, Bostwick D, Bergstralh E, Young CY (2001) Neuroendocrine cells in human prostate over-express the anti-apoptosis protein survivin. Prostate 48:7–15
30. Jongsma J, Oomen MH, Noordzij MA, Van Weerden WM, Martens GJ, van der Kwast TH, Schroder FH, van Steenbrugge GJ (2000) Androgen deprivation of the PC-310 [correction of prohormone convertase-310] human prostate cancer model system induces neuroendocrine differentiation. Cancer Res 60:741–748
31. Allen FJ, Van Velden DJ, Heyns CF (1995) Are neuroendocrine cells of practical value as an independent prognostic parameter in prostate cancer? Br J Urol 75:751–754
32. Tan MO, Karaoglan U, Celik B, Ataoglu O, Biri H, Bozkirli I (1999) Prostate cancer and neuroendocrine differentiation. Int Urol Nephrol 31:75–82
33. Cerovic SJ, Brajuskovic GR, Vukotic Maletic VD, Micic SR (2004) Neuroendocrine differentiation in prostate cancer. Vojnosanit Pregl 61:513–518
34. Cindolo L, Cantile M, Franco R, Chiodini P, Schiavo G, Forte I, Zlobec I, Salzano L, Botti G, Gidaro S, Terracciano L, Cillo C Parallel determination of neuroD1, chromogranin-A, KI67 and androgen receptor expression in surgically treated prostate cancers. Int Braz J Urol 37:57–66
35. Falkmer S, Askensten U, Grimelius L, Abrahamsson PA (1990) Cytochemical markers and DNA content of neuroendocrine cells in carcinoma of the prostate gland during tumour progression. Acta Histochem Suppl 38:127–132
36. Cohen RJ, Glezerson G, Haffejee Z (1991) Neuro-endocrine cells—a new prognostic parameter in prostate cancer. Br J Urol 68:258–262
37. Collado B, Gutierrez-Canas I, Rodriguez-Henche N, Prieto JC, Carmena MJ (2004) Vasoactive intestinal peptide increases vascular endothelial growth factor expression and neuroendocrine differentiation in human prostate cancer LNCaP cells. Regul Pept 119:69–75
38. Humez S, Monet M, Legrand G, Lepage G, Delcourt P, Prevarskaya N (2006) Epidermal growth factor-induced neuroendocrine differentiation and apoptotic resistance of androgen-independent human prostate cancer cells. Endocr Relat Cancer 13:181–195
39. di Sant'Agnese PA (2001) Neuroendocrine differentiation in prostatic carcinoma: an update on recent developments. Ann Oncol 12 (Suppl 2):S135–S140
40. Ahlgren G, Pedersen K, Lundberg S, Aus G, Hugosson J, Abrahamsson PA (2000) Regressive changes and neuroendocrine differentiation in prostate cancer after neoadjuvant hormonal treatment. Prostate 42:274–279
41. Hirano D, Okada Y, Minei S, Takimoto Y, Nemoto N (2004) Neuroendocrine differentiation in hormone refractory prostate cancer following androgen deprivation therapy. Eur Urol 45:586–592, discussion 592

Virchows Arch (2012) 461:109–116
DOI 10.1007/s00428-012-1273-4

ORIGINAL ARTICLE

Anterior gradient protein 2 (AGR2) is an independent prognostic factor in ovarian high-grade serous carcinoma

S. Darb-Esfahani · F. Fritzsche · G. Kristiansen · W. Weichert · J. Sehouli · I. Braicu · M. Dietel · C. Denkert

Received: 16 May 2012 / Revised: 15 June 2012 / Accepted: 20 June 2012 / Published online: 3 July 2012
© Springer-Verlag 2012

Abstract Ovarian high-grade serous carcinoma (HGSC, type 2 ovarian carcinoma) is a poor prognosis cancer with limited therapeutic options. We aimed to investigate the expression pattern and prognostic potential of the metastasis-promoting protein anterior gradient 2 (AGR2) in primary HGSC. Immunohistochemistry was applied to a cohort of 124 primary HGSCs using tissue microarrays. Additionally, in 48 type 1 carcinomas (low-grade serous (LGSC), endometrioid (EC), clear cell (CCC), and mucinous carcinoma (MC)), AGR2 expression was investigated in an exploratory approach. A strong expression of AGR2 was seen in 15 HGSCs (12.1 %) and was significantly linked to shortened overall survival (OS, $p=0.011$) and also for progression-free survival (PFS, $p=0.001$) in the setting of adjuvant platinum-based chemotherapy (CTX). Multivariate survival analysis including age, stage, and residual tumor after surgery revealed that AGR2 expression was an independent prognostic marker for OS ($p=0.001$) and PFS ($p=0.001$) in HGSC. In type 1 carcinomas, AGR2 was significantly increased as compared to HGSC ($p=0.001$) and was seen in subsets of all histological types, low-grade serous LGSC, EC, CCC, and MC. In particular, strong diffuse staining was seen in LGSC and MC. There was no association between AGR2 and estrogen receptor expression in ovarian type 1 or type 2 carcinomas. AGR2 expression identifies highly aggressive HGSC with a compromised prognosis for which novel therapeutic options are needed. Our data strongly support the further evaluation of AGR2 as a therapeutic target and a potential marker for response to platinum-based CTX in this tumor entity.

Keywords High-grade serous carcinoma · Ovarian · AGR2 · Prognosis

S. Darb-Esfahani (✉) · M. Dietel · C. Denkert
Institute of Pathology, Charité Universitätsmedizin Berlin,
Charitéplatz 1,
10117 Berlin, Germany
e-mail: silvia.darb-esfahani@charite.de

F. Fritzsche
Institute of Pathology Enge,
Zürich, Switzerland

G. Kristiansen
Institute of Pathology, Universitätsklinikum Bonn,
Bonn, Germany

W. Weichert
Institute of Pathology, Universitätsklinikum Heidelberg,
Heidelberg, Germany

J. Sehouli · I. Braicu
Department of Gynecology, Charité Campus Virchow Klinikum,
Charité Universitätsmedizin Berlin,
Berlin, Germany

Introduction

Epithelial ovarian cancer is a heterogeneous group of neoplasms that is constituted of five major histological types, high-grade serous (HGSC), low-grade serous (LGSC), endometrioid (EC), clear cell (CCC), and mucinous carcinoma (MC). HGSC, together with undifferentiated, high-grade endometrioid carcinoma, and cacinosarcoma constitute the so-called type 2 group of ovarian carcinomas whereas LGSC, EC G1-2, CCC, and MC are grouped as type 1 tumors, according to the dualistic model of ovarian carcinogenesis (reviewed in [1]). This theoretical classification, which should not replace the histological terms in widespread use, helps to separate ovarian carcinomas that are often low stage and more slowly progressive and has defined intraovarian precursor lesions (borderline tumors), from the aggressive high-grade tumors. During the last decade, profound differences in molecular profiles, precursor lesions, response to chemotherapy (CTX), and prognosis

have been described for these histological subtypes (reviewed in [2]). HGSC constitutes the major subtype (approximately 70 %) of all ovarian carcinomas. Molecularly, it is characterized by a high rate of genomic instability and p53 alterations [3]. Patient prognosis in general is unfavorable: 75 % of patients are diagnosed in a late stage when the carcinoma has already disseminated in the peritoneal cavity. Radical surgery and adjuvant platinum-based CTX is the standard of care for all ovarian carcinomas to date [4]. However, although 75 % of ovarian cancer patients initially respond to CTX, 75 % of these will relapse and ultimately die of their disease. Novel therapeutic options are therefore needed. The evaluation of novel biomarkers within molecularly and morphologically defined subgroups bears the potential to identify molecules and pathways as targets for a specific cancer therapy.

Anterior gradient protein 2 (AGR2) was first described in *Xenopus laevis* where it plays a role during early neural development [5]. In humans, AGR2 is predominantly found in tissues with mucus-secreting or endocrine cells [6]. It is a member of the protein disulfide isomerase family of endoplasmic reticulum-resident proteins. Although its exact physiological function is not known, AGR2 has been implicated in the folding of proteins as a chaperone protein [6]. It became of interest in cancer research, when a differential expression was found in estrogen receptor (ER)-positive breast cancer cell lines [7]. Since then, elevated AGR2 has been seen in subsets of breast [8–11], prostate [12–14], non-small cell lung [15], pancreatic [16], and hepatic adenocarcinomas [17], in some entities along with an impact on prognosis [8–11, 14]. In breast and prostate adenocarcinoma, AGR2 was under the control of ER or androgen receptor expression [11, 13]. Upregulation of AGR2 enhances classical hallmarks of cancer, such as metastasis, invasion, colony formation, and proliferation (reviewed in [6]).

In ovarian cancer, where ER signaling also has a prognostic implication as we previously showed [18, 19], AGR2 has not yet been investigated in a larger cohort. We therefore determined the expression pattern, the potential prognostic role, and the relationship with ER expression in all major subtypes of ovarian carcinoma.

Methods

Study population This study included 124 patients with primary HGSC who underwent radical surgery between 1991 and 2007 with the aim of total cytoreduction at the Department of Gynecology and Obstetrics (Charité Universitätsmedizin Berlin). Resection specimens were formalin fixed and paraffin embedded for diagnostic purposes at the Institute of Pathology of the Charité. Hematoxylin/eosin (HE)-stained slides were reevaluated according to histology by an experienced gynecopathologist (SDE). Typing as HGSC was performed as suggested by McCluggage taking into account growth pattern, nuclear polymorphism, and mitotic count [20]. As expected from this tumor subtype, most cases were high-stage tumors (Fédération Internationale de Gynécologie et d'Obstétrique (FIGO) stages III–IV, n=110, 88.7 %). Data on residual tumor mass were available for 92 patients (74 %). The majority of patients had been treated with standard adjuvant platinum-based CTX (n=109/114, 95.6 %), and two patients (1.8 %) with FIGO I tumor stage have not received adjuvant CTX. Data on overall survival (OS) were available for all patients. Median OS in patients alive after follow-up was 45.0 months (range 2.5–162.3 months), and 46 patients died during follow-up (37.1 %). Data on progression-free survival (PFS) were available for 111 patients (88.7 %; median PFS in nonprogressive patients 32.1, range 0.5–127.8 months). The distribution of clinicopathological parameters in the study cohort is shown in Table 1. We additionally investigated a group of type 1 carcinomas, consisting of 16 LGSCs, 15 ECs G1-2, 9 CCCs, and 8 MCs.

Table 1 Characteristics of the study group

	Number (%)
Total	124 (100 %)
Age	
≤60 years	63 (50.8)
>60 years	61 (49.2)
pT	
pT1	12 (9.7)
pT2	8 (6.4)
pT3	104 (83.9)
pN	
pN0	35 (28.2)
pN1	67 (54.0)
pNx	22 (17.8)
FIGO stage	
FIGO I	8 (6.5)
FIGO II	6 (4.8)
FIGO III	100 (80.6)
FIGO IV	10 (8.1)
Residual tumor	
No	60 (65.2)
Yes	32 (34.8)
Missing	32 (25.8 of total)
CTX	
Platinum-based CTX	109 (95.6)
Other CTX	3 (2.6)
No CTX	2 (1.8)[a]
Missing	10 (8.1 of total)

[a]FIGO I

Immunohistochemistry For tissue microarrays (TMA) construction, representative tumors areas were marked on HE-stained slides by a pathologist, and two to four tissue cores (diameter 1.5 mm) subsequently punched out the respective donor paraffin blocks using a tissue microarrayer (Beecher Instruments, Woodland, WI, USA). Cores from 40 to 60 carcinomas were placed in recipient paraffin blocks. Immunohistochemistry staining of TMA sections was performed according to standard procedures as described earlier [21]. A mouse monoclonal antibody was raised against full-length recombinant AGR2 (clone 1c3, Abnova, GmbH, Heidelberg, Germany) was used in a dilution of 1:50. 3,3′-diaminobenzidine peroxide substrate (DAB^+) was used as a chromogen. Stained slides were scanned and evaluated using the TMA evaluator software from VM Scope GmbH (Berlin, Germany). The percentage of positive tumors cells was scored as 0 (0 %), 1 (0–10 %), 2 (11–50 %), 3 (51–80 %), or 4 (80–100 %), and the staining intensity was scored as 0 (negative), 1 (weak), 2 (moderate), or 3 (strong). The strongest, not necessarily the predominant intensity, was scored. The multiplication of the intensity and percentage scores resulted in an immunoreactivity score (IRS), which ranged from 0 to 12.

Statistical evaluation Statistical analyses were performed with SPSS Statistics 19 (SPSS Inc., Chicago, IL, USA) and GraphPad Prism v.5 (La Jolla, CA, USA). Associations were tested by Fisher's exact, chi-square or Mann–Whitney test, as indicated. Survival analysis was performed using the Kaplan–Meier method or Cox regression for multivariate testing. All p values were calculated two tailed, and p values <0.05 were considered as significant.

Results

Expression pattern of AGR2 in HGSC A significant number of HGSC were completely negative for AGR2 (n=84, 67.7 %). In the remaining carcinomas, staining was either weak to moderate diffuse (Fig. 1a, b) or patchy with groups of positive cells distributed throughout the tumor. Fifteen tumors (12.1 %) revealed groups of strongly stained cells usually constituting 10–50 % of all tumor cells, with two cases revealing 50–80 % of strongly stained cells (Fig. 1c). Staining was strictly cytoplasmic. The use of an IRS yielded one group of completely negative tumors (IRS=0, n=84), one group with intermediate expression (IRS=1–4, n=26), and a high expression group (IRS=6–9, n=14), with the latter group being identical to the group defined simply by strong staining intensity with the exception of a single case with moderate staining in 50–80 % of cells (IRS=6). We therefore decided to continue our subsequent analyses using only staining intensity as a grouping variable. In the diagram (Fig. 1d), the distribution of staining results is displayed. No relevant staining signals were obtained in tumor stroma or inflammatory cells. AGR2 expression was not associated with age, tumor, nodal, or FIGO stage; residual tumor after surgery; or type of CTX (p>0.05, not shown).

Impact of AGR2 expression on patient survival AGR2 expression was subsequently tested for a prognostic effect in HGSC. Kaplan–Meier analysis revealed that patients with AGR2-negative tumors had an OS quite similar to those with AGR2 weakly or moderately expressing carcinomas (Fig. 2a). Only a strong AGR2 expression resulted in a clearly worse OS. The same effect was seen for PFS (Fig. 2b). When we stratified our study cohort into a group of strong AGR2 expression (AGR2 high) and a group of negative, weak, and moderate expression (AGR2 low), patients with AGR2-low carcinomas had a mean survival of 106.17 months as opposed to 47.23 months in patients with AGR2-high carcinomas (p=0.011, Fig. 2c). Mean survival until progression was reduced from 38.71 months in patients with AGR2 low-expressing tumors to 12.38 months in case of a high AGR2 expression (p=0.001, Fig. 2d). A multivariate Cox regression analysis including patient age, FIGO stage, and residual tumor after surgery demonstrated that high AGR2 expression was an independent prognostic marker, both for OS (hazard ratio (HR)=2.60, p=0.023) and PFS (HR=3.89, p=0.001, Table 2).

Correlation with ER expression As a regulation of AGR2 by ER has been reported in breast cancer, the association of AGR2 expression with ER and progesterone receptor (PR) expression was determined on the protein and mRNA level; these data had been determined previously in our study cohort [18, 19]. There was no association of AGR2 expression (high vs. low) with ERα (gene name ESR1) or PR mRNA expression as determined by quantitative reverse transcription polymerase chain reaction, neither on the continuous level (Mann–Whitney test, p=0.438 and p=1.000, respectively) nor with dichotomized ESR1 and PR mRNA expression groups (Fisher's exact test, p=0.320 and p=0.633, respectively). AGR2 expression was also not associated with ER or PR protein expression (Fisher's exact test, p=0.588 and p=0.584, respectively). The use of other cutoffs for AGR2 expression also did not show any association (p>0.05, data not shown).

AGR2 expression in other histological subtypes In an exploratory approach, we analyzed the expression of AGR2 in 16 LGSCs, 8 MCs, 15 G1-2 ECs, and 9 CCCs. Contrarily to HGSC, a strong staining throughout the whole tumor was noted in some LGSC and MC (Fig. 3a, b). AGR2-high expression was found in 15 (12.1 %) of HGSC, in 4 (25 %) of LGSC, in 5 (35.7 %) of EC, in 1 (11.1 %) of CCC, and 5 (62.5 %) of MC (Fig. 3c). No association of

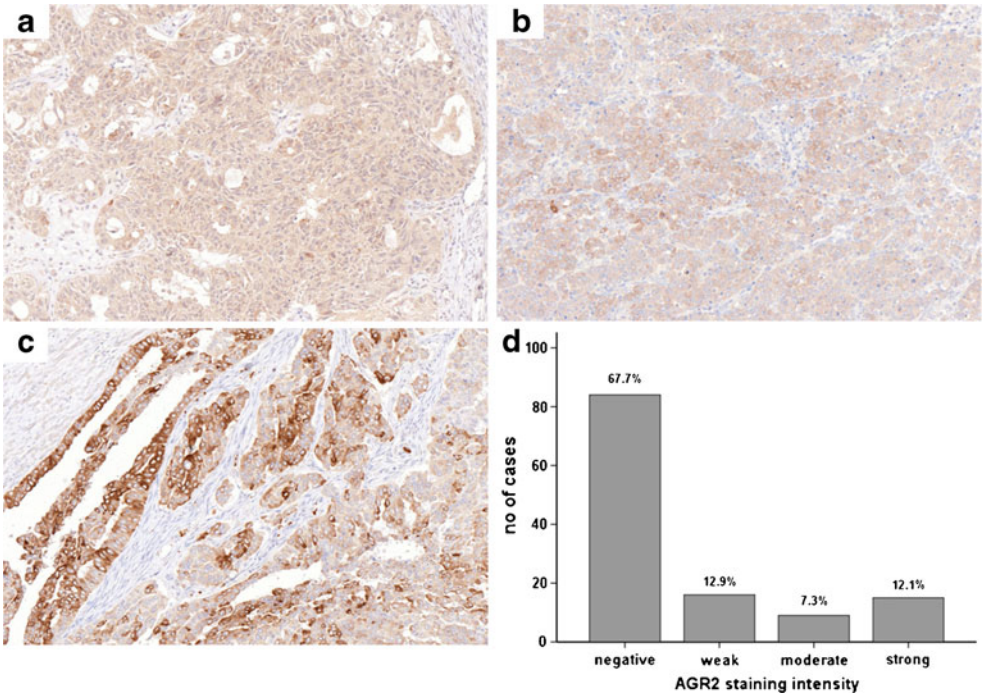

Fig. 1 Expression pattern of AGR2 in HGSC. **a** Solid tumor masses with weak diffuse AGR2 expression, **b** weak to moderate staining, **c** invasive sheets and glands of HGSC with weak background expression of AGR2 and patchy groups of strongly stained tumor cells, and **d** staining intensity groups in HGSC

AGR2 expression with either ER or PR protein or mRNA expression was seen within the histological subtypes of type 1 carcinomas (not shown).

Discussion

In this study, we investigated the expression pattern and the prognostic impact of the metastasis-associated protein AGR2 in HGSC. Strong AGR2 expression was seen in a subset of tumors with exceptionally shortened OS and PFS. The prognostic impact of AGR2 expression was independent of patient age, stage, and residual tumor mass. We further gained evidence that AGR2 is highly expressed in a significant rate of type 1 carcinomas, especially EC, LGSC, and MC.

To our knowledge, this is the first study investigating AGR2 protein expression in a larger cohort of ovarian carcinomas and therefore also the first study to reveal a prognostic significance in HGSC. Elevated AGR2 transcript levels were first detected in ovarian cancer specimens using gene array profiling, especially in the mucinous subtype [22, 23]. Recently, increased AGR2 protein has also been detected in the serum of patients and holds potential as a screening marker [24, 25]. The latter study also provided a preliminary immunohistochemical investigation of AGR2 expression in a group of 15 serous and mucinous carcinomas and found almost all tumors to be positive, whereas in our cohort, a significant proportion of tumors, especially HGSC, were completely negative. Differences in staining protocol and interpretation may account for this. In contrast to AGR2, its ortholog AGR3, which is implicated in growth and metastasis of ER-dependent breast cancers [26], has already been investigated in ovarian carcinoma [27, 28] and, interestingly, was a favorable prognostic factor in HGSC and LGSC. Although in each of those studies including ours less than 10 specimens of MC were evaluated, a consensus on a diffuse expression of AGR2 and/or AGR3 in this histological subtype is evident. Our study additionally shows that also in EC and LGSC, high AGR2 expression is often present and that even CCC may be AGR2 positive, however less frequently. As AGR2 is predominantly found in mucus-secreting or endocrine cells in normal tissue [6], AGR2 expression in ovarian carcinoma may be related to the extent of mucus secretion, which is highest in MC, but also found in subsets of the other histological types. The reasons for the differential expression of AGR2 in ovarian carcinoma subtypes remain to be clarified. Taking together all reports on AGR2/3 expression in ovarian carcinomas, the further evaluation as diagnostic biomarkers and potential therapeutic targets in all histological subtypes is promising; however, due to the rarity of type 1 tumors, these should potentially be investigated in a multicenter setting.

In our study, only HGSC with strong overexpression of AGR2 turned out to constitute a special prognostic subgroup. This is in contrast to the situation in breast cancer, where AGR2 mRNA and protein expression have already been systematically evaluated repeatedly. Here, a clear deterioration of the prognosis was evident even when no more than 1 % of tumor cells were stained, as compared to completely negative cases and patient prognosis declined with a growing rate of

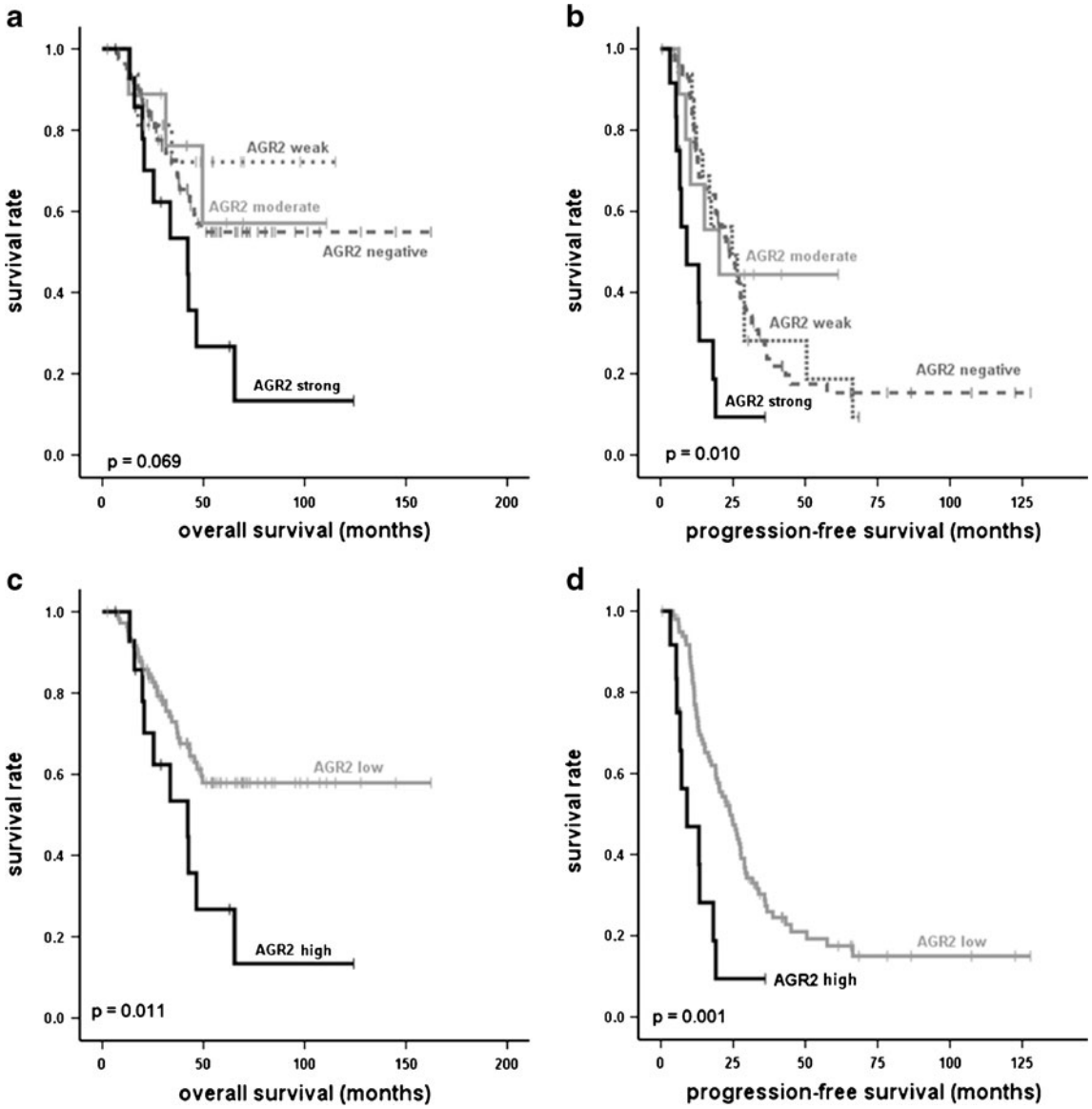

Fig. 2 Survival analysis: OS (**a**) and PFS (**b**) using four groups of AGR2 expression. OS (**c**) and PFS (**d**) after stratifying the cohort into a group with AGR2-low (negative, weak, or moderate staining) and AGR2-high expression (strong staining). *p*: log rank test

positive tumor cells in a dose-dependent manner [8, 9]. Moreover, a clear prognostic impact of AGR2 seemed to be restricted to ER-positive breast cancers [8, 11]. The different impact of AGR2 expression in HGSC and breast cancer might be explained by an apparently differing regulation in both cancer types. In breast cancer, there is a strong association of AGR2 and ER expression [8–10], apparently due to a transcriptional regulation of AGR2 by ER [11]. Although we and others previously showed that a significant subset of ovarian carcinomas including HGSC reveals ER and PR expression [18, 19], we did not find a link between hormone receptor status and AGR2 expression in our cohort. AGR2 therefore plays an ER-independent role in HGSC, similarly to hepatic fibrolamellar and pancreatic adenocarcinoma [16, 17].

Physiological stress seems to constitute an alternative regulatory pathway for induction of AGR2, independently from steroid hormone receptor function. Thus, serum/oxygen depletion [29], UV-induced DNA damage [30], or endoplasmic reticulum-related stress [16] have been found to upregulate AGR2 in various cell culture models. In breast cancer cells, an intact extracellular signal-regulated kinase/mitogen-activated protein kinase pathway was necessary for the upregulation of AGR2 by serum depletion [29]. Alterations are also common in HGSC [3]. Stressful conditions due to reduced blood supply are seen in all solid cancers [31] and might be potential regulators of AGR2 upregulation in HGSC, too.

Our finding of a negative prognostic impact of AGR2 may be explained by its described function in tumor

Table 2 Survival analysis

	Univariate			Multivariate	
	No. of events/no. of cases	Mean survival, months (SE)	*p* (log rank)	HR (95 % CI)	*p*
Overall survival					
Age (per year)	–	–	–	1.02 (0.99–1.05)	0.301
AGR2 expression					
Low	36/109	106.17 (7.39)	0.011	1	0.023
High	10/15	47.23 (10.34)		2.60 (1.14–5.91)	
FIGO stage					
FIGO I–II	6/19	81.49 (9.89)	0.208	1	0.689
FIGO III–IV	55/135	85.66 (7.56)		1.34 (0.32–5.69)	
Residual tumor					
No	22/72	89.07 (6.63)	0.009	1	0.010
Yes	20/38	55.05 (7.44)		2.47 (1.25–4.91)	
Progression-free survival					
Age (per year)	–	–	–	1.00 (0.98-1.03)	0.823
AGR2 expression					
Low	72/99	38.71 (4.58)	0.001	1	0.001
High	10/12	12.63 (2.73)		3.89 (1.73–8.77)	
FIGO stage					
FIGO I–II	7/16	65.53 (11.55)	0.002	1	0.135
FIGO III–IV	92/120	30.30 (3.46)		4.53 (0.63–32.86)	
Residual tumor					
No	49/69	37.06 (5.23)	0.009	1	0.019
Yes	30/36	20.95 (3.78)		1.83 (1.10–3.04)	

SE standard error; *HR* hazard ratio, *CI* confidence interval

biology. Cells with the upregulation of AGR2 gain a metastatic, proliferative, and invasive phenotype, which all constitute features of highly aggressive tumors. For instance, transfection of benign rat mammary tumor cells with AGR2 results in the development of lung metastasis after transferral of cells into the mammary fat pad in syngeneic hosts

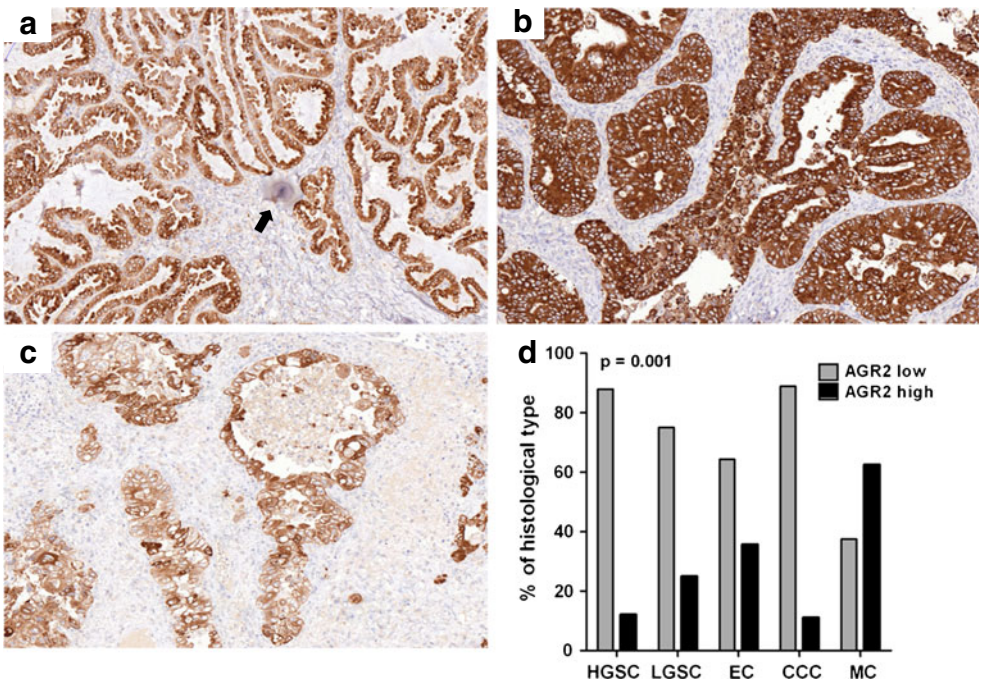

Fig. 3 Expression pattern of AGR2 in different histological types of ovarian carcinoma. **a** Strong diffuse staining in a LGSC (*arrow*: psammoma body), **b** strong diffuse staining in a moderately differentiated MC, **c** CCC with tubulocystic growth pattern and strong AGR2 expression, and **d** rates of AGR2 high expression (strong staining) in the five major histological ovarian carcinoma types. *p*: chi-square test

[16, 32, 33]. An increased proliferative and invasive capacity was seen in breast and pancreatic cancer cells after forced expression of AGR2 [34]. In HGSC, striking individual differences in survival exist, which to date cannot sufficiently be predicted by morphological features or molecular markers. AGR2 might contribute to the aggressiveness of certain ovarian carcinomas, and AGR2 expression might also serve as a prognostic marker. Furthermore, our finding of a significantly shortened survival until disease relapse points to a role of AGR2 in CTX resistance, as PFS in HGSC is largely dependent on response to adjuvant CTX and OS is further dependent on response to second and third line CTX [4]. In pancreatic cancer cells, a direct relationship between AGR2 expression and response to gemcitabine has been established in vitro and in vivo [33]; interestingly, AGR3, which seems to have similar tumor-promoting properties as AGR2, has been implicated with cisplatin resistance in ovarian cancer [27]. In the light of our results, it would be intriguing to functionally investigate the role of AGR2 in CTX response in ovarian HGSC.

In conclusion, we demonstrate that the metastasis-related protein AGR2 is highly expressed in a subset of ovarian HGSC of the ovary that shows a particularly unfavorable prognosis. In HGSC, as opposed to breast cancer, AGR2 expression does not seem to be under transcriptional control of ER. We further show a high expression of AGR2 in subsets of LGSC, EC, CCC, and especially MC. Our data strongly encourage the further evaluation of AGR2 as a therapeutic target molecule and a potential response predictor to platinum-based CTX in this tumor entity.

Acknowledgments We thank Mrs. Petra Wachs for her excellent technical assistance.

Conflict of interest The authors declare that they have no conflict of interest.

References

1. Bast RC Jr, Hennessy B, Mills GB (2009) The biology of ovarian cancer: new opportunities for translation. Nat Rev Cancer 9:415–428
2. Prat J (2012) Ovarian carcinomas: five distinct diseases with different origins, genetic alterations, and clinicopathological features. Virchows Arch 460:237–249
3. Cancer Genome Atlas Research Network (2011) Integrated genomic analyses of ovarian carcinoma. Nature 474:609–615
4. Thigpen T, duBois A, McAlpine J, DiSaia P, Fujiwara K, Hoskins W, Kristensen G, Mannel R, Markman M, Pfisterer J, Quinn M, Reed N, Swart AM, Berek J, Colombo N, Freyer G, Gallardo D, Plante M, Poveda A, Rubinstein L, Bacon M, Kitchener H, Stuart GC, Gynecologic Cancer InterGroup (2011) First-line therapy in ovarian cancer trials. Int J Gynecol Cancer 21:756–762
5. Sive HL, Hattori K, Weintraub H (1989) Progressive determination during formation of the anteroposterior axis in *Xenopus laevis*. Cell 58:171–180
6. Brychtova V, Vojtesek B, Hrstka R (2011) Anterior gradient 2: a novel player in tumor cell biology. Cancer Lett 304:1–7
7. Thompson DA, Weigel RJ (1998) hAG-2, the human homologue of the *Xenopus laevis* cement gland gene XAG-2, is coexpressed with estrogen receptor in breast cancer cell lines. Biochem Biophys Res Commun 251:111–116
8. Innes HE, Liu D, Barraclough R, Davies MP, O'Neill PA, Platt-Higgins A, deSilva RS, Sibson DR, Rudland PS (2006) Significance of the metastasis-inducing protein AGR2 for outcome in hormonally treated breast cancer patients. Br J Cancer 94:1057–1065
9. Barraclough DL, Platt-Higgins A, de Silva RS, Barraclough R, WinstanleyJ WCR, Rudland PS (2009) The metastasis-associated anterior gradient 2 protein is correlated with poor survival of breast cancer patients. Am J Pathol 175:1848–1857
10. Fritzsche FR, Dahl E, Pahl S, Burkhardt M, Luo J, Mayordomo E, Gansukh T, Dankof A, Knuechel R, Denkert C, Winzer KJ, Dietel M, Kristiansen G (2006) Prognostic relevance of AGR2 expression in breast cancer. Clin Cancer Res 12:1728–1734
11. Hrstka R, Nenutil R, Fourtouna A, Maslon MM, Naughton C, Langdon S, Murray E, Larionov A, Petrakova K, Muller P, Dixon MJ, Hupp TR, Vojtesek B (2010) The pro-metastatic protein anterior gradient-2 predicts poor prognosis in tamoxifen-treated breast cancers. Oncogene 29:4838–4847
12. Kristiansen G, Pilarsky C, Wissmann C, Kaiser S, Bruemmendorf T, Roepcke S, Dahl E, Hinzmann B, Specht T, Pervan J, Stephan C, Loening S, Dietel M, Rosenthal A (2005) Expression profiling of microdissected matched prostate cancer samples revealsCD166/MEMD and CD24 as new prognostic markers for patient survival. J Pathol 205:359–376
13. Bu H, Bormann S, Schäfer G, Horninger W, Massoner P, Neeb A, Lakshmanan VK, Maddalo D, Nestl A, Sültmann H, Cato AC, Klocker H (2011) The anterior gradient 2 (AGR2) gene is overexpressed in prostate cancer and may be useful as a urine sediment marker for prostate cancer detection. Prostate 71:575–587
14. Maresh EL, Mah V, Alavi M, Horvath S, Bagryanova L, Liebeskind ES, Knutzen LA, Zhou Y, Chia D, Liu AY, Goodglick L (2010) Differential expression of anterior gradient gene AGR2 in prostate cancer. BMC Cancer 10:680
15. Fritzsche FR, Dahl E, Dankof A, Burkhardt M, Pahl S, Petersen I, Dietel M, Kristiansen G (2007) Expression of AGR2 in non small cell lung cancer. Histol Histopathol 22:703–708
16. Dumartin L, Whiteman HJ, Weeks ME, Hariharan D, Dmitrovic B, Iacobuzio-Donahue CA, Brentnall TA, Bronner MP, Feakins RM, Timms JF, Brennan C, Lemoine NR, Crnogorac-Jurcevic T (2011) AGR2 is a novel surface antigen that promotes the dissemination of pancreatic cancer cells through regulation of cathepsins B and D. Cancer Res 71:7091–7102
17. Vivekanandan P, Micchelli ST, Torbenson M (2009) Anterior gradient-2 is overexpressed by fibrolamellar carcinomas. Hum Pathol 40:293–299
18. Sinn BV, Darb-Esfahani S, Wirtz RM, Budczies J, Sehouli J, Chekerov R, Dietel M, Denkert C (2011) Evaluation of a hormone receptor-positive ovarian carcinoma subtype with a favourable prognosis by determination of progesterone receptor and oestrogen receptor 1 mRNA expression in formalin-fixed paraffin-embedded tissue. Histopathology 59:918–927
19. Darb-Esfahani S, Wirtz RM, Sinn BV, Budczies J, Noske A, Weichert W, Faggad A, Scharff S, Sehouli J, Oskay-Ozcelik G, Zamagni C, De Iaco P, Martoni A, Dietel M, Denkert C (2009) Estrogen receptor 1 mRNA is a prognostic factor in ovarian carcinoma: determination by kinetic PCR in formalin-fixed paraffin-embedded tissue. Endocr Relat Cancer 16:1229–1239
20. McCluggage WG (2008) My approach to and thoughts on the typing of ovarian carcinomas. J Clin Pathol 61:152–163

21. Noske A, Weichert W, Niesporek S, Röske A, Buckendahl AC, Koch I, Sehouli J, Dietel M, Denkert C (2008) Expression of the nuclear export protein chromosomal region maintenance/exportin 1/Xpo1 is a prognostic factor in human ovarian cancer. Cancer 112:1733–1743
22. Marquez RT, Baggerly KA, Patterson AP, Liu J, Broaddus R, Frumovitz M, Atkinson EN, Smith DI, Hartmann L, Fishman D, Berchuck A, Whitaker R, Gershenson DM, Mills GB, Bast RC Jr, Lu KH (2005) Patterns of gene expression in different histotypes of epithelial ovarian cancer correlate with those in normal fallopian tube, endometrium, and colon. Clin Cancer Res 11:6116–6126
23. Wamunyokoli FW, Bonome T, Lee JY, Feltmate CM, Welch WR, Radonovich M, Pise-Masison C, Brady J, Hao K, Berkowitz RS, Mok S, Birrer MJ (2006) Expression profiling of mucinous tumors of the ovary identifies genes of clinicopathologic importance. Clin Cancer Res 12:690–700
24. Rice GE, Edgell TA, Autelitano DJ (2010) Evaluation of midkine and anterior gradient 2 in a multimarker panel for the detection of ovarian cancer. J Exp Clin Cancer Res 29:62
25. Edgell TA, Barraclough DL, Rajic A, Dhulia J, Lewis KJ, Armes JE, Barraclough R, Rudland PS, Rice GE, Autelitano DJ (2010) Increased plasma concentrations of anterior gradient 2 protein are positively associated with ovarian cancer. Clin Sci (Lond) 118:717–725
26. Fletcher GC, Patel S, Tyson K, Adam PJ, Schenker M, Loader JA, Daviet L, Legrain P, Parekh R, Harris AL, Terrett JA (2003) hAG-2 and hAG-3, human homologues of genes involved in differentiation, are associated with oestrogen receptor-positive breast tumours and interact with metastasis gene C4.4a and dystroglycan. Br J Cancer 88:579–585
27. Gray TA, Maclaine NJ, Michie CO, Bouchalova P, Murray E, Howie J, Hrstka R, Maslon MM, Nenutil R, Vojtesek B, Langdon S, Hayward L, Gourley C, Hupp TR (2012) Anterior gradient-3: a novel biomarker for ovarian cancer that mediates cisplatin resistance in xenograft models. J Immunol Methods 378:20–32
28. King ER, Tung CS, Tsang YT, Zu Z, Lok GT, Deavers MT, Malpica A, Wolf JK, LuKH BMJ, Mok SC, Gershenson DM, Wong KK (2011) The anterior gradient homolog 3 (AGR3) gene is associated with differentiation and survival in ovarian cancer. Am J Surg Pathol 35:904–912
29. Zweitzig DR, Smirnov DA, Connelly MC, Terstappen LW, O'Hara SM, Moran E (2007) Physiological stress induces the metastasis marker AGR2 in breast cancer cells. Mol Cell Biochem 306:255–260
30. Pohler E, Craig AL, Cotton J, Lawrie L, Dillon JF, Ross P, Kernohan N, Hupp TR (2004) The Barrett's antigen anterior gradient-2 silences the p53 transcriptional response to DNA damage. Mol Cell Proteomics 3:534–547
31. Harris AL (2002) Hypoxia—a key regulatory factor in tumour growth. Nat Rev Cancer 2:38–47
32. Liu D, Rudland PS, Sibson DR, Platt-Higgins A, Barraclough R (2005) Human homologue of cement gland protein, a novel metastasis inducer associated with breast carcinomas. Cancer Res 65:3796–3805
33. Ramachandran V, Arumugam T, Wang H, Logsdon CD (2008) Anterior gradient 2 is expressed and secreted during the development of pancreatic cancer and promotes cancer cell survival. Cancer Res 68:7811–7818
34. Vanderlaag KE, Hudak S, Bald L, Fayadat-Dilman L, Sathe M, Grein J, Janatpour MJ (2010) Anterior gradient-2 plays a critical role in breast cancer cell growth and survival by modulating cyclin D1, estrogen receptor-alpha and survivin. Breast Cancer Res 12:R32

Virchows Arch (2012) 461:117–122
DOI 10.1007/s00428-012-1265-4

ORIGINAL ARTICLE

Role of tumor-associated macrophages and angiogenesis in desmoid-type fibromatosis

Stefhanie Romero · Justyna Szafranska · Eliovel Cabrera · Allan Gonzalez · Ana Peiró · Jaume Llauger · Luis Ortega · Silvia Bague · Belén Canet · Inigo Espinosa · Jaime Prat

Received: 2 March 2012 / Revised: 8 May 2012 / Accepted: 13 June 2012 / Published online: 29 June 2012
© Springer-Verlag 2012

Abstract Desmoid-type fibromatosis (DTF) is a rare soft tissue tumor with fibroblastic features affecting two to four individuals per million population per year. Despite its bland microscopic appearance, the tumor behaves aggressively. Although unable to metastasize, DTF tends to recur and local recurrences in anatomically critical sites can be fatal. Tumor-associated macrophages (TAM) play an important role in tumor development through the activation of angiogenesis, particularly in cases of epithelial malignancies. The aim of this study is to investigate the prognostic significance of TAMs and the number of microvessels in DTF. Tumor macrophages (CD163), microvessel density (CD31), and beta-catenin were investigated on 69 primary DTF cases with follow-up information. *CTNNB1* mutations were also studied. High density of tumor macrophages and high number of microvessels were associated with a significantly worse recurrence-free survival (P=0.03 and P=0.007, respectively). There was a significant correlation between microvessel density and CD163 macrophages (P=0.02). Furthermore, combination of high number of tumor macrophages and high microvessel density greatly improved the statistical significance (P=0.000005). Macrophages and microvessels may play an important role in the biologic behavior of DTF. This finding could help in the clinical management of patients with DTF.

Keywords Desmoid-type fibromatosis · Macrophages · Angiogenesis · Survival

S. Romero · J. Szafranska · E. Cabrera · A. Gonzalez · S. Bague · B. Canet · I. Espinosa · J. Prat
Department of Pathology, Hospital de la Santa Creu i Sant Pau, Institute of Biomedical Research (IIB Sant Pau), Autonomous University of Barcelona,
Barcelona, Spain

A. Peiró
Department of Orthopedic Surgery, Hospital de la Santa Creu i Sant Pau,
Barcelona, Spain

J. Llauger
Department of Radiology, Hospital de la Santa Creu i Sant Pau,
Barcelona, Spain

L. Ortega
Department of Pathology, Hospital Clínico San Carlos,
Madrid, Spain

J. Prat (✉)
Department of Pathology, Hospital de la Santa Creu i Sant Pau, Autonomous University of Barcelona,
Sant Quintí 87-89,
08041 Barcelona, Spain
e-mail: jprat@santpau.cat

Introduction

Desmoid-type fibromatosis (DTF) is a rare, locally invasive soft tissue tumor with fibroblastic–myofibroblastic features. Although unable to metastasize, desmoid-type fibromatoses often recur and they can rarely cause death when they invade or compress a vital structure, such as occurs with tumors in the root of the neck and within the abdomen [1]. There are currently no well-established prognostic factors beyond size, site, and the extent and adequacy of initial excision that can assist in the management of patients, especially in terms of follow-up. The identification of new prognostic factors, particularly ones that are relevant to the biology of DTF, will therefore be of clinical value in the management of these patients.

Many studies have shown that tumor-associated macrophages (TAMs) play an important role in tumor development and progression [2–4]. These macrophages produce cytokines that promote tumor growth, angiogenesis, extracellular matrix breakdown, invasion, and metastases. The

formation of new blood vessels has been correlated with prognosis in different types of tumors [5–10]. In addition, several studies have shown an association between number of TAMs and microvessel density [10–12].

In this study, we evaluated if there is a statistically significant correlation between TAMs, microvessel density, and clinical outcome in DTF.

Material and methods

Tissue samples

Paraffin-embedded samples of 69 specimens from 69 different patients with desmoid-type fibromatosis were obtained from the Tumor Tissue Bank and the Surgical Pathology files of the Hospital de la Santa Creu i Sant Pau, Barcelona, Spain and from the Hospital Clínico Universitario San Carlos, Madrid, Spain. The 69 specimens represent biopsy or resection of the primary disease, and the date of the diagnosis ranged from 1995 to 2009. For 12 cases, material from recurrent lesions was available. Follow-up information was available in 58 cases. Tumors were examined and classified using the histopathological criteria recommended by the World Health Organization. Cases in which patients were diagnosed with familial adenomatous polyposis (FAP) or had a family history of FAP were excluded; therefore, only sporadic desmoid tumors were ultimately evaluated.

Tissue microarray design

Two tissue microarrays (TA88 and TA98) were made using a tissue microarray workstation (Beecher Instruments, Sun Prairie, WI, USA). For each DTF case, a block with viable tumor was chosen. Hyalinized, myxoid, and hypocellular areas were avoided. Only high or moderately cellular areas were chosen. A 0.6-mm tissue core was taken from these areas in each of the blocks and inserted into the TA88 and TA98 tissue microarray blocks. To confirm the presence of the original tumor area, a hematoxylin and eosin section was analyzed.

Immunohistochemical analysis

Slides were cut at 4 μm. Deparaffination and antigen retrieval were done in a PT Link module (DAKO, Glostrup, Denmark) and immunohistochemistry was done in a Dako Autostainer (DAKO, Glostrup, Denmark). The primary antibodies used were CD31 (mouse monoclonal JC70A, prediluted, DAKO), CD163 (mouse monoclonal 10D6, 1/100, Novocastra, CA, USA) and β-catenin (mouse monoclonal β-catenin-1, prediluted, DAKO). Antigen retrieval solution was PT Link High pH. For CD31 and CD163, an additional incubation was done with EnVision Linker mouse (DAKO). Visualization system used was EnVision+FLEX (DAKO). Detection was done with DAB/HRP and hematoxylin as a counter stain. A tumor-associated macrophage identified by CD163 was defined as a cell with abundant cytoplasm, a dendritic pattern, and a round or oval nuclei. Microvessel density was determined by counting the number of CD31-positive microvessels in an entire 0.6-mm core. A microvessel was defined as any endothelial cell or endothelial cell cluster staining positive for CD31. Scoring criteria are shown in Table 1.

CTNNB1 genotyping

Mutations of the beta-catenin gene (*CTNNB1*) were assessed by PCR amplification followed by sequencing analyses. The exon 3 of *CTNNB1* was amplified by PCR using the oligonucleotide primers P3 (5′-GATTTGATGGAGTTGGACATGG-3′) and P4 (5′-TGTTCTTGAGTGAAGGACTGAG-3′). After this first-round amplification, 1 μL of the PCR product was reamplified by nested PCR, using a set of amplimers, P1 (5′-AGTCACTGGCAGCAACAGTC-3′) and P2 (5′-TCTTCCTCAGGATTGCCTT-3′). PCR conditions were as described previously; annealing temperatures were 55 °C for primers P3 and P4 and 52 °C for primers P1 and P2. The PCR products were purified using the exoSAP-IT (USB, Cleveland, OH, USA) and subjected to direct sequencing using ABI PRISM™ big Dye terminator v1.1 cycle sequencing Kit (Applied Biosystems, Foster City, CA, USA). Sequencing fragments were detected by capillary electrophoresis using an automated ABI PRISM 310 Genetic Analyzer (Applied Biosystems).

Statistical analysis

Statistical analysis was done using WinSTAT, a statistics add-in for Microsoft Excel, where the Kaplan–Meier method was used for survival analysis. Analysis of time to recurrence (recurrence-free survival (RFS)) was calculated

Table 1 Scoring criteria for MVD (CD31), macrophages (CD163), and β-catenin

	CD31 (MVD)	CD163 (macrophages)	β-catenin
Score 1	≤9 cells/0.6 mm	≤25 cells/0.6 mm	Negative; nuclear staining in <1 % of tumor cell/0.6 mm
Score 2	>9 cells/0.6 mm	>25 cells/0.6 mm	Positive; nuclear staining in ≥1 % of tumor cell/0.6 mm

from initial surgery for the primary desmoids to the first recurrence. Cox regression analysis was used to study the relationship between survival and the different variables. The following variables were introduced into the analysis: age, sex, tumor location, tumor size, surgical margins status, *CTNNB1* mutations, β-catenin expression, and co-expression of CD163 and CD31 in DTF cases. A value of $P \leq 0.05$ was considered statistically significant.

Results

Cases

A series of 69 paraffin-embedded primary desmoid-type fibromatoses were used for the construction of the tissue microarrays. Clinical details are described in Table 2. There was a slight predominance of female patients, with a female to male ratio of ~1.3:1. The average age of the patients at the time of initial diagnosis was 41 years (ranging from 13 to 94 years). Size was known in 45 cases and ranged from 1 to 27 cm (average, 7 cm). The most common location in this series was superficial trunk (27, 39 %), followed by upper and lower extremities (22, 31 %), neck (10, 15 %), and deep trunk/mesentery (10, 15 %). Information about resection margins was available for 41 patients. Margins were positive in 30 (73 %) tumors and negative in 11 (27 %) tumors. Univariate analysis showed that male patients and an extremity tumor location were significantly associated with an increased propensity for local recurrence ($P=0.02$ and $P=0.0001$, respectively; Table 3).

Table 2 Clinicopathologic features of 69 DTFs

Total no. of patients	69 (%)
Age ($n=69$; 13–94 years; median, 41)	
Sex ($n=69$)	
Female	39 (57)
Male	30 (43)
Size ($n=45$; 1–27 cm; median, 7)	
Location ($n=69$)	
Superficial trunk	27 (39)
Lower extremities	16 (23)
Neck	10 (15)
Deep trunk/mesentery	10 (15)
Upper extremities	6 (8)
Resection limits ($n=41$)	
Affected	30 (73)
Not affected	11 (27)

Table 3 Univariate analysis of different clinicopathological features for RFS in desmoid-type fibromatosis cases

Factors	5RFS rate % (*N* of cases)	*P*
Age		
≤30	44 (9)	0.7
>30 to ≤50	34 (27)	
>50	49 (22)	
Sex		
Female	55 (32)	0.026
Male	22 (26)	
Tumor location		
Superficial trunk	78 (24)	0.0001
Extremity	5 (19)	
Neck	61 (10)	
Deep trunk/mesentery	92 (5)	
Tumor size		
≤7 cm	32 (21)	0.4
>7 cm	16 (19)	
Resection limits		
Affected	11 (27)	0.1
Not affected	32 (10)	
Mutation		
T41A	40 (30)	0.6
S45F	0 (7)	
WT (no mutation)	50 (8)	
β-catenin protein		
Positive	42 (46)	0.7
Negative	38 (12)	
CD163 (macrophages)		
Positive	21 (26)	0.03
Negative	57 (26)	
CD31 (MVD)		
Positive	26 (26)	0.007
Negative	53 (28)	

5RFS 5-year recurrence-free survival rate in percentage (number of cases)

Expression of CD31 (MVD) and CD163 (TAM) in DTF

In order to investigate microvessel density (MVD) in patients with DTF, a vascular marker (CD31) was used to mark the endothelial cells. There was considerable variation in MVD across the different cases of DTF where it ranged from 0 to 33 per 0.6 mm core (mean, 9; Fig. 1). To quantify the amount of tumor-associated macrophages, we used CD163, a relatively specific marker for macrophages. The staining signal was located in the membrane and cytoplasm but not in the nucleus (Fig. 1). Tumor-associated macrophages ranged from 3 to 84/0.6 mm (mean, 25). There was a significant correlation between microvessel density and CD163-macrophages ($P=0.02$). CD163 and CD31 immunostaining was done on whole tissue sections of selected

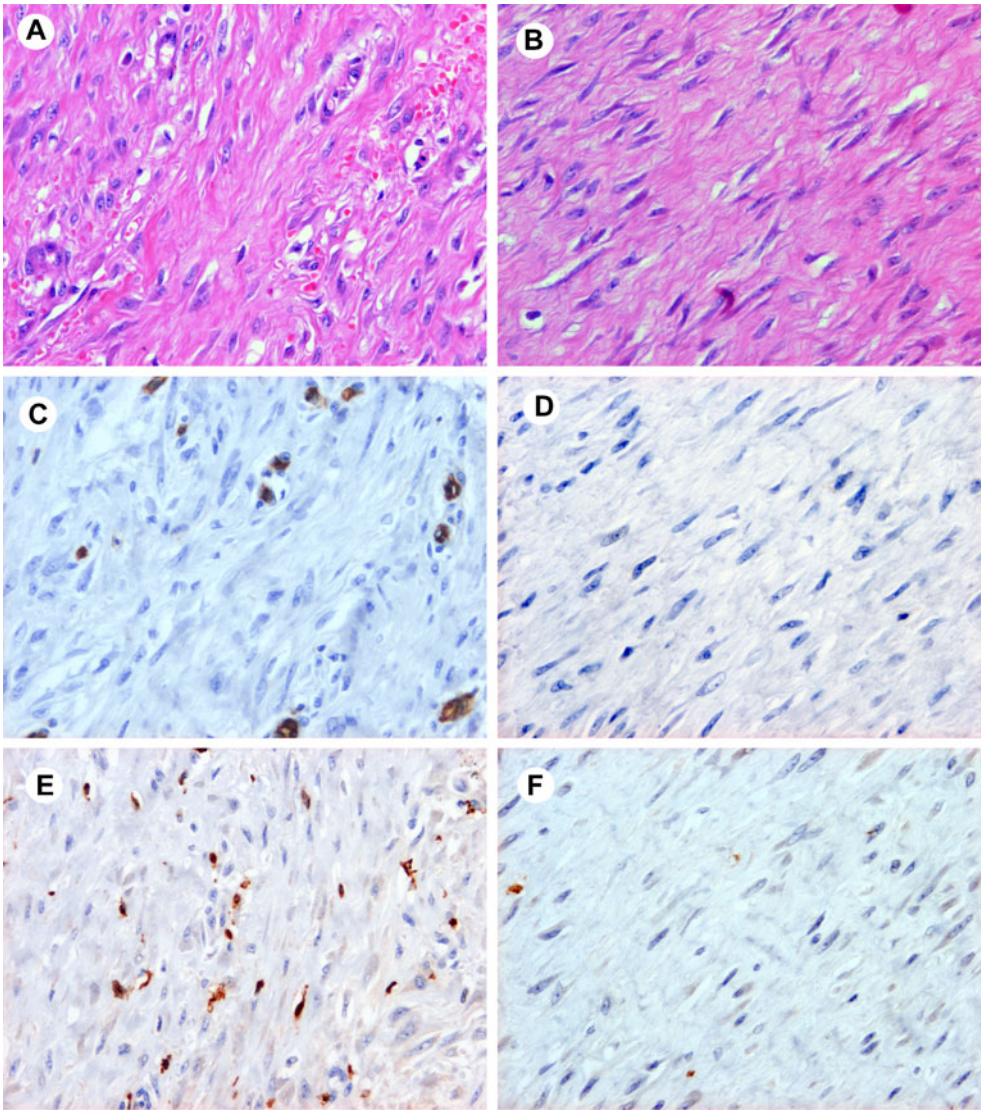

Fig. 1 Representative images showing a DTF case (**a**, H&E) with high MVD (**c**, CD31) and dense infiltrate of macrophages (**e**, CD163). A DTF case (**b**, H&E) with low MVD (**d**, CD31) and sparse infiltrate of macrophages (**f**, CD163)

cases of desmoid-type fibromatosis that showed dense or sparse CD163-positive macrophage infiltrates and high or low microvessel density. There seems to be a high degree of spatial uniformity in the intratumoral macrophage density and in the intratumoral number of microvessels within the high or moderately cellular areas. We next examined the consistency in macrophage infiltrate and MVD by comparing these features in 12 primary DTF and their corresponding recurrent lesions. The presence of TAMs, as measured by CD163 staining, and the level of MVD did not remain stable between primary and recurrent lesions (data not shown).

Prognosis of TAMs and MVD in DTF

Cases were stratified based on whether they displayed greater or less than the mean MVD and TAMs. RFS was used as an endpoint measurement for Kaplan–Meier analysis. Patients with high MVD (>9 microvessels/0.6 mm) had a higher probability to recur than patients with low MVD (n=54, P=0.007; Fig. 2a). Also, patients with DTF showing dense CD163-positive macrophages (>25/0.6 mm) had worse recurrence-free survival than patients with low macrophage infiltrate (n=52, P=0.03; Fig. 2b). Furthermore, the 12 cases that had high MVD and dense macrophage infiltrate showed a very strong correlation with poor patient outcome compared to the 38 cases that had either singly high MVD or dense macrophage infiltrate, or low for both (P=0.000005; Fig. 2c). In the multivariate analysis incorporating age, sex, tumor location, tumor size, surgical margins status, *CTNNB1* mutations, β-catenin expression, and co-expression of CD163 and CD31, the presence of high MVD and dense macrophage infiltrate was selected as the feature most predictive of recurrence (P=0.008).

CTNNB1 mutations and nuclear expression of B-catenin

Mutational information was available in 47 patients. A mutation in exon 3 of the *CTNNB1* gene was identified in

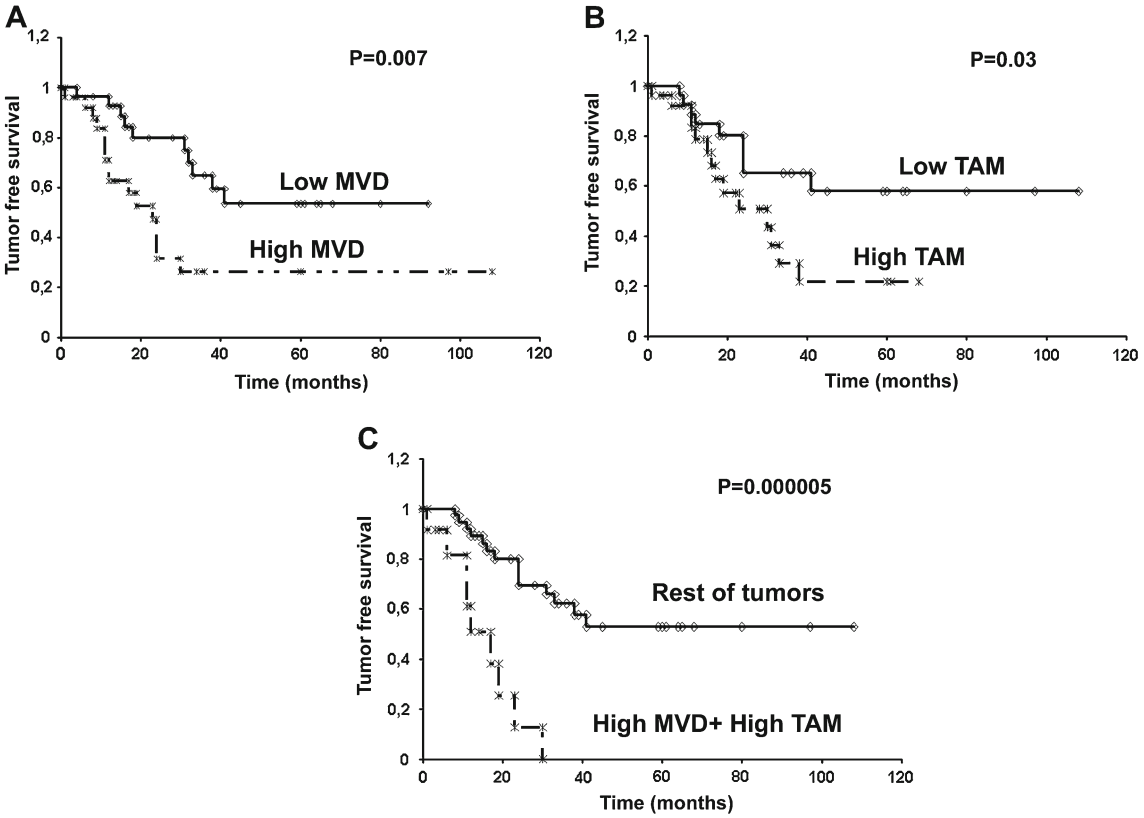

Fig. 2 **a** Kaplan–Meier plot showing that patients with a high MVD (>9/0.6 mm core) have a higher tendency to recur than patients with low MVD (≤9/0.6 mm core; $P=0.007$). **b** Kaplan–Meier plot showing that patients with high number of tumor-associated macrophages (TAM; >25/0.6 mm core) have a higher probability to recur than those with sparse infiltrate of macrophages (≤25/0.6 mm core; $P=0.030$). **c** Kaplan–Meier plot showing that patients with a high density of microvessels (>9/0.6 mm core) and a dense infiltrate of macrophages (>25/0.6 mm core) have a higher tendency to recur than the rest of the patients ($P=0.000005$)

39 cases (83 %). Four different point mutations in three different codons were found in all mutated cases: T41A ($n=30$, 77 %), S45F ($n=7$, 18 %), S45P ($n=1$, 2.5 %), and T40S ($n=1$, 2.5 %). There was no correlation between any specific mutation and prognosis (Table 3). Nuclear β-catenin expression was observed in 81 % of desmoid samples (56/69). Mutation of the *CTNNB1* gene was found in the majority of β-catenin negative cases (9/13; 70 %).

Discussion

TAMs can promote tumor development through activation of angiogenesis [2–4, 13]. In fact, TAMs and microvessel density are associated with adverse prognosis in several tumors [5–7, 10, 14, 15]. We have analyzed the role of tumor angiogenesis and tumor-associated macrophages in primary desmoid-type fibromatosis; a tumor with a high tendency to recur. Our results show that the density of microvessels and tumor-associated macrophages were predictive of recurrences. Of note, the combination of microvessel density and tumor-associated macrophages improved the prognostic significance. All together suggest that macrophages and microvessels may play an important role in the clinical behavior of desmoid-type fibromatosis.

Desmoid-type fibromatosis is a mesenchymal tumor that exhibits evidence of fibroblastic–myofibroblasltic differentiation. Local recurrence is frequent and histological examination alone does not permit accurate prediction of the clinical outcome. There are currently no well-established prognostic factors. Prognostic factors including age, tumor size, tumor location, and the extent and adequacy of initial excision remain controversial [1, 16–18]. In the 69 DTF cases studied in the current report, only tumor location and sex correlated with recurrence-free survival. Tumors located in extremities and male patients were associated with an increased propensity for local recurrence.

Thus, the identification of novel prognostic factors, particularly ones that are relevant to the oncobiology of desmoid-type fibromatosis, will therefore be of clinical value in the management of these patients. Recently, the presence of specific mutations in the β-catenin gene (*CTNNB1*) has been associated with local recurrence in sporadic desmoid-type fibromatosis. *CTNNB1* 45 F mutations significantly correlated with increased desmoids tumor recurrence [19]. In our cases, although tumors with *CTNNB1* 45 F

mutations showed poorer prognosis than tumors with *CTNNB1* 41A mutations, the difference was not significant.

Our findings suggest that CD163 macrophages and CD31 microvessels play an important role in the pathogenesis of DTF and suggest a relationship between macrophages and angiogenesis. A previous study suggested that microvessel density was not prognostic of clinical outcome in desmoid-type fibromatosis [20]. The small number of desmoid-type fibromatosis cases (33) or the variability of the morphology of the areas selected for each case may explain why the association between microvessel density and poor clinical prognosis in desmoid-type fibromatosis was not apparent in that study.

The relationship between TAMs and angiogenesis has been implicated in the tumorigenesis of several carcinomas and sarcomas [10, 11]. Espinosa et al., demonstrated that colony-stimulating factor 1 (CSF1)-associated macrophages highly correlated with microvessel density and poor prognosis in nongynecological leiomyosarcoma cases [10]. In addition, Kubota et al. showed that CSF1 depletion in a mouse model of osteosarcoma resulted in the suppression of tumor angiogenesis [21]. All together suggest that anti-angiogenic molecules or therapies that prevent the attraction of macrophages into the tumor stroma may help in the management of desmoid-type fibromatosis patients.

In summary, our results indicate that high microvessel density predicts poor outcome in desmoid-type fibromatosis. When combining high microvessel density with dense macrophage infiltrate, an even stronger prognostic correlation with patient outcome was obtained. Therapies that act on cancer cells but also targeting non-neoplastic cells may help in the management of these patients.

Acknowledgments This work was supported by grant from the Spanish Group for Sarcoma Research (GEIS; ref. GEIS/2008).

Conflicts of interest The authors declare no conflicts of interest.

References

1. Weiss SW, Goldblum JR (2008) Fibromatoses. In: Weiss SW, Goldblum JR (eds) Ezinger and Weiss's soft tissue tumors, 5th edn. Mosby, Inc, St Louis, pp 227–256
2. Condeelis J, Pollard JW (2006) Macrophages: obligate partners for tumor cell migration, invasion, and metastasis. Cell 124(2):263–266
3. Lewis CE, Pollard JW (2006) Distinct role of macrophages in different tumor microenvironments. Cancer Res 66(2):605–612
4. Qian BZ, Pollard JW (2010) Macrophage diversity enhances tumor progression and metastasis. Cell 141(1):39–51
5. Frank RE, Saclarides TJ, Leurgans S, Speziale NJ, Drab EA, Rubin DB (1995) Tumor angiogenesis as a predictor of recurrence and survival in patients with node-negative colon cancer. Ann Surg 222(6):695–699
6. Hollingsworth HC, Kohn EC, Steinberg SM, Rothenberg ML, Merino MJ (1995) Tumor angiogenesis in advanced stage ovarian carcinoma. Am J Pathol 147(1):33–41
7. Olivarez D, Ulbright T, DeRiese W, Foster R, Reister T, Einhorn L, Sledge G (1994) Neovascularization in clinical stage A testicular germ cell tumor: prediction of metastatic disease. Cancer Res 54 (10):2800–2802
8. Weidner N, Carroll PR, Flax J, Blumenfeld W, Folkman J (1993) Tumor angiogenesis correlates with metastasis in invasive prostate carcinoma. Am J Pathol 143(2):401–409
9. Weidner N, Semple JP, Welch WR, Folkman J (1991) Tumor angiogenesis and metastasis–correlation in invasive breast carcinoma. N Engl J Med 324(1):1–8
10. Espinosa I, Edris B, Lee CH, Wei Cheng H, Gilks CB, Wang Y, Montgomery KD, Varma S, Li R, Marinelli RJ, West RB, Nielsen T, Beck AH, van de Rijn M (2011) CSF1 expression in nongynecological leiomyosarcoma is associated with increased tumor angiogenesis. Am J Pathol 179 (4):2100–7
11. Lin EY, Li JF, Gnatovskiy L, Deng Y, Zhu L, Grzesik DA, Qian H, Xue XN, Pollard JW (2006) Macrophages regulate the angiogenic switch in a mouse model of breast cancer. Cancer Res 66 (23):11238–11246
12. Leek RD, Lewis CE, Whitehouse R, Greenall M, Clarke J, Harris AL (1996) Association of macrophage infiltration with angiogenesis and prognosis in invasive breast carcinoma. Cancer Res 56 (20):4625–4629
13. Espinosa I, Jose Carnicer M, Catasus L, Canet B, D'Angelo E, Zannoni GF, Prat J Myometrial invasion and lymph node metastasis in endometrioid carcinomas: tumor-associated macrophages, microvessel density, and HIF1A have a crucial role. Am J Surg Pathol 34 (11):1708-1714
14. Beck AH, Espinosa I, Edris B, Li R, Montgomery K, Zhu S, Varma S, Marinelli RJ, van de Rijn M, West RB (2009) The macrophage colony-stimulating factor 1 response signature in breast carcinoma. Clin Cancer Res 15(3):778–787
15. Lee CH, Espinosa I, Vrijaldenhoven S, Subramanian S, Montgomery KD, Zhu S, Marinelli RJ, Peterse JL, Poulin N, Nielsen TO, West RB, Gilks CB, van de Rijn M (2008) Prognostic significance of macrophage infiltration in leiomyosarcomas. Clin Cancer Res 14 (5):1423–1430
16. Pritchard DJ, Nascimento AG, Petersen IA (1996) Local control of extra-abdominal desmoid tumors. J Bone Joint Surg Am 78 (6):848–854
17. Easter DW, Halasz NA (1989) Recent trends in the management of desmoid tumors. Summary of 19 cases and review of the literature. Ann Surg 210(6):765–769
18. McKinnon JG, Neifeld JP, Kay S, Parker GA, Foster WC, Lawrence W Jr (1989) Management of desmoid tumors. Surg Gynecol Obstet 169(2):104–106
19. Lazar AJ, Tuvin D, Hajibashi S, Habeeb S, Bolshakov S, Mayordomo-Aranda E, Warneke CL, Lopez-Terrada D, Pollock RE, Lev D (2008) Specific mutations in the beta-catenin gene (CTNNB1) correlate with local recurrence in sporadic desmoid tumors. Am J Pathol 173(5):1518–1527
20. Kuhnen C, Helwing M, Rabstein S, Homann HH, Muller KM (2005) Desmoid-type fibromatosis (aggressive fibromatosis). Pathologe 26(2):117–126
21. Kubota Y, Takubo K, Shimizu T, Ohno H, Kishi K, Shibuya M, Saya H, Suda T (2009) M-CSF inhibition selectively targets pathological angiogenesis and lymphangiogenesis. J Exp Med 206 (5):1089–1102

Virchows Arch (2012) 461:123–128
DOI 10.1007/s00428-012-1268-1

ORIGINAL ARTICLE

BIRC2 amplification in squamous cell carcinomas of the uterine cervix

M. Choschzick · A. M. Tabibzada · F. Gieseking · L. Woelber · F. Jaenicke · G. Sauter · R. Simon

Received: 4 October 2011 / Revised: 1 June 2012 / Accepted: 13 June 2012 / Published online: 26 June 2012
© Springer-Verlag 2012

Abstract Oncogene amplification is a key step in cell transformation towards malignancy. Chromosomal aberrations involving the long arm of chromosome 11, including amplifications at 11q13 and 11q22, have been previously reported in cervical cancer. While the role of the *CCND1* gene as the driver gene for 11q13 amplification is well established in different tumor types, the significance of the 11q22 amplicon is less clear. The 11q22 amplicon corresponds to several putative target genes including the apoptose inhibitor *BIRC2*, recently detected as amplified in cervical cancer cell lines. To better understand the distribution and frequency of 11q amplification sites in uterine cervical carcinomas, we analyzed *BIRC2* and *CCND1* copy number changes using fluorescence in situ hybridization in a tissue microarray containing 238 cervical cancers. High-level amplification of *BIRC2* was found in 12.9 % of tumors. Amplification of *BIRC2* in cervical carcinomas was homogeneous as shown in corresponding whole tissue sections of amplified tumors at the tissue microarray. *BIRC2* amplification was significantly more frequent than *CCND1* amplification (2.1 %) in our cohort ($p<0.01$), and amplification of both genes were independent from each other. *BIRC2* amplification was associated with younger-patient age ($p<0.05$) and squamous cell differentiation ($p=0.025$) of cervix carcinomas. However, *BIRC2* copy number changes were not related to tumor stage, grading and nodal status of cervical cancers. In conclusion, *BIRC2* is amplified in a subset of squamous cell carcinoma of the uterine cervix. Further studies are necessary to evaluate possible prognostic effects of *BIRC2* copy number gains in cervical carcinomas.

Keywords BIRC2 · c-IAP · Amplification · Cervical carcinoma

M. Choschzick (✉) · A. M. Tabibzada · G. Sauter · R. Simon
Department of Pathology,
University Medical Centre Hamburg-Eppendorf,
Martinistr. 52,
20246 Hamburg, Germany
e-mail: mchoschz@uke.uni-hamburg.de

F. Gieseking · L. Woelber · F. Jaenicke
Department of Gynaecology,
University Medical Centre Hamburg-Eppendorf,
Hamburg, Germany

Introduction

Human papillomavirus (HPV) infection plays a pivotal role in cervical cancer development as shown in numerous studies [1, 2]. Despite this, deregulation of additional cellular signaling pathways is necessary for transformation towards malignancy. Amplification of oncogenes might be a key step in this process. Commonly amplified chromosomal regions in cervical carcinomas are located at 1q, 3q, 5p, 8q, 11q, and 20q [3–7]. So far, little is known about possible candidate oncogenes at the long arm of chromosome 11. At 11q13, the regulator protein cyclin D1 (CCND1) is generally accepted as a biologically relevant amplification target. CCND1 promotes as cofactor of cyclin-dependent kinases progression through G1-S-phase of the cell cycle via phosphorylation and inactivation of the retinoblastoma protein [8]. Chromosomal *CCND1* aberrations can be observed in a variety of cancer types including carcinomas of the uterine cervix [9, 10]. Imoto et al. [11] first reported on an amplicon at 11q22 comprising the baculoviral IAP repeat-containing protein 2 (*BIRC2*) gene in cervical cancer cell lines as well as in primary carcinomas of the uterine cervix. Recently, high resolution array CGH revealed the same amplicon at 11q22 containing the *BIRC* gene cluster in the cervical cancer cell Ca Ski [12]. *BIRC2* encodes for the protein c-IAP1 which is a member of the inhibitor-of-apoptosis family [13]. The c-IAPs play a role as caspase inhibitors

and co-factors in the tumor necrosis factor (TNF) signaling pathway. Down-regulation of c-IAP1 through activation of the Akt pathway results in apoptosis of endometrium cancer cell lines [14]. Several studies have shown that the 11q22 amplicon is not restricted to cervical cancer but also occurred in carcinomas of the lung and esophagus [15, 16].

To explore the potential significance of *BIRC2* and *CCND1* amplification in cancer of the uterine cervix, we analyzed a tissue microarray containing 238 cervical carcinoma specimens by FISH and correlated the results with clinicopathological prognostic parameters. Our results indicate a possible important role of the *BIRC2* amplicon in the development of a subset of cervical carcinomas.

Materials and methods

Cervix cancer tissue microarray

A total of 238 formalin-fixed (buffered neutral aqueous 4 % solution), paraffin-embedded cervical carcinomas with a median patient age of 47.5 (range 23–85) years were assembled in a tissue microarray (TMA) format as previously described [17]. Briefly, we punched one tissue cylinder per case with a diameter of 0.6 mm from representative tumor areas of a "donor" tissue block using a home-made semiautomatic robotic precision instrument. Tumor specimens (217) were analyzable for *BIRC2* and 193 specimens for *CCND1* by fluorescence in situ hybridization (FISH). Homogeneity analysis of *BIRC2* was carried out by hybridization of corresponding whole tissue sections of amplified tumors at the TMA. The use of these human tissues for protein expression and FISH studies was approved by the local ethics committee of the University of Hamburg.

FISH analysis

A FISH probe was generated from genomic clone RP11-864 G5 (length 186 kB) containing the entire *BIRC2* gene. The probe was labeled with digoxigenin-dUTP by nick translation (Invitrogen). A commercially available pericentromeric probe for chromosome 11 was used as reference (CEP 11 D11Z1 SpectrumOrange, Abbott, Downers Grove, IL, USA). The probe combination for FISH of the *CCND1* gene was LSI Cyclin D1 (11q13) SpectrumOrange/CEP 11 SpectrumGreen (order # 05J41-001). For dual-color FISH analysis, 4-μm sections of the cervical cancer tissue microarray blocks were transferred to an adhesive-coated slide system (Instrumedics, Hackensack, NJ, USA). For proteolytic slide pretreatment, a commercial kit was used (Paraffin pretreatment reagent kit; Vysis). Before hybridization, tissue microarray sections were deparaffinized, air dried, and dehydrated in 70 %, 85 %, and 100 % ethanol followed by denaturation for 5 min at 74 °C in 70 % formamide-2× SSC solution. After overnight hybridization at 37 °C in a humidified chamber, slides were washed and counterstained with 0.2 mmol/l 40,6-diamidino-2-phenylindole in an antifade solution. Detection of the digoxigenin-labeled probe was conducted using fluorescent antibody enhancer set (Roche) containing an FITC-conjugated antibody. For each tissue spot, the predominant gene and centromere copy numbers in the tumor cell nuclei were estimated. Differences between arrayed and analyzed tumor spots were either due to missing tissue samples on the tumor tissue microarray or lack of interpretable FISH signals.

A tumor was considered amplified if the ratio of *BIRC2*/centromere 11 and *CCND1*/centromere 11, respectively, was ≥2.0. Ratios of >1.0 and <2.0 were considered as gains and a ratio of ≤1.0 as normal.

CCND1 immunohistochemistry

Standard indirect immunoperoxidase procedures were used for the detection of CCND1 according to the recommendations of the manufacturer (DAKO; clone SP4). The CCND1 staining intensity and the fraction of stained tumor cells were recorded for each tissue spot. The staining intensity was estimated in a 4-step scale (0, no staining; 1+, faint intensity; 2+, moderate intensity; and 3+, strongest intensity). The fraction of stained cells was scored according to the following criteria: score 0 (no stained cells), score 1 (≤25 % stained cells), score 2 (≤50 % stained cells), score 3 (≤75 % stained cells), and score 4 (>75 % stained cells). A final immunohistochemistry (IHC) result was calculated from these scores. Negative, no staining at all; weak, intensity 1+, or intensity 2+ in ≤50 % of cells, or intensity 3+ in <25 % of cells; moderate, intensity 2+ in 50 % to 75 % of cells, or intensity 3+ in 25 % to 50 % of cells; and strong, intensity 2+ in >75 % of cells, or intensity 3+ in >50 % of cells.

Statistics

The Pearson χ^2 test was used to determine the correlation between gene amplification status of carcinomas and clinicopathologic parameters as well as CCND1 IHC. The Student's *t* test was used for the analysis of metric parameters. Analysis was performed using R statistical software package for Windows (version 2.7.2; R Foundation for statistical computing).

Results

BIRC2 and *CCND1* amplification

Tables 1 and 2 summarize the results of *BIRC2* and *CCND1* FISH analysis of 238 cervical carcinomas. *BIRC2* FISH

Table 1 Associations between *BIRC2* and *CCND1* amplification status of cervical carcinomas and associated clinicopathological tumor characteristics

	BIRC2 amplification status			*CCND1* amplification status				
	Analyzed (*n*)	*N* (%)	*A* (%)	Analyzed (*n*)	*N* (%)	*G* (%)	*A* (%)	*p* value
All samples	217	189 (87.1)	28 (12.9)	193	182 (94.3)	7 (3.6)	4 (2.1)	<0.01
Patient age (years)								
Median	47	49	35.5	47	47	50	57.5	<0.01[a]/0.046[b]
Average	49.2	50.9	37.9	49.1	48.9	49.9	57.3	
Histological type								
Squamous cell carcinoma	165	139 (84.2)	26 (15.8)	149	139 (93.3)	7 (4.7)	3 (2.0)	0.025[a]
Adenosquamous carcinoma	18	17 (94.4)	1 (5.6)	15	15	0	0	
Adenocarcinoma	29	28 (96.6)	1 (3.4)	27	26 (96.3)	0	1 (3.7)	
Others	5	5	0	2	2	0	0	
Tumor stage								
pT1a1	1	0	1	1	0	1	0	n.s.
pT1a2	2	2	0	2	2	0	0	
pT1b1	109	91 (83.5)	18 (16.5)	95	90 (94.7)	3 (3.2)	2 (2.1)	
pT1b2	22	22	0	20	20	0	0	
pT2a	17	16 (94.1)	1 (5.9)	17	17	0	0	
pT2b	51	44 (86.3)	7 (13.7)	43	39 (90.7)	3 (7.0)	1 (2.3)	
pT3a	6	6	0	6	6	0	0	
pT3b	1	1	0	1	1	0	0	
pT4	5	4 (80.0)	1 (20.0)	5	5	0	0	
Nodal stage								
N0	156	133 (85.3)	23 (14.7)	140	134 (95.7)	5 (3.6)	1 (0.7)	n.s.
N1	58	53 (91.4)	5 (8.6)	50	45 (90.0)	2 (4.0)	3 (6.0)	
Grading								
G1	7	7	0	3	3	0	0	n.s.
G2	89	78 (87.6)	11 (12.4)	83	77 (92.8)	4 (4.8)	2 (2.4)	
G3	113	96 (85.0)	17 (15.0)	98	93 (94.9)	3 (3.1)	2 (2.0)	
Tumor diameter								
Median (mm)	31	32	30	32	32	40	48	0.02[b]
Average (mm)	36.5	36.9	33.4	37.1	36.6	39.5	52.8	

N normal, *A* amplified, *G* gain, *n.s.* not significant

[a] *BIRC2* amplified vs. *BIRC2* normal

[b] *BIRC2* amplified vs. *CCND1* amplified

analysis was successful in 217 arrayed tissue samples. Amplification of *BIRC2* was found in 28 of 217 (12.9 %) tumors. Amplification levels were usually high with an average of 18.1 FISH signals per nucleus and an average ratio of 6.9. Homogeneity analysis was performed on all *BIRC2* amplified cervical carcinomas at the TMA by using corresponding whole tissue sections for FISH analysis. *BIRC2* amplification was homogeneous in the 28 at the TMA detected tumors. Figure 1 illustrates a representative example.

Table 2 Gene copy number and copy number ratio of 28 *BIRC2*-amplified cervical carcinomas and 4 cervical carcinomas with *CCND1* amplification

	Amplified tumors	Copy number			Ratio			*p* value
		Median	Average	Range	Median	Average	Range	
BIRC2	28	25	18.1	6.5–25	5.5	6.9	2.1–12.5	0.0013
CCND1	4	6.5	6.5	4–9	3.25	3.25	2–4.5	

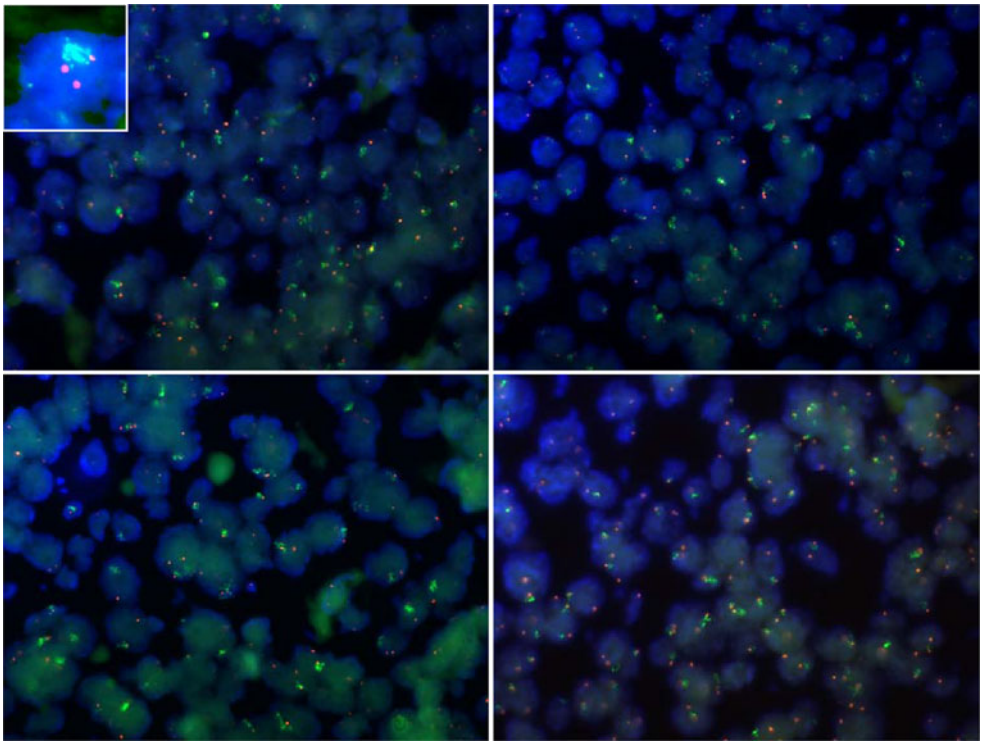

Fig. 1 Representative example of *BIRC2* FISH analysis in squamous cell carcinoma of the cervix: homogeneous BIRC2 amplification in four different tumor areas (*green signals* indicate BIRC2 copy number and *red signals* indicate copy number of chromosome 11)

Copy number alterations of *CCND1* occurred in 11 of 193 (5.7 %) interpretable cervical carcinoma samples including amplification in 4 (2.1 %) tumors and gains in 7 (3.6 %) tumors according to our predefined criteria. All *CCND1* amplified tumors only showed low-level copy number gains with <10 FISH signals per nucleus. *CCND1* amplification was statistically less frequent and the average ratio significantly lower than in tumors with amplifications of the *BIRC2* gene ($p<0.01$, each).

Furthermore, we studied the immunohistochemical expression of CCND1 in our data set (Table 3). In general, carcinomas of the uterine cervix with gains and/or CCND1 amplification showed significantly enhanced CCND1 staining intensity ($p=0.003$). Nevertheless, 3 of 4 *CCND1* amplified carcinomas exhibited no or only weak CCND1 expression.

Table 3 Analysis of immunohistochemical CCND1 expression compared to *CCND1* gene copy number in cervical carcinomas ($n=184$)

CCND1 IHC	***CCND1*** amplification status			
	Normal (%)	Gain (%)	Amplification (%)	*p* value
Negative	103 (59.5)	2 (28.6)	2 (50.0)	0.003
Weak	39 (22.5)	0	1 (25.0)	
Moderate	30 (17.3)	4 (57.1)	0	
Strong	1 (0.6)	1 (14.3)	1 (25.0)	
Total	173	7	4	184

We did not detect any tumors with co-amplification of *BIRC2* and *CCND1* in our examination of 181 tumor samples which were analyzable for both gene loci by FISH (Table 4). Only three tumors with *CCND1* copy number gains were simultaneously *BIRC2* amplified. There was no statistical difference between the observed (1.7 %) and the expected (0.8 %; based on the frequencies of individual amplifications) co-occurrence frequency of *BIRC2* amplification and *CCND1* copy number changes ($p=0.3$).

Clinicopathological associations

Clinicopathological features of cervical carcinomas with *BIRC2* and *CCND1* amplification/gains are given in Table 1. Patients with *BIRC2* amplified tumors were younger compared to patients with *BIRC2* disomy or *CCND1* amplification ($p<0.01$ and $p=0.046$, respectively). There was no association between *BIRC2* amplification status and tumor stage, tumor diameter, nodal status, or grading

Table 4 Occurence of co-amplifications of *BIRC2* and *CCND1* in 181 assessable cervical carcinomas

BIRC2	***CCND1***			*p* value
	Normal (%)	Gain (%)	Amplification (%)	
Normal (%)	149 (87.6)	4 (57.1)	4 (100)	0.3
Amplification (%)	21 (12.4)	3 (42.9)	0 (0)	
Total	170	7	4	181

of cervical carcinomas. *BIRC2* amplification was preferentially observed in squamous cell carcinomas of the cervix (p=0.025). Only one adenocarcinoma and one adenosquamous carcinoma showed amplification of *BIRC2*. The number of *CCND1* amplifications and *CCND1* gains was, in general, too low for further statistical analysis. *CCND1* amplified carcinomas were mostly observed in older patients with locally advanced tumors. The tumor diameter of *CCND1*-amplified carcinomas was higher than in *BIRC2*-amplified carcinomas. However, there were no obvious associations to pT category, nodal stage, grading, and histological subtype of cervical carcinomas.

Discussion

Gene amplification is an important mechanism for protein overexpression and oncogene activation in tumor cells [18]. Structural and numerical alterations of chromosome 11 have been reported in up to 48 % of cervical carcinomas [19]. In the majority of cases, these alterations occur as deletions of the region 11q23-qter. Nevertheless, copy number gains have also been found at 11q12-q23 [5].

The comparably high number of analyzed tumor samples at our TMA enabled a comprehensive survey of *BIRC2* and *CCND1* aberrations in cervical cancer and correlation with clinicopathological data. In the present study, 12.9 % of cervical cancers showed high level amplification of the *BIRC2* gene. This observation is in line with results recently achieved by Imoto et al. [11] describing *BIRC2* amplification in a small series of 5 of 27 (18.5 %) cervical cancer specimens. Taken together, the results of both studies suggest that *BIRC2* is amplified in a relevant proportion of cervical carcinomas. In contrast, *CCND1* aberrations were only detected in 11 of 184 (6 %) cervical carcinomas including four amplified tumors. Furthermore, amplification of the *BIRC2* locus occurred independently from *CCND1* amplifications in our study. Homogeneity of *BIRC2* amplification in cervical cancer as shown in this analysis also clearly indicates that our results are biologically significant. All these observations argue for an important and specific role of *BIRC2* in tumorigenesis of a subset of cervical carcinomas. *BIRC2* is located at 11q22 in the close proximity to *BIRC1*. The protein products of both genes (c-IAP1 and c-IAP2) play a role in the complex signal transduction system of the NF-κB pathway [20]. NF-κB proteins comprise a family of seven transcription factors which are responsible for regulation of different cellular functions including anti-apoptotic mechanisms [21]. TNFα receptor activation leads to unmasking cytosolic retained inactive NF-κB proteins which are translocated to the nucleus for binding at specific DNA target sites. The c-IAP proteins associate in this signaling cascade with TNF receptor-associated factors (TRAFs) and exert E3 ligase activities for ubiquinitation of downstream effectors and degradation of NF-κB inhibitory proteins [20]. The oncogenic capacities of the NF-κB pathway are rather complex, but the induction of caspase inhibitory proteins seems to be a key event [22, 23]. It may be hypothesized, that BIRC2 amplification and overexpression may constitutively activate the anti-apoptotic NF-κB signaling cascade and, therefore, promote tumor development. Further experimental data are required to pinpoint this assumption.

Remarkably, *BIRC2* amplification was strongly associated to squamous cell phenotype of cervical carcinomas and younger patient age. In contrast to adenocarcinomas which are more connected to HPV 18 infection, squamous cell carcinoma are mostly HPV 16 associated [24]. HPV integration into the host genome is associated with complex chromosomal rearrangements including DNA amplification inside and outside of the insertion locus [25–27]. Interestingly, Peter et al. detected 11q22 amplification in 2 out of 34 cervical carcinomas, both of which squamous cell carcinomas and associated to HPV 16. In the same study, eight cervical adenocarcinomas showed no 11q22 aberrations, while four of these tumors were associated with HPV 18. Thus, it may be speculated that specific types of HPV 16 perhaps in younger patients preferentially lead to amplification of 11q22 in a subgroup of cervical squamous cell carcinomas.

There are only few studies engaged in *CCND1* amplification frequency in carcinomas of the uterine cervix. In the present study, frequency of CCND1 alterations (5.7 %) was lower than in earlier publications (13.5 % and 24 %) [9, 28]. Methodological factors and differences in sample composition, as well as size of the examined data set, may be causative for the varying results. However, the rate of cervical carcinomas with positive CCND1 expression (40.4 %) in our examination was similar to previous analyses [29, 30]. Furthermore, we only found a loose correlation between immunohistochemically detectable expression and *CCND1* amplification status. This observation is in line with the results of Cheung et al. [28]. The exact role of CCND1 alterations in cervical cancer has not yet been determined. Our findings suggest that other mechanisms as amplification might be responsible for de-regulation of CCND1 expression in cervical carcinomas. The tendency to increased tumor diameters and older patient age in *CCND1* amplified tumors might be interpreted as late event in genetic instable tumors.

In summary, *BIRC2* is amplified in a subgroup of squamous-cell differentiated cervical carcinomas especially in younger women. *BIRC2* amplification is more frequent and independent from *CCND1* copy number changes in cervical cancer. Further studies will be necessary to confirm the clinicopathological relevance of *BIRC2* amplification in cervical cancer.

Conflict of interest statement We declare that we have no conflict of interest.

References

1. zur Hausen H (2002) Papillomaviruses and cancer: from basic studies to clinical application. Nat Rev Cancer 2:342–350
2. Pett M, Coleman N (2007) Integration of high-risk human papillomavirus: a key event in cervical carcinogenesis? J Pathol 212:356–367
3. Hidalgo A, Baudis M, Petersen I et al (2005) Microarray comparative genomic hybridization detection of chromosomal imbalances in uterine cervix carcinoma. BMC Cancer 5:77
4. Heselmeyer K, Schrock E, du Manoir S et al (1996) Gain of chromosome 3q defines the transition from severe dysplasia to invasive carcinoma of the uterine cervix. Proc Natl Acad Sci U S A 93:479–484
5. Huang FY, Kwok YK, Lau ET et al (2005) Genetic abnormalities and HPV status in cervical and vulvar squamous cell carcinomas. Cancer Genet Cytogenet 157:42–48
6. Wilting SM, Snijders PJ, Meijer GA et al (2006) Increased gene copy numbers at chromosome 20q are frequent in both squamous cell carcinomas and adenocarcinomas of the cervix. J Pathol 209:220–230
7. Atkin NB (1997) Cytogenetics of carcinoma of the cervix uteri: a review. Cancer Genet Cytogenet 95:33–39
8. Sherr CJ (1996) Cancer cell cycles. Science 274:1672–1677
9. Singh RK, Dasgupta S, Bhattacharya N et al (2005) Deletion in chromosome 11 and Bcl-1/Cyclin D1 alterations are independently associated with the development of uterine cervical carcinoma. J Cancer Res Clin Oncol 131:395–406
10. Diehl JA (2002) Cycling to cancer with cyclin D1. Cancer Biol Ther 1:226–231
11. Imoto I, Tsuda H, Hirasawa A et al (2002) Expression of cIAP1, a target for 11q22 amplification, correlates with resistance of cervical cancers to radiotherapy. Cancer Res 62:4860–4866
12. Lockwood WW, Coe BP, Williams AC et al (2007) Whole genome tiling path array CGH analysis of segmental copy number alterations in cervical cancer cell lines. Int J Cancer 120:436–443
13. Rothe M, Pan MG, Henzel WJ et al (1995) The TNFR2-TRAF signaling complex contains two novel proteins related to baculoviral inhibitor of apoptosis proteins. Cell 83:1243–1252
14. Gagnon V, St-Germain ME, Parent S et al (003) Akt activity in endometrial cancer cells: regulation of cell survival through cIAP-1. Int J Oncol 23:803–810
15. Imoto I, Yang ZQ, Pimkhaokham A et al (2001) Identification of cIAP1 as a candidate target gene within an amplicon at 11q22 in esophageal squamous cell carcinomas. Cancer Res 61:6629–6634
16. Dai Z, Zhu WG, Morrison CD et al (2003) A comprehensive search for DNA amplification in lung cancer identifies inhibitors of apoptosis cIAP1 and cIAP2 as candidate oncogenes. Hum Mol Genet 12:791–801
17. Sauter G, Simon R, Hillan K (2003) Tissue microarrays in drug discovery. Nat Rev Drug Discov 2:962–972
18. Albertson DG (2006) Gene amplification in cancer. Trends Genet 22:447–455
19. Kirchhoff M, Rose H, Petersen BL et al (1999) Comparative genomic hybridization reveals a recurrent pattern of chromosomal aberrations in severe dysplasia/carcinoma in situ of the cervix and in advanced-stage cervical carcinoma. Genes Chromosomes Cancer 24:144–150
20. Wajant H, Scheurich P (2011) TNFR1-induced activation of the classical NF-kappaB pathway. FEBS J 278:862–876
21. Zheng C, Yin Q, Wu H (2011) Structural studies of NF-kappaB signaling. Cell Res 21:183–195
22. Luo JL, Kamata H, Karin M (2005) IKK/NF-kappaB signaling: balancing life and death—a new approach to cancer therapy. J Clin Invest 115:2625–2632
23. Karin M, Cao Y, Greten FR et al (2002) NF-kappaB in cancer: from innocent bystander to major culprit. Nat Rev Cancer 2:301–310
24. Iwasawa A, Nieminen P, Lehtinen M et al (1996) Human papillomavirus DNA in uterine cervix squamous cell carcinoma and adenocarcinoma detected by polymerase chain reaction. Cancer 77:2275–2279
25. Wagatsuma M, Hashimoto K, Matsukura T (1990) Analysis of integrated human papillomavirus type 16 DNA in cervical cancers: amplification of viral sequences together with cellular flanking sequences. J Virol 64:813–821
26. Winder DM, Pett MR, Foster N et al (2007) An increase in DNA double-strand breaks, induced by Ku70 depletion, is associated with human papillomavirus 16 episome loss and de novo viral integration events. J Pathol 213:27–34
27. Thorland EC, Myers SL, Gostout BS et al (2003) Common fragile sites are preferential targets for HPV16 integrations in cervical tumors. Oncogene 22:1225–1237
28. Cheung TH, Yu MM, Lo KW et al (2001) Alteration of cyclin D1 and CDK4 gene in carcinoma of uterine cervix. Cancer Lett 166:199–206
29. Carreras R, Alameda F, Mancebo G et al (2007) A study of Ki-67, c-erbB2 and cyclin D-1 expression in CIN-I, CIN-III and squamous cell carcinoma of the cervix. Histol Histopathol 22:587–592
30. Bae DS, Cho SB, Kim YJ et al (2001) Aberrant expression of cyclin D1 is associated with poor prognosis in early stage cervical cancer of the uterus. Gynecol Oncol 81:341–347

Virchows Arch (2012) 461:129–139
DOI 10.1007/s00428-012-1267-2

ORIGINAL ARTICLE

PI3KCA mutations and/or PTEN loss in Her2-positive breast carcinomas treated with trastuzumab are not related to resistance to anti-Her2 therapy

Mattia Barbareschi · Lucia Veronica Cuorvo · Salvatore Girlando · Emma Bragantini · Claudio Eccher · Elena Leonardi · Antonella Ferro · Alessia Caldara · Renza Triolo · Chiara Cantaloni · Nicola Decarli · Enzo Galligioni · Paolo Dalla Palma

Received: 18 February 2012 / Revised: 28 May 2012 / Accepted: 13 June 2012 / Published online: 29 June 2012
© Springer-Verlag 2012

Abstract The purpose of this study is to evaluate whether activating mutations of the p110α catalytic subunit of class A phosphoinositide 3-kinases (*PI3KCA*) or complete loss of phosphatase and tensin homolog (PTEN) is associated with response to anti-human epidermal growth factor receptor 2 (Her2) treatment in breast cancer (BC). We analysed *PI3KCA* hot-spot mutations and PTEN immunohistochemical expression in 129 Her2-positive infiltrating BC treated with trastuzumab, including 26 cases treated with neoadjuvant therapy, 48 metastatic infiltrating breast cancer (IBC; MBC) and 55 early-stage IBC, with complete clinical information (mean follow-up 37, 66 and 32 months, respectively). *PI3KCA* hot-spot mutations were observed in 25 cases (19 %): 12 (9 %) in exon 9 and 13 (10 %) in exon 20. No correlations were observed between mutations and pathological and biological parameters. In patients treated with neoadjuvant therapy and in MBC, we did not observe any relationship with response to trastuzumab-based therapy. PTEN loss was observed in 24 out of 86 informative cases (28 %), 3 (13 %) of which were also mutated for *PI3KCA*. PI3K pathway activation, defined as *PI3KCA* mutation and/or PTEN loss, was not associated with response to treatment or clinical outcome in MBC. *PI3KCA* mutation and/or PTEN loss should not exclude patients from potentially beneficial anti-Her2 therapy.

Keywords Breast cancer · Her2 · Trastuzumab · *PI3KCA* mutation · PTEN loss

M. Barbareschi (✉) · L. V. Cuorvo · S. Girlando · E. Bragantini · E. Leonardi · C. Cantaloni · N. Decarli · P. D. Palma
Unit of Surgical Pathology, Laboratory of Molecular Pathology, Trentino Biobank, S. Chiara Hospital, Trento, Italy
e-mail: mattia.barbareschi@apss.tn.it

C. Eccher
Bruno Kessler Foundation, Trento, Italy

A. Ferro · A. Caldara · R. Triolo · E. Galligioni
Unit of Medical Oncolgy, S. Chiara Hospital, Trento, Italy

Introduction

Human epidermal growth factor receptor 2 (Her2) is a tyrosine kinase receptor, which is overexpressed or amplified in 20 to 25 % of infiltrating breast carcinomas (IBC), which may behave more aggressively. Her2 overexpression may lead to increased receptor homo/heterodimerization, which induces phosphorylation of the intracellular domain, leading in turn to activation of many downstream signalling molecules, including class A phosphoinositide 3-kinases (PI3K)/AKT. Activated PI3K catalyzes the phosphorylation of inositol lipids to produce phosphatidylinositol-3,4,5-trisphosphate (PIP3), which in turn, as a negative feedback mechanism, is dephosphorylated to PIP2 by phosphatase and tensin homolog (PTEN). PIP3 activates the serine/threonine kinase AKT which in turn phosphorylates and regulates the mammalian target of rapamycin (mTOR).

Trastuzumab, a humanized monoclonal antibody targeting the extracellular domain of Her2, has good therapeutic efficacy in patients with Her2-positive IBC. Trastuzumab is effective in neoadjuvant therapy, in cases of metastatic breast cancer (MBC) and in the adjuvant setting in early-stage IBC.

However, not all patients benefit from trastuzumab-based therapy, and a relevant percentage shows an initial resistance to trastuzumab.

The underlying antitumoural mechanisms of trastuzumab are complex and not completely understood [1]. The hypothesized mechanisms include inhibition of Her2 homo/heterodimerization, Her2 endocytosis and degradation or reduced shedding of the extracelluar domain, leading to downregulation of downstream signalling through the PI3K–AKT pathway. An alternative mechanism of action could be related to the fact that trastuzumab, being an intact monoclonal antibody, may recruit Fc-competent immune effector cells and the other components of antibody-dependent cell-mediated cytotoxicity, leading to tumour cell death [2].

Several lines of evidence suggest that Her2-independent activation of the PI3K–AKT pathway may be related to resistance to trastuzumab [3–5]. Aberrations of the components of the PI3K–AKT pathway are frequent in IBC, including activating mutations of the p110α catalytic subunit of PI3K (*PI3KCA*) and PTEN loss, which have been described in 9 to 45 % of cases [6–17] and 4 to 28 % of cases [18–21], respectively. The vast majority of *PIK3CA* mutations, comprising approximately 90 % of cases, are clustered at two hot-spot regions in exon 9 (E542K and E545K) and exon 20 (H1047R and H1047L) encoding the helical and kinase domains, respectively [6–17]. *PI3KCA* mutations are among the most common genetic aberrations in human IBC and have generally been reported as more frequent in node-negative [8, 17], estrogen receptor (ER)-positive and Her2-negative IBC [8–10, 14, 22–24], but data are not consistent. Controversies exist also concerning the prognostic value of *PI3KCA* mutations: most authors report favourable relation with survival [9, 10, 25, 26] but again data are not consistent [14, 27, 28] probably due to the heterogeneity of the investigated series and to possible different pathogenetic significance of mutations occurring at different sites in the molecule [7]. *PI3KCA* mutations have also been indicated as possible markers for poor response to trastuzumab [21, 27–29], but data are still not conclusive [5, 27, 30, 31]. Preclinical studies also suggest that the *PI3KCA* gene could be a target for new drugs [32] suggesting the possibility to combine anti-Her2 therapy with different inhibitors targeting PI3K, TORC1, AKT or EGFR [33, 34].

In the present study, we analyse *PI3KCA* mutations at hot-spots in exon 9 and exon 20 and PTEN expression in a retrospective series of Her2-positive IBC treated with trastuzumab (26 cases treated with neoadjuvant therapy, 48 metastatic IBC and 55 early-stage IBC), investigating their frequency and their relationship with clinical and pathological parameters and response to trastuzumab treatment.

Material and methods

Patients and tumour samples

We retrospectively evaluated 129 Her2-positive IBC which had been treated with trastuzumab at the Santa Chiara Hospital of Trento Italy between 2000 and 2010. The study has been approved by the ethical committee of the Santa Chiara Hospital. The investigated cases include three groups of patients: 26 primary IBC treated with neoadjuvant trastuzumab therapy, 48 advanced MBC and 55 early-stage IBC treated with adjuvant therapy. Complete follow-up information was available for all cases; mean follow-up was 37, 66 and 32 months for the above three groups of patients. Neoadjuvant therapy consisted of doxorubicin and trastuzumab for three courses followed by paclitaxel and trastuzumab for 4 cycles followed by cyclophosphamide, methotrexate, fluorouracil associated with trastuzumab (according to NOAH trial regimen). In MBC patients, the first-line therapy consisted of trastuzumab associated with taxanes (weekly paclitaxel or docetaxel). All early-stage IBC patients received adjuvant trastuzumab for 1 year after surgery. All patients showing positive estrogen receptors also received hormonal therapy with tamoxifen±ovarian ablation if in premenopausal status and with aromatase inhibitors if in postmenopausal status. All cases were reviewed by a pathologist (MB). For each case, one representative tissue block was selected for further analyses. The percentage of tumour cells in each block was visually estimated, and only cases with more that 50 % of tumour cell content were included in the study.

For patients affected by primary IBC treated with neoadjuvant trastuzumab, pathological response at surgery was scored as: (a) *complete*, if no invasive residual disease in breast and axilla was found, (b) *partial*, if the residual tumour burden was inferior to the clinically estimated tumour diameter and (c) *absent*, if the residual tumour burden was identical or higher than the clinically estimated tumour diameter (stable or progressive disease). For MBC, response to therapy was evaluated clinically. The different pathological characteristics of the whole group of cases are shown in Table 1, and the characteristics of the three different series are illustrated in Tables 2, 3 and 4.

Her2 immunoreactivity was evaluated using the HercepTest kit (DakoCytomation, Glostrup, Denmark) according to the manufacturer's FDA-approved procedures, using manual or computer-assisted assessment [35]. All cases with Her2 score 2+ were further investigated with fluorescent in situ hybridization using the *HER2* FISH pharmDx™ kit (DakoCytomation). Tumours with a *HER2*/Cep17 ratio ≥2.2 were considered as amplified.

In all cases, ER, progesterone receptor (PgR) and Ki67 were evaluated using 6 F11 (Leica, Novocastra, Newcastle, UK), Pgr636 (DakoCytomation) and MIB1 (Leica, Novocastra) antibodies, respectively [36]. Ki67 labelling index was

Table 1 Clinical–pathologic characteristics of the whole series of Her2-positive IBC according to mutational status of *PI3KCA*

	Total	mt Ex 9 *PI3KCA*	%	mt Ex 20 *PI3KCA*	%	WT *PI3KCA*	%
Cases	129	12	9.3	13	10	104	81
Histotype							
Ductal	115	11	9.5	11	9.5	93	80.8
Lobular	10	1	10	0		9	90
Other	4	0		2	50	2	50
Tumour size							
T1	42	3	7.1	7	16.7	32	76.2
T2	63	8	12.7	4	6.3	51	81
T3–T4	22	1	4.5	2	9.1	19	83.4
Not known	2	0		0		2	100
Nodal status							
Negative	40	5	12.5	6	15	29	72.5
Positive	88	7	8	7	8	74	84
Not known	1					1	100
Hormone receptor status[a]							
ER positive	73	7	9.6	9	12.4	57	78
ER negative	56	5	8.9	4	7.1	47	84
Not known							
PgR positive	58	4	6.9	6	10.3	48	82.7
PgR negative	71	8	11.3	7	9.9	56	78.8
Proliferative activity[b]							
Ki67 high	119	12	10	13	11	94	79
Ki67 low	7	0		0		7	100
Not known	3	0		0		3	100

[a]Hormone receptor status was defined as positive for ER and PgR if at least 1 % reactive cells were seen

[b]Proliferative activity was scored as high if Ki67-reactive cells were at least 25 %

evaluated manually in the peripheral areas of all tumours. In case of marked heterogeneity, Ki67 labelling was also evaluated using computer-assisted image analysis [37]. Cases with at least 1 % reactive cells were considered positive for ER and PgR. Ki67 labelling was scored as high if at least 25 % reactive cells were counted. A subset of 34 cases out of the series of advanced MBC and 52 out of 55 cases treated with adjuvant therapy were immunostained for PTEN, using the 138G6 antibody (Cell Signaling Technology, Celbio, Italy). PTEN immunohistochemistry was scored as absent (complete PTEN loss) when no immunostaining was observed in spite of positive internal controls, or positive, if any degree of cytoplasmic and nuclear staining was observed. In 14 cases, PTEN could not be evaluated because of lack of available histological samples or inadequate internal control immunostaining.

Mutational analysis

Sample DNA extraction

Five 10-μm sections were cut from each paraffin-embedded tumour block. Slides were deparaffinized twice with 1 mL of xylene, vortexed and centrifuged. The supernatant was removed and then washed with 1 mL absolute ethanol. The samples were resuspended in 180 μl lysis buffer containing 20 μl proteinase K. DNA was isolated with the Qiamp DNA mini-kit (Qiagen, Valencia, CA) and was incubated overnight at 56 °C at 300 rpm.

Real-time polymerase chain reaction amplification

Briefly, DNA fragments were amplified using RT-PCR with primers specific for exon 9 and exon 20 of the *PI3KCA* gene, designed to allow the identification of the following mutations: E542K, E545K and Q546K in exon 9 and M1043I, H1047R, H1047L, G1049S and G1049R in exon 20 (Diatech Pharmacogenetics, Jesi, Italy). Each mix contained 5× buffer Mg^{2+}-free, 50 mM Mg^{2+} solution, 10 mM of each dNTP, 1 μl of specific primers, EvaGreen dye (20× in water), 5 U/μl Hot Star Taq DNA Polymerase and 100 ng genomic DNA in a 50-μl final volume. The mixture was denatured for 3 min at 95 °C and underwent 40 cycles: at 95 °C for 20 s, at 57 °C for 30 s and at 72 °C for 30 s, followed by a final step for 6 min at 60 °C for the acquisition the green signal.

Table 2 Clinical–pathologic characteristics of the series of Her2-positive IBC treated with neoadjuvant trastuzumab therapy according to mutational status of *PI3KCA*

	Total	mt Ex 9 *PI3KCA*	%	mt Ex 20 *PI3KCA*	%	WT *PI3KCA*	%
Cases	26	1	3.8	3	11.5	22	84.6
Mean follow-up	37						
Histotype							
Ductal	26	1	3.8	3	11.5	22	84.6
Tumour size							
T1							
T2	15	1	6.6	1	6.6	13	86.6
T3–T4	11	0		2	18.2	9	81.8
Nodal status							
Negative	7	1	14.3	1	14.3	5	7.1
Positive	19	0		2	10.5	17	89.4
Hormone receptor status							
ER positive	13	0		2	15.4	11	84.6
ER negative	13	1	7.7	1	7.7	11	84.6
Not known							
PgR positive	11	0		1	9.1	9	81.8
PgR negative	15	1	6.6	2	13.3	13	86.6
Proliferative activity							
Ki67 high	23	1	4.3	3	13	19	82.6
Ki67 low	2	0		0		2	100
Not known	1	0		0		1	100

Pyrosequencing

Each sample submitted for pyrosequencing was prepared utilizing 3 μl streptavidin sepharose (GE Healthcare, Buckinghamshire, UK), 37 μl PyroMark binding buffer (Qiagen), 20 μl MB water (Qiagen) and 20 μl biotinylated PCR product. The plate was mixed and incubated for 15 min on a shaking table at 1,400 rpm. In the second step, the binding solutions were released into 40 μl of annealing buffer containing the respective sequencing primer. Primers were annealed to the target after incubation at 80 °C for 2 min and allowed to cool to room temperature prior to pyrosequencing. PyroGold reagents were used for the pyrosequencing reaction, and the signal was analysed using the PyroMark Q96 ID system (Qiagen). The software analyses the bioluminescence produced at the end of the enzymatic reactions, of which the intensity is proportional to the number of incorporated nucleotides. Positive controls were cases with known *PI3KCA* mutational status. The results of the experiments were interpreted according to the cut-offs provided by the manufacturer (Diatech Pharmacogenetics). For exon 9 mutations, the cutoff nucleotide substitution values to define a case as mutated were: E542K A>5 %, E545K A >10 %, Q546K G>10 % and Q546K A>5 %. For exon 20 mutations, the cut-off nucleotide substitution values to define a case as mutated were: M1043I T>10 %, M1043I A>10 %, H1047R C>12 %, H1047L A>10 %, G1049S G>6 % and G1049R T>5 %.

Statistical methods

Statistical analysis was performed using the SPSS 15.0 software for Windows (SPSS Inc., Chicago, IL). In the groups of primary IBC treated with neoadjuvant trastuzumab therapy and MBC groups, we evaluated the possible association of *PI3KCA* mutations/PTEN loss with response to therapy; in the series of MBC, we evaluated also their relation with overall and disease-free survival (DFS). No survival analysis was performed in early IBC because of the short follow-up (all patients are alive and disease free).

Contingency tables were used to analyse the relationships between the categorical variables: absence/presence of mutation/loss of PTEN vs. pathological and biological parameters. Fisher's exact test (2×2 tables) and chi-square test (general contingency tables) were used to test the significance of the association between two classifications. Kaplan–Meier survival analysis with log-rank test was used to determine the difference in DFS and overall survival between groups. All tests were two sided. The statistical significance level was chosen at 5 %. All analyses were performed blinded to the study endpoints.

Table 3 Clinical–pathologic characteristics of the series of Her2-positive MBC treated with trastuzumab therapy according to mutational status of *PI3KCA*

	Total	mt Ex 9 *PI3KCA*	%	mt Ex 20 *PI3KCA*	%	WT *PI3KCA*	%
Cases	48	3	6.25	2	4.1	43	85.6
Mean follow-up	66						
Histotype							
Ductal	43	3	7	2	4.6	38	88.4
Lobular	3	0		0		3	100
Other	2	0		0		2	100
Tumour size							
T1	15	1	6.6	2	13.3	12	80
T2	22	1	4.5	0		21	95.4
T3–T4	10	1	10	0		9	90
Not known	1	0		0		1	100
Nodal status							
Negative	10	1	10	2	20	7	70
Positive	37	2	5.4	0		35	94.6
Not known	1					1	100
Hormone receptor status							
ER positive	23	2	8.7	1	4.3	20	87
ER negative	25	1	4	1	4	23	92
Not known							
PgR positive	16	1	6.6	0		15	193.7
PgR negative	32	1	3.1	2	6.3	29	90.6
Proliferative activity							
Ki67 high	43	3	7	2	4.6	37	86
Ki67 low	3	0		0		3	100
Not known	2					2	100

Results

Clinical outcome of the patients

In the series of patients treated with neoadjuvant trastuzumab therapy, 11 (42 %) showed complete pathological response, 14 (54 %) partial pathological response and 1 (4 %) showed stable disease. At a mean follow-up of 37 months, 3 patients died of disease, 3 were alive with relapsing disease and 20 were alive without evidence of disease.

In the series of patients affected by MBC treated with trastuzumab therapy, 4 (8 %) showed complete clinical response, 18 (38 %) partial clinical response with more than 50 % reduction of the tumour, 14 (29 %) partial clinical response with less than 50 % reduction of the tumour, 8 (17 %) stable disease and 3 (6 %) showed progressive disease. In responsive cases (complete and partial responses), median response duration was 9.5 months with two patients having durable complete response over 3 years of trastuzumab treatment. At a mean follow-up of 66 months, 39 patients died of disease, 7 were alive with disease and 2 were alive without evidence of disease. In the series of 55 early-stage IBC treated with adjuvant therapy at a mean follow-up of 32 months, all patients were alive without evidence of relapse.

Frequency of *PI3KCA* mutations and relationships with pathological and biological characteristics

In the whole series of 129 IBC, *PI3KCA* mutations were observed in 25 cases (19 %): 12 (9 %) in exon 9 (2 Q546K and 10 E545K) and 13 (10 %) in exon 20 (1 H1047L and 12 H1047R; Fig. 1). *PI3KCA* mutations were observed in 15 % of locally advanced IBC treated with neoadjuvant therapy, in 10 % of MBC and in 29 % of early-stage IBC treated with adjuvant trastuzumab therapy. The relationships between *PI3KCA* mutation and pathological and biological characteristics are shown in Table 1 for the whole series and in Tables 2, 3 and 4 for the three different groups of patients. No statistically significant correlations were observed between mutations and pathological and biological parameters. In particular, we did not observe any relationship with histological type, nodal status and hormone receptor status.

Table 4 Clinical–pathologic characteristics of the series of Her2-positive IBC treated with adjuvant trastuzumab therapy according to mutational status of *PI3KCA*

	Total	mt Ex 9 *PI3KCA*	%	mt Ex 20 *PI3KCA*	%	WT *PI3KCA*	%
	55	8	14.6	8	14.6	39	70.9
Mean follow-up (months)	32						
Histotype							
Ductal	46	7	15.2	6	13	33	71.7
Lobular	7	1	14.3	0	0	6	85.7
Other	2			2	100	0	
Tumour size							
T1	27	2	7.4	5	18.5	20	74
T2	26	6	23	3	11.5	17	65.3
T3–T4	1					1	1
Not known	1					1	1
Nodal status							
Negative	23	3	13	3	13	17	74
Positive	32	5	15.6	5	15.6	22	68.8
Not known							
Hormone receptor status							
ER positive	37	5	13.5	6	16.2	26	70.3
ER negative	18	3	16.6	2	11.1	13	72.2
Not known							
PgR positive	31	3	9.7	5	16.1	23	74.2
PgR negative	24	5	20.8	3	12.5	16	66.6
Not known							
Proliferative activity							
Ki67 high	53	8	15.1	8	15.1	47	88.7
Ki67 low	2					2	100

Association of *PI3KCA* mutation with response to therapy and clinical outcome

In the series of patients treated with *neoadjuvant therapy*, *PI3KCA* mutations were observed in 3 out of the 11 cases with complete pathological response (three exon 20 H1047R mutations with 14.1, 33.9 and 71.2 % substitution frequency, respectively) and in 1 out of 14 cases with partial response (one exon 9 Q546K mutation with 19.5 % substitution frequency) (Table 5). These data suggest that *PI3KCA* mutations are not a major determinant of trastuzumab resistance because even cases with very high percentages of the mutated allele showed complete pathological response.

In the series of *metastatic breast carcinomas*, *PI3KCA* mutations were observed in 3 out of the 29 cases with partial clinical response (two exon 9 E545K mutations with substitution frequency of 11.6 and 38.4 % respectively, and one exon 20 H1047R mutation with 28.1 % substitution frequency) and in 1 out of 10 cases with stable/progressive disease (exon 20 H1047R mutation with 21.1 % substitution frequency; Table 6). No gene mutations were observed in the four patients showing complete clinical responses. These data suggest that *PI3KCA* mutations are not a major determinant of trastuzumab resistance in metastatic IBC treated with trastuzumab. Survival analysis in metastatic IBC showed that *PI3KCA* mutations are not related to adverse clinical outcome. However, the survival analysis has limited statistical power due to the limited number of investigated cases.

PTEN expression and PI3K mutation

PTEN immunohistochemical expression was evaluable in 86 cases and ranged from complete loss of reactivity in tumour cells, in spite of positive internal controls, to various degrees of immunoreactivity (Fig. 2). PTEN loss was observed in 24 (28 %) cases, 3 (13 %) of which were also mutated for *PI3KCA*. PTEN immunostaining was observed in 62 (72 %) cases, 17 (27 %) of which showed PI3K mutation. These data show that in the present series of IBC, PTEN loss, although less frequent in cases with concurrent *PI3KCA* mutation (13 versus 27 %), was not mutually exclusive with *PI3KCA* mutation.

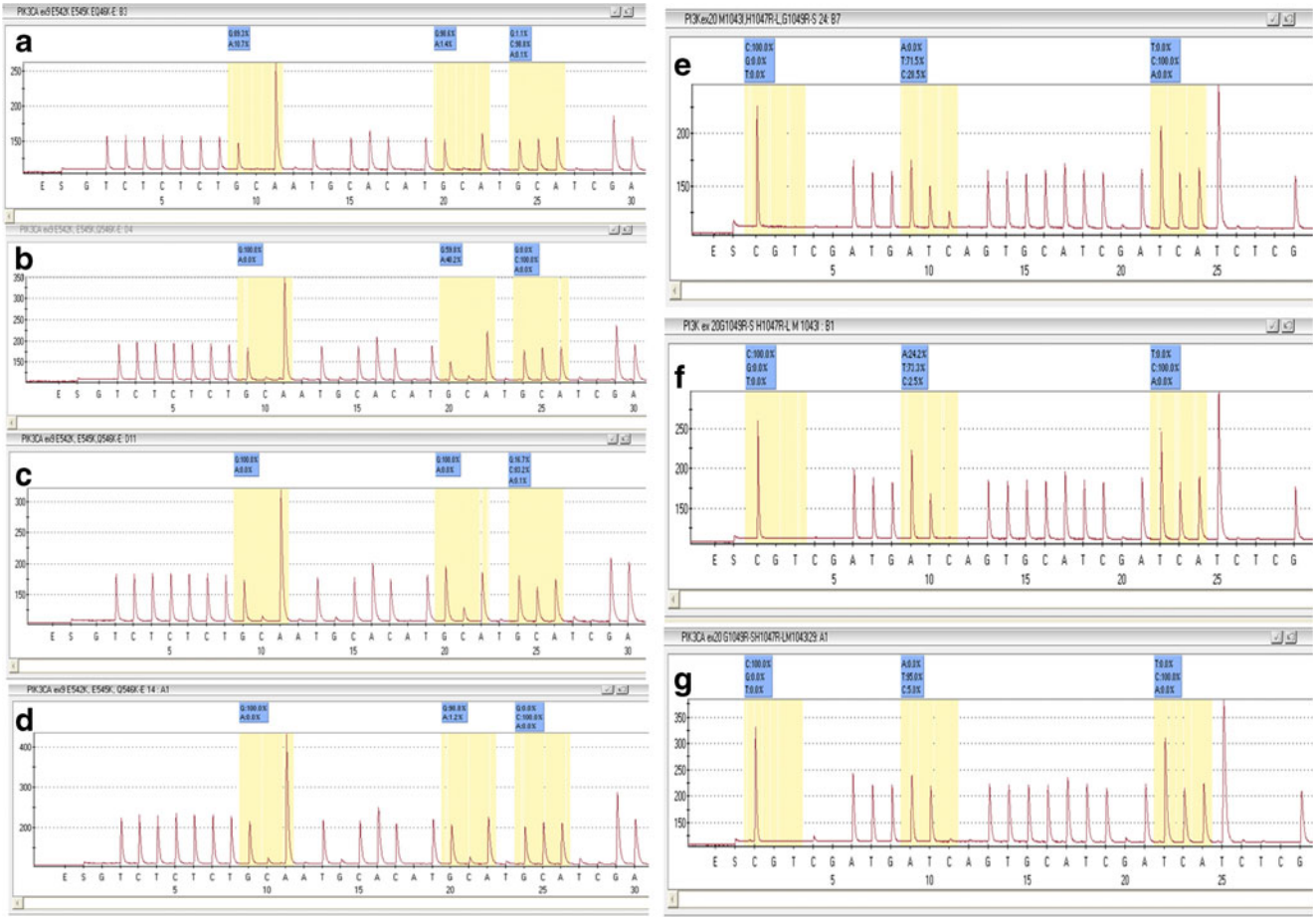

Fig. 1 Pyrosequencing reports of five different cases with **a** exon 9 E542K mutation, **b** exon 9 E545K mutation, **c** exon 9 Q546E mutation, **d** exon 9 wild-type genotype, **e** exon 20 H1047R mutation, **f** exon 20 H1047L mutation and **g** exon 20 wild-type genotype

Combined evaluation of *PI3KCA* mutation and PTEN loss in relation to clinical outcome in metastatic breast carcinomas

PTEN immunostaining could be evaluated in 34 of the 48 MBC, 10 of which showed complete PTEN loss. *PI3KCA* mutations were observed in 1 out of these 10 cases with complete PTEN loss and in 3 of the 24 cases with PTEN expression. PI3K pathway activation, defined as PTEN loss and/or *PI3KCA* mutation, was seen in 13 out of these 34 cases, including 1 case with complete clinical response, 5

Table 5 Relation between *PI3KCA* mutations and therapy responses in the series of patients treated with neoadjuvant trastuzumab

	Total	mt Ex 9 *PI3KCA*	mt Ex 20 *PI3KCA*	wt*PI3KCA*
Pathological response	26			
Stable disease	3 (11.5 %)	0	0	3
Partial responder	12 (46.1 %)	0	1	11
Complete responder	11 (42.3 %)	1	2	8

mt Ex 9 PI3KCA mutation in exon 9 of the *PI3KCA* gene, *mt Ex 20 PI3KCA* mutation in exon 20 of the *PI3KCA* gene, *wtPI3KCA* wild-type *PI3KCA* gene

Table 6 Relation between PI3K mutation and response therapy in the series of 48 patients with MBC treated with trastuzumab

Clinical response	Total	mt Ex 9 *PI3KCA*	mt Ex 20 *PI3KCA*	wt*PI3KCA*
Progressive disease	3 (6.2 %)			3
Stable disease	8 (16.6 %)		1	7
Partial responder >50 %[a]	18 (37.5 %)	1		17
Partial responder <50 %[b]	14 (29.2 %)	1	1	12
Complete responder	4 (8.3 %)			4
NV	1 (2.1 %)	1		0

mt Ex 9 PI3KCA mutation in exon 9 of the *PI3KCA* gene, *mt Ex 20 PI3KCA* mutation in exon 20 of the *PI3KCA* gene, *wtPI3KCA* wild-type *PI3KCA* gene

[a] Partial response with residual tumour burden inferior to 50 % of the clinically estimated initial tumour diameter

[b] Partial response with residual tumour burden greater than 50 % of the clinically estimated initial tumour diameter

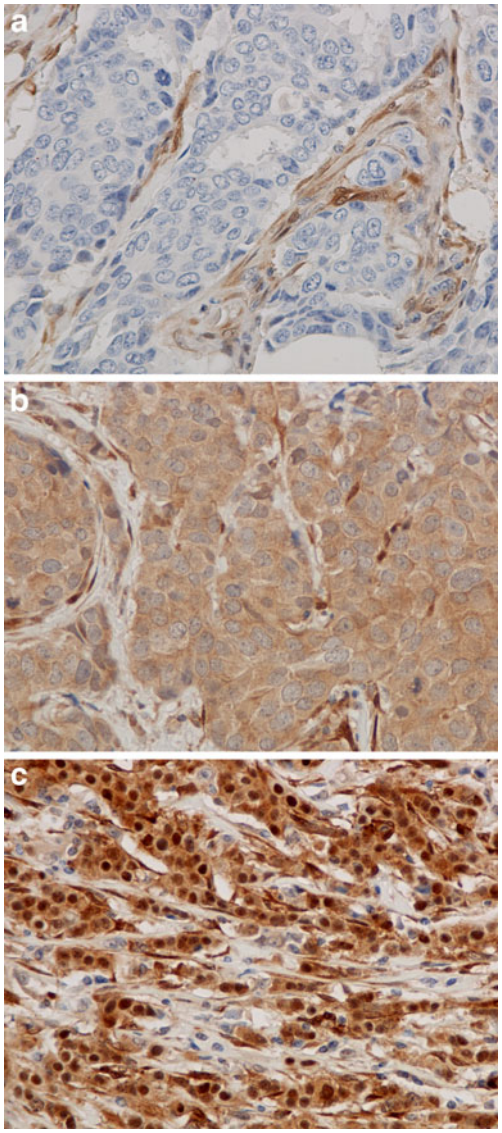

Fig. 2 Different levels of PTEN immunohistochemical expression in breast carcinomas, ranging from complete absence in tumour cells with concurrent positive internal controls (**a**) to mild cytoplasmic positivity (**b**), to strong cytoplasmic and nuclear reactivity (**c**)

cases with prominent clinical response (>50 % reduction in tumour burden) and 5 cases with partial clinical response (<50 % reduction in tumour burden), and in 2 cases with stable disease (Table 7). These data suggest that PI3K pathway activation is not a major determinant of trastuzumab resistance in MBC.

Discussion

Our present study on 129 Her2-positive IBC treated with trastuzumab, analysed with the highly specific and sensitive pyrosequencing technique, shows that *PI3KCA* mutations occur in 19 % of cases and are not related to pathological features of the tumours. In retrospective analyses of small groups of MBC and locally advanced IBC treated with neoadjuvant trastuzumab, we show that *PI3KCA* mutations are not related to response to treatment. In a subset of cases, we also show that *PI3KCA* mutations are not mutually exclusive with PTEN expression loss, and that, in MBC, PI3K pathway activation, defined as *PI3KCA* mutation and/or PTEN loss, is not associated with response to treatment. Survival analysis in the group of MBC shows that neither *PI3KCA* mutations nor PI3K/PTEN pathway activation is related to clinical outcome, but the limited number of investigated cases could have precluded the study to reach statistical significance.

Table 7 PI3K pathway activation, defined as *PI3KCA* mutation and/or PTEN loss in relation with clinical response in the series of MBC (34 informative cases)

	Cases with wt*PI3KCA* and PTEN expression	Activated PI3K pathway (mt*PI3KCA* and/or PTEN loss)
Progressive disease	3	–
Stable disease	6	2
Partial responder >50 %[a]	13	5
Partial responder <50 %[b]	9	5
Complete responder	3	1

wtPI3KCA wild-type *PI3KCA* gene, *mtPI3KCA* mutated *PI3KCA* gene

[a] Partial response with residual tumour burden inferior to 50 % of the clinically estimated initial tumour diameter

[b] Partial response with residual tumour burden greater than 50 % of the clinically estimated initial tumour diameter

The reported frequency of *PI3KCA* mutation in literature is quite variable, ranging from 15 [30] to 29 % [38]. This wide range of frequencies in Her2-positive IBC could in part be related to the limited number of investigated cases in some studies, to the different analytical methods used, or could be related to differences between population groups. The latter is a well-known phenomenon, which has been observed not only between different ethnic groups, such as for example frequency of EGFR mutations lung carcinoma in Western and Japanese populations, but also within the same ethnic group, such as *B-raf* mutations and *PTC/Ret* translocations in thyroid carcinomas [38, 39]. In a previous study of a consecutively collected series of IBC from the same geographical area (Trentino, Northeast Italy), we observed a frequency of *PI3KCA* mutation (26 % mutated cases) which is slightly higher than the one observed in the present study [7]. This difference might be related to the different composition of the two series, as the previous series included mainly Her2-negative ER-positive IBC, while the present one includes only Her2-positive cases,

with a higher percentage of ER-negative cases. Several studies have indeed shown that *PI3KCA* mutation is more frequent in ER-positive and Her2-negative IBC [8–10, 14, 22–24] suggesting that in these cases PI3K/AKT pathway activation occurs through a Her2-independent mechanism. However, discordances exist, and other studies have either not found such associations or even provided opposite results, such as an association between *PI3KCA* mutations and Her2 overexpression [13]. Comparison between the different studies is extremely difficult as the inclusion criteria are different. Moreover, since the pathogenetic role of mutations in different regions of the *PI3KCA* gene could provide different activating effects, with potentially different pathogenetic and clinic relevance [7], further studies, and possibly a meta-analysis of currently available data, should further investigate these relationships.

The most intriguing aspect of the study of *PI3KCA* mutations is their possible role as predictive markers of resistance to anti-Her2 therapy, either using trastuzumab or the reversible dual kinase inhibitor lapatinib, which is active also against EGFR. Preclinical and preliminary data suggest that *PI3KCA* mutations might predict resistance to anti-Her2 therapy [5, 21, 27–29]. The study of Razis et al. [28] is of particular interest as it includes a series of partly Her2-positive and partly Her2-negative metastatic IBC treated with trastuzumab: in Her2-negative cases, *PI3KCA* mutations were not related to time to progression, while in the Her2-positive group, a strong and independent association between *PI3KCA* mutations and worse prognosis was found. However, data are still not conclusive, and some studies suggest that *PI3KCA* mutations are not associated with response or clinical outcome [31, 39] or are of limited predictive value [5, 30]. Our present study shows that *PI3KCA* mutations occur in patients responding to trastuzumab treatment (i.e. four neoadjuvant patients and five MBC patients), further supporting the hypothesis that *PI3KCA* mutations do not exclude the possibility of clinical benefit to trastuzumab therapy.

Previous reports suggested that *PI3KCA* mutation and PTEN loss are mutually exclusive [13]. However, in our study 3 (12.5 %) out of 24 PTEN-negative IBC showed also *PI3KCA* mutation, as also reported by Perez-Tenor et al. [10] and Wang et al. [31]. The reason for this redundancy in the activation of the PI3K pathway is not clear, but could be related to different yet unknown cross-talk mechanisms between different pathways, or to an additive effect of these two activating hits along the same metabolic pathway.

The lack of a clear-cut relationship between *PI3KCA* mutation and therapeutic response to anti-Her2 agents can be interpreted in the light of the complex and poorly understood mechanisms of action of trastuzumab. First, resistance could be related to the fact that the PI3K/AKT signalling pathway is very complex and may be improperly constitutionally activated at several levels with different mechanisms, which, beside *PI3KCA* mutation, potentially include loss of PTEN expression, *PI3KCA* gene amplification, mutations or amplification of *AKT*, deregulation of mTOR activity, altered expression of p70S6K, etc. In particular, PTEN loss has been associated with resistance to anti-Her2 therapy in cell lines and patients [21, 27, 28, 30, 38]. The combined evaluation of alterations of the PI3K/AKT pathway at several levels could provide a rationale for combining anti-Her2 therapy with PI3K/AKT inhibitors [29, 40]. Preliminary data indeed show that concurrent evaluation of *PI3KCA* mutations and PTEN and p70S6K expression may identify patients without PI3K/AKT pathway activation who could benefit more from trastuzumab-based therapy [27, 28, 30, 31]. However, in our small series of MBC, PI3K/PTEN pathway activation was not related to clinical response to trastuzumab, and further studies are needed to clarify this issue. Alternatively, the fact that *PI3KCA* mutated cases may respond to trastuzumab therapy could be interpreted in the light of the possible role of trastuzumab in determining antibody-dependent cell-mediated cytotoxicity. Trastuzumab is an intact monoclonal antibody which, binding to the Her2 molecule, could elicit antibody-dependent cellular cytotoxicity which could lead to tumour cell necrosis and hence clinical/pathological response [41–43].

In conclusion, our study shows that *PI3KCA* mutations are frequent in Her2-positive breast cancer and that there is no significant correlation with response to trastuzumab-based therapy. The study also shows that PI3K pathway activation, defined as PTEN loss and/or *PI3KCA* mutation, is not associated with response to treatment or with clinical outcome. Since most reported series of IBC treated with anti-Her2 treatment are small and the possible variables influencing the results are many, including the confounding effects of the patients' background treatments [5], an effort should be undertaken to pool all data together to perform a meta-analysis and possibly to study PI3K pathway activation mechanisms in a more comprehensive way, including also less frequently studied biomarkers such as *AKT* mutation and phosphorylation status, mTOR and p70S6K expression levels. More importantly, the value of the combined use of trastuzumab with different inhibitors targeting the PI3K pathway at different levels needs to be tested. Finally, our data show that *PI3KCA* mutation and/or PTEN loss are not criteria to exclude patients from potentially beneficial anti-Her2 therapy.

Acknowledgments This study has been supported by grants of the Provincia Autonoma di Trento, Italy and of the Fondazione Cassa di Risparmio di Trento e Rovereto, Italy.

Conflict of interest We declare that we have no conflict of interest.

References

1. Clifford A, Hudis MD (2007) Trastuzumab—mechanism of action and use in clinical practice. N Engl J Med 357:39–51
2. Bailey TA, Luan H, Clubb RJ, Naramura M, Band V, Raja SM, Band H (2011) Mechanisms of Trastuzumab resistance in ErbB2-driven breast cancer and newer opportunities to overcome therapy resistance. J Carcinog 10:28
3. Yakes FM, Chinratanalab W, Ritter CA, King W, Seelig S, Arteaga CL (2002) Herceptin-induced inhibition of phosphatidylinositol-3 kinase and Akt is required for antibody-mediated effects on p27, cyclin D1, and antitumor action. Cancer Res 62:4132–4141
4. Mills GB, Kohn E, Lu Y, Eder A, Fang X, Wang H, Bast RC, Gray J, Jaffe R, Hortobagyi G (2003) Linking molecular diagnostics to molecular therapeutics: targeting the PI3K pathway in breast cancer. Semin Oncol 30(5 Suppl 16):93–104
5. Esteva FJ, Guo H, Zhang S, Santa-Maria C, Stone S, Lanchbury JS, Sahin AA, Hortobagyi GN, Yu D (2010) PTEN, PIK3CA, p-AKT, and p-p70S6K status: association with trastuzumab response and survival in patients with HER2-positive metastatic breast cancer. Am J Pathol 177:1647–1656
6. Lopez-Knowles E, O'Toole SA, McNeil CM, Millar EK, Qiu MR, Crea P, Daly RJ, Musgrove EA, Sutherland RL (2010) PI3K pathway activation in breast cancer is associated with the basal-like phenotype and cancer-specific mortality. Int J Cancer 126:1121–1131
7. Barbareschi M, Buttitta F, Felicioni L, Cotrupi S, Barassi F, Del GM, Ferro A, Dalla PP, Galligioni E, Marchetti A (2007) Different prognostic roles of mutations in the helical and kinase domains of the PIK3CA gene in breast carcinomas. Clin Cancer Res 13:6064–6069
8. Kalinsky K, Heguy A, Bhanot UK, Patil S, Moynahan ME (2011) PIK3CA mutations rarely demonstrate genotypic intratumoral heterogeneity and are selected for in breast cancer progression. Breast Canc Res Treat 129:635–643
9. Maruyama N, Miyoshi Y, Taguchi T, Tamaki Y, Monden M, Noguchi S (2007) Clinicopathologic analysis of breast cancers with PIK3CA mutations in Japanese women. Clin Cancer Res 13:408–414
10. Perez-Tenorio G, Berglund F, Esguerra MA, Nordenskjold B, Rutqvist LE, Skoog L, Stal O (2006) Cytoplasmic p21WAF1/CIP1 correlates with Akt activation and poor response to tamoxifen in breast cancer. Int J Oncol 28:1031–1042
11. Stemke-Hale K, Gonzalez-Angulo AM, Lluch A, Neve RM, Kuo WL, Davies M, Carey M, Hu Z, Guan Y, Sahin A, Symmans WF, Pusztai L, Nolden LK, Horlings H, Berns K, Hung MC, van de Vijver MJ, Valero V, Gray JW, Bernards R, Mills GB, Hennessy BT (2008) An integrative genomic and proteomic analysis of PIK3CA, PTEN, and AKT mutations in breast cancer. Cancer Res 68:6084–6091
12. Lerma E, Catasus L, Gallardo A, Peiro G, Alonso C, Aranda I, Barnadas A, Prat J (2008) Exon 20 PIK3CA mutations decreases survival in aggressive (HER-2 positive) breast carcinomas. Virchows Arch 453:133–139
13. Saal LH, Holm K, Maurer M, Memeo L, Su T, Wang X, Yu JS, Malmstrom PO, Mansukhani M, Enoksson J, Hibshoosh H, Borg A, Parsons R (2005) PIK3CA mutations correlate with hormone receptors, node metastasis, and ERBB2, and are mutually exclusive with PTEN loss in human breast carcinoma. Cancer Res 65:2554–2559
14. Li SY, Rong M, Grieu F, Iacopetta B (2006) PIK3CA mutations in breast cancer are associated with poor outcome. Breast Canc Res Treat 96:91–95
15. Buttitta F, Felicioni L, Barassi F, Martella C, Paolizzi D, Fresu G, Salvatore S, Cuccurullo F, Mezzetti A, Campani D, Marchetti A (2007) PIK3CA mutation and histological type in breast carcinoma: high frequency of mutations in lobular carcinoma. J Pathol 208:350–355
16. Benvenuti S, Frattini M, Arena S, Zanon C, Cappelletti V, Coradini D, Daidone MG, Pilotti S, Pierotti MA, Bardelli A (2008) PIK3CA cancer mutations display gender and tissue specificity patterns. Hum Mutat 29:284–288
17. Liedtke C, Cardone L, Tordai A, Yan K, Gomez HL, Figureoa LJ, Hubbard RE, Valero V, Souchon EA, Symmans WF, Hortobagyi GN, Bardelli A, Pusztai L (2008) PIK3CA-activating mutations and chemotherapy sensitivity in stage II–III breast cancer. Breast Canc Res 10:R27
18. Tsutsui S, Inoue H, Yasuda K, Suzuki K, Higashi H, Era S, Mori M (2005) Reduced expression of PTEN protein and its prognostic implications in invasive ductal carcinoma of the breast. Oncology 68:398–404
19. Gonzalez-Angulo AM, Ferrer-Lozano J, Stemke-Hale K, Sahin A, Liu S, Barrera JA, Burgues O, Lluch AM, Chen H, Hortobagyi GN, Mills GB, Meric-Bernstam F (2011) PI3K pathway mutations and PTEN levels in primary and metastatic breast cancer. Mol Cancer Ther 10:1093–1101
20. Gori S, Sidoni A, Colozza M, Ferri I, Mameli MG, Fenocchio D, Stocchi L, Foglietta J, Ludovini V, Minenza E, De Angelis V, Crino L (2009) EGFR, pMAPK, pAkt and PTEN status by immunohistochemistry: correlation with clinical outcome in HER2-positive metastatic breast cancer patients treated with trastuzumab. Ann Oncol 20:648–654
21. Berns K, Horlings HM, Hennessy BT, Madiredjo M, Hijmans EM, Beelen K, Linn SC, Gonzalez-Angulo AM, Stemke-Hale K, Hauptmann M, Beijersbergen RL, Mills GB, van de Vijver MJ, Bernards R (2007) A functional genetic approach identifies the PI3K pathway as a major determinant of trastuzumab resistance in breast cancer. Canc Cell 12:395–402
22. Bachman KE, Argani P, Samuels Y, Silliman N, Ptak J, Szabo S, Konishi H, Karakas B, Blair BG, Lin C, Peters BA, Velculescu VE, Park BH (2004) The PIK3CA gene is mutated with high frequency in human breast cancers. Canc Biol Ther 3:772–775
23. Boyault S, Drouet Y, Navarro C, Bachelot T, Lasset C, Treilleux I, Tabone E, Puisieux A, Wang Q (2012) Mutational characterization of individual breast tumors: TP53 and PI3K pathway genes are frequently and distinctively mutated in different subtypes. Breast Canc Res Treat 132:23–39
24. Michelucci A, Di CC, Lami A, Collecchi P, Caligo A, Decarli N, Leopizzi M, Aretini P, Bertacca G, Porta RP, Ricci S, Della RC, Stanta G, Bevilacqua G, Cavazzana A (2009) PIK3CA in breast carcinoma: a mutational analysis of sporadic and hereditary cases. Diagn Mol Pathol 18:200–205
25. Ellis MJ, Lin L, Crowder R, Tao Y, Hoog J, Snider J, Davies S, DeSchryver K, Evans DB, Steinseifer J, Bandaru R, Liu W, Gardner H, Semiglazov V, Watson M, Hunt K, Olson J, Baselga J (2010) Phosphatidyl-inositol-3-kinase alpha catalytic subunit mutation and response to neoadjuvant endocrine therapy for estrogen receptor positive breast cancer. Breast Canc Res Treat 119:379–390
26. Dupont JJ, Laenkholm AV, Knoop A, Ewertz M, Bandaru R, Liu W, Hackl W, Barrett JC, Gardner H (2011) PIK3CA mutations may be discordant between primary and corresponding metastatic disease in breast cancer. Clin Cancer Res 17:667–677
27. Lai YL, Mau BL, Cheng WH, Chen HM, Chiu HH, Tzen CY (2008) PIK3CA exon 20 mutation is independently associated with a poor prognosis in breast cancer patients. Ann Surg Oncol 15:1064–1069
28. Razis E, Bobos M, Kotoula V, Eleftheraki AG, Kalofonos HP, Pavlakis K, Papakostas P, Aravantinos G, Rigakos G, Efstratiou I, Petraki K, Bafaloukos D, Kostopoulos I, Pectasides D, Kalogeras KT, Skarlos D, Fountzilas G (2011) Evaluation of the association of PIK3CA mutations and PTEN loss with efficacy of trastuzumab

therapy in metastatic breast cancer. Breast Canc Res Treat 128:447–456
29. Junttila TT, Akita RW, Parsons K, Fields C, Lewis Phillips GD, Friedman LS, Sampath D, Sliwkowski MX (2009) Ligand-independent HER2/HER3/PI3K complex is disrupted by trastuzumab and is effectively inhibited by the PI3K inhibitor GDC-0941. Canc Cell 15:429–440
30. Dave B, Migliaccio I, Gutierrez MC, Wu MF, Chamness GC, Wong H, Narasanna A, Chakrabarty A, Hilsenbeck SG, Huang J, Rimawi M, Schiff R, Arteaga C, Osborne CK, Chang JC (2011) Loss of phosphatase and tensin homolog or phosphoinositol-3 kinase activation and response to trastuzumab or lapatinib in human epidermal growth factor receptor 2-overexpressing locally advanced breast cancers. J Clin Oncol 29:166–173
31. Wang L, Zhang Q, Zhang J, Sun S, Guo H, Jia Z, Wang B, Shao Z, Wang Z, Hu X (2011) PI3K pathway activation results in low efficacy of both trastuzumab and lapatinib. BMC Canc 11:11
32. Brunner-Kubath C, Shabbir W, Saferding V, Wagner R, Singer CF, Valent P, Berger W, Marian B, Zielinski CC, Grusch M, Grunt TW (2011) The PI3 kinase/mTOR blocker NVP-BEZ235 overrides resistance against irreversible ErbB inhibitors in breast cancer cells. Breast Canc Res Treat 129:387–400
33. Miller TW, Rexer BN, Garrett JT, Arteaga CL (2011) Mutations in the phosphatidylinositol 3-kinase pathway: role in tumor progression and therapeutic implications in breast cancer. Breast Canc Res 13:224
34. Eichhorn PJ, Gili M, Scaltriti M, Serra V, Guzman M, Nijkamp W, Beijersbergen RL, Valero V, Seoane J, Bernards R, Baselga J (2008) Phosphatidylinositol 3-kinase hyperactivation results in lapatinib resistance that is reversed by the mTOR/phosphatidylinositol 3-kinase inhibitor NVP-BEZ235. Cancer Res 68:9221–9230
35. Cantaloni C, Tonini RE, Eccher C, Morelli L, Leonardi E, Bragantini E, Aldovini D, Fasanella S, Ferro A, Cazzolli D, Berlanda G, Dalla PP, Barbareschi M (2011) Diagnostic value of automated Her2 evaluation in breast cancer: a study on 272 equivocal (score 2+) Her2 immunoreactive cases using an FDA approved system. Appl Immunohistochem Mol Morphol 19:306–312
36. Barbareschi M, Girlando S, Mauri FM, Forti S, Eccher C, Mauri FA, Togni R, Dalla PP, Doglioni C (1994) Quantitative growth fraction evaluation with MIB1 and Ki67 antibodies in breast carcinomas. Am J Clin Pathol 102:171–175
37. Fasanella S, Leonardi E, Cantaloni C, Eccher C, Bazzanella I, Aldovini D, Bragantini E, Morelli L, Cuorvo LV, Ferro A, Gasperetti F, Berlanda G, Dalla PP, Barbareschi M (2011) Proliferative activity in human breast cancer: Ki-67 automated evaluation and the influence of different Ki-67 equivalent antibodies. Diagn Pathol 6(Suppl 1):S7
38. Xu BH, Jiang ZF, Chua D, Shao ZM, Luo RC, Wang XJ, Liu DG, Yeo W, Yu SY, Newstat B, Preston A, Martin AM, Chi HD, Wang L (2011) Lapatinib plus capecitabine in treating HER2-positive advanced breast cancer: efficacy, safety, and biomarker results from Chinese patients. Chin J Canc 30:327–335
39. Girlando S, Cuorvo LV, Bonzanini M, Morelli L, Amadori P, Dalla PP, Barbareschi M (2011) High prevalence of B-RAF mutation in papillary carcinoma of the thyroid in north-east Italy. Int J Surg Pathol 8:173–176
40. Lu CH, Wyszomierski SL, Tseng LM, Sun MH, Lan KH, Neal CL, Mills GB, Hortobagyi GN, Esteva FJ, Yu D (2007) Preclinical testing of clinically applicable strategies for overcoming trastuzumab resistance caused by PTEN deficiency. Clin Cancer Res 13:5883–5888
41. Park S, Jiang Z, Mortenson ED, Deng L, Radkevich-Brown O, Yang X, Sattar H, Wang Y, Brown NK, Greene M, Liu Y, Tang J, Wang S, Fu XY (2010) The therapeutic effect of anti-HER2/neu antibody depends on both innate and adaptive immunity. Canc Cell 18:160–170
42. Mohsin SK, Weiss HL, Gutierrez MC, Chamness GC, Schiff R, DiGiovanna MP, Wang CX, Hilsenbeck SG, Osborne CK, Allred DC, Elledge R, Jenny C, Chang JC (2005) Neoadjuvant Trastuzumab induces apoptosis in primary breast cancers. J Clin Oncol 23:2460–2468
43. Varchetta S, Gibelli L, Oliviero V, Nardini E, Gennari R, Gatti G, Silva LS, Villani N, Tagliabue E, Menard S, Costa A, Fannioni FF (2007) Element related to enterogenity of antibody-dependent cell cytotoxicity in patients under Trastuzumab therapy for primary operable breast cancer overexpressing Her2. Cancer Res 67:11991–11999

Virchows Arch (2012) 461:141–148
DOI 10.1007/s00428-012-1276-1

ORIGINAL ARTICLE

Stromal p16 expression differentiates endometrial polyp from endometrial hyperplasia

Suzuko Moritani · Shu Ichihara · Masaki Hasegawa · Akari Iwakoshi · Sakae Murakami · Tomoko Sato · Tomomitsu Okamoto · Yoshio Mori · Hajime Kuhara · Steven G. Silverberg

Received: 2 January 2012 / Revised: 23 May 2012 / Accepted: 25 June 2012 / Published online: 7 July 2012
© Springer-Verlag 2012

Abstract Endometrial polyps are very common benign endometrial lesions, but their pathogenesis is poorly understood, except for a few studies indicating the possibility of benign stromal neoplasm. Although the histopathological diagnosis of endometrial polyp on a surgical specimen is straightforward, it is often difficult to differentiate endometrial polyp from endometrial hyperplasia on a biopsy or curettage specimen. Presently, there is no immunohistochemical marker helpful in this differential diagnosis. In this study, we examined p16 expression in 35 endometrial polyps and 33 cases of endometrial hyperplasia that included 16 simple hyperplasias, 14 complex atypical hyperplasias, and 3 complex hyperplasias without atypia. Stromal p16 expression differed significantly between the two groups; it was seen in 31 (89 %) endometrial polyps, but in only 1 (3 %) endometrial hyperplasia. The percentage of p16-positive stromal cells ranged from 10 to 90 % (mean, 47 %) and the positive cells tended to be distributed around glands. Six cases of endometrial hyperplasia within an endometrial polyp were also examined and all cases showed stromal p16 expression. There was no difference in glandular p16 expression between endometrial polyps 33 (94 %) and hyperplasia 27 (82 %). The p16-immunoreactivity was mostly confined to metaplastic epithelial cells in both groups. Stromal p16 expression might be a peculiar characteristic of endometrial polyp and constitute a useful marker for the diagnosis, especially in fragmented specimens from biopsy or curettage. Stromal p16 expression might be a reflection of p16-induced cellular senescence, which has been documented in several benign mesenchymal neoplasms.

Keywords Endometrial polyp · p16 · Endometrial hyperplasia · Stromal p16 expression

S. Moritani (✉) · S. Ichihara · M. Hasegawa
Department of Advanced Diagnosis, Division of Pathology,
Nagoya Medical Center,
4-1-1, Sannomaru, Naka-ku,
Nagoya, Aichi 460-0001, Japan
e-mail: MoritaniS@aol.com

A. Iwakoshi
Department of Pathology,
Nagoya University Graduate School of Medicine,
Nagoya, Japan

S. Murakami · T. Sato
Department of Pathology, Social Insurance Chukyo Hospital,
Nagoya, Japan

T. Okamoto
Department of Obstetrics and Gynecology,
Social Insurance Chukyo Hospital,
Nagoya, Japan

Y. Mori
Department of Pathology, Chuno Kosei Hospital,
Seki, Japan

H. Kuhara
Department of Pathology, Toyokawa Municipal Hospital,
Toyokawa, Japan

S. G. Silverberg
Department of Pathology, University of Maryland Medical Center,
Baltimore, MD, USA

Introduction

The endometrial polyp is a relatively common gynecologic lesion that can cause abnormal genital bleeding. It can occur at any age, but many of the patients are perimenopausal [1]. Endometrial polyp is the most frequent endometrial lesion occurring in patients who are taking tamoxifen therapy for breast cancer [2].

The histological diagnosis of endometrial polyp in a hysterectomy specimen is usually not difficult due to its easily recognized characteristic polypoid configuration. The glands within the polyp vary in size and shape and frequently show cystic dilatation, and their distribution is rather random compared with normal endometrial glands. The stroma of the polyp is typically fibrotic and contains thick-walled blood vessels [3]. However, histological diagnosis of endometrial polyp on curettage or biopsy specimens is difficult. The polypoid configuration of the lesion is not always apparent because of the fragmented nature of the specimens. Indeed, according to a classical study by Winkler et al. [4], endometrial polyp is commonly overdiagnosed as endometrial hyperplasia. Interobserver agreement with respect to the diagnosis of endometrial hyperplasia has also been reported as very low, especially when the amount of tissue was not adequate and the lesion contained elements of an endometrial polyp [5]. The confusion between endometrial hyperplasia, especially simple hyperplasia, and endometrial polyp seems to result from the close resemblance in glandular morphology of these two lesions. The only hallmark for histological differentiation between the two lesions is the difference in stromal appearance. The thick-walled blood vessels in endometrial polyps are relatively easy to recognize and their vascular pattern is different from that of endometrial hyperplasia, which has small spiral artery-like blood vessels. The long axis of endometrial glands arranged parallel to the surface epithelium was recently reported to be a useful histological feature for diagnosing endometrial polyp [6]. However, there has been no useful immunohistochemical marker to differentiate endometrial polyp from endometrial hyperplasia.

Recently, during workup of endometrial serous adenocarcinomas associated with endometrial polyps, we noticed stromal p16 expression in endometrial polyps. Although the stromal component of endometrial polyp has been described as "neoplastic" in some textbooks [7, 8], the histopathological and immunohistochemical characteristics of the stromal cells in endometrial polyps are poorly understood. In this study, we examined and compared the stromal p16 expression in endometrial polyps and endometrial hyperplasia, and its significance for differential diagnosis between these lesions.

Materials and methods

Thirty-five cases of endometrial polyp and 33 cases of endometrial hyperplasia were retrieved from the surgical pathology file of Social Insurance Chukyo Hospital from August 2008 to April 2011 and the consultation files of SM. Patient ages ranged from 32 to 83 years (mean±SD, 54.63±14.10, median 54.6) for endometrial polyp and from 17 to 69 years (mean±SD, 49.20±10.18, median 49) for endometrial hyperplasia, respectively (p=0.0789). Of the 35 cases of endometrial polyp, 17, 10, 7, and 1 were diagnosed in a hysterectomy, curettage, hysteroscopic polypectomy, and autopsy specimen, respectively. Of the 33 cases of endometrial hyperplasia, 18 and 15 were in a hysterectomy or curettage specimen, respectively. In this study, we did not include any cases of which the histological differential diagnosis between endometrial polyp and endometrial hyperplasia was ambiguous. For the cases of endometrial polyp in a curettage specimen, we only selected those in which polypoid configuration, and fibrous stroma with thick-walled blood vessels were clearly identified. Polyp size was measured for all except for curettage specimens. The presence and type of epithelial metaplasia within a polyp and hyperplasia were described. For the cases that had metaplastic changes, the proportion of metaplastic epithelia was estimated. We also selected six cases of endometrial hyperplasia within a polyp. Patient age ranged from 29 to 62 years (mean±SD, 42.67±13.24, median, 41). A simple hyperplasia without atypia should not be diagnosed in a polyp [8], we only selected complex hyperplasia with or without atypia within a polyp. As controls, four cases of endometrial stromal sarcoma, four cases of adenosarcoma, and 23 cases of endometrioid adenocarcinoma were selected from the same files.

A representative slide from each case was selected and 4-μm-thick sections were cut for immunohistochemistry. After dewaxing and rehydrating, the sections were treated in citrate buffer (10 mM, pH 6.0) in an autoclave (121 °C). Immunohistochemical staining was performed using anti-Human p16INK4a antibody (clone E6H4, prediluted, mtm laboratories AG, Heidelberg, Germany) and the CINtec Histology kit, following the manufacturer's instructions. The percentage of positive cells and the location of positive signals (nuclear or cytoplasmic) visually estimated for both glandular and stromal components of all lesions. A cut-off index was arbitrarily defined as the presence of more than 10 % immunoreactive cells. The estimated percentages were categorized as 0 for <10 % positive cells, 1 for ≥10 % or more but <25 %, 2 for ≥25 % or more but <50 %, and 3 for ≥50 %.

Results

The clinicopathological features of the endometrial polyps and endometrial hyperplasias included in this study are summarized in Table 1. Endometrial polyps ranged in size from 3 to 45 mm (mean±SD 14.06±1.78 mm, median 10 mm). Polyps were classified according to Malpica et al. [9]. Eighteen (51 %) endometrial polyps had proliferative-type endometrial glands and relatively hypercellular stroma,

Table 1 Histological and immunohistochemical features of endometrial polyp and hyperplasia

	Endometrial polyp		Endometrial hyperplasia	
n	35		33	
Age* (years)	32–83 (54.63±2.45)		17–69 (49.2±10.18)	
Size (mm)	3–45 (14.06±1.78)		–	
Histologic type	Hyperplastic	18 (51 %)	Simple without atypia	16 (48 %)
	Atrophic	13 (37 %)	Complex atypical	14 (42 %)
	Functional	3 (9 %)	Complex without atypia	3 (10 %)
	Mixed	1 (3 %)		
Metaplasia	Tubal	32 (91 %)	Tubal	25 (76 %)
	Eosinophilic	2 (5 %)	Eosinophilic	9 (27 %)
	Mucinous	1 (3 %)	Mucinous	0
	Morular	0	Morular	3 (10 %)
	Surface pap/syn	0	Surface pap/syn	1 (3 %)
Stromal p16 **	31 (89 %)		1 (3 %)	
Glandular p16 ***	33 (94 %)		27 (82 %)	

Surface pap/syn surface papillary/syncytial change

*P=0.0789, **P<0.01, ***P=0.1108

corresponding to a hyperplastic polyp. Thirteen (37 %) endometrial polyps had glands with low proliferative activity and fibrotic hypocellular stroma, corresponding to atrophic polyp, and three (9 %) showed secretory changes, corresponding to functional polyp. The single remaining endometrial polyp had a mixed endometrial and endocervical-type epithelium, corresponding to mixed polyp. All ten curettage specimens of endometrial polyps showed thick-walled blood vessels in the stroma and/or three sides lined by endometrial surface epithelium. Various kinds of epithelial metaplasia were seen in various proportions in 32 (91 %) of the 35 endometrial polyps. The most frequent metaplasia was tubal metaplasia, seen in 32 cases (91 %), followed by eosinophilic cell change (two cases, 5 %) and mucinous change (one case, 3 %). Tubal metaplasia occupied less than 10 % of the glands within a polyp in five cases (16 %), 10 % or more and less than 25 % in 7 (22 %), 25 % or more and less than 50 % in 6 cases (19 %), and 50 % or more in 14 cases (43 %). Eosinophilic cell change occupied less than 20 % of the glands in two cases.

Sixteen (48 %) of the 33 endometrial hyperplasia cases were simple hyperplasia without atypia, 14 (42 %) were complex atypical hyperplasia, and 3 (10 %) were complex hyperplasia without atypia. Various types of epithelial metaplasia were seen in various proportions in 28 (85 %) cases of endometrial hyperplasia. The most frequent metaplasia was tubal metaplasia, seen in 25 cases (75 %), followed by eosinophilic cell change (nine cases, 27 %), morular metaplasia (three cases, 10 %), and surface papillary/syncytial change (one case, 3 %). Tubal metaplasia occupied less than 10 % of the glands within hyperplastic lesions in two cases (8 %), 10 % or more and less than 25 % in seven (28 %), 25 % or more and less than 50 % in nine cases (36 %), and 50 % or more in seven cases (28 %). Eosinophilic cell change occupied less than 20 % of the glands within hyperplastic lesion in seven cases (78 %).

Of six endometrial hyperplasia cases within a polyp, two were complex hyperplasias without atypia, and four complex hyperplasias with atypia. All but one case of complex hyperplasia without atypia showed tubal metaplasia ranging in proportion from less than 10 to 90 %. Morular metaplasia was seen in one complex hyperplasia with atypia.

Stromal p16 expression was found in 31(89 %) of 35 endometrial polyps. The immunoreactivity was located in the nucleus (Fig. 1). The percentage of positive stromal cells ranged from 10 to 90 % (mean, 47 %; median, 40 %). The stromal p16 immunoreactivity score was 1 in 3 cases, 2 in 15 cases, and 3 in 13 cases (Table 2). In cases with less than 50 % stromal cells positive, the p16-positive cells tended to be distributed around glands, but in some cases they clustered evenly within the stroma. The p16-positive stromal cells were distributed diffusely within the polyp from the surface onto the deeper portions. Even in the four negative cases, a small number of positive stromal cells were noted sporadically. Two of the four negative cases were atrophic polyps and the other two were hyperplastic polyps. Stromal p16 expression did not differ between the histological types of endometrial polyp or according to patient age. In hysterectomy and autopsy cases, there were no p16-positive stromal cells in the endometrium. In the curettage specimens, stromal p16 expression was seen exclusively in the fragments derived from endometrial polyp.

Stromal p16 expression was positive in only 1 (3 %) of 33 endometrial hyperplasia cases. Thus, there was a statistically significant difference in stromal p16 expression between endometrial polyp and endometrial hyperplasia (P< 0.01). In 28 (87.5 %) of 32 negative cases, there were absolutely no p16-positive cells in the stroma. A small number of positive cells were noted in the remaining four

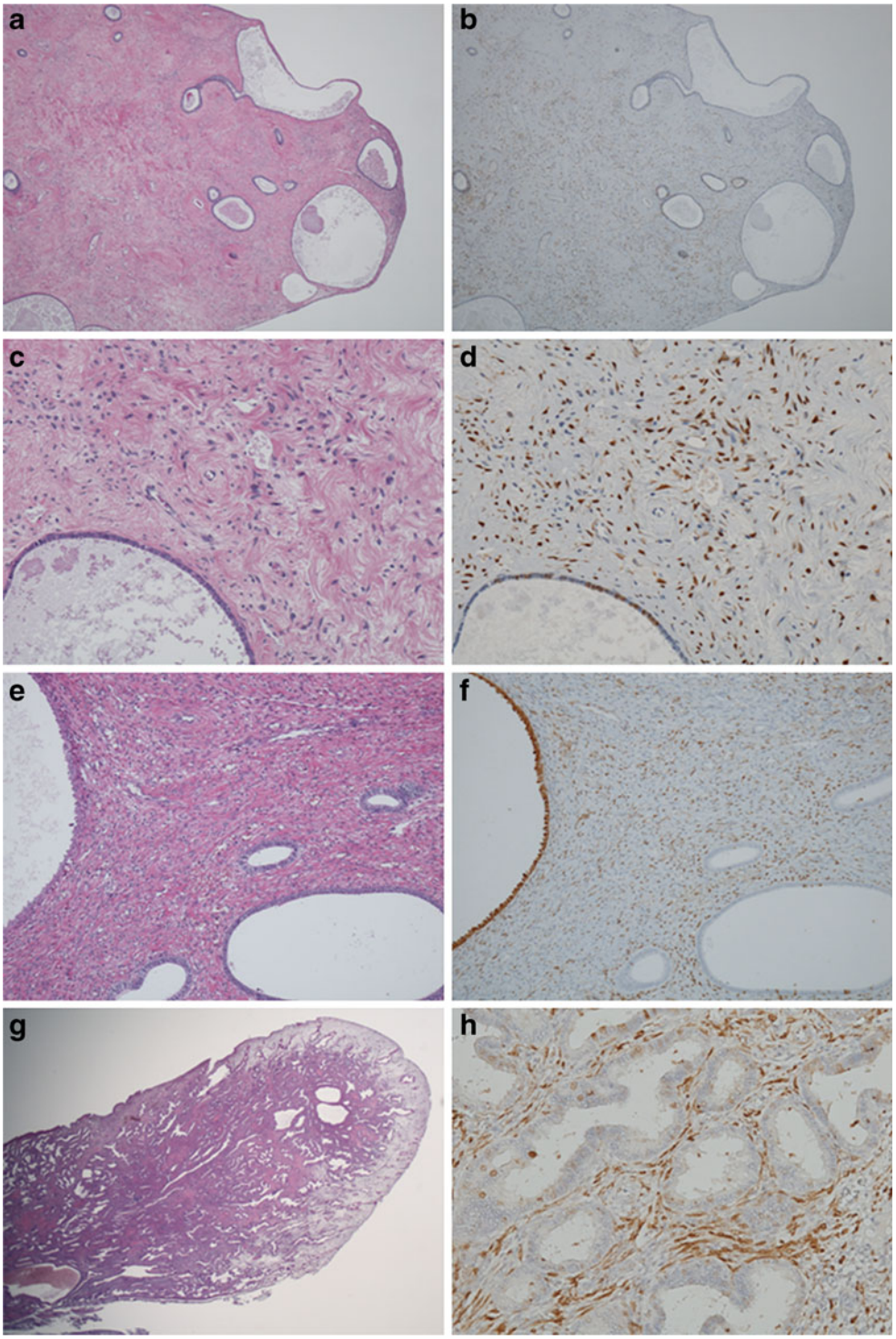

Fig. 1 Stromal p16 expression in endometrial polyps. **a**–**d** Atrophic polyp. The polyp has fibrotic hypocellular stroma and cystically dilated glands lined by inactive epithelial cells. More than 50 % of the stromal cells are positive for p16. **e**, **f** Hyperplastic polyp. The polyp has abundant stromal cells and proliferative-type endometrial glands. More than 50 % of the stromal cells are positive for p16. A cystically dilated gland with tubal metaplasia (left side) also showed p16. **g**, **h** Functional polyp. The polyp has tortuous secretory-type endometrial glands. Most of the stromal cells are positive for p16

negative cases, three of which were simple hyperplasia, and the other complex atypical hyperplasia. The only case with stromal p16 expression was a hysterectomy sample with simple hyperplasia without atypia. In this case, the hyperplastic endometrium showed multiple polypoid excrescences. The p16-positive stromal cells were located in the superficial part of the stroma, just beneath the surface epithelium covering the polypoid excrescences.

In all six cases of endometrial hyperplasia within polyps, the typical fibrous stroma characteristic to endometrial polyps was identified at least focally. Stromal p16 expression was positive in all six endometrial hyperplasias within polyps. Two cases were scored as 1, 3 as 2, and one case was scored as 3 (Table 2). In two cases, the p16-positive stromal cells tended to be distributed near the surface of the polypoid excrescences, where the stroma was somewhat fibrous,

Table 2 The proportion of p16-positive stromal and glandular cells

	Score 0	Score 1	Score 2	Score 3	Total
Stromal p16 expression					
Endometrial polyp *	4	3	15	13	35
Endometrial hyperplasia *	32	1	0	0	33
Endometrial hyperplasia within polyp	0	3	2	1	6
ESS/adenosarcoma	4	2	0	2	8
Glandular p16 expression					
Endometrial polyp **	5	9	7	14	35
Endometrial hyperplasia **	4	7	10	12	33
Endometrial hyperplasia within polyp	3	0	1	2	6

Score 0 the positive cells are less than 10 %, *Score 1* the positive cells are 10 % or more and less than 25 %, *Score 2* the positive cells are 25 % or more and less than 50 %, *Score 3* The positive cells are 50 % or more, *ESS* endometrial stromal sarcoma

*$P<0.01$; **$P=0.8009$

unlike cellular non-fibrous stroma of the typical endometrial hyperplasia (Fig. 2a, b). In the other four cases, p16-positive stromal cells were distributed randomly but tended to occur in areas where characteristic fibrous stroma was evident. There was no significant difference in the proportion of p16-positive stromal cells between complex hyperplasia with and without atypia. The existence of p16-positive stromal cells seemed to reflect the persistence of original stromal cells of an endometrial polyp. The proportion of p16-positive stromal cells decreased where non-fibrous cellular stroma predominated. There were no p16-positive stromal celsl in the non-polypoid areas of the same specimens in all the six cases.

There was no stromal p16 expression in any of the 23 cases of endometrioid adenocarcinoma. The neoplastic endometrial stromal cells in two of four endometrial stromal sarcomas and two of four adenosarcomas were positive for p16 (Table 2). One endometrial stromal sarcoma and one adenosarcoma showed focal p16 positivity in about 10 % of the tumor cells. The other adenosarcoma showed sarcomatous overgrowth and 90 % of the tumor cells were positive for p16. The other endometrial stromal sarcoma showed focal p16 positivity in about 50 % of the tumor cells.

Glandular p16 expression was noted in 33 cases (94 %) of endometrial polyp and 27 cases (82 %) of endometrial hyperplasia (Fig. 3a–d). The immunoreactivity was located both in nuclei and cytoplasm. Most of the positive epithelial cells showed tubal metaplasia in both endometrial polyp and hyperplastic areas, and all foci of eosinophilic cell change and surface papillary/syncytial change were p16 positive (Fig. 3e, f). We found p16 expression in morular metaplasia in one case of complex hyperplasia with atypia within a polyp. Atypical epithelial cells without metaplastic changes were negative in all 14 cases of complex atypical hyperplasia. Epithelial p16 expression seemed to be almost exclusively located in tubal metaplasia, eosinophilic cell change, and surface papillary/syncytial change, and the percentage of p16-positive epithelial cells closely reflected the degree of these metaplastic changes. There was no difference in epithelial p16 expression between endometrial polyp and hyperplasia ($P=0.1108$). Glandular p16 expression was seen in five of six cases of endometrial hyperplasia within polyps and the immunoreactivity was mostly confined to metaplastic epithelial cells.

Discussion

P16 is a very useful immunohistochemical marker in the area of gynecological pathology [10]. The strong nuclear and cytoplasmic immunoreactivity in high-risk HPV-associated cervicovaginal neoplasms greatly helps in differentiating these neoplasms from problematic benign mimics [11, 12]. Recently p16 expression was found to be positive in most endometrial serous adenocarcinomas and it is now widely used as a sensitive and discriminating marker of

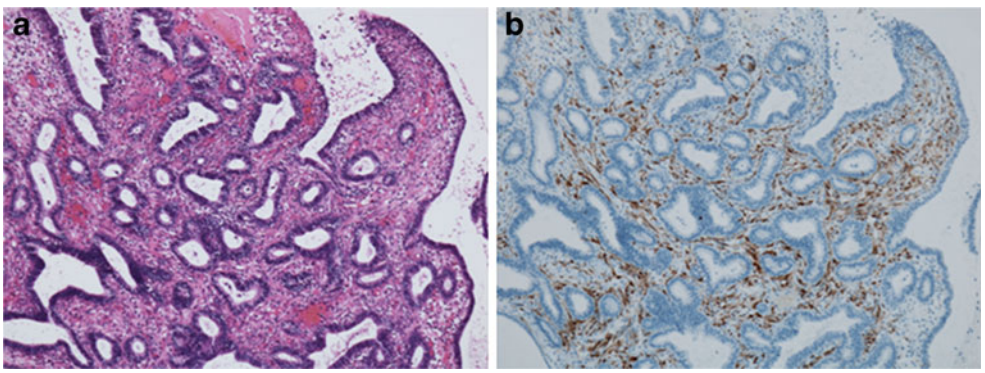

Fig. 2 Stromal p16 expression in endometrial hyperplasia within polyps. **a**, **b** P16-positive stromal cells in the surface. Unlike pure endometrial hyperplasia, the stroma is fibrous

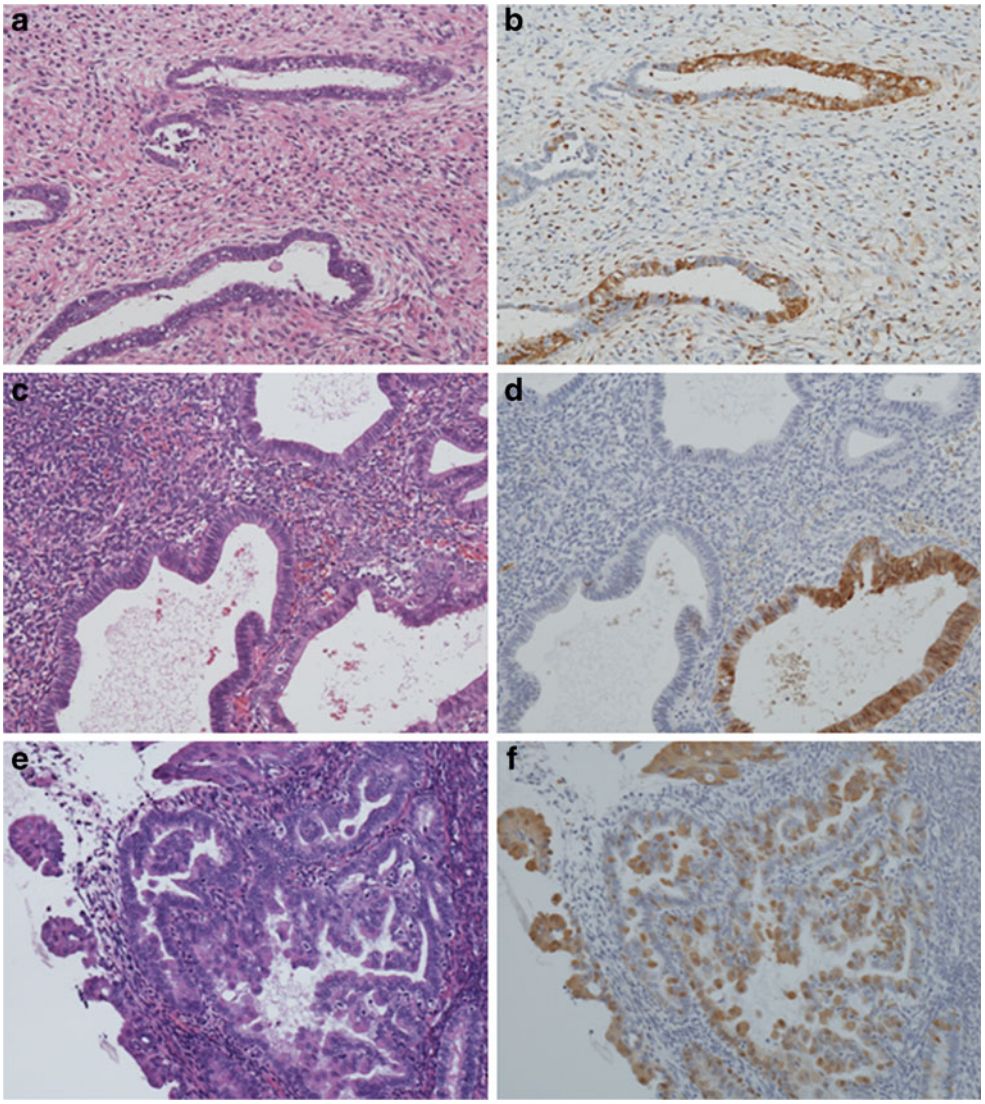

Fig. 3 Glandular p16 expression in endometrial polyp and hyperplasia. **a**, **b** Endometrial polyp. P16 is positive in tubal metaplasia and the stromal cells. **c**, **d** Simple hyperplasia without atypia. The gland at the lower right corner is positive for p16, and shows tubal metaplasia. All stromal cells are negative for p16. **e**, **f** Complex atypical hyperplasia with eosinophilic cell change. P16 is positive in the epithelial cells with eosinophilic metaplasia

endometrial serous adenocarcinoma and its precursor, endometrial intraepithelial carcinoma (EIC) [13, 14]. Compared with studies on p16 immunohistochemistry in epithelial lesions, there have been very few studies applying p16 immunohistochemistry to stromal gynecologic lesions except for leiomyosarcoma and undifferentiated endometrial sarcoma [15, 16]. More diffuse and stronger p16 staining was seen in leiomyosarcoma than in leiomyoma. In the present study, we found prominent p16 expression in the stromal cells of endometrial polyps, regardless of patient age, and the histological type of the polyp. There was a marked difference in stromal p16 expression between endometrial polyp and endometrial hyperplasia. We consider stromal p16 expression in endometrial polyps to be very characteristic and useful in differentiating endometrial polyp from endometrial hyperplasia.

In our study, nearly half of the cases consisted of non-surgical samples. Although the accuracy of diagnosis in these non-surgical cases, especially of polyp and simple hyperplasia without atypia, may be questioned, we selected these cases very carefully, paying attention to the histological features of polyp, and excluded any ambiguous cases. In both surgical and non-surgical samples, stromal p16 expression was seen almost exclusively in endometrial polyps. In addition, stromal p16 expression was seen only in fragments derived from an endometrial polyp in curettage specimens. We consider p16 immunohistochemistry especially useful in the pathological diagnosis of endometrial polyp on fragmented curettage specimens.

Recent studies using endometrial biopsy and curettage specimens showed relatively high interobserver agreement for a diagnosis of endometrial polyp [17, 18]. However, poorer agreement was seen in cases of endometrial intraepithelial neoplasia (EIN) arising in a polyp with or without extensive metaplastic changes [18]. To make a diagnosis of EIN or complex hyperplasia within a polyp, benign components of the polyp should be recognized and it should be regaded as the reference point. In our study, stromal p16

expression was also seen in all six cases of endometrial hyperplasia within a polyp. The p16-positive stromal cells tended to occur in the areas where characteristic fibrous stroma of the polyp persisted, which makes p16 immunohistochemistry useful in that it highlights the characteristic stroma. It is of interest that only one case of simple hyperplasia without atypia showed focal stromal p16 expression. This case showed multiple polypoid excrescences and p16-positive cells were seen in the surface of polypoid excrescences. Stromal p16 expression might be at least partly related to the polypoid growth of endometrium.

P16 is a cyclin-dependent kinase-4 inhibitor that is encoded by a gene localized on chromosome 9p21 within the INK4a/ARF locus. The role of p16 in tumorigenesis is variable and the significance of its overexpression differs from tumor to tumor [19]. P16 overexpression occurs in tumours along at least two different mechanisms. The first is an abnormality in the Rb pathway. Normally, p16 inactivates CDK4/6, blocking phosphorylation of Rb, and induces cell cycle arrest. Loss of this p16 function allows uncontrolled cellular proliferation [20]. Some malignant tumors, such as malignant peripheral nerve sheath tumor, have been reported not to express p16, in association with loss of the p16 gene [20]. Paradoxically, other malignant tumours show p16 overexpression, the well-known example being HPV-related neoplasms. The HPV oncoprotein E7 inactivates Rb, which results in the release of p16 from its negative feedback control and an increase in the level of p16 protein [21]. Some HPV-unrelated malignant tumors also overexpress p16, which has been explained by a positive feedback mechanism caused by deregulation of Rb [22]. The second situation of p16 overexpression is related to another important function of p16, oncogene-induced senescence (OIS). P16 induces cellular senescence in response to oncogene expression, and induces cell cycle arrest [23]. This mechanism is well exemplified in some benign tumors such as nevi, neurofibroma, and schwannoma. These tumors overexpress p16 and show senescence-associated acidic β-galactosidase activity, BRAF mutations, and growth arrest [23]. As the malignant counterparts of these tumors are negative for p16, overexpression of p16 in benign tumors seems to control proliferation and protect the tumor cells from malignant transformation [24]. As an endometrial polyp is a benign lesion, stromal p16 expression in an endometrial polyp is likely explained by this second mechanism of p16 overexpression. There is limited information on p16 expression in malignant endometrial stromal tumors, notably endometrial stromal sarcoma. However, a very limited study showed lower expression of p16 in endometrial stromal sarcoma than in leiomyosarcoma and undifferentiated endometrial sarcoma [16]. As it is of interest to explore whether or not the function of p16 as a tumor-suppressor gene is lost in malignant endometrial stromal tumors, we also examined p16 expression in four cases of endometrial stromal sarcoma and four cases of adenosarcoma and of both two cases were positive for p16. The staining pattern was focal in three cases and diffuse in one case, which was an adenosarcoma with stromal overgrowth. As the staining pattern of p16 in malignant endometrial stromal cells was quite variable, the significance of p16 immunorectivity in these cases remains to be clarified.

Although endometrial polyp is considered to be a benign stromal neoplasm, the data to support this hypothesis are limited. Fletcher et al. reported clonal 6p21 rearrangement restricted to the mesenchymal component of an endometrial polyp [25]. Cin et al. found amplification of the HMGIC gene in endometrial polyps and identified HMGIC expression in the nuclei of the stromal cells in endometrial polyps [26]. The HMGIC gene is known to be expressed in benign mesenchymal tumors, but has rarely been reported in malignant tumors [26].

There have been a few immunohistochemical studies focusing on endometrial stromal cells. Normally functioning endometrial stromal cells are positive for calretinin [27, 28]; its immunoreactivity has been reported to be negative or reduced in the stroma of dysfunctional bleeding, postmenopausal, ectopic, hyperplastic, and neoplastic endometrium including polyp [27]. CD34 is positive in the stromal cells of the basalis of normal endometrium, and increased in dysfunctional uterine bleeding and endometrial polyp [28]. These studies imply stromal cell alteration in various endometrial abnormalities whether or not they are neoplastic. As our study here focused only on endometrial polyp and endometrial hyperplasia, it is unclear whether p16 expression in endometrial polyps indicates neoplastic stromal proliferation or non-neoplastic stromal abnormalities. To clarify this issue, whether or not the stromal proliferation is clonal must be elucidated.

The mechanism and significance of p16 overexpression in non-neoplastic gynecological lesions are poorly understood. Horree et al. found that p16 was consistently expressed in endometrial tubal metaplasia [29]. In their study, p16 expression was paralleled by aberrant expression of cell cycle proteins and resembled the pattern of p16 expression frequently seen in endometrial carcinomas. They proposed endometrial tubal metaplasia to be a potential premalignant endometrial lesion [29]. P16 has also been reported to be expressed in endocervical tubal metaplasia [30], but as this is a very common epithelial change, it is not clear from the very small numbers of cases reported whether or not all tubal metaplasia are premalignant lesions. In our study, in addition to p16 expression in almost all foci of tubal metaplasia, eosinophilic cell change and surface syncytial change were also p16-positive. Although the mechanism of endometrial metaplasia is still unknown, it seems likely that p16 plays some role in the altered endometrial glandular differentiation.

Acknowledgments This work was supported by a grant-in-aid for clinical research from the National Hospital Organization of Japan.

Conflict of interest statement The authors declare that they have no conflict of interest.

References

1. Silverberg SG (1992) Endometrial polyp and hyperplasias. In: Silverberg SG, Kurman RJ (eds) Tumors of the uterine corpus and gestational trophoblastic disease. Atlas of tumor pathology. Third series. Fascicle 3. Armed Forces Institute of Pathology, Washington, pp 15–45
2. Reslová T, Tosner J, Resl M et al (1999) Endometrial polyps. A clinical study of 245 cases. Arch Gynecol Obstet 262:133–139
3. Silverberg SG (2000) Problems in the differential diagnosis of endometrial hyperplasia and carcinoma. Mod Pathol 13:309–327
4. Winkler B, Alvarez S, Richart RM et al (1984) Pitfalls in the diagnosis of endometrial hyperplasia. Obstet Gynecol 64:185–193
5. Allison KH, Reed SD, Voigt LF et al (2008) Diagnosing endometrial hyperplasia: why is it so difficult to agree? Am J Surg Pathol 32:691–698
6. Kim KR, Peng R, Ro JY et al (2004) A diagnostically useful histopathologic feature of endometrial polyp. The long axis of endometrial glands arranged parallel to surface epithelium. Am J Surg Pathol 28:1057–1062
7. Huang E, Hornstein MD, Stewart EA et al (2011) Evaluation of the cyclic endometrium and benign endometrial disorders. In: Crum CP, Nucci MR, Lee KR (eds) Diagnostic gynecologic and obstetric pathology, 2nd edn. Elsevier Saunders, Philadelphia, pp 407–456
8. McCluggage WG (2011) Benign diseases of the endometrium. In: Kurmann RJ, Ellenson LH, Ronnett BM (eds) Blaustein's pathology of the female genital tract, 6th edn. Springer, New York, pp 307–358
9. Malpica A, Deavers MT, Euscher E (2010) Benign endometrial conditions. In: Malpica A, Deavers MT, Euscher E (eds) Biopsy interpretation of the uterine cervix and corpus. Lippincott Williams & Wilkins, Philadelphia, pp 117–144
10. O'Neill CJ, McCluggage WG (2006) p16 expression in the female genital tract and its value in diagnosis. Adv Anat Pathol 13:8–15
11. Keating JT, Cviko A, Riethdorf S et al (2001) Ki-67, Cyclin E, and $p16^{INK4}$ are complimentary surrogate biomarkers for human papilloma virus-related cervical neoplasia. Am J Surg Pathol 25:884–891
12. Klaes R, Friedrich T, Ridder R et al (2002) $p16^{INK4a}$ immunohistochemistry improves interobserver agreement in the diagnosis of cervical intraepithelial neoplasia. Am J Surg Pathol 26:1389–1399
13. Chiesa-Vottero A, Malpica A, Deavers MT, Broaddus R, Nuovo GJ, Silva EG (2007) Immunohistochemical overexpression of p16 and p53 in uterine serous carcinoma and ovarian high-grade serous carcinoma. Int J Gynecol Pathol 26:328–333
14. Yemelyanova A, Ji H, Shih JM et al (2009) Utility of p16 expression for distinction of uterine serous carcinomas from endometrial endometrioid and endocervical adenocarcinomas. Immunohistochemical analysis of 201 cases. Am J Surg Pathol 33:1504–1514
15. Gannon BR, Manduch M, Childs TJ (2007) Differential immunoreactivity of p16 in leiomyosarcomas and leiomyoma variants. Int J Gynecol Pathol 27:68–73
16. D'Angelo E, Prat J (2010) Uterine sarcomas: a review. Gynecol Oncol 116:131–139
17. Carlson JW, Mutter GL (2008) Endometrial intraepithelial neoplasia is associated with polyps and frequently has metaplastic change. Histopathology 53:325–332
18. Marotti JD, Glatz K, Parkash V, Hecht JL (2011) International internet-based assessment of observer variability for diagnostically challenging endometrial biopsies. Arch Pathol Lab Med 135:464–470
19. Romagosa C, Simonetti S, López-Vincente L et al (2011) $p16^{Ink-4a}$ overexpression in cancer: a tumor suppressor gene associated with senescence and high-grade tumors. Oncogene 30:2087–2097
20. Serrano M (1997) The tumor suppressor protein p16INK4a. Exp Cell Res 237:7–13
21. Munger K, Werness BA, Dyson N, et al (1989) Complex formation of human papillomavirus E7 proteins with the retinoblastoma tumor suppressor gene product. EMBO J 4099–4105.
22. Schwartz B, Avivi-Green C, Polak-Charcon S (1998) Sodium butyrate induces retinoblastoma protein dephosphorylation, p16 expression and growth arrest of colon cancer cells. Mol Cell Biochem 188:21–30
23. Michaloglou C, Vredeveld LCW, Soengas MS et al (2005) $BRAF^{E600}$-associated senescence-like cell cycle arrest of human naevi. Nature 436:720–724
24. Sabah M, Cummins R, Leader M et al (2006) Loss of p16(INK4A) expression is associated with allelic imbalance/loss of heterozygosity of chromosome 9p21 in microdissected malignant peripheral nerve sheath tumors. Appl Immunohistochem Mol Morphol 14:97–102
25. Fletcher JA, Pinkus JL, Lage JM et al (1992) Clonal 6p21 rearrangement is restricted to the mesenchymal component of an endometrial polyp. Genes Chrom Cancer 5:260–263
26. Cin PD, Wanschura S, Kazmierczak B et al (1998) Amplification and expression of the *HMGIC* gene in a benign endometrial polyp. Genes Chrom Cancer 22:95–99
27. Moghrabi HA, Elkeilani A, Thomas JM et al (2007) Calretinin: an immunohistochemical marker for the normal functional endometrial stroma and alterations of the immunoreactivity in dysfunctional uterine bleeding. Path Res Pract 203:79–83
28. Mai KT, Teo I, Moghrabi HA et al (2008) Calretinin and CD34 immunoreactivity of the endometrial stroma in normal endometrium and change of the immunoreactivity in dysfunctional uterine bleeding with evidence of 'disordered endometrial stroma'. Pathology 40:493–499
29. Horree N, Heintz APM, Sie-Go DMDS et al (2007) p16 is consistently expressed in endometrial tubal metaplasia. Cell Oncol 29:37–45
30. Murphy N, Heffron CCBB, King B et al (2004) $p16^{INK4a}$ positivity in benign, premalignant and malignant cervical glandular lesions: a potential diagnostic problem. Virchows Arch 445:610–615

Virchows Arch (2012) 461:149–156
DOI 10.1007/s00428-012-1277-0

ORIGINAL ARTICLE

Down-staging (<pT2) of urothelial cancer at cystectomy after the diagnosis of detrusor muscle invasion (pT2) at diagnostic transurethral resection (TUR): is prediction possible?

Willemien Beukers · Titia Meijer · Cornelis J. Vissers · Joost L. Boormans · Ellen C. Zwarthoff · Geert J. L. H. van Leenders

Received: 16 April 2012 / Revised: 30 May 2012 / Accepted: 25 June 2012 / Published online: 10 July 2012
© The Author(s) 2012. This article is published with open access at Springerlink.com

Abstract Urothelial cell carcinoma (UCC) with musculus detrusor (MD) invasion is treated by cystectomy. Subsequent pathologic evaluation of cystectomies does not reveal MD invasion (<pT2) in a subgroup of patients. Our objective was to identify features at diagnostic transurethral resection (TUR) predicting down-staging (<pT2) at cystectomy. Patients with pathologically confirmed MD invasion at TUR followed by cystectomy for UCC without (neo-) adjuvant therapy were included (N=106). Slides of both TUR and cystectomy specimens were reviewed, and survival analyses were performed. In total, 27/106 (26 %) tumors were down-staged at cystectomy, of which 13 (12 %) had no residual tumor (pT0). There was no significant difference in age, gender, time interval between TUR and operation, number of slides sampled, and presence of TUR scar between down-staged (<pT2) and pT2 UCC. At review of TUR specimens (N=52) with UCC initially diagnosed as pT2, MD invasion was not confirmed in eight cases (15 %). One case showed extensive histiocytic reaction misinterpreted as UCC; in four cases, muscularis mucosae had been considered MD, and in three cases, desmoplastic reaction mimicked MD. No histologic parameter at TUR was significantly associated with down-staging at cystectomy. Overall and disease-specific survival was not statistically different in down-staged and pT2 UCC. In conclusion, down-staging of UCC (<pT2) at cystectomy occurred in 26 %. At review of diagnostic TURs, MD invasion was not confirmed in 15 %. No clinical or pathologic parameter was predictive for down-staging at cystectomy. There was no difference in survival between down-staged and pT2-staged UCC.

Keywords Cystectomy · Urothelial cell carcinoma · Down-staging · pT0

W. Beukers · T. Meijer · C. J. Vissers · E. C. Zwarthoff · G. J. L. H. van Leenders (✉)
Department of Pathology, Josephine Nefkens Institute, Erasmus MC,
PO Box 2040, 3000 CA Rotterdam, The Netherlands
e-mail: g.vanleenders@erasmusmc.nl

J. L. Boormans
Department of Urology, Erasmus MC,
Rotterdam, The Netherlands

Introduction

Bladder cancer is the fourth most common cancer in males and ninth most common cancer in females [1]. The majority of bladder tumors primarily appear as non-muscle invasive disease (<pT2), whereas 20 % of urothelial carcinomas (UCCs) are infiltrating the musculus detrusor (MD) at presentation. Up to 25 % of initially non-muscle invasive tumors will eventually progress to MD invasive disease. Tumors limited to the mucosa (pTa/pT1) are conservatively treated, while bladder cancer infiltrating within or beyond the MD (≥pT2) requires aggressive treatment [2, 3]. After radical surgery, the 5-year recurrence free-survival of ≥pT2 UCC is only 56–58 % [4, 5]. Accurate pathologic staging of UCC at diagnostic transurethral resection (TUR) specimens is, therefore, an important parameter to determine the optimal therapy for individual patients.

Although accurate pathological staging at diagnostic TUR is pivotal for therapeutic decision-making, definite tumor stage can only be perceived after pathologic evaluation of cystectomy specimens. In a substantial number of patients, no invasion in the MD is identified at cystectomy, prompted by MD invasion at diagnostic TUR. These patients either show residual UCC without stromal invasion

(pTa), UCC with invasion of the lamina propria (pT1), carcinoma in situ (CIS) (pTis), or no residual tumor at all (pT0). Down-staging of UCC to pT0 in cystectomy specimens is reported in 5 to 20 % [6–10]. Although down-staging is a well-known feature, it can be confronting for patient, urologist, and pathologist, raising the question whether the initial diagnosis prompting radical surgery was adequate.

Several pathologic features might mimic MD invasion of UCC. Infiltration of the muscularis mucosae (MM) and extensive desmoplastic stromal reaction can both be misinterpreted as MD invasion. Furthermore, it is not well-established whether UCC located directly adjacent to but not within the MD should be staged as pT2 disease. The objective of the present study was (a) to identify clinical and pathological features of UCC at diagnostic TUR, which correspond with down-staging at cystectomy and (b) to investigate the clinical outcome of patients with down-staged UCC after cystectomy.

Material and methods

Study population

In this study, we included patients with pathologically confirmed MD invasion at diagnostic TUR, followed by cystectomy for UCC without neo-adjuvant chemotherapy or radiotherapy. All patients were treated for UCC of the urinary bladder at Erasmus MC, location Dijkzigt, between June 1989 and May 2010. Patients were routinely followed up every 3 months on the first 2 years after cystectomy, semiannually on the third to fifth year, and subsequently at 12-month intervals. In case of progression, patients were followed up every 3 months. Loco-regional recurrent disease or distant metastases were assessed by CT of the abdomen and pelvis, chest X-rays, and bone scans (if indicated). Death was reported by treating physicians or general practitioner. Follow-up was defined as time from operation to event or last patient contact. Patients that deceased from other causes than bladder cancer, or that were lost to follow-up, were censored at the date of last contact. All clinical data were collected retrospectively from the electronic patient database.

Pathologic review

Slides of cystectomies and diagnostic TUR specimens were retrieved from the archives and reviewed by a urogenital pathologist (GvL). Initial diagnoses had been made by a group of general clinical pathologists. At review, stage and grade were reassigned according the UICC 2002 TNM staging system and the WHO grading system 1973 and 2004, respectively. The following additional pathological parameters were recorded at review of the cystectomy specimens: number of slides of the urinary bladder sampled, presence of a TUR scar, and presence of CIS. At review of the diagnostic TUR specimens, the depth of invasion was established paying special attention to potential pitfalls such as MM invasion, extensive desmoplastic stromal reaction, invasion adjacent to but not within the MD, and invasion in between MD bundles. If classification was uncertain based on routine haematoxylin and eosin staining (HE), immunohistochemistry was performed. In case MD invasion was not obvious despite histology and additional immunohistochemistry, the tumor was classified as pT1 (N=1), which is similar to our approach in daily practice, in which these tumors are reported as “pT1 at least.” The use of the samples for research purposes was approved by the Erasmus MC Medical Ethics Committee according to the Medical Research Involving Human Subjects Act (MEC-2004-261).

Immunohistochemistry

Formalin-fixed, paraffin-embedded tissue sections (5 μm) from TUR specimens were cut and mounted on aminoacetylsilane-coated slides (Starfrost, Berlin, Germany). Sections were deparaffinised in EZprep (Roche Diagnostics, Indianapolis, IN, USA). For all antibodies, heat-induced epitope retrieval was performed in CC1 buffer (high pH) (Roche Diagnostics) for 64 min. The slides were incubated with monoclonal Desmin antibody (clone DE-R-11; 1:50; Novocastra, Newcastle, UK) or monoclonal keratin 7 antibody (clone OV-TL 12/30; 1:1,000; Biogenex, San Ramon, CA, USA) at 36 °C for 32 min, followed by amplification using UltraView Universal DAB detection kit (Roche Diagnostics). All reactions were performed in an automatic BenchMark Ultra device (Roche Diagnostics). Finally, the slides were counterstained, dehydrated, cleared in xylene, and mounted in Pertex (Histolab Products, Gothenburg, Sweden).

Statistical analysis

For comparison of continuous and categorical parameters of the pT2 and the down-staged group at cystectomy, Mann–Whitney and Fisher's exact test were performed, respectively. Kaplan–Meier curves with log-rank analysis were used for comparison of survival. A p value <0.05 was considered statistically significant. All analyses were performed using the Predictive Analytics Software 17 (SPSS Inc., Chicago, IL, USA).

Results

Patient characteristics

Between May 1989 and June 2010, a total of 160 patients had undergone cystectomy for a urothelial malignancy at Erasmus MC, comprising of 135 (84.4 %) males and 25 (15.6 %) females (Table 1). The mean age of the patients at operation was 62.4 years (range 33.2–82.5 years). The majority of male patients had undergone a radical cystoprostatectomy (N=128; 94.8 %), which was combined by a left (N=4), right (N=4), or bilateral (N=1) nephro-ureterectomy. Four (3.0 %) male patients had been treated by simple cystectomy, of whom three had undergone a previous radical prostatectomy for prostate adenocarcinoma. Three men (2.2 %) had been treated by partial cystectomy. A total of 17 (68 %) female patients had undergone a cysto-hysterectomy with adnexa extirpation, combined with a left (N=1) or right (N=1) nephro-ureterectomy. Eight (32 %) females had been treated with simple cystectomy (Table 1).

The clinical indication for cystectomy was UCC with MD invasion (≥cT2) in 137 patients (85.7 %), therapy-resistant recurrence of superficial high grade pTa/pT1 UCC and/or CIS (N=17; 10.6 %), involvement of the prostatic urethra by superficial high grade UCC/CIS (N=4; 2.5 %), a very large superficial UCC (pTa; N=1; 0.6 %), and urothelial CIS combined with sigmoid adenocarcinoma with potential involvement of the urinary bladder (N=1; 0.6 %). Of the 137 patients who had been operated for MD invasion, 23 (16.8 %) patients had undergone neo-adjuvant therapy and 8 (5.8 %) had clinical MD invasion without pathological confirmation. For further analysis, we included the remaining 106 (77.4 %) patients who had pathologically confirmed MD invasion (≥pT2) at diagnostic TUR, followed by cystectomy without neo-adjuvant therapy.

Table 1 Clinical characteristics of 160 patients operated for urothelial cell carcinoma

N=160	No. of patients (%)
Age (median; range)	62.4 (33.2–82.5)
Sex	
Male	135 (84)
Female	25 (16)
Type of operation	
Male	
Radical cystoprostatectomy	128 (95)
With nephro-ureterectomy	9
Simple cystectomy	4 (3)
Partical cystectomy	3 (2)
Female	
Cysto-hysterectomy with adnexa extirpation	17 (68)
With nephro-ureterectomy	2
Simple cystectomy	8 (32)
Indication for cystectomy	
Musculus detrusor invasion	137 (86)
Therapy-resistant recurrent pTa/pT1 or CIS	17 (11)
Involvement of the prostatic urethra by UCC/CIS	4 (2)
Very large superficial high grade UCC	1 (0.5)
Urothelial CIS combined with sigmoid adenocarcinoma	1 (0.5)

UCC urothelial cell carcinoma, *HG* high grade, *CIS* carcinoma in situ

Characterization of down-staged UCC

Of the 106 patients with ≥pT2 UCC at TUR, histologic evaluation of the cystectomy specimen revealed 13 cases (12.3 %) without residual tumor (pT0), 5 (4.7 %) with CIS only, 3 (2.8 %) with pTa, 6 (5.7 %) with pT1, 33 (31.1 %) with pT2, 37 (34.9 %) with pT3, and 9 (8.5 %) with pT4 disease. Therefore, 27 (25.5 %) cases had lower stage UCC at cystectomy, then at initial diagnostic TUR, which showed ≥pT2 disease (Table 2). No statistically significant difference in age (p=0.64), gender (p=1.00), or number of days between diagnostic TUR and operation (p=0.96) existed

Table 2 Tumor characteristics of 106 patients with ≥pT2 on diagnostic transurethral resection (TUR), followed by cystectomy for urothelial cell carcinoma without (neo-) adjuvant therapy

N=106	No. of patients (%)
Stage	
pT0	13 (12)
pTis	5 (5)
pTa	3 (3)
pT1	6 (6)
pT2	33 (31)
>pT2	46 (43)
Concomitant CIS	16
Grade	
WHO 1973	
No tumor	13 (12)
G1	0 (0)
G2	9 (9)
G3	79 (79)
WHO 2004	
No tumor	13 (12)
PUNLMP	0 (0)
LG	0 (0)
HG	88 (88)

CIS carcinoma in situ, *PUNLMP* papillary urothelial neoplasm of low malignant potential, *LG* low grade, *HG* high grade

Table 3 Clinical (N=106) and pathologic (N=58) characteristics of down-staged (<pT2) and ≥pT2 urothelial carcinoma at cystectomy

No.	Clinico-pathologic variable	Down-staged <pT2	≥pT2	p value
106	Age (median; range)	64.9 (35.1–73.9)	64.1 (33.2–82.5)	0.64
	Male/female (%)	23:4 (85/15)	68:11 (86/14)	1.00
	Time after TUR (days) (median; range)	57 (15–113)	55 (12–220)	0.96
58	Number slides (median; range)	10 (3–33)	10 (2–23)	0.62
	TUR reaction (%)	20/27 (74)	17/31 (55)	0.13

Review of pathologic cystectomy characteristics was performed only on the down-staged (<pT2) and pT2 urothelial cancers

TUR transurethral resection

between down-staged (<pT2) and concordantly staged (≥pT2) cystectomies (Table 3).

To investigate whether down-staging was due to difference in sampling, we histologically reviewed all cystectomy slides of ≤pT2 UCC. Stages pT3 and pT4 were not evaluated (N=46). In two cases, slides were not available for review, leaving a total of 58 cases for analysis. The mean number of slides sampled from the urinary bladder was ten in both the down-staged and the concordantly staged pT2 group (p=0.62). Histological reaction to previous TUR was found in 20/27 (74 %) cases of the down-staged group as compared to 17/31 (55 %) cases in the pT2 group (p=0.13), indicating that under-sampling of the cystectomy specimen was not the cause of tumor down-staging after operation (Table 3).

In order to find histological features at diagnostic TUR that corresponded with down-staging at cystectomy, we reviewed all diagnostic TUR slides of the 58 patients with ≤pT2 UCC. Six cases were not available for review, leaving 52 cases for further analysis. At review, one case showed extensive histiocytic infiltration while no UCC was found in the diagnostic TUR specimen, which was verified with

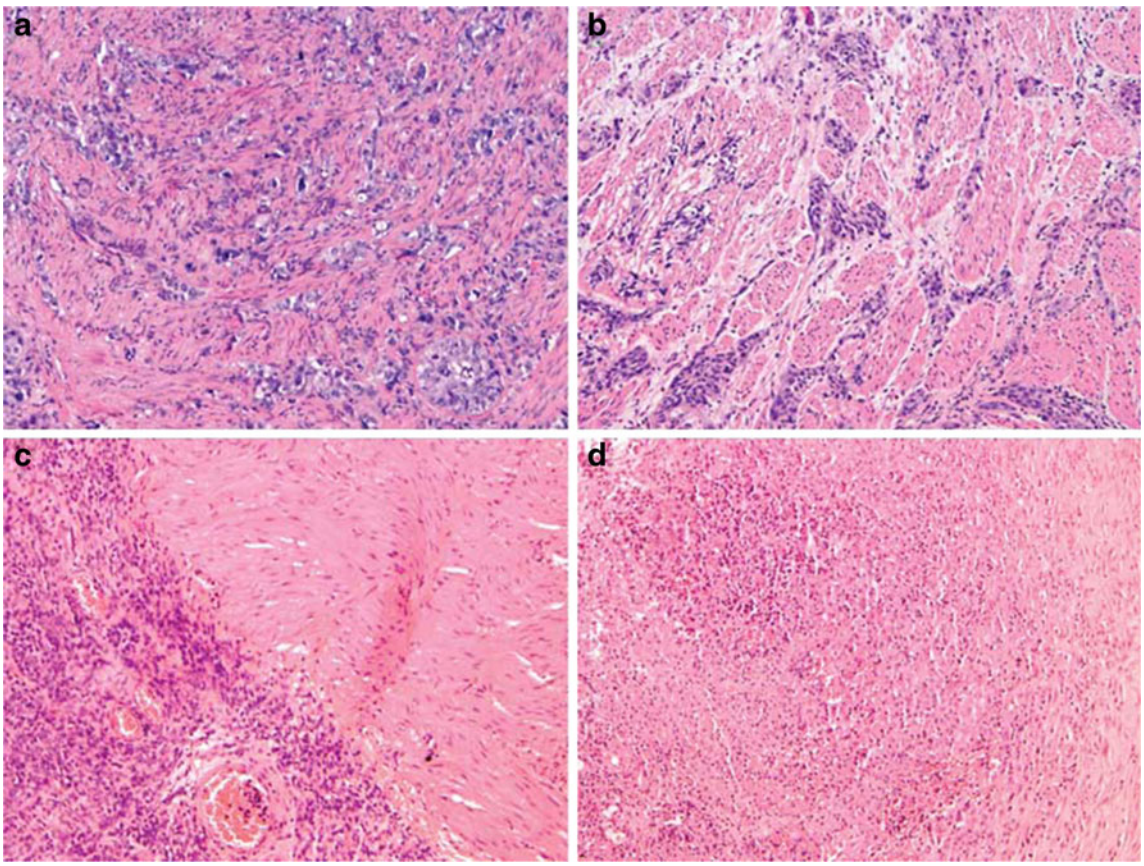

Fig. 1 Assessment of urothelial cell carcinoma invasion in relation to the musculus detrusor. **a**, **b** Urothelial carcinoma invading in between musculus detrusor fascicles. **c** Urothelial cancer located adjacent to but no in between musculus detrusor fascicles. **d** Histiocytic reaction after previous diagnostic transurethral resection, misinterpreted as urothelial cancer invading the musculus detrusor. HE; original magnifications ×100

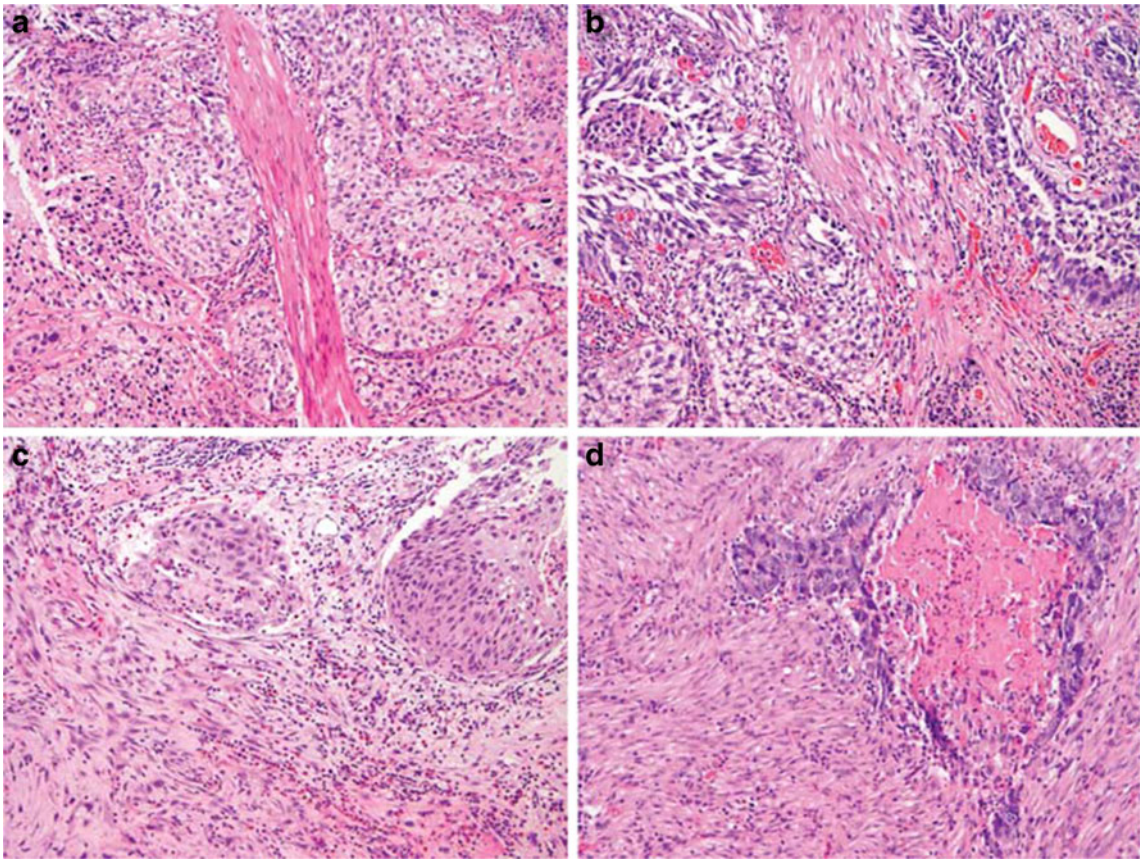

Fig. 2 Pitfalls of urothelial cell carcinoma invasion of musculus detrusor. **a**, **b** Muscularis mucosae fascicles mimicking musculus detrusor. **c**, **d** Extensive desmoplastic stromal reaction misinterpreted as musculus detrusor invasion. HE; original magnifications ×100

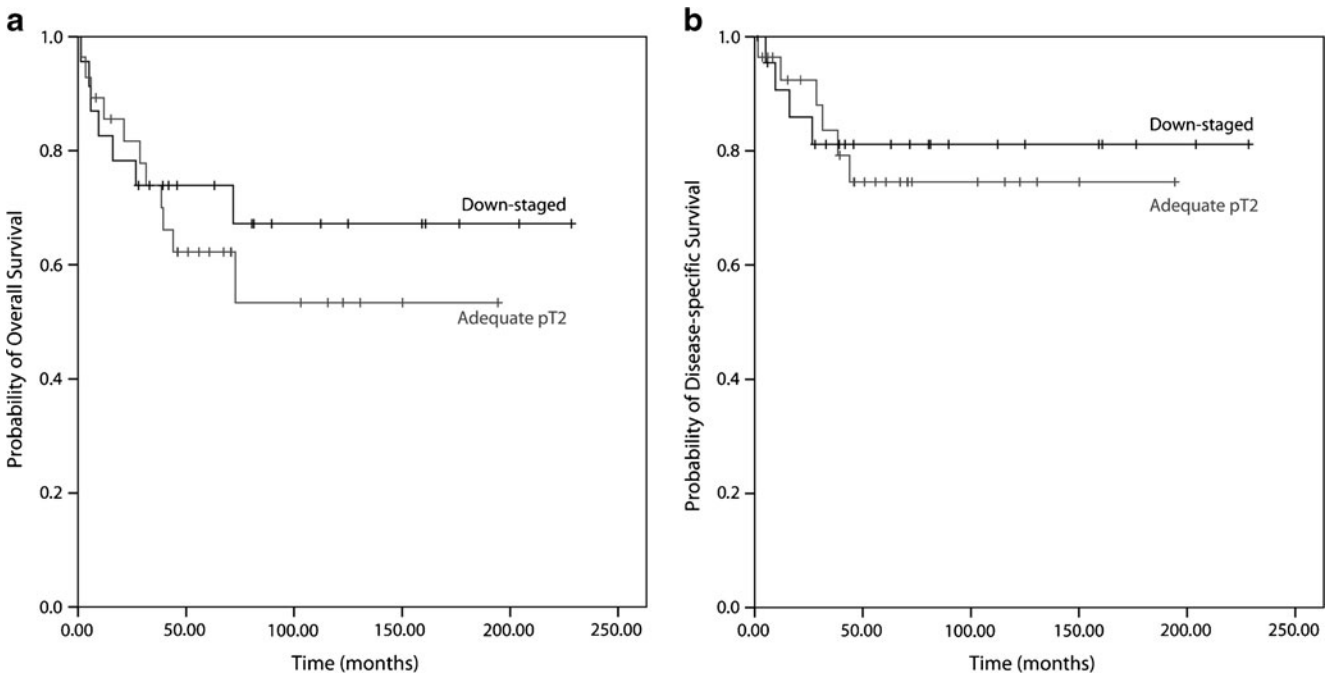

Fig. 3 Survival analysis of down-staged and pT2-staged urothelial cell carcinoma after cystectomy. There was no difference in overall **a** (p=0.53) or disease-specific **b** (p=0.76) survival of patients with <pT2 versus pT2 urothelial cancer at cystectomy

negative immunohistochemical Ker7 staining (Fig. 1). This case was incorrectly diagnosed as UCC at the time of diagnosis; subsequent cystoprostatectomy indeed did not reveal UCC (pT0). In the remaining 51 cases, grade according to WHO 1973 (p=0.28) or 2004 (p=0.26), and concomitant CIS (p=0.55) were not associated with down-staging at cystectomy. Of the tumors, 40/51 (78.4 %) demonstrated invasion into the MD, 4 (7.8 %) showed tumor adjacent to the MD but not in between the muscle fascicles, and 7 (13.5 %) did not reveal invasion up to MD bundles convincingly (Fig. 2). Of these seven cases, four (7.7 %) showed invasion in between small smooth muscle fascicles, which were not characteristic for MD, but could represent MM and three (5.8 %) demonstrated extensive desmoplastic stromal reaction without tumor infiltration into the MD. The desmoplastic stromal reaction was probably interpreted as MD invasion at initial diagnosis (Fig. 3). In four cases, Desmin immunohistochemistry expression was used to facilitate identification of smooth muscle fascicles at review, in case of cauterization or differentiation with desmoplastic stromal reaction. There was no significant relation of the type of tumor invasion in the TUR specimen and the subsequent findings at cystectomy (Table 4).

Survival analysis

The mean follow-up of the pT2 group and the down-staged group was 61.6 and 70.9 months, respectively. To investigate whether patients who were down-staged at cystectomy had a favorable outcome versus those with stage pT2 at cystectomy, survival analysis was performed. We excluded 9/60 (15 %) patients with positive regional lymph nodes from the analysis, i.e., 4/27 (14.8 %) in the down-staged group and 5/33 (15.2 %) in the pT2 group. There was no significant difference in overall (p=0.53) and disease-specific (p=0.76) survival between the adequately staged and down-staged group (Fig. 3).

Discussion

In a significant number of cases, urologists and pathologists are confronted with UCC down-staged (<pT2) at cystectomy, although operation was prompted by an MD invasive tumor at diagnostic TUR. Down-staging at cystectomy might have several causes, such as successful neo-adjuvant therapy, complete UCC resection at TUR, or false-positive diagnosis at TUR. In the present study, we investigated the incidence and the possible origin of down-staging in a well-defined cohort of 106 cystectomy patients, of whom operation was prompted by pathologic MD invasion at diagnostic TUR and who had not undergone neo-adjuvant therapy.

We found down-staging at cystectomy in 26 % of the study population. In 12 %, no residual UCC (pT0) was identified, which is in line with numbers (6–20 %) reported by others [6–9]. Age, gender, and interval between TUR and operation were not statistically different between concordantly staged pT2 and the down-staged group. Since the number of slides sampled at grossing and frequency of identifying a TUR scar at microscopic evaluation of cystectomy specimens was similar in both groups, down-staging was not due to sampling error.

At review of the diagnostic TUR specimens, in 12 out of 52 (23.1 %) cases, UCC infiltration into the MD could not be confirmed. Discrepancy with the original TUR staging was caused by false interpretation of (a) histiocytic reaction as invasive UCC (1.9 %), (b) invasion of the MM as MD invasion (7.7 %), (c) extensive desmoplastic stromal reaction as MD (5.8 %), and (d) UCC impinging upon the MD as invasion into the MD (7.7 %). As far as we know, the latter subtle distinction has not been subject of study yet. If UCC adjacent to MD would be classified as pT2 disease, as is often done in pathologic practice, the prevalence of down-staging UCC at review of TUR specimens was 15.4 % (8/52). Interestingly, this percentage of staging discordance is in line with the percentage of original pT1 UCC up-staged to pT2 disease at review, indicating that inter-observer variability is also existing in assessing MD invasion [11]. Distinguishing between MM and MD invasion at diagnostic TUR is a well-known challenge in surgical pathology, which is hampered

Table 4 Pathologic characteristics of urothelial cell carcinoma at diagnostic transurethral resections (TUR) in the down-staged (N=21) and adequately pT2-staged group (N=30)

N=51	Down-staged N (%)	Adequate pT2 N (%)	p value
G2/G3	2/19 (10/90)	7/23 (23/77)	0.28
LG/HG	0/21 (0/100)	3/27 (10/90)	0.26
Concomitant CIS	8 (38)	9 (30)	0.55
Desmoplastic stromal reaction	0 (0)	3 (100)	N/A
MM invasion	2 (50)	2 (50)	1.00
Adjacent to MD	2 (50)	2 (50)	1.00
In between MD fascicles	17 (43)	23 (57)	1.00

LG low grade, *HG* high grade, *CIS* carcinoma in situ, *MM* muscularis mucosae, *MD* musculus detrusor

by problems in tissue orientation and potential MM hyperplasia. In addition, MD-infiltrating tumors may partially destruct muscle fibers, leaving thin residual MD bundles resembling MM [12]. Despite these difficulties, accurate recognition of MD invasion is crucial for patient treatment according to the current guidelines. Immunohistochemical expression of the cytoskeletal protein Smoothelin is reported to be stronger in MD than in MM [13–15]. Therefore, additional immunohistochemistry using Smoothelin can be useful in differentiating both muscle layers. While variable Smoothelin expression patterns can be appreciated when both layers are present in the same specimen, its value in classifying a limited amount of smooth muscle fibers in small specimens remains to be established. Therefore, we decided not to include this marker in the current study. Finally, extensive desmoplastic myofibroblastic reaction evoked by UCC invasion might histologically mimic MD [16]. In this case, immunohistochemical detection of Desmin is helpful to distinguish myofibroblasts from MD smooth muscle cells [17].

No statistically significant difference in overall and disease-specific survival was found between the down-staged and concordantly staged pT2 group. Interestingly, the percentage of patients with positive lymph nodes was similar between the two groups as well. Regarding the patients with pT0 disease, survival after cystectomy was not different from the patients with higher tumor stages. This is in accordance with the findings of Thrasher et al. [18]. This implicates that MD invasive UCC at diagnostic TUR with down-staging at cystectomy should still be regarded as pT2 disease. The clinical significance of pT0 disease at cystectomy is, however, still under debate. Volkmer et al. excluded patients with neo-adjuvant therapy and found a significantly better disease-specific survival in patients with pT0 disease at cystectomy versus patients with maximal pT2a disease at cystectomy [19]. Likewise, Tilki et al. investigated a group of 4,430 patients treated with radical cystectomy and found significantly better clinical outcomes in patients with pT0 disease than those with clinical and pathological stage T2 [20]. These results are conflicting with the findings in our study, which could be explained by the fact that in our study a relatively small number of patients were included.

This relatively low number of patients is a limitation of this study and was due to our strict selection criteria, i.e., exclusion of non-urothelial cancer such as squamous carcinoma and adenocarcinoma, presence of neo-adjuvant therapy, availability of slides for review, and omitting high-stage disease (pT3/4) from analysis. Nevertheless, to the best of our knowledge, this is the first study specifically investigating the nature of down-staging in UCC, in which we retrospectively demonstrate 15 % inter-observer variability in the diagnosis of clinically decisive MD invasion. For practical purposes, important lessons can be drawn from this study. First, UCC invasion directly adjacent to MD bundles can be classified as pT2 disease at TUR since down-staging in this group did not occur more frequently than in UCC with invasion into the MD fascicles. Secondly, the presence of pT2 disease at cystectomy in patients with MM invasion or extensive desmoplastic stromal reaction yet no MD invasion at TUR as well as the significant inter-observer variability of T1-2 staging raises the question whether the current clinicopathologic guidelines for treatment of invasive UCC can be optimized. Herr performed a re-staging TUR in patients with histologically proven pT2 disease [21]. If re-staging revealed pT0 or pT1 disease, patients were offered immediate cystectomy or careful follow-up. Interestingly, the 10-year disease-specific survival was similar in both groups with significantly better survival in patients with pT0 as compared to pT1 tumor at re-staging. Since cystectomy is a surgical procedure with 90-day complication rates as high as 46 % and peri-operative mortality ranging from 1 to 4 % [3, 22], further studies on the use of re-TUR and imaging modalities for the treatment and follow-up as alternative for radical operation in a subgroup of UCC patients are mandatory.

In conclusion, we have shown that 26 % of patients with initial pT2 stage at diagnostic TUR were down-staged at subsequent cystectomy. No clinical or pathologic parameters could be identified that were associated with down-staging (<pT2) of UCC at cystectomy. Review of diagnostic TUR specimens revealed inter-observer variability, with pT2 to <pT2 in 15 % of the cases. No difference in survival was found in patients with down-staged versus pT2 UCC at cystectomy.

Conflict of interest The authors declare that they have no conflict of interest.

Open Access This article is distributed under the terms of the Creative Commons Attribution License which permits any use, distribution, and reproduction in any medium, provided the original author(s) and the source are credited.

References

1. Jemal A, Siegel R, Ward E, Hao Y, Xu J, Murray T, Thun MJ (2008) Cancer statistics, 2008. CA Cancer J Clin 58:71–96
2. Colombel M, Akaza H, Bohle A, Palou J, Buckley R, Lamm D, Brausi M, Witjes JA, Persad R (2008) Epidemiology, staging, grading, and risk stratification of bladder cancer. Eur Urol Suppl 7:618–626
3. Morgan TM, Keegan KA, Clark PE (2011) Bladder cancer. Curr Opin Oncol 23:275–282
4. Ghoneim MA, Abdel-Latif M, el-Mekresh M, Abol-Enein H, Mosbah A, Ashamallah A, el-Baz MA (2008) Radical cystectomy for carcinoma of the bladder: 2,720 consecutive cases 5 years later. J Urol 180:121–127

5. Shariat SF, Karakiewicz PI, Palapattu GS, Lotan Y, Rogers CG, Amiel GE, Vazina A, Gupta A, Bastian PJ, Sagalowsky AI, Schoenberg MP, Lerner SP (2006) Outcomes of radical cystectomy for transitional cell carcinoma of the bladder: a contemporary series from the Bladder Cancer Research Consortium. J Urol 176:2414–2422
6. Dalbagni G, Genega E, Hashibe M, Zhang ZF, Russo P, Herr H, Reuter V (2001) Cystectomy for bladder cancer: a contemporary series. J Urol 165:1111–1116
7. Lee SE, Jeong IG, Ku JH, Kwak C, Lee E, Jeong JS (2004) Impact of transurethral resection of bladder tumor: analysis of cystectomy specimens to evaluate for residual tumor. Urology 63:873–877
8. Amling CL, Thrasher JB, Frazier HA, Dodge RK, Robertson JE, Paulson DF (1994) Radical cystectomy for stages Ta, Tis and T1 transitional cell carcinoma of the bladder. J Urol 151:31–35
9. Stein JP, Lieskovsky G, Cote R, Groshen S, Feng AC, Boyd S, Skinner E, Bochner B, Thangathurai D, Mikhail M, Raghavan D, Skinner DG (2001) Radical cystectomy in the treatment of invasive bladder cancer: long-term results in 1,054 patients. J Clin Oncol 19:666–675
10. Svatek RS, Shariat SF, Novara G, Skinner EC, Fradet Y, Bastian PJ, Kamat AM, Kassouf W, Karakiewicz PI, Fritsche HM, Izawa JI, Tilki D, Ficarra V, Volkmer BG, Isbarn H, Dinney CP (2011) Discrepancy between clinical and pathological stage: external validation of the impact on prognosis in an international radical cystectomy cohort. BJU Int 107:898–904
11. Bol MG, Baak JP, Buhr-Wildhagen S, Kruse AJ, Kjellevold KH, Janssen EA, Mestad O, Ogreid P (2003) Reproducibility and prognostic variability of grade and lamina propria invasion in stages Ta, T1 urothelial carcinoma of the bladder. J Urol 169:1291–1294
12. Ro JY, Ayala AG, el-Naggar A (1987) Muscularis mucosa of urinary bladder. Importance for staging and treatment. Am J Surg Pathol 11:668–673
13. Miyamoto H, Sharma RB, Illei PB, Epstein JI (2010) Pitfalls in the use of smoothelin to identify muscularis propria invasion by urothelial carcinoma. Am J Surg Pathol 34:418–422
14. Paner GP, Brown JG, Lapetino S, Nese N, Gupta R, Shen SS, Hansel DE, Amin MB (2010) Diagnostic use of antibody to smoothelin in the recognition of muscularis propria in transurethral resection of urinary bladder tumor (TURBT) specimens. Am J Surg Pathol 34:792–799
15. Paner GP, Shen SS, Lapetino S, Venkataraman G, Barkan GA, Quek ML, Ro JY, Amin MB (2009) Diagnostic utility of antibody to smoothelin in the distinction of muscularis propria from muscularis mucosae of the urinary bladder: a potential ancillary tool in the pathologic staging of invasive urothelial carcinoma. Am J Surg Pathol 33:91–98
16. Cheng L, Montironi R, Davidson DD, Lopez-Beltran A (2009) Staging and reporting of urothelial carcinoma of the urinary bladder. Mod Pathol 22:S70–S95
17. Council L, Hameed O (2009) Differential expression of immunohistochemical markers in bladder smooth muscle and myofibroblasts, and the potential utility of desmin, smoothelin, and vimentin in staging of bladder carcinoma. Mod Pathol 22:639–650
18. Thrasher JB, Frazier HA, Robertson JE, Paulson DF (1994) Does of stage pT0 cystectomy specimen confer a survival advantage in patients with minimally invasive bladder cancer? J Urol 152:393–396
19. Volkmer BG, Kuefer R, Bartsch G Jr, Straub M, de Petriconi R, Gschwend JE, Hautmann RE (2005) Effect of a pT0 cystectomy specimen without neoadjuvant therapy on survival. Cancer 104:2384–2391
20. Tilki D, Svatek RS, Novara G, Seitz M, Godoy G, Karakiewicz PI, Kassouf W, Fradet Y, Fritsche HM, Sonpavde G, Izawa JI, Ficarra V, Lerner SP, Schoenberg M, Stief CG, Dinney CP, Skinner E, Lotan Y, Sagalowsky AI, Reich O, Shariat SF (2010) Stage pT0 at radical cystectomy confers improved survival: an international study of 4,430 patients. J Urol 184:888–894
21. Herr HW (2001) Transurethral resection of muscle-invasive bladder cancer: 10-year outcome. J Clin Oncol 19:89–93
22. Morgan TM, Clark PE (2010) Bladder cancer. Curr Opin Oncol 22:242–249

Virchows Arch (2012) 461:157–162
DOI 10.1007/s00428-012-1270-7

ORIGINAL ARTICLE

ERG rearrangement in local recurrences compared to distant metastases of castration-resistant prostate cancer

Veit J. Scheble · Gregor Scharf · Martin Braun · Christian Ruiz · Susanna Stürm · Karen Petersen · Rudi Beschorner · Alexander Bachmann · Tobias Zellweger · Falko Fend · Glen Kristiansen · Lukas Bubendorf · Nicolas Wernert · Zaki Shaikhibrahim · Sven Perner

Received: 20 January 2012 / Revised: 17 April 2012 / Accepted: 13 June 2012 / Published online: 6 July 2012
© Springer-Verlag 2012

Abstract Castration-resistant prostate cancer is the second most common cause of cancer death and results in a median survival of less than 2 years. In prostate cancer, fusions between *TMPRSS2* and *ERG* are common. The *ERG* rearrangement prevalence in local recurrent castration-resistant prostate cancer compared to distant metastatic prostate cancer is unknown. We investigated the frequency of *ERG* rearrangement in local recurrent castration-resistant prostate cancer compared to distant metastatic prostate cancer, and assessed for associations between androgen receptor (*AR*) amplification and *ERG* rearrangement status. Samples from 134 patients diagnosed with prostate cancer (84 local recurrent castration resistant prostate cancer, 55 distant metastatic prostate cancer) were assessed for their *ERG* rearrangement and *AR* amplification status by fluorescence in situ hybridization. Statistical analysis was performed using the χ^2 test. We found that the *ERG* rearrangement occurs at a significantly lower frequency in distant metastatic prostate cancer (25 %) than in local recurrent castration-resistant prostate cancer (45 %). The *AR* amplification frequencies were 45 and 35 % in local recurrent castration-resistant prostate cancer and distant metastatic prostate cancer, respectively. The *ERG* rearrangement occurred at a lower frequency in distant metastatic prostate cancer compared to local recurrent castration-resistant prostate cancer.

Veit J. Scheble and Gregor Scharf equally contributed to this study.
Zaki Shaikhibrahim and Sven Perner have equal contribution as senior authors.

V. J. Scheble · G. Scharf · K. Petersen · F. Fend · S. Perner
Institute of Pathology, University Hospital Tuebingen,
Tuebingen, Germany

V. J. Scheble
Medical Clinic II, University Hospital Tuebingen,
Tuebingen, Germany

R. Beschorner
Institute for Brain Research, Comprehensive Cancer Center,
University Hospital Tuebingen,
Tuebingen, Germany

C. Ruiz · S. Stürm · L. Bubendorf
Institute for Pathology, University Hospital Basel,
Basel, Switzerland

M. Braun · S. Perner
Institute of Pathology, Department of Prostate Cancer Research,
University Hospital Bonn,
Bonn, Germany

M. Braun · G. Kristiansen · N. Wernert · Z. Shaikhibrahim · S. Perner (✉)
Institute of Pathology, University Hospital Bonn,
Sigmund-Freud-Str. 25,
53127 Bonn, Germany
e-mail: sven.perner1972@gmail.com

A. Bachmann
Department of Urology, University Hospital Basel,
Basel, Switzerland

T. Zellweger
Division of Urology, St. Claraspital,
Basel, Switzerland

Keywords *ERG* rearrangement · Androgen receptor · Prostate cancer · Castration-resistant prostate cancer · Hormone refractory prostate cancer · Metastatic cancer

Introduction

Castration-resistant prostate cancer (CRPC) is the second most common cause of male cancer-related death [1], and is known to be associated with a median survival of less than 2 years [2]. Recurrent gene fusions, occurring between the androgen-regulated gene *TMPRSS2* and the ETS transcription factor *ERG*, are one of the most common genomic alterations in locally defined prostate cancer (PCa) [3, 4]. Since their discovery, the potential clinical utilization of the *ERG* rearrangements in PCa has been studied extensively [5–7]. The *ERG* rearrangements have been reported to be specific to PCa [8], and are reported to occur in about 15–80 % of PCa [3, 9, 10] depending on the cohort design and the histological subtypes of PCa [11, 12]. While the *ERG* rearrangements are believed to be an early and clonal event in PCa progression [13, 14], other molecular events such as androgen receptor (*AR*) or *PTEN* copy number status vary during disease progression [15]. Moreover, *AR* amplifications have been reported to occur almost exclusively in CRPC [16, 17].

As only few studies have addressed the *ERG* rearrangement in CRPC (Table 1) [18–23], we aimed in this study to investigate the frequency of *ERG* rearrangement in CRPC in the view of comparing the frequency of the rearrangement in local recurrent CRPC (recurrent CRPC) to distant metastatic PCa (metastatic CRPC). Furthermore, we aimed at assessing the potential associations between the *AR* amplification and the *ERG* rearrangement status.

Materials and methods

This study has been approved by the institutional ethical review board of the University Hospital Tuebingen, Germany.

Cohorts

We assessed tissue samples from a cohort of 134 patients diagnosed with PCa (84 samples recurrent CRPC, 55 samples metastatic CRPC). Thirty-nine patients were treated surgically at the University Hospital of Tuebingen in Germany, and 95 patients were treated surgically at the University Hospital of Basel in Switzerland. The samples were then separated into two subcohorts, one consisting of 84 samples from recurrent CRPC and the other consisting of 55 samples from metastatic CRPC. The metastatic CRPC subcohort consisted of 42 samples from bone metastases, 9 samples from CNS metastases and 4 samples from other metastatic sites. For 5 cases both primary tumour and metastatic tissue were available. Due to the small number of cases, these were not evaluated separately. Before the appearance of the local recurrence, all patients had received hormone ablation either surgically (orchiectomy) or chemically (steroid treatment) or combined.

Tissue microarrays

Tuebingen cohort

Tissue microarrays (TMAs) were constructed as described earlier [8]. Formalin-fixated, paraffin-embedded cancer specimen were cut in 3-μm-thick sections, mounted on slides and stained with hematoxylin and eosin (H&E). Subsequently, the PCa and normal prostatic tissues were differently marked on the H&E slide (GS and VJS). We then designed TMAs using the software TMADesigner (Alphelys, Plaisir, France). TMA

Table 1 ERG rearrangement in recurrent and metastatic CRPC in literature

ERG+	Cases	%	Study	Cohort description
recurrent CRPC				
18	52	34.6	Rickman et al. [22]	
22	58	37.9	Leinonen et al. [20]	
28	76	36.8	Saramaki et al. [23]	
68	186	36.6	Total	
metastatic CRPC				
11	29	37.9	Cai et al. [18]	rtPCR instead of FISH analysis
15	43	34.9	Han et al. [19]	Cohort description provides little detail
10	27	37.0	Mehra et al. [21]	Cohort description provides little detail
36	99	36.4	Total	

recurrent CRPC local recurrent castration resistant prostate cancer, *metastatic CRPC* distant metastatic prostate cancer, *ERG+* number of cases revealing an *ERG* rearrangement, *rtPCR* real-time polymerase chain reaction, *FISH* fluorescence in situ hybridization

recipient blocks were constructed using a semiautomatic tissue array instrument (Beecher Instruments, Sun Prairie, WI, USA). Three cores per case with a diameter of 0.6 mm from representative tumour regions were included. Recipient blocks were cut into 3-μm-thick sections and placed onto superfrost slides.

Basel cohort

The Basel TMA was constructed as described previously [24]. Briefly, cancer regions were marked on an H&E slide, and two to three cores per tumour with a diameter of 0.6 mm were taken. Castration resistance was defined as palliative transurethral resection due to local recurrence despite ongoing androgen withdrawal.

For both cohorts we used three cores per surgical specimen, cases were excluded if there was too little tumour tissue available. Cases that were not assessable due to technical issues have been excluded before we performed statistical analysis. Whenever possible, we randomly selected for three different TUR-P pieces, avoiding TUR material with heat-related or mechanical artifacts. Due to the TUR technique, multifocality was no longer detectable. We avoided sampling errors as far as possible by punching three cores per patient.

FISH Probes

The *ERG* rearrangement status was evaluated by fluorescence in situ hybridization (FISH), applying a break apart assay as described previously [12]. For the androgen receptor amplification status, we performed an amplification FISH assay with one red target probe (RP11-479J1, Invitrogen, Paisley, UK) and a green reference probe covering a stable region on chromosome X (RP11-308F2, Invitrogen). We assessed for amplifications semi-quantitatively by comparing the number of red signals (*AR* target region) to the number of corresponding green signals (reference region). A red/green ratio greater than 2:1 up to 5:1 was defined as low level amplification. Red/green ratios greater than 5:1 were defined as high-level amplifications. All TMA slides were analyzed under a ×63 oil immersion objective using a fluorescence microscope (Zeiss, Jena, Germany) equipped with appropriate filters, a charge-coupled device camera and the FISH imaging and capturing software Metafer 4 (Metasystems, Altlussheim, Germany). FISH evaluation was independently performed by two experienced observers (VJS and GS). At least 100 nuclei per case were assessed.

Statistical analysis

In order to test the significance of the differences in the *ERG* rearrangement frequencies and the *AR* amplification status between recurrent CRPC and metastatic CRPC, we performed the χ^2 test. We then determined Cramèrs V to measure the effect size of our findings.

Results

Out of 84 recurrent CRPC specimens, we found *ERG* rearranged cases at a frequency of 45 % (38 out of 84; 95 % CI, 34–56 %; Figs. 1a and 2b). More specifically, 13 cases (34 %) showed an *ERG* rearrangement through insertion and 25 cases (66 %) via deletion (Fig. 1a). In the recurrent CRPC samples, *AR* amplification was found in 38 out of 84 (45 %; 95 % CI, 34–56 %) cases (Figs. 1c and 2a).

Within 55 metastatic CRPC specimens, we found a frequency of 14 out of 55 (25 %; 95 % CI, 14–39 %) *ERG* rearranged cases (Figs. 1b and 2b). More specifically, six cases (43 %) showed an *ERG* rearrangement through insertion and eight cases (57 %) revealed rearrangement via deletion (Fig. 1b). Furthermore, we assessed the cases for the *AR* amplification and found an amplified *AR* status in 19 out of 55 (35 %; 95 % CI, 22–48 %) assessable cases (Figs. 1d and 2a).

Within the five cases with both primary tumour and metastatic sites available, we found intrafocal homogeneity regarding the *ERG* rearrangement status—all cases showed a normal status without *ERG* rearrangement both in primary tumour and metastatic site. For *AR* one case showed heterogeneity with a normal status in the primary tumour and amplification in the metastasis, three cases were normal both in primary and metastatic focus and one showed an amplification of *AR* both in the prostate and the metastatic site.

Statistical analysis using the χ^2 test revealed that the *ERG* rearrangement occurs at a significantly lower frequency in metastatic CRPC than recurrent CRPC ($p=0.018$). In *AR* amplification status, χ^2 analysis revealed no significant difference between metastatic CRPC and recurrent CRPC ($p=0.21$). We then determined the effect size by calculating Cramèrs V, which equals 0.2.

Discussion

The *ERG* rearrangement frequency in PCa is reported in several studies, and it varies widely (15–80 %), depending on cohort design [3, 9, 10]. A few studies investigated the *ERG* rearrangement prevalence in CRPC, but each of the studies mentioned in Table 1 has its inconsistencies [18–23]. Thus, the *ERG* rearrangement frequency in CRPC remains vague, in particular the frequency of rearrangement in recurrent CRPC compared to metastatic CRPC. In this study, FISH assessment of two independent CRPC cohorts consisting of recurrent CRPC and metastatic CRPC revealed frequency of 45 and 25 % *ERG* rearranged cases,

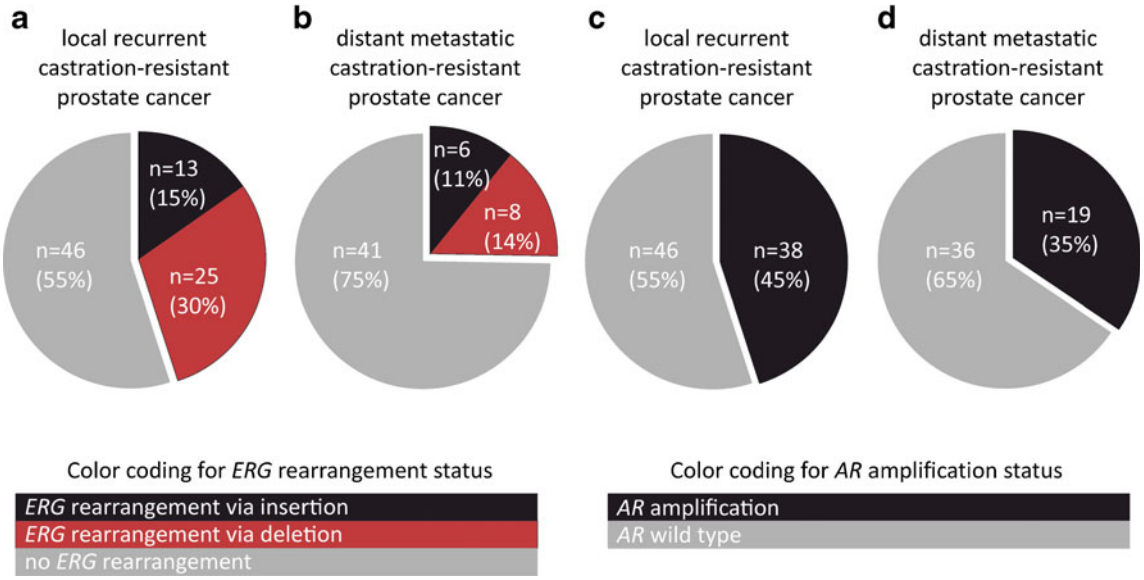

Fig. 1 **a**–**d** Pie chart displaying *ERG* rearrangement and *AR* amplification prevalences in local recurrent and distant metastatic prostate cancer

respectively. Previous studies reported *ERG* rearrangement frequencies between 34.6 and 37.9 % in recurrent CRPC, and 34.9 to 37.9 % in metastatic CRPC cohorts (Table 1). The differences in *ERG* rearrangement frequencies between our study and the previously reported studies (Table 1) are due to the fact that we have used the same experimental setting for the evaluation of both recurrent CRPC and metastatic CRPC simultaneously with a clear cohort definition. In all prior studies mentioned, the *ERG* rearrangement frequency in either recurrent CRPC or metastatic CRPC was assessed, but never compared directly. Furthermore, it partially remains unclear, whether local recurrences or distant metastases of CRPC were examined. We have to admit that our results might be influenced by various differences between the Basel and the Tuebingen subcohort, such as different medical treatments or differences in lifestyle. On the other hand, the *AR* amplification prevalence in our cohorts matches the range of amplification frequencies described in earlier studies, both in metastatic CRPC and recurrent CRPC [17, 25–27].

Earlier studies reported that the *ERG* rearrangement is an early and clonal event during tumour progression [13, 14]. However, our results show a lower frequency of *ERG* rearrangement in the most advanced stage of disease, metastatic CRPC, than in recurrent CRPC. Due to the design of our study, we currently can only speculate on the cause of the differences: A plausible explanation may be that the sensitivity to androgen might be higher in the prostatic region compared to other regions or the blood circulatory system. Thus, the androgen-dependent serine protease *TMPRSS2* might be more active in the prostate and in the prostatic lymphatic region compared to distant organs. As a result, a negative selection of androgen-dependent *ERG* rearranged PCa might occur in a subset of distant metastases. Another possible explanation is that *ERG* promotes the local invasiveness of PCa, but has no influence on metastatic spread.

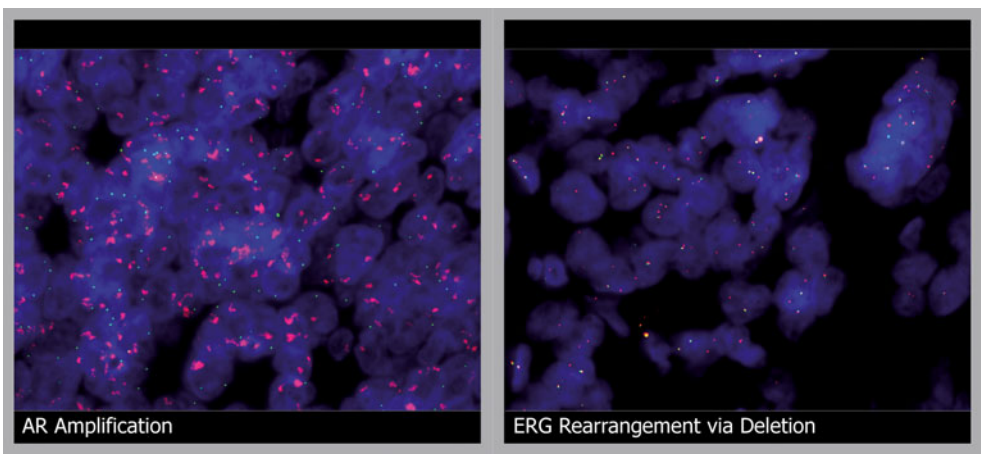

Fig. 2 **a** FISH images showing a high-level amplification of the androgen receptor (*red clusters*) compared to the centromere of chromosome X (*green signals*). **b** FISH image showing an *ERG* rearrangement via deletion represented by one overlapping red and green signal (wild-type allele) and one single red signal per nucleus with a loss of the second green signal, indicating a gene fusion

Several other factors might be causative for these findings as well: Clinical features such as different medicinal treatments, molecular factors such as interindividual molecular and genetic variations as well as environmental and lifestyle events diverging between different cohorts. Taken together, our findings that *ERG* rearrangement occurs at a lower frequency in metastatic CRPC compared to recurrent CRPC may have clinical implications that remain to be studied and may potentially be utilized in the future as a stratification tool for prediction or therapy.

In summary, we examined local recurrent and distant metastatic PCa for the *ERG* rearrangement status and found a lower frequency of *ERG* rearrangement in distant metastatic prostate cancer compared to local recurrent prostate cancer. In contrast, there is no significant difference for *AR* amplification status between these two groups. This is the first study to compare these two divisions of advanced prostate cancer. Our surprising results may potentially be used in clinical decision settings.

Acknowledgments We thank Christine Beschorner for the exceptional technical support and Veit Scharf for helpful contributions to statistical analyses. This work was supported by a grant of the German Research Foundation [Deutsche Forschungsgemeinschaft (DFG), Emmy-Noether-Program, PE1179/2-1], the Wilhelm-Sander-Stiftung (grant no. 2011.077.1) and the Rudolf-Becker-Foundation to SP, a junior grant of the University Hospital of Tuebingen (fortüne-Programme) to VJS and by a grant of the DFG (WE1104/11-1) and German Cancer Aid (Deutsche Krebshilfe, 107827) to NW.

Conflict of interest The Brigham and Women's Hospital and the University of Michigan have filed a patent on ETS gene rearrangements in prostate cancer, on which SP is co-inventor and the diagnostic field of use has been licensed to GenProbe Inc. GenProbe has neither played a role in the design and conduct of the study, nor in the collection, analysis or interpretation of the data and no involvement in the preparation, review or approval of the manuscript.

References

1. Attard G, Sarker D, Reid A, Molife R, Parker C, de Bono JS (2006) Improving the outcome of patients with castration-resistant prostate cancer through rational drug development. Br J Cancer 95(7):767–774. doi:10.1038/sj.bjc.6603223
2. Appleman LJ (2010) Castration-refractory prostate cancer: new therapies, new questions. Oncology (Williston Park) 24(14):1318–1319, 1326
3. Mosquera JM, Mehra R, Regan MM, Perner S, Genega EM, Bueti G, Shah RB, Gaston S, Tomlins SA, Wei JT, Kearney MC, Johnson LA, Tang JM, Chinnaiyan AM, Rubin MA, Sanda MG (2009) Prevalence of *TMPRSS2-ERG* fusion prostate cancer among men undergoing prostate biopsy in the United States. Clin Cancer Res 15(14):4706–4711. doi:10.1158/1078-0432.CCR-08-2927
4. Tomlins SA, Rhodes DR, Perner S, Dhanasekaran SM, Mehra R, Sun XW, Varambally S, Cao X, Tchinda J, Kuefer R, Lee C, Montie JE, Shah RB, Pienta KJ, Rubin MA, Chinnaiyan AM (2005) Recurrent fusion of *TMPRSS2* and ETS transcription factor genes in prostate cancer. Science 310(5748):644–648. doi:10.1126/science.1117679
5. Salami SS, Schmidt F, Laxman B, Regan MM, Rickman DS, Scherr D, Bueti G, Siddiqui J, Tomlins SA, Wei JT, Chinnaiyan AM, Rubin MA, Sanda MG (2011) Combining urinary detection of TMPRSS2: ERG and CaP3 with serum PSA to predict diagnosis of prostate cancer. Urol Oncol. doi:10.1016/j.urolonc.2011.04.001
6. He H, Magi-Galluzzi C, Li J, Carver P, Falzarano S, Smith K, Rubin MA, Zhou M (2011) The diagnostic utility of novel immunohistochemical marker ERG in the workup of prostate biopsies with "atypical glands suspicious for cancer". Am J Surg Pathol 35 (4):608–614. doi:10.1097/PAS.0b013e31820bcd2d
7. Rice KR, Chen Y, Ali A, Whitman EJ, Blase A, Ibrahim M, Elsamanoudi S, Brassell S, Furusato B, Stingle N, Sesterhenn IA, Petrovics G, Miick S, Rittenhouse H, Groskopf J, McLeod DG, Srivastava S (2010) Evaluation of the *ETS*-related gene mRNA in urine for the detection of prostate cancer. Clin Cancer Res 16(5):1572–1576. doi:10.1158/1078-0432.CCR-09-2191
8. Scheble VJ, Braun M, Beroukhim R, Mermel CH, Ruiz C, Wilbertz T, Stiedl AC, Petersen K, Reischl M, Kuefer R, Schilling D, Fend F, Kristiansen G, Meyerson M, Rubin MA, Bubendorf L, Perner S (2010) ERG rearrangement is specific to prostate cancer and does not occur in any other common tumor. Mod Pathol 23(8):1061–1067. doi:10.1038/modpathol.2010.87
9. Braun M, Scheble V, Menon R, Scharf G, Wilbertz T, Petersen K, Beschorner C, Reischl M, Kuefer R, Schilling D, Stenzl A, Kristiansen G, Rubin M, Fend F, Perner S (2011) Relevance of cohort design for studying the frequency of the ERG rearrangement in prostate cancer. Histopathology (in press)
10. Tomlins SA, Bjartell A, Chinnaiyan AM, Jenster G, Nam RK, Rubin MA, Schalken JA (2009) ETS gene fusions in prostate cancer: from discovery to daily clinical practice. Eur Urol 56 (2):275–286. doi:10.1016/j.eururo.2009.04.036
11. Guo CC, Dancer JY, Wang Y, Aparicio A, Navone NM, Troncoso P, Czerniak BA (2011) TMPRSS2-ERG gene fusion in small cell carcinoma of the prostate. Hum Pathol 42(1):11–17. doi:10.1016/j.humpath.2010.05.026
12. Scheble VJ, Braun M, Wilbertz T, Stiedl AC, Petersen K, Schilling D, Reischl M, Seitz G, Fend F, Kristiansen G, Perner S (2010) ERG rearrangement in small cell prostatic and lung cancer. Histopathology 56(7):937–943. doi:10.1111/j.1365-2559.2010.03564.x
13. Perner S, Mosquera JM, Demichelis F, Hofer MD, Paris PL, Simko J, Collins C, Bismar TA, Chinnaiyan AM, De Marzo AM, Rubin MA (2007) *TMPRSS2-ERG* fusion prostate cancer: an early molecular event associated with invasion. Am J Surg Pathol 31(6):882–888. doi:10.1097/01.pas.0000213424.38503.aa00000478-200706000-00008
14. Perner S, Svensson MA, Hossain RR, Day JR, Groskopf J, Slaughter RC, Jarleborn AR, Hofer MD, Kuefer R, Demichelis F, Rickman DS, Rubin MA (2010) ERG rearrangement metastasis patterns in locally advanced prostate cancer. Urology 75(4):762–767. doi:10.1016/j.urology.2009.10.010
15. Feldman BJ, Feldman D (2001) The development of androgen-independent prostate cancer. Nat Rev Cancer 1(1):34–45
16. Bubendorf L, Kononen J, Koivisto P, Schraml P, Moch H, Gasser TC, Willi N, Mihatsch MJ, Sauter G, Kallioniemi OP (1999) Survey of gene amplifications during prostate cancer progression by high-throughout fluorescence in situ hybridization on tissue microarrays. Cancer Res 59(4):803–806
17. Visakorpi T, Hyytinen E, Koivisto P, Tanner M, Keinanen R, Palmberg C, Palotie A, Tammela T, Isola J, Kallioniemi OP (1995) In vivo amplification of the androgen receptor gene and progression of human prostate cancer. Nat Genet 9(4):401–406. doi:10.1038/ng0495-401
18. Cai C, Wang H, Xu Y, Chen S, Balk SP (2009) Reactivation of androgen receptor-regulated *TMPRSS2:ERG* gene expression in castration-resistant prostate cancer. Cancer Res 69(15):6027–6032. doi:10.1158/0008-5472.CAN-09-0395

19. Han B, Mehra R, Lonigro RJ, Wang L, Suleman K, Menon A, Palanisamy N, Tomlins SA, Chinnaiyan AM, Shah RB (2009) Fluorescence in situ hybridization study shows association of PTEN deletion with ERG rearrangement during prostate cancer progression. Mod Pathol 22(8):1083–1093. doi:10.1038/modpathol.2009.69
20. Leinonen KA, Tolonen TT, Bracken H, Stenman UH, Tammela TL, Saramaki OR, Visakorpi T (2010) Association of SPINK1 expression and *TMPRSS2:ERG* fusion with prognosis in endocrine-treated prostate cancer. Clin Cancer Res 16(10):2845–2851. doi:10.1158/1078-0432.CCR-09-2505
21. Mehra R, Tomlins SA, Yu J, Cao X, Wang L, Menon A, Rubin MA, Pienta KJ, Shah RB, Chinnaiyan AM (2008) Characterization of *TMPRSS2*-ETS gene aberrations in androgen-independent metastatic prostate cancer. Cancer Res 68(10):3584–3590. doi:10.1158/0008-5472.CAN-07-6154
22. Rickman DS, Chen YB, Banerjee S, Pan Y, Yu J, Vuong T, Perner S, Lafargue CJ, Mertz KD, Setlur SR, Sircar K, Chinnaiyan AM, Bismar TA, Rubin MA, Demichelis F (2010) ERG cooperates with androgen receptor in regulating trefoil factor 3 in prostate cancer disease progression. Neoplasia 12(12):1031–1040
23. Saramaki OR, Harjula AE, Martikainen PM, Vessella RL, Tammela TL, Visakorpi T (2008) *TMPRSS2:ERG* fusion identifies a subgroup of prostate cancers with a favorable prognosis. Clin Cancer Res 14(11):3395–3400. doi:10.1158/1078-0432.CCR-07-2051
24. Ruiz C, Holz DR, Oeggerli M, Schneider S, Gonzales IM, Kiefer JM, Zellweger T, Bachmann A, Koivisto PA, Helin HJ, Mousses S, Barrett MT, Azorsa DO, Bubendorf L (2011) Amplification and overexpression of vinculin are associated with increased tumour cell proliferation and progression in advanced prostate cancer. J Pathol 223(4):543–552. doi:10.1002/path.2828
25. Brown RS, Edwards J, Dogan A, Payne H, Harland SJ, Bartlett JM, Masters JR (2002) Amplification of the androgen receptor gene in bone metastases from hormone-refractory prostate cancer. J Pathol 198(2):237–244. doi:10.1002/path.1206
26. Linja MJ, Savinainen KJ, Saramaki OR, Tammela TL, Vessella RL, Visakorpi T (2001) Amplification and overexpression of androgen receptor gene in hormone-refractory prostate cancer. Cancer Res 61(9):3550–3555
27. Koivisto P, Kononen J, Palmberg C, Tammela T, Hyytinen E, Isola J, Trapman J, Cleutjens K, Noordzij A, Visakorpi T, Kallioniemi OP (1997) Androgen receptor gene amplification: a possible molecular mechanism for androgen deprivation therapy failure in prostate cancer. Cancer Res 57(2):314–319

Virchows Arch (2012) 461:163–168
DOI 10.1007/s00428-012-1283-2

ORIGINAL ARTICLE

In oral squamous cell carcinoma, high FAK expression is correlated with low P53 expression

Pablo Rosado · Paloma Lequerica-Fernández · Ignacio Peña · Laura Alonso-Durán · Juan C. de Vicente

Received: 6 January 2012 / Revised: 21 June 2012 / Accepted: 2 July 2012 / Published online: 12 July 2012
© Springer-Verlag 2012

Abstract Focal adhesion kinase (FAK) and p53 have been associated with metastatic activity and a poor prognosis in oral squamous cell carcinoma (OSCC). Recently, a feedback mechanism in which FAK regulates p53 has been proposed. The present study aims to determine the role of p53 in FAK regulation in these tumors. FAK and p53 expression was examined by immunohistochemistry in normal oral mucosa and in 67 oral squamous cell carcinomas. $p16^{INK4a}$ was also studied in view of its association with human papillomavirus infection. The association between FAK and p53 was subsequently analyzed. FAK expression in OSCCs was heterogeneous: 22 (33 %) cases showed weak expression, 16 (24 %) showed moderate expression, and 22 (33 %) cases showed high expression. Regarding p53, 31 of 67 (46 %) available tumor specimens showed negative staining, and 36 of 67 (54 %) showed positive nuclear staining for p53. FAK expression was inversely correlated with p53 expression (Fisher's exact test, $p=0.005$). There was no association between $p16^{INK4a}$ and p53 or FAK expression. In conclusion, our results support the hypothesis that FAK activity might be involved in the down-regulation of p53 expression in OSCC.

Keywords FAK · p53 · $p16^{INK4a}$ · Oral squamous cell carcinoma · Immunohistochemistry

P. Rosado
Department of Oral and Maxillofacial Surgery,
Hospital de Cabueñes,
Gijón, Asturias, Spain

P. Lequerica-Fernández
Department of Analysis and Biochemistry, Hospital San Agustín,
Avilés, Spain

I. Peña · J. C. de Vicente (✉)
Department of Oral and Maxillofacial Surgery,
Facultad de Medicina y Odontología, Universidad de Oviedo,
Hospital Universitario Central de Asturias,
c/ Catedrático José Serrano s/n.,
33006 Oviedo, Asturias, Spain
e-mail: jvicente@uniovi.es

L. Alonso-Durán · J. C. de Vicente
Instituto Universitario de Oncología del Principado de Asturias,
Oviedo, Asturias, Spain

Introduction

Focal adhesion kinase (FAK) is a protein tyrosine kinase located in the cytoplasm, which has been shown to play an important role in the onset, progression, and development of metastasis of cancer of the breast [1], colorectum [2], liver [3], endometrium [4], esophagus [5], stomach [6], larynx [7], lung [8], ovary [9], prostate [10], and thyroid [11]. These studies have correlated the increased expression of FAK with metastatic activity and poor prognosis. We have also recently studied FAK expression in oral squamous cell carcinoma (OSCC) by means of immunohistochemistry and have found a significant association with neck node metastasis and survival.

There is strong evidence that FAK signaling pathways can stimulate tumor progression and metastasis formation through the regulation of cell migration, apoptosis, invasion, and angiogenesis [4]. Its role in tumor development has been linked to different factors. On the one hand, the expression of FAK has been associated with cell proliferation through activation of cyclin D1 [12]. On the other, some studies have shown that FAK-dependent signaling can promote changes in cell shape and formation of invadopodia, leading to an invasive cell phenotype [13–15]. Recently, FAK has been involved in cell survival by interacting with p53 and inhibiting anoikis [16]. Golubovskaya et al. [17] were the first to find direct binding of FAK to p53 protein. Moreover, it has been proposed that a feedback regulation mechanism functions between these proteins [18].

Inactivation of the p53 gene by means of mutation, deletion, or binding to viral proteins has been demonstrated in oral cancers in up to 40–50 % of cases [19]. Mutated p53 can repress promoter activity of certain anti-apoptosis and cell cycle-associated genes. Several studies have suggested a possible role for this protein in patient prognosis in OSCC, although a recent meta-analysis revealed that these are inconclusive [20].

So far, no studies exploring a possible relationship between FAK and p53 in oral carcinomas have been performed. OSCC is the sixth most common human neoplasm accounting for 3 % of all newly diagnosed cancers [21]. The main accepted risk factors are tobacco and alcohol consumption, but recently high-risk subtypes of the human papillomaviruses (HPV) have also been postulated to play a role [22]. As a result, a distinction can be made between "traditional" and HPV-associated oral cancer patients. The former are typically older than 50 years, usually male, and their tumors are characterized by high levels of EGFR expression, mutant p53, and generally poor outcome. Conversely, patients with HPV-associated head and neck squamous cell carcinomas are typically younger, more likely to be never-smokers/never-drinkers, have tumors mainly located at the oropharynx and characterized by wild-type p53, $p16^{INK4a}$ overexpression, and have a more favorable outcome [23]. Persistent high-risk HPV infections may promote malignant transformation of stratified squamous epithelium, which is mediated by inactivation of p53 and pRb by the viral gene products E6 and E7 [24]. The inactivation of pRb results in overexpression of $p16^{INK4a}$ [25], a cyclin-dependent kinase inhibitor and G1/S cell cycle phase checkpoint regulator and a marker of HPV E7-mediated functional inactivation of pRb. The method of HPV detection in tumor tissue includes the polymerase chain reaction, in situ hybridization for HPV DNA and E6/E7 messenger RNA, and immunohistochemistry for $p16^{INK4a}$ [26]. Its expression is easily detectable by immunohistochemistry and it has been proposed as a biomarker that would allow unambiguous identification of tumors related to HPV infection [27].

This study aims to determine the role of p53 in FAK regulation in OSCC and the immunohistochemical expression of $p16^{INK4a}$.

Materials and methods

Tissue microarray

An OSCC tissue microarray (TMA) was constructed similar to the arrays previously described [28]. The TMA was built with institutional review board approval from archived formalin-fixed, paraffin-embedded tissue samples (Department of Pathology at the Hospital Universitario Central de Asturias) from 69 patients whose surgical procedures took place between 1990 and 1992. A pathologist reviewed the original archived hematoxylin–eosin-stained slides. At least three samples of each donor tissue block were taken to adequately represent each case. The TMA also contained morphologically normal oral mucosa samples, which were obtained from non-oncological patients undergoing oral surgery. In order to ascertain the histopathological diagnosis and the adequacy of tissue sampling, a section from each microarray was stained with hematoxylin and eosin and examined by light microscopy.

Fifty-four patients were male and 15 were female. The mean age was 61 years (range, 24–87 years). All patients underwent radical surgery and, in all cases, resection margins were free of tumor. Postoperative radiotherapy was administered to 31 (45 %) patients. The characteristics of the patients studied and the clinical and pathological features of their tumors are provided in Table 1. The stage of disease was determined after the surgical resection of the tumor according to the TNM system of the International Union Against Cancer (7th edition) [29].

Immunohistochemistry

The OSCC TMA was evaluated for FAK and p53 expression using immunohistochemical staining. Briefly, 4-μm-thick TMA sections were cut and dried on capillary-gap glass slides (Dako Cytomation). The sections were deparaffinised with standard xylene and hydrated through graded alcohols into water. Antigen retrieval was performed using Target Retrieval Solution pH 6.0 in PTLink (Dako). Staining was done at room temperature on an automatic staining workstation (Dako Autostainer Plus) with mouse IgG anti-FAK monoclonal antibody clone 4.47 (Upstate Biotechnology Inc, Lake Placid, NY, USA) at 1:250 dilution for 1 h and 30 min, anti-p53 IgG monoclonal antibody (clone DO-7, DakoCytomation, Carpinteria, CA, USA) at 1:50 dilution for 45 min, and prediluted mouse monoclonal anti-$p16^{INK4a}$ antibody clone E6H4 (MTM Laboratories, Westborough, MA, USA) at 50 mmol/L for 30 min. The Dako EnVision Flex+Visualization System (Dako Autostainer) was used. Counterstaining with hematoxylin for 1 min was the final step. Following staining, the slides were dehydrated through graded alcohols and mounted with a coverslip using a standard medium. Negative controls, consisting of slides stained with omission of the primary antibody, were also included. Colon adenocarcinoma, breast carcinoma, and endometrium samples were used as positive controls for FAK, p53, and $p16^{INK4a}$, respectively.

The slides were viewed randomly, without clinical data, by two of the authors. FAK staining was

Table 1 Clinical features in 67 patients with oral squamous cell carcinoma

Variable	No. of patients	Percent (%)
Age (years)		
Median (range)	59 (24–87)	
Gender		
Male	52	77.6
Female	15	22.4
Site		
Lip	3	4.5
Tongue	28	41.8
Floor of mouth	18	26.9
Gum	8	11.9
Buccal	6	9.0
Palate	4	6.0
Size T		
T1	18	26.9
T2	27	40.3
T3	6	9.0
T4	16	23.9
Nodes N		
N0	42	62.7
N1	13	19.4
N2	12	17.9
N3	0	0
Stage TNM		
I	13	19.4
II	18	26.9
III	12	17.9
IV	24	35.8
Tumor differenciation		
Poor	0	0
Moderate	14	20.9
Well	53	79.1

cytoplasmic with equal intensity in all tumor cells within a tumor sample. FAK immunostaining was scored based on the percentage of stained cells into four categories: no expression (score 0; 0 % of stained cells), low expression (score 1; 1–33 % of stained cells), moderate expression (score 2; 34–66 %), and high expression (score 2; >67 % of stained cells). For the p53, according to literature [23, 24], we considered that it was overexpressed when more than 10 % of the tumor cells showed nuclear staining. Below this cutoff, the expression was considered negative. For $p16^{INK4a}$, staining of tumor cell nuclei and/or cytoplasm was interpreted as positive. Slides were scored for the percentage of $p16^{INK4a}$-stained cells from 0 to 4+.

Statistical analyses

All statistical analyses were performed using the PASW statistical software, version 18. Cross-tabulation analyses were performed using Pearson chi-square (χ^2) and Fisher exact (for tables with values <5) tests for comparison between categorical variables. All tests were two-sided. *P* values less than 0.05 were considered to be statistically significant.

Results

Expression of FAK in OSCC specimens

FAK expression in OSCCs was observed in 60 (90 %) out of 67 cases (Fig. 1). This expression was heterogeneous: 22 (33 %) cases showed weak expression, 16 (24 %) moderate expression, and 22 (33 %) cases showed high expression. FAK was strongly expressed in the cytoplasm and on the cell membrane. FAK staining was negligible in tumor stromal tissue.

Expression of p53 in OSCC samples

Thirty-one of 67 (46 %) available tumor specimens were negative for p53, and 36 of 67 (54 %) showed positive nuclear staining for p53 in more than 10 % of tumor cells (Fig. 2). The immunoreactivity was weaker in the center of infiltrating tumor nests or cords, whereas it was stronger and more diffuse in the peripherally located cells.

Expression of $p16^{INK4a}$ in OSCC samples

Immunohistochemical analysis showed that 21 % (14 of 67) of the cases were positive for $p16^{INK4a}$, while the remaining

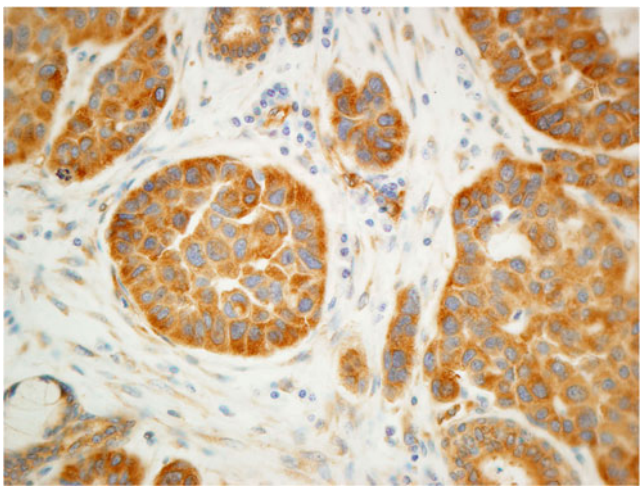

Fig. 1 Immunohistochemical study of FAK in oral squamous cell carcinoma. Intense cytoplasmic staining in tumor nests. Original magnifications, ×400

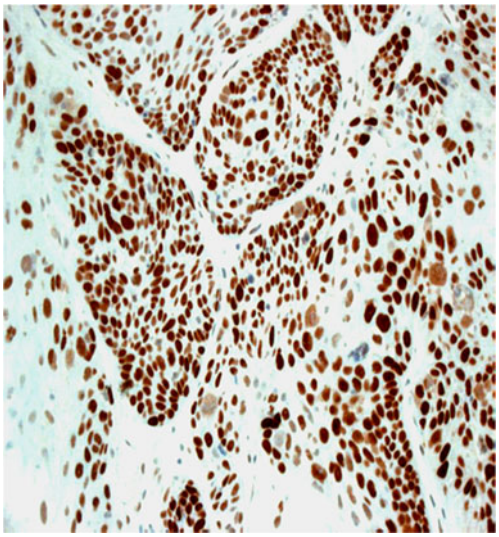

Fig. 2 Immunohistochemical study of p53 in oral squamous cell carcinoma. Original magnifications, ×200

53 tumor samples were negative (Fig. 3). In all positive cases, the immunoreactivity was focal, which we interpreted as negative because $p16^{INK4a}$-positive foci are found in many squamous cell carcinomas negative for high-risk HPV.

Relationship between p53, FAK, and $p16^{INK4a}$ staining

The relationship between p53 and FAK is summarized in Table 2. The immunoreactivity for FAK showed a negative correlation with nuclear expression of p53 (Fisher's exact test, $p=0.005$). Thus, p53-negative OSCC significantly more frequently showed overexpression of FAK than p53-positive OSCC. There was no statistically significant correlation between $p16^{INK4a}$ expression and p53 or FAK expression.

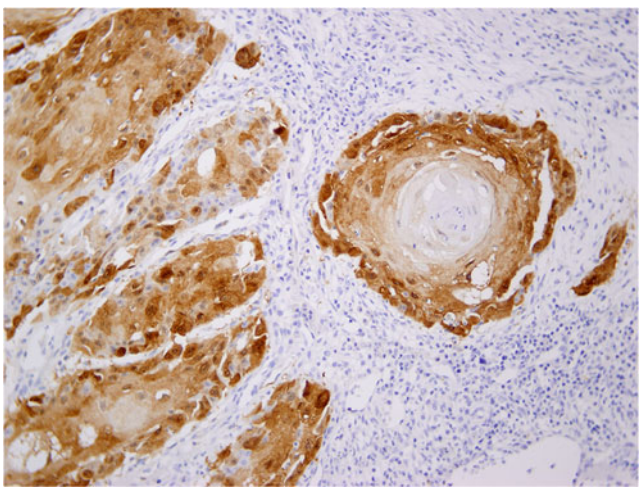

Fig. 3 Immunohistochemical study of $p16^{INK4a}$ in oral squamous cell carcinoma. Original magnifications: ×200

Table 2 FAK and p53 expression in OSCC patients (Fisher's exact test, $p=0.005$)

		p53-stained cells		
		0–9 %	10–100 %	Total
Fak-stained cells	Low expression (< 33 %)	8 (28.5 %)	20 (71.5 %)	28
	High expression (≥ 33 %)	25 (64 %)	14 (36 %)	39
	Total	33	34	67

Discussion

FAK has different roles in cancer development with different mechanisms involved [30]. First, FAK is an important regulator of cell migration and angiogenesis which are both required for cancer cell invasion and metastasis as it controls the dynamic regulation of focal adhesions, cadherin dependent cell–cell adhesions, and actin structure in the cell periphery. Second, FAK is involved in remodeling of the actin cytoskeleton by modulating RHO-GTPase pathways [31]. Third, it has been implicated in matrix metalloproteinase expression which is involved in tumor cell invasion. Fourth, FAK mediates adhesion-dependent survival (known as anoikis), which is often lost in tumor cells. Finally, studies have indicated that FAK has a direct role in tumor growth through the ERK–MAPK pathway.

Although little is known about FAK regulation, some authors have shown that p53 can inhibit the transcriptional activity of FAK promoter both in vitro [32] and in vivo [33] and have suggested that p53 can suppress metastasis through down-regulation of FAK. Moreover, a feedback regulation mechanism has been proposed in which FAK regulates p53 via FERM-induced degradation: FERM binds to p53, and FERM-enhanced Mdm2-dependent p53 ubiquitination decreases p53 transcriptional functions [16].

P53 protein is normally present in cells at a very low level and has a very short half-life (around 20 min). Therefore, it is hard to detect in normal tissue by immunohistochemistry [30]. However, when mutated resulting in a defect in the degradation pathway or by binding to viral proteins, p53 protein remains more stable and can be detected by immnohistochemistry. p53 immunohistochemistry has been widely used as a surrogate marker for p53 mutation. However, the correlation is not perfect because immunohistochemistry results are strongly dependent on the selected antibodies and fixation procedures.

Only few studies have analyzed in vivo whether or not loss of p53 function contributes to abnormal FAK expression. In 2005, Rodrigo et al. [34] studied by immunohistochemistry how the loss of p53 function influences FAK

expression in squamous cell carcinomas of the larynx. Their results showed no relationship between the expressions of these molecules. More recently, Golubovskaya studied also by immunohistochemistry a population-based series of breast carcinomas. They found that FAK expression and p53 mutation are positively correlated and FAK-positive carcinomas are 2.5 times more likely to be p53-mutation-positive than FAK-negative tumors [35].

The present study reports on the possible role of FAK in p53 regulation in OSCC. Our results show a negative correlation between the expression of these two molecules, contrasting with studies performed in breast and endometrial cancer that have found a positive correlation between them [35, 36]. Lim et al. [37] proposed a model for FAK regulation of p53. Proline-rich kinase-2 (Pyk2) and FAK are protein-tyrosine kinases that contain an N-terminal 4.1, ezrin, radixin, moesin (FERM) domain. Lim et al. [37] showed that Pyk2 promotes cell proliferation and survival through FERM domain-mediated nuclear translocation, p53 binding, and enhanced Mdm2-dependent p53 ubiquitination leading to p53 inhibition. Thus, loss of FAK expression leads to elevated p53 levels. However, adaptative or compensatory elevation of Pyk2 levels may counteract p53 activation, leading to a reduction in p53 and p21 levels and allowing for cell cycle re-initiation. Interestingly, the cellular and environmental context may dictate whether FAK or Pyk2 FERM domains function as positive or negative regulators. This is due to the fact that FAK FERM overexpression can inhibit FAK tyrosine phosphorylation in trans [38] and block FAK signaling, promoting cytokine gene expression [39].

As the cases included in this study might have been infected by high-risk HPV, we determined the immunoexpression of $p16^{INK4a}$. Despite molecular evidence that $p16^{INK4a}$ overexpression is due to functional disruption of pRb by E7, a small subset of HPV-negative tumors overexpress p16, indicating alternative mechanisms of p16 overexpression. HPV-positive tumors are commonly associated with $p16^{INK4a}$ overexpression, whereas tumors not associated with HPV are rarely p16-positive [40]. In fact, p16 immunohistochemistry reportedly has 100 % sensitivity in screening for transcriptionally active HPV infection; however, with a specificity of 79 %, alternative HPV-independent mechanisms of $p16^{INK4a}$ overexpression have to be considered [26].

Kumar et al. [41] showed that the rate of p53 mutation is quite low in HPV-associated OSCC, and Karsai et al. found that loss of $p16^{INK4a}$ expression is associated with aberrant expression of p53, which is more prevalent in the hypopharynx and in the most advanced stage tumors [42]. In our study, 54 % of tumors showed overexpression of p53, but only 23 % of tumors were $p16^{INK4a}$-positive, and there was no correlation between their expressions. The negative correlation between p53 mutation and over-expression and HPV strengthens the etiologic role of HPV in OSCC [43].

In conclusion, we found a negative correlation between p53 and FAK expression. Further studies are needed to clarify the role of FAK, both in patient survival and in p53 regulation in OSCC.

Acknowledgments This work was supported by a grant for scientific research from the Ministry of Health, Spain (Instituto de Salud Carlos III, PI070675).

Conflict of interest We declare that we have no conflict of interest.

References

1. Garcia S, Dales JP, Charafe-Jauffret E, Carpentier-Meunier S, Andrac-Meyer L, Jacquemier J, Andonian C, Lavaut MN, Allasia C, Bonnier P, Charpin C (2007) Overexpression of c-Met and of the transducers PI3K, Fak and JAK in breast carcinomas correlates with shorter survival and neoangiogenesis. Int J Oncol 31:49–58
2. Lark AL, Livasy CA, Calvo B, Caskey L, Moore DT, Yang X, Cance WG (2003) Overexpression of focal adhesion kinase in primary colorectal carcinomas and colorectal liver metastases: immunohistochemistry and real-time PCR analyses. Clin Cancer Res 9:215–222
3. Itoh S, Maeda T, Shimada M, Aishima S, Shirabe K, Tanaka S, Maehara Y (2004) Role of expression of focal adhesion kinase in progression of hepatocellular carcinoma. Clin Cancer Res 10:2812–2817
4. Zhao J, Guan JL (2009) Signal transduction by focal adhesion kinase in cancer. Cancer Metastasis Rev 28:35–49
5. Miyazaki T, Kato H, Nakajima M, Sohda M, Fukai Y, Masuda N, Manda R, Fukuchi M, Tsukada K, Kuwano H (2003) Fak overexpression is correlated with tumour invasiveness and lymph node metastasis in oesophageal squamous cell carcinoma. Br J Cancer 89:140–145
6. Su JM, Gui L, Zhou YP, Zha XL (2002) Expression of focal adhesion kinase and alpha5 and beta1 integrins in carcinomas and its clinical significance. World J Gastroenterol 8:613–618
7. Aronsohn MS, Brown HM, Hauptman G, Kornberg LJ (2003) Expression of focal adhesion kinase and phosphorylated focal adhesion kinase in squamous cell carcinoma of the larynx. Laryngoscope 113:1944–1948
8. Hsu NY, Chen CY, Hsu CP, Lin TY, Chou MC, Chiou SH, Chow KC (2007) Prognostic significance of expression of nm23-H1 and focal adhesion kinase in non-small cell lung cancer. Oncol Rep 18:81–85
9. Judson PL, He X, Cance WG, Van Le L (1999) Overexpression of focal adhesion kinase, a protein tyrosine kinase, in ovarian carcinoma. Cancer 86:1551–1556
10. Rovin JD, Frierson HF Jr, Ledinh W, Parsons JT, Adams RB (2002) Expression of focal adhesion kinase in normal and pathologic human prostate tissues. Prostate 53:124–132
11. Kim SJ, Park JW, Yoon JS, Mok JO, Kim YJ, Park HK, Kim CH, Byun DW, Lee YJ, Jin SY, Suh KI, Yoo MH (2004) Increased expression of focal adhesion kinase in thyroid cancer: immunohistochemical study. J Korean Med Sci 19:710–715
12. Zhao JH, Reiske H, Guan JL (1998) Regulation of the cell cycle by focal adhesion kinase. J Cell Biol 143:1997–2008
13. Haskell H, Natarajan M, Hecker TP, Ding Q, Stewart J Jr, Grammer JR, Gladson CL (2003) Focal adhesion kinase is expressed in the angiogenic blood vessels of malignant astrocytic tumors in vivo and

promotes capillary tube formation of brain microvascular endothelial cells. Clin Cancer Res 9:2157–2165
14. Hauck CR, Hsia DA, Ilic D, Schlaepfer DD (2002) v-Src SH3-enhanced interaction with focal adhesion kinase at beta 1 integrin-containing invadopodia promotes cell invasion. J Biol Chem 277:12487–12490
15. Hsia DA, Mitra SK, Hauck CR, Streblow DN, Nelson JA, Ilic D, Huang S, Li E, Nemerow GR, Leng J, Spencer KS, Cheresh DA, Schlaepfer DD (2003) Differential regulation of cell motility and invasion by FAK. J Cell Biol 160:753–767
16. Lim ST, Chen XL, Lim Y, Hanson DA, Vo TT, Howerton K, Larocque N, Fisher SJ, Schlaepfer DD, Ilic D (2008) Nuclear Fak promotes cell proliferation and survival through FERM-enhanced p53 degradation. Mol Cell 29:9–22
17. Golubovskaya VM, Finch R, Cance WG (2005) Direct interaction of the N terminal domain of focal adhesion kinase with the N-terminal transactivation domain of p53. J Biol Chem 280:25008–25021
18. Cance WG, Golubovskaya VM (2008) Focal adhesion kinase versus p53: apoptosis or survival? Sci Signal 1:pe22
19. Friedrich RE, Giese M, Riethdorf S, Loning T (2000) P53-mutation in smears of oral squamous cell carcinoma. Anticancer Res 20:4927–4930
20. Tandon S, Tudur-Smith C, Riley RD, Boyd MT, Jones MT (2010) A systematic review of p53 as a prognosis factor of survival in squamous cell carcinoma of the four main anatomical subsites of head and neck. Cancer Epidemiol Biomarkers Prev 19:574–587
21. Choi S, Myers JN (2008) Molecular pathogenesis of oral squamous cell carcinoma: implications for therapy. J Dent Res 87:14–32
22. Psyrri A, DiMaio D (2008) Human papillomavirus in cervical and head-and-neck cancer. Nat Clin Pract Oncol 5:24–31
23. Harris SL, Thorne LB, Seaman WT, Hayes DN, Couch ME, Kimple RJ (2011) Association of p16(INK4a) overexpression with improved outcomes in young patients with squamous cell cancers of the oral tongue. Head Neck 33:1622–1627
24. Santos M, Montagut C, Mellado B, García A, Ramón y Cajal S, Cardesa A, Puig-Tintoré LM, Ordi J (2004) Immunohistochemical staining for p16 and p53 in premalignant and malignant epithelial lesions of the vulva. Int J Gynecol Pathol 23:206–214
25. Riethdorf S, Neffen EF, Cviko A, Löning T, Crum CP, Riethdorf L (2004) p16INK4A expression as biomarker for HPV 16-related vulvar neoplasias. Hum Pathol 35:1477–1483
26. Thomas J, Primeaux T (2012) Is p16 immunohistochemistry a more cost-effective method for identification of human papilloma virus-associated head and neck squamous cell carcinoma? Ann Diagn Pathol 16:91–99
27. Klussmann JP, Gültekin E, Weissenborn SJ, Wieland U, Dries V, Dienes HP, Eckel HE, Pfister HJ, Fuchs PG (2003) Expression of p16 protein identifies a distinct entity of tonsillar carcinomas associated with human papillomavirus. Am J Pathol 162:747–753
28. Kononen J, Bubendorf L, Kallioniemi A, Bärlund M, Schraml P, Leighton S, Torhorst J, Mihatsch MJ, Sauter G, Kallioniemi OP (1998) Tissue microarrays for high-throughput molecular profiling of tumor specimens. Nat Med 4:844–847
29. Edge SB, Compton CC (2010) The American Joint Committee on Cancer: the 7th edition of the AJCC cancer staging manual and the future of TNM. Ann Surg Oncol 17:1471–1474
30. Grabenbauer GG, Mühlfriedel CH, Rödel F, Niedobitek G, Hornung J, Rödel C, Martus P, Iro H, Kirchner T, Steininger H, Sauer R, Weidenbecher M, Distel L (2000) Squamous cell carcinoma of the oropharynx: ki-67 and p53 can identify patients at high risk for local recurrence after surgery and postoperative radiotherapy. Int J Radiat Oncol Biol Phys 48:1041–1050
31. Sittel C, Ruiz S, Volling P, Kvasnicka HM, Jungehülsing M, Eckel HE (1999) Prognostic significance of Ki-67 (MIB1), PCNA and p53 in cancer of the oropharynx and oral cavity. Oral Oncol 35:583–589
32. Golubovskaya V, Kaur A, Cance W (2004) Cloning and characterization of the promoter region of human focal adhesion kinase gene: nuclear factor kappa B and p53 binding sites. Biochim Biophys Acta 1678:111–125
33. Golubovskaya VM, Finch R, Kweh F, Massoll NA, Campbell-Thompson M, Wallace MR, Cance WG (2008) p53 regulates FAK expression in human tumor cells. Mol Carcinog 47:373–382
34. Rodrigo JP, Cabanillas R, Secades P, Canel M, Chiara MD, Suárez C (2007) Relationship between FAK and P53 expression in squamous cell carcinomas of the larynx. Acta Otorrinolaringol Esp 58:347–351
35. Golubovskaya VM, Conway-Dorsey K, Edmiston SN, Tse CK, Lark AA, Livasy CA, Moore D, Millikan RC, Cance WG (2009) FAK overexpression and p53 mutations are highly correlated in human breast cancer. Int J Cancer 125:1735–1738
36. Livasy CA, Moore D, Cance WG, Lininger RA (2004) Focal adhesion kinase overexpression in endometrial neoplasia. Appl Immunohistochem Mol Morphol 12:342–345
37. Lim ST, Miller NLG, Nam JO, Chen XL, Lim Y, Schlaepfer DD (2010) Pyk2 inhibition of p53 as an adaptative and intrinsic mechanism facilitating cell proliferation and survival. J Biol Chem 285:1743–1753
38. Cohen LA, Guan JL (2005) Residues within the first subdomain of the FERM-like domain in focal adhesion kinase are important in its regulation. J Biol Chem 280:8197–8207
39. Schlaepfer DD, Hou S, Lim ST, Tomar A, Yu H, Lim Y, Hanson DA, Uryu SA, Molina J, Mitra SK (2007) Tumor necrosis factor-alpha stimulates focal adhesion kinase activity required for mitogen-activated kinase-associated interleukin 6 expression. J Biol Chem 282:17450–17459
40. Weinberger PM, Yu Z, Haffty BG, Kowalski D, Harigopal M, Brandsma J, Sasaki C, Joe J, Camp RL, Rimm DL, Psyrri A (2006) Molecular classification identifies a subset of human papillomavirus-associated oropharyngeal cancers with favorable prognosis. J Clin Oncol 24:736–747
41. Kumar B, Cordell KG, Lee JS, Worden FP, Prince ME, Tran HH, Wolf GT, Urba SG, Chepeha DB, Teknos TN, Eisbruch A, Tsien CI, Taylor JM, D'Silva NJ, Yang K, Kurnit DM, Bauer JA, Bradford CR, Carey TE (2008) EGFR, p16, HPV Titer, Bcl-xL and p53, sex, and smoking as indicators of response to therapy and survival in oropharyngeal cancer. J Clin Oncol 26:3128–3137
42. Karsai S, Abel U, Roesch-Ely M, Affolter A, Hofele C, Joos S, Plinkert PK, Bosch FX (2007) Comparison of p16(INK4a) expression with p53 alterations in head and neck cancer by tissue microarray analysis. J Pathol 211:314–322
43. Chen SF, Yu FS, Chang YC, Fu E, Nieh S, Lin YS (2012) Role of human papillomavirus infection in carcinogenesis of oral squamous cell carcinoma with evidences of prognostic association. J Oral Pathol Med 41:9–15

Virchows Arch (2012) 461:169–175
DOI 10.1007/s00428-012-1272-5

ORIGINAL ARTICLE

Alpha-methylacyl-coenzyme A racemase expression in neuroendocrine neoplasms of the stomach

Alexey Annenkov · Ken Nishikura · Koji Domori · Yoichi Ajioka

Received: 5 April 2012 / Revised: 25 May 2012 / Accepted: 20 June 2012 / Published online: 11 July 2012
© The Author(s) 2012. This article is published with open access at Springerlink.com

Abstract The enzyme alpha-methylacyl-coenzyme A racemase plays an important role in the beta-oxidation of branched-chain fatty acid and its derivatives. It has been used to detect prostatic adenocarcinoma and high-grade intraepithelial neoplasia, and recently also as a marker for other neoplasms, including those of the genitourinary system, breast, upper and lower gastrointestinal tract and their precursor lesions. We assessed expression of alpha-methylacyl-coenzyme A racemase by immunohistochemistry in neuroendocrine tumours of the stomach to determine differences in the incidence and pattern of expression among different types of gastric neuroendocrine tumours. While none of the grade 1 neuroendocrine tumours were immunoreactive, 67 % of grade 2 neuroendocrine tumours and 90 % of neuroendocrine carcinomas were positive for alpha-methylacyl-coenzyme A racemase. Furthermore, an adenocarcinoma component was found in 72.5 % (37 of 51) of neuroendocrine carcinomas, whereas none of the grade 1 and 2 neuroendocrine tumours contained an adenocarcinoma component. In 83 % of neuroendocrine carcinomas, the adenocarcinoma component was positive for alpha-methylacyl-coenzyme A racemase, and both adenocarcinoma and neuroendocrine carcinoma components stained positively in 78 % of these cases. Our results indicate that alpha-methylacyl-coenzyme A racemase is a useful marker for distinguishing between grade 1 (negative) and grade 2 neuroendocrine tumours, and neuroendocrine carcinoma of the stomach (frequently positive). Different patterns of alpha-methylacyl-coenzyme A racemase expression between gastric neuroendocrine tumours and neuroendocrine carcinoma suggest that these might develop via different tumourigenic pathways.

Keywords Alpha-methylacyl-coenzyme A racemase · Stomach · Neuroendocrine tumour · Neuroendocrine carcinoma

Introduction

Neuroendocrine neoplasms generally show characteristic histological features, such as trabecular, sheet-like and solid alveolar architecture, and neuroendocrine granules in the cytoplasm of tumour cells, which sometimes contain hormonal products. According to the latest World Health Organization (WHO) classification of digestive system tumours (fourth edition, 2010), gastric neuroendocrine neoplasms are divided into neuroendocrine tumour (NET) and carcinoma (NEC), and the former is further divided into grade 1 NET (NET G1) and grade 2 NET (NET G2). This classification is based on the proliferative activity of tumour cells. NET G1, NET G2 and NEC of the stomach correspond to what was formerly called carcinoid tumour (synonymous with well-differentiated endocrine tumour), atypical carcinoid tumour and endocrine cell carcinoma (synonymous with small cell carcinoma), respectively. Gastric NET G1 is usually composed of uniform small cells with little atypia, limited growth within the submucosa and rare angioinvasion or distal metastasis, corresponding clinically with low-grade malignant potential and favourable

The first two authors (AA and KN) contributed equally to this work.

A. Annenkov · K. Domori · Y. Ajioka
Division of Molecular and Diagnostic Pathology, Graduate School of Medical and Dental Sciences, Niigata University, Niigata, Japan

K. Nishikura (✉)
Division of Molecular and Functional Pathology, Graduate School of Medical and Dental Sciences, Niigata University, 1-757 Asahimachi-dori, Chuo-ku, Niigata 951-8510, Japan
e-mail: knishi@med.niigata-u.ac.jp

prognosis. NET G2 is also known as a malignant carcinoid and sometimes demonstrates aggressive biological behaviour [1]. NEC is predominantly composed of atypical cells, larger than those of NET with conspicuous mitotic figures, and demonstrates aggressive biological behaviour with frequent angioinvasion, distant metastasis and poor prognosis. Ki67 and p53 are reported to be helpful markers to distinguish between neuroendocrine cell neoplasms, but the histopathological distinction between NET G1 and NET G2, or between NET G2 and NEC [2], remains difficult.

Alpha-methylacyl-coenzyme A racemase (AMACR) is an enzyme that plays an important role in the beta-oxidation of branched-chain fatty acids and their derivatives [3–5]. AMACR was originally identified in mitochondria and peroxisomes of rat liver cells. Given the involvement of AMACR in the metabolism of lipids, it was speculated that overexpression of this protein might lead to alterations in the balance of cellular oxidants, which in turn might contribute to the pathogenesis of neoplasms. AMACR has been primarily used to detect prostatic adenocarcinoma and high-grade intraepithelial neoplasia [6, 7], and recently also as a differential and prognostic marker of several other neoplasms and their precursor lesions, including those from the prostate, genitourinary system, breast and upper and lower GI tract [7–21].

As yet, only two reports have considered AMACR expression in neuroendocrine neoplasms [17, 22], and only five reports mention AMACR expression in gastric neoplasms [18–21, 23]. These studies found that AMACR expression distinguishes between adenoma and/or ordinary adenocarcinoma and non-neoplastic conditions, and that AMACR expression may depend on tumour differentiation. However, none of these studies mention gastric NET or NEC. The aim of our study was to clarify the differences in the incidence and patterns of immunohistochemically determined expression of AMACR between NET G1, NET G2 and NEC of the stomach.

Materials and methods

Case selection

For the present study, 82 cases of gastric neuroendocrine neoplasms, registered between 1985 and 2011 at the Division of Molecular and Functional Pathology, Niigata University Graduate School of Medical and Dental Sciences, Niigata City, Japan, were selected. The tumours came from 1 Russian and 80 Japanese patients, who had undergone endoscopic resection or surgical resection without systemic adjuvant therapy. All samples had been fixed in 10 % formalin solution and embedded in paraffin. Clinical information was obtained from the medical records of each patient.

Endocrine differentiation of tumour cells was confirmed by diffuse and intense immunoreactivity of at least one of well-known endocrine markers, including chromogranin A, synaptophysin and neural cell adhesion molecule (NCAM, CD56).

The neuroendocrine cell neoplasms were divided into three groups according to the 2010 WHO classification [1]: (1) NET G1 (22 cases), with a mitotic count of less than two per ten high-power fields (HPF) and/or a Ki67 index ≤2 %; (2) NET G2 (9 cases), with a mitotic count of 2–20 per ten HPF and/or a Ki67 index of 3–20 %; and (3) NEC (51 cases), with a mitotic count >20 per ten HPF and/or a Ki67 index >20 %. The study was approved by the ethics committee of Niigata University Graduate School of Medical and Dental Sciences.

Histological diagnosis

The diagnosis of gastric neuroendocrine neoplasms was confirmed by two pathologists (AA and KN), who reviewed the clinical information and histological slides. The histological analysis recorded the following: depth of tumour invasion, lymphatic invasion, angioinvasion, mitotic frequency and lymph node metastasis. Lymphatic invasion and angioinvasion were confirmed via immunostaining for D2-40 and CD34.

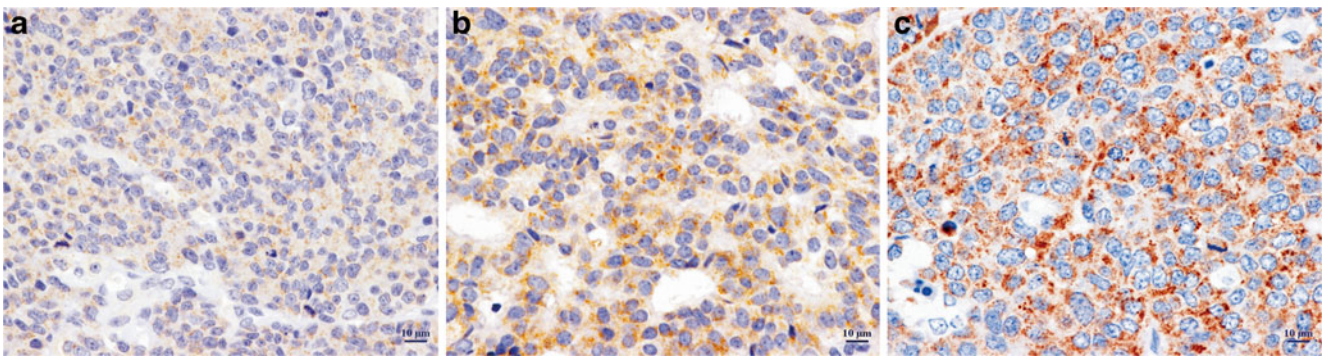

Fig. 1 Intensity of AMACR immunohistochemical staining; weak (**a**), intermediate (**b**) and strong (**c**)

Table 1 Clinicopathological features of neuroendocrine neoplasms of the stomach

	NET G1 (n=22)	NET G2 (n=9)	NEC (n=51)	p value		
				NET G1 vs NET G2	NET G1 vs NEC	NET G2 vs NEC
Sex, male/female	12:10	7:2	40:11	NS	NS	NS
Age (years), average±standard deviation	57.6±11.7	56.8±15.0	69.6±9.8	NS	0.001	0.01
Tumour size (mm), median (quartile range)	6 (4–10)	20 (8–30)	48.5 (30–61)	NS	<0.001	0.002
mp invasion	0/22 (0 %)	4/9 (44 %)	39/51 (76 %)	0.005	<0.001	NS
Mitosis (per ten HPF), mean (range)	0 (0–1)	2 (1–4)	25 (15–43)	<0.001	<0.001	<0.001
Lymphatic invasion	0/22 (0 %)	6/9 (67 %)	47/51 (92 %)	<0.001	<0.001	NS
Angioinvasion	0/22 (0 %)	4/9 (44 %)	39/51 (76 %)	0.005	<0.001	NS
LN metastasis	0/9 (0 %)	3/5 (60 %)	33/48 (69 %)	NS	<0.001	NS

NET neuroendocrine tumour, *NEC* neuroendocrine carcinoma, *NS* not significant, *mp* muscularis propria, *HPF* high-power field, *LN* lymph node

Immunohistochemistry

The most invasive area of each tumour was selected, and the corresponding paraffin block was cut into consecutive 3-μm sections for immunostaining, after a representative haematoxylin and eosin (H&E) section was stained.

Immunohistochemical analysis was performed via the high polymer method, using the Histofine MAX-PO (MULTI) kit (Nichirei Biosciences Inc., Tokyo, Japan). Sections were deparaffinized and rehydrated, then microwaved at 98 °C for seven cycles of 3 min (i.e. for synaptophysin, CD34, D2-40, and AMACR) or autoclaved at 121 °C for 20 min (i.e. for Ki-67, chromogranin A, NCAM and p53) in 10 mmol/L of citrate buffer (pH 6.0, for all antibodies except AMACR) or 1 mmol/L Tris–EDTA buffer (pH 9.0, for AMACR) to retrieve antigenic activity. Endogenous peroxidase activity was blocked by 0.3 % hydrogen peroxide in methanol for 20 min. In all sections, except Ki-67, non-specific binding was blocked with 10 % normal serum. Sections were incubated overnight with the following primary antibodies: mouse monoclonal antibodies against chromogranin A (DAK-A3, dilution at 1:500, Dako, Glostrup, Denmark), NCAM (1B6, 1:100, Novocastra, Newcastle, UK), CD34 (QBEnd-10, 1:200, Dako), D2-40 (D2-40, 1:200, Signet Laboratories, Dedham, MA, USA), p53 (PAb1801, 1:40, Novocastra) and Ki67 (MIB-1, 1:200, Dako), as well as rabbit monoclonal antibodies against synaptophysin (1:100, Dako) and AMACR (p504s, clone 13H4, 1:100, Dako). Sections were then incubated with Histofine Simple Stain MAX-PO (MULTI) (Nichirei Biosciences Inc.) for 30 min at room temperature. Antibody–antigen reactivity was visualized with diaminobenzidine, and sections were lightly counterstained with haematoxylin. Finally, the sections were dehydrated with graded ethanol and xylene and mounted with coverslips.

Interpretation of AMACR immunohistochemical expression

Sections from ten cases of prostate cancer served as positive control for AMACR, whereas sections incubated with non-immune mouse IgG served as negative controls. AMACR expression was considered positive when the cytoplasm of >5 % of tumour cells was stained. Positive AMACR staining was divided into

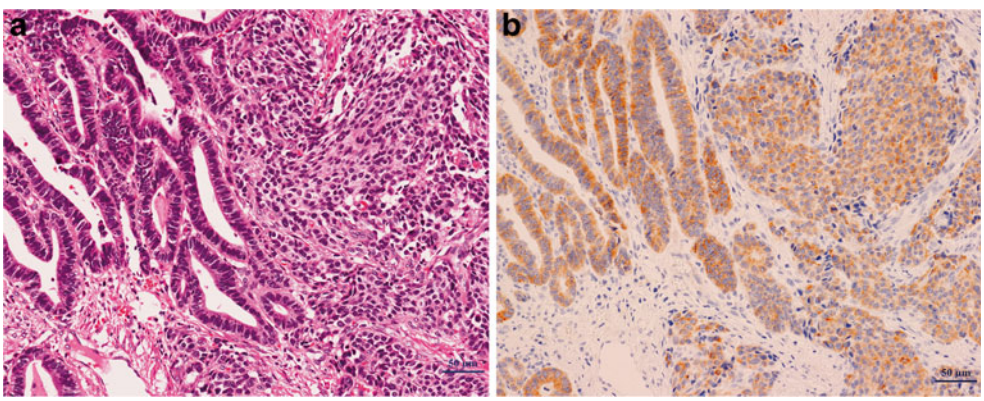

Fig. 2 Immunoexpression of AMACR in adenoNEC case. The adenocarcinoma part and NEC part showed histologic continuity (**a**) and similar strong immunoexpression pattern of AMACR (**b**)

Table 2 AMACR expression in neuroendocrine neoplasms of the stomach

Type of tumour	Number	AMACR expression				*p* value
		Weak	Intermediate	Strong	Total	
NET G1	22	0	0	0	0	<0.001
NET G2	9	3 (33.3 %)	1 (11.1 %)	2 (22.2 %)	6 (66.7 %)	
NEC	51	7 (13.7 %)	16 (31.4 %)	23 (45.1 %)	46 (90.2 %)	

NET neuroendocrine tumour, *NEC* neuroendocrine carcinoma

three patterns: strong (intense and granular cytoplasmic stain), weak (faint and diffuse cytoplasmic stain) and intermediate (mixture of strong and weak patterns) (Fig. 1).

Interpretation of Ki67 index and p53 immunohistochemical expression

The Ki67 index was determined via MIB-1 antibody staining and was expressed as a percentage of 1,000 tumour cells counted in areas with strongest nuclear labelling ("hot spots"). Expression of p53 protein was classified as follows: (−) negative, (+) scattered positive cells, (++) focal aggregates of positive cells and (+++) positive cells occurring in most tumour cells. The staining patterns (++) and (+++) were considered as overexpression of p53 protein, consistent with our previous report [2].

Statistical analysis

Differences between groups were determined via Fisher's exact and χ^2 tests. All statistical analyses were conducted with PASW statistics 17.0 (SPSS Japan Inc. Tokyo, Japan). A $p<0.05$ was considered statistically significant.

Results

Clinicopathological features

The clinicopathological features of the studied endocrine neoplasms of the stomach are summarized in Table 1. The three types of gastric neuroendocrine neoplasm demonstrated significant differences in tumour size, invasion into the muscular layer or deeper, mitosis, lymphatic invasion, angioinvasion and lymph node metastasis.

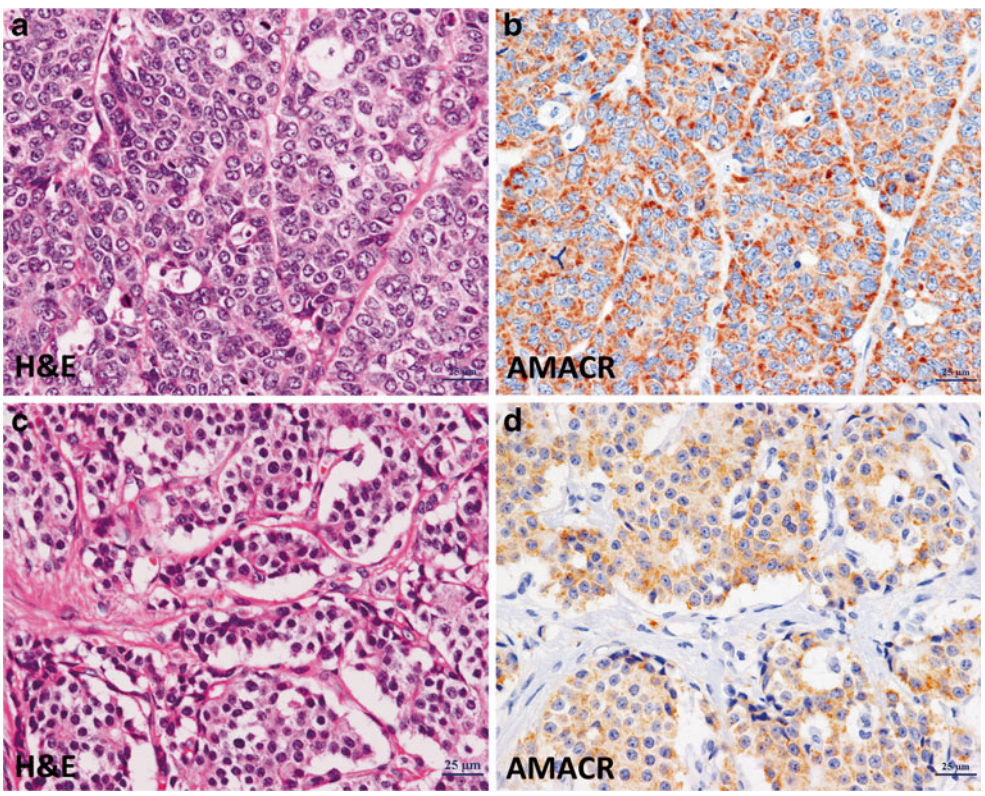

Fig. 3 Immunohistochemical staining of NEC and NET G2. NEC (**a**, H&E) demonstrates strong immunoexpression of AMACR (**b**), and NET G2 (**c**, H&E) shows intermediate intensity of AMACR expression (**d**)

Table 3 Relationship between the AMACR-positive and AMACR-negative cases of NEC and clinical features

	AMACR positive	AMACR negative
Tumour size (mm), median (quartile range)	49 (18–61)	57 (20–60)
mp invasion	35/46 (76 %)	4/5 (80 %)
Lymphatic invasion	43/46 (93 %)	4/5 (80 %)
Angioinvasion	35/46 (76 %)	4/5 (80 %)
LN metastasis	30/43 (70 %)	3/5 (60 %)

mp muscularis propria, *NEC* neuroendocrine carcinoma, *LN* lymph node

Histological features

An adenocarcinoma component was associated with 37 of 51 (73 %) NEC cases (adenoNEC), and 12 of 37 (32.4 %) cases were diagnosed as mixed adenoneuroendocrine carcinoma (MANEC), a special type of adenoNEC with either component of adenocarcinoma and NEC exceeding 30 % according to the current WHO classification [1]. The remaining 14 cases demonstrated NEC without any signs of adenocarcinoma. Specifically, the adenocarcinoma component that was associated with NEC was limited to the mucosa (68 %, 25 of 37) or submucosa (32 %, 12 of 37), and 34 of 37 cases (92 %) were of well to moderately differentiated adenocarcinoma. Furthermore, 89 % of the differentiated adenocarcinoma components were histologically continuous with NEC components in the submucosal layer (Fig. 2). Conversely, no NET G1 or G2 cases contained an adenocarcinoma component (0 of 22 and 0 of 9).

AMACR expression in the non-neoplastic epithelium

AMACR was not expressed in the non-neoplastic gastric mucosa surrounding each tumour. Intestinal metaplasia was weakly positive for AMACR staining in <5 % of cells of the 9 % of cases that were considered negative.

AMACR expression in NET G1, NET G2 and NEC

AMACR expression levels in gastric neuroendocrine tumours are summarized in Table 2. While none of the NET G1 cases expressed AMACR (0 of 22), 67 % (six of nine) of NET G2 cases expressed AMACR. Specifically, there was strong staining in 33 % (two of six), intermediate staining in 17 % (one of six) and weak staining in 50 % (three of six) of NET G2 (Fig. 3). Furthermore, AMACR was expressed in 90 % (46 of 51) of NEC cases, where 50 % (23 of 46) showed strong staining, 35 % (15 of 46) showed intermediate staining and 15 % (7 of 46) weak staining. Of the NEC cases associated with adenocarcinoma (adenoNEC), the adenocarcinoma component expressed AMACR in 84 % (31 of 37) and the NEC in 89 % (33 of 37). In adenoNEC cases, there was no significant difference in AMACR expression between MANEC and non-MANEC (91.6 vs 80.0 %). Interestingly, 93 % (13 of 14) of NEC without an adenocarcinoma component was positive for AMACR. The adenocarcinoma and NEC components were both positive in 78 % (29 of 37) of cases (Fig. 2). The AMACR expression status was concordant between the adenocarcinoma and NEC component in 83.8 % (31 of 37) of cases, both positive in 78 % (29 of 37) and both negative in 5.5 % (2 of 37) (Fig. 2). For adenoNEC cases, AMACR staining was concordant between the adenocarcinoma and NEC components in 52 % (15 of 29), and the staining patterns were similar (i.e. strong–intermediate, intermediate–weak) in 86 % (25 of 29) of cases. AMACR staining was strong for both adenocarcinoma (15 of 31, 48 %) and NEC (23 of 46, 50 %) (Fig. 2). There were no significant differences between the AMACR-positive and AMACR-negative NEC, and NET G2 cases with respect to clinical features, including tumour size, depth of invasion, lymphatic invasion, angioinvasion and lymph node metastasis (Table 3).

Correlations between Ki67-index, p53 expression and AMACR expression

Expression of p53 and Ki67 index are presented in Table 4. Overexpression of p53 and AMACR expression correlated in neuroendocrine tumours of the stomach. In NET G1 cases, both p53 and AMACR were negative. In NEC cases, p53 overexpression (67 %) and AMACR expression (90 %)

Table 4 Correlation between Ki67 index, p53 overexpression and AMACR positivity in neuroendocrine neoplasms of the stomach

Type of tumour	Ki67 index, mean (range)	p53 overexpression (*n*)	AMACR positivity (*n*)
NET G1	1.7 % (1.5–2)	0 (0/22)	0 (0/22)
NET G2	7.2 % (4.5–10)	0 (0/9)	66.7 % (6/9)
NEC	67.1 % (55.4–78.9)	66.7 % (34/51)	90.2 % (46/51)

NET neuroendocrine tumour, *NEC* neuroendocrine carcinoma

often concurred (67 %). However, in NET G2 cases without overexpression of p53, 67 % (six of nine) of cases expressed AMACR. The Ki67 showed a linear correlation with AMACR expression in NET G1, NET G2 and NEC.

Discussion

Although AMACR is expressed in numerous tumour types, its expression has never been studied in neuroendocrine neoplasms of the digestive system. There are only two papers showing significant AMACR expression in neuroendocrine neoplasms of the lung. In the present study, the incidence and pattern of immunohistochemical expression of AMACR in NET G1, NET G2 and NEC of the stomach were investigated.

AMACR overexpression has been observed in prostate and colorectal carcinomas, and linked to a high-fat diet [13]. However, the exact mechanism by which a high-fat diet might contribute to tumourigenesis in these organs remains unclear. Furthermore, AMACR expression may not be limited to tumours linked to dietary factors and may be involved in carcinogenesis via a degradation pathway of branched-chain fatty acids, or an epiphenomenon. The pathologenetic link between dietary branched-chain fatty acids and cancer has not yet been determined, and it remains unclear why branched-chain fatty acids appear to be more carcinogenic than straight-chain fatty acids. Some investigators have speculated that the overexpression of AMACR may lead to alteration in the balance of cellular oxidants, resulting in the production of reactive oxygen species, which leads to oxidative stress, and then DNA damage [24].

In the present study, we found that AMACR expression was significantly higher in NEC (90 %) and NET G2 (67 %) than in NET G1 (0 %), and that AMACR expression correlated with the Ki67 index (Table 4). These findings suggest that AMACR might be a good marker for differentiating between these neoplasms. Overexpression of p53 has been considered to be the best marker to distinguish between NEC and NET. Indeed, 67 % of our NEC but no NET cases overexpressed p53. Furthermore, AMACR was more often positive than p53 (90 vs 67 %) in NEC, and furthermore, AMACR was expressed in 67 % of NET G2, suggesting that AMACR may better discriminate between grade 1 and 2 gastric neuroendocrine neoplasms (i.e. not only between NEC and NET, but also between NET G1 and NET G2). Only a few studies have been performed regarding the prognostic significance of AMACR expression in gastric tumours, and it is still controversial [18–20]. We did not find a correlation between aggressive features, such as lymphatic invasion or lymph node metastasis, and AMACR expression in NET G2 and NEC. This may be due to the small number of samples, and future study with a higher number of cases, especially of NET G2, might clarify this issue.

Many gastric NET cases are formed by aggregation of endocrine cell micronests, predominantly composed of enterochromaffin-like cells, and caused by the trophic effect of hypergastrinemia, which occurs upon extensive atrophy of the fundic gland mucosa [25]. Patterns of AMACR expression concurred between adenocarcinoma and NEC components of adenoNEC. The absence of an adenocarcinoma component in NET G1 and G2 cases might suggest not only the histological features, but also the tumourigenic pathway between NET and NEC are different. The possibility that NEC originates from a preceding adenocarcinoma component might be considered.

Shilo et al. reported overexpression of AMACR in pulmonary neuroendocrine tumours, with AMACR expression in 72 % (31 of 43) of typical carcinoids, 52 % (15 of 29) of atypical carcinoids, 70 % (16 of 23) of large cell neuroendocrine carcinomas and 51 % (32 of 63) of small cell carcinomas [22]. Jiang et al. reported that pulmonary small cell carcinomas (zero of five) and pulmonary carcinoid tumours (zero of ten) are negative for AMACR [17]. These data suggest that the malignant potential of pulmonary carcinoids is different from that of gastric carcinoids, as reflected in AMACR staining.

One important limitation of our study is that we used a small number of specimens, especially of NET G2, and therefore, additional studies are necessary to further clarify the overexpression of AMACR in the development of NEC and NET G2, as well as the use of AMACR in differentiating between various neuroendocrine neoplasms of the stomach.

Acknowledgments The authors would like to thank Mr. Naoyuki Yamaguchi, Ms. Kazue Kobayashi and all of the staff at the Division of Molecular and Diagnostic Pathology, Niigata University Graduate School of Medical and Dental Sciences, for their assistance. This study was funded by the Division of Molecular and Diagnostic Pathology, Niigata University Graduate School of Medical and Dental Sciences.

Conflict of interest The authors declare that they have no conflict of interest.

Open Access This article is distributed under the terms of the Creative Commons Attribution License which permits any use, distribution, and reproduction in any medium, provided the original author(s) and the source are credited.

References

1. The International Agency for Research on Cancer et al (2010) WHO classification of tumours of the digestive system (IARC WHO classification of tumours), 4th edn. World Health Organization, Geneva, pp 13–14

2. Nishikura K, Watanabe H, Iwafuchi M et al (2003) Carcinogenesis of gastric endocrine cell carcinoma: analysis of histopathology and p53 gene alteration. Gastric Cancer 6:203–209
3. Schmitz W, Fingerhut R, Conzelmann E (1994) Purification and properties of an alpha-methylacyl-CoA racemase from rat liver. Eur J Biochem 222:313–323
4. Ferdinandusse S, Denis S, IJlst L et al (2000) Subcellular localization and physiological role of alpha-methylacyl-CoA racemase. J Lipid Res 41:1890–1896
5. Clayton PT (2001) Clinical consequences of defects in peroxisomal beta-oxidation. Biochem Soc Trans 29:298–305
6. Xu J, Stolk JA, Zhang X et al (2000) Identification of differentially expressed genes in human prostate cancer using subtraction and microarray. Cancer Res 60:1677–1682
7. Jiang Z, Woda BA, Rock KL et al (2001) P504S: a new molecular marker for the detection of prostate carcinoma. Am J Surg Pathol 25:1397–1404
8. Jiang Z, Fanger GR, Banner BF et al (2003) A dietary enzyme: alpha-methylacyl-CoA racemase/P504S is overexpressed in colon carcinoma. Cancer Detect Prev 27:422–426
9. Chen ZM, Ritter JH, Wang HL (2005) Differential expression of alpha-methylacyl coenzyme A racemase in adenocarcinomas of the small and large intestines. Am J Surg Pathol 29:890–896
10. Lin A, Weiser MR, Klimstra DS et al (2007) Differential expression of alpha-methylacyl-coenzyme A racemase in colorectal carcinoma bears clinical and pathologic significance. Hum Pathol 38:850–856
11. Marx A, Simon P, Simon R et al (2008) AMACR expression in colorectal cancer is associated with left-sided tumour localization. Virchows Arch 453:243–248
12. Lisovsky M, Falkowski O, Bhuiya T (2006) Expression of alpha-methylacyl-coenzyme A racemase in dysplastic Barrett's epithelium. Hum Pathol 37:1601–1606
13. Dorer R, Odze RD (2006) AMACR immunostaining is useful in detecting dysplastic epithelium in Barrett's esophagus, ulcerative colitis, and Crohn's disease. Am J Surg Pathol 30:871–877
14. Marx A, Wandrey T, Simon P et al (2009) Combined alpha-methylacyl coenzyme A racemase/p53 analysis to identify dysplasia in inflammatory bowel disease. Hum Pathol 40:166–173
15. Zhou M, Roma A, Magi-Galluzzi C (2005) The usefulness of immunohistochemical markers in the differential diagnosis of renal neoplasms. Clin Lab Med 25:247–257
16. Witkiewicz AK, Varambally S, Shen R et al (2005) Alpha-methylacyl-CoA racemase protein expression is associated with the degree of differentiation in breast cancer using quantitative image analysis. Cancer Epidemiol Biomarkers Prev 14:1418–1423
17. Jiang Z, Fanger GR, Woda BA et al (2003) Expression of alpha-methylacyl-CoA racemase (P504s) in various malignant neoplasms and normal tissues: a study of 761 cases. Hum Pathol 34:792–796
18. Lee WA (2006) Alpha-methylacyl-CoA-racemase expression in adenocarcinoma, dysplasia and non-neoplastic epithelium of the stomach. Oncology 71:246–250
19. Cho EY, Kim KM, Park CK et al (2007) AMACR is highly expressed in gastric adenomas and intestinal-type carcinomas. APMIS 115:713–718
20. Truong CD, Li W, Feng W et al (2008) Alpha-methylacyl-CoA racemase expression is upregulated in gastric adenocarcinoma: a study of 249 cases. Int J Clin Exp Pathol 1:518–523
21. Huang W, Zhao J, Li L et al (2008) a-Methylacyl coenzyme A racemase is highly expressed in the intestinal-type adenocarcinoma and high-grade dysplasia lesions of the stomach. Histol Histopathol 23:1315–1320
22. Shilo K, Dracheva T, Mani H et al (2007) Alpha-methylacyl CoA racemase in pulmonary adenocarcinoma, squamous cell carcinoma, and neuroendocrine tumours: expression and survival analysis. Arch Pathol Lab Med 131:1555–1560
23. Nozawa Y, Nishikura K, Ajioka Y et al (2012) Relationship between alpha-methylacyl coenzymeA racemase expression and mucin phenotype in gastric cancer. Hum Pathol 43:878–887
24. Lloyd MD, Darley DJ, Wierzbicki AS et al (2008) Alpha-methylacyl-CoA racemase—an 'obscure' metabolic enzyme takes centre stage. FEBS J 275:1089–1102
25. Itsuno M, Watanabe H, Iwafuchi M et al (1989) Multiple carcinoids and endocrine cell micronests in type A gastritis —their morphology, hystogenesis, and natural history. Cancer 63:881–890

Virchows Arch (2012) 461:177–183
DOI 10.1007/s00428-012-1271-6

ORIGINAL ARTICLE

Frozen section diagnosis in donor liver biopsies: observer variation of semiquantitative and quantitative steatosis assessment

Stefan Biesterfeld · Jasmin Knapp · Fernando Bittinger · Heiko Götte · Martin Schramm · Gerd Otto

Received: 14 July 2011 / Revised: 27 February 2012 / Accepted: 20 June 2012 / Published online: 8 July 2012
© Springer-Verlag 2012

Abstract Donor livers are not generally accepted for liver transplantation if intraoperative frozen section histology on wedge biopsies provides evidence for more severe steatosis. In this reliability study, assessment of steatosis in donor liver biopsies by different approaches (frozen sections vs. paraffin sections; macrovesicular steatosis vs. microvesicular steatosis), different observers, and different evaluation methods (conventional microscopy vs. point grid analysis on digital microphotographs) was compared. One hundred twenty consecutive donor liver biopsies were investigated. Intraoperative diagnosis was made on hematoxylin and eosin (H&E)-stained frozen sections. The residual portion of each biopsy was analyzed later on H&E-, diastase-resistant PAS-, and Elastica van Gieson-stained paraffin sections. Microvesicular steatosis and macrovesicular steatosis were classified semiquantitatively into 5 % steps. Additionally, point grid counting was applied on ten digital microphotographs per slide. The values for steatosis revealed a wide range of data between 0 and 70 or 85 % (mean values, 12.0–18.3 %), considering all types of specimens. The results of the two observers were highly correlated for macrovesicular steatosis ($r \geq 0.925$) and for microvesicular steatosis ($r \geq 0.880$). The values for macrovesicular and microvesicular steatosis, however, showed poor correlation ($r \leq 0.581$). The rate of agreement between the two observers ranged between 84.2 and 95.8 % (κ, 0.763–0.937), depending on the threshold setting. For point grid analysis, significantly lower mean values and ranges for both types of steatosis compared to conventional histopathology were found ($p < 0.001$). Comparing the results of point grid analysis with those of conventional histopathology, a relatively loose correlation was found (r, 0.581–0.779). Intraoperative histology remains a reliable and highly relevant method for the assessment of steatosis in liver donor grafts. It represents one important component in the decision-finding whether or not a donor liver should be accepted and should possibly be combined with results of preoperative computed tomography imaging. Considering our data, macrovesicular and microvesicular steatosis should be analyzed separately due to the limited correlation between them.

Keywords Liver · Steatosis · Transplantation pathology · Histopathology · Image analysis · Reliability

S. Biesterfeld (✉) · M. Schramm
Department of Cytopathology,
Heinrich Heine University of Düsseldorf,
Moorenstr. 5,
40225 Düsseldorf, Germany
e-mail: Stefan.Biesterfeld@med.uni-duesseldorf.de

J. Knapp · F. Bittinger
Institute of Pathology, University of Mainz,
Mainz, Germany

H. Götte
Institute of Medical Biostatistics, Epidemiology and Informatics (IMBEI), University of Mainz,
Mainz, Germany

G. Otto
Department of Transplantation Surgery, University of Mainz,
Mainz, Germany

Introduction

Significant liver steatosis means a risk factor for severe complications after major hepatic surgery. Cases with hepatic steatosis showed an up to twofold increased risk for postoperative complications and those with at least 30 % steatosis also had an almost threefold increased risk of postoperative death [1–3]. Similar results have also been reported for liver transplantation. While mild steatosis did not affect the clinical result [4–7], more severe steatosis

influenced the graft function and the short-term and long-term outcome of the patients [8–26]. As a consequence, donor livers with more severe steatosis are not generally accepted. However, there is no consensus about a suitable threshold of steatosis: whereas in some institutions donor livers with a degree of steatosis of 25–30 % [8, 22] are declined, those with steatosis up to 50–60 % have been accepted by others [23, 27]. The prognosis of the allograft function also depends on additional factors, such as cold and warm ischemia time, type and duration of intensive care treatment and medication of the donor, and finally numerous recipient factors. Therefore, it has been stated that donor livers should not be declined depending on the degree of steatosis alone [2, 14, 28].

Due to the limited period of time between explantation and transplantation, the analysis of frozen section histology on wedge biopsies has been widely accepted as standard procedure for the assessment of steatosis. However, the interpretation mode has not yet been standardized. Mostly, quite rough cutoff points for grouping (0–30, 30–60, >60 %) have been applied. Further, there is no consensus if the degree of steatosis in general or the degree of macrovesicular or microvesicular steatosis in particular is to be used as a variable. Additionally, aspects of interobserver reliability must also be taken into account. Furthermore, it has to be considered that a biopsy may not always reflect the degree of steatosis in the whole organ [29], for example, due to the phenomenon of focal steatosis [30]. Finally, the effects of tissue fixatives [31] or the use of different staining methods [27, 32, 33] might further influence the results.

In this study, the assessment of steatosis of donor liver biopsies using different approaches (frozen sections vs. paraffin sections; macrovesicular steatosis vs. microvesicular steatosis), different observers, and different evaluation methods were compared. From our data, we conclude that both types of steatosis can be interpreted with substantial reliability in frozen sections and in paraffin sections. However, macrovesicular and microvesicular steatosis revealed an only limited correlation and thus represent independent phenomena with probably independent clinical meaning.

Patients and methods

Patients

One hundred twenty consecutive intraoperative donor liver biopsies, provided by the German Organ Transplantation Foundation (DSO), were investigated. Histopathological analysis was performed at the Institute of Pathology of the Johannes Gutenberg University of Mainz where 24-h pathology on-call service is available. We received the specimens as unfixed ice-cooled subcapsular wedge biopsies measuring 0.7–2 cm in longest diameter.

Methods

After macroscopic description of size, color, and consistency, biopsies were snap-frozen in liquid nitrogen. The intraoperative diagnosis was made on representative hematoxylin and eosin (H&E)-stained, 4-μm-thick frozen sections. Without impact on the transplantation process, the residual portion of each biopsy was formalin-fixed and later analyzed using H&E-, diastase-resistant PAS-, and Elastica van Gieson-stained paraffin sections. Evaluation of the slides was performed by two independent observers. The original diagnoses had been made by observer 1, one of the chief consultants of the institution. Observer 2 who has a position as resident was introduced into the principles of steatosis assessment by observer 1 and by a second independent chief consultant and performed the evaluation of the slides retrospectively. For standardized interpretation, we investigated the slides in a conventional light microscope as follows. Ten consecutive viewing fields in the length axis of the biopsy were interpreted using the ×20 and the ×40 objective magnification. Per viewing field, the rates of liver cells with macrovesicular and microvesicular steatosis [34] were estimated separately in 5 % steps (0, 1, 5, 10, 15 %, etc.), and the mean values of the ten fields were taken as final scaling values for the respective type of steatosis.

For point grid counting [35], ten digital microphotographs of each H&E-stained slide were stored at 40-fold objective magnification using the software package Adobe Photoshop CS2 9.0. The first field of view was chosen in the longest diameter of the biopsy close to the end. In order to prevent overlapping images, steps along the longitudinal axis of the biopsy measuring 1.5 viewing fields were chosen for each new image. This procedure was continued until all images had been grabbed. A grid with 24 crosspoints (6×4) was superimposed on each image (Fig. 1). Considering only cells being in touch with a crosspoint, the number of hepatocytes with macrovesicular or microvesicular fat vacuoles and the total number of hepatocytes were counted manually, resulting in up to 240 counts per slide. Hits on connective tissue or bile duct epithelium were not considered.

Statistical analysis

To analyze the relationship between the different assessments of steatosis, the following statistical variables were calculated:

- The coefficient of correlation (r) was used to analyze interrelationships in uncategorized data.
- Cohen's kappa value (κ) [36] that enables the comparison of categorized data was used for better comparability with previous studies. The κ values were interpreted according to Landis and Koch [37] as slight (0–0.2), fair (0.21–0.4), moderate (0.41–0.6), substantial (0.61–0.8), or almost perfect (>0.8).

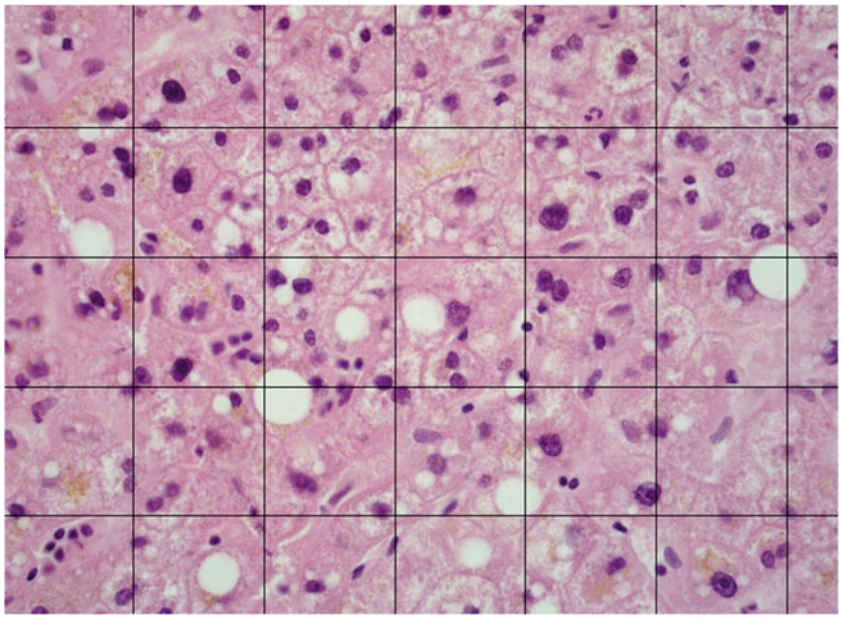

Fig. 1 Principle of point grid analysis. A grid of six horizontal and four vertical lines is superimposed to an H&E-stained slide of a liver biopsy. Only those hepatocytes found on the 24 crosspoints of the lines are considered for evaluation

- For compact data illustration, a factor analysis was performed (for details, see [38]). In brief, the original data are rearranged to a smaller two-dimensional set of factors on a scale between −1 and +1 as source variables for the observed interrelations in the data. The nearer the relative positions of the factors are, the closer the respective variables are correlated. Thus, a two-dimensional (*x*/*y*) diagram of a factor analysis sums up the results of many correlations and of various multifield tables in a visual way.
- In Bland–Altman plots [39], the mean values of two assessments (*x*-axis) and the differences between them (*y*-axis) were presented. Considering a respective threshold, usually the ±2 SD level around the mean value, outliers and trends in the data distribution may be detected more easily.

Results

Conventional histopathology

Macrovesicular steatosis and microvesicular steatosis revealed a wide range of data (Table 1). The mean values ranged between 12.0 and 14.2 % for macrovesicular steatosis and between 15.8 and 18.3 % for microvesicular steatosis; the standard deviations were well comparable. A high correlation between the results of the two observers could be confirmed by correlation analysis (Table 2) for macrovesicular steatosis (*r*, 0.925–0.984) and for microvesicular steatosis (*r*, 0.880–0.953). The degrees of macrovesicular and microvesicular steatosis were quite independent from each other (Table 3): the coefficients of correlation between the two types of steatosis were significantly lower than those found for interobserver analysis (*r*, 0.490–0.581). The close correlation of the assessments of the two observers and the only loose interrelationship between the degree of macrovesicular and microvesicular steatosis are further illustrated in Fig. 2.

In a few cases, outlying values occurred. Focusing on the clinically more important macrovesicular steatosis, in six cases of frozen section analysis (=5.0 %) and in three cases of paraffin section analysis (=2.5 %), the two observers came to differences exceeding the respective ±2 SD interval (Figs. 3 and 4). Comparing the results on frozen sections

Table 1 Mean values, standard deviations, and ranges of steatosis assessment in 120 wedge biopsies of donor livers

Observer/method	Mean	SD	Min	Max
Macrovesicular steatosis				
Observer 1, frozen section	12.0	15.8	0	60
Observer 1, paraffin section	12.2	16.0	0	70
Observer 2, frozen section	14.2	15.4	0	50
Observer 2, paraffin section	13.8	16.4	0	60
Point grid analysis, frozen section	3.4	5.5	0	31.5
Point grid analysis, paraffin section	2.8	5.0	0	23.7
Microvesicular steatosis				
Observer 1, frozen section	15.8	16.4	0	80
Observer 1, paraffin section	15.8	16.8	0	85
Observer 2, frozen section	15.9	16.4	0	80
Observer 2, paraffin section	18.3	15.8	0	70
Point grid analysis, frozen section	5.4	4.9	0	29.0
Point grid analysis, paraffin section	3.3	3.9	0	21.6

All values are given in percent

Table 2 Coefficients of correlation (*r*) for the assessment of steatosis of 120 wedge biopsies of donor livers by two observers, comparing different types of specimens

	Observer 1, frozen section	Observer 1, paraffin section	Observer 2, frozen section	Observer 2 paraffin section	Point grid analysis, frozen section	Point grid analysis, paraffin section
Observer 1, frozen section	–	*0.953*	*0.942*	*0.880*	*0.665*	*0.618*
Observer 1, paraffin section	0.984	–	*0.931*	*0.919*	*0.651*	*0.691*
Observer 2, frozen section	0.947	0.939	–	*0.908*	*0.688*	*0.669*
Observer 2, paraffin section	0.925	0.932	0.946	–	*0.637*	*0.746*
Point grid analysis, frozen section	0.780	0.779	0.808	0.809	–	*0.581*
Point grid analysis, paraffin section	0.792	0.807	0.799	0.867	0.785	–

Values for macrovesicular steatosis are rendered in normal font, while values for microvesicular steatosis are rendered in italics

and on paraffin sections per observer, we found four more severe differences for observer 1 (=3.3 %) and two for observer 2 (=1.7 %). It has to be considered, however, that the ±2 SD interval was significantly lower for observer 1 (SD, 2.9 vs. 5.3 %).

Additionally, we calculated the agreement of the two observers after data categorization (Table 4). Thresholds were set after 10 and 30 %, resulting in the three groups of "<10," "10–30," and ">30 %," or after 30 and 60 %, resulting in the three groups of "<30," "30–60," and ">60 %." The rate of agreement ranged between 84.2 and 95.8 % (κ, 0.763–0.937, "substantial" or "almost perfect", respectively).

Point grid analysis

The data distribution of the point grid analysis (Table 1) revealed significantly lower mean values and ranges compared to conventional histopathology (*U* test: $p<0.001$). Additionally, lower values were found for the coefficients of correlation, comparing the results with those of conventional histopathology for macrovesicular steatosis (*r*, 0.779–0.867) and for microvesicular steatosis (*r*, 0.581–0.746) (Table 2; Fig. 2). The intraobserver reproducibility was tested on 20 randomly chosen cases. Evaluating frozen sections and paraffin sections separately, an almost linear relation was found for macrovesicular steatosis ($r=0.992$) and for microvesicular steatosis ($r=0.971$).

Discussion

Histological assessment on liver biopsies remains the principal approach to quantify hepatic steatosis in the donor liver, but bears controversial issues such as sampling error, different methods of tissue processing, intraobserver and interobserver variation, and finally discrepancies encountered when visual and morphometric results are compared. In addition to this, macrosteatotic and microsteatotic alterations

Table 3 Coefficients of correlation (*r*) for the assessment of steatosis of 120 wedge biopsies of donor livers by two observers, correlating the values for macrovesicular steatosis and for microvesicular steatosis

	Observer 1, frozen section	Observer 1, paraffin section	Observer 2, frozen section	Observer 2, paraffin section	Point grid analysis, frozen section	Point grid analysis, paraffin section
Observer 1, frozen section	0.509	0.490	0.521	0.432	0.377	0.304
Observer 1, paraffin section	0.528	0.515	0.525	0.450	0.389	0.314
Observer 2, frozen section	0.554	0.540	0.575	0.485	0.399	0.325
Observer 2, paraffin section	0.581	0.577	0.576	0.571	0.423	0.423
Point grid analysis, frozen section	0.355	0.351	0.352	0.321	0.334	0.197
Point grid analysis, paraffin section	0.510	0.526	0.485	0.590	0.334	0.395

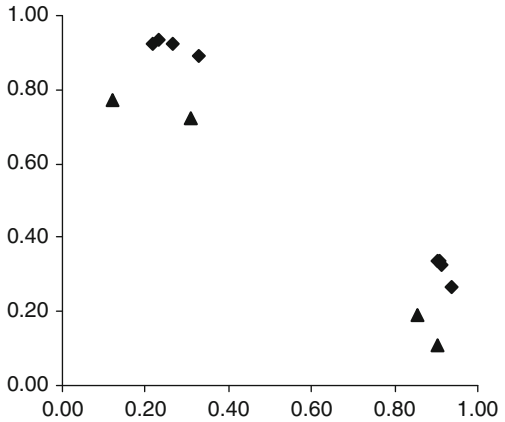

Fig. 2 Factor analysis of steatosis assessment of 120 wedge biopsies of donor livers. *Left*/*top* microvesicular steatosis, *right*/*bottom* macrovesicular steatosis. *Rectangles* represent the four data sets of conventional microscopy, *triangles* represent the two data sets of point grid analysis. Explained cumulative proportion of variance, 85.2 %

clearly need to be distinguished. With the exception of sampling error, this study focuses on these principal issues, especially on the reliability of steatosis assessment under intraoperative conditions.

Comparing frozen sections and paraffin sections, only slight differences were found: The results for evaluating macrovesicular and microvesicular steatosis were highly correlated (r>0.88, κ>0.76) and are well comparable to those of two previous studies [11, 40] which reported κ values >0.8 for the comparison of macrovesicular steatosis, microvesicular steatosis, or steatosis in general, respectively. Concerning intraobserver and interobserver variation of

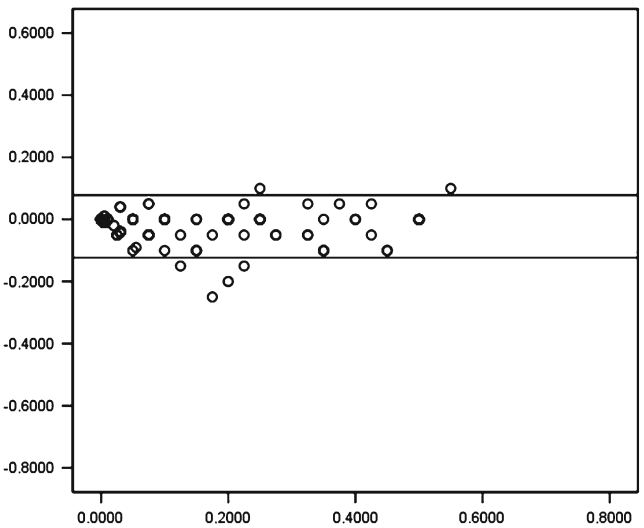

Fig. 3 Bland–Altman plots for the interobserver reproducibility of macrovesicular steatosis assessment of 120 wedge biopsies of donor livers on frozen sections. *Abscissa* mean value of the two assessments. *Ordinate* difference between the two assessments. The *horizontal lines* represent the thresholds of the ±2 SD interval. Mean difference, 2.5 %; SD, 5.5 %

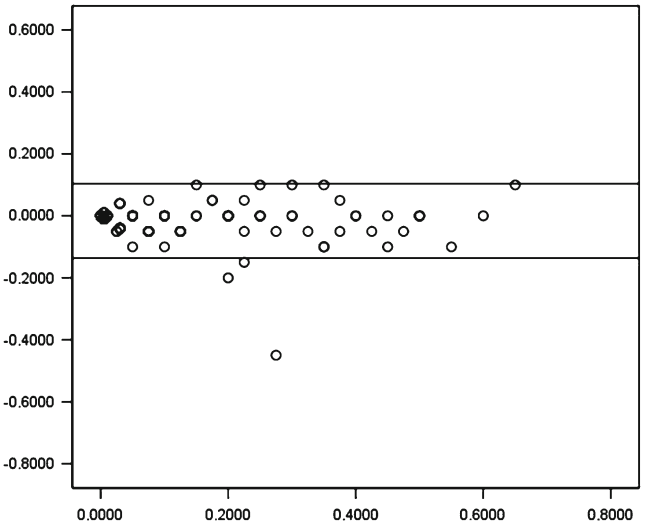

Fig. 4 Bland–Altman plots for the interobserver reproducibility of macrovesicular steatosis assessment of 120 wedge biopsies of donor livers on paraffin sections. *Abscissa* mean value of the two assessments. *Ordinate* difference between the two assessments. The *horizontal lines* represent the thresholds of the ±2 SD interval. Mean difference, 1.6 %; SD, 6.0 %

steatosis assessment, comparably sparse data exist [35, 41–44]. Well comparable κ values for interobserver agreement between 0.51 and 0.71 or between 0.42 and 0.65 for intraobserver agreement, respectively, have been reported. In our study, the overwhelming majority of specimens in the evaluation of the slides by a second independent observer led to very similar results as compared to the original assessment on the date of liver explantation, resulting in κ values >0.76. Our comparably high κ values might be due to the fact that the degree of steatosis has not been roughly estimated but has been calculated as the mean value of steatosis in a defined number of viewing fields evaluated separately in 5 % steps. As a result of the separate assessment of macrovesicular and microvesicular steatosis, the weak correlation of both forms of steatosis deserves further consideration. However, that issue has not been systematically

Table 4 Agreement analysis and kappa statistics (κ) for the assessment of macrovesicular and microvesicular steatosis of 120 wedge biopsies of donor livers in three groups

Thresholds for grouping	Rate of agreement and κ value			
	Macrovesicular steatosis		Microvesicular steatosis	
Frozen sections				
10/30 %	88.3 %	0.825	84.2 %	0.763
30/60 %	95.0 %	0.925	95.8 %	0.937
Paraffin sections				
10/30 %	89.2 %	0.838	85.0 %	0.776
30/60 %	94.2 %	0.913	95.0 %	0.925

compared and described yet. The only weak correlation between both types of steatosis (r, 0.490–0.581) underlines the need for separate assessment of both types of steatosis. This is not only important regarding their different impacts on graft function but may also have different underlying pathophysiological mechanisms leading to consequences in the treatment of prospective organ donors. To overcome methodological limitations of conventional histology by computed image analysis or by point grid analysis will not clearly improve diagnostics. Up to now, there is no evidence that point grid analysis could be superior to conventional histopathology. Further, its use in routine pathology would require a modified scaling for "mild," "moderate," or "severe" steatosis: our finding that conventional histopathology resulted in almost 3.75-fold values for macrosteatosis and microsteatosis as compared to point grid analysis fits well with those of other groups who reported average values between 2.70-fold and 3.78-fold investigating biopsies from donor livers [45] or from cases with metabolic syndrome [46] or hepatitis C [47, 48]. From the point of view of transplantation pathology, it should be further noted that, for the moment, the application of an image analytical technique will be too time-consuming under the conditions of intraoperative diagnostics. Possibly, digitalization of microscopic slides will open a field of computer-assisted or even automated intraoperative microscopy in the nearer future.

In the context of clinical decision-making as to whether a donor liver should be accepted for transplantation or not, a comprehensive interpretation of intraoperative steatosis assessment could be supplemented by results from preoperative imaging. Unfortunately, results on hepatic sonography showed a limited sensitivity for the prediction of steatosis and contradictory results concerning specificity [24, 49]. Applying unenhanced computed tomography (CT), however, at least two studies gave evidence that the calculation of the ratio of attenuation values in the liver to those in the spleen could be clinically used as a valid noninvasive method to evaluate hepatic steatosis preoperatively for donor livers [50], also regarding the aspect of macrovesicular steatosis [51].

From our point of view, the use of intraoperative histology remains a reliable and most important method for the assessment of steatosis in liver donor grafts, if well-defined criteria are used and as far as methodological limitations are considered in data interpretation. Following our data, it can be reliably applied also on frozen sections and definitely implies a separate determination of macrovesicular or microvesicular steatosis. For clinical purposes, it remains the most important component for the acceptance of a donor liver, especially in cases with a limited macroscopic quality [52], and may be combined with results of preoperative CT imaging. Validation of steatosis assessment by analyzing the clinical course of the recipients after transplantation is highly recommended and should be performed on our patient group in the near future.

Conflict of interest We declare that we have no conflicts of interest.

References

1. Behrns KE, Tsiotos GG, de Souza NF, Krishna MK, Ludwig J, Nagorney DM (1998) Hepatic steatosis as a potential risk factor for major hepatic resection. J Gastrointest Surg 2:292–298
2. McCormack L, Petrowsky H, Jochum W, Furrer K, Clavien PA (2007) Hepatic steatosis is a risk factor for postoperative complications after major hepatectomy. A matched case–control study. Ann Surg 245:923–930
3. de Meijer VE, Kalish BT, Puder M, IJzermans JNM (2010) Systematic review and meta-analysis of steatosis as a risk factor in major hepatic resection. Brit J Surg 97:1331–1339
4. Veteläinen R, van Vliet A, Gouma DJ, van Gulik TM (2007) Steatosis as a risk factor in liver surgery. Ann Surg 245:20–30
5. Soejima Y, Shimada M, Suehiro T (2003) Use of steatotic graft in living donor liver transplantation. Transplantation 76:344–348
6. Hayashi M, Fujii K, Kiuchi T, Uryuhara K, Kasahara M, Takatsuki M, Takeichi T, Kitade H, Sugimoto T, Uemoto S, Asonuma K, Egawa H, Fujita S, Inomata Y, Tanaka K (1999) Effects of fatty infiltration of the graft on the outcome of living-related liver transplantation. Transplant Proc 31:403
7. Ito T, Kiuchi T, Egawa H, Kaihara S, Oike F, Ogura Y, Fujimoto Y, Ogawa K, Tanaka K (2003) Surgery-related morbidity in living donors of right-lobe liver graft: lessons from the first 200 cases. Transplantation 76:158–163
8. Crowley H, Lewis WD, Gordon F, Jenkins R, Khettry U (2000) Steatosis in donor and transplant liver biopsies. Hum Pathol 31:1209–1213
9. Ploeg RJ, D'Alessandro AM, Knechtle SJ, Stegall MD, Pirsch JD, Hoffmann RM, Sasaki T, Sollinger HW, Belzer FO, Kalayoglu M (1993) Risk factors for primary dysfunction after liver transplantation—a multivariate analysis. Transplantation 55:807–813
10. Salizzoni M, Franchello A, Zamboni F, Ricchiuti A, Cocchis D, Fop F, Brunati A, Cerutti E (2003) Marginal grafts: finding the correct treatment for fatty livers. Transplant Int 16:486–493
11. d'Alessandro E, Calabrese F, Gringeri E, Valente M (2010) Frozen-section diagnosis in donor livers: error rate estimation of steatosis degree. Transplant Proc 42:2226–2228
12. Todo S, Demetris AJ, Makowka L, Teperman L, Podesta L, Shaver T, Tzakis A, Starzl TE (1989) Primary nonfunction of hepatic allografts with preexisting fatty infiltration. Transplantation 47:903–905
13. d'Alessandro AM, Kalayoglu M, Sollinger HW, Hoffmann RM, Reed A, Knechtle SJ, Pirsch JD, Hafez GR, Lorentzen D, Belzer FO (1991) The predictive value of donor liver biopsies for the development of primary nonfunction after orthotopic liver transplantation. Transplantation 51:157–163
14. Chui AKK, Shi LW, Rao ARN, Verran DJ, Painter D, Koorey D, McCaughan GW, Sheil AGR (2000) Donor fatty (steatotic) liver allografts in orthotopic liver transplantation: a revisit. Transplant Proc 32:2101–2102
15. Ureña MA, Moreno Gonzalez E, Romero CJ, Ruiz-Delgado FC, Moreno Sanz C (1999) An approach to the rational use of steatotic donor livers in liver transplantation. Hepatogastroenterology 46:1164–1173
16. Angelico M (2005) Donor liver steatosis and graft selection for liver transplantation: a short review. Eur Rev Med Pharmacol Sci 9:295–297

17. Reddy MS, Bhati C, Neil D, Mirza DF, Manas DM (2008) National Organ Retrieval Imaging System: results of the pilot study. Transpl Int 21:1036–1044
18. Markin RS, Wisecarver JL, Radio SJ, Stratta RJ, Langnas AN, Hirst K, Shaw BW (1993) Frozen section evaluation of donor livers before transplantation. Transplantation 56:1403–1409
19. Strasberg SM, Howard TK, Molmenti EP, Hertl M (1994) Selecting the donor liver: risk factors for poor function after orthotopic liver transplantation. Hepatology 20:829–838
20. Zamboni F, Franchello A, David E, Rocca G, Ricchiuti A, Lavezzo B, Rizzetto M, Salizzoni M (2001) Effect of macrovescicular steatosis and other donor and recipient characteristics on the outcome of liver transplantation. Clin Transplant 15:53–57
21. Verran D, Kusyk T, Painter D, Fisher J, Koorey D, Strasser S, Stewart G, McCaughan G (2003) Clinical experience gained from the use of 120 steatotic donor livers for orthotopic liver transplantation. Liver Transpl 9:500–505
22. Yoo HY, Molmenti E, Thuluvath PJ (2003) The effect of donor body mass index on primary graft non-functional, retransplantation rate, and early graft and patient survival after liver transplantation. Liver Transpl 9:72–78
23. Ureña MA, Ruiz-Delgado FC, González EM, Segurola CL, Romero CJ, García IG, González-Pinto I, Gómez Sanz R (1998) Assessing risk of the use of livers with macro- and microsteatosis in a liver transplant program. Transplant Proc 30:3288–3291
24. Adani GL, Baccarani U, Sainz-Barriga M, Lorenzin D, Bresadola V, Risaliti A, Avellini C, Trevisan G, De Candia A, Bresadola F (2006) The role of hepatic biopsy to detect macrovacuolar steatosis during liver procurement. Transpl Proc 38:1404–1406
25. Yoong KF, Gunson BK, Neil DA, Mirza DF, Mayer AD, Buckels JA, McMaster P (1999) Impact of donor liver microvesicular steatosis on the outcome of liver retransplantation. Transplant Proc 31:550–551
26. Salizzoni M, Franchello A, Zamboni F, Ricchiuti A, Cocchis D, Fop F, Brunati A, Cerutti E (2003) Marginal grafts: finding the correct treatment for fatty livers. Transpl Int 16:486–493
27. Frongillo F, Avolio AW, Nure E, Mulè A, Pepe G, Magalini SC, Agnes S (2009) Quantification of degree of steatosis in extended criteria donor grafts with standardized histological techniques: implications for graft survival. Transplant Proc 41:1268–12172
28. Doyle MBM, Vachharajani N, Wellen JR, Anderson CD, Lowel JA, Shenoy S, Brunt EM, Chapman WC (2010) Short- and long-term outcomes after steatotic liver transplantation. Arch Surg 145:653–660
29. Ratziu V, Charlotte F, Heurtier A, Gombert S, Giral P, Bruckert E, Grimaldi A, Capron F, Poynard T, LIDO Study Group (2005) Sampling variability of liver biopsy in non-alcoholic fatty liver disease. Gastroenterology 128:1898–1906
30. Kammen BF, Pacharn P, Thoeni RF, Lu Y, Qayyum A, Coakly F, Gooding CA, Brasch RC (2001) Focal fatty infiltration of the liver: analysis of prevalence and CT findings in children and young adults. Am J Roentgenol 177:1035–1039
31. di Donato D, Brasaemle DL (2003) Fixation methods for the study of lipid droplets by immunofluorescence microscopy. J Histochem Cytochem 51:773–780
32. Fukumoto S, Fujimoto T (2002) Deformation of lipid droplets in fixed samples. Histochem Cell Biol 118:423–428
33. Fiorini RN, Kirtz J, Periyasamy B, Evans Z, Haines JK, Cheng G, Polito C, Rodwell D, Shafizadeh SF, Zhou X, Campbell C, Birsner J, Schmidt M, Lewin D, Chavin KD (2004) Development of an unbiased method for the estimation of liver steatosis. Clin Transplant 18:700–706
34. Crawford JM (2007) Basic mechanisms in hepatopathology. In: Burt AD, Portmann BC, Ferrell LD (eds) MacSween's pathology of the liver. Churchill Livingstone/Elsevier, Philadelphia, p 88
35. Franzén L, Ekstedt M, Kechagias S, Bodin L (2005) Semi quantitative evaluation overestimates the degree of steatosis in liver biopsies: a comparison to stereological point counting. Mod Pathol 18:912–916
36. Cohen J (1960) A coefficient of agreement for nominal scales. Educ Psychol Meas 20:37–46
37. Landis JR, Koch GG (1977) The measurement of observer agreement for categorical data. Biometrics 33:159–174
38. Sun DQ, Feng CH, Böcking A, Biesterfeld S (1994) Principal component analysis. A factor analytical technique for the determination of interobserver variation in histomorphologic tumor grading. Anticancer Res 14:1525–1528
39. Bland JM, Altman DG (1995) Comparing methods for measurement: why plotting difference against standard method is misleading. Lancet 346:1085–1087
40. Fiorentino M, Vasuri F, Ravaiolo M, Ridolfi L, Grigioni WF, Pinna AD, d'Errico-Grigioni A (2009) Predictive value of frozen-section analysis in the histological assessment of steatosis before liver transplantation. Liver Transpl 15:1821–1825
41. Theodossi A, Skene AM, Portmann B, Knill-Jones RP, Patrick RS, Tate RA, Kealey W, Jarvis KJ, O'Brian DJ, Williams R (1980) Observer variation in assessment of liver biopsies including analysis by kappa statistics. Gastroenterology 79:232–241
42. Younossi ZM, Gramlich T, Liu YC, Matteoni C, Petrelli M, Goldblum J, Rybicki L, McCullough AJ (1998) Non-alcoholic fatty liver disease: assessment of variability in pathologic interpretations. Mod Pathol 11:560–565
43. Bedossa P, Bioulac-Sage P, Callard P, Chevallier M, Degott C, Deugnier Y, Fabre M, Reynes M, Voigt JJ, Serge Zafrani E, the french METAVIR cooperative study group (1994) Intraobserver and interobserver variations in liver biopsy interpretation in patients with chronic hepatitis C. Hepatology 20:15–20
44. Auger J, Schoevaert D, Martin ED (1986) Comparative study of automated morphometric and semiquantitative estimations of alcoholic liver steatosis. Anal Quant Cytol Histol 8:56–62
45. Marsman H, Matsushita T, Dierkhising R, Kremers W, Rosen C, Burgart L, Nyberg S (2004) Assessment of donor liver steatosis: pathologist or automated software? Hum Pathol 35:430–435
46. Turlin B, Ramm GA, Purdiem DM, Laine F, Perrin M, Deugnier Y, Macdonald GA (2008) Assessment of hepatic steatosis: comparison of quantitative and semiquantitative methods in 108 liver biopsies. Liver Int 29:530–535
47. Kumar D, Farrell GC, Fung C, George G (2002) Hepatitis C virus genotype 3 is cytopathic to hepatocytes: reversal of hepatic steatosis after sustained therapeutic response. Hepatology 36:1266–1272
48. Rawlins SR, El-Zammar O, Zinkievich JM, Newman N, Levine RA (2010) Digital quantification is more precise than traditional semiquantitation of hepatic steatosis: correlation with fibrosis in 220 treatment-naive patients with chronic hepatitis C. Dig Dis Sci 55:2049–2057
49. Hepburn MJ, Vos JA, Fillman EP, Lawitz EJ (2005) The accuracy of the report of hepatic steatosis on ultrasonography in patients infected with hepatitis C in a clinical setting: a retrospective observational study. BMC Gastroenterol 5:14
50. Iwasaki M, Takada Y, Hayashi M, Minamiguchi S, Haga H, Maetani Y, Fujii K, Kiuchi T, Tanaka K (2004) Non-invasive evaluation of graft steatosis in living donor liver transplantation. Transplantation 78:1501–1505
51. Limanond P, Raman SS, Lassman C, Sayre J, Ghobrial RM, Busuttil RW, Saab S, Lu DSK (2004) Macrovesicular hepatic steatosis in living related liver donors: correlation between CT and histological findings. Radiology 230:276–280
52. Rey JW, Wirges U, Dienes HP, Fries JWU (2009) Hepatic steatosis in organ donors: disparity between surgery and histology? Transplant Proc 41:2557–2560

Virchows Arch (2012) 461:185–193
DOI 10.1007/s00428-012-1263-6

ORIGINAL ARTICLE

Training increases concordance in classifying pulmonary adenocarcinomas according to the novel IASLC/ATS/ERS classification

Arne Warth · Judith Cortis · Ludger Fink · Annette Fisseler-Eckhoff · Helene Geddert · Thomas Hager · Klaus Junker · Gian Kayser · Julia Kitz · Florian Länger · Alicia Morresi-Hauf · German Ott · Iver Petersen · Albrecht Stenzinger · Alex Soltermann · Saskia Ting · Verena Tischler · Ekkehard Vollmer · Philipp A. Schnabel · Wilko Weichert · on behalf of the Pulmonary Pathology Working Group of the German Society of Pathology

Received: 17 February 2012 / Revised: 5 June 2012 / Accepted: 6 June 2012 / Published online: 23 June 2012
© Springer-Verlag 2012

Abstract The International Association for the Study of Lung Cancer (IASLC), the American Thoracic Society (ATS), and the European Respiratory Society (ERS) proposed a classification for lung adenocarcinomas (ADC) based on the predominant growth pattern. This classification has been shown to have prognostic and maybe even predictive impact. However, until now, the reproducibility of this classification has not been sufficiently demonstrated. Digital images of 40 selected ADC cases were shown twice to members of the Pulmonary Pathology Working Group of the German Society of Pathology. Each time a teledialogue-based survey on the classification was performed. Between the voting procedures, salient features of the novel classification were presented and discussed in detail by its

Philipp A. Schnabel and Wilko Weichert contributed equally to this work.

A. Warth (✉) · J. Cortis · A. Stenzinger · P. A. Schnabel · W. Weichert
Institute of Pathology, University Hospital Heidelberg,
Im Neuenheimer Feld 224,
69120 Heidelberg, Germany
e-mail: arne.warth@med.uni-heidelberg.de

L. Fink
Institute of Pathology and Cytology,
Wetzlar, Germany

A. Fisseler-Eckhoff
Institute of Pathology and Cytology, Horst Schmidt Hospital,
Wiesbaden, Germany

H. Geddert
Institute for Pathology, St. Vincentius Hospital,
Karlsruhe, Germany

T. Hager · S. Ting
Institute of Pathology and Neuropathology, University Hospital,
Essen, Germany

K. Junker
Institute of Pathology, Hospital Bremen Mitte,
Bremen, Germany

G. Kayser
Institute of Pathology, University Hospital,
Freiburg, Germany

J. Kitz
Institute of Pathology, University Hospital,
Göttingen, Germany

F. Länger
Institute of Pathology, University Hospital,
Hannover, Germany

A. Morresi-Hauf
Institute of Pathology, Asklepios Hospital,
München-Gauting, Germany

G. Ott
Institute of Clinical Pathology, Robert Bosch Hospital,
Stuttgart, Germany

I. Petersen
Institute of Pathology, University Hospital,
Jena, Germany

A. Soltermann · V. Tischler
Institute of Surgical Pathology, University Hospital,
Zürich, Switzerland

E. Vollmer
Institute of Clinical & Experimental Pathology,
Research Center Borstel, Leibniz Center for
Medicine and Biosciences,
Borstel, Germany

members. The mean percentages of consensual votes per pattern ranged between 59.6 and 75 %, with lepidic and solid being the pattern with the most discordant and concordant votes, respectively. The other patterns ranged in between (papillary 65.8 %; acinar 67.8 %; micropapillary 74.2 %). The extent of disagreement decreased after the educational session. This decrease, however, was heterogeneous for the different patterns with acinar being the pattern with the strongest improvement. The overall number of abstentions decreased significantly after the educational session ($p<0.001$) as well. The IASLC/ATS/ERS classification of lung ADC can be applied with reasonable consensus even for difficult cases in a nationwide context. The reproducibility evidently improves following educational sessions, even among experienced lung pathologists. Worldwide harmonization is clearly the next step on the way to a clinically meaningful, internationally accepted use of this novel prognostic and potentially predictive tool in lung pathology.

Keywords Pulmonary adenocarcinoma · Classification · Subtyping · Reproducibility

Introduction

Pulmonary carcinomas are very frequent neoplasms, heading cancer death statistics for both sexes in the western world [1]. Of these, the most prevalent tumor type is adenocarcinoma (ADC) accounting for approximately half of all lung cancers.

As well as in other neoplasms, a reliable estimation of patient survival probability is crucial in pulmonary tumors, since the selection of conventional therapy regimens, administered in the palliative or adjuvant setting, is largely based on the estimated risk of the patient to die of the disease in a given time frame. For lung cancer, the cornerstone of clinical survival estimation is stage categorization. Besides tumor staging, tumor grade as determined by the pathologist on the basis of conventional histomorphology is a reliable predictor of survival in a broad variety of solid human tumor entities and strongly influences clinical decision making, e.g., in breast cancer, prostate cancer, or sarcomas [2–4]. However, up to now, grading in lung cancer has largely been performed without internationally accepted criteria and without any clinical impact. Similarly, histological subtyping in some regard is not very well standardized in pulmonary ADC either. In response, several groups have tried to establish standardized subtyping and grading schemes for lung cancer [5, 6]. On the basis of these new data, an international multidisciplinary expert panel of the International Association for the Study of Lung Cancer (IASLC), the American Thoracic Society (ATS), and the European Respiratory Society (ERS) has proposed a novel classification system for ADC. This system is based on the evaluation of ADC architecture and is intended to facilitate standardized tumor grading [6]. ADC are now categorized according to their predominant growth pattern. The independent prognostic impact of this classification across all tumor stages has subsequently been confirmed by us and others in large ADC cohorts from Europe, Australia, and the USA [7–10]. Thus, grading of pulmonary ADC on the basis of the predominant pattern will very likely enter clinical decision making in the near future. However, prior to the application of this classification in routine diagnostics, it is mandatory to validate this classification in terms of reliability and reproducibility when used by different evaluators, outside a well-defined study setting. This implies that all pathologists involved in lung pathology need to share the same criteria regarding the evaluation of tumor architecture as outlined by the IASLC/ATS/ERS consensus. In order to provide a nationwide basis for this issue, the Pulmonary Pathology Working Group of the German Society of Pathology organized a meeting to introduce and discuss the novel classification, to test for reproducibility among pulmonary pathologist, and to identify potential problems and pitfalls which should be further clarified. Here, we present the results of this meeting, provide information on the level of agreement/disagreement in the evaluation of selected complex patterns among a large group of pulmonary pathologists, and assess the impact of expert discussions and training in this context.

Material and methods

Participants of the meeting and selection of cases

The annual autumn meeting of the Pulmonary Pathology Working Group of the German Society of Pathology took place from the 25th to 26th November 2011 at the Thoracic Hospital Heidelberg, Germany. The meeting was attended by a total of 77 pathologists and clinicians with a special interest in pulmonary pathology. Prior to the meeting, all participants were asked to provide digital images of difficult patterns of pulmonary ADC to the organizing committee (AW, PAS). A total of five institutions followed our call for photomicrographs of complicated patterns. The organizing committee in Heidelberg supplemented some additional cases to allow for a total of 40 images for the test sessions.

Test setting

The meeting started with a 1-h state of the art lecture by one of the authors of the IASCL/ATS/ERS classification (Prof. Keith Kerr, Royal Infirmary Hospital, Aberdeen, Scotland). Subsequently, all interested pathologists were asked to

participate in an anonymous teledialogue-based study (TED) to vote for the predominant pattern (lepidic, acinar, papillary, micropapillary, or solid) of 40 selected ADC images (30 s per image; only H&E stains). Images were presented as beamer projections to the audience and all participants agreed to the manner and quality of the presentation. On day 1, 27 pathologists took part in the evaluation round, while on day 2, 24 pathologists participated. To avoid any bias, votes were given anonymously. All images as well as the votes for the predominant pattern can be seen and evaluated again using the following link: http://www.klinikum.uni-heidelberg.de/Online-Tutorial-for-Pulmonary-Adenocarcinoma-Subtyping.125267.0.html.

All participants also had the chance to abstain if indecisive. The TED results were not reported to the participants. The first TED round was subsequently followed by specific lectures of expert pulmonary pathologists (AFE, KJ, IP, PAS, FL) concerning all five patterns (25 min each), which were intensively discussed with the audience. The following day, the same pictures of all 40 cases were presented again to the participating pathologists in a second TED round (same conditions) in order to test for resolved or still evident problems in pattern definition according to the IASLC/ATS/ERS consensus.

Statistics

Differences in pattern classification between both evaluation rounds as well as differences in the percentages of voters who did abstain to classify the respective patterns were compared with the non-parametric Wilcoxon test for paired sample analysis. p values<0.05 were considered significant. All statistics were done with SPSS Statistics 19 (IBM, Ehningen, Germany) and with GraphPad Prism 4.03 (GraphPad Software, La Jolla, CA, USA).

Results

Designation of the predominant patterns

The number of votes per case for predominantly lepidic, acinar, papillary, micropapillary, and solid growth patterns for both evaluation rounds was noted. The predominant pattern was designated by definition as the pattern which attained the highest number of votes in the second evaluation round after the discussions. Only if votes for two patterns were equal in the second evaluation, the first evaluation round was included for the calculation in order to designate the predominant pattern.

This resulted in 6 (15 %) cases with a predominantly lepidic, 15 (37.5 %) cases with a predominantly acinar, 10 cases (25 %) with a predominantly papillary, 6 (15 %) cases with a predominantly micropapillary, and 3 (7.5 %) cases with a predominantly solid pattern of ADC. The uneven distribution of cases in the respective pattern groups is explained by the fact that obviously some patterns were deemed more problematic than others by the contributors of cases; these patterns were therefore overrepresented in the test set. In order to allow for a direct comparison of the results with the standards defined, the following sections are headed by a short definition of each pattern according to the IASLC/ATS/ERS.

Problems and pitfalls in the definition of predominant lepidic growth

According to definition, lepidic growth consists of neoplastic cells growing along pre-existing alveolar structures. Papillary or micropapillary patterns and intraalveolar tumor cells are absent [6].

In the first round, 57.4 % of voters classified lepidic predominant cases as being lepidic, and this value increased insignificantly to 59.6 % of voters in the second round (Fig. 1, Table 1; p=1.0). This was the lowest number of consensual votes for all patterns. The most frequent problems occurred in the separation of lepidic from papillary (misclassified by 13.9 % of voters) and acinar (misclassified by 7.6 % of voters) differentiation. The former problem is depicted exemplarily in one of the cases, were the votes for lepidic and papillary were equal in the second evaluation round (Fig. 2a). The number of participants who abstained from voting in the lepidic group was 16.8 %, the highest of all patterns.

Problems and pitfalls in the definition of predominant acinar growth

According to the consensus definition, acinar growth consists of glands which are round to oval-shaped with a central luminal space surrounded by tumor cells. Acinar structures may also consist of aggregates of tumor cells with peripheral nuclear polarization and with central cytoplasm without a clear lumen. When the alveolar architecture is lost and/or myofibroblastic stroma is present, invasive acinar adenocarcinoma is considered present. Cribriform arrangements are also regarded as a pattern of acinar adenocarcinoma [6].

Acinar predominant cases were classified as being acinar by 51.4 % of voters in the first evaluation round (Fig. 1, Table 1). This value increased significantly (p=0.001) to 67.8 % of voters in the second evaluation round. The most problematic pattern to delineate was lepidic with 8.7 % of voters misclassifying, followed by solid (4.9 %) and papillary growth (4.5 %). The separation between acinar and lepidic can be quite challenging, most likely as a consequence of different appraisals concerning the maintenance or the loss of alveolar

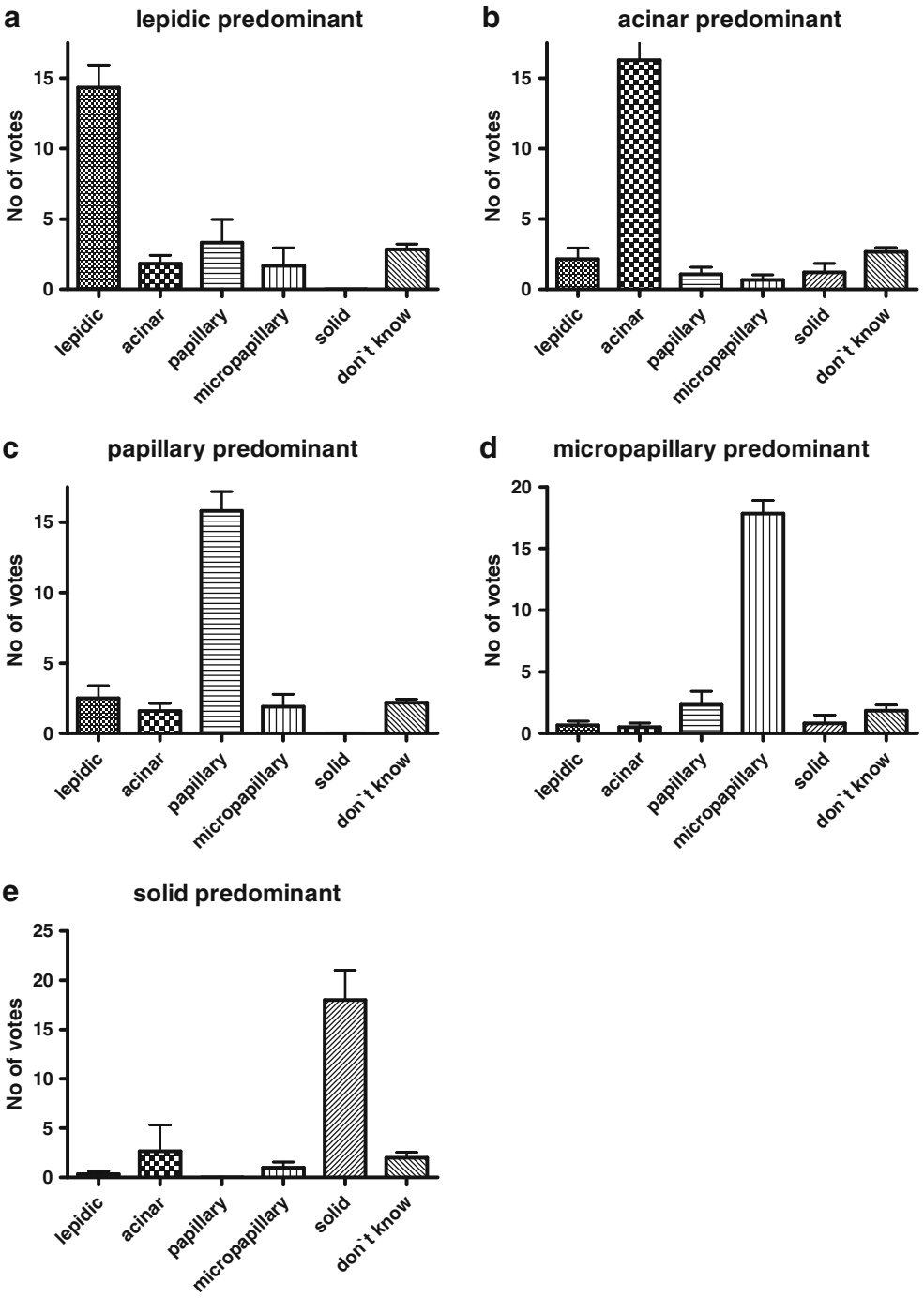

Fig. 1 Number of voters per pattern in the second evaluation round for lepidic predominant (**a**), acinar predominant (**b**), papillary predominant (**c**), micropapillary predominant (**d**), and solid predominant (**e**) cases

structures. Additional histochemical stains can be helpful in this regard. Two typical problematic cases from our set with initially almost equal number of votes for both patterns are shown in Fig. 2b, e.

Problems and pitfalls in the definition of predominant papillary growth

According to the consensus classification, papillary architecture is characterized by growth of columnar cells along central fibrovascular cores. If a tumor has lepidic growth but the alveolar spaces are filled with papillary structures, the tumor is classified as papillary ADC. Myofibroblastic stroma is not needed to diagnose this pattern [6].

Papillary predominant cases were classified as papillary by 63.2 % of pathologists participating in the first round (Fig. 1, Table 1). The proportion of voters who classified these cases as papillary increased insignificantly to 65.8 % in the second round (p=0.887). Following lepidic, this pattern was the second most complicated to classify. Specific

Table 1 Medians, quartiles, means, standard deviations, and percentages of voters per pattern

Predominant growth	Voters	Cases	Median lepidic	Quartiles	Mean lepidic	SD	% of votes	Median acinar	Quartiles	Mean acinar	SD	% of votes	Median papillary	Quartiles	Mean papillary	SD
Lepidic first round	27	6	**15**	**13–18.5**	**15.5**	**3.1**	**57.4**	3	2–5	3.3	1.6	12.3	2.5	0–4.5	2.3	2.3
Lepidic second round	24	6	**14.5**	**10–18.5**	**14.3**	**3.9**	**59.6**	1.5	0.5–3.5	1.8	1.5	7.6	2	0–8	3.3	4.0
Acinar first round	27	15	1	0–6	2.9	3.2	10.6	**14**	**11–18**	**13.9**	**5.3**	**51.4**	1	0–3	1.8	2.4
Acinar second round	24	15	0	0–5	2.1	3.2	8.7	**18**	**11–20**	**16.3**	**5.3**	**67.8**	0	0–2	1.1	1.9
Papillary first round	27	10	0	0–5	2.5	4.0	9.3	0.5	0–3	1.5	2.3	5.4	**17.5**	**12–22**	**17.1**	**5.3**
Papillary second round	24	10	2	0–5.5	2.5	2.9	10.4	1	0.5–2	1.6	1.7	6.7	**16.5**	**11.5–19.5**	**15.8**	**4.4**
Micropapillary first round	27	6	0.5	0–2	0.8	1.2	3.0	1	0–2	1.0	1.1	3.7	1.5	0.5–4.5	2.2	1.9
Micropapillary second round	24	6	0.5	0–1.5	0.7	0.8	2.9	0	0–1.5	0.5	0.8	2.1	2	0–5	2.3	2.7
Solid first round	27	3	0	/	0.0	0.0	0.0	1	/	3.3	4.9	12.2	0	/	0.0	0.0
Solid second round	24	3	0	/	0.3	0.6	1.2	0	/	2.7	4.6	11.2	0	/	0.0	0.0

Predominant growth	% of votes	Median micropapillary	Quartiles	Mean micropapillary	SD	% of votes	Median solid	Quartiles	Mean solid	SD	% of votes	Median abstentions	Quartiles	Mean abstentions %	SD	% of votes
Lepidic first round	8.6	0	0–4	1.3	2.8	4.9	0	0–0	0.0	0.0	0.0	4.5	1.5–7.5	4.5	3.0	16.8
Lepidic second round	13.9	0.5	0–4.5	1.7	3.1	7.2	0	0–0	0.0	0.0	0.0	2.5	2–4	2.9	1.0	11.7
Acinar first round	6.7	0	0–1	0.9	1.9	3.3	0	0–5	3.3	5.6	12.1	4	3–6	4.2	2.1	15.9
Acinar second round	4.5	0	0–1	0.7	1.4	2.8	0	0–2	1.2	2.4	4.9	3	2–4	2.6	1.2	11.3
Papillary first round	**63.2**	0.5	0–2.5	1.8	3.7	7.0	0	0–0	0.0	0.0	0.0	4	2.5–5.5	4.1	1.8	15.1
Papillary second round	**65.8**	1	0–3	1.9	2.8	7.9	0	0–0	0.0	0.0	0.0	2	1.5–3	2.2	0.8	9.2
Micropapillary first round	8.1	**16**	**13–23.5**	**17.5**	**4.8**	**64.8**	0	0–4	1.3	2.8	4.8	5	1.5–6	4.2	2.3	15.6
Micropapillary second round	9.6	**17**	**16–20.5**	**17.8**	**2.6**	**74.2**	0	0–2.5	0.8	1.6	3.3	2	0.5–3	1.9	1.2	7.9
Solid first round	0.0	0	/	0.0	0.0	0.0	**22**	/	**19.7**	**4.0**	**73.0**	4	/	4.0	1.0	14.8
Solid second round	0.0	1	/	1.0	1.0	4.2	**21**	/	**18.0**	**5.2**	**75.0**	2	/	2.0	1.0	8.4

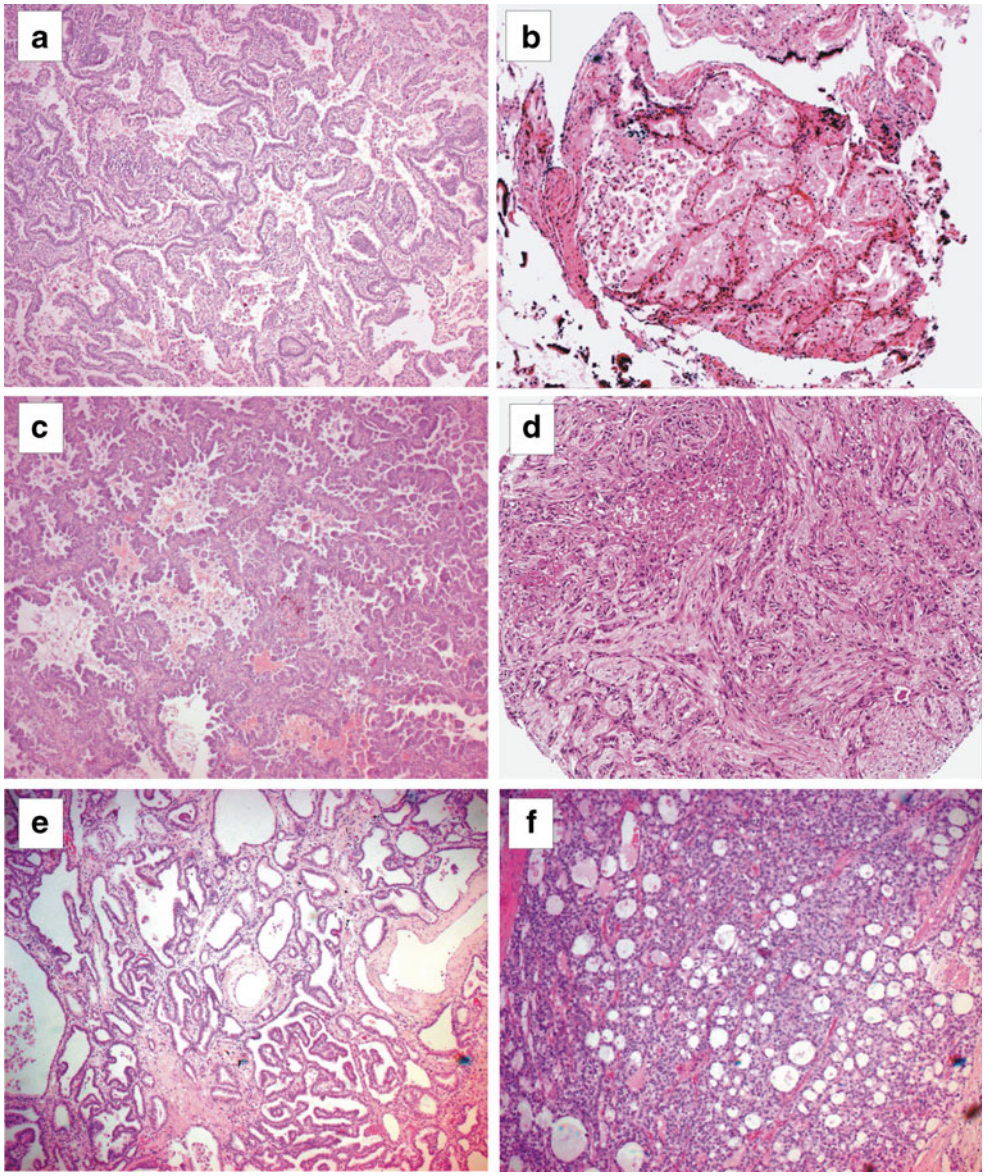

Fig. 2 Exemplary images of cases with difficulties in pattern classification. **a** The problem in the delineation of cross cut alveolar walls from true papillae in the separation of lepidic from papillary growth. We believe that this case is still lepidic. **b** A problematic case in the separation between lepidic and acinar differentiation. In such cases, the presence of desmoplastic stroma whose visualization can be enhanced by the use of elastic stains is helpful to decide whether the alveolar structure is still maintained or already lost. **c** An exemplary case to depict difficulties in the separation between papillary structures from micropapillary growth. Here some of the secondary structures still have fibrovascular cores while others had not. In this case, we would opt for micropapillary predominance. **d** Parts of a predominant "collapsed" acinar ADC with extensive desmoplastic stromal reaction. The aggregates of tumor cells tend to have peripheral nuclear polarization with central cytoplasm. However, clear lumina are hardly visible. This obviously is challenging with respect to the separation of acinar and solid growth. **e** A case with difficulties in the separation of acinar from lepidic structures. Since the overall architecture is largely maintained, one might rather classify this case as lepidic predominant. **f** A case where solid tumor cell nests contain a moderate amount of lumina. In such cases, problems in the differential between acinar and solid growth may occur. One might rather classify this case as acinar (cribriform) predominant. For further examples with comments for all cases of this study, please refer to the online tutorial mentioned in the text

problems arouse with lepidic (10.4 % of voters), micropapillary (7.9 %), and acinar (6.4 %) misclassifications. A problematic case depicting the difficult differential between papillary and micropapillary is shown in Fig. 2c (see below).

Problems and pitfalls in the definition of predominant micropapillary growth

According to the IASLC/ATS/ERS definition, micropapillary growth is characterized by tumor cells growing in micropapillary

tufts which lack fibrovascular cores. The tumor cells may appear detached and/or connected to alveolar walls. The tumor cells are usually small and cuboidal with minimal nuclear atypia. Ring-like glandular structures which "float" within alveolar spaces are regarded as micropapillary as well [6].

The predominantly micropapillary pattern was classified as micropapillary by 64.8 % of voters in the first round. This value increased insignificantly to 74.2 % of voters in the second evaluation round (Fig. 1, Table 1; $p=0.194$). This pattern thereby was the second most reliable to classify. Misclassifications usually occurred in the differential diagnosis from papillary growth, usually when both differentiation patterns were intermixed in one area (Fig. 2c).

Problems and pitfalls in the definition of predominant solid growth

According to the consensus criteria, solid growth is characterized by polygonal tumor cells forming sheets which lack other recognizable patterns of adenocarcinoma, i.e., acinar, papillary, micropapillary, or lepidic growth [6]. The solid pattern was the easiest to classify and the one with the highest percentages of consensual votes in both the first round (73 %) as well as the second round (75 %) (Fig. 1, Table 1; $p=0.564$). When problems occurred, they were usually with acinar growth (11.2 % of misclassifications) either when nests of cells without clearly discernable lumina were present or in cribriform tumor areas. The former issue is depicted in Fig. 2d, the latter in Fig. 2f. In addition, problems in the differential diagnosis of solid versus micropapillary pattern (4.2 %) occurred in cases where the alveolar spaces were filled with discohesive tumor cell aggregates. It must be mentioned that pure solid ADC diagnosis in the routine setting requires mucin stains, which were not used in this study for reasons of practicability (preselection of cases was done including mucin stains).

Accuracy of classification

As mentioned above, educational sessions improved identification of acinar as well as micropapillary patterns (Fig. 3). For lepidic, papillary, and solid growth, the single discussion session did not result in a statistically significant improvement of consensus. As a consequence, the overall number of misclassifications decreased only slightly but significantly ($p=0.001$, Fig. 3). As a second important consequence of the discussions, the number of participants who did initially abstain from voting for a specific pattern decreased in all pattern groups as well as overall (Fig. 3). These differences were statistically significant for acinar ($p=0.006$) and papillary ($p=0.010$) patterns and for the overall classification ($p<0.001$). The differences failed to reach statistical significance for lepidic ($p=0.104$), micropapillary ($p=0.056$), and solid growth ($p=0.109$).

Discussion

The novel IASLC/ATS/ERS classification of lung ADC has been shown to have impact on overall, disease-specific, and disease-free survival in several retrospectively analyzed patient cohorts from all over the world [7–10]. In addition, there are hints that this classification based on predominant patterns might have predictive value with respect to radio/chemotherapy response [9]. All this strongly points to the potential clinical usefulness of this simple, cheap, and effective way to classify these neoplasms.

However, prior to clinical use, harmonization of diagnostic standards and testing for reproducibility of such a novel classification is mandatory. Specifically, it is essential to show that intra- and interobserver reproducibility is adequate and that the classification can reliably be used in daily routine practice. To test for these factors and to improve the conformity of pattern interpretation, we held a nationwide meeting of pulmonary pathologists in Heidelberg, Germany, where we discussed difficult cases and probed for our respective standards. Our study aimed to measure agreement in the interpretation of complex patterns among a large group of pulmonary pathologists. To address this, the selection of specific tumor areas by photomicrographs was chosen as the most reliable approach. We did not aim for an emulation of the real world diagnostic setting. The latter has been done in a complementary study which we recently published on this topic [11], which comprised of a full slide evaluation of 100 unselected cases by a limited number of reviewers, while in the present study we focused on the presentation of a smaller number of selected problematic tumor areas with a higher number of voters (up to 27). It is evident that a selected photomicrograph shows only small parts of a tumor compared to full slide evaluation, which might influence the interobserver agreement reported.

The way the "reference" for the designation of the predominant pattern was set in our study merits discussion. We feel that the best way to define such a reference is to rely on the majority votes of a large number of pulmonary pathologists after they discussed the novel IASLC/ATS/ERS classification together. Alternative strategies to define the "correct" pattern classification, notably the use of an "expert opinion" as standard, have limitations given that for some of the cases a majority of trained pulmonary pathologists might have a different opinion than the "expert panel". In addition, the "expert" approach would not allow for the incorporation of a variety of different views.

In our present study, we demonstrate that the evaluation of histological patterns in pulmonary ADC leads to a quite

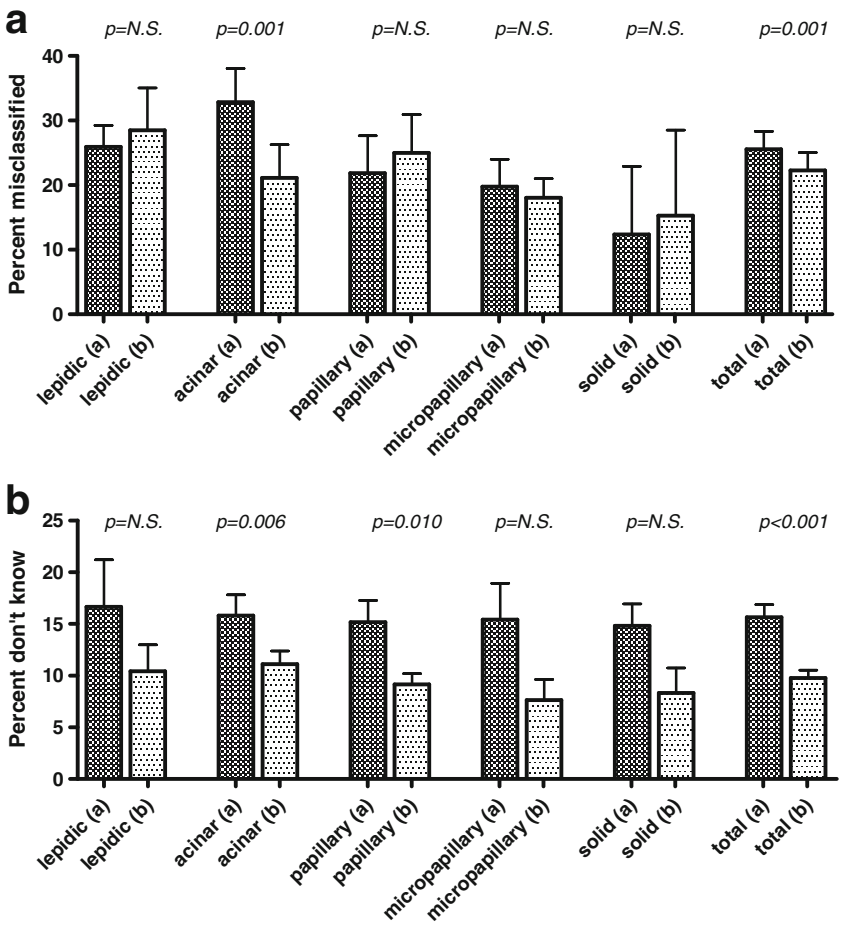

Fig. 3 Percentage of voters per pattern (**a**) as well as percentage of voters who abstained (**b**) overall and per pattern. N.S. = not significant

fair overall consensus. The notion that the consensus for the predominant pattern is indeed surprisingly high is in line with our data from the only other yet published study on this topic [11]. When focusing on difficult cases, we found that especially separation of lepidic and papillary patterns but also the clear-cut separation of both patterns from the acinar pattern is quite hard to achieve with a sufficiently high consensus level. The observation that papillary growth is difficult to determine and somewhat hard to delineate from lepidic growth (true papillae versus cross sections of branching alveolar walls) and micropapillary growth (often intermixed with papillary growth) is also supported from our previous work [11]. Solid growth did not pose any problems. In contrast, lepidic growth was problematic to evaluate when only difficult cases were considered, specifically the distinction from papillary growth (see above) and acinar growth (neoplastic acini with desmoplastic stroma versus pre-existing alveolar structures with thickened septa) was tricky. In the previous study on unselected cases, the consensus results for the lepidic pattern were fairly high [11]. This discrepancy might be explained by the fact that specifically in difficult tumor areas (as selected in this study) lepidic predominant pattern can be very challenging.

In our study, we demonstrated that training sessions for pattern classification are beneficial in two regards. First, they significantly decrease the number of evaluators who are unsure how to classify a given growth pattern and therefore providing support in the daily diagnostic challenge. Second, training sessions increase consensus [11]. Also for other tumor entities, including Gleason grade in prostate cancer [12], Elston–Ellis grade in breast cancer [13], and grading of sarcomas [14], training significantly increases the quality of the histopathological evaluation of grading schemes. Our data underline the value of expert discussions in order to ultimately improve the consensus of ADC pattern classification among pathologists. However, the modesty of improvement also indicates that for specific problems in pattern definition, we still have to do a more in-depth training effort either slide based or based on photomicrographs.

Our study shows that consensus approaches are possible on a nationwide level and provide a useful starting point for further discussions on this topic. However, what we clearly need is an international harmonization of pattern evaluation and a comparison with the results presented here. To support this, we set up a website in English dedicated to this topic:

(http://www.klinikum.uni-heidelberg.de/Online-Tutorial-for-Pulmonary-Adenocarcinoma-Subtyping.125267.0.html).

The website includes a database of ADC images (including the ones used in this study) and participants might give their own opinion on specific difficult cases. It can be easily reached through the homepage of the Institute of Pathology of the University Heidelberg. After the vote for the predominant pattern, one can see the consensus pattern according to all other participators Pathologists all over the world are very much invited to upload images of difficult ADC pattern to be included into the database. Thereby, we hope to contribute to the necessary discussions in this field of pathology. Such approaches have been shown to be successful in comparable fields of diagnostic surgical pathology such as Gleason grading in core needle biopsies [12].

In summary, we found that the novel IASLC/ATS/ERS classification of lung ADC can be applied with reasonable concordance even in difficult cases. In addition, we confirmed that discussions and training might overcome insecurities on how to classify and increase the congruence.

Conflicts of interest None.

References

1. Jemal A, Siegel R, Xu J, Ward E (2010) Cancer statistics. CA Cancer J Clin 60:277–300
2. Coindre JM (2006) Grading of soft tissue sarcomas: review and update. Arch Pathol Lab Med 130:1448–1453
3. Cross SS (1998) Grading and scoring in histopathology. Histopathology 33:99–106
4. Gleason DF, Mellinger GT (1974) Prediction of prognosis for prostatic adenocarcinoma by combined histological grading and clinical staging. J Urol 111:58–64
5. Langer CJ, Besse B, Gualberto A et al (2010) The evolving role of histology in the management of advanced non-small-cell lung cancer. J Clin Oncol 28:5311–5320
6. Travis WD, Brambilla E, Noguchi M et al (2011) International association for the study of lung cancer/american thoracic society/european respiratory society international multidisciplinary classification of lung adenocarcinoma. J Thorac Oncol 6:244–285
7. Russell PA, Wainer Z, Wright GM et al (2011) Does lung adenocarcinoma subtype predict patient survival?: a clinicopathologic study based on the new international association for the study of lung cancer/american thoracic society/european respiratory society international multidisciplinary lung adenocarcinoma classification. J Thorac Oncol 6:1496–1504
8. Sica G, Yoshizawa A, Sima CS et al (2010) A grading system of lung adenocarcinomas based on histologic pattern is predictive of disease recurrence in stage I tumors. Am J Surg Pathol 34:1155–1162
9. Warth A, Muley T, Meister M et al (2012) The novel histologic IASLC/ATS/ERS classification of invasive pulmonary adenocarcinoma is a stage-independent predictor of survival. J Clin Oncol 30:1438–1446
10. Yoshizawa A, Motoi N, Riely GJ et al (2011) Impact of proposed IASLC/ATS/ERS classification of lung adenocarcinoma: prognostic subgroups and implications for further revision of staging based on analysis of 514 stage I cases. Mod Pathol 24:653–664
11. Warth A, Stenzinger A, von Brünneck A-C et al (2012) Interobserver variability in the application of the novel IASLC/ATS/ERS classification. Europ Resp J. doi:10.1183/09031936.00219211
12. Kronz JD, Silberman MA, Allsbrook WC et al (2000) A web-based tutorial improves practicing pathologists' Gleason grading of images of prostate carcinoma specimens obtained by needle biopsy: validation of a new medical education paradigm. Cancer 89:1818–1823
13. Robbins P, Pinder S, de Klerk N et al (1995) Histological grading of breast carcinomas: a study of interobserver agreement. Hum Pathol 26:873–879
14. Coindre JM, Trojani M, Contesso G et al (1986) Reproducibility of a histopathologic grading system for adult soft tissue sarcoma. Cancer 58:306–309

Virchows Arch (2012) 461:195–204
DOI 10.1007/s00428-012-1269-0

ORIGINAL ARTICLE

Feasibility and clinical utility of intraoperative consultation with frozen section in osseous lesions

Murat Sezak · Basak Doganavsargil · Burcin Kececi · Mehmet Argin · Dundar Sabah

Received: 18 December 2011 / Revised: 26 May 2012 / Accepted: 13 June 2012 / Published online: 8 July 2012
© Springer-Verlag 2012

Abstract Intraoperative consultation (IOC) with frozen section (FS) allows the surgeon to make therapy decisions during the operation. However, there is relatively little information on the use of IOC in skeletal lesions. We performed a retrospective study to examine the indications for IOC and compare the histological findings of FS and permanent paraffin section (PS) results to determine its clinical benefits. Ninety-seven consecutive cases evaluated between 2008 and 2011 were retrieved from IOC archives of our Pathology Department. In 79 % of the cases, there was no prior core needle biopsy (CNB), and IOC was performed to confirm the clinical or radiological diagnosis. In 5 (5 %) cases, no definitive result could be obtained with FS, and diagnosis was deferred. The reasons for a deferred diagnosis (DD) included poor section quality in two lipomatous lesions and the sample heterogeneity in the others. When adjusted for DD, FS and PS results showed 100 % concordance in terms of discriminating "benign vs. malignant" and defining diagnostic categories as "benign non-tumoral," "benign tumoral/tumor-like," "malignant primary tumor," "malignant metastatic tumor," or "hematopoietic malignancy." The presence of non-sclerotic osseous tissues does not have a significant adverse impact on the FS section quality and diagnosis made by FS. Thus, sections with diagnostic value can be obtained from bone lesions via FS. In this study, specific diagnoses were made in 88 % of the cases. We believe that IOC with FS can be safely performed in tertiary referral centers where there is a multidisciplinary team working in collaboration.

Keywords Frozen section · Intraoperative consultation · Skeletal lesions · Bone tumor

M. Sezak (✉) · B. Doganavsargil
Department of Pathology, Ege University Faculty of Medicine, 35100 Bornova, Izmir, Turkey
e-mail: murat.sezak@ege.edu.tr

B. Kececi · D. Sabah
Department of Orthopaedics Surgery, Ege University Faculty of Medicine, Izmir, Turkey

M. Argin
Department of Radiodiagnostics, Ege University Faculty of Medicine, Izmir, Turkey

Introduction

The frozen section (FS) technique is utilized for intraoperative consultation (IOC) in many fields of surgical pathology. The major indication of FS is to obtain a diagnosis of an unknown pathological process to distinguish malignant from benign lesions intraoperatively [1]. It is also used to determine the adequacy of resection margins, tumor spreading, lymph node status [2], presence of residual tumor or recurrences, and to identify the content and/or adequacy of the specimen for definitive diagnosis. The reported concordance rate between FSs and permanent paraffin sections (PS) vary between 89 % and 98.3 % in many organ systems [3–10]. However, there is relatively little information regarding the use and efficacy of IOC in bone pathology [11–13].

Tumors or tumor-like lesions of bone and, in particular, primary malignant bone tumors are uncommon lesions that require a multidisciplinary approach for proper diagnosis and management. The diagnostic approach to a bone lesion requires a comprehensive clinical history, physical examination, and radiological evaluation. Moreover, it is essential that suspicious lesions undergo a histopathologic assessment and are treated accordingly [14]. Percutaneous core needle biopsy (CNB) has widely been accepted as the standard diagnostic

tool for such lesions due to its relative ease of application, safety, and cost-effectiveness [15]. In light of the CNB results, benign or metastatic lesions are managed with follow-up and/or treatment by lesional surgery, whereas certain primary sarcomas of the bone (e.g., osteosarcoma, Ewing sarcoma) are treated with neoadjuvant chemotherapy and/or radiotherapy followed by wide resection and limb-salvage surgery. In cases of inadequate material or a suspicious diagnosis in CNB, an open biopsy is recommended.

In the majority of the bone lesions, the histopathologic diagnosis and treatment decisions are generally made prior to curative surgery. IOC is primarily used in bone pathology to assess the efficacy of biopsy [16] by ascertaining whether the obtained diagnostic tissue is sufficient for the evaluation of the permanent section. Other indications include confirming an infection when septic loosening is suspected in joint prosthesis [17–19] and evaluating bone marrow margins to rule out intramedullary tumor extension [20,21].

We conducted a retrospective study at our regional tertiary referral centre to review our IOC experience, evaluate the clinical indications for IOC, compare the concordance rates of FS with PS results, determine the number of cases where it was possible to establish a specific diagnosis, and determine the effect of tissue content on section quality and its ability to yield a diagnosis.

Materials and methods

In this study, we reviewed 97 consecutive cases retrieved from IOC archives of our Pathology Department FS files between 2008 and 2011.

Intraoperative consultation

In our center, clinical and radiological findings of all the bone lesions are evaluated by a multidisciplinary council consisting of an orthopedic surgeon, a pathologist, a radiologist, medical and radiation oncologists, and nuclear medicine specialists. The primary objective of the IOC for the selected cases was also identified in this council.

All of the samples were performed, in accordance with open biopsy procedures for suspicious malignant bone lesions, by a surgical team experienced in orthopedic oncology. Pathological assessment was either performed by or in consultation with pathologists competent in osseous pathologies.

Preparation of FS

Tissue samples consisting of trabecular bone fragments with minimal thickness or soft tissue components representing the lesion were selected for freezing and subsequent cutting. Large cortical bone fragments were not sampled even if they were present in the material. In order to reduce the amount of tissue with in evitable freezing artifacts in permanent sections, the tissue was not completely frozen unless the first sample was inadequate for defining the lesion. Selected tissues were frozen at −35 °C with Thermo Scientific Cryotome FSH and fixed with 80 % alcohol for 1 min after 4–8 μm thick sections were obtained. Manual hematoxylin-eosin staining was performed as follows: 1 min of hematoxylin staining, rinsing with distilled water, 5 s of differentiation with acid alcohol, rinsing, 30 s of eosin staining, rinsing, alcohol dehydratation, and xylene treatment to increase transparency and mounting with Entellan.

Reporting of IOC findings

Cases were initially evaluated for the diagnostic adequacy of material and subsequently categorized as “benign non-tumoral,” “benign tumoral/tumor-like,” “malignant primary sarcoma,” “metastatic tumor,” or “hematopoietic malignancy” as previously discussed in the above mentioned multidisciplinary council to determine the type of therapeutic surgery. When frozen sections were equivocal in diagnosis, the case was assigned a “deferred diagnosis” (DD) status. Subsequent PS was performed for definitive diagnosis. In most of studied subjects, the IOC also provided a comment regarding the final diagnosis (e.g., benign, tumor/tumor-like lesion, consistent with fibrous dysplasia).

Evaluation of the technical quality of the FS

All FS samples were retrospectively evaluated and their tissue content (presence of bone and/or soft tissue) was recorded. The section quality was also semi-quantitatively classified as “good quality” if it was comparable with permanent sections, or “low quality” if the sections were too thick, fragmented, corrugated, or if the staining was suboptimal for evaluating nuclear and cytoplasmic details. The effect of tissue content on section quality and its ability to yield a diagnosis were also examined.

Comparison of FS and PS results and statistical analysis

Clinical and radiological data, the indication for IOC, as well as FS, PS, and CNB results were retrieved from the files of the departments of Orthopedics, Radiodiagnostics, and Pathology. The SPSS 13.0 software was used for descriptive analyses and kappa calculations.

Results

A total of 97 subjects (48 female, 49 male) with a mean age of 33.2 years (22.1 SD) were included in the study.

Table 1 IOC indications

	Frozen section results						
	Benign		Malignant			DD	Total n, (%)
	Non-tumoral	Tumoral/tumorlike lesion	Primary sarcoma	Metastatic	Hematopoietic Tm		
IOC performed for diagnosis and treatment							
To confirm the clinical/radiological diagnosis in cases without a prior CNB							77 (79 %)
Excluding primary malignancy in benign considered cases	7	29	2	1		1	40 (41.2 %)
Excluding primary malignancy in suspected cases of metastasis				7	1		8 (8.2 %)
Identify the cause of pathologic fracture	6	5	1	4	1		17 (17.5 %)
Determining the cause of prosthetic loosening (infection/tumor recurrence)	9	2				1	12 (12.4 %)
To confirm the clinical/radiological diagnosis and tumor spread in cases with a prior CNB							20 (20.6 %)
Cases with non-diagnostic CNB	3	1	1			2[a]	7 (7.2 %)
Cases with disconcordant clinical and radiological findings with CNB[a]		6					6 (6.2 %)
Cases in which the benign-malignant discrimination cannot be made with CNB						1	1 (1 %)
Lymph node evaluation (evaluation of primary bone tumor spread)	3		2				5 (5.1 %)
Surgical margin evaluation (evaluation of primary bone tumor spread)			1				1 (1 %)
Total	28	43	7	12	2	5	97 (100 %)

DD Deferred diagnose

[a] Two intraosseous lipoma cases

Diagnoses by FS were 71 benign (73 %), 21 malignant (22 %), and 5 DD (5 %).

IOC was performed for diagnosis and treatment in 91 cases and for the evaluation of tumoral spread in 6 previously diagnosed cases. The indications for IOC and FS results are shown in Table 1. Of the 91 cases undergoing IOC for diagnostic and therapeutic purposes, 14 had CNB prior to IOC. Of these, seven had inadequate non-diagnostic biopsies, and six underwent open biopsy/IOC due to discordance between the CNB diagnosis with clinical and radiological findings; in one case, the reason was the failure to discriminate between malignant and benign histology. For the six cases, the results of FS were consistent with CNB and the lesions were excised/or curetted in the same session as the diagnosis of "benign tumor/tumor-like lesion category". The diagnosis remained unchanged after subsequent excision/curettage specimens. In two cases with non-diagnostic CNB, and one additional case in which the benign-malign discrimination could not be made by CNB, the FS also failed to yield a diagnosis and these cases were referred to as a "DD." Subsequent PS of the former two cases provided diagnoses of intraosseous lipomas.

In the 77 patients who did not have a CNB, indications for IOC included: (1) to exclude primary malignancy in a case of "benign" diagnosis on clinical and radiological grounds (n=40, 52 %); (2) to identify the cause of pathological fracture (n=17, 22 %); (3) to exclude primary bone malignancy in cases with clinically suspected carcinoma metastasis (n=8, 10 %); and (4) to determine the cause of prosthetic loosening (infection/tumor recurrence) (n=12, 16 %) (Table 1). Among the "pre-IOC benign considered" cases, 16 involved patients under 10 years of age who required general anesthesia for CNB, and in five cases, the lesion was located in the acetabulum, where it was technically difficult to reach with CNB. In this group, one case was diagnosed as pleomorphic sarcoma, whereas another was diagnosed as squamous cell carcinoma metastasis, although both were initially diagnosed as osteomyelitis on a clinical and/or radiological basis. An additional case suspicious for "osteoblastoma" was radiologically diagnosed as pleomorphic sarcoma by FS. Among the 17 cases sent for IOC to identify the cause of pathological fracture, six cases were determined to be malignant, whereas one was revealed as a primary sarcoma.

Of the 97 total samples, 28 were classified as benign/non-tumoral (29 %), 43 as benign tumor/tumor-like lesion (44 %), 2 as malignant tumor of hematopoietic origin (2 %), and 12 as metastatic carcinoma (12.4 %). Seven cases were diagnosed as malignant primary sarcoma, of which four were primary diagnoses and three were metastases and/or surgical margin invasion by a primary bone sarcoma (Table 2). A diagnosis of prosthetic infection was made in six cases with prosthetic loosening (infection/tumor recurrence group) in the benign non-tumoral group. However, in one case, in tissues selected for FS, the appearance was suggestive of reactive-reparative changes related with prosthetic wear and tear but failed to prove infection, whereas the remaining tissue subsequently submitted for PS showed prosthetic infection.

In five cases (5 %), no definitive result could be obtained with FS (DD) (proportion=0, 0515 with exact confidence interval=0.017–0.12). DD cases were diagnosed as chondroblastoma, giant cell tumor, chondrosarcoma, and intraossous lipoma in two cases according to their PS results. A comparison between FS and PS showed a 100 % concordance (kappa=1) following adjustment for DD, both with regard to the technique's ability to discriminate between benign and malignant lesions and in terms of diagnostic category. A comparison between the techniques for

Table 2 Comparison of FS/PS diagnostic categories

			Frozen section results						Total
			Benign		Malignant			DD	
			Non-tumoral	Tumoral Tumorlike	Primary sarcoma	Hematopoietic Tm	Metastatic		
Parafine section results	Benign	Non-tumoral	28 100 %						28
		Tumoral/Tumorlike		43 91.5 %				4	47
	Malignant	Primary sarcoma			7[a] 87.5 %			1	8
		Hematopoietic Tm				2 100 %			2
		Metastatic					12 100 %		12
	Total		28	43	7	2	12	5	97

DD Deferred diagnose

[a] Three case of primary sarcoma was sent to IOC for evaluation of invasion/metastasis after neoadjuvant treatment

Table 3 Details of diagnostic categories in respect to frozen section and paraffin section results

			Paraffin section results											
			Benign—tumor/tumorlike											Benign - Non Tumoral
			Chondroma	Chondroblastoma	Osteoblastoma	Giant cell tumor	Desmoplastic fibroma	Non-ossifying fibroma	Fibrous dysplasia	Bone cysts	Giant cell reparatif granuloma	Lipoma	Langerhans Cell Histiocytosis	Normal Tissue/ non Diagnostic
Frozen section results	Benign—tumor/tumorlike	Chondroma	3											
		Chondroblastoma		4										
		Osteoblastoma			1									
		Giant Cell Tumor				4								
		Desmoplastic fibroma												
		Non-ossifying fibroma						4						
		Fibrous dysplasia					1		5					
		Bone cysts								9				
		Giant cell reparatif granuloma								1	2			
		Lipoma												
		Langerhans cell histiocytosis											8	
		Probably benign tm				1								
	Benign—non-tumoral	Normal tissue/non-diagnostic												2
		Osteomyelitis												
		Reparatif changes												
		Prostheses infection												
		Callus												
		Cyst hydatic												
		Non-metastatic LN												
	Malign primary	Pleomorphic sarcoma												
		Chondrosarcoma												
		Metastatic LN/invasion (primary)												
	Malign other	Lymphoma												
		Plasma cell myeloma												
		Carcinoma metastasis												
		DD		1		1						2		
	Parafine section results total		3	5	1	5	1	4	5	10	2	2	8	2

			Paraffin section results													
			Benign - Non Tumoral						Malign Primary			Malign Other				
			Osteomyelit	Reparatif Changes	Prostheses Infection	Callus	Cyst Hydatic	Non Metastatic LN	Pleomorphic Sarcoma	Chondrosarcoma	Metastatic LN/ invasion (primary)	Lymphoma	Plasma Cell Myeloma	Carcinoma Metastasis	Frozen Section Results Total
Frozen section results	Benign—tumor/ tumorlike	Chondroma													3
		Chondroblastoma													4
		Osteoblastoma													1
		Giant Cell Tumor													4
															0

Table 3 (continued)

		Paraffin section results												
		Benign - Non Tumoral						Malign Primary			Malign Other			
		Osteomyelit	Reparatif Changes	Prostheses Infection	Callus	Cyst Hydatic	Non Metastatic LN	Pleomorphic Sarcoma	Chondrosarcoma	Metastatic LN/ invasion (primary)	Lymphoma	Plasma Cell Myeloma	Carcinoma Metastasis	Frozen Section Results Total
	Desmoplastic fibroma													
	Non-ossifying fibroma													4
	Fibrous dysplasia													6
	Bone cysts													9
	Giant cell reparatif granuloma													3
	Lipoma													0
	Langerhans cell histiocytosis													8
	Probably benign tm													1
Benign—non-tumoral	Normal tissue/non-diagnostic													2
	Osteomyelitis	2												2
	Reparatif changes	2	11	1										14
	Prostheses infection			5										5
	Callus				1									1
	Cyst hydatic					1								1
	Non-metastatic LN						3							3
Malign primary	Pleomorphic sarcoma							3	1					4
	Chondrosarcoma													0
	Metastatic LN/ invasion (primary)									3				3
Malign other	Lymphoma										1			1
	Plasma cell myeloma											1		1
	Carcinoma metastasis												12	12
	DD								1					5
Parafine section results total		4	11	6	1	1	3	3	2	3	1	1	12	97

DD Deferred diagnose

definitive diagnosis obtained from the FS and PS records showed that a final diagnosis could be achieved in 85 of the 97 cases (88 %) (Table 3). Five of these 12 low concordance cases were DD cases. Among the other seven cases, one case was diagnosed as pleomorphic cell sarcoma through FS, PS showing a dedifferentiated chondrosarcoma. Other diagnostic entities with low concordance were fibrous lesions, giant cell lesions, and reparative tissues with a heterogeneous character. In two cases classified as having reparative changes with FS, on PS osteomyelitis or prosthesis infection were diagnosed. When the effects of section quality on FS results were examined, "good quality" was obtained in 79 cases (81 %) and "low quality" in 18 (19 %) (Table 4). Of these low quality cases, 11 samples (21 %) contained bone tissue and 7 (16 %) consisted of soft tissue alone. The presence of bone tissue in the sample did not have a significant effect on the section quality (p=0.541). Of the soft tissue samples with low section quality, two had non-evaluable tissue content with a diagnosis of intraosseous lipoma in paraffin sections.

Discussion

As suggested by Rosai [22], FS is a crucial but difficult procedure requiring experience, a good knowledge of clinical medicine and pathology, an ability to make quick decisions under time constraints, good judgment skills, an attitude that is conservative but not excessively so, and an awareness of methodological limitations.

In the present study, 92 of 97 cases exhibited full-concordance between FS and PS in terms of discriminating benign versus malignant. Similar results were also achieved in categorizing the lesions as "benign non-tumoral," "benign tumoral/tumor-like," "malignant primary tumor," "malignant metastatic tumor," or "hematopoietic malignancy". The concordance rate was 100 % following adjustment for five cases with DD (deferral rate, 5 %). Regarding the final diagnosis, a specific diagnosis could be made in 88 % of the cases. Overall, our results were comparable with the published approximate concordance, discordance, and deferral rates of 98 %, 2 %, and 4 %, respectively, for many organ systems [5]. Although there is relatively little information on the concordance rates in bone pathology, previous studies report a diagnostic accuracy varying between 90 % and 96.5 %, and a specific diagnosis between 85.9 % and 86.3 % [2,13,23], which is very similar to our findings.

Despite the reassuring results, the role of IOC in bone pathology is limited in clinical practice, largely due to histopathological evaluation with CNB and the therapeutic decision made prior to curative surgery. Furthermore, primary bone sarcomas, such as osteosarcoma and Ewing sarcoma, are treated with neoadjuvant chemoradiotherapy prior to surgical resection. During the study period of 3 years, 611 CNB evaluations were conducted in our center. However, review of the IOC cases over the same period showed that in 65 of 97 cases, FS was preferred for diagnostic purposes (i.e., benign considered cases, suspected metastasis cases, pathological fractures). Most centers can assess clinically and radiologically unsuspected cases where the multidisciplinary team opts for curettage or total excision without a CNB. This approach may also apply to some of our cases. This is also one of the reasons for the relatively high number of IOC cases without a core needle biopsy in our series, many of which were referred to our center for surgery without performing a CNB beforehand. For those clinically and radiologically unsuspicious cases, if the decision is in favor of curettage or total excision without a CNB, IOC is used as a "histological check" before final surgery. In benign assessed deep-seated tumoral/tumor-like lesions or very young patients who require general anesthesia for CNB, this approach is also preferred. Twenty-one of the 40 cases which were considered benign exhibited these features. As a result of this approach, two cases, which were initially evaluated as "osteomyelitis," were finally diagnosed as osteosarcoma and squamous cell carcinoma. One case involved tissue that was located within the acetabulum and was previously considered to be an "aggressive osteoblastoma"; this case was also initially diagnosed as osteosarcoma by FS. An additional primary sarcoma was found

Table 4 FS section quality/FS tissue content and diagnostic ability of FS

Frozen section quality					
	Tissue type		Total	FS diagnose	
	Soft tissue	Bony tissue		Diagnosed	DD
Low	7[a]	11	18	16	2[a]
	15.9 %	20.8 %	18.6 %	88.9 %	11.1 %
High	37	42	79	76	3
	84.1 %	79.2 %	81.4 %	96.2 %	3.8 %
Total	44	53	97	92	5
	45.4 %	54.6 %	100.0 %	94.8 %	5.2 %

DD Deferred diagnose, *FS* Frozen section

[a]Two intraosseous lipoma cases

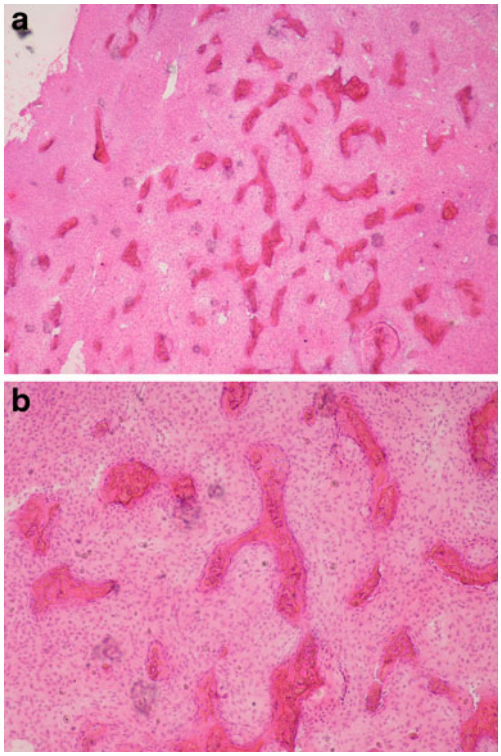

Fig. 1 **a**–**b** Osteofibrous dysplasia: preserved architecture of properly cut metaplastic bone. Note the few hematoxylin remains (**a** HE. ×40, **b** HE. ×200)

among the pathological fracture group. Thus, the diagnosis of primary sarcoma with FS provided the surgical team with the opportunity to design a detailed treatment plan consisting of neoadjuvant therapy following resection to be undertaken under elective conditions. When prior CNBs were discordant with clinical and radiological findings, IOC confirmed the prior CNB diagnosis. In the "benign tumor/tumor-like lesion category," FS was used as an alternative to open biopsy and enabled the surgeon to complete the therapeutic surgery (excision or curettage) during the same session. However, in 2 of 7 cases with non-diagnostic CNB, FS did not provide a diagnosis. Due to the lipomatous

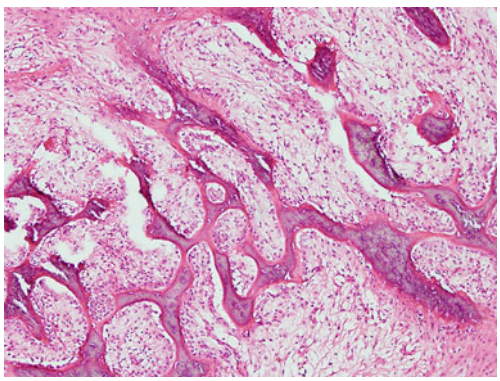

Fig. 2 Fracture healing: cellular details of osteoblasts. The osteoclasts are easily observed (HE. ×200)

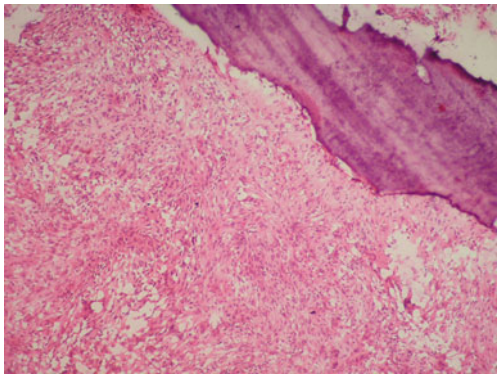

Fig. 3 Fibrous cortical defect: Note the thick cortical bone and preserved cortico-medullary junction (HE. ×200)

nature of the lesions, both cases were classified as "DD" due to technical limitations. The other three samples in the DD category were chondroblastoma, giant cell tumor, and low grade chondrosarcoma according to their subsequent PS results. The failure to make a diagnosis with FS in these samples was due to the tissue characteristics, which required multiple samples, rather than poor section quality. However, in one prosthetic infection case, which was "missed" by FS, the tissues selected for freezing were not representative; however, the FS diagnosis could have been resolved by submitting additional tissue or the specimen entirely, although the pathological foci in subsequent PS were small and could just as easily have been overlooked.

The common belief shared by many surgical pathologists is that frozen section examination is not feasible on osseous lesions due to difficulties associated with histological assessment and tissue consistency, i.e., hardness. However, many bone lesions and tumors are associated with bone lysis and bone-forming tumors usually do not cause formation of sclerotic bone. Samples may contain cortical bone and/or hard tissue fragments. Sampling from soft and tiny trabecular regions rather than peripheral sclerotic zones, which are likely reactive or cortical bone in nature and therefore unsuitable for the preparation of thin sections,

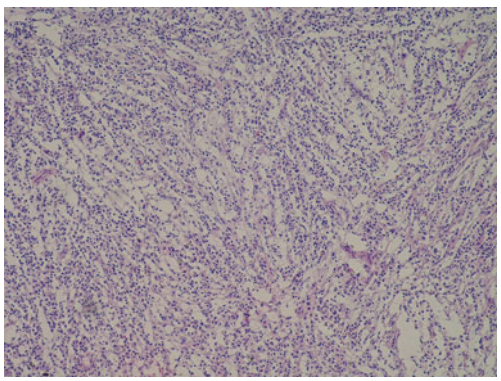

Fig. 4 Reparative tissue: poor quality section. Note the artifactual bubbles and lines due to freezing artifacts (HE. ×200)

may help to overcome this problem. In our study, FS sampling was performed accordingly, and in 95 samples (98 %), diagnostic findings were evident.

It should be noted that undecalcified trabeculae provide smoother FS sections compared to PS (Figs. 1a, b, 2, 3, 4). Technically, paraffin and undecalcified bone present significant differences in hardness. The main objective of tissue follow-up is to achieve similar tissue consistency (similar to the hardness of paraffin) throughout the sample, which is a prerequisite for smooth sectioning. In this regard, the similar consistency of frozen embedding medium, frozen tissue, and bone allows for smoother sectioning with FS for tissues containing tiny bone trabeculae in comparison with (undecalcified trabeculae) PS. In our series, among 11 low-quality samples that contained bone trabeculae, only one was not properly prepared due to thick bone tissue, and intense freezing artifacts resulting from significant stromal bleeding and edema affected the remaining samples (Fig. 4). Increased water content within the tissue, such as bleeding and edema, is associated with poorer section quality. Nevertheless, apart from those two "intraosseous lipoma" cases in which the diagnosis was deferred for technical reasons, it was still possible to obtain a diagnosis with FS in all osseous tissue bearing "low quality" sections. However, although the presence of osseous tissues does not have a significant adverse impact on the diagnosis made by FS, it may be impossible to harvest good quality sections from adipose tissue during frozen examination since adipose tissue does not freeze. Bui et al. [12] observed a similar limitation for adipocytic lesions as well as myxoid lesions and recommend pursuing cytology in conjunction with histopathology for these cases.

Technological advances in the last three decades have resulted in the advancement and development of novel pathological examination methods and auxiliary techniques. However, with the exception of a few tumor types, the use of these techniques in bone lesion and tumors is less common, rendering the traditional hematoxylin-eosin staining the predominant method of histological diagnosis. Therefore, good quality tissue samples from bone tissue obtained at FS may still provide significant diagnostic information similar to PS.

IOC would certainly be useful in the assessment of suspicious areas of invasion or metastasis after neoadjuvant treatment followed by wide resection, as well as for determining the etiology of a pathologic fracture, the cause of prosthetic loosening [16–18], and the adequacy of CNB and open biopsies [19–21]. It may also be suitable for cases that are not easily accessible—such as those involving the acetabulum—which carry increased risk of fracture with CNB, those located under thick sclerotic/cortical bone, or those that may not yield adequate tissue for sampling with CNB, such as cystic lesions. If a primary malignancy of the bone is excluded, a definitive treatment can be administered during the same session. The importance of a multidisciplinary approach and provision of adequate clinical and radiological data to the pathologist should be underscored to avoid from erroneous diagnostic conclusions at IOC because of the well-known heterogeneous characteristics of bone lesions.

Conclusion

In addition to the indications reported in the literature, FS can be used in lesions thought to be metastatic and in cases of pathological fractures. The FS technique can also be used to obtain histopathological data in cases with inadequate biopsy results. In cases where radiological findings are discordant with CNB results, in cases where open biopsy is indicated and in "clinically and radiologically" unsuspected cases where the multidisciplinary team opts for curettage or total excision without a CNB. In cases where primary bone sarcoma is excluded, final surgical treatment can be performed during the same session. When FS examination reveals primary bone sarcoma or defers diagnosis, it can be considered as an open biopsy and treatment is planned after PS results are obtained. It must be kept in mind that patients with suspected primary bone sarcoma are not good candidates for IOC and should always be evaluated with prior CNB instead.

The final diagnosis was obtained in 87.6 % of all the cases via FS, and we believe it is possible to obtain sections with diagnostic value from bone lesions via FS. We suggest that IOC with FS can be safely performed in tertiary referral centers or in sites with a comprehensive multidisciplinary team—including an orthopedic surgeon experienced in orthopedic oncology, pathology specialists competent in skeletal pathologies, a radiologist, medical and radiation oncologists, and nuclear medicine specialists—working in collaboration.

Conflict of interest We declare that we have no conflict of interest.

References

1. Acs G, Baloch ZW, LiVolsi VA (2002) Intraoperative consultation: an historical perspective. Semin Diagn Pathol 19(4):190–191
2. Ahmad Z, Barakzai MA, Idrees R, Bhurgri Y (2008) Correlation of intra-operative frozen section consultation with the final diagnosis at a referral center in Karachi, Pakistan. Indian J Pathol Microbiol 51(4):469–473
3. Howanitz PJ, Hoffman GG, Zarbo RJ (1990) The accuracy of frozen-section diagnoses in 34 hospitals. Arch Pathol Lab Med 114(4):355–359

4. Dalal BL, Malik AK, Datta BN (1979) Frozen section diagnosis—a review of 1051 cases. Indian J Cancer 16(2):59–65
5. Zarbo RJ, Hoffman GG, Howanitz PJ (1991) Interinstitutional comparison of frozen-section consultation. A College of American Pathologists Q-Probe study of 79,647 consultations in 297 North American institutions. Arch Pathol Lab Med 115(12):1187–1194
6. White VA, Trotter MJ (2008) Intraoperative consultation/final diagnosis correlation: relationship to tissue type and pathologic process. Arch Pathol Lab Med 132(1):29–36
7. Coffey D, Kaplan AL, Ramzy I (2005) Intraoperative consultation in gynecologic pathology. Arch Pathol Lab Med 129(12):1544–1557
8. Johnston EI, Beach RA, Waldrop SM, Lawson D, Cohen C (2006) Rapid intraoperative immunohistochemical evaluation of sentinel lymph nodes for metastatic breast carcinoma. Appl Immunohistochem Mol Morphol 14(1):57–62
9. LiVolsi VA, Baloch ZW (2005) Use and abuse of frozen section in the diagnosis of follicular thyroid lesions. Endocr Pathol 16 (4):285–293
10. Adesina AM (2005) Intraoperative consultation in the diagnosis of pediatric brain tumors. Arch Pathol Lab Med 129(12):1653–1660
11. Mirra JM, Brien EW, Luck JV Jr (1997) Intraoperative pathologic consultation (IOC) for tumors of the bone. Chir Organi Mov 82 (1):7–31
12. Bui MM, Smith P, Agresta SV, Cheong D, Letson GD (2008) Practical issues of intraoperative frozen section diagnosis of bone and soft tissue lesions. Cancer Control 15(1):7–12
13. Estrada-Villasenor EG, Cedillo ED, Gonzalez LM, Martinez GR (2007) Accuracy of intraoperative consultation for bone tumors: experience in an orthopedic hospital. J Orthop Sci 12(2):123–126
14. Folpe AL, Inwards CY (2010) Bone and soft tissue pathology. Saunders/Elsevier, Philadelphia
15. Mankin HJ, Mankin CJ, Simon MA (1996) The hazards of the biopsy, revisited. Members of the Musculoskeletal Tumor Society. J Bone Joint Surg Am 78(5):656–663
16. Bruns J, Delling G, Henne-Bruns D, Hossfeld DK (2008) Biopsy of tumors of the musculoskeletal system. Dtsch Arztebl Int 105 (27):492–497
17. Bori G, Soriano A, Garcia S, Gallart X, Mallofre C, Mensa J (2009) Neutrophils in frozen section and type of microorganism isolated at the time of resection arthroplasty for the treatment of infection. Arch Orthop Trauma Surg 129(5):591–595
18. Feldman DS, Lonner JH, Desai P, Zuckerman JD (1995) The role of intraoperative frozen sections in revision total joint arthroplasty. J Bone Joint Surg Am 77(12):1807–1813
19. Nunez LV, Buttaro MA, Morandi A, Pusso R, Piccaluga F (2007) Frozen sections of samples taken intraoperatively for diagnosis of infection in revision hip surgery. Acta Orthop 78(2):226–230
20. Meyer MS, Spanier SS, Moser M, Scarborough MT (1999) Evaluating marrow margins for resection of osteosarcoma. A modern approach. Clin Orthop Relat Res (363):170–175
21. Ashford RU, McCarthy SW, Scolyer RA, Bonar SF, Karim RZ, Stalley PD (2006) Surgical biopsy with intra-operative frozen section. An accurate and cost-effective method for diagnosis of musculoskeletal sarcomas. J Bone Joint Surg Br 88(9):1207–1211
22. Rosai J (1996) Chapter 1 introduction in: Ackerman's Surgical Pathology eighth Ed. Mosby 7–8
23. Shah MS, Garg V, Kapoor SK et al (2003) Fine-needle aspiration cytology, frozen section, and open biopsy: relative significance in diagnosis of musculoskeletal tumors. J Surg Orth Adv 12:203–207

Virchows Arch (2012) 461:205–210
DOI 10.1007/s00428-012-1274-3

ORIGINAL ARTICLE

Chondroclasts are mature osteoclasts which are capable of cartilage matrix resorption

H. J. Knowles · L. Moskovsky · M. S. Thompson · J. Grunhen · X. Cheng · T. G. Kashima · N. A. Athanasou

Received: 25 January 2012 / Revised: 8 May 2012 / Accepted: 25 June 2012 / Published online: 11 July 2012
© Springer-Verlag 2012

Abstract Multinucleated cells termed chondroclasts have been observed on the deep surface of resorbed hyaline cartilage but the relationship of these cells to macrophages and osteoclasts and their role in rheumatoid arthritis (RA) and other arthritic conditions is uncertain. Multinucleated cells in RA and other arthritic conditions showing evidence of cartilage resorption were characterised immunohistochemically for expression of macrophage/osteoclast markers. Mature human osteoclasts formed from circulating monocytes and tissue macrophages were cultured for up to 4 days on slices of human cartilage and glycosaminoglycan (GAG) release was measured. Multinucleated cells resorbing unmineralised cartilage were seen in osteoarthritis, RA, septic arthritis, avascular necrosis and in four cases of giant cell tumour of bone that had extended through the subchondral bone plate. Chondroclasts expressed an osteoclast-like phenotype (TRAP+, cathepsin K+, MMP9+, CD14−, HLA-DR−, CD45+, CD51+ and CD68+). Both macrophages and osteoclasts cultured on cartilage released GAG. These findings indicate that chondroclasts have an osteoclast-like phenotype and that mature human osteoclasts are capable of cartilage matrix resorption. Resorption of unmineralised subchondral cartilage by chondroclasts and macrophages can be a feature of joint destruction in inflammatory and non-inflammatory arthropathies as well as inflammatory and neoplastic subchondral bone lesions.

Keywords Osteoclast · Chondroclast · Cartilage · Resorption

Abbreviations

RANKL	Receptor activator of nuclear factor kappa B ligand
M-CSF	Macrophage-colony stimulating factor
MMP	Matrix metalloproteinase
TRAP	Tartrate-resistant acid phosphatase
OA	Osteoarthritis
GAG	Glycosaminoglycan

Introduction

Resorption or degradation of the deep surface of joint cartilage is seen in a number of pathological conditions, including inflammatory and non-inflammatory arthropathies as well as primary and secondary epiphyseal tumours and infections involving overlying cartilage. Multinucleated cells termed chondroclasts have been identified at sites of mineralised and non-mineralised articular hyaline cartilage erosion in the rheumatoid joint [1–3]. These cells have not been characterised in other arthritic conditions and remain poorly defined in terms of their relationship to other matrix-resorbing cells, particularly osteoclasts.

Osteoclasts are multinucleated cells which form part of the mononuclear phagocyte system [4]. These cells are specialised to carry out mineralised matrix resorption and are formed, in the presence of receptor activator of nuclear factor kappa B ligand (RANKL) and macrophage-colony stimulating factor (M-CSF), by fusion of CD14+ cells found

H. J. Knowles · M. S. Thompson · J. Grunhen · X. Cheng · T. G. Kashima · N. A. Athanasou (✉)
Nuffield Department of Orthopaedics, Rheumatology and Musculoskeletal Sciences, University of Oxford, Oxford OX 7LD, UK
e-mail: nick.athanasou@ndorms.ox.ac.uk

H. J. Knowles · M. S. Thompson · J. Grunhen · X. Cheng · T. G. Kashima · N. A. Athanasou
Department of Pathology, Nuffield Orthopaedic Centre, Oxford OX 7LD, UK

L. Moskovsky
Department of Pathology, Semmelweiss University, Budapest, Hungary

in monocyte and macrophage populations [5, 6]. Osteoclasts exhibit a number of specific ultrastructural, immunophenotypic and functional features [4]. Isolated mature osteoclasts have not been shown to be capable of cartilage matrix resorption and these cells are unable to carry out lacunar resorption of a demineralised bone matrix [7]. Osteoclasts are thought to resorb the organic matrix of bone principally through the production of acid proteases, such as cathepsin K, rather than neutral matrix collagenases [4, 8]; however, osteoclasts are known to produce some types of matrix metalloproteinases (MMPs), some of which, like cathepsin K, have been shown to play a role in cartilage matrix resorption [9–11].

In this study, our aim has been to characterise the nature of multinucleated cartilage-resorbing cells which have been termed chondroclasts. We have analysed a number of subchondral lesions showing evidence of cartilage resorption from cases of inflammatory and non-inflammatory arthritis, as well as other lesions, including infections and epiphyseal primary and metastatic bone tumour, in order to determine phenotypic characteristics of chondroclasts. To investigate the precise relationships between chondroclasts, osteoclasts and macrophages, we have also sought by cell culture to determine whether osteoclasts and macrophages are capable of cartilage matrix resorption.

Materials and methods

Phenotypic analysis of chondroclasts

Pathological bone and joints specimens showing evidence of cartilage resorption by multinucleated cells were obtained from files of the Nuffield Orthopaedic Centre, Oxford. These specimens were processed routinely for histology and included 15 cases of rheumatoid arthritis of the knee, 15 cases of osteoarthritis (OA) of the knee, 5 cases of septic arthritis (hip and knee joint), 5 cases of avascular necrosis of the hip, 4 cases of giant cell tumour of bone, 2 cases of osteosarcoma and 3 cases of metastatic carcinoma. The tissues were fixed in formalin and 5-μm sections of paraffin-embedded tissue were stained with haematoxylin–eosin. This study was approved by the Oxford Clinical Research Ethics Committee (C01.071).

Immunohistochemistry, using an indirect immunoperoxidase technique, was carried out with the monoclonal antibodies PD7/26, CR3/43, KP1 (all from Dako UK), NCL-CD14, NCL-CD51, (both from Leica Microsystems UK), 24-9C5 (Invitrogen), 182-12GJ and 56-2A4 (both from Daiichi Fine Chemical, Toyama, Japan) to determine expression of the macrophage/osteoclast markers CD45, HLA-DR, CD68, CD14, CD51, tartrate-resistant acid phosphatase (TRAP), cathepsin K and matrix metalloproteinase 9 (MMP-9), respectively. Immunohistochemistry for CD14, CD68 and CD51 was also carried out on macrophage and osteoclast cultures on cartilage (see below) to confirm the identity of cultured cells.

Cell cultures of macrophages and osteoclasts on cartilage

Morphologically intact normal human knee articular cartilage (derived from above knee amputation specimens carried out for primary bone tumour in young patients) provided the substrate for cell culture of macrophages and osteoclasts. Slices of cartilage were stored at −80 °C and then cut to approximately 3×3-mm squares before being placed in the wells of a 96-well tissue culture plate containing alpha MEM culture medium (Lonza, Wokingham, UK) supplemented with 10 % heat-inactivated FBS, 50 IU/ml Penicillin, 50 μg/ml streptomycin sulphate (Invitrogen, Paisley, UK) and 2 mM L-Glutamine (Lonza).

Peripheral blood mononuclear cells were isolated from buffy coat blood using Histopaque. CD14+ monocytes were selected using an AutoMACS cell separator (Miltenyi Biotech, Surrey, UK) as previously described [12]. CD14+ cells were seeded onto cartilage slices at 0.25×10^6 cells/well. Non-adherent cells were removed after 2 h. CD14+ monocyte-derived macrophages were incubated with 25 ng/ml M-CSF (R&D, Abingdon, UK) for 4 days. To generate osteoclasts, CD14+ cells were incubated with 25 ng/ml M-CSF and 50 ng/ml RANKL (Pepro-tech, UK), with medium and cytokines replaced every 3–4 days, for 14–16 days. Osteoclasts were also cultured on dentine slices to confirm active lacunar resorption.

Human osteoclasts were obtained directly by curettage from two cases of GCTB, a tumour known to contain large numbers of mature human osteoclasts [13, 14], and cultured for 48 h on the cartilage slices. Giant cells were also isolated from a case of pigmented villonodular synovitis, as previously described [15].

Glycosaminoglycan release from cartilage

Glycosaminoglycan (GAG) release from cartilage was measured using the dimethylmethylene blue (DMB) assay [16]. Four-day conditioned media from monocytes or mature osteoclasts on cartilage was spun down to remove cell debris. Ten microlitres media was mixed with 250 μl DMB reagent and the absorbance measured at 525 nm. The GAG concentration was read from a chondroitin sulphate standard curve and normalised to cartilage weight.

Results

Chondroclast resorption of cartilage

Multinucleated cells actively resorbing the subchondral bone plate and the deep surface of articular cartilage (chondroclasts)

were seen in all the lesions examined (Fig. 1a, b). These multinucleated cells were found on the surface of mineralised articular hyaline cartilage and on the deep surface of unmineralised articular cartilage where the subchondral bone plate had been completely resorbed. In some areas, multinucleated cells were found in contiguous areas of resorption of unmineralised cartilage and mineralised subchondral cartilage and bone. Numerous multinucleated cells resorbing cartilage were seen in GCTBs that had extended through the subchondral bone plate (Fig. 1c, d). Scattered macrophage-like mononuclear cells were also present at sites of cartilage and bone resorption in all the above lesions.

Antigenic phenotype of chondroclasts

Immunohistochemical analysis showed that the multinucleated cells resorbing cartilage expressed an osteoclast phenotype [17], being CD14−, HLA-DR−, CD45+, CD68+ CD51+, TRAP+, cathepsin K+ and MMP9+ (Table 1, Fig. 1b). Some, but not all, of the mononuclear macrophage-like cells at sites of cartilage resorption also expressed an osteoclast phenotype, with others expressing a macrophage phenotype (i.e. CD14+, HLA-DR+ and CD51−).

Cartilage matrix resorption by osteoclasts and macrophages

CD14+ macrophages and osteoclasts formed in vitro from CD14+ monocyte precursors stimulated GAG release when cultured on cartilage (Fig. 2). These cultures also exhibited MMP13 activity (data not shown). When osteoclast and macrophage cell cultures on cartilage slices were fixed in formalin and processed for histology, it was found that these cells expressed the immunophenotypic markers characteristic of macrophages (CD68+, CD14+ and CD51−) and osteoclasts (CD68+, CD14− and CD51+) respectively. Confirmation that mature human osteoclasts are capable of releasing GAG from cartilage in vitro is shown in cultures of GCTB-derived osteoclasts which showed increased GAG release relative to controls (Fig. 3). It was also noted that osteoclast-like giant cells isolated from a case of PVNS were capable of releasing GAG from cartilage (Fig. 3).

Discussion

Bromley and Woolley were the first to characterise multinucleated cells resorbing mineralised and unmineralised articular cartilage at sites of subchondral erosion in rheumatoid knee joints [1–3]. They noted that these multinucleated cells (chondroclasts) contained intracellular vacuoles, phagocytosed collagen fibres and lysosomal bodies in which there was histochemically demonstrable acid phosphatase, an enzyme marker of cells of the mononuclear phagocyte system. Ultrastructural studies showed that cytoplasmic extensions into cartilage of these chondroclasts were noted, but structures similar to the specialised ruffled border and sealing zone elaborated by a resorbing osteoclast were not identified.

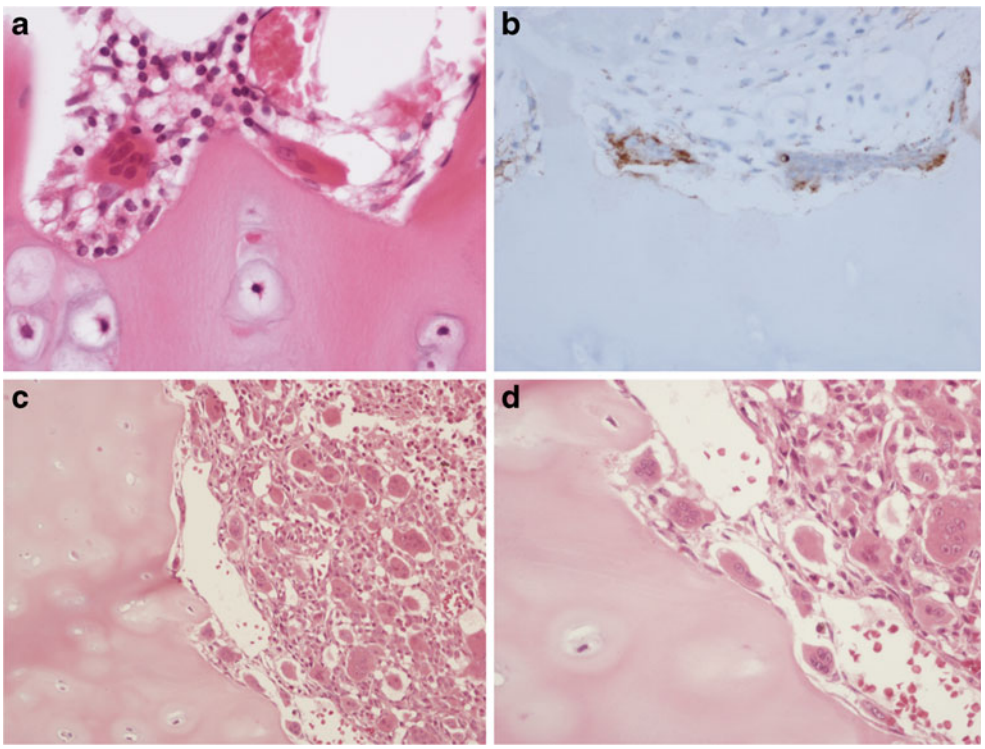

Fig. 1 **a** Chondroclasts resorbing OA articular cartilage, **b** CD51 expression by chondroclasts and **c** low-power and **d** high-power view of osteoclasts in giant cell tumour of bone resorbing articular cartilage

Table 1 Phenotypic markers on subchondral mononuclear and multinucleated cells

	Osteoclast	Chondroclast	Macrophage[a]
CD68	+	+	+
CD45	+	+	+
CD14	−	−	+
CD51	+	+	-
HLA-DR	−	−	+
TRAP	+	+	−
Cathepsin K	+	+	−
MMP-9	+	+	−

[a] Some mononuclear macrophage-like cells at sites of cartilage resorption expressed an osteoclast phenotype (see text)

In this study, multinucleated cells which resorb unmineralised articular hyaline cartilage were found in both inflammatory and non-inflammatory arthritic conditions; these cells were also noted in epiphyseal tumours and inflammatory lesions that had extended through the subchondral bone plate into overlying cartilage. These multinucleated cells expressed the specific phenotypic features of osteoclasts, being CD51+, CD14−, HLA-DR−, TRAP+, cathepsin K+ and MMP9+ [4, 17]. Multinucleated cells expressing some of the histochemical and ultrastructural characteristics of osteoclasts have been noted in cartilage at sites of endochondral bone formation in the growth plate and maturing skeleton of experimental animals and in deer antlers and other tissues [18–22]. These cells have been designated chondroclasts, although this term has been used rather loosely in these studies to include multinucleated cells that resorb the mineralised cartilage found at sites of new bone formation; as contact with bone mineral is thought to be the stimulus for osteoclast resorption, it is expected that osteoclasts would be able to resorb calcified cartilage. Ruffled border formation is observed in osteoclasts on calcified bone

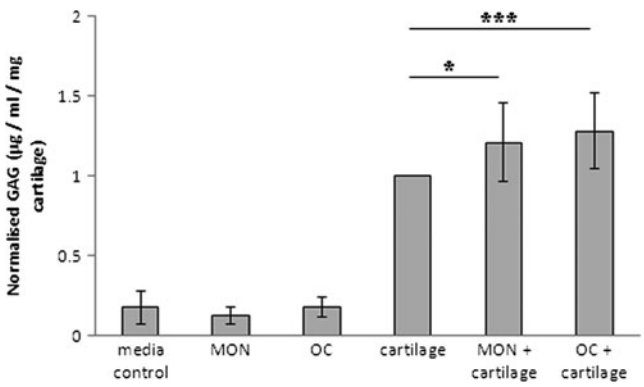

Fig. 2 CD14+ monocyte-derived macrophages (*MON*) and in vitro-differentiated human osteoclasts (*OC*) stimulate GAG release from cartilage $p<0.05$, $p<0.005$ versus cartilage control

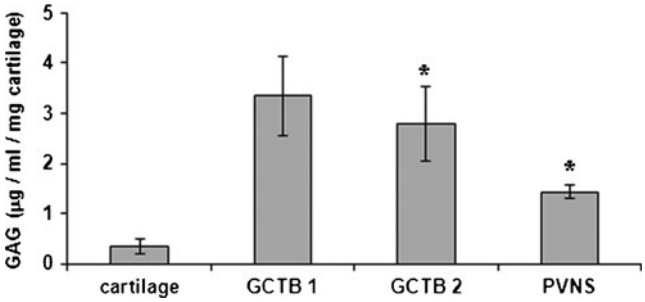

Fig. 3 Osteoclast-like giant cells from GCTB and PVNS stimulate GAG release from cartilage in vitro. *$p<0.05$ versus cartilage control

and decalcified bone slices in cultures of bone marrow macrophages, cultures of osteoclast-like cells on cartilage slices do not show a true ruffled border. These cells have irregular cell projections and a clear zone-like structure but do not have a true ruffled border. These results suggest that the mineral component of bone may determine terminal osteoclast differentiation [23].

Several studies have shown that substrate composition has a major effect on bone resorption by osteoclasts. Osteoclasts do not resorb bone covered by an unmineralised layer of osteoid but are able to resorb bone that is rendered anorganic [7, 24, 25]. Osteoclasts do not form a ruffled border or clear zone on a poorly calcified or cartilage substrate [1, 2, 23] and it has been suggested that bone cells, such as osteoblasts initiate the process of bone resorption by releasing collagenase that degrades the organic matrix leading to exposure of mineral to osteoclast contact [7, 26–28]. The mRNA for MMP-1 has been localised in osteoblasts, osteocytes and chondrocytic cells but not osteoclasts [8]. Osteoclasts, however, are capable of resorbing both the organic and inorganic components of bone [29]; these cells release cysteine proteinases such as cathepsin K which break down collagen in the acid microenvironment of the resorption lacuna; various neutral MMPs, including MMP13, are also thought to play a role in osteoclast lacunar resorption in specific pathological conditions [9].

We noted that chondroclasts shared many of the specific phenotypic features of osteoclasts. These cells elaborated the tartrate-resistant isoform of acid phosphatase, as well as cathepsin K and MMP-9, osteoclast-associated enzymes which break down the organic matrix of bone and cartilage [10, 11, 30]. Supportive evidence for chondroclasts and osteoclasts being closely related is also provided by our finding that mature human osteoclasts are capable of releasing GAG from hyaline cartilage. Numerous osteoclastic giant cells are found in GCTB, an osteolytic epiphyseal bone tumour that can involve overlying articular cartilage. GCTB contains mononuclear stromal cells that are known to have collagenase activity [31]. Evidence that chondroclasts, like osteoclasts, may play a role in joint pathology comes from our observation that PVNS-derived giant cells also released GAG from cartilage. PVNS is a lesion which

contains numerous macrophages and giant cells which have an osteoclast phenotype [15]; in addition, as inflammatory macrophages and tumour-associated macrophages are known to differentiate into osteoclast [32, 33], it is possible that these mononuclear cells in subchondral pathological lesions may have differentiated into chondroclasts as well as regarding cartilage directly. Mononuclear cells expressing an osteoclast-like (CD14− and CD51+) and a macrophage-like (CD14+ and CD51−) antigenic phenotype were also noted at sites of cartilage resorption. Cell culture results showed that CD14+ monocyte-derived macrophages are capable of releasing GAG from cartilage. Osteoclasts form from CD14+ macrophage precursors in the presence of RANKL and M-CSF [4, 6], and it is possible that these subchondral CD14+ cells represent the mononuclear precursor cell population that differentiates into the osteoclasts and chondroclasts that resorb bone/mineralised cartilage and unmineralised cartilage, respectively.

RANKL is required for osteoclast formation and it has been shown that both RANKL and osteoprotegerin (OPG), the decoy receptor for RANKL, are found in areas of cartilage resorption [34]. Bone resorption is markedly reduced by inhibitors of osteoclast formation and activity. Accelerated cartilage resorption by chondroclasts has been noted in mice lacking OPG [35]. Bisphosphonates and inhibitors of cathepsin K prevent cartilage loss in animal models of inflammatory and degenerative joint disease [36, 37]. Our findings indicate that chondroclasts are closely related to osteoclasts and that these cells may play a role in joint destruction in inflammatory and non-inflammatory arthritis, suggesting that there may be a role for anti-osteoclast therapies in controlling cartilage destruction.

Acknowledgments We wish to thank Mrs C Lowe for typing the manuscript and R. Taylor for providing the PVNS cells. This study was supported by the Rosetrees Charitable Trust and EuroBoNet a Network of Excellence, funded by the European Union.

Conflict of interest We declare that we have no conflict of interest.

References

1. Bromley M, Woolley DE (1984) Histopathology of the rheumatoid lesion. Identification of cell types at sites of cartilage erosion. Arthritis Rheum 27:857–863
2. Bromley M, Woolley DE (1984) Chondroclasts and osteoclasts at subchondral sites of erosion in the rheumatoid joint. Arthritis Rheum 27:968–975
3. Bromley M, Bertfield H, Evanson JM, Woolley DE (1985) Bidirectional erosion of cartilage in the rheumatoid knee joint. Ann Rheum Dis 44:676–681
4. Novack DV, Teitelbaum SL (2008) The osteoclast: friend or foe? Annu Rev Pathol 3:457–484
5. Fujikawa Y, Quinn JM, Sabokbar A, McGee JO, Athanasou NA (1996) The human osteoclast precursor circulates in the monocyte fraction. Endocrinology 137:4058–4060
6. Quinn JM, Elliott J, Gillespie MT, Martin TJ (1998) A combination of osteoclast differentiation factor and macrophage colony stimulating factor is sufficient for both human and mouse osteoclast formation in vitro. Endocrinology 139:4424–4427
7. Chambers TJ, Thomson BM, Fuller K (1984) Effect of substrate composition on bone resorption by rabbit osteoclasts. J Cell Sci 70:61–71
8. Fuller K, Chambers TJ (1995) Localisation of mRNA for collagenase in osteocytic, bone surface and chondrocytic cells but not osteoclasts. J Cell Sci 108:2221–2230
9. Andersen TL, del Carmen OM, Kirkegaard T, Lenhard T, Foged NT, Delaissé JM (2004) A scrutiny of matrix metalloproteinases in osteoclasts: evidence for heterogeneity and for the presence of MMPs synthesized by other cells. Bone 35:1107–1119
10. Murphy G, Lee MH (2005) What are the roles of metalloproteinases in cartilage and bone damage? Ann Rheum Dis 64:44–47
11. Cawston TE, Young DA (2010) Proteinases involved in matrix turnover during cartilage and bone breakdown. Cell Tissue Res 339:221–235
12. Knowles H, Athanasou NA (2008) Acute hypoxia and osteoclast activity: a balance between enhanced resorption and increased apoptosis. J Pathol 218:256–264
13. Chambers TJ, Fuller K, McSheehy PM, Pringle JA (1985) The effects of calcium regulating hormones on bone resorption by isolated human osteoclastoma cells. J Pathol 145:297–305
14. Lau YS, Sabokbar A, Gibbons CLMH, Athanasou NA (2005) Phenotypic and molecular studies on giant cell tumours of bone and soft tissues. Hum Pathol 36:945–954
15. Taylor R, Kashima TG, Knowles H, Gibbons CL, Whitwell D, Athanasou NA (2011) Osteoclast formation and function in pigmented villonodular synovitis. J Pathol 225:151–156
16. Riley GP, Harrall RL, Constant CR, Chard MD, Cawston TE, Hazleman BL (1994) Glycosaminoglycans of human rotator cuff tendons: changes with age and in chronic rotator cuff tendinitis. Ann Rheum Dis 53:367–376
17. Maggiani F, Forsyth R, Hogendoorn PCW, Krenacs T, Athanasou NA (2011) Immunophenotype of osteoclasts and macrophage polykaryons. J Clin Pathol 64:701–705
18. Lewinson D, Sibermann (1992) Chondroclasts and endothelial cells collaborate in the process of cartilage resorption. Anat Rec 233:504–514
19. Shibata S, Suzuki S, Yamashita Y (1997) An ultrastructural study of cartilage resorption at the site of initial endochondral bone formation in the fetal mouse mandibular condyle. J Anat 191:65–76
20. Szuwart T, Kierdorf H, Kierdorf U, Clemen G (2002) Histochemical and ultrastructural studies of cartilage resorption and acid phosphatise activity during antler growth in fallow deer (*Dama dama*). Anat Rec 268:66–72
21. Nordahl J, Andersson G, Reinholt FP (1998) Chondroclasts and osteoclasts in bones of young rats: comparison of ultrastructural and functional features. Calcif Tissue Int 63:401–408
22. Arana-Chavez VE, Bradaschia-Correa V (2009) Clastic cells: mineralized tissue resorption in health and disease. Int J Biochem Cell Biol 41:446–450
23. Suzumoto R, Takami M, Sasaki T (2005) Differentiation and function of osteoclasts cultured on bone and cartilage. J Electron Microsc (Tokyo) 54:529–540
24. Yovich S, Seydel U, Papadimitriou JM, Nicholson GC, Wood DJ, Zheng MH (1998) Evidence that failure of osteoid bone matrix resorption is caused by perturbation of osteoclast polarization. Histochem J 30:267–273
25. Shimizu H, Sakamoto S, Sakamoto M (1989) Matrix collagen of devitalized bone is resistant to osteoclastic bone resorption. Connect Tissue Res 20:169–175

26. Chambers TJ, Fuller K (1985) Bone cells predispose bone surfaces to resorption by exposure of mineral to osteoclastic contact. J Cell Sci 76:155–165
27. Fuller K, Gallagher AC, Chambers TJ (1991) Osteoclast resorption-stimulating activity is associated with the osteoblast cell surface and/or the extracellular matrix. Biochem Biophys Res Commun 27:67–73
28. Holiday LS, Welgus HG, Flixzar CJ, Veith GM, Jeffrey JJ, Gluck SL (1997) Initiation of osteoclast bone resorption by interstitial collagenase. J Biol Chem 29:22053–22058
29. Blair HC, Kahn AJ, Crouch EC, Jeffrey JJ, Teitelbaum SL (1986) Isolated osteoclasts resorb the organic and inorganic components of bone. J Cell Biol 102:1164–1172
30. Dejica VM, Mort JS, Laverty S, Percival MD, Antoniou J, Zukor DJ, Poole AR (2008) Cleavage of type II collagen by cathepsin K in human osteoarthritic cartilage. Am J Pathol 173:161–169
31. Cowan RW, Mak I, Colterjohn N, Singh G, Chent M (2009) Collagenase expression and activity in the stromal cell from giant cell tumour of bone. Bone 44:865–871
32. Quinn JMW, McGee JO'D, Athanasou NA (1998) Human tumour-associated macrophages differentiate into osteoclastic bone-resorbing cells. J Pathol 184:31–36
33. Fujikawa Y, Sabokbar A, Neale S, Athanasou NA (1996) Human osteoclast formation and bone resorption by monocytes and synovial macrophages in rheumatoid arthritis. Ann Rheum Dis 55:1–7
34. Komuro H, Olee T, Kuhn K, Quach J, Brinson DC, Shikhman A, Valbracht J, Creighton-Achermann L, Lotz M (2001) The osteoprotegerin/receptor activator of nuclear factor kappaB/receptor activator of nuclear factor kappaB ligand system in cartilage. Arthritis Rheum 44:2768–2776
35. Ota N, Takaishi H, Kosaki N, Takito J, Yoda M, Tohmonda T, Kimura T, Okada Y, Yasuda H, Kawaguchi H, Matsumoto M, Chiba K, Ikegami H, Toyama Y (2009) Accelerated cartilage resorption by chondroclasts during bone fracture healing in osteoprotegerin-deficient mice. Endocrinology 150:4823–4834
36. Strassle BW, Mark L, Leventhal L, Piesla MJ, Jian Li X, Kennedy JD, Glasson SS, Whiteside GT (2010) Inhibition of osteoclasts prevents cartilage loss and pain in a rat model of degenerative joint disease. Osteoarthr Cartil 18:1319–1328
37. Svelander L, Erlandsson-Harris H, Astner L, Grabowska U, Klareskog L, Lindstrom E, Hewitt E (2009) Inhibition of cathepsin K reduces bone erosion, cartilage degradation and inflammation evoked by collagen-induced arthritis in mice. Eur J Pharmacol 613:155–162

Virchows Arch (2012) 461:211–219
DOI 10.1007/s00428-012-1257-4

ORIGINAL ARTICLE

Virtual CT autopsy in clinical pathology: feasibility in clinical autopsies

Saskia E. Westphal · Jonas Apitzsch · Tobias Penzkofer · Andreas H. Mahnken · Ruth Knüchel

Received: 5 January 2012 / Revised: 29 April 2012 / Accepted: 21 May 2012 / Published online: 23 June 2012
© Springer-Verlag 2012

Abstract For the past century, autopsy techniques in clinical pathology have not changed significantly, while autopsy rates are declining. Modern imaging techniques offer interesting prospects of supportive post-mortem diagnostic investigation. In a prospective study of 29 autopsy cases, complimentary virtual autopsy using unenhanced post-mortem computed tomography (pmCT) was performed. We analysed in a prospective cohort study 29 unenhanced pmCT scans, generated prior to autopsy. Clinical information regarding clinical history and circumstances of death were provided. The objective of the study was to find consistency and/or discrepancy between virtual autopsy and conventional autopsy findings regarding cause of death and death-related diagnoses, reconstruction of the pathogenetic mechanisms involved, side diagnoses and CPR (cardiopulmonary resuscitation)- or death-related post-mortem changes. Accuracy of pmCT for cause of death was 68 % and the positive predictive value (PPV) was 75 %. Regarding the pathogenetic mechanisms, accuracy of pmCT was 21 % and PPV was 29 %. The combined diagnostic yield of autopsy and pmCT was 133 % compared to autopsy only. Modern imaging techniques give an opportunity for post-mortem diagnostics to complete but not yet replace traditional autopsy. We could show that in two out of three cases, the cause of death found by pmCT matched the diagnosis from classical autopsy. While both disciplines, pathology and radiology, will profit from the mutual exchange of data, it seems a realistic aim to strive for virtual autopsy possibly further supported by biopsies and contrast-enhanced pmCT as an alternative to the classical clinical autopsy. A combination of both methods enhances diagnostic quality and completeness of the autopsy report.

Keywords Autopsy study · Autopsy rate Germany · Europe · Virtual autopsy · CT · pmCT

Electronic supplementary material The online version of this article (doi:10.1007/s00428-012-1257-4) contains supplementary material, which is available to authorized users.

S. E. Westphal · R. Knüchel
Department of Pathology, RWTH Aachen University Hospital, Aachen, Germany

J. Apitzsch · T. Penzkofer · A. H. Mahnken
Clinic for Diagnostic and Interventional Radiology, RWTH Aachen University Hospital, Aachen, Germany

T. Penzkofer · A. H. Mahnken
Applied Medical Engineering, Helmholtz Institute of Biomedical Engineering, RWTH Aachen, Aachen, Germany

R. Knüchel (✉)
Department of Pathology, RWTH Aachen University Hospital, Pauwelsstr. 30,
52074 Aachen, Germany
e-mail: rknuechel-clarke@ukaachen.de

Introduction

Autopsy is an essential tool for student and pathology resident teaching. At the same time, it is a valuable performance measure for any hospital [1]. Autopsy can be of great importance regarding economic and legal consequences for hospitals and clinicians [2]. In the long term, decline in autopsy rates must lead to a lack of accuracy of mortality statistics, on which the financial support of specific research areas are based. In Europe, autopsy rates have been declining [3–6]. In the USA, Australia and Asia, trends are the same [7–9]. Influential factors include request rates by

clinicians, laws determining legal autopsy consent, and consent rates [10].

Autopsy methods used by departments of pathology all over the world have not changed much during the past century. Basically, pathologists rely on macroscopic organ morphology and microscopic examination. As diagnostic methods have changed and improved significantly in the field of radiologic imaging, our aim was to find out whether medical autopsy pathology benefits from modern diagnostic imaging.

In forensic medicine, post-mortem imaging has a long tradition. New imaging techniques, such as spiral multislice computed tomography (CT) and magnetic resonance imaging (MRI), offer excellent utilities for post-mortem examination. Forensic research groups in Europe, the UK, USA, Australia and Asia attend to the concept of post-mortem imaging [11–15].

In medical autopsy pathology, post-mortem imaging has not yet been used to an extent comparable to forensic pathology. Our goal was to investigate the potential of unenhanced post-mortem CT (pmCT) imaging for virtual autopsy. Native CT autopsy imaging in comparison to full autopsy, to our knowledge, has only rarely been used in non-forensic settings [16]. Often, MRI is used in combination with pmCT [17–19]. MRI is more time consuming and more expensive than CT, and the availability of MRI scanners is limited. Therefore, a systematic evaluation of the feasibility and accuracy of finding the cause of death with native pmCT in comparison to the results of conventional autopsy was conducted.

The objectives for virtual autopsy were to provide the examiner with sufficient material to report on the following topics:

1. Cause of death
2. Death-related diagnoses
3. Reconstruction of pathogenetic mechanisms involved
4. Unspecific findings (post-mortem changes, changes related to CPR)
5. Side diagnoses

Materials and methods

This study was conducted at a German university hospital. The study was approved by the local ethics committee.

We included in this prospective study 29 randomly selected cases of deceased persons delivered to the Department of Pathology for conventional autopsy. Sex ratio was *f*/*m*=10:19. Mean age at death was 59 years, ranging from 0 months to 91 years. The cases comprised 17 deaths on a standard hospital ward, eight deaths in an intensive care unit, two deaths in the emergency room, one intrauterine death and one death at home. The manner of death was due to natural cause in all cases.

We used the combination of imaging and classical autopsy prospectively whenever feasible, i.e. availability of CT for consented classical autopsies.

Virtual autopsy

Before conventional autopsy, at a mean time of 50 h (±40 h) after death, the body was wrapped (arms attached laterally) in an artefact-free body bag in the supine position, placed in the CT gantry, and scanned from head to toe with a 64 dual-source CT scanner (SOMATOM Definition, Siemens, Forchheim, Germany) with 64×0.6 mm collimation, a tube voltage of 120 kV and an effective tube current-time product of 160 mAs_{eff}. From raw data, axial images with 5- and 1-mm slice thickness and a recon increment of 4 or 0.7 mm were reconstructed using medium smooth (B30f) and sharp (B60f) convolution kernels. Including positioning of the body on the scanner, the duration of the average pmCT scan was 10 min. After reconstruction of the raw data, the reconstructed images were transferred to a Picture Archiving and Communication System (iSite Radiology, Philips Medical Systems, the Netherlands). The CT scanner was used out of working hours (before 0730 or after 1800 hours).

Afterwards, the pictures were evaluated by two experienced general radiologists with no previous experience of post-mortem imaging. The clinical information given by the autopsy request form was provided to radiologists before image interpretation. The radiologists reported their findings in a standard form, including the neurocranium, thorax, abdomen and extremities.

Conventional autopsy

The autopsy was performed in a standardized form (accredited Department of Pathology, IS0/IEC 17020) by experienced pathologists at a mean time of 62 h (±45 h) after death. All three body cavities (neurocranium, thorax and abdomen) were opened except in two cases. In one case, only cardiac autopsy was consented. In one case of systemic echinococcosis, classical clinical autopsy was omitted due to infection hazard. Following complete autopsy, the autopsy findings were demonstrated to the clinicians requesting the autopsy. The clinical picture was correlated with findings at autopsy.

Statistical analysis

Statistical analysis was conducted using Microsoft® Office Excel 2003 (Microsoft Corporation, Redmond, WA, USA). All cases in which pmCT and autopsy were performed were included in the statistical analysis (n=28).

Results

The results are structured according to the report about the Swiss Virtopsy® project published in 2003 [20]. The results of pmCT and conventional autopsy were compared with regard to the detection of

1. Cause of death
2. Death-related diagnoses
3. Reconstruction of pathogenetic mechanisms involved
4. Unspecific findings (post-mortem changes, changes related to CPR)
5. Side diagnoses

The cause of death was distributed as shown in Table 1, with predominance of diseases of the circulatory system, infectious diseases and diseases of the respiratory system. Summing up the total number of diagnoses found at autopsy in combination with pmCT, 33 % additional diagnoses were found using pmCT (190 at autopsy, 124 with both methods and 103 with pmCT only). Including CPR-related and post-mortem changes, the combined diagnostic yield was 48 % higher than without pmCT (190 at autopsy only, 128 at both autopsy and pmCT, 154 additional diagnoses with pmCT). The distribution in the diagnostic groups is shown in Table 2 and visualized in Fig. 1.

Table 1 Autopsy and radiology cause of death

	Autopsy		pmCT	
	n	%	*n*	%
Reported cause of death				
Cardiac failure	12	43	8	42
Haemorrhage	7	25	6	32
Cardiorespiratory failure	2	7	1	5
Multi-organ failure	2	7	1	5
Acute respiratory failure	2	7	1	5
Lung emboli	1	4	1	5
Meningoencephalitis	1	4	0	0
None proven (intrauterine death)	1	4	1	5
Total[a]	28		19	
Diagnostic group				
Diseases of the circulatory system	22	54	18	69
Infectious and parasitic diseases	6	15	0	0
Diseases of the respiratory system	4	10	4	15
Diseases of the digestive system	2	5	1	4
Neoplasms	2	5	2	8
Diseases of the nervous system	2	5	1	4
Congenital malformations, deformations and chromosomal abnormalities	1	2	0	0
Injury, poisoning and certain other consequences of external causes	1	2	0	0
None proven (intrauterine death)	1	2	1	4
Total[b]	41		26	

[a] One case excluded (no autopsy due to infection risk)

[b] Sum exceeds number of patients because in some cases, several systems/pathologies were involved equally

1. Cause of death

   The cause of death was assigned to a specific site or pathology, e.g. cardiac failure, cardiorespiratory failure, acute respiratory failure, multi-organ failure or haemorrhage, whenever possible. In one case of intrauterine death, no cause of death could be proved by either method.

   In 19 of 28 cases, the cause of death diagnosis after pmCT matched the diagnosis after conventional autopsy (Table 3).

2. Death-related diagnoses

   Five-percent more death-relevant diagnoses were found in the combination of classical autopsy and pmCT (122 at autopsy, plus six with pmCT). In a case of multiple myeloma with multiple osteoblastic and osteolytic lesions, the lesions were found with pmCT as well as after macroscopic examination in classical autopsy (Fig. 2).

   With pmCT, atherosclerosis of cerebral arteries was found in one of five cases with cerebral atherosclerosis in classical autopsy. In one case of fatal subarachnoidal haemorrhage, the haemorrhage was visible with pmCT (Fig. 2). In one case of meningoencephalitis and circumscript subarachnoidal haemorrhage, the haemorrhage was not visible with pmCT. Brain lesions, such as Alzheimer's disease, in two cases and a small haemorrhage were missed with pmCT.

   Generalised atherosclerosis with calcification was found in 13 cases with equal results of pmCT and classical autopsy. Coronary sclerosis was identified with pmCT in 16 of 19 cases at classical autopsy. In six cases, in which coronary sclerosis was associated with myocardial infarction and cardiac failure, the cardiac cause of death was diagnosed correctly with regard to characteristic changes of the organs on a balance of probabilities. There were no false-positive findings of coronary sclerosis with pmCT. One basilary artery aneurysm was missed with pmCT, as well as one out of three other aneurysms.

   In our patient cohort, thromboses were missed with unenhanced pmCT images in one case of an in-stent thrombosis and two cases of bypass thrombosis.

   In our study, out of 12 cases of cardiac failure in clinical autopsy, ten cases were diagnosed correctly by use of pmCT. There were no false-positive findings for cardiac failure. Although myocardial lesions (infarction, myocarditis) were not visible with pmCT, cardiac failure was diagnosed correctly from death-associated diagnoses, such as coronary atherosclerosis, organ congestion and pleural effusions. Myocardial hypertrophy was reported at

Table 2 Distribution of diagnoses

	Number	Percent	Autopsy	Autopsy+pmCT	pmCT
Circulatory system	162	34	66	76	20
Musculoskeletal system and connective tissue	65	14	17	8	40
Digestive system	45	10	25	11	9
Respiratory system	43	9	18	8	17
Genitourinary system	27	6	12	11	4
Neoplasms	19	4	14	2	3
Diseases of the blood and blood-forming organs	14	3	6	2	6
Infectious and parasitic diseases	12	3	9	3	0
Nervous system	9	2	9	0	0
Injury and other consequences of external causes	8	2	4	1	3
Endocrine, nutritional and metabolic diseases	7	1	4	2	1
Congenital malformations, deformations and chromosomal abnormalities	6	1	6	0	0
Unspecific/post-mortem changes	55	12	0	4	51
Total	472		190	128	154

autopsy in 19 cases, but only in ten cases with pmCT. One left ventricular aneurysm was missed with pmCT.

Ground glass attenuation was diagnosed with pmCT in 12 cases. The pathomorphologic findings in those cases in classical autopsy were acute pulmonary congestion in nine cases, pulmonary oedema in three cases, hyaline membranes and pneumonia in one case, severe bacteremia in one case and bone marrow embolisation in one case. Seven out of nine cases of pulmonary emphysema were missed with pmCT. Mixed dust pneumoconiosis was found with pmCT due to calcified lesions in two cases (100 %).

There were one false-positive, one true-positive and two false-negative diagnoses of pneumonia in pmCT. Pleural effusions were found with pmCT in 19 cases, compared to 18 cases at autopsy. A small pneumothorax was found with pmCT in three cases, which had been missed at autopsy.

Fluid with a density of more than 50 HU in one of the body cavities or preformed spaces (ventricles, pericardium) was found in eight cases with pmCT. The finding correlated with the autopsy finding of haemorrhage in all cases (intraabdominal haemorrhage in five cases, pericardial tamponade in two cases, intraventricular haemorrhage in one case) (Fig. 2). Diffuse haemorrhage, as present in one case, was not visible with pmCT.

3. Reconstruction of the pathogenetic mechanism

The reconstruction of the pathogenetic mechanism using pmCT was correct in 5 of 28 cases, i.e. three cases of intraabdominal haemorrhage, one case of intracranial haemorrhage and one case of pulmonary embolism (Table 4). In one case (intrauterine death), the cause of death and the pathogenetic mechanism remained unclear after both pmCT and classical autopsy. In most cases, the site of death could be assigned to the lung or the heart correctly with pmCT, but the exact cause of organ failure remained unclear. At traditional autopsy, the cause of organ failure could be defined precisely by means of histologic examination and assessment of characteristic macroscopic tissue changes, such as yellow necrosis of myocardial tissue with hemorrhagic margin in case of myocardial infarction. Differing results in the reconstruction of the pathogenetic mechanism were found in a case of severe bacterial infection of the lungs and in cases of cardiac failure due to myocarditis or myocardial infarction with or without pericardial tamponade, as well as chronic ischaemic cardiomyopathy or chronic heart transplant vasculopathy. One case of dilated cardiomyopathy was missed with pmCT, and death

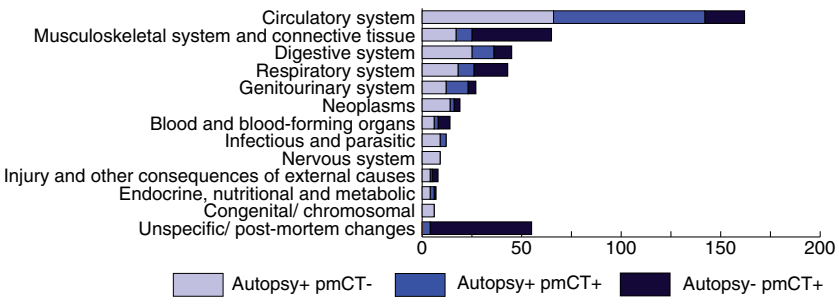

Fig. 1 Distribution of diagnoses (*light blue*, diagnoses found at autopsy/missed with pmCT; *ink blue*, diagnoses found with both methods; *dark blue*, diagnoses found with pmCT/missed at autopsy)

Table 3 Cross-tabulation cause of death in pmCT vs. classical autopsy

Cause of death (CoD)			Classical autopsy				
			CoD found			CoD not found	
			(A+C)	22		(B+D)	6
pmCT	CoD found A+B=	23	A (true pos)=	18		B (false pos)=	5
	CoD not found C+D=	5	C (false neg)=	4		D (true neg)=	1
			Total A+B+C+D				28
Sensitivity=			85.71 %				
Specificity=			14.29 %				
Positive predictive value=			75 %		95 % CI=	55.100 to 88.000%	
Negative predictive value=			25 %		95 % CI =	4.5587 to 69.935%	
Accuracy=			67.86 %				

was assigned to myocardial hypertrophy. In one case of respiratory distress, the pulmonary oedema was found, but atelectasis had been missed with pmCT, and therefore, the pathogenetic mechanism remained unclear. In one case of COPD, heart failure was correctly found as the cause of death, but the pathogenetic mechanism with right heart failure due to COPD was not reconstructed correctly. In three cases of haemorrhage, haematoperitoneum was found with pmCT, but the exact localisation of the bleeding site was missed. In one case of diffuse bleeding, the haemorrhage was missed with pmCT. Two cases of bronchopneumonia and one case of meningoencephalitis were missed with pmCT. In one case of sepsis after chemotherapy, death was attributed to cardiopulmonary insufficiency, while at autopsy, multi-organ failure was believed to be the cause of death. In one case of respiratory failure, the radiologists suspected air embolism to be the cause of death; therefore, the reconstruction of the pathogenetic mechanism differed from the autopsy result as well.

4. Unspecific findings

After the combination of pmCT with classical autopsy, more than ten times more unspecific death-related and CPR-related diagnoses were documented (4 at classical autopsy, 51 additional with pmCT). Cardiopulmonary resuscitation and putrefaction may cause artefacts on pmCT images. Rib fractures are usually examined during classical autopsy but were missed on macroscopic examination in two cases. One case of multiple rib fractures was missed with pmCT. One sternum fracture was found with both methods; one was missed at autopsy.

Gas in the cardiovascular system was found in ten cases with pmCT, associated with CPR before death in seven cases. Aerobilia was described in eight cases with pmCT, as well as six cases of subcutaneous emphysema. None of these findings were documented at clinical autopsy.

5. Side diagnoses

After a combination of side diagnoses found at classical autopsy and additional diagnoses found with pmCT, 35 % additional diagnoses were found (202 at classical autopsy, 70 additional diagnoses with pmCT). With pmCT, hernias were seen in five cases. Traditional autopsy revealed no hernia. Muscle atrophy was found in three cases with pmCT, compared to five cases at autopsy.

Neoplastic lesions were reported by the radiologists; missed at autopsy were one lipoma and two cartilaginous exostoses. On the other hand, at autopsy, one rectum carcinoma, one colon carcinoma, one renal cell carcinoma, one prostate carcinoma, one transitional cell carcinoma and ten cases of low-grade intraepithelial neoplasia of the colon, as well as one pulmonary metastasis of a squamous cell carcinoma, were reported, which were missed with pmCT. Radiologists reported one false-positive "tumour" in the pleural cavity, which at autopsy proved to be coagulated blood.

Calcified lesions, such as cholecystolithiasis, were visible with pmCT in three of five cases at autopsy. Prostate enlargement was diagnosed in two cases with pmCT, compared to three cases at autopsy. Two cases of mixed dust pneumoconiosis were diagnosed with pmCT, in agreement with autopsy findings.

Organ size and configuration as well as hypodense lesions, such as cysts, could be assessed with pmCT. Myocardial hypertrophy was diagnosed with pmCT in 10 of 18 cases at autopsy. Goitre was found with pmCT in one of four cases in conformity with autopsy. Hepatosplenomegaly was found with pmCT in three of four cases at autopsy. Fatty liver was found in one case in agreement with autopsy, as well as liver or kidney cysts in five cases.

Fluid accumulations (anasarca, ascites) were diagnosed in seven cases with pmCT, compared to six cases at autopsy. One small pneumothorax was found with pmCT, which was not visible at autopsy. Thirteen

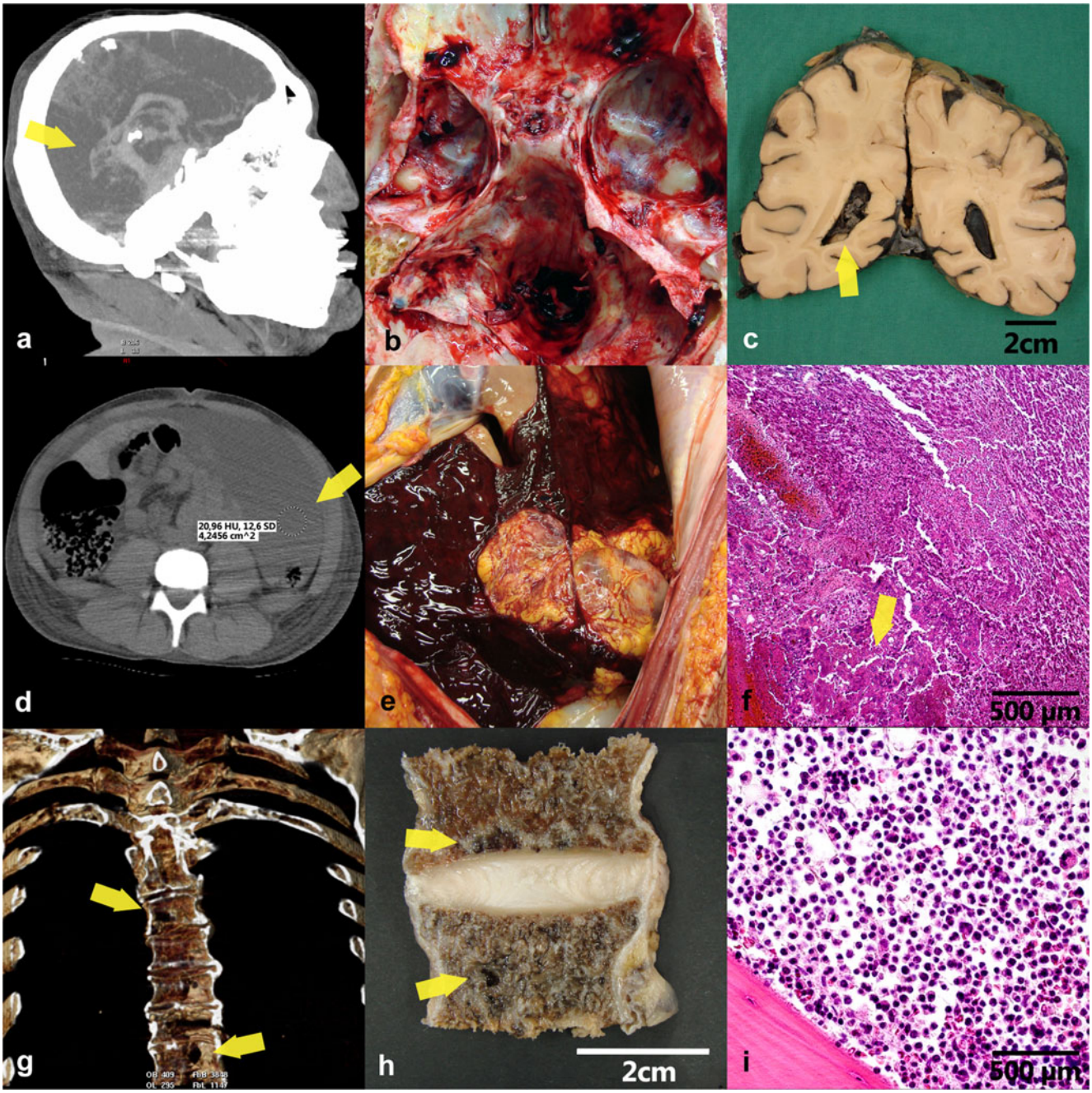

Fig. 2 **a** Subarachnoid and intraventricular haemorrhage, visible as hyperdense fluid with pmCT (*arrow*); **b** macroscopic view of skull base with haemorrhage; **c** macroscopic view of brain slice with subarachnoid and intraventricular haemorrhage (*arrow*, ventricle); **d** abdominal pmCT with intraabdominal haemorrhage, visible as hyperdense fluid with pmCT (*arrow*); **e** Macroscopic view of haematoperitoneum (*top*, liver; *middle right*, transverse colon and omentum; *down*, colon descendens); **f** hemorrhagic metastasis of chorion carcinoma in liver (*arrow*, chorion carcinoma cells); **g** three-dimensional reconstruction of spine and ribs with multiple osteolyses (*arrows*); **h** macroscopic view of vertebral bodies with osteolyses (*arrows*); **i** microscopic view of plasmocytoma cells in bone marrow

skeletal degenerations and four cases of arthroses, one of herniated vertebral disc, one of a bone cyst and one cartilaginous exostosis, were missed at autopsy.

See complete results online as supplementary material in Supplementary Table 1 (items 1–4) and Supplementary Table 2 (item 5).

Discussion

The basic methods of clinical autopsy technique including macroscopic and microscopic examination have not changed much since Virchow's time. We discuss whether radiologic imaging is capable of providing valid information

Table 4 Cross-tabulation Pathogenetic mechanism in pmCT vs. classical autopsy

Pathogenetic Mechanism (PM)			Classical autopsy			
			PM found		PM not found	
			(A+C)	15	(B+D)	13
pmCT	PM found A+B=	17	A (true pos)=	5	B (false pos)=	12
	PM not found C+D=	11	C (false neg)=	10	D (true neg)=	1
			Total A+B+C+D			28
Sensitivity=			33.33 %			
Specificity=			7.69 %			
Positive predictive value=			29.41 %	95 % CI=	13.279 to 53.133 %	
Negative predictive value=			9.09 %	95 % CI=	1.6232 to 37.735 %	
Accuracy=			21.43 %			

for diagnosing the cause of death with certainty and reliability and if pmCT adds value to the classical autopsy. Finally, a short outlook on future perspectives is given.

The diagnosis of the cause of death after pmCT matched the diagnosis after autopsy in two out of three of our cases (Table 3). The discrepancy rate of 1/3 is similar to the discrepancy rate of 30 % reported by Roberts et al. [21] and the major discrepancy rate of 12.5–40 % (depending on type of pathology) by Wichmann et al. [16]. Weustink et al. [17] report a discrepancy rate of 23 % with minimal invasive autopsy, consisting of pmCT, MRI and biopsy. The positive predictive value (PPV) of 75 % (Table 3) is obviously not representative for the wide range of diagnoses found. The PPV would ideally be calculated per diagnosis, which would require a much larger sample size.

Other publications on post-mortem imaging report difficulties in finding artery occlusions, myocardial infarctions and pulmonary lesions [22, 23].

The results show that coronary thromboses and in-stent thromboses and myocardial infarction were not found with pmCT in any case. Nevertheless, in all cases of coronary or in-stent thrombosis with myocardial infarction, a cardiac cause of death was diagnosed correctly with pmCT by deduction from associated diagnoses (congestion, coronary atherosclerosis, pleural effusion). Therefore, although the pathogenetic mechanism could not be reconstructed in full detail by the radiologist, the cause of death was diagnosed correctly. The lung is subject to post-mortem sedimentation of blood, which causes density shifts (internal livores) and makes the differentiation between pneumonia and pulmonary oedema difficult. In our study, there was only one false-positive finding of pneumonia. Still, it is difficult to correlate pathologic findings of the lung and the radiologic finding of ground glass attenuation, which not only may partly correlate with pulmonary pathologies but may partly also be caused by internal livores of the lung [24].

In contrast to artery occlusions, myocardial infarctions and pulmonary lesions, haemorrhage and haematoma can be differentiated from other liquids due to their high attenuation in pmCT (unclotted blood, 30–45 HU; clotted blood, .45–70 HU [25]). In our study, in cases of fatal haemorrhage, the intracavital bleeding was recognized equally well with pmCT and macroscopic examination. Organ sizes and configurations as well as cysts could be assessed with pmCT (myocardial hypertrophy, goitre, hepatosplenomegaly, fatty liver, liver and kidney cysts). There was a discrepancy in diagnosis of myocardial hypertrophy between radiologists and pathologists (19 at classical autopsy, 10 with pmCT). This discrepancy might be due to the poor contrast between myocardium and left ventricular lumen in unenhanced pmCT, which makes the differentiation between myocardial hypertrophy and left ventricular dilation difficult for the radiologist. Moreover, post-mortal contraction of the ventricles limits the appraisal of the imaging findings. These shortcomings caused the misinterpretation in the cause of death due to dilated cardiomyopathy, in which the myocardial hypertrophy was reported from pmCT, but dilation of the left ventricle was missed.

While dilation of heart cavities can be easily detected in vivo using contrast-enhanced CT in pmCT, the assessment of cardiac myopathy can be hindered by collapse of the heart cavities and lack of clear delineation of the myocardium due to the missing contrast agent. This is a possible explanation for the discrepancy between autopsy and pmCT findings.

A complete autopsy includes external examination for the documentation of sure signs of death (rigour mortis, livores, putrefaction, injuries not compatible with life) and other external findings. Livores and putrefaction are visible with pmCT as internal livores and intravascular gas [24]. Nevertheless, rigour mortis or punction marks cannot be assessed with pmCT. Therefore, the external examination cannot be completely replaced by imaging methods.

Information on organ colour, not only characteristic for myocardial infarction, but also other characteristic colour changes such as icterus, antracosis or colour of ascites, pleural or pericardial effusion, bile, stomach and intestinal content and “nutmeg liver” (sign of chronic passive congestion of the liver) are not visible.

The results show that the reconstruction of the pathogenetic mechanism is still challenging (Table 4). In the study, the attempt of the radiologists to reconstruct the pathogenetic mechanism was dismissed when it was not identical with the pathogenetic mechanism reconstructed by the pathologists. Probably, in some constellations, there is more than one valid interpretation of findings. Therefore, the discrepancies may be due to different focuses on the pathologies found. The presentation of the autopsy findings to the clinical colleagues requesting autopsy and the interdisciplinary discussion of case progression and autopsy findings imply an important, possibly decisive, advantage to the pathologists. Thus, an interdisciplinary discussion of pmCT findings with autopsy findings and clinical progression of every case would be desirable for the most valid diagnosis of cause of death.

There are special areas in which pmCT may even prove superior to classical autopsy: The results show that pmCT is an excellent tool for assessment and documentation of calcified and bone lesions. Histological assessment of calcified tissue is extremely time consuming, as it is necessary to decalcify tissues prior to sectioning. Furthermore, the comparison of imaging autopsy findings with findings of intravital clinical examinations, such as coronary angiography, is very simple and readily accessible for clinicians. The extremities and the joints are examined only on very rare occasions, in order not to mutilate the body. Pathologies of the musculoskeletal system, especially of the viscerocranium and the extremities, are therefore easily missed by conventional autopsy. Fractures can be missed with both methods when there is no dislocation or haemorrhage [16, 25]; therefore, a combination of both methods gives most valid results. In cases of metallic implants, beam hardening artefacts occur on pmCT images, impairing assessment of underlying structures.

Vessels and organs are opened for macroscopic examination at autopsy. Therefore, air accumulations, such as subcutaneous emphysema, intravascular or intrapericardiac air and aerobilia, are more efficiently visualized and documented with pmCT than at macroscopic examination.

The same applies to small pleural effusions and small pneumothoraces, which were seen on radiological images, but not found at clinical autopsy. With the opening of the body cavities, pressure is released; thus, lesions depending on intracavital pressure such as hiatal or inguinal hernia become invisible at macroscopic examination but are easily recognized with pmCT. The presence of catheters and tracheal tubes can be documented three-dimensionally with pmCT, as well as the site of catheter tip or tracheal tube.

Unlike at conventional autopsy, the data generated with pmCT stay stored and are readily accessible afterwards for repeated examination. Compared to CT images from living patients, with pmCT, we do not have to deal with motion artefacts or limitation of dose of radiation. In contrast to notes or pictures taken at autopsy, the images acquired with pmCT are a three-dimensional snapshot not limited by the point of view or knowledge of the individual generating them.

In the future, a method to overcome diagnostic difficulties resulting from lack of inspiration and dependent density may be post-mortem ventilation [26]. With the use of contrast enhancement, post-mortem imaging of the cardiovascular system might become equal, if not superior, to macroscopic examination, as a bleeding site might be found by extravasation of the contrast agent. In cases of haemorrhage from an unknown site, pmCT angiography could help to find an extravasation site at macroscopic examination and support macroscopic findings. The diagnostic problems concerning myocardial hypertrophy with pmCT could be overcome with contrast filling of the heart cavities. Also, the above-mentioned assessment of in-stent stenosis, in-stent thrombosis, coronary artery occlusion and aneurysms might become possible. Still, signs of intravitality of the lesions would yet need confirmation by macroscopic and histologic analysis, in order to exclude artificial extravasation or post-mortem blood clots.

Conclusion

It is amazing how much we already see on unenhanced post-mortem CT images. Concluding from our observations, unenhanced virtual autopsy represents a valuable tool for documentation of pathologic findings such as calcified lesions of the cardiovascular system, bone fractures, lesions of the musculoskeletal system, air accumulations and herniations. Therefore, pmCT complements traditional autopsy techniques. The combination of both methods enhances the diagnostic quality and completeness of the autopsy report. Furthermore, imaging data can be acquired and stored in a less observer-dependent manner to be re-evaluated ad libitum. In addition to traditional autopsy findings, visualization of pathomorphologic findings by post-mortem imaging is likely to be appreciated by clinicians and students. The acceptance of virtual autopsy as a complementary method to traditional autopsy by clinicians needs to be further evaluated.

We believe that many limitations of pmCT will be overcome in the future with the help of post-mortem angiography and CT-guided biopsy from areas of special interest. Furthermore, by interdisciplinary discussion of the results, pathologists and radiologists will get an opportunity to correlate their diagnoses with clinical findings and experience a learning curve interpreting post-mortem imaging and reconstructing the underlying pathogenetic mechanism. In order to avoid systematic errors and to define the limitations

of pmCT accurately, traditional autopsy should always be performed as a gold standard. As an instrument of clinical quality control, resident training in pathology and student teaching, traditional autopsy is still unsurpassed.

Acknowledgments The authors would like to thank Bernd Sellhaus, Marc Britz and Wim Haas.

Disclosures None.

Conflict of interest The authors declare that they have no conflict of interest.

References

1. Horowitz RE, Naritoku WY (2007) The autopsy as a performance measure and teaching tool. Hum Pathol 38:688–695
2. Krukemeyer MG, Driesch C, Dankof A, Krenn V, Hansen D, Dietel M (2007) Necessity of increasing autopsy frequency following the introduction of DRGs. Pathologe 28:294–298
3. Brinkmann B, Du CA, Vennemann B (2002) Recent data for frequency of autopsy in Germany. Dtsch Med Wochenschr 127:791–795
4. Chariot P, Witt K, Pautot V, Porcher R, Thomas G, Zafrani ES, Lemaire F (2000) Declining autopsy rate in a French hospital: physician's attitudes to the autopsy and use of autopsy material in research publications. Arch Pathol Lab Med 124:739–745
5. Lindstrom P, Janzon L, Sternby NH (1997) Declining autopsy rate in Sweden: a study of causes and consequences in Malmo, Sweden. J Intern Med 242:157–165
6. Start RD, McCulloch TA, Benbow EW, Lauder I, Underwood JC (1993) Clinical necropsy rates during the 1980s: the continued decline. J Pathol 171:63–66
7. Harrington DE, Sayre EA (2010) Managed care and measuring medical outcomes: did the rise of HMOs contribute to the fall in the autopsy rate? Soc Sci Med 70:191–198
8. Anon. (2004) The decline of the hospital autopsy: a safety and quality issue for healthcare in Australia. Med J Aust 180:281–285
9. Ishiko T (1989) Decline of autopsy rates in Japan and the significance of autopsy in gastric carcinoma. Gan To Kagaku Ryoho 16:1920–1924
10. Burton JL, Underwood J (2007) Clinical, educational, and epidemiological value of autopsy. Lancet 369:1471–1480
11. Persson A, Jackowski C, Engstrom E, Zachrisson H (2008) Advances of dual source, dual-energy imaging in postmortem CT. Eur J Radiol 68:446–455
12. Rutty GN (2007) Are autopsies necessary? The role of computed tomography as a possible alternative to invasive autopsies. Rechtsmedizin 17:21–28
13. Woodward PJ, Sohaey R, Harris DP, Jackson GM, Klatt EC, Alexander AL, Kennedy A (1997) Postmortem fetal MR imaging: comparison with findings at autopsy. AJR Am J Roentgenol 168:41–46
14. O'Donnell C, Woodford N (2008) Post-mortem radiology—a new sub-speciality? Clin Radiol 63:1189–1194
15. Shiotani S, Kohno M, Ohashi N, Yamazaki K, Nakayama H, Ito Y, Kaga K, Ebashi T, Itai Y (2002) Hyperattenuating aortic wall on postmortem computed tomography (PMCT). Radiat Med 20:201–206
16. Wichmann D, Obbelode F, Vogel H, Hoepker WW, Nierhaus A, Braune S, Sauter G, Pueschel K, Kluge S (2012) Virtual autopsy as an alternative to traditional medical autopsy in the intensive care unit: a prospective cohort study. Ann Intern Med 156:123–130
17. Weustink AC, Hunink MG, van Dijke CF, Renken NS, Krestin GP, Oosterhuis JW (2009) Minimally invasive autopsy: an alternative to conventional autopsy? Radiology 250:897–904
18. Stawicki SP, Gracias VH, Schrag SP, Martin ND, Dean AJ, Hoey BA (2008) The dead continue to teach the living: examining the role of computed tomography and magnetic resonance imaging in the setting of postmortem examinations. J Surg Educ 65:200–205
19. Ikeda G, Yamamoto R, Suzuki M, Ishikawa H, Kikuchi K, Shiotani S (2007) Postmortem computed tomography and magnetic resonance imaging in a case of terminal-stage small cell lung cancer: an experience of autopsy imaging in tumor-related death. Radiat Med 25:84–87
20. Thali MJ, Yen K, Schweitzer W, Vock P, Boesch C, Ozdoba C, Schroth G, Ith M, Sonnenschein M, Doernhoefer T, Scheurer E, Plattner T, Dirnhofer R (2003) Virtopsy, a new imaging horizon in forensic pathology: virtual autopsy by postmortem multislice computed tomography (MSCT) and magnetic resonance imaging (MRI)—a feasibility study. J Forensic Sci 48:386–403
21. Roberts IS, Benamore RE, Benbow EW, Lee SH, Harris JN, Jackson A, Mallett S, Patankar T, Peebles C, Roobottom C, Traill ZC (2012) Post-mortem imaging as an alternative to autopsy in the diagnosis of adult deaths: a validation study. Lancet 379:136–142
22. Jackowski C, Schweitzer W, Thali M, Yen K, Aghayev E, Sonnenschein M, Vock P, Dirnhofer R (2005) Virtopsy: postmortem imaging of the human heart in situ using MSCT and MRI. Forensic Sci Int 149:11–23
23. Pflederer T, Marwan M, Schepis T, Ropers D, Seltmann M, Muschiol G, Daniel WG, Achenbach S (2010) Characterization of culprit lesions in acute coronary syndromes using coronary dual-source CT angiography. Atherosclerosis 211:437–444
24. Shiotani S, Kohno M, Ohashi N, Yamazaki K, Nakayama H, Watanabe K, Oyake Y, Itai Y (2004) Non-traumatic postmortem computed tomographic (PMCT) findings of the lung. Forensic Sci Int 139:39–48
25. Lubner M, Menias C, Rucker C, Bhalla S, Peterson CM, Wang L, Gratz B (2007) Blood in the belly: CT findings of hemoperitoneum. Radiographics 27:109–125
26. Germerott T, Preiss US, Ebert LC, Ruder TD, Ross S, Flach PM, Ampanozi G, Filograna L, Thali MJ (2010) A new approach in virtopsy: postmortem ventilation in multislice computed tomography. Leg Med (Tokyo) 12:276–279

Virchows Arch (2012) 461:221–225
DOI 10.1007/s00428-012-1266-3

CASE REPORT

Transdifferentiation of pituitary thyrotrophs to lactothyrotrophs in primary hypothyroidism: case report

Mark E. Jentoft · Robert Y. Osamura · Kalman Kovacs · Ricardo V. Lloyd · Bernd W. Scheithauer

Received: 31 May 2012 / Accepted: 13 June 2012 / Published online: 3 July 2012
© Springer-Verlag 2012

Abstract Primary hypothyroidism causes adenohypophysial hyperplasia via stimulation by hypothalamic thyrotropin-releasing hormone (TRH). The effect was long thought to simply result in thyroid-stimulating hormone (TSH) and prolactin (PRL) cell hyperplasia, an increase in TSH and PRL blood levels with resultant pituitary enlargement, often mimicking adenoma. Recently, it was shown that transformation of growth hormone (GH) cells into TSH cells takes place in both clinical and experimental primary hypothyroidism. Such shifts from one cell to another with a concomitant change in hormone production are termed "transdifferentiation" and involve the gradual acquisition of morphologic features of thyrotrophs ("somatothyrotrophs"). We recently encountered a unique case of pituitary hyperplasia in a 40-year-old female with primary hypothyroidism wherein increased TSH production was by way of PRL cell recruitment. The resultant "lactothyrotrophs" maintained TSH cell morphology (cellular elongation and prominence of PAS-positive lysosomes) but expressed immunoreactivity for both hormones. No co-expression of GH was noted nor was thyroidectomy cells seen. This form of transdifferentiation has not previously been described.

Keywords Transdifferentiation · Hypothyroidism · Pituitary hyperplasia · Thyrotroph · Lactotroph · Lactothyrotroph

Bernd W. Scheithauer is deceased.

M. E. Jentoft · B. W. Scheithauer
Department of Laboratory Medicine and Pathology, Mayo Clinic, Rochester, MN, USA

K. Kovacs
Department of Laboratory Medicine, St. Michael's Hospital, University of Toronto, Toronto, ON, Canada

R. V. Lloyd
Department of Pathology, University of Wisconsin School of Medicine and Public Health, Madison, WI, USA

R. Y. Osamura
Teikyo University Chiba Medical Center, Chiba, Japan

M. E. Jentoft (✉)
Department of Laboratory Medicine and Pathology, Mayo Clinic, 200 First Street, SW, Rochester, MN 55905, USA
e-mail: jentoft.mark@mayo.edu

Introduction

Primary hypothyroidism has been shown to be associated with increased blood TSH and PRL levels, which often normalize after treatment with thyroid hormones [1, 2]. Hypothyroidism-induced pituitary hyperplasia is a well-documented phenomenon known to result from lack of feedback-inhibition by thyroid hormones. Decreased circulating levels of T3 (triiodothyronine) and T4 (thyroxine) lead to the hypersecretion of both TSH and PRL, the stimulatory result of hypothalamic TRH [3]. PRL is known to be secreted in response to TRH and is the basis for hyperprolactinemia in the setting of primary hypothyroidism [4, 5]. Originally, "one cell–one hormone" was the paradigm of adenohypophysial pathophysiology. With the recognition of plurihormonal pituitary adenomas [6], the concept was abandoned, a pattern also justified upon the demonstration of transdifferentiation, the conversion of one cell type to another with simultaneous secreting of two different hormones, in both the clinical and experimental

setting. A classic example is primary hypothyroidism wherein one sees somatotrophs transform to so-called "somatothyrotrophs," GH cells co-secreting GH and TSH [7]. Such transdifferentiation also occurs in experimentally induced primary hypothyroidism in dogs and rats [8, 9]. Herein, we describe a form of transdifferentiation not reported to date.

Clinical history

The patient is a 40-year-old female with longstanding primary hypothyroidism and poor medication compliance. She presented with a 4-month history of constant, gradually worsening headaches and occasional double and/or blurred vision. On computer tomographic (CT) and magnetic resonance imaging (MRI) scans (Fig. 1), a 1-cm sellar mass thought to represent a pituitary adenoma was seen to cause superior displacement of the optic chiasm. Within a month of surgery, the blood PRL level was 54 ng/mL (normal 3–30 ng/mL); the mild elevation was thought to be due to pituitary stalk compression. Serum TSH levels had been markedly elevated at over 800 μIU/mL (normal 0.4-4.5 μIU/mL) but were presently normal due to recent, short-term compliance in taking Synthroid. Blood cortisol, luteinizing hormone (LH) and follicle-stimulating hormone (FSH) levels were normal.

Materials and methods

A transsphenoidal resection was undertaken in hopes of relieving headaches and avoiding chiasmal damage. Upon incising the dura, soft, somewhat lobulated yellow tissue was seen. The lesion was debulked until more normal-appearing pituitary tissue remained. Initial assessment of the specimen revealed abnormal pituitary tissue but not an adenoma as had been clinically suspected. The possibility of thyrotroph hyperplasia was entertained since acinar architecture, despite expansion, was relatively preserved.

Results

On consultative review of the specimen, the pituitary tissue revealed the usual morphologic heterogeneity of adenohypophysial cell types (Fig. 2) but was associated with conspicuous acinar expansion. Affected acini featured cytologically monomorphous, chromophobic cells, often elongate and extending across the variably expanded acini. Periodic acid-Schiff staining demonstrated cytoplasmic lysosomes of varying size within their cytoplasm (Fig. 3). Also of note were small numbers of psammomatous calcifications. Immunohistochemistry (avidin–biotin–peroxidase complex method) revealed the full spectrum of pituitary hormones. Antibody sources and dilutions of the pituitary battery consisting of TSH, PRL, GH, adrenocorticotropin (ACTH), LH, and FSH as well as control methods are described elsewhere [10]. The monotonous cells, both within expanded acini as well as in the surrounding pituitary, were immunopositive for TSH and to a lesser extent PRL. Cells staining for GH, ACTH, LH and FSH were normal in distribution.

Immunohistochemistry for transcription factors and techniques are as follows; Pit-1 (polyclonal antibody; dilution, 1:100; sc-442; Santa Cruz) and GATA-2 (polyclonal antibody; dilution, 1:100; sc-1235; Santa Cruz). The sections were deparaffinized in xylene, dehydrated in graded ethanol, and endogenous peroxidase activity was blocked with 0.3 % hydrogen peroxide in methanol. They were then soaked and autoclaved for 5 min in the antigen retrieval solution, Citra-Plus Reagent (pH 6.0, BioGenex) at 121 °C, allowed to cool to room temperature and washed with 0.01 M phosphate-buffered saline (PBS). The sections were treated with primary antibodies overnight at 4 °C. After washing in 0.01 M PBS, sections were incubated with biotinylated anti-rabbit, anti-

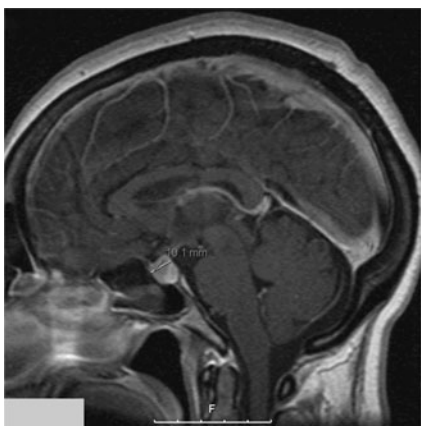

Fig. 1 MRI scan demonstrating an enlargement of the pituitary gland with mild suprasellar extension nearly abutting the optic chiasm

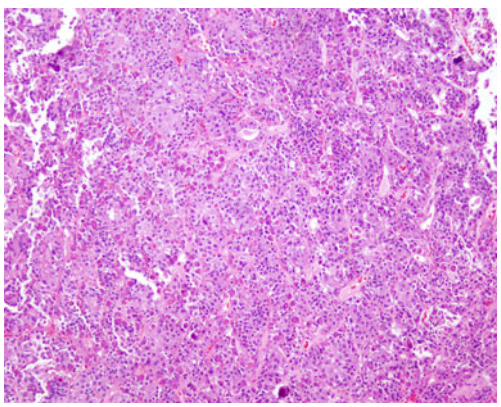

Fig. 2 (H&E) Heterogeneous mixture of adenohypopysial cell types seen as are occasional scattered calcifications

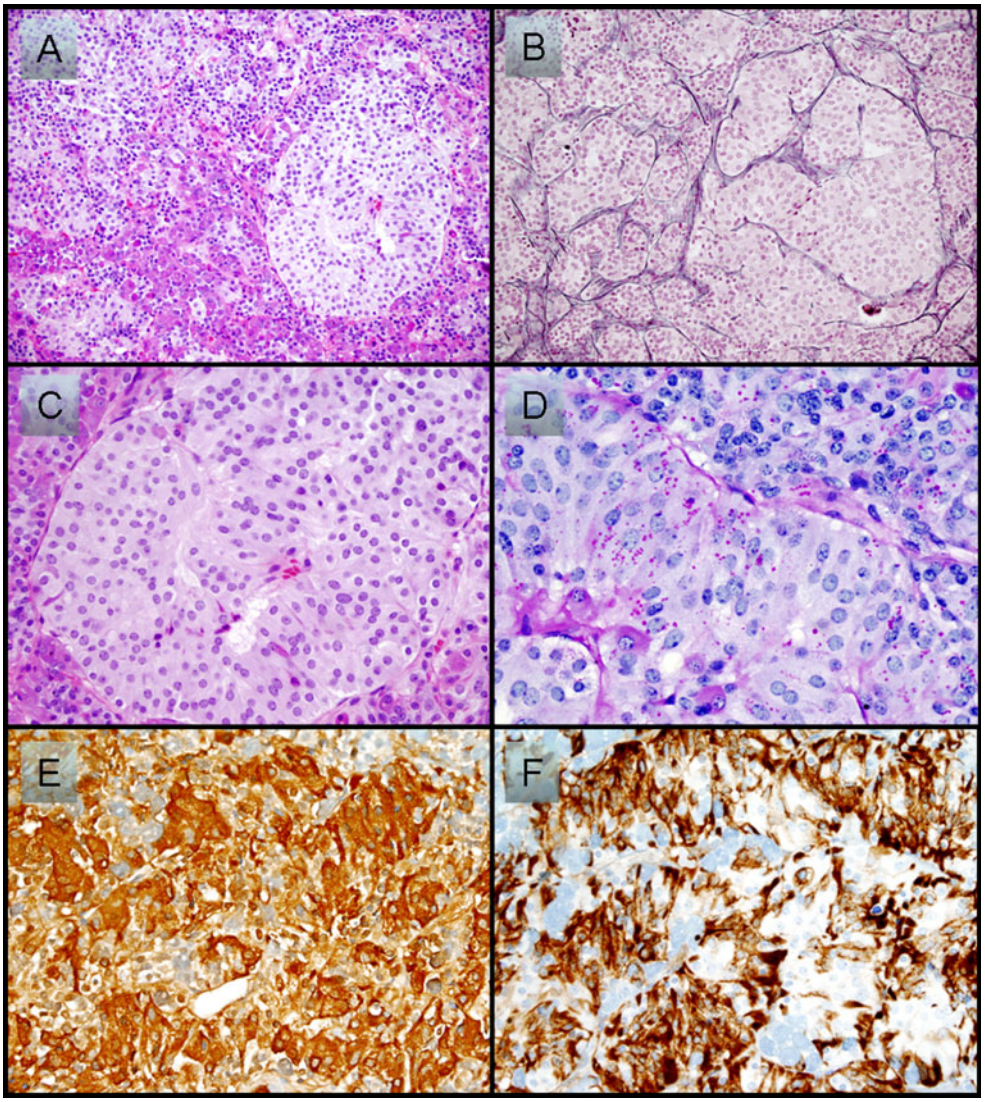

Fig. 3 (H&E) Expanded acinus of chromophobic cells seen in associated background admixture of other adenohypophysial cells (**a**); (Reticulin) acinar architecture expanded and intact (**b**; H&E) elongate, monotonous, chromophobic cells expanding an acinus (**c**); (PAS) PAS-positive cytoplasmic globules, a common feature of TSH cells, represent lysosomes (**d**) note staining in the same population of elongate hyperplastic cells in expanded acini for TSH (**e**) and PRL (**f**) hyperplastic cells in expanded acini (**a**, **c** H&E; **b** Gomori reticulin; **d** periodic acid-Schiff; **e**, **f** immunohistochemical stains)

mouse or anti-goat secondary antibody (1:50 dilution; Jackson Immuno-Research, Laboratories, West Grove, PA) for 1 h at room temperature. The immunohistochemical reaction was developed using a Vectastain ABC kit (Vector Laboratories, Inc., Burlingame, CA), and antigens were visualized by treatment of the slide with 50 mM Tris–HCl buffer (pH 7.6) containing 0.3 % 3,3-diaminobenzidine (DAB) and 0.03 % H_2O_2 for 3–5 min at room temperature.

Dual immunohistochemical staining was performed to determine colocalization for TSH and PRL; the methods for dual immunohistochemical staining are described elsewhere [11]. Dual staining for TSH and PRL was noted within some cells in the hyperplastic acini (Fig. 4).

Discussion

Our case is an example of adenohypophysial hyperplasia occurring in the setting of primary hypothyroidism. It has its basis not only in TSH cell (thyrotroph) and PRL cell (lactotroph) hyperplasia but is known to involve transdifferentiation of GH cells (somatotrophs) to ones secreting both GH and TSH [7]. Such cells are termed "thyrosomatotrophs." While these biphenotypic cells stain for both hormones, they ultrastructurally have come to resemble thyrotrophs. The present case differs from this response. The hyperplastic cells in our case morphologically resembled thyrotrophs in being elongate in configuration and containing abundant, sizable lysosomes. Furthermore, the second hormone expressed was not GH but PRL. As expected in hypothyroidism, preoperative serum elevations of both TSH and PRL were noted. The presence of rare psammoma bodies in normal adenohypophysis, a feature in our case, is a reflection of hyperprolactinemia. They are seen in 10 % of prolactinomas [12] and have previously been documented in combined lactotroph and thyrotroph hyperplasia in the setting of primary hypothyroidism [5]. Psammoma bodies are also a feature of the pituitary in the neonatal period, which is characterized by PRL elevations [13, 14].

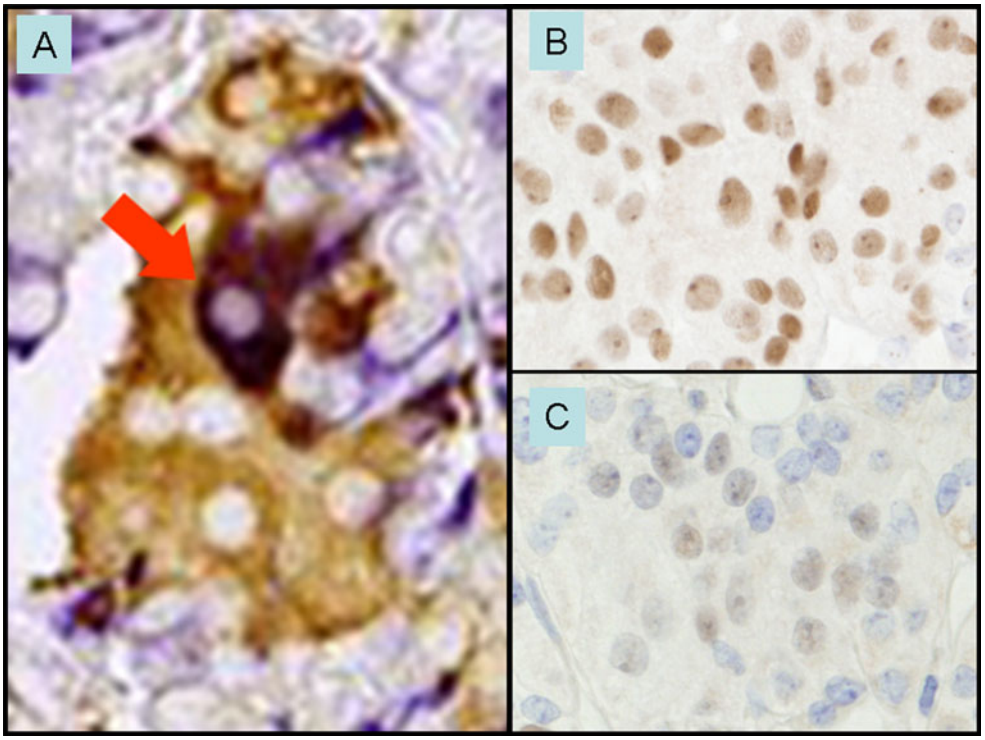

Fig. 4 Dual immunohistochemical staining (**a**) performed for TSH (*brown*) and PRL (*blue*); dual positive cell present within hyperplastic lobules as represented by the *arrow*; immunohistochemical staining for transcription factors in the areas of hyperplasia; nuclei strongly positive for Pit-1 (**b**) weakly positive for GATA-2 (**c**)

The literature clearly indicates that combined thyrotroph and lactotroph cell hyperplasia occurs in the setting of primary hypothyroidism. It has been well documented histologically, immunohistochemically and at the biochemical level [3, 5, 15]. This results in pituitary enlargement as well as increases in blood TSH and PRL levels which often resolves after replacement therapy [3, 15]. On occasion, however, mass effect and hormone elevations persist and necessitate surgical intervention [5].

Two main mechanisms appear to contribute to increased blood PRL levels and lactotroph hyperplasia in primary hypothyroidism. Both involve stimulatory effects upon lactotrophs, one being the hypothalamic-releasing hormone TRH and the other effect of interruption of down flow of hypothalamic dopamine ("stalk section effect"). Inhibition of PRL secretion, the physiologic effect of dopamine, results in mild to moderately elevated PRL levels [4]. In addition, TRH is known to stimulate lactotrophs. As a result, blood PRL levels are elevated in up to 20 % of patients with primary hypothyroidism [4]. Both of these mechanisms likely contributed to hyperprolactinemia in our case. It is of note that TRH-R1 receptor-deficient mice have decreases in both blood PRL levels and pituitary PRL mRNA when compared to control mice [16]. In comparison, suckling produces less of an increase in both [16]. In yet another study, TRH-deficient mice demonstrated significantly decreased pituitary PRL mRNA levels in response to primary hypothyroidism [17]. The levels normalized with thyroid hormone replacement, leading to the conclusion that the reduction in PRL mRNA level seen in TRH-deficient mice was also the result of primary hypothyroidism. Interestingly, such TRH-deficient mice had normal blood and pituitary concentrations of PRL [17]. A TRH receptor-inactivating mutation causing lack of TRH binding was recently reported in a child and resulted in lack of an increase in TSH and PRL following intravenous TRH administration. As in the TRH-deficient mice, this patient's blood PRL levels were also within normal limits [18]. Reports, such as these, show that TRH is indeed involved in the regulation of PRL, although the extent to which it does remains unclear.

The mechanism by which TRH induces TSH and PRL gene expression is unclear, but there is evidence that TRH activates calcium–calmodulin-dependent protein kinase cascade in pituitary cells [19]. Thyrotroph hyperplasia in our case is undoubtedly the result of TRH elevation, itself the result of primary hypothyroidism. Although TRH likely played a role in increasing serum PRL levels, pituitary enlargement with resultant stalk section effect may have further promoted PRL secretion.

Transdifferentiation in pathologic states is an uncommon event. In normal physiology, it is well-known to occur in pregnancy wherein GH cells transform to PRL cells, an event reversed postpartum or upon cessation of breastfeeding [20, 21]. Although primary hypothyroidism is the only documented pathophysiologic example [5], it may be that GH-to-PRL cell transformation occurs in estrogen-mediated prolactin cell hyperplasia. Interestingly, LH/FSH cell transition to ACTH cells in gonadotropic adenomas has also been documented, although this phenomenon is rare [22, 23]. TSH, GH, and PRL cells are particularly prone to undergo transdifferentiation, which may be a reflection of their

cytogenesis. All three share the common transcription factor Pit1 [5]. This explains the multi-hormonal immunophenotype pattern (GH, PRL, and TSH) of pituitary in acromegaly-associated pituitary adenomas [24]. Recent studies have also shown that TTF-1 regulates PRL and GH transcription in the GH3 tumor cell line, suggesting that it may also be involved in transdifferentiation of cells expressing PRL, GH, and possibly TSH [25]. The hyperplastic cells in our case were strongly positive for Pit-1 and less intensely for GATA-1 (Fig.4). It has been reported that Pit-1 promotes the differentiation of the pituitary cells to GH, PRL, and TSH [26].

In any event, regardless of the mechanisms underlying TSH and PRL cell hyperplasia, our case provides an example of adenohypophysial transdifferentiation in primary hypothyroidism. The hybrid cells (lactothyrotrophs) have not previously been described.

Acknowledgments The authors express appreciation to the Jarislowsky and Lloyd Carr-Harris Foundations for their generous support of our research. We also thank Mrs. Denise Chase for the excellent secretarial support.

Conflict of interest The authors declare that they have no conflict of interest.

References

1. Hung W, Fitz CR, Lee ED (1990) Pituitary enlargement due to lingual thyroid gland and primary hypothyroidism. Pediatr Neurol 6:60–62
2. Raber W, Gessl A, Nowotny P, Vierhapper H (2003) Hyperprolactinaemia in hypothyroidism: clinical significance and impact of TSH normalization. Clin Endocrinol 58:185–191
3. Alves C, Alves AC (2008) Primary hypothyroidism in a child simulating a prolactin-secreting adenoma. Childs Nerv Syst 24:1505–1508
4. Kronenberg HMMS, Polonsky KS, Larsen PR (2008) Williams textbook of endocrinology. Saunders Elsevier, Philadelphia, 2008
5. Pioro EP, Scheithauer BW, Laws ER Jr, Randall RV, Kovacs KT, Horvath E (1988) Combined thyrotroph and lactotroph cell hyperplasia simulating prolactin-secreting pituitary adenoma in long-standing primary hypothyroidism. Surg Neurol 29:218–226
6. Scheithauer BW, Horvath E, Kovacs K, Laws ER Jr, Randall RV, Ryan N (1986) Plurihormonal pituitary adenomas. Semin Diagn Pathol 3:69–82
7. Vidal S, Horvath E, Kovacs K, Cohen SM, Lloyd RV, Scheithauer BW (2000) Transdifferentiation of somatotrophs to thyrotrophs in the pituitary of patients with protracted primary hypothyroidism. Virchows Arch 436:43–51
8. Diaz-Espineira MM, Mol JA, van den Ingh TS, van der Vlugt-Meijer RH, Rijnberk A, Kooistra HS (2008) Functional and morphological changes in the adenohypophysis of dogs with induced primary hypothyroidism: loss of TSH hypersecretion, hypersomatotropism, hypoprolactinemia, and pituitary enlargement with transdifferentiation. Domest Anim Endocrinol 35:98–111
9. Radian S, Coculescu M, Morris JF (2003) Somatotroph to thyrotroph cell transdifferentiation during experimental hypothyroidism - a light and electron-microscopy study. J Cell Mol Med 7:297–306
10. Yamada S, Sano T, Stefaneanu L, Kovacs K, Aiba T, Sawano S, Shishiba Y (1993) Endocrine and morphological study of a clinically silent somatotroph adenoma of the human pituitary. J Clin Endocrinol Metab 76:352–356
11. Inada K, Oda K, Utsunomiya H, Itoh J, Osamura RY (1992) Immunohistochemical analysis of GH-producing adenomas–with special emphasis on plurihormonality of individual tumor cells by double staining. Tokai J Exp Clin Med 17:213–222
12. Scheithauer BW (1984) Surgical pathology of the pituitary: the adenomas. Part I Pathol Annu 19(Pt 1):317–374
13. Groisman GM, Amar M, Polak-Charcon S (1999) Microcalcifications in the anterior pituitary gland of the fetus and the newborn: a histochemical and immunohistochemical study. Hum Pathol 30:199–202
14. Terada T, Stefaneanu L (1996) Vanishing psammoma bodies in the anterior pituitary of the human newborn: an immunohistochemical and histometric study. Endocr Pathol 7:151–157
15. Hopper NW, Albanese A (2005) Primary hypothyroidism in a child mimicking a pituitary macroadenoma. Horm Res 63:61–64
16. Rabeler R, Mittag J, Geffers L, Ruther U, Leitges M, Parlow AF, Visser TJ, Bauer K (2004) Generation of thyrotropin-releasing hormone receptor 1-deficient mice as an animal model of central hypothyroidism. Mol Endocrinol 18:1450–1460
17. Yamada M, Shibusawa N, Ishii S, Horiguchi K, Umezawa R, Hashimoto K, Monden T, Satoh T, Hirato J, Mori M (2006) Prolactin secretion in mice with thyrotropin-releasing hormone deficiency. Endocrinology 147:2591–2596
18. Collu R, Tang J, Castagne J, Lagace G, Masson N, Huot C, Deal C, Delvin E, Faccenda E, Eidne KA, Van Vliet G (1997) A novel mechanism for isolated central hypothyroidism: inactivating mutations in the thyrotropin-releasing hormone receptor gene. J Clin Endocrinol Metab 82:1561–1565
19. Murao K, Imachi H, Cao WM, Yu X, Tokumitsu H, Inuzuka H, Wong NC, Shupnik MA, Kobayashi R, Ishida T (2004) Role of calcium-calmodulin-dependent protein kinase cascade in thyrotropin (TSH)-releasing hormone induction of TSH and prolactin gene expression. Endocrinology 145:4846–4852
20. Scheithauer BW, Sano T, Kovacs KT, Young WF Jr, Ryan N, Randall RV (1990) The pituitary gland in pregnancy: a clinicopathologic and immunohistochemical study of 69 cases. Mayo Clin Proc 65:461–474
21. Vidal S, Horvath E, Kovacs K, Lloyd RV, Smyth HS (2001) Reversible transdifferentiation: interconversion of somatotrophs and lactotrophs in pituitary hyperplasia. Mod Pathol 14:20–28
22. Egensperger R, Scheithauer BW, Horvath E, Kovacs K, Giannini C, Young WF, Lloyd R, Atkinson J, Nippoldt TB (2001) Cushing's disease due to plurihormonal adrenocorticotropic hormone and gonadotropin-producing pituitary adenoma. Acta neuropathologica 102:398–403
23. Ikeda H, Yoshimoto T, Kovacs K, Horvath E (1995) Cushing's disease due to female gonadotroph adenoma of the pituitary. Clin Endocrinol 43:383–386
24. Salehi F, Cohen S, Syro LV, Uribe H, Horvath E, Kovacs K, Asa SL (2006) Plurihormonality in pituitary adenomas associated with acromegaly. Endocr Pathol 17:291–296
25. Lee NO, Son YJ, Kim JG, Ha CM, Yun CH, Lim HL, Park JW, D'Elia AV, Damante G, Lee BJ (2007) TTF-1 regulates growth hormone and prolactin transcription in the anterior pituitary gland. Biochem Biophys Res Commun 362:193–199
26. Osamura RY, Oda K, Utsunomiya H, Inada K, Umemura S, Shibuya M, Katakami H, Voss JW, Mayo KE, Rosenfeld MG (1993) Immunohistochemical expression of PIT-1 protein in pituitary glands of human GRF transgenic mice: its relationship with hormonal expressions. Endocr J 40:133–139

Virchows Arch (2012) 461:227–229
DOI 10.1007/s00428-012-1264-5

LETTER TO THE EDITOR

Intestinal metaplasia and colonization of endometriosis in a case of an appendiceal mucinous neoplasm

Louis Libbrecht · Christophe Snauwaert · Martine De Vos · Karel Geboes · Claude Cuvelier · Liesbeth Ferdinande

Received: 1 June 2012 / Accepted: 13 June 2012 / Published online: 27 June 2012
© Springer-Verlag 2012

Intestinal endometriosis is reported in 15–37 % of patients with pelvic endometriosis [1]. Making a correct diagnosis can be challenging for clinicians as well as for pathologists as this disease is able to mimic other pathologies such as inflammatory bowel disease, infectious etiologies, or neoplasms. The appendix is less commonly involved than the small or large intestine. Endometriosis of the appendix is often asymptomatic and discovered as an incidental finding, but it may also present as an acute or chronic appendicitis, occasionally with the formation of an inflammatory mass, mimicking a neoplasm [1]. A few case reports describe the development of obstructive mucocoeles secondary to endometriosis of the appendix. These mucin-filled cystic dilatations of the appendix were lined by normal epithelium without hyperplastic or neoplastic changes [2]. We report the case of an appendiceal mucinous neoplasm in association with endometriosis in a 48-year-old woman. The appendiceal lesion was an incidental finding in this patient who underwent imaging for an episode of pancreatitis. Surgery was performed. Microscopic examination demonstrated that the cystic lesion was covered by a mucosa with serrated and dilated crypts that assumed L- and inverted T-shapes (Fig. 1). The crypts were lined by columnar epithelial cells with low-grade atypia. With the presence of extra-appendiceal acellular mucin, this lead to the diagnosis of a low-grade mucinous neoplasm with low risk of recurrence [3]. In addition, the wall of the appendix showed numerous foci of endometriosis consisting of endometrial glands embedded in variable amounts of endometrial stroma, confirmed with ER and CD10 immunohistochemistry (not shown). Interestingly, some of the glandular structures that were embedded in the endometrial stroma were lined by mucinous epithelium, very similar to the epithelium observed in the appendiceal mucinous neoplasm. Immunohistochemistry demonstrated CK7 expression in the normal endometrial epithelium and CK20 expression in the mucinous epithelium. Two theories could explain this finding.

Firstly, the epithelium of the appendiceal mucinous neoplasm colonizes the endometrial glands of the appendiceal endometriosis. In intestinal endometriosis, endometrial glands can merge with the surface epithelium and be continuous with it [1, 4]. Secondly, the endometrial glands undergo metaplastic mucinous changes. Mucinous metaplasia in endometriosis is a well-known phenomenon, although it more often mimics endocervical epithelium. Intestinal-type mucinous metaplasia with goblet cells and Paneth cells has been described, but is rare [5]. In our opinion, both explanations can account for the observations in this case. In a few glands, both types of epithelium were continuous. The transition between the normal endometrial epithelium and the mucinous epithelium was very abrupt. Focally, some Paneth cells were present. The glands were dilated and showed serrated growth pattern. Similar cytological and architectural characteristics as recognized in the neoplasm and the sharp demarcation between both types of epithelium suggest that the mucinous changes of the epithelium are due to colonization of the endometrial glands (Figs. 2, 3, 4, and 5). In other areas, the

L. Libbrecht · K. Geboes · C. Cuvelier · L. Ferdinande (✉)
Department of Pathology, Ghent University Hospital,
De Pintelaan 185,
9000 Ghent, Belgium
e-mail: Liesbeth.Ferdinande@UGent.be

C. Snauwaert · M. De Vos
Department of Gastroenterology, Ghent University Hospital,
De Pintelaan 185,
9000 Ghent, Belgium

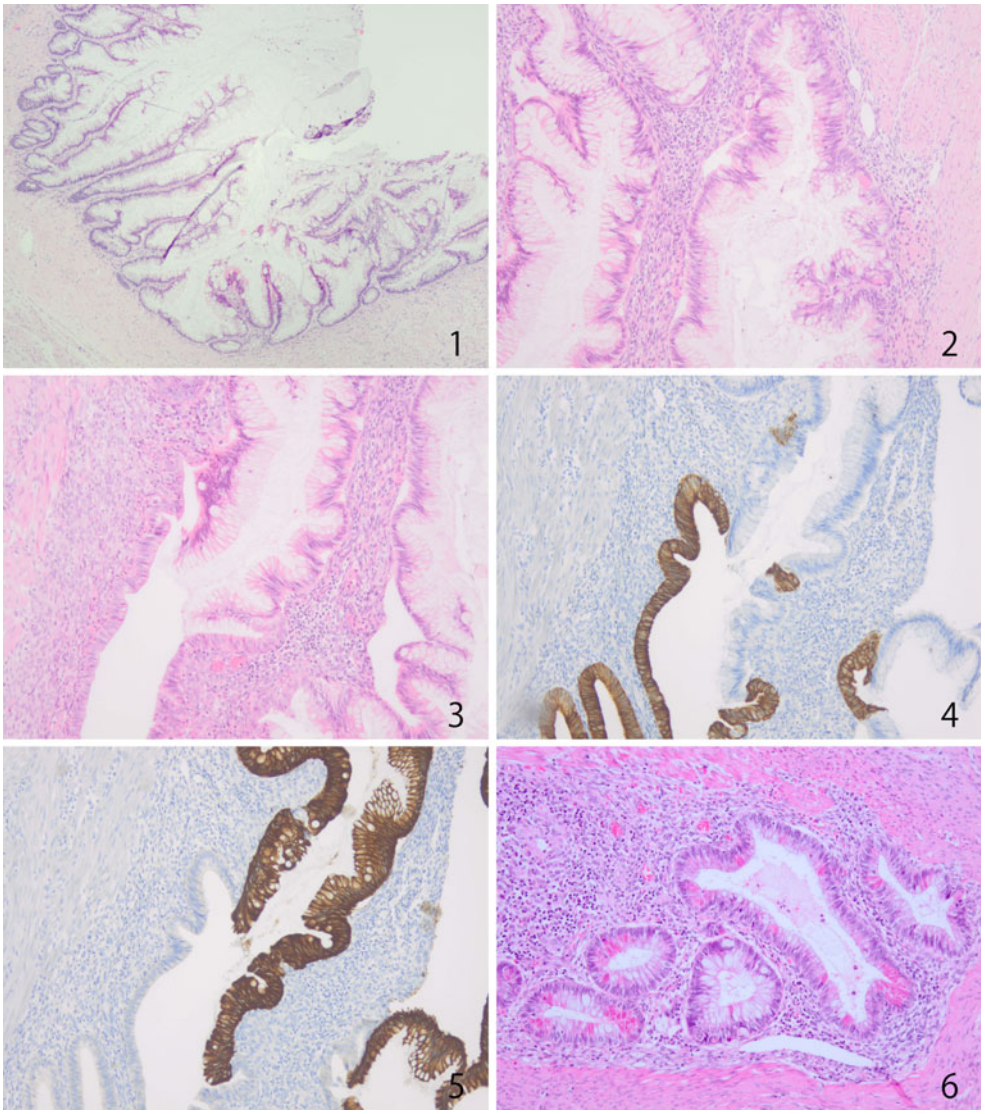

Figs. 1–6 *1* Low-grade mucinous neoplasm with low risk of recurrence (haematoxylin-eosin). *2–5* The appendiceal mucinous neoplasm colonizes the glands of the appendiceal endometriosis. In these areas, an abrupt transition between both types of epithelium is observed with different immunohistochemical profiles (*2–3* haematoxylin-eosin, *4* CK7 immunohistochemistry, *5* CK20 immunohistochemistry). *6* Intestinal-type mucinous metaplasia of the appendiceal endometriosis with mucinous cells and Paneth cells (haematoxylin-eosin)

glands did not display complex serrated architecture and the epithelium consisted of an equal mixture of mucinous cells and Paneth cells. Probably, these areas represent metaplastic changes, featuring intestinal-type mucinous metaplasia (Fig. 6).

In the context of mucinous appendiceal neoplasms, it is important not to consider the glands lined by mucinous epithelium as invasive neoplastic glands, but as metaplastic or colonized endometrial glands. The lack of nuclear atypia and desmoplastic reaction and the presence of endometrial stroma surrounding the glands are in favor of the latter.

In contrast to the previously described mucocoeles, the development of the appendiceal mucinous neoplasm was probably not a consequence of the endometriosis as it concerns a true neoplasm with more complex pathogenesis than merely an obstructive problem. Whether there is an association between the endometrial metaplasia and the mucinous neoplasm, however, remains unclear. Endometrial metaplasia may arise as a response to hormonal or other stimuli and it cannot be excluded that in this case the mucinous metaplasia in the endometrial glands was induced by the vicinity of a mucinous neoplasm and its growth factors.

References

1. Yantiss RY, Clement PB, Young RH (2001) Endometriosis of the intestinal tract. A study of 44 cases of a disease that may cause diverse challenges in clinical and pathologic evaluation. Am J Surg Pathol 25:445–454
2. Driman DK, Melega DE, Vilos GA, Plewes EA (2000) Mucocele of the appendix secondary to endometriosis. Report of two

cases, one with localized pseudomyxoma peritonei. Am J Clin Pathol 113:860–864
3. Pai RK, Beck AH, Norton JA, Longacre TA (2009) Appendiceal mucinous neoplasms. Clinicopathologic study of 116 cases with analysis of factors predicting recurrence. Am J Surg Pathol 33:1425–1439
4. Ponsford Tipps AM, Weidner N (2011) Colonization of intestinal endometriosis by benign colonic mucosa: a pattern potentially misdiagnosed as invasive mucinous carcinoma. Int J Surg Pathol 19:259–262
5. Mai KT, Burns BF (1999) Development of dysplastic mucinous epithelium from endometriosis of the appendix. Histopathology 35:368–372

Virchows Arch (2012) 461:231–243
DOI 10.1007/s00428-012-1287-y

REVIEW AND PERSPECTIVES

Understanding molecular mechanisms in peritoneal dissemination of colorectal cancer

Future possibilities for personalised treatment by use of biomarkers

E. M. V. de Cuba · R. Kwakman · M. van Egmond · L. J. W. Bosch · H. J. Bonjer · G. A. Meijer · E. A. te Velde

Received: 24 April 2012 / Revised: 5 July 2012 / Accepted: 6 July 2012 / Published online: 24 July 2012
© Springer-Verlag 2012

Abstract When colorectal cancer (CRC) metastasizes, this is mostly to the liver via the portal circulation. In addition, 10–25 % of CRC patients eventually show metastases in the peritoneum. A selection of these patients is treated with cytoreductive surgery (CRS) and hyperthermic intraperitoneal chemotherapy (HIPEC). However, several clinical needs still exist in which biomarkers could play an important role. Relatively little is known about the biology of peritoneal spread of CRC. The development of peritoneal metastases (PM) involves several steps, including: detachment of malignant cells; anoikis evasion; attachment to and invasion of the peritoneal surface ultimately ending in a colonization phase in which the malignant cells thrive in the newly formed niche. In this paper, we provide an overview of molecules associated with peritoneal dissemination and explore the clinical possibilities of these candidate biomarkers. A literature search was conducted using the PubMed database of the U.S. National Library of Medicine and Medline to identify studies on the biological behaviour of PM of CRC. In a series of over 100 studies on PM published between 1990 and 2010, IGF-1, HIF1α, VEGF, EGFR and ITGB1 emerge as the most interesting candidates for possible clinical application. Even though these promising candidate biomarkers have been identified, all of these require extensive further validation prior to clinical application. Yet, the pace of the omics revolution makes that the question is not if, but when biomarkers will be introduced to improve diagnosis and ultimately outcome of patients with PM due to CRC.

Keywords Peritoneal metastases · Colorectal cancer · Cytoreductive surgery · HIPEC · Biomarkers · Targets

E. M. V. de Cuba · R. Kwakman · M. van Egmond · H. J. Bonjer · E. A. te Velde (✉)
Department of Surgical Oncology,
VU University Medical Center, Amsterdam,
De Boelelaan 1117,
1081 HV Amsterdam, The Netherlands
e-mail: e.tevelde@vumc.nl

L. J. W. Bosch · G. A. Meijer
Department of Pathology,
VU University Medical Center, Amsterdam,
De Boelelaan 1118,
1081 HZ Amsterdam, The Netherlands

Introduction

Colorectal carcinoma (CRC) is a major health problem, being the third most common cancer worldwide. Each year, more than 1 million people develop CRC, and over 600,000 patients die of this cancer, despite improvements in diagnostic and treatment modalities [1]. Approximately half of CRC patients develop metastases, mainly to the liver via the portal vein system [2, 3]. Another category of distant metastases from CRC are those to the peritoneum, i.e., peritoneal metastases (PM). In up to 25 % of patients with metastatic CRC, the peritoneum is the sole site of metastasis [3, 4]. Untreated PM is associated with poor survival of about 6–12 months, while systemic chemotherapy alone does not appear to yield any clinically significant survival benefit [5, 6].

In the early 1990s, a treatment with a curative intent for patients with PM of CRC, without evidence of distant metastasis to other sites, was introduced. This consists of debulking surgery (cytoreductive surgery [CRS]) combined with heated intra-peritoneal chemotherapy (HIPEC) [7, 8]. This approach is based on the hypothesis that peritoneal

dissemination is a form of local rather than systemic spread, which in theory makes PM amenable to a form of local disease control, i.e., surgery [9]. This theory is further supported by the observation that a subgroup of patients, in whom no residual macroscopic tumour is left after resection, shows a 5-year survival of 35–45 % [10]. This is equal to the survival of patients undergoing resection for liver metastasis, which to date is part of the standard of care for liver metastases of colorectal origin (CRLM) [3, 10, 11].

Thus, patients with resectable metastatic colorectal cancer, either to the liver or the peritoneum, have benefitted from the aggressive surgical management. However, because treatment with CRS and HIPEC has a morbidity and mortality rate of 15–18 % and 5 %, respectively, it is of utmost importance to be able to carefully select those patients who will benefit most from this treatment [4, 5, 10, 12]. In addition, major challenges in diagnosing and treating PM remain. For example, most early peritoneal lesions are smaller than 1 cm, and as such not visible on pre-operative computed tomography (CT) or positron emission tomography (PET) scans, which hampers both timely diagnosis and adequate monitoring of patients with PM [12]. Furthermore, the chemotherapy that is used in HIPEC is still based on the "one size fits all" principle, without any biological stratification.

At present, the selection of patients is made roughly on clinical parameters and intra-operative findings. Based on the hypothesis that the phenotype, and thus clinical behaviour, of PM in CRC is driven by underlying biological mechanisms, readouts of disease biology (i.e., biomarkers) will be of help for more refined identification of suitable patients. Additionally, adequate targets may be of great value in prognosis assessment, imaging and guidance of therapy.

The aim of the present paper is therefore to provide an overview of promising molecular changes reported to be involved in peritoneal dissemination of CRC and to evaluate the potential for clinical application of these biomarkers.

Materials and methods

A literature search was conducted using the PubMed database of the U.S. National Library of Medicine and Medline using the following keywords: peritoneal metastasis, CRC, biological behaviour, detachment, motility, anoikis, attachment, invasion, angiogenesis, proliferation, epithelial to mesenchymal transition (EMT), immunohistochemistry (IHC), proteins, HIPEC and combinations of these keywords. These search terms were used in order to include as many articles as possible on the subject. Additional papers were included by cross-referencing from papers retrieved in the first search.

Articles from 1990 up to 2010 on biomarkers in PM of CRC were included for individual review, and only so when fitting the scope of this paper. A second reader conducted additional review when necessary. Studies on ovarian, gastric, and carcinoma of the pancreas spread to the peritoneum were included for review as well. Reports on in vivo, in vitro as well as ex vivo experiments were included.

Results

The process of metastasis in general comprises different phases: First, tumour cells detach from the primary tumour, second, they migrate to the distant site, and third they adapt to the new microenvironment, i.e., niche, and grow out [13, 14].

The niche in question, the peritoneum, is the surface of the abdominal wall. It is made up of a single layer of mesothelial cells on a basement membrane supported by a connective tissue or stroma compartment, also referred to as the submesothelium, which forms the niche for PM. This submesothelium consists of stromal cells and extracellular matrix (ECM), which is composed of laminin, collagen, fibronectin, proteoglycan and elastin [15].

Cellular mechanisms involved in peritoneal spread

Below, candidate biomarkers are discussed in the order of the sequential steps of the metastatic process. However, as considerable interactions exist between these processes, this classification is by no means absolute.

Detachment and increased motility

Upon detachment from the primary CRC, in addition to anoikis evasion, tumour cells have to enable motility in order to reach the target organ [16]. This is acquired by downregulation of cell–cell adhesion molecules (CAMs) and changes in the cytoskeleton, such as the extension of lammellipodia and filopodia [17].

Cell–cell adhesion molecules include the integrin family of proteins, cadherins, selectins and members of the immunoglobulin superfamily (e.g., ICAM and VCAM), which are discussed in Section 3. Also, other adhesion molecules, like CDH2, and cell surface molecules with signal transduction function, like epidermal growth factor receptor (EGFR) and c-MET play a role here [18]. These phenotypic alterations that take place during invasion, with tumour cells exhibiting reduced adhesion and increased motility, are also referred to as EMT [17, 19]. In the context of PM, the molecule TWIST is reported to be involved in this process.

Twist homolog 1 (TWIST)

TWIST is a transcription factor that is most abundantly expressed in tissues of mesodermal origin. TWIST is known as an EMT trigger [13, 14]. Studies aiming to block the function of TWIST by siRNA in ovarian adenocarcinoma cells have shown suppression of adhesion molecules and matrix metalloproteinases (MMPs). Levels of migration, invasion and adhesion to peritoneal mesothelium were significantly lower in siTWIST cells, supporting that downregulation of TWIST could, in theory, ultimately inhibit peritoneal dissemination [20].

Met proto-oncogene (c-MET)

c-MET is a proto-oncogene that encodes for the hepatocyte growth factor receptor (HGFR). It has tyrosine kinase activity and is essential in embryonic development and wound healing [21]. Activation of MET by hepatocyte growth factor (HGF) initiates an invasive growth program [22], which physiologically occurs during embryonic development and organ regeneration, but that is hijacked by cancer cells to promote invasion [23]. Abnormal MET expression in cancer has been linked to poor survival in several malignancies, including CRC [24]. c-MET was found to play an important role in peritoneal dissemination of ovarian carcinoma (OvCa) cells in culture, most probably through an $\alpha5\beta1$ integrin-dependent mechanism [25]. Using tissue microarrays (TMAs), cell lines and animal models, the role of c-MET in PM of OvCa was investigated. The disease specific survival of patients with high c-MET protein expression was significantly lower than those with low expression (N=138). In experiments using ECM components, primary mesothelial cells, full-thickness human peritoneum and in vivo mouse peritoneum, marked inhibition of dissemination was noted by siRNA targeting c-MET [25, 26]. Furthermore, a reduction in $\alpha5\beta1$ protein and mRNA, accompanied by a reduction in MMP2 and MMP9 activity, was noted [25]. As such, theoretically c-MET represents a very attractive candidate biomarker of PM formation risk as well as a possible therapeutic target in prevention of peritoneal dissemination.

Epidermal growth factor receptor

EGFR is a cell surface protein and when its ligand binds, a signalling cascade starts that leads to cell proliferation [3, 10, 11, 26]. Activation of EGFR is thought to promote the downregulation of E-cadherin, causing disruption of adherens junctions, through induction of MMP9. This interaction has been investigated in OvCa by blocking with an siRNA directed against MMP9 [27]. This study involved two cell lines and tissue samples from 146 primary OvCas, including 17 paired samples of primary tumour and PM. Treatment with recombinant MMP9 or transient expression of MMP9 was sufficient to regain function and reduce E-cadherin levels in the cell lines, which subsequently caused a migratory and invasive response. These findings were validated by IHC on TMAs containing patient material, which exhibited co-localization of activated EGFR and MMP9 accompanied by E-cadherin loss [27]. Clinically elevated levels of both EGFR and MMP9 have been associated with worse survival [28–30].

Other markers associated with detachment and increased motility in in vitro and in vivo studies in the context of PM are HGF, RHOA and CDH2 [24, 27, 31–34]. However, the clinical significance of up- or downregulation of these specific genes in PM of CRC remains to be verified.

Anoikis evasion

Anoikis is a form of programmed cell death that takes place when cells detach from the surrounding ECM, thereby loosing integrin–ligand interactions, as occurs during tumour cell invasion [13, 35]. In normal tissue anoikis is critical in maintaining tissue homeostasis by preventing tissue proliferation in unwanted sites. Evading anoikis is a condition for cancer cells to survive and is believed to be an essential step in metastasis [36, 37]. This also is the case during the process of PM formation where detached cells exhibit anchorage independent growth, meaning that they are able to survive without intact cell–cell signalling, a requisite for cell survival in normal cells [38]. In PM, this is most likely achieved by forming tumour cell clusters and retaining the ability to proliferate in cell clusters, as opposed to the adherence to platelets as described in haematogenous spread [35, 39].

In peritoneal spread, two molecules are reported to play a role in anoikis evasion.

Kallikrein-related peptidases

The process of evading anoikis in PM involves the activation of the kallikrein-related peptidases (KLKs), a group of serine proteases. There are 15 proteins belonging to the kallikrein family [40]. Known functions of the KLKs include degradation of ECM molecules, contributing to activation of growth factors and proteases. One of the most well-known KLKs, utilized in diagnosis and follow-up of prostate cancer, is KLK3 or prostate-specific antigen (PSA) [41]. Interestingly, there is a link between cell clustering and KLK expression. Cell clustering is a frequent event in OvCa ascites, which may contribute to anoikis evasion [40]. The aggregation of these malignant cells was associated with a higher protein expression of KLK7 [40]. Hence, it is assumed that treatment response is, at least partly, governed by anoikis resistance under the influence of KLK7. Further investigation revealed that $\alpha5\beta1$ integrins and KLK7

co-express in OvCa. Based on these findings, an association between KLK7 levels and PM via cell aggregates and α5β1 integrin-mediated cell adhesion was assumed. Several integrin inhibitors, such as Volociximab [42, 43] are currently under development and are of interest as targeted therapy in PM, based not only on the abovementioned results but also on a proof of principle study with blocking of β1 integrin (ITGB1) in a murine and ex vivo peritoneal model, described under "Adhesion to peritoneal surface" [44].

KLKs have also been investigated as prognostic markers in CRC in primary tumours. A higher KLK 7 protein expression was found to be associated with a shorter overall and disease free survival in a study containing 105 patients [45, 46]. In addition, analysis of a panel of KLKs shows overexpression of KLK5, KLK7 and KLK 14 to be prognostically relevant in patients with primary CRC in a multivariate analysis [46].

V-Src sarcoma viral oncogene homolog (Src)

Src is a tyrosine kinase that is described as a key player in cell-matrix contact-mediating focal adhesions, in cell–cell contact-mediating adherens junctions and in cell-anchorage dependent signalling [39, 47]. A Src-dependent mechanism has been reported that provides transient protection of colonic epithelial cells from anoikis [48]. Using a Src-specific inhibitor, loss of protection from anoikis was shown in various experiments [48, 49]. CRC cell line experiments have shown that enforced Src expression increases resistance to anoikis [50]. As well as having a role in anoikis evasion, upregulation of c-SRC causes adherent cells to scatter and to extend their lamellipodia, thus making tumour cells highly motile [50]. In a murine model, blocking of Src showed reduced peritoneal dissemination compared to control transfectants. These results support the hypothesis that c-SRC may play a role in detachment and motility of CRC cells.

Adherence to peritoneal surface

After evasion of anoikis, detached malignant cells will have to adhere to the peritoneal surface to be able to ultimately invade and colonize the peritoneum. Adherence to the peritoneal surface depends largely on the interaction between malignant cells and ECM components through integrins, cadherins, and cell-adhesion molecules.

Integrins

Integrins are a family of receptors that play a major role in cell-ECM attachment and signalling. Integrins may also play a role in attachment of malignant cells to the peritoneum. The integrin family consists of 24 members, and function in different combinations of α and β subunits [2, 18]. Integrins are expressed on epithelial as well as endothelial cells, leukocytes and platelets. Altered expression patterns of integrins are frequently associated with a malignant phenotype, supporting invasive and metastatic behaviour [51, 52].

One of the integrins involved is the ITGB1. In a surgical trauma animal model, blocking ITGB1 caused less tumour cells to adhere to the peritoneum, followed by impaired outgrowth of tumours. These results were confirmed in an ex vivo peritoneal and in vivo mesothelial model. This suggests a role for integrins in the adherence and growth of tumour cells on (surgically traumatized) peritoneum [44]. Another integrin, α5β3, has been identified in PM of pancreatic cancer. It is the primary receptor for Cyr61, one of the molecules described under "Inducing Angiogenesis". The experiments involving this receptor–ligand couple were carried out on a murine pancreatic cancer model, using microarray analysis, reverse transcription-polymerase chain reaction (RT-PCR) and IHC to confirm the results [33]. With IHC, co-localization of Cyr61 and α5 was observed, suggesting that the interaction between Cyr61 and α5β3 promotes the formation of PM [33].

Cadherin 1 (CDH1 or E-cadherin)

This protein is part of the cadherin family of cell adhesion molecules, consisting of glycoproteins that mediate cell–cell adhesion in epithelial cells. Reduced cell surface expression of this protein has been observed in many cancers, including oesophageal, colon, breast and OvCa [53]. As a consequence these cells show easy disaggregation, facilitating invasion and metastasis [39, 54].

In PM of CRC one in vivo study has been described with a LoVo clone showing E-cadherin downregulation to be associated with metastasis [55]. These cells formed a primary colon carcinoma in the host model, which was then resected. Seven out of ten mice showed isolated mesenteric lymph node metastases, not peritoneal carcinomatosis, after resection, compared to ten disease-free mice in the control group.

In an OvCa model, however, downregulation of E-cadherin by siRNA was followed by upregulation of α5β1integrin [34]. In this study, intra-peritoneal administration of an α5β1integrin antibody significantly reduced ascites and the number of metastases compared to the control group [34]. In a cohort of 107 OvCa patients, the overexpression of α5-integrin correlated with worse survival [34]. Altogether, these findings imply an effect of downregulation of E-cadherin through an integrin-mediated pathway.

Intercellular adhesion molecule 1 (ICAM-1)

The ICAMs are a subfamily of the immunoglobulin superfamily of cell adhesion molecules. ICAM 1 is one of five ICAMs [18]. The role of ICAM 1 has been investigated in a

pneumoperitoneum-simulated environment using a CRC cell line and a mesothelial cell monolayer [56]. In this study, increased adhesion of CRC cells to the stimulated mesothelium was observed [56]. In an attachment assay to detect MMP's activity in naive (unstimulated) mesothelium, it was confirmed that increased expression of ICAM-1 led to increased adhesion of malignant cells [57]. Moreover, the link between ICAM1-CD43 interaction and MMP production was analysed on invasion of attached cells. An increase in adhesion and invasion was noted, which was manifested by an increase in MMP expression [57].

Epithelial cell adhesion molecule (Ep-CAM)

Ep-CAM is a type 1 transmembrane glycoprotein and not structurally related to the four major families of cell adhesion molecules [58]. Ep-CAM is frequently highly expressed in malignancies of epithelial origin, including CRC [58, 59].

In peritoneal dissemination of OvCa the expression of Ep-CAM in primary, metastatic and recurrent epithelial OvCa was studied [60]. Using real-time PCR (qRT-PCR) and IHC in patient material and cell lines, high expression of Ep-CAM was detected in all three disease stages, with a significant difference in Ep-CAM expression levels between metastatic, recurrent and chemotherapy-resistant OvCa compared to normal ovarian epithelium [60].

CD 44 molecule (CD44)

The protein encoded by the CD44 gene is a cell surface glycoprotein that plays a role in cell-adhesion, cell–cell interaction and migration. It is a receptor for hyaluronic acid and can interact with MMPs and collagens as well. It participates in several cellular functions, one of which is metastasis [61].

Alternative splicing of CD44 pre-mRNA results in different isoforms of the protein. In CRC, CD44 exon v6 splice variants are present in advanced stages of disease [62, 63].

In PM, in vitro adhesion assays have been performed with the use of mesothelial cell cultures and OvCa cells. A CD44 monoclonal antibody partially inhibited adhesion of tumour cells to the mesothelium. In nude mice, treatment with CD44 monoclonal antibody led to significantly less tumour implants on the peritoneal surface [61]. Although some adhesion of OvCa cells to the mesothelial layer still occurred, albeit to a lesser extent, it ultimately lead to less PM [61, 64].

Interactions have also been reported between chemokine receptors present on malignant cells and targets in the mesothelium in OvCa. Examples of this mechanism are the binding of CXCR4 to CXCL12 and the binding of MUC16 to Mesothelin [65, 66].

Altogether, these data suggest that the blocking of these attachment-mediating molecules could be of clinical importance. For example, in the peri-operative window, blocking of these candidates could lead to less implantation and subsequently less tumour outgrowth [44, 56, 57, 61].

Invasion of the peritoneum

Proteolytic enzymes to degradate the ECM are necessary for tumour cells to be able to invade beyond the basement membrane. These enzymes are secreted by tumour cells themselves or by the stromal cells surrounding them [67]. ECM degrading metallopeptidases (MMPs) have been extensively linked to this step in peritoneal dissemination [13].

Matrix metallopeptidases (MMPs)

Proteins of the MMP family break down the ECM in normal physiological processes as well as in disease, including cancer [68]. MMPs facilitate invasion of the tumour cells into the nearby stroma by degrading multiple types of ECM proteins. They play a role in metastasis of CRC, including in liver- and lung metastases [68, 69].

In gastric carcinoma, overexpression of MMP7 in primary tumours, as seen by IHC and RT-PCR, was an independent risk factor for formation of PM [16]. In OvCa, overexpression of MMP9 was reported to promote a migratory and invasive phenotype in functional experiments performed in two OvCa cell lines [27]. Altogether, the invasion of the peritoneal surface by cancer cells has been linked to altered MMP2, MMP7 and MMP9 expression in several gastrointestinal tract malignancies [16, 27, 69–71]. For this reason, attempts have been made to treat PM with MMP inhibitors. Indeed, inhibition of MMPs with the drug Batimastat in rats inhibited development of CRC metastasis [72]. However, intra-peritoneal administration of this drug resulted in marked peritoneal inflammation and ascites, reason why no clinical studies with Batimastat in humans have been initiated to date.

In addition, the Wilms' tumour gene protein 1 (WT1) and TIMP2 are also reported to promote invasion. Contact between malignant cells and the submesothelial collagen results in WT1 overexpression and subsequent invasion in OvCa [73]. Furthermore, decreased invasive capacity is observed after blocking WT1 by siRNA [73]. TIMP-2 is a tissue inhibitor of metalloproteinases, for which a twofold upregulation of TIMP-2 mRNA was observed in the PM of CRC patients, next to upregulation of HIF-1α and IGF-1 that are described below [74]. TIMP-2 is part of the TIMP gene family and proteins encoded by this gene are inhibitors of the MMPs [75]. In contrast to other TIMP family members, TIMP-2 also has the ability to directly suppress the proliferation of endothelial cells [76].

Several other genes have also been implicated in invasion of the peritoneum. These include c-MET[23, 32], ITGB1 [38, 44, 77, 78] and CDH1 [61], which have been discussed previously under "Adhesion to the peritoneal surface".

The colonization phase — survival in the new niche

Sustaining proliferative signalling, enabling replicative immortality and evading growth suppressors

One of the most fundamental characteristics of malignant cells is their ability to sustain proliferation. Cancer cells can achieve this by various methods, such as producing growth factors and receptors for autocrine stimulation and by stimulating the tumour-associated stroma to deliver various growth factors [79]. Additionally, changing receptor and downstream signalling facilitates ligand-independent signalling, also leading to proliferation induction [13]. In this category, IGF-1, VEGF and HIF1α have been reported in PM.

Insulin like growth factor 1 (IGF-1)

IGF-1 is part of a family of peptides that play important roles in growth and development in mammals [80]. In a microarray study on PM and liver metastasis from CRC patients, IGF-1 mRNA was exclusively and fairly consistently overexpressed in PM when compared to liver metastasis [74]. Conversely, circulating levels of insulin-like growth factor binding protein 3 (IGFBP3), an endogenous antagonist of IGF-1, correlates with slower progression in patients with metastatic CRC [81, 82]. Both of these findings imply a role for IGF-1 in the formation of PM and underline that gene expression profiles differ per site of metastasis [74, 81].

Inducing angiogenesis

As with all cells, cancer cells are in need of nutrients for survival and 150–180 μm is the maximum distance at which these nutrients can diffuse from blood vessels. Beyond this distance the tumour cannot proliferate without active angiogenesis, since the resulting hypoxia induces apoptosis [13, 83, 84]. One of the mechanisms used by cancer cells to overcome this limitation is the induction of angiogenesis, a process in which genes like hypoxia inducible factor 1 (HIF1) and vascular endothelial growth factor (VEGF) play a role [13, 83, 85].

Hypoxia inducible factor (HIF) 1

Hypoxia within the tumour microenvironment can induce angiogenesis by release of HIF1, which regulates production of VEGF [83, 85].

In the same study discussed above, 20 colorectal adenocarcinomas and eight high-grade appendiceal adenocarcinomas were analysed for genome wide mRNA expression using oligonucleotide microarrays. Site-specific gene expression profiles were observed. A twofold upregulation of HIF1α specific for PM was noted in this cohort, next to TIMP-2 and IGF1, which were discussed above [74]. HIF1α has also been described as being upregulated in primary CRC when compared to normal mucosa [83].

Vascular endothelial growth factor and VEGF receptor (VEGFR)

VEGF has been extensively described as one of the most important angiogenic factors in solid tumours [13]. An IHC study of PM tissue samples from patients with adenocarcinoma of the appendix or colon demonstrated that higher VEGF expression was associated with a worse clinical prognosis. However, no significant correlation was noted between micro-vessel density and survival [86]. Mutations in VEGF, as well as the tumour suppressor gene p53 have been shown to play a role in metastasis of CRC [2]. About 50 % of patients with metastatic disease are known to be positive for both mutations in p53 and VEGF [2, 87]. VEGF targeted therapies are clinically widely used in combination with chemotherapeutic agents in patients with histologically confirmed CRC metastasis and measurable disease in the absence of absolute contraindications [87]. In a PM of CRC murine model, blocking of VEGFR with DC101, a VEGFR-2 specific antibody, has been shown to have a negative effect not only on angiogenesis but also on the proliferation of both tumour cells and endothelial cells, effectively showing significantly reduced intra-abdominal tumour burden and ascites formation [88–90].

Immune aggregates and VEGF

As an alternative mechanism for the pathogenesis of PM, one paper described the preferential attachment of malignant cells to immune aggregates in the omentum. In a murine model using several cell lines, including one OvCa cell line, these immune aggregates in the omentum were noted to have a complex network of capillaries with a high vascular density [91]. The mesothelial cells overlying these immune aggregates were observed to be hypoxic and VEGF-A production co-localized with these hypoxic regions. This mechanism was hypothesised to contribute to the survival of these tumour cells on the peritoneum, due to apparent constitutive readiness of the vasculature in the immune aggregates to expand [91, 92]. Interestingly, these immune

aggregates have also been observed in humans [93–97]. Theoretically, their presence and reported make-up could form a plausible explanation for the attachment of free cancer cells to these sites in the peritoneal surface.

Cysteine-rich protein 61 (Cyr61)

Cyr61, already referred to above, is a secreted matricellular protein that binds to integrins [98]. The connective tissue growth factor, cysteine-rich protein, and nephroblastoma overexpressed gene (CCN) family consists of six members that play a role in processes such as fibrosis, angiogenesis and wound healing [98]. Overexpression of Cyr61 in tumour cells has been linked to PM in pancreatic cancer [33]. Cyr61 is the ligand for the α5β3 integrin, described under "Attachment to peritoneum". Therefore, Cyr61 is known to activate both angiogenesis and cell–cell attachment related signalling pathways in PM [33].

Molecules such as CD44 and α5β3 have also been linked to angiogenesis in disseminated disease in several experiments [33, 61, 64]. These results are mostly based on comparative genomic hybridization and IHC (validation) studies in pancreatic, colorectal and OvCa.

Taken together, these findings support an important role of angiogenesis in the process of peritoneal dissemination. For this reason, interfering with angiogenesis has been investigated as a method for treating PM. In nude mice, inhibition of growth of PM of CRC was demonstrated when intra-peritoneally injected tumour cells were treated with the angiogenesis inhibitor TNP-470 [99]. TNP-470 inhibits methionine aminopeptidase type II, which causes proliferation of endothelial cells [99–101]. The TNP-470 treated mice in this study had significantly less tumour foci intraperitoneally, smaller tumours and a longer survival compared to the control group [99]. These effects are similar to those that have been reported in the aforementioned VEGFR-blocking experiments, suggesting that anti-angiogenic therapy holds promise in the treatment of PM.

A summary of the process of peritoneal dissemination and the proposed effects of the identified molecules in PM of CRC is depicted in Fig. 1. Of all the described molecules, albeit highly experimental, several show not

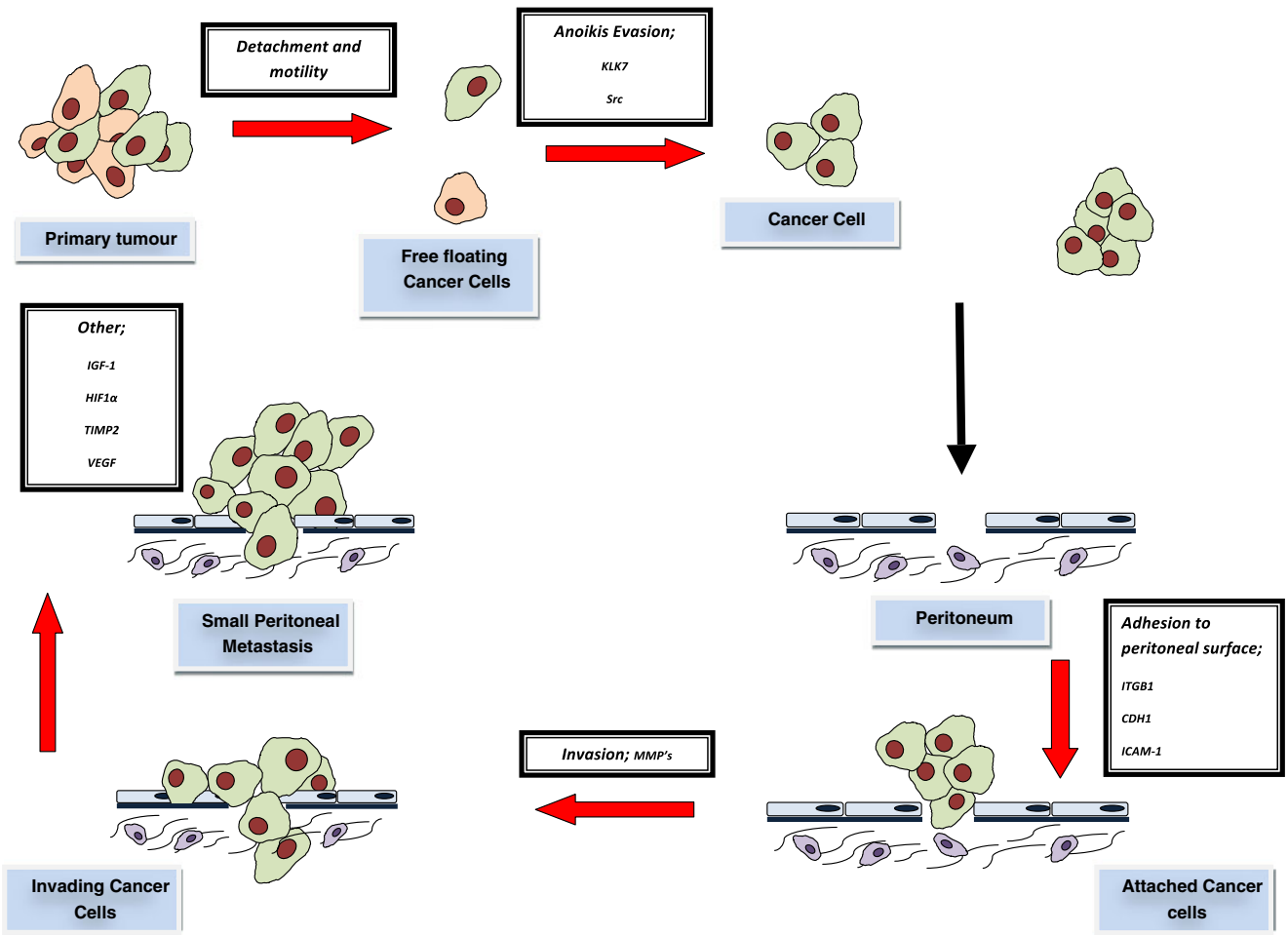

Fig. 1 Roles of the identified molecules in PM of CRC per dissemination step

only biological relevance, but have been shown to have either a prognostic effect in PM or hold promise as a therapeutic target in the future (Table 1).

Discussion

PM of CRC, but also other malignancies, form a serious threat for the patient's survival. While systemic drug therapy has only limited effect on the patient's outcome, the best option for changing the clinical course is aggressive surgery in combination with HIPEC. At least a subset of patients has been demonstrated to benefit from this approach. Yet despite the reported survival benefit reported after CRS and HIPEC in patients with PM of CRC, several unmet clinical needs still exist, mainly in the field of diagnostics. Basically, they fall apart into three topics. A first major issue is the challenge to be able to diagnose the presence of PM earlier, at a stage when the disease is less widespread. Secondly, there is a need for diagnostic tools to discriminate between patients who are likely to benefit from this intensive treatment, and those that will not, and thus would be exposed to the risk of

Table 1 Summary of targets with possibility for clinical implementation in PM in the future

Promising target in PM	Biological relevance in PM	Difference with CRLM	Prognostic relevance	Possible therapeutic implications
IGF-1	Growth factor	Yes, >2-fold change in mRNA [74]	Not clear	Monoclonal antibody Figitumumab [107, 108]
KLK7	Anoikis Evasion	Not clear	Yes, worse overall survival in CRC [45, 46]	Inhibition of KLK7 would lead to less evasion of anoikis [40]. However, interaction with α5β1 integrin, thus integrin inhibitors such as Volociximab may also be of interest [42, 43].
HIF1	Angiogenesis	Yes, >2-fold change in mRNA [74]	Not clear, trend was observed	HIF1 inhibitors could potentially be of interest in PM. HIF1 upregulation seems also to be specific for PM [74, 109]
VEGF	Angiogenesis	No	Yes, high VEGF expression correlated to worse survival [86]	Currently anti-VEGF antibody therapies already in use in clinical setting, very promising for clinical application [87].
Cyr61	Angiogenesis	No	Not clear	Is the ligand for α5β3. If possibility for blocking this interaction blocking of attachment to peritoneal surface ensues and subsequent angiogenesis is inhibited [33].
TWIST	Detachment and motility	No	Not clear	In experimental model blocking of TWIST showed less migration, invasion and adhesion to peritoneal surface. In theory powerful inhibition of PM formation [20].
c-MET	Detachment and motility	No	Yes, higher expression of c-MET correlated to worse survival [24]	In multiple experimental models blocking of c-MET showed marked inhibition of dissemination. Theoretically attractive therapeutic target [25].
EGFR	Detachment and motility	No	Not clear	Cetuximab is a clinical grade antibody already widely in use for metastasized CRC. No clinical data on specific EGFR inhibition in PM is available.
Integrins	Adhesion molecule	Not clear	Not clear	In multiple experimental models blocking of integrins showed marked inhibition of dissemination. Theoretically attractive therapeutic target [44, 77, 78]. Several integrin inhibitors currently under development [42, 43].
ICAM-1	Adhesion molecule	Not clear	Not clear	Highly experimental, dubious if therapeutically significant. Theoretically blocking of ICAM-1 leads to less PM due to less attachment to peritoneum [56].
Ep-CAM	Adhesion molecule	Not clear	Yes, higher expression of Ep-CAM correlated to worse survival [60]	Dubious if therapeutically significant. Theoretically blocking of Ep-CAM leads to less PM due to less attachment to peritoneum.
CD44	Adhesion molecule	Not clear	Yes, exon v6 variant in advanced disease [62, 63]	Highly experimental, dubious if therapeutically significant. Blocking of CD44 does not completely block attachment to peritoneum in experimental model [61].
MMPs	Proteolytic enzyme	No	Yes, higher expression of MMP7 in primary tumour independent risk factor for PM [16].	In experimental model, treatment with Batimastat showed inhibition of PM. However serious adverse events reported, thus no clinical studies to date [72].

morbidity and mortality of this treatment in vain. A third, but perhaps more remote goal, is to arrive, even in this disease state, to a more personalised approach. In an ideal situation the cytoreductive drugs used during HIPEC would be more in tune with the biological characteristics of the individual tumour, rather than the current "one size fits all" approach.

A common denominator in trying to achieve these goals is making use of relevant information on the biology of the disease process, because these biological mechanisms ultimately dictate the clinical phenotype. This biological information can be read out from patient samples at the DNA, RNA or protein level, but in principle also by molecular imaging modalities. These reporter molecules are then referred to as biomarkers. As the present review shows, the field of biomarkers for these three indications is still rather in its infancy. Most observations concern initial proof of concept studies, there is hardly any validation in independent series, and no prospective stratification studies yet. Most work has been done on retrospectively collected tissue samples, and limited efforts have been conducted to develop assays that would work in clinical diagnostic settings. Moreover, the field of molecular imaging of PM is still in its early days.

More specifically, with respect to biomarkers for early detection of PMs, several clinical studies have shown that a lower peritoneal cancer index (PCI) — i.e., the amount of PM present at the start of treatment — as well as the extent to which the surgeon has succeeded in removing all PM, are both strongly associated with disease outcome after CRS and HIPEC for PM of CRC [4, 10, 102]. Yet, detection of small lesions remains a challenge, making pre- and intra-operative assessment of the extent of PM difficult [12]. Recently, targeted imaging strategies have been applied in PM of OvCa by means of intra-operative tumour specific fluorescent imaging using a Folate Receptor-α-targeted fluorescent agent [103]. This allows for a more precise resection of small lesions that are otherwise overlooked [103]. Theoretically, similar approaches could work in PM of CRC, e.g., targeting molecules like EGFR and VEGFR. As for pre-operative imaging, alternative PET-tracers to 18-FDG could provide the additional accuracy needed for timely diagnosis of PM. However, challenges here also exist in the fact that the currently available pre-operative imaging modalities such as CT, PET and MRI come with technical limitations, such as a maximum resolution of the obtained image.

After meticulous analysis of the available literature we have to conclude that currently the only targets that have the potential to be assessed in a clinical setting in the near future are IGF1, TIMP2, HIF1 and VEGF. These are the only known targets to have been solely extracted by analysis of PM of CRC in two separate studies [74, 86]. It is also known that HIF1 regulates production of VEGF [83, 85], making VEGF, an even more interesting target. As to biomarkers for the prediction of response to CRS and HIPEC for PM of CRC — i.e., discriminating between patients that may and patients that probably will not benefit from the treatment — only VEGF has been reported to be associated with outcome after CRS and HIPEC [86]. Yet, all four markers currently lack enough promise for translation on short notice into a diagnostic test of use in a clinico-pathological setting in the assessment of material acquired from PM of CRC (Table 2).

With respect to personalised therapy approaches, currently little data exist on candidate biomarkers for prediction of response to mitomycin C (MMC), despite the fact that this drug has been around for quite some time. Interestingly, MMC based functional assays are used for the diagnosis of Fanconi anaemia, a rare hereditary disorder in which the function of one of several genes in the Fanconi pathway is disrupted. So far, however, no clear role for the Fanconi pathway has been established in CRC. Also, other biomarkers that may be associated with response to cross-linking agents have not yet been evaluated in CRC PM [104]. To date, established targeted therapies in CRC include drugs against EGFR, like Cetuximab, or anti-angiogenic drugs like Bevacuzimab. For the former drug, a number of biomarkers exist, of which KRAS mutation status is most established, while for the latter so far no good biomarkers have been established [105, 106]. Remarkably, most of the molecules involved have not yet been reported as having an effect on survival in PM of CRC, except for VEGF.

Table 2 Targets extracted from PM of CRC studies and possible clinical implications

Target expressed in HIPEC patient material from PM of CRC	Possible clinical implementation	Correlation with outcome of HIPEC patients after treatment with CRS and HIPEC
IGF-1 [74, 107, 108]	Therapeutic	Unknown
TIMP2 [16, 74]	Possible stratification tool	Unknown
HIF1 [74, 84]	Possible stratification tool Therapeutic	Unknown
VEGF [86, 87]	Possible stratification tool Therapeutic	Yes [86]

Areas for further investigation

The present review of literature suggests that there is opportunity for both discovery studies and further validation of the identified candidates for implementation in treatment stratification in patients with PM of CRC. Mainly the lack of genome-wide studies on well-defined patient cohorts poses an interesting avenue of research to identify other molecules possibly omitted by the thus far implemented candidate based approach.

Several other aspects of metastasis also require further elucidation. One of which is acquiring insight into the differences or similarities between the biology of primary colorectal tumours versus their corresponding metastases. Secondly, a better understanding of metastasis promoting features of the peritoneal environment itself, including tumour–stroma interaction.

Conclusions

Currently, several promising candidates have been identified that may have potential for use as a biomarker in PM of CRC, but all of these require extensive further validation. Therefore, rapid changes in clinical decision-making and therapy design based on current data would be premature. Yet, the pace of the omics revolution makes that the question is not *if* — but *when* — biomarkers will be introduced to improve diagnosis and ultimately outcome of patients with PM due to CRC. This will certainly have the potential for a significant reduction in treatment related morbidity and mortality in this population by bringing the right treatment to the right patient.

Conflict of interest The authors declare that they have no conflict of interest.

References

1. Parkin DM, Bray F, Ferlay J, Pisani P (2005) Global cancer statistics, 2002. CA Cancer J Clin 55(2):74–108
2. Bird NC, Mangnall D, Majeed AW (2006) Biology of colorectal liver metastases: a review. J Surg Oncol 94(1):68–80
3. Koppe MJ, Boerman OC, Oyen WJG, Bleichrodt RP (2006) Peritoneal carcinomatosis of colorectal origin. Ann Surg 243 (2):212–222
4. Maggiori L, Elias D (2010) Curative treatment of colorectal peritoneal carcinomatosis: current status and future trends. Eur J Surg Oncol 36(7):599–603
5. Cao C, Yan TD, Black D, Morris DL (2009) A systematic review and meta-analysis of cytoreductive surgery with perioperative intraperitoneal chemotherapy for peritoneal carcinomatosis of colorectal origin. Ann Surg Oncol 16(8):2152–2165
6. Klaver YLB, Lemmens VEPP, Creemers GJ, Rutten HJT, Nienhuijs SW, de Hingh IHJT (2011) Population-based survival of patients with peritoneal carcinomatosis from colorectal origin in the era of increasing use of palliative chemotherapy. Ann Oncol 22(10):2250–2256
7. Sugarbaker PH (1995) Patient selection and treatment of peritoneal carcinomatosis from colorectal and appendiceal cancer. World J Surg 19(2):235–240
8. Sugarbaker PH, Jablonski KA (1995) Prognostic features of 51 colorectal and 130 appendiceal cancer patients with peritoneal carcinomatosis treated by cytoreductive surgery and intraperitoneal chemotherapy. Ann Surg 221(2):124–132
9. Cavaliere F, De Simone M, Virzì S et al (2011) Prognostic factors and oncologic outcome in 146 patients with colorectal peritoneal carcinomatosis treated with cytoreductive surgery combined with hyperthermic intraperitoneal chemotherapy: Italian multicenter study S.I.T.I.L.O. Eur J Surg Oncol 37(2):148–154
10. Verwaal VJ (2003) Randomized trial of cytoreduction and hyperthermic intraperitoneal chemotherapy versus systemic chemotherapy and palliative surgery in patients with peritoneal carcinomatosis of colorectal cancer. J Clin Oncol 21(20):3737–3743
11. Abdalla EK, Vauthey J-N, Ellis LM, Ellis V, Pollock R, Broglio KR, Hess K, Curley SA (2004) Recurrence and outcomes following hepatic resection, radiofrequency ablation, and combined resection/ablation for colorectal liver metastases. Annals of Surgery 239(6):818–825, discussion 825–7
12. Verwaal VJ, Zoetmulder FAN (2004) Follow-up of patients treated by cytoreduction and chemotherapy for peritoneal carcinomatosis of colorectal origin. Eur J Surg Oncol (EJSO) 30(3):280–285
13. Hanahan D, Weinberg RA (2011) Hallmarks of cancer: the next generation. Cell 144(5):646–674
14. Nguyen DX, Bos PD, Massagué J (2009) Metastasis: from dissemination to organ-specific colonization. Nat Rev Cancer 9 (4):274–284
15. van der Wal JBC, Jeekel J (2007) Biology of the peritoneum in normal homeostasis and after surgical trauma. Colorectal Dis 9 (Suppl 2):9–13
16. Yonemura Y, Endou Y, Fujita H, Fushida S, Bandou E, Taniguchi K, Miwa K, Sugiyama K, Sasaki T (2000) Role of MMP-7 in the formation of peritoneal dissemination in gastric cancer. Gastric Cancer 3(2):63–70
17. Yilmaz M, Christofori G (2009) EMT, the cytoskeleton, and cancer cell invasion. Cancer Metastasis Rev 28(1–2):15–33
18. Paschos KA, Canovas D, Bird NC (2009) The role of cell adhesion molecules in the progression of colorectal cancer and the development of liver metastasis. Cell Signal 21(5):665–674
19. Guarino M, Rubino B, Ballabio G (2007) The role of epithelial–mesenchymal transition in cancer pathology. Pathology 39 (3):305–318
20. Terauchi M, Kajiyama H, Yamashita M et al (2007) Possible involvement of TWIST in enhanced peritoneal metastasis of epithelial ovarian carcinoma. Clin Exp Metastasis 24(5):329–339
21. Ma PC, Maulik G, Christensen J, Salgia R (2003) c-Met: structure, functions and potential for therapeutic inhibition. Cancer Metastasis Rev 22(4):309–325
22. Gentile A, D'Alessandro L, Lazzari L, Martinoglio B, Bertotti A, Mira A, Lanzetti L, Comoglio PM, Medico E (2008) Met-driven invasive growth involves transcriptional regulation of Arhgap12. Oncogene 27(42):5590–5598
23. Boccaccio C, Comoglio PM (2006) Invasive growth: a MET-driven genetic programme for cancer and stem cells. Nat Rev Cancer 6(8):637–645
24. Osada S, Matsui S, Komori S et al (2010) Effect of hepatocyte growth factor on progression of liver metastasis in colorectal cancer. Hepatogastroenterology 57(97):76–80

25. Sawada K, Radjabi AR, Shinomiya N et al (2007) c-Met overexpression is a prognostic factor in ovarian cancer and an effective target for inhibition of peritoneal dissemination and invasion. Cancer Res 67(4):1670–1679
26. Davies RL, Grosse VA, Kucherlapati R, Bothwell M (1980) Genetic analysis of epidermal growth factor action: assignment of human epidermal growth factor receptor gene to chromosome 7. Proc Natl Acad Sci U S A 77(7):4188–4192
27. Cowden Dahl KD, Symowicz J, Ning Y, Gutierrez E, Fishman DA, Adley BP, Stack MS, Hudson LG (2008) Matrix metalloproteinase 9 is a mediator of epidermal growth factor-dependent E-cadherin loss in ovarian carcinoma cells. Cancer Res 68 (12):4606–4613
28. Nicosia SV, Bai W, Cheng JQ, Coppola D, Kruk PA (2003) Oncogenic pathways implicated in ovarian epithelial cancer. Hematol Oncol Clin North Am 17(4):927–943
29. Davidson B, Goldberg I, Gotlieb WH, Kopolovic J, Ben-Baruch G, Nesland JM, Berner A, Bryne M, Reich R (1999) High levels of MMP-2, MMP-9, MT1-MMP and TIMP-2 mRNA correlate with poor survival in ovarian carcinoma. Clin Exp Metastasis 17 (10):799–808
30. Kamat AA, Fletcher M, Gruman LM, Mueller P, Lopez A, Landen CN, Han L, Gershenson DM, Sood AK (2006) The clinical relevance of stromal matrix metalloproteinase expression in ovarian cancer. Clin Cancer Res 12(6):1707–1714
31. Gentile A, Trusolino L, Comoglio PM (2008) The Met tyrosine kinase receptor in development and cancer. Cancer Metastasis Rev 27(1):85–94
32. Benvenuti S, Comoglio PM (2007) The MET receptor tyrosine kinase in invasion and metastasis. J Cell Physiol 213(2):316–325
33. Holloway SE, Beck AW, Girard L, Jaber MR, Barnett CC Jr, Brekken RA, Fleming JB (2005) Increased expression of Cyr61 (CCN1) identified in peritoneal metastases from human pancreatic cancer. J Am Coll Surg 200(3):371–377
34. Sawada K, Mitra AK, Radjabi AR et al (2008) Loss of E-cadherin promotes ovarian cancer metastasis via 5-integrin, which is a therapeutic target. Cancer Res 68(7):2329–2339
35. Douma S, Van Laar T, Zevenhoven J, Meuwissen R, Van Garderen E, Peeper DS (2004) Suppression of anoikis and induction of metastasis by the neurotrophic receptor TrkB. Nature 430(7003):1034–1039
36. Chiarugi P, Giannoni E (2008) Anoikis: a necessary death program for anchorage-dependent cells. Biochem Pharmacol 76 (11):1352–1364
37. Horbinski C, Mojesky C, Kyprianou N (2010) Live free or die. Am J Pathol 177(3):1044–1052
38. Gimond C, van Der Flier A, van Delft S, Brakebusch C, Kuikman I, Collard JG, Fässler R, Sonnenberg A (1999) Induction of cell scattering by expression of beta1 integrins in beta1-deficient epithelial cells requires activation of members of the rho family of GTPases and downregulation of cadherin and catenin function. J Cell Biol 147(6):1325–1340
39. Weinberg RA (2006) The biology of cancer. 1st ed. 850. Garland Science, Taylor & Francis Group, LLC. New York, NY USA
40. Dong Y, Tan OL, Loessner D, Stephens C, Walpole C, Boyle GM, Parsons PG, Clements JA (2010) Kallikrein-related peptidase 7 promotes multicellular aggregation via the 5 1 integrin pathway and paclitaxel chemoresistance in serous epithelial ovarian carcinoma. Cancer Res 70(7):2624–2633
41. Stamey TA, Yang N, Hay AR, McNeal JE, Freiha FS, Redwine E (1987) Prostate-specific antigen as a serum marker for adenocarcinoma of the prostate. N Engl J Med 317(15):909–916
42. Bhaskar V, Zhang D, Fox M, Seto P, Wong MHL, Wales PE, Powers D, Chao DT, DuBridge RB, Ramakrishnan V (2007) A function blocking anti-mouse integrin alpha5beta1 antibody inhibits angiogenesis and impedes tumor growth in vivo. J Transl Med 5:61
43. Ramakrishnan V, Bhaskar V, Law DA et al (2006) Preclinical evaluation of an anti-alpha5beta1 integrin antibody as a novel anti-angiogenic agent. J Exp Ther Oncol 5(4):273–286
44. Oosterling SJ, van der Bij GJ, Bögels M, Raa ST, Post JA, Meijer GA, Beelen RHJ, Egmond MV (2008) Anti-β1 integrin antibody reduces surgery-induced adhesion of colon carcinoma cells to traumatized peritoneal surfaces. Ann Surg 247(1):85–94
45. Talieri M, Mathioudaki K, Prezas P, Alexopoulou DK, Diamandis EP, Xynopoulos D, Ardavanis A, Arnogiannaki N, Scorilas A (2009) Clinical significance of kallikrein-related peptidase 7 (KLK7) in colorectal cancer. Thromb Haemost. doi:10.1160/TH08-07-0471
46. Talieri M, Li L, Zheng Y, Alexopoulou DK, Soosaipillai A, Scorilas A, Xynopoulos D, Diamandis EP (2009) The use of kallikrein-related peptidases as adjuvant prognostic markers in colorectal cancer. Br J Canc 100(10):1659–1665
47. Kim LC, Song L, Haura EB (2009) Src kinases as therapeutic targets for cancer. Nat Rev Clin Oncol 6(10):587–595
48. Hofmann C, Lippert E, Falk W, Schölmerich J, Rogler G, Obermeier F (2009) Primary human colonic epithelial cells are transiently protected from anoikis by a Src-dependent mechanism. Biochem Biophys Res Commun 390(3):908–914
49. Windham TC, Parikh NU, Siwak DR, Summy JM, McConkey DJ, Kraker AJ, Gallick GE (2002) Src activation regulates anoikis in human colon tumor cell lines. Oncogene 21(51):7797–7807
50. Sakamoto M, Takamura M, Ino Y, Miura A, Genda T, Hirohashi S (2001) Involvement of c-Src in carcinoma cell motility and metastasis. Jpn J Cancer Res 92(9):941–946
51. Felding-Habermann B (2003) Integrin adhesion receptors in tumor metastasis. Clin Exp Metastasis 20(3):203–213
52. Varner JA, Cheresh DA (1996) Integrins and cancer. Curr Opin Cell Biol 8(5):724–730
53. Guilford P, Hopkins J, Harraway J, McLeod M, McLeod N, Harawira P, Taite H, Scoular R, Miller A, Reeve AE (1998) E-cadherin germline mutations in familial gastric cancer. Nature 392(6674):402–405
54. Birchmeier W, Weidner KM, Hülsken J, Behrens J (1993) Molecular mechanisms leading to cell junction (cadherin) deficiency in invasive carcinomas. Semin Cancer Biol 4(4):231–239
55. Pocard M, Debruyne P, Bras-Gonçalves R, Mareel M, Dutrillaux B, Poupon MF (2001) Single alteration of p53 or E-cadherin genes can alter the surgical resection benefit in an experimental model of colon cancer. Dis Colon Rectum 44(8):1106–1112
56. Ziprin P, Ridgway PF, Peck DH, Darzi AW (2003) Laparoscopic enhancement of tumour cell binding to the peritoneum is inhibited by anti-intercellular adhesion molecule-1 monoclonal antibody. Surg Endosc 17(11):1812–1817
57. Alkhamesi NA, Roberts G, Ziprin P, Peck DH (2007) Induction of proteases in peritoneal carcinomatosis, the role of ICAM-1/CD43 interaction. Biomark Insights 2:377–384
58. Balzar M, Winter MJ, de Boer CJ, Not Available SVL (1999) The biology of the 17-1A antigen (Ep-CAM). J Mol Med 77(10):699–712
59. Xie X, Wang C-Y, Cao Y-X, Wang W, Zhuang R, Chen L-H, Dang N-N, Fang L, Jin B-Q (2005) Expression pattern of epithelial cell adhesion molecule on normal and malignant colon tissues. WJG 11(3):344–347
60. Bellone S, Siegel ER, Cocco E, Cargnelutti M, Silasi D-A, Azodi M, Schwartz PE, Rutherford TJ, Pecorelli S, Santin AD (2009) Overexpression of epithelial cell adhesion molecule in primary, metastatic, and recurrent/chemotherapy-resistant epithelial ovarian cancer. Int J Gynecol Canc 19(5):860–866
61. Lessan K, Aguiar DJ, Oegema T, Siebenson L, Skubitz AP (1999) CD44 and beta1 integrin mediate ovarian carcinoma cell adhesion to peritoneal mesothelial cells. Am J Pathol 154(5):1525–1537

62. Herrlich P, Pals S, Ponta H (1995) CD44 in colon cancer. Eur J Cancer 31A(7–8):1110–1112
63. Mulder JW, Wielenga VJ, Polak MM, van den Berg FM, Adolf GR, Herrlich P, Pals ST, Offerhaus GJ (1995) Expression of mutant p53 protein and CD44 variant proteins in colorectal tumorigenesis. Gut 36(1):76–80
64. Cannistra SA, Kansas GS, Niloff J, DeFranzo B, Kim Y, Ottensmeier C (1993) Binding of ovarian cancer cells to peritoneal mesothelium in vitro is partly mediated by CD44H. Cancer Res 53 (16):3830–3838
65. Kajiyama H, Shibata K, Terauchi M, Ino K, Nawa A, Kikkawa F (2008) Involvement of SDF-1alpha/CXCR4 axis in the enhanced peritoneal metastasis of epithelial ovarian carcinoma. Int J Cancer 122(1):91–99
66. Gubbels JAA, Belisle J, Onda M et al (2006) Mesothelin-MUC16 binding is a high affinity, *N*-glycan dependent interaction that facilitates peritoneal metastasis of ovarian tumors. Mol Cancer 5 (1):50
67. Kataoka H, Tanaka H, Nagaike K, Uchiyama S, Itoh H (2003) Role of cancer cell–stroma interaction in invasive growth of cancer cells. Hum Cell 16(1):1–14
68. Vihinen P, Kähäri V-M (2002) Matrix metalloproteinases in cancer: prognostic markers and therapeutic targets. Int J Cancer 99 (2):157–166
69. Yamada T, Oshima T, Yoshihara K et al (2010) Overexpression of MMP-13 gene in colorectal cancer with liver metastasis. Anticancer Res 30(7):2693–2699
70. Sc EJCB, D GRP, Sc RGB, Sc TRB, Sc MMB, Sc PZB (2010) Investigation of tumor–peritoneal interactions in the pathogenesis of peritoneal metastases using a novel ex vivo peritoneal model1. J Surg Res 164(2):e265–e272
71. Peng L, Xing X, Li W, Qu L, Meng L, Lian S, Jiang B, Wu J, Shou C (2009) PRL-3 promotes the motility, invasion, and metastasis of LoVo colon cancer cells through PRL-3-integrin β1-ERK1/2 and-MMP2 signaling. Mol Cancer 8(1):110
72. Aparicio T, Kermorgant S, Dessirier V, Lewin MJ, Lehy T (1999) Matrix metalloproteinase inhibition prevents colon cancer peritoneal carcinomatosis development and prolongs survival in rats. Carcinogenesis 20(8):1445–1451
73. Barbolina MV, Adley BP, Shea LD, Stack MS (2008) Wilms tumor gene protein 1 is associated with ovarian cancer metastasis and modulates cell invasion. Cancer 112(7):1632–1641
74. Varghese S, Burness M, Xu H, Beresnev T, Pingpank J, Alexander HR (2007) Site-specific gene expression profiles and novel molecular prognostic factors in patients with lower gastrointestinal adenocarcinoma diffusely metastatic to liver or peritoneum. Ann Surg Oncol 14(12):3460–3471
75. Hojilla CV, Mohammed FF, Khokha R (2003) Matrix metalloproteinases and their tissue inhibitors direct cell fate during cancer development. Br J Cancer 89(10):1817–1821
76. NCBI (ed) TIMP2 TIMP metallopeptidase inhibitor 2 [*Homo sapiens*]. Gene, NCBI.
77. Raa ST, Oosterling SJ, van der Kaaij NP, van den Tol MP, Beelen RHJ, Meijer S, van Eijck CHJ, van der Sijp JRM, van Egmond M, Jeekel J (2005) Surgery promotes implantation of disseminated tumor cells, but does not increase growth of tumor cell clusters. J Surg Oncol 92(2):124–129
78. van der Bij GJ, Oosterling SJ, Beelen RHJ, Meijer S, Coffey JC, van Egmond M (2009) The perioperative period is an underutilized window of therapeutic opportunity in patients with colorectal cancer. Ann Surg 249(5):727–734
79. Bhowmick NA, Neilson EG, Moses HL (2004) Stromal fibroblasts in cancer initiation and progression. Nature 432(7015):332–337
80. Kjeldsen T, Andersen AS, Wiberg FC, Rasmussen JS, Schäffer L, Balschmidt P, Møller KB, Møller NP (1991) The ligand specificities of the insulin receptor and the insulin-like growth factor I receptor reside in different regions of a common binding site. Proc Natl Acad Sci U S A 88(10):4404–4408
81. Fuchs CS, Goldberg RM, Sargent DJ, Meyerhardt JA, Wolpin BM, Green EM, Pitot HC, Pollak M (2008) Plasma insulin-like growth factors, insulin-like binding protein-3, and outcome in metastatic colorectal cancer: results from Intergroup Trial N9741. Clin Cancer Res 14(24):8263–8269
82. Goldberg RM (2003) A randomized controlled trial of fluorouracil plus leucovorin, irinotecan, and oxaliplatin combinations in patients with previously untreated metastatic colorectal cancer. J Clin Oncol 22(1):23–30
83. Greijer AE, Delis-van Diemen PM, Fijneman RJA, Giles RH, Voest EE, Hinsbergh VWM, Meijer GA (2008) Presence of HIF-1 and related genes in normal mucosa, adenomas and carcinomas of the colorectum. Virchows Arch 452(5):535–544
84. Nijkamp MW, Hoogwater FJH, Steller EJA, Westendorp BF, van der Meulen TA, Leenders MWH, Rinkes IHMB, Kranenburg O (2010) CD95 is a key mediator of invasion and accelerated outgrowth of mouse colorectal liver metastases following radiofrequency ablation. J Hepatol 53(6):1069–1077
85. Wu Y, Jin M, Xu H, Shimin Z, He S, Wang L, Zhang Y (2010) Clinicopathologic significance of HIF-1α, CXCR4, and VEGF expression in colon cancer. Clin Dev Immunol 2010:1–10. doi:10.1155/2010/537531
86. Logan-Collins JM, Lowy AM, Robinson-Smith TM, Kumar S, Sussman JJ, James LE, Ahmad SA (2007) VEGF expression predicts survival in patients with peritoneal surface metastases from mucinous adenocarcinoma of the appendix and colon. Ann Surg Oncol 15(3):738–744
87. Hurwitz H, Fehrenbacher L, Novotny W et al (2004) Bevacizumab plus irinotecan, fluorouracil, and leucovorin for metastatic colorectal cancer. N Engl J Med 350(23):2335–2342
88. Shaheen RM, Ahmad SA, Liu W, Reinmuth N, Jung YD, Tseng WW, Drazan KE, Bucana CD, Hicklin DJ, Ellis LM (2001) Inhibited growth of colon cancer carcinomatosis by antibodies to vascular endothelial and epidermal growth factor receptors. Br J Cancer 85(4):584–589
89. Bruns CJ, Shrader M, Harbison MT, Portera C, Solorzano CC, Jauch K-W, Hicklin DJ, Radinsky R, Ellis LM (2002) Effect of the vascular endothelial growth factor receptor-2 antibody DC101 plus gemcitabine on growth, metastasis and angiogenesis of human pancreatic cancer growing orthotopically in nude mice. Int J Cancer 102(2):101–108
90. Bruns CJ, Liu W, Davis DW, Shaheen RM, McConkey DJ, Wilson MR, Bucana CD, Hicklin DJ, Ellis LM (2000) Vascular endothelial growth factor is an in vivo survival factor for tumor endothelium in a murine model of colorectal carcinoma liver metastases. Cancer 89(3):488–499
91. Sorensen EW, Gerber SA, Sedlacek AL, Rybalko VY, Chan WM, Lord EM (2009) Omental immune aggregates and tumor metastasis within the peritoneal cavity. Immunol Res. doi:10.1007/s12026-009-8100-2
92. Gerber SA, Rybalko VY, Bigelow CE, Lugade AA, Foster TH, Frelinger JG, Lord EM (2006) Preferential attachment of peritoneal tumor metastases to omental immune aggregates and possible role of a unique vascular microenvironment in metastatic survival and growth. Am J Pathol 169(5):1739–1752
93. Beelen RHJ, Oosterling SJ, van Egmond M, van den Born J, Zareie M (2005) Omental milky spots in peritoneal pathophysiology (spots before your eyes). Perit Dial Int 25(1):30–32
94. Beelen RH (1992) Role of omental milky spots in the local immune response. Lancet 339(8794):689
95. Krist LF, Koenen H, Calame W, van der Harten JJ, van der Linden JC, Eestermans IL, Meyer S, Beelen RH (1997) Ontogeny of milky spots in the human greater omentum: an immunochemical study. Anat Rec 249(3):399–404

96. Yildirim A, Aktaş A, Nergiz Y, Akkuş M (2010) Analysis of human omentum-associated lymphoid tissue components with S-100: an immunohistochemical study. Rom J Morphol Embryol 51 (4):759–764
97. Yildirim A, Akkus M, Nergiz Y, Yuruker S (2004) Immunohistochemical analysis of CD31, CD36, and CD44 antigens in human omentum. Saudi Med J 25(3):308–312
98. Babic AM, Kireeva ML, Kolesnikova TV, Lau LF (1998) CYR61, a product of a growth factor-inducible immediate early gene, promotes angiogenesis and tumor growth. Proc Natl Acad Sci U S A 95(11):6355–6360
99. Fan Y-F, Huang Z-H (2002) Angiogenesis inhibitor TNP-470 suppresses growth of peritoneal disseminating foci of human colon cancer line Lovo. WJG 8(5):853–856
100. Griffith EC, Su Z, Niwayama S, Ramsay CA, Chang YH, Liu JO (1998) Molecular recognition of angiogenesis inhibitors fumagillin and ovalicin by methionine aminopeptidase 2. Proc Natl Acad Sci U S A 95(26):15183–15188
101. Hines J, Ju R, Dutschman GE, Cheng Y-C, Crews CM (2010) Reversal of TNP-470-induced endothelial cell growth arrest by guanine and guanine nucleosides. J Pharmacol Exp Ther 334 (3):729–738
102. Yan TD (2006) Systematic review on the efficacy of cytoreductive surgery combined with perioperative intraperitoneal chemotherapy for peritoneal carcinomatosis from colorectal carcinoma. J Clin Oncol 24(24):4011–4019
103. van Dam GM, Themelis G, Crane LMA, et al (2011) Intraoperative tumor-specific fluorescence imaging in ovarian cancer by folate receptor-α targeting: first in-human results. Nature Medicine 17:1–6
104. Van der Speeten K, Stuart OA, Chang D, Mahteme H, Sugarbaker PH (2011) Changes induced by surgical and clinical factors in the pharmacology of intraperitoneal mitomycin C in 145 patients with peritoneal carcinomatosis. Cancer Chemother Pharmacol 68(1):147–156
105. De Roock MD W, De Vriendt MSc V, MD NN, MD PFC, MD PST (2011) KRAS, BRAF, PIK3CA, and PTEN mutations: implications for targeted therapies in metastatic colorectal cancer. Lancet Oncology 12(6):594–603
106. Prahallad A, Sun C, Huang S, Di Nicolantonio F, Salazar R, Zecchin D, Beijersbergen RL, Bardelli A, Bernards R (2012) Unresponsiveness of colon cancer to BRAF(V600E) inhibition through feedback activation of EGFR. Nature 483(7387):100–103
107. Olmos D, Postel-Vinay S, Molife LR et al (2010) Safety, pharmacokinetics, and preliminary activity of the anti-IGF-1R antibody figitumumab (CP-751,871) in patients with sarcoma and Ewing's sarcoma: a phase 1 expansion cohort study. Lancet Oncol 11(2):129–135
108. Haluska P, Worden F, Olmos D, Yin D, Schteingart D, Batzel GN, Paccagnella ML, de Bono JS, Gualberto A, Hammer GD (2010) Safety, tolerability, and pharmacokinetics of the anti-IGF-1R monoclonal antibody figitumumab in patients with refractory adrenocortical carcinoma. Cancer Chemother Pharmacol 65 (4):765–773
109. Nijkamp MW, van der Bilt JDW, de Bruijn MT, Molenaar IQ, Voest EE, van Diest PJ, Kranenburg O, Borel Rinkes IHM (2009) Accelerated perinecrotic outgrowth of colorectal liver metastases following radiofrequency ablation is a hypoxia-driven phenomenon. Ann Surg 249(5):814–823

Virchows Arch (2012) 461:245–257
DOI 10.1007/s00428-012-1281-4

REVIEW AND PERSPECTIVES

EML4-ALK testing in non-small cell carcinomas of the lung: a review with recommendations

Erik Thunnissen · Lukas Bubendorf · Manfred Dietel · Göran Elmberger · Keith Kerr · Fernando Lopez-Rios · Holger Moch · Wlodzimierz Olszewski · Patrick Pauwels · Frédérique Penault-Llorca · Giulio Rossi

Received: 13 April 2012 / Revised: 21 June 2012 / Accepted: 2 July 2012 / Published online: 24 July 2012
© The Author(s) 2012. This article is published with open access at Springerlink.com

Abstract In non-small cell lung cancer, epidermal growth factor receptor gene mutations and anaplastic lymphoma kinase (ALK) gene rearrangements have a major impact upon the level of response to treatment with specific tyrosine kinase inhibitors. This review describes the molecular basis of ALK inhibition, summarizes current data on the effectiveness and safety of ALK inhibition therapy, describes the different testing methodologies with their advantages and disadvantages, provides a suggested testing algorithm and puts forward a proposal for an external quality assessment program in ALK testing.

Keywords Anaplastic lymphoma kinase · Rearrangement · Crizotinib · Algorithm · Guidelines · Non-small cell lung cancer

Electronic supplementary material The online version of this article (doi:10.1007/s00428-012-1281-4) contains supplementary material, which is available to authorized users.

E. Thunnissen (✉)
Department of Pathology, VU University Medical Centre,
Amsterdam, The Netherlands
e-mail: e.thunnissen@vumc.nl

L. Bubendorf
Institute for Pathology, University Hospital Basel,
Basel, Switzerland

M. Dietel
Institute for Pathology, Charité,
Charité Campus Mitte,
Berlin, Germany

G. Elmberger
Department of Pathology, Solna, Karolinska University Hospital,
Stockholm, Sweden

K. Kerr
Department of Pathology, Aberdeen University Medical School,
Aberdeen, Scotland, UK

F. Lopez-Rios
Laboratorio de Dianas Terapéuticas, Centro Integral Oncológico
Clara Campal, Hospital Universitario Sanchinarro,
Madrid, Spain

H. Moch
Institute for Surgical Pathology, Universitätsspital Zurich,
Zurich, Switzerland

W. Olszewski
Department of Pathology,
Maria Sklodowska-Curie Institute of Oncology,
Warszawa, Poland

P. Pauwels
Department of Pathology, Antwerp University Hospital,
Edegem, Belgium

F. Penault-Llorca
Department of Pathology, Centre Jean Perrin,
Clermont-Ferrand, France

G. Rossi
Sezione di Anatomia Patologica, Azienda Policlinico di Modena,
Modena, Italy

Introduction

In 2008, lung cancer was the most commonly diagnosed cancer and caused the highest number of cancer-related deaths [1]. Currently, only 10–15 % of lung cancer patients will be cured [2]. Strategies to maximize treatment benefit have centred on individualizing treatment according to the molecular profile of the disease [3, 4]. Mutations of the epidermal growth factor receptor (EGFR) gene have a major impact upon the level of response to treatment with tyrosine kinase inhibitors [5]. In addition to mutations in the EGFR gene, alterations in hepatocyte growth factor receptor (MET), vascular endothelial growth factor (VEGF), VEGF receptor, GTPase KRAS (KRAS), receptor tyrosine protein kinase erbB-2 (HER2), echinoderm microtubule-associated protein-like 4-anaplastic lymphoma kinase (EML4-ALK), phosphatidylinositol-4,5-bisphosphate 3-kinase catalytic subunit alpha isoform, serine/threonine protein kinase B-raf, insulin-like growth factor 1 receptor [6], ROS1 [7], and the KIF5B and RET fusion gene [8, 9] have also been implicated as oncogenic drivers in the pathogenesis of non-small cell lung cancer (NSCLC), especially adenocarcinoma.

In 2007, Soda et al. [10] reported that a small inversion within chromosome 2p results in the formation of a fusion gene comprising portions of the EML4 gene and ALK in NSCLC cells. A recently developed MET inhibitor (PF-02341066, crizotinib; Pfizer) was shown to also inhibit ALK [11, 12]. Phase I [13, 14] and II [15, 16] studies have revealed encouraging data [14], leading to an accelerated approval of crizotinib by the FDA in August 2011 [16]. Pathologists will play a key role in the identification of aberrations of ALK in NSCLC. The aim of this article is to provide information on how ALK alterations in NSCLC can be detected, with an emphasis on the uncertainties regarding methodology.

Molecular basis of ALK inhibition therapy

Transforming rearrangements of the ALK gene were first identified in anaplastic large cell lymphomas [17, 18], and subsequently in inflammatory myofibroblastic tumours [19] and a subset of NSCLC [10]. An inversion event on the short arm of chromosome 2, resulting in the fusion of ALK gene with the EML4 gene locus, is the most common aberration of the ALK gene in lung cancer (Fig. 1) [10]. This rearrangement leads to the production of a chimeric protein, which has constitutive ALK kinase activity [14]. Over ten EML4-ALK variants have been identified in lung cancer so far, as well as other fusion partners TFG and KIF5B [20]. In addition, as single fluorescence in situ hybridization (FISH) signals (3′) are also associated with a positive response to crizotinib treatment, it seems that small deletions of 5′ end of the ALK gene may also occur [14, 21].

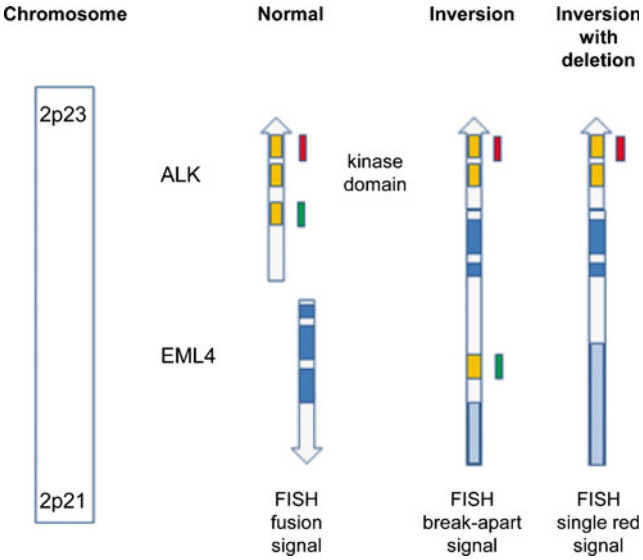

Fig. 1 Signal pattern of Vysis ALK Break Apart FISH Kit. ALK and EML4 are located on chromosome 2p21–2p23. Note that EML4 is normally on the opposite strand to ALK, and that both probes on the ALK gene (*red orange* and *green*) are close together, explaining the FISH fusion signal. The EML4-ALK fusion gene is the result of an inversion of the N-terminal portion of EML4 with the kinase domain of ALK [10]. This inversion leads to an increased distance between the red orange and green probes. A deletion of the proximal part combined with the inversion explains the single red orange signal. The EML4-ALK fusion protein has a fully functional ALK kinase domain and has gain-of-function properties [5, 10]. Cells are considered ALK FISH positive when there is: (1) ≥1 set of red and green signals that are ≥2 signal diameters apart, or (2) a single red signal without a corresponding green signal in addition to fused (normal) signals. A sample is considered negative if <5 cells (<10 %) are positive and positive if >25 cells (>50 %) are positive. A sample is considered equivocal if 5–25 cells (10–50 %) are positive

Current estimates suggest that the EML4-ALK fusion is present in approximately 3–6 % of adenocarcinomas, depending upon on the population studied and the ALK detection methods used [22, 23].

Clinical characteristics associated with the EML4-ALK gene fusion are adenocarcinoma histology, never/light smoking history and younger age [24–26]. However, these characteristics are not shared by all carriers. The ALK fusion has also been detected in older patients (aged 76 years) with a smoking history [24]. Therefore, clinical characteristics are insufficient and molecular testing is necessary to determine ALK status [27].

ALK-positive tumours have been detected in all histological subtypes of adenocarcinoma, but especially in solid signet-ring cell and mucinous cribriform patterns [24, 28–31].

Effectiveness and safety of ALK inhibition therapy

Crizotinib is the most advanced ALK inhibitor in clinical development [3]. In ALK-positive patients (n=119), an

overall response rate (complete responses + partial responses) of 61 % (95 % CI, 52–70 %), a clinical benefit rate (complete responses + partial responses + stable disease) of 88 % and a preliminary median progression-free survival of 10 months (95 % CI, 8–15 months) have been shown [13]. The median overall survival has not been reached. In a retrospective case-match analysis, Shaw et al. [32] found that ALK-positive NSCLC patients had a longer overall survival rate after crizotinib as second- or third-line therapy. Crizotinib seems to show poor penetration of the blood–brain barrier [33].

Crizotinib is well tolerated, with reported treatment-related adverse events of nausea (46 %), vision disorder (45 %), vomiting (39 %) and diarrhoea (29 %), mostly of grade 1/2. Grade 3/4 adverse events were reported in 15 % of patients (mostly increased alanine aminotransferase, dyspnoea and neutropenia) [13].

A proportion of ALK-positive patients with NSCLC (in most studies <10 %) continue to show progressive disease in spite of crizotinib treatment [15, 34]. Several mechanisms of resistance have been suggested to explain this lack of efficacy: (1) ALK kinase domain mutations (found in 4/11 samples); (2) copy number gain of the ALK gene rearrangement (found in 2/11 samples); (3) EGFR/KRAS mutations (found in 3/11 samples) [35]. Some patients never showed (intrinsic resistance) and some initially showed (acquired resistance) a response to treatment [35].

Neither percentage of positive cells nor signal copy number appears to be predictive of benefit from ALK inhibition treatment [21]. In other words, using ALK FISH, there is no greater likelihood of a treatment response to crizotinib in a patient with a sample showing nearly 100 % positivity than for a patient with a sample showing just above the positivity threshold. However, it is still important to know the percentage of positive cells to determine whether the threshold has been reached.

Detection of ALK gene rearrangements

Increasing availability of targeted agents with selective biomarkers has introduced new challenges in NSCLC diagnosis [36]. Issues related to small sample diagnostics, the interaction between pulmonologists and pathologists, tissue management and required clinical information have recently been described [37]. Current diagnostic approaches to detect ALK rearrangements include immunohistochemistry (IHC), FISH and reverse transcriptase polymerase chain reaction (RT-PCR). Unpublished information from pilot studies suggests that ALK fusions may be demonstrated with massive parallel sequencing. However, sufficient details for an adequate comparison with FISH are currently lacking.

Tissue management

With personalized tumour medicine in mind, tissue sample size should be maximized whenever feasible. In addition, tissue handling, processing and sectioning should be standardized to minimize wastage and optimize use of tissue for staining procedures and PCR-based molecular tests. Histological and cytological specimens are both potentially suitable for ALK testing. Currently, the only clinically validated test to determine ALK status is the Vysis/Abbott ALK FISH break apart test. However, this test and the interpretation algorithm are only designed and validated for histopathological use on intact formalin-fixed paraffin-embedded (FFPE) tissue biopsies or resection specimens. If cytological material is to be used, laboratories must take steps to validate their testing methodology.

Tumour tissue should preferentially be taken from metastases if access is less dangerous. Sampling of these sites ensures that the more important fraction of total tumour cell burden is collected. Furthermore, potential heterogeneity problems within the primary tumour are avoided when sampling metastases.

Standardized tissue and cell processing

Tissue handling steps have recently been described [37]. While so-called ‘reflex’ IHC and molecular testing provides a rapid diagnosis, it should be avoided if tissue resources are marginal. In anticipation of obligatory biomarker testing, an algorithm for reflex block cutting could be employed.

If the initial tissue sample is small, some (three to four) additional sections (extra spare cut sections) may be taken to avoid tissue loss by recutting. The quality of some epitopes and DNA/RNA may be lost (within hours/days) when sections are not immediately used [38–40]. Various treatments for the cut sections may prevent oxidation [37].

An algorithm that laboratory staff may find useful when handling lung biopsies is presented in Electronic supplementary material (ESM 1).

Clinical diagnostic tests

IHC

Immunohistochemical detection of the ALK protein has considerable potential as a screening tool to test NSCLC samples for ALK rearrangements. The biological premise is that the translocation or inversion of part of the ALK gene with its numerous possible partners leads to over-expression of the ALK protein, and therefore overactivity of the ALK tyrosine kinase. This protein ALK tyrosine kinase is the target of crizotinib. It therefore makes sense to assess the drug target directly.

IHC has several advantages over either an ISH method (especially when based on fluorescent probes) or an approach based upon mRNA (RT-PCR) to detect the actual rearrangement. These advantages are that it is cheap, rapid and easily integrated into a diagnostic protocol and familiar to all pathologists. Although IHC is only minimally quantitative, in practice it is used as a semiquantitative test [41]. However, challenges with IHC are: (1) the tissue preparation; (2) the choice of antibody; (3) the signal enhancement system; (4) the scoring system.

Pre-analytical phase Currently, the role that pre-analytical issues, like fixative and duration of fixation, may have on ALK epitope preservation has not been evaluated. However, compared to what has been observed for other antibodies [39], here the pre-analytical steps appear to be particularly critical and mistakes are irremediable. False-negative cases may be due to poor fixation. Such issues may be of particular concern in surgically resected tumours, where a gradient in positivity can be observed due to the gradient in fixative penetration in the sample [42]. Ultimately, any test for abnormal ALK genes in NSCLC is likely to be most important in small biopsy or cytology samples, where intra-sample heterogeneity is less likely to be appreciated because fewer cells are present, but where the possibility of heterogeneity of expression may lead to a false-negative test.

Analytical phase One of the particular challenges in IHC detection is that the protein concentrations in ALK-rearranged NSCLC are relatively low. Standard detection methodology, as used in the identification of ALK-rearranged anaplastic lymphomas, is inadequate for the detection of all cases of ALK-rearranged NSCLC. Currently, there are three primary antibodies commonly referred to in the published literature; clone 5A4 (Novocastra, Leica, but also available pre-diluted from Abcam), ALK1 (Dako) and D5F3 (Cell Signalling Technology). Experience with the first two antibodies is widest, and more success (and excellent comparison with the outcome of FISH testing for the rearrangement) has resulted from their use with detection systems with a substantial degree of signal amplification (Leica/Novocastra Novolink, Dako Advance, Tyramide, Envision+, Ventana i-view). For more details, see Tables 1 and 2. If using FISH as the gold standard, use of these antibodies in this way has resulted in both a very high negative predictive value (all IHC-negative cases are also FISH-negative) and high positive predictive values (90–100 % probability of being FISH positive when IHC is strongly positive) [23, 24, 43–51]. For more details, see "Concordance between IHC and FISH" section. Good concordance has also been shown between RT-PCR and the antibodies ALK1 [22, 44] and 5A4 [45]. With current knowledge, all IHC positive (+/++/+++) cases would be best screened with FISH to confirm probable rearrangement.

In the literature (Table 1) and in the experience of the authors, there is some variation in the best concentrations of various primary antibodies and the antigen retrieval methodology. Personal experience with the 5A4 clone has found better results with pH6- when compared to pH9-buffered solution.

Comparing primary antibodies is very difficult since there are few published studies with comparative data. One study did compare the D5F3 clone with the ALK1 clone and found the former far superior [49], but the latter was not used with any special detection amplification. At this moment, it is very difficult to reach a conclusion from the literature; there may be a marginally better performance from the 5A4 clone when compared to the ALK1 clone, borne out by anecdotal experience, but it must be emphasized that other variations in study methodology make comparison problematic.

Post-analytical phase In NSCLC, ALK-rearranged staining is cytoplasmic. It may have a granular character, and in some cases there may be membrane accentuation. Opinions differ as to the degree of staining heterogeneity that may be encountered. Whilst some assert that it is generally homogeneous in tumours, others, including the authors, have certainly seen variation in staining intensity in sections of surgically resected tumours (see comment above regarding fixation).

One of the most neglected issues in the literature is the question of definitions of degree of staining. Many studies do not even indicate how different grades of staining were defined. There is no clear consensus on this matter. Prospectively, it may be of value to determine a so-called histoscore (H-score) utilizing the proportion of tumour cells showing each different intensity (+, ++ and +++) of staining. Assessment of staining intensity is very subjective. The use of successive microscope objectives with related spatial resolutions as a physical aid in establishing intensity (as first applied on HER2 by Ruschoff et al. [50]) may lead to more uniformity in intensity scoring. Strong staining (+++) is clearly visible using a ×2 or ×4 objective, moderate staining (++) requires a ×10 or ×20 objective to be clearly seen, whilst weak staining (+) cannot be seen until a ×40 objective is used. This approach is called the modified H-score. Frequently used scoring systems are presented in Table 2.

For the time being, the modified H-score is recommended because it will allow sufficient detail for comparison with other studies. It may turn out that a more simplified scoring system is suitable as well. Ultimately, studies are required where prospectively determined IHC scores can be directly related to clinical outcomes in patients treated with crizotinib.

Table 1 IHC protocols described in the literature

	Antibody	Source	HIER	Dilution	Incubation	Detection system
Yi et al. [46]	ALK1	Dako	EDTA, pH 8, 30 min	1/100	30 min at RT	Advance (Dako)
Yang et al. [43]	ALK1	Dako	EDTA, pH 8, 30 min	1/100	30 min at RT	Advance (Dako)
Paik et al. [47]	5A4	Abcam	CC1 (Ventana), 1 h	1/30	2 h at 42 °C	i-view (Ventana)
McLeer-Florin et al. [48]	5A4	Abcam	CC1 (Ventana), 1 h	1/50	2 h at 37 °C	i-view (Ventana)
Hofman et al. [45]	5A4	Abcam	pH 9, 40 min, 97 °C	1/50	30 min RT	EnVision Flex (Dako)
Kim et al. [27]	5A4	Novocastra	CC1 100 °C, 20 min	1/30	2 h at 42 °C	i-view (Ventana)
Mino-Kenudson et al. [49]	D5F3 D9E4	CST CST	EDTA pH 8 pressure cooker	1/500[a] 1/100[b]	Overnight	EnVision+ (Dako)
	ALK1	Dako		1/50[a] 1/2[b]		

HIER heat-induced epitope retrieval, *EDTA* ethylenediaminetetraacetic acid, *RT* room temperature, *CST* cell signaling technology

[a] For anaplastic large cell lymphomas

[b] For lung adenocarcinomas and inflammatory myofibroblastic tumours

Pathologists should be aware of various artefacts that may lead to false-positive staining; these are generic issues, not necessarily specific to ALK IHC. The possibility of false-negative tests can be guarded against, at least to some extent, by the use of positive control material with every test staining run. Such material may not be readily available, and it is important that the control material is from ALK-rearranged NSCLC or similar and has the same levels of ALK protein epitopes. ALK-rearranged lymphomas are not suitable as a control because he protein epitope level is much higher than in NSCLC, thus giving false confidence of sufficient staining.

Table 2 IHC scoring systems

	Score			
	0	1+	2	3
Yi et al. [46]	No staining	Faint cytoplasmic staining	Moderate smooth cytoplasmic staining	Intense granular cytoplasmic staining in ≥10 % of tumour cells
Kim et al. [27]	No staining	Faint or weak staining intensity with >5 % tumour cells or any staining intensity with ≤5 % tumour cells [a]	Moderate staining >intensity with >5 % tumour cells [b]	Strong and granular staining intensity with >5 % tumour cells [c]

[a] Average of 14.7 % positively stained cells

[b] Average of 58.2 % positively stained cells

[c] Average of 97.3 % positively stained cells

FISH

The majority of clinical studies examining ALK mutations have used FISH. In the USA, prescription of crizotinib is dependent upon the use of the Vysis ALK Break Apart FISH Probe Kit (Abbott Molecular, Inc.) [16]. Although FISH can be performed on FFPE tumour specimens and detect multiple ALK fusion variants [28], there are various challenges related to the FISH technique, e.g. the break apart red and green signals indicating ALK rearrangements (Fig. 2) can be subtle and occasionally difficult to recognize.

Pre-analytical phase A protocol for cytology is provided in ESM 2.

Processing and sectioning—For an effective procedure for surgical specimens, it is recommended that embedded tissues do not exceed 2 cm in length and 3 mm in thickness. Samples should be processed according to a standard protocol.

In practice, ALK testing works well on 3- to 5-μm sections. A minor preference exists for a thickness of 5 μm. Sections should be mounted on coated slides to prevent cleavage artefacts and washing off during the procedure. Sections should be dried at 60 °C for 1 h or at 45 °C overnight.

The maximum storage time for tissue or cell block sections should be 1–6 months (based on the authors' experience) and 6–12 months for conventional cytological specimens [52] to avoid hybridization failure and either false-negative or false-positive results. A protective coating

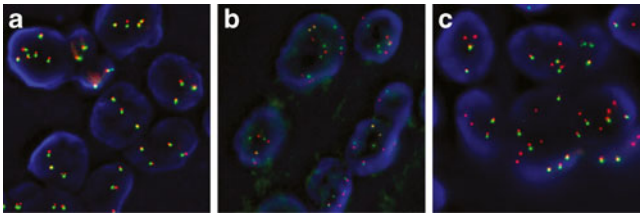

Fig. 2 Representative examples of ALK FISH findings in three pulmonary adenocarcinomas (Vysis ALK Break Apart FISH probe). All three carcinomas show increased ALK copy number. **a** Normal signals, no rearrangement. Note that some of the signals are fused and produce a yellow signal, while others have *green* and *red* signals in close proximity. **b** One or two break apart signals per nucleus, indicative of inversion. **c** Single red signals, indicative of inversion and deletion. Note that the cancer cells in **b** and **c** contain both rearranged and normal ALK signals. Cells are considered ALK FISH positive when there is: (1) ≥1 set of red and green signals that are ≥2 signal diameters apart, or (2) a single red signal without a corresponding green signal in addition to fused (normal) signals. A sample is considered negative if <5 cells (<10 %) are positive and positive if >25 cells (>50 %) are positive. A sample is considered equivocal if 5–25 cells (10–50 %) are positive

of paraffin to histological sections prevents loss of antigenicity caused by photo-oxidation and drying of the tissues [37]. In order to avoid problems of irregular or background staining of histological specimens, it is essential to deparaffinize the samples properly [37].

Relocation of tumour cells by a software-driven automated stage is highly desirable for 'restrained' cytological specimens with a tumour cell proportion of <50 %. This allows precise distinction of the tumour cells from admixed benign cells and facilitates review of the results at the microscope.

Analytical phase

Method—Use of diagnostic kits certified by the FDA (Abbott Vysis ALK Break Apart FISH Probe Kit, Abbott Molecular, Inc.) is recommended. The package insert contains a detailed protocol of the technical procedures and interpretation. In practice, the Vysis kit has some limitations: (1) appropriate optical filters are required for the probes used; (2) the green signal may fade earlier than the red signal, increasing the likelihood of false-positive single-red signals. Other, not yet FDA-approved, FISH assays are commercially available (e.g. ZytoLight® SPEC ALK/EML4 TriCheck™ Probe, ZytoVision). Every assay should undergo validation in the laboratory before clinical implementation. This validation can be conducted with five to ten positive and five to ten negative cases. The results are compared with a reference centre, and concordance of at least 95 % should be obtained. In addition, laboratories should participate in external quality assessment schemes as soon as they become available. When a laboratory authorized to conduct FISH adopts another bright-field ISH for diagnostic purposes, an internal validation can be conducted in the laboratory comparing the new technique with FISH. Again, a concordance of 95 % must be obtained. This 95 % threshold may change in time, after more experience is gained with the external quality assessment. The use of standardized kits requires strict adherence to the manufacturers' instructions, i.e. without any deviation.

A minimum norm for ALK experience is not known yet, but for Her2 it was suggested that at least 150 ISH cases per annum (minimum of 100 breast and 50 gastric cases by ISH per annum) would be the optimal volume to ensure quality and cost effectiveness [53] (see "Proposal for an external quality assessment program" section).

The number of annual tests considered optimal for guaranteeing the technical sufficiency of a laboratory is 150 ISH tests on any type of tumour [51]. Analysis of complete histological sections is recommended in order to minimize signal loss on the Z-axis. In FISH procedures, it is essential to use fluorescence filters with excitation and emission wavelengths appropriate to the fluorochromes of the probes contained in the kit.

Controls—With ISH techniques, the case for study serves as a control when consistently presenting signals, both in tumour cells and in the accompanying normal cells. Nevertheless, the use of separate controls is strongly advised. A pre-hybridization assessment of digestion is useful in difficult samples (e.g. very small biopsies with low tumour content).

Post-analytical phase

Assessment of the results—A pathologist should interpret the results. When other persons score the specimens, they should be well trained and experienced in histo- and cytomorphology. In such a case, a pathologist should coordinate, validate, review and sign off the interpretation. A total of 50 nuclei should be scored using an epifluorescence microscope equipped with a DAPI, a Spectrum Orange, Spectrum Green and double-filter set, using a ×60–100 oil immersion objective lens. The spectral orange probe is mostly called the 'red probe/signal' in the literature, and this terminology has been used throughout the manuscript.

Assessment must be conducted exclusively on nuclei with sufficient hybridization quality, in a consecutive

manner, and with the microscope focus adjusted to each nucleus in order to correctly identify all the signals present in the nucleus of the cells.

When conducting FISH as an ISH technique, given the difficulty of dark-field assessment, the following are recommended:

a. Cells are considered ALK FISH positive when: (1) at least one set of red and green signals have a distance between the signal borders of ≥2 diameters of the largest of the two signals (break apart of the two differently coloured probes indicates gene fusion by inversion), or (2) when there is a single red signal without a corresponding green signal in addition to fused (normal) signals (indicating gene fusion by inversion and deletion) (Figs. 1 and 2). Note that a single green signal without a corresponding red signal is considered negative. Similarly, an increased copy number of non-rearranged ALK genes with fused signals corresponds to polysomy of chromosome 2 or ALK amplification, but is negative for rearrangement.
b. A sample is considered negative if <5 cells (<10 %) are positive and positive if >25 cells (>50 %) are positive.
c. A sample is considered equivocal if 5–25 cells (10–50 %) are positive. In this case, a second reader should evaluate the slide. If the average of the two readings contains at least 15 % positive cells, the sample is considered ALK FISH positive. It should be kept in mind that the digestion time needs to be adjusted for some samples. Examples of typical FISH findings are shown in Fig. 2.

During interpretation, the spatial distribution of the distance between the two signals in the *Z*-direction also needs to be taken into account. In cases of only one signal, adjusting the plane of focus (by turning the microscrew) is frequently necessary when using the conventional FISH microscope. An advantage of a digitized automatic FISH analysis system is that fluorescent images may be compressed in the *Z*-direction (*Z*-stacks), often making this automated stage more convenient than live microscopy. The presence of all signals in one horizontal plane facilitates scoring and review, and allows permanent documentation. In our experience, a positive scoring result that cannot convincingly be illustrated by fluorescence photography is of questionable value.

Cytological specimens offer the advantage of analysing entire cells/nuclei containing all chromosomal signals. Instead, a part of the nuclei in histological tissue sections are truncated, leading to a lower number of fluorescence signals, and this effect depends on the section thickness.

Note that in most ALK-positive samples, not all alleles are abnormal (e.g. only one in a disomic cell or one or two in tetrasomic cells). Typically, there is one predominant type of rearrangement in one sample (either break apart or deletion). Great variability in signal patterns within one sample might suggest technical artefacts.

There is evidence that ALK rearrangements are truly diffuse rather than heterogeneous within ALK-positive tumours [21, 54]. First, IHC typically shows diffuse ALK expression in ALK-positive tumours [47, 55]. Second, the distribution of cell positivity by FISH is diffuse; there are no discrete foci of ALK rearrangements within a tumour [21, 54]. This suggests that any observed variability is not biological, but rather caused by technical factors.

Given the presumed homogeneous distribution of ALK rearrangements, the percentage of FISH-positive cells in an ALK-positive tumour lying between 20 and 80 %, and not reaching 100 % may appear contrary. The ‘single red’ signal is found in a higher fraction of tumour cells than the ‘break apart’ signal [21]. This discrepancy can readily be explained by the distribution of signals in three-dimensional space and their projection by the assessing pathologist to the horizontal plane. A separated signal can be located anywhere on a virtual sphere around the other signal. In a disomic tumour cell with one rearranged ALK gene copy, the probability of detecting break apart signals in the two-dimensional projection may therefore not exceed 25–30 %.

In the authors' experience, the minimum number of tumor cells required in histological specimens is at least 100, as approximately half will not be stained with the fluorescence probes for reasons related to the stereological analysis. Less than 40 tumor cells/neoplastic nuclei with FISH signals are unreliable for determining positivity.

Increased ALK gene copy number (3 to >6 gene copies), which is mostly due to polysomy of chromosome 2, has been reported in 80 % of NSCLC [56]. In cases of polysomy, one rearranged signal per nucleus is sufficient for a ‘positive’. High gene copy number of non-rearranged ALK does not appear to influence response to crizotinib. A possible predictive value of the copy number of the rearranged ALK gene in tumour cells and its influence on the

level of ALK protein expression remains to be investigated.

Overall, interpretation of the ALK FISH analysis is more complex than for other FISH assays, e.g. with amplifications or interchromosomal translocation. This is due to the fact that: (1) fusion inversion occurs on the same chromosome arm—in contrast to fusion processes in SYT-SSX and BCR-ABL FISH tests, for example, where genes from different chromosomes are involved; (2) in some ALK wild-type cells (especially with larger nuclei or after prolonged digestion) the red and green signals may be slightly separated and the fusion to yellow fluorescence is not apparent; (3) the process of cutting and subsequent signal separation may lead to a low number of false-positive break apart signals in cells without the ALK fusion. These characteristics mean that a low threshold of positive cells can still select patients who will react to ALK inhibitor treatment. However, this complexity highlights the need for specific training and experience with ALK FISH.

Personnel—The number of laboratory technicians who conduct tests and the number of pathologists who interpret them must be as low as possible in order to guarantee the effectiveness of the undertaking. Both the technicians and the pathologists must have undergone training. For assessing the post-analytical (interpretation) phase, correlation with the reference result of at least 95 % in 10–20 cases is recommended. Periodically, the aforesaid training should be refreshed in dedicated working sessions.

Report—While the report should be adapted to the different information systems used in different hospitals, it must include, at minimum, the data presented in Table 3. The recommended turnaround time is <7 working days.

FISH is not feasible in all laboratories and the results are not always clear. McLeer-Florin et al. [48] reported that 19 % of cases analyzed by FISH were not interpretable.

Concordance between IHC and FISH

The results from the three larger FISH/IHC concordance studies have shown that in FISH-negative cases, IHC is always negative (i.e. 100 % concordance) [46, 47, 57]. This complete concordance is also seen between a positive FISH result and an IHC 3+ score [46, 47, 57]. Very good concordance levels between FISH and IHC have also been demonstrated by Jokoji et al. [58]. McLeer-Florin et al. [48] also found good concordance between FISH and IHC. In their research, the Novocastra 5A4 antibody was used. The authors suggested using IHC to evaluate the cases that were not interpretable by FISH.

Some of the panel have had different experiences: namely that it is possible to have a sample that is IHC 3+ and FISH negative. In one such patient, a response to Crizotinib was seen (E.T.). Also a sample may be FISH positive and IHC negative. Some discordant results have been observed in tumours expressing ALK with a weak (1+) to moderate (2+) signal. Table 4 provides a summary of published articles comparing ALK analysis by FISH and IHC.

PCR-based molecular assays

RT-PCR provides a highly sensitive technique in which a very low copy number of RNA molecules can be detected. As for EML4/ALK the forward and backward primers are

Table 3 Recommended data in a report on ALK testing by in situ hybridization

Clinical information
Patient identification
Identification of doctor making request
Dates of request and test
Identification of sample (case and block number)
Type of sample[a]
Anatomical origin
Gross specimen handling/molecular method
Date block received by laboratory
Block used for analysis
Probe used (supplier, approval by FDA or other agency)
Method of assessment (semi-quantitative, image analysis)
Threshold for positivity
Microscopy/molecular results
Number of nuclei assessed
Results
Positive (%)
Presence or absence of patterns indicating rearrangement (specify whether split or single)
Negative (% of translocated cells, if any)
Presence or absence of patterns indicating rearrangement
Inconclusive: Explanations for inconclusive answers[b]
Conclusion
Molecular test outcome and interpretation
Rearrangement associated with sensitivity
Name and signature of the pathologist(s) responsible for the investigation

[a] For example, bronchial–transbronchial biopsy, surgical specimen, core needle biopsy, transbronchial fine needle aspiration, effusion cytology or other

[b] For example, possible false-negatives due to low fraction of tumour cells or uncertain fixation time

Table 4 Summary of published articles comparing ALK analysis by FISH and IHC

Reference	Antibody	Source	Detection method	Samples, *n*	ALK+		ALK−		Comments
					FISH	IHC	FISH	IHC	
Shaw et al. [25]	ALK1	Dako	n.a.	NSCLC, 141	19 (13 %)	19 (13 %)	n.a.	n.a.	Only FISH+ cases were confirmed with IHC
Boland et al. [44]	ALK1	Dako	n.a.	NSCLC, 335	6 (1.8 %)	6 (1.8 %)	n.a.	n.a.	The 6 cases testing positive using IHC were positive with FISH. 8 of the IHC ALK− cases were also tested using FISH. All were negative
Rodig et al. [24]	ALK1	Dako	EnVision +	Adeno, 358	20 (5.6 %)	n.a.	n.a.	n.a.	8 of the 10 FISH ALK+ cases with sufficient tissue were also IHC ALK+ (sensitivity=80 %); 1 case ALK– by FISH was ALK+ by IHC
Mino-Kenudson et al. [49]	ALK1	Dako	EnVision +	Adeno, 153	22 (14.3 %)	n.a.	n.a.	n.a.	Sensitivity and specificity of IHC were 67 and 97 %, respectively
	D5F3	Cell ST	EnVision +	Adeno, 153	22 (14.3 %)	n.a.	n.a.	n.a.	Sensitivity and specificity of IHC were 100 and 99 %, respectively
Yi et al. [46]	ALK1	Dako	Advance	Adeno, 101	10 (9.9 %)	11[a] (10.9 %)	91 (90.1 %)	90[a] (89.1 %)	Of the 10 FISH+ cases, 8 were IHC 3+, 1 was IHC 2+ and 1 was IHC +; of the 91 FISH– cases, 2 were IHC 2+, 20 were IHC 1+, 69 were IHC 0; sensitivity and specificity[a] of IHC were 90 and 97.8 %, respectively
Paik et al. [47]	5A4	Novocastra	i-view	NSCLC, 453	19 (4.2 %)[a]	26 (5.7 %)	434 (95.8 %)	427[a] (94.3 %)	Of the 19 FISH+ cases, 16 were IHC 3 +, 3 were IHC 2+; of the 434 FISH− cases, 7 were IHC 2+, 14 were IHC 1 +, 413 were IHC 0; sensitivity and specificity[a] of IHC were 100 and 92.5 %, respectively
Mitsudomi et al. [64]	5A4	Santa Cruz	EnVision +	NSCLC, 345	n.a.	12 (3.5 %)	n.a.	n.a.	All these 12 IHC ALK+ cases were also FISH ALK+; all IHC ALK– cases were also FISH ALK–
Martinez et al. [65]	D5F3	Cell ST	n.a.	NSCLC, 71	6 (8.5 %)	n.a.	n.a.	n.a.	All FISH ALK– negative cases were also IHC ALK–. 4/6 FISH ALK+ cases were also ALK IHC+; 1 case was IHC ALK–; 1 sample could not be analysed.
Paik et al. [66]	5A4	Novocastra	n.a.	NSCLC, 735	28 (3.8 %)	35 (4.8 %)	707 (96.2 %)	700 (95.2 %)	Of all cases, 15 were IHC 3+, 20 were IHC 2+, 20 IHC 1+, 700 were IHC0; all IHC0/1+ were ALK FISH–, all IHC 3+ cases were ALK FISH+, and 13 of the 20 IHC 2+ were FISH+; sensitivity and specificity[a] of IHC were 100 and 96.2 %, respectively
				Adeno, 395	27 (6.8 %)	n.a.	368 (93.2 %)	n.a.	
McLeer-Florin et al. [48]	5A4	Abcam	i-view	Adeno, 441	n.a.	29 (6.5 %)	n.a.	n.a.	Of 81 cases with interpretable IHC and FISH results, 21 were FISH ALK+; of these 21 cases, 19 were IHC ALK+ and 2 were IHC doubtfully positive; of the 60 FISH ALK– cases, 1 was IHC ALK+ and 59 were IHC ALK–
Yang et al. [43]	ALK1	Dako	Advance	Adeno, 300	22/216 (10.2 %)	32 (10.7 %)[a]	194/216 (89.8 %)	268 (89.3 %)	All IHC 0 cases were FISH ALK– and all IHC 3+ were FISH ALK+; 96.9 % of IHC 1+ cases were FISH ALK− and 85.7 % of IHC 2+ cases were FISH ALK+

IHC scores of 0 and 1+ are regarded as negative; scores of 2+ or 3+ as positive

Adeno adenocarcinomas, *ALK* anaplastic large cell kinase, *FISH* fluorescence in situ hybridization, *IHC* immunohistochemistry, *n.a.* not available, *NSCLC* non-small cell lung cancer, *ALK+/–* positive/negative results for ALK rearrangement

[a] Using FISH as the gold standard

complementary to gene fragments, which are normally on opposite strands, the specificity is high. RT-PCR can be used on mRNA/cDNA to directly detect EML4-ALK; hence, it does not suffer from the problems inherent in interpreting FISH or IHC. Therefore, it has been used as a gold standard to assess the sensitivity and specificity of IHC [55], FISH [55, 59] and CISH [27, 59]. It has also been used as a stand-alone test instead of FISH or IHC [60].

However, RT-PCR has several disadvantages that make it unlikely to become the standard test for this mutation. Firstly, good quality RNA is required [59]: some of the amplicons are more than 1,000 bp in size and require proper cryopreservation of tumour samples that may be lacking in routine practice [55]. In FFPE sections, RT-PCR above 300 bp is not reliable. Secondly, multiplex systems are required because of the wide variations in fusion types [59]. Thirdly, only known alterations can be tested (at least 10 are currently known for ALK) [20]. Furthermore, the clinical relevance of multiplex RT-PCR is unclear because so far in all clinical trials FISH has been used to identity ALK-positive patients. RT-PCR is included in the diagnostic algorithm proposed by Just et al. [55], but only after IHC and FISH have been performed, and only as a source of further information on the ALK fusion variant and expression level, rather than for diagnosis.

RT-PCR for ALK mutation testing is being offered by some commercial vendors (e.g. Response Genetics, Inc., in the USA); however, it is not clear how reliable these tests are. The panel strongly suggested that any such tests should involve pathologists early in the development and should be diagnostically orientated.

Testing algorithm

In the National Consensus from Spain [61], ALK rearrangement testing is recommended in patients with advanced NSCLC who are negative for the EGFR mutation (all histological subtypes in non-smokers; non-squamous-cell carcinoma subtype in current or ex-smokers). In contrast, the most recent NCCN guidelines (version 1.2012) [62] recommend ALK rearrangement testing concurrent with EGFR mutation testing for adenocarcinomas, large cell carcinomas and NSCLC NOS. This differs from recent guidelines in Switzerland [63] and France (French National Cancer Institute; INCa) [48] proposing ALK testing only by FISH and only in EGFR-negative KRAS-negative adenocarcinoma patients.

Since phase II and III clinical trials with crizotinib in ALK-positive patients have used FISH, this technique should be considered the ‘gold standard’ for determining ALK positivity. However, following successful validation with large series and different antibodies, IHC could also become a good screening method.

The authors agree that more data for an evidence-based algorithm are needed. It is possible that the algorithm presented in Fig. 3 may in the future be the algorithm of choice.

Proposal for an external quality assessment program

For optimal ALK mutation testing in NSCLC, the quality of the sample, the analytical procedure and the reporting of the test result are crucial (Table 3). European quality assessment projects will examine different steps of ALK mutation testing.

One important ongoing quality assurance project in Europe is the FALKE (Fusion of EML4-ALK epidemiology Evaluation) project. This initiative was set up by the German Society of Pathology for German-speaking countries. The basis of this ring trial is to test 1,000 samples from NSCLC patients. For the FALKE project, it was decided to test all NSCLC and not to focus on adenocarcinoma. For all samples, ALK IHC and ALK FISH will be performed.

In 2012, the European Society of Pathology (ESP) will run two external quality assessment programs for lung cancer. Registration will take place through the ESP website (QA activities: http://esp-pathology.org/).

In the first round, starting March 2012, ALK FISH and optional ALK IHC will be offered. The pre-validated tissue microarray slides will have both positive and negative controls (n ≥10). The second round, in September 2012, will offer assessment of ALK1, EGFR and KRAS on tissue microarray samples. Participation is voluntary. Laboratories meeting the predefined performance threshold will be listed on the ESP website.

Conclusions

For the personalized treatment of patients with NSCLC, it is necessary to sample as much tumour tissue as possible.

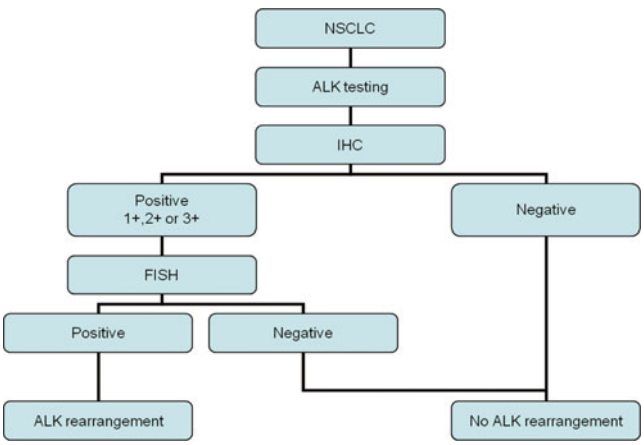

Fig. 3 Possible ALK testing algorithm in NSCLC if IHC becomes fully validated

Adequate clinical information is essential for the optimal tissue management.

Patients with ALK fusion adenocarcinomas confirmed by FISH have been shown to respond favourably to crizotinib treatment, and a phase III trial is currently ongoing. However, the question of how best to select patients that may benefit from crizotinib treatment remains to be answered.

There is evidence that IHC could be useful and less expensive than FISH. Some of the difficulties in interpreting FISH results may be alleviated by automated procedures.

Whether FISH or IHC becomes the primary method of ALK mutation testing in Europe, it is clear that rigorous quality assessment is of the utmost importance to ensure reliable results and appropriate patient selection.

Acknowledgments We would like to extend our thanks to Pfizer for sponsoring the consensus meeting. Also, we would like to gratefully acknowledge the help of Monika Leonhardt and Paul Lavender, archimed medical communication AG, Zofingen, Switzerland, for writing support sponsored by Pfizer.

Conflict of interest This paper was produced following a consensus meeting on 22 November 2011, Zurich, organized and sponsored by Pfizer. L.B., G.R., K.K. and F.P.-L. have worked as consultants/advisers to Pfizer. K.K. has worked in the speaker's bureau, and L.B. and F.P.-L. have received research funding.

Open Access This article is distributed under the terms of the Creative Commons Attribution License which permits any use, distribution, and reproduction in any medium, provided the original author(s) and the source are credited.

References

1. Jemal A, Bray F, Center MM, Ferlay J, Ward E, Forman D (2011) Global cancer statistics. CA Cancer J Clin 61:69–90
2. Berghmans T, Pasleau F, Paesmans M, Bonduelle Y, Cadranel J, Cs Toth I, Garcia C, Giner V, Holbrechts S, Lafitte JJ, Lecomte J, Louviaux I, Markiewicz E, Meert AP, Richez M, Roelandts M, Scherpereel A, Tulippe C, Van Houtte P, Van Schil P, Wachters C, Westeel V, Sculier JP (2012) Surrogate markers predicting overall survival for lung cancer: ELCWP recommendations. Eur Respir J 39:9–28
3. Gaughan EM, Costa DB (2011) Genotype-driven therapies for non-small cell lung cancer: focus on EGFR, KRAS and ALK gene abnormalities. Ther Adv Med Oncol 3:113–125
4. Hamburg MA, Collins FS (2010) The path to personalized medicine. N Engl J Med 363:301–304
5. Horn L, Pao W (2009) EML4-ALK: honing in on a new target in non-small-cell lung cancer. J Clin Oncol 27:4232–4235
6. Janku F, Garrido-Laguna I, Petruzelka LB, Stewart DJ, Kurzrock R (2011) Novel therapeutic targets in non-small cell lung cancer. J Thorac Oncol 6:1601–1612
7. Takeuchi K, Soda M, Togashi Y, Suzuki R, Sakata S, Hatano S, Asaka R, Hamanaka W, Ninomiya H, Uehara H, Lim Choi Y, Satoh Y, Okumura S, Nakagawa K, Mano H, Ishikawa Y (2012) RET, ROS1 and ALK fusions in lung cancer. Nat Med 18:378–381
8. Kohno T, Ichikawa H, Totoki Y, Yasuda K, Hiramoto M, Nammo T, Sakamoto H, Tsuta K, Furuta K, Shimada Y, Iwakawa R, Ogiwara H, Oike T, Enari M, Schetter AJ, Okayama H, Haugen A, Skaug V, Chiku S, Yamanaka I, Arai Y, Watanabe SI, Sekine I, Ogawa S, Harris CC, Tsuda H, Yoshida T, Yokota J, Shibata T (2012) KIF5B-RET fusions in lung adenocarcinoma. Nat Med 18:375–377
9. Ju YS, Lee WC, Shin JY, Lee S, Bleazard T, Won JK, Kim YT, Kim JI, Kang JH, Seo JS (2012) A transforming KIF5B and RET gene fusion in lung adenocarcinoma revealed from whole-genome and transcriptome sequencing. Genome Res 22:436–445
10. Soda M, Choi YL, Enomoto M, Takada S, Yamashita Y, Ishikawa S, Fujiwara S, Watanabe H, Kurashina K, Hatanaka H, Bando M, Ohno S, Ishikawa Y, Aburatani H, Niki T, Sohara Y, Sugiyama Y, Mano H (2007) Identification of the transforming EML4-ALK fusion gene in non-small-cell lung cancer. Nature 448:561–566
11. Christensen JG, Zou HY, Arango ME, Li Q, Lee JH, McDonnell SR, Yamazaki S, Alton GR, Mroczkowski B, Los G (2007) Cytoreductive antitumor activity of PF-2341066, a novel inhibitor of anaplastic lymphoma kinase and c-Met, in experimental models of anaplastic large-cell lymphoma. Mol Cancer Ther 6:3314–3322
12. Zou HY, Li Q, Lee JH, Arango ME, McDonnell SR, Yamazaki S, Koudriakova TB, Alton G, Cui JJ, Kung PP, Nambu MD, Los G, Bender SL, Mroczkowski B, Christensen JG (2007) An orally available small-molecule inhibitor of c-Met, PF-2341066, exhibits cytoreductive antitumor efficacy through antiproliferative and antiangiogenic mechanisms. Cancer Res 67:4408–4417
13. Camidge DR, Bang BR, Kwak EL, Shaw A, lafrate AJ, Maki RG, Solomon J, Ou SI, Salgia R, Wilner K, Costa DB, Shapiro GI, LoRusso P, Stephenson P, Tang Y, Ruffner K, Clark JW (2011) Progression-free survival (PFS) from a phase I study of crizotinib (PF-02341066) in patients with *ALK*-positive non-small cell lung cancer (NSCLC). J Clin Oncol 29:suppl. abstr. 2501
14. Kwak EL, Bang YJ, Camidge DR, Shaw AT, Solomon B, Maki RG, Ou SH, Dezube BJ, Janne PA, Costa DB, Varella-Garcia M, Kim WH, Lynch TJ, Fidias P, Stubbs H, Engelman JA, Sequist LV, Tan W, Gandhi L, Mino-Kenudson M, Wei GC, Shreeve SM, Ratain MJ, Settleman J, Christensen JG, Haber DA, Wilner K, Salgia R, Shapiro GI, Clark JW, Iafrate AJ (2010) Anaplastic lymphoma kinase inhibition in non-small-cell lung cancer. N Engl J Med 363:1693–1703
15. Crino L, Kim D, Riely G, Janne PA, Blackhall DR, Camidge V, Hirsch V, Mok T, Solomon B, Park K, Gadgeel M, Martins R, Han J, De Pas TM, Bottomley A, Polli A, Petersen J, Tassell VR, Shaw A (2011) Initial phase II results with crizotinib in advanced *ALK*-positive non-small cell lung cancer (NSCLC): PROFILE 1005. J Clin Oncol 29:suppl. abstract 7514
16. Food and Drug Administration (2011) Summary review (application number: 202570Orig1s000). Food and Drug Administration, Silver Spring
17. Lamant L, Meggetto F, al Saati T, Brugieres L, de Paillerets BB, Dastugue N, Bernheim A, Rubie H, Terrier-Lacombe MJ, Robert A, Rigal F, Schlaifer D, Shiuta M, Mori S, Delsol G (1996) High incidence of the t(2;5)(p23;q35) translocation in anaplastic large cell lymphoma and its lack of detection in Hodgkin's disease. Comparison of cytogenetic analysis, reverse transcriptase-polymerase chain reaction, and P-80 immunostaining. Blood 87:284–291
18. Morris SW, Kirstein MN, Valentine MB, Dittmer KG, Shapiro DN, Saltman DL, Look AT (1994) Fusion of a kinase gene, ALK, to a nucleolar protein gene, NPM, in non-Hodgkin's lymphoma. Science 263:1281–1284
19. Pulford K, Lamant L, Espinos E, Jiang Q, Xue L, Turturro F, Delsol G, Morris SW (2004) The emerging normal and disease-related roles of anaplastic lymphoma kinase. Cell Mol Life Sci 61:2939–2953
20. Sasaki T, Rodig SJ, Chirieac LR, Janne PA (2010) The biology and treatment of EML4-ALK non-small cell lung cancer. Eur J Cancer 46:1773–1780
21. Camidge DR, Theodoro M, Maxson DA, Skokan M, O'Brien T, Lu X, Doebele RC, Baron AE, Varella-Garcia M (2012) Correlations between the percentage of tumor cells showing an ALK (anaplastic

lymphoma kinase) gene rearrangement, ALK signal copy number, and response to crizotinib therapy in ALK fluorescence in situ hybridization-positive nonsmall cell lung cancer. Cancer. doi:10.1002/cncr.27411
22. Takeuchi K, Choi YL, Soda M, Inamura K, Togashi Y, Hatano S, Enomoto M, Takada S, Yamashita Y, Satoh Y, Okumura S, Nakagawa K, Ishikawa Y, Mano H (2008) Multiplex reverse transcription-PCR screening for EML4-ALK fusion transcripts. Clin Cancer Res 14:6618–6624
23. Takeuchi K, Choi YL, Togashi Y, Soda M, Hatano S, Inamura K, Takada S, Ueno T, Yamashita Y, Satoh Y, Okumura S, Nakagawa K, Ishikawa Y, Mano H (2009) KIF5B-ALK, a novel fusion oncokinase identified by an immunohistochemistry-based diagnostic system for ALK-positive lung cancer. Clin Cancer Res 15:3143–3149
24. Rodig SJ, Mino-Kenudson M, Dacic S, Yeap BY, Shaw A, Barletta JA, Stubbs H, Law K, Lindeman N, Mark E, Janne PA, Lynch T, Johnson BE, Iafrate AJ, Chirieac LR (2009) Unique clinicopathologic features characterize ALK-rearranged lung adenocarcinoma in the western population. Clin Cancer Res 15:5216–5223
25. Shaw AT, Yeap BY, Mino-Kenudson M, Digumarthy SR, Costa DB, Heist RS, Solomon B, Stubbs H, Admane S, McDermott U, Settleman J, Kobayashi S, Mark EJ, Rodig SJ, Chirieac LR, Kwak EL, Lynch TJ, Iafrate AJ (2009) Clinical features and outcome of patients with non-small-cell lung cancer who harbor EML4-ALK. J Clin Oncol 27:4247–4253
26. Varella Garcia ea (2011) ALK diagnostics (session MTE36.1)14th World Conference on Lung Cancer, Amsterdam
27. Kim H, Yoo SB, Choe JY, Paik JH, Xu X, Nitta H, Zhang W, Grogan TM, Lee CT, Jheon S, Chung JH (2011) Detection of ALK gene rearrangement in non-small cell lung cancer: a comparison of fluorescence in situ hybridization and chromogenic in situ hybridization with correlation of ALK protein expression. J Thorac Oncol 6:1359–1366
28. Yoshida A, Tsuta K, Nakamura H, Kohno T, Takahashi F, Asamura H, Sekine I, Fukayama M, Shibata T, Furuta K, Tsuda H (2011) Comprehensive histologic analysis of ALK-rearranged lung carcinomas. Am J Surg Pathol 35:1226–1234
29. Popat S, Gonzalez D, Min T, Swansbury J, Dainton M, Croud JG, Rice AJ, Nicholson AG (2012) ALK translocation is associated with ALK immunoreactivity and extensive signet-ring morphology in primary lung adenocarcinoma. Lung Cancer 75:300–305
30. Inamura K, Takeuchi K, Togashi Y, Nomura K, Ninomiya H, Okui M, Satoh Y, Okumura S, Nakagawa K, Soda M, Choi YL, Niki T, Mano H, Ishikawa Y (2008) EML4-ALK fusion is linked to histological characteristics in a subset of lung cancers. J Thorac Oncol 3:13–17
31. Sakairi Y, Nakajima T, Yasufuku K, Ikebe D, Kageyama H, Soda M, Takeuchi K, Itami M, Iizasa T, Yoshino I, Mano H, Kimura H (2010) EML4-ALK fusion gene assessment using metastatic lymph node samples obtained by endobronchial ultrasound-guided transbronchial needle aspiration. Clin Cancer Res 16:4938–4945
32. Shaw A, Yeap B, Solomon B, Riely G, lafrate AJ, Shapiro GI, Costa DB, Butaney M, Ou S, Maki RG, Bang YJ, Varella-Garcia M, Salgia R, Wilner KD, Kulig K, Selaru P, Tang Y, Kwak EL, Clark JW, Camidge DR (2011) Impact of crizotinib on survival in patients with advanced, ALK-positive NSCLC compared with historical controls. J Clin Oncol 29:abstract 7507
33. Costa DB, Kobayashi S, Pandya SS, Yeo WL, Shen Z, Tan W, Wilner KD (2011) CSF concentration of the anaplastic lymphoma kinase inhibitor crizotinib. J Clin Oncol 29:e443–e445
34. Scagliotti G, Stahel RA, Rosell R, Thatcher N, Soria JC (2012) ALK translocation and crizotinib in non-small cell lung cancer: an evolving paradigm in oncology drug development. Eur J Cancer 48:961–973
35. Doebele RC, Pilling AB, Aisner D, Kutateladze TG, Le AT, Weickhardt AJ, Kondo KL, Linderman DJ, Heasley LE, Franklin WA, Varella-Garcia M, Camidge DR (2012) Mechanisms of resistance to crizotinib in patients with ALK gene rearranged non-small cell lung cancer. Clin Cancer Res 18:1472–1482
36. Kerr KM (2012) Personalized medicine for lung cancer: new challenges for pathology. Histopathology 60:531–546
37. Thunnissen E, Kerr KM, Herth FJ, Lantuejoul S, Papotti M, Rintoul RC, Rossi G, Skov BG, Weynand B, Bubendorf L, Katrien G, Johansson L, Lopez-Rios F, Ninane V, Olszewski W, Popper H, Jaume S, Schnabel P, Thiberville L, Laenger F (2012) The challenge of NSCLC diagnosis and predictive analysis on small samples. Practical approach of a working group. Lung Cancer 76:1–18
38. Atkins D, Reiffen KA, Tegtmeier CL, Winther H, Bonato MS, Storkel S (2004) Immunohistochemical detection of EGFR in paraffin-embedded tumor tissues: variation in staining intensity due to choice of fixative and storage time of tissue sections. J Histochem Cytochem 52:893–901
39. DiVito KA, Charette LA, Rimm DL, Camp RL (2004) Long-term preservation of antigenicity on tissue microarrays. Lab Invest 84:1071–1078
40. Oyama T, Ishikawa Y, Hayashi M, Arihiro K, Horiguchi J (2007) The effects of fixation, processing and evaluation criteria on immunohistochemical detection of hormone receptors in breast cancer. Breast Cancer 14:182–188
41. Prinsen CF, Klaassen CH, Thunnissen FB (2003) Microarray as a model for quantitative visualization chemistry. Appl Immunohistochem Mol Morphol 11:168–173
42. Werner M, Chott A, Fabiano A, Battifora H (2000) Effect of formalin tissue fixation and processing on immunohistochemistry. Am J Surg Pathol 24:1016–1019
43. Yang P, Kulig K, Boland JM, Erickson-Johnson MR, Oliveira AM, Wampfler J, Jatoi A, Deschamps C, Marks R, Fortner C, Stoddard S, Nichols F, Molina J, Aubry MC, Tang H, Yi ES (2012) Worse disease-free survival in never-smokers with ALK+ lung adenocarcinoma. J Thorac Oncol 7:90–97
44. Boland JM, Erdogan S, Vasmatzis G, Yang P, Tillmans LS, Johnson MR, Wang X, Peterson LM, Halling KC, Oliveira AM, Aubry MC, Yi ES (2009) Anaplastic lymphoma kinase immunoreactivity correlates with ALK gene rearrangement and transcriptional up-regulation in non-small cell lung carcinomas. Hum Pathol 40:1152–1158
45. Hofman P, Ilie M, Hofman V, Roux S, Valent A, Bernheim A, Alifano M, Leroy-Ladurie F, Vaylet F, Rouquette I, Validire P, Beau-Faller M, Lacroix L, Soria JC, Fouret P (2011) Immunohistochemistry to identify EGFR mutations or ALK rearrangements in patients with lung adenocarcinoma. Ann Oncol. doi:10.1093/annonc/mds137
46. Yi ES, Boland JM, Maleszewski JJ, Roden AC, Oliveira AM, Aubry MC, Erickson-Johnson MR, Caron BL, Li Y, Tang H, Stoddard S, Wampfler J, Kulig K, Yang P (2011) Correlation of IHC and FISH for ALK gene rearrangement in non-small cell lung carcinoma: IHC score algorithm for FISH. J Thorac Oncol 6:459–465
47. Paik JH, Choe G, Kim H, Choe JY, Lee HJ, Lee CT, Lee JS, Jheon S, Chung JH (2011) Screening of anaplastic lymphoma kinase rearrangement by immunohistochemistry in non-small cell lung cancer: correlation with fluorescence in situ hybridization. J Thorac Oncol 6:466–472
48. McLeer-Florin A, Moro-Sibilot D, Melis A, Salameire D, Lefebvre C, Ceccaldi F, de Fraipont F, Brambilla E, Lantuejoul S (2012) Dual IHC and FISH testing for ALK gene rearrangement in lung adenocarcinomas in a routine practice: a French study. J Thorac Oncol 7:348–354
49. Mino-Kenudson M, Chirieac LR, Law K, Hornick JL, Lindeman N, Mark EJ, Cohen DW, Johnson BE, Janne PA, Iafrate AJ, Rodig SJ (2010) A novel, highly sensitive antibody allows for the routine

detection of ALK-rearranged lung adenocarcinomas by standard immunohistochemistry. Clin Cancer Res 16:1561–1571
50. Ruschoff J, Dietel M, Baretton G, Arbogast S, Walch A, Monges G, Chenard MP, Penault-Llorca F, Nagelmeier I, Schlake W, Hofler H, Kreipe HH (2010) HER2 diagnostics in gastric cancer-guideline validation and development of standardized immunohistochemical testing. Virchows Arch 457:299–307
51. Bartlett AI, Starcyznski J, Robson T, Maclellan A, Campbell FM, van de Velde CJ, Hasenburg A, Markopoulos C, Seynaeve C, Rea D, Bartlett JM (2011) Heterogeneous HER2 gene amplification: impact on patient outcome and a clinically relevant definition. Am J Clin Pathol 136:266–274
52. Savic S, Glatz K, Schoenegg R, Spieler P, Feichter G, Tamm M, Bubendorf L (2006) Multitarget fluorescence in situ hybridization elucidates equivocal lung cytology. Chest 129:1629–1635
53. Bartlett JM, Starczynski J, Atkey N, Kay E, O'Grady A, Gandy M, Ibrahim M, Jasani B, Ellis IO, Pinder SE, Walker RA (2011) HER2 testing in the UK: recommendations for breast and gastric in-situ hybridisation methods. J Clin Pathol 64:649–653
54. Camidge DR, Kono SA, Flacco A, Tan AC, Doebele RC, Zhou Q, Crino L, Franklin WA, Varella-Garcia M (2010) Optimizing the detection of lung cancer patients harboring anaplastic lymphoma kinase (ALK) gene rearrangements potentially suitable for ALK inhibitor treatment. Clin Cancer Res 16:5581–5590
55. Just PA, Cazes A, Audebourg A, Cessot A, Pallier K, Danel C, Vacher-Lavenu MC, Laurent-Puig P, Terris B, Blons H (2011) Histologic subtypes, immunohistochemistry, FISH or molecular screening for the accurate diagnosis of ALK-rearrangement in lung cancer: a comprehensive study of Caucasian non-smokers. Lung Cancer 76(3):309–315
56. Salido M, Pijuan L, Martinez-Aviles L, Galvan AB, Canadas I, Rovira A, Zanui M, Martinez A, Longaron R, Sole F, Serrano S, Bellosillo B, Wynes MW, Albanell J, Hirsch FR, Arriola E (2011) Increased ALK gene copy number and amplification are frequent in non-small cell lung cancer. J Thorac Oncol 6:21–27
57. Yang P (2011) Anaplastic lymphoma kinase (ALK) status and clinical outcomes by IHC and FISH: a reterospective study of never-smoker, adenocarcinoma lung cancer cases. Lung Cancer 71:S26–S28
58. Jokoji R, Yamasaki T, Minami S, Komuta K, Sakamaki Y, Takeuchi K, Tsujimoto M (2010) Combination of morphological feature analysis and immunohistochemistry is useful for screening of EML4-ALK-positive lung adenocarcinoma. J Clin Pathol 63:1066–1070
59. Yoshida A, Tsuta K, Nitta H, Hatanaka Y, Asamura H, Sekine I, Grogan TM, Fukayama M, Shibata T, Furuta K, Kohno T, Tsuda H (2011) Bright-field dual-color chromogenic in situ hybridization for diagnosing echinoderm microtubule-associated protein-like 4-anaplastic lymphoma kinase-positive lung adenocarcinomas. J Thorac Oncol 6:1677–1686
60. Li C, Fang R, Sun Y, Han X, Li F, Gao B, Iafrate AJ, Liu XY, Pao W, Chen H, Ji H (2011) Spectrum of oncogenic driver mutations in lung adenocarcinomas from East asian never smokers. PLoS One 6:e28204
61. Garrido P, de Castro J, Concha A, Felip E, Isla D, Lopez-Rios F, Paz-Ares L, Ramirez J, Sanz J, Gomez JJ (2012) Guidelines for biomarker testing in advanced non-small-cell lung cancer. A national consensus of the Spanish Society of Medical Oncology (SEOM) and the Spanish Society of Pathology (SEAP). Clin Transl Oncol 14:338–349
62. National Comprehensive Cancer Network (2011) NCCN Flash Update: NCCN Guidelines Updated. National Comprehensive Cancer Network, Fort Washington
63. Rothschild S, Zippelius A, Betticher DC, Bubendorf L, Gugger M, Savic S, Soltermann A, Letovanec I, Diebold J, Henzi M-T, Brutsche M, Pless M, Gautschi O (2011) Neue Therapiekonzepte beim Bronchuskarzinom. Schweiz Med Forum 11:7
64. Mitsudomi T, Tomizawa K, Horio Y, Hida T, Yatabe Y (2011) Comparison of high sensitive IHC, FISH, and RT-PCR direct sequencing for detection of ALK translocation in lung cancer. J Clin Oncol 29:abstract 7534
65. Martinez P, Hernandez-Losa J, Castellvi J, Tallada N, Cedres S, Montero MA, Rodriguez-Freixinos V, Nuñez I, Argiles G, Mulet-Margalef N, Torrejon D, Ramon y Cajal S, Felip E (2011) ALK rearrangement in a selected population of advanced non-small cell lung cancer patients: FISH and inmunohistochemistry diagnostic methods, prevalence, and clinical outcomes. J Clin Oncol 29:abstr 7566
66. Paik JH, Choi CM, Kim H, Jang SJ, Choe G, Kim DK, Kim HJ, Yoon H, Lee CT, Jheon S, Choe JY, Chung JH (2011) Clinicopathologic implication of ALK rearrangement in surgically resected lung cancer A proposal of diagnostic algorithm for ALK-rearranged adenocarcinoma. Lung Cancer 76(3):403–409

Virchows Arch (2012) 461:259–269
DOI 10.1007/s00428-012-1248-5

ORIGINAL ARTICLE

Systematic comparison of tissue fixation with alternative fixatives to conventional tissue fixation with buffered formalin in a xenograft-based model

Thorben Nietner · Tiantom Jarutat · Alfred Mertens

Received: 26 February 2012 / Revised: 22 April 2012 / Accepted: 2 May 2012 / Published online: 20 July 2012
© The Author(s) 2012. This article is published with open access at Springerlink.com

Abstract In our study we systematically compared the alternative fixatives acidified formal alcohol (AFA), PAXgene®, HOPE®, and combinations of AFA or formalin with ultrasound treatment to standard (buffered) formalin fixation. We examined general morphology and detectability of protein structures by immunohistochemistry of the membrane receptors epidermal growth factor receptor (EGFR), insulin-like growth factor 1 receptor (IGF-1R), and phosphorylated human epidermal growth factor receptor 2 (phospho-HER2). In order to allow for stringent comparability of different fixation techniques, we used matched mouse xenograft tumor samples from three different human cancer cell lines (colon, ovarian, and non-small cell lung cancer), either fixed conventionally with formalin or an alternative fixative. Tissue morphology after fixation with AFA and PAXgene® was comparable to formalin-fixed paraffin-embedded tissue (FFPET) morphology. Ultrasound fixations resulted in slightly inferior morphology and HOPE® fixation preserved morphology only poorly compared to FFPET in this system. None of the tested alternative fixatives enabled immunohistochemical detectability of all three targets in the same manner as FFPET. Pronounced staining was possible for EGFR and IGF-1R with all alternative fixatives but HOPE®, and phospho-HER2 staining was only noteworthy with formalin-ultrasound-fixed tissue. Therefore, the use of alternative fixatives comes with the need for careful validation of obtained IHC results individually for each target.

Keywords Formalin fixation · Immunohistochemistry · AFA · HOPE® · PAXgene® · Ultrasound

Introduction

Antibody-based therapeutics and targeted therapies in oncology have achieved great importance in recent years. With the ongoing development of personalized healthcare, pathologists are in need of specific diagnostics, often based on protein detection in patients' tissue. Tissue diagnostics in biomedical research and routine practice are either performed with fresh frozen tissue or with formalin-fixed tissue, which has been used in histopathology for decades, firstly mentioned by Blum in 1893 [1, 2]. The advantages of formalin are firstly the antibacterial and antiviral effect, which protects laboratory personnel from infections and secondly the complete fixation of the tissue due to the chemical properties of formaldehyde [3]. However, formalin is toxic and its cross-linking effect on tissue structures often makes specific bioanalysis of proteins and nucleic acids difficult [4–9]. Therefore, powerful fixation techniques are

Thorben Nietner and Tiantom Jarutat contributed equally to this work.

Electronic supplementary material The online version of this article (doi:10.1007/s00428-012-1248-5) contains supplementary material, which is available to authorized users.

T. Nietner
University of Hohenheim,
70593 Stuttgart, Germany
e-mail: thorben.nietner@googlemail.com

T. Jarutat · A. Mertens (✉)
Roche Diagnostics GmbH,
Nonnenwald 2,
82377 Penzberg, Germany
e-mail: alfred.mertens@roche.com

T. Jarutat
e-mail: tiantom.jarutat@roche.com

needed which can produce highly conserved tissues from which an analysis for every target is possible.

In the past years, many alternative fixation studies have been carried out, most of them dealing with one novel or optimized fixative in comparison to standard formalin, but only a few studies on many different fixatives were conducted. Comparative studies between formalin and an alternative fixative for example, were about Streck's tissue fixative [9], Bouin's fixative [10], methacarn [11], ethanol [5], HOPE® [12–18], and UMFIX [8, 19, 20]. Broad-ranging studies on various fixatives for example have been from Prento and Lyon [21] in 1997 (Histochoice, Kryofix, Mirsky's fixative, NoTox, Omnifix II, Streck's Tissue Fixative/Tissue-Tek, Clarke's ethanol-acetic acid, and ethanol) and from Atkins et al. [7] in 2004 (Bouin's fixative, AFA, PreFer, and Pen-fix).

The aim of this study was to compare standard buffered formalin fixation (3.9 % formaldehyde, *w/v*) to fixation with acidified formal alcohol (AFA), which is widely used in France, with HOPE® fixation [12–18], with the recently introduced non-cross-linking fixative PAXgene® [22, 23] and with combinations of AFA and formalin with ultrasound treatment, since ultrasound-accelerated tissue fixation has been reported for formalin fixation previously [24–28]. In order to allow for stringent comparability of the different fixation techniques matched mouse xenograft tumor samples were used. The samples were removed in the exact same manner with minimized ischemia ranging at most to 60 s and standardized fixation parameters such as duration or temperature were applied.

On the other hand, the study was aligned to routine histopathology and downstream workflows in pathological laboratories

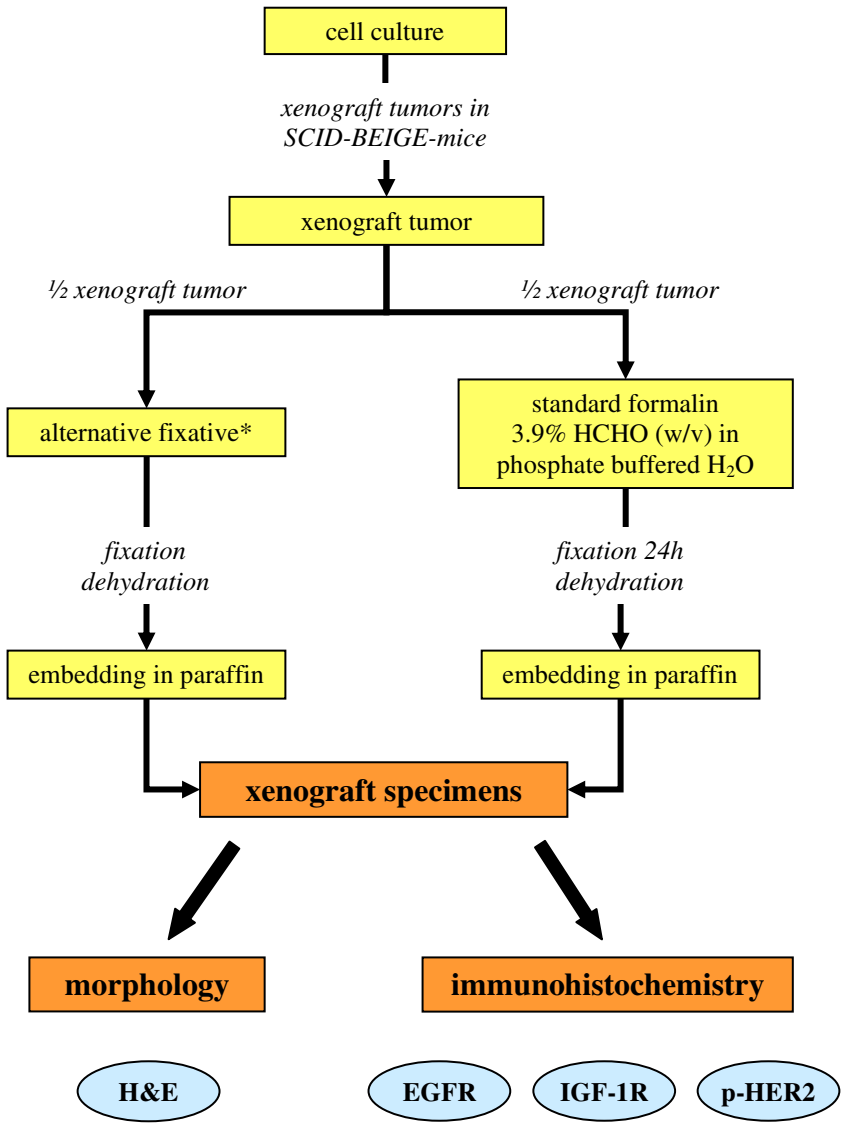

Fig. 1 Experimental setup

as much as possible. Therefore, alternative fixations were coupled to the usual dehydration process, subsequent paraffin embedding and fully automated immunohistochemistry on the BenchMark XT instrument (Ventana Medical Systems; Tucson, USA), which at the same time enabled maximized standardization. Comparison of alternative fixatives was also oriented to immunohistochemical targets which have significant impact on patient care as well as to exploratory tissue biomarkers. Immunohistochemistry was applied for epidermal growth factor receptor (EGFR) as an established target in cancer diagnostics, insulin-like growth factor 1 receptor (IGF-1R) as an exploratory marker and phosphorylated human epidermal growth factor receptor 2 (phospho-HER2) as a signal transduction marker in order to test detectability of phosphorylated antigens.

Material and methods

In the study, the alternative fixatives AFA, PAXgene®, HOPE®, and combinations of AFA or formalin with ultrasound treatment were compared to standard (buffered) formalin fixation. For this comparison tumor samples obtained from mouse xenograft tissue models of the human cancer cell lines COLO-205, OVCAR-5, and NCI-H322M were used. For every alternative fixative at least five xenografts of every cell line from five different mice were generated. In order to systematically compare all fixatives with formalin, one half of every tumor underwent fixation in standard formalin and the other half of this tumor was fixed in one of the alternative fixatives (Fig. 1). For comparison of alternative fixation with formalin fixation both H&E staining and IHC staining of the membrane receptors EGFR, IGF-1R, and phospho-HER2 were performed (Fig. 1).

For detailed methodology of the study and fixation protocols please refer to Supplementary file 1. Staining protocols of IHC targets on the BenchMark XT instrument (Ventana Medical Systems; Tucson, USA) are included in Supplementary file 2.

Results

In an initial screen, we selected the best fixation conditions for fixation of xenografts with AFA, AFA-ultrasound, formalin-ultrasound, PAXgene®, and HOPE® by evaluation of tissue preservation/tissue morphology. It was assumed that a fixation which allows good preservation of morphological details would be beneficial for IHC analyses.

Morphology

H&E-stained sections of NCI-H322M xenograft tissue of all tested fixatives are shown in Fig. 2. Preservation of xenograft tissue structures was comparable to standard formalin fixation after fixation with AFA for 24 h, PAXgene®, and ultrasound fixation with AFA and formalin (both for 7 h). Tissue structures were well preserved for the abovementioned fixatives and, in the cases of AFA 24 h, PAXgene®, and AFA-ultrasound fixation, more nuclear details like nucleoli and mitoses were detectable (Fig. 2a–c). HOPE® fixation however, led to decreased morphological detail compared to standard formalin fixation, in which many nuclei developed a characteristic condensed and polygonal shape. Furthermore, the cytoplasm of some cells was shrunken to a considerably larger extent than with the standard FFPET method and typical tissue architecture was partially destroyed after fixation with HOPE®, visible in artificial fissures (Fig. 2e).

Immunohistochemistry

Optimization of immunohistochemical staining methods

Immunohistochemical assay parameters like deparaffinization and antigen retrieval times were optimized individually for each fixative other than standard formalin for maximal IHC signal over background when analyzing xenografts from COLO-205 cells. The resulting modified protocols were then applied accordingly to the other xenograft models. In summary, for fixation with AFA, PAXgene®, and AFA-ultrasound, manual deparaffinization led to better staining results (intensity and quantity) than the automatic deparaffinization using the BenchMark XT for all tested IHC targets. In most of the cases, antigen retrieval times were shorter or of the same duration as for the use of standard formalin-fixed tissue. For the detailed methodology and results refer to Supplementary file 3.

Immunohistochemical staining of EGFR, IGF-1R, and phospho-HER2

EGFR Staining of EGFR obtained from fixation with AFA, AFA-ultrasound, and PAXgene® resulted in very intense staining with more cells stained than in standard formalin-fixed tissue. For AFA and AFA-ultrasound the EGFR staining was comparable for all three xenograft models (COLO-205, OVCAR-5, and NCI-H322M) and, in comparison to standard formalin, more intensive in all cases with a good counterstaining and detailed nuclear morphology (Fig. 3d–i). PAXgene® fixation led to better staining results of EGFR for all xenograft models (Fig. 3a–c); whereas the difference to standard formalin was smallest for COLO-205 xenografts. Fixation with formalin-ultrasound led to slightly stronger EGFR staining intensity with a few more cells stained in OVCAR-5 and NCI-H322M xenografts and to the same EGFR staining intensity with more cells stained (~5–10 %) for COLO-205 xenografts compared to standard formalin fixation (Fig. 3j–o). The detection of EGFR was not

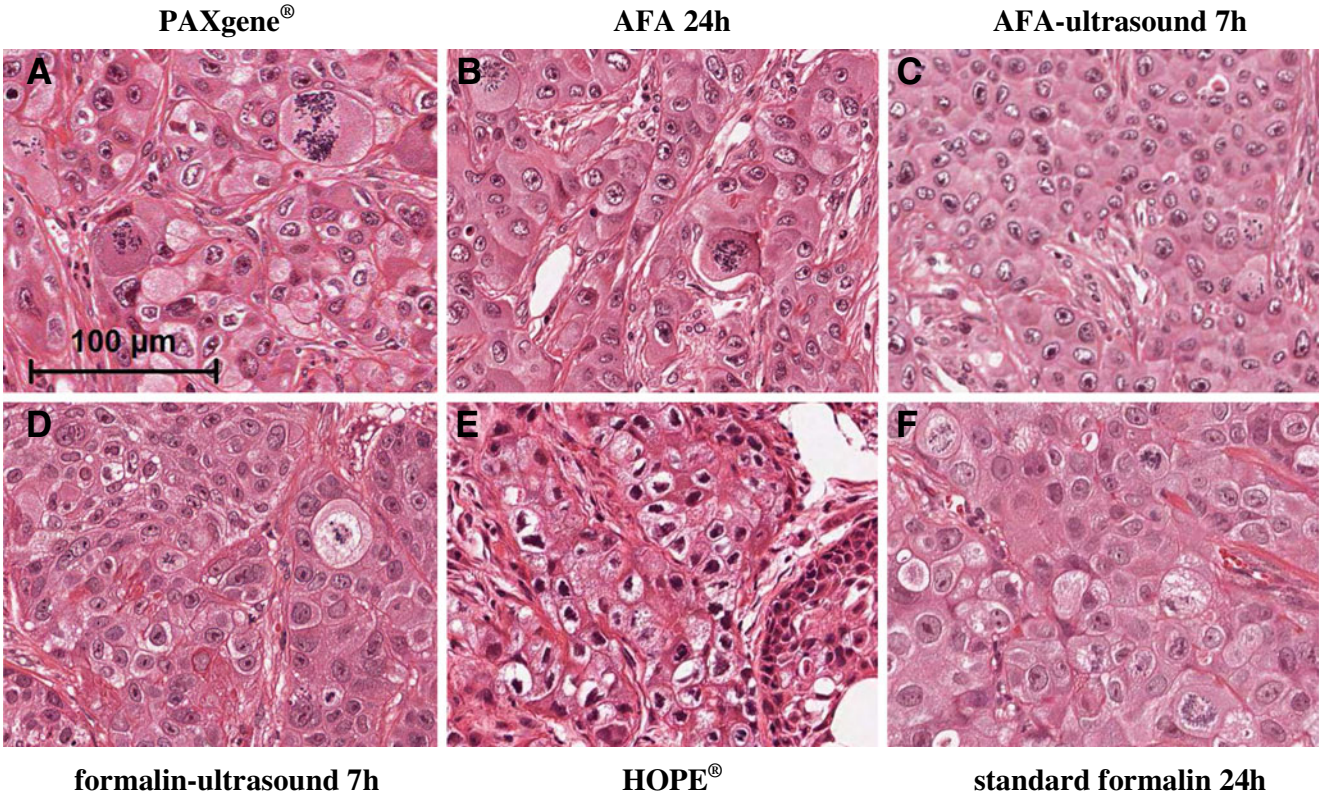

Fig. 2 H&E staining of NCI-H322M xenografts **a** PAXgene®, **b** AFA 24 h, **c** AFA-ultrasound 7 h, **d** formalin-ultrasound 7 h, **e** HOPE®, **f** standard formalin 24 h

possible for tissue that was fixed with HOPE® due to unspecific staining, which also occurred when performing a negative control with an IgG control antibody.

IGF-1R Detection of IGF-1R was possible with all alternatively fixed tissues. The best results, which were nearly comparable to the IGF-1R staining of standard formalin-fixed tissue, were achieved with COLO-205 xenografts fixed with AFA, AFA-ultrasound, and PAXgene®. However, for NCI-H322M and OVCAR-5 xenografts, quantity of IGF-1R staining was less for tissue fixed with AFA, AFA-ultrasound, and PAXgene® than for standard formalin-fixed tissue (Fig. 4a–i and p–r). Formalin-ultrasound-fixed tissue showed an IGF-1R staining which was comparable to staining results of standard formalin-fixed tissue (Fig. 4j–l and p–r). HOPE®-fixed tissue showed a more intense IGF-1R staining (Fig. 4m) with fewer cells stained than the standard formalin-fixed tissue for all three xenograft models. Nevertheless, HOPE®-fixed OVCAR-5 and NCI-H322M xenografts (Fig. 4, N+O) showed cells with condensed shape and shrunken cytoplasm, which made histopathological evaluation difficult.

Phospho-HER2 The immunohistochemistry of p-HER2 only led to noteworthy staining with formalin-ultrasound-fixed tissue. p-HER2 staining intensity in formalin-ultrasound-fixed tissue (Fig. 5j–l) was comparable to staining intensity of standard formalin-fixed tissue (Fig. 5p–r), whereas the staining quantity in all three xenograft models over all the tumors was less for formalin-ultrasound-fixed tissue. HOPE® fixation led to a weak membrane staining of p-HER2 and to an unspecific cytoplasmic staining for all three xenograft models (Fig. 5m–o). HOPE®-fixed OVCAR-5 xenografts (Fig. 5n) had a decreased morphology which did not allow a histopathological evaluation for p-HER2 staining. No significant staining of p-HER2 could be observed after fixation with AFA, AFA-ultrasound, and PAXgene® (Fig. 5a–i).

All results of the study are summarized in Table 1, showing the results for morphology and the different immunohistochemical targets. Evaluation of IHC experiments with complete scoring is included in Supplementary file 4.

Discussion

In the present study we demonstrate that careful validation of the usage of alternative fixatives has to be done as the impact on the biomarker results obtained by IHC in relation to standard formalin fixation is significant. A comparison of fixation with formalin, AFA, PAXgene®, HOPE®, and ultrasound accelerated fixation with formalin and AFA was

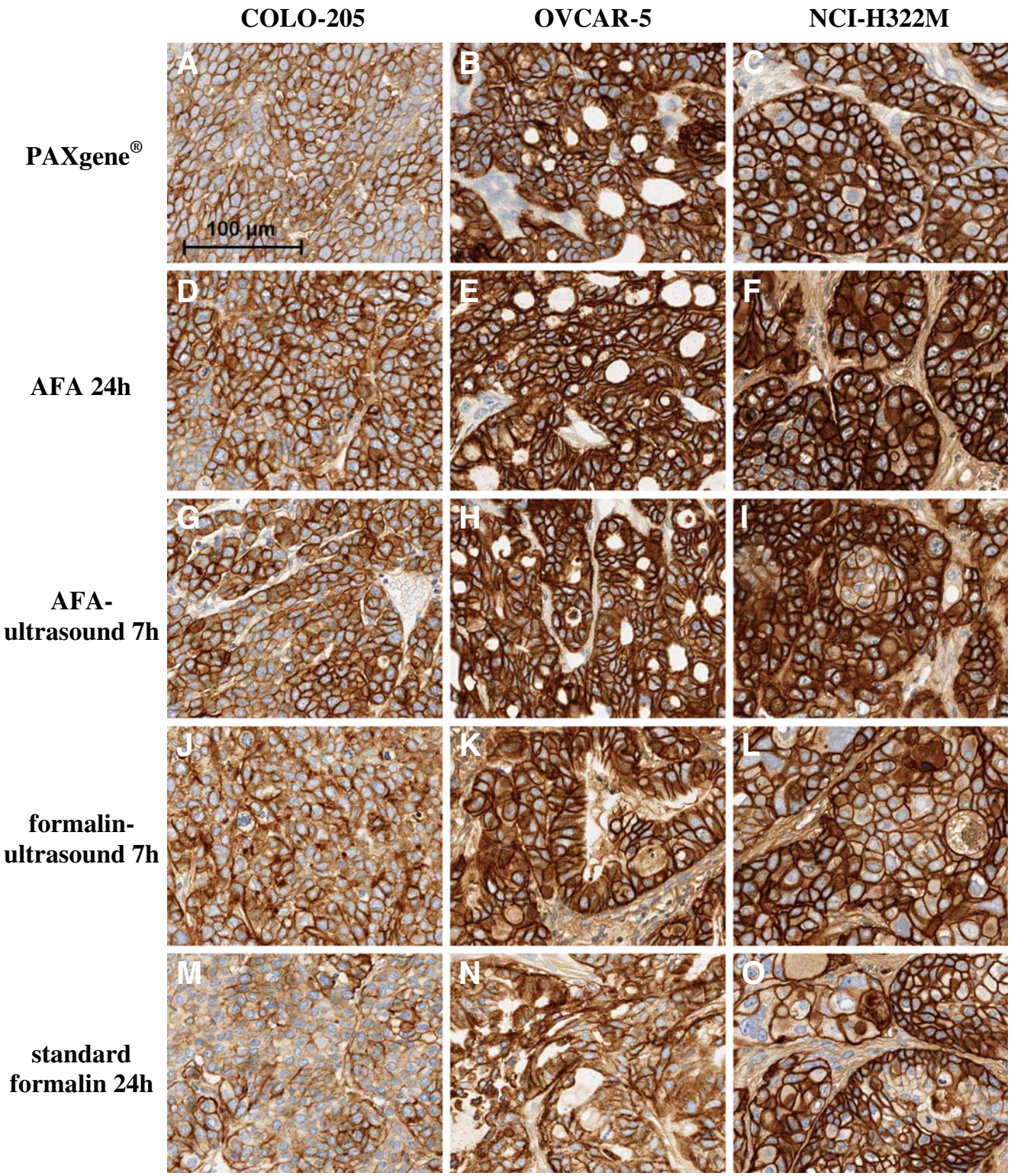

Fig. 3 IHC staining with anti-EGFR of different xenograft tissues fixed with alternative fixation methods and standard formalin. All pictures are shown in the same scale (*100-µm scale bar picture top left*)

performed on the basis of tissue morphology and immunohistochemical detection of three membrane receptors (EGFR, IGF-1R, and p-HER2). For each fixative five mouse xenograft tumors of three different human cancer cell line models from five different mice have been analyzed. The use of xenograft tissue enabled a direct comparison with human cellular background in a consistency (controlled ischemia, controlled cut halves and infiltration of the

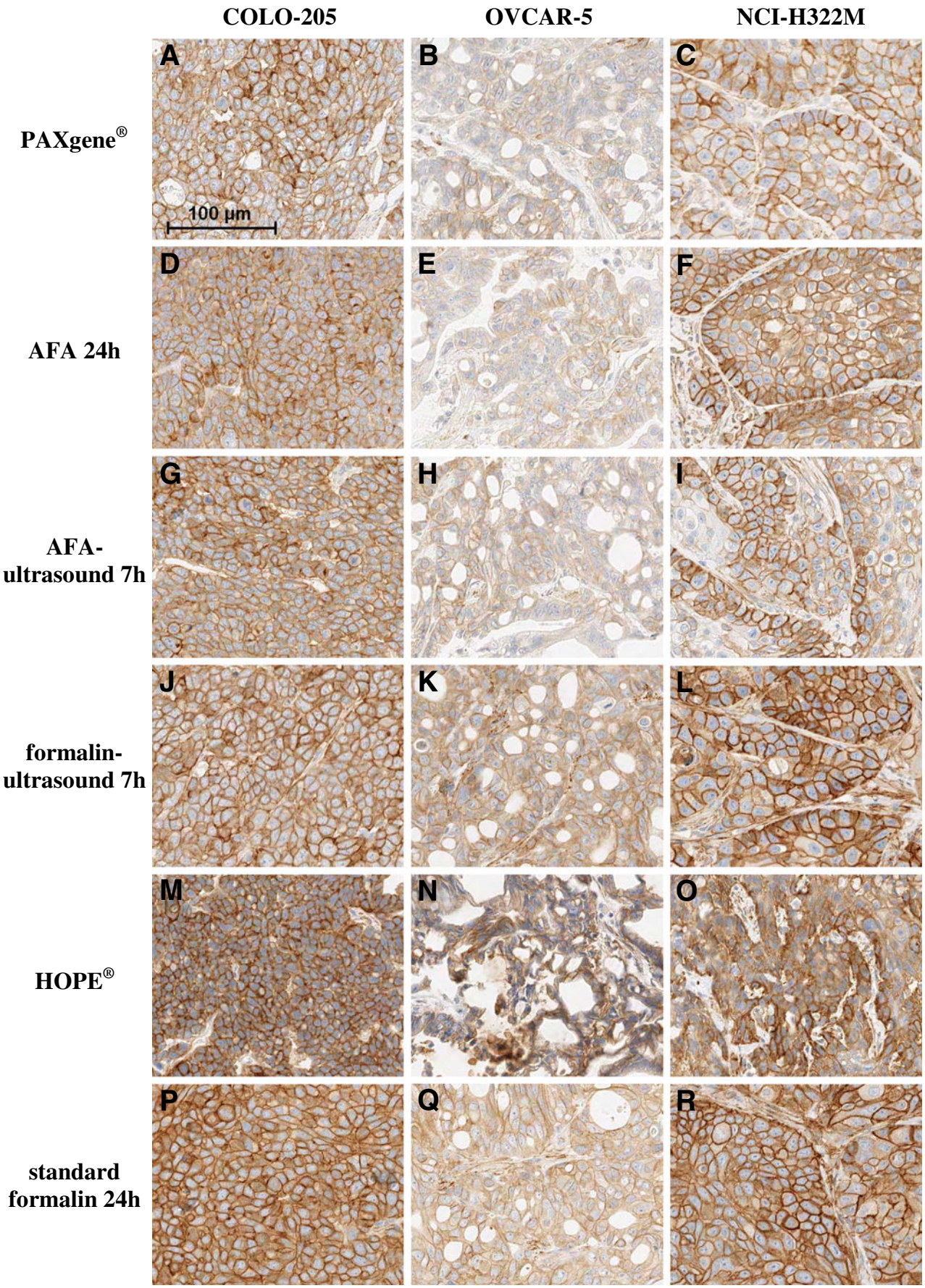
COLO-205
OVCAR-5
NCI-H322M
PAXgene®
AFA 24h
AFA-ultrasound 7h
formalin-ultrasound 7h
HOPE®
standard formalin 24h
A
B
C
D
E
F
G
H
I
J
K
L
M
N
O
P
Q
R
100 µm

◀ **Fig. 4** IHC staining with anti-IGF-1R of different xenograft tissues fixed with alternative fixation methods and standard formalin. All pictures are shown in the same scale (*100-μm scale bar picture top left*)

fixative to small sample sizes) which would not be achievable with diagnostic human tissue (as biopsies would be too valuable). To our knowledge, this is the first study on alternative fixation with AFA-ultrasound compared to fixation with buffered formalin in a systematic model system.

Morphology of alternatively fixed tissue

This study clearly showed that the morphology of xenograft tissue was well preserved after fixation with AFA for 24 h, AFA-ultrasound for 7 h, PAXgene® (complete fixation duration 5 h), and formalin-ultrasound for 7 h. The detailed nuclear morphology after fixation with AFA is consistent to the results of Foster et al. [3] who describe that nuclear chromatin structure is better preserved after ethanol fixation than after formalin fixation, since AFA consists of 75 % ethanol (plus 18 % water, 5 % acetic acid, and 2 % formaldehyde solution, meaning 8 g formaldehyde/L). With regard to PAXgene®, our results are concordant to the results from Kap et al. [22], who reported on well-preserved human tissue morphology after PAXgene® fixation in most of the cases.

However, in our study, tissue morphology of xenografts after fixation with HOPE® was not preserved as well as after standard formalin fixation, in contrast to recently published results of fixation of human tissue with HOPE® [17, 18], despite extensive testing of different parameters following manufacturer's recommendations. The artificial fissures of HOPE®-fixed tissue, like in our study, have also been mentioned from Olert et al. [12].

Immunohistochemical detectability in alternatively fixed tissue

Immunohistochemical detectability of EGFR, IGF-1R, and phospho-HER2 in our study was the best for tissue fixed with standard formalin throughout all xenograft tumor models. We observed that fixation with AFA (with or without ultrasound sonication) and PAXgene® led to a more intense and quantitative staining of EGFR than formalin fixation, were nearly comparable to formalin fixation for IGF-1R analyses, but surprisingly gave no significant signal in immunohistochemical detection of p-HER2. Our results are consistent to the results of the study on EGFR detectability in alternatively fixed tumor tissue from Atkins et al. [7]. They describe that staining of EGFR in tissue fixed with AFA for 24 h and buffered formalin for 24 h had a comparable performance up to 9 months storage after fixation and that EGFR staining in AFA 24 h-fixed tissue was slightly better compared to buffered formalin-fixed tissue after 12 months storage. However, our additionally performed immunohistochemistry of IGF-1R and p-HER2 in AFA- and formalin-fixed tissue emphasize that not in all cases is AFA as powerful as formalin as a fixative in histopathology.

Especially the unavailable signal for detection of the phospho-site of HER-2 in AFA-fixed tissue does not concur in the experience that total HER2 IHC shows a higher signal in alcohol-fixed specimens. This has to be seen critical in the background of the comparison of results obtained with the non-formalin fixatives to formalin, because there are indications that probing phosphorylated states of therapeutical targets might be more precise in predicting therapeutic response, as presence of phosphorylation surrogates an actively signaling pathway. Therefore, one should carefully validate the performance of alcohol-based fixatives when using it as an alternative to formalin in immunohistochemistry in each case.

For HOPE® fixation we could not achieve IHC results comparable to formalin fixation concerning the three selected receptors. The reasons might lie in the HOPE® fixation procedure for some reason not being amenable to the xenograft model system. Furthermore, we cannot concur with the statement from Olert et al. [12] and Goldman et al. [30] that HOPE®-fixed tissues do not require any pretreatment for immunohistochemistry since we only detected IGF-1R and p-HER2 with IHC in HOPE®-fixed tissue after antigen retrieval with CC1 buffer and CC2 buffer, respectively.

The best results in comparison to standard formalin fixation were achieved with formalin-ultrasound fixation in our study, whereupon staining of p-HER2 in formalin-ultrasound-fixed tissue was not as quantitative as in standard formalin-fixed tissue. However, we do not see underfixation of tissue with formalin-ultrasound as an issue here because detectability of EGFR and IGF-1R was consistently comparable to formalin fixation without ultrasound (standard formalin), but we assume that ultrasound itself could be a reason for the difference. Besides the enhanced reactivity and diffusion of formaldehyde in the tissue [25–27], ultrasound treatment may also trigger chemical reactions or may influence chemical reactions in certain directions [31–34]. One hypothesis could be that phosphorylated proteins are more sensitive to ultrasound treatment than other proteins.

IHC methodology and alternative fixatives

On the one hand, the often-stated better protein quality and antigenicity of alternatively fixed tissue [4, 5, 9, 11, 35, 36] in our opinion, has to be limited. Our results (improved detection of EGFR with protease treatment in AFA/PAXgene®-fixed tissue, improved detection of IGF-1R with CC1 buffer incubation in AFA/PAXgene®/HOPE®-fixed tissue) imply that also for alternatively fixed tissue, an epitope unmasking pretreatment—the so-called antigen retrieval—can improve immunohistochemical detectability. Similar results have been

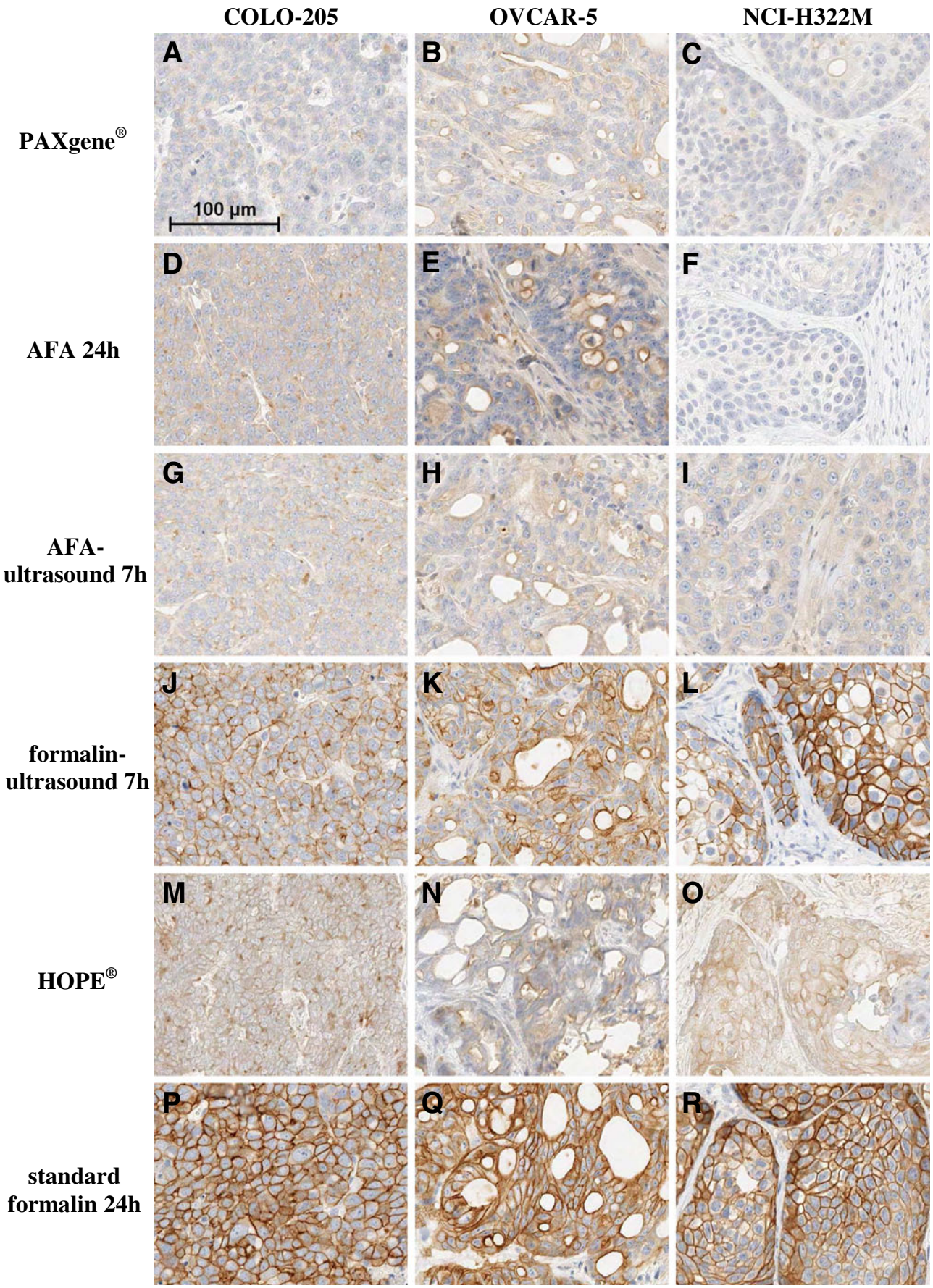
COLO-205
OVCAR-5
NCI-H322M
PAXgene®
AFA 24h
AFA-ultrasound 7h
formalin-ultrasound 7h
HOPE®
standard formalin 24h
A
B
C
D
E
F
G
H
I
J
K
L
M
N
O
P
Q
R
100 µm

◀ **Fig. 5** IHC staining with anti-phospho-HER2 of different xenograft tissues fixed with alternative fixation methods and standard formalin. All pictures are shown in the same scale (*100-μm scale bar picture top left*)

reported from Nassiri et al. [20] in a study on the alternative fixative UMFIX and from Prento and Lyon [21] in a study on several alternative fixatives. Besides the need for optimized antigen retrieval for alternatively fixed tissue, we observed that one-step on-instrument deparaffinization from alternatively fixed tissue on the BenchMark XT platform led to worse results in immunohistochemistry.

On the other hand, we applied IHC assays, which had been optimized for standard formalin-fixed tissue and thus probably probe denatured epitopes, to alternatively fixed tissue, as we wanted to test alternative fixation methods with regard to performance in routine histopathology. A potential superiority of the alternative fixatives in preserving immuno-detectability of native or conformational epitopes, that might be lost during standard formalin fixation, remains to be elucidated in further studies.

In addition to continuative IHC analyses of more proteins, also comprehensive techniques focusing on detection

Table 1 Summary of results

a) Morphology

Morphology	
more details, better preservation of tissue architecture ↑	PAXgene®, AFA
	standard formalin, AFA-ultrasound, formalin-ultrasound
	HOPE®

b) Immunohistochemistry: Manual Deparaffinization

Immunohistochemistry			
	EGFR	**IGF-1R**	**p-HER2**
pronounced staining ↑	PAXgene®, AFA, AFA-ultrasound	**standard formalin**, formalin-ultrasound	**standard formalin**
	formalin-ultrasound	PAXgene®, AFA, AFA-ultrasound	formalin-ultrasound
	standard formalin	HOPE®	HOPE®
	HOPE® (not possible)		PAXgene®, AFA, AFA-ultrasound

c) Immunohistochemistry: Automatic Deparaffinization (not performed for HOPE® fixed tissue)

Immunohistochemistry			
	EGFR	**IGF-1R**	**p-HER2**
pronounced staining ↑	**standard formalin**, formalin-ultrasound	**standard formalin**	**standard formalin**
	AFA, AFA-ultrasound	formalin-ultrasound	formalin-ultrasound
		AFA, AFA-ultrasound	PAXgene®, AFA, AFA-ultrasound
	PAXgene®	PAXgene®	

of various proteins present in fixed tissue, like proteomics-based approaches, could be beneficial [37, 38]. Such approaches have already been applied for the fixative PAXgene® [23] and are showing great potential. Nevertheless, the differing results of alternative fixatives to buffered formalin in IHC could be an indicator, that also with other protein/immuno-based methods (proteomics like MALDI mass spectrometry and protein microarrays or also Western Blot and ELISA) a careful validation and interpretation of the collected data has to be carried out.

Conclusions

In summary, fixation of xenograft tissue with standard formalin resulted in the best immunohistochemical detectability of the chosen membrane receptors when deparaffinization is performed with the BenchMark XT autostainer. When manual deparaffinization is applied, alternatively fixed tissues show both more intense staining (EGFR) and decreased staining (IGF-1R, p-HER2). While most of the alternative fixatives preserved histomorphology, HOPE®-fixed tissue showed decreased morphology. With regard to clinical routine, it is important to know that IHC staining in alternatively fixed tissue may be dependent on the deparaffinization technique (manual vs. automatic) used. Therefore, the use of alternative fixation methods comes with the need to verify the performance of IHC assays individually for each target.

Acknowledgments We are grateful to Prof. Dr. Ralf Huss and Prof. Dr. Wolfgang Schwack for helpful advices and collaborative support. We thank Adriana Zabarella for support in IHC techniques and Christa Bielmeier and Gunther Muth for support in preparing xenograft tumor samples. The authors also thank Dr. Alexandra Farfsing and Dr. Corinna Wolf for useful discussion and valuable comments on the manuscript.

Conflict of interest Thorben Nietner was employee at Roche Diagnostics GmbH during performance of experimental studies.

Open Access This article is distributed under the terms of the Creative Commons Attribution License which permits any use, distribution, and reproduction in any medium, provided the original author(s) and the source are credited.

References

1. Blum F (1893) Der formaldehyd als haertungsmittel. Z wiss Mikrosk 10:314–315
2. Blum F (1896) Ueber wesen und wert der formolhärtung. Anat Anz 11:718–727
3. Foster CS, Gosden CM, Ke YQ (2006) Primer: tissue fixation and preservation for optimal molecular analysis of urologic tissues. Nat Clin Pract Urol 3:268–278
4. Warmington AR, Wilkinson JM, Riley CB (2000) Evaluation of ethanol-based fixatives as a substitute for formalin in diagnostic clinical laboratories. J Histotechnol 23:299–308
5. Gillespie JW, Best CJ, Bichsel VE, Cole KA, Greenhut SF, Hewitt SM, Ahram M, Gathright YB, Merino MJ, Strausberg RL, Epstein JI, Hamilton SR, Gannot G, Baibakova GV, Calvert VS, Flaig MJ, Chuaqui RF, Herring JC, Pfeifer J, Petricoin EF, Linehan WM, Duray PH, Bova SG, Emmert-Bucket MR (2002) Evaluation of non-formalin tissue fixation for molecular profiling studies. Am J Pathol 160:449–457
6. Srinivasan M, Sedmak D, Jewell S (2002) Effect of fixatives and tissue processing on the content and integrity of nucleic acids. Am J Pathol 161:1961–1971
7. Atkins D, Reiffen KA, Tegtmeier CL, Winther H, Bonato M, Störkel S (2004) Immunohistochemical detection of EGFR in paraffin-embedded tumor tissues: variation in staining intensity due to choice of fixative and storage time of tissue sections. J Histochem Cytochem 52:893–901
8. Gugic D, Nassiri M, Nadji M, Morales A, Vincek V (2007) Novel tissue preservative and tissue fixative for comparative pathology and animal research. J Exp Anim Sci 43:271–281
9. Burns JA, Li Y, Cheney CA, Ou Y, Franlin-Peifer LL, Kuklin N, Zhang ZQ (2009) Choice of fixative is crucial to successful immunohistochemical detection of phosphoproteins in paraffin-embedded tumor tissues. J Histochem Cytochem 57:257–264
10. Ananthanarayanan V, Pins MR, Meyer RE, Gann PH (2005) Immunohistochemical assays in prostatic biopsies processed in Bouin's fixative. J Clin Pathol 58:322–324
11. Van der Loos CM (2007) A focus on fixation. J Biotech Histochem 82:141–154
12. Olert J, Wiedorn KH, Goldmann T, Kühl H, Mehraein Y, Scherthan H, Niketeghad F, Vollmer E, Müller MA, Müller-Navia J (2001) HOPE fixation: a novel fixing method and paraffin-embedding technique for human soft tissues. Pathol Res Pract 197:823–826
13. Goldman T, Wiedorn KH, Kühl H, Olert J, Branscheid D, Pechovsky D, Zissel G, Galle J, Müller-Quernheim J, Vollmer E (2002) Assessment of transcriptional gene activity in situ by application of HOPE-fixed, paraffin embedded tissues. Pathol Res Pract 198:91–95
14. Wiedorn KH, Olert J, Stacy RAP, Goldman T, Kühl H, Matthus J, Vollmer E, Bosse A (2002) HOPE—a new fixing technique enables preservation and extraction of high molecular weight DNA and RNA of >20 kb from paraffin embedded tissues. Pathol Res Pract 198:735–740
15. Sen Gupta R, Hillemann D, Kubica T, Zissel G, Müller-Quernheim J, Galle J, Vollmer E, Goldmann T (2003) HOPE-Fixation enables improved PCR-based detection and differentiation of *Mycobacterium tuberculosis* complex in paraffin-embedded tissues. Pathol Res Pract 199:619–623
16. Goldmann T, Burgemeister R, Sauer U, Loeschke S, Lang D, Branscheid D, Zabel P, Vollmer E (2006) Enhanced molecular analyses by combination of the HOPE-technique and laser microdissection. Diagn Pathol 1:2
17. Kothmaier H, Rohrer D, Stacher E, Quehenberger F, Becker KF, Popper HH (2011) Comparison of formalin-free tissue fixatives. A proteomic study testing their application for routine pathology and research. Arch Pathol Lab Med 135:744–752
18. Braun M, Menon R, Nikolov P, Kirsten R, Petersen K, Schilling D, Schott C, Gundisch S, Fend F, Becker KF, Perner S (2011) The HOPE fixation technique—a promising alternative to common prostate cancer biobanking approaches. BMC Cancer 11:511. doi:10.1186/1471-2407-11-511
19. Nadji M, Nassiri M, Vincek V, Kanhoush R, Morales AR (2005) Immunohistochemistry of tissue prepared by a molecular-friendly fixation and processing system. Appl Immunohistochem Mol Morphol 13:277–282

20. Nassiri M, Ramos S, Zohourian H, Vincek V, Morales AR, Nadji M (2008) Preservation of biomolecules in breast cancer tissue by a formalin-free histology system. J Clin Pathol 8:1
21. Prento P, Lyon H (1997) Commercial formalin substitutes for histopathology. J Biotech Histochem 72:273–282
22. Kap M, Smedts F, Oosterhuis W, Winther R, Christensen N, Reischauer B, Viertler C, Groelz D, Becker KF, Zatloukal K, Langer R, Slotta-Huspenina J, Bodo K, de Jong B, Oelmuller U, Riegman P (2011) Histological assessment of PAXgene tissue fixation and stabilization reagents. PLoS One 6(11):1–10
23. Ergin B, Meding S, Langer R, Kap M, Viertler C, Schott C, Ferch U, Riegman P, Zatloukal K, Walch A, Becker KF (2010) Proteomic analysis of PAXgene-fixed tissues. J Prot Res 9:5188–5196
24. Yasuda K, Yamashita S, Shiozawa M, Aiso S, Yasui Y (1992) Application of ultrasound for tissue fixation: combined use with microwave to enhance the effect of chemical fixation. Acta Histochem Cytochem 25:237–244
25. Stephanis CG, Hatiris JG, Mourmouras DE (1998) Acceleration of formaldehyde reactions with proteins due to ultrasound. Ultrason Sonochem 5:33–35
26. Chu WS, Furusato B, Wong K, Sesterhenn IA, Mostofi FK, Wei MQ, Zhu Z, Abbondanzo SL, Liang Q (2005) Ultrasound-accelerated formalin fixation of tissue improves morphology, antigen and mRNA preservation. Mod Pathol 18:850–863
27. Chu WS, Liang Q, Tang Y, King R, Wong K, Gong M, Wei M, Liu J, Feng SH, Lo SC, Andriko JA, Orr M (2006) Ultrasound-accelerated tissue fixation/processing achieves superior morphology and macromolecule integrity with storage stability. J Histochem Cytochem 54:503–513
28. Chen Q, Zou X, Cheng J, Wu J (2007) Application of ultrasound in preparing pathological sections to reduce processing time. Ultrasonics 47:78–81
29. von Ahlfen S, Missel A, Bendrat K, Schlumpberger M (2007) Determinants of RNA quality from FFPE samples. PLoS One 2 (12):e1261. doi:10.1371/journal.pone.0001261
30. Goldman T, Vollmer E, Gerdes J (2003) What's cooking? Detection of important biomarkers in HOPE-fixed, paraffin-embedded tissues eliminates the need for antigen retrieval. Corresp Am J Pathol 163:6
31. Kawai N, Iino M (2003) Molecular damage to membrane proteins induced by ultrasound. Ultrasound Med Biol 29:609–614
32. Shkumatov VM, Adzerikho IE, Lesnikovich JA, Cherniavsky EA (2004) Effect of ultrasound on structure and functional properties of antithrombin III and proteins of PPSB complex. Biochemistry (Mosc) 69:195–200
33. Hickenboth CR, Moore JS, White SR, Sottos NR, Baudry J, Wilson SR (2007) Biasing reaction pathways with mechanical force. Nature 446:423–427
34. Filippov AV, Gröbner G, Antzutkin ON (2010) Aggregation of amyloid Aβ(1–40) peptide in perdeuterated 2,2,2-trifluoroethanol caused by ultrasound sonication. Magn Reson Chem 48:427–434
35. Bassarova AV, Popov AA (1998) Immunohistochemical detection of p53—effect of fixation and methods of antigen retrieval. Folia Histochem Cytobiol 36:127–132
36. Goldstein NS, Hewitt SM, Taylor CR, Yaziji H, Hicks DG (2007) Recommendations for improved standardization of immunohistochemistry. Appl Immunohistochem Mol Morphol 15:124–133
37. Becker KF, Taylor CR (2011) "Liquid morphology": immunochemical analysis of proteins extracted from formalin-fixed paraffin-embedded tissues: combining proteomics with immunohistochemistry. Appl Immunohistochem Mol Morphol 19(1):1–9
38. Rauser S, Deininger SO, Suckau D, Höfler H, Walch A (2010) Approaching MALDI molecular imaging for clinical proteomic research: current state and fields of application. Expert Rev Proteomics 7(6):927–941

Virchows Arch (2012) 461:271–282
DOI 10.1007/s00428-012-1282-3

ORIGINAL ARTICLE

EGFR and HER2–Akt–mTOR signaling pathways are activated in subgroups of salivary gland carcinomas

Shioto Suzuki · Yoh Dobashi · Hiroshi Minato · Ryosuke Tajiri · Tomokazu Yoshizaki · Akishi Ooi

Received: 13 April 2012 / Revised: 11 June 2012 / Accepted: 2 July 2012 / Published online: 25 July 2012
© Springer-Verlag 2012

Abstract Salivary gland carcinomas encompass a wide spectrum of histological entities. To identify candidate therapeutic targets and innovative treatment options for these carcinomas, we examined epidermal growth factor receptor (EGFR), phosphorylated EGFR (p-EGFR), HER2, and phosphorylated forms of Akt (p-Akt) and mammalian target of rapamycin (p-mTOR) in 47 salivary gland tumors using immunohistochemistry. EGFR overexpression was found in 51 % of the tumors (24/47); in particular, EGFR overexpression occurred in mucoepidermoid (seven out of seven) and salivary duct carcinomas (9/12). Although *EGFR* amplification was not detected by fluorescence in situ hybridization analysis, increased copy number due to polysomy of chromosome 7, which houses *EGFR*, was observed in 4 of the 24 tumors with EGFR overexpression; this polysomy occurred most frequently in salivary duct carcinomas (three out of nine). HER2 overexpression was observed in 21 % (10/47) of all tumors; in these 10 tumors, *HER2* gene amplification was found in seven cases. p-Akt was found in 51 % (24/47) of all tumors, most frequently in mucoepidermoid carcinomas (six out of seven). p-mTOR was found in 57 % of the latter (four out of seven). Consequently, different signaling cascades were found activated: (1) an EGFR/HER2(–Akt)–mTOR-dependent axis, with gene gains of *HER2* and/or *EGFR*, activated in salivary duct carcinoma and carcinoma ex pleomorphic adenoma; (2) an EGFR(–Akt)–mTOR-dependent pathway activated in mucoepidermoid carcinoma or acinic cell carcinoma, without HER2 or EGFR gene alterations; and (3) an Akt-dependent pathway without EGFR/HER2 activation in other types. These findings indicate that phosphoprotein mapping of components in the EGFR/HER2–Akt–mTOR pathways may be a useful guide to select appropriate targeting regimens.

Keywords EGFR · HER2 · Akt · mTOR · Salivary gland carcinoma

S. Suzuki · R. Tajiri · A. Ooi
Department of Molecular and Cellular Pathology,
Kanazawa University Graduate School of Medical Science,
13-1 Takara-machi,
Kanazawa, Ishikawa 920-8640, Japan

S. Suzuki (✉)
Division of Pathology and Laboratory Medicine,
Iwata City Hospital,
Iwata, Shizuoka 438-8550, Japan
e-mail: shiosuzuki-path@umin.net

Y. Dobashi
Department of Pathology, Saitama Medical Center,
Jichi Medical University,
Saitama 330-8503, Japan

H. Minato
Department of Pathology and Laboratory Medicine,
Kanazawa Medical University,
Kanazawa, Ishikawa 920-0293, Japan

T. Yoshizaki
Department of Otolaryngology—Head and Neck Surgery,
Kanazawa University Graduate School of Medical Science,
Kanazawa, Ishikawa 920-8641, Japan

Introduction

Salivary gland carcinomas are rare malignant tumors for which it is difficult to assess prognostic factors (0.4–2.6 cases per 100,000) [1]. Moreover, the histopathology of these tumors is diverse; the World Health Organization (WHO) classification describes at least 24 different types of salivary gland carcinoma [1]. The different types of salivary gland carcinoma can be assigned to distinct prognostic groups; for example, acinic cell carcinomas are usually low-grade tumors and salivary duct carcinomas are usually high-grade tumors. In addition, 33 % of salivary duct carcinomas will recur locally, and 46 % will give rise

to distant metastases [1]. Moreover, other types of salivary gland carcinoma tend to have an unpredictable clinical course, despite recent progress in diagnostic strategies and surgical and chemotherapeutic interventions [1]. These facts highlight the need for optimized treatment of those carcinomas with aggressive behavior, through tailored therapeutic approaches.

A potentially effective approach to tailored treatment of aggressive tumors is to inhibit the function of growth factor receptors, because aberrant expression of growth factors is often associated with metastasis, advanced disease, and poor prognosis in a variety of human tumors [2, 3]. Among the myriad of growth factor receptors, two—epidermal growth factor receptor (EGFR; erbB1) and HER2 (erbB2)—have been extensively studied in salivary gland carcinomas [4–11].

EGFR is a 170-kDa membrane glycoprotein that is encoded by the *EGFR* gene, which is located on chromosome 7p12. Many strategies for inhibiting EGFR have been and are being developed, and several such strategies are in clinical use [12–16]. A regimen involving a monoclonal anti-EGFR antibody (cetuximab, panitumumab) has been established for the treatment of colorectal and head and neck cancers that overexpress EGFR [12, 16]. Additionally, several activating mutations within the tyrosine kinase domain of EGFR have been discovered, and these mutations can be used to identify non-small cell lung carcinomas (NSCLC) that respond to tyrosine kinase inhibitors (TKIs), including gefitinib and erlotinib [13]. Other molecular alterations, including gene amplification or chromosomal polysomy, also promote tumorigenesis [14], and some of these alterations have been associated with a higher response rate to TKIs in NSCLC [15]. Although one third of salivary gland carcinomas overexpress EGFR, little is known about the status of the *EGFR* gene and EGFR protein activation in these carcinomas [4–9].

HER2 is a 185-kDa membrane glycoprotein that is encoded by the *HER2* gene, which is located on chromosome 17q12. Accumulated evidence from studies on breast carcinoma has led to the consensus that *HER2* gene amplification and HER2 overexpression are biomarkers for assessing responsiveness to targeted therapy with a humanized monoclonal anti-HER2 antibody, trastuzumab [2, 17]. However, in the clinic, a substantial population of cases shows equivocal expression of HER2 upon immunohistochemical analysis (IHC); in these cases, initial IHC followed by gene amplification analysis by fluorescence in situ hybridization (FISH) has become standard [17]. Although it has been suggested that HER2 overexpression is an indicator of poor prognosis of salivary duct carcinomas [5] and mucoepidermoid carcinomas [10], this claim is controversial [4]. Furthermore, only a few studies have focused on genetic alterations of *EGFR* and *HER2* [7, 18], and therefore, the significance of such alterations in salivary gland carcinomas remains unclear.

Akt and mammalian target of rapamycin (mTOR) function downstream of EGFR and HER2, and both Akt and mTOR seem to be critical transmitters of the oncogenic signal in tumors (Fig. 1) [19–21]. We found that the EGFR–Akt–mTOR pathway is constitutively active in defined subsets of NSCLC [19, 20] and mTOR to be a possible determinant of nodal metastasis [19]. In this sense, Akt and mTOR, like EGFR and HER2, may be suitable therapeutic targets. However, to our knowledge, only one study on salivary carcinoma, specifically on adenoid cystic carcinoma, has focused on p-Akt [22], and no such studies have focused on mTOR.

Accordingly, detailed information with respect to the participation of EGFR and HER2 signaling through Akt and mTOR will help further the development of rational clinical strategies. With this goal in mind, we analyzed (1) activation of the EGFR and HER2 proteins, (2) *EGFR* and *HER-2* copy number, and (3) activation of the Akt–mTOR pathway. The functional involvement of EGFR and HER2 signaling in salivary gland carcinomas was evaluated with particular focus on the aggressive subtypes, i.e., salivary duct carcinoma, mucoepidermoid carcinoma, and carcinoma ex pleomorphic adenoma.

Materials and methods

Tissue samples

We examined samples from 47 salivary gland carcinomas; these tumor samples were obtained from 47 consecutive

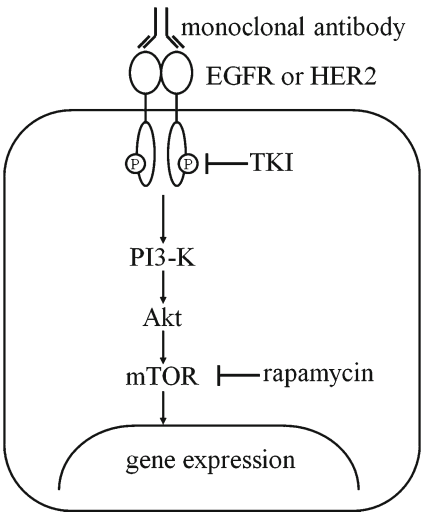

Fig. 1 Schematic presentation of the signaling pathway from the growth factor receptor through the Akt/mTOR effectors. *EGFR* epidermal growth factor receptor, *mTOR* mammalian target of rapamycin, *PI3K* phosphatidylinositol 3-kinase, *TKI* tyrosine kinase inhibitor

surgeries performed between 1995 and 2010 at the Department of Otolaryngology—Head and Neck Surgery, Kanazawa University. The subjects included 24 male and 23 female patients with a mean age of 59.2 years (median, 63 years; range, 28–83 years). For each tumor, the stage of extension was assessed according to the system for staging primary tumor/regional lymph nodes/distant metastasis described in the AJCC Cancer Staging Manual [23]. The 47 tumors were classified as follows: 11 were pT1, 24 were pT2, and 12 were pT3; 12 cases were classified as lymph node-negative (pN0), 11 were lymph node-positive (pN1/2), and the pN status was unknown in the other 24 cases because lymph node dissection was not performed at surgery.

According to the WHO classification [1], the specimens were classified as salivary duct carcinoma (n=12), mucoepidermoid carcinoma (n=7), carcinomas ex pleomorphic adenoma (n=7), acinic cell carcinoma (n=6), adenoid cystic carcinoma (n=5), myoepithelial carcinoma (n=3), basal cell adenocarcinoma (n=2), epithelial–myoepithelial carcinoma (n=2), lymphoepithelial carcinoma (n=2), or adenocarcinoma, NOS (n=1). All seven cases of mucoepidermoid carcinoma were classified as low grade [1]. The seven cases of carcinoma ex pleomorphic adenoma comprised of four salivary duct carcinomas, two adenocarcinomas, NOS, and one mucoepidermoid carcinoma. This laboratory study was approved by the Institutional Review Board at Kanazawa University, and written informed consent was obtained from all patients.

Immunohistochemical analysis

All tissue samples were processed using standard methods, and serial sections were used for IHC. Sections were autoclaved for epitope retrieval and stained with primary antibodies. Antibodies against the following antigens were used: the cytoplasmic domain of EGFR (clone EGFR.25, Novocastra, Newcastle upon Tyne, UK) 1:100 dilution, HER2 (polyclonal, Nichirei, Tokyo, Japan) 1:400, phosphorylated form of EGFR (p-EGFR^{Tyr1068}, polyclonal; Invitrogen, Carlsbad, CA, USA) 1:50, p-Akt^{Ser473} (clone 193 H12, Cell Signaling Technology, Beverly, MA, USA) 1:300, and p-mTOR^{Ser2448} (clone 49 F9, Cell Signaling Technology) at 1:100 dilution. The sensitivity and the specificity of these antibodies for use in IHC analysis of cancerous tissue specimens have been validated by us and others in previous studies [8, 19, 24]. All primary antibodies were visualized using a CSAII kit (Catalyzed Signal Amplification System 2; Dako, Glostrup, Denmark) according to the manufacturer's instructions.

Immunohistochemical staining was evaluated by the three authors (SS, YD, AO). As in previous studies by us and others, in tumor sections immunohistochemically stained for anti-EGFR or anti-HER2, membranous expression was scored as follows: score 0, no staining or staining in <10 % of tumor cells; score 1, faint and partial staining in ≥10 % of tumor cells; score 2, weak to moderate complete membrane staining in ≥10 % of tumor cells; and score 3, strong complete membrane staining in ≥10 % of tumor cells [7, 11, 18, 19, 24]. Scores of 2 or 3 were classified as overexpression because it is widely recognized that only the samples with scores of 2 or 3 in IHC analyses are frequently associated with amplification of the *EGFR* or *HER2* gene [11, 17, 19, 20]. For the other primary antibodies, results were evaluated as significant, when clear staining with higher intensity than in non-neoplastic cells was observed, or not significant. The IHC result for each antibody was considered positive when more than 10 % of the neoplastic cells had significant staining [8, 19].

Fluorescence in situ hybridization

Of the 47 tumors examined, 27 tumors overexpressed EGFR and/or HER2; each of these 27 tumors was subjected to FISH analysis to assess *EGFR* and/or *HER2* copy number. FISH probes for the *EGFR* (7p12) and *HER2* (17q12) loci were generated using two bacterial artificial chromosomes, RP11-339F13 and RP11-62 N23, respectively [24]. These probes were labeled with SpectrumOrange using a nick translation reagent kit (Abbott, Abbott Park, IL, USA). In order to standardize chromosome number in each sample, a SpectrumGreen-labeled pericentromeric probe (Abbott) was also used on each FISH preparation; two such probes, one specific for chromosome 7 and the other for chromosome 17, were used. FISH was performed using standard methods as previously described [24]. The tissue sections were counterstained with 4′,6-diamidine-2′-phenylindole dihydrochloride and *p*-phenylenediamine in phosphate-buffered saline and glycerol (DAPI II) (Abbott) and examined under a fluorescence microscope (Olympus, Tokyo, Japan) equipped with a Triple Bandpass Filter set (Abbott) to discriminate DAPI II, SpectrumOrange, and SpectrumGreen. The number of *EGFR, HER2*, and centromeric signals were counted in each cancer cell nucleus, and the signals were evaluated using the following definitions: definite gene clusters were regarded as high-level amplification for both *EGFR* and *HER2*. In addition, an *EGFR*/centromere ratio greater >2.0 or an average *EGFR* gene copy number >4.0 was interpreted as positive, i.e., an amplification event [25]. In contrast, a *HER2*/centromere ratio >2.2 or an average *HER2* gene copy >6.0 was interpreted as positive, i.e., an amplification event [26]. Increased gene copy number due to polysomy was defined as the presence in more than 50 % of the tumor cells of more than two gene signals accompanied by an identical number of centromeric signals on which the target gene is located [19]. FISH images were

taken using a charged coupled device camera and stored on a personal computer.

Statistical analysis

StatView software (version 5.0; Abacus Concepts, Berkeley, CA, USA) was used for the data analysis. The correlations between immunohistochemical scores were assessed with the χ^2 and Fisher's exact tests. For all tests, statistical significance was defined as a probability value less than 0.05.

Agreement among observers for the interpretation of IHC specimens was assessed by kappa (κ) statistics [27]. In accordance with the criteria of Landis and Koch [28], the κ-values were divided into several classes to evaluate the degree of agreement: $\kappa<0.00$, poor; $0.00<\kappa\leq0.20$, slight; $0.20<\kappa\leq0.40$, fair; $0.40<\kappa\leq0.60$, moderate; $0.60<\kappa\leq0.80$, substantial; and $0.80<\kappa\leq1.00$, nearly perfect.

Results

IHC

We examined the expression and phosphorylation status of EGFR, HER2, and two downstream effector molecules, Akt and mTOR, using IHC. The results of the IHC analysis are summarized in Table 1; the tumors were grouped according to histological type. Overall inter-observer agreement was nearly perfect (the lowest $\kappa=0.84$: 95 % confidence interval, 0.76–0.92 for EGFR).

In tumor cells, positive EGFR staining was confined mainly to the plasma membrane, occasionally with associated cytoplasmic staining. Weak staining was occasionally observed in non-neoplastic ductal, acinar, and stromal cells; however, the intensity of this staining was much weaker than that in tumor cells (Fig. 2). Expression of EGFR was found in 79 % (37/47) of all cases. Of the EGFR-positive cases, 14 showed strong staining (score 3), 10 had intermediate staining (score 2), and 13 had weak staining (score 1). EGFR overexpression (defined as scores of 2 or 3) occurred more frequently in mucoepidermoid carcinoma (seven out of seven) and salivary duct carcinoma (9/12) than in all other types of salivary gland carcinoma (8/28); this difference was statistically significant (the mucoepidermoid and salivary duct carcinomas vs all others, $p=0.0002$).

Positive p-EGFR immunohistochemical staining was found at the plasma membrane and in the cytoplasm of tumor cells. p-EGFR staining was observed in 25 cases (53 %) including large proportion of mucoepidermoid carcinomas (six out of seven) and adenoid cystic carcinomas (three out of five).

Since it has been described that overexpressed HER2 is generally accompanied by HER2 activation [29], we evaluated its expression. HER2 staining was observed in tumor cells mainly at the plasma membrane, with occasional cytoplasmic staining (Fig. 2). Overexpression of HER2 was found in 21 % (10/47) of all cases. With respect to histological types, overexpression of HER2 was found in some salivary duct carcinomas (6/12), some carcinomas ex pleomorphic adenoma (three out of seven), and one myoepithelial carcinoma (one out of three), but not in the other types (0/25).

Positive p-Akt staining was found predominantly in the cytoplasm and, occasionally, in the nucleus of tumor cells

Table 1 Immunohistochemical analysis of 47 tumors

Histological subtypes	EGFR score			p-EGFR		HER2 score			p-Akt		p-mTOR		Total
	3+2	1	0	(+)	(−)	3+2	1	0	(+)	(−)	(+)	(−)	
Salivary duct carcinoma	9	0	3	5	7	6	1	5	6	6	10	2	12
Mucoepidermoid carcinoma	7	0	0	6	1	0	0	7	6	1	4	3	7
Carcinoma ex pleomorphic adenoma	3	2	2	4	3	3	0	4	3	4	5	2	7
Acinic cell carcinoma	0	3	3	3	3	0	0	6	1	5	3	3	6
Adenoid cystic carcinoma	1	3	1	3	2	0	0	5	3	2	2	3	5
Myoepithelial carcinoma	0	3	0	1	2	1	0	2	2	1	1	2	3
Basal cell adenocarcinoma	1	1	0	2	0	0	0	2	1	1	0	2	2
Epithelial–myoepithelial carcinoma	0	1	1	1	1	0	0	2	1	1	2	0	2
Lymphoepithelial carcinoma	2	2	0	2	0	0	0	2	1	1	0	2	2
Adenocarcinoma, NOS	1	0	0	0	1	0	0	1	0	1	0	1	1
Total	24	13	10	27	20	10	1	36	24	23	27	20	47

(+) positive for expression of p-Akt or p-mTOR, *p-EGFR* phosphorylated epidermal growth factor receptor, *mTOR* mammalian target of rapamycin

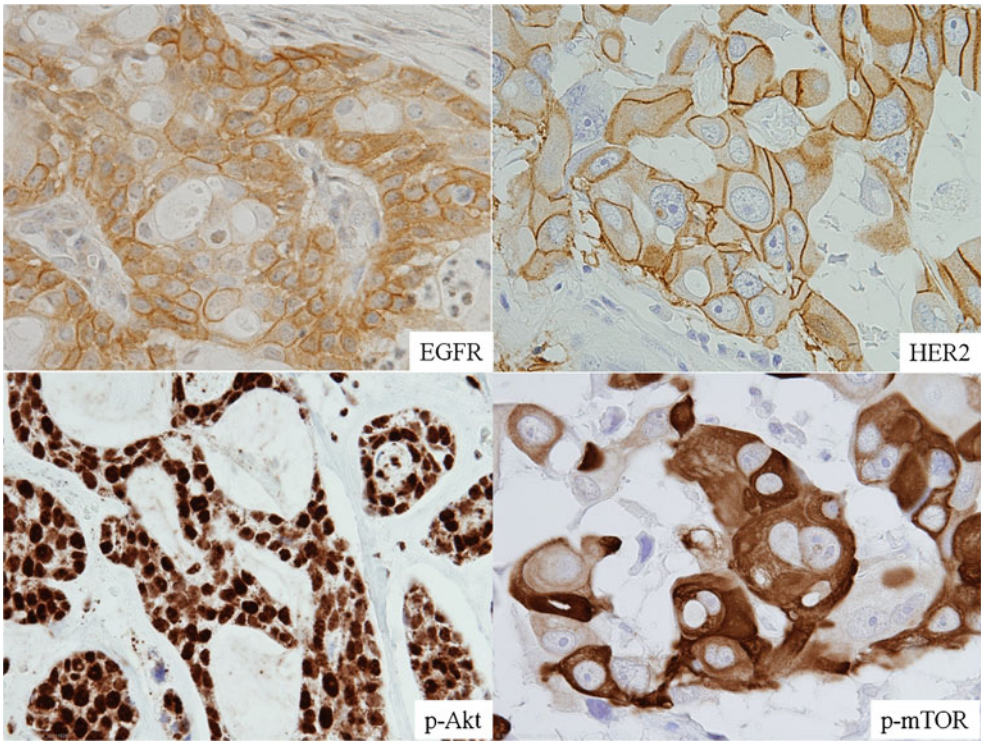

Fig. 2 Immunohistochemical staining of the EGFR and HER2 proteins, as well as downstream signaling intermediates, in representative cases. Positive staining for EGFR or HER2 was confined almost exclusively to the plasma membrane of tumor cells, but occasionally there was associated cytoplasmic staining. Staining for p-Akt and p-mTOR was mainly observed respectively in the nuclei and the cytoplasm of tumor cells. *EGFR* epidermal growth factor receptor, *p-mTOR* phosphorylated mammalian target of rapamycin

(Fig. 2). p-Akt staining was found in 51 % (24/47) of all tumors and was present in most mucoepidermoid carcinomas (six out of seven) and adenoid cystic carcinomas (three out of five).

Positive p-mTOR staining was observed in the cytoplasm and also in the nuclei of tumor cells (Fig. 2). Expression of p-mTOR was found in 57 % (27/47) of all tumors, and it was present in almost every salivary duct carcinoma (10/12) and most carcinomas ex pleomorphic adenoma (five out of seven) and mucoepidermoid carcinomas (four out of seven); p-mTOR staining was found in less than half of the tumors in all other classes (8/21), but these differences were not statistically significant (the former three types vs all other types, p=0.0206).

Correlations between staining patterns

EGFR and HER2 In consecutively stained serial sections (Fig. 3), the areas of EGFR and HER2 staining partially overlapped within a single tumor nodule in seven cases (five cases of salivary duct carcinomas and two cases of carcinoma ex pleomorphic adenoma). In addition, co-expression of these proteins in one cell was occasionally observed.

EGFR and p-EGFR p-EGFR-positive cell groups were generally found in areas of extensive EGFR expression (Fig. 3). Furthermore, 68 % of EGFR-positive cases (EGFR score 1–3, 25/37) showed p-EGFR expression, and conversely, p-EGFR expression was not observed in any EGFR-negative cases (EGFR score 0, 0/10). These results indicate that EGFR expression is a prerequisite for EGFR activation. Accordingly, p-EGFR staining was seen more frequently in mucoepidermoid and salivary duct carcinomas, which frequently exhibited EGFR overexpression; specifically six of seven mucoepidermoid carcinomas were p-EGFR-positive, and 5 of 12 salivary duct carcinomas were p-EGFR-positive. Tumors that overexpressed EGFR (EGFR score 2 or 3, 18/24) were significantly more likely (p= 0.0034, Table 2) to have p-EGFR-positive cells than tumors that did not overexpress EGFR (EGFR score 0 and 1, 7/23). Therefore, EGFR overexpression most often but not always accompanied p-EGFR expression.

p-EGFR and p-Akt Nineteen tumors were p-EGFR-positive but HER2-negative. p-Akt was positive in 11 of these 19 cases. Hence, EGFR staining, regardless of HER2 staining, was associated with p-Akt staining in up to 58 % of the cases. Consistently, the p-EGFR-positive areas in those 11 tumors overlapped with the p-Akt-positive areas (Fig. 3).

HER2 and p-Akt There were four tumors that were HER2-positive but p-EGFR-negative. p-Akt staining was positive in two of these, suggesting that, in the absence of the EGFR signaling, HER2 might activate p-Akt. However, HER2 and p-Akt staining in these two cases only partially overlapped.

p-EGFR/HER2 and p-Akt Six tumors were p-EGFR-positive and HER2-positive. Of these six tumors, three showed p-Akt staining, and in two of these, the areas of p-Akt staining almost completely overlapped with p-EGFR

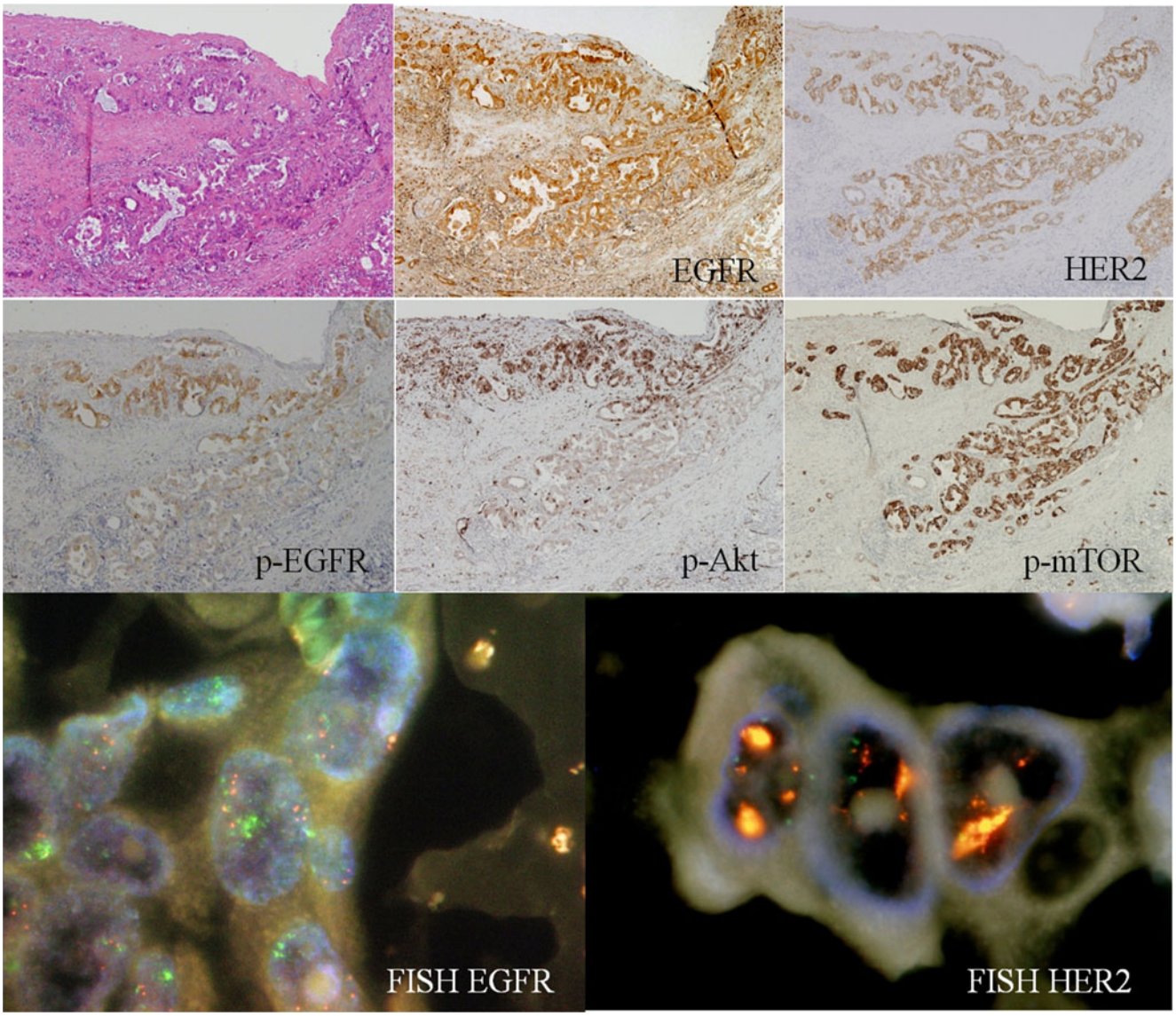

Fig. 3 Hematoxylin and eosin staining (HE), immunohistochemical staining for proteins of the EGFR/HER2 and their downstream signaling intermediates, and *EGFR/HER2* gene alterations. A case of salivary duct carcinoma showed co-overexpression of EGFR (score 2) and HER2 (score 3), and the areas of EGFR overexpression partially overlapped those of HER2 overexpression. The p-EGFR-positive areas were restricted to areas within broader EGFR overexpressing areas. The areas with p-EGFR or HER2 staining tended to overlap with areas of p-Akt and p-mTOR staining, respectively. FISH revealed *EGFR* gene copy gain due to chromosome 7 polysomy and high-level *HER2* gene amplification. *EGFR* epidermal growth factor receptor, *FISH* fluorescence in situ hybridization, *mTOR* mammalian target of rapamycin, *p-EGFR* phosphorylated EGFR

Table 2 Relationship between overexpression of EGFR or HER2 and expression of p-Akt or p-mTOR

	p-EGFR			p-Akt			p-mTOR		
	(+)	(−)		(+)	(−)		(+)	(−)	
EGFR									
(+)	18	6		14	10		14	10	
(−)	7	16	$p=0.0034$	10	13	$p=0.3868$	13	10	$p>0.9999$
HER2									
(+)	6	4		5	5		9	1	
(−)	19	18	$p=0.7298$	19	18	$p>0.9999$	18	19	$p=0.0292$

staining, whereas HER2 and p-Akt staining only partially overlapped.

p-Akt and p-mTOR Of 24 p-Akt-positive cases, 12 were p-mTOR-positive. However, 15 of 23 p-Akt-negative cases were also p-mTOR-positive. This suggests that mTOR signaling was induced by both Akt-dependent and Akt-independent mechanisms.

Gene alteration and protein expression of EGFR and HER2 and phosphorylation of downstream molecules

FISH was performed in 27 cases in which overexpression of EGFR, HER2, or both was observed. The results are summarized in Table 3.

EGFR Among 24 cases exhibiting EGFR overexpression, no *EGFR* amplification was detected. However, *EGFR* gene copy gain due to chromosome 7 polysomy was present in four of these cases (three salivary duct carcinomas and one lymphoepithelial carcinoma), and all showed p-EGFR staining consistent with EGFR activation.

HER2 Among the 10 cases exhibiting HER2 overexpression, *HER2* amplification was observed in seven cases, including five salivary duct carcinomas (five out of six) and two cases of carcinoma ex pleomorphic adenoma (two out of three).

EGFR and HER2 Nine cases (six salivary duct carcinomas, two carcinomas ex pleomorphic adenomas, and one lymphoepithelial carcinoma) showed *HER2* amplification, chromosome 7 polysomy, or both. Among these cases, two salivary duct carcinomas had both chromosome 7 polysomy and *HER2* amplification (Fig. 3). In these two cases, expression of both proteins overlapped. Furthermore, focal co-expression of EGFR and HER2 was observed in single cells in one of these. Of the other seven cases, two (one salivary duct carcinoma and one lymphoepithelial carcinoma) showed chromosome 7 polysomy only, and five cases (three salivary duct carcinomas and two carcinomas ex pleomorphic adenoma) showed *HER2* gene amplification only.

Correlation between status of EGFR/HER2 and their downstream signaling intermediates in each histological type

The activation of EGFR and HER2 was evaluated by assessing p-EGFR signal and HER2 overexpression, respectively, using IHC [29]. Cases were stratified into four categories: p-EGFR(+) and HER2(+), p-EGFR(+) and HER2(−), p-EGFR(−) and HER2(+), and p-EGFR(−) and HER2(−). Results were evaluated for each histological type of tumor with five or more cases (Fig. 4).

In the 12 cases of salivary duct carcinoma, p-EGFR was expressed in five cases, three of which harbored chromosome 7 polysomy, and HER2 was overexpressed in six cases, five of which harbored *HER2* amplification. All but one of the cases showing p-EGFR expression, HER2 overexpression, or both (eight cases in total) were p-mTOR positive. In contrast, p-Akt staining was observed in only four of these. Among the seven cases of mucoepidermoid carcinoma, six showed p-EGFR staining, but not HER2 overexpression, and p-Akt or p-mTOR staining in five and four cases, respectively.

In carcinoma ex pleomorphic adenoma (seven cases), p-EGFR staining was found in four cases, and three of these were accompanied by HER2 overexpression. All four cases were positive for p-mTOR, but p-Akt was positive in only two cases. None of the cases showed evidence of *EGFR* copy

Table 3 Immunohistochemical phenotypes of and genetic alterations in tumors showing evidence of *EGFR* or *HER2* gene alteration

No.	Age	Sex	Histological type	EGFR			HER2		p-Akt	p-mTOR
				IHC	FISH	p-EGFR	IHC	FISH		
1	83	M	Salivary duct carcinoma	3	Polysomy	+	3	Amp(+)	−	+
2	68	M	Salivary duct carcinoma	2	Polysomy	+	3	Amp(+)	+	+
3	68	M	Lymphoepithelial carcinoma	3	Polysomy	+	0	Disomy	−	−
4	65	M	Salivary duct carcinoma	3	Polysomy	+	3	Disomy	+	+
5	68	M	Salivary duct carcinoma	3	Disomy	−	3	Amp(+)	−	+
6	74	M	Salivary duct carcinoma	0	Disomy	−	3	Amp(+)	−	+
7	79	M	Salivary duct carcinoma	2	Disomy	−	3	Amp(+)	+	+
8	47	W	Carcinoma ex pleomorphic adenoma	1	Disomy	+	3	Amp(+)	+	+
9	57	M	Carcinoma ex pleomorphic adenoma	2	Disomy	+	3	Amp(+)	−	+

EGFR epidermal growth factor receptor, *IHC* immunohistochemistry, *FISH* fluorescence *in situ* hybridization, *pEGFR* phosphorylation of EGFR, *amp* gene amplification

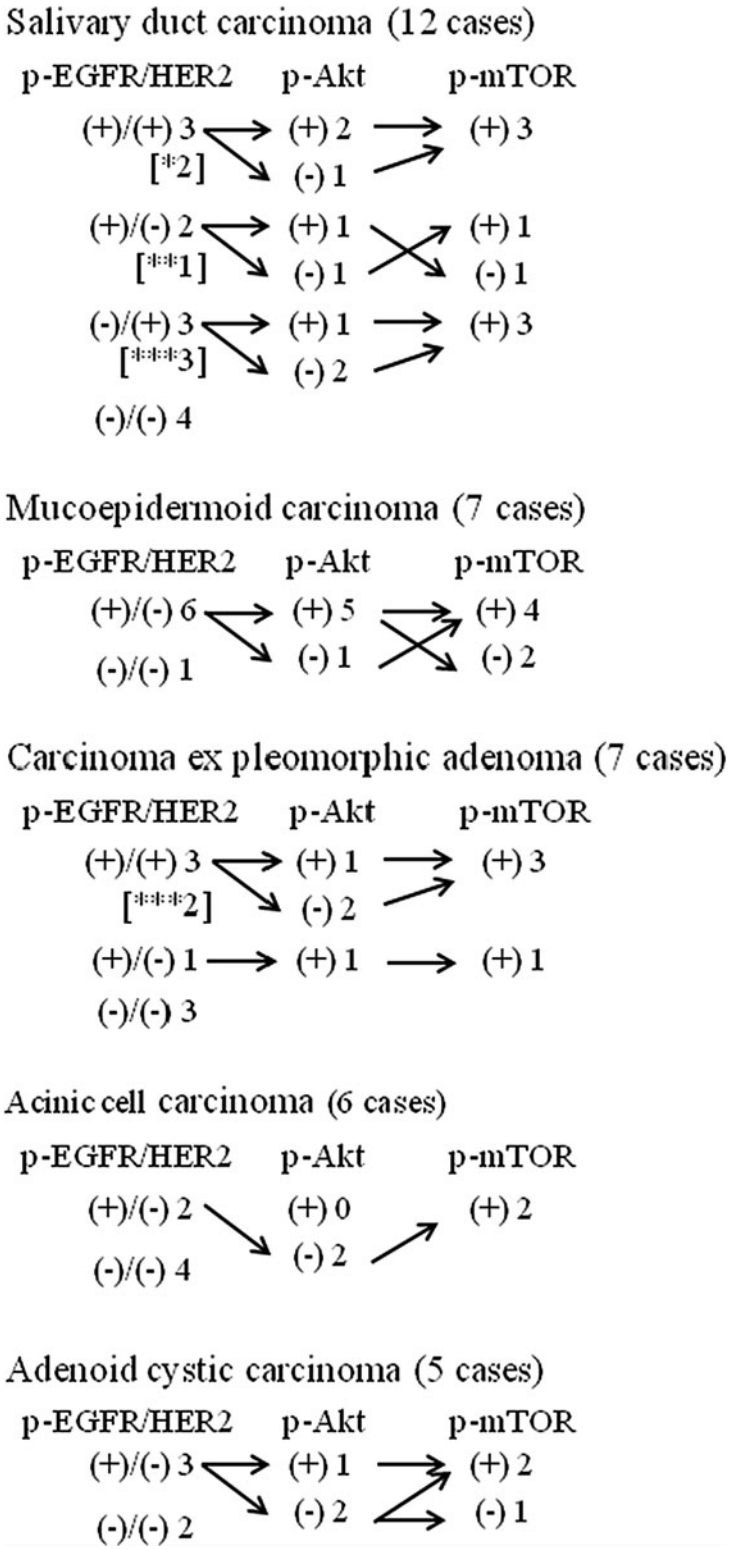

Fig. 4 Results of immunohistochemical analysis in representative histological subtypes. One asterisk: Cases showing both EGFR gene gain and HER2 gene amplification; two asterisks: cases showing EGFR gene gain; three asterisks: cases showing HER2 gene amplification

number gain; instead, two cases showed evidence of *HER2* amplification. In acinic cell carcinomas (six cases), p-EGFR was positive in two cases, and both showed p-mTOR staining; however, p-Akt was negative in both cases. Moreover, HER2 overexpression was not observed in any of these cases.

In adenoid cystic carcinomas (five cases), p-EGFR was positive in three cases; p-Akt was positive in one of these three cases, and p-mTOR in two. HER2 overexpression was not observed in any of the adenoid cystic carcinomas.

In carcinomas of all histological types listed above, p-EGFR(−) and HER2(−) cases accounted for 38 % (14/37, ranging from 14 % [one out of seven] in mucoepidermoid carcinoma to 67 % [four out of six] in acinic cell carcinoma). Among these 14 cases, p-Akt staining was positive in seven cases (two adenoid cystic carcinomas, two salivary duct carcinomas, one acinic cell carcinoma, one carcinoma ex pleomorphic adenoma, and one mucoepidermoid carcinoma), and p-mTOR staining was found in two (salivary duct carcinoma and acinic cell carcinoma) of these.

Altogether, three signal transduction pathways were identified (Fig. 5). The first is the EGFR/HER2–(Akt)–mTOR pathway: 7 of 12 salivary duct carcinomas and four of seven carcinomas ex pleomorphic adenoma exhibited signs of activation of this pathway associated with gene gains of *EGFR* and/or *HER2*. The second is an EGFR(–Akt)–mTOR-dependent pathway: five of seven mucoepidermoid carcinomas, two of six acinic cell carcinomas, and two of five adenoid cystic carcinomas exhibited signs of activation of this pathway without increased gene copy number of *EGFR* or *HER2*. The last pathway is p-Akt-dependent but unrelated to EGFR or HER2 and mostly p-mTOR negative.

Discussion

A large body of evidence links overexpression of EGFR, HER2, or both to malignancy in a wide array of human tumors [2, 3]; therefore, EGFR and HER2 and downstream effector molecules are promising candidates as targets for effective therapies. Drugs targeting EGFR [12–16], HER2 [2], and mTOR [30] are available, and Akt inhibitors have also been assessed in clinical trials as treatments for solid tumors [31]. Although salivary gland carcinomas are in general not highly aggressive, they constitute a biologically heterogeneous group, and depending on the histological types, they are occasionally life-threatening [1]. Therefore, patients should be treated based on their unique phenotype. However, there are very few studies that provide a comprehensive picture of the expression or activation status, or gene alteration status of components in the EGFR/HER2–Akt–mTOR pathways in human salivary gland carcinomas. The present study was intended to provide phosphoprotein mapping of this pathway as a potentially promising guide for the selection of appropriate targeting regimens.

Our results offer insight into the role of EGFR- and HER2-mediated signaling. Past studies have described the frequency of EGFR expression in salivary gland carcinomas, ranging from 36 to 85 %, depending on the selection of histological types and the diversity in the scoring criteria used in IHC analyses [4–9]. Here, we observed EGFR expression in 79 % (37/47) of all cases and found overexpression in specific histological types, e.g., mucoepidermoid carcinoma (seven out of seven) and salivary duct carcinoma (9/12). p-EGFR staining was consistently observed in these two histological types. Therefore, the monoclonal antibody against EGFR, cetuximab, might be a candidate for targeted treatment of patients with either mucoepidermoid or salivary duct carcinoma.

Although the mutations in the TK domain of *EGFR* that are frequently found in lung cancer were rare in salivary gland carcinomas [13, 32], recent studies of lung and colonic carcinomas indicate that a high level of chromosome 7 polysomy, which goes along with increased *EGFR* copy number, may also function as a biomarker for responsiveness to TKIs [15, 33]. If this is the case, salivary gland carcinoma might also be successfully treated with TKIs. Regarding numerical aberrations of the *EGFR* gene, there has been only one report describing polysomy of chromosome 7 in salivary duct carcinomas [7]. In the current study, chromosome 7 polysomy was present in four cases (three salivary duct carcinomas and one lymphoepithelial carcinoma), corresponding to 9 % of all cases. Hence, more

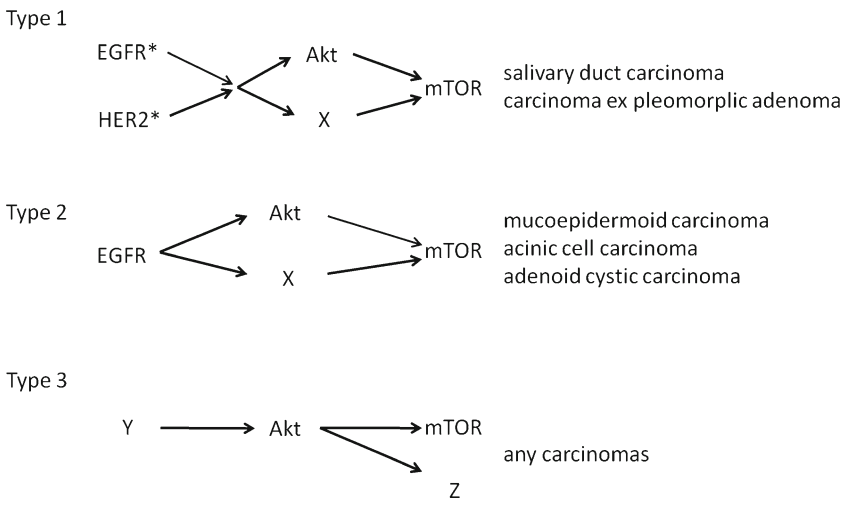

Fig. 5 Putative signaling pathways active in salivary gland carcinomas. *EGFR* epidermal growth factor receptor, *mTOR* mammalian target of rapamycin, *X* responsible kinase(s) for mTOR other than Akt, *Y* growth factor receptor(s) other than EGFR or HER2, *Z* substrate(s) of Akt other than mTOR. *Asterisk* indicates increase of gene copy by amplification or polysomy

extensive exploration of *EGFR* aberrations may contribute to effective and optimal EGFR-targeted therapy with TKIs.

Past studies revealed HER2 overexpression in 10–38 % of salivary gland carcinomas [4–7, 10, 11]. We found this in 21 % of all 47 cases, restricted to salivary duct carcinomas (50 %), carcinomas ex pleomorphic adenoma (43 %), and myoepithelial carcinomas (33.3 %). Unlike EGFR, antibodies against the phosphorylated form of HER2 have not been widely used on paraffin-embedded sections. A previous study of human mammary epithelial cells showed that the basal phosphorylation level of HER2 increased due to enhanced HER2 autophosphorylation, cross-phosphorylation by EGFR, or even through increased autocrine stimulation of HER2 heterodimers [29]. Thus, we interpreted the HER2 overexpression observed in the current study as being equivalent to HER2 activation.

Unlike *EGFR* gene amplification, *HER2* gene amplification was often (70 % of HER2-overexpressing tumors) responsible for HER2 overexpression; *HER2* amplification occurred most frequently in salivary duct carcinomas (42 %, 5/12 cases), and the frequency was higher than that (12 %) in the previous study [7]. In addition, we observed *HER2* gene amplification in 29 % (two out of seven) of carcinomas ex pleomorphic adenoma; interestingly, *HER2* gene amplification in carcinomas ex pleomorphic adenoma has not been reported previously. Although it was not clear whether gene gains of *EGFR* or *HER2* influence the pattern of activation of downstream molecules, tumors harboring *EGFR* or *HER2* gene gains generally showed activation of EGFR or HER2, as well as the Akt/mTOR axis.

Only two studies [7, 18] on the relationship between *EGFR* and *HER2* gene alterations in salivary gland carcinomas have been published. One study showed that three out of eight *HER2*-amplified tumors harbored chromosome 7 polysomy (*EGFR* gene copy gain) [7]. Two of seven *HER2*-amplified tumors harbored chromosome 7 polysomy in our study, and co-expression of EGFR and HER2 proteins within a tumor nodule was confirmed by immunohistochemical analysis; focal co-expression on a cell-by-cell basis was observed in one case. These cases showed mTOR activation.

From a therapeutic point of view, inhibiting EGFR or HER2 alone is not optimal for effective inhibition of tumor cells, highlighting the need for multipoint intervention. For this purpose, general assessment of effector protein activation through phosphoprotein study needs to be performed. The status of p-Akt in salivary gland carcinomas has not been evaluated extensively. One study revealed a high frequency (86 %) of p-Akt expression in adenoid cystic carcinomas based on IHC [22]. However, that study did not focus on other histological types nor on the expression or the activation status of EGFR or HER2 [22]. In the current study, p-Akt staining was found in 51 % of all 47 cases, in 58 % of the cases showing EGFR activation, and in 50 % of the cases showing HER2 activation. Moreover, p-Akt was frequently seen in mucoepidermoid carcinomas (six out of seven), and five of these six p-Akt-positive mucoepidermoid carcinomas showed evidence of EGFR phosphorylation. Indeed, in these cases, the area showing positive p-EGFR staining tended to overlap with the areas of p-Akt staining.

The mTOR protein is a critical downstream modulator of Akt and is an appealing therapeutic target because it has an established inhibitor, rapamycin [30, 34]. However, no previously published pathological study focused on mTOR in salivary gland carcinomas. We found that mTOR is activated in 57 % of all 47 tumors, notably in a high percentage of salivary duct carcinomas (83 %). These findings indicate that, in a significant percentage of this subset, mTOR is activated, and therefore, tailored treatment with rapamycin may be considered.

The correlation between the activation patterns of EGFR/HER2 and Akt, or between the activation patterns of Akt and mTOR, was not entirely consistent in the current study, possibly due to complex cross-talk between pathways. For example, although Akt is a major positive regulator of mTOR, ras-extracellular signal-regulated kinase 1/2 also converges to mTOR [34]. Another possibility is that activation of Akt by p-EGFR or activation of mTOR by p-Akt may be executed in a transient manner, and thus, histopathological evidence of simultaneous activation of these kinases may be difficult to detect in fixed tissue specimens.

Overall, dysregulation of the kinase-driven EGFR/HER2(–Akt)–mTOR pathway might constitute a critical mechanism underlying the pathology of a substantial fraction of salivary gland carcinomas, although other signaling pathways including c-kit and Wnt/β-catenin signaling pathways might be involved in p-EGFR-negative and HER2-negative cases [1]. Moreover, we teased out specific categories that could be defined by the activation profiles of this axis and, therefore, found three types of signal transduction cascades (Fig. 5).

The first category of tumors involve a EGFR/HER2(–Akt)–mTOR-dependent pathway that is frequently associated with *EGFR* and/or *HER2* gene gains. Theoretically, cocktails of monoclonal antibodies against EGFR, cetuximab, or anti-HER2, trastuzumab, or possibly, a dual inhibitor of both EGFR and HER2, e.g., lapatinib [35], combined with rapamycin, could be candidate treatments for the tumors in this group. Moreover, EGFR-TKIs and/or an Akt inhibitor could be useful depending on the presence of *EGFR* gene gains or Akt activation, respectively.

The second category of tumors involved a EGFR(–Akt)–mTOR-dependent pathway, but no gene gains. This category of tumors may be sensitive to combination regimens involving anti-EGFR agents and rapamycin directed against mTOR.

The last category comprises Akt-dependent carcinomas that do not depend on signals from EGFR or HER2. This

particular subset of tumors could be candidates for treatment with Akt inhibitors, e.g., perifosin [31].

The present study on archival tissues of salivary gland carcinomas provides a detailed description of EGFR and/or HER2 activation via the mTOR pathway, and overall these findings provide insight into possibilities for treatment regimens for salivary gland carcinomas that involve tailored combination therapies.

Acknowledgments This study was financial supported by The Japanese Ministry of Education, Sports, Science and Culture, Young Scientists B 22790340 (SS), No. C 23590409 (YD), C 22590310 (AO), and the Smoking Research Foundation (YD).

Conflict of interest The authors declare that they have no conflict of interest.

References

1. Barnes L, Eveson J, Reichart P, Sidransky D (eds) (2005) World Health Organization classification of tumours. Pathology and genetics of head and neck tumours. IARC, Lyon. pp 209–253
2. Ross JS, Fletcher JA (1998) The HER-2/neu oncogene in breast cancer: prognostic factor, predictive factor, and target for therapy. Oncologist 3:237–252
3. Mayer A, Takimoto M, Fritz E, Schellander G, Kofler K, Ludwig H (1993) The prognostic significance of proliferating cell nuclear antigen, epidermal growth factor receptor, and mdr gene expression in colorectal cancer. Cancer 71:2454–2460
4. Ettl T, Schwarz S, Kleinsasser N, Hartmann A, Reichert TE, Driemel O (2008) Overexpression of EGFR and absence of C-KIT expression correlate with poor prognosis in salivary gland carcinomas. Histopathology 53:567–577
5. Williams MD, Roberts D, Blumenschein GR Jr, Temam S, Kies MS, Rosenthal DI, Weber RS, El-Naggar AK (2007) Differential expression of hormonal and growth factor receptors in salivary duct carcinomas: biologic significance and potential role in therapeutic stratification of patients. Am J Surg Pathol 31:1645–1652
6. Locati LD, Perrone F, Losa M, Mela M, Casieri P, Orsenigo M, Cortelazzi B, Negri T, Tamborini E, Quattrone P, Bossi P, Rinaldi G, Bergamini C, Calderone RG, Liberatoscioli C, Licitra L (2009) Treatment relevant target immunophenotyping of 139 salivary gland carcinomas (SGCs). Oral Oncol 45:986–990
7. Williams MD, Roberts DB, Kies MS, Mao L, Weber RS, El-Naggar AK (2010) Genetic and expression analysis of HER-2 and EGFR genes in salivary duct carcinoma: empirical and therapeutic significance. Clin Cancer Res 16:2266–2274
8. Sorensen KB, Godballe C, de Stricker K, Krogdahl A (2006) Parotid carcinoma: expression of kit protein and epidermal growth factor receptor. J Oral Pathol Med 35:286–291
9. Vered M, Braunstein E, Buchner A (2002) Immunohistochemical study of epidermal growth factor receptor in adenoid cystic carcinoma of salivary gland origin. Head Neck 24:632–636
10. Press MF, Pike MC, Hung G, Zhou JY, Ma Y, George J, Dietz-Band J, James W, Slamon DJ, Batsakis JG et al (1994) Amplification and overexpression of HER-2/neu in carcinomas of the salivary gland: correlation with poor prognosis. Cancer Res 54:5675–5682
11. Glisson B, Colevas AD, Haddad R, Krane J, El-Naggar A, Kies M, Costello R, Summey C, Arquette M, Langer C, Amrein PC, Posner M (2004) HER2 expression in salivary gland carcinomas: dependence on histological subtype. Clin Cancer Res 10:944–946
12. Bourhis J, Lefebvre JL, Vermorken JB (2010) Cetuximab in the management of locoregionally advanced head and neck cancer: expanding the treatment options? Eur J Cancer 46:1979–1989
13. Lynch TJ, Bell DW, Sordella R, Gurubhagavatula S, Okimoto RA, Brannigan BW, Harris PL, Haserlat SM, Supko JG, Haluska FG, Louis DN, Christiani DC, Settleman J, Haber DA (2004) Activating mutations in the epidermal growth factor receptor underlying responsiveness of non-small-cell lung cancer to gefitinib. N Engl J Med 350:2129–2139
14. Hirsch FR, Herbst RS, Olsen C, Chansky K, Crowley J, Kelly K, Franklin WA, Bunn PA Jr, Varella-Garcia M, Gandara DR (2008) Increased EGFR gene copy number detected by fluorescent in situ hybridization predicts outcome in non-small-cell lung cancer patients treated with cetuximab and chemotherapy. J Clin Oncol 26:3351–3357
15. Felip E, Rojo F, Reck M, Heller A, Klughammer B, Sala G, Cedres S, Peralta S, Maacke H, Foernzler D, Parera M, Mocks J, Saura C, Gatzemeier U, Baselga J (2008) A phase II pharmacodynamic study of erlotinib in patients with advanced non-small cell lung cancer previously treated with platinum-based chemotherapy. Clin Cancer Res 14:3867–3874
16. Cunningham D, Humblet Y, Siena S, Khayat D, Bleiberg H, Santoro A, Bets D, Mueser M, Harstrick A, Verslype C, Chau I, Van Cutsem E (2004) Cetuximab monotherapy and cetuximab plus irinotecan in irinotecan-refractory metastatic colorectal cancer. N Engl J Med 351:337–345
17. Wolff AC, Hammond ME, Schwartz JN, Hagerty KL, Allred DC, Cote RJ, Dowsett M, Fitzgibbons PL, Hanna WM, Langer A, McShane LM, Paik S, Pegram MD, Perez EA, Press MF, Rhodes A, Sturgeon C, Taube SE, Tubbs R, Vance GH, van de Vijver M, Wheeler TM, Hayes DF (2007) American Society of Clinical Oncology/College of American Pathologists guideline recommendations for human epidermal growth factor receptor 2 testing in breast cancer. J Clin Oncol 25:118–145
18. Vidal L, Tsao MS, Pond GR, Cohen EE, Cohen RB, Chen EX, Agulnik M, Hotte S, Winquist E, Laurie S, Hayes DN, Ho J, Dancey J, Siu LL (2009) Fluorescence in situ hybridization gene amplification analysis of EGFR and HER2 in patients with malignant salivary gland tumors treated with lapatinib. Head Neck 31:1006–1012
19. Dobashi Y, Suzuki S, Kimura M, Matsubara H, Tsubochi H, Imoto I, Ooi A (2011) Paradigm of kinase-driven pathway downstream of epidermal growth factor receptor/Akt in human lung carcinomas. Hum Pathol 42:214–226
20. Suzuki S, Igarashi S, Hanawa M, Matsubara H, Ooi A, Dobashi Y (2006) Diversity of epidermal growth factor receptor-mediated activation of downstream molecules in human lung carcinomas. Mod Pathol 19:986–998
21. Armengol G, Rojo F, Castellvi J, Iglesias C, Cuatrecasas M, Pons B, Baselga J, Ramon y Cajal S (2007) 4E-binding protein 1: a key molecular "funnel factor" in human cancer with clinical implications. Cancer Res 67:7551–7555
22. de Lima Mde D, Marques YM, Alves Sde M Jr, Freitas VM, Soares FA, de Araujo VC, Pinto Ddos S Jr, Mantesso A (2009) MDM2, P53, P21WAF1 and pAKT protein levels in genesis and behaviour of adenoid cystic carcinoma. Cancer Epidemiol 33:142–146
23. Edge SB, Byrd D, Compton CC, Fritz AG, Greene FL et al (eds) (2010) AJCC cancer staging manual, 7th edn. Springer-Verlag, New York
24. Ooi A, Zen Y, Ninomiya I, Tajiri R, Suzuki S, Kobayashi H, Imoto I, Dobashi Y (2010) Gene amplification of ERBB2 and EGFR in adenocarcinoma in situ and intramucosal adenocarcinoma of Barrett's esophagus. Pathol Int 60:466–471
25. Varella-Garcia M (2006) Stratification of non-small cell lung cancer patients for therapy with epidermal growth factor receptor inhibitors: the EGFR fluorescence in situ hybridization assay. Diagn Pathol 1:19

26. Walker RA, Bartlett JM, Dowsett M, Ellis IO, Hanby AM, Jasani B, Miller K, Pinder SE (2008) HER2 testing in the UK: further update to recommendations. J Clin Pathol 61:818–824
27. Thomson TA, Hayes MM, Spinelli JJ, Hilland E, Sawrenko C, Phillips D, Dupuis B, Parker RL (2001) HER-2/neu in breast cancer: interobserver variability and performance of immunohistochemistry with 4 antibodies compared with fluorescent in situ hybridization. Mod Pathol 14:1079–1086
28. Landis JR, Koch GG (1977) The measurement of observer agreement for categorical data. Biometrics 33:159–174
29. Wolf-Yadlin A, Kumar N, Zhang Y, Hautaniemi S, Zaman M, Kim HD, Grantcharova V, Lauffenburger DA, White FM (2006) Effects of HER2 overexpression on cell signaling networks governing proliferation and migration. Mol Syst Biol 2:54
30. Pantuck AJ, Seligson DB, Klatte T, Yu H, Leppert JT, Moore L, O'Toole T, Gibbons J, Belldegrun AS, Figlin RA (2007) Prognostic relevance of the mTOR pathway in renal cell carcinoma: implications for molecular patient selection for targeted therapy. Cancer 109:2257–2267
31. Unger C, Berdel W, Hanauske AR, Sindermann H, Engel J, Mross K (2010) First-time-in-man and pharmacokinetic study of weekly oral perifosine in patients with solid tumours. Eur J Cancer 46:920–925
32. Dahse R, Driemel O, Schwarz S, Dahse J, Kromeyer-Hauschild K, Berndt A, Kosmehl H (2009) Epidermal growth factor receptor kinase domain mutations are rare in salivary gland carcinomas. Br J Cancer 100:623–625
33. Moroni M, Veronese S, Benvenuti S, Marrapese G, Sartore-Bianchi A, Di Nicolantonio F, Gambacorta M, Siena S, Bardelli A (2005) Gene copy number for epidermal growth factor receptor (EGFR) and clinical response to antiEGFR treatment in colorectal cancer: a cohort study. Lancet Oncol 6:279–286
34. Dobashi Y, Watanabe Y, Miwa C, Suzuki S, Koyama S (2011) Mammalian target of rapamycin: a central node of complex signaling cascades. Int J Clin Exp Pathol 4:476–495
35. Chan SK, Hill ME, Gullick WJ (2006) The role of the epidermal growth factor receptor in breast cancer. J Mammary Gland Biol Neoplasia 11:3–11

Virchows Arch (2012) 461:283–290
DOI 10.1007/s00428-012-1290-3

ORIGINAL ARTICLE

Cancer of unknown primary originating from oropharyngeal carcinomas are strongly correlated to HPV positivity

Pamela Zengel · Gerald Assmann · Martin Mollenhauer · Andreas Jung · Karl Sotlar · Thomas Kirchner · Stephan Ihrler

Received: 30 November 2011 / Revised: 2 July 2012 / Accepted: 23 July 2012 / Published online: 2 August 2012
© Springer-Verlag 2012

Abstract Human papillomavirus (HPV)-associated oropharyngeal squamous cell carcinoma (OSCC) has been identified as a distinct entity within squamous cell carcinoma of the head and neck. It is associated with special characteristics and is preponderantly restricted to palatial tonsils and base of tongue. These primary locations have for long been associated with the clinical situation of cancer of unknown primary (CUP). In order to investigate the putative relationship between CUP and HPV, we investigated 26 patients who initially presented as CUP and were finally diagnosed with carcinomas of these two locations. Twenty-one cases proved to be positive for high-risk HPV. Primary carcinomas were small and frequently presented in a submucosal location. HPV-positive carcinomas, presented more often in women, showed atypical basaloid differentiation and correlated to cystic lymph node metastases. This study demonstrates an over-representation of HPV-associated OSCC in patients who were initially diagnosed with CUP. This finding indicates a strong relationship between HPV-association and CUP in OSCC. The frequent manifestation as CUP is presumably caused by the unusual predisposition for small size and submucosal location combined with early lymphatic metastization. In order not to miss clinically occult carcinomas, consequent interdisciplinary cooperation in combination with meticulous histological workup is mandatory.

Keywords HPV · CUP · Oropharyngeal carcinoma · Lymphoepithelial carcinoma · p16

Introduction

The majority of squamous cell carcinomas of the head and neck (HNSCC) are attributable to chronic alcohol and/or tobacco abuse [1, 2]. In the last 10 years, an enormous amount of knowledge has been accumulated regarding the significance of high-risk human papillomavirus (HPV) in oropharyngeal carcinoma [3, 4]. In contrast to HNSCC associated with alcohol and/or tobacco, high-risk HPV-associated oropharyngeal squamous cell carcinoma (OSCC) are characterised by the following typical clinical, histological and molecular aspects: occurrence at younger age on average, frequent absence of classical risk factors, correlation with oral sexual habits, strong predilection for the palatial tonsils and the base of tongue, unusual basaloid or lymphoepithelial histological differentiation instead of squamous differentiation, higher degree of radiosensitivity and overall better survival [5–10].

The multi-step process of infection of squamous epithelial by high-risk HPV involves obligatory contact to the basal membrane, which might be enabled by the reticulated nature

The results were presented at the meeting of the German Society of Pathology in Leipzig 2011.

Pamela Zengel and Gerald Assmann contributed equally to this work.

P. Zengel (✉)
Department of Otorhinolaryngology, Head and Neck Surgery, Grosshadern Medical Center, Ludwig Maximilian University, Marchioninistrasse 15,
81377 Munich, Germany
e-mail: pamela.zengel@med.uni-muenchen.de

G. Assmann · M. Mollenhauer · A. Jung · K. Sotlar · T. Kirchner · S. Ihrler
Institute of Pathology, Ludwig Maximilian University, Munich, Germany

M. Mollenhauer
Institute of Pathology, Technical University of Munich, Munich, Germany

S. Ihrler
Laboratory for Dermatohistology and Oral pathology, Munich, Germany

of the cryptal epithelium [11]. High-risk HPV subtype 16, which affects crucial molecular pathways in squamous cells through its viral oncoproteins E6 and E7 [12], has been identified in about 90 % of these carcinomas [13]. E7 binds to the retinoblastoma protein, leading to a release of the transcription factor E2F which causes an upregulation of p16 in the infected epithelial cells [14, 15]. The resulting immunohistological overexpression of p16 has been suggested as a diagnostically valuable surrogate biomarker of oncogenic HPV infection [16, 17]. A recent Swedish study documents a seven-fold increase of HPV-associated tonsillar carcinoma during the years 1970–2006 [18]. This increased incidence has been primarily attributed to a change in sexual habits [6].

Due to these major differences, in particular in clinical presentation, molecular carcinogenesis and better prognosis, HPV-associated oropharyngeal carcinoma is now regarded as a new entity, distinct from classic alcohol- and tobacco-associated HNSCC [19–21].

In approximately 3–9 % of all metastasized HNSCC, the primary carcinoma cannot be detected despite thorough clinical and radiological examinations that resulted in the clinical situation of cervical cancer of unknown primary (CUP) [22–25]. In many cases following the initial presentation as cervical CUP, the clinically occult primary tumour can finally be detected in the palatinal tonsils, the base of tongue, the nasopharynx or rarely in other locations. Therefore, bilateral tonsillectomy and biopsies in the base of tongue and in the nasopharynx have long been recommended in cases of cervical CUP [23, 26].

The two anatomical regions of palatinal tonsils and of base of tongue, therefore, play a paramount role both in the new entity of HPV-associated OSCC and in the clinical setting of cervical CUP. Regarding the extensive literature accumulated on HPV-associated OSCC, it is remarkable that only few data statistically support association with cervical CUP. In order to investigate this relationship, we decided to study clinical, histological and molecular aspects of 26 consecutive patients who initially presented as cervical CUP and were finally diagnosed with primary carcinomas of the palatinal tonsils and the base of tongue.

Materials and methods

Materials

The retrospective analysis involved 26 patients of the Department of Otorhinolaryngology, Head and Neck Surgery at the Ludwig Maximilian University in Munich, Germany between the years 1994 and 2009 who initially presented with cervical lymph node metastases and occult primary tumours. All patients underwent clinical investigation, computer tomography of the head and neck, thorax and abdomen, and endoscopy of the pharynx, larynx, trachea, bronchi and oesophagus without detection of a primary tumour (cervical CUP). Diagnostic lymph node dissection was performed to confirm the malignancy of the disease. Then, diagnostic tonsillectomy and multifocal biopsies in the base of the tongue and the nasopharynx were performed. Lastly, patients underwent selective or modified radical neck dissection. All cases were included in which a primary carcinoma was finally detected in the palatinal tonsils (n=12) or in the base of tongue (n=14). The tumour specimens were independently reviewed by two expert oral pathologists (GA and SI).

Clinical data from patient files were used to ascertain age, sex, and risk factors associated with tobacco and alcohol. Patient age ranged from 45 to 86 years, with a median of 62, and the gender breakdown consisted of 18 males and eight females. Clinical follow-up was not part of the study objectives.

Methods

Surgical specimens from the tonsils and the base of tongue were completely embedded and processed in serial sections in order to enhance detection of small tumours. The pathological workup consisted of: dominant tumour differentiation as either lymphoepithelial (with abundant intraepithelial lymphocytes), basaloid syn: transitional or squamous; maximum size of the primary tumour and of the largest lymph node metastasis; presence of microscopic involvement of the superficial mucosa and of macroscopic cysts in nodal metastases.

Immunohistological and molecular studies were performed on the primary tumour (in four small tumours, molecular studies had to be performed on the nodal metastases). Tissue sections were immunostained with antibodies against p16, p53, pan-keratin and Ki67 using a Ventana Bench Mark XT and Ventana reagents according to slightly modified standard protocols of the manufacturer [27].

A positive result of p16 immunostaining was defined as strong nuclear and cytoplasmic reaction in the majority of tumour cells and a negative result as none or minor reaction in some scattered tumour cells. HPV was detected and subtyped by E6 nested multiplex polymerase chain reaction, as described elsewhere [28]. Briefly, a nested-PCR assay with degenerate E6/E7 consensus primers and with type-specific primers for the detection and typing of HPV genotypes 6/11, 16, 18, 31, 33, 35, 39, 42, 43, 44, 45, 51, 52, 56, 58, 59, 66 and 68 was performed. Furthermore, all cases were tested for the presence of Ebstein-Barr virus (EBV)-encoded RNA antigen to detect an infection with EBV by in situ hybridization on a Ventana BenchMark XT with Ventana reagents applying Ventana protocols. The significance of experimental data was quantified using the Excel software (Microsoft Corp., Redmond, WA) to calculate Student's t test, Fischer's exact test and odds ratio. For comparative groups in which the unadjusted value of the directly calculated odds ratio was 0 due to a zero size sample; all group values were adjusted by 0.5 to provide a

more meaningful result. In particular, the groups involving no HPV-negative women and no HPV-negative non-smokers were adjusted.

Results

Clinical, (immuno)-histological and molecular data are summarised in Table 1.

Primary tumour

The average size of the primary tumour was 1.1 cm in the tonsils (0.3–2.4 cm) and 0.8 cm in the base of the tongue (0.2–2.2 cm). In 17 of the 26 cases (65 %), the size of the primary tumour was 1.0 cm or less (Figs. 1c and 2a, b). In many cases, serial sectioning and additional immunohistological staining with pan-keratin, p16 and/or Ki67 proved to be helpful or necessary for the detection, especially of small carcinomas

Table 1 Clinical, histological and molecular pathological characterisation of 26 cases of metastasized and initially occult carcinoma (CUP) of palatinal tonsils and base of tongue

No.	Clinical data		LN metastasis			Primary tumour			(Immuno-)histological/molecular analysis			
	Age/sex	Risk factors[a]	Size[b] (in cm)	Kind of nd	Cystic	Localization	Size (in cm)	Infiltration of mucosa	Histological differentiation[c]	HR-HPV PCR[d]	p16 IH[e]	EBV-ISH[f]
1	64 m	yes	4,0	mrnd	No	Tonsil	0.8	No	Basaloid	−	−	−
2	*56 m*	*no*	*4,0*	*mrnd*	*Yes*	*Tonsil*	*0.8*	*No*	*Basaloid*	+	+	−
3	*70 f*	*yes*	*2,8*	*snd*	*Yes*	*Tonsil*	*0.4*	*No*	*Basaloid*	+	+	−
4	*82 f*	*no*	*4,0*	*mrnd*	*Yes*	*Tonsil*	*2.4*	*No*	*Basaloid/squamous*	+	+	−
5	66 m	yes	2,2	snd	No	Tonsil	0,3	No	Basaloid	−	−	−
6	*54 m*	*no*	*6,3*	*mrnd*	*Yes*	*Tonsil*	*0,8*	*No*	*Lymphoepithelial*	+	+	−
7	*64 m*	*yes*	*2,2*	*snd*	*No*	*Tonsil*	*0,3*	*No*	*Lymphoepithelial*	+	+	−
8	*75 m*	*no*	*5,0*	*mrnd*	*Yes*	*Tonsil*	*1,4*	*Yes*	*Basaloid*	+	+	−
9	*49 f*	*no*	*0,5*	*snd*	*No*	*Tonsil*	*2,3*	*Yes*	*Basaloid*	+	+	−
10	*56 f*	*yes*	*1,2*	*snd*	*No*	*Tonsil*	*1,8*	*Yes*	*Basaloid*	+	+	−
11	*65 f*	*no*	*1,3*	*snd*	*No*	*Tonsil*	*0,4*	*No*	*Basaloid*	+	+	−
12	*48 m*	*no*	*3,5*	*snd*	*Yes*	*Tonsil*	*1,5*	*Yes*	*Basaloid*	+	+	−
13	*62 m*	*no*	*2,3*	*snd*	*No*	*Tongue base*	*2,2*	*Yes*	*Basaloid/squamous*	+	+	−
14	*52 m*	*yes*	*2,2*	*snd*	*Yes*	*Tongue base*	*1,6*	*Yes*	*Basaloid*	+	+	−
15	*68 m*	*no*	*2,5*	*snd*	*Yes*	*Tongue base*	*0,3*	*No*	*Basaloid*	+	+	−
16	57 m	yes	4,0	mrnd	Yes	Tongue base	0,5	No	Basaloid	−	−	−
17	*86 m*	*dn*	*3,3*	*snd*	*No*	*Tongue base*	*0,4*	*No*	*Basaloid*	+	+	−
18	62 m	yes	[g]	snd	[g]	Tongue base	0,3	No	Lymphoepithelial	−	−	−
19	50 m	*dn*	2,2	snd	No	Tongue base	0,3	No	Lymphoepithelial	−	−	−
20	*54 m*	*yes*	*2,7*	*snd*	*Yes*	*Tongue base*	*1,2*	*Yes*	*Basaloid*	+	+	−
21	*57 m*	*dn*	*3,3*	*snd*	*Yes*	*Tongue base*	*1,8*	*Yes*	*Basaloid*	+	+	−
22	*78 f*	*no*	*5,5*	*mrnd*	*Yes*	*Tongue base*	*0.5*	*No*	*Lymphoepithelial*	+	+	−
23	*53 m*	*yes*	*3,2*	*snd*	*No*	*Tongue base*	*0.3*	*No*	*Basaloid*	+	+	−
24	*46 f*	*yes*	*1,4*	*snd*	*No*	*Tongue base*	*0.9*	*No*	*Basaloid*	+	+	−
25	*73 f*	*no*	*2,2*	*snd*	*No*	*Tongue base*	*0.4*	*Yes*	*Basaloid*	+	+	−
26	*76 m*	*no*	*2,2*	*snd*	*No*	*Tongue base*	*0.6*	*No*	*Basaloid*	+	+	−

Cases set in italics are tumours with HPV association

m male, *f* female, *LN* lymph node, *dn* data not available

[a] abuse of alcohol and/or tobacco

[b] size of largest lymph node metastasis;

nd neck dissection, *mrnd* modified radical neck dissection, *snd* selective neck dissection

[c] Dominant type of histological differentiation

[d] Detection of high-risk HPV in PCR

[e] Immunohistochemistry for p16

[f] EBV in situ hybridisation

[g] lymph node metastases were extracted outside of our reference

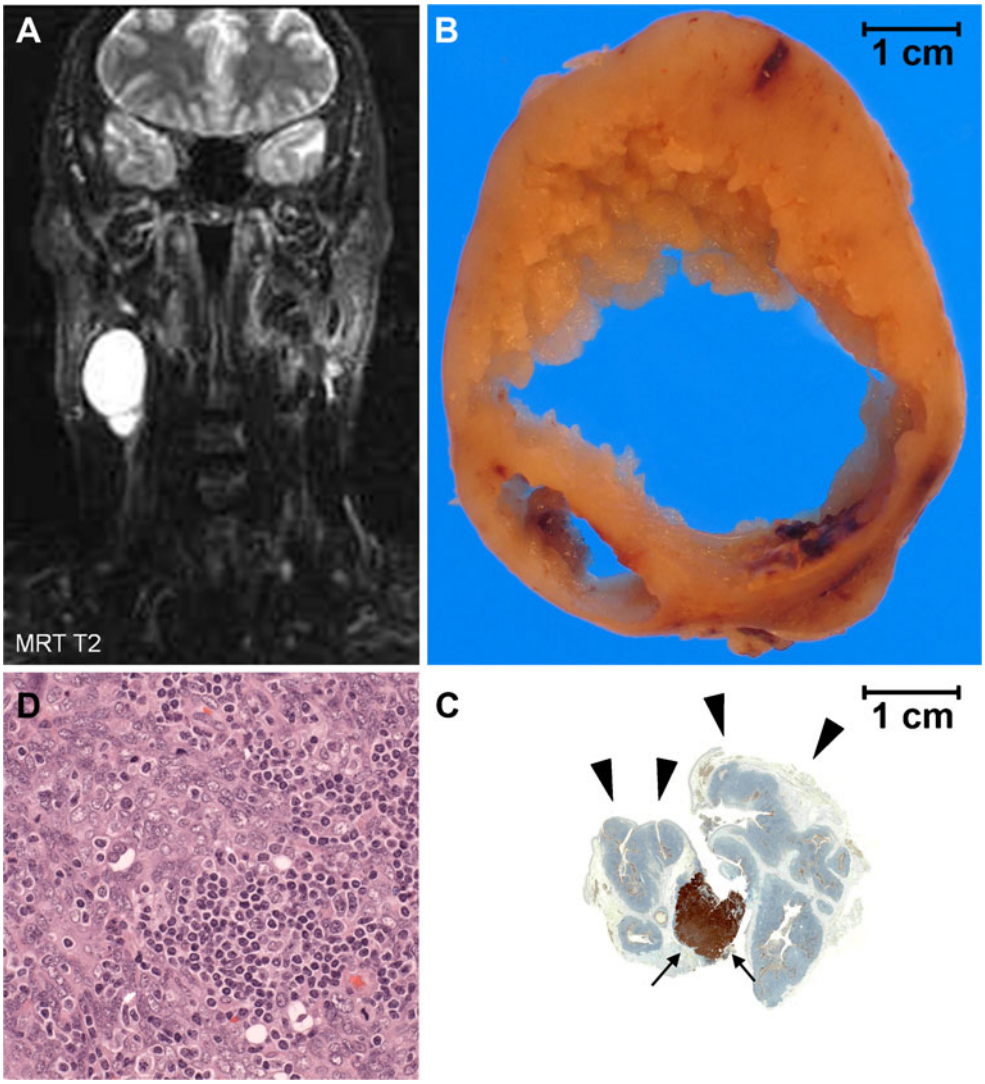

Fig. 1 **a** a 54 year old male patient (case no. 6) with a large cystic cervical lesion in magnetic resonance tomography, T2-weighted image; **b** Macroscopic image of a cystic lymph node metastasis (6.3 cm); **c** Ipsilateral palatial tonsil (*arrowheads*: surface epithelium) with a small, deep and submucosal located HPV-associated carcinoma (p16-positive: *brown*; *arrows*; 0.8 cm; identical magnification to **b**); **d**: Lymphoepithelial histological differentiation of the tonsillar carcinoma

and/or of carcinomas with lymphoepithelial differentiation resembling reticulated cryptal epithelium (Figs. 1c, d and 2b). Eight of the 12 tumours of the tonsils (67 %) and nine of the 14 tumours of the base of tongue (64 %) were completely devoid of infiltration of the superficial mucosa (Figs. 1c and 2a, b).

Histological differentiation revealed a continuum from lymphoepithelial to basaloid and conventional squamous type (usually non-keratinizing), often with a mixture of different patterns (Fig. 3). The quantitatively dominant pattern was lymphoepithelial in 19 %, basaloid in 74 % and squamous in 7 % of the cases.

Lymph node metastases

The average size of the largest lymph node metastasis (2.9 cm; 3.1 cm in tonsillar and 2.7 cm in base of the tongue carcinoma) was significantly larger than the average size of the primary tumours (0.9 cm, $p \leq 0.001$ (tonsils) $p \leq 0.0001$ (base of tongue)). With the exception of only two cases (nos. 9 and 10, Table 1), all lymph node metastases were generally larger than the respective primary tumours (Table 1; Fig. 1). Macroscopic cysts in lymph node metastases were present in 12 of the 26 cases (46 %; 50 % in tonsillar and 43 % in base of the tongue carcinoma; Fig. 1a, b). The spectrum of histological differentiation in the lymph node metastases was equivalent to the spectrum in the primary tumours (Fig. 3). In all cases in which the primary tumour was located in the tonsils, the lymph node metastasis was ipsilateral. In the cases in which the primary tumour was located in the base of tongue, lymph node metastasis was ipsilateral in nine cases and ipsilateral and contralateral in four cases. We performed modified radical neck dissection in seven cases and selective neck dissection in 19 cases.

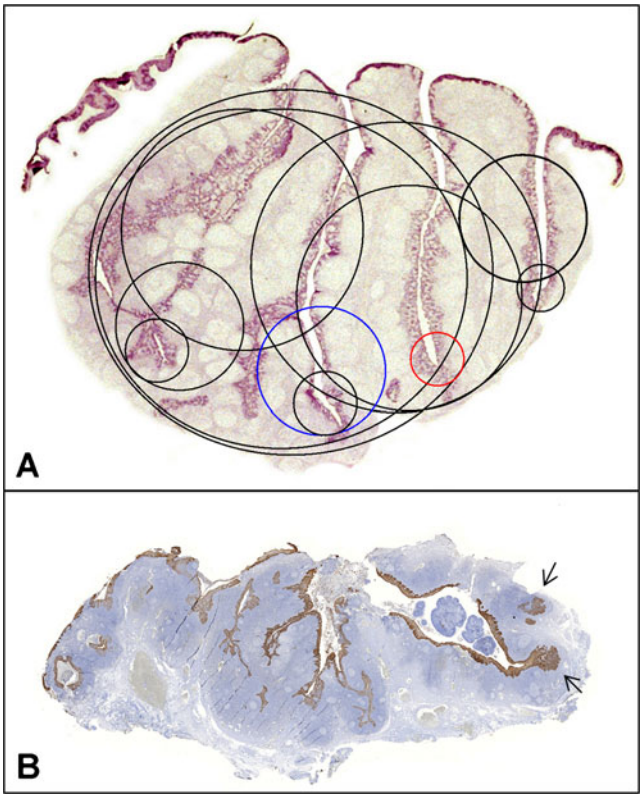

Fig. 2 **a** All ten HPV-positive tonsillar carcinomas are projected onto a regular palatial tonsil (pan-Keratin), corresponding to relative size and topographical location. *Red circle*: case no. 11 (Fig. 2b); *blue circle*: case no. 6 (Fig. 1c). **b** Small HPV-associated carcinoma (case no. 11; 0.4 cm), developing from the base of a tonsillar crypt (*arrows*; pan-Keratin)

Status of HPV and EBV

Twenty-one of the 26 cases (81 %) showed both immunohistological overexpression of p16 and molecular proof of high-risk HPV (83 % in tonsillar and 79 % in base of the tongue carcinoma), whereas 19 % showed negative results for both techniques. Molecular subtyping showed high-risk HPV type 16 in 18 cases, type 33 in two and type 58 in one case. Analysis for EBV (based on in situ hybridization) was negative in all cases (Table 1).

Comparison of tonsillar and base of the tongue carcinomas

Comparing carcinomas from the tonsils and the base of the tongue, no relevant differences were found concerning the average size of the primary tumour or the lymph nodes, the spectrum of histological differentiation or the presence of risk factors or cystic metastases. Whereas base of the tongue carcinomas mostly involved the full thickness of the lymphoepithelial tissue, in seven of the 12 tonsillar carcinomas (58 %), tumours were restricted to the bottom half of the tonsils adjacent to or in direct contact to the crypts (Figs. 1c and 2a, b).

Comparison of HPV status

Both general comparison as well as statistical analysis of HPV status was hampered by the fact that only five of the 26 cases proved to be HPV-negative (two in the tonsils and three in the base of the tongue; Table 1). For this reason, tonsillar and base of the tongue carcinomas were combined for this analysis.

HPV-positive and HPV-negative carcinomas showed a minor difference concerning the average size of the primary tumour (1.1 cm in HPV-positive versus 0.4 cm in HPV-negative carcinomas) but no difference in the average size of the largest lymph node metastasis (2.9 cm in HPV-positive versus 3.1 cm in HPV-negative carcinomas). Both groups showed a comparable spectrum of the histomorphological differentiation.

Relevant differences between HPV-positive and HPV-negative carcinomas were present for the following aspects:

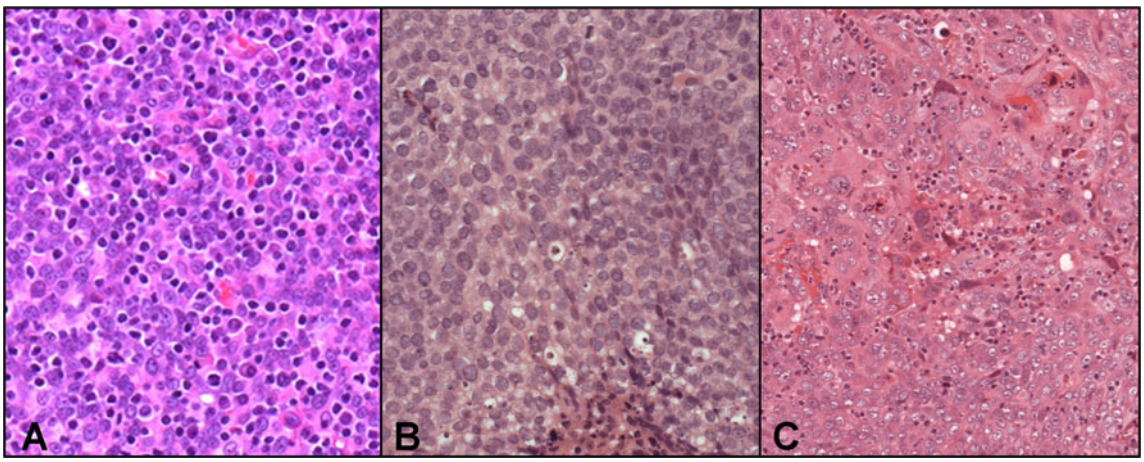

Fig. 3 Atypical, continuous histological spectrum of HPV-associated oropharyngeal carcinoma: Dominance of lymphoepithelial (**a**) and basaloid (**b**) differentiation. Rarely squamous (usually non-keratinizing) differentiation (**c**)

All eight female patients had HPV-positive carcinomas (100 %), whereas thirteen of the 18 male patients had HPV-positive carcinomas (72 %), resulting in an odds ratio of 7.08 (95 %CI) and Fisher's exact test of $p=0.13$. The risk factors tobacco and/or alcohol were present in all five HPV-negative cases (100 %) but only in 32 % of HPV-positive cases, providing an odds ratio of 15 (95 %CI) and p value of 0.03. Cystic nodal metastases were present in 20 % of HPV-negative carcinomas but in 52 % of HPV-positive carcinomas (corresponding to 92 % HPV-positivity in those cases with cystic lymph node metastasis), corresponding to an odds ratio of 3.0 and $p=0.29$.

Discussion

HPV-associated OSCC has been identified as a distinct entity with clinical, histological, molecular, prognostic and therapeutic characteristics that are distinct from classical HNSCC associated with tobacco and/or alcohol [19, 20, 29]. One of these characteristics is the preponderant topographical restriction to the palatinal tonsils and the base of tongue [10, 30]. These two special locations, on the other hand, have for long been known to be the predominant sites of occult primary carcinomas in cases of cervical CUP [24–26]. This parallelism leads to the consideration of whether a causal relationship exists between HPV positivity and cervical CUP. This clinically important question has not been sufficiently investigated in the existing literature.

Correlation between HPV-association and CUP

To the best of our knowledge, this is the first study demonstrating an over-representation of HPV-associated carcinoma in a large cohort of OSCC that presented as cervical CUP. Eighty percent of our 26 CUP cases with subsequent histological detection of occult tonsillar and base of the tongue carcinomas proved to be positive for high-risk HPV in the majority for type 16. This ratio surpasses by far the average rate of HPV-positivity of 51 % (from 39 to 84 %) of HNSCC in these two special sites, independent of CUP [20, 31, 32].

So far, a relationship between HPV-positivity and CUP had only been addressed in the inverse direction by Weiss et al. [33]. Their study demonstrated that 33 % of HPV-associated tonsillar and base of tongue carcinoma clinically presented as cervical CUP, surpassing the reported figures of 3–9 % CUP in HNSCC in general, independent of HPV status [23]. In summary, the data of our study and of the study by Weiss et al. [33] together strongly support a positive relationship between HPV-association and CUP in OSCC. The following aspects contribute to this relationship.

It has been shown that HPV-associated OSCC generally tend to be small, as indicated by a dominance of low pT-stages (pT1/pT2) [18, 31]. However, detailed data on the exact tumour size are lacking. Our investigation demonstrates for the first time that the majority of occult HPV-associated carcinoma in CUP is small or very small in size between 0.3 and 1.0 cm, rendering preoperative clinical or radiological detection of these carcinomas difficult or impossible (Table 1; Figs. 1 and 2).

In parallel, it has been postulated that HPV-associated OSCC develop from basal cells of the reticulated cryptal epithelium as a result of their susceptibility for productive infection with high-risk HPV, analogous to the well-understood situation in the transitional epithelium of the cervix uteri and anorectal zone [32]. Our demonstration of a deep, submucous location of small carcinomas for the most part in contact to basal parts of crypts (Fig. 2) strongly supports this postulated development both in the tonsils and the base of tongue. This pathogenetic development from lymphoepithelial cryptal epithelium correlates to the high rate of basaloid and lymphoepithelial histologic differentiation of these tumours (Figs. 1d and 3).

Unexpectedly for their small size, HPV-associated OSCC are characterised by a high rate of lymph node metastases at the time of clinical diagnosis (65–93 %). In particular, large and cystically transformed lymph node metastases are a strong indicator for HPV-association (92 % in our study) [18, 31]. This strong tendency for early lymphatic metastization, in combination with frequent small size and deep, submucosal location, combines to contribute to the frequent clinical presentation of those carcinomas as cervical CUP, both in the tonsils and the base of tongue. The reasons for the frequent, early and rapid lymphatic metastization remain unclear and necessitate further investigation.

HPV-negative OSCC can, in a minority of cases, also present clinically as cervical CUP with or without cystic lymph node metastases, manifest as small and submucosal tumours and show atypical histological differentiation, all features which appear to be typical for HPV-associated

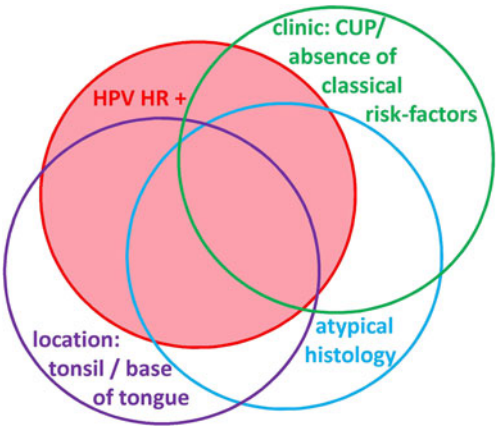

Fig. 4 The entity of HPV-associated oropharyngeal carcinoma is characterised by a variable overlap of typical, however not specific or obligate clinical and histomorphological criteria

HNSCC. As illustrated in Fig. 4, all these criteria are typical and diagnostically important; however, they are neither obligatory nor sufficient for the determination of HPV-association. In this complex clinicopathological constellation, further immunohistological and/or molecular studies are therefore often necessary.

Clinical-pathological algorithm for detection of occult carcinomas

Regarding the special prognostic and therapeutic implications of HPV-associated oropharyngeal carcinoma, their frequent clinical presentation as cervical CUP necessitates a consequent search for any occult primary tumour. In cases of cervical CUP with one or more of these clinical (absence of classical risk factors) and/or histological characteristics (cystic transformation of nodal metastases; atypical histological differentiation), additional immunohistological (p16) and/or molecular studies should be performed in the lymph node metastasis to prove or exclude HPV association. In case of HPV-positivity, a recommendation should be given in the pathology report for diagnostic tonsillectomy and meticulous biopsies in the base of the tongue, as there is a high likelihood that occult primary carcinoma may be situated in one of these two locations. In contrast, HPV-associated carcinoma only rarely develops in the nasopharynx [34].

Regarding the small size and deep location of the majority of these carcinomas, a meticulous histological workup of the surgical specimens is necessary in order not to miss these carcinomas. The palatinal tonsils must be completely embedded, often combined with serial sections. Additional immunohistological staining (keratin, p16, Ki67) can assist in the detection, especially of small carcinomas with lymphoepithelial differentiation, which resemble physiological cryptal epithelium (Figs. 1, 2, and 3a).

This algorithm for a consequent search for occult primary carcinomas demands intense communication between clinicians and pathologists. Deficits in this communication may lead to a failure in detecting occult carcinomas, resulting in a prolonged or life-long situation of cervical CUP, which harbours the risk of insufficient or improper treatment such as overly aggressive adjuvant radiotherapy or ultimately resulting in severe adverse psychological effects.

Summary

This study strongly supports a causal relationship between HPV-associated oropharyngeal carcinoma and the clinical situation of cervical CUP. This relationship is due to the unusually small size of many of these carcinomas in a deep, submucous location, combined with frequent and early lymphatic metastization. Due to the unique prognostic and therapeutic specialities of HPV-associated OSCC and the severe negative psychological consequences resulting from a life-long CUP condition, early and consequent interdisciplinary cooperation is mandatory to effectively detect occult primary tumours.

Acknowledgments This investigation was supported by a grant of "Wissenschaftliches Herausgeberkollegium der Münchener Medizinischen Wochenschrift e.V.", Grant 2007.

Conflict of interest We declare that we have no conflict of interest.

References

1. Williams HK (2000) Molecular pathogenesis of oral squamous carcinoma. Mol Pathol 53(4):165–172
2. Vokes EE, Weichselbaum RR, Lippman SM, Hong WK (1993) Head and neck cancer. N Engl J Med 328(3):184–194. doi:10.1056/NEJM199301213280306
3. Haraf DJ, Nodzenski E, Brachman D, Mick R, Montag A, Graves D, Vokes EE, Weichselbaum RR (1996) Human papilloma virus and p53 in head and neck cancer: clinical correlates and survival. Clin Cancer Res 2(4):755–762
4. Smith EM, Ritchie JM, Summersgill KF, Hoffman HT, Wang DH, Haugen TH, Turek LP (2004) Human papillomavirus in oral exfoliated cells and risk of head and neck cancer. J Natl Cancer Inst 96(6):449–455
5. Ritchie JM, Smith EM, Summersgill KF, Hoffman HT, Wang D, Klussmann JP, Turek LP, Haugen TH (2003) Human papillomavirus infection as a prognostic factor in carcinomas of the oral cavity and oropharynx. Int J Cancer 104(3):336–344. doi:10.1002/ijc.10960
6. D'Souza G, Agrawal Y, Halpern J, Bodison S, Gillison ML (2009) Oral sexual behaviors associated with prevalent oral human papillomavirus infection. J Infect Dis 199(9):1263–1269. doi:10.1086/597755
7. Rosenquist K, Wennerberg J, Schildt EB, Bladstrom A, Goran Hansson B, Andersson G (2005) Oral status, oral infections and some lifestyle factors as risk factors for oral and oropharyngeal squamous cell carcinoma. A population-based case–control study in southern Sweden. Acta Otolaryngol 125(12):1327–1336. doi:10.1080/00016480510012273
8. Frisch M, Biggar RJ (1999) Aetiological parallel between tonsillar and anogenital squamous-cell carcinomas. Lancet 354 (9188):1442–1443. doi:10.1016/S0140-6736(99)92824-6
9. Gillison ML, D'Souza G, Westra W, Sugar E, Xiao W, Begum S, Viscidi R (2008) Distinct risk factor profiles for human papillomavirus type 16-positive and human papillomavirus type 16-negative head and neck cancers. J Natl Cancer Inst 100(6):407–420. doi:10.1093/jnci/djn025
10. Mannarini L, Kratochvil V, Calabrese L, Gomes Silva L, Morbini P, Betka J, Benazzo M (2009) Human Papilloma virus (HPV) in head and neck region: review of literature. Acta Otorhinolaryngol Ital 29(3):119–126
11. Schiller JT, Day PM, Kines RC Current understanding of the mechanism of HPV infection. Gynecol Oncol 118 (1 Suppl): S12–S17. doi:10.1016/j.ygyno.2010.04.004
12. zur Hausen H (1999) Papillomaviruses in human cancers. Proc Assoc Am Physicians 111(6):581–587
13. Klussmann JP, Weissenborn SJ, Wieland U, Dries V, Kolligs J, Jungehuelsing M, Eckel HE, Dienes HP, Pfister HJ, Fuchs PG

(2001) Prevalence, distribution, and viral load of human papillomavirus 16 DNA in tonsillar carcinomas. Cancer 92(11):2875–2884. doi:10.1002/1097-0142(20011201)92:11

14. Andl T, Kahn T, Pfuhl A, Nicola T, Erber R, Conradt C, Klein W, Helbig M, Dietz A, Weidauer H, Bosch FX (1998) Etiological involvement of oncogenic human papillomavirus in tonsillar squamous cell carcinomas lacking retinoblastoma cell cycle control. Cancer Res 58(1):5–13
15. Munger K, Basile JR, Duensing S, Eichten A, Gonzalez SL, Grace M, Zacny VL (2001) Biological activities and molecular targets of the human papillomavirus E7 oncoprotein. Oncogene 20 (54):7888–7898. doi:10.1038/sj.onc.1204860
16. Geisler SA, Olshan AF, Weissler MC, Cai J, Funkhouser WK, Smith J, Vick K (2002) p16 and p53 Protein expression as prognostic indicators of survival and disease recurrence from head and neck cancer. Clin Cancer Res 8(11):3445–3453
17. Klussmann JP, Gultekin E, Weissenborn SJ, Wieland U, Dries V, Dienes HP, Eckel HE, Pfister HJ, Fuchs PG (2003) Expression of p16 protein identifies a distinct entity of tonsillar carcinomas associated with human papillomavirus. Am J Pathol 162(3):747–753
18. Nasman A, Attner P, Hammarstedt L, Du J, Eriksson M, Giraud G, Ahrlund-Richter S, Marklund L, Romanitan M, Lindquist D, Ramqvist T, Lindholm J, Sparen P, Ye W, Dahlstrand H, Munck-Wikland E, Dalianis T (2009) Incidence of human papillomavirus (HPV) positive tonsillar carcinoma in Stockholm, Sweden: an epidemic of viral-induced carcinoma? Int J Cancer 125(2):362–366. doi:10.1002/ijc.24339
19. D'Souza G, Kreimer AR, Viscidi R, Pawlita M, Fakhry C, Koch WM, Westra WH, Gillison ML (2007) Case–control study of human papillomavirus and oropharyngeal cancer. N Engl J Med 356(19):1944–1956. doi:10.1056/NEJMoa065497
20. Klussmann JP, Dinh S, Guntinas-Lichius O, Wittekindt C, Weissenborn S, Wieland U, Dienes HP, Hoffmann T, Smith E, Turek L, Speel EJM, Pfister HJ (2004) HPV-assoziierte Tonsillenkarzinome. Ein Update. HNO 52(3):208–218
21. Klussmann JP, Weissenborn SJ, Wieland U, Dries V, Eckel HE, Pfister HJ, Fuchs PG (2003) Human papillomavirus-positive tonsillar carcinomas: a different tumor entity? Med Microbiol Immunol 192(3):129–132. doi:10.1007/s00430-002-0126-1
22. Begum S, Gillison ML, Ansari-Lari MA, Shah K, Westra WH (2003) Detection of human papillomavirus in cervical lymph nodes: a highly effective strategy for localizing site of tumor origin. Clin Cancer Res 9(17):6469–6475
23. Guntinas-Lichius O, Peter Klussmann J, Dinh S, Dinh M, Schmidt M, Semrau R, Mueller R-P (2006) Diagnostic work-up and outcome of cervical metastases from an unknown primary. Acta Otolaryngol 126(5):536–544
24. Desai PC, Jaglal MV, Gopal P, Ghim SJ, Miller DM, Farghaly H, Jenson AB (2009) Human papillomavirus in metastatic squamous carcinoma from unknown primaries in the head and neck: a retrospective 7 year study. Exp Mol Pathol 87(2):94–98. doi:10.1016/j.yexmp. 2009.04.003
25. Compton AM, Moore-Medlin T, Herman-Ferdinandez L, Clark C, Caldito GC, Wang XI, Thomas J, Abreo FW, Nathan CO (2011) Human papillomavirus in metastatic lymph nodes from unknown primary head and neck squamous cell carcinoma. Otolaryngol Head Neck Surg 145(1):51–57. doi:10.1177/0194599811400385
26. Koch WM, Bhatti N, Williams MF, Eisele DW (2001) Oncologic rationale for bilateral tonsillectomy in head and neck squamous cell carcinoma of unknown primary source. Otolaryngol Head Neck Surg 124(3):331–333. doi:10.1067/mhn.2001.114309
27. Ihrler S, Weiler C, Hirschmann A, Sendelhofert A, Lang S, Guntinas-Lichius O, Arnold G, Zietz C, Harrison JD (2007) Intraductal carcinoma is the precursor of carcinoma ex pleomorphic adenoma and is often associated with dysfunctional p53. Histopathology 51(3):362–371. doi:10.1111/j.1365-2559.2007.02736.x
28. Sotlar K, Diemer D, Dethleffs A, Hack Y, Stubner A, Vollmer N, Menton S, Menton M, Dietz K, Wallwiener D, Kandolf R, Bultmann B (2004) Detection and typing of human papillomavirus by e6 nested multiplex PCR. J Clin Microbiol 42(7):3176–3184. doi:10.1128/JCM.42.7.3176-3184.2004
29. Klussmann JP, Weissenborn SJ, Wieland U, Dries V, Eckel HE, Pfister HJ, Fuchs PG (2003) Human papillomavirus-positive tonsillar carcinomas: a different tumor entity? Med Microbiol Immunol 192(3):129–132
30. Nguyen NP, Chi A, Nguyen LM, Ly BH, Karlsson U, Vinh-Hung V Human papillomavirus-associated oropharyngeal cancer: a new clinical entity. QJM 103 (4):229–236. doi:10.1093/qjmed/hcp176
31. Attner P, Du J, Nasman A, Hammarstedt L, Ramqvist T, Lindholm J, Marklund L, Dalianis T, Munck-Wikland E The role of human papillomavirus in the increased incidence of base of tongue cancer. Int J Cancer 126 (12):2879–2884. doi:10.1002/ijc.24994
32. Syrjanen S (2004) HPV infections and tonsillar carcinoma. J Clin Pathol 57(5):449–455
33. Weiss D, Koopmann M, Rudack C Prevalence and impact on clinicopathological characteristics of human papillomavirus-16 DNA in cervical lymph node metastases of head and neck squamous cell carcinoma. Head Neck 33 (6):856–862. doi:10.1002/hed.21548
34. Lo EJ, Bell D, Woo J, Li G, Hanna EY, El-Naggar AK, Sturgis EM Human papillomavirus & WHO type I nasopharyngeal carcinoma. Laryngoscope 120 Suppl 4:S185. doi:10.1002/lary.21649

Virchows Arch (2012) 461:291–298
DOI 10.1007/s00428-012-1275-2

ORIGINAL ARTICLE

DNA ploidy may be a prognostic marker in stage I and II serous adenocarcinoma of the endometrium

Manohar Pradhan · Ben Davidson · Vera Maria Abeler · Håvard Emil Danielsen · Claes Göran Tropé · Gunnar Balle Kristensen · Björn Åke Risberg

Received: 27 April 2012 / Revised: 11 June 2012 / Accepted: 25 June 2012 / Published online: 24 July 2012
© The Author(s) 2012. This article is published with open access at Springerlink.com

Abstract In patients with serous adenocarcinoma (SAC) of the endometrium, we evaluated the prognostic importance of clinicopathological parameters, DNA ploidy, and immunoexpression of p53, estrogen receptor (ER), progesterone receptor (PR), and Ki-67. In a series of 73 stage I and II SAC, DNA ploidy analysis was performed on hysterectomy specimens using DNA image cytometry. Immunohistochemical analysis of p53, ER, PR, and Ki-67 expression was additionally performed. In the review of the histological slides by three gynecologic pathologists, the presence of a serous component was not agreed upon in 17 (23 %) cases. The remaining 56 cases, consisting of pure SAC or SAC mixed with endometrioid adenocarcinoma, were further analyzed. Tumor recurrence was observed in 14 patients, and 28 patients died during the follow-up period. Patients with diploid (n=19), aneuploid (n=29), and tetraploid (n=8) tumor had 5-year recurrence rates of 10, 38, and 53 %, respectively (p=0.09). A DNA ploidy parameter, 5c exceeding rate, was found to be a prognostic marker for recurrence (p=0.03), progression-free survival (p<0.01), and overall survival (p=0.02). Immunoexpression of p53, ER, PR, and Ki-67 did not have prognostic value, and the same was true for FIGO stage, lymphovascular invasion, the extent of myometrial invasion, and lymphadenectomy. The histological diagnosis of SAC may be difficult in some cases. Established clinicopathological parameters do not seem to be strong prognosticators in stage I and II disease. A DNA ploidy parameter, 5c exceeding rate, may be a prognostic marker in this patient group and should be further validated in larger series.

Keywords Serous adenocarcinoma · Endometrial carcinoma · DNA ploidy · p53 · Estrogen receptor · Progesterone receptor

M. Pradhan · H. E. Danielsen · G. B. Kristensen · B. Å. Risberg
Institute for Medical Informatics, Oslo University Hospital, Oslo, Norway

M. Pradhan · B. Davidson · V. M. Abeler
Department of Pathology, Oslo University Hospital, Oslo, Norway

M. Pradhan · H. E. Danielsen
Center for Cancer Biomedicine, University of Oslo, Oslo, Norway

B. Davidson · C. G. Tropé
The Medical Faculty, University of Oslo, Oslo, Norway

H. E. Danielsen
Department of Informatics, University of Oslo, Oslo, Norway

C. G. Tropé · G. B. Kristensen
Department of Gynecological Oncology, Oslo University Hospital, Oslo, Norway

B. Å. Risberg (✉)
Department of Pathology, The Norwegian Radium Hospital, Oslo University Hospital, Montebello, 0310 Oslo, Norway
e-mail: BRB@ous-hf.no

Introduction

Endometrial carcinoma (EC), the most common gynecological malignancy in the Western world, is considered to be a relatively less aggressive tumor with a good prognosis. Nearly 30 years ago, Lauchlan and Hendrickson et al. recognized a distinct histological type, serous adenocarcinoma (SAC), which has a more aggressive behavior [1, 2]. SAC is a rare tumor accounting for 4–10 % of all EC [3, 4]. SAC usually arises from atrophic endometrium and therefore

occurs in relatively older women [3, 5]. SAC differs from endometrioid adenocarcinoma (EAC) in a number of respects; estrogen receptor (ER) and progesterone receptor (PR), usually present in normal endometrium and EAC, are less frequently expressed in SAC [6]. The mutation of *TP53*, coding for the tumor suppressor p53, is considered to be an early event in SAC as the mutation has been demonstrated in intraepithelial carcinoma [7]. Ki-67, a nuclear protein associated with cell proliferation, is more extensively expressed in SAC compared to EAC [8]. In contrast to EAC, SAC has not been found to be associated with *PTEN* and *KRAS* mutation or microsatellite instability [9]. Recent gene expression studies have demonstrated different profiles in SAC compared to EAC grade 1 and 2 [10]. SAC is associated with DNA aneuploidy, and most of the tumors show a DNA index >1.60 and a higher 5c exceeding rate (5c ExR) than EAC [11].

The incidence of recurrence after primary therapy is higher in SAC than EAC [12, 13]. Furthermore, SAC is more often diagnosed at advanced stage compared to EAC [3]. In spite of its rarity, SAC has been shown to be responsible for 39 % of all EC-related deaths [4]. However, in an accumulated multinational series of 8,033 EC patients, SAC was found in 323 cases (4 %) with 80 % overall 5-year survival in stage I patients [3]. This indicates that a substantial number of SAC patients have a good prognosis, but reliable prognostic indicators are lacking. In the present study, we evaluated the prognostic role of clinicopathological parameters, DNA ploidy, and immunohistochemical markers in stage I and II SAC.

Materials and methods

This is a study of consecutive patients with SAC of the endometrium referred to the Norwegian Radium Hospital from October 1998 to December 2007. Altogether, 215 patients were diagnosed with SAC in the period, out of which 73 stage I and II cases were available for DNA ploidy and histological review in hysterectomy specimen. The specimens were retrieved from the archives of the Department of Pathology. Data regarding FIGO stage (2009), the extent of myometrial invasion, and lymphovascular invasion (LVI) were retrieved from pathological reports. Clinical data were provided by the Department of Gynecologic Oncology. Data on patient death were acquired from the death register of the Central Bureau of Statistics, which is based on the transmitted death certificates by the patient's physician. Simple and radical hysterectomies were performed in 60 and 13 cases, respectively. In 29 patients, infracolic omentectomy was performed. Both pelvic and paraaortic lymphadenectomy were done in 16 cases and only pelvic lymphadenectomy in 26 cases. Twenty-three patients received adjuvant chemotherapy, ten patients received radiotherapy, and five patients received both. Patients with recurrence were treated with chemotherapy (six cases), radiotherapy (five cases), hormonal therapy (one case), both chemotherapy and radiotherapy (two cases), chemotherapy and antihormonal treatment (one case), and all three therapeutic modalities (two cases). Ethical approval for the study was obtained from the Regional Committee for Medical and Health Research Ethics, Southeastern Norway.

Histologic review

All H&E slides from the area from which DNA ploidy and immunohistochemical analysis were performed were independently reviewed by three experienced gynecological pathologists (BD, BR, and VA). The World Health Organization recommendation [14] was used to classify the tumors. Pure SAC and SAC mixed with EAC were entered in the study. Discrepant cases were discussed at a consensus session.

DNA image cytometry

Using thick 50-μm sections from paraffin-embedded blocks from hysterectomy specimens, a monolayer of cells was prepared on a slide. After staining with the Feulgen method, nuclear DNA content was measured indirectly using Ploidy Work Station (Room4, Crowborough, UK). DNA ploidy histograms were created using PWS classifier (Room4, Crowborough, UK). The histograms were classified as diploid, aneuploid (DNA index, DI, 1.06–1.89 and >2.10), tetraploid (DI 1.90–2.10), and polyploid. DNA ploidy-related parameters such as DI, 5c ExR, and 9c exceeding rate (9c ExR) of the tumors were also noted. A detailed description of the procedure, DNA content measurement, and histogram classification criteria are given elsewhere [11].

Immunohistochemistry

From the formalin-fixed, paraffin-embedded tissue blocks of the hysterectomy specimen, 4–5-μm thick sections were cut and stained using a Dako Autostainer. Sections were deparaffinized, and epitopes were unmasked using Dako PT link with high pH buffer for 20 min. Endogenous peroxidase was blocked using EnVision FLEX Peroxidase-Blocking Reagent. The sections were incubated with primary mouse monoclonal antibodies against p53 (1:5,000, Santa Cruz Biotechnology, Inc., Santa Cruz, CA), ER (1:200, Novocastra Laboratories Ltd, Newcastle-upon-Tyne, UK), PR (1:300, Novocastra Laboratories Ltd.), and Ki-67 (1:200, DakoCytomation, Glostrup, Denmark) for

Table 1 Recurrence rate, progression-free survival, and overall survival based on clinical and pathological parameters in patients with stage I and II serous adenocarcinoma

Variables	Categories	Number of patients (%)	Number of recurrence (%)	Number of death (%)	5-year recurrence rate±SE (%)	5-year PFS		5-year OS	
						5-year PFS ±SE (%)	*p* value[a]	5-year OS ±SE (%)	*p* value[a]
Age	<72	28 (50)	6 (21)	9 (32)	26±10	59±11	<0.01	69±10	<0.01
	≥72	28 (50)	8 (29)	19 (68)	32±10	38±11		56±10	
Stage	IA	43 (77)	10 (23)	19 (44)	29±8	52±10	NS	69±8	NS
	IB	8 (14)	1 (13)	5 (63)	17±15	25±20		38±17	
	II	5 (9)	3 (60)	4 (80)	60±22	40±22		40±22	
Myometrial invasion	No invasion	10 (18)	2 (20)	3 (30)	32±21	68±21	NS	90±10	NS
	<Half myometrium	34 (61)	9 (26)	17 (50)	30±9	45±11		60±9	
	>Half myometrium	12 (21)	3 (25)	8 (67)	28±14	38±15		42±14	
Adjuvant therapy	Chemotherapy	19 (34)	6 (32)	8 (42)	40±14	60±14	0.02	78±10	0.04
	Radiotherapy	10 (18)	0	3 (30)	–[b]	79±13		80±13	
	Both	2 (4)	0	0	–[b]	–[b]		–[b]	
	No adjuvant therapy	25 (45)	8 (32)	17 (68)	42±13	22±10		42±10	

PFS progression-free survival, *OS* overall survival, *SE* standard error, *NS* not significant

[a] Overall *p* value by log-rank test

[b] No statistics were computed because all cases were censored

30 min. EnVision FLEX+ Mouse (LINKER) was applied for 15 min for signal amplification. After applying Dako EnVision FLEX+HRP for 30 min, diluted DAB chromogen was applied for 10 min. The slides were counterstained with hematoxylin and mounted. Relevant positive and negative controls were used with each antibody, with satisfactory results. In mixed tumors, expression was scored only in the serous component. Based on percentage of cells showing immunoexpression, slides were scored as negative (0–10 %), weakly positive (11–50 %), and strongly positive (51–100 %).

Statistical analysis

Predictive Analytics SoftWare statistics 18 (SPSS Inc., Chicago, IL) was used for statistical analysis. All statistical tests were two-sided, and p value <0.05 was considered as statistically significant. Progression-free survival (PFS) was calculated from the hysterectomy date to recurrence or 31 March 2009. Both recurrence and death due to any cause were considered as an event for PFS. Overall survival (OS) was calculated from the date of surgery to death or 31 March 2011 using death due to any cause as an event. For survival analysis, median value was used as cutoff for age, 5c ExR, and 9c ExR. The Kaplan–Meier method was used to calculate the 5-year recurrence rate, PFS, and OS. Log-rank test was used for univariate survival analysis.

Results

Histological review

After review and consensus discussion, all three or two of the three pathologists agreed on the SAC diagnosis in 56 cases, which were included in further analyses. We used the reviewed diagnosis as the basis for the present study as it was found to be better in predicting prognosis in EC [15].

Patient characteristics

The median age of patients with SAC was 73 years (mean, 72; range, 56–89 years). There were 43 patients diagnosed at stage IA, 8 at stage IB, and 5 at stage II (Table 1). There was no myometrial invasion in 10 cases, invasion of less than half the myometrial thickness in 34 cases, and more than half in 12 cases. LVI was present in 17 cases. Recurrence was detected in 14 patients, of whom 2 had recurrence in the vagina, 5 in the pelvis, and 7 outside the pelvis. The majority of recurrences occurred in the first year after operation (eight cases); the earliest detected was after 3 months.

Table 2 Recurrence rate, progression-free survival, and overall survival based on DNA ploidy and immunohistochemical markers in patients with stage I and II serous adenocarcinoma

Variables	Categories	Number of patients (%)	Number of recurrences (%)	Number of death (%)	5-year recurrence rate±SE (%)	5-year PFS		5-year OS	
						5-year PFS ±SE (%)	*p* value[a]	5-year OS ±SE (%)	*p* value[a]
DNA ploidy	Diploid	19 (34)	2 (11)	7 (37)	10±7	61±13	NS	71±11	NS
	Aneuploid	29 (52)	8 (28)	15 (52)	38±13	43±12		64±9	
	Tetraploid	8 (14)	4 (50)	6 (75)	53±19	38±17		38±17	
5c ExR[b]	<2.28 %	28 (50)	4 (14)	10 (36)	15±7	58±11	<0.01	66±9	0.02
	≥2.28 %	28 (50)	10 (36)	18 (64)	48±13	39±11		59±10	
9c ExR[b]	<0.07 %	27 (48)	5 (19)	12 (44)	28±10	51±11	NS	65±9	NS
	≥0.07 %	29 (52)	9 (31)	16 (55)	33±11	45±12		59±10	
P53	Negative (≤10 %)	11 (21)	3 (27)	6 (55)	73±13	62±15	NS	82±12	NS
	Weak (11–50 %)	8 (15)	0	2 (25)	–[c]	75±15		75±15	
	Strong (51–100 %)	34 (64)	11 (32)	20 (59)	59±11	34±10		49±9	
ER	Negative (≤10 %)	33 (63)	9 (27)	17 (52)	67±10	40±10	NS	54±9	NS
	Weak (11–50 %)	13 (25)	4 (31)	9 (69)	67±14	54±14		69±13	
	Strong (51–100 %)	6 (12)	1 (17)	1 (17)	83±15	83±15		83±15	
PR	Negative (≤10 %)	38 (73)	7 (18)	20 (53)	80±7	50±10	NS	58±8	NS
	Weak (11–50 %)	12 (23)	6 (50)	7 (58)	35±18	31±16		58±14	
	Strong (51–100 %)	2 (4)	0	0	–[c]	–[c]		–[c]	
Ki-67	Negative (≤10 %)	1 (2)	0	1 (100)	–[c]	–[c]	NS	–[c]	NS
	Weak (11–50 %)	21 (46)	9 (43)	16 (76)	51±12	27±11		47±11	
	Strong (51–100 %)	24 (52)	2 (8)	8 (33)	90±7	74±9		75±9	

PFS progression-free survival, *OS* overall survival, *SE* standard error, *5c ExR* 5c exceeding rate, *9c ExR* 9c exceeding rate, *ER* estrogen receptor, *PR* progesterone receptor, *NS* not significant

[a] Overall *p* value by log-rank test

[b] Median cutoff was used to group the cases

[c] No statistics were computed because all cases were censored

DNA ploidy

The mean and median CVs of the diploid peaks were 3.02 and 2.80, respectively. The mean number of nuclei analyzed was 1,005 (median, 1,192; range, 280–2,546). The majority of tumors (n=29, 52 %) were aneuploid, of which 2 cases had DI≤1.20 and 27 cases had DI> 1.20. Tetraploidy and diploidy were detected in 8 (14 %) and 19 (34 %) tumors, respectively (Table 2). Median 5c ExR was 2.28 (mean, 6.08 %; range, 0–72.82 %). Median 9c ExR was 0.07 (mean, 0.42 %; range, 0–13.76 %).

Immunohistochemistry

Immunohistochemistry was performed in 53 cases for p53, 52 cases for ER and PR, and 46 cases for Ki-67. The majority of tumors (n=34, 64 %) had strong nuclear expression of

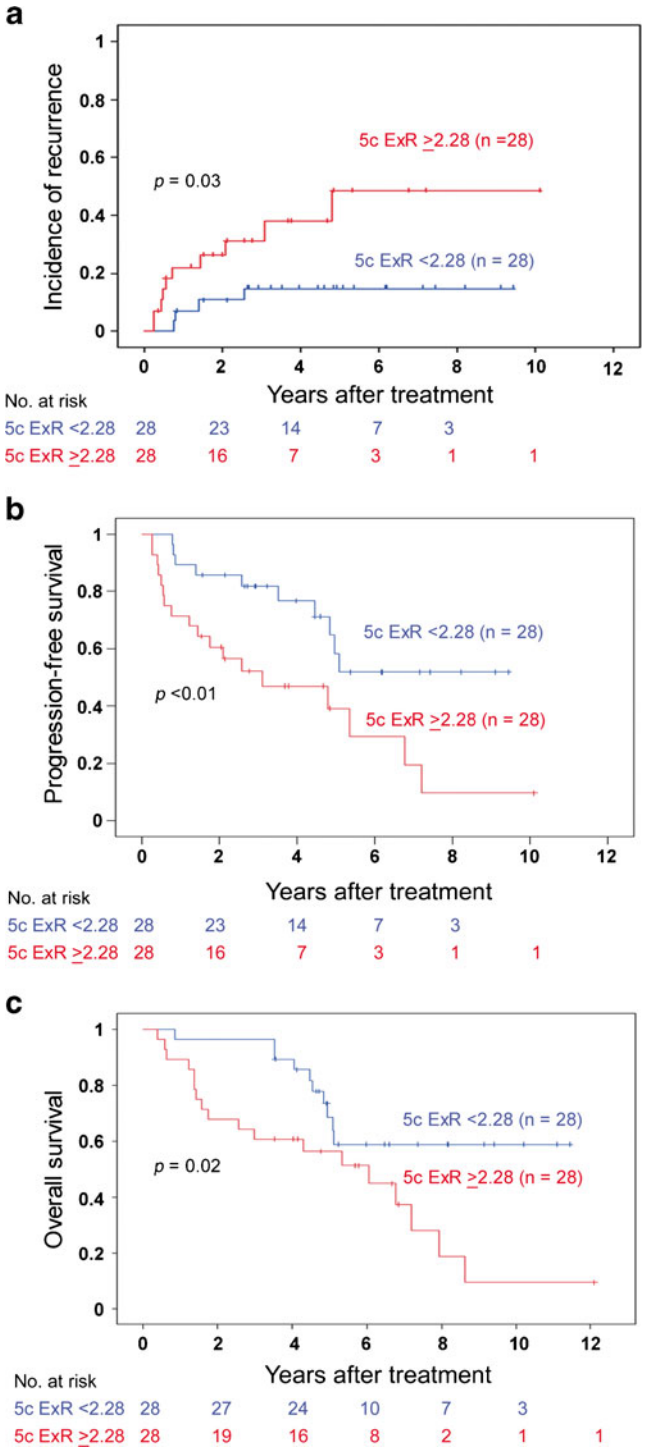

Fig. 1 Recurrence rate, progression-free survival, and overall survival based on 5c exceeding rate in patients with serous adenocarcinoma stage I and II

p53 in >50 % of cells. ER and PR expression in >50 % of cells was found in six (12 %) and two (4 %) tumors, respectively. Ki-67 score >50 % was seen in 24 (52 %) cases (Table 2).

Survival analysis

Altogether, 14 patients had recurrent disease, and 28 patients died during the follow-up period. The 5-year PFS and OS for all cases were 48±9 and 62±7 %, respectively. Patients with aneuploid and tetraploid tumors had a higher recurrence rate and lower 5-year PFS and OS compared to patients with diploid tumors (Table 2). DNA ploidy approached, but did not reach statistical significance for recurrence (p=0.09). A DNA ploidy parameter, 5c ExR, was found to be prognostic for 5-year recurrence rate (p=0.03), PFS (p<0.01), and OS (p=0.02; Table 2, Fig. 1). p53, ER, PR, and Ki-67 expression was unrelated to prognosis. Stage, the extent of myometrial invasion, LVI, lymphadenectomy, and the extent of hysterectomy failed to show prognostic significance (Table 1). Shorter 5-year PFS (22 %) and OS (42 %) were observed for patients who did not receive any form of adjuvant therapy. Notably, patients who received radiotherapy as adjuvant treatment had no recurrences.

Discussion

In this study, we evaluated the prognostic importance of various clinical, pathological, DNA ploidy, and immunohistochemical markers in early-stage SAC. The only significant prognostic marker we found was the 5c ExR, a parameter that can simply be extracted from a DNA ploidy analysis. The explanation is that 5c ExR is high in proliferating tetraploid tumors and aneuploid tumors with high DI. Non-diploid tumors with low S-phase fraction and diploid tumors show low 5c ExR. Therefore, less aggressive non-diploid tumors are separated from highly aggressive tumors. Earlier, Strang et al. reported that 5c ExR is a prognostic parameter in patients with EC [16]. In our previous study, in which exclusively endometrioid carcinoma was analyzed, 5c ExR (1 % as a cutoff) failed to show prognostic importance [13]; however, when the cutoff was changed to 2.28, same as in this series, 5c ExR was a prognostic indicator (unpublished data). Therefore, 5c ExR can be an objective DNA ploidy parameter for patients with endometrial carcinoma. Additionally, 5c ExR has also been found to be a prognostic parameter in other cancers, e.g., non-small cell lung carcinoma, uterine cervical carcinoma, neuroendocrine tumors, and ependymoma [17–20]. There was also a tendency, though not statistically significant, for patients with diploid tumors to have lower recurrence rate and increased overall survival. Kato et al. investigated 30 patients with SAC in all stages and found no association between aneuploidy and survival [21].

SAC is usually diagnosed based on morphology alone. However, some tumors are difficult to classify due to overlapping features between SAC and EAC [22–24]. We

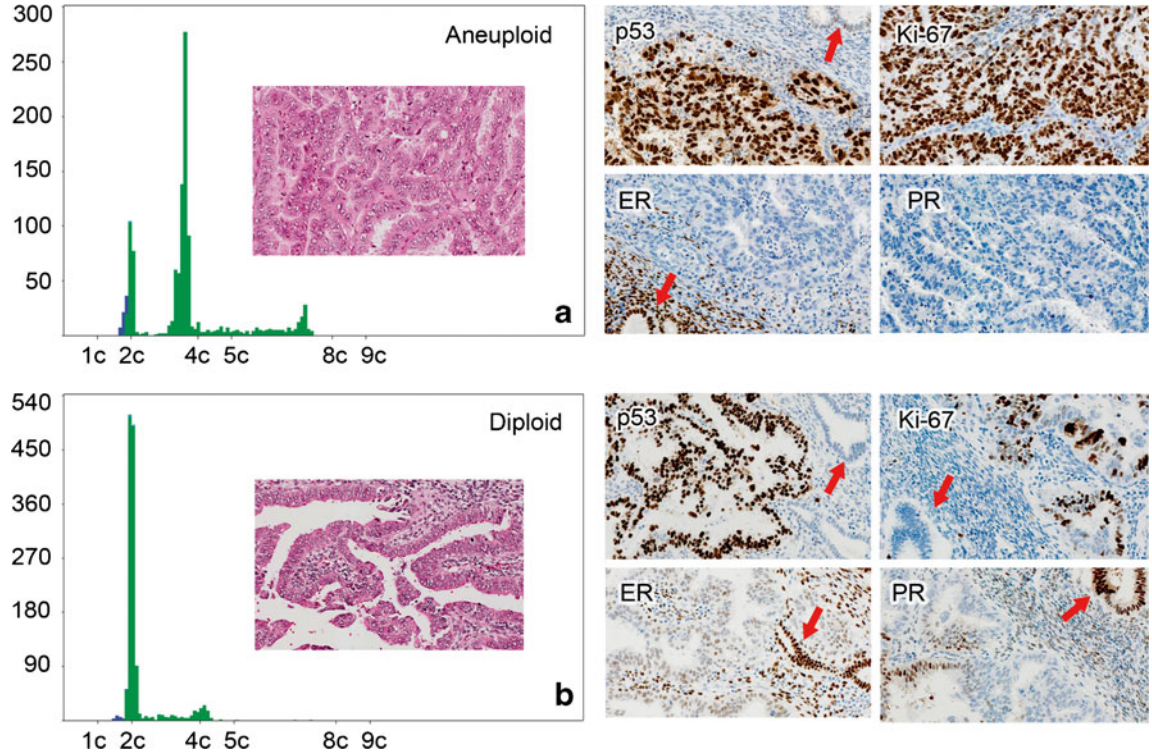

Fig. 2 **a** DNA ploidy histogram of an aneuploid serous adenocarcinoma showing high 5c ExR, strongly positive p53, and Ki-67 expression and negative staining for estrogen and progesterone receptors. **b** A diploid serous adenocarcinoma with low 5c ExR showing strong expression of p53 and Ki-67 and weak expression of estrogen and progesterone receptors. Benign glands are marked with *red arrows*

observed lack of agreement in a substantial number of cases at consensus session. This indicates that SAC, even after being a distinct entity for more than 30 years, is not so easy to diagnose morphologically in a certain number of cases. Nordström et al. reported that 12 % of EC were reclassified as SAC following histological review of 266 cases [25]. The differential diagnosis of SAC included both benign and malignant lesions, including EAC with small non-villous papillae, papillary CAC, and malignant mullerian mixed tumors [26]. Therefore, there is a need for ancillary techniques for SAC diagnosis. Many pathologists use overexpression of p53 and Ki-67 together with underexpression of ER and PR as additional diagnostic aids (Fig. 2). Since SAC is associated with aneuploidy with DI >1.60, DNA ploidy might also be a potential parameter supporting the diagnosis [11]. There are reports on markers such as insulin-like growth factor II mRNA-binding protein 3 which may be useful in this differential diagnosis [27].

In EC, stage, myometrial invasion, and LVI are established prognostic parameters [28]. However, these parameters had no prognostic role in our series. Grade and depth of myometrial invasion did not predict prognosis in SAC in an earlier study, and these tumors are currently not graded [21]. Goff et al. analyzed 50 cases of SAC and similarly found no prognostic importance for the depth of myometrial invasion [29].

p53 mutation is considered to be an early event in SAC since it is found in serous intraepithelial carcinoma [7]. Usually, mutation leads to overexpression of mutant p53 protein which can be detected using immunohistochemistry. However, nonsense mutation leads to total absence of protein expression [30]. Although overexpression of p53 has been reported to be a prognostic factor in EC [31], p53 immunostaining was not informative of disease outcome in the present series of SAC. This finding is similar to the observation by Alkushi et al. where p53 overexpression was not a prognostic indicator in patients with SAC but was of prognostic importance in the analysis of patients with low-grade EAC [32]. p53 expression may be helpful in morphologically ambiguous cases due to the higher rate of overexpression in SAC [22]. ER and PR are expressed in normal endometrial tissue, as well as in the majority of EAC, mainly of low grade. In SAC, ER and PR expression was found to be lower than in EAC [33]. ER and PR expression was unrelated to prognosis in our series. High expression of Ki-67, a proliferation marker, was shown to be associated with poor prognosis in patients with EC [31]. However, Ki-67 had no prognostic value in our series of SAC.

In conclusion, established clinicopathological parameters and immunohistochemical markers do not provide prognostic information for patients in SAC stage I and II with high risk of

recurrence and death of disease. A DNA ploidy parameter, 5c exceeding rate, may be a prognostic marker in this patient group and should be further validated in larger series.

Acknowledgments The authors thank Erika Thorbjørnsen, Signe Eastgate, Jeanne D' Arc Karerwa, and Ellen Hellesylt for their technical assistance in DNA ploidy analysis and immunohistochemistry. Special thanks to Odd Røyne and Yunyong Wang for database management and clinical data entry, respectively. This work was supported by Radium Hospital Foundation.

Conflict of interest The authors declare no conflict of interest.

Open Access This article is distributed under the terms of the Creative Commons Attribution License which permits any use, distribution, and reproduction in any medium, provided the original author(s) and the source are credited.

References

1. Hendrickson M, Ross J, Eifel P, Martinez A, Kempson R (1982) Uterine papillary serous carcinoma: a highly malignant form of endometrial adenocarcinoma. Am J Surg Pathol 6:93–108
2. Lauchlan SC (1981) Tubal (serous) carcinoma of the endometrium. Arch Pathol Lab Med 105:615–618
3. Creasman WT, Odicino F, Maisonneuve P, Quinn MA, Beller U, Benedet JL, Heintz AP, Ngan HY, Pecorelli S (2006) Carcinoma of the corpus uteri. FIGO 26th Annual Report on the Results of Treatment in Gynecological Cancer. Int J Gynaecol Obstet 95 (Suppl 1):S105–S143
4. Hamilton CA, Kapp DS, Chan JK (2008) Clinical aspects of uterine papillary serous carcinoma. Curr Opin Obstet Gynecol 20:26–33
5. Abeler VM, Kjørstad KE (1990) Serous papillary carcinoma of the endometrium: a histopathological study of 22 cases. Gynecol Oncol 39:266–271
6. Halperin R, Zehavi S, Habler L, Hadas E, Bukovsky I, Schneider D (2001) Comparative immunohistochemical study of endometrioid and serous papillary carcinoma of endometrium. Eur J Gynaecol Oncol 22:122–126
7. Sherman ME, Bur ME, Kurman RJ (1995) p53 in endometrial cancer and its putative precursors: evidence for diverse pathways of tumorigenesis. Hum Pathol 26:1268–1274
8. Kallakury BV, Ambros RA, Hayner-Buchan AM, Sheehan CE, Malfetano JH, Ross JS (1998) Cell proliferation-associated proteins in endometrial carcinomas, including papillary serous and endometrioid subtypes. Int J Gynecol Pathol 17:320–326
9. Lax SF (2004) Molecular genetic pathways in various types of endometrial carcinoma: from a phenotypical to a molecular-based classification. Virchows Arch 444:213–223
10. Chen Y, Yao Y, Zhang L, Li X, Wang Y, Zhao L, Wang J, Wang G, Shen D, Wei L, Zhao J (2011) cDNA microarray analysis and immunohistochemistry reveal a distinct molecular phenotype in serous endometrial cancer compared to endometrioid endometrial cancer. Exp Mol Pathol 91:373–384
11. Pradhan M, Abeler VM, Danielsen HE, Tropé CG, Risberg BÅ (2006) Image cytometry DNA ploidy correlates with histological subtypes in endometrial carcinomas. Mod Pathol 19:1227–1235
12. Sood BM, Jones J, Gupta S, Khabele D, Guha C, Runowicz C, Goldberg G, Fields A, Anderson P, Vikram B (2003) Patterns of failure after the multimodality treatment of uterine papillary serous carcinoma. Int J Radiat Oncol Biol Phys 57:208–216
13. Pradhan M, Abeler VM, Danielsen HE, Sandstad B, Tropé CG, Kristensen GB, Risberg BÅ (2012) Prognostic importance of DNA ploidy and DNA index in stage I and II endometrioid adenocarcinoma of the endometrium. Ann Oncol 23:1178–84
14. Silverberg SG, Kurman RJ, Nogales F, Mutter GL, Kubik-Huch RA, Tavassoli FA (2003) Tumours of uterine corpus. In: Tavassoli FA, Devilee P (eds) World Health Organization Classification of Tumours: Pathology and Genetics. Tumours of the breast and female genital organs. IARC Press, Lyon, pp 218–232
15. Baak JP, Snijders W, van Diermen B, van Diest PJ, Diepenhorst FW, Benraadt J (2003) Prospective multicenter validation confirms the prognostic superiority of the endometrial carcinoma prognostic index in international Federation of gynecology and obstetrics stage 1 and 2 endometrial carcinoma. J Clin Oncol 21:4214–4221
16. Strang P, Stenkvist B, Bergström R, Stendahl U, Valdes C, Tribukait B (1991) Flow cytometry and interactive image cytometry in endometrial carcinoma. A comparative and prognostic study. Anticancer Res 11:783–788
17. Grote HJ, Friedrichs N, Pomjanski N, Guhde HF, Reich O, Böcking A (2001) Prognostic significance of DNA cytometry in carcinoma of the uterine cervix FIGO stage IB and II. Anal Cell Pathol 23:97–105
18. Maounis NF, Chorti M, Apostolakis E, Ellina E, Blana A, Aggelidou M, Dritsas I, Markidou S (2006) Prognostic impact of deoxyribonucleic acid (DNA) image analysis cytometry and immunohistochemical expression of Ki67 in surgically resected non-small cell lung cancers. Cancer Detect Prev 30:507–514
19. Onguru O, Ulutin C, Celasun B, Gunhan O (2003) DNA ploidy and nuclear morphometry in adult intracranial ependymomas. Clin Neuropathol 22:266–272
20. Raatz H, Böcking A, Hauptmann S (2004) Prognostic impact of DNA-image-cytometry in neuroendocrine (carcinoid) tumours. Cell Oncol 26:81–88
21. Kato DT, Ferry JA, Goodman A, Sullinger J, Scully RE, Goff BA, Fuller AF Jr, Rice LW (1995) Uterine papillary serous carcinoma (UPSC): a clinicopathologic study of 30 cases. Gynecol Oncol 59:384–389
22. Garg K, Leitao MM Jr, Wynveen CA, Sica GL, Shia J, Shi W, Soslow RA (2010) p53 overexpression in morphologically ambiguous endometrial carcinomas correlates with adverse clinical outcomes. Mod Pathol 23:80–92
23. Faratian D, Stillie A, Busby-Earle RM, Cowie VJ, Monaghan H (2006) A review of the pathology and management of uterine papillary serous carcinoma and correlation with outcome. Int J Gynecol Cancer 16:972–978
24. Murray SK, Young RH, Scully RE (2000) Uterine endometrioid carcinoma with small nonvillous papillae: an analysis of 26 cases of a favorable-prognosis tumor to be distinguished from serous carcinoma. Int J Surg Pathol 8:279–289
25. Nordström B, Strang P, Lindgren A, Bergström R, Tribukait B (1996) Carcinoma of the endometrium: do the nuclear grade and DNA ploidy provide more prognostic information than do the FIGO and WHO classifications? Int J Gynecol Pathol 15:191–201
26. Clement PB, Young RH (2004) Non-endometrioid carcinomas of the uterine corpus: a review of their pathology with emphasis on recent advances and problematic aspects. Adv Anat Pathol 11:117–142
27. Zheng W, Yi X, Fadare O, Liang SX, Martel M, Schwartz PE, Jiang Z (2008) The oncofetal protein IMP3: a novel biomarker for endometrial serous carcinoma. Am J Surg Pathol 32:304–315
28. Abeler VM, Kjørstad KE (1991) Endometrial adenocarcinoma in Norway. A study of a total population. Cancer 67:3093–3103
29. Goff BA, Kato D, Schmidt RA, Ek M, Ferry JA, Muntz HG, Cain JM, Tamimi HK, Figge DC, Greer BE (1994) Uterine papillary serous carcinoma: patterns of metastatic spread. Gynecol Oncol 54:264–268

30. Mineta H, Borg A, Dictor M, Wahlberg P, Akervall J, Wennerberg J (1998) p53 mutation, but not p53 overexpression, correlates with survival in head and neck squamous cell carcinoma. Br J Cancer 78:1084–1090
31. Salvesen HB, Iversen OE, Akslen LA (1999) Prognostic significance of angiogenesis and Ki-67, p53, and p21 expression: a population-based endometrial carcinoma study. J Clin Oncol 17:1382–1390
32. Alkushi A, Lim P, quino-Parsons C, Gilks CB (2002) Markers of proliferative activity are predictors of patient outcome for low-grade endometrioid adenocarcinoma but not papillary serous carcinoma of endometrium. Mod Pathol 15:365–371
33. Alkushi A, Kobel M, Kalloger SE, Gilks CB (2010) High-grade endometrial carcinoma: serous and grade 3 endometrioid carcinomas have different immunophenotypes and outcomes. Int J Gynecol Pathol 29:343–350

Virchows Arch (2012) 461:299–304
DOI 10.1007/s00428-012-1285-0

ORIGINAL ARTICLE

Gliomatosis peritonei is associated with frequent recurrence, but does not affect overall survival in patients with ovarian immature teratoma

Na Ra Yoon · Jeong-Won Lee · Byoung-Gie Kim · Duk-Soo Bae · Insuk Sohn · Chang Ohk Sung · Sang Yong Song

Received: 24 March 2012 / Revised: 2 July 2012 / Accepted: 6 July 2012 / Published online: 21 July 2012
© Springer-Verlag 2012

Abstract Gliomatosis peritonei (GP) is commonly associated with ovarian teratoma and is not thought to have an adverse prognostic effect. However, the prognostic impact and characteristics of GP remain to be clarified. In this study, we investigated the clinicopathologic features of ovarian teratoma associated with GP, and we further compared ovarian immature teratoma (IT) with GP to ovarian IT without GP. During the study period, there were a total of 16 ovarian teratomas associated with GP. Among them, 15 cases were ovarian ITs of various grades. When ovarian IT with GP (n=15) was compared to ovarian IT without GP (n=27), it was found that ovarian IT patients with GP had larger tumor size (median, 19 vs. 13 cm; P<0.001), more frequent recurrence (40 %, 6/15 vs. 3.7 %, 1/27; P=0.005), and frequently elevated preoperative CA-125 level (100 %, 12/12 vs. 50 %, 10/20; P=0.004). All recurrences occurred within 2 years of the initial surgery. Survival curves indicated that ovarian IT patients with GP had significantly shorter recurrence-free survival compared to those without GP (P= 0.002). The 2-year recurrence-free survival rates were 59.3 and 96.3 % in IT with GP and IT without GP, respectively. However, all but one case of IT with GP are currently alive. In conclusion, GP is an adverse prognostic factor characterized by frequent recurrence in patients with ovarian IT.

Keywords Gliomatosis peritonei · Ovarian teratoma · Recurrence · Prognosis

Abbreviations

GP	Gliomatosis peritonei
IT	Immature teratoma
BEP	Bleomycin, etoposide, and cisplatin
GFAP	Glial fibrillary acidic protein

Introduction

Gliomatosis peritonei (GP) is a very rare entity characterized by disseminated implants composed of mature glial tissue in the peritoneal cavity. GP is almost exclusively associated with ovarian teratoma, usually immature teratoma [1–4]. Ovarian teratoma with GP is usually regarded as advanced disease (stage III) [5]. However, GP has long been thought not to have an adverse prognostic effect, and the prognosis of an immature teratoma (IT) with GP is better than would be expected based on grading of the primary tumor [6, 7]. However, the prognostic significance of GP and characteristics of patients with GP have still not been clarified because studies reported in the literature were performed in a small sample or are isolated case reports over a short-term

N. R. Yoon · S. Y. Song (✉)
Department of Pathology, Samsung Medical Center,
Sungkyunkwan University School of Medicine,
50 Ilwon-dong, Gangnam-gu,
Seoul 135-710, South Korea
e-mail: yoda.song@samsung.com

J.-W. Lee · B.-G. Kim · D.-S. Bae
Department of Obstetrics and Gynecology, Samsung Medical Center, Sungkyunkwan University School of Medicine,
Seoul, South Korea

I. Sohn
Samsung Cancer Research Institute,
Seoul, South Korea

C. O. Sung (✉)
Department of Pathology, Asan Medical Center, University of Ulsan College of Medicine,
86 Asanbyeongwon-gil, Pungnap-2 dong, Songpa-Gu,
138-736 Seoul, South Korea
e-mail: co.sung@amc.seoul.kr

follow-up period. In addition, few studies have made a direct comparison of clinicopathologic features between IT with GP and IT without GP. It was recently demonstrated that GP is genetically unrelated to the associated teratoma, but is probably derived from nonteratomatous cells via metaplasia of submesothelial cells [8], and multiple tumors arising in the patients with immature teratomas and GP are independent rather than the result of tumor spread [9]. A few instances of GP have also been associated with growing teratoma syndrome after chemotherapy [4, 10, 11]. These findings suggest a difference in clinicopathologic features between IT with GP and IT without GP.

ITs with GP predominantly affect young women and adolescents. Therefore special consideration for limited surgery is needed. However, there is no standard treatment for GP because of its rarity, and there is debate with regard to whether or not omentectomy should be mandatory. Patients with high-grade (grade 2 or 3 in a three-tiered grading system) IT are most often treated with cisplatin-based chemotherapy after the initial operation. Cisplatin-based chemotherapy regimens have dramatically improved the prognosis of IT [12, 13]. The most common combination chemotherapy regimen is BEP (bleomycin, etoposide, and cisplatin). However, most cases of GP were reported before the BEP protocol was widely used. In addition, the prognostic role of omentectomy has rarely been studied. In this study, we investigated the clinicopathologic features of patients with ovarian teratomas associated with GP and compared the characteristics of ITs with GP to those of ITs without GP in patients who all were uniformly treated at single institution between 1995 and 2010.

Materials and methods

Patients

This study included 16 patients with ovarian teratomas with GP and 27 patients with ovarian ITs without GP who were diagnosed at Samsung Medical Center (Seoul, Korea) between January 1995 and August 2010. No cases were excluded, and all patients were treated uniformly according to the institutional treatment protocol. All high-grade ITs and a few low grade (grade 1) ITs with capsular rupture were treated with chemotherapy (BEP regimen) after initial surgery. ITs were graded according to published guidelines [14]. All cases were staged surgically with or without omentectomy. In patients who did not undergo omentectomy, the diagnosis of GP was made based on multiple omental/peritoneal biopsies that were performed for any suspicious lesions during the operation. Clinicopathologic features were reviewed retrospectively from medical or pathological records. Tumor size was measured in two dimensions using the gross specimen and the largest dimension was used for analysis. The median follow-up period was 2,547 (range, 428 to 6,362) days for ITs with GP, and 2,085 (range, 250 to 4,919) days for ITs without GP.

Recurrence evaluation

During the course of regular follow-up after the initial surgery, newly growing masses detected on radiographs including CT and/or MRI were considered recurrences, but the development of another teratoma in the contralateral ovary was not.

Immunohistochemistry

Surgical specimens were fixed in 10 % buffered formalin and embedded in paraffin. Sections were cut to a thickness of 4 μm, and immunohistochemistry was performed by standard methods using an avidin–biotin complex. Deparaffinized sections were treated with 3 % hydrogen peroxide in order to block endogenous peroxidase activity. Primary antibody against glial fibrillary acidic protein (GFAP; dilution 1:3,000; Biogenex, CA, USA) was used.

Statistical analysis

Various clinicopathologic parameters including age, tumor size, grade, initial surgery (omentectomy), chemotherapy, recurrence, and preoperative CA-125 level were included for analysis. Correlations were examined using either Pearson's χ^2 or Fisher's exact test, as appropriate. Continuous values such as patient age and tumor size were analyzed using the Mann–Whitney U test. Recurrence-free survival and overall survival were measured from the date of initial surgery to the date of first recurrence or death until January 2012. Survival curves were generated using the Kaplan–Meier method, and survival curves were compared using the log-rank test. All tests were two-sided and P values less than 0.05 were considered statistically significant. Statistical analysis was performed using Stata/IC statistical software (version 12, StataCorp Ltd., TX, USA).

Results

Characteristics of ovarian teratoma with GP

During the study period, there were a total of 16 ovarian teratomas associated with GP. The median patient age was 15 years (range, 4 to 38), and the mean tumor size was 19.8 cm (median, 18 cm; range, 15 to 36). Among the 16 ovarian teratomas associated with GP, all but one case were associated with immature teratomas of various grades (grade 1, four cases; grade 2, two cases; grade 3, nine cases). GP was

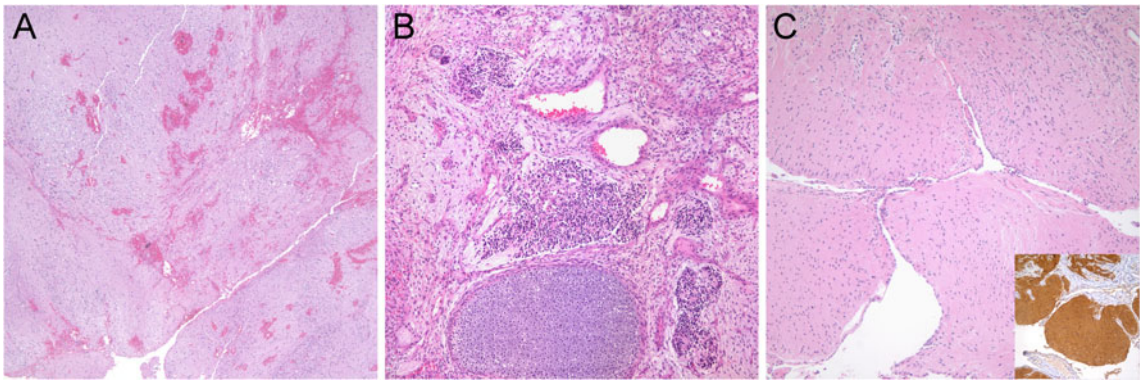

Fig. 1 A recurrent mass composed of mature glial tissue (**a**). Immature teratoma of ovary (**b**) with gliomatosis peritonei (**c**). Strong immunoreactivity for glial fibrillary acidic protein in gliomatosis peritonei (**c**, *inset*)

identified during the initial surgery in 15 of the 16 total patients. In the remaining case, GP was identified during the second operation performed due to a recurrent mass in the abdomen after chemotherapy for grade 3 IT.

During the follow-up period, six patients (37.5 % of 16 patients) experienced a recurrence (diaphragm and/or liver surface in five patients; omentum in one patient). Among them, five patients underwent a second operation, and all recurrent masses were composed of mature glial tissues (Fig. 1a). The remaining patient refused further treatment and died 536 days after the initial diagnosis. Representative figures for ovarian IT with GP are given in (Fig. 1b). GFAP immunostaining highlighted mature glial tissue in the GPs (Fig. 1c).

Clinicopathologic features of IT with GP compared to those of IT without GP

Because almost all cases of GP were associated with IT, we selected ITs without GP diagnosed in the same time period and treated with the same treatment modality for comparative analysis. During the study period, 27 patients were diagnosed with ovarian IT without GP. When the two groups were compared with various clinicopathologic factors, tumor size ($P<0.001$), recurrence rate ($P=0.005$), and preoperative CA-125 elevation ($P=0.004$) were found to differ significantly (Table 1). IT patients with GP had larger tumors (median of 19 cm vs. median of 13 cm), more frequent recurrence (40 %, 6/15 vs. 3.7 %, 1/27), and an elevated preoperative CA-125 level (100 %, 12/12 vs. 50 %, 10/20) compared to IT patients without GP.

We also compared the tumor size in our patients with those in 18 published reports of ovarian ITs with GP (33 cases total) [2–4, 6, 10, 11, 15–24]. The mean tumor size of the 33 previously reported cases was 20.9 cm (median, 21 cm; range, 11.5 to 32). The tumor size of previously reported cases of ovarian IT with GP did not differ from the tumor size in our patients ($P=0.360$), and was significantly larger than the tumor size of ITs without GP that included in this study ($P<0.001$; Fig. 2).

Table 1 Clinicopathologic features of ovarian immature teratomas (ITs) with gliomatosis peritonei (GP) compared to ovarian ITs without GP

	Total no.	IT with GP	IT without GP	*P* value
Age, median	42	13 years (from 4 to 29)	18 years (from 2 to 38)	0.237
Tumor size, median	42	19 cm (from 15 to 36)	13 cm (from 4 to 23)	<0.001
Grade				
Low (grade 1)	14	4 (26.7 %)	10 (37.0 %)	0.495
High (grade 2 or 3)	28	11 (73.3 %)	17 (63.0 %)	
Initial surgery				
With omentectomy	19	8 (53.3 %)	11 (40.7 %)	0.432
Without omentectomy	23	7 (46.6 %)	16 (59.3 %)	
Chemotherapy				
Yes	30	13 (86.7 %)	17 (63.0 %)	0.158
No	12	2 (13.3 %)	10 (37.0 %)	
Relapse				
Yes	7	6 (40.0 %)	1 (3.7 %)	0.005
No	35	9 (60.0 %)	26 (96.3 %)	
Initial CA-125				
Elevated	22	12 (100.0 %)	10 (50.0 %)	0.004
Normal	10	0 (0.0 %)	10 (50.0 %)	

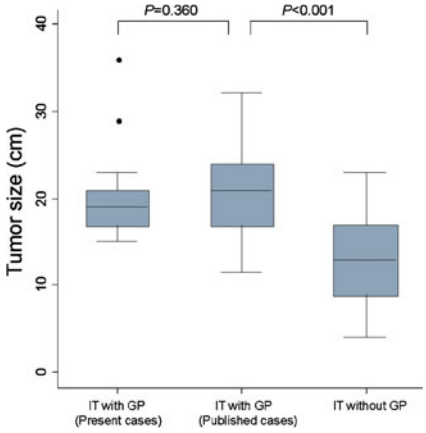

Fig. 2 Tumor sizes of ovarian immature teratoma with gliomatosis peritonei (n=15) and ovarian immature teratoma without gliomatosis peritonei (n=27) in this study were compared with published cases of ovarian immature teratoma with gliomatosis peritonei (n=33). (*IT*, immature teratoma; *GP*, gliomatosis peritonei)

Impact of GP on the survival of patients with ovarian IT

Survival curves for each group (IT with GP vs. IT without GP) differed significantly in terms of recurrence-free survival (P=0.002, Fig. 3a). All recurrences occurred within 2 years of the initial surgery. The 2-year recurrence-free survival rates were 59.3 and 96.3 % in the IT with GP and IT without GP groups, respectively. When the cases were restricted to high-grade IT, there was also a significant difference in recurrence-free survival (P=0.011, Fig. 3b). However, overall survival did not differ between the two groups. All patients with IT without GP survived, and only one IT patient with GP died due to the tumor 536 days after the initial surgery.

Comparison of characteristics between recurring and non-recurring ITs with GP

Various clinicopathologic factors including age, tumor size, grade, initial surgery (omentectomy or not), and chemotherapy after surgery (received or not) were analyzed in order to identify characteristics that differed between patients who experienced recurrence of their IT with GP and those who did not. None of the tested factors differed significantly between the two groups, and omentectomy was not associated with tumor recurrence (P=1.000). Of six patients who experienced a recurrence, half underwent omentectomy, as did 55.5 % of nine patients who did not experience recurrence. Patients with ITs with GP that recurred tended to have larger tumors than patients who did not experience a recurrence; however, this tendency was not statistically significant (P=0.083).

Discussion

In this study, we investigated the clinicopathologic features of ovarian teratoma with GP, and we demonstrated the prognostic impact of GP in patients with IT. GP has long been known for its association with a good outcome [6, 7]. However, in this study, we found that GP was associated with frequent recurrence and shorter recurrence-free survival in patients with IT, although it did not affect overall patient survival.

A recent large study of mature and immature extracranial teratomas in children conducted by the UK Children's Cancer Study Group included 54 ovarian ITs, and reported that 3 of 10 (30 %) patients with ovarian IT with GP experienced a recurrence compared with 2 of 44 (4.5 %) ovarian ITs

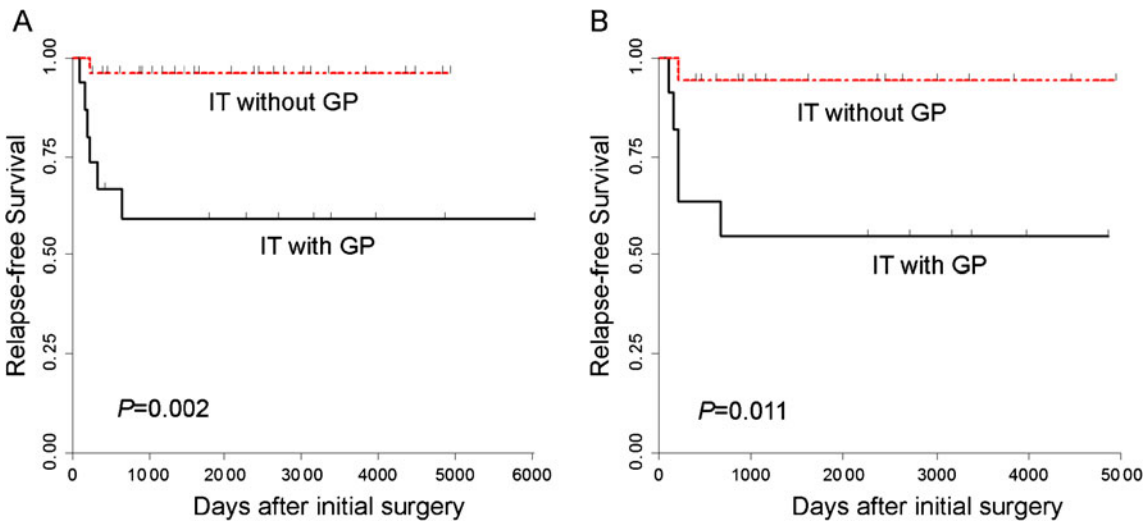

Fig. 3 Recurrence-free survival curves showing the impact of gliomatosis peritonei in all patients with ovarian immature teratomas (**a**) and in patients of ovarian immature teratoma with high-grade (grade≥2) (**b**). (*IT*, immature teratoma; *GP*, gliomatosis peritonei)

without GP (P=0.0389) [5]. They also indicated that there were no deaths among the ovarian teratoma patients. A recent study of 34 immature ovarian teratomas diagnosed at a single institution found that 4 of 34 (12 %) ITs recurred and the 2-year progression-free survival rate was 87.1 % [25], although there was no mention of whether or not GP was included. In the present study, the 2-year recurrence-free survival rate was 59.3 %. Overall, the previous findings strongly suggest that GP is associated with frequent recurrence, and this is confirmed by our series of IT with GP patients, which is the largest study reported to date.

Although GP did not affect overall survival in our series, it was important clinically because frequent recurrence in patients with GP led to a second operation in most cases. In this study, all tumors recurred during chemotherapy or within a short time after chemotherapy. This finding may suggest that at least some of the recurrent GPs were associated with the conversion of a metastatic immature teratoma into a mature tumor as a result of chemotherapy. Therefore, complete removal of the tumor during the initial surgery may be important for preventing recurrence after chemotherapy. However, in this study, most recurrences were found in the liver and/or the diaphragmatic surface. This finding may explain why radical surgery including omentectomy did not prevent recurrence in our study. However, elimination of as many lesions as possible during surgery may be important because a few cases of GP showed adverse outcomes, which were commonly associated with recurrence and malignant transformation, such as glioblastoma [15, 23], and a few recurrences were a form of growing teratoma syndrome [4].

In this study, we compared the IT patients with GP to those without GP in order to identify characteristics unique to IT patients with GP. We found that IT with GP was characterized by larger tumor size as well as frequent recurrence compared to IT without GP. Smaller (<15 cm) ovarian teratomas are usually associated with benign status [26], and tumor size correlates with survival and stage [27]. These findings seem to be consistent with our findings showing that ITs with GP tended to be larger than ITs without GP because IT with GP was usually considered advanced disease. In addition, the elevated CA-125 levels observed in all IT patients with GP may also be related to the presence of a large, widespread tumor.

In conclusion, GP was associated with frequent recurrence and shorter recurrence-free survival in patients with ovarian IT, and ovarian IT with GP was characterized by larger tumor size and frequent elevation of the preoperative CA-125 level. Therefore, identification of GP in ovarian ITs is important and it should be classified as a distinctive entity.

Conflict of interest statement We declare that we have no conflict of interest.

References

1. Chaung JH, Chen L (1992) Ovarian teratoma with gliomatosis peritonei. J Pediatr Surg 27:662–664
2. Hamada Y, Tanano A, Sato M, Tsuji M, Sakaida N, Okamura A, Hioki K (1998) Ovarian teratoma with gliomatosis peritonei: report of two cases. Surg Today 28:223–226
3. Nielsen SN, Scheithauer BW, Gaffey TA (1985) Gliomatosis peritonei. Cancer 56:2499–2503
4. Umekawa T, Tabata T, Tanida K, Yoshimura K, Sagawa N (2005) Growing teratoma syndrome as an unusual cause of gliomatosis peritonei: a case report. Gynecol Oncol 99:761–763
5. Mann JR, Gray ES, Thornton C, Raafat F, Robinson K, Collins GS, Gornall P, Huddart SN, Hale JP, Oakhill A (2008) Mature and immature extracranial teratomas in children: the UK Children's Cancer Study Group Experience. J Clin Oncol 26:3590–3597
6. Robboy SJ, Scully RE (1970) Ovarian teratoma with glial implants on the peritoneum. An analysis of 12 cases. Hum Pathol 1:643–653
7. Stephany JD, Green VS, Gonzalez OR (2004) Pathologic quiz case: an abdominopelvic mass in a 13-year-old adolescent girl. Predominantly mature cystic teratoma with minimal immature neuroglia and gliomatosis peritonei. Arch Pathol Lab Med 128:705–706
8. Kwan MY, Kalle W, Lau GT, Chan JK (2004) Is gliomatosis peritonei derived from the associated ovarian teratoma? Hum Pathol 35:685–688
9. Best DH, Butz GM, Moller K, Coleman WB, Thomas DB (2004) Molecular analysis of an immature ovarian teratoma with gliomatosis peritonei and recurrence suggests genetic independence of multiple tumors. Int J Oncol 25:17–25
10. Hsieh YL, Liu CS (2009) Progression from an immature teratoma with miliary gliomatosis peritonei to growing teratoma syndrome with nodular gliomatosis peritonei. Pediatr Neonatol 50:78–81
11. Mrabti H, El Ghissassi I, Sbitti Y, Amrani M, Hachi H, Errihani H (2011) Growing teratoma syndrome and peritoneal gliomatosis. Case Rep Med 2011:123527
12. Culine S, Lhomme C, Kattan J, Michel G, Duvillard P, Droz JP (1995) Pure malignant immature teratoma of the ovary: the role of chemotherapy and second-look surgery. Int J Gynecol Cancer 5:432–437
13. Williams SD, Blessing JA, Moore DH, Homesley HD, Adcock L (1989) Cisplatin, vinblastine, and bleomycin in advanced and recurrent ovarian germ-cell tumors. A trial of the Gynecologic Oncology Group. Ann Intern Med 111:22–27
14. O'Connor DM, Norris HJ (1994) The influence of grade on the outcome of stage I ovarian immature (malignant) teratomas and the reproducibility of grading. Int J Gynecol Pathol 13:283–289
15. Dadmanesh F, Miller DM, Swenerton KD, Clement PB (1997) Gliomatosis peritonei with malignant transformation. Mod Pathol 10:597–601
16. England RA, deSouza NM, Kaye SB (2007) Gliomatosis peritonei: MRI appearances and its potential role in follow up. Br J Radiol 80:e101–104
17. Harms D, Janig U, Gobel U (1989) Gliomatosis peritonei in childhood and adolescence. Clinicopathological study of 13 cases including immunohistochemical findings. Pathol Res Pract 184:422–430
18. Khan J, McClennan BL, Qureshi S, Martell M, Iyer A, Bokhari SJ (2005) Meigs syndrome and gliomatosis peritonei: a case report and review of literature. Gynecol Oncol 98:313–317
19. Lipskar AM, Rothstein DH, Soffer SZ, Edelman M, Glick RD (2009) Intrathoracic glial implants in a child with gliomatosis peritonei. J Pediatr Surg 44:1817–1820

20. Luesley DM, Monypenny IJ, Fielding JW, Chan KK (1983) Gliomatosis peritonei associated with ovarian teratomas. Case report. Br J Obstet Gynaecol 90:668–670
21. Moukarram H, Chia KV (2006) Conservative treatment of an immature ovarian teratoma with gliomatosis peritonei. J Obstet Gynaecol 26:277–278
22. Muller AM, Sondgen D, Strunz R, Muller KM (2002) Gliomatosis peritonei: a report of two cases and review of the literature. Eur J Obstet Gynecol Reprod Biol 100:213–222
23. Shefren G, Collin J, Soriero O (1991) Gliomatosis peritonei with malignant transformation: a case report and review of the literature. Am J Obstet Gynecol 164:1617–1620, discussion 1620–1611
24. Truong LD, Jurco S 3rd, McGavran MH (1982) Gliomatosis peritonei. Report of two cases and review of literature. Am J Surg Pathol 6:443–449
25. Vicus D, Beiner ME, Clarke B, Klachook S, Le LW, Laframboise S, Mackay H (2011) Ovarian immature teratoma: treatment and outcome in a single institutional cohort. Gynecol Oncol 123:50–53
26. Herbst AL (1992) Neoplastic disease of the ovary. In: Herbst AL, Mishell DR, Stenchever MA, Droegemueller W (eds) Comprehensive gynecology. Mosby Year Book, St. Louis, pp 937–988
27. Norris HJ, Zirkin HJ, Benson WL (1976) Immature (malignant) teratoma of the ovary: a clinical and pathologic study of 58 cases. Cancer 37:2359–2372

Virchows Arch (2012) 461:305–312
DOI 10.1007/s00428-012-1286-z

ORIGINAL ARTICLE

BRCA1-methylated sporadic breast cancers are BRCA-like in showing a basal phenotype and absence of ER expression

Amanjit Bal · Sangeeta Verma · Kusum Joshi · Anuj Singla · Ravi Thakur · Sunil Arora · Gurpreet Singh

Received: 6 April 2012 / Revised: 25 June 2012 / Accepted: 6 July 2012 / Published online: 21 July 2012
© Springer-Verlag 2012

Abstract *BRCA1* mutations have been associated with hereditary breast cancer only. Recent studies indicate that a subgroup of sporadic breast cancer might also be associated with reduction in BRCA1 mRNA levels and protein expression. However, the mechanism of reduced mRNA and protein expression is yet not fully elucidated. This study aims to assess BRCA1 protein expression and the role of *BRCA1* promoter methylation in sporadic breast cancer in North Indian population and to correlate these with known prognostic factors and molecular profiles of breast cancer. BRCA1 protein expression was normal (>50 % tumour cells) in 41 (43 %) cases, reduced (20–50 % tumour cells) in 33 (35 %) cases and absent/markedly reduced (<20 % tumour cells) in 21 (22.1 %) cases. Cases which were negative for BRCA1 protein were more frequently positive for basal markers (29 versus 5 %) and were more often ER-negative (62 versus 39 %) than BRCA1-positive tumours. Methylation of *BRCA1* promoter region was seen in 11/45 cases (24 %). All 11 cases showing *BRCA1* methylation had absent (eight cases) or reduced (three cases) BRCA1 protein expression. BRCA1 protein-negative tumours were more frequently basal marker-positive and ER-negative, highlighting the 'BRCAness' of sporadic breast cancer with loss of BRCA1 protein expression through promoter hypermethylation similar to hereditary breast cancer with BRCA1 mutations. Loss of BRCA1 in sporadic breast cancer suggests that therapeutics targeting BRCA1 pathway in hereditary breast cancer like PARP inhibitors might be used as therapeutic targets for sporadic breast tumours.

Keywords BRCA1 · Sporadic breast cancer · Basal-like breast cancer · Triple negative breast cancer

A. Bal (✉) · S. Verma · K. Joshi · R. Thakur
Department of Histopathology, Post Graduate Institute of Medical Sciences & Research (PGIMER),
Sector 12,
Chandigarh 160012, India
e-mail: docaman5@hotmail.com

A. Singla · S. Arora
Department of Immunopathology, Post Graduate Institute of Medical Sciences & Research (PGIMER),
Sector 12,
Chandigarh 160012, India

G. Singh
Department of General Surgery, Post Graduate Institute of Medical Sciences & Research (PGIMER),
Sector 12,
Chandigarh 160012, India

Introduction

The *BRCA1* gene located on the long (q) arm of chromosome 17 at position 21 belongs to a class of tumour suppressor genes. BRCA1 protein expression controls and regulates cell growth and division. Mutations in BRCA1 gene have been associated with breast and ovarian cancer. The most coherent data on *BRCA1* are available from hereditary breast cancers only. Mutations of *BRCA1* are thought to account for approximately 45 % of families with a significantly high breast cancer incidence and at least 80 % of families with an increased incidence of both early-onset breast and ovarian cancers [1].

Majority of breast cancers are 'sporadic' (non-hereditary). No evidence of *BRCA1* mutations have been found in sporadic breast cancers. However, the demonstration of a

reduction in BRCA1 mRNA levels and methylation of the *BRCA1* promoter region in breast cancer cells compared with normal breast epithelium suggests a potential role of *BRCA1* in sporadic tumours. Decreased BRCA1 mRNA expression is also significantly associated with acquisition of metastatic capacity in sporadic breast cancer [2]. These results indicate that a certain level of normally functioning *BRCA1* is required for the maintenance of negative growth regulatory mechanisms in breast epithelial cells.

In the absence of germline mutations, it has been anticipated that somatic *BRCA1* mutations and allelic imbalance (AI) would be found to contribute to sporadic breast carcinogenesis. Surprisingly, somatic *BRCA1* gene mutations and AI have not been found in sporadic breast tumours [3–5]. For these reasons, the involvement of the *BRCA1* genes in sporadic breast tumours has been questioned. An alternative mechanism for BRCA1 inactivation has been suggested to be gene silencing by epigenetic mechanisms. Hypermethylation of CpG island promoters is known to be strongly associated with gene silencing. Once established, methylation is passed on to daughter cells during DNA replication by the activity of DNA methyltransferases, thereby conserving the overall pattern of methylated CpG islands [6].

A considerable amount of research is going on to elucidate the role of BRCA1 protein expression in sporadic breast tumours; however, there are conflicting results in various studies. In this study, we studied the association of BRCA1 protein expression with known prognostic parameters and the molecular profile of human breast cancer. We also addressed the role of *BRCA1* promoter methylation in decreased protein expression.

Materials and methods

A total of 95 cases of lumpectomies or mastectomies for invasive breast cancer received over a period of 2 years were included in the study. Cases with adequate material (in the form of adequate representative viable tumour in the sections or the specimen) were studied. Cases with family history of breast cancer, those which had been treated by chemotherapy prior to the surgery and those with previous history of lumpectomy followed by mastectomy for residual disease, were excluded.

Morphological examination

All cases were processed for paraffin sections for routine haematoxylin and eosin staining and immunohistochemistry. The histological type, tumour size, nuclear grade, mitoses, in situ component, necrosis, lymphovascular emboli (LVE) and nodal status was noted. A section showing tumour as well as normal mammary gland was selected for immunohistochemical studies.

Immunohistochemistry

The selected sections were cut and mounted on poly-*l*-lysine-coated glass slides. Immunohistochemistry was performed using CK8/18(Novacastra, Clone NCL-5D3, 1:100), CK14 (Novacastra, Clone NCL-LL002, 1:100), CK 5/6 (Dako, Clone D5/16B4, 1:50), ER (Dako, Clone 1D5, 1:20), PR (Dako, Clone PgR636 1:50), Her2/neu (Dako, Polyclonal, 1:250) and BRCA1 (Biocare Medical, Clone MS110, 1:25).

Molecular classification

The cases of invasive breast carcinoma were classified into molecular subtypes using the following immunohistochemical markers: oestrogen receptor (ER), progesterone receptor (PR), Her-2/neu and cytokeratins (CK), CK8/18 for luminal phenotype and CK5/6 and CK4/14 for basal phenotype [7]. For CK 8/18, 5/6 and 4/14, cytoplasmic and membranous immunoreactivity even in 1 % of tumour cells was taken as positive. For oestrogen and progesterone receptors, the intensity of nuclear staining was graded as weak, moderate or strong. Moderate or strong nuclear staining in >10 % tumour cells was taken as positive. Her2/neu immunostaining was considered positive when strong (3+) complete membranous staining was observed in at least 30 % of tumour cells, whereas cases with 0 to 2+ staining were regarded as negative.

BRCA 1 immunostaining

The sections were deparaffinized in xylene and rehydrated in a series of graded alcohol. Blocking of endogenous peroxidase was done for 5 min with Biocare's Peroxidazed 1, and antigen retrieval was performed by heating in a pressure cooker. To block non-specific staining, sections were incubated for 10-15 min at room temperature with background Sniper (Biocare). Incubation with primary antibody was done for 60 min at room temperature followed by incubation with polymer for 30 min and by incubation with biotinylated secondary antibody for 40 min. Di-amino benzidene was used as a chromogen.

BRCA1 methylation

BRCA1 methylation status was assessed in 45 cases. The tumour samples of primary breast cancer patients, who underwent surgery, were collected and stored at −80 °C for further use. DNA was extracted from the frozen

tumour tissues by Qiagen DNeasy Blood & Tissue Kit (Catalog No. 69504) according to the manufacturer's instructions. Final elution was done in 50 μl of elution buffer. The quality and integrity of DNA from tissues was checked by electrophoresis on 0.8 % agarose gel, quantitated spectrophotometrically and stored at −20 °C until further use.

Methylation-specific PCR

As per the protocol provided by the manufacturer, DNA samples (500 ng) were modified with sodium bisulfite that converts the unmethylated cytosine but not the methylated ones to uracil (EZ DNA Methylation-Gold™ Kit, Zymo Research Catalog No. D5005)**.** The bisulfite-treated DNA was amplified using specific primers for methylated and unmethylated alleles. The sequence of the primers was as follows:

Methylated: F: 5′-CCGTGGCAACGGAAAAGCGC -3′, R: 5′-AGCGAGCTCACGCCGCGCAG-3′

Unmethylated: F: 5′-CCGTGGCAACGGAAAAGCGC -3′, R: 5′-AGCGAGCTCACGCCGCGCAG-3′

PCR was carried out in a total volume of 20 μL containing 20 pM of each primer pair, 0.4 μl of 10 mM dNTPs, 0.8 μl of 25 mM $MgCl_2$, 2 μl of 10× Taq buffer and 1.5 U of Taq DNA polymerase (Fermentas). Each PCR reaction underwent initial denaturation at 95 °C for 5 min and 35 cycles of the following profile: 30 s at 95 °C, 30 s at optimal temperature and 1 min at 72 °C followed by a final 10-min extension at 72 °C. Fully methylated DNA (provided with the kit) and DNA from lymphocytes from healthy individuals were used as positive controls for methylated and unmethylated DNA, respectively. A template control without DNA was included in each PCR assay. After amplification, products were electrophoresed using 2.5 % agarose gels, stained with ethidium bromide and visualized under UV illumination.

Statistical analysis

Correlation among variables in the univariate analysis was determined by Pearson chi-square test and Fisher's exact test. Significance was assumed at p value <0.05.

Results

Clinicopathological parameters

The age of the patients (n=95) ranged from 29 to 81 years with a mean of 53.3 years. The majority of cases (55 %) were>50 years and 45 % were below 50 years of age. The largest dimension of the tumour ranged from 1 to 8 cm. Twenty-four percent of tumours were<2 cm (pT1), 73 % of tumours were in the range of 2–5 cm (pT2) and 3 % tumours were greater than 5 cm (pT3) in largest dimensions.

The most frequent histological subtype was infiltrating ductal carcinoma, not otherwise specified (IDC-NOS, 89 cases). There were two cases of invasive lobular carcinoma (ILC), three cases of invasive papillary carcinoma and one case each of mucinous carcinoma and metaplastic carcinoma. The majority of tumours (56 %) were classified as infiltrating ductal carcinoma, NOS grade II, followed by grade III (19 %), and the remaining 14 % of cases were grade I tumours. Both cases of ILC were grade I tumours. One case of invasive papillary carcinoma was classified as grade I and the remaining two cases as grade II. The mucinous carcinoma was a grade I tumour and the metaplastic carcinoma was a grade III tumour. Fifty-two percent of cases did not have axillary lymph node metastasis. In 28 % of cases, there were less than four lymph nodes involved, and in the remaining 20 % cases, more than four lymph nodes were involved. Lymphovascular emboli were seen in five of 17 grade I tumours, 27 of 58 grade II tumours and eight of 20 grade III tumours.

Molecular phenotyping

Based on ER/PR/Her-2 neu expression, 95 cases were categorized into four subgroups [7] (Fig. 1): ER + and/or PR + and HER2− (44 cases), ER + and/or PR + and HER2+ (14 cases), ER − and/or PR − and HER2+ (20 cases) and ER−, PR − and HER2− (triple negative, 17 cases). All cases demonstrated immunoreactivity for the luminal CK8/18. Additionally, 10 % of these tumours showed expression of the basal markers: six cases (6 %) were positive for both CK14 and CK5/6 and four (4 %) were positive for only CK5/6. Out of the 17 triple negative cases, eight were positive for one of the basal markers. The remaining two cases with basal marker expression were Her2 +.

BRCA 1 protein expression

Interpretation of BRCA 1 immunostaining

Staining of normal breast epithelial cells on the tumour sections and/or normal breast tissue sections from the same breast was used as control. BRCA1 expression in the benign epithelial cells in the samples was detected as a strong, dark brown, dotted nuclear stain. No cytoplasmic expression was observed in these cells. BRCA1 expression was also observed in tumour-infiltrating lymphocytes present in the sections. Staining in breast cancer cells was predominantly localized to the nucleus, but the intensity of staining varied from strong to absent.

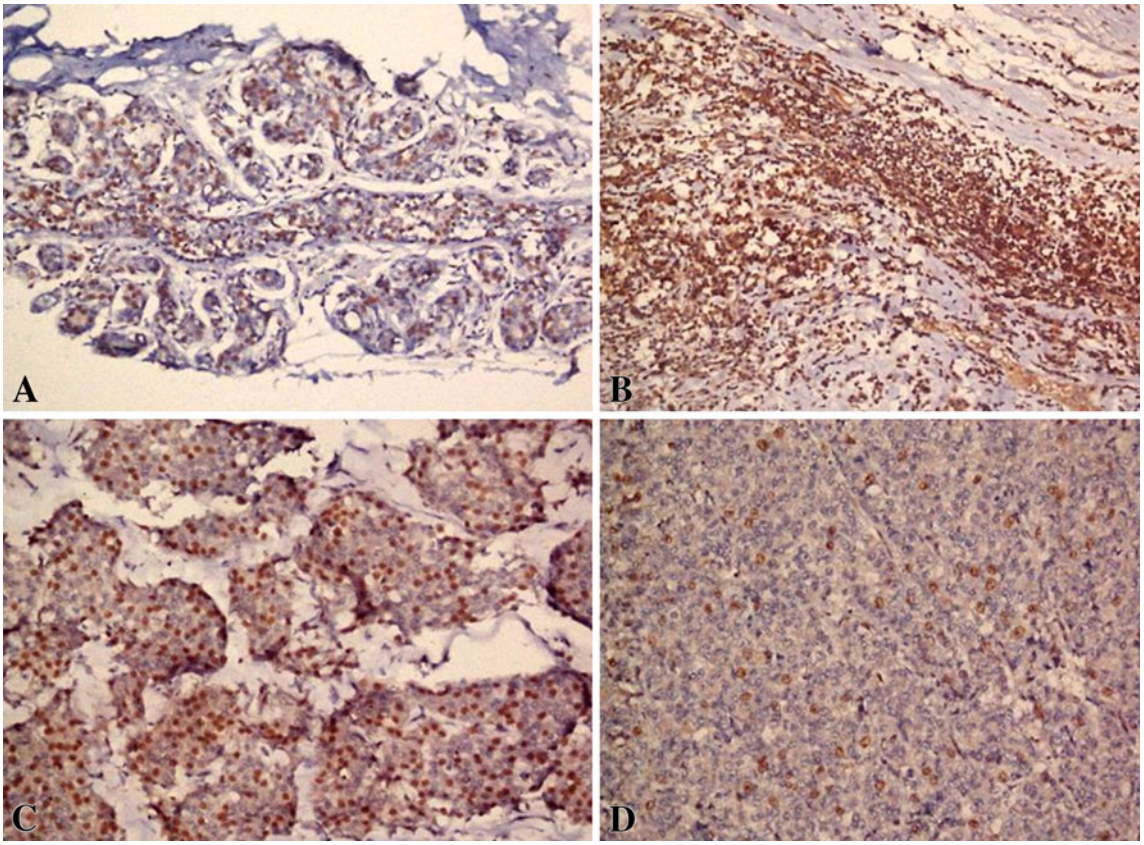

Fig. 1 Photomicrographs showing **a** BRCA1 positivity in normal breast lobule, **b** BRCA1 positivity in lymphocytes, **c** level 3 BRCA1 positivity and **d** level 1 BRCA1 positivity (BRCA1 immunostain)

The protein expression levels in tumour sections were assessed as follows:

Level 3 (normal expression): when the immunoreactivity was comparable to that of the normal breast epithelium or moderate to strong nuclear staining in >50 % of tumour cells

Level 2 (reduced expression): when the staining was clearly weaker than normal surrounding cells or moderate to strong nuclear staining in 20 to 50 % of tumour cells

Level 1 (absent/markedly reduced expression): when there was no staining or weak nuclear staining in <20 % of tumour cells

BRCA1 protein expression was assessed in all 95 cases. BRCA1 protein expression was normal (level 3, >50 % tumour cells) in 41 (43 %) cases; it was reduced (level 2, 20–50 % tumour cells) in 33 (35 %) cases and absent/markedly reduced (level 1, <20 % tumour cells) in 21 (22 %) cases (Fig. 1).

Comparison of BRCA1 protein expression with existing prognostic factors

The level of expression of BRCA1 protein in the tumour samples was compared with existing prognostic factors as depicted in Table 1. BRCA1 staining was not statistically significantly correlated with various histological and clinical prognostic factors. BRCA1 expression was compared in different subtypes of breast cancer; out of 21 cases showing loss of BRCA1 expression, 19 cases were IDC-NOS and one case each of metaplastic carcinoma and invasive papillary carcinoma. Among the BRCA1-negative tumours, 26 % cases were grade III, which is higher than the percentage of BRCA1-positive grade III tumours (19 %). The BRCA1-negative tumours had a higher percentage of basal marker positivity (29 versus 5 %), and this association was statistically significant (p=0.007). BRCA1 nuclear staining correlated with basal marker expression in each grade of tumours; grade III tumours significantly more often showed basal marker expression (p=0.007) as shown in Table 2. None of the grade I tumours expressed basal markers and the association among grade II tumours was not statistically significant (p=0.51 and p=0.49, respectively).

ER-negative status seemed to be more frequent in the BRCA1-negative group as compared to BRCA1-positive group (62 versus 39 %), though this association was not found to be statistically significant (p=0.83).

Table 1 Comparison of BRCA1 protein expression with existing prognostic factors

		BRCA (95 cases)				
		Negative (21)		Positive (74)		*p* value
Size	<2 cm	4	19.0 %	18	24.3 %	0.77
	>2 cm	17	81.0 %	56	75.7 %	
Grade	I	3	14.3 %	14	18.9 %	0.76
	II	12	57.1 %	46	62.2 %	
	III	6	28.6 %	14	18.9 %	
DCIS	Absent	9	42.9 %	35	47.3 %	0.80
	Present	12	57.1 %	39	52.7 %	
LN	No	11	52.4 %	39	52.7 %	0.85
	Yes	10	47.6 %	35	47.3 %	
LVE	Present	10	47.6 %	30	40.5 %	0.62
	Absent	11	52.4 %	44	59.5 %	
ER	Negative	13	61.9 %	29	39.2 %	0.083
	Positive	8	38.1 %	45	60.8 %	
Her-2	Negative	15	71.4 %	47	63.5 %	0.6
	Positive	6	28.6 %	27	36.5 %	
Basal markers	Negative	15	71.4 %	70	94.6 %	0.007
	Positive	6	28.6 %	4	5.4 %	

Methylation of BRCA1 gene and protein expression

Hypermethylation of the *BRCA1* was assayed in 45 primary sporadic breast tumours. Cases were selected with respect to BRCA1 protein expression profile (15 cases with absent BRCA1 protein expression, 15 cases with reduced BRCA1 protein expression and 15 cases with normal BRCA1 protein expression) on immunohistochemistry. Methylation was detected in 11/45 (24 %) tumours. Figure 2 shows methylation-specific PCR (MSP) analysis of breast tumours. Lane 1 shows a 50-bp ladder as molecular weight marker; lanes 2, 3, 5, 9 and 11 show the presence of methylated DNA in tumour. Lane 13 shows a positive methylated DNA control and lane 12 shows a negative control.

Out of these 11 cases showing methylation, eight cases were those without BRCA1 expression (level 1) and three were cases with reduced BRCA1 expression (level 2) (Fig. 3). If level 2 and level 1 BRCA1 expressions are taken together, all cases (100 %) of reduced BRCA1 expression showed BRCA1 promoter methylation. None of the tumours with normal BRCA1 expression on immunohistochemistry was methylated. The association between BRCA1 protein expression and *BRCA1* methylation was found to be statistically significant ($p=0.003$).

Table 2 Comparison between BRCA1 nuclear staining and basal marker expression in each grade of tumours

			CK classification		*p* value
			Luminal	Basal	
BRCA-positive	Grade	I	16/20	0	0.51
		II	42/52	2/3	0.49
		III	12/13	2/7	0.007

Association of *BRCA1* promoter methylation with clinicopathological and immunohistochemical prognostic parameters

A statistically significant correlation was found between *BRCA1* methylation and ER status ($p=0.002$) and with basal marker expression ($p=0.02$) as shown in Table 3. Ninety percent of tumours with *BRCA1* methylation were ER-negative as compared to 35.3 % unmethylated tumours, and this difference was statistically significant. A significant difference was also found in terms of basal marker expression; 36 % of tumours with *BRCA1* methylation expressed one of the basal markers, whereas only 6 % of unmethylated tumours were positive for basal markers. The rest of the parameters did not show any significant association. Patients with *BRCA1* promoter methylated tumours were younger than those with unmethylated tumours (54.5 vs 35.3 %, $p=0.21$) and the majority (81.8 %) of the methylated tumours were of >2 cm in size ($p=0.45$). Another difference between the two groups was a higher frequency of high-grade tumours showing methylation (45.5 vs 17.6 %), though this association was not statistically significant ($p=0.06$).

Triple negative and BRCA1 expression (17 cases)

All the triple negative cases were distributed according to their grade, BRCA1 protein expression and basal marker expression. Among nine cases of grade III, five cases (29.4 %) revealed basal marker positivity, and these cases were also found to be negative for BRCA1 protein expression. One case expressed basal markers as well as BRCA1 protein. Among eight grade II cases, two expressed basal markers, out of which one revealed absent BRCA1 expression. None of the triple negative cases were grade I. Eight TN cases were analysed for BRCA1 methylation, six of which showed methylation.

Discussion

BRCA1 gene is a tumour suppressor gene and is linked with key metabolic processes such as DNA damage repair, regulation of gene expression and cell cycle control. A major function of *BRCA1* is in double-strand break repair by homologous recombination (HR), a DNA repair mechanism that uses the sister chromatid as a template and repairs double-strand breaks in an error-free manner. Deficiencies

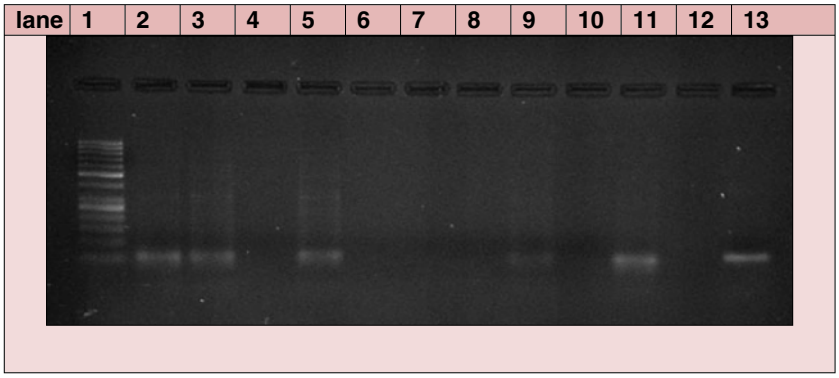

Fig. 2 MSP analysis of BRCA1 promoter region in breast tumours. *Lane 1* shows a 50-bp ladder as molecular weight marker; *lanes 2*, *3*, *5*, *9* and *11* show the presence of methylated DNA in the tumour. *Lane 13* shows positive methylated DNA control and *lane 12* shows the negative control

in homology-directed DNA repair cause high levels of genomic instability that increases the risk of tumorigenesis. Furthermore, *BRCA1* interacts with p53, OCT-/POU2F1 or ZBRK1 and participates in controlling the genes involved in the cell cycle: CDNK1A and GADD45. Alterations of *BRCA1* that impair such functions lead to increased proliferation and chromosomal instability [8].

It has been shown that germline mutations are associated with inherited forms of breast cancer, but somatic mutations are very rare in the sporadic forms of breast cancer. However, several studies demonstrated loss of heterozygosity and a reduced level or absence of *BRCA1* mRNA and protein in a subset of sporadic breast cancer, suggesting that transcriptional and/or posttranscriptional repression of BRCA1 may be involved in the development of sporadic breast cancer [9–11]. One of the common mechanisms of functional inactivation of tumour suppressor genes in cancer cells is aberrant DNA hypermethylation of CpG islands in the promoter region of the gene that is associated with loss of gene expression. Similarities between the morphology and molecular biology of sporadic breast cancers with hypermethylation of *BRCA1* and inherited *BRCA1* breast cancer have led to the concept of 'BRCAness' [12, 13].

Cells with BRCA1 dysfunction are extremely sensitized to the inhibition of poly (ADPribose) polymerase (PARP) enzymatic activity, either alone or when combined with DNA-damaging agents relative to isogenic cells with an intact BRCA pathway. The impairment of base excision repair by PARP inhibitors is highly effective in cells deficient in HR, such as in tumours with loss of BRCA1 function, however, it is not lethal in cells with alternative mechanisms of DNA repair, thus providing a therapeutic opportunity [14, 15]. The model for sensitivity to PARP inhibition is dependent upon HR deficiency rather than inherited BRCA mutation. Therefore, PARP inhibitors might be applicable to sporadic tumours with loss of function of BRCA1 due to hypermethylation or other impairments of the HR pathway.

A few studies have assessed BRCA1 protein expression in sporadic breast cancer using immunohistochemistry [16, 17] In our study, BRCA1 expression was assessed in 95 cases and was found to be normal in 41 (43.1 %) cases, reduced in 33 (38 %) cases and absent/markedly reduced in 21 (22 %) cases. The BRCA1-negative breast cancer had a higher percentage of basal marker positivity (29 versus 5 %). ER-negative status was found to be more frequent in the BRCA1-negative group as compared to the BRCA1-positive

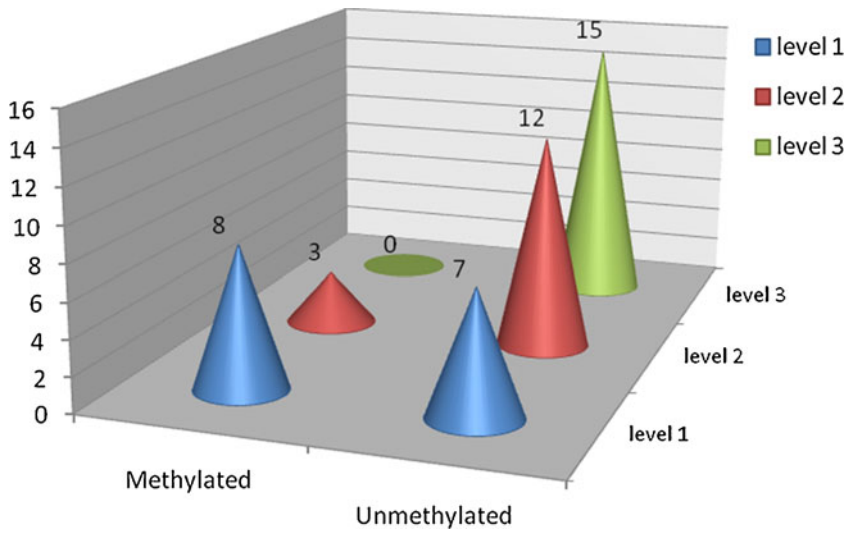

Fig. 3 Association between BRCA1 protein expression and BRCA1 methylation (p=0.003)

Table 3 Association of BRCA1 methylation with clinicopathological and immunohistochemical prognostic parameters

Features		BRCA1 promoter				*p* value
		Methylated (11)		Unmethylated (34)		
Age	<50	6	54.5 %	12	35.3 %	0.21
	>50	5	45.5 %	22	64.7 %	
Size	<2 cm	2	18.2 %	9	26.5 %	0.45
	>2 cm	9	81.8 %	25	73.5 %	
Grade	I	0	0.0 %	9	26.5 %	0.06
	II	6	54.5 %	19	55.9 %	
	III	5	45.5 %	6	17.6 %	
DCIS	Absent	3	27.3 %	19	55.9 %	0.09
	Present	8	72.7 %	15	44.1 %	
LN	No	5	45.5 %	16	47.1 %	0.6
	Yes	6	54.5 %	18	52.9 %	
LV emboli	Present	7	63.6 %	11	32.4 %	0.06
	Absent	4	36.4 %	23	67.6 %	
ER	Negative	10	90.9 %	12	35.3 %	0.002
	Positive	1	9.1 %	22	64.7 %	
Her-2	Negative	7	63.6 %	21	61.8 %	0.6
	Positive	4	36.4 %	13	38.2 %	
Basal markers	Negative	7	63.6 %	32	94.1 %	0.02
	Positive	4	36.4 %	2	5.9 %	

group (62 versus 39 %). Lambie et al. [18] demonstrated a statistically significant inverse correlation between nuclear expression of BRCA1 and histological grade; higher-grade carcinomas were associated with a progressive loss of expression of BRCA1 (p=0.002). In contrast, our study did not demonstrate such inverse relationship with the tumour grade. BRCA1 expression was also compared in different histological subtypes of breast cancer. Lambie et al. [18] also reported a significant association between BRCA1 nuclear expression and the proportion of medullary, atypical medullary and high-grade carcinomas IDC-NOS. However, in our study, cases showing loss of BRCA1 expression were predominantly high-grade IDC-NOS and one case each of metaplastic and invasive papillary carcinoma. There was no case of medullary carcinoma.

Unlike sporadic cancers, where basal-like cancer represents around 15 % of invasive cancers [19, 20], 80–90 % of cancers arising in *BRCA1* germline mutation carriers are of the basal-like subtype [19]. Expression microarray analyses have also indicated strong similarities in gene expression between *BRCA1* familial cancers and sporadic basal-like cancers [21, 22]. This phenotypic overlap has raised the possibility that inactivation of *BRCA1* gene function may also underlie sporadic basal-like cancers and that loss of *BRCA1* gene function may have an etiological role in the development of the basal-like phenotype. Some studies have examined *BRCA1* in unselected sporadic breast cancer, identifying both methylation of the *BRCA1* promoter in 10–15 % of cancers and loss of BRCA1 expression in a number of breast cancers [23, 24]. The incidence of *BRCA1* methylation has appeared to be more common in cancers with a high histological grade and with a triple negative phenotype, suggesting that BRCA1 methylation could underlie basal-like cancers [25]. However, recent studies examining the basal-like subtype specifically have generated conflicting results, and it is presently unclear whether *BRCA1* gene is dysfunctional in these cancers [26]. Data from this study reveal that loss of BRCA1 expression correlates with the expression of basal cytokeratins and thus may play a significant role in the pathogenesis of sporadic basal-like breast tumours.

In breast cancer, more than 40 genes have been shown to be inactivated by methylation, including those involved in DNA repair, cell cycle regulation, tumour suppression, cell adhesion and cell signalling [27–29]. The identification of these methylated genes has significantly contributed to elucidate the molecular pathways which are altered in breast carcinoma and provided potential targets for molecular detection. In this study, *BRCA1* methylation was detected in 24 % of the cases which had absent to reduced BRCA1 protein expression. None of the tumours with normal BRCA1 expression on IHC had methylation of the *BRCA1* promoter. The association between BRCA1 protein expression and *BRCA1* promoter methylation was statistically significant (p=0.003) as was the correlation between *BRCA1* promoter methylation and ER status (p=0.002) and the basal marker expression (p=0.02). In the literature, hypermethylation of the *BRCA1* promoter has been observed in 11–32 % of sporadic breast cancers [30]. It has previously been suggested that *BRCA1*-methylated tumours might phenocopy familial BRCA1 tumours [31]. In support of this notion, we observed the absence of ER expression to be significantly associated with *BRCA1* methylation (p= 0.004), a well-established characteristic of familial BRCA1 tumours. In Indian literature, Mirza et al. [32] reported *BRCA1* to be methylated in 13 of 50 (26 %) tumours. Of these, ten cases were analysed for BRCA1 protein expression and eight showed loss or reduced expression of BRCA1 protein. They also observed the absence of ER expression to be significantly associated with *BRCA1* methylation (p=0.024). From the same centre in India, Raju Bagadi et al. [33] reported *BRCA1* methylation in 15/54 (28 %) cases, which was also associated with lack of ERα expression and nodal metastasis.

Conclusions

This study highlights the role of *BRCA1* gene in sporadic breast cancer. BRCA1 protein-negative tumours showed a

statistically significant association with basal marker expression and ER-negative status, thereby highlighting the 'BRCAness' of sporadic breast cancer with loss of BRCA1 protein expression and promoter hypermethylation similar to hereditary breast cancer with BRCA1 mutations. Loss of BRCA1 in sporadic breast cancer implies that therapeutics targeting the BRCA1 pathway in hereditary breast cancer like PARP inhibitors might also be applicable to sporadic breast tumours.

Conflict of interest The authors declare that they have no financial or non-financial conflict of interests.

References

1. Easton DF, Bishop DT, Ford D (1993) Genetic linkage analysis in familial breast and ovarian cancer: results from 214 families. The Breast Cancer Linkage Consortium. Am J Hum Genet 52:678–701
2. Claus EB, Schildkraut JM, Thompson WD (1996) The genetic attributable risk of breast and ovarian cancer. Cancer 77:2318–2324
3. Futreal PA, Liu Q, Shattuck-Eidens D, Cochran C, Harshman K, Tavtigian S (1994) BRCA1 mutations in primary breast and ovarian carcinomas. Science 266:120–122
4. Lancaster JM, Wooster R, Mangion J et al (1996) BRCA2 mutations in primary breast and ovarian cancers. Nat Genet 13:238–240
5. Johnson SM, Shaw JA, Walker RA (2002) Sporadic breast cancer in young women: prevalence of loss of heterozygosity at p53, BRCA1 and BRCA2. Int J Cancer 98:205–209
6. Herman JG, Baylin SB (2003) Gene silencing in cancer in association with promoter hypermethylation. N Engl J Med 349:2042–2054
7. Kim MJ, Ro JY, Ahn SH et al (2006) Clinicopathologic significance of the basal-like subtype of breast cancer: a comparison with hormone receptor and Her2/neuoverexpressing phenotypes. Hum Pathol 37:1217–1226
8. DeVargas RL, Michor F (2011) Evolutionary dynamics of BRCA1 alterations in breast tumorigenesis. J Theor Biol 273:207–215
9. Valentin MD, da Silva SD, Privat M, Alaoui-Jamali M, Bignon YB (2012) Molecular insights on basal-like breast cancer. Breast Canc Res Treat 2012 Jan 11 [Epub ahead of print]
10. Santarosa M, Maestro R (2012) BRACking news on triple-negative/basal-like breast cancers: how BRCA1 deficiency may result in the development of a selective tumor subtype. Cancer Metastasis Rev 31:131–142
11. Warmoes M, Jaspers JE, Pham TV et al (2012) Proteomics of mouse BRCA1-deficient mammary tumors identifies DNA repair proteins with diagnostic and prognostic value in human breast cancer. Mol Cell Proteomics 2012 Feb 24 [Epub ahead of print]
12. Da Pang, Zhao Y, Xue W et al (2011) Methylation profiles of the BRCA1 promoter in hereditary and sporadic breast cancer among Han Chinese. Med Oncol 2011 Nov 11 [Epub ahead of print]
13. Ibragimova I, Cairns P (2011) Assays for hypermethylation of the *BRCA1* gene promoter in tumor cells to predict sensitivity to PARP-inhibitor therapy. Meth Mol Biol 780:277–291
14. Jaspers JE, Rottenberg S, Jonkers J (2009) Therapeutic options for triple negative breast cancers with defective homologous recombination. Biochim Biophys Acta 1796:266–280
15. Tutt A, Robson M, Garber JE et al (2010) Oral poly(ADP-ribose) polymerase inhibitor olaparib in patients with BRCA1 or BRCA2 mutations and advanced breast cancer: a proof of-concept trial. Lancet 376:235–244
16. Taylor J, Lymboura M, Pace PE et al (1998) An important role for BRCA1 in breast cancer progression is indicated by its loss in a large proportion of non-familial breast cancers. Int J Cancer 79:334–342
17. Rakha EA, El-Sheikh SE, Kandil MA et al (2008) Expression of BRCA1 protein in breast cancer and its prognostic significance. Hum Pathol 39:857–865
18. Lambie H, Miremadi A, Pinder SE et al (2003) Prognostic significance of BRCA1 expression in sporadic breast carcinomas. J Pathol 200:207–213
19. Nielsen TO, Hsu FD, Jensen K (2004) Immunohistochemical and clinical characterization of the basal-like subtype of invasive breast carcinoma. Clin Cancer Res 10:5367–5374
20. Abd El-Rehim DM, Pinder SE, Paish CE (2004) Expression of luminal and basal cytokeratins in human breast carcinoma. J Pathol 203:661–671
21. Foulkes WD, Ingunn MS, Chappuis PO et al (2003) Germline BRCA1 mutations and a basal epithelial phenotype in breast cancer. J Natl Cancer Inst 95:19
22. Singha AK, Pandey A, Tewarib M, Shukla HS, Pandey HP (2011) Epigenetic silencing of BRCA1 gene associated with demographic and pathologic factors in sporadic breast cancer: a study of an Indian population. Eur J Cancer Prev 20:478–483
23. Ben GR, Hachana M, Ziadi S et al (2011) Contribution of epigenetic alteration of BRCA1 and BRCA2 genes in breast carcinomas in Tunisian patients. Canc Epidemiol Oct 4, (Epub ahead of print)
24. Jones PA, Baylin SB (2002) The fundamental role of epigenetic events in cancer. Nat Rev Genet 3:415–428
25. Birgisdottir V, Stefansson OA (2006) Epigenetic silencing and deletion of the BRCA1 gene in sporadic breast cancer. Breast Cancer Res 8:R38
26. Foulkes WD, Stefansson IM, Chappuis PO et al (2003) Germline BRCA1 mutations and a basal epithelial phenotype in breast cancer. J Natl Cancer Inst 95:1482–1485
27. Esteller M (2002) CpG island hypermethylation and tumor suppressor genes: a booming present, a brighter future. Oncogene 21:5427–5440
28. Baylin SB, Ohm JE (2006) Epigenetic gene silencing in cancer: a mechanism for early oncogenic pathway addiction? Nat Rev Cancer 6:107–116
29. Esteller M, Silva JM, Dominguez G, Bonilla F, Matias-Guiu X, Lerma E (2000) Promoter hypermethylation and BRCA1 inactivation in sporadic breast and ovarian tumors. J Natl Cancer Inst 92:564–569
30. Xu CF, Brown MA, Chambers JA et al (1995) Distinct transcription start sites generate two forms of BRCA1 mRNA. Hum Mol Genet 4:2259–2264
31. Catteau A, Morris JR (2002) BRCA1 methylation: a significant role in tumour development? Semin Cancer Biol 12:359–371
32. Mirza S, Sharma G, Prasad CP et al (2007) Promoter hypermethylation of TMS1, BRCA1, ERα and PRB in serum and tumor DNA of invasive ductal breast carcinoma patients. Life Sci 81:280–287
33. Raju Bagadi SA, Prasad CP, Kaur J et al (2008) Clinical significance of promoter hypermethylation of RASSF1A, RARβ2, BRCA1 and HOXA5 in breast cancers of Indian patients. Life Sci 82:1288–1292

Virchows Arch (2012) 461:313–322
DOI 10.1007/s00428-012-1289-9

ORIGINAL ARTICLE

Keratin expression in breast cancers

Mu-Min Shao · Siu Ki Chan · Alex M. C. Yu · Christopher C. F. Lam · Julia Y. S. Tsang · Philip C. W. Lui · Bonita K. B. Law · Puay-Hoon Tan · Gary M. Tse

Received: 7 March 2012 / Revised: 28 May 2012 / Accepted: 23 July 2012 / Published online: 1 August 2012
© Springer-Verlag 2012

Abstract Cytokeratin (CK) immunohistochemistry can play an important role in breast carcinoma evaluation. We evaluated the expression of a panel of commonly used CKs in a large cohort of breast cancers and assessed its correlation with other biomarkers and breast cancer subtypes. Expression of CK7, CK8, CK18 and CK19 was observed in more than 90 % of all breast carcinomas in this study, confirming their efficacy in immunohistochemical identification of breast cancer. A combination of CK8 and CK7 gave the highest sensitivity for detection of a minute number of breast cancer cells. Expression of other CKs, including CK5/6, CK14 and CK20, correlated positively with high tumour grade. The expression of CK5/6 and CK14 in a significant number of high-grade tumours raised concern regarding the use of absence of their expression to identify breast carcinoma. For identification of the basal subtype, CK5/6 gave a higher detection rate than CK14. CK20 expression was found more frequently than reported in previous studies, might constitute an indicator of poor prognosis and may be associated with the molecular apocrine subtype. This study highlights the diagnostic and prognostic relevance of the unique CK expression patterns in breast cancer.

Keywords Breast cancer · Cytokeratin · Immunohistochemistry · CK20

M.-M. Shao
Department of Pathology, Shenzhen Affiliated Hospital, Guangzhou University of Traditional Chinese Medicine, Shenzhen, China

S. K. Chan
Department of Pathology, KwongWah Hospital, Hongkong, Hong Kong

A. M. C. Yu · C. C. F. Lam · J. Y. S. Tsang · G. M. Tse
Department of Anatomical and Cellular Pathology, Prince of Wales Hospital, The Chinese University of Hong Kong, Hongkong, Hong Kong

P.-H. Tan
Department of Pathology, Singapore General Hospital, Singapore, Singapore

P. C. W. Lui
Department of Pathology, Union Hospital, Hongkong, Hong Kong

B. K. B. Law
Breast Center, Union Hospital, Hongkong, Hong Kong

G. M. Tse (✉)
Department of Anatomical and Cellular Pathology, Prince of Wales Hospital,
NganShing Street, Shatin,
Hongkong, Hong Kong
e-mail: gmktse@gmail.com

Introduction

Immunohistochemical assessment of members of the cytokeratin (CK) family has been used in the histopathological evaluation of breast carcinoma. CKs constitute two of the six types of intermediate filaments in mammalian cells (the other four are desmin, vimentin, glial fibrillary acidic protein (GFAP) and neurofilament). Twenty different types have been identified: CK 1 to 20 [1, 2]. They can be subgrouped into a high molecular weight and a low molecular weight subgroup, or into acidic or basic types based on their isoelectric points. In general, CK9 to CK20 are called type I CKs, whereas CK1 to CK8 are called type II CKs. Type I CKs are encoded on chromosome 17q whereas type II CKs are encoded on chromosome 12q [3–6].

In normal breast tissue, CK5 and CK14 are expressed in myoepithelial cells. CK7, CK8, CK18 and CK19 are expressed in the ductal epithelium. CK20 is not detectable

in breast epithelium [7]. During the development of malignancy, the original CK profile of the cell is frequently retained. As a result, different types of breast cancers are sometimes characterized according to a purported cell of origin within the breast, based on differential CK expression patterns.

In current practice, evaluation of CK profiles is used for the detection of small tumour foci in sentinel lymph nodes or other metastatic sites [8, 9]. Cytokeratin expression is also helpful in differentiating between specific breast cancer subtypes [10–16], and as prognostic indicator [17–20]. Despite extensive analysis of expression of individual CK's in breast cancer, only a few large studies have been published on the use of CK panels. Immunohistochemical studies on large case series have shown the added value of assessing the expression of combinations of biomarkers rather than individual markers [21]. As CK expression is important in the differential diagnostic workup of breast cancer and given its heterogeneity, a thorough evaluation of CK expression in different breast cancer subtypes is essential. This should be based on a large cohort, allowing accurate analysis of even less common subtypes and cancers showing low CK expression. In the present study, the correlation between the expression of various CKs, other important biomarkers and histological and molecular subtypes, was analysed.

Materials and methods

Patient data

The histological files of two of the involved institutions were searched for breast carcinomas over periods of 3 and 7 years, respectively. All cases for which excision specimens were available were included. Haematoxylin and eosin (H&E)-stained 4-μm slides of the corresponding tumour blocks were reviewed by two of the authors. The diagnosis and histotypes were confirmed using the WHO criteria [22], and the tumours were graded according to Bloom and Richardson [22]. Patient details and clinical information including patient age and lymph node involvement were retrieved from medical records.

Tissue microarray construction

Cellular areas of the tumours were selected and marked on the H&E slides, and sampled for tissue microarray (TMA) construction. Two to three 1.5-mm-tissue cores were obtained from paraffin blocks of each case, depending on tumour cellularity. The TMAs were assembled with a tissue arrayer (Beecher Instruments, Silver Springs, MD). Forty-one composite TMA blocks, each containing up to 54 tissues cores, were constructed. Serial 4-μm sections were cut onto Superfrost Plus glass slides (Menzel-Glaser, Germany). One section from each tissue array block was stained with H&E and reviewed to confirm that representative tumour samples were included in the TMA blocks.

Immunohistochemistry and scoring

TMA slides were subjected to immunohistochemical staining for CKs and other biomarkers. The biomarker panel included antibodies against ER, PR, HER2, Ki-67, p63, c-Kit, chromogranin (CG), synaptophysin (Syn) and EGFR. The CK panel included CK5/6, CK7, CK8, CK14, CK18, CK19 and CK20. Slides were deparaffinized, rehydrated and subjected to antigen retrieval. Immunohistochemical staining of all markers was performed using a BenchMark XT-automated slide-staining instrument (Ventana, Arizona, USA) with Ultraview Universal DAB dectection kit (Ventana, Arizona, USA). The slides were then counterstained with haematoxylin. Details of the antibodies and staining conditions used are listed in Table 1.

The TMA slides were scored for staining intensity and area stained by two of the authors blinded to the clinical information and staining results for other markers. For ER, PR, Ki-67 and p63, staining was nuclear; for Syn and CG, staining was cytoplasmic; for CK5/6, CK7, CK8, CK14, CK18, CK19, CK20 and C-Kit, staining was both cytoplasmic and membranous; for EGFR and HER2, staining was membranous. The staining was considered positive when there was moderate to strong nuclear immunoreactivity in≥ 1 % of tumour cells for ER and PR. HER2 immunostaining was evaluated as 0, 1+, 2+ and 3+ according to the ASCO guidelines [23]. Tumours with 3+ staining were considered positive for HER2. For Ki-67, high expression was defined arbitrarily as 15 % or more of tumour cells showing moderate to strong immunoreactivity. For all other markers, a positive reaction was scored when 5 % or more cells showed strong/moderate staining.

The tumours were also classified into the five different molecular subtypes using immunohistochemical results as surrogate criteria as follows:

Luminal A: ER+and/or PR+, HER2−;
Luminal B: ER+and/or PR+, HER2+;
HER2: ER−, PR−, HER2+, CK5/6±;
Basal: ER−, PR−, HER2−, (triple negative), CK5/6 and/or EGFR+;
Unclassified: ER−, PR−, HER2−, (triple negative), CK5/6− and EGFR−.

Statistical analysis

The findings were analyzed using the statistical software SPSS for Windows, Version 16. Spearman correlation was

Table 1 Antibodies for Immunohistochemical analysis of TMA

Marker	Manufacture	Dilution	Clone	Antigen retrieval (microwave)	Incubation	
					Time (min)	Temp (°C)
ER	Ventana	Pre-diluted	SP1	EDTA pH 8	32	37
PR	Ventana	Pre-diluted	1E2	EDTA pH 8	32	37
CG	Biogenex	1:600	LK2H10	Citrate pH 6	32	37
Syn	Ventana	Pre-diluted	SP11	EDTA pH 8	32	37
Ki67	Ventana	Pre-diluted	30-9	EDTA pH 8	32	37
HER2	Ventana	Pre-diluted	4B5	EDTA pH 8	16	37
C-kit	Dako	1:300	104D2	EDTA pH 8	32	37
EGFR	Ventana	Pre-diluted	3 C6	EDTA pH 8	32	37
p63	Ventana	Pre-diluted	4A4	EDTA pH 8	32	37
CK5/6	Dako	1:40	D5/6 B4	EDTA pH 8	32	37
CK14	Neomarkers	1:100	LL002	EDTA pH 8	32	37
C-kit	Dako	1:300	104D2	EDTA pH 8	32	37
EGFR	Ventana	Pre-diluted	3 C6	EDTA pH 8	32	37
p63	Ventana	Pre-diluted	4A4	EDTA pH 8	32	37
CK7	Dako	Pre-diluted	OV-TL 12/30	EDTA pH 8	32	37
CK8	Dako	Pre-diluted	TS1	EDTA pH 8	32	37
CK18	Dako	Pre-diluted	DC-10	EDTA pH 8	32	37
CK19	Dako	Pre-diluted	RCK108	EDTA pH 8	32	37
CK20	Dako	Pre-diluted	Ks20.8	Pepsin digest	32	37

used to test for association of CK expression with tumour grade and lymph node status. Pearson's correlation was used to test for the association of all the markers and the histotypes and molecular subtypes. A p value of <0.05 was taken to reflect statistical significance.

Results

A total of 575 cases of breast cancer were included in this study. The age range of patients was 22 to 102 years (mean 55 years). Overall 167 cases (29.0 %) were grade I, 244 cases (42.5 %) were grade II and 164 cases (28.5 %) were grade III. Lymph node metastases were found in 190 cases (33.0 %). As to the histotypes, 435 cases (75.7 %) were infiltrating duct carcinoma not otherwise specified (IDC NOS). Eight cases (1.4 %) showed apocrine features, 87 (15.1 %) were mucinous carcinoma, 11 (2.0 %) were infiltrating lobular carcinoma, 9 (1.5 %) were medullary-like carcinoma, 5 (0.9 %) were metaplastic carcinoma and 28 (4.8 %) were other minor subtypes. Using the immunohistochemical marker expression as surrogate for molecular classification, 446 cases (77.5 %) were luminal A, 50 (8.7 %) were luminal B, 35 (6.1 %) were HER2 and 44 (7.7 %) were triple negative, including 19 (3.3 %) basal like and 25 (4.4 %) unclassified cancers.

Expression of biomarkers

The overall expression rate of each of the biomarkers was: ER: 471 cases (81.9 %), PR: 445 cases (77.4 %), HER2: 85 cases (14.7 %), high Ki-67: 236 cases (41 %), p63: 29 cases (5 %), EGFR: 53 cases (9.2 %), c-Kit: 120 cases (20.8 %), CG: 32 cases (5.6 %) and Syn: 59 cases (10.3 %). The expression rate of each biomarker stratified by grade is shown in Table 2. ER and PR were significantly and more frequently expressed in low-grade tumours (96.4 % in grade I, 86.9 % in grade II and 59.8 % in grade III tumours for ER; 89.8 % in grade I, 78.3 % in grade II and 63.4 % in grade III tumours for PR; $p<0.001$ for both). In contrast, the expression of HER2, EGFR, Ki-67, c-Kit and p63 was significantly associated with higher tumour grade ($p<0.001$ for all markers except p63 with $p=0.001$).

Expression of CKs and correlation analysis

The number of cases expressing the different CKs was for CK5/6 39 (6.8 %), CK7 532 (92.5 %), CK8 566 (98.4 %), CK14 26 (4.5 %), CK18 566 (98.4 %), CK19 539 (93.7 %) and CK20 10 (1.7 %). Figure 1 shows representative staining patterns of CKs. The expression rate of each CK stratified by grade is shown in Table 2. CKs could be grouped into two groups according to the frequency of expression. A

Table 2 Summary of expression rate for cytokeratins panel

Grade	No.	CK5/6		CK7		CK8		CK14		CK18		CK19		CK20	
		n	%	*n*	%	*n*	%	*n*	%	*n*	%	*n*	%	*n*	%
I	167	4	2.4	151	90.4	162	97	5	3	162	97	155	92.8	0	0
II	244	13	5.3	222	91	240	98.4	8	3.3	240	98.4	231	94.7	4	1.6
III	164	22	13.4	159	97	164	100	13	7.9	164	100	153	93.3	6	3.7
Total	575	39	6.8	532	92.5	566	98.4	26	4.5	566	98.4	539	93.7	10	1.7
Correlation coefficient (*p* value)		0.144 (0.001)		0.083 (0.049)		NS		NS		NS		NS		0.116 (0.009)	

ns not significant

'high expression' group (>90 % of all cancers positive irrespective of tumour grade) comprised of CK7, CK8, CK18 and CK19. The expression of CK7, but not of CK8, CK18 and CK19, showed a weak positive correlation with tumour grade (r=0.083, p=0.049) and a weak negative correlation with patient age (r=−0.084, p=0.044). In contrast, CK5/6, CK14 and CK20 composed the 'low expression' group (<15 % of all cancers positive). They showed a

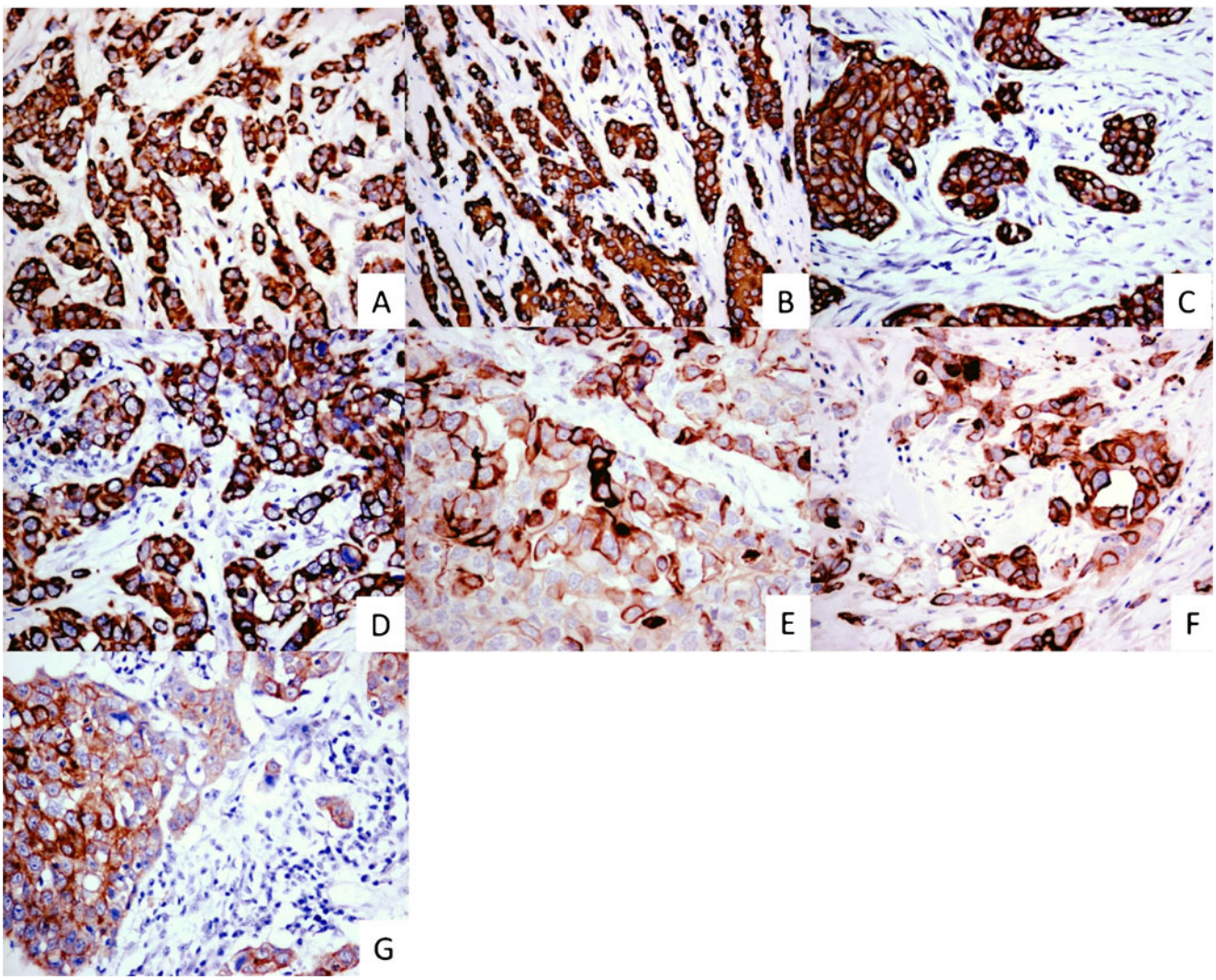

Fig. 1 Representative staining of CK7 (**a**), CK8 (**b**), CK18 (**c**), CK19 (**d**), CK5/6 (**e**), CK14 (**f**) and CK20 (**g**)

much lower overall expression rate (<7 %) but higher with high grade (<14 %). CK5/6 and CK20 expression also showed a stronger positive correlation with tumour grade than CK7 (r=0.144, p=0.001 for CK5/6 and r=0.110, p=0.009 for CK20). CK14 expression showed a negative correlation with lymph node status (r=−0.107, p=0.011).

Comparing CKs with other biomarkers (Table 3), CK5/6 expression correlated with negative ER, PR and high/positive Ki-67, EGFR, p63 and c-Kit expression (r=−0.186, -0.166, 0.281, 0.375, 0.454 and 0.371, respectively, all with p<0.001). Similarly, CK14 expression correlated weakly with negative ER (r=−0.11, p=0.008), HER2 (r=−0.082, p=0.05) and high/positive Ki-67, EGFR, p63 and c-Kit expression (r=0.146, 0.273, 0.396 and 0.272, respectively, all with p<0.001). CK20 expression correlated with negative ER (r=−0.104, p=0.013), PR (r=−0.116, p=0.005) but positive HER2 (r=0.162, p<0.001) expression.

In the 'high expression' CK group, expression of CK8, CK18 and CK19 showed similar correlation patterns with the biomarker panel: correlation with positive ER, PR and HER2 and low/negative Ki-67, EGFR, p63 and c-Kit expression (Table 3). CK18 expression correlated weakly with negative CG expression (r=−0.096, p=0.022). CK19 expression also correlated weakly with negative CG and Syn expression (r=−0.087, p=0.037 and r=−0.108, p=0.009, respectively). In addition, CK7 expression correlated with positive HER2 (r=0.139, p=0.001), but negative CG (r=−0.118, p=0.005) and Syn (r=−0.202, p=<0.001) expression.

The correlation between expressions of different CKs is listed in Table 3. Expression of CK5/6 and CK14 was strongly correlated (r=0.659, p<0.001). This was found also for CK8, CK18 and CK19 (r=0.694 between CK8 and CK18; r=0.507 between CK8 and CK19 and r=0.591 between CK18 and CK19, all with p<0.001). Furthermore, a significant negative correlation was found between expression of CK5/6 and CK14 as a group and of CK8, CK18 and CK19 as a group, in agreement with the obligatory heteropolymer patterns (CK14 partnering with CK5/6; CK18 or CK19 partnering with CK8). In line with previous reports showing more variable expression of CK7 in breast carcinoma as compared to that of CK8,18 and 19 [24], we found a weaker correlation of CK7 expression with that of CK8, CK18 and CK19 (r=0.365, 0.368 and 0.370, respectively, all with p<0.001). In addition, CK7 expression was not correlated with that of CK5/6 and of CK14. Interestingly, expression of CK20 did not show any correlation with that of any other CKs.

The use of combinations of 'high expression' CKs for immunohistochemical identification of breast carcinoma

In breast cancer, CKs have been used as markers to detect circulating tumour cells and micrometastases. We analysed the expression rate of the frequently used 'high expression' CKs and investigated whether their combination might improve immunohistochemical detection of breast cancer. The combination of CK8 and CK18 was expressed in 98.4 % of cases and the expression rate in breast cancer stratified by grade was at least 97 %. For CK7 and CK19, overall expression rates of 92.5 and 93.7 %, respectively, were

Table 3 Summary of correlation among cytokeratins and other biomarkers

	Correlation coefficient (p value)						
	CK5/6	CK14	CK7	CK8	CK18	CK19	CK20
ER	−0.186 (<0.001)	−0.11 (0.008)	ns	0.156 (<0.001)	0.214 (<0.001)	0.161 (<0.001)	−0.104 (0.013)
PR	−0.166 (<0.001)	ns	ns	0.145 (<0.001)	0.258 (<0.001)	0.161 (<0.001)	−0.116 (0.005)
HER2	ns	−0.082 (0.05)	0.139 (0.001)	0.086 (0.039)	0.086 (0.04)	0.108 (0.001)	0.162 (<0.001)
Ki67	0.281 (<0.001)	0.146 (<0.001)	ns	−0.114 (0.006)	−0.233 (<0.001)	−0.236 (<0.001)	ns
EGFR	0.375 (<0.001)	0.273	ns	−0.147 (<0.001)	−0.182 (<0.001)	−0.097 (0.002)	ns
P63	0.454 (<0.001)	0.396 (<0.001)	ns	−0.132 (0.001)	−0.207 (<0.001)	−0.153 (<0.001)	ns
c-kit	0.371 (<0.001)	0.272 (<0.001)	ns	−0.142 (0.001)	−0.261 (<0.001)	−0.13 (0.002)	ns
Syn	ns	ns	−0.202 (<0.001)	ns	ns	−0.087 (0.037)	ns
CG	ns	ns	−0.118 (0.005)	ns	−0.096 (0.022)	−0.108 (0.009)	ns
CK14	0.659 (<0.001)	–	–	–	–	–	–
CK7	ns	ns	–	–	–	–	–
CK8	−0.219 (<0.001)	−0.113 (0.007)	0.365 (<0.001)	–	–	–	–
CK18	−0.322 (<0.001)	−0.194 (<0.001)	0.368 (<0.001)	0.694 (<0.001)	–	–	–
CK19	−0.179 (<0.001)	ns	0.37 (<0.001)	0.507 (<0.001)	0.591 (<0.001)	–	–
CK20	ns	ns	ns	ns	ns	ns	–

ns not significant

found. Combining two CKs, CK8+CK18, CK8+CK19 or CK18+CK19 did not showed any increase in expression rate (data not shown) while CK7 combined with CK8 or CK18 demonstrated an increased overall expression rate to 99 % (Table 4). If the threshold for calling a tumour positive for any CK would be increased from 5 to 60 %, the overall expression rates of CK7, CK8, CK18 and CK19 in breast cancer would be 83.8, 96.5, 90.8 and 82.1 %, respectively (Table 4). Combining CK7+CK8 would increase the expression rate to 98.1 % while a combined CK7+CK18 gave an expression rate of only 95.1 %. Of note, when the expression of CKs in the metastatic lymph nodes was analysed, combined CK7+CK8 continued to show the highest expression rate (96.1 % using a 60 % cutoff; Table 4).Interestingly, when the tumours were stratified by grade, combined CK7+CK8 did not show increased expression rate in grade I tumours but the expression rate was increased in grade III tumours (CK8 alone=96.3 % and CK7+CK8=100 %). The expression rate using CK7+CK18 was only 93.9 % in grade III tumours. Similar results were also observed in metastatic lymph nodes (data not shown).

CKs expression in histological subtypes of breast carcinoma

The expression rate of CKs was analysed in different histological subtypes (Table 5). Again, CK8 showed the highest expression rate (> 98 %) in all different histological subtypes. The expression rates of CK7, CK18 and CK19 were slightly lower than that of CK8. Except in metaplastic carcinoma (80 % positive for CK7 and 60 % positive for CK18/CK19), the expression rates for these CKs ranged from 88–100 % in all other histological subtypes. Notably, CK18 and CK19 expression showed a significant negative correlation with metaplastic carcinoma ($r=-0.189$, $p<0.001$ and $r=-0.130$, $p=0.002$, respectively). While the group of 'high expression' CKs were positive in most histological subtypes, the group of 'low expression' CKs showed a restricted pattern of expression. Expression of CK5/6 was mainly found in medullary-like and metaplastic carcinomas (66.7 %, $r=0.095$, $p=0.023$ and 40 %, $r=0.126$, $p=0.003$, respectively). For all other subtypes, the expression rate of CK5/6 was <10 %. The expression pattern of CK14 was similar to CK5/6 but with a lower expression rate, and CK14 expression occurred only in metaplastic carcinoma (40 %, $r=0.16$, $p<0.001$) but not in medullary-like carcinoma. CK20 expression was rare in most histological subtypes with only 1.4 % cases expressing CK20 in IDC NOS and none in most others. However, it was the only CK that was strongly expressed in 50 % of carcinomas with apocrine features ($r=0.428$, $p<0.001$.

CK expression in molecular subtypes of breast carcinomas

Further analysis of CK expression in different molecular subtypes revealed an over 90 % expression rate of CK7 and CK8 in all molecular subtypes (Table 5). A significant negative correlation of CK8 expression was found with triple negative breast cancer (TNBC) ($r=-0.122$, $p=0.003$). CK18 and CK19 also showed a >90 % expression rate in luminal A, luminal B and HER2 subtypes but only ≤80 % in triple negative subtypes. They were found to be associated positively with luminal A subtype but negatively with TNBC (CK18: luminal A subtype, $r=0.148$, $p<0.001$; triple negative subtype, $r=-0.302$, $p<0.001$ and CK19: luminal A subtype, $r=0.085$, $p=0.042$; triple negative subtype, $r=-0.169$, $p<0.001$). On the contrary, CK5/6 and CK14 showed high expression rates in TNBC (25 and 11 %, respectively) with significant associations (CK5/6: $r=0.209$, $p<0.001$ and CK14: $r=0.095$, $p=0.023$). Furthermore, CK5/6 expression was also negatively correlated with luminal A subtype ($r=-0.104$, $p=0.013$). CK20 expression was found in <10 % of all molecular subtypes. Despite its low frequency compared with other 'low expression' CKs, CK20 showed

Table 4 Expression rate of high expression CKs with different cutoff

Cut-off	Grade	CK7, %	CK8, %	CK18, %	CK19, %	CK7+CK8, %	CK7+CK18, %
Primary tumour							
5 %	I	90.4	97.0	97.0	92.8	97.6	97.6
	II	91.0	98.4	98.4	94.7	99.2	98.0
	III	97	100	100	93.3	100	100
	Overall	92.5	98.4	98.4	93.7	99.0	98.4
60 %	I	82.0	95.8	94.6	86.2	97.6	95.8
	II	83.6	97.1	91.4	84.0	99.2	95.5
	III	86.0	96.3	79.9	75.0	100	93.9
	Overall	83.8	96.5	90.8	82.1	98.1	95.1
Metastatic lymph nodes							
5 %	Overall	92.9	100	98.4	95.3	100	100
60 %	Overall	80.5	91.3	80.5	80.5	96.1	92.1

Table 5 Summary of cytokeratins expression in special histologic and molecular subtypes of breast cancer

	% (correlation coeficient, *p* value)	CK5/6	CK7	CK8	CK14	CK18	CK19	CK20
Histologic subtypes	Infiltrating duct carcinoma NOS	6.8 (ns)	92.3 (ns)	98.1 (ns)	4.7 (ns)	96.3 (ns)	93.4 (ns)	1.4 (ns)
	Infiltrating lobular carcinoma	9.1 (ns)	90.9 (ns)	100 (ns)	9.1 (ns)	100 (ns)	100 (ns)	0 (ns)
	Mucinous carcinoma	0 (ns)	90.8 (ns)	98.9 (ns)	0 (ns)	98.9 (ns)	98.9 (ns)	0 (ns)
	Medullary-like carcinoma	66.7 (0.095, 0.023)	100 (ns)	100 (ns)	11.1 (ns)	88.9 (ns)	88.9 (ns)	0 (ns)
	Metaplastic carcinoma	40 (0.126, 0.003)	80 (ns)	100 (ns)	40 (0.160, <0.001)	60 (−0.187, <0.001)	60 (−0.130, 0.002)	0 (ns)
	IDC with apocrine feature	0 (ns)	100 (ns)	100 (ns)	0 (ns)	100 (ns)	87.5 (ns)	50 (0.438, <0.001)
Molecular subtypes	Luminal A	5 (−0.104, 0.013)	91 (ns)	99 (ns)	5 (ns)	98 (0.148, <0.001)	95 (0.085, 0.042)	1 (-0.152, <0.001)
	Luminal B	4 (ns)	96 (ns)	100 (ns)	0 (ns)	100 (ns)	96 (ns)	4 (ns)
	HER 2	6 (ns)	100 (ns)	97 (ns)	0 (ns)	97 (ns)	94 (ns)	9 (0.136, 0.001)
	Triple negative group	25 (0.209, <0.001)	93 (ns)	93 (−0.122, 0.003)	11 (0.095, 0.023)	77 (−0.302, <0.001)	80 (−0.169, <0.001)	5 (ns)

ns not significant

the highest expression rate in HER2 subtype (9 % for CK20 vs 6 % for CK5/6 and 0 % for CK14). Importantly, a positive correlation with HER2 subtype was demonstrated only for CK20 expression but not for the others (r=0.136, p=0.001).

Molecular classification of breast carcinomas using basal CKs

Within the group of TNBC, the expression rate of basal CKs, namely CK5/6 and CK14 was 25 and 11 %, respectively. Furthermore, most of the breast cancers that expressed CK14 in the triple negative group also expressed CK5/6 (four of five cases, 80 %). In this group, the expression rate of EGFR was 75 %. Using a combination of EGFR or CK5/6 expression as immunohistochemical definition of basal-like subtype classified 43.2 % of triple negative breast cancers as basal subtype (11.4 % expressed only CK5/6, 18.2 % expressed only EGFR and 13.6 % co-expressed both markers), whereas if CK14 or EGFR are used, this would be 36.4 % (4.5 % expressed only CK14, 25 % expressed only EGFR and 6.9 % co-expressed both markers). In fact, only 2.2 % of TNBC expressed CK14 without CK5/6 or EGFR expression. Hence, CK5/6 was more sensitive than CK14 in the identification of basal like breast cancer in the current cohort.

Discussion

CK expression in breast cancer can be divided into three groups according to the expression rates and correlation patterns. One group includes CK7, CK8, CK18 and CK19 showing high expression rates (>90 %). The other group comprises CK5/6 and CK14 with low expression rates (<15 %). CK20, which appears to be distinct from CK5/6 and CK14, but also showing a low expression rate, composes the third group. Within these respective groups, there was significant correlation among members of the same group and similar correlation patterns with other biomarkers.

A clinically important role for the 'high expression' group of CKs is the detection of small amounts of breast cancer tissue. The overall expression rate of CK19 reported in breast cancer was high, ranging from 89 to 92 % [7, 25]. The presence of CK19 mRNA has been considered a reliable and sensitive marker for the detection of metastasis in sentinel lymph nodes [8, 26, 27]. In the current series, its overall expression rate was 93.7 %, and there was no difference according to grade of the tumours. However, CK19 was expressed in only 60 % of metaplastic carcinomas. This same observation was also made by others [8, 25, 28]. Using CK19 as the sole marker to detect minute foci of breast cancer may result in missing some of them. In our case series, CK8 was found to have the highest expression rate of >98 % irrespective of grade and tumour subtypes and might be a better marker for breast cancer detection. In most diagnostic scenarios, the quantity of malignant cells is limited. If the threshold for calling a case positive for the expression of a CK is increased from 5 to 60 %, the overall expression rate of CK8 and CK19 decreases to 96.5 and 82.1 %, respectively. Only 75 % of grade three tumours would then be CK19 positive. To improve the likelihood of detecting minute amounts of cancer tissue, CK8 might be complemented by CK7 (Table 4). Combined CK7+CK8 would achieve a 98.1 and 100 % expression rate in all cases and grade III tumours, respectively. Hence in samples with

little cancer tissue, CK7+CK8 might have a better sensitivity in detecting breast cancer than CK19 or CK8 alone, particularly for high-grade breast cancers.

In the course of diagnostic histopathology, the need frequently arises to differentiate between florid epithelial hyperplasia and low-grade atypical epithelial proliferation (atypical epithelial hyperplasia or low-grade carcinoma in situ), particularly in architecturally complex lesions like papillary lesions or complex sclerosing lesions. CKs have long been thought to be useful in this differentiation. While benign hyperplasia is usually positive for CK5/6 and CK14, the atypical to low-grade malignant epithelium tends to be negative [15, 29]. In the current series, the expression rate of CK5/6 and CK14 in grade 1/2 breast cancers was 4.1 and 3.1 %, respectively, but considerably higher (13.4 and 7.9 %, respectively) in grade 3 cancer. Thus the absence of expression of both CK5/6 and CK14 identifies low-grade breast cancer relative to florid epithelial hyperplasia. In high-grade cancer, assessment of CK5/6 and CK14 expression would have a lower specificity.

The initial description of molecular subtypes of breast cancer was based on microarray profiling [30, 31]. The basal subtype has been the focus of intense investigations, and many different profiles have been proposed for the immunohistochemical classification of this group. Apart from being triple negative, additional immunohistochemical criteria include expression of CK5/6 [16], CK14 [11] or both CK5/6 and CK14 [32]. Other definitions involve other markers, including expression of CK5/6 and/or EGFR [12, 33] as in this study, or combinations of CK5, p63 and p-cadherin [34], or basal CK, EGFR and osteonectin [35]. We show that the expression of most of these markers is correlated (Tables 4 and 5). Irrespective of the combinations, basal CK5/6 and CK14 remain key markers with the majority of CK14-positive cases and also in CK5/6 positive cases. Using EGFR with CK5/6 yielded a total of 43.2 % as of basal subtype. If CK14 is added, the basal subtype increases by 2.2 %. The expression rates of CK5/6 and CK14 were similar in metaplastic carcinoma but the CK14 expression rate was lower in medullary-like carcinoma. These findings point to CK14 as a marker for only a subset of the basal subtype. Overall, CK5/6 showed a higher sensitivity for the basal subtype than CK14 (58 vs 21 %), similar to the reported range of 58–62 % [12, 35, 36].

Besides serving as a diagnostic marker, basal CKs has also been reported to be related to TNBC prognosis with TNBC expressing either or both CK5/6 and EGFR having adverse outcome [17]. Others reported CK cocktail 34βE12 but not CK5/6 to be associated with improved overall survival [19]. These apparently conflicting results require further investigation. We found expression of CK5/6 and CK14 to be negatively correlated with ER and PR expression and positively correlated with high Ki-67, indicative of poor prognosis.

In the current cohort, 1.7 % of tumours expressed CK20. There was no association of CK20 with any other CK. Lack of CK20 expression is usually taken as characteristic for breast cancer and together with CK7 expression is commonly used for the diagnosis of metastatic breast carcinoma [7]. The small but probably not entirely negligible number of CK20-positive cases should be borne in mind. Of note, all CK20-positive cases were of intermediate to high grade, were negative for ER and PR but positive for HER2. It would thus appear that CK20 carries prognostic significance. In fact, CK20 gene expression had been reported to be associated with increased stage, metastases and lower overall survival in breast cancer [18, 20]. The CK20-positive group was also strongly associated with apocrine features and HER2 subtype. Interestingly, these features of CK20-positive tumours were also shared by a recently identified molecular subtype with poor prognosis, which has been called the molecular apocrine group [37]. It is tempting to speculate that the application of CK20 can help to identify this special subtype immunohistochemically. More investigation is required to clarify the significance of CK20 in breast cancer.

In summary, we show that CK expression is useful as an adjunct in the diagnosis, classification and prognostication of breast cancer. CK7 and CK8 in combination allow better detection of minute quantities of breast cancer than CK19, in particular for high-grade tumours. Caution is needed in the use of CK5/6 and CK14 to differentiate low-grade breast cancer from usual epithelial hyperplasia, as CK5/6 and CK14 are expressed in a significanct number of high-grade breast cancers. In the immunohistochemical classification of molecular groups, CK5/6 appeared more sensitive than CK14 for the basal subtype. Finally, despite the low expression rate, CK20 expression could be an indicator of poor prognosis in breast cancer and implicated in the molecular apocrine subytpe.

Conflict of interest The authors declare that they have no conflict of interest.

Reference

1. Moll R, Franke WW, Schiller DL, Geiger B, Krepler R (1982) The catalog of human cytokeratins: patterns of expression in normal epithelia, tumors and cultured cells. Cell 31(1):11–24
2. Moll R, Zimbelmann R, Goldschmidt MD, Keith M, Laufer J, Kasper M, Koch PJ, Franke WW (1993) The human gene encoding cytokeratin 20 and its expression during fetal development and in gastrointestinal carcinomas. Differentiation 53(2):75–93
3. Bader BL, Jahn L, Franke WW (1988) Low level expression of cytokeratins 8, 18 and 19 in vascular smooth muscle cells of human umbilical cord and in cultured cells derived therefrom, with

an analysis of the chromosomal locus containing the cytokeratin 19 gene. Eur J Cell Biol 47(2):300–319
4. Popescu NC, Bowden PE, DiPaolo JA (1989) Two type II keratin genes are localized on human chromosome 12. Hum Genet 82 (2):109–112
5. Romano V, Bosco P, Rocchi M, Costa G, Leube RE, Franke WW, Romeo G (1988) Chromosomal assignments of human type I and type II cytokeratin genes to different chromosomes. Cytogenet Cell Genet 48(3):148–151
6. Rosenberg M, Fuchs E, Le Beau MM, Eddy RL, Shows TB (1991) Three epidermal and one simple epithelial type II keratin genes map to human chromosome 12. Cytogenet Cell Genet 57(1):33–38
7. Chu PG, Weiss LM (2002) Keratin expression in human tissues and neoplasms. Histopathology 40(5):403–439
8. Alvarenga CA, Paravidino PI, Alvarenga M, Dufloth R, Gomes M, Zeferino LC, Schmitt F (2011) Expression of CK19 in invasive breast carcinomas of special histological types: implications for the use of one-step nucleic acid amplification. J Clin Pathol 64 (6):493–497
9. Effenberger KE, Borgen E, Eulenburg CZ, Bartkowiak K, Grosser A, Synnestvedt M, Kaaresen R, Brandt B, Nesland JM, Pantel K, Naume B (2011) Detection and clinical relevance of early disseminated breast cancer cells depend on their cytokeratin expression pattern. Breast Cancer Res Treat 125(3):729–738
10. Boecker W, Moll R, Dervan P, Buerger H, Poremba C, Diallo RI, Herbst H, Schmidt A, Lerch MM, Buchwalow IB (2002) Usual ductal hyperplasia of the breast is a committed stem (progenitor) cell lesion distinct from atypical ductal hyperplasia and ductal carcinoma in situ. J Pathol 198(4):458–467
11. Jones C, Ford E, Gillett C, Ryder K, Merrett S, Reis-Filho JS, Fulford LG, Hanby A, Lakhani SR (2004) Molecular cytogenetic identification of subgroups of grade III invasive ductal breast carcinomas with different clinical outcomes. Clin Cancer Res 10 (18 Pt 1):5988–5997
12. Nielsen TO, Hsu FD, Jensen K, Cheang M, Karaca G, Hu Z, Hernandez-Boussard T, Livasy C, Cowan D, Dressler L, Akslen LA, Ragaz J, Gown AM, Gilks CB, van de Rijn M, Perou CM (2004) Immunohistochemical and clinical characterization of the basal-like subtype of invasive breast carcinoma. Clin Cancer Res 10(16):5367–5374
13. Rakha EA, El-Sayed ME, Green AR, Paish EC, Lee AH, Ellis IO (2007) Breast carcinoma with basal differentiation: a proposal for pathology definition based on basal cytokeratin expression. Histopathology 50(4):434–438
14. Reisenbichler ES, Balmer NN, Adams AL, Pfeifer JD, Hameed O (2011) Luminal cytokeratin expression profiles of breast papillomas and papillary carcinomas and the utility of a cytokeratin 5/p63/ cytokeratin 8/18 antibody cocktail in their distinction. Mod Pathol 24(2):185–193
15. Tan PH, Aw MY, Yip G, Bay BH, Sii LH, Murugaya S, Tse GM (2005) Cytokeratins in papillary lesions of the breast: is there a role in distinguishing intraductal papilloma from papillary ductal carcinoma in situ? Am J Surg Pathol 29(5):625–632
16. van de Rijn M, Perou CM, Tibshirani R, Haas P, Kallioniemi O, Kononen J, Torhorst J, Sauter G, Zuber M, Kochli OR, Mross F, Dieterich H, Seitz R, Ross D, Botstein D, Brown P (2002) Expression of cytokeratins 17 and 5 identifies a group of breast carcinomas with poor clinical outcome. Am J Pathol 161(6):1991–1996
17. Cheang MC, Voduc D, Bajdik C, Leung S, McKinney S, Chia SK, Perou CM, Nielsen TO (2008) Basal-like breast cancer defined by five biomarkers has superior prognostic value than triple-negative phenotype. Clin Cancer Res 14(5):1368–1376
18. Cheng CW, Yu JC, Wang HW, Huang CS, Shieh JC, Fu YP, Chang CW, Wu PE, Shen CY (2010) The clinical implications of MMP-11 and CK-20 expression in human breast cancer. Clin Chim Acta 411 (3–4):234–241
19. Mehta R, Jain RK, Sneige N, Badve S, Resetkova E (2010) Expression of high-molecular-weight cytokeratin (34betaE12) is an independent predictor of disease-free survival in patients with triple-negative tumours of the breast. J Clin Pathol 63(8):744–747
20. Wang SM, Huang DM, Li B, Ruan JD (2009) Association of CK20 expression with the progression, metastasis and prognosis of breast cancer. Xi Bao Yu Fen Zi Mian Yi Xue Za Zhi 25(8):706–707
21. Rakha EA, Reis-Filho JS, Ellis IO (2010) Combinatorial biomarker expression in breast cancer. Breast Cancer Res Treat 120(2):293–308
22. Elston CW, Ellis IO (1991) Pathological prognostic factors in breast cancer. I. The value of histological grade in breast cancer: experience from a large study with long-term follow-up. Histopathology 19(5):403–410
23. Wolff AC, Hammond ME, Schwartz JN, Hagerty KL, Allred DC, Cote RJ, Dowsett M, Fitzgibbons PL, Hanna WM, Langer A, McShane LM, Paik S, Pegram MD, Perez EA, Press MF, Rhodes A, Sturgeon C, Taube SE, Tubbs R, Vance GH, van de Vijver M, Wheeler TM, Hayes DF (2007) American Society of Clinical Oncology/College of American Pathologists guideline recommendations for human epidermal growth factor receptor 2 testing in breast cancer. J Clin Oncol 25(1):118–145
24. Malzahn K, Mitze M, Thoenes M, Moll R (1998) Biological and prognostic significance of stratified epithelial cytokeratins in infiltrating ductal breast carcinomas. Virchows Arch 433 (2):119–129
25. Delgallo WD, Rodrigues JR, Bueno SP, Viero RM, Soares CT (2010) Cell blocks allow reliable evaluation of expression of basal (CK5/6) and luminal (CK8/18) cytokeratins and smooth muscle actin (SMA) in breast carcinoma. Cytopathology 21(4):259–266
26. Schem C, Maass N, Bauerschlag DO, Carstensen MH, Loning T, Roder C, Batic O, Jonat W, Tiemann K (2009) One-step nucleic acid amplification-a molecular method for the detection of lymph node metastases in breast cancer patients; results of the German study group. Virchows Arch 454(2):203–210
27. Tsujimoto M, Nakabayashi K, Yoshidome K, Kaneko T, Iwase T, Akiyama F, Kato Y, Tsuda H, Ueda S, Sato K, Tamaki Y, Noguchi S, Kataoka TR, Nakajima H, Komoike Y, Inaji H, Tsugawa K, Suzuki K, Nakamura S, Daitoh M, Otomo Y, Matsuura N (2007) One-step nucleic acid amplification for intraoperative detection of lymph node metastasis in breast cancer patients. Clin Cancer Res 13(16):4807–4816
28. Tot T (2000) The cytokeratin profile of medullary carcinoma of the breast. Histopathology 37(2):175–181, d
29. Moriya T, Kozuka Y, Kanomata N, Tse GM, Tan PH (2009) The role of immunohistochemistry in the differential diagnosis of breast lesions. Pathology 41(1):68–76
30. Sorlie T, Perou CM, Tibshirani R, Aas T, Geisler S, Johnsen H, Hastie T, Eisen MB, van de Rijn M, Jeffrey SS, Thorsen T, Quist H, Matese JC, Brown PO, Botstein D, Eystein Lonning P, Borresen-Dale AL (2001) Gene expression patterns of breast carcinomas distinguish tumor subclasses with clinical implications. Proc Natl Acad Sci U S A 98(19):10869–10874
31. Sorlie T, Tibshirani R, Parker J, Hastie T, Marron JS, Nobel A, Deng S, Johnsen H, Pesich R, Geisler S, Demeter J, Perou CM, Lonning PE, Brown PO, Borresen-Dale AL, Botstein D (2003) Repeated observation of breast tumor subtypes in independent gene expression data sets. Proc Natl Acad Sci U S A 100 (14):8418–8423
32. Bankfalvi A, Ludwig A, De-Hesselle B, Buerger H, Buchwalow IB, Boecker W (2004) Different proliferative activity of the glandular and myoepithelial lineages in benign proliferative and early malignant breast diseases. Mod Pathol 17(9):1051–1061
33. Dawood S, Hu R, Homes MD, Collins LC, Schnitt SJ, Connolly J, Colditz GA, Tamimi RM (2011) Defining breast cancer prognosis based on molecular phenotypes: results from a large cohort study. Breast Cancer Res Treat 126(1):185–192

34. Matos I, Dufloth R, Alvarenga M, Zeferino LC, Schmitt F (2005) p63, cytokeratin 5, and P-cadherin: three molecular markers to distinguish basal phenotype in breast carcinomas. Virchows Arch 447(4):688–694
35. Lakhani SR, Reis-Filho JS, Fulford L, Penault-Llorca F, van der Vijver M, Parry S, Bishop T, Benitez J, Rivas C, Bignon YJ, Chang-Claude J, Hamann U, Cornelisse CJ, Devilee P, Beckmann MW, Nestle-Kramling C, Daly PA, Haites N, Varley J, Lalloo F, Evans G, Maugard C, Meijers-Heijboer H, Klijn JG, Olah E, Gusterson BA, Pilotti S, Radice P, Scherneck S, Sobol H, Jacquemier J, Wagner T, Peto J, Stratton MR, McGuffog L, Easton DF (2005) Prediction of BRCA1 status in patients with breast cancer using estrogen receptor and basal phenotype. Clin Cancer Res 11 (14):5175–5180
36. Bhargava R, Beriwal S, McManus K, Dabbs DJ (2008) CK5 is more sensitive than CK5/6 in identifying the "basal-like" phenotype of breast carcinoma. Am J Clin Pathol 130(5):724–730
37. Farmer P, Bonnefoi H, Becette V, Tubiana-Hulin M, Fumoleau P, Larsimont D, Macgrogan G, Bergh J, Cameron D, Goldstein D, Duss S, Nicoulaz AL, Brisken C, Fiche M, Delorenzi M, Iggo R (2005) Identification of molecular apocrine breast tumours by microarray analysis. Oncogene 24(29):4660–4671

Virchows Arch (2012) 461:323–331
DOI 10.1007/s00428-012-1280-5

ORIGINAL ARTICLE

Atypical angioimmunoblastic T-cell lymphomas masquerading as systemic polyclonal B-immunoblastic proliferation

Bhavesh Papadi · Jacek M. Polski · David R. Clarkson · Theresa O. Liu-Dumlao

Received: 15 March 2012 / Revised: 21 June 2012 / Accepted: 27 June 2012 / Published online: 12 July 2012
© Springer-Verlag 2012

Abstract Angioimmunoblastic T cell lymphoma (AITL) is a relatively rare peripheral T cell lymphoma derived from follicular T helper cells. AITL has a varied presentation, both clinically and morphologically. AITL can pose a diagnostic challenge as it may be difficult to identify and characterize the neoplastic cells among the polymorphous infiltrates composed of polyclonal B immunoblasts and plasma cells. In AITL, the reactive B cell and plasma cell proliferation is secondary to dysregulated secretion of cytokines such as interleukin-6 by the neoplastic follicular T helper cells. SPBIP is a condition of unknown etiopathogenesis characterized by systemic involvement by polyclonal B immunoblasts and plasma cells. We report two cases of AITL, which are presented with atypical findings making it difficult to diagnose. The cases had features similar to SPBIP. Our cases highlight the importance of screening cases of polyclonal plasmacytosis and SPBIP like cases for underlying AITL.

Keywords Angioimmunoblastic T cell lymphoma · Polyclonal B immunoblastic proliferation

Introduction

Angioimmunoblastic T cell lymphoma (AITL) is a peripheral T cell lymphoma (PTCL) arising from follicular T helper cells [1]. It is a disease of middle-aged and elderly individuals [2] and characterized by very high incidence of Epstein–Barr virus (EBV) infection [3]; constitutional symptoms such as fever, night sweats, weight loss, and other symptoms depending upon the organ system involved [4]; and generalized lymphadenopathy with frequent involvement of spleen, liver, skin, and bone marrow [2]. Morphologically, lymph nodes show partial to complete effacement of lymph node architecture. The lymph node infiltrate ranges from polymorphic cells composed of immunoblasts, plasma cells, eosinophils, small lymphocytes, and follicular dendritic cells (FDC) to a monotonous infiltrate of atypical lymphoma cells, often with clear cytoplasm. Numerous arborizing blood vessels are usually seen [5, 6].

The diagnosis of AITL can be very challenging, especially at an early stage in the disease evolution, when the lymph node architecture is relatively preserved with many hyperplastic lymphoid follicles and the lymphoma cells are not readily identifiable. This is complicated by the fact that AITL retains some functional characteristics of non-neoplastic follicular T helper cells, such as the capacity to secrete cytokines like interleukin (IL)-6 and to stimulate immune cell growth and thus, AITL is associated with obscuring non-neoplastic immune cells [7]. As a result, identifying AITL presents two sets of challenges. The first is identifying AITL cases that present with partial effacement of architecture, hyperplastic germinal centers, and minimal expansion of FDC and separating them from reactive conditions. The second challenge is identifying AITL cases without readily identifiable CD10-positve lymphoma cells or FDC expansion and separating them from PTCL, unspecified. Once lymphoma is suspected, the most useful histological features to distinguish AITL from PTCL, unspecified are prominent vascularity, proliferation of follicular T helper cells, CD10-positive cells, EBV infection, and florid FDC proliferation [8]. Follicular T helper cells have emerged as a distinct helper T cell subset residing in reactive

B. Papadi · J. M. Polski (✉)
Department of Pathology, University of South Alabama,
2451 Fillingim Street,
Mobile, AL 36617, USA
e-mail: jpolski@usouthal.edu

D. R. Clarkson · T. O. Liu-Dumlao
Department of Hematology-Oncology, University of South Alabama Mitchell Cancer Institute,
Mobile, AL 36604, USA

germinal centers of lymph node and providing help to B cells. Consequently, several markers characteristically expressed by these follicular T helper cells can be used in the diagnostic practice. The markers include cell surface molecules CXCR5, CD154, PD-1 (CD279), ICOS, CD200, as well as cytoplasmic SAP, chemokine CXCL13, and transcription factors Bcl-6 and MAF [9]. While molecular studies can generally detect clonal T cell receptor (TCR) rearrangement, about 10–20 % of cases do not show any clonal TCR gene rearrangements [10, 11]. Also, clonal immunoglobulin heavy chain (IgH) gene rearrangements can be seen in addition to clonal TCR gene rearrangements in some cases of AITL [12].

AITL may be categorized into three overlapping architectural patterns, as described by Attygalle et al. [8]. In pattern I, there is partial preservation of lymph nodal architecture with hyperplastic follicles and a polymorphous paracortical infiltrate. Pattern II presents with depleted follicles and may have Castleman disease-like features. Pattern III presents with complete effacement of architecture, accompanied by perivascular proliferation of FDC. Cases intermediate between AITL and PTC, unspecified have been also described [8].

Systemic polyclonal B Immunoblastic proliferation (SPBIP) is a very rare atypical lymphoproliferative disorder with only a handful cases of SPBIP published in the literature [13–16]. SPBIP can present with a subacute onset of symptoms such as fever, dyspnea, malaise, weakness, and other symptoms depending on the organ systems involved. The process can involve lymph nodes, bone marrow, spleen, thymus, liver, kidneys, thyroid, adrenal glands, lungs, and skin. There may be evidence of infection reflecting either an initiating event or immunodeficiency secondary to the atypical proliferation process. The disease process is characterized by a systemic involvement by proliferating polyclonal B immunoblasts and plasma cells. There may be lymphocytosis with the presence of immunoblasts and plasma cells in the peripheral blood. The uncontrolled production of immunoglobulins may result in polyclonal gammaglobulinemia. The etiopathogenesis of SPBIP is unknown. While the cells appear polyclonal by immunoglobulin expression or gene rearrangement studies, clonality was demonstrated by cytogenetic studies in some cases [13, 16]. It is not entirely clear whether these proliferations are neoplastic or reactive in nature. It is also not clear if SPBIP is related to so-called polyclonal lymphomas [17]. Although SPBIP responds to corticosteroid therapy or chemotherapy, untreated or even treated cases can be fatal. Treatment with corticosteroids alone or in combination with cytotoxic agents can quickly induce complete remission with resolution of lymphadenopathy and normalization of peripheral blood picture [14, 15].

AITL and SPBIP share many clinical and morphologic features and especially an exuberant polyclonal B immunoblast and plasma cell proliferation. Extensive immunophenotypic, cytogenetic, and molecular testing is sometimes necessary to distinguish between AITL and SPBIP. We report our experience with two cases of AITL that initially presented with unexplained, massive, and systemic B immunoblastic and plasmacytic proliferation mimicking SPBIP.

Clinical history

Case 1

A 55-year-old African-American female with a past medical history of diabetes mellitus and hypertension first presented to her primary care physician with lymphadenopathy. A cervical lymph node biopsy was performed at an outside institution and showed atypical lymphoid hyperplasia. Approximately 5 days later, she was admitted to a hospital with weakness, dizziness, dyspnea, diffuse lymphadenopathy (inguinal, cervical, axillary, and retroperitoneal lymph nodes), hemoptysis, and bleeding gums. A complete blood count showed a leukocyte count of 29.1×10^9/L, hemoglobin 94 g/L, hematocrit 28 %, and platelet count of 10×10^9/L. Blood serology was negative for antinuclear antibodies, human immunodeficiency virus, acute cytomegalovirus infection, and acute EBV infection. Platelet-associated antibodies were detected. The patient was found to have polyclonal gammaglobulinemia with elevated serum IgG, IgA, IgM, and IgE. A repeat cervical lymph node biopsy and a bone marrow aspirate and biopsy were performed. The lymph node, peripheral blood, and bone marrow aspirate samples were studied by flow cytometric analysis. Gene rearrangement studies were performed on the peripheral blood and lymph node specimens. A diagnosis of SPBIP was suspected at this time. The patient was treated with methylprednisolone, dexamethasone, vincristine, and cyclophosphamide. The treatment resulted in complete clinical response with nonpalpable lymph nodes and normal peripheral blood findings.

About 2 months after her initial presentation, the patient was readmitted with a white blood cell count of 27.9×10^9/L and 38 % atypical lymphocytes. Peripheral blood flow cytometry demonstrated the presence of abnormal B immunoblasts. She was again treated with the same regimen of intravenous corticosteroids and chemotherapy and subsequently responded clinically.

A year later, she was admitted again with generalized lymphadenopathy. An axillary lymph node biopsy was performed. This time, the findings were more consistent with AITL. The patient received therapy with cyclophosphamide, adriamycin, vincristine, and prednisolone (CHOP) and remained in remission for 12 months. At the time of

evaluation for bone marrow transplantation, a positron emission tomography scan revealed uptake in the colon and colonoscopy revealed adenocarcinoma of the colon. A colectomy was performed and the patient received adjuvant chemotherapy with fluoruracil, oxaliplatin, and has remained disease free of her colon carcinoma. Fourteen months after receiving CHOP, she has again relapsed with adenopathy in the supraclavicular area and biopsy affirmed recurrence of AITL.

Case 2

A 70-year-old Caucasian female presented to her primary physician with a 2-week history of weakness, drenching sweats, early satiety, postprandial nausea, and vomiting, and 15 % weight loss. A complete blood count showed a leukocyte count of 24.7×10^9/L, hemoglobin 123 g/L, hematocrit 37 %, and a platelet count of 238×10^9/L. She had elevated serum IgG of 45.5 g/L. Serum and urine protein electrophoresis did not reveal evidence of monoclonal gammopathy. A computer tomography scan of chest and abdomen revealed enlargement of mediastinal, periaortic, and pericaval lymph nodes and mild splenomegaly. Review of peripheral smear was significant for plasmacytosis. Bone marrow aspirate and biopsy procedure, as well as right inguinal lymph node excision biopsy, were performed. Flow cytometry and gene rearrangement studies were performed on specimens of peripheral blood, bone marrow, and lymph node. The diagnosis of AITL was made, and the patient was treated with frontline chemotherapy with CHOP regimen. Interval evaluation showed persistent low level of disease in the bone marrow and low level of hypermetabolic uptake in the spleen. She received more chemotherapy with continued response on re-evaluation and proceeded to autologous stem cell transplantation. The patient remains free of disease 15 months from initial presentation.

Materials and methods

Histologic and immunohistochemical studies

Fresh biopsy tissue was fixed in 10 % neutral-buffered formalin, embedded in paraffin and sectioned at 3 μm. Sections were stained with hematoxylin and eosin for morphological evaluation. Immunohistochemical analysis was performed on the paraffin sections with the following antibodies: CD2, CD3, CD4, CD5, CD7, CD8, CD10, CD19, CD20, CD21, CD23, CD45, CD79a, PAX5, CXCL13, and PD-1/CD279. The immunohistochemical analysis was performed on an automated immunostainer with a streptoviridin–biotin peroxidase detection system, preceded by microwave antigen retrieval in citrate buffer.

Flow cytometric immunophenotyping

Four- or eight-color flow cytometry was performed on Canto II flow cytometer (BD Bioscience, San Jose, CA, USA). The data was analyzed by FACSDiva software (BD Bioscience). The following monoclonal antibodies were utilized: CD2, CD3, CD4, CD5, CD7, CD8, CD10, CD11c, CD13, CD14, CD15, CD16, CD19, CD20, CD22, CD23, CD25, CD33, CD34, CD36, CD38, CD45, CD56, CD57, CD61, CD71, CD103, CD117, CD138, Kappa, Lambda, FMC-7, and human leukocyte antigen (HLA)-DR (BD Bioscience).

Epstein–Barr virus in situ hybridization

A test utilizing alkaline phosphatase-conjugated detection chemistry to localize fluorescein-labeled oligonucleotide probes against EBER1 RNA was performed on paraffin-embedded tissue at Mayo Medical Laboratories (Rochester, MN, USA) as previously described [18].

Molecular analysis

A polymerase chain reaction based analysis was done on peripheral blood, bone marrow aspirate, and paraffin-embedded tissue at Mayo Medical Laboratories for clonal IgH and TCR gene rearrangements as previously described [19].

Results

Case 1

The initial cervical lymph node biopsy showed a partial effacement of the nodal architecture by interfollicular proliferation of B immunoblasts and plasma cells with a number of residual follicles with hyperplastic germinal centers (Fig. 1a and b). No increase in vascularity was appreciated. Cervical lymph node flow cytometry revealed 30 % B immunoblasts/plasma cells with expression of CD45 (moderate), CD19 (moderate), CD38 (bright), CD56 (dim), CD71 (dim), HLA-DR, and polytypic cytoplasmic light chains without surface light chain expression (Fig. 1c and d). No aberrant T cell phenotypes were detected by flow cytometry. The T cells were CD10 negative (Fig. 1e and f). Gene rearrangement studies performed on the lymph node were negative for clonal IgH gene rearrangement. However, clonal TCR gene rearrangement was detected in the lymph node.

Peripheral blood revealed numerous immunoblasts of intermediate to large size, round to oval nucleus with prominent nucleoli. Bone marrow aspirate and biopsy were hypercellular with a diffuse infiltration by immunoblasts and plasma cells. The peripheral blood flow cytometry

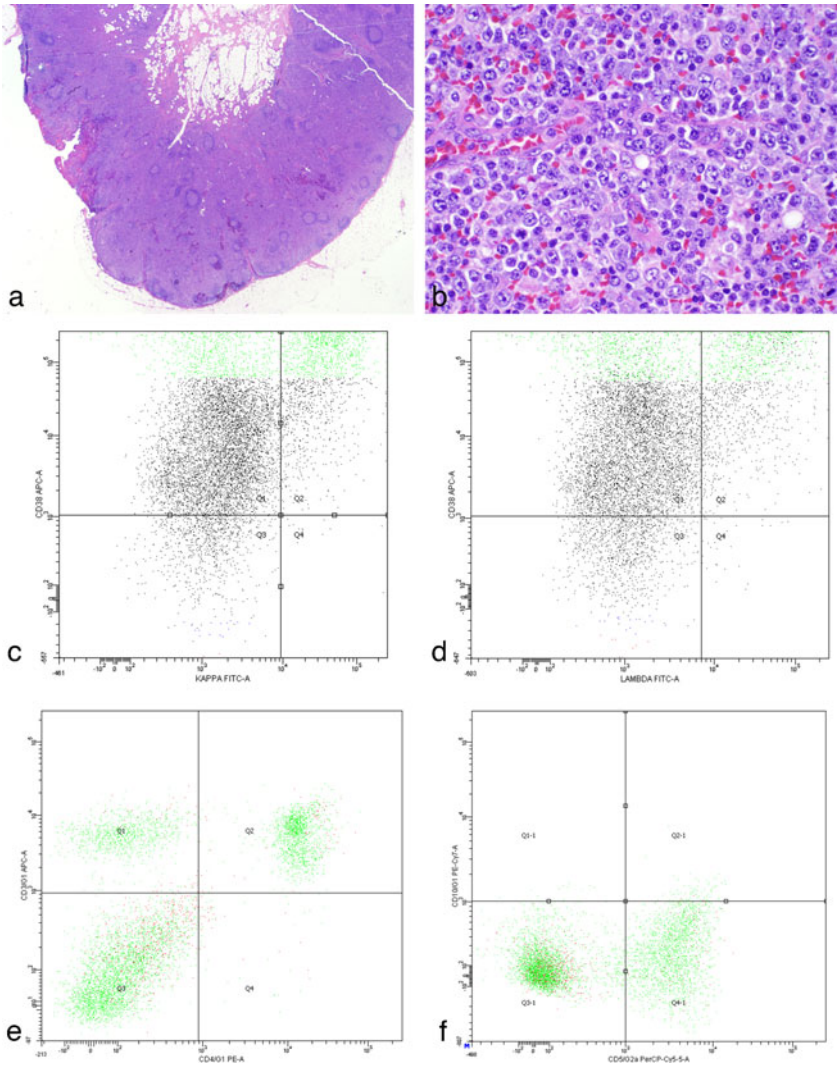

Fig. 1 Case 1: cervical lymph node with interfollicular atypical proliferation and preservation of hyperplastic follicles; hematoxylin and eosin (H&E) stain, magnification ×10 (**a**). High-power view of cervical lymph node showing immunoblasts and plasma cells; H&E stain, magnification ×400 (**b**). Flow cytometry reveals B immunoblasts/plasma cells strongly positive for CD38 with polytypic cytoplasmic light chains (**c** and **d**). Flow cytometry reveals T cells with no abnormal expression of CD3 or CD4 (**e**). Flow cytometry reveals T cells with no abnormal expression of CD10 (**f**)

revealed 27 % B immunoblasts/plasma cells with expression of CD45 (moderate), CD19 (moderate), CD38 (bright), CD56 (dim), CD71 (dim), HLA-DR, and polytypic cytoplasmic light chains without surface light chain expression. Bone marrow aspirate flow cytometry showed 34 % cells with the same phenotype. A cytogenetic study of peripheral blood was unsuccessful with the failure of cells to grow.

The axillary lymph node biopsy showed a diffuse and polymorphic infiltrate comprising small- and intermediate-sized atypical lymphoid cells, immunoblasts, and numerous plasma cells. Only rare, atrophic follicles with inconspicuous FDC were seen (Fig. 2a). There were occasional arborizing blood vessels with plump endothelial cells (Fig. 2b). Rare atypical cells had clear cytoplasm (Fig. 2c). The atypical T-cells expressed CD2, CD3, CD4, CD5, CD7, PD-1/CD279, TCR beta F1, and partial CXCL13, but not CD10 (Fig. 2d and e). Epstein–Barr virus in situ hybridization (EBV-ISH) revealed rare scattered cells containing EBV (Fig. 2f). Rare small follicles and numerous interfolicular immunoblasts were demonstrated by the CD20 stain (Fig. 2g). CD21 staining revealed irregular and mildly expanded FDC mesh works with some encircling of vessels (Fig. 2h). Flow cytometric analysis showed small polyclonal B cells (22 %), large polyclonal B cells (16 %), and T cells with apparently normal phenotype. The large B cells represented polyclonal activated B cells with immunoblastic or plasmacytic differentiation and expressed CD45, CD19, CD22, CD38, CD71, CD138, HLA-DR, FMC-7, and polytypic cytoplasmic kappa and lambda light chains. This immunophenotype was similar to that previously described for immunoblasts/plasma cells in the peripheral blood, bone marrow, and cervical lymph node. Molecular studies revealed no clonal IgH gene rearrangements, but clonal TCR gene rearrangement was detected. Cytogenetic studies done on the lymph node tissue revealed no abnormalities.

Case 2

Peripheral blood smear showed increased numbers of plasma cells (Fig. 3a). Bone marrow was hypercellular for age

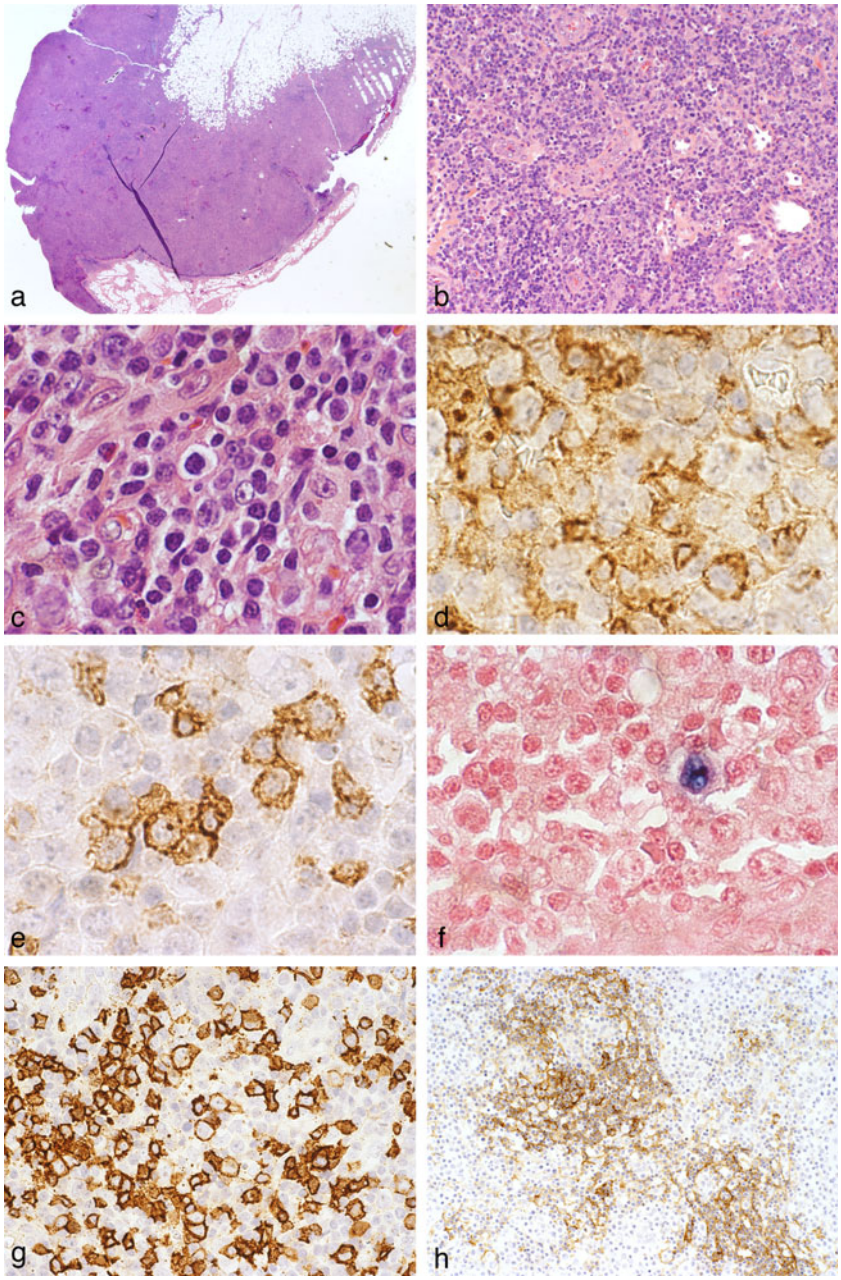

Fig. 2 Case 1: axillary lymph node with diffuse atypical proliferation and rare, indistinct follicles, H&E stain, magnification ×10 (**a**). Higher-power view of axillary lymph node showing vascular proliferation and polymorphous infiltrate, H&E stain, magnification ×200 (**b**). Atypical lymphoid cells with clear cytoplasm, H&E stain, magnification ×1000 (**c**). Atypical lymphoid cells positive for CD4, magnification ×1,000 (**d**). Atypical lymphoid cells positive for PD-1/CD279, magnification ×1,000 (**e**). Rare lymphoid cells positive for EBER, magnification ×1,000 (**f**). Immunoblasts positive for CD20, magnification ×400 (**g**). Mild expansion of follicular dendritic cells positive for CD21, magnification ×200 (**h**)

with marked plasma cell infiltration (Fig. 3b). The peripheral blood flow cytometry revealed 27 % plasma cells. The plasma cells were characterized by the expression of CD45 (bright), CD19, CD23 (dim), CD38, CD71, CD138, HLA-DR, and cytoplasmic polytypic light chains (Fig. 3c and d). There was no surface light chain expression. The bone marrow flow cytometry revealed 21 % plasma cells. The phenotype of bone marrow plasma cells was similar to that described above except for additional weak expression of CD56.

The inguinal lymph node biopsy showed architectural effacement with multiple vague but complex lymphoid nodules composed of variably sized lymphoid cells, immunoblasts, and plasma cells (Fig. 4a). There was mildly increased vascularity with rare arborizing vessels (Fig. 4b). Rare abnormal follicles were present with irregular germinal centers and absent mantle zones. Rare atypical cells had clear cytoplasm (Fig. 4c). A number of small or large lymphoid cells were positive for CD2, CD3, CD4, CD5, CD7, TCR beta F1, and PD-1/CD279, although no significant staining was noted for CD10 or CXCL13 (Fig. 4d and e). EBV-ISH revealed numerous cells containing EBV (Fig. 4f). There were numerous CD20-positive immunoblasts and markedly expanded CD21-positive FDC mesh works (Fig. 4g and h).

The inguinal lymph node flow cytometry revealed a predominance of T cells. A few polyclonal B cells and plasma cells were also detected. The B cells had a normal

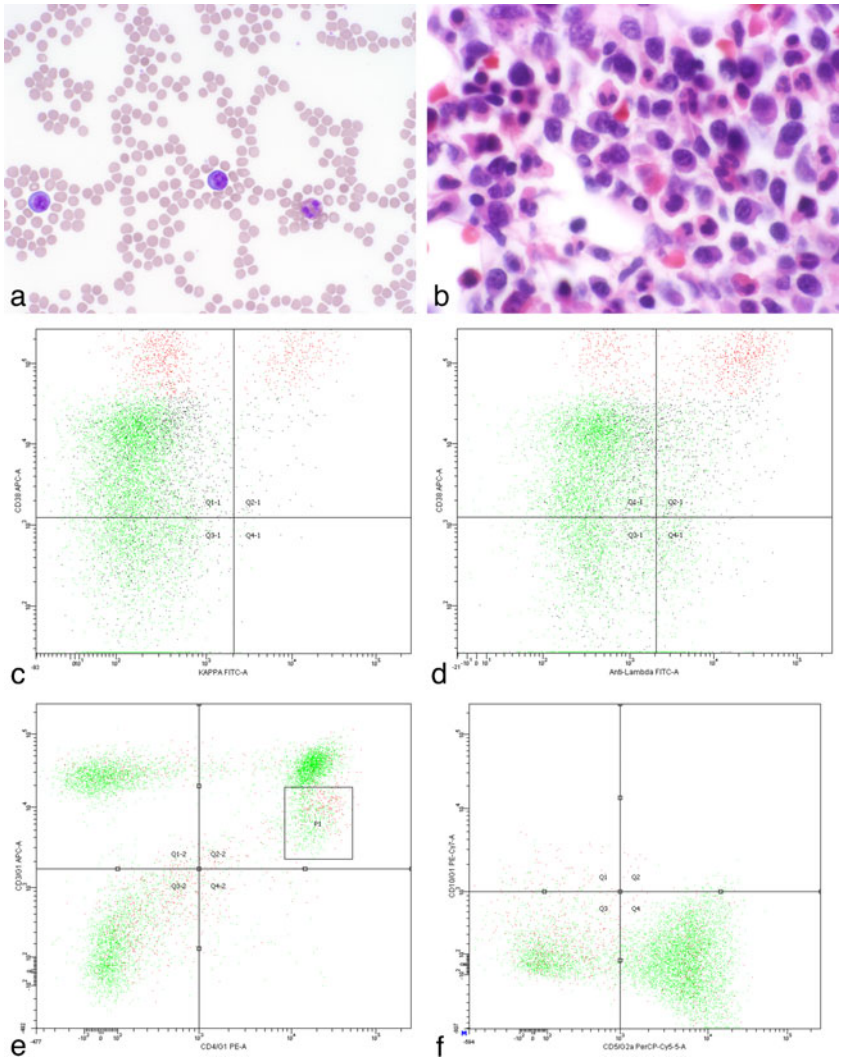

Fig. 3 Case 2: peripheral blood smear with circulating plasma cells, Wright stain, magnification ×400 (**a**). Bone marrow with increase in plasma cells, H&E stain, magnification ×1,000 (**b**). Flow cytometry reveals immunoblasts/plasma cells strongly positive for CD38 with polytypic cytoplasmic light chains (**c** and **d**). Flow cytometry performed on the inguinal lymph node reveals a subset of CD4 positive T cells with slightly weak expression of CD3 (**e**). The T cells have no abnormal expression of CD10 (**f**)

phenotype. A small population of CD4-positive T cells had slightly weaker expression of CD3 (Fig. 3e). No other T cell abnormalities were detected. The T cells were CD10 negative (Fig. 3f). While peripheral blood and bone marrow did not reveal any T cell clonality, inguinal lymph node had clonal TCR gene rearrangement. Cytogenetic studies performed on bone marrow aspirate were negative.

A follow-up bone marrow aspirate and biopsy, done 5 months after initial presentation, showed low level involvement of the bone marrow aspirate by lymphoma and the lymphoma cells had weak expression of CD3 by flow cytometry, similar to that previously detected in the inguinal lymph node.

Discussion

The diagnosis of AITL in the above cases was difficult due to a predominance of numerous polyclonal B immunoblasts or plasma cells in all the specimens examined, including blood and bone marrow, paucity of atypical cells, and lack of significant immunophenotypic T cell abnormalities. Case 1 was especially difficult as the flow cytometric studies failed to detect abnormal T cell immunophenotype and there was no expression of CD10 in T-cells typically seen in AITL [20]. Unfortunately, CD10 expression is neither sensitive nor specific for detection of AITL [20, 21]. Due to those factors, the initial presentation in case 1 was initially considered to be SPBIP. Later, clonal TCR gene rearrangement studies suggested a possibility of PTCL. In retrospect, it was pattern I of AITL. The relapse in case 1 had morphologhic findings more typical for AITL, and specifically pattern II. Case 2 was somewhat easier to diagnose as flow cytometry revealed a subset of CD4-positive T-cells with slightly weaker expression of CD3. That was the sole immunophenotypic abnormality and no CD10 expression was seen in this case. The immunoperoxidase studies were helpful and demonstrated increased staining for PD-1/CD279 in the atypical infiltrate in both cases. Weak CXCL13 staining was present in case 1, but absent in case 2. It is well

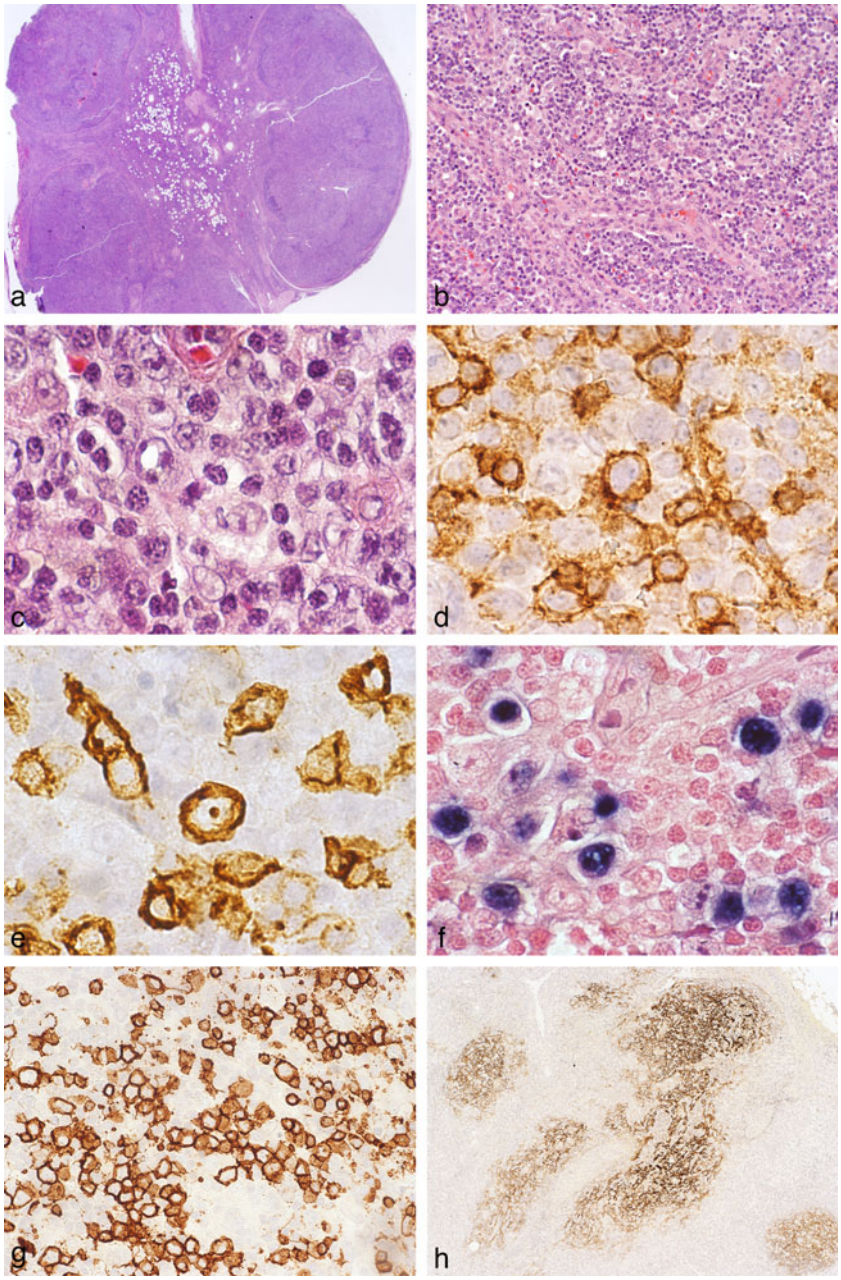

Fig. 4 Case 2: inguinal lymph node with a vaguely nodular atypical proliferation, H&E stain, magnification ×10 (**a**). Higher power view of inguinal lymph node showing vascular proliferation and polymorphous infiltrate, H&E stain, magnification ×200 (**b**). Rare atypical lymphoid cells, some with clear cytoplasm, H&E stain, magnification ×1,000 (**c**). Atypical lymphoid cells positive for CD4, magnification ×1,000 (**d**). Atypical lymphoid cells positive for PD-1/CD279, magnification ×1,000 (**e**). Lymphoid cells positive for EBER, magnification ×1,000 (**f**). Immunoblasts positive for CD20, magnification ×400 (**g**). Marked expansion of follicular dendritic cells positive for CD21, magnification ×40 (**h**)

established that markers of follicular helper T-cells, PD-1/CD279, and CXCL13, are helpful in the diagnosis of AITL [9, 22, 23]. The morphologic findings in case 2 were intermediate between pattern I (hyperplastic follicles) and pattern II (involuted follicles).

The molecular studies were contributory in both cases and revealed clonal TCR gene rearrangements and positivity for EBER in lymph node specimens from both cases. Of interest, while initial bone marrow in case 2 was very abnormal with marked plasmacytosis and similar to that reported in some bone marrows in patients with AITL [24], no involvement by lymphoma was found by flow cytometry or molecular studies at that time. This suggests that plasmacytosis is a secondary and systemic change rather than a local response to AITL.

The above cases highlight the importance of a high degree of suspicion for underlying AITL in lymph nodes with interfollicular or diffuse polyclonal plasma cell and/or immunoblastic proliferations, especially when a clonal T cell population is detected. Since neoplastic cells may be scattered and in extremely small numbers, when the suspicion is high, subtle abnormalities on the flow cytometry should be thoroughly investigated. Immunoperoxidase stains for CD10 and follicular T cell markers such as PD-1/CD279 and CXCL13 can be helpful, but may not be always conclusive as in the above cases.

Sometimes, a pathologist will be faced with peripheral blood or bone marrow specimens from patients with AITL before evaluating lymph nodes diagnostic for AITL. The extent of secondary plasmacytosis in those specimens can be very striking and potentially misleading as previously documented [24]. One should consider AITL in the long list of differential diagnosis of polyclonal plasmacytosis. Among other conditions, systemic polyclonal plasmacytosis can be seen in infections, drug reactions, hyperimmunization, toxins, serum sickness, Hodgkin lymphoma, autoimmune diseases, idiopathic conditions, and the previously mentioned SPBIP [25–36]. However, SPBIP is a diagnosis of exclusion and one needs to investigate alternative causes for polyclonal plasmacytosis or B immunoblastic proliferation before making a diagnosis of SPBIP.

In summary, ALTL should be considered a type of IL-6 syndrome as it has many clinical and pathologic features shared with other conditions associated with increased secretion of IL-6 [37].

Conflict of interest The authors declare that they have no conflict of interest.

References

1. Attygalle AD, Al Jehani R, Diss TC et al (2002) Neoplastic T-cells in angioimmunoblastic T-cell lymphoma express CD10. Blood 99:627–633
2. Swerdlow SH, Campo E, Harris NL et al (2008) WHO classification of tumours of haematopoietic and lymphoid tissues. IARC press, Lyon
3. Dunleavy K, Wilson WH, Jaffe ES (2007) Angioimmunoblastic T-cell lymphoma: pathobiological insights and clinical implications. Curr Opin Hematol 14:348–353
4. Lachenal F, Berger F, Ghesquieres H et al (2007) Angioimmunoblastic T-cell lymphoma. Clinical and laboratory features at diagnosis in 77 patients. Medicine 86:282–292
5. Frizzera G, Moran EM, Rappaport H (1974) Angio-immunoblastic lymphadenopathy with dysproteinaemia. Lancet 1(7866):1070–1073
6. Dogan A, Attygalle AD, Kyriakou C (2003) Angioimmunoblastic T-cell lymphoma. Br J Hematol 121:681–691
7. Warnke RA, Jones D, Hsi ED (2007) Morphologic and immunophenotypic variants of nodal T-cell lymphomas and T-cell lymphoma mimics. Am J Clin Pathol 127:511–527
8. Attygalle AD, Chuang SS, Diss TC et al (2007) Distinguishing angioimmunoblastic T-cell lymphoma from peripheral T-cell lymphoma, unspecified, using morphology, immunophenotype and molecular genetics. Histopathology 50:498–508
9. Gaulard P, de Leval L (2011) Follicular helper T cells: implications in neoplastic hematopathology. Semin Diagn Pathol 28:202–213
10. O'Connor NT, Crick JA, Wainscoat JS et al (1986) Evidence for monoclonal T-lymphocyte proliferation in angioimmunoblastic lymphadenopathy. J Clin Pathol 39:1229–1232
11. Lipford EH, Smith HR, Pittaluga S et al (1987) Clonality of angioimmunoblastic lymphadenopathy and implications for its evolution to malignant lymphoma. J Clin Invest 79:637–642
12. Feller AC, Griesser H, Schilling CV et al (1988) Clonal gene rearrangement patterns correlate with immunophenotype and clinical parameters in patients with angioimmunoblastic lymphadenopathy. Am J Pathol 133:549–556
13. Baker AM, Davis DW, Berg KK (2001) Polyclonal systemic immunoblast proliferation: an unusual hematologic entity presenting as a medical examiner case. J Forensic Sci 46(1):156–159
14. Peterson LC, Kueck B, Arthur DC et al (1988) Systemic polyclonal immunoblastic proliferations. Cancer 61:1350–1358
15. Poje EJ, Soori GS, Weisenburger DD (1992) Systemic polyclonal B-immunoblastic proliferation with marked peripheral blood and bone marrow plasmacytosis. Am J Clin Pathol 98:222–226
16. Peterson L, Marcerelli A, Arthur D et al (1998) Systemic polyclonal immunoblastic proliferation: a distinct atypical lymphoproliferative disorder. Mod Pathol 11:138A
17. McGrath MS (1991) EBV negative polyclonal lymphoma: identification of a new HIV-associated disease process. J Acquir Immune Defic Syndr 4(4):408–415
18. Chang KL, Chen YY, Shibata D et al (1992) Description of an in situ hybridization methodology for detection of Epstein–Barr virus RNA in paraffin-embedded tissues with a survey of normal and neoplastic tissues. Diagn Mol Pathol 1:246–255
19. Van Dongen JJ, Langerak AW, Bruggemann M et al (2003) Design and standardization of PCR primers and protocols for detection of clonal immunoglobulin and T-cell receptor gene recombinations in suspect lymphoproliferations: report of the BIOMED-2 Concerted Action BMH4-CT98-3936. Leukemia 17(12):2257–2317
20. Chen W, Kesler MV, Karandikar NJ et al (2006) Flow cytometric features of angioimmunoblastic T-cell lymphoma. Cytometry B Clin Cytom 70B:142–148
21. Cook J, Craig F, Swerdlow S (2003) Benign CD10-positive T cells in reactive lymphoid proliferations and B-cell lymphomas. Mod Pathol 16(9):879–885
22. Yu H, Shahsafaei A, Dorfman D (2009) Germinal-center T-helper cell markers PD-1 and CXCL13 are both expressed by neoplastic cells in angioimmunoblastic T-cell lymphoma. Am J Clin Pathol 131:33–41
23. Grogg K, Attygale A, Macon W et al (2006) Expression of CXCL13, a chemokine highly upregulated in germinal center T-helper cells, distinguishes angioimmunoblastic T-cell lymphoma from peripheral T-cell lymphoma, unspecified. Mod Pathol 19:1101–1107
24. Grogg K, Morice WG, Macon WR (2007) Spectrum of bone marrow findings in patients with angioimmunoblastic T-cell lymphoma. Br J Hematol 137(5):416–422
25. Koduri PR, Naides SJ (1996) Transient blood plasmacytosis in parvovirus B19 infection: a report of two cases. Ann Hematol 72:49–51
26. Barnett EV, Stone G, Swisher SN et al (1963) Serum sickness and plasmacytosis: a clinical, immunologic and hematologic analysis. Am J Med 35:113–122
27. Komiya I, Kuriya S (1991) Perpheral blood plasmacytosis in a patient with infectious mononucleosis-like illness. Eur J Hematol 46:61–62
28. Kothol RC, Hamilton HE (1981) Azathioprine-induced plasmacytosis. JAMA 246:2193
29. Gorden L, Smith C, Graber SE (1991) Case report: marked plasmacytosis and immunoglobulin abnormalities following infusion of streptokinase. Am J Med Sci 301:186–189
30. Moake JL, Ladry PR, Oren ME et al (1974) Transient peripheral plasmacytosis. Am J Clin Pathol 62:8–15
31. Barker BE, Farnes P, LaMarche PH (1966) Peripheral blood plasmacytosis following systemic exposure to *Phytolacca americana* (pokeweed). Pediatrics 38:490–493

32. Gawoski J, Ooi W (2003) Dengue fever mimicking plasma cell leukemia. Arch Pathol Lab Med 127:1026–1027
33. Kojimaa M, Murayamab K, Igarashib T et al (2007) Bone marrow plasmacytosis in idiopathic plasmacytic lymphadenopathy with polyclonal hyperimmunoglobulinemia: a report of four cases. Pathol Res Pract 203(11):789–794
34. Kass L, Votaw ML (1975) Eosinophilia and plasmacytosis of the bone marrow in Hodgkin's disease. Am J Clin Pathol 64(2):248–250
35. Lee J, Chang J, Cho Y et al (2005) A case of reactive plasmacytosis mimicking multiple myeloma in a patient with primary Sjogren's syndrome. J Korean Med Sci 20:506–508
36. Ohno H, Tanaka H, Sakai H et al (2005) Polyclonal proliferation of plasma cells associated with marked hypergammaglobulinemia in an elderly patient. Int J Hematol 81:62–65
37. Akira S, Taga T, Kishimoto T (1993) Interleukin-6 in biology and medicine. Adv Immunol 54:1–78

Virchows Arch (2012) 461:333–337
DOI 10.1007/s00428-012-1288-x

ORIGINAL ARTICLE

Epithelial cell adhesion molecules and epithelial mesenchymal transition (EMT) markers in Ewing's sarcoma family of tumors (ESFTs). Do they offer any prognostic significance?

Isidro Machado · José A. López-Guerrero · Samuel Navarro · Marco Alberghini · Katia Scotlandi · Piero Picci · Antonio Llombart-Bosch

Received: 23 May 2012 / Accepted: 16 July 2012 / Published online: 17 August 2012
© Springer-Verlag 2012

Abstract Epithelial marker and adhesion molecule expression has been reported in Ewing's sarcoma family of tumors (ESFTs), although the prognostic significance has not been assessed systematically. We performed immunohistochemical analysis of epithelial cell adhesion molecule and epithelial mesenchymal transition markers on 415 genetically confirmed ESFTs. Survival analyses were performed in 217 patients. The atypical histological subtype expressed a high proportion of the epithelial markers compared with conventional and PNET variants. We observed that expression of desmoplakin ($p<0.001$) and PI3K ($p=0.003$) was higher in disseminated than in localized disease. Multivariate analysis showed that desmoplakin and pGSK3β constitute independent good prognostic factors for progression free survival (PFS), while ZO-1 and Snail represent independent good prognostic factors for overall survival (OS). In contrast, CK8/18 represents an independent poor prognostic factor for OS and the radiotherapy treatment group demonstrated an independent poor prognostic factor for PFS and OS. Although the expression of pan-cytokeratin has been previously highlighted in a significant proportion of ESFT, its expression did not reveal prognostic significance in the present series. Considering the results of prognostic analysis herein reported, we strongly recommend a prospective validation of at least the immunomarkers with prognostic significance (desmoplakin, ZO-1, CK8/18, pGSK3β, and Snail) in prospective series that include localized and disseminated tumors.

Keywords Ewing's sarcoma · Epithelial markers · Prognostic significance

The authors wish to dedicate this article to the memory of Prof. Marco Alberghini who sadly passed away while this paper was in press.

I. Machado
Pathology Department, Instituto Valenciano de Oncología, Valencia, Spain

J. A. López-Guerrero
Laboratory of Molecular Biology, Instituto Valenciano de Oncología, Valencia, Spain

S. Navarro · A. Llombart-Bosch (✉)
Pathology Department, University of Valencia, Avda Blasco Ibañez, 15, 46010 Valencia, Spain
e-mail: antonio.llombart@uv.es

M. Alberghini
Pathology Department, Rizzoli Institute, Bologna, Italy

K. Scotlandi · P. Picci
Laboratory of Experimental Oncology, Rizzoli Institute, Bologna, Italy

Introduction

Epithelial marker and adhesion molecule expression has been reported in Ewing's sarcoma family of tumors (ESFTs) [1–6], although the prognostic significance has not been assessed systematically in a large series of genetically confirmed tumors. The aim of the present study is to determine if epithelial cell adhesion molecules and epithelial mesenchymal transition (EMT) expression offer any prognostic significance in a large series of ESFT.

Table 1 Immunohistochemical study: antibodies, source, and dilution

Antibodies	Source	Dilution
CK (AE1/AE3)	Dako	1/50
CK8/18	Novocastra	1/50
CK 34β12	Novocastra	1/50
E-cadherin	Novocastra	1/20
Claudin	Zymed	1/100
Occludin	Zymed	1/100
Desmoglein 1	Santa Cruz	1/200
Desmoplakin	Santa Cruz	1/100
ZO-1	Zymed	1/50
Snail	Abgent	1/100
Slug	Abgent	1/100
PI3K	Santa Cruz	1/50
GSK3β	Santa Cruz	1/400
P-GSK3β	Santa Cruz	1/100
AKT1,2	Santa Cruz	1/400
AKT1,2,3	Santa Cruz	1/400

Material and methods

In the present study, we performed immunohistochemical (IHC) analysis of epithelial cell adhesion molecule and EMT markers (Table 1) on 415 genetically confirmed ESFT retrieved from the prognostic and therapeutic targets in the Ewing's family of tumors (PROTHETS) and EuroBoNet European projects. The immunostaining score was classified as non-informative, negative (mild in <5 %), or positive: 1+ (mild in 5–10 %), 2+ (moderate in 10–50 %), and 3+ (intense in >50 %); mainly cytoplasmic, paranuclear, or membranous staining. All sections were independently evaluated by three pathologists (IM, SN, and ALLB). Any differences were resolved by agreement.

Survival analyses were performed in 217 patients with localized disease and available follow-up using Kaplan–Meier method with log-rank tests and Cox proportional hazards models [7]. Detailed clinical and follow-up data

Table 2 Immunoexpression of epithelial cell adhesion molecules and EMT markers n=415

Immunohistochemical markers	Negative (%)	Positive (%)
Claudin	91 (24)	285 (76)
E-cadherin	368 (97)	10 (3)
Desmoglein	151 (51)	147 (49)
Desmoplakin	271 (72)	106 (28)
Occludin	88 (24)	287 (76)
ZO-1	42 (11)	333 (89)
CK8/18	207 (88)	28 (12)
CK34β12	220 (96)	9 (4)
CK (AE1/AE3)	305 (80)	76 (20)
p-GSK3β	93 (26.9)	253 (73.1)
Snail	102 (27.9)	263 (72.1)
Slug	58 (15.7)	311 (84.3)
GSK3β	42 (11.3)	330 (88.7)
AKT1,2,3	52 (14.2)	314 (85.8)
AKT1,2	143 (40.3)	212 (59.7)
PI3K	192 (52.5)	174 (47.5)

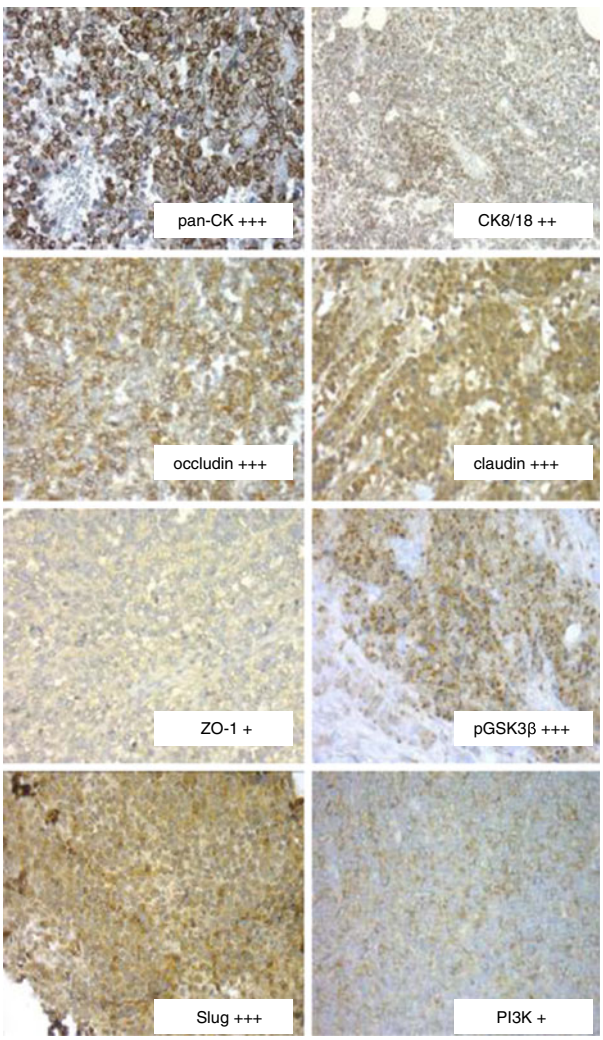

are described in studies by López-Guerrero et al. [7] and Llombart-Bosch et al. [8].

Results

IHC expression results are summarized in Table 2. Although the statistical analysis did not reveal significant results, the atypical histological subtype expressed a high proportion of the epithelial markers compared with conventional and PNET variants. We observed that expression of desmoplakin ($p<0.001$) and PI3K ($p=0.003$) was higher in disseminated (disseminated primary tumors, recurrences, and metastasis) than in localized disease. However, in the univariate analysis, the association of the expression of epithelial and adhesion molecules with progression free survival (PFS) and overall survival (OS) in localized tumors revealed that desmoplakin represents an independent good prognostic factor for both PFS and OS (Fig. 1). Multivariate analysis (Table 3) showed that desmoplakin and pGSK3β constitute independent good prognostic factors for PFS, while ZO-1 and Snail represent independent good prognostic factors for OS. CK8/18 represents an independent poor prognostic factor for OS and the radiotherapy treatment group demonstrated an independent poor prognostic factor for PFS and OS.

Discussion

Comparative expression of epithelial markers and adhesion molecules with other ESFT series has been previously described, indicating heterogenous expression of epithelial markers across the diverse series [1–6]. In particular, Srivastava et al. [5] described follow-up information in 12 well-documented ESFT that stained strongly for pan-keratin with ultrastructural confirmation. This study showed that keratin-positive ESFT may represent a more aggressive subset of the ESFT group of tumors [5]. However, in additional series, Kavalar et al. [9] demonstrated that pan-CK immunoexpression ($p=0.934$) had no statistically significant impact on survival [9]. In fact, although pan-cytokeratin expression has been highlighted in a significant proportion of ESFT in several studies [1–6], in the present series, similar to Kavalar et al. [9], its expression did not reveal prognostic significance. Nevertheless, CK8/18 immunoexpression represents, at least in the present series, an independent poor prognostic factor for OS in localized ESFT, similar to that described by Makino T et al. [10] in squamous cell carcinoma of the esophagus, where CK8/18 immunoexpression represents a poor prognostic factor for OS [10]. As far as we know, prognostic significance of low molecular weight CK (CK8/18) in other series of sarcomas or mesenchymal tumors has not been described.

Parameters	n	Events	%PFS	P
Claudin				
Negative	57	28	46	0.565
Positive	138	60	48	
E-Cadherin				
Negative	189	88	46	0.090
Positive	6	0	100	
Desmoglein				
Negative	111	51	49	0.641
Positive	74	35	44	
Desmoplakin				
Negative	157	79	44	0.032
Positive	38	9	66	
Occludin				
Negative	68	31	51	0.419
Positive	126	57	46	
ZO				
Negative	30	17	39	0.141
Positive	163	72	48	
CAM5.2				
Negative	153	69	49	0.337
Positive	18	9	24	
CK34BE12				
Negative	161	74	47	0.922
Positve	5	2	60	
CK				
Negative	160	75	47	0.693
Positive	36	15	46	

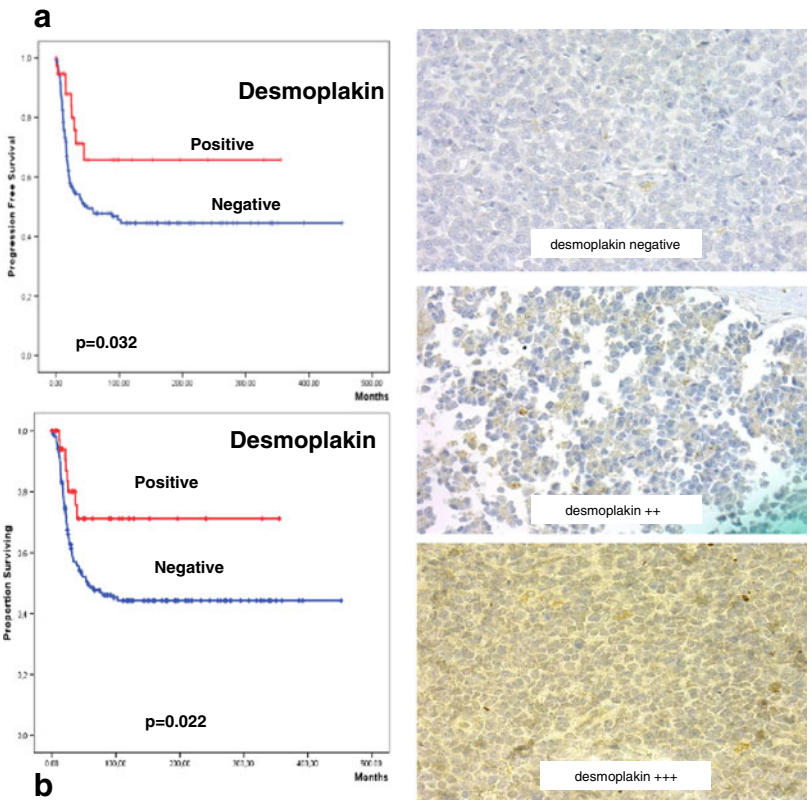

Fig. 1 Association of the expression of adhesion molecules and cytokeratins with progression free survival (**a**) and overall survival (**b**) ($n=217$). Univariate analysis

Table 3 Association of the expression of adhesion molecules, cytokeratins, and EMT markers with progression free survival (A) and overall survival (B)

Parameters	HR [95 % CI HR]	*p*
A[a]		
Desmoplakin		
Negative	1	0.044
Positive	0.49 [0.24–0.98]	
pGSK3B		
Negative	1	0.026
Positive	0.57 [0.34–0.94]	
Treatment		
Surgery group	1	0.036
Radiotherapy group	1.8 [1.03–3.01]	
B[b]		
Treatment		
Surgery group	1	0.006
Radiotherapy group	2.2 [1.3–3.9]	
CAM5.2		
Negative	1	0.034
Positive	2.3 [1.1–5.0]	
ZO-1		
Negative	1	0.006
Positive	0.44 [0.24–0.79]	
Snail		
Negative	1	<0.0001
Positive	0.34 [0.2–0.56]	

Multivariate analysis

[a] N=164. Variables included: type of treatment, lobular pattern, desmoplakin, and pGSK3β

[b] N=152. Variables included: type of treatment, lobular pattern, desmoplakin, ZO, Snail, CAM5.2

Although Schuetz et al. [4] described a very detailed study of adhesion molecules (desmoplakin, claudin, occludin, ZO-1, E-cadherin, and desmoglein) in ESFT, to our knowledge, this is the first study to report the prognostic involvement of these markers as well as EMT markers in ESFT. In the present series, desmoplakin and ZO-1 immunoexpression represent an independent good prognostic factor in localized ESFT. Our data are analogous with previous studies in other human tumors suggesting that reduced desmoplakin immunoreactivity is associated with an unfavorable prognosis as reported by Papagerakis et al. [11] proposing that downregulation of desmoplakin expression may represent a useful marker for evaluating the risk of metastasis in human carcinomas. Indeed, additional studies in sarcomas need to be performed in order to confirm the prognostic significance of this marker as well as other adhesion molecules (ZO-1) in mesenchymal neoplasms.

EMT markers have been implicated in sarcomagenesis, and particularly, the Snail family of transcription factors has been implicated in neural crest development, apoptosis, and neoplastic EMT [12]. Snail is a marker of malignancy in epithelial tumors and a prognostic study in gastric cancer demonstrated that overall survival rate of gastric cancer patients with high Snail expression was significantly lower than those patients with low Snail expression [13]. However, in sarcomas, this protein expression has been not systematically studied. Sharili et al. [14] have suggested a link between Snail2 expression and metastasis in osteosarcomas—this being the first study where Snail2 has been associated with sarcoma progression. This study shows that Snail2 may be a useful prognostic marker for osteosarcoma [14]. In the present series, in contrast with carcinomas [13] and sarcomas series [14], Snail expression represents an independent good prognostic factor for OS. The present study confirms the results of Lopez-Guerrero et al. [7] where radiotherapy groups (with surgery and/or chemotherapy) represent an adverse prognostic factor for OS and PFS, probably due to the presence of inoperable cases with advanced disease.

Considering the results for prognostic analysis herein reported, we strongly recommend a prospective validation of at least the immunomarkers having prognostic significance (desmoplakin, ZO-1, CK8/18, pGSK3β, and Snail) in independent series including localized and disseminated tumors of ESFT and other sarcoma series.

Acknowledgments This study was supported by prognostic and therapeutic targets in the Ewing's family of tumors, contract 503036, and EuroBoNet, European network to promote research into uncommon cancers in adults and children, contract 018814.

Conflict of interest None.

References

1. Folpe AL, Goldblum JR, Rubin BP, Shehata BM, Liu W, Dei Tos AP, Weiss SW (2005) Morphologic and immunophenotypic diversity in Ewing family tumors: a study of 66 genetically confirmed cases. Am J Surg Pathol 29(8):1025–1033
2. Gu M, Antonescu CR, Guiter G, Huvos AG, Ladanyi M, Zakowski MF (2000) Cytokeratin immunoreactivity in Ewing's sarcoma: prevalence in 50 cases confirmed by molecular diagnostic studies. Am J Surg Pathol 24(3):410–416
3. Collini P, Sampietro G, Bertulli R, Casali PG, Luksch R, Mezzelani A, Sozzi G, Pilotti S (2001) Cytokeratin immunoreactivity in 41 cases of ES/PNET confirmed by molecular diagnostic studies. Am J Surg Pathol 25(2):273–274
4. Schuetz AN, Rubin BP, Goldblum JR, Shehata B, Weiss SW, Liu W, Wick MR, Folpe AL (2005) Intercellular junctions in Ewing sarcoma/primitive neuroectodermal tumor: additional evidence of epithelial differentiation. Mod Pathol 18(11):1403–1410
5. Srivastava A, Rosenberg AE, Selig M, Rubin BP, Nielsen GP (2005) Keratin positive Ewing's sarcoma: an ultrastructural study of 12 cases. Int J Surg Pathol 13(1):43–50
6. Machado I, Navarro S, López-Guerrero JA, Alberghini M, Picci P, Llombart-Bosch A (2011) Epithelial marker expression does not rule out a diagnosis of Ewing's sarcoma family of tumours. Virchows Arch 459(4):409–414
7. López-Guerrero JA, Machado I, Scotlandi K, Noguera R, Pellín A, Navarro S, Serra M, Calabuig-Fariñas S, Picci P, Llombart-Bosch A (2011) Clinicopathological significance of cell cycle regulation

markers in a large series of genetically confirmed Ewing's sarcoma family of tumors. Int J Cancer 128(5):1139–1150
8. Llombart-Bosch A, Machado I, Navarro S, Bertoni F, Bacchini P, Alberghini M, Karzeladze A, Savelov N, Petrov S, Alvarado-Cabrero I, Mihaila D, Terrier P, Lopez-Guerrero JA, Picci P (2009) Histological heterogeneity of Ewing's sarcoma/PNET: an immunohistochemical analysis of 415 genetically confirmed cases with clinical support. Virchows Arch 455(5):397–411
9. Kavalar R, Pohar Marinsek Z, Jereb B, Cagran B, Golouh R (2009) Prognostic value of immunohistochemistry in the Ewing's sarcoma family of tumors. Med Sci Monit 15(8):CR442–CR452
10. Makino T, Yamasaki M, Takeno A, Shirakawa M, Miyata H, Takiguchi S, Nakajima K, Fujiwara Y, Nishida T, Matsuura N, Mori M, Doki Y (2009) Cytokeratins 18 and 8 are poor prognostic markers in patients with squamous cell carcinoma of the oesophagus. Br J Cancer 101(8):1298–1306
11. Papagerakis S, Shabana AH, Pollock BH, Papagerakis P, Depondt J, Berdal A (2009) Altered desmoplakin expression at transcriptional and protein levels provides prognostic information in human oropharyngeal cancer. Hum Pathol 40(9):1320–1329
12. Subramaniam MM, Navarro S, Llombart-Bosch A (2011) Immunohistochemical study of correlation between histologic subtype and expression of epithelial-mesenchymal transition-related proteins in synovial sarcomas. Arch Pathol Lab Med 135(8):1001–1009
13. He H, Chen W, Wang X, Wang C, Liu F, Shen Z, Xu J, Gu J, Sun Y (2012) Snail is an independent prognostic predictor for progression and patient survival of gastric cancer. Cancer Sci. doi:10.1111/j.1349-7006.2012.02295.x
14. Sharili AS, Allen S, Smith K, Hargreaves J, Price J, McGonnell I (2011) Expression of Snail2 in long bone osteosarcomas correlates with tumour malignancy. Tumour Biol 32(3):515–526

Virchows Arch (2012) 461:339–343
DOI 10.1007/s00428-012-1295-y

CASE REPORT

Clear cell sarcoma expressing a novel chimerical transcript *EWSR1 exon 7/ATF1 exon 6*

Egle Gineikiene · Dmitrij Seinin · Birute Brasiuniene · Andrius Brazaitis · Laimonas Griskevicius · Arturas Jakubauskas

Received: 23 May 2012 / Revised: 3 July 2012 / Accepted: 26 July 2012 / Published online: 11 August 2012
© Springer-Verlag 2012

Abstract Clear cell sarcoma harbours recurrent translocation, resulting in *EWSR1*/*ATF1* or less commonly *EWSR1*/*CREB1* fusion. To date, six types of *EWSR1*/*ATF1* fusion have been reported, of which three are in-frame and encode functional proteins. We present a reverse transcription - polymerase chain reaction analysis of a tumour near the hallux of the right foot. The sequencing of obtained fragments revealed the presence of a novel chimerical transcript—the in-frame fusion between *EWSR1* exon 7 and *ATF1* exon 6 that represents the fourth in-frame type of *EWSR1*/*ATF1* fusion identified in clear cell sarcomas.

Keywords Clear cell sarcoma · Chimerical transcript · *EWSR1*/*ATF1* · qPCR

E. Gineikiene · B. Brasiuniene · L. Griskevicius · A. Jakubauskas (✉)
Hematology, Oncology and Transfusion Medicine Center,
Vilnius University Hospital Santariskiu Klinikos,
Santariskiu 2,
Vilnius 08661, Lithuania
e-mail: arturas.jakubauskas@santa.lt

D. Seinin
National Center of Pathology,
Vilnius University Hospital Santariskiu Klinikos,
P. Baublio 5,
Vilnius 08406, Lithuania

A. Brazaitis
Center of Radiology,
Vilnius University Hospital Santariskiu Klinikos,
Santariskiu 2,
Vilnius 08661, Lithuania

L. Griskevicius
Clinics of Internal, Family Medicine and Oncology,
Faculty of Medicine, Vilnius University,
M.K. Ciurlionio 21,
Vilnius 03101, Lithuania

Introduction

Clear cell sarcoma (CCS), first described in 1965 [1], is perhaps the rarest clinicopathologic entity among mesenchymal tumours. Clear cell sarcoma mainly affects adolescents and young adults with female sex predominance. The most common locations of CCS are the foot and ankle. Other sites of involvement include the knee, thigh, hand, neck, trunk and, rarely, retroperitoneum and bone. So-called clear cell sarcoma of the kidney is a different entity [2] and should not be confused with CCS.

CCS displays morphologic or immunohistochemical features very similar to malignant melanoma, which is the most important differential diagnostic consideration. These two malignancies have overlapping immunohistochemical characteristics: expression of S-100 protein and melanocytic markers as HMB-45, Melan A and microphthalmia transcription factor. The tumour usually does not express cytokeratin, epithelial membrane antigen, desmin or smooth muscle actin [3]. However, CCS has been shown to be characterised by two recurrent chromosomal translocations *t* (*12*;*22*) (*q13*;*q12*) and *t* (*2*;*22*) (*q34*;*q12*), which do not occur in melanoma [4]. The most common chromosomal translocation *t* (*12*;*22*) (*q13*;*q12*) results in fusion of the *EWSR1* gene on 22q12 and the *ATF1* gene on 12q13. Less frequently, a chromosomal translocation *t* (*2*;*22*) (*q34*;*q12*) has been found which results in the *EWSR1*/*CREB1* fusion gene. These characteristic cytogenetic changes are considered to play a pivotal role in the development of CCS.

To date, six types of *EWSR1*/*ATF1* fusion and a single type of *EWSR1*/*CREB1* fusion have been described [4, 5]. Type 1 (*EWSR1 exon 8*/*ATF1 exon 4*; GenBank/EMBL/DDBJ accession no. JF290487), type 2 (*EWSR1 exon7*/*ATF1 exon 5*; GenBank/EMBL/DDBJ accession no. JF290488) and type 3 (*EWSR1 exon10*/*ATF1 exon 5*) are in-frame fusions and encode functional proteins. The other types of *EWSR1*/*ATF1* fusion—type 4 (*EWSR1 exon 7*/

ATF1 exon 7), type 5 (*EWSR1 exon 7*/*ATF1 exon 4*; GenBank/EMBL/DDBJ accession no. JN202448) and type 6 (*EWSR1 exon 9*/*ATF1 exon 4*; GenBank/EMBL/DDBJ accession no. JN202449)—are out-of-frame fusions and were identified only once, together with type 1 and type 2 transcripts (Fig. 1) [5, 6].

Clinical history

A 42-year-old male patient with no familial history of cancer presented with a 1-year history of painful lump near the hallux of the right foot. The lump was resected, and the patient was referred to our hospital for detailed examination and further treatment. The diagnosis of CCS was confirmed by biopsy, using the criteria from the WHO classification of tumours of soft tissues and bone [7]. Nuclear magnetic resonance imaging revealed a subcutaneous tumour mass 13×11 mm in size, accumulating contrast, near the first interphalangeal joint and flexor hallucis brevis muscle (Fig. 2a). Bone destruction was not observed. Computed tomography (CT) indicated mediastinal lymphadenophathy and metastases to the lungs (Fig. 2b) and omentum. The patient received three cycles of doxorubicin-based chemotherapy. Six months later, CT showed new metastases in inguinal lymph nodes and bones. High-dose ifosfamide monotherapy was started with palliative intent. The patient died 2 months later.

Materials and methods

Tumour samples and immunohistochemistry

Formalin-fixed and paraffin-embedded (FFPE) samples of tumour were presented for morphological and immunohistochemical analysis. FFPE sections were stained with haematoxylin and eosin and antibodies to S-100, HMB-45, Melan A, smooth muscle cell actin (SMA), CD34 and Pancytokeratin (Clones AE1/AE3) (Dako, Glostrup, Denmark).

RT-PCR analysis and sequencing

Total RNA was extracted from FFPE sections containing 90 % tumour cells. The extraction was performed using PureLink FFPE Total RNA Isolation Kit as described (Invitrogen, Carlsbad, CA, USA). RNA (1 μg) was reverse-transcribed in a 20-μl reaction volume using random hexamers and First Strand cDNA Synthesis Kit (Fermentas, Vilnius, Lithuania) according

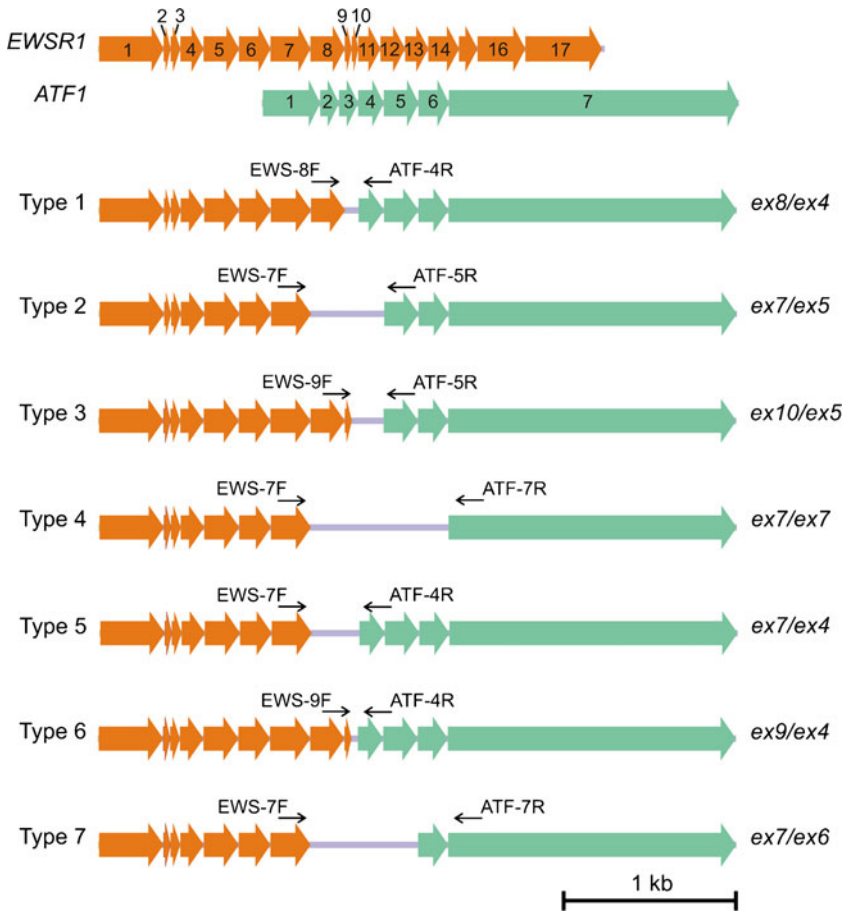

Fig. 1 *EWSR1*/*ATF1* fusion transcript types. *Orange* and *green arrows* indicate exons of *EWSR1* and *ATF1*, respectively. *Black arrows* indicate placement of primers used in this study

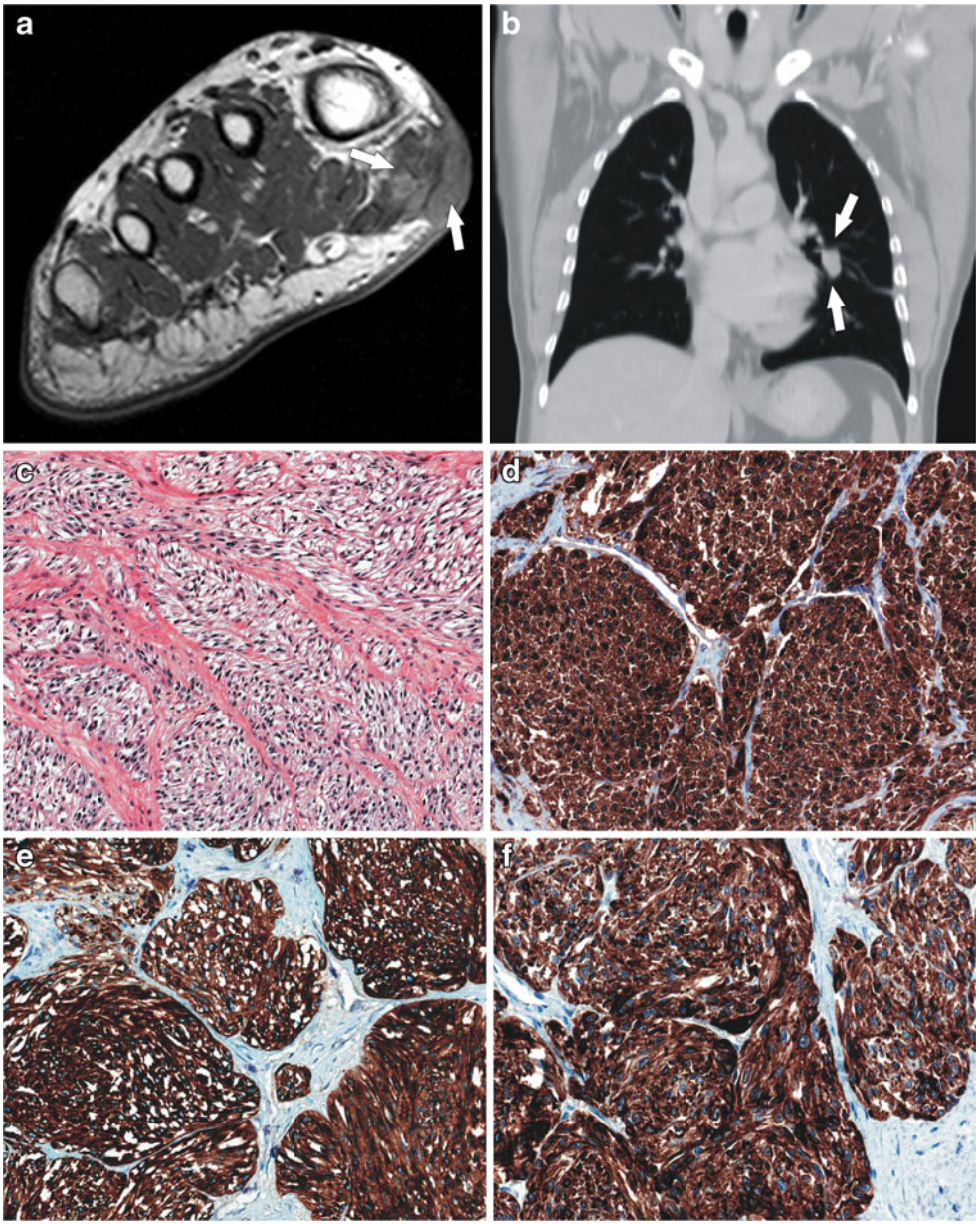

Fig. 2 Radiological images and histopathology. **a** Nuclear magnetic resonance image of the tumour mass (indicated by *white arrows*). **b** Computed tomography image showing the left lung metastasis (indicated by *white arrows*). **c** Haematoxylin–eosin staining of tumour sample; cytoplasmic immunoreactivities to **d** S100 protein; **e** HMB-45; **f** Melan A (all original magnifications ×200)

the vendor's recommendations, and after reaction, it was diluted up to 100 μl with deionised water.

The integrity of extracted mRNA was evaluated by running a polymerase chain reaction (PCR) for a 150-bp fragment of the ubiquitously expressed ubiquitin C gene with primers UBC-F and UBC-R [5]. Five different specific PCRs (four reactions for each type of *EWSR1*/*ATF1* chimerical transcript and one reaction for *EWSR1*/*CREB1* [4]) were performed using the earlier reported forward and reverse primers and reaction conditions [5]. RT-PCR products were visualised on a 2 % agarose gel electrophoresis using SYBR Green I (Fig. 3a).

The resultant RT-PCR fragment was purified by incubation with Exonuclease I and FastAP™ Thermosensitive Alkaline Phosphatase (Fermentas) as recommended by the vendor. Nucleotide sequences were generated using BigDye Terminator v1.1 Chemistry (Applied Biosystems, Foster City, CA, USA), and data were collected on Genetic Analyzer 3500(Applied Biosystems). The public interface of BLAST software at the National Center for Biotechnology Information (Bethesda, MD, USA) was used for analysis of sequence data [8].

Results

Histologically, the tumour was composed of nests of spindle-shaped and polygonal neoplastic cells with eosinophilic or clear cytoplasm. Nests of tumour cells were surrounded by fibrous septa. The neoplastic cell nuclei were vesicular with prominent nucleoli (Fig. 2c). The degree of nuclear polymorphism was low. The mitotic rate was three to

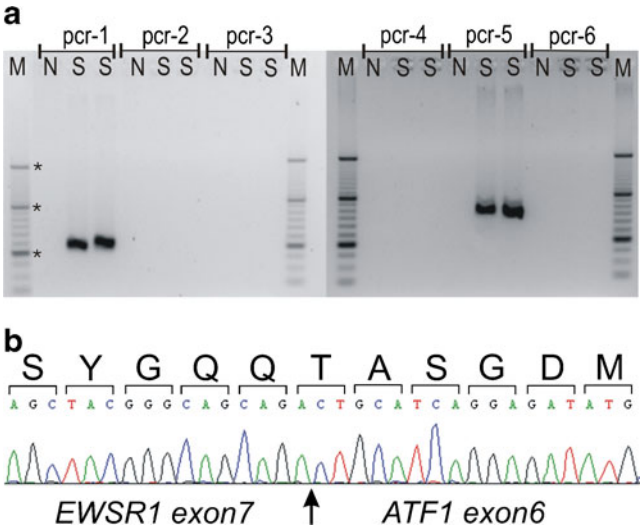

Fig. 3 Detection and identification of a novel *EWSR1*/*ATF1* chimerical transcript. **a** Agarose gel image (*inverted*). pcr-1 indicate PCR using UBC-F and UBC-R primer pair; pcr-2 indicate PCR using EWS-7F and ATF-5R primer pair; pcr-3 indicate PCR using EWS-8F and ATF-4R primer pair; pcr-4 indicate PCR using EWS-9F and ATF-5R primer pair; pcr-5 indicate PCR using EWS-7F and ATF-7R primer pair. pcr-6 indicate PCR using EWS-7F and CREB-7R primer pair. *N* and *S* show no template control and sample experiments, respectively. *M*, O'RangeRuler 50 bp DNA Ladder (Fermentas) molecular mass marker. The reference bands (indicated by *asterisk*) represent 1,000 bp (*top*), 500 bp (*middle*) and 200 bp (*bottom*) mass standards. **b** Partial sequencing chromatogram of chimerical transcript. Junction point of *EWSR1* and *ATF1* coding sequences indicated by *arrow*

five mitoses/ten high-power fields. The immunohistochemical examination showed tumour cells expressing protein S-100 (90 % of tumour cells) (Fig. 2d) and antigens associated with melanin synthesis: cytoplasmic immunoreactivity for HMB-45 (100 % of tumour cells) (Fig. 2e) and Melan A (100 % of tumour cells) (Fig. 2f). Tumour cells were negative for SMA, CD34 and Pancytokeratin (data not shown).

To determine the presence of either *EWSR1*/*ATF1* or *EWSR1*/*CREB1* fusion transcripts, RT-PCR analysis of total RNA isolated from tumour sample was performed. Agarose gel electrophoresis indicated that primers EWS-7F and ATF-7R amplified ≥300-bp-long fragment (Fig. 3a). Other primer combinations were negative. The calculated size of expected amplicon of out-of-frame fusion *EWSR1 exon 7*/*ATF1 exon 7* was 122 bp. Therefore, we considered alternative exon junctions: in the case of *EWSR1 exon 7*/*ATF1 exon 6* fusion, the resultant PCR fragment would have been 282-bp long and, in the case of *EWSR1 exon 8*/*ATF1 exon 7* fusion, the resultant PCR fragment would have been 303-bp long. To clarify this position, we purified and sequenced the resultant PCR fragment using the same primers, which showed the presence of a chimerical transcript of an in-frame fusion *EWSR1 exon 7*/*ATF1 exon 6* (Fig. 3b). The fusion sequence was deposited in the GenBank/EMBL/DDJB databases under accession no. JN624779.

Discussion

Approximately 15–20 % of sarcomas carry chromosomal translocations resulting in fusion genes. The fusion proteins frequently act as transcription factors, upregulating the expression of genes responsible for tumour growth [9]. Sarcomas with fusion genes have been classified in different ways, e.g. according to the genes participating in chromosomal translocation, the structural and functional features of each fusion gene or the variability of chimerical transcripts produced by the same fusion partners. Sarcomas with fusion genes usually harbour a single chimerical transcript, with the exception of synovial sarcoma and CCS. One report described the presence of two variant fusion genes, *SS18*/*SSX1* and *SS18*/*SSX2*, in tumour samples of 10 % of synovial sarcomas [10]. The translocation *t* (*X*;*18*) (*p11*;*q11*) resulted in the fusion of the *SS18* gene on chromosome 18 with either the *SSX1* or *SSX2* gene on the same chromosome X but with different breakpoint localizations. Each translocation resulted in a single chimerical transcript but in separate cell subpopulations of the tumour. This finding indicates that genetically variant subclones exist in synovial sarcoma.

The chromosomal translocation *t* (*12*;*22*) (*q13*;*q12*) resulting in a fusion of the *EWSR1* gene on chromosome 22q12 and the *ATF1* gene on chromosome 12q13, differentiates CCS from malignant melanoma or other tumours of a neuroectodermal or mesenchymal origin. CCS has been reported to harbour multiple types of the *EWSR1*/*ATF1* chimerical transcripts resulting from a single chromosomal rearrangement in one tumour [6]. Two different chimerical transcripts resulting from the same *EWSR1*/*ATF1* fusion are frequently observed in CCS. To date, two chimerical types have been found in more than one third of CCS [4], and two reports described the presence of three [6] and even four chimerical types [5]. This phenomenon suggests that post-transcriptional alternative splicing is taking place [4–6]. We have reported unequal quantitative distribution of different chimerical transcripts in a tumour [5]. Apparently, the *EWSR1* gene is very adaptable regarding the final structure of chimerical transcripts. Exons 7, 8, 9, 10 and 12 may serve as the fusion sites for tumours with different frequencies in different sarcomas. In the case of CCS, the exon 8 followed by the exon 7 have been identified as the most frequent fusion sites [6].

RT-PCR analysis of the present case of CCS revealed the presence of a novel *EWSR1 exon 7*/*ATF1 exon 6* fusion, which we propose to be designated as type 7. This concerns an in-frame fusion which most likely encodes a functional chimerical transcription factor since the conserved bZIP transcription factor domain [11] of cyclic AMP-dependent transcription factor ATF1 is encoded by exon 6 and exon 7 of the *ATF1* gene. This case expands the variability of the *EWSR1*/*ATF1* chimerical transcripts that result from chromosomal translocation *t* (*12*;*22*) (*q13*;*q12*) in CCS.

Conflict of interest We declare that we do not have conflict of interest.

References

1. Enzinger FM (1965) Clear-cell sarcoma of tendons and aponeuroses. An analysis of 21 cases. Cancer 18:1163–1174
2. Argani P, Perlman EJ, Breslow NE, Browning NG, Green DM, D'Angio GJ, Beckwith JB (2000) Clear cell sarcoma of the kidney: a review of 351 cases from the National Wilms Tumor Study Group Pathology Center. Am J Surg Pathol 24:4–18
3. Dim DC, Cooley LD, Miranda RN (2007) Clear cell sarcoma of tendons and aponeuroses: a review. Arch Pathol Lab Med 131:152–156
4. WangW-L ME, Zhang W, Hernandez VS, Tuvin D, Garcia L, Lev DC, Lazar AJ, López-Terrada D (2009) Detection and characterization of *EWSR1*/*ATF1* and *EWSR1*/*CREB1* chimeric transcripts in clear cell sarcoma (melanoma of soft parts). Mod Pathol 22:1201–1209. doi:10.1038/modpathol.2009.85
5. Jakubauskas A, Valceckiene V, Andrekute K, Seinin D, Kanopka A, Griskevicius L (2011) Discovery of two novel *EWSR1*/*ATF1* transcripts in four chimerical transcripts-expressing clear cell sarcoma and their quantitative evaluation. Exp Mol Pathol 90:194–200. doi:10.1016/j.yexmp.2010.12.005
6. Panagopoulos I, Mertens F, Dêbiec-Rychter M, Isaksson M, Limon J, Kardas I, Domanski HA, Sciot R, Perek D, Crnalic S, Larsson O, Mandahl N (2002) Molecular genetic characterization of the *EWS*/*ATF1* fusion gene in clear cell sarcoma of tendons and aponeuroses. Int J Cancer 99:560–567. doi:10.1002/ijc.10404
7. Fletcher CDM, Unni KK, Mertens F (eds) (2002) World Health Organization classification of tumours: pathology and genetics of tumours of soft tissue and bone. IARC, Lyon
8. Johnson M, Zaretskaya I, Raytselis Y, Merezhuk Y, McGinnis S, Madden TL (2008) NCBI BLAST: a better web interface. Nucleic Acids Res 36:W5–W9. doi:10.1093/nar/gkn201
9. Bovee JV, Hogendoorn PC (2009) Molecular pathology of sarcomas: concepts and clinical implications. Virchows Arch 456:193–199
10. Yang K, Lui WO, Xie Y, Zhang A, Skytting B, Mandahl N, Larsson C, Larsson O (2002) Co-existence of *SYT–SSX1* and *SYT–SSX2* fusions in synovial sarcomas. Oncogene 21:4181–4190
11. Hurst HC (1995) Transcription factors 1: bZIP proteins. Protein Profile 2:101–168

Virchows Arch (2012) 461:345–350
DOI 10.1007/s00428-012-1298-8

CASE REPORT

Thyroid-like follicular carcinoma of the kidney: report of two cases with detailed immunohistochemical profile and literature review

Lara Alessandrini · Matteo Fassan · Marina Paola Gardiman · Andrea Guttilla · Fabio Zattoni · Tommaso Prayer Galletti · Filiberto Zattoni

Received: 19 June 2012 / Revised: 25 July 2012 / Accepted: 2 August 2012 / Published online: 17 August 2012
© Springer-Verlag 2012

Abstract Thyroid-like follicular carcinoma of the kidney (TLFC) is an unusual histological variant of renal cell carcinoma not included in the current WHO classification of renal tumors. Its morphological features resemble a large spectrum of benign and malignant renal and extra-renal conditions which should be ruled out in the diagnostic process. Because TLFC outcome is different from the other variants of renal cell carcinoma, the exploration for disease-specific markers is mandatory. The aim of the present paper is to illustrate the histological characteristics and immunohistochemical profile of two new cases along with a brief review of the literature.

Keywords Renal cell carcinoma · Oncology · Thyroid-like follicular carcinoma · Immunohistochemistry

Introduction

Thyroid-like follicular carcinoma of the kidney (TLFC) is an unusual histologic type of renal cell carcinoma, which morphologically closely mimics follicular carcinoma of the thyroid. First described in 1996 [1], only further 10 cases have been described so far [2–6]. The relevance of this peculiar histologic variant relies on its morphological resemblance to a large spectrum of benign and malignant renal and extra-renal conditions. As a consequence, an erroneous diagnosis could result in inadequate therapeutic solutions.

Given the relevance for the introduction of disease-specific markers, we report two cases of TLFC focusing on their immunohistochemical profile. A brief review of the previous published cases is also discussed.

L. Alessandrini · M. Fassan · M. P. Gardiman (✉)
Department of Medicine, Surgical Pathology and Cytopathology Unit, University Hospital of Padua,
Via Aristide Gabelli,
61-35121 Padua (PD), Italy
e-mail: marinapaola.gardiman@sanita.padova.it

M. Fassan
Department of Surgical Oncology and Gastroenterology Sciences, General Oncology Unit, University of Padua,
Padua (PD), Italy

A. Guttilla · F. Zattoni · T. P. Galletti · F. Zattoni
Department of Surgical Oncology and Gastroenterology Sciences, Urology Unit, University of Padua,
Padua (PD), Italy

Clinical history

Case 1

A 76-year-old white man with a past medical history significant for hypertension, atrial fibrillation, and prostate cancer underwent radical prostatectomy and adjuvant radiotherapy in 2007. The patient was admitted at the Urology Department of Padua University Hospital for hematuria in May 2011. An abdominal ultrasound showed the presence of a left kidney mass. The CT scan revealed a round moderately hyperdense and well-vascularized solid mass of about 5 cm with a necrotic central area at the upper pole of the left kidney and the presence of some enlarged lymph nodes (the largest of 17 mm) below the diaphragm pillars and in the para-aortic and interaortocaval area. The patient was submitted to an open radical left nephrectomy and he was discharged after 7 days. The gross specimen (measures of the kidney: 10×5.5×5 cm) showed a well-circumscribed round mass measuring 4.5 cm in its largest diameter. On cut surface, the lesion was pale yellow to whitish, with focal hemorrhagic zones. Focal extension into perinephric adipose tissue was grossly evident and subsequently confirmed

by microscopic examination. Neither invasion of renal pelvis nor macroscopic invasion of the renal vein was found. A single (non-metastatic) para-aortic lymph node was histologically confirmed. The patient is alive without signs of tumor relapse at an 11-month follow-up.

Case 2

A renal mass was incidentally discovered during an ultrasound exam (that showed normal internal genitalia) in a 41-year-old white woman with a past medical history significant of: (a) Hodgkin's lymphoma (treated with splenectomy, chemotherapy, and radiotherapy); (b) right video-assisted laparoscopic ovariectomy (benign serous cyst); (c) post-RT hypothyroidism; and (d) sinus tachycardia (treated with beta blockers). She subsequently performed a CT scan that highlighted the presence at the inferior pole of the right kidney of a 5-cm fluid-filled round mass. The lack of enhancement after contrast and the presence of septa were confident with a final radiological diagnosis of a hemorrhagic cyst or complex cysts. A subsequent MRI confirmed the presence of a round right kidney mass of about 5 cm with solid septa. On December 2011, the patient underwent to a robotic-assisted partial nephrectomy. The postoperative course was uneventful and the patient was discharged after 9 days. The gross specimen exhibited a well-circumscribed yellow-tan lesion (4.3 cm in its largest diameter) with cystic–hemorrhagic areas. The patient is alive without signs of tumor relapse at a 4-month follow-up.

Materials and methods

Surgical specimens were sampled according to the current protocols [7]. Formalin-fixed, paraffin-embedded tissue samples were obtained, and 4-μm sections were stained with hematoxylin and eosin.

Immunohistochemical analysis was performed using the Bond ™ Polymer Refine Detection System (Leica Microsystems, Newcastle upon Tyne, UK). A large panel of primary antibodies was used (source and solutions): cytokeratin 7 (Dakocytomation, Glostrup, Denmark; 1:800); cytokeratin 19 (Dakocytomation;1:100); cytokeratin 20 (Dakocytomation; 1:50); 34βE12 (Novocastra labs ltd, Newcastle upon Tyne, UK; 1:100); thyroid transcription factor 1 (TTF-1; Dakocytomation; 1:200); Thyroglobulin (TG; Dakocytomation; 1:50); galectin-3 (Cell Marque Corporation, Rocklin, CA; 1:50); Hector Battifora Mesothelial cell 1 (HBME-1; Cell Marque Corporation; 1:50); epithelial membrane antigen (EMA; Dakocytomation; 1:500); Vimentin (Novocastra labs ltd; 1:200); chromogranin (Dakocytomation; 1:100); synaptophysin (Dakocytomation; 1:400); CD56 (Novocastra labs ltd; 1:100); CD10 (Diagnostic Biosystems, Pleasanton, CA; 1:50); E-cadherin (Dakocytomation;1:200); renal cell carcinoma (RCC; Novocastra labs ltd; 1:100); neuron specific enolase (NSE; Dakocytomation; 1:200); carcino embryonic antigen (CEA; Biogenex, Fremont CA; 1:200); *Ulex europaeus* lectin (Ulex; Vector laboratories, Burlingame, CA; 1:50); and Wilm's tumor 1 (WT-1; Dakocytomation, 1:200).

Sections were lightly counterstained with hematoxylin. Appropriate positive and negative controls were run concurrently for all the applied antisera.

Results

Both tumors were histologically characterized by a striking follicular architecture composed of macro- and microfollicles filled with eosinophilic amorphous colloid-like material that mirrored follicular carcinoma of the thyroid (Fig. 1a, b, c). Follicles were lined by cuboidal cells with scant eosinophilic cytoplasm and round to oval nuclei with evenly distributed chromatin (Fig. 1d). Occasional nucleoli were also detected at high magnification. Mitotic activity was absent. Patchy lymphoid aggregates, focal areas of papillary differentiation (Fig. 1a), hemorrhagic zones, and cholesterol crystals were present. In case 1, the predominant follicular pattern was focally interrupted by solid areas of pseudosarcomatoid appearance, without well-formed follicles. The cells showed elongated cytoplasm with round–oval nuclei and mild atypia (Fig. 1d). Histologic examination of the single para-aortic lymph node revealed no metastasis. Surgical excision margins of case 2 were not involved by neoplasia.

In both lesions, immunohistochemical analysis showed identical results (Fig. 2). The tumor exhibited strong and diffuse cytoplasmic/membranous reactivity for cytokeratins (CKs) 7 (Fig. 2d) and 19, vimentin, and EMA (Fig. 2a), whereas CK 20 was not expressed. Focal staining for 34βE12 (Fig. 2b) and E-cadherin was detected. Histogenetic markers for follicular cell origin (TG and TTF-1) and markers usually overexpressed in thyroid malignancies (HBME-1 and galectin-3) were negative, as were markers of neuroendocrine differentiation (CD56, synaptophysin, chromogranin, and NSE). Tumor cells did not show any immunostaining for WT-1, CD10 (Fig. 2c), RCC, CEA, and Ulex.

Clinicopathologic characteristics and immunohistochemical profile of the present cases and the previously reported ones are listed in Table 1.

Discussion

TLFC is an unusual histological variant of renal cell carcinoma not included in the current WHO classification of renal

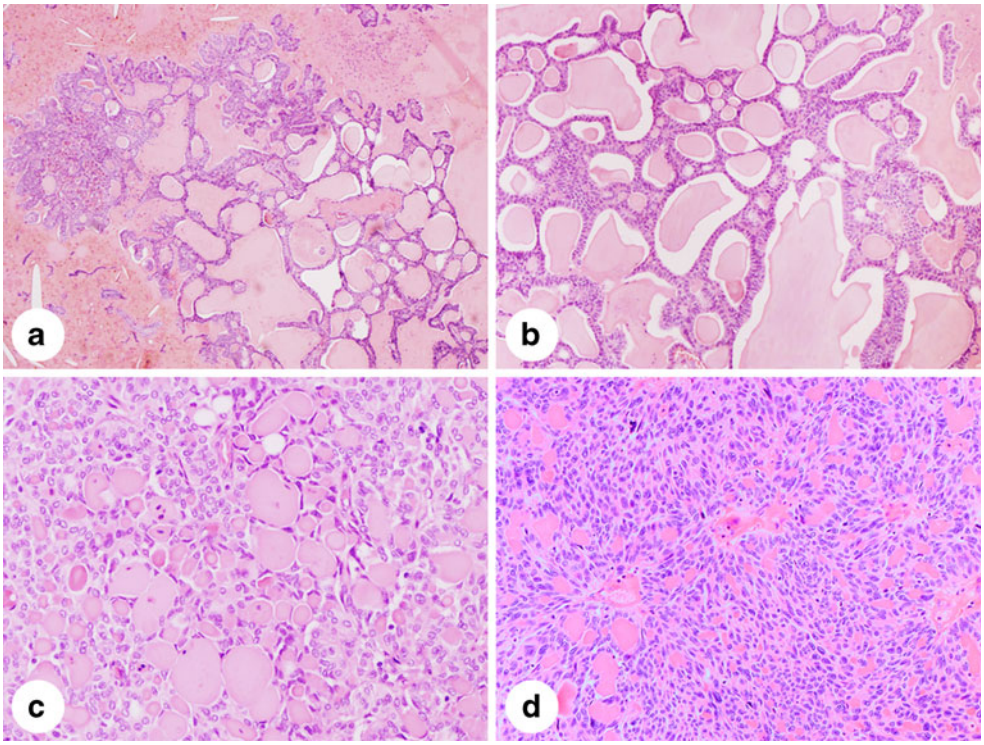

Fig. 1 Follicular architecture of both neoplasms composed of macro- and microfollicles filled with colloid-like material. **a** Area with papillary differentiation, hematoxylin and eosin (original magnification ×50). **b** Hematoxylin and eosin (original magnification ×100). **c** Follicles were lined by cuboidal cells with scant eosinophilic cytoplasm and round to oval nuclei with evenly distributed chromatin**,** Hematoxylin and eosin (original magnification ×200). **d** Solid areas of pseudosarcomatoid changes with mild nuclear atypia, Hematoxylin and eosin (original magnification ×100)

tumors and is a matter of debate within the pathologists' community [8, 9]. Its morphological features resemble a large spectrum of benign and malignant renal and extra-renal conditions which should be ruled out in the diagnostic process.

The striking follicular architecture featured by the presented cases and by those previously reported prompts differential diagnosis with a metastasis from a well-differentiated primary tumor of the thyroid. Renal metastasis of thyroid follicular carcinoma is a rare event, with only few cases described (usually associated to widespread neoplastic diffusion) [10–16]. Moreover, metastatic thyroid tumors usually preserve a thyroid-specific immunoprofile [17]. A

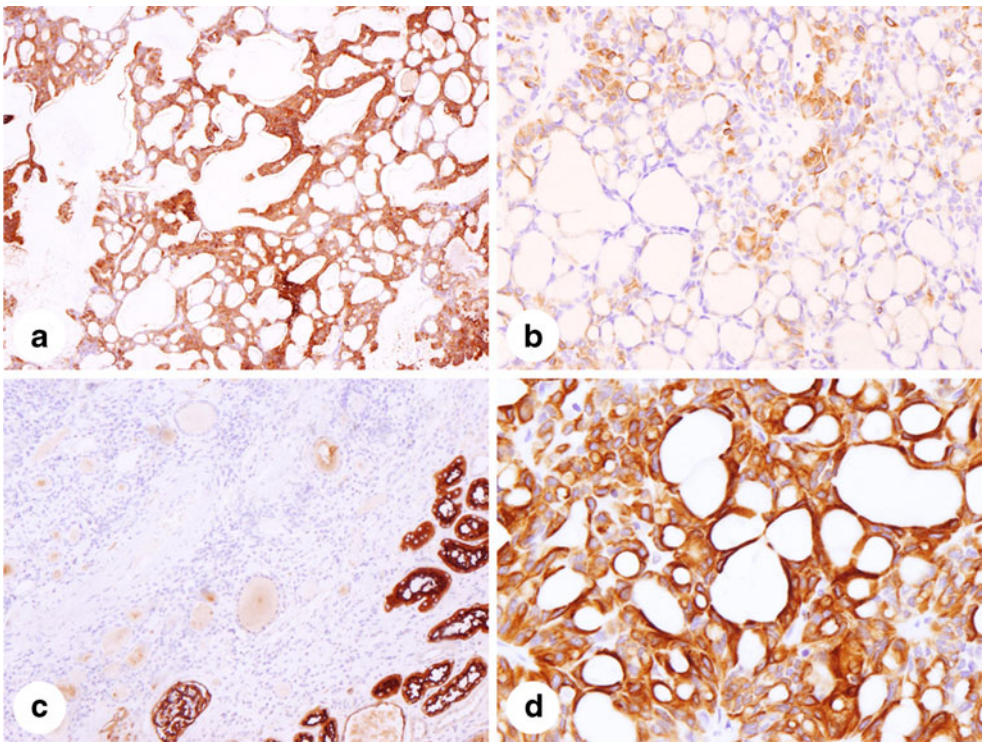

Fig. 2 Immunophenotype of thyroid-like follicular carcinoma; **a** Strong immunoreactivity for EMA (original magnification ×50); **b** Focal 34βE12 positivity (original magnification ×200); **c** Neoplastic cells were CD10 negative (*upper left*) compared with CD10 positive normal renal tissue (*lower right*) (original magnification ×80); **d** Strong and diffuse immunoreactivity for CK7 (original magnification ×320)

Table 1 Clinicopathologic characteristics and immunohistochemical profile of the present cases and the previously reported ones

Reference no./ no. of cases	Age (years)/ Gender	Clinical presentation	Tumor size (cm)	Location	pTNM	Follow-up (months)	Negative immunohistochemical markers	Positive immunohistochemical markers
1-1 case	39/F	Abdominal pain	1.5	Right kidney/ lower pole	pT1aN0	18	CD15	TG, estrogen receptor
2-6 cases	53/F	Incidental	2.1	Right kidney/ mid-pole	pT1aNX	54	PAX-2, RCC, CD10, WT1Ksp-cadherin, α-methyl-CoA racemase, vimentin, CD56, CD57, TG, TTF-1	CK 7 (1 case)
	29/F	Incidental	1.9	Right kidney/ upper pole	pT1aNX	84		
	45/M	Incidental	3.5	Right kidney/ lower pole	pT1aN1	17		
	83/M	Incidental	2.1	Left kidney/ lower pole	pT1aNX	48		
	35/M	Incidental	3.0	Right kidney/ mid-pole	pT1aNX	20		
	50/M	Incidental	4.0	Right kidney/ mid-pole	pT1aN0	7		
3-1 case	32/F	Incidental	11.8	Right kidney/ lower and mid-pole	pT2NX	6	CK 34βE12, CK7, CK19, CK20, CD15, EMA, CEA, TG, TTF-1	CK AE1/AE3, CD10, CK 35βH11 (focal), vimentin (focal)
4-1 case	29/F	Incidental	5.0	Left Kidney/ mid-pole	PT1bN0M1	60	CD10, CD117, TG, TTF-1	CAM 5.2, Ck7, CK20, vimentin
5-1 case	34/F	Flank pain, Gross hematuria	6.2	Right kidney/ mid-pole	pT1bN2M1	3	CK 20, TG, TTF-1, CD10, CD117, RCC, CEA, WT-1, p63, α-methyl-CoA racemase,	in lung: PAX-2, PAX-8, CK 7, CK 5, vimentin, EMA, N-cadherin in kidney: PAX-2, vimentin, CK7
6- 1 case	31/F	Flank pain, weight loss and gross hematuria	4.0	Left kidney/ upper-mid-pole	pT1aN0	21	CK20, CD10, TG, TTF-1, α-methyl-CoA racemase,	CK AE1/AE3, CK7, CK19,vimentin, RCC, Galectin-3, HBME-1,PAX-2
Present 2 cases	76/M	Gross hematuria	4.5	Left kidney/ upper pole	pT1bN0	11	CK20, CD10, RCC, CEA, WT-1, Chromogranin, Synaptophysin,CD56, NSE, TG, TTF-1, Galectin-3, HBME-1, *Ulex europaeus* lectin	CK7, CK19, EMA, vimentin, 34βE12 (focal), E-cadherin (focal)
	41/F	Incidental	4.3	Right kidney/ inferior pole	pT1bNX	4		

thorough clinical and histopathological workup is therefore mandatory to definitely exclude a thyroid metastasis, especially in cases with clinical and/or immunophenotypic unexpected findings [4, 8, 9].

In patient #1, an endocrinological screening was performed after the pathological report, and any thyroid disease was excluded. Patient #2 was clinically followed for hypothyroidism, and all her subsequent diagnostic workup was negative for a primitive thyroid neoplasm.

In both cases, the negative immunostaining for thyroglobulin, TTF-1, HBME-1, and galectin-3 helped exclude a thyroid primary neoplasm.

In fact, nuclear reactivity for TTF-1 is constantly present in follicular cell-derived benign and malignant thyroid lesions. When used in combination with TG, TTF-1 is an effective marker for thyroid origin [17]. Overall in the thyroid, HBME-1 stains mostly follicular-derived malignant tumors, including well-differentiated and poorly differentiated carcinomas, with a variable sensitivity and specificity in different series [17]. Galectin-3 is one of the members of a family of non-integrin galactoside-binding lectins that may be a helpful tool to distinguish preoperatively benign from malignant follicular thyroid nodules [18].

Thyroidization of the kidney should also be considered in the differential diagnosis: this is a benign process that extensively involves the kidney, most frequently as a consequence of end-stage renal diseases or pyelonephritis. It is characterized by atrophic distal tubules and collecting ducts with colloid-like material in the lumen. Thyroidization can be easily distinguished from TLFC since the former is diffuse and bilateral, with clinical evidence of an underlying end-stage disease, whereas the latter is a well-circumscribed, unilateral, incidentally discovered mass [19].

In our female patient, a hypothetical metastasis from a malignant ovarian lesion has been ruled out. The gynecological evaluation she had before the operation was negative for ovarian masses. Struma ovarii is a germ cell tumor of the ovary mainly composed of thyroid tissue: malignant transformation is rare and localized to the liver, peritoneum, and omentum [20]. Commonly mentioned diagnostic features (optical clearing, grooves, pseudoinclusions, and mitoses) were absent in our lesion, along with TTF-1 staining, which is always present in metastatic struma [20]. WT-1 negative immunostaining was helpful to exclude serous and small cell carcinoma of the ovary [21, 22]: areas with papillary structures detected in our case could remind of papillary serous carcinoma, whereas small cell carcinoma form follicle-like spaces that almost always contain eosinophilic fluid.

Among the others, unusual renal tumors and also carcinoid tumors of the kidney should be excluded. These tumors are also very infrequent and are histologically similar to their counterparts in other organ sites. The tumor cells have abundant amphophilic cytoplasm, salt and pepper chromatin, and are arranged in an insular, nested, acinar, trabecular, or pseudoglandular pattern. Focal areas of tubular differentiation with dense eosinophilic secretions, similar to follicular architecture of our cases, could be found, but complete negative staining for neuroendocrine markers (CD56, NSE, chromogranin, and synaptophysin) allowed us to exclude this diagnostic hypothesis.

Primary epithelial tumors of the kidney could have focal zones of tubular architecture and/or contain dense eosinophilic material, but it is usually a limited finding in clear cell or papillary carcinoma [23, 24], oncocytoma, and metanephric adenoma. In TLFC, the neoplasia is entirely composed of variably sized tubules, many of which are filled with colloid-like material.

In cases when the differential diagnosis is not straightforward, an appropriate panel of immunohistochemical markers is available, including CD10, vimentin, high molecular weight keratins, CKs 7, 19, and 20, E-cadherin, and *U. europaeus* lectin [25]. The presented immunophenotypic profile is similar to the other cases reported in literature (Table 1; CK7+, CK 19+, CK20−, 34BE12+, E-cadherin+, vimentin+, CD10 −), except for the case by Jung et al. which showed positivity for CD10 [3] and the first case reported which was unexpectedly TG-positive despite the negative clinical and serum tests [1]. The distribution pattern of the above-mentioned markers, together with *U. europaeus* lectin, was investigated by Kim and colleagues to prove its usefulness in the discrimination among common epithelial kidney tumors [25]. The immunohistochemical profile characteristic of each histologic variant of renal cell neoplasm was different from the one of TLFC [25].

Of interest, also in an intrahepatic cholangiocarcinoma [26] and in five breast tumors [27], a remarkable follicular architecture resembling thyroid neoplasms has been reported. In all these cases, there was no clinical evidence of a previous and/or concomitant thyroid disease, and immunohistochemical markers for follicular cell origin (TG and TTF-1) were negative [26, 27].

In conclusion, the peculiar immunophenotype of this newly defined entity, along with the absence of a specific genetic alteration [2–4], underlines the importance of a wide-spectrum panel of markers to discriminate from metastases from thyroid or ovary tumors and to differentiate these neoplasms from other primary kidney tumors. A correct histolopathologic definition of these tumors may avoid unnecessary ancillary treatments and has important prognostic and clinical implications [28, 29].

Acknowledgments The authors thank Dr. P.R. Valentini for her invaluable technical assistance.

Conflict of interest The authors have no conflict of interest to declare.

References

1. Angell SK, Pruthi R, Freiha FS (1996) Primary thyroid-like carcinoma of the kidney. Urology 48:632–635
2. Amin MB, Gupta R, Ondrej H et al (2009) Primary thyroid-like follicular carcinoma of the kidney: report of 6 cases of a histologically distinctive adult renal epithelial neoplasm. Am J Surg Pathol 33:393–400
3. Jung SJ, Chung JI, Park SH et al (2006) Thyroid follicular carcinoma-like tumor of kidney: a case report with morphologic, immunohistochemical, and genetic analysis. Am J Surg Pathol 30:411–415
4. Sterlacci W, Verdorfer I, Gabriel M et al (2008) Thyroid follicular carcinoma-like renal tumor: a case report with morphologic, immunophenotypic, cytogenetic, and scintigraphic studies. Virchows Arch 452:91–95
5. Dhillon J, Tannir NM, Matin SF, Tamboli P, Czerniak BA, Guo CC (2011) Thyroid-like follicular carcinoma of the kidney with metastases to the lungs and retroperitoneal lymph nodes. Hum Pathol 42:146–150
6. Khoja HA, Almutawa A, Binmahfooz A et al (2012) Papillary thyroid carcinoma-like tumor of the kidney: a case report. Int J Surg Pathol 20:411–415
7. Srigley JR, Amin MB, Delahunt B et al (2010) Protocol for the examination of specimens from patients with invasive carcinoma of renal tubular origin. Arch Pathol Lab Med 134:e25–e30
8. Insabato L, Ben-Dor D, Galliani CA et al (2009) Primary thyroid and thyroid-like follicular carcinoma of the kidney versus solitary metastatic carcinoma of the thyroid: a vexing issue. Virchows Arch 454:717–718
9. Sterlacci W, Mikuz G (2009) Primary thyroid-like renal tumor or renal metastasis from the thyroid? Virchows Arch 455:97–98
10. Abe K, Hasegawa T, Onodera S, Oishi Y, Suzuki M (2002) Renal metastasis of thyroid carcinoma. Int J Urol 9:656–658
11. Takayasu H, Kumamoto Y, Terawaki Y et al (1968) A case of bilateral renal tumor originating from a thyroid carcinoma. J Urol 100:717–719
12. Okada Y, Nonomura M, Terachi T et al (1979) Unilateral and solitary renal metastasis from well differentiated thyroid carcinoma initially treated 22 years before. Acta Urol Jpn 25:1043–1047
13. Davis RI, Corson JM (1979) Renal metastases from well differentiated follicular thyroid carcinoma. Cancer 43:265–268
14. Johnson MW, Morettin LB, Sarles HE et al (1982) Follicular carcinoma of the thyroid metastatic to the kidney 37 years after resection of the primary tumor. J Urol 127:114–116
15. Tur GE, Asanuma Y, Sato T et al (1994) Resection of metastatic thyroid carcinomas to the liver and the kidney: report of a case. Jpn J Surg 24:844–848
16. Garcia-Sanchis L, Lopez-Aznar D, Oltra A et al (1999) Metastatic follicular thyroid carcinoma to the kidney: a case report. Clin Nucl Med 24:48–50
17. Fischer S, Asa SL (2008) Application of immunohistochemistry to thyroid neoplasms. Arch Pathol Lab Med 132:359–372
18. Bartolazzi A, Orlandi F, Saggiorato E et al. Italian Thyroid Cancer Study Group (ITCSG) (2008) Galectin-3-expression analysis in the surgical selection of follicular thyroid nodules with indeterminate fine-needle aspiration cytology: a prospective multicentre study. Lancet Oncol 9:543–549
19. Laberke HG, Klingebiel T, Quack G (1983) A contribution to the morphology and pathogenesis of thyroid-like lesions in the kidney. Pathol Res Pract 176:284–296
20. Robboy SJ, Shaco-Levy R, Peng RY et al (2009) Malignant struma ovarii: an analysis of 88 cases, including 27 with extraovarian spread. Int J Gynecol Pathol 28:405–422
21. Shimizu M, Toki T, Takagi Y et al (2000) Immunohistochemical detection of the Wilms' tumor gene (WT1) in epithelial ovarian tumors. Int J Gynecol Pathol 19:158–163
22. McCluggage WG, Oliva E, Connolly LE et al (2004) An immunohistochemical analysis of ovarian small cell carcinoma of hypercalcemic type. Int J Gynecol Pathol 23:330–336
23. Fadare O, Lam S, Rubin C, Renshaw IL, Nerby CL (2010) Papillary renal cell carcinoma with diffuse clear cells and thyroid-like macrofollicular areas. Ann Diagn Pathol 14:284–291
24. Ohe C, Kuroda N, Pan CC et al (2010) A unique renal cell carcinoma with features of papillary renal cell carcinoma and thyroid-like carcinoma: a morphological, immunohistochemical and genetic study. Histopathology 57:494–497
25. Kim MK, Kim S (2002) Immunohistochemical profile of common epithelial neoplasms arising in the kidney. Appl Immunohistochem Mol Morphol 10:332–338
26. Fornelli A, Bondi A, Jovine E, Eusebi V (2010) Intrahepatic cholangiocarcinoma resembling a thyroid follicular neoplasm. Virchows Arch 456:339–342
27. Eusebi V, Damiani S, Ellis IO et al (2003) Breast tumor resembling the tall cell variant of papillary thyroid carcinoma. Am J Surg Pathol 27:1114–1118
28. Patard JJ, Leray E, Rioux-Leclercq N et al (2005) Prognostic value of histologic subtypes in renal cell carcinoma: a multicenter experience. J Clin Oncol 23:2763–2771
29. Amin M, Amin MB, Tamboli P et al (2002) Prognostic impact of histologic subtyping of adult renal epithelial neoplasms: an experience of 405 cases. Am J Surg Pathol 26:281–291

Virchows Arch (2012) 461:351
DOI 10.1007/s00428-012-1260-9

ERRATUM

Erratum to: Classification of types of intraductal papillary-mucinous neoplasm of the pancreas: a consensus study

Toru Furukawa · Günter Klöppel · Volkan Adsay · Jorge Albores-Saavedra · Noriyoshi Fukushima · Akira Horii · Ralph H. Hruban · Yo Kato · David S. Klimstra · Daniel S. Longnecker · Jutta Lüttges · G. Johan A. Offerhaus · Michio Shimizu · Makoto Sunamura · Arief Suriawinata · Kyoichi Takaori · Suguru Yonezawa

Published online: 26 July 2012
© Springer-Verlag 2012

Erratum to: Virchows Arch (2005) 447:794–799
DOI 10.1007/s00428-005-0039-7

The original version of this paper unfortunately contained an error.

N. Volkan Adsay's name was incorrectly abbreviated, thus, impacting PubMed citation. **The name "Volkan Adsay N" should be "Adsay, V".**
In addition, Toru Furukawa's present affiliation and e-mail address is given below.

The online version of the original article can be found at http://dx.doi.org/10.1007/s00428-005-0039-7.

T. Furukawa (✉) · A. Horii
Department of Molecular Pathology, Tohoku University School of Medicine, 2-1 Seiryomachi, Aoba-ku,
Sendai, 980-8575, Japan
e-mail: furukawa@mail.tains.tohoku.ac.jp

G. Klöppel · J. Lüttges
Department of Pathology, University of Kiel,
Kiel, Germany

V. Adsay
Department of Pathology, Wayne State University,
Detroit, MI, USA

J. Albores-Saavedra
Department of Pathology, LSU Health Sciences Center,
Shreveport, LA, USA

N. Fukushima
Department of Pathology, Tokyo Medical College,
Tokyo, Japan

R. H. Hruban
Departments of Pathology and Oncology,
The Sol Goldman Pancreatic Cancer Research Center,
The Johns Hopkins Medical Institutions,
Baltimore, MD, USA

Y. Kato
Department of Pathology, Cancer Institute,
Japanese Foundation for Cancer Research,
Tokyo, Japan

D. S. Klimstra
Department of Pathology, Memorial Sloan-Kettering Cancer Center,
New York, NY, USA

D. S. Longnecker · A. Suriawinata
Department of Pathology, Dartmouth-Hitchcock Medical Center,
Lebanon, NH, USA

G. J. A. Offerhaus
Department of Pathology, Academic Medical Center,
Amsterdam, The Netherlands

M. Shimizu
Department of Pathology, Saitama Medical School,
Saitama, Japan

M. Sunamura
Department of Gastroenterological Surgery,
Tohoku University School of Medicine,
Sendai, Japan

K. Takaori
Department of General and Gastroenterological Surgery,
Osaka Medical College,
Osaka, Japan

S. Yonezawa
Department of Human Pathology, Field of Oncology, Kagoshima University Graduate School of Medical and Dental Sciences,
Kagoshima, Japan

Present Address:
T. Furukawa
Institute for Integrated Medical Sciences,
Tokyo Women's Medical University,
8-1 Kawada-cho, Shinjuku-ku,
Tokyo, 162-8666, Japan
e-mail: furukawa.toru@twmu.ac.jp

Virchows Arch (2012) 461:353–354
DOI 10.1007/s00428-012-1294-z

ERRATUM

Erratum to: FGFR1 expression and gene copy numbers in human lung cancer

Lukas H. Kohler · Masoud Mireskandari · Thomas Knösel · Annelore Altendorf-Hofmann · Almut Kunze · Andreas Schmidt · Norbert Presselt · Yuan Chen · Iver Petersen

Published online: 7 August 2012
© Springer-Verlag 2012

Erratum to: Virchows Arch (2012) 461:49–57
DOI 10.1007/s00428-012-1250-y

There was an error in the original version of Fig. 7 representing the DNA imbalances of the 4 lung cancer subtypes as detected by conventional CGH. For large cell lung cancer (LCLC), the ideogram of chromosome 9 together with the histograms of DNA gains and losses was shown and not chromosome 8 harbouring the FGFR1 locus.

The corrected version with the chromosome 8 histogram (see new figure), however, indicates an identical finding, i.e. that chromosome 8p is more often affected by deletions than DNA gains.

The online version of the original article can be found at http://dx.doi.org/10.1007/s00428-012-1250-y.

L. H. Kohler · M. Mireskandari · T. Knösel · Y. Chen · I. Petersen (✉)
Institute of Pathology, Jena University Hospital,
Friedrich-Schiller-University,
Ziegelmuehlenweg 1,
07740 Jena, Germany
e-mail: Iver.Petersen@med.uni-jena.de

A. Altendorf-Hofmann
Department of General and Visceral and Vascular Surgery,
Jena University Hospital, Friedrich-Schiller-University,
Erlanger Allee 101,
07740 Jena, Germany

A. Kunze · A. Schmidt
Department of Pathology, Central Clinic Bad Berka,
Robert-Koch-Allee 9,
99438 Bad Berka, Germany

N. Presselt
Department of Thoracic and Vascular Surgery,
Central Clinic Bad Berka,
Robert-Koch-Allee 9,
99437 Bad Berka, Germany

Present Address:
T. Knösel
Institute of Pathology, Ludwig-Maximilian-University,
Thalkirchner Strasse 36,
80337 Munich, Germany

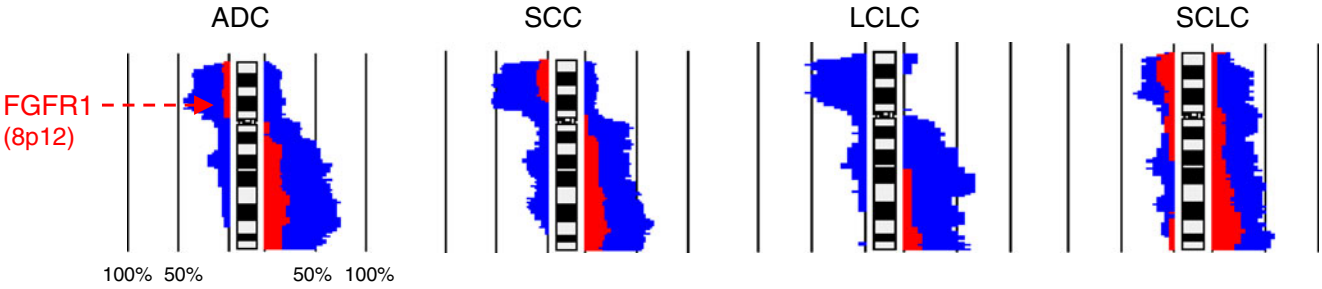

Fig. 7 DNA imbalances of lung cancer subtypes according to conventional comparative genomic hybridization/CGH (compiled from data of Petersen I in Travis et al. 2004, [30]). Cases with DNA gains were represented by the histogram on the *right side* of the chromosome ideogram, cases with DNA loss on the *left side*. The data indicated that 8p deletions are at least as frequent as DNA gains with pronounced gains (indicated by the *red colour*) as putative correlates of an amplification being undetectable in the NSCLC subtypes

Virchows Arch (2012) 461:355–365
DOI 10.1007/s00428-012-1292-1

ORIGINAL ARTICLE

LGR4 and LGR6 are differentially expressed and of putative tumor biological significance in gastric carcinoma

Jan Simon Steffen · Eva Simon · Viktoria Warneke · Katharina Balschun · Matthias Ebert · Christoph Röcken

Received: 14 May 2012 / Revised: 18 July 2012 / Accepted: 23 July 2012 / Published online: 2 August 2012
© Springer-Verlag 2012

Abstract Gastric cancer (GC) is one of the most common causes of cancer-related deaths worldwide. We investigated the differential expression and putative tumor biological significance of five G-protein-coupled receptors (GPCRs) in GC, i.e., LGR4, LGR6, GPR34, GPR160, and GPR171. Based on our previous microarray analyses, we identified five candidate genes in human GC samples. Real-time RT-PCR was carried out to validate their expression in malignant and non-malignant tissues on an independent collective comprising 32 GC patients with and without lymph node metastases. Selected protein targets LGR4 and LGR6 were further validated on paraffin-embedded sections of ten intestinal and ten poorly cohesive (diffuse)-type GCs and their corresponding non-malignant tissue using immunohistochemistry. Additionally, the putative tumor biological significance of LGR4 and LGR6 was studied using tissue microarrays obtained from a cohort of 481 GC patients. On transcriptional level, GPR34, GPR160, and GPR171 were not differentially expressed in GC compared with non-neoplastic mucosa. LGR4 and LGR6 were up-regulated on transcriptional (real-time RT-PCR) and translational (immunohistochemistry) levels in GC. Furthermore, in tissue microarray analysis, LGR6 expression was significantly associated with local tumor growth (T-category; $p=0.04$) and correlated with patient survival. LGR4 expression was significantly correlated with nodal spread (N-category; $p=0.025$). Our systematic analysis indicates that LGR4 and LGR6 may play a role in GC biology. Future studies will have to demonstrate whether these are also putative diagnostic, prognostic, and/or therapeutic targets for GC.

Keywords LGR4 · LGR6 · GPCR · Gastric cancer

Introduction

Despite a declining incidence in many Western countries, gastric cancer (GC) remains the fourth most common cancer worldwide with about one million new cases per year. It is also one of the most common causes for cancer-related deaths, ranking second behind lung cancer [1, 2]. The prognosis of GC is determined by the tumor stage at the time of the diagnosis [3]. As long as the tumor is restricted to the mucosa, surgery promises excellent outcome. However, in many Western countries, the majority of GCs are diagnosed at an advanced stage, when tumor cells have already reached the muscularis propria, limiting treatment options [4]. Following diagnosis, perioperative chemotherapy has become standard of care in Germany [5]. In the palliative setting, trastuzumab can be applied in GC overexpressing Her2/neu [6]. Despite these advancements, not all patients are eligible for currently available targeted therapies or perioperative chemotherapy, and novel treatment targets and predictive biomarkers are still urgently needed. For this purpose, G-protein-coupled receptors (GPCRs) are promising candidates. They represent the largest group of cell surface

Electronic supplementary material The online version of this article (doi:10.1007/s00428-012-1292-1) contains supplementary material, which is available to authorized users.

J. S. Steffen · E. Simon · V. Warneke · K. Balschun · C. Röcken
Institute of Pathology, Christian-Albrechts-University, Kiel, Germany

M. Ebert
Department of Medicine II, Faculty of Clinical Medicine Mannheim, University of Heidelberg, Mannheim, Germany

C. Röcken (✉)
Department of Pathology, Christian-Albrechts-University, Arnold-Heller-Str. 3/14, 24105 Kiel, Germany
e-mail: christoph.roecken@uksh.de

receptors and about 40 % of all drugs currently used in medicine, target GPCRs [7]. GPCRs consist of a single polypeptide chain with seven transmembrane domains [8]. They are involved in a broad range of physiological processes and signal transduction systems, including immune response, hormone and enzyme release, or blood pressure regulation [9]. Furthermore, there is ample evidence now that GPCRs are involved in tumor cell biology and few are even expressed in stem cells [10]: LGR5 was recently identified as a putative cancer stem cell marker of gastric and colon cancer [11, 12].

In previous studies, we systematically searched for GPCRs differentially expressed in GC using gene array technology [9]. Fifty-two GPCRs and GPCR-related genes were up- or down-regulated in node-positive GC, including LGR5, GPR34, GPR160, and GPR171. Follow-up studies demonstrated that the expression of LGR5 in the tumor center and invasion front of GC correlated significantly with the local tumor growth (T-category) and the nodal spread (N-category). Furthermore, patients with $LGR5^{+}$ GCs had a shorter median survival (28.0±8.6 months) than patients with $LGR5^{-}$ GCs (54.5±6.3 months) [13]. LGR5 is a Wnt-signaling molecule and has two homologues, LGR4 and LGR6, which share approximately 50 % sequence homology with LGR5 [14]. LGR4 and LGR5 bind R-spondins and associate with the Frizzled/LrpWnt receptor complex. Conditional deletion of LGR4 and LGR5 in the mouse gut impairs Wnt target gene expression and results in the rapid demise of intestinal crypts, thus phenocopying Wnt pathway inhibition [15]. While the expression pattern of LGR5 in GC was investigated recently, little is known about the differential expression of its two homologues. In this study, we aimed to fill this gap of information by further exploring the putative biological significance of *LGR4*, *LGR6*, *GPR34*, *GPR160*, and *GPR171* in GC.

Material and methods

Subjects

Unfixed, fresh frozen tissue was available from an independent series of 32 intestinal-type GCs and corresponding non-malignant tissue. Patients were selected considering age, gender, tumor type, and nodal status. A total of 16 cases were node-positive (N1), and 16 cases were node-negative (N0). Poorly cohesive (diffuse)-type carcinomas were not included in the validation cohort since our initial gene array analyses were done only on intestinal-type GCs [9].

Formalin-fixed and paraffin-embedded malignant and corresponding non-malignant tissues of 20 GC cases were retrieved from the archives of the Institute of Pathology of the Christian-Albrechts-University Kiel. The cases were selected according to age, gender, and tumor type. All patients were operated at the University Hospital Schleswig-Holstein (1997–2009). The patient characteristics are summarized in Table 1.

For TMA construction, an independent cohort of 481 GC patients was retrieved from the archive of the Institute of Pathology of the Christian-Albrechts-University. These patients had undergone either total or partial gastrectomy for adenocarcinomas of the stomach or esophago-gastric junction. Each resection specimen had undergone histological examination by trained surgical pathologists. The time

Table 1 Characteristics of patients studied by polymerase chain reaction (PCR) and immunohistochemistry (IHC)

	PCR		IHC	
	Male	Female	Male	Female
Mean age [years (range)]	64 (45–81)	71 (54–87)	72 (54–84)	69 (55–80)
Total [*n*]	20	12	10	10
Tumor type				
Intestinal [*n*]	20	12	5	5
Poorly cohesive [*n*]	–	–	5	5
T-category				
pT1 [*n*]	3	–	3	2
pT2 [*n*]	12	8	5	3
pT3 [*n*]	2	4	1	2
pT4 [*n*]	3	–	1	3
N-category				
pN0 [*n*]	10	6	7	5
pN1 [*n*]	7	5	–	3
pN2 [*n*]	3	–	2	1
pN3 [*n*]	–	1	1	1

of patient death was obtained from the *Epidemiological Cancer Registry* of the state Schleswig-Holstein, Germany. Follow-up data of patients still alive were retrieved from hospital records and by contacting the general practitioners.

Ethics statement

All tissue samples were obtained as part of a diagnostic or therapeutic surgery carried out after the patient gave written informed consent. Patients offering samples for the study were pseudonymized and analyzed anonymously, so no individual-related data are contained in the data base. The study was approved by the local ethics committee of the University Hospital in Kiel, Germany (ref. number D 453/10).

Real-time reverse transcriptase polymerase chain reaction (RT-PCR)

Total RNA was isolated from cryoconserved tissues using Ambion's mirVana miRNA Isolation Kit (Applied Biosystems, Darmstadt, Germany), followed by a DNase treatment with Turbo DNA-free kit (Ambion). cDNA synthesis was performed using the Transcriptor First Strand cDNA Synthesis Kit (Roche Diagnostics GmbH, Mannheim, Germany). Primers were obtained by BioTeZ Berlin-Buch GmbH, Berlin, Germany (LGR6, GPR160, GPR34) and biomers.net, Ulm, Germany (LGR4, GPR171). The following primer sequences were chosen: *LGR4* 5′GGC TGA GTG CTT TGC AGT CT, 5′CCT CCG TCA AGC TGT TGT C; *LGR6* 5′CCA AGG ACA GTT TCC CAA AA, 5′ GAC TCC TCA TCATCA AGG TGA A; *GPR34* 5′CGG TGA AAG GTT GCG ACT AT, 5′GGT TGG TCG CTA TGA TTG GT; *GPR160* 5′CGA CAG CCA TCG ATC CTC, 5′AGC GAG AGC GGT TCC TTC, *GPR171* 5′ATT CCG CTC AAA GGT CAC TG, 5′TCC AGT AAG GCC AGA ATT GG. Real-time RT-PCR was carried out using the Maxima™ SYBR Green qPCR Master Mix (Fermentas GmbH, St. Leon-Rot, Germany) and the LightCycler 480 system by Roche Diagnostics (Mannheim, Germany). Three housekeeping genes were selected as reference genes, which have especially been established for the used GC collective: *Homo sapiens succinate dehydrogenase complex*, *subunit A*, *flavoprotein* (*Fp*) (*SDHA*), *Homo sapiens calpain 2* (*CAPN2*), and *Cyclophilin C* (*CYCC*). The appropriateness of these genes has been proven by geNorm in advance. Each setting included two none template controls (no cDNA in PCR) in order to detect unspecific products or primer dimerization. All experiments were performed in duplicates.

Histology

For histological analyses, tissue samples were fixed in 10 % neutralized formalin and embedded in paraffin. Deparaffinized sections were stained using hematoxylin and eosin (H&E). Gastric carcinoma was classified according to the WHO classification [16]. The pTNM stage was determined according to the seventh edition of the international union against cancer [17].

Tissue microarray construction

Formalin-fixed and paraffin-embedded tissue samples were used to generate tissue microarrays as described previously [9]. Three representative tumor-bearing core cylinders were obtained from each paraffin donor block and transferred into the recipient paraffin block. Successful transfer of tumor tissue was confirmed microscopically using H&E-stained sections. Four-micrometer sections of the resulting tumor tissue microarray block were cut for further analysis.

Immunohistochemistry

For immunohistochemistry, formalin-fixed and paraffin-embedded sections were used. Prior to immunostaining, sections were deparaffinized in xylol for 20 min and rehydrated in a descending alcohol series. Antigen retrieval was carried out with ethylenediaminetetraacetic acid (95 °C) and washed in Tris-buffered saline. Subsequently, slides were incubated with the primary antibody (LGR4: polyclonal rabbit, 1:100, Atlas Antibodies, Stockholm, Sweden; LGR6: polyclonal rabbit, 1:800, antibodies-online GmbH, Aachen, Germany) in a moist chamber at room temperature for 30 min and afterwards at 4 °C overnight. The N-Histofine Simple Stain MAX PO system (Nichirei Biosciences Inc., Tokyo, Japan) served as the secondary antibody and was additionally used as carrier for the polymerase. Staining was carried out by utilizing a diaminobenzidine (DAB) substrate (Vector Laboratories Inc. Burlingame, USA). Counterstaining was performed with hemalaun. Sections were coverslipped with EZ-Mount™ (Thermo Scientific Anatomical Pathology, Runcorn, UK) after counterstaining. Omission of primary antibodies served as a negative control.

Statistical analysis

Statistical analysis was carried out with Microsoft Excel 2010 (Microsoft Deutschland GmbH, Unterschleißheim) and PASW Statistics 18 (IBM Deutschland GmbH, Ehningen). An immunoreactivity scoring system (IRS) consisting of two categories was established for interpretation of immunohistochemical data. Briefly, category A documented the intensity of immunostaining as 0 (no immunostaining), 1 (weak), 2 (moderate), and 3 (strong). Category B documented the percentage of immunoreactive cells as 0 (negative), 1 (scattered positive cells; ≤ 1 %), 2 (2–10 % positive cells), 3 (11–50 %), 4 (51–80 %) and 5 (>80 %). The addition of categories A and B resulted in a score ranging from 0 to 8. Cases with an IRS≥2

were considered as positive, and those with an IRS<2 as negative. Correlation of immunohistochemical staining with patient characteristics was performed with Fisher's exact test. Differences in terms of patient survival were assessed by the log-rank test. Results are presented as Kaplan–Meier curves. Statistical comparison of paired groups (e.g., the IRS of malignant and non-malignant tissues of the same patient) was evaluated with a paired two-sided *t*-test. Independent groups (e.g. node-positive vs. node-negative carcinomas) were analyzed using an unpaired two-sided *t*-test. Real-time RT-PCR data were logarithmized to obtain approximately normally distributed data. *P*-values<0.05 were considered as statistically significant, and *p*-values<0.001 as highly significant.

Results

Differential expression of GPCRs in malignant and non-malignant gastric tissues

In the first experiment, we aimed to validate the differential expression of our six prime candidates (*LGR4*, *LGR6*, *GPR34*, *GPR160*, and *GPR171*) in GC. mRNA was extracted from corresponding unfixed neoplastic and non-neoplastic gastric mucosae of 32 intestinal-type GCs. Real-time RT-PCR demonstrated that *LGR4* mRNA was significantly up-regulated in GC compared with corresponding non-neoplastic mucosa (p=0.0271). Interestingly, *LGR6* mRNA was markedly up-regulated. However, this did not reach statistical significance (p=0.0567). The mRNA expression of *GPR34*, *GPR160*, and *GPR171* showed no difference between GC and corresponding non-neoplastic mucosa of the same patients (Fig. 1).

Differential expression of GPCRs in node-positive and node-negative gastric cancer tissues

Next, we analyzed the mRNA expression in the primary tumor tissue of 16 node-positive and 16 node-negative intestinal-type GCs. None of our five target genes showed significant differences between metastatic and non-metastatic primary tumors (data not shown).

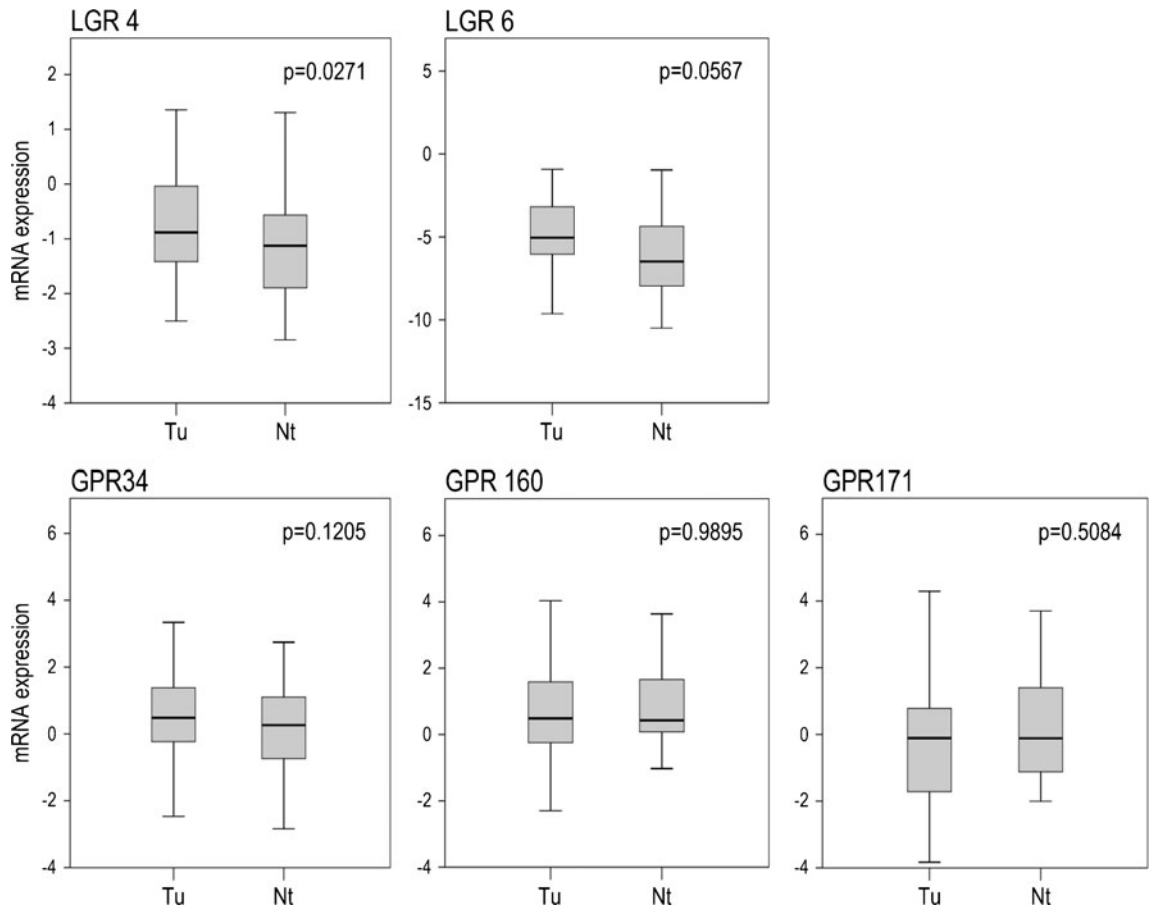

Fig. 1 mRNA expression levels of five target genes in malignant (*Tu*) and non-malignant (*Nt*) tissues. *P*-values were calculated with a paired two-sided *t*-test

Expression pattern of LGR4 and LGR6 in non-neoplastic and neoplastic gastric tissues

The differential expression of LGR4 and LGR6 was then explored on the translational level in GC by immunohistochemistry, now also including poorly cohesive-type GCs. Twenty GCs (ten poorly cohesive and ten intestinal types) were retrieved from the archive and forwarded to immunostaining. Immunostaining was carried out on large tissue sections enclosing neoplastic and non-neoplastic gastric mucosae. Comparing the IRS of neoplastic and non-malignant tissues by applying a paired *t*-test, LGR4 was significantly overexpressed in intestinal-type malignant tissue compared to non-neoplastic foveolar epithelium ($p=0.027$). Thirteen (65 %) cases showed cytoplasmatic immunostaining for LGR4 (Fig. 2a) including eight intestinal- and five poorly cohesive-type carcinomas. Additionally, nuclear positivity was observed in three samples (one intestinal and two diffuse GCs). LGR4 immunoreactive epithelial cells in non-malignant tissue were only found in six cases (30 %). However, positive staining was frequently observed in glandular cells of the non-neoplastic mucosa. Anti-LGR6 staining delivered eight (40 %) positive GCs (Fig. 2d), allocated into six intestinal-type and two poorly cohesive-type GCs. The LGR6 expression (IRS value) in intestinal-type tumor tissue significantly exceeded expression in non-neoplastic foveolar epithelium ($p=0.017$). The non-malignant foveolar epithelium was LGR6-positive in six (30 %) cases. Similar to LGR4, LGR6 was partially expressed by non-neoplastic gastric gland epithelia. In most GCs as well as in all sections of non-neoplastic gastric mucosa, detached LGR4- and LGR6-positive stromal cells were found (Fig. 2b, e). Additionally, in six cases, LGR6-positive vessels were observed in neoplastic as well as in non-neoplastic tissue.

Putative tumor biological significance of LGR4 and LGR6 in gastric cancer

Next, we explored the putative tumor biological significance of LGR4 and LGR6 by immunostaining of tissue microarrays obtained from formalin-fixed and paraffin-embedded tumor samples of 481 GC patients.

$LGR4^+$ tumor cells were found in 206 of 481 (43 %) patients. A strong cytoplasmic immunoreaction was observed in 12 (2.5 %) cases and a weak to moderate staining in 159 (33.1 %) cases. In addition, 17 % of the positive cases exhibited a nuclear immunostaining. Two hundred seventy five tumors (57 %) lacked LGR4 immunoreactivity. Next, we studied the correlation between the expression of LGR4 and various clinico-pathological patient characteristics (Table 2). The expression of LGR4 by tumor cells correlated with nodal spread ($p=0.025$). Subgroup analysis demonstrated this effect being restricted to poorly cohesive-type carcinomas (Table 4).

$LGR6^+$ tumor cells were found in 153 of 481 (32 %) patients. A strong cytoplasmic immunoreaction was observed in 7 (1.5 %) cases and a weak to moderate staining in 146 (30 %) cases. Three hundred twenty eight tumors (68 %) lacked LGR6 immunoreactivity. Next, we studied the correlation between the expression of LGR6 and various clinico-pathological patient characteristics (Table 2). The expression

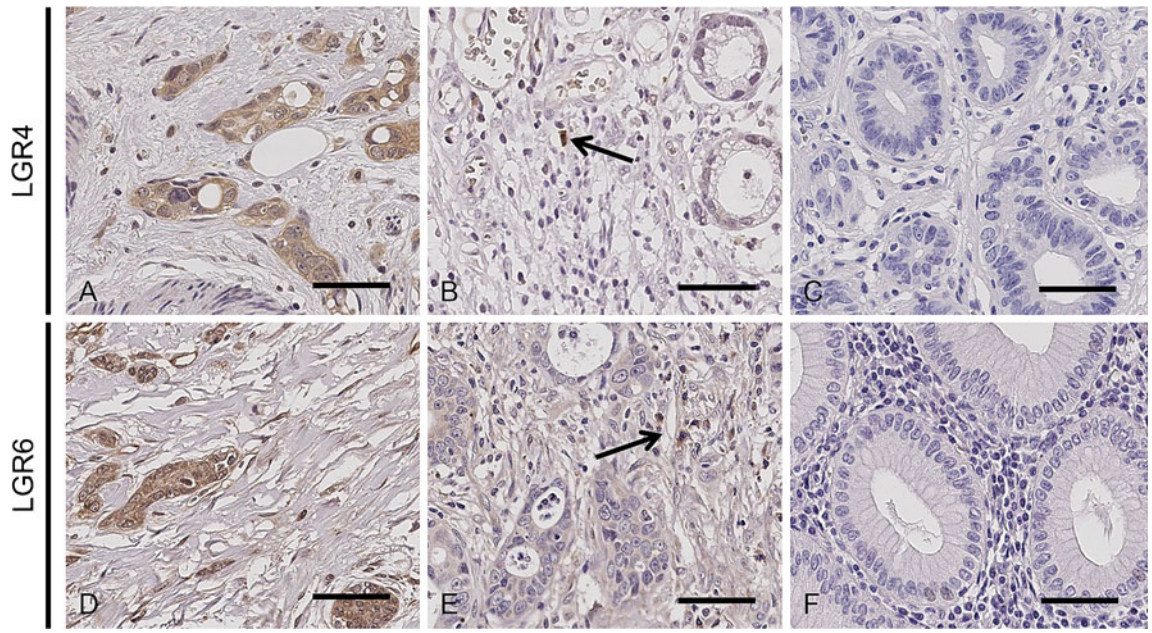

Fig. 2 Moderate LGR4- and LGR6-positive cytoplasmatic staining in intestinal-type gastric carcinoma (**a**, **d**). LGR4- and LGR6-negative gastric carcinoma, positive immunoreaction in detached stromal cells (*arrows*) (**b**, **e**). Negative control (**c**, **f**). *Scale bar*: **a**–**f**: 50 μm. Original magnifications: ×400

Table 2 Entire study cohort: assessment of LGR4 and LGR6 expression in tissue microarrays and correlation with clinico-pathological patient characteristics. *P*-values were calculated with Fisher's exact test

	Total	LGR4 negative	LGR4 positive	*p*-value	Total	LGR6 negative	LGR6 positive	*p*-value
Patients, *n* (%)	481	275 (57)	206 (43)		481	328 (68)	153 (32)	
Age (MV±SD)		67±11.4	68±10.3			68±11.2	67±10.4	
Age in years, *n* (%)				0.44				0.259
< 65	177	105 (59)	72 (41)		177	115 (65)	62 (35)	
≥ 65	285	158 (55)	127 (45)		285	200 (70)	85 (30)	
Gender, *n* (%)				0.925				0.086
Male	298	171 (57)	127 (43)		303	198 (65)	105 (35)	
Female	183	104 (57)	79 (43)		178	130 (73)	48 (27)	
Tumor type, *n* (%)				0.228				0.071
Intestinal	207	114 (55)	93 (45)		207	129 (62)	78 (38)	
Poorly cohesive	220	134 (61)	86 (39)		220	159 (72)	61 (28)	
Mixed	51	25 (49)	26 (51)		51	37 (73)	14 (27)	
Localization, *n* (%)				0.365				0.453
Proximal	146	78 (53)	68 (47)		145	95 (66)	50 (34)	
Distal	317	184 (58)	133 (42)		318	220 (69)	98 (31)	
T-category, *n* (%)				0.406				0.04
pT1	59	32 (54)	27 (46)		60	34 (57)	26 (43)	
pT2	56	34 (61)	22 (39)		55	32 (58)	23 (42)	
pT3	190	116 (61)	74 (39)		190	140 (74)	50 (26)	
pT4	175	92 (53)	83 (47)		175	121 (69)	54 (31)	
T-category grouped, *n* (%)				1.000				0.006
pT1/pT2	115	66 (57)	49 (43)		115	66 (57)	49 (43)	
pT3/pT4	365	208 (57)	157 (43)		365	261(72)	104 (28)	
Lymph nodes, *n* (%)				0.541				0.828
No metastases	137	81 (59)	56 (41)		137	95 (69)	42 (31)	
Metastases	338	189 (56)	149 (44)		338	230 (68)	108 (32)	
N-category, *n* (%)				0.025				0.512
pN0	137	81 (59)	56 (41)		137	95 (69)	42 (31)	
pN1	69	45 (65)	24 (35)		69	51 (74)	18 (26)	
pN2	81	47 (58)	34 (42)		82	56 (68)	26 (32)	
pN3a	117	69 (59)	48 (41)		117	81 (69)	36 (31)	
pN3b	71	28 (39)	43 (61)		70	42 (60)	28 (40)	
Grade, *n* (%)				0.38				0.105
G1/G2	111	67 (60)	44 (40)		113	70 (62)	43 (38)	
G3/G4	351	194 (55)	157 (45)		349	245 (70)	104 (30)	

of LGR6 by tumor cells correlated with local tumor growth (p=0.040) and was more frequently observed in early stage carcinomas (p=0.006). Interestingly, LGR4 and LGR6 were both more commonly expressed by intestinal-type GCs. However, this did not reach statistical significance.

The subgroup analyses (Tables 3 and 4) demonstrated that the expression of LGR4 in poorly cohesive-type GC correlated significantly with the N-category. Among intestinal cases, $LGR6^+$ tumor cells were more prevalent in male patients. However, this difference did not reach statistical significance (p=0.092).

Co-expression of LGR4 and LGR6 was observed in 98 cases allocated to 49 intestinal-type, 37 poorly cohesive-type, and 12 mixed-type carcinomas. Co-expression of LGR4 and LGR6 did not correlate with local tumor growth or nodal spread (Online Resource 1).

Survival analysis

Next, we explored the influence of LGR4 and LGR6 expression on patient survival (Fig. 3). GC patients with LGR6-positive tumors lived longer than patients with

Table 3 Intestinal-type gastric carcinomas: assessment of LGR4 and LGR6 expression in tissue microarrays and correlation with clinicopathological patient characteristics. *P*-values were calculated with Fisher's exact test

	Total	LGR4 negative	LGR4 positive	*p*-value	Total	LGR6 negative	LGR6 positive	*p*-value
Patients, *n* (%)	207	114 (55)	93 (45)		207	129 (62)	78 (38)	
Age (MV ± SD)		69±9.9	68±10.5			70±10.0	68±10.2	
Age in years, *n* (%)				0.360				0.085
< 65	64	32 (50)	32 (50)		64	34 (53)	30 (47)	
≥ 65	135	78 (58)	57 (42)		135	90 (67)	45 (33)	
Gender, *n* (%)				0.514				0.092
Male	157	84 (54)	73 (46)		159	94 (59)	65 (41)	
Female	50	30 (60)	20 (40)		48	35 (73)	13 (27)	
Localization, *n* (%)				0.770				0.653
Proximal	77	43 (56)	34 (44)		76	45 (59)	31 (41)	
Distal	121	64 (53)	57 (47)		122	77 (63)	45 (37)	
T-category, *n* (%)				0.988				0.262
pT1	37	20 (54)	17 (46)		38	22 (58)	16 (42)	
pT2	33	19 (58)	14 (42)		32	16 (50)	16 (50)	
pT3	87	48 (55)	39 (45)		87	60 (69)	27 (31)	
pT4	50	27 (54)	23 (46)		50	31 (62)	19 (38)	
T-category grouped, *n* (%)				1.000				0.097
pT1/pT2	70	39 (56)	31 (44)		70	38 (54)	32 (46)	
pT3/pT4	137	75 (55)	62 (45)		137	91 (66)	46 (34)	
Lymph nodes, *n* (%)				0.556				0.650
No metastases	72	42 (58)	30 (42)		72	47 (65)	25 (35)	
Metastases	132	70 (53)	62 (47)		132	81 (61)	51 (39)	
N-stage, *n* (%)				0.496				0.906
pN0	72	42 (58)	30 (42)		72	47 (65)	25 (35)	
pN1	36	20 (56)	16 (44)		35	22 (63)	13 (37)	
pN2	37	18 (49)	19 (51)		38	22 (58)	16 (42)	
pN3a	43	26 (60)	17 (40)		43	28 (65)	15 (35)	
pN3b	16	6 (37.5)	10 (62.5)		16	9 (56)	7 (44)	
Grade, *n* (%)				0.200				1.000
G1/G2	106	63 (59)	43 (41)		108	67 (62)	41 (38)	
G3/G4	92	46 (50)	46 (50)		90	56 (62)	34 (38)	

LGR6-negative tumors (mean survival: LGR6-positive 28± 32 months, LGR6-negative 19±23 months; $p=0.052$). The subgroup analyses showed that the difference in patient survival was mainly restricted to poorly cohesive-type GCs (Fig. 3). No difference was found between patients with LGR4-positive and LGR4-negative tumors.

$LGR4^+/LGR6^+$ carcinomas had a better survival rate than $LGR4^-/LGR6^-$ carcinomas (Online Resource 2). However, in log-rank (Mantel–Cox) test, this effect did not reach statistical significance ($p=0.321$).

Finally, patient survival correlated significantly with tumor type ($p=0.007$), T-category ($p<0.001$), the presence of lymph node metastases ($p<0.001$), N-category ($p<0.001$), and tumor grade ($p<0.001$; data not shown). On multivariate analysis, LGR6 was not an independent prognosticator of patient survival.

LGR4, LGR5, and LGR6 expression in non-neoplastic gastric mucosa

Finally, we tested the hypothesis whether LGR4 and LGR6 are expressed in gastric stem cells. Serial sections of non-neoplastic gastric mucosa were stained with antibodies directed against LGR4, LGR5, and LGR6. LGR4 and LGR6 immunostaining was not found in LGR5 immunoreactive cells, and they are thus unlikely to stain gastric stem cells (Fig 4).

Table 4 Poorly cohesive-type gastric carcinomas: assessment of LGR4 and LGR6 expression in tissue microarrays and correlation with clinicopathological patient characteristics. *P*-values were calculated with Fisher's exact test

	Total	LGR4 negative	LGR4 positive	*p*-value	Total	LGR6 negative	LGR6 positive	*p*-value
Patients, *n* (%)	220	134 (61)	86 (39)		220	159 (72)	61 (28)	
Age (MV ± SD)		64±11.6	68±10.4			66±11.7	67±10.1	
Age in years, *n* (%)				0.120				0.878
< 65	96	64 (67)	32 (33)		96	70 (73)	26 (27)	
≥ 65	115	64 (56)	51(44)		115	82 (71)	33 (29)	
Gender, *n* (%)				0.581				0.653
Male	111	70 (63)	41 (37)		113	80 (71)	33 (29)	
Female	109	64 (59)	45 (41)		107	79 (74)	28 (26)	
Localization, *n* (%)				0.198				0.596
Proximal	53	28 (53)	25 (47)		53	37 (70)	16 (30)	
Distal	160	101 (63)	59 (37)		160	118 (74)	42 (26)	
T-category, *n* (%)				0.084				0.441
pT1	17	11 (65)	6 (35)		17	10 (59)	7 (41)	
pT2	15	9 (60)	6 (40)		15	10 (67)	5 (33)	
pT3	85	60 (71)	25 (29)		85	65 (76)	20 (24)	
pT4	103	54 (52)	49 (48)		103	74 (72)	29 (28)	
T-category grouped, *n* (%)				1.000				0.202
pT1/pT2	32	20 (62.5)	12 (37.5)		32	20 (62.5)	12 (37.5)	
pT3/pT4	188	114 (61)	74 (39)		188	139 (74)	49 (26)	
Lymph nodes, *n* (%)				0.745				1.000
No metastases	52	33 (63)	19 (37)		52	38 (73)	14 (27)	
Metastases	167	100 (60)	67 (40)		167	121 (72)	46 (28)	
N-category, n (%)				0.013				0.299
pN0	52	33 (63)	19 (37)		52	38 (73)	14 (27)	
pN1	29	23 (79)	6 (21)		30	26 (87)	4 (13)	
pN2	33	21 (64)	12 (36)		33	24 (73)	9 (27)	
pN3a	60	38 (63)	22 (37)		60	43 (72)	17 (28)	
pN3b	45	18 (40)	27 (60)		44	28 (64)	16 (36)	

Discussion

The poor prognosis of GC is a major issue in gastrointestinal oncology. Most GCs are diagnosed at an advanced stage when local resection is no longer a therapeutic option [2, 18, 19], with nodal spread being the most important prognostic factor [19]. Inevitably, the search for new factors contributing to the pathogenesis of lymph node metastases and the detection of new therapeutic targets is of outstanding importance. GPCRs are prime candidates for novel cancer prevention and treatment strategies since they play an important role in regulating physiological and pathophysiological processes. These receptors form the largest family of human membrane-bound proteins and represent a target for more than 40 % of all drugs used in medicine [7].

In our present study, we explored and aimed to validate the differential expression and putative tumor biological significance of five GPCRs. Four GPCRs, i.e., LGR6, GPR34, GPR160, and GPR171, were depicted from a list of differentially expressed genes detected by gene array analysis of three node-positive vs. three node-negative intestinal-type gastric carcinomas published previously by our group [9]. We added LGR4 to this list, as LGR4 shares homology with LGR5 and LGR6, which both were found by gene array analysis. Interestingly, while we were unable to validate the differential expression of GPR34, GPR160, and GPR171, both LGR4 and LGR6 were found to be up-regulated in GC tissue compared with corresponding non-neoplastic tissue. Furthermore, using immunohistochemistry, we provide evidence that the expression of LGR4 correlates with nodal spread and of LGR6 inversely with local tumor growth. Interestingly, in TMA analysis, we found a positive impact of LGR6 expression on patient survival in poorly cohesive-type carcinomas. Thus, both LGR4 and LGR6 are probably involved in gastric cancer biology.

The leucine-rich repeat-containing G-protein-coupled receptors (LGR4, LGR5, and LGR6) are interesting GPCRs. Their functions as well as their ligands are still widely unknown [12, 20], even though it was recently shown that

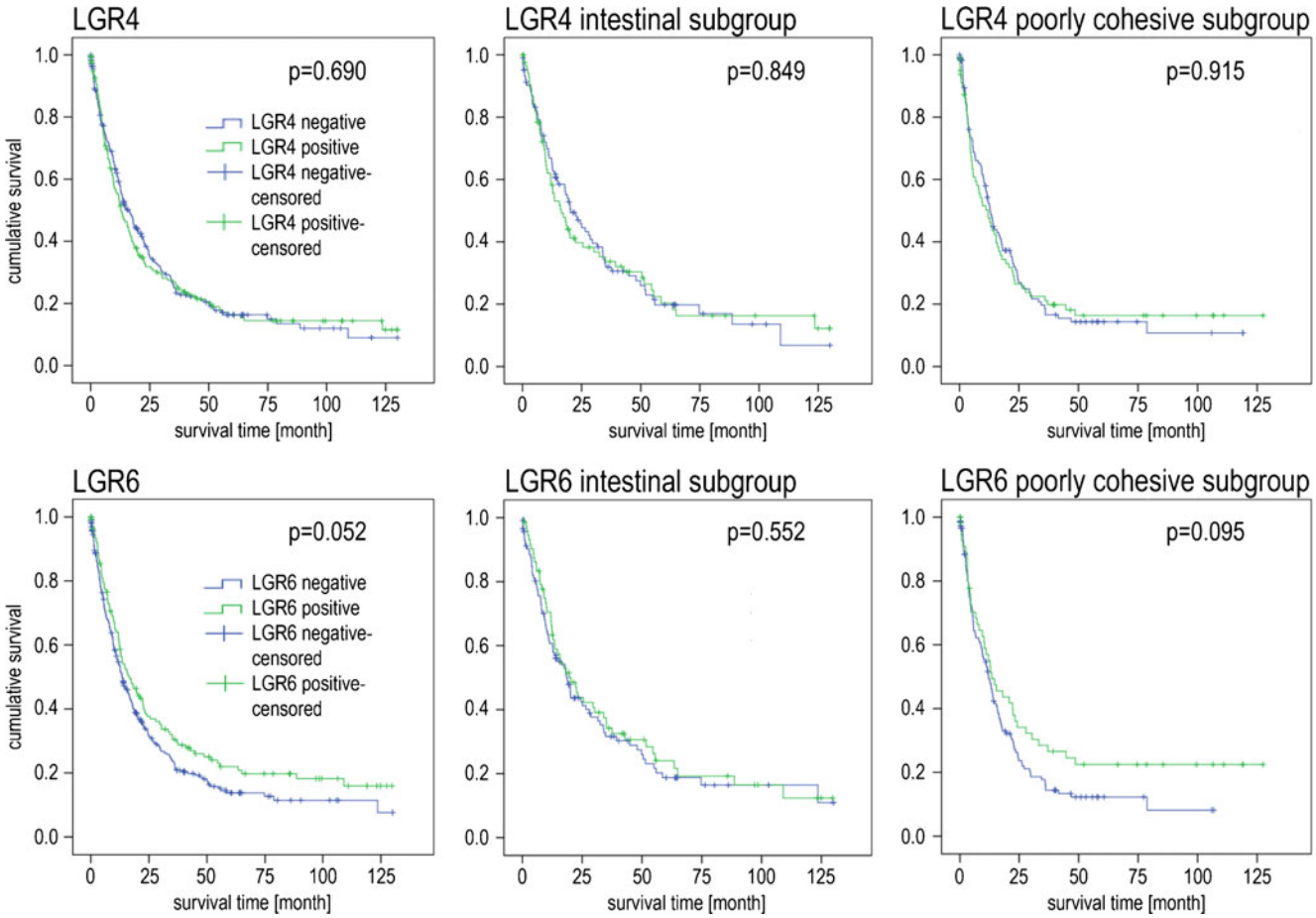

Fig. 3 Patient survival depending on LGR4 and LGR6 expression depicted by Kaplan–Meier curves. *P*-values were calculated using the log-rank (Mantel–Cox) test

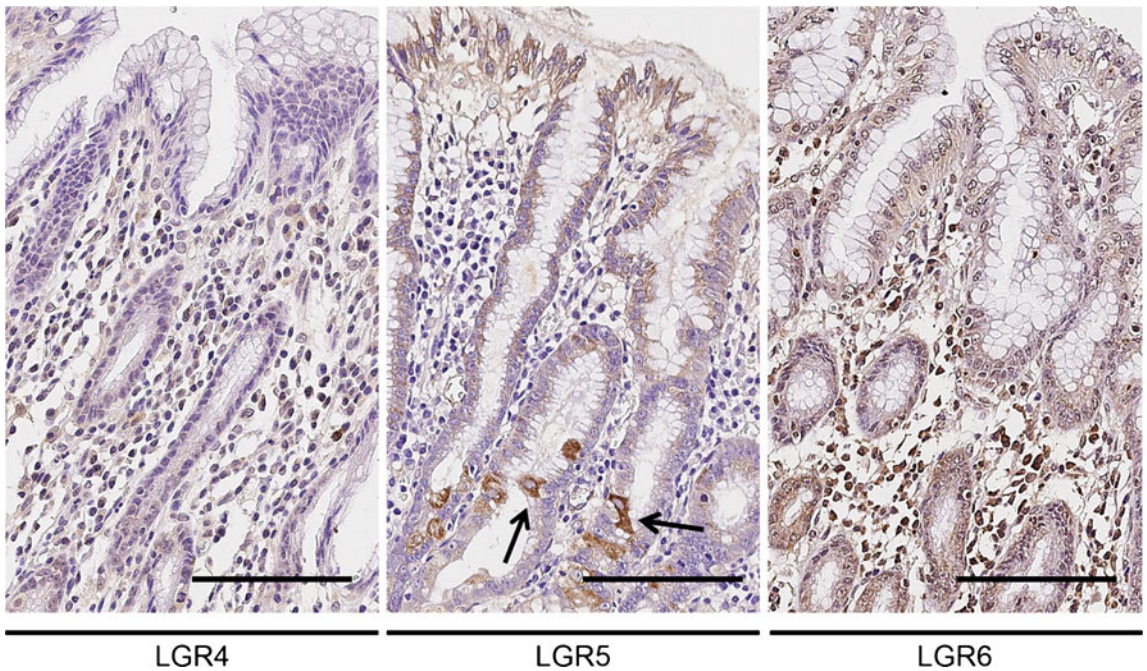

Fig. 4 Immunostaining of LGR4, LGR5, and LGR6 in non-neoplastic mucosa. Serial sections were obtained from a sample of non-neoplastic gastric mucosa. LGR5-positive staining was observed in putative gastric stem cells (*arrows*). In contrast to that, putative mucosal stem cells did not immunoreact with antibodies directed against LGR4 or LGR6. *Scale bar*: 100 μm. Original magnifications: ×200

R-spondin growth factors are able to bind LGR4 and LGR5 and, in this manner, interact with the Wnt pathway [21, 22]. LGRs have been previously reported to be of biological relevance in different physiological and pathophysiological processes. The importance of LGR5 as a marker of putative gastrointestinal stem cells and cancer stem cells in hepatogastrointestinal carcinomas was reported recently by our group [13]. LGR5 is expressed at the tumor center and the invasion front of GCs and correlates with local tumor growth and nodal spread. *LGR4* appears to be involved in fundamental embryonic development processes of all germinal sheets as was shown by Mazerbourg et al. [20]. LGR4 is broadly expressed in various highly proliferative tissues without being restricted to stem cell populations [12]. This is notable having in mind that its relative LGR5 was proven recently to be a stem cell marker in gastric and intestinal mucosae [11, 23] (Fig. 4). Gao et al. observed LGR4 overexpression promoting invasiveness and metastasis of colorectal carcinoma and postulated this gene being a potential marker for metastases and poor prognosis [24, 25]. Nevertheless, in log-rank (Mantel–Cox) test, we did not find an impact of LGR4 expression on survival of GC patients. As recently reported, LGR4 seems to be part of the Wnt pathway in the intestine [22, 26]. Due to this function, the receptor is hypothesized to be a potential new therapeutic target for intestinal cancers [26]. Our systematic analysis indicates that *LGR4* also plays a role in GC biology. Future studies will have to demonstrate whether it is also a putative diagnostic, prognostic, and/or therapeutic target for GC. Interestingly, in some GCs, we found a nuclear immunoreaction for LGR4. This observation is worth being subject of further research as nuclear immunostaining has already been published in connection with other GPCRs and their signaling pathways [27].

LGR6 is expressed in multiple tissues, e.g. brain, thymus, kidney, spleen, heart, and intestine [14]. This receptor was shown to mark a population of Wnt-independent stem cells in the skin, which is located in a certain domain of the hair follicle, just below the sebaceous gland [11, 28]. These stem cells seem to be involved in wound repair and hair follicle development [11, 12, 28]. Leushacke and Barker described the perspective to utilize isolated LGR6-positive stem cells for epithelial culture. These cells may have potential for new clinical treatment strategies of skin disorders [11]. However, in our patient cohort, LGR6 was not found in the stem cell niche of non-neoplastic gastric mucosa and did not colocalize with LGR5 immunoreactive cells. Thus, at present, we have no evidence of LGR6 being a stem cell marker in the stomach (Fig. 4).

Collectively, our current and previous findings lend support to the hypothesis that members of the LGR family of GPCRs, notably LGR4, LGR5, and LGR6, are differentially expressed in GCs and are tumor biologically relevant. While LGR5 might be a stem cell marker, the functions of LGR4 and LGR6 are unknown. Both LGR4 and LGR6 have potential in terms of diagnostics and therapy of GC, but they will need to be subject to future research. Further studies into this topic are urgently warranted.

Acknowledgments We would like to thank Sandra Krüger for her excellent technical support. This study was supported by grants from Deutsche Forschungsgemeinschaft (Ro 1173/12).

Conflict of interest The authors declare that they have no conflict of interest.

Disclosures There are no potential conflicts (financial, professional, or personal) to disclose that are relevant to the manuscript.

References

1. Krejs GJ (2010) Gastric cancer: epidemiology and risk factors. Dig Dis 28:600–603
2. Garlipp B, Schwalenberg J, Adolf D, Lippert H, Meyer F (2011) Epidemiology, surgical management and early postoperative outcome in a cohort of gastric cancer patients of a tertiary referral center in relation to multi-center quality assurance studies. Pol Przegl Chir 83:123–134
3. Crew KD, Neugut AI (2006) Epidemiology of gastric cancer. World J Gastroenterol 12:354–362
4. Correa P, Piazuelo MB, Camargo MC (2006) Etiopathogenesis of gastric cancer. Scand J Surg 95:218–224
5. Moehler M, Al-Batran SE, Andus T et al und AWMF (2011) German S3-guideline "Diagnosis and treatment of esophagogastric cancer". Z Gastroenterol 49:461–531
6. Bang YJ, Van Cutsem E, Feyereislova A, Chung HC, Shen L, Sawaki A, Lordick F, Ohtsu A, Omuro Y, Satoh T, Aprile G, Kulikov E, Hill J, Lehle M, Rüschoff J, Kang YK und Investigators, ToGA Trial (2010) Trastuzumab in combination with chemotherapy versus chemotherapy alone for treatment of HER2-positive advanced gastric or gastro-oesophageal junction cancer (ToGA): a phase 3, open-label, randomised controlled trial. Lancet 376:687–697
7. Böhme I, Beck-Sickinger AG (2009) Illuminating the life of GPCRs. Cell Commun Signal 7:16
8. Pierce KL, Premont RT, Lefkowitz RJ (2002) Seven-transmembrane receptors. Nat Rev Mol Cell Biol 3:639–650
9. Ingold B, Simon E, Ungethüm U, Kuban RJ, Müller BM, Lupp A, Neumann U, Ebert MP, Denkert C, Weichert W, Schulz S, Röcken C (2010) Vascular CXCR4 expression—a novel antiangiogenic target in gastric cancer? PLoS One 5:e10087
10. Schmuck R, Warneke V, Behrens HM, Simon E, Weichert W, Röcken C (2011) Genotypic and phenotypic characterization of side population of gastric cancer cell lines. Am J Pathol 178:1792–1804
11. Leushacke M, Barker N (2011) LGR5 and LGR6 as markers to study adult stem cell roles in self-renewal and cancer. Oncogene. doi:10.1038/onc.2011.479
12. Barker N, Clevers H (2010) Leucine-rich repeat-containing G-protein-coupled receptors as markers of adult stem cells. Gastroenterology 138:1681–1696
13. Simon E, Petke D, Böger C, Behrens HM, Warneke V, Ebert M, Röcken C (2012) The spatial distribution of LGR5(+) cells correlates with gastric cancer progression. PLoS One 7:e35486

14. Hsu SY, Kudo M, Chen T, Nakabayashi K, Bhalla A, van der Spek PJ, van Duin M, Hsueh AJ (2000) The three subfamilies of leucine-rich repeat-containing G protein-coupled receptors (LGR): identification of LGR6 and LGR7 and the signaling mechanism for LGR7. Mol Endocrinol 14:1257–1271
15. de Lau W, Barker N, Low TY, Koo BK, Li VS, Teunissen H, Kujala P, Haegebarth A, Peters PJ, van de Wetering M, Stange DE, van Es JE, Guardavaccaro D, Schasfoort RB, Mohri Y, Nishimori K, Mohammed S, Heck AJ, Clevers H (2011) LGR5 homologues associate with Wnt receptors and mediate R-spondin signalling. Nature 476:293–297
16. Bosman FT, Carneiro F, Hruban RH, Theise ND (2010) WHO classification of tumors of the digestive system, 4th edn. International Agency for Research on Cancer, Lyon
17. Sobin LH, Gospodarowicz MK, Wittekind C (2010) International Union Against Cancer (UICC) TNM classification of malignant tumors, 7th edn. Wiley-Liss, New York
18. Bornschein J, Kandulski A, Selgrad M, Malfertheiner P (2010) From gastric inflammation to gastric cancer. Dig Dis 28:609–614
19. Carl-McGrath S, Ebert M, Röcken C (2007) Gastric adenocarcinoma: epidemiology, pathology and pathogenesis. Cancer therapy 5:877–894
20. Mazerbourg S, Bouley DM, Sudo S, Klein CA, Zhang JV, Kawamura K, Goodrich LV, Rayburn H, Tessier-Lavigne M, Hsueh AJ (2004) Leucine-rich repeat-containing, G protein-coupled receptor 4 null mice exhibit intrauterine growth retardation associated with embryonic and perinatal lethality. Mol Endocrinol 18:2241–2254
21. Birchmeier W (2011) Stem cells: orphan receptors find a home. Nature 476:287–288
22. Carmon KS, Gong X, Lin Q, Thomas A, Liu Q (2011) R-spondins function as ligands of the orphan receptors LGR4 and LGR5 to regulate Wnt/beta-catenin signaling. Proc Natl Acad Sci U S A 108:11452–11457
23. Barker N, van Es JH, Kuipers J, Kujala P, van den Born M, Cozijnsen M, Haegebarth A, Korving J, Begthel H, Peters PJ, Clevers H (2007) Identification of stem cells in small intestine and colon by marker gene LGR5. Nature 449:1003–1007
24. Gao Y, Kitagawa K, Hiramatsu Y, Kikuchi H, Isobe T, Shimada M, Uchida C, Hattori T, Oda T, Nakayama K, Nakayama KI, Tanaka T, Konno H, Kitagawa M (2006) Up-regulation of GPR48 induced by down-regulation of p27Kip1 enhances carcinoma cell invasiveness and metastasis. Cancer Res 66:11623–11631
25. Gao Y, Shan ZY, Wang H, Zhang HM, Teng WP (2009) Inhibitory effect of shRNA targeting GPR48 on invasion and metastasis of human cervical carcinoma cell line HeLa. Ai Zheng 28:104–107
26. Mustata RC, Van Loy T, Lefort A, Libert F, Strollo S, Vassart G, Garcia MI (2011) LGR4 is required for Paneth cell differentiation and maintenance of intestinal stem cells ex vivo. EMBO Rep 12:558–564
27. Gobeil F, Fortier A, Zhu T, Bossolasco M, Leduc M, Grandbois M, Heveker N, Bkaily G, Chemtob S, Barbaz D (2006) G-protein-coupled receptors signalling at the cell nucleus: an emerging paradigm. Can J Physiol Pharmacol 84:287–297
28. Snippert HJ, Haegebarth A, Kasper M, Jaks V, van Es JH, Barker N, van de Wetering M, van den Born M, Begthel H, Vries RG, Stange DE, Toftgård R, Clevers H (2010) LGR6 marks stem cells in the hair follicle that generate all cell lineages of the skin. Science 327:1385–1389

Virchows Arch (2012) 461:367–377
DOI 10.1007/s00428-012-1303-2

ORIGINAL ARTICLE

ARID1A expression loss in gastric cancer: pathway-dependent roles with and without Epstein–Barr virus infection and microsatellite instability

Hiroyuki Abe · Daichi Maeda · Rumi Hino · Yuya Otake · Maya Isogai · Aya Shinozaki Ushiku · Keisuke Matsusaka · Akiko Kunita · Tetsuo Ushiku · Hiroshi Uozaki · Yoko Tateishi · Tsunekazu Hishima · Yoshiaki Iwasaki · Shumpei Ishikawa · Masashi Fukayama

Received: 22 March 2012 / Revised: 9 August 2012 / Accepted: 10 August 2012 / Published online: 23 August 2012
© Springer-Verlag 2012

Abstract The AT-rich interactive domain 1A gene (ARID1A), which encodes one of the subunits in the Switch/Sucrose Nonfermentable chromatin remodeling complex, carries mutations and is responsible for loss of protein expression in gastric carcinoma, particularly with Epstein–Barr virus (EBV) infection and a microsatellite instability-high phenotype. We used immunohistochemistry to investigate the significance of ARID1A loss in 857 gastric carcinoma cases, including 67 EBV(+) and 136 MLH1-lost gastric carcinomas (corresponding to a microsatellite instability-high phenotype). Loss of ARID1A expression was significantly more frequent in EBV(+) (23/67; 34 %) and MLH1-lost (40/136; 29 %) gastric carcinomas than in EBV(−)MLH1-preserved (32/657; 5 %) gastric carcinomas ($P<0.01$). Loss of ARID1A correlated with larger tumor size, advanced invasion depth, lymph node metastasis, and poor prognosis in EBV(−)MLH1-preserved gastric carcinoma. A correlation was found only with tumor size and diffuse-type histology in MLH1-lost gastric carcinoma, but no correlation was observed in EBV(+) gastric carcinoma. Loss of ARID1A expression in EBV(+) gastric carcinoma was highly frequent in the early stage of gastric carcinoma, although EBV infection did not cause downregulation of ARID1A: EBV-positive nasopharyngeal carcinomas ($n=8$) and lymphomas ($n=15$) failed to show loss of ARID1A, and EBV infection did not cause loss of ARID1A in gastric carcinoma cell lines. Taken together, loss of ARID1A may be an early change in carcinogenesis and may precede EBV infection in gastric epithelial cells, while loss of ARID1A promotes cancer progression in gastric cancer cells without EBV infection or loss of MLH1 expression. Loss of ARID1A has different and pathway-dependent roles in gastric carcinoma.

Keywords ARID1A · Epstein–Barr virus · Gastric cancer · Microsatellite instability · MLH1

H. Abe · D. Maeda · R. Hino · Y. Otake · M. Isogai · A. S. Ushiku · K. Matsusaka · A. Kunita · T. Ushiku · H. Uozaki · S. Ishikawa · M. Fukayama (✉)
Department of Pathology, Graduate School of Medicine, The University of Tokyo, Hongo 7-3-1, Tokyo 113-0033, Japan
e-mail: mfukayama-tky@umin.net

Y. Otake
Division of Central Clinical Research Laboratory, Nissay Hospital, Osaka, Japan

Y. Tateishi · T. Hishima
Department of Pathology, Tokyo Metropolitan Cancer and Infectious diseases Center, Komagome Hospital, Tokyo, Japan

Y. Iwasaki
Department of Surgery, Tokyo Metropolitan Cancer and Infectious diseases Center, Komagome Hospital, Tokyo, Japan

Introduction

Gastric cancer (GC) is one of the most common malignancies in the world, particularly in East Asia [1]. The prognosis of advanced-stage GC is still poor, and investigation of pathological features and molecular mechanisms according to its specific subtypes is mandatory to develop more effective therapies for individuals with GC. Epstein–Barr virus (EBV)-associated

GC (EBV(+) GC) shows monoclonal growth of EBV-infected stomach epithelial cells, accounting for nearly 10 % of GCs. Its typical morphology is a poorly differentiated carcinoma with massive infiltration of lymphocytes, generally referred to as lymphoepithelioma-like carcinoma. The molecular mechanism is also distinctive [2–4], i.e., EBV(+) GC is a representative of GCs showing a CpG island methylator phenotype [5, 6], as well as GCs with high microsatellite instability (MSI). The latter GC subtype (MSI-high GC) is mostly caused by loss of MLH1 expression due to promoter methylation of the *MLH1* gene [7, 8].

Recent genome-wide sequencing studies have demonstrated that the *AT-rich interactive domain 1A gene* (*ARID1A*) is frequently mutated in EBV(+) GC and MSI-high GC [9, 10]. ARID1A is one of the subunits of the Switch/Sucrose Nonfermentable (SWI/SNF) chromatin remodeling complex and is currently thought to behave like a tumor suppressor gene [11–15]. Previous studies have identified an *ARID1A* rearrangement in primary breast cancer and an *ARID1A* deletion in a lung cancer cell line [12]. Mutation of *ARID1A* has been demonstrated in carcinomas of the ovary, for example, in approximately half of the clear-cell subtype and in 30 % of the endometrioid subtype, but in none of the serous or mucinous subtypes [13, 14]. Most *ARID1A* mutations are insertion/deletion mutations. This leads to truncation of ARID1A protein, and such a type of protein is assumed to be prone to degradation. *ARID1A* gene mutation correlated closely with loss of ARID1A expression (ARID1A loss) as assessed by immunohistochemistry even in the absence of mutation in other alleles [9, 14, 16], and ARID1A loss can be used as a surrogate marker for the gene mutations. One-third of endometrioid carcinomas of the uterine corpus and adenocarcinomas/adenosquamous carcinomas of the uterine cervix also showed ARID1A loss [17–19], but *ARID1A* mutation and ARID1A loss were not frequent in carcinomas of other organs [20].

To clarify the significance of ARID1A in GC, we performed immunohistochemistry of ARID1A using high-throughput tissue microarray (TMA) of GC, with special attention to two subtypes, EBV(+) GC and MSI-high GC. In addition, we also evaluated ARID1A expression in other types of EBV-associated malignancies, such as nasopharyngeal carcinomas and lymphomas. Furthermore, an experimental approach using genetically engineered EBV was applied to investigate the relationship between EBV infection and ARID1A expression in GC.

Materials and methods

Tissue samples

Formalin-fixed and paraffin-embedded GC tissues were obtained from the Department of Pathology, Tokyo University Hospital, and the Department of Pathology, Tokyo Metropolitan Cancer and Infectious Diseases Center, Komagome Hospital (893 cases). Biopsy samples of nasopharyngeal carcinomas (eight cases) and lymphomas (15 cases) were also obtained from the Tokyo University Hospital. Lymphoma samples included six diffuse large B cell lymphomas, four EBV-associated lymphoproliferative disorders, three Hodgkin lymphomas, one extranodal NK/T cell lymphoma, nasal-type, and one peripheral T cell lymphoma, unspecified. All tumors were retrieved from the archives of each institution.

For immunohistochemistry, TMAs were designed from paraffin tissue blocks of GCs, each made by punching out 2-mm-diameter cores of tumors from the block. At least two cores were obtained from each case. For clinicopathological analyses, all of the cases, including both early (T1 or Tis) and advanced (T2 or more) carcinomas, were used. For prognostic analyses, we used a subset of advanced carcinoma cases (n=254) with information about prognosis. Correlations of ARID1A expression status with the following clinical and pathological variables were evaluated: gender, age, size and location of the tumor, histological type (Lauren classification [21]), histological invasion depth, lymphatic and venous invasion, lymph node metastasis, EBV-encoded small RNA in situ hybridization (EBER-ISH) status, and MLH1 expression status. Negative immunostaining of MLH1 (MLH1-loss) was used as a marker of MSI-high GC [7, 8].

Some uterine endometrioid carcinomas have ARID1A-negative areas adjacent to positive areas, and the mutation is thought to arise in clones within the tumors [17]. To assess the distribution of positive and negative tumor cells in EBV(+) GC, whole sections of EBV(+) GC (45 cases) were stained for ARID1A. This study was approved by the ethics committee of each institution (Tokyo University Hospital and Komagome Hospital).

GC cell lines and EBV infection

GC cell lines MKN1, MKN74, TMK1, and SNU719 were used in the present study. MKN1 and MKN74 were obtained from Riken Bioresource Center Cell Bank (Tsukuba, Japan). TMK1 was a gift from Prof. W. Yasui (Hiroshima University). SNU719 cells were derived from EBV(+) GC and obtained from the Korean Cell Line Bank (Seoul, Korea). The cell lines were cultured in RPMI-1640 (Nacalai Tesque, Kyoto, Japan) supplemented with 10 % fetal bovine serum, penicillin (40 units/mL), and streptomycin (50 μg/mL) at 37 °C in a 5 % CO_2 incubator.

EBV-negative GC cell lines MKN1, MKN74, and TMK1 were infected with recombinant EBV using the cell-to-cell contact method as previously described [22]. Briefly, a Burkitt's lymphoma cell line, Akata, was modified to produce recombinant EBV, in which the

neomycin-resistant gene was inserted and was used as a source of the virus. Recombinant EBV was a gift from Prof. K. Takada (Hokkaido University). After removal of Akata cells, GC cells were subjected to bulk selection with G418 (Sigma Aldrich, St. Louis, MO, USA), yielding EBV-infected GC cell lines. To confirm EBV infection, noncoding small RNA of the EBV latent gene *EBER1* was evaluated using reverse transcription–polymerase chain reaction as previously described [23]. Cell blocks were then made from the cultured cells with and without EBV infection; cells were fixed with 4 % paraformaldehyde, collected, and embedded in paraffin using agarose as an embedding medium [24].

Western blotting

Whole cell extracts were prepared from GC cell lines, and Western blotting was performed as previously described [25]. The primary antibodies used were rabbit polyclonal anti-ARID1A (HPA005456, dilution 1:1,000; Sigma-Aldrich) and goat polyclonal anti-actin (sc-1616, dilution 1:1,000; Santa Cruz Biotechnology, Santa Cruz, CA, USA).

Immunohistochemistry and EBER-ISH

Immunohistochemistry was applied to tissue microarrays, cell blocks, and whole sections using the VECSTATIN ABC kit (Vector Laboratories, Burlingame, CA, USA) and DAB+Chromogen (Dako, Glostrup, Denmark) using the peroxidase method. The primary antibodies used were rabbit polyclonal anti-ARID1A (HPA005456, dilution 1:200; Sigma-Aldrich) and mouse monoclonal anti-MLH1 (550838, clone G168-15, dilution 1:50; BD Pharmingen, Franklin Lakes, NJ, USA). For ARID1A, the sections were autoclaved for 10 min in citrate buffer (pH 6) for antigen retrieval. For MLH1, the sections were microwaved for 15 min in citrate buffer (pH 6). Tumors were regarded as positive for ARID1A and MLH1 if tumor cells showed nuclear immunoreactivity. Non-neoplastic cells, such as fibroblasts, endothelial cells, and lymphocytes, served as internal positive controls for ARID1A. Lymphocytes in a germinal center and normal epithelium in the proliferative zone served as internal positive controls for MLH1.

EBER-ISH was performed on paraffin sections using a fluorescein isothiocyanate (FITC)-labeled peptide nucleic acid probe (Y5200; Dako) and anti-FITC (V0403, dilution 1:200; Dako).

Immunohistochemistry and EBER-ISH results were evaluated independently by two pathologists (H.A. and D.M.). Cores devoid of tumor tissues or inappropriate immunostaining results for evaluation (e.g., no staining of internal control cells) were excluded from analyses.

Statistical analysis

The chi-square test was used to examine the distribution of two variables—i.e., two or oligo-valued data. The unpaired *t* test was used to test for differences in tumor size and patient age. Overall survival and disease-free survival data were plotted by Kaplan–Meier methods, and *P* values were determined by the log-rank test. Prognostic factors were also analyzed by multivariate analyses (Cox proportional hazards model). *P* values less than 0.05 were considered statistically significant.

Table 1 The relationships between ARID1A expression and clinicopathological factors in gastric cancer

	ARID1A		
	Positive	Negative	*P* value
Gender			
Male	534	59	0.15
Female	229	35	
Age[a] (years)	64.1±11.6	66.5±10.4	0.06
Tumor location			
U	198	40	0.003*
M	300	23	
L	260	31	
Tumor size[a] (mm)	61±39	75±39	<0.001*
Invasion depth			
Early[b]	209	14	0.009*
Advanced	554	80	
Lauren's classification			
Intestinal	356	39	0.32
Diffuse	402	55	
Lymphatic invasion			
Negative	282	25	0.046*
Positive	479	69	
Venous invasion			
Negative	261	18	0.003*
Positive	500	76	
Lymph node metastasis			
Negative	303	30	0.10
Positive	435	63	
EBV			
Negative	719	71	<0.001*
Positive	44	23	
MLH1			
Negative	96	40	<0.001*
Positive	667	54	

U upper, *M* middle, *L* lower, *EBV* Epstein–Barr virus

*$P < 0.05$ were defined as statistically significant

[a] Mean±standard deviation

[b] Early means Tis or T1 in tumor node metastasis classification

Results

Correlation of ARID1A loss with EBV infection and MLH1 loss

The results of the immunohistochemical investigations are presented in Table 1. In total, 857 of 893 cases in the TMAs were appropriate for immunohistochemical evaluation. Of these 857 GC cases, EBER-ISH revealed positive signals in 67 (8 %), and immunohistochemistry showed MLH1-loss in 136 (16 %). Only three cases of EBV(+) GC were negative for MLH1 expression.

ARID1A expression was determined by nuclear staining. Stromal cells, such as lymphocytes, fibroblasts, and endothelial cells, showed positive nuclear staining and served as a positive internal control (Fig. 1). Loss of ARID1A expression was observed in 23 of 67 cases of EBV(+) GC (34 %) and in 40 of 136 cases of MLH1-lost GC (29 %), whereas loss of ARID1A expression was observed in 32 of 657 cases of EBV(−)MLH1-preserved GC (5 %). Thus, ARID1A loss was significantly frequent in EBV(+) GC and MLH1-lost GC ($P<0.01$, $P<0.01$, respectively).

Clinicopathological characteristics of ARID1A loss in EBV (+) GC, MLH1-lost GC, and EBV(−)MLH1-preserved GC

The relationships between loss of ARID1A expression and other clinicopathological factors were analyzed (Table 1). ARID1A loss correlated with tumor location, larger tumor size, advanced invasion depth, as well as with frequent lymphatic and venous invasion. Gastric carcinoma cases were then classified into three subgroups: EBV(+) GC ($n=67$), MLH1-lost GC ($n=136$), and EBV(−)MLH1-preserved GC ($n=657$), followed by clinicopathological analysis in each group (Table 2). Of 67 cases of EBV (+) GC, three showed MLH1-loss, and these exceptional

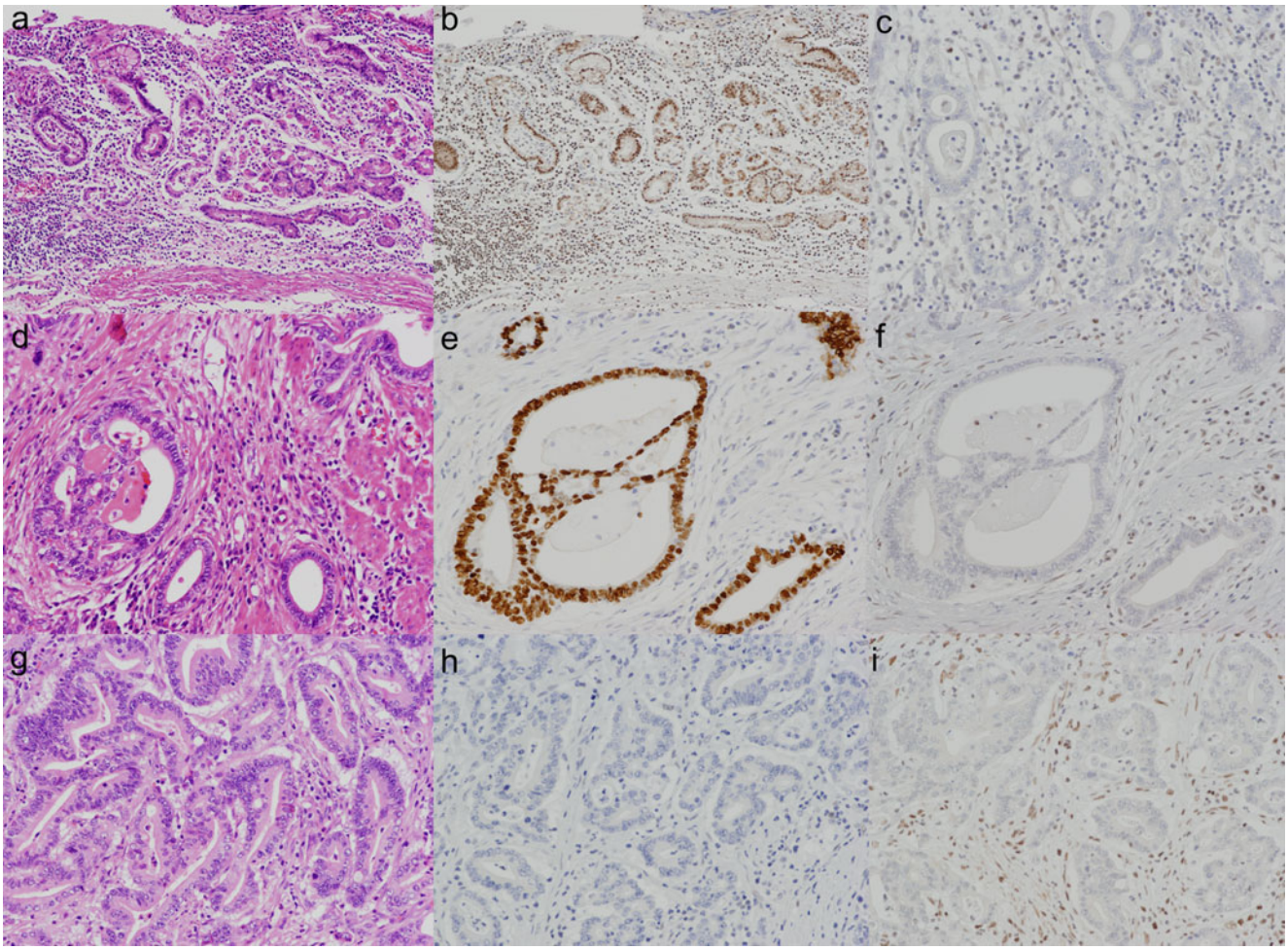

Fig. 1 ARID1A immunohistochemistry in non-neoplastic and neoplastic stomachs. **a** H&E of non-neoplastic gastric mucosa and **b** preserved ARID1A in gastric epithelial and stromal cells. **c** ARID1A-negative gastric carcinoma. **d** H&E of EBV-positive gastric carcinoma with **e** positive EBV-encoded small RNA signals in the nuclei and **f** ARID1A-loss. **g** H&E of EBV-negative gastric carcinoma with **h** MLH1-loss and **i** ARID1A-loss

Table 2 The relationships between ARID1A expression and clinicopathological factors in gastric cancer classified by EBV and MLH1 status

	EBV(+) (n=67)			MLH1-loss (n=136)			EBV(−) MLH1-preserved (n=657)		
	ARID1A			ARID1A			ARID1A		
	Positive	Negative	P value	Positive	Negative	P value	Positive	Negative	P value
Gender									
Male	35	17	0.06	61	20	0.14	439	23	0.84
Female	9	6		35	20		186	9	
Age[a] (years)	60.5±10.7	63.8±9.9	0.23	69.1±11.0	69.9±10.0	0.70	63.7±11.5	63.9±10.3	0.91
Tumor location									
U	24	15	0.32	27	11	0.40	149	14	0.08
M	17	5		29	8		254	11	
L	3	3		40	21		217	7	
Tumor size (mm)[a]	55±40	67±49	0.32	61±31	78±37	0.007*	61±40	76±35	0.04*
Invasion depth									
Early[b]	18	10	0.84	17	4	0.26	175	1	0.002*
Advanced	26	13		79	36		450	31	
Lauren's classification									
Intestinal	13	10	0.28	65	20	0.04*	279	10	0.13
Diffuse	30	13		30	20		343	22	
Lymphatic invasion									
Negative	25	13	0.98	31	9	0.25	226	4	0.006*
Positive	19	10		65	31		397	28	
Venous invasion									
Negative	23	11	0.73	22	6	0.30	216	2	<0.001*
Positive	21	12		74	34		407	30	
Lymph node metastasis									
Negative	26	13	0.84	31	12	0.68	246	6	0.01*
Positive	18	10		59	27		360	26	

U upper, *M* middle, *L* lower

*P<0.05 were defined as statistically significant

[a] Mean±standard deviation

[b] Early means Tis or T1 in tumor node metastasis classification

cases were included in both EBV(+) GC and MLH1-lost GC for this analysis. No clinicopathological factor was associated with ARID1A loss in EBV(+) GC. ARID1A loss correlated only with larger tumor size and diffuse-type histology in MLH1-lost GC. However, ARID1A loss correlated with larger tumor size, advanced invasion depth, frequent lymphatic invasion, venous invasion, and lymph node metastasis in EBV(−)MLH1-preserved GC.

When the frequencies of ARID1A loss were compared between early and advanced carcinoma, ARID1A loss was also observed in EBV(+) GC (10/28 vs 13/39, P=0.84). However, ARID1A loss was more common in advanced carcinomas (31/481) than in early carcinomas in EBV (−)MLH1-preserved GC (1/176) (P=0.002).

Relationship between ARID1A expression loss and prognosis

The effect of ARID1A loss on survival was analyzed in 254 cases of advanced carcinomas (T2 or more). Immunohistochemistry was appropriate for evaluation in 250 cases, including eight EBV(+) GC and 36 MLH1-lost GC. In this series, only one case of EBV(+) GC was found to show MLH1 loss, and this case was included in both EBV(+) GC and MLH1-lost GC for the analysis. ARID1A loss was observed in 3 of 8 cases of EBV (+) GC (38 %), in 10 of 36 cases of MLH1-lost GC (28 %), and in 13 of 207 cases of EBV(−)MLH1-preserved GC (6 %). In each subtype, the frequencies of ARID1A loss were comparable with those in the whole cases.

Patients with ARID1A loss tended to show poorer prognosis, although this was not statistically significant

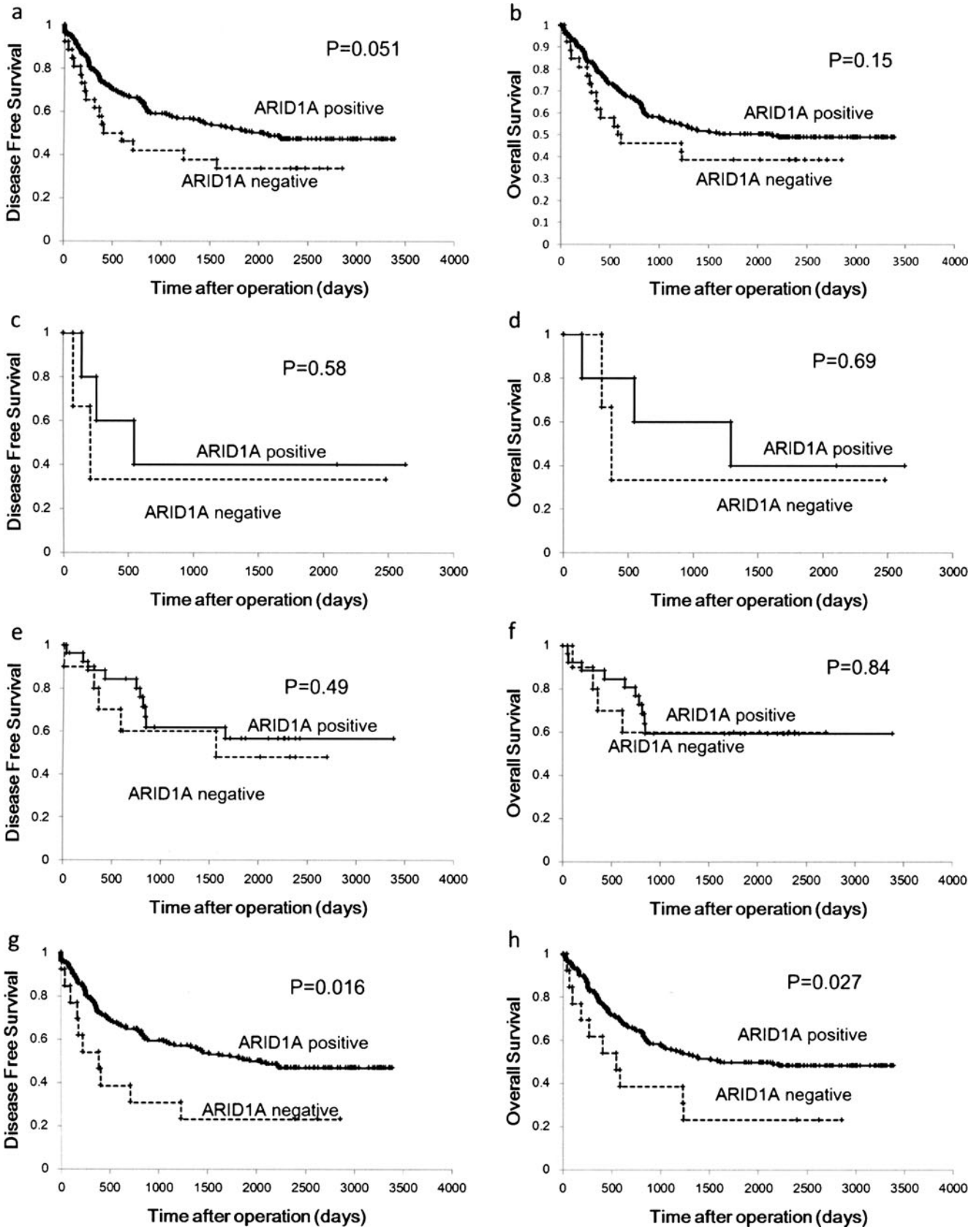
a
Disease Free Survival
P=0.051
ARID1A positive
ARID1A negative
Time after operation (days)
b
Overall Survival
P=0.15
ARID1A positive
ARID1A negative
Time after operation (days)
c
Disease Free Survival
P=0.58
ARID1A positive
ARID1A negative
Time after operation (days)
d
Overall Survival
P=0.69
ARID1A positive
ARID1A negative
Time after operation (days)
e
Disease Free Survival
P=0.49
ARID1A positive
ARID1A negative
Time after operation (days)
f
Overall Survival
P=0.84
ARID1A positive
ARID1A negative
Time after operation (days)
g
Disease Free Survival
P=0.016
ARID1A positive
ARID1A negative
Time after operation (days)
h
Overall Survival
P=0.027
ARID1A positive
ARID1A negative
Time after operation (days)

◀ **Fig. 2** Survival curves of ARID1A-positive and -negative gastric carcinoma. Disease-free survival and overall survival curves in all of the gastric carcinoma (**a** and **b**, respectively), EBV(+) gastric carcinoma (**c** and **d**, respectively), MLH1-lost gastric carcinoma (**e** and **f**, respectively), and EBV(−)MLH1-preserved gastric carcinoma cases (**g** and **h**, respectively). Loss of ARID1A expression significantly correlates with worse disease-free survival and overall survival in EBV(−)MLH1-preserved gastric carcinoma

(Fig. 2a, b). The prognostic analyses of each subtype failed to demonstrate a correlation between ARID1A loss and disease-free survival or overall survival in both EBV (+) GC and MLH1-lost GC, although the number of the cases was relatively small (Fig. 2c–f). Conversely, in EBV(−)MLH1-preserved GC, patients with ARID1A loss had a significantly shorter disease-free survival (P=0.016) and overall survival (P=0.027) (Fig. 2g, h). Multivariate analysis showed that ARID1A loss was an independent prognostic factor in both disease-free survival and overall survival in EBV(−)MLH1-preserved GC (Table 3).

ARID1A loss and EBV infection

Since ARID1A-loss was found to be highly frequent in the early stage of EBV(+) gastric carcinoma, the significance of ARID1A-loss was further evaluated in the whole section of EBV(+) GC and other types of EBV-associated malignancies.

To assess the distribution of ARID1A expression within an individual cancer tissue, whole sections of EBV(+) GC in the first series of TMA were evaluated in parallel by immunohistochemistry. All 45 cases of EBV(+) GC were either diffusely positive or totally negative for ARID1A in the entire lesion, except for one case which consisted of two discrete components of ARID1A-positive and -negative cells side by side (Fig. 3).

Table 3 Prognostic analysis of clinicopathological factors in EBV(−) MLH1-preserved gastric cancer

	Number of cases	Disease-free survival		Overall survival	
		Univariate analysis P value	Multivariate analysis P value	Univariate analysis P value	Multivariate analysis P value
Gender					
Male	139	0.56		0.077	
Female	68				
Age (years)					
>65	101	0.54		0.19	
≦65	106				
Tumor location					
U	61	0.49		0.60	
M	68				
L	74				
Tumor size (mm)					
>60	109	<0.001*	<0.001*	<0.001*	<0.001*
≦60	98				
Lauren's classification					
Intestinal	77	0.34		0.81	
Diffuse	130				
Lymphatic invasion					
Negative	16	0.002*	0.073	0.015*	0.48
Positive	191				
Venous invasion					
Negative	19	0.003*	0.20	0.010*	0.25
Positive	188				
Lymph node metastasis					
Negative	39	<0.001*	0.016*	<0.001*	0.024*
Positive	168				
ARID1A expression					
Negative	13	0.016*	0.039*	0.027*	0.048*
Positive	194				

U upper, *M* middle, *L* lower

*P<0.05 were defined as statistically significant

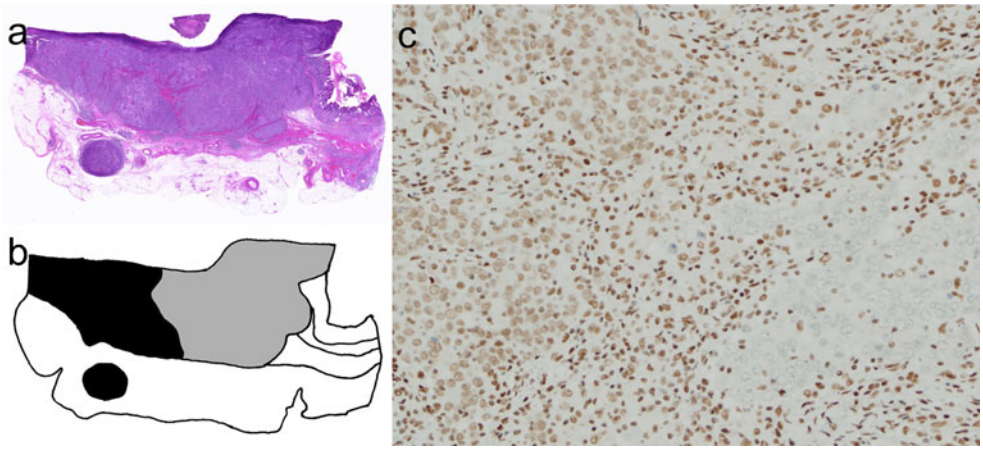

Fig. 3 A case of EBV(+) gastric carcinoma showing both ARID1A-positive and -negative components. **a** H&E staining of a whole section of gastric carcinoma. **b** Schematic representation of distribution of ARID1A-positive and -negative carcinoma cells within the tumor. *Black region* indicates ARID1A-positive carcinoma cells. *Gray region* indicates ARID1A-negative carcinoma cells. Note two discrete components positioned side by side. **c** ARID1A immunohistochemistry. High-magnification view of the border of ARID1A-positive and -negative components

To evaluate whether ARID1A loss was specific to EBV (+) GC among EBV-associated malignancies, ARID1A expression was evaluated in EBV-positive nasopharyngeal carcinomas (n=8) and lymphomas (n=15). There was no case showing loss of ARID1A expression (Fig. 4).

In the following experimental approach, we tried to determine whether EBV infection induces ARID1A loss in GC cells. Three EBV(−) cell lines and one EBV(+) GC cell line showed positive expression of ARID1A. Using the Akata system of EBV infection, three EBV(−) GC cell lines were infected with EBV, in which the neomycin-resistant gene was integrated, and EBV-infected GC cell lines were successfully established. Western blot analysis showed that ARID1A expression was preserved after EBV infection (Fig. 5a). Investigating cell blocks immunohistochemically, we noted ARID1A expression in GC cell lines irrespective of EBV infection (Fig. 5b, c).

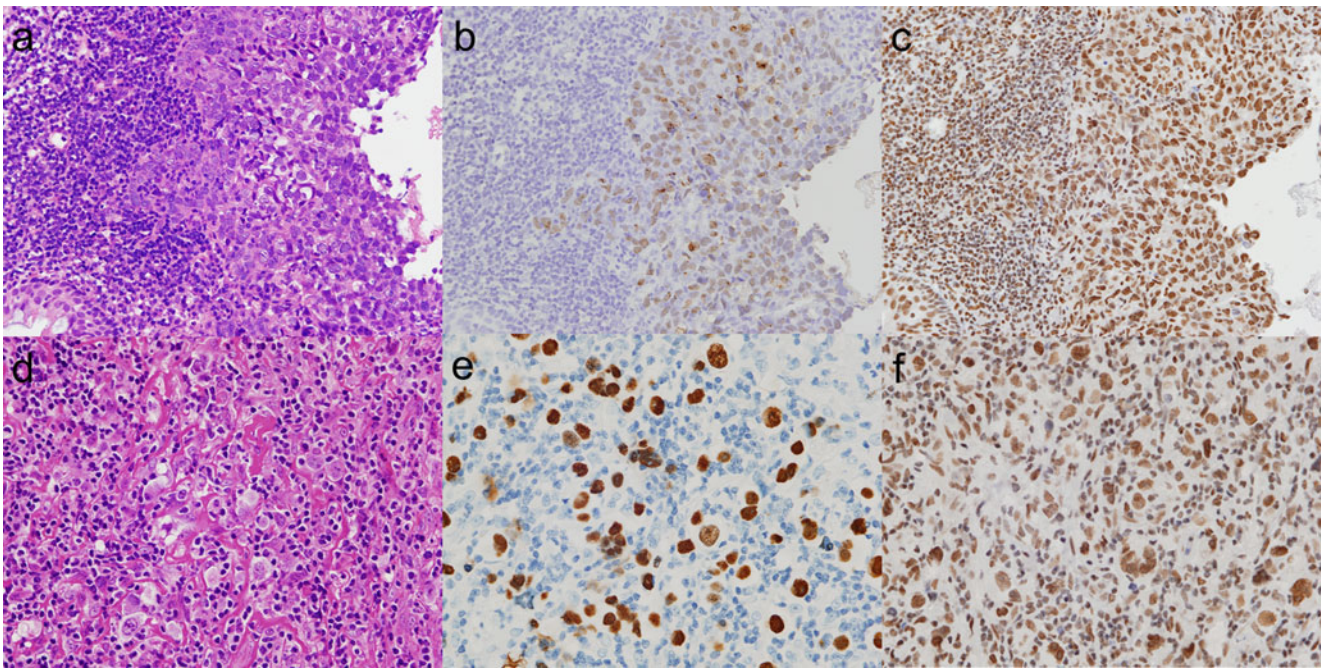

Fig. 4 ARID1A expression in EBV-associated malignancies other than gastric carcinoma. **a**–**c** Nasopharyngeal carcinoma. **d**–**f** Diffuse large B-cell lymphoma. **a**, **d** H&E staining. **b**, **e** EBER-ISH. **c**, **f** ARID1A immunohistochemistry

Discussion

ARID1A is one of the accessory subunits of the SWI/SNF chromatin remodeling complex, and is believed to provide specificity to this complex in the regulation of gene expression by binding to AT-rich DNA sequences [11]. *ARID1A* mutation and loss of ARID1A protein expression have been found to be highly frequent in carcinomas of the ovary and uterus, and with considerable frequency in subtypes of GCs. The presence of mutations is strongly correlated with the loss of ARID1A expression, even if the mutation is accompanied by a wild-type allele. Previous studies have reported loss of ARID1A expression in 100 % (9/9) [16] and 73 % (27/37) [14] of clear cell carcinomas of the ovary with *ARID1A* gene mutation. Wang et al. recently demonstrated *ARID1A* mutation and ARID1A loss in specific subtypes of GC, EBV(+) GC and MSI-high GC [9]. Performing immunohistochemistry for ARID1A and high-throughput TMA of 857 cases of GC, we found that in a Japanese population, ARID1A loss occurs in GC (11 %), with preference for EBV(+) GC and MLH1-lost GC (corresponding to MSI-high GC), the percentage amounting to 34 and 29 %, respectively. There were two new findings: First, the frequencies of ARID1A loss in the early and advanced stages were different when comparing the three groups. This suggests that the timing of ARID1A loss may be different in each subgroup. Second, ARID1A loss was correlated with multiple parameters of tumor aggressiveness in EBV(−)MLH1-preserved GC, such as larger tumor size, advanced invasion depth, frequent vessel invasion, and lymph node metastasis. ARID1A loss was confirmed to be a negative indicator of disease-free survival and overall survival for the patients with advanced GC. These facts clearly demonstrate that ARID1A loss is responsible for cancer progression in EBV(−)MLH1-preserved GC.

The significance of ARID1A loss or mutation in cancer is now subject to intensive investigation. Induction of ARID1A expression suppressed cellular proliferation of the cell lines of gastric, ovarian clear cell, and uterine endometrioid carcinoma harboring *ARID1A* mutation. Knockdown of ARID1A in gastric and ovarian cell lines with wild-type *ARID1A* increased cellular proliferation [10, 15]. These facts are compatible with our studies, in which we found that ARID1A-loss was prognostically unfavorable for patients with EBV(−)MLH1-preserved GC. On the other hand, Wang et al. reported that ARID1A expression loss was associated with better prognosis in gastric carcinoma [9]. In that study, the discrepancy might be explained by the possibility that the cases with loss of ARID1A included more EBV(+) GC and MSI-high GC. EBV(+) and MSI-high GC show a better prognosis than other types of gastric carcinomas [2, 26]. The significance of ARID1A-loss might be different in the three subgroups, as demonstrated in the present study.

In our recent study on the DNA methylation epigenotype with Illumina's Infinium BeadArray [27], two high methylation groups were found to exist: EBV-negative and EBV-positive. In that study, *MLH1* methylation and EBV infection were mutually exclusive, and GC cases with *MLH1* methylation belonged to the EBV-negative/high methylation group. In the present study, immunohistochemistry of MLH1 also revealed a relationship between MLH1 loss and EBV infection, which has also been reported by others [28]. In the MLH1-lost subgroup, the effect of ARID1A loss was limited as compared with that in the EBV(−)MLH1-preserved subgroup as described above. Because loss of MLH1 expression results in a MSI-high phenotype, *ARID1A* mutations in this subgroup are mostly considered to be caused by a slippage error on the short repeats of four to seven mononucleotides in the coding region [9]. A

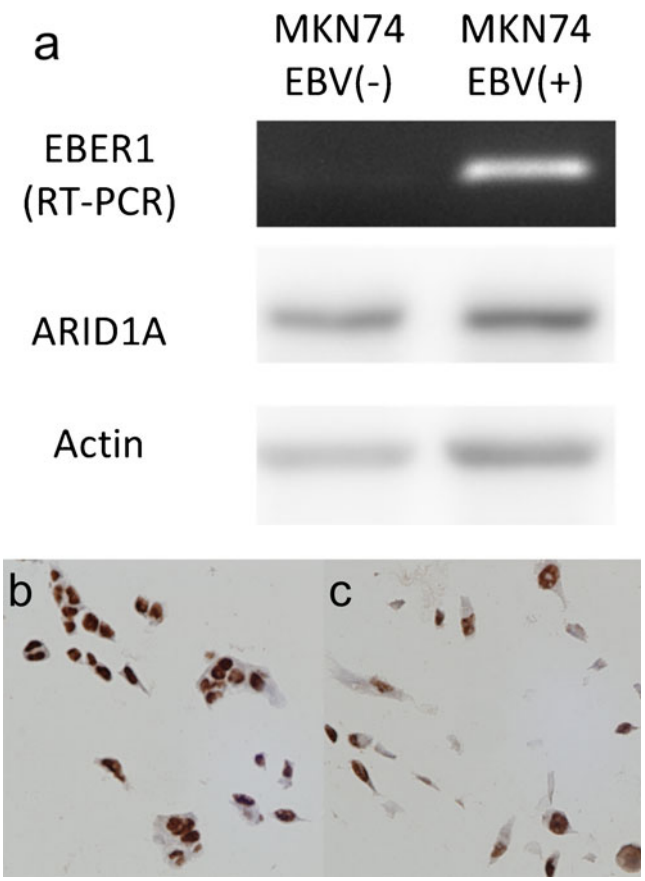

Fig. 5 Effect of EBV infection on ARID1A expression in gastric carcinoma cell lines. **a** ARID1A expression in MKN74 with and without EBV infection. *Upper column*: reverse transcription–polymerase chain reaction of EBER1. *Middle column*: Western blot of ARID1A. *Lower column*: Western blot of Actin. **b**, **c** Immunohistochemistry for ARID1A expression in cell blocks of parental MKN74 cells (**b**) and MKN74 cells with EBV infection (**c**). No difference in ARID1A expression was observed, as demonstrated by Western blotting (**a**) and by immunohistochemistry of cell blocks (**b**, **c**)

previous study revealed that loss of BRG1 or BRM, which are subunits of the SWI/SNF complex, cause DNA methylation in the promoter region of CD44 and E-cadherin [29]. Thus, ARID1A loss in this subset might also play a role in promoting epigenetic abnormalities through dysfunction of the SWI/SNF complex.

The clinicopathological characteristics associated with ARID1A loss were totally different in EBV(+) GC. The frequency rate of ARID1A loss in early carcinomas was nearly as high as that in advanced carcinomas, and no factor was correlated with loss of expression. In addition, the clonal nature of ARID1A loss was confirmed by immunohistochemistry of the whole section. One case had ARID1A-positive and -negative components within tumor, but the components appeared to be colliding. Furthermore, ARID1A loss was not observed in EBV-associated malignant neoplasms other than stomach neoplasms, and using the Akata infection system, we confirmed that EBV infection did not cause loss of expression in GC cell lines. These findings suggest that epithelial cells with ARID1A loss constitute one precursor lesion of the stomach for EBV infection and subsequent cancer development. Epithelial cells with ARID1A loss might be more susceptible to EBV infection. Alternatively, ARID1A loss, cooperating with EBV infection, may accelerate CpG-island methylation on the promoter region of DNA, which then forms the EBV-positive/high epigenotype in the infected stomach cells [27].

In the present study, ARID1A loss was frequent in EBV (+) GC or MLH1-lost (MSI-high) GC; both of which are known to show the CpG island methylator phenotype. The significance of ARID1A loss is different and may be pathway-dependent in EBV(+) GC, MLH1-lost GC, and EBV(−)MLH1-preserved GC. ARID1A loss is a negative predictor for the prognosis of patients with EBV(−)MLH1-preserved GC. Further studies are necessary to clarify the role of ARID1A loss, in association with the function of SWI/SNF complex, in the formation of EBV-negative and EBV-positive high epigenotypes.

Acknowledgments This work was supported by a grant-in-aid for scientific research (20249022) from the Ministry of Education, Culture, Science, Sports, and Technology, Japan.

Conflict of interest The authors declare that they have no conflict of interest.

References

1. Jemal A, Center MM, DeSantis C, Ward EM (2010) Global patterns of cancer incidence and mortality rates and trends. Cancer Epidemiol Biomarkers Prev 19:1893–1907
2. Fukayama M (2010) Epstein–Barr virus and gastric carcinoma. Pathol Int 60:337–350
3. Kang GH, Lee S, Kim WH, Lee HW, Kim JC, Rhyu MG, Ro JY (2002) Epstein–barr virus-positive gastric carcinoma demonstrates frequent aberrant methylation of multiple genes and constitutes CpG island methylator phenotype-positive gastric carcinoma. Am J Pathol 160:787–794
4. Chong JM, Sakuma K, Sudo M, Ushiku T, Uozaki H, Shibahara J, Nagai H, Funata N, Taniguchi H, Aburatani H, Fukayama M (2003) Global and non-random CpG-island methylation in gastric carcinoma associated with Epstein–Barr virus. Cancer Sci 94:76–80
5. Chang MS, Uozaki H, Chong JM, Ushiku T, Sakuma K, Ishikawa S, Hino R, Barua RR, Iwasaki Y, Arai K, Fujii H, Nagai H, Fukayama M (2006) CpG island methylation status in gastric carcinoma with and without infection of Epstein–Barr virus. Clin Cancer Res 12:2995–3002
6. Hino R, Uozaki H, Murakami N, Ushiku T, Shinozaki A, Ishikawa S, Morikawa T, Nakaya T, Sakatani T, Takada K, Fukayama M (2009) Activation of DNA methyltransferase 1 by EBV latent membrane protein 2A leads to promoter hypermethylation of PTEN gene in gastric carcinoma. Cancer Res 69:2766–2774
7. Leung SY, Yuen ST, Chung LP, Chu KM, Chan AS, Ho JC (1999) hMLH1 promoter methylation and lack of hMLH1 expression in sporadic gastric carcinomas with high-frequency microsatellite instability. Cancer Res 59:159–164
8. Fleisher AS, Esteller M, Wang S, Tamura G, Suzuki H, Yin J, Zou TT, Abraham JM, Kong D, Smolinski KN, Shi YQ, Rhyu MG, Powell SM, James SP, Wilson KT, Herman JG, Meltzer SJ (1999) Hypermethylation of the hMLH1 gene promoter in human gastric cancers with microsatellite instability. Cancer Res 59:1090–1095
9. Wang K, Kan J, Yuen ST, Shi ST, Chu KM, Law S, Chan TL, Kan Z, Chan AS, Tsui WY, Lee SP, Ho SL, Chan AK, Cheng GH, Roberts PC, Rejto PA, Gibson NW, Pocalyko DJ, Mao M, Xu J, Leung SY (2011) Exome sequencing identifies frequent mutation of ARID1A in molecular subtypes of gastric cancer. Nat Genet 43:1219–1223
10. Zang ZJ, Cutcutache I, Poon SL, Zhang SL, McPherson JR, Tao J, Rajasegaran V, Heng HL, Deng N, Gan A, Lim KH, Ong CK, Huang D, Chin SY, Tan IB, Ng CC, Yu W, Wu Y, Lee M, Wu J, Poh D, Wan WK, Rha SY, So J, Salto-Tellez M, Yeoh KG, Wong WK, Zhu YJ, Futreal PA, Pang B, Ruan Y, Hillmer AM, Bertrand D, Nagarajan N, Rozen S, Teh BT, Tan P (2012) Exome sequencing of gastric adenocarcinoma identifies recurrent somatic mutations in cell adhesion and chromatin remodeling genes. Nat Genet 44:570–574
11. Wilson BG, Roberts CW (2011) SWI/SNF nucleosome remodellers and cancer. Nat Rev Cancer 11:481–492
12. Huang J, Zhao YL, Li Y, Fletcher JA, Xiao S (2007) Genomic and functional evidence for an ARID1A tumor suppressor role. Genes Chromosomes Cancer 46:745–750
13. Jones S, Wang TL, Shih IM, Mao TL, Nakayama K, Roden R, Glas R, Slamon D, Diaz LA, Vogelstein B, Kinzler KW, Velculescu VE, Papadopoulos N (2010) Frequent mutations of chromatin remodeling gene ARID1A in ovarian clear cell carcinoma. Science 330:228–231
14. Wiegand KC, Shah SP, Al-Agha OM, Zhao Y, Tse K, Zeng T, Senz J, McConechy MK, Anglesio MS, Kalloger SE, Yang W, Heravi-Moussavi A, Giuliany R, Chow C, Fee J, Zayed A, Prentice L, Melnyk N, Turashvili G, Delaney AD, Madore J, Yip S, McPherson AW, Ha G, Bell L, Fereday S, Tam A, Galletta L, Tonin PN, Provencher D, Miller D, Jones SJ, Moore RA, Morin GB, Oloumi A, Boyd N, Aparicio SA, Shih IM, Mes-Masson AM, Bowtell DD, Hirst M, Gilks B, Marra MA, Huntsman DG (2010) ARID1A mutations in endometriosis-associated ovarian carcinomas. N Engl J Med 363:1532–1543
15. Guan B, Wang TL, Shih IM (2011) ARID1A, a factor that promotes formation of SWI/SNF-mediated chromatin remodeling, is a

tumor suppressor in gynecologic cancers. Cancer Res 71:6718–6727
16. Maeda D, Mao TL, Fukayama M, Nakagawa S, Yano T, Taketani Y, Shih IM (2010) Clinicopathological significance of loss of ARID1A immunoreactivity in ovarian clear cell carcinoma. Int J Mol Sci 11:5120–5128
17. Guan B, Mao TL, Panuganti PK, Kuhn E, Kurman RJ, Maeda D, Chen E, Jeng YM, Wang TL, Shih IM (2011) Mutation and loss of expression of ARID1A in uterine low-grade endometrioid carcinoma. Am J Surg Pathol 35:625–632
18. Wiegand KC, Lee AF, Al-Agha OM, Chow C, Kalloger SE, Scott DW, Steidl C, Wiseman SM, Gascoyne RD, Gilks B, Huntsman DG (2011) Loss of BAF250a (ARID1A) is frequent in high-grade endometrial carcinomas. J Pathol 224:328–333
19. Katagiri A, Nakayama K, Rahman MT, Rahman M, Katagiri H, Ishikawa M, Ishibashi T, Iida K, Otsuki Y, Nakayama S, Miyazaki K (2012) Frequent loss of tumor suppressor ARID1A protein expression in adenocarcinomas/adenosquamous carcinomas of the uterine cervix. Int J Gynecol Cancer 22:208–212
20. Jones S, Li M, Parsons DW, Zhang X, Wesseling J, Kristel P, Schmidt MK, Markowitz S, Yan H, Bigner D, Hruban RH, Eshleman JR, Iacobuzio-Donahue CA, Goggins M, Maitra A, Malek SN, Powell S, Vogelstein B, Kinzler KW, Velculescu VE, Papadopoulos N (2012) Somatic mutations in the chromatin remodeling gene ARID1A occur in several tumor types. Hum Mutat 33:100–103
21. Lauren P (1965) The two histological main types of gastric carcinoma: diffuse and so-called intestinal-type carcinoma. An attempt at a histo-clinical classification. Acta Pathol Microbiol Scand 64:31–49
22. Imai S, Nishikawa J, Takada K (1998) Cell-to-cell contact as an efficient mode of Epstein–Barr virus infection of diverse human epithelial cells. J Virol 72:4371–4378
23. Iwasaki Y, Chong JM, Hayashi Y, Ikeno R, Arai K, Kitamura M, Koike M, Hirai K, Fukayama M (1998) Establishment and characterization of a human Epstein–Barr virus-associated gastric carcinoma in SCID mice. J Virol 72:8321–8326
24. Mansy SS (2004) Agarose cell block: innovated technique for the processing of urine cytology for electron microscopy examination. Ultrastruct Pathol 28:15–21
25. Shinozaki A, Sakatani T, Ushiku T, Hino R, Isogai M, Ishikawa S, Uozaki H, Takada K, Fukayama M (2010) Downregulation of microRNA-200 in EBV-associated gastric carcinoma. Cancer Res 70:4719–4727
26. Lawes DA, SenGupta S, Boulos PB (2003) The clinical importance and prognostic implications of microsatellite instability in sporadic cancer. Eur J Surg Oncol 29:201–212
27. Matsusaka K, Kaneda A, Nagae G, Ushiku T, Kikuchi Y, Hino R, Uozaki H, Seto Y, Takada K, Aburatani H, Fukayama M (2011) Classification of Epstein–Barr virus-positive gastric cancers by definition of DNA methylation epigenotypes. Cancer Res 71:7187–7197
28. Grogg KL, Lohse CM, Pankratz VS, Halling KC, Smyrk TC (2003) Lymphocyte-rich gastric cancer: associations with Epstein–Barr virus, microsatellite instability, histology, and survival. Mod Pathol 16:641–651
29. Banine F, Bartlett C, Gunawardena R, Muchardt C, Yaniv M, Knudsen ES, Weissman BE, Sherman LS (2005) SWI/SNF chromatin-remodeling factors induce changes in DNA methylation to promote transcriptional activation. Cancer Res 65:3542–3547

Virchows Arch (2012) 461:379–383
DOI 10.1007/s00428-012-1307-y

ORIGINAL ARTICLE

A distinctive epitheliomesenchymal biphasic tumor in the duodenum: the first case of duodenoblastoma?

F. Poizat · C. de Chaisemartin · E. Bories · J. R. Delpero · L. Xerri · J. F. Flejou · G. Monges

Received: 18 January 2012 / Revised: 19 July 2012 / Accepted: 23 August 2012 / Published online: 8 September 2012
© Springer-Verlag 2012

Abstract Epitheliomesenchymal biphasic neoplasms are extremely rare in the duodenum, and most of these are carcinosarcomas. Miettinen et al. (Am J Surg Pathol 33:1370–7, 2009) recently reported three cases of a novel distinctive epitheliomesenchymal biphasic tumor of the stomach in young adults. In view of the resemblance to other childhood blastomas, they proposed to refer to this entity as a gastroblastoma. Since none of the components were sufficiently atypical, the gastroblastoma seemed more comparable to this kind of tumor than carcinosarcomas or other aggressive and malignant biphasic tumors. This report describes a duodenal location of a similar epitheliomesenchymal biphasic tumor in a 22-year-old woman. To our knowledge, this is the first reported case occurring primarily in the duodenum and might be the first case of "duodenoblastoma."

Keywords Epitheliomesenchymal biphasic tumor · Duodenoblastoma · Gastroblastoma · Carcinosarcoma · Duodenum

F. Poizat (✉) · L. Xerri · G. Monges
Department of Biopathology, Paoli Calmettes Institut,
232 Bd Sainte Marguerite,
13009 Marseille, France
e-mail: poizatf@marseille.fnclcc.fr

C. de Chaisemartin · J. R. Delpero
Department of Surgery, Paoli Calmettes Institut,
232 Bd Sainte Marguerite,
13009 Marseille, France

E. Bories
Department of Endoscopy, Paoli Calmettes Institut,
232 Bd Sainte Marguerite,
13009 Marseille, France

J. F. Flejou
Department of Pathology, Saint Antoine Hospital,
184 rue du Faubourg Saint Antoine,
75571 Paris Cedex 12, Paris, France

Introduction

In 2009, after a review of several gastrointestinal sarcomas, Miettinen et al. [1] identified a novel distinctive epitheliomesenchymal biphasic tumor of the stomach. They described three cases, arising in the stomachs of young adults. Following this publication, another case has been reported [8].

Our report describes a similar tumor in a young woman. However, it was located in the duodenum. Although the morphology was close to what Miettinen described for gastroblastoma, we noticed some differences in the expression profile of immunohistochemical markers. To our knowledge, this tumor is not a carcinosarcoma or other biphasic malignant or locally aggressive tumor. Therefore, we propose to classify this novel distinctive epitheliomesenchymal biphasic tumor as described by Miettinen and to report it as duodenoblastoma.

Clinical history

In June 2010, a 22-year-old woman checked in with a severe case of melena. She had no particular medical history but had recently delivered a baby. Gastroduodenoscopy followed by endoultrasonography revealed an ulcerated and hemorrhagic tumor located in the muscular layer of the proximal duodenum (Fig. 1). This 37-mm mass protruded into the duodenal lumen and was superficially ulcerated (Fig. 2). No locoregional lymphadenopathy was found. The patient underwent partial resection of the distal duodenum. Preoperative observations confirmed that the tumor was located at the free border of the descending duodenum and did not show any adhesion to nearby organs. The tumor was completely resected. The patient is still in full remission 16 months after surgery.

Fig. 1 Abdominal computed tomography scan showing a 37-mm mass protruded into the duodenum lumen

Materials and methods

The tumor was histologically examined, and patient follow-up was obtained from the electronic medical records. After surgical removal, the tumor was sampled and fixed in a 30 % ethanol-formaldehyde solution. It was then entirely embedded in paraffin. Paraffin sections (5 μm) were cut and processed for hematoxylin–eosin–safranin or immunohistochemical staining.

Primary sources of antibodies and dilutions used in the immunohistochemical studies are shown in Table 1. Immunohistochemical staining was performed using a Dako Autostainer (DakoCytomation, Trappes, France) and horseradish peroxidase-labeled secondary antibodies, with diaminobenzinidine or 3-amino-9-ethyl-carbazole as chromogens. Staining controls were either external or internal, depending on the antibody used.

Pathological findings

The tumor was an intramural 37-mm-diameter lesion within the wall of the duodenum. It was nodular, and the overlaying duodenal mucosa was ulcerated (Fig. 2). The cut surface was white and flaky without any hemorrhagic areas.

Histological examination showed a multinodular biphasic and grossly well-circumscribed tumor, infiltrating the muscularis propria, extending to the duodenal serosa, and pushing up the duodenal mucosa (Fig. 3). At low magnification, the main

Table 1 Antibodies used and related results

Antigen	Dilution	Source	Spindle cell component (%)	Epithelial component (%)
Alpha-smooth muscle actin	1/250	Dako Denmark A/S	+	−
AE1/AE3	1/100	Dako Denmark A/S	−	+
Caldesmone	1/50	Dako Denmark A/S	−	−
Calrétinine	1/200	Invitrogen Ltd., UK	−	−
CD10	1/20	Visionbiosystems Novacastra	−	−
CD117	1/350	Dako Denmark A/S	−	−
CD56	1/50	Visionbiosystems Novacastra	−	−
CD99	1/40	Dako Denmark A/S	+	+
Chromogranine A	1/1000	Dako Denmark A/S	−	−
Keratin 20	Undiluted	Dako Denmark A/S	−	−
Keratin 5/6	Undiluted	Dako Denmark A/S	−	−
Keratin 7	Undiluted	Dako Denmark A/S	−	+
Desmin	1/50	Dako Denmark A/S	+	−
DOG1	1/200	Dako Denmark A/S	−	−
EMA	1/200	Dako Denmark A/S	−	−
Ki67	Undiluted	Dako Denmark A/S	20	20
P-63	1/50	Dako Denmark A/S	−	−
Estrogen receptor	Undiluted	Dako Denmark A/S	−	−
Progesterone receptor	Undiluted	Dako Denmark A/S	+	−
S100 protein	Undiluted	Dako Denmark A/S	−	−
Synaptophysin	Undiluted	Dako Denmark A/S	−	−
Vimentine	1/500	Dako Denmark A/S	+	−

Fig. 2 Resected specimen showing a 37-mm-diameter ulcerated, polypoid tumor located in the duodenum

component consisted of small spindle and round cells, with a high nucleocytoplasmic ratio, without any particular differentiation. A second component was epithelioid, consisting of cohesive lobulated cells, without glandular or squamous differentiation. Nuclear atypia or necrosis was not found. Mitotic activity varied up to a maximum of nine mitoses per 50 HPF. There was a very discrete collagenous stroma creating a fascicular architecture (Fig. 4).

The result of the immunohistochemical study is listed in Table 1. The spindle cell component was positive for vimentin and desmin. In some areas, it was positive for smooth muscle actin, but negative for PS100, KIT, DOG1, CD34, and neuroendocrine markers (synaptophysin, chromogranin A, and CD56). The epithelial component was positive for pan-keratin AE1/AE3 and keratin 7 (Fig. 5). The maximum proliferation index (Mib1-Ki67) was estimated at 20 % in some areas. Staining for progesterone receptor was positive, but negative for estrogen receptor. The molecular analysis provided no evidence for a SYT/SSX translocation.

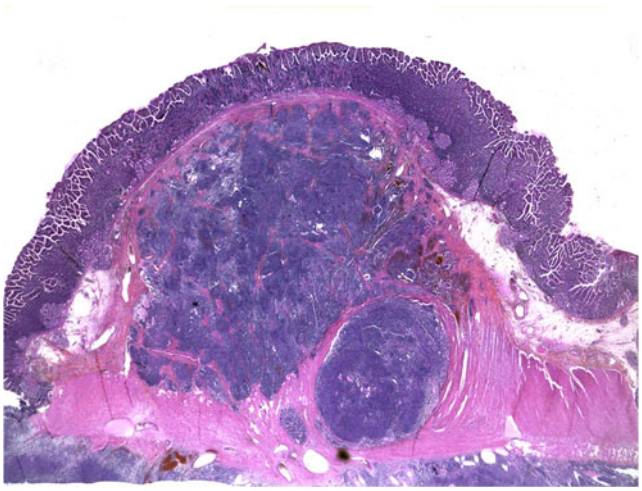

Fig. 3 Multinodular and roughly limited tumor, infiltrating the muscularis propria, extending to the duodenal serosa, and pushing out the duodenal mucosa

Discussion

Spindle cell tumors of the intestine are rare and represent 10 % of malignant tumors of the small intestine and 0.1 % of the large intestine [2]. Most of these tumors are gastrointestinal stromal tumor (GIST), metastases from melanoma or sarcoma. Moreover, epitheliomesenchymal biphasic neoplasms are extremely rare in the duodenum, and most of these are high-grade carcinosarcomas [5, 6, 9]. Duodenal synoviosarcomas with confirmatory molecular analysis of the SYT/SSX translocation have also been reported [3, 4].

We report a duodenal epitheliomesenchymal biphasic neoplasm without the cellular differentiation or nuclear atypia, justifying a diagnosis of carcinosarcoma or other malignancy. Our case presents clinical and morphological features similar to those of the "novel distinctive epitheliomesenchymal tumor of the stomach of young adults," recently described by Miettinen et al. [1]. They described three cases which occurred in the stomach of young adults and proposed to call these tumors gastroblastomas, in analogy to other childhood biphasic neoplasms for which the term blastoma is used. These three cases were grossly multinodular or lobulated. One tumor formed an exophytic polyp, and the two others were ulcerated and transmural.

These tumors had two components: uniform oval and spindled cells in diffuse sheets and clusters or cords of epithelial cells, occasionally forming glandular structures. The epithelial component was positive for keratin, partly for keratin 7 and negative for keratins 5/6 and 20 and epithelial membrane antigen. The mesenchymal component was positive for vimentin and CD10. Both of the two components were negative for smooth muscle actin, desmin, CD34, CD 99, estrogen receptor, KIT, PS100, p63, calretinin, chromogranin, synaptophysin, CDX2, and thyroid transcription factor. None of the three cases demonstrated SS18 gene rearrangement by FISH.

The tumors described by Miettinen [1] and our case share the similar clinicopathological features: occurrence in young adults, relatively large tumor size, multinodular shape, two components with low-grade features and relatively low-mitotic activity, low overall atypia, and absence of conspicuous nuclear pleomorphism.

However, we found some immunohistochemical differences with the gastroblastoma; the mesenchymal component of our case was positive for desmin, CD99, and smooth muscle actin and negative for CD10. Moreover, the tumor expressed progesterone receptor, but this might have been related to the fact that the patient was postpartum. The expression of desmin

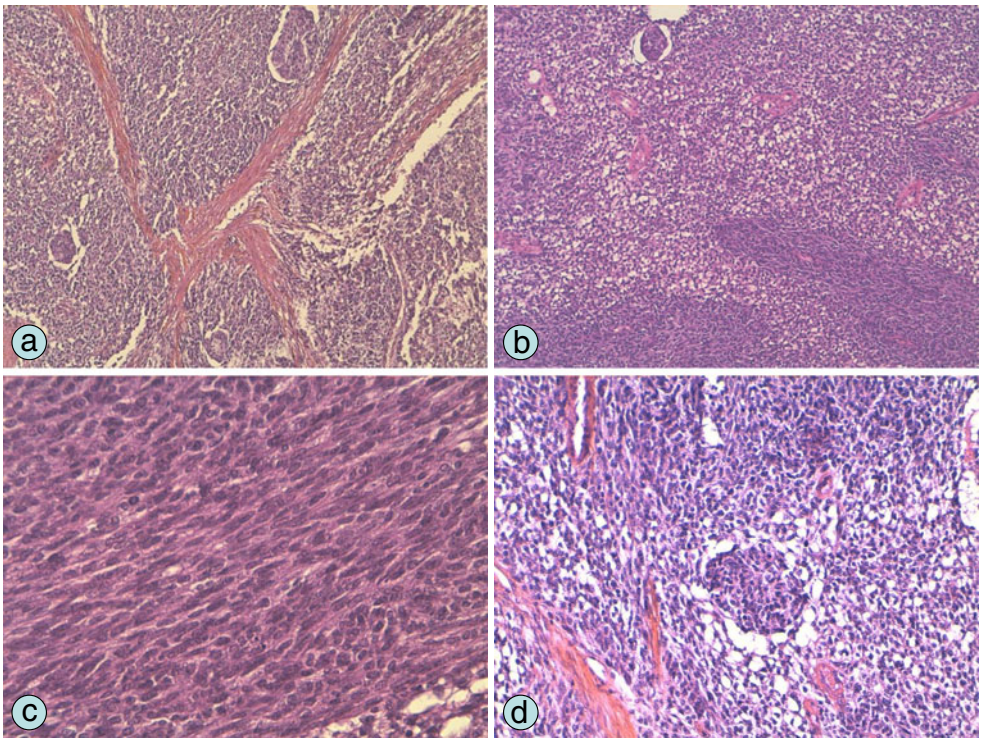

Fig. 4 Most of the tumor is composed of spindle cells, with some clusters of epithelioid cells (**a**, **b**). The two components show no nuclear atypia, uniform cytology with little mitotic activity (**c**, **d**)

and smooth muscle actin might suggest a diagnosis of a leiomyosarcoma, which was not compatible with the presence of epithelial cell nests. However, despite these immunochemical differences, the clinicopathological features so closely resemble those of gastroblastoma that we consider our case to be similar to those described by Miettinen.

The differential diagnosis of a low-grade malignant biphasic tumor of the duodenum comprises teratoma, mixed tumor (myoepithelioma) [1], GIST, pancreatoblastoma [7] in an ectopic pancreas, and gangliocytic paraganglioma. Teratoma would display more specific differentiation and would occur in younger patients. Mixed tumors (myoepitheliomas) of

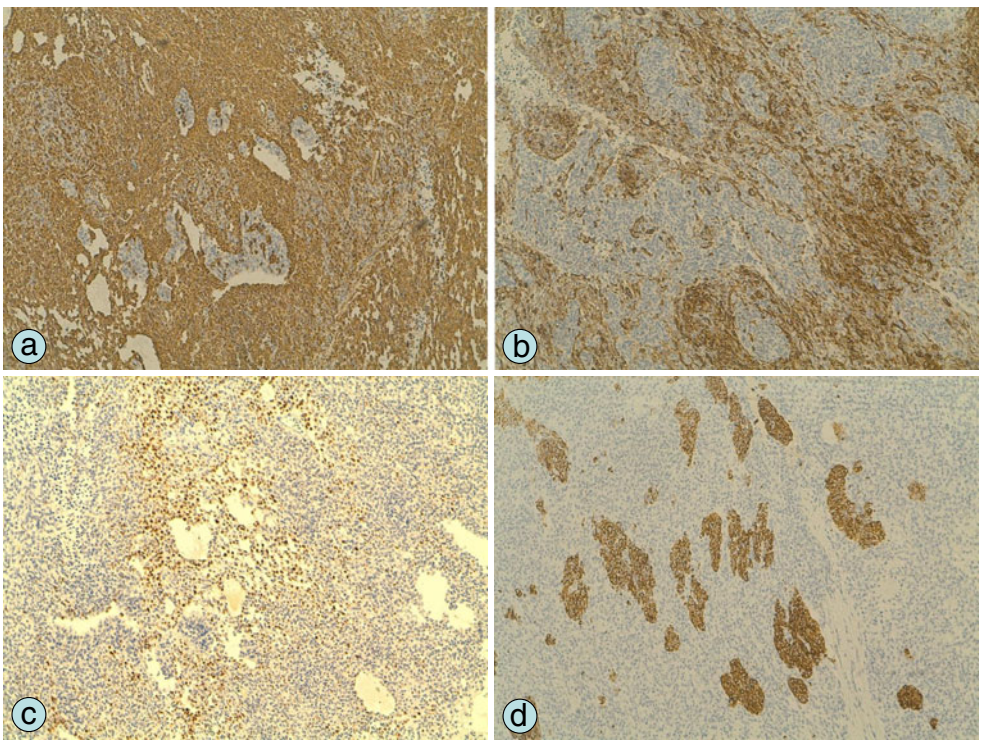

Fig. 5 Immunohistochemical features. The spindle cell component was positive for vimentin (**a**), smooth muscle actin (**b**), and progesterone receptor (**c**). The epithelial elements were positive for keratin 7 (**d**)

salivary gland or skin adnexal are not likely to occur in the gastrointestinal tract. A GIST is excluded because the tumor lacked immunoreactivity for KIT and DOG1. The morphology lacked distinct squamoid nests or acinar differentiation, excluding a diagnosis of pancreatoblastoma. Lack of expression of neuroendocrine markers excluded gangliocytic paraganglioma.

Our patient is still in full remission 16 months after surgery, with no evidence of tumor recurrence on surveillance CT scans. Of Miettinen's cases, the three patients were reported as alive, including one without any recurrence for 14 years. This suggests that these tumors should be considered as of low-grade malignancy.

Conclusion

We report an epitheliomesenchymal biphasic tumor in the duodenum that differs from other digestive biphasic tumors such as carcinosarcoma, synoviosarcoma, or teratoma. Four cases of gastric location have been recently described in the literature, and our case is both clinically and morphologically very similar to these. Although the immunohistochemical profile is slightly different, we believe this tumor to be similar to the gastroblastoma described by Miettinen.

Conflict of interest None.

References

1. Miettinen M, Dow N, Lacosta J, Sobin LH (2009) A distinctive novel epitheliomesenchymal biphasic tumor of the stomach in young adults ("Gastroblastomas"): a series of 3 cases. Am J Surg Pathol 33:1370–7
2. Miettinen M, Fletcher CDM, Kindblom LG, Tsui WMS (2010) Mesenchymal tumours of the small intestine. In: Hamilton SR, Aaltonen LA (eds) World Health Organisation. Classification of tumors. Pathology and Genetics, Tumours of the digestive system. IARC Press, Lyon, pp 115–116
3. Garcia Ruiz S, Jimenez Rodriguez RM, Alcaide Leon P, Alamo Martinez JM, Suarez Artacho G, Gomez Bravo MA (2010) Synovial two-phase sarcoma in third portion of the duodenum: clinical case and review of the literature. Rev Esp Enferm Dig 102 (1):62–3
4. Schreiber-Facklam H, Bode-Lesniewska B, Frigerio S, Flury R (2007) Primary monophasic synovial sarcoma of the duodenum with SYT/SSX2 type of translocation. Human Path 38(6):946–9
5. Kench JG, Frommer DJ (1997) Sarcomatoid carcinoma of the ampulla of Vater. Pathology 29:89–91
6. Kijima H, Takeshita T, Suzuki H, Tanahashi T, Suto A, Izumika H et al (1999) Carcinosarcoma of the ampulla of Vater: a case report with immunohistochemical and ultrastructural studies. Am J Gastroenterol 94:3055–9
7. Cavallini A, Falconi M, Bortesi L, Crippa S, Barugola G, Butturini G (2009) Pancreatoblastomas in adults: a review of literature. Pancreatology 9(1–2):73–80
8. Shin DH, Lee JH, Kang HJ, Choi KU, Kim JY et al (2010) Novel epitheliomesenchymal biphasic stomach tumour (gastroblastoma) in a 9-year-old: morphological, ultrastructural and immunohistochemical findings. J Clin Pathol 63:270–274
9. Sunagawa H, Inamine S, Watanabe M, Kawakami K, Toyama T, Zaha H et al (2009) Carcinosarcoma of the duodenum: report of a case. Surg Today 39(10):892–6

Virchows Arch (2012) 461:385–392
DOI 10.1007/s00428-012-1299-7

ORIGINAL ARTICLE

The significantly reduced number of interstitial cells of Cajal in chagasic megacolon (CM) patients might contribute to the pathophysiology of CM

Sheila Jorge Adad · Gisele Barbosa e Silva · Alessandro Adad Jammal

Received: 5 June 2012 / Revised: 22 July 2012 / Accepted: 2 August 2012 / Published online: 16 August 2012
© Springer-Verlag 2012

Abstract In addition to neurons, interstitial cells of Cajal (ICC) play an important role in coordinating intestinal motility with a pacemaker function. This study aimed to quantitatively analyze ICC, neurons, and muscular area, the latter to correct for quantitation errors resulting from dilation in case of a megacolon and from the dispersion of ICC that can be attributed to muscular hypertrophy. We analyzed 30 colon samples: ten chagasic megacolon (CM), ten chagasic colons without megacolon (CXM), and ten nonchagasic control patients (NC). We measured the area of muscularis propria and counted the number of neurons of the myenteric plexus in a histological section of an intestinal ring and the number of ICC at the level of the myenteric plexus and circular muscle layer, the latter in a section immunohistochemically stained for CD117. Muscular hypertrophy occurred only in the CM group. Compared to the NC group, we found in the CM group a statistically significant reduction of 80 % in the number of neurons, 60 % in the number of ICC in the myenteric plexus, and 38 % in the area of circular muscle. In the CXM group, these numbers were highly variable, and their reduction, less pronounced. We conclude that the number of ICC is significantly reduced in CM patients, and that this might contribute to the pathophysiology of CM. However, the development of CM requires severe denervation, whereas CXM generally exhibits less than 50 % denervation, favoring the hypothesis that the reduction in ICC number is, in part, a consequence of denervation.

Keywords Chagas disease · Chagasic megacolon · Enteric nervous system · Morphometric neuron analysis · Interstitial cells of Cajal · Muscular hypertrophy

S. J. Adad (✉) · G. B. e Silva
Discipline of Special Pathology,
Universidade Federal do Triângulo Mineiro (UFTM),
Av. Getúlio Guaritá, 130,
CEP 38025-440 Uberaba, MG, Brazil
e-mail: sheila.adad@gmail.com

A. A. Jammal
Universidade de Uberaba (UNIUBE),
Av. Nenê Sabino, 1801,
CEP 38055-500 Uberaba, MG, Brazil

Introduction

The World Health Organization estimates that there are 15 million people afflicted by Chagas disease in Latin America, with an annual incidence of 41,200 new cases and 12,500 annual deaths due to heart disease and digestive complications. With increasing population movement, Chagas disease has become a global challenge; nonendemic areas, including Europe and Japan, have reported cases of this disease, and it is estimated that there are currently more than 300,000 individuals infected with *Trypanosoma cruzi* in the USA [1]. Megacolon is the second most common manifestation of the digestive form of Chagas disease, which is found in 5–10 % of chronic Chagas patients in central Brazil. The digestive form of Chagas disease represents a model of intestinal denervation that affects digestive tract motility [2], and its study may help to further our understanding of other diseases that result in dysmotility.

The pathogenesis of chagasic megacolon has been linked to intramural denervation, particularly of the myenteric plexus [3–5], which impairs organ motility and dilation over time and is occasionally associated with organ elongation [3]. Köberle [3, 6] devised a way to correct neuronal counts for dispersion caused by dilation of the megacolon, which

often expands to three to four times its normal perimeter. According to Köberle [3], colon denervation in excess of 55 % could induce the development of megacolon, and denervation exceeding 90–95 % could result in megaesophagus, which was confirmed by Adad et al. [4, 5]. Notably, occasionally, a correction of neuronal counts was required to account for neuronal hypertrophy [5].

Recently, in addition to neurons, the interstitial cells of Cajal (ICC) have been demonstrated to play an important role in coordinating intestinal motility, functioning as pacemakers [7–9] that generate slow-wave activity [9, 10] and act as intermediaries in the spatial coordination of the neural activity of smooth muscle [11, 12]. Abnormalities in the ICC population have been reported in several intestinal motility disorders such as Hirschsprung's disease [13], congenital hypertrophic pyloric stenosis [14, 15], chronic idiopathic intestinal pseudo-obstruction [16], and slow-transit constipation [10]. Wedel et al. [10] evaluated patients with slow-transit constipation and megacolon (Hirschsprung's disease and congenital hypoganglionosis) and found a reduction of ICC with concomitant loss of neurons, suggesting a mutual influence between ICC and the enteric nervous system. According those results, ICC might "play a crucial role in the pathophysiology of colorectal motility disorders." However, the authors note that "there is no clear cutoff between controls and patients" with slow-transit constipation, as both groups have overlapping ICC values, "suggesting that a decreased number of ICC per se do not necessarily lead to symptoms of chronic constipation" [10].

Regarding the assessment of ICC in chagasic megacolon, we found only three studies [17–19]. However, none of these studies corrected for the dispersion of ICC and neurons induced by the dilation of the megacolon. Hagger et al. [17] and Geraldino et al. [18] noted that decreased ICC can promote the development of megacolon. However, a reduction of ICC in the colon does not necessarily induce megacolon development. Also, it is important to analyze ICC and neuron counts using a systematic and quantitative approach. The ICC in normal human tissues, which have an apoptotic rate of 1–2 %, are completely renewed every 6 months [20] and thus can easily regenerate. In contrast, neurons are postmitotic cells that do not regenerate in mature tissues after injury and elimination, despite functional compensation by noninjured neurons. Intense denervation can occur during the acute phase of Chagas disease, but megacolon generally develops several decades later, with slow and age-related loss of neurons, accompanied by the functional overloading and exhaustion of the residual neurons [3]. The slow, chronic, inflammation-induced destruction of neurons, which persists during the chronic phase, also contributes to denervation [4, 21].

This study aimed to quantitatively analyze ICC, neurons, and muscular area to correct for quantitation errors resulting from dilation in the megacolon and from the dispersion of ICC attributed to muscular hypertrophy. We, furthermore, investigated the possible correlation of these variables between the chagasic megacolon (CM) and chagasic colons without megacolon (CXM) groups, with the CXM group representing a transitional stage between normal and CM states.

Materials and methods

Colon tissue samples from 30 adults obtained from surgery (CM) or necropsy [CM, CXM, and nonchagasic control patients (NC)] were obtained for analysis and grouped as follows: ten from CM patients, ten CXM patients, and ten from NC; all patient ages were statistically similar (CM=54±13, CXM=52±16, and NC=57±21 years of age). The diagnosis of Chagas disease was based on a positive result in at least two of the following three blood and/or pericardial fluid reactions: ELISA, passive hemagglutination, and indirect immunofluorescence for *T. cruzi*. The diagnosis of megacolon was established from clinical (intestinal constipation frequently accompanied by complications, such as fecaloma and volvulus) and radiological data (opaque enema showing dilation and loss of haustration, possibly accompanied by lengthening of the colon, and/or single X-ray of the abdomen showing fecaloma and intestinal dilation).

A ring from the rectosigmoid transition was extracted, no more than 6 h after death or surgery, and the external perimeter and thickness of the muscularis propria were measured. The samples were then fixed in 4 % formaldehyde and processed for paraffin embedding.

Serial histological sections (7 μm) were cut; one was hematoxylin–eosin stained for overall evaluation; one was Masson's trichrome stained to measure the area of muscularis propria; one was Giemsa stained for neuronal counting, and one was immunohistochemically CD117 (c-kit) stained for ICC counts (DakoCytomation Code A4502 1:400 dilution; polymer technique). Chronic myositis was diagnosed when a mononuclear infiltrate associated with degeneration and/or necrosis of myocytes were found. Chronic ganglionitis was diagnosed when a mononuclear infiltrate was found within the ganglia of the myenteric plexus.

As the intestinal perimeter is much larger in the CM group compared to the NC group (Fig. 1) which causes dispersion of neurons, using a standard area for neuronal count in different groups would induce errors in these cell numbers. To correct for this potential error, we counted all of the neurons within the myenteric plexus in the Giemsa-stained section of a complete intestinal ring. For the CM group, in which neuronal hypertrophy (enlargement of the perikaryon of neurons) is detected, a correction factor was

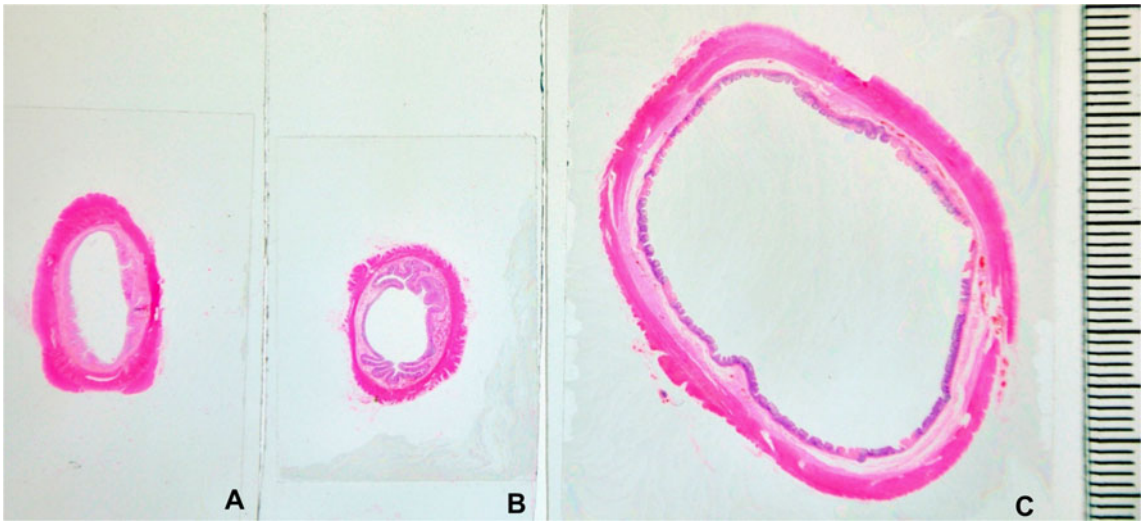

Fig. 1 Histological sections of intestinal rings, showing similar perimeters in a nonchagasic control intestine (**a**) and a chagasic intestine without megacolon (**b**), which have significantly smaller perimeters than that of chagasic patients with megacolon (**c**), highlighting the need for counting neurons throughout the ring in order to correct for the dispersion of these cells resulting from intestinal dilation

applied as described previously [5]. This correction factor was calculated by dividing the average ganglion cell diameter in the NC group (15.53 μm) by the average in the CM group (28.42 μm). This factor (0.62) was then multiplied by the number of neurons for each case in the CM group. ICC were counted at the level of the myenteric plexus and the circular muscle layer in half of a section ring due to technical immunohistochemical difficulties that limited the preservation of the entire ring within a single histological section. After counting, the resulting cell number was doubled to account for the uncounted half of section ring and for comparison to the number of neurons. The percentage neuron and ICC loss in each case was calculated, e.g., for neurons by subtracting from the average number of neurons in the NC group the number of neurons found in each case, divided by the average number of neurons of the NC group×100.

Immunohistochemistry

The sections were deparaffinized and rehydrated though a graded alcohol series ending in distilled water. The sections were then subjected to heat-induced antigen retrieval by immersion in a heat-resistant container filled with Tris-buffered solution containing EDTA and treatment in a pressure cooker for 30 min. Endogenous peroxidase activity was blocked by incubation with 3 % solution of H_2O_2 for 15 min. Immunostaining was performed using the polymer technique (Novolink, Novocastra), according to the manufacturer's protocols. ICC and mast cells were c-kit positive. Mast cells were round with a round central nucleus and served as an internal control. ICC exhibited a fusiform cell body with two or more processes; both nucleated cells and c-kit-positive elongated structures were considered ICC.

The measure of muscular areas was made directly on Masson's trichrome-stained histological sections with the aid of a graphic-measuring table coupled with a semiautomatic image analyzing system (MOP-Videoplan, Eletronik Kontron, Germany). First, the inner contour of the circular muscle layer and then the outer contour of the longitudinal muscle layer were outlined to measure the area (in square millimeters) of the muscularis propria. This measurement accounts for acute bowel distension due to excessive gas and fecal accumulation, which could alter the perimeter of the intestine and the thickness of muscular layer without changing its area.

For statistical analysis, the variables were evaluated using GraphPad Instat version 3.0. For variables with normal distribution, an analysis of variance was performed using Bartlett's test to assess the homogeneity of variance and the Kolmogorov–Smirnov test to assess whether the distribution was normal. Variables that did not exhibit normal distribution and/or heteroscedastic distribution were compared using the Kruskal–Wallis test. For all of the tests, the statistical significance was defined as $p<0.05$. Ethical approval for the study protocols was obtained from the research ethics committee of the Universidade Federal do Triângulo Mineiro, Uberaba, MG, Brazil.

Results

The neuron and ICC counts and the area of muscularis propria of each case are shown in box 1. The comparison between the mean values of each group is shown in Table 1.

Box 1 The patients' age as well as the intestinal perimeter, muscular layer thickness, area of the muscularis propria, number of interstitial cells of Cajal in the circular muscle layer and myenteric plexus and number of neurons in the myenteric plexus in a histological section of a full intestinal ring of the rectum-sigmoid transition, according to the study groups

Case	Group	Age (years)	Intestinal perimeter (cm)	Muscular layer thickness (mm)	Muscular layer area (mm^2)	ICC in muscular layer	ICC in plexus	Neurons[a]
02	CM	65	8.9	3.0	233	1,468	160	166
03	CM	64	15.9	2.0	202	1,606	184	59
04	CM	58	14.3	2.0	260	852	64	89
05	CM	54	14.5	2.5	291	816	32	09
08	CM	49	12.3	1.5	206	1,796	244	26
09	CM	70	25.2	3.0	763	880	382	68
10	CM	55	16.1	1.0	197	834	102	06
11	CM	30	17.5	3.0	438	228	200	27
12	CM	34	16.8	2.0	366	904	370	32
13	CM	63	12.7	2.5	306	894	250	28
39	CXM	49	6.6	1.5	124	1,530	234	311
40	CXM	43	6.8	1.5	99	1,462	388	291
41	CXM	66	4.5	1.0	62	1,564	422	184
42	CXM	47	4.7	1.0	57	1,036	288	246
43	CXM	57	8.0	1.0	75	1,662	342	135
44	CXM	70	6.0	1.0	94	978	312	198
45	CXM	56	8.6	0.5	104	1,602	308	159
46	CXM	22	3.9	2.0	80	1,694	314	182
47	CXM	36	7.2	1.0	90	1,992	414	140
48	CXM	72	9.6	0.5	55	1,216	698	239
61	NC	76	4.8	2.0	95	1,902	592	247
62	NC	54	6.2	1.0	67	1,846	436	197
63	NC	79	4.7	1.0	61	426	332	253
64	NC	85	10.8	0.5	95	1,696	684	317
65	NC	53	12.4	0.5	119	1,828	376	238
66	NC	47	5.4	1.0	63	1,922	386	259
67	NC	34	6.9	1.5	103	1,936	570	296
68	NC	22	13.4	0.5	66	1,572	468	278
69	NC	46	8.0	1.0	78	1,536	638	175
70	NC	70	4.7	1.0	63	1,952	570	339

NC nonchagasic patients, *CXM* chagasic patients without megacolon, *CM* chagasic patients with megacolon

[a] The number of neurons obtained in each case of the CM group was multiplied by a correction factor (0.62) to account for the enlargement of the perikaryon of neurons found in the CM group

We found that the intestinal perimeter, the muscularis propria thickness, and the muscularis propria area of the CM samples significantly increased compared to the NC and CXM samples ($p<0.05$), between which there were no significant differences. These data indicate that, in CM, the development of permanent dilation is accompanied by muscular hypertrophy.

In the CM samples, the number of neurons in the myenteric plexus was significantly reduced in comparison with both NC and CXM samples ($p<0.05$). The average percentage of denervation in the CM samples was 80 %, and in only 1 case, the loss of neurons was less than 55 % (in this case, the patient had been constipated for a year only). Neuronal loss in the CXM group was highly variable (ranging from 0 to 47 %, with an average of 20 %), which might explain why the difference between the CXM and NC groups was not statistically different ($p=0.07$), indicating just a trend (Table 1). Chronic ganglionitis was observed in nine (90 %) cases of the CM group and in four (40 %) cases of the CXM group, but not in the NC group. Chronic myositis was observed in nine (90 %) cases of the CM group and in two (20 %) of the CXM group, but not in the NC group (Fig. 2a–c).

Table 1 The mean values of the intestinal circumference, muscularis propria thickness, muscularis propria area, number of interstitial cells of Cajal in the circular muscle layer and myenteric plexus region and number of neurons in the myenteric plexus in a histological section of a full intestinal ring of the rectum-sigmoid transition, according to the study groups

	NC		CXM		CM	
	(n=10)		(n=10)		(n=10)	
	x ± SD	Med (min–max)	x ± SD	Med (min–max)	x ± SD	Med (min–max)
Intestinal perimeter[a]	7.7±3.3	6.6 (4.7–13.4)	6.6±1.9	6.7 (3.9–9.6)	15.4±4.3*, **	15.2 (8.9–25.2)
Muscular thickness[a]	1.0±0.5	1.0 (0.5–2)	1.1±0.5	1.0 (0.5–2)	2.3±0.7*, **	2.3 (1–3)
Muscular area[b]	81±21	73 (61–119)	84±22	85 (55–124)	326±172	276 (197–763)*
ICC muscular[a]	1,662±459	1,837 (426–1,952)	1,474±313	1,547 (978–1992)	1,028±463*, **	887 (228–1,796)
ICC plexus[a]	505±121	519 (332–684)	372±129	328 (234–698)	199±118*, **	192 (32–382)
Number of neurons[a]	260±51	256 (175–339)	209±61	191 (135–311)	51±48*, **	30 (06–166)

NC nonchagasic patients, *CXM* chagasic patients without megacolon, *CM* chagasic patients with megacolon, x ± *SD* mean and standard deviation, *Med* median, *min* minimum value, *max* maximum value

*p<0.05, statistically significant difference, CM vs NC; **p<0.05 statistically significant difference, CM vs CXM

[a] ANOVA

[b] Kruskal–Wallis test

There was a significant reduction in the ICC counts at the level of the myenteric plexus in the CM group compared to both the NC and CXM groups (p<0.05). However, although the ICC count was slightly lower in the CXM group than in the NC group, the difference was not statistically significant (p>0.05). The reduction of ICC counts in the CM group was more significant at the level of the plexus (average reduction of 60 %) than in the circular muscle layer (average reduction of 38 %). In the circular muscle layer, we observed a significant decrease in the ICC count in the CM group only relative to the NC group (p<0.05), which did not differ statistically from the CXM group (p>0.05) (Table 1, Fig. 2d–f).

Figure 3 shows the reduction in the number of neurons and ICC in CM and CXM groups compared to the NC group, which was found more striking in regard of the number of neurons. The CXM group seems to be an intermediate group between CM and NC.

Discussion

To our knowledge, this is the first study of ICC in the colon of Chagas patients without overt megacolon. It is also the first study to morphometrically evaluate CM and to study simultaneously the muscular hypertrophy and the number of ICC and neurons in the myenteric plexus. Additionally, counting cells in a complete intestinal ring in each case, instead of counting them in an identical area sample for all cases, allowed us to correct the neuron and ICC dispersion due to intestinal dilation and muscular hypertrophy of the megacolon.

The CM and CXM groups demonstrated significantly different ICC counts at the level of the myenteric plexus, but not in the circular muscle layer. The significant difference in ICC counts observed predominantly in the level of the myenteric plexus, where there was concurrent reduction of neurons, might suggest that the loss of ICC occurs after denervation, as the enteric neurons and the ICC are interdependent [10]. Furthermore, during the development and progression of Chagas disease, a population of ICC might have been simultaneously destroyed with enteric neurons as a result of ganglionitis, either during the acute phase or slowly during the chronic phase. At this phase, although the parasite load is low, it is nonetheless persistent [4, 21–24], providing constant and chronic antigenic stimulus to the immune system, favoring ganglial inflammation by cross reaction between antigens of *T. cruzi* and neuronal antigens [25–27].

Previous studies have only quantitated ICC in chagasic individuals with megacolon [17–19]. Our data, demonstrating a reduction of ICC in the level of the myenteric plexus in the CM group compared to the NC group, are consistent with previous findings by Hagger et al. [17], Geraldino et al. [18], and Iantorno et al. [19]. However, we detected a reduction—albeit less significant—in the number of ICC in the muscular layer, consistent with previous findings by Hagger et al. [17] and Geraldino et al. [18], but in contrast to those by Iantorno et al. [19]. Surprisingly, Iantorno et al. [19] found an increase in ICC in the muscular layer of the CM group compared to the NC group. These authors suggested that this finding could represent a compensatory mechanism and further commented that the ICC in the muscular layer are more

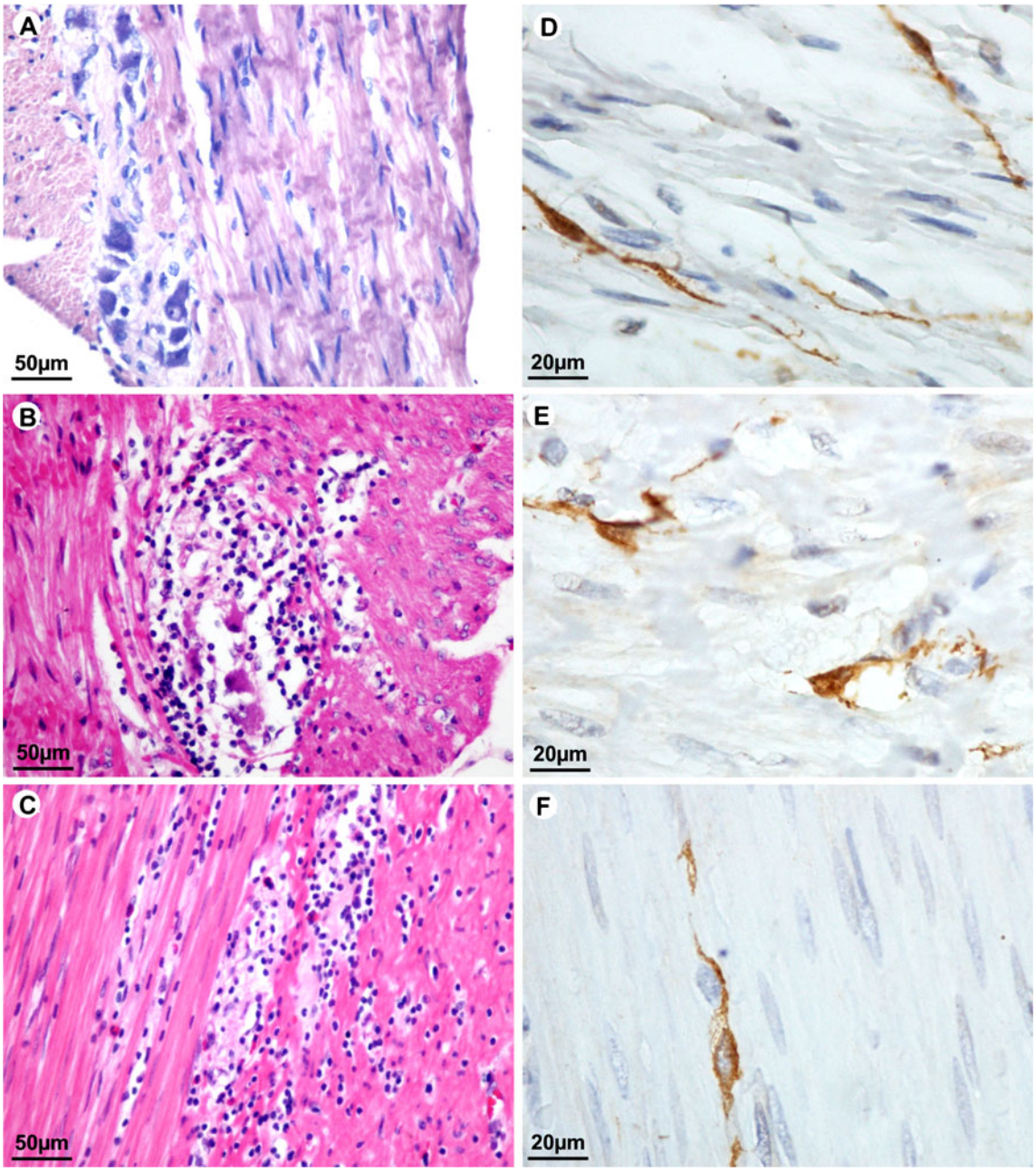

Fig. 2 **a** Ganglia of the myenteric plexus with several normal neurons surrounded by the normal muscular layer of the colon of nonchagasic patient (Giemsa, ×400); **b** myositis with concurrent moderate ganglionitis, involving neurons in the chagasic intestine without megacolon (hematoxylin and eosin (H & E), ×400); **c** mild ganglionitis and myositis and absence of neurons in a chagasic intestine with megacolon (H & E, ×400). **d**–**f** c-Kit immunoreactivity marking the interstitial cells of Cajal *in brown* in the circular muscle layer; **d** colon of nonchagasic patient; **e** colon of chagasic patient without megacolon; **f** chagasic megacolon (×100); note fewer ICC in the chagasic megacolon in comparison to nonchagasic and chagasic without megacolon

distal from the main inflammatory site in Chagas disease—the myenteric plexus. However, such results could at most account for a minor reduction in ICC, not an increase in ICC counts. Despite the regenerative capacity of ICC, myositis exists during the chronic phase of Chagas disease [4, 21], which contributes to the reduction of the ICC population.

Although muscle hypertrophy has been previously described and demonstrated in chagasic megaesophagus, there has been no morphometric characterization of the colon. In previous morphometric studies, we assessed cases from the current study, and an increase in the fibrous tissue in muscular layer of CM was observed [28, 29]. The connective tissue,

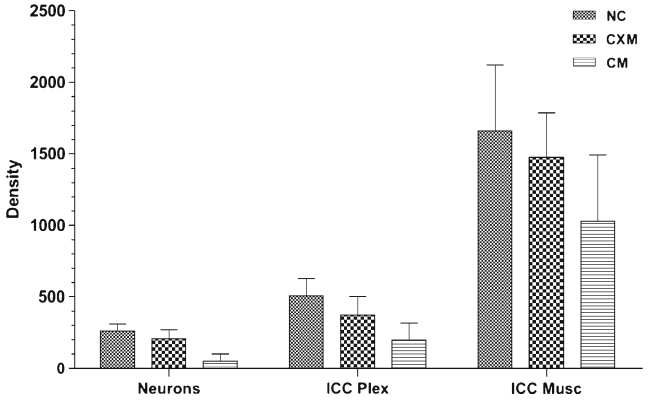

Fig. 3 Neurons and interstitial cells of Cajal density in the colon, according to the study groups. *ICC plex* ICC in level of the myenteric plexus, *ICC musc* ICC in the circular muscle layer, *NC* nonchagasic patients, *CXM* chagasic patients without megacolon, *CM* chagasic patients with megacolon

which accounted for 0.16 % of the muscle layer in the NC group, increased to 4 % in CM group [28]. Considering that, in the current study, we demonstrated a critical enlargement of 400 % in muscularis propria area in the CM group compared to the NC and CXM groups, it was predominantly due to muscular hypertrophy/hyperplasia. Had a compensatory hyperplasia of ICC occurred in the muscular layer in the CM cases, we would have detected such an increase in the number of ICC. This, however, did not occur, and we counted the ICC in half of an intestinal ring in all groups, rather than in equal areas in all three groups, consistent with the methods of other studies [17–19]. The paradoxical increase of ICC found in CM cases by Iantorno et al. [19] might be explained by mast cells, which are also c-kit positive. Mast cells progressively increase in number in CM patients [28, 29] and may have been included in the authors' ICC counts. Another explanation might be the distribution of ICC in different regions of the colon. Iantorno et al. [19] did not specify which region of the fragment was removed in cases of CM and idiopathic megacolon. They state that the distribution of ICC is relatively uniform in the human colon. However, data regarding the distribution of ICC in normal colon are contradictory; a study by Lyford el al. [30] argues for uniform distribution; however, studies by Horisawa et al. [31] and Hagger et al. [32] indicate that the distribution is heterogeneous.

Similar corrective studies could be performed to validate the results of previous studies that found a denervation and reduction of ICC in other diseases, such as idiopathic megacolon [19, 33], Hirschsprung's disease and congenital hypoganglionosis [10], or in patients with slow-transit constipation [10], as none of these studies corrected for ICC and/or neuron counts as a result of their dispersion during intestinal dilation. If the ICC reduction in these diseases is as significant as in chagasic megacolon cases, similar differences should be found. Regardless, Wedel et al. [10] highlights the overlap between the ICC values in the control group and slow-transit constipation, suggesting that the reduced ICC counts do not necessarily lead to symptoms of chronic constipation. Sanders et al. [12] suggest that the loss of ICC, which generates slow waves, reduces the myogenic regulation of motility, "but intact neural reflexes may compensate, to some extent, for loss of myogenic regulation and provide a means for propulsive behavior in tissues lacking pacemaker ICC and slow waves."

This study in chagasic megacolon indicates that diseases, which course with motility disorders, may have a reduced number of both neurons and ICC. However, the development of chagasic megacolon requires severe denervation, and the reduction of ICC may be, in part, a consequence of denervation. For this reason, we suggest that quantitative analysis of ICC should be associated to neuronal count.

Acknowledgments We would like to thank Dr. Uilho Antonio Gomes for his assistance with our statistical analyses. This paper was completed with financial support from Conselho Nacional de Desenvolvimento Científico e Tecnológico (CNPq) and Fundação de Amparo à Pesquisa de Minas Gerais (FAPEMIG).

Conflict of interest None.

References

1. Coura JR, Viñas PA (2010) Chagas disease: a new worldwide challenge. Nature 465(7301):S6–S7
2. Meneghelli UG (2004) Chagasic enteropathy. Rev Soc Bras Med Trop 37:252–260
3. Köberle F (1968) Chagas' disease and Chagas' syndromes: the pathology of American trypanosomiasis. Adv Parasitol 6:63–116
4. Adad SJ, Andrade DCS, Lopes ER, Chapadeiro E (1991) Contribuição ao estudo da anatomia patológica do megaesôfago chagásico. Rev Inst Med Trop São Paulo 33:445–450
5. Adad SJ, Cançado CG, Etchebehere RM, Teixeira VP, Gomes UA, Chapadeiro E, Lopes ER (2001) Neuron count reevaluation in the myenteric plexus of chagasic megacolon after morphometric neuron analysis. Virchows Arch 438:254–258
6. Köberle F (1961) Patologia y anatomia patologica de la enfermedad de Chagas. Bol Ofic Sanit Panamer 51:404–428
7. Thuneberg L (1982) Interstitial cells of Cajal: intestinal pacemaker cells? Adv Anat Embryol Cell Biol 71:1–130
8. Faussone-Pellegrini MS (1992) Histogenesis, structure and relationships of interstitial cells of Cajal (ICC): from morphology to functional interpretation. Eur J Morphol 30:137–148
9. Sanders KM (1996) A case for interstitial cells of Cajal as pacemakers and mediators of neurotransmission in the gastrointestinal tract. Gastroenterology 111:492–515
10. Wedel T, Spiegler J, Soellner S, Roblick UJ, Schiedeck TH, Bruch HP, Krammer HJ (2002) Enteric nerves and interstitial cells of Cajal are altered in patients with slow-transit constipation and megacolon. Gastroenterology 123:1459–1467
11. Farraway L, Ball AK, Huizinga JD (1995) Intercellular metabolic coupling in canine colon musculature. Am J Physiol 268:C1492–C1502

12. Sanders KM, Ordög T, Koh SD, Torihashi S, Ward SM (1999) Development and plasticity of Interstitial Cells of Cajal. Neurogastroenterol Motil 11:311–338
13. Yamataka A, Kato Y, Tibboel D, Murata Y, Sueyoshi N, Fujimoto T, Nishiye H, Miyano T (1995) A lack of intestinal pacemaker (c-kit) in aganglionic bowel of patients with Hirschsprung's disease. J Pediatr Surg 30:441–444
14. Yamataka A, Fujiwara T, Kato Y, Okazaki T, Sunagawa M, Miyano T (1996) Lack of intestinal pacemaker (C-KIT-positive) cells in infantile hypertrophic pyloric stenosis. J Pediatr Surg 31:96–98
15. Vanderwiden JM, Liu H, De Laet MH, Vanderhaeghen JJ (1996) Study of the interstitial cells of Cajal in infantile hypertrophic pyloric stenosis. Gastroenterology 111:279–288
16. Isozaki K, Hirota S, Miyagawa J, Taniguchi M, Shinomura Y, Matsuzawa Y (1997) Deficiency of c-kit+cells in patients with a myopathic form of chronic idiopathic intestinal pseudo-obstruction. Am J Gastroenterol 92:332–334
17. Hagger R, Finlayson C, Kahu F, Oliveira R, Chimelli L, Kumar D (2000) A deficiency of interstitial cells of Cajal in Chagasic megacolon. J Auton Nerv Syst 80:108–111
18. Geraldino RS, Ferreira AJ, Lima MA, Cabrine M, Ramirez LE (2006) Interstitial cells of Cajal in patients with chagasic megacolon originating from a region of old endemicity. Pathophysiology 13:71–74
19. Iantorno G, Bassotti G, Kogan Z, Lumi CM, Cabanne AM, Fisogni S, Varrica LM, Bilder CR, Munoz JP, Liserre B, Morelli A, Villanacci V (2007) The enteric nervous system in chagasic and idiopathic megacolon. Am J Surg Pathol 31:460–468
20. Gibbons SJ, De Giorgio R, Pellegrini MS, Garrity-Park MM, Miller SM, Schmalz PF, Young-Fadok TM, Larson DW, Dozois EJ, Camilleri M, Stanghellini V, Szurszewski JH, Farrugia G (2009) Apoptotic cell death of human interstitial cells of Cajal. Neurogastroenterol Motil 21:85–93
21. Côbo EC, Silveira TP, Micheletti AM, Crema E, Adad SJ (2012) Research on *Trypanosoma cruzi* and analysis of inflammatory infiltrate in esophagus and colon from chronic chagasic patients with and without mega. J Trop Med 2012:232646. Epub 2011 Oct 30
22. Vago AR, Macedo AM, Adad SJ, Reis DA, Corrêa-Oliveira R (1996) PCR detection of *Trypanosoma cruzi* DNA in oesophageal tissues of patients with chronic digestive Chagas' disease. Lancet 348:891–892
23. Vago AR, Andrade LO, Leite AA, Reis DA, Macedo AM, Adad SJ, Tostes S Jr, Moreira MCV, Brasileiro Filho G, Pena DJ (2000) Genetic characterization of *Trypanosoma cruzi* directly from tissues of patients with chronic Chagas disease. Am J Pathol 156:1805–1809
24. Vago AR, Silva DM, Adad SJ, Correa-Oliveira R, D'Avila Reis D (2003) Chronic Chagas disease: presence of parasite DNA in the oesophagus of patients without megaesophagus. Trans Rev Soc Trop Med Hyg 97:308–309
25. Ribeiro dos Santos R, Marquez JO, Von Gal Furtado CC, Ramos de Oliveira JC, Martins AR, Köberle F (1979) Antibodies against neurons in chronic Chagas' disease. Tropenmed Parasitol 30:19–23
26. Teixeira ML, Rezende Filho J, Figueredo F, Teixeira AR (1980) Chagas disease selective affinity and cytotoxicity of *Trypanosoma cruzi*-immune lymphocytes to parasympathetic ganglion cells. Mem Inst Oswaldo Cruz 75:33–45
27. Van Voorhis WC, Schlekewy L, Trong HL (1991) Molecular mimicry by *Trypanosoma cruzi*: the F1-160 epitope that mimics mammalian nerve can be mapped to a 12-amino acid peptide. Proc Natl Acad Sci USA 88:5993–5997
28. Pinheiro SW, Rua AMO, Etchebehere RM, Cançado CG, Chica JEL, Lopes ER, Adad SJ (2003) Morphometric study of the fibrosis and mast cells count in the circular colon musculature of chronic Chagas patients with and without megacolon. Rev Soc Bras Med Trop 36:461–466
29. Da Silveira AB, Adad SJ, Correa-Oliveira R, Furness JB, D'Avila Reis D (2007) Morphometric study of eosinophils, mast cells, macrophages and fibrosis in the colon of chronic chagasic patients with and without megacolon. Parasitology 134:789–796
30. Lyford GL, He CL, Soffer E, Hull TL, Strong SA, Senagore AJ, Burgart LJ, Young-Fadok T, Szurszewski JH, Farrugia G (2002) Pan-colonic decrease in interstitial cells of Cajal in patients with slow transit constipation. Gut 51:496–501
31. Horisawa M, Watanabe Y, Torihashi S (1998) Distribution of c-Kit immunopositive cells in normal human colon and in Hirschsprung's disease. J Pediatr Surg 33:1209–1214
32. Hagger R, Gharaie S, Finlayson C, Kumar D (1998) Regional and transmural density of interstitial cells of Cajal in human colon and rectum. Am J Physiol 275:G1309–G1316
33. Lee JI, Park H, Kamm MA, Talbot IC (2005) Decreased density of interstitial cells of Cajal and neuronal cells in patients with slow-transit constipation and acquired megacolon. J Gastroenterol Hepatol 20:1292–1298

Virchows Arch (2012) 461:393–398
DOI 10.1007/s00428-012-1291-2

ORIGINAL ARTICLE

Hepatic stellate cells are involved in the pathogenesis of acute-on-chronic liver failure (ACLF)

Archana Rastogi · Chhagan Bihari · Rakhi Maiwall · Arvind Ahuja · Manoj Kumar Sharma · Ashish Kumar · Shiv Kumar Sarin

Received: 10 February 2012 / Revised: 9 July 2012 / Accepted: 23 July 2012 / Published online: 11 August 2012
© Springer-Verlag 2012

Abstract ACLF is a condition with varied acute and chronic underlying etiologies and high mortality. Hepatic stellate cells (HSCs) are known to play an important role in hepatic fibrogenesis. Experimental data suggest that HSCs also display characteristics of hepatic stem/progenitor cells (HPCs). We investigated the number of activated HSC and their relationship to HPCs in ACLF in comparison to acute and chronic stages of other liver diseases. Immunohistochemical analysis of the number of activated HSCs and HPCs was performed in liver biopsies of 70 cases of ACLF and in the biopsies of patients with cirrhosis (45), acute hepatitis (25), chronic hepatitis (25), and normal live-related liver transplantation (LDLT) donor biopsies (15). The number of α-SMA-positive HSCs was assessed both quantitatively and semi-quantitatively. Keratin-19 (K19)-positive HPCs were estimated semi-quantitatively, and we looked for correlations between numbers of HSCs and HPCs. We found significantly more α-SMA activated HSCs/1,000 hepatocytes in ACLF biopsies (231±91) than in biopsies of patients with acute hepatitis (147±77), cirrhosis (73±35), chronic hepatitis (66±30), and normal LDLT donor biopsies (25±10), respectively ($p<0.0001$). A significant correlation between the presence of HPCs and ACLF versus other etiologies of liver disease was found ($p<0.001$). There was a significant correlation between the numbers of HPCs and of activated HSCs ($p<0.001$). ACLF is associated with more significant HSC activation than in acute hepatitis and other chronic liver diseases. There is a significant relationship between the presence of HSCs and that of HPCs, indicating a possible dynamic role of HSCs in liver regeneration and pathobiology of ACLF.

Keywords ACLF · Stellate cells · Immunohistochemistry · α-SMA · Progenitor cells · K19

Introduction

Liver failure can develop either as acute liver failure in the absence of any preexisting liver disease, as chronic decompensation of an end-stage liver disease (ESLD), or as an acute deterioration of known or unknown chronic liver disease—the acute-on-chronic liver failure (ACLF) [1].

ACLF represents a newly described complication of cirrhosis that has received considerable attention recently because of its impressive presentation, high mortality, and impact on transplant allocation [2]. Due to donor scarcity, other approaches have been proposed, particularly cellular-based procedures using hepatic stem/progenitor cells (HPCs) [3]. There is paucity of histologic data in ACLF. Previous studies have emphasized the importance of liver biopsy in prognostication and determining the outcome by determining the extent of necrosis, liver damage, and fibrosis [1]. Recent focus is on the mechanisms of activation and differentiation of human HPCs and the interaction with their probable niche, and a liver biopsy can further provide vital information in this regard.

Liver fibrosis is widely acknowledged as a damaging process in long-term liver disease. Hepatic stellate cells (HSCs) are known to play an important role in the development of fibrosis and its progression to cirrhosis; however, their role in liver failure is not clear. Activated hepatic

All authors contributed in conceiving and developing the manuscript.

A. Rastogi (✉) · C. Bihari · A. Ahuja
Department of Pathology, Institute of Liver and Biliary Sciences,
D-1, Vasant Kunj,
New Delhi 110070, India
e-mail: drarchanarastogi@gmail.com

R. Maiwall · M. K. Sharma · A. Kumar · S. K. Sarin
Department of Hepatology, Institute of Liver and Biliary Sciences,
D-1, Vasant Kunj,
New Delhi 110070, India

stellate cells convert from vitamin-A-storing cells to contractile myofibroblastic cells responsible for extracellular matrix (ECM) production in the injured liver. There is growing evidence mainly from the experimental studies that HSCs possess signaling pathways required for stem/progenitor cell functions [4, 5].

To the best of our knowledge, none of the previous studies have tried to elucidate the role of HSCs in ACLF. We undertook this study to compare the number of activated HSC in ACLF with that in other acute and chronic stages of liver diseases and to determine their relationship with HPCs.

Patient selection

ACLF cases (70) were diagnosed by the APASL criteria. The APASL's definition of ACLF is "acute hepatic insult manifesting as jaundice and coagulopathy, complicated within 4 weeks by ascites and/or encephalopathy in a patient with previously diagnosed or undiagnosed chronic liver disease" [6].

Chronic hepatitis (25) included in the study was viral hepatitis, with fibrosis stage of 2–3 according to the modified Ishak's system [7]. Chronic hepatitis represents a series of liver disorders of varying causes and severity in which hepatic inflammation and necrosis continue for at least 6 months [8].

Acute hepatitis represents liver disorders in which hepatic inflammation and necrosis last for less than 6 months. Of acute hepatitis with compatible histology, 25 cases were included in the present study.

In the study were also included 45 cases of cirrhosis. Cirrhosis is a condition that is defined histopathologically by the development of fibrosis and architectural distortion with formation of regenerative nodules. It has a variety of clinical manifestations and complications [8].

Grading of necroinflammatory activity and fibrosis staging in chronic hepatitis and cirrhosis was done by a modification of the Ishak system [7].

Methods

Liver biopsy

All of the biopsies in the ACLF group were done by transjugular approach, except for two cases in which explant liver sections were available for immunohistochemistry. Mean biopsy length was 12 mm. Formalin fixed, paraffin-embedded serial sections of the liver biopsies of ACLF group were reviewed retrospectively. The pathologist was blinded to all clinical and histological findings, and liver biopsies of the five study groups (ACLF, acute hepatitis, chronic hepatitis, cirrhosis, and normal LDLT donor biopsies) were randomly numbered before immunohistochemical analysis.

Immunohistochemistry

Activated HSCs were stained by immunohistochemistry (IHC) using a monoclonal antibody for α-smooth muscle actin (α-SMA) (ready to use, clone HHF35, Biogenex, CA, USA); hepatic progenitor cells (HPCs) were assessed by anti-keratin 19 (K19) (ready to use, clone RCK 108, Biogenex, CA, USA).

Immunohistochemical staining was performed by peroxidase-enzyme-labeled streptavidin-biotin (LSAB) detection method using Polymer-HRP kit (Biogenex, San Ramon, USA) with diaminobenzidine (DAB) as a chromogen and Meyer's hematoxylin for contrasting. Muscle cells of small arterial profiles in the portal tracts served as a positive internal control. Negative control was performed by leaving out the primary antibody during the staining procedure.

Sections taken on poly-L-lysine-coated slides were deparaffinized. Endogenous peroxidase blocking was done by 3 % hydrogen peroxide in distilled water for 10 min. Heat retrieval was done in Tris buffer solution (TBS) (PH 6.0) in two cycles for 2 min half power and then full power, respectively, in microwave and cooled at room temperature. Protein block was applied for 5 min. Treatment with primary antibody with positive control was done for 1 h, secondary antibody for 20 min, and tertiary (streptavidin) for 20 min. TBS rinse was done after each step. Sections were treated with DAB for 10 min and counterstained with hematoxylin.

Assessment of activated HSCs

Both quantitative and semi-quantitative methods were used to assess the number of activated HSCs.

Quantitative assessment was expressed as the "hepatic stellate cell index" (HSCI), i.e., the number of HSCs per 1,000 hepatocytes [9]. Activated HSCs were counted using oil immersion objective (×1,000) of an Olympus BX51 microscope.

Semi-quantitative assessment was done by determining the percentage of α-SMA-positive HSCs in the perisinusoidal spaces (modification of Schmitt-Graff et al.) [10]. HSCs were counted in specific areas of liver biopsy, in ≥5 fields each of perivenular area, intermediate area, and periportal areas using ×100 and ×200 magnification.

Grading on a scale of 0–4 was performed: with 0, no staining; 1 (up to 10 % of sinusoidal surface showing activated HSCs); 2 (11–30 %); 3 (31–70 %); and 4 (71–100 %). Grades 3 and 4 were considered significant for statistical analysis.

HPCs were also semi-quantitatively estimated on a scale of 0–4, by counting HPCs at ×200 magnification in three to five

non-overlapping fields (0—no cells, 1—1–10 HPCs, 2—11–30 HPCs, 3—31–70 HPCs, 4—>70 HPCs). HPCs were distinguished from intermediate hepatocytes by their smaller size, scanty cytoplasm, and more intense K19 immunostaining [3].

Statistical analysis

Correlation of HSCs/1,000 hepatocytes was done with the etiologic groups (HBV reactivation, alcoholic hepatitis superimposed on alcoholic liver disease, acute viral infection on chronic liver disease, and cryptogenic).

The number of activated HSCs was compared between two groups by the Mann–Whitney test and among more than two groups by the Kruskal–Wallis test. HPC activation in ACLF versus other groups was determined by Pearson's Chi-square test. The relationship between HSCs and HPCs was assessed by the Kruskal–Wallis test. Correlation of HSCs with etiology in ACLF was done by Kruskal–Wallis test. A p value <0.001 was considered to indicate significant difference.

Results

Demographic and biochemical characteristics

A total of 165 liver biopsies of an equal number of patients and 15 normal living donor transplantation biopsies were included in this study.

The mean age of ACLF patients was 46.1±13.2 years (median 47 years, range 13–71 years), with male predominance (male to female 5:2). Mean serum bilirubin and albumin levels were 20.5±11.3 mg/dl and 2.2±0.4 g/dl, respectively.

The mean age of chronic hepatitis patients was 40.1±14.3 years, with a male-to-female ratio of 17:8; for acute hepatitis, the mean age was 39±17 years, and the male-to-female ratio was 18:7; for cirrhosis, the mean age was 46.4±10.4 years, and the male-to-female ratio was 24:21.

Etiology of acute insult and chronic liver disease in ACLF

Chronic liver disease was due to hepatitis B virus (n=23), alcohol (n=23), and cryptogenic (6), and HCV, NASH, PBC, and autoimmune hepatitis were the underlying etiology in the rest. Acute decompensation was due to viral etiology (n=32), alcohol (n=19), drugs (n=5), and unknown in the rest. Major etiologic groups were reactivation of chronic hepatitis B (n=19) and acute alcoholic hepatitis superimposed on alcoholic liver disease (n=19) (Table 3).

Acute hepatitis comprised of HAV (8), HEV (8), HBV (7), and drug induced (2). The chronic hepatitis group comprised HBV (17), HCV (7), and combined HBV and HCV (1), and the cirrhosis patients were of ALD (6), HBV (13), HCV (21), NASH (4), and cryptogenic (1).

Histological characteristics of ACLF

All of the cases showed histological features of acute and chronic hepatitis in variable combinations as described in our previous study [1]. Ballooning or eosinophilic degeneration of hepatocytes, cellular and canalicular cholestasis, ductular proliferation and ductular bile plugs, variable degree of parenchymal necrosis/collapse, lobular inflammation, apoptosis, sinusoidal cell activation along with the features of chronic liver disease as periportal fibrous extensions, bridging fibrosis or cirrhosis, pericellular fibrosis, and interface activity were seen in the ACLF biopsies (Fig. 1a, b).

Activated HSCs as detected by α-SMA immunohistochemistry

HSCI was highest (231±91) for the ACLF group as compared to 147±77, 66±30, 73±35, and 25±10 for acute hepatitis,

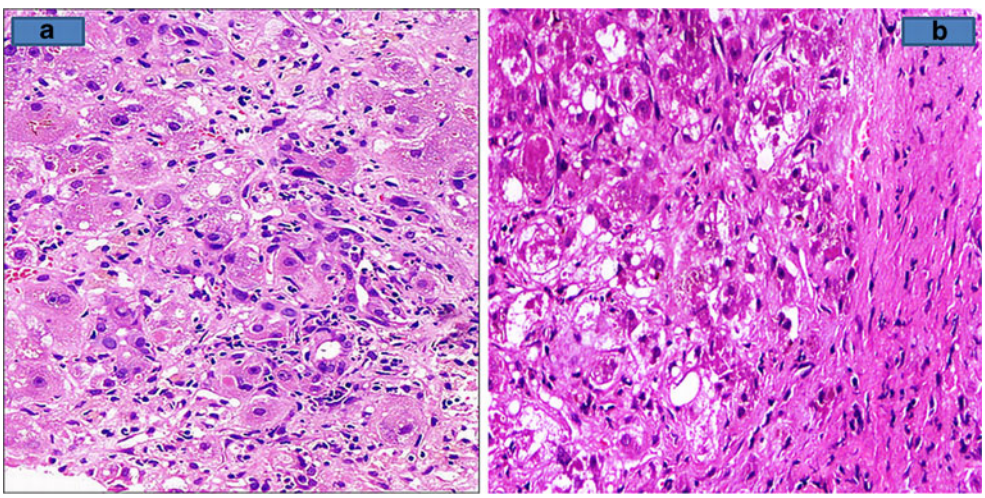

Fig. 1 **a** H&E-stained section showing periportal fibrous extensions, pericellular fibrosis and interface activity, eosinophilic degeneration of hepatocytes, and cellular and canalicular cholestasis (×200). **b** H&E-stained section showing fibrous bands, ballooning degeneration hepatocytes with Mallory hyaline bodies, cellular/canalicular cholestasis, and eosinophilic degeneration (×200)

Table 1 Hepatic stellate cell index (HSCI) in ACLF and other groups

α-SMA immunostained activated HSCs	ACLF	Acute hepatitis	Cirrhosis	Chronic hepatitis	Normal	*P* value
HSCs/1,000 hepatocytes	231±91	147±77	73±35	66±30	25±10	$P<0.0001$
Zone 1 HSCs (%)	58±12	42±17	31±17	18±10	8±4	$P<0.0001$
Zone 2 HSCs (%)	44±14	25±14	17±11	11±6	7±4	$P<0.0001$
Zone 3 HSCs (%)	50±14	39±17	23±13	15±9	8±4	$P<0.0001$

chronic hepatitis, cirrhosis, and normal LDLT biopsies, respectively ($p<0.001$). Mean HSC percentage was significantly higher in all of the three acinar areas in ACLF in comparison to the other groups ($p<0.001$) (Table 1) (Fig. 2a–d).

Semi-quantitative analysis revealed a significantly higher number of cases with activated stellate cells (high grade) in periportal, intermediate, and perivenular areas in the ACLF group ($p<0.001$) (Table 2).

In ACLF, there was no significant correlation of the number of HSCs/1,000 hepatocytes with any of the etiologic groups ($p=0.95$).

Relationship of activated HSCs with HPCs

There was a significant correlation between the number of K19-positive HPCs and ACLF in comparison with other etiologies of liver disease ($p<0.001$). There was a significant correlation between the number of HPCs and number of HSCs/1,000 hepatocytes (Table 3). Along with an increase in the number of HSCs, the number of HPCs increased significantly (Table 4).

Discussion

This is the first study to analyze HSC activation and its correlation with HPCs in ACLF. Immunohistochemical analysis of the number of activated HSCs as detected by α-SMA staining and HPC activation as detected by K19 immunostaining in ACLF was compared in biopsies of liver diseases of different stages including acute hepatitis, chronic hepatitis, cirrhosis, and normal LDLT. The number of activated HSC was significantly higher in the ACLF as compared to the other groups. Activated HSCs were observed in decreasing frequency in ACLF, acute hepatitis, cirrhosis, chronic hepatitis, and normal LDLT donor biopsies, respectively. There was a significant correlation between the number of HSCs and that of HPCs, which suggests that they play a role in liver regeneration. None of the previous studies have explored HSC activation and their correlation with liver regeneration in ACLF.

There are limited data on the entity of ACLF, but in recent years, this syndrome has gained a lot of interest, and at present, considerable efforts are ongoing to better

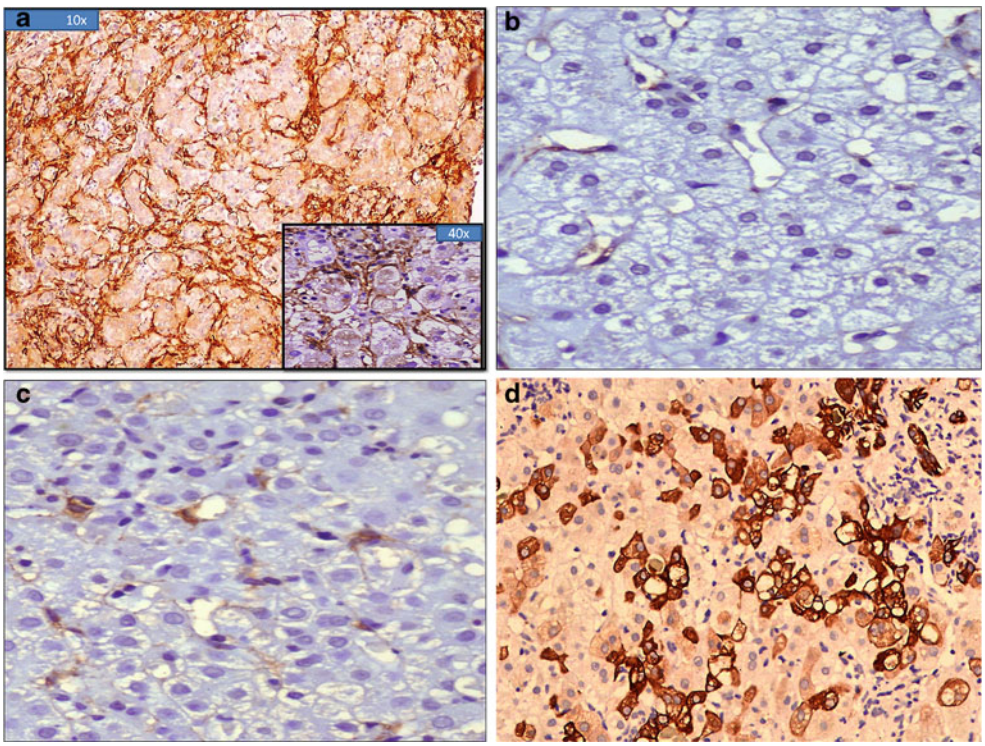

Fig. 2 **a** α-SMA immunohistochemistry showing activated HSCs in ACLF (×100), with SMA-positive stellate cell in inset (×400). **b** Minimal SMA expression seen on a biopsy of chronic viral hepatitis (×200). **c** Focal mild SMA (hepatic stellate cell activation) on a biopsy of acute viral hepatitis (×200). **d** K19 immunohistochemistry showing a fair number of HPCs and intermediate hepatocytes in ACLF (×200)

Table 2 Zonal HSCs% comparison among disease groups

Liver biopsy groups	%Biopsies showing high-grade (grade 3–4) α-SMA expression in HSCs		
	Zone 1	Zone 2	Zone 3
ACLF	69/70(98.6 %)	63/70(90 %)	65/70(92.9 %)
Acute hepatitis	18/25(72 %)	6/25(24 %)	15/25(60 %)
Chronic hepatitis	2/25(8 %)	0/25(0 %)	2/25(8 %)
Cirrhosis	21/45(46.7 %)	2/45(4.4 %)	9/45(20 %)
Normal	0	0	0

Table 4 Correlation of HSCs/1,000 hepatocytes with HPCs

HPCs (K19 IHC)	Hepatic stellate cells/1,000		
	Number	Median (range)	*p* value[a]
0	17	30 (20–160)	<0.001
1	80	75 (20–400)	
2	25	120 (30–400)	
3	44	210 (100–400)	
4	8	220 (150–300)	

[a] Kruskal–Wallis test

characterize the syndrome, to gain further insight into its pathophysiology, and to optimize therapy [2]. ACLF is potentially reversible, and early and accurate diagnosis and prognosis of patients are of critical importance for optimal management.

There is a paucity of literature on liver biopsy in ACLF. A recent study by our group [1] has highlighted the role of liver biopsy features as outcome predictors. Liver biopsies in ACLF display features of acute injury and chronic liver diseases with/without necrosis, in varying combinations and with variable severity. Hepatocyte ballooning, eosinophilic degeneration, rosette formation, apoptosis, fatty change, cholestasis (hepatocyte, canalicular, bile ductular, and ducts), lobular inflammation, portal inflammation, Mallory–Denk body, several foci of confluent necrosis with or without bridging necrosis with portal/periportal fibrosis, ductular proliferation, pericellular fibrosis, and cholangiolitis can all be seen in these biopsies [1]. Extensive necrosis, ductular cholestasis, eosinophilic degeneration of hepatocytes, and advanced fibrosis have been shown to be important histological predictors of poor outcome [1].

In the normal liver, HSCs comprise approximately 1.4 % of total liver volume and are present at a ratio of about 3.6 to 6 cells per 100 hepatocytes (or 1:20) [11, 12]. It is widely accepted that HSCs contribute to liver fibrosis. HSC cells reside within the perisinusoidal space of Disse in the liver that is lined by parenchymal cells and fenestrated sinusoidal endothelial cells (SECs). HSCs can develop into myofibroblast-like cells that synthesize extracellular matrix proteins and contribute to liver fibrosis [11, 13–15]. Activated HSCs loose lipid droplets stored in their cytoplasm, proliferate, and gain abundant microfilaments that consist mainly of α-smooth muscle actin (α-SMA) [16]. Activated hepatic stellate cells are identified by using a specific monoclonal antibody to detect cytoplasmic alpha smooth muscle actin (alpha-SMA), which is not present in quiescent cells [17].

Table 3 Etiological classification of ACLF patients (n=70)

Etiology of chronic liver disease	Etiology of acute insult	
Hepatitis B (n=23)	Reactivation of hepatitis B	(n=19)
	Acute viral hepatitis	(n=4)
Alcohol (n=23)	Acute alcoholic hepatitis	(n=19)
	Acute viral hepatitis	(n=4)
Cryptogenic (n=6)	Acute viral hepatitis	(n=2)
	Drugs	(n=2)
	Unknown	(n=2)
NASH, HCV, PBC, AIH (n=18)	Acute viral hepatitis	(n=3)
	Drugs	(n=3)
	Unknown	(n=12)

There are scarce animal experimental data suggesting that mesenchymal cells such as stellate cells physically interact with oval cells and induce signals in them [18]. A recent study has shown that stellate cells of the rat liver display characteristics of stem/progenitor cells. They express CD133 (cluster designation 133) and Oct4 (octamer 4), markers expressed on pluripotent stem cells, which supports the notion that HSCs can differentiate into hepatocyte-like and endothelial-like cells in vitro and points to the role of HSCs in liver regeneration [19]. Another experimental study has provided similar information that HSCs are directly involved in restoration of liver mass even in vivo [20]. Savitza et al. have highlighted the interrelationship between stellate cells, β-catenin-dependent Wnt signaling, and the Notch signaling, which are considered to characterize the stem cell niche for HPCs. Stellate cells have also been shown to possess signaling pathways required for stem cell functions such as hedgehog and β-catenin-dependent Wnt signaling in other studies [21].

Recently, a clinical study in acute liver failure (ALF) patients has provided evidence of increased α-SMA expression, increased stiffness as measured by transient elastography, and increased serum TIMP and MMP levels [22] and has thus raised several questions regarding the role of stellate cells in liver failure such as the role of hepatocellular death in HSC activation and fibrogenesis. Also, there is a recent interest in HSCs as they display characteristics of stem cells. Our study also highlights that HSCs probably have an important role in liver regeneration.

Relevance of molecular signaling pathways for HSCs and their role on stem cell proliferation, differentiation, and their niche is unclear. It is of utmost importance to investigate the interactions of HSCs with other postulated characteristics of the stem cell niche, such as Notch and Wnt signaling in liver failure.

Future studies in a similar cohort of human liver diseases of different etiologies and stages using immunohistochemical markers and molecular studies for death signaling, HPCs, and their niche and HSCs are needed to confirm these initial observations and might provide further insight into liver injury and repair mechanisms and may help to improve therapeutic interventions in these currently untreatable human liver diseases.

Conclusion

ACLF is associated with higher numbers of activated HSC in comparison to acute hepatitis and chronic liver diseases. There is a significant relationship between the number of HSCs and of HPCs, indicating a possible dynamic role of HSCs in liver regeneration and pathobiology of ACLF.

Acknowledgment Technical Staff, Department of Pathology.

Conflicts of interest We declare that we have no conflict of interest.

References

1. Rastogi A, Kumar A, Sakhuja P et al (2011) Liver histology as predictor of outcome in patients with acute-on-chronic liver failure (ACLF). Virchows Arch 459(2):121–127
2. Laleman W, Verbeke L, Meersseman P et al (2011) Acute-on-chronic liver failure: current concepts on definition, pathogenesis, clinical manifestations and potential therapeutic interventions. Expert Rev Gastroenterol Hepatol 5(4):523–537
3. Sancho-Bru P, Najimi M, Caruso M, Pauwelyn K, Cantz T, Forbes S, Roskams T, Ott M, Gehling U, Sokal E, Verfaillie CM, Muraca M (2009) Stem and progenitor cells for liver repopulation: can we standardize the process from bench to bedside? Gut 58:594–603
4. Sicklick JK, Li Y-X, Choi SS, Qi Y et al (2005) Role for hedgehog signaling in hepatic stellate cell activation and viability. Lab Investig 85:1368–1380
5. Kordes C, Sawitza I, Häussinger D (2008) Canonical Wnt signaling maintains the quiescent stage of hepatic stellate cells. Biochem Biophys Res Commun 367:116–123
6. Sarin SK, Kumar A, Almeida J et al (2009) Acute on chronic liver failure (ACLF): consensus recommendations of the Asia Pacific Association for the Study of the Liver (APASL). Hepatol Int 3:269–282
7. Ishak K, Baptista A, Bianchi L et al (1995) Histological grading and staging of chronic hepatitis. J Hepatol 22:696–699
8. Fauci AS, Brauwald E, Kasper DL(2005) Harrison's principle of internal medicine, 17th ed. Amazon
9. Horwath E, Kovacs K, Ross RC (1973) Liver ultrastructure in methotrexate treatment of psoriasis. Arch Dermatol 108:427–428
10. Schmitt-Graff A, Kruger S, Bochard F et al (1991) Modulation of alpha smooth muscle actin and desmin expression in perisinusoidal cells of normal and diseased human livers. Am J Pathol 138:1233–1242
11. Geerts PD (2001) History, heterogeneity, developmental, biology, and functions of quiescent hepatic stellate cells. Sem Liver Dis 21:311–335
12. Roger KM (2007) Hepatic stellate cells and liver fibrosis. Arch Pathol Lab Med 131:1728–1734
13. Friedman SL (2008) Hepatic stellate cells: protean, multifunctional, and enigmatic cells of the liver. Physiol Rev 88:125–172
14. Burt AD (1999) Pathobiology of hepatic stellate cells. J Gastroenterol 34:299–304
15. Brenner DA, Waterboer T, Choi SK et al (2000) New aspects of hepatic fibrosis. J Hepatol 32(1 Suppl):32–38
16. Cassiman D, Libbrecht L, Desmet V et al (2002) Hepatic stellate cell/myofibroblast subpopulations in fibrotic human and rat livers. J Hepatol 36:200–209
17. Tsukada S, Parsons CJ, Rippe RA (1996) Mechanisms of liver fibrosis. J Hepatol 25(5):677–683
18. Paku S, Schnur J, Nagy P et al (2001) Origin and structural evolution of the early proliferating oval cells in rat liver. Am J Pathol 158:1313–1323
19. Tanaka M, Itoh T, Tanimizu N et al (2011) Liver stem/progenitor cells: their characteristics and regulatory mechanisms. J Biochem 149(3):231–239
20. Yang L, Jung Y, Omenetti A et al (2008) Fate-mapping evidence that hepatic stellate cells are epithelial progenitors in adult mouse livers. Stem Cells 26:2104–2113
21. Sawitza I, Kordes C, Reister S et al (2009) The niche of stellate cells within rat liver. Hepatology 50(5):1617–1624
22. Dechêne A, Sowa JP, Robert K et al (2010) Acute liver failure is associated with elevated liver stiffness and hepatic stellate cell activation. Hepatology 52(3):1008–1016

Virchows Arch (2012) 461:399–403
DOI 10.1007/s00428-012-1304-1

ORIGINAL ARTICLE

Tumor architecture exerts no bias on nuclear grading in breast cancer diagnosis

Braulio Mora · Dario Bombari · Stephan C. Schaefer · Marcus Schmidt · Jean-Francois Delaloye · Fred Mast · Hans-Anton Lehr

Received: 20 June 2012 / Revised: 14 August 2012 / Accepted: 16 August 2012 / Published online: 31 August 2012
© The Author(s) 2012. This article is published with open access at Springerlink.com

Abstract We recently reported that nuclear grading in prostate cancer is subject to a strong confirmation bias induced by the tumor architecture. We now wondered whether a similar bias governs nuclear grading in breast carcinoma. An unannounced test was performed at a pathology conference. Pathologists were asked to grade nuclei in a PowerPoint presentation. Circular high power fields of 27 invasive ductal carcinomas were shown, superimposed over low power background images of either tubule-rich or tubule-poor carcinomas. We found (a) that diagnostic reproducibility of nuclear grades was poor to moderate (weighed kappa values between 0.07 and 0.54, 27 cases, 44 graders), but (b) that nuclear grades were not affected by the tumor architecture. We speculate that the categorized grading in breast cancer, separating tubule formation, nuclear pleomorphism, and mitotic figure counts in a combined three tier score, prevents the bias that architecture exerts on nuclear grades in less well-controlled situations.

Keywords Confirmation bias · Cancer grading · Nuclear pleomorphism · Architecture · Cognitive psychology

B. Mora · H.-A. Lehr (✉)
Institute of Pathology, CHUV,
Lausanne, Switzerland
e-mail: hansanton.lehr@yahoo.de

B. Mora
e-mail: brauliomora@gmail.com

D. Bombari · F. Mast
Department of Psychology, University of Bern,
Bern, Switzerland

D. Bombari
e-mail: db2838@columbia.edu

F. Mast
e-mail: fred.mast@psy.unibe.ch

S. C. Schaefer
Institute of Pathology, Inselspital,
Bern, Switzerland
e-mail: stephan.schaefer@pathology.unibe.ch

M. Schmidt
Department of Gynecology and Obstetrics, University of Mainz,
Mainz, Germany
e-mail: Marcus.Schmidt@unimedizin-mainz.de

J.-F. Delaloye
Department of Gynecology and Obstetrics, CHUV,
Lausanne, Switzerland
e-mail: Jean-Francois.Delaloye@chuv.ch

Introduction

Despite major advances in our understanding of breast cancer biology and the advent of novel diagnostic tools to predict survival and treatment response of breast cancer patients (i.e., MIB-1, IGkG, genetic tests, etc.) [1–3], time-honored tumor grading has been confirmed as one of the most reliable prognostic and predictive markers [4]. Grading of breast carcinomas is based on three histomorphological criteria: degree of tubular differentiation, nuclear pleomorphism, and mitotic figure count [5, 6]. Recently, we found that nuclear grading in prostate cancer is subject to a strong confirmational bias induced by the tumor architecture: pathologists unconsciously assigned grades for nuclear pleomorphism that matched the Gleason grade—irrespective of nuclear morphology [7, 8]. This phenomenon is of little clinical consequence in prostate cancer, where prognosis is predicted by tumor architecture and not by nuclear grade [7]. However, we wondered whether the same heuristic phenomenon could be operative in the grading of breast cancer, potentially leading to a clinically relevant loss of prognostic/predictive information.

Methods

In analogy to the prostate cancer experiments [8], we prepared a PowerPoint presentation, where circular images of high power fields (HPF, Ø0.62 mm) of 27 invasive ductal carcinomas were superimposed over low power background images with the tumor architecture. The photographs were taken from a historical collection of cases from 1993 to 1995 at the University of Mainz [2, 4], for which specific patient consent had been obtained. No patient identifiers were known. In a random order, each HPF image was shown twice, once superimposed over a background image of a well-differentiated, tubule-rich carcinoma and once superimposed over an image of a poorly differentiated, tubule-poor carcinoma (Fig. 1a). In order to avoid recognition of the HPFs after the first presentation, the circular images belonging to the same case were rotated and flipped using Photoshop (Adobe, CS3, St. Jose, CA). With permission from the organizers of the joint annual meeting of the Austrian and the Swiss Societies of Pathology in Feldkirch in November 2010, this presentation was shown to the audience of a plenary session. Each HPF was displayed for 7 s, followed by a 1-s transition in which the background image of the next case was shown (Fig. 1b). The 7 s was chosen based on previous experience with a similar experimental setup, where nuclei were displayed on a computer screen for 8 s, and where the pathologists spoke out loud the nuclear grade at an average of 4–5 s into the 8-s interval. The presentation of the 60 HPF hence lasted exactly for 8 min. The experiment had not been announced (it "spontaneously" replaced a talk that was printed in the program book). In a brief introduction, pathologists were asked to grade nuclear pleomorphism of the projected HPFs on a five-tier scale (1, 1–2, 2, 2–3, and 3) and note the grades on a form that they found on their seats. No information was given concerning the true aim of the experiment. In particular, no mention was made of the background images. It was hence left to the "imagination" of the participants to assume that the background images belonged to the high power fields. This was the exact same experimental situation that we had used before in the prostate cancer experiments in which we had found a strong architectural bias on nuclear grading [8]. The only additional information that was asked from the participants was the number of years in practice. Statistical analyses included weighed kappa analyses and paired *t* tests (www.wessa.net).

Results

Fifty-eight of the conference attendees (70–80) participated in the experiment. Data from 14 participants were discarded since they did not rate all HPFs. Thirty-six of the remaining 44 raters indicated the number of years of experience. The reliability of nuclear grade assignment ranged from moderate to good for about half of the HPFs (n=14, weighed kappa values 0.25–0.54) and poor for the other half of the HPFs (n=13, weighed kappa values 0.07–0.25). Grading consistency was not affected by the years of professional experience (data not shown).

Average nuclear grades assigned to the HPFs superimposed over tubule-rich backgrounds (2.10±0.63) were comparable to average grades assigned to the same HPFs superimposed over tubule-poor backgrounds (2.15±0.62), suggesting that tumor architecture did not influence nuclear grade assignment. Also, the difference of the tubular differentiation of the background images did not influence nuclear grades (1.92±0.63 for 16 HPFs presented before pure tubular backgrounds vs. 2.00±0.67 for the same HPFs presented before solid backgrounds, n.s.).

We also found that the professional experience of the participants had no influence on the results: neither did we see any effect of tubule formation on nuclear grades in n=11 beginners (1–3 years of professional experience; 2.03±0.42 vs. 1.99±0.44), in n=13 more experienced pathologists (4–10 years of experience; 2.13±0.48 vs. 2.16±0.47), nor in n=12 "old-timers" with more than 10 years of experience (2.11±0.46 vs. 2.15±0.47). These results are shown in a graphic form in Fig. 2.

Fig. 1 PowerPoint presentation showing high power fields superimposed over different architectural backgrounds. Using a beamer, HPFs of 27 invasive ductal carcinomas were projected in the plenary lecture hall of a pathology conference. Unknown to the participants, each high power filed was shown twice, superimposed once over a well-differentiated, tubule-rich background image and once over a poorly differentiated, tubule-poor background image (**a**). In order to avoid recognition, high power fields were flipped and rotated within their circular inset (**a**). The presentation was automatically timed to show each HPF for 7 s. Between HPFs, the background image of the next case was shown for 1 s (**b**). Pathologists were asked to assign nuclear grades for each HPF and note their grade on a form that they found on their seats. The present figure was specifically created for this publication to demonstrate the principle, but using only a limited set of only four high power fields, each shown twice, superimposed over the distinct (tubule-rich or tubule-poor) background images. In the original presentation, a total of n=27 cases were randomly presented

Discussion

The principal finding of this experiment is that grading of nuclear pleomorphism in invasive ductal breast carcinoma is not affected by the tumor architecture. This finding is unexpected, as it does not confirm our prior observations in prostate carcinomas [7, 8]. In these previous studies, we found that nuclear grade assignment was unconsciously affected by a powerful confirmation bias induced by the tumor architecture. In Bombari's study [8], each of 20

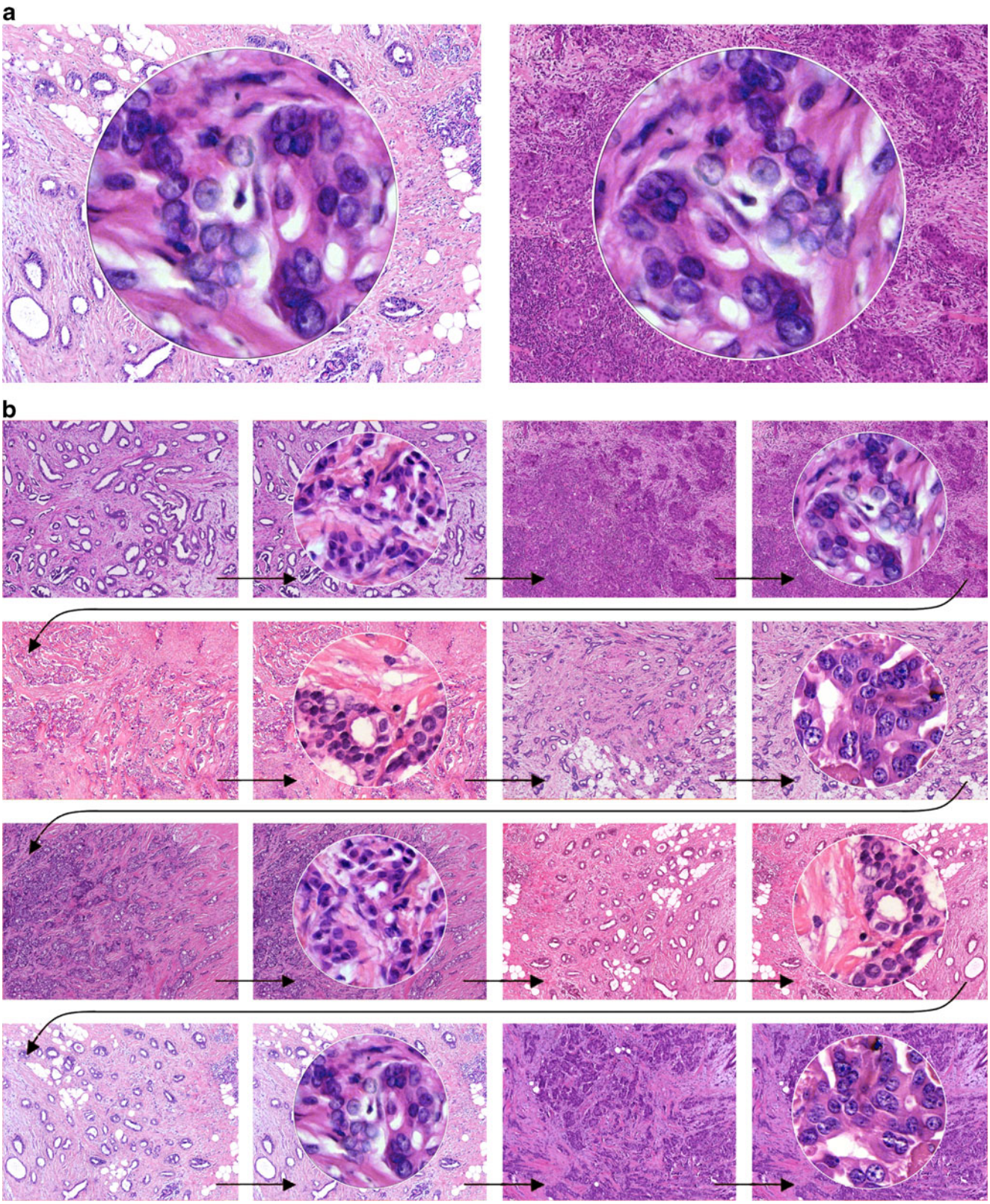

pathologists was assigned lower pleomorphism grades to the nuclei of high power fields when these had been superimposed over a background of a tubule-rich carcinoma (Gleason pattern 3) and significanly higher grades when the same high power fields were shown a little later superimposed over an image of a cribriform or solid carcinoma (Gleason

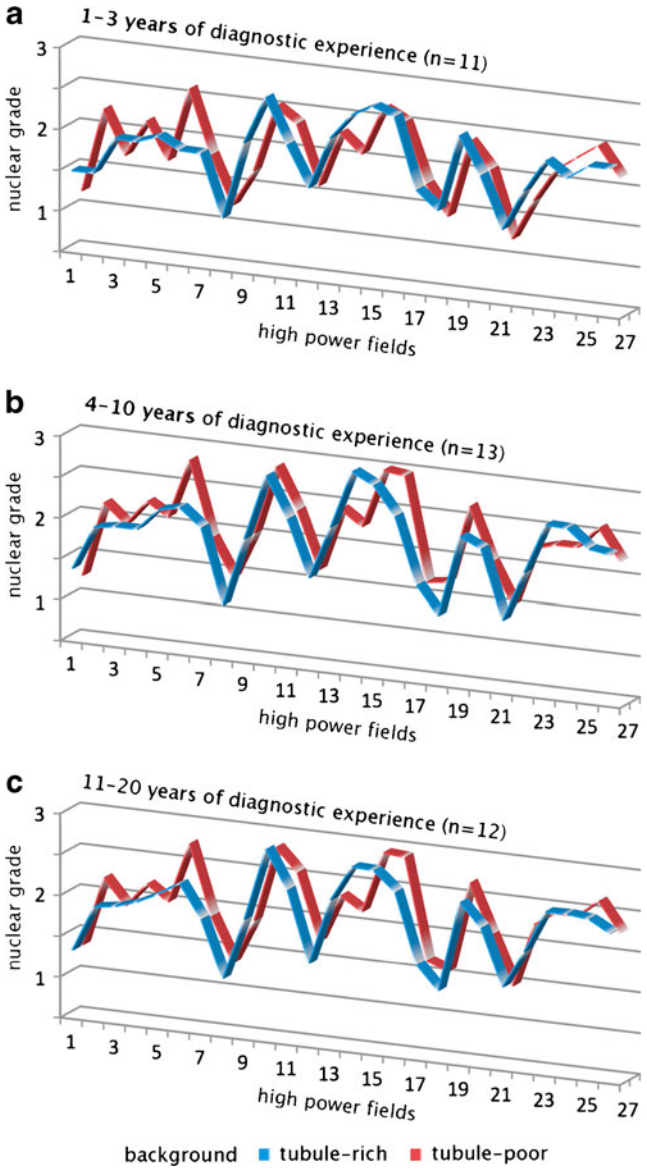

Fig. 2 Nuclear grades assigned to 27 pairs of high power fields superimposed over tubule-rich (*blue*) or tubule-poor (*red*) backgrounds. The data are shown for three subgroups of pathologists with various years of experience. **a** 1–3 years of experience, $n=11$; **b** 4–10 years of experience, $n=13$; **c** 11–20 years of experience, $n=12$. Note that for most high power fields, pathologists assigned similar nuclear grades, largely unaffected by the architecture of the background images

patterns 4 or 5). Tracking pathologists' eye fixations further showed that depending on the tumor architecture of the background image, pathologists looked at different nuclei within the high power fields: they fixated on smaller nuclei with evenly distributed, pale chromatin when the background showed a Gleason 3 pattern and on larger, hyperchromatic nuclei when the background was a Geason 4 or 5 pattern [8]. However, this selection of nuclei that "matched the expectation" accounted for only about one tenth of the total grade gravitation, suggesting that nuclear selection represents an unconscious strategy of our minds to vindicate the confirmation bias induced by the tumor architecture [8].

In the present study, we found that this powerful confirmation bias is not operative in breast cancer grading, even though the participants had exactly the same chance to explore tumor architecture and nuclear pleomorphism on the projected tumor images as they had in the previous experiments on prostate cancers [8]. In analogy to well-established modes of avoiding optical illusions by the adherence to strict guidelines and rules in aviation [9], we assume that the rigid grading system of breast cancer that was initially established by Bloom and Richardson [5] and later modified by Elston and Ellis [6] effectively prevents cross-category biases. By experience, pathologists know that in breast cancer, architecture and nuclear grade do not necessarily go along hand in hand. For instance, lobular carcinomas show no tubular differentiation (grade 3), but usually little nuclear pleomorphism (grade 1). In contrast, every pathologist has seen carcinomas with "ugly" nuclei (grade 3), but with more or less well-formed tubular architecture (grade 1). In breast cancer diagnosis, it hence poses no "conflict" for our minds to see small, round, and pale nuclei and correctly assign them a grade 1 even though the low power image in the background displays an architecturally undifferentiated (grade 3) carcinoma without any formation of tubules. In this context, it should be noticed that the pathologists who participated in the study all practice in Austria and in Switzerland, where the adherence to the three tier Bloom and Richardson grading system is generally very high. Also, it may be of interest to note that most pathologists in these two countries practice in a rather "generalist" approach, with only few departments being organized in subspeciality services, and that the session, in which the experiment was performed, had no particular breast focus. This suggests that the results of our study can be applied to most diagnostic pathologists.

In this experiment, we have focussed on the degree of tubule formation as leading architectural pattern. Another histological feature that may have potentially biased the partcipants is the relative amount of stroma between tumor cells. Pathologists tend to be quite vigilant to morphological cues that contribute, sometimes quite unconsciously, to the interpretation of the complex image on the H&E-stained slide. These cues are not always easily quantifiable, such as the percent of tubule formation or the number of mitotic figures, but are often quite subjective in nature, such as the presence and the extent of necrosis, the type and amount of peritumoral stroma, or the peritumoral lymphocytic response, to name only a few of the more obvious features. In a less well-controlled situation, as we have identified recently in prostate cancer grading [7, 8], such additional morphological features will likely affect overall cancer grading. However, the findings of the present study, where tubule formation did not affect nuclear grading (Fig. 2), suggest that in breast cancer grading, where the well-standardized and

widely applied Bloom and Richardson criteria separate architectural features from nuclear features and from mitotic figure counts, stroma will likely not affect nuclear grading.

The second observation that we made in the present study is that grade assignment to nuclei in high power fields is surprisingly inaccurate. We used weighed kappa analysis to quantify the consistency of grade assignment to the 27 pairs of high power fields. The interobserver reliability was poor in about half of the cases (weighed kappa values below 0.25) and moderate to good in the other half of the cases (kappa values between 0.25 and 0.54). We acknowledge that the experimental setup used in this study had a different primary aim. Also, grade assignment on a single projected high power field certainly does not reflect the situation that pathologists encounter during routine cancer grading, where they scan thousands of nuclei during nuclear grade assignment and not only those in one high power field. Nevertheless, our findings correlated rather well with kappa scores for interobserver reliability of nuclear pleomorphism in prior reports (range 0.3 to 0.4) that have underscored the limitations of this particular component of the grading system in breast cancer [10–12].

To conclude, we found that a cognitive bias induced by the tumor architecture does not govern nuclear grading in breast cancer diagnosis. Even though more research is needed to determine the exact conditions under which this confirmation bias unfolds, the present observation is relevant in that it suggests that adherence to strict guidelines, notably categorized grading, has the capacity to effectively counteract errors due to inconscious mental shortcuts in histological cancer grading.

Acknowledgments The study was supported by a grant of the Swiss Science Foundation (FNS 3220030–120417, to Hans-Anton Lehr and Fred Mast).

Conflict of interest The authors declare that they have no conflict of interest.

Open Access This article is distributed under the terms of the Creative Commons Attribution License which permits any use, distribution, and reproduction in any medium, provided the original author(s) and the source are credited.

References

1. Cattoretti G, Becker MH, Key G et al (1992) Monoclonal antibodies against recombinant parts of the Ki-67 antigen (MIB 1 and MIB 3) detect proliferating cells in microwave-processed formalin-fixed paraffin sections. J Pathol 168:357–363
2. Schmidt M, Hellwig B, Hammad S et al (2012) A comprehensive analysis of human gene expression profiles identifies stromal immunoglobulin κ C as a compatible prognostic marker in human solid tumors. Clin Cancer Res 18:2695–2703
3. Kelly CM, Bernard PS, Krishnamurthy S et al (2012) Agreement in risk prediction between the 21-gene recurrence score assay (Oncotype DX(R)) and the PAM50 Breast Cancer Intrinsic Classifier™ in early-stage estrogen receptor-positive breast cancer. Oncologist 17:492–498
4. Schmidt M, Böhm D, von Törne C et al (2008) The humoral immune system has a key prognostic impact in node-negative breast cancer. Cancer Res 68:5405–5413
5. Bloom HJG, Richardson WW (1957) Histological grading and prognosis in breast cancer. Br J Cancer 11:359–377
6. Elston EW, Ellis IO (1993) Pathological prognostic factors in breast cancer. I. The value of histological grade in breast cancer. Experience from a large study with long-term follow-up. Histopathology 19:403–410
7. Fandel TM, Pfnür M, Schäfer SC et al (2008) Do we truly see what we think we see? The role of cognitive bias in pathological interpretation. J Pathol 216:193–200
8. Bombari D, Mora B, Schaefer SC, Mast F, Lehr HA (2012) What was I thinking? Eyetracking experiments underscore the bias that architecture exerts on nuclear grading in prostate cancer grading. PLoS ONE 7:e38023
9. Matthews S and members of the CFIT-ALAR action group (2000) FSF approach and landing accident reduction briefing note 5.3—visual illusions, Flight Safety Digest 19:103–109 (www.mtc.gob.pe/portal/transportes/aereo/…/fsd_aug-nov00_bn5-3.pdf)
10. Frierson HF Jr, Wolber RA, Berean KW et al (1995) Interobserver reproducibility of the Nottingham modification of the Bloom and Richardson histologic grading scheme for infiltrating ductal carcinoma. Am J Clin Pathol 103:195–198
11. Sikka M, Agarwal S, Bhatia A (1999) Interobserver agreement of the Nottingham histologic grading scheme for infiltrating duct carcinoma breast. Indian J Cancer 36:149–153
12. Meyer JS, Alvarez C, Milikowski C, Olson N et al (2005) Breast carcinoma malignancy grading by Bloom-Richardson system vs proliferation index: reproducibility of grade and advantages of proliferation index. Mod Pathol 18:1067–1078

Virchows Arch (2012) 461:405–417
DOI 10.1007/s00428-012-1279-y

ORIGINAL ARTICLE

Morphological parameters of flat epithelial atypia (FEA) in stereotactic vacuum-assisted needle core biopsies do not predict the presence of malignancy on subsequent surgical excision

Simonetta Bianchi · Benedetta Bendinelli · Isabella Castellano · Quirino Piubello · Giuseppe Renne · Maria Grazia Cattani · Domenica Di Stefano · Giovanna Carrillo · Licia Laurino · Alessandra Bersiga · Carmela Giardina · Stefania Dante · Carla Di Loreto · Carmela Quero · Concetta Maria Antonacci · Domenico Palli · VANCB Study Group

Received: 16 February 2012 / Revised: 26 April 2012 / Accepted: 27 June 2012 / Published online: 1 September 2012
© Springer-Verlag 2012

Abstract Flat epithelial atypia (FEA) may represent the earliest precursor of low-grade breast cancer and often coexists with more advanced atypical proliferative breast lesions such as atypical ductal hyperplasia (ADH) and lobular intraepithelial neoplasia (LIN). The present study aims to investigate the association between morphological parameters of FEA and presence of malignancy at surgical excision (SE) and the clinical significance of the association of FEA

S. Bianchi (✉)
Division of Pathological Anatomy, Department of Medical and Surgical Critical Care, AOU Careggi, University of Florence, Largo G.A. Brambilla 3, 50134 Florence, Italy
e-mail: simonetta.bianchi@unifi.it

B. Bendinelli · D. Palli
Molecular and Nutritional Epidemiology Unit, Cancer Research and Prevention Institute (ISPO), Florence, Italy

I. Castellano
Division of Pathological Anatomy, Department of Biomedical Sciences and Human Oncology, University of Turin, Turin, Italy

Q. Piubello
Pathological Anatomy Unit, OCM, Azienda Ospedaliera Universitaria Integrata di Verona, Verona, Italy

G. Renne
Division of Pathology and Laboratory Medicine, European Institute of Oncology, Milan, Italy

M. G. Cattani
Pathological Anatomy Unit, Bellaria Hospital, Bologna, Italy

D. Di Stefano
Division of Pathological Anatomy, Department of Neurological Sciences, St Andrea Hospital, "La Sapienza" University, Rome, Italy

G. Carrillo
Pathological Anatomy Unit, AORN Cardarelli Hospital, Naples, Italy

L. Laurino
Pathological Anatomy Unit, General Hospital of Treviso, Treviso, Italy

A. Bersiga
Pathological Anatomy Unit, Istituti Ospitalieri di Cremona, Cremona, Italy

C. Giardina
Department of Pathological Anatomy, University of Bari, Bari, Italy

S. Dante
Pathological Anatomy Unit, Hospital of Vicenza, Vicenza, Italy

C. Di Loreto
Division of Pathological Anatomy, Department of Medical and Biological Sciences, University of Udine, Udine, Italy

C. Quero
Department of Pathology, National Cancer Institute Giovanni Paolo II, Bari, Italy

C. M. Antonacci
Pathological Anatomy Unit, Sacco Hospital, Milan, Italy

with ADH and/or LIN. This study included 589 cases of stereotactic 11-gauge vacuum-assisted needle core biopsy (VANCB), reporting a diagnosis of FEA, ADH or LIN with subsequent SE from 14 pathology departments in Italy. Available slides were reviewed, with 114 (19.4 %) showing a malignant outcome at SE. Among the 190 cases of pure FEA, no statistically significant association emerged between clinical–pathological parameters of FEA and risk of malignancy. Logistic regression analyses showed an increased risk of malignancy according to the extension of ADH among the 275 cases of FEA associated with ADH (p=0.004) and among the 34 cases of FEA associated with ADH and LIN (p=0.02). In the whole series, a statistically significant increased malignancy risk emerged according to mammographic R1–R3/R4–R5 categories (OR=1.56; p=0.04), extension (OR=1.24; p=0.04) and grade (OR=1.94; p=0.004) of cytological atypia of FEA. The presence of ADH was associated with an increased malignancy risk (OR=2.85; p<0.0001). Our data confirm the frequent association of FEA with ADH and/or LIN. A diagnosis of pure FEA on VANCB carries a 9.5 % risk of concurrent malignancy and thus warrants follow-up excision because none of the clinical–pathological parameters predicts which cases will present carcinoma on SE.

Keywords Breast · Flat epithelial atypia · Stereotactic vacuum-assisted needle core biopsy · Surgical excision · Malignancy

Introduction

Widespread implementation of mammography screening programmes and the introduction of digital mammography in the pre-clinical diagnosis of breast lesions have led to an increasing number of core biopsies (CB) performed for non-palpable nodules and microcalcifications. In the diagnostic assessment of microcalcifications, stereotactic 11-gauge vacuum-assisted needle core biopsy (VANCB) has a lower underestimation rate for malignancy than stereotactic 14-gauge needle core biopsy (NCB) [1]. On CB performed for indeterminate or suspicious microcalcifications, a lesion designated as flat epithelial atypia (FEA) is frequently diagnosed.

FEA, for which the term ductal intraepithelial neoplasia grade 1a (DIN1a) is also used, was introduced by the World Health Organization (WHO) Working Group on the Pathology and Genetics of Tumors of the Breast [2] with the aim of unifying columnar cell lesions with low-grade of cytological atypia, characteristically without complex architectural atypia in the form of arcades, bars, Roman bridges, tufts or micropapillae that are essential in distinguishing this lesion from atypical ductal hyperplasia (ADH or DIN1b). For FEA, a variety of terms has been proposed [3]. Azzopardi [4] introduced the term clinging carcinoma in situ for this lesion, which can be mistaken for either normal breast tissue or fibrocystic breast change.

Although the biological and clinical significance of FEA is still far from completely understood, emerging histological and molecular evidence suggests that FEA may represent the earliest morphologically identifiable non-obligatory precursor of low-grade breast cancer [5, 6]. In fact, FEA often coexists with more advanced atypical proliferative breast lesions such as ADH and atypical lobular hyperplasia (LIN1/ALH) or low-grade ductal carcinoma in situ (DCIS, particularly micropapillary and cribriform type), lobular carcinoma in situ (LIN2/LCIS), tubular carcinoma and invasive lobular carcinoma (ILC) [7–12]. Otherwise, the possibility that columnar cell lesions in general and FEA in particular significantly elevate breast cancer risk is at the moment not well supported [13, 14].

From a clinical point of view, a diagnosis of FEA on CB, pure or in association with more advanced atypical proliferative breast lesions, impacts on the management of these patients. Based on the underestimated malignancy rates of patients with a CB diagnosis of FEA, the prevailing recommendation remains surgical excision (SE) [15].

The aims of our study were to evaluate: (1) if morphological parameters of pure FEA can predict malignancy (DCIS or invasive carcinoma) in subsequently performed SE, (2) the frequency of association of FEA with more advanced atypical proliferative breast lesions such as ADH and/or lobular intraepithelial neoplasia (LIN) and (3) the clinical significance of ADH and or LIN associated with FEA in terms of finding DCIS or invasive carcinoma in subsequently performed SE.

Materials and methods

The study population of a large Italian multi-institutional series of stereotactic VANCB, performed using an 11-gauge stereotactic vacuum-assisted device (Mammotome®, Ethicon Endo-Surgery, Breast Care, Norderstedt, Germany), has been previously reported [1]. Of 22 institutions participating in that study, 14 agreed to proceed with a histological review of all VANCB and SE specimens: eight from Northern Italy, three from Central Italy and three from Southern Italy. Institutional review board approvals were obtained for the study from each participating centre.

Pathology departments participating in the study were asked to retrieve from their archival files all available slides of consecutive B3 cases from VANCB specimens related to the study period [1] and reported in the original histological diagnosis as FEA, atypical epithelial proliferation of ductal type/ADH and LIN. In all participating pathology departments, once a

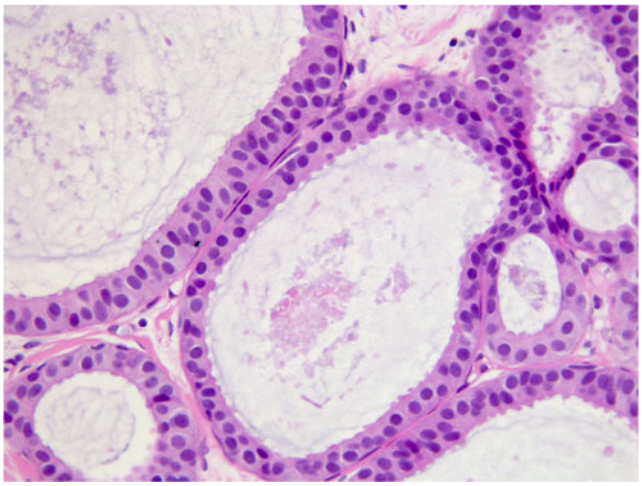

Fig. 1 Pure flat epithelial atypia: dilated acinar unit lined by a single cell layer of columnar epithelial cells that show mild cytological atypia characterized by relatively round and monotonous nuclei

diagnosis of FEA was considered, at least three additional levels of sectioning of VANCB, generally taken approximately at 25 μm apart, were routinely performed in view of the possibility of coexisting more advanced atypical proliferative breast lesions such as ADH and LIN1/ALH. Only VANCB cases with subsequent SE were included in this study.

Radiology departments participating in the study were asked to provide for each case the age of patient, mammographic pattern (microcalcifications versus other patterns), mammographic category according to BI-RADS (Breast Imaging Reporting and Data System) five-point (R1-R5) classification system [16], number of tissue cores obtained (12, 13–20, 21+) and presence of residual microcalcifications on post-stereotactic VANCB radiograms.

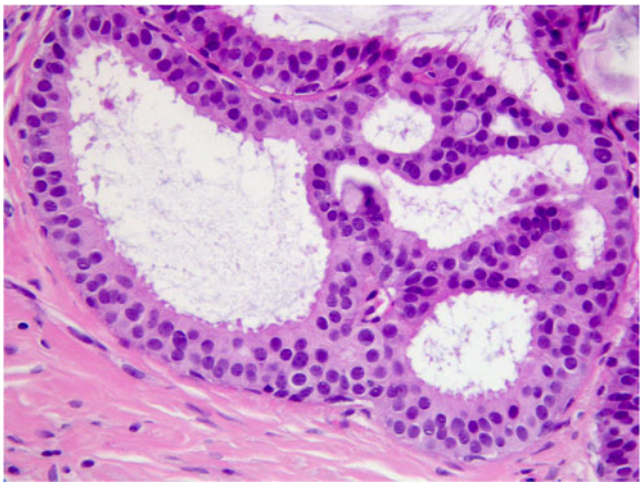

Fig. 3 Atypical ductal hyperplasia arising in a background of flat epithelial atypia: part of the acinus is lined by only a few layers of atypical cells (*left*); on the *right*, the acinus shows a more complex architectural atypia with formation of bridges and fenestrations. Atypical ductal hyperplasia is composed of cells cytologically identical to those in the areas of flat epithelial atypia

An electronic spreadsheet to record clinical, radiological and histological data was used. Each pathologist participating in the study reviewed all haematoxylin & eosin (H&E) and immunohistochemically stained slides, when routinely obtained, of his/her own VANCB cases. The following morphological parameters were evaluated: (a) presence of determinant microcalcifications within the index lesion, (b) presence of unrelated microcalcifications, (c) patterns of FEA (cystically dilated glands, blunt duct adenosis (BDA) resembling pattern on low power, presence of apocrine features as reported by Kunju et al. [11]), (d) grade of cytological atypia of FEA: mild atypia (characterized by relatively round or ovoid rather than elongated nuclei with

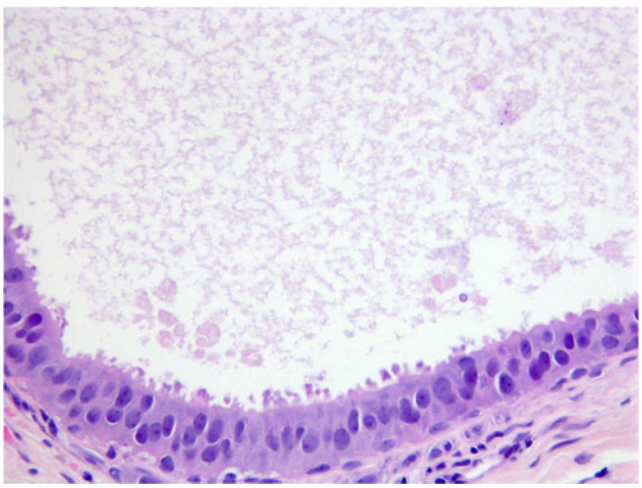

Fig. 2 Pure flat epithelial atypia formed from columnar cells showing mild (*left* and *right*) to moderate (*centre*) nuclear atypia with an increased nuclear–cytoplasmic ratio

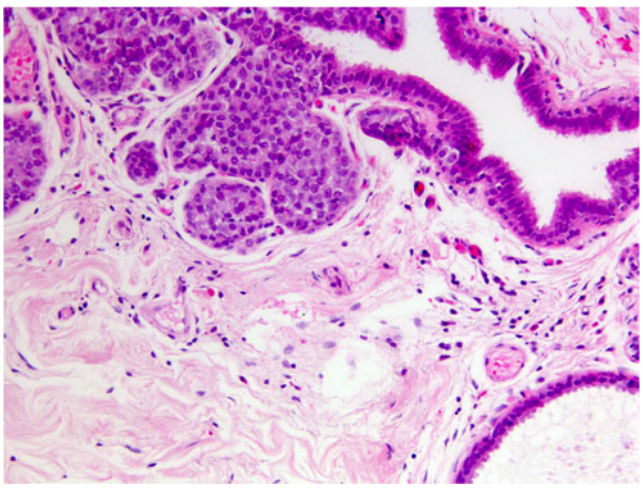

Fig. 4 Terminal duct lobular unit concurrently affected by lobular intraepithelial neoplasia (*left*), columnar cell change (*centre* and *right*) and flat epithelial atypia (*lower right*)

Table 1 Distribution of the final histological outcomes after surgical excision and percentages of malignancy according to the VANCB-reviewed histological diagnoses among 589 study cases of pure or associated FEA. Heterogeneity p value <0.0001

Mention of FEA at VANCB	Diagnosis at surgical excision				Total
	Benign, *N*	Atypia, *N*	Malignancy		
			N	%	
Pure FEA	73	99	18	9.5	190 (32.2 %)
FEA + ADH	72	128	75	27.3	275 (46.7 %)
FEA + LIN	17	60	13	14.4	90 (15.3 %)
FEA + ADH + LIN	5	21	8	23.5	34 (5.8 %)
Total	167 (28.4 %)	308 (52.3 %)	114 (19.4 %)		589 (100 %)

a slight increase in the nuclear/cytoplasmic ratio, finely dispersed chromatin or slight margination of chromatin, variably prominent nucleoli and loss of polarity) or moderate atypia (characterized by enlarged, more oval nuclei with cytologically atypical features including mild to moderate pleomorphism, prominent nucleoli, some clumping of chromatin and increased nuclear/cytoplasmic ratio) as described by Pinder et al. [17, 18], (e) patterns of ADH (cribriform, micropapillary, solid or with presence of apocrine features) according to Kunju et al. [11], (f) patterns of LIN (LIN1/ALH or LIN2/LCIS), (g) presence of chronic inflammation and (h) presence of stromal changes including fibrosis and myxoid change.

FEA was diagnosed according to strict morphological criteria [2, 19]: variably distended acini lined by one to several layers of monotonous, mildly or moderately atypical, cuboidal to columnar cells growing in an exclusively flat pattern in the complete absence of architecturally atypical intraluminal proliferations. The presence of a single atypical intraluminal structure as arcade, bar, Roman bridge, tuft or micropapillary formation was considered enough for a diagnosis of FEA associated with concomitant ADH.

ADH was diagnosed using combined histological and cytological criteria as established by Page and Rogers [20]: a proliferative lesion that fulfils some but not all qualitative criteria for a diagnosis of intraductal carcinoma, i.e. evenly spaced cells with hyperchromatic nuclei coexisting with patterns of usual ductal hyperplasia or columnar cell changes, producing a partial involvement of glandular structure by neoplastic cells. In CB histology, technical issues hamper the application of quantitative criteria in diagnosing ADH [21].

In the histological revision, LIN was subdivided into atypical lobular hyperplasia (LIN1/ALH) and lobular carcinoma in situ (LIN2/LCIS). LIN1/ALH was defined by filling and distension of fewer than half of the terminal duct units of a lobule with uniform small dyscohesive cells, evenly spaced, with round nuclei and minimal pleomorphism. LIN2/LCIS was diagnosed when more than half of the acini in the terminal duct units were completely filled or distended [22]. The presence of a single lobule with morphological characteristics of LIN1 or LIN2 was considered sufficient for a diagnosis of FEA associated with LIN. The extent of involvement was determined by evaluating the number of large ducts and/or terminal duct lobular units affected by FEA, ADH and LIN as described by Ely et al. [23] and Wagoner et al. [24]. Cases were divided according the number of foci affected in: (a) cases confined to one focus, (b) cases limited to two foci, (c) cases limited to three foci and (d) cases with four or more foci. The reviewed VANCB final diagnoses were coded into seven categories as follows: pure FEA, pure ADH, pure LIN, FEA + ADH, FEA + LIN, ADH + LIN, FEA + ADH + LIN.

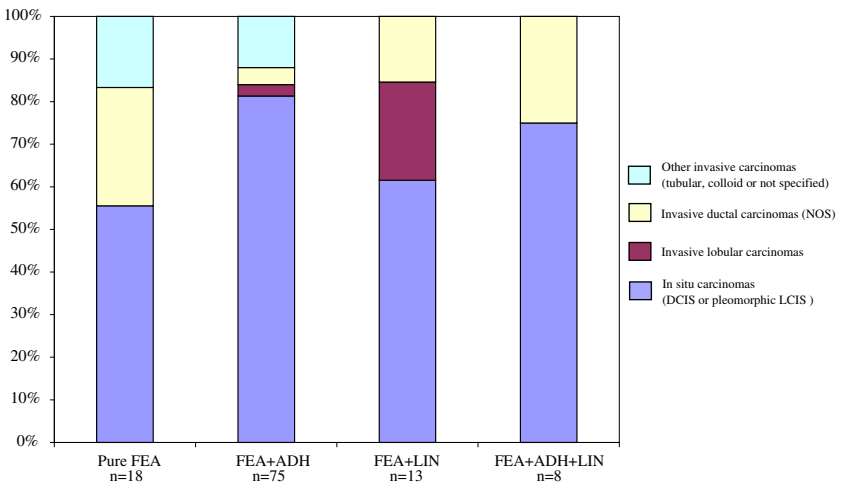

Fig. 5 Percentage distribution of the histological types and grade (nuclear grade for DCIS and histological grade for invasive carcinomas) of malignancies, as diagnosed at surgical excision, according to VANCB diagnosis

Table 2 Distribution of 190 patients with a VANCB diagnosis of pure FEA according to the final histological outcome at surgical excision (malignancy yes/no) and several FEA-related variables. ORs from logistic analyses (95 % CIs and *p* values) for each variable as estimate of malignant breast cancer risk are also reported based on a model including terms for age and grade of cytological atypia of FEA

		Malignancy at surgical excision			Logistic analysis		
		Yes	No	*p* value	OR	95 % CI	*p*
Mammographic category[a]	R2–R3	8	105		1		
	R4–R5	10	67	0.17	2.15	0.78–5.77	0.14
Mammographic pattern	Microcalcifications[b]	18	167				
	Other	0	5	1.00[c]	–	–	–
Determinant microcalcifications	Yes	15	158		1		
	No	3	14	0.21[c]	2.57	0.64–10.43	0.19
Number of cores	12	3	33				
	13–20	14	135				
	>20	1	4	0.52[c]	1.14[d]	0.34–3.81	0.83
Chronic inflammation	Yes	2	21		1		
	No	16	151	1.00[c]	1.33	0.82–6.39	0.72
Stromal changes	Yes	6	63		1		
	No	12	109	0.78	1.40	0.49–4.01	0.53
Pattern of FEA	BDA resembling pattern (reference)	7	52		1		
	Cystically dilated glands	11	105		–	–	–
	Apocrine features	0	15	0.46[c]	–	–	–
FEA with apocrine features	Yes	0	15		1		
	No	18	157	0.37[c]	–	–	–
Extension of FEA	1 focus	3	36				
	2 foci	2	40				
	3 foci	6	44				
	4+ foci	7	52	0.59[c]	1.23[d]	0.78–1.94	0.37
Extension of FEA (dichotomous)	1–2 foci	5	76		1		
	3+ foci	13	96	0.18	1.99	0.67–5.91	0.21
Cytological atypia of FEA	Mild grade	9	123		1		
	Moderate grade	9	49	0.06	2.41	0.90–6.45	0.08

[a] R2 mammographic category was reported in 1 case (0.5 %) and R5 mammographic category was reported in 4 cases (2.1 %)

[b] In 48 cases (25.9 %), complete removal of microcalcifications was obtained; among them, two cases of malignancy were assessed at surgical excision

[c] *p* values from Fisher exact tests

[d] Variable included as an ordinal term in the logistic model.

In each pathology department participating in the study, histology reports and slides of subsequent SE were collected. Each local pathologist reviewed all H&E slides of subsequent SE of his/her VANCB cases included in the study and reported them as: (a) malignant lesions specifying histotype, histological grade, size and lymph node status for invasive carcinoma, nuclear grade and size for DCIS and size for pleomorphic lobular carcinoma in situ, (b) atypical lesions specifying if FEA, ADH, ALH, LCIS were pure or in association and (c) benign lesions. Pathologists were asked to select for each VANCB case one or more representative H&E-stained slides and, where appropriate, IHC-stained slides of the lesion to be reviewed jointly by the panel of 14 pathologists participating in the study. The selected slides of all VANCB cases included in the study were reviewed during a meeting organized at the Division of Pathological Anatomy of the University of Florence in September 2010 to obtain concordance on the diagnosis on each VANCB. Slides were reviewed using the Leica

Table 3 Frequency of several FEA- and ADH-related variables among 275 patients with a VANCB diagnosis of combined FEA and ADH according to histological outcome at surgical excision (malignant yes/no). ORs from logistic analyses (95 % CIs and *p* values) for each variable as estimate of malignant breast cancer risk are also reported

		Malignancy at surgical excision			Logistic analysis		
		Yes	No	*p* value	OR[b]	95 % CI	*p*
Mammographic category[a]	R3	31	102		1		
	R4–R5	44	98	0.15	1.52	0.86–2.68	0.15
Mammographic pattern	Microcalcifications[d]	75	193		1		
	Other	0	7	0.20[e]	–	–	–
Determinant microcalcifications	Yes	96	188		1		
	No	6	12	0.59[e]	1.54	0.51–4.69	0.45
Number of cores	12	11	33				
	13–20	62	158				
	>20	2	8	0.81[e]	0.91[c]	0.46–1.79	0.78
Chronic inflammation	Yes	15	36		1		
	No	60	164	0.70	0.83	0.40–1.71	0.61
Stromal changes	Yes	29	74		1		
	No	46	126	0.80	0.95	0.53–1.71	0.87
Pattern of FEA	BDA resembling pattern (reference)	28	83		1		
	Cystically dilated glands	45	114		1.15	0.64–2.06	0.64
	Apocrine features	2	3	0.68[e]	2.83	0.40–20.21	0.30
FEA with apocrine features	Yes	2	3		1	0.06–2.24	0.27
	No	73	197	0.62[e]	0.38	0.06–2.66	0.33
Extension of FEA	1 focus	8	34				
	2 foci	14	53				
	3 foci	15	38				
	4+ foci	38	75	0.16	1.17[c]	0.88–1.56	0.28
Extension of FEA (dichotomous)	1–2 foci	22	87		1		
	3+ foci	53	113	0.03	1.35	0.71–2.56	0.36
Cytological atypia of FEA	Mild grade	45	138		1		
	Moderate grade	30	62	0.16	1.50	0.84–2.67	0.17
Pattern ADH	Cribriform (reference)	31	103		1		
	Micropapillary	41	86		1.72	0.97–3.07	0.06
	Solid	2	7		1.07	0.20–5.67	0.94
	Apocrine features	1	4	0.40[e]	1.24	0.13–12.4	0.85
ADH with apocrine features	Yes	1	4		1		
	No	74	196	1.00[e]	2.69	0.21–34.56	0.45
Extension of ADH	1 focus	15	64				
	2 foci	22	66				
	3 foci	13	38				
	4+ foci	25	32	0.01	1.45[c]	1.12–1.86	0.004
Extension of ADH (dichotomous)	1–2 foci	37	130		1		
	3+ foci	38	70	0.02	1.85	1.06–3.23	0.03

[a] R5 mammographic category was reported in six (2.2 %) cases, while no cases were reported as R2 mammographic category

[b] Adjusted for age, grade of cytological atypia of FEA, pattern of ADH, extension of ADH

[c] Variable included as an ordinal term in the logistic model

[d] In 50 (18.7 %) cases, complete removal of microcalcifications was obtained; among them, five cases of malignancy were assessed after surgical excision

[e] *p* values from Fisher exact test

DMD108 digital microscope (Leitz Microsystems, Wetzlar, Germany) connected to a high-resolution data projector. In cases for which concordance was not reached, a majority diagnosis was established. No information about SE follow-up was provided during the panel revision. For the present analyses, only cases with a VANCB diagnosis of FEA (pure FEA, FEA + ADH, FEA + LIN, FEA + ADH + LIN) were considered.

Statistical analysis

The distribution of the histological diagnoses reported for the 859 VANCB specimens was calculated. The distribution of the histological diagnoses after SE (benign, atypical or malignant lesion) was also established as well as the percentage of cases with malignancy (according to each specific diagnosis at VANCB).

For all cases with a diagnosis of FEA (pure or associated with other lesions), the distribution according to the following variables was calculated: mammographic category (R2–R3, R4–R5), mammographic pattern (microcalcifications, other), determinant microcalcifications (yes, no), number of cores (12, 13–20, >20), chronic inflammation (yes/no), stromal changes (yes/no), pattern of FEA (blunt duct adenosis resembling pattern, cystically dilated glands, apocrine features), extension of FEA (one focus, two foci, three foci, four foci or more), grade of cytological atypia of FEA (mild, moderate), pattern of ADH (cribriform, micropapillary, solid or with presence of apocrine features), extension of ADH (one focus, two foci, three foci, four foci or more), pattern of LIN (ALH/LIN1 or LCIS/LIN2), extension of LIN (one focus, two foci, three foci, four foci or more). *P* values from chi-square test or Fisher exact test were also calculated. Mean age at VANCB diagnosis according to malignant outcome (*p* values from between-mean comparison *t* tests) was also calculated. Logistic regression models were used to compute odd ratios (ORs) and 95 % confidence intervals (95 % CIs) for each FEA-related variable as estimate of malignant breast cancer risk. Logistic regression analyses were performed separately for a diagnosis on VANCB of pure FEA, of FEA + ADH, of FEA + LIN and of FEA + ADH + LIN. Logistic models were adjusted for age at VANCB diagnosis of the cases, grade of cytological atypia of FEA, pattern and extension of ADH or LIN or both, respectively.

Logistic regression analyses were also performed for all cases including a VANCB diagnosis of FEA (pure FEA or FEA + ADH or FEA + LIN or FEA + ADH + LIN). Logistic models were adjusted for age at VANCB diagnosis, grade of cytological atypia of FEA and co-presence of ADH or LIN.

Results

A total of 859 histologically reviewed VANCB cases with a subsequent SE were available including pure FEA (Figs. 1 and 2) (*N*=190, 22.1 %), pure LIN (*N*=149, 17.3 %), pure ADH (*N*=108, 12.6 %), FEA associated with ADH (Fig. 3) (*N*=275, 32.0 %), FEA associated with LIN (Fig. 4) (*N*=90, 10.5 %), ADH associated with LIN (*N*=13, 1.5 %) and FEA associated with both ADH and LIN (*N*=34, 4.0 %).

Of 589 (68.6 %) cases with FEA (190 pure FEA and 399 FEA associated with ADH or LIN or ADH + LIN), 167 (28.3 %) had a benign, 308 (52.3 %) an atypical (including LIN1 and LIN2) and 114 (19.4 %) a malignant outcome diagnosed on subsequent SE. A total of 18 malignancies among pure FEA, 75 malignancies among FEA + ADH, 13 malignancies among FEA + LIN and 8 malignancies among FEA + ADH + LIN were diagnosed on SE, resulting in underestimation rates of 9.5, 27.3, 14.4 and 23.5 % respectively (Table 1; heterogeneity *p* value <0.0001). As shown in Fig. 5, DCIS was the most frequent malignancy at SE among all the types of VANCB diagnosis. The median age of patients with pure FEA was 50.7 years, 51.9 years for FEA + ADH, 49.9 years for FEA + LIN and 52.6 years for FEA + ADH + LIN (data not shown).

In Tables 2, 3, 4 and 5, the distribution of cases with a VANCB diagnosis of pure FEA, FEA + ADH, FEA + LIN and FEA + ADH + LIN, respectively, according to malignancy upon SE, and several FEA and/or ADH and/or LIN-related variables is reported together with the results of multivariate analyses. The risk of malignancy in women with moderate cytological atypia showed a trend towards being increased (Table 2) compared with that of women with mild cytological atypia (χ^2 test, p=0.06). The suggestion was confirmed by logistic regression analysis (OR 2.41; p=0.08). The suggestion that complete removal of microcalcifications was less frequently associated with malignancy (two cases out of 48 or 4.2 % showing malignancy at surgery) than incomplete removal was not statistically significant (16 out of 142 or 11.3 %).

In Table 3 (FEA + ADH), an increased risk of malignancy according to the extension of ADH emerged in a model adjusted for age, grade of cytological atypia of FEA and pattern of ADH (OR 1.45, *p* value 0.004). In Table 4 (FEA + LIN), an increased risk of malignancy in patients with a moderate grade of cytological atypia of FEA compared to patients with a mild grade of cytological atypia emerged (OR 5.22, *p* value 0.03). In Table 5 (FEA + ADH + LIN), an increased risk of malignancy according to the extension of ADH emerged (OR 6.71, *p* value 0.02).

According to Table 6, women in the mammographic category R4–R5 had an increased risk of malignancy compared with those in R2–R3 category (OR 1.56, 95 % CI

Table 4 Frequency of several FEA- and LIN-related variables among 90 patients with a VANCB diagnosis of FEA associated with L IN according to histological outcome at surgical excision (malignant yes/no). ORs from logistic analyses (95 % CIs and *p* values) for each variable as estimate of malignant breast cancer risk are also reported

		Malignancy at surgical excision			Logistic analysis		
		Yes	No	*p* value	OR[b]	95 % CI	*p*
Mammographic category[a]	R3	6	42		1		
	R4–R5	7	35	0.57	1.58	0.42–5.95	0.5
Mammographic pattern	Microcalcifications[d]	11	73		1		
	Other	2	4	0.21[e]	4.57	0.61–34.52	0.14
Determinant microcalcifications	Yes	12	58		1		
	No	1	9	0.28[e]	0.16	0.02–1.63	0.12
Number of cores	12	2	7				
	13–20	9	63				
	>20	23	7	0.47[e]	1.70[c]	0.32–9.20	0.54
Chronic inflammation	Yes	3	7		1		
	No	10	70	0.15[e]	0.38	0.07–2.08	0.27
Stromal changes	Yes	4	28		1		
	No	9	49	0.77[e]	1.06	0.25–4.46	0.94
Pattern of FEA	BDA resembling pattern (reference)	2	29		1		
	Cystically dilated glands	8	48		3.52	0.61–20.35	0.16
	Apocrine features	3	0	0.002[e]	–	–	–
FEA with apocrine features	Yes	3	0		1	–	–
	No	10	77	0.002[e]	–	–	–
Extension of FEA	1 focus	6	27				
	2 foci	1	21				
	3 foci	2	12				
	4+ foci	4	17	0.50[e]	0.92[c]	0.53–1.58	0.75
Extension of FEA (dichotomous)	1-2 foci	7	48		1		
	3+ foci	6	29	0.56	1.06	0.29–3.85	0.93
Cytological atypia of FEA	Mild grade	9	70		1		
	Moderate grade	4	7	0.05[e]	5.22	1.16–23.53	0.03
Pattern of LIN	LIN1/ALH	10	42		1		
	LIN2/LCIS	3	35	0.22[e]	0.38	0.09–1.53	0.17
Extension of LIN	1 focus	3	22				
	2 foci	3	19				
	3 foci	3	14				
	4+ foci	4	22	0.98[e]	1.26[c]	0.73–2.19	0.41
Extension of LIN (dichotomous)	1–2 foci	6	41		1		
	3+ foci	7	36	0.64	1.58	0.45–5.58	0.48

[a] R5 mammographic category was reported in one (1.1 %) case, while no cases were reported as R2 mammographic category

[b] Adjusted for age, cytological atypia of FEA, pattern of LIN, extension of LIN

[c] Variable included as an ordinal term in the logistic model.

[d] In 17 (20.2 %) cases, complete removal of microcalcifications was obtained; among them, no cases of malignancy were assessed after surgical excision

[e] *p* values from Fisher exact tests

Table 5 Frequency of several FEA-, ADH- and LIN-related variables among 34 patients with a VANCB diagnosis of FEA associated with ADH and LIN according to histological outcome after surgical excision (malignant yes/no). ORs from logistic analyses (95 % CIs and *p* values) for each variable as estimate of malignant breast cancer risk are also reported

		Malignancy at surgical excision			Logistic analysis		
		Yes	No	*p* value	OR[b]	95 % CI	*p*
Mammographic category[a]	R3	4	12		1		
	R4	4	14	1.00[e]	1.51	0.08–28.34	0.78
Mammographic pattern	Microcalcification[d]	8	25		1		
	Other	0	1	1.00	–	–	–
Determinant microcalcifications	Yes	7	19		1		
	No	1	7	0.64[e]	2.89	0.09–89.38	0.54
Number of cores	12	1	3				
	13–20	6	21				
	>20	1	2	1.00[e]	0.85[c]	0.09–7.97	0.88
Chronic inflammation	Yes	1	1		1		
	No	7	25	0.42[e]	1.09	0.003–474.86	0.98
Stromal changes	Yes	3	5		1		
	No	5	21	0.36[e]	0.05	0.001–2.23	0.12
Pattern of FEA	BDA-resembling pattern (reference)	3	8		1		
	Cystically dilated glands	4	16		0.47	0.02–10.90	0.64
	Apocrine features	1	2	0.72[e]	–	–	–
Apocrine features of FEA	Yes	1	2		1		
	No	7	24	1.00[e]	0.06	0.001–3.40	0.17
Extension of FEA	1 focus	2	8				
	2 foci	0	7				
	3 foci	1	2				
	4+ foci	5	9	0.31[e]	0.59[c]	0.16–2.19	0.43
Extension of FEA (dichotomous)	1–2 foci	2	15		1		
	3+ foci	6	11	0.22[e]	0.60	0.03–10.36	0.72
Cytological atypia of FEA	Mild grade	5	22		1		
	Moderate grade	3	4	0.32[e]	1.35	0.11–17.24	0.82
Pattern ADH	Cribriform (reference)	3	11		1		
	Micropapillary	3	10		4.79	0.14–170.30	0.39
	Solid	1	1		–	–	–
	Apocrine features	1	4	0.85[e]	–	–	–
Apocrine features of ADH	Yes	1	4		1		
	No	7	22	1.00[e]	0.16	0.01–4.29	0.27
Extension of ADH	1 focus	2	15				
	2 foci	0	6				
	3 foci	1	2				
	4+ foci	5	3	0.02[e]	6.71[c]	1.30–34.77	0.02
Extension of ADH (dichotomous)	1–2 foci	2	21		1		
	3+ foci	6	5	0.007[e]	86.38	2.26–>999.9	0.02

Table 5 (continued)

		Malignancy at surgical excision			Logistic analysis		
		Yes	No	*p* value	OR[b]	95 % CI	*p*
Pattern of LIN	LIN1/ALH	3	16		1		
	LIN2/LCIS	5	10	0.42[e]	3.12	0.33–29.64	0.32
Extension of LIN	1 focus	1	6				
	2 foci	3	6				
	3 foci	0	5				
	4+ foci	4	9	0.51[e]	0.46[c]	0.13–1.61	0.23
Extension of LIN (dichotomous)	1–2 foci	4	12		1		
	3+ foci	4	14	1.00[e]	0.04	0.001–1.68	0.09

[a] No cases were reported as R2 or R5 mammographic category

[b] Adjusted for age, cytological atypia of FEA, pattern of ADH, extension of ADH, pattern of LIN, extension of LIN

[c] Variable included as an ordinal term in the logistic model.

[d] In 12 (36.4 %) cases, complete removal of microcalcifications was obtained; among them, two cases of malignancy were assessed after surgical excision

[e] *p* values from Fisher exact tests

1.01–2.39, *p* value 0.04). Women with an extension of FEA of three foci or more had an increased risk of malignancy compared with those with one or two foci (OR 1.73, 95 % CI 1.10–2.73, *p* value 0.02). Women with moderate grade of cytological atypia had an increased risk of malignancy compared with those with mild grade of cytological atypia (OR 1.94, 95 % CI 1.24–3.04, *p* 0.004). While the association of LIN with FEA at VANCB (FEA + LIN or FEA + ADH + LIN) did not modulate the risk of a malignant outcome, the association of ADH (FEA + ADH or FEA + ADH + LIN) was a strong predictor of malignancy at SE (OR 2.85, 95 % CI 1.78–4.58, $p<0.0001$). The mean age of women with malignancy at SE was significantly higher than that of women with a non-malignant outcome (53.4 vs 50.7 years, $p=0.001$).

Discussion

Our study, although limited by its retrospective design, to the best of our knowledge, represents the largest series published to date of FEA, pure or in association with more advanced lesions such as ADH and or LIN, diagnosed on stereotactic 11-gauge VANCB with subsequent follow-up surgical excision. It may contribute to the assessment of the clinical and biological significance of pure FEA and to the management of patients with VANCB diagnosis of pure FEA. All VANCB cases were histologically reviewed and diagnoses were agreed by the panel of 14 pathologists participating in the study using non-ambiguous terminology [25, 26].

Pure FEA

On CB performed for indeterminate or suspicious microcalcifications, a lesion designated as flat epithelial atypia is increasingly recognized and diagnosed [1]. The preoperative histological diagnosis of FEA poses a management dilemma for the clinician. Although there is no definitive agreement at present on the clinical management of FEA (underestimation rates for CB diagnosis of pure FEA reported in the literature vary from 0 to 67 % [13]), the currently prevailing recommendation is that it warrants follow-up surgical excision [1, 27]. A few studies in the published literature support the follow-up observation for the management of pure FEA [26, 28, 29]. A recent review [15] reported a pooled underestimation rate of 12 % for FEA in VANCB (in good agreement with our 12.7 % [1]) compared to 17 % in studies restricted to NCB (difference not statistically significant). Consequently, the authors concluded that surgical excision should be considered. On the other hand, the data reported mostly concern small series (range 1–60 cases), partly published only in abstract form, mostly lacking standardized terminology (including pure FEA and FEA with ADH and or LIN). No single or a combination of clinical, radiological or pathological criteria clearly identified a subset of pure FEA cases at low risk of malignancy. Thus, our results and other recent data [27] justify the conclusion that the presence of pure FEA on VANCB warrants follow-up excision.

The identification of FEA also poses a diagnostic challenge to the pathologist, particularly in CB, because FEA with mild cytological atypia may be subtle and care should be taken not to overlook the lesion or to

Table 6 Frequency of several FEA-related variables among 589 patients with a mention of FEA in the VANCB diagnosis (pure FEA or FEA associated with ADH or LIN or ADH + LIN) according to histological outcome after surgical excision (malignant yes/no). ORs from logistic analyses (95 % CIs and *p* values) for each variable as estimate of malignant breast cancer risk are also reported

		Malignancy at surgical excision			Logistic analysis		
		Yes	No	*p* value	OR[b]	95 % CI	*p*
Mammographic category[a]	R2–R3	49	261		1		
	R4-R5	65	214	0.02	1.56	1.01–2.39	0.04
Mammographic pattern	Microcalcifications[d]	112	458		1		
	Other	2	17	0.55[e]	0.55	0.12–2.52	0.44
Determinant microcalcifications	Yes	103	423		1		
	No	11	52	0.69	1.01	0.49–2.10	0.98
Pattern of FEA	BDA-resembling pattern (reference)	40	172		1		
	Cystically dilated glands	68	283		1.18	0.75–1.86	0.48
	Apocrine features	6	20	0.88	1.90	0.68–5.29	0.22
Apocrine features of FEA	Yes	6	20		1		
	No	108	455	0.62	0.59	0.22–1.56	0.28
Extension of FEA	1 focus	19	105				
	2 foci	17	121				
	3 foci	24	96				
	4+ foci	54	153	0.01	1.24[c]	1.02–1.50	0.04
Extension of FEA (dichotomous)	1–2 foci	36	226		1		
	3+ foci	78	249	0.002	1.73	1.10–2.73	0.02
Cytological atypia of FEA	Mild grade	68	353		1		
	Moderate grade	46	122	0.02	1.94	1.24–3.04	0.004
Number of cores	12	17	76				
	13–20	91	377				
	>20	6	21	0.9	1.05[c]	0.63–1.74	0.85
Chronic inflammation	Yes	21	65		1		
	No	93	410	0.2	0.79	0.44–1.39	0.41
Stromal changes	Yes	42	170		1		
	No	72	305	0.83	0.96	0.61–1.49	0.84
Association with ADH	Yes	83	226		1		
	No	31	249	<0.0001	2.85	1.78–4.58	<0.0001
Association with LIN	Yes	21	103		1		
	No	93	372	0.44	1.32	0.75–2.33	0.34

[a] R2 mammographic category was reported in one (0.2 %) case and R5 mammographic category was reported in 11 (1.9 %) cases

[b] Adjusted for age, cytological atypia of FEA, co-presence of ADH and/or LIN

[c] Variable included as an ordinal term in the logistic model.

[d] In 127 (22.3 %) cases, complete removal of microcalcifications was obtained; among them, nine cases of malignancy were assessed after surgical excision

[e] *p* values from Fisher exact tests

over-diagnose it and reporting as atypical any columnar cell lesion [17, 18].

Our results confirm previous reports [11, 25–27] that almost all patients (185/190, 97.4 %) with pure FEA are

asymptomatic and that microcalcifications are the main determinant in 91 % (173/190) of cases. As earlier studies reported [11], we found moderate to severe chronic inflammation in 12 % of pure FEA cases (23/190) and stromal changes, including myxoid change and fibrosis in 36.3 % (69/190), of which the significance remains to be clarified.

FEA associated with ADH

Although FEA may occur as pure lesion, a large proportion (275/589 or 46.7 %) is associated with ADH, in agreement with earlier reports [11, 12, 26, 27, 30]. The association of FEA with ADH has an important impact on clinical management as for ADH on CB the need for surgical excision is unanimously recognized [31]. The positive predictive value for malignancy of FEA associated with ADH on CB significantly increases when compared to that of pure FEA [11, 26]. We found that 27.3 % (75/275) of FEA associated with ADH showed a malignancy at follow-up SE. Our study confirms the strong association between FEA and ADH on CB. Our data, together with data from other observational [26] and molecular studies [5–6] support the hypothesis that FEA represents the earliest precursor of low-grade ductal carcinoma, both in situ and invasive [19].

FEA associated with LIN

Some investigators have reported the coexistence of FEA and LIN in the same surgical specimen, particularly in cases of tubular carcinoma [7, 32, 33]. Recently, Abdel-Fatah et al. [8] found that columnar cell lesions, predominantly FEA, and LIN coexist in 60 % of cases of ILC, suggesting that the loss of E-cadherin expression may switch on the development of lobular differentiation, and proposed an evolutionary pathway of ILC through columnar cell lesions on the basis of histological evidence and common genetic changes.

We found FEA associated with LIN in 15.3 % (90/589) of cases, in agreement with data reported by Levoue et al. [27], which results in a malignancy underestimation rate of 14.4 %.

FEA associated with ADH and LIN

In 5.8 % (34/589) of our cases, we found FEA associated both with ADH and LIN, resulting in an underestimation rate of malignancy of 23.5 %, which is closer to the underestimation rate of FEA + ADH (27.3 %) than that of FEA + LIN (14.4 %). This indicates that ADH determines the natural history of the lesion. In FEA associated with both ADH and LIN, the extension of ADH seems to be strongly associated with the risk of malignancy.

Taken together, in our series 19.4 % (114/589) of cases with a mention of FEA (pure FEA and/or FEA associated to ADH and/or LIN) showed a malignancy at subsequent SE. The risk of malignancy increased along with the mammographic category, the extension of FEA and the grade of cytological atypia of FEA, while the association with ADH was a strong predictor of malignancy. The median age of patients with pure FEA was slightly younger than that of patients with FEA + ADH and FEA + ADH + LIN (50.7, 51.9 and 52.6 years, respectively) but slightly older compared to those with FEA + LIN (49.9 years, as reported earlier) [11, 26].

Conclusion

None of the studied parameters of pure FEA can predict the risk of malignancy in a subsequent SE. A trend was found only for the grade of cytological atypia (mild versus moderate) and incomplete removal of microcalcifications.

In FEA associated with ADH or ADH and LIN, the risk of malignancy increases along with increasing extension of ADH. In FEA associated with LIN, the risk of malignancy is higher in case of moderate cytological atypia of FEA. The risk of malignancy in FEA increased according to mammographic category, extension of FEA and grade of cytological atypia of FEA.

A diagnosis of pure FEA on VANCB warrants SE because, on the basis of clinical–pathological parameters, it is impossible to predict which cases are associated with carcinoma. The absence of residual microcalcifications on post-VANCB mammography does not exclude the presence of an associated malignancy at SE: we found malignancy in 4 % (2/48), 10 % (5/50) and 16.7 % (2/12) of cases with complete removal of microcalcifications by VANCB in pure FEA, FEA + ADH and FEA + ADH + LIN, respectively.

We therefore confirm the frequent association of FEA with more advanced atypical proliferative breast lesions such as ADH and/or LIN [17–19, 34] and support the recommendation proposed by several authors [25, 30] that deeper levels of CB with pure FEA should be examined in order to detect or exclude the co-existence of more advanced breast lesions. The findings concerning the frequent association of FEA with more advanced atypical proliferative breast lesions support the hypothesis that FEA, together with ADH and LIN, belongs to the family of precursor lesions of low grade in situ and invasive breast cancer [5, 8] as the earliest precursor recognized to date.

Acknowledgments Pathologists contributing to VANCB Study Group: Antonacci CM (Milano), Bersiga A (Cremona), Bianchi S (Firenze), Carrillo G (Napoli), Castellano I (Torino), Cattani MG (Bologna), Dante S (Vicenza), Di Loreto C (Udine), Di Stefano D (Roma), Ferrero G (Cremona), Giardina C (Bari), Laurino L (Treviso), Piubello Q (Verona), Querzoli P (Ferrara), Renne G (Milano), Sapino

A (Torino), Vezzosi V (Firenze). Radiologists contributing to VANCB Study Group: Amadori S (Milano), Ambrogetti D (Firenze), Balestrieri N (Treviso), Bazzocchi M (Udine), Bodini MT (Cremona), Cassano E (Milano), Durando M (Torino), Festa R (Napoli), Guerrieri AM (SARIS, Bari), Maggian P (Vicenza), Mariscotti G (Torino), Mattei M (Roma), Montemezzi S (Verona), Saguatti G (Bologna), Scalabrin U (Vicenza), Trasente I (Napoli), Ventrella V (Bari)

Funding source This work was supported by a grant from the "Ente Cassa di Risparmio" of Florence-Italy.

Conflict of interest The authors declare that they have no conflict of interest.

References

1. Bianchi S, Caini S, Renne G et al (2011) Positive predictive value for malignancy on surgical excision of breast lesions of uncertain malignant potential (B3) diagnosed by stereotactic vacuum-assisted needle core biopsy (VANCB): a large multi-institutional study in Italy. Breast 20:264–270
2. Tavassoli FA, Hoefler H, Rosai J et al (2003) Intraductal proliferative lesions. In: Tavassoli FA, Devilee P (eds) Pathology and genetics of tumours of the breast and female genital organs. IARC, Lyon, pp 63–73
3. Monfair F (2010) Flat ductal intraepithelial neoplasia of the breast. A review of diagnostic criteria, differential diagnoses, molecular genetic findings, and clinical relevance. It is time to appreciate the Azzopardi concept. Arch Pathol Lab Med 133:879–892
4. Azzopardi JP (1979) Problems in breast pathology. Saunders, London, pp 193–203
5. Simpson PT, Gale T, Reis-Filho JS et al (2005) Columnar cell lesions of the breast: the missing link in breast cancer progression? A morphological and molecular analysis. Am J Surg Pathol 29:734–746
6. Bombonati A, Sgroi DC (2011) The molecular pathology of breast cancer progression. J Pathol 223:307–317
7. Brogi E, Oyama T, Koerner FC (2001) Atypical cystic lobules in patients with lobular neoplasia. Int J Surg Pathol 9:201–206
8. Abdel-Fatah TMA, Powe DG, Hodi Z et al (2007) High frequency of coexistence of columnar cell lesions, lobular neoplasia, and low grade ductal carcinoma in situ with invasive tubular carcinoma and invasive lobular carcinoma. Am J Surg Pathol 31:417–426
9. Collins LC, Achacoso NA, Nekhlydov L et al (2007) Clinical and pathologic features of ductal carcinoma in situ associated with the presence of flat epithelial atypia: an analysis of 543 patients. Mod Pathol 20:1149–1155
10. Leibl S, Regitnig P, Monfair F (2007) Flat epithelial atypia (DIN 1a, atypical columnar change): an underdiagnosed entity very frequently coexisting with lobular neoplasia. Histopathology 50:859–865
11. Kunju LP, Kleer CG (2007) Significance of flat epithelial atypia on mammotome core needle biopsy: should it be excised? Hum Pathol 38:35–41
12. Lee TYJ, MacIntosh RF, Rayson D et al (2010) Flat epithelial atypia on breast needle core biopsy: a retrospective study with clinical–pathological correlation. Breast J 16:377–383
13. Boulos FI, Dupont WD, Simpson JF et al (2008) Histologic associations and long-term cancer risk in columnar cell lesions of the breast. A retrospective cohort and a nested case–control study. Cancer 113:2415–2421
14. Aroner SA, Collins LC, Schnitt SJ et al (2010) Columnar cell lesions and subsequent breast cancer risk: a nested case–control study. Breast Cancer Res 12:R61, http://breast-cancer-research.com/content/12/4/R61
15. Verschuur-Maes AHJ, Van Deurzen CHM, Monninkhof EM et al (2012) Columnar cell lesions on breast needle biopsies: is surgical excision necessary? A systematic review. Ann Surg 255:259–265
16. Lazarus E, Mainiero MB, Schepps B et al (2006) BI-RADS lexicon for US and mammography: interobserver variability and positive predictive value. Radiology 239:385–391
17. Pinder SE, Reis-Filho JS (2007) Non-operative breast pathology: columnar cell lesions. J Clin Pathol 60:1307–1312
18. Pinder SE, Provenzano E, Reis-Filho JS (2007) Lobular in situ neoplasia and columnar cell lesions: diagnosis in breast core biopsies and implications for management. Pathology 39:208–216
19. Schnitt SJ, Vincent-Salomon A (2003) Columnar cell lesions of the breast. Adv Anat Pathol 10:113–124
20. PageDL Rogers LW (1992) Combined histologic and cytologic criteria for the diagnosis of mammary atypical ductal hyperplasia. Hum Pathol 23:1095–1097
21. Rosen PP, Hoda SA (2010) Breast pathology: diagnosis by needle core biopsy. Lippincott Williams & Wilkins, Philadelphia
22. Cangiarella J, Guth A, Axelrod D et al (2008) Is surgical excision necessary for the management of atypical lobular hyperplasia and lobular carcinoma in situ diagnosed on core needle biopsy? A report of 38 cases and review of the literature. Arch Pathol lab Med 32:979–983
23. Ely KA, Carter BA, Jensen RA et al (2001) Core biopsy of the breast with atypical ductal hyperplasia. A probabilistic approach to reporting. Am J Surg Pathol 25:1017–1021
24. Wagoner MJ, Laronga C, Acs G (2009) Extent and histologic pattern of atypical ductal hyperplasia present on core needle biopsy specimens of the breast can predict ductal carcinoma in situ in subsequent excision. Am J Clin Pathol 131:112–121
25. Martel M, Barron-Rodriquez P, Tolgay Ocal I et al (2007) Flat DIN 1 (flat epithelial atypia) on core needle biopsy: 63 cases identified retrospectively among 1751 core biopsies performed over an 8-year period (1992–1999). Virchows Arch 451:883–891
26. Piubello Q, Parisi A, Eccher A et al (2009) Flat epithelial atypia on core needle biopsy: which is the right management? Am J Surg Pathol 33:1078–1084
27. Lavoué V, Roger CM, Poilblanc M et al (2011) Pure flat atypia (DIN 1a) on core needle biopsy: study of 60 biopsies with follow-up surgical excision. Breast Cancer Res Treat 125:121–126
28. Senetta R, Campanino PP, Mariscotti G et al (2009) Columnar cell lesions associated with breast calcifications on vacuum-assisted core biopsies: clinical, radiographic, and histological correlations. Mod Pathol 22:762–769
29. Noel JC, Buxant F, Engohan-Aloghe C (2010) Immediate surgical resection of residual microcalcifications after a diagnosis of pure flat epithelial atypia on core biopsy: a word of caution. Surg Oncol 19:243–246
30. Chivukula M, Bhargava R, Tseng G et al (2009) Clinicopathologic implications of "flat epithelial atypia" in core needle biopsy specimens of the breast. Am J Clin Pathol 131:802–808
31. Sudarshan M, Meguerditchian AN, Mesorulle B et al (2011) Flat epithelial atypia of the breast: characteristics and behaviours. Am J Surg 201:245–250
32. Rosen PP (1999) Columnar cell hyperplasia is associated with lobular carcinoma in situ and tubular carcinoma. Am J Surg Pathol 23:1561
33. Sahoo S, Recant WM (2005) Triad of columnar cell alteration, lobular carcinoma in situ, and tubular carcinoma of the breast. Breast J 11:140–142
34. Lerwill MF (2008) Flat epithelial atypia of the breast. Arch Pathol Lab Med 132:615–621

Virchows Arch (2012) 461:419–423
DOI 10.1007/s00428-012-1312-1

ORIGINAL ARTICLE

Flat epithelial atypia with and without atypical ductal hyperplasia: to re-excise or not. Results of a 5-year prospective study

Ikechukwu Uzoaru · Bradley R. Morgan · Zheng G. Liu · Frank J. Bellafiore · Farah S. Gaudier · Jeanne V. Lo · Kourosh Pakzad

Received: 31 July 2012 / Revised: 27 August 2012 / Accepted: 31 August 2012 / Published online: 8 September 2012
© Springer-Verlag 2012

Abstract Flat epithelial atypia (FEA) of the breast have a tendency to calcify and, as such, are becoming increasingly detected by mammography. There is no consensus yet on whether to excise these lesions or not after diagnosis on core needle biopsies (CNB). We reviewed 3,948 cases of breast CNB between June 2004 and June 2009 correlating histomorphologic, radiological, and clinical features. There were 3.7 % (145/3,948) pure FEA and 1.5 % (58/3,948) concomitant FEA and atypical ductal hyperplasia (ADH). In the pure FEA population, 46.2 % (67/145) had microcalcifications on mammography with 65.5 % (95/145) of patients undergoing subsequent excisional biopsies with the following findings: benign 20 % (19/95), ADH 37.9 % (36/95), ductal carcinoma in situ (DCIS) 1.1 % (1/95), and DCIS and invasive ductal carcinoma (IDC) 2.1 % (2/95). In the concomitant FEA and ADH group, 86.2 % (50/58) patients had microcalcifications on radiograph with 74.1 % (43/58) of patients undergoing subsequent excisions with: benign 23.3 % (10/43), DCIS 9.3 % (4/43), DCIS and IDC 4.7 % (2/43), DCIS + lobular carcinoma in situ + invasive lobular carcinoma 2.3 % (1/43), and tubular carcinoma 2.3 % (1/43). The incidence of carcinoma in the FEA + ADH group is 18.6 % (8/43) and 3.2 % (3/95) for the pure FEA group. This difference is statistically significant (p=0.0016). The relative risk of carcinoma in the ADH + FEA group versus the pure FEA group is 6.4773, with 95 % CI of 1.8432 and 22.76 24. Five-year mean follow-up in the unexcised pure FEA did not show any malignancies. These findings suggest that pure FEA has a very low association with carcinoma, and these patients may benefit from close clinical and mammographic follow-up while the combined pure FEA and ADH cases may be re-excised.

Keywords Breast · Flat epithelial atypia · Core needle biopsies · Re-excision of flat epithelial atypia · Breast calcifications and densities

Introduction

Flat epithelial atypia (FEA), as defined by the World Health Organization (WHO), is an intraductal alteration of the terminal duct lobular units characterized by replacement of the native epithelium by one layer or three to five layers of mildly atypical cells [1]. The affected ducts are often dilated and contain flocculent material or microcalcifications. It is believed that FEA is the same lesion originally described in 1979 by John G. Azzopardi as "clinging carcinoma (CC), monomorphous type" [2]. However, in recent times, FEA is becoming increasingly recognized due to greater awareness of its morphological features and the increased use of mammographic breast screening. Moreover, FEA has been shown to be a neoplastic lesion at the molecular level [3, 4]. FEA as defined by the WHO encompasses a variety of atypical beast lesions previously known by various appellations including atypical cystic lobules [5], small ectatic ducts lined by atypical cells with apocrine snouts [6], atypical cystic duct [7, 8], columnar alteration with prominent apical snouts and secretions [9–11], DIN flat type [3, 12,

This work was presented in part as an abstract poster at the San Antonio Breast Cancer Symposium on December 12, 2010 in San Antonio Texas, USA.

I. Uzoaru (✉) · B. R. Morgan · Z. G. Liu · F. J. Bellafiore · F. S. Gaudier · J. V. Lo · K. Pakzad
Department of Pathology, Carle Foundation Hospital, Urbana, IL 61801, USA
e-mail: ike.uzoaru@carle.com

13], and columnar cell change with atypia [14–16]. The contentious issue with FEA is what to do with it after a diagnosis on core needle biopsy (CNB) since there is no consensus yet whether to re-excise these lesions or not. We report herein our findings in a review of 3,948 cases of consecutive breast core needle biopsies between 2004 and 2009 carrying diagnoses of FEA, columnar change/hyperplasia with atypia, combined FEA and atypical ductal hyperplasia (ADH), and their corresponding excisional biopsy findings.

Methods

Beginning January 2004, the pathologists in the Department of Pathology at Carle Foundation Hospital, Urbana, Illinois, USA adopted the policy of group review of breast biopsies. Particular emphasis was placed on FEA and other atypical breast lesions. These cases were reviewed by at least two pathologists and in most cases, by all pathology staff around a six-headed microscope (Olympus BH51®). These cases were then logged into the laboratory information system database (Softpart ©). The database was queried in the latter part of June 2009 to determine the number of cases of pure FEA and FEA plus ADH on CNBs. The findings on CNBs are correlated with the corresponding excisional biopsies where available. All CNBs showing ductal carcinoma in situ (DCIS), invasive ductal carcinoma (IDC), invasive lobular carcinoma (ILC), or other forms of breast cancer were excluded from the study. Diagnosis of FEA was made based on the 2003 WHO definition [1]. The medical records were also reviewed, and patients who had any previous breast cancer were eliminated from the study. Demographic and clinical information including age, mammographic/radiologic information, and findings of the subsequent excisional biopsies whenever available were also obtained from the medical records. The CNBs were grouped into two: (1) pure FEA where FEA was the most advanced atypical lesion in the breast core biopsy; and (2) FEA plus ADH group with ADH as the most advanced atypical lesion. The subsequent excisional biopsy findings whenever available were correlated with the corresponding CNB cases in the two groups. Some cases, where additional levels were obtained that resulted in an upgrade to a more atypical lesion or carcinoma, were eliminated from this study.

The core needle biopsy processes are as follows: For calcifications as well as masses not seen on ultrasound, the area is sampled via 9-gauge ATEC system (Hologic Corp., Indianapolis, IN©) and a Lorad Table (Hologic Corp, Indianapolis, IN©). After written informed consent and local anesthesia, the area of interest is targeted under stereotactic guidance, and correct needle is documented on both pre- and post-fire stereo pair images. Several (usually 5–12) cores are obtained. For calcifications, the core samples are radiographed during the procedure to ensure target calcifications have been sampled. A metallic microclip marker is placed at the site of biopsy. Post clip placement mammography is obtained following the procedure to document correct clip position. For masses sampled under ultrasound, the lesion is sampled either using vacuum-assisted technique or not. For both modalities, written informed consent is obtained and local anesthesia is used. For vacuum-assisted technique, an 11-gauge ATEC (Hologic Corp., Indianapolis, IN©) system is used with several (usually 5–12) cores being obtained. For non-vacuum-assisted technique, a 14-gauge Achieve (CareFusion, San Diego, CA) needle system is used with usually 5–7 core samples obtained. Metallic microclip markers are placed at the areas of biopsy and confirmed with post clip placement mammography.

Clinical and mammographic follow-up in the 50 unexcised pure FEAs was obtained from the electronic medical records of these patients.

Results

A total of 3,948 breast CNBs were performed and evaluated between June 2004 and June 2009. There were 3.7 % (145/3,948) cases of pure FEA (age range 33–82 years, median 49 years, mean 54 years) (Fig. 1) and 1.5 % (58/3,948) cases of concomitant FEA and ADH (age range 34–83 years, median 51.5 years, mean 54 years). In the pure FEA group, 65.5 % (95/145) patients had subsequent excisional biopsies. Of these 95 patients, 71 % (67/95) had microcalcifications and the rest had mammographic densities/masses.

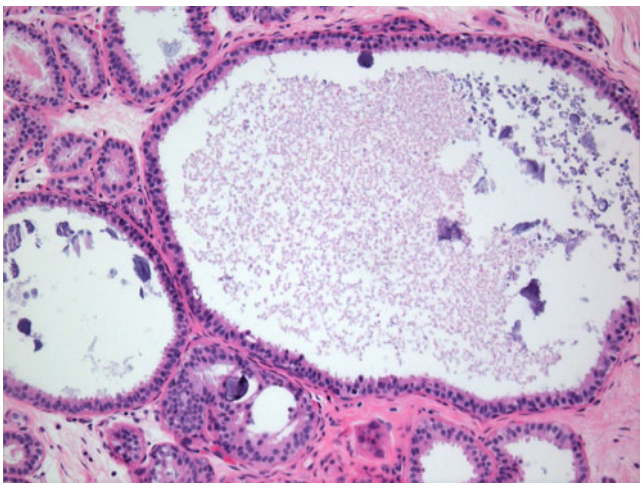

Fig. 1 CNB of breast showing FEA with dilated ducts lined by ovoid atypical cells containing flocculent material and calcifications. H&E ×200

Excisional biopsy findings in this group included: benign/fibrocystic changes 20 % (19/95), FEA 35.8 % (34/95), ADH 37.9 % (36/95), low nuclear grade DCIS1.1 % (1/95) (Fig. 2), and DCIS and well-differentiated IDC 2.1 % (2/95) (Fig. 3).

In the concomitant FEA and ADH group (n=58), 86.2 % (50/58) had microcalcifications and 74.1 % (43/58) of the patients underwent subsequent excisional biopsies with the following findings: benign/fibrocystic changes 23.3 % (10/43), DCIS 9.3 % (4/43), DCIS and IDC 4.6 % (2/43), DCIS and ILC 2.3 % (1/43), and tubular carcinoma 2.3 % (1/43). The mean ages of the pure FEA and the FEA plus ADH group are homogeneous with no statistical difference (p=0.3446) using t test. The incidence of carcinoma in the ADH plus FEA and pure FEA group is 18.6 % (8/43) and 3 % (3/95), respectively. The relative risk of carcinoma findings in the ADH plus FEA group versus the pure FEA group is 6.4773 (95 % CI 1.8432, 22.7624), p=0.0016 (Fisher's exact test). Women in the ADH plus FEA group are six times more likely to be diagnosed with carcinoma compared to the pure FEA group.

The DCIS seen in the excision of one of the cases of pure FEA measured 4.0 mm with low nuclear grade and cribriform architecture without necrosis. The other two cases of invasive ductal carcinoma were both of low grade (grade 1/3 Nottingham Histologic Score) and measured 0.8×0.8 cm and 1.3×0.7 cm, respectively. The decision to re-excise in the pure FEA patients was mainly from the preference of the patient. Follow-up in the unexcised pure FEA cases in the form of yearly mammograms was available in 33 patients. Seventeen patients were lost to follow-up. The follow-up period ranged from 3 to 8 years with a mean of 5 years. The 33 patients for whom follow-up studies were available did not show any evidence of malignancy.

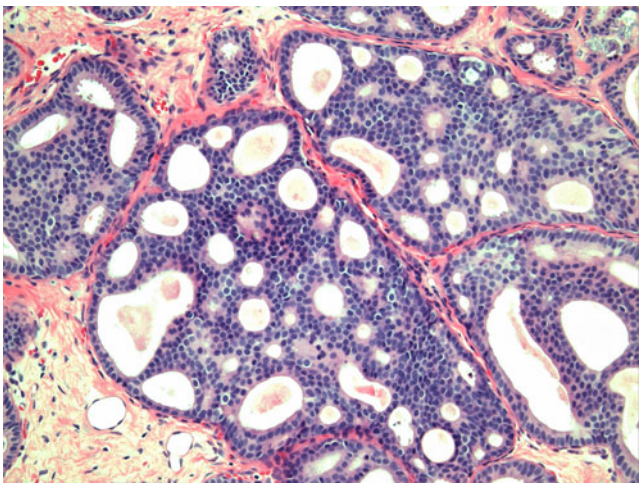

Fig. 2 Re-excision of FEA showing cribriform DCIS low nuclear grade. H&E, ×200

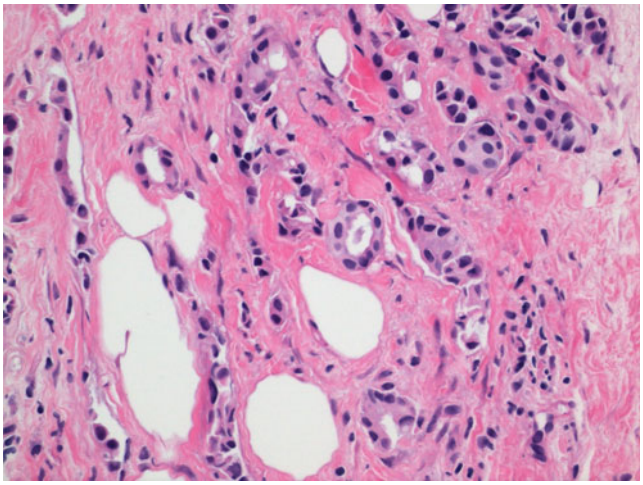

Fig. 3 Re-excision of FEA showing grade 1/3 invasive ductal carcinoma. H&E, ×200

Discussion

Our study shows a pure FEA rate of 3.7 % and a combined FEA and ADH rate of 1.5 % of which there were 3 and 20 % carcinoma rates, respectively. Puibello and colleagues [17] found a similar rate of 3.7 and 1.2 % for pure FEA and combined FEA plus ADH, respectively, in a retrospectively review of 875 core needle biopsies performed using the 11-gauge biopsy gun. Puibello and associates also found a younger median age group for the pure FEA group compared with the combined FEA plus ADH group, an observation reported by Kunju and Kleer[18]. We did not see any statistical difference between the age groups of patients with pure FEA and those in the combined FEA and ADH groups in our study.

It is now generally accepted that FEA is the earliest morphologic precursor of breast cancer and, together with ADH and DCIS, is the non-obligate precursor of invasive and metastatic ductal carcinoma. Morphologic and epidemiologic factors appear to support this hypothesis [19–21]. More light has been shed on the evolutionary relationship between FEA, ADH, DCIS, and invasive ductal carcinoma. Moinfar and associates in the first ever study of genetic abnormalities in FEA showed a high rate of loss of heterozygosity (LOH) at chromosomes 16q in FEA which is also manifested in the adjacent low-grade in situ lesions and low-grade invasive ductal carcinoma [3]. Dabbs and associates also showed LOH in FEA (columnar cell change with atypia/atypical columnar cell hyperplasia) [4]. Similarly, Buerger et al. [22] showed frequent loss of 16q in low-grade DCIS and 13q loss including amplifications of 17q12 and 11q13 in high-grade DCIS. O'Connell and colleagues [23] demonstrated loss of 16 q as a hot spot in ADH which is most frequently related to low-grade rather than high-grade DCIS. More recently, Simpson and colleagues

[24] in a comprehensive CGH based study showed that FEA, ADH, DCIS, and invasive ductal carcinoma (low and intermediate nuclear grade) are an evolutionary continuum in the breast cancer tumorigenesis and progression of the molecular luminal A and B categories [25, 26]. In our study, no high-grade DCIS or IDC was seen in the patients who had cancer on subsequent excisional biopsies in the pure FEA and FEA plus ADH groups.

Moinfar [27] has recently proposed adopting the DIN terminology (low or high grade) as the all encompassing term for all the flat lesions of the breast that had enjoyed various appellations. Interestingly, the WHO classification [1] uses DIN1a as a synonym for FEA. Moinfar [27] argues that the DIN terminology points out the flat, ductal phenotype and neoplastic nature of the lesions with no significant intraluminal proliferations. Furthermore, the term DIN eliminates the use of the alarming term of "cancer" or "carcinoma in situ" in flat lesions including DCIS, and unifies the intraepithelial neoplasia of the breast as commonly seen in other organ systems. Our cases of FEA showed mild nuclear atypia. However, there were cases that looked more atypical than others with more prominent nucleoli without intraluminal proliferations or frankly high-grade nuclei.

What still remains a contentious issue with FEA is the lack of a generally accepted mode of treatment of patients after a diagnosis is made on CNB. Kunju and Kleer [18], in a review of 60 core biopsies, found carcinoma rates of 21 and 38 % in the pure FEA and pure ADH groups, respectively. They concluded that FEA shows a risk of upgrade to carcinoma similar to that of ADH and a follow-up excision in FEA cases. Piubello and associates [17] found no evidence of carcinoma in 20 excisional biopsies of the 33 pure FEA in their review. They recommended close radiologic follow-up in these patients diagnosed with pure FEA. Jara-Lazaro and associates [28] recommended excisional biopsy for pure FEA after a review of several published cases in the literature showing up to 22 % of ductal carcinoma after excisional biopsies. Senetta et al. [29] and de Mascarel et al. [30] did not find any cancer associated with pure FEA in their studies and did not recommend excisional biopsies. All these cases are limited by their small sample sizes. Verschuur-Maes et al. [31] in a retrospective review of 4,164 breast CNBs found 311 columnar cell lesions consisting of 221 columnar lesions without atypia, 69 with atypia, and 21 mixed columnar cell lesions and ADH. Their progression risks were 2 % for columnar cell lesions without atypia, 18 % for columnar cell lesion with atypia, and 22 % for columnar cell lesions and ADH. In a cohort-retrospective review of 80 cases of in situ carcinoma with a mean follow-up period of 17.5 years, Eusebi and associates [32] found only two cases of recurrent well-differentiated DCIS in 32 CC with monomorphous nuclei 3 and 9 years, respectively, after the initial breast biopsies. Both recurrences showed no evidence of disease after subsequent re-excisions 19 and 26 years, respectively, after the initial biopsies. Similarly, Bijker et al. [33], with a median follow-up of 5.4 years, found no recurrences in 59 cases of well-differentiated DCIS with clinging architecture. They recommended close follow-up of these patients after local excisions. More recently, Yamaguchi et al. [34], in a retrospective review of 2,358 breast CNB spanning 4 years, found a pure FEA rate of 0.72 % (17/2,358) and combined FEA + ADH rate of 0.76 % (18/2,358). Subsequent excisions performed in 53 cases revealed malignancy rates in the pure FEA and combined FEA + ADH groups of one out of eight (1/8) and seven out of ten (7/10), respectively, with recommendation to re-excise the combined FEA + ADH and watch the cases of pure FEA. These findings in the rates of malignancy on re-excision of the CNBs are similar to our cases where ADH was the most common finding after excisional biopsies of pure FEA (38 %), and a 3 % ductal carcinoma rate and the FEA plus ADH group, on the other hand, showed a carcinoma incidence of 20 %. Greater than 90 % of our patients who had subsequent excisional breast biopsies had their lesions removed less than 80 days after the original CNBs. This suggests that the FEA most likely coexisted with the more atypical lesions that were found on subsequent excisional biopsies. The tumors found on excision of the pure FEAs were small and of low grade, and whether to subject patients to excisional biopsies for small low-grade tumors that may progress slowly and may not have a fatal course is debatable. Furthermore, the available follow-up in the unexcised pure FEA cases failed to show any malignancies albeit with a short follow-up period. However, the possibility of selection bias in favor of less extensive/less suspicious lesions cannot be completely excluded due to small population size and variability of method of follow-up.

In conclusion, FEA on CNB has a low predictive value for breast carcinoma on subsequent surgical excisional biopsy, and it is more often associated with ADH. FEA appears to have a natural sequential progression to ADH and subsequently to frank breast carcinoma. Women in the FEA plus ADH group were six times more likely to be diagnosed with carcinoma compared to the pure FEA group. It might be prudent for these patients to have clinical and mammographic follow-up and re-excise those cases that have concomitant ADH. Further studies with larger sample sizes and longer follow-up periods may be needed to further determine what management steps to undertake in patients diagnosed with pure FEA.

Acknowledgments The authors wish to thank Dr. Maria Muyot for help with the statistical analyses.

Conflict of interest The authors declare that they have no conflict of interest.

References

1. Tavassoli FA, Hoofer H, Rosai J, Holland R, Ellis IO, Schnitt SJ, Booker W, Heywang-Köbrunner MF, Lakhani SR (2003) Intraductal proliferative lesions. In: Tavassoli FA, Devilee P (eds) World Health Organization classification of tumours: Tumours of the breast and female genital tract organs IARC. Lyon, France, pp 63–73
2. Azzopardi JG (1979) Clinging carcinoma. In: Azzopardi JG, Ahmed A, Millis RR (eds) Problems in breast pathology. Saunders, Philadelphia, pp 193–203
3. Moinfar F, Man YG, Bratthauer GL, Ratschek M, Tavassoli FA (2000) Genetic abnormalities in mammary ductal intraepithelial neoplasia-flat type ("clinging ductal carcinoma in situ"): a simulator of normal mammary epithelium. Cancer 88:2072–2081
4. Dabbs DJ, Carter G, Fudge M, Peng Y, Siralsky P, Finkelstein S (2006) Molecular alterations in columnar cell lesions of the breast. Mod Pathol 19:344–349
5. Koerner FC, Oyama T, Maluf H (2001) Morphological observations regarding the origins of atypical cystic lobules (low grade clinging carcinoma of flat type). Virchows Arch 439:523–530
6. Goldstein NS, O'Malley BA (1997) Cancerization of small ectatic ducts of the breast by ductal carcinoma in situ cells with apocrine snouts. A lesion associated with tubular carcinoma. Am J Clin Pathol 107:561–566
7. Kusama R, Fujimori M, Matsuyama I et al (2000) Clinicopathologic characteristics of atypical cystic duct (ACD) of the breast: assessment of ACD as a precancerous lesion. Pathol Int 50:793–800
8. Tsuchiya S (1998) Atypical ductal hyperplasia, atypical lobular hyperplasia, and interpretation of a new borderline lesion. Jpn J Cancer Clin 44:548–555
9. Fraser JL, Raza S, Chorny K, Connolly JL, Schnitt SJ (1998) Columnar alteration with prominent apical snouts and secretions: a spectrum of changes frequently present in breast biopsies performed for microcalcifications. Am J Surg Pathol 22:1521–1527
10. Oyama T, Iijima K, Takei H (2000) Atypical cystic lobule of the breast: an early stage of low grade ductal carcinoma in situ. Breast Cancer 7:326–331
11. Dessauvagie B, Zhao W, Heel-Miller KA, Harvey J, Bentel JM (2007) Characterization of columnar cell lesions of the breast: immunophenotypic analysis of columnar alteration of lobules with prominent apical snouts and secretions. Hum Pathol 38:284–292
12. Bratthauer G, Tavassoli FA (2004) Assessment of lesions coexisting with various grades of ductal intraepithelial neoplasia of the breast. Virchows Arch 444:340–344
13. Martel M, Barron-Rodriguez P, Ocal IT, Dotto J, Tavassoli FA (2007) Flat DIN 1(flat epithelial atypia) on core needle biopsy: 63 cases identified retrospectively among 1,751 cores over an 8 year period (1992-1999). Virchows Arch 451:883–891
14. Turashvili G, Hayes M, Gilks B, Watson P, Aparichio S (2008) Are columnar cell lesions the earliest histologically detectable non-obligate precursor of breast cancer? Virchows Arch 452:589–598
15. Schnitt SJ, Vincent-Salomon A (2007) Columnar cell lesions of the breast. Adv Anat Pathol 10:113–124
16. Tan PH, Ho BC-S, Selvarajan S, Yap WM, Hanby A (2008) Pathological diagnosis of columnar cell lesions of the breast: are there issues of reproducibility? J Clin Pathol 58:705–709
17. Puibello Q, Parisi A, Eccher A, Barbazeni G, Franchini Z, Iannucci A (2009) Flat epithelial atypia on core needle biopsy—which is the right management? Am J Surg Pathol 33:1078–1084
18. Kunju LP, Kleer CG (2007) Significance of flat epithelial atypia on mammotome core needle biopsy: should it be excised? Hum Pathol 38:35–41
19. Oyama T, Maluf H, Koerner F (1999) Atypical cystic lobules: an early stage in the formation of low grade ductal carcinoma in situ. Virchows Arch 435:413–421
20. Wellings SR, Jensen HM, Marcum RG (1975) An atlas of subgross anatomy of the human breast with special reference to possible precancerous lesions. J Natl Cancer Inst 55:231–273
21. Lerwill MF (2008) Flat epithelial atypia of the breast. Arch Pathol Lab Med 132:615–621
22. Buerger H, Mommers EC, Littman R et al (2001) Ductal invasive G2 and G3 carcinomas of the breast are the end stages of at least two different lines of genetic evolution. J Pathol 194:165–170
23. O'Connell P, Pekkel V, Fuqua SA, Osborne CK, Clark GM (1998) Analysis of loss of heterozygosity in 399 premalignant breast lesions at 15 genetic loci. J Natl Cancer Inst 90:697–703
24. Simpson PT, Gale T, Reis-Filho JS et al (2005) Columnar cell lesions of the breast: the missing link in breast cancer progression? A morphologic and molecular analysis. Am J Surg Pathol 29:734–746
25. Sotiriou C, Soek-Ying N, McShane LM et al (2003) Breast cancer classification and prognosis based on gene expression profiles from a population-based study. Proc Natl Acad Sci USA 100 (18):10393–10398
26. Bombonati A, Sgroi DC (2011) The molecular pathology of breast cancer progression. J Pathol 223:307–317
27. Moinfar F (2010) Flat ductal intraepithelial neoplasia of the breast: evolution of Azzopardi's "clinging" concept. Sem Diagn Pathol 27:37–48
28. Jara-Lazaro AR, Tse GM, Tan PH (2009) Columnar cell lesions of the breast: an update and significance on core biopsy. Pathology 41 (1):18–27
29. Senetta R, Campanino PP, Mariscotti G et al (2009) Columnar cell lesions associated with breast calcifications on vacuum assisted core biopsies: clinical, radiographic, and histologic correlations. Mod Pathol 22:762–769
30. de Mascarel I, Brouste V, Asad-Syed M, Hurtevent G, MacGrogan G (2011) All atypia diagnosed at stereotactic vacuum assisted breast biopsy do not need surgical excision. Mod Pathol 9:1198–1206
31. Verschuur-Maes AHJ, Witkamp AJ, De Bruin PC, Van Der Wall E, Van Priest PJ (2011) Progression risk of columnar cell lesions of the breast diagnosed in core. Int J Cancer 129:2674–2680
32. Eusebi V, Feudale E, Foschini MP et al (1994) Long-term follow-up of in situ carcinoma of the breast. Sem Diagn Pathol 11(3):223–235
33. Bijker N, Peterse JL, Duchateau L et al (2001) Risk factors for recurrence and metastases after breast-conserving therapy for ductal carcinoma in situ: analysis of European Organization for Research and Treatment of Cancer Trial 10853. J Clin Oncol 19:2263–2271
34. Yamaguchi R, Tanaka M, Tse GM et al (2012) Pure flat epithelial atypia is uncommon in subsequent breast excisions for atypical epithelial proliferation. Cancer Sci 103(8):1580–1585

Virchows Arch (2012) 461:425–431
DOI 10.1007/s00428-012-1311-2

ORIGINAL ARTICLE

Higher cytoplasmic and nuclear poly(ADP-ribose) polymerase expression in familial than in sporadic breast cancer

Marie-Luise Klauke · Nicoline Hoogerbrugge · Jan Budczies · Peter Bult · Judith Prinzler · Cornelia Radke · J. Han J. M. van Krieken · Manfred Dietel · Carsten Denkert · Berit Maria Müller

Received: 27 January 2012 / Revised: 17 July 2012 / Accepted: 29 August 2012 / Published online: 12 September 2012
© Springer-Verlag 2012

Abstract Poly(ADP-ribose) polymerase 1 (PARP) is a key element of the single-base excision pathway for repair of DNA single-strand breaks. To compare the cytoplasmic and nuclear poly(ADP-ribose) expression between familial (BRCA1, BRCA2, or non BRCA1/2) and sporadic breast cancer, we investigated 39 sporadic and 39 familial breast cancer cases. The two groups were matched for hormone receptor status and human epidermal growth factor receptor 2 status. Additionally, they were matched by grading with a maximum difference of ±1 degree (e.g., G2 instead of G3). Cytoplasmic PARP (cPARP) expression was significantly higher in familial compared to sporadic breast cancer (P=0.008, chi-squared test for trends) and a high nuclear PARP expression (nPARP) was significantly more frequently observed in familial breast cancer (64 %) compared with sporadic breast cancer (36 %) (P=0.005, chi-squared test). The overall PARP expression was significantly higher in familial breast cancer (P=0.042, chi-squared test). In familial breast cancer, a combination of high cPARP and high nPARP expression is the most common (33 %), whereas in sporadic breast cancer, a combination of low cPARP and intermediate nPARP expression is the most common (39 %). Our results show that the overall PARP expression in familial breast cancer is higher than in sporadic breast cancer which might suggest they might respond better to treatment with PARP inhibitors.

Keywords PARP · Poly(ADP-ribose) polymerase · Breast cancer · BRCA mutation · Hereditary breast cancer

J. Budczies · J. Prinzler · M. Dietel · C. Denkert · B. M. Müller (✉)
Institute of Pathology, Charité University Hospital, Campus Mitte, Charitéplatz 1, 10117 Berlin, Germany
e-mail: berit.mueller@charite.de

M.-L. Klauke
Radboud University Nijmegen Medical Centre, Geert Grooteplein-Zuid 10, 6525 GA Nijmegen, the Netherlands

N. Hoogerbrugge
Department of Human Genetics, Radboud University Nijmegen Medical Centre, Geert Grooteplein-Zuid 10, 6525 GA Nijmegen, the Netherlands

P. Bult · J. H. J. M. van Krieken
Department of Pathology, Radboud University Nijmegen Medical Centre, PO Box 9101, 6500 HB Nijmegen, the Netherlands

C. Radke
Institute of Pathology, DRK Kliniken Berlin Westend, Spandauer Damm 130, 14050 Berlin, Germany

Abbreviations

HR	Hormone receptor
IDC	Invasive ductal carcinoma
ILC	Invasive lobular carcinoma

Introduction

In the USA in 2012 about 226,870 women will be diagnosed with breast cancer, which makes breast cancer the most common cancer in women, and with 39,510 estimated deaths, breast cancer is the second most frequent cause of cancer death in women [1]. About 5–10 % of these cases can be related to a hereditary or familial form of breast cancer

[2]. There are several types of mutation found in this type of breast cancer, but the best studied are the BRCA1 and BRCA2 mutations, which were discovered in the 1990s and are located on chromosome 17q and 13q, respectively [3], and account for about 20–50 % of all familial breast cancers [4].

The proteins encoded by the BRCA1 and BRCA2 genes play an important role in the repair of double-strand breaks and initiation of homologous recombination in damaged DNA. Carriers of a mutated form of BRCA are heterozygous for this gene and have a higher susceptibility for carcinogenesis through loss of heterozygosity. The susceptibility for carcinogenesis further increases as BRCA-associated tumors more often seem to express mutated versions of the tumor suppressor genes TP53 and c-erbB2 [5, 6].

BRCA-mutated tumors are often histologically poorly differentiated (grade 3) and show a more aggressive phenotype, for example, high mitotic counts and decreased tubular formation. This may explain the poor prognosis of patients carrying the mutated gene in the germ line [7].

Furthermore, the majority of BRCA1-mutated breast cancers is triple negative, i.e., no expression of estrogen- and progesterone receptor and no amplification of the Her2 gene, and highly proliferative, which leads to a comparably high response rate to certain kinds of chemotherapy. Nevertheless, there is a high recurrence rate [8].

Current therapeutic strategies for triple-negative breast cancer are focused on chemotherapy, in some cases augmented with radiotherapy or treatment with biologicals [9]. Because the overall prognosis is not very promising, there is a need for new treatment approaches, which should be selective for the tumor and have an acceptable side effect pattern. Beside other agents like platinum in neoadjuvant chemotherapy [10], poly(ADP-ribose) polymerase (PARP) inhibitors seem to be highly effective agents for tumors in patients with BRCA-mutated genes [11].

PARP-1 (PARP) is the most studied and founding member of the PARP family which contains 17 other proteins that are present in various cell compartments. It is located primarily in the nucleus and its functions range from regulation of gene expression and chromatin structure to an important role in metabolism. But the most important function, which is the reason PARP inhibitors were developed, is the role of PARP-1 in the repair of DNA single-strand breaks via the single-base excision pathway [12, 13].

Inhibition of PARP will lead to an accumulation of single-strand breaks, which would turn into double-strand breaks after cell division. Because tumor cells of patients with a BRCA mutation are BRCA deficient, they would not be able to repair these double-strand breaks. Finally, this would lead to apoptosis of the tumor cells [14]. This mechanism is thought to be highly selective and would not affect normal tissues of the patients because only tumor cells are completely BRCA deficient [15].

In vitro studies showed a more than 1,000-fold higher sensitivity for PARP inhibitors in the cell lines with BRCA1 and BRCA2 mutations compared to wild-type breast cancer cells [11]. In phases 1 and 2 trials, PARP inhibitors have proven to be effective in women with BRCA1 and BRCA2 mutations who were resistant to normal chemotherapy [11, 16]. But the first PARP inhibitor to enter a clinical phase 3 trial, iniparib, failed to meet the goals of the trial. Subsequent research implied that iniparib might not be a PARP inhibitor but seems to non-selectively modify cysteine-containing proteins in tumor cells [17].

In the light of these studies, more basic research studies needs to be done to improve our knowledge of PARP and its localization in order to allow the development of more PARP-specific inhibitors. This study focuses on possible differences in PARP localization between hereditary and non-hereditary breast cancer tissue samples.

Materials and methods

Study population

To determine the PARP expression in familial breast cancer, we analyzed formalin-fixed paraffin-embedded tissue of 47 patients from the Department of Pathology of the Radboud University Nijmegen Medical Centre.

The core biopsies were arranged in two tissue microarrays, together with samples of liver tissue for adequate orientation. We had to exclude eight cases from the final analysis due to lack of tumor in the tissue microarrays. The final cohort consisted of 24 BRCA1-mutated-, 8 BRCA2-mutated-, 2 non-BRCA-mutated cases, and 5 cases in which mutation analysis had not been yet performed at the moment of study inclusion.

The sporadic breast cancer tissue samples were provided by the Institute of Pathology of the Charité University Hospital. They were matched with the 39 familial cases by hormone receptor status and human epidermal growth factor receptor 2 (HER2) status. Additionally, they were matched by grading with a maximum difference of ±1 degree (e.g., G2 instead of G3). Matching between cohorts was executed using the statistical language R [18]. Of the tumors, 30 matched exactly with respect to grading, while there was a difference of ±1 for the other nine.

Immunohistochemical staining and histopathological examination

Immunohistochemical staining on the tissue microarrays was performed using standard procedures. To detect PARP

residues in the samples, a monoclonal-purified mouse anti-human PARP antibody (1:1,500; clone 7D3–6; BD Pharmingen, San Diego, CA) was used. As detection system, a peroxidase/DAKO system (Dako REALTM Detection System, peroxidase/3,3-diaminodbenzidine positive, rabbit/mouse; Dako, Glostrup, Denmark) was used.

Stained slides were digitized and virtually examined with the VM Slide Explorer 2009 (VMscope GmbH, Berlin, Germany). Nuclear PARP (nPARP) and cytoplasmic PARP (cPARP) expression patterns were evaluated in terms of the nuclear and cytoplasmic intensity (negative, weak, moderate, and strong) and the percentage of stained tumor cells (0 to 100 %, with 10 % intervals).

The intensity and percentage of positive tumor cells were used to calculate an immunoreactivity score (IRS), which was divided into three subgroups defined as low (IRS 0–2), intermediate (IRS 3–4), and high (IRS 6–12) expression [19]. To get an impression of the overall PARP staining, nuclear and cytoplasmic PARP expression patterns were combined. Nuclear and cytoplasmic PARP expression received one point for an IRS of 0–2, two points for an IRS of 3–4, and three points for an IRS of 6–12. In order to determine the overall PARP expression, the points given for nPARP and cPARP expression were added and the result was defined as low (0–2 points), intermediate (3–4 points), and high (5–6 points) overall PARP expression.

Information about the histological grading was extracted from the pathology reports. If the information was not available, the tumor tissue was regraded on the TMA.

Statistical evaluation

Statistical analysis was carried out using the PASW Statistics 18 program (IBM, Armonk, New York). For the evaluation, the familial and sporadic subgroups were compared regarding the cytoplasmic, nuclear, and overall PARP expression. Differences between the subgroups were assessed using the chi-squared test and the chi-squared test for trends. P values <0.05 were considered statistically significant.

Results

Study cohort

The clinicopathological characteristics of the cohort are listed in Table 1. The mean age at diagnosis of patients with familial breast cancer was 45±11 years and of patients with sporadic breast cancer was 65±12 years.

The tumor samples showed different cytoplasmic and nuclear PARP expression patterns, which were categorized as low, intermediate, or high, as recently described [19]. Figure 1a shows tumor tissue with a negative (low) cytoplasmic and negative (low) nuclear PARP expression, Fig. 1b shows tumor cells with intermediate cytoplasmic and low nuclear PARP expression, and Fig. 1c shows a high cytoplasmic and low nuclear PARP expression.

Table 1 Tumor characteristics (including histological grading, tumor size, nodal status, hormone receptor status, HER2 status, histological tumor type, and mutation status) of the familial and sporadic breast cancer samples

	Familial BC	Sporadic
Histological grading		
G1	3 (7.7 %)	4 (10.3 %)
G2	27 (69.2 %)	18 (46.2 %)
G3	9 (23.1 %)	17 (43.6 %)
Tumor size pT		
pT 1	22 (56.4 %)	15 (38.5 %)
pT 2	10 (25.6 %)	20 (51.3 %)
pT 3	4 (10.3 %)	3 (7.7 %)
pT 4	1 (2.6 %)	0
Missing	(5.1 %)	1 (2.6 %)
Nodal status		
N0	20 (51.3 %)	28 (71.8 %)
N+	15 (38.5 %)	8 (20.5 %)
Missing	4 (10.3 %)	3 (7.7 %)
Hormone receptor status		
HR+	21 (53.8 %)	21 (53.8 %)
HR−	18 (46.2 %)	18 (46.2 %)
HER2 status		
HER2+	1 (2.6 %)	1 (2.6 %)
HER2−	38 (97.4 %)	38 (97.4 %)
Histological tumor type		
IDC	36 (92.3 %)	35 (89.7 %)
ILC	3 (7.7 %)	4 (10.3 %)
Mutation status		
BRCA 1	24 (61.5 %)	–
BRCA 2	8 (20.5 %)	–
Non-BRCA1/2	2 (5.1 %)	–
Mutation not known	5 (12.9 %)	–

Comparison of cPARP expression in familial and sporadic breast cancer

As shown in Fig. 2, the cytoplasmic PARP expression in familial breast cancer was low in 33 %, intermediate in 26 %, and high in 41 % of cases. In contrast, cPARP in sporadic breast cancer was low in 59 %, intermediate in 26 %, and high in 15 % of cases. Statistical analysis showed that cPARP expression was significantly higher in familial compared to sporadic breast cancer (P=0.008, chi-squared test for trends).

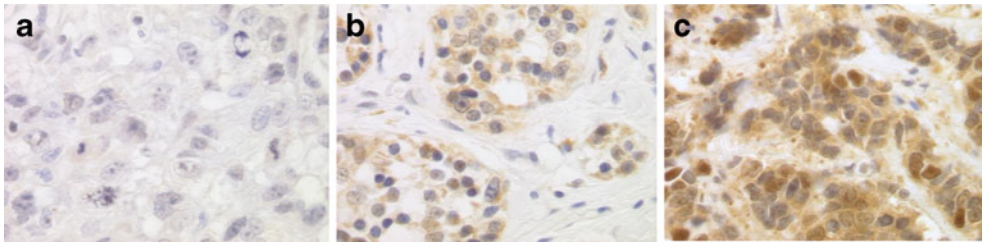

Fig. 1 Tumor cells with different PARP expression patterns: **a** negative (*low*) cytoplasmic and negative (*low*) nuclear PARP expression; **b** intermediate cytoplasmic and low nuclear PARP expression; and **c** high cytoplasmic and low nuclear PARP expression

Comparison of nPARP expression in familial and sporadic breast cancer

Figure 3 shows that the nuclear PARP expression in familial breast cancer was low in 13 %, intermediate in 23 %, and high in 64 % of cases. Compared to that, the nPARP expression in sporadic breast cancer was low in 5 %, intermediate in 59 %, and high in 36 % of cases. Familial breast cancer showed a significant higher nPARP expression than sporadic breast cancer (P=0.005, chi-squared test). In comparison, non-familial breast cancer showed more intermediate nPARP expression (59 %) than familial breast cancer (23.1 %).

Comparison of the overall PARP expression in familial and sporadic breast cancer

The overall PARP expression, a combination of cPARP and nPARP expression, in familial breast cancer was low in 8 %, intermediate in 41 %, and high in 51 % of cases. In sporadic breast cancer, the overall PARP expression was low in 5 %, intermediate in 69 %, and high 26 % of cases (Fig. 4). Familial breast cancer showed a significantly higher overall PARP expression (P=0.042, chi-squared test). There was no significant correlation between cPARP, nPARP, or the overall PARP expression and other clinicopathological parameters (results not shown).

Correlation of cPARP and nPARP expression in familial and sporadic breast cancer

Figure 5 shows that familial breast cancer samples exhibited low PARP expression pattern in 11 cases, in 15 cases either cPARP or nPARP was high and in 13 cases cPARP and nPARP were high. On the contrary, sporadic breast cancer showed low PARP expression in 23 cases, in 12 cases either cPARP or nPARP was high and only in 4 cases cPARP as well as nPARP expression was high. Table 2 compares cPARP and nPARP expression in breast cancer, regardless of familial or sporadic origin. It shows that 17 % of cases had high nPARP but low cPARP expression and 7 % had high cPARP but low to intermediate nPARP expression.

Taken together, the results suggest that sporadic breast cancer more often exhibits a low PARP expression pattern, whereas in familial breast cancer, high PARP expression is more common (P=0.009, chi-squared test). No significant correlation between the clinicopathological parameters or the BRCA mutation status and PARP expression patterns (data not shown) was found.

Discussion

Our study shows that cPARP expression is significantly higher in familial than in sporadic breast cancer. In familial

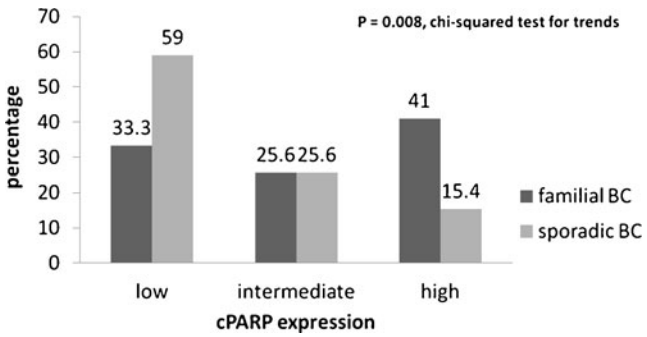

Fig. 2 cPARP expression (*low*, *intermediate*, and *high*) in familial and sporadic breast cancer. cPARP expression was significantly more often high in familial breast cancer and more often low in sporadic breast cancer (P=0.008, chi-squared test for trends)

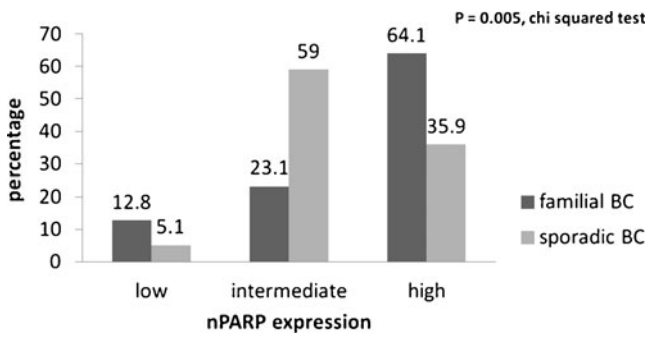

Fig. 3 nPARP expression (*low*, *intermediate*, and *high*) in familial and sporadic breast cancer. nPARP expression was significantly higher in familial breast cancer than in sporadic breast cancer (P=0.005, chi-squared test)

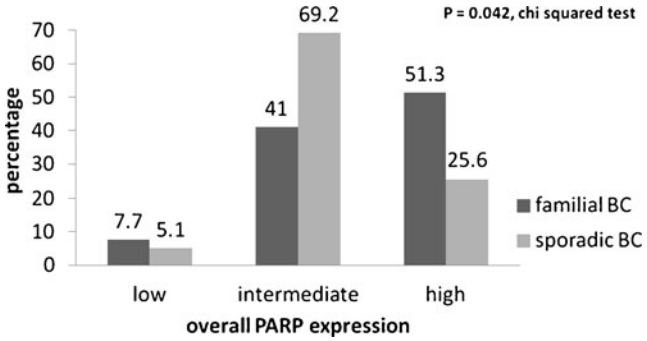

Fig. 4 Overall PARP expression (*low*, *intermediate*, and *high*) in familial and sporadic breast cancer. The overall PARP expression was significantly higher in familial breast cancer than in sporadic breast cancer (P=0.042, chi-squared test)

breast cancer, the number of samples with intermediate nPARP expression was lower, but cases with low or high nPARP expression were more frequent. The overall PARP expression was significantly higher in familial breast cancer. Additionally in familial breast cancer, a combination of high cPARP and high nPARP expression is most common, whereas in sporadic breast cancer, a combination of low cPARP and intermediate nPARP expression is most common.

PARP expression in familial and sporadic breast cancer has been investigated by several others. Domagala et al. included 130 BRCA1-associated and 594 BRCA1 non-related breast cancer tissue samples in their study. Immunohistochemical staining and evaluation showed that the BRCA1-associated tumor samples more often exhibited a low nPARP expression. cPARP expression was low in most cases, but more frequent in the BRCA1-associated group, similar to our results [20]. The differences in cPARP and

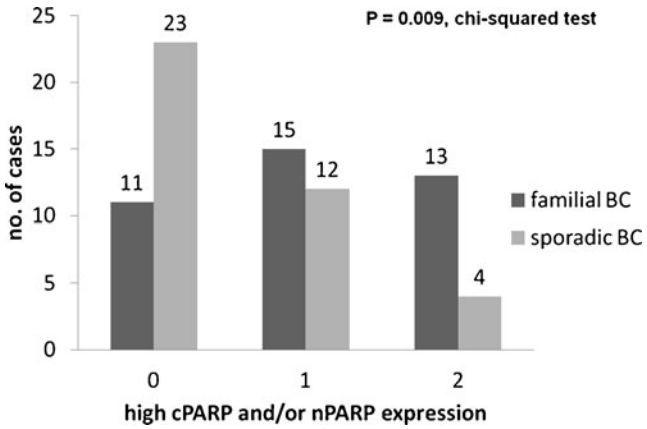

Fig. 5 Combined cPARP and nPARP expression defining three different groups in which either none (0) of the two, one (1), or both (2) were highly expressed, showing that in familial breast cancer more often one of the two or both were highly expressed and in sporadic breast cancer mostly neither cPARP nor nPARP were highly expressed (P=0.009, chi-squared test)

Table 2 Comparison of cPARP and nPARP expression levels

nPARP	cPARP			
	Low	Intermediate	High	Total
Low	5 (6.4 %)	1 (1.3 %)	1 (1.3 %)	7 (9 %)
Intermediate	18 (23.1 %)	10 (12.8 %)	4 (5.8 %)	31 (41 %)
High	13 (16.7)	9 (11.5 %)	17 (21.8 %)	39. (50 %)
Total	36 (46.2 %)	20 (25.6 %)	22 (28.2 %)	78 (100 %)

nPARP expression are evident but cannot be explained with our study design.

Another study done by Ozretić et al. included tissue samples from 93 BRCA1/2-associated and 53 sporadic breast cancers [21]. Consistent with our findings, Ozretić et al. found high nPARP expression more frequently in BRCA1/2-associated cases. In contrast to our results, they did not observe cytoplasmic staining. They also observed significantly higher nPARP expression in hormone receptor-positive cases, whereas other studies showed higher PARP expression in hormone receptor negative samples than in hormone receptor-positive samples [19, 22]. Our study did not show any correlation between PARP expression and hormone receptor status or other clinicopathological parameters.

The differences in results between those two studies and ours may be due to different PARP antibodies used. Domagala et al. also used a different scoring system (multiplicative quickscore) than Ozretić et al. and us (immunoreactivity score). Another difference between the studies is that we included different kinds of familial breast cancer cases (BRCA1, BRCA2, and non-BRCA1/2) while Domagala et al. and Ozretić et al. only included BRCA1- and BRCA2-mutated tumors. In addition, we used a case–control approach, matching cases according to size, grade, HR status, and HER2 status, whereas Ozretić et al. and Domagala et al. used different selection criteria.

In a recent review on the various functions of PARP-1, its dominant role in DNA repair is highlighted [23]. In response to genotoxic stress, PARP relocates to the site of DNA damage to induce DNA repair in several different ways, e.g., PARylation and subsequently p53 activation. BRCA-mutated cases might have more DNA damage. This might explain why cPARP and nPARP expression is higher in familiar breast cancer cases. This hypothesis is supported by Ossovskaya et al. who demonstrated that loss of a DNA repair pathway can be compensated by upregulation of alternative DNA repair mechanisms. We contend that also the PARP pathway may be upregulated due to the loss of a DNA repair pathway [22]. The resulting higher PARP levels in turn induce downregulation of, e.g., BRCA2 expression, through interaction with the BRCA2 promoter [24]. Newer

data suggest that PARP inhibition can also downregulate BRCA1, which in turn downregulates homologous recombination. Cells which show low BRCA expression, e.g., BRCA-mutated breast cancer cells, have defects in the homologous recombination pathway [25]. A study by Patel et al. showed that PARP-1 plays an important role in nonhomologous end joining in these cells, which finally contributes to the genomic instability arisen from the use of PARP inhibitors [25–27].

In a recent study of sporadic breast cancer in the neoadjuvant setting, we reported a correlation between high cPARP expression and high-grade histological characteristics, unfavorable long-term prognosis, and better response to neoadjuvant chemotherapy [19]. In our present study, cPARP expression was higher in familial breast cancers. As breast cancer prognosis depends on parameters such as estrogen receptor expression, tumor size, and nodal status [28, 29], which were different between the patient groups in these studies, the lack of consistency between these studies does not come as a surprise. In order determine the potential of PARP as a prognostic factor in hereditary and non-hereditary breast cancer, a large case–control study will be necessary.

Patients with a higher PARP expression might also respond better to neoadjuvant chemotherapy. This idea might be supported by a study from Arun et al. which showed that hereditary breast cancer, especially BRCA1, is associated with higher pCR rates after neoadjuvant systemic chemotherapy [30]. In order to confirm this hypothesis, studies including PARP expression and response to neoadjuvant chemotherapy in hereditary and non-hereditary breast cancer are needed.

Although our study showed promising results, there are still some limitations to it. In order to make a statement about the long-term prognosis in the two groups, it would have been beneficial to include survival data and probably even larger group sizes. As the genetic testing has not been performed for the cohort of clinically sporadic breast cancer cases, it might be possible that a few familial breast cancer cases are present in this group. In addition, the cohort of familial breast cancer was not homogenous, and BRCA testing had not been performed for five cases. It might therefore be interesting for further study purposes to differentiate between different types of familial breast cancer, especially in the context of a study from Kurian et al. that showed that women who tested negative for an BRCA1 or BRCA2 mutation are not at high enough risk to be kept under routine surveillance [27]. But in combination with the PARP expression and the probable prognostic implication of that, it might be interesting to further investigate differences in PARP expression between hereditary and familial breast cancer.

In conclusion, our results show that the overall PARP expression is higher in familial breast cancer than in sporadic breast cancer, which suggests that they might respond better to treatment with PARP inhibitors. In order to reveal the potential of PARP as a prognostic factor and predictor of response to PARP inhibitors, further research needs to be done.

Acknowledgments We would like to thank Petra Wachs and Ines Koch for their excellent technical assistance as well as Martina Eickmann, Catarina Liebscher, and Britta Dahl for proofreading.

Conflict of interests The authors declare that they have no conflict of interest.

References

1. Siegel R, Naishadham D, Jemal A (2012) Cancer statistics, 2012. CA Cancer J Clin 62(1):10–29
2. Lee E-H, Park SK, Park B, Kim S-W, Lee MH, Ahn SH, Son BH, Yoo K-Y, Kang D (2010) Effect of BRCA1/2 mutation on short-term and long-term breast cancer survival: a systematic review and meta-analysis. Breast Cancer Res Treat 122(1):11–25
3. Murphy CG, Moynahan ME (2010) BRCA gene structure and function in tumor suppression: a repair-centric perspective. Cancer J 16(1):39–47
4. Bane A, O'Malley FP (2006) Familial breast cancer. In: Kuhn B (ed) Breast pathology. Churchill Livingstone Elsevier, Philadelphia, pp 241–248
5. Osin PP, Lakhani SR (1999) The pathology of familial breast cancer immunohistochemistry and molecular analysis. Breast Cancer Res 1(1):36–40
6. Turner N, Tutt A, Ashworth A (2004) Hallmarks of 'BRCAness' in sporadic cancers. Nat Rev Cancer 4(10):814–819
7. van der Groep P, van der Wall E, van Diest P (2011) Pathology of hereditary breast cancer. Cell Oncol (Dordr) 34(2):71–88
8. Anders C, Carey LA (2008) Understanding and treating triple-negative breast cancer. Oncology (Williston Park) 22(11):1233–1243
9. Goldhirsch A, Wood WC, Coates AS, Gelber RD, Thürlimann B, Senn HJ, Panel M (2011) Strategies for subtypes dealing with the diversity of breast cancer: highlights of the St Gallen International Expert Consensus on the primary therapy of early breast cancer 2011. Ann Oncol 22(8):1736–1747
10. Byrski T, Gronwald J, Huzarski T, Grzybowska E, Budryk M, Stawicka M, Mierzwa T, Szwiec M, Wisniowski R, Siolek M, Dent R, Lubinski J, Narod S (2010) Pathologic complete response rates in young women with BRCA1-positive breast cancers after neoadjuvant chemotherapy. J Clin Oncol 28(3):375–379
11. Fong PC, Boss DS, Yap TA, Tutt A, Wu P, Mergui-Roelvink M, Mortimer P, Swaisland H, Lau A, O'Connor MJ, Ashworth A, Carmichael J, Kaye SB, Schellens JHM, de Bono JS (2009) Inhibition of poly(ADP-ribose) polymerase in tumors from BRCA mutation carriers. N Engl J Med 361(2):123–134
12. Leung M, Rosen D, Fields S, Cesano A, Budman DR (2011) Poly (ADP-ribose) polymerase-1 inhibition: preclinical and clinical development of synthetic lethality. Mol Med 17(7–8):854–862
13. Schreiber V, Amé J, Dollé P, Schultz I, Rinaldi B, Fraulob V, Ménissier-de Murcia J, de Murcia G (2002) Poly(ADP-ribose) polymerase-2 (PARP-2) is required for efficient base excision DNA repair in association with PARP-1 and XRCC1. J Biol Chem 277(25):23028–23036
14. Calvert H, Azzariti A (2011) The clinical development of inhibitors of poly(ADP-ribose) polymerase. Ann Oncol 22(suppl 1): i53–i59

15. Annunziata CM, O'Shaughnessy J (2010) Poly (ADP-ribose) polymerase as a novel therapeutic target in cancer. Clin Cancer Res 16(18):4517–4526
16. Tutt A, Robson M, Garber JE, Domchek SM, Audeh MW, Weitzel JN, Friedlander M, Arun B, Loman N, Schmutzler RK, Wardley A, Mitchell G, Earl H, Wickens M, Carmichael J (2010) Oral poly (ADP-ribose) polymerase inhibitor olaparib in patients with BRCA1 or BRCA2 mutations and advanced breast cancer: a proof-of-concept trial. Lancet 376(9737):235–244
17. Patel AG, De Lorenzo SB, Flatten KS, Poirier GG, Kaufmann SH (2012) Failure of iniparib to inhibit poly(ADP-ribose) polymerase in vitro. Clin Cancer Res 18(6):1655–1662
18. Development Core Team R (2011) R: a language and environment for statistical computing. R Foundation for Statistical Computing, Vienna
19. von Minckwitz G, Müller BM, Loibl S, Budczies J, Hanusch C, Darb-Esfahani S, Hilfrich J, Weiss E, Huober J, Blohmer JU, du Bois A, Zahm D-M, Khandan F, Hoffmann G, Gerber B, Eidtmann H, Fend F, Dietel M, Mehta K, Denkert C (2011) Cytoplasmic poly (adenosine diphosphate ribose) polymerase expression is predictive and prognostic in patients with breast cancer treated with neoadjuvant chemotherapy. J Clin Oncol 29(16):2150–2157
20. Domagala P, Huzarski T, Lubinski J, Gugala K, Domagala W (2011) PARP-1 expression in breast cancer including BRCA1-associated triple negative and basal-like tumors: possible implications for PARP-1 inhibitor therapy. Breast Cancer Res Treat 127 (3):861–869
21. Ozretić L, Rhiem K, Huss S, Wappenschmidt B, Markiefka B, Sinn P, Schmutzler RK, Buettner R (2011) High nuclear poly (adenosine diphosphate-ribose) polymerase expression is predictive for BRCA1- and BRCA2-deficient breast cancer. J Clin Oncol 29(34):4586–4588
22. Ossovskaya V, Chou Koo I, Kaldjian EP, Alvares C, Sherman BM (2010) Upregulation of poly (ADP-ribose) polymerase-1 (PARP1) in triple-negative breast cancer and other primary human tumor types. Genes Cancer 1(8):812–821
23. Krishnakumar R, Kraus WL (2010) The PARP side of the nucleus: molecular actions, physiological outcomes, and clinical targets. Mol Cell 39(1):8–24
24. Wang J, Bian C, Li J, Couch FJ, Wu K, Zhao RC (2008) Poly (ADP-ribose) polymerase-1 down-regulates BRCA2 expression through the BRCA2 promoter. J Biol Chem 283(52):36249–36256
25. Hegan DCLY, Stachelek GC, Crosby ME, Bindra RS, Glazer PM (2010) Inhibition of poly(ADP-ribose) polymerase down-regulates BRCA1 and RAD51 in a pathway mediated by E2F4 and p130. Proc Natl Acad Sci U S A 107(5):2201–2206
26. Patel AGSJ, Kaufmann SH (2011) Nonhomologous end joining drives poly(ADP-ribose) polymerase (PARP) inhibitor lethality in homologous recombination-deficient cells. Proc Natl Acad Sci U S A 108(8):3406–3411
27. Kurian AW, Gong GD, John EM, Johnston DA, Felberg A, West DW, Miron A, Andrulis IL, Hopper JL, Knight JA, Ozcelik H, Dite GS, Apicella C, Southey MC, Whittemore AS (2011) Breast cancer risk for noncarriers of family-specific BRCA1 and BRCA2 mutations: findings from the breast cancer family registry. J Clin Oncol 29(34):4505–4509
28. Elston C, Ellis I (1991) Pathological prognostic factors in breast cancer. I. The value of histological grade in breast cancer: experience from a large study with long-term follow-up. Histopathology 19(5):403–410
29. Subramanian A, Salhab M, Mokbel K (2008) Oestrogen producing enzymes and mammary carcinogenesis: a review. Breast Cancer Res Treat 111(2):191–202
30. Arun B, Bayraktar S, Liu DD, Gutierrez Barrera AM, Atchley D, Pusztai L, Litton JK, Valero V, Meric-Bernstam F, Hortobagyi GN, Albarracin C (2011) Response to neoadjuvant systemic therapy for breast cancer in BRCA mutation carriers and noncarriers: a single-institution experience. J Clin Oncol 29(28):3739–3746

Virchows Arch (2012) 461:433–439
DOI 10.1007/s00428-012-1293-0

ORIGINAL ARTICLE

Morphological and molecular characteristics of nested melanoma of the elderly (evolved lentiginous melanoma)

Ilaria Pennacchia · Simone Garcovich · Rita Gasbarra · Alvaro Leone · Vincenzo Arena · Guido Massi

Received: 21 February 2012 / Revised: 11 July 2012 / Accepted: 23 July 2012 / Published online: 15 August 2012
© Springer-Verlag 2012

Abstract We identified a group of melanocytic lesions with an architectural pattern very similar to that of a junctional nevus: cells mostly grouped in distinct nests, more or less of the same size and shape, and regularly distributed along the dermoepidermal junction. In contrast with these nevus-like features, these neoplasms display additional details which are incompatible with a diagnosis of junctional nevus. These include areas of lentiginous array with focal pagetoid spread of melanocytes above the junction; marked cytological atypia, such as nuclear enlargement, hyperchromasia, nuclear membrane thickening and with a mild degree of cellular pleomorphism. Moreover, these lesions mostly developed on severely sun-damaged skin of old patients. Using a four-probe fluorescence in situ hybridization (FISH) assay targeting RREB1, MYB, Cep6, and CCND1, we found that seven of the eight propositus cases showed chromosomal aberrations consistent with the standardized FISH diagnostic criteria for melanoma. Instead, the five junctional nevi that served as controls were negative in this test. These findings underline the utility of correlating clinical–pathological observations with FISH analysis for diagnosing correctly as melanoma these malignant neoplasms, which closely simulate a junctional nevus.

Keywords Nested · Melanoma · Nevi · FISH

I. Pennacchia and S.Garcovich equally contributed to this work.

I. Pennacchia (✉) · V. Arena · G. Massi
Department of Pathology, Catholic University Medical School, Rome, Italy
e-mail: ilaria.pennacchia@libero.it

S. Garcovich
Department of Dermatology, Catholic University Medical School, Rome, Italy

R. Gasbarra · A. Leone
Department of Pathology, Forlanini Hospital, Rome, Italy

Introduction

We have identified a group of melanocytic lesions of which the architectural pattern strikingly resembles that of a common junctional melanocytic nevus. The neoplastic cells are predominantly organized in nests, mostly roundish and discrete, more or less of the same size and shape, and evenly scattered along the dermoepidermal junction. These reassuring architectural features give a first impression at scanning magnification of a junctional nevus, but these lesions display other details which are unquestionably in conflict with the seemingly benign nature of these tumors [1–7]. Significant cytological atypia is observed: cells are either hyperchromatic, with small lymphocyte-like nuclei and barely distinguishable cytoplasm or large-sized, with a thick and irregular nuclear membrane, coarse chromatin, and prominent nucleoli. Occasionally, areas of lentiginous melanocytic proliferation are noted, along with focal pagetoid spread of atypical cells within the epidermis [8–11]. Moreover, a closer view at higher magnification shows the presence of a subtle but indisputable cellular pleomorphism. Finally, these lesions have mostly developed on severely sun-damaged skin of old patients. We present in this paper eight cases with the above-mentioned cytoarchitectural features, which we investigated from a morphological point of view but also with the Vysis LSI RREB/LSI MYB/LSICCND1/CEP6 fluorescence in situ hybridization (FISH) in order to confirm a diagnosis of melanoma of these lesions. This four-probe multicolor FISH assay detects genetic abnormalities in chromosomes 6 and 11 and currently provides a means to discriminate melanoma from nevi with a sensitivity of 86.7 % and a specificity of 95.4 %. The four chromosomal loci and the specific genes targeted by the

FISH assay include 6p25 (RREB1), 6q23 (MYB), 11q13 (cyclin D1), and Cep6 (the centromeric portion of chromosome 6) [12–14].

Materials and methods

We selected eight propositus cases of melanocytic neoplasms containing the following conflicting histological characteristics:

1. Prevalence of a nested pattern, with mostly roundish and clear cut nests, regularly shaped and sized, evenly scattered along the dermoepidermal junction. In some cases, however, focal areas with large, bizarrely shaped, and irregularly confluent melanocytic nests could be found as well.
2. Sharp circumscription by discrete nests at both extremities of the lesions.
3. The presence of focal areas with lentiginous proliferation of melanocytes at the dermoepidermal junction.
4. Occasional pagetoid scattering of melanocytes both at the center and the edges of lesions and also above areas in which single melanocytes predominated.
5. Presence of features of marked cytological atypia, namely, either hyperchromatic cells, with small lymphocyte-like nuclei and an almost undetectable rim of cytoplasm or large cells, with thick and irregular nuclear membranes, prominent nucleoli, and clumped chromatin. A mild degree of cellular pleomorphism was detectable, too.
6. Absence of epidermal atrophy, expansive nodules, and significant mitotic activity.
7. Presence of a variable degree of solar elastosis in all but one case.
8. All lesions were more than 5 mm in diameter and less than 1 mm in thickness.
9. Adult/old age of patient (range 37–90 years).

Control cases

Five cases of junctional nevi without any hints of malignancy were used as controls.

Fluorescence in situ hybridization (FISH)

FISH analysis on the eight propositus cases and five controls was carried out on 3–4 μm thick sections from formalin-fixed, paraffin-embedded tissue samples. From each specimen, two slides were obtained, one for H&E staining, the other for FISH analysis. On the H&E stained sections, regions with predominance of melanocytic cells over stromal cells were marked using a diamond-tipped scribe. The same areas were scribed on the corresponding unstained slides. Deparaffination was carried out by baking the unstained slides for 4–5 h at 75 °C and subsequently immersing them in Coplin jars containing xylene, first at 60 °C for 1 h and then at room temperature for 20 min. Slides afterwards underwent two passages in absolute alcohol, each time for 20 min. Before hybridization, sections were pretreated with 1× SSC pH 6.3 at 80±1 °C for 35 min and digested with 25 mg/ml protease at 37 °C for 10 min. Slides were then rinsed in purified water for 3 min and immersed three times in 70 %, 85 %, and 100 % ethanol, respectively, each time for 2 min. The following DNA probes (Abbott Laboratories) were used: the RREB1 (6p25) probe, labeled with Spectrum Red; the MYB (6q23) probe, labeled with SpectrumGold; the CCND1 (11q13) probe, labeled with SpectrumGreen; and the CEP 6 probe, labeled with SpectrumAqua. Hybridization was performed using the HYBrite machine (Abbott Laboratories). Ten microliters of probe in hybridization buffer was applied to each slide which was subsequently covered with a coverslip and sealed with rubber cement. The slides were codenatured with the probe mixture at 73 °C for 5 min and then hybridized for ≥16 h at 37 °C. Slides were then washed in 2× SSC/0.3 % NP40 for 2 min at room temperature, counterstained with 10 μl of DAPI 1 (Abbott) and finally examined under a fluorescence microscope (Olympus BX61), equipped with appropriate excitation and emission filters, allowing visualization of aqua, green, gold, and red fluorescent signals and DAPI counterstaining. For each case, 30 cells from a minimum of three different regions previously located within the tumor were scored for the four FISH probes. To determine melanoma status, four parameters were calculated:

1. Average CCND1 signals per nucleus,
2. Average MYB signals per nucleus,
3. Percentage of nuclei with abnormal RREB1, and
4. Percentage of nuclei with loss of MYB relative to CEP6.

Specimens were defined as “Melanoma FISH positive” if one of the following from the manufacturer's established criteria was fulfilled:

1. Average CCND1 signals per nuclei or average MYB signals per nuclei ≥2.5,
2. Percent loss of MYB relative to CEP6 ≥31 %, and
3. Percentage of abnormal nuclei for RREB1 ≥63 %.

Specimens were classified as “FISH negative” if none of the criteria mentioned above were met.

DNA extraction and BRAF mutational analysis

Two or more sections of paraffin-embedded tissue (the number varied depending on the concentration of tumor

cells in the sample) were manually microdissected by an expert pathologist with a sterile razor and genomic DNA was extracted with a QIAamp DNA mini extraction kit following the manufacturer's protocol (Qiagen). Amplification of BRAF was performed by PCR with the AmpliTaq kit (Applied Biosystems) using the following primers: BRAF F: 5′-CCTAAACTCTTCATAATGCTT-3′ BRAF R: 5′-ATAGCCTCAATTCTTACCAT-3′. The PCR products were treated with exonuclease/shrimp alkaline phosphatase (Exo/Sap USB) and sequenced with the same PCR primers using the 3.1 BigDye Terminator Cycle Sequencing Ready reaction kit (Applied Biosystems). The sequencing reactions were purified with the XTerminator solution (Applied Biosystems) and run by capillary gel electrophoresis in an ABI PRISM 310 Genetic Analyzer (Applied Biosystems). PCR reactions were performed at least twice and sequence analyses were performed in forward and reverse orientations.

Immunohistochemistry

Immunohistochemical staining for cyclin D1 (clone SP4-R), S-100 (clone 4C4.9), p16, Melanoma Associated Antigen (clone KBA.62), and Anti-Human Melanosome (Clone HMB-45) was performed using the Ventana BenchMark XT (Ventana, Tucson, AZ) (Fig. 3a, b, c).

Results

Clinical characteristics

All the eight propositus cases occurred in females, with a median age of 65.6 years (range 37–90 years). Four of the eight cases were on the trunk, three on the lower extremities, and one on the forearm. Of the five control cases of junctional nevi, four were from females, with a median patient age of 34.8 years (range 26–53 years). Three cases were from the trunk and two from the extremities.

Histological findings

Histologically (Table 2), all lesions were mostly well-circumscribed with sharp margins and characterized by a striking nested pattern (Fig. 1), suggesting at scanning magnification a diagnosis of junctional nevus. Nests were mostly small, nevus-like, clear cut, and evenly spaced along the junction. However, a few alarming details indicative of malignancy were present as well. All cases but one showed a mild to severe degree of solar elastosis, with even confluent masses of elastotic fibers replacing the normal collagen bundles. A few areas of lentiginous proliferation with focal pagetoid ascent of melanocytes, more consistent with a diagnosis

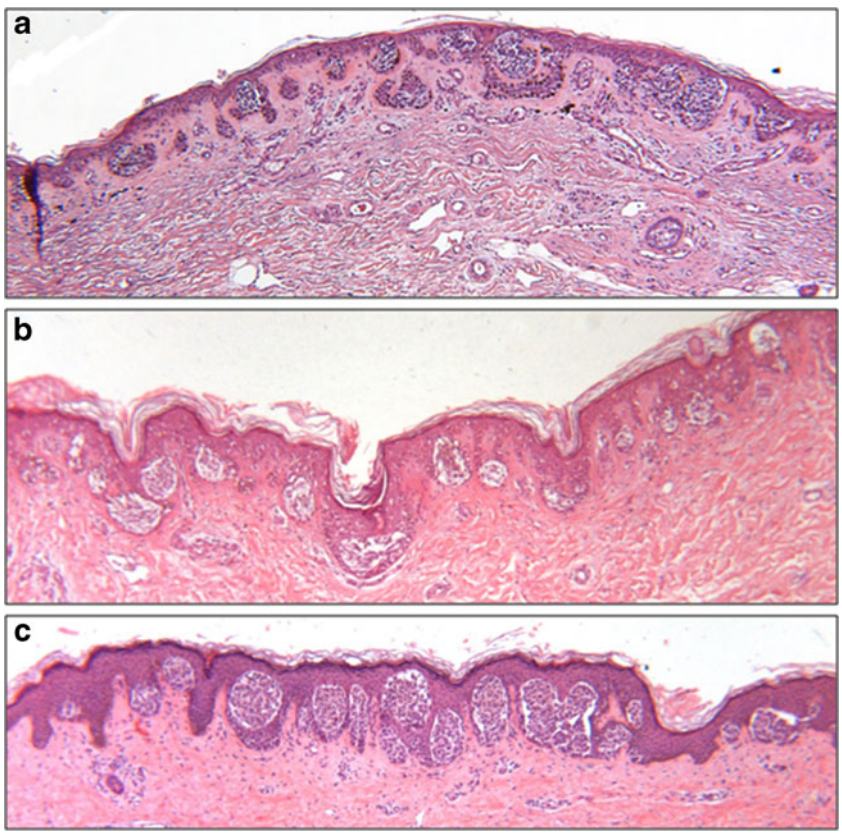

Fig. 1 A panel showing the striking nested pattern throughout the entire span of the lesion

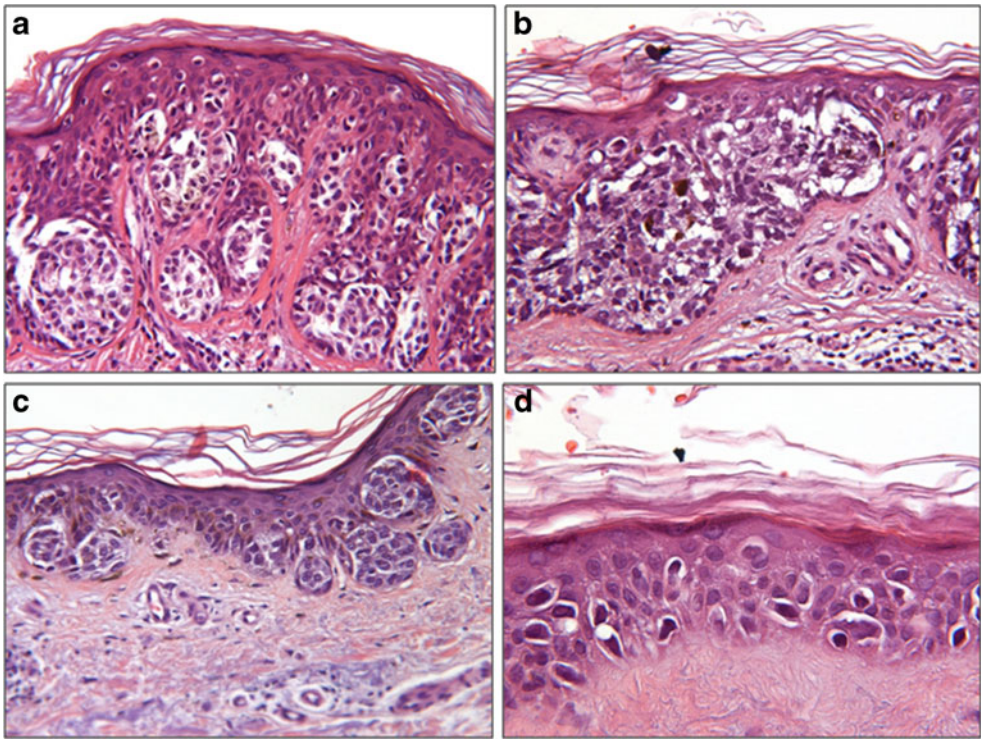

Fig. 2 Some of the hints of malignancy observed in the lesions (see text for details)

of melanoma in situ, were found as well. Some cytological atypia along with mild cellular plemorphism was also present. Cells were small, lymphocytic-like, highly hyperchromatic with barely distinguishable cytoplasm (Fig. 2). In some cases, a second population of large melanocytes with vesicular nuclei, irregularly thickened nuclear membranes, and prominent nucleoli was also found. Occasionally, nests were larger and widely confluent in bizarrely shaped masses of cells. Moreover, they sometimes varied significantly in size, shape, and content of pigment. No or scant inflammatory infiltrate was seen in the cases. In case no. 3 additional serial sections were made revealing a clear-cut invasive malignant melanoma of about 0.3 mm in thickness.

FISH results

Regarding FISH analysis, results were obtained using an Excel-based analysis algorithm for data elaboration supplied by the producing company and are plotted in Table 1. Seven of the eight cases proved positive in the test (Fig. 3d). The alteration in the RREB1 site was the most frequently observed abnormality in our nested melanoma cases (Table 1). In contrast, the five cases of junctional melanocytic nevus used as control were all negative by FISH, no genome anomalies were registered, and reference values were always well below cutoff values.

Table 1 Clinical data and FISH results

Case	Age	Sex	Dim (mm)	RREB1 percentage of nuclei with signal ≠ 2≥63	MYB ≥2.5 amplification (average)	CCND1 ≥2.5 amplification (average)	Percentage loss of MYB ≥31	FISH results
1	90	F	10	88.1	4.1	3	33	Positive
2	61	F	7	50	1.9	1.5	2	Negative
3	37	F	8	50	2.7	2.5	5.6	Positive
4	49	F	12	78	2.5	1.9	49	Positive
5	67	F	>30	87.8	2.1	2.1	24.2	Positive
6	76	F	10	88.9	1.5	1.7	41.5	Positive
7	80	F	6	78	2.8	2.2	25	Positive
8	65	F	10	63.8	2.4	2.1	19.6	Positive

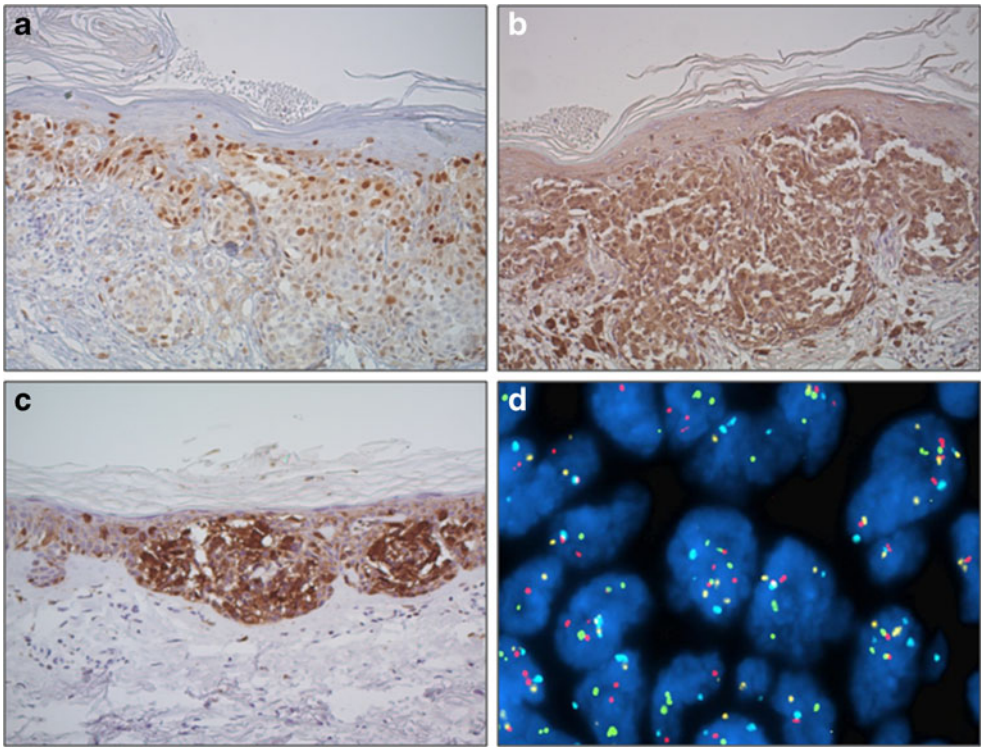

Fig. 3 Immunohistochemistry for cyclin D1 (**a**), melan-A (**b**), and HMB45 (**c**). **d** FISH analysis image

BRAF results

Cases no. 1, 2, and 7 showed the BRAF V600E mutation, whereas all the others were normal.

Discussion

The cases of our study have in common a striking nested junctional pattern highly suggestive at scanning magnification of a diagnosis of a benign nevus. Cells are mostly arranged in roundish nests evenly aligned at the dermoepidermal junction. Nests are mostly clear-cut and regularly sized and shaped. There is no doubt that in routine histological examination these lesions might be misdiagnosed as junctional nevi. However, the clinical setting is definitely not compatible with a junctional nevus. Patients are old and the neoplasms appear on severely sun-damaged skin. Moreover, the lesions are unusually large in most of the cases. Furthermore, from a histological point of view, major cytological details conflict with a diagnosis of

Table 2 Histological characteristics

No.	Shoulders	Elastosis	Atrophy	Lentiginous array[a]	Cytological atypia	Confluence of nest	Pagetoid spread[b]	Inflammatory infiltrate	Pigment distribution
1	Lentiginous	++	No	++	++	Yes	+	+	Irregular
2	Nested	++	No	++	+	Yes	+	+/−	Irregular
3	Nested	+	No	−	+	Yes	+	+/−	Regular
4	Nested	No	No	−	+	Yes	++	No	Irregular
5	Lentiginous	+	No	++	+++	Yes	++	+	Irregular
6	Nested	+++	No	+/−	+	Yes	+	No	Regular
7	Nested	++	No	+	++	Yes	+	No	Regular
8	lentiginous	++	No	+	+++	Yes	+	No	Regular

The values reported (insignificant or not detectable finding −, low +, moderate ++, and severe +++) were independently assessed by 2 different observers (IP-VA) and confirmed by a senior pathologist (GM)

[a] Lentiginous arrangement was considered (+) when present for a third of the span of the lesional epidermis, (++) for half of the span, and (+++) for more than half

[b] Pagetoid spread was judged as (+) when 1–3 melanocytes were present for 1 mm of epidermis, (++) for 3–5 melanocytes, and (+++) for more than 5. Other cytological or architectural details were judged simply presence or absence

junctional nevus [1–3, 5, 7]. The most important of these is the presence of diffuse hyperchromasia of the cells inside the nests. Nuclei are small, lymphocyte-like, hyperchromatic as well as clumped. In some cases, a second population of large cells with a thickened nuclear membrane and large and basophilic nucleoli is found as well. At high power, a subtle but unquestionable cellular pleomorphism is also present. A further aspect contradicting a diagnosis of benign melanocytic nevus is the presence of a few cells with atypical features scattered above the junction. The pagetoid spread involves not only the center of the lesions but also the lateral portion of the neoplasms and even areas where junctional nests are not present at all. In some cases, a major feature is the presence of a lentiginous pattern of growth alternating with a nested one [8–10]. Melanocytes are aligned in single units along the junction with skip areas of irregular distribution. In all, these junctional lesions fulfill most criteria for a diagnosis of melanoma despite their striking nested pattern. Obviously, these lesions have to be distinguished from a form of junctional or compound dysplastic nevus, which can also occur in older patients and is usually larger than 5 mm in diameter [15–17]. However, in the cases we present, a diagnosis of malignant melanoma rather than dysplastic nevus was favored mostly on the basis of the following histological features: (1) predominance of melanocytic cells with a significant cytological atypia; (2) absence of lamellar fibroplasia in the papillary dermis which is typical of Clark nevus; and (3) presence of severe solar elastosis, which makes the diagnosis of dysplastic nevus highly improbable. This notwithstanding, in order to corroborate the diagnosis of melanoma, we further evaluated these lesions with a FISH assay for diagnosis in melanoma which currently provides a sensitivity of 86.7 % and a specificity of 95.4 % in discriminating benign and malignant melanocytic neoplasms [12–14, 18–20]. This assay revealed chromosomal alterations indicative of melanoma in all but one of our cases, whereas all control cases were negative. In our opinion, the subset of melanoma we presented here represents an evolved stage of the so-called lentiginous melanoma, an entity which was firstly described by King et al. in 2005 [8–10]. The term "lentiginous melanoma" defines a group of slowly progressing melanoma typically found on the trunk and proximal extremities of middle-aged and older patients. Its histological pattern is characterized by a broad lentiginous proliferation of atypical melanocytes occasionally gathered in nests, with focal pagetoid spread and nonsignificant dermal fibroplasia. In the paper by Newman et al. [11], a FISH study was conducted on 19 cases of lentiginous melanoma, of whom 16 (84 %) were positive by the test. Hence, in the same way, we propose to label as nested melanoma the subgroup of neoplasms closely mimicking a junctional nevus that we first described here. We firmly believe these lesions should be studied carefully through serial sections as they might not only reveal areas of more conventional melanoma but also an invasive component into the papillary dermis, as happened in one of our lesions. Regarding clinical treatment, reexcision of these lesions is highly recommended (Table 2).

Conclusions

Our observations support the notion that a small but distinct group of melanomas closely simulate junctional nevi because of their nested architecture. The striking nested pattern which characterizes this new entity, compared with the prominent lentiginous proliferation with only focal nesting of lentiginous melanoma, makes it a very dangerous diagnostic trap. In view of the strong similarity to a junctional nevus, these lesions are more likely to be misinterpreted as benign than cases of lentiginous melanoma, given that the lentiginous growth pattern itself represents a major hint of malignancy. A diagnosis of nested melanoma can be suspected when considering some additional clinical and histological clues, namely, old age of the patient, large lesion, presence of severe sun damage, atypical cytological features, focal pagetoid spread, and lentiginous pattern of melanocytic proliferation. These clues should induce the pathologist to perform additional evaluation with FISH technique with which we found chromosomal alterations consistent with melanoma in all but one of our cases. All the lesions consisted of junctional melanocytic proliferations in the initial sections, but additional serial sections showed an invasive component in one case. Making the correct diagnosis of melanoma in these cases is not only an academic matter as the misinterpretation of these lesions could have serious implications for treatment and prognosis.

Conflict of interest None.

References

1. Zembowicz A, McCusker M, Chiarelli C et al (2001) Morphological analysis of nevoid melanoma, a study of 20 cases with a review of the literature. Am J Dermatopathol 23:167–175
2. Schmoeckel C, Castro CE, Braun-Falco O (1985) Nevoid malignant melanoma. Arch Dermatol Res 277:362–369
3. McNutt NS, Urmacher C, Halamian J et al (1985) Naevoid malignant melanoma: morphologic patterns and immunohistochemical reactivity. J Cutan Pathol 22:502–517
4. Blessing K, Evans AT, Al-Nafuss A (1983) Verrucous naevoid and keratotic melanoma: a clinicopathological study of 20 cases. Histopathology 23:455–458
5. Kossard S, Wilkinson B (1997) Small cell (naevoid) melanoma. A clinicopathologic study of 131 cases. Australas J Dermatol 38 (Suppl):S54–S58
6. Kossard S, Wilkinson B (1995) Nucleolar organiser regions and image analysis nuclear morphometry of small cell naevoid melanoma. J Cutan Pathol 23:132–136

7. Blessing K, Grant JJH, Sanders DSA et al (2000) Small cell malignant melanoma, a variant of naevoid melanoma: clinicopathological features and histological differential diagnosis. J Clin Pathol 53:591–595
8. King R, Page RN, Googe PB et al (2005) Lentiginous melanoma: a histologic pattern of melanoma to be distinguished from lentiginous nevus. Mod Pathol 18:1397–1401
9. Kossard S (2002) Atypical lentiginous junctional naevi of the elderly and melanoma. Australas J Dermatol 43:93–101
10. Kossard S, Commens C, Symons M et al (1991) Lentinginous dysplastic naevi in the elderly: a potential precursor for malignant melanoma. Australas J Dermatol 32:27–37
11. Newman MD, Mirzabeigi M, Gerami P (2009) Chromosomal copy number changes supporting the classification of lentiginous junctional melanoma of the elderly as a subtype of melanoma. Mod Pathol 22:1258–1262
12. Gerami P, Mafee M, Lurtsbarapa T et al (2010) Sensitivity of fluorescence in situ hybridization for melanoma diagnosis using RREB1, MYB, Cep6, and 11q13 probes in melanomas. Arch Dermatol 146(3):273–278
13. Gaiser T, Kutzner H, Palmedo G et al (2010) Classifying ambiguous melanocytic lesions with FISH and correlation with clinical long-term follow-up. Mod Pathol 23:413–419
14. Gerami P, Zembowicz A (2011) Update on fluorescence in situ hybridization in melanoma. State of the Art. Arch Pathol Lab Med 135:830–837
15. Kim JC, Murphy GF (2000) Dysplastic melanocytic nevi and prognostically indeterminate nevomelanomatoid proliferations. Clin Lab Med 20:691–712
16. Sagebiel RW (1985) Histopathology of precursor melanocytic lesions. Am J Surg Pathol 9(Suppl):41–52
17. Skender-Kalnenas TM, English DR, Heenan PJ (1995) Benign melanocytic lesions: risk markers or precursors of cutaneous melanoma? J Am Acad Dermatol 33:1000–1007
18. Gerami P, Beilfuss B, Haghighat Z et al (2011) Fluorescence in situ hybridization as an ancillary method for the distinction of desmoplastic melanomas from sclerosing melanocytic nevi. J Cutan Pathol 38:329–334
19. Gammon B, Beilfuss B, Guitart J et al (2011) Fluorescence in situ hybridization for distinguishing cellular blue nevi from blue nevus-like melanoma. J Cutan Pathol 38:335–341
20. Pouryazdanparast P, Haghighat Z, Beilfuss BA et al (2011) Melanocytic nevi with an atypical epithelioid cell component: clinical, histopathologic, and fluorescence in situ hybridization findings. Am J Surg Pathol 35:1405–1412

Virchows Arch (2012) 461:441–448
DOI 10.1007/s00428-012-1309-9

ORIGINAL ARTICLE

Loss of microRNA-200a and c, and microRNA-203 expression at the invasive front of primary cutaneous melanoma is associated with increased thickness and disease progression

Léon C. van Kempen · Karin van den Hurk · Vladimir Lazar · Stefan Michiels · Véronique Winnepenninckx · Marguerite Stas · Alan Spatz · Joost J. van den Oord

Received: 23 July 2012 / Revised: 16 August 2012 / Accepted: 27 August 2012 / Published online: 6 September 2012
© Springer-Verlag 2012

Abstract Loss of E-cadherin expression in melanoma correlates with increased tumor thickness and reduced disease-free survival. The molecular mechanisms underpinning its differential expression in melanoma tissue remain elusive. MicroRNAs (miRNAs) have been implicated in tumor progression and regulation of E-cadherin expression. Here, we demonstrate a significant correlation between tumor thickness and loss of expression of miR-200a, miR-200c, and miR-203 in a series of 23 frozen primary melanomas, where it was confirmed in two subsequent validation series (series 1: six nevi, 15 primary

Electronic supplementary material The online version of this article (doi:10.1007/s00428-012-1309-9) contains supplementary material, which is available to authorized users.

L. C. van Kempen (✉) · A. Spatz
Lady Davis Institute for Medical Research,
Jewish General Hospital,
LDI-E447, 3755 Cote Ste-Catherine,
Montreal, QC, Canada H3T 1E2
e-mail: leon.vankempen@mcgill.ca

L. C. van Kempen · A. Spatz
Department of Pathology, McGill University,
Jewish General Hospital,
Montreal, Canada

A. Spatz
Department of Oncology, McGill University,
Jewish General Hospital,
Montreal, Canada

K. van den Hurk · V. Winnepenninckx
Department of Pathology, GROW-School for Oncology and Developmental Biology, Maastricht University Medical Center,
Maastricht, The Netherlands

V. Lazar
Division of Functional Genomics, Gustave-Roussy Institute,
Villejuif, France

S. Michiels
Division of Biostatistics and Epidemiology,
Gustave-Roussy Institute,
Villejuif, France

S. Michiels
Breast Cancer Translational Research Laboratory,
Institut Jules Bordet, Université Libre de Bruxelles,
Brussels, Belgium

M. Stas
Division of Surgical Oncology, University Hospitals,
Katholieke Universiteit Leuven,
Leuven, Belgium

J. J. van den Oord
Laboratory of Morphology and Molecular Pathology,
University Hospitals, Katholieke Universiteit Leuven,
Leuven, Belgium

L. C. van Kempen · M. Stas · A. Spatz · J. J. van den Oord
EORTC Melanoma Group,
Brussels, Belgium

L. C. van Kempen
Department of Pathology,
Radboud University Nijmegen Medical Centre,
Nijmegen, The Netherlands

melanomas, and 16 metastases; series 2: 11 matched pairs of primary melanomas and metastases). Decreased levels of miR-200a, miR-200c, and miR-203 correlated with increasing thickness in the combined validation series (P=0.024, 0.033, and 0.031, respectively). In addition, progressive loss of miR-200a expression with disease progression was observed in series 1 (P<0.001) and in series 2 (P=0.029). MiR-200 in situ hybridization and E-cadherin immunohistochemistry demonstrated reduced expression of both at the deep invasive margin of the tumor. Furthermore, a functional validation study using an anti-miR200 strategy demonstrated that loss of miR-200 expression in melanoma cell lines reduced E-cadherin expression. Collectively, our data point towards an important role for miR-200 and miR203 expression in regulating E-cadherin during melanoma progression.

Keywords E-cadherin · Melanoma progression · Melanoma thickness · Mesenchymal characteristics · MicroRNA 200 family

Introduction

Epithelial–mesenchymal transition (EMT) is associated with increased malignancy of carcinomas [1]. EMT increases migratory and invasive capacities of tumor cells and can prevent apoptosis and senescence. Dissolution of E-cadherin-mediated adhesion is a key preliminary step in EMT. Throughout tumor progression, melanoma cells accumulate mesenchymal characteristics [2–4]. In culture, loss of E-cadherin correlates with the metastatic potential of melanoma cells and with the ability of keratinocytes to modulate expression of melanoma progression markers like MelCAM [5]. Accumulation of mesenchymal traits by melanoma cells in tissue is not as evident as in cell lines. This is not only because of the enormous cytological variation between primary cutaneous melanomas, but also because phenotypic differences within a given melanoma in which mesenchymal-like spindle cell areas may alternate with areas in which the melanoma cells assume a more epithelial-like aspect. Furthermore, invasive melanoma cells in tissue commonly lack spindle morphology [6]. Loss of E-cadherin expression has been reported to correlate with increased thickness [7] and reduced survival [8]. However, E-cadherin expression in melanoma may be quite heterogeneous [9].

Canonical and noncanonical Wnt signaling modulate E-cadherin expression [10]. Fibroblast growth factor, Hedgehog, transforming growth factor β (TGFβ), and noncanonical Wnt signals synergistically induce EMT regulators, such as, Snail, Slug, TWIST, and the E-cadherin repressors ZEB1 and 2. High Snail protein expression is observed in melanoma [11] and can induce immune suppression via induction of regulatory T cells and impairment of dendritic cell function [12]. Our previously published gene expression study in primary melanoma demonstrated a correlation between overexpression of Snail and poor 4-year distant metastasis-free survival (DMFS) [13] and supported the hypothesis that mesenchymal traits of melanoma cells is associated with poor prognosis.

In addition to Wnt signaling, E-cadherin expression can be modulated by differential expression of microRNAs (miRNAs). MiR-9 directly targets the E-cadherin encoding messenger, CDH1 [14]. Conversely, miR-200 family members (miR-141; miR-200a, b and c; and miR-429) target transcriptional repressors of E-cadherin, i.e., ZEB1 and ZEB2, in breast, ovarian, and pancreatic cancers [15–17] and various tumor cell lines [18]. Although target prediction algorithms predicted little overlap in the targets of miR-200 family members, experimental approaches suggested that their sets of targets are highly overlapping [18].

Using a large set of fresh frozen nevi, primary melanomas, and melanoma metastases, we demonstrate that expression of miR-200a and miR-200c correlate with melanoma thickness and metastasis. These findings were validated by quantitative PCR, miRNA in situ hybridization, and functional validation studies. Collectively, our data support the hypothesis that loss of miR-200 and miR-203 expression in melanoma increases mesenchymal characteristics and that this can contribute to progression.

Materials and methods

Tissues

All tissue samples were retrieved from the pathology archives at the University Hospital Leuven, Leuven, Belgium. The pertinent histological and clinical features are listed in Supplemental Tables S1–S3. Representative tissue parts were snap frozen in liquid nitrogen-cooled isopentane and stored at −80 °C until used. Sampling, storage, and use of these samples were performed according to requirements of the Local Ethical Committee. For miRNA in situ hybridization, formalin-fixed and paraffin-embedded tissue blocks were retrieved from pathology archives of the Radboud University Nijmegen Medical Centre. Tissues were obtained according to local ethical guidelines and approved by the local regulatory committee.

Preparation of total RNA and cDNA for miRNA profiling

Depending on the size of the sample, 20 to 40 sections (10 μm) were cut from frozen tissue blocks containing more than 75 % melanoma or nevus cells as evaluated from hematoxylin and eosin-stained sections. Sections were lysed immediately in 1 ml TRIzol (Invitrogen) and RNA was extracted subsequently according to the manufacturer's protocol. Absence of DNA contamination and RNA integrity

were analyzed on a Bioanalyzer (Agilent Technologies). RNA integrity number (RIN) higher than 7.5 and, in most cases, higher than 9 were obtained.

Total RNA (8 ng) was reverse transcribed using 50 nM stem–loop RT primer and MultiScribe Reverse Transcriptase (Life Technologies) according to the manufacturer's protocol. The expression of total 158 mature human miRNAs was analyzed using specific miRNA primers available from Life Technologies (Supplemental Table S4).

Real-time quantitative PCR

Real-time PCR was performed using the standard TaqMan protocol using Applied Biosystems reagents and an Applied Biosystems 7900 High Throughput Sequence Detection System. All reactions were run in duplicate. Mean Treshold Cycle (Ct) value was determined as median of two reads. In order to provide robust data, only values below 32 Ct were considered as specific and values above 32 CT were considered as missing data. This resulted in the exclusion of 29 miRNAs for further analyses, leaving a total of 129 miRNAs in the discovery phase of the study (Supplemental Table S4). Change in expression was determined by calculating the 2^{-ddCt} value [19]. MiRNA expression was normalized to let-7a expression. Normalization to any calibrator sample had very low influence on the overall data (data not shown), demonstrating high quality total RNA purification.

Statistical analysis

The Pearson correlation coefficient between the normalized Ct value of a miRNA and primary tumor thickness was determined. A stratified correlation coefficient was calculated for the analysis of association between expression and tumor thickness after combining all data from the two validation series, thereby controlling for possible batch effects [20]. DMFS was defined as the time interval between the diagnosis of the primary cutaneous melanoma and a distant metastasis and statistical differences assessed by a logrank test. Patients alive without distant metastasis or who died of causes not related to melanoma were censored at the date of last follow-up or at the date of death, respectively. An analysis of variance was applied to test for the difference in expression between nevi, tumors, and metastases. The paired *t* test was used for paired analysis of miRNA expression in the matched series of primary melanomas and metastases. Because of multiple testing, *p* values were adjusted for the False Discovery Rate (FDR) criterion [21]. *P* values from the stratified correlation analyses are based on an empirical permutation distribution and were not further adjusted. The *t* test for equality of means for independent samples (equal variance not assumed, two-tailed) was used to determine the difference in CDH1 expression in cell lines after miR-200c silencing.

In situ hybridization for miR-200c and E-cadherin immunohistochemistry

Consecutive tissue sections of formalin-fixed and paraffin-embedded primary melanomas ($n=10$) were prepared. MiRNA in situ hybridization was performed on 6-μm sections according to our previously described protocol [22] with minor modifications. A 5′- and 3′-end digoxigenin-labeled LNA/DNA oligonucleotide designed to hybridize to miR-200c ([18]; 5′-CCATCATTACCCGGCTGTATTA, underlined nucleotides indicate LNA bases, Exiqon, Vedbaek, Denmark) was hybridized to the tissue section overnight at 55 °C. MiR-200c was visualized using alkaline phosphatase-conjugated anti-digoxigenin Fab fragments (Roche), nitro blue tetrazolium, and 5-bromo-4-chloro-3′-indolyphosphate. The consecutive 4-μm sections were stained for E-cadherin as described previously [23].

MiR-200c silencing

E-cadherin-expressing human melanoma cell lines 888Mel, 1 F6, and SK-Mel28 were cultured as described previously [23, 24]. Exponentially growing cells were transfected with 20 nM thioacetylated LNA–DNA oligo towards miR-200c (5′-CCATCATTACCCGGCTGT ATTA) or a thioacetylated LNA–DNA scrambled oligo (Exiqon) using X-tremeGENE siRNA transfection reagent (Roche) according to the supplier's protocol. Two days after transfection, cells were harvested and plated in a 6-well plate at 60 % confluence and the transfection protocol repeated. The remaining cells were used for total RNA extraction (NucleoSpin RNA II, Macherey-Nagel, Düren, Germany). A total of three transfections were performed. cDNA was prepared using 0.5 μg total RNA, oligo-dT primers, and Moloney Murine Leukemia Virus Reverse Transcriptase (Promega) according to the supplier's protocol. cDNA was diluted five times and 5 μl was used for qPCR using Power SYBR Green Universal Master Mix (Applied Biosystems), and a CDH1-specific primer pair (NM_004360.3, 5′-ATGAGTGTCCCC CGGTATCTT and 5′-CAGCCGCTTTCAGATTTTCATC) in 25 μl. All samples were normalized for GAPDH expression (NM_002046.3, 5′-GAACCTGACCTGCCGTCTAG, 5′-CCTGCTTCACCACCTTCTTGA). A preliminary primer validation study revealed that the slope of the standard curves for both CDH1 and GAPDH was between 2.9 and 3.2. Normalized Ct values for CDH1 expression for scrambled and anti-miR-200 oligo-transfected cells at $t=0$ was set at 100 % and used to calculate change in CDH1 expression for all other time points. The experiment was performed three times in triplicate.

Table 1 Pearson correlation coefficient between normalized Ct values and tumor thickness

Name	*p* value[a]	FDR[b]	Correlation[c]
miR-203	0.000	0.002	0.788
miR-205	0.000	0.018	0.713
miR-200b	0.001	0.026	0.698
miR-200a	0.002	0.056	0.661
miR-130b	0.002	0.056	−0.606
miR-200c	0.004	0.067	0.582
miR-335	0.004	0.067	0.581
miR-150	0.004	0.068	0.574
miR-106a	0.006	0.079	−0.553
miR-17-5p	0.007	0.079	−0.550
miR-302c*	0.007	0.079	0.585

[a] Pearson correlation between expression and tumor thickness

[b] *P* value adjusted for the false discovery rate

[c] A positive correlation indicates that miRNA expression decreases with tumor thickness

* the standard annotation to identify that this is the miR302 passenger strand

Results

Discovery phase for miRNAs associated with progression

For the discovery phase of the study, miRNAs were isolated from fresh frozen primary cutaneous melanomas from 23 different patients (median Breslow thickness 3.68 mm; range 0.44–15.64; Table S1). Of these patients, 12 patients did not develop distant metastases during a follow-up of at least 4 years. Expression of 159 different miRNAs was measured in triplicate by qPCR. Thirty miRNAs were subsequently excluded from further analyses because reproducible quantification failed. Statistical analyses of the remaining 129 miRNAs (Supplemental Table S4) identified 11 miRNAs which expression strongly correlated with tumor thickness ($p<0.01$ and FDR<0.08, Table 1). The most significant miRNA was miR-203: its expression strongly decreased with increasing tumor thickness ($p<0.001$, FDR<0.002).

Two miRNAs demonstrated a significant correlation with DMFS or death due to the disease. Loss of miR-203 expression was associated with reduced DMFS (logrank $p=0.006$), whereas increased expression of miR-130b was associated with better DMFS (logrank $p=0.008$). However, for both miRNAs, the FDR was high (FDR=0.25).

Validation phase: unmatched and matched series

To replicate the possible associations with progression, we subsequently analyzed expression of nine miRNAs (miR-17.5p, 106a, 130b, 150, 200a, 200c, 203, 205, and 335) in a second unmatched series of melanocytic lesions (six acquired nevi, 15 primary melanomas (median thickness 4.20 mm, range 0.94–9.28), and 16 melanoma metastases). qPCR analyses revealed significantly different expressions of miR-200a, miR-200c, and miR-203 (Fig. 1; ANOVA, $p<0.001$, FDR<0.001), with miR-203 being the most significant. To confirm the progressive decrease in expression with progression to metastasis, their expression was determined in a third matched set of 11 primary cutaneous melanomas (median thickness 4.27 mm, range 0.59–5.57) and their corresponding locoregional ($n=10$) or distant ($n=3$) metastases (Supplemental Table S3). A paired *t* test confirmed a significant difference for miR-200a ($p=0.029$, FDR<0.08), but not for miR-203 ($p=0.08$) and miR-200c ($p=0.07$). However, the expressions of the three miRNAs were very highly correlated between each other (all three pairwise correlation coefficients>0.84, $p<0.002$).

We next analyzed whether expression of the three miRNAs correlated with tumor thickness by combining the two validation studies (26 primary melanomas, median thickness 4.1 mm (range 0.59–9.28)). For each miRNA, a correlation coefficient stratified by series was calculated in order to control possible batch effects [20] and found a significant correlation with tumor thickness for each miRNA ($p=0.024$, 0.033, and 0.031 for miR-200a, miR-200c, and miR-203, respectively).

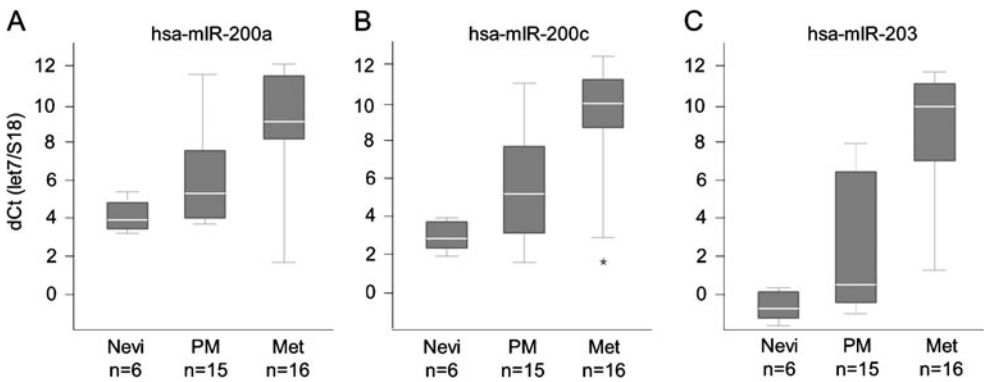

Fig. 1 Box plot presentation of miR-200a, miR-200c, and miR-203 expression in nevi, melanoma, and melanoma metastases. Ct values for the miRNAs in nevi, melanoma, and melanoma metastases were normalized to Let7 and 18S and expressed as 2^{-Ct}

In situ detection of miR-200c and E-cadherin expression in primary melanoma

It has been established previously that downregulation of miR-200a and miR-200c increases ZEB1/2 expression and that it downregulates E-cadherin expression in vitro [25]. To demonstrate this correlation in melanoma tissue, a chromogenic in situ hybridization assay for miR-200c was performed using a LNA–DNA oligo [18]. A total of ten superficial spreading primary melanomas with clear vertical growth phase were analyzed. Consecutive tissue slides were stained for E-cadherin. Strong miR-200c and E-cadherin expressions were observed in epidermis and hair follicles of the skin and served as an internal positive control. This strong and positive correlation between miR-200c and E-cadherin expressions in nontumor tissue strongly suggests specific hybridization signals. These analyses demonstrated that loss of miR-200c expression coincides with loss of E-cadherin expression in all tumors analyzed. The weakest hybridization signal at the deep invasive margin of the melanoma (Fig. 2, representative staining) confirmed the progressive loss of miR-200c with increasing thickness. Loss of miR-200c and E-cadherin expression did not correlate with clear mesenchymal cell morphology: cells lacking E-cadherin did not display an obvious spindled shape. However, a case of spindle cell melanoma was entirely negative (Supplemental Fig. S1).

Downregulation of miR-200 in melanoma cell lines

To demonstrate a possible causal relation between loss of miR-200c and E-cadherin expressions, E-cadherin expressing melanoma cell lines 888Mel, 1 F6, and SKMel28 were transfected with a LNA–DNA oligo that was previously shown to antagonize miR-200c [18]. Three rounds of transfection with anti-miR-200c resulted in decreased CDH1 expression in all three cell lines, whereas transfection with the scrambled control LNA–DNA oligo did not (Fig. 3). At 6 days post-transfection, mean CDH1 expression was reduced to 43 % (SEM=5.8, n=3, P=0.008) in 1F6 cells compared to scrambled control (Fig. 3a), 44 % for 888Mel cells (SEM=6.9, n=3, P=0.014, Fig. 3b), and 60 % in SKMel28 cells (SEM=6.9, n=3, P=0.031, Fig. 3c). These data suggest a causal relationship between miR-200c and E-cadherin expressions in melanoma. Additional transfections did not further decrease CDH1 expression and expression returned to normal levels within 1 week after the last transfection (data not shown).

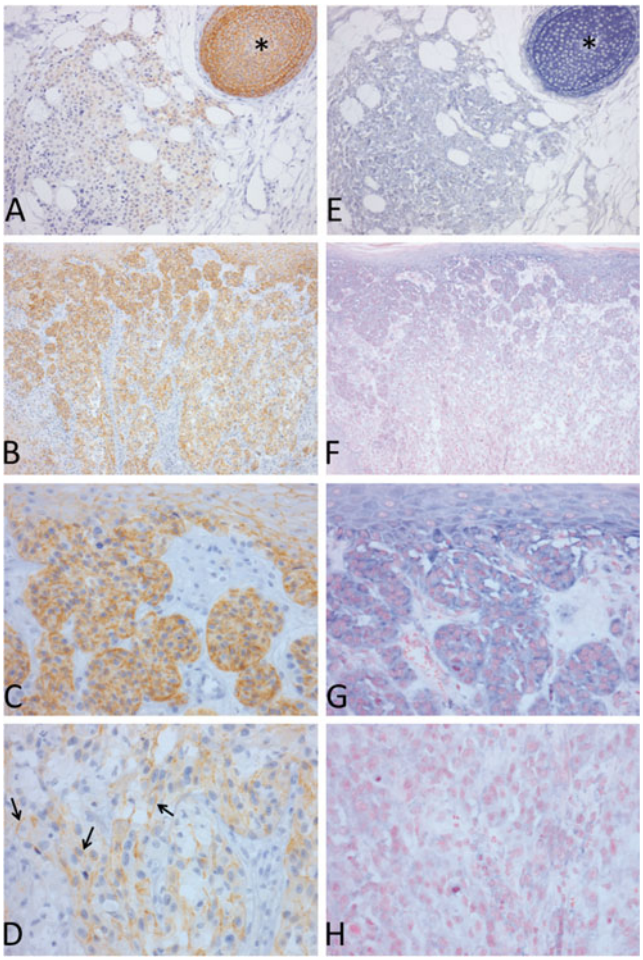

Fig. 2 In situ detection of miR-200 and E-cadherin. Consecutive tissue sections were subjected to E-cadherin immunohistochemistry (**a**–**d**) and miR-200c in situ hybridization (**e**–**h**). A subcutaneous metastasis (**a**, **e**) displays no E-cadherin (**a**) and miR-200c (**e**), whereas high E-cadherin (*red AEC staining*) and miR-200 expression (*blue NBT-BCIP staining*) was observed in the adjacent hair shaft (*asterisk*). In primary melanoma (**b**–**f**), a progressive loss of both E-cadherin (**b**) and miR-200c (**f**) can be seen with increasing thickness. At higher power view of the subepidermal component (**c**, **g**), clear membranous E-cadherin staining of the overlying epidermis and strong membranous staining of melanoma cells can be seen (**c**). Strong miR-200c expression was observed in epidermis and melanoma cells (**g**). In the deep dermal component, low and predominantly membranous E-cadherin expression was detected (**d**, *arrow*) but miR-200c expression was not observed (**h**)

Discussion

In this study, we demonstrate that loss of miR-200a, miR-200c, and miR-203 expression in melanoma correlates with tumor thickness, and their progressive loss in a series of matched primary tumors and associated metastases strongly suggest a possible association with disease progression. Loss of miR-200c and E-cadherin expression was exclusively observed that the invasive front and in in vitro experiments support a causal relation between loss of miR-200c and E-cadherin expression.

Loss of miR-200 family members in melanoma has been described previously [26], but not in the context of tumor thickness, localization of expression with the tumor, and

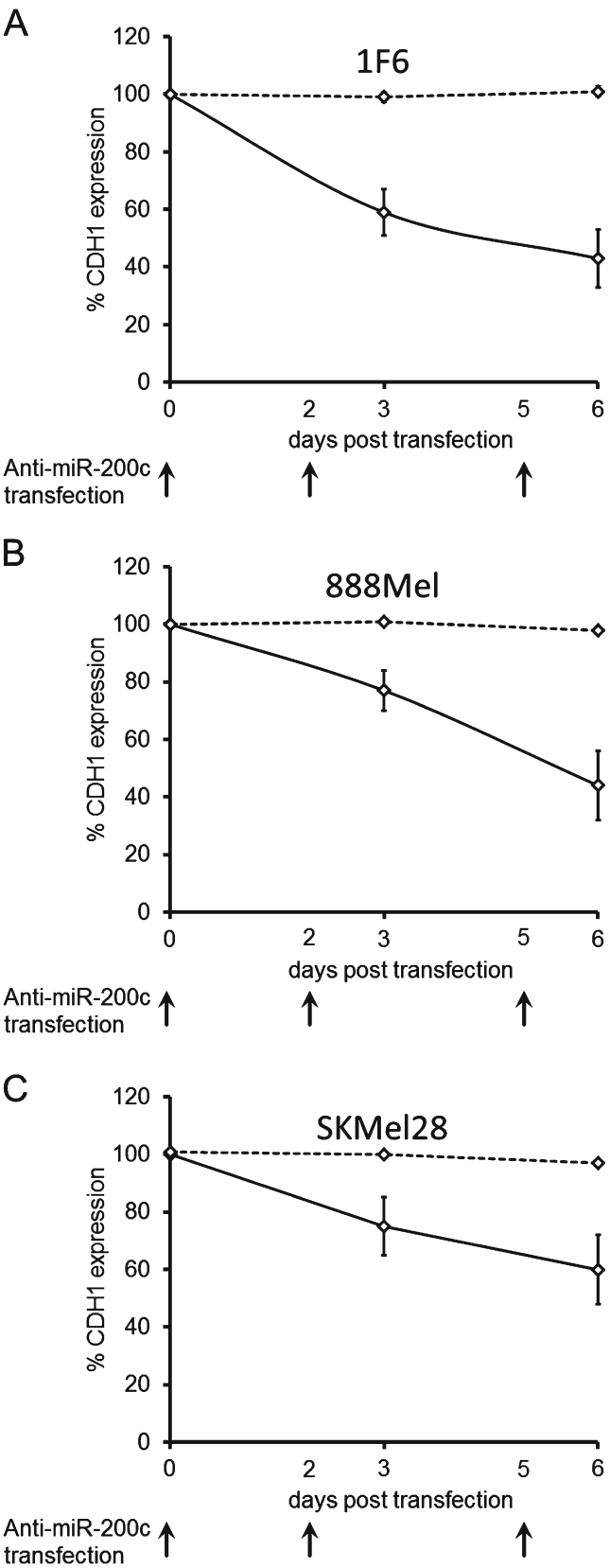

Fig. 3 Anti-miR-200c reduced E-cadherin expression in melanoma. Consecutive rounds of transfection of three different E-cadherin-expressing melanoma cell lines 1F6 (**a**), 888Mel (**b**), and SKMel28 (**c**) with the LNA–DNA oligo-targeting miR-200c resulted in a progressive decrease in E-cadherin (CDH1) expression as measured by qPCR in all cell lines (*solid line*) compared to scrambled control transfected cells (*dashed line*).Six days after transfection, mean CDH1 expression levels in 1F6, 888Mel, and SKMel28 cells were reduced to 43 % (P=0.008), 44 % (P=0.014), and 60 % (P=0.031) of that of control cells, respectively. *Arrows* indicate time points of transfection. Data is expressed as the percentage of expression of scrambled control transfected cells. *Error bars* indicate the standard deviation of three different experiments, each in triplicate

progression towards a metastatic melanoma phenotype. Recently, reduced expression of miR-200 family members was observed in a series of melanoma metastases compared to a series of unrelated primary melanoma [27]. Our work significantly refines these observations by visualizing the gradual loss of miR-200c and E-cadherin expression in primary melanoma, with maximal loss of expression at the most invasive component of the tumor. Furthermore, using pairs of melanoma metastases and the primary melanomas from which they originated, we could demonstrate loss of miR-200a, c, and miR-203 expression with advanced stages of disease for individual. Therefore, our data support the hypothesis that loss miR-200a, c, and miR-203 correlates with melanoma progression towards metastases.

The mechanism by which loss of miR-200a, c, and miR-203 contributes to melanoma metastasis remains elusive and their role in metastasis is subject of debate. Previous observations suggest that miR-200c expression can suppress migration of carcinoma cells [18, 25, 28, 29]. However, in melanoma cell lines, miR-200 family members do not inhibit cell migration but have profound effects on melanoma cell morphology and mode of melanoma cell invasion in 3D matrices [30]. MiR-200c overexpression drives the nonmesenchymal amoeboid form of invasion in type I collagen gels [30]. A different study demonstrated that melanoma cells can express markers of amoeboid invasion at the invasive front of melanomas, which most often consists of cells without a spindled morphology [6]. In that study, miR-200c expression was not analyzed. Our data, however, demonstrate that loss of miR-200c expression occurs at the invasive front and argues that miR-200c-mediated ameboid invasion in 3D culture models with its known limitations [31] is not representative for melanoma invasion in tissue. A recent study using a breast cancer cell line suggests a biphasic role of miR-200 family members in metastasis in which their expression can hinder tumor cell dissemination and entry into circulation but that it can support outgrowth at a secondary site [32]. Our data, however, demonstrate that loss of miR-200c expression occurs at the invasive front and that its expression in metastases is significantly lower compared to primary lesion from which it originated. This may suggests that the metastases originated from the miR-200-negative cells at the invasive front. The discrepancies between our data, miR-200c-mediated mode of invasion in 3D culture models, and the

possible biphasic effect of the expression of miR-200 family members in melanoma warrants further investigations.

The contribution of miR-200 a and c to tumor progression most likely extends beyond its ability to modulate invasion via the ZEB/miR-200/E-cadherin axis. Our data demonstrate a very strong correlation between miR-200a, c, and miR-203 expressions. ZEB1, in addition to repressing E-cadherin transcription, also represses miR-203 expression [17]. It has been proposed that miR-203 is a key molecule repressing expression of epithelial differentiation by 'stemness'-related genes [33, 34], such as, the stem cell-related transcription factors *BMI1* [35] and *SOX2* [17]. Expression of Sox2 has been documented in melanoma cells with presumed stem cell or tumor-initiating characteristics, in particular, at the invasive front of primary cutaneous melanoma [36, 37]. A stem cell-like phenotype is associated with the cell's ability to grow in an anchorage-independent manner. Loss of miR200a and c may, therefore, be important for cells to acquire this ability. Although we were not able to maintain long-term down regulation of miR200c expression using anti-miR-200c that allowed us to test if loss of miR-200c loss increased colony formation in soft agar (data not shown), others have demonstrated that forced expression of miR-200c in A375 melanoma cells reduced their capacity to grow in soft agar [27]. This suggests that loss of miR-200c could indeed promote anchorage-independent growth. The observations that ZEB1 expression is necessary for TrkB-mediated suppression of anoikis in rat intestinal epithelial and kidney cells [38] and that TrkB expression is predominantly observed in the invasive growth component of melanoma [39] lend further support to additional effects of disturbing the ZEB-miR200 equilibrium beyond that of modulating E-cadherin-mediated cell adhesion in melanoma cells.

Our results demonstrate a clear and highly significant correlation between loss of miR-200a, c, and miR-203 expression at the invasive front of melanoma, which is casually related to loss of E-cadherin expression. Expression of these miRNAs is strongly reduced in melanoma metastases compared to the matched primary tumors. Several lines of research point to a variety of effects of miR-200 activity in different tumor types and cell lines. If and how these are relevant for melanoma progression warrants further investigations.

Conflict of interest None.

References

1. Thiery JP, Acloque H, Huang RY, Nieto MA (2009) Epithelial–mesenchymal transitions in development and disease. Cell 139:871–890
2. Na YR, Seok SH, Kim DJ, Han JH, Kim TH, Jung H, Lee BH, Park JH (2009) Bone morphogenetic protein 7 induces mesenchymal-to-epithelial transition in melanoma cells, leading to inhibition of metastasis. Cancer Sci 100:2218–2225
3. Nurmenniemi S, Sinikumpu T, Alahuhta I, Salo S, Sutinen M, Santala M, Risteli J, Nyberg P, Salo T (2009) A novel organotypic model mimics the tumor microenvironment. Am J Pathol 175:1281–1291
4. Yang J, Price MA, Li GY, Bar-Eli M, Salgia R, Jagedeeswaran R, Carlson JH, Ferrone S, Turley EA, McCarthy JB (2009) Melanoma proteoglycan modifies gene expression to stimulate tumor cell motility, growth, and epithelial-to-mesenchymal transition. Cancer Res 69:7538–7547
5. Hsu MY, Wheelock MJ, Johnson KR, Herlyn M (1996) Shifts in cadherin profiles between human normal melanocytes and melanomas. J Investig Dermatol Symp Proc 1:188–194
6. Sanz-Moreno V, Gaggioli C, Yeo M, Albrengues J, Wallberg F, Viros A, Hooper S, Mitter R, Feral CC, Cook M, Larkin J, Marais R, Meneguzzi G, Sahai E, Marshall CJ (2011) ROCK and JAK1 signaling cooperate to control actomyosin contractility in tumor cells and stroma. Cancer Cell 20:229–245
7. Jaeger J, Koczan D, Thiesen HJ, Ibrahim SM, Gross G, Spang R, Kunz M (2007) Gene expression signatures for tumor progression, tumor subtype, and tumor thickness in laser-microdissected melanoma tissues. Clin Cancer Res 13:806–815
8. Tucci MG, Lucarini G, Brancorsini D, Zizzi A, Pugnaloni A, Giacchetti A, Ricotti G, Biagini G (2007) Involvement of E-cadherin, beta-catenin, Cdc42 and CXCR4 in the progression and prognosis of cutaneous melanoma. Br J Dermatol 157:1212–1216
9. George E, Polissar NL, Wick M (2010) Immunohistochemical evaluation of p16INK4A, E-cadherin, and cyclin D1 expression in melanoma and Spitz tumors. Am J Clin Pathol 133:370–379
10. Katoh M (2011) Network of WNT and other regulatory signaling cascades in pluripotent stem cells and cancer stem cells. Curr Pharm Biotechnol 12:160–170
11. Poser I, Dominguez D, de Herreros AG, Varnai A, Buettner R, Bosserhoff AK (2001) Loss of E-cadherin expression in melanoma cells involves up-regulation of the transcriptional repressor Snail. J Biol Chem 276:24661–24666
12. Kudo-Saito C, Shirako H, Takeuchi T, Kawakami Y (2009) Cancer metastasis is accelerated through immunosuppression during Snail-induced EMT of cancer cells. Cancer Cell 15:195–206
13. Winnepenninckx V, Lazar V, Michiels S, Dessen P, Stas M, Alonso SR, Avril MF, Ortiz Romero PL, Robert T, Balacescu O, Eggermont AM, Lenoir G, Sarasin A, Tursz T, van den Oord JJ, Spatz A (2006) Gene expression profiling of primary cutaneous melanoma and clinical outcome. J Natl Cancer Inst 98:472–482
14. Ma L, Young J, Prabhala H, Pan E, Mestdagh P, Muth D, Teruya-Feldstein J, Reinhardt F, Onder TT, Valastyan S, Westermann F, Speleman F, Vandesompele J, Weinberg RA (2010) miR-9, a MYC/MYCN-activated microRNA, regulates E-cadherin and cancer metastasis. Nat Cell Biol 12:247–256
15. Bendoraite A, Knouf EC, Garg KS, Parkin RK, Kroh EM, O'Briant KC, Ventura AP, Godwin AK, Karlan BY, Drescher CW, Urban N, Knudsen BS, Tewari M (2010) Regulation of miR-200 family microRNAs and ZEB transcription factors in ovarian cancer: evidence supporting a mesothelial-to-epithelial transition. Gynecol Oncol 116:117–125
16. Tryndyak VP, Beland FA, Pogribny IP (2009) E-cadherin transcriptional down-regulation by epigenetic and microRNA-200 family alterations is related to mesenchymal and drug-resistant phenotypes in human breast cancer cells. Int J Cancer 126:2575–2583
17. Wellner U, Schubert J, Burk UC, Schmalhofer O, Zhu F, Sonntag A, Waldvogel B, Vannier C, Darling D, zur HA, Brunton VG, Morton J, Sansom O, Schuler J, Stemmler MP, Herzberger C, Hopt U, Keck T, Brabletz S, Brabletz T (2009) The EMT-activator ZEB1 promotes tumorigenicity by repressing stemness-inhibiting microRNAs. Nat Cell Biol 11:1487–1495
18. Park SM, Gaur AB, Lengyel E, Peter ME (2008) The miR-200 family determines the epithelial phenotype of cancer cells by

targeting the E-cadherin repressors ZEB1 and ZEB2. Genes Dev 22:894–907
19. Livak KJ, Schmittgen TD (2001) Analysis of relative gene expression data using real-time quantitative PCR and the 2(−Delta Delta C(T)) method. Methods 25:402–408
20. Kraft P, Schadt E, Aten J, Horvath S (2003) A family-based test for correlation between gene expression and trait values. Am J Hum Genet 72:1323–1330
21. Benjamini Y, Hochberg Y (1995) Controlling the false discovery rate: a practical and powerful approach to multiple testing. J R Stat Soc Ser B 57:289–300
22. van Kempen LC, Rijntjes J, Mamor-Cornelissen I, Vincent-Naulleau S, Gerritsen MJ, Ruiter DJ, van Dijk MC, Geffrotin C, van Muijen GN (2008) Type I collagen expression contributes to angiogenesis and the development of deeply invasive cutaneous melanoma. Int J Cancer 122:1019–1029
23. Alexaki VI, Javelaud D, Van Kempen LC, Mohammad KS, Dennler S, Luciani F, Hoek KS, Juarez P, Goydos JS, Fournier PJ, Sibon C, Bertolotto C, Verrecchia F, Saule S, Delmas V, Ballotti R, Larue L, Saiag P, Guise TA, Mauviel A (2010) GLI2-mediated melanoma invasion and metastasis. J Natl Cancer Inst 102:1148–1159
24. van Muijen GN, Cornelissen LM, Jansen CF, Figdor CG, Johnson JP, Brocker EB, Ruiter DJ (1991) Antigen expression of metastasizing and non-metastasizing human melanoma cells xenografted into nude mice. Clin Exp Metastasis 9:259–272
25. Gregory PA, Bert AG, Paterson EL, Barry SC, Tsykin A, Farshid G, Vadas MA, Khew-Goodall Y, Goodall GJ (2008) The miR-200 family and miR-205 regulate epithelial to mesenchymal transition by targeting ZEB1 and SIP1. Nat Cell Biol 10:593–601
26. Schultz J, Lorenz P, Gross G, Ibrahim S, Kunz M (2008) MicroRNA let-7b targets important cell cycle molecules in malignant melanoma cells and interferes with anchorage-independent growth. Cell Res 18:549–557
27. Xu Y, Brenn T, Brown ER, Doherty V, Melton DW (2012) Differential expression of microRNAs during melanoma progression: miR-200c, miR-205 and miR-211 are downregulated in melanoma and act as tumour suppressors. Br J Cancer 106:553–561
28. Burk U, Schubert J, Wellner U, Schmalhofer O, Vincan E, Spaderna S, Brabletz T (2008) A reciprocal repression between ZEB1 and members of the miR-200 family promotes EMT and invasion in cancer cells. EMBO Rep 9:582–589
29. Korpal M, Lee ES, Hu G, Kang Y (2008) The miR-200 family inhibits epithelial-mesenchymal transition and cancer cell migration by direct targeting of E-cadherin transcriptional repressors ZEB1 and ZEB2. J Biol Chem 283:14910–14914
30. Elson-Schwab I, Lorentzen A, Marshall CJ (2010) MicroRNA-200 family members differentially regulate morphological plasticity and mode of melanoma cell invasion. PLoS One 5
31. Sabeh F, Shimizu-Hirota R, Weiss SJ (2009) Protease-dependent versus -independent cancer cell invasion programs: three-dimensional amoeboid movement revisited. J Cell Biol 185:11–19
32. Korpal M, Ell BJ, Buffa FM, Ibrahim T, Blanco MA, Celia-Terrassa T, Mercatali L, Khan Z, Goodarzi H, Hua Y, Wei Y, Hu G, Garcia BA, Ragoussis J, Amadori D, Harris AL, Kang Y (2012) Direct targeting of Sec23a by miR-200 s influences cancer cell secretome and promotes metastatic colonization. Nat Med 17:1101–1108
33. Lena AM, Shalom-Feuerstein R, Rivetti DV, Aberdam D, Knight RA, Melino G, Candi E (2008) miR-203 represses 'stemness' by repressing DeltaNp63. Cell Death Differ 15:1187–1195
34. Yi R, Poy MN, Stoffel M, Fuchs E (2008) A skin microRNA promotes differentiation by repressing 'stemness'. Nature 452:225–229
35. Hsu SD, Lin FM, Wu WY, Liang C, Huang WC, Chan WL, Tsai WT, Chen GZ, Lee CJ, Chiu CM, Chien CH, Wu MC, Huang CY, Tsou AP, Huang HD (2011) miRTarBase: a database curates experimentally validated microRNA-target interactions. Nucleic Acids Res 39:D163–D169
36. Laga AC, Lai CY, Zhan Q, Huang SJ, Velazquez EF, Yang Q, Hsu MY, Murphy GF (2011) Expression of the embryonic stem cell transcription factor SOX2 in human skin: relevance to melanocyte and merkel cell biology. Am J Pathol 176:903–913
37. Laga AC, Zhan Q, Weishaupt C, Ma J, Frank MH, Murphy GF (2011) SOX2 and nestin expression in human melanoma: an immunohistochemical and experimental study. Exp Dermatol 20:339–345
38. Smit MA, Peeper DS (2011) Zeb1 is required for TrkB-induced epithelial–mesenchymal transition, anoikis resistance and metastasis. Oncogene 30:3735–3744
39. Innominato PF, Libbrecht L, van den Oord JJ (2001) Expression of neurotrophins and their receptors in pigment cell lesions of the skin. J Pathol 194:95–100

Virchows Arch (2012) 461:449–455
DOI 10.1007/s00428-012-1297-9

ORIGINAL ARTICLE

Morphological and immunological changes in the skin of autopsied women with AIDS

Renata Beatriz Silva · Laura Penna Rocha · Laís Resende Cardoso de Souza · Humberto Aparecido Faria · Janaínna Grazielle Pacheco Olegário · Maria Helena Soares · Mara Lúcia Fonseca Ferraz · Rosana Rosa Miranda Corrêa · Vicente de Paula Antunes Teixeira · Camila Lourencini Cavellani

Received: 24 April 2012 / Revised: 19 June 2012 / Accepted: 31 July 2012 / Published online: 16 August 2012
© Springer-Verlag 2012

Abstract Acquired immunodeficiency syndrome (AIDS) is characterized by decreased immunity, making a patient more susceptible to opportunistic infections which can have cutaneous manifestations. The aim of this study was to evaluate the local immunity of the skin through morphological and immunohistochemical analysis. Skin samples of 52 women, 27 without AIDS and 25 with AIDS, autopsied in an academic referral hospital in Brazil were evaluated. The autopsy reports and medical records were reviewed, and histochemical Hematoxylin–eosin, Picrosirius red, and Verhoeff stains as well as morphometric (Image J and KS-300 Kontron-Zeiss) and immunohistochemical (S-100 and anti-IgA) analyses of the skin were performed. Women with AIDS presented a thinner epidermis than women without AIDS (33.33 [12.00–317.66] vs 67.42 [12.00–530.02] μm; $p<0.001$), with a lower number of epithelial cell layers (4.00 [2.00–11.00] vs 4.00 [2.00–16.00]; $p<0.001$), a smaller cell diameter (12.92 [6.00–28.87] vs 24.32 [6.00–33.12] μm; $p<0.001$), and a lower number of Langerhans cells (LC) (12.58 [0.00–81.74] vs 31.44 [0.00–169.77] LC/mm^2; $p<0.001$). The dermis contained more collagen fibers (8.20 % [2.40–19.40] vs 6.30 % [0.40–13.90]; $p<0.001$). Some of these parameters were negatively correlated with viral load and positively correlated with the number of CD4+ T-lymphocytes. We conclude that a decrease of the local skin immunity in women with AIDS may contribute to the development of skin lesions.

Keywords AIDS · Atrophy · Immunity · Skin

R. B. Silva · L. P. Rocha · L. R. C. de Souza · H. A. Faria · J. G. P. Olegário · M. H. Soares · M. L. F. Ferraz · R. R. M. Corrêa · V. d. P. A. Teixeira · C. L. Cavellani (✉)
General Pathology Division,
Triangulo Mineiro Federal University,
Rua Frei Paulino 30, Bairro Abadia,
CEP: 38025-180, Uberaba, Minas Gerais, Brazil
e-mail: camila@patge.uftm.edu.br

Introduction

Acquired immunodeficiency syndrome (AIDS) is characterized by decreased immunity, making the patient more susceptible to opportunistic infections and cutaneous manifestations, especially in countries where the availability of antiretroviral therapy is limited [1, 2]. Skin involvement in AIDS comprises neoplasia, infections, and inflammatory disorders [3].

The immune response to infectious agents occurs through two mechanisms known as innate immunity and adaptive immunity. The first is provided by natural barriers such as the skin tissue, mucosa, and lymphoid tissue; the latter is related to the production of antibodies and cytokines by B lymphocytes and CD4+ and CD8+ T-lymphocytes [4]. In this context, morphological and immunological alterations of the skin may indicate a decrease of both innate and adaptive immunity of the skin. Therefore, the study of skin samples of autopsied patients presents an opportunity to gain knowledge of this organ and its changes in patients with AIDS.

The epidermis is a continuously renewed stratified epithelium. It is mostly composed of keratinocytes, but 5 to 10 % of the cells are Langerhans cells (LC) and melanocytes [5]. The LC found in the epidermis have functions which include antigen presentation and the stimulation of a T-cell response. During AIDS, there is a decrease of LC in the epidermis [6] and in other stratified epithelia such as the esophagus [7–9], uterine cervix [10], and the oral mucosa [11].

Keratinocytes represent the body's "first line of defense" from the outside environment, and as such they are the first responders to injury. After injury, keratinocytes become activated, secreting various cytokines and growth factors as well as responding to cytokines and growth factors as part of the mounting inflammatory response [12]. Several adhesion molecules are involved in the migration of circulating T cells to the tissues, but the memory lymphocytes which infiltrate the skin express the cutaneous lymphocyte antigen, a surface glycoprotein that allows the arrival of lymphocytes in the skin [13]. Both Th1 and Th2 responses are well developed in the skin, but in most inflammatory cutaneous diseases the predominant response is Th1 [14]. Despite humoral immunity being less active in the skin, it is relevant to evaluate the influence of AIDS on the expression of immunoglobulins in the epidermis.

Epidemiological data have shown a progressive incidence of the infection caused by the human immunodeficiency virus (HIV), and in most cases, the disease is associated with heterosexual transmission [15], which results in a substantial increase of cases in women [16]. Studies of women with AIDS have demonstrated a reduction in the thickness of the cervical [10, 17] and esophageal epithelia [8, 9], which suggest altered innate immunity since the epithelial cells constitute a physical barrier important to the defense against pathogens [18]. As the skin contains a stratified squamous epithelium [19], similar to the one which covers the external portion of the uterine cervix and of the esophagus, we expected to find in our study a thinner epidermis in women with AIDS.

Patients with advanced HIV infection frequently have a CD4+ T-lymphocyte count of <200 cells/mm^3, high levels of RNA virus in the plasma, and clinical manifestations indicating severe immunodeficiency [20]. The higher the level of the viral load, the lower the CD4+ T-lymphocyte count and the greater the risk of developing AIDS [21]. Therefore, our study intended to verify whether the morphological and immunological alterations described in other organs [8–10, 17] also occur in the skin of AIDS patients, as well as the influence of the viral load and the CD4+ T-lymphocyte count on these alterations.

Methods

This study was approved by Triângulo Mineiro Federal University Research Ethics Committee on 06/08/07 (approval number 902). The reports of 330 autopsies, conducted between 1984 and 2008 at the General Hospital of Triângulo Mineiro Federal University in the state of Minas Gerais, Brazil, were reviewed. We selected those from 52 women aged between 16 and 54 in order to compose two groups: (1) women without AIDS (n=27) and (2) women with AIDS (n=25). Although Triangulo Mineiro Federal University offers services for various regions of Minas Gerais state and also to other states, all patients in this study, with and without AIDS, were from Minas Gerais state. Cases with an incomplete autopsy report or with chronic metabolic or infectious diseases that might influence the findings were excluded. Data concerning age, body mass index (BMI), cause of death, and macroscopic alterations of the skin were collected from the autopsy reports, whereas the use of antiretroviral therapy and the values of the last viral load tests and CD4+ T-lymphocyte cell count were collected from medical records.

We recovered the results of these exams from only 11 patients with AIDS since they started being taken care of in this hospital only in 1998. Moreover, some patients requested care only in the terminal phase of their disease, leaving insufficient time to conduct these tests. Patients with and without AIDS were matched according to age, BMI, and cause of death in order to avoid the confounding effects of these variables.

All patients with AIDS observed in this study died during the post-highly active antiretroviral therapy (HAART) era (after 1996) [20]. Some patients autopsied before 1997 were assigned to the group without AIDS because the number of patients without AIDS autopsied in post-HAART era, with age, BMI value, and cause of death matching our patients with AIDS, was insufficient.

AIDS diagnosis was made by evidence of at least one AIDS-defining disease presented by a patient [22]. All patients without AIDS were HIV-negative. In this study, the causes of death were grouped into cardiovascular, infectious, digestive, neoplastic, and others [23].

Skin fragments from the anterior thoracic region of women selected for this study were obtained from the General Pathology Division archives. This region was chosen because it is an area protected from the harmful effects of ultraviolet irradiation. The skin samples were macroscopically and microscopically normal. They had been submitted to histological processing, and for the study, we cut serially sections from the available paraffin blocks at 4 μm for histochemical and immunohistochemical studies. In order to account for tangential cutting, the morphology of dermal papillae and of cell layers (basal, spindle, granular, and corneal) was observed. Cases in which the epidermal morphology indicated that the sections were not perpendicular to the surface were excluded. Hematoxylin–eosin (H&E) staining was carried out for the morphometric analysis of epidermis thickness, Picrosirius red was used for the quantitative analysis of collagen fibers, and Verhoeff stain was used for the measurement of elastic tissue.

Image J Program (an interactive analysis system) was used to measure epidermal thickness, which was measured by tracing five straight lines on different parts of each field

to be analyzed [8–10, 17] Along each line, the number of keratinocyte nuclei was counted in order to determine the number of cell layers in the epidermis. The average cell diameter was obtained by dividing the epidermal thickness by the number of keratinocyte nuclei in each measure.

To investigate the amount of collagen fibers in the dermis, Picrosirius red stained fragments were examined under polarized light and quantified by Image J software. To analyze elastic fibers, skin samples stained with Verhoeff stain were examined under a conventional light microscope and quantified by an image analysis system, KS-300 (Kontron-Zeiss®).

To evaluate the number of Langerhans cells, antibody Anti-S100 (Dako®) was used at a concentration of 1/400; IgA was quantified using antibody anti-IgA (Erviegas®) at a concentration of 1/1,000. For antigen retrieval, heating in sodium citrate buffer was utilized for the antibody Anti-S100 and trypsin digestion for anti-IgA. For blocking of non-specific staining, bovine serum albumin was used. The primary antibodies were incubated for 2 h and processed through LSAB+System-HRP (DAKO®); diaminobenzidine (DAB) was used as substrate-chromogen.

Immunostained LC were quantified by conventional light microscopy along the length of the specimen and the number expressed/area (mm^2). To determine the quantity of immunostained IgA in the dermis, the DAB-stained area was measured using KS-300 (Kontron-Zeiss®) software.

Statistical analysis was carried out using the SigmaStat 2.03® program. In cases of normal distribution and similar variances, Student's *t*-test was employed; otherwise, we used Mann–Whitney (*T*) test. Correlation between both variables with abnormal distribution was determined through Spearman (rS) tests, respectively. We considered statistically significant values at $p<0.05$.

Results

The age range of both groups was 30–39 years. The average BMI in the non-AIDS group was 23.22±6.82 kg/m^2 and in the AIDS group it was 21.67±5.24 kg/m^2 ($p=0.364$). The frequency of causes of death from cardiovascular, infectious, neoplastic, and other causes in women without AIDS and with AIDS were nine (33.33 %), 11 (40.74 %), two (7.40 %), and five (18.51 %) versus nine (36.00 %), nine (36.00 %), two (8.00 %), and five (20.00 %), respectively.

Macroscopic alterations in the skin were observed in four (14.80 %) women without AIDS and in seven (28.00 %) women with AIDS. Among these changes, eschar, ulcer, crusted lesion, scaly lesion, verrucous lesion, and nocardiosis in skin were reported in the autopsy records of one (3.70 %), two (7.40 %), one (3.70 %), 0, 0, and 0 patient without AIDS and of two (8.00 %), one (4.00 %), 0, 2 (8.00 %), one (4.00 %), and one (4.00 %) patient with AIDS, respectively.

Antiretroviral therapy was taken by 14 (56.00 %) women with AIDS, but in most cases, the treatment compliance was insufficient.

Women with AIDS showed significantly reduced epidermal thickness, number of keratinocyte layers, and keratinocyte diameter than women without AIDS (Table 1; Fig. 1).

Women with AIDS had a significantly higher percentage of dermal collagen fibers than women without AIDS, but the density of elastic fibers was not different (Table 2).

The number of LC was significantly smaller in patients with AIDS. A lower IgA-immunoreactive area was observed in the dermis in the group with AIDS, but this did not reach statistical significance (Table 3; Fig. 2).

In the group of patients with AIDS, the mean CD4+ T-lymphocyte count was 43.00 cells/mm^3 (7.00–517.00), and the mean viral load was 595.00 copies/ml (233.00–15,019.00) of blood. A significant negative correlation was observed between the viral load and the thickness of the epidermis (rS, −0.157; $p<0.001$), the number of cell layers (rS, −0.0618; $p=0.00986$), the average cell diameter (rS, −0.144; $p<0.001$), the IgA-immunoreactive area (rS, −0.243; $p<0.001$), and the LC number (rS, −0.484; $p<0.001$) in the epidermis of patients with AIDS. There was a significant positive correlation between the number

Table 1 Thickness, number of cell layers, and cell diameter of epidermis of women autopsied from 1984 to 2008

Groups	Number, *n* (%)	Thickness (μm)[a]	Number of cells layers[b]	Cell diameter (μm)[c]
		Med (min–max)		
Without AIDS	27 (51.92)	67.42 (12.00–530.02)	4.00 (2.00–16.00)	24.32 (6.00–33.12)
With AIDS	25 (48.08)	33.33 (12.00–317.66)	4.00 (2.00–11.00)	12.92 (6.00–28.87)
Total	52 (100)			

Med median, *min* minimum, *max* maximum

[a] $T=11{,}389{,}145.000$, $p<0.001$

[b] $T=14{,}752{,}322.000$, $p<0.001$

[c] $T=11{,}015{,}860.000$, $p<0.001$

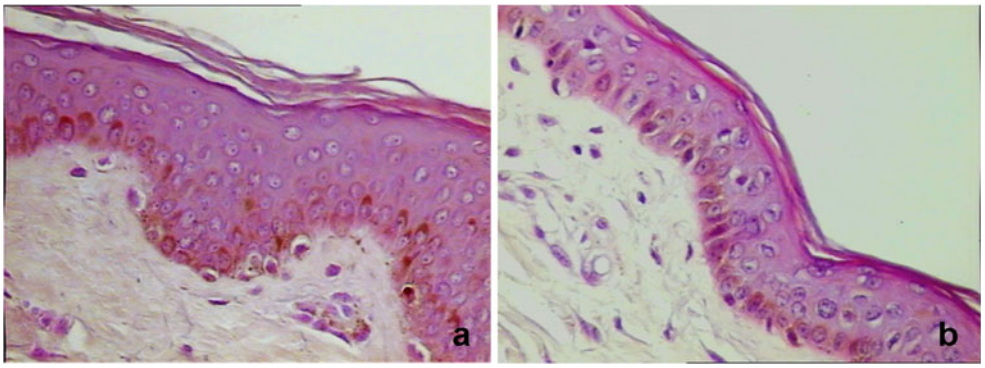

Fig. 1 Epidermal thickness of women autopsied from 1984 to 2008 (H&E, ×800). **a** Women without AIDS, **b** women with AIDS

of CD4+ T-lymphocytes (cell/mm^3) and the thickness of epidermis (rS, 0.0964; $p<0.001$), the number of cell layers (rS, 0.145; $p<0.001$), and the LC (rS, 0.276; $p<0.001$) in patients with AIDS.

Discussion

Women have been more intensely infected by AIDS in the 25 to 39 age range and still show increasing indices of incidence in practically every age range, but the incidence rates have stabilized during the last decade [24]. The average age in both groups observed in this study represents the age at which women are mostly infected by the syndrome.

There was no significant difference in BMI values between the groups of women with and without AIDS, which avoided a possible influence of this parameter on the thickness of the epidermis.

Causes of death were similar in patients with and without AIDS, which is important because some causes of death, such as neoplastic, are related to weight loss [25, 26], which might influence the thickness of the epidermis.

Skin changes were more frequent in patients with AIDS, in agreement with the literature. The decrease in immunity, caused by this syndrome, makes the patient more susceptible to opportunistic infections and cutaneous manifestations [1].

Table 2 Percentage of collagen and elastic fibers in dermis of women autopsied from 1984 to 2008

Groups	Number, *n* (%)	Dermis collagen fibers (%)[a] Med (min–max)	Dermis elastic fibers (%)[b] Med (min–max)
Without AIDS	27 (51.92)	6.30 (0.40–13.90)	5.72 (0.48–32.18)
With AIDS	25 (48.08)	8.20 (2.40–19.40)	5.98 (0.18–20.17)
Total	52 (100)		

Med median, *min* minimum, *max* maximum

[a] $T=146{,}956.000$, $p<0.001$

[b] $T=165{,}888.500$, $p=0.962$

Epidermal thickness was significantly reduced in patients with AIDS, which is in agreement with the results obtained in studies on cervical [10, 17] and esophageal [8, 9] epithelia in women with AIDS. This atrophy of the epidermis is caused by a significant reduction in the number of cell layers, which may be related to the cytopathogenic effect of HIV infection, which induces apoptosis [27]. HIV cytopathogenesis is associated with the entrance of osmotically active monovalent cations, K+and Na+, into the infected cells since the virus is capable of disturbing the transport of ions through the plasma membrane [28, 29]. The most common HIV cytopathogenic effect, in vitro, is called ballooning degeneration, in which cells swell beyond the limits of membrane integrity, hence suffering cell lysis [30]. Another contributing factor to epidermis atrophy was the reduction of cell diameter, which indicates that the virus might compromise the synthesis and/or the function of cell components.

The percentage of collagen fibers in the dermis was significantly increased in patients with AIDS compared with patients without AIDS. The HIV cytopathogenic effect, immunodepression, and occurrence of co-infections might induce alterations in the tissue microenvironments, including changes in cytokine production, increasing the inflammatory and fibrogenic activities [31].

The elastic fibers are responsible for skin contraction and their quantity is likely to diminish with age, exposure to solar radiation, and other factors [32]. AIDS-related parameters did not influence the quantity of elastic fibers in the dermis.

Women with AIDS presented a significantly lower number of LC in the epidermis than those not infected by the retrovirus, which is in agreement with the literature [33, 34]. Several hypotheses attempt to explain the LC loss during viral infections. LCs may be infected directly by HIV, causing cellular death, which is related to the immediate cytopathogenic effect of the virus [35, 36]. Alternatively, the antigen presenting LC may migrate from the epithelium to regional lymphoid tissues to mount an immune response [37], reducing the density of the epithelial LCs.

Table 3 Number of LC in the epidermis and quantity of IgA in the dermis of women autopsied from 1984 to 2008

Groups	Number, *n* (%)	Langerhans cells/mm^{2a} Med (min–max)	Quantity of IgA (%)^{b} Med (min–max)
Without AIDS	27 (51.92)	31.44 (0.00–169.77)	22.78 (2.35–77.33)
With AIDS	25 (48.08)	12.58 (0.00–81.74)	21.87 (2.03–74.92)
Total	52 (100)		

Med median, *min* minimum, *max* maximum

[a] T=230,873.500, p<0.001

[b] T=530,580.500, p=0.462

HIV infection induces activation and dysfunction of B cells, resulting in hypergammaglobulinemia [38–40]. However, the resulting antibodies are not HIV antigen specific [38, 41, 42]. Although we expected an increase of IgA in the dermis, lower but not statistically significant values were found in the group with AIDS. This reduction of IgA in the dermis might contribute to the occurrence of opportunistic cutaneous infections in patients infected with AIDS because the high amount of immunoglobulin secreted during AIDS is not specific, although some retain neutralizing functions [43].

Increase of viral load precedes the decrease of the number of CD4+ T-lymphocytes as high plasma HIV RNA levels indicate worse prognosis [44, 45]. The possible relationship between viral load and dermatological alterations in patients with AIDS is not entirely clear, but it is thought that HIV may alter LC and keratinocytes, which may increase skin vulnerability to several diseases [46, 47]. We observed a significant negative correlation between the viral load and epidermal thickness, the number of cell layers, the average cell diameter, and the IgA and LC in the epidermis of patients with AIDS, which suggests that the higher the viral load, the lower the local skin immunity.

Advanced stages of cutaneous diseases in AIDS are associated with very low CD4+ T-lymphocyte count. [32]. Moreover, several studies show a negative correlation between CD4+ T-lymphocyte count and dermatological diseases [48–50]. However, we found in the epidermis of AIDS patients a significant positive correlation between the CD4+ T-ymphocyte count and epidermal thickness, number of cell layers, and number of LC. These data suggest that the higher the CD4+ T-lymphocyte count, the higher the local skin immunity is.

Our data suggest that AIDS reduces local skin immunity. This might interfere with the constitution and the natural immune function of the skin, enhancing the impact of harmful agents during the course of the disease. A better understanding of silent skin changes during AIDS would be valuable not only for the production of cosmetics, topical therapeutic applications, and external physical therapeutic modalities but also to better understand how to cure a wide variety of dermatological lesions in patients with AIDS.

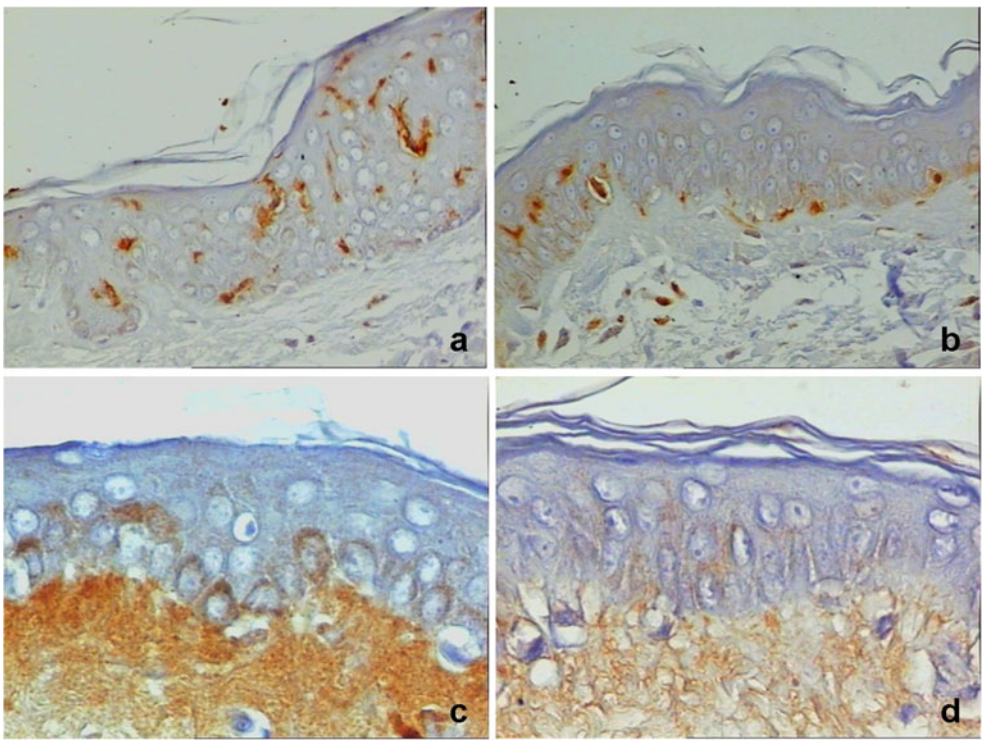

Fig. 2 Immunostained LC in the epidermis and IgA in the dermis of women autopsied from 1984 to 2008. **a** LC in women without AIDS (Anti-S100, ×800), **b** LC in women with AIDS (Anti-S100, ×800), **c** quantity of IgA in women without AIDS (Anti-IgA, ×1,600), **d** quantity of IgA in women with AIDS (Anti-IgA, ×1,600)

Acknowledgments This study was conducted at the General Pathology Division of the Triângulo Mineiro Federal University, Uberaba, Minas Gerais, Brazil, with grants from Conselho Nacional de Desenvolvimento Científico e Tecnológico, Coordenação de Aperfeiçoamento de Pessoal de Nível Superior, Fundação de Amparo à Pesquisa do Estado de Minas Gerais, and Fundação de Ensino e Pesquisa de Uberaba.

Conflict of interest The authors declare that they have no conflict of interest.

References

1. Coldiron BM, Bergstresser PR (1989) Prevalence and clinical spectrum of skin disease in patients with human immunodeficiency virus. Arch Dermatol 125:357–361
2. Ramdial PK (2000) Selected topics in HIV-associated skin pathology. Curr Diagn Pathol 6:113–124
3. Gomides MD, Berbert AL, Mantese SA, Rocha A, Ferreira MS, Borges AS (2002) Skin diseases in patients with AIDS: study in 55 cases in Uberlândia, MG, Brazil. Rev Assoc Med Brás 48:36–41
4. Machado PRL, Araújo MIA, Carvalho L, Carvalho EM (2004) Immune response mechanisms to infections. An Bras Dermatol 79:647–664
5. Kanitakis J (2002) Anatomy, histology and immunohistochemistry of normal human skin. Eur J Dermatol 12:390–401
6. Tschachler E, Groh V, Popovic M, Mann DL, Konrad K, Safai B, Eron L, diMarzo VF, Wolff K, Stingl G (1987) Epidermal Langerhans cells: a target for HTLV-III/LAV infection. J Invest Dermatol 88:233–237
7. Charton-Bain MC, Terris B, Dauge MC, Marche C, Walker F, Bouchaud O, Xerri L, Potet F (1999) Reduced number of Langerhans cells in oesophageal mucosa from AIDS patients. Histopathology 34:399–404
8. Rocha L, Silva R, Olegário J, Corrêa R, Teixeira V, Cavellani C (2010) Esophageal epithelium of women with AIDS: thickness and local immunity. Pathol Res Pract 206:248–252
9. Rocha LP, de Melo E, Silva AT, Gomes NC, Faria HA, Silva RB, Olegário JG, Corrêa RR, Teixeira VPA, Cavellani CL (2011) The influence of gender and of aids on the immunity of autopsied patients' esophagus. AIDS Res Hum Retroviruses 27:511–518
10. Cavellani CL, Rocha LP, da Silva Rosa SC, Oliveira LF, Faria HA, Olegario JG, Correa RR, Teixeira Vde P (2011) The influence of AIDS on the morphometric and immune status of the uterine cervix of autopsied patients. Curr HIV Res 9:606–612
11. Spörri B, von Overbeck J, Brand CU, Schmidli J, Sanchez ML, Grunow R, Braathen LR (1994) Reduced number of Langerhans cells in oral mucosal washings from HIV-1 seropositives. J Oral Pathol Med 23:399–402
12. Morasso MI, Tomic-Canic M (2005) Epidermal stem cells: the cradle of epidermal determination, differentiation and wound healing. Biol Cell 97:173–183
13. Santamaria-Babí LF (2004) CLA+T cells in cutaneous diseases. Eur J Dermatol 14:13–18
14. Norris DA (2010) Estrutura e função da pele. In: Ausiello D, Goldman L (eds) Cecil - Tratado de Medicina Interna, 23rd edn. Elsevier, Rio de Janeiro, p 3378
15. Simon V, Ho D, Karim Q (2006) HIV/AIDS epidemiology, pathogenesis, prevention, and treatment. Lancet 358:489–504
16. Brito AM, Castilho EA, Szwarcwald CL (2001) AIDS and HIV infection in Brazil: a multifaceted epidemic. Rev Soc Bras Med Trop 34:207–217
17. Guimarães JV, Salge AK, Penha DS, Murta EF, Saldanha JC, Castro EC, Dos Reis MA, Teixeira VPA (2007) Thickness of the cervical epithelium of autopsied patients with acquired immunodeficiency syndrome. Ann Diag Pathol 11:258–261
18. Wagner C, Isermann K, Fehrenbach H, Roeder T (2008) Molecular architecture of the fruit fly's airway epithelial immune system. BMC Genomics 9:446
19. Murphy G (1997) Histology of the skin. In: Elenitsas R, Jaworsky C, Johnson B (eds) Lever's histopathology of the skin. Lippincott-Raven, Philadelphia, pp 5–50
20. Nobre V, Braga E, Rayes A, Serufo JC, Godoy P, Nunes N, Antunes CM, Lambertucci JR (2003) Opportunistic infections in patients with AIDS admitted to an university hospital of the Southeast of Brazil. Rev Inst Med Trop São Paulo 45:69–74
21. Canini SR, Reis RB, Pereira LA, Gir E, Pelá NT (2004) HIV/AIDS patients' quality of life: a literature review. Rev Lat Am Enfermagem 12:940–945
22. Center for Disease Control (CDC) (2002) Deaths among persons with AIDS through. In: HIV/AIDS surveillance supplemental report 8 (1). http://www.cdc.gov/hiv/stats/hasrsupp.htm. Accessed 11 Nov 2010.
23. Reis MA, Costa RS, Ferraz AS (1995) Causes of death in renal transplant recipients: a study of 102 autopsies from 1968 to 1991. J R Soc Med 88:24–27
24. Fonseca MGP, Bastos FI (2007) Twenty-five years of the AIDS epidemic in Brazil. Cad Saúde Pública 23:333–344
25. Bosaeus I, Daneryd P, Lundholm K (2002) Dietary intake, resting energy expenditure, weight loss and survival in cancer patients. J Nutr 132:3465S–3466S
26. Inui A (2002) Cancer anorexia–cachexia syndrome: current issues in research and management. CA Cancer J Clin 52:72–91
27. Laurent-Crawford AG, Krust B, Muller S, Rivière Y, Rey-Cuillé MA, Béchet JM, Montagnier L, Hovanessian AG (1991) The cytopathic effect of HIV is associated with apoptosis. Virology 185:829–839
28. Choi B, Gatti PJ, Haislip AM, Fermin CD, Garry RF (1998) Role of potassium in human immunodeficiency virus production and cytopathic effects. Virology 247:189–199
29. Voss TG, Fermin CD, Levy JA, Vigh S, Choi B, Garry RF (1996) Alteration of intracellular potassium and sodium concentrations correlates with induction of cytopathic effects by human immunodeficiency virus. J Virol 70:5447–5454
30. Levy JA (1993) Pathogenesis of human immunodeficiency virus infection. Microbiol Rev 57:183–289
31. Verma S (2006) Haart attenuates liver fibrosis in patients with HIV/HCV co-infection: fact or fiction? J Antimicrob Chemother 58:496–501
32. Josephine M, Issac E, George A, Ngole M, Albert SE (2006) Patterns of skin manifestations and their relationships with CD4 counts among HIV/AIDS patients in Cameroon. Int J Dermatol 45:280–284
33. Belsito DV, Sanchez MR, Baer RL, Valentine F, Thorbecke GJ (1984) Reduced Langerhans' cell Ia antigen and ATPase activity in patients with the acquired immunodeficiency syndrome. N Engl J Med 310:1279–1282
34. Braathen LR, Ramirez G, Kunze RO, Gelderblom H (1987) Langerhans cells as primary target cells for HIV infection. Lancet 2:1094
35. Lehner T, Hussain L, Wilson J, Chapman M (1991) Mucosal transmission of HIV. Nature 353:709
36. Brown KN, Trichel A, Barratt-Boyes SM (2007) Parallel loss of myeloid and plasmacytoid dendritic cells from blood and lymphoid tissue in simian AIDS. J Immunol 178:6958–6967
37. Olaitan A, Johnson MA, MacLean A, Poulter LW (1996) The distribution of immunocompetent cells in the tract of HIV-positive women. AIDS 10:759–764

38. Lane HC, Masur H, Edgar LC, Whalen G, Rook AH, Fauci AS (1983) Abnormalities of B-cell activation and immunoregulation in patients with the acquired immunodeficiency syndrome. N Engl J Med 309:453–458
39. Bélec L, Dupré T, Prazuck T, Tévi-Bénissan C, Kanga JM, Pathey O, Lu XS, Pillot J (1995) Cervicovaginal overproduction of specific IgG to human immunodeficiency virus (HIV) contrasts with normal or impaired IgA local response in HIV infection. J Infect Dis 172:691–697
40. Notermans DW, de Jong JJ, Goudsmit J, Bakker M, Roos MT, Nijholt L, Cremers J, Hellings JA, Danner SA, de Ronde A (2001) Potent antiretroviral therapy initiates normalization of hypergammaglobulinemia and a decline in HIV type 1-specific antibody responses. AIDS Res Hum Retroviruses 17:1003–1008
41. Yarchoan R, Redfield RR, Broder S (1986) Mechanisms of B cell activation in patients with acquired immunodeficiency syndrome and related disorders. J Clin Invest 78:439–447
42. Shirai A, Cosentino M, Leitman-Klinman SF, Klinman DM (1992) Human immunodeficiency virus infection induces both polyclonal and virus-specific B cell activation. J Clin Invest 89:561–566
43. Nara P (1996) Humoral immunity to HIV-1: lethal force or Trojan horse? In: Gupta S (ed) Immunology of HIV infection. Plenum, New York, pp 243–276
44. Saag MS, Holodniy M, Kuritzkes DR, O'Brien WA, Coombs R, Poscher ME, Jacobsen DM, Shaw GM, Richman DD, Volberding PA (1996) HIV viral load markers in clinical practice. Nat Med 2:625–627
45. Piatak M, Saag MS, Lifson JA (1993) High levels of HIV-1 in plasma during all stages infection determined by competitive PCR. Science 259:1749–1754
46. Dann FJ, Tabibian P (1995) Cutaneous diseases in human immunodeficiency virus infected patients referred to the UCLA Immunosuppression Skin Clinic: reasons for referral and management of select diseases. Cutis 55:85–98
47. Sadick NS (1993) Clinical and laboratory evaluation of AIDS trichopathy. Int J Dermatol 32:33–38
48. Jensen BL, Weismann K, Sindrup JH, Sondergaard J, Schmidt K (2000) Incidence and prognostic significance of skin disease in patients with HIV/AIDS: a 5-year observational study. Acta Derm Venereol 80:140–143
49. Jing W, Ismail R (1999) Mucocutaneous manifestations of HIV infection: a retrospective analysis of 145 cases in a Chinese population in Malaysia. Int J Dermatol 38:457–463
50. Uthayakumar S, Nandwani R, Drinkwater T, Nayagam AT, Darley CR (1997) The prevalence of skin disease in HIV infection and its relationship to the degree of immunosuppression. Br J Dermatol 137:595–598

Virchows Arch (2012) 461:457–466
DOI 10.1007/s00428-012-1302-3

ORIGINAL ARTICLE

Expression patterns of emmprin and monocarboxylate transporter-1 in ovarian epithelial tumors

Miyoko Fukuoka · Makoto Hamasaki · Kaori Koga · Hiroyuki Hayashi · Mikiko Aoki · Tatsuhiko Kawarabayashi · Shingo Miyamoto · Kazuki Nabeshima

Received: 7 March 2012 / Revised: 28 July 2012 / Accepted: 9 August 2012 / Published online: 28 August 2012
© Springer-Verlag 2012

Abstract Emmprin is a transmembrane glycoprotein known as a matrix metalloproteinase inducer and is highly up-regulated in malignant cancer cells. The monocarboxylate transporters (MCTs) are responsible for H^+-linked transport of monocarboxylates across the cell membrane. It was recently demonstrated that proper plasma membrane localization and activity of MCTs require the presence of emmprin as a chaperone and that MCT-1 also acts as chaperone for emmprin. The objectives of this study were to clarify emmprin and MCT-1 expression patterns in ovarian epithelial tumors and to elucidate the clinicopathological significance of co-localization of the two molecules. Immunohistochemical analysis of 205 epithelial tumors indicated that emmprin is always localized in cell membranes but its distribution differs according to tumor type: in lateral membranes in 89 % of adenomas, in lateral and basal membranes in 76 % of borderline tumors, and in membranes surrounding the entire cell in 98 % of carcinomas. Most carcinomas in situ also showed a lateral and basal expression pattern. In only 21 % of the carcinomas, the cells expressing membranous MCT-1 showed co-localized emmprin expression. Poor co-localization of the two molecules was more frequently found in serous carcinomas. However, the overall survival was not significantly different for the good and poor co-localization carcinoma groups. These findings indicate that the emmprin expression pattern might discriminate between invasive carcinomas and borderline tumors including carcinoma in situ. Moreover, there may be an as yet unidentified regulatory mechanism(s), for localization of MCT-1 and emmprin in cell membranes in vivo.

Keywords Emmprin · MCT-1 · Expression pattern · Ovarian epithelial tumors · Immunohistochemistry

Introduction

Epithelial ovarian cancer is a frequent cause of cancer death in women because it is usually first detected in the metastatic phase of the disease [1]. Matrix metalloproteinases (MMPs), which comprise a family of zinc-dependent proteolytic enzymes, have a central role in the progression of tumors, and degradation of the extracellular matrix by MMPs and energy production via glycolysis are both critical for tumor invasion and growth.

Emmprin is a transmembrane glycoprotein known as an MMP inducer [2], which stimulates peritumoral fibroblasts to produce MMP. Emmprin, also known as basigin and CD147, is a cell surface glycoprotein of the immunoglobulin superfamily that is highly up-regulated in malignant cancer cells [3, 4]. Emmprin is functionally associated with monocarboxylate transporters (MCTs). The MCT family has 14 members, including isoforms 1, 2, 3, and 4, which are responsible for the H^+-linked transport of monocarboxylates such as lactic acid across the membrane. The underlying molecular events involved in MCT regulation are poorly understood; however, it was recently demonstrated that the

Electronic supplementary material The online version of this article (doi:10.1007/s00428-012-1302-3) contains supplementary material, which is available to authorized users.

M. Fukuoka · M. Hamasaki · K. Koga · H. Hayashi · M. Aoki · K. Nabeshima (✉)
Department of Pathology, Faculty of Medicine, Fukuoka University,
7-45-1 Nanakuma, Jonan-ku,
Fukuoka 814-0180, Japan
e-mail: kaznabes@fukuoka-u.ac.jp

M. Fukuoka · T. Kawarabayashi · S. Miyamoto
Department of Obstetrics and Gynecology, Faculty of Medicine, Fukuoka University,
Fukuoka, 812-0180, Japan

proper plasma membrane expression and activity of MCTs, particularly MCT-1 and MCT-4, in vitro require the presence of emmprin as a chaperone [5]. Interestingly, silencing of MCT-1 led to maturation arrest of CD147 in its core glycosylated form, demonstrating that MCT-1 also acts as chaperone for CD147 [6]. However, the clinicopathological significance of co-localization of emmprin and MCTs in ovarian epithelial tumors has been hardly explored [7]. The objectives of this study using ovarian epithelial tumors were to clarify the expression patterns of emmprin and MCT-1 and to elucidate the clinicopathological significance of co-localization of the two molecules.

Material and methods

Tissue samples

The study material comprised a total of 205 patients with ovarian epithelial tumors including 48 ovarian adenomas (age range, 10–83 years; mean, 45.2 years), 48 ovarian borderline tumors (age range, 17–86 years; mean, 48.3), and 109 ovarian carcinomas (age range, 29–86 years; mean, 55.8) obtained from the ovarian tumor files kept at the Department of Pathology, Fukuoka University Hospital. The 205 patients had been treated at the Department of Obstetrics and Gynecology, Fukuoka University Hospital between April 1993 and April 2005. Six normal ovarian control specimens were obtained from early stage cervical cancer patients and leiomyoma patients with a mean age of 58 ± 9 years (range 46–67), who underwent surgery during the same period. Anonymous use of redundant tissue is part of the standard treatment agreement with patients at our hospital when no objection is expressed. The study protocol was approved by the Ethics Committee of Fukuoka University. Tumor tissue specimens for laser capture microdissection or western blotting were frozen in liquid nitrogen and kept at −80 °C until use.

Pathological evaluation

The surgically resected specimens were fixed routinely in 10 % formalin and processed into paraffin blocks for histopathological examination. The histopathological type was determined according to the 2003 World Health Organization classification [8]. The histological grading of carcinomas was determined according to the Silverberg grading system [9].

Immunohistochemistry

For immunoperoxidase staining of formalin-fixed, paraffin-embedded tissue sections, a dextran polymer-based method (for emmprin) and a standard biotin–streptavidin method (for MCT-1) were used. Briefly, after nonspecific protein binding sites were blocked with 5 % nonfat dry milk in Tris-buffered saline, pH 7.6 (TBS) for 1 h at room temperature (RT), sections were incubated with mouse anti-emmprin monoclonal antibody (R&D Systems, Minneapolis, MN, USA) used at a 1:100 dilution overnight at 4 °C or with anti-MCT-1 goat polyclonal antibody (Santa Cruz Biotechnology, Santa Cruz, CA, USA) used at a 1:20 dilution for 1 h at RT. The sections were then washed in TBS and incubated with Histofine reagent (Nichirei Biosciences, Tokyo, Japan) for 1 h for emmprin or with biotinylated anti-goat rabbit IgG (Vector Laboratories, Burlingame, CA, USA) for 30 min at RT for MCT-1. The sections were then washed in TBS and incubated with streptavidin-horseradish peroxidase pre-diluted (BD Pharmingen™, Franklin Lakes, NJ, USA) for 30 min at RT for MCT-1. The reaction was visualized by using horseradish peroxidase and 3,3′-diamino-benzidine (DAKO, Carpinteria, CA, USA) or alkaline phosphatase and naphthol AS-BI phosphate (Sigma, St Louis, MO, USA).

The immunohistochemical specificity of the emmprin antibody was confirmed by two types of negative controls: substituting mouse non-immune IgG for the primary antibody and omitting the primary antibody in the staining protocol. Antigen competition controls using anti-MCT-1 antibody absorbed with a fivefold excess of MCT-1 N-terminal peptide antigen (Santa Cruz Biotechnology) were also performed. Epithelioid sarcoma and malignant mesothelioma tissues were used as positive controls for emmprin and MCT-1, respectively (Supplementary Fig. 1).

Stained sections were evaluated semiquantitatively by two independent observers (M.F. and K.N.), who were blinded to the clinical data. Immunostaining was considered negative if less than 10 % of the tumor cells were stained. In specimens considered positive, staining of the tumor was quantitated on a scale from 1 to 4 based on the percentage of positively stained tumor cells, as described previously [10]. The scale was structured as follows: 1+=10–24%; 2+=25–49%; 3+=50–74%; and 4+=≥75 %. As to the localization of reactivity, a membranous or a combined membranous and cytoplasmic reactivity was interpreted as positive. The emmprin expression patterns and co-localization of emmprin with MCT-1 were also evaluated.

Protein extraction from frozen tissue samples and western blotting

Western blotting was performed using frozen tumor tissues, not identical but closely matched in the subtypes of tumors, including ovarian carcinomas from 12 patients (age range, 49–80 years; mean, 58) and ovarian adenomas from 6 patients (age range, 27–82 years; mean, 54.8). Proteins

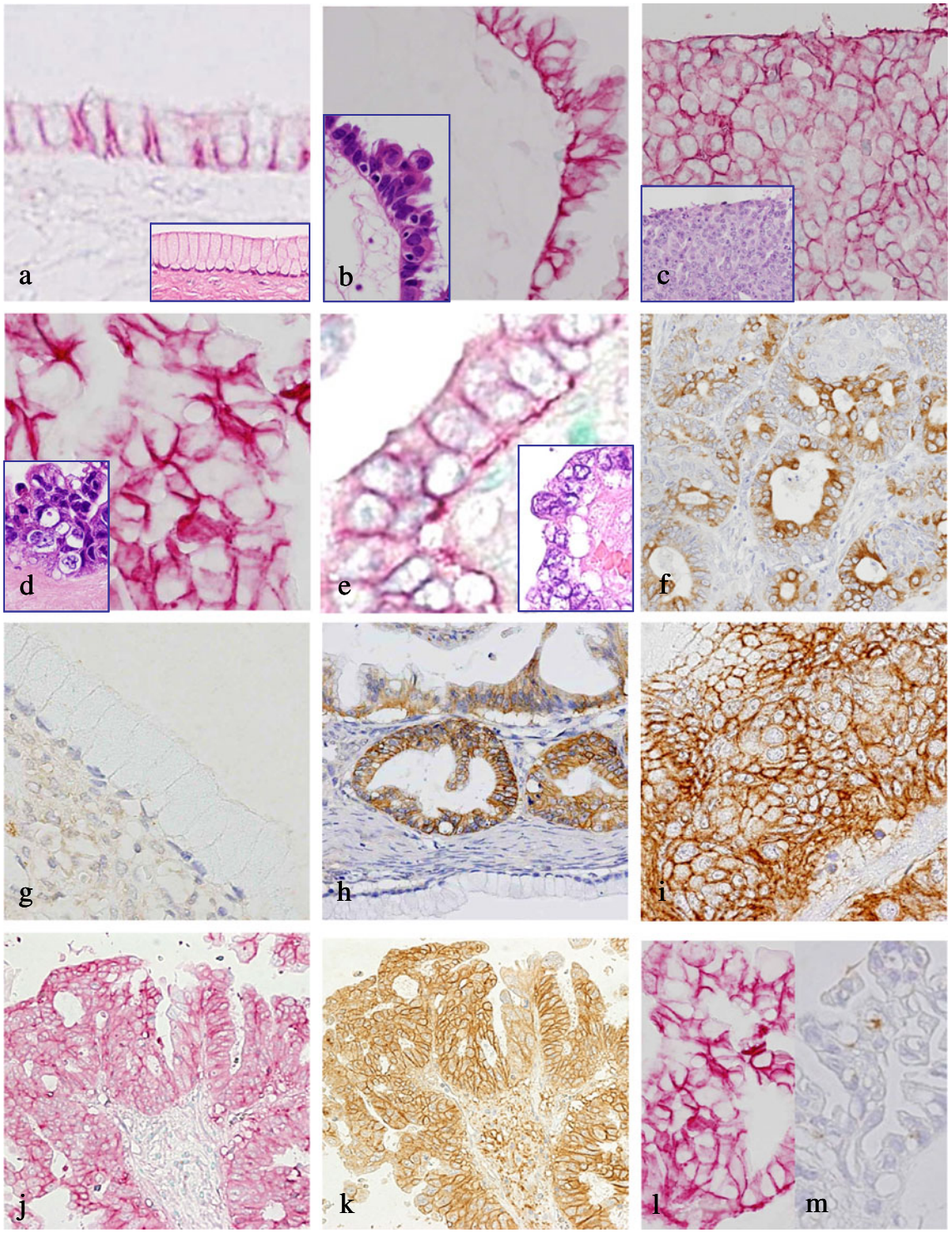

Fig. 1 Immunohistochemical expression of emmprin and MCT-1 in ovarian epithelial tumors: adenomas (**a**, **g**), borderline tumors (**b**, **h**), carcinomas in situ (**d**, **e**), and carcinomas (**c**, **i**). **a** Adenoma cells showed emmprin immunoreactivity in lateral cell membranes. **b** Borderline tumors showed emmprin immunoreactivity in lateral and basal membranes. **c** Carcinoma cells showed emmprin immunoreactivity in membranes surrounding all the cells. Most carcinomas in situ showed emmprin immunoreactivity in lateral and basal membranes (**e**), but in only one case, reactivity was seen in membranes surrounding all the cells (**d**). *Insets* in **a**–**e**, HE (hematoxylin–eosin) staining. **f** EMA was expressed irregularly and focally in apical parts of carcinomas. **g** Adenoma cells were negative for MCT-1, while stromal cells were occasionally positive (40 %). Borderline tumors (**h**) and carcinomas (**i**) showed immunoreactivity in the cytoplasm and around the cell membranes. Expressions of emmprin and MCT-1 showed good co-localization in some tumors (**j**, **k**) and poor localization in others (**l**, **m**). **j**, **l** Emmprin; **k**, **m** MCT-1. Original magnifications: **b**, **c**, **f**, **h**–**k**—×200; **a**, **d**, **e**, **g**, **l**, **m**—×400

including emmprin and MCT-1 were extracted from tissue samples using a homogenizer (Polytron-aggregate; Kinematica, Lucerne, Switzerland) in a lysis buffer containing 10 mM Tris HCl (pH 7.5), 15 mM NaCl, 2 mM ethylenediaminetetraacetic acid, 1 % Triton X-100, and protease inhibitors (Complete Mini; Roche Applied Sciences, Penzberg, Germany) on ice for 30 min. The extracts were clarified by centrifugation at 14,000 rpm for 10 min and subjected to sodium dodecyl sulfate-polyacrylamide gel electrophoresis after measurement of their protein concentrations with the Bio-Rad Protein Assay (Bio-Rad, Hercules, CA, USA). After electrophoresis, the proteins were transferred electrophoretically to an Immobilon membrane (Millipore, Bedford, MA, USA), as described previously [11]. Nonspecific protein binding sites were blocked with 5 % non-fat dry milk in 0.05 % Tween-20/TBS, pH 7.6 (TBS-T) at 37 °C for 1 h, and the membrane was incubated overnight at 4 °C with mouse anti-emmprin monoclonal antibody (R&D Systems) or rabbit anti-MCT-1 polyclonal antibody (Alpha Diagnostic International, San Antonio, TX, USA). After washing with TBS-T, the membrane was incubated for 1 h with peroxidase-conjugated anti-mouse (for emmprin) and anti-rabbit (for MCT-1) IgG. Color was developed with chemiluminescence reagents according to the instructions supplied by the manufacturer (DuPont NEN, Boston, MA, USA). The bands on the film were subjected to image analysis with NIH ImageJ version 1.44. Student's *t* test was used for all statistical analyses.

Laser capture microdissection

Laser capture microdissection (LCM) was performed with the Pixcell IIe LCM system (Arcturus Engineering Inc., Mountain View, CA, USA) as described previously [12]. Frozen sections were cut and attached to uncharged microscope slides for each sample. Immediately after dehydration and staining (HistoGene; Arcturus), slides were processed with the Pixell IIe LCM system, followed by collection of microdissected cells with CapSure Macro LCM Caps (Arcturus Engineering Inc.).

RNA extraction, cDNA synthesis, and real-time quantitative RT-PCR

Total RNA was isolated from frozen tissue specimens, with the illustra RNAspin Mini RNA Isolation Kit (GE Healthcare Bio-Sciences, Piscataway, NJ, USA), according to the instructions supplied by the manufacturer. Next, the cDNA was synthesized from 1 μg of total RNA, with the First-Strand cDNA Synthesis Kit (GE Healthcare Bio-Sciences). Three gene-specific oligonucleotide primer pairs were purchased for emmprin, MCT-1, and glyceraldehyde-3-phosphate dehydrogenase (GAPDH) (Takara Bio, Otsu, Japan). The primer pairs used for RT-PCR analysis were intron-spanning—for emmprin: 5′-TGTCACTGACTGGGCCTGGTA-3′ (forward) and 5′-GCCTCCATGTTCAGGTTCTCAA-3′ (reverse); for MCT-1: 5′-TGTGGAATGCTGTCCTGTCCTC-3′ (forward) and 5′-TGATGCCCATGCCAATGAA-3′ (reverse); and for GAPDH: 5′-GCACCGTCAAGGCTGAGAAC-3′ (forward) and 5′-TGGTGAAGACGCCAGTGGA-3′ (reverse). Real-time monitoring of PCR reactions was performed with the Light-Cycler system (Roche Applied Science, Indianapolis, IN, USA) and SYBR® Premix Ex Taq™II (Takara Bio), according to the instructions supplied by the manufacturers. Each assay was performed three times to verify the results. Student's *t* test was used for statistical analysis of the normalized values for ovarian cancers and adenomas.

Statistical analysis

Associations between categorical factors were evaluated with the χ^2 test or Fisher's exact test. Survival curves were plotted with the Kaplan–Meier method, and *P* values were calculated with the log rank test. Univariate analysis was performed by using Cox's proportional hazards regression analysis. Statistical comparison between clinical stage and pathological grades was performed with the Kruskal–Wallis test. A *P* value of <0.05 was considered to denote a statistically significant difference. All statistical evaluations were performed with the Stat View statistical software for Windows version 5.0 (SAS Institute Inc., Cary, NC, USA).

Results

The clinicopathological characteristics of patients with ovarian carcinomas

Table 1 summarizes the clinicopathological characteristics of the 109 patients with ovarian carcinomas. The pathological diagnosis identified 39 cases of serous cystadenocarcinoma, 16 of mucinous cystadenocarcinoma, 27 of endometrioid adenocarcinoma, 18 of clear cell adenocarcinoma, 3 of squamous cell carcinoma, and 6 of malignant mixed epithelial tumors. Lymph node metastasis and recurrence were found in 18 cases (19 %) and 30 cases (28 %), respectively, in a follow-up period of 1–115 months (mean, 51.2 months). The residual tumor size after primary debulking surgery was 0 in 76 cases (70 %), less than 1 cm in 3 cases (3 %), and more than 1 cm in 30 cases (28 %). Advanced stages (III, IV), high grade (3), and the presence of residual tumor, peritoneal dissemination, and lymph node metastasis were significantly associated with shorter survival. Adenomas comprised 33 cases of mucinous cystadenoma and 15 cases of serous cystadenoma, and borderline tumors

Table 1 Univariate analysis of overall survival for ovarian carcinoma patients and correlation of clinicopathological parameters with emmprin/MCT-1 co-localization

Variable	Number of patients	Univariate analysis			Co-localization		
		RR	95 % CI	*P* value	Poor	Good	*P* value
All cases	109						
Age (years)							
<50	39 (36)				30	9	
>50	70 (64)	1.97	0.88–4.41	0.098	57	13	0.753
FIGO stage							
I	50 (46)				38	12	
II	12 (11)	7.96	1.33–47.7	0.023	9	3	
III	35 (32)	21.5	4.99–92.7	<0.005	32	3	
IV	11 (10)	41.2	8.57–198.	<0.005	8	3	0.269
Grade							
1	43 (49)				33	10	
2	26 (30)	2.04	0.86–4.84	0.105	22	4	
3	19 (21)	2.58	1.09–6.08	0.031	18	1	0.217
Histology							
Serous carcinomas	39 (36)	1.57	0.77–3.20	0.218	36	3	
Nonserous carcinomas	70 (64)				52	18	0.039
Residual tumors							
No	78 (72)				60	18	
Yes	31 (28)	3.55	1.77–7.15	<0.005	26	5	0.395
Peritoneal dissemination							
No	59 (55)				45	14	
Yes	48 (45)	8.08	3.30–19.8	<0.005	40	8	0.509
Lymph node metastasis							
No	75 (81)				57	18	
Yes	18 (19)	4.29	1.94–9.47	<0.005	16	2	0.379
Ascites (ml)							
<500	79 (77)				61	18	
>500	23 (27)	1.65	0.73–3.75	0.23	20	3	0.196

RR risk ratio, *CI* confidence interval

comprised 36 cases of mucinous, 9 cases of serous, 1 case of endometrioid, and 2 cases of mixed tumor.

Immunohistochemical expression of emmprin

Emmprin expression was positive in 27/48 (56 %) of adenomas, 45/48 (94 %) of borderline tumors, and 108/109 (99 %) carcinomas (Table 2). Emmprin was localized in the cell membranes of all positive tumors, but its distribution was quite different according to the tumor type. It was present in only the lateral membranes in 24/27 (89 %) of adenomas (Fig. 1a) and in the lateral and basal membranes in 34/45 (76 %) of borderline tumors (Fig. 1b), while 98 % (107/109) of carcinomas showed emmprin immunoreactivity surrounding all the cells (Fig. 1c; Table 2). The difference in expression patterns in these three types of tumors was significant ($P<0.01$, Kruskal–Wallis test; Table 2). In 15 cases of carcinoma in situ, only one tumor showed emmprin expression surrounding all the cells (Fig. 1d), while the others exhibited its reactivity in lateral and basal membranes as was seen in most borderline tumors (Fig. 1e). Moreover, most of the emmprin-expressing carcinomas

Table 2 Expression patterns of emmprin in ovarian epithelial tumors

	Number of cases		Expression pattern (% positive)		
	Total	Positive	Lateral	Basolateral	Surrounding
Adenoma	48	27	24 (89)*	3 (11)	0
Borderline tumor	48	45	7 (15)	34 (76)*	4 (9)
Carcinoma	109	108	0	1 (1)	107 (98)*

*$P<0.01$ by Kruskal–Wallis test

(104/109, 95 %) were scored 3+ or 4+ (high expression group), while 25 % (12/48) and 65 % (31/48), respectively, of emmprin-expressing adenomas and borderline tumors belonged to the high expression group; the differences among these three different types of tumors were statistically significant ($P<0.01$, Fisher's exact test; Fig. 2a). As a nonspecific membrane protein control, epithelial membrane antigen (EMA) expression was also examined in carcinomas and its expression pattern was focal and irregular, quite different from that of emmprin (Fig. 1f). No emmprin immunoreactivity was found in normal ovarian tissues except for granulosa cells (data not shown).

Immunohistochemical expression of MCT-1

Positive MCT-4 immunoreactivity was observed in none of the ovarian epithelial tumors including adenomas, borderline tumors, and carcinomas (data not shown). Most adenoma cells were also negative for MCT-1 (Fig. 1g), whereas borderline tumors (Fig. 1h) and carcinomas (Fig. 1i) exhibited positive membrane and cytoplasmic reactivity to MCT-1. MCT-1 reactivity was also detected in the tumor stroma in 40 % (19/48) of adenomas (Fig. 1g). Panels b and c of Fig. 2 show a summary of MCT-1 immunostaining results for ovarian epithelial tumors. Positive MCT-1 expression in cell membranes was seen in 4 % (2/48) of adenomas, 21 % (10/48) of borderline tumors, and 41 % (45/109) of carcinomas, and the difference between adenomas and carcinomas was statistically significant ($P<0.01$, Fisher's exact test; Fig. 2b). Tumors with high MCT-1 expression (scores 3 and 4) were identified in 2 % (1/48) of adenomas, 13 % (6/48) of borderline tumors, and 19 % (21/109) of carcinomas, and the difference between adenomas and carcinomas was statistically significant ($P<0.01$, Fisher's exact test; Fig. 2c). No MCT-1 immunoreactivity was found in normal ovarian tissues except for granulosa cells (data not shown).

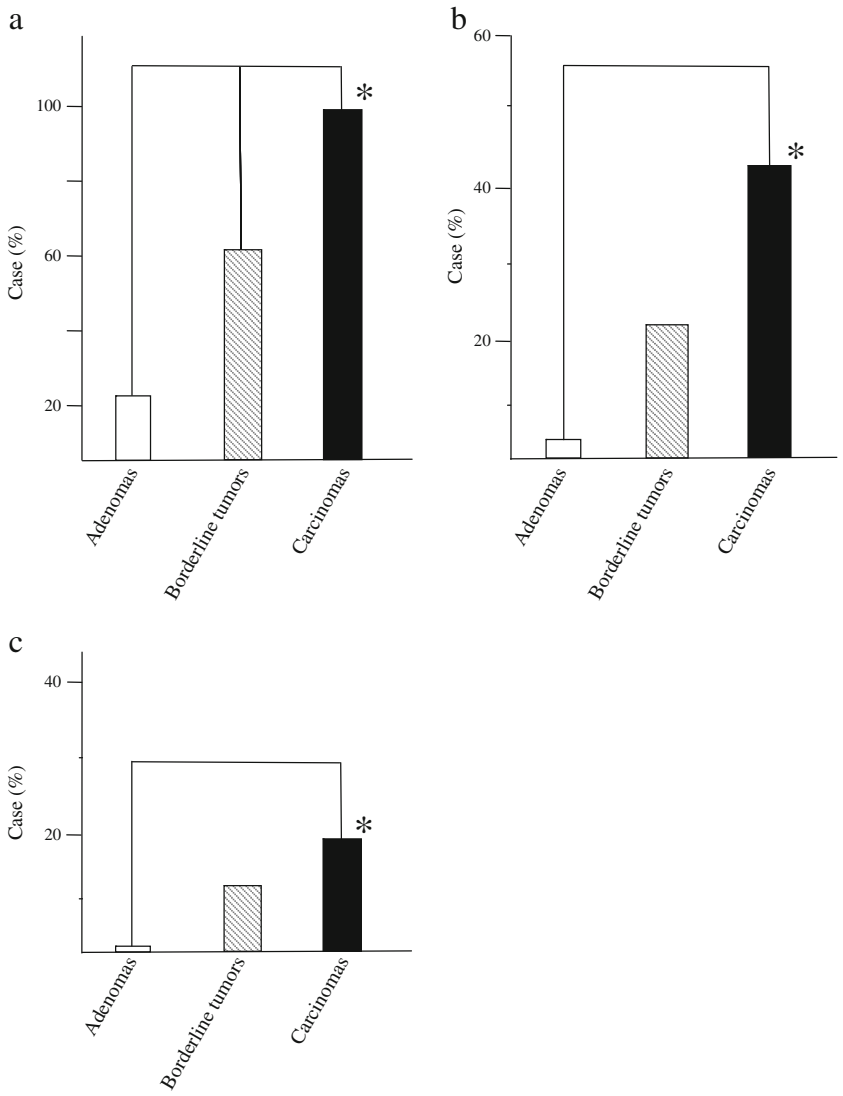

Fig. 2 Semiquantitative analysis of emmprin and MCT-1 expression in adenomas, borderline tumors, and carcinomas. Numbers of tumors with high levels of emmprin expression (scores 3 and 4) (**a**) are shown for adenomas, borderline tumors, and carcinomas. Numbers of MCT-1 positive tumors (**b**) or those of tumors expressing high levels of MCT-1 (**c**) are shown for adenomas, borderline tumors, and carcinomas. *$P<0.01$ by Fisher's exact test

Co-localization of emmprin and MCT-1

Co-localization of emmprin and MCT-1 in carcinomas was analyzed next. Some carcinomas expressed both emmprin and MCT-1 in the same parts of the tumors, as was demonstrated immunohistochemically in serial sections (Fig. 1j, k), while others showed expression of only emmprin but not of MCT-1 (Fig. 1l, m). Parts which expressed MCT-1 but not emmprin were extremely rare. Figure 3a summarizes the results of this co-localization analysis. Good co-localization of emmprin and MCT-1, which was defined by identical immunostaining scores for emmprin and MCT-1 or with a difference of only 1 and shown as black columns in Fig. 3a, was observed in 23 carcinomas (21 %), whereas 86 carcinomas (79 %) showed poor co-localization. The two groups of carcinomas, expressing good or poor co-localization of emmprin and MCT-1, showed no statistical differences in overall survival of patients (Fig. 3b), nor in clinicopathological parameters except for the histological type (Table 1). Serous carcinomas were significantly more associated with carcinomas showing poor co-localization, while 30 cases of recurrent carcinomas also showed a similar rate (8/30, 27 %) of co-localization of emmprin and MCT-1 (Table 3). In 95 % (21/22) of the cases with poor co-localization, a different expression pattern of emmprin and MCT-1 was found with emmprin expressed in cell membranes, while MCT-1 was found diffused in the cytoplasm.

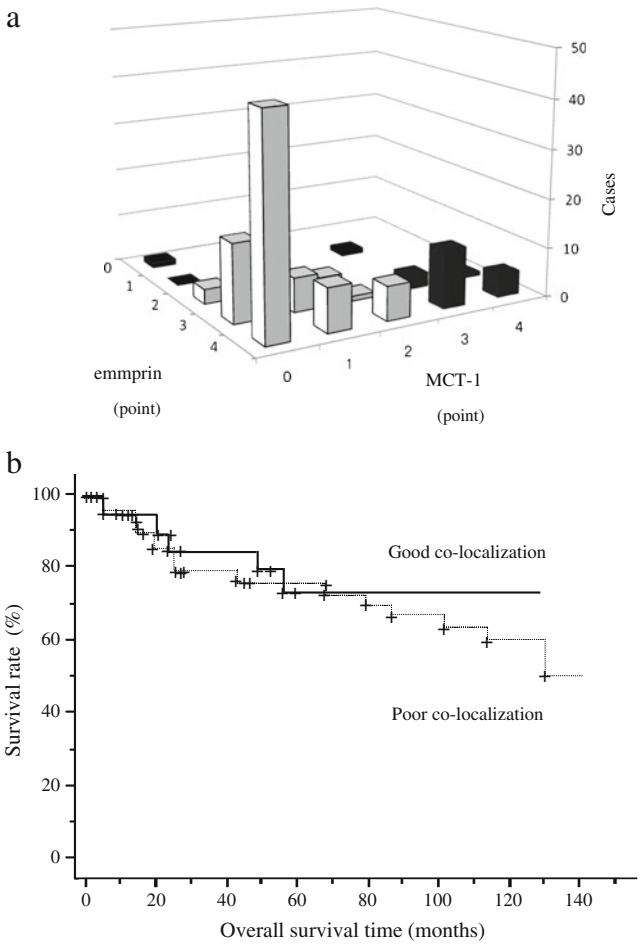

Fig. 3 Co-localization of emmprin and MCT-1 (**a**). *Black columns* show tumors with good co-localization of emmprin and MCT-1, while *white columns* represent tumors with poor co-localization. Overall survival of patients with tumors showing good or poor co-localization of emmprin and MCT-1 (**b**). No significant difference was found between the two groups of patients

Expression of emmprin and MCT-1 mRNAs and proteins in ovarian epithelial tumors

Expression levels of emmprin and MCT-1 mRNA were also examined in 14 frozen tissue samples (4 or 5 adenomas and 10 carcinomas) by means of real-time RT-PCR. The expression levels of emmprin and MCT-1 mRNA, although higher in ovarian carcinomas than in adenomas, were not statistically significantly different (Fig. 4a).

Expression levels of emmprin and MCT-1 proteins were also examined in 18 frozen tissue samples (6 adenomas and 12 carcinomas) by means of western blotting. MCT-1 was expressed as a 48-kDa band, while emmprin appeared as 58 and 45 kDa bands, possibly due to different levels of glycosylation or proteolytic degradation [11, 13]. All carcinomas expressed both emmprin and MCT-1 proteins (Fig. 4b), with expression levels that were both higher than those of adenomas, although the differences were not statistically significant between the two types of tumors (Fig. 4c).

Discussion

To the best of our knowledge, this study is the first to show that immunohistochemical expression patterns of emmprin might be useful for differentiating invasive carcinomas from borderline tumors including in situ adenocarcinomas. Moreover, in regard to co-localization of emmprin and MCT-1, we found that ovarian carcinomas could be divided into two groups. One comprises tumors that co-express these two molecules in the cell membrane of most of the carcinoma cells (the good co-localization group). The others consist of tumors with more than 50 % of the carcinoma cells expressing only emmprin and not MCT-1 (the poor co-localization group). Although the two groups did not show significant differences in overall survival, our findings indicate that emmprin expression in cell membranes in vivo does not always need co-expression of MCT-1 but that MCT-1 expression in membranes may need the co-expression of emmprin.

We also found that emmprin is differently expressed in cell membranes depending on the type of tumor.

Table 3 Expression of emmprin and MCT-1 in recurrent ovarian tumors

Expression	No. of patients (%)
Total	30
Emmprin	
High expression	26 (87)
Low expression	4 (13)
MCT-1	
High expression	7 (23)
Low expression	23 (77)
Co-localization	
Good	8 (27)
Poor	22 (73)

Furthermore, the expression pattern in most of the in situ carcinomas was the same as that in borderline tumors. Thus, emmprin expression surrounding the entire cell membrane was almost always restricted to invasive carcinomas. This pattern of expression was due not only to loss of cellular polarity in carcinoma cells, but possibly also to a mechanism specific to emmprin, since a mucin-like glycoprotein, EMA, was expressed irregularly and focally in cell membranes, especially around the apical membranes, even in carcinomas. A similar occurrence of differences in localization in ovarian tumors according to tumor type was also reported for aquaporin-5 (AQP5), a family member of small membrane transport proteins that act primarily as water selective pores [14]. AQP5 is mainly localized in the basolateral membrane of benign tumor cells, the apical and

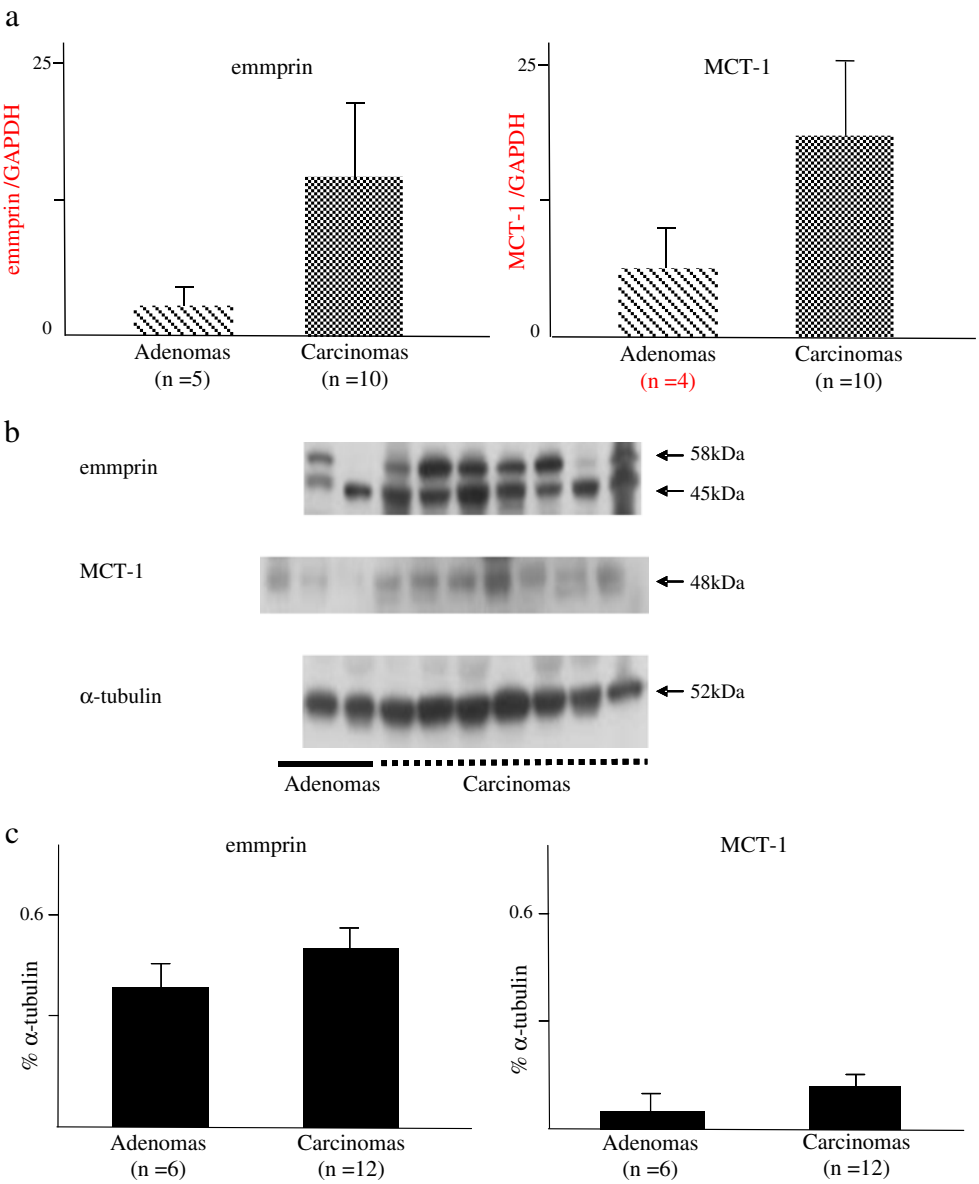

Fig. 4 Detection by real-time RT-PCR and western blotting of emmprin and MCT-1 in tissue extracts from adenomas and carcinomas. **a** Emmprin and MCT-1 mRNAs were both expressed at higher levels in ovarian carcinomas than in adenomas. **b** The 45- and 58-kDa bands of emmprin and the 48-kDa band of MCT-1 can be seen in both tumor extracts, although their intensities were stronger in carcinomas than adenomas. **c** Semiquantitative analysis of emmprin and MCT-1protein expressions by means of image analysis

basolateral membrane of borderline cells and scattered in the membrane of malignant cells, while the normal ovarian epithelium shows almost no or weak staining for this protein. However, the mechanism involved in this difference in localization of AQP5 is still unknown [14]. As for emmprin localization within cells, a sorting signal consisting of Leu-252 in its C-terminal domain has been identified by using extensive mutagenesis [15]. This signal dictates basolateral localization of emmprin in MDCK cells but is not recognized by the retinal pigment epithelium, resulting in a reversed apical localization of emmprin in this epithelium [15, 16]. These findings suggest the presence of a cell type-specific recognition mechanism for the Leu-252-based signal. It seems that this recognition mechanism is maintained or somewhat altered in ovarian adenomas and borderline tumors, respectively, and probably malfunctions in carcinomas.

In vitro studies have demonstrated that the co-presence or co-expression of emmprin is critical for cell membrane localization and activity of MCTs. On the other hand, maturation and cell surface expression of emmprin depends on MCT expression [6, 17]. In COS and HeLa cells, MCT transfection caused accumulation of expressed protein in a perinuclear compartment, whereas co-transfection with emmprin enabled expression of active MCT-1 and MCT-4 in the cell membrane [17]. In Lovo cells, emmprin and MCT-1 co-localized on the cell surface, and anti-human CD147/emmprin mouse monoclonal antibody (MEM-M6/1) inhibited the association of these molecules, resulting in the prevention of lactate uptake and release and a reduction in intracellular pH [18]. Emmprin/basigin co-localized with MCT-1 and MCT-4 on the A375 melanoma cell membrane, while silencing of emmprin/basigin in A375 cells by siRNA clearly eliminated the expression of MCT-1 and MCT-4 and their co-localization with emmprin/basigin and dramatically reduced the glycolysis rate, the level of extracellular pH, and the production of ATP [19]. Co-expression of emmprin and MCT-1 was also observed in vivo and was significantly associated with lymph node and/or distant metastases in cervical adenocarcinomas (P=0.033). However, no statistically significant associations with survival data were found [20]. In gastric carcinomas, MCT-1/emmprin co-expression was associated with advanced gastric carcinoma, Lauren's intestinal type, TNM staging, and lymph node metastasis [21]. Co-expression of emmprin with MCT-1 in ovarian carcinomas was reported by two groups [5, 7]. In one of these studies, a substantial number of MCT-1-positive cases were negative for emmprin, prompting the authors to suggest that MCT-1 plasma membrane expression in tumors may depend on an as yet unidentified regulatory protein [5]. In our study, however, emmprin was highly expressed in cell membranes in 95 % of carcinomas, while in about 80 % of carcinomas, MCT-1 was much less highly expressed in the cell membrane than was emmprin (poor co-localization group). Carcinoma cells expressing emmprin in cell membranes and MCT-1 in the cytoplasm were also observed (data not shown). There may thus be a mechanism by which emmprin is expressed in cell membranes independently of MCT-1, as well as a mechanism to prevent the translocation of MCT-1 from the cytoplasm to cell membranes even in the presence of emmprin. A study by another group showed frequent co-expression of emmprin with MCT-1 in both primary and metastatic epithelial ovarian cancer cells by immunofluorescence labeling [7]. In their study, emmprin expression was mainly cell membrane-associated, but also with distinct positive cytoplasmic staining, and MCT-1 immunostaining was mainly cytoplasmic. These staining patterns were interpreted as co-expression. However, in our study, we focused on membranous expression of emmprin and MCT-1, and a membranous or a combined membranous and cytoplasmic reactivity was interpreted as positive. Our study is the first to examine in ovarian carcinomas whether co-localization of emmprin with MCT-1 is associated with overall survival and other clinicopathological parameters. Poor co-localization occurred significantly more frequently in serous carcinomas, but overall survival and progression-related parameters were not different between the good and poor co-localization groups of carcinomas.

The relationship between emmprin expression and patient survival has remained controversial. Increased expression of emmprin in colorectal carcinomas showed a significant correlation with poor disease-specific survival [22]. Similarly, positive emmprin expression in bladder carcinomas was significantly associated with stage, grade, recurrence, progression, and death of patients [23]. However, it was also reported that low membranous emmprin expression in high grade ovarian carcinomas or low cytoplasmic staining in serous carcinomas is an independent predictor of poor 10-year disease-related survival [24]. More interestingly, it has been shown that emmprin expression in carcinoma cells in effusions and solid lesions does not correlate with disease outcome for ovarian carcinomas, but that emmprin expression in stromal cells of primary tumors and in endothelial cells of all solid tumors correlated with poor survival [25]. In our study, most of the carcinomas (95 %) expressed high levels of emmprin, and thus the emmprin expression level did not correlate with patient survival. Emmprin was also sometimes expressed in tumor stroma, which might have reduced the difference in emmprin protein expression between carcinomas and adenomas in whole tissue extracts, but the stromal expression level was not associated with patient outcome or tumor progression (data not shown). While emmprin expression seems to be involved in tumor progression in view of its diverse biological functions and high levels of expression in both

primary and recurrent ovarian tumors, its association with survival of patients with ovarian carcinomas needs to be further explored.

Acknowledgments We wish to thank Ms. K. Yano, Ms. H. Fukagawa, and Ms. M. Onitsuka for their expert technical assistance with immunohistochemical staining and in vitro studies. This work was supported in part by a grant from the Research Center for Advanced Molecular Medicine, Fukuoka University.

Conflict of interest The authors declare that they have no conflict of interest.

References

1. Torng PL, Mao TL, Chan WY, Huang SC, Lin CT (2004) Prognostic significance of stromal metalloproteinase-2 in ovarian adenocarcinoma and its relation to carcinoma progression. Gynecol Oncol 92:559–567
2. Biswas C, Zhang Y, DeCastro R, Guo H, Nakamura T, Kataoka H, Nabeshima K (1995) The human tumor cell-derived collagenase stimulatory factor (renamed EMMPRIN) is a member of the immunoglobulin superfamily. Cancer Res 55:434–439
3. Toole BP (2003) Emmprin (CD147), a cell surface regulator of matrix metalloproteinase production and function. Curr Top Dev Biol 54:371–389
4. Nabeshima K, Iwasaki H, Koga K, Hojo H, Suzumiya J, Kikuchi M (2006) Emmprin (basigin/CD147): matrix metalloproteinase modulator and multifunctional cell recognition molecule that plays a critical role in cancer progression. Pathol Int 56:359–367
5. Pinheiro C, Reis RM, Ricardo S, Longatto-Filho A, Schmitt F, Baltazar F (2010) Expression of monocarboxylate transporters 1, 2, and 4 in human tumours and their association with CD147 and CD44. J Biomed Biotechnol 2010:427694
6. Deora AA, Philp N, Hu J, Bok D, Rodriguez-Boulan E (2005) Mechanisms regulating tissue-specific polarity of monocarboxylate transporters and their chaperone CD147 in kidney and retinal epithelia. Proc Natl Acad Sci U S A 102:16245–16250
7. Chen H, Wang L, Beretov J, Hao J, Xiao W, Li Y (2010) Co-expression of CD147/EMMPRIN with monocarboxylate transporters and multiple drug resistance proteins is associated with epithelial ovarian cancer progression. Clin Exp Metastasis 27:557–569
8. Tavassoli FA, Devilee P (2003) Pathology and genetics of tumours of the breast and female genital organs. International Agency for Research on Cancer, Oxford, Oxford University Press [distributor], Lyon
9. Silverberg SG (2000) Histopathologic grading of ovarian carcinoma: a review and proposal. Int J Gynecol Pathol 19:7–15
10. Hayashi H, Nabeshima K, Aoki M, Hamasaki M, Enatsu S, Yamauchi Y, Yamashita Y, Iwasaki H (2010) Overexpression of IQGAP1 in advanced colorectal cancer correlates with poor prognosis—critical role in tumor invasion. Int J Cancer 126:2563–2574
11. Koga K, Aoki M, Sameshima T, Hamasaki M, Egawa N, Seiki M, Toole BP, Suzumiya J, Nabeshima K (2011) Synthetic emmprin peptides inhibit tumor cell–fibroblast interaction-stimulated upregulation of MMP-2 and tumor cell invasion. Int J Oncol 39:657–664
12. Nakayama M, Bennett CJ, Hicks JL, Epstein JI, Platz EA, Nelson WG, De Marzo AM (2003) Hypermethylation of the human glutathione S-transferase-pi gene (GSTP1) CpG island is present in a subset of proliferative inflammatory atrophy lesions but not in normal or hyperplastic epithelium of the prostate: a detailed study using laser-capture microdissection. Am J Pathol 163:923–933
13. Koga K, Nabeshima K, Aoki M, Kawakami T, Hamasaki M, Toole BP, Nakayama J, Iwasaki H (2007) Emmprin in epithelioid sarcoma: Expression in tumor cell membrane and stimulation of MMP-2 production in tumor-associated fibroblasts. Int J Cancer 120:761–768
14. Yang JH, Shi YF, Cheng Q, Deng L (2006) Expression and localization of aquaporin-5 in the epithelial ovarian tumors. Gynecol Oncol 100:294–299
15. Deora AA, Gravotta D, Kreitzer G, Hu J, Bok D, Rodriguez-Boulan E (2004) The basolateral targeting signal of CD147 (EMMPRIN) consists of a single leucine and is not recognized by retinal pigment epithelium. Mol Biol Cell 15:4148–4165
16. Marmorstein AD, Bonilha VL, Chiflet S, Neill JM, Rodriguez-Boulan E (1996) The polarity of the plasma membrane protein RET-PE2 in retinal pigment epithelium is developmentally regulated. J Cell Sci 109(Pt 13):3025–3034
17. Kirk P, Wilson MC, Heddle C, Brown MH, Barclay AN, Halestrap AP (2000) CD147 is tightly associated with lactate transporters MCT1 and MCT4 and facilitates their cell surface expression. EMBO J 19:3896–3904
18. Baba M, Inoue M, Itoh K, Nishizawa Y (2008) Blocking CD147 induces cell death in cancer cells through impairment of glycolytic energy metabolism. Biochem Biophys Res Commun 374:111–116
19. Su J, Chen X, Kanekura T (2009) A CD147-targeting siRNA inhibits the proliferation, invasiveness, and VEGF production of human malignant melanoma cells by down-regulating glycolysis. Cancer Lett 273:140–147
20. Pinheiro C, Longatto-Filho A, Pereira SM, Etlinger D, Moreira MA, Jube LF, Queiroz GS, Schmitt F, Baltazar F (2009) Monocarboxylate transporters 1 and 4 are associated with CD147 in cervical carcinoma. Dis Markers 26:97–103
21. Pinheiro C et al (2009) The prognostic value of CD147/EMMPRIN is associated with monocarboxylate transporter 1 co-expression in gastric cancer. Eur J Cancer 45:2418–2424
22. Buergy D et al (2009) Prognostic impact of extracellular matrix metalloprotease inducer: immunohistochemical analyses of colorectal tumors and immunocytochemical screening of disseminated tumor cells in bone marrow from patients with gastrointestinal cancer. Cancer 115:4667–4678
23. Zhong WD et al (2010) Extracellular matrix metalloproteinase inducer expression has an impact on survival in human bladder cancer. Cancer Epidemiol 34:478–482
24. Sillanpaa S et al (2007) Prognostic significance of extracellular matrix metalloproteinase inducer and matrix metalloproteinase 2 in epithelial ovarian cancer. Tumour Biol 28:280–289
25. Davidson B, Goldberg I, Berner A, Kristensen GB, Reich R (2003) EMMPRIN (extracellular matrix metalloproteinase inducer) is a novel marker of poor outcome in serous ovarian carcinoma. Clin Exp Metastasis 20:161–169

Virchows Arch (2012) 461:467–474
DOI 10.1007/s00428-012-1249-4

ORIGINAL ARTICLE

Retrospective analysis of survival in muscle-invasive bladder cancer: impact of pT classification, node status, lymphovascular invasion, and neoadjuvant chemotherapy

Amber M. D'Souza · Kamal S. Pohar · Tahir Arif · Susan Geyer · Debra L. Zynger

Received: 15 February 2012 / Revised: 27 April 2012 / Accepted: 8 May 2012 / Published online: 23 August 2012
© Springer-Verlag 2012

Abstract A range of studies have analyzed prognostic factors in bladder cancer. However, prior cohorts have included heterogeneous pT classification at biopsy and others were derived from large, multi-institutional clinical trials over the span of many years. Our objective was to analyze prognostic factors in a recent radical cystectomy (RC) cohort at a single institution and evaluate outcomes based on current practice patterns. A retrospective analysis of overall survival (OS) was conducted on 180 RC patients with biopsy proven pT2 disease between 2007–2010. Increasing pT classification was a negative predictor of survival. pT was grouped into three categories with pT0/a/is/1/2a surviving longer than pT2b/3a/3b, and pT4 having the worst prognosis. Subclassifying pT2 and pT3 showed no statistically significant difference in survival. Lymphovascular invasion (LVI) and node positivity correlated with decreased OS. Patients treated with neoadjuvant chemotherapy (NAC) had a higher incidence of pT0, yet pN1+ was more common and NAC was not associated with improved OS. This investigation provides reference OS values for patients with pathologically diagnosed muscle-invasive bladder cancer based on current medical guidelines outside the context of a clinical trial. pT4 was the strongest negative predictor of survival, followed by pN1+, the group pT2b/3a/3b, and presence of LVI. NAC patients were noted to have a higher frequency of low pT classification, yet more frequent node positivity, suggesting that pT classification in NAC patients may not accurately reflect remaining tumor burden.

Keywords Bladder cancer · Survival · Stage · Lymph node · Neoadjuvant

A portion of the content of this study was presented as a platform presentation at the annual USCAP meeting in Vancouver, Canada in March 2012.

A. M. D'Souza · T. Arif · D. L. Zynger (✉)
Department of Pathology,
The Ohio State University Medical Center,
410 W 10th Ave 401 Doan Hall,
Columbus, OH 43210, USA
e-mail: debra.zynger@osumc.edu

K. S. Pohar
Department of Urology,
The Ohio State University Medical Center,
Columbus, OH, USA

S. Geyer
Department of Hematology,
The Ohio State University Medical Center,
Columbus, OH, USA

Introduction

Bladder cancer is the second most common genitourinary malignancy in the United States [1]. It is estimated that 69,250 people will be diagnosed and 14,990 will die of bladder cancer in 2011 [2]. While only approximately one third of patients have muscle-invasive disease, these patients have a significantly greater risk of metastasis, progression, and death [3].

Radical cystectomy (RC) with pelvic lymphadenectomy is currently the standard of care for treating muscle-invasive disease. However, with persistent failure rates of 30-45 % from surgery alone, interest in neoadjuvant chemotherapy (NAC) arose [4]. The poor survival in muscle-invasive disease may be attributed to micrometastasis already present at the time of diagnosis, which NAC could possibly treat. Level 1 evidence for NAC is based on methotrexate, vincristine, doxorubicin, and cisplatin (MVAC), with cisplatin described as the single most effective chemotherapeutic agent against urothelial carcinoma of the bladder [5, 6].

A range of studies have analyzed prognostic factors in bladder cancer. Canter et al. [7] illustrated that increasing age, advanced pathological classification, and positive lymph nodes (LN) were adversely associated with cancer-specific survival. The Southwest Oncology Group Intergroup trial concluded that increased survival was associated with cisplatin based NAC, completion of RC, and removing a minimum number of LN [3]. However, much of the data are from large, multi-institutional clinical trials over the span of many years while others cohorts include patients with both muscle-invasive and non-muscle invasive disease [5–7]. The study is unique in that we analyzed a recent, large, single institution RC cohort restricted to pathologically proven muscle-invasive disease at biopsy to assess survival outcomes in current day practice.

Materials and methods

Data were collected from all patients who had a RC at this institution from 2007 to 2010. Pathology reports from RC and bladder biopsy/transurethral resections (TUR) were reviewed. Parameters obtained included gender, age, cT classification prior to RC, NAC usage, regimen, and number of cycles received, pT classification at TUR and RC, grade at RC and TUR, number of nodes resected, nodal status, presence of lymphovascular invasion (LVI) and/or carcinoma in situ (CIS) at TUR and RC, surgical margin status, and date of death. LVI information was available for all but three patients due to inaccessible TUR reports. Patients that received NAC regardless of number of cycles or regimen were designated as having received NAC. Exclusion criteria for NAC included renal insufficiency precluding treatment with cisplatin and Eastern Cooperative Oncology Group performance status ≥3. NAC was given at our hospital or an outside facility. RC was offered to almost all patients with pT2 disease (tumor invasive into the muscularis propria) with very few determined to be non-surgical candidates.

Pathologic classification was based upon AJCC seventh edition definitions [8]. The cohort for analyses was restricted to patients with TUR of pT2 to ensure consistency. A central review of all 180 RC cases was completed by one pathologist (D.L.Z.). Stage-based response (SBR) was defined as a decrease in pT between TUR (pT2) and RC (<pT2). Nodal involvement was recorded as pN0 if all nodes were negative or pN1+ if any nodes were positive. Patients with no nodes removed (pNX) were excluded from survival analysis using nodal involvement as a factor.

Overall survival (OS) was defined as time from RC to date of death due to any cause or date of last chart review. Surviving subjects were censored at the time of last chart review in time-to-event analyses. Kaplan–Meier survival curves were used to evaluate differences in OS between groups. Cox regression models were used to model OS based on RC pT classification, nodal involvement, NAC use, and SBR. Survival analyses included univariate and multivariable modeling. Due to limited numbers in some subgroups, 95 % confidence intervals (CI) for survival estimates at given time points were used to assess variability and differences between groups in lieu of formal comparisons. Prognostic utility of collapsed subgroups based on RC pT classification were explored and analyzed in a similar manner. Comparisons between groups were evaluated using chi-square tests or Fisher exact tests if fewer than five subjects in a cell. Differences in continuous measures between groups were evaluated using two-sample *t* tests or Kruskal–Wallis tests if comparing across more than two subgroups. Logistic regression was used to measure significance of prediction factors against binary response variables. Given the hypothesis-generating nature of these analyses for potential prospective studies, multiple comparison corrections were not used, and statistical significance was declared at $P<0.05$.

Results

The study reviewed all patients who had RC for primary bladder carcinoma at our institution between 2007–2010 ($n=305$). At TUR, 180 patients were pT2. All statistics were performed on these 180 patients.

Table 1 outlines the clinicopathological characteristics of the cohort. In 2007, 7.1 % (2/28) of patients received NAC, which increased to 40.8 % (20/49) in 2008, 53.1 % (26/49) in 2009, and 59.3 % (32/54) in 2010 as in recent years use of NAC is strongly encouraged for every candidate patient.

Figure 1a depicts OS by RC stage ($P<0.00001$). pT4a (invasion of prostatic stroma, uterus, or vagina) was comparable to pT4b (invasion of pelvic or abdominal wall) and pT0 (no evidence of tumor) similar to pTis (carcinoma in situ), therefore these groups were combined (pT4a/pT4b and pT0/is) and are each reflected by only one curve. OS rate (1.5 years) (95 % CI) based on stage was pT0/pTis, 80 % (65–98 %); pT1 (subepithelial invasion), 77 % (54–100 %); pT2a, 80 % (62–100 %); pT2b, 61 % (43–87 %); pT3a (microscopic perivesicular fat invasion), 58 % (42–81 %); pT3b (macroscopic perivesicular fat invasion), 43 % (25–72 %); pT4, 12 % (4–35 %). Estimates are not given for pTa (noninvasive papillary carcinoma) given that there was only one pTa patient. Based on the World Health Organization/International Society of Urologic Pathology grading system included in the seventh edition of AJCC, 139 patients (77.2 %) were high grade at RC. Five patients (2.8 %) were low grade at RC and 36 patients (20 %) did not have a grade given due to no residual tumor or predominance of glandular/squamous differentiation.

Table 1 Cohort characteristics of patients receiving RC between 2007 and 2010 for pT2 bladder cancer

	Number (%)
Total	180 patients
Mean age (years)	67.1 (range 23–87)
Sex	34 F (18.9 %), 146 M (81.1 %)
NAC	81 (45.0 %)
Gemcitabine/cisplatin	41
MVAC	22
Other	18
Mean number of completed cycles	3.9
LVI	78 (44.1 %)
Mean LN count at RC	31.3 (range 0–77)
Positive margin at RC	24 (13.3 %)
Deaths	76 (42.2 %)
Mean surviving follow-up (days)	406.4 (range 207–1,619)
pT at RC	
pT0	27 (15.0 %)
pTa	1 (0.6 %)
pTis	7 (3.9 %)
pT1	12 (6.7 %)
pT2a	18 (10.0 %)
pT2b	23 (12.8 %)
pT3a	33 (18.3 %)
pT3b	28 (15.6 %)
pT4	31 (17.2 %)
pN at RC	
pN0	123 (68.3 %)
pN1+	54 (30.0 %)
pNX	3 (1.7 %)
SBR	45 (25.0 %)

Subclassifying pT2 revealed no difference in OS (P=0.18). Subclassifying pT3 showed a non-statistically significant separation in curves (P=0.09). Restricting subclassification to the pN0 population did not yield a significant difference among pT2 and pT3 subcategories (P=0.8 and P=0.57, respectively). OS (1.5 years) (95 % CI) based on substage for pN0 patients was pT2aN0, 84 % (65–100 %); pT2bN0, 74 % (55–100 %); pT3aN0, 59 % (40–86 %); pT3bN0, 63 % (41–96 %). Median OS (95 % CI) in months was pT3a, 28.3 (15.3—not applicable (NA)); pT3b, 13.0 (7.9—NA); and pT4, 8.4 (4.0–13.9). Sufficient deaths did not occur in the remaining stages to calculate median OS with CI.

Graphically, there were noted similarities in survival distribution, with certain pT classifications having comparable survival rates across different time points. pT was collapsed into three groups for additional analysis, with pT0/a/is/1/2a surviving longer than pT2b/3a/3b and pT4 having the worst survival (P<0.00001) (Fig. 1b). OS (1.5 years) (95 % CI) were pT0/a/is/1/2a, 79 % (68–92 %); pT2b/3a/3b, 53 % (41–67 %); pT4, 12 % (4–35 %).

SBR was shown to have improved OS (P=0.00043) with a 1.5-year OS (95 % CI) of 79 % (67–95 %) vs. 45 % (37–56 %) without SBR (Fig. 1c).

Nodal involvement was strongly associated with poor outcome (P<0.00001) (Fig. 1d). OS (1.5 years) (95 % CI) were 66 % (56–76 %) for pN0 and 30 % (19–48 %) for pN1+. Median OS (95 % CI) was 11 months (9.2–17.8) in pN1+ and could not be calculated for pN0 due to insufficient deaths. pN1+ was not restricted to high pT, as 4.5 % of the cohort and 14.8 % of the pN1+ group were pT0 (n=1), pTis (n=1), pT1 (n=2), and pT2a (n=4).

Of the patients, 44.1 % had LVI. Figure 1e demonstrates OS based on presence of LVI (P<0.0001). OS (1.5 years) (95 % CI) was 70 % (60–82 %) without LVI versus 33 % (23–48 %) with LVI. When analyzing LVI and nodal status together, 50.0 % (87/174) of patients had no LVI/pN0, 6.3 % (11/174) no LVI/pN1+, 19.0 % (33/174) LVI/pN0, and 24.7 % (43/174) LVI/pN1+ with 1.5-year OS (95 % CI) of no LVI/pN0, 78 % (68-89 %); LVI/pN0, 38 % (23-61 %); no LVI/pN1+, 28 % (9-82 %); and LVI/pN1+, 30 % (17-51 %). Distribution of number of LN for the subgroups showed no statistical significant difference (P=0.28) (mean number of LN: no LVI/pN0, 31.8; LVI/pN0, 29.9; no LVI/pN1+, 37.3; and LVI/pN1+, 28.3). Number of LN removed was not a significant predictor of nodal status (P=0.65) or LVI (P=0.14).

Of the patients, 38.2 % (68/178) had CIS on TUR or RC. OS (95 % CI) in months was 22.7 (14.9—NA) without CIS verses 19.9 (13.9—NA) with CIS (P=0.889), demonstrating no statistically significant difference.

Tables 2 and 3 reveal characteristics of patients that received NAC verses immediate RC. More NAC patients were cT3/4 (42/81, 51.9 % vs. 45/99, 45.5 %). More frequent decrease in T classification comparing cT prior to RC versus pT at RC in the NAC group was observed (45.7 % vs. 24.2 %). There was a higher incidence of NAC patients with pT0 (23.5 % vs. 8.1 %) and the low pT group pT0/a/is/1/2a (45.7 % vs. 28.3 %). However, in each cT group, there were more pN1+ patients with a history of NAC, although this difference was not statistically significant (P=0.63 for cT2; P=0.21 for cT3; P=0.24 for cT4). Of note, all eight patients that had low RC pT (pT0/a/is/1/2a) with pN1+ disease were in the NAC group (representing 9.9 % of the NAC group). Of these eight patients, three have died with a median follow-up in the remaining five living patients of 14 months. There was no significant difference in OS (P=0.746) based on use of NAC (Fig. 1f) with median OS (95 % CI) in months as 24.0 (15.6—NA) with NAC and 22.2 (14.0—NA) for RC alone. OS (1.5 years) (95 % CI) was 58 % (46–72 %) in the NAC group and 50 % (40–63 %) with no NAC and the 3-year OS (95 % CI) was 31 % (15–63 %) with

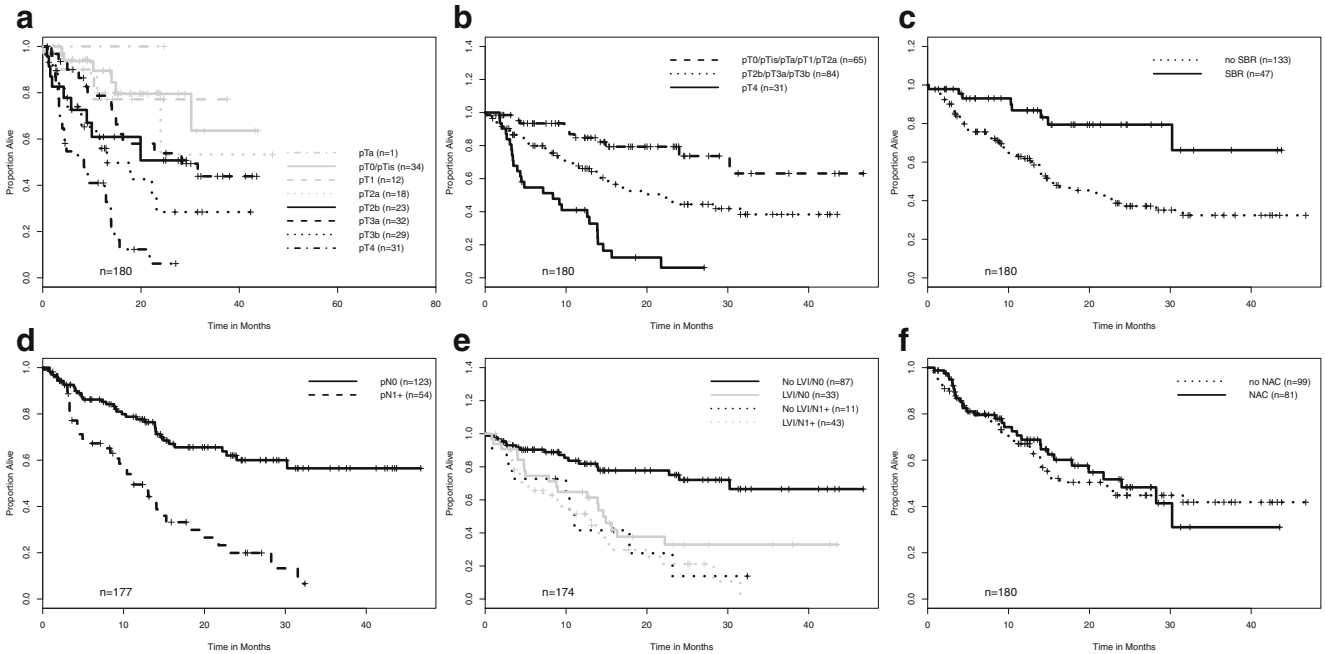

Fig. 1 Survival analysis showing survival time in months for the proportion of patients remaining alive. **a** OS for RC pT classification ($P<0.00001$). **b** OS by collapsed RC pT classification ($P<0.0001$). **c** OS by SBR ($P=0.000426$). **d** OS by RC Nodal status (three patients were pNX and were not included) ($P<0.00001$). **e** OS by LVI and node status ($P<0.0001$) status. **f** OS by NAC status ($P=0.746$)

NAC compared to 42 % (31–56 %) without NAC. An additional consideration when interpreting OS is the time interval from TUR to RC which was on average 56.6 days longer for patients receiving NAC. We also attempted to see if there was a survival benefit with NAC for certain stage groups, with no benefit identified.

On multivariable analysis, pT4 followed by high RC pT group and positive nodes were negative prognostic factors (Table 4). SBR was not significant in the multivariable setting. Although SBR was a significant prognostic univariate factor, it was actually the RC pT0/a/is/1/2a group that conferred an improved OS. SBR was a surrogate of this pT group, without the inclusion of pT2a. When LVI was combined with RC pT, it was a significant prognostic factor, but nodal status was a stronger predictor of OS. This was confirmed looking at all subsets models. NAC was not a significant factor of OS across all pT classifications, collapsed pT groups, nodal status, SBR, and did not impact the other prognostic indicators. Thus, only RC pT, pT groupings, and nodal status remained significant in multivariable analysis.

Discussion

Muscularis propria-invasive bladder cancer has been associated with significant risk of progression, metastasis, and death [3]. Standard of care for ≥ pT2 disease is RC with lymphadenectomy, with increasing usage of NAC [4, 5, 9]. Past studies have evaluated different prognostic markers in order to stratify survival. Factors such as use of NAC, completion of RC, and extended LN dissection have been shown to improve survival, whereas advanced pT and LN metastases were linked to poor outcomes [3, 7]. Our aim was to analyze prognostic factors of bladder cancer in RC. This study is relevant in that it reflects a contemporary cohort at a single institution with similar surgical practices. Unlike previous reports, analysis was restricted to patients with TUR proven pT2 disease to ensure consistency within the cohort. The data provide reference OS values for patients with pathologically diagnosed muscle-invasive bladder cancer based on current medical guidelines outside the context of a clinical trial.

Over 50 % of patients at our institution had pT3/4 disease at RC. Not surprisingly, the OS of 57.8 % for the cohort was low. Incidence of pT3/4 disease from other single institutions ranged from 30 % to 53 % [10–13]. Of note, these studies had widely variable accrual lengths and included all RC patients, compared to only pT2 disease at TUR in our cohort [10–13]. We demonstrated a statistically significant relationship between pT classification at RC and OS. Similar to previous publications, pT4 had the worst OS (12 % at 1.5 years), with T4a and T4b disease behaving comparably [14, 15]. There was a non-statistical separation in survival

Table 2 NAC versus immediate RC

	NAC (n=81)	Immediate RC (n=99)
Mean age (years)	65.6	68.3
Mean LN count at RC	33.1	29.4
Positive margin at RC	11 (13.6 %)	13 (13.1 %)
Mean TUR to RC duration (days)	140.4 (range 0–478)	83.8 (range 0–336)
SBR (n=45)	27 (33.3 %)	18 (18.2 %)
pTN at RC		
pT0N0 (n=26)	18 (22.2 %)	8 (8.1 %)
pT0N1+ (n=1)	1 (1.2 %)	0
pTaN0 (n=1)	1 (1.2 %)	0
pTisN0 (n=6)	1 (1.2 %)	5 (5.1 %)
pTisN1+ (n=1)	1 (1.2 %)	0
pT1N0 (n=10)	3 (3.7 %)	7 (7.1 %)
pT1N1+ (n=2)	2 (2.5 %)	0
pT2aN0 (n=14)	6 (7.4 %)	8 (8.1 %)
pT2aN1+ (n=4)	4 (4.9 %)	0
pT2bN0 (n=17)	8 (9.9 %)	9 (9.1 %)
pT2bN1+ (n=6)	2 (2.5 %)	4 (4.0 %)
pT3aN0 (n=24)	3 (3.7 %)	21 (21.2 %)
pT3aN1+ (n=8)	5 (6.2 %)	3 (3.0 %)
pT3aNX (n=1)	0	1 (1.0 %)
pT3bN0 (n=14)	4 (4.9 %)	10 (10.1 %)
pT3bN1+ (n=12)	6 (7.4 %)	6 (6.1 %)
pT3bNX (n=2)	0	2 (2.0 %)
pT4N0 (n=11)	5 (6.2 %)	6 (6.1 %)
pT4N1+ (n=20)	11 (13.6 %)	9 (9.1 %)

curves between pT3a and pT3b and no difference in OS for pT2a and pT2b. Limiting analysis to the pN0 population did not show a difference in survival. Prior investigations have found no difference in recurrence free survival (RFS) for pT3 substages except within pN0 in which pT3aN0 had improved RFS compared to pT3bN0 [16, 17]. The literature

Table 3 cT within NAC versus immediate RC group

cT prior to RC (n=180)	NAC (n=81)	Immediate RC (n=99)
cT2 (n=96)	39/81 (48.1 %)	57/99 (57.6 %)
cT3 (n=54)	20/81 (24.7 %)	34/99 (34.3 %)
cT4 (n=30)	22/81 (27.2 %)	8/99 (8.1 %)
cT>pT at RC (n=61)	37/81 (45.7 %)	24/99 (24.2 %)
cT2 prior to RC, pN1+ at RC (n=11)	9/39 (23.1 %)	2/57 (3.5 %)
cT3 prior to RC, pN1+ at RC (n=14)	8/20 (40.0 %)	6/34 (17.6 %)
cT4 prior to RC, pN1+ at RC (n=16)	13/22 (59.1 %)	3/8 (37.5 %)

Table 4 Multivariate analysis of prognostic factors

Factor	Hazard ratio	95 % CI	P value
pT group			
pT2b/3a/3b	2.19	1.11–4.32	0.023
pT4	5.57	2.63–11.77	0.000007
pN classification			
pN1+	2.01	1.21–3.35	0.007
NAC status			
NAC	0.90	0.56–1.47	0.68

reports conflicting results regarding RFS for pT2 subcategories [18, 19]. A limitation of subclassifying pT3 tumors is that it is based on gross impression of fat invasion, making standardization difficult. Similarly, subclassifying pT2 is somewhat subjective because it reflects an estimation of the depth of muscularis propria invasion. Demonstrating a survival benefit within these substages was also limited by the number of patients and number of deaths that occurred, especially within the pT2 population. We found OS between pT0, pTa, pTis, and pT1 to be comparable, although analysis was limited by small numbers and few deaths. There is contradictory published data comparing pT0 to pTa/Tis [20, 21]. Nonetheless, pT0 has improved survival compared to ≥pT1 at RC [20]. Based on similarities in survival distribution, pT were collapsed into pT0/a/is/1/2a, pT2b/3a/3b, and pT4 groups, representing a novel simplified model for bladder cancer OS. There was a statistically significant difference between these three groups, with pT0/a/is/1/2a patients surviving longer than pT2b/3a/3b, and pT4 disease having the worst survival. Moreover, on multivariable analysis, RC pT group pT2b/3a/3b remained a strong negative predictor of OS.

Our investigation indicates that patients with SBR (pT2 at TUR and <pT2 at RC) have improved OS, with a 1.5-year survival rate of 79 % vs. 45 % without SBR. There is limited data regarding the prognostic implications of SBR as most studies focus on complete pT response (pT0). When comparing SBR as a potential prognostic factor versus a three-tiered RC pT group, the collapsed pT group was a stronger indicator of OS. This illustrates that SBR is a surrogate to analyze lower RC pT, without the inclusion of pT2a. Thus, our data indicate that a stage of ≤pT2a is a stronger prognostic factor and may be more relevant to describe the effectiveness of a treatment than SBR and/or complete pT response. It is also interesting to note that presence of SBR is not specific to patients with NAC: 18.2 % of the RC cohort also had a decrease from pT stage at TUR to pT stage at RC. This illustrates that use of BCG therapy as well as physically debulking the tumor during TUR may play a role in downstaging tumors. While previous studies have used downstaging or a complete pT response as an indicator of successful use of NAC, our study demonstrates that

downstaging is not limited to this population of patients and may be relevant in the immediate RC cohort.

Of our cohort, 30 % was pN1+ at RC and represented a significant negative predictor of survival. Nodal status impacting prognosis has been well illustrated in the literature [3, 7, 10, 15, 22, 23]. At 1.5 years after RC, 66 % of our patients with pN0 were alive versus 30 % with pN1+, consistent with published outcomes [3, 7, 10, 15, 22, 23]. Abdel-Latif et al. [23] demonstrated a 3-year RFS of 78 % with pN0 versus 38 % with positive nodes. Moreover, Stein et al. [10] found a 69 % 5-year OS with pN0 verses 31 % with pN1+. One limitation in the ability to compare our results with other institutions is that as a tertiary care center, we treat more patients with high stage and positive nodal disease. Our institution also routinely uses extended lymph node dissection, which is not practiced in all hospitals. While pN1+ was a predictor of poor outcome, an important finding of our analysis was that positive nodes were not limited to high pT disease, with 4.5 % of patients having pN1+ with ≤pT2a disease.

Almost half of the cohort had LVI. LVI did not impact survival in node positive patients; however, LVI was a negative predictor of survival in the pN0 group. There is data illustrating LVI at RC as an independent predictor of survival and recurrence in bladder cancer [24, 25]. Shariat et al. [26] studied pN0 RC patients and demonstrated that LVI was strongly associated with clinical outcome. The finding of pN0 patients with LVI and poor survival raises the possibility that the nodal resection was less substantial in this group. However, our data showed that LN number was comparable. A second possibility is that the LN metastases may not have been present for histologic assessment, in that either the tumor was cut through and discarded during processing or that the metastatic deposit is still embedded in paraffin and was not available for microscopic examination. A third possibility is that a diagnostic error occurred in which the pathologist did not identify the positive LN. A past article compared histologic impression versus keratin immunohistochemistry to detect micrometastasis in node negative bladder cancer, with no identified missed metastases [27]. We hypothesize that these patients may have a different path of tumor spread, for example, directly to non-regional lymph nodes or bone marrow. Future research is required to understand the mechanism by which patients come to have pathologically identified LVI and negative nodes and the biologic relevance of these findings.

Between the NAC vs. non-NAC groups, age and surgical parameters such as number of LN and margin status were comparable. However, there was extensive heterogeneity in type of NAC given, number of cycles, medical setting (tertiary care center vs. community practice) and time between NAC and RC, reflecting the current variable practice patterns. With NAC, we observed more frequent decrease of T classification comparing cT prior to RC and pT at RC (45.7 % vs. 24.2 %), increased pT0 (23.5 % vs. 8.1 %) and a higher rate of SBR (33.3 % vs. 18.2 %). High pT (≥pT2b) at RC occurred less often with NAC (34.6 % vs. 56.6 %). Similarly, previous authors have demonstrated that NAC is associated with more frequent complete pathologic response than RC alone (33–38 % vs. 5–15 %) [3, 12, 20, 28, 29]. However, we did not identify a statistically significant increase in OS in NAC patients (NAC OS 22 vs. 24 months without NAC). Literature regarding the survival advantage of NAC is controversial, but evidence from clinical trials suggests a benefit of up to 5.5 % [3, 28–34]. Perhaps to achieve this benefit, NAC must be better standardized as is done in a clinical trial and therefore our data does not discredit the use of neoadjuvant chemotherapy in patients with muscle-invasive bladder cancer. Surprisingly, pN1+ was more common in NAC patients (39.5 % vs. 22.2 %). For each cT classification, more node positivity was seen in the NAC cohort, although this difference was not statistically significant. Moreover, we identified a group of pN1+ patients with a low pT (≤pT2a). All patients in this group received NAC, with deaths observed. These findings suggest that focusing on pT classification or the frequency of decreased cT to pT at RC without the corresponding node status in NAC patients may not be fully indicative of a tumor's potential lethality, a concept not discussed in the literature. As NAC has consistently been shown to decrease pT at RC, systemic chemotherapy could have utility in the treatment of non-muscle-invasive, BCG refractory patients that are not ideal surgical candidates or have limited life expectancy.

Limitations of this investigation included its retrospective nature, short follow-up, limited number of patients, and multiple surgeons. Another consideration was potential bias between NAC and non-NAC groups. Poor renal function and performance status excluded patients from NAC. Age was slightly higher in the non-NAC group, which in conjunction with the NAC exclusionary criteria should help eliminate a bias of unhealthier patients receiving NAC. NAC was heterogeneous, as previously discussed. Other histopathological factors which may have prognostic significance, such as tumor multifocality and grade, were not analyzed. Lastly, being a tertiary care center with potentially higher cT/pT tumor, more positive nodes, routine use of extended LN dissection, and frequent use of NAC, our data may not be representative of other patient cohorts.

Conclusions

We performed a retrospective single institutional study of muscle-invasive bladder cancer at RC. Negative prognostic factors in bladder cancer included pT4, pT2b/3a/3b disease,

pN1+, and LVI. Collapsing pT into pT0/a/is/1/2a, pT2b/3a/3b, and pT4 was a stronger predictor of survival than SBR. pN0 patients with LVI had decreased OS. The presence of positive nodes at RC was not limited to high pT disease with pN1+ seen in NAC patients with low RC pT. pT0 and SBR were more common in patients with a history of NAC, although use of NAC was not associated with increased OS. Our findings may be more indicative of outcomes outside the context of a clinical trial and highlight the variability of multidisciplinary management in bladder cancer in its current usage today.

Conflicts of interest statement We declare that we have no conflict of interest.

Funding/financial disclosures None

References

1. American Cancer Society (2010) Cancer Facts and Figures 2010. http://www.cancer.org/acs/groups/content/@epidemiologysurveilance/documents/document/acspc-026238.pdf . Accessed 3 January 2012
2. National Cancer Institute (2010). Bladder Cancer Information. http://www.cancer.gov/cancertopics/types/bladder. Accessed 3 January 2012
3. Grossman HB, Natale RB, Tangen CM et al (2003) Neoadjuvant chemotherapy plus cystectomy compared with cystectomy alone for locally advanced bladder cancer. N Engl J Med 349:859–866
4. Kaufman DS, Shipley WU, Feldman AS (2009) Bladder cancer. Lancet 374:239–249
5. Logothetis CJ, Dexeus FH, Finn L et al (1990) A prospective randomized trial comparing MVAC and CISCA chemotherapy for patients with metastatic urothelial tumors. J Clin Oncol 8:1050–1055
6. von der Maase H, Hansen SW, Roberts JT et al (2000) Gemcitabine and cisplatin versus methotrexate, vinblastine, doxorubicin, and cisplatin in advanced or metastatic bladder cancer: results of a large, randomized, multinational, multicenter, phase III study. J Clin Oncol 18:3068–3077
7. Canter D, Long C, Kutikov A, Plimack E et al (2011) Clinicopathological outcomes after radical cystectomy for clinical T2 urothelial carcinoma: further evidence to support the use of neoadjuvant chemotherapy. BJU Int 107:58–62
8. Edge SB, Byrd DR, Comptom CC (2010) American Joint Committee on Cancer. AJCC Cancer Staging Manual, Seventh Edition. Springer, New York, pp 497–502
9. Fedeli U, Fedewa SA, Ward EM (2011) Treatment of muscle invasive bladder cancer: evidence from the National Cancer Database, 2003 to 2007. J Urol 185:72–78
10. Stein JP, Lieskovsky G, Cote R et al (2001) Radical cystectomy in the treatment of invasive bladder cancer: long-term results in 1,054 patients. J Clin Oncol 19:666–675
11. Madersbacher S, Hochreiter W, Burkhard F et al (2003) Radical cystectomy for bladder cancer today—a homogeneous series without neoadjuvant therapy. J Clin Oncol 21:690–696
12. Weight CJ, Garcia JA, Hansel DE et al (2009) Lack of pathologic down-staging with neoadjuvant chemotherapy for muscle-invasive urothelial carcinoma of the bladder: a contemporary series. Cancer 115:792–799
13. Manoharan M, Katkoori D, Kishore TA et al (2009) Outcome after radical cystectomy in patients with clinical T2 bladder cancer in whom neoadjuvant chemotherapy has failed. BJU Int 104:1646–1649
14. Pollack A, Zagars GK, Cole CJ et al (1995) The relationship of local control to distant metastasis in muscle invasive bladder cancer. J Urol 154:2059–2063
15. Honma I, Masumori N, Sato E et al (2004) Local recurrence after radical cystectomy for invasive bladder cancer: an analysis of predictive factors. Urology 64:744–748
16. Tilki D, Svatek RS, Karakiewicz PI et al (2010) pT3 Substaging is a prognostic indicator for lymph node negative urothelial carcinoma of the bladder. J Urol 184:470–474
17. Sonpavde G, Khan MM, Svatek RS et al (2011) Prognostic risk stratification of pathological stage T3N0 bladder cancer after radical cystectomy. J Urol 185:1216–1221
18. Yu RJ, Stein JP, Cai J et al (2006) Superficial (pT2a) and deep (pT2b) muscle invasion in pathological staging of bladder cancer following radical cystectomy. J Urol 176:493–8
19. Boudreaux KJ Jr, Clark PE, Lowrance WT et al (2009) Comparison of American Joint Committee on Cancer pathological stage T2a versus T2b urothelial carcinoma: analysis of patient outcomes in organ confined bladder cancer. J Urol 181:540–545
20. Tilki D, Svatek RS, Novara G et al (2010) Stage pT0 at radical cystectomy confers improved survival: an international study of 4,430 patients. J Urol 184:888–894
21. Amling CL, Thrasher JB, Frazier HA et al (1994) Radical cystectomy for stages Ta, Tis and T1 transitional cell carcinoma of the bladder. J Urol 151:31–35
22. Ghoneim MA, El-Mekresh MM, Mokhtar AA et al (2000) A predictive model of survival after radical cystectomy for carcinoma of the bladder. BJU Int 85:811–816
23. Abdel-Latif M, Abol-Enein H, El-Baz M et al (2004) Nodal involvement in bladder cancer cases treated with radical cystectomy: incidence and prognosis. J Urol 172:85–89
24. Lotan Y, Gupta A, Shariat SF et al (2005) Lymphovascular invasion is independently associated with overall survival, cause-specific survival, and local and distant recurrence in patients with negative lymph nodes at radical cystectomy. J Clin Oncol 23:6533–6539
25. Quek ML, Stein JP, Nichols PW et al (2005) Prognostic significance of lymphovascular invasion of bladder cancer treated with radical cystectomy. J Urol 174:103–106
26. Shariat SF, Svatek RS, Tilki D et al (2010) International validation of the prognostic value of lymphovascular invasion in patients treated with radical cystectomy. BJU Int 105:1402–1412
27. Yang XJ, Lecksell K, Eptsein JI (1999) Can immunohistochemistry enhance the detection of micrometasasis in pelvic lymph nodes from patients with high-grade urothelial carcinoma of the bladder? Am J Clin Pathol 112:649–653
28. International Collaboration of Trialists (1999) Neoadjuvant cisplatin, methotrexate, and vinblastine chemotherapy for muscle-invasive bladder cancer: a randomised controlled trial. Lancet 354:533–540
29. Sonpavde G, Goldman BH, Speights VO et al (2009) Quality of pathologic response and surgery correlate with survival for patients with completely resected bladder cancer after neoadjuvant chemotherapy. Cancer 115:4104–4019
30. Sherif A, Rintala E, Mestad O et al (2002) Neoadjuvant cisplatin-methotrexate chemotherapy for invasive bladder cancer—Nordic cystectomy trial 2. Scand J Urol Nephrol 36:419–425
31. Advanced Bladder Cancer Meta-analysis Collaboration (2003) Neoadjuvant chemotherapy in invasive bladder cancer: a systematic review and meta-analysis. Lancet 361:1927–1934

32. Sherif A, Holmberg L, Rintala E et al (2004) Neoadjuvant cisplatinum based combination chemotherapy in patients with invasive bladder cancer: a combined analysis of two Nordic studies. Eur Urol 45:297–303
33. Advanced Bladder Cancer (ABC) Meta-analysis Collaboration (2005) Neoadjuvant chemotherapy in invasive bladder cancer: update of a systematic review and meta-analysis of individual patient data advanced bladder cancer (ABC) meta-analysis collaboration. Eur Urol 48:202–205
34. International Collaboration of Trialists (2011) International phase III trial assessing neoadjuvant cisplatin, methotrexate, and vinblastine chemotherapy for muscle-invasive bladder cancer: long-term results of the BA06 30894 trial. J Clin Oncol 29:2171–2177

Virchows Arch (2012) 461:475–481
DOI 10.1007/s00428-012-1300-5

ORIGINAL ARTICLE

Cartilage tumour progression is characterized by an increased expression of heparan sulphate 6*O*-sulphation-modifying enzymes

Cathelijn J. F. Waaijer · Carlos E. de Andrea · Andrew Hamilton · Jolieke G. van Oosterwijk · Sally E. Stringer · Judith V. M. G. Bovée

Received: 20 February 2012 / Revised: 29 July 2012 / Accepted: 3 August 2012 / Published online: 18 August 2012
© Springer-Verlag 2012

Abstract Chondrosarcomas are malignant cartilage-forming tumours that can arise centrally (in the medulla) or peripherally (at the surface) of the bone. They are classified into three histological grades which correspond to the clinical severity. Previous studies by our group have shown altered signal transduction of the fibroblast growth factor and Wnt signalling pathways during peripheral chondrosarcoma progression. Heparan sulphate (HS) is a glycosaminoglycan that facilitates receptor binding of multiple growth factors, in which the sulphation of 6*O* position plays a pivotal role. 6*O*-Sulphation occurs through three HS 6*O*-sulphotransferases (HS6ST1-3) and is fine-tuned by two endosulphatases (SULF1-2) that remove 6*O*-sulphate groups. We have investigated whether the expression of HS6STs and SULFs changes during chondrosarcoma progression and have determined 6*O*-sulphation levels in two chondrosarcoma cell lines. Immunohistochemistry on tissue microarrays of chondrosarcomas showed that HS6ST3 and SULF1 were highly expressed in most chondrosarcomas, whereas SULF2 expression was absent in most cases. HS6ST1 and HS6ST2 expression are significantly increased during chondrosarcoma progression, which suggest that 6*O*-sulphation is increased during progression. This was confirmed in one grade III chondrosarcoma cell line, which showed a dramatically increased 6*O*-sulphation compared to an articular chondrocyte cell line by HPLC; another cell line showed an increased expression of one 6*O*-sulphated HS disaccharide. In conclusion, our results show increased HS6ST1 and HS6ST2 expression during chondrosarcoma progression and increased HS 6*O*-sulphation in vitro. As 6*O*-sulphation plays an important role in signal transduction, altered HS6ST expression might be associated with changes in signal transduction pathways in chondrosarcoma progression.

Keywords Chondrosarcoma · Heparan sulphate · 6*O*-Sulphation · Bone tumours · Immunohistochemistry

C. J. F. Waaijer · C. E. de Andrea · J. G. van Oosterwijk · J. V. M. G. Bovée (✉)
Department of Pathology, Leiden University Medical Center, Albinusdreef 2, PO Box 9600, L1-Q, 2300 RC Leiden, The Netherlands
e-mail: j.v.m.g.bovee@lumc.nl

A. Hamilton · S. E. Stringer
Cardiovascular Medicine, School of Biomedicine, Faculty of Medical and Human Sciences, Manchester Academic Health Science Centre (CMFT), University of Manchester, 46 Grafton Street, Manchester M13 9NT, UK

Introduction

Chondrosarcomas (CS) are malignant cartilage-forming tumours that can arise centrally (in the medulla) or peripherally (at the surface) of the bone. Both types can originate from benign precursor lesions, called enchondromas (central) or osteochondromas (peripheral). Chondrosarcomas are histologically classified into three grades which correspond to the clinical severity [1]. We have previously shown altered signal transduction during chondrosarcoma progression. Fibroblast growth factor (FGF) signalling positively correlates with

increasing histological grade in peripheral cartilage tumours, whereas Wnt signalling is attenuated in both central and peripheral tumours [2–4].

Osteochondromas are caused by inactivation of one of the exostosin (*EXT*) genes [5, 6]. EXT is involved in the biosynthesis of heparan sulphate proteoglycans (HSPGs), elongating the heparan sulphate (HS) chains attached to proteoglycan cores. HSPGs are present on the cell surface and in the extracellular matrix, where they, among other functions, act as co-receptors for growth factors [7, 8]. HS chains consist of alternating units of an uronic acid (UA) which can be sulphated on the 2*O* position and a glucosamine (GlcNAc) which can be sulphated on *N*, 3*O* and 6*O* positions. Each modification of the chain only occurs on some of the disaccharides and results in a domain structure with regions high in sulphation that interact with protein ligands, interspersed with less-sulphated regions.

EXT inactivation is absent in central cartilaginous tumours [4]. Instead central tumours carry heterozygous mutations in isocitrate dehydrogenase (*IDH*) 1 or *IDH2* in more than 50 % of all cases, while peripheral cartilage tumours do not carry *IDH* mutations [9, 10]. Both IDH1 and IDH2 are involved in cellular metabolism. Recent studies suggest that while *IDH* (in the case of central tumours) and *EXT* (peripheral tumours) cause the formation of benign cartilaginous tumours, malignant transformation is a process unrelated to these mutations, and the mechanisms underlying this process are as yet unknown but might be similar [10–12].

In other tumour types, it has been found that HS chain modifications can play a role in tumour progression by influencing HS-ligand binding [13, 14]. One of these modifications is 6*O*-sulphation which is mediated by three HS 6*O*-sulphotransferases (HS6ST1-3) that attach sulphate groups to the 6*O* position of glucosamine groups in the HS chain [15]. In addition, two endosulphatases, SULF1 and SULF2, play a role in fine-tuning the 6*O*-sulphation pattern by removing 6*O*-sulphate groups [16, 17].

The level and pattern of 6*O*-sulphation of HS chains have been shown to affect their binding capacity to different growth factors (as reviewed by Lamanna et al. [18]). For example, 6*O*-sulphation inhibits the binding of Wnt and BMP to their respective receptors but, on the other hand, is a requisite for the binding of FGF to its receptor. Altered signal transduction during chondrosarcoma progression might therefore be (partially) mediated by the changes in HS 6*O*-sulphation.

Therefore, we investigated whether the expression of the HS6STs and SULFs differs with increasing histological grade in cartilage tumours and whether the levels of HS 6*O*-sulphation are altered in high-grade chondrosarcoma cell lines in order to elucidate the role of HS 6*O*-sulphation in chondrosarcoma progression.

Materials and methods

Construction of TMAs

The tissue microarrays (TMAs) used in this study were constructed as described [19]. A total of 153 formalin-fixed, paraffin-embedded enchondroma (six), osteochondroma (11), central chondrosarcoma [91 samples, composed of 42 grade I (CCSI), 36 grade II (CCSII) and 13 grade III (CCSIII)] and peripheral chondrosarcoma samples [45, composed of 31 peripheral chondrosarcomas grade I (PCSI), 11 grade II (PCSII) and three grade III (PCSIII)] diagnosed between 1985 and 2008 were retrieved from the archives of the departments of pathology at Leiden University Medical Center (Leiden, The Netherlands) and Onze Lieve Vrouwe Gasthuis (Amsterdam, The Netherlands). Diagnosis was re-evaluated before inclusion. Three representative 2-mm cores were punched from every tumour sample and transferred to the recipient block using TMA Master (3DHISTECH, Budapest, Hungary). In addition, cores from skin, colon, tonsil, prostate, breast carcinoma, spleen and liver were included for control and orientation purposes. Follow-up data on metastasis-free and overall survival were collected. The mean follow-up period was 9 years. On a total of 153 patients in our sample set, 11 patients developed metastases, 28 presented with local recurrences and 22 died. In order to compare protein expression to normal cartilage, separate paraffin sections of articular cartilage ($n=5$) and growth plate (four post-natal and one foetal) were included as well. Articular cartilage and growth plates were acquired from pathological specimens that are not related to cartilaginous tumours. All samples were handled according to the ethical guidelines as described in the Code for Proper Secondary Use of Human Tissue in The Netherlands of the Dutch Federation of Medical Scientific Societies (www.federa.org).

Immunohistochemistry

Immunohistochemistry was performed and the slides were scanned using Mirax Desk instrument (3DHISTECH) as described in [19]. An overview of the used antibodies, positive controls, antigen retrieval and dilution is given in Table 1. The staining of the TMAs was scored on a 0–7 scale based on staining intensity (1=weak, 2=moderate and 3=strong) added to the percentage of the positive cells (1=0–24 %, 2=25–49 %, 3=50–74 % and 4=75–100 %) by two independent observers (CJFW and CEdA) [20].

Cell culture

The articular chondrocyte cell line LBPVA [21] and chondrosarcoma cell lines CH2879 [22] and OUMS27 [23] (both CCSIII) were cultured in RPMI 1640 (Invitrogen, Breda, The Netherlands) supplemented with 20 % foetal calf serum

Table 1 Overview of used antibodies

Antigen	Species and clone	Positive control	Antigen retrieval	Dilution	Manufacturer
HS6ST1	Mouse monoclonal, 9L832	Kidney	Citrate pH 6.0	1:200	US Biological
HS6ST2	Rabbit polyclonal	Prostate	Citrate pH 6.0, 5 % elk milk	1:200	Sigma Aldrich
HS6ST3	Rabbit polyclonal	Kidney	Citrate pH 6.0, 5 % elk milk	1:50	Abcam
SULF1	Goat polyclonal	Testis	Citrate pH 6.0	1:50	Abcam
SULF2	Mouse monoclonal, 2B4	Squamous cell lung carcinoma	Citrate pH 6.0	1:100	AbD Serotec

(Invitrogen), 2 % P/S (Invitrogen) and 1 % GlutaMAX (Invitrogen). At 70–80 % confluency, the cells were harvested and HS disaccharide analysis was performed as described in [24].

Statistical analysis

Results were analysed by the PASW 17.0 for Windows software package (SPSS Inc., Chicago, IL, USA). The differences in relative HS disaccharide expression as measured by SAX–HPLC were analysed by independent samples Student's *t* tests. Trends in immunohistochemical scores between histological grades were evaluated by ANOVA followed by post-hoc test for linear trend. Survival (metastasis-free, disease-free and overall survival) was compared between a high and low expression group using Kaplan Meier survival analysis. High expression was defined as a score of the median or higher and low expression as a score below the median. P values<0.05 were considered significant for all analyses.

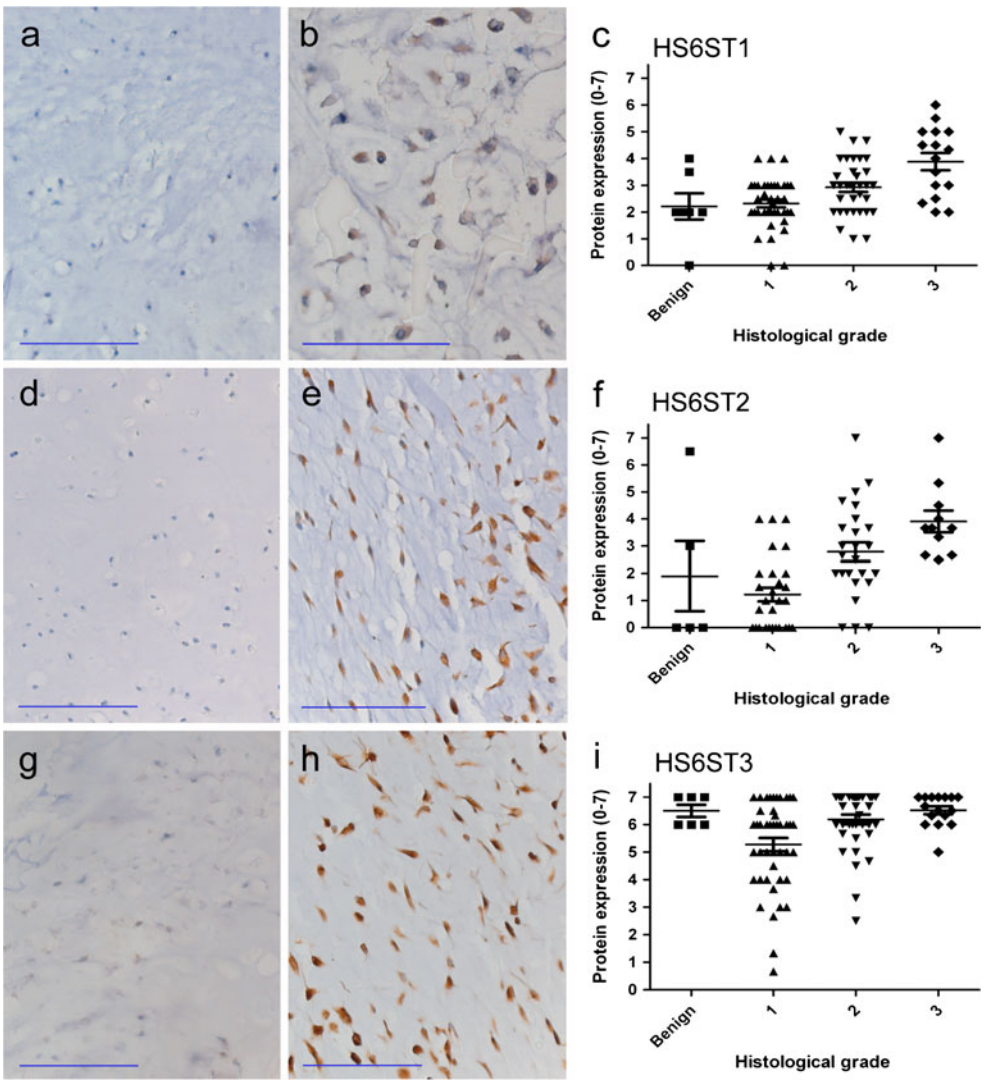

Fig. 1 HS6ST protein expression in cartilage tumour tissue shows a correlation of HS6ST1 and HS6ST2 expressions with histological grade. **a** Grade I central chondrosarcoma negative for HS6ST1. **b** Moderately strong HS6ST1 expression in a grade II peripheral chondrosarcoma. **c** HS6ST1 expression grouped by histological grade shows a strong correlation between expression and histological grade ($p<0.001$). **d** Grade I central chondrosarcoma negative for HS6ST2. **e** Strong HS6ST2 expression in grade II central chondrosarcoma. **f** HS6ST2 expression is correlated with increasing histological grade ($p=0.033$). **g** Weak HS6ST3 expression in grade I central chondrosarcoma. **h** Strong HS6ST3 expression in grade II central chondrosarcoma. **i** High HS6ST3 expression in most cases. *Blue bars* indicate 10 μm; *error bars* represent standard error of the mean (SEM)

Results

Expression of heparan sulphate 6*O*-sulphotransferases

We performed immunohistochemistry to assess the expression of the HS6STs, which attach sulphate groups to the HS chain on the 6*O* position of glucosamine. As the expression of all enzymes was highly similar between central and peripheral cartilage tumours, the results of central and peripheral tumours were combined (data not shown).

In general, while HS6ST3 was expressed strongly in almost all cartilage tumours, HS6ST1 and HS6ST2 were expressed at lower levels, although some, especially high-grade tumours, showed high expression (Fig. 1a–f). Expression in normal cartilage was absent or low, similar to the expression detected in low-grade samples (data not shown). For HS6ST1 and HS6ST2, a trend for an increased score with increasing histological grade was present ($p<0.001$ and $p=0.033$, respectively). Although on average HS6ST3 expression was reduced in grade I chondrosarcomas compared to the other grades, immunohistochemical scores did not show a significant trend with increasing histological grade (Fig. 1g–h). Normal cartilage samples showed moderately strong expression of HS6ST3 (data not shown).

As histological grade is negatively correlated with survival in chondrosarcoma patients [1], we assessed whether there were differences in survival (metastasis-free, disease-free and overall survival) between patients with high expression of HS6ST1 and HS6ST2 and patients with low expression. However, no correlation with metastasis-free, disease-free or overall survival was found (data not shown).

Expression of endosulphatases

We examined the expression of SULF1 and SULF2, the two endosulphatases that are able to remove 6*O*-sulphate groups after they have been attached to the HS chain by HS6STs. Whereas SULF1 was expressed strongly in almost all cartilage tumours, SULF2 expression was rare (Fig. 2). Although the median expression of SULF1 seemed to increase with increasing histological grade, no significant trend was observed ($p=0.193$). SULF2 was expressed only in a small number of tumours, and expression was highly focal (Fig. 2d–f). SULF2 expression was absent in normal cartilage (data not shown).

HS disaccharide analysis of chondrosarcoma cell lines

To further study 6*O*-sulphation in chondrosarcomas, the relative HS disaccharide content of two high-grade central chondrosarcoma cultures and one articular chondrocyte cell line was analysed. The results showed an increased expression of 6*O*-sulphated HS disaccharides (UA-GlcNAc 6S and UA-GlcNS 6S) in CH2879 (CCS grade III) in comparison to the articular chondrocyte cell line (Fig. 3a). Another CCS grade III cell line, OUMS27, showed an increased UA-GlcNAc 6S expression, although the change was not as large as in CH2879. After regrouping the disaccharide distribution by its sulphation type, CH2879 showed a significantly increased

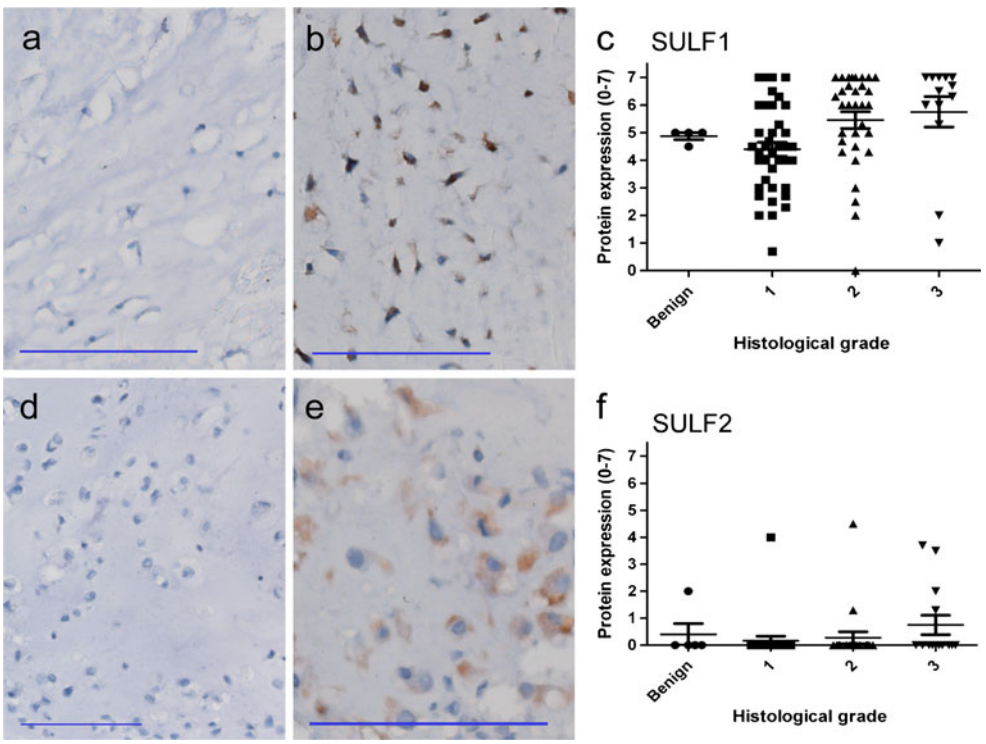

Fig. 2 High SULF1 and low SULF2 protein expression in cartilage tumours. **a** Grade I central chondrosarcoma negative for SULF1. **b** Moderate to strong expression of SULF1 in a grade III central chondrosarcoma. **c** SULF1 expression is not significantly correlated to histological grade. **d** Grade III central chondrosarcoma negative for SULF2. **e**) Grade II central chondrosarcoma showing focal expression of SULF2. **f** Most cartilage tumours are negative for SULF2. *Blue bars* indicate 10 μm; *error bars* represent SEM

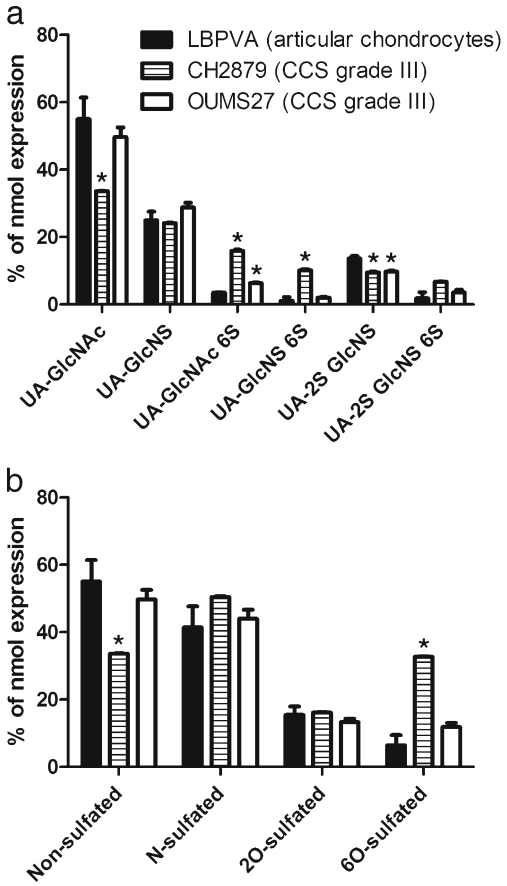

Fig. 3 Increased 6*O*-sulphation in a grade III central chondrosarcoma cell line compared to articular chondrocytes. **a** Relative HS disaccharide expression as determined by SAX–HPLC in CH2879 (cell line CCS grade III), OUMS27 (cell line CCS grade III) and LBPVA (cell line normal articular chondrocytes) shows significantly increased relative expression of the 6*O*-sulphated UA-GlcNAc 6S and UA-GlcNS 6S disaccharides and simultaneous decreased expression of the UA-GlcNAc and UA-2S GlcNS disaccharides in CH2879, and the significantly increased expression of UA-GlcNAc 6S and decreased expression of UA-2S GlcNS in OUMS27, compared to the relative disaccharide expression in the LBPVA cell line. **b** HS 6*O*-sulphation level is markedly increased in the CH2879 cell line compared to the LBPVA articular chondrocyte cell line, but not in the OUMS27 chondrosarcoma cell line. *Asterisks* denote a p value<0.05 compared to normal articular chondrocytes; *error bars* represent SEM

total 6*O*-sulphation compared to the articular chondrocytes (Fig. 3b). In OUMS27, the total 6*O*-sulphation levels were not significantly increased. In both cell lines, the expression of the *N*- and 2*O*-sulphated UA-2S-GlcNS disaccharide was reduced compared to the articular chondrocytes (Fig. 3a). In addition, the total relative expression of non-sulphated disaccharides was reduced in CH2879 (Fig. 3b).

Discussion

Previously, our group has reported increased FGF signalling and decreased Wnt signalling with malignant progression of chondrosarcoma [2–4]. The degree and the pattern of 6*O*-sulphation of HS chains play an important role in determining the capacity of HS chains to facilitate growth factor-receptor binding [14, 15]. In the case of 6*O*-sulphation, this is achieved by a delicate balance of heparan sulphate 6*O*-sulphotransferases (HS6ST1-3) attaching sulphate groups to the 6*O* position and 6*O*-endosulfatases (SULF1-2) removing some of these sulphate groups. Different studies have highlighted the importance of 6*O*-sulphation in tumourigenesis, especially by examining the role of SULF expression in tumours [13, 25, 26].

Our study showed that the expression of HS6ST1 and HS6ST2 was increased in chondrosarcoma with increasing histological grade. This suggests that 6*O*-sulphation also increases during chondrosarcoma progression. Conversely, HS6ST3 is generally highly expressed in most chondrosarcoma samples, so 6*O*-sulfotransferase activity is likely to be present in most chondrosarcomas. However, the HS6STs have been shown to have different substrate preferences for trisulphated sequences on one hand and disaccharides lacking 2*O*-sulphate groups on the other [27, 28]. Therefore, changes in the expression of one HS6ST could lead to distinct differences in the structure of the HS chain, even though another HS6ST is ubiquitously present. The 6*O*-sulphation can be modified by endosulphatases (SULF1 and SULF2) that can, in turn, remove 6*O*-sulphate groups after addition to the HS chain by HS6STs. SULF1 expression was high in almost all samples. Conversely, SULF2 was not expressed in most cases. Although the expression of HS6ST1 and HS6ST2 increased with increasing histological grade [1], the expression was not correlated to metastasis-free, disease-free or overall survival. This is probably due to the relatively small disease-related morbidity and mortality in chondrosarcoma and, therefore, also in our set of patients [1].

The combination of positive correlation of both HS6ST1 and HS6ST2 with histological grade raises the question as to whether 6*O*-sulphation is increased during malignant progression as well. As the isolation of HS disaccharides from cartilage cryosections proved to be technically unfeasible, cell lines were used even though they may be a sub-optimal biological model because HS sulphation is very tissue- and environment-specific [29–31]. Disaccharide analysis of two high-grade chondrosarcoma cell lines showed the increased expression of two 6*O*-sulphated disaccharides in one high-grade CS cell line and of one 6*O*-sulphated disaccharide in the other cell line. The total 6*O*-sulphation was markedly increased in the former high-grade CS cell line, but the latter cell line did not show this pattern. The relative expression of *N*- and 2*O*-sulphated disaccharides was reduced in both cultures, which is likely due to the relatively increased expression of 6*O*-sulphated disaccharides. In conclusion, the results suggest that 6*O*-sulphation could be upregulated in high-grade chondrosarcomas, although the degree of 6*O*-sulphation is variable.

Studies on the role of HS 6*O*-sulphation in growth factor-receptor binding have shown that an increase in 6*O*-sulphation leads to increased FGF and decreased Wnt receptor binding [18]. We here show increased HS6ST expression and increased 6*O*-sulphation during malignant progression of chondrosarcoma, which might underlie the previously reported increased FGF and decreased Wnt signalling during chondrosarcoma progression [2, 3].

In conclusion, this study shows that with malignant progression in chondrosarcoma, there is an increased expression of two HS 6*O*-sulphotransferases, HS6ST1 and HS6ST2. Our results point to an increased 6*O*-sulphation during the process of progression, which might act as an upstream mechanism influencing the activity of signalling pathways such as FGF and Wnt pathways and, in this way, play a role in chondrosarcoma progression.

Acknowledgments We thank Andrea Facchini (Istituto Ortopedico Rizzoli, Bologna, Italy) for the donation of the LBPVA cell line, Antonio Llombart-Bosch (Valencia University, Spain) for the CH2879 cell line and Toshiyuki Kunisada (Okayama University Medical School, Japan) for the OUMS27 cell line. We would also like to thank Armin Walter (Onze Lieve Vrouwe Gasthuis, Amsterdam, The Netherlands) for kindly providing patient samples. We would also like to gratefully acknowledge Pancras Hogendoorn, Christianne Reijnders, Steve Rosen (University of California, San Diego, CA, USA) and Jacob van den Born (University Medical Center Groningen, The Netherlands) for their fruitful discussion. Lastly, we would like to thank Klaas van der Ham for his photographic assistance and Inge Briaire-de Bruijn and Dorien van der Geest for their expert technical assistance. This work was supported by The Netherlands Organisation for Scientific Research (917-76-315 to JVMGB and CJFW) and the European Network of Excellence EuroBoNet grant number 018814 (LSHC-CT-2006-018814 to CJFW and CEdA).

Conflict of interest The authors declare that they have no conflicts of interest.

References

1. Fletcher CD, Unni KK, Mertens F (eds) (2002) World Health Organization classification of tumours. Pathology and genetics of tumours of soft tissue and bone. IARC, Lyon
2. Bovee JV, van den Broek LJ, Cleton-Jansen AM, Hogendoorn PC (2000) Up-regulation of PTHrP and Bcl-2 expression characterizes the progression of osteochondroma towards peripheral chondrosarcoma and is a late event in central chondrosarcoma. Lab Invest 80:1925–1934
3. Hameetman L, Rozeman LB, Lombaerts M, Oosting J, Taminiau AH, Cleton-Jansen AM, Bovée JV, Hogendoorn PC (2006) Peripheral chondrosarcoma progression is accompanied by decreased Indian Hedgehog signalling. J Pathol 209:501–511
4. Schrage YM, Hameetman L, Szuhai K, Cleton-Jansen AM, Taminiau AH, Hogendoorn PC, Bovée JV (2009) Aberrant heparan sulfate proteoglycan localization, despite normal exostosin, in central chondrosarcoma. Am J Pathol 174:979–988
5. Ahn J, Ludecke H-J, Lindow S, Horton WA, Lee B, Wagner MJ, Horsthemke B, Wells DE (1995) Cloning of the putative tumour suppressor gene for hereditary multiple exostoses (EXT1). Nature Genet 11:137–143
6. Wuyts W, Van Hul W, Wauters J, Nemtsova M, Reyniers E, Van Hul E, De Boulle K, De Vries BB, Hendrickx J, Herrygers I, Bossuyt P, Balemans W, Fransen E, Vits L, Coucke P, Nowak NJ, Shows TB, Mallet L, Van den Ouweland AM, McGaughran J, Halley DJ, Willems P (1996) Positional cloning of a gene involved in hereditary multiple exostoses. Hum Mol Genet 5:1547–1557
7. Bernfield M, Gotte M, Park PW, Reizes O, Fitzgerald ML, Lincecum J, Zako M (1999) Functions of cell surface heparan sulfate proteoglycans. Annu Rev Biochem 68:729–777
8. Rodgers KD, San Antonio JD, Jacenko O (2008) Heparan sulfate proteoglycans: a GAGgle of skeletal-hematopoietic regulators. Dev Dyn 237:2622–2642
9. Amary MF, Bacsi K, Maggiani F, Damato S, Halai D, Berisha F, Pollock R, O'Donnell P, Grigoriadis A, Diss T, Eskandarpour M, Presneau N, Hogendoorn PC, Futreal A, Tirabosco R, Flanagan AM (2011) IDH1 and IDH2 mutations are frequent events in central chondrosarcoma and central and periosteal chondromas but not in other mesenchymal tumours. J Pathol 224:334–343
10. Pansuriya TC, van Eijk R, d'Adamo P, van Ruler MA, Kuijjer ML, Oosting J, Cleton-Jansen AM, van Oosterwijk JG, Verbeke SL, Meijer D, van Wezel T, Nord KH, Sangiorgi L, Toker B, Liegl-Atzwanger B, San-Julian M, Sciot R, Limaye N, Kindblom LG, Daugaard S, Godfraind C, Boon LM, Vikkula M, Kurek KC, Szuhai K, French PJ, Bovee JV (2011) Somatic mosaic IDH1 and IDH2 mutations are associated with enchondroma and spindle cell hemangioma in Ollier disease and Maffucci syndrome. Nat Genet 43:1256–1261
11. de Andrea CE, Hogendoorn PC (2012) Epiphyseal growth plate and secondary peripheral chondrosarcoma: the neighbours matter. J Pathol 226:219–228
12. de Andrea CE, Reijnders CM, Kroon HM, de Jong D, Hogendoorn PC, Szuhai K, Bovee JV (2012) Secondary peripheral chondrosarcoma evolving from osteochondroma as a result of outgrowth of cells with functional EXT. Oncogene 31:1095–1104
13. Backen AC, Cole CL, Lau SC, Clamp AR, McVey R, Gallagher JT, Jayson GC (2007) Heparan sulphate synthetic and editing enzymes in ovarian cancer. Br J Cancer 96:1544–1548
14. Tatrai P, Egedi K, Somoracz A, van Kuppevelt TH, Ten DG, Lyon M, Deakin JA, Kiss A, Schaff Z, Kovalszky I (2010) Quantitative and qualitative alterations of heparan sulfate in fibrogenic liver diseases and hepatocellular cancer. J Histochem Cytochem 58:429–441
15. Habuchi H, Tanaka M, Habuchi O, Yoshida K, Suzuki H, Ban K, Kimata K (2000) The occurrence of three isoforms of heparan sulfate 6-*O*-sulfotransferase having different specificities for hexuronic acid adjacent to the targeted *N*-sulfoglucosamine. J Biol Chem 275:2859–2868
16. Morimoto-Tomita M, Uchimura K, Werb Z, Hemmerich S, Rosen SD (2002) Cloning and characterization of two extracellular heparin-degrading endosulfatases in mice and humans. J Biol Chem 277:49175–49185
17. Dhoot GK, Gustafsson MK, Ai X, Sun W, Standiford DM, Emerson CP Jr (2001) Regulation of Wnt signaling and embryo patterning by an extracellular sulfatase. Science 293:1663–1666
18. Lamanna WC, Kalus I, Padva M, Baldwin RJ, Merry CL, Dierks T (2007) The heparanome–the enigma of encoding and decoding heparan sulfate sulfation. J Biotechnol 129:290–307
19. Pansuriya TC, Oosting J, Krenacs T, Taminiau AH, Verdegaal SH, Sangiorgi L, Sciot R, Hogendoorn PC, Szuhai K, Bovee JV (2011) Genome-wide analysis of Ollier disease: is it all in the genes? Orphanet J Rare Dis 6:2
20. Bovée JV, Cleton-Jansen AM, Kuipers-Dijkshoorn N, van den Broek LJ, Taminiau AH, Cornelisse CJ, Hogendoorn PC (1999) Loss of heterozygosity and DNA ploidy point to a diverging

genetic mechanism in the origin of peripheral and central chondrosarcoma. Genes Chrom Cancer 26:237–246
21. Grigolo B, Roseti L, Neri S, Gobbi P, Jensen P, Major EO, Facchini A (2002) Human articular chondrocytes immortalized by HPV-16 E6 and E7 genes: maintenance of differentiated phenotype under defined culture conditions. Osteoarthr Cartil 10:879–889
22. Gil-Benso R, Lopez-Gines C, Lopez-Guerrero JA, Carda C, Callaghan RC, Navarro S, Ferrer J, Pellin A, Llombart-Bosch A (2003) Establishment and characterization of a continuous human chondrosarcoma cell line, ch-2879: comparative histologic and genetic studies with its tumor of origin. Lab Invest 83:877–887
23. Kunisada T, Miyazaki M, Mihara K, Gao C, Kawai A, Inoue H, Namba M (1998) A new human chondrosarcoma cell line (OUMS-27) that maintains chondrocytic differentiation. Int J Cancer 77:854–859
24. Reijnders CM, Waaijer CJ, Hamilton A, Buddingh EP, Dijkstra SP, Ham J, Bakker E, Szuhai K, Karperien M, Hogendoorn PC, Stringer SE, Bovee JV (2010) No haploinsufficiency but loss of heterozygosity for EXT in multiple osteochondromas. Am J Pathol 177:1946–1957
25. Lai JP, Sandhu DS, Shire AM, Roberts LR (2008) The tumor suppressor function of human sulfatase 1 (SULF1) in carcinogenesis. J Gastrointest Cancer 39:149–158
26. Lemjabbar-Alaoui H, van Zante A, Singer MS, Xue Q, Wang YQ, Tsay D, He B, Jablons DM, Rosen SD (2010) Sulf-2, a heparan sulfate endosulfatase, promotes human lung carcinogenesis. Oncogene 29:635–646
27. Chen E, Stringer SE, Rusch MA, Selleck SB, Ekker SC (2005) A unique role for 6-*O* sulfation modification in zebrafish vascular development. Dev Biol 284:364–376
28. Smeds E, Habuchi H, Do AT, Hjertson E, Grundberg H, Kimata K, Lindahl U, Kusche-Gullberg M (2003) Substrate specificities of mouse heparan sulphate glucosaminyl 6-*O*-sulphotransferases. Biochem J 372:371–380
29. Tekotte H, Engel M, Margolis RU, Margolis RK (1994) Disaccharide composition of heparan sulfates: brain, nervous tissue storage organelles, kidney, and lung. J Neurochem 62:1126–1130
30. Toida T, Yoshida H, Toyoda H, Koshiishi I, Imanari T, Hileman RE, Fromm JR, Linhardt RJ (1997) Structural differences and the presence of unsubstituted amino groups in heparan sulphates from different tissues and species. Biochem J 322(Pt 2):499–506
31. Warda M, Toida T, Zhang F, Sun P, Munoz E, Xie J, Linhardt RJ (2006) Isolation and characterization of heparan sulfate from various murine tissues. Glycoconj J 23:555–563

Virchows Arch (2012) 461:483–487
DOI 10.1007/s00428-012-1318-8

ORIGINAL ARTICLE

Gastric neuroendocrine cell hyperplasia and type 1 tumours occurring within gastric hyperplastic polyps

Runjan Chetty · Pelvender Gill · Parassar Mugon · Jyotsna Shrimankar · Caroline Hughes

Received: 13 June 2012 / Revised: 6 September 2012 / Accepted: 15 September 2012 / Published online: 26 September 2012
© Springer-Verlag Berlin Heidelberg 2012

Abstract We wish to highlight the unusual occurrence of gastric neuroendocrine cell hyperplasia and type I neuroendocrine tumours within three hyperplastic polyps. In all cases, the neuroendocrine component was present within and between the hyperplastic foveolar glands of the polyps and overall formed the minor part of the polyps. Two of the patients presented with epigastric pain and the other with fatigue from anaemia, and on endoscopy, all three were found to have superficially ulcerated gastric polyps in the body (cases 1 and 2) and fundus (case 3). Two of the cases had serologically proven autoimmune atrophic gastritis, while the third case had histological evidence of an atrophic gastritis, most likely also autoimmune in aetiology. Cases 1 and 3 had single hyperplastic polyps, while case 2 had three polyps. All polyps showed linear neuroendocrine cell hyperplasia within hyperplastic foveolar epithelium both at the surface and within deeper-situated glands. Neuroendocrine immunohistochemistry highlighted the neuroendocrine cell hyperplasia. The bulk of the neuroendocrine component was restricted to hyperplastic mucosa forming the polyps. Non-hyperplastic adjacent mucosa showed less prominent neuroendocrine cell hyperplasia. It is unclear whether the two pathologies occurred simultaneously or independently. The common feature and causal link is atrophic gastritis, which predisposed the gastric mucosa to the development of both neuroendocrine cell hyperplasia and tumours, and hyperplastic polyps.

Keywords Gastric hyperplastic polyp · Neuroendocrine cell hyperplasia · Neuroendocrine tumour · Atrophic gastritis

R. Chetty (✉) · P. Gill · C. Hughes
Department of Cellular Pathology, Biomedical Research Centre,
Nuffield Department of Clinical Laboratory Sciences,
Oxford University Hospitals, University of Oxford,
Level 1, Academic Centre, John Radcliffe Hospital, Headley Way,
Oxford OX3 9DU, UK
e-mail: runjan.chetty@gmail.com

P. Mugon
Central Health Laboratory,
Candos, Mauritius

J. Shrimankar
Department of Pathology, University Hospital of North Tees,
North Tees and Hartlepool NHS Foundation Trust,
Hardwick,
Stockton-on-Tees, UK

Gastric hyperplastic polyps are relatively common and are usually encountered as a reactive condition to mucosal injury and/or inflammation. This is noted particularly in association with autoimmune atrophic gastritis and, less commonly in *Helicobacter pylori* chronic gastritis and in post-antrectomy stomachs. Hyperplastic polyps are also encountered infrequently in rare forms of chronic gastritis such as cytomegalovirus gastritis, lymphocytic gastritis, amyloid deposition, Zollinger–Ellison syndrome and gastric antral vascular ectasia [1–3]. While they represent a discrete entity, gastric hyperplastic polyps have been associated with both adenomatous/flat dysplasia, and adenocarcinoma usually within the adjacent non-polyp mucosa [1–3].

Although uncommon, neuroendocrine cell hyperplasia and tumours are well described in the stomach. Clearly defined clinicopathological associations exist for the different types of gastric neuroendocrine tumours [4–6]. Linear neuroendocrine hyperplasia and tumours (so-called type I tumours) are pathognomonic of atrophic gastritis.

Both hyperplastic polyps and neuroendocrine cell hyperplasia and tumours thus occur in the milieu of gastric atrophy and injury and are well recognised in this context as separate entities.

We present three cases with atrophic gastritis and gastric hyperplastic polyps associated with neuroendocrine cell hyperplasia and an accompanying neuroendocrine tumour both within the hyperplastic polyps. Adjacent non-hyperplastic

gastric mucosa did not show prominent neuroendocrine cell hyperplasia as compared to the hyperplastic foveolar epithelium. The occurrence and coexistence of hyperplastic neuroendocrine cells and type I tumours within gastric hyperplastic polyps have not been described previously, to the best of our knowledge.

Materials and methods

Cases 1 and 2 were referred for a second opinion to one of the authors (RC). All materials were received in 10 % neutral buffered formalin, processed routinely, and hematoxylin and eosin (H&E)-stained sections were produced. Immunohistochemistry was performed on the paraffin-embedded, formalin-fixed tissue for the following: chromogranin (Dako-Cytomation, Ely, UK; dilution 1/50), synaptophysin (Dako; 1/200), gastrin (Leica/Novocastra, Newcastle-on-Tyne, UK; 1/200), serotonin (Leica/Novocastra; prediluted), somatostatin (Leica; 1/2,000), CD56 (Leica; 1/80), pan-cytokeratin (Dako; 1/40) and Ki-67 (Leica; 1/200).

In addition to the three study cases, five other random gastric hyperplastic polyps were examined morphologically and immunohistochemically for neuroendocrine cells.

Results

Results of clinicopathological assessment are presented in Table 1.

Clinical information

Case 1 A 45-year old male complained of epigastric pain and, on endoscopy, was found to have an ulcerated mucosal polypoid lesion in the body of his stomach, measuring 25 mm that was snared and submitted for pathological evaluation. The patient was also found to have a microcytic anaemia due to blood loss from the gastric ulcerated area. He had autoantibodies to parietal cells, but gastrin levels were not determined.

Case 2 This was a 72-year-old man who also had epigastric pain, melaena and anaemia. He was found to have a large polypoid mass together with two smaller polyps, in the fundus and body. He underwent a partial gastrectomy because of the clinical suspicion of malignancy and the multiplicity of polyps and, 1 year post-operatively, is well and disease-free. Autoimmune serology and serum gastrin levels were not performed.

Case 3 This was a 33-year-old female who presented with fatigue and found to have a microcytic anaemia and vitamin B12 deficiency. In the investigation of the cause of the anaemia, endoscopy revealed marked gastric atrophy in the body and fundus together with a small polyp in the fundus.

She had positive serology for anti-parietal cell antibodies; however, anti-intrinsic factor antibodies were negative. She was also noted to have hypergastrinaemia at this time (gastrin level >400 units). Endoscopy showed a normal antrum and a fundic polyp. The polyp was removed, and the fundus, body and antrum were biopsied.

None of the patients had Zollinger–Ellison syndrome or multiple endocrine neoplasia type I (MEN-I), clinically and by relevant imaging. They also did not have a family history of any polyposis syndrome.

Gross findings

Case 1 The submitted polyp was tan-coloured, measured 23×15 mm and showed surface ulceration.

Case 2 A partial gastrectomy excised a large polypoid lesion measuring 25×18 mm, and two smaller polyps, 13×8 and 12×7 mm, respectively, were also noted. The surface of the largest polyp showed pinpoint hemorrhagic foci but no obvious ulceration. Deep to this polyp, the gastric wall appeared firmer and thickened. This area was sampled extensively.

Case 3 The polyp that was submitted for histological evaluation along with the biopsies, measured 10×10 mm and appeared tan-coloured.

Microscopy

All three cases had features typical of hyperplastic polyps (Fig. 1a–c). There was foveolar hyperplasia with irregular cystic dilatation of glands. Foci of intestinal metaplasia were

Table 1 Clinicopathological features

Case	Age	Gender	Site	Polyp size (mm)	NET size (mm)	Resection	Autoantibodies	Gastrin levels
1	45	Male	Body	23	20	Polypectomy	Anti-parietal cell	Not done
2	72	Male	Fundus/body	25	4	Partial gastrectomy	Not done	Not done
3	33	Female	Fundus/body	10	5	Polypectomy	Anti-parietal cell, anti-intrinsic factor	>400 units

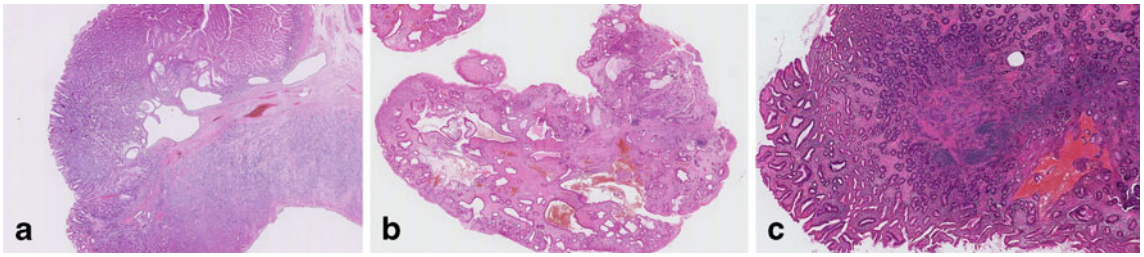

Fig. 1 **a**–**c** Low power images of the polyps from the three cases. There is surface ulceration and dilated tortuous glands typical of hyperplastic polyps. The neuroendocrine component is within the hyperplastic polyp as aggregates between the hyperplastic tubules

noted in all three hyperplastic polyps but most prominent in cases 2 and 3. The stroma appeared acutely inflamed with oedema; granulation tissue and evidence of chronic inflammation with lymphoid aggregates were also present. Several prominent ectatic vessels were also present in the lamina propria. Several (but not all) hyperplastic glands within the polyps and surface mucosa showed linear neuroendocrine cell hyperplasia (Fig. 2a–c). The neuroendocrine cells were clearly visible as linear runs or rows along the abluminal aspect of the hyperplastic glands in both superficial and deep aspects of the polyps. Although not every hyperplastic gland showed neuroendocrine cell hyperplasia, the majority of glands directly above and within the neuroendocrine tumours showed the most obvious linear neuroendocrine cell hyperplasia. Immediately adjacent mucosa did not show the same striking neuroendocrine cell hyperplasia (in case 1, non-hyperplastic mucosa was present at the base of the polypectomy specimen; in the remaining two cases, ample adjacent mucosa was available from the gastrectomy specimen and biopsy material). The neuroendocrine hyperplasia in adjacent mucosa was more evident in sections stained with neuroendocrine markers. Within the lamina propria, micronodules, trabeculae and sheets of neuroendocrine cells were noted between hyperplastic, dilated glands. These cells were uniform with eosinophilic cytoplasm and monotonous nuclei with typical "salt and pepper" chromatin distribution. The neuroendocrine tumours extended into the submucosa in cases 1 and 2. In case 3, oblique sectioning precluded definitive comment on submucosal penetration. The neuroendocrine component occupied 90 % of the polyp in case 1, 10 % in case 2 and 50 % in case 3.

In addition in case 2, the adjacent mucosa showed mainly low-grade dysplasia with focal areas of high-grade dysplasia. The dysplastic epithelium contained occasional neuroendocrine cells, but there was no linearity to the arrangement and

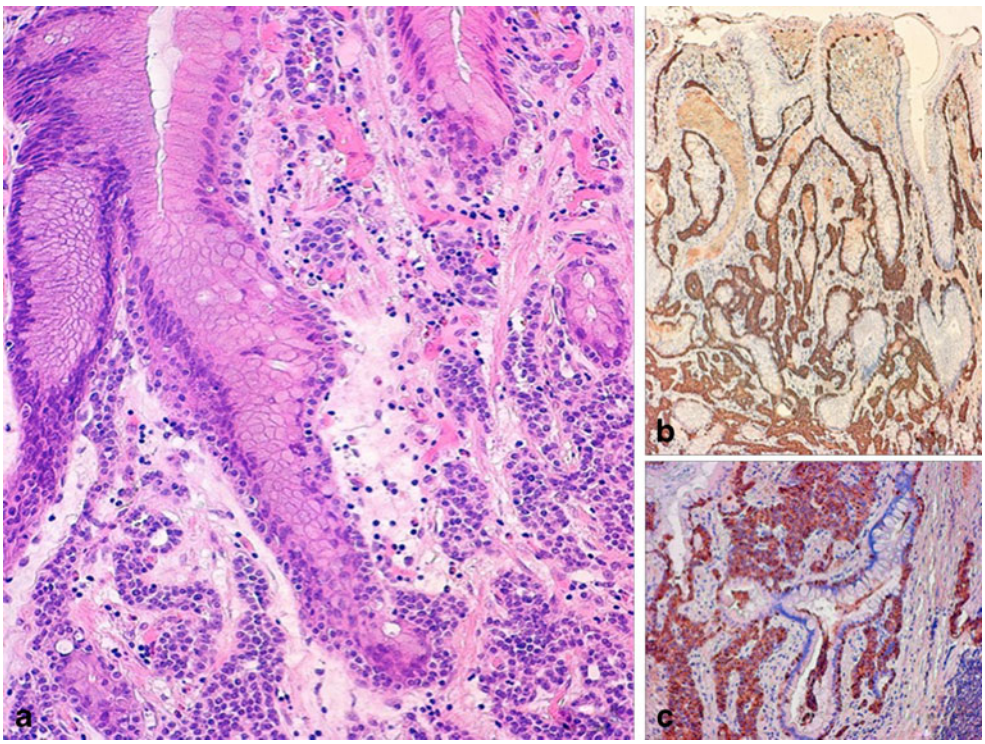

Fig. 2 **a**–**c** The hyperplastic glands display single cell, linear neuroendocrine hyperplasia in both cases (**a**, from case 1). Neuroendocrine tumour cells are present within the lamina propria between hyperplastic glands. Chromogranin stain highlights the extent of neuroendocrine cell hyperplasia within the hyperplastic polyps (**b**, from case 1; and **c**, from case 3)

was not interpreted as hyperplastic. An adenocarcinoma was not present.

The adjacent, non-polyp/non-hyperplastic mucosa in all three cases showed evidence of atrophic chronic gastritis with loss of and/or very occasional parietal cells. There was an associated chronic inflammation with lymphoid aggregates, intestinal metaplasia and so-called "antralization" of the body and fundus because of the absence of oxyntic mucosa. *H. pylori* organisms were not identified in all three cases. The neuroendocrine cell hyperplasia was predominantly noted in areas containing hyperplastic polyps and was not prominent in normal non-hyperplastic-appearing gastric mucosa remote to the polyps, either on H&E or neuroendocrine immunohistochemical markers.

In case 1, there were three mitoses per 10 high-power fields (HPF), and the Ki-67 proliferation index was 16 %, making this a grade 2 neuroendocrine tumour.

Case 2 contained one mitotic figure per 10 HPF and a Ki-67 index of less than 2 % and was therefore a grade 1 neuroendocrine tumour.

Case 3 was graded as a grade 2 neuroendocrine tumour with one mitotic figure per 10 HPF but a Ki-67 index of 4 %.

The neuroendocrine component of both polyps was strongly positive for chromogranin (Fig. 3a, b), synaptophysin, CD56 and cytokeratin. Gastrin, serotonin and somatostatin were all negative.

The five control hyperplastic polyps did not show any evidence of linear neuroendocrine cell hyperplasia on H&E sections or with neuroendocrine cell markers. In fact, fewer neuroendocrine cells were identified within the hyperplastic foveolar glands of the polyps compared to normal adjacent gastric mucosa.

Discussion

Neuroendocrine tumours of the stomach are said to be of three types. Type I occurs in the presence of achlorhydric, atrophic body gastritis or autoimmune gastritis associated with pernicious anaemia. This represents the most common type of gastric neuroendocrine tumour and is gastrin-dependent. Type II occurs in the setting of Zollinger–Ellison syndrome that is associated with MEN-I and is gastrin-dependent, and type III is a sporadic form that develops without antecedent specific gastric pathology and is gastrin-independent. It is also well known that there is a temporal sequence or evolution from neuroendocrine hyperplasia through to tumour, especially in types I and II [4–6]. Enterochromaffin–like cell hyperplasia occurs in the body and fundus of the stomach and is seen either autoimmune chronic atrophic gastritis or in patients with MEN-I. Thus, types I and II gastric neuroendocrine tumours are associated with precursor neuroendocrine cell hyperplasia. In both these clinical contexts, there are definite provoking circumstances for neuroendocrine cell hyperplasia. Two of the three patients in this paper had both serologic evidence of autoimmune atrophic gastritis, but all three patients had histological features consistent with atrophic gastritis. Although case 2 did not have appropriate autoimmune serology performed, the histological features (including neuroendocrine cell hyperplasia and the absence of *H. pylori* organisms) favoured an autoimmune aetiology. None of the patients reported herein had any evidence of MEN-I clinically or histologically. The unusual feature of the neuroendocrine tumour in case 2 was the high Ki-67 index (16 %). In general, type I gastric neuroendocrine tumours have a low proliferation index although, in rare cases, it may be high and the tumours maybe of grade 2 lesions [7]. Type III neuroendocrine tumour is not usually accompanied by neuroendocrine cell hyperplasia and is usually a low- to high-grade tumour.

There is a report of a case of juvenile polyposis of the stomach with accompanying hypergastrinemia [8]. The gastrectomy specimen of this case showed multiple hyperplastic-type polyps with G cell hyperplasia in the polyp and in adjacent normal mucosa (in antral glands).

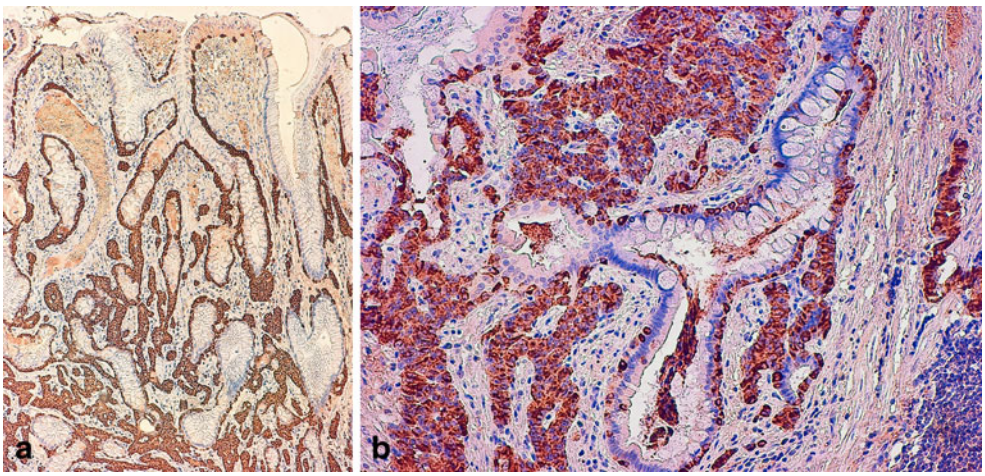

Fig. 3 **a**, **b** The neuroendocrine component of both polyps was strongly positive for chromogranin

The authors ascribed the increase in G cells to changes in cell migration patterns [8]. While this argument is appealing, neuroendocrine cell hyperplasia does not appear to be part of the same hyperplastic/reactive process involving both foveolar epithelium in gastric hyperplastic polyps since the five random polyps selected as "control" cases failed to show any neuroendocrine hyperplasia.

In a recent study on patients with autoimmune metaplastic atrophic gastritis, Park and colleagues demonstrated that hyperplastic polyps occurred in 57.5 % of patients while 19 % of patients had well differentiated neuroendocrine tumours [9].

Any proposed pathogenetic mechanism linking hyperplastic polyps with neuroendocrine cell hyperplasia is speculative and conjectural. While there does not appear to be an obvious direct causal link between the two pathologies, it is likely that they both arose within atrophic gastric mucosa that is stimulated by hypergastrinaemia. It should also be noted that the hyperplastic polyp can predominate, and the neuroendocrine component may be masked, especially in biopsy samples. The neuroendocrine hyperplasia may have preceded, occurred concurrently or even appeared after the hyperplastic polyps. Some glands may have contained linear neuroendocrine cell hyperplasia as a result of the atrophic gastritis, and the foveolar hyperplasia occurred as a secondary phenomenon. It may also be possible that the neuroendocrine cell hyperplasia or tumour stimulated the foveolar epithelium in a paracrine fashion.

This paper highlights the unusual coexistence of gastric hyperplastic polyps and neuroendocrine cell hyperplasia together with an underlying neuroendocrine tumour within the hyperplastic glands of the polyp. Surrounding mucosa that was not hyperplastic did not show as prominent neuroendocrine cell proliferation as within the hyperplastic mucosa. Although it is unclear precisely how these two pathologies are pathogenetically linked, it is likely that gastric atrophy and hypergastrinaemia are important. The novel aspect of this report is the coexistence of the hyperplastic polyp, neuroendocrine hyperplasia and neuroendocrine tumour within the same lesion, a phenomenon that has not, to the best of our knowledge, been described before.

Conflict of interest We declare that we have no conflict of interest.

References

1. Abraham SC, Singh VK, Yardley JH, Wu T (2001) Hyperplastic polyps of the stomach: associations with histologic patterns of gastritis and gastric atrophy. Am J Surg Pathol 25:500–507
2. Abraham SC (2002) Gastric polyps: classification and meaning. Pathology Case Rev 7:2–11
3. Jain R, Chetty R (2009) Gastric hyperplastic polyps: a review. Dig Dis Sci 54:1839–6
4. Klöppel G, Anlauf M, Perren A (2007) Endocrine precursor lesions of gastroentero-pancreatic neuroendocrine tumors. Endocr Pathol 18:150–5
5. Rindi G, Luinetti O, Cornaggia M, Capella C, Solcia E (1993) Three subtypes of gastric argyrophil carcinoid and the gastric neuroendocrine carcinoma: clinicopathologic study. Gastroenterology 104:994–1006
6. Solcia E, Fiocca R, Villani L, Luinetti O, Capella C (1995) Hyperplastic, dysplastic, and neoplastic enterochromaffin-like cell proliferations of the gastric mucosa. Classification and histogenesis. Am J Surg Pathol 19(Suppl 1):S1–7
7. Christopoulos C, Papavassiliou E (2005) Gastric neuroendocrine tumors: biology and management. Ann Gastroenterol 18:127–40
8. Papay KD, Falck VG, Poulsen SS et al (2010) Juvenile polyposis of the stomach—a novel cause of hypergastrinemia. Nat Rev Gastroenterol Hepatol 7:583–8
9. Park JY, Cornish TC, Lam-Himlin D, Shi C, Montgomery E (2010) Gastric lesions in patients with autoimmune metaplastic gastritis (AMG) in a tertiary care setting. Am J Surg Pathol 34:1591–8

Virchows Arch (2012) 461:489–494
DOI 10.1007/s00428-012-1308-x

ORIGINAL ARTICLE

Foveolar cells phagocytose apoptotic neutrophils in chronic active *Helicobacter pylori* gastritis

R. A. Caruso · F. Fedele · C. Di Bella · E. Mazzon · L. Rigoli

Received: 9 February 2012 / Revised: 3 August 2012 / Accepted: 23 August 2012 / Published online: 5 September 2012
© Springer-Verlag 2012

Abstract The recognition and removal of apoptotic inflammatory cells by tissue macrophages and non-professional phagocytes, in a process called efferocytosis, is required for resolution of inflammation and is actively anti-inflammatory. We have previously demonstrated phagocytosis of apoptotic neutrophils by tumor cells in human gastric carcinoma, but to date, there have been no studies investigating this process in chronic active *Helicobacter pylori* gastritis. Biopsy specimens from 28 subjects with or without *H. pylori* infection and active inflammation were examined and graded according to the updated Sydney system. Light microscopy, electron microscopy, and Terminal Deoxynucleotidyltransferase-Mediated UTP End Labeling staining were used to identify apoptosis. *H. pylori* infection was detected by histology and by molecular assay in 16 out of 28 cases. DNA from paraffin-embedded gastric biopsies was amplified using primers specific for cagA, for the cag "empty site" as well as for the s and m alleles of vacA. The more virulent cagA-positive strains were found in five out of nine patients with chronic active gastritis. The vacA s1/m1 and s2/m1 genotypes were more common in nine patients with chronic active gastritis, while the vacA s2/m2 genotype was more frequent in seven patients with chronic inactive gastritis. Apoptotic neutrophils were also detected within the cytoplasmic vacuoles of the foveolar cells of nine cases with chronic active gastritis. Transmission electron micrographs revealed further apoptotic neutrophils within spacious phagosomes of foveolar cells in a similar manner to those described in late-phase efferocytosis both in vivo and in vitro. These new observations expand the morphological spectrum of gastritis in patients infected with more virulent *H. pylori* strains, compatible with an anti-inflammatory role for the gastric epithelial cells in their removal of apoptotic neutrophils during active chronic gastritis.

Keywords *H. pylori* gastritis · Neutrophil apoptosis · Efferocytosis · Electron microscopy

R. A. Caruso (✉) · F. Fedele
Department of Human Pathology, School of Medicine,
University of Messina,
Messina, Italy
e-mail: rosariocaruso@tin.it

C. Di Bella · L. Rigoli
Department of Pediatrics, School of Medicine,
University of Messina,
Messina, Italy

E. Mazzon
Department of Clinical and Experimental Medicine
and Pharmacology, School of Medicine, University of Messina,
Messina, Italy

Introduction

Helicobacter pylori colonizes the human stomach and establishes a long-term infection of the gastric mucosa [1]. The persistent colonization induces gastritis and is associated with the development of peptic ulcer disease, atrophic gastritis, and gastric cancer [2]. The pathobiology of *H. pylori* gastritis is peculiar in many aspects. *H. pylori* gastritis is characterized by severe, acute, and chronic inflammation, which might last for decades if not treated properly [2, 3]. Persistent active inflammation with neutrophil infiltration is exceptional in other organs or biological systems. Activated neutrophils generate reactive oxygen and nitrogen species, which are mutagenic and carcinogenic, therefore having serious biological implications [4].

Phagocytosis of apoptotic cells, also known as efferocytosis, is an essential feature of immune responses [5, 6]. Failure to do so will result in disintegration of the apoptotic cell via a process called secondary necrosis and subsequent uncontrolled leakage of the contents of dying cells, resulting

in a propagated inflammatory response [7]. While the macrophage and dendritic cells are considered to be the most important cells involved in apoptotic cell removal, including that of apoptotic neutrophils, many lines of evidence suggest an important role for non-professional "neighboring" cells with phagocytic capacity (such as epithelial cells, endothelial cells, and fibroblasts) [7–10].

Although neutrophils are well known to play an important role in *H. pylori* gastritis, of which their presence marks the activity and severity, few data are available regarding the clearance mechanism of apoptotic neutrophils in *H. pylori* gastritis.

In the present study, using Terminal Deoxynucleotidyltransferase-Mediated UTP End Labeling (TUNEL) assay and electron microscopy, we showed intrafoveolar apoptotic neutrophils in *H. pylori* chronic active gastritis. These results are discussed in relation to recent studies on efferocytosis, in vivo and in vivo.

Subjects and methods

Study subjects and sampling

Twenty-eight patients scheduled for upper endoscopy were enrolled prospectively from the Department of Internal Medicine between December 2006 and February 2007 at the University Hospital of Messina. The study protocol was approved by the ethics committee of the University Hospital of Messina (Messina, Italy). None of the subjects had taken any antibiotics, proton-pump inhibitors, H2 antagonists, non-steroidal anti-inflammatory drugs, or corticosteroids 2 months prior to this study. After obtaining a written informed consent, upper endoscopy was performed, and endoscopic findings were recorded. The protocol included the collection of six biopsy specimens (four for diagnosis and two for electron microscopy) from the gastric antrum and corpus.

For light microscopy, four biopsy specimens were fixed in 10 % buffered formalin and embedded in paraffin. We graded the histopathological findings of gastritis (glandular atrophy, intestinal metaplasia, mononuclear cells, neutrophils, *H. pylori* density) on a scale of 0 (normal), 1 (mild), 2 (moderate), and 3 (marked) using the visual analog scale of the updated Sydney system [3]. All cases were histologically examined by two of the authors (RAC and FF). If their opinions differed, the specimens were jointly reconsidered until a consensus was reached.

TUNEL assay

TUNEL assay was conducted by using a TUNEL detection kit according to the manufacturer's instruction (Apotag, HRP kit DBA, Milan, Italy). Briefly, sections were incubated with 15 μg/ml proteinase K for 15 min at room temperature and then washed with PBS. Endogenous peroxidase was inactivated by 3 % H2O2 for 5 min at room temperature and then washed with PBS. Sections were immersed in terminal deoxynucleotidyltransferase (TdT) buffer containing deoxynucleotidyl transferase and biotinylated dUTP in TdT buffer, incubated in a humid atmosphere at 37 °C for 90 min, and then washed with PBS. The sections were incubated at room temperature for 30 min with anti-horseradish peroxidase-conjugated antibody, and the signals were visualized with diaminobenzidine. Sections of human tonsil and human small intestine, as well as a control tissue provided with the ApoTag kit, were the positive controls.

Genomic DNA extraction from paraffin-embedded gastric biopsies

DNA was extracted from formalin-fixed, paraffin-embedded tissue blocks. Sections of a total of 30–60 μm thickness were deparaffinized with xylene as previously described [11]. Then, total DNA was extracted using the QIAamp Tissue kit (Qiagen, Hilden, Germany) with standard protocols.

PCR amplification

PCR was performed to detect the cagA and cag empty site, and the signal sequence (s1 and s2) and middle region (m1 and m2) alleles of the vacA gene, as previously described [12] using the primers listed in Table 1 and the following conditions: 30 cycles of 94 °C for 1 min, 55 °C for 1 min, and 72 °C for 1 min. The amplified genes were analyzed by electrophoresis in a 2 % gel with ethidium bromide.

Electron microscopy

For electron microscopy, two biopsies (one from the gastric antrum and one from the corpus) were immediately fixed in 3 % phosphate-buffered glutaraldeyde pH 7.4 and post-fixed in 1 % osmium tetroxide. Semi-thin araldite-embedded sections were stained with toluidine blue for selection of fields. For

Table 1 Primers used in this study

Region	Primer	Nucleotide sequence	bp	Reference
cagA	cagA-F	gat aac agg caa gct ttt gag g	349	[23]
	cagA-R	ctg caa aag att gtt tgg cag a		
cag empty site	Luni-1	aca ttt tgg cta aat aaa cgc tg	535	[23]
	R5280	ggt tgc acg cat ttt ccc tta atc		
vacAs1 and *vacAs2*	Va1-F	atg gaa ata caa caa aca cac	*s1* 259	[23]
	Va1-R	ctg ctt gaa tgc gcc aaa c	*s2* 289	
vacAm1	Va3-F	ggt caa aat gcg gtc atg g	290	[23]
	Va3-R	cca ttg gta cct gta gaa ac		
vacAm2	Va4-F	gga gcc cca gga aac att g	352	[23]
	Va4-R	cat aac tag cgc ctt gca c		

electron microscopy, ultrathin sections were double-stained with uranyl acetate and lead citrate; they were then examined and photographed in a Zeiss EM 902 electron microscope.

Statistical analyses

To examine the relationship between *H. pylori* genotypes and gastritis activity, Fisher's exact test was performed owing to the small sample size in some groups. A p value <0.05 was considered statistically significant.

Results

H. pylori colonization and histopathological diagnosis

Of the 28 patients with gastric symptoms, 16 were positive for *H. pylori*, detected by histology as well as by PCR. Seven out of 16 positive cases revealed chronic gastritis without activity, characterized by mononuclear cell infiltration consisting of various amounts of lymphocytes, plasma cells, mast cells, and macrophages in the lamina propria but without the presence of neutrophils. Nine out of the 16 positive cases revealed active gastritis. In these cases, mucosal biopsies revealed a regenerative epithelium, with neutrophil infiltration of the lamina propria around non-colonized renewal zone epithelium of gland necks or beneath infected epithelium (Fig. 1). Neutrophils were also found inside the epithelium and formed small collections (microabscesses) in the lumen of the foveolae. Some intraepithelial neutrophils exhibited apoptotic changes such as chromatin condensation and cell shrinkage (Fig. 2) and were TUNEL positive (Fig. 3). One to three apoptotic neutrophils were found within the cytoplasmic vacuole of a foveolar cell (Fig. 2). This phenomenon was particularly extensive in four out of nine cases (Figs. 2 and 3) and was accompanied by cytoplasmic mucin depletion, nuclear pseudostratification, and occasional mitoses (Fig. 2). Of the nine patients with chronic active gastritis, five harbored cagA-positive strains (Table 2). *H. pylori* strains belonged to the vacAs1/m1 genotype in seven cases and vacAs1/m2 genotype in two cases (Table 2). The vacA s1/m1 and s2/m1 genotypes were significantly more common in nine patients with chronic active gastritis, while the vacAs2/m2 genotype was more frequent in seven patients with chronic inactive gastritis (Table 3).

Twelve patients with non-ulcer dyspepsia showed histologic normal mucosa and were not infected with *H. pylori*.

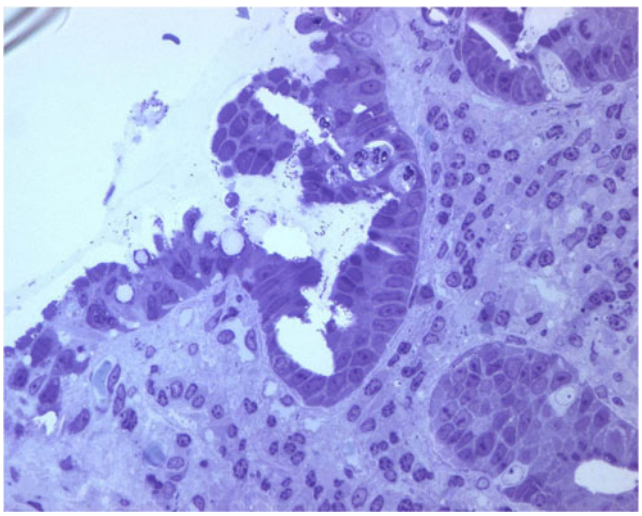

Fig. 1 Chronic active *H. pylori* gastritis. Apoptotic neutrophils showing chromatin condensation are found within large vacuoles of foveolar cells. Semi-thin section; toluidine blue; ×400

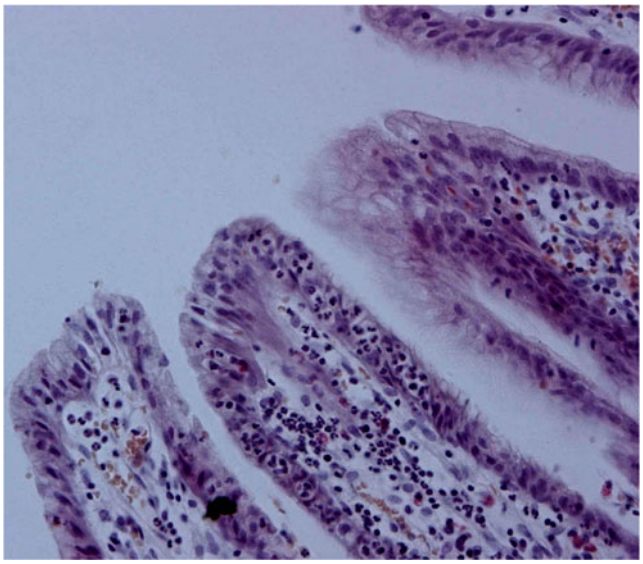

Fig. 2 The affected gastric mucosa shows depletion of mucin and heavy infiltration of foveolar cells by neutrophils. One to three apoptotic neutrophils are contained in cytoplasmic vacuoles of foveolar cells. H & E×200

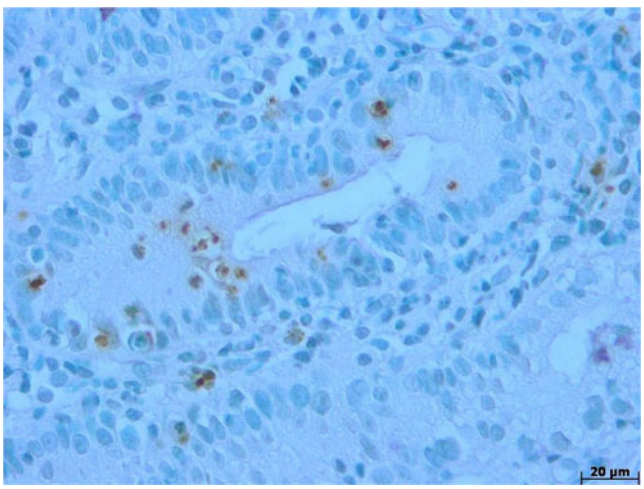

Fig. 3 TUNEL-positive neutrophils are detected within cytoplasmic vacuoles of foveolar cells. ×400

Table 2 *H. pylori* genotypes in the nine patients with chronic active gastritis

Patient	cagA genotype	vacA genotype
1	Positive	s1/m1
2	Negative	s1/m1
3	Positive	s1/m1
4	Negative	s1/m1
5	Positive	s1/m1
6	Positive	s1/m1
7	Positive	s1/m1
8	Negative	s2/m1
9	Negative	s2/m1

No granulocytes and only sparse mononuclear cells (mostly lymphocytes and macrophages) were observed in the lamina propria by both light and electron microscopies, while virtually no imononuclear cells were detected inside the epithelium apart from occasional lymphocytes.

Electron microscopy

By electron microscopy, interepithelial neutrophils exhibited the characteristic equipment of discrete primary and secondary granules, glycogen, and lipid bodies. Other neutrophils were present within spacious phagosomes of epithelial cells and showed apoptotic changes. Ultrastructural signs of early apoptotic changes included nuclear chromatin separation into dense and electron-lucent areas, rounded nuclear profiles, preservation of cytoplasmic granules, and maintenance of cell membrane integrity (Fig. 4). Late apoptotic morphology was characterized by cell shrinkage, tightly packed cytoplasmic granules, and uniform collapsed nucleus (Fig. 5). Several cytoplasmic organelles including lysosomes were found in the vicinity of phagosomes (Fig. 5).

Discussion

Our histologic data show apoptotic neutrophils within cytoplasmic vacuoles of foveolar cells in chronic active *H. pylori* gastritis. To investigate neutrophil apoptosis, we chose three independent techniques: light microscopy with H & E staining, TUNEL staining, and electron microscopy. At the light microscopic level, apoptotic cells may be recognized by their typical condensed chromatin and reduced cell volume [13]. Electron microscopy is still considered the "gold standard" for the identification of apoptotic cells [14]. Moreover, the inter- or intraepithelial localization of neutrophils is easily recognized by electron microscopy, whereas this recognition is difficult by light microscopy. At the electron

Table 3 *H. pylori* genotypes in 16 patients with *H. pylori* chronic gastritis

	Chronic inactive gastritis; score 0/1 (N=7)	Chronic active gastritis; score 2/3 (N=9)	*P* value
cagA+	0	5	<0.01
vacA			
s1/m1	0	7	
s2/m1	1	2	
s2/m2	6	0	<0.01

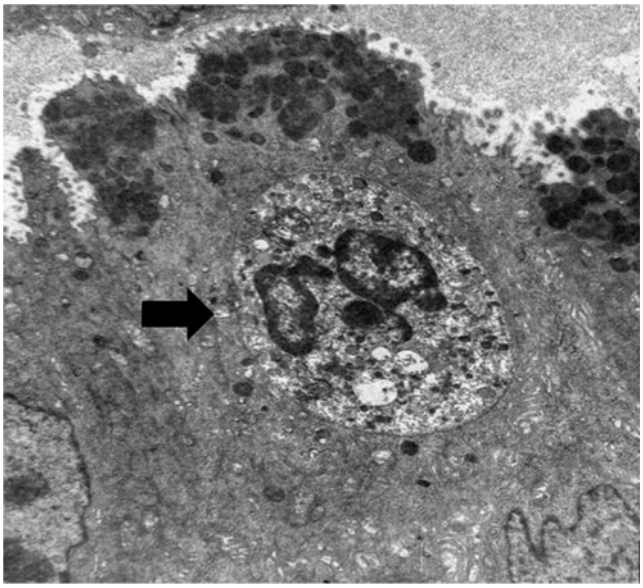

Fig. 4 Ultrastructural features of an apoptotic neutrophil (*arrow*) within the phagosome of a foveolar cell. The phagocytized neutrophil shows early apoptotic changes including nuclear chromatin separation into dense and electron-lucent areas, preservation of cytoplasmic granules, glycogen granule depletion, cytoplasmic vacuoles. ×10,000

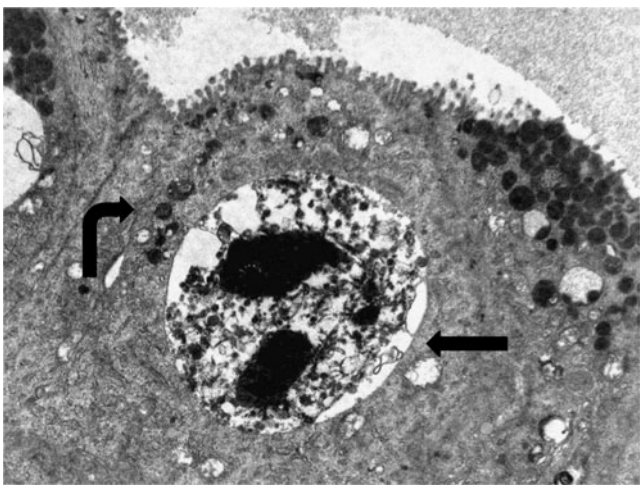

Fig. 5 Neutrophil showing late apoptotic changes is noted within a spacious phagosome of a foveolar cell (*arrow*). Note mucin granule depletion and concentration of lysosomes near phagosome (*curved arrow*). ×10,000

microscopy level, neutrophils showed tightly packed cytoplasmic granules, condensed nuclear chromatin, and, especially, uniform and collapsed nucleus, which has been outlined as the defining morphological feature of an apoptotic cell [14]. Furthermore, the tissue specimens in our study were put into formalin or glutaraldehyde for fixation immediately after endoscopic biopsy so that no accumulation of apoptotic cells after removal from the organism was possible. Several molecular approaches have been devised for detection of apoptotic neutrophils in tissues. The TUNEL technique, which is based on enzymatic incorporation of labeled nucleotides at sites where DNA fragmentation has occurred, is commonly used [14]. However, the TUNEL staining is not specific to apoptotic cells (e.g., necrotic cells also exhibit DNA fragmentation) [14]. Hence, in this study, our ultrastructural analysis served as complement to, as well as validation of, the TUNEL technique.

Emperipolesis has been defined as a random passage of different types of cells through the cytoplasm of another cell without any important change on either the host or invading cells [15]. It differs from phagocytosis in that an engulfed cell only temporarily exists within another cell [16]. We rule out the possibility that the presence of neutrophils within foveolar cell is merely due to emperipolesis, because these neutrophils were apoptotic, as revealed by electron microscopy and TUNEL assay.

The pattern of apoptotic neutrophils within vacuoles of foveolar cells most closely resembles that seen in efferocytosis: a dynamic process characterized by phagocytosis of apoptotic cells [5, 6, 17, 18]. Our ultrastructural data, such as spacious phagosomes containing apoptotic neutrophils and concentration of lysosomes around the phagosomes, are also morphologic hallmarks of late-phase efferocytosis described in vivo and in vitro [18].

In our previous studies, we also showed apoptotic neutrophil phagocytosis by tumor cells in human gastric carcinomas [19]. Taken together, our results confirm and extend earlier findings demonstrating intraepithelial apoptotic neutrophils, likely due to efferocytosis, not only in foveolar epithelium in chronic active *H. pylori* gastritis, but also in neoplastic epithelial cells of human gastric carcinomas.

Our data, resulting from *H. pylori* genotype analyses from paraffin-embedded biopsies, showed a significative association between neutrophil activity and more virulent *H. pylori* strains such as cagA-positive as well as vacAs1/m1 and vacAs2/m1 strains. These distinct *H. pylori* genotypes were also associated with the neutrophil efferocytosis phenomenon.

There are conflicting data both in vitro and in vivo regarding the mechanisms leading to the induction of neutrophil apoptosis by *H. pylori*. Neutrophils are constitutively programmed to undergo apoptosis, and such a process limits their pro-inflammatory potential and leads to rapid and non-phlogistic recognition by macrophages [8]. The possibility that *H. pylori* increases the lifespan of neutrophils, by preventing the natural occurring apoptosis, thus causing the prolongation of the phlogistic process, has been recently suggested [20, 21]. However, there are a few studies regarding the clearance mechanism of apoptotic neutrophils in *H. pylori* gastritis. Therefore, the exact mechanisms involved in mediating neutrophil efferocytosis by foveolar cells observed in vivo during infection with more virulent *H. pylori* strains remain not well determined to date. Our findings, however, suggest that foveolar epithelium might be an active participant in the removal of apoptotic neutrophils and therefore plays an important role in the modulation of neutrophil inflammation in patients infected with more virulent *H. pylori* strains.

One of the hallmarks of chronic active gastritis caused by *H. pylori* infection is the infiltration of neutrophils into the gastric mucosa [22]. However, other infections and inflammatory conditions (e.g., syphilis and Crohn's disease, reactive gastropathy with focal activity) may be responsible for the presence of neutrophils in gastric mucosa [22]. A complete understanding of neutrophil efferocytosis phenomenon by gastric foveolar cells will require further studies to assess its specificity among the different forms of gastritis.

In summary, through the use of light and electron microscopies and TUNEL staining, the present study provides evidence of intrafoveolar apoptotic neutrophils in chronic active *H. pylori* gastritis. These findings are compatible with a late phase of neutrophil efferocytosis by foveolar cells and suggest a role in the removal of apoptotic neutrophils during active gastritis caused by more virulent *H. pylori* strains. Further studies will be required to fully evaluate the clinical significance of our findings and to determine the specificity of this morphologic change.

Conflict of interest statement The authors declare that they have no conflict of interest.

References

1. Blaser MJ (1997) Ecology of *Helicobacter pylori* in the human stomach. J Clin Invest 100:759–762
2. Correa P, Piazuelo MB (2008) Natural history of *Helicobacter pylori* infection. Dig Liver Dis 40:490–496
3. Dixon MF, Genta RM, Yardley JH, Correa P et al (1996) Classification and grading of gastritis. The updated Sydney system. Am J Surg Pathol 20:1161–1181
4. Lonkar P, Dedon PC (2011) Reactive species and DNA damage in chronic inflammation: reconciling chemical mechanisms and biological fates. Int J Cancer 128:1999–2009
5. deCathelineau AM, Henson PM (2003) The final step in programmed cell death: phagocytes carry apoptotic cells to the grave. Essays Biochem 39:105–117
6. Gardai SJ, McPhillips KA, Frasch SC, Janssen WJ, Starefeldt A, Murphy-Ullrich JE, Bratton DL, Oldenborg PA, Michalak M,

Henson PM (2005) Cell-surface calreticulin initiates clearance of viable or apoptotic cells through trans-activation of LRP on the phagocyte. Cell 123:321–334
7. Savill J, Fadok V (2000) Corpse clearance defines the meaning of cell death. Nature 407:784–788
8. Savill JS, Wyllie AH, Henson JE, Walport MJ, Henson PM, Haslett C (1989) Macrophage phagocytosis of aging neutrophils in inflammation. Programmed cell death in the neutrophil leads to its recognition by macrophages. J Clin Invest 83:865–875
9. Sexton DW, Al-Rabia M, Blaylock MG, Walsh GM (2004) Phagocytosis of apoptotic eosinophils but not neutrophils by bronchial epithelial cells. Clin Exp Allergy 34:1514–1524
10. Monks J, Rosner D, Geske FJ, Lehman L, Hanson L, Neville MC, Fadok VA (2005) Epithelial cells as phagocytes: apoptotic epithelial cells are engulfed by mammary alveolar epithelial cells and repress inflammatory mediator release. Cell Death Differ 12:107–114
11. Fan H, Gulley ML (2001) DNA extraction from paraffin-embedded tissues. Methods Mol Med 49:1–4
12. Mukhopadhyay AK, Kersulyte D, Jeong JY, Datta S et al (2000) Distinctiveness of genotypes of *Helicobacter pylori* in Calcutta, India. J Bacteriol 182:3219–3227
13. Payne CM, Glasser L, Tischler ME, Wyckoff D, Cromey D, Fiederlein R, Bohnert O (1994) Programmed cell death of the normal human neutrophil: an in vitro model of senescence. Microsc Res Tech 28:327–344
14. Kroemer G, Galluzzi L, Vandenabeele P, Abrams J et al (2009) Classification of cell death: recommendations of the Nomenclature Committee on Cell Death 2009. Cell Death Differ 16:3–11
15. Humble JG, Jaynee WHM, Pulvertaft RJ (1956) Biological interaction between lymphocyte and other cells. Br J Hematol 2:283–294
16. Xia P, Wang S, Guo Z, Yao X (2008) Emperipolesis, entosis and beyond: dance with fate. Cell Res 18:705–707
17. Fiorentini C, Falzano L, Fabbri A, Stringaro A, Logozzi M, Travaglione S, Contamin S, Arancia G, Malorni W, Fais S (2001) Activation of rho GTPases by cytotoxic necrotizing factor 1 induces macropinocytosis and scavenging activity in epithelial cells. Mol Biol Cell 12:2061–2073
18. Zhou Z, Yu X (2008) Phagosome maturation during the removal of apoptotic cells: receptors lead the way. Trends Cell Biol 18:474–485
19. Caruso RA, Muda AO, Bersiga A, Rigoli L, Inferrera C (2002) Morphological evidence of neutrophil–tumor cell phagocytosis (cannibalism) in human gastric adenocarcinomas. Ultrastruct Pathol 26:315–321
20. Cappon A, Babolin C, Segat D et al (2010) *Helicobacter pylori*-derived neutrophil-activating protein increases the lifespan of monocytes and neutrophils. Cell Microbiol 12:754–764
21. Oldani A, Cormont M, Hofman V et al (2009) *Helicobacter pylori* counteracts the apoptotic action of its VacA toxin by injecting the CagA protein into gastric epithelial cells. PLoS Pathog 5:e1000603
22. Rugge M, Pennelli G, Pilozzi E, Fassan M et al (2011) Gastritis: the histology report. Dig Liver Dis 43(Suppl 4):S373–S384
23. Secka O, Antonio M, Berg DE, Tapgun M et al (2011) Mixed infection with cagA positive and cagA negative strains of *Helicobacter pylori* lowers disease burden in The Gambia. PLoS One 6:e27954

Virchows Arch (2012) 461:495–504
DOI 10.1007/s00428-012-1319-7

ORIGINAL ARTICLE

Serrated polyps of the colon: how reproducible is their classification?

Arzu Ensari · Banu Bilezikçi · Fatima Carneiro · Gülen Bülbül Doğusoy · Ann Driessen · Ayşe Dursun · Jean-François Flejou · Karel Geboes · Gert de Hertogh · Anne Jouret-Mourin · Cord Langner · Irıs D. Nagtegaal · Johan Offerhaus · Janina Orlowska · Ari Ristimäki · Julian Sanz-Ortega · Berna Savaş · Maria Sotiropoulou · Vincenzo Villanacci · Nazmiye Kurşun · Fred Bosman

Received: 2 May 2012 / Revised: 20 August 2012 / Accepted: 17 September 2012 / Published online: 6 October 2012
© Springer-Verlag Berlin Heidelberg 2012

Abstract For several years, the lack of consensus on definition, nomenclature, natural history, and biology of serrated polyps (SPs) of the colon has created considerable confusion among pathologists. According to the latest WHO classification, the family of SPs comprises hyperplastic polyps (HPs), sessile serrated adenomas/polyps (SSA/Ps), and traditional serrated adenomas (TSAs). The term SSA/P with dysplasia has replaced the category of mixed hyperplastic/adenomatous polyps (MPs). The present study aimed to evaluate the reproducibility of the diagnosis of SPs based

A. Ensari (✉) · B. Savaş
Department of Pathology, Ankara University Medical School, Sihhiye,
Ankara, Turkey
e-mail: ensariarzu@gmail.com

B. Bilezikçi
Department of Pathology, Ankara Guven Hospital,
Ankara, Turkey

F. Carneiro
Institute of Molecular Pathology and Immunology of the University of Porto (IPATIMUP),
Porto, Portugal

F. Carneiro
Medical Faculty and Centro Hospitalar São João,
Porto, Portugal

G. B. Doğusoy
Department of Pathology, Group Florence Nightingale Hospitals,
Istanbul, Turkey

A. Driessen
Department of Pathology, Maastricht University Medical Center,
Maastricht, The Netherlands

A. Dursun
Department of Pathology, Gazi Medical Faculty,
Ankara, Turkey

J.-F. Flejou
Department of Pathology, Saint-Antoine Hospital, AP-HP, Pierre et Marie Curie Medical School,
Paris, France

G. de Hertogh
Department of Pathology, KU Leuven,
Leuven, Belgium

K. Geboes
Universiteit Gent,
Ghent, Belgium

A. Jouret-Mourin
Department of Pathology, Cliniques Universitaires St Luc, UCL,
Brussels, Belgium

C. Langner
Institute of Pathology, Medical University of Graz,
8036, Graz, Austria

I. D. Nagtegaal
Department of Pathology,
Radboud University Nijmegen Medical Center,
Nijmegen, The Netherlands

J. Offerhaus
Department of Pathology, University Medical Center Utrecht,
H04.312, PB 85500, 3508 GA, Utrecht, The Netherlands

J. Orlowska
Department of Pathology, Maria Sklodowska-Curie Memorial Cancer Centre and Institute of Oncology,
Warsaw, Poland

A. Ristimäki
Department of Pathology, HUSLAB and Haartman Institute,
Helsinki University Central Hospital,
Helsinki, Finland

on currently available diagnostic criteria and interactive consensus development. In an initial round, H&E slides of 70 cases of SPs were circulated among participating pathologists across Europe. This round was followed by a consensus discussion on diagnostic criteria. A second round was performed on the same 70 cases using the revised criteria and definitions according to the recent WHO classification. Data were evaluated for inter-observer agreement using Kappa statistics. In the initial round, for the total of 70 cases, a fair overall kappa value of 0.318 was reached, while in the second round overall kappa value improved to moderate (kappa=0.557; $p<0.001$). Overall kappa values for each diagnostic category also significantly improved in the final round, reaching 0.977 for HP, 0.912 for SSA/P, and 0.845 for TSA ($p<0.001$). The diagnostic reproducibility of SPs improves when strictly defined, standardized diagnostic criteria adopted by consensus are applied.

Keywords Serrated polyp · Diagnosis · Criteria · Kappa statistics

Introduction

The term "serrated polyp" is used as a generic name for polyps demonstrating saw tooth-like infolding of the surface and crypt epithelium. The family of serrated polyps (SPs) comprises hyperplastic polyps (HPs), sessile serrated adenomas/polyps (SSA/Ps), and traditional serrated adenomas (TSAs) according to the latest WHO classification [1], in which the term "SSA/P with dysplasia" is preferred instead of the category of mixed hyperplastic/adenomatous polyps (MPs) [2]. The most common members of the SP family, HPs, comprise 80–90 % of all serrated polyps and are found throughout the colon and rectum, yet with distal predominance. Histologically, HPs are characterized by simple elongated crypt architecture and narrow crypt bases resembling normal mucosa, with proliferative activity confined to the basal third of the crypts [1, 3–6]. SSA/Ps, on the other hand, account for 8–20 % of serrated polyps with a predilection for the right colon. Their diagnosis is based mainly on crypt architectural features including serration, dilatation, horizontal orientation, L-shape or inverted T-form at the base of the crypts [1, 3–9], which furthermore show an asymmetrical proliferation zone and goblet cell or gastric foveolar cell differentiation [10]. The rarest type of SPs, TSA, has a protuberant growth pattern with a complex villiform configuration and premature crypt formation, defined as "ectopic crypt" [1, 5, 9, 11].

Lack of consensus in pathological diagnosis and classification in the past two decades resulted in publications in which polyps with almost identical morphology were reported with different diagnostic terms [12–15]. Hence, the molecular data that were created on the "serrated neoplasia" pathway have been rather inconsistent [16–21]. An accurate diagnosis of SPs is, therefore, crucial for a better understanding of the biology of the different entities, their specific molecular characteristics, and a better definition of the risk for malignant neoplasia that they incur. Only when this has been clarified can accurate risk assessment and adequate surveillance approaches be adopted. In daily practice, reproducibility of histopathological lesions in the serrated polyp family has been perceived as less than optimal [22–30]. We therefore designed a European study aiming to find answers to the following questions:

1. How reproducible are the diagnoses of serrated polyps?
2. What is the impact of a standardized classification (i.e., WHO classification) on diagnostic reproducibility?
3. Which criteria are used for diagnosis, how reproducible are they, and what is their discriminative value?

Materials and methods

Twenty European pathologists, all members of the Digestive Diseases Working Group of European Society of Pathology and all with special interest and experience in gastrointestinal pathology, were invited to participate in the study. Cases diagnosed as SPs (28 HPs, 25 SSA/Ps, 11 TSAs, and six MPs) in the original sign-outs were retrieved from the pathology archives of Ankara, Graz, and Warsaw. None of the features as size, location, or biopsy orientation was

A. Ristimäki
Genome-Scale Biology, Research Program Unit,
University of Helsinki,
Helsinki, Finland

J. Sanz-Ortega
Departamento de Anatomia Patologuca, Facultad de Medicina,
Universidad Complutense de Madrid, Instituto de Investigación
Sanitaria del Hospital Clínico San Carlos (IdISSC),
Madrid, Spain

M. Sotiropoulou
Department of Pathology, Alexandra Hospital,
Athens, Greece

V. Villanacci
Department of Pathology, Spedali Civili Brescia,
Brescia, Italy

N. Kurşun
Department of Biostatistics, Ankara University Medical School,
Ankara, Turkey

F. Bosman
University Institute of Pathology,
University of Lausanne Medical Center,
Lausanne, Switzerland

considered in the selection of cases in order to simulate a real-life experience for participating pathologists. Thus, the cases comprised a mixture of polyps with characteristic features and those with features hampering an ambiguous diagnosis. The aim was to assess the histological criteria and classification without any supportive information to avoid bias in morphological assessment. Consequently, the original sign-out diagnoses, size, and location of the polyps were not provided on the worksheet.

We used the definitions and diagnostic criteria available in the literature by 2008 [3–9] when the study was initiated, prior to the last edition of the WHO blue book [1]. Thus, diagnostic categories comprised of HP, SSA/P, TSA, and MP when a final diagnosis could be made, while a category of unclassified polyp (UCP) was used for a case for which a participant could not make a final diagnosis, e.g., due to inadequate sampling or poor orientation [31, 32]. Diagnostic categories are presented in Fig. 1. The participants were requested to provide a diagnosis and to indicate which of the nine categories of diagnostic criteria, comprising epithelial serration (surface/upper crypt/lower crypt), crypt dilatation (upper/lower crypt), crypt architectural changes (horizontal crypts, crypt branching, inverted crypts), mitotic activity (upper/lower crypt), mature goblet cell distribution (upper/lower crypt), gastric epithelium (lower crypt), nuclear features (hyperchromasia, elongation, pseudostratification, vesicular nucleus, prominent nucleolus), cytoplasmic eosinophilia, and dysplasia (low/high grade), were present in the lesion. The final diagnosis (HP, SSA/P, TSA, MP, or UCP) was determined according to the diagnoses made by the majority of participants for each case.

The study was designed to allow an assessment of diagnostic reproducibility before and after introduction of the latest WHO classification [1]. The initial round of observations included 20 pathologists and a total of 70 cases. To initiate this process, the group first evaluated 15 cases of SPs retrieved from the files of the Department of Pathology, Ankara University Medical School, including round table discussions based on the initial observations and focusing on diagnostic criteria and terminology in order to establish a common language and a standardized diagnostic approach. A further 55 cases were then provided by three centers (Ankara, Graz, and Warsaw) to allow in-depth analysis of reproducibility and diagnostic criteria on a total of 70 cases, permitting reliable Kappa analysis. Subsequent to the publication of the 4th edition of WHO Classification of Tumors of the Digestive System [1], the same group (four members could not participate, leaving a total of 16 assessors) reassessed the 70 case series using the WHO diagnostic categories and proposed criteria, which constituted the second round. The worksheets for the second round contained the initial diagnostic categories of HP, SSA/P, TSA, and MP in order to allow comparisons between the two rounds, but the participants were informed that the category of MP in their previous assessment corresponded to the new category of SSA/P with dysplasia, in line with the WHO classification. The participants were requested to diagnose such cases as SSA/P with dysplasia, including a qualification of the

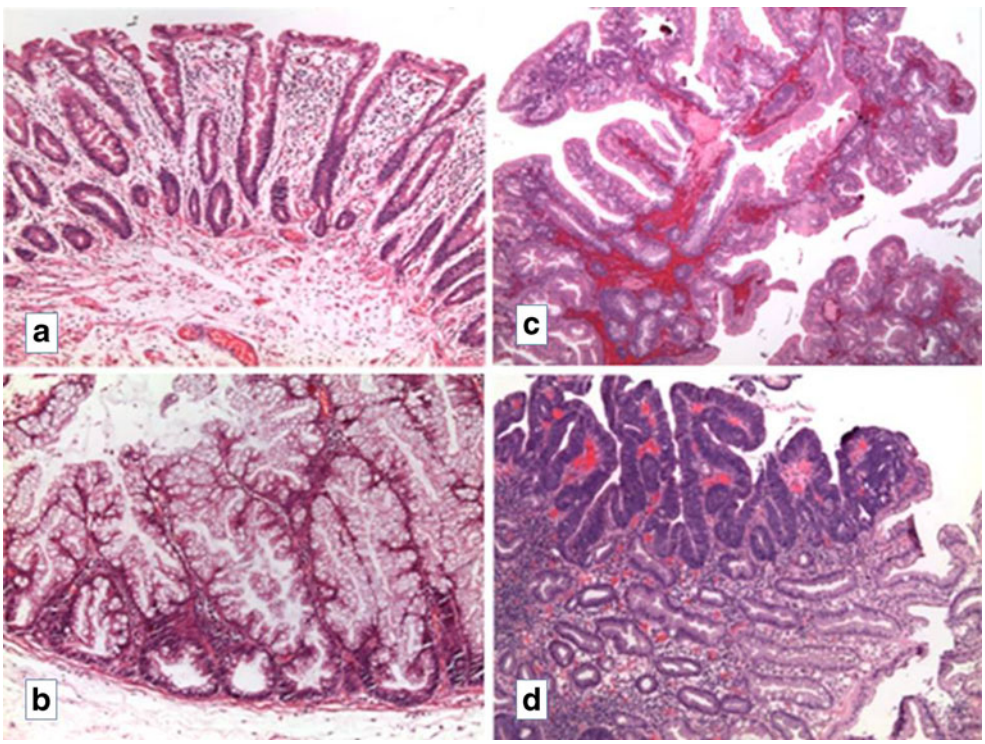

Fig. 1 SP categories including **a** HP (H&E, ×200), **b** SSA/P (H&E, ×200), **c** TSA (H&E, ×100), and **d** MP (H&E, ×100)

degree of dysplasia (low or high grade). Dysplasia was not further classified as adenomatous or serrated, although nuclear features comprising hyperchromasia, elongation, and pseudostratification are considered as diagnostic for "adenomatous" dysplasia, while vesicular nucleus, prominent nucleolus, and cytoplasmic eosinophilia are indicative of "serrated" dysplasia according to the WHO [1].

To define the most reproducible and discriminative criteria for each diagnostic category of SPs, all participants registered on the excel sheets as to which of the predefined diagnostic criteria they regarded as the most relevant.

Statistical analysis

Kappa statistics was performed in the Department of Biostatistics, Ankara University Medical School, by the same biostatistician (NK) for each round using SPSS for Windows 15.0 for paired (between two observers) and overall (group) inter-observer agreement and for intra-observer agreement. Comparisons between the initial and the second round were assessed using the Wilcoxon signed ranks tests. Analysis of the criteria was performed using chi-square tests and by means of proportions of positive judgements method for agreement levels [33]. Kappa values were grouped as poor (<0.2), fair (0.21–0.40), moderate (0.41–0.60), good (0.61–0.80), and perfect (>0.80). A p value less than 0.05 was considered as significant.

Results

Initial round: how reproducible are the diagnoses of SPs?

In the initial round, 44 % (n=31) of the 70 cases were diagnosed as HP, 40 % (n=28) as SSA/P, 10 % (n=7) as TSA, and 6 % (n=4) as MP by the majority of the observers.

The overall kappa value for the first 15 cases was poor with a kappa value of 0.202 (CI lower 0.147–CI upper 0.256; p<0.001), while overall kappa values for each diagnostic category were 0.315 for HP, 0.223 for SSA/P, 0.181 for TSA (p<0.001), and 0.107 for MP (p>0.05).

Following consensus discussions, on the additional 55 cases a fair inter-observer agreement was achieved with an overall kappa value of 0.349 (CI lower 0.320–CI upper 0.377; p<0.001). Kappa values for each diagnostic category were 0.443 for HP, 0.323 for SSA/P, 0.512 for TSA (p< 0.001), and 0.235 for MP (p=0.01), respectively.

Finally, on the full 70-case set, a fair overall kappa of 0.318 (CI lower 0.293–CI upper 0.343; p<0.001) was reached; also, for each diagnostic category, kappa values were fair, reaching to 0.415 for HP, 0.301 for SSA/P, 0.433 for TSA (p<0.001), and 0.221 for MP (p=0.01).

Second round: the impact of WHO classification on reproducibility

In the second round, a re-evaluation of all 70 cases was performed by 16 of the initial 20 participants using WHO criteria. A diagnosis of HP was made on 43 % (n=30), SSA/P on 46 % (n=32), TSA in 10 % (n=7), and MP on 1 % (n=1) of the cases. One HP was diagnosed as SSA/P and three MPs as SSA/P with dysplasia, while the diagnoses of 30 HPs, 28 SSA/Ps, seven TSAs, and one MP remained unchanged (Fig. 1d). No case was classified as UCP by the majority in either round, but 49 % (n=33) of the cases received this diagnosis from between one to three observers.

Overall kappa value was moderate (kappa=0.557; CI lower 0.532–CI upper 0.612, p<0.001), while kappa values were significantly higher than the previous observations for each diagnostic category: 0.977 for HP, 0.912 for SSA/P, 0.845 for TSA, and 0.158 for MP (p<0.001). Paired and overall agreements for all rounds and diagnostic categories are summarized in Table 1.

Intra-observer agreement for each diagnostic category was evaluated with respect to the initial and final rounds of assessments made by each of the 16 observers for the total of 70 cases. Kappa values ranged between 0.013 and 1.00 (Table 2). The overall agreement between the initial and second round of diagnoses for all cases was 0.79 (p< 0.0001), while the kappa value was 0.855 for HP, 0.767 for SSA/P, 0.841 for TSA, and 0.386 for MP (p<0.001). Kappa analysis was not performed for UCP as this cannot be considered as a diagnostic category. Examples of cases which were renamed after the final round are presented in Fig. 2.

How reproducible and discriminative are the histologic criteria?

Firstly, the analysis of histological criteria revealed perfect and near-perfect agreement on epithelial serration in the upper crypts (kappa=0.97), serration of the surface epithelium (kappa=0.83), mitosis in the lower crypts (kappa= 0.79), goblet cells in the upper crypts (kappa=0.77), and dilatation of upper crypts (kappa=0.72) in contrast to crypt architectural features, which yielded fair to moderate agreement and to nuclear features that resulted in only fair agreement between the observers (Table 3).

Secondly, the association of the criteria to each diagnostic category was analyzed by recording the frequencies of the criteria selected by the observers for each diagnostic category in every case using proportions of positive judgements method [33]. The presence of dilatation, mature goblet cells in upper crypts (p=0.01), and epithelial serration (p<0.05) were significantly associated with a diagnosis of HP, while epithelial serration, crypt dilatation, presence of mature

Table 1 Paired and overall agreement for all cases and for each diagnostic category

	All cases	HP	SSA	TSA	MP
Initial round (total, n=70)					
Overall kappa	0.318	0.415	0.301	0.433	0.221
Paired kappa (min–max)	0.03–0.93	0.08–0.75	0.05–0.82	0.09–0.93	0.03–0.88
p value	<0.001	<0.001	<0.001	<0. 001	0.014
Second round (total, n=70)					
Overall kappa	0.557	0.977	0.912	0.845	0.158
Paired kappa (min–max)	0.09–1.00	0.11–1.00	0.09–1.00	0.21–1.00	0.09–1.00
p value	<0.001	<0.001	<0.001	<0.001	0.014

goblet cells in lower crypts (p<0.001), crypt architectural changes (p<0.001), vesicular nucleus (p<0.001), and prominent nucleolus (p<0.01) were significantly associated with a diagnosis of SSA/P. TSA, on the other hand, was determined by the presence of epithelial serration in lower crypts (p< 0.001), mitotic activity in upper crypts (p<0.001), nuclear features of atypia (p<0.001), cytoplasmic eosinophilia (p< 0.001), presence of low-grade dysplasia (p<0.001), crypt branching (p<0.01), ectopic crypts (p<0.05), and gastric epithelium in lower crypts (p<0.05) (Table 4). Most discriminatory criteria for each diagnostic category are presented in Fig. 3. Low-grade dysplasia was diagnosed in 3.2 % of HP, 24.4 % of SSA/P, 81.3 % of TSA, 22.4 % of MP, and 27.3 % of UCP, while high-grade dysplasia was found in 2.2 % of SSA/P, 3.1 % of TSA, 22.5 % of MP, and 5.5 % of UCP. Among SSA/Ps with dysplasia, 69.8 % showed "serrated" dysplasia, while 30.2 % had "adenomatous" dysplasia as determined by the associated cytological features. Adenomatous dysplasia was more frequent in TSAs (59.7 %) in comparison to "serrated" dysplasia (40.3 %), similar to MPs of which 26.1 % had "adenomatous" and 17.96 % had "serrated" dysplasia.

Table 2 Intra-observer agreement between the initial and final rounds of assessments on 70 cases

Observer	HP	SSA/P	TSA	MP
1	0.550[a]	0.573[a]	0.297[b]	1.00[c]
2	0.826[c]	0.750[d]	0.628[d]	0.665[d]
3	0.492[a]	0.295[b]	0.716[d]	–
4	0.424[a]	0.378[b]	0.237[b]	–
5	0.672[d]	0.746[d]	0.530[a]	0.203[e]
6	1.00[c]	1.00[c]	1.00[c]	1.00[c]
7	0.453[a]	0.557[a]	0.480[a]	0.800[d]
8	0.659[d]	0.621[d]	0.925[c]	0.549[a]
9	0.632[d]	0.465[a]	0.497[a]	0.379[b]
10	0.909[c]	0.857[c]	0.873[c]	1.00[c]
11	0.013[e]	0.287[b]	0.156[e]	0.071[e]
12	0.733[d]	0.576[a]	0.647[d]	0.488[a]
13	0.726[d]	0.549[a]	0.573[a]	–
14	0.603[a]	0.627[d]	0.056[e]	–
15	0.672[d]	0.746[d]	0.531[a]	0.245[b]
16	0.822[c]	0.793[d]	1.00[c]	1.00[c]

[a] Moderate
[b] Fair
[c] Perfect
[d] Good
[e] Poor

Discussion

This study presents a European initiative aiming to improve the reproducibility of histological diagnoses of SPs. The poor overall inter-observer agreement for 15 cases studied initially led us to repeat the assessment after a consensus discussion on 70 cases, which improved the agreement from poor to fair, highlighting the significance of a standardized approach supported by a consensus discussion.

Introduction of the WHO classification through a second consensus meeting led to a further improvement in overall agreement for the whole group, and perfect agreement was achieved for the categories HP, SSA/P, and TSA.

Few studies [22–30] have addressed the question of reproducibility in the diagnosis of SPs (Table 5). Those that evaluated inter-observer agreement had a major drawback as they used the term "serrated adenoma" for all serrated polyps except HP, possibly due to the poorly defined criteria to distinguish SSA from TSA, available at time of publication [22, 24]. However, Farris et al. [23], in an approach similar to ours, evaluated the diagnostic concordance of five GI pathologists on 185 SPs comprising 92 HPs, 74 SSAs, and 19 TSAs. The observers were provided with a list of criteria for SSA and TSA in the first round, which revealed moderate overall agreement, while clinical information including size and localization of the polyps caused no change on the level of agreement in the second round. Following a consensus conference, the agreement was evaluated on a different but smaller series and revealed moderate agreement for HP and SSA and near-perfect agreement for TSA. Their

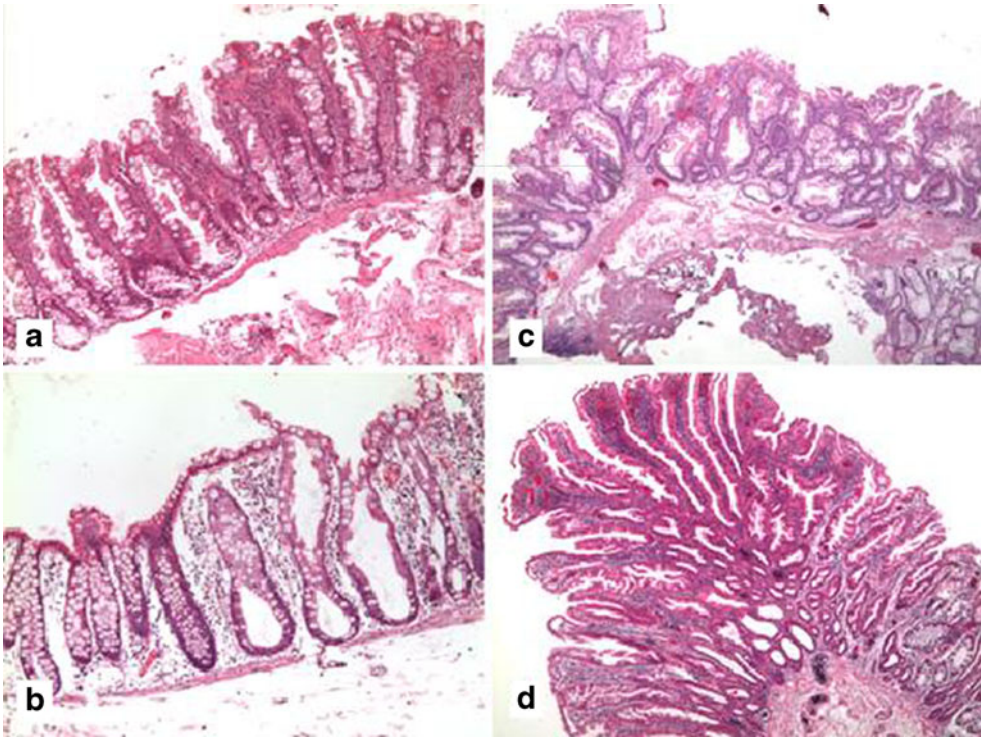

Fig. 2 Examples of cases which were renamed after the final round. **a** HP renamed as SSA/P (H&E, ×200), **b** HP renamed as SSA/P (H&E, ×200), **c** SSA/P renamed as TSA (H&E, ×100), **d** MP renamed as SSA/P with dysplasia (H&E, ×100)

study design is similar to ours with respect to the consecutive rounds of evaluation followed by consensus discussions to achieve the best possible agreement between the observers. In contrast to our study, they did not evaluate the reproducibility of the diagnostic criteria.

Table 3 Agreement of observers for diagnostic criteria

Diagnostic criteria	Kappa value
Epithelial serration in upper crypts	0.9661
Surface epithelial serration	0.8328
Mitosis in lower crypts	0.7928
Goblet cells in upper crypts	0.7666
Dilatation in upper crypts	0.7189
Dilatation in lower crypts	0.5658
Goblet cells in lower crypts	0.4841
Epithelial serration in lower crypts	0.4307
Crypt branching	0.4165
Nuclear elongation	0.3780
Nuclear pseudostratification	0.3719
Horizontal crypts	0.3671
Nuclear hyperchromasia	0.3553
Cytoplasmic eosinophilia	0.3370
Prominent nucleolus	0.3258
Vesicular nucleus	0.3217
Dysplasia—low grade	0.2631
Mitosis in upper crypts	0.2533
Ectopic crypts	0.2104
Gastric epithelium in lower crypts	0.2044
Inverted crypts	0.1745
Dysplasia—high grade	0.0405

Our study was conducted in a blind fashion regarding the size and localization of the polyps in order to analyze the morphological criteria in a more stringent way, devoid of any bias. It is, on the other hand, generally accepted that diagnosis of polyps with intermediate features that lie on a continuum between HP and SSA/P may require clinical information, and for such polyps, pathologists may be more inclined to make a diagnosis of SSA/P when the polyp is large and localized in the right colon. However, additional clinical information failed to have any effect on the diagnostic accuracy of the observers in two previous studies [23, 27]. We believe that the histopathological diagnosis of a polyp should not depend upon the size or the localization of the lesion. However, for unclassified non-dysplastic serrated polyps with intermediate features or in case of sampling error, pathologists need to know the size and localization of the lesion before making a diagnosis. Although a diagnosis of serrated polyp "unclassified" is recommended by WHO [1], improvement in our diagnostic skills together with the use of standardized criteria will help to better classify such borderline cases and avoid unnecessary utilization of the unclassified category.

The third issue that was raised by the initiative was to define the most reproducible and discriminative criteria for each type of serrated polyp. Although many publications utilize similar criteria in the diagnosis of SPs, there are considerable variations in histologic features as well as

Table 4 Diagnostic criteria discriminative for each SP category

Criteria	HP (%)	SSA/P (%)	TSA (%)	MP (%)
Epithelial serration				
Upper crypt	98.8*	95.75	94.05	99.5
Lower crypt	25.0	70.1***	64.2***	43.4
Dilatation				
Upper crypt	64.8*	72.2	69.6	81.9
Lower crypt	23.5	88.75***	62.55	77.5
Architectural features				
Horizontal crypts	4.0	67.5***	31.4	40.5
Crypt branching	8.5	62.95***	52.3**	66.4
Inverted crypts	7.0	24.8	11.6	14.5
Ectopic crypts	4.0	20.05	88.6 *	12.8
Mitosis				
Upper crypt	5.0	18.15	63.8***	43.45
Lower crypt	68.15	78.4	77.3	79.5
Mature goblet cell				
Upper crypt	77.4**	76.85	71.55	82.4
Lower crypt	40.1	57.7 ***	38.2	63.45
Gastric epithelium	14.4	22.15	22.0 *	25.8
Nuclear features				
Hyperchromasia	18.0	39.0	83.6***	76.2***
Elongation	11.1	42.35	86.85***	83.25***
Pseudostratification	17.5	40.6	90.85***	88.5***
Vesicular nucleus	18.1	43.7***	45.4	53.4
Prominent nucleolus	21.5	45.45***	67.2	64.7
Cytoplasmic eosinophilia	10.3	23.25	78.35***	46.8
Dysplasia				
Low grade	3.3	24.45	81.85***	72.4***
High grade	0	1.56	3.1	22.55**

*$p \leq 0.05$; **$p \leq 0.01$; ***$p \leq 0.001$

definitions and terminology in many others, particularly for SSA/P [4, 10, 18]. The first approach of standardization came from Bariol et al. [22], who evaluated the diagnostic utility of histologic criteria attributed to serrated adenomas in a series of cases including hyperplastic polyps, serrated adenomas, admixed polyps, and conventional adenomas. In their study, surface epithelial dysplasia, surface epithelial tufting, increased surface mitosis, and epithelial serration in more than 20–50 % of crypts were the criteria with the highest kappa values for the diagnosis of serrated adenoma. They did not, however, assess how consistently different observers could distinguish serrated adenoma from other polyps, nor did they further classify their cases as sessile and traditional serrated adenomas.

In a more recent attempt to distinguish HP from SSA, Sandmeier and colleagues [27] assessed 102 SPs and tested the reproducibility of Snover's criteria [5]. They, too, blinded the observers to the clinical information in order to avoid any bias in the histopathological interpretation. As in our study, they found architectural changes together with the various cell types including goblet cells, undifferentiated cells, and gastric foveolar cells in basal crypts to be the most useful criteria to distinguish SSA from HP. Also, Farris et al. [23] concluded that architectural rather than cytological features are most helpful in distinguishing SSA from HP, whereas cytological features like nuclear elongation and stratification are more useful in distinguishing TSA from other serrated lesions. Of the WHO criteria, the most discriminatory for HP were serration, dilatation, and presence of mature goblet cells in the upper crypts, whereas the presence of these features in the lower crypt zone was significantly consistent with a diagnosis of SSA/P together with the architectural features, such as horizontal crypts and crypt branching, and nuclear features, including vesicular nucleus and prominent nucleolus. TSA, on the other hand, was associated with ectopic crypts and crypt branching as well as nuclear features comprising hyperchromasia, elongation, pseudostratification, and cytoplasmic eosinophilia. These findings confirm that architectural rather than cytologic features are diagnostically useful and also that nuclear features are more reproducible than architectural criteria.

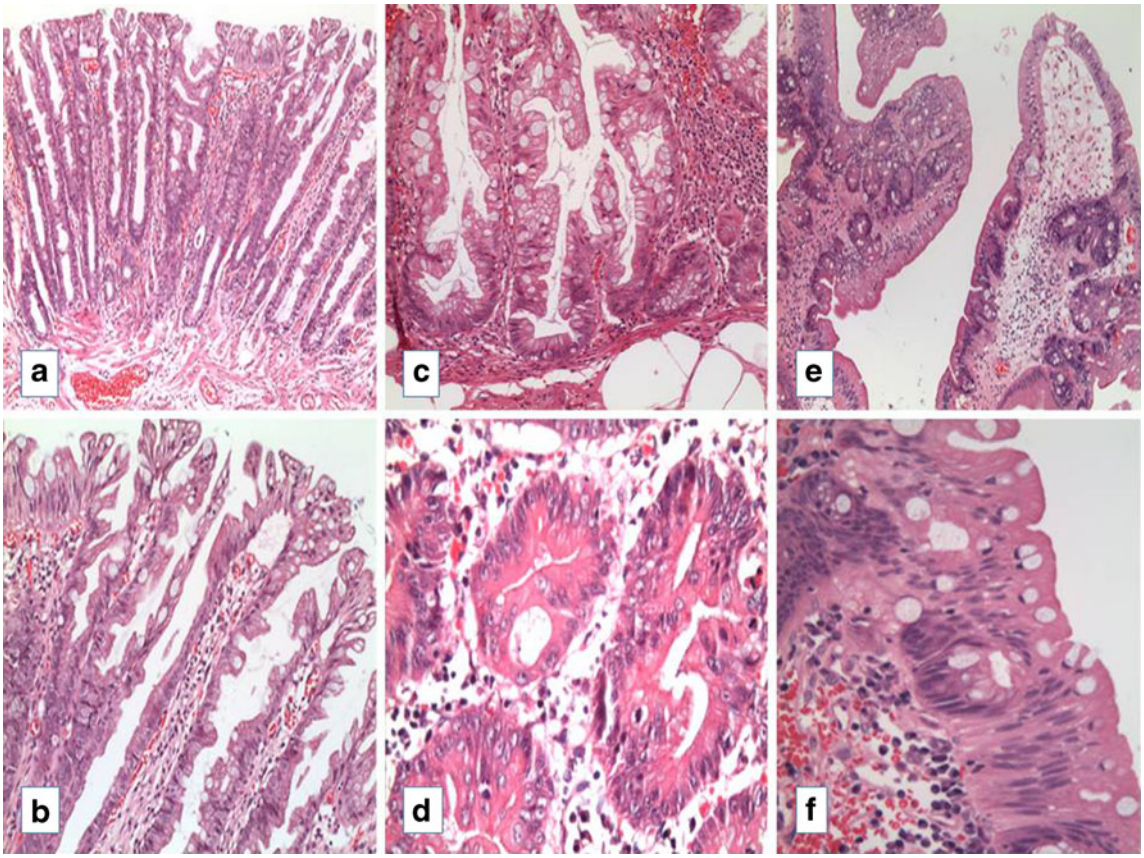

Fig. 3 Most discriminatory criteria for each diagnostic category. **a**, **b** Serration, dilatation, and mature goblet cells in upper crypts in HP (H&E, ×100 and×200, respectively). **c**, **d** Serration, dilatation, horizontal shape in lower crypts and vesicular nuclei with nucleoli in SSA/P (H&E, ×200 and×400, respectively). **e**, **f** Ectopic crypts, cytoplasmic eosinophilia, pseudostratification, nuclear elongation and hyperchromasia in TSA (H&E, ×100 and×400, respectively)

On similar grounds, the Working Group on Gastrointestinal Pathology of the German Society of Pathology [34] proposed that the SSA/P architectural features should be present in at least two different crypts, not necessarily adjacent, although the new WHO definition of SSA/P requires two or three contiguous crypts with these features [1]. There is no evidence base for either view, but it is safe to postulate that several crypts close together should be a

Table 5 Summary of publications on reproducibility of the diagnoses of SPs

Publication (reference number)	Cases	Results
Bariol et al. 2003 [22]	255 polyps (72 HPs, 9 SAs, 4 MPs, 170 conventional adenomas), 2 observers	Kappa for diagnostic criteria ranging from −0.029 to 0.852
Sandmeier et al. 2007 [27]	102 SPs (58 HPs, 7 SSAs, 5 TSAs, 3 MPs, 29 UCPs)	Criteria for HP vs. SSA, no kappa
Glatz et al. 2007 [26]	20 SPs (8HPs, 4 TSAs, 4 SSAs, 4 tubulovillous adenomas), 168 participants (Internet-based quiz)	High variation in SSA, no kappa
Farris et al. 2008 [23]	185 SPs (92 HPs, 74 SSAs, 19 TSAs), 5 observers	Kappa=0.55
Bustamente-Balen et al. 2009 [28]	195 SPs (187 HPs, 8 SAs), 2 observers	Kappa=0.14
Wong et al. 2009 [24]	60 polyps (26 SAs, 11 HPs, 6 MPs, 12 conventional adenomas, 5 other polyps), 4 observers	Kappa=0.38
Khalid et al. 2009 [25]	40 SPs (comprised of HPs and SSAs and all originally diagnosed HPs), 3 observers	Kappa=0.16
Gunia et al. 2011 [29]	19 SPs (8 SSAs, 3 TSAs, 8 inflammatory polyps), 3 observers/trainees	Kappa=0.29–0.65
Present study	70 SPs (28 HPs, 25 SSA/Ps, 11 TSAs, 6 MPs)	Kappa=0.557, 0.977 for HP, 0.912 for SSA/P, and 0.845 for TSA

minimal criterium, which was however not assessed in our study.

Two types of dysplasia have been observed in SSA/Ps: "adenomatous" dysplasia and "serrated" dysplasia, the latter characterized by round cells with eosinophilic cytoplasm, vesicular nuclei, and prominent nucleoli [1, 20, 35]. SSA/Ps with dysplasia were probably classified as "mixed polyps" in the past [2, 5, 6, 32, 36], a term used for lesions with distinct foci of adenomatous epithelium and hyperplastic/serrated architecture. WHO [1] recommends the term "SSA/P with dysplasia" in order to emphasize that the dysplastic part of the lesion never shows APC mutations as found in adenomatous epithelium but rather presents with MSI resulting from methylation of MLH-1. In our study, a small number of cases, almost half of which showed dysplastic foci, were diagnosed as MP in the first round, whereas a diagnosis of SSA/P with high-grade dysplasia was made for these cases in the second round. Surprisingly, however, there was one particular case which was persistently diagnosed as MP in both rounds by the majority of the participants who apparently felt that dysplastic SSA/P category does not always coincide with polyps showing truly and distinctly mixed features. For the latter ones, a category of MP would seem legitimate.

In the present study, although dysplasia was graded as low and high without further classification into adenomatous or serrated types, the histological criteria used in the study already comprised features of serrated dysplasia such as vesicular nuclei, prominent nucleoli, and eosinophilic cytoplasm, as well as features of adenomatous dysplasia characterized by pseudostratification, nuclear byperchromasia, and elongation [1]. An evaluation of these criteria demonstrated that the majority of SSA/Ps possessed features of "serrated" dysplasia. Although their original description involves dysplastic epithelium, TSAs lack mitotic activity in the tall columnar epithelial cells with pencillate nuclei and eosinophilic cytoplasm and are therefore not truly dysplastic in the sense of tubular or villous adenomas [1]. The high rate of low-grade dysplasia in the TSA group suggests that the epithelial lining of TSAs was misinterpreted as low-grade dysplastic by the majority of the observers due to its resemblance to adenomatous epithelium. The low-grade dysplasia observed in a small percentage of HPs seems to correspond with a mucin-poor variant of HP presenting with regenerative epithelium that can be misinterpreted as dysplasia.

In conclusion, the results of the study show that consensus discussions on a sufficiently large SP collection improve inter-observer agreement, which was further improved when the new WHO classification was introduced. Furthermore, architectural criteria appear as most reliable for an accurate diagnosis of a SP. However, even when a consensus classification such as that provided by the WHO is applied, the reproducibility of the histopathological diagnosis on a SP remains imperfect.

Conflict of interest The authors declare that they have no conflict of interest.

References

1. Snover DC, Ahnen DJ, Burt RW, Odze RD (2010) Serrated polyps of the colon and rectum and serrated polyposis. In: Bosman FT, Carneiro F, Hruban RH, Theise ND (eds) WHO classification of tumours of the digestive system, 4th edn. IARC, Lyon, pp 160–165
2. Longacre TA, Fenoglio-Preiser CM (1990) Mixed hyperplastic adenomatous polyps/serrated adenomas. A distinct form of colorectal neoplasia. Am J Surg Pathol 14:524–537
3. Torlakovic E, Skovlund E, Snover DC, Torlakovic G, Nesland JM (2003) Morphologic reappraisal of serrated colorectal polyps. Am J Surg Pathol 27:65–81
4. Higuchi T, Sugihara K, Jass JR (2005) Demographic and pathological characteristics of serrated polyps of colorectum. Histopathology 47:32–40
5. Snover DC, Jass JR, Fenoglio-Preiser C, Batts KP (2005) Serrated polyps of the large intestine: a morphologic and molecular review of an evolving concept. Am J Clin Pathol 124:380–391
6. Cunningham KS, Riddell RH (2006) Serrated mucosal lesions of the colorectum. Curr Opin Gastroenterol 22:48–53
7. Goldstein NS (2006) Serrated pathway and APC (conventional)-type colorectal polyps: molecular–morphologic correlations, genetic pathways, and implications for classification. Am J Clin Pathol 125:146–153
8. Torlakovic E, Snover DC (2006) Sessile serrated adenoma: a brief history and current status. Crit Rev Oncog 12:27–39
9. Torlakovic EE, Gomez JD, Driman DK et al (2008) Sessile serrated adenoma (SSA) vs. traditional serrated adenoma (TSA). Am J Surg Pathol 32:21–29
10. Hirano H, Ajioka Y, Watanabe H et al (2004) Bidirectional gastric differentiation in cellular mucin phenotype (foveolar and pyloric) in serrated adenoma and hyperplastic polyp of the colorectum. Pathol Int 54:401–407
11. Noffsinger AE (2009) Serrated polyps and colorectal cancer: new pathway to malignancy. Annu Rev Pathol 4:343–364
12. Goldstein NS, Bhanot P, Odish E, Hunter S (2003) Hyperplastic-like colon polyps that preceded microsatellite-unstable adenocarcinomas. Am J Clin Pathol 119:778–796
13. Hirono H, Ajioka Y, Watanabe H, Baba Y, Tozawa E, Nishikura K, Mukai G, Honma T, Aoyagi Y (2004) Bidirectional gastric differentiation in cellular mucin phenotype (foveolar and pyloric) in serrated adenoma and hyperplastic polyp of the colorectum. Pathol Int 54:401–407
14. Li SC, Burgart L (2007) Histopathology of serrated adenoma, its variants, and differentiation from conventional adenomatous and hyperplastic polyps. Arch Pathol Lab Med 131:440–445
15. Bauer VP, Papaconstantinou HT (2008) Management of serrated adenomas and hyperplastic polyps. Clin Colon Rectal Surg 21:273–279
16. Jass JR, Young J, Leggett BA (2000) Hyperplastic polyps and DNA microsatellite unstable cancers of the colorectum. Histopathology 37:295–301
17. Jass JR, Young J, Leggett BA (2002) Evolution of colorectal cancer: change of pace and change of direction. J Gastroenterol Hepatol 17:17–26
18. Jass JR (2005) Serrated adenoma of the colorectum and the DNA-methylator phenotype. Nat Clin Pract Oncol 2:398–405
19. O'Brien MJ, Yang S, Mack C et al (2006) Comparison of microsatellite instability, CpG island methylation phenotype, BRAF and KRAS status in serrated polyps and traditional adenomas indicates

separate pathways to distinct colorectal carcinoma end points. Am J Surg Pathol 30:1491–1501
20. Goldstein NS (2006) Small colonic microsatellite unstable adenocarcinomas and high-grade epithelial dysplasias in sessile serrated adenoma polypectomy specimens: a study of eight cases. Am J Clin Pathol 125:132–145
21. Jass JR (2007) Classification of colorectal cancer based on correlation of clinical, morphological and molecular features. Histopathology 50:113–130
22. Bariol C, Hawkins NJ, Turner JJ, Meagher AP, Williams DB, Ward RL (2003) Histopathological and clinical evaluation of serrated adenomas of the colon and rectum. Mod Pathol 16(5):417–423
23. Farris AB, Misdraji J, Srivastava A, Muzikansky A, Desphande V, Lauwers GY, Mino-Kenudson M (2008) Sessile serrated adenoma. Challenging discrimination from other serrated colonic polyps. Am J Surg Pathol 32:30–35
24. Wong NACS, Hunt LP, Novelli MR, Shepard NA, Warren BF (2009) Observer agreement in the diagnosis of serrated polyps of the large bowel. Histopathology 55:63–66
25. Khalid O, Radaideh S, Cummings OW, O'Brien MJ, Goldblum JR, Rex DK (2009) Reinterpretation of histology of proximal colon polyps called hyperplastic in 2001. World J Gastroenterol 15:3767–3770
26. Glatz K, Pritt B, Glatz D, Harmann A, O'Brien MJ, Blaszyk H (2007) A multinational, internet-based assessment of observer variability in the diagnosis of serrated colorectal polyps. Am J Clin Pathol 127:938–945
27. Sandmeier D, Seelentag W, Bouzourene H (2007) Serrated polyps of the colorectum: is sessile serrated adenoma distinguishable from hyperplastic polyp in daily practice? Virchows Arch 450:613–618
28. Bustamente-Balen M, Bernet L, Cano R, Morell L, Lopez A (2009) Assessing the reproducibility of the microscopic diagnosis of sessile serrated adenoma of the colon. Rev Esp Enferm Dig (Madrid) 101:258–264
29. Gunia S, Berg T, Gradhand E, Becker S (2011) Knowledge of the anatomical polyp location might bias the pathological classification of histologically equivocal colorectal serrated polyps—a consensus study performed by pathology trainees. Path Res Pract 207:116–120
30. Denis B, Peters C, Chapelain C, Kleinclaus I, Fricker A, Wild R, Auge B, Gendre I, Perrin P, Chatelain D, Flejou JF (2009) Diagnostic accuracy of community pathologists in the interpretation of colorectal polyps. Eur J Gastroenterol Hepatol 21:1153–1160
31. Chung SM, Chen YT, Panczykowski A, Schamberg N, Klimstra DS, Yantiss RK (2008) Serrated polyps with "intermediate features" of sessile serrated polyp and microvesicular hyperplastic polyp: a practical approach to the classification of nondysplastic serrated polyps. Am J Surg Pathol 32:407–412
32. Ensari A, Bosman FT, Offerhaus GJA (2010) The serrated polyp: getting it right! J Clin Pathol 63:665–668
33. Landis JR, Koch GG (1977) The measurement of observer agreement for categorical data. Biometrics 33:159–174
34. Aust DE, Baretton GB (2010) Serrated polyps of the colon and rectum (hyperplastic polyps, sessile serrated adenomas, traditional serrated adenomas, and mixed polyps)—proposal for diagnostic criteria. Virchows Arch 457:291–297
35. Sheridan TB, Fenton H, Lewin MR et al (2006) Sessile serrated adenomas with low- and high-grade dysplasia and early carcinomas: an immunohistochemical study of serrated lesions "caught in the act". Am J Clin Pathol 126:564–571
36. Hamilton SR, Vogelstein B, Kudo S et al (2000) Carcinoma of the colon and rectum. In: Hamilton SR, Aaltonen IA (eds) Tumours of the digestive system. WHO classification of tumours. IARC, Lyon, pp 113–114

Virchows Arch (2012) 461:505–512
DOI 10.1007/s00428-012-1296-x

ORIGINAL ARTICLE

A combination of smears and cell block preparations provides high diagnostic accuracy for endobronchial ultrasound-guided transbronchial needle aspiration

Guillaume Gauchotte · Jean-Michel Vignaud · Olivier Ménard · Marie-Pierre Wissler · Yves Martinet · Joëlle Siat · Christophe Paris · Christelle Clément-Duchêne

Received: 28 May 2012 / Revised: 20 July 2012 / Accepted: 1 August 2012 / Published online: 16 August 2012
© Springer-Verlag 2012

Abstract Endobronchial ultrasound-guided transbronchial needle aspiration has demonstrated its accuracy in the diagnostic workup of enlarged mediastinal lymph nodes. In addition to conventional smears, the use of liquid-based cytology (LBC) and cell block preparations (CBP) has been introduced more recently. The aim of our study was to determine the performance of each of the different techniques, separately and combined, in terms of diagnostic yield and sensitivity. A total of 290 consecutive patients were included. The pathological examination was based on smear cytology, LBC, and CBP. Adequate sampling was defined by the presence of pathological material or lymphocytes. The global diagnostic yield was 82.7 % and the sensitivity was 89.1 %. The diagnostic yield was 72.8 % for smears, 78.8 % for LBC, and 69.9 % for CBP. The combination of smears with CBP significantly increased diagnostic yield (p=0.01) and sensitivity (p=0.006), but not the combination of smears with LBC (yield: p=0.07; sensitivity: p=0.13). The combination of the three techniques further increased yield (p=0.007) and sensitivity (p=0.006), compared with smears alone. CBP were more sensitive than smears for both diagnoses of carcinoma (p=0.01) and granulomatous inflammation (p=0.048). Conversely, LBC was less sensitive than smears for granulomatous inflammation (p=0.004), but the difference was not significant for carcinoma (p=0.42). CBP, as a complement to smears, increases diagnostic yield and sensitivity for both diagnoses of carcinoma and granulomatous inflammation. LBC, if used alone, increases the risk of a false-negative result.

Keywords Endobronchial ultrasound-guided transbronchial needle aspiration · Transbronchial needle aspiration · Cytology · Cell block · Sarcoidosis · Lung cancer · Mediastinal lymph node

G. Gauchotte · J.-M. Vignaud · M.-P. Wissler
Department of Pathology, CHU Nancy,
Nancy, France

G. Gauchotte · J.-M. Vignaud · C. Paris · C. Clément-Duchêne
Faculty of Medicine, INSERM U954,
Nancy, France

O. Ménard · Y. Martinet · C. Clément-Duchêne
Department of Respiratory Diseases, CHU Nancy,
Nancy, France

J. Siat
Department of Thoracic Surgery, CHU Nancy,
Nancy, France

C. Paris
Department of Occupational Diseases, CHU Nancy,
Nancy, France

G. Gauchotte (✉)
Service d'Anatomie et Cytologie Pathologiques, Hôpital Central,
CHU de Nancy,
29, avenue du Maréchal De Lattre de Tassigny,
54000 Nancy, France
e-mail: g.gauchotte@chu-nancy.fr

Introduction

Lung cancer is the leading cause of cancer death in France with a 5-year survival rate of 15 %. Only 20 % of cases of lung cancers benefit from curative surgical treatment. Precise staging has great importance to decide the best therapeutic strategy. Mediastinoscopy [1] has been the gold standard for a long time in the diagnosis of enlarged mediastinal lymph nodes but explores a limited number of lymph node stations. More recently, endobronchial ultrasound-guided transbronchial needle aspiration (EBUS-TBNA) has demonstrated its usefulness in the diagnosis of benign

as well as malignant mediastinal or hilar lymph nodes and in lung cancer staging [2–6].

EBUS-TBNA is an accurate, minimally invasive, and cost-effective method for the diagnosis of mediastinal or hilar adenopathy and staging in lung cancer [7]. It has been shown to be equivalent to classical mediastinal biopsy [8], with a sensitivity ranging from 81 % to 98 % [7–9]. The specimens collected during EBUS-TBNA were classically limited to conventional smears, providing good inter-observer reproducibility [6]. Liquid-based cytology (LBC) was reported as a promising alternative to conventional cytology [10]. With the EBUS-TBNA method, small tissue cores can also be obtained. These fragments are paraffin-embedded and analyzed on cell block preparations (CBP). An efficient analysis can be carried out using this method, conserving histological architecture and allowing immunohistochemical and molecular analysis [10, 11].

We hypothesized that combining smears, LBC, and CBP would improve the sensitivity of EBUS-TBNA. The aim of this study was therefore to determine the performance of each of the different techniques (smears, LBC, and CBP), separately and combined, in terms of yield and sensitivity.

Methods

Patients

Between July 2009 and July 2011, 290 consecutive patients were included in the study at the Respiratory Department of the Medical University Hospital of Nancy (France). EBUS-TBNA was performed for the diagnosis of enlarged mediastinal nodes or for the staging of lung cancer in the presence of enlarged (by computed tomography, CT) and/or hypermetabolic (positron emission tomography/computed tomography, PET/CT) lymph node(s). The patients provided written consent after receipt of information about the benefits and the risks of this method (institutional review board approval: number DC2008-459, Comité de Protection des Personnes Est-III).

EBUS-TBNA and sampling

All exams were performed by the same operator (OM). Conventional flexible bronchoscopy was first performed. Then, EBUS was started using the Olympus BF UC160F-OL8. Each nodal station was located using ultrasound imaging. Lymph nodes with a short axis larger than 10 mm were sampled. Three punction biopsies were performed at each level with a dedicated 22-gauge needle. On-site adequacy assessment was not performed during EBUS-TBNA. Half of the aspirate was expelled onto glass smears. Alternatively, one slide was air-dried, and the following slide was immediately fixed with CytoRAL (RAL; Marcillac, France). For each aspirate, an average of eight smears was obtained. Smears were available for all patients. The residue of the needle content of each aspirate was expelled in CytoRich (Thermo Fisher Scientific; Waltham, USA), an ethanol-based fixative. This allowed performing LBC on 193 patients and cell blocks/CBP on 276 patients. At the end of EBUS-TBNA, bronchial aspirates were systematically collected for bacteriological analysis.

Sample analysis

Air-dried smears were stained with May–Grunwald–Giemsa (MGG), and fixed smears were stained with Harris–Shorr coloration (Harris hematoxylin, Oxoid, Basingstoke, UK; Shorr staining solution, Merck KGaA, Darmstadt, Germany). LBC was performed from a CytoRich-fixed material with an Autocyte automate (Tripath; Burlington, VT, USA). In the presence of tissue microfragments in CytoRich fixative, 5-μm paraffin-embedded tissue sections were processed from cell blocks and stained with hematoxylin and eosin. Grocott's methenamine silver stain and Ziehl–Neelsen stain were used in case of granulomatous inflammation. The cases were reviewed by two experienced pathologists (JMV, GG).

Statistical analysis

The diagnostic yield was defined by obtaining adequate material, consisting of either pathological material or a significant number of lymphocytes, indicating adequate sampling of a lymph node. The diagnostic yield was calculated for the whole series, considering each cytological and histological method, and each lymph node station.

Sensitivity and negative predictive value (NPV) were calculated, globally and for each technique. True positivity was defined by the assessment of a diagnosis with EBUS-TBNA; false negativity was defined by the absence of diagnosis during a contributive EBUS-TBNA (presence of lymphocytes), when a different diagnostic method resulted

Fig. 1 **a** Small cell carcinoma, diagnosed by smears with MGG staining (*left*, ×400) and sections of paraffin-embedded samples (*right*, ×200, H&E). Primitive lung adenocarcinoma: **b** cluster of atypical carcinomatous cells on smears (MGG, ×400); **c** cell block preparation: tumor cells forming glandular lumens (*left*, H&E, ×400), staining for TTF1 antigen (*right*, IHC, ×400). **d** Colonic adenocarcinoma metastasis: *left*, CytoRich-fixed CBP obtained from 22G needle (H&E, ×40); *right*, glandular carcinomatous structures consistent with a colonic adenocarcinoma (H&E, ×400). **e** Squamous cell carcinoma: CBP (H&E, ×200); *inset*, staining for p63 (IHC, ×200). **f** Small B-cell lymphoma: on smears with MGG staining, presence of small- to medium-sized lymphocytes containing slightly irregular nuclei (×400); *inset*, diffuse staining with CD20 (IHC, ×400). Sarcoidosis: **g** granuloma composed of epithelioid cells on conventional cytology (Harris-Shorr, ×400); **h** epithelioid and giant cells granuloma in CBP (H&E, ×400)

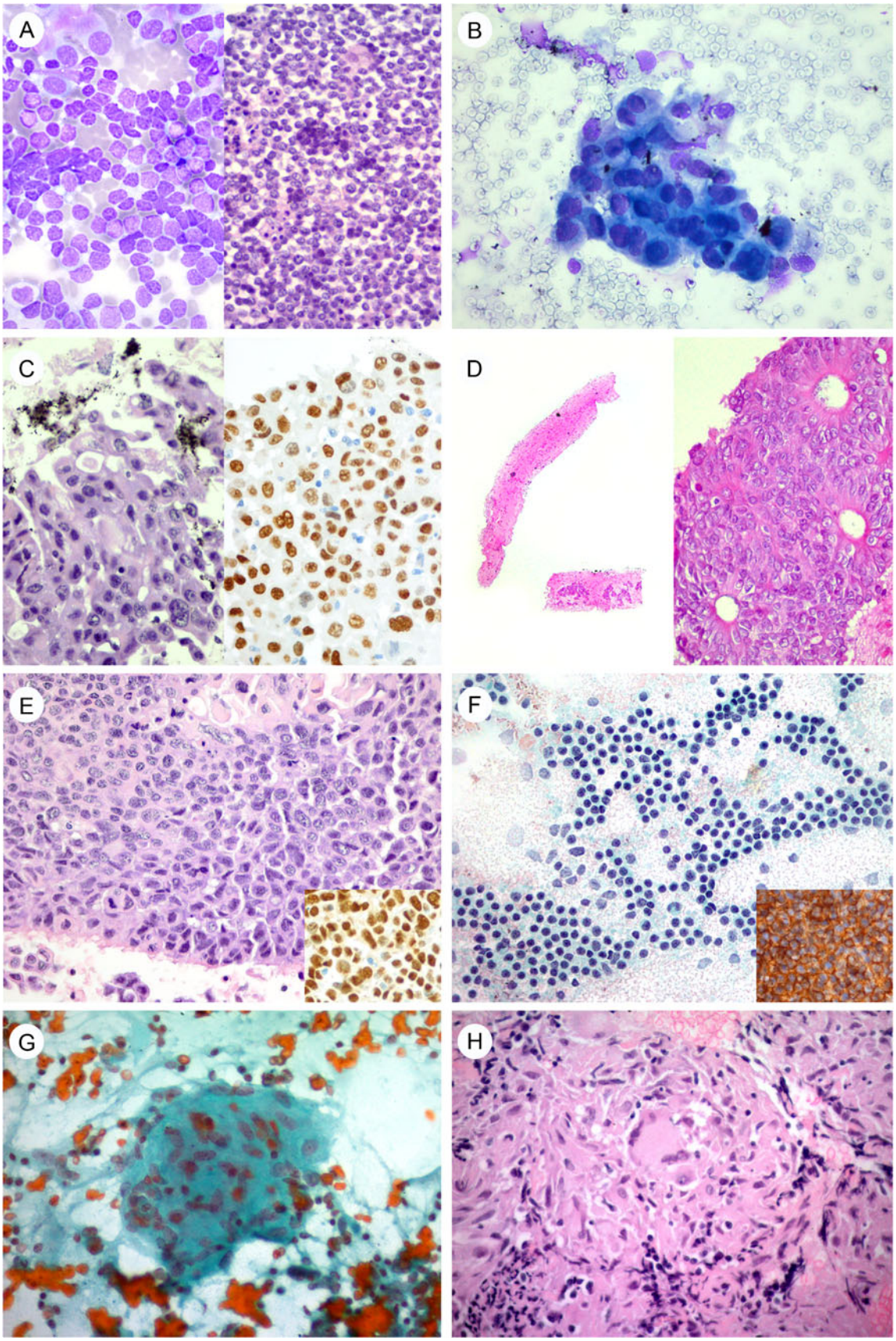
A
B
C
D
E
F
G
H

in a diagnosis. True negativity was defined by the absence of a diagnosis and the absence of evolution within a 6-month clinical and radiological follow-up. The diagnosis was not verified by other methods in order to avoid unnecessary invasive exams; therefore, no false positive cases were identified, resulting in 100 % specificity and positive predictive value.

Statistical analysis was performed using R-project software, version 2.11.1 (R Development Core Team, http://www.R-project.org), using 95 % confidence interval (CI 95 %). Chi-square test was used for qualitative variables and Wilcoxon–Mann–Whitney test was used for quantitative variables. A p-value$\leq$0.05 was considered as statistically significant.

Results

Clinical data

A total of 290 patients were included in our study, corresponding to the sampling of 493 lymph node stations (1.7 stations for each EBUS-TBNA). The mean age was 61.6 years (20–89). The indications for performing an EBUS-TBNA were a suspicion of lung cancer with mediastinal or hilar metastatic lymph nodes (159 patients, 54.8 %), isolated enlarged mediastinal lymph nodes (126 patients, 43.4 %), and mediastinal tumors (four patients, 1.4 %). No data were available for one patient (0.3 %).

Global diagnostic yield and diagnoses

For the 240 patients examined, the analysis showed either pathological material (147 patients, 50.7 %) or normal lymphocytes (93 patients, 32 %), resulting in a diagnostic yield of 82.7 %. The average size of lymph nodes was 29.8 mm (min, 10 mm; max, 60 mm). The yield correlated positively with the size of lymph nodes (p=0.004).

EBUS-TBNA diagnosed carcinoma in 118 patients (40.8 %), comprising of small-cell lung carcinoma (SCLC; 9.7 %), non small-cell lung carcinoma not otherwise specified (7.6 %), adenocarcinoma (13.8 %), squamous cell carcinoma (9.7 %), lymphomas (0.7 %), granulomatous inflammation (9.0 %), and non-specific inflammatory tissue (0.3 %) (Fig. 1).

A significant number of lymphocytes were observed in the smears of 93 patients, confirming the successful sampling of lymph nodes, but without any pathological material. Follow-up was available for 63 of these 93 patients. Eighteen false-negative cases were identified, which were assessed by a second EBUS-TBNA in two cases, lobectomy with mediastinal lymph node dissection in five cases, mediastinal biopsy in four cases, computed tomography-guided biopsy in one case, three biopsies of other organs in three cases, two bacteriological samples in two cases, and biopsy during flexible bronchoscopy in one case. These 18 false-negative cases comprised of nine carcinomas, eight granulomatous inflammations, and one lymphoma. This resulted in a global sensitivity of 89.1 % and a negative predictive value of 71.4 %. In these false-negative cases, EBUS-TBNA provided only lymphocyte-containing cytological samples (smears and/or LBC) in six cases, only CBP in one case, and both cytological samples and CBP in 11 cases.

In the 50 remaining cases, neither pathological material nor lymphocytes were found, with only blood and/or bronchial cells, indicating the failure of lymph node sampling.

Lymph node stations

The yield sorted by lymph node station was 76.3 % (95 % CI, 72.3–80.0). Of the 172 punction biopsies, seven were performed at the subcarinal station, 94 at the 4R station, 41 at the 4L station, and 41 at the 10R station (Table 1).

Comparison of the technical methods

Smears were performed in all cases, LBC in 193 cases, and CBP in 276 cases. The yield sorted by cytological or histological methods was as follows: 72.8 % (95 % CI, 77.5–86.7) for smears, 78.8 % (95 % CI, 72.3–84.3) for LBC, and 69.9 % (95 % CI, 64.1–75.3) for CBP (Table 2). The combination of the three techniques significantly increased the yield compared to smears or CBP alone (p=0.007 and p=0.0007, respectively). In addition to smears, the use of CBP significantly increased the yield (p=0.01), but not the use of LBC (p=0.07).

Tables 3 and 4 show the comparison of sensitivity and negative predictive value between smears, LBC, and CBP and for each diagnostic category. The combination of the three types of samples significantly increased sensitivity compared with smears or LBC alone (p=0.006 and p=4.10^{-5}, respectively). Most notably, the combined use of smears and CBP significantly increased sensitivity compared with smears taken alone (p=0.0006), but not the combined use of smears and LBC (p=0.13). CBP were significantly more sensitive than smears both for the diagnoses of carcinoma (p=0.01) and granulomatous inflammation (p=0.048). LBC was less sensitive than smears for the diagnosis of granulomatous inflammation (p=0.004), but without a significant difference for carcinoma (p=0.42).

Discussion

EBUS-TBNA is a safe and effective method for the exploration of mediastinal adenopathies

EBUS-TBNA was proven to be an efficient, safe, and cost-effective method to explore mediastinal and hilar enlarged

Table 1 Diagnostic yield according to lymph node stations

Site	Number, *n*	+ (%)	95 % CI	Ly (%)	95 % CI	Y (%)	95 % CI
2R	11	54.5	23.4–83.3	0.0	0–28.5	54.5	23.4–83.3
2L	3	100.0	29.2–100	0.0	0–70.8	100.0	29.2–100
4R	123	42.3	33.4–51.5	34.1	25.8–43.2	76.4	67.9–83.6
4L	60	25.0	14.7–37.9	43.3	30.6–56.8	68.3	55.0–79.7
7	215	38.1	40.0–55.4	41.9	35.2–48.8	80.0	74.0–85.1
10R	58	31.0	28.5–60.3	39.7	27.0–53.4	70.7	57.3–81.9
10L	4	25.0	0.6–80.6	25.0	0.6–80.6	50.0	6.8–93.2
11R	5	40.0	5.3–85.3	60.0	14.7–94.7	100.0	47.8–100
11L	7	57.1	22.3–95.7	28.6	3.7–71.0	85.7	42.1–99.6
12L	3	33.3	0.8–90.6	33.3	0.8–90.6	66.7	9.4–99.2
12R	2	100.0	15.8–100	0.0	0–84.2	100.0	15.8–100
Ptf	2	100.0	15.8–100	0.0	0–84.2	100.0	15.8–100
Total	493	38.1	33.8–42.6	38.1	33.8–42.6	76.3	72.3–80.0

+ positive diagnosis, *Ly* no diagnosis but with presence of lymphocytes, *Y* yield, *Ptf* posterior tracheal face

lymph nodes [2–6, 12]. This method is presently replacing classical mediastinoscopy [8]. In our study, EBUS-TBNA was performed in 54.8 % of the cases in the context of a lung tumor in order to determine lung cancer stage or to obtain a diagnosis for a lung tumor when the tumor was not accessible to classical endobronchial or transparietal biopsy. The global diagnostic yield was higher than 80 %, in line with the data available in the literature [10, 13], underlining the conclusion that it is not necessary to use more invasive diagnostic methods. For 43.4 % of patients, EBUS-TBNA was performed to explore enlarged isolated mediastinal lymph nodes, mostly leading to a diagnosis of granulomatous inflammation (suggestive of sarcoidosis or tuberculosis) and also lymphoma and rare metastatic carcinoma (colonic and kidney). No complications occurred in our series, confirming the safety of this method.

Global sensitivity was high, about 90 %. The highest sensitivity was obtained for carcinoma (91 %) and the lowest for granulomatous inflammation (77 %) and lymphoma (67 %). False-negative diagnoses were assessed in most cases through standard histological examination of mediastinal lymphadenectomy samples, during surgical treatment, or by mediastinal biopsy. In the literature, sensitivity ranges from 81 % to 98 % for a diagnosis of carcinoma [7, 8, 14–18] and 83 % for sarcoidosis [19]. For lung carcinoma staging, maximal sensitivity is obtained by combining EBUS-TBNA with mediastinal biopsy, the former allowing sampling of lymph node stations difficult to access through mediastinoscopy [12]. The combination of EBUS-TBNA and mediastinal biopsy, which is more invasive and expensive, should be limited to selected indications, depending on pre-operative radiological data. Wallace et al. have reported an alternative method, combining endobronchial with transesophageal fine-needle aspiration. With this method, they reported 93 % sensitivity [18].

Table 2 Diagnostic yield comparison between smears, liquid-based cytology, and cell block preparations

Procedure	% vs %	*P*-value
Smears vs LBC	77.4[a] vs 78.8	0.75
Smears vs CBP	72.8 vs 69.9	0.51
CBP vs LBC	77.6 vs 78.8	0.28
Smears vs smears *and* LBC	77.4[a] vs 84.6	0.07
Smears vs smears *and* CBP	72.8 vs 81.4	0.01*
Smears vs Global	72.8 vs 82.8	0.007*
LBC vs Global	78.8 vs 86.7[a]	0.37
CBP vs Global	69.9 vs 82.8	0.0007*

*$p<0.05$ (statistically significant)

[a] Exclusion of exams 1–95, for which no LBC was performed

The combination of CBP with conventional cytology increases diagnostic yield

We show that combining CBP and smears, but not LBC and smears, increases the diagnostic yield versus smear cytology alone. Fragments of lymph node tissue, although very small, allow a comfortable and reliable histological analysis. Our results are in line with the study of Sanz-Santoz et al., who reported a nearly 7 % increased yield using CBP ("cyto-blocks") [20]. In our study, the combination of the three techniques increased the yield up to 10 %. However, the diagnostic yield of CBP only was lower than that of conventional smears. Consequently, CBP is an efficient complement to conventional cytology but cannot replace it. A higher yield might be obtained in the future with the development of optimized dedicated needles for EBUS. Indeed although some lymph nodes are easily targeted, aspirates can be low on diagnostic material, most notably concerning tumors containing an abundant fibrous stroma or for fibrosing inflammatory processes. In contrast, it is worth noting that the sensitivity of

Table 3 Diagnostic yield, sensitivity, and negative predictive value of smears, liquid-based cytology, and cell block preparations

Procedure	Yield	95 % CI	Diagnosis	Sensitivity (%)	95 % CI	NPV (%)	95 % CI
Smears	72.8 % (211/290)	77.5–86.7	Carcinoma (all types)	81.3	73.3–87.8	81.6	73.7–88.0
			Small cell carcinoma	92.9	76.4–99.1	98.1	93.2–99.8
			Granuloma	50.0	24.7–75.3	92.7	86.2–96.8
			Lymphoma	33.3	0.8–90.6	98.1	93.2–99.8
			Total	76.8	68.9–83.4	75.6	67.4–82.5
LBC	78.8 % (152/193)	72.3–84.3	Carcinoma (all types)	86.6	77.3–93.1	87.8	79.2–93.7
			Small cell carcinoma	86.4	65.1–97.1	96.3	89.7–99.2
			Granuloma	4.5	0.1–22.8	79.0	69.7–86.5
			Lymphoma	33.3	0.8–90.6	97.5	91.4–99.7
			Total	68.2	58.5–76.9	69.9	60.6–78.2
CBP	69.9 % (193/276)	64.1–75.3	Carcinoma (all types)	93.0	86.6–96.9	88.4	78.4–94.9
			Small cell carcinoma	92.9	76.5–99.1	96.8	89.0–99.6
			Granuloma	82.8	64.2–94.2	92.4	83.2–97.5
			Lymphoma	66.7	9.4–99.2	98.4	91.3–100.0
			Total	90.4	84.4–94.7	81.3	70.7–89.4
Total	82.8 % (240/290)	77.9–86.9	Carcinoma (all types)	90.9	83.4–95.8	83.3	70.7–92.1
			Small cell carcinoma	93.3	77.9–99.2	95.7	85.5–99.5
			Granuloma	76.5	58.8–89.3	84.9	72.4–93.3
			Lymphoma	66.7	9.4–99.2	97.8	88.5–99.9
			Total	89.1	83.3–93.4	71.4	58.7–82.1

Table 4 Sensitivity and negative predictive value comparison between smears, liquid-based cytology, and cell block preparations according to diagnosis

Procedure	Sensitivity		NPV	
	% vs %	*P*-value	% vs %	*P*-value
Smears vs LBC				
Global	76.8 vs 68.2	0.17	75.6 vs 69.9	0.39
Carcinoma	81.3 vs 86.6	0.42	81.6 vs 87.8	0.30
Granuloma	50.0 vs 4.5	0.004*	92.7 vs 79.0	0.007*
Smears vs CBP				
Global	76.8 vs 90.4	0.003*	75.6 vs 81.3	0.43
Carcinoma	81.3 vs 93.0	0.01*	81.6 vs 88.4	0.30
Granuloma	50.0 vs 82.8	0.048*	92.7 vs 98.4	0.82
LBC vs CBP				
Global	68.2 vs 90.4	2.10^{-5}*	69.9 vs 81.3	0.11
Carcinoma	86.6 vs 93.0	0.21	87.8 vs 88.4	0.90
Granuloma	4.5 vs 82.8	2.10^{-7}*	79.0 vs 98.4	0.03*
Smears vs smears *and* LBC	76.8 vs 75.9	0.13	75.6 vs 53.4	0.32
Smears vs smears *and* CBP	76.8 vs 91.6	0.0006*	75.6 vs 73.3	0.77
Smears vs total	76.8 vs 89.1	0.006*	75.6 vs 71.4	0.66
LBC vs total	68.2 vs 89.1	4.10^{-5}*	69.9 vs 71.4	0.97
CBP vs total	90.4 vs 89.1	0.85	81.3 vs 71.4	0.24
Carcinoma vs granuloma				
Smears	81.3 vs 50.0	0.01*	81.6 vs 92.7	0.02*
LBC	86.6 vs 4.5	9.10^{-13}*	87.8 vs 79.0	0.16
CBP	93.0 vs 82.8	0.17	88.4 vs 92.4	0.62
Total	90.9 vs 76.5	0.06	83.3 vs 84.9	0.97

*$p<0.05$ (statistically significant)

cytology in EBUS-TBNA is very high for SCLC (Table 3). This might be explained by its high cellularity, the absence of fibrous stroma, and the poor cohesiveness of the tumor cells, which facilitates their aspiration. The use of larger needles might increase the diagnostic yield. However, Nakajima et al. showed that the yield of a 21G needle is equivalent to that of a 22G needle; moreover, it led to more contamination of the sample with blood [21]. An alternative approach was reported by Franke et al., who used a 21G forceps introduced in the orifice obtained after sampling with a 22 G needle, resulting in a higher diagnostic yield, with minimal hemorrhagic complications [22].

CBP are more sensitive than conventional and liquid-based cytology

To our knowledge, the expected sensitivity gain by using other methods than conventional cytology in EBUS-TBNA has not yet been reported. Relative to the yield, sensitivity is a more accurate means of evaluating the diagnostic performance of a diagnostic method as yield does not take into account the potential risk of a false-negative result. We show here that the combination of the three sample types significantly increases sensitivity compared with smears only. This sensitivity gain cannot be attributed to LBC use but is due to the possibility to analyze tissue micro-fragments fixed in CytoRich. LBC did not significantly increase sensitivity, even if fragments were picked from the same container. CBP sensitivity was significantly higher than cytology both for the diagnoses of carcinoma and granulomatous inflammation. Thus, although the diagnostic yield of histological samples is not very high, they provide a real gain in terms of sensitivity. Due to a higher risk of a false-negative result, a negative EBUS-TBNA without CBP should be interpreted more carefully than a case for which paraffin-embedded fragments of normal lymph node parenchyma are present. An additional advantage is that immunohistochemistry can be performed on paraffin-embedded tissues, a very useful tool to make an accurate diagnosis. This material can also be used successfully for molecular biological studies, screening for *EGFR* and *ALK* mutation, a major parameter for the treatment of lung adenocarcinoma [11, 23]. Samples from our EBUS-TBNA were successfully used for molecular analyses in 90 % of cases (data not shown).

Cytology without CBP incurs an increased risk of a false-negative result

We show that smears not combined with CBP run a higher risk of a false-positive result upon a diagnosis of carcinoma and even more so in granulomatous inflammation (Table 4). Moreover, it must be underlined that LBC resulted in very low sensitivity for the diagnosis of sarcoidosis and other types of granulomatous inflammation (sensitivity of smears, 50 %; LBC, 4.5 %). This might be explained by the relative lack of cellular cohesiveness in granulomas and the difficulty in identifying single epitheloid cells on such a preparation. Conversely, epithelioid cells are easily identified on CBP, in which the granulomatous architecture is conserved. Even though EBUS-TBNA has been shown in a randomized trial to be an efficient method for the diagnosis of granulomatous inflammation [19], the risk of a false-negative result should be kept in mind when interpreting an EBUS-TBNA case. When CBP are not available in case of a suspicion of sarcoidosis or tuberculosis, a new EBUS-TBNA or other investigations should be considered before excluding these diagnoses.

Conclusion

In conclusion, the combination of conventional cytology with histological sections from paraffin-embedded samples significantly increases diagnostic yield and sensitivity, both for carcinoma and granulomatous inflammation. Conversely, smears and LBC, used without CBP, increase the risk of a false-negative result, most notably in the case of a granulomatous inflammation. Our results should incite operators to systematically collect material in liquid fixative milieu in addition to conventional smears.

Acknowledgments The authors thank Chantal Letang and all the teams of the Department of Pathology (Hôpital Central, CHU Nancy) for technical support and Mrs. Jacqueline Zevnick for reviewing the manuscript.

Conflict of interest The authors have no conflict of interest to disclose.

References

1. Luke WP, Pearson FG, Todd TR, Patterson GA, Cooper JD (1986) Prospective evaluation of mediastinoscopy for assessment of carcinoma of the lung. J Thorac Cardiovasc Surg 91:53–56
2. Gu P, Zhao YZ, Jiang LY, Zhang W, Xin Y, Han BH (2009) Endobronchial ultrasound-guided transbronchial needle aspiration for staging of lung cancer: a systematic review and meta-analysis. Eur J Cancer 45:1389–1396
3. Herth F, Becker HD, Ernst A (2004) Conventional vs endobronchial ultrasound-guided transbronchial needle aspiration: a randomized trial. Chest 125:322–325
4. Herth FJ, Becker HD, Ernst A (2003) Ultrasound-guided transbronchial needle aspiration: an experience in 242 patients. Chest 123:604–607
5. Lee HS, Lee GK, Kim MS, Lee JM, Kim HY, Nam BH, Zo JI, Hwangbo B (2008) Real-time endobronchial ultrasound-guided transbronchial needle aspiration in mediastinal staging of non-small cell lung cancer: how many aspirations per target lymph node station? Chest 134:368–374
6. Skov BG, Baandrup U, Jakobsen GK, Kiss K, Krasnik M, Rossen K, Vilmann P (2007) Cytopathologic diagnoses of fine-needle aspirations from endoscopic ultrasound of the mediastinum:

reproducibility of the diagnoses and representativeness of aspirates from lymph nodes. Cancer 111:234–241. doi:10.1002/cncr.22866
7. Yasufuku K, Chiyo M, Koh E, Moriya Y, Iyoda A, Sekine Y, Shibuya K, Iizasa T, Fujisawa T (2005) Endobronchial ultrasound guided transbronchial needle aspiration for staging of lung cancer. Lung Cancer 50:347–354
8. Yasufuku K, Pierre A, Darling G, de Perrot M, Waddell T, Johnston M, da Cunha Santos G, Geddie W, Boerner S, Le LW, Keshavjee S (2011) A prospective controlled trial of endobronchial ultrasound-guided transbronchial needle aspiration compared with mediastinoscopy for mediastinal lymph node staging of lung cancer. J Thorac Cardiovasc Surg 142:1393–1400. doi:10.1016/j.jtcvs.2011.08.037, e1391
9. Vincent BD, El-Bayoumi E, Hoffman B, Doelken P, DeRosimo J, Reed C, Silvestri GA (2008) Real-time endobronchial ultrasound-guided transbronchial lymph node aspiration. Ann Thorac Surg 85:224–230
10. Delattre C, Fournier C, Bouchindhomme B, Renaud F, Escande F, Ramon P, Copin MC (2011) Endoscopic ultrasound guided transbronchial fine needle aspiration: a French Department of Pathology's 4-year experience. J Clin Pathol 64:1117–1122. doi:10.1136/jclinpath-2011-200382
11. Garcia-Olive I, Monso E, Andreo F, Sanz-Santos J, Taron M, Molina-Vila MA, Llatjos M, Castella E, Moran T, Bertran-Alamillo J, Mayo-de-Las-Casas C, Queralt C, Rosell R (2012) Endobronchial ultrasound-guided transbronchial needle aspiration for identifying EGFR mutations. Eur Respir J 35:391–395
12. Annema JT, Versteegh MI, Veselic M, Welker L, Mauad T, Sont JK, Willems LN, Rabe KF (2005) Endoscopic ultrasound added to mediastinoscopy for preoperative staging of patients with lung cancer. JAMA 294:931–936
13. Eckardt J, Petersen HO, Hakami-Kermani A, Olsen KE, Jorgensen OD, Licht PB (2009) Endobronchial ultrasound-guided transbronchial needle aspiration of undiagnosed intrathoracic lesions. Interact Cardiovasc Thorac Surg 9:232–235
14. Hwangbo B, Kim SK, Lee HS, Kim MS, Lee JM, Kim HY, Lee GK, Nam BH, Zo JI (2009) Application of endobronchial ultrasound-guided transbronchial needle aspiration following integrated PET/CT in mediastinal staging of potentially operable non-small cell lung cancer. Chest 135:1280–1287
15. Rintoul RC, Skwarski KM, Murchison JT, Wallace WA, Walker WS, Penman ID (2005) Endobronchial and endoscopic ultrasound-guided real-time fine-needle aspiration for mediastinal staging. Eur Respir J 25:416–421
16. Sun W, Song K, Zervos M, Pass H, Cangiarella J, Bizekis C, Crawford B, Wang BY (2010) The diagnostic value of endobronchial ultrasound-guided needle biopsy in lung cancer and mediastinal adenopathy. Diagn Cytopathol 38:337–342. doi:10.1002/dc.21195
17. Szlubowski A, Kuzdzal J, Kolodziej M, Soja J, Pankowski J, Obrochta A, Kopinski P, Zielinski M (2009) Endobronchial ultrasound-guided needle aspiration in the non-small cell lung cancer staging. Eur J Cardiothorac Surg 35:332–335, discussion 335-336
18. Wallace MB, Pascual JM, Raimondo M, Woodward TA, McComb BL, Crook JE, Johnson MM, Al-Haddad MA, Gross SA, Pungpapong S, Hardee JN, Odell JA (2008) Minimally invasive endoscopic staging of suspected lung cancer. JAMA 299:540–546
19. Tremblay A, Stather DR, Maceachern P, Khalil M, Field SK (2009) A randomized controlled trial of standard vs endobronchial ultrasonography-guided transbronchial needle aspiration in patients with suspected sarcoidosis. Chest 136:340–346
20. Sanz-Santos J, Serra P, Andreo F, Llatjos M, Castella E, Monso E (2012) Contribution of cell blocks obtained through endobronchial ultrasound-guided transbronchial needle aspiration to the diagnosis of lung cancer. BMC Cancer 12:34. doi:10.1186/1471-2407-12-34
21. Nakajima T, Yasufuku K, Takahashi R, Shingyoji M, Hirata T, Itami M, Matsui Y, Itakura M, Iizasa T, Kimura H (2011) Comparison of 21-gauge and 22-gauge aspiration needle during endobronchial ultrasound-guided transbronchial needle aspiration. Respirology 16:90–94. doi:10.1111/j.1440-1843.2010.01871.x
22. Franke KJ, Bruckner C, Szyrach M, Ruhle KH, Nilius G, Theegarten D (2012) The contribution of endobronchial ultrasound-guided forceps biopsy in the diagnostic workup of unexplained mediastinal and hilar lymphadenopathy. Lung 190:227–232
23. Santis G, Angell R, Nickless G, Quinn A, Herbert A, Cane P, Spicer J, Breen R, McLean E, Tobal K (2011) Screening for EGFR and KRAS mutations in endobronchial ultrasound derived transbronchial needle aspirates in non-small cell lung cancer using COLD-PCR. PLoS One 6:e25191. doi:10.1371/journal.pone.0025191

Virchows Arch (2012) 461:513–519
DOI 10.1007/s00428-012-1317-9

ORIGINAL ARTICLE

Invasion of the inner and outer layers of the visceral pleura in pT1 size lung adenocarcinoma measuring ≤3 cm: correlation with malignant aggressiveness and prognosis

Makoto Hamasaki · Fumiaki Kato · Kaori Koga · Hiroyuki Hayashi · Mikiko Aoki · Yoshihiro Miyake · Akinori Iwasaki · Kazuki Nabeshima

Received: 29 March 2012 / Revised: 17 July 2012 / Accepted: 6 September 2012 / Published online: 22 September 2012
© Springer-Verlag 2012

Abstract Visceral pleural invasion (VPI) is defined as penetration by cancer cells of the elastic layer of the pleura. The purpose of this retrospective study was to compare the effect of invasion of the inner elastic layer of the pleura on survival to that of invasion of the outer elastic layer. One hundred twenty-four pT1 size lung adenocarcinomas were examined for visceral pleural invasion, which was classified into three types: no pleural invasion (NPI), invasion of the inner elastic layer only (IEL), and invasion of both inner and outer elastic layers (OEL). The relationship between the types of VPI and the prognosis was analyzed by univariate and multivariate analyses. Seventy-three (59 %) cancers showed NPI, while 51 cancers showed invasion of the pleura [(IEL) in 26 (21 %), OEL in 25 (20 %)]. The 5-year survival was 81, 60, and 37 % for patients with NPI, IEL, and OEL, respectively. Survival was poorest in patients with OEL ($P<0.01$). Invasion of the outer elastic layer was also significantly associated with lymph node metastasis and frequent lymphatic involvement, micropapillary pattern, higher stromal invasion grade, and presence of small cluster invasion within tumors. Univariate analysis showed a significant relationship between invasion of the outer elastic layer and poor prognosis. However, multivariate analysis identified lymph node metastasis as the most significant predictor of poor prognosis. Analysis of invasion of the inner and outer visceral pleura is important; invasion of the outer elastic layer correlates with poor prognosis in pT1 size lung adenocarcinomas.

Keywords Lung cancer · Pleura · Visceral pleura · Elastic lamina · Pleural invasion · Tumor aggressiveness

M. Hamasaki · F. Kato · K. Koga · H. Hayashi · M. Aoki · K. Nabeshima (✉)
Department of Pathology, Fukuoka University School of Medicine and Hospital,
7-45-1 Nanakuma, Jonan-ku,
Fukuoka 814-0180, Japan
e-mail: kaznabes@fukuoka-u.ac.jp

F. Kato · A. Iwasaki
Department of Thoracic Surgery, Fukuoka University School of Medicine and Hospital,
Fukuoka, Japan

Y. Miyake
Department of Preventive Medicine and Public Health, Fukuoka University School of Medicine,
Fukuoka, Japan

Background

Visceral pleural invasion (VPI) increases the T category of lung cancers and is one of the most important prognostic factors in lung cancer [1–5]. Both tumor–node–metastasis (TNM) staging systems of the International Union Against Cancer (UICC, seventh edition) [6] and the Japan Lung Cancer Society (JLCS, sixth edition) classify VPI into the following stages: pl0, lung tumor with no pleural involvement beyond its elastic layer; pl1, lung tumor that extends beyond the elastic layer of the visceral pleura but is not exposed on the pleural surface; and pl2, lung tumor that is exposed on the pleural surface but does not involve adjacent anatomic structures. Anatomically, however, the visceral pleura comprises two elastic layers: one is the thick elastic layer beneath the submesothelial layer (the outer elastic layer), and another is the thin elastic layer in close to the pulmonary parenchyma (the inner elastic layer) [6]. Both the UICC and JLCS TNM staging systems do not mention the exact elastic layer for the above definitions of VPI and staging of lung cancer. Infiltration of the most prominent elastic layer has been introduced as the international recommendation [6]. The outer elastic layer is more easily recognized than the inner elastic layer, because no elastic fibers are located between the pleural surface and the outer elastic

layer. Several studies reported that VPI represented the unequivocal penetration of tumor cells beyond the elastic layer [4, 5, 7]. In this regard, the prognostic difference of penetration of the two elastic layers has not been investigated even in the above articles. There is only one study that intended to standardize or establish internationally acceptable guidelines for the diagnosis of VPI with respect to the two elastic layers [8]. However, the authors could not find any significant difference in the patients' survival based on the invasion of the elastic layers, and their conclusion was that differential evaluation of the tumor infiltration depth according to the elastic layers is not practical. In the present study, we evaluated VPI for each elastic layer and correlated these with the survival of patients with pT1 size lung adenocarcinomas.

Materials and methods

Patients

We reviewed 126 pT1 size lung adenocarcinomas (≤3 cm) that had been surgically resected at the Department of Thoracic Surgery, Fukuoka University Hospital, between January 1993 and December 2002. The study protocol was approved by the Ethics Committee of Fukuoka University. Anonymous use of redundant tissue is part of the standard treatment agreement with patients in our hospital when no objection is expressed. The pathological stage was determined according to the TNM classification of malignant tumors, seventh edition (International Union Against Cancer). We excluded two patients with tumors, in which pleural invasion was difficult to diagnose because of artificial damage of tissue associated with the preparation of intraoperative frozen diagnosis. Thus, 124 cases were available for investigating the relationship between pleural invasion and survival.

Pathologic evaluation

The surgically resected specimens were fixed routinely in 10 % formalin, and the whole tumor nodules were processed into paraffin blocks for histopathological examination. Tissue sections were cut 4 μm thick, including the largest cut surface of the tumor and stained with hematoxylin and eosin, elastica-van-Gieson, and orcein stains. The tumors were histopathologically classified according to the novel IASLC/ATS/ERS consensus classification [9]. Lymphatic and vascular involvements were immunohistochemically confirmed using D2-40 and anti-CD31 antibodies, which detect lymph and vascular

Table 1 Characteristics of patients with lung adenocarcinoma

	All cases (%)
n	126
Age (years)	
<65	60 (48)
≥65	66 (52)
Gender	
M	55 (44)
F	71 (56)
Type of resection	
Lobectomy	93 (74)
Limited surgery	33 (26)
Histological subtypes	
Adenocarcinoma in situ	4 (3)
Minimally invasive adenocarcinoma	2 (2)
Lepidic predominant	3 (2)
Acinar predominant	21 (17)
Papillary predominant	73 (58)
Micropapillary predominant	11 (9)
Solid predominant	5 (4)
Invasive mucinous adenocarcinoma	7 (6)
Pleural invasion[a]	
NPI	73 (59)
IEL	26 (21)
OEL	25 (20)
Pathologic N status	
N0	103 (82)
N1	9 (7)
N2	14 (11)

NPI no pleural invasion, *IEL* invasion of the internal elastic layer, *OEL* invasion of the outer elastic layer

[a] Pleural invasion was determined histopathologically in 124 tumors as described in "Materials and methods"

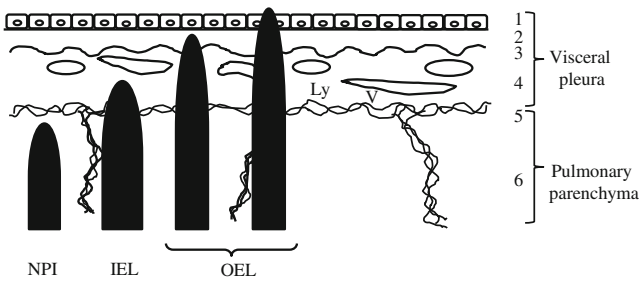

Fig. 1 Scheme diagram illustrating the different types of visceral pleural invasion (VPI) in lung cancers based on the two elastic layers of the pleura. The pl0 tumors show NPI and IEL, which do not penetrate the outer elastic layer, while pl1 tumors show OEL, which penetrates the outer elastic layer. The pl2 tumors represent those with invasion of the visceral pleural surface, but no involvement of the parietal pleura. *1* Mesothelial layer, *2* submesothelial layer, *3* outer elastic layer (superficial elastic layer), *4* subpleural layer, *5* inner elastic layer (deep fibroelastic layer), *6* pulmonary parenchyma. *Ly* lymphatics, *V* blood vessels, *NPI* no pleural invasion, *IEL* invasion of the inner elastic layer only, *OEL* invasion of both inner and outer elastic layers (modified from [8])

endothelial cells, respectively. Immunohistochemical staining was performed as described previously [10].

The clinicopathological parameters analyzed in this study included age, gender, tumor size, lymph node metastasis, stromal invasion grade (SIG), micropapillary pattern (MPP), small cluster invasion (SCI), lymphatic and vascular permeation, and pleural invasion. SCI was defined as single or small clusters of invading carcinoma cells seen at the invasive margin of the tumor within the fibrotic focus [10, 11]. The small clusters appear to have separated from acinar or papillary structures of

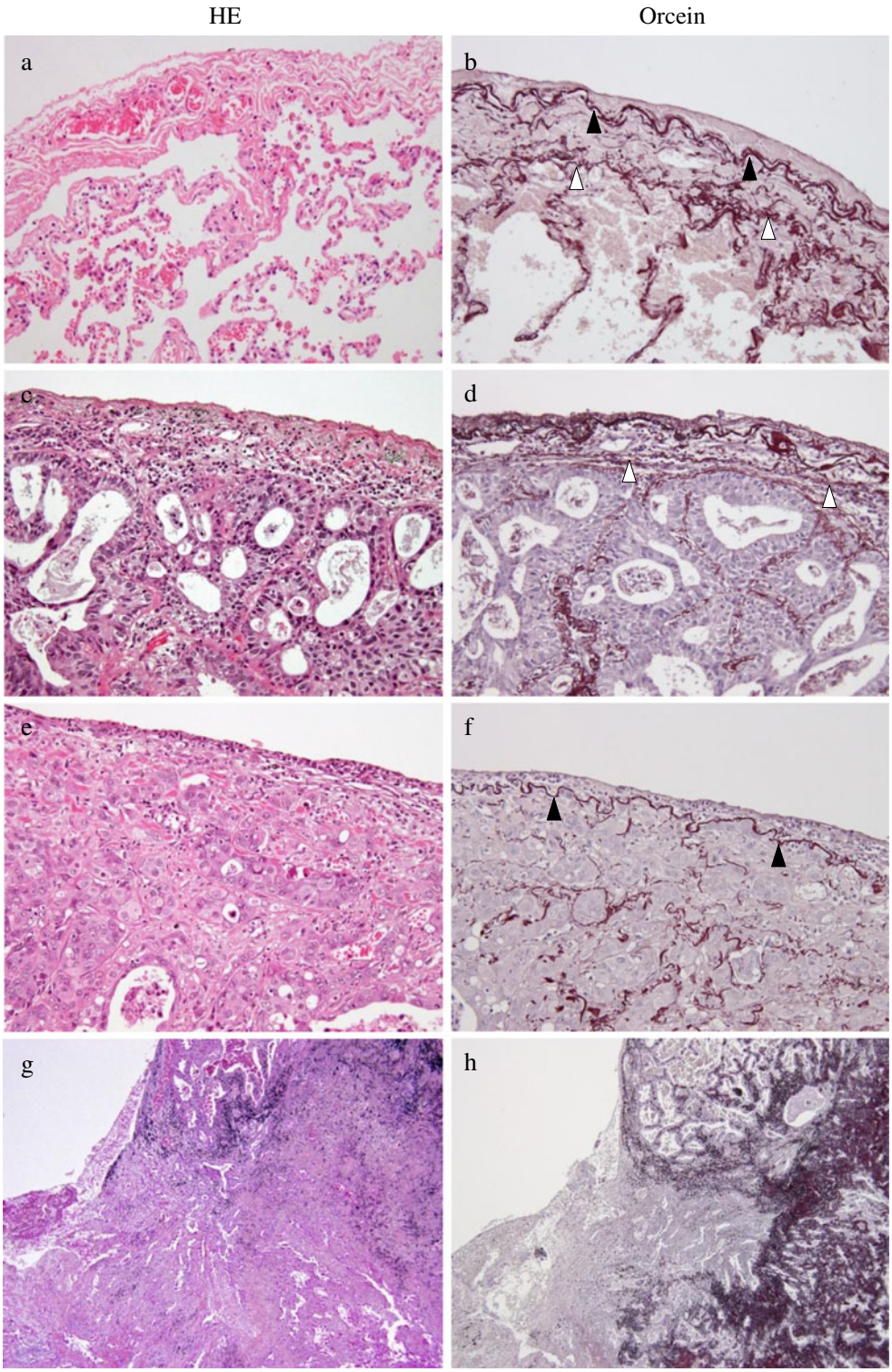

Fig. 2 Morphology of visceral pleura and pleural invasion. The slightly thickened pleura contains fibrocollagenous layer and lymphatic and blood vessels (**a**). The two elastic layers are stained with orcein. The outer elastic layer is thick and continuous (*black arrowheads*) while the inner elastic layer is thin and occasionally discontinuous (*white arrowheads*). Note the presence of lymphatic and blood vessels between these two elastic layers (**b**). Carcinoma cells do not invade the inner elastic layer (*white arrowheads*) (**c**, **d**). Carcinoma cells invade the inner elastic layer but do not penetrate the outer elastic layer (*black arrowheads*) (**e**, **f**). Carcinoma cells penetrate the outer elastic layer and are present on the pleural surface (**g**, **h**)

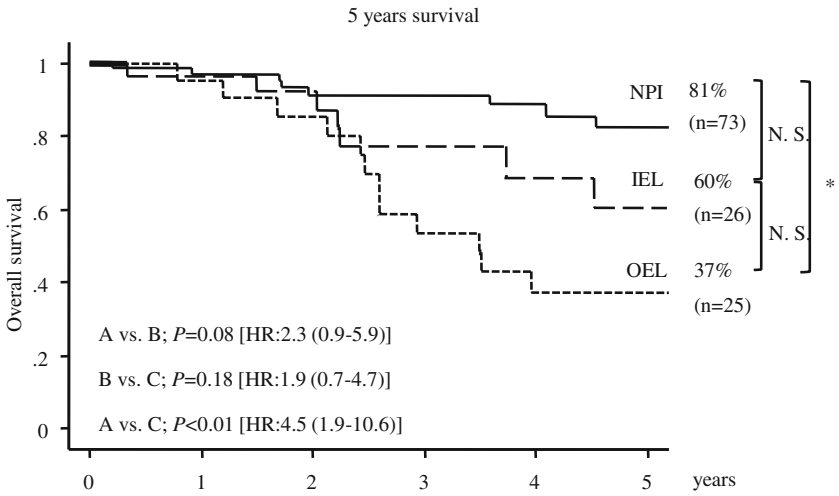

Fig. 3 Five-year overall survival curves for patients with lung adenocarcinoma according to the type of visceral pleural invasion (NPI, IEL, and OEL). Survival is poorest in patients with the outer layer penetration, and difference in survival between NPI and OEL was statistically significant. There was no significant difference in survival of patients with types (NPI and IEL) and (IEL and OEL). *NPI* no pleural invasion, *solid line*; *IEL* invasion of the internal elastic layer, *dashed line*; *OEL* invasion of the outer elastic layer, *dotted line*; *N.S.* not significant

tumors due to dedifferentiation. The details of the scoring system of SIG and MPP were described previously [11].

Statistical analysis

Summary statistics were obtained using standard methods and statistical analysis software StatView for Windows version 5.0 (SAS Institute Inc., Cary, NC, USA). The relationships between several clinicopathological parameters and histopathological subgroups were evaluated using the χ^2 test and Fisher's exact test. Survival curves were plotted using the Kaplan–Meier method, and differences in survival were determined by log-rank analysis. Univariate analysis was conducted for each clinicopathological parameter. Multivariate analysis with the Cox proportional hazard model was used to determine the independent prognostic factors. A P value less than 0.05 was considered statistically significant.

Results

Table 1 summarizes the clinicopathological characteristics of patients. This study included 126 patients (55 men and 71 women) with a mean age of 64 years (range, 28–85 years), and 60 patients (48 %) were less than 65 years old. Histopathological subtypes included adenocarcinoma in situ (4/126, 3 %), minimally invasive adenocarcinoma (2/126, 2 %), lepidic predominant (3/126, 2 %), acinar predominant (21/126, 17 %), papillary predominant (73/126, 58 %), micropapillary predominant (11/126, 9 %), solid predominant (5/126, 4 %), and invasive mucinous adenocarcinoma (7/126, 6 %). The subtypes of invasive adenocarcinoma showed no significant differences in terms of the extent of pleural invasion. Lobectomy was performed in 93 patients (74 %), and limited surgery was performed in 33 cases (26 %). Regional lymph node dissection was performed in all patients, and lymph node metastasis was diagnosed in 23 patients (18 %). The pleura has two elastic layers (Fig. 2a, b): the outer (Fig. 2b, black arrowheads) and inner (Fig. 2b, white arrowheads) layers, which can be identified with elastic fiber stains. VPI was classified into three types [no pleural invasion (NPI), invasion of the internal elastic layer (IEL), and invasion of the outer elastic layer (OEL)] according to modification of the scoring system by Warth et al. [8] (Figs. 1 and 2). NPI showed no invasion of pleural elastic layers; the tumor cells were adjacent to the inner elastic layer (deep fibroelastic layer) but did not penetrate it (Fig. 2c, d). IEL represented invasion of the inner elastic layer by tumor cells, but no penetration of the outer elastic layer (superficial elastic layer) (Fig. 2e, f). OEL represented invasion of the outer elastic layer by tumor cells (Fig. 2g, h). Of the 124 cases, 73 cases were classified as NPI (Figs. 1 and 2c, d, 59 %), 26 cases as IEL (Figs. 1 and 2e, f, 21 %), and 25 cases as OEL (Figs. 1 and 2g, h, 20 %). The latter group included four cases in which the tumor cells extended on to the surface of the visceral pleura.

The survival rates at 5 years for patients with NPI, IEL, and OEL were 81, 60, and 37 %, respectively (Fig. 3). Invasion of the inner elastic layer did not influence overall survival in pT1 size lung adenocarcinomas [hazard ratio

Table 2 Relationship between pleural invasion and lymph node metastasis

	Lymph node metastasis		
	n	(+)	(−)
NPI	73	9 (12.3 %)	64 (87.6 %)*
IEL	26	3 (11.5 %)	23 (88.4 %)**
OEL	25	11 (44.0 %)	14 (56.0 %)

NPI no pleural invasion, *IEL* invasion of the internal elastic layer, *OEL* invasion of the outer elastic layer

*P=0.003, compared with OEL, by χ^2 test; **P=0.01, compared with OEL, by χ^2 test

Table 3 Relationship between pleural invasion and lymphovascular involvement

	n	Pleura				Tumor			
		Lymphatic invasion		Blood vessel invasion		Lymphatic invasion		Blood vessel invasion	
		(+)	(−)	(+)	(−)	(+)	(−)	(+)	(−)
NPI	73	0 (0 %)	73 (100 %)	0 (0 %)	73 (100 %)	16 (22 %)	57 (78 %)*	8 (11 %)	65 (89 %)#
IEL	26	1 (4 %)	25 (96 %)	0 (0 %)	26 (100 %)	5 (19 %)	21 (81 %)$	6 (23 %)	20 (77 %)
OEL	25	4 (16 %)	16 (64 %)	2 (8 %)	23 (92 %)	20 (80 %)	5 (20 %)	10 (40.0 %)	15 (60 %)

NPI no pleural invasion, *IEL* invasion of the internal elastic layer, *OEL* invasion of the outer elastic layer

*$P<0.01$, compared with lymphatic invasion in tumor of OEL, by χ^2 test; #$P<0.01$, compared with tumor vessel invasion in tumor of OEL, by χ^2 test; \$$P<0.01$, compared with lymphatic invasion in tumor of OEL, by χ^2 test

(HR) 2.3, 95 % confidence interval (CI) 0.9–5.9, $P=0.08$]. However, invasion of the outer elastic layer correlated more significantly with shorter survival than of the internal elastic layer (HR 4.5, 95 % CI 1.9–10.6, $P<0.01$) (Fig. 3).

Table 2 shows the relationship between the type of VPI and lymph node metastasis. Lymph node metastasis was more common in patients with tumors of type OEL than those with NPI or IEL type tumors. Furthermore, lymphatic involvement within the tumor, especially in or around the fibrotic foci, was significantly more frequent in patients of OEL than NPI and IEL, while that in the pleura did not show significant differences between the two types (Table 3). Vascular involvement in the tumor was also significantly different between NPI and OEL. Furthermore, in IEL and OEL, lymphatic involvement within the tumor correlated significantly with more frequent lymph node metastasis, while vascular involvement did not ($P=0.002$) (Table 4). However, no significant differences were found between patients with N1 and N2 metastasis in terms of pleural invasion and lymphatic involvement. MPP, SIG (grade 3), and SCI were significantly more frequently observed in tumors with VPI of OEL than NPI (Table 5). No significant differences were found between NPI and IEL and IEL and OEL (Table 5).

Univariate analysis showed significant relations between survival of patients with pT1 size lung adenocarcinoma and lymph node metastasis ($P<0.01$), SIG ($P=0.01$), MPP ($P=0.03$), SCI ($P<0.01$), and VPI with penetration of the outer elastic layer ($P<0.01$). Multivariate analysis that included clinicopathological parameters identified lymph node metastasis ($P=0.02$) as independent and significant prognostic factors (Table 6).

Table 4 Correlation between lymphatic involvement in the tumor with lymph node metastasis in IEL and OEL

	Ly			V			Total
	(+)	(−)	*P*	(+)	(−)	*P*	
N0	13	24	0.002	12	25	0.8	37
N1+N2	12	2		4	10		14

IEL invasion of the internal elastic layer, *OEL* invasion of the outer elastic layer

Discussion

So far, only one report by Warth et al. has analyzed the significance of pleural invasion in relation to invasion of the inner versus the outer elastic layers [8]. The authors used a new scoring system to define tumor infiltration depth in each elastic layer. However, in their study, no significant relationship was found between the patients' survival and the tumor infiltration depth [8]. Our study is the first to report that prognosis was significantly poorer for patients with pT1 size lung adenocarcinomas invading the outer elastic layer of the pleura than those invading the inner elastic layer. The different outcomes in internal and external elastic invasion subgroups between the study of Warth et al. and ours can be explained at least in some parts by the completely different methodology. Their methodology different from ours includes (1) no lymph node metastasis was

Table 5 Correlation between pleural invasion and micropapillary pattern, stromal invasion grade, and small cluster invasion

	n	Tumor (%)		
		MPP-positive	SIG grade 3	SCI-positive
NPI	73	42/73 (57.5)*	42/73 (57.5)#	34/73 (46.6)$
IEL	26	17/26 (65.3)	20/26 (77.0)	17/26 (65.3)
OEL	25	22/25 (88.0)	24/25 (96.0)	22/25 (88.0)

MPP micropapillary pattern, *SIG* stromal invasion grade, *SCI* small cluster invasion, *NPI* no pleural invasion, *IEL* invasion of the internal elastic layer, *OEL* invasion of the outer elastic layer

*$P<0.001$, compared with MPP-positive OEL; #$P<0.001$, compared with OEL of the same grade; \$$P<0.001$, compared with SCI-positive OEL

Table 6 Results of univariate analysis

	Univariate analysis		Multivariate analysis	
	Hazard ratio (95 % CI)	*P* value	Hazard ratio (95 % CI)	*P* value
Age (≥65 years)	1.78 (0.84–3.75)	0.13		
Gender (F)	1.11 (0.54–2.27)	0.79		
Tumor size (≥2 cm)	1.82 (0.86–3.82)	0.12		
Lymph node metastasis (positive)	3.16 (1.45–6.88)	<0.01	3.12 (1.22–7.95)	0.02
SIG (grade 3)	6.29 (1.48–26.67)	0.01	3.08 (0.53–17.80)	0.21
MPP (positive)	2.87 (1.10–7.51)	0.03	1.70 (0.48–6.02)	0.41
SCI (positive)	4.40 (1.68–11.53)	<0.01	1.72 (0.48–6.20)	0.41
Lymphatic involvement in tumor (positive)	2.40 (1.16–4.96)	0.02	0.94 (0.36–2.44)	0.89
Vascular involvement in tumor (positive)	1.78 (0.85–3.89)	0.15		
Pleural invasion (OEL)	3.34 (1.57–7.07)	<0.01	1.82 (0.70–4.78)	0.22

CI confidence interval, *SIG* stromal invasion grade, *MPP* micropapillary pattern, *SCI* small cluster invasion, *OEL* invasion of the outer elastic layer

admitted to the case selection; 2) tumor size was not a selective criterion; 3) not only adenocarcinoma but also squamous cell carcinoma and other histological types of NSCLC were included; (4) the median follow-up was 40.6 months; and (5) no other clinicopathological factors except for the depth of pleural invasion were analyzed for a correlation with survival.

VPI is ordinarily defined as tumor extension beyond the elastic layer of the visceral pleura, regardless of its invasion of the pleural surface [4, 12]. The visceral pleura comprises two elastic layers that are easily recognized with elastic stains: one is the thick and continuous elastic layer beneath the submesothelial layer (the outer elastic layer), and the other is the thin and discontinuous elastic layer, which attaches to the alveolar septal elastic fibers (the inner elastic fiber) [6, 13]. It is a well-known fact that elastic layers are frequently duplicated or even triplicated, making it quite hard to recognize them. Furthermore, lung cancers, especially subpleural tumors, often cause pleural puckering, and the visceral pleural elastic layer could be invaded in three patterns: (1) without eliciting any secondary changes, (2) with prominent elastic reduplication and inflammatory infiltrates, and (3) with thick fibroblastic proliferation [6, 14]. In our study, the inner elastic layer sometimes became ill-defined and difficult to recognize even in sections prepared with elastin staining mostly due to the fibrous thickening of the visceral pleura and collapsed alveolar septal elastic fibers (Fig. 2g, h). Even in such occasions, the outer elastic layer could be recognized more easily than the inner elastic layer, because the former was thicker, continuous, and located close to the pleural surface. Moreover, in the tumor with entirely fused thick elastic layers, invasion of the outer elastic layer could be assessed by detecting carcinoma cells, which completely penetrated the elastic layer and reached outside of it. Therefore, the outer elastic layer is the more convenient and efficient landmark than the inner elastic layer.

The reported incidence of VPI in resected nonsmall cell lung carcinomas (NSCLCs) is between 16.2 and 26.8 % [3, 15–17]. VPI is an important prognostic factor in stage I and stage II NSCLCs [3, 5, 16]. However, it is not clear why VPI is associated with a poor prognosis. Previous studies indicated that VPI was significantly correlated with more extensive mediastinal lymph node involvement [3, 17]. Also, several studies reported that VPI is associated with N2 lymph node metastases [3, 16, 18]. These reports support the notion that VPI correlates with tumor invasion and metastasis through the subpleural lymphatics into the mediastinal lymph nodes. Anatomically, the visceral pleura contains many lymphatic and blood vessels sandwiched between the inner and outer elastic layers (subpleural layer) (Fig. 1). Based on these results, we speculated that adenocarcinomas with VPI penetrate the inner elastic layer and invade the lymphatic and blood vessels in the subpleural layer, leading to frequent lymph node metastasis compared with adenocarcinomas without VPI. In our study, however, the frequency of lymphovascular involvement in the pleura was not significantly different among the three types of VPI. In contrast, the frequency of lymphatic involvement in the tumor (in or around the central scar) was significantly higher in OEL than NPI and IEL (Table 3). Lymph node metastasis was found mostly in intrapulmonary and hilar nodes, and only five patients had skip metastasis to the mediastinal nodes. Furthermore, in VPI-positive cases (IEL and OEL), presence of lymphatic involvement in the tumor was also significantly associated with lymph node metastasis (Table 4). Thus, VPI might reflect poor prognosis not by pleural lymphatic involvement but by the presence of lymphatic involvement within the primary tumor itself. The lymphatic involvement in patients with stage I NSCLC is

reported to be indicative of tumor invasiveness [16, 19]. Furthermore, we divided tumors in our study into pT1a and pT1b size and analyzed them about the VPI, frequency of lymphovascular involvement in the pleura or in the tumor, and survival. Significantly more tumors with NPI (no pleural invasion) were found in pT1a tumors than pT1b tumors ($P<0.01$). The lymphatic involvement tended to be found more frequently in pT1b tumors than pT1a tumors, but their difference was not significant. Moreover, the depth of VPI was not significantly different between pT1a and pT1b tumors (data not shown).

We reported previously that high grade stromal invasion significantly correlated with shorter overall survival in patients with pT1 size adenocarcinomas and that MPP-positive tumors with stromal invasion grade 3 (SIG 3) were significantly associated with poorer prognosis than MPP-negative tumors with SIG 3 [10, 11]. Moreover, the presence of SCI also correlated with high grade stromal invasion, MPP, lymphatic involvement, and lymph node metastasis, leading to shorter survival. These results suggested that MPP, SIG, and SCI reflect tumor aggressiveness and invasiveness in pT1 size lung adenocarcinoma. In the present study, the presence of MPP, SIG, and SCI was significantly associated with invasion of the outer elastic layer of the pleura (OEL). Moreover, univariate analysis indicated that lymph node metastasis ($P<0.01$), SIG ($P=0.01$), MPP ($P=0.03$), SCI ($P<0.01$), and VPI ($P<0.01$) were related with shorter survival (Table 6). Considered together, invasion of the outer elastic layer seems to reflect high tumor invasiveness and aggressive behavior of pT1 size lung adenocarcinoma.

In conclusion, the present study demonstrated that the outer elastic layer of the pleura is a more useful landmark for the diagnosis of VPI than the inner elastic layer: (1) it is easier to recognize the outer layer of the pleura than the inner layer with elastic stain. (2) Invasion of the outer elastic layer of the pleura correlates with shorter survival and seems to reflect the invasiveness and aggressiveness of pT1 size lung adenocarcinomas. Thus, the routine use of elastic stains is suggestive in case of questionable pleural invasion in daily practice.

Acknowledgments We thank Ms. M. Onitsuka for the excellent technical assistance in immunohistochemical staining. This work was supported in part by a grant from the Research Center for Advanced Molecular Medicine, Fukuoka University.

Conflict of interest The authors declare no conflict of interest.

References

1. Brewer LA, Bai AF, Little JN, Rabago YPG (1958) Carcinoma of the lung; practical classification for early diagnosis and surgical treatment. J Am Med Assoc 166:1149–1155
2. Ichinose Y, Yano T, Asoh H, Yokoyama H, Yoshino I, Katsuda Y (1995) Prognostic factors obtained by a pathologic examination in completely resected non-small-cell lung cancer. An analysis in each pathologic stage. J Thorac Cardiovasc Surg 110:601–605
3. Manac'h D, Riquet M, Medioni J, Le Pimpec-Barthes F, Dujon A, Danel C (2001) Visceral pleura invasion by non-small cell lung cancer: an underrated bad prognostic factor. Ann Thorac Surg 71:1088–1093
4. Shimizu K, Yoshida J, Nagai K, Nishimura M, Yokose T, Ishii G, Nishiwaki Y (2004) Visceral pleural invasion classification in non-small cell lung cancer: a proposal on the basis of outcome assessment. J Thorac Cardiovasc Surg 127:1574–1578
5. Butnor KJ, Cooper K (2005) Visceral pleural invasion in lung cancer: recognizing histologic parameters that impact staging and prognosis. Adv Anat Pathol 12:1–6
6. Travis WD, Brambilla E, Rami-Porta R, Vallieres E, Tsuboi M, Rusch V, Goldstraw P (2008) Visceral pleural invasion: pathologic criteria and use of elastic stains: proposal for the 7th edition of the TNM classification for lung cancer. J Thorac Oncol 3:1384–1390
7. Butnor KJ, Vollmer RT, Blaszyk H, Glatz K (2007) Interobserver agreement on what constitutes visceral pleural invasion by non-small cell lung carcinoma: an internet-based assessment of international current practices. Am J Clin Pathol 128:638–647
8. Warth A, Muley T, Herpel E, Pfannschmidt J, Hoffmann H, Dienemann H, Schirmacher P, Schnabel PA (2010) A histochemical approach to the diagnosis of visceral pleural infiltration by non-small cell lung cancer. Pathol Oncol Res 16:119–123
9. Travis WD et al (2011) International Association for the Study of Lung Cancer/American Thoracic Society/European Respiratory Society: international multidisciplinary classification of lung adenocarcinoma: executive summary. Proc Am Thorac Soc 8:381–385
10. Kawakami T, Nabeshima K, Hamasaki M, Iwasaki A, Shirakusa T, Iwasaki H (2009) Small cluster invasion: a possible link between micropapillary pattern and lymph node metastasis in pT1 lung adenocarcinomas. Virchows Arch 454:61–70
11. Kawakami T, Nabeshima K, Makimoto Y, Hamasaki M, Iwasaki A, Shirakusa T, Iwasaki H (2007) Micropapillary pattern and grade of stromal invasion in pT1 adenocarcinoma of the lung: usefulness as prognostic factors. Mod Pathol 20:514–521
12. Osaki T, Nagashima A, Yoshimatsu T, Yamada S, Yasumoto K (2004) Visceral pleural involvement in nonsmall cell lung cancer: prognostic significance. Ann Thorac Surg 77:1769–1773, discussion 1773
13. Hiroshima K et al (2009) Malignant pleural mesothelioma: clinicopathology of 16 extrapleural pneumonectomy patients with special reference to early stage features. Pathol Int 59:537–545
14. Gallagher B, Urbanski SJ (1990) The significance of pleural elastica invasion by lung carcinomas. Hum Pathol 21:512–517
15. Hung JJ, Wang CY, Huang MH, Huang BS, Hsu WH, Wu YC (2007) Prognostic factors in resected stage I non-small cell lung cancer with a diameter of 3cm or less: visceral pleural invasion did not influence overall and disease-free survival. J Thorac Cardiovasc Surg 134:638–643
16. Shimizu K, Yoshida J, Nagai K, Nishimura M, Ishii G, Morishita Y, Nishiwaki Y (2005) Visceral pleural invasion is an invasive and aggressive indicator of non-small cell lung cancer. J Thorac Cardiovasc Surg 130:160–165
17. Takizawa T, Terashima M, Koike T, Watanabe T, Kurita Y, Yokoyama A, Honma K (1998) Lymph node metastasis in small peripheral adenocarcinoma of the lung. J Thorac Cardiovasc Surg 116:276–280
18. Kang JH, Kim KD, Chung KY (2003) Prognostic value of visceral pleura invasion in non-small cell lung cancer. Eur J Cardiothorac Surg 23:865–869
19. Harada M, Hato T, Horio H (2011) Intratumoral lymphatic vessel involvement is an invasive indicator of completely resected pathologic stage I non-small cell lung cancer. J Thorac Oncol. 6:48-54

Virchows Arch (2012) 461:521–530
DOI 10.1007/s00428-012-1321-0

ORIGINAL ARTICLE

HER3 overexpression is a prognostic indicator of extrahepatic cholangiocarcinoma

Hee Jin Lee · Joon-Yong Chung · Stephen M. Hewitt · Eunsil Yu · Seung-Mo Hong

Received: 28 May 2012 / Revised: 20 August 2012 / Accepted: 21 September 2012 / Published online: 2 October 2012
© Springer-Verlag Berlin Heidelberg 2012

Abstract Members of the HER (ERBB) receptor protein tyrosine kinase family play an important role in regulating cellular division, proliferation, differentiation, and migration and have prognostic significance in a number of cancers. Here, we sought to define their role in extrahepatic cholangiocarcinoma (EHCC). HER2 and HER3 protein expression was studied in 230 EHCC cases using a tissue microarray and compared with clinicopathological variables, including the survival of EHCC patients. HER3 was predominantly localized to the cytoplasm, whereas HER2 exhibited a membranous expression pattern. Overexpression of HER2 and HER3 was observed in 6 % (13/224) and 39 % (90/230) of EHCCs, respectively. Membranous HER2 overexpression occurred more frequently in intraductal papillary neoplasms with an associated invasive carcinoma than in tubular adenocarcinomas (P=0.02). HER3 protein was more commonly overexpressed in nodular and infiltrative than in papillary tumors (P=0.03). HER3 overexpression was associated with decreased survival in both univariate (P=0.01) and multivariate (P=0.008) analyses, whereas HER2 overexpression was not associated with survival. HER2 and HER3 are overexpressed in subsets of EHCC patients. Notably, HER3 overexpression is correlated with decreased patient survival, suggesting that HER3 constitutes a prognostic factor as well as a potential candidate for targeted therapy.

H. J. Lee · E. Yu · S.-M. Hong (✉)
Department of Pathology, Asan Medical Center,
University of Ulsan College of Medicine,
388-1, Pungnap-dong, Songpa-gu,
Seoul 138-736, Korea
e-mail: smhong28@gmail.com

J.-Y. Chung · S. M. Hewitt
Applied Molecular Pathology Laboratory
and Tissue Array Research Program, Laboratory of Pathology,
National Cancer Institute, National Institutes of Health,
Bethesda MD, USA

Keywords Extrahepatic · Bile duct · Cholangiocarcinoma · HER2 · HER3 · Immunohistochemistry · Prognosis

Introduction

Extrahepatic cholangiocarcinoma (EHCC) is a malignant epithelial neoplasm of the biliary tract, from the hepatic hilum to the distal bile duct, that accounts for 70–90 % of all cholangiocarcinomas [1]. EHCC is a relatively uncommon cancer in Western countries but is more prevalent in Eastern Asian countries, including Korea [1–3]. Surgical resection of the tumor is the only curative therapeutic modality for patients with EHCC but can be applied only in a limited number of patients with localized or locally advanced disease [4]. The 5-year survival rate of EHCC patients following surgical resection is approximately 20 % [5]. Several neoadjuvant therapies, including chemotherapy, radiation therapy, and photodynamic therapy, have been extensively studied, but none have yielded significant survival advantages for EHCC patients [1, 6]. Therefore, identification of new biomarkers for early detection and/or development of new therapeutic regimens based on a better understanding of the biological mechanisms of this deadly disease are essential for decreasing mortality among EHCC patients.

Epidermal growth factor receptors (EGFRs) are members of a membrane receptor protein tyrosine kinase family that includes HER1 (ErbB1/EGFR), HER2 (ErbB2), HER3 (ErbB3), and HER4 (ErbB4). After binding ligands, EGFRs are activated by receptor homo- or heterodimerization, resulting in the phosphorylation of various downstream substrates, which mediate intracellular signal transduction. EGFR signaling pathways play an important role in regulating cell division, proliferation, differentiation, and migration [7]. The EGFR family member HER3 lacks intrinsic protein tyrosine kinase activity [8]. However, binding of

neuregulin family ligands enables HER3 to form functional heterodimers with EGFR or HER2 that act through the cytoplasmic domain of HER3 to exert tyrosine phosphorylation activity [9]. Thus, by heterodimerizing with other EGFR proteins, HER3 can participate in diverse signal transduction cascades and regulate various cellular processes [7, 9]. The development of tyrosine kinase inhibitors of EGFR or HER2 was initially considered a promising strategy for blocking EGFR or HER2 pathways in several solid cancers, including breast and lung cancers. However, evidence suggests that HER3 may be responsible for the resistance to these therapeutic regimens, which often develops [10]. Overexpression of HER3 has been reported in several malignant neoplasms in gastrointestinal tract organs, including gastric [11–13], colorectal [14–19], and ampulla of Vater [18] cancers. Although a few studies have demonstrated HER2 expression in cholangiocarcinoma, showing that it is relatively infrequent in these tumors [20–23], there have been no comprehensive studies of HER2 and HER3 expression in EHCCs. In the current study, we analyzed HER2 and HER3 protein expression in 230 EHCC cases using tissue microarray immunohistochemistry. We demonstrate that HER3 expression in EHCC constitutes a prognostic factor.

Materials and methods

Patients and tumor samples

The study population consisted of 230 patients with surgically resected EHCCs treated at Asan Medical Center, University of Ulsan College of Medicine, in Seoul, South Korea, between 1991 and 2005. Carcinomas with an epicenter in the extrahepatic bile duct were included in this study, whereas carcinomas from the ampulla of Vater or pancreas were not. Carcinomas arising in the gallbladder or intrahepatic bile duct with extension to the extrahepatic bile duct were also excluded. Information regarding the age and gender of patients, surgical procedure, survival time, and survival status was obtained by reviewing EHCC patients' medical records. Data pertinent to location, size, and growth pattern of the tumor were obtained from surgical pathology reports. Materials were obtained with appropriate human protection approval from the Institutional Review Board of the Asan Medical Center (Project Number 2011–0734). Information regarding post-operative radiation, chemotherapy, and performance status of patients was not analyzed in this study.

Tissue microarray construction

Tissue microarrays were constructed from archival formalin-fixed, paraffin-embedded tissue blocks as previously described [24]. Briefly, 230 extrahepatic cholangiocarcinoma cases and 12 normal extrahepatic bile ducts were included. A representative area was carefully selected for each tumor or normal biliary epithelia from a hematoxylin-and-eosin-stained section of a donor block. Each case was represented by two to four 1.5-mm-diameter cores.

Immunohistochemistry and scoring

Immunohistochemistry was performed on 4-μm-thick tissue microarray sections as previously described [25]. Briefly, tissue sections were deparaffinized and hydrated in xylene and serially diluted ethanol, respectively. Endogenous peroxidase was blocked by incubation in 3 % H_2O_2 for 10 min. Antigen retrieval was performed in a steam pressure cooker using preheated antigen retrieval buffer, pH 6 (Dako, Glostrup, Denmark), at 95 °C for 10 min. Non-specific binding of antibodies was minimized by incubating sections with Protein Block (Dako) for 15 min. Microarrays were incubated at room temperature for 30 min with rabbit polyclonal anti-HER2 (c-erbB2, A0485; 1:750 dilution; Dako) or overnight at 4 °C with mouse monoclonal anti-HER3 (RTJ.2, 1:500 dilution; Santa Cruz, CA, USA). Antigen–antibody reactions were detected with an LSAB+peroxidase kit (Dako) and 3,3′-diaminodbenzidine (Dako). Negative controls were composed of identically treated histologic sections with the omission of primary antibodies. Immunostained sections were lightly counterstained with hematoxylin, dehydrated in ethanol, and cleared in xylene. We did not perform immunohistochemistry for Her2 and Her3 on full sections. Tissue core representativity might be a concern, but certainly for 1.5-mm cores previous studies have demonstrated that two to four tissue cores are representative with 95–97 % concordance rate [62].

HER2 protein expression was scored on a scale of 0 to 3 using the following gastric cancer staging system [26]: 0, no reactivity or membranous reactivity in less than 10 % of cells; 1+, faint/barely perceptible membranous reactivity in ≥10 % of cells or reactivity in only part of the cell membrane; 2+, weak to moderate complete or basolateral membranous reactivity in ≥10 % of tumor cells; 3+, strong complete or basolateral membranous reactivity in ≥10 % of tumor cells. Cases receiving a HER2 score of 3+ were considered positive for HER2 expression.

The results of immunohistochemical staining for HER3 were scored based on the intensity of staining as 0 (negative), 1 (weak), or 2 (strong), and the percentage of positive epithelial cells as 0 (<5 %), 1 (6–25 %), 2 (26–50 %), 3 (51–75 %), or 4 (>76 %). A Histo-score was generated as the product of intensity and area. The Histo-score was then dichotomized into no/lower expression (Histo-score, 0–6) and overexpression (Histo-score, 8).

Statistical analysis

Statistical analyses were performed using SPSS version 17 (SPSS Inc., Chicago, IL, USA). Associations between categorical variables were examined using Pearson's chi-square and Fisher's exact tests. Survival curves were calculated by the Kaplan–Meier method, and statistical significance was evaluated using the log-rank test and the Cox proportional hazards regression model. $P<0.05$ was considered as statistically significant.

Results

Clinicopathological characteristics of cases

The clinicopathological characteristics of cases are summarized in Table 1. Patient age ranged from 30 to 84 years (mean, 60.9 years). Of the 230 patients, 164 were men and 66 were women. Tumor size ranged from 0.5 to 6 cm (mean, 2.5 cm). Thirty-one cases were pT1 tumors, 84 were pT2, 91 were pT3, and 24 were pT4. The length of patient follow-up time ranged from 1 to 127 months, and median survival time at last follow-up was 22 months.

HER2 and HER3 expression

HER2 protein expression patterns were analyzed in tumors from a total of 224 EHCC patients using tissue microarray immunohistochemistry. Information regarding six patients was excluded from the HER2 analysis because their tissue microarray cores were either detached or folded during the HER2 immunohistochemical staining procedure. Representative images of the expression of HER2 and HER3 in EHCC tumors and normal biliary epithelial cells are shown in Fig. 1. All 12 samples of normal biliary epithelial cells did not show immunoreactivity for either HER2 or HER3. HER3 was predominantly distributed in a cytoplasmic pattern, whereas HER2 was mainly localized to the cell membrane in EHCC cases. HER2 and HER3 overexpression was observed in 6 % (13/224 cases) and 39 % (90/230 cases) of EHCCs, respectively. Only the histological subtype was significantly associated with HER2 overexpression ($P=0.02$). Specifically, intraductal papillary neoplasms with associated invasive carcinoma cases showed significantly more HER2 overexpression than other histological subtypes, including tubular adenocarcinoma, adenosquamous carcinoma, intestinal type adenocarcinoma, and mucinous carcinoma, which did not express HER2 (Table 2). HER3 protein was more commonly overexpressed in nodular and infiltrative tumors than in papillary tumors ($P=0.03$). HER3 overexpression was more frequent in cases without than in cases with invasion of the pancreas ($P=0.02$).

Table 1 Clinicopathologic characteristics of patients with EHCC

Variables	No. of patients
Mean age	230
60.9 years	
Gender	
Male	164
Female	66
Mean tumor size	230
2.5 cm	
Location	
Perihilar	106
Distal	118
Diffuse	6
Histologic subtype	
Tubular adenocarcinoma	193
Intraductal papillary neoplasm with an associated invasive carcinoma	15
Intestinal type adenocarcinoma	9
Mucinous carcinoma	4
Adenosquamous carcinoma	6
Clear cell carcinoma	1
Signet ring cell carcinoma	1
Sarcomatoid carcinoma	1
pT classification	
pT1	31
pT2	84
pT3	91
pT4	24
Lymph node metastasis	
Present	76
Absent	154
Hepatic invasion	
Present	10
Absent	220
Pancreatic invasion	
Present	104
Absent	126
Duodenal invasion	
Present	24
Absent	206
Perineural invasion	
Present	167
Absent	63
Vascular invasion	
Present	71
Absent	159

Among 13 HER2-overexpressing EHCCs, seven (54 %) showed HER3 overexpression. There was a significant

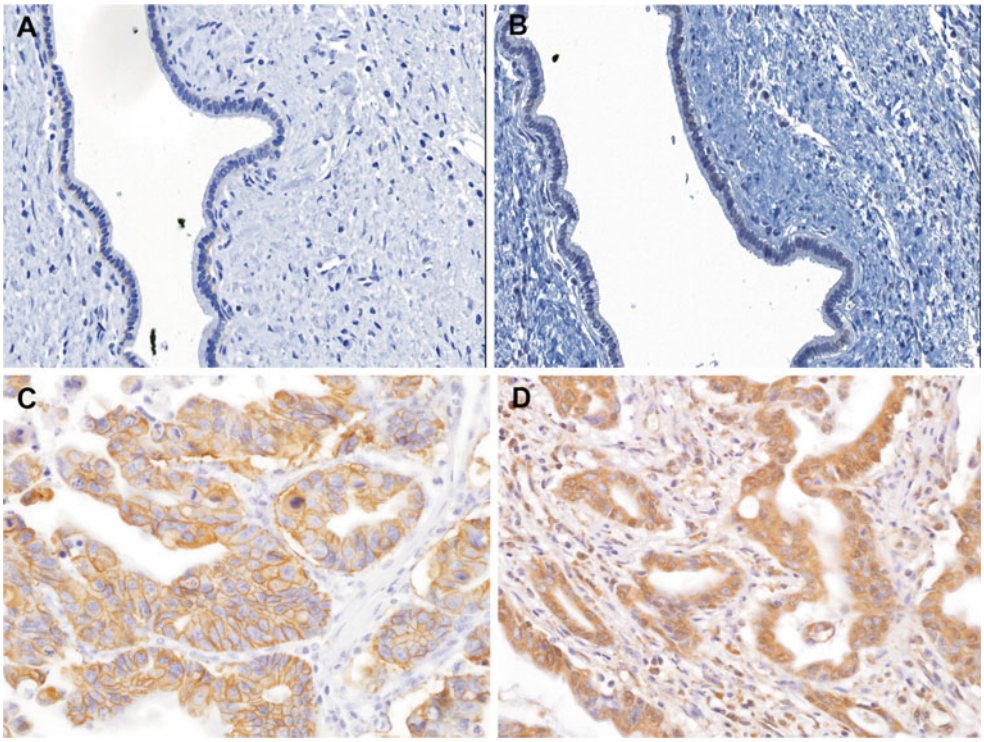

Fig. 1 Representative immunohistochemical staining of HER2 and HER3 in EHCC. Normal bile duct epithelia show negativity for HER2 (**a**) and HER3 (**b**). Cholangiocarcinoma show strong and complete membranous expression of HER2 (**c**) and diffuse and strong cytoplasmic HER3 immunopositivity (**d**)

correlation between cases with HER2 overexpression and those with HER3 overexpression (R=0.24, P<0.001) but not between HER2 and HER3 co-overexpression and clinicopathological parameters (Table 3).

Survival analysis

Median survival of patients with HER3 overexpression (24.0 months) was significantly worse than that of patients with no/lower HER3 expression (31.9 months; P=0.01, log-rank test; Fig. 2a). The 1-, 3-, and 5-year survival rates in the HER3-overexpression group were 82.2, 22.6, and 13.9 %, respectively, whereas the corresponding rates in the no/lower HER3-expression group were 82.6, 40.5, and 31.2 %.

There was no significant difference in survival between patients with HER2 overexpression (median survival, 25.9 months) and those without HER2 expression (median survival, 27.8 months; P=0.17, log-rank test; Fig. 2b).

Median survival of EHCC patients with both HER2 and HER3 overexpression (24.8 months) tended to be lower than that in patients without HER2 and HER3 co-overexpression (28.0 months; P=0.08; Fig. 2c), but this did not reach statistical significance.

Association between survival and other clinicopathological factors

The relationships between other clinicopathological variables and survival are summarized in Table 4. Of these additional clinicopathological variables, tumor differentiation status (P<0.001), pT classification (P=0.01), lymph node metastasis (P<0.001), liver invasion (P=0.01), and vascular invasion (P=0.02) were also significantly associated with survival. In contrast, survival was not associated with gender (P=0.38), tumor location (P=0.47), growth pattern (P=0.09), pancreatic invasion (P=0.24), duodenal invasion (P=0.07), perineural invasion (P=0.36), or resection margin status (P=0.10).

Multivariate analysis of clinicopathological factors

The independent prognostic significance of HER3 expression as well as of other clinicopathological parameters was determined by applying the Cox proportional hazards model (Table 5). HER3 overexpression (P=0.007), differentiation (P=0.002), liver invasion (P=0.03), and lymph node metastasis (P=0.002) remained as prognostic factors.

Discussion

In this study, we observed overexpression of HER2 and HER3 protein in a subset of EHCCs, with about 6 % of EHCC cases overexpressing HER2 (13/224) and 39 % (90/230) overexpressing HER3. In addition, we found HER3 overexpression to be an independent prognostic factor in EHCC patients. HER3 is unique among members of the

Table 2 Comparison between HER2 and HER3 immunohistochemical staining results and clinicopathologic factors in EHCC

Variable	Total no. of cases	HER2 expression (%)	*P*-value	Total no. of cases	HER3 expression (%)	*P*-value
Gender			0.36			0.46
Male	161	11 (6.8)		164	67 (40.9)	
Female	63	2 (3.2)		66	23 (34.8)	
Location			0.18			0.21
Perihilar	101	9 (8.9)		106	48 (45.3)	
Distal	117	4 (3.4)		118	40 (33.9)	
Diffuse	6	0 (0.0)		6	2 (33.3)	
Growth pattern			0.39			0.03*
Papillary	22	1 (4.5)		23	4 (17.4)	
Nodular	14	2 (14.3)		14	8 (57.1)	
Infiltrative	188	10 (5.3)		193	78 (40.4)	
Differentiation			1			0.13
Well differentiated	63	4 (6.3)		66	32 (48.5)	
Moderately differentiated	123	7 (5.7)		125	46 (36.8)	
Poorly differentiated	38	2 (5.3)		39	12 (30.8)	
Histologic subtype			0.02*			0.64
Tubular adenocarcinoma	188	8 (4.3)		193	73 (37.8)	
Intraductal papillary neoplasm with an associated invasive carcinoma	14	5 (35.7)		15	7 (46.7)	
Intestinal type adenocarcinoma	9	0 (0.0)		9	5 (55.6)	
Mucinous carcinoma	4	0 (0.0)		4	1 (25.0)	
Adenosquamous carcinoma	6	0 (0.0)		6	2 (33.3)	
Clear cell carcinoma	1	0 (0.0)		1	1 (100.0)	
Signet ring cell carcinoma	1	0 (0.0)		1	0 (0.0)	
Sarcomatoid carcinoma	1	0 (0.0)		1	1 (100.0)	
pT classification			0.35			0.08
pT1	29	3 (10.3)		31	16 (51.6)	
pT2	82	6 (7.3)		84	38 (45.2)	
pT3	89	4 (4.5)		91	27 (29.7)	
pT4	24	0 (0.0)		24	9 (37.5)	
Duodenal invasion			0.37			1
Absent	200	13 (6.5)		206	81 (39.3)	
Present	24	0 (0.0)		24	9 (37.5)	
Hepatic invasion			1			0.74
Absent	215	12 (5.6)		220	87 (39.5)	
Present	9	1 (11.1)		10	3 (30.0)	
Pancreatic invasion			0.15			0.02*
Absent	121	10 (8.3)		126	58 (46.0)	
Present	103	3 (2.9)		104	32 (30.8)	
Perineural invasion			0.2			0.13
Absent	62	6 (9.7)		63	30 (47.6)	
Present	162	7 (4.3)		167	60 (35.9)	
Vascular invasion			0.56			0.56
Absent	154	10 (6.5)		159	60 (37.7)	
Present	70	3 (4.3)		71	30 (42.3)	
Lymph node metastasis			1			0.67
Absent	153	9 (5.9)		154	62 (40.3)	
Present	71	4 (5.6)		76	28 (36.8)	

Table 2 (continued)

Variable	Total no. of cases	HER2 expression (%)	*P*-value	Total no. of cases	HER3 expression (%)	*P*-value
Resection marginal status			1			0.15
Negative	173	10 (5.8)		176	64 (36.4)	
Positive	51	3 (5.9)		54	26 (48.1)	
Stage grouping			0.46			0.4
Stage IA	24	3 (12.5)		25	12 (48.0)	
Stage IB	60	3 (5.0)		60	28 (46.7)	
Stage IIA	58	3 (5.2)		58	18 (31.0)	
Stage IIB	58	4 (6.9)		63	23 (36.5)	
Stage III	24	0 (0.0)		24	9 (37.5)	

*$P<0.05$ (significant)

HER receptor tyrosine kinase family in that it lacks intrinsic tyrosine kinase activity but it does contain six consensus phosphotyrosine sites, which bind the SH2 domain of the three regulatory subunits of phosphoinositide-3-kinase (PI3K) [27, 28]. Binding of HER3 can activate the PI3K/Akt signaling pathway, which is a critical regulator of many cellular processes. HER2-mediated transformation of epithelial cells is associated with the activation of the PI3K/Akt signaling pathway in breast cancer. Several targeted therapeutics, including trastuzumab, a monoclonal antibody against the extracellular domain of HER2, and lapatinib, an EGFR/HER2 tyrosine kinase inhibitor, have been approved for use in the treatment of HER2-overexpressing breast cancers. It has been proposed that inhibition of HER3 phosphorylation and blockade of the PI3K/Akt signaling pathway are required in order to obtain a tumor suppression effect despite differences in the operating mechanisms of these therapeutic agents [29]. HER2–HER3 heterodimerization plays a key role in HER2-mediated transformation, tumor progression, and drug resistance [29]. Previous studies on loss of HER3 expression in HER2-dependent cells have demonstrated reduced PI3K signaling and decreased cell proliferation, suggesting that HER3 is essential for HER2-driven carcinogenesis [30, 31]. Treatment of HER2-amplified tumors with tyrosine kinase inhibitors results in a compensatory increase in HER3 expression, membranous HER3 localization, and decreased HER3 dephosphorylation [32]. MET-dependent phosphorylation of HER3 has been identified as one mechanism of resistance to EGFR inhibitors in lung cancer [33]. A recent study demonstrated that blocking both HER2 and HER3 inhibits the PI3K/Akt pathway more effectively than blocking HER2 or HER3 alone, suggesting that also HER3 should be inhibited in patients with HER2- and PI3K-dependent cancers in order to completely block the PI3K/Akt pathway [29]. Our group previously demonstrated that the Akt pathway is activated in a large proportion of EHCCs (84 %) [24]. In the present study, we demonstrate that HER3 is overexpressed in 39 % of EHCC cases. Considering the current study and the results of previous studies of breast cancers and EHCCs, we hypothesize that application of a therapeutic regimen for blocking HER3, such as AMG888, together with HER2 inhibitors and PI3K inhibitors might be effective in a subset of EHCC patients with activated Akt and HER3.

HER3 overexpression has been identified in malignant neoplasms from several organs, including melanoma, and prostate, colorectal, lung, ovarian, and gastric cancers [17, 30, 34–38]. In addition, HER3 overexpression has been reported to be associated with a worse outcome in melanomas and lung and gastric cancers [34, 38, 39]. Although HER3 is specifically required for HER2-driven tumorigenesis and has been extensively studied in the HER2-amplified subtype of breast cancers, other types of cancer also show higher HER3 expression without accompanying HER2 overexpression [30, 40]. In these tumors, HER3 may function as an allosteric activator of other members of the HER receptor tyrosine kinase family, such as EGFR [41–43]. EGFR expression has been reported in 8–57 % of cholangiocarcinomas, and patients with EGFR-positive tumors showed worse clinical outcome than those with EGFR-negative cancers [20, 23, 44, 45]. The absence of a survival difference in patients with HER2 overexpression and the significantly shorter survival in patients with HER3 overexpression, as demonstrated in this

Table 3 Comparison of results of immunohistochemical staining for HER2 and HER3 co-expression with clinicopathologic factors in EHCC

Variable	Total no. of cases	HER2 and HER3 co-overexpression (%)	*P*-value
Gender			0.2
Male	161	7 (4.3)	
Female	63	0 (0.0)	
Location			0.09
Perihilar	101	6 (5.9)	
Distal	117	1 (0.9)	
Diffuse	6	0 (0.0)	
Growth pattern			0.36
Papillary	22	0 (0.0)	
Nodular	14	1 (7.1)	
Infiltrative	188	6 (3.2)	
Differentiation			1
Well differentiated	63	2 (3.2)	
Moderately differentiated	123	4 (3.3)	
Poorly differentiated	38	1 (2.6)	
Histologic subtype			0.12
Tubular adenocarcinoma	188	4 (2.1)	
Intraductal papillary neoplasm with an associated invasive carcinoma	14	3 (21.4)	
Intestinal type adenocarcinoma	9	0 (0.0)	
Mucinous carcinoma	4	0 (0.0)	
Adenosquamous carcinoma	6	0 (0.0)	
Clear cell carcinoma	1	0 (0.0)	
Signet ring cell carcinoma	1	0 (0.0)	
Sarcomatoid carcinoma	1	0 (0.0)	
pT classification			0.66
pT1	29	1 (3.4)	
pT2	82	4 (4.9)	
pT3	89	2 (2.2)	
pT4	24	0 (0.0)	
Duodenal invasion			0.61
Absent	200	7 (3.5)	
Present	24	0 (0.0)	
Hepatic invasion			1
Absent	215	7 (3.3)	
Present	9	0 (0.0)	
Pancreatic invasion			0.46
Absent	121	5 (4.1)	
Present	103	2 (1.9)	
Perineural invasion			0.4
Absent	62	3 (4.8)	
Present	162	4 (2.5)	
Vascular invasion			0.44
Absent	154	6 (3.9)	
Present	70	1 (1.4)	
Lymph node metastasis			1
Absent	153	5 (3.3)	
Present	71	2 (2.8)	
Resection marginal status			1
Absent	173	5 (2.9)	
Present	51	2 (3.9)	
Stage grouping			0.94
Stage IA	24	1 (4.2)	
Stage IB	60	2 (3.3)	
Stage IIA	58	2 (3.4)	
Stage IIB	58	2 (3.4)	
Stage III	24	0 (0.0)	

study, suggest a possible link between shorter survival time in the HER3-overexpression group and EGFR–HER3 heterodimerization in a subset of these patients. These patients may benefit from a therapeutic regimen that includes other types of HER inhibitors, including erlotinib, cetuximab, and lapatinib, which have been investigated recently in cholangiocarcinomas [46–50].

HER2 overexpression in cholangiocarcinomas has been explored in various studies and has shown to vary widely (between 5 and 76 %) [20, 51–57]. These discrepancies might be explained by the lack of a standardized methodology, different standards of interpretation, or differences in tumor location. In recent reports, the HER2 expression rate in resected EHCCs was reported to be 5 to 10 % [20, 23, 45, 52]. The approximately 6 % HER2 expression rate identified in the current study is in agreement with these previous studies. Consistent with some previous reports, we found a higher HER2 overexpression rate in intraductal papillary neoplasm with an associated invasive carcinoma than in other histological types [20, 45, 54]. Although the HER2 overexpression rate is not exceptionally high in EHCCs, a subset of patients with HER2 overexpression might benefit from HER2-targeted monoclonal therapy.

The recently updated (7th edition) American Joint Committee on Cancer Staging Manual divided EHCCs into perihilar and distal bile duct cancers [58]. The term “distal bile duct cancers” was applied to cancers distal to the insertion of the cystic duct. This division reflects the growing evidence for distinct biological patterns in perihilar and distal EHCCs

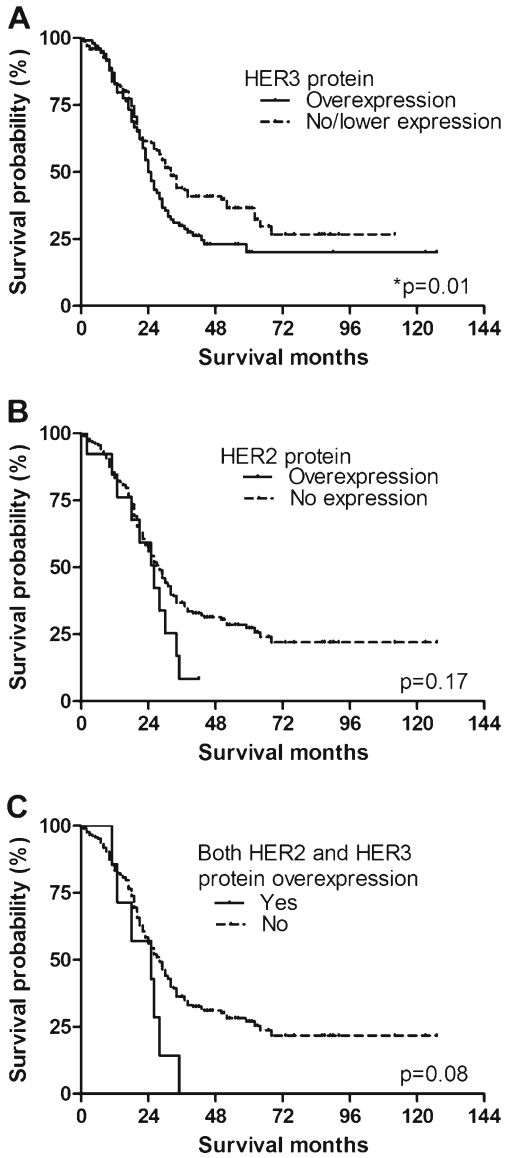

Fig. 2 Survival curves stratified by HER2 and HER3 expression in EHCC patients. **a** Median survival in patients in the HER3-overexpression group (24.0 months) was significantly shorter than that for patients in the no/lower HER3-expression group (31.9 months; P=0.01, log-rank test). **b** Survival was not significantly different between patients in the HER2-overexpression group (25.9 months) and the no/lower HER2-expression group (27.8 months; P=0.17, log-rank test). **c** Median survival in EHCC patients with both HER2 and HER3 co-overexpression (24.8 months) was marginally different from that in patients without HER2 and HER3 co-overexpression (28.0 months; P=0.08)

[59–61]. However, in our study, the proportions of HER2 and HER3 overexpression were similar in perihilar and distal bile duct cancer groups.

In conclusion, HER2 and HER3 proteins are overexpressed in subsets of EHCCs. HER3 overexpression is correlated with decreased patient survival and therefore constitutes a prognostic factor and a potential therapeutic target in patients with EHCCs.

Table 4 Univariate analysis of pathologic features affecting survival in EHCC patients

Variable	Characteristics	Median survival time (month)	*P*-value	95 % confidence interval	
				Lower	Upper
HER2 expression	Low	27.8	0.17	24.2	31.4
	High	25.9		18.6	33.2
HER3 expression	Low	31.9	0.01*	27.3	36.5
	High	24.0		22.0	26.0
Gender	Male	28.4	0.38	24.8	32.0
	Female	21.8		15.0	28.6
Location	Perihilar	24.8	0.47	21.1	28.4
	Distal	30.0		25.5	34.5
	Diffuse	12.0		0	42.7
Growth pattern	Papillary	50.0	0.09		
	Nodular	30.0		10.8	49.2
	Infiltrative	25.9		22.2	29.6
Differentiation	Well	34.0	<0.001*	24.0	44.0
	Moderate	26.8		22.5	31.2
	Poor	17.5		11.0	24.0
pT classification	pT1	44.0	0.01*		
	pT2	24.9		22.2	27.6
	pT3	25.9		19.0	32.9
	pT4	27.0		14.5	39.5
Perineural invasion	Absent	28.9	0.36	21.8	36.0
	Present	26.1		21.8	30.4
Vascular invasion	Absent	28.9	0.02*	22.9	34.9
	Present	26.1		20.9	31.2
Duodenal invasion	Absent	26.9	0.07	23.6	30.2
	Present	27.0		14.5	39.5
Liver invasion	Absent	28.0	0.01*	24.9	31.1
	Present	17.5		0.0	35.7
Pancreas invasion	Absent	26.1	0.24	21.6	30.6
	Present	27.0		22.2	31.8
Resection margin status	Negative	28.8	0.1	24.9	32.7
	Positive	23.1		17.5	28.7
Lymph node metastasis	Absent	30.0	<0.001*	27.0	33.0
	Present	18.2		15.5	20.9

*P<0.05 (significant)

Table 5 Multivariate analysis for prognosis in EHCC

Variable	*P*-value	Relative risk	95 % confidence interval
HER3 expression	0.007*	1.6	1.14–2.26
Differentiation	0.002*	1.52	1.16–2.00
pT classification	0.066	1.21	0.99–1.48
Vascular invasion	0.646	1.1	0.75–1.62
Liver invasion	0.025*	2.47	1.12–5.45
Lymph node metastasis	0.002*	1.81	1.25–2.65

Duodenal invasion was not included because it was a covariate with pT classification

*P<0.05 (significant)

Acknowledgments We thank Ylaya Kris for technical assistance.

Conflict of interest The authors declare that they have no conflict of interest.

References

1. Malhi H, Gores GJ (2006) Cholangiocarcinoma: modern advances in understanding a deadly old disease. J Hepatol 45:856–867
2. Hong SM, Kim MJ, Pi DY, Jo D, Cho HJ, Yu E, Ro JY (2005) Analysis of extrahepatic bile duct carcinomas according to the New American Joint Committee on Cancer staging system focused on tumor classification problems in 222 patients. Cancer 104:802–810
3. Nagakawa T, Kayahara M, Ikeda S, Futakawa S, Kakita A, Kawarada H, Matsuno M, Takada T, Takasaki K, Tanimura H, Tashiro S, Yamaoka Y (2002) Biliary tract cancer treatment: results from the Biliary Tract Cancer Statistics Registry in Japan. J Hepatobiliary Pancreat Surg 9:569–575
4. Seyama Y, Makuuchi M (2007) Current surgical treatment for bile duct cancer. World J Gastroenterol 13:1505–1515
5. Nathan H, Pawlik TM, Wolfgang CL, Choti MA, Cameron JL, Schulick RD (2007) Trends in survival after surgery for cholangiocarcinoma: a 30-year population-based SEER database analysis. J Gastrointest Surg 11:1488–1496, discussion 1496–1487
6. Thomas MB (2007) Biological characteristics of cancers in the gallbladder and biliary tract and targeted therapy. Crit Rev Oncol Hematol 61:44–51
7. Sithanandam G, Anderson LM (2008) The ERBB3 receptor in cancer and cancer gene therapy. Cancer Gene Ther 15:413–448
8. Guy PM, Platko JV, Cantley LC, Cerione RA, Carraway KL 3rd (1994) Insect cell-expressed p180erbB3 possesses an impaired tyrosine kinase activity. Proc Natl Acad Sci U S A 91:8132–8136
9. Citri A, Yarden Y (2006) EGF-ERBB signalling: towards the systems level. Nat Rev Mol Cell Biol 7:505–516
10. Hsieh AC, Moasser MM (2007) Targeting HER proteins in cancer therapy and the role of the non-target HER3. Br J Cancer 97:453–457
11. Poller DN, Spendlove I, Baker C, Church R, Ellis IO, Plowman GD, Mayer RJ (1992) Production and characterization of a polyclonal antibody to the c-erbB-3 protein: examination of c-erbB-3 protein expression in adenocarcinomas. J Pathol 168:275–280
12. Sanidas EE, Filipe MI, Linehan J, Lemoine NR, Gullick WJ, Rajkumar T, Levison DA (1993) Expression of the c-erbB-3 gene product in gastric cancer. Int J Cancer 54:935–940
13. Slesak B, Harlozinska A, Porebska I, Bojarowski T, Lapinska J, Rzeszutko M, Wojnar A (1998) Expression of epidermal growth factor receptor family proteins (EGFR, c-erbB-2 and c-erbB-3) in gastric cancer and chronic gastritis. Anticancer Res 18:2727–2732
14. Ciardiello F, Kim N, Saeki T, Dono R, Persico MG, Plowman GD, Garrigues J, Radke S, Todaro GJ, Salomon DS (1991) Differential expression of epidermal growth factor-related proteins in human colorectal tumors. Proc Natl Acad Sci U S A 88:7792–7796
15. Maurer CA, Friess H, Kretschmann B, Zimmermann A, Stauffer A, Baer HU, Korc M, Buchler MW (1998) Increased expression of erbB3 in colorectal cancer is associated with concomitant increase in the level of erbB2. Hum Pathol 29:771–777
16. Kapitanovic S, Radosevic S, Slade N, Kapitanovic M, Andelinovic S, Ferencic Z, Tavassoli M, Spaventi S, Pavelic K, Spaventi R (2000) Expression of erbB-3 protein in colorectal adenocarcinoma: correlation with poor survival. J Cancer Res Clin Oncol 126:205–211
17. Kountourakis P, Pavlakis K, Psyrri A, Rontogianni D, Xiros N, Patsouris E, Pectasides D, Economopoulos T (2006) Prognostic significance of HER3 and HER4 protein expression in colorectal adenocarcinomas. BMC Cancer 6:46. doi:1471-2407-6-46
18. Friess H, Wang L, Zhu Z, Gerber R, Schroder M, Fukuda A, Zimmermann A, Korc M, Buchler MW (1999) Growth factor receptors are differentially expressed in cancers of the papilla of Vater and pancreas. Ann Surg 230:767–774, discussion 774–765
19. Friess H, Yamanaka Y, Kobrin MS, Do DA, Buchler MW, Korc M (1995) Enhanced erbB-3 expression in human pancreatic cancer correlates with tumor progression. Clin Cancer Res 1:1413–1420
20. Yoshikawa D, Ojima H, Iwasaki M, Hiraoka N, Kosuge T, Kasai S, Hirohashi S, Shibata T (2008) Clinicopathological and prognostic significance of EGFR, VEGF, and HER2 expression in cholangiocarcinoma. Br J Cancer 98:418–425
21. Su WC, Shiesh SC, Liu HS, Chen CY, Chow NH, Lin XZ (2001) Expression of oncogene products HER2/Neu and Ras and fibrosis-related growth factors bFGF, TGF-beta, and PDGF in bile from biliary malignancies and inflammatory disorders. Dig Dis Sci 46:1387–1392
22. Harder J, Waiz O, Otto F, Geissler M, Olschewski M, Weinhold B, Blum HE, Schmitt-Graeff A, Opitz OG (2009) EGFR and HER2 expression in advanced biliary tract cancer. World J Gastroenterol 15:4511–4517
23. Shafizadeh N, Grenert JP, Sahai V, Kakar S (2010) Epidermal growth factor receptor and HER-2/neu status by immunohistochemistry and fluorescence in situ hybridization in adenocarcinomas of the biliary tree and gallbladder. Hum Pathol 41:485–492
24. Chung JY, Hong SM, Choi BY, Cho H, Yu E, Hewitt SM (2009) The expression of phospho-AKT, phospho-mTOR, and PTEN in extrahepatic cholangiocarcinoma. Clin Cancer Res 15:660–667
25. Takikita M, Xie R, Chung JY, Cho H, Ylaya K, Hong SM, Moskaluk CA, Hewitt SM (2011) Membranous expression of Her3 is associated with a decreased survival in head and neck squamous cell carcinoma. J Transl Med 9:126. doi:1479-5876-9-126
26. Hofmann M, Stoss O, Shi D, Buttner R, van de Vijver M, Kim W, Ochiai A, Ruschoff J, Henkel T (2008) Assessment of a HER2 scoring system for gastric cancer: results from a validation study. Histopathology 52:797–805
27. Soltoff SP, Carraway KL 3rd, Prigent SA, Gullick WG, Cantley LC (1994) ErbB3 is involved in activation of phosphatidylinositol 3-kinase by epidermal growth factor. Mol Cell Biol 14:3550–3558
28. Prigent SA, Gullick WJ (1994) Identification of c-erbB-3 binding sites for phosphatidylinositol 3′-kinase and SHC using an EGF receptor/c-erbB-3 chimera. EMBO J 13:2831–2841
29. Garrett JT, Olivares MG, Rinehart C, Granja-Ingram ND, Sanchez V, Chakrabarty A, Dave B, Cook RS, Pao W, McKinely E, Manning HC, Chang J, Arteaga CL (2011) Transcriptional and posttranslational up-regulation of HER3 (ErbB3) compensates for inhibition of the HER2 tyrosine kinase. Proc Natl Acad Sci U S A 108:5021–5026
30. Lee-Hoeflich ST, Crocker L, Yao E, Pham T, Munroe X, Hoeflich KP, Sliwkowski MX, Stern HM (2008) A central role for HER3 in HER2-amplified breast cancer: implications for targeted therapy. Cancer Res 68:5878–5887
31. Holbro T, Beerli RR, Maurer F, Koziczak M, Barbas CF 3rd, Hynes NE (2003) The ErbB2/ErbB3 heterodimer functions as an oncogenic unit: ErbB2 requires ErbB3 to drive breast tumor cell proliferation. Proc Natl Acad Sci U S A 100:8933–8938
32. Sergina NV, Rausch M, Wang D, Blair J, Hann B, Shokat KM, Moasser MM (2007) Escape from HER-family tyrosine kinase inhibitor therapy by the kinase-inactive HER3. Nature 445:437–441
33. Engelman JA, Zejnullahu K, Mitsudomi T, Song Y, Hyland C, Park JO, Lindeman N, Gale CM, Zhao X, Christensen J, Kosaka T, Holmes AJ, Rogers AM, Cappuzzo F, Mok T, Lee C, Johnson BE, Cantley LC, Janne PA (2007) MET amplification leads to gefitinib resistance in lung cancer by activating ERBB3 signaling. Science 316:1039–1043
34. Reschke M, Mihic-Probst D, van der Horst EH, Knyazev P, Wild PJ, Hutterer M, Meyer S, Dummer R, Moch H, Ullrich A (2008) HER3 is a determinant for poor prognosis in melanoma. Clin Cancer Res 14:5188–5197

35. Lozano JJ, Soler M, Bermudo R, Abia D, Fernandez PL, Thomson TM, Ortiz AR (2005) Dual activation of pathways regulated by steroid receptors and peptide growth factors in primary prostate cancer revealed by factor analysis of microarray data. BMC Genomics 6:109. doi:1471-2164-6-109
36. Sun M, Behrens C, Feng L, Ozburn N, Tang X, Yin G, Komaki R, Varella-Garcia M, Hong WK, Aldape KD, Wistuba II (2009) HER family receptor abnormalities in lung cancer brain metastases and corresponding primary tumors. Clin Cancer Res 15:4829–4837
37. Simpson BJ, Weatherill J, Miller EP, Lessells AM, Langdon SP, Miller WR (1995) c-erbB-3 protein expression in ovarian tumours. Br J Cancer 71:758–762
38. Begnami MD, Fukuda E, Fregnani JH, Nonogaki S, Montagnini AL, da Costa WL, Soares FA Jr (2011) Prognostic implications of altered human epidermal growth factor receptors (HERs) in gastric carcinomas: HER2 and HER3 are predictors of poor outcome. J Clin Oncol 29:3030–3036
39. Yi ES, Harclerode D, Gondo M, Stephenson M, Brown RW, Younes M, Cagle PT (1997) High c-erbB-3 protein expression is associated with shorter survival in advanced non-small cell lung carcinomas. Mod Pathol 10:142–148
40. Kluger HM, DiVito K, Berger AJ, Halaban R, Ariyan S, Camp RL, Rimm DL (2004) Her2/neu is not a commonly expressed therapeutic target in melanoma—a large cohort tissue microarray study. Melanoma Res 14:207–210
41. Ueno Y, Sakurai H, Tsunoda S, Choo MK, Matsuo M, Koizumi K, Saiki I (2008) Heregulin-induced activation of ErbB3 by EGFR tyrosine kinase activity promotes tumor growth and metastasis in melanoma cells. Int J Cancer 123:340–347
42. Engelman JA, Janne PA, Mermel C, Pearlberg J, Mukohara T, Fleet C, Cichowski K, Johnson BE, Cantley LC (2005) ErbB-3 mediates phosphoinositide 3-kinase activity in gefitinib-sensitive non-small cell lung cancer cell lines. Proc Natl Acad Sci U S A 102:3788–3793
43. Soler M, Mancini F, Meca-Cortes O, Sanchez-Cid L, Rubio N, Lopez-Fernandez S, Lozano JJ, Blanco J, Fernandez PL, Thomson TM (2009) HER3 is required for the maintenance of neuregulin-dependent and -independent attributes of malignant progression in prostate cancer cells. Int J Cancer 125:2565–2575
44. Jan YY, Yeh TS, Yeh JN, Yang HR, Chen MF (2004) Expression of epidermal growth factor receptor, apomucins, matrix metalloproteinases, and p53 in rat and human cholangiocarcinoma: appraisal of an animal model of cholangiocarcinoma. Ann Surg 240:89–94
45. Nakazawa K, Dobashi Y, Suzuki S, Fujii H, Takeda Y, Ooi A (2005) Amplification and overexpression of c-erbB-2, epidermal growth factor receptor, and c-met in biliary tract cancers. J Pathol 206:356–365
46. Philip PA, Mahoney MR, Allmer C, Thomas J, Pitot HC, Kim G, Donehower RC, Fitch T, Picus J, Erlichman C (2006) Phase II study of erlotinib in patients with advanced biliary cancer. J Clin Oncol 24:3069–3074
47. Dragovich T, Huberman M, Von Hoff DD, Rowinsky EK, Nadler P, Wood D, Hamilton M, Hage G, Wolf J, Patnaik A (2007) Erlotinib plus gemcitabine in patients with unresectable pancreatic cancer and other solid tumors: phase IB trial. Cancer Chemother Pharmacol 60:295–303
48. Paule B, Herelle MO, Rage E, Ducreux M, Adam R, Guettier C, Bralet MP (2007) Cetuximab plus gemcitabine–oxaliplatin (GEMOX) in patients with refractory advanced intrahepatic cholangiocarcinomas. Oncology 72:105–110
49. Andre T, Reyes-Vidal JM, Fartoux L, Ross P, Leslie M, Rosmorduc O, Clemens MR, Louvet C, Perez N, Mehmud F, Scheithauer W (2008) Gemcitabine and oxaliplatin in advanced biliary tract carcinoma: a phase II study. Br J Cancer 99:862–867
50. Safran H, Miner T, Resnick M, Dipetrillo T, McNulty B, Evans D, Joseph P, Plette A, Millis R, Sears D, Gutman N, Kennedy T (2008) Lapatinib/gemcitabine and lapatinib/gemcitabine/oxaliplatin: a phase I study for advanced pancreaticobiliary cancer. Am J Clin Oncol 31:140–144
51. Aishima SI, Taguchi KI, Sugimachi K, Shimada M, Tsuneyoshi M (2002) c-erbB-2 and c-Met expression relates to cholangiocarcinogenesis and progression of intrahepatic cholangiocarcinoma. Histopathology 40:269–278
52. Altimari A, Fiorentino M, Gabusi E, Gruppioni E, Corti B, D'Errico A, Grigioni WF (2003) Investigation of ErbB1 and ErbB2 expression for therapeutic targeting in primary liver tumours. Dig Liver Dis 35:332–338
53. Chow NH, Huang SM, Chan SH, Mo LR, Hwang MH, Su WC (1995) Significance of c-erbB-2 expression in normal and neoplastic epithelium of biliary tract. Anticancer Res 15:1055–1059
54. Endo K, Yoon BI, Pairojkul C, Demetris AJ, Sirica AE (2002) ERBB-2 overexpression and cyclooxygenase-2 up-regulation in human cholangiocarcinoma and risk conditions. Hepatology 36:439–450
55. Terada T, Ashida K, Endo K, Horie S, Maeta H, Matsunaga Y, Takashima K, Ohta T, Kitamura Y (1998) c-erbB-2 protein is expressed in hepatolithiasis and cholangiocarcinoma. Histopathology 33:325–331
56. Ukita Y, Kato M, Terada T (2002) Gene amplification and mRNA and protein overexpression of c-erbB-2 (HER-2/neu) in human intrahepatic cholangiocarcinoma as detected by fluorescence in situ hybridization, in situ hybridization, and immunohistochemistry. J Hepatol 36:780–785
57. Voravud N, Foster CS, Gilbertson JA, Sikora K, Waxman J (1989) Oncogene expression in cholangiocarcinoma and in normal hepatic development. Hum Pathol 20:1163–1168
58. Edge SB, Byrd DR, Compton CC, Fritz AG, Greene FL, Trotti AI (2010) AJCC cancer staging manual. Springer, New York
59. Nakeeb A, Pitt HA, Sohn TA, Coleman J, Abrams RA, Piantadosi S, Hruban RH, Lillemoe KD, Yeo CJ, Cameron JL (1996) Cholangiocarcinoma. A spectrum of intrahepatic, perihilar, and distal tumors. Ann Surg 224:463–473, discussion 473–465
60. DeOliveira ML, Cunningham SC, Cameron JL, Kamangar F, Winter JM, Lillemoe KD, Choti MA, Yeo CJ, Schulick RD (2007) Cholangiocarcinoma: thirty-one-year experience with 564 patients at a single institution. Ann Surg 245:755–762
61. Argani P, Shaukat A, Kaushal M, Wilentz RE, Su GH, Sohn TA, Yeo CJ, Cameron JL, Kern SE, Hruban RH (2001) Differing rates of loss of DPC4 expression and of p53 overexpression among carcinomas of the proximal and distal bile ducts. Cancer 91:1332–1341
62. Watanabe A, Cornelison R, Hostetter G (2005) Tissue microarrays: applications in genomic research. Expert Rev Mol Diagn 5:171–181

Virchows Arch (2012) 461:531–540
DOI 10.1007/s00428-012-1320-1

ORIGINAL ARTICLE

Cribriform adenocarcinoma of minor salivary glands may express galectin-3, cytokeratin 19, and HBME-1 and contains polymorphisms of *RET* and *H-RAS* proto-oncogenes

Jan Laco · Kateřina Kamarádová · Pavla Vítková · Eva Sehnálková · Šárka Dvořáková · Eliška Václavíková · Vlasta Sýkorová · Jana Kašpírková · Alena Skálová · Aleš Ryška

Received: 13 June 2012 / Accepted: 20 September 2012 / Published online: 28 September 2012
© Springer-Verlag Berlin Heidelberg 2012

Abstract The aim of the study was to further elucidate the immunohistochemical and genetic characteristics of cribriform adenocarcinoma of minor salivary glands (CAMSG). The study comprised five CAMSG from two males and three females, aged 21–72 years. Four tumors were localized at the base of tongue and one in the floor of mouth. At the time of diagnosis, four tumors had metastasised to regional lymph nodes. After tumor resection, two patients were treated by radiotherapy and one by chemoradiotherapy. During the follow-up (median 14 months), two patients developed lymph node metastasis. Microscopically, all tumors showed cribriform, papillary, follicular, and microcystic growth patterns. The tumor cells displayed vesicular nuclei with intranuclear grooves. Immunohistochemically, all tumors showed expression of cytokeratin (CK) 7, CK8, CK18, vimentin, smooth muscle actin, calponin, S-100 protein, and p16 protein. In addition, we observed expression of galectin-3, CK19, and HBME-1, but not of thyroglobulin and TTF-1. No mutations of *RET*, *BRAF*, *K-RAS*, *H-RAS*, and *N-RAS* proto-oncogenes were detected. However, in *RET* proto-oncogene, we found polymorphisms Gly691Ser (exon 11) and Ser904Ser (exon 15) in one case, p.Leu769-Leu (exon 13) in one case, and variant p.IVS14-24 G/A of intron 14 in two cases, and in *H-RAS* proto-oncogene we found polymorphism 81 T-C (exon 1) in three cases. Thyroglobulin and TTF-1 are the only useful markers in the differential diagnosis between CAMSG and papillary thyroid carcinoma as both tumors may express galectin-3, CK19, and HBME-1. The *RET*, *H-RAS*, and *N-RAS* proto-oncoogenes are not mutated in CAMSG.

Keywords Salivary gland · Tongue · Cribriform adenocarcinoma · *RET* proto-oncogene · *H-RAS* proto-oncogene

J. Laco (✉) · A. Ryška
The Fingerland Department of Pathology, Charles University Faculty of Medicine and Faculty Hospital,
Sokolska 581,
500 05, Hradec Králové, Czech Republic
e-mail: lacoj@lfhk.cuni.cz

K. Kamarádová
Department of Pathology and Molecular Medicine, Charles University 2nd Faculty of Medicine and Faculty Hospital Motol, Prague, Czech Republic

P. Vítková
Department of Pathology, Hospital České Budějovice, Budweis, Czech Republic

E. Sehnálková
Department of Pathology, Silesian Hospital, Opava, Czech Republic

Š. Dvořáková · E. Václavíková · V. Sýkorová
Department of Molecular Endocrinology, Institute of Endocrinology, Prague, Czech Republic

J. Kašpírková · A. Skálová
Bioptic Laboratory, Pilsen, Czech Republic

A. Skálová
Department of Pathology, Charles University Faculty of Medicine, Pilsen, Czech Republic

Introduction

Cribriform adenocarcinoma of minor salivary gland (CAMSG) origin is the term proposed by Skálová et al. [1] for the tumor previously known as cribriform adenocarcinoma of the tongue. CAMSG is a very rare tumor, occurring predominantly but not exclusively in the posterior

tongue, in patients without a gender or age predilection. The tumor often presents with cervical lymph node metastases, which may be even the first manifestation of the disease [1]. However, despite advanced locoregional status, the prognosis of CAMSG seems to be favorable—no tumor-related death has been reported so far [1–3].

The microscopic hallmark of CAMSG is the appearance of tumor cell nuclei, which closely resemble "ground glass" or "Orphan Annie eyes" nuclei of papillary thyroid carcinoma (PTC). In addition, polymorphous low-grade adenocarcinoma of salivary glands (PLGA) is the principal differential diagnosis of CAMSG. Some of the previous reports of PLGAs occurring in the tongue and presenting with lymph node metastases may actually represent examples of CAMSG [4].

In spite of the microscopic similarities between CAMSG and PTC, the question on whether or not they have molecular genetic and immunohistochemical characteristics in common has not been addressed. PTC is characterized by the frequent presence of *RET/PTC*rearrangements and $BRAF^{V600E}$ mutation and immunohistochemically by the invariable expression of thyroglobulin and thyroid transcription factor-1 (TTF-1) and variable positivity of galectin-3, cytokeratin 19 (CK19), and human mesothelial cell-1 (HBME-1), which are commonly used in differential diagnostics [5–7]. In the study by Skálová et al. [1], the authors noticed in CAMSG only focal expression of CK19 (up to 5 % of tumor cells) in nine of 12 tumors, whereas thyroglobulin and TTF-1 were consistently not expressed. In addition, they did not find any mutations in the genes studied, including *BRAF*, *K-RAS*, *c-kit*, and *PDGFRα* [1].

The aim of our study was to report five additional cases of CAMSG with the purpose to confirm and eventually extend knowledge on the immunohistochemical and molecular genetic profile of this rare tumor by focusing on the expression of galectin-3 and HBME-1 and on the detection of mutations in *BRAF*, *K-RAS*, *N-RAS*, *H-RAS*, and *RET* proto-oncogenes, the latter of which had not been analyzed yet in CAMSG.

Materials and methods

All five cases of CAMSG were retrieved from the consultation files of the authors (J.L., A.R., A. S.). The paraffin blocks for immunohistochemical and molecular genetic analysis were available in all cases. The tissue specimens had been immediately fixed in 10 % formalin, routinely processed, embedded in paraffin, and stained with hematoxylin–eosin (H&E). As a control group, we included five cases of PLGA of salivary glands.

Immunohistochemical study

Four-micrometer-thick sections were cut from paraffin blocks, mounted on slides coated with 3-aminopropyltriethoxy-silane, deparaffinized in xylene, and rehydrated in descending grades (100 to 70 %) of ethanol. The primary antibodies used are listed in Table 1. Staining for HBME-1 and thyroglobulin was done manually. Antigen retrieval for thyroglobulin was performed using 0.003 % ficin for 30 min at ambient temperature. For HBME-1, the tissue was processed in a microwave vacuum histoprocessor (RHS 1, Milestone, Sorisole, Italy) at pH 6.0 at 120 °C for 4 min. Endogenous peroxidase activity was inhibited by immersing the sections in 3 % hydrogen peroxide. After incubation with the antibodies, the sections were subjected to EnVision+Dual Link System-HRP (Dako, Glostrup, Denmark). Finally, the reaction was visualized using 3-3′-diaminobenzidine and the slides were counterstained with hematoxylin. The detection of epidermal growth factor receptor (EGFR) and p16 was performed using EGFR pharmDx™ kit (Dako) and CINtec® $p16^{INK4a}$ Histology Kit (mtm laboratories, Heidelberg, Germany), respectively, according to the instructions of the manufacturers. Staining for all other antigens was performed using a BenchMark Ultra immunostainer (Roche, Basel, Switzerland), with an Ultra View Universal DAB Detection Kit and Bluing Reagent as visualization reagent and chromogen. Appropriate positive and negative controls were used.

Detection of human papillomaviruses

For human papillomavirus (HPV) studies, genomic DNA was isolated from formalin-fixed, paraffin-embedded tissue. Special precautions were taken to prevent HPV DNA microcontamination. Briefly, 5-μm-thick sections were cut from the blocks. A new microtome blade was used each time a new case was sectioned. DNA was extracted by the QIAsymphony DNA Mini Kit (Qiagen, Hilden, Germany) according to the manufacturer's protocol. The quality of isolated DNA was checked by polymerase chain reaction (PCR) that amplifies a set of control genes [8]. HPV DNA detection was performed using a set of several PCRs with different primers to cover a wide detection range of predominantly high- and low-risk HPV types. For all samples, the primer's systems CPSGB, GP5+/GP6+, and MY09/11, targeting both L1 and E1 regions, were used as previously described [9]. To avoid false negative results because of loss of L1 and/or E1 regions during the HPV DNA integration into host genome, PCR targeting HPV oncogenes E6 and E7 of the six most prevalent HR-HPV types, namely, types 16, 18, 31, 33, 35, and 45, was performed [10]. Furthermore, INNO-LiPA HPV Genotyping Kit Extra (Innogenetics NV, Gent, Belgium) was run in order to reveal possible multiple HPV-type infections. All PCRs were run on the cycler GeneAmp PCR System 9700 (PE/ Applied Biosystem, Forster City, CA, USA). Amplicons were analyzed in 2 % agarose gel with ethidium bromide. Positive PCR samples were genotyped by hybridization to type specific probes or sequenced and compared to BLAST databases. Positive and negative controls were included in every single run.

Table 1 List of primary antibodies

Antibody	Clone	Dilution	Source
Calponin	CALP	1:500	Dako (Glostrup, Denmark)
CK	AE1/AE3	1:100	Dako (Glostrup, Denmark)
CK5/6	D5/16 B4	1:100	Dako (Glostrup, Denmark)
CK7	OV-TL 12/30	1:50	Dako (Glostrup, Denmark)
CK8	35βH11	1:1	Dako (Glostrup, Denmark)
CK18	DC 10	1:50	Dako (Glostrup, Denmark)
CK19	RCK 108	1:100	Dako (Glostrup, Denmark)
CK20	K_s 20.8	1:25	Dako (Glostrup, Denmark)
Cyclin D1	SP4	1:50	Dako (Glostrup, Denmark)
EGFR	2-18C9	–	Dako (Glostrup, Denmark)
EMA	E29	1:800	Dako (Glostrup, Denmark)
Galectin-3	9C4	1:400	Novocastra/Leica (Newcastle Upon Tyne, UK)
HBME-1	HBME-1	1:12	Abcam (Cambridge, UK)
Her2	4B5	Pre-diluted	Ventana/Roche (Basel, Switzerland)
Ki-67	MIB-1	1:50	Dako (Glostrup, Denmark)
S-100 protein	polyclonal	1:1,500	Dako (Glostrup, Denmark)
SMA	1A4	Pre-diluted	Ventana (Basel, Switzerland)
p16 protein	E6H4	–	mtm laboratories (Heidelberg, Germany)
p53 protein	DO-7	1:300	Dako (Glostrup, Denmark)
p63 protein	4A4	Pre-diluted	Ventana/Roche (Basel, Switzerland)
Thyroglobulin	polyclonal	1:800	Dako (Glostrup, Denmark)
TTF-1	8G7G3/1	1:25	Dako (Glostrup, Denmark)
Vimentin	V9	1:400	Dako (Glostrup, Denmark)

CK cytokeratin, *EGFR* epidermal growth factor receptor, *EMA* epithelial membrane antigen, *SMA* smooth muscle actin, *TTF-1* thyroid transcription factor-1

Molecular genetic study

The mutation analysis was performed under informed consent. Somatic DNA was isolated in each case from formalin-fixed, paraffin-embedded tissue blocks and analyzed for *RET* proto-oncogene mutations. Five-micrometer-thick tissue sections were deparaffinized using sequential washes with xylene and absolute ethanol. Samples were digested using protease K and DNA was extracted using QIAamp DNA Blood Mini Kit (Qiagen, Hilden, Germany). After measurement of the DNA concentration and DNA/protein ratio, the DNA was used for PCR amplification. The primers and conditions specific for PCR amplifications and sequencing of exons 10, 11, 13, 14, 15, and 16 of the *RET* proto-oncogene and exon 15 of the *BRAF* proto-oncogene were used as previously described [11, 12]. For sequenase reaction, the previously purified PCR products (Agencourt Ampure kit, Beckman Coulter, Brea, CA, USA), unlabelled primers, and DTCS Quick Start kit (Beckman Coulter) were used. Subsequently, the PCR products were re-purified (Agencourt CleanSEQ kit, Beckman Coulter), sequenced on a CEQ 8000 sequencing machine (Beckman Coulter, Brea, CA, USA), and analyzed by CEQ 8000 sequencing software. Sequence traces were compared with *RET* reference sequence (NG_007489.1).

Sequences of *H-RAS*, *K-RAS*, and *N-RAS* proto-oncogenes in exons 1 and 2 (designated as H1, H2, K1, K2, N1, and N2) were amplified to generate 282-, 358-, 340-, 250-, 232-, and 268-bp fragments, respectively, using the primer pairs as previously described for H1, H2 [13] and N1, N2 [14]. The primer pairs for the amplification of *K-RAS* proto-oncogene were 5′-GAT ACA CGT CTG CAG TCA ACT G-3′ and 5′-GGT CCT GCA CCA GTA ATA TGC-3′ for K1 and 5′-GTC TTT TCA AGT CCT TTG CCC-3′ and 5′-CAC AAA GAA AGC CCT CCC CA-3′ for K2 [13–15]. For each PCR, 30 ng of DNA was amplified with 0.1 μM of each primer, 160 μM deoxynucleotide triphosphates, 0.25 U Gold AmpliTaq Perkin Polymerase, 1 mM (H2), 1.5 mM (H1), 2 mM (K1, K2, N1) or 3 mM (N2) $MgCl_2$, and 1× PCR buffer II (10 mM Tris–HCl, pH 8.3; 50 mM KCl) in a final volume of 15 μL. The cycling conditions were: denaturation step at 94 °C for 2 min and at 95 °C for 20 s, followed by 5 cycles of denaturation at 95 °C for 20 s, annealing at 62.5 °C for 30 s, primer extension at 72 °C for 1 min, 40 cycles of denaturation at 95 °C for 30 s, annealing at 57.5 °C (H1, H2, K1, K2) or 56.4 °C (N1, N2) for 40 s, primer extension at 72 °C for 1 min, and one final runoff extension at 72 °C for 10 min. The PCR reactions were carried out in thermocycler TGradient 96 (Biometra, Goettingen, Germany). All PCR products were visualized by electrophoresis in 1.5 % agarose gel with ethidium bromide. Then, sequenase reaction

and sequencing procedure was similar to *RET* proto-oncogene analysis.

Results

Clinical data

The clinicopathological data of the CAMSG patients are summarized in Table 2. The studied cases comprised of two males and three females with unremarkable personal history, aged 21–72 years (median 55 years) at the time of diagnosis. Four tumors were localized at the base of tongue (one left, three right) and one in the floor of mouth close to the left sublingual gland. Four tumors were well circumscribed, measuring 25–60 mm (median 36 mm) in greatest diameter. One advanced tumor infiltrated the adjacent palatine tonsil and epiglottis. At the time of presentation, four patients had ipsilateral regional lymph node metastases, in two cases as first manifestation of the disease. None of the patients had distant metastases. All patients underwent radical resection of the tumor with negative margins. In four patients, regional lymph node dissection was performed. Adjuvant radiotherapy was indicated in two patients and one patient was treated by chemoradiotherapy with cisplatin in monotherapy. The follow-up period ranged 4–45 months (median 14 months). All patients are alive. In three patients, no evidence of locoregional recurrence was found, whereas one patient had developed ipsilateral lymph node metastasis 37 months after removal of the primary tumor and one patient featured ipsilateral lymph node metastases at 5 and 15 months, respectively, after resection of the primary tumor.

The diagnoses of the referring pathologists in cases 1–3 and in case 5 were metastasizing papillary thyroid carcinoma, cribriform adenocarcinoma, and polymorphous low-grade adenocarcinoma. In case 4, the original diagnosis was "proliferating pleomorphic adenoma" and no further treatment was judged necessary. The lymph node lesion which developed 37 months after removal of the primary tumor was misdiagnosed as a metastasis of papillary thyroid carcinoma. Total thyreoidectomy was performed but carcinoma was not found. Subsequently, the lymph node was sent for second opinion and the diagnosis of metastasizing cribriform adenocarcinoma was established. Biopsies taken at that time from the nasopharynx, base of tongue, and palatine tonsils were negative. Therefore, the original tumor was finally reviewed and diagnosed as cribriform adenocarcinoma. Thus, the correct diagnosis took 45 months.

The control cases of PLGA comprised two males and three females, aged 28–73 years (median 51 years). Four tumors were localized on the hard palate and one case occurred in the right retromolar region of the oral cavity. The tumors appeared well circumscribed and measured 12–35 mm (median 23 mm) in greatest diameter (stage pT1 or pT2). None of the patients featured regional lymph node or distant metastases on clinical examination. All tumors had been treated by surgical resection with negative margins, and in two patients dissection of ipsilateral cervical lymph nodes had been performed (stage pN0). None of the patients received adjuvant chemo/radiotherapy. The follow-up period ranged 10–77 months (median 51 months). All patients

Table 2 Clinicopathological data of the patients

	Case 1	Case 2	Case 3	Case 4	Case 5
Sex/age (years)	Male/21	Female/72	Male/55	Female/52	Female/68
Initial presentation	LN metastasis	Primary tumor	Primary tumor	Primary tumor	LN metastasis
Tumor localization	Base of tongue	Base of tongue	Base of tongue	Floor of mouth	Base of tongue
Tumor size (mm)	Large tumor; infiltration of tonsil and epiglottis	60	25	30	42
Nodal status	Positive	Positive	Positive	NA	Positive
pTNM	pT4a pN2b	pT4a pN1	pT2 pN2a	pT2 pNX	pT3 pN2b
Adjuvant treatment	Chemoradiotherapy with cisplatin	Radiotherapy	Radiotherapy	None	None
Follow-up duration (months)	8	4	14	45	15
Follow-up status	Alive; NED	Alive; NED	Alive; NED	Alive; LN metastasis at 37 months	Alive; LN metastases at 5 and 15 months
Original diagnosis	Metastasis of PTC	CAMSG	PLGA	Pleomorphic adenoma; metastasis of PTC	Metastasis of PTC

CAMSG cribriform adenocarcinoma of minor salivary gland, *LN* lymph node, *NA* not available, *NED* no evidence of disease, *PLGA* polymorphous low-grade adenocarcinoma, *PTC* papillary thyroid carcinoma

are alive and none developed locoregional recurrence of the tumor.

Histopathological findings

Grossly, all five CAMSG were gray–white in color, without areas of necrosis. Microscopically, all CAMSGs were covered by normal squamous epithelium, which was ulcerated in one case (case 3). No connection between the surface epithelium and the tumor tissue was seen, but close relationship to a salivary gland was obvious in two cases (cases 3 and 4). The tumors were predominantly solid, composed of variably sized nodules (Fig. 1a), which were separated by irregular and often hyalinized fibrous bands with areas of old and recent hemorrhage and chronic inflammation. In addition, there were intermingled areas of tubular and cribriform (Fig. 1b), papillary (Fig. 1c), follicular, and microcystic growth pattern. The follicular/microcystic spaces contained pale to eosinophilic material with scalloped margins, which stained with alcian blue. Not infrequently, the tumor nodules were separated from the neighboring fibrous stroma by irregular clefts (Fig. 1d), which contained erythocytes and were lined by cells with hyperchromatic nuclei and deeply eosinophilic cytoplasm (Fig. 2a). The tumor cells, however, were generally uniform in size and shape and showed little atypia. They had a moderate amount of pale to eosinophilic cytoplasm and round to oval slightly enlarged overlapping vesicular nuclei with occasional nucleoli and intranuclear grooves (Fig. 2b). Nuclear pseudoinclusions/cytoplasmic invaginations were not observed. The mitotic activity was less than five mitoses per ten high power fields (HPFs). No atypical mitoses were found. Scattered microcalcifications were seen in one case (case 4). Multinucleated giant cells were not present. Angioinvasion was found in four cases (cases 1, 2, 3, and 5), whereas perineural spread was evident in only one case (case 3). Necrosis was absent. The microscopic appearance of cervical lymph node metastases was identical to that of the primary tumors. No transcapsular spread of metastasizing tumor cells was found.

The microscopic appearance of control cases was that of typical PLGA. The tumors were arranged in solid and cribriform growth patterns, occasionally creating a target-like appearance. No peripheral clefts were identified. Some tumor cells had pale nuclei but not to the extent seen in CAMSG. The mitotic activity was minimal (less than two mitoses per ten HPFs). No atypical mitoses were found. No angioinvasion was found, but in three cases perineural spread of tumor cells was evident. Necrosis was absent in all cases.

Immunohistochemical findings

The results of immunohistochemical analysis of CAMSG cases are listed in Table 3. All tumors showed strong diffuse or focal expression of cytokeratins (AE1/AE3), CK7, CK8, CK18, vimentin, smooth muscle actin (SMA), calponin (Fig. 3a), and S-100 protein (Fig. 3b). The basal/myoepithelial cell markers, i.e., CK5/6 (Fig. 3c) and p63 protein, were variably expressed in all tumors, frequently at the periphery

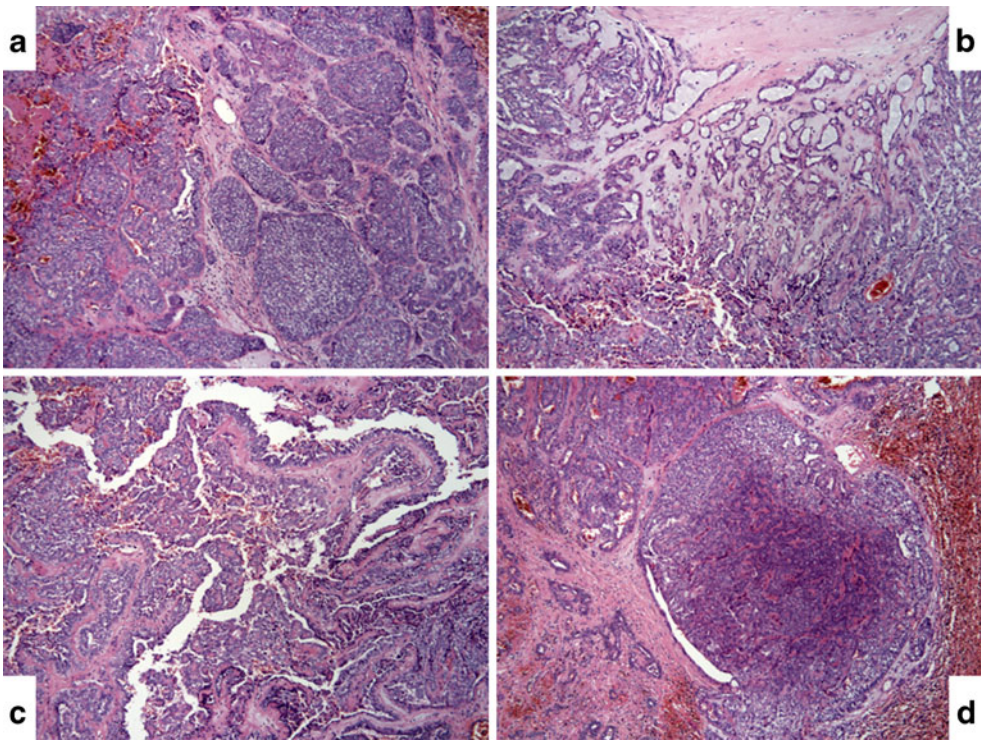

Fig. 1 The tumor shows variable architecture—there are areas of **a** nodular, **b** tubular and cribriform, and **c** papillary growth pattern. **d** Nodules are separated from the fibrous stroma by irregular clefts (H&E, original magnification (**a**–**d**) ×100)

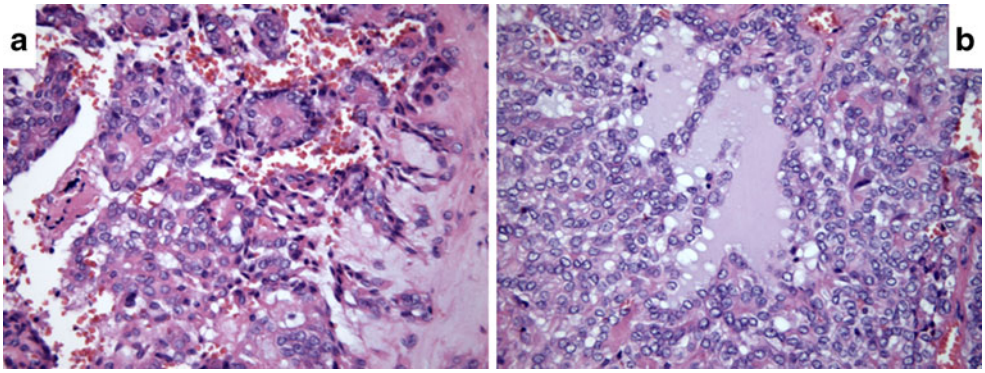

Fig. 2 **a** Peripheral clefts are lined by cells with hyperchromatic nuclei and deeply eosinophilic cytoplasm. **b** Follicles contain pale eosinophilic material with scalloped margins and are lined by cells with overlapping vesicular nuclei with occasional nucleoli and intranuclear grooves (H&E, original magnification (**a**, **b**) ×400)

of the tumor nodules. The Ki-67 proliferation index was less than 25 %. All five tumors showed nuclear and cytoplasmic p16 protein expression, in two cases (cases 1 and 3) in up to 40–50 % of tumor cells (Fig. 3d) and in one case (5) it was observed in up to 90 % of tumor cells. Notably, the overlying squamous epithelium was devoid of any p16 staining in all cases. Importantly, the tumors showed variable expression of galectin-3 (Fig. 4a), CK19 (Fig. 4b), HBME-1 (Fig. 4c), and cyclin D1 (Fig. 4d). The staining for CK20, EGFR, Her2, thyroglobulin, and TTF-1 was consistently negative.

There was a significant overlap in the immunohistochemical profile between CAMSG and PLGA cases. All PLGAs showed diffuse expression of CKs, CK7, CK8, CK18, and vimentin, and conversely, all were negative with CK20, EGFR, and Her-2/neu. In addition, there was a variable expression of calponin, p16 protein, p53 protein, p63 protein, CK5/6, EMA, S-100 protein, SMA, and cyclin D1. Finally, all cases of PLGA were consistently negative for thyroglobulin and for TTF-1, but we noticed diffuse expression of galectin-3 in five cases and variable expression of CK19 in two cases and of HBME-1 in three cases, respectively.

Detection of human papillomaviruses and molecular genetic analysis HPV DNA was not found in any of the CAMSG and PLGA cases.

In the CAMSG group, no somatic mutations in the studied exons of *RET*, *BRAF*, *K-RAS*, *H-RAS*, and *N-RAS* proto-oncogenes were detected. However, in *RET* proto-oncogene, we observed heterozygous polymorphism Gly691Ser in exon 11 (case 4), heterozygous polymorphism p.Leu769Leu in exon 13 (case 1), heterozygous polymorphism Ser904Ser in exon 15 (case 4), and the intronic variant p.IVS14-24 G/A of intron 14 (cases 3 and 4), respectively. In addition, we found homozygous (case 2) and heterozygous (cases 4 and 5) polymorphisms 81 T-C in exon 1 of the *H-RAS* proto-oncogene, respectively.

In the PLGA group, the analysis of exons 13, 14, and 15 of the *RET* proto-oncogene and of exons 1 and 2 of *H-RAS* proto-oncogene repeatedly failed. However, no mutations or polymorphisms of *BRAF*, *K-RAS*, *N-RAS*, and *RET* (exons 10, 11, and 16) proto-oncogenes were found.

Discussion

Cribriform adenocarcinoma of minor salivary gland origin was recently shown to belong to the ever-expanding spectrum of salivary gland tumors [1]. The neoplasm was originally described by Michal et al. [2] in 1999 under the term "cribriform adenocarcinoma of the tongue" on a small series of eight tumors, all affecting the tongue. Despite the finding that all eight tumors were thyroglobulin-negative, a possible

Table 3 Results of immunohistochemical analysis (as percentage of positive tumor cells)

	Case 1	Case 2	Case 3	Case 4	Case 5
Calponin	100	100	40	20	80
CK	100	100	100	100	100
CK5/6	30	20	10	5	5
CK7	100	100	100	90	100
CK8	100	80	80	90	90
CK18	100	80	90	80	100
CK19	100	80	90	0	90
CK20	0	0	0	0	0
Cyclin D1	40	20	5	0	30
EGFR	0	0	0	0	0
EMA	0	10	0	0	0
Galectin-3	50	100	30	100	100
HBME-1	50	100	40	40	30
Her2	0	0	0	0	0
Ki-67	10	5	5	20	25
p16 protein	50	10	40	20	90
p53 protein	30	10	5	0	40
p63 protein	10	10	5	5	5
S-100 protein	100	100	100	100	100
SMA	90	90	20	40	20
Thyroglobulin	0	0	0	0	0
TTF-1	0	0	0	0	0
Vimentin	100	100	100	100	100

CK cytokeratin, *EGFR* epidermal growth factor receptor, *EMA* epithelial membrane antigen, *SMA* smooth muscle actin, *TTF-1* thyroid transcription factor-1

origin from the thyroglossal duct *anlage* was proposed at that time.

The incidence of CAMSG is difficult to ascertain, but it seems to be a very rare tumor. Only one case report [3] was published between 1999 and 2011, when Skálová et al. [1] published the largest series so far comprising of 23 new cases. Very recently, additional case reports were published by Borowski-Borowy et al. [16] and by Čoček et al. [17]. Thus, together with our five cases, there are 39 well-documented cases of CAMSG at the moment. Anecdotally, at least four cases of bona fide CAMSG were reported in the past as examples of polymorphous low-grade adenocarcinoma [4] or under the designation "tubular adenocarcinoma" [18] and "papillary carcinoma of minor salivary gland" [19]. If Skálová et al. [1] have identified the 23 cases among more than 5,000 salivary gland tumors in their archives and we have found our five cases among approximately 500 salivary gland tumors examined since 2000 at our institution, the relative frequency of CAMSG could be about 0.5–1.0 % of all salivary gland tumors.

A detailed analysis of the 39 published cases of CAMSG (including our five cases) revealed the following characteristics of this tumor entity [1–3, 16, 17]. The tumors occurred in 16 males and 19 females (data not available in four patients), aged 21–85 years (median age approximately 57 years). The 21-year-old male from our series appears to be the youngest patient reported so far. The (base of the) tongue seems to be the principal localization of CAMSG as 29/39 (74 %) of cases herein presented mostly as a painless swelling or in one case as a polypoid mass [3]. A total of ten cases occurred elsewhere in the oral cavity/oropharynx (three palate, three palatine tonsil, two retromolar mucosa, one floor of mouth, and one upper lip). This observation, together with the consistent absence of thyroglobulin and TTF-1 expression in the tumor cells, strongly argues against the originally proposed origin of CAMSG from thyroglossal duct *anlage* at the base of tongue [2]. Interestingly, no case of CAMSG affecting major salivary glands has been reported so far.

The characteristic feature of CAMSG seems to be the tendency for early dissemination to cervical lymph nodes, which were affected in 29/39 (74 %) patients at initial presentation [1–3, 16, 17]. However, despite frequent positive nodal status, the prognosis of CAMSG appears to be relatively favorable—although the tumor may recur locally. No tumor-related death was reported during the follow-up period lasting up to 13 years [1–3, 16, 17].

All CAMSGs reported so far showed a similar microscopic appearance. The tumors had infiltrative margins and displayed nodular, papillary, follicular/microcystic, tubular, and cribriform architecture. Except for the cells lining peripheral clefts (considered to be presumably artifactual), which had irregular hyperchromatic nuclei and deeply eosinophilic cytoplasm, the tumors were composed of one cell type, characterized by a small to moderate amount of pale to eosinophilic cytoplasm and round to oval slightly enlarged overlapping vesicular nuclei with occasional nucleoli and intranuclear grooves. Generally, there is at most mild cytological

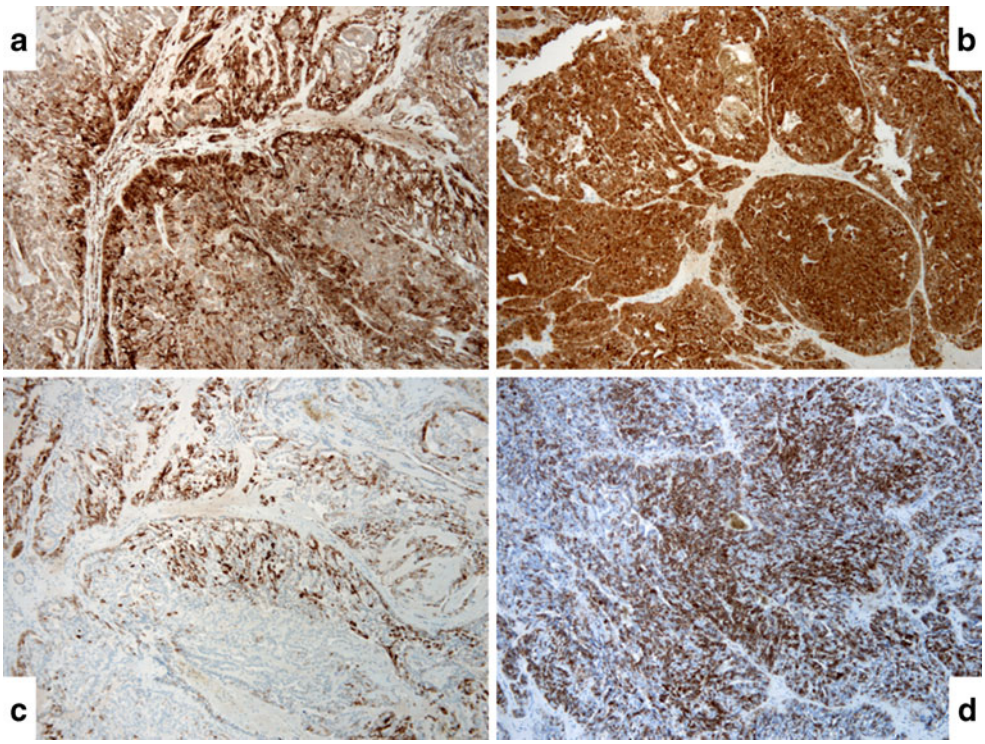

Fig. 3 Tumor cells show diffuse expression of **a** calponin and **b** S-100 protein and focal positivity of **c** cytokeratins 5/6 and **d** p16 protein (original magnification (**a**–**d**) ×100)

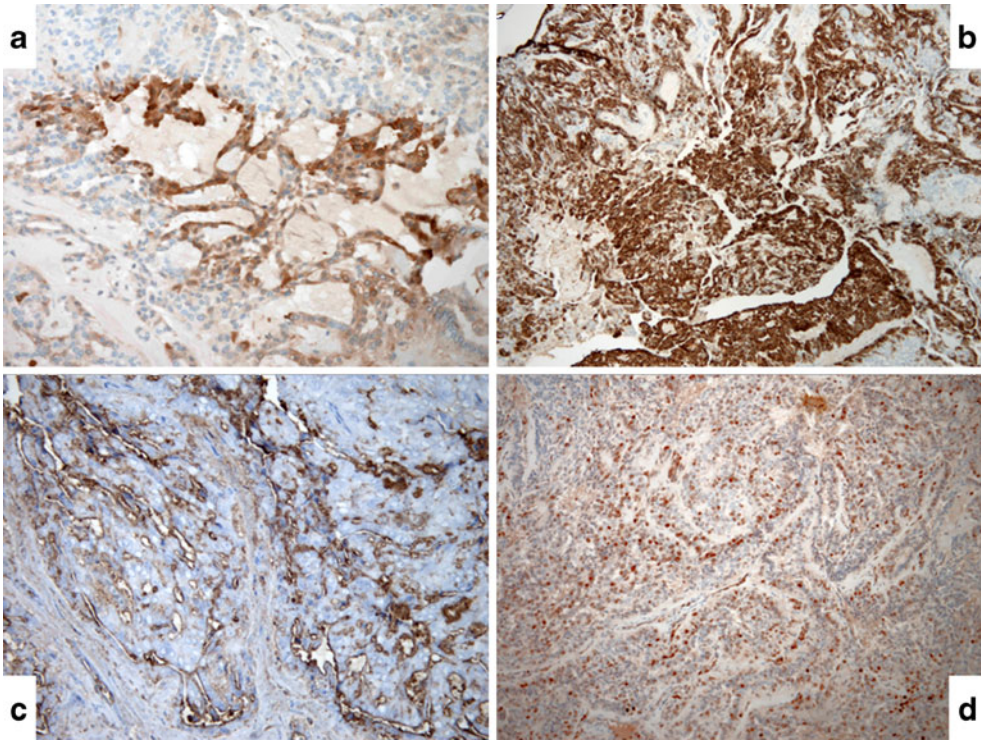

Fig. 4 Tumor cells show **a** focal cytoplasmic expression of galectin-3, **b** nearly diffuse cytoplasmic expression of cytokeratin 19, **c** focal membranous/apical expression of HBME-1, and **d** focal nuclear expression of cyclin D1 (original magnification ×100 (**b**, **d**), ×200 (**a**), and ×400 (**c**))

atypia and low mitotic activity. Thus, CAMSG closely resemble PTC. Interestingly, intranuclear pseudoinclusions and giant multinucleated cells are not observed in CAMSG. Similarly, microcalcifications have been found only exceptionally (one case in Michal's series [2] and one in our case). While angioinvasion has been a common finding, perineural spread was rarely seen. Ultrastructurally, the tumor cells displayed microvilli on the apical borders and microfilaments in the cytoplasm [1, 2]. These are features of so-called secretory myoepithelial cells (also termed myosecretory cells), which have been detected also in lobular carcinoma of the breast [20].

Immunohistochemically, CAMSG shows diffuse expression of CK, CK7, CK8, CK18, vimentin, and S-100 protein. There is also a significant expression of basal/abluminal and/or myoepithelial cell markers, i.e., SMA, calponin, CK5/6, and p63 protein. Whereas Skálová et al. [1] observed only very focal expression of CK19 in nine of 12 tumors, we found nearly diffuse expression of this marker in four cases. In addition, we demonstrated significant positivity of galectin-3 and HBME-1 in all five tumors. This finding is important since all three markers are commonly expressed in PTC and are routinely used in its differential diagnosis [5–7]. All cases of CAMSG reported so far have been consistently negative for thyroglobulin and/or TTF-1 [1–3, 16, 17].

In CAMSG, Skálová et al. [1] noticed the expression of p16 protein and HPV DNA in most cases with a variable proportion of positive cells (ranging from 5 to 60 %), including one case with diffuse expression. Only the latter case also harbored HPV DNA, specifically of type 33 with weak expression of HPV 18. We observed variable expression of p16 protein in all five tumors, but HPV DNA was not found. Moreover, with the exception of a small study by Vageli et al. [21], all studies testing for HPV DNA in salivary gland tumors have reported negative results [22–24]. Accordingly, we have not detected HPV DNA in the PLGA control cases. As p16 protein overexpression may be induced by cellular senescence and activation of proto-oncogenes in HPV-unrelated lesions/tumors [25, 26], we hypothesize that the p16 expression observed in CAMSG may be related to polymorphisms of *RET* and *H-RAS* proto-oncogenes found in our cases.

Little is known about molecular genetic changes in CAMSG. Skálová et al. [1] did not find any mutations in the *BRAF*, *K-RAS*, *c-kit*, and *PDGFRα* proto-oncogenes in ten tumors, of which tissue was available for analysis. Similarly, we did not find any mutation in the *BRAF*, *K-RAS*, and *N-RAS* proto-oncogenes. However, we observed heterozygous polymorphisms in *RET* proto-oncogene: Gly691Ser in exon 11, p.Leu769Leu in exon 13, Ser904Ser in exon 15, and the variant p.IVS14-24 G/A of intron 14. The *RET* proto-oncogene plays a very important role in the pathogenesis of medullary thyroid carcinoma and of PTC, and its polymorphisms seem to have a relevant role in modifying the course of the disease [6, 7, 27–29]. Furthermore, we detected in CAMSG homozygous and heterozygous polymorphisms 81 T-C in exon 1 of the *H-RAS* proto-oncogene. The presence of the *H-RAS* 81 T-C polymorphism was reported in association with aneuploidy, higher amounts of total *H-RAS* mRNA expression, higher amounts of p21 isoform, and a higher fraction of neoplastic cells in S phase [30]. It has been

suggested that the *H-RAS* 81 T-C polymorphism might induce aneuploidy through overexpression of the active p21 isoform in follicular tumors of the thyroid gland [30].

The differential diagnosis of CAMSG includes PLGA and PTC. PLGA usually occurs on the palate and metastasizes only rarely. Microscopically, it often shows target-like appearance, frequently contains clear cells and less frequently mucoid cells, and the tumor cell nuclei do not show a striking ground glass appearance. On the contrary, CAMSG occurs in tongue in most cases and shows a strong tendency for early lymphogenous dissemination. Microscopically, CAMSG is composed of only one cell type and the tumor cell nuclei are typically of ground glass appearance. In addition, the presence of peripheral clefts appears to be characteristic for CAMSG. On the other hand, we observed a significant overlap in the immunohistochemical profile between PLGA and CAMSG, including expression of galectin-3, CK19, and HBME-1, indicating that none of these markers can be used in differential diagnostics. Furthermore, we did not find any difference in the molecular genetic characteristics between PLGA and CAMSG in the analyzed exons of the studied proto-oncogenes.

Another differential diagnosis of CAMSG is PTC, particularly in the case of nodal metastasis. In addition, PTC arising from lingual thyroid may be considered when one is dealing with a primary tumor, but this is a rare event. In CAMSG, colloid is absent and the eosinophilic material present in follicular areas is rather pale in contrast with the deeply eosinophilic colloid seen in the follicular variant of PTC. In addition, giant multinucleated cells are not observed in CAMSG and psammoma bodies are found only exceptionally. Unlike PTC, the CAMSG is composed of secretory myoepithelial cells. Most importantly, CAMSG is consistently negative with both thyroglobulin and TTF-1 [1–3, 16, 17]. However, one must be alert to the fact that both CAMSG and PTC may show variable expression of galectin-3, CK19, and HBME-1 as shown in our cases.

In summary, we report five additional cases of CAMSG with immunohistochemical and molecular genetic analysis. The finding of galectin-3, CK19, and HBME-1 expression in CAMSG is of particular importance for differential diagnostics versus PTC. The *RET*, *B-RAF*, *K-RAS*, *N-RAS*, and *H-RAS* proto-oncogenes were not mutated, but we found several polymorphisms in the *RET* and *H-RAS* proto-oncogenes that could modify some characteristics of CAMSG. The immunohistochemical and molecular genetic profiles of CAMSG and PLGA are similar, and based on their different biological behavior and microscopical appearance, we propose to consider CAMSG as a separate salivary gland tumor entity distinct from PLGA.

Acknowledgments The authors thank Mrs. M. Žáková for her excellent technical support and Vladimír Hořava Jr., M.D., Šárka Solecká, M.D., Tomáš Vaněk, M.D., Jana Hatlová, M.D., and Radomír Lána, M.D., for kindly providing patients' (cases 4 and 5) clinicopathological data. This study was supported by the project PRVOUK of Charles University in Prague, Czech Republic, and by grant IGA MH CR NT 13901–4.

Conflict of interest The authors declare that they have no conflict of interest.

References

1. Skálova A, Šíma R, Kašpírková-Němcová J et al (2011) Cribriform adenocarcinoma of minor salivary gland origin principally affecting the tongue: characterization of new entity. Am J Surg Pathol 35:1168–1176
2. Michal M, Skálová A, Simpson RHW et al (1999) Cribriform adenocarcinoma of the tongue: a hitherto unrecognized type of adenocarcinoma characteristically occurring in the tongue. Histopathology 35:495–501
3. Prasad KC, Kaniyur V, Pai RR, Nesari SS (2004) Pedunculated cribriform adenocarcinoma of the base of the tongue. Ear Nose Throat J 83:62–64
4. Perez-Ordonez B, Linkov I, Huvos AG (1998) Polymorphous low-grade adenocarcinoma of minor salivary glands: a study of 17 cases with emphasis on cell differentiation. Histopathology 32:521–529
5. Laco J, Ryška A, Čáp J, Čelakovský P (2008) Expression of galectin-3, cytokeratin 19, neural cell adhesion molecule and E-cadherin in certain variants of papillary thyroid carcinoma. Cesk Patol 44:103–107
6. Nikiforova MN, Nikiforov YE (2008) Molecular genetics of thyroid cancer: implications for diagnosis, treatment and prognosis. Expert Rev Mol Diagn 8:83–95
7. Lloyd RV, Buehler D, Khanafshar E (2011) Papillary thyroid carcinoma variants. Head Neck Pathol 5:51–56
8. van Dongen JJ, Langera AW, Bruggemann M et al (2003) Design and standardisation of PCR primers and protocols for detection of clonal immunoglobulin and T-cell receptor gene recombinations in suspect lymphoproliferations: report of the BIOMED-2 Concerted Action BMH4-CT98-3936. Leukemia 17:2257–2317
9. Kazakov DV, Němcová J, Mikyškova I, Bělousová IE, Vazmitel M, Michal M (2007) Human papillomavirus in lesions of anogenital mammary-like glands. Int J Gynecol Pathol 26:475–480
10. Hagmar B, Johansson B, Kalantari M, Petersson Z, Skyldberg B, Walaas L (1992) The incidence of HPV in a Swedish series of invasive cervical carcinoma. Med Oncol Tumor Pharmacother 9:113–117
11. JindřichováŠ VJ, Vlček P, Neradilová M, Němec J, Bendlová B (2004) Screening of six risk exons of the RET proto-oncogene in families with medullary thyroid carcinoma in the Czech Republic. J Endocrinol 183:257–265
12. Sýkorová V, DvořákováŠ RA et al (2011) $BRAF^{V600E}$ mutation in the pathogenesis of a large series of papillary thyroid carcinoma in Czech Republic. J Endocrinol Invest 33:318–324
13. Quiros RM, Ding HG, Gattuso P, Prinz RA, Xu X (2005) Evidence that one subset of anaplastic thyroid carcinomas are derived from papillary carcinomas due to BRAF and p53 mutations. Cancer 103:2261–2268
14. Carta C, Moretti S, Passeri L et al (2006) Genotyping of an Italian papillary thyroid carcinoma cohort revealed high prevalence of BRAF mutations, absence of RAS mutations and allowed the detection of a new mutation of BRAF oncoprotein (BRAF (V599lns)). Clin Endocrinol (Oxf) 64:105–109

15. Vasko V, Ferrand M, di Cristofaro J, Carayon P, Henry JF, de Micco C (2003) Specific pattern of RAS oncogene mutations in follicular thyroid tumors. J Clin Endocrinol Metab 88:2745–2752
16. Borowski-Borowy P, Dyduch G, Papla B, Gabryś I, Składzień J, Okoń K (2011) Cribriform adenocarcinoma of the tongue. Pol J Pathol 62:168–171
17. Čoček A, Hronková K, Voldánová J et al (2011) Cribriform adenocarcinoma of the base of tongue and low-grade, polymorphous adenocarcinomas of the salivary glands. Oncol Lett 2:135–138
18. Yajima M, Yamazaki T, Minemura T, Kotani A (1989) Tubular adenocarcinoma of the apex of the tongue. J Oral Maxillofac Surg 47:86–88
19. Crocker TP, Kreutner A, Othersen HB, Garvin J (1983) Papillary adenocarcinoma of minor salivary gland origin in a child. Arch Otolaryngol 109:827–831
20. Del Vecchio M, Foschini MP, Peterse JL, Eusebi V (2005) Lobular carcinoma of the breast with hybrid myoepithelial and secretory ("myosecretory") cell differentiation. Am J Surg Pathol 29:1530–1536
21. Vageli D, Sourvinos G, Ioannou M, Koukoulis GK, Spandidos DA (2007) High-risk human papillomavirus (HPV) in parotid lesions. Int J Biol Markers 22:239–244
22. Atula T, Grénman R, Klemi P, Syrjänen S (1998) Human papillomavirus, Epstein–Barr virus, human herpesvirus 8 and human cytomegalovirus involvement in salivary gland tumours. Oral Oncol 34:391–395
23. Rommel B, de Villiers EM, Dürst M, Bartnitzke S, Bullerdiek J (1991) Failure to detect human papillomavirus sequences at the 3p21 rearrangement site in pleomorphic adenomas. Cancer Genet Cytogenet 52:187–191
24. Seethala RR, Thompson LD, Gnepp DR et al (2012) Lymphadenoma of the salivary gland: clinicopathological and immunohistochemical analysis of 33 tumors. Mod Pathol 25:26–35
25. Ben-Porath I, Weinberg RA (2005) The signals and pathways activating cellular senescence. Int J Biochem Cell Biol 37:961–976
26. Romagosa C, Simonetti S, López-Vicente L et al (2011) $p16^{Ink4a}$ overexpression in cancer: a tumor suppressor gene associated with senescence and high-grade tumors. Oncogene 30:2087–2097
27. Weinhaeusel A, Scheuba C, Lauss M et al (2008) The influence of gender, age, and RET polymorphisms on C-cell hyperplasia and medullary thyroid carcinoma. Thyroid 18:1269–1276
28. Sromek M, Czetwertyńska M, Skasko E, Zielińska J, Czapczak D, Steffen J (2010) The frequency of selected polymorphic variants of the RET gene in patients with medullary thyroid carcinoma and in the general population of central Poland. Endocr Pathol 21:178–185
29. Ceolin L, Siqueira DR, Romitti M, Ferreira CV, Maia AL (2012) Molecular basis of medullary thyroid carcinoma: the role of RET polymorphisms. Int J Mol Sci 13:221–239
30. Castro P, Soares P, Gusmao L, Seruca R, Sobrinho-Simoes M (2006) H-RAS 81 polymorphism is significantly associated with aneuploidy in follicular tumors of the thyroid. Oncogene 25:4620–4627

Virchows Arch (2012) 461:541–551
DOI 10.1007/s00428-012-1323-y

ORIGINAL ARTICLE

Time-dependent biological differences in molecular markers of high-grade urothelial cancer over 7 decades (ras proteins, pTEN, uPAR, PAI-1 and MMP-9)

Jorunn Litlekalsoy · Jens G. Hostmark · Daniela Elena Costea · Martin Illemann · Ole Didrik Laerum

Received: 8 August 2012 / Revised: 11 September 2012 / Accepted: 25 September 2012 / Published online: 6 October 2012
© Springer-Verlag Berlin Heidelberg 2012

Abstract The aim of this study was to evaluate changes and correlations between various molecular markers related to growth regulation and invasiveness in urothelial carcinomas in samples collected from 1932 to 2004. Paraffin-embedded autopsy/biopsy tissues from 144 patients were stained with antibodies against H–K–N ras proteins, pTEN protein, urokinase plasminogen activator receptor (uPAR), plasminogen activator inhibitor-1 (PAI-1) and matrix metalloproteinase-9 (MMP-9) and analyzed by in situ hybridization. Statistical analysis was performed by SPSS using cross tabulation and logistic regression. While the presence of K-ras, N-ras, PAI-1, and loss of pTEN increased over the last few decades, uPAR expression decreased during the same period. The increase in K-ras expression associated positively with the increase in expression of the other two ras proteins, H-ras and N-ras, and the loss of pTEN. A strong positive correlation was also observed between PAI-1 and uPAR, PAI-1 and previously detected markers, EGFR (epidermal growth factor receptor) and p53. Presence of uPAR was found to be positively associated with p16 expression. Multivariate analysis with clinical parameters revealed a positive correlation between PAI-1 expression and tumour grade, CkHMW (high molecular weight cytokeratin) and tumour grade, CkHMW and metastasis, EGFR and metastasis. mRNA could be detected in samples from the last 50 years while older samples were negative, indicating its complete degradation during longer storage. In conclusion, increased accumulation of K-ras, N-ras, and PAI-1 together with loss of pTEN in bladder carcinomas of grades II and III seems to be more dominant in recent times, suggesting an altered malignant potential in these neoplasms.

Keywords Tissue microarrays · Urothelial carcinomas · RAS · pTEN · uPAR · PAI-1

J. Litlekalsoy · D. E. Costea · O. D. Laerum
The Gade Institute, Section for Pathology, University of Bergen, 5021 Bergen, Norway

J. Litlekalsoy · J. G. Hostmark
Department of Surgical Sciences, University of Bergen, 5021 Bergen, Norway

J. G. Hostmark
Surgical Clinic, Department of Urology, Haukeland University Hospital, 5021 Bergen, Norway

M. Illemann
The Finsen Laboratory, Biocenter, Rigshospitalet, 2100 Copenhagen, Denmark

M. Illemann
Biotech Research and Innovation Centre (BRIC), University of Copenhagen, 2200 Copenhagen, Denmark

O. D. Laerum
Department of Pathology, Haukeland University Hospital, 5021 Bergen, Norway

J. Litlekalsoy (✉)
Department of Pathology/The Gade Institute, Section of pathology, Haukeland University Hospital, 5021 Bergen, Norway
e-mail: Jorunn.Litlekalsoy@gades.uib.no

Introduction

Urothelial carcinomas of the bladder are generally known to develop through divergent pathways of tumourigenesis. While low-grade papillary tumours seldom become muscle-invasive, they have frequently mutated genes contributing to a constantly activated receptor tyrosine kinase ras pathway. High-grade invasive and metastasizing tumours, in addition, have loss of function of p53, pTEN and retinoblastoma protein

pathways [1, 2]. The *RAS* gene that encodes p21/ras consists of three families, *H-RAS*, *K-RAS* and *N-RAS*. These genes are converted to active oncogenes by point mutations leading to amino acid substitutions at positions 12, 13 or 61 and are together with p53 mutations the most frequent genetic alterations detected in human neoplasms. The ras proteins were among the first proteins identified that can regulate cell growth and are responsible for cell survival, proliferation, differentiation and apoptosis that can be detrimental for both normal and cancer cells. The incidence of *RAS* gene activation and mutation in human cancers varies greatly [3]. In bladder cancer the frequency of mutations in *RAS* genes has been controversial, where both low and high frequency of mutations have been reported. Point mutations and genetic instability in polymorphic sites in the *RAS* genes are, however proposed to be an early event in bladder tumour genesis [4, 5].

The pTEN (MMACI) gene located at 10q23 is considered a tumour suppressor gene since it normally induces cell cycle arrest and apoptosis. pTEN encodes a multifunctional phosphatase which is known to be mutated or deleted in many human cancers, including gliomas, breast, prostate, lung, thyroid and endometrial carcinomas. This gene is also reported to show loss of heterozygosity (LOH) in bladder cancer, and more frequently in muscle-invasive transitional cell carcinomas (TCC) [6]. The functions of pTEN at the cell membrane are reasonably well understood, while the roles of pTEN in the nucleus are less clear. Mutations or deletions of pTEN DNA occur at moderate frequency in human primary bladder cancers and bladder cancer cell lines (~30 %). Tsuruta et al. [7] have demonstrated that pTEN deficiency usually is associated with Akt and ERK activation, enlarged cell size and tissue hyperplasia with tumour formation. It has also been reported that mice deficient of pTEN in the urothelium develop bladder cell hyperplasia and carcinomas [7].

Muscular invasion leading to local dissemination and metastasis is another key event in the tumour progression, being mediated by proteolytic factors which degrade basement membranes and the extracellular matrix. The urokinase plasminogen activator (uPA) system represents a family of serine proteases, which plays an important role in tumour invasion, in addition to its general role in tissue remodelling. High endogenous levels of uPA and its receptor uPAR are also associated with advanced metastatic cancers. Surprisingly, high expression of its main inhibitor, PAI-1 may further stimulate tumour dissemination. Various MMPs are also known to act as key players in tumour invasion and metastasis. They promote intravasation and regulate the relationship between tumour cells and host tissue stroma subsequent to extravasation [8, 9].

Since combinations of such biomarkers seem to be critical for tumour progression, we have examined them in archival paraffin embedded autopsy material collected for 10–70 years. Human life style and exposure to various carcinogenic agents are thought to have a major impact on human neoplasia. Still, it has been difficult to assess the relative importance and contribution of different carcinogenic components on human tumourigenesis over time. Recent improvements in immunohistochemical and molecular methods have enabled direct comparisons on paraffin embedded tumour specimens over a rather long time period. By assessing many different tumour markers related to growth regulation and invasiveness, we show here that the occurrence of some key biological features of invasive urothelial carcinomas differed significantly over time. This strongly indicates that invasive bladder carcinomas in this 70-year observation period might be initiated and developed through different molecular pathways. In addition, we show that stored paraffin-embedded samples of urothelial carcinomas can be used for detection of mRNA as long as 50 years after collection, but by longer storage time their usefulness for in situ hybridization is limited.

Materials and methods

Patient material and tissue

Paraffin-embedded autopsy/biopsy tissue collected between 1932 and 2004 with invasive urothelial cancer (WHO grade II and III) from 144 patients was included as previously described [10]. Available normal tissue obtained from the same autopsies served as controls. Variables as age, gender, metastasis, time from diagnoses till death and time from death until autopsy were recorded (Table 1). For use of control biopsy material from the recent years, ethical clearance was given by the Regional Ethical Committee (REK No. 12226) and informed consent was provided.

Table 1 Patient data

Period	Autopsies	Biopsies	Grade II	Grade III	Metastases	Mean (SEM) age [years]	Females % of total
1932–1948	14	4	7	11	6	67.3 (2.6)	27.8
1950–1959	25	5	18	12	12	66.4 (2.1)	40.0
1960–1970	41		15	26	18	72.9 (1.4)	39.0
1990–2004	42	13	5	50	31	72.1 (1.2)	34.6

Partly compiled from BJU 99:1013–1019

Tissue microarray technique

TMA were created by manually transferring three cores of 1,0 mm in diameter from the archival paraffin embedded tissue blocks representing each donor (patient) to an empty recipient paraffin block by use of a custom-made instrument (Beecher Instruments, Silver Springs, MD). On the basis of hematoxylin and eosin-stained whole mount sections from the representative paraffin blocks, the most cellular parts of the tumour and the area devoid of necrosis were selected.

Immunohistochemistry

The TMA blocks were cut in 5-μm paraffin sections and stained with antibodies against H-ras, K-ras, N-ras, pTEN, uPAR, PAI-1 and MMP-9 protein as described previously [10]. The sections were deparaffinized and various treatments were used for antigen retrieval (see Table 2 for details). After application of the primary antibody, visualization was performed according to standard streptavidin–biotin method were the substrate system consists of an HRP substrate buffer containing hydrogen peroxide and concentrated diaminobenzidine (DAB) using ChemMate Detection Kit (DAKO, Copenhagen, Denmark) or followed by a method using NovaRED Substrate Kit (SK-4800 Vector Laboratories, USA). All slides were counterstained with hematoxylin. Sections of tissue microarray made of 12 different tissues (six cores each) together with paraffin embedded sections of HeLa cells, all reported to express one or more of our chosen proteins, served as control tissue (Table 3). To uncover non-specific binding of the monoclonal antibodies, extra sections in which the primary antibody was omitted served as negative controls.

In vitro transcription and in situ hybridisation

Antisense and sense uPAR-riboprobes were generated from plasmids pHUR04 and pHUR06 [11], incorporating ^{35}S-labelled UTP (NEN, Boston, MA) by in vitro transcription using T3/T7/Sp6 RNA polymerases (Roche, Basel, Switzerland). The DNA templates were digested with DNase (Promega, Madison, WI). Unincorporated ^{35}S-labelled UTP and DNA were removed using RNeasy MinElute Cleanup kit (Qiagen, Hilden, Germany). The ^{35}S-radioactivity concentration of the probes was adjusted by dilution to 250,000 cpm/μl. Paraffin section of 3 μm were cut under RNase free conditions deparaffinised with xylene, hydrated, washed with PBS (130 mM NaCl, 7 mM Na_2HPO_4, 3 mM NaH_2PO_4, pH 7.0) and pre-treated with TEG-buffer (10 mM Tris, 0.5 mM EDTA, pH 9.0) for 10 min at 98°C. Sections were then dehydrated in ethanol/water solutions. Next, 4 μl of the ^{35}S-labelled RNA probe (~500,000 cpm/slide for biopsies collected after 1990 or ~1,000,000 cpm/slide for biopsies collected before 1990) were added to 16 μl of a

Table 2 Antibodies

Antigen	Specificities of protein antibodies	Purchaser	Dilution	Pre-treatment
H-ras (F235) (sc-29)	Monoclonal H-ras p21	Santa Cruz Biotechnology Inc. Europe	1:50, 60 min, room temperature	Microwave treatment for 10 min at 750 W and 20 min at 500 W in mmol/l citrate buffer, pH 6
K-ras (NCC-RAS-00) sc-58463	Monoclonal K-ras p21	Santa Cruz Biotechnology Inc. Europe	1:100, 60 min, room temperature	Microwave treatment for 10 min at 750 W and 20 min at 500 W in mmol/l citrate buffer, pH 6
N-ras (F155) sc-31	Monoclonal N-ras p21	Santa Cruz Biotechnology Inc. Europe	1:50, 60 min, room temperature	Microwave treatment for 10 min at 750 W and 20 min at 500 W in mmol/l citrate buffer, pH 6
pTen (A2B1) sc-7974	Monoclonal AA 388-400	Santa Cruz Biotechnology Inc. Europe	1:50, 60 min, room temperature	Microwave treatment for 10 min at 750 W and 20 min at 500 W in mmol/l citrate buffer, pH 6
uPAR (R2)	Monoclonal Domain 3	Finsen Laboratory, Rigshospitalet Copenhagen, Denmark	1:2,000, 60 min, room temperature	Proteinase K treatment for 15 min
PAI-1[a,b]	Polyclonal	Finsen Laboratory, Rigshospitalet Copenhagen, Denmark	1:500, 60 minutes room temperature	Microwave treatment for 10 min at 750 W and 20 min at 500 W in TE-buffer pH9
MMP-9 (A0150)	Polyclonal AA 146-159	Dako Cytomation, DK-2600 Glostrup Denmark	1:1,000, 120 minutes room temperature	Microwave treatment for 10 min at 750 W and 20 min at 500 W in 10 mmol/L citratbuffer pH6

[a] Biochem. J. (1998) 329, 55–63

[b] AJP (2003) 163(5)

Table 3 Positive controls

	H-ras	K-ras	N-ras	pTEN	uPAR	PaI-1	MMP-9
Adenocarcinoma in pancreas	+	+	+	–	+[a]	–	+[b]
Normal pancreas	+	+	+	+	–	–	–
Squamous cell carcinoma	–	–	–	–	+[c]	+[d]	–
Transitional cell carcinoma	+	+	+	–	+	+[d]	+[e]
Bile duct carcinoma	+	+	+	–[f]	+[g]	–	+[h]
Gastric adenocarcinoma	+	–	+	–	+[i]	–	–
Normal appendix	+	+[j]	+	+[k]	–	–	+[h]
Mammary carcinoma	+	–	+	+	+[c]	–	–
Glioblastoma	+	+	+	+	+[j]	–	–
Adenocarcinoma of colon	+	–	+	–	+	+[a]	–
Normal liver	+	–	+[l]	+	–	–	–
Clear cell carcinoma of the kidney	+	–	–	+	–	–	–
HeLa cells	+	+	+	–	–	+	–

[a] Positive in connective tissue

[b] Some positive granulocytes (at border of tumour)

[c] Positive in tumour and connective tissue

[d] Positive in tumour

[e] Positive granulocytes and macrophages

[f] Negative tumour, positive in nerves

[g] Postivie in connective tissue around glands

[h] Some positive granulocytes

[i] Postive in connective tissue around tumour and glands

[j] Positive around blood vessels

[k] Positive in nerves and connective tissue

[l] Positive in kupffer cells, hepatocytes negative

hybridisation mixture (50 % deionised formamid, 10 % dextran sulphate, 1 μg/μlt-RNA, 0.02 % (wt/vol) Ficoll 400, 0.02 % (wt/vol) polyvinilpyrrolidone, 0.02 % (wt/vol) bovine serum albumin (BSA) Fraction V, 10 mM DTT, 300 mM NaCl, 0.5 mM EDTA, 10 mM Tris–HCl and 10 mM $NaPO_4$, pH 6.8) was incubated for 16–18 h at 55° C in a humidified chamber. The sections were washed twice with sodium citrate buffer (SSC, 150 mM NaCl; 150 mM sodium citrate, pH 7.0) containing 0.1 % SDS and 10 mM DTT. Sections were washed in sequence, 10 min for each step: 2× SSC, 0.5× SSC and 0.2× SSC, then incubated with RNase A (20 mg/ml in 500 mM NaCl, 1 mM EDTA, 10 mM Tris–HCl, pH 7.2) at 44°C for 10 min to remove nonspecifically bound riboprobe, and subsequently washed in 0.2× SSC as specified earlier. Sections were dehydrated in ethanol solution containing 300 mM ammonium acetate, soaked in an autoradiographic emulsion (ILFORD Imaging UK Limited, Mobberley, UK) and exposed for 7 days (biopsies collected after 1990) or 21 days (biopsies collected before 1990) at 4°C after which the sections were developed. Finally the sections were counterstained with Mayer's haematoxylin and eosin, dehydrated with ethanol and mounted.

Evaluation of staining results

Immunohistochemical staining

Presence of (H–K–N) ras, pTEN, PAI-1, uPAR and MMP-9 proteins were recorded as positive or negative by two of the authors (O.D.L. and J.L). The pTEN staining was located mainly in the cytoplasm, while the ras proteins were detected in the membrane of tumour cells. PAI-1 was located in the cellular cytoplasm and membrane both in the tumour and connective tissue. uPAR was located in the cellular cytoplasm and membrane, around blood vessels and glands, and in connective tissue around tumour. MMP-9 expression was located in the membrane of the tumour cells and in granulocytes and macrophages at the border of tumour. The proportion of positive cells was recorded by a grading system where + denoted 1–10 %, + + 10–50 %, and +++ 50–100 % of the cells. Available normal tissue from both the tumour slides and tissue from other organs collected from the autopsies served as controls. If cores in the tissue microarrays were lost during the process or the score otherwise was difficult to perform, new whole mount sections were stained in replacement.

In situ hybridisation

The hybridisation signal was found primarily in cancer cells but also in stromal cells. The strength of the signal varied with high/low count of the radioactive probes and different time of developing. The recording of positive/negative signals were made by two of the authors (O.D.L. and M.I.).

Statistics

Statistical evaluation was performed using Statistical Package for the Social Sciences (SPSS) program version 12 (SPSS Inc., Chicago, IL). To determine if there was a significant trend across the time for the expression of the variables tested in the study the chi-square test for independence (linear-by-linear association) was used. For this purpose the variable expressing the period of time the tissues were collected ('years in groups') was categorized in four groups: 1932–1948, 1950–1959, 1960–1970, and 1990–2004. The chi-square test (Spearman correlation) was also used to investigate whether there was any relationship between the expressions of the markers tested in the study. Logistic regression was further used to estimate the strength of the associations between different markers or between markers and the time of collection.

Results

Protein detection

Expression of ras proteins in the tumour sections showed variation over time. H-ras showed quite low expression in the oldest material collected (1932–1948), with highest expression (73 % of cases) in tissues collected between1950 and 1959 (Figs. 1a and 2a), and then gradually decreasing towards more recent years. K-ras was also mostly expressed by tumours collected in 1932–1948 (63 % of cases). Although no visible trend towards increased or decreased expression over time could be observed (Figs. 1b and 2b), the cross-tabulation analysis revealed a positive correlation between K-ras expression and the time period the tissue was collected ($p=0.018$). A nonsignificant increase in positivity was observed for N-ras expression towards recent years of collection (Figs. 1c and 2c). Significant correlations were found between N-ras expression and H-ras expression ($p=0.002$) with an odds ratio (OR) of 3.84 (Tables 4 and 5), as well as between N-ras and K-ras expression ($p=0.021$, OR=2.85).

Forty five percent of the bladder tumours from 1932 to 1948 stained negatively for A2B1 antibody that identifies pTEN (Fig. 1d). The loss of pTEN was as low as 34 % in tumours from 1950 to1959, but increased to 69 % in 1960–1970s and to 59 % in 1990–2004 (Fig. 1d). Cross-tabulation analysis revealed a trend of positive correlation between pTEN loss and the time of tissue collection ($p=0.020$). A positive correlation was found by both cross-tabulation and logistic regression between loss of pTEN and K-ras expression, with a high OR of 4.850 (Tables 4 and 5).

Both markers of the plasminogen activation system were found expressed by both tumour cells and normal host cells at the tumour front (connective tissue, macrophages and granulocytes as presented in Table 6). The highest fraction of positive cases for uPAR expression was seen in tumours from 1932 to 1948 (Fig. 1e). A nonsignificant decrease was observed in the percentage of tumours expressing uPAR over time towards the more recent years (Figs. 1e and 2d). In contrast, PAI-1 expression was found to be positively correlated with uPAR expression by both cross-tabulation and logistic regression analyses ($p=0.009$ and 0.002, respectively). The OR of having a positive tumour for PAI-1 when uPAR was positive, was of 3.74. The variation in time of PAI-1 expression was found statistically significant by both cross-tabulating and logistic regression ($p=0.001$ and $p=0.010$, respectively), with the odds of finding a positive PAI-1 tumour in the more recent years of 1.69 (Figs. 1f and 2e).

Only three out of 154 tumours showed positive staining for MMP-9 in the malignant tissue or the invasion front. MMP-9 was generally expressed in granulocytes and was abundantly present in these in 14 of the cases. As a general observation, the staining was rather weak in the older material.

Normal tissue controls

Paraffin wax-embedded autopsy tissue from normal organs was tested for the selected tumour markers. This tissue included connective and fatty tissue, tissue from thyroid gland, smooth muscular, leukocytes, heart, lungs, uterine cervix, normal urinary bladder epithelium, appendix, lymph nodes, endometrium, ureter and ovaries, placenta, liver, brain, kidneys, bone marrow and prostate. The A2B1 antibody showed expression of pTEN in almost all normal tissue with exception of samples from the kidney, lung and brain, which were found negative with one sample each. The H-ras protein was also found expressed in most of the normal tissue samples, except for samples with connective and fatty tissue and samples from the brain. In the prostate and uterus the expression of the protein was found around glands. All samples of normal tissue were negative for K-ras expression except for one sample from the heart that showed a positive staining. The expression of N-ras protein in the normal tissue was found in one sample of decidual tissue from the placenta, in the tubuli of the kidneys (two samples), in endometrial and myometric tissue of the uterus (one sample) and in one sample from the prostate. The normal samples were all largely negative for the expression of PAI-1. Positive staining was seen in the trophoblast of one sample from placenta, in the connective tissue in one sample from the kidney and one sample of connective

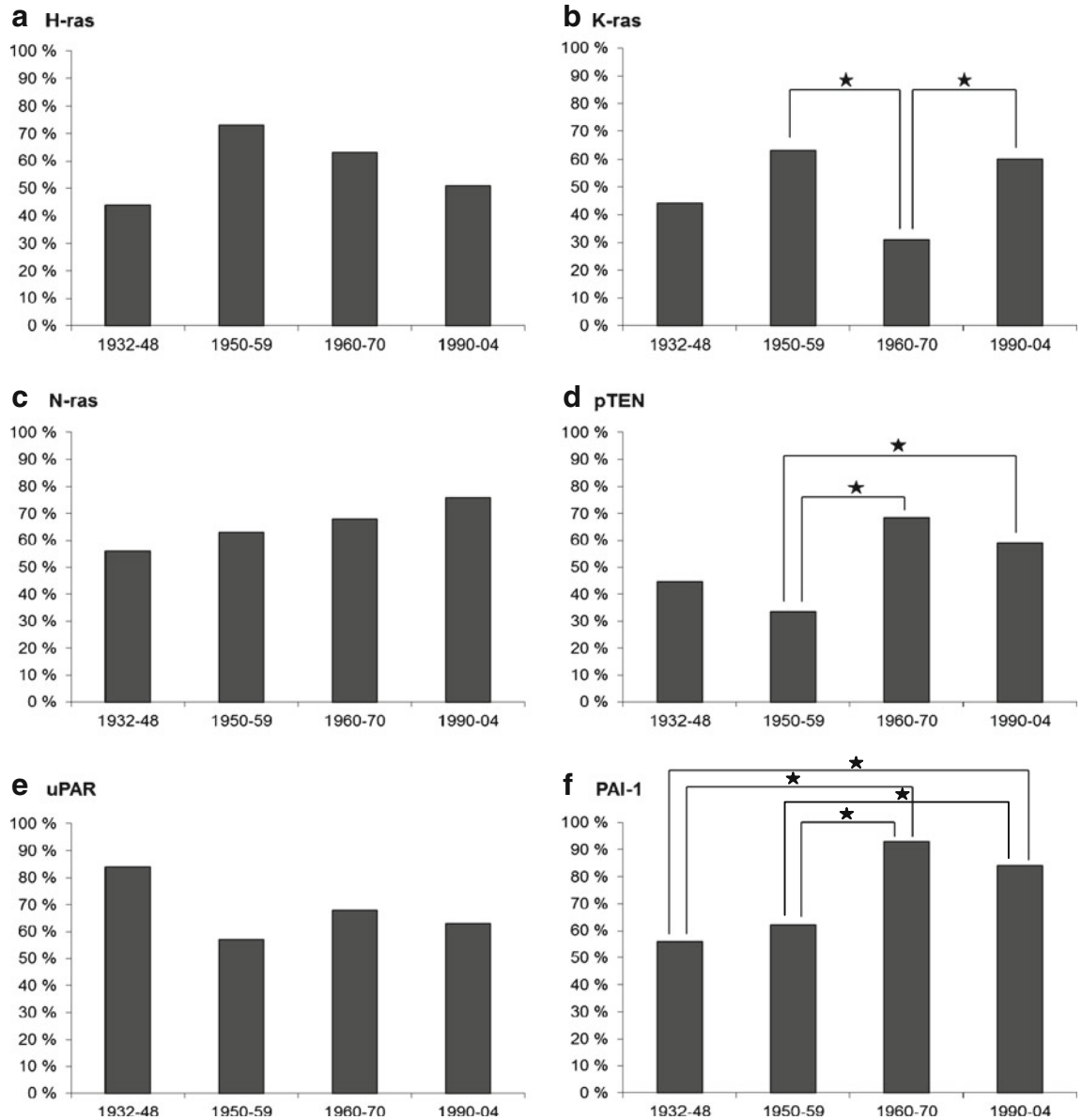

Fig. 1 Positive score (percentage) of H–K–N-ras expression (**a**, **b**, **c**), pTEN loss (negative score) (**d**), uPAR (**e**) and PAI-1 (**f**) expression in the tumour tissue. The significance ≤0.05 between the different time groups is labeled (*filled star*)

tissue. The normal tissue samples stained with uPAR were also found largely negatively expressed. Positive staining was seen in one sample of connective tissue from liver and prostate and in two samples from the kidneys and lungs.

Time-dependent trends in protein expression

Tumours diagnosed in the period 1960–2004 showed higher proportions of PAI-1 and N-ras positivity as well as more frequent pTEN deletion than tumours collected earlier. H-ras, K-ras and uPAR did not show a consistent pattern, but K-ras positive tumours increased during the time period 1932–2004 (Fig. 1). Twelve different tumour markers (including data from [10]) were taken together and analyzed in this study, and Table 7 gives a list of markers that have increased/decreased by more than 10 % in the period 1932–2004. The table displays relative change in percent and proportion from 2004 to 1932 for the actual markers.

Correlations to tumour grade and metastasis

Based on a new, more complex logistic regression analysis including both new and formerly collected markers, a positive correlation was found between PAI-1 positive score and tumour grade (p=0.003) with an OR=4.76 (Table 8). CkHMW score was found to positively correlate with the

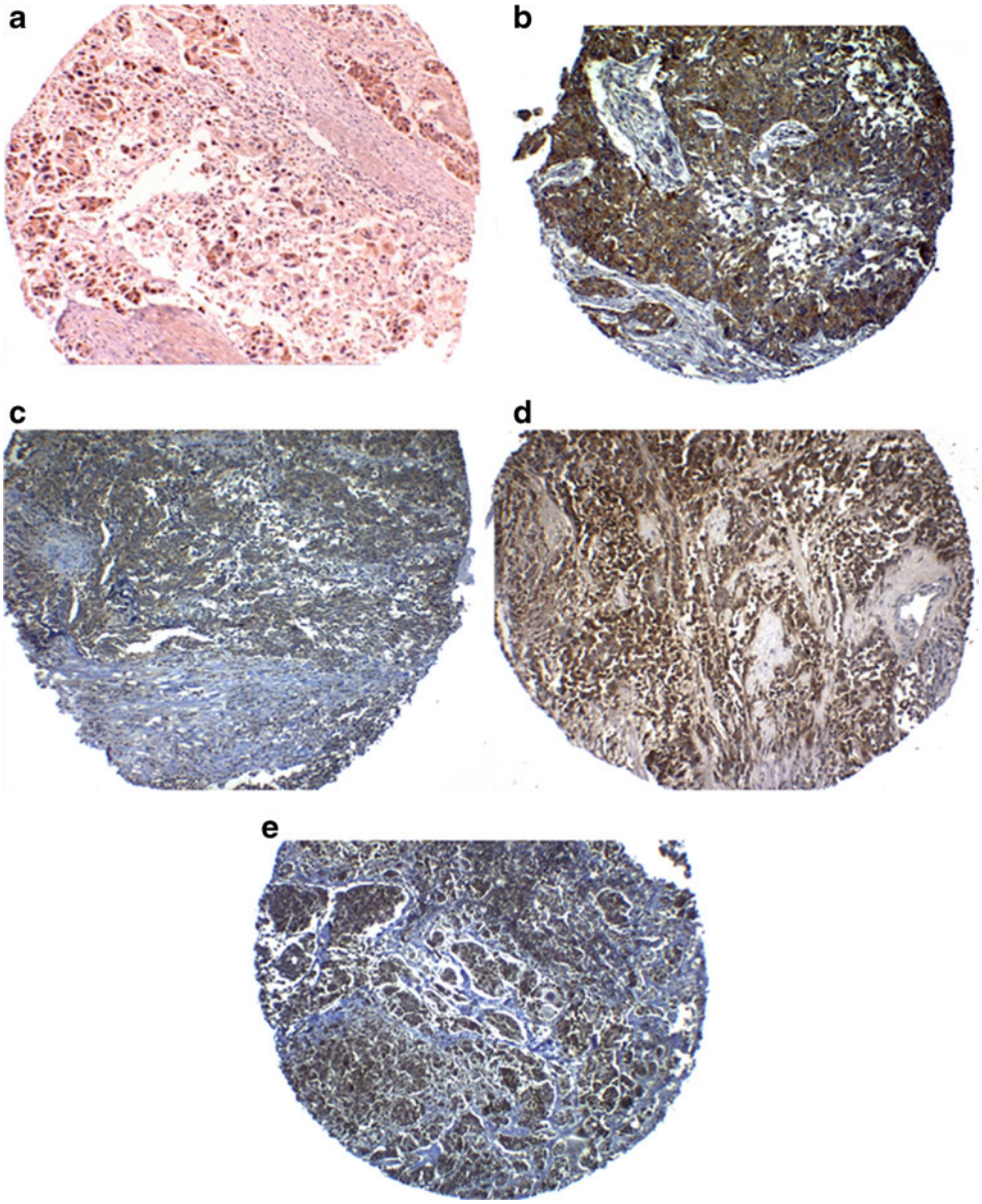

Fig. 2 Tissue microarrays (*TMA*) of invasive urothelial carcinoma from autopsies/biopsies (×10): **a** H-ras staining in autopsy tissue from 1957, **b** K-ras staining in autopsy tissue from 1966, **c** N-ras staining in biopsy tissue from 1995, **d** uPAR staining in autopsy tissue from 1990, **e** PAI-1 staining in autopsy tissue from 1999

Table 4 Correlations detected by cross-tabulation analysis

Marker	Associated marker/parameter	*p* value
N-ras	K-ras	0.026
	H-ras	<0.01
	PAI-1	0.016
K.ras	pTEN	<0.01
	years in groups	0.018
pTEN	years in groups	0.020
uPAR	PAI-1	0.009
PAI-1	years in groups	0.001
PAI-1	p53[a]	0.022

[a] Associations with markers previously detected by Litlekalsoy et al. [10]

Table 5 Associations and the odds ratio detected by logistic regression analysis

Marker	Associated marker/parameter	*p* value	Odds ratio
N-ras	H-ras	0.002	3.84
N-ras	K-ras	0.021	2.85
K-ras	pTEN	<0.01	4.85
PAI-1	uPAR	0.002	3.74
PAI-1	years in groups	0.010	1.69
PAI-1	EGFR[a]	0.011	3.58
PAI-1	p53[a]	0.004	4.64
uPAR	p16[a]	0.027	2.58

[a] Associations with markers previously detected by Litlekalsoy et al. [10]

Table 6 Percent of cell types with expression of uPAR and PAI-1 in the tumour tissue

Years	1932–1948		1950–1959		1960–1970		1990–2004	
	uPAR	PAI-1	uPAR	PAI-1	uPAR	PAI-1	uPAR	PAI-1
Cancer cells	20	100	59	100	54	100	50	100
Myofibroblasts	94	20	83	11	86	11	83	9
Macrophages	0	10	0	0	4	0	9	5
Granulocytes	20	0	24	0	11	0	15	0

occurrence of metastasis, as previously also found ($p<0.001$, OR=5.177). In addition, we found a new positive association of EGFR and Ck7 with metastasis ($p=0.016$, OR=3.22 and $p=0.009$, OR=3.70, respectively; Table 8).

mRNA detection of uPAR

In newer autopsies (collected in 1990s) uPAR mRNA could easily be detected. Here strong hybridisation signals for uPAR mRNA was found primarily in cancer cells (Fig. 3a–b and Table 9) and in some stromal cells (not shown). uPAR mRNA in samples collected during the 1960s had a weaker hybridisation signal and was only seen in some tumour cells located throughout the tissue, (Fig. 3c–d and Table 9). The two non-overlapping antisense probes gave for all samples tested, similar hybridisation signal and the corresponding sense probes were all negative (data not shown). It was not possible to detect uPAR mRNA in two samples collected from autopsies performed in the 1930s (data not shown).

Discussion

Urothelial carcinoma is one of the human cancers where external exposure to chemical agents was first recognised [12]. However, since detailed information about lifelong exposure to different chemical compounds and/or physical agents over different time periods is usually not available, it has been difficult to assess the relative importance of different carcinogens.

In this study, we have tried another approach. Due to recent improvements in immunohistochemical methods, including procedures for demasking of different epitopes in paraffin embedded tissue, it has become possible to compare tumour material directly even after a very long period has elapsed [10]. When looking at the expression of all markers over time on TCC, including all earlier available data [10], the expression of K-ras, N-ras, p53 protein and PAI-1, as well as pTEN deletion have become more frequent in the recent years, while H-ras, p16 and Ck 7 expressions were roughly constant. In contrast, the expression of uPAR and EGFR was found to be less frequent in the most recent decade investigated, especially CkHMW showing a dramatic decrease in the last decade (Table 7). Since it has been previously demonstrated that CkHMW is a sensitive marker for high-grade invasive urothelial carcinomas [13], our finding might imply that TCC had a different, more invasive phenotype in earlier times. On the other hand, the increase in proportions of tumours expressing other markers of malignant behaviour in recent decades, like K-ras, N-ras, and PAI-1, as well as loss of pTEN does not support this view. More likely, the etiological factors leading to TCC have changed over time, and the different exposures could have led to a different phenotype of cancers with the same histological pattern.

Archival tissue of urothelial tumours showed an elevated expression of K-ras, N-ras, PAI-1 and loss of pTEN in more recent years, and low expression in the older material back to the 1930s. In parallel, the expression of uPAR had an opposite

Table 7 Relative change and proportion of positive tumours in the earliest decade (1990–2004) compared with the oldest tumours (1932–1948)

Marker	Relative change (%)	Proportion
N-ras	20	1.35
K-ras	16	1.36
pTEN deletion	15	1.34
uPAR	−21	0.75
PAI-1	28	1.50
p53[a]	19	1.38
EGFR[a]	−18	0.78
CkHMW[a]	−60	0.33

[a] Markers previously detected by Litlekalsoy et al. [10]

Table 8 Associations and odds ratio detected by logistic regression analysis between various markers and tumour grade or occurrence of metastasis

Marker	Grade/metastasis	*p* value	Odds ratio
PAI-1	Grade	0.032	4.76
CkHMW[a]	Metastasis	<0.001	5.17
EGFR[a]	Metastasis	0.016	3.22
Ck7[a]	Metastasis	0.009	3.70

[a] Associations with markers previously detected by Litlekalsoy et al. [10]

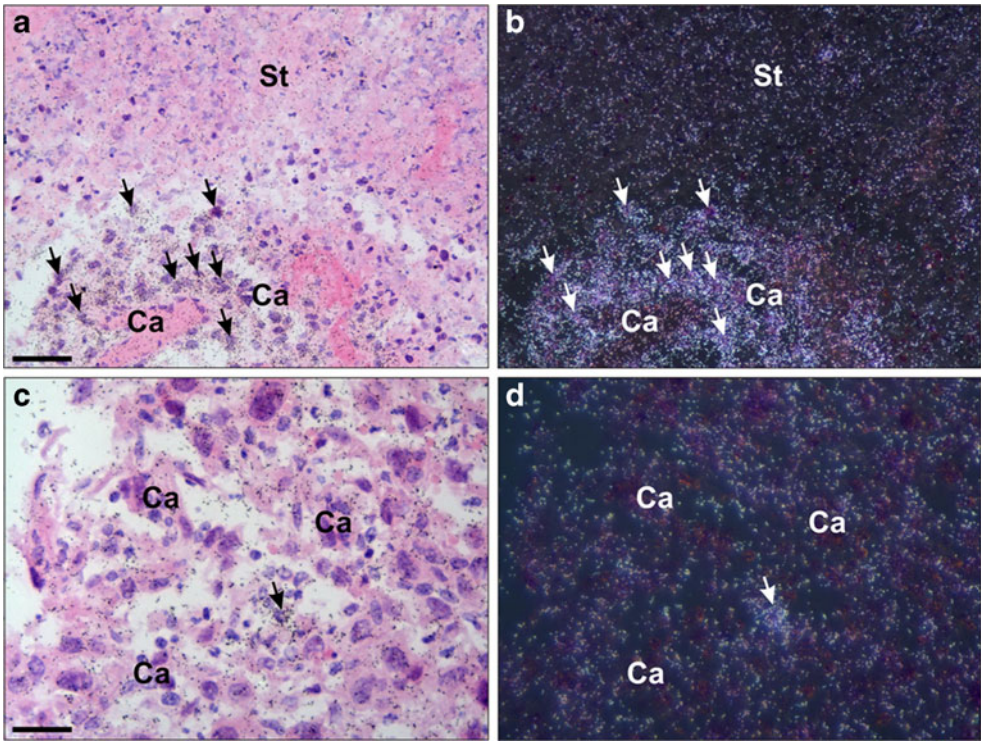

Fig. 3 uPAR in situ hybridisation of whole autopsies of human bladder cancer. Sections of a human bladder collected in the 1990s (**a**, **b**) and the 1960s (**c**, **d**) were processed for uPAR in situ hybridisation. The uPAR-mRNA signal is seen as *black silver grains* in bright-field illumination (**a** and **c**) and as *white spots* in dark-field illumination (**b** and **d**). In the autopsy from 1990s, strong uPAR mRNA hybridisation signal was found in primarily cancer cells (*arrows* in **a** and **b**), whereas uPAR mRNA hybridisation signal in autopsies from the 1960s were only found in some few cancer cells located throughout the tissue (*arrows* in **c** and **d**). Bars: **a** ~40 μm, **c** ~20 μm

pattern and was decreasing through the same time span, indicating that the older material seems to be rather well preserved. It is also interesting that the positive score of H-ras and Ck 7 seems to remain stable (as one could expect) through the entire period, and in this manner can serve as a control for both the staining process and the quality of the paraffin embedded tissue

Comparisons between tumours occurring over such a long time span are for natural reasons limited by the availability of clinical and other relevant information from the earliest periods. Patient data available for such studies on archival material going far back in time are scarce and often absent. In addition, one can never exclude the possibility of sampling errors, since inclusion criteria for therapy were highly different at that time as compared to the present-day clinical situation. Still, significant results may give valuable hints to how biological features of urothelial carcinoma may vary over time.

In Norway, there are no available data on bladder cancer mortality before 1951. Both the incidence and survival have increased since 1965 for both sexes. Although the general trends are more stable during the last decade, mortality has been slowly declining for 20 years [14].

Generally, bladder cancer is described as a malignancy with a long latency time. The reported mean duration of the latent period varies from 18 to 44 years [15]. Mean life expectancy has steadily increased from 1930 to 2000, and this might be an important reason for the increase of bladder cancer incidence. The patient awareness of symptoms and better treatment modalities has also improved the chances of survival. In 1930 the per-operative mortality for cystectomies was much higher than today. This is reflected by the fact that mortality has decreased although the incidence has increased in Western Europe from 1970 to 2005 [16]. Better diagnostics and treatment today might only cure the less malignant tumours, leaving the most malignant ones to be lethal.

It has earlier been shown that extraction and mutational analysis of fragments of DNA can be performed on archival human urothelial cancers from autopsy material which dates equally long back in time. For example, with magnetic bead extraction, mutational analysis (sequencing) can be performed on different exons of *TP53*. Thus, molecular analyses on paraffin embedded material from malignant tumours may be performed after storage many decades back in time [17]. Since there was an overlap between the material used for DNA

Table 9 Intensity of uPAR mRNA hybridisation signal in whole biopsies of bladder cancer

Biopsy no	Year collected	uPAR mRNA
1	1939	–
2	1939	–
5	1960	+
6	1965	+
8	1990	+
9	1992	++
10	1994	+++
11	1998	++

– no signal detected; + few sporadic cells; ++ several cells; +++ many cells

analyses and our present material, this further supports that key cell components may be preserved over so long periods.

The ras-signalling pathway has been given considerable attention because of its important role in carcinogenesis and as a target for anticancer therapy. Oncogenic mutations in the *RAS* gene are reported to be present in about 30 % of all human cancers. In addition to mutated activation, amplified *RAS* genes are leading to constitutively active proteins and overexpression in some tumours [18, 19]. Generally, the expression of H-ras was low in the earliest period, but otherwise revealed no particular time-dependent pattern, and the expression of K-ras was highly variable over time, while N-ras showed a steady increase in the period 1932 to 2004 (Fig. 1, Table 7)

The early stage tumours (Ta) are representing about 75–85 % of the initial neoplasms are often characterized by gain-of-function mutations in classical oncogenes as *RAS* and FGFR3 while flat carcinoma in situ (Tis) and invasive tumours (phenotypic late stage) are characterized by loss-of-function mutations in tumour suppressor genes as *TP53*, RB and pTEN [20]. pTEN gene alterations with deletion are associated with aggressive tumour phenotypes, and are among the most commonly altered tumour suppressor genes in solid cancers. Similar to N-ras expression, a lack of pTEN protein was seen in 40 % of the tumours in three of the different time groups, with an increasing pattern from 1932 to 2004 (Table 7, Fig. 1).

Generally, high concentrations of proteolytic components are correlated with poor outcome in many different cancer types. In some model systems PAI-1 may inhibit uPA and reduce invasion and metastasis. However, other studies have shown that overexpression of this inhibitor, alone or together with uPA/uPAR are capable to promote rather than inhibit tumour cell invasion and migration [21–23]. In the present tumour material, the expression of PAI-1 was found to exceed 50 % in all the four time groups and the expression increased moderately from 1932 to 2004, (Table 7, Fig. 1). Whereas PAI-1 was found mainly expressed in the cancer cells, uPAR was more frequently expressed in the myofibroblasts. In addition, the expression of the protein distributed among the different cell types was found to be rather stable through the entire period from 1932 to 2004 (Table 6). Since MMP-9 expression was negative in the majority of tumour samples, it is unlikely that the uPA/uPAR directly influences MMP9. In addition, there were no significant time differences in uPAR.

Taken together, accumulation of K-ras, N-ras, and PAI-1 together with loss of pTEN in bladder carcinomas of grade II and III seems to be more dominant in recent time, suggesting a higher malignant potential in these neoplasms. Our findings are conformal with an interplay between oncogenic alteration (mutations and/or overexpression) and deletion of tumour suppressor genes in the dysregulation of cell signalling causing tumourigenesis and cancer progression [24]. This suggests that invasive bladder carcinomas are initiated and developed through interplay between human life style patterns and environmental factors which may contribute to develop different phenotypes of urinary bladder carcinomas with the same histological pattern.

Acknowledgements We thank Mrs. Turid Gulbrandsen for technical assistance with the immunohistochemical staining procedures and Ms. Randi Hope Lavik for assistance with the tables and figures. We are also very grateful to Dr. Heike Immervoll for her guidance in TMA modelling and to Mrs. Öznur Turan for expert technical assistance with in situ hybridisations, and Mr John Post for photographical assistance. This project was supported by the Uro-Bergen fund and the Norwegian Cancer Society.

References

1. Matsushita K, Cha EK, Matsumoto K, Baba S, Chromecki TF, Fajkovic H, Sun M, Karakiewicz PI, Scherr DS, Shariat SF (2011) Immunohistochemical biomarkers for bladder cancer prognosis. Int J Urol 18(9):616–629. doi:10.1111/j.1442-2042.2011.02809.x
2. Shariat SF, Zlotta AR, Ashfaq R, Sagalowsky AI, Lotan Y (2007) Cooperative effect of cell-cycle regulators expression on bladder cancer development and biologic aggressiveness. Mod Pathol Off J U S Can Acad Pathol Inc 20(4):445–459. doi:10.1038/modpathol.3800757
3. Przybojewska B, Jagiello A, Jalmuzna P (2000) H-RAS, K-RAS, and N-RAS gene activation in human bladder cancers. Cancer Genet Cytogenet 121(1):73–77
4. Ayan S, Gokce G, Kilicarslan H, Ozdemir O, Yildiz E, Gultekin EY (2001) K-RAS mutation in transitional cell carcinoma of urinary bladder. Int Urol Nephrol 33(2):363–367
5. Vageli D, Kiaris H, Delakas D, Anezinis P, Cranidis A, Spandidos DA (1996) Transcriptional activation of H-ras, K-ras and N-ras proto-oncogenes in human bladder tumors. Cancer Lett 107 (2):241–247
6. Aveyard JS, Skilleter A, Habuchi T, Knowles MA (1999) Somatic mutation of PTEN in bladder carcinoma. Br J Cancer 80(5–6):904–908. doi:10.1038/sj.bjc.6690439
7. Tsuruta H, Kishimoto H, Sasaki T, Horie Y, Natsui M, Shibata Y, Hamada K, Yajima N, Kawahara K, Sasaki M, Tsuchiya N, Enomoto K, Mak TW, Nakano T, Habuchi T, Suzuki A (2006) Hyperplasia and carcinomas in Pten-deficient mice and reduced PTEN protein in human bladder cancer patients. Cancer Res 66 (17):8389–8396. doi:10.1158/0008-5472.CAN-05-4627
8. Dass K, Ahmad A, Azmi AS, Sarkar SH, Sarkar FH (2008) Evolving role of uPA/uPAR system in human cancers. Cancer Treat Rev 34(2):122–136. doi:10.1016/j.ctrv.2007.10.005
9. Stamenkovic I (2000) Matrix metalloproteinases in tumor invasion and metastasis. Semin Cancer Biol 10(6):415–433. doi:10.1006/scbi.2000.0379
10. Litlekalsoy J, Vatne V, Hostmark JG, Laerum OD (2007) Immunohistochemical markers in urinary bladder carcinomas from paraffin-embedded archival tissue after storage for 5–70 years. BJU Int 99(5):1013–1019. doi:10.1111/j.1464-410X.2006.06699.x
11. Pyke C, Kristensen P, Ralfkiaer E, Grondahl-Hansen J, Eriksen J, Blasi F, Dano K (1991) Urokinase-type plasminogen activator is expressed in stromal cells and its receptor in cancer cells at invasive foci in human colon adenocarcinomas. Am J Pathol 138(5):1059–1067
12. WHO (1999) Some chemicals that cause tumours of the kidney or urinary bladder in rodents and some other substances. IARC Monogr Eval Carcinog Risks Hum 73:14–683

13. Varma M, Morgan M, Amin MB, Wozniak S, Jasani B (2003) High molecular weight cytokeratin antibody (clone 34betaE12): a sensitive marker for differentiation of high-grade invasive urothelial carcinoma from prostate cancer. Histopathology 42(2):167–172
14. kreftregister Dn (2007) Cancer in norway
15. Matanoski GM, Elliot EA (1981) Bladder cancer epidemiology. Epidemiol Rev 3:203–228
16. Ferlay J, Randi G, Bosetti C, Levi F, Negri E, Boyle P, La Vecchia C (2008) Declining mortality from bladder cancer in Europe. BJU Int 101(1):11–19. doi:10.1111/j.1464-410X.2007.07239.x
17. Litlekalsoy J (2009) Molecular investigations on archival tissues. VDM Verlag Dr. Muller Aktiengesellschaft & Co. KG, Saarbrucken, Germany
18. Adjei AA (2001) Blocking oncogenic Ras signaling for cancer therapy. J Natl Cancer Inst 93(14):1062–1074
19. Chesa PG, Rettig WJ, Melamed MR, Old LJ, Niman HL (1987) Expression of p21 ras in normal and malignant human tissues: lack of assosiation with proliferation and malignancy. Proc Natl Acad Sci USA 84:3234–3238
20. Cordon-Cardo C (2008) Molecular alterations associated with bladder cancer initiation and progression. Scand J Urol Nephrol Suppl 218:154–165. doi:10.1080/03008880802291915
21. Carroll VA, Binder BR (1999) The role of the plasminogen activation system in cancer. Semin Thromb Hemost 25(2):183–197
22. Cherrington JM, Strawn LM, Shawver LK (2000) New paradigms for the treatment of cancer: the role of anti-angiogenesis agents. Adv Cancer Res 79:20–27
23. Noel A, Maillard C, Rocks N, Jost M, Chabottaux V, Sounni NE, Maquoi E, Cataldo D, Foidart JM (2004) Membrane associated proteases and their inhibitors in tumour angiogenesis. J Clin Pathol 57(6):577–584
24. Oxford G, Theodorescu D (2003) The role of Ras superfamily proteins in bladder cancer progression. J Urol 170(5):1987–1993. doi:10.1097/01.ju.0000088670.02905.78

Virchows Arch (2012) 461:553–559
DOI 10.1007/s00428-012-1310-3

ORIGINAL ARTICLE

Bcl-2 expression indicates better prognosis of Merkel cell carcinoma regardless of the presence of Merkel cell polyomavirus

Helka Sahi · Virve Koljonen · Heli Kavola · Caj Haglund · Erkki Tukiainen · Harri Sihto · Tom Böhling

Received: 12 April 2012 / Revised: 2 August 2012 / Accepted: 29 August 2012 / Published online: 14 September 2012
© Springer-Verlag 2012

Abstract Merkel cell carcinoma (MCC) is an aggressive dermal tumour of neuroendocrine origin. The recently found Merkel cell polyomavirus (MCV) integrates clonally in the tumour genome, which suggests an important role in the pathogenesis of the disease. Previous small-scale studies have detected anti-apoptotic protein bcl-2 in 80 % of MCC tumours, but its correlation to the prognosis of MCC remains controversial. Our aim was to clarify the correlation of immunohistochemical expression of bcl-2 to MCV presence and MCC prognosis. We analyzed 116 primary MCC specimens with corresponding clinical data by immunohistochemistry for bcl-2. The presence of MCV DNA had been analyzed by quantitative PCR for 108 tumours. The correlations were analyzed statistically. Of the primary MCC samples, 85 % were bcl-2 positive. No significant differences in MCV DNA occurred between the bcl-2-positive and bcl-2-negative tumours. Local and systemic metastasis was more common in patients with bcl-2 negative tumours (33 %) than in patients with bcl-2-positive tumours (12 %; $p=0.04$) at the time of diagnosis. The mean overall survival was higher in patients with bcl-2-positive tumours than of those with negative tumours (mean survival 1,814 days (5.0 years) vs. 769 days (2.1 years), $p=0.01$). Bcl-2 positivity indicates better clinical stage at the time of diagnosis and a longer survival in MCC.

Keywords Merkel cell carcinoma · Bcl-2 · Apoptosis · Merkel cell polyomavirus

H. Sahi · V. Koljonen · H. Kavola · E. Tukiainen
Department of Plastic and Reconstructive Surgery,
Helsinki University Hospital,
Helsinki, Finland

H. Sahi · T. Böhling
Department of Pathology, Helsinki University and HUSLAB,
Helsinki, Finland

V. Koljonen
Institute of Clinical Medicine, Department of Surgery,
Helsinki University Hospital,
Helsinki, Finland

C. Haglund
Department of Gastroenterological Surgery,
Helsinki University Hospital,
Helsinki, Finland

H. Sihto
Laboratory of Molecular Oncology, Biomedicum Helsinki,
Helsinki, Finland

H. Sahi (✉)
Department of Plastic Surgery, Töölö Hospital,
P.O. Box 266, 0029 HUS Helsinki, Finland
e-mail: helka.sahi@helsinki.fi

Introduction

Merkel cell carcinoma (MCC) is a rare but potentially lethal neuroendocrine carcinoma of the skin [1]. The molecular pathogenesis of MCC remains unclear but alterations have been found in the function of major cell cycle control pathways of the p53 protein family and the retinoblastoma protein [2, 3]. Another important step in the tumourigenesis of MCC seems to be the intrinsic inhibition of apoptosis regulated by proteins such as the bcl-2 family and survivin [4–7]. Recently, survivin was found to have a critical role in the survival of Merkel cell polyomavirus (MCV)-positive MCC cells [8], thus serving as a potential therapeutic target in the treatment of MCC.

MCV was discovered in 2008 by Feng et al. and has been observed in approximately 70 to 80 % of the MCCs worldwide [9–11]. The importance of MCV infection is not yet fully understood, but the clonal integration pattern of the viral genome indicates its role in the early pathogenesis of

the carcinoma [9]. The expression of viral DNA differs between MCCs in different patient groups, peaking in the immunosuppressed [12, 13] and correlating with the geographical location in terms of sun exposure [14]. It was recently suggested by Bhatia et al. [15] that MCC can be divided into two subgroups that are different in the amount of MCV DNA. These subgroups differ in their expression of tumour-associated molecules, for example the retinoblastoma protein and p53 [16]. The presence MCV DNA has also been linked to a better prognosis in our previous study [17].

Bcl-2 is an anti-apoptotic proto-oncogene regulating the intrinsic pathway of apoptosis, which includes crucial changes in mitochondrial functions [18–20]. It seems to promote cell survival by inhibiting apoptosis, i.e. programmed cell death [21]. Overexpression of bcl-2 is a common finding in malignancies, e.g. in many lymphomas and various solid tumours [17, 21]. According to two small-scale studies, it occurs in approximately two thirds of MCC [4, 5].

The mechanisms responsible for up-regulation of bcl-2 remain unknown. Bcl-2 expression is in general a sign of poor prognosis, but it seems to correlate with better prognosis and higher differentiation in some solid tumours, such as non-small cell lung cancer [22, 23]. In regard to MCC, no data on either of these correlations has been noted [4, 5]. To the best of our knowledge, no study has compared the integration of MCV DNA to the expression of bcl-2 protein.

Our objective was to examine by immunohistochemistry the expression of bcl-2 in a large cohort of primary MCC samples. The main emphasis was to elucidate potential differences in bcl-2 expression between MCV-positive and MCV-negative MCCs. We also reviewed possible correlation of bcl-2 expression with clinical behaviour and prognosis of MCC, in order to assess whether bcl-2 might serve as a clinically useful prognostic marker.

Patients and methods

The study was conducted in two phases. In phase I, 30 tumour samples were randomly selected and stained for bcl-2. They were evaluated to determine the quality of the stain and to find the most accurate way of classifying it. In phase II, a tissue array containing 417 spots from tumour tissue samples of 137 patients was stained for bcl-2 and reviewed in terms of clinical data and MCV expression, when available.

Patients, clinical data and tissue samples

Data on patients diagnosed with MCC in Finland during 1979–2004 were obtained from the Finnish Cancer Registry and the files of Helsinki University Hospital. Detailed data on patient and tumour characteristics, like tumour size, location, local recurrence, local and systemic metastasis and survival were obtained from the hospital and primary health care centre files. The stage of the disease at the time of diagnosis was defined according to the American Joint Committee on Cancer staging system criteria (Table 1). The demographic data of these patients are presented in Table 2.

Formalin-fixed, paraffin-embedded tissue blocks of patients included in this survey were retrieved from the archives of pathology departments. The histology of the tumour samples was re-evaluated in a blinded fashion by one of the authors with special expertise in MCC pathology (T. Böhling). Sections were stained with haematoxylin and eosin and by immunohistochemistry with antibodies for cytokeratin-20 (CK-20; DakoCytomation, Glostrup, Denmark) and thyroid transcription factor-1 (TTF-1; Novocastra, Balliol Business Park West, Benton Lane, Newcastle Upon Tyne, UK). A diagnosis of MCC was made when the morphology was compatible with MCC, CK-20 expression was positive and staining for TTF-1 was negative. The longest axis of the tumour was measured from H&E stained slides.

For phase I, one slide per tumour block of each patient was randomly selected from 30 patients for bcl-2 staining. For phase II, we utilised a multi-tissue array with 471 cores from 137 tumours. Some of the specimens included in the array were derived from the tumour samples used in phase I or from the tumour samples of patients that had been included in our previous study on the clinical features of MCC with MCV infection [15]. The tissue microarray block consisted of two or more 0.7 mm diameter cores from each tumour. Most patients of phase I were also included in phase II.

Individual cores in the arrays that showed no tumour cells present in the specimen, or detachment of the specimen from its position in the array, or folds in the specimen were excluded. At least one representative spot was available for 116 patients.

Immunohistochemistry

Four-micrometre-thick tissue sections were deparaffinised in xylene and rehydrated through graded ethanol and distilled water. For antigen retrieval, slides were treated in a pretreatment module (LabVision Corp., Fremont, CA, USA) in Tris–HCl buffer (pH 8.5) for 20 min at 98 °C. Staining of sections was performed in an Autostainer 480 (Lab Vision Corp.) using Dako REAL EnVision Detection System, Peroxidase/DAB+, Rabbit/Mouse (Dako, Glostrup, Denmark). In brief, the sections were treated with 0.3 % Dako REAL Peroxidase-Blocking solution to block endogenous peroxidase for 5 min. Subsequently, sections were incubated with a bcl-2 antibody (Dako Glostrup Denmark, Catalog number

Table 1 The American Joint Committee on Cancer staging system criteria for MCC [35]

Stage			Lymph node		Extracutaneous invasion	Systemic metastasis
			Microscopic evaluation	Clinical evaluation		
I	Primary lesion≤2 cm	A	–	–	–	–
		B	Not applied	–	–	–
II	Primary lesion>2 cm	A	–	–	–	–
		B	Not applied	–	–	–
		C	–	–	+	–
III	Positive lymph node	A	+	–	+/–	–
		B	+/–	+	+/–	–
IV	Systemic metastasis		+/–	+/–	+/–	+

M 0887, 1:100) for 1 h, followed by a 30-min incubation with peroxidase-conjugated Dako REAL EnVision/HRP, rabbit/mouse (ENV) reagent. Final visualisation was carried out by incubation with Dako REAL DAB+ Chromogen for 10 min. Between each step of the staining procedure, slides were washed with PBS-0.04 %–Tween20. The sections were counterstained with Meyer's haematoxylin, washed in tap water for 10 min and mounted in an aqueous mounting medium (Aquamount, BDH, Poole, UK).

Interpretation of stainings

Phase I: The staining results were analysed and recorded as negative or positive by consensus between two investigators (T.B. and H.S.). Positive cases were scored as weak or strong. A sample of bcl-2-positive porcine kidney served as a positive control to minimise interassay variation.

Phase II: For statistical analysis, the few cases showing weak positive staining were included in the negative group.

Table 2 Clinical characteristics of the 116 MCC patients (phase II)

Characteristics	Number (%)
Age (years)	
Mean	77
Range	35–100
Gender	
Male	33 (28)
Female	83 (72)
Location of primary tumour	
Head and neck	61 (53)
Trunk	8 (7)
Lower extremities	24 (21)
Upper extremities	23 (20)
Size of primary tumour (cm)	
<2.0	69 (59)
≥2.0	47 (41)
Metastasis at time of diagnosis	
Yes	15 (13)
No	101 (87)
Overall survival (days)	
Mean	1,661
Range	5–8101

Evaluation of MCV expression

The MCV detection had been carried out in our previous study. The presence of MCV DNA in tumour samples was analysed in DNA extracted from representative deparaffinised tumour sections, and the quantitation of MCV DNA was done using real-time PCR, as described in detail elsewhere [15]. The presence of MCV DNA had been determined in 108 (93 %) of the 116 tumour samples.

Statistical analysis

Statistical analysis was conducted with NCSS 2007 [24]. p values less than 0.05 were considered statistically significant. Correlations between bcl-2 expression and tumour size, location, stage of disease at diagnosis, local recurrence and metastasis and MCV DNA status (when available) were calculated with Fisher's exact test.

Overall survival was calculated from the date of diagnosis to the date of death, with censoring of subjects who were alive on August 1, 2008, when data collection for the study was closed. Fisher's exact test was used for testing the correlation between bcl-2 expression and absolute survival. The correlation between bcl-2 expression and overall survival in days was evaluated by Kaplan–Meier analysis with log rank testing. An institutional ethics committee approved the study protocol, and permission to analyse the tissue samples was obtained from the National Agency for Medicolegal Affairs, Finland.

Results

Phase I: Of the 30 tumour samples, 23 (77 %) were immunohistochemically positive for bcl-2. In the positive cases, all tumour cells were stained. Staining intensity was strong in 18 (60 %) of the 30 samples.

Phase II: Of the microarray samples, 85 % (99/116) were bcl-2 positive (Figs. 1 and 4) and 15 % (17/116) negative (Figs. 2, 3 and 4). The mean age of patients with bcl-2-negative tumours was 81.8 years and of those with bcl-2-positive tumours 76.2 years (p=0.053). Gender spectrum was similar in both groups (Table 2).

The tumour diameter ranged from 3 to 85 mm, with a mean size of 20.3 mm. Of the bcl-2-positive tumours, 63 % were ≤2 cm in diameter, whereas in bcl-2-negative tumours, the percentage was only 41 %. This difference did not reach statistical significance (p=0.114).

Local and systemic metastasis was more common in patients with bcl-2-negative tumours (33 %) than in patients with bcl-2-positive tumours (12 %; p=0.044) at the time of diagnosis. The tendency to local recurrence did not differ significantly between the groups.

No statistically significant correlation was found between bcl-2 and MCV DNA presence: Of the 99 bcl-2-positive samples, 80 % were MCV positive, and 75 % of the 17 bcl-2-negative samples were MCV positive (p=0.737). None of the patients with bcl-2-negative tumours survived to the end of data collection, while 22 % of the patients with bcl-2-positive tumours were alive at that point (p=0.039).

The mean follow-up was 1,661 days (4.6 years) ranging from 5 to 8,101 days. The mean overall survival was longer for patients with bcl-2-positive tumours than for those with negative tumours (mean survival 1,814 vs. 769 days, p=0.010). The Kaplan–Meier analysis of overall survival showed a statistically significant difference between the bcl-2-positive and bcl-2-negative groups (p=0.0017; Fig. 5).

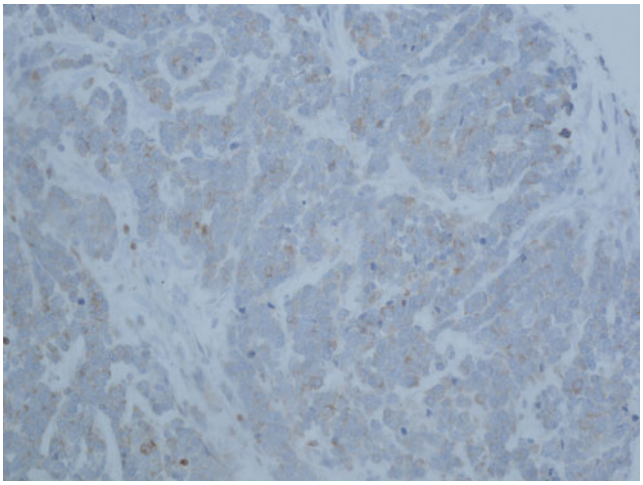

Fig. 2 A negative bcl-2 immunostain in Merkel cell carcinoma (original magnification × 200)

Discussion

We examined by immunohistochemistry expression of the anti-apoptotic proto-oncogene bcl-2 in 116 Merkel cell carcinoma tissue samples. Bcl-2 expression overall was frequent, 85 % of the samples being bcl-2 positive. Bcl-2-positive cases were significantly more often of lower disease stage, i.e. less frequent metastatic spread at the time of diagnosis (p=0.044). Bcl-2-positive cases showed significantly better survival than bcl-2-negative cases (p=0.021). Patients with bcl-2-positive tumours showed a statistically significant difference of 1,044 days in mean overall survival (p=0.010). The difference in overall survival

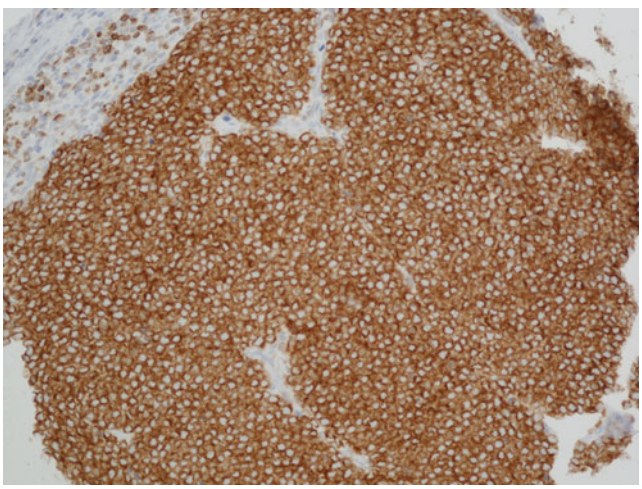

Fig. 1 A strong positive bcl-2 immunostain in Merkel cell carcinoma (original magnification × 200)

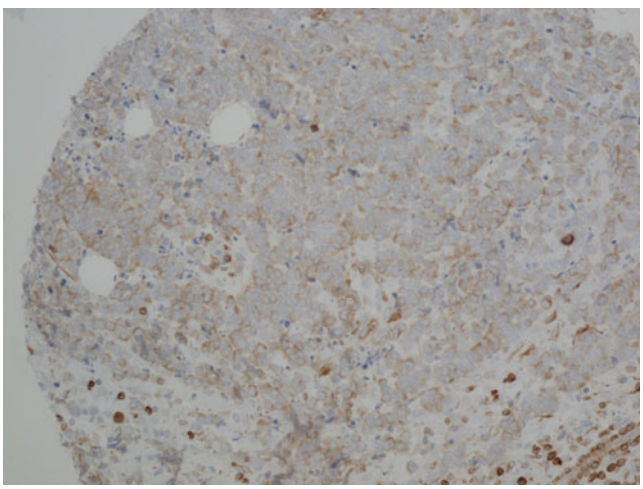

Fig. 3 A weak positive bcl-2 immunostain in Merkel cell carcinoma (original magnification × 200)

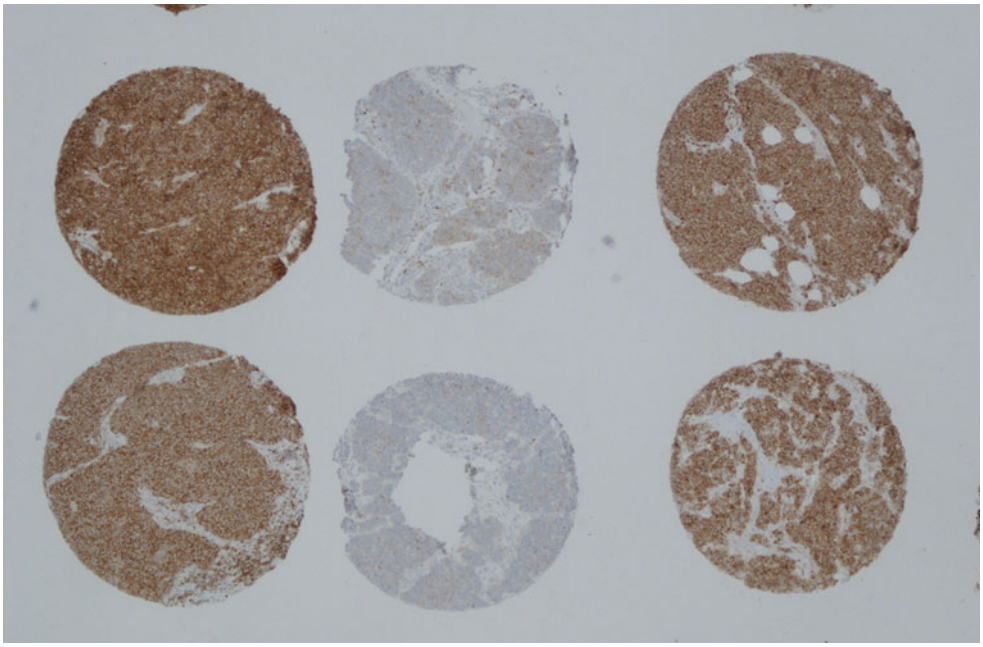

Fig. 4 Section of the MCC multi-tissue array stained for bcl-2: negative samples surrounded by strongly positive samples (original magnification × 40)

was also statistically significant in Kaplan–Meier analysis (p=0.0017). Neither of the earlier small-scale studies of Feinmesser et al. (25 cases) and Kennedy et al. (15 cases) found a significant relationship between bcl-2 expression and survival.

Nuclear overexpression of bcl-2 as well as that of the anti-apoptotic protein survivin would be expected to be associated with worse prognosis [7]. Our finding of the opposite might be explained by the modulation of the effects of bcl-2 by phosphorylation and also by simultaneous expression of various related proteins such as bax or c-kit which constitute important regulators of bcl-2 function [25–28]. Alternatively, tumour progression might render the tumour independent of bcl-2, other molecular events becoming responsible for more aggressive tumour behaviour. A hint in this direction is the fact that in this study, patients with bcl-2-negative tumours were older than patients with bcl-2-positive tumours.

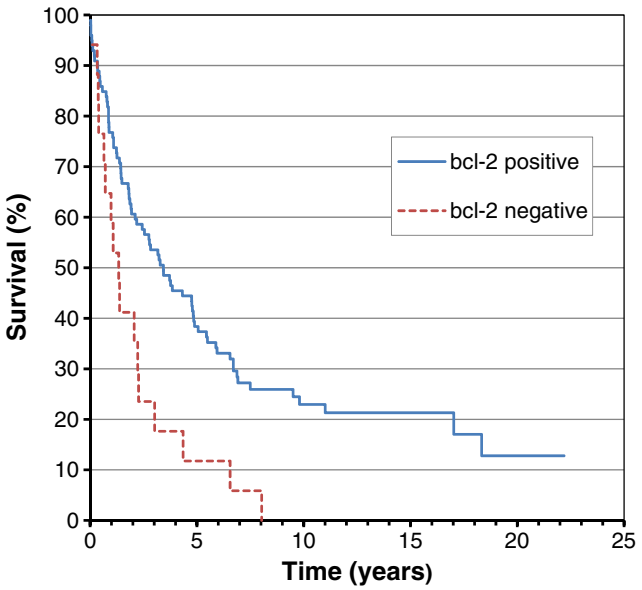

Fig. 5 Kaplan–Meier analysis on the overall cumulative survival of patients with bcl-2-positive MCC (*blue line*) and patients with bcl-2-negative MCC (*red dash line*) in years, p=0.0017

MCV becomes oncogenic through integration of the viral DNA in the genome of the host cell, followed by truncation of the large viral T antigen (LTA) [29]. LTA is crucial for viral replication [29]. It has been speculated that truncation of LTA plays an important part in the tumourigenesis of MCC because persisting replication of MCV would eventually lead to lysis of the host cell, or to such major disruptions in the host genome that apoptosis could no longer be avoided [3, 30]. Overexpression of anti-apoptotic proteins might thus favour such disruption and eventually make the host cell susceptible for tumour defense mechanisms. The role of LTA truncation in MCC tumourigenesis might in part explain how the overexpression of an anti-apoptotic proto-oncogene paradoxically is associated with less aggressive behaviour.

Polyomaviruses often target the p53 protein [31]. The LTA has a p53-binding domain, but the truncation of the LTA inactivates its ability to bind p53 [29]. Also, mutations of the *p53* gene itself are only seen in MCV-negative tumours. These observations suggest that p53 might have a role in the tumourigenesis of MCC independent of MCV infection [16]. p53 is involved in controlling bcl-2 [32, 33], and its inactivation could theoretically lead to overexpression of bcl-2 protein.

A recent study by Bhatia et al. [15] suggests that, according to the abundance of MCV DNA, MCC can be subdivided into two groups which show differences in their expression of molecules involved in tumour regulation. This suggestion has, however, been met with doubt [34]. Closer investigation of the pathogenesis of MCC in terms of anti-apoptotic and cell cycle control proteins and epigenetics might shed some light on this issue.

In previous studies [4, 5], the assessment of immunohistochemical bcl-2 expression has been quite variable. Kennedy et al. classified the tumours according to four levels of bcl-2 staining intensity. Feinmesser et al. used semiquantitative scoring of the immunostaining taking staining intensity (four levels), as well as the percentage of immunostained cells (five levels) into consideration. We noted in phase I of this study that in a bcl-2-positive MCC, the tumour cells are all stained. We suggest that our dichotomous approach, distinguishing the clearly bcl-2-positive cases (diffusely positive regardless of intensity) from the bcl-2-negative cases, is to be preferred.

Tumour size has been established as the most reliable prognostic marker in MCC. We found no correlation between tumour size and bcl-2 status even though bcl-2 expression was associated with better prognosis. Bcl-2 expression was also associated with lower disease stage at the time of diagnosis. Eventually, bcl-2 expression might become a clinically useful parameter, in terms of prognosis or treatment choice. In conclusion, bcl-2 expression in MCC is associated with better prognosis and lower disease stage at the time of diagnosis. Bcl-2 expression is not correlated with MCV status of the tumours.

Conflict of interest The authors declare that they have no conflict of interest.

References

1. Koljonen V, Bohling T, Granhroth G, Tukiainen E (2003) Merkel cell carcinoma: a clinicopathological study of 34 patients. Eur J Surg Oncol 229:607–610
2. Koljonen V, Tukiainen E, Haglund C, Bohling T (2006) Cell cycle control by p21, p27 and p53 in Merkel cell carcinoma. Anticancer Res 26:2209–2212
3. Houben R, Schrama D, Becker JC (2009) Molecular pathogenesis of Merkel cell carcinoma. Exp Dermatol 18:193–198
4. Kennedy MM, Blessing K, King G, Kerr KM (1996) Expression of bcl-2 and p53 in Merkel cell carcinoma. An immunohistochemical study. Am J Dermatopathol 18:273–277
5. Feinmesser M, Halpern M, Fenig E, Tsabari C, Hodak E, Sulkes J et al (1999) Expression of the apoptosis-related oncogenes bcl-2, bax, and p53 in Merkel cell carcinoma: can they predict treatment response and clinical outcome? Hum Pathol 30:1367–1372
6. Hanahan D, Weinberg RA (2000) The hallmarks of cancer. Cell 100:57–70
7. Kim J, McNiff JM (2008) Nuclear expression of survivin portends a poor prognosis in Merkel cell carcinoma. Mod Pathol 21:764–769
8. Arora R, Shuda M, Guastafierro A, Feng H, Toptan T, Tolstov Y et al (2012) Survivin is a therapeutic target in merkel cell carcinoma. Sci Transl Med 4:133ra56
9. Feng H, Shuda M, Chang Y, Moore PS (2008) Clonal integration of a polyomavirus in human Merkel cell carcinoma. Science 319:1096–1100
10. Kassem A, Schopflin A, Diaz C, Weyers W, Stickeler E, Werner M et al (2008) Frequent detection of Merkel cell polyomavirus in human Merkel cell carcinomas and identification of a unique deletion in the VP1 gene. Cancer Res 68:5009–5013
11. Becker JC, Houben R, Ugurel S, Trefzer U, Pfohler C, Schrama D (2009) MC polyomavirus is frequently present in Merkel cell carcinoma of European patients. J Invest Dermatol 129:248–250
12. Sahi H, Kukko H, Böhling T, Tukiainen E, Sihto H, Joensuu H et al (2010) Unusually young Merkel cell carcinoma patients are Merkel cell polyomavirus positive and frequently immunocompromised. Eur J Plast Surg 33:349–353
13. Koljonen V, Kukko H, Pukkala E, Sankila R, Bohling T, Tukiainen E et al (2009) Chronic lymphocytic leukaemia patients have a high risk of Merkel-cell polyomavirus DNA-positive Merkel-cell carcinoma. Br J Cancer 101:1444–1447
14. Garneski KM, Warcola AH, Feng Q, Kiviat NB, Leonard JH, Nghiem P (2009) Merkel cell polyomavirus is more frequently present in North American than Australian Merkel cell carcinoma tumors. J Invest Dermatol 129:246–248
15. Bhatia K, Goedert JJ, Modali R, Preiss L, Ayers LW (2010) Merkel cell carcinoma subgroups by Merkel cell polyomavirus DNA relative abundance and oncogene expression. Int J Cancer 126:2240–2246
16. Sihto H, Kukko H, Koljonen V, Sankila R, Bohling T, Joensuu H (2011) Merkel cell polyomavirus infection, large T antigen, retinoblastoma protein and outcome in Merkel cell carcinoma. Clin Cancer Res 17:4806–4813
17. Sihto H, Kukko H, Koljonen V, Sankila R, Bohling T, Joensuu H (2209) Clinical factors associated with Merkel cell polyomavirus infection in Merkel cell carcinoma. J Natl Cancer Inst 101:938–945
18. Tsujimoto Y, Croce CM (1986) Analysis of the structure, transcripts, and protein products of bcl-2, the gene involved in human follicular lymphoma. Proc Natl Acad Sci U S A 83:5214–5218
19. Hockenbery D, Nunez G, Milliman C, Schreiber RD, Korsmeyer SJ (1990) Bcl-2 is an inner mitochondrial membrane protein that blocks programmed cell death. Nature 348:334–336
20. Leverkus M, Diessenbacher P, Geserick P (2008) FLIP ing the coin? Death receptor-mediated signals during skin tumorigenesis. Exp Dermatol 17:614–622
21. Kroemer G (1997) The proto-oncogene Bcl-2 and its role in regulating apoptosis. Nat Med 3:614–620
22. Ikegaki N, Katsumata M, Minna J, Tsujimoto Y (1994) Expression of bcl-2 in small cell lung carcinoma cells. Cancer Res 54:6–8
23. Pezzella F, Turley H, Kuzu I, Tungekar MF, Dunnill MS, Pierce CB et al (1993) bcl-2 protein in non-small-cell lung carcinoma. N Engl J Med 329:690–694
24. Hintze J (2009) NCSS, NCSS, LLC. Kaysville, Utah. www.ncss.com
25. Reed JC (1994) Bcl-2 and the regulation of programmed cell death. J Cell Biol 124:1–6
26. Moll I, Gillardon F, Waltering S, Schmelz M, Moll R (1996) Differences of bcl-2 protein expression between Merkel cells and Merkel cell carcinomas. J Cutan Pathol 23:109–117
27. Su LD, Fullen DR, Lowe L, Uherova P, Schnitzer B, Valdez R (2002) CD117 (KIT receptor) expression in Merkel cell carcinoma. Am J Dermatopathol 24:289–293
28. Oltvai ZN, Milliman CL, Korsmeyer SJ (1993) Bcl-2 heterodimerizes in vivo with a conserved homolog, Bax, that accelerates programmed cell death. Cell 74:609–619

29. Shuda M, Feng H, Kwun HJ, Rosen ST, Gjoerup O, Moore PS et al (2008) T antigen mutations are a human tumor-specific signature for Merkel cell polyomavirus. Proc Natl Acad Sci U S A 105:16272–16277
30. Olavarrieta L, Hernandez P, Krimer DB, Schvartzman JB (2002) DNA knotting caused by head-on collision of transcription and replication. J Mol Biol 322:1–6
31. Pipas JM, Levine AJ (2001) Role of T antigen interactions with p53 in tumorigenesis. Semin Cancer Biol 11:23–30
32. Miyashita T, Reed JC (1995) Tumor suppressor p53 is a direct transcriptional activator of the human bax gene. Cell 80:293–299
33. Ortega S, Malumbres M, Barbacid M (2002) Cyclin D-dependent kinases, INK4 inhibitors and cancer. Biochim Biophys Acta 1602:73–87
34. Houben R, Schrama D, Alb M, Pfohler C, Trefzer U, Ugurel S et al (2010) Comparable expression and phosphorylation of the retinoblastoma protein in Merkel cell polyoma virus-positive and negative Merkel cell carcinoma. Int J Cancer 126:796–798
35. (2010) Merkel cell carcinoma. In: Edge SB, Byrd DR, Compton CC, et al. (eds) AJCC cancer staging manual, 7th ed. Springer, New York, 315-323

Virchows Arch (2012) 461:561–570
DOI 10.1007/s00428-012-1306-z

ORIGINAL ARTICLE

Malignant fibrous histiocytoma and fibrosarcoma of bone: a re-assessment in the light of currently employed morphological, immunohistochemical and molecular approaches

Salvatore Romeo · Judith V. M. G. Bovée · Herman M. Kroon · Roberto Tirabosco · Cristina Natali · Lucia Zanatta · Raf Sciot · Fredrik Mertens · Nick Athanasou · Marco Alberghini · Karoly Szuhai · Pancras C. W. Hogendoorn · Angelo Paolo Dei Tos

Received: 9 May 2012 / Revised: 30 July 2012 / Accepted: 22 August 2012 / Published online: 22 September 2012
© Springer-Verlag 2012

Abstract Malignant fibrous histiocytoma (MFH) and fibrosarcoma (FS) of bone are rare malignant tumours and contentious entities. Sixty seven cases labelled as bone MFH (57) and bone FS (10) were retrieved from five bone tumour referral centres and reviewed to determine whether recent advances allowed for reclassification and identification of histological subgroups with distinct clinical behaviour. A panel of immunostains was applied: smooth muscle actin, desmin, h-caldesmon, cytokeratin AE1–AE3, CD31, CD34, CD68, CD163, CD45, S100 and epithelial membrane antigen. Additional fluorescence in situ hybridisation and immunohistochemistry were performed whenever appropriate. All cases were reviewed by six bone and soft tissue pathologists and a consensus was reached. Follow-up for 43 patients (median 42 months, range 6–223 months) was available. Initial histological diagnosis was reformulated in 18 cases (26.8 %). Seven cases were reclassified as leiomyosarcoma, six as osteosarcoma, three as myxofibrosarcoma and one each as

Electronic supplementary material The online version of this article (doi:10.1007/s00428-012-1306-z) contains supplementary material, which is available to authorized users.

S. Romeo · L. Zanatta · A. P. Dei Tos (✉)
Department of Pathology, Treviso Regional Hospital,
Piazza Ospedale 1,
31100 Treviso, Italy
e-mail: apdeitos@ulss.tv.it

J. V. M. G. Bovée · P. C. W. Hogendoorn
Department of Pathology, Leiden University Medical Center,
Leiden, The Netherlands

H. M. Kroon
Department of Radiology, Leiden University Medical Center,
Leiden, The Netherlands

R. Tirabosco
Department of Pathology, Royal National Orthopaedic Hospital,
London, UK

C. Natali
Department of Pathology, Rovigo Regional Hospital,
Rovigo, Italy

R. Sciot
Department of Pathology, Leuven University,
Leuven, Belgium

F. Mertens
Department of Clinical Genetics, Lund University Hospital,
Lund, Sweden

N. Athanasou
Department of Pathology, Nuffield Orthopaedic Center,
Oxford, UK

M. Alberghini
Department of Pathology, Rizzoli Orthopaedic Institute,
Bologna, Italy

K. Szuhai
Department of Molecular Cell Biology,
Leiden University Medical Center,
Leiden, The Netherlands

embryonal rhabdomyosarcoma and interdigitating dendritic cell sarcoma. One case showed a peculiar biphasic phenotype with epithelioid nests and myofibroblastic spindle cells. Among the remaining 48 cases, which met the WHO criteria for bone FS and bone MFH, we identified five subgroups. Seven cases were reclassified as undifferentiated pleomorphic sarcoma (UPS) and 11 as UPS with incomplete myogenic differentiation due to positivity for at least one myogenic marker. Six were reclassified as spindle cell sarcoma not otherwise specified. Among the remaining 24 cases, we identified a further two recurrent morphologic patterns: eight cases demonstrated a myoepithelioma-like phenotype and 16 cases a myofibroblastic phenotype. One of the myoepithelioma-like cases harboured a *EWSR1–NFATC2* fusion. It appears that bone MFH and bone FS represent at best exclusion diagnoses.

Keywords Bone neoplasm · Fibrosarcoma of bone · Malignant fibrous histiocytoma of bone · Classification

Introduction

The 2002 WHO classification of tumours of soft tissue and bone significantly differs from the previous ones by integrating immunophenotypic as well as genetic information into tumour definition. Advances in the understanding of the genetics and biology allowed for a better separation of distinct clinical entities with specific clinical, biological and histopathological features. This has been extensively done for malignant fibrous histiocytoma (MFH) of soft tissue [1] and more recently also for adult fibrosarcoma (FS) of soft tissue [2] while no significant changes were introduced in the classification of FS and MFH arising primarily in bone [3]. Both are distinguished from osteosarcoma by the absence of malignant osteoid deposition [3]. According to the 2002 WHO classification, bone FS was defined as a 'malignant spindle cell neoplasm of bone in which the tumor cells are typically organised in a fascicular or herringbone pattern' [3]. Bone MFH was defined as a 'malignant neoplasm composed of fibroblasts and pleomorphic cells with a prominent storiform pattern' [3]. The recognition of these two entities is thus currently based on the mere presence of a growth pattern and not by the cellular differentiation. Remarkably, such patterns (i.e. herring-bone pattern and storiform pattern) have been shown—in soft tissue tumours—to be present in several different clinicopathologic entities and therefore their identification should not represent the only clue to diagnosis [3, 4]. We hypothesised that the absence of 'stringent criteria' might have resulted over the years in the inclusion of distinctively unrelated clinical entities under the diagnostic 'umbrella' of bone FS and bone MFH. To test this, we retrieved and reviewed cases previously diagnosed as bone FS and bone MFH from the archive of five European bone tumour referral centres. We reclassified a quarter of the cases and subdivided the rest into five subgroups and finally tested whether these subgroups may have any prognostic impact.

Materials and methods

Tumour samples

Formalin-fixed, paraffin-embedded samples from tumours originally diagnosed between 1990 and 2009 as MFH (n=57) and FS (n=10) of bone were collected in context of the research activities of EuroBoNeT, a Framework Program 6-funded network of excellence devoted to the study of the pathology and biology of bone tumours. Only paraffin blocks from cases with preserved antigenic properties (i.e. positivity of the internal positive controls) were included in the study.

The original pathology reports along with haematoxylin–eosin-stained original slides were reviewed by the local pathologist to identify representative blocks. New haematoxylin–eosin (HE)-stained slides were centrally prepared for morphological revision. Clinical information was reviewed and updated.

Histological revision was conducted in two steps: first, digitalised HE slides were allocated on a web repository to be accessed by a panel of pathologists trained in bone and soft tissue tumours pathology (SR, RT, PCWH, APDT, RS and MA). HE slides were scanned with the SCANSCOPE XT (automated high-throughput scanning—APERIO, San Diego, USA) 200× magnification and allocated on a web repository. Each file was 4–6 Gb in size.

A consensus joint microscopy session was subsequently held in order to reach a final diagnosis on each case (SR, JVMGB, NA, RT, PCWH and APDT). This included the review of the immunohistochemical stains as well as of radiological imaging. Incidentally, the members of the two sessions changed; nonetheless, every case was reviewed for at least one session by each pathologist.

All samples were handled in a coded fashion, and all procedures were performed according to the ethical guidelines of each contributing institution.

Radiological review

A radiological review was conducted in parallel with the pathological revision by a radiologist specifically trained in the radiological assessment of bone tumours (HMK). Radiological imaging, including plain radiography, CT scan, bone scans and MR, was available for 50 patients. Evaluated parameters included the margins of the lesion, extension in soft tissue, presence and extension of mineralisation, heterogeneity of the lesion and possible signs of Paget disease or bone infarct.

Pathology review

Cases were re-classified based on the guidelines proposed in the 2002 WHO classification for soft tissue tumours [3]. Cases which met the WHO 2002 classification criteria for bone MFH and bone FS, therefore in the absence of a specific classic line of differentiation (i.e. leiomyosarcomas), were subdivided into five subgroups based on the presence/absence of pleomorphism, myoepithelioma-like features and myofibroblastic features according to the diagnostic algorithm outlined in Fig. 1. Myoepithelioma-like features were defined as presence of small/medium size epithelioid and/or spindle cells, featuring ovoid nuclei, sharp cytoplasmic borders and abundant pericellular collagen deposition. 'Myoepithelioma-like' terminology was used because none of the cases from this study fulfilled the minimum immunohistochemical criteria for myoepithelioma, i.e. the co-reactivity for EMA, with or without cytokeratin, together with either S100 or GFAP or both [5].

Myofibroblastic features were defined as presence of spindle cells, arranged in a storiform or fascicular pattern of growth, featuring tapering nuclei, pale cytoplasm with indistinct borders and set in stroma alternating myxoid and collagenised areas. Neoplastic cells featured immunopositivity for smooth muscle actin and tended to be negative for both desmin and h-caldesmon staining. Grading was done on a two-tiered scale (high and low grade, respectively).

Immunohistochemistry

The following panel of immunohistochemical stains was applied to each case: smooth muscle actin (SMA), desmin, h-caldesmon, cytokeratin AE1/AE3, CD31, CD34, CD68, CD163, CD45, S100 and epithelial membrane antigen (EMA) (details regarding these and second-line immunostains are shown in Table 1). Additional fluorescence in situ hybridisation (FISH) and immunohistochemistry were performed, when appropriate, to confirm/reject alternative diagnoses. All the tumours were scored using the sum of intensity of signal (possible range—0 = no expression; 1 = weak expression; 2 = moderate expression; 3 = strong expression) and the number of positive cells (% tumour cells—0=0 %; 1=1–25 %; 2=26–50 %, 3=51–75 %; 4= 76–100 %). The intracellular (nuclear, cytoplasmic and membranous) and the intra-tumoural (matrix-rich areas or cellular areas) localisation of immunoreactivity were noted.

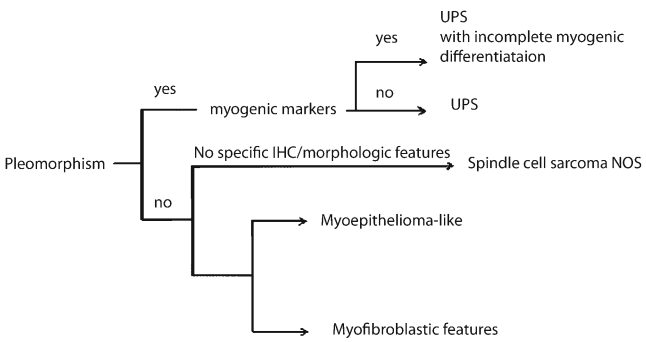

Fig. 1 Diagnostic algorithm used to subclassify cases which met the 2002 classification criteria for bone FS or bone MFH

Interphase FISH

Rearrangement of the *EWSR1* and *FUS* genes has been shown to be recurrent in myoepitheliomas of bone and soft tissue [5]. To assess this rearrangement, FISH using specific break-apart probes (Vysis LSI EWSR1 Dual Colour Break Apart Probe and Vysis LSI FUS Dual Color Break Apart Probe; Vysis, Downers Grove, IL, USA) was performed on all cases displaying myoepithelioma-like phenotype [5]. Furthermore, in order to rule out a diagnosis of synovial sarcoma, both cases displaying myoepithelioma-like phenotype as well as the cases grouped as spindle cell sarcoma NOS were tested for SS18 (previously known as SYT) rearrangement with specific break-apart probes (LSI SYT Dual Colour Break Apart Rearrangement Probe; Vysis). In brief, 5-μm paraffin-embedded tissue sections were used. Hybridisation was performed according to the manufacturer's protocol. Slides were mounted and counterstained with anti-fade DAPI (Vysis), visualised using an epifluorescence microscope (Olympus BX61) and analysed with a FISH Analysis software (Cytovision 4.5.1; Genetix, New Milton, UK); 200 interphase cells were analysed. One case (MFH19) showed a break-apart signal and amplification of the proximal *EWSR1* probe. As such pattern has been described to occur in association with *EWSR1–NFATC2* fusion, this rearrangement was tested via interphase FISH with a set of BAC probes, as previously reported [6]: RP5-994O24 for *NFATC2* and CTA-984 G1 for *EWSR1*.

Statistics

Follow-up was available for 43 patients (median 42 months, range 6–223 months).

Overall survival was evaluated with Kaplan–Meier curves. SPSS 15 software package was used. Given the limited numbers and the heterogeneity of the cases (i.e. treatments, size of the tumour and margins), only overall survival of cases without metastases at presentation were analysed.

Results

Clinical features

The median age of the patients in the entire cohort was 56 years (range 23–85), and men were more often affected

Table 1 Details of the antibodies used for immunohistochemistry

Antibody	Clone	Source	Dilution	AR
EMA	E29	Dako, Glostrup, Denmark	Prediluted	Flex (Dako)
CKAE1/AE3	Monoclonal AE1/AE3	Dako, Glostrup, Denmark	Prediluted	Flex (Dako)
SMA	Monoclonal 1°4	Dako, Glostrup, Denmark	Prediluted	Flex (Dako)
DESM	Monoclonal D33	Dako, Glostrup, Denmark	Prediluted	Flex (Dako)
CD34	QBend-10	Dako, Glostrup, Denmark	Prediluted	Flex (Dako)
CD31	Monoclonal JC70A	Dako, Glostrup, Denmark	Prediluted	Flex (Dako)
CD163	Monoclonal 10D6	Neomarkers	1/100	Flex (Dako)
Clusterin	Monoclonal NCL	Novocastra	1/100	Flex (Dako)
CD21	Monoclonal 1F8	Dako, Glostrup, Denmark	Prediluted	Flex (Dako)
Calponin	Monoclonal CALP	Dako, Glostrup, Denmark	1/200	Flex (Dako)
CD35	Monoclonal BER-MAC-DRP	Dako, Glostrup, Denmark	1/50	Flex (Dako)
CD10	56C6	Neomarkers	1/10	Flex (Dako)
CD68	PGM1	Dako, Glostrup, Denmark	Prediluted	Flex (Dako)
S100	Polyclonal	Dako, Glostrup, Denmark	Prediluted	Flex (Dako)
CD99	Monoclonal MIC2 clone 12E7	Dako, Glostrup, Denmark	Prediluted	Flex (Dako)
GFAP	Monoclonal 6F2	Dako, Glostrup, Denmark	1/1,000	Flex (Dako)
CD45	LCA-Monoclonal 2B11+PD7/26	Dako, Glostrup, Denmark	Prediluted	Flex (Dako)
INI1	Monoclonal BAF 47 (INI1)	BD	1/25	Flex (Dako)
TLE1	Monoclonal anti-TLE (M-101)	Santa Cruz Biotech	1/50	Flex (Dako)

(men/women 2.4:1) (Supplementary Table). Two cases, MFH 19 and MFH27, had received radiation therapy for a primary non-Hodgkin lymphoma of bone and endometrial carcinoma, respectively. The time interval between irradiation and bone tumour occurrence was 7 and 30 years, respectively.

Radiological review

The largest tumour diameter ranged from 2 to 25 cm. At the time of diagnosis, soft tissue extension was present in 82 % (28/34 radiologically evident) and metastasis in 14 % of the cases. A previous history of bone infarct and Paget disease was reported and radiologically confirmed for cases MFH89 and MFH72, respectively (Fig. 2). Previous fibrous dysplasia in the same bone occurred in case MFH75.

Pathology review

All the evaluated cases were morphologically high-grade sarcomas. Out of 67 cases, 18 were re-classified using existing WHO 2002 criteria for bone and soft tissue sarcomas as leiomyosarcoma (seven cases), osteosarcoma (six cases), myxofibrosarcoma (three cases), embryonal rhabdomyosarcoma (one case) and interdigitated dendritic cell (IDC) sarcoma (one case) (Table 2). MFH91 showed a unique biphasic morphology with epithelioid cells (Fig. 3a) positive for both CK AE1–3 staining (Fig. 3b) surrounded by elongated spindle cells positive for SMA (Fig. 3c).

The remaining cases met the WHO criteria for MFH or FS of bone. Among these 48 cases, five different patterns were distinguished: undifferentiated pleomorphic sarcoma (UPS), UPS with incomplete myogenic differentiation, spindle cell sarcoma not otherwise specified (NOS), myoepithelioma-like sarcoma and myofibroblastic-like sarcoma.

Leiomyosarcoma of bone

Seven cases were re-classified as primary bone leiomyosarcoma (Fig. 3d), one of which was previously diagnosed as FS; the remaining six cases were previously diagnosed as MFH. Median age at presentation was 63 years (range 29–84; male/female ratio 4:3) (Table 2). The lower limbs were most often affected, followed by the pelvis (ratio 2.5:1) (Table 2). One of the cases occurred in association with a previous bone infarction (MFH89) (Fig. 2). Histological features were overlapping with those of soft tissue leiomyosarcomas. More specifically, tumours were made up of a proliferation of intersecting elongated spindle cells with eosinophilic, fibrillary cytoplasm with blunt-ended nuclei (Fig. 3d). Diffuse nuclear pleomorphism was present in two cases and focal in the remaining cases. Necrosis was present in all samples in less than 50 % of the tumour. Immunohistochemistry showed, in all seven cases, positivity for SMA (Fig. 3e) (Supplementary Table) and at least one other myogenic marker; either desmin (Fig. 3f) or h-caldesmon (Supplementary Table). EMA and CK AE1–AE3

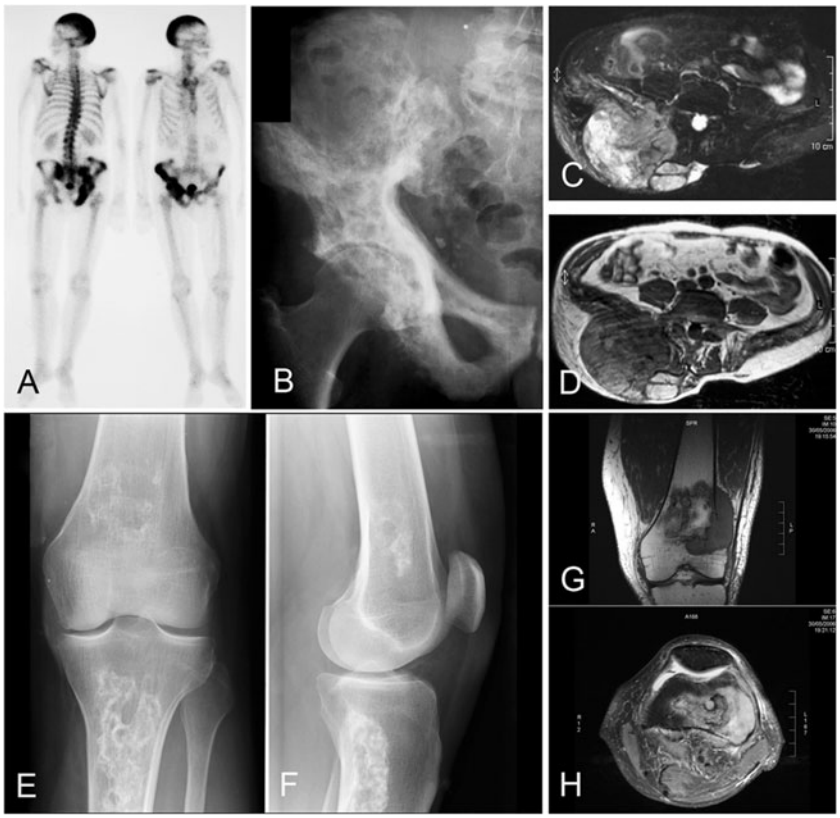

Fig. 2 Two tumours were radiologically confirmed to be secondary to Paget disease and bone infarct, respectively. **a** Bone scintigraphy showing markedly increased uptake of the radiopharmacon in the skull and right side of the pelvis. **b** Antero-posterior conventional radiograph of the right side of the pelvis. Structural changes are pathognomonic for Paget disease. Osteolytic lesion in the proximal part of the right iliac bone consistent with secondary sarcomatous degeneration. **c**, **d** Axial MR: T1-weighted (**c**) and T2-weighted (**d**) images demonstrating a large lesion arising from the right iliac bone with predominantly intermediate signal intensity on the T1-weighted image and predominantly high signal intensity on the T2-weighted image. Large accompanying posterior soft tissue mass is present, too. **e**, **f** Antero-posterior and lateral conventional radiographs of the knee demonstrating mixed osteolytic and sclerotic lesions in the distal part of the femur and proximal part of the tibia. The appearance is classic for areas of bone infarction. **g**, **h** Coronal T1-weighted (**g**) and axial T2-weighted images depicting the lesion in the distal femur. In addition to the centrally located bone infarct, there is a lesion with apparent cortical destruction and soft tissue extension with intermediate signal intensity on the T1-weighted coronal image, and predominantly high signal intensity on the axial T2-weighted image. These findings indicate secondary sarcomatous degeneration of the bone infarct

were found positive in five and four cases each (both positive in two) (Supplementary Table). The two pleomorphic cases were also tested for myogenin, to rule out pleomorphic rhabdomyosarcoma, which proved negative.

Table 2 Results of the reclassification of MFH and FS of bone

New diagnosis	No. of cases	Age range (median)	Gender (male/female ratio)	Location (axial/upper limbs/lower limbs)
Leiomyosarcoma	7	29–84 (63)	4/3	2/0/5
Osteosarcoma	6	25–70 (51)	4/0	0/0/4
Myxofibrosarcoma	3	39–68 (44)	2/1	0/0/3
Interdigitating dendritic cell sarcoma	1	30	Male	Unknown
Embryonal rhabdomyosarcoma	1	82	Female	Upper limb
Biphasic sarcoma	1	29	Male	Upper limb
Myoepihelioma-like	8	32–85 (70)	3/4	2/0/5
Myofibroblastic	16	36–78 (54)	13/3	3/2/11
Spindle cell NOS	6	51–76 (60)	4/1	2/0/4
UPS	7	49–68 (53)	3/2	0/1/3
UPS with myogenic	11	23–77 (43)	5/4	2/1/5

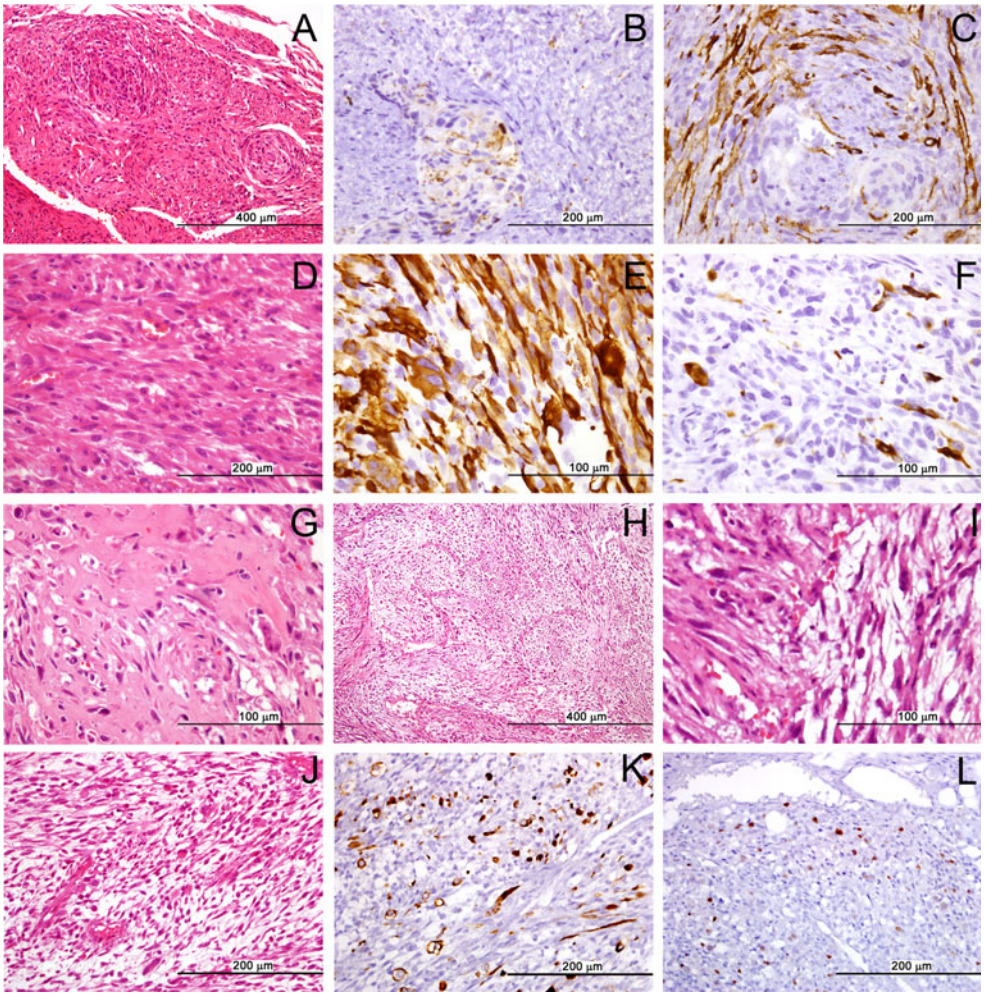

Fig. 3 One case was showing a unique biphasic phenotype, with epithelioid cells arranged in nests surrounded by elongated spindle cells (**a**). Epithelioid cells were positive for CK AE1–3 (**b**) while spindle cells were positive for SMA (**c**). More than a quarter of the cases were reclassified as leiomyosarcomas, due to their morphology (**d**) and the positivity for either desmin (**e**) and or heavy caldesmon (**f**), **g** osteosarcoma, **h**–**i** myxofibrosarcoma and **j** embryonal rhabdomyosarcoma, showing focal positivity for desmin (**k**) and myogenin (**l**)

Osteosarcoma

Five cases previously diagnosed as MFH of bone were reclassified as conventional osteosarcoma (Fig. 3g) and one case previously diagnosed as FS was reclassified as teleangiectatic osteosarcoma. Median age at presentation was 51 years (range 25–70). All four osteosarcomas with known location were affecting the lower limbs. All patients were men. Main diagnostic clue was represented by the presence of unequivocal deposition of malignant osteoid, detected in all six cases (Table 2).

Myxofibrosarcoma of bone

Three cases originally diagnosed as bone MFH were reclassified as myxofibrosarcoma of bone (Fig. 3h and i). Median age at presentation was 44 years (range 39–68; male/female ratio 2:1). All cases were involving the lower limbs (Table 2). Histologically, tumours were composed by a spindle cell proliferation set in an abundant extracellular myxoid matrix alternating with more cellular areas with scant and denser extracellular matrix. In the myxoid areas, elongated curvilinear thin-walled blood vessels were found. Neoplastic cells were often pleomorphic with occasional pseudolipoblasts. All immunostains of the standard panel proved negative with the exception of scattered SMA positive neoplastic cells (Supplementary Table).

Other rare entities

Two cases were reclassified as IDC sarcoma and embryonal spindle cell rhabdomyosarcoma, respectively. The IDC sarcoma, previously diagnosed as bone MFH, was made up of elongated cells with eosinophilic cytoplasm interspersed with mononuclear inflammatory cells. The standard immunohistochemistry panel showed positivity only for S100 protein; second-line immunostains were all negative, including CD21, CD23, CD35, CD1a, clusterin, MITF1, HMB45, GFAP and MelanA. We favoured the diagnosis of IDC versus other 'dendritic' neoplasm based on the absence of any other specific markers. Melanoma and malignant peripheral nerve sheath tumour were excluded due to the absence of primary lesions and/or predisposing conditions. Furthermore, second-line melanoma markers were negative and GFAP was also negative.

One case diagnosed as FS was reclassified as embryonal spindle cell rhabdomyosarcoma. This tumour contained elongated and occasional 'tadpole' cells with densely eosinophilic cytoplasm with abundant myxoid extracellular matrix deposition (Fig. 3j). Immunostains showed widespread positivity for desmin and diffuse nuclear myogenin expression (Fig. 3k and l).

UPS with or without incomplete myogenic differentiation

Eighteen cases showed diffuse and severe pleomorphism with absence of a recognisable line of differentiation; they were grouped as UPS (seven cases) (Fig. 4m) or as UPS with incomplete myogenic differentiation (11 cases) (Fig. 4k) when showing at least patchy or focal positivity for one single myogenic marker (i.e. one marker among SMA, heavy caldesmon and desmin, usually SMA) (Fig. 4l).

Median age of occurrence for UPS and UPS with partial myogenic differentiation was 53 (range 49–68) and 43 years (range 23–77), respectively. Lower limbs and males were more often affected in both (Table 2).

Spindle cell sarcoma NOS

Three cases previously diagnosed as FS of bone and three previously diagnosed as MFH of bone were grouped as spindle cell sarcoma NOS. The median age was 60 years (range 51–76); men were more often affected (4:1). Four were located in the femur, one in the pelvis and one in a thoracic vertebra. They were made up of spindle cells, showing no marked pleomorphism (Fig. 4j). Focal storiform pattern and fascicular growth, but no herringbone growth pattern, were found. The standard panel of immunostains failed in demonstrating any line of differentiation. Interphase FISH for SS18 rearrangement and TLE1 staining were performed in all cases to exclude a synovial sarcoma and were negative.

Myoepithelioma-like sarcoma

These tumours were composed of small epithelioid and/or spindle cells, featuring a sharp cytoplasmatic border surrounded by abundant pericellular collagen (Fig. 4a). Immunostains for EMA and CK AE1–AE3 (Fig. 4b) were often

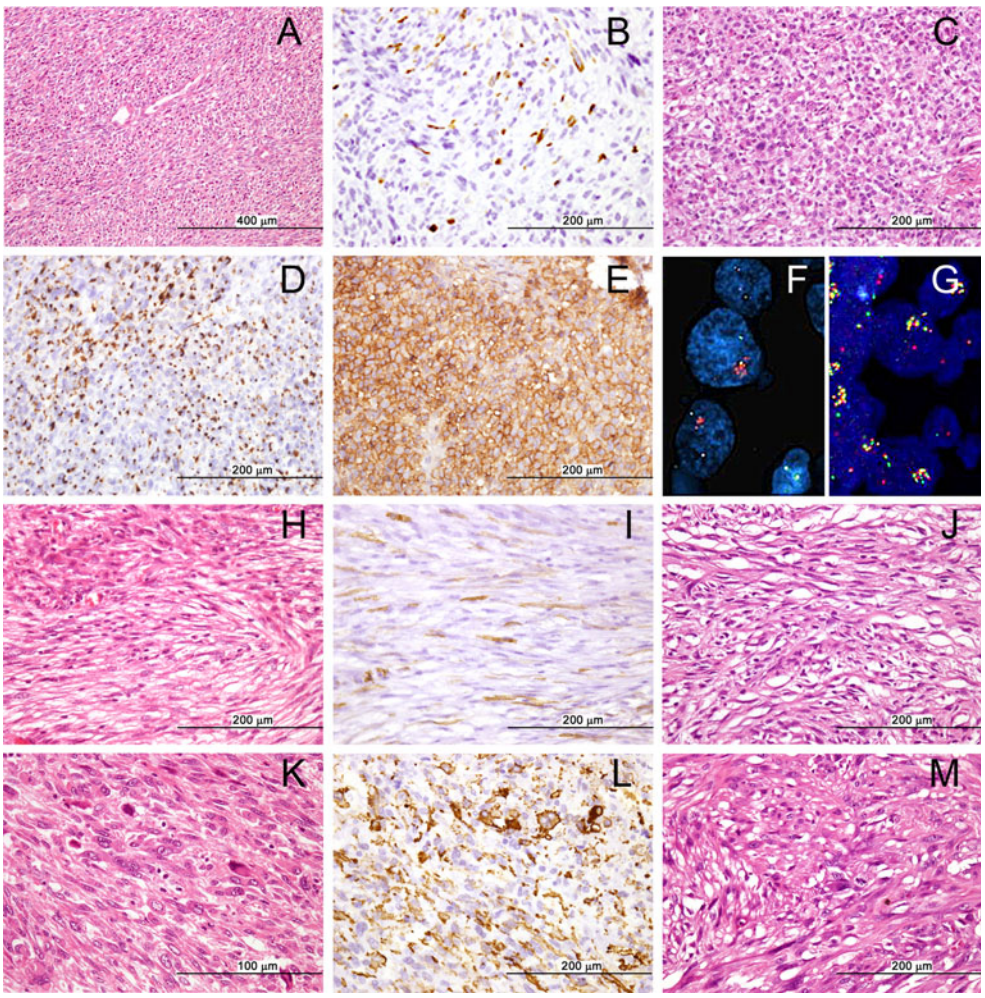

Fig. 4 Some cases not showing any specific lineage of differentiation were reclassified as **a**–**b** myoepithelioma-like sarcoma. Among myoepithelioma-like sarcoma case, MFH19 (**c**–**f**) showed diffuse positivity for CK AE1–3 (**d**) and CD99 (**e**) and rearrangement of EWSR1 with amplification of the proximal 5′ probe shown by interphase FISH with a split-apart probe set for EWSR1 (**f**) and a characteristic fusion and amplification with NFATC2 shown by interphase FISH with a co-localisation probe set for EWSR1–NFATC2 (**g**). The remaining cases were classified as **h**–**i** myofibroblastic sarcoma, characterised by positivity for SMA (**i**), **j** spindle cell sarcoma NOS, **k** UPS with partial myogenic differentiation due for the positivity for SMA (**l**) and UPS without partial myogenic differentiation (**m**)

positive but no staining for S100 was observed. To confirm/rule out a full-blown myoepithelioma, second-line immunohistochemistry was performed including immunostains for GFAP and calponin. The former stain was negative in all cases while calponin was focally positive in two cases (MFH1 and MFH19).

Furthermore, the *EWSR1* gene was assessed by interphase FISH in seven cases. One case (MFH19) (Fig. 4f) showed a split signal of the two probes flanking the *EWSR1* locus and multiple signals for the telomeric probe reflecting a genomic amplification of 5′ part of *EWSR1* (Fig. 4f). Such an amplification pattern has been previously observed [6] to be associated with *NFTAC2* gene rearrangement resulting in an in-frame *EWSR1–NFATC2* fusion. This case showed diffuse positivity for CK AE1–3 (Fig. 4d) and EMA. Second-line immunostains showed diffuse positivity for CD99 (Fig. 4e), patchy positivity for calponin and negativity for chromogranin, CD56, CD20 and p63. The presence of *EWSR1–NFATC2* fusion was confirmed also in our case (Fig. 4g).

This patient had previously (7 years before) received radiotherapy for a non-Hodgkin lymphoma of bone and was alive with no evidence of disease at 64 months' follow-up.

None of the remaining cases showed rearrangements of either *EWSR1* or *FUS*.

Prompted by the results in MFH19, CD99 staining was performed also in all the seven remaining myoepithelioma-like sarcomas and found to be diffusely positive in three of them.

Epithelioid morphology together with the positivity for epithelial markers (CK AE1–3 and EMA) prompted us also to rule out a possible synovial sarcoma or an epithelioid sarcoma. Neither *SS18 (SYT)* rearrangement, as assessed by interphase FISH, nor loss of INI1 nuclear staining, as assessed by immunohistochemistry, was found in 6/6 and 8/8 cases, respectively. The presence of other primary epithelial cancers was excluded in all patients.

Myofibroblastic-like sarcoma

The myofibroblastic-like sarcomas were made up of spindle cells, more often arranged in a storiform pattern or with a tissue culture-like appearance (Fig. 4h). Pleomorphism was mostly absent or only focally present. Immunostaining showed varying patterns of SMA positivity, ranging from isolated, weakly stained neoplastic cells to diffuse positivity (Fig. 4i). Desmin and h-caldesmon were negative.

None of the reviewed cases showed neoplastic cells positive for either CD68 or CD163 or LCA. However, as highlighted by these stains, a moderate, often intense, intra- and peri-tumoural inflammatory infiltrate was always present together with CD68 and CD163 positive multinucleated giant cells. ALK was negative in all cases.

Clinical features and overall survival data

The present study cohort was heterogeneous with regard to original tumour burden, stage at presentation, margin status at surgery and therapeutic regime. Furthermore, follow-up was not available for all the cases (Supplementary Table). Analysis of the survival curves in patients without metastasis at presentation did not reveal any significant differences.

Discussion

Bone MFH and FS are contentious entities and few extensive or recent reports are available in the literature. Nishida et al. [7] reported a series of 81 cases of bone MFH diagnosed at the Mayo Clinic between 1910 and 1993. Our study differs from previous ones both in reviewing cases previously diagnosed either as bone MFH or as bone FS and for the application of the 2002 WHO classification criteria, as well as using immunohistochemistry and molecular genetics to further analyse the tumours. This resulted in reclassification of a substantial (>25 %) number of cases.

Not surprisingly, the vast majority of reclassified cases (13 out of 18) were osteosarcomas and bone leiomyosarcomas. Bone leiomyosarcomas may be easily overlooked if smooth muscle differentiation is not morphologically suspected and subsequent appropriate immunostaining is not performed: misdiagnosis as either bone MFH or bone FS, depending on the degree of cytological pleomorphism, may occur [8]. Cases occurring as secondary to either radiation or bone infarct have been reported [8, 9], and we here report an additional leiomyosarcoma of bone secondary to bone infarct [9].

Osteosarcoma is the most common primary malignant bone tumour. Its diagnosis is based on the microscopical identification of osteoid produced by malignant cells in a distinct clinical and radiological setting. Since osteoid deposition may be focal and scant, it may be overlooked and therefore the proper diagnosis is not rendered, most often when dealing with needle biopsies [10]. Particular attention should be paid to the presence of mineralisation on the imaging, therefore confirming that radiological evaluation still plays a major role in the diagnostic workout of bone lesions [10]. Finally, it is worthy to remark that since only focal osteoid deposition may be found, sampling errors may occur and therefore the diagnosis of osteosarcoma may not be rendered [10]. This may occasionally have occurred in our case series, too.

We were able to identify three examples of primary myxofibrosarcoma of bone. Since myxoid MFH has been widely used in the past as an alternative label for myxofibrosarcoma [11–13], it is very likely that the case reported by Nishida et al. [7] as myxoid MFH would now be reclassified as myxofibrosarcoma of bone. As for myxofibrosarcoma of soft tissue, the

bone cases in this study showed a broad intra-tumoural heterogeneity with respect to cellularity and pleomorphism, with morphologically low-grade malignant areas juxtaposed to high-grade malignant areas [1]. It is important to emphasise that reclassification of myxoid MFH into myxofibrosarcoma is not just a renaming exercise since the metastatic rate of soft tissue high-grade myxofibrosarcoma is lower than that observed in other subtypes of pleomorphic sarcoma [14]. Two of the presented three cases, for which metastases were not present at diagnosis, showed a longer overall survival when compared to the other groups. Larger numbers should be evaluated to test whether there is a significantly better prognosis for this group of tumours, but in consideration of the extreme rarity, such a goal appears considerably difficult to attain.

Cases that did not match with conventional clinicopathologic entities and met the 2002 WHO criteria for MFH or FS of bone were subclassified in five subgroups. One subgroup included lesions that we agreed to label descriptively as 'myoepithelioma-like neoplasms'. These cases morphologically showed a striking resemblance to malignant myoepithelioma. Major differences were the absence of a myxoid background and the fact that none matched the most typical immunohistochemical criteria for myoepithelioma, i.e. the coreactivity for EMA ± cytokeratin and either S100 or GFAP [5]. Remarkably, one of the cases (MFH19) showed rearrangement of the *EWSR1* gene. The positivity for CD99 and the particular rearrangement of *EWSR1*, namely amplification of the 5′ part of *EWSR1*, prompted us to evaluate the presence of a *EWSR1–NFATC2* fusion [6]. Using interphase FISH, we confirmed the *EWSR1–NFATC2* fusion in this myoepithelioma-like tumour, therefore widening the range of phenotypes reported for this specific translocation in bone tumours [6], and further supporting the relationship of this group of lesions with typical primary bone myoepithelial lesions. In the study from Bahrami et al. [2], some of the cases previously diagnosed as soft tissue fibrosarcomas were reclassified as either monophasic synovial sarcoma or solitary fibrous tumour. No such cases were encountered here. Remarkably, Verbeke et al. [15] in a study focused on the reappraisal of cases previously diagnosed as primary bone haemangiopericytoma actually reclassified several cases as examples of bone monophasic synovial sarcomas and bone solitary fibrous tumour. Cases with prominent HPC-like vascular organisation were not present in our series.

Pleomorphic undifferentiated sarcomas represented less than half of the unclassified tumours, a remarkable proportion of which showed incomplete myogenic differentiation. Expression of smooth muscle markers is known to occur in cases previously labelled as bone MFH [16] and also electron microscopic examination shows that myofibroblasts are often present in this tumour [17–19]. As UPS with myogenic differentiation of soft tissue are known to be associated with a worse prognosis [14], we investigated a possible correlation between the presence of incomplete myogenic differentiation and outcome. In contrast with what has been reported in soft tissue, we actually found an opposite trend. Whether this difference may be related to a different mesenchymal cell of origin (i.e. mesenchymal stem cells, the supposed cells of origin of sarcoma, have different plasticity according to the tissue they have been isolated from [20]) and/or distinct microenvironment cannot currently be established due to the low number bias and the absence of a uniform treatment regimen.

For a subset of the cases of the present study (n=11), karyotypes based on conventional chromosome banding analysis have been reported [21]. They all showed complex karyotypes and neither the overall pattern (ploidy level, degree of complexity) nor specific cytogenetic features distinguished any of the subtypes [21]. This indicates that potential genotype–phenotype correlations between morphologic subtypes among so-called MFH of bone are beyond the resolution level of chromosome banding. Further, more detailed genetic studies are warranted.

In the 2002 WHO classification, it was stated that based on its rarity further subclassification of bone MFH is substantially useless [3]. Until now, both so-called MFH and FS of bone have been treated similarly to osteosarcoma. In our series, a substantial proportion of cases previously diagnosed as bone MFH and bone FS were reclassified as another type of sarcoma (i.e. leiomyosarcoma and myxofibrosarcoma). Since both leiomyosarcoma and UPS may be treated systemically with alternative drugs (i.e. gemcitabine alone or in combination with taxotere) [22, 23], a more precise classification is reasonably expected to impact also on the choice of the most appropriate therapeutic option. In this light, it should be emphasised that the correct classification requires a certain skill set and expertise; therefore, bone tumours should be sent to specialist clinics for the most accurate diagnosis and treatment. We identified two groups of lesions (myoepithelial-like and myofibroblastic-like) that may well represent distinctive subgroups that will deserve further characterisation through accrual of a larger number of cases.

Acknowledgments We would like to thank M. Niero for her expert technical assistance and I. Carraretto for fruitful discussion. This study was funded by EuroBoNeT, a European Commission-granted European Network of excellence for studying the pathology and genetics of bone tumours.

Conflict of interest statement We declare that we have no conflict of interest.

References

1. Dei Tos AP (2006) Classification of pleomorphic sarcomas: where are we now? Histopathology 48(1):51–62

2. Bahrami A, Folpe AL (2010) Adult-type fibrosarcoma: a reevaluation of 163 putative cases diagnosed at a single institution over a 48-year period. Am J Surg Pathol 34(10):1504–1513
3. Fletcher CDM, Unni KK, Mertens F (2002) WHO Classification of tumours. Pathology & genetics of tumours of soft tissue and bone. IARC, Lyon
4. Fletcher CDM (1992) Pleomorphic malignant fibrous histiocytoma: fact or fiction? A critical reappraisal based on 159 tumors diagnosed as pleomorphic sarcoma. Am J Surg Pathol 16:213–228
5. Antonescu CR, Zhang L, Chang NE, Pawel BR, Travis W, Katabi N et al (2010) EWSR1–POU5F1 fusion in soft tissue myoepithelial tumors. A molecular analysis of sixty-six cases, including soft tissue, bone, and visceral lesions, showing common involvement of the EWSR1 gene. Gene Chromosomes Canc 49(12):1114–1124
6. Szuhai K, Ijszenga M, de Jong D, Karseladze A, Tanke HJ, Hogendoorn PC (2009) The NFATc2 gene is involved in a novel cloned translocation in a Ewing sarcoma variant that couples its function in immunology to oncology. Clin Cancer Res 15 (7):2259–2268
7. Nishida J, Sim FH, Wenger DE, Unni KK (1997) Malignant fibrous histiocytoma of bone. A clinicopathologic study of 81 patients. Cancer 79(3):482–493
8. Antonescu CR, Erlandson RA, Huvos AG (1997) Primary leiomyosarcoma of bone: a clinicopathologic, immunohistochemical, and ultrastructural study of 33 patients and a literature review. Am J Surg Pathol 21(11):1281–1294
9. Petra M, Gibbons CL, Athanasou NA (2002) Leiomyosarcoma of bone arising in association with a bone infarct. Sarcoma 6(1):47–50
10. Raymond AK, Ayala AG, Knuutila S (2002) Conventional osteosarcoma. In: Fletcher CDM, Unni KK, Mertens F (eds) World Health Organization classification of tumours. Pathology and genetics of tumours of soft tissue and bone. IARC, Lyon, pp 264–270
11. Angervall L, Kindblom LG, Merck C (1977) Myxofibrosarcoma. A study of 30 cases. Acta Pathol Microbiol Scand A 85A(2):127–140
12. Weiss SW, Enzinger FM (1977) Myxoid variant of malignant fibrous histiocytoma. Cancer 39:1672–1685
13. Mentzel T, Calonje E, Wadden C, Camplejohn RS, Beham A, Smith MA et al (1996) Myxofibrosarcoma. Clinicopathologic analysis of 75 cases with emphasis on the low-grade variant. Am J Surg Pathol 20(4):391–405
14. Fletcher CD, Gustafson P, Rydholm A, Willen H, Akerman M (2001) Clinicopathologic re-evaluation of 100 malignant fibrous histiocytomas: prognostic relevance of subclassification. J Clin Oncol 19(12):3045–3050
15. Verbeke SL, Fletcher CD, Alberghini M, Daugaard S, Flanagan AM, Parratt T et al (2010) A reappraisal of hemangiopericytoma of bone; analysis of cases reclassified as synovial sarcoma and solitary fibrous tumor of bone. Am J Surg Pathol 34(6):777–783
16. Ueda T, Araki N, Mano M, Myoui A, Joyama S, Ishiguro S et al (2002) Frequent expression of smooth muscle markers in malignant fibrous histiocytoma of bone. J Clin Pathol 55(11):853–858
17. Erlandson RA, Antonescu CR (2004) The rise and fall of malignant fibrous histiocytoma. Ultrastruct Pathol 28(5–6):283–289
18. Antonescu CR, Erlandson RA, Huvos AG (2000) Primary fibrosarcoma and malignant fibrous histiocytoma of bone—a comparative ultrastructural study: evidence of a spectrum of fibroblastic differentiation. Ultrastruct Pathol 24(2):83–91
19. Montgomery E, Fisher C (2001) Myofibroblastic differentiation in malignant fibrous histiocytoma (pleomorphic myofibrosarcoma): a clinicopathological study. Histopathology 38(6):499–509
20. Bernardo ME, Emons JA, Karperien M, Nauta AJ, Willemze R, Roelofs H et al (2007) Human mesenchymal stem cells derived from bone marrow display a better chondrogenic differentiation compared with other sources. Connect Tissue Res 48(3):132–140
21. Mertens F, Romeo S, Bovée JVMG, Tirabosco R, Athanasou NA, Alberghini M et al (2011) Reclassification and subtyping of so-called malignant fibrous histiocytoma of bone: comparison with cytogenetic features. Clin Sarcoma Res 1(1):10
22. Maki RG, Wathen JK, Patel SR, Priebat DA, Okuno SH, Samuels B et al (2007) Randomized phase II study of gemcitabine and docetaxel compared with gemcitabine alone in patients with metastatic soft tissue sarcomas: results of sarcoma alliance for research through collaboration study 002. J Clin Oncol 25(19):2755–2763 [corrected]
23. Hensley ML, Maki R, Venkatraman E, Geller G, Lovegren M, Aghajanian C et al (2002) Gemcitabine and docetaxel in patients with unresectable leiomyosarcoma: results of a phase II trial. J Clin Oncol 20(12):2824–2831

Virchows Arch (2012) 461:571–580
DOI 10.1007/s00428-012-1315-y

ORIGINAL ARTICLE

Whole genome and transcriptome amplification: practicable tools for sustainable tissue biobanking?

Adriana von Teichman · Martina Storz · Susanne Dettwiler · Holger Moch · Peter Schraml

Received: 29 March 2012 / Revised: 24 August 2012 / Accepted: 3 September 2012 / Published online: 25 September 2012
© Springer-Verlag 2012

Abstract The use of whole genome amplification (WGA) and whole transcriptome amplification (WTA) techniques enables the enrichment of DNA and RNA from very small amounts of tissue. Here, we tested the suitability of WGA and WTA for tumor tissue biobanking. DNA and RNA from 13 standardized and seven non-standardized frozen and 12 formalin-fixed, paraffin-embedded (FFPE) clear cell renal cell carcinoma specimens (>9 years old) served to test the robustness of the WGA and WTA products by reidentifying von Hippel–Lindau (*VHL*) gene mutations known to exist in these samples. The enrichment of DNA and RNA from frozen tissue was up to 1,291-fold and 423-fold, respectively. The sizes and yields (10- to 73-fold) of the amplified DNA obtained from the 12 FFPE samples were generally lower. The quality of the RNA from the FFPE samples was too low to reliably perform WTA. Our results demonstrate that frozen tumor tissue is very suitable for WGA and WTA. All 20 VHL mutations were verified with WGA. Notably, we were able to show that 18 of the 20 (90 %) *VHL* mutations are also transcribed. In FFPE tumor tissue, 8 of 12 cases (67 %) showed the expected mutations after the first WGA. Accurate WTA with FFPE material is sophisticated and strongly depends on the modification and degradation status of the fixed tissue. We conclude that for sustainable tissue biobanking, the use of WGA and WTA is a unique opportunity to provide researchers with sufficient amounts of nucleic acids, preferably from limited frozen tissue material.

Keywords WGA · WTA · Tissue biobank · *VHL* gene · Mutation analysis

A. von Teichman · M. Storz · S. Dettwiler · H. Moch · P. Schraml (✉)
Institute of Surgical Pathology, University Hospital Zurich, Schmelzbergstrasse 12,
8091 Zurich, Switzerland
e-mail: peter.schraml@usz.ch

Introduction

Tumor tissue biobanks represent an ideal platform for translational research. Large tumor tissue collections exist in pathology institutes at universities in which thousands of tissue samples are stored. In general, tumor tissue samples are formalin-fixed and paraffin-embedded (FFPE). The volume of archived tissue samples is limited by the size of the paraffin block and varies between a few cubic millimeter (fine needle biopsies) and 1–2 cm^3.

Due to formalin fixation, the molecular structures in FFPE material become modified, degraded, and cross-linked [1] and are of limited value, particularly when high-throughput technologies, such as DNA microarrays, deep sequencing, or mass spectrometry, are to be applied. As a result, frozen tumor tissue samples not required for diagnostic purposes are routinely collected in parallel in many pathology institutes.

According to the recommendations of the TuBAFrost consortium [2], approximately 0.5 cm^3 is the ideal size for collecting frozen tumor tissue samples in a tumor tissue biobank. This is also in line with our standardized operating procedure for freezing and processing tumor tissues which was established at the Central Tissue Biobank at the University Hospital of Zurich [3].

Depending on the organ and the surgical resection specimen that a tumor originated from, residual tissue fragments available for the biobank may be very small. Furthermore, it is expected that ongoing optimization of surgical dissection techniques and cancer screening tests will lead to a further increase of micro-biopsy samples in the biobanks. Subsequently, although the demand for tumor tissue in the cancer research community is rising, the tissue material available for research projects will become more and more limited in the near future. In addition, once tumor samples have been depleted, these samples are no longer available for further

studies. As a consequence, biobank managers are forced to look for suitable strategies to help prevent the wasting of valuable tumor tissue material. The amplification of whole genomes and transcriptomes of tumor tissue samples may be such an approach.

Several companies offer commercially available kits which allow the amplification of the human genome and transcriptome up to over 1,000-fold [4–6]. In this study, we evaluated the suitability of a whole genome amplification (WGA) and a whole transcriptome amplification (WTA) kit for tumor tissue biobanking using tissue from FFPE and frozen clear cell renal cell carcinoma (ccRCC) specimens. The GenomePlex® WGA2 kit (Sigma-Aldrich) is based on the random fragmentation of genomic DNA and conversion of the resulting small fragments to PCR-amplifiable DNA molecules flanked by universal priming sites. In the whole transcriptome amplification kit (WTA2, Sigma-Aldrich), RNA undergoes a single-step conversion into cDNA fragments flanked by universal priming sites followed by a subsequent PCR amplification of the resulting cDNA library using universal oligonucleotide primers. The accuracy and robustness of the WGA and WTA products were tested using RCC samples with known von Hippel–Lindau (*VHL*) mutations [7].

Materials and methods

Tissue and nucleic acid extraction

Twenty frozen and 12 FFPE unrelated ccRCC specimens with known *VHL* mutations [7] were selected for this study to test whether WGA and WTA are applicable to tissues that were treated differently and of a different age. Thirteen of the 20 samples were frozen according to a standardized procedure [3] which was established at our institute in 2006 and were expected to serve as "positive controls". The remaining seven tissues were collected before 2006 using non-standardized protocols. The 12 FFPE ccRCC specimens were between 9 and 19 years of age. The *VHL* mutations are listed in Tables 1 and 2. Hematoxylin and eosin-stained (HE) sections were reviewed by one pathologist (H.M.). All tumor samples contained at least 70 % tumor cells. Magnified HE sections of three tumors are shown in Fig. 1. DNA and RNA were isolated from one and five 20 μm frozen sections, respectively, using the DNeasy Blood and Tissue and the RNeasy Mini Kits (Qiagen, Hilden, Germany), respectively. DNA and RNA from FFPE tissue were isolated from three punched tissue cylinders (diameter 0.6 mm) using the EZ1 DNA Tissue kit (Qiagen) and an RNA extraction protocol [8], respectively. The concentrations of the obtained nucleic acids were measured using the Nanodrop (Thermo Fisher Scientific, Waltham, MA, USA).

Whole genome and transcriptome amplification

The GenomePlex® WGA2 and WTA2 tissue kits (Sigma-Aldrich, St. Louis, MO, USA) were used to amplify the genomes and transcriptomes of both frozen and FFPE tissue. We used between 8 and 38 ng of DNA and RNA from frozen tissue, and 100 ng of DNA from FFPE material as input for the WGA and the WTA, respectively. The quality of the amplified DNA was analyzed on 1.5 % agarose gels. The amplified products were purified using the MinElute PCR Purification Kit (Qiagen), and the concentrations were measured using the Nanodrop.

VHL mutation analysis

PCR of the three *VHL* exons in the amplified genomes was performed as previously described [9]. One hundred nanograms of amplified DNA was used as template.

Using the Primer3 online program, new primers were designed to analyze the *VHL* mutations in the amplified transcriptomes. One primer pair (forward: 5′-gagtacggccct gaagaaga-3′; reverse: 5′-ggcacaaataattcagtttggtt-3′; 350 bp) spanned exons 1 and 2. The second primer pair (forward: 5′-acacgatgggcttctggtta-3′; reverse: 5′-tcaatctcccatccgttgat-3′; 271 bp) spanned exons 2 and 3. One hundred nanograms of amplified cDNA was used as template.

Sequencing of the PCR products was performed by the dideoxy chain-termination method using the BigDye® Terminator v1.1 Cycle Sequencing kit (Applied Biosystems). Forward and reverse primers used for the PCR were also used for sequencing. Cycle sequencing products were analyzed using the AbiPrism 3100 Genetic analyzer (Applied Biosystems).

A second PCR was performed if no amplified product or no *VHL* mutation was obtained. If the result was not in accordance with the expected result, the original DNA or RNA was subjected to a second or third WGA or WTA, respectively. The products underwent *VHL*-PCR and DNA sequencing as described above.

Results

Whole genome amplification

Between 8 and 35 ng of DNA was used as template for the whole genome amplification of frozen ccRCC tissue. The sizes of the resulting PCR products ranged between 100 and 1,000 bp (Fig. 2a). A DNA yield between 2.98 and 17.36 μg of DNA was obtained. Seventeen samples had more than 10 μg of DNA which is equivalent to a 300- to 1,291-fold enrichment. There were no significant differences in the amplified DNA sizes and the yields between tissue samples

Table 1 WGA and WTA results with frozen ccRCC tissue

Year of sample	*VHL* mutation	Starting amount DNA (ng)	DNA yield (μg)	OD 260/280	Fold enrichment	Result	Starting amount RNA (ng)	cDNA yield (μg)	OD 260/280	Fold enrichment	Result
1992	c.492_511del/p.Gln164Glnfs	11	11.40	1.93	1,037	Correct (1st WGA)	15	4.2	2.10	275	Sequence n.a. (1st WTA)
											No mutation (2nd WTA)
2004	c.263_264GG > CT/p.Trp88Ser	19	2.98	1.88	157	Correct (1st WGA)	38	10.1	1.99	267	Correct (1st WTA)
2004	c.400G > T/p.Glu134X	17	5.48	1.89	322	Correct (1st WGA)	30	8.8	1.94	298	No mutation (1st WTA)
											Correct (2nd WTA)
2004	c.300_308del/p.Thr-100_Pro103delinsThr	18	12.11	1.91	673	Correct (1st WGA)	35	7.1	1.94	202	Correct (1st WTA)
2005	c.473T > G/p.Leu158Arg	14	6.06	1.92	433	Correct (1st WGA)	20	7.2	1.96	369	Correct (1st WTA)
2005	c.484T > C/p.Cys162Arg	15	13.27	1.93	885	Correct (1st WGA)	18	6.2	2.11	343	Correct (1st WTA)
2005	c.512delA/p.Lys171Serfs	11	10.32	1.93	938	Correct (1st WGA)	32	9.2	2.00	288	Correct (1st WTA)
2006	c.255_256GC > TA/ p.LeuPro85_86LeuThr	10	11.38	1.94	1,138	Correct (1st WGA)	22	9.1	1.90	423	Correct (1st WTA)
2006	c.234delT/p.Asn78Asnfs	8	10.33	1.92	1,291	Correct (1st WGA)	25	9.5	2.11	374	Correct (1st WTA)
2006	c.232_250del/p.Asn78fs	35	10.49	1.9	300	Correct (1st WGA)	22	4.6	1.98	211	Correct (1st WTA)
2006	c.599_600delGG/p.Arg200fs	26	11.99	1.91	461	No mutation (1st WGA) Correct (2nd WGA)	31	9.7	1.97	309	Correct (1st WTA)
2006	c.562_565del/p.Leu188fs	18	12.00	1.92	667	Correct (1st WGA)	22	8.6	1.95	386	Correct (1st WTA)
2006	c.240T > A/p.Ser80Arg	15	11.22	1.89	748	Correct (1st WGA)	21	6.8	1.96	330	No PCR product (1st WTA)
											Correct (2nd WTA)
2006	c.277G > C/p.Glu93Arg	20	11.21	1.91	561	Correct (1st WGA)	31	8	1.96	255	Correct (1st WTA)
2006	c.208G > T/p.Glu70X	20	11.41	1.9	571	Correct (1st WGA)	31	7.9	1.99	253	No PCR product (1st WTA)
											Correct (2nd WTA)
2007	c.266T > C/p.Leu89Pro	14	14.20	1.98	1,014	No mutation (1st WGA) Correct (2nd WGA)	21	7.3	2.01	340	Correct (1st WTA)
2007	c.421_430dup/p.Gly144Glufs	18	13.26	1.99	737	No mutation (1st WGA)	38	8.9	1.97	237	Sequence n.a. (1st WTA)
						Correct (2nd WGA)					No mutation (2nd WTA)
2007	c.484T > /p.Cys162Arg	19	17.36	1.89	914	No mutation (1st WGA) Correct (2nd WGA)	28	9	2.08	319	Correct (1st WTA)
2007	c.458T > C/p.Leu153Pro	19	13.74	1.96	723	No mutation (1st WGA)	38	11.8	2.02	315	No mutation (1st WTA)
						Correct (2nd WGA)					Correct (2nd WTA)
2007	c.564-565GG > AT/p.LeuGlu188_189LeuX	19	16.63	1.98	875	No mutation (1st WGA)	38	14.9	2.01	397	Sequence n.a. (1st WTA)
						Correct (2nd WGA)					Correct (2nd WTA)

n.a. not analyzable

Table 2 WGA results with FFPE ccRCC tissue

Year of sample	*VHL* mutation	Starting amount DNA (ng)	DNA yield (µg)	OD 260/280	Fold enrichment	Result
1993	c.491_494delAGGT/p.Gln164fs	100	2.89	1.8	29	Correct (1st WGA)
1994	c.257C > A/p.Pro86His	100	1.26	2.01	13	Correct (1st WGA)
1995	c.389T > A/p.Val130Asp	100	1.1	1.71	11	Different mutation (1st WGA)
						No mutation (2nd WGA)
1995	c.472C > G/p.Leu158Val	100	3.19	1.89	32	Correct (1st WGA)
1995	c.374_380del/p.His125fs	100	1.93	1.83	19	Correct+additional mutation (1st WGA)
						Correct (2nd WGA)
1997	c.234T > A/p.Asn78Lys	100	1.04	1.68	10	Correct (1st WGA)
2000	c.468_470delTAC/p.Tyr156	100	6.01	1.85	60	No mutation (1st WGA)
						Correct (2nd WGA)
2000	c.409delG/p.Val137fs	100	4.5	1.86	45	Correct (1st WGA)
2001	c.323insC/p.Arg108fs	100	4.26	1.87	43	Correct (1st WGA)
2002	c.234T > G/p.Asn78Lys	100	3.5	1.78	35	Correct (1st WGA)
2002	c.452T > C/p.Ile151Thr	100	7.26	1.88	73	Correct + additional mutation (1st WGA)
						Correct (2nd WGA)
2003	c.264G > T/p.Trp88Cys	100	2.2	1.78	22	Correct (1st WGA)

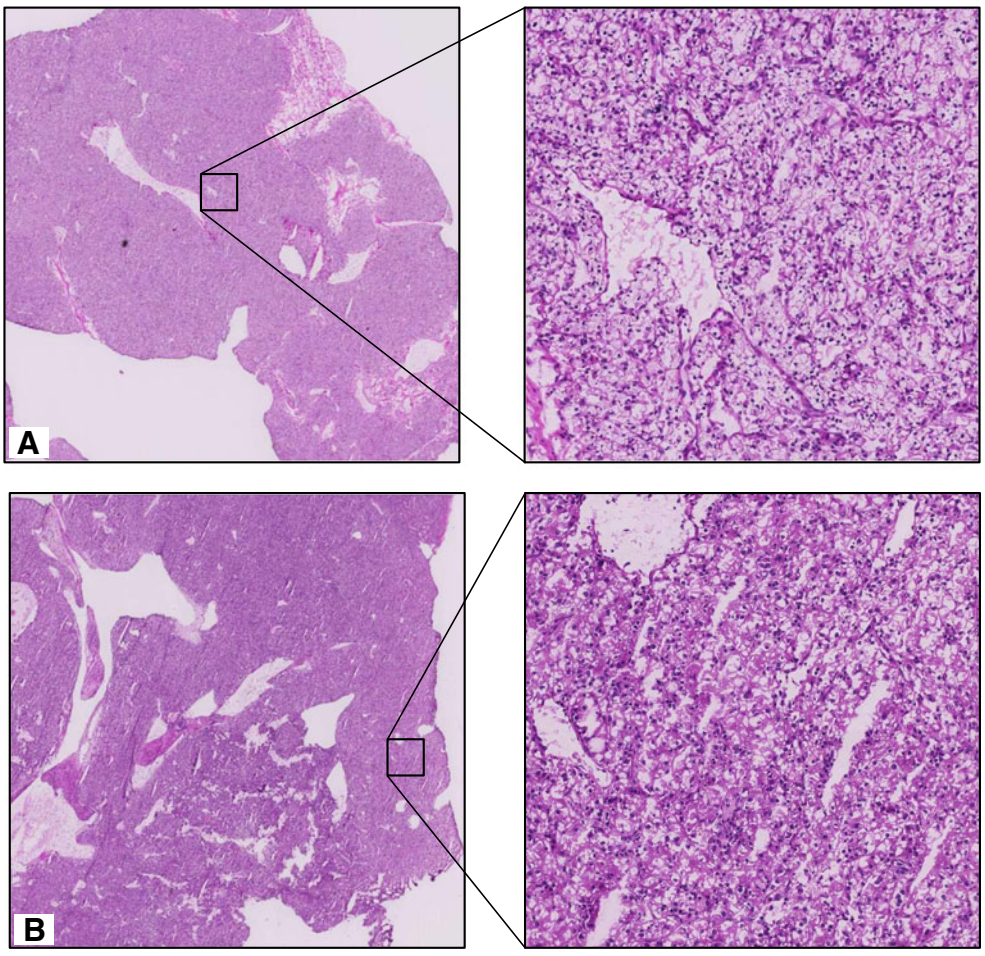

Fig. 1 HE sections of two homogenous ccRCC cases with strongly dominating *VHL* wildtype sequences. Tumors with *VHL* mutations c.458T>C/p.Leu153Pro and c.564-565GG>AT/p.Leu-Glu188-189LeuX, respectively. Details are shown in Table 1

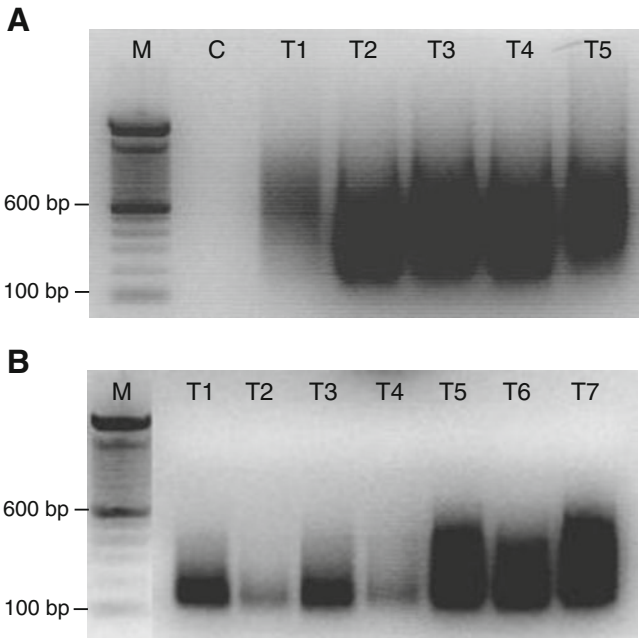

Fig. 2 A 1.5 % agarose gel with WGA products of DNA isolated from five frozen ccRCCs (**a**) and of DNA isolated from seven FFPE ccRCCs (**b**). *M*, 100 bp DNA ladder; *C*, negative control (no DNA template); *T1*, tumor 1, etc

collected under standardized and non-standardized conditions. The detailed results are shown in Table 1.

In contrast to the frozen tissue samples, the sizes and yields of the genomic DNA amplification products obtained from the 12 FFPE ccRCC samples varied significantly among each other and were generally lower (Fig. 2b). As recommended by the supplier, 100 ng of DNA from each of the ccRCC samples was used as input for the whole genome amplification. The DNA yields were between 1.04 and 7.26 μg, which is equivalent to a 10- to 73-fold enrichment. Details are listed in Table 2.

Whole transcriptome amplification

Fifteen to 38 ng of RNA, extracted from the same 20 frozen ccRCC samples, was used for the whole transcriptome amplification. The quality of the amplified cDNA was not analyzed. Between 4.2 and 14.9 μg of amplified cDNA was obtained after the WTA, which is a 202- to 423-fold enrichment. The sizes and yields of amplified cDNA obtained from standardized and non-standardized tissue sets were comparable. The results are shown in Table 1.

We also intended to perform WTA with the same 12 FFPE ccRCC samples used for WGA. However, as we were not able to amplify sufficient amounts of the two PCR products from the original RNA extracts (Fig. 3), particularly the 350 bp fragment which spans the *VHL* exons 1 and 2, we decided to omit this analysis.

VHL mutation analysis of WGA products

The WGA products served as DNA templates for *VHL* exon-specific PCRs. For each sample, only the primer pair covering the known mutated exon was used. Fourteen of the 20 (70 %) amplified DNA samples showed the correct mutation after the first WGA. The WGA of six samples using the original DNA preparation from tissues was repeated because the expected *VHL* mutation was not visible in the DNA sequence. However, it is important to note that in the original DNA of these six ccRCC cases, the *VHL* wild-type sequence was strongly dominating and the mutated sequence was underrepresented. The *VHL* mutations of two tumors are illustrated in Figs. 4 and 5. The results of the WGA are shown in Table 1.

The genomes of all of the 12 ccRCC FFPE samples were successfully amplified. After the first WGA, eight (67 %) of these showed the expected mutations. Two cases showed the expected mutations and an additional *VHL* mutation. Of the last two cases, one had no mutation and the other had a different *VHL* mutation. After repeating the WGA with the original DNA samples of the four tumors that showed discrepant results, three had the correct mutation and one had no mutation. The results are shown in Table 2. An example of a *VHL* mutation identified in the original DNA and after WGA of one ccRCC is shown in Fig. 4a and b, respectively.

VHL mutation analysis of WTA products

To see whether a *VHL* gene affected with a mutation is also transcribed in ccRCC, the WTA products of the 20 frozen ccRCC were subjected to a PCR which specifically amplifies *VHL* expressed alleles. Surprisingly, 13 of 20 (65 %) *VHL* mutations were confirmed as transcribed after the first WTA and five (25 %) after the second PCR or the second WTA. Six of the 20 analyzed ccRCCs had frameshift mutations which probably lead to a loss of function of the VHL protein (pVHL). The frameshift mutations identified in the genomic DNA of the two ccRCC samples could not be verified in the corresponding WTA products. The transcribed *VHL* mutations of two tumors are shown in Figs. 4c and 5c. The results are listed in Table 1.

Discussion

In this study, we demonstrate that WGA and WTA are well suited to sufficiently and accurately enrich DNA and RNA from frozen tumor tissue. The whole amplification of genomes and transcriptomes of nucleic acids extracted from FFPE tumor tissues, however, has limitations. Below, we address some critical points which are of general importance if these methods are used to amplify DNA and RNA from

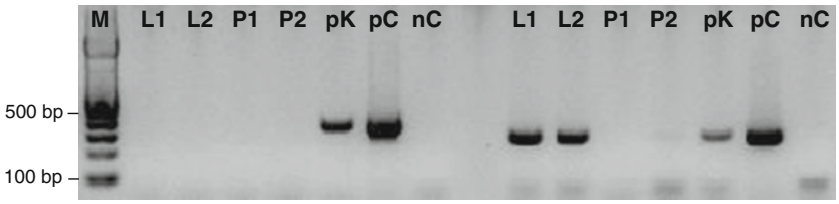

Fig. 3 Reverse transcription-PCR analysis of the 350 bp (exon 1/2) and the 271 bp (exon 2/3) *VHL* fragments. *M*, 100 bp DNA ladder; *L1* and *L2*, FFPE normal liver; *P1* and *P2*, FFPE normal prostate; *pK*, WTA amplified cDNA control from frozen normal kidney; *pC*, plasmid containing the whole *VHL* coding sequence (positive control); *nC*, negative control (no cDNA template)

cancer tissue. For tumor tissue biobanking, these technologies may help to permanently provide sufficient amounts of high quality nucleic acids from limited and valuable tumor tissue material for research purposes.

Mutated *VHL* alleles are commonly transcribed in ccRCC

It is widely accepted that in ccRCC, *VHL* inactivation follows the two-hit mechanism with loss of the chromosomal 3p arm and a mutation of *VHL* in the remaining allele. Recently, we showed that *VHL* mutations may exert different impacts on pVHL's functionality [7] provided that the mutated gene is expressed. Several data exist about pVHL expression in ccRCC [10–15], but the expression status of mutated *VHL* alleles has not been reported to date. Here, we were able to demonstrate that most of the *VHL* mutated alleles are transcribed, regardless of their mutation type. It is, consequently, conceivable that the location and the type

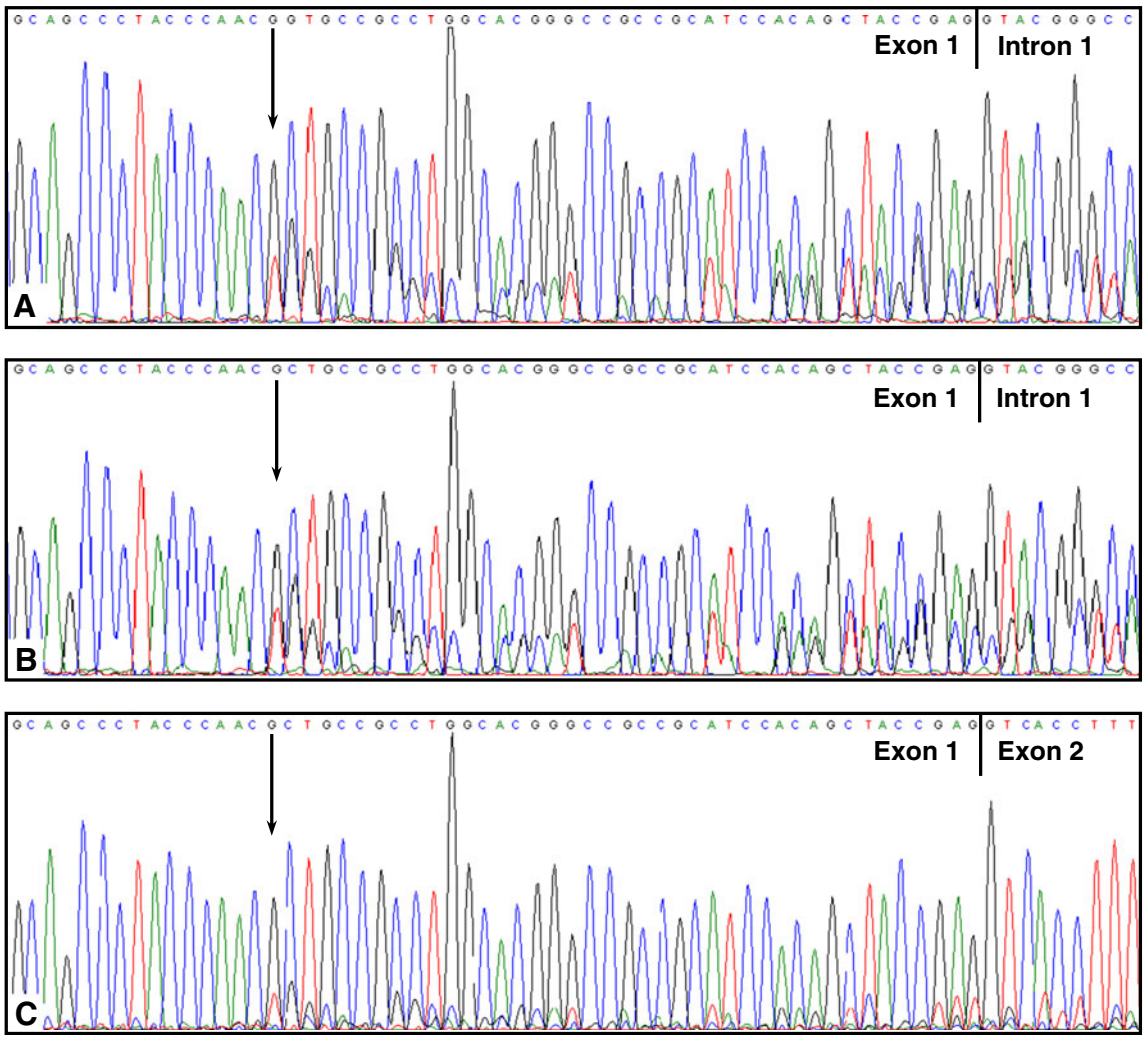

Fig. 4 *VHL* mutation c.300_308del/p.Thr100_Pro103delinsThr in the original DNA of one ccRCC patient (**a**), after WGA (**b**), and after WTA (**c**). The mutation site is denoted by an *arrow*. The boundaries between exon 1/intron 1 and exon 1/exon 2 are indicated

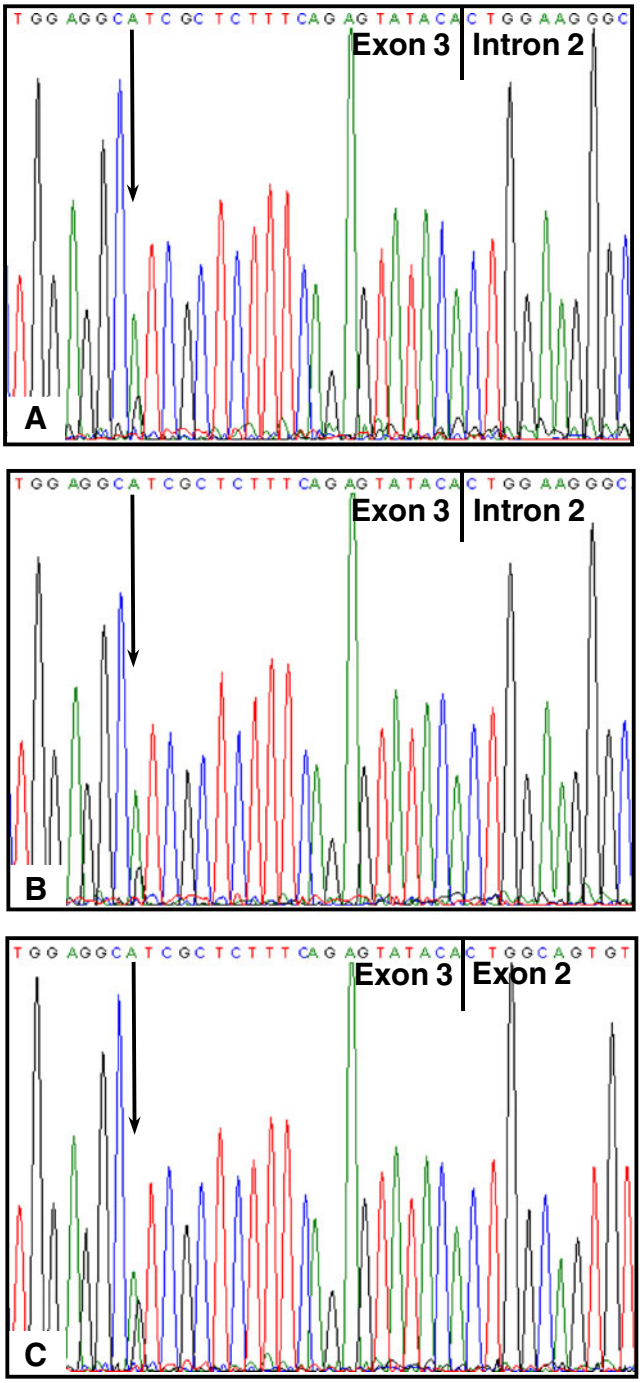

Fig. 5 *VHL* mutation c.484T>C/p.Cys162Arg in the original DNA of one ccRCC patient (**a**), after WGA (**b**), and after WTA (**c**). The sequence is shown in reverse and the mutation site is denoted by an *arrow*. The boundaries between exon 3/intron 2 and exon 3/exon 2 are indicated

of a *VHL* mutation may have dramatic effects on the multi-adaptor functions of pVHL [16] as well as on tumor behavior and response to targeted therapies. Although evidence of mutant pVHL expression in ccRCC has not been reported, previous immunohistochemistry data indicate the presence of pVHL in the majority of ccRCC [10–15].

WGA of DNA extracted from frozen tumor tissue

The DNA obtained after WGA was up to 1,300-fold enriched which is in the range described by the supplier. After the first WGA, the expected *VHL* mutation was present in 14 of 20 samples but absent in six samples. After repeating the WGA from original tissue DNA, all six cases showed the correct *VHL* mutation. In all 20 samples, even in the six ccRCC cases in which the *VHL* mutated sequences were significantly underrepresented, the sizes of the resulting sequence peaks of both the wild-type and the mutated *VHL* sequences obtained after WGA were comparable with those of the original, unamplified DNA (see Fig. 4). As the tumor specimen used for the WGA and sequence analyses consisted of more than 70 % tumor cells, we believe that the observed underrepresention of *VHL* mutations in the six ccRCC is a matter of genetic heterogeneity of the tumor cells. Intratumoral heterogeneity was described in a former study in which *VHL* deletions were analyzed [17]. We conclude that in tumor types that are more heterogeneous than RCC, underrepresented gene sequence alterations may frequently be missed after WGA if whole sections are used for DNA extraction. To minimize this problem, DNA should be extracted from micro-dissected or punched tumor areas rather than from whole tumor sections.

WGA of DNA extracted from FFPE tumor tissue

Although the starting amount of DNA extracted from FFPE ccRCC tissue was 100 ng, the enrichment of DNA was about tenfold lower when compared to WGA with DNA extracted from frozen tumor tissue. WGA with 10 ng of DNA resulted in significantly less amplification product (data not shown). Two-thirds of the samples had the correct mutation after the first WGA. Discrepant results were obtained from the four remaining cases that had either different, additional, or no *VHL* mutations. After a second, separate WGA, three of these cases showed the correct mutation and only one case (with a different mutation after the first WGA) had no mutation. It is known that the frequency of damaged bases can vary considerably due to the fixation time and the modifying effects of formalin on DNA in tissue [18, 19]. Therefore, the results obtained from a mutation analysis should be interpreted with care. In a previous comprehensive *VHL* mutation study, we could not validate the results from approximately 10 % of the formalin-fixed ccRCC samples [7]. At least two independent rounds of PCR and sequencing were performed to distinguish between real and artificial mutations.

A previous study showed that FFPE tissue is less accurate than frozen material for determining mutations in tumors [20]. If WGA is to be performed with DNA from FFPE tumor material, we suggest that two separate parallel WGA

rounds using DNA from original tissue are carried out to select bad from good quality tissue specimens. As a quality control of the whole genome amplified DNA, any exonic sequence can be PCR-amplified and sequenced. If the two obtained sequences are well analyzable and identical, then the integrity of the WGA DNA is given. In case of a discrepancy between the sequences, a third WGA, PCR, and sequencing analysis should be included and compared with the first two sequences. If this third WGA sequence corresponds to one of the others, these two may be used for further molecular analyses. If, however, three different results are obtained, this tissue sample should not be considered for further analyses. The proposed strategy for testing the quality of WGA products is schematically illustrated in Fig. 6.

To further minimize PCR artifacts, the use of non-cross-linking fixatives may be an alternative to buffered formalin as the quality of the nucleic acids seems to be similar to those derived from frozen tissue [21, 22]. A further option may be to treat DNA isolated from FFPE tissue with uracil-DNA glycosylase to reduce uracil lesions which are the major cause of sequence artifacts [23].

WTA of RNA extracted from frozen tumor tissue

The enrichment of amplified cDNA varied only between 200- and 400-fold, indicating a uniform WTA of all 20 RNA samples. With the exception of two ccRCC samples, which had *VHL* frameshift mutations in the original DNA, the expected *VHL* mutations were found to be transcribed in

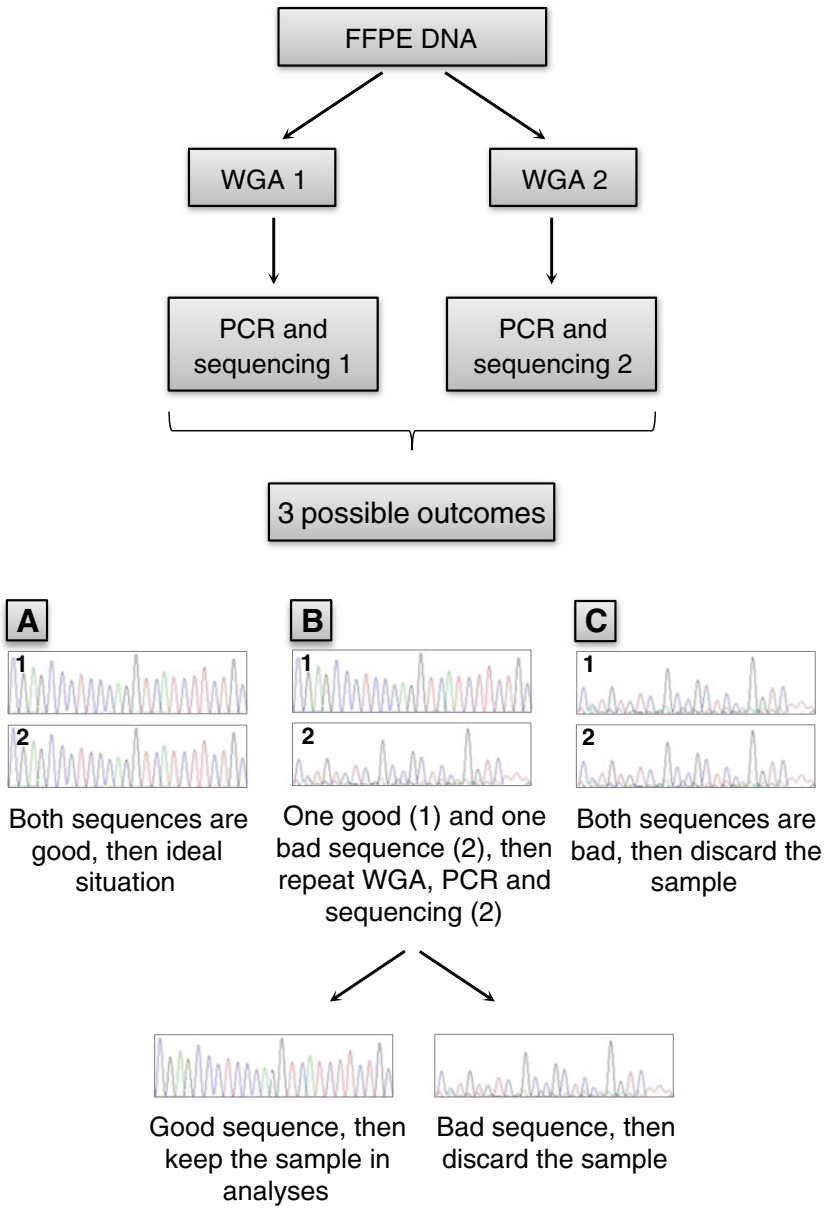

Fig. 6 Proposed strategy to test the quality of DNA from WGA products derived from FFPE tissue. The original DNA is used for additional WGA rounds

the remaining 18 ccRCC samples. To our knowledge, there are no studies to date demonstrating that *VHL* mutations are expressed at the RNA level in sporadic ccRCC, regardless of the mutation type.

In 7 of 20 cases, the *VHL* mutation could not be evaluated after the first WTA. After repeating the WTA, the *VHL* mutations were found in five cases but were not visible in two samples. Not only technical problems (no PCR product of the *VHL* fragment or non-analyzable sequence) but also *VHL* mutations, which can lead to the downregulation or even to the loss of RNA expression, may explain the discrepant findings. These results demonstrate that whole transcriptomes from frozen tissues are linearly amplified and are applicable for gene expression, specific gene mutation, as well as RNA-Seq analyses.

WTA of RNA extracted from FFPE tumor tissue

As already outlined for DNA, the quality of the RNA extracted from FFPE material is similarly low and, therefore, of limited value for molecular analysis [24]. The amplification of sequences becomes increasingly problematic with the size of the PCR product. To ensure that only cDNA was being amplified, we worked with primer pairs that spanned two *VHL* exons. The sizes of the PCR fragments were, however, too large to amplify sufficient amounts of DNA for sequence analysis. As it was suggested in other studies [1, 25, 26], our results imply that a successful WTA-based mutation analysis of FFPE tissue is strongly dependent on the chosen size of the PCR fragment to be analyzed and the age of the tissue sample.

WGA and WTA for economic tumor tissue biobanking?

WGA and WTA technologies can help to provide sufficient amounts of high quality nucleic acids from valuable tumor tissue material for research purposes in tumor tissue biobanking. By using fixed and non-fixed ccRCC nucleic acids with known *VHL* mutations, we demonstrate that nucleic acids from frozen tumor tissue are most suitable for WGA and WTA. The severity of the modification and degradation of nucleic acids in FFPE tumor tissue often differs and thus hampers the accurate amplification. Additional rounds of WGA or WTA and validation experiments lead to increased costs. In Switzerland, one WGA costs approximately 10 Swiss Francs and one WTA is about eight times more expensive. The routine use of WGA and WTA for large tumor tissue biobanks, which receive thousands of tissue samples annually, would cause an enormous financial burden on a biobank's budget, in terms of manpower, consumables, freezers, space, and logistics. In contrast, research projects usually focus on analyzing a few dozen up to several hundred tissue samples of one specific tumor type, which represents only a tiny part of the whole inventory of a large tumor tissue biobank. The use of WGA and WTA should be restricted to those tissue samples, preferably frozen ones, required for approved research projects. This would help to keep the costs within an affordable limit. Furthermore, to financially fund tumor tissue biobanks, it will be of utmost importance for cancer research scientists to include costs for tissue biobanking, such as sampling, storing, and processing as well as the costs for WGA and WTA in grant applications if they intend to work with DNA and RNA from cancer tissue.

Conclusions

Our data indicate that both WGA and WTA are feasible with nucleic acids extracted from frozen and FFPE tissue. Nevertheless, the use of the latter has certain limitations and the results should be interpreted with caution. Although standardized procedures are required to guarantee the high quality of frozen tissue collections, it seems that non-standardized protocols formerly used for snap freezing native tissue samples do not negatively influence the outcome of WGA and WTA.

Acknowledgments This study was supported by the Zurich Cancer League, the Foundation for Research in Science and the Humanities at the University of Zurich, and the Swiss National Science Foundation (3238BO-103145).

Conflict of interest There is no conflict of interest to declare.

References

1. Lassmann S, Kreutz C, Schoepflin A, Hopt U, Timmer J, Werner M (2009) A novel approach for reliable microarray analysis of microdissected tumor cells from formalin-fixed and paraffin-embedded colorectal cancer resection specimens. J Mol Med 87:211–224
2. Morente MM, Mager R, Alonso S, Pezzella F, Spatz A, Knox K, Kerr D, Dinjens WN, Oosterhuis JW, Lam KH, Oomen MH, van Damme B, van de Vijver M, van Boven H, Kerjaschki D, Pammer J, Lopez-Guerrero JA, Llombart Bosch A, Carbone A, Gloghini A, Teodorovic I, Isabelle M, Passioukov A, Lejeune S, Therasse P, van Veen EB, Ratcliffe C, Riegman PH (2006) TuBaFrost 2: standardising tissue collection and quality control procedures for a European virtual frozen tissue bank network. Eur J Cancer 42:2684–2691
3. Steu S, Baucamp M, von Dach G, Bawohl M, Dettwiler S, Storz M, Moch H, Schraml P (2008) A procedure for tissue freezing and processing applicable to both intra-operative frozen section diagnosis and tissue banking in surgical pathology. Virchows Arch 452:305–312
4. Clement-Ziza M, Gentien D, Lyonnet S, Thiery JP, Besmond C, Decraene C (2009) Evaluation of methods for amplification of picogram amounts of total RNA for whole genome expression profiling. BMC Genom 10:246
5. Gonzalez-Roca E, Garcia-Albeniz X, Rodriguez-Mulero S, Gomis RR, Kornacker K, Auer H (2010) Accurate expression profiling of very small cell populations. PLoS One 5:e14418

6. Navin N, Hicks J (2011) Future medical applications of single-cell sequencing in cancer. Genome Med 3:31
7. Rechsteiner MP, von Teichman A, Nowicka A, Sulser T, Schraml P, Moch H (2011) VHL gene mutations and their effects on hypoxia inducible factor HIFalpha: identification of potential driver and passenger mutations. Cancer Res 71:5500–5511
8. Bode B, Frigerio S, Behnke S, Senn B, Odermatt B, Zimmermann DR, Moch H (2006) Mutations in the tyrosine kinase domain of the EGFR gene are rare in synovial sarcoma. Mod Pathol 19:541–547
9. von Teichman A, Comperat E, Behnke S, Storz M, Moch H, Schraml P (2011) VHL mutations and dysregulation of pVHL- and PTEN-controlled pathways in multilocular cystic renal cell carcinoma. Mod Pathol 24:571–578
10. Kivela AJ, Parkkila S, Saarnio J, Karttunen TJ, Kivela J, Parkkila AK, Bartosova M, Mucha V, Novak M, Waheed A, Sly WS, Rajaniemi H, Pastorekova S, Pastorek J (2005) Expression of von Hippel-Lindau tumor suppressor and tumor-associated carbonic anhydrases IX and XII in normal and neoplastic colorectal mucosa. World J Gastroenterol 11:2616–2625
11. Osipov V, Keating JT, Faul PN, Loda M, Datta MW (2002) Expression of p27 and VHL in renal tumors. Appl Immunohistochem Mol Morphol 10:344–350
12. Schraml P, Hergovich A, Hatz F, Amin MB, Lim SD, Krek W, Mihatsch MJ, Moch H (2003) Relevance of nuclear and cytoplasmic von Hippel Lindau protein expression for renal carcinoma progression. Am J Pathol 163:1013–1020
13. Corless CL, Kibel AS, Iliopoulos O, Kaelin WG Jr (1997) Immunostaining of the von Hippel-Lindau gene product in normal and neoplastic human tissues. Hum Pathol 28:459–464
14. Sakashita N, Takeya M, Kishida T, Stackhouse TM, Zbar B, Takahashi K (1999) Expression of von Hippel–Lindau protein in normal and pathological human tissues. Histochem J 31:133–144
15. Los M, Jansen GH, Kaelin WG, Lips CJ, Blijham GH, Voest EE (1996) Expression pattern of the von Hippel-Lindau protein in human tissues. Lab Invest 75:231–238
16. Frew IJ, Krek W (2008) pVHL: a multipurpose adaptor protein. Sci Signal 1:pe30
17. Moch H, Schraml P, Bubendorf L, Richter J, Gasser TC, Mihatsch MJ, Sauter G (1998) Intratumoral heterogeneity of von Hippel-Lindau gene deletions in renal cell carcinoma detected by fluorescence in situ hybridization. Cancer Res 58:2304–2309
18. Agell L, Hernandez S, de Muga S, Lorente JA, Juanpere N, Esgueva R, Serrano S, Gelabert A, Lloreta J (2008) KLF6 and TP53 mutations are a rare event in prostate cancer: distinguishing between Taq polymerase artifacts and true mutations. Mod Pathol 21:1470–1478
19. Quach N, Goodman MF, Shibata D (2004) In vitro mutation artifacts after formalin fixation and error prone translesion synthesis during PCR. BMC Clin Pathol 4:1
20. Verhoest G, Patard JJ, Fergelot P, Jouan F, Zerrouki S, Dreano S, Mottier S, Rioux-Leclercq N, Denis MG (2012) Paraffin-embedded tissue is less accurate than frozen section analysis for determining VHL mutational status in sporadic renal cell carcinoma. Urol Oncol 30:469–475
21. Moelans CB, Oostenrijk D, Moons MJ, van Diest PJ (2011) Formaldehyde substitute fixatives: effects on nucleic acid preservation. J Clin Pathol 64:960–967
22. Turashvili G, Yang W, McKinney S, Kalloger S, Gale N, Ng Y, Chow K, Bell L, Lorette J, Carrier M, Luk M, Aparicio S, Huntsman D, Yip S (2011) Nucleic acid quantity and quality from paraffin blocks: defining optimal fixation, processing and DNA/RNA extraction techniques. Exp Mol Pathol 92:33–43
23. Do H, Dobrovic A (2012) Dramatic reduction of sequence artefacts from DNA isolated from formalin-fixed cancer biopsies by treatment with uracil-DNA glycosylase. Oncotarget 3:546–558
24. Klopfleisch R, Weiss AT, Gruber AD (2011) Excavation of a buried treasure—DNA, mRNA, miRNA and protein analysis in formalin fixed, paraffin embedded tissues. Histol Histopathol 26:797–810
25. Huijsmans CJ, Damen J, van der Linden JC, Savelkoul PH, Hermans MH (2010) Comparative analysis of four methods to extract DNA from paraffin-embedded tissues: effect on downstream molecular applications. BMC Res Notes 3:239
26. Ribeiro-Silva A, Zhang H, Jeffrey SS (2007) RNA extraction from ten year old formalin-fixed paraffin-embedded breast cancer samples: a comparison of column purification and magnetic bead-based technologies. BMC Mol Biol 8:118

Virchows Arch (2012) 461:581–588
DOI 10.1007/s00428-012-1313-0

ORIGINAL ARTICLE

Rosette-forming glioneuronal tumor — evidence of stem cell origin with biphenotypic differentiation

S. Chakraborti · A. Mahadevan · A. Govindan · A. Bhateja · S. Dwarakanath · H. R. Aravinda · A. A. Phalguni · V. Santosh · T. C. Yasha · P. Rout · S. Sampath · S. K. Shankar

Received: 24 May 2012 / Revised: 7 August 2012 / Accepted: 3 September 2012 / Published online: 13 September 2012
© Springer-Verlag 2012

Abstract Rosette-forming glioneuronal tumor (RGNT) of the fourth ventricle is a new addition to the WHO classification of central nervous system tumors. To date, 72 cases have been described in literature. In the present study, we report the clinical and imaging features, with detailed histopathological and immunohistochemical profile, of eight cases. Confocal microscopic evidence of stem cell origin with biphenotypic, glial and neurocytic differentiation is presented with a comprehensive review of literature.

Keywords Glioneuronal tumor · Rosette-forming glioneuronal tumor · GFAP · Synaptophysin · CD133 · Stem cell · Confocal microscopy

Introduction

Rosette-forming glioneuronal tumor (RGNT) of the fourth ventricle was designated as a new tumor entity in the 2007 issue of World Health Organization Classification of Tumors of the Central Nervous System [1]. This mixed neuronal–glial tumor is rare and benign, with a female predilection [1]. Originally described by Kuchelmeister and colleagues [2] as a dysembryoblastic neuroepithelial tumor of the cerebellum, it was in 2002, that Komori et al. [3] in a large series of 11 cases, elaborated on the histological, immunohistochemical and ultrastructural features of this biphenotypic tumor. To date, 72 cases of RGNT have been published in the medical literature [3–41]. In this study,

S. Chakraborti
Department of Pathology, Kasturba Medical College, Mangalore, Karnataka, India

A. Mahadevan (✉) · V. Santosh · T. C. Yasha · S. K. Shankar
Department of Neuropathology, National Institute of Mental Health and Neurosciences, Hosur Road, Bangalore, Karnataka, India 560 029
e-mail: anita_mahadevan@yahoo.com

A. Mahadevan
e-mail: amahadevan@nimhans.kar.nic.in

A. Govindan
Department of Pathology, Government Medical College, Kozhikode, Kerala, India

A. Bhateja
Sita Bhateja Hospial, Bangalore, Karnataka, India

S. Dwarakanath · S. Sampath
Department of Neurosurgery, National Institute of Mental Health and Neurosciences, Bangalore, Karnataka, India

H. R. Aravinda
Department of Neuroimaging and Interventional Radiology, National Institute of Mental Health and Neurosciences, Bangalore, Karnataka, India

A. A. Phalguni
Department of Neurophysiology, National Institute of Mental Health and Neurosciences, Bangalore, Karnataka, India

P. Rout
Department of Pathology, St John's Medical College and Hospital, Bangalore, Karnataka, India

we present our experience of eight cases with clinicoradiological and immunohistochemical features and provide evidence of its stem cell origin with biphenotypic differentiation, based on confocal microscopic features.

Material and methods

There were eight cases of RGNT in our neuropathology archives diagnosed between 2007 and 2011. The paraffin embedded sections were stained with hematoxylin and eosin stain for routine histological evaluation. Immunohistochemistry was performed on representative sections using indirect immunoperoxidase method with antibodies to glial fibrillary acid protein (GFAP; monoclonal, 1:50 dilution, BioGenex, USA), Synaptophysin (Syn; polyclonal, 1:50 dilution, Dako, USA), MIB-1 (monoclonal, 1:30 dilution, BioGenex, USA) in all cases and CD133 (polyclonal, 1:10, ABCAM, USA) and NeuN (1:100, monoclonal, Millipore, MA, USA), depending on the availability of tissues. The clinical features, histology and immunohistochemical features of the eight cases were tabulated in Table 1.

Double labeling was carried out using GFAP (monoclonal, 1:200) detected by secondary antibody tagged to FITC, and Syn (polyclonal, 1:200) detected with secondary antibody conjugated to Cy3. For triple labeling, GFAP was detected by FITC, Syn by Cy3 and stem cell marker CD133 (polyclonal, 1:10) by secondary antibody tagged to Cy5. Sections were viewed and images captured using a laser scanning confocal microscope (DMIRE-TCS Leica, Germany) with different excitation filters (514 nm for Cy3, 488 nm for FITC and 633 nm for Cy5 fluorochromes, respectively). Emission bandwidth of 495–540 nm for FITC, 550–620 nm for Cy3 and 630–700 nm for Cy5 was maintained to avoid any non-specific overlap of emission frequencies. The channel detecting Cy3 and Cy5 were assigned red and blue color, respectively. All images were captured under 20× magnifications at a constant PMT (photo multiplier tube) voltage of 557 V and each image was averaged four times. The image format was kept constant at 1,024×1,024 pixel resolution.

Results

The age range of the patients in this study was 7–59 years (mean: 25.8 years), with male predominance (M/F=3:1; Table 1). Six cases presented with headache, followed by vomiting in five cases, ataxia and papilledema in four cases. One of the cases presented with scholastic decline, progressive deterioration of vision, hand tremors, dysarthria and difficulty in walking. The duration of symptoms ranged from 2 months to 4 years. In three cases, the tumor was located in the fourth ventricle (Case 4, Fig. 1a–c), in two cases within the third ventricle (Case 2, Fig. 1d), and one case each in right cerebellum, medulla oblongata and vermis.

Magnetic resonance imaging showed the lesions to be hypointense on T1W, hyperintense on T2W, not inverting on FLAIR in Cases 2, 4 and 6 (Case 4, Fig. 1a–c), with patchy enhancement in Case 4 and irregular ring enhancement in Case 6. In Cases 5 and 8, the lesions were iso- to hypointense on T1W, hyperintense on T2W, with moderate and heterogenous enhancement, respectively, on contrast administration. However, Case 1 did not show any contrast enhancement. Obstructive hydrocephalus was noted in Cases 3 and 6. Computed tomogram in Case 7 revealed a cystic lesion with hypodense centre and hyperdense periphery, enhancing on contrast.

Histopathological examination of the tumor in all cases showed biphasic morphology. Cellular areas consisted of neurocytic rosettes with small, monomorphic, round tumor cells, having dense nuclei and scant cytoplasm, arranged in rosettoid pattern with central, anuclear, eosinophilic neurofibrillary stroma (Fig. 2a,b). At places, perivascular arrangement of tumor cells formed rosettes (Fig. 2c). The intervening paucicellular areas with pilocytic morphology, were composed of astrocytic cells having bipolar piloid processes, along with Rosenthal fibres and eosinophilic granular bodies (Fig. 2d). In three cases (Cases 3, 4 and 5), the glial component exhibited microcystic change with foci of mucoid matrix, along with oligodendroglial-like cells around the microcystic areas in one (Case 3). No Rosenthal fibres or eosinophilic granular bodies were seen in Case 6. Only one case showed glomeruloid vascular proliferation and focal necrosis (Case 2). No mature ganglionic element was noted in any of the cases examined. Diligent search did not reveal any mitotic figures.

Immunohistochemical studies demonstrated strong positivity of synaptophysin in the tumor cell cytoplasm and neuropil in the neurocytic and perivascular rosettes in all the cases (Fig. 2e). NeuN immunostaining exhibited focal positivity in occasional cells lining the rosettes (Case 2 and 3) (Fig. 2e, inset) and inter-rosette areas in a single case (Case 3). GFAP expression was confined to the pilocytic/glial component of the tumor (Fig. 2f). Only two cases showed focal and weak positivity of GFAP in the neurocytic component (Case 1, 2 and 5). MIB-1 expression ranged from <1 % to 3 % (Fig. 2g), and in a single case (Case 5), it reached 6 % focally. CD133 immunostaining revealed positivity in the glial component of all the cases stained (Cases 2, 3 and 5) (Fig. 2h), with focal labeling of cells in both perivascular and neurocytic rosettes in Cases 3 and 5, and neurocytic rosettes alone in Case 2 (Fig. 2h, inset).

Confocal microscopy was performed to localize the markers of glial and neuronal lineage and stem cells, if

Table 1 Clinicopathological summary of eight cases in the present series

Caseno	Age (years)/ sex	Clinical features	Duration of symptoms (months)	Site	Magnetic resonance imaging/Computed tomogram	Histology	Immunohistochemistry				
							Synaptophysin	GFAP	CD133	NeuN	MIB-1
1	16/M	Headache	12	Third ventricle	Hypointense on T1 and hyperintense on T2, non-enhancing on contrast	Neurocytic and perivascular rosettes, intervening pilocytic glial component. Calcification. No mitosis.	Strong positivity in neurocytic and perivascular rosettes	Strong positivity in glial component, focal and weak positivity in neurocytic zones	Not done	Not done	2–3 %
2	42/F	Headache, vomiting, diplopia, mild papilledema	4	Posterior third ventricle	Hypointense on T1 and hyperintense on T2	Neurocytic and perivascular rosettes, intervening pilocytic glial component, glomeruloid vascular proliferation, focal necrosis. No mitosis.	Strong positivity in neurocytic and perivascular rosettes	Strong positivity in glial component, focal and weak positivity in neurocytic zones	Positive in glial component and focally positive in neurocytic rosettes	Focally positive in cells lining the rosettes	2–3 %
3	59/M	Ataxia, vomiting	2	Right Cerebellum	Hypointense on T1 and hyperintense on T2, solid-cystic, with mild obstruc tive hydrocephalus	Neurocytic and perivascular rosettes, intervening pilocytic glial component, microcystic areas with oligodendroglial-like cells, focal mucoid matrix. No mitosis.	Strong positivity in neurocytic and perivascular rosettes	Strong positivity in glial component, negative in neurocytic zones	Positive in glial component and focally positive in perivascular and neurocytic rosettes	Occasional cells positive in rosettes and inter-rosette areas	<1 % in predominant areas, focally 3 %
4	7/M	Headache, vomiting	24	Fourth ventricle	Hypointense on T1 and hyperintense on T2, patchy enhancement	Perivascular rosettes, intervening pilocytic glial component, focal mucoid matrix and microcystic change. No mitosis.	Positivity in perivascular and neurocytic rosettes	Strong positivity in glial zones and focal, weak positivity in neurocytic zones	Not done	Negative	<1 %
5	22/M	Headache, ataxia, vomiting	4	Fourth ventricle and cerebellum	Iso- to hypointense on T1 and hyperintense on T2, solid, moderate enhancement	Neurocytic and perivascular rosettes, intervening pilocytic glial component, focal mucoid matrix and microcystic change. No mitosis.	Strong positivity in neurocytic and perivascular rosettes	Strong positivity in glial component, focal and weak positivity in neurocytic zones	Positive predominantly in glial component and in the rosettes	Not done	3 – 6 %
6	19/M	Scholastic decline, visual disturbance, hand tremors, dysarthria, difficulty in walking, papilledema	48	Medulla oblongata, expanding the inferior cerebellar peduncle and extending into cisterna magna	Hypointense on T1 and hyperintense on T2, with small, irregular, ring enhancement and obstructive hydrocephalus	Neurocytic and perivascular rosettes, intervening fibrillary glial stroma. No mitosis.	Positivity in neurocytic and perivascular rosettes	Positive in the fibrillary glial component	Not done	Not done	<1 %
7	18/F	Headache, ataxia, papilledema	2	Cerebellar vermis	Cystic with hypodense centre and hyperdense periphery, enhancing on contrast	Neurocytic and perivascular rosettes, intervening pilocytic glial component. No mitosis.	Strong positivity in neurocytic and perivascular rosettes	Strong positivity in glial component, focal and weak positivity in neurocytic zones	Not done	Not done	Not done
8	24/M	Headache, vomiting, ataxia, papilledema	3	Fourth ventricle	Iso- to hypointense on T1 and hyperintense on T2, heterogenous enhancement	Neurocytic and perivascular rosettes, intervening pilocytic glial component. No mitosis.	Not done	Not done	Not done	Not done	Not done

Fig. 1 Case 4: T2 weighted imaging shows tumor in the fourth ventricle (arrow, **a**), T1 weighted contrast scan show patchy contrast enhancement along the periphery (arrow, **b**) and on CISS 3D sequences (**c**) is seen as a large hypointense lesion filling up the expanded fourth ventricle. CISS 3D sequences in mid-saggital plane from Case 2 (**d**) shows a hypointense lesion within the posterior third ventricle (*arrow*)

any, in the different tumor components. The predominant glial component of the tumor exhibited green fluorescence (FITC) and enveloped the perivascular rosettes (Figs. 2j and 3a). The red fluorescence (Cy3) of Syn was essentially confined to the perivascular and neurocytic rosettes, though scattered Syn labeled cells were found in the inter-rosette glial zones (Figs. 2i and 3b,f). In the neurocytic rosettes, the neurofibrillary matrix forming the core, had few entrapped glial fibres and occasional astrocytes (Fig. 2j,k). In contrast, the perivascular rosettes demonstrated intermingling of neurocytic (Cy3) and several glial cells (FITC) (Figs. 2i–k and 3a,b,d).

On triple labeling for stem cells (CD133, blue fluorescence, Cy5) in addition to glial (GFAP, green fluorescence, FITC) and neuronal lineage (Synaptophysin, red fluorescence, Cy3) abundant co-localization of stem cell marker was evident in the glial areas interposed between the neurocytic rosettes (Fig. 3e–h). Similar feature was also noted, though to a lesser degree within the perivascular rosettes, in contrast to minimal co-localization in the neurocytic rosettes (Fig. 3a–d). The fibrillary neuropil rosette is lightly stained by Syn and lacked CD133 positive stem cells migrating through it. These features suggest CD133 labeled stem cell population was predominantly present in the inter-rosette glial zones, and to a lesser extent in the neurocytic component. The rosette-forming glial neuronal tumors of the fourth ventricle appear to be evolving from a bi-potential stem cell population in the periventricular ontogenically stem cell rich area.

Post-operatively, none of the cases received adjuvant therapy, and all were lost for follow-up after 6 months.

Discussion

To date, 72 cases of RGNT have been published in the medical literature [3–41], of which, review of 17 cases is described in World Health Organization Classification of Tumors of the Central Nervous System, 2007 [1]. Available clinicopathological data in 63 cases was reviewed. In the published series, the mean age at presentation was 31.1 years (age range, 6–79 years), with maximum number of cases in second decade (30.2 %), followed by the fourth (22.2 %) and third decades (19.04 %). This tumor has mild female predilection (M/F=1:1.7), unlike the present series in which male predominance was documented (six out of eight cases, Table 1). The male predominance seen in the present study is probably due to small sample size. The commonest symptoms recorded were headache (47.3 %), followed by ataxia (21.8 %), diplopia (10.9 %), tinnitus (7.2 %), blurred vision, seizures, anisocoria and cranial nerve palsy in 3.6 % of cases each. Eight (12.7 %) cases were asymptomatic or incidentally discovered [4, 6, 10, 12, 18, 26, 39].

RGNT, though originally described in the fourth ventricle, is not restricted to that site alone. Literature review showed that fourth ventricle (in 53.9 % cases) was the most frequent site of occurrence, followed by cerebellar vermis (14.3 %), pineal region (11.1 %) and cerebellum (7.9 %). Occasional cases are reported in dorsal pons [3], thalamus [3, 21], left cerebellopontine angle [12], brain stem [14, 38], intramedullary C2–T4 [4, 15], third ventricle [16, 23, 35, 36, 38], septum pellucidum [35] and optic chiasma in a known case of neurofibromatosis-1 [17]. Multifocal growth pattern in the form of satellite lesions [3, 7, 12] and panventriclular involvement is on record [23].

On MR imaging, RGNT are iso/hypointense on T1-weighted and hyperintense on T2-weighted sequences [12], similar to the present study. Out of 52 cases, in which neuroimaging data was available, the tumor was solid in 42.3 % of the cases, solid-cystic in 28.8 % of the cases and entirely cystic in 25 % of the cases. Calcification was noted in 21.2 % of the cases, unlike our study. Lack of contrast enhancement was seen in 30.8 % of the cases and focal enhancement in 25 % of the cases, and minimal enhancement in 11.5 % cases. Less common enhancement patterns included ring-like [4, 15], dot-like [25] and curvilinear patterns [14].

Histologically, RGNT is characterized by biphasic architecture, composed of two distinct cell lineages, a neurocytic

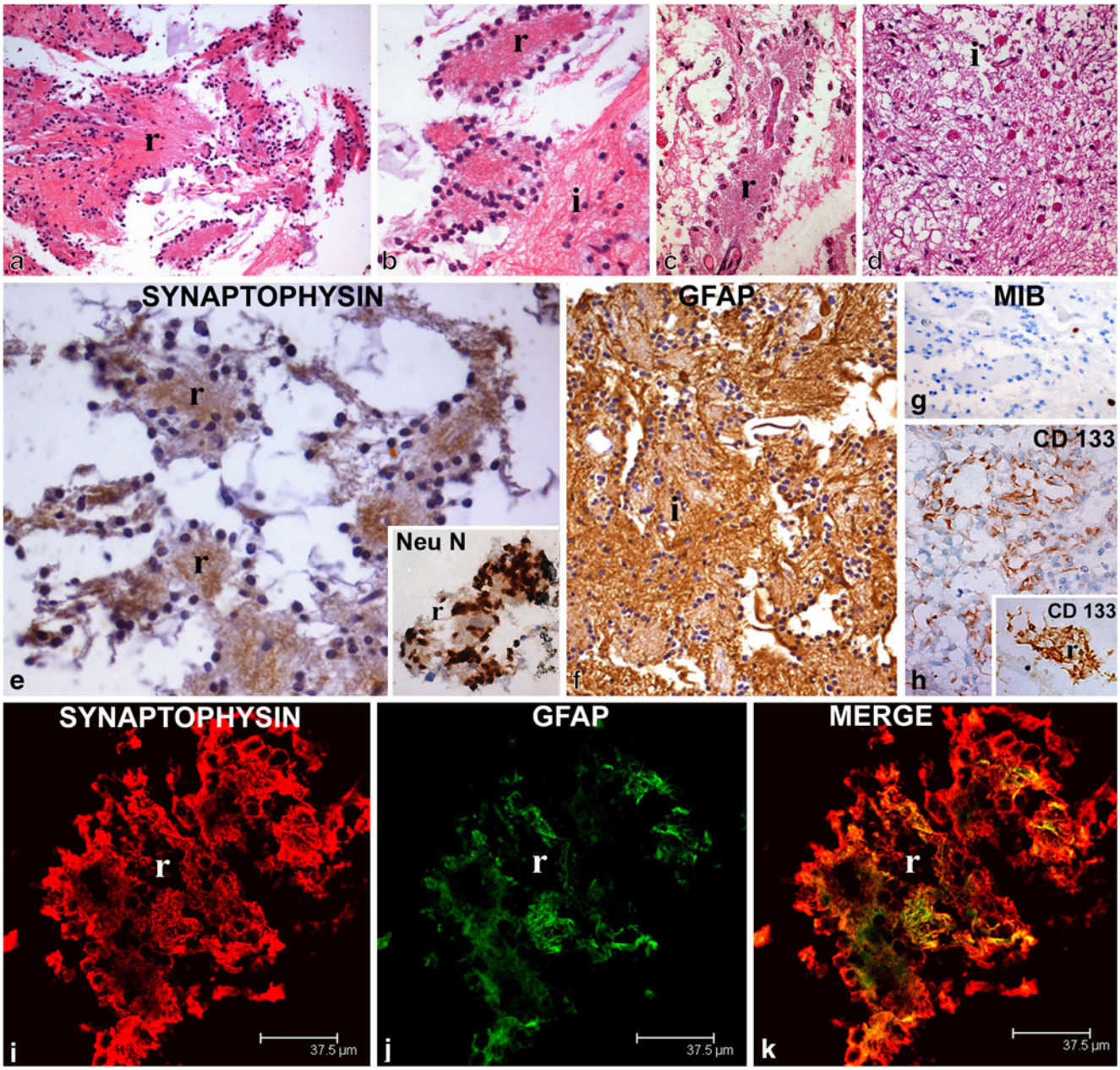

Fig. 2 Case 2: microphotographs reveal a low-grade tumor composed of neurocytic and perivascular rosettes (**a**–**c**) and areas with pilocytic astrocytoma-like morphology, the latter being rich in eosinophillic granular bodies (**d**). Rosettes have central anuclear, fibrillary neuropil bordered by small, monomorphic, tumor cells (neurocytic rosettes, **b**). Some of the rosettes have perivascular arrangement of tumor cells (**c**). The neurocytic and perivascular rosettes have synaptophysin positive core (**e**). Focally the tumor cells composing the neurocytic rosettes are immunopositive for NeuN (**e**, *inset*). The glial component is strongly labeled by GFAP (**f**). MIB-1 labeling index (**g**) is very low. CD133 positivity is seen in the glial component (**h**), with focal labeling of cells in neurocytic rosettes (**h**, *inset*). Double fluorescent labeling with synaptophysin (Cy3, **i**) and GFAP (FITC, **j**) reveal dual expression of neuronal and glial marker in the rosettes (merged image, **k**). (**a** HE, ×100; **b** HE, ×240; **c** HE, ×240; **d** HE, ×200; **e** Syn, ×400; **e** *inset*: NeuN, ×300; **f** GFAP, ×200; **g** MIB-1, ×240; **h** CD133, ×200; **h** *inset*: CD133, ×200; **i**–**k** magnification: scale bar; *r* rosettes, *i* inter-rosette)

component forming neurocytic rosettes and perivascular rosettes expressing Syn [1, 42] and negative for S-100 and GFAP [3]. NeuN immunopositivity in the rosette forming cells is reported as focal [7] to absent [4, 42] in concordance to our findings. The GFAP/S-100 positive glial component, which dominates, typically exhibits features of pilocytic astrocytoma [1, 3, 42]. Similar to one our cases (Case 2), oligodendroglial-like cells were also seen in other studies [3, 27]. Such oligodendroglial-like cells were negative for synaptophysin [3, 27] and GFAP [3], and showed variable cytoplasmic positivity to S-100 [3]. Confocal evidence of co-expression of glial marker GFAP and neuronal markers

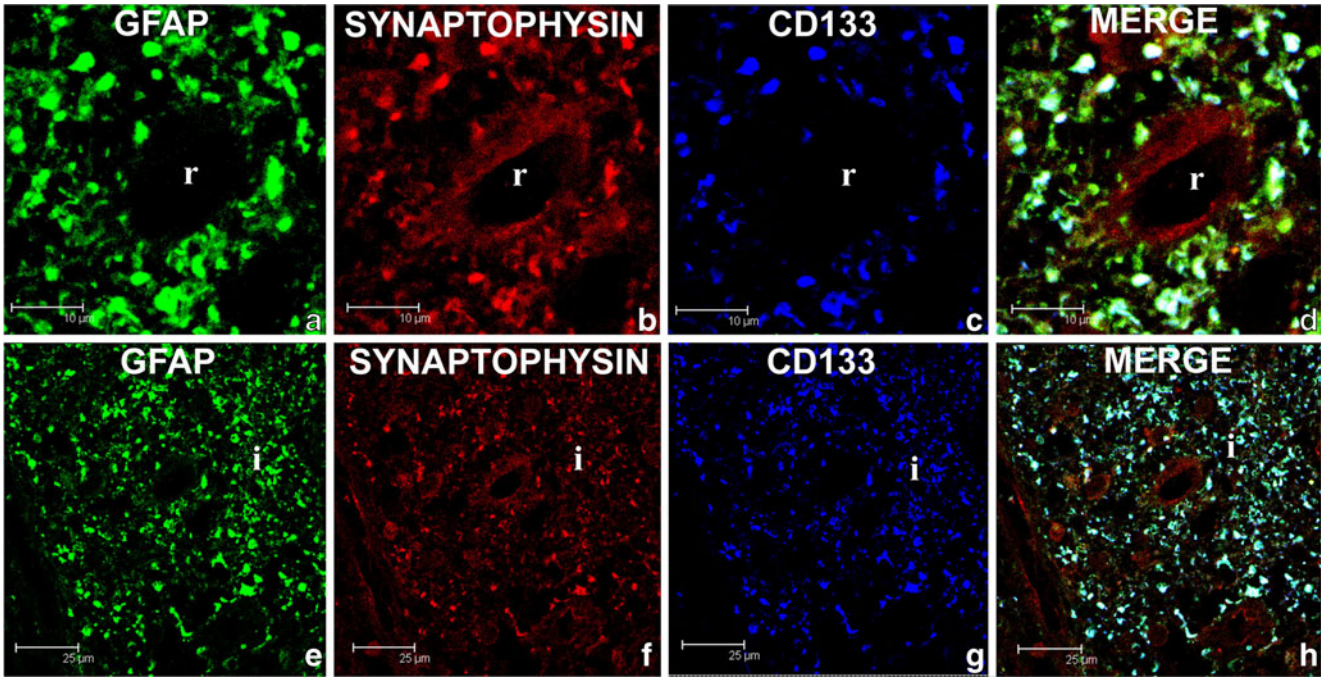

Fig. 3 Case 1: triple labeling with GFAP (FITC; **a**, **e**), synaptophysin (Cy3; **b**, **f**) and stem cell marker CD133 (Cy5; **c**, **g**) with merging (**d**, **h**) were viewed under confocal microscope. The perivascular rosettes (*r*), demonstrated glial component highlighted by FITC (**a**) in addition to neuronal cells (**b**). Abutting the vessel wall, synaptophysin positive neuropil processes are seen. However a few glial cells exhibited co-localization of synaptophysin (**b**) and CD133 (**c**) seen as white fluorescence on merging (**d**) reflecting pluripotent nature of the cells. In the inter-rosette zones (**i**), cells were predominantly glial (**e**) with interspersed cells expressing both synaptophysin (**f**) and CD133 (**g**, **h**). (**a**–**h** magnification: scale bar; *r* rosettes, *i* inter-rosette)

Syn in the tumor cells in addition to stem cell marker CD133, suggest biphenotypic differentiation from a common cell line, as in periventricular stem cells. Similar to CD34 positive hematopoietic stem cells, CD133 is considered a marker of stem cells in diverse normal tissues including endothelial progenitors, myogenic cells, prostatic epithelial stem cells, neural stem cells (NSC), and in tumors such as leukemias, several epithelial cancers, gliomas and medulloblastomas [43]. The NSCs are localized specifically in the subventricular zone of the lateral ventricle wall and the subgranular zone of the hippocampal dentate gyrus. A subset of these cells are characterized as positive for LeX, CD133, GFAP and Nestin, and exhibit self-renewal and multi-lineage neural potentiality and differentiation into neuronal, astrocytic, ependymal and oligodendroglial cell lines [44].

Floating neurons though not a feature of RGNT, have been reported in two cases [27], while Lu et al. [16] documented coexisting RGNT and dysembryoblastic neuroepithelial tumor (DNET). Thrombosis of blood vessels [7] and endothelial proliferation [7, 27] have also been described occasionally. Focal necrosis, as seen in Case 1, has yet not been described in earlier studies. MIB-1 index is low (1.8±0.75 [SD]; range, 0–3.8 %) [29]. Only a single case with high MIB-1 labeling index of 20 %, with high mitotic activity and glomeruloid vascular proliferation is on record [37].

Genetic analysis of RGNT has revealed mutation in PIK3CA gene [36], presence of wild-type genetic sequences in exon 4 of both IDH1 (R132) and IDH2 (R172) genes by polymerase chain reaction [35, 42], intact neurofibromatosis type 1 (NF1) gene [18] and no 1p19q loss by fluorescent in situ hybridization [23, 35]. The molecular analysis for the presence of KIAA1549-BRAF fusions did not reveal the presence of any cDNA amplification products [32].

Komori et al. [3] confirmed the glia and neurocytic nature of the tumor cells ultrastructurally. The glial cells had heterochromatic nuclei with dense glial filaments within the cytoplasm while the neurocytic cells had sparse nuclear chromatin, free ribosomes, scattered profiles of rough endoplasmic reticulum, prominent Golgi apparatus and lamellar mitochondria. The neuropil was comprised of loose cytoplasmic processes containing longitudinally arrayed microtubules, with sparse dense core granules [3].

Histologically, the differential diagnosis includes ganglioglioma, desmoplastic infantile ganglioglioma, DNET and papillary glioneuronal tumors (PGNT), which can be reasonably excluded by clinical and histological features. Another close differential which is radiologically indistinguishable from diffuse gliomas is rosetted glioneuronal tumor/glioneuronal tumor with neuropil-like islands [42]. This tumor involving the cerebral hemispheres is composed of coarsely fibrillary or gemistocytic astroglial and ganglionic

components, abrupt transition with round or ovoid neuropil-like islands, along with nuclear atypia, cortical infiltration, mitosis and MIB-1 labeling of 1–18.1 % [45].

The available follow-up data in 45 cases has revealed no recurrence in 39 cases (86.7 %) (duration of follow-up: 2 to 162 months), following biopsy, debulking, gross total or subtotal resection. In the case reported by Wang et al., with intraventricular dissemination, no progression was seen even after 7 months following biopsy and radiotherapy [23]. In only three cases, following gross total resection, recurrence occurred after 4, 9 [36] and 10 years [21]. Hence, surgery alone, that is gross or subtotal resection, is the treatment of choice of this benign tumor with female preponderance.

It is hypothesized that the tumor originates from the pluripotential cells of the subependymal plate, capable of divergent differentiation towards glial and neuronal lineages [11]. In this study, we demonstrate by confocal microscopy evidence for biphenotypic differentiation of stem cells in the evolution of this phenotypic form of benign glioneuronal tumor. In an earlier study from our Institute, we have observed similar phenomenon in PGNT [46], suggesting a common ontogenic evolution. Similar studies focusing on stem cell participation in other glioneuronal tumors will provide an insight into the evolution and biological behavior of these tumors.

Confocal microscopy with double and triple immunolabeling demonstrated co-localization of stem cell marker predominantly with glial and to lesser extent neurocytic component. This depicts that the terminally differentiated glial and neurocytic tumor cells also express the stem cell marker CD133. The findings also suggest that rosette-forming glial neuronal tumors probably evolve from a bipotent stem cell population in the periventricular ontogenically stem cell rich area.

Acknowledgement We acknowledge the technical assistance (with photographic illustrations) of Ms. V. Rajasakti, Mr. Prasanna Kumar, Mr. Shivaji Rao and Mr. K. Manjunath, Human Brain Tissue Repository, Department of Neuropathology, National Institute of Mental Health and Neurosciences, Bangalore, India.

Conflict of interest The authors declare that they have no conflict of interest. The authors state that the research was not funded/sponsored by any organization.

References

1. Hainfeller JA, Scheithauer BW, Giangaspero F, Rosenblum MK (2007) Rosette-forming glioneuronal tumor of the fourth ventricle. In: Louis DN, Ohgaki H, Weistler OD, Cavenee WK (eds) WHO classification of tumors of the central nervous system. International Agency for Research on Cancer, Lyon, pp 115–116
2. Kuchelmeister K, Demirel T, Schlörer E, Bergman M, Gullotta F (1995) Dysembryoblastic neuroepithelial tumor of the cerebellum. Acta Neuropathol 89:385–390
3. Komori T, Scheithaeur BW, Hirose T (2002) A rosette-forming glioneuronal tumor of the fourth ventricle: infratentorial form of dysembryoblastic neuroepithelial tumor? Am J Surg Pathol 26:582–591
4. Preusser M, Dietrich W, Czech T, Prayer D, Budka H, Hainfellner JA (2003) Rosette-forming glioneuronal tumor of the fourth ventricle. Acta Neuropathol 106:506–508. doi:10.1007/s00401-003-0758-2
5. Albanese A, Mangiola A, Pompucci A, Sabatino G, Gessi M, Lauriola L, Anile C (2005) Rosette-forming glioneuronal tumor of the fourth ventricle: report of a case with clinical and surgical implications. J Neurooncol 71:195–197. doi:10.1007/s11060-004-1375-1
6. Adachi J, Nishikawa R, Hirose T, Matsutani M (2005) Mixed neuronal–glial tumor of the fourth ventricle and successful treatment of postoperative mutism with bromocriptine: case report. Surg Neurol 63:375–379. doi:10.1016/j.surneu.2004.05.039
7. Jacques TS, Eldridge C, Patel A, Saleem NM, Powell M, Kitchen ND, Thom M, Revesz T (2006) Mixed glioneuronal tumor of the fourth ventricle with prominent rosette formation. Neuropathol Appl Neurobiol 32:217–220. doi:10.1111/j.1365-2990.2005.00692.x
8. Johnson M, Pace J, Burroughs JF (2006) Fourth ventricle rosette-forming glioneuronal tumor. Case report. J Neurosurg 105:129–131
9. Vajtai I, Arnold M, Kappeler A, Jeless O, Lukes A, Mariani L, Paulus W (2007) Rosette-forming glioneuronal tumor of the fourth ventricle: report of two cases with a differential diagnostic overview. Pathol Res Pract 203:613–619. doi:10.1016/j.prp. 2007.04.009
10. Tan CC, Gonzales M, Veitch A (2008) Clinical implications of the infratentorial rosette-forming glioneuronal tumor: case report. Neurosurgery 63:E175–E176. doi:10.1227/01.NEU.0000319638.62586.52
11. Pimentel J, Resende M, Vaz A, Reis AM, Campos A, Carvalho H, Honavar M (2008) Rosette-forming glioneuronal tumor: pathology case report. Neurosurgery 62:E1162–E1163. doi:10.1227/01.NEU.0000315283.97499.A3
12. Marhold F, Preusser M, Dietrich W, Prayer D, Czech T (2008) Clinicoradiological features of rosette-forming glioneuronal tumor (RGNT) of the fourth ventricle: report of four cases and literature review. J Neurooncol 90:301–308. doi:10.1007/s11060-008-9661-y
13. Joseph V, Wells A, Kuo YH, Halcrow S, Brophy B, Scott G, Manavis J, Swift J, Blumbergs PC (2009) The 'rosette-forming glioneuronal tumor' of the fourth ventricle. Neuropathology 29:309–314. doi:10.1111/j.1440-1789.2008.00953.x
14. Amemiya S, Shibahara J, Aoki S, Takao H, Ohtomo K (2008) Recently established entities of central nervous system tumors: review of radiological findings. J Comput Assist Tomogr 32:279–285. doi:10.1097/RCT.0b013e31814ce981
15. Anan M, Inoue R, Ishii K, Abe T, Fujiki M, Kobayashi H, Goya T, Nakazato Y (2009) A rosette-forming glioneuronal tumor of the spinal cord: the first case of a rosette-forming glioneuronal tumor originating from the spinal cord. Hum Pathol 40:898–901. doi:10.1016/j.humpath.2008.11.010
16. Lu JQ, Scheithauer BW, Sharma P, Scott JN, Parney IF, Hader W, Burger PC, Clark AW (2009) Multifocal complex glioneuronal tumor in an elderly man: an autopsy study: case report. Neurosurgery 64: E1193–E1195. doi:10.1227/01.NEU.0000345640.40566.48
17. Scheithauer BW, Silva AI, Ketterling RP, Pula JH, Lininger JF, Krinock MJ (2009) Rosette-forming glioneuronal tumor: report of a chiasmal-optic nerve example in neurofibromatosis type 1: special pathology report. Neurosurgery 64:E771–E772. doi:10.1227/01.NEU.0000340979.81362.F3
18. Kinno M, Ishizawa K, Shimada S, Masaoka H, Doi M, Seyama S, Komori T, Hirose T (2009) Cytology is a useful tool for the diagnosis of rosette-forming glioneuronal tumor of the fourth ventricle: a report of two cases. Cytopathology 40:898–901. doi:10.1111/j.1365-2303.2008.00619.x
19. Zhu JJ, Xiong J, Wang Y, Cheng HX, Mao Y, Gao MS, Li C (2009) Rosette-forming glioneuronal tumor of fourth ventricle: report of two cases. Zhonghua Bing Li Xue Za Zhi 38:850–851

20. Ma XM, Li YL, Liu HM, Xu Y, Chen B (2009) Rosette-forming glioneuronal tumor of the fourth ventricle: report of two cases. Zhonghua Bing Li Xue Za Zhi 38:778
21. Ghosal N, Furtado SV, Hegde AS (2009) Rosette forming glioneuronal tumor pineal gland and tectum: an intraoperative diagnosis on smear preparation. Diagn Cytopathol 38:590–593. doi:10.1002/dc.21269
22. Li YM, Li WQ, Pan Y, Lu YC, Long NY, Tao XF, Yu HY (2009) Rosette-forming glioneuronal tumor of the fourth ventricle with previous intratumoral haemorrhage: case report and review of the literature. J Int Med Res 37:958–966
23. Wang Y, Xiong J, Chu SG, Liu Y, Cheng HX, Wang YF, Zhao Y, Mao Y (2009) Rosette-forming glioneuronal tumor: report of an unusual case with intraventricular dissemination. Acta Neuropathol 118:813–819. doi:10.1007/s00401-009-0569-1
24. Arai A, Sasayama T, Tamaki M, Sakagami Y, Enoki E, Ohbayashi C, Kohmura E (2010) Rosette-forming glioneuronal tumor of the fourth ventricle—case report. Neurol Med Chir (Tokyo) 50:224–228. doi:10.2176/nmc.50.224
25. Luan S, Zhuang D, Sun L, Huang FP (2010) Rosette-forming glioneuronal tumor (RGNT) of the fourth ventricle: case report and review of literature. Clin Neurol Neurosurg 112:362–364. doi:10.1016/j.clineuro.2010.01.006
26. Shah MN, Leonard JR, Perry A (2010) Rosette-forming glioneuronal tumors of the posterior fossa. J Neurosurg Pediatr 5:98–103. doi:10.3171/2009.7.PEDS09113
27. Frydenberg E, Laherty R, Rodriguez M, Ow-Yang M, Steel T (2010) A rosette-forming glioneuronal tumor of the pineal gland. J Clin Neurosci 17:1326–1328
28. Rainov NG, Wagner T, Heidecke V (2010) Rosette-forming glioneuronal tumor of the fourth ventricle. Cen Eur Neurosurg 71:219–221
29. Solis OE, Mehta RI, Lai A, Mehta RI, Farchoukh LO, Green RM, Cheng JC, Natarajan S, Vinters HV, Cloughesy T, Yong WH (2010) Rosette-forming glioneuronal tumor: a pineal region case with IDH1 and IDH2 mutation analyses and literature review of 43 cases. J Neurooncol 102:477–484. doi:10.1007/s11060-010-0335-1
30. Podlesek D, Geiger K, Hendry DJ, Schackert G, Krex D (2011) Rosette-forming glioneuronal tumor of the fourth ventricle in an elderly patient. J Neurooncol 103:727–731. doi:10.1007/s11060-010-0408-1
31. Yin B, Liu L, Chen XR, Li K, Geng DY (2011) Rosette-forming glioneuronal tumor of the fourth ventricle. J Neuroradiol. doi:10.1016/j.neurorad.2011.02.004
32. Gessi M, Waha A, Setty P, Waha A, Pietsch T (2011) Analysis of KIAA1549-BRAF fusion status in a case of rosette-forming glioneuronal tumor of the fourth ventricle (RGNT). Neuropathology 31:654–657. doi:10.1111/j.1440-1789.2011.01220.x
33. Fushimi Y, Miyasaki A, Taki H, Aoyama K, Hirato J, Kanagaki M, Togashi K (2011) Rosette-forming glioneuronal tumor of the fourth ventricle with bilateral olivary degeneration. Jpn J Radiol 29:445–448. doi:10.1007/s11604-011-0566-x
34. Karafin M, Jallo GI, Ayars M, Eberhart CG, Rodriguez FJ (2011) Rosette forming glioneuronal tumor in association with Noonan syndrome: pathobiological implications. Clin Neuropathol 30:297–300. doi:10.5414/NP300374
35. Xiong J, Liu Y, Chu SG, Chen H, Chen HX, Mao Y, Wang Y (2011) Rosette-forming glioneuronal tumor of the septum pellucidum with extension to the supratentorial ventricles: Rare case with genetic analysis. Neuropathology. doi:10.1111/j.1440-1789.2011.01261.x
36. Ellezam B, Theeler BJ, Luthra R, Adesina AM, Aldape KD, Gilbert MR (2011) Recurrent PIK3CA mutations in rosette-forming glioneuronal tumor. Acta Neuropathol. doi:10.1007/s00401-011-0886-z
37. Matyja E, Grajkowska W, Nauman P, Ozieblo A, Bonicki W (2011) Rosette-forming glioneuronal tumor of the fourth ventricle with advanced microvascular proliferation — a case report. Neuropathology 31:427–432. doi:10.1111/j.1440-1789.2010.01168.x
38. Sharma P, Swain M, Padua MD, Ranjan A, Lath R (2011) Rosette-forming glioneuronal tumors: A report of two cases. Neurol India 59:276–280. doi:10.4103/0028-3886.79148
39. Hsu C, Kwan G, Lau Q, Bhuta S (2012) Rosette-forming glioneuronal tumour: Imaging features, histopathological correlation and a comprehensive review of literature. Br J Neurosurg. doi:10.3109/02688697.2012.655808
40. Gao C, Xie R, Cao XY, Huang FP (2009) Rosette-forming glioneuronal tumor of the fourth ventricle. A rare neoplasm of the central nervous system. Neurosciences (Riyadh) 14:292–293
41. Alturkustani M, Ang LC (2012) Rosette-forming glioneuronal tumour of the 4th ventricle in a NF1 patient. Can J Neurol Sci 39:95–96
42. Rosenblum MK (2007) The 2007 WHO classification of nervous system tumors: newly recognized members of the mixed glioneuronal group. Brain Pathol 17:308–313. doi:10.1111/j.1750-3639.2007.00079.x
43. Brescia P, Richichi C, Pelicci G (2012) Current strategies for identification of glioma stem cells: adequate or unsatisfactory? J Oncol. doi:10.1155/2012/376894
44. Ma DK, Bonaguidi MA, Ming GL, Song H (2009) Adult neural stem cells in the mammalian central nervous system. Cell Res 19:672–682. doi:10.1038/cr.2009.56
45. Edgar MA, Rosenblum MK (2007) Mixed glioneuronal tumors: recently described entities. Arch Pathol Lab Med 131:228–233. doi:10.1043/1543-2165(2007) 131
46. Govindan A, Mahadevan A, Bhat DI, Arivazhagan A, Chakraborti S, Suja MS, Phalguni AA, Sampath S, Chandramouli BA, Shankar SK (2009) Papillary glioneuronal tumor – evidence of stem cell origin with biphenotypic differentiation. J Neurooncol 95:71–80. doi:10.1007/s11060-009-9893-5

Virchows Arch (2012) 461:589–599
DOI 10.1007/s00428-012-1301-4

ORIGINAL ARTICLE

Survivin, MMP-2, MT1-MMP, and TIMP-2: their impact on survival, implantation, and proliferation of endometriotic tissues

Ambrogio P. Londero · Angelo Calcagno · Tiziana Grassi · Stefania Marzinotto · Maria Orsaria · Carlo Alberto Beltrami · Diego Marchesoni · Laura Mariuzzi

Received: 19 April 2012 / Revised: 9 August 2012 / Accepted: 9 August 2012 / Published online: 6 September 2012
© Springer-Verlag 2012

Abstract In order to study survivin, matrix metalloproteinases (MMP-2), membranous type 1 matrix metalloproteinase (MT1-MMP), and tissue inhibitor metalloproteinase-2 (TIMP-2) expression immunohistochemically in endometriotic tissues and normal endometrium, our retrospective study considered 194 patients affected by endometriosis and 71 patients with normal endometrium. Tissue microarrays were created from paraffin-embedded blocks; immunohistochemistry was used to assess protein expression. In endometriotic tissues, survivin was expressed at a higher level than in normal endometrium; its glandular expression level was higher in non-ovarian than in ovarian endometriotic tissues and lower in stromal components. Endometrial tissues from women without endometriosis and endometriotic tissues had different matrix metalloproteinase expression profiles. MMP-2 and MT1-MMP correlated with TIMP-2 in endometriotic tissues. Furthermore, in endometriotic tissues, expression of survivin, aurora B kinase, and Ki-67 showed a significant positive correlation, which indicates a role in cellular proliferation that could be closely linked to its anti-apoptotic activity in endometriosis development. Our results imply a role for matrix metalloproteinases in endometriosis invasiveness; correlation of their expression with that of TIMP-2 underscores its possible key regulatory role.

Keywords Endometriosis · Survivin · Matrix metalloproteinase-2 · Membranous type 1 matrix metalloproteinase · Tissue inhibitor metalloproteinase-2 · Tissue microarrays

Abbreviations

ABK	Aurora B kinase
APC	Adenomatous polyposis coli
ASRM	American Society of Reproductive Medicine
ET	Endometriotic tissue
IAP	Inhibitor of apoptosis protein
IQR	Interquartile range
MMP-2	Matrix metalloproteinase-2
MMP	Matrix metalloproteinase
MT1-MMP	Membranous type 1 matrix metalloproteinase
PR	Progesterone receptor
TIMP-2	Tissue inhibitor metalloproteinase-2
TMA	Tissue microarray

Introduction

Endometriosis is characterized by the presence of endometrial stroma and glands outside the uterus cavity. The mechanism underlying its initiation and progression has still not been fully clarified; however, it is thought to be principally caused by retrograde menstruation followed by ectopic establishment of endometrium-like cells, which acquire the ability to survive, implant, and proliferate [1].

Ambrogio P. Londero and Angelo Calcagno equally contributed to this work.

Electronic supplementary material The online version of this article (doi:10.1007/s00428-012-1301-4) contains supplementary material, which is available to authorized users.

A. P. Londero · A. Calcagno (✉) · T. Grassi · D. Marchesoni
Clinic of Obstetrics and Gynecology, University of Udine,
Piazzale SM della Misericordia,
15-33100 Udine, Italy
e-mail: angelo_calcagno@hotmail.com

S. Marzinotto · M. Orsaria · C. A. Beltrami · L. Mariuzzi
Institute of Pathology, University of Udine,
33100 Udine, Italy

Increased expression of anti-apoptotic proteins may contribute to ectopic endometrial tissue localization [2–4]; spontaneous apoptosis in ectopic endometrial tissue decreases in women with endometriosis [5, 6]. Survivin—a member of the inhibitor of apoptosis (IAP) protein family—can regulate both cell proliferation and apoptosis [7].

Survivin also influences cell proliferation because of its close interaction with aurora B kinase. In fact, M phase-specific phosphorylation of histone H3 at threonine 3 recruits the chromosomal passenger complex to chromatin to activate aurora B kinase; this interaction is mediated by survivin [8]. Physiological interaction between aurora B kinase and survivin is essential for accurate chromosome segregation and completion of cytokinesis [9]. Upregulation of survivin/aurora B kinase cascade has been described in colon cancer development [10], but no studies on this pathway have been done with endometriotic tissue.

Matrix metalloproteinases are highly homologous proteolytic zinc enzymes responsible for the degradation of extracellular matrix components (collagen, proteoglycans, fibronectin, and laminin) [11]. Matrix metalloproteinase-2 (MMP-2) degrades type IV collagen and may affect endometriosis adhesion and invasion [11]; it is activated in two steps: a latent MMP-2 precursor is cleaved by membranous type 1 matrix metalloproteinase (MT1-MMP) to produce an MMP-2 intermediate, which then autocatalytically converts itself into mature MMP-2 [12]. Unlike soluble matrix metalloproteinases (MMPs), MT1-MMP is localized on cell surface; its increased expression activates cell-surface MMP-2, a process that is involved in cell invasion [11]. In the extracellular matrix, natural inhibitors—tissue inhibitors of metalloproteinases (TIMPs)—regulate MMP activities. Tissue inhibitor metalloproteinase-2 (TIMP-2) has a dual role in controlling MMP-2 activation. The TIMP-2–MT1-MMP complex is needed to activate inhibitor-free pro-MMP-2 [13]. TIMP-2 also inhibits MMP-2 by forming stable complexes with its active site [14]. Thus, the balance between free MT1-MMP and the MT1-MMP–TIMP-2 complex apparently decide the degree of MMP-2 activation [15].

MMP regulation in human endometrium is complex and influenced by steroids, growth factors and cytokines [16]. Progesterone exposure has been shown in in vitro studies to suppress endometrial MMP protein and mRNA expression [17]. Bruner-Tran et al. have shown that progesterone inhibition of endometrial MMPs during the secretory phase appears to be deficient in women with endometriosis [18].

Chung et al. has demonstrated mRNA expression of MMP-2, MT1-MMP, and TIMP-2 in endometriotic tissues, in eutopic endometrium from healthy patients, and in those affected by endometriosis and found that eutopic endometrium from women with endometriosis was more invasive and prone to peritoneal implantation due to strong mRNA expression of MMP-2 and MT1-MMP and low mRNA expression of TIMP-2 [11]. Other authors have also associated MMP-2 with endometriosis invasion [19, 20].

The aim of this study was to examine survivin, MMP-2, MT1-MMP, and TIMP-2 protein expression immunohistochemically in ovarian and non-ovarian endometriotic tissues and to compare them to normal endometrium. We also correlated our new results, in terms of survivin, MMP-2, MT1-MMP, and TIMP-2 semiquantitative immunohistochemical expression, with data already published by our group on this tissue microarray (TMA) model (aurora B kinase, Ki-67, and PRs) [21] (Supplemental data).

Materials and methods

A TMA model was used, as previously described, to analyze immunohistochemical staining of survivin, MMP-2, MT1-MMP, TIMP-2, and to compare them to immunohistochemistry patterns of aurora B kinase, Ki-67, and PRs [21]. The only difference was the addition of 43 new controls. In all, we identified 220 women in the registry of the University Hospital of Udine Pathology Department who received histopathological diagnoses of endometriosis between January 2000 and December 2009; of these, 194 met the established criteria [21] and were included in the study. We included all Caucasian women of fertile age at the time of intervention. Exclusion criteria were menopause, climacteric, and use of hormone therapy during the year before surgery. For these 194 women, 438 paraffin blocks of ET were available; one 1.5-mm diameter tissue core punch per block was performed. The final TMA included at least two samples per patient.

As control, eutopic endometrial tissue was obtained from formalin-fixed paraffin-embedded endometrial sections from all women who underwent hysterectomy for leiomyoma from 2006 to 2010; 71 samples met the inclusion criteria previously described. We included all Caucasian women of fertile age at the time of intervention with regular menses and without known endometrial pathology, histological diagnosis of adenomyosis, or use of any hormone medication during the year before surgery [21]. According to their menses dates and histological confirmation using Noyes criteria [22], 29 of these patients were in follicular phase (proliferative endometrium) and 42, in luteal phase (secretory endometrium).

The types of clinical data collected have been previously described [21]. Staging was determined according to the American Society of Reproductive Medicine (ASRM) classification of endometriosis [23]. This study was conducted according to the Declaration of Helsinki and with internal review board approval.

The TMA preparation process and the immunohistochemical staining of PR, aurora B kinase, and Ki-67 have been previously described [21]. Here, we report a brief

summary of immunohistochemical staining procedure for survivin, MMP-2, MT1-MMP, and TIMP-2. Blocks were cut into 4-μm sections and collected on glass slides. Deparaffinized rehydrated sections were incubated with H_2O_2 for 10 min to block endogenous peroxidase activity. Antigen retrieval was performed in citrate buffer at pH 6 and 98 °C. The sections were rinsed in PBS and then incubated overnight in a wet chamber at 4 °C with the following primary antibodies: mouse anti-MMP-2 (Ab-4 clone A-Gel VC2, NeoMarkers, Biocompare, South San Francisco, CA, USA; diluted 1:50), polyclonal anti-MT1-MMP (Millipore, ab6004, Billerica, MA, USA; diluted 1:100), monoclonal mouse anti-human-TIMP-2 (Millipore, MAB3310; diluted 1:200), and anti-survivin (Abcam, ab469, Cambridge, UK; diluted 1:1,500) [4, 24, 25]. A Dako REAL™ EnVision™ Dako Rabbit/Mouse (Dako, K5007, Glostrup, Denmark) was used as second antibody. Horseradish peroxidase activity was detected using Dako REAL™ DAB + Chromogen (Dako, K5007) as substrate for 3 min in accordance with the manufacturer's instructions. Sections were counterstained with hematoxylin with cover slip. The positive control used for survivin was lung tumor; for MMP2, normal colon; for MT1-MMP, human prostate; and for TIMP-2, colon carcinoma. Sections incubated with non-immune rabbit serum instead of primary antibody were used as negative controls.

A semiquantitative analysis of the immunohistochemical staining was performed independently by two pathologists. Staining was semiquantitatively evaluated as H-score (product of percentage of positive-stained cells and intensity score—evaluated as strong (3), moderate (2), and weak (1)—giving a possible range of 0–300) as previously described [21]. Glands were considered separately from stroma for all markers. The number of positive cells was obtained by counting at least 500 stromal cells or 100 epithelial cells [21].

Data were analyzed using R (version 2.14.0). A $p<0.05$ was considered significant. For all proteins analyzed, staining was investigated in terms of percentage of positive cells and H-score. Normality of variables was tested with the Kolmogorov–Smirnov test. Non-parametric data were presented with median values and IQR, whereas parametric data were described with mean values and standard deviations. The Kruskal–Wallis test and the one-way ANOVA for continuous variables were used for variance analysis where appropriate. To compare multiple categorical variables, the Chi-square test was used. For bivariate analysis, the following statistical tests were applied: Wilcoxon test, Student's *t* test, Spearman's rho, and Kendall's tau for continuous variables; Chi-square and Fisher exact test for categorical variables. Because of statistically significant age difference between patients and controls, it was necessary to evaluate the results by univariate and multivariate logistic regression with age correction.

Results

Description of the population

Women affected by endometriosis were significantly younger than controls and had lower parity (Table 1). The most common initial indication for surgery in endometriosis group was the presence of an ovarian mass (82 %), followed by chronic pelvic pain (12 %), and other causes (6 %). Disease stage, using ASRM classification, was III or IV in 81 % of cases. Last menses date was used to identify and compare patients with endometriosis who underwent surgery during follicular or luteal phases. We found no significant differences between protein expression profiles of

Table 1 Characteristics of the population: eutopic endometrium and endometriotic tissues

	Ovarian ET	Non-ovarian ET	Controls (endometrium)	*p*
Age	39.36 (±9.38)	35.56 (±7.86)	42.93 (±5.23)	<0.05
Gravidity	1 (0–2)	1 (0–2)	2 (1–3)	<0.05
<39	0 (0–1)	0 (0–0)	2 (1–2)	<0.05
≥39	1 (1–2)	2 (1–3)	2 (1–3)	<0.05
Parity	1 (0–1)	1 (0–2)	2 (1–3)	<0.05
<39	0 (0–0)	0 (0–0)	1 (1–2)	<0.05
≥39	1 (1–2)	2 (1–2)	2 (1–3)	<0.05
Phases				
Follicular phase	57 % (201/353)	55 % (47/85)	40.85 % (29/71)	<0.05
Luteal phase	43 % (152/353)	45 % (38/85)	59.15 % (42/71)	<0.05
Endometriosis location				
Ovarian endometriosis	81 % (353/438)			
Pelvic endometriosis		11 % (48/438)		
Non-pelvic endometriosis		5 % (24/438)		
Bowel endometriosis		3 % (13/438)		

endometriotic tissue removed during follicular phase and those removed during luteal phase.

Cellular and subcellular staining location

Glands and stroma were positive for survivin immunostaining in endometriotic tissues and normal endometrium. In stromal components, staining was localized to nuclei only in both endometriotic tissues and normal endometrium. Glandular staining was restricted to nuclei in proliferative endometrium but was both cytoplasmic and nuclear in endometriotic tissues and in secretory endometrium (Fig. 1). As survivin expression rates in nuclear and cytoplasmic glandular components of secretory endometrium and endometriotic tissues were not significantly different (p=n.s.), we only reported the nuclear data. In both glands and stroma, MMP-2, MT1-MMP, and TIMP-2 stained the cytoplasm only (Fig. 2).

Survivin expression in endometriotic tissues

In non-ovarian endometriotic tissues, the survivin H-score in the glandular component was higher than that in ovarian endometriotic tissues, proliferative, or secretory endometrium ($p<0.05$; Tables 2, 3 and 4). In ovarian endometriotic tissues, the survivin H-score in glandular components was higher than that in proliferative and secretory endometrium but only statistically significant when compared with proliferative endometrium in multivariate logistic regression with age correction ($p<0.05$; Table 3). In ovarian endometriotic tissues, stromal component survivin was more highly expressed in ovarian endometriotic tissues than in non-ovarian endometriotic tissues ($p<0.05$), but the difference was not significant after multivariate analysis ($p=0.074$; Table 3). In endometriotic tissues, results did not show significant differences in survivin H-scores between follicular and luteal phases (Table 2).

MT1-MMP, MMP-2, and TIMP-2 expression

Table 2 shows differences between proliferative and secretory endometrium (see p value ([b])). MT1-MMP in glandular and stromal components ($p<0.05$) and TIMP-2 in glandular component of secretory endometrium were more highly expressed than that in proliferative endometrium ($p=0.056$); stromal component MMP-2 in secretory endometrium was less expressed than that in proliferative endometrium ($p<0.05$). MT1-MMP, MMP-2, and TIMP-2 were more highly expressed in endometriotic tissues than in eutopic endometrium ($p<0.05$) (Table 2).

MT1-MMP was significantly more expressed in glandular component of ovarian and non-ovarian endometriotic tissues than in proliferative or secretory endometrium, even after correcting for age in multivariate logistic regression analysis ($p<0.05$) (Tables 4 and 5). MT1-MMP was also significantly more expressed in stromal components of ovarian and non-ovarian endometriotic tissues than in proliferative endometrium ($p<0.05$) (Tables 4 and 5).

MMP-2 was expressed at a higher level in the glandular component of ovarian endometriotic tissues than in other locations (non-ovarian endometriotic tissues, proliferative, and secretory endometrium; $p<0.05$) and at a higher level in stromal ovarian endometriotic tissues than in non-ovarian endometriotic tissues or secretory endometrium ($p<0.05$; Tables 4 and 5). MMP-2 was also expressed at a significantly higher level in the glandular component of non-ovarian endometriotic tissues than in proliferative and secretory endometrium ($p<0.05$), but the comparisons lost statistical significance after correction for patients' ages ($p=0.077$ and $p=0.053$, respectively; Fig. 3).

TIMP-2 was expressed more in glandular and stromal components of ovarian and non-ovarian endometriotic tissues than in proliferative or secretory endometrium ($p<0.05$; Tables 4 and 5). Moreover, TIMP-2 was expressed in glandular components of non-ovarian endometriotic tissues at higher levels than in ovarian endometriotic tissues (Table 4).

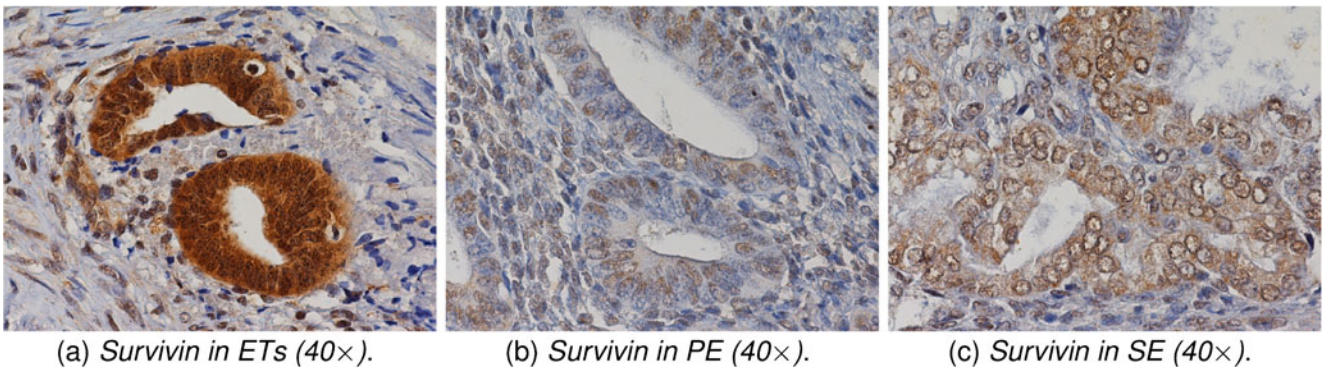

Fig. 1 Examples of survivin expression. Survivin immunostaining in endometriotic tissues (**a**) is more pronounced than in normal endometrium (**b**–**c**). Moreover, in ET and in secretory endometrium (**a**–**c**), survivin expression in the glandular component is both cytoplasmic and nuclear but is restricted to the nuclei in the proliferative endometrium (**b**)

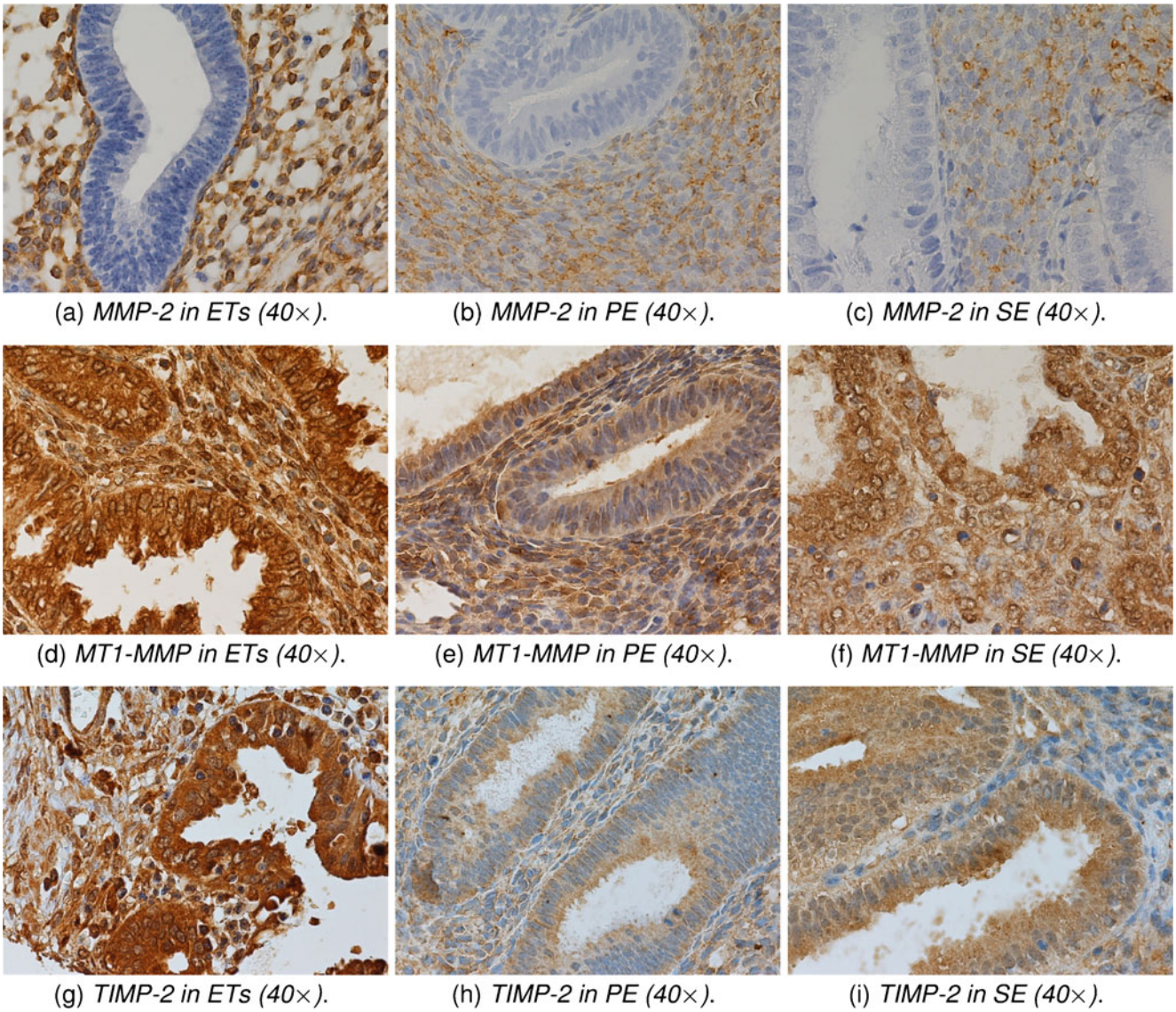

Fig. 2 Examples of MMP-2, MT1-MMP, and TIMP expression. MMP-2, MT1-MMP, and TIMP immunostaining in endometriotic tissues are exclusively cytoplasmic, in both glands and stroma

Table 2 H-score values of MMP1, MMP2, TIMP 1, and survivin in eutopic endometrium and endometriotic tissues

	Ovarian ET	Non-ovarian ET	Proliferative endometrium	Secretory endometrium	p^a	p^b
MT1-MMP gland	210 (180–270)	210 (180–270)	20 (10–42.5)	180 (140–270)	<0.05	<0.05
MT1-MMP stroma	210 (140–270)	210 (145–270)	100 (50–140)	180 (140–270)	<0.05	<0.05
MMP-2 gland	270 (140–270)	30 (0–120)	0 (0–0)	0 (0–0)	<0.05	NA
MMP-2 stroma	270 (240–270)	270 (180–270)	270 (240–270)	140 (120–270)	<0.05	<0.05
TIMP-2 gland	180 (180–270)	180 (180–270)	180 (80–180)	180 (90–270)	<0.05	0.056
TIMP-2 stroma	180 (180–270)	180 (180–270)	140 (40–180)	120 (57–180)	<0.05	0.826
Survivin gland	180 (140–270)	270 (180–270)	120 (50–140)	160 (57.5–240)	<0.05	0.104
Survivin stroma	100 (20–165)	40 (10–100)	100 (20–140)	40 (10–100)	<0.05	0.126

[a] Kruskal–Wallis test

[b] Wilcoxon test between proliferative and secretory endometrium

Table 3 Expression of survivin in eutopic endometrium and endometriotic tissues

	OR (CI 95 %)	*p*	OR (CI 95 %)[a]	*p*
Survivin gland				
Ovarian ET	Referral		Referral	
Non-ovarian ET	6.38 (2.16–18.84)	<0.05	7.39 (2.46–22.17)	<0.05
Proliferative endometrium	0.11 (0.04–0.33)	<0.05	0.11 (0.03–0.32)	<0.05
Secretory endometrium	0.56 (0.28–1.14)	0.111	0.5 (0.25–1.04)	0.063
Survivin stroma				
Ovarian ET	Referral		Referral	
Non-ovarian ET	0.5 (0.26–0.98)	<0.05	0.54 (0.27–1.06)	0.074
Proliferative endometrium	0.94 (0.42–2.08)	0.870	0.91 (0.41–2.02)	0.809
Secretory endometrium	0.54 (0.27–1.08)	0.081	0.5 (0.25–1.01)	0.052

Univariate and multivariate logistic regression ([a] with age correction) comparing ovarian versus other localization

Correlation between MT1-MMP, MMP-2, TIMP-2, and survivin

The first analytic groups considered all endometriotic tissues together since all correlations among MT1-MMP, MMP-2, TIMP-2, and survivin were similar in ovarian and non-ovarian endometriotic tissues (Table 6). Endometriotic tissues showed no significant correlation between MT1-MMP and survivin H-scores (Table 6). However, MT1-MMP was significantly correlated with TIMP-2 in glandular

Table 4 Different expressions of MMPs and TIMP-2 between non-ovarian endometriotic tissue (referral) and other locations

	OR (CI 95 %)	*p*	OR (CI 95 %)[a]	*p*
Survivin gland				
Ovarian ET	0.16 (0.05–0.46)	<0.05	0.14 (0.05–0.41)	<0.05
Non-ovarian ET	Referral		Referral	
Proliferative endometrium	0.02 (0–0.08)	<0.05	0.01 (0–0.06)	<0.05
Secretory endometrium	0.09 (0.03–0.3)	<0.05	0.07 (0.02–0.24)	<0.05
Survivin stroma				
Ovarian ET	1.99 (1.02–3.89)	<0.05	1.85 (0.94–3.65)	0.074
Non-ovarian ET	Referral		Referral	
Proliferative endometrium	1.86 (0.72–4.82)	0.199	1.68 (0.64–4.4)	0.291
Secretory endometrium	1.08 (0.45–2.55)	0.867	0.92 (0.38–2.24)	0.857
MT1-MMP gland				
Ovarian ET	0.69 (0.33–1.45)	0.324	0.7 (0.33–1.5)	0.362
Non-ovarian ET	Referral		Referral	
Proliferative endometrium	0.01 (0–0.06)	<0.05	0.01 (0–0.06)	<0.05
Secretory endometrium	0.29 (0.11–0.73)	<0.05	0.3 (0.12–0.79)	<0.05
MT1-MMP stroma				
Ovarian ET	1.07 (0.61–1.87)	0.822	1.12 (0.63–1.97)	0.707
Non-ovarian ET	Referral		Referral	
Proliferative endometrium	0.03 (0–0.23)	<0.05	0.03 (0–0.25)	<0.05
Secretory endometrium	0.65 (0.3–1.45)	0.297	0.72 (0.32–1.64)	0.437
TIMP-2 gland				
Ovarian ET	0.37 (0.12–1.08)	0.070	0.28 (0.09–0.85)	<0.05
Non-ovarian ET	Referral		Referral	
Proliferative endometrium	0.10 (0.03–0.36)	<0.05	0.06 (0.02–0.24)	<0.05
Secretory endometrium	0.18 (0.05–0.60)	<0.05	0.09 (0.03–0.34)	<0.05
TIMP-2 stroma				
Ovarian ET	0.99 (0.44–2.25)	0.986	0.84 (0.36–1.93)	0.678
Non-ovarian ET	Referral		Referral	
Proliferative endometrium	0.13 (0.05–0.38)	<0.05	0.10 (0.03–0.29)	<0.05
Secretory endometrium	0.13 (0.05–0.36)	<0.05	0.09 (0.03–0.25)	<0.05

In mono- and multivariate logistic regression, we considered as dependent variables H-score values over the 50th percentile of the distribution

[a]Age correction

Table 5 Different expressions of MMPs and TIMP-2 between ovarian endometriotic tissues (referral) and other locations

	OR (CI95%)	*p*	OR (CI95%)[a]	*p*
MT1-MMP gland				
Ovarian ET	Referral		Referral	
Non-ovarian ET	1.46 (0.69–3.07)	0.324	1.42 (0.67–3.02)	0.362
Proliferative endometrium	0.01 (0–0.08)	<0.05	0.01 (0–0.08)	<0.05
Secretory endometrium	0.42 (0.21–0.85)	<0.05	0.43 (0.21–0.89)	<0.05
MT1-MMP stroma				
Ovarian ET	Referral		Referral	
Non-ovarian ET	0.94 (0.53–1.65)	0.822	0.9 (0.51–1.59)	0.707
Proliferative endometrium	0.03 (0–0.21)	<0.05	0.03 (0–0.21)	<0.05
Secretory endometrium	0.61 (0.31–1.21)	0.157	0.65 (0.33–1.29)	0.214
MMP-2 gland				
Ovarian ET	Referral		Referral	
Non-ovarian ET	0.11 (0.05–0.21)	<0.05	0.09 (0.04–0.18)	<0.05
Proliferative endometrium	0.01 (0–0.1)	<0.05	0.01 (0–0.1)	<0.05
Secretory endometrium	0.01 (0–0.07)	<0.05	0.01 (0–0.08)	<0.05
MMP-2 stroma				
Ovarian ET	Referral		Referral	
Non-ovarian ET	0.5 (0.27–0.95)	<0.05	0.48 (0.25–0.91)	<0.05
Proliferative endometrium	2.81 (0.35–22.39)	0.330	2.85 (0.36–22.77)	0.322
Secretory endometrium	0.25 (0.09–0.71)	<0.05	0.26 (0.09–0.76)	<0.05
TIMP-2 gland				
Ovarian ET	Referral		Referral	
Non-ovarian ET	2.74 (0.92–8.14)	0.070	3.52 (1.16–10.67)	<0.05
Proliferative endometrium	0.28 (0.12–0.63)	<0.05	0.23 (0.10–0.53)	<0.05
Secretory endometrium	0.48 (0.23–1.02)	0.057	0.33 (0.15–0.75)	<0.05
TIMP-2 stroma				
Ovarian ET	Referral		Referral	
Non-ovarian ET	1.01 (0.44–2.28)	0.986	1.19 (0.52–2.75)	0.678
Proliferative endometrium	0.13 (0.06–0.31)	<0.05	0.12 (0.05–0.28)	<0.05
Secretory endometrium	0.14 (0.06–0.29)	<0.05	0.10 (0.05–0.23)	<0.05

In mono- and multivariate logistic regression, we considered as dependent variables H-score values over the 50th percentile of the distribution

[a]Age correction

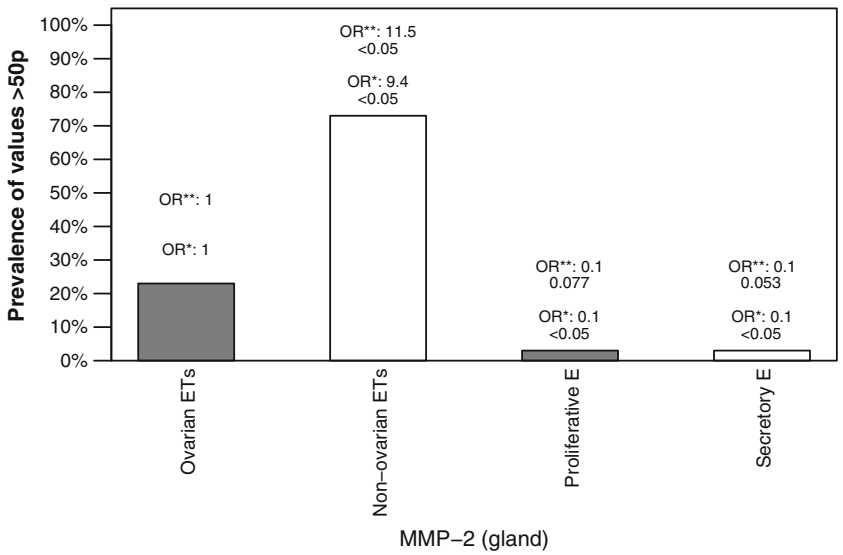

Fig. 3 Expression of MMP-2 in the glandular component of ovarian endometriotic tissues and other locations. In the graph, the *bar plots* show the prevalence of values higher than the median value ($p>50$) of the H-score distribution. The odds ratios (*OR*) and *p* values at the *top of the bars* refer to univariate (*single asterisk*) and multivariate (*double asterisks*) logistic regression analysis (corrected for patients' ages) where the dependent variable is the prevalence of values higher than the median value of the related distribution

Table 6 Correlation of MT1-MMP, MMP-2, or TIMP-2 with survivin or TIMP-2 (Spearman's rho and related *p* values)

	Survivin	*p*	TIMP-2	*p*
Endometriotic tissues				
MT1-MMP (gland)	0.111	0.160	0.150	<0.05
MT1-MMP (stroma)	0.005	0.944	0.211	<0.05
MMP-2 (gland)	−0.310	<0.05	−0.204	<0.05
MMP-2 (stroma)	0.160	<0.05	−0.044	0.530
TIMP-2 (gland)	0.333	<0.05	N/A	N/A
TIMP-2 (stroma)	0.096	0.194	N/A	N/A
Proliferative endometrium				
MT1-MMP (gland)	0.283	0.145	0.358	0.061
MT1-MMP (stroma)	0.373	0.051	0.053	0.073
MMP-2 (gland)	N/A	N/A	N/A	N/A
MMP-2 (stroma)	−0.527	0.064	−0.568	<0.05
TIMP-2 (gland)	0.643	<0.05	N/A	N/A
TIMP-2 (stroma)	0.700	<0.05	N/A	N/A
Secretory endometrium				
MT1-MMP (gland)	0.519	<0.05	0.489	<0.05
MT1-MMP (stroma)	0.483	<0.05	0.440	<0.05
MMP-2 (gland)	N/A	N/A	N/A	N/A
MMP-2 (stroma)	0.164	0.558	0.349	0.203
TIMP-2 (gland)	0.484	<0.05	N/A	N/A
TIMP-2 (stroma)	0.586	<0.05	N/A	N/A

and stromal components of endometriotic tissues and secretory endometrium. H-scores of MMP-2 and survivin in glandular components of endometriotic tissues showed significant negative correlation but not in glandular components of secretory and proliferative endometrium. MMP-2 and survivin H-scores showed significant positive correlation in the stromal component of endometriotic tissues, but not in stromal components of secretory and proliferative endometrium. However, we found positive correlations between TIMP-2 and survivin H-scores in glandular components of endometriotic tissues, secretory, and proliferative endometrium; whereas their scores in the stromal component were only significantly correlated in proliferative and secretory endometrium and not significantly in endometriotic tissues (Table 6). MMP2 and TIMP-2 had a significant negative correlation in proliferative endometrial stroma.

In the second analytic group, we correlated the new studied proteins—Ki-67, aurora B kinase, and PR—to better understand their role in endometriosis, using relevant data from a previous published study [21]. Results are reported in the supplemental data: supplemental Table 1, Supplemental Fig. 1, Supplemental Fig. 2, and Supplemental Fig. 3. The three major results were the following: a significant positive correlation in endometriotic tissues among expression of survivin, aurora B kinase, and Ki-67; a significant positive correlation between Ki-67 and MMP-2 H-score in glandular components of non-ovarian endometriotic tissues; and significant negative correlations of PR H-scores with MT1-MMP and MMP-2 (Supplemental Table 1, Supplemental Fig. 1, Supplemental Fig. 2, and Supplemental Fig. 3).

Discussion

In endometriotic tissues, survivin was expressed at a higher level than in normal eutopic endometrium; its glandular expression level was higher in non-ovarian than in ovarian endometriotic tissues, but lower in the stromal component. In endometriotic tissues, expression of survivin, aurora B kinase and Ki-67 was positively correlated. Eutopic endometrium from women without endometriosis and endometriotic tissues had different matrix metalloproteinase expression profiles, and MMPs in endometriotic tissues were expressed at higher levels than in normal eutopic endometrium. Moreover, MMP expression correlated with PR, survivin, Ki-67, and TIMP in endometriotic tissues.

Survivin expression in endometriotic tissues

We confirmed the different subcellular localization of survivin shown in previous studies (Fig. 1) [26]. Survivin has different functions in cytokinesis, proliferation, and inhibition of apoptosis mediated by interaction with caspases [27]. During mitosis, survivin localizes to different components of the mitotic apparatus to regulate the proliferation mechanism. The exclusive nuclear location in proliferative endometrium may be explained by the prominent role of survivin in highly proliferative tissues. Caspase family proteins act in the cytoplasm to degrade contents of the cell upon activation of the death pathway; they are inhibited by interaction with the IAP family proteins [27]. As a consequence, the nuclear and cytoplasmic location of survivin in the glandular component of the secretory endometrium may be explained by the need to maintain a balance between low proliferation and apoptosis. Similarly, if the nuclear location of survivin in the glandular component of endometriotic tissues could be explained by its role in cell proliferation, its cytoplasmic location could be related to anti-apoptotic activity, leading to endometriotic tissue survival.

The staining pattern of survivin in eutopic endometrium reportedly differs between during proliferative and secretory phases [26, 28]. Moreover, survivin expression in endometriotic cells seems to be cycle-independent [26]. Our data confirm this loss of cyclic variation in survivin expression in endometriotic cells, but we did not find a significant difference in survivin expression between proliferative and secretory endometrium.

We confirmed previous reports of high expression levels of survivin in endometriotic tissue [4, 28] (Tables 2, 3, and

4). Ueda et al. investigated the biological role of survivin in endometriosis and found that survivin was highly expressed, especially in non-ovarian locations, suggesting that these endometriotic cells escape apoptosis by expressing high levels of survivin [4]. In comparing protein expression between ovarian and non-ovarian specimens, we found that survivin H-scores in glandular components were higher in non-ovarian than in ovarian endometriotic tissues but lower in the stroma (Table 3).

Cyclic expression of survivin in normal endometrial cells suggests that *survivin* gene expression is influenced by steroid hormones and downregulated by increased progesterone in luteal phase [26]; in fact, we found a negative (if not significant) correlation between survivin and PRs. Mesenchymal cells are essential in directing the growth, differentiation, and function of epithelium [29]. Zhang and colleagues found that the presence of stromal paracrine factors produced by normal endometrial stromal cells mediated the effect of progesterone on endometriotic glandular cells in vitro [26]. They also found endometriotic stromal cells to lose the ability to regulate apoptotic signaling in endometriotic glandular cells that grow in ectopic foci [26], while the endometriotic glandular component does not lose responsiveness to paracrine factors produced by endometrial stromal cells in vitro [26].

The higher survivin H-score in ovarian stroma than in non-ovarian endometriotic tissue locations implies a different role for the stroma in determining cell survival in these two forms of endometriosis (Table 2). Because the glandular component of endometriosis seems not to lose normal responsiveness to paracrine factors, less survivin in the glandular component of ovarian endometriotic tissues than in non-ovarian ones could be explained by paracrine regulation determined by the ovarian milieu (Tables 2 and 3). Certainly, we need further in vitro studies to test and expand this hypothesis.

MT1-MMP, TIMP-2, and MMP-2 and their expression

Tissue remodeling is important because establishment of endometriotic lesions requires endometrial cells to adhere and invade through the peritoneal mesothelium. The MMP family was investigated because its components break down and repair extracellular matrix and are involved in the menstrual cycle regulation [30]. In the literature, there is no agreement on differences in the expression of MMP-2 among endometriotic tissues and eutopic endometrium from women affected or unaffected by endometriosis [11, 19, 31–33]. However, endometriotic tissues seem to express more MMP-2 than do eutopic endometrium [31, 33]. Although the subcellular locations of MMP-2, MT1-MMP, and TIMP-2 are still not clear in endometriosis, we found cytoplasmic location for these proteins (Fig. 2); we also found that MMP-2 expression is increased in endometriotic tissues compared with that in eutopic endometrium of women unaffected by endometriosis. Our data also show that the glandular component of non-ovarian endometriotic tissues presented less MMP-2 than ovarian endometriotic tissues, while stromal component H-scores did not register significant differences when peritoneal and bowel endometriosis are considered separately (Tables 4 and 5).

Furthermore, similarly to Chung et al., we found levels of MT1–MMP (responsible for activation of MMP-2) to be more elevated in endometriotic tissues than in eutopic endometrium of women without endometriosis (Table 4 and 5) [11].

In accordance with the findings of Sotnikova et al., we found higher TIMP-2H-scores in endometriotic tissues than in eutopic endometrium of women without endometriosis (Tables 2, 4, and 5) [31]. TIMP-2 inhibits MMP activity and selectively interacts with MT1-MMP to facilitate the cell-surface activation of pro-MMP-2 [15], which together imply that TIMP-2 participates in regulating endometriotic cell invasion. Higher expression of MT1-MMP, TIMP-2, and MMP-2 in endometriotic tissues than in normal endometrium could be related to extracellular remodeling associated with endometriotic invasion. In normal endometrium, we also found (as expected) varying positive correlations between H-scores of TIMP-2 and MT1-MMP ($p<0.05$) or MMP-2 (p=n.s.). We also found a significant negative correlation between TIMP-2 and MMP-2 in glandular components of endometriotic tissues and proliferative endometrial stroma, which suggests a key role for TIMP-2 in regulating the MMP pathway among endometrium and endometriotic tissues. This possibly relates this negative correlation to a function for TIMP-2 in endometriotic glandular cells that reduces MMP remodeling activity and inactivates MMP-2. The loss of significant negative correlation in endometriotic stroma could be related to a deregulated MMP pathway.

Ueda et al. found survivin and MMPs to be simultaneously upregulated and hypothesized that these two pathways contribute to survival and invasion of endometriosis [4]. Accordingly, we found significant positive correlation between MMP-2 and survivin in stromal components of endometriotic tissues but found them to be negatively correlated in glandular components of endometriotic tissues. This might indicate a still efficient regulatory mechanism in the glandular component of endometriotic tissues, which is associated to a deregulated stroma. We also found significant positive correlations between survivin and MT1-MMP or TIMP-2 in the stromal component of proliferative and secretory endometrium that were lost in stromal components of endometriotic tissues.

These results, together with previous reports, are best explained, in our opinion, by endometriosis development requiring highly modified stroma/glandular interaction [26].

Correlation with Ki-67, aurora B kinase, and PR

Correlating our results in terms of expression of MT1-MMP, TIMP-2, MMP2, and survivin with previously published data [21] relies on our conviction that cellular proliferation, hormonal environment, anti-apoptotic factors, and stability of extracellular matrix are all closely involved in endometriosis development.

We found different significant negative correlations between PR and MT1-MMP or MMP-2 among endometriotic tissues, secretory, and proliferative endometrium (Supplemental Table 1, Supplemental Fig. 2). We also found significant positive correlation of PR with TIMP-2 glandular H-scores in proliferative endometrium. The significant correlations found between PR and TIMP-2 were in accordance with the previous literature, where progestins have been found to downregulate MMP expression [34, 35]. The only exception was a significant positive correlation of PR with MMP-2 stromal H-score in endometriotic tissues. This and previous findings also agree with the previous literature, which found that ectopic endometriotic stromal cells failed to mediate progesterone response in endometriotic epithelial cells and with the theory of progesterone resistance as a component of endometriosis development [26].

In general, no correlation was found between MMP proteins studied and Ki-67. Nevertheless, in glandular components of non-ovarian endometriotic tissues, we found a significant positive correlation between Ki-67 and MMP-2, which implied that non-ovarian locations might have more aggressive forms of endometriosis (Supplemental Fig. 3).

We hypothesized a direct role for survivin in cell proliferation control in endometriosis after finding a significant correlation between survivin and aurora B kinase (Supplemental Fig. 1). In fact, aurora B kinase is involved in mitosis; its interaction with survivin is reportedly essential in cell-cycle control [9]. Survivin stimulates aurora B kinase activity and helps correctly target aurora B kinase to its substrates during the cell cycle, thus providing a mechanism with which survivin exerts its function in human cells. We have not found in the literature any data correlating survivin and aurora B kinase in endometriotic tissue.

Although the aurora B kinase H-score was higher in proliferative endometrium than in endometriotic tissues [21] and the survivin H-score was higher in endometriotic tissues than in proliferative endometrium (Table 2), we detected, for the first time, a significant positive correlation between the expression of these two proteins in the endometriosis glandular component (Supplemental Fig. 1A). While lacking statistical evidence, aurora B kinase and survivin expression seem to correlate positively in both stromal and glandular components of normal endometrium, although no correlation was found in the endometriotic stromal component. The latter could be related to a stromal impairment that could deregulate survivin function in ectopic endometrial stroma (Supplemental Fig. 1A).

Conclusions

Despite the retrospective nature of our study, we feel that the large number of cases reinforces our data analysis. To our knowledge, this is the first time this protein expression pattern has been investigated. We studied the expression of survivin, MT1-MMP, MMP-2, and TIMP-2 immunohistochemically, according to their localization in ovarian and non-ovarian endometriosis, in TMA-containing specimens from 194 women. The correlation of these new data with data from our previous study leads us to suppose roles for survivin in cell proliferation among endometriotic tissues, and for MMP-2, MT1-MMP, and TIMP-2 in endometriosis invasiveness. Our hypothesis, conclusions, and aims are based on data from a TMA study; future in vivo studies could validate our data.

Acknowledgments We are grateful to Dr. Enrica Stella for her help in this study, Matteo De Luca for the technical assistance in realizing TMA, and to Dr. Serena Bertozzi for her help in preparation of this manuscript. Dr. Giorgio Zaccagna, Dr. Guido Borgna and Dr. Marco Pittino are thanked for their helpful collaboration. This study was financially supported by the University of Udine.

Conflict of interest The authors declare that they have no potential conflicts of interest relevant to this article.

References

1. Leyendecker G, Kunz G, Noe M, Herbertz M, Mall G (1998) Endometriosis: a dysfunction and disease of the archimetra. Hum Reprod Update 4:752–762
2. Fujino K, Ueda M, Takehara M et al (2006) Transcriptional expression of survivin and its splice variants in endometriosis. Mol Hum Reprod 12:383–388. doi:10.1093/molehr/gal042
3. Fauvet R, Poncelet C, Hugol D, Lavaur A, Feldmann G, Daraï E (2003) Expression of apoptosis-related proteins in endometriomas and benign and malignant ovarian tumours. Virchows Arch 443:38–43. doi:10.1007/s00428-003-0813-3
4. Ueda M, Yamashita Y, Takehara M et al (2002) Survivin gene expression in endometriosis. J Clin Endocrinol Metab 87:3452–3459
5. Imai A, Takagi A, Tamaya T (2000) Gonadotropin-releasing hormone analog repairs reduced endometrial cell apoptosis in endometriosis in vitro. Am J Obstet Gynecol 182:1142–1146
6. Gebel HM, Braun DP, Tambur A, Frame D, Rana N, Dmowski WP (1998) Spontaneous apoptosis of endometrial tissue is impaired in women with endometriosis. Fertil Steril 69:1042–1047
7. Ai Z, Yin L, Zhou X, Zhu Y, Zhu D, Yu Y, Feng Y (2006) Inhibition of survivin reduces cell proliferation and induces apoptosis in human endometrial cancer. Cancer 107:746–756. doi:10.1002/cncr.22044
8. Kelly AE, Ghenoiu C, Xue JZ, Zierhut C, Kimura H, Funabiki H (2010) Survivin reads phosphorylated histone H3 threonine 3 to

activate the mitotic kinase Aurora B. Science 330:235–239. doi:10.1126/science.1189505
9. Musacchio A (2010) Molecular biology. Surfing chromosomes (and Survivin). Science 330:183–184, doi:10.1126/science.1197261.
10. Chu Y, Yao PY, Wang W et al (2010) Aurora B kinase activation requires survivin priming phosphorylation by PLK1. J Mol Cell Biol. doi:10.1093/jmcb/mjq037
11. Chung HW, Lee JY, Moon HS, Hur SE, Park MH, Wen Y, Polan ML (2002) Matrix metalloproteinase-2, membranous type 1 matrix metalloproteinase, and tissue inhibitor of metalloproteinase-2 expression in ectopic and eutopic endometrium. Fertil Steril 78:787–795
12. Will H, Atkinson SJ, Butler GS, Smith B, Murphy G (1996) The soluble catalytic domain of membrane type 1 matrix metalloproteinase cleaves the propeptide of progelatinase A and initiates autoproteolytic activation. Regulation by TIMP-2 and TIMP-3. J Biol Chem 271:17119–17123
13. Zucker S, Drews M, Conner C et al (1998) Tissue inhibitor of metalloproteinase-2 (TIMP-2) binds to the catalytic domain of the cell surface receptor, membrane type 1-matrix metalloproteinase 1 (MT1-MMP). J Biol Chem 273:1216–1222
14. Strongin AY, Collier I, Bannikov G, Marmer BL, Grant GA, Goldberg GI (1995) Mechanism of cell surface activation of 72-kDa type IV collagenase. Isolation of the activated form of the membrane metalloprotease. J Biol Chem 270:5331–5338
15. Murphy G (2011) Tissue inhibitors of metalloproteinases. Genome Biol 12:233. doi:10.1186/gb-2011-12-11-233
16. Kokorine I, Marbaix E, Henriet P, Okada Y, Donnez J, Eeckhout Y, Courtoy PJ (1996) Focal cellular origin and regulation of interstitial collagenase (matrix metalloproteinase-1) are related to menstrual breakdown in the human endometrium. J Cell Sci 109(Pt 8):2151–2160
17. Osteen KG, Keller NR, Feltus FA, Melner MH (1999) Paracrine regulation of matrix metalloproteinase expression in the normal human endometrium. Gynecol Obstet Invest 48(Suppl 1):2–13
18. Bruner-Tran KL, Eisenberg E, Yeaman GR, Anderson TA, McBean J, Osteen KG (2002) Steroid and cytokine regulation of matrix metalloproteinase expression in endometriosis and the establishment of experimental endometriosis in nude mice. J Clin Endocrinol Metab 87:4782–4791
19. Uzan C, Cortez A, Dufournet C, Fauvet R, Siffroi JP, Daraï E (2004) Eutopic endometrium and peritoneal, ovarian and bowel endometriotic tissues express a different profile of matrix metalloproteinases-2, -3 and -11, and of tissue inhibitor metalloproteinases-1 and -2. Virchows Arch 445:603–609. doi:10.1007/s00428-004-1117-y
20. Ria R, Loverro G, Vacca A, Ribatti D, Cormio G, Roccaro AM, Selvaggi L (2002) Angiogenesis extent and expression of matrix metalloproteinase-2 and -9 agree with progression of ovarian endometriomas. Eur J Clin Invest 32:199–206
21. Calcagno A, Grassi T, Mariuzzi L et al (2011) Expression patterns of Aurora A and B kinases, Ki-67 and the estrogen and progesterone receptors determined using an endometriosis tissue microarray model. Hum Reprod 26:2731–2741. doi:10.1093/humrep/der264
22. Noyes R, Hertig A, Rock J (1950) Dating the endometrial biopsy. Fertil Steril 1:3–25
23. ASRM (1997) Revised American Society for Reproductive Medicine classification of endometriosis: 1996. Fertil Steril 67:817–821
24. Dilly M, Hambruch N, Shenavai S et al (2011) Expression of matrix metalloproteinase (MMP)-2, MMP-14 and tissue inhibitor of matrix metalloproteinase (TIMP)-2 during bovine placentation and at term with or without placental retention. Theriogenology 75:1104–1114. doi:10.1016/j.theriogenology.2010.11.019
25. Mazzoni A, Pashley DH, Tay FR et al (2009) Immunohistochemical identification of MMP-2 and MMP-9 in human dentin: correlative FEI-SEM/TEM analysis. J Biomed Mater Res A 88:697–703. doi:10.1002/jbm.a.31920
26. Zhang H, Li M, Zheng X, Sun Y, Wen Z, Zhao X (2009) Endometriotic stromal cells lose the ability to regulate cell-survival signaling in endometrial epithelial cells in vitro. Mol Hum Reprod 15:653–663. doi:10.1093/molehr/gap069
27. Tamm I, Wang Y, Sausville E, Scudiero DA, Vigna N, Oltersdorf T, Reed JC (1998) IAP-family protein survivin inhibits caspase activity and apoptosis induced by Fas (CD95), Bax, caspases, and anticancer drugs. Cancer Res 58:5315–5320
28. Konno R, Yamakawa H, Utsunomiya H, Ito K, Sato S, Yajima A (2000) Expression of survivin and Bcl-2 in the normal human endometrium. Mol Hum Reprod 6:529–534
29. Donjacour AA, Cunha GR (1991) Stromal regulation of epithelial function. Cancer Treat Res 53:335–364
30. Gaide Chevronnay HP, Selvais C, Emonard H, Galant C, Marbaix E, Henriet P (2012) Regulation of matrix metalloproteinases activity studied in human endometrium as a paradigm of cyclic tissue breakdown and regeneration. Biochim Biophys Acta 1824:146–156. doi:10.1016/j.bbapap. 2011.09.003
31. Sotnikova NY, Antsiferova YS, Posiseeva LV, Shishkov DN, Posiseev DV, Filippova ES (2010) Mechanisms regulating invasiveness and growth of endometriosis lesions in rat experimental model and in humans. Fertil Steril 93:2701–2705. doi:10.1016/j.fertnstert.2009.11.024
32. Di Carlo C, Bonifacio M, Tommaselli GA, Bifulco G, Guerra G, Nappi C (2009) Metalloproteinases, vascular endothelial growth factor, and angiopoietin 1 and 2 in eutopic and ectopic endometrium. Fertil Steril 91:2315–2323. doi:10.1016/j.fertnstert.2008.03.079
33. Wenzl RJ, Heinzl H (1998) Localization of matrix metalloproteinase-2 in uterine endometrium and ectopic implants. Gynecol Obstet Invest 45:253–257
34. Mönckedieck V, Sannecke C, Husen B et al (2009) Progestins inhibit expression of MMPs and of angiogenic factors in human ectopic endometrial lesions in a mouse model. Mol Hum Reprod 15:633–643. doi:10.1093/molehr/gap063
35. Bruner-Tran KL, Zhang Z, Eisenberg E, Winneker RC, Osteen KG (2006) Down-regulation of endometrial matrix metalloproteinase-3 and -7 expression in vitro and therapeutic regression of experimental endometriosis in vivo by a novel nonsteroidal progesterone receptor agonist, tanaproget. J Clin Endocrinol Metab 91:1554–1560. doi:10.1210/jc.2005-2024

Virchows Arch (2012) 461:601–605
DOI 10.1007/s00428-012-1314-z

CASE REPORT

Neonatal hyperimmune T-cell reaction mimicking T-cell non-Hodgkin's lymphoma following BCG and hepatitis B co-vaccination

Snjezana Dotlic · Semir Vranic · Gordana Jakovljevic · Ivana Ilic · Mirjana M. Kardum-Paro · Stefan D. Dojcinov

Received: 30 June 2012 / Revised: 23 August 2012 / Accepted: 3 September 2012 / Published online: 12 September 2012
© Springer-Verlag 2012

Abstract We describe a case of a 2-week-old male infant who presented with a rapidly enlarging inguinal mass after having received both the bacille Calmette–Guérin (BCG) and hepatitis B vaccines at birth. The clinical picture raised suspicion of a neoplasm, and an excision biopsy was performed. It showed complete effacement of the lymph node architecture by a diffuse proliferation of monomorphic, mitotically active, and medium-sized T-cell blasts with strong expression of CD99. Coalescent necrotizing granulomas were also seen. The lymph node culture was negative for BCG. Upon expert review and additional molecular diagnostics, the initial pathological diagnosis of lymphoblastic T-cell lymphoma was changed to ectopic BCG lymphadenitis and hyperimmune post-vaccinal reaction. The atypical T-cell proliferation was most likely a result of the adjuvant effects of the co-administered vaccines. Post-vaccinal reactions usually involve the injection site or result in localized lymph node enlargements in the areas draining the inoculation site. This case highlights the importance of the clinical context for accurate interpretation of the pathological findings. In the setting of post-vaccinal lymphadenopathy, a biopsy is rarely needed but, when performed, should be interpreted with great caution.

Keywords BCG lymphadenitis · Blastic T-cell proliferation · Post-vaccinal reaction · Immunohistochemistry

S. Dotlic (✉) · I. Ilic
Department of Pathology and Cytology,
University Hospital Centre Zagreb,
10000 Zagreb, Croatia
e-mail: sdotlic30@gmail.com

S. Vranic
Department of Pathology, Clinical Center of the
University of Sarajevo,
Sarajevo, Bosnia and Herzegovina

G. Jakovljevic
Department of Hematology and Oncology, Pediatric Clinic,
Children's Hospital Zagreb,
Zagreb, Croatia

M. M. Kardum-Paro
Institute of Clinical Chemistry and Laboratory Medicine,
University Hospital Merkur,
Zagreb, Croatia

S. D. Dojcinov
All Wales Lymphoma Panel, University Hospital of Wales,
Cardiff, UK

Introduction

Bacille Calmette–Guérin (BCG)-associated lymphadenitis usually involves the ipsilateral, axillary, supraclavicular, or cervical lymph nodes following BCG vaccination [1]. This uncommon post-vaccinal complication is associated with risk factors such as young age, high vaccine concentration, vigor of administration, and immune-suppressed settings [1]. The enlarged lymph nodes usually spontaneously regress, but in a minority of cases, they may suppurate and drain through the overlying skin. Presentation is mostly within 6 months from vaccination. The involved lymph nodes are often up to 2 cm in diameter but could also be massively enlarged [1, 2]. The diagnosis is clinical and management conservative, so biopsies are seldom taken. The histological appearances are of suppurative granulomatous inflammation with a rich infiltrate of small lymphocytic T cells.

Hepatitis B vaccine at birth is being added to routine immunization protocols in many countries. Most reactions

associated with this vaccine are confined to the injection site, resulting in cutaneous lymphoid hyperplasia [3]. Lymphadenopathy is exceedingly rare and is due to polyclonal growth of both B and T cells [3].

We present a case of an infant who developed inguinal lymphadenopathy following BCG and hepatitis B immunization at birth. The unusual clinical and challenging pathological features of this post-vaccinal reaction (PVR) had initially resulted in a diagnosis of lymphoma.

Clinical history

A 2-week-old immunocompetent male baby without a history of HIV infection presented with an isolated right inguinal mass rapidly growing to a diameter of 3 cm over a period of 1 week. At birth, he had received consecutively the BCG and hepatitis B (Engerix B®) vaccines as part of the routine immunization protocol in Croatia. At presentation, the only detected abnormality was a mildly elevated erythrocyte sedimentation rate, but otherwise the baby was well. An ultrasound scan revealed a conglomerate of lymph nodes in the right inguinal region. As lymphadenopathy was not in the lymphatic drainage area of the vaccination sites, there was high clinical suspicion of malignancy.

Materials and methods and results

Histopathology

A fine needle aspiration showed atypical lymphoid cells suspicious of lymphoma. The bone marrow aspirate showed no abnormality on flow cytometrical examination. A 2-cm lymph node was excised which macroscopically appeared homogeneous and showed small foci of necrosis. Histologically, the architecture of the lymph node was completely effaced (Fig. 1a). There was a diffuse infiltrate of medium-sized, regular, and mitotically active lymphoid blasts (Fig. 1c). Coalescent palisading granulomas with copious necrosis were also noted, but no acid-fast bacilli could be identified (Fig. 1b).

Immunohistochemistry and molecular diagnostics

The immunostains highlighted effacement of the lymph node architecture. The diffuse proliferation of blasts was of T-cell phenotype with virtually no residual B-cell areas (the lack of CD20-positive cells, Fig. 1d). There was a considerable restriction to the expression of CD8 over CD4 (Fig. 1g–h). The majority of the cells had an activated cytotoxic TIA1/granzyme B/perforin-positive phenotype (Fig. 1i) in a background of abundant evenly distributed histiocytes (CD68 positive, Fig. 1j). No aberrant loss of T-cell markers including CD2, CD3, CD5, CD7, and CD43 was seen (Fig. 1e–f). There were scattered CD30-positive blasts (Fig. 1k). However, most cells showed strong expression of CD99 (Fig. 1l) and a high proliferation index of 90 % as assessed by Ki-67 immunostaining (Fig. 1). These atypical features prompted the local pathologist to make a diagnosis of T-cell lymphoma, probably of lymphoblastic type. Upon expert review, additional immunohistochemistry showed no expression of TdT, CD34, CD10, or CD117. Epstein–Barr virus-encoded RNA was not detected by in situ hybridization. The polymerase chain reaction using the Biomed-2 T-cell receptor beta and gamma primers showed reproducible polyclonal smears.

The lymph node culture was negative for BCG but grew *Gemella morbillorum*, a streptococcus-like anaerobic bacterium rarely associated with disease in humans. EBV and CMV serology were negative. These overall findings were interpreted as BCG lymphadenitis with reactive hyperimmune PVR. The baby received antibiotic therapy. The ultrasound and whole-body MRI scans performed after 2 months showed no evidence of lymphadenopathy or organomegaly. Eight months after the event, the child remains well, with no signs of disease.

Discussion

This case of unusual hyperimmune PVR and ectopic BCG lymphadenitis highlights several problems which have caused substantial concerns for both clinicians and pathologists. As a consequence of the atypical clinical and particularly pathological findings, a malignant diagnosis was seriously entertained.

While the literature data on the clinical and pathological appearances of PVRs are scanty, the information available is useful in preventing diagnostic errors [4, 5]. Studies of peripheral lymphadenopathy in children highlight the clinical features which point to a high likelihood of underlying malignancy. These include lymphadenopathy of more than 2 cm, more than 4 weeks in duration, supraclavicular involvement, and abnormal laboratory and radiological findings [2, 6]. For pathologists, the difficulty in interpreting the histology of PVRs partly stems from the fact that they are quite rare. Most are managed empirically by clinicians and pathologists who exceptionally rarely see biopsies from these patients [1]. In most cases, PVRs involve the injection site [1]. Lymphadenopathy is relatively uncommon. A variety of histologically brisk and sometimes blastic hyperimmune reactions are usually associated with small pox, measles, and tetanus vaccines [7, 8].

BCG lymphadenitis in very young patients is also uncommon with an incidence estimated at 4–31 cases per 10,000

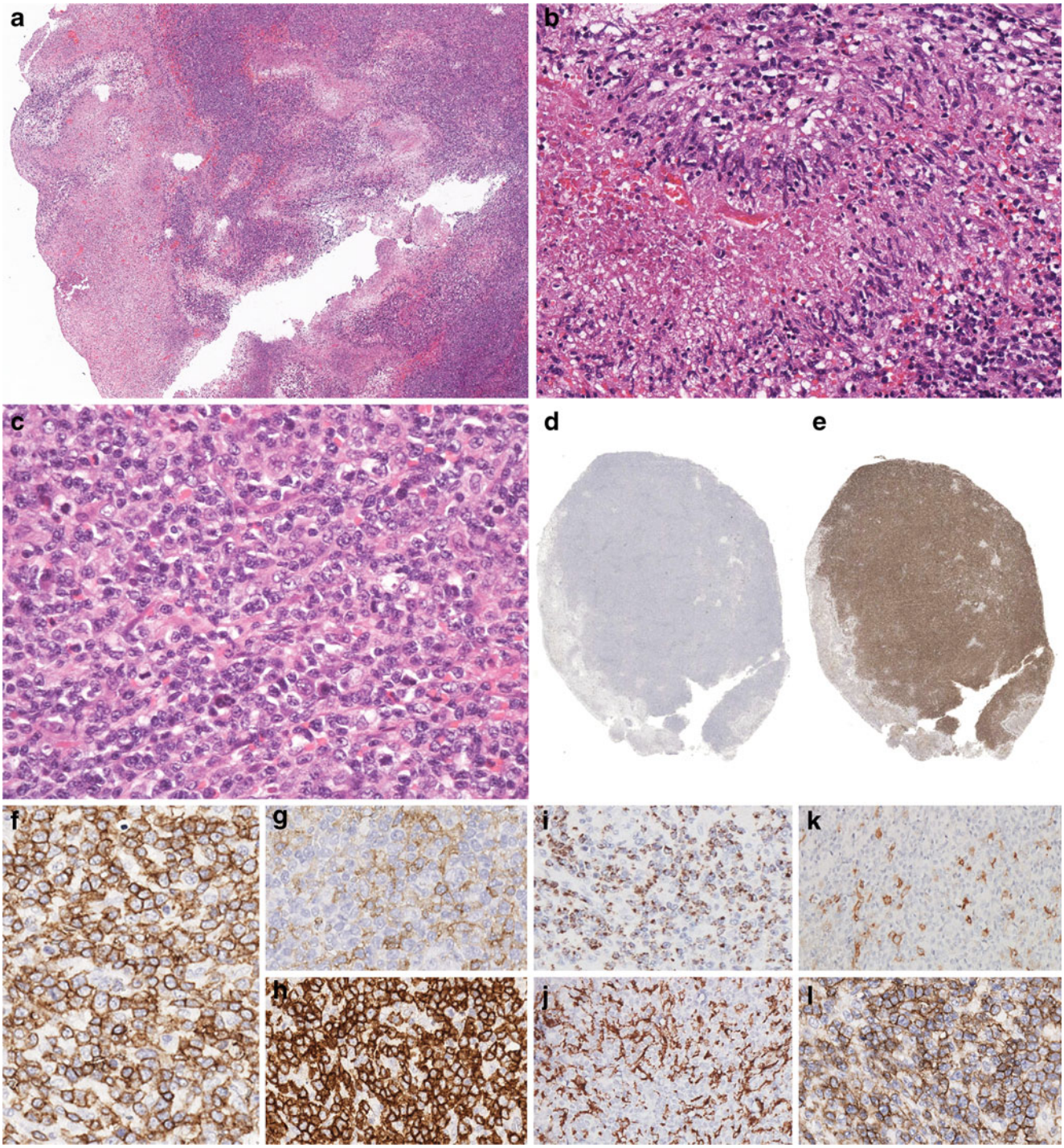

Fig. 1 Histological features. **a** Lymph node with effaced architecture and a large necrotic area. **b** Serpiginous granulomas with peripheral palisading of histiocytes. **c** Diffuse infiltrate of medium-sized and large lymphoid blasts with mitotic activity. **d** CD20 shows no evidence of any B-cell infiltrate. **e** CD3 highlights a diffuse proliferation of T cells. **f** CD3 outlines a range of cell sizes including medium-sized and large blasts. **g** CD4 highlights few positive cells; the cells showing weak expression of CD4 are histiocytes. **h** The T-cell infiltrate is restricted to expression of CD8. **i** Most cells are positive for TIA1. **j** Large numbers of CD68-positive histiocytes are present. **k** There are scattered CD30-positive blasts. **l** Most of the T cells are positive for CD99. H & E, original magnification: **a**, **d**, **e**×10, **b**×40, **c**×400, **f**–**l**×200

vaccinated subjects under the age of 1 year. There is significant geographical variation pointing to varied susceptibility of different populations [9]. It usually takes 2–6 weeks after vaccination to develop and, in 95 % of cases, presents itself as ipsilateral, mostly axillary lymphadenopathy. Notably, in the remaining 5 % of cases, lymphadenopathy develops in

areas outside the lymphatic drainage of the inoculation site and may involve the inguinal nodes, as in our case [10, 11]. The risks for BCG lymphadenitis are associated with the dose, strain of vaccine, vigor of application, age, underlying immunosuppression, and HIV infection [1]. The clinical aspect is important, and typically there are no significant systemic symptoms. BCG is isolated in two thirds of cases, and saprophytic and anaerobic flora of different types is often detected [12]. Likewise, acid-fast bacilli are not universally identified by special stains, and diagnosis should not rely on their histological identification [4]. *G. morbillorum*, as seen in our case, rarely causes clinical symptoms. The typical histological appearances of BCG lymphadenitis may not differ from cases of tuberculous lymphadenitis. In addition, abundant suppuration associated with granulomatous inflammation is also seen [4]. There is a background T-cell infiltrate composed of small lymphocytes. In our case, the diffuse proliferation of atypical lymphoid blasts with effacement of the lymph node architecture, as well as the clinical presentation with massive lymphadenopathy in an unusual site, prompted the pathologist to consider a diagnosis of lymphoma. Our patient was immunocompetent, with no history of HIV infection.

In our case, the baby also received hepatitis B vaccine concurrently with the BCG. Most PVRs associated with the hepatitis B vaccine are confined to the injection site. They are rare and result in cutaneous lymphoid hyperplasia of B-cell phenotype or a polyclonal proliferation of B-cell and T-cell subsets [3, 13]. It is thus unlikely that the extent of blastic T-cell reaction would have been associated specifically to the hepatitis B vaccine. It is possible that the co-administration and the adjuvant effect of both vaccines together played the key role in eliciting a blastic T-cell proliferation. The additional complicating feature in this case was the expression of CD99. Within the T-cell lineage, this is frequently associated with lymphoblastic lymphoma/leukemia [14]. However, it may not be widely appreciated that CD99 is expressed on all T cells, but the level of expression depends on the level of maturation and also cell subset. Most studies of CD99 expression in T cells have assessed it by means of flow cytometry. As it is much less sensitive, low levels of expression may not be identifiable by immunohistochemistry on tissue samples. Not only normal CD4+ memory T cells abundantly express CD99, but also CD8+ cells, in particular those with a cytotoxic phenotype [15, 16]. This can potentially result in erroneous interpretation of the nature of the lymphoid proliferation as neoplastic [17]. As T-lymphoblastic leukemia was considered in this case in the differential diagnosis, while spontaneous remission has been reported in the literature, this is exceptionally rare in adults and even more so in children [18, 19]. In addition, the activated cytotoxic phenotype of this T-cell lymphoproliferation would be highly unusual in acute lymphoblastic leukemia.

In summary, the clinical context is of paramount importance for accurate interpretation of the pathological features. In conjunction with PVRs, both pathologists and clinicians should be aware of the uncommon features such as massive lymphadenopathy outside the lymphatic drainage areas of the injection site and extensive blastic, hyperimmune T-cell reaction. Familiarity with reactive T-cell phenotypes including the expression of CD99 is also important. Even with the atypical site of presentation of this PVR, the biopsy and concerns it raised could have been avoided altogether as the spectrum of clinical features commonly associated with malignancy was absent. In the context of exuberant and atypical PVR, it would be prudent to look for evidence of underlying immunodeficiency.

Conflict of interest The authors declare no conflicts of interest.

References

1. Goraya JS, Virdi VS (2002) Bacille Calmette–Guérin lymphadenitis. Postgrad Med J 78:327–329
2. Karadeniz C, Oguz A, Ezer U, Oztürk G, Dursun A (1999) The etiology of peripheral lymphadenopathy in children. Pediatr Hematol Oncol 16:525–531
3. Maubec E, Pinquier L, Viguier M et al (2005) Vaccination-induced cutaneous pseudolymphoma. J Am Acad Dermatol 52:623–629
4. Al-Bhlal LA (2000) Pathologic findings for bacille Calmette–Guérin infections in immunocompetent and immunocompromised patients. Am J Clin Pathol 113:703–708
5. Al-Bhlal LA (2001) Fine-needle aspiration cytology of postvaccinial disseminated bacille Calmette–Guerin infection. Diagn Cytopathol 24:333–335
6. Oguz A, Karadeniz C, Temel EA, Citak EC, Okur FV (2006) Evaluation of peripheral lymphadenopathy in children. Pediatr Hematol Oncol 23:549–561
7. Kennedy JS, Frey SE, Yan L et al (2004) Induction of human T cell-mediated immune responses after primary and secondary smallpox vaccination. J Infect Dis 190:1286–1294
8. Akosa AB, Ali MH, Khoo CT, Evans DM (1990) Angiolymphoid hyperplasia with eosinophilia associated with tetanus toxoid vaccination. Histopathology 16:589–593
9. Dommergues MA, de La Rocque F, Guy C et al (2009) Local and regional adverse reactions to BCG-SSI vaccination: a 12-month cohort follow-up study. Vaccine 27:6967–6973
10. Nieminen T, Salo E (2004) Lymphadenitis in the left groin due to bacille Calmette–Guerin (BCG) vaccination. Duodecim 120:2247–2250
11. Moëll C, Wiebe T, Hallberg T (1983) Bcg vaccination as a cause of multifocal osteomyelitis in a 12-year-old girl. Acta Paediatr Scand 72:153–155
12. Brehmer W, Falkenberg N, Hussels H, Otto HS, Preussler H, Waldschmidt J (1977) Regional suppurative lymphadenitis after BCG vaccination. Dtsch Med Wochenschr 102:1251–1255
13. Atalar H, Sarifakioglu E, Dener C, Yanik B, Koktener A, Bayrak R (2008) Cutaneous lymphoid hyperplasia and reactive lymphadenopathy induced by hepatitis B vaccination. Eur J Dermatol 18:188–189

14. Dworzak MN, Fröschl G, Printz D et al (2004) CD99 expression in T-lineage ALL: implications for flow cytometric detection of minimal residual disease. Leukemia 18:703–708
15. Dworzak MN, Fritsch G, Buchinger P et al (1994) Flow cytometric assessment of human MIC2 expression in bone marrow, thymus, and peripheral blood. Blood 83:415–425
16. Alberti I, Bernard G, Rouquette-Jazdanian AK et al (2002) CD99 isoforms expression dictates T cell functional outcomes. FASEB J 16:1946–1948
17. Park CK, Shin YK, Kim TJ, Park SH, Ahn GH (1999) High CD99 expression in memory T and B cells in reactive lymph nodes. J Korean Med Sci 14:600–606
18. Ceesay MM, Vadher B, Tinwell B, Goderya R, Sawicka E (2008) Spontaneous remission of T lymphoblastic lymphoma. J Clin Pathol 61:955–957
19. Yoruk A, Erguven M, Celiker E et al (2008) Spontaneous remission of acute lymphoblastic leukemia with mediastinal mass. Pediatr Hematol Oncol 25:181–186

Virchows Arch (2012) 461:607–608
DOI 10.1007/s00428-012-1316-x

LETTER TO THE EDITOR

Endosalpingiosis can mimic malignant glands and result in a false positive mesorectal resection margin

Dimas Suárez-Vilela · Francisco Miguel Izquierdo · Jose Ramón Riera-Velasco · Juliana Escobar-Stein

Received: 20 August 2012 / Accepted: 6 September 2012 / Published online: 21 September 2012
© Springer-Verlag 2012

To the editor:

Total mesorectal excision (TME) is a superior surgical modality for the treatment of rectal cancer, as local recurrence rates can be reduced from 30–40 % without TME to <5 % with TME [1].

Pathologists play a key role in the evaluation of these specimens, including the quality assurance of surgical performance as well as evaluation of the circumferential radial margin (CRM). Accurate determination of CRM status is essential, since this is the single most important factor for predicting the risk of local recurrence in patients with rectal cancer [1, 2].

We have studied a case of a woman with a carcinoma of the rectum that showed glandular structures of uncertain origin on the CRM. Immunohistochemical marker studies showed that those glands corresponded to endosalpingiosis (ES) rather than tumor involvement of the CRM.

Our case was a stenosing adenocarcinoma in a 64-year-old woman localized in the sigmoid colon, 20 cm from the anus. An intraluminal metal prosthesis was required, and a segmental laparoscopic surgical resection of the sigmoid was performed. The surgical specimen contained a well-differentiated adenocarcinoma measuring 3×3 cm in size that did not involve any of the surgical margins. The tumor stage was pT3, pN0, pMx. On follow-up endoscopy, a new tumor was found in the rectum at 7 cm from the anal line. This neoplasm consisted of a well-differentiated adenocarcinoma. The patient was treated with a long course of neoadjuvant chemoradiotherapy prior to a low-anterior rectal resection. The TME specimen received measured 6 cm in length. On gross study, a remnant tumor was not found, but upon histological examination, isolated glands of a well-differentiated adenocarcinoma were present in the mucosa and submucosa. The lymph nodes of the mesorectum (MR) were free of tumor metastases. At the peritoneum-free CRM, some small glands and psammomatous microcalcifications were present (Fig. 1a). These glands were lined by a single layer of cuboidal or columnar epithelial cells with eosinophilic cytoplasms and vesicular nuclei containing a tiny nucleolus (Fig. 1b). Cilia were focally found on the luminal border of the epithelial cells in one gland (Fig. 1b). Periglandular stroma was densely collagenous with some fibroblastic cells. In the mesenchymal component, neither foamy macrophages nor hemosiderin was found. These glands raised the question of a differential diagnosis with neoplastic structures with post-therapy, and an immunohistochemical study was performed. The glands showed cytoplasmic immunoreactivity for CKAE1-AE and CK7, and nuclear reactivity for estrogen receptors (Fig. 1c) and Wilms tumor 1 antigen (WT1) (Fig. 1d), but not for CK20, CD10, CDX2, calretinin, CEA, and progesterone receptors. Periglandular stromal cells were slightly positive for CD10 and progesterone receptors, but not for the other markers.

Histological and immunohistochemical features of these glands corresponded to ES rather than infiltration by adenocarcinoma. ES is characterized by the presence of benign glands lined by tubal-type epithelium that usually involve the pelvis and lower abdominal peritoneum and pelvis, and para-aortic lymph nodes in women [3]. This a nonneoplastic process, which is generally considered to be derived from

D. Suárez-Vilela · J. R. Riera-Velasco · J. Escobar-Stein
Department of Anatomía Patológica, Hospital Valle del Nalón,
Polígono de Riaño, s/n,
33920 Riaño (Langreo), Asturias, Spain

F. M. Izquierdo (✉)
Department of Anatomía Patológica,
Complejo Asistencial Universitario de León,
Altos de la Nava s/n,
24008 León, Spain
e-mail: fizquierdog@saludcastillayleon.es

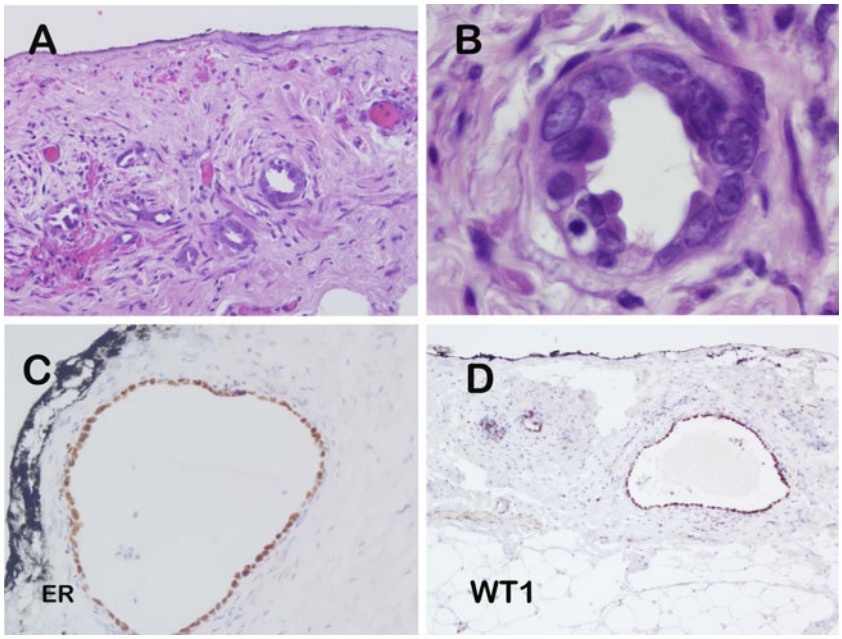

Fig 1 **a** Small glands localized less than 1 mm away of the circumferential radial margin of the mesorectum. **b** The glands are lined by cuboidal or columnar epithelium with vesicular nuclei and small nucleoli. Some cells show cilia on the luminal surface. **c** Nuclear positivity for estrogen receptors in dilated glands. **d** Nuclear staining for *WT1* in glands of different sizes

the so-called secondary müllerian system, is almost always an incidental finding on microscopic examination [3]. To our knowledge, cases of ES involving peritoneal-free CRM of the MR have not been described, although this entity has been reported in sigmoid colon and appendix [3, 4]. We believe that ES and other entities derived from the secondary müllerian system such as endocervicosis and endometriosis should be kept in mind when the MR, the CRM, and the lymph nodes of a surgical specimen of rectal carcinoma are microscopically examined in cases of female patients. When such glands are found in these locations and are not adequately interpreted, a false positive diagnosis of tumor involvement of CRM could be the result. In general, a conventional histological examination will suffice to resolve this differential diagnosis, in as much as these glands do not show significant nuclear atypia. If necessary, immunohistochemical study with a panel of antibodies including CK7, CK20, CDX2, CD10, WT1, ER, and PR is helpful in order to resolve this diagnostic problem, as the glands derived from müllerian epithelium display an immunophenotype different from that of rectal adenocarcinoma. The glands of the carcinomas of rectum express CK20 and CDX2 but not the other antigens, whereas the benign glands and the periglandular stroma do not express CK20 or CDX2 but are positive for some of the other markers of the panel [5–8].

Conflict of interest The authors declare that they have no conflict of interest.

References

1. Parfitt JR, Driman DK (2007) The total mesorectal excision specimen for rectal cancer: a review of its pathological assessment. J Clin Pathol 60:849–855
2. Boch SL, Nagtegaal ID (2012) The importance of the pathologist's role in assessment of the quality of the mesorectum. Curr Colorectal Cancer Rep 8:90–98
3. Clement PB, Young RH (1999) Florid cystic endosalpingiosis with tumor-like manifestations. A report of four cases including the first reported cases of transmural endosalpingiosis of uterus. Am J Surg Pathol 23:166–175
4. McCluggage WG, Clements WDB (2001) Endosalpingiosis of the colon and appendix. Histopathology 39:645–646
5. Mittal K, Soslow R, McCluggage WG (2008) Application of immunohistochemistry to gynaecologic pathology. Arch Pathol Lab Med 132:402–423
6. Ordi J, Romagosa C, Tavassoli FA, Nogales F, Palacin A, Condom E, Torné A, Cardesa A (2003) CD10 expression in epithelial tissues and tumors of the gynecological tract: a useful marker in the diagnosis of mesonephric, trophoblastic and clear cell tumors. Am J Surg Pathol 27:178–186
7. Clement PB (2007) The pathology of endometriosis: a survey of the many faces of a common disease emphasizing diagnostic pitfalls and unusual and newly appreciated aspects. Adv Anat Pathol 14:241–260
8. Bárcena C, Oliva E (2011) WT1 expression in the female genital tract. Adv Anat Pathol 18:454–465

Virchows Arch (2012) 461:609–619
DOI 10.1007/s00428-012-1330-z

INVITED EDITORIAL

Congenital malformations: from superstition to understanding

J. Bruce Beckwith

Received: 29 September 2012 / Accepted: 11 October 2012 / Published online: 26 October 2012
© Springer-Verlag Berlin Heidelberg 2012

Throughout most of human history, congenital anomalies were perceived as omens, portents, or punishments of supernatural origin. This concept is reflected in the term "monster," probably derived from the Latin verb *monstrare* (to show or reveal). Other explanations for congenital abnormalities included witchcraft, astrological configurations, or emotional experiences of the pregnant mother. Malformed humans and animals also inspired many of the characters populating the literature, mythology, art, and religion of every culture.

By the eighteenth century superstition still dominated public conceptions of malformations, but this topic was beginning to attract serious attention from physicians and scientists. Abnormalities such as conjoined twins were a popular subject for anatomists, who produced some superb morphological studies. However, scientific investigation of causes and mechanisms of abnormal development were delayed because of persisting support for the concept of preformation of embryos. Toward the end of the century, epigenesis finally achieved acceptance by leading scientists, opening the door to the investigation of normal and abnormal development.

By the dawn of the nineteenth century, a foundation had been established for the study of abnormal development, which was destined to become one of the most productive of biomedical sciences. The ultimate mechanisms of normal and abnormal development are now explored at the molecular level, and the lives of countless individuals born with malformations have been greatly enhanced by advances in medicine and surgery. No other biomedical science provides a more colorful and instructive illustration of the long journey from superstition to understanding. The older literature in this field, in addition to its historical interest, is a source of knowledge and information of unique value for scientists and practitioners.

J. B. Beckwith (✉)
Department of Pathology and Human Anatomy,
Loma Linda University,
Loma Linda, CA, USA
e-mail: beckwithbrowning@earthlink.net

Ancient and primitive cultures

Accurate depictions of malformations that are clearly based upon actual cases are included in the art, folklore, and literature of many cultures (Fig. 1). Other figures, such as mermaids, cyclops, chimeras, and multiheaded and janiform monsters, though possibly inspired by cases of malformation, are embellished or distorted in their description and artistic representation. While most anomalous cases engendered negative reactions, some were esteemed as divinities or shamans. Achondroplasia and other forms of dwarfism are portrayed as divinities in the art of ancient Egypt and Greece [1] as well as pre-Hispanic cultures of Central and South America (Fig. 2).

Birth defects were interpreted as omens or portents in many early cultures. For example, Babylonian–Assyrian cuneiform tablets include an extensive catalog of anomalies believed to represent omens, some of which are clearly based upon observation of actual cases. For example, "If a woman gives birth and the anus is closed, the land will suffer famine" [2].

1500–1650: the age of prodigy books

The sixteenth century was described by Jean Céard [3] as "the golden age of prodigy books," reflecting the popularity of illustrated books, manuscripts, and broadsides depicting malformed humans and animals as omens or portents of profound supernatural significance. The quintessential prodigy book

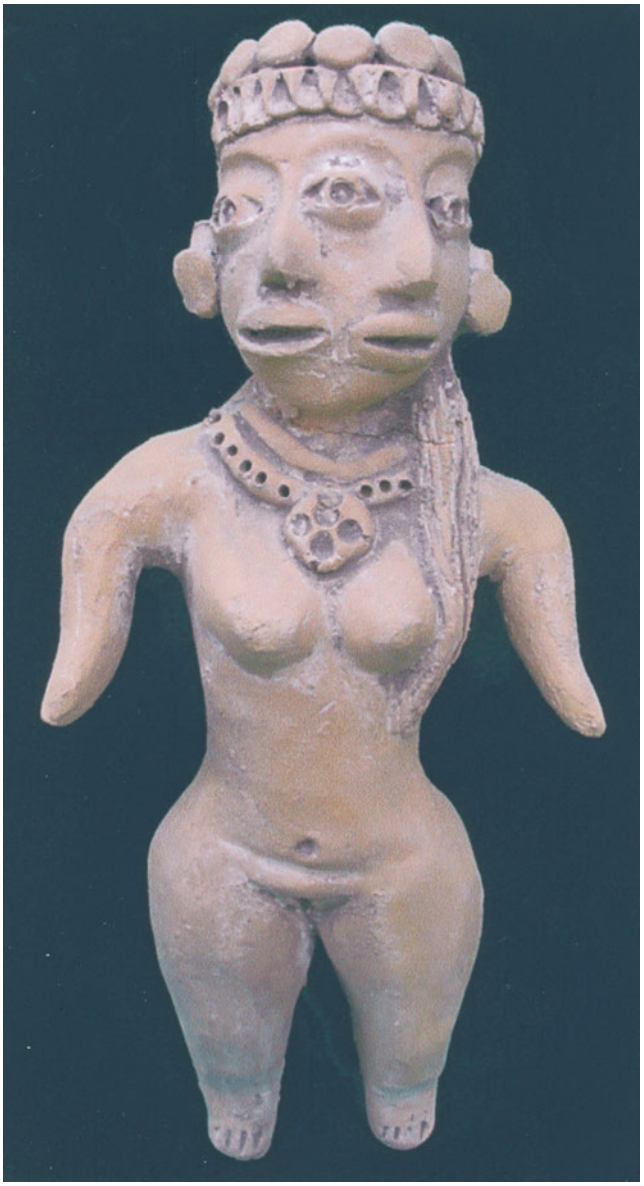

Fig. 1 *Diprosopus triophthalmos* precolumbian figurine from Mexico. Author's collection; reproduction of an original in the museum of anthropology in Mexico City, a generous gift from Dr. P.V. Mayoral, pathologist at the Children's Hospital in that city

Fig. 2 Achondroplasia. Moche figural vessel, ca. 200–300 C.E. 32-cm tall. Author's collection

was the 1557 chronicle of Conrad Lycosthenes (1518–1565) [4]. This thick folio, embellished by some 1,500 woodcut illustrations, is a compendium of unusual natural phenomena both real and alleged, spanning the history of the world from the temptation of Eve to the year of publication. Particular emphasis was upon the temporal association of anomalous births of humans or animals with significant historical events. Though most "monsters" described in this work are either fictional or imaginatively embellished, it also includes some reasonably accurate depictions of conjoined twins, limb anomalies, and other malformations. A reprint of the 1557 German edition makes this fascinating work accessible to modern readers.

Somewhat less credulous than the work of Lycosthenes was the 1573 treatise on monsters and prodigies by the great pioneer of French surgery, Ambroise Paré (1510–1590) [5]. Accurately depicted anomalies observed by Paré and other contemporary observers are presented, but these were not distinguished from fictional or imaginatively embellished abnormalities. This work is readily available to modern readers in reprinted versions, including the fine scholarly French edition of Céard [6] and the English translation by Pallister [7]. The 1554 treatise by Jakob Rueff (1500–1558), intended for midwives [8], includes a chapter on teratological cases. Brief descriptions and simple woodcuts accurately depicting conjoined twins, limb reduction defects, and

other anomalies are presented along with fictitious cases copied from other sources.

Several notable works devoted to malformations appeared during the first half of the seventeenth century. Most notable of these was the posthumously published *Monstrorum Historia* of Ulysses Aldrovandi (1522–1605) [9]. This elegant folio volume features 366 attractive woodcut illustrations, many full pages depicting a wide variety of malformations in humans and plant and animal species. Excellent depictions of actual specimens are included along with substantial numbers of apocryphal ones. An emerging scientific approach to this subject is reflected in the organization of the book according to pattern or site of abnormality, such as rostral duplications and dwarfism. The 1634 and subsequent editions of the treatise of Fortunio Liceti (1577–1657) [10] are notable for their attractive copper engravings. This work was primarily concerned with the presumed significance of anomalies rather than their accurate depiction, with numerous impossible or inaccurate representations such as human-quadruped chimeras. However, it contains a few accurately depicted cases, including an apparent example of trisomy 13 (Fig. 3). The 1609 monograph of Johann Georg Schenck [11] (d. 1620) features some excellent depictions of malformations in humans and animals (Fig. 4) in addition to numerous inaccurate or fanciful ones typical of works from this era.

Some of the earliest recorded postmortem examinations involved cases of malformation. The 1507 treatise on postmortem examinations of Antonio Benevieni (1443–1502) includes several cases of malformed infants [12]. The first reported necropsy in the western hemisphere was performed in 1533 on conjoined twins who died shortly after delivery. The examination was requested by clergy in order to determine if the twins had one soul or two [13].

Mid-seventeenth to early eighteenth century: transition toward a science

This period begins with a shining moment in the history of teratology. On page 233 of his pioneering 1651 treatise on embryology [14], William Harvey, after describing the upper lip of human fetuses as completing its formation from separate elements, suggested that failure of this process was the likely mechanism of development for congenitally cleft lip. Harvey's recognition that the study of embryology could provide the keys to understanding the causes and mechanisms of abnormal development was over a century ahead of his time. General acceptance of this view was delayed by strong support for the concept of preformation of embryos, defended by Haller, Buffon and other influential authorities of the eighteenth century. The works of Roe [15] and Tort [16] describe the vigorous intellectual debates during the latter part of that century that culminated in general acceptance of epigenesis as the mechanism of normal and abnormal development.

Though superstition and religion still dominated the subject of birth defects, early steps toward scientific teratology

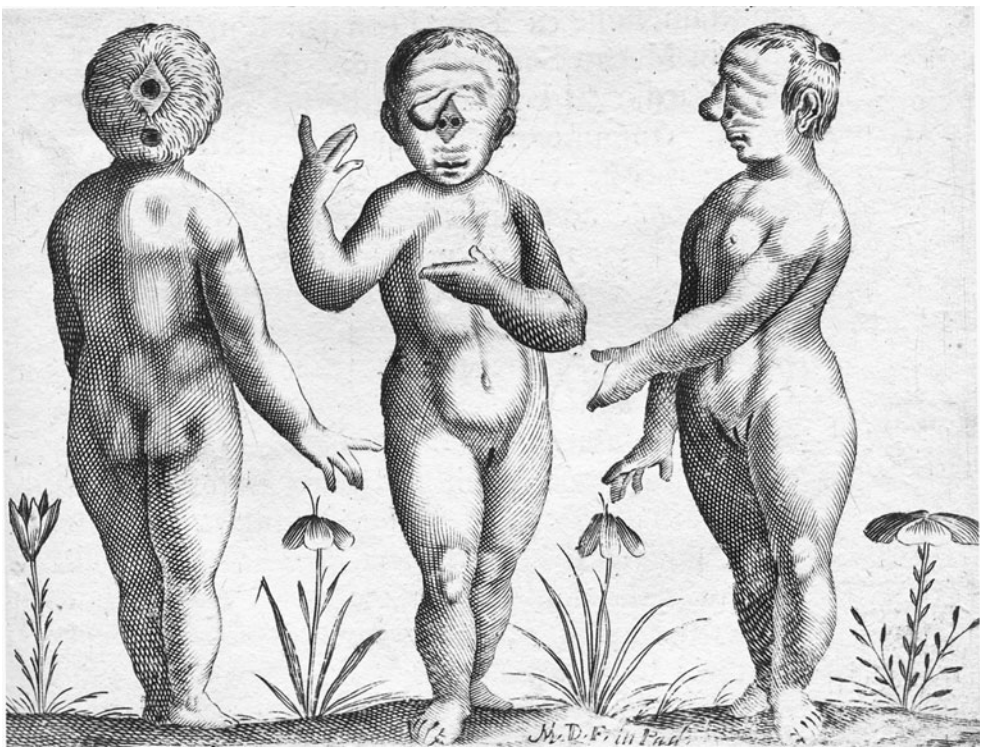

Fig. 3 Figure on page 133 of Liceti's 1634 treatise on monsters [10]. Infant born in Fermo, Italy in 1624. Drawing by an unnamed artist who observed the infant both before and after death. The combination of cyclopia with a midline scalp defect is suggestive of trisomy 13

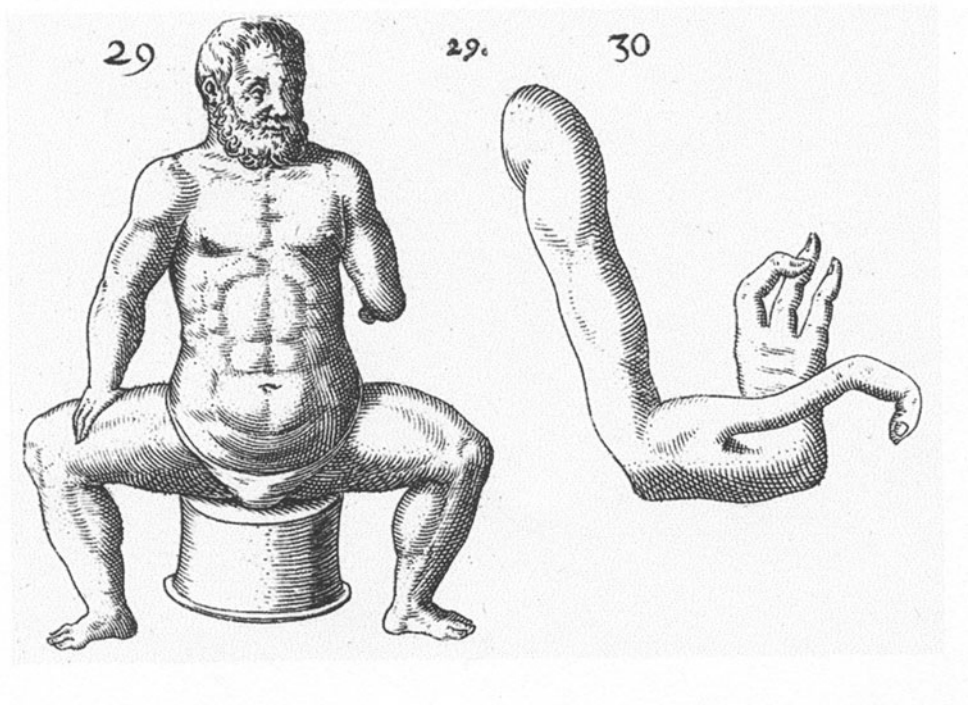

Fig. 4 Accurately depicted examples of limb anomalies from Schenck's 1609 treatise [11]

were manifested by an increasing proportion of accurately described cases and greatly improved quality of published descriptions and illustrations.

Mid-eighteenth to early nineteenth centuries: the golden age of gross teratology

During the second half of the eighteenth century, the study of the gross anatomy of malformation entered a new golden age, one that would continue through the early decades of the nineteenth century. During that period, when gross anatomy was the leading medical science, morphological studies of malformation attained levels of excellence rarely seen today. Advances in anatomical techniques and in medical and scientific illustration produced a rich heritage of magnificently illustrated works, many of which have never been surpassed. Numerous splendid monographs described specific patterns of malformation, such as that published in 1791 by Samuel Thomas Sömmerring (1755–1830) [17], featuring 12 engraved copperplates, six of which depicted a series of rostral duplications progressing from midline facial cleft through various degrees of diprosopus to dicephalus, a pioneering demonstration that patterns of malformation could be arranged and classified in a meaningful manner.

Albrecht von Haller (1708–1777), a dominant figure in scientific medicine for much of this century, has been credited by some authors as the founder of scientific teratology. The third volume of his *Opera Minora,* published in

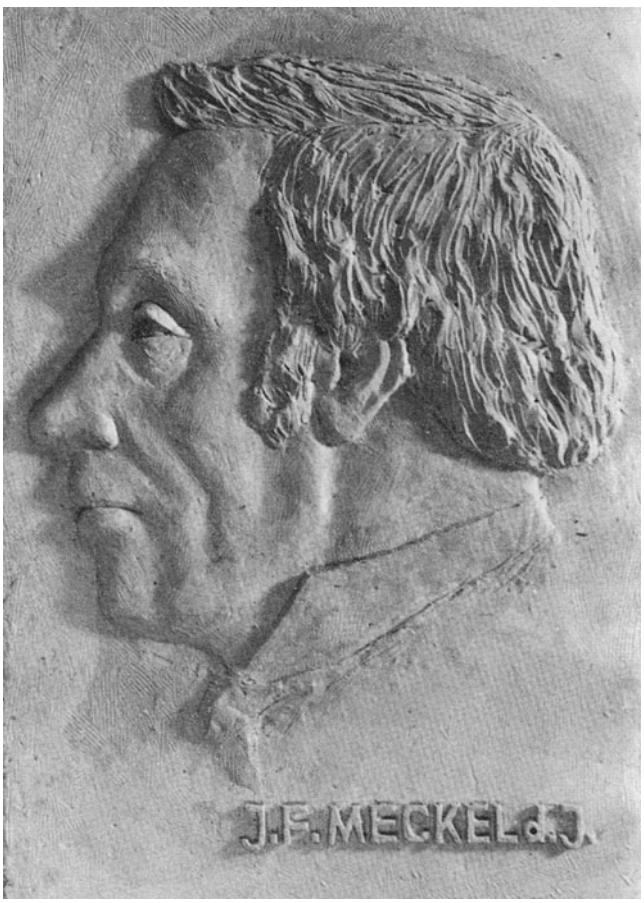

Fig. 5 J. F. Meckel the Younger. Soft tissue reconstruction of Meckel's facial features, based in part on remnants of his skull exhumed in 1967. From Schierhorn [26]

1768 [18], largely devoted to the topic of malformations, has been described by some historians as the beginning of scientific teratology. Haller's emphasis upon accurate descriptions and depictions of cases and his influential role in the eradication of fanciful and inaccurate descriptions from the literature of science were influential in preparing the way for scientific teratology. However, his strong support of preformation during the latter decades of his life contributed to the delay in linking the topic of malformation to embryology. Vigorous debates during the eighteenth century, as mentioned above, stimulated scientific interest in the genesis of malformations and led to the general acceptance of the concept of epigenesis by the end of the century.

Nineteenth and early twentieth century: teratology becomes a science

This century witnessed the emergence of teratology as a recognized scientific discipline inextricably linked to the study of embryonic development. Much of the credit for establishing the union of teratology and embryology belongs to Johann Friedrich Meckel the younger (1781–1833, the last and greatest of the dynastic trio of great Meckel anatomists) [19–21] (Fig. 5). The remarkable intelligence and technical skill of the Meckel triumvirate was unfortunately combined with significant emotional instability in their adult years [22]. While the younger Meckel was apparently a likeable and popular person in his early years, his forceful and arrogant personality led to difficult relationships with many colleagues in later life [23].

Meckel's early interest in the problem of malformation was reflected in his 1802 graduation dissertation devoted to congenital cardiac malformations and his pioneering 1809 study of the developmental significance of the ileal diverticulum bearing his name [24]. But his most important contribution was the epoch-making *Handbuch der pathologischen Anatomie,* published in two volumes from 1812 to 1818 [25]. This work is now generally credited as the beginning of scientific teratology [19, 26]. Though not reflected in its title, volume 1 and the first 221 pages of volume 2 were devoted entirely to malformations. This was the first work to present a systematic approach to the entire spectrum of human anomalies, but its most important contribution was its emphasis upon the embryological mechanisms of abnormal development. Meckel recognized that malformations represented deviations from normal development and that extensive study of normal embryology must precede a true understanding of birth defects. He clearly

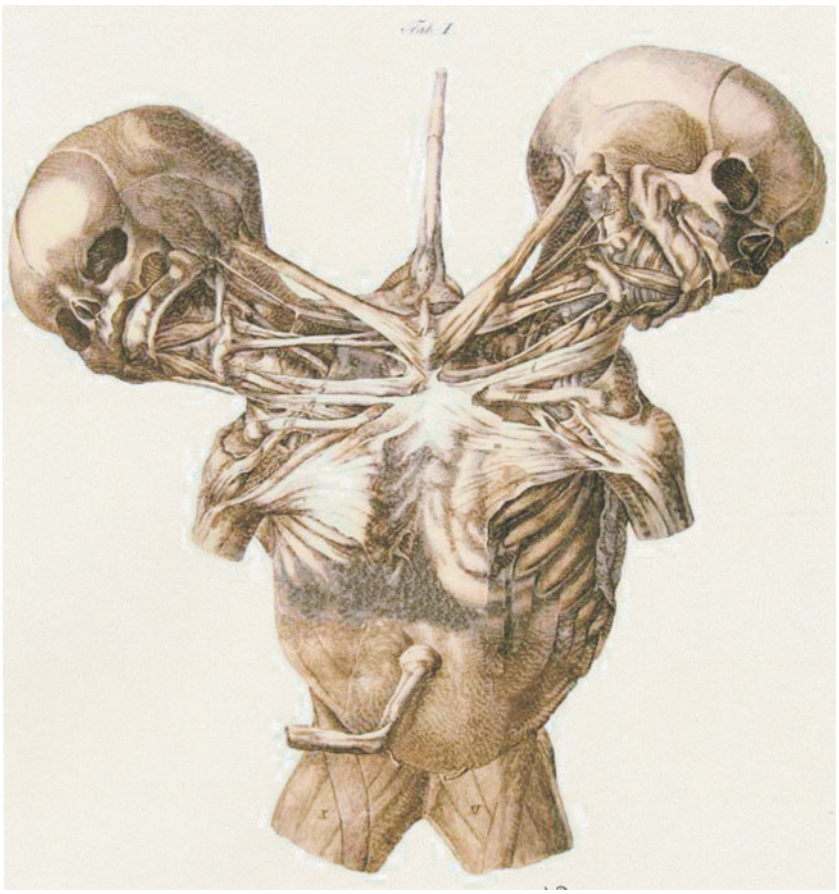

Fig. 6 *Dicephalus tribrachius* conjoined twins. Portion of plate 1 in Meckel's monograph on conjoined twins [27]. This figure exemplifies the excellence of anatomical dissection and illustration in many older publications

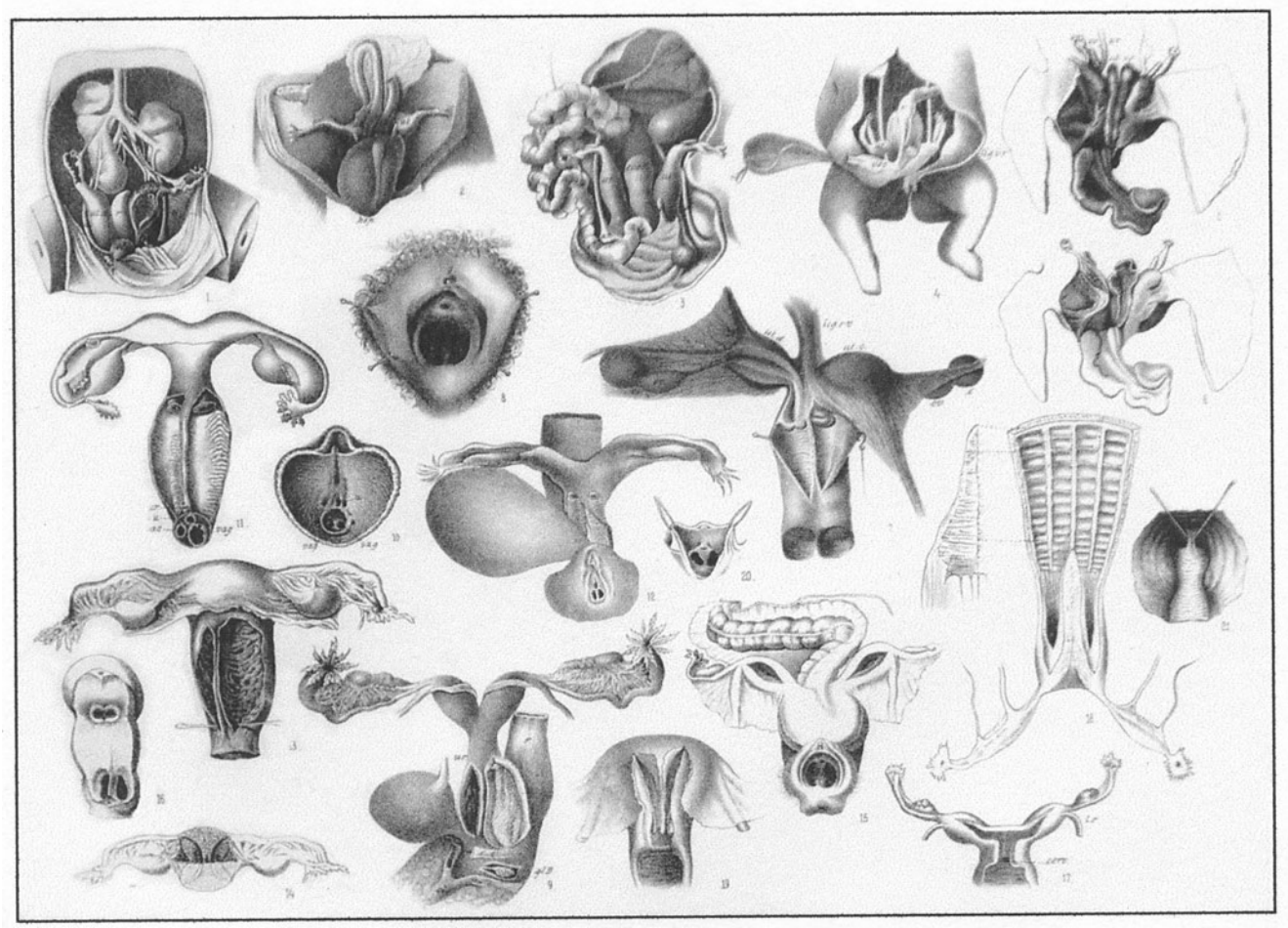

Fig. 7 Anomalies of the genital and urinary tracts. Plate 41 in Ahlfeld's superb atlas of malformations [39]

recognized the importance of developmental arrest, though placing excessive emphasis upon deficient or excessive formative energy (*Bildungskraft*) as the most important factor leading to structural defects. The concept of developmental arrest had been suggested by William Harvey in 1651, but not until Meckel's work did the study of malformations become inseparably linked to embryology.

In his remaining two decades, Meckel published numerous major contributions to the study of malformations. Most notable of these were his 1815 monograph on conjoined twinning [27] (Fig. 6), his splendidly illustrated atlas of pathological anatomy of several organ systems [28], and many contributions to journals, mostly in *Deutsches Archiv für die Physiologie* (1815–1823) and *Archiv für Anatomie und Physiologie* (1826–1832), both of which he edited. Klunker's valuable study of Meckel's scientific work, describing extant specimens from his teratological museum with color illustrations of many specimens, is available online [29].

Two other epochal contributions to this field followed in the 1830s. The best known and most influential of these was the treatise of Isidore Geoffroy Saint-Hilaire (1805–1861), referred to in this paper as "Geoffroy." His work consisted of three text volumes and an atlas published from 1832 to 1837 [30]. Isidore's father, Étienne (1772–1844), was a prominent and controversial figure in the history of French biology during the early decades of the nineteenth century [31], whose vigorous pursuit of unifying principles governing anatomical structure and development led to a monograph on malformations as clues to these general laws [32]. Isidore's treatise, probably stimulated by his father and written during the early years of his career, provided a comprehensive survey of the entire spectrum of malformations that emphasized anatomy, nomenclature, and classification more than pathogenesis. It introduced the term "teratology" for the scientific study of congenital anomalies and proposed numerous new terms for specific abnormalities, many of which have been perpetuated. This work proved immensely popular and played a major role in fostering scientific interest in the field of malformations. After completing this work, Isidore devoted his efforts to comparative anatomy, with only minor contributions to the literature of teratology.

A work comparable in excellence to that of Geoffroy was the 1832 treatise on malformations of domestic and

agricultural animals by Ernst Friedrich Gurlt (1794–1882) [33]. Comprising part 2 of a treatise devoted to the pathological anatomy of species of interest to veterinarians, the text was accompanied by 25 lithographed plates featuring 136 finely executed figures illustrating a wide spectrum of malformations. This work remains one of the best descriptive works on mammalian teratology today. It was the first treatise to apply the Linnean binomial system of taxonomy to the entire spectrum of malformations. Geoffroy adopted this approach to classification of malformations in the second volume of his treatise, published in 1836. Gurlt published another superb treatise on veterinary teratology near the end of his long career [34]. This work features 20 finely lithographed plates with 119 figures, most of which depict the internal anatomy of malformations, adding to its value as a companion to the 1832 atlas, which was mostly devoted to external malformations.

The above foundation works were followed by a vast literature on descriptive and experimental teratology during the remainder of the nineteenth century, including many textbooks, monographs, dissertations, and atlases that remain invaluable resources for modern science and medicine. Works dealing with individual malformation categories are too numerous to mention here. Two examples of the many unique cases of permanent value to science include Fattori's depiction of a fetus containing two internal parasitic twins, one in the abdominal cavity and the other in the pelvis [35] (Fig. 7), and that of Baart de la Faille [36] concerning a fetus with twin parasitic fetuses attached to its palatal region (Figs. 8 and 9).

The next few paragraphs describe important general texts and atlases that feature numerous illustrations and descriptions of important cases of malformation. These collective works are invaluable for those seeking rare or instructive cases from the older literature. Though most are in languages other than English, the fine illustrations make them worthwhile even for those unable to appreciate the accompanying text. Most are relatively rare, but some are available in reprint form, as indicated in the reference list, and many others are being added to readily accessible digital archives. Regrettably, the folded plates, the crowning feature of most works in this field, have been scanned in the folded state in most currently available digital volumes, and colored plates are often reproduced in black and white.

The splendid atlas by Willem Vrolik (1801–1862) [37], the illustrated companion to his two-volume textbook of teratology [38], consists of 101 beautifully lithographed plates, with accompanying text in both Latin and Dutch. Covering a wide spectrum of anomalies from the literature as well as specimens in the Vrolik Museum at the University of Amsterdam, this work is an invaluable resource of permanent value. Vrolik's textbook deserves a place of honor in the literature of teratology, though its influence was limited by its having been published only in Dutch.

The text and large folio atlas of Friedrich Ahlfeld (1843–1929) [39], though less well known than that of Vrolik, is one of the great treasures of teratology. Its 49 plates with 750 finely lithographed figures, printed on heavy stock, make it an invaluable resource (Fig. 7). The illustrations depict instructive, unique, or important cases selected from the literature, unpublished museum specimens, or cases studied by Ahlfeld. External, skeletal, and visceral anomalies are included. The text volumes indicate the source of each figure and discuss its salient features. This work does not include all patterns of human malformation but includes excellent coverage of conjoined twinning and other duplication anomalies, clefts of various body parts, urogenital abnormalities, cyclopia, microcephaly, and various other anomalies. Ahlfeld, a prominent German obstetrician with a deep interest in teratology, possessed a superb library of teratological works, the nineteenth century portion of which has been maintained intact in the Welch Library of the Johns Hopkins University School of Medicine.

Friedrich August von Ammon (1799–1861) published in 1842 a splendid atlas of malformations that are of

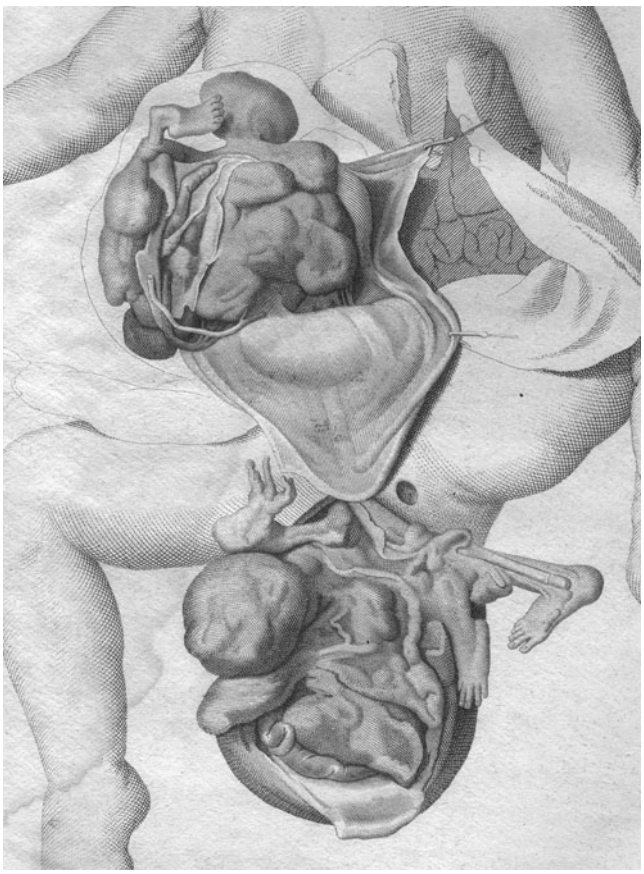

Fig. 8 *Twin foeti in foetu*, described and depicted in the 1815 folio monograph of Fattori [35]. Portion of figure on plate 1. This female fetus, delivered at 7 months gestation, contained two fetal inclusions, one in the abdomen and another in the pelvic cavity. Feet and other fetal structures are clearly identifiable in each mass

particular interest to surgeons [40]. Its 34 copperplates of elephant folio size feature 574 finely stipple-engraved and outline figures depicting a wide array of malformations, mostly chosen from the previous literature. Figures were selected for their potential surgical interest and are organized in useful fashion. Facial clefts, urogenital anomalies, anorectal atresias, parasitic twins, and limb duplications are among the abnormalities depicted and discussed in this impressive work.

One of the most valuable resources for descriptive human teratology is the text and atlas of August Förster (1822–1865) [41]. This deceptively slender volume provides authoritative coverage of all major malformations, both external and visceral. It features succinct descriptions and simple but instructive line drawings by the author, a pathologist who was also a trained artist. Its 26 plates depict the essential features of hundreds of instructive cases from the literature and the author's experience. Its excellent critical bibliography, the first of its kind, has been the basis for most subsequent bibliographies of teratology.

Adolph Wilhelm Otto (1786–1845), one of the first pathologists with a particular interest in malformations, published a magnificent folio volume describing 600 specimens in the anatomical museum in Breslau [42]. This large folio volume is one of the great treasures in the history of the field. Its 30 copperplates, one partially colored, feature 146 figures depicting a variety of human malformations. Its 129 pages of Latin text provide detailed descriptions of each specimen, especially valuable because they include details concerning internal anatomy revealed by complete dissection of most specimens. Much rewarding work remains to be done on this work, which describes malformation complexes "discovered" in recent years and likely contains descriptions of syndromes yet to be recognized. This as well as Ottos' other significant contributions to teratology were the topic of an excellent study by Kampf [43].

An invaluable source of information on conjoined twins was a series of four lengthy articles by George Jackson Fisher (1825–1893) [44], accompanied by 30 engraved plates containing a total of 126 figures from the preceding literature. The fourth article included five plates depicting thoracopagic variants that were to be discussed in a fifth and final paper that was never published. This work includes detailed descriptions and fine illustrations from original sources that are now difficult if not impossible to find.

Cesare Taruffi (1821–1902), the first professor of pathology at the University of Bologna, published a series of eight volumes on the history of teratology from 1881 to 1894 [45]. Taruffi intended to continue this work with volumes on internal malformations, but these were never published. However, it remains by far the most extensive and detailed source of information on the history of teratology from the Renaissance to the latter decades of the nineteenth century. Taruffi mentions virtually every work previously published in this field. The first four volumes are most useful, covering the general history of teratology and the vast literature on conjoined twins. Despite its unique value, this work presents frustrating challenges. With the exception of occasional

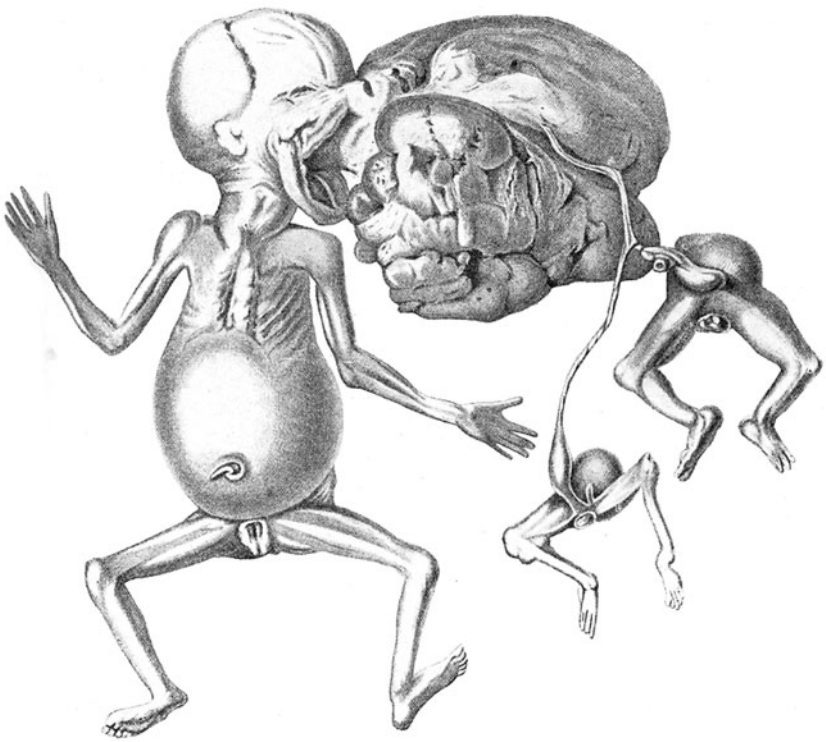

Fig. 9 *Epignathus* parasitic twins in a female fetus of 5 months, reported in a rare monograph by Baart de la Faille [36]. Original not available; figure from Schatz [21], who suggested this was a case of parasitic triplets, of which the pharyngeal component represent the third parasite. Later restudy of the original specimen by Marchand [31] suggested that the pharyngeal mass represented rostral portions of twins whose caudal portions are obvious

small line drawings, it has no illustrations. More importantly, it contains numerous typographical errors. The author's writing style is sometimes difficult to follow, even for native speakers of Italian. Despite these shortcomings, Taruffi's magnum opus contains vast amounts of information that is available nowhere else. This is the work I usually consult first when researching a topic in antiquarian teratology. A particularly useful feature is the inclusion of hundreds of tables summarizing details of cases reported by previous authors. Volume 4 contains a collective subject and author index to the first four volumes, while the remaining volumes contain only subject indexes for that volume.

A notable work that provides authoritative coverage of literature of the entire nineteenth century is the *Manual of Antenatal Pathology and Hygiene: The Embryo* [46], published in 1904 by John William Ballantyne (1861–1923). Ballantyne, an obstetrician with a profound interest in pathology, carried out postmortem examinations of numerous deformed fetuses and infants. A meticulous scholar, he was familiar with the literature of teratology in all the major languages of Europe. Some chapters in this work remain today the best discussions of specific malformations ever published. This book is a delight to read and is embellished by excellent photographs and drawings of personally studied cases.

Experimental teratology has its roots in this century. The studies of Camille Dareste (1822–1899) are the most influential pioneer in this field and are described by Fischer [47].The second edition of Dareste's summary work [48] provides an authoritative overview of this field up to the end of the nineteenth century.

Twentieth century and the dawn of the molecular age

The first half of this century witnessed significant expansion of knowledge in descriptive and experimental teratology. A notable contribution covering much of this period was the encyclopedic treatise on the morphology of malformations begun by Ernst Schwalbe (1871–1920) [49] and continued after Schwalbe's death under the editorship of Georg B. Gruber (1884–1960). The first two parts, written entirely by Schwalbe, were published in 1906 and 1907, respectively. Part 1 is devoted to historical and general considerations, while part 2 is a particularly valuable review of the complex topic of conjoined twinning. Part 3 is organized into three sections dealing with malformation types, organ systems, and body regions, issued in nineteen fascicles published from 1909 to 1958, and index fascicle for part 3 was published in 1960, completing this monumental work. Despite its complex organization, this treatise of 3,885 pages, with more than 2,000 illustrations, is an indispensable resource for information on both descriptive and experimental teratology of humans and other vertebrates in the first half of the twentieth century. By mid-century, major progress had been made in experimental embryology, epidemiology, teratogenetic mechanisms, cytogenetic studies, and characterization of dysmorphic syndromes. A general overview of this era is included in Gruber's separate historical study [50].

The elucidation of the structure of DNA in 1953 inaugurated the age of molecular biology, in which the mechanisms of abnormal development are explored at fundamental levels previously viewed as unattainable. New discoveries and concepts are revealed at a pace that exceeds the capacity of the printing press. Concepts are often developed, expanded, and superseded almost overnight, and an adequate history of this period can only be written by a future generation.

In the present era, when it is difficult if not impossible to keep abreast of new knowledge in most fields of science, the writings of past generations might seem of value only to historians. But the literature of teratology created by past generations is a resource of permanent value to medicine and science. Works from the golden age of gross anatomy and pathology contain superb depictions and descriptions of rare anomalies that are an invaluable source of gross anatomical information. In addition, the older literature includes descriptions of numerous unique specimens that reveal key information concerning specific malformation patterns. The older literature is also essential for determining whether a particular abnormality is new or changing in incidence. Descriptions of the lives of persons born with various malformations prior to the development of effective surgical amelioration can be helpful in making management decisions such as surgical separation of certain patterns of conjoined twinning. It is hoped that the present review will prove helpful to those wishing to explore this valuable and fascinating resource.

References

1. Dasen V (1993) Dwarfs in ancient Egypt and Greece. Clarendon, Oxford
2. Jastrow M Jr (1914) Babylonian–Assyrian birth-omens and their cultural significance. Religionsgeschichtliche Versuche und Vorarbeiten, Bd. 15, Heft 5:[i]-vi, 1–86
3. Céard J (1977) La nature et les prodiges. L'insolite au XVI^{e} siècle, en France. Librairie Droz, Geneva, A second edition was issued in 1996, with insignificant additions and in much smaller format than the original
4. Lycosthenes K (1557) Prodigiorum ac ostentorum chronicon. Henricum Petri, Basel, A German edition published the same year, entitled "Wunderwerck oder Gottes unergründtliches Vorbilden", is available in a facsimile edition published by Georg Olm in 2007

5. Paré A (1573) Deux livres de chirurgie. I. De la generation de l'homme. II. Des monstres tant terrestres que marins avec leurs portraits. André Wechel, Paris
6. Céard J (1971) Ambroise Paré. Des monstres et prodigies, Édition critique et commentée. Librairie Droz, Geneva
7. Pallister JL (1982) Ambroise Paré. On monsters and marvels. Translated with an introduction and notes. University of Chicago Press, Chicago
8. Rueff J (1554) De conceptu et generatione hominis. Christoph Froschouer, Zürich, German edition issued the same year. Reprint edition illustrated by Jost Ammann published in Frankfurt in 1580 and 1587. Modern reprint of the 1587 edition published in 1980 by Medicina Rara. An English translation, first published in 1637 and available in modern reprint, omits most of the section dealing with monsters
9. Aldrovandi U (1642) Monstrorum Historia. Nicolai Tebaldini, Bologna, A reprint edition, in a somewhat smaller format than the original folio volume, was published in 2002 by Nino Aragno Editore
10. Liceti F (1634) De Monstrorum Caussis, Natura, et Differentiis, Libri Duo, 2nd edn. Paulum Frambottum, Padua, The first edition was published in 1616 without illustrations. An excellent third edition, with an appendix by Gerard Blasius, was published in 1665 by Andreae Frisii, Amsterdam. A French translation of the 1665 edition, with excellent reproduction of the plates, was included in Jean Palfyn's *Description Anatomique des Parties de la Femme, qui Servent à la Generation,* published in Leyden in 1708. An abbreviated reprint of portions of Liceti's text in French, with comments by Francois Houssay, was published by Editions Hippocratique in 1937
11. Schenck JG (1609) Monstrorum historia memorabilis. Matthiae Becker, Frankfurt
12. Benivieni A (1507) De abditis nonnullis ac mirandis morborum et sanitationum causis. Translation by Charles Singer, with biographical appreciation by Esmond L. Long. Charles C, Thomas, Springfield, 1954
13. Chavarria AP (1924) The Siamese twins of Española. The first known post-mortem examination in the New World. Ann Med Hist 6:297–302
14. Harvey W (1651) De generatione animalium. Typis du-Gardianis; impensis Octaviani Pulleyn in Coemeterio Paulino, London
15. Roe SA (1981) Matter, life and generation. Eighteenth-century embryology and the Haller–Wolff debate. Cambridge University Press, Cambridge
16. Tort P (1980) L'ordre et les monstres. Le débat sur l'origine des deviations anatomiques au XVIIIe siècle. Le Sycamore, Paris
17. Sömmerring ST (1791) Abbildungen und Beschreibungen einiger Misgeburten die sich ehemals auf dem anatomischen Theater zu Kassel befanden. Universitätsbehandlung, Mainz, Enke's important study of this work, including a reprint of the original, was published in 2000 by Schwabe & Co., Basel
18. von Haller A (1768) Operum anatomici argumenti minorum, Tomus tertius. Francisci Grasset, Lausanne
19. Clark O (1969) The contribution of J. F. Meckel, the Younger, to the science of teratology. J Hist Med 24:310–322
20. Meader RG (1937) The Meckel dynasty in medical education. Yale J Biol Med 10:1–29
21. Schatz F (1900) Die Gefässverbindungen der Placentakreisläufe eineiiger Zwillinge, ihre Entwicklung und ihre Folgen. Arch Gynäkol 60:Tafel V
22. Marchand F (1912) Über den Epignathus (Fall II) von Baart de la Faille. Arch Entwicklugsmechanik Organ 35:189–209
23. Beneke R (1934) Johann Fredrich Meckel der Jüngere. Beitr. z. Gesch. d. Universität Halle-Wittenberg, Band 3
24. Meckel JF (1809) Ueber die Divertikel am Darmkanal. Archiv Physiol 9:421–453
25. Meckel JF (1812–1818) Handbuch der pathologischen Anatomie. Carl Heinrich Reclam, Leipzig
26. Schierhorn H (1984) Johann Friedrich Meckel d. J. als Begründer der wissenschaftlichen Teratologie. Gegenbaurs Morphol Jahrb 130:399–439
27. Meckel JF (1815) De duplicitate monstrosa commentarius. Halle and Berlin, Librariis Orphanotrophei. 96 p., 8 plates
28. Meckel JF (1817–26) Tabulae anatomico-pathologicae. Leipzig. IF Gleditsch
29. Klunker UR (2003) Bestand und Identität der human-teratologischen Präparate in den Meckel'schen Sammlungen under besonderer Berücksichtigung des wissenschaftlichen Werkes von Johann Friedrich Meckel dem Jüngeren (1781–1833). Diss. Med. Fak. Der Martin-Luther-Universität Halle-Wittenberg. Available online at http://sundoc.bibliothek.uni-halle.de/diss-online/03/03H116/prom.pdf
30. Geoffroy St.-Hilaire I (1832–1837) Histoire des anomalies de l'organisation chez l'homme et les animaux. J-B Baillière, Paris. 3 volumes plus atlas of 20 plates
31. Le Guyader H (2004) Geoffroy Saint-Hilaire: a visionary naturalist. University of Chicago Press, Chicago
32. Geoffroy St.-Hilaire É (1822) Philosophie anatomique. Des Monstruosités Humaines. Paris, Chez l,auteur
33. Gurlt EF (1832) Lehrbuch der pathologischen Anatomie der Haus-Säugethiere, Zweiter Teil, welcher die Classification, Beschreibung und Anatomie der Missgeburten enthält. Mit Atlas. G. Reimer, Berlin
34. Gurlt EF (1877) Ueber thierische Missgeburten. Ein Beitrag zur pathologischen Anatomie und Entwickelungs-Geschichte. August Hirschwald, Berlin
35. Fattori S (1815) De feti che racchiudono feti. Tipografia Giovanni Capelli, Pavia
36. Baart de la Faille J (1874) Jets over den Epignathus. Groningen. (Rare monograph, not available to the present author. Depicted by Schatz Arch. Gynaekol. 60: Taf. V, 1900)
37. Vrolik W (1849) Tabulae ad illustrandam embryogenesin hominis et mammalium tam naturalem quam abnormem. GMP Londonck, Amsterdam, A German edition, issued by T.O. Weigel of Leipzig in 1854, consists of unsold sets of the Amsterdam edition, with a new title page. An English translation, published by Greenwood Genetics Center in 2004, makes the text more accessible to modern readers, with suboptimal reproduction of the plates
38. Vrolik W (1840–1842) Handboek der ziektekundige ontleedkunde. Eerste deel, Tweede deel, Aangeborene gebreken. Johannes Müller, Amsterdam
39. Ahlfeld F (1880, 1882) Die Missbildungen des Menschen. Fr. Wilh. Grunow, Leipzig. Abschnitt 1 (1880). Text pages 1–144, Atlas plates 1–23. Abschnitt 2 (1882) Text pages 145–297, Atlas plates 24–49
40. von Ammon FA (1842) Die angeborenen chirurgischen Krankheiten des Menschen in Abbildungen dargestellt. F.A. Herbig, Berllin
41. Förster A (1861) Die Missbildungen des Menschen systematisch dargestellt. Friedrich Mauke, Jena. Text and Atlas with 26 lithographed plates containing 524 figures. A second edition, issued posthumously in 1865, contains identical text and figures
42. Otto AW (1841) Monstrorum sexcentorum descriptio anatomica. Ferdinand Hirt, Breslau
43. Kampf K (1987) Teratologie als Vorstufe einer Entwicklungsgeschichte. A.W. Otto (1786–1845) und sein "Museum Monstrorum" Breslau 1841. Band 47 in Arbeiten der Forschungsstelle des Instituts für Geschichte der Medizin der Universität zu Köln. p 243
44. Fisher GJ (1865–8) Diploteratology, an essay on compound human monsters. Trans Med Soc State N Y 1865, 232–268; 1866, 207–296; 1867, 396–430; 1868, 276–306

45. Taruffi C (1881–1894) Storia della teratologia, Tomo I–VIII. Regia Tipografica, Bologna
46. Ballantyne JW (1904) Manual of antenatal pathology and hygiene. The Embryo. William Green and Sons, Edinburgh, The American edition published by William Wood and Sons in 1905 is identical to the Edinburgh one except for the title page. An excellent facsimile reprint was published by Greenwood Genetics Center in 1991
47. Fischer J-L (1994) Leben und Werk von Camille Dareste (1822–1899), Schöpfer der experimentellen Teratologie. Acta Historica Leopoldina, No. 21, Deutsche Akademie der Naturforscher Leopoldina, Halle/Salle
48. Dareste C (1891) Recherches sur la producton artificielle des Monstruosités, ou Essais de tératogénie expérimentale. Paris, C. Reinwald
49. Schwalbe E, Gruber GB (eds) (1906–60) Morphologie der Missbildungen des Menschen und der Tiere. Gustav Fischer, Jena
50. Gruber GB (1963–4) Studien zur Historik der Teratologie. Zentralblatt f. allgemeine Pathologie u. Pathol Anat 105:293–316 and 106:512–562

Virchows Arch (2012) 461:621–628
DOI 10.1007/s00428-012-1326-8

ORIGINAL ARTICLE

Colorectal carcinoma grading by quantifying poorly differentiated cell clusters is more reproducible and provides more robust prognostic information than conventional grading

Valeria Barresi · Luca Reggiani Bonetti · Giovanni Branca · Carmela Di Gregorio · Maurizio Ponz de Leon · Giovanni Tuccari

Received: 26 June 2012 / Revised: 5 September 2012 / Accepted: 27 September 2012 / Published online: 24 October 2012
© Springer-Verlag Berlin Heidelberg 2012

Abstract The most widely used system to define the histological grade of colorectal carcinoma (CRC) is based on the degree of gland formation. This system suffers from significant interobserver variability which may limit its prognostic value and consequently better standardized criteria for the assessment of histological grading of CRC are needed. The present study aims to evaluate and to compare, in a cohort of postsurgical pTNM stage I CRC, conventional histological grading, and a novel grading system based on the number of poorly differentiated clusters of neoplastic cells, in terms of interobserver reproducibility, prognostic significance on progression-free survival, and association with other clinicopathological characteristics. Grading with both systems was performed by two pathologists independently and blinded to the clinicopathological data. Interobserver agreement was higher when grade was assessed by counting poorly differentiated clusters than by assessing the relative proportion of the glandular component. Contrary to conventional grading, the novel system provided significant prognostic information in terms of progression-free survival and was significantly associated with budding, invasive growth, lymphatic invasion, and occult nodal metastases of CRC. In conclusion, our findings suggest that a tumor grading system based on the number of poorly differentiated clusters is more reproducible and provides better prognostic stratification of pTNM stage I CRC patients than conventional grading.

Keywords Colorectal cancer · Grading · Stage I · Poorly differentiated clusters · Nodal occult metastases

V. Barresi · G. Branca · G. Tuccari
Department of Human Pathology, University of Messina, Messina, Italy

L. Reggiani Bonetti · C. Di Gregorio
Department of Laboratory Integrated Activities, Anatomic Pathology and Legal Medicine, University of Modena and Reggio Emilia, Modena, Italy

M. Ponz de Leon
Department of Internal Medicine, University of Modena and Reggio Emilia, Modena, Italy

V. Barresi (✉)
Dipartimento di Patologia Umana, Policlinico G. Martino, Pad D, Via Consolare Valeria, 98125 Messina, Italy
e-mail: vbarresi@unime.it

Introduction

Colorectal carcinoma (CRC) is one of the leading causes of cancer death in Western Europe and in the USA [1]. At present, postsurgical tumor node metastasis (pTNM) stage is regarded as the main prognostic factor for its clinical course [2, 3] and therapy protocols for CRC largely depend on the pTNM stage at the time of the initial diagnosis. At pTNM stage I, CRC is confined within the muscular wall of the large bowel in the absence of nodal or distant metastases, and has a 5-year survival rate of approximately 80–90 % [1, 4]. As a consequence, stage I CRC is treated by surgery only, while adjuvant therapy is limited to CRC at a higher TNM stage. However, a proportion of patients with stage I CRC show progressive disease and develop locoregional or distant metastases with ultimately adverse outcome [4]. Hence, there is a need for prognostic markers which identify patients with stage I CRC who are at increased risk of progression and who may benefit from adjuvant therapy. Identification of histological or immunohistochemical prognostic parameters which may be easily determined on cancer tissue taken from the initial surgical specimen would serve this purpose [5–9]. Histological grading is a significant prognostic factor for CRC, independent of TNM

stage [10, 11]. At present, the most widely used and accepted standard for CRC grading is based upon the degree of gland formation but this approach suffers from significant interobserver variability [12–14], which limits its utility for prognostic purposes [14]. Interobserver disagreement related to this system might be caused by a lack of objective parameters to assess the relative proportion of the glandular component.

In an effort to standardize the criteria for histological grading of CRC, a novel grading system, based upon the number of cancer cell clusters, composed of ≥5 cancer cells, and lacking a gland-like structure (poorly differentiated clusters), was recently proposed [15]. In stages II and III, CRC grading based on counting poorly differentiated clusters appeared less subjective and provided better prognostic information than conventional grading [15]. Based upon these results, we aimed to analyze in pTNM stage I CRC the prognostic significance, the interobserver variability, as well as the association with other clinicopathological parameters of this novel grading system in comparison with conventional grading according to the World Health Organization (WHO) criteria [16, 17]. We also compared the predictive value of both grading systems for on the presence of occult metastases in lymph nodes in pTNM stage I CRC.

Materials and methods

Thirty-six cases of surgically resected pTNM stage I CRCs with progressive disease within 5 years from the initial diagnosis were selected from the Cancer Registry of Modena, Italy and from the files of the Department of Human Pathology of the University of Messina, Italy. Furthermore, 82 pTNM stage I cases without evidence of progressive disease 5 years after the initial diagnosis were included in the study, constituting a cohort of a total of 118 cases (65 male and 53 female patients; age range, 43–89 years; mean age, 69.78 years). The tumors were subdivided into three groups: CRCs located in the right colon, including caecum, ascending colon, and transversum; CRCs in the left colon, including descending colon and sigma, and rectal carcinoma. None of the patients had received chemotherapy.

All tumor tissue samples had been formalin-fixed and paraffin-embedded and sections had been stained with haematoxylin and eosin (H&E). Pathological staging had been performed according to the pTNM system (v7) [18]. According to depth of infiltration, tumors were subdivided into pT1 (invading the submucosa) and pT2 (invading muscularis propria) [18]. In addition, in pT1 cases, the depth of infiltration within the submucosa was assessed and classified according to the Kikuchi system into sm1 (invasion of the upper third of the submucosa), sm2 (invasion of the middle third of the submucosa) and sm3 (invasion of the lower third of the submucosa) [19].

For each case, the growth pattern (expanding vs. infiltrative), perineural invasion, and tumor budding were also assessed. Tumor budding was defined as isolated single cancer cells or clusters of cells composed of three to five elements in the stroma of the actively invasive margin of the tumor [20]. After choosing one field where budding was most intensive, a budding count was made at ×200 magnification, with a count of less than five foci considered negative, and a count of five or more as positive [21].

Lymphatic invasion (L) as well as the presence of occult metastases in the regional lymph nodes had been investigated in all the cases. Specifically, L was assessed by immunohistochemical staining of lymphatic vessels recognized by the D2–40 antibody and defined as the presence of clusters or single neoplastic cells within the lumen of D2–40 stained vessels [9]. Detection of occult nodal metastases was performed using immunohistochemistry as previously described [22], after review of H&E-stained sections by three pathologists yielded no cases with lymph node metastases. To this end, lymph nodes were serially sectioned, and at 200 μ intervals 4 μ sections were mounted, dewaxed and either stained with haematoxylin-eosin or immunohistochemically using a monoclonal antihuman pan-cytokeratin antibody (DAKO CK, Carpinteria, CA, USA). Immunohistochemistry was carried out with the streptavidin–biotin method and antibody binding was visualized using amino-ethyl carbazole as chromogen. Occult nodal metastatic disease was defined as single or small clusters of tumor cells or neoplastic glands, less than 2 mm in size, detected by immunohistochemistry [18]. According to the definition of the American Joint Committee on Cancer, metastatic deposits with a diameter between 2 and 0.2 mm were classified as micrometastases, and those less than 0.2 mm in diameter as isolated tumor cells (ITC) [18]. Cases showing nodal micrometastases or ITC were all considered as $pN0_{micro+}$ for the present study [23].

The number of retrieved lymph nodes was also recorded for each case. A cutoff value of 12 nodes was used in order to assess whether the number of retrieved nodes had any effect on patient outcome.

Histological grading

For each case, histological grading based on glandular differentiation and on poorly differentiated cell clusters counting was performed on H&E stained sections, prepared from a longitudinal tissue sample of the whole tumor including its deepest part. The median number of slides examined per patient was 2 (range, 1–4). Histological grading based on glandular differentiation was assessed according to WHO criteria [16, 17].

According to the definition of Ueno et al. [15], poorly differentiated clusters are defined as cancer cell clusters in tumor stroma composed of ≥5 cancer cells and lacking a gland-like structure. Poorly differentiated clusters in each

Table 1 Clinicopathological characteristics in 118 analyzed colorectal carcinomas, according to the development of disease progression

Parameter	Patients	
	Absence of disease progression after 5 years (n=82)	Disease progression within 5 years (n=36)
Mean age	69.45±10.09	70.55±7.6
Sex		
M	46	19
F	36	17
Site		
Right colon	26	3
Left colon	38	13
Rectum	18	20
Grade WHO		
Low grade	77	34
High grade	5	2
Grade PDC		
G1	56	12
G2	19	14
G3	7	10
Cancer growth		
Expanding	60	7
Infiltrative	22	29
Tumor budding		
Absent	60	13
Present	22	23
Perineural invasion		
Absent	62	9
Present	20	36
Number of retrieved nodes		
<12	55	25
≥12	26	11
pT		
pT1	15	5
sm1	10	2
sm2	5	0
sm3	0	3
pT2	67	31
pN		
$pN0_{micro-}$	78	10
$pN0_{micro+}$	4	26
L		
Absent	77	9
Present	5	27

PDC poorly differentiated clusters

CRC were quantified according to the procedure previously described [15]. In detail, the whole tumor including its advancing edge was first scanned at a lower-power magnification to identify the area with the highest number of poorly differentiated clusters. Next, the clusters were counted using a ×20 objective lens (i.e., a microscopic field with a diameter of 1 mm), on a Zeiss microscope. Tumors with <5.5 to 9 and ≥10 clusters were classified as grade 1 (G1), grade 2 (G2), and grade 3 (G3), respectively. Two pathologists (VB and LRB) established the histological grade, using as a reference the image shown in the paper by Ueno et al. [15], and blinded to the clinicopathological data. In case of disagreement, consensus was reached by examination using a double-headed microscope.

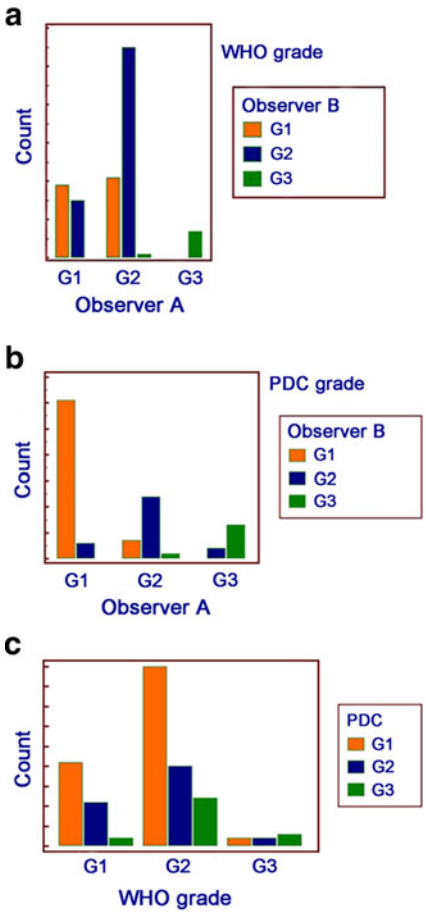

Fig. 1 **a** Interobserver reproducibility in the assessment of histological grading based on glandular differentiation, according to WHO criteria. Variability mainly involved the definition of G1 and G2 cases, while that of G3 cancers was more consistent. **b** Interobserver reproducibility in the assessment of histological grading based on poorly differentiated clusters. Variability mainly involved the definition of G2 carcinomas, while that of G1 and G3 cancers was more consistent. **c** Comparison between histological grading based on glandular differentiation and on poorly differentiated clusters in the cases of our cohort. Discordance between the two systems involved all three grades

Statistical analyses

Fleiss–Cohen's weighted k statistics were used for the assessment of interobserver variability in tumor grading; K

Table 2 Statistical correlations between WHO grade and the various clinicopathological parameters of the 118 CCRs, investigated through chi-square and Fisher's exact tests

Parameter	WHO grade		*P*
	Low grade	High grade	
Gender			
Male	61	4	NS
Female	50	3	
Site			
Right colon	25	4	NS
Left colon	48	3	
Rectum	38	0	
Tumor growth			
Expanding	62	5	NS
Infiltrative	49	2	
Tumor budding			
Absent	71	2	NS
Present	40	5	
Perineural invasion			
Absent	86	3	NS
Present	25	4	
pT			
pT1	20	0	NS
pT2	91	7	
pN			
$pN0_{micro-}$	83	5	NS
$pN0_{micro+}$	28	2	
L			
Absent	81	5	NS
Present	30	2	
Disease progression within 5 years			
Not	77	5	NS
Yes	34	2	

NS not significant

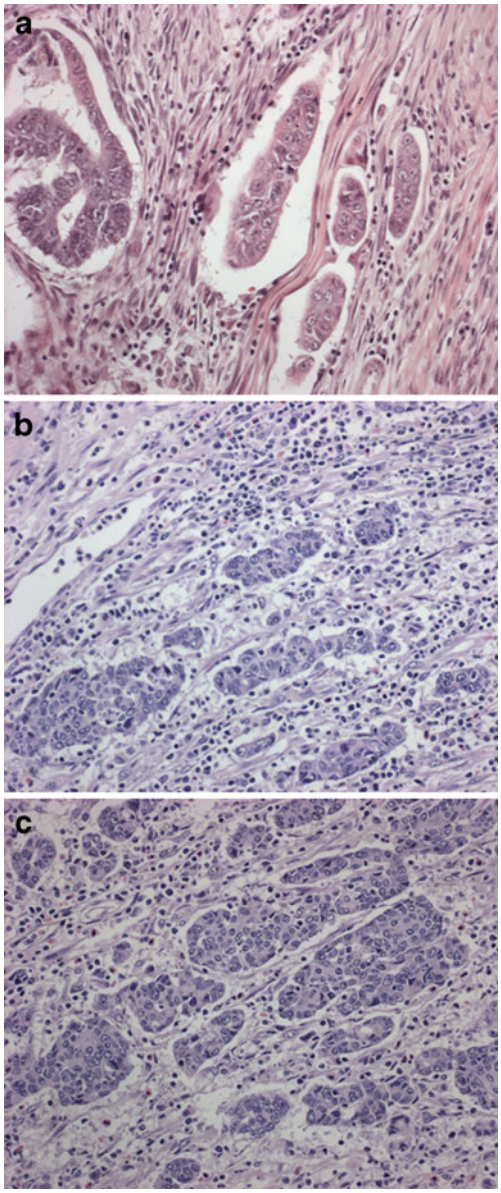

Fig. 2 **a** Histological grading based on poorly differentiated clusters: **a** G1 colorectal carcinoma, showing less than five poorly differentiated clusters in a microscopic filed of a ×20 objective lens (haematoxylin and eosin stain; original magnification, ×200); **b** G2 colorectal cancer, with eight poorly differentiated clusters in a microscopic filed of a ×20 objective lens (haematoxylin and eosin stain; original magnification, ×200); **c** G3 colorectal cancer, with more than 10 poorly differentiated clusters in a microscopic field of a ×20 objective lens (haematoxylin and eosin stain; original magnification, ×200)

statistics was applied in order to compare the two methods of grading.

Chi-square and Fisher's exact tests were carried out to investigate the statistical correlations between the two histological grading systems and the various clinicopathological parameters, including site of the tumors, depth of infiltration in the colonic wall (pT and sm), pattern of growth, tumor budding, perineural invasion, lymphatic invasion, occult nodal disease, and disease progression.

The area under receiver operating characteristic (ROC) curve was calculated to verify the prediction accuracy of each grading system regarding the presence of nodal occult disease ($pN0_{micro+}$) and the risk of progression of the tumor.

The impact of the various histological parameters on the progression-free survival of the patients was assessed by the Kaplan–Meier method, with entry date as the date of primary surgery. The end point was defined as the duration of survival to disease progression (metastatic disease) of CRC. Follow-up ranged between 9 and 154 months. The Mantel–Cox log-rank test was applied to assess the strength of association between time to progression and each of the histological parameters (pT stage, submucosal invasion, pattern of growth, histological grade based on glandular formation, histological grade based on poorly differentiated clusters, tumor budding, perineural invasion, lymphatic invasion, $pN0_{micro+}$, number of

Table 3 Statistical correlations between histological grading based on poorly differentiated clusters grade and the various clinicopathological parameters of the 118 CCRs, investigated through chi-square test

Parameter	Grading based on poorly differentiated clusters			*P*
	G1	G2	G3	
Gender				
Male	38	18	9	NS
Female	30	15	8	
Site				
Right colon	18	6	5	NS
Left colon	28	18	5	
Rectum	22	9	7	
Tumor growth				
Expanding	43	19	5	0.041
Infiltrative	25	14	12	
Tumor budding				
Absent	56	13	4	<0.0001
Present	12	20	13	
Perineural invasion				
Absent	54	25	10	NS
Present	14	8	7	
pT				
pT1	10	8	2	NS
pT2	58	25	15	
SM				
sm1	7	5	0	NS
sm2	3	1	1	
sm3	0	2	1	
pN				
$pN0_{micro-}$	61	20	7	<0.0001
$pN0_{micro+}$	7	13	10	
L				
Absent	56	22	8	0.008
Present	12	11	9	
Disease progression within 5 years				
Not	56	19	7	0.0009
Yes	12	14	10	

NS not significant

retrieved lymphnodes) as a single variable. Subsequently, a multivariate analysis (Cox regression model) was used to determine the independent effect of each significant variable.

A $P<0.05$ was considered as statistically significant. Data were analyzed using the SPSS package version 6.1.3 (SPSS Inc., Chicago, IL, USA).

Results

The clinicopathological characteristics of the CRCs included in the study in relation to prognosis are shown in Table 1. Conventional grading of the tumors in our cohort resulted in 34 well differentiated (grade 1), 77 moderately differentiated (grade 2), and 7 poorly differentiated (grade 3) CRCs, corresponding to 111 low-grade and 7 high-grade carcinomas according to the 2010 WHO classification [17]. Interobserver agreement in the assessment of conventional grading was moderate when using the WHO three-tiered grading system (*K*, 0.431) [16]. Disagreement mainly concerned well and moderately differentiated tumors, whereas reproducibility was higher in the identification of poorly differentiated cases (Fig. 1a). The interobserver agreement increased to good (*K*, 0.715) when the two-tiered system proposed in the 2010 WHO classification was applied [17]. Conventional grading did not correlate with the various clinico-pathological parameters (Table 2).

The grading system based upon poorly differentiated cell clusters resulted in 68 grade 1 (Fig. 2a), 33 grade 2 (Fig. 2b), and 17 grade 3 (Fig. 2c) CRCs. Interobserver agreement in grading using this approach was good (*K*, 0.776), interobserver variability mainly concerning grade 2 tumors (Fig. 1b). Discordance in grading between the pathologists concerned five CRCs with a mucinous component of less than 50 %. In these cases, the divergent histological grade depended upon the inclusion or exclusion in the count of poorly differentiated clusters of the groups of cells within the mucus. Consensus was reached following the decision to exclude the mucinous component from the count.

Comparison of the two grading systems by *K* statistics resulted in poor concordance (*K*, 0.080), the disagreement involving all three grades (Fig. 1c). High histological grade assessed by counting poorly differentiated cell clusters significantly correlated with infiltrative growth ($P=0.041$), tumor budding ($P<0.0001$), $pN0_{micro+}$ ($P<0.0001$), and lymphatic invasion ($P=0.008$; Table 3). In addition, the novel histological grade but not the conventional grade was significantly correlated with disease evolution, patients showing disease progression having a higher grade tumor than those without evidence of disease progression 5 years after the initial diagnosis ($P=0.0009$; Table 3).

The predictive value of histological grade on the presence of occult nodal metastases and the risk of disease progression was higher when assessed by the novel grading system than by conventional grading. Specifically, with reference to the predictive value on occult nodal metastases, the area under ROC curve was 0.751 ($P=0.0001$) for grading based on poorly differentiated clusters, while it was 0.505 ($P=0.8513$) for WHO grading. Regarding the predictive value on progression risk, the area under ROC curve was 0.690 for grading based on poorly differentiated clusters ($P=0.0001$), while it was 0.503 ($P=0.9081$) for WHO grading.

Univariate analyses revealed that localization in the rectum, deeper submucosal invasion (sm3) for pT1 cancers, an infiltrative growth pattern, the presence of tumor budding, lymphatic invasion, occult nodal metastases, as well as high

Table 4 Univariate and multivariate analyses for progression-free survival in 118 TNM stage I colorectal carcinomas

Parameter	X^2	*df*	*P*	β	SE	Exp (β)
Univariate analysis						
Age	0.09634	1	0.7563			
Site	13.2567	2	0.0013			
pT	0.2096	1	0.6471			
sm	25.17	2	<0.0001			
Grade PDC	15.9902	2	0.0003			
WHO grade	0.003066	1	0.9558			
Tumor Budding	14.9747	1	0.0001			
Tumor growth	18.235	1	<0.0001			
Perineural invasion	0.000015	1	0.9968			
Lymphatic invasion	74.5385	1	<0.0001			
Nodal occult disease	81.9622	1	<0.0001			
Number of retrieved nodes	0.01757	1	0.8945			
Multivariate analysis						
Lymphatic invasion			0.0001	1.6884	0.4932	5.4106
Nodal occult disease			0.0006	1.8106	0.4853	6.1142

PDC poorly differentiated clusters

histological grade based on poorly differentiated clusters, but not WHO grade, were significant negative prognostic parameters (Table 4; Fig. 3a and b). Multivariate analysis confirmed lymphatic invasion and occult nodal metastases as independent prognostic parameters (P=0.0006, P=0.0001; Table 4).

Discussion

In the past, a variety criteria, including architecture, the presence of glandular structures, the pattern of invasion, cytological features and the number of mitoses have been proposed in attempts to get to a reproducible histological grading of CRC [24–26]. The most widely used system at present for grading CRC is based on the degree of gland formation, while other features, such as the invasiveness or tumor architecture, are considered as independent factor [27]. In particular, according to the WHO classification of tumors of the digestive system [16], histological grade of CRC is defined by considering the percentage of the tumor showing formation of gland-like structures: well differentiated (grade 1) CRCs exhibiting glandular structures in more than 95 % of the tumor, moderately differentiated (grade 2) CRCs 50–95 %, poorly differentiated (grade 3) cancers 5–50 % and undifferentiated (grade 4) less than 5 % glandular structures [16]. In addition, in the fourth edition of the WHO classification, it has been proposed to group grades 1 and 2 as "low-grade" and grades 3 and 4 as "high grade" CRCs [17]. The weakness of this grading system is that the estimation of the degree of gland formation and as a consequence assignment of a grade are rather subjective [12–14], and lead to significant interobserver variability and limit the prognostic significance of the histological grade [14]. Further increasing the subjectivity is that according to the WHO criteria, in heterogeneous tumors, grade should be established considering the least differentiated component, the size of the area to be considered not being specified [17].

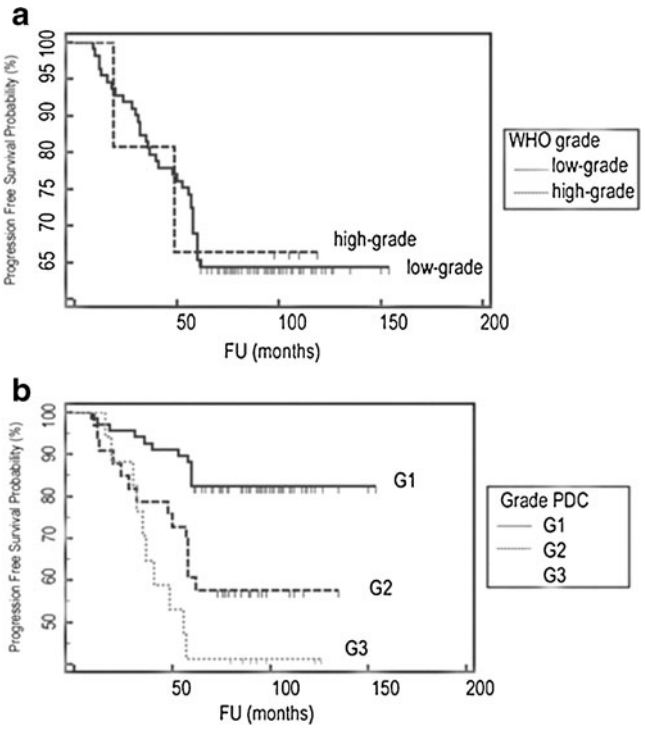

Fig. 3 **a** Kaplan–Meier curves showing that progression-free survival does not differ on the basis of WHO grade in patients with stage I colorectal carcinomas. **b** Kaplan–Meier curves showing that progression-free survival is significantly longer in patients with stage I colorectal cancers characterized by low histological grade assessed by counting PDC

Given the need to standardize the criteria for the assessment of histological grade in CRC, a novel system, based on the count of poorly differentiated clusters has been recently proposed [15]. Based upon the evidence that this system has a higher reproducibility than conventional grading in stages II and III tumors [15], in the present study we compared the interobserver reproducibility and prognostic value of the novel and conventional grading systems in a cohort of pTNM stage I CRCs in order to assess whether the novel grading system might identify patients at higher risk of progression. We demonstrate that also in stage I CRC, the interobserver reproducibility of the novel grading system is higher than that of the conventional system, which might be related to the better standardization of novel system. We found moderate interobserver agreement with three-tiered conventional system [16], variability mainly involving the distinction between well- and moderately differentiated CRCs, and it improved to good when the recently suggested two-tiered system [17] was applied. Good interobserver agreement with higher *K* value was using the novel grading system, although variability remained in the assessment of all three grades. Interestingly, one cause of disagreement in the novel system appeared to be CRCs with a mucinous component. In the original paper which proposes counting poorly differentiated cell clusters for CRC grading [15], the authors included cases with a mucinous component representing more than 50 % of the tumor but they did not specify whether their count of poorly differentiated clusters included mucinous areas or not [15]. Our patient series did not include mucinous CRCs, but some cases had a mucinous component of less than 50 % of the tumor. Assessors disagreed in grading these tumors as inclusion or exclusion of mucinous areas in counting poorly differentiated clusters that had not been agreed upon. Consensus was reached at the double-headed microscope following the decision to exclude mucinous areas, as according to WHO criteria the presence of a mucinous component should be mentioned separately in the histological report of CRC and should not be included in the grading [17].

We found poor concordance when comparing the two histological grading approaches. By conventional grading, most cases (65 %) were moderately differentiated (G2), 29 % were well differentiated (G1), and only 6 % were poorly differentiated (G3). In contrast, using the novel grading system 28 % CRCs were G2 while G1 increased to 58 % and G3 to 14 %. Thus, the novel grading system reduces the number of G2 cases and increases the number of G1 tumors.

Although interobserver reproducibility of conventional grading increased when passing from a three-tiered to a two-tiered system [17], it did not correlate with clinicopathological features, in line with the findings in stage II and III CRCs [15]. We clearly show that also in stage pTNM I CRC tumor grading based on poorly differentiated cell clusters, but not conventional grading, significantly correlates with histological parameters associated with bad prognosis, such as infiltrative growth, tumor budding, and lymphatic vessel invasion. In addition, novel grading provides a significant negative, although not independent, prognostic marker in stage I CRC. We also observed a significant correlation between high novel but not conventional histological grade and the presence of occult nodal metastases, defined as the presence of metastatic deposits detected by immunohistochemistry or reverse transcription polymerase chain reaction and measuring less than 2 mm in greatest extent in otherwise node negative (pN0) cancers [20, 27–30]. Occult nodal metastases recently received increased attention as a significant prognostic factor for risk of recurrence in patients with pN0 CRC [23, 31]. Our data show that occult nodal metastases represent an independent negative prognostic parameter in pTNM stage I CRC patients. We speculate that the novel histological grade represents a more efficient tool to than the time-consuming and costly evaluation of occult nodal metastases to identify pTNM stage I CRC patients at increased risk of disease progression. Furthermore, novel histological grading might be applied to assess the risk of nodal involvement, in case of conservative local excision approaches for low rectal carcinoma when nodes cannot be examined or their number is lower than the recommended 12 necessary for accurate staging.

In conclusion, we show that also in pTNM stage I CRC the novel tumor grading system based on counting poorly differentiated cell clusters is more reproducible than conventional grading. This grading system deserves to be reassessed in larger cohorts of CRCs to further test its reproducibility and prognostic value and its significance in CRC histological subtypes. Novel grading constitutes an additional histological tool to select stage I CRC patients who might benefit from adjuvant systemic treatment.

Acknowledgments We wish to thank Associazione Italiana Ricerca Cancro (AIRC) for financial support.

Conflict of interest statement We declare that we have no conflict of interest.

References

1. Landis SH, Murray T, Bolden S (1999) Cancer statistics. Cancer J Clin 49:8–31
2. Wiggers T, Arends JW, Schutter B et al (1988) A multivariate analysis of pathologic prognostic indicators in large bowel cancer. Cancer 61:386–395
3. Wu XC, Chen VW, Steele B et al (2001) Subsite-specific incidence rate and stage of disease in colorectal cancer by race, gender, and age group. Cancer 92:2547–2554
4. Di Gregorio C, Fante R, Roncucci L et al (1996) Clinical features, frequency and prognosis of Dukes' A colorectal carcinoma: a population-based investigation. Eur J Cancer 32A:1957–1962
5. Barresi V, Reggiani-Bonetti L, Di Gregorio C et al (2010) Stage I colorectal carcinoma: vascular endothelial growth factor (VEGF)

immunohistochemical expression, microvessel density and their correlation with clinical outcome. Virchows Arch 457:11–19
6. Barresi V, Ieni A, Reggiani-Bonetti L, Di Gregorio C et al (2011) Neutrophil gelatinase-associated lipocalin (NGAL): a new prognostic marker in stage I colorectal carcinoma? Hum Pathol 42:1720–1726
7. Barresi V, Reggiani-Bonetti L, Di Gregorio C et al (2011) Lymphatic vessel density and its prognostic value in stage I colorectal carcinoma. J Clin Pathol 64:6–12
8. Barresi V, Reggiani-Bonetti L, Di Gregorio C et al (2011) Neutrophil gelatinase-associated lipocalin (NGAL) and matrix metalloproteinase-9 (MMP-9) prognostic value in stage I colorectal carcinoma. Pathol Res Pract 207:479–486
9. Barresi V, Reggiani-Bonetti L, Vitarelli E et al (2012) Immunohistochemical assessment of lymphovascular invasion in stage I colorectal carcinoma: prognostic relevance and correlation with nodal micrometastases. Am J Surg Pathol 36:66–72
10. Freedman LS, Macaskill P, Smith AN (1984) Multivariate analysis of prognostic factors for operable rectal cancer. Lancet 29:733–736
11. Fisher ER, Sass R, Palekar A et al (1989) Dukes' classification revisited. Findings from the National Surgical Adjuvant Breast and Bowel Projects (Protocol R-01). Cancer 64:2354–2360
12. Blenkinsopp WK, Stewart-Brown S, Blesovsky L et al (1981) Histopathology reporting in large bowel cancer. J Clin Pathol 34:509–513
13. Thomas GDH, Dixon MF, Smeeton NC et al (1983) Observer variation in the histological grading of rectal carcinoma. J Clin Pathol 36:385–391
14. Chandler I, Houlston RS (2008) Interobserver agreement in grading of colorectal cancers-findings from a nationwide web-based survey of histopathologists. Histopathology 52:494–499
15. Ueno H, Kajiwara Y, Shimazaki H et al (2012) New criteria for histologic grading of colorectal cancer. Am J Surg Pathol 36:193–201
16. Hamilton SR, Volgelstein B, Kudo S et al (2000) Carcinoma of the colon and rectum. In: Hamilton SR, Aaltonen LA (eds) Pathology and genetics of tumours of the digestive system. IARC Press, Lyon, pp 110–111
17. Hamilton SR, Bosman FT, Boffetta P (2010) Carcinoma of the colon and rectum. In: Bosman T, Carneiro F, Hruban RH, Theise ND (eds) WHO classification of tumours of the digestive system. IARC Press, Lyon, pp 138–139
18. Sobin L, Gospodarowicz M, Wittekind C (2009) TNM classification of malignant tumours. Wiley, New York
19. Kikuchi R, Takano M, Takagi K et al (1995) Management of early invasive colorectal cancer. Risk of recurrence and clinical guidelines. Dis Colon Rectum 38:1286–1895
20. Morodomi T, Isomoto H, Shirouzu G et al (1989) An index for estimating the probability of lymph node metastasis in rectal cancers. Lymph node metastasis and the histopathology of actively invasive regions of cancers. Cancer 63:539–643
21. Ueno H, Mochizuki H, Hashiguchi Y et al (2004) Preoperative parameters expanding the indication of sphincter preserving surgery in patients with advanced low rectal cancer. Ann Surg 239:34–42
22. Reggiani Bonetti L, Di Gregorio C et al (2011) Lymph node micrometastasis and survival of patients with stage I (Dukes' A) colorectal carcinoma. Scand J Gastroenterol 46:881–886
23. Lips DJ, Koebrugge B, Liefers GJ et al (2011) The influence of micrometastases on prognosis and survival in stage I–II colon cancer patients: the Enroute study. BMC Surg 11:11
24. Stewart FW, Spies JW (1929) Biopsy histology in the grading of rectal carcinoma. Am J Pathol 5:109–115
25. Dukes C (1937) Histological grading of rectal cancer. Proc R Soc Med 30:371–376
26. Grinnell RS (1939) The grading and prognosis of carcinoma of the colon and rectum. Ann Surg 109:500–533
27. Compton CC, Fielding LP, Burgart LJ et al (2000) Prognostic factors in colorectal cancer. College of American Pathologists consensus statement 1999. Arch Pathol Lab Med 124:979–994
28. Nicastri DG, Doucette JT, Godfrey TE et al (2007) Is occult lymph node disease in colorectal cancer patients clinically significant? A review of the relevant literature. J Mol Diagn 9:563–571
29. Greenson JK, Isenhart CE, Rice R et al (1994) Identification of occult micrometastases in pericolic lymph nodes of Duke's B colorectal cancer patients using monoclonal antibodies against cytokeratin and CC49. Correlation with long-term survival. Cancer 73:563–569
30. Hayashi N, Ito I, Yanagisawa A, Kato Y et al (1995) Genetic diagnosis of lymph node metastasis in colorectal cancer. Lancet 345:1257–1259
31. Mescoli C, Albertoni L, Pucciarelli S et al (2012) Isolated tumor cells in regional lymph nodes as relapse predictors in stage I and II colorectal cancer. J Clin Oncol 30:965–971

Virchows Arch (2012) 461:629–638
DOI 10.1007/s00428-012-1324-x

ORIGINAL ARTICLE

Correlation of immunohistochemical staining p63 and TTF-1 with EGFR and K-ras mutational spectrum and diagnostic reproducibility in non small cell lung carcinoma

Erik Thunnissen · Evan Boers · Daniëlle A. M. Heideman · Katrien Grünberg · Dirk J. Kuik · Arnold Noorduin · Matthijs van Oosterhout · Divera Pronk · Cees Seldenrijk · Hannie Sietsma · Egbert F. Smit · Robertjan van Suylen · Jan von der Thusen · Bart Vrugt · Anne Wiersma · Birgit I Witte · Michael den Bakker

Received: 23 June 2012 / Revised: 11 September 2012 / Accepted: 25 September 2012 / Published online: 12 October 2012
© Springer-Verlag Berlin Heidelberg 2012

Abstract For treatment purposes, distinction between squamous cell carcinoma and adenocarcinoma is important. The aim of this study is to examine the diagnostic accuracy on lung cancer small biopsies for the distinction between adenocarcinoma and squamous cell carcinoma and relate these to immunohistochemical and *KRAS* and *EGFR* mutation analysis. An interobserver study was performed on 110 prospectively collected biopsies obtained by bronchoscopy or transthoracic needle biopsy of patients with non-small cell lung cancer. The diagnosis was correlated with

E. Thunnissen (✉) · D. A. M. Heideman · K. Grünberg · D. Pronk
Department of Pathology, VU University Medical Center,
De Boelelaan 1117,
1081 HV, Amsterdam, The Netherlands
e-mail: e.thunnissen@vumc.nl

D. A. M. Heideman
e-mail: dam.heideman@vumc.nl

K. Grünberg
e-mail: k.grunberg@vumc.nl

D. Pronk
e-mail: d.pronk@vumc.nl

E. Boers
Department of Pathology, Isala klinieken,
Stilobadstraat 3,
Overijssel, The Netherlands
e-mail: j.e.boers@isala.nl

D. J. Kuik · B. I. Witte
Department of Epidemiology and Biostatistics, VUmc,
Amsterdam, The Netherlands

D. J. Kuik
e-mail: Dj.kuik@vumc.nl

B. I. Witte
e-mail: b.witte@vumc.nl

A. Noorduin
Department of Pathology,
Laan van Londen 1800,
3317 DA, Dordrecht, The Netherlands
e-mail: anoorduyn@paldordrecht.nl

M. van Oosterhout · C. Seldenrijk
Department of Pathology, St. Antonius Ziekenhuis,
Koekoekslaan 1,
3435 CM, Nieuwegein, The Netherlands

M. van Oosterhout
e-mail: m.van.oosterhout@antoniusziekenhuis.nl

C. Seldenrijk
e-mail: k.seldenrijk@antoniusziekenhuis.nl

H. Sietsma
Department of Pathology, UMCG, Martiniziekenhuis,
Van Swietenplein 1,
9700 RM, Groningen, The Netherlands
e-mail: j.sietsma@mzh.nl

E. F. Smit
Department of Pulmonology, VU University Medical Center,
De Boelelaan 1117,
1081 HV, Amsterdam, The Netherlands
e-mail: ef.smit@vumc.nl

R. van Suylen
Department of Pathology, AZM,
P. Debyelaan 25,
6229 HX, Maastricht, The Netherlands
e-mail: rj.van.suylen@yahoo.com

J. von der Thusen
Department of Pathology AMC,
Meibergdreef 9,
1105 AZ, Amsterdam, The Netherlands
e-mail: j.vonderthusen@rbht.nhs.uk

immunohistochemical (IHC) analysis for markers of adeno- (TTF1 and/or mucin positivity) and squamous cell differentiation (P63 and CK5/6) as well as *KRAS* and *EGFR* mutation analysis. Eleven observers independently read H&E-stained slides of 110 cases, resulting in a kappa value of 0.55±0.10. The diagnosis non-small cell lung cancer not otherwise specified was given on average on 29.5 % of the biopsies. A high concordance was observed between hematoxylin–eosin-based consensus diagnosis (≥8/11 readings concordant) and IHC markers. In all cases with *EGFR* (n=1) and *KRAS* (n=20) mutations, adenodifferentiation as determined by IHC was present and p63 staining was absent. In 2 of 25 cases with a consensus diagnosis of squamous cell carcinoma, additional stainings favored adenodifferentation, and a *KRAS* mutation was present. P63 is most useful for distinction between *EGFR*/*KRAS* mutation positive and negative patients. In the diagnostic work-up of non-small cell lung carcinoma the limited reproducibility on small biopsies is optimized with immunohistochemical analysis, resulting in reliable delineation for predictive analysis.

Keywords Adenocarcinoma · Squamous cell carcinoma · Lung cancer · Reproducibility · Immunohistochemistry · Mutation analysis

Introduction

Until recently, for practical purposes, pulmonary carcinoma was divided in small cell lung cancer (SCLC) and non-small cell lung cancer (NSCLC). However, distinguishing squamous cell carcinoma (SqCC) from non-SqCC, the latter comprising adenocarcinoma and large cell carcinoma, has become increasingly more important as international guidelines (National Comprehensive Cancer Network, American Society Clinical Oncology, and European Society Medical Oncology) advise against the use of bevacizumab in SqCC for safety reasons. In addition, in adenocarcinoma pemetrexed has superior efficacy compared to SqCC based on the results of recent phase III trials [1–4]. Furthermore, driver mutations such as activating epidermal growth factor receptor (EGFR) mutations [5, 6] and EML4-Alk rearrangements are predominantly found in non-SqCC [7]. Based on the results of recent phase I/II and III trials in patients with these genomic alterations, treatment with tyrosine kinase inhibitors is the treatment of choice [7, 8]. Thus, for a rational strategy in genomic diagnostics in NSCLC, the reliable distinction between non-SqCC and SqCC is of paramount importance.

The WHO pathology classification is based on the standard histochemical hematoxylin–eosin (H&E) staining. In the current WHO classification, confirmatory immunohistochemical typing is only required for the diagnosis of large cell neuroendocrine carcinoma [9]. The use of special histochemical stains to demonstrate the presence of luminal and intracytoplasmic mucin droplets is optional. Most lung cancers are diagnosed by biopsy or cytology. However, most of the initial reproducibility studies were performed on resection specimen [10–12]. Interestingly, the diagnosis on biopsy does not always reflect the diagnosis on the corresponding resection specimen [13, 14]. In biopsy studies on SqCC and adenocarcinoma, reproducibility improves with the use of a mucin stain [15, 16]. Recently, a multidisciplinary classification of adenocarcinoma has been described, with additional staining for subtyping of NSCLC [17–19]. The data supporting the immunohistochemical approach was obtained in a subgroup of lower stage lung cancer patients by comparison from biopsies with resection of the same patients [20–22]. Moreover, the assumption is made that with this categorization of NSCLC into adenocarcinoma and squamous cell carcinoma, the associated mutations are also defined within these subgroups. Overall, the questions arises how good (1) the diagnostic accuracy is for NSCLC typing on biopsies in current routine practice and (2) the immunohistochemical approach delineates the category with EGFR and KRAS mutations. The aim of this study is to examine the diagnostic accuracy on lung cancer biopsies for the distinction between adenocarcinoma and SqCC and relate these to immunohistochemical and *KRAS* and *EGFR* mutation analysis. To this end, an interobserver study was performed on prospectively collected biopsies obtained by bronchoscopy or transthoracic needle biopsy.

Materials and methods

In a multicenter cross-sectional study, seven laboratories prospectively sampled bronchoscopic or transthoracic biopsies obtained in the diagnostic work-up of 110 patients with primary pulmonary non-small cell lung carcinoma. In each

B. Vrugt
Department of Pathology, Martiniziekenhuis,
Van Swietenplein 1,
9728 NT, Groningen, The Netherlands
e-mail: bart.vrugt@usz.ch

A. Wiersma
Department of Pathology,
Wagnerlaan 55,
6815 AD, Arnhem, The Netherlands
e-mail: awiersma@alysis.nl

M. den Bakker
Department of Pathology, Erasmus MC,
Dr. Molewaterplein 50,
3015 GE, Rotterdam, Netherlands
e-mail: m.denbakker@erasmusmc.nl

Present Address:
B. Vrugt
Institut für Klinische Pathologie, Universitäts Spital Zürich,
Schmelzbergstrasse 12,
8091 Zürich, Switzerland

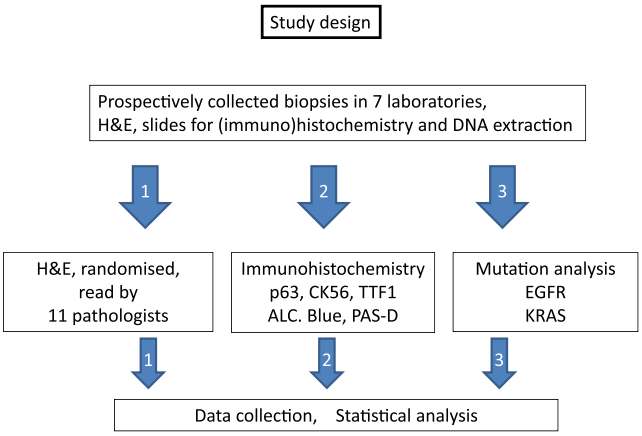

Fig. 1 Schematic representation of study design

laboratory, at least 10 biopsies were collected. Study design is shown in Fig. 1. All samples were used in compliance with the respective institutional ethical regulations. H&E-stained sections were randomized, divided in three sets, and independently read by 11 pathologists, members of Dutch pulmonary pathology group. Histotyping was performed according to the WHO classification [9] and recorded as adenocarcinoma, NSCLC favor adenocarcinoma, SqCC, NSCLC favor SqCC, or NSCLC not otherwise specified (NOS).

Immunohistochemistry was performed as described before [23]. For NKX2.1/TTF1 clones, 8G7G3/1 or SPT24 were used, and for p63, 4A4 alone or in combination with Y4A3 was used. Mucin staining was performed by diastase periodic acid–schiff (PAS-D) and Alcian blue methods according to routine procedure. The immunohistochemically stained slides were scored for intensity (from 0 to 3, 0=negative, 1=weak, 2=moderate, and 3= strongly positive) and percentage of positive tumor cells with 10 % increments by one observer (ET). For each immunohistochemical stain, a total score was obtained by multiplying intensity and percentage positive tumor cells. Cases with adenocarcinoma differentiation were defined as those with a TTF-1 score of >30. Cases with SqCC differentiation were defined as those with a p63 score of >240. As p63 may occasionally stain adenocarcinomas with scattered cells with variable intensity and because SqCC is strongly positive for p63 in all basal and parabasal (but not in the more mature) tumor cells, this threshold was chosen because it clearly delineates SqCC from adenocarcinoma differentiation [19]. For TTF1, a positive threshold of >30 was used, as even minor staining is associated with adenodifferentiation. Mucin stains were scored as positive or negative, requiring at least two tumor cells in the biopsy with distinct intracytoplasmic mucin droplets to designate this staining positive.

After submission of the H&E readings, the outcome of the (immuno)histochemical stains were read by one observer (ET), and mutation analysis were submitted to the central database for statistical analysis.

Mutation analysis was performed for *KRAS* and *EGFR* using high-resolution melting assay followed by cycle sequencing of products with an aberrant melt curve at the Department of Pathology (VU University Medical Center, Amsterdam, The Netherlands), as described previously [24, 25]. Mutation analysis was performed blinded for the histological and IHC data. The mutation data were submitted to the central database for statistical analysis.

Statistical analysis

Frequency distributions and kappa scores were calculated for 11 observers and 5 categories with SPSS package version 15 (JK). H&E diagnosis was defined as "consensus" if eight or more readings were concordant; cases failing to reach consensus were considered "NSCLC NOS." As marker for adenodifferentiation TTF1 or mucin positivity was used, while positivity for p63 was used as squamous differentiation. Chi-2 tests were performed for frequency distribution; $p<0.05$ was considered significant.

Results

H&E-based pathology diagnoses

Eleven observers independently read H&E stained slides of 110 prospectively collected cases. The distribution over the five categories is shown in Table 1. The mean of the frequency of morphological diagnosis by the 11 observers were for definite adenocarcinomas, 19.8 %; probable adenocarcinoma, 13.6 %; definite SqCC, 18.6 %; probable SqCC, 18.6 %; and NSCLC not otherwise specified (NOS), 29.5 %. For a distinction into three categories: definite adenocarcinoma, definite SqCC, and other groups combined the kappa value was 0.53±0.11. For another composition of three categories, combining the definite and probable adenocarcinoma in one group, the definite and probable SqCC in the second group, and the NSCLC NOS in the third group, the kappa value was 0.44±0.10.

The diagnosis NSCLC NOS was given on average on 29 % of the biopsies. After combining the definite and probable adenocarcinomas as well as the definite and probable SqCCs, 15 cases were unanimously diagnosed as adenocarcinoma and 14 as SqCC. In total, 32 cases were diagnosed at least adenocarcinoma once without a diagnosis of SqCC, and 36 cases diagnosed as SqCC without a diagnosis of adenocarcinoma. In 43 % of the cases, at least one of the 11 diagnosis consisted of adenocarcinoma and SqCC. The five most ambiguous cases had at least either four squamous cell and three adenocarcinoma diagnosis or vice versa, with each twice NSCLC NOS

Table 1 For the H&E diagnosis of diagnosis by 11 pathologists on 110 cases, mean, standard deviation (SD) and range, immunohistochemical staining support for adenocarcinoma and squamous cell carcinomas are shown for the five categories

H&E diagnosis	Mean±SD	Range	Staining support for adenocarcinoma (%)	Staining support for squamous cell carcinoma (%)
Adenocarcinoma	19.8±5.1 %	11.8–27.3 %	32.0	6.0
Probably adenocarcinoma	13.6±7.4 %	3.6–30.0 %	17.5	7.9
NSCLC-NOS	29.5±8.0 %	10–37.3 %	28.1	27.1
Probably squamous cell carcinoma	18.6±5.0 %	13.6–29.1 %	11.0	27.7
Squamous cell carcinoma	18.6±6.3 %	4.5–30 %	11.4	31.3

NSCLC-NOS non-small cell lung carcinoma not otherwise specified

(Immuno)histochemistry

Mucin staining with Alcian blue and PAS-D was concordant in 91 % of the cases, while Alcian blue positivity with PAS-D negativity was seen in seven cases and vice versa in three cases ($p=10^{-14}$). Immunohistochemical evidence of adeno-differentiation (TTF1-positive and/or mucin-positive) was present in 56 of 110 cases, with both stains positive in 17 cases ($p=0.03$).

For all diagnosis of 11 pathologists, the immunohistochemical phenotype related to H&E categories is shown in Table 1. It is noteworthy that, for the expected phenotype based on H&E diagnosis "probably" and "certain," a similar fraction of opposite immunohistochemical phenotype is present. For squamous cell carcinoma, the opposite phenotype from expected is higher than for adenocarcinoma.

In 4 of 101 cases, the additional stains showed positivity for squamous as well as adeno-differentiation and in another 10 of 101 cases special stains were negative.

Prediction

Of 106 of the 110 specimens, sufficient tissue was left for mutation analysis. Mutation analysis was successful in 101/of 106 (95 %) of cases for both *EGFR* and *KRAS*, and in one case, only *EGFR* analysis was successful, while *KRAS* could not be determined due to the limited amount of DNA. In four cases, DNA was of insufficient quality. In the 101 cases, 20 *KRAS* mutations (20 %) and 1 *EGFR* (1 %) mutation were detected. Twenty-three percent of the biopsies were obtained by a transthoracic approach, with a slightly higher mutation rate (35 %) than central (bronchoscopic) biopsies (17 %, $p=0.07$). The case with *EGFR* mutation was unanimously diagnosed as "certain adenocarcinoma." In the H&E-based consensus diagnosis, mutations were found more frequently in adenocarcinoma and in the NSCLC NOS group than in SqCC ($p=0.002$). The distribution of the H&E diagnosis over the five categories was not associated with mutations ($p=0.63$). The presence of mucin was

Table 2 Distribution of H&E-based consensus diagnosis, immunohistochemistry (for adeno- and squamous differentiation +/−), and mutation analysis (yes/no) is shown

			Mutation yes		Mutation no		Total
			IHC adeno combi		IHC adeno combi		
			+	−	+	−	
H&E consensus diagnosis[a]	Adenocarcinoma	P63+	0	0	0	2	2
		P63−	11	0	10	1	22
	NSCLC, NOS	P63+	0	0	1	21	22
		P63−	8	0	15	7	30
	Squamous cell carcinoma	P63+	0	0	3	17	20
		P63−	2	0	1	2	5
Total			21	0	30	50	101

IHC adeno combination consisted of at least one positive marker: TTF1, and/or mucin (PAS-D and/or Alcian blue)

[a] H&E-based consensus diagnosis obtained with ≥8/11 readings concordant; adenocarcinoma represents the IASLC/ATS/ERS classification categories adenocarcinoma and NSCLC favor adenocarcinoma, while squamous cell carcinoma represents squamous cell carcinoma and NSCLC, favor squamous cell carcinoma

Table 3 Test characteristics [sensitivity, specificity, positive predictive value (Pos. PV), and negative predictive value (Neg. PV)] for presence of *EGFR* or *KRAS* mutation is shown for H&E consensus diagnosis and IHC subtyping of NSCLC

Test	Sensitivity	Specificity	Pos. PV	Neg. PV
H&E consensus diagnosis non squamous [a]	90.5 %	28.8 %	25.0 %	92.0 %
TTF1 [b]	76.2 %	73.8 %	43.2 %	92.2 %
CK7 [b]	95.2 %	63.8 %	40.8 %	98.1 %
P63 [b]	0 %	45.0 %	0 %	63.2 %
CK5/6 [b]	4.8 %	53.8 %	2.6 %	68.3 %
PAS-D[c]	52.4 %	86.3 %	50.0 %	87.3 %
Alcean Blue[c]	61.9 %	83.8 %	50 %	89.3 %
Combination Adeno 1 (TTF1 and/or Mucin+)	100 %	62.5 %	41.2 %	100 %
Combination Adeno 2 (TTF1, mucin and/or CK7+)	100 %	56.3 %	37.5 %	100 %
Combination Squamous	4.8 %	45.0 %	2.2 %	64.3 %

The combination ADENO 1 consisted of at least one positive marker of TTF1, or mucin (PAS-D and/or Alcian blue). In the combination Adeno 2 CK7 was added. The IHC combination squamous consisted of at least one positive marker p63, CK56

[a] H&E-based consensus diagnosis (≥8/11 readings concordant), else undetermined

[b] The thresholds for positive immunohistochemistry were set for p63 at >240, implying strong positivity in most of the tumor cells and for TTF-1 >30

[c] A mucin stain is positive with staining in intracytoplasmic vacuoles of at least two tumor cells

associated with *KRAS* mutation ($p<0.001$). All mutation positive cases were negative for p63, and 16 (76 %) were positive for TTF1.

In Table 2, the distribution of H&E-based consensus diagnosis (≥8/11 readings concordant), markers for adeno- and squamous differentiation and mutation analysis is shown. In all cases with *EGFR* and *KRAS* mutations, adenodifferentiation was present. The sensitivity, specificity, positive and negative predictive value for presence of mutation analysis for H&E and immunohistochemical characterization are shown in Table 3.

In 22 of 24 cases with a consensus diagnosis of adenocarcinoma, additional stains support the adenodifferentiation. In 20 of 25 cases with a consensus diagnosis of SqCC, immunohistochemical differentiation was concordant. In three of the five remaining cases, adenodifferentiation was present; in two out of these three cases, a *KRAS* mutation was observed. Each pathologist diagnosed at least once a case as (probable) SqCC, which had an adenocarcinoma phenotype in the additional stains. Apparently, a squamoid appearance is present in some NSCLC biopsies, leading to the erroneous impression of squamous differentiation and diagnosis of SqCC on H&E, while additional stains favor adenocarcinoma.

Discussion

Rational clinical management of patients with advanced NSCLC requires an unequivocal pathological diagnosis as treatment decisions are increasingly based on histological and molecular subtyping. In particular, the distinction between squamous and non-squamous histology is of importance. This study clearly demonstrates that (1) distinction between adenocarcinoma and SqCC on H&E-stained sections solely is not possible in about 30 % of the cases, (2) refinement is possible with the use of additional immunohistochemical stains, thereby (3) delineating a group with a higher probability of harboring *EGFR* and *KRAS* mutations and potentially EML4-Alk rearrangements, findings important for treatment allocation.

Basically, the kappa values and the fraction of NSCLC-NOS are in line with previous reports [13, 15]. Importantly, our results validate the International Association for the Study of Lung Cancer, American Thoracic Society, and European Respiratory Society (IASLC/ATS/ERS) classification in demonstrating that refinement of the diagnosis in cases of undertermined NSCLC is possible with additional (immuno)histochemical stains [17], which is also in keeping with the study of Pardo et al. in resected large cell carcinomas of the lung and of others [18–20, 22, 26–31].

As three different types of examination were performed on the same biopsies (see Fig. 1), three combinations of two examinations may be compared. Firstly, the immunohistochemical distinction between adenocarcinoma and mutation analysis reveals that all *KRAS* and *EGFR* mutations were only present in p63-negative NSCLC cases. This observation is in line with the concept that these mutations do not occur in immunohistochemically defined SqCC.

Secondly, comparing H&E diagnosis with additional stains reveal high concordancy for adenocarcinoma in 22 of 24 (92 %) and SqCC in 20 of 25 (80 %). The H&E NSCLC NOS group (<8/11 same diagnosis) comprised 53 of 101 cases with evidence for adeno or squamous differentiation in 46 of 53 cases (77 %). Twenty percent of the

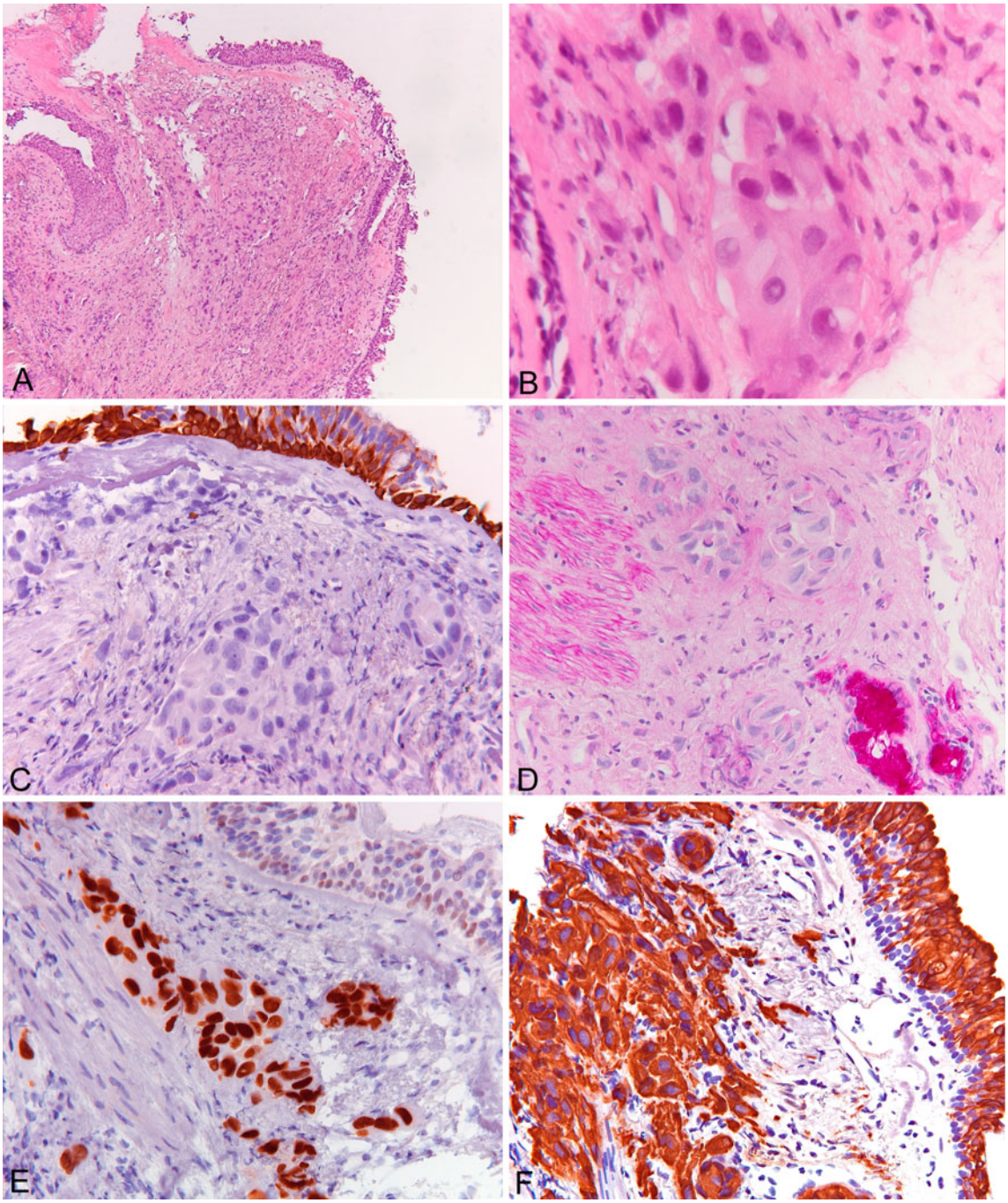

Fig. 2 Biopsy with non-small cell lung carcinoma, squamoid appearance H&E (**a**, **b**), p63 (**c**), mucin stain PAS-D (**d**), TTF1 (**e**), and CK7 (**f**). p63 −, PAS-D−, TTF1+, and CK7+ positive combination

consensus SqCCs (≥8/11) were not supported by immunohistochemical "squamous" differentiation (i.e. p63−), part of these cases (3 out of 5) may be seen as biopsy examples of poorly differentiated adenocarcinoma with a "squamoid" appearance, (Figs. 2 and 3). The existence of a squamoid appearance is recognized in diagnostic pathology, but examples are difficult to find in the literature. Recently, Rekhtman and colleagues [32] reported resection specimen with squamoid morphology and *EGFR* or *KRAS* mutations, which in hindsight were either poorly differentiated adenocarcinomas or adenosquamous carcinomas. Clearly, the use of strict morphological criteria in diagnosing SqCC on H&E is required comprising the presence of cytoplasmic keratinization and/or intercellular bridges. Distinct keratinization is, in our experience, infrequently seen in biopsies of squamous cell lung carcinoma, in

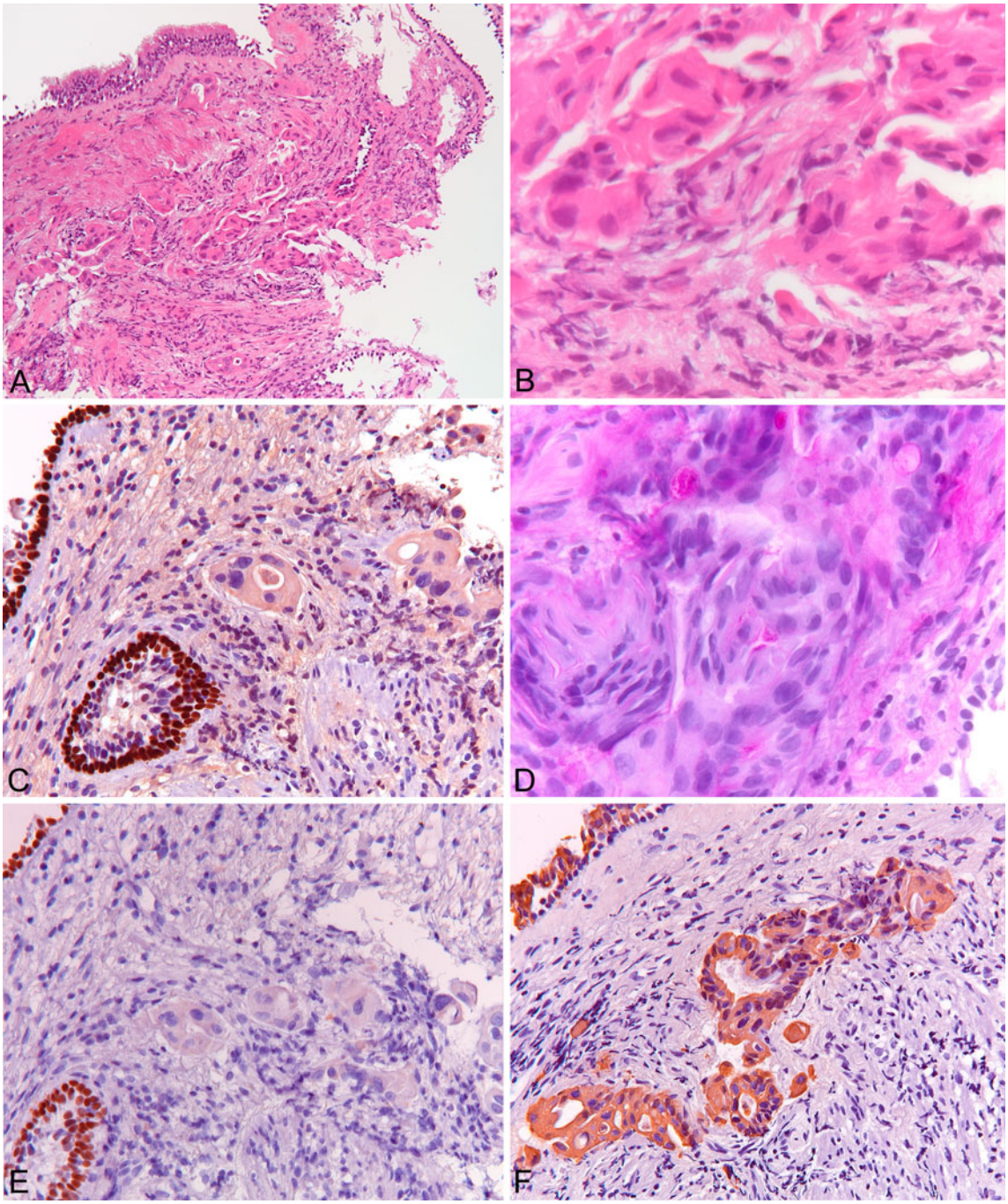

Fig. 3 Biopsy with non-small cell lung carcinoma, squamoid appearance H&E (**a**, **b**), p63 (**c**), mucin stain PAS-D (**d**), TTF1 (**e**), and CK7 (**f**). The p63−, PAS-D+, TTF1−, and CK7+ positive combination. Both cases apparently have squamoid appearance, but immunohistochemically show adenodifferentiation and contained *KRAS* mutation

contrast to, e.g., SqCC of the head and neck region. Conversely, H&E consensus diagnosis of adenocarcinoma with p63 positivity was less frequently found (8 %). The combined adeno- and squamous cell differentiation in the additional stains was low (4 %), comparable to the frequency of adenosquamous carcinomas in resection specimens [33, 34].

Thirdly, comparing H&E diagnosis with mutation analysis: 52 % of the mutations were present in the consensus adenocarcinoma group and 38 % in the NSCLC NOS group, showing that selection for mutation analysis on biopsies should not be restricted to adenocarcinomas alone. Moreover, in 2 of 25 (8 %) consensus diagnosis of squamous cell carcinomas, a *KRAS* mutation was found, while the

additional stains did not support squamous differentiation in these cases. As this frequency of 8 % KRAS mutation in biopsies is higher than expected based on resection specimen, the suggestion arises that H&E diagnosis alone on biopsies (i.e., without immunohistochemistry) is not the best way to characterize poorly differentiated NSCLC. As *EGFR* mutations are reported in low frequency in squamous cell carcinomas [35–41], and these studies did not report the use of immunohistochemical stains, one may wonder whether these *EGFR*-mutant "squamous" tumors may have been misclassified adenosquamous or poorly differentiated adenocarcinomas.

Immunohistochemical markers for squamous differentiation are p63, 34βE12, desmocollin CK5/6, and p40 [42, 43]. In our study, p63 with a threshold for strong positive staining in ≥80 % tumor cell nuclei had slightly better performance than CK5/6, and as the combination of both had no additional value, p63 alone appears to be sufficient to demonstrate squamous differentation [27]. This high threshold is easy applicable and the reason for the high specificity.

The low fraction of *EGFR* mutations is explained as a chance phenomenon rather than an analytic shortcoming, since we use a highly sensitive mutational assay with an analytical sensitivity of 5 % in combination with manual microdissection for cases with a low fraction of tumor cells [24, 25]. Moreover, the fraction of KRAS mutations is in line with other studies [44].

In this study, the presence of at least two tumor cells with distinct intracytoplasmic mucin droplets was used as criterion to consider mucin staining to be positive. The WHO uses five tumor cells in at least two HPF in resection specimen [9]. We feel that our approach in biopsies is pragmatic. Moreover, the presence of mucin was associated with *KRAS* mutations, as shown previously [45, 46].

In future clinical trials where the histological diagnosis (non-)squamous cell carcinoma is used as triage for different chemotherapy regimen, the use of additional stains for histological diagnosis may shed more light on the relation histology/chemotherapy [47]. The term non-squamous may be used in the clinic, but is not recommended for routine pathology diagnosis.

In conclusion, in the diagnostic work-up of non-small cell lung carcinoma, the limited reproducibility on small biopsies is optimized with immunohistochemical analysis, resulting in reliable delineation for predictive analysis. The use of additional staining added to H&E is advised.

Disclosure and conflict of interest Lilly provided funding for part of the mutation analysis, without any restrictions and honorary for advisory board meeting (Thunnissen) to "Stichting Research Fonds Pathologie" (=non-commercial pathology VU University Medical center-linked entity).

References

1. Scagliotti GV, Parikh P, von Pawel J, Biesma B, Vansteenkiste J, Manegold C, Serwatowski P, Gatzemeier U, Digumarti R, Zukin M, Lee JS, Mellemgaard A, Park K, Patil S, Rolski J, Goksel T, de Marinis F, Simms L, Sugarman KP, Gandara D (2008) Phase III study comparing cisplatin plus gemcitabine with cisplatin plus pemetrexed in chemotherapy-naive patients with advanced-stage non-small-cell lung cancer. J Clin Oncol 26(21):3543–3551
2. Johnson DH, Fehrenbacher L, Novotny WF, Herbst RS, Nemunaitis JJ, Jablons DM, Langer CJ, DeVore RF, Gaudreault J, Damico LA, Holmgren E, Kabbinavar F (2004) Randomized phase II trial comparing bevacizumab plus carboplatin and paclitaxel with carboplatin and paclitaxel alone in previously untreated locally advanced or metastatic non-small-cell lung cancer. J Clin Oncol 22(11):2184–2191
3. Sandler A, Gray R, Perry MC, Brahmer J, Schiller JH, Dowlati A, Lilenbaum R, Johnson DH (2006) Paclitaxel-carboplatin alone or with bevacizumab for non-small-cell lung cancer. N Engl J Med 355(24):2542–2550
4. Reck M, von Pawel J, Zatloukal P, Ramlau R, Gorbounova V, Hirsh V, Leighl N, Mezger J, Archer V, Moore N, Manegold C (2010) Overall survival with cisplatin-gemcitabine and bevacizumab or placebo as first-line therapy for nonsquamous non-small-cell lung cancer: results from a randomised phase III trial (AVAiL). Ann Oncol 21(9):1804–1809
5. Lynch TJ, Bell DW, Sordella R, Gurubhagavatula S, Okimoto RA, Brannigan BW, Harris PL, Haserlat SM, Supko JG, Haluska FG, Louis DN, Christiani DC, Settleman J, Haber DA (2004) Activating mutations in the epidermal growth factor receptor underlying responsiveness of non-small-cell lung cancer to gefitinib. N Engl J Med 350(21):2129–2139
6. Pao W, Miller VA, Politi KA, Riely GJ, Somwar R, Zakowski MF, Kris MG, Varmus H (2005) Acquired resistance of lung adenocarcinomas to gefitinib or erlotinib is associated with a second mutation in the EGFR kinase domain. PLoS Med 2(3):e73
7. Kwak EL, Bang YJ, Camidge DR, Shaw AT, Solomon B, Maki RG, Ou SH, Dezube BJ, Janne PA, Costa DB, Varella-Garcia M, Kim WH, Lynch TJ, Fidias P, Stubbs H, Engelman JA, Sequist LV, Tan W, Gandhi L, Mino-Kenudson M, Wei GC, Shreeve SM, Ratain MJ, Settleman J, Christensen JG, Haber DA, Wilner K, Salgia R, Shapiro GI, Clark JW, Iafrate AJ (2010) Anaplastic lymphoma kinase inhibition in non-small-cell lung cancer. N Engl J Med 363(18):1693–1703
8. Mok TS, Wu YL, Thongprasert S, Yang CH, Chu DT, Saijo N, Sunpaweravong P, Han B, Margono B, Ichinose Y, Nishiwaki Y, Ohe Y, Yang JJ, Chewaskulyong B, Jiang H, Duffield EL, Watkins CL, Armour AA, Fukuoka M (2009) Gefitinib or carboplatin-paclitaxel in pulmonary adenocarcinoma. N Engl J Med 361(10):947–957
9. Travis WD, Brambilla E, Muller-Hermelink KM (2004) Pathology and genetics: tumours of the lung, pleura, thymus and heart. IARC, Lyon
10. Yesner R (1985) Large cell carcinoma of the lung. Semin Diagn Pathol 2(4):255–269
11. Roggli VL, Vollmer RT, Greenberg SD, McGavran MH, Spjut HJ, Yesner R (1985) Lung cancer heterogeneity: a blinded and randomized study of 100 consecutive cases. Hum Pathol 16(6):569–579
12. Feinstein AR, Wells CK (1982) Lung cancer staging. A critical evaluation. Clin Chest Med 3(2):291–305
13. Thomas JS, Lamb D, Ashcroft T, Corrin B, Edwards CW, Gibbs AR, Kenyon WE, Stephens RJ, Whimster WF (1993) How reliable is the diagnosis of lung cancer using small biopsy specimens?

Report of a UKCCCR Lung Cancer Working Party. Thorax 48 (11):1135–1139
14. Edwards SL, Roberts C, McKean ME, Cockburn JS, Jeffrey RR, Kerr KM (2000) Preoperative histological classification of primary lung cancer: accuracy of diagnosis and use of the non-small cell category. J Clin Pathol 53(7):537–540
15. Burnett RA, Howatson SR, Lang S, Lee FD, Lessells AM, McLaren KM, Nairn ER, Ogston S, Robertson AJ, Simpson JG, Smith GD, Tavadia HB, Walker F (1996) Observer variability in histopathological reporting of non-small cell lung carcinoma on bronchial biopsy specimens. J Clin Pathol 49(2):130–133
16. Burnett RA, Swanson Beck J, Howatson SR, Lee FD, Lessells AM, McLaren KM, Ogston S, Robertson AJ, Simpson JG, Smith GD (1994) Observer variability in histopathological reporting of malignant bronchial biopsy specimens. J Clin Pathol 47(8):711–713
17. Travis WD, Brambilla E, Noguchi M, Nicholson AG, Geisinger KR, Yatabe Y, Beer DG, Powell CA, Riely GJ, Van Schil PE, Garg K, Austin JHM, Asamura H, Rusch VW, Hirsch FR, Scagliotti G, Mitsudomi T, Huber RM, Ishikawa Y, Jett J, Sanchez-Cespedes M, Sculier JP, Takahashi T, Tsuboi M, Vansteenkiste J, Wistuba I, Yang PC, Aberle D, Brambilla C, Flieder D, Franklin W, Gazdar A, Gould M, Hasleton P, Henderson D, Johnson B, Johnson D, Kerr K, Kuriyama K, Lee JS, Miller VA, Petersen I, Roggli V, Rosell R, Saijo N, Thunnissen E, Tsao M, Yankelewitz D (2011) International association for the study of lung cancer/american thoracic society/european respiratory society international multidisciplinary classification of lung adenocarcinoma. J Thorac Oncol 6(2):244–285
18. Rossi G, Pelosi G, Graziano P, Barbareschi M, Papotti M (2009) A reevaluation of the clinical significance of histological subtyping of non-small-cell lung carcinoma: diagnostic algorithms in the era of personalized treatments. Int J Surg Pathol 17(3):206–218
19. Rossi G, Papotti M, Barbareschi M, Graziano P, Pelosi G (2009) Morphology and a limited number of immunohistochemical markers may efficiently subtype non-small-cell lung cancer. J Clin Oncol 27(28):e141–e142
20. Loo PS, Thomas SC, Nicolson MC, Fyfe MN, Kerr KM (2010) Subtyping of undifferentiated non-small cell carcinomas in bronchial biopsy specimens. J Thorac Oncol 5(4):442–447
21. Nicholson AG, Gonzalez D, Shah P, Pynegar MJ, Deshmukh M, Rice A, Popat S (2010) Refining the diagnosis and EGFR status of non-small cell lung carcinoma in biopsy and cytologic material, using a panel of mucin staining, TTF-1, cytokeratin 5/6, and P63, and EGFR mutation analysis. J Thorac Oncol 5(4):436–441
22. Rossi G, Marchioni A, Milani M, Scotti R, Foroni M, Cesinaro A, Longo L, Migaldi M, Cavazza A (2004) TTF-1, cytokeratin 7, 34betaE12, and CD56/NCAM immunostaining in the subclassification of large cell carcinomas of the lung. Am J Clin Pathol 122 (6):884–893
23. Galleges Ruiz MI, Floor K, Steinberg SM, Grunberg K, Thunnissen FB, Belien JA, Meijer GA, Peters GJ, Smit EF, Rodriguez JA, Giaccone G (2009) Combined assessment of EGFR pathway-related molecular markers and prognosis of NSCLC patients. Br J Cancer 100(1):145–152
24. Heideman DAM, Thunnissen FB, Doeleman M, Kramer D, Verheul HM, Smit EF, Postmus PE, Meijer CJLM, Meijer GA, Snijders PJF (2009) A panel of high resolution melting (HRM) technology-based assays with direct sequencing possibility for effective mutation screening of EGFR and K-ras genes. Cell Oncol 31(5):329–333
25. Kramer D, Thunnissen FB, Gallegos-Ruiz MI, Smit EF, Postmus PE, Meijer CJ, Snijders PJ, Heideman DA (2009) A fast, sensitive and accurate high resolution melting (HRM) technology-based assay to screen for common K-ras mutations. Cell Oncol 31(3):161–167
26. Pardo J, Martinez-Penuela AM, Sola JJ, Panizo A, Gurpide A, Martinez-Penuela JM, Lozano MD (2009) Large cell carcinoma of the lung: an endangered species? Appl Immunohistochem Mol Morphol 17(5):383–392
27. Terry J, Leung S, Laskin J, Leslie KO, Gown AM, Ionescu DN (2010) Optimal immunohistochemical markers for distinguishing lung adenocarcinomas from squamous cell carcinomas in small tumor samples. Am J Surg Pathol 34(12):1805–1811
28. Au NHC, Gown AM, Cheang M, Huntsman D, Yorida E, Elliott WM, Flint J, English J, Gilks CB, Grimes HL (2004) P63 expression in lung carcinoma: a tissue microarray study of 408 cases. Appl Immunohistochem Mol Morphol 12(3):240–247
29. Tan D, Li Q, Deeb G, Ramnath N, Slocum HK, Brooks J, Cheney R, Wiseman S, Anderson T, Loewen G (2003) Thyroid transcription factor-1 expression prevalence and its clinical implications in non-small cell lung cancer: a high-throughput tissue microarray and immunohistochemistry study. Hum Pathol 34(6):597–604
30. Nicholson A, Gonzalez D, Shah P, Pynegar M, Deshmukh M, Rice A, Popat S (2010) Refining the diagnosis and EGFR status of non-small cell lung carcinoma in biopsy and cytologic material, using a panel of mucin staining, TTF-1, cytokeratin 5/6, and P63, and EGFR mutation analysis. J Thorac Oncol 5:436–441
31. Pelosi G, Fraggetta F, Pasini F, Maisonneuve P, Sonzogni A, Iannucci A, Terzi A, Bresaola E, Valduga F, Lupo C, Viale G (2001) Immunoreactivity for thyroid transcription factor-1 in stage I non-small cell carcinomas of the lung. Am J Surg Pathol 25 (3):363–372
32. Rekhtman N, Paik PK, Arcila ME, Tafe LJ, Oxnard GR, Moreira AL, Travis W, Zakowski MF, Kris MG, Ladanyi M (2012) Clarifying the spectrum of driver oncogene mutations in biomarker-verified squamous carcinoma of lung: lack of EGFR/KRAS and presence of PIK3CA/AKT1 mutations. Clin Cancer Res 18:1167–1176
33. Ohtsuka K, Ohnishi H, Fujiwara M, Kishino T, Matsushima S, Furuyashiki G, Takei H, Koshiishi Y, Goya T, Watanabe T (2007) Abnormalities of epidermal growth factor receptor in lung squamous-cell carcinomas, adenosquamous carcinomas, and large-cell carcinomas: tyrosine kinase domain mutations are not rare in tumors with an adenocarcinoma component. Cancer 109 (4):741–750
34. Sartori G, Cavazza A, Sgambato A, Marchioni A, Barbieri F, Longo L, Bavieri M, Murer B, Meschiari E, Tamberi S, Cadioli A, Luppi F, Migaldi M, Rossi G (2009) EGFR and K-ras mutations along the spectrum of pulmonary epithelial tumors of the lung and elaboration of a combined clinicopathologic and molecular scoring system to predict clinical responsiveness to EGFR inhibitors. Am J Clin Pathol 131(4):478–489
35. Qin BM, Chen X, Zhu JD, Pei DQ (2005) Identification of EGFR kinase domain mutations among lung cancer patients in China: implication for targeted cancer therapy. Cell Res 15(3):212–217
36. Han SW, Kim TY, Hwang PG, Jeong S, Kim J, Choi IS, Oh DY, Kim JH, Kim DW, Chung DH, Im SA, Kim YT, Lee JS, Heo DS, Bang YJ, Kim NK (2005) Predictive and prognostic impact of epidermal growth factor receptor mutation in non-small-cell lung cancer patients treated with gefitinib. J Clin Oncol 23(11):2493–2501
37. Cappuzzo F, Hirsch FR, Rossi E, Bartolini S, Ceresoli GL, Bemis L, Haney J, Witta S, Danenberg K, Domenichini I, Ludovini V, Magrini E, Gregorc V, Doglioni C, Sidoni A, Tonato M, Franklin WA, Crino L, Bunn PAJ, Varella-Garcia M (2005) Epidermal growth factor receptor gene and protein and gefitinib sensitivity in non-small-cell lung cancer. J Natl Cancer Inst 97(9):643–655
38. Chou TY, Chiu CH, Li LH, Hsiao CY, Tzen CY, Chang KT, Chen YM, Perng RP, Tsai SF, Tsai CM (2005) Mutation in the tyrosine kinase domain of epidermal growth factor receptor is a predictive

and prognostic factor for gefitinib treatment in patients with non-small cell lung cancer. Clin Cancer Res 11(10):3750–3757
39. Park S, Holmes-Tisch AJ, Cho EY, Shim YM, Kim J, Kim HS, Lee J, Park YH, Ahn JS, Park K, Janne PA, Ahn MJ (2009) Discordance of molecular biomarkers associated with epidermal growth factor receptor pathway between primary tumors and lymph node metastasis in non-small cell lung cancer. J Thorac Oncol 4(7):809–815
40. Gandara DR, Grimminger P, Mack PC, Lara PNJ, Li T, Danenberg PV, Danenberg KD (2010) Association of epidermal growth factor receptor activating mutations with low ERCC1 gene expression in non-small cell lung cancer. J Thorac Oncol 5(12):1933–1938
41. Park SH, Ha SY, Lee JI, Lee H, Sim H, Kim YS, Hong J, Park J, Cho EK, Shin DB, Lee JH (2009) Epidermal growth factor receptor mutations and the clinical outcome in male smokers with squamous cell carcinoma of lung. J Korean Med Sci 24 (3):448–452
42. Bishop JA, Teruya-Feldstein J, Westra WH, Pelosi G, Travis WD, Rekhtman N (2012) p40 (DeltaNp63) is superior to p63 for the diagnosis of pulmonary squamous cell carcinoma. Mod Pathol 25:405–415
43. Pelosi G, Fabbri A, Bianchi F, Maisonneuve P, Rossi G, Barbareschi M, Graziano P, Cavazza A, Rekhtman N, Pastorino U, Scanagatta P, Papotti M (2012) DeltaNp63 (p40) and thyroid transcription factor-1 immunoreactivity on small biopsies or cell-blocks for typing non-small cell lung cancer: a novel two-hit, sparing-material approach. J Thorac Oncol 7(2):281–290
44. Suzuki Y, Orita M, Shiraishi M, Hayashi K, Sekiya T (1990) Detection of ras gene mutations in human lung cancers by single-strand conformation polymorphism analysis of polymerase chain reaction products. Oncogene 5(7):1037–1043
45. Marchetti A, Buttitta F, Pellegrini S, Chella A, Bertacca G, Filardo A, Tognoni V, Ferreli F, Signorini E, Angeletti CA, Bevilacqua G (1996) Bronchioloalveolar lung carcinomas: K-ras mutations are constant events in the mucinous subtype. J Pathol 179(3):254–259
46. Finberg KE, Sequist LV, Joshi VA, Muzikansky A, Miller JM, Han M, Beheshti J, Chirieac LR, Mark EJ, Iafrate AJ (2007) Mucinous differentiation correlates with absence of EGFR mutation and presence of KRAS mutation in lung adenocarcinomas with bronchioloalveolar features. J Mol Diagn 9 (3):320–326
47. Scagliotti G, Brodowicz T, Shepherd FA, Zielinski C, Vansteenkiste J, Manegold C, Simms L, Fossella F, Sugarman K, Belani CP (2011) Treatment-by-histology interaction analyses in three phase III trials show superiority of pemetrexed in nonsquamous non-small cell lung cancer. J Thorac Oncol 6(1):64–70

Virchows Arch (2012) 461:639–646
DOI 10.1007/s00428-012-1338-4

ORIGINAL ARTICLE

The presence of sinusoidal CD163$^+$ macrophages in lymph nodes is associated with favorable nodal status in patients with breast cancer

Aaron S. Mansfield · Paivi Heikkila · Karl von Smitten · Jukka Vakkila · Marjut Leidenius

Received: 30 August 2012 / Revised: 2 October 2012 / Accepted: 29 October 2012 / Published online: 13 November 2012
© Springer-Verlag Berlin Heidelberg 2012

Abstract As macrophages are some of the first cells to encounter metastatic tumor cells in sentinel lymph nodes (SLN) and natural killer (NK) cells are critical to the cytotoxicity of abnormal cells, we sought to determine if these cell populations were altered in the presence of nodal metastasis. We used immunohistochemistry to assess the SLN of 47 patients with breast cancer (36 with nodal metastasis and 11 without nodal metastasis) and 10 control lymph nodes. We assessed metastatic areas and nonmetastatic areas separately for CD163, a marker of macrophages, and ANK-1, a marker for precursors of activated NK cells. Positively stained cells were manually counted in multiple high-power fields and averaged. Groups were compared with the Kruskal–Wallis test. Spearman rank order test was used for correlations. There was a lower frequency of CD163$^+$ macrophages in the SLN of patients with breast cancer (median, 11.0 %; range, 4.1–20.4 %) than controls (median, 16.5 %; range, 8.9–19.6 %; p=0.002). There were no differences in the expression of ANK between patients with cancer (median, 1.4 %; range, 0.23–6.3 %) and controls (median, 1.5 %; range, 0.60–5.4 %; p=0.5). In patients with nodal metastasis, the accumulation of CD163$^+$ cells in the sinuses correlated negatively with CD8$^+$ tumor-infiltrating lymphocytes (r^2=0.23; p=0.001). These results suggest that the reduction of CD163$^+$ macrophages in the sinuses of the SLN is associated with nodal metastasis and may have a role in regional immunity.

Keywords Breast cancer · Macrophages · Natural killer cells · Lymph nodes

A. S. Mansfield (✉)
Medical Oncology, Mayo Clinic,
200 First Street SW,
Rochester, MN 55905, USA
e-mail: Mansfield.aaron@mayo.edu

P. Heikkila
Department of Pathology, Helsinki University Central Hospital,
Helsinki, Finland

K. von Smitten · M. Leidenius
Breast Surgery Unit, Helsinki University Central Hospital,
Helsinki, Finland

J. Vakkila
Hematology Research Unit, Helsinki University Central Hospital,
Helsinki, Finland

Introduction

Breast cancer is the most common female malignancy, and the role of the immune system in the pathogenesis and metastasis of this disease is becoming increasingly understood. Accumulating evidence suggests that the adaptive immune system has an important role in the prevention of metastatic spread to regional tumor-draining lymph nodes. Our recent studies on the sentinel lymph nodes (SLN) of patients with breast cancer indicate that there is suppression of regional immunity with the spread of cancer to the SLN [1, 2]. Metastasis to the SLN correlated with the accumulation of immunosuppressive regulatory T cells [1, 3, 4] and the absence of mature dendritic cells [2]. Furthermore, alterations in regional immunity in early stage breast cancer have been correlated with worse disease-free survival [5].

In addition to the adaptive immune system that includes T and B cells and specialized antigen-presenting dendritic cells, cells of the innate immune system have a large presence in lymph nodes. Macrophages are a critical component of the innate immune system responsible for phagocytosis of self and foreign materials. In lymph nodes, macrophages are scattered in paracortical T cell areas, but the vast majority of macrophages occupy the medullary cords and line the capsule and trabeculae [6] that are primary sites for tumor cell arrest upon regional lymph node metastases [7, 8].

Natural killer (NK) cells are part of the innate immune system that distinguish healthy cells from abnormal ones and lyse cells that are transformed or infected with virus [9]. NK cells not only share a common mechanism of cytotoxicity with T cells, but they have been shown to have features of the adaptive immune system in a murine model, such as memory and reactivation [10]. Precursors of activated NK cells express ANK-1, a neuronal cell adhesion molecule [11]. These precursors represent only a quarter of the NK cells in the peripheral blood, but are the majority of NK cells within normal and cancerous solid tissues [11]. In lymph nodes, ANK-1^+ cells are preferentially located in the central area of germinal centers, in proximity with $CD3^+$ T cells [11].

Metastasis to lymph nodes is one of the strongest predictors of survival in patients with breast cancer [12–14]. Axillary lymph node clearance has been replaced by SLN biopsy at many centers in the setting of the appropriate clinical stage [15]. Improved selectivity in lymph node dissection has resulted in a more detailed analysis of the removed nodes and greater attention is being paid to the immune status of these nodes. SLN are unique in that they represent the sites of T cell activation and early metastasis. As such, these nodes are ideal for investigations of tumor immunology in breast cancer.

Our aim in this study was to determine if there was a derangement in regional innate immunity in breast cancer. As macrophages are some of the first cells to encounter metastatic tumor cells in the SLN and NK cells are critical to the cytotoxicity of abnormal cells, we sought to determine if these cell populations were altered in the presence of nodal metastasis. In our previous studies, we focused on the cells of the adaptive immune system [1, 2], and in this report, we have explored the frequency and location of macrophages and NK cells in the SLN and related the findings with the metastatic status of the patients. Macrophages were identified with CD163 that is a cell surface receptor involved with the clearance of hemoglobin–haptoglobin complexes [16]. CD163 is almost exclusively expressed by macrophages that accumulate in the sinuses of lymph nodes [17]. We used ANK-1 as an NK cell marker that identifies a subpopulation of mature NK cells that can infiltrate solid tissues and lymph nodes [11].

Patients, materials, and methods

We used the SLN of 47 patients with breast cancer treated at the Breast Surgery Unit of Helsinki University Hospital between 2001 and 2003. A prospectively collected database was searched to select patients without nodal metastases and patients with varying sizes of nodal metastases. These patients were selected based on the availability of non-SLN for future investigations. These patients had either tumor-negative SLN (n=11) or tumor-positive SLN (n=36), as defined by the International Union Against Cancer (UICC) TNM classification system. The clinicopathological data of these patients are summarized in Table 1. We also classified patients by estrogen receptor (ER) status, progesterone receptor status, and MIB-1, as described previously [18]. Also, SLN from 10 control patients who underwent SLN biopsy due to a false-positive core needle biopsy were examined. The control patients had premalignant conditions like lobular neoplasia in situ or atypical ductal hyperplasia, but not ductal carcinoma in situ or invasive breast cancer.

The SLN were histologically assessed intraoperatively using serial sectioning and immunohistochemistry [19, 20] and postoperatively by review by a trained pathologist. Following intraoperative analysis, tissue samples were fixed in formalin, embedded in paraffin, and stored in a tissue bank for future retrieval.

Formalin-fixed, paraffin-embedded lymph nodes were sectioned into 3- to 4-μm slices and affixed on glass slides. Samples were heated for half an hour at 56 °C, then

Table 1 Patient and tumor characteristics

	SLN+	SLN−
Number	36	11
Age[a]	60 (49–70)	54 (48–70)
Type		
Ductal	20	5
Lobular	14	3
Other	2	3
Tumor size[a] (mm)	16 (14–23)	17 (14–22)
Tumor stage		
T1	26	6
T2	10	5
Tumor grade		
I	8	4
II	24	3
III	4	4
ER		
Positive	34	9
Negative	2	2
PR		
Positive	23	8
Negative	13	3
MIB-1		
Positive	15	5
Negative	21	6

There were no statistical differences between the groups. MIB-1 ≥5 % was considered positive

ER estrogen receptor, *PR* progesterone receptor, *MIB-1* proliferation index

[a] Data are presented as the median (range)

deparaffinized in xylene, rehydrated in a graded alcohol series, and washed in water. For antigen retrieval, CD163 samples were microwaved for a total of 20 min in an ethylenediaminetetraacetic acid buffer. ANK-1 samples were microwaved for a total of 20 min in a citric acid buffer, pH 6.0. Endogenous peroxidase activity was quenched in a bath of methanol and hydrogen peroxide for 30 min. Antibodies against CD163 (NCL-CD163; Novocastra, Newcastle upon Tyne, UK) and ANK-1 (provided by Dr. Nik Vujanovic, University of Pittsburgh Cancer Center, Pittsburgh, PA, USA [11]) were incubated with specimens overnight at concentrations of 1:400 and 1:100, respectively, at 4 °C. The Envision Advance-Kit (Dako, Glostrup, Denmark) was used for the detection of CD163 and the TSA-INDIRECT-Kit NEL700 (PerkinElmer, Waltham, MA, USA) was used for the detection of ANK-1. Peroxidase activity was localized for all samples using a bath of 3-amino-9-ethylcarbazole and hydrogen peroxide for 15 min. Samples were counterstained with Harris hematoxylin for 30 s and mounted.

Positively stained cells in the nonmetastatic regions of the lymph nodes were quantified as the percentage of all cells in a minimum of three high-power fields (×400 magnification) and averaged. We scored areas with the greatest accumulation of positively stained cells on scanning at lower magnification. Nonmetastatic regions were used to allow comparison of lymphocytes between patients with and without metastasis. Additionally, the average number of positively stained cells per high-power field was determined in areas of metastasis; however, with the exception of two patients, it was not possible to assess immune cell infiltrates in samples with micrometastatic (<2 mm) nodal disease. For cells that expressed ANK-1, we recorded if they were primarily distributed in germinal centers, if they clustered elsewhere, or if they scattered throughout the SLN. Two investigators assessed each sample (PH with either AM or ML). A Nikon Eclipse 80i microscope was used for data analysis and image acquisition. We compared these results to the expression of indoleamine 2,3-dioxygenase (IDO), a tryptophan-degrading enzyme that inhibits T cell proliferation, and markers of T cells (CD3), cytotoxic T cells (CD8), regulatory T cells (Foxp3), and plasmacytoid dendritic cells (CD123) using the methodology we described previously [1, 2].

JMP (SAS Institute Inc., Cary, NC, USA) was used for statistical analysis. Basic statistics were used to analyze our grouped data. Since the data were nonparametric, the Mann–Whitney *U* test and the Kruskal–Wallis test were used to compare the groups based on nodal status. Tukey's multiple comparison test was used if the Kruskal–Wallis test was significant. Logistic regression analyses were performed to assess the predictive effect each stain had on nodal status. The Spearman rank order correlation coefficient was used to determine if there was a correlation between the stains.

Results

$CD163^+$ macrophages reside in marginal and medullary sinuses in the SLN with and without metastasis

Nodal $CD163^+$ cells had the morphologic appearance of macrophages. $CD163^+$ cells were absent from paracortical T cell areas and primarily localized to the marginal and medullary sinuses of the SLN (Fig. 1). SLN without metastasis from patients with breast cancer did not differ from control lymph nodes and normal cellular structure was preserved. The cellular composition of lymph nodes with metastases was evaluated at tumor-free sites where normal nodal architecture was not distorted. Similar to tumor-free nodes, $CD163^+$ cells accumulated almost entirely at sinuses lining capsule and trabeculae and were virtually absent from paracortical T cell areas of the SLN with metastasis.

Metastasis to the SLN is associated with low frequency of $CD163^+$ macrophages in marginal sinuses

In the SLN of patients with breast cancer, the frequency of $CD163^+$ macrophages (median, 11.0 %; range, 4.1–22.4 %) was lower than in controls (median, 16.5 %; range, 8.9–19.6 %; $p=0.002$) (Fig. 2a). Furthermore, in patients with breast cancer, there was a lower proportion of $CD163^+$ macrophages in the SLN with metastases (SLN+) (median, 10.5 %; range, 4.1–20.4 %) than in the SLN without metastases (SLN−) (median, 13.8 %; range, 10.0–22.4 %; $p=0.002$) (Fig. 2b). The difference in accumulation of $CD163^+$ macrophages in the SLN between controls and SLN+ was significant ($p=0.004$), but the difference between controls and SLN− was not. Logistic regression analysis demonstrated that CD163 expression was predictive of nodal status ($p=0.02$).

IDO^+ macrophages are frequent in cancer patients but do not associate with lymph node metastases

In our previous study, we observed that IDO expression occurred predominately in macrophages located in the perisinusoidal areas, both around medullary and marginal sinuses [1]. Additionally, we reported a trend towards a higher frequency of IDO^+ cells in the SLN of patients with breast cancer than controls ($p=0.08$). Since $CD163^+$ and IDO^+ cells colocalize to the same nodal compartments, some of the IDO^+ cells may represent $CD163^+$ cells. We were not able to perform double stainings for the markers, but we combined data from our previous project with the present one to determine correlations between IDO and CD163 and ratios of IDO^+/10 $CD163^+$ cells among our groups. The expression of IDO and CD163 did not correlate in controls or in cancer patients, indicating that these markers are independently regulated. There was a lower ratio of $IDO^+/CD163^+$ cells in controls (1 IDO^+ cell/10 $CD163^+$

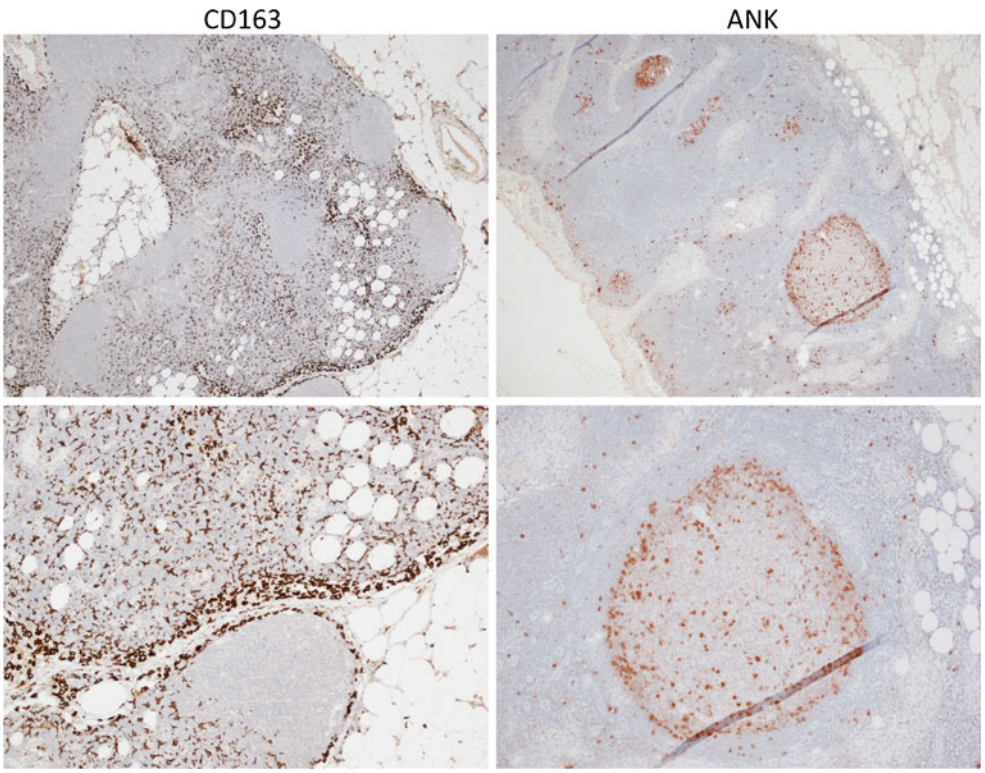

Fig. 1 Representative micrographic images of each stain. The *top row* represents low-power images (×40) and the *bottom row* represents high-power images (×100) representative for each stain. These samples were from patients without nodal metastasis

cells) than in patients with cancer (3.5 IDO$^+$ cells/10 CD163$^+$ cells; p=0.005), but the difference in the ratios between SLN− (2.9 IDO$^+$ cells/10 CD163$^+$ cells) and SLN+ (3.7 IDO$^+$ cells/10 CD163$^+$ cells) patients was insignificant (p=0.13; Fig. 3a).

High Foxp3$^+$ and low CD163$^+$ frequencies are characteristic of metastatic SLN in breast cancer

In our previous study [1], the frequency of Foxp3$^+$ cells was shown to be increased in metastatic SLN compared to tumor-free SLN (p=0.02). We compared the ratios of Foxp3 to CD163 to see if this ratio was more predictive than either marker alone. Foxp3$^+$ and CD163$^+$ cell counts did not correlate with one another in controls or in patients with cancer, showing that their expression in the SLN are not related. However, there was a lower ratio of Foxp3$^+$/CD163$^+$ in controls (6:1,000) than in patients with breast cancer (17:1,000; p <0.0001). Additionally, there was a lower ratio of Foxp3$^+$/CD163$^+$ cells in SLN− (11:1,000) than in SLN+ (20:1,000; p=0.003; Fig. 3b). When we compared Foxp3 expression, CD163 expression, and the ratio of Foxp3$^+$/1,000 CD163$^+$ cells in a multivariate analysis for nodal stage, all three retained significance (p<0.001 for each).

In one of our earlier reports [2], we determined the frequencies of immature (CD1a$^+$) and mature (CD208$^+$) myeloid and plasmacytoid (CD123$^+$) dendritic cells and various subsets of T cells (CD4$^+$, CD8$^+$, and Foxp3$^+$) that all resided mainly in paracortical T cell areas. We correlated

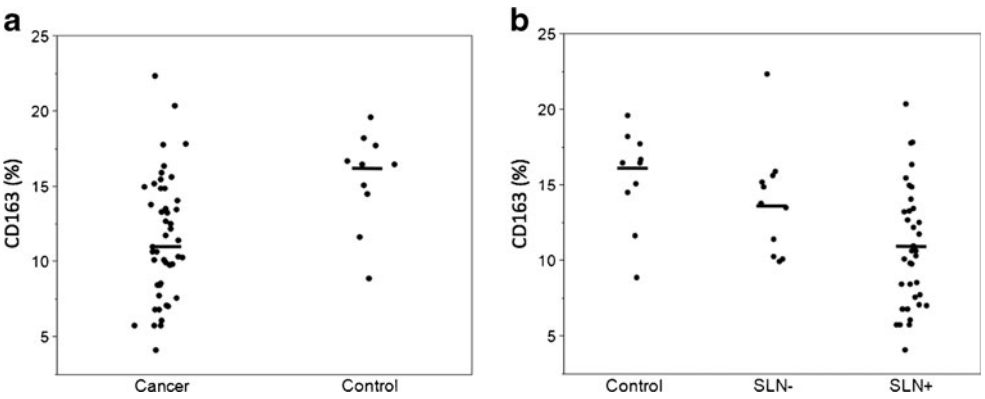

Fig. 2 Expression of CD163 by groups. The figure demonstrates the percent expression of CD163 between the groups. The *dots* represent samples and the *bars* represent medians for each group. There were fewer CD163$^+$ macrophages in the SLN of breast cancer patients than controls (p=0.002) (**a**). SLN+ demonstrated fewer CD163$^+$ cells than controls (p=0.004) (**b**)

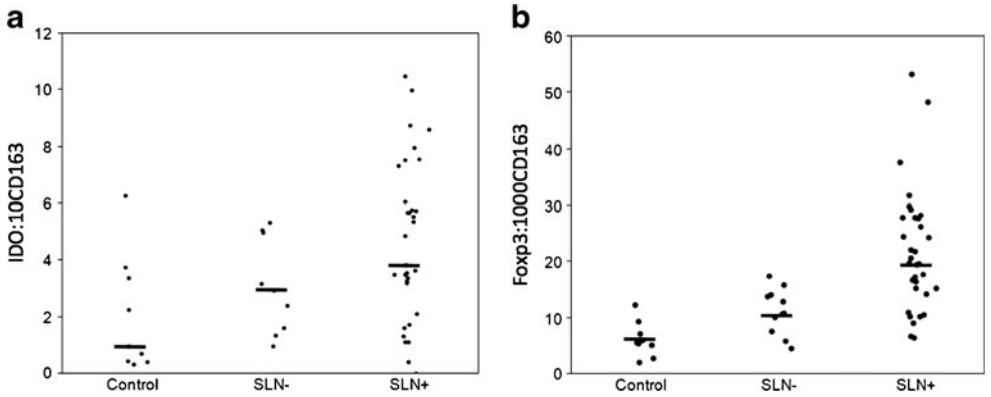

Fig. 3 Ratios of IDO/10 CD163 and Foxp3/1,000 CD163 by group. **a** The ratios of IDO/10 CD163 by group with *bars* at the medians. There was a significantly higher ratio of IDO/10 CD163 in patients with cancer compared to controls ($p=0.005$). **b** The ratios of Foxp3/1,000 CD163 by group with *bars* at the medians. There was a significantly higher ratio of Foxp3/1,000 CD163 SLN+ compared to SLN− and controls ($p<0.0001$)

the number of CD163$^+$ cells with these cell counts, but none of the correlations were significant (data not shown).

ANK-1$^+$ cells localized to follicles and germinal centers

Similar to previous studies [11], ANK-1$^+$ cells were located in germinal centers when abundant (Fig. 1); however, in cases with a low proportion of ANK-1$^+$ cells, these cells were observed as small clusters or sparsely scattered in the paracortical areas of the SLN. There were no statistically significant differences observed in the accumulation of ANK-1$^+$ cells in the SLN between cancer patients (median, 1.4 %; range, 0.23–6.3 %) and controls (median, 1.5 %; range, 0.60–5.4 %; $p=0.92$) (Fig. 4a) nor between SLN+ (median, 1.2 %; range, 0.23–6.2 %) and SLN− (median, 1.4 %; range, 0.31–6.3 %; $p=0.5$; Fig. 4b). ANK-1 was not a predictor of nodal status based on logistic regression analysis. There were no differences between patients with cancer and controls in the distribution of ANK-1$^+$ cells between germinal centers, clusters or scattered, nor between SLN+ and SLN− (data not shown). There was a higher proportion of ANK-1$^+$ cells in subjects with a primarily germinal center distribution (median, 2.0 %; range, 0.67–6.3 %) compared to those that clustered elsewhere (median, 1.1 %; range, 0.51–1.9 %) and those that scattered throughout the SLN (median, 0.71 %; range, 0.31–1.6 %; $p<0.0001$). There were no correlations between ANK-1$^+$ cells and any of the studied cell subsets, including CD163$^+$ cells, dendritic cell subsets, and T cell subsets.

In patients with nodal disease, the frequency of CD163$^+$ and IDO$^+$ cells correlated negatively with infiltration of metastases by T cells

In patients with nodal metastases, the tumor area in the SLN was studied separately and infiltration of T cell subsets was determined. There was a trend of a negative correlation of the frequency of CD163$^+$ cells in the sinuses of the SLN with infiltration of nodal metastases by CD3$^+$ cells ($r^2=0.23$, $p=0.06$; Fig. 5a) and CD8$^+$ cells ($r^2=0.49$, $p=0.001$; Fig. 5b). There was no correlation of ANK-1$^+$ cells in the SLN with infiltration of nodal metastases by lymphocytes ($r^2=0.01$, $p=0.71$; Fig. 5c). Additionally, the presence of IDO$^+$ cells in the sinuses of the SLN was negatively but insignificantly ($r=-0.527$, $p=0.053$) correlated with infiltration of nodal metastases by CD3$^+$ T cells.

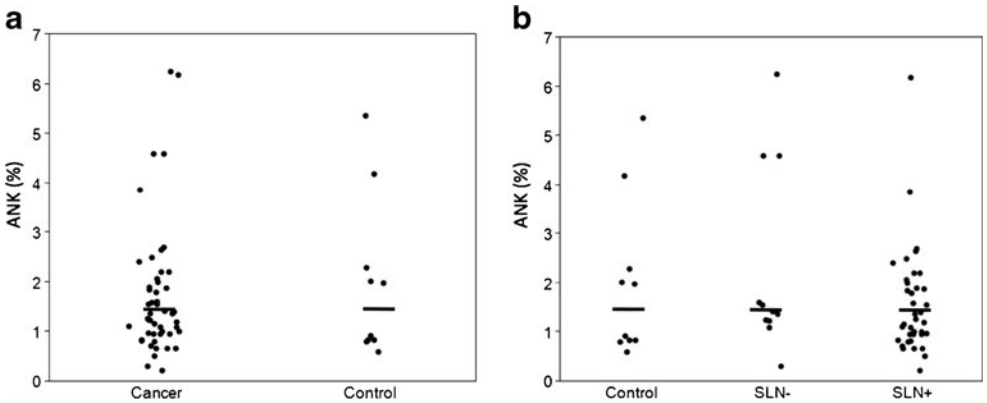

Fig. 4 Expression of ANK by groups. The figure demonstrates the percent expression of ANK between the groups. The *dots* represent samples and the *bars* represent medians for each group. There were no statistically significant differences observed in the accumulation of ANK-1$^+$ cells in the SLN between cancer patients ($p=0.92$) (**a**) nor between SLN+ and SLN− ($p=0.5$) (**b**)

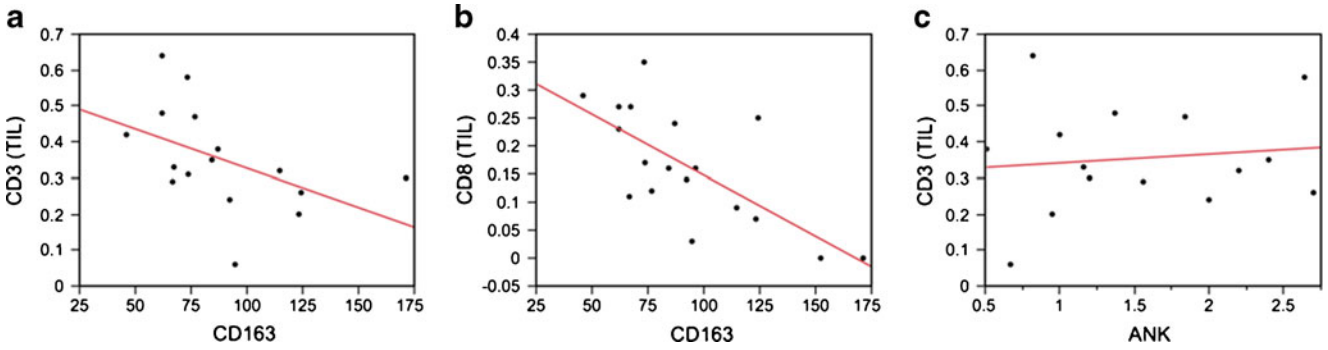

Fig. 5 Correlation of CD163 and ANK-1 with TIL. The correlation of sinusoidal CD163$^+$ cells in the SLN with CD3 TIL (r^2=0.23, p=0.06; **a**) and CD8 TIL (r^2=0.49, p=0.001; **b**) are displayed. Additionally, the correlation of ANK-1$^+$ cells in the SLN with nodal involvement with the frequency of CD3 TIL (r^2=0.01, p=0.71; **c**) is shown

Clinicopathologic features

No statistically significant correlations were found between the frequencies of CD163 or ANK-1 accumulation and age, tumor grade, tumor type, location, T stage, and stage or diameter of the tumor in SLN+ or SLN−.

Discussion

We observed fewer CD163$^+$ macrophages in the SLN of patients with breast cancer, especially in those with nodal metastasis, than in controls. In other words, the presence of CD163$^+$ cells in the perisinusoidal areas of the SLN may be protective against metastasis. On the other hand, breast cancer seemed to promote the sinusoidal expression of IDO in CD163$^+$ macrophages since the ratio between the number of IDO$^+$ cells and CD163$^+$ cells was significantly higher in cancer patients than in controls. Even though we cannot formally exclude the possibility that the increase of IDO expression occurred in cells other than CD163$^+$ macrophages, the colocalization of IDO and CD163 in sinusoidal areas and the morphological similarities between CD163-expressing and IDO-expressing cells strongly suggest that increases in IDO occurred mainly in CD163$^+$ macrophages. Since the increase of sinusoidal IDO expression did not associate with the presence of nodal metastasis but merely with the presence of cancer, the data suggest that, in draining lymph nodes of cancer patients, a large proportion of sinusoidal CD163$^+$ macrophages begin to express IDO in response to factors secreted or released into the lymph nodes by distant cancer. We speculate that, in the absence of nodal metastasis, the CD163$^+$/IDO$^-$ cell population may be higher to protect patients from tumor dissemination. Once metastasis occurs, the function of the macrophages likely changes, possibly due to paracrine influences, and the IDO$^+$ population increases. In our previous study, we found that, in tumor-free nodes, sinusoidal IDO expression correlated with the presence of paracortical Foxp3$^+$ cells [1]. Thus, it appears that the frequency of sinusoidal IDO$^+$ macrophages is regulated by cancer cell-derived factors in the lymph nodes and that the number Foxp3$^+$ regulatory T cells increase in paracortical T cell areas thereafter, depending on the expression of IDO in sinusoidal macrophages.

Lymph node metastasis correlated both with the reduction of sinusoidal CD163$^+$ macrophages and induction of paracortical Foxp3$^+$ cells [1]. Since Foxp3$^+$ and CD163$^+$ cell counts did not correlate with each other, the reduction of CD163$^+$ macrophages in cancer patients is not directly related to the presence of Foxp3$^+$ T cells in the paracortex of the SLN. Whether the observed changes in metastatic lymph nodes are due to the locally infiltrated cancer cells or are due to the actual promotion of invasion is not clear based on our present data. It could be that lymph node invasion occurs more easily in those patients that have reduced sinusoidal CD163$^+$ macrophage counts in response to cancer-derived lymph nodes and that paracortical Foxp3 expression further promotes the growth of infiltrated tumor cells. We are in the process of exploring tumor-free draining lymph nodes from the same patients and the results of that analysis will clarify this issue further.

Tumor-associated macrophages (TAM) in breast cancer demonstrate an M2 polarization [21], and CD163$^+$ macrophages have been shown to be a marker of macrophage induction by Th2 cytokines IL-4 and IL-13 [22]. These TAM are believed to support tumor growth, promote angiogenesis, and suppress adaptive immunity [23] For example, in invasive ductal carcinoma of the breast, accumulation of macrophages has been associated with worse disease-free survival and prognosis [24]. Our findings suggest that CD163$^+$ macrophages in the sinuses of tumor-draining lymph nodes are associated with a favorable nodal stage. Yet, in metastatic lymph nodes, a higher frequency of CD163$^+$ cells was associated with fewer infiltrating T cells and cytotoxic T cells in nodal metastases. As many of these CD163$^+$ macrophages were of the same morphology and in

the same SLN compartment as the IDO$^+$ cells in our previous studies, these macrophages likely represent an M2 type and promote immunosuppression. Tumor-infiltrating lymphocytes (TIL), both CD3$^+$ and CD8$^+$, have been related to improved survival in a meta-analysis in patients with solid tumors [25]. On the other hand, TIL of nodal metastases have not received much attention, although their presence has been correlated with disease-free survival in melanoma in one study [26]. Thus, it appears that, depending on the location and the local microenvironment, the presence of CD163$^+$ macrophages in cancer patients may be associated with beneficial or less desired immune reactions.

We found no differences in the frequency or distribution of ANK-1$^+$ NK cells between the SLN of patients with breast cancer and controls. NK cells are not a homogenous population and roughly 75 % of NK cells do not express ANK-1. We were interested in studying the ANK-1$^+$ population since those NK cells have the capacity to infiltrate tumor tissues and, in the lymph nodes, are found in proximity to T cells residing in germinal centers [6]. Even though we did not find any differences in the pattern of distribution or frequency of ANK-1$^+$ cells in metastatic and nonmetastatic SLN, the remarkable differences in the distribution pattern between various individuals and SLN were interesting. Currently, very little is known about the role of ANK-1$^+$ NK cells in germinal centers. Since ANK-1$^+$ frequencies correlated with the presence of ANK-1$^+$ cells in germinal centers of T cell areas, the nature of interaction between ANK-1$^+$ NK cells and T cells in metastatic lymph nodes requires further exploration. It has been shown that NK activity is reduced in the periphery in patients with breast cancer [27].

There are a number of limitations in our patient material. Especially, the number of SLN− cancer patients was very small, just 11. Therefore, the possibility of type II error cannot be excluded. It is difficult to extrapolate the significance of these findings on survival, as most of our patients had early stages of disease and, for this reason, there have been too few survival events to correlate with our findings. Also, the patients were selected based primarily on their nodal status and irrespective of the histological subtype and tumor grade. For these reasons, patients with invasive lobular cancer were over-represented, resulting in over-representation of ER$^+$ tumors in the present study. Therefore, we do not know how well our results reflect the immunological status of ER$^-$ patients. Also, we used SLN from patients with premalignant conditions like atypical ductal hyperplasia or lobular carcinoma in situ as controls. These control nodes may already have immunological alterations and, therefore, cannot be regarded as normal. However, to date, no changes in the immune profile of the SLN from patients with such premalignant conditions have been reported. Furthermore, we quantified our results manually based on our scan of representative areas. As such, we could not be blinded to the group the samples belong to; however, a whole-section automated digital image analysis may have quantified aberrant expression of markers by tumor and would not have allowed us to separate nonmetastatic regions from metastases.

In conclusion, these results indicate that reduction of CD163$^+$ macrophages in the sinuses of the SLN is associated with nodal invasion of tumor cells in breast cancer patients; however, in the SLN with metastasis, greater numbers of CD163$^+$ cells correlated with fewer infiltrating CD8$^+$ T cells in nodal metastases. Although the frequency of CD163$^+$ and IDO$^+$ cells were not correlated with each other, patients with breast cancer had higher ratios of IDO$^+$/CD163$^+$ cells than controls. Even though there was no correlation of ANK-1$^+$ expression and nodal status, there was a higher frequency of ANK-1$^+$ cells when these cells were distributed among germinal centers in metastatic lymph nodes. Whether the downregulation of CD163$^+$ macrophages in the SLN with metastasis represents a mechanism or marker of metastasis requires further investigation. We are the first to suggest that decreased frequency of sinusoidal CD163$^+$ macrophages may have a role in nodal dissemination of breast cancer.

Conflict of interest We declare that we have no conflict of interest.

References

1. Mansfield AS, Heikkila PS, Vaara AT, von Smitten KA, Vakkila JM, Leidenius MH (2009) Simultaneous Foxp3 and IDO expression is associated with sentinel lymph node metastases in breast cancer. BMC Cancer 9:231
2. Mansfield AS, Heikkila P, von Smitten K, Vakkila J, Leidenius M (2011) Metastasis to sentinel lymph nodes in breast cancer is associated with maturation arrest of dendritic cells and poor co-localization of dendritic cells and CD8(+) T cells. Virchows Arch 459:391–398
3. Matsuura K, Yamaguchi Y, Osaki A, Ohara M, Okita R, Emi A, Murakami S, Arihiro K (2009) FOXP3 expression of micrometastasis-positive sentinel nodes in breast cancer patients. Oncol Rep 22:1181–1187
4. Matsuura K, Yamaguchi Y, Ueno H, Osaki A, Arihiro K, Toge T (2006) Maturation of dendritic cells and T-cell responses in sentinel lymph nodes from patients with breast carcinoma. Cancer 106:1227–1236
5. Kohrt HE, Nouri N, Nowels K, Johnson D, Holmes S, Lee PP (2005) Profile of immune cells in axillary lymph nodes predicts disease-free survival in breast cancer. PLoS Med 2:e284
6. Angel CE, Chen CJ, Horlacher OC, Winkler S, John T, Browning J, MacGregor D, Cebon J, Dunbar PR (2009) Distinctive localization of antigen-presenting cells in human lymph nodes. Blood 113:1257–1267
7. Chambers AF, Groom AC, MacDonald IC (2002) Dissemination and growth of cancer cells in metastatic sites. Nat Rev Cancer 2:563–572

8. Nathanson SD (2003) Insights into the mechanisms of lymph node metastasis. Cancer 98:413–423
9. Lanier LL (2008) Evolutionary struggles between NK cells and viruses. Nat Rev Immunol 8:259–268
10. Sun JC, Beilke JN, Lanier LL (2009) Adaptive immune features of natural killer cells. Nature 457:557–561
11. Li S, Xu J, Makarenkova VP, Tjandrawan T, Vakkila J, Reichert T, Gooding W, Lagenaur CF, Achim CL, Chambers WH, Herberman RB, Whiteside TL, Vujanovic NL (2004) A novel epitope of N-CAM defines precursors of human adherent NK cells. J Leukoc Biol 76:1187–1199
12. Mansour EG, Ravdin PM, Dressler L (1994) Prognostic factors in early breast carcinoma. Cancer 74:381–400
13. Nemoto T, Vana J, Bedwani RN, Baker HW, McGregor FH, Murphy GP (1980) Management and survival of female breast cancer: results of a national survey by the American College of Surgeons. Cancer 45:2917–2924
14. Rosen PP, Groshen S, Saigo PE, Kinne DW, Hellman S (1989) Pathological prognostic factors in stage I (T1N0M0) and stage II (T1N1M0) breast carcinoma: a study of 644 patients with median follow-up of 18 years. J Clin Oncol 7:1239–1251
15. Leidenius MH, Krogerus LA, Toivonen TS, von Smitten KA (2005) Sentinel node biopsy is not sensible in breast cancer patients with large primary tumours. Eur J Surg Oncol 31:364–368
16. Kristiansen M, Graversen JH, Jacobsen C, Sonne O, Hoffman HJ, Law SK, Moestrup SK (2001) Identification of the haemoglobin scavenger receptor. Nature 409:198–201
17. Martens JH, Kzhyshkowska J, Falkowski-Hansen M, Schledzewski K, Gratchev A, Mansmann U, Schmuttermaier C, Dippel E, Koenen W, Riedel F, Sankala M, Tryggvason K, Kobzik L, Moldenhauer G, Arnold B, Goerdt S (2006) Differential expression of a gene signature for scavenger/lectin receptors by endothelial cells and macrophages in human lymph node sinuses, the primary sites of regional metastasis. J Pathol 208:574–589
18. Leidenius MH, Vironen JH, Heikkila PS, Joensuu H (2010) Influence of isolated tumor cells in sentinel nodes on outcome in small, node-negative (pT1N0M0) breast cancer. Ann Surg Oncol 17:254–262
19. Leidenius MH, Krogerus LA, Toivonen TS, Von Smitten KJ (2003) The feasibility of intraoperative diagnosis of sentinel lymph node metastases in breast cancer. J Surg Oncol 84:68–73
20. Leikola JP, Toivonen TS, Krogerus LA, von Smitten KA, Leidenius MH (2005) Rapid immunohistochemistry enhances the intraoperative diagnosis of sentinel lymph node metastases in invasive lobular breast carcinoma. Cancer 104:14–19
21. Sica A, Schioppa T, Mantovani A, Allavena P (2006) Tumour-associated macrophages are a distinct M2 polarised population promoting tumour progression: potential targets of anti-cancer therapy. Eur J Cancer 42:717–727
22. Gordon S (2003) Alternative activation of macrophages. Nat Rev Immunol 3:23–35
23. Mantovani A, Marchesi F, Porta C, Sica A, Allavena P (2007) Inflammation and cancer: breast cancer as a prototype. Breast 16 (Suppl 2):S27–S33
24. Tsutsui S, Yasuda K, Suzuki K, Tahara K, Higashi H, Era S (2005) Macrophage infiltration and its prognostic implications in breast cancer: the relationship with VEGF expression and microvessel density. Oncol Rep 14:425–431
25. Gooden MJ, de Bock GH, Leffers N, Daemen T, Nijman HW (2011) The prognostic influence of tumour-infiltrating lymphocytes in cancer: a systematic review with meta-analysis. Br J Cancer 105:93–103
26. Mihm MC Jr, Clemente CG, Cascinelli N (1996) Tumor infiltrating lymphocytes in lymph node melanoma metastases: a histopathologic prognostic indicator and an expression of local immune response. Lab Invest 74:43–47
27. Dewan MZ, Takada M, Terunuma H, Deng X, Ahmed S, Yamamoto N, Toi M (2009) Natural killer activity of peripheral-blood mononuclear cells in breast cancer patients. Biomed Pharmacother 63:703–706

Virchows Arch (2012) 461:647–653
DOI 10.1007/s00428-012-1327-7

ORIGINAL ARTICLE

BMI1 expression identifies subtypes of Merkel cell carcinoma

Maria Kouzmina · Valtteri Häyry · Junnu Leikola · Caj Haglund · Tom Böhling · Virve Koljonen · Jaana Hagström

Received: 12 May 2012 / Revised: 31 July 2012 / Accepted: 28 September 2012 / Published online: 11 October 2012
© Springer-Verlag Berlin Heidelberg 2012

Abstract Merkel cell carcinoma (MCC) is a rare cutaneous neuroendocrine carcinoma. The aims of this study were to investigate the expression of the transcription factors B-lymphoma Moloney murine leukaemia virus insertion (BMI1), myelocytomatosis viral oncogene homologue (c-Myc) and Snail in MCC tumour specimens and to examine the relationship of these markers to Merkel cell polyoma virus (MCV). The study comprised of 133 patients with primary MCC. The expression of BMI1, Snail and c-Myc protein was assessed by immunohistochemistry and compared with clinical parameters, MCV status and patient survival. The presence of MCV was inversely correlated with the expression of BMI1 protein. Tumours expressing BMI1 protein more often presented with lymph node metastases. Snail protein expression was decreased in cases with metastatic dissemination. This study identified two subgroups of MCC: tumours expressing BMI1 but negative for MCV DNA and tumours negative for BMI1 expression but positive for MCV. Importantly, BMI1-positive cases often presented with lymph node metastases. Combined, these results suggest that subtypes of this malignancy exist.

Keywords Merkel cell carcinoma · BMI1 · Merkel cell polyoma virus

Abbreviations

AJCC	American Joint Committee on Cancer
BMI1	B-lymphoma Moloney murine leukaemia virus insertion
CK-20	Cytokeratin-20
c-Myc	Myelocytomatosis viral oncogene homologue
DNA	Deoxyribonucleic acid
LT3	Large T 3
MCC	Merkel cell carcinoma

Virve Koljonen and Jaana Hagström contributed equally to this work.

M. Kouzmina (✉)
Department of Oral and Maxillofacial Surgery, Helsinki University Central Hospital,
P.O. Box 263, Kasarminkatu 11-13,
00029 HUS, Helsinki, Finland
e-mail: maria.kouzmina@fimnet.fi

V. Häyry
Department of Otorhinolaryngology—Head and Neck Surgery, Helsinki University Central Hospital,
Helsinki, Finland

J. Leikola · V. Koljonen
Department of Plastic Surgery, Helsinki University Central Hospital,
Helsinki, Finland

C. Haglund
Department of Gastroenterological Surgery, Helsinki University Central Hospital,
Helsinki, Finland

T. Böhling
Department of Pathology, Helsinki University and HUSLAB,
Helsinki, Finland

M. Kouzmina · V. Häyry · V. Koljonen
Institute of Clinical Medicine, Helsinki University,
Helsinki, Finland

J. Hagström
Department of Pathology/Haartman Institute and HUSLAB,
Helsinki University Central Hospital,
Helsinki, Finland

J. Hagström
Department of Oral Pathology, University of Helsinki,
Helsinki, Finland

MCV	Merkel cell polyoma virus
PCR	Polymerase chain reaction
TTF-1	Thyroid transcription factor-1
UVB	Ultraviolet B

Introduction

Merkel cell carcinoma (MCC) is an aggressive cutaneous neuroendocrine malignancy. Over the years, a lively academic discussion on the cell of origin of MCC has been conducted in the literature. The non-neoplastic Merkel cells of the skin have characteristics of both epidermal and neuroendocrine cells. Szeder et al. provided evidence favouring an origin from the neural crest in view of the absence of expression in prenatal MCs of NT-3, an important mediator in neural crest development and in sensory neurogenesis [1]. MCs contain desmosomes and express cytokeratin 20, unlike melanocytes which migrate from the neural crest and do not contain cytokeratin or desmosomes. This suggests that the MC is a modified keratinocyte (as reviewed by Lucarz and Brand [2].) Both these characteristics support the hypothesis that Merkel cells are derived from the neural crest [3, 4] and are of epidermal origin [5, 6].

Current data support the view, however, that MCC is derived from primitive pluripotent epidermal cells, rather than from non-neoplastic Merkel cells [7, 8]. This cell of origin hypothesis is supported by numerous reports describing MCC with squamous and sarcomatous [9], eccrine [10], leiomyosarcomatous [11], rhabdomyoblastic [12] and fibrosarcomatous differentiation [13]. Merkel cells undergo slow turnover and are replaced by cells originating from epidermal stem cells, not through proliferation of differentiated Merkel cells [14]. This is corroborated by the finding that mitoses do not occur in human adult Merkel cells [15, 16].

The cancer stem cell hypothesis states that cancer is composed of a heterogeneous mix of malignant cells and a fraction of these express stem cell markers [17, 18]. Furthermore, only these cancer stem cells are thought to have the potential of initiating tumour growth, hence causing tumour recurrence after treatment [19]. A vast amount of clinical research on tumours of varied origin, representing most embryonic germ layers, proves that the expression of stem cell genes is often a sign of aggressive disease [20]. Still, the molecular biology of cancer stem cells is not fully understood. Abbas and Bhawan studied the expression of stem cell markers (cytokeratins 15 and 19 and nestin) in 11 MCC samples [21]. The absence of cytokeratin 15 and nestin expression in all tumour samples, together with the absence of both markers in non-neoplastic Merkel cells, provides an additional common immunohistochemical feature between MCC and the Merkel cell.

Stem cell markers, such as B-lymphoma Moloney murine leukaemia virus insertion (BMI1), myelocytomatosis viral oncogene homologue (c-Myc) and Snail, have been used to identify cancer stem cells. The polycomb protein BMI1 has served as a cancer stem cell marker in several types of tumour, especially skin cancer (both basal cell carcinoma and squamous cell carcinoma), melanoma and medulloblastoma [22, 23]. The BMI1 protein is part of a large polycomb complex, regulating stem cell maintenance through epigenetic regulation, particularly histone methylation and subsequent gene promoter suppression [24]. C-Myc has been identified as a regulator of epidermal stem cell homeostasis [25], and c-Myc signalling is interconnected with the BMI1 pathway [26]. Snail, a zinc-finger transcription factor, is essential for the formation of neural crest and is a key regulator of epithelial–mesenchymal transition. In addition, it is involved in wound healing, fibrosis and skin development [27].

The recently discovered Merkel cell polyoma virus (MCV) is a possible causative agent for MCC [28]. It is found in 24–89 % of MCCs [29–32], but its role in the carcinogenesis of MCC is still partly unknown. However, a strong causal role of MCV in the pathogenesis of MCC is suggested by monoclonal integration and truncation of a large T viral antigen in MCC cells [28, 33].

The main limitation in applying the cancer stem cell hypothesis in clinical diagnostics is the lack of a single marker for a tumour stem cell. Rather, a plethora of markers have been identified, all more or less specific for a certain type of tumour or tissue [34]. Therefore, in this study, we focused on screening MCC samples for stem cell markers of epidermal, neural and neural crest origin, based on the previous and current cell of origin hypothesis, and on comparing the stem cell marker expression with MCV status.

Materials and methods

The study protocol was approved by the Ethics Committee of Helsinki University Central Hospital. The Ministry of Health and Social Affairs granted permission to collect patient data and the National Authority for Medicolegal Affairs to collect tissue samples.

Patients, clinical data and tissue samples

Data of patients diagnosed with MCC in Finland during 1979–2004 were obtained from the Finnish Cancer Registry. The study material comprised of 133 primary MCC tumour samples obtained from 133 patients. Detailed data of patients and tumour characteristics, including tumour size, location, stage of disease at time of diagnosis, local recurrence, local and systemic metastasis and survival, were obtained from hospital and primary health care centre files.

Table 1 summarises the clinicopathological data of these patients.

Formalin-fixed, paraffin-embedded tumour tissue blocks of patients included in this survey were retrieved from the archives of the Department of Pathology. The histology of the tumour samples was re-evaluated without knowledge of clinical or molecular data by one of the authors with special expertise in MCC pathology (TB). For diagnostic purposes, the samples were stained for cytokeratin-20 (CK-20, Dako-Cytomation, Glostrup, Denmark) and thyroid transcription factor-1 (TTF-1; Novocastra, Balliol Business Park West, Benton Lane, Newcastle Upon Tyne, UK). Requirements for a diagnosis of MCC were morphology compatible with MCC at light microscopy and expression of CK-20 but not of TTF-1. Maximum tumour dimension was measured from the available haematoxylin–eosin-stained slides.

Table 1 Clinical characteristics of patients and primary tumours

Gender	
Male	39
Female	94
Age (years)	
≤50	3
51–69	28
70+	102
Primary tumour location	
Head and neck	75
Lower extremities	26
Upper extremities	24
Trunk	8
Primary tumour size(mm)	
≤20	95
>20	38
Stage[a] at presentation	
I	90 (68 %)
II	28 (21 %)
III	11 (8 %)
IV	4 (3 %)
Presence of MCV DNA in tumour samples (n=115)	
Yes	86
No	29
Course of disease	
No dissemination	72
Metastatic dissemination	61
Only local recurrence	16
Regional lymph basin	26
Systemic metastasis	19
Outcome	
Alive	23
Dead	110

[a] Staging according to the American Joint Committee on Cancer (AJCC) staging system criteria

The presence of MCV DNA was tested for in DNA extracted from representative deparaffinised tumour sections as described elsewhere [31]. Quantitation of MCV DNA was done using real-time PCR with hydrolysis probes and primers specific for the viral LT3 coding region in a LightCycler 480 instrument (Roche Diagnostics GmbH, Mannheim, Germany). A formalin-fixed, paraffin-embedded sample of normal skin was retrieved for double immunostaining of BMI1 and CK-20 to examine BMI1 expression in Merkel cells of normal skin.

Patients were retrospectively staged according to the AJCC staging system [35]. In brief, patients with primary MCC with no clinical or pathological evidence of regional or distant metastases were divided into two stages: stage I for primary tumours ≤20 mm and stage II for primary tumours >20 mm. Stages I and II were further divided into substages A and B according to the method of nodal evaluation; microscopic evaluation of draining lymph nodes was substaged as A, those evaluated clinically as B. For patients with histologically proven micrometastasis, stage was defined as IIIA; this included all tumour sizes. Stage IV comprised of tumours of any size and regional lymph node status with systemic spread of metastasis. None of the stage IV patients included in this study had lymph node metastases recorded in their clinical files. The follow-up started on the date of diagnosis of MCC and ended on the date of death or the closing date of the study (24 March 2010).

Immunohistochemistry

Tissue sections (4 μ) were deparaffinised in xylene, rehydrated through a graded alcohol series and treated in a PT-module (LabVision UK Ltd., Runcorn, UK) in Tris–HCl buffer (pH 8.5) for 20 min at 98 °C and with 0.3 % Dako REAL peroxidase-blocking solution (Dako-Cytomation, Glostrup, Denmark) for 5 min to block endogenous peroxidase. Immunostaining was performed by mouse monoclonal c-Myc (9E10) antibody (Santa Cruz, CA, USA, diluted 1:400 in Dako REAL antibody diluent, Biohit, Helsinki, Finland), mouse monoclonal anti-BMI1 antibody (ab 14389) (Abcam, Cambridge, UK, 1:400) and rabbit polyclonal anti-Snail antibody (ab17731) (Abcam, 1:2,000), followed by a 30-min incubation with the Dako REAL EnVision/HRP detection system. Finally, slides were visualised using Dako REAL DABþ chromogen (10 min). Between each step, washing was done with PBS 0.04 % in Tween20. Slides were counterstained with Meyer's haematoxylin and mounted in a mounting medium (Aquamount, BDH, Poole, UK). In every immunohistochemical staining series, a specific positive control was used. As negative controls, sections incubated without primary antibody were used.

Evaluation of immunostainings

For every marker, one representative section of each tumour was analysed, and the whole tumour area was interpreted. The slides were evaluated separately by two researchers (JH and MK) unaware of patients' status. In case of discrepancy, a consensus score was used. The frequency of immunopositive tumour cells was evaluated from the stained sections. The expression of the studied proteins was evaluated by scoring the percentage of stained tumour cells. In one patient, BMI1 immunohistochemistry was repeatedly unsuccessful, bringing the number of BMI1-stained samples down to 132.

Statistical analysis

Statistical analysis was conducted with NCSS 2007 (NCSS Statistical Software, Kaysville, UT, USA) and SPSS statistics 19.0 software (IBM Corporation, NY, USA). p values less than 0.05 were considered significant. The expression of BMI1, Snail and c-Myc was compared with gender, tumour size and location, local recurrence and metastatic dissemination. The Mann–Whitney U test was used to compare numerical values between two groups. Spearman rank correlation was used to analyse two numerical variables. The chi-square test was used when valid, to compare categorical variables.

For 115 samples (87 %), MCV status could be determined. The statistical association between the presence of MCV DNA and immunoexpression of Snail and BMI1 and c-Myc was evaluated with the Mann–Whitney U test.

Results

Tables 2 and 3 summarise the results of immunohistochemistry, and examples of immunoexpression are presented in Fig. 1.

BMI1 in MCC

When present, BMI1 staining was nuclear and usually strong and homogeneous throughout the sample. BMI1 protein was expressed in 66 (50.0 %) of the samples and 66 (50.0 %) were totally negative, as detailed in Table 2. The frequency of BMI1-positive tumour cells ranged from 2.0 to 99.0 %, with a mean of 28.0 %. Table 3 presents the BMI1 expression stratified by tumour staging.

Table 2 Expression of stem cell markers BMI1, Snail and c-Myc in 133 Merkel cell carcinoma samples

	Negative staining (n)	Positive staining (n)
BMI1	66	66
c-Myc	40	93
Snail	0	133

The frequency of BMI1-positive tumour cells was compared with the presence of MCV in the same samples. BMI1 protein expression was found in 66.0 % of MCV-negative and 45.0 % of MCV-positive cases. Based on the results observed in the Mann–Whiney U test, we defined a positive BMI1 protein expression status at a cut-off of 5 % and applied this in subsequent statistical analyses. Using the chi-square test, positive BMI1 protein expression status thus defined correlated with lymph node metastases (p=0.023) and inversely correlated with MCV (p=0.010).

An inverse correlation between BMI1 protein expression and MCV was observed. The mean frequency of BMI1-positive tumour cells was 11.2 % in MCV-positive and 20.8 % in MCV-negative cases (p=0.029).

At the time of diagnosis, 11 patients presented with regional lymph node metastases and all were at stage III. Nine of these tumours were positive and two negative for BMI1. There was no statistically significant difference in survival between patients with BMI1-positive and BMI1-negative tumours.

BMI1 in Merkel cells of normal skin

To provide a framework for our observations on BMI1 in MCC, we also investigated BMI1 expression in non-neoplastic Merkel cells of the skin. We performed double immunohistochemical staining for BMI1 and CK-20 on sections of normal skin and found that these markers co-localise in some cells (Fig. 2). However, not all BMI1-positive cells expressed CK-20 and vice versa, suggesting that BMI1 is expressed in some normal Merkel cells. Keratinocytes expressing CK-20 were abundant in the basal cell layer of the epidermis and around the adnexal bodies. In contrast to MCC samples, occasionally also nuclear expression of BMI1 was seen in the epidermis.

Snail and c-Myc in MCC

Nuclear expression of Snail was observed in all 133 samples. The frequency of immunoreactive tumour cells was high, ranging from 10.0 to 98.0 % (mean 87.0 %). Interestingly, the mean frequency of Snail-positive tumour cells was higher in cases with local disease (87.8 %) than in cases with metastases (81.9 %) (p=0.002). Cytoplasmic c-Myc expression was observed in 93 (70.0 %) of the samples. The frequency of positive tumour cells ranged from 2.0 to 98.0 % (mean 32.0 %). No statistically significant correlation was found between Snail or c-Myc and MCV.

Table 3 BMI1 expression stratified by Merkel cell carcinoma stages

	BMI1 expression						
	BMI1 negative	BMI1 immunopositivity[a]					Number of cases
	BMI1 0; number of cases (%)	BMI1 1–≤5 %; number of cases (%)	BMI1 5–10 %; number of cases (%)	BMI1 11–35; number of cases (%)	BMI 36–70; number of cases (%)	BMI 71–100; number of cases (%)	
Stage 1	41 (45.6)	7 (7.8)	18 (20)	8 (8.9)	9 (10)	7 (7.8)	90
Stage 2	21 (75)	–	5 (17.9)	1 (3.6)	1 (4)	–	28
Stage 3	2 (18)	–	4 (36.4)	3 (27.3)	0 (0)	2 (18)	11
Stage 4	3(75)	–	–	–	1 (25)	–	4
Number of cases	67 (50)	7 (5)	27 (20)	12 (9)	11 (8)	9 (7)	133

[a] Evaluated by scoring the percentage of positive tumour cells

Discussion

In this study, we analysed the protein expression of BMI1, Snail and c-Myc in 133 primary MCC samples. In addition to reporting the expression of the specific stem cell markers, we also correlated the results with clinical parameters. We established a significant correlation between expression of BMI1 and absence of MCV DNA. We also observed increased lymph node metastases in BMI1-positive cases. These observations suggest that a subpopulation of MCCs is not dependent on MCV as a causative agent and this subgroup has different clinical features.

BMI1 protein expression has been reported in a series of 32 samples of MCC, 75.0 % of which showed nuclear and cytoplasmic BMI1 expression [36]. In our material, the number of BMI1-positive tumours was smaller (50.0 %), a difference attributed to the use of different reagents (antibodies), but also different samples: Brunner et al. studied 32 samples, and only six of these were clinically stage II and III. With our samples, we could perform statistical analyses encompassing tumour stage and MCV status.

We did not find a causative link between BMI1 and MCC. However, BMI1 might contribute to the pathogenesis of MCC through a mechanism independent of MCV. The role of BMI1 in carcinogenesis is complex. Overexpression of BMI1 is associated with resistance to apoptotic cues in human foreskin keratinocytes and immortalisation of human dermal keratinocytes and human dermal papilla cells [37]. High BMI1 expression is found in malignant melanoma, although decreased BMI1 expression is linked to clinical progression [38]. BMI1 is constitutively expressed in normal skin; similar findings of BMI1 expression in skin have been reported by Reinisch et al. [39].

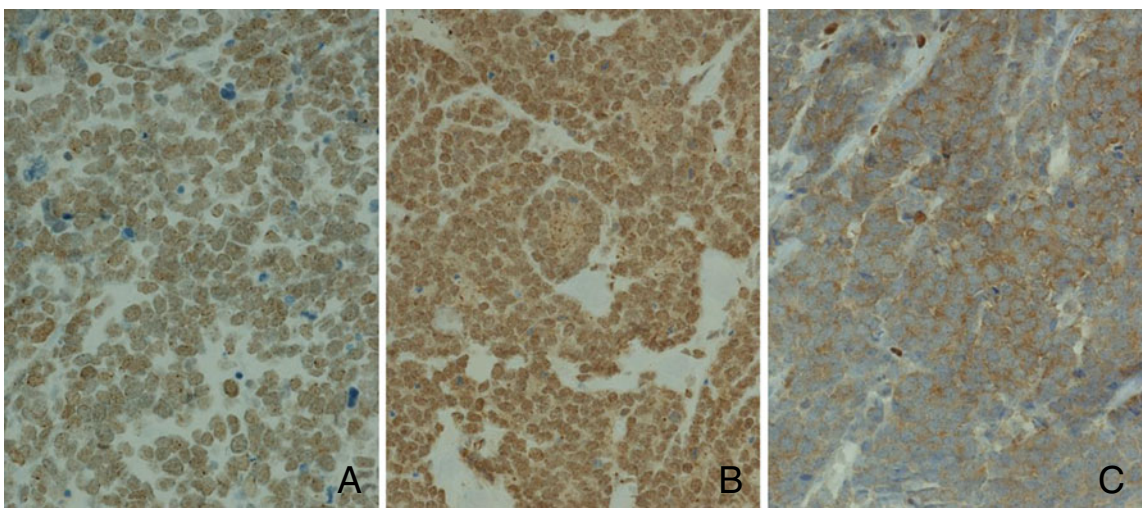

Fig. 1 BMI1 immunoreactivity (**a**), Snail immunoreactivity (**b**) and c-Myc cytoplasmic immunoreactivity (**c**) in Merkel cell carcinoma (original magnification ×400)

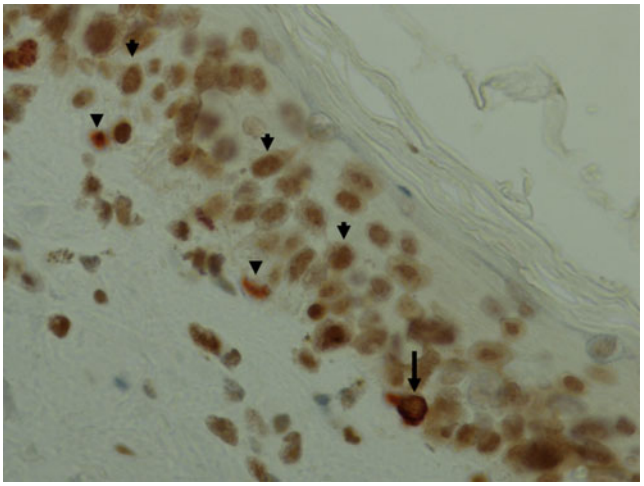

Fig. 2 Double immunostaining for CK-20 (*brown*, *short arrow*) and BMI1 (*red*, *arrowhead*) on a normal skin tissue sample. Double stained cell marked with a *long arrow*. CK-20 immunoreactive cells are located mainly in the epidermis and BMI1-positive cells are stromal (original magnification ×200)

Clinical and epidemiological evidences suggest a role for UV radiation in the pathogenesis of MCC. Miller and Rabkin [40] found a link between the incidence of MCC and ultraviolet B (UVB) exposure. Indirect evidence for UV exposure as an aetiological factor is that MCC usually occurs on sun-damaged skin of the head and neck regions [41]. The tumours are often in close proximity to other lesions of actinically damaged skin. In one study, cellular depletion of BMI1 led to enhanced sensitivity of glioma cells to apoptosis induced by UV irradiation [42]. In cultured keratinocytes, BMI1 overexpression rendered cells resistant to UVB-induced apoptotic cues [43]. BMI1 is capable of transforming cultured cells, although this requires normal nuclear localisation of the protein. If nuclear localisation motifs are disrupted, BMI1 remains cytoplasmic and presumably inactive. However, the transcriptional suppression activity of BMI1 is reported to be independent of subnuclear localisation [44]. Our results are in accordance with previous studies on BMI1 conducted in other types of malignancies. Our results support the previous finding of frequent expression of BMI1 in MCC samples [36] and link BMI1 expression to the MCV status. This correlation supports the notion that BMI1 involvement in the pathogenesis of MCC might be independent of MCV.

We found a statistically significant correlation between high Snail protein expression and local stage of disease at presentation. We emphasise that this association should be taken cautiously: statistical significance does not necessarily reflect biological significance and this should be further investigated. In many cancers, Snail protein expression is indicative of the epithelial–mesenchymal transition and invasive disease, and it has been shown to correlate with clinicopathological features of aggressive/advanced disease, although this is not always the case [45]. Even though in our material high Snail expression seemed paradoxically correlated with local disease, it is important to note that we found a high frequency of tumour cells expressing Snail in the vast majority of our samples, underscoring the involvement of the epithelial–mesenchymal transition in MCC.

In conclusion, our finding of the absence of BMI1 protein expression in MCV-positive MCCs suggests that novel mechanisms, differing from canonical non-viral malignant transformation models, exist in the pathogenesis and progression of this disease. In our view, the expression in MCC of BMI1 and Snail, transcription factors regulating stem cell function, supports the cancer stem cell theory in MCC.

Acknowledgments The authors thank Päivi Peltokangas, Tuire Koski and Elina Aspiala for excellent technical assistance. Harri Sihto is thanked for MCV analysis and Timo Pessi for assistance with statistical analysis. Funding of this study was from departmental sources only.

Conflict of interest Each author declares no financial conflicts of interest with regard to the data presented in this manuscript.

References

1. Szeder V, Grim M, Kucera J et al (2003) Neurotrophin-3 signaling in mammalian Merkel cell development. Dev Dyn 228:623–629
2. Lucarz A, Brand G (2007) Current considerations about Merkel cells. Eur J Cell Biol 86:243–251
3. Winkelmann RK (1977) The Merkel cell system and a comparison between it and the neurosecretory or APUD cell system. J Invest Dermatol 69:41–46
4. Grim M, Halata Z (2000) Developmental origin of avian Merkel cells. Anat Embryol (Berl) 202:401–410
5. Sidhu GS, Chandra P, Cassai ND (2005) Merkel cells, normal and neoplastic: an update. Ultrastruct Pathol 29:287–294
6. Compton CC, Regauer S, Seiler GR et al (1990) Human Merkel cell regeneration in skin derived from cultured keratinocyte grafts. Lab Invest 63:233–241
7. Brown JA, Smoller BR (2009) Merkel cell carcinoma: what is it, what will it do and where will it go? What role should the pathologist play in reporting this information? J Cutan Pathol 36:924–927
8. Calder KB, Smoller BR (2010) New insights into Merkel cell carcinoma. Adv Anat Pathol 17:155–161. doi:10.1097/PAP.0b013e3181d97836
9. Hwang JH, Alanen K, Dabbs KD et al (2008) Merkel cell carcinoma with squamous and sarcomatous differentiation. J Cutan Pathol 35:955–959
10. Saeb-Lima M, Montante-Montes de Oca D, Albores-Saavedra J (2008) Merkel cell carcinoma with eccrine differentiation: a clinicopathologic study of 7 cases. Ann Diagn Pathol 12:410–414
11. Cooper L, Debono R, Alsanjari N et al (2000) Merkel cell tumour with leiomyosarcomatous differentiation. Histopathology 36:540–543
12. Eusebi V, Damiani S, Pasquinelli G et al (2000) Small cell neuroendocrine carcinoma with skeletal muscle differentiation: report of three cases. Am J Surg Pathol 24:223–230
13. Tan KB, Murali R, Karim RZ et al (2008) Merkel cell carcinoma with fibrosarcomatous differentiation. Pathology 40:314–316
14. Van Keymeulen A, Mascre G, Youseff KK et al (2009) Epidermal progenitors give rise to Merkel cells during embryonic development and adult homeostasis. J Cell Biol 187(1):91–100

15. Vaigot P, Pisani A, Darmon YM et al (1987) The majority of epidermal Merkel cells are non-proliferative: a quantitative immunofluorescence analysis. Acta Derm Venereol 67:517–520
16. Moll I, Zieger W, Schmelz M (1996) Proliferative Merkel cells were not detected in human skin. Arch Dermatol Res 288:184–187
17. Ezeh UI, Turek PJ, Reijo RA et al (2005) Human embryonic stem cell genes OCT4, NANOG, STELLAR, and GDF3 are expressed in both seminoma and breast carcinoma. Cancer 104:2255–2265. doi:10.1002/cncr.21432
18. Monk M, Holding C (2001) Human embryonic genes re-expressed in cancer cells. Oncogene 20:8085–8091. doi:10.1038/sj.onc.1205088
19. Al-Hajj M (2007) Cancer stem cells and oncology therapeutics. Curr Opin Oncol 19:61–64. doi:10.1097/CCO.0b013e328011a8d6
20. Ailles LE, Weissman IL (2007) Cancer stem cells in solid tumors. Curr Opin Biotechnol 18:460–466. doi:10.1016/j.copbio.2007.10.007
21. Abbas O, Bhawan J (2011) Expression of stem cell markers nestin and cytokeratin 15 and 19 in cutaneous malignancies. J Eur Acad Dermatol Venereol 25:311–316. doi:10.1111/j.1468-3083.2010.03791.x
22. Leung C, Lingbeek M, Shakhova O et al (2004) Bmi1 is essential for cerebellar development and is overexpressed in human medulloblastomas. Nature 428:337–341. doi:10.1038/nature02385
23. Mihic-Probst D, Kuster A, Kilgus S et al (2007) Consistent expression of the stem cell renewal factor BMI-1 in primary and metastatic melanoma. Int J Cancer 121:1764–1770. doi:10.1002/ijc.22891
24. Bracken AP, Dietrich N, Pasini D et al (2006) Genome-wide mapping of Polycomb target genes unravels their roles in cell fate transitions. Genes Dev 20:1123–1136. doi:10.1101/gad.381706
25. Ambler CA, Maatta A (2009) Epidermal stem cells: location, potential and contribution to cancer. J Pathol 217:206–216. doi:10.1002/path.2468
26. Guney I, Wu S, Sedivy JM (2006) Reduced c-Myc signaling triggers telomere-independent senescence by regulating Bmi-1 and p16(INK4a). Proc Natl Acad Sci U S A 103:3645–3650. doi:10.1073/pnas.0600069103
27. Nakamura M, Tokura Y (2011) Epithelial–mesenchymal transition in the skin. J Dermatol Sci 61:7–13. doi:10.1016/j.jdermsci.2010.11.015
28. Feng H, Shuda M, Chang Y et al (2008) Clonal integration of a polyomavirus in human Merkel cell carcinoma. Science 319:1096–1100
29. Foulongne V, Kluger N, Dereure O et al (2008) Merkel cell polyomavirus and Merkel cell carcinoma, France. Emerg Infect Dis 14:1491–1493
30. Becker JC, Houben R, Ugurel S et al (2009) MC polyomavirus is frequently present in Merkel cell carcinoma of European patients. J Invest Dermatol 129:248–250
31. Sihto H, Kukko H, Koljonen V et al (2009) Clinical factors associated with Merkel cell polyomavirus infection in Merkel cell carcinoma. J Natl Cancer Inst 101:938–945
32. Garneski KM, Warcola AH, Feng Q et al (2009) Merkel cell polyomavirus is more frequently present in North American than Australian Merkel cell carcinoma tumors. J Invest Dermatol 129:246–248
33. Shuda M, Feng H, Kwun HJ et al (2008) T antigen mutations are a human tumor-specific signature for Merkel cell polyomavirus. Proc Natl Acad Sci U S A 105:16272–16277
34. Alison MR, Lim SM, Nicholson LJ (2011) Cancer stem cells: problems for therapy? J Pathol 223:147–161. doi:10.1002/path.2793
35. Edge SB, Byrd DR, Compton CC (eds) (2010) Merkel cell carcinoma. Springer, New York, pp 315–323
36. Brunner M, Thurnher D, Pammer J et al (2008) Expression of VEGF-A/C, VEGF-R2, PDGF-alpha/beta, c-kit, EGFR, Her-2/Neu, Mcl-1 and Bmi-1 in Merkel cell carcinoma. Mod Pathol 21:876–884
37. Haga K, Ohno S, Yugawa T et al (2007) Efficient immortalization of primary human cells by p16INK4a-specific short hairpin RNA or Bmi-1, combined with introduction of hTERT. Cancer Sci 98:147–154. doi:10.1111/j.1349-7006.2006.00373.x
38. Bachmann IM, Puntervoll HE, Otte AP et al (2008) Loss of BMI-1 expression is associated with clinical progress of malignant melanoma. Mod Pathol 21:583–590. doi:10.1038/modpathol.2008.17
39. Reinisch CM, Uthman A, Erovic BM et al (2007) Expression of BMI-1 in normal skin and inflammatory and neoplastic skin lesions. J Cutan Pathol 34:174–180. doi:10.1111/j.1600-0560.2006.00587.x
40. Miller RW, Rabkin CS (1999) Merkel cell carcinoma and melanoma: etiological similarities and differences. Cancer Epidemiol Biomarkers Prev 8:153–158
41. Tai PT, Yu E, Winquist E et al (2000) Chemotherapy in neuroendocrine/Merkel cell carcinoma of the skin: case series and review of 204 cases. J Clin Oncol 18:2493–2499
42. Li J, Gong LY, Song LB et al (2010) Oncoprotein Bmi-1 renders apoptotic resistance to glioma cells through activation of the IKK-nuclear factor-kappaB pathway. Am J Pathol 176:699–709. doi:10.2353/ajpath.2010.090502
43. Lee K, Adhikary G, Balasubramanian S et al (2008) Expression of Bmi-1 in epidermis enhances cell survival by altering cell cycle regulatory protein expression and inhibiting apoptosis. J Invest Dermatol 128:9–17. doi:10.1038/sj.jid.5700949
44. Cohen KJ, Hanna JS, Prescott JE et al (1996) Transformation by the Bmi-1 oncoprotein correlates with its subnuclear localization but not its transcriptional suppression activity. Mol Cell Biol 16:5527–5535
45. Becker KF, Rosivatz E, Blechschmidt K et al (2007) Analysis of the E-cadherin repressor Snail in primary human cancers. Cells Tissues Organs 185:204–212. doi:10.1159/000101321

Virchows Arch (2012) 461:655–661
DOI 10.1007/s00428-012-1328-6

ORIGINAL ARTICLE

Potentially clinically relevant prostate cancer is found more frequently after complete than after partial histopathological processing of radical cystoprostatectomy specimens

H. M. Fritsche · A. Aziz · F. Eder · W. Otto · S. Denzinger · W. F. Wieland · M. May · F. Hofstädter · A. Hartmann · M. Burger

Received: 7 June 2012 / Revised: 3 September 2012 / Accepted: 29 September 2012 / Published online: 9 October 2012
© Springer-Verlag Berlin Heidelberg 2012

Abstract Incidental prostate cancer is often found in cystoprostatectomy specimens. The presence of a clinically significant tumour has an impact on follow-up strategies. In prostatectomy specimen for prostate cancer, whole-mount sections improve diagnostic accuracy. The present study compares detection of incidental prostate cancer in complete to routine processing. We included 295 consecutive patients who underwent radical cystoprostatectomy. Between 01/1995 and 12/2003 (period I), specimens of 129 patients were partially processed, whereas between 01/2004 and 03/2009 (period II), specimens of 166 patients were completely processed. Incidental prostate cancer was detected overall in 91 (30.8 %) patients. Prostate cancer was detected in 24 (18.6 %) patients in period 1 and in 67 (40.4 %) patients in period 2 ($p<0.001$). Potentially clinically significant prostate cancer was detected in 12 (9.2 %) and 29 (17.5 %) patients, respectively ($p=0.044$). Complete embedding and processing of cystoprostatectomy specimen yield significantly more potentially clinically relevant prostate cancers. The present data suggest that notably in younger men the specimens should be completely processed.

Keywords Urothelial carcinoma · Incidental · Prostate cancer · Cystectomy · Cystoprostatectomy

HM Fritsche and A Aziz contributed equally.

H. M. Fritsche (✉) · A. Aziz · W. Otto · S. Denzinger · W. F. Wieland
Department of Urology, Caritas St. Josef Medical Centre, University of Regensburg,
Landshuter Str. 65,
93053 Regensburg, Germany
e-mail: hans-martin.fritsche@ukr.de

F. Eder · F. Hofstädter
Department of Pathology, University of Regensburg, Regensburg, Germany

M. May
Department of Urology, St. Elisabeth-Hospital, Straubing, Germany

A. Hartmann
Department of Pathology, University of Erlangen, Erlangen, Germany

M. Burger
Department of Urology, University of Würzburg, Würzburg, Germany

Introduction

Radical cystoprostatectomy is the standard of care treatment for muscle-invasive urothelial carcinoma of the bladder and has also been recommended in early invasive bladder cancer in the presence of carcinoma in situ or recurrence following bladder-sparing approaches by control transurethral resection and adjuvant intravesical therapy with BCG [1, 2]. While from an oncological point of view cystoprostatectomy is the standard of care, its impact on quality of life is significant. Aside from the general morbidity related to such invasive surgery, two factors dominate among the long-term consequences. Firstly, cystoprostatectomy implies the need for urinary diversion, incontinent variants especially impairing quality of life [3], and secondly, cystoprostatectomy with complete removal of the prostate has inherent repercussions on sexual function. Radical prostatectomy damages the nerve plexus surrounding the lateral and ventral aspect of the prostate and the neurovascular bundle positioned posterolaterally to the prostate, innervating the corpora cavernosa and mediating erectile function [2].

Accordingly, surgical approaches entirely sparing the prostate have been proposed but are not recommended by major guidelines due to the possible occurrence of urothelial carcinoma involving the prostatic urethra as well as incidental prostate cancer [1]. While nerve-sparing techniques are more commonly accepted, prostate-sparing approaches harbour the risk of leaving significant prostatic cancer in situ [4].

The issue of incidental prostate cancer is a relevant problem; rates of 18 to 51 % have been described in cystoprostatectomy specimens [4–10]. As incidental prostate cancer is very common in the general population and is regarded insignificant in most cases, prostate cancer in cystoprostatectomy specimen is not always of clinical concern. The definition of insignificant prostate cancer has evolved over time: generally, a tumour volume of less than 0.5 cm^3, a Gleason score of less than 7 and a tumour stage confined to the prostate (no extraprostatic extension, no seminal vesicle invasion or lymph node involvement, negative surgical margins) define insignificant cancer cases [11, 12]. While prostate cancer with more favourable characteristics may have no influence on post-cystoprostatectomy management and follow-up, significant incidental prostate cancer warrants the regular monitoring of prostate-specific antigen (PSA) and an awareness of the potential need to take respective measurements should levels rise.

While the detection of incidental prostate cancer in cystoprostatectomy specimens is of great clinical importance, detection rates depend significantly on the technique used in histopathological processing. In many institutions, protocols for processing the prostate in cystoprostatectomy specimens do not demand the assessment of the entire organ. In contrast, protocols for processing prostatectomy specimens resected for known prostate cancer require complete processing of the whole gland. While the latter method is more complex and time consuming, significantly improved diagnostic accuracy has been reported for complete versus partial processing of prostatectomy specimens [11, 13]. Likewise, higher accuracy has been suggested for complete versus partial processing of prostates in cystoprostatectomy specimens [9, 10]; however, no comparative data on this issue have been reported as yet. The present analysis aimed at comparing detection rates of potentially clinically significant incidental prostate cancer in cystoprostatectomy specimens dependent on complete versus partial processing in the most homogenous series reported to date.

Patients and methods

Patients

Subsequent to institutional review board approval, we reviewed the prospectively collected institutional bladder cancer database and selected a cohort of 295 consecutive patients who had undergone cystoprostatectomy for invasive bladder cancer at the Department of Urology, Caritas St. Josef Medical Centre, University of Regensburg, Germany, between 01/1995 and 03/2009. Indication for radical cystoprostatectomy was muscle-invasive urothelial carcinoma of the bladder or recurrent Ta, T1 or CIS refractory to transurethral resection with or without intravesical chemo- or immunotherapy. Patients with known prostate cancer, clinical suspicion of prostate cancer (positive digital rectal exam and/or PSA levels above 4 ng/ml), preceding neoadjuvant chemotherapy or radiotherapy were excluded. All patients underwent open radical cystectomy with complete prostatectomy and lymph node dissection of at least the external iliac and obturator fields.

Pathologic evaluation

The specimens were stained with blue dye and fixed with a solution of 5 % buffered formalin. Both seminal vesicles were removed and processed separately in all cases. Between 01/1995 and 12/2003 (period of time 1 [POT1]), specimens of 129 patients were partially processed, i.e. removal of ink-stained apical margins, serial sectioning perpendicular to the ink, embedding of three sections of each side in partial blocks and one transverse slice cut perpendicular to the rectal surface. Between 01/2004 and 03/2009 (period of time II [POT2]), specimens of 166 patients were completely processed, i.e. removal of ink-stained apical margins as described earlier and processing of the entire gland including all ink-stained margins using whole-mount sections with 4-mm slices for full histopathological assessment. All areas of prostate cancer were circled with a pen (Fig. 1). The extracapsular tumour spread, positive surgical margins, seminal vesicle involvement and Gleason score were all documented. Staging was performed according to the 2009 revision (7th edition) of the American Joint Committee on Cancer—Union Internationale contre le Cancer TNM classification. Grade was assessed according to the 2005 modification of the International Society of Urological Pathology/World Health Organization. The specimens of the patients who underwent radical cystoprostatectomy before the AJCC/IUCC and ISUP modifications in 2009 and 2005, respectively, were reviewed by an experienced uropathologist. Prostate cancer volume was estimated by the focus diameter in POT1 and determined by the grid method in POT2 as described by May et al. [14]. The grid method is carried out using a transparent grid subdivided into several small squares with each square measuring exactly 1 mm^2. Areas of the different tumour foci were estimated, added on each slide and multiplied by 4 mm, giving the height of the single section and thus yielding approximate volumes (in mm^3) of the space occupied by

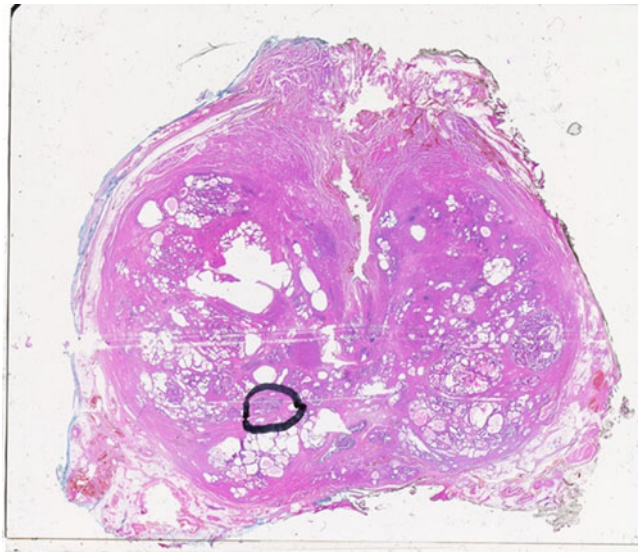

Fig. 1 Exemplary whole-mounted sectioned prostate with marked incidental prostate cancer

prostatic tissue between two adjacent slides. Addition of the volumes of the single slides and final multiplication with a shrinkage factor of 1.3 completed the calculation of prostate cancer volume, which was documented as being less than or equal to or higher than 0.5 mm^3.

In accordance with clinical and pathological criteria, potentially clinically significant prostate cancer was defined by any of the following parameters: tumour volume≥0.5 cm^3, capsular penetration, seminal vesicle infiltration, Gleason score≥7, positive surgical margins or lymph node metastases [11, 15].

Follow-up

Patients were followed up every 3 to 4 months for the first year after cystoprostatectomy, every 6 months from the second through to the fifth year and annually thereafter. The follow-up consisted of history, physical examination, routine blood work and serum chemistry studies including PSA and sonographic evaluation of the upper urinary tract. Elective bone scans, chest scan or computed tomography and magnetic resonance imaging were performed whenever potentially clinically indicated. Biochemical recurrence of prostate cancer was defined as PSA levels above 0.1 ng/ml. Macroscopic recurrence of malignancy was defined as occurrence of gross tumour at the site of surgery or distant lymph nodes or the event of distant metastasis. Cause of death was determined by chart review corroborated by death certificates. Any of the cited conditions was attributed to prostate cancer in case of a suggestive PSA level and other clinical findings found to be suggestive as judged by the investigators.

Statistical analysis

Fisher's exact test was used to evaluate the association between categorical variables and Mann–Whitney *U*-test was used to evaluate the association between variables with continuous distribution. All reported *p*-values are two-sided and statistical significance was set at 0.05. Analyses were performed with SPSS version 17.0 (SPSS, IBM, Somers, NY, USA).

Results

Median age was 68 years (IQR 15); median PSA was 2.4 ng/ml (IQR 0.8). The patient groups treated in POT1 and POT2 did not differ with regard to age (p=0.129) or preoperative PSA level (p=0.156).

Prostate cancer was detected in 91 of 295 patients (30.8 %; Table 1). Stratified to POT1 and POT2, incidental prostate cancer was detected in 24 (19 %) and 67 (40 %) patients, respectively (p<0.001). Potentially clinically significant prostate cancer was detected in 12 (9 %) and 29 (18 %) patients in POT1 and POT2, respectively (p=0.044). A prostate cancer volume≥0.5 cm^3 was detected in 11 (8 %) and 17 (10 %) patients in POT1 and POT2, respectively (p=0.062). Prostate cancer staged ≥ pT2b was detected in 13 (10 %) and 32 (19 %) patients in POT1 and POT2, respectively (p<0.001). Gleason≥7 was detected in four (3 %) and 15 (9 %) in POT1 and 2, respectively (p=0.039). Positive surgical margins due to prostate cancer were detected in one (1 %) and six (4 %) patients in POT1 and POT2, respectively (p=0.112).

Within a median follow-up of 4.6 years, one patient died of progressive prostate cancer. No further patient showed a biochemical recurrence. Neither adjuvant hormonal therapy nor local radiotherapy had to be performed in any of the patients.

Discussion

Why is the detection of incidental prostate cancer in cystoprostatectomy specimens important?

Apart from rare indications, cystoprostatectomy is performed for muscle-invasive bladder cancer or for high-risk non-muscle-invasive bladder cancer. However, many patients and clinicians are faced with prostate cancer as an additional malignancy. Prostate cancer not only increases the subjective burden of disease on the patient but can also potentially require increased attention throughout the follow-up. While many cases of prostate cancer are judged as "insignificant", some may indeed be significant and

Table 1 Patient and tumour characteristics of 295 patients with radical cystoprostatectomy due to urothelial carcinoma of the bladder and clinically unsuspected prostate cancer, stratified by the method of histopathological processing

Parameters	Number of patients (%)			*p*-value
	Overall	Partial sampling	Complete sampling	
All patients	295	129	166	
Median age (years)	68	67	68	0.129
Median PSA (ng/ml)	2.4	2.5	2.2	0.156
Incidental PC	91 (30.8)	24 (18.6)	67 (40.4)	<0.001
Potentially clinically significant PC	41 (13.9)	12 (9.3)	29 (17.5)	0.044
PC volume≥0.5 cm^3	28 (9.5)	11 (8.5)	17 (10.2)	0.062
Gleason score >6	19 (6.4)	4 (3.1)	15 (9.0)	0.039
pT ≥pT2b	45 (15.3)	13 (10.1)	32 (19.3)	<0.001
R1	7 (2.4)	1 (0.8)	6 (3.6)	0.112

PC prostate cancer

require specific measurements such as local radiotherapy and androgen deprivation therapy, which bring inherent side effects. This implies two requirements for the management of cystoprostatectomy. Firstly, the rate of incomplete removal of prostate cancer during cystoprostatectomy needs to remain feasibly low, and secondly the presence of prostate cancer has to be detected in the histopathological workup of cystoprostatectomy specimens.

The first requirement is met by respective assessment by digital rectal examination and detection of PSA prior to cystoprostatectomy and by radical resection of the prostate. Due to the functional advantages of nerve-sparing cystoprostatectomy by leaving the periprostatic sheath, the procedure is viewed as critical by many surgeons [4] as it harbours the risk of leaving prostate cancer in situ [1, 5]. While a surgeon will be aware of this problem and may opt against nerve-sparing cystoprostatectomy in the confirmed presence of prostate cancer, incidental prostate cancer will only be brought to attention by the pathologist. The high occurrence of incidental prostate cancer leaves the second requirement, i.e. the detection of prostate cancer in histopathological workup, all the more important.

Is incidental prostate cancer in cystoprostatectomy a relevant problem?

According to the high overall incidence of prostate cancer, incidental prostate cancer in cystoprostatectomy specimens is frequent; the two latest publications on this topic show rates of up to 50 %. Revelo [7], Pettus [9] and Mazzucchelli reported an overall rate of incidental prostate cancer of up to nearly 50 % [10]. These recently reported, relatively high numbers are contrasted by decisively lower rates of incidental prostate cancer in other series. Lee, for example, observed 4 % in 250 patients, the lowest rate of incidental prostate cancer reported to date [16]. Moutzouris found incidental prostate cancer in 27 % of 57 patients [17]. Abdelhady reported 28 % in 204 patients, with potentially clinically significant prostate cancer being found in 8 % of patients based on Gleason≥7, extracapsular extension and positive surgical margins [18]. While the ethnicity of prostate cancer incidence has been suggested by Lee as an explanation for the stark contrast observed, Pettus and Mazzucchelli refer to obvious differences in the mode of histopathological processing between various series [9, 10, 16].

Does the mode of histopathological processing matter?

The accuracy of pathological assessment has been reported to depend on the technique of histopathological processing in prostate specimens resected for known prostate cancer [11, 12]. There are, in essence, two protocols used to process the prostate in cystoprostatectomy specimens. While partial protocols do not require the assessment of the entire organ, many institutions use protocols, which require the complete processing of the entire prostate. A direct and exact comparison is difficult, however, due to the lack of universal standards. Lee and Moutzouris mention complete transverse sections obtained at 5-mm intervals from apex to base [16, 17]. Abdelhady refers to "routine pathological examination" [18].

Those series reporting decisively higher rates of incidental prostate cancer seem to differ in histopathological processing. Revelo describes the distal 2 to 3 mm of the apex to have been embedded as a shave margin or radially sectioned in a cone-like fashion and the prostate to have been transversely sectioned in approximately 5-mm slices and entirely submitted in whole mounts [7]. Mazzucchelli reports the removal of apex, base and seminal vesicles and submission for routine histological examination; the remaining prostate was step-sectioned at 3- or 5-mm intervals and examined as whole-mount sections [10].

Do variations in incidental prostate cancer relate to these differences in histopathological processing?

One must bear in mind that further parameters have to be taken into account when comparing the results of different series, e.g. the varying number of pathologists involved in

assessment, the ethnicity of patients or the differing volume of cystoprostatectomy in each centre.

What novelties do the present data bring to the paradigm and which of these needs to be taken into account?

To date, the two principal modes of processing have not been compared. We compared two consecutive cohorts of cystoprostatectomy from one institution differing only in time period of cystoprostatectomy and mode of histopathological processing. We believe that several factors ensure the homogeneity of our data and that no differences between the cohorts (apart from mode of processing) bias our results. Firstly, no changes in surgical technique or screening for prostate cancer had been implemented between the time periods, which might have influenced the radicality of tumour resection or prostate cancer detection during preoperative workup [1]. Secondly, the basic character of our centre did not change and all patients were subjected to cystoprostatectomy under the close supervision of an experienced urologist (WFW). Thirdly, all cystoprostatectomy specimens were assessed by two experienced uropathologists (FH and AH) in close coordination; so, whilst a certain intra-observer variation may be present, no major inter-observer variation should bias the present results. The homogeneity of the cohorts is strengthened by the lack of differences in patient and tumour characteristics with the exception of incidental prostate cancer.

As detection rates of overall and potentially clinically significant prostate cancer in period I and period II are in keeping with previous series which used partial and complete embedding processing, respectively, our data strongly suggest that the different modes of histopathological processing provide the explanation for these differences. Decisive factors for the detection rates are the histopathologic examination by

Table 2 Literature on incidental prostate cancer in RCP, including year of publication, patients' characteristics, tumour characteristics and method of histopathological processing (modified from Damiano et al. [5])

Reference	Year of publication	Number of patients	Mean age of patients (years)	Number of PC (%)	Number of significant PC (% of PC)	Method of sampling	Thickness of slices (mm)
Winfield et al. [19]	1987	80	64	22 (28)	11 (50)	Complete	N/A
Pritchett et al. [20]	1988	165	65	45 (27)	N/A	Partial	N/A
Montie et al. [21]	1989	84	62	33 (46)	6 (15)	Complete	4–5
Kabalin et al. [22]	1989	66	64	25 (38)	3 (12)	Complete	3
Abbas et al. [23]	1996	40	64	18 (45)	N/A	Partial	2–3
Moutzouris et al. [17]	1999	59	67	16 (27)	N/A	Complete	5
Aydin et al. [24]	1999	121	67	17 (14)	N/A	N/A	N/A
Yang et al. [25]	1999	49	68	16 (33)	N/A	Complete	3
Conrad et al. [26]	2001	133	60	58 (44)	11 (19)	Complete	3
Prange et al. [27]	2001	89	64	41 (48)	4 (10)	Complete	4
Ward et al. [28]	2004	129	69	30 (23)	18 (60)	N/A	N/A
Revelo et al. [7]	2004	121	67	50 (41)	24 (48)	Complete	5
Kouriefs et al. [6]	2005	128	N/A	23 (18)	N/A	N/A	N/A
Delongchamps et al. [29]	2005	141	62	20 (14)	14 (70)	Complete	4
Ruffion et al. [8]	2005	100	62	51 (51)	22 (43)	Complete	2.5
Lee et al. [16]	2006	248	63	10 (4)	N/A	Complete	5
Rocco et al. [30]	2006	63	67	34 (54)	12 (35)	Complete	3
Abdelhady et al. [18]	2006	204	67	58 (28)	18 (31)	Complete	N/A
Winkler et al. [31]	2007	97	N/A	58 (60)	31 (53)	Complete	2
Hosseini et al. [32]	2007	50	63	7 (14)	4 (57)	Partial	N/A
Weizer et al. [33]	2007	35	65	16 (46)	4 (25)	N/A	N/A
Pettus et al. [9]	2007	235	70	113 (48)	39 (35)	Complete	5
Mazzucchelli et al. [10]	2008	248	68	123 (50)	23 (19)	Complete	3
Gakis et al. [4]	2010	95	68	26 (27)	7 (27)	Complete	4–5
Fritsche et al.	2011	291	67	25 (16)/66 (40)	12 (48)/29 (44)	Partial/ complete	4

N/A not available, *PC* prostate cancer

whole-mount-sections and the thickness of the examined slices (Table 2).

The major limitation of the present study is that the follow-up is too short to derive the real impact of prostate sampling. As such, no conclusions can be drawn on the true clinical significance of the cases detected. As potentially clinically significant prostate cancer was defined as generally accepted, we think that the respective results are valid. However, despite the strong comparability of both cohorts (except for the time of cystoprostatectomy and mode of histopathological processing), the present data do not originate from a randomized trial. As no such trial is to be expected, given the inherent ethical and methodological hurdles associated with such a project, we believe the results of the present approach to be valid.

Conclusions

The first comparative data on partial versus complete embedding processing of cystoprostatectomy specimens suggest the latter to increase detection rates of overall potentially clinically significant prostate cancer decisively. As the diagnosis of prostate cancer in cystoprostatectomy specimens has major clinical implications, the present data warrant further studies with longer follow-up and suggest the consideration of complete embedding processing especially in younger men.

Acknowledgments We thank Patrick Goldsworthy for his excellent assistance.

Conflict of interest None of the authors has any disclosure or conflict of interest.

References

1. Stenzl A, Cowan NC, De Santis M, Kuczyk MA, Merseburger AS, Ribal MJ, Sherif A, Witjes JA, European Association of Urology (2011) The updated EAU guidelines on muscle-invasive and metastatic bladder cancer. Eur Urol 59:1009–1018
2. Babjuk M, Oosterlinck W, Sylvester R, Kaasinen E, Böhle A, Palou-Redorta J, Roupret M, European Association of Urology (2011) EAU guidelines on non-muscle-invasive urothelial carcinoma of the bladder. Eur Urol 59:997–1008
3. Nagele U, Anastasiadis AG, Stenzl A, Kuczyk M (2011) Radical cystectomy with orthotopic neobladder for invasive bladder cancer: a critical analysis of long-term oncological, functional, and quality of life results. World J Urol. doi:10.1007/s00345011064 94
4. Gakis G, Schilling D, Bedke J et al (2010) Incidental prostate cancer at radical cystoprostatectomy: implications for apex-sparing surgery. BJU Int 105:468–471
5. Damiano R, Di Lorenzo G, Cantiello F et al (2007) Clinicopathological features of prostate adenocarcinoma incidentally discovered at time of radical cystectomy: an evidence based analysis. Eur Urol 52:648–657
6. Kouriefs C, Fazili T, Masood S, Naseem MS, Mufti GR (2005) Incidentally detected prostate cancer in cystoprostatectomy specimens. Urol Int 275:213–216
7. Revelo MP, Cookson MS, Chang SS, Shook MF, Smith JA Jr, Shappell SB (2004) Incidence and location of prostate and urothelial carcinoma in prostates from cystoprostatectomies: implications for possible apical sparing surgery. J Urol 171:646–651
8. Ruffion A, Manel A, Massoud W et al (2005) Preservation of prostate during radical cystectomy: evaluation of prevalence of prostate cancer associated with bladder cancer. Urology 65:703–707
9. Pettus JA, Al-Ahmadie H, Barocas DA, Koppie TM, Herr H, Donat SM, Dalbagni G, Reuter VE, Olgac S, Bochner BH (2008) Risk assessment of prostatic pathology in patients undergoing radical cystoprostatectomy. Eur Urol 53:370–375
10. Mazzucchelli R, Barbisan F, Scarpelli M, Lopez-Beltran A, van der Kwast TH, Cheng L, Montironi R (2009) Is incidentally detected prostate cancer in patients undergoing radical cystoprostatectomy clinically significant? Am J Clin Pathol 131:279–283
11. Heidenreich A, Bellmunt J, Bolla M, European Association of Urology et al (2011) EAU guidelines on prostate cancer. Part 1: screening, diagnosis, and treatment of clinically localised disease. Eur Urol 59:61–71
12. van der Kwast TH, Amin MB, Billis A, Prostate Cancer Group ISUP et al (2011) International Society of Urological Pathology (ISUP) Consensus Conference on Handling and Staging of Radical Prostatectomy Specimens. Working group 2: T2 substaging and prostate cancer volume. Mod Pathol 24:16–25
13. Sehdev AE, Pan CC, Epstein JI (2011) Comparative analysis of sampling methods for grossing radical prostatectomy specimens performed for nonpalpable (stage T1c) prostatic adenocarcinoma. Hum Pathol 32:494–499
14. May M, Siegsmund M, Hammermann F, Loy V, Gunia S (2007) Visual estimation of the tumour volume in prostate cancer: a useful means for predicting biochemical-free survival after radical prostatectomy? Prostate Cancer Prostatic Dis 10:66–71
15. Epstein JI, Walsh PC, Carmichael M, Brendler CB (1994) Pathologic and clinical findings to predict tumor extent of nonpalpable (stage T1c) prostate cancer. JAMA 271:368–374
16. Lee SH, Chang PL, Chen SM, Sun GH, Chen CL, Shen BY, Wu YS, Tsui KH (2006) Synchronous primary carcinomas of the bladder and prostate. Asian J Androl 8:357–359
17. Moutzouris G, Barbatis C, Plastiras D, Mertziotis N, Katsifotis C, Presvelos V, Theodorou C (1999) Incidence and histological findings of unsuspected prostatic adenocarcinoma in radical cystoprostatectomy for transitional cell carcinoma of the bladder. Scand J Urol Nephrol 33:27–30
18. Abdelhady M, Abusamra A, Pautler SE, Chin JL, Izawa JI (2007) Clinically significant prostate cancer found incidentally in radical cystoprostatectomy specimens. BJU Int 99:326–329
19. Winfield HN, Reddy PK, Lange PH (1987) Coexisting adenocarcinoma of prostate in patients undergoing cystoprostatectomy for bladder cancer. Urology 30:100–101
20. Pritchett TR, Moreno J, Warner NE et al (1988) Unsuspected prostatic adenocarcinoma in patients who have undergone radical cystoprostatectomy for transitional cell carcinoma of the bladder. J Urol 139:1214–1216
21. Montie JE, Wood DP Jr, Pontes JE, Boyett JM, Levin HS (1989) Adenocarcinoma of the prostate in cystoprostatectomy specimens removed for bladder cancer. Cancer 63:381–385
22. Kabalin JN, McNeal JE, Price HM, Freiha FS, Stamey TA (1989) Unsuspected adenocarcinoma of the prostate in patients undergoing cystoprostatectomy for other causes: incidence, histology and morphometric observations. J Urol 141:1091–1094
23. Abbas F, Hochberg D, Civantos F, Soloway M (1996) Incidental prostatic adenocarcinoma in patients undergoing radical cystoprostatectomy for bladder cancer. Eur Urol 30:322–326

24. Aydin O, Cosar EF, Varinli S, Bugdatci R, Tansung Z (1999) Prostatic intraepithelial neoplasia in prostate specimens: frequency, significance and relationship to the sampling of the specimen (a retrospective study of 121 cases). Int Urol Nephrol 31:687–697
25. Yang CR, Ou YC, Ho HC et al (1999) Unsuspected prostate carcinoma and prostatic intraepithelial neoplasm in Taiwanese patients undergoing cystoprostatectomy. Mol Urol 3:33–39
26. Conrad S, Hautmann SH, Henke RP et al (2001) Detection and characterization of early prostate cancer by six systematic biopsies and fine needle aspiration cytology in prostates from bladder cancer patients. Eur Urol 39:25–29
27. Prange W, Erbersdobler A, Hammerer P et al (2001) High-grade prostatic intraepithelial neoplasia in cystoprostatectomy specimens. Eur Urol 39:30–31
28. Ward JF, Bartsch G, Sebo TJ, Pinggera GM, Blute ML, Zincke H (2004) Pathologic characterization of prostate cancers with a very low serum prostate specific antigen (0–2 ng/mL) incidental to cystoprostatectomy: is PSA a useful indicator of clinical significance? Urol Oncol 22:40–47
29. Delongchamps NB, Mao K, Theng H, Zerbib M, Debre B, Peyromaure M (2005) Outcome of patients with fortuitous prostate cancer after radical cystoprostatectomy for bladder cancer. Eur Urol 48:946–950
30. Rocco B, de Cobelli O, Leon ME et al (2006) Sensitivity and detection rate of a 12-core transperineal prostate biopsy: preliminary report. Eur Urol 49:827–833
31. Winkler MH, Livni N, Mannion EM, Hrouda D, Christmas T (2007) Characteristics of incidental prostatic adenocarcinoma in contemporary radical cystoprostatectomy specimens. BJU Int 99:554–558
32. Hosseini SY, Danesh AK, Parvin M et al (2007) Incidental prostatic adenocarcinoma in patients with PSA less than 4 ng/mL undergoing radical cystoprostatectomy for bladder cancer in Iranian men. Int Braz J Urol 33:167–173
33. Weizer AZ, Shah RB, Lee CT et al (2007) Evaluation of the prostate peripheral zone/capsule in patients undergoing radical cystoprostatectomy: defining risk with prostate capsule sparing cystectomy. Urol Oncol 25:460–464

Virchows Arch (2012) 461:663–668
DOI 10.1007/s00428-012-1325-9

ORIGINAL ARTICLE

MicroRNA expression profiles of seminoma from paraffin-embedded formalin-fixed tissue

Z. Bing · S. R. Master · J. W. Tobias · D. A. Baldwin · X. W. Xu · J. E. Tomaszewski

Received: 23 April 2012 / Revised: 20 August 2012 / Accepted: 27 September 2012 / Published online: 14 October 2012
© Springer-Verlag Berlin Heidelberg 2012

Abstract In this study, we used microRNA (miRNA) microarrays in an unbiased screen for aberrantly expressed miRNAs in seminoma, a primitive type of germ cell tumor. Formalin-fixed and paraffin-embedded (FFPE) surgical samples from 11 cases of normal testicular tissue resected for nonneoplastic causes and from 11 cases of seminoma were assessed for miRNA expression. Normal testicular tissue and seminoma were paired by race. We found 112 miRNAs to be differentially expressed between seminoma and normal testicular tissue; 52 miRNAs were overexpressed, and 60, downregulated in seminoma. We did not observe significant differences between black and white populations in our race-paired study. The upregulation of the expression of hsa-mir-21, hsa-mir-372, hsa-mir-373, has-mir-221, and hsa-mir-222 was validated by reverse transcription and real-time PCR. Hsa-mir-372 was upregulated around 1,270-fold (95 % confidence interval (CI) 525.2–3,064.8; p=8.1e-5 by Mann–Whitney U test). Hsa-mir-373 was upregulated around 1,530-fold (95 % CI 620.5–3,785.6; p=8.0e-5 by Mann–Whitney U test), consistent with previous reports, indicating that the miRNAs in FFPE are well preserved, and FFPE can be a valuable source for the miRNA study of seminoma. In addition, expression of hsa-mir-21 (12.2-fold, 0.0095), hsa-mir-221 (3.8-fold, 0.014) and hsa-mir-222 (3.8-fold, 0.019) was found elevated in seminoma compared to normal testicular tissue.

Keywords Seminoma · miRNA microarray

Z. Bing (✉) · S. R. Master · D. A. Baldwin · X. W. Xu
Department of Pathology and Laboratory Medicine, 6 Founders, Hospital of the University of Pennsylvania,
3400 Spruce Street,
Philadelphia, PA 19104, USA
e-mail: bingz@uphs.upenn.edu

J. W. Tobias
Penn Bioinformatics Core, University of Pennsylvania,
1313 Blockley Hall, 423 Guardian Drive,
Philadelphia, PA 19104, USA

J. E. Tomaszewski
Pathology and Anatomic Sciences, SUNY at Buffalo,
Buffalo, NY, USA

Introduction

Testicular germ cell tumors (TGCT) are the most common malignancies in men in the second to fourth decades of life. The overall incidence of TGCT has increased from 3.35 per 100,000 to 4.84 per 100,000 men from 1973 to 1998 [1], with an estimated 7,500 new cases of germ cell tumor each year [2]. As germ cell tumors represent a unique group of tumors that originate from a common precursor and with primitive (including embryonal carcinoma and seminoma) as well as more differentiated subtypes containing several cell lineages (such as extraembryonic lineages in case of yolk sac tumors and choriocarcinomas and embryonic lineages in case of teratoma), they provide a unique system for the study of tumor proliferation and differentiation.

Mature microRNAs (miRNA) are small RNAs about 20–22 nucleotides in length. Experimental data show that miRNAs are key players in stem cell self-renewal as well as in differentiation. Recently, it has been shown that miRNAs play an essential role in tumorigenesis [3]. miRNAs can function as tumor suppressors or oncogenes. miRNA-372 and miRNA-373 were found to play a critical role in the tumorigenesis of testicular germ cells [4]. To establish the expression profile of seminoma and study whether paraffin embedded tissue can be used as a

tissue source for miRNA profiling, we assessed miRNA expression using paraffin-embedded and formalin-fixed tissue in array analyses.

Materials and methods

Materials

Formalin-fixed and paraffin-embedded (FFPE) tissue samples from 11 cases of testicular tissue resected for nonneoplastic causes and 11 cases of seminoma were retrieved from the archives of the Hospital of the University of Pennsylvania and were assessed for miRNA expression. The clinical information is listed in Table 1. This study was approved by the University of Pennsylvania Institutional Review Board.

RNA extraction

Three 25 μm FFPE tissue sections per sample were used to extract total RNA, following the RecoverAll Total Nucleic Acid Isolation protocol (Ambion no. 1975). Total RNA was further purified by ammonium acetate/ethanol precipitation overnight. Total RNA yield was determined by NanoDrop ND-1000 spectrophotometry. The integrity of miRNA was assessed with Agilent's 2100 bioanalyzer in conjunction with an RNA LabChip kit (Agilent no. 5065–4476). Of each sample, 5 μg of total RNA was used for miRNA microarray.

miRNA microarrays

Targets were prepared using the miRCURY Labeling kit (Exiqon) according to the manufacturer's instructions. Briefly, 5 μg of total RNA was added to 2 μl of dye (Cy3 and Cy5 separately for each sample). After labeling, the RNA was hybridized to a microarray. A corresponding dye-swap sample pair was hybridized to a second microarray. Glass slide microarrays were an expanded version of the RAKE miRNA array previously described, and the same principles for oligomer probe design and printing conditions were used. The array probe sequences are available as GEO platform GPL3699 (www.ncbi.nlm.nih.gov/projects/geo/) and correspond to the active, mature sequences of the miRNAs. These include 754 synthetic miRNA probes corresponding to 219 human, 34 rat, 59 mouse, 10 *Arabidopsis thaliana*, and 422 candidate and predicted human and mouse miRNAs. Hybridization was carried out at 42 °C. Slides were scanned at 5-μM resolution using GenePix 4000B laser scanner (Axon) at a power level of 100 % and PMT sensitivity of 700 for the detection of 530-nm

Table 1 Case selections and diagnoses

Case	Age	Race	Diagnosis	Pathologic stage
N01	22	B*	Gunshot wound	NA
N02	20	B	Gunshot wound	NA
N03	23	B	Gunshot wound	NA
N04	27	C*	Motor vehicle accident	NA
N05	47	C	Motor vehicle accident	NA
N06	63	C	Prostate cancer	NA
N07	32	C	Necrotizing fasciitis	NA
N08	42	C	Motor vehicle accident	NA
N09	32	C	Trauma	NA
N10	20	C	Trauma	NA
N11	21	C	Trauma	NA
S01	42	B	Seminoma, 11.5 cm, with lymphovascular invasion	pT2 Nx Mx
S02	32	B	Seminoma, 2.5 cm	PT1Nx Mx
S03	86	B	Seminoma, 8.0 cm, with spermatic cord invasion	pT3 Nx Mx
S04	51	C	Seminoma, 2.5 cm	PT1Nx Mx
S05	52	C	Seminoma, 7.0 cm	PT1Nx Mx
S06	46	C	Seminoma, 2.5 cm	PT1Nx Mx
S07	24	C	Seminoma, 6.0 cm, with lymphovascular invasion	PT2Nx Mx
S08	32	C	Seminoma, 5.5 cm	PT1Nx Mx
S09	43	C	Mixed germ cell tumors with seminoma, YST, EC	pT2 Nx Mx
S10	51	C	Seminoma, three nodules, 1.9, 1.8, and 1.0 cm	pT2 Nx Mx
S11	28	C	Seminoma, 11.5 cm, with lymphovascular invasion	pN1Nx Mx

NA not applicable

fluorescence and 750 nm for the detection at 635 nm. Image quantification was performed in GenePix Pro.

Data analysis

GenePix results (GPR) files were imported into GeneSpring (Agilent Technologies, version 7.31), and the on-chip replicate signal intensities (quadruplicate spots of a particular miRNA sequence) were averaged for each identifier (miRNA sequence). Expression data were first normalized to control for variations in array spot morphology among the individual arrays by dividing the average seminoma signal for a given miRNA identifier by the average normal testicle signal for that miRNA. Each array was subsequently normalized to the median of this ratio for all non-control genes. In this way, dye-swapped pairs were rendered comparable across arrays by scaling each such that the median in all is equal. The data were next filtered by removing control spots, removing those spots with expression values lower than 2 of the pairs ("absence of value" filter), and finally removing those spots flagged in the GPR file as poor spots. This was done to remove from consideration those identifiers that were not of biological relevance for the sake of comparison between seminoma and normal testicular tissue. After the application of these filters, the ratios (average, dye-swapped PTC signal/average, dye-swapped goiter signal) of 466 different identifiers representing 253 different miRNAs were imported into an Excel spreadsheet, where the data were log2 transformed. Significance analysis of microarrays (SAM, version 3.0b) was applied using a one-class design with 500 permutations and accepting a false discovery rate of <5 %. SAM results are reported as the computed fold change for seminoma/normal testis, score (d), indicating the *t*-statistic for likelihood of difference between classes, and the *q* value, indicating the lowest false discovery rate at which the gene is called significant (http://www-tat.stanford.edu/~tibs/SAM/).

Real-time reverse transcription PCR

Real-time quantitative reverse transcription (RT)-PCR was performed on an iCycler (Bio-Rad) using individual TaqMan® miRNA assays (Applied Biosystems) according to the manufacturer's instructions. For each reverse transcription 10 ng of total RNA was used with validated specific miRNA primers for each miRNA (miR-372, miR-373, and miRNA-21) along with U6B snRNA (Applied Biosystems) as a control. The stem-loop RT primer specifically hybridizes to a mature miRNA molecule and is reverse transcribed with a MultiScribe reverse transcriptase. The RT products are then quantified using TaqMan® PCR assays (Applied Biosystems), following the manufacturer's protocol on Bio-Rad iCycler instrument. The mean number of cycles (C_T) was determined from triplicate reactions. Delta C_T was calculated as $C_T$miRNA−C_TU6B. Relative gene expression was calculated as $2^{-(\text{delta } C_T)}$ and multiplied by 10^6 for data presentation as previously described [5]. Mann–Whitney *U* test was used to assess statistical significance of differences between the relative miRNA expression levels in seminoma compared to normal testicular tissue.

Results

Distinct expression profile of miRNAs in seminoma

In FFPE tissue samples, we identified significant differences in miRNA expression between normal testicular tissue and seminoma using the statistical analysis of microarrays approach with a false discovery rate of 5 %. In seminoma, 52 miRNAs were overexpressed, and 60 miRNAs were downregulated (Table 2). There were ten miRNAs that demonstrated close to or less than threefold upregulation in seminoma: miR-372, miR-373, miR-290, miR-422b, miR-21, miR-342, miR-222, miR-221, and miR-373*. In seminoma, the nine significantly downregulated miRNAs included miR34a, miR-293, miR-105-1.2, miR-30a-as, miR-217, miR-196-1, miR-196-2, miR-99, and miR-106a.

RT-PCR validation

In order to confirm the results of our miRNA microarray analysis from formalin-fixed, paraffin-embedded tissue, we

Table 2 Selected dysregulated miRNAs in seminoma compared to benign testicular tissue

miRNA	Fold change
Hsa-mir-372	145.7
Hsa-mir-373	74.5
miR-21	6.2
miR-342	4.2
Hsa-mir-222	3.9
Has-mir-221	3.9
Has-mir-150	3.0
miR-130b	2.9
miR-130a	2.8
miR-106b	2.6
Hsa-mir-183	2.6
Hsa-mir-25	2.6
Hsa-mir-17	−1.4
Hsa-mir-30a	−1.5
Hsa-mir-100	−2.0
miR-15a	−2.4
miR-106a	−3.3
Has-mir-217	−4.4

Table 3 miRNA validation data

miRNA	No. of N	No. of seminoma	Fold (S/N)	*p* values (Mann–Whitney *U* test)
miR-21	11	11	12.2	0.0095
miR-221	10	10	3.8	0.014
miR-222	10	10	3.8	0.019
miR-372	11	11	1,268.7	8.1e-05
miR-373	11	11	1,532.7	8.0e-05

N benign testicular tissue, *S* seminoma

performed semi-quantitative RT-PCR for a group of miRNAs including miR-372, miR-373, miR-21, miR-221, and miR-222 in paired normal testicular and seminoma tissue samples (Table 3, Fig. 1). The expression patterns of these miRNAs were concordant in all of these cases; miR-372 was upregulated around 1,270-fold (95 % confidence interval (CI) 525.2–3,064.8; p=8.1e-5 by Mann–Whitney U test) (Fig. 1a) and miR-373 around 1,530-fold (95 % CI 620.5–3,785.6; p=8.0e-5 by Mann–Whitney U test) (Fig. 1b), which is consistent with previous reports [4, 6]. Interestingly, miR-21 (Fig. 1c), miR-221 (Fig. 1d), and miR-222 (Fig. 1e) were the first to be reported as upregulated, but their function in the pathogenesis of seminoma is yet to be elucidated.

Discussion

Type II testicular germ cell tumors include seminoma and non-seminomatous germ cell tumor (GCT). Intratubular germ cell neoplasia unclassified (ITGCNU) is a precursor of type II testicular germ cell tumors and was first described by Skakkebaek in 1972 [7]. ITGCNU is abundant in tissue surrounding a primary GCT up to 82 % of cases [8]. To avoid contamination with ITGCNU, we sought to use as control tissues testicular tissue samples resected for nonneoplastic causes but matched for race.

The mechanisms responsible for the progression of ITGCNU to invasive cancer is poorly understood [9] and needs to be further studied. To investigate the expression of miRNAs in this process, microdissection of fresh frozen tissues and single cell miRNA amplification [10] have been employed. Isolation and profiling of miRNA have been successfully performed on FFPE [11, 12] on many different tissue types [13–16], but not on testicular germ cell tumors. In this study, we present evidence showing that miRNAs in FFPE testicular tissues, including seminoma, are well preserved, and the results obtained are consistent with those from fresh tissue samples [4, 17].

We observed a marked increase of expression of miRNA-372 and miRNA-373, consistent with previous reports [4, 6, 17]. The microRNA-371-373 (miR-371-373) cluster was initially identified as specifically expressed in human embryonic stem cells [18] and was believed to be involved in stem cell pluripotency [19, 20].

Upregulation of miR-372 and miR-373 could conceivably be involved in the pathogenesis of these tumors [4, 21] through a P53-related mechanism. The majority of testicular germ cell tumors overexpress wild-type P53 [22, 23] which inhibits CDK. miR-372 and miR-373 might counteract this effect of overexpression of wild-type P53 by downregulating the expression of the tumor suppressor LATS2. Interestingly, the upregulation of miR-371-373 cluster may contribute to cisplatin resistance, probably by counteracting wild-type P53-induced senescence or differentiation capacity [24]. In addition, miR-373 has been reported to promote tumor invasion and metastasis by suppression of CD44 [25]. Our study confirms their upregulation in seminoma, and also, that FFPE can be used to study miRNA expression in human tumors. It is noteworthy that the levels of expression

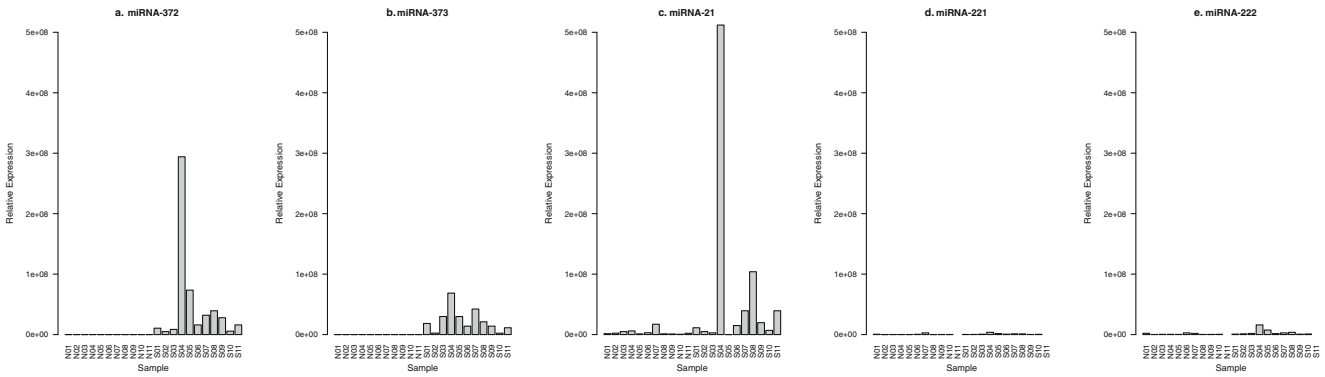

Fig. 1 Real-time RT-PCR confirmation of some of upregulated miRNAs in seminoma compared to benign testicular tissue. Relative expression levels of miRNA-372 and miRNA-373, miRNA-21, miRNA-221, and miRNA-222 in the cases used for the array analysis (Table 1) calculated as a function of U6B control are as follows: $2-(\text{delta } C_T)\times 10^6$, as previously described [5]. Signals for seminoma are labeled as *Sxx*, and signals for benign testicular tissue are labeled as *Nxx*. *p* values calculated by Mann–Whitney *U* test for each miRNA in seminoma compared to benign testicular tissue are listed in Table 3

of different miRNAs, especially miR-21, in seminoma vary greatly. Whether this is biologically relevant is undetermined. However, it has been reported that miRNA preservation in FFPE is storage time dependent potentially due to non-specific hybridization and/or degradation [26, 27].

We furthermore found overexpression of miR-21, miR-221, and miR-222. miR-21 was elevated >12-fold compared to the nonneoplastic testicular tissue. miR-21 expression has been shown to be increased in multiple tumors [28] including tumors from the brain [29], breast [30], colon [31], pancreas [5, 32], and thyroid [16]. miR-21 may be involved in the regulation of self-renewal of spermatogonial stem cells (SSC). Niu et al. showed that transient inhibition of miR-21 in SSC-enriched germ cell cultures increased apoptosis and significantly decreased the number of donor-derived colonies of spermatogenesis in transplantation experiments in mouse testes [33]. In addition, miR-21 was regulated by ETV5, a transcription factor known to play an important role in SSC self-renewal. miR-21 targets major pathways regulating cell survival including mitochondrial apoptosis and the PI3K-AKT-mTOR pathway as well as P53 and Ras [28]. The ubiquitous expression of miR-21 and its role in the cancer initiation, cell transformation, and cancer cell invasion and metastasis make it a potential target for therapeutic intervention. It has been shown that miR-21 can be silenced by antisense oligonucleotides and synthetic analogs of miR-21 [34, 35]. The expression of miR-21 in non-seminomatous tumors and its expression in chemoresistant germ cell tumors have not been studied as yet.

miR-221 and miR-222 have been reported to be upregulated in melanoma, glioblastoma, lung cancer, hepatocellular carcinoma, papillary tumors of the thyroid, pancreatic cancer, and prostate carcinoma [36–40]. It has been shown that phosphatase and tensin homolog (PTEN) is a target of miR-221/222, and upregulated PTEN expression suppressed AKT activity and increased radiation-induced apoptosis, resulting in enhanced radiosensitivity of tumor cells [41, 42]. Whether overexpression of miR-221/222 is related to the radiation sensitivity of seminoma needs further study. Also, the role of upregulation of miRNA-21, miRNA-221, and miRNA-222 in the development of seminoma needs further investigation.

In summary, we have utilized FFPE material to study miRNA expression patterns in primary testicular seminomas. We found upregulation of miRNA-372 and miR-373, confirming previous reports that employed fresh tissue. This indicates that FFPE can be a valuable source for this type of study. In addition, we identified and validated upregulation of the expression of several novel miRNAs, including miR-21 and miR-221/222. miRNA's role in the development of germ cell tumors has not been fully elucidated and merits further study.

Acknowledgments We thank Aihua Liu for the technical support.

Conflict of interest None.

References

1. McGlynn KA, Devesa SS, Sigurdson AJ et al (2003) Trends in the incidence of testicular germ cell tumors in the United States. Cancer 97(1):63–70
2. Iczkowski KA, Butler SL (2006) New immunohistochemical markers in testicular tumors. Anal Quant Cytol Histol 28(4):181–187
3. Cowland JB, Hother C, Gronbaek K (2007) MicroRNAs and cancer. APMIS 115(10):1090–1106
4. Voorhoeve PM, le Sage C, Schrier M et al (2006) A genetic screen implicates miRNA-372 and miRNA-373 as oncogenes in testicular germ cell tumors. Cell 124(6):1169–1181
5. Lee EJ, Gusev Y, Jiang J et al (2007) Expression profiling identifies microRNA signature in pancreatic cancer. Int J Cancer 120 (5):1046–1054
6. Palmer RD, Murray MJ, Saini HK et al (2010) Malignant germ cell tumors display common microRNA profiles resulting in global changes in expression of messenger RNA targets. Cancer Res 70 (7):2911–2923
7. Skakkebaek NE (1972) Possible carcinoma-in-situ of the testis. Lancet 2(7776):516–517
8. Heidenreich A, Weissbach L, Holtl W et al (2001) Organ sparing surgery for malignant germ cell tumor of the testis. J Urol 166 (6):2161–2165
9. Di Vizio D, Cito L, Boccia A et al (2005) Loss of the tumor suppressor gene PTEN marks the transition from intratubular germ cell neoplasias (ITGCN) to invasive germ cell tumors. Oncogene 24(11):1882–1894
10. Tang F, Hajkova P, Barton SC et al (2006) MicroRNA expression profiling of single whole embryonic stem cells. Nucleic Acids Res 34(2):e9
11. Lehmann U (2010) MicroRNA-profiling in formalin-fixed paraffin-embedded specimens. Methods Mol Biol 667:113–125
12. Liu A, Xu X (2011) MicroRNA isolation from formalin-fixed, paraffin-embedded tissues. Methods Mol Biol 724:259–267
13. Luzna P, Gregar J, Uberall I et al (2011) Changes of microRNAs-192, 196a and 203 correlate with Barrett's esophagus diagnosis and its progression compared to normal healthy individuals. Diagn Pathol 6(1):114
14. Niyazi M, Zehentmayr F, Niemoller OM et al (2011) MiRNA expression patterns predict survival in glioblastoma. Radiat Oncol 6:153
15. Snowdon J, Zhang X, Childs T et al (2011) The microRNA-200 family is upregulated in endometrial carcinoma. PLoS One 6(8): e22828
16. Tetzlaff MT, Liu A, Xu X et al (2007) Differential expression of miRNAs in papillary thyroid carcinoma compared to multinodular goiter using formalin fixed paraffin embedded tissues. Endocr Pathol 18(3):163–173
17. Gillis AJ, Stoop HJ, Hersmus R et al (2007) High-throughput microRNAome analysis in human germ cell tumours. J Pathol 213(3):319–328
18. Suh MR, Lee Y, Kim JY et al (2004) Human embryonic stem cells express a unique set of microRNAs. Dev Biol 270(2):488–498
19. Judson RL, Babiarz JE, Venere M et al (2009) Embryonic stem cell-specific microRNAs promote induced pluripotency. Nat Biotechnol 27(5):459–461
20. Wang Y, Baskerville S, Shenoy A et al (2008) Embryonic stem cell-specific microRNAs regulate the G1-S transition and promote rapid proliferation. Nat Genet 40(12):1478–1483

21. Voorhoeve PM, le Sage C, Schrier M et al (2007) A genetic screen implicates miRNA-372 and miRNA-373 as oncogenes in testicular germ cell tumors. Adv Exp Med Biol 604:17–46
22. Lowe SW, Ruley HE, Jacks T, Housman DE (1993) p53-dependent apoptosis modulates the cytotoxicity of anticancer agents. Cell 74 (6):957–967
23. Lutzker SG (1998) P53 tumour suppressor gene and germ cell neoplasia. APMIS 106(1):85–89
24. Port M, Glaesener S, Ruf C et al (2011) Micro-RNA expression in cisplatin resistant germ cell tumor cell lines. Mol Cancer 10:52
25. Huang Q, Gumireddy K, Schrier M et al (2008) The microRNAs miR-373 and miR-520c promote tumour invasion and metastasis. Nat Cell Biol 10(2):202–210
26. Rentoft M, Fahlen J, Coates PJ et al (2011) miRNA analysis of formalin-fixed squamous cell carcinomas of the tongue is affected by age of the samples. Int J Oncol 38(1):61–69
27. Siebolts U, Varnholt H, Drebber U et al (2009) Tissues from routine pathology archives are suitable for microRNA analyses by quantitative PCR. J Clin Pathol 62(1):84–88
28. Li S, Liang Z, Xu L, Zou F (2012) MicroRNA-21: a ubiquitously expressed pro-survival factor in cancer and other diseases. Mol Cell Biochem 360(1–2):147–158
29. Chan JA, Krichevsky AM, Kosik KS (2005) MicroRNA-21 is an antiapoptotic factor in human glioblastoma cells. Cancer Res 65 (14):6029–6033
30. Frankel LB, Christoffersen NR, Jacobsen A et al (2008) Programmed cell death 4 (PDCD4) is an important functional target of the microRNA miR-21 in breast cancer cells. J Biol Chem 283(2):1026–1033
31. Asangani IA, Rasheed SA, Nikolova DA et al (2008) MicroRNA-21 (miR-21) post-transcriptionally downregulates tumor suppressor Pdcd4 and stimulates invasion, intravasation and metastasis in colorectal cancer. Oncogene 27(15):2128–2136
32. Nagao Y, Hisaoka M, Matsuyama A et al (2012) Association of microRNA-21 expression with its targets, PDCD4 and TIMP3, in pancreatic ductal adenocarcinoma. Mod Pathol 25(1):112–121
33. Niu Z, Goodyear SM, Rao S et al (2011) MicroRNA-21 regulates the self-renewal of mouse spermatogonial stem cells. Proc Natl Acad Sci U S A 108(31):12740–12745
34. Elmen J, Lindow M, Silahtaroglu A et al (2008) Antagonism of microRNA-122 in mice by systemically administered LNA-antimiR leads to up-regulation of a large set of predicted target mRNAs in the liver. Nucleic Acids Res 36(4):1153–1162
35. Krutzfeldt J, Rajewsky N, Braich R et al (2005) Silencing of microRNAs in vivo with 'antagomirs'. Nature 438(7068):685–689
36. Felicetti F, Errico MC, Segnalini P, Mattia G, Care A (2008) MicroRNA-221 and −222 pathway controls melanoma progression. Expert Rev Anticancer Ther 8(11):1759–1765
37. le Sage C, Nagel R, Egan DA et al (2007) Regulation of the p27 (Kip1) tumor suppressor by miR-221 and miR-222 promotes cancer cell proliferation. EMBO J 26(15):3699–3708
38. Liang Y (2008) An expression meta-analysis of predicted microRNA targets identifies a diagnostic signature for lung cancer. BMC Med Genomics 1:61
39. Miller TE, Ghoshal K, Ramaswamy B et al (2008) MicroRNA-221/222 confers tamoxifen resistance in breast cancer by targeting p27Kip1. J Biol Chem 283(44):29897–29903
40. Zhao JJ, Lin J, Yang H et al (2008) MicroRNA-221/222 negatively regulates estrogen receptor alpha and is associated with tamoxifen resistance in breast cancer. J Biol Chem 283(45):31079–31086
41. Garofalo M, Di Leva G, Romano G et al (2009) miR-221&222 regulate TRAIL resistance and enhance tumorigenicity through PTEN and TIMP3 downregulation. Cancer Cell 16(6):498–509
42. Zhang C, Kang C, Wang P et al (2011) MicroRNA-221 and −222 regulate radiation sensitivity by targeting the PTEN pathway. Int J Radiat Oncol Biol Phys 80(1):240–248

Virchows Arch (2012) 461:669–676
DOI 10.1007/s00428-012-1333-9

ORIGINAL ARTICLE

Primary benign vascular tumors and tumorlike lesions of the kidney: a clinicopathologic analysis of 15 cases

Vikas Mehta · Vijayalakshmi Ananthanarayanan · Tatjana Antic · Thomas Krausz · John Milner · Girish Venkataraman · Maria M. Picken

Received: 24 August 2012 / Revised: 8 October 2012 / Accepted: 15 October 2012 / Published online: 23 October 2012
© Springer-Verlag Berlin Heidelberg 2012

Abstract Primary benign vascular lesions of the kidney are uncommonly encountered in routine surgical pathology practice. They can, however, mimic malignancy or be an incidental finding adjacent to a malignancy. Fifteen specimens harboring 16 primary benign renal lymphatic/vascular lesions were identified from our files from 1999 to 2011 and subjected to a detailed pathologic evaluation and clinicopathologic correlation. Clinical and demographic data were available for all the 15 cases. There were ten males and five female patients with age range of 33–74 years (mean 54 years). Lesions ranged from 0.5 cm to 40 cm (average, 6.6 cm). There were six arteriovenous malformations (AVMs), four hemangiomas, three anastomosing hemangiomas, two lymphangiomas, and one solid intravascular papillary endothelial hyperplasia (IPEH). Five AVMs were located in the kidney parenchyma and one in the pelviureteric system. Additional associated lesions ranged from renal stones to renal cell carcinoma in two cases (one lymphangioma and one AVM). One AVM was associated with a capillary hemangioma in the vicinity, and another with a history of renal cell carcinoma in the contralateral kidney. Capillary hemangiomas and lymphangiomas were noninfiltrative and lacked cytological atypia and mitotic activity. Except for a renal pelvic AVM, all other renal AVMs radiologically mimicked malignancy. The patients had undergone partial or radical nephrectomies except for the renal pelvic AVM which was laparoscopically excised. To the best of our knowledge, none of the cases had any syndromic/systemic associations. Benign vascular lesions of the kidney are rarely seen in routine surgical pathology practice, partly because a vast majority of them are medically treated by embolization. However, lesions mimicking renal malignancy are subjected to surgery. They may exist as isolated lesions or coexist with malignant lesions either in the ipsilateral or the contralateral kidney.

Keywords Benign vascular lesions · Hemangioma · Anastomosing hemangioma · Arteriovenous malformations

V. Mehta · G. Venkataraman · M. M. Picken (✉)
Department of Pathology, Loyola University Medical Center, Maywood, IL, USA
e-mail: mpicken@lumc.edu

J. Milner
Department of Urology, Loyola University Medical Center, Maywood, IL, USA

V. Ananthanarayanan · T. Antic · T. Krausz
Department of Pathology, University of Chicago, Chicago, IL, USA

Introduction

Vascular lesions of the kidney are seen infrequently in surgical pathology practice and only single case reports are encountered in literature. Most of the published literature on renal vascular lesions has originated from interventional radiology and urology. Brown et al. found only 25 cases of vascular tumor and tumorlike lesions of the kidney [1]. Montgomery and Epstein described six cases of a new variant of a benign vascular tumor involving the kidneys, perinephric adipose tissue, and testes, which they designated anastomosing hemangioma [2]. Arteriovenous malformations (AVMs) are typically subjected to therapeutic embolization and nephrectomy is rarely performed. However, vascular lesions of kidney, especially AVMs, may mimic renal cell carcinoma. The present study documents 15 cases with 16 unusual renal lesions of vascular origin, six of which include renal and perirenal AVMs. We describe the clinical presentation and pathology with an emphasis on the differential diagnosis and coexisting or underlying lesions so as to better discriminate them from other much more common renal epithelial and mesenchymal lesions.

Materials and methods

Using electronic medical review, 15 specimens harboring 16 primary benign renal vascular/lymphatic lesions were identified from files from our institutions between 1999 and 2012. After obtaining Institutional Review Board approval, the cases were subjected to a detailed pathologic evaluation and clinicopathologic correlation. The cases were reviewed by two different pathologists and the tumors were classified according to the 2002 World Health Organization Classification of Tumors of Soft tissue and Bone [3]. The histological characteristics of the lesions, their pathologic associations, and respective radiologic appearances were obtained from patient's medical records. Immunostains for CD34, HMB-45, SMA as well as special stain for elastic fibers and Verhoeff's Van Gieson (EvG) were performed using commercially available antibodies, microwave heat-induced epitope retrieval, and the Dako EnVision detection system (Dako Corp, Carpinteria, CA), when indicated.

Results

The clinical features of the 15 studied cases are summarized in Table 1. Demographic data were available for all the 15 cases. There were ten male and five female patients (M:F=2:1) with age range of 33–74 years (mean 54 years). The radiologic finding in most cases was the presence of either a cystic (five cases) or a solid (ten cases) mass suspicious for neoplasia. Lesions ranged from 0.5 cm to 40 cm (average, 6.6 cm). There were six AVMs, four hemangiomas, three anastomosing hemangiomas, two lymphangiomas, and one solid intravascular papillary endothelial hyperplasia (IPEH) (i.e., Masson's hemangioma). To the best of our knowledge, none of the cases had any syndromic/systemic associations.

AVMs occurred in three males and three females, with size ranging from 2 cm to 9.2 cm (average, 3.8 cm). The age of the patients with AVMs ranged from 33 to 74 years (mean, 59 years). Five AVMs were located in the renal parenchyma and one in the pelviureteric system. Associated lesions included capillary hemangioma in the vicinity (one case), papillary renal cell carcinoma (one case), and clear cell renal cell carcinoma in the contralateral kidney (one case). The microscopic features of these renal vascular malformations were identical to those of their soft tissue counterparts, consisting of an admixture of abnormally arranged thick- and thin-walled vessels, resembling malformed veins, venules, arteries, and arterioles, occasionally with associated thrombosis. There were no cellular elements in between these vascular channels (Fig. 1a and b). EvG stain (Fig. 1c) highlights the elastic lamina in the arterial channels. Variable amount of smooth muscle was within their walls (Fig. 1d). Except for the renal pelvic AVM, all other lesions radiologically mimicked malignancy. In all cases, the patients underwent a partial or radical nephrectomy, except for the renal pelvic AVM, which was laparoscopically excised. Clinical follow-up was available for

Table 1 Clinical and demographic data of 15 patients

No.	Age (year)	Sex	Diagnosis	Size (cm)	Additional findings	Operation	Follow up (months)
1	58	F	AVM	4	None	Right radical nephrectomy	36
2	33	F	AVM	9.2	Renal infarcts	Left radical nephrectomy	68
3	74	F	AVM	3.4	CYSTIC papillary RCC TYPE 1	Left partial nephrectomy	12
4	62	M	AVM	2.4	None	Left open partial nephrectomy, repair of left renal artery aneurysm	9
5	47	M	AVM	2	None, clear cell RCC in contralateral kidney	Partial right nephrectomy	112
6	61	M	AVM and hemangioma	AVM=2; Hemangioma=0.9	None	Laparoscopic right nephroureterectomy	NA
7	60	M	Hemangioma	0.5	Clear cell RCC	Radical nephrectomy	88
8	39	F	Hemangioma	1.8	None	Partial right nephrectomy	13
9	63	M	Hemangioma	9	Renal stone	Laparoscopic drainage of renal cyst	89
10	49	M	Anastomosing hemangioma	2.0	ESRD	Radical nephrectomy	3
11	55	M	Anastomosing hemangioma	0.6	ESRD, papillary adenomas	Radical nephrectomy	3
12	45	M	Anastomosing hemangioma	1.9	ESRD	Radical nephrectomy	12
13	46	M	Lymphangioma	40	Clear cell RCC	Right radical nephrectomy; resection of intraabdominal cyst	58
14	55	F	Lymphangioma	2.8	Benign renal cyst	Laparoscopic renal cystectomy	144
15	48	M	IPEH	2.2	None	Partial nephrectomy	132

5/6 patients, ranging from 9 to 112 months (mean 47 months). None of the patients showed recurrence.

The hemangiomas ranged from 0.5 to 9 cm in size (average, 3.4 cm). The age of the patients ranged from 39 to 63 years (mean, 56 years). Morphologically, circumscribed vascular lesion was identified within the renal cortex surrounded by atrophic tubules (Fig. 1e and f). At a higher magnification, the lesion was composed of a generally well-demarcated but unencapsulated proliferation of capillary-sized blood vessels, lined by flattened to ovoid endothelial cells with very scant intervening stroma. Unlike their soft tissue and cutaneous counterparts, these cases lacked a well-defined lobular growth pattern. Immunoperoxidase staining for CD34 highlighting the endothelial cells confirmed the vascular origin of the lesion (not shown).

The Masson's hemangioma was arising in an intrarenal hematoma. Histological examination of the lesion revealed a relatively circumscribed variably cellular lesion. There was no definite encapsulation. At the periphery of the lesion, the tumor cells were disposed in a compact arrangement with solid sheets of uniformly spindle-to-polygonal cells with indistinct cell borders (Fig. 2a). Closer to the center of the tumor, there were large ectatic vascular spaces filled with loosely lying single cells admixed with extravasated red blood cells (RBCs) and arranged focally in the form of broad, interlacing, and anastomotic retiform cords of cells with focal pseudopapillary formations (Fig. 2b). The lining cells of the aforementioned pseudopapillae consisted of a prominent flat–spindle and sometimes oval cells, with the morphologic appearance resembling typical endothelial cells (Fig. 2c). In many areas, the cores of these papillae were hyalinized (Fig. 2d). In addition, there were foci of extracellular hyaline material resembling fibrin, admixed with RBCs. Congo red stain was negative for amyloid. There was no significant necrosis, mitoses, or pleomorphism to suggest a malignant lesion. All the lining cells were strongly positive for CD31 (Fig. 2e) and focally positive for CD34 (Fig. 2f). The stains for pan keratin, CK 7, smooth muscle actin, HMB45, and S100 were all negative. Based on morphology and immunophenotype, the lesion was diagnosed as ‘atypical solid papillary endothelial hyperplasia’ (PEH, Masson's hemangioma) arising in an intrarenal hematoma.

The anastomosing hemangiomas ranged in size from 0.6 to 2.0 cm. The histological examination revealed vaguely “spleen-like” proliferation of anastomosing vascular channels lined by bland endothelial cells. Extramedullary hematopoiesis was seen in all the three cases. In one case, the lesion extended to the adjacent adrenal gland (Fig. 3a, b, and c).

The lymphangiomas ranged from 2.8 to 40 cm (mean, 21.4 cm). The age of the patients ranged from 46 to 55 years (mean, 50.5 years). Additional associated lesions were renal cell carcinoma in one case and benign renal cyst in another. Microscopically, the lymphangiomas show thin-walled cystic spaces filled with proteinaceous fluid. Cyst walls contain irregular smooth-muscle elements, and foci of lymphocyte clusters appear inside and between some cystic spaces. Cysts were lined by attenuated endothelial cells (Fig. 3c and d). The immunostains for D2-40 were performed and supported the diagnosis (Fig. 3e).

Discussion

While most of pathology literature on benign vascular lesions has focused on soft tissue and skin, little attention has been paid to primary vascular renal lesions. Most renal vascular lesions are diagnosed radiologically and are managed with embolization. Therefore, such lesions are rarely encountered in general surgical pathology practice. However, not all vascular lesions have a typical radiology. In our series, five out of six cases of AVM, one out of four cases of hemangioma, and one out of two cases of lymphangioma were suspicious for or associated with a malignancy.

Abnormal communications between the arteries and veins can be congenital or acquired. While congenital lesions are termed “arteriovenous malformations” (AVMs), acquired renal arteriovenous communications are often termed renal “arteriovenous fistulas” (AVFs). AVMs of the urinary tract are very uncommon and the majority are identified during the evaluation of gross hematuria [4, 5]. AVFs can be secondary or idiopathic. The former are typically associated with percutaneous renal surgery and biopsies. In contrast, idiopathic renal AVFs are typically associated with renal artery aneurysms [6] and are thought to arise from the spontaneous erosion or rupture of a renal artery into a nearby renal vein. Idiopathic renal AVFs are rare and represent less than 3 % of renal AVMs. On the other hand, congenital renal AVMs are classified as cirsoid or cavernous types. Congenital cirsoid AVMs, the most common type, which was also observed in our patients, have a dilated, corkscrew appearance, resembling varicose veins. If bilateral, they may lead to renal failure necessitating renal transplantation [7]. Embolization of an AVM in one of the patient (case 2) in this series led to extensive infarction of the kidney, necessitating a nephrectomy. It is noteworthy that the lesion in another case of AVM was interpreted radiologically as a lymphoma or a transitional cell carcinoma (case 3). Thus, a subset of AVMs may mimic malignancy.

The role of humoral factors in the pathogenesis of AVMs [8] has been investigated. To this end, angiogenic factors, like astrocytic VEGF, have been demonstrated in children with recurrent cerebral AVMs. Polymorphism in the IL-6 promoter and elevated IL-6 in the vicinity of cerebral vascular tissue has been shown to induce MMP-3 and MMP-9 expression, which in turn, increased proliferation and migration of cerebral endothelial cells, thus promoting development of AVMs [9]. In two of our patients, we encountered hemangiomas adjacent to

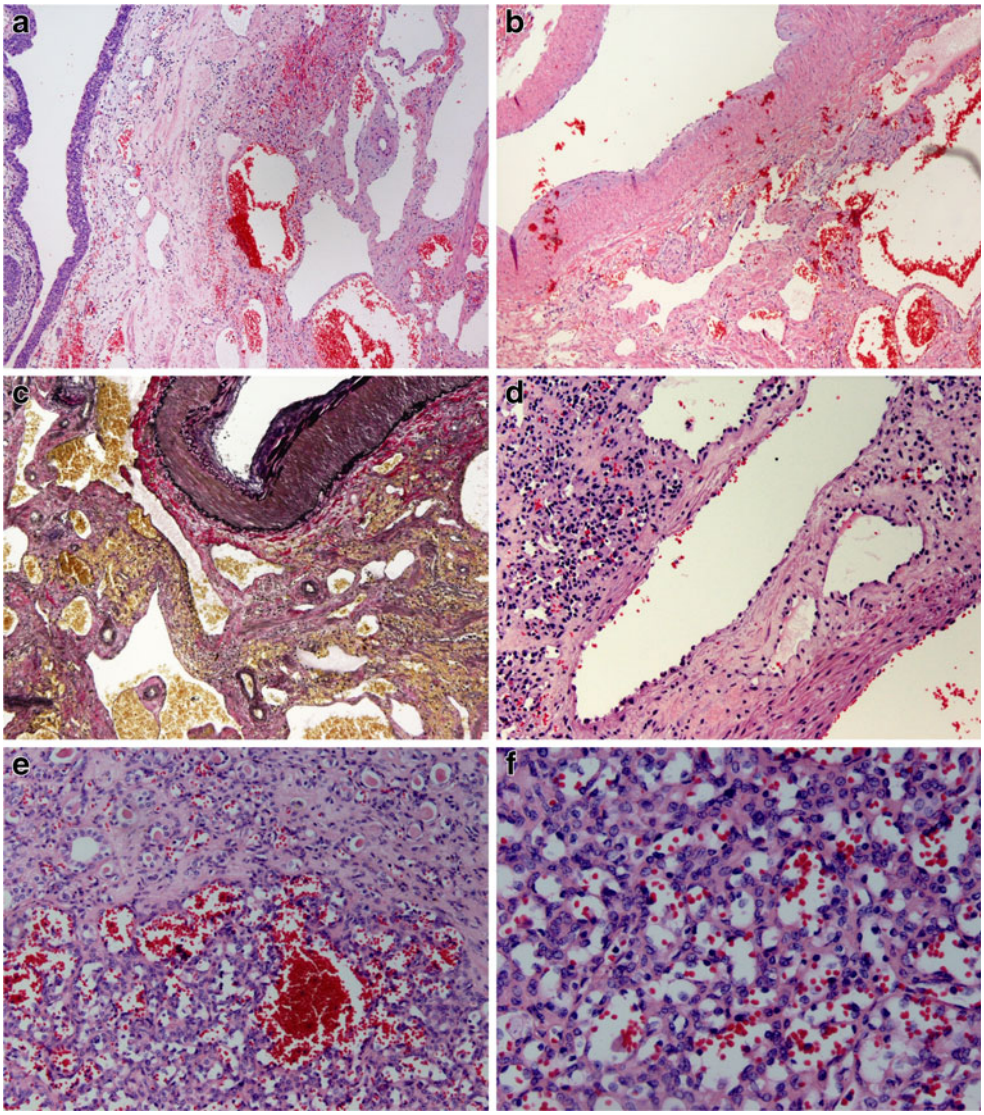

Fig. 1 **a** Low power view of the AVM in case 1. Typical tortuous, large vascular channels are evident adjacent to the pelvic urothelium. **b** Medium power of the same case 1. The smooth muscle within the wall of the anastomotic channels is evident. **c** Elastic Van Gieson stain demonstrating very minimal staining of the elastic lamina within the walls of these abnormal vessels. In contrast, a normal muscular artery close to the pelvis shows a typical double-layered staining pattern of the internal and external elastic laminae. **d** Medium power view of the cystic AVM. There was no evidence of coexisting RCC in the ipsilateral kidney. **e** and **f** Low and high power views of the capillary hemangioma seen adjacent to the hyalinized RCC in case 6. Note the presence of thyroidization in the adjacent tubules indicative of end-stage changes in **f**. **a** Hematoxylin and eosin, ×40; **b** hematoxylin and eosin, ×100; **c** elastic Van Gieson, ×100; **d** hematoxylin and eosin, ×100; **e** and **f** hematoxylin and eosin, ×100 and× 400, respectively

AVMs and renal cell carcinomas (RCCs). It is plausible that angiogenic factors secreted by these lesions promote the development of new vascular proliferations in their vicinity.

AVMs (or AVFs) occurring in the setting of malignancy have also been reported [10, 11]. Involvement of the renal vein and parasitic tumor vessels are relatively common in RCC. There are anecdotal reports of an IVC thrombus associated with renal AVM in the absence of identifiable malignancy [12]. There was no evidence for an IVC thrombus in any of our cases.

Pelviureteric AVMs are very rare with less than five reported cases in the literature [4, 13, 14]. Mishal reported AVM mimicking a parapelvic cyst [14]. One of our cases also was misclassified initially as a benign cyst. Hence, careful microscopic examination and immunohistochemistry are needed in order to establish a correct diagnosis. Angiomyolipomas which also contain abnormal thick-walled vessels may need to be considered in the differential diagnosis. In AVM involving the renal pelvic adipose tissue, the presence of islands of adipose tissue entrapped in between tortuous vascular channels may superficially resemble an angiomyolipoma (AML). Conversely, fat-poor and/or epithelioid angiomyolipoma may superficially mimic AVM. AVFs may also develop within AMLs. Immunohistochemical stains like HMB45 may be helpful in resolving difficult cases. Cystic renal lesions such as cystic nephroma-mixed epithelial and stromal tumor of the kidney may also mimic AVM. However, AVFs following radiofrequency ablation are also common.

Anastomosing hemangioma is a recently described rare neoplasm displaying some overlapping features with both sinusoidal hemangioma and hobnail hemangioma of soft tissue and skin. Microscopically, anastomosing hemangioma are solitary, mostly well demarcated, capillary-sized vascular proliferations supported by scattered large feeding and draining blood vessels forming a sievelike pattern [2]. Larger lesions demonstrated lobulated patterns with scattered areas of

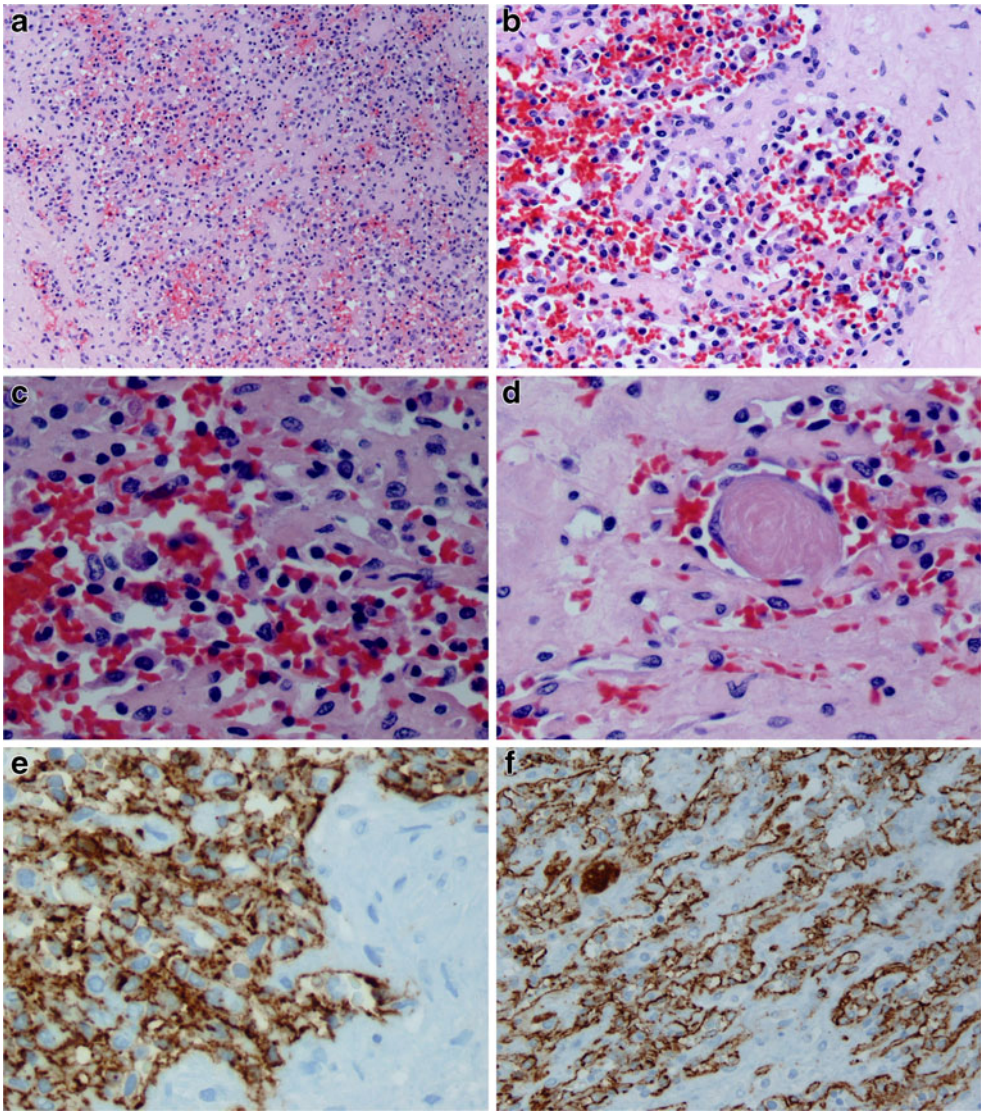

Fig. 2 **a** Low power view of the solid atypical PEH in case 15. *Solid areas* of the tumor are evident in the periphery. **b** At a higher power, broadly anastomotic network of tumors cells with cystic spaces are noted. The cystic spaces are filled with RBCs and tumor cells which appear oval to spindle in shape with minimal pleomorphism. There were no mitoses elsewhere in the tumor. **c** At high magnification, spindly to flattened cells are lining these vascular spaces. **d** Scattered hyalinized cores of the pseudopapillae lined by attenuated endothelium were the only clue to an IPEH. The hyaline material was negative for Congo red, ruling out amyloid. **e** and **f** These vascular spaces are positive for CD31 and CD34, respectively, supporting the vascular histogenesis of this lesion. **a** Hematoxylin and eosin, ×40; **b** hematoxylin and eosin, ×100; **c** hematoxylin and eosin, ×400; **d** and **f** Immunoperoxidase, ×100

stromal edema and/or stromal hyalinization with deposition of collagen and nonendothelial supporting cells between proliferating capillaries [2]. Extramedullary hematopoiesis composed predominantly of nucleated RBC precursors is generally present. They also found hyaline globules of endothelial cells in two of their six cases. Such globules have been described in cutaneous and soft tissue vascular lesions such as glomeruloid or papillary hemangioma [15, 16] and in Kaposi sarcoma [17], angiosarcoma [18], granulation tissue [17], pyogenic granuloma [17], and littoral cell angioma of the spleen [19] but no globules of this sort were described in the more recent report of renal capillary hemangiomas by Brown et al. [1]. Similar to the study by Brown et al., we saw no hyaline globules in our cases of anastomosing hemangiomas or vice versa.

Capillary hemangiomas are benign vascular lesions described in various locations including the skin, soft tissues, and breast [20–22]. In addition, they have been reported in association with rare syndromes like Klippel–Trenaunay and Sturge–Weber syndromes [23]. Büttner et al. recently reported hemangiomas in 8.8 % of the end-stage kidneys [24]. However, there are no reports of capillary hemangiomas occurring in the vicinity of AVM (as seen in case 6) or RCCs (as seen in case 7). Interestingly, in case 7, the background kidney showed features of end-stage pathology. While RCCs have been described to occur in the setting of end-stage kidneys [25, 26], our case represents the first report of a hemangioma and RCC coexisting in an end-stage kidney. Thus, systematic and adequate sampling of end-stage kidneys is needed in order to detect various coexisting lesions.

Lymphangiomas are rare benign tumors that are congenital malformations of the lymphatic system. While most lymphangiomas occur in the neck (75 %) or axilla (20 %), these lesions have also been described to occur in other sites including the retroperitoneum, mediastinum, mesentery, omentum, colon,

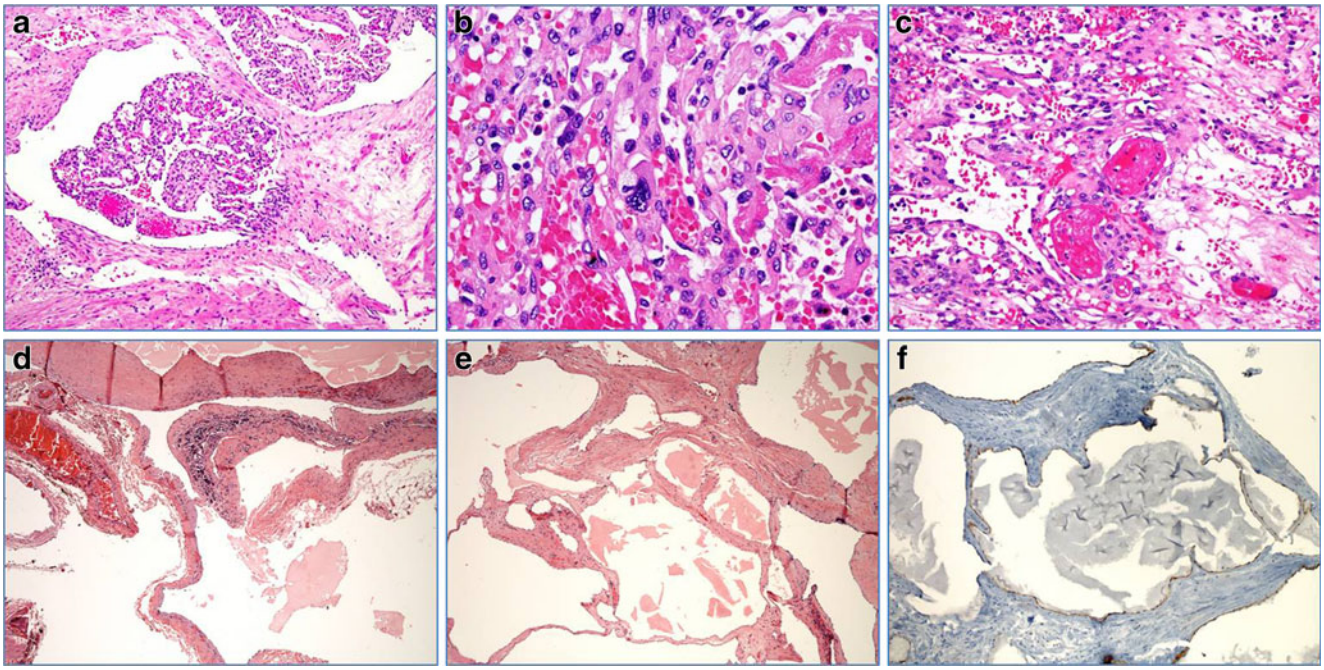

Fig. 3 **a** Intravascular growth pattern of anastomosing hemangioma demonstrating vaguely lobular architecture. **b** At a higher power, extramedullary hematopoiesis is noted. **c** Vascular thrombi are a common feature in these tumors. **d** and **e** Microscopic examination of a lymphangioma of the kidney revealing endothelial-lined cystic spaces containing lymph fluid separated by thin walls with incomplete muscle layer and lymphocytic infiltration. **f** D2-40 immunostain highlights cystic spaces lined by attenuated endothelium. **a** Hematoxylin and eosin, ×40; **b** hematoxylin and eosin, ×400; **c** hematoxylin and eosin, ×100; **d** and **e** hematoxylin and eosin, ×40

and pelvis [27]. Renal lymphangiomas are rare and are thought to arise from dilated lymphatic channels or developmental malformations of the lymphatic system. Most renal lymphangiomas are focal lesions, but diffuse renal lymphangiomatosis may occur. These generally appear as unilocular or multilocular cysts on cross-sectional imaging. Case reports have described lymphangiomas with a solid appearance on sonography [28]. In these cases, the masses are sonographically echogenic due to the reverberations that occur between microscopic lymph spaces and surrounding connective tissue. Grossly, lymphangiomas are thin-walled cystic masses with a smooth gray, pink, tan, or yellow external surface. On cut section, they vary in appearance and may contain large macroscopic interconnecting cysts (often referred to as cystic hygroma or cystic lymphangioma) or microscopic cysts (cavernous lymphangioma) [29]. The cysts may contain chylous, serous, hemorrhagic, or mixed fluid [30]. Histologically, dilated lymphatic spaces are lined with attenuated endothelial cells resembling the cells that line normal lymphatics. The lymphatic spaces are usually filled with proteinaceous eosinophilic fluid. The supporting stroma is composed of collagen and may contain lymphocytes and lymphoid aggregates [29]. Importantly, perirenal lymphangiomas, in particular, typically collapse after excision making identification of previously radiologically detected lesion difficult. Hence, awareness of such lesions is important.

IPEH is a rare peculiar entity characterized by exuberant endothelial proliferation within the lumen of medium-sized veins reported to occur mainly in the skin and soft tissues [31], although cases have been reported in the breast [32]. There are three broad categories of IPEH: a primary form, which occurs within any vessel in the body, unrelated to trauma; a secondary form, which arises within a preexisting vascular lesion such as hemangioma or varices; and an extravascular form that is known to originate within hematomas [33]. Morphologically, the typical IPEH of the soft tissue usually occurs within a thrombosed muscular artery, and microscopy shows numerous fronds and papillae lined by endothelial cells filling up cystic spaces. While there are two reports of IPEH occurring in the renal sinus [34] and within a thrombosed renal vein [35], there is only one report, to date, of an PEH within the renal parenchyma per se [36]. Our case (case # 15, Table 1) was neither intravascular nor papillary in its architecture. We identified only structures resembling papillae with fibrin cores, lined by an attenuated endothelium. Such old lesions may be mistaken for Kaposi's sarcoma or even angiosarcoma [32], depending on the cellularity of the lesion. Kaposi's sarcoma can be identified based on the presence of multifocal lesions in most cases and serology for HIV and the infiltrative nature of the tumor will help distinguish this lesion clearly from IPEH which is typically well circumscribed and unifocal.

Typical papillary features may not be obvious when a PEH arises in a hematoma within a solid organ. Indeed, in long-standing lesions, the papillae may fuse to form a broad

anastomotic network of vessels and cells embedded within connective tissue, which is exactly what we see in our case. At the same time, we cannot entirely rule out the possibility that the current lesion did not develop from a preexisting capillary hemangioma within the kidney, given that we could not document history of prior hematoma, either by radiology or clinical history. Considering that the patient was noted to have renal stone disease, this could possibly represent a risk factor for development of hematoma in the kidney which subsequently gave rise to the IPEH. However, the more important fact is to avoid misinterpretation of old IPEHs with tufting and solid pattern as angiosarcoma. The differential diagnosis may include: spindle cell hemangioendothelioma, Kaposi's sarcoma, juxtaglomerular cell tumor, glomus tumor, epithelioid hemangioma, Kaposiform hemangioendothelioma, hemangioblastoma, AML (epithelioid variants), and low-grade angiosarcoma. Branton et al., in their series on 17 cases of IPEH involving the breast, summarized that features helpful in distinguishing IPEH from angiosarcoma include circumscription of the lesion, intravascular location or association with thrombus, and papillary architecture without significant cytologic atypia or areas of solid growth [32]. Although our case showed circumscription, there was no evidence of an investing vascular wall to support origin from within a vessel lumen. Furthermore, immunostains supported the endothelial origin of the spindly tumor cells.

In conclusion, surgical pathologists need to be aware of the fact that vascular renal lesions may have varied morphology. With increase in radiologic studies, previously rare and unusual lesions may be seen more often. Awareness of these entities can help to better discriminate them from other much more common renal epithelial and mesenchymal lesions.

Acknowledgments This study was presented in the 101st annual conference of the United States and Canadian Academy of Pathology, February 2012.

Conflict of interest None.

References

1. Brown JG, Folpe AL, Rao P, Lazar AJ, Paner GP, Gupta R et al (2010) Primary vascular tumors and tumor-like lesions of the kidney: a clinicopathologic analysis of 25 cases. Am J Surg Pathol 34:942–9
2. Montgomery E, Epstein JI (2009) Anastomosing hemangioma of the genitourinary tract: a lesion mimicking angiosarcoma. Am J Surg Pathol: 33:1364–9
3. Fletcher CDM, Unni KK, Mertens F (eds) (2002) World Health Organization classification of tumours. Pathology and Genetics of Tumours of Soft Tissue and Bone IARC, Lyon
4. Tang CN, Law IC, Iu PP, Yip AW (1997) Arteriovenous malformation of the ureter—a rare cause of haematuria. Br J Urol: 80:500–1
5. Varela ME (1928) Aneurisma arteriovenosa de los vasos renales yasistolia consecutiva. Rev Med Latino-Amer: 14:3244
6. Majwal TK, Ismail A, Alaqily R (2002) Renal artery stenosis associated with saccular aneurysm and arterio-venous fistula. J Invasive Cardiol: 14:411–3
7. Riedlinger WF, Kissane JM, Gibfried M, Liapis H (2004) Congenital bilateral renal arteriovenous malformation: an unrecognized cause of renal failure. Pediatr Dev Pathol: 7:285–9
8. Sonstein WJ, Kader A, Michelsen WJ, Llena JF, Hirano A, Casper D (1996) Expression of vascular endothelial growth factor in pediatric and adult cerebral arteriovenous malformations: an immunocytochemical study. J Neurosurg: 85:838–45
9. Chen Y, Pawlikowska L, Yao JS, Shen F, Zhai W, Achrol AS et al (2006) Interleukin-6 involvement in brain arteriovenous malformations. Ann Neurol: 59:72–80
10. Rangel A, Albarran H, Gomez-Orta F, Soriano M, Badui E (1997) A case of giant arteriovenous shunt in a renal carcinoma. Rev Invest Clin: 49:277–80
11. Ueno Y, Mizusawa H, Ishizuka O, Igawa Y, Nisizawa O, Uehara T (1999) A case of transitional cell carcinoma presenting as rupture of a renal arteriovenous malformation. Hinyokika Kiyo: 45:707–9
12. Harada H, Togashi M, Abe T, Takeyama Y, Seki T, Ohashi N (2000) Renal arteriovenous malformation with thrombus in the inferior vena cava. Int J Urol: 7:310–2
13. Turkeri LN, Daudi I, Abraham JL, Wojtowycz AR, Haas GP (1998) Cirsoid arteriovenous malformation of kidney presenting as a mass suggestive of malignancy. Int J Urol: 5:96–8, discussion 9
14. Mishal J, Leibovici O, Bregman L, London D, Yoffe B, Sherer Y (2001) Huge renal arteriovenous malformation mimicking a simple para-pelvic cyst. Urol Int: 66:49–50
15. Chan JK, Fletcher CD, Hicklin GA, Rosai J (1990) Glomeruloid hemangioma. A distinctive cutaneous lesion of multicentric Castleman's disease associated with POEMS syndrome. Am J Surg Pathol: 14:1036–46
16. Lee H, Meier FA, Ma CK, Ormsby AH, Lee MW (2008) Eosinophilic globules in 3 cases of glomeruloid hemangioma of the head and neck: a characteristic offering more evidence for thanatosomes with or without POEMS. Am J Dermatopathol: 30:539–44
17. Fukunaga M, Silverberg SG (1991) Hyaline globules in Kaposi's sarcoma: a light microscopic and immunohistochemical study. Mod Pathol: 4:187–90
18. Vuletin JC, Wajsbort RR, Ghali V (1990) Primary retroperitoneal angiosarcoma with eosinophilic globules. A combined light-microscopic, immunohistochemical, and ultrastructural study. Arch Pathol Lab Med: 114:618–22
19. Michal M, Skalova A, Fakan F, Koza V, Svojgrova M (1993) Littoral cell angioma of the spleen. A case report with ultrastructural and immunohistochemical observations. Zentralbl Pathol: 139:361–5
20. Hoda SA, Cranor ML, Rosen PP (1992) Hemangiomas of the breast with atypical histological features. Further analysis of histological subtypes confirming their benign character. Am J Surg Pathol: 16:553–60
21. Nagar H, Marmor S, Hammar B (1992) Haemangiomas of the breast in children. Eur J Surg: 158:503–5
22. Mentzel T, Calonje E, Fletcher CD (1994) Vascular tumors of the skin and soft tissue. Overview of newly characterized entities and variants. Pathologe: 15:259–70
23. Schofield D, Zaatari GS, Gay BB (1986) Klippel–Trenaunay and Sturge–Weber syndromes with renal hemangioma and double inferior vena cava. J Urol: 136:442–5
24. Maike Büttner MD VKM, Kathrin Brunner MD, Arndt Hartmann MD, Kerstin Amann MD, Abbas Agaimy MD (2012) Benign mesenchymal tumors and tumor-like lesions in end-stage renal disease. Histopathology (Accepted article).

25. Farivar-Mohseni H, Perlmutter AE, Wilson S, Shingleton WB, Bigler SA, Fowler JE Jr (2006) Renal cell carcinoma and end stage renal disease. J Urol: 175:2018–20
26. Tickoo SK, dePeralta-Venturina MN, Harik LR, Worcester HD, Salama ME, Young AN et al (2006) Spectrum of epithelial neoplasms in end-stage renal disease: an experience from 66 tumor-bearing kidneys with emphasis on histologic patterns distinct from those in sporadic adult renal neoplasia. Am J Surg Pathol: 30:141–53
27. Singh S, Baboo ML, Pathak IC (1971) Cystic lymphangioma in children: report of 32 cases including lesions atrrare sites. Surgery: 69:947–51
28. Kim JK, Ahn HJ, Kim KR, Cho KS (2002) Renal lymphangioma manifested as a solid mass on ultrasonography and computed tomography. J Ultrasound Med: 21:203–6
29. Wiess SW GJ (2001) Soft tissue tumors. 4th ed. St. Louis, MO: Mosby
30. Ros PR, Olmsted WW, Moser RP Jr, Dachman AH, Hjermstad BH, Sobin LH (1987) Mesenteric and omental cysts: histologic classification with imaging correlation. Radiology: 164:327–32
31. Kuo T, Sayers CP, Rosai J (1976) Masson's "vegetant intravascular hemangioendothelioma": a lesion often mistaken for angiosarcoma: study of seventeen cases located in the skin and soft tissues. Cancer: 38:1227–36
32. Branton PA, Lininger R, Tavassoli FA (2003) Papillary endothelial hyperplasia of the breast: the great impostor for angiosarcoma: a clinicopathologic review of 17 cases. Int J Surg Pathol: 11:83–7
33. O'Hara CD, Nascimento AG (2003) Endothelial lesions of soft tissues: a review of reactive and neoplastic entities with emphasis on low-grade malignant ("borderline") vascular tumors. Adv Anat Pathol: 10:69–87
34. Johraku A, Miyanaga N, Sekido N, Ikeda H, Michishita N, Saida Y et al (1997) A case of intravascular papillary endothelial hyperplasia (Masson's tumor) arising from renal sinus. Jpn J Clin Oncol: 27:433–6
35. Akhtar M, Aslam M, Al-Mana H, Bamefleh H, Al-Khateeb SS, Lindstedt E (2005) Intravascular papillary endothelial hyperplasia of renal vein: report of 2 cases. Arch Pathol Lab Med: 129:516–9
36. Garber BB, Prestipino AJ, Pollack HM, Levine SR, Whitmore KE (1990) Masson's tumor of the kidney: a new renal lesion. J Urol: 143:344–6

Virchows Arch (2012) 461:677–685
DOI 10.1007/s00428-012-1322-z

ORIGINAL ARTICLE

Absence of TCL1A expression is a useful diagnostic feature in splenic marginal zone lymphoma

Enrico Munari · Marianna Rinaldi · Achille Ambrosetti · Massimiliano Bonifacio · Angela Bonalumi · Marco Chilosi · Alberto Zamò

Received: 17 May 2012 / Revised: 30 August 2012 / Accepted: 25 September 2012 / Published online: 14 October 2012
© The Author(s) 2012. This article is published with open access at Springerlink.com

Abstract Splenic marginal zone lymphoma (SMZL) is a low-grade lymphoma showing a rather nonspecific immunophenotype. Gene expression profiling studies suggested that TCL1A could be a marker of SMZL, but reported data are conflicting. We evaluated TCL1A expression in a series of spleen and bone marrow samples involved by SMZL and correlated the findings with other immunophenotypical, morphological, and clinical data. In addition, we evaluated the expression of TCL1A in a series of spleens and lymph nodes involved by lymphomas that might mimic SMZL (13 nodal marginal zone lymphomas (NMZL), 39 follicular lymphomas (FL), 30 B-cell chronic lymphocytic leukemias (B-CLL), 31 mantle cell lymphomas (MCL), 1 lymphoplasmacytic lymphoma) and 15 bone marrow specimens involving hairy cell leukemia (HCL). TCL1A staining was negative in 24/31 cases of SMZL (77 %); 27/31 MCL and all B-CLL were positive for TCL1A; 32/34 cases of nodal FL (96 %) and all five splenic FL were positive for TCL1A, although at a lower intensity. Eight of 13 NMZL were positive for TCL1A, often showing a heterogeneous staining pattern. All HCL samples were strongly positive for TCL1A. No correlation was found between the pattern of splenic infiltration, TCL1A expression, and the clinical course. TCL1A-positive SMZL showed a higher rate of DBA44 staining compared to the negative ones, and this difference was statistically significant (Fisher test, single-tailed, $p=0.0397$). Our data support the use of TCL1A in the panel of diagnostic markers used in the differential diagnosis of splenic low-grade B-cell lymphoma; a possible prognostic value, however, needs a larger series to be established.

Keywords Splenic marginal zone lymphoma · TCL1A · Immunohistochemistry · Differential diagnosis

E. Munari · M. Chilosi · A. Zamò (✉)
Department of Pathology and Diagnostics,
Section of Anatomic Pathology, University of Verona,
P.le Scuro 10,
37134 Verona, Italy
e-mail: alberto.zamo@univr.it

M. Rinaldi · A. Ambrosetti · M. Bonifacio · A. Bonalumi
Department of Medicine, Section of Haematology,
University of Verona,
P.le Scuro 10,
37134 Verona, Italy

Introduction

Splenic B-cell marginal zone lymphoma is a rare entity, accounting for less than 2 % of all lymphoid malignancies; it shows an indolent clinical course, although 10 % of cases progress to diffuse large B cell lymphoma [1]. The diagnosis of SMZL relies on a combination of histopathological analysis and immunophenotyping of the spleen samples, although bone marrow biopsies are frequently the first and often the only sample analyzed by pathologists, since splenectomy is not clinically required in a large percentage of patients [2].

A commercially available specific marker of SMZL is lacking, and the immunophenotypical profile of SMZL is currently mainly defined on the basis on the lack of expression of markers associated with its mimickers (follicular lymphoma, mantle cell lymphoma, B-cell chronic lymphocytic leukemia/small lymphocytic lymphoma, hairy cell leukemia), including CD5, CD10, CD23, cyclin D1, CD25, CD11c, and Annexin A1 to name just a few. However, both SMZL and its mimickers can occasionally show an aberrant phenotype (e.g., expression of CD5 and/or CD23 in SMZL or lack of CD10 in follicular lymphomas (FL)), making a final diagnostic decision more difficult. The detection of the deletion of 7q might help, because it is rare in other lymphoma subtypes, while it is present in about 30–40 % of SMZL [3, 4]; its detection, however, might be

impractical for routine testing and is not completely specific. So far, the only reliable marker of marginal zone differentiation is IRTA-1 [5–7], but the antibody is not commercially available. Differentiating SMZL from other lymphomas is even more problematic in bone marrow biopsies, where neoplastic cells can be scarce, morphologic criteria are less solid, the immunophenotype might differ, and genetic analysis might not work. Myeloid cell nuclear differentiation antigen (MNDA) has recently been described as a sensitive (although not completely specific) marker of nodal and splenic marginal zone lymphomas, that might be useful both in primary sites and in the bone marrow [8].

Although not widely used, TCL1A is a helpful marker in lymphoma characterization [9]. *TCL1A* (T-cell leukemia/lymphoma 1A) is a proto-oncogene member of a multigene family that includes *TCL1B* and *MTCP1* [10]. *TCL1A* maps to the 14q32.1 locus and has been shown to enhance the activity of the Akt kinase, which plays a central role in regulating cellular survival [11, 12]. In T-cell prolymphocytic leukemia, *TCL1A* acts like a classic oncogene through constitutive activation [13]. The oncogenic role of TCL1A in B-cell malignancies is less well understood: while in murine models it appears to retain a major function in the development of B-cell tumors [14], in humans, such a role is less clear.

Herling et al. reported the expression of TCL1A in a high percentage of precursor B acute lymphoblastic leukemia/lymphoblastic lymphoma, Burkitt lymphoma, and mantle cell lymphoma, while FL showed positive staining in 57 % of cases [9]. Leich et al. correlated TCL1A expression with the presence of the t(14;18) translocation in FL, with 84 % of translocation-positive cases showing TCL1A expression, while 80 % of t(14;18)-negative FL without BCL2 protein expression were also TCL1A negative [15]. These data support the hypothesis that TCL1A expression is down-regulated in B-cell tumors resembling a late B-cell program.

The present literature reports conflicting data regarding the expression of TCL1A in SMZL. Herling and co-workers [9] reported a small series of ten SMZL, which were all negative for TCL1A; variable expression of *TCL1A* mRNA was instead reported by Aggarwal et al. [16]. In a series published by Ruiz-Ballesteros et al., the protein appears to be expressed by immunohistochemistry in 80 % of cases (14/20) [17].

In this study, we analyzed the expression of TCL1A in a series of 31 consecutive cases of SMZL, which to our knowledge is the largest series so far; for 25 patients, matched bone marrow biopsies were available. Morphological, immunophenotypical, and clinical data were collected and correlated. Our data support the use of TCL1A in the diagnostic workup for SMZL.

Methods

Cases

Thirty-one consecutive cases of SMZL were retrieved from the archives of the Department of Pathology and Diagnostics, University of Verona. For 25 cases, one or more matched bone marrow biopsies were available.

Clinical data were available for 24 SMZL cases and included age at diagnosis, gender, spleen size, presence of autoimmune phenomena, hemoglobin, white cell count, presence of neoplastic circulating cells, presence of M component, albumin and LDH values, HBV and HCV serology, liver and nodal involvement, overall survival (OS), and disease-free survival (DFS).

Nine cases of non-Hodgkin lymphoma involving the spleen were used as controls, including five follicular lymphomas (FL), one mantle cell lymphoma (MCL), one small B-cell lymphoma/chronic lymphocytic leukemia (B-CLL/SLL), one hairy cell leukemia (HCL), and one lymphoplasmacytic lymphoma (LPL). Five normal spleen specimens (removed after traumatic injury) were also included in the study. We also added a series of lymph node cases involving lymphomas that might mimic SMZL (13 NMZL, 34 FL, 29 B-CLL/SLL, 30 MCL) and 15 bone marrow specimens involving hairy cell leukemia, which might be a differential diagnostic problem when only minimal involvement is present.

Morphological classification

Cases were classified morphologically as described by Isaacson et al. [18]. Spleen specimens were divided into three groups according to the main pattern of neoplastic infiltration: "nodular" (white pulp effaced by tumor cells with scant red pulp infiltration), "nodular/diffuse" (marked expansion of tumor cells with variable nodular/intrasinusoidal involvement of the red pulp), and "primarily diffuse" (white pulp completely effaced with massive red pulp involvement) [18–20]. In bone marrow biopsies, the neoplastic infiltrate was defined as "sinusoidal" (rows of at least three to four cells positive for B-cell markers inside sinusoids), "interstitial" (small and discohesive groups of cells dispersed in the bone marrow interstitium), and "nodular pattern" (neoplastic cells organized in nodules that may be associated with an interstitial and/or sinusoidal component).

Construction of tissue microarrays

Three tissue microarrays were built using a manual arrayer (Beecher Instruments). After morphological evaluation and marking of proper areas in H&E-stained slides, three 2-mm cores were taken from each block. All slides were scanned using the D-SIGHT device (Menarini Diagnostics, Florence, Italy).

Immunohistochemistry

Immunohistochemical staining was performed using an autostainer (Leica Bond Max) using the following antibodies: CD5, CD20, Ki67, cyclin D1, CD123, TCL1, T-bet, DBA44, BCL2, BCL6, CD23, ANXA1, MNDA, and GCET1 (Table 1). MNDA and GCET1 antibodies were kindly provided by Dr. Roncador (CNIO, Madrid, Spain). Double staining was performed as previously described [21].

Statistical analysis

Fisher exact test (one-sided and two-sided) was used for statistical analysis.

Results

Clinical data

Clinical data were available for 24 cases. Mean age was 62 years (range 48–79). All cases presented with splenomegaly (spleen mean main axis 22 cm, range 15–30) and all underwent splenectomy for diagnostic and therapeutic purposes. Fourteen of 24 cases (58 %) presented with liver enlargement and 17/24 with lymphadenopathy. In all patients with an available bone marrow trephine biopsy, an involvement was demonstrated.

Other relevant findings were lymphocytosis (11/24 patients, 45 %), anemia (7/24, 29 %), thrombocytopenia (14/24, 58 %), presence of serum M component (10/24, 41 %), and autoimmune phenomena (8/24, 33 %); 2/24 (8 %) patients resulted HCV positive and other two (8 %) HBV positive. One third of patients (8/24, 33 %) presented an IPI score of 3–4, while 15/24 (62 %) an IPI score of 1–2; data were not available for one case. Seven of 24 (29 %) presented LDH values above normal range; 3/24 (12 %) presented an albumin concentration below 35 g/L. Sixteen of 24 patients (66 %) had normal values of albumin, LDH, and hemoglobin; 3/24 patients (12 %) had one of these three values outside the normal range, 3/24 patients (12 %) had two abnormal values, and 2/24 (8 %) had all three values outside the reference range.

As a first line of therapy, 9/24 (37 %) patients were treated with chemotherapy, consisting of alkylating agents with or without rituximab besides splenectomy; the remaining 15 patients underwent splenectomy alone. Of these, 11 underwent chemotherapy as second-line therapy. The mean follow-up period was 69 months (range 6–233). During the follow-up period, 5/24 patients (20 %) died because of the lymphoma, after a mean period of 80 months (range 49–110); 9/24 (37 %) patients presented signs of disease progression. At the time of the last clinical observation, 7/24 patients (29 %) were free from disease after chemotherapy/splenectomy.

Table 1 Antibodies used in the study

Antigen	Clone	Producer	Dilution
CD5	4C7	Labvision	1:150
CD20	L26	Dako	1:250
Ki67	MM1	Novocastra	1:50
TCL1A	27D6/20	MBL	1:500
T-bet	4B10	Santa Cruz	1:100
CCND1	SP4	Neomarkers	1:10
CD123	7 G3	BD	1:100
DBA44	DBA44	Dako	1:20
BCL2	124	Dako	1:40
BCL6	LN22	Novocastra	1:10
CD23	1B12	Novocastra	1:100
ANXA1	B01P	Abnova	1:100
MNDA	235	CNIO	Pure supernatant
GCET1	RAM341	Abcam/CNIO	1:500

Morphological classification

In the spleen, a nodular pattern of infiltration was present in 8/31 cases (26 %), a nodular/diffuse pattern in 15/31 cases (48 %), and a primarily diffuse pattern in 8/31 cases (26 %). In bone marrow biopsies, we found a mixed nodular/interstitial/sinusoidal pattern in 9/25 cases (36 %), nodular/sinusoidal in 5/25 (20 %), interstitial/sinusoidal in 4/25 (16 %), nodular/interstitial in 1/25 (4 %), purely sinusoidal in 3/25 (12 %), and purely interstitial in 3/25 (12 %) (Table 2). We detected a secretive differentiation in 4/31 cases (13 %); neoplastic involvement of the liver was documented in 13/31 cases (42 %).

Immunohistochemistry

Normal spleen (Fig. 1a, CD20 staining depicted in Fig. 1b) showed the typical targetoid staining for TCL1A (Fig. 1c), with germinal center cells stained at intermediate intensity, mantle cells strongly stained, and marginal zone cells unstained. MNDA, as previously described, stained both mantle and marginal zone cells (Fig. 1d).

In SMZL (Fig. 2a, CD20 staining depicted in Fig. 2b), TCL1A staining was negative in 24/31 cases (77 %) (Fig. 2c); MNDA was positive in 29/31 cases (94 %) (Fig. 2d). In the bone marrow (Fig. 3a, CD20 staining depicted in Fig. 3b), TCL1A staining was negative in 21/25 cases (84 %) (Fig. 3c); MNDA was positive in 22/25 cases (88 %) (Fig. 3d). Out of the five cases that were positive for TCL1A on spleen specimens and were paired with bone marrow biopsies, four resulted positive for TCL1A also in the bone marrow biopsy (for two cases with spleen samples bone marrow biopsies were not available). In the bone marrow, MNDA was also positive in myeloid cells, thus requiring the

Table 2 Synopsis of histopathological and immunohistochemical results

Case	Splenic pattern	Bone marrow pattern	CD5	CD20	Ki67	TCL1A		MNDA		T-bet	DBA44	Bcl2	Bcl6
						Spleen	BM	Spleen	BM				
2	N	NIS	−	+++	−	−	−	+	+ w	−	−	++	−
4	N	NA	−	++	−	−	NA	+	NA	−	−	+	−
14	N	NA	−	+++	−	−	NA	+	NA	−	−	++	−
28	N	IS	−	+++	−	−	−	+	+ w	−	−	+++	−
30	N	IS	−	+++	−	−	−	++	+	NA	−	++	−
1	ND	NS	−	++	−	−	−	+	+ w	−	−	−	−
6	ND	NS	−	++	−	−	−	++	+ w	−	−	+	−
11	ND	I	−	+++	++	−	−	++	+ w	−	−	+++	−
21	ND	S	−	+++	−	−	−	+	+ w	−	−	+++	+
23	ND	NIS	−	+++	−	−	−	+	+ w	++	−	+++	+
26	ND	NIS	−	+++	+	−	−	+	+ w	−	−	++	−
27	ND	NS	−	+++	−	−	−	+	+ w	−	−	+++	−
29	ND	NIS	−	+++	+	++	+	−	−	NA	−	++	−
31	D	NA	−	+++	−	++	NA	+	NA	+++	NA	++	NA
5	D	NIS	−	++	−	−	−	+	−	−	−	+	−
16	D	NS	−	+++	−	−	−	++	+ w	−	−	+++	−
17	D	S	−	+++	−	−	−	+	+ w	−	−	++	−
25	D	NA	−	++	−	−	NA	+	NA	+	−	+	−
20	D	NIS	−	+++	−	−	−	+	+ w	−	+	++	−
12	D	S	−	+++	−	−	−	+	+ w	−	++	+++	−
9	D	I	−	+++	++	++	−	+	+ w	+++	+++	++	−
15	ND	NIS	−	+++	−	−	−	+	+ w	−	+	+++	−
18	ND	NI	−	++	−	−	−	−	−	++	+	++	−
13	ND	IS	−	+++	−	++	+	+	+ w	−	+	+++	−
10	ND	NA	−	+++	−	+++	NA	+	NA	−	+	+++	−
7	ND	NA	−	+++	−	−	NA	+	NA	−	++	++	−
22	ND	I	−	+++	−	−	−	+	+	+++	++	+	+
24	ND	IS	−	+++	−	−	−	+	+ w	+++	+++	−	+
19	N	NS	−	++	−	−	−	+	+	−	+	+++	−
3	N	NIS	−	+++	−	++	+ w	+	+ w	−	+	++	−
8	N	NIS	+	+++	−	++	+	+	+ w	−	++	++	−

Cases ordered by pattern and DBA44 staining. Case numbers according to chronological order. Splenic pattern of infiltration: *N* nodular, *ND* nodular/diffuse, *D* diffuse. Bone marrow pattern of infiltration: *N* nodular, *I* interstitial, *S* sinusoidal. Immunostain evaluation, percentage of positive cells: −, <10 %; +, 11–35 %; ++, 36–75 %; +++, >75 %; *NA* not available, *w* weak, *BM* bone marrow

use of double staining for MNDA and CD20 to correctly score B cells.

Thirteen of 30 (43 %) cases showed a variable degree of staining for DBA44, although only 5/30 (17 %) in more than 35 % of cells. Five of the six TCL1A-postive cases where also DBA44 positive (83 %), while 8/24 TCL1A-negative cases showed expression of DBA44 (33 %). This difference was not statistically significant using a two-sided Fisher exact test ($p=0.0606$) but became significant when using a single-tailed test ($p=0.0397$). T-bet resulted positive in 7/31 cases (22 %), while ANXA1, cyclin D1, and CD123 were invariably negative. In one case, the neoplastic cells were CD5 positive, but negative for CD23, cyclin D1, and TCL1A; thus, a splenic localization of CLL/SLL or MCL was reasonably excluded. TCL1A-positive cases showed no apparent peculiarities when compared to the negative ones; the staining was present usually only in part of the cells (36–75 % in six of seven cases) and with variable intensity (Fig. 4a).

Among lymph node cases involved by lymphomas that might mimic SMZL, 8/13 (61 %) of NMZL showed a positive but heterogeneous staining with a “mosaic-like”

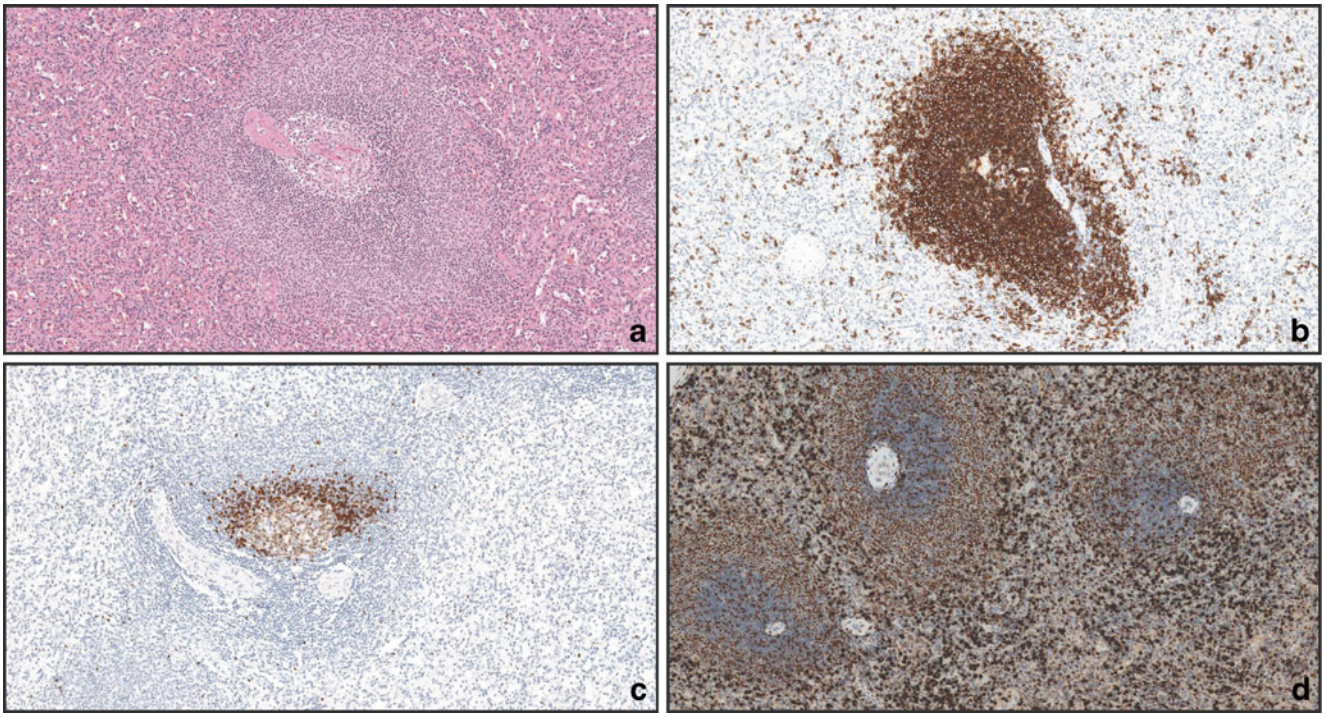

Fig. 1 Normal spleen parenchyma. **a** Normal spleen parenchyma, H&E (×10); **b** CD20 (×10); **c** TCL1A highlights mantle cells and scattered germinal center cells but results negative in marginal zone cells (×10); **d** MNDA (×10)

pattern (Fig. 4b). Twenty-seven of 30 MCL as well as all CLL/SLL (29/29) stained strongly and diffusely for TCL1A (three MCL cases showed a weak or heterogeneous staining that was scored as negative), while 32/34 cases of FL (94 %) were positive for TCL1A. All HCL bone marrow trephine biopsies (15/15) were positive for TCL1A. All spleen

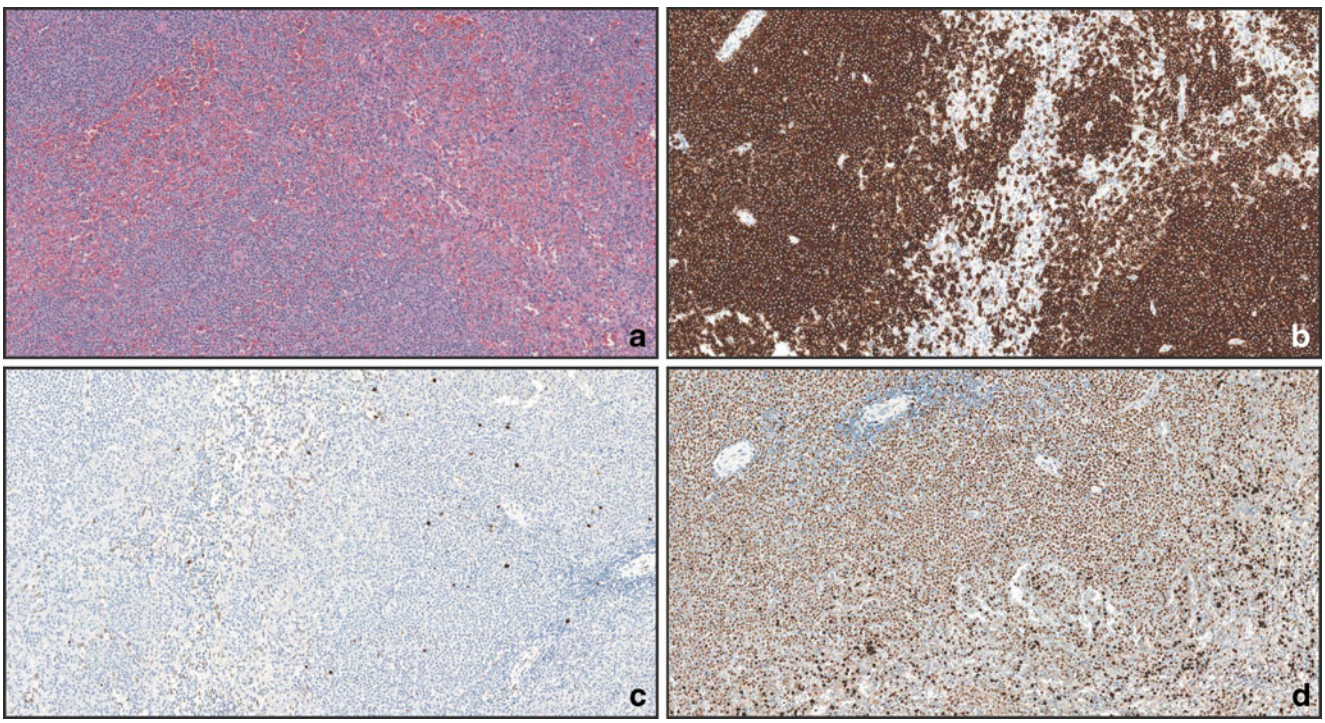

Fig. 2 Spenic marginal zone B-cell lymphoma, nodular and diffuse pattern of infiltration. **a** H&E (×10); **b** CD20 (×10); **c** TCL1A results negative in the neoplastic cells (×10); **d** MNDA results positive in the neoplastic component (×10)

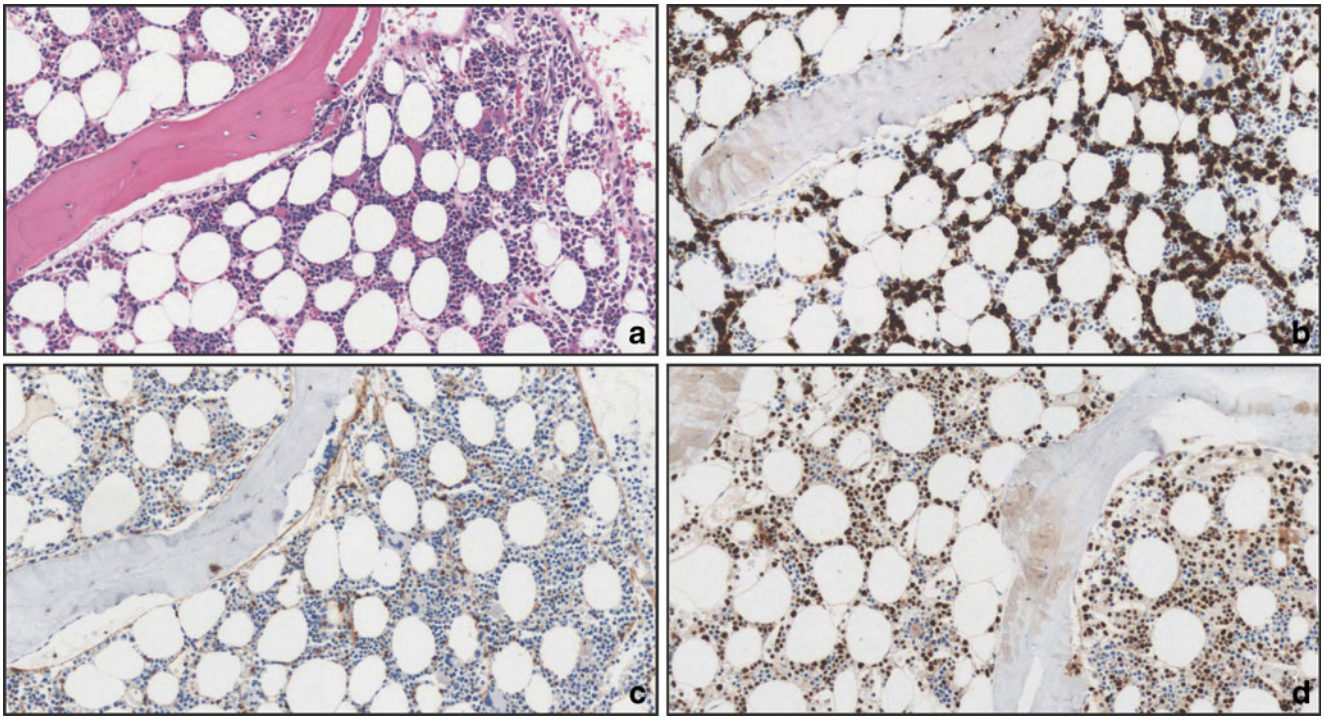

Fig. 3 Bone marrow involvement by splenic marginal zone B-cell lymphoma showing a prevalently interstitial pattern of infiltration. **a** H&E (×20); **b** CD20 (×20); **c** TCL1A (×20); **d**: MNDA (×20)

samples involved by other lymphoma/leukemia subtypes (five FL, one B-CLL, one MCL, one HCL, one LPL) stained positive for TCL1A.

Clinicopathological correlation

No correlation was found between the type of splenic infiltration and the clinical course, including OS and DFS. We did not find any statistically significant correlation between TCL1A expression and the primarily diffuse pattern seen in 7/31 cases, nor with disease progression. In fact, we did not find any difference in terms of TCL1A expression among cases with a diffuse pattern of splenic infiltration compared to those with a nodular or nodular and diffuse pattern.

Discussion

Due to the lack of specific markers, splenic marginal zone B-cell lymphoma is still a diagnosis of exclusion. The use of a large number of markers, even negative, allows exclusion of morphologically similar entities and thus improves diagnostic reliability. The problem is more pertinent when analyzing bone marrow specimens, since the diagnostic criteria are less reliable, and morphological evaluation is sometimes of limited help. Since only a part of the patients with SMZL

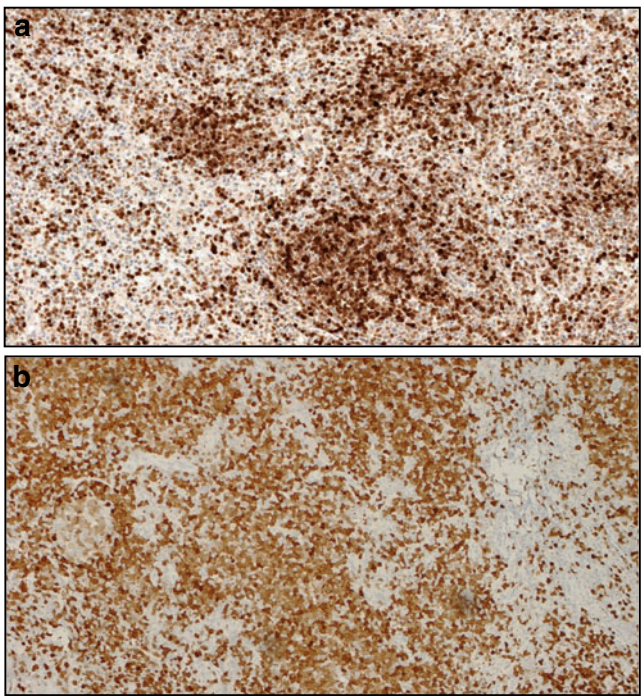

Fig. 4 Examples of TCL1A-positive cases of splenic and nodal marginal zone lymphoma. **a** Example of a TCL1A-positive splenic marginal zone lymphoma (×10); **b** example of a TCL1A-positive nodal marginal zone lymphoma (×10); a residual non-neoplastic germinal center is also present

undergo splenectomy before a bone marrow biopsy is taken, these specimens are often the first (and frequently the only) samples available for evaluation.

In this paper, we analyzed the expression of TCL1A in SMZL, a marker that is lost in marginal zone differentiation of normal B cells [9], the mRNA of which was detected at high levels in SMZL [22] although current literature is conflicting regarding its expression as detected by immunohistochemistry. In addition, we analyzed matched spleen and bone marrow samples and described the morphological and immunohistochemical findings in both. We also analyzed possible correlations with clinical parameters such as disease progression, albumin, hemoglobin, and LDH values.

Our series of cases showed an indolent course and good prognosis, similar to previously published studies. Only 5/24 patients (21 %) for whom clinical data were available died because of lymphoma, after a median interval of 80 months (range 49–110). Nine of 24 patients (37 %) underwent disease progression, three of whom developed transformation to diffuse large B-cell lymphoma.

Morphologically, a purely diffuse pattern was present in 8/31 (26 %) of spleen samples of SMZL, while the majority showed a classical nodular pattern with or without red pulp involvement. Three of the purely diffuse cases were also positive for DBA44 and, based on the 2008 WHO criteria, would fit in the provisional category called "splenic B-cell lymphoma, unclassifiable," which includes a subcategory called splenic diffuse red pulp lymphoma. DBA44 was not restricted to the purely diffuse subtypes, however, since also ten other cases with mixed or nodular patterns showed a variable degree of expression (Table 2). Moreover, four cases with a purely diffuse pattern were DBA44 negative, supporting the view that this marker might not be strictly associated with a diffuse pattern of infiltration. A recent series of splenic diffuse red pulp lymphomas, however, included also cases which were DBA44 negative [23]. Interestingly, we found a higher rate of expression of DBA44 in TCL1A-positive cases, since five of the six (83 %) TCL1A-positive cases where also DBA44 positive, while 8/24 (33 %) TCL1A-negative cases showed expression of DBA44 to some extent. This association was not statistically significant using a two-tailed Fisher test ($p=0.0606$). Since we wanted to test the positive association between TCL1A and DBA44, a one-tailed test might be appropriate which turned out to be significant ($p=0.0397$). The small number of cases did not allow a more powerful statistical approach, but the high prevalence of double-positive cases is intriguing and warrants further investigation of the hypothesis that DBA44-positive cases might be different from the negative ones, irrespective of the growth pattern.

On the bone marrow biopsies, we confirmed what was reported so far in the literature [24] concerning the presence of a sinusoidal pattern of infiltration, which we observed (often associated with nodular and interstitial aggregates) in 80 % of cases. Regarding other immunophenotypic markers, all cases were negative for CD10, CD23, CD123, cyclin D1, and ANXA1. CD5 appeared positive in one case only, which was negative for CD23 and CCND1 excluding other entities such as MCL and B-CLL.

In our series, TCL1A was negative in almost 80 % of cases of SMZL. This finding is at variance with the high levels of mRNA of *TCL1A* detected in another series [22]. Several explanations are possible for this curious phenomenon, including low translation rate of mRNA and fast protein degradation. The reported positive staining in 80 % of SMZL [17] is more difficult to explain, also considering variations in the techniques used.

The absence of TCL1A staining seems a useful feature in defining SMZL: while in fact only 7/31 (22 %) of cases of SMZL showed positive staining for TCL1A, among cases of lymphomas that might mimic SMZL, 8/13 (61 %) of NMZL showed a mosaic-like, heterogeneously positive staining, while all nodal B-CLL/SLL (29/29) and 27/30 (90 %) nodal MCL showed strong and diffuse positivity for TCL1A (the remaining three MCL cases showed a weak or heterogeneous staining). Moreover, 32/34 nodal cases of FL (94 %) and all HCL bone marrow trephine biopsy (15/15) stained positive for TCL1A. In the spleen, five FL, one MCL, one B-CLL/SLL, one HCL, and one LPL also showed expression of TCL1A.

As previously said, among the five cases that were positive for TCL1A on spleen specimens and had paired bone marrow biopsies, one case was negative in the bone marrow biopsy. This asymmetry might be due to the interaction between neoplastic cells with the bone marrow microenvironment or simply to a lower technical performance on de-calcified samples (however, a few positive cells were always detectable).

In a study conducted in 2006 by Herling et al. [25], the expression of TCL1 has been evaluated on a series of 213 cases of CLL/SLL; in 90 % of the cases, expression of TCL1 was found by flow cytometry, immunohistochemistry, and western blotting. The highest level of expression obtained was lower than that observed in T-cell prolymphocytic leukemia (T-PLL), but correlated with expression of ZAP-70 and presence of wild-type *IGHV* genes. In splenic marginal zone B-cell lymphomas, this latter correlation has never been directly proven, but indirect evidence comes from studies that demonstrated that the presence of wild-type *IGHV* genes correlates with the presence of deletion of 7q31 [26] and that such a deletion correlates in turn with the expression of TCL1A in SMZL [17]. Further studies are therefore needed to verify this hypothesis.

In a multicenter study conducted by the Intergruppo Italiano Linfomi, Arcaini et al. [27] suggested, on a large series of consecutively diagnosed SMZL (309 cases), three parameters predictive for a shorter survival: hemoglobin less than 120 g/L, albumin less than 35 g/L, and LDH above normal values. These authors proposed a prognostic model which considers three groups: in particular, low risk (no adverse factors), intermediate risk (one adverse factor), and high risk (two or

three parameters out of normal range). We did not find any correlation between the high risk group and the expression of TCL1A, although a statistically significant correlation ($p<0.05$) is present if the three abnormal parameters are taken together and correlated with TCL1A-positive staining. TCL1A expression might therefore be a predictor of shorter survival, but the low number of TCL1A-positive cases does not allow a powerful statistical analysis.

Recently, Kanellis et al. [8] evaluated the expression of MNDA in a broad spectrum of lymphoid neoplasias, reporting that all of the 20 cases of SMZL tested were positive for this marker. In our series, we found this antigen expressed in 94 % of cases. We can confirm the usefulness of this marker, with the caveat of a strong expression in myeloid cells that might impair the recognition of the MNDA-positive lymphoid infiltrate, especially in the interstitial pattern of infiltration. In our opinion, the use of a double staining procedure, using a membrane/cytoplasmic B-cell marker such as CD20, greatly facilitates the evaluation of MNDA. Interestingly, one of the two splenic MNDA-negative cases was DBA44 positive, and the other was TCL1A positive; moreover, one case that was MNDA negative only in the bone marrow showed a diffuse pattern in the spleen. In consideration of these data and of those concerning DBA44 previously discussed, we propose to investigate the hypothesis that aberrant phenotypic/morphologic features tend to cluster together. We hypothesize that besides classical SMZL and the relatively well-described "diffuse red pulp lymphoma," there might be a third group displaying a classical (i.e., nonpurely diffuse) pattern but showing an aberrant phenotype. The clinical and biological significance of this group, however, needs to be investigated on a larger series and possibly using high-throughput technologies to identify specific molecular signatures. In conclusion, our data support the use of TCL1A in the panel of diagnostic markers used in the differential diagnosis of splenic low-grade B-cell lymphoma; a possible biological and/or prognostic significance of this marker and the possible existence of a novel group of splenic lymphomas with an aberrant phenotype, however, need evaluation of a larger series.

Acknowledgments This study was supported in part by AIRC and Fondazione Cariverona. We thank Giovanna Roncador for providing GCET1 and MNDA antibodies.

Conflict of interest We declare that we have no conflict of interest.

Open Access This article is distributed under the terms of the Creative Commons Attribution License which permits any use, distribution, and reproduction in any medium, provided the original author(s) and the source are credited.

References

1. Iannitto E, Minardi V, Callea V, Stelitano C, Calvaruso G, Tripodo C, Quintini G, De Cantis S, Ambrosetti A, Pizzolo G, Franco V, Florena AM, Abbadessa V (2006) Assessment of the frequency of additional cancers in patients with splenic marginal zone lymphoma. Eur J Haematol 76(2):134–140. doi:10.1111/j.1600-0609.2005.00578.x
2. Thieblemont C, Davi F, Noguera ME, Briere J (2011) Non-MALT marginal zone lymphoma. Curr Opin Hematol 18(4):273–279. doi:10.1097/MOH.0b013e3283477815
3. Andersen CL, Gruszka-Westwood A, Ostergaard M, Koch J, Jacobsen E, Kjeldsen E, Nielsen B (2004) A narrow deletion of 7q is common to HCL, and SMZL, but not CLL. Eur J Haematol 72(6):390–402. doi:10.1111/j.1600-0609.2004.00243.x
4. Matutes E, Oscier D, Montalban C, Berger F, Callet-Bauchu E, Dogan A, Felman P, Franco V, Iannitto E, Mollejo M, Papadaki T, Remstein ED, Salar A, Sole F, Stamatopoulos K, Thieblemont C, Traverse-Glehen A, Wotherspoon A, Coiffier B, Piris MA (2008) Splenic marginal zone lymphoma proposals for a revision of diagnostic, staging and therapeutic criteria. Leukemia 22(3):487–495. doi:10.1038/sj.leu.2405068
5. Falini B, Agostinelli C, Bigerna B, Pucciarini A, Pacini R, Tabarrini A, Falcinelli F, Piccioli M, Paulli M, Gambacorta M, Ponzoni M, Tiacci E, Ascani S, Martelli MP, Favera RD, Stein H, Pileri SA (2012) IRTA1 is selectively expressed in nodal and extranodal marginal zone lymphomas. Histopathology. doi:10.1111/j.1365-2559.2012.04289.x
6. Falini B, Tiacci E, Pucciarini A, Bigerna B, Kurth J, Hatzivassiliou G, Droetto S, Galletti BV, Gambacorta M, Orazi A, Pasqualucci L, Miller I, Kuppers R, Dalla-Favera R, Cattoretti G (2003) Expression of the IRTA1 receptor identifies intraepithelial and subepithelial marginal zone B cells of the mucosa-associated lymphoid tissue (MALT). Blood 102(10):3684–3692. doi:10.1182/blood-2003-03-0750
7. Miller I, Hatzivassiliou G, Cattoretti G, Mendelsohn C, Dalla-Favera R (2002) IRTAs: a new family of immunoglobulinlike receptors differentially expressed in B cells. Blood 99(8):2662–2669
8. Kanellis G, Roncador G, Arribas A, Mollejo M, Montes-Moreno S, Maestre L, Campos-Martin Y, Rios Gonzalez JL, Martinez-Torrecuadrada JL, Sanchez-Verde L, Pajares R, Cigudosa JC, Martin MC, Piris MA (2009) Identification of MNDA as a new marker for nodal marginal zone lymphoma. Leukemia 23 (10):1847–1857. doi:10.1038/leu.2009.108
9. Herling M, Patel KA, Hsi ED, Chang KC, Rassidakis GZ, Ford R, Jones D (2007) TCL1 in B-cell tumors retains its normal b-cell pattern of regulation and is a marker of differentiation stage. Am J Surg Pathol 31(7):1123–1129. doi:10.1097/PAS.0b013e31802e2201
10. Pekarsky Y, Koval A, Hallas C, Bichi R, Tresini M, Malstrom S, Russo G, Tsichlis P, Croce CM (2000) Tcl1 enhances Akt kinase activity and mediates its nuclear translocation. Proc Natl Acad Sci U S A 97(7):3028–3033. doi:10.1073/pnas.040557697
11. Laine J, Kunstle G, Obata T, Sha M, Noguchi M (2000) The protooncogene TCL1 is an Akt kinase coactivator. Mol Cell 6 (2):395–407
12. Croce CM (1999) Role of TCL1 and ALL1 in human leukemias and development. Cancer Res 59(7 Suppl):1778s–1783s
13. Isobe M, Russo G, Haluska FG, Croce CM (1988) Cloning of the gene encoding the delta subunit of the human T-cell receptor reveals its physical organization within the alpha-subunit locus and its involvement in chromosome translocations in T-cell malignancy. Proc Natl Acad Sci U S A 85 (11):3933–3937

14. Bichi R, Shinton SA, Martin ES, Koval A, Calin GA, Cesari R, Russo G, Hardy RR, Croce CM (2002) Human chronic lymphocytic leukemia modeled in mouse by targeted TCL1 expression. Proc Natl Acad Sci U S A 99(10):6955–6960. doi:10.1073/pnas.102181599. 99/10/6955 [pii]
15. Leich E, Zamo A, Horn H, Haralambieva E, Puppe B, Gascoyne RD, Chan WC, Braziel RM, Rimsza LM, Weisenburger DD, Delabie J, Jaffe ES, Fitzgibbon J, Staudt LM, Mueller-Hermelink HK, Calaminici M, Campo E, Ott G, Hernandez L, Rosenwald A (2011) MicroRNA profiles of t(14;18)-negative follicular lymphoma support a late germinal center B-cell phenotype. Blood 118 (20):5550–5558. doi:10.1182/blood-2011-06-361972
16. Aggarwal M, Villuendas R, Gomez G, Rodriguez-Pinilla SM, Sanchez-Beato M, Alvarez D, Martinez N, Rodriguez A, Castillo ME, Camacho FI, Montes-Moreno S, Garcia-Marco JA, Kimby E, Pisano DG, Piris MA (2009) TCL1A expression delineates biological and clinical variability in B-cell lymphoma. Mod Pathol 22 (2):206–215. doi:10.1038/modpathol.2008.148
17. Ruiz-Ballesteros E, Mollejo M, Mateo M, Algara P, Martinez P, Piris MA (2007) MicroRNA losses in the frequently deleted region of 7q in SMZL. Leukemia 21(12):2547–2549. doi:10.1038/sj.leu.2404853
18. Isaacson PG, Matutes E, Burke M, Catovsky D (1994) The histopathology of splenic lymphoma with villous lymphocytes. Blood 84(11):3828–3834
19. Mollejo M, Menarguez J, Lloret E, Sanchez A, Campo E, Algara P, Cristobal E, Sanchez E, Piris MA (1995) Splenic marginal zone lymphoma: a distinctive type of low-grade B-cell lymphoma. A clinicopathological study of 13 cases. Am J Surg Pathol 19(10):1146–1157
20. Schmid C, Kirkham N, Diss T, Isaacson PG (1992) Splenic marginal zone cell lymphoma. Am J Surg Pathol 16(5):455–466
21. Chilosi M, Zamo A, Brighenti A, Malpeli G, Montagna L, Piccoli P, Pedron S, Lestani M, Inghirami G, Scarpa A, Doglioni C, Menestrina F (2003) Constitutive expression of DeltaN-p63alpha isoform in human thymus and thymic epithelial tumours. Virchows Arch 443(2):175–183. doi:10.1007/s00428-003-0857-4
22. Ruiz-Ballesteros E, Mollejo M, Rodriguez A, Camacho FI, Algara P, Martinez N, Pollan M, Sanchez-Aguilera A, Menarguez J, Campo E, Martinez P, Mateo M, Piris MA (2005) Splenic marginal zone lymphoma: proposal of new diagnostic and prognostic markers identified after tissue and cDNA microarray analysis. Blood 106(5):1831–1838. doi:10.1182/blood-2004-10-3898
23. Kanellis G, Mollejo M, Montes-Moreno S, Rodriguez-Pinilla SM, Cigudosa JC, Algara P, Montalban C, Matutes E, Wotherspoon A, Piris MA (2010) Splenic diffuse red pulp small B-cell lymphoma: revision of a series of cases reveals characteristic clinico-pathological features. Haematologica 95(7):1122–1129. doi:10.3324/haematol.2009.013714
24. Boveri E, Arcaini L, Merli M, Passamonti F, Rizzi S, Vanelli L, Rumi E, Rattotti S, Lucioni M, Picone C, Castello A, Pascutto C, Magrini U, Lazzarino M, Paulli M (2009) Bone marrow histology in marginal zone B-cell lymphomas: correlation with clinical parameters and flow cytometry in 120 patients. Ann Oncol 20 (1):129–136. doi:10.1093/annonc/mdn563
25. Herling M, Patel KA, Khalili J, Schlette E, Kobayashi R, Medeiros LJ, Jones D (2006) TCL1 shows a regulated expression pattern in chronic lymphocytic leukemia that correlates with molecular subtypes and proliferative state. Leukemia 20(2):280–285. doi:10.1038/sj.leu.2404017
26. Novara F, Arcaini L, Merli M, Passamonti F, Zibellini S, Rizzi S, Rattotti S, Rumi E, Pascutto C, Vetro A, Astori C, Boveri E, Lucioni M, Paulli M, Zuffardi O, Lazzarino M (2009) High-resolution genome-wide array comparative genomic hybridization in splenic marginal zone B-cell lymphoma. Hum Pathol 40 (11):1628–1637. doi:10.1016/j.humpath.2009.01.025
27. Arcaini L, Lazzarino M, Colombo N, Burcheri S, Boveri E, Paulli M, Morra E, Gambacorta M, Cortelazzo S, Tucci A, Ungari M, Ambrosetti A, Menestrina F, Orsucci L, Novero D, Pulsoni A, Frezzato M, Gaidano G, Vallisa D, Minardi V, Tripodo C, Callea V, Baldini L, Merli F, Federico M, Franco V, Iannitto E (2006) Splenic marginal zone lymphoma: a prognostic model for clinical use. Blood 107(12):4643–4649. doi:10.1182/blood-2005-11-4659

Virchows Arch (2012) 461:687–697
DOI 10.1007/s00428-012-1335-7

ORIGINAL ARTICLE

Histopathological, immunohistochemical and molecular spectrum of myoepithelial tumours of soft tissues

Bharat Rekhi · Mukund Sable · Nirmala A. Jambhekar

Received: 7 July 2012 / Revised: 6 September 2012 / Accepted: 18 October 2012 / Published online: 25 October 2012
© Springer-Verlag Berlin Heidelberg 2012

Abstract Primary soft tissue myoepithelial tumours (METs) are rare. Recent studies have shown *EWSR1* rearrangement in certain METs. We present clinicopathological, immunohistochemical and molecular features of 14 primary soft tissue METs. Fourteen tumours, five benign and nine malignant, occurred in 12 men and two women, with an age range of 18–60 years (mean, 39.2); in upper extremities, four (29 %); chest wall, three (21 %); paraspinal region, three (21 %); pelvis, two (14 %) and lower extremities, two (14 %). Tumour size varied from 2 to 21.6 cm (mean, 8.7). Microscopically, most tumours were at least focally circumscribed. Morphological heterogeneity was noted, commonest patterns being cord-like and diffuse arrangement of polygonal cells in a myxoid stroma. By immunohistochemistry, tumours were positive for epithelial membrane antigen (EMA) (10/12, 83 %), cytokeratin (CK)/MNF116 (3/12, 25 %), p63 (7/10, 70 %), CD10 (4/6, 67 %), calponin (6/6, 100 %), S-100P (11/13, 85 %), glial fibrillary acidic protein (GFAP) (6/12, 50 %), smooth muscle actin (SMA) (3/9, 33 %), INI1/SMARCB1 (6/10, 60 %), brachyury (0/11), CD34 (0/5) and vimentin (4/4, 100 %), implying 93 % positivity for at least one epithelial marker. *EWSR1* gene rearrangement was detected in 3/6 (50 %) METs (one benign and two malignant) and in an eccrine porocarcinoma which was included for reasons of comparison. Outcome details were available for six patients all surgically treated; three tumours (two malignant and one benign) resected with unknown marginal status recurred; two patients died and a single patient with myoepithelial carcinoma, who underwent a wide excision, is disease-free. This study illustrates the wide morphological spectrum of soft tissue METs, including benign and malignant subtypes. EMA and S-100P are optimal markers that should be supplemented with broad spectrum keratins, such as AE1/AE3, along with p63, GFAP and calponin in case of need but the results must be correlated with morphological features. Brachyury is useful in separating parachordoma/myoepithelioma from chordoma. *EWSR1* rearrangement mostly occurs in METs that are deep-seated, irrespective of benign or malignant behaviour. Most malignant METs are INI1 negative.

Keywords Soft tissue myoepithelioma · Soft tissue myoepithelial carcinoma · *EWSR1* rearrangement · FISH · Parachordoma

B. Rekhi (✉) · M. Sable · N. A. Jambhekar
Department of Pathology, Tata Memorial Hospital, Parel, Mumbai, India
e-mail: rekhi.bharat@gmail.com

Introduction

Myoepithelial tumours (METs), including myoepithelioma and myoepithelial carcinoma, are rare in the musculoskeletal system. According to the World Health Organisation (WHO) Classification of soft tissue tumours, myoepithelioma, mixed tumour and parachordoma constitute a common spectrum of tumours, in which mixed tumour is composed of epithelial and myoepithelial elements within a hyalinised or chondromyxoid stroma, myoepithelioma of myoepithelial cells which lack ductal differentiation and parachordoma displays clear cells [1]. Subsequent to the initial study of 19 mixed tumours and myoepitheliomas of soft tissues by Kilpatrick et al. [2], others have documented case reports and series, expanding upon the histomorphological spectrum and immunohistochemical profile of METs [3–8]. The literature on genetic alterations in soft tissue myoepitheliomas is scarce, with initial studies on deregulated expression of *PLAG1* and *HMGA2* in METs, which had been found in the morphologically identical pleomorphic adenomas of salivary gland [9, 10].

However, the genetic profile of soft tissue myoepithelioma appears to be heterogeneous [11].

Recently, *EWSR1* gene rearrangements, leading to formation of a fusion transcript, were identified in some METs [12–14]. Subsequently, other clinicopathological studies on soft tissue METs reported *EWSR1* rearrangements [15, 16]. Recently, an unusual primary intraosseous myoepithelioma arising in the iliac bone and displaying prominent squamous differentiation as well as trisomy of 11, 15 and 17 with del (16q) and del (22q11), but lacking *EWSR1* gene rearrangement, was documented [17]. *EWSR1*-negative myoepithelial carcinoma of soft tissue has also been recently reported [18]. The purpose of the present study is to present the varying histomorphological patterns of soft tissue METs, including the immunohistochemistry (IHC) profile in order to identify optimal IHC markers for its differential diagnosis. The results of *EWSR1* rearrangement in seven soft tissue METs and one skin adnexal tumour are also reported.

Materials and methods

Eighteen tumours either diagnosed as a soft tissue MET (myoepithelioma or myoepithelial carcinoma) or with MET as one of the differential diagnosis, primarily involving soft tissues with or without adjacent tissues, were retrieved over a 7-year period (2002–2011) from our pathology database. METs of head and neck region, including salivary gland tumours and mixed tumours of skin, including chondroid syringomas or adnexal tumours displaying ductal differentiation were excluded, resulting in 14 study cases. The criteria for malignancy included at least moderate nuclear atypia, with or without mitotic counts, exceeding 2–3/10 high power field [5]. All cases were reviewed by BR with MR. FISH results were interpreted by BR.

Clinical information was obtained from the hospital case files and electronic medical records. Radiological details were obtained from the Picture Archiving and Communications System (PACS) at Centricity (GE Healthcare, USA). The series consisted of biopsies (3), resection specimens (5) and six consultation cases, for which paraffin blocks with or without slides (6) were available. The resection specimens included widely excised specimens with grossly and microscopically free tumour resection margins (R0) and marginal excision specimens with grossly free but microscopically involved tumour resection margins (R1). Tumour resections with unavailable marginal status were designated as Rx.

IHC was performed by immunoperoxidase method using a MACH 2 Universal HRP-Polymer detection kit (Biocare, CA, USA), including 3′-3′-diaminobenzidine tetrahydrochloride as the chromogen. Appropriate positive and negative controls were included. The details of the markers identified by the various antibodies are listed in Table 1.

Table 1 List of various antibody markers in the present study

Sr no.	Antibody marker	Clonality, clone	Dilution	Antigen retrieval	Manufacturer
1	Epithelial membrane antigen (EMA)	Monoclonal, E29	1:1,200	Pepsin (enzymatic)	Dako, Produkionsveg, Glostrup, Denmark
2	Cytokeratin (CK)	Monoclonal, MNF116	1:200	Pronase (enzymatic)	Dako
3	S100-P	Polyclonal	1:600	Pepsin (enzymatic)	Dako
4	Glial fibrillary acid protein (GFAP)	Polyclonal	1:800	Pepsin (enzymatic)	Dako
5	p63	Monoclonal, 4A4	1:200	Heat Pascal (Tris–EDTA)	Dako
6	CD10	Monoclonal, 56C6	1:50	Heat Pascal (Tris–EDTA)	Biocare, PA, USA
7	Calponin	Monoclonal, CALP	1:50	Heat microwave (sodium citrate)	Dako
8	Vimentin	Monoclonal, V9	1:400	Heat microwave (Tris–EDTA)	Dako
9	Smooth muscle actin (SMA)	Monoclonal, IA4	1:300	Enzymatic (pepsin)	Dako
10	Brachyury/'T'	Polyclonal	1:300	Heat, pressure cooker (sodium citrate)	Santa Cruz Biotechnology, Inc, Santa Cruz, CA, USA
11	INI1/SMARCB1	Monoclonal ,3E10	1:600	Heat, pressure cooker (sodium citrate)	Acris, GmbH, Herford ,Germany
12	High molecular weight cytokeratin (HMWCK)	Monoclonal ,34βE12	1:200	Heat microwave (sodium citrate)	Dako
13	CD34	Monoclonal, QBEnd 10	1:100	Heat microwave (sodium citrate)	Dako

Table 2 Clinicopathological features of 14 METs, primarily involving soft tissues

Sr no.	Age/ sex	Site	Histopathological features		Immunohistochemical results	Treatment	Outcome
			Cell arrangement	Matrix			
1	41/M	Extradural, D10	Sheets, clusters	Myxoid	CK+, HMWCK+, S-100P+, GFAP+, p63+, CD10+, SMA−	NK	NK
2[a]	18/M	Inguinal	Sheets	Myxohyaline	EMA−, CK−, S-100P+, GFAP−, calponin+, SMA−, BU−, INI1+	NK	NK
3[b]	44/M	Paraspinal, D12-L2	Cords, trabeculae, reticular, clusters	Myxoid	EMA+, CK−, S-100P+, GFAP+, p63+, SMA+, BU−	Surgical resection (R1)	Recurrence, AWD (13 months)
4[b,c]	37/F	Forearm	Alveolar, nesting, pseudo-acinar/ rosetting	Collagenous	CK+, EMA−, S-100P+, GFAP+, p63+, calponin+, SMA+, vimentin+, BU−, INI1−	Surgical resection (Rx)	FOD (33 months)
5[b,c]	60/M	Chest wall	Cords, trabeculae, pseudo-acinar/rosetting	Hyaline	EMA+, CK−, S-100P+, GFAP+, p63+, calponin+, BU−, INI1+, Ki-67–10 %,	Surgical resection (Rx, R0)	Recurrence, AWD (4 months)
6[c]	58/M	Pelvis	Sheets, nesting	Myxochondroid	EMA+, CK−, S-100P+, GFAP−, p63−, CD10−, SMA-vimentin+, BU−, INI1+	Surgical resection (Rx, R0)	Recurrence, metastasis (lymph nodes, lungs) AWD (27 months)
7[c]	21/M	Arm	Sheets, nesting	Myxoid	EMA+, S-100P+, GFAP+, CD10+, SMA−, BU−, INI1−	Surgical resection (Rx)	NK
8[c]	35/F	Forearm	Sheets, trabeculae, cords	Collagenous	EMA+, CK−, S-100P−, GFAP−, BU−, INI1−	Surgical resection (R0)	FOD (85 months)
9[a,c]	27/M	Paraspinal, D6–D9	Cords, clusters	Hyaline, osteochondroid	EMA+, CK−, S-100P−, GFAP−, p63+, CD10+, calponin+, SMA-vimentin+, BU−, INI1+	Surgical resection (R1)	Presented with metastasis (lung) DOD (1 months)
10[c]	30/M	Pelvis	Cords, trabeculae	Myxohyaline	EMA+, CK−, S-100P+, GFAP−, BU−, INI1+	NK	NK
11[a,c]	60/M	Chest wall	Palisades	Myxohyaline	CK+, p63+, GFAP−, CD10+, SMA+, BU−, INI1+	Surgical resection (Rx)	Presented with metastasis (lung), outcome, NK
12	45/M	Thigh	Cords, reticular	Myxoid	EMA+, S-100P+, GFAP+p63+, calponin+, vimentin+, BU−, INI1−	Surgical resection (R0)	On FU
13[a]	38/m	Chest wall	Diffuse, cords, clusters	Hyaline, calcification	EMA+, CK−, S-100P+, p63−, CD10−, calponin+	Surgical resection (R0)	On FU
14	36/M	Palm	Clusters	Myxoid	EMA+, CK−, S-100P+, p63−, SMA−	Surgical resection (Rx)	NK

M male, *F* female, *CK* cytokeratin, + positive, − negative, *HMWCK* high molecular weight cytokeratin, *EMA* epithelial membrane antigen, *GFAP* glial fibrillary acidic protein, *SMA* smooth muscle actin, *BU* brachyury (T), *NK* not known, *Rx* surgical resection with unknown marginal status, *R0* surgical resection with clear margins, *R1* surgical resection, grossly free and microscopically with positive margin, *FOD* free of disease, *AWD* alive with disease, *FU* follow-up

[a] Cases where EWSR1 rearrangement was not detected

[b] Cases where *EWSR1* rearrangement was detected

[c] Malignant/myoepithelial carcinoma

Fluorescence in situ hybridisation (FISH) study with a LSI EWSR1 dual colour break apart probe (ZytoLight SPEC EWSR1 dual colour break apart probe) was performed on 4-μm paraffin sections. The sections were counterstained with 4′-6-diamidino-2-phenylindole (DAPI) and examined with a fluorescence microscope (Axio Imager Z1, Carl Zeiss, Germany), using AxioCam MRc 5 camera and AxioVision Rel 4.5 software. A tumour sample was considered positive if more than 15 % of the analysed 100 cells showed rearrangement signal break apart [19].

Results

Fourteen tumours occurred in 12 men and two women (M:F, 6:1), with an age range of 18–60 years (mean, 39.2, median, 37.5). Tumours most commonly occurred in the upper extremities (4, 29 %), including forearm (2), arm (1) and palm (1), followed by chest wall (3, 21 %), paraspinal/extradural region (3, 21 %), pelvis (2, 14 %) and lower extremities (2, 14 %), including groin (1) and thigh (1). Nine tumours involved deep soft tissues, with or without adjacent bones, whilst five tumours involved the skin. One skin adnexal tumour that showed the *EWSR1* rearrangement and had originated on the forearm was included for reasons of comparison.

On magnetic resonance imaging (MRI), the tumours were of variable size and mostly lobulated, heterogeneous and hyperintense on T2-weighed and STIR images. A single case showed peripheral inhomogeneous enhancement. One case presented with lung metastasis, detected on computed tomography. Tumour size, known in nine cases, varied from 2 to 21.6 cm (mean, 8.7, median, 7).

All 11 patients with known treatment details underwent surgical resection, R0 in three, R2 in two and Rx in six cases. Two of six patients who initially underwent Rx resections subsequently underwent R0 resection, in view of residual disease. Of seven cases with available follow-up, three developed tumour recurrence and two cases, lung metastasis. Three patients were alive with disease over 4 to 27 months, two patients were free of disease over 33 and 85 months and a single patient, who presented with metastasis, died of disease within a month, despite a R0 resection.

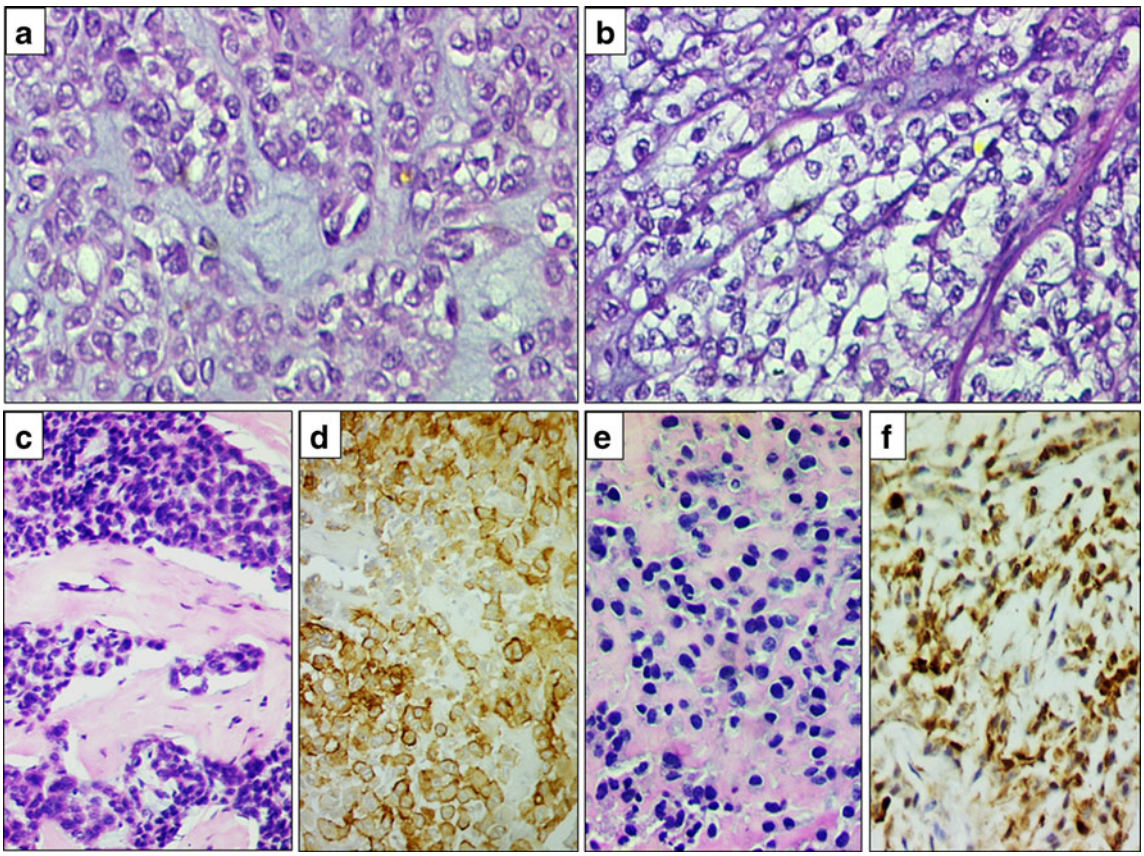

Fig. 1 **a** Case 1. Histopathological features of a classical myoepithelioma/parachordoma. Polygonal cells arranged in a nesting pattern and embedded in a myxoid stroma. **b** Areas comprising clear cells. **c** Case 8. Tumor cells arranged in nesting, cord-like and pseudo-acinar/rosetting pattern in a collagenous matrix. **d** The same tumor displaying EMA positivity. **e** Case 10. Plasmacytoid tumor cells in a hyaline/sclerotic matrix. **f** The same tumor displaying S-100P positivity. **a** H&E ×400. **b** H&E ×400. **c** H&E ×200. **d** DAB ×400. **e** H&E ×400. **f** DAB ×400

Pathological findings

Grossly, the MET were often well-defined with grey-white, glistening/myxoid, cystic to fleshy cut surfaces. Microscopically, most tumours were at least focally circumscribed in ten cases and infiltrating in four cases. Tumours were mostly multinodular. Various tumour cell arrangements were noted, including cord-like (7), sheet-like/diffuse (6), clusters (5), nests/lobules (3), trabeculae (3), pseudo-acinar/rosetting, without ductal formation (2), alveolar (1), rhythmic palisades (1) and predominantly reticular (1). The stroma was variable and mostly myxoid (5), followed by hyaline/sclerotic (3), myxohyaline (3), collagenous (2), myxochondroid (1) and osteochondroid (1). Calcification was observed in two tumours, including a single case that displayed mineralised bone formation. Varying proportions of diverse cell types were noted, mostly polygonal/epithelioid (12), followed by clear (5), spindle (5), plasmacytoid (1), rhabdoid (2) and small round (1) cell types.

Nine of the 14 (64 %) tumours fulfilled criteria of malignancy, justifying a diagnosis of myoepithelial carcinoma. Mitotic figures were absent in all five myoepitheliomas and varied from ten to 50/10 hpf in nine myoepithelial carcinomas, all accompanied with at least moderate (seven cases) to marked (two cases) nuclear atypia. Perineural invasion was identified in a single case. The skin adnexal tumour was a circumscribed dermal tumour, composed of infiltrating nests of basaloid tumour cells which exhibited focal squamous and clear cell differentiation with prominent duct formation and intervening sclerosis and focal cystic change. There were readily identifiable mitoses, moderate nuclear atypia and focal tumour necrosis, justifying a diagnosis of eccrine porocarcinoma.

Immunohistochemical findings

By immunohistochemistry, tumour cells were variably positive for epithelial membrane antigen (EMA) (10/

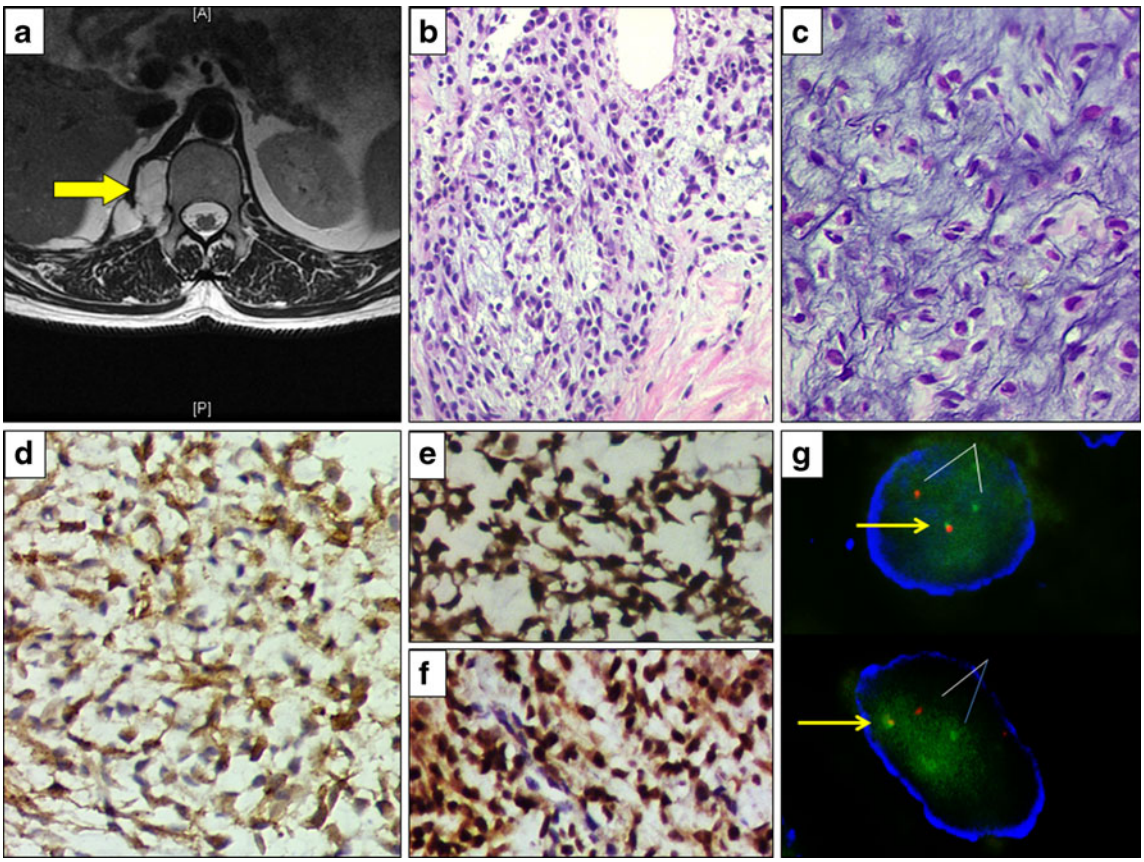

Fig. 2 Case 2. **a** Magnetic resonance imaging (MRI) findings. Axial T2-weighed image showing a lobulated, hyperintense mass in right paravertebral region involving the psoas muscle, expanding the neural foramen of D12 to L2 vertebrae. **b** Histopathological features. Polygonal to spindly cells in clusters and cords, embedded in a myxoid stroma. **c** Tumor cells on higher magnification. **d** EMA positivity. **e** Diffuse S-100P positivity. **f** Diffuse p63 positivity. **g** *EWSR1* rearrangement detected in the form of split signal (*double arrows*) in tumor cells, in contrast to single-fused signals (*pointed arrow*). **b** H&E ×200. **c** H&E ×400. **d** DAB ×400. **e** DAB ×400. **f** DAB ×400. **g** DAPI ×1,000

12, 83 %), cytokeratin (CK)/MNF116 (3/12, 25 %), p63 (7/10, 70 %), CD10 (4/6, 67 %), calponin (6/6, 100 %), S-100P mostly diffusely (11/13, 85 %), glial fibrillary acidic protein (GFAP) (6/12, 50 %), smooth muscle actin (SMA) (3/9, 33 %), INI1/SMARCB1 (6/10)(60 %), brachyury (0/11), CD34 (0/5), vimentin (4/4, 100 %) and high molecular weight cytokeratin (HMWCK), the latter positive in an isolated case. Thirteen of 14 (93 %) tumours were positive for at least one epithelial marker. The eccrine porocarcinoma was diffusely AE1/AE3-, CK5/6- and p63-positive and focally positive for EMA and CEA, especially in the ducts. S-100P was positive in rare cells. GFAP was negative. We tested six cases displaying polygonal cells for expression of INI1/SMACRB1 and observed negative expression in 40 % of these tumours.

Interphase cytogenetic findings by FISH

Amongst ten cases with sections available, six cases could be evaluated, and *EWSR1* gene rearrangement was detected in three METs (cases 3, 4 and 5) and in the eccrine porocarcinoma but not in three other METs (Table 2, Figs. 1, 2, 3, 4, 5 and 6).

Discussion

This study describes certain established [1, 2] clinicopathological features of soft tissue METs, including male preponderance, wide age range (mean 39.2, median 37.5) and upper extremities as the commonest afflicted site. We found more cases of a myoepithelial carcinoma (9) than myoepithelioma (5) presumably due to our centre being a tertiary cancer referral centre.

The innate differentiational plasticity of myoepithelial cells results in a wide histopathological spectrum, including various architectural patterns, cell types and stromal reactions, as also noted in this study. The commonest histopathological pattern was that of a circumscribed lesion composed of epithelioid cells arranged in cords and sheets in a myxoid stroma. Less common features were presence of mineralised osteoid, cellular palisades, rosetting arrangement, alveolar arrangement and plasmacytoid- and rhabdoid-like cells [2–6]. Previous authors [2–5] included tumours with ductal differentiation (mixed tumours), but our study excluded mixed tumours. The wide histopathological spectrum led to a long list of differential diagnoses in

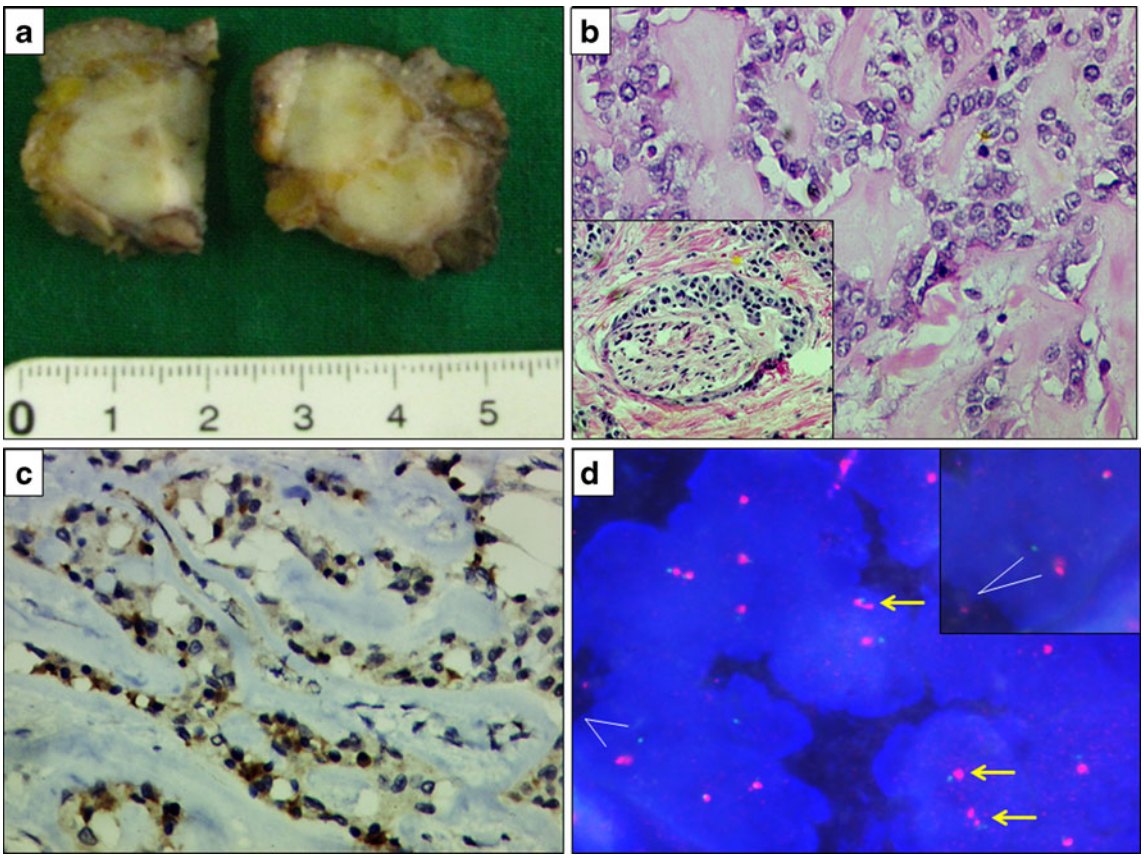

Fig. 3 Case 5. **a** Grossly, a multinodular tumor with a grey-white cut surface and translucent hue. **b** Microscopy (same case). Tumor cells arranged in cords within a hyaline stroma. *Inset*: perineurial invasion. **c** GFAP positivity. D. *EWSR1* rearrangement detected. **b** H&E ×400, inset H&E ×400. **c** DAB ×400

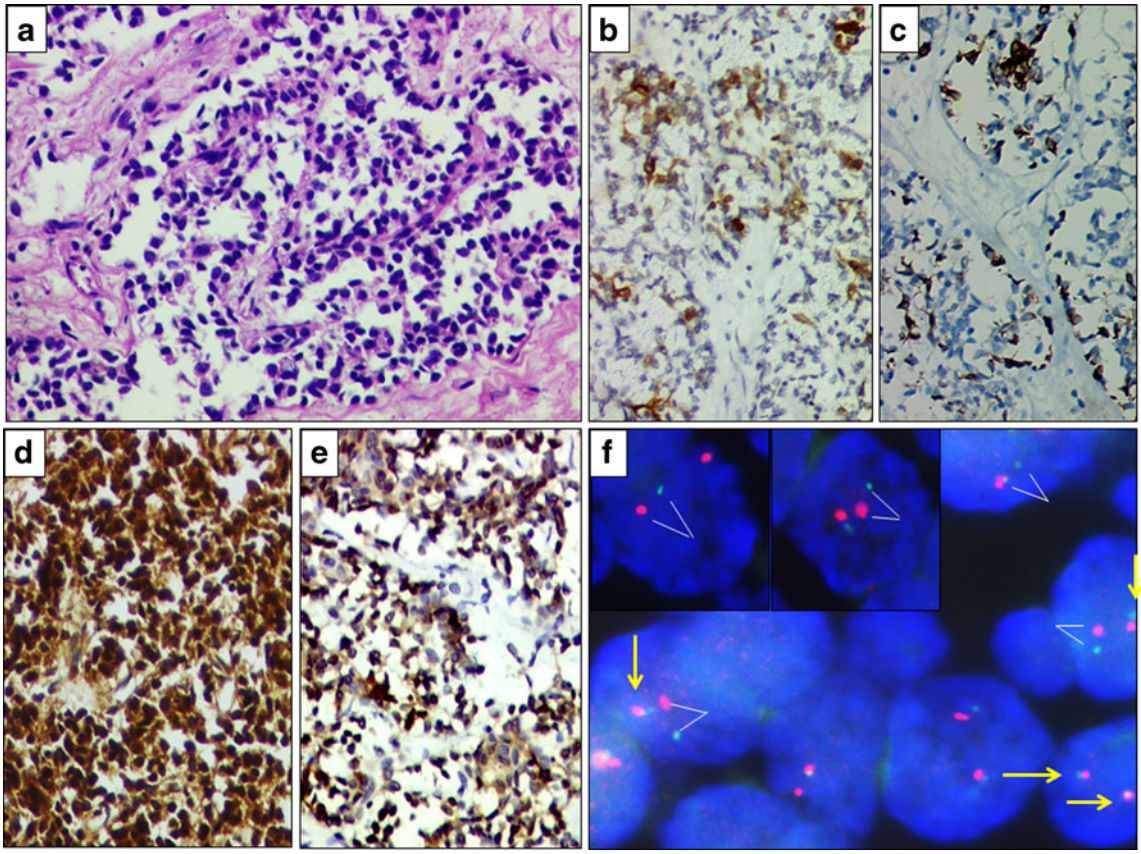

Fig. 4 Histopathological features of a myoepithelial carcinoma (Case 4). **a** Small round cells arranged in an alveolar pattern, within a collagenous stroma. **b** Focal CK positivity. **c** Focal GFAP positivity. **d** Diffuse S-100P positivity. **e** SMA positivity. **f** *EWSR1* rearrangement detected, including the *insets*, in the form of split signal (*double arrows*) in tumor cells, in contrast to single-fused signals (*pointed arrow*). **a** H&E ×200. **b** DAB ×400. **c** DAB ×400. **d** DAB ×400. **e** DAB ×400. **f** DAPI ×1,000

individual cases, including epithelioid sarcoma (ES), extraskeletal myxoid chondrosarcoma (EMC), epithelioid malignant peripheral nerve sheath tumour (MPNSTs), ossifying fibromyxoid tumour (OFMT), round cell/myxoid liposarcoma and metastatic carcinoma and chordoma, the latter when the axial skeleton is affected and clear cells are found. Of the three cases that we excluded as ESs, two showed focal myxoid areas resulting in a diagnosis of a myoepithelial carcinoma. ES with myxoid change has been reported [20]. The presence of clear cells in five tumours led to a differential diagnosis of chordoma, notably in two tumours occurring in the paraspinal region.

Various differential diagnoses in different cases were further objectively ruled out with IHC results. A combination of epithelial markers, including EMA and cytokeratins, along with S-100P or GFAP was found to constitute the optimal IHC panel for supporting a diagnosis of a MET [14]. The percentages of cases expressing EMA, CK (MNF116), S-100P and GFAP in the present study tumours were 83 %, 25 %, 85 % and 50 %, respectively. Whilst at least one of the epithelial markers was positive in 93 % of the tumours, 79 % expressed diffuse S-100P, with or without GFAP generally in agreement with earlier studies [3, 5] EMA appeared as a more robust epithelial marker than CK (MNF116). Diffuse S100-P and EMA generally ruled out an EMC, as reported earlier [5, 14] although others observed S-100P and EMA expression in 40 % EMCs [21]. In three of our cases, either expression of epithelial markers or of S-100P and GFAP was absent. These tumours were, nonetheless, diagnosed as METs based on histopathological features and expression of other supportive myoepithelial markers, notably p63, calponin and CD10. The two latter markers have been found useful in salivary gland METs in different studies [22, 23]. As calponin, vimentin is a highly sensitive marker but less specific, but absence of expression of these markers makes a diagnosis of myoepithelial neoplasm less likely [22]. SMA was positive in 33 % of the tumours, similar to a previous study [5]. In view of the presence of clear cells in five tumours, with chordoma as a differential, brachyury/T, a specific marker for axial and extra axial chordomas, was tested [24, 25]. It was negative in all 11 tested tumours, supporting the notion that parachordomas/METs/mixed tumours are different from axial or extra-axial chordomas [24, 26, 27]. CD34 negativity in all five tumours

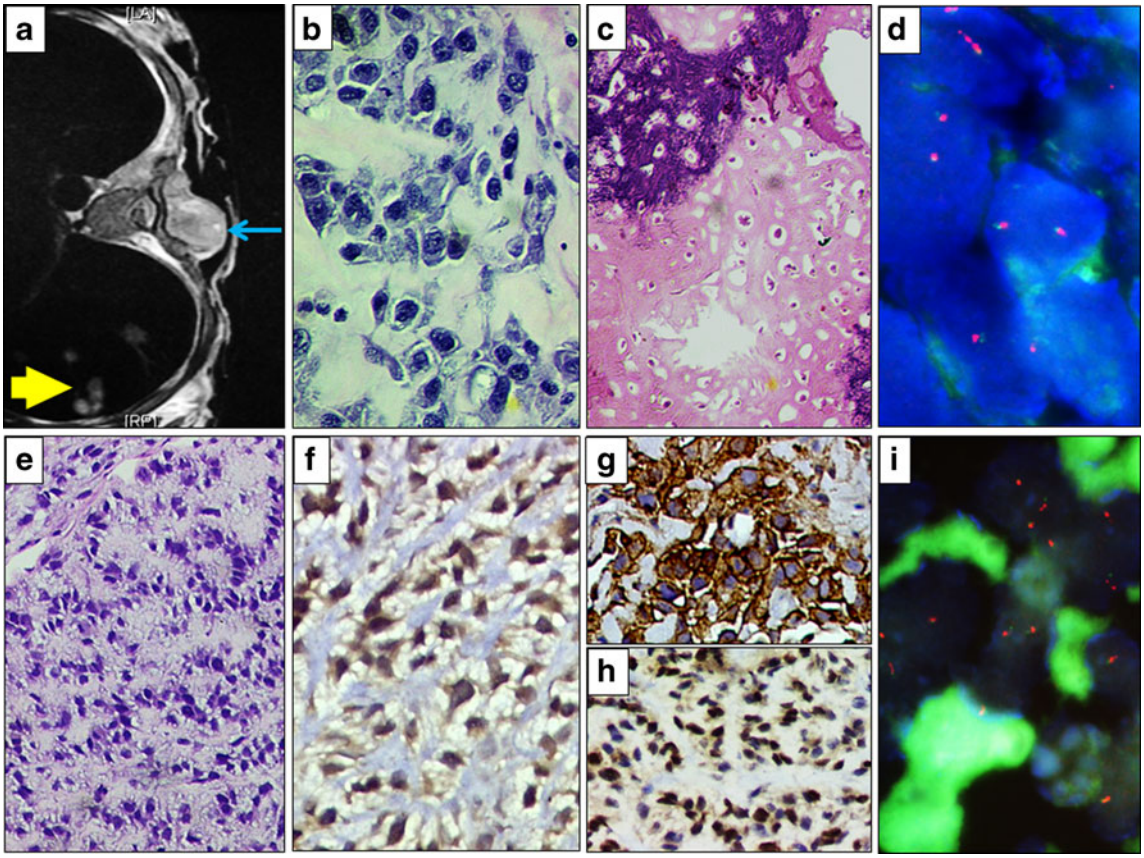

Fig. 5 **a** Case 9. MRI AXT2 image showing a large, hyperintense, lobulated mass lesion in the back extending from D6 to D9, extending into the left paraspinal region and intraspinally, causing compression of the spinal cord (*arrow*). Additionally, multiple lung nodules noted, suggestive of metastases (*arrow head*). **b** Infiltrating tumor cells, exhibiting moderate to marked nuclear atypia in a hyaline/sclerotic stroma. **c** Osteochondroid matrix with calcification. **d** *EWSR1* rearrangement not detected (all fused signals). **e** Case 11. Tumor cells arranged in rhythmic palisades within myxohyaline stroma. **f** CK positivity. **g** CD10 positivity. **h** p63 positivity. **i** *EWSR1* rearrangement not detected. **b** H&E ×400. **c** H&E ×200. **d** DAPI ×1,000. **e** H&E ×400. **f** DAB ×400. **g** DAB ×400. **h** DAB ×400. **i** DAPI ×1,000

for which a diagnosis of ES was considered indicates its value in differentiation METs from ES that frequently is CD34 positive [28].

Absence of expression of INI1 has been proposed as highly sensitive and specific for diagnosis of ESs and extra-renal rhabdoid tumours [29]. Morphologically, ES rarely shows variable cell morphology with matrix formation as is often found in METs. Even though epithelial markers may be expressed, ESs and extra-renal rhabdoid tumours rarely display S-100P or GFAP positivity which helps in the differential with MET. Conversely, CD34 expression is found in some ESs, but not in METs [28].

Genetic alterations in soft tissue METs were not well understood and are still rarely documented. The morphologically similar pleomorphic adenoma of salivary glands display frequent rearrangements of *PLAG1* and *HMGA2*, but this was not found in soft tissue mixed tumours, including METs [11]. Recently, Baharami et al. [30] documented *PLAG1* rearrangement mostly in mixed tumours of skin and soft tissues that displayed ductal differentiation and they concluded that only those mixed tumours of skin and soft tissues that displayed ductal differentiation are genetically linked to mixed salivary gland tumours. Matsuyama et al. [31] did not find immunohistochemical expression of PLAG1 or fusion transcripts involving PLAG1 in any MET and concluded that METs of skin and soft tissues are genetically different from mixed salivary gland tumours. Recently, *EWSR1* gene rearrangements have been found in METs [12–16]. In addition to Ewing sarcoma/PNET, *EWSR1* gene rearrangements have been observed in desmoplastic small round cell tumour, clear cell sarcoma, angiomatoid fibrous histiocytoma, myxoid liposarcoma and EMC, a close differential diagnosis of a MET [32–34]. In the present study, *EWSR1* rearrangement was detected in three of six (50 %) METs, including a single myoepithelioma and two myoepithelial carcinomas, but not in a single ES. Antonescu et al. [14] observed *EWSR1* gene rearrangement in 45 % METs, including mixed tumours, and concluded that *EWSR1* rearrangement is a more common genetic alteration in METs outside the salivary gland and

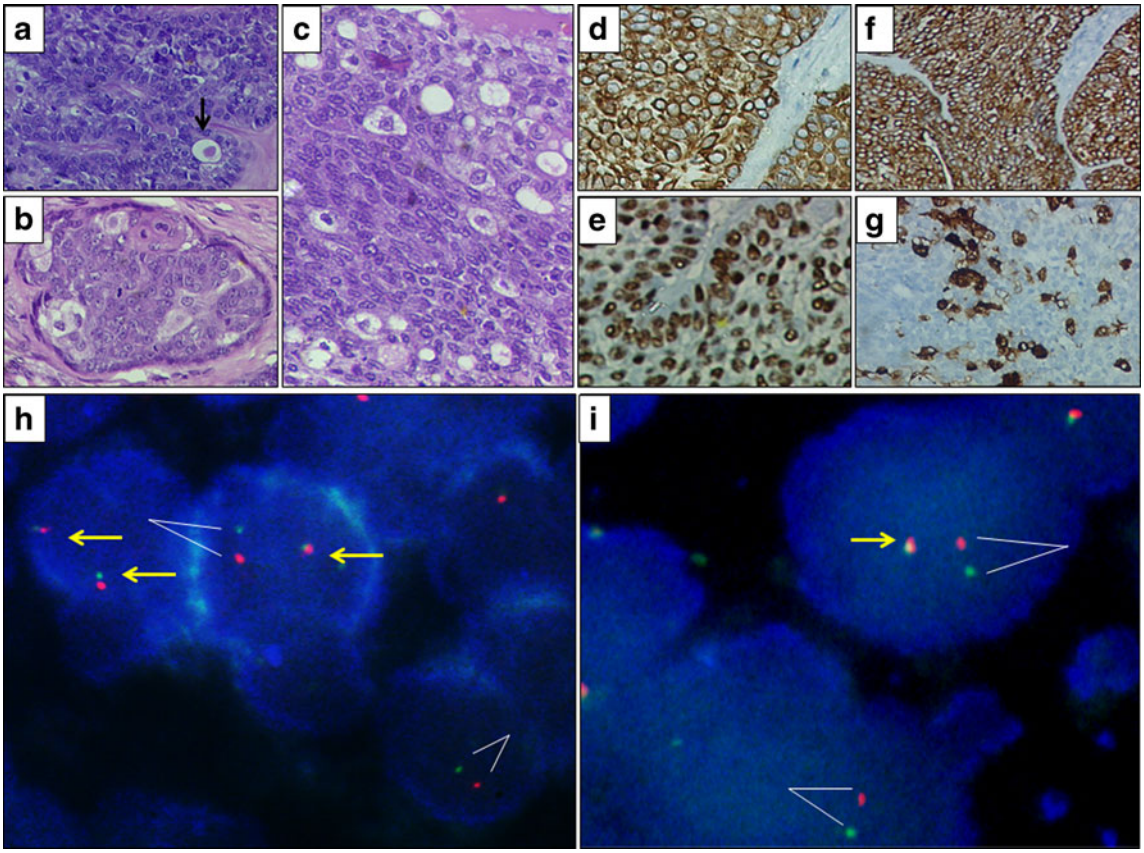

Fig. 6 **a**–**c** Eccrine porocarcinoma. Histopathological features include squamous differentiation, focal clearing with duct formation (*arrow*). **d**. AE1/AE3 positivity. **e** P63 positivity. **f** CK5/6 positivity. **g** EMA positivity highlighting ducts. **h**–**i**. *EWSR1* rearrangement detected. **a**–**c** H&E ×400. **d** DAB ×200. **e** DAB ×400. **f** DAB ×200. **h**–**i** DAPI ×1,000

that *EWSR1*-negative tumours were more often benign, superficially located and show ductal differentiation. Flucke et al. [15, 16] noted *EWSR1* rearrangement in 44 % cutaneous METs, (including those with ductal differentiation) and in 25 % myoepitheliomas. We did not detect *EWSR1* rearrangement in two myoepithelial carcinomas. Other studies documented *EWSR1*-negative myoepithelial carcinoma, associated with poor outcome [18]. Our *EWSR1*-positive METs did not behave differently from *EWSR1*-negative METs. We found an ES of myxoid type to be *EWSR1*-negative, whereas the eccrine porocarcinoma displayed *EWSR1* rearrangement as earlier reported [35].

We observed absence of INI1 expression in 1/3 *EWSR1*-positive tumours, unlike three *EWSR1*-negative tumours that did express INI1. It would be worth testing the possibility that lack of INI1 expression correlates with *EWSR1* rearrangement in soft tissue METs. INI1 negativity has been observed in myoepithelial carcinomas [36] and in extraskeletal myxoid sarcomas of a series of 96 EWSR1 rearranged sarcomas [37].

EWSR1-positive METs show various histological patterns as observed by Antonescu et al. [14] including small blue cells in solid sheets, tumours with epithelioid or rhabdoid appearance and tumours composed of spindle cells in a sclerotic stroma. Our *EWSR1*-positive tumours included two benign and two malignant tumours that displayed polygonal cells in a myxohyaline matrix, spindly and polygonal cells in a myxoid matrix, small round cells in an alveolar arrangement in a collagenous stroma and polygonal cells in a sclerotic matrix. Whilst Antonescu et al. [14] observed *EWSR1* rearrangement more in intraosseous METs, a recently documented pelvic myoepithelioma, with prominent osteochondroid matrix, was found to be *EWSR1*-negative [17]. Furthermore, Antonescu et al. [14] identified *EWSR1–PBX* and *EWSR1–POUF1* fusion transcripts in certain METs and Flucke et al. [16] documented *EWSR1–ATF* chimeric transcript in a case of a pelvic myoepithelioma.

In conclusion, we found that MET in soft tissue shows a wide histopathological spectrum with EMA and S-100P constituting a basic diagnostic IHC panel. Inclusion of broad spectrum cytokeratins, such as AE1/AE3 along with p63, GFAP, calponin, CK5/6 and SMA, can be helpful especially in cases where morphology is equivocal for MET and the basic IHC panel is non-contributory. Brachyury/T can help in differentiating myoepithelioma/parachordoma from a chordoma. Forty percent of METs, mostly malignant types,

are INI1/SMARCB1-negative. *EWSR1* rearrangement is a significant genetic alteration in soft tissue METs, irrespective of benign or malignant behaviour. Musculoskeletal METs do not have genetic aberrations in common with mixed salivary gland tumours.

Acknowledgments The support of Immunohistochemistry laboratory of our Department is acknowledged. We thank Smita Mumbarkar, Jyoti Bodke and Ragni Mohite from molecular pathology laboratory, ACTREC, Khargar, Navi Mumbai for performing cytogentic test (FISH).

Conflict of interest None.

References

1. Kilpatrick SE, Limon J (2002) Mixed tumor/myoepithelioma/parachordoma. In: Fletcher CDM, Unni K, Mertens F (eds) World Health Organization classification of tumors. IARC, Lyon, pp 198–199
2. Kilpatrick SE, Hitchcock MG, Kraus MD, Calonje E, Fletcher CD (1997) Mixed tumors and myoepitheliomas of soft tissue: a clinicopathologic study of 19 cases with a unifying concept. Am J Surg Pathol 21:13–22
3. Michal M, Miettinen M (1999) Myoepitheliomas of the skin and soft tissues. Virchows Arch 434:393–400, Report of 12 cases
4. Bisceglia M, Cardone M, Fantasia L, Cenacchi G, Pasquinelli G (2001) Mixed tumors, myoepitheliomas, and oncocytomas of the soft tissues are likely members of the same family: a clinicopathologic and ultrastructural study. Ultrastruct Pathol 25:399–418
5. Hornick JL, Fletcher CD (2003) Myoepithelial tumors of soft tissue: a clinicopathologic and immunohistochemical study of 101 cases with evaluation of prognostic parameters. Am J Surg Pathol 27:1183–1196
6. Hornick JL, Fletcher CD (2004) Cutaneous myoepithelioma: a clinicopathologic and immunohistochemical study of 14 cases. Hum Pathol 35:14–24
7. Stojsić Z, Brasanac D, Bacetić D, Janković R, Drndarević N (2006) Soft tissue myoepithelial carcinoma. Vojnosanit Pregl 63:611–614
8. Lee JR, Georgi DE, Wang BY (2007) Malignant myoepithelial tumor of soft tissue: a report of two cases of the lower extremity and a review of the literature. Ann Diagn Pathol 11:190–198
9. Kas K, Voz ML, Roijer E, Astrom AK, Meyen E, Stenman G, Van de Ven WJ (1997) Promoter swapping between the genes for a novel zinc finger protein and beta-catenin in pleomorphic adenomas with t(3;8)(p21;q12) translocations. Nat Genet 15:170–174
10. Martins C, Fonseca I, Roque L, Pereira T, Ribeiro C, Bullerdiek J, Soares J (2005) *PLAG1* gene alterations in salivary gland pleomorphic adenoma and carcinoma ex-pleomorphic adenoma: a combined study using chromosome banding, in situ hybridization and immunocytochemistry. Mod Pathol 18:1048–1055
11. Hallor KH, Teixeira MR, Fletcher CD, Bizarro S, Staaf J, Domanski HA, von Steyern FV, Panagopoulos I, Mandahl N, Mertens F (2008) Heterogeneous genetic profiles in soft tissue myoepitheliomas. Mod Pathol 21:1311–1319
12. Brandal P, Panagopoulos I, Bjerkehagen B, Gorunova L, Skjeldal S, Micci F, Heim S (2008) Detection of a t(1;22)(q23;q12) translocation leading to an *EWSR1–PBX1* fusion gene in a myoepithelioma. Genes Chromosomes Cancer 47:558–5564
13. Brandal P, Panagopoulos I, Bjerkehagen B, Heim S (2009) t (19;22)(q13;q12) Translocation leading to the novel fusion gene *EWSR1–ZNF444* in soft tissue myoepithelial carcinoma. Genes Chromosomes Cancer 48:1051–1056
14. Antonescu CR, Zhang L, Chang NE, Pawel BR, Travis W, Katabi N, Edelman M, Rosenberg AE, Nielsen GP, Dal Cin P, Fletcher CD (2010) EWSR1–POU5F1 fusion in soft tissue myoepithelial tumors. A molecular analysis of sixty-six cases, including soft tissue, bone, and visceral lesions, showing common involvement of the *EWSR1* gene. Genes Chromosomes Cancer 49:1114–1124
15. Flucke U, Palmedo G, Blankenhorn N, Slootweg PJ, Kutzner H, Mentzel T (2011) *EWSR1* gene rearrangement occurs in a subset of cutaneous myoepithelial tumors: a study of 18 cases. Mod Pathol 24:1444–1450
16. Flucke U, Mentzel T, Verdijk MA, Slootweg PJ, Creytens DH, Suurmeijer AJ, Tops BB (2012) EWSR1-ATF1 chimeric transcript in a myoepithelial tumor of soft tissue: a case report. Hum Pathol 43:764–768
17. Rekhi B, Amare P, Gulia A, Baisane C, Patil A, Agarwal S, Puri A, Jambhekar NA (2011) Primary intraosseous myoepithelioma arising in the iliac bone and displaying trisomies of 11, 15, 17 with del (16q) and del (22q11)—a rare case report with review of literature. Path Res Pract 207:780–785
18. Aparicio MA, López-Barea F, Cruz JJ, Macías MDCG, Hernández T, de Alava E (2012) Soft tissue myoepithelial carcinoma without *EWSR1* gene rearrangement and poor outcome. A case report. Rev Esp Patol 45:58–63
19. Bridge RS, Rajaram V, Dehner LP, Pfeifer JD, Perry A (2006) Molecular diagnosis of Ewing sarcoma/primitive neuroectodermal tumor in routinely processed tissue: a comparison of two FISH strategies and RT-PCR in malignant round cell tumors. Mod Pathol 19:1–8
20. Flucke U, Hulsebos TJ, van Krieken JH, Mentzel T (2010) Myxoid epithelioid sarcoma: a diagnostic challenge. A report on six cases Histopathology 57:753–759
21. Flucke U, Tops BB, Verdijk MA, van Cleef PJ, van Zwam PH, Slootweg PJ, Bovée JV, Riedl RG, Creytens DH, Suurmeijer AJ, Mentzel T (2012) NR4A3 rearrangement reliably distinguishes between the clinicopathologically overlapping entities myoepithelial carcinoma of soft tissue and cellular extraskeletal myxoid chondrosarcoma. Virchows Arch 460:621–628
22. McHugh JB, Visscher DW, Barnes EL (2009) Update on selected salivary gland neoplasms. Arch Pathol Lab Med 133:1763–1774
23. Kane SV, Bagwan IN (2010) Myoepithelial carcinoma of the salivary glands: a clinicopathologic study of 51 cases in a tertiary cancer center. Arch Otolaryngol Head Neck Surg 136:702–712
24. Tirabosco R, Mangham DC, Rosenberg AE, Vujovic S, Bousdras K, Pizzolitto S et al (2008) Brachyury expression in extra-axial skeletal and soft tissue chordomas: a marker that distinguishes chordoma from mixed tumor/myoepithelioma/parachordoma in soft tissue. Am J Surg Pathol 32:572–580
25. Jambhekar NA, Rekhi B, Dikshit R, Agarwal M, Puri A (2010) Revisiting chordoma with brachyury, a "new age" marker—analysis of a validation study on 51 cases. Arch Pathol Lab Med 134:1181–1187
26. Fisher C, Miettinen M (1997) Parachordoma: a clinicopathologic and immunohistochemical study of four cases of an unusual soft tissue neoplasm. Ann Diagn Pathol 1:3–10
27. Folpe A, Agoff SN, Willis J, Weiss SW (1999) Parachordoma is immunohistochemically and cytogenetically distinct from axial chordoma and extraskeletal myxoid chondrosarcoma. Am J Surg Pathol 23:1059–1067
28. Rekhi B, Gorad BD, Chinoy RF (2008) Clinicopathological features with outcomes of a series of conventional and proximal-type epithelioid sarcomas, diagnosed over a period of 10 years at a tertiary cancer hospital in India. Virchows Arch 453:141–153
29. Hornick JL, Dal Cin P, Fletcher CD (2009) Loss of INI1 expression is characteristic of both conventional and proximal-type epithelioid sarcoma. Am J Surg Pathol 33:542–550

30. Bahrami A, Dalton JD, Krane JF, Flether CDM (2012) A subset of cutaneous and soft tissue mixed tumors is genetically linked to their salivary gland counterpart. Genes Chromosomes Cancer 51:140–148
31. Matsuyama A, Hisaoka M, Hashimoto H (2012) PLAG1 expression in mesenchymal tumors: an immunohistochemical study with special emphasis on the pathogenetical distinction between soft tissue myoepithelioma and pleomorphic adenoma of the salivary gland. Pathol Intl 62:1–7
32. Kumar R, Rekhi B, Shirazi N, Gawde D, Pais A, Aamre P, Jambhekar NA (2008) Spectrum of cytomorphological features, including literature review, of an extraskeletal myxoid chondrosarcoma with t (9; 22) (q22; q11.2) translocation in one case. Diagn Cytopathol 36:868–875
33. Noguchi H, Mitsuhashi T, Seki K, Tochigi N, Tsuji M, Shimoda T, Hasegawa T (2010) Fluorescence in situ hybridization analysis of extraskeletal myxoid chondrosarcomas using EWSR1 and NR4A3 probes. Hum Pathol 41:336–342
34. Romeo S, Dei Tos AP (2010) Soft tissue tumors associated with EWSR1 translocation. Virchows Arch 456:219–234
35. Jin Y, Jin C, Mertens F, Persson B, Jonsson N (1998) Characterization of a malignant eccrine poroma by cytogenetic and fluorescence in situ hybridization techniques. Cancer Genet Cytogenet 102:100–103
36. Hollmann TJ, Hornick JL (2011) INI1-deficient tumors: diagnostic features and molecular genetics. Am J Surg Pathol 35:e47–e63
37. Kohashi K, Oda Y, Yamamoto H, Tamiya S, Oshiro Y, Izumi T, Taguchi T, Tsuneyoshi M (2008) SMARCB1/INI1 protein expression in round cell soft tissue sarcomas associated with chromosomal translocations involving EWS: a special reference to SMARCB1/INI1 negative variant extraskeletal myxoid chondrosarcoma. Am J Surg Pathol 32:1168–1174

Virchows Arch (2012) 461:699–703
DOI 10.1007/s00428-012-1329-5

ORIGINAL ARTICLE

Juvenile trabecular ossifying fibroma: an update

Pieter J. Slootweg

Received: 27 August 2012 / Revised: 26 September 2012 / Accepted: 4 October 2012 / Published online: 10 October 2012
© Springer-Verlag Berlin Heidelberg 2012

Abstract Fibro-osseous lesions are characterized by the presence of bone marrow that has changed into fibrous tissue and that contains mineralized material of varying appearances. Because of overlapping clinical, radiological, and histopathological features, their classification has evoked much discussion. The current classification recognizes fibrous dysplasia, ossifying fibroma, and osseous dysplasia. Juvenile trabecular ossifying fibroma is a rare variant of ossifying fibroma that is clinically characterized by rapid growth that may suggest malignancy. A series of 15 cases is reported with emphasis on a hitherto unnoticed histological feature that may be helpful in recognizing this lesion.

Keywords Maxillofacial bone pathology · Fibro-osseous lesions · Juvenile trabecular ossifying fibroma

Introduction

The current classification of maxillofacial fibro-osseous lesions encompasses fibrous dysplasia (FD), ossifying fibroma (OF), and osseous dysplasia [1, 2]. Although the separation of FD from OF has been disputed in the past [3], the demonstration of a specific molecular alteration in FD that has not been detected in OF has definitely proven that FD and OF are different entities. Activating missense mutations of the gene encoding the α subunit of the stimulatory G protein are a consistent finding in FD and have diagnostic significance in distinguishing FD from the other maxillofacial fibro-osseous lesions [4, 5].

P. J. Slootweg (✉)
Department of Pathology 824, Radboud University Nijmegen Medical Center,
PO box 9101, 6500 HB Nijmegen, Netherlands
e-mail: p.slootweg@pathol.umcn.nl

Juvenile trabecular (JTrOF) is a recently identified subtype of OF [6]. This lesion is rare and therefore not yet clinicopathologically well defined. In the present paper, a series of 15 cases of JTrOF with long-term follow-up is presented with the emphasis on histological features that define the place of this entity within the area of maxillofacial bone pathology.

Material and methods

Cases are from the author's hospital and consultation practice. Clinical data and radiographs were provided by the referring clinicians. For recent cases, the referring clinicians were asked for an update of follow-up. Relevant clinical data of the cases are listed in Table 1. Cases 1–9 have been included in previous reports on maxillofacial fibro-osseous lesions [7] but are included in this series because of updated follow-up and analysis of the defining histological features of JTrOF. From all cases, histological slides from paraffin-embedded and routinely processed material were available; with the exception of case 8 also from the recurrences. One recent case (case 15) was analyzed for presence of the mutation in the GNAs gene that is diagnostic for FD. No mutation was observed (further details not published).

Results

Clinical data

The series consisted of six males and nine females. In nine cases, the lesion was localized in the maxilla; the others involved the mandible. Mean age of diagnosis was 13.8 years. As far as could be retrieved from the available clinical data, clinically conspicuous jaw swelling was the

Table 1 List of cases

Case number	Gender	Site	Age (years)	Follow-up
1	M	Maxilla	15	Not available
2	F	Mandible	30	Recurrence after 3.5 years and 10 years, thereafter NED for 22 years
3	F	Maxilla	10	NED for 30 years
4	M	Maxilla	3	NED for 13 years
5	F	Maxilla	9	NED for 5 years
6	F	Maxilla	14	NED for 2 years
7	M	Mandible	14	Lost to follow-up
8	M	Maxilla	14	Recurrence after 2 years, thereafter NED for 4 years
9	M	Mandible	25	Recurrence after 4 months, thereafter NED for 3 years.
10	F	Mandible	11	Not available
11	F	Maxilla	6	NED for 3 years, then discharged from follow-up
12	M	Maxilla	3	Recent case
13	F	Mandible	7	Recent case
14	F	Mandible	22	NED for 1 year
15	F	Maxilla	25	Recent case

NED No evidence of disease

most prominent symptom, sometimes causing gross facial disfigurement (Fig. 1). Radiographs showed a mainly radiolucent lesion with an expanded cortical rim and a sharp demarcation from the uninvolved adjacent structures, compatible with a benign expanding intraosseous lesion. Cortical perforation and invasive growth in facial soft tissues was not observed (Fig. 2).

Some patients mentioned a history of persisting growth over several years, either due to a "wait and see" approach based on a preliminary diagnosis of fibrous dysplasia or because of a patient's delay. In other cases, a rapid growth over a time span of only a few months was reported.

Treatment consisted of surgery not extending beyond what was needed to remove the pathologic tissue; excision of adjacent normal tissue only being done when needed for functional or cosmetic reasons. Sometimes, surgery was done after incisional biopsy; in other cases, treatment consisted of excisional biopsy only. Follow-up data as listed in Table 1 indicate that this approach led to permanent cure, although sometimes after a second surgical intervention. Mostly, this recurrence was due to the outgrowth of residual tumor left behind after initial treatment.

Pathology

Material submitted for pathology varied. In some cases, the lesion was removed in fragments of varying size. In other cases, a partial maxillectomy or mandibulectomy was done, especially in patients with large tumors. Some cases showed

Fig. 1 Tumor causing gross swelling of left mandible (Case13)

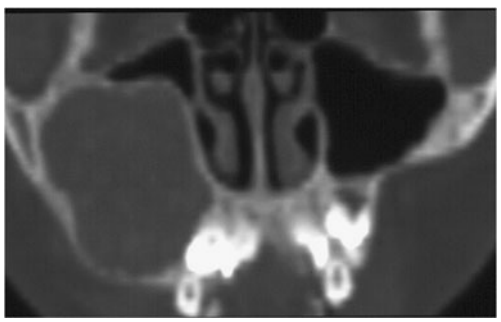

Fig. 2 Radiograph shows well defined lucent lesion in right maxilla. The clear demarcation is evident (Case 11)

Fig. 3 Cut surface showing thin brown curvilinear strands (Case 15)

at their cut surface a characteristic pattern of curvilinear thin brown strands (Fig. 3). In tumors that were excised with a rim of surrounding tissue, a clear demarcating border was visible to the naked eye (Fig. 4).

Histopathologically, all cases were characterized by a loose fibroblastic tissue with areas of collagen condensation. Subsequent deposition of minerals led to the formation of trabeculae of woven bone lined by a dense rim of swollen osteoblasts that appeared to be incorporated in the expanding osteoid (Fig. 5). Another typical feature was the variation in cellularity, more or less cellular areas separated from each other by thin elongated strands of hemorrhage with clusters of multinucleated cells of the osteoclastic type, and pseudocystic stromal degeneration (Figs. 6 and 7). These strands formed the microscopical substrate of the grossly visible curvilinear brown strands mentioned above. Mitotic figures were present in both the fibroblasts as well as in the bone-rimming osteoblasts, sometimes up to three in one high power field, but there was no significant atypia (Fig. 8). The lesions were sharply demarcated from their surroundings, either by a fibrous capsule or by a rim of

Fig. 4 Cut surface showing sharp demarcation from adjacent jaw bone that contains a first mandibular deciduous molar tooth and its permanent successor, the first premolar as tooth-germ in its bony crypt (Case 13)

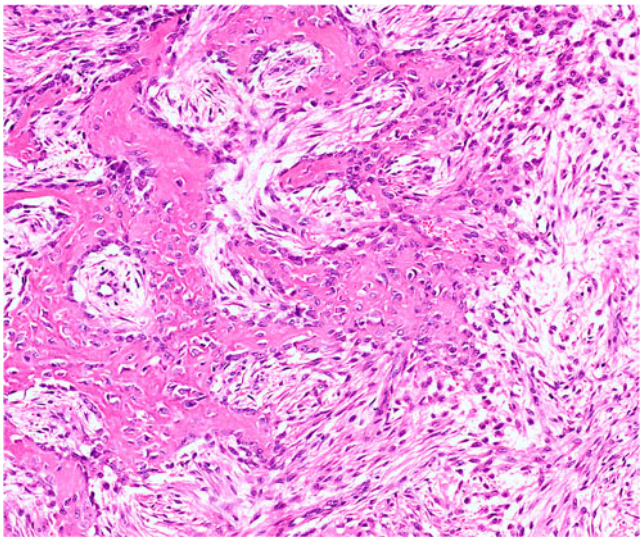

Fig. 5 Photomicrograph showing bony trabeculae densely rimmed with osteoblasts and osteoid incorporating adjacent stromal fibroblasts

preexistent bone that showed remodeling as reaction to the neighboring expanding neoplasm (Fig. 9).

Both osteoid formation engulfing adjacent osteoblasts and hemorrhagic edematous strands with osteoclasts were universally observed. In addition to these common features, some lesions had areas with a more mature appearance: collagenous tissue with plump bony fragments lacking a rim of active osteoblasts and containing only a few inactive osteocytes (Fig. 10). Moreover, a gradual transition from slender bony trabeculae to osseous spherules could occasionally be observed. In case of recurrence, no essential changes in the histological picture were observed other than a slight increase in more mature areas as described above.

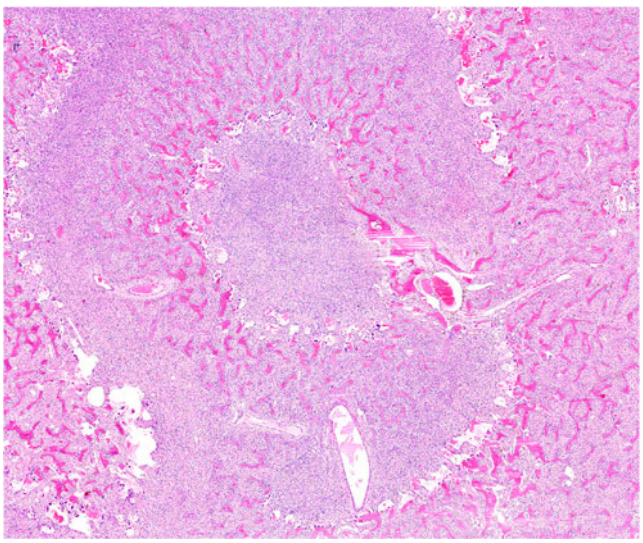

Fig. 6 Low power view showing the histological counterpart of Fig. 3. It seems as if immature areas are expanding at the expense of the more mature areas at their periphery

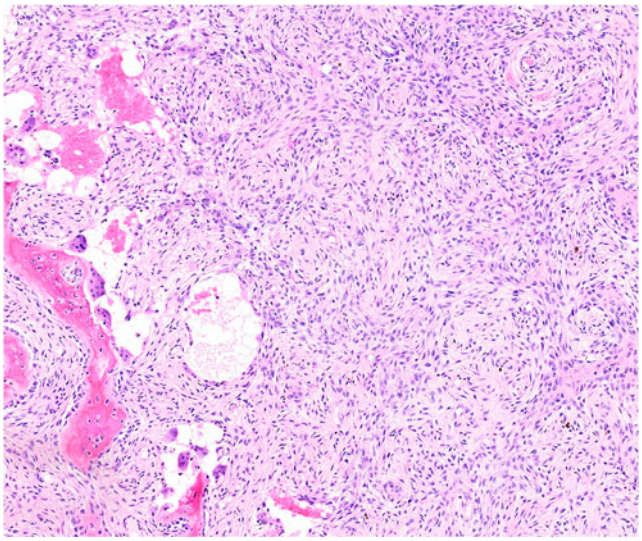

Fig. 7 At larger magnification, fibrocellular tissue with cell-rich bony trabeculae is separated from less cellular and more mature bone by a rim of osteoclasts, hemorrhage, and pseudocystic stromal degeneration

Discussion

In the current WHO classification, JTrOF is defined as a lesion that consists of cell-rich fibrous tissue containing bands of cellular osteoid without osteoblastic rimming together with slender trabeculae of immature bone containing coarse lacunae with plump osteocytes and lined by a dense rim of enlarged osteoblasts. Sometimes, these trabeculae may anastomose to form a lattice. Mitoses are present, especially in the cell-rich areas. Additional but less typical features are multinucleated giant cells, pseudocystic stromal degeneration, and hemorrhages [8].

In view of the data obtained from the current series, this definition ignores that multinucleated giant cells, pseudocystic stromal degeneration, and hemorrhage are not distributed randomly and independently from each other throughout the lesion but that they cluster and form elongated curvilinear strands that are even visible with the naked eye as thin brown lines. Therefore, the WHO definition as cited above should be rephrased by changing the status of the above-mentioned features until now classified as additional but less typical into highly specific.

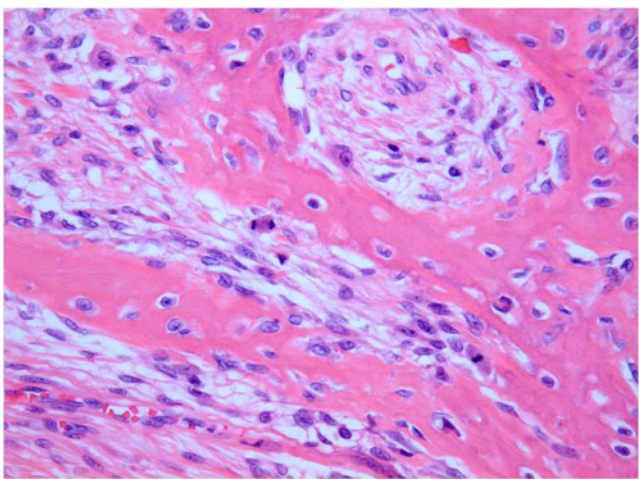

Fig. 8 At high magnification, mitotic activity is apparent, picture showing two mitotic figures in one high power field (×40)

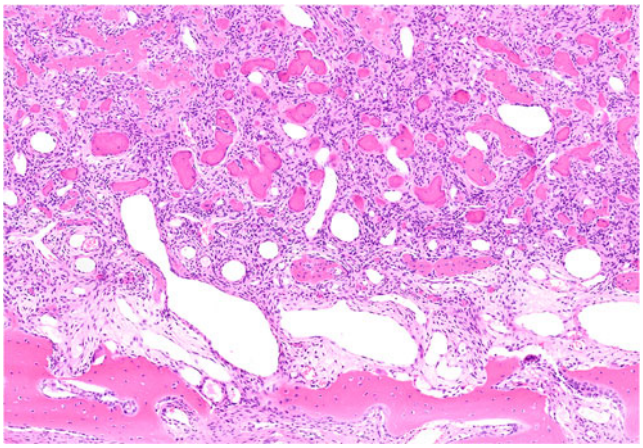

Fig. 9 The sharp demarcation at the radiographs is reflected in the corresponding histology. There is no merging of lesional bone with adjacent preexistent jaw bone as is seen in fibrous dysplasia

Recognition of this pattern that is not reflected in the radiographic appearance of the lesion is extremely helpful in defining the uniqueness of JTrOF within the group of fibro-osseous lesions and other bone-forming disorders that may occur in the maxillofacial skeleton as none of them displays these thin, garland-like curvilinear strands of edema, hemorrhage, and osteoclasts. Emphasizing this point is not an idle exercise on semantics or nosology but is asking

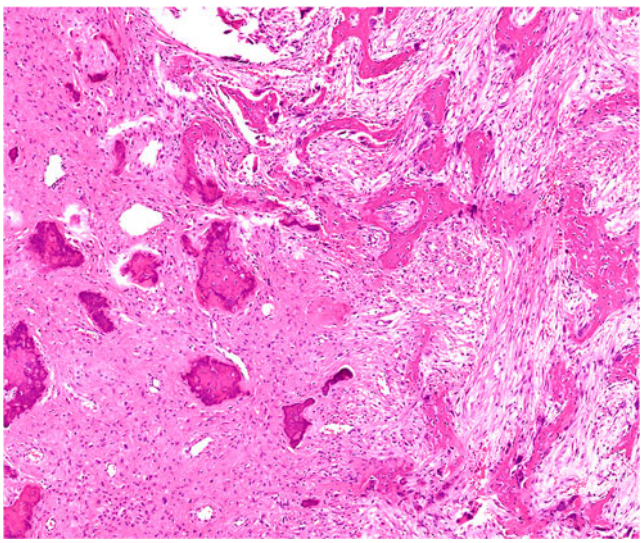

Fig. 10 Occasionally, immature areas (*right side*) merge with less cellular and more fibrous areas in which the bone is coarser and contains shrunken osteocytes

the attention of pathologists for a reliable diagnostic tool which especially concerns the distinction of JTrOF from osteosarcoma. Both lesions may show rapid and apparently aggressive growth and show a cellular, bone-forming tissue on biopsy; mistaking JTrOF for osteosarcoma has serious consequences for the patient: extensive surgery and possibly also chemotherapy for a lesion that can be cured with conservative excision as shown by the cases presented in this report.

Conflict of interest I declare that I have no conflict of interest.

References

1. Brannon RB, Fowler CB (2001) Benign fibro-osseous lesions: a review of current concepts. Adv Anat Pathol 8:126–143
2. Slootweg PJ (1996) Maxillofacial fibro-osseous lesions: classification and differential diagnosis. Semin Diagn Pathol 13:104–112
3. Voytek TM, Ro JY, Eideken J et al (1995) Fibrous dysplasia and cemento-ossifying fibroma. A histologic spectrum. Am J Surg Pathol 19:775–781
4. Pollandt K, Engels C, Kaiser E, Werner M, Delling G (2001) Gsα gene mutations in monostotic fibrous dysplasia of bone and fibrous dysplasia-like low-grade central osteosarcoma. Virchows Arch 439:170–175
5. Toyosawa S, Yuki M, Kishino M et al (2007) Ossifying fibroma vs fibrous dysplasia of the jaw: molecular and immunological characterization. Mod Pathol 20:389–396
6. El-Mofty SK (2002) Psammomatoid and trabecular juvenile ossifying fibroma of the craniofacial skeleton: two distinct clinicopathologic entities. Oral Surg Oral Med Oral Pathol Oral Radiol Endod 93:296–304
7. Slootweg PJ, Panders AK, Koopmans R, Nikkels PGJ (1994) Juvenile ossifying fibroma. An analysis of 33 cases with emphasis on histopathological aspects. J Oral Pathol Med 23:385–388
8. Slootweg PJ, El-Mofty SK (2005) Ossifying fibroma. In: Barnes L, Eveson JW, Reichart PA, Sidransky D (eds) World Health Organization classification of tumours. Pathology and genetics of tumours of the head and neck. IARC, Lyon, pp 319–320

Virchows Arch (2012) 461:705–711
DOI 10.1007/s00428-012-1331-y

ORIGINAL ARTICLE

Histological characteristics of the human femoral head in patients with femoral neck fracture

Takashi Sakai · Daiki Iwana · Nobuo Nakamura · Takashi Nishii · Masaki Takao · Tetsu Watanabe · Hideki Yoshikawa · Nobuhiko Sugano

Received: 15 March 2012 / Revised: 28 August 2012 / Accepted: 15 October 2012 / Published online: 20 October 2012
© Springer-Verlag Berlin Heidelberg 2012

Abstract The reparative reaction including angiogenesis and osteogenesis in human bone after an ischemic event remains unknown. To investigate the reparative reaction in human bone, the distribution of tartrate resistant acid phosphatase (TRAP)-positive cells and the expressions of hypoxia inducible factor-1α (HIF-1α), vascular endothelial growth factor (VEGF), fibroblast growth factor-2 (FGF-2), and CD31 were observed around the fracture site in 101 hips in 100 patients with femoral neck fracture. These 17 men and 83 women had a mean age of 80 years (range, 58–97 years). Of the hips, 17 were Garden stage 3, and 84 were Garden stage 4. The mean duration from fracture to surgery was 6.3 days (range, 1–14 days). Hematoxylin–eosin staining, TRAP staining, and immunohistochemistry using anti-HIF-1α, anti-VEGF anti-FGF-2, and anti-CD31 antibodies were performed for the coronal section of the retrieved whole femoral heads. TRAP-positive cells were detected near the trabecular bone around the fracture site in ten hips (10 %). HIF-1α expression was detected in 41 hips (41 %), mainly in the endothelial cells of the vessels. VEGF showed diffuse cytoplasmic staining of the mononuclear cells in the edematous area in 39 hips (39 %) while FGF-2 was detected in the cytoplasm of mononuclear cells in the bone marrow in 82 hips (82 %). CD31 was expressed in the bone marrow vessels in 35 hips (35 %). There were significant differences in HIF-1α expression relative to the duration between the fracture and the surgery, and in CD31 expression relative to Garden stage. HIF-1α expression was detected around the fracture site in the early period after fracture and CD31 expression was detected more frequently in Garden 3 hips while VEGF and FGF-2 expressions were detected regardless of Garden classification.

Keywords Femoral neck fracture · Tartrate resistant acid phosphatase (TRAP) · Hypoxia inducible factor-1α (HIF-1α) · Vascular endothelial growth factor (VEGF) · Fibroblast growth factor-2 (FGF-2) · CD31

Each author certifies that his or her institution has approved the human protocol for this investigation and that all investigations were conducted in conformity with ethical principles of research.

T. Sakai (✉) · M. Takao · H. Yoshikawa
Department of Orthopaedic Surgery,
Osaka University Graduate School of Medicine,
2-2, Yamadaoka,
565-0871, Suita, Japan
e-mail: tsakai-osk@umin.ac.jp

D. Iwana · N. Nakamura
Department of Orthopaedic Surgery, Kyowakai Hospital,
Suita, Japan

T. Nishii · N. Sugano
Department of Orthopaedic Medical Engineering,
Osaka University Graduate School of Medicine,
Suita, Japan

T. Watanabe
Department of Orthopaedic Surgery,
Toyonaka-Watanabe Hospital,
Toyonaka, Japan

Introduction

Osteogenesis and angiogenesis are closely associated with the reparative process in damaged bone [1]. The reparative reaction of nontraumatic osteonecrosis of the femoral head (ONFH) in the late stage has been elucidated using human femoral head samples [2–4]. The reparative reaction in the early phase of human ONFH remains unclear, and to investigate is difficult because human femoral head samples are harvested during surgery such as arthroplasty. Almost all

samples show progressing stages, and a long time has passed since osteonecrosis occurred. On the other hand, whether animal osteonecrosis is the same as human osteonecrosis is questionable because the blood supply around the femoral head and the anatomy of the experimental animal models are different from those of humans.

Femoral neck fracture (FNF) is a common trauma in elderly individuals. When the blood supply to the femoral head is impaired in a fracture event, the reduction or disruption of blood supply to the bone, i.e., hypoxia, leads to death of the bone marrow and trabecular bone, and in some cases, eventual late segmental collapse [5]. The reparative reaction to the fracture affects the clinical course in FNF [6]. In the reparative process, osteoblasts and osteoclasts perform the important function of repairing the fracture site, in this case, the femoral neck.

Angiogenesis is also an important part of the reparative reaction in FNF. A close relationship between blood vessels and bone formation has already been recognized in damaged bone areas [6]. It has been reported that pro-angiogenic factors often stimulate osteocytes and enhance bone repair [7]. Hypoxia inducible factor-1α (HIF-1α) is one of the pro-angiogenic transcription factors that is stabilized and activated under hypoxic conditions, and it regulates vascular endothelial growth factor (VEGF) that controls angiogenesis [8]. VEGF and fibroblast growth factor-2 (FGF-2) have emerged as prominent control factors for angiogenesis and thus as therapeutic tools to enhance neovascularization [9, 10]. CD31 is also expressed in the endothelial cells of the bone marrow vessels and has been used for the evaluation of angiogenesis [11]. Although there is one report that HIF-1 and VEGF have been activated during fracture repair in a rat fracture model [12], there are no reports of HIF-1α, VEGF, FGF-2, or CD31 expression in the reparative reaction of human bone fractures including FNF.

The aim of the present study was to elucidate the distribution of tartrate-resistant acid phosphatase (TRAP)-positive cells and the expressions of HIF-1α, VEGF, FGF-2, and CD31 around the fracture site of the femoral head in patients with FNF, as the reparative reaction after an ischemic event in human bone, and to elucidate the relationship between the histological findings and clinical factors including duration between fracture and surgery, and Garden's classification [5].

Patients and methods

Patients

The design of this study was approved by our institutional review board. A total of 101 femoral heads from 100 patients with FNF who underwent hip bipolar endoprosthesis were studied. Prior to surgery, informed consent was obtained from all patients regarding the planned investigations of the retrieved femoral head. The patients were 83 women and 17 men with a mean age of 80 years (range, 58–97 years). The mean duration from fracture until surgery was 6.3 days (range, 1–14 days). Radiologic staging according to Garden's classification criteria [5] was stage 3 in 17 hips and stage 4 in 84 hips. Before the fracture, six hips received vitamin D and five hips received bisphosphonate. The fracture site was on the coronal section of the whole femoral head with FNF (Fig. 1).

As controls, three femoral heads from one male and two female patients with chondrosarcoma of the acetabulum bone were investigated (control A). Although these control femoral heads were resected as wide resection therapy, they showed no malignancy or no abnormal histology. In addition, 20 femoral heads from 20 patients with hip osteoarthritis were also investigated (control B) because these femoral heads were damaged at the articular surface, but blood supply was maintained until a femoral neck osteotomy was done during total hip arthroplasty. The osteotomy site was investigated in the femoral heads of controls A and B (Fig. 1).

Femoral head retrieval and sample preparation

The 124 whole femoral heads (101 FNF and 23 controls) were fixed in formalin and decalcified in ethylenediaminetetraacetic acid (pH 7.4). Afterwards, the femoral heads were cut on the coronal plane, embedded in paraffin and cut into 5-μm sections. The specimens were deparaffinized by ascending alcohol concentrations and heated with citrate buffer (Dako REAL™ Target Retrieval Solution, Glostrup, Denmark, 1:10).

TRAP staining

TRAP staining was performed on all femoral heads using a TRAP staining kit (Cell Garage, Tokyo, Japan) at room temperature. Slides were counterstained with hematoxylin and embedded in aqueous permanent mounting medium (Dakocytomation, Carpinteria, CA). An osteoclast was defined as a TRAP-positive cell with more than three nuclei that existed around the trabecular bone.

Immunohistochemistry

Endogenous peroxidase was inactivated using 90 % methanol and 30 % hydrogen peroxide. Specimens were rinsed three times in Tris-buffered saline and buffer and then nonspecific antigens were blocked with 10 % goat normal antiserum (Histofine, Nichirei Biosciences, Tokyo, Japan) for 30 min. The following antibodies were used in all decalicified femoral heads at the specified dilutions: a rabbit monoclonal IgG against HIF-1α (Epitomics, Burlingame, CA; 1:100), a rabbit monoclonal IgG against an N-terminal

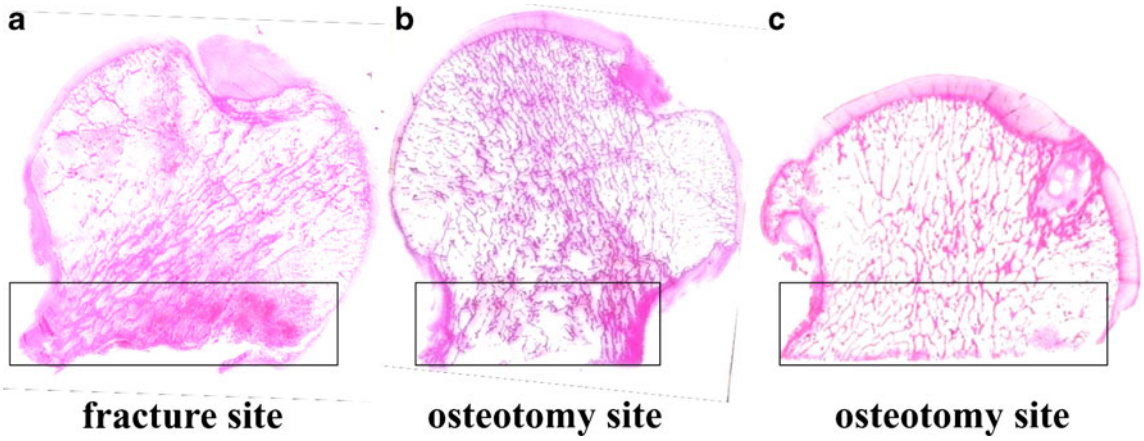

Fig. 1 Coronal section of the whole femoral head (H & E, ×1 magnification). **a** Femoral neck fracture. **b** Femoral head resected in the wide resection for chondrosarcoma of acetabular bone (control A). **c** Osteoarthritis (control B)

epitope of human VEGF (Diagnostic BioSystems, Pleasanton, CA; 1:100), a rabbit polyclonal IgG against FGF-2 (Santa Cruz Biotechnology, Santa Cruz, CA; 1:100), and a rabbit monoclonal IgG against CD31 (Epitomics, Burlingame, CA; 1:100) applied as the primary antibodies at 4 °C for 24 h. After rinsing with Tris-buffered saline, an anti-rabbit secondary antibody (Histofine) was applied for 30 min, and then streptavidin-labeled peroxidase (Histofine) was applied for 20 min. After the specimens were immersed in Tris–HCl buffer (pH 8.0), detection of HIF-1α, VEGF, FGF-2, and CD31 was performed using 3.3′-diaminobenzidine tetrahydrochloride (Wako, Tokyo, Japan). Finally, slides were counterstained with hematoxylin. Negative controls were performed using normal rabbit IgG (Santa Cruz Biotechnology, Santa Cruz, CA; 1:100).

Histological estimation

Histological estimation of TRAP-positive cells and immunoreactivity was performed using ×100 magnified histology around the fracture site. Two independent observers (TS, DI) evaluated the stained specimens. Histological estimation was discussed by all of the authors to reach an overall consensus. We then investigated the relationships between these histological results and the clinical characteristics, including age, gender, duration between fracture and surgery, and Garden stage.

Statistical analysis

The chi-squared test or Fisher's exact probability test was used for the analysis of the relationship between the histological results and the clinical characteristics, including gender and Garden stage. The Mann–Whitney *U* test was used for the analysis of the relationship between the histological results, and age and duration between fracture and surgery. Statistical analyses were conducted using SPSS software for Windows (version 20; IBM, Armonk, NY). A P value of <0.05 was considered to indicate a significant difference.

Results

TRAP-staining and immunoreactivity of HIF-1α, VEGF, FGF-2, and CD31

TRAP-positive cells were detected around the fracture in ten hips (10 %) (Fig. 2). TRAP-positive multinucleated cells

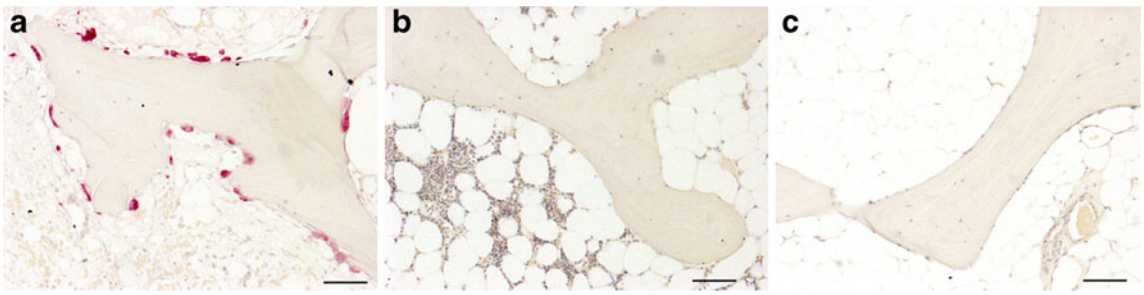

Fig. 2 TRAP staining. **a** TRAP-positive cells were detected around the trabecular bone around the fracture site in FNF. **b** There were no TRAP-positive cells around the osteotomy site in control A. **c** Control B (bar, 100 μm)

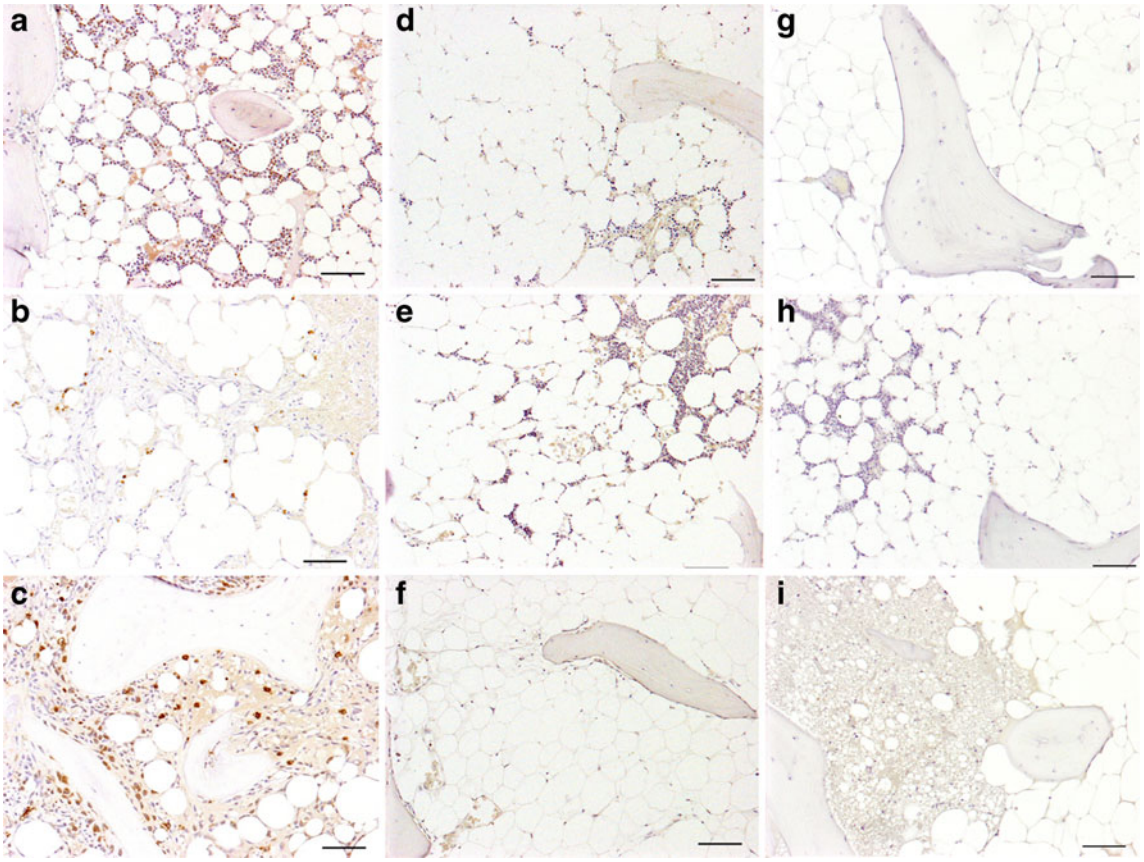

Fig. 3 Immunohistochemical staining. **a** HIF-1α expression was detected on the endothelial cells around the fracture site. **b** VEGF was expressed in the cytoplasm of the mononuclear cells in the edematous area. **c** FGF-2 was expressed in the cytoplasm of the mononuclear cells in the bone marrow widely. In control A (**d** HIF-1α, **e** VEGF, **f** FGF-2) and control B (**g** HIF-1α, **h** VEGF, **i** FGF-2), there were no positive cells (bar, 100 μm)

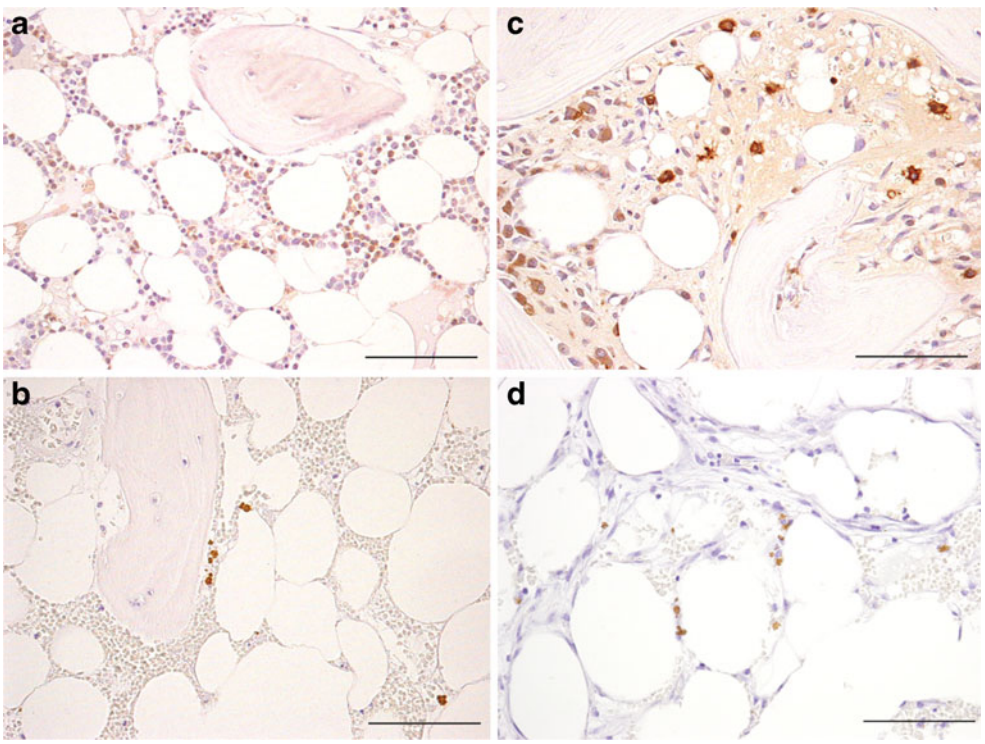

Fig. 4 Immunohistochemical staining for FNF. **a** HIF-1α. **b** VEGF. **c** FGF-2. **d** CD31. (bar, 100 μm)

were detected near the trabecular bone. No new appositional trabecular bone at the fracture site was detected. In controls, no TRAP-positive cells were detected around the osteotomy site in all three patients with metastatic tumors or all 20 patients with hip osteoarthritis.

Around the fracture site, HIF-1α expression was detected in the cytoplasm of the mononuclear cells, which were mainly endothelial cells, in 41 hips (41 %) (Figs. 3 and 4). VEGF protein was expressed in the cytoplasm of the mononuclear cells in the edematous area in 39 hips (39 %) (Figs. 3 and 4). FGF-2 was detected in the cytoplasm of the mononuclear cells in the bone marrow in 82 hips (82 %) (Figs. 3 and 4). CD31 was expressed in the bone marrow vessels in 35 hips (35 %) (Fig. 4). There were no cells that were positive for HIF-1α, VEGF, or FGF-2 expression around the osteotomy site in all controls.

Histological estimation and clinical characteristics

Although there were no significant differences in TRAP staining, VEGF expression, or FGF-2 expression concerning age, gender, duration between fracture and surgery, or vitamin D and/or bisphosphonate intake, there were significant differences in HIF-1α concerning duration between fracture and surgery (positive: 4.9±2.6 days vs negative: 7.2±3.0 days; $P=0.0004$) (Table 1). There were also significant differences in CD31 concerning Garden classification (positive: Garden 3/4, 13/22 hips vs negative, 4/62 hips; $P=0.000$). There were no significant differences in TRAP staining or immunohistochemistry of HIF-1α, VEGF, and FGF-2 between Garden stage 3 and stage 4 hips.

Table 1 Clinical characteristics and histological findings

	TRAP (n=101 hips)		
	Positive	Negative	P value
Gender (M/F)	4/15	13/69	0.40[a]
Age (years)	81.9±8.4	79.7±8.5	0.39[b]
Duration after fracture (days)	7.3±3.5	6.1±2.9	0.14[b]
Garden's stage (3/4)	6/13	11/71	0.06[c]
	HIF-1α (n=101 hips)		
	Positive	Negative	P value
Gender (M/F)	9/32	8/52	0.26[c]
Age (years)	78.9±9.7	81.0±7.5	0.39[b]
Duration after fracture (days)	4.9±2.6	7.2±3.0	0.0004[b]
Garden's stage (3/4)	8/33	9/51	0.55[c]
	VEGF (n=101 hips)		
	Positive	Negative	P value
Gender (M/F)	4/35	13/49	0.13[a]
Age (years)	80.7±8.3	79.8±8.6	0.74[b]
Duration after fracture (days)	6.1±2.6	6.4±3.3	0.82[b]
Garden's stage (3/4)	5/34	12/50	0.39[c]
	FGF-2 (n=101 hips)		
	Positive	Negative	P value
Gender (M/F)	17/65	0/19	0.02[a]
Age (years)	79.5±8.9	82.9±5.5	0.09[b]
Duration after fracture (days)	6.1±3.1	7.0±2.5	0.19[b]
Garden's stage (3/4)	13/69	4/15	0.40[a]
	CD31 (n=101 hips)		
	Positive	Negative	P value
Gender (M/F)	7/28	10/56	0.54[c]
Age (years)	79.9±9.1	80.2±8.2	0.73[b]
Duration after fracture (days)	6.4±2.7	6.2±3.2	0.54[b]
Garden's stage (3/4)	13/22	4/62	0.00[a]

A P value of <0.05 was considered as significant differences

[a] Fisher's exact probability test

[b] Mann–Whitney U test

[c] Chi-square test

Discussion

After FNF occurs, secondary osteonecrosis of the femoral head and late segmental collapse will develop due to rupture of the feeding arteries, including the femoral circumflex artery. Although the exact reparative reaction mechanism in the human femoral head remains unknown, the repair process probably takes place as bone remodeling coupled with osteoclastic resorption and bone formation. Interactions occur within the intraosseous vascular system and during the process of osteogenesis [13].

Angiogenesis is another important process in the reparative reaction in FNF. The major pathophysiological condition regulating angiogenesis is hypoxia, which upregulates HIF-1α, VEGF, and FGF-2 expressions in the tissue repair process [8, 14, 15]. HIF-1α has been identified as the master regulator of the transcriptional response to oxygen deprivation in healthy and transformed cell lines [16], and regulates the expression of numerous target genes that control angiogenesis, such as, VEGF [8, 17]. VEGF, a pro-angiogenic growth factor, regulates the recruitment, survival and activity of endothelial cells, osteoblasts and osteoclasts, and contributes to the major mechanism by which angiogenesis and osteogenesis are tightly coupled during bone repair [7, 9, 18]. The inhibition of VEGF activity disrupts the bone repair of femoral fractures and cortical bone defects in mice [19, 20].

HIF-1α expression was detected more frequently in the early period of the reparative process after fracture in the restricted area compared with VEGF and FGF-2 expressions. These findings are representative for the early expression of HIF-1α followed by VEGF expression [8] and FGF-2 expression [14, 15] under hypoxic conditions in FNF in humans. The process of angiogenesis induction might have already begun to wane in the late phase of the reparative process. Hypoxia may induce the upregulation of HIF-1α expression around the fracture site and the upregulation of

VEGF expression in the mononuclear cells in the edematous area, which enhances angiogenesis.

CD31 expression was not always detected in femoral head samples in human FNF, and CD31 expression was detected more frequently in Garden 3 hips. Roche et al. have showed that CD31 staining was absent in some unequivocal barium-filled bone marrow vessels of mice [11]. CD31 staining for the blood vessels of bone marrow may depend on various factors including blood vessel damage, animal type, and patient age.

Clinical, genetic, and basic research studies have revealed that the FGFs, including FGF-2, also function as important regulators of bone development, remodeling, and repair [21–23]. The distribution of VEGF and FGF2 showed similar patterns in ONFH [3, 24, 25]. Recombinant human FGF-2 microspheres have been reported to prevent the collapse of ONFH in a rabbit model [26] and a combination of vascular bundle implantation and FGF-2 administration has been shown to improve surgical angiogenesis in necrotic bone [10]. FGF-2 also increases osteoclastic bone remodeling [27, 28]. In the present study, FGF-2 was expressed in the bone marrow cells around the fracture site. Thus, FGF-2 protein may also be an important angiogenesis regulator in the reparative reaction in FNF.

Although there were no significant differences in local VEGF expression relative to the duration between fracture and surgery in the present study, in the systemic angiogenic response during bone healing, VEGF and FGF-2 serum concentrations in patients with long bone fractures increase within 2 weeks after the fracture [29, 30]. VEGF and FGF-2 expressions may differ between intraosseous lesions and serum.

The present study revealed the distribution of TRAP-positive cells and HIF-1α, VEGF, FGF-2, and CD31 expression around the fracture site of the femoral head in human FNF. TRAP-positive cells did not show any relation with the duration between fracture and surgery or Garden's stage. HIF-1α expression was detected at the endothelial cells of the blood vessels in the early period of the reparative process after fracture, and CD31 expression was detected more frequently in Garden 3 hips, whereas VEGF was detected in the cytoplasm of mononuclear cells in the edematous area and FGF-2 was detected in the cytoplasm of mononuclear cells in the bone marrow regardless of Garden stage. These results contribute to understanding the molecular processes in the reparative reaction in FNF and to potentially accelerating the reparative reaction by local therapeutic intervention.

Acknowledgments The institution of one of the authors (NS) has received funding from a grant from the Japanese Investigation Committee under the auspices of the Ministry of Health and Welfare. We thank Mrs. Mari Shinkawa, Miss Yasuko Taniguchi, Miss Takako Shizuka, and Miss Mizuki Nakata for the technical support of sample preparation.

Conflict of interest There is no conflict of interest in the present study.

References

1. Trueta J (1963) The role of the vessels in osteogenesis. J Bone Joint Surg Br 45:402–418
2. Sakai T, Sugano N, Nishii T, Haraguchi K, Ochi T, Ohzono K (2000) MR findings of necrotic lesions and the extralesional area of osteonecrosis of the femoral head. Skeletal Radiol 29:133–141
3. Plenk H Jr, Gstettner M, Grosschmidt K, Breitenseher M, Urban M, Hoffman S (2001) Magnetic resonance imaging and histology of repair in femoral head osteonecrosis. Clin Orthop Relat Res 386:42–53
4. Li W, Sakai T, Nishii T, Nakamura N, Takao M, Yoshikawa H, Sugano N (2009) Distribution of TRAP-positive cells and expression of HIF-1α, VEGF, and FGF-2 in the reparative reaction in patients with osteonecrosis of the femoral head. J Orthop Res 27:694–700
5. Garden RS (1964) Stability and union in subcapital fractures of the femur. J Bone Joint Surg Br 46:630–647
6. Sugano N, Masuhara K, Nakamura N, Ochi T, Hirooka A, Hayami Y (1996) MRI of early osteonecrosis of the femoral head after transcervical fracture. J Bone Joint Surg Br 78-B:253–257
7. Carano RA, Filvaroff EH (2003) Angiogenesis and bone repair. Drug Discov Today 8:980–989
8. Kim HH, Lee SE, Chung WJ (2002) Stabilization of hypoxia-inducible factor-1alpha is involved in the hypoxic stimuli-induced expression of vascular endothelial growth factor in osteoblastic cells. Cytokine 17:14–27
9. Street J, Bao M, de Guzman L et al (2002) Vascular endothelial growth factor stimulates bone repair by promoting angiogenesis and bone turnover. Proc Natl Acad Sci U S A 15:9656–9661
10. Nakamae A, Sunagawa T, Ishida O, Suzuki O, Yasunaga Y, Hachisuka H, Ochi M (2004) Acceleration of surgical angiogenesis in necrotic bone with a single injection of fibroblast growth factor-2 (FGF-2). J Orthop Res 22:509–513
11. Roche B, David V, Vanden-Bossche A, Peyrin F, Malaval L, Vico L, Lafage-Proust M (2012) Structure and quantification of microvascularisation within mouse long bones: what and how should we measure? Bone 50:390–399
12. Komatsu DE, Hadjiargyrou M (2004) Activation of the transcription factor HIF-1 and its target genes, VEGF, HO-1, iNOS, during fracture repair. Bone 34:680–688
13. Trueta J, Harrison MHM (1953) The normal vascular anatomy of the femoral head in adult man. J Bone Joint Surg Am 35:442–461
14. Calvani M, Rapisarda A, Uranchimeg B, Shoemaker RH (2006) Hypoxic induction of an HIF-1alpha-dependent bFGF autocrine loop drives angiogenesis in human endothelial cells. Blood 107:2705–2717
15. Egger M, Schgoer W, Beer AG et al (2007) Hypoxia up-regulates the angiogenic cytokine secretoneurin via an HIF-1α and basic FGF-dependent pathway in muscle cells. FASEB J 21:2906–2923
16. Wiener CM, Booth G, Semenza GL (1996) In vivo expression of mRNAs encoding hypoxia inducible factor. Biochem Biophys Res 225:485–488
17. Dai Y, Xu M, Wang Y, Pasha Z, Li T, Ashraf M (2007) HIF-1alpha induced-VEGF overexpression in bone marrow stem cells protects cardiomyocytes against ischemia. J Mol Cell Cardiol 42:1036–1044
18. Peng H, Wright V, Usas A et al (2002) Synergistic enhancement of bone formation and healing by stem cell-expressed VEGF and bone morphogenetic protein-4. J Clin Invest 110:751–759

19. Gerber HP, Vu TH, Ryan AM et al (1999) VEGF couples hypertrophic cartilage remodeling, ossification and angiogesis during endochondral bone formation. Nat Med 6:623–628
20. Haigh JJ, Gerber HP, Ferrara N, Wagner EF (2000) Conditional inactivation of VEGF-A in areas of collagen2a1 expression results in embryonic lethality in the heterozygous state. Development 7:1445–1453
21. Boyce BF, Hughes DE, Wright KR et al (1999) Recent advances in bone biology provide insight into the pathogenesis of bone diseases. Lab Invest 79:83–94
22. Goldfarb M (1996) Functions of fibroblast growth factors in vertebrate development. Cytokine Growth Factor Rev 7:311–325
23. Marie P, Debiais F, Cohen-Solal M, de Vernejoul MC (2000) New factors controlling bone remodeling. Joint Bone Spine 67:150–156
24. Varoga D, Drescher W, Pufe M, Groth G, Pufe T (2009) Differential expression of vascular endothelial growth factor in glucocorticoid-related osteonecrosis of the femoral head. Clin Orthop Relat Res 467:3273–3282
25. Radke S, Battmann A, Jatzke S, Eulert J (2006) Expression of the angiomatrix and angiogenic proteins CYR61, CTGF, and VEGF in osteovecrosis of the femoral head. J Othop Res 24:945–952
26. Kuroda Y, Akiyama H, Kawanabe K, Tabata Y, Nakamura T (2010) Treatment of experimental osteonecrosis of the hip in adult rabbits with a single local injection of recombinant human FGF-2 microspheres. J Bone Miner Metab 28:608–616
27. Collin-Osdoby P, Rothe L, Bekker S et al (2002) Basic fibroblast growth factor stimulates osteoclast recruitment, development, and bone pit resorption in association with angiogenesis in vivo on the chick chorioallantoic membrane and activates isolated avian osteoclast resorption in vitro. J Bone Miner Res 17:1859–1871
28. Warren SM, Brunet LJ, Harland RM et al (2003) The BMP antagonist noggin regulates cranial suture fusion. Nature 422:625–629
29. Sarahrudi K, Thomas A, Braunsteiner T, Wolf H, Vecsei V, Aharinejad S (2009) VEGF serum concentrations in patients with long bone fractures: a comparison between impaired and normal fracture healing. J Orthop Res 27:1293–1297
30. Weiss S, Zimmermann G, Pufe T, Varoga D, Henle P (2009) The systemic angiogenic response during bone healing. Arch Orthop Trauma Surg 129:989–997

Virchows Arch (2012) 461:713–715
DOI 10.1007/s00428-012-1332-x

CASE REPORT

Bilateral Sertoli cell tumors of the testis—a likely new extracolonic manifestation of familial adenomatous polyposis

Guang-Qian Xiao · Roberto C Granato · Pamela D. Unger

Received: 14 August 2012 / Revised: 24 September 2012 / Accepted: 15 October 2012 / Published online: 23 October 2012
© Springer-Verlag Berlin Heidelberg 2012

Abstract Testicular Sertoli cell tumors are rare and usually sporadic and unifocal. The large cell calcifying Sertoli cell tumor variant is known to be associated with Carney and Peutz–Jeghers syndromes and can be bilateral in these patient populations. There has been no documented association of Sertoli cell tumor with familial adenomatous polyposis (FAP) in the literature. The case presented is a bilateral Sertoli cell tumor occurring in a 34-year-old patient with FAP. The tumor had a conventional Sertoli cell tumor morphology, but with different morphology in the left and right sites. Beta-catenin immunostain showed strong nuclear reactivity in the tumor cells but not the nonneoplastic Sertoli cells. The presence of bilaterality as well as overexpression of beta-catenin by this tumor supports an association of the development of Sertoli cell tumor with the patient's FAP syndrome and adenomatous polyposis coli inactivation.

Keywords Sertoli cell tumor · Testis · Familial adenomatous polyposis

Introduction

Sertoli cell tumor is an infrequent sex cord-stromal tumor of the testis, accounting for less than 1 % of all testicular tumors. The vast majority of Sertoli cell tumors are sporadic. Rare cases have been associated with genetic syndromes, namely, androgen insensitivity syndrome [1], Carney syndrome [2], and Peutz–Jeghers syndrome [3]. Familial adenomatous polyposis (FAP) is an inherited colorectal cancer syndrome characterized by the early onset of hundreds to thousands of adenomas throughout the large bowel. The association of Sertoli cell tumor with FAP has never been documented in the literature. We herein present a case of bilateral Sertoli cell tumor in a patient with FAP. This is the first to describe Sertoli cell tumor in FAP.

G.-Q. Xiao (✉) · P. D. Unger
Department of Pathology, Mount Sinai School of Medicine,
One Gustave L. Levy Place, Box 1194,
New York, NY 10029, USA
e-mail: guang-qian.xiao@mountsinai.org

R. C. Granato
Department of Urology, Mount Sinai School of Medicine,
New York, NY 10029, USA

Clinical history

A 34-year-old male patient with history of FAP had subtotal colectomy at age of 15. Since then, he has been followed by yearly endoscopy, which, on multiple occasions, showed tubular adenoma polyps in the sigmoid colon and rectum. There is no other significant past medical history. His mother has FAP. His two siblings are without disease. Recently, he presented with bilateral testicular masses. Physical examination was otherwise unremarkable without coexisting other abnormalities associated with FAP. No hormone-related symptoms or feminization was noted in the patient. Bilateral testicular nodules were subsequently enucleated and were sent for intraoperative frozen assessment. The frozen diagnosis for both lesions was low-grade lesion favoring Sertoli cell tumor. The postoperative course was uneventful.

Materials and methods

Two portions of $2.5 \times 1.8 \times 1.2\text{-cm}^3$ in greatest dimension tan-brown tissue were received from left and right testes. Examination of the specimens revealed 1.4 cm (left) and 1.3 cm (right) in greatest dimension round, variegated white-tan, homogenous solid lesions surrounded by normal-looking testicular parenchyma. There was no tissue necrosis or hemorrhage. Both specimens were entirely submitted for microscopic examination.

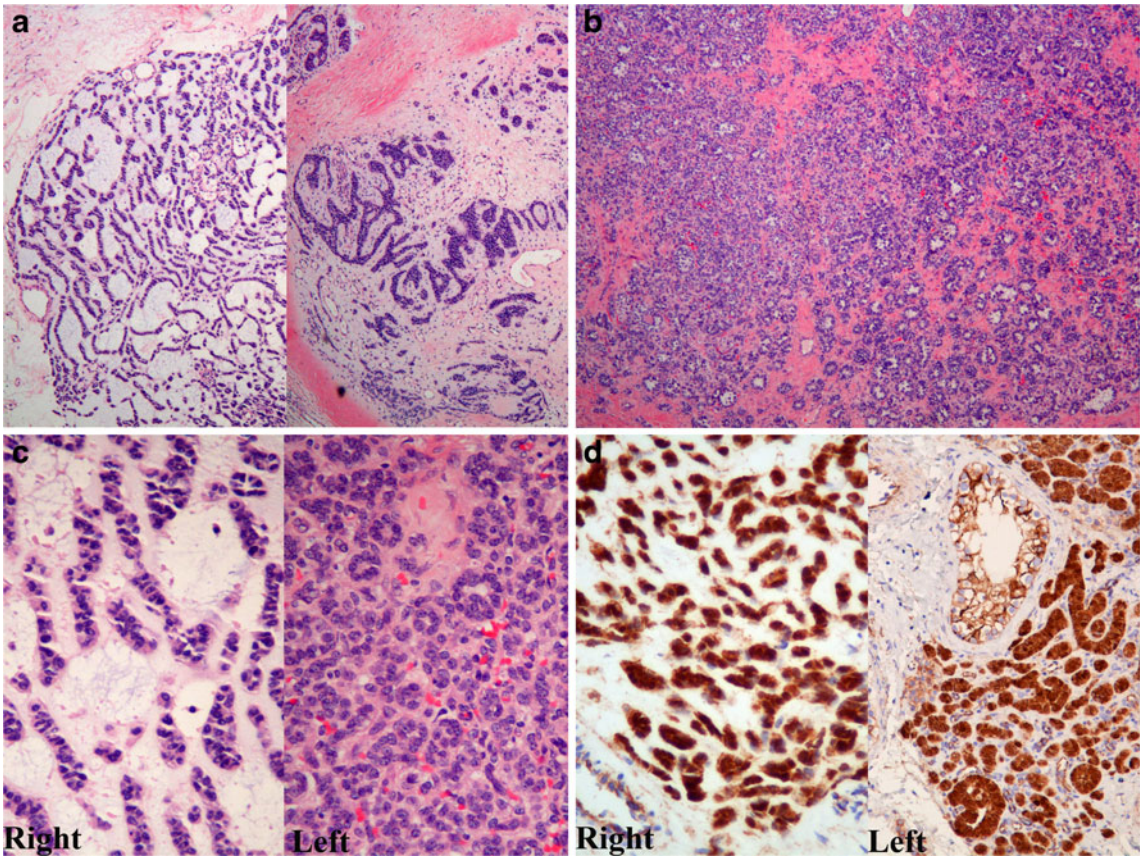

Fig. 1 **a** The right testicular tumor is predominantly composed of elongated solid tubular pattern. The associated stroma is myxoid or sclerotic (hematoxylin–eosin, original magnification ×60). **b** The left tumor cells are loosely organized into small rounded hollow tubules (hematoxylin–eosin, original magnification ×60). **c** The neoplastic cells of both sides are monotonous with small uniform bland rounded or oval nuclei, dense chromatin, and scant cytoplasm. The nucleoli are inconspicuous (original magnification ×300). **d** The tumor cells of both sides display strong nuclear reactivity with beta-catenin. The germ cells and nonneoplastic Sertoli cells show no nuclear reactivity with beta-catenin (original magnification ×300)

Results

Microscopically, the right testicular tumor was predominantly composed of elongated solid tubules. The associated stroma was myxoid or sclerotic (Fig. 1a). The neoplastic cells of the left site tumor were loosely organized into small hollow tubules (Fig. 1b). The tumor cells of both sites shared similar cytological features; they were monotonous and bland with uniform small rounded or oval nuclei, dense chromatin, and scant cytoplasm (Fig. 1c). The nucleoli were inconspicuous and mitoses were absent. Within both tumors, occasional entrapped seminiferous tubules containing Sertoli cells only were seen. No calcification or large eosinophilic Sertoli tumor cells either inside or outside the tumor were seen. The surrounding seminiferous tubules of both testes showed normal spermatogenesis. No associated germ cell tumor elements or intratubular neoplasia was observed. The histological diagnosis for both tumors was Sertoli cell tumor.

Immunohistochemical stains revealed the tumor to be focally positive for inhibin and calretinin and negative for PLAP and AFP. These findings were consistent with Sertoli cell tumor. In addition, the tumor cells showed strong nuclear reactivity with beta-catenin, whereas beta-catenin nuclear reactivity was absent in the germ cells and nonneoplastic Sertoli cells (Fig. 1d).

Discussion

It is known that systemic syndromes may be associated with Sertoli cell tumors. They have been reported in patients with Carney, Peutz–Jeghers, and androgen insensitivity syndromes [1–5]. Most of these tumors are the large cell calcifying variant. Familial adenomatous polyposis is an autosomal, dominant colorectal cancer syndrome, caused by a germline mutation and inactivation in the adenomatous polyposis coli (APC) gene on chromosome 5q21. It is characterized by hundreds of adenomatous colorectal polyps, with an almost inevitable progression to colorectal cancer at an average age of 35 to 40 years [6]. Mutations

in APC, a multifunctional tumor suppressor, have also been related to the development of various extracolonic neoplasms, including soft tissue tumors (e.g., desmoid tumor and osteoma) and gastric and duodenal adenomas [7–9]. Although no clinical cases of testicular germ cell tumors have been reported in FAP patients, some infantile yolk sac tumors have been demonstrated to contain APC mutation [10]. Nevertheless, no association between Sertoli cell tumor and FAP syndrome or APC alteration has been previously addressed or studied. The bilaterality of Sertoli cell tumor in this FAP patient appears beyond a casual sporadic coincidence and suggests a causal relation between germline APC mutation and Sertoli cell tumor. It has recently been elucidated that APC is an essential negative regulator of Wnt/beta-catenin signaling [11, 12]. Activation of the Wnt/beta-canin pathway caused by APC inactivation has been shown to be sufficient for intestinal tumorigenesis and related to the increased risk of development of desmoid tumors and other FAP-related neoplasms [13] In one recent study, overactive beta-catenin signaling has been shown to cause testicular Sertoli cell tumor development in the mouse [14]. In another study with a mouse model that specifically expresses a truncated form of APC in Sertoli cells, no tumorigenesis was observed [15]. The discrepancy between the findings of these two mouse models as well as human patients might be due to the difference of the fine-tuning of Wnt/beta-catenin pathway, APC mutations, and/or the onset time of APC loss. In our patient, in comparison with the nonneoplastic Sertoli cells, the overexpression of beta-catenin in the Sertoli cell tumor, similar to desmoid tumor, provides molecular evidence supporting the probable association of tumorigenesis of these Sertoli cell tumors with the germline line APC mutation. The molecular mechanism of Sertoli cell tumor, its relation with APC germline mutation, and the role of APC mutation in this tumor warrant further investigation. It is also of interest to see whether or not APC inactivation is involved in the development of non-FAP-related Sertoli cell tumors.

In conclusion, a case of bilateral Sertoli cell tumor in a FAP patient is presented. The bilaterality and overexpression of beta-catenin in this tumor strongly imply an association between these two events. The case illustrated here adds an additional tumor manifestation to the FAP syndrome. Further study is warranted to evaluate the molecular basis of APC alteration in the tumorigenesis of Sertoli cell tumor.

Conflict of interest We declare that we have no conflict of interest.

References

1. Rutgers JL, Scully RE (1991) The androgen insensitivity syndrome (testicular feminization): a clinicopathologic study of 43 cases. Int J Gynecol Pathol 10(2):126–144
2. Washecka R, Dresner MI, Honda SA (2002) Testicular tumors in Carney's complex. J Urol 167(3):1299–1302
3. Young RH, Koelliker DD, Scully RE (1998) Sertoli cell tumors of the testis, not otherwise specified: a clinicopathologic analysis of 60 cases. Am J Surg Pathol 22(6):709–721
4. Ulbright TM, Amin MB, Young RH (2007) Intratubular large cell hyalinizing Sertoli cell neoplasia of the testis: a report of 8 cases of a distinctive lesion of the Peutz-Jeghers syndrome. Am J Surg Pathol 31(6):827–835
5. Baksu A, Kabukcuoglu F, Baksu B, Goker N et al (2004) Bilateral sertoli cell adenoma and serous cyst in a patient with androgen insensitivity syndrome. Eur J Obstet Gynecol Reprod Biol 114 (1):104–107
6. Galiatsatos P, Foulkes WD (2006) Familial adenomatous polyposis. Am J Gastroenterol 101(2):385–398
7. Escobar C, Munker R, Thomas JO et al (1012) Update on desmoid tumors. Ann Oncol 23(3):562–569
8. Wijn MA, Keller JJ, Giardiello FM et al (2007) Oral and maxillofacial manifestations of familial adenomatous polyposis. Oral Dis 13(4):360–365
9. Bülow S, Björk J, Christensen IJ et al (2004) Duodenal adenomatosis in familial adenomatous polyposis. The DAF Study Group. Gut 53:381–386
10. Kato N, Shibuya H, Fukase M, Tamura G, Motoyama T (2006) Involvement of adenomatous polyposis coli (APC) gene in testicular yolk sac tumor of infants. Hum Pathol 37:48–53
11. Tejpar S, Michils G, Denys H (2005) Analysis of Wnt/Beta catenin signalling in desmoid tumors. Acta Gastroenterol Belg 68(1):5–9
12. Aoki K, Taketo MM (2007) Adenomatous polyposis coli (APC): a multi-functional tumor suppressor gene. J Cell Sci 120:3327–3335
13. Lips DJ, Barker N, Clevers H et al (2009) The role of APC and beta-catenin in the aetiology of aggressive fibromatosis (desmoid tumors). Eur J Surg Oncol 35(1):3–10
14. Chang H, Guillou F, Taketo MM et al (2009) Overactive beta-catenin signaling causes testicular Sertoli cell tumor development in the mouse. Biol Reprod 81(5):842–849
15. Tanwar PS, Zhang L, Teixeira JM (2011) Adenomatous polyposis coli (APC) is essential for maintaining the integrity of the seminiferous epithelium. Mol Endocrinol 25(10):1725–1739

Virchows Arch (2012) 461:717–719
DOI 10.1007/s00428-012-1336-6

LETTER TO THE EDITOR

Metastasis of endometrial adenocarcinoma in a primary lung adenocarcinoma

Aurélie Pelissier-Komorek · Wassila El Alami-Thomas · Daniela Lebrun · Marie Danièle Diebold

Received: 12 October 2012 / Accepted: 23 October 2012 / Published online: 31 October 2012
© Springer-Verlag Berlin Heidelberg 2012

Dear Sir,

To our knowledge, we report the first case of a metastasis of an endometrial adenocarcinoma in a pulmonary adenocarcinoma. A 72-year-old woman presented to our department with minimal metrorrhagia. The patient was diagnosed 6 years earlier with a mediastinal follicular lymphoma stage 3A according to Ann Arbor classification. Taking into account the characteristics of the lymphoma, therapy abstinence was decided, but the patient was followed up with regular laboratory monitoring l and computed tomography (CT) scans. The mediastinal lymphadenopathy remained stable. A pelvic sonogram made during the gynecology consultation showed a thick endometrium, and biopsies were taken. Histopathological examination of the samples led to a diagnosis of a well-differentiated (grade 1) endometrioid adenocarcinoma.

The pelvic MRI showed myometrial infiltration without penetration of the serosa and right external iliac lymph nodes of 2 cm diameter. Chest CT revealed a single well-defined 24-mm mass located in the Fowler segment of the right lung (Fig. 1) which was not seen on previous scans. FDG PET/CT gave rise to a suspicion of a hypermetabolic pulmonary focus.

The lesion was not accessible by bronchoscopy, making trans-bronchial biopsy impossible. A diagnostic right lower lobe resection was performed. Macroscopic examination revealed a white-gray solitary nodular mass, measuring $20 \times 20 \times 16$ mm in the lung parenchyma. Microscopy revealed the association of two types of malignant tissues. The predominant type presented the typical architectural and cytological pattern of lepidic lung adenocarcinoma. In this area, lining the alveolar lumen, cells were cuboid cylindrical with large irregular nuclei and eosinophilic or clear cytoplasm. Alcian blue staining revealed the presence of extracellular mucins. Within this tumor, a 9-mm nodule of a different malignant tissue was found, characterized by glandular architecture with cavities lined with high cylindrical cells with basophilic, elongated, and nucleolated nuclei (Fig. 2).

By immunohistochemistry, the two components were distinct. Tumor cells of the main mass were positive for thyroid transcriptor factor 1 (TTF-1) and cytokeratin 7 (CK7), but negative for estrogen receptor (ER) and progesterone receptor (PR). Inversely, the cells of the minor focus were negative for TTF-1 and CK7 but positive for ER/PR (Fig. 2). A final histological diagnosis was made of metastasis of endometrial adenocarcinoma in a primary lung adenocarcinoma. No metastases were found in other organs. The endometrial cancer was stage IVB according to the FIGO classification, and neoadjuvant chemotherapy based on taxol–carboplatin was initiated.

The association in a single tumor mass of a primary cancer containing metastatic tissue is a phenomenon called tumor-to-tumor metastasis. Tumor-to-tumor metastasis and collision tumor have been confounded in some publications, and the incidence of the former cannot be deduced from the number of cases reported [1]. Collision tumor is the term used for the presence of two histologically distinct primary

A. Pelissier-Komorek (✉)
Department of Obstetric Gynecology,
University Hospital of Reims,
45 rue Cognacq Jay,
51100 Reims, France
e-mail: a.komorek@gmail.com

A. Pelissier-Komorek · D. Lebrun
Department of Oncology, Institut Jean Godinot,
Avenue du Général Koenig,
51100 Reims, France

W. El Alami-Thomas · M. D. Diebold
Department of Pathological Anatomy,
University Hospital of Reims,
Avenue du Général Koenig,
51100 Reims, France

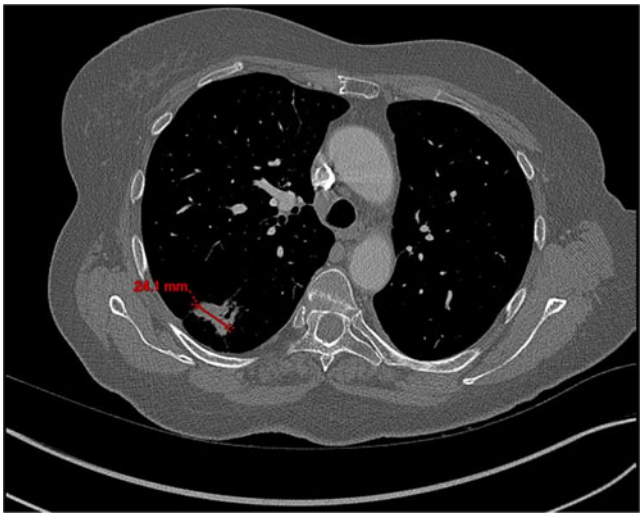

Fig. 1 Pulmonary parenchymal condensation zone of 24.1 mm at the right Fowler segment on sagittal scanner, parenchymal window

tumors in a single location in a single or two adjacent organs. Campbell et al. [2] defined the following strict criteria for a diagnosis of tumor-to-tumor metastasis:

1. More than one primary tumor must exist in the patient
2. The recipient tumor should be a benign or malignant lesion
3. The malignancy of the donor tumor must be proven
4. The metastatic neoplasm should be a true metastasis with established growth in the recipient tumor, not the result of contiguous growth ("collision tumor")
5. Tumors that have metastasized to a lymph node with a preexisting malignant lymphoma are excluded

Our case satisfies all the criteria for tumor-to-tumor metastasis. Berent reported the first case of tumor-to-tumor metastasis in 1902, which was a squamous epithelial cancer of the lower jaw to a primary renal cell carcinoma [3]. The most common recipient tumor is renal cell carcinoma, and

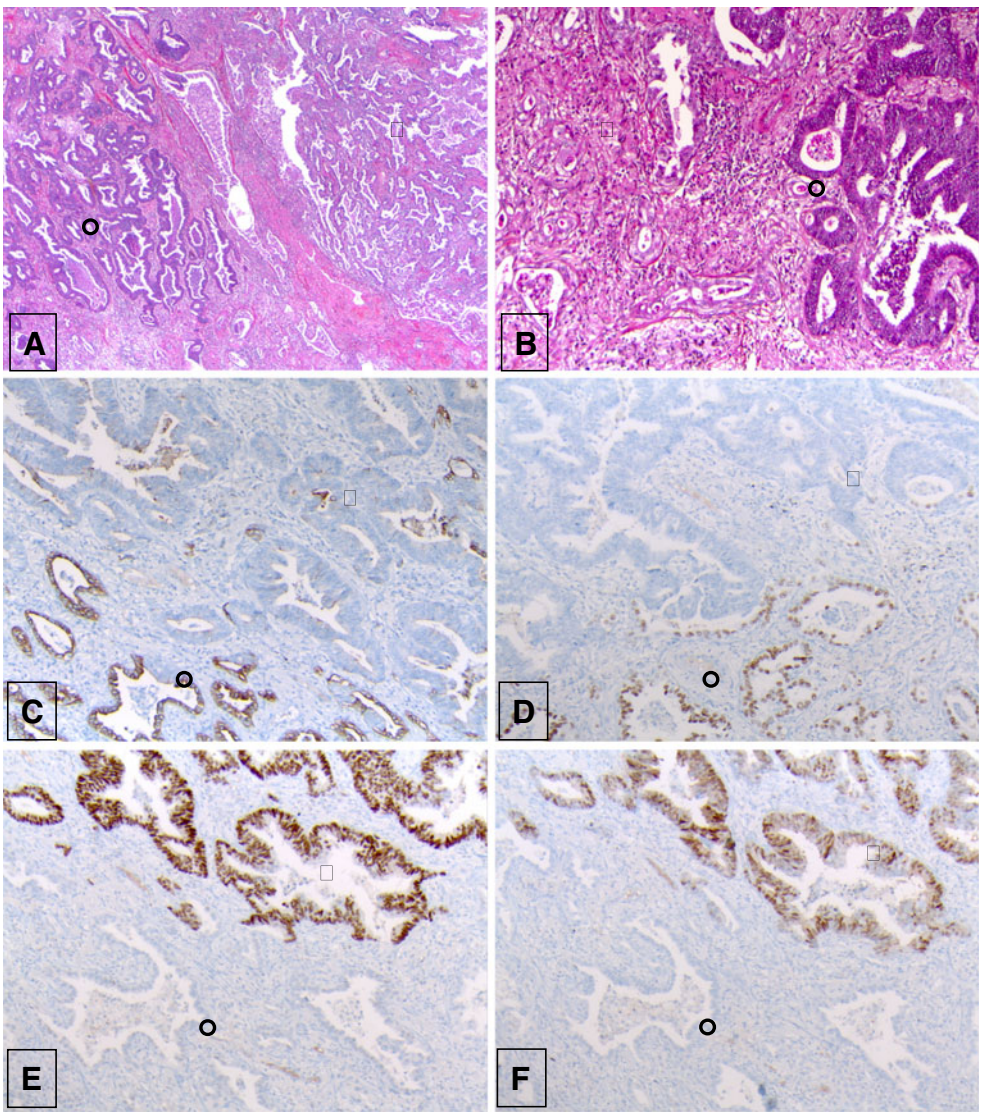

Fig. 2 **a** (×2.5), **b** (×10) Highlighting of a lepidic component (*circle*) and tubulopapillary component (*rectangle*) within the same tumor foci with staining HPS; **c** CK7 immunostains (×10); **d** TTF1 immunostains (×10); **e** ER immunostains (×10); **f** PR immunostains (×10)

the most common donor cancers are the lung, prostate, and thyroid. In the literature, only 50 cases of cancer-to-cancer metastasis [4] and about 60 cases of metastases from cancer to benign tumors have been reported. When the recipient tumor is benign, the most frequently reported association is metastasis from breast carcinoma to intracranial meningioma [4]. Most (72 %) endometrial cancers are diagnosed in stage I, and only 3 % are stage IV [5]; distant metastases are rare. Preferred sites in the order of frequency are the abdominal cavity, liver, and finally, lung. To our knowledge, we described the first case of endometrial cancer metastasis in a lung cancer. The recipient tumor properties may explain why circulating cells present in lymphatic and blood vascular system might preferentially develop there, through hypervascularity promoted by tumor angiogenesis, of which renal carcinoma is a clear example. Low activity of the immune system in a malignant tumor has also been incriminated. The concomitant lymphoma in our patient might have provided a favorable host environment.

References

1. Aggarwal N, Amin RM, Chung D, Parwani AV (2012) Tumor-to-tumor metastasis: case report of a pulmonary adenocarcinoma metastatic to a clear cell renal cell carcinoma. Pathol Res Pract 208:50–52
2. Campbell LV Jr, Gilbert E, Chamberlain CR Jr, Watne AL (1968) Metastases of cancer to cancer. Cancer 22:635–643
3. Berent W (1902) Seltene mestatasenbildung. Zentralbl Allg Pathol 13:406–410
4. Möller MG, Gribbin T, Ebrom S, Padula G, Fitzgerald TL (2005) Breast cancer metastatic to renal cell carcinoma. Surgery 14:577–579
5. Jemal A, Murray T, Ward E, Samuels A, Tiwari RC, Ghafoor A (2005) Cancer statistics, 2005. CA Cancer J Clin 55:10–30

Virchows Arch (2012) 461 (Suppl 1):S1–S332
DOI 10.1007/s00428-012-1284-1

ABSTRACTS

ESP Abstracts 2012

Free Papers

Monday, 10 September 2012, 17.00–19.00, Congress Hall
OFP-01 Oral Free Paper Session Breast Pathology I

OFP-01-001

A study of Sperm-associated Antigen 5 (SPAG5) in predicting response to Anthracycline (ATC)/Platinum Chemotherapies (CT) in breast (BC) & Ovarian Cancers (OVC)

T. Abdel-Fatah*, G. Ball, S. McArdle, P. Moseley, I. Seyer, A. Green, I. Ellis, S. Chan
*Nottingham City Hospital, Dept. of Clinical Oncology, United Kingdom

Objective: SPAG5 plays an essential role in cell cycle progression. In this study the molecular and clinicopathological functions of SPAG5 was investigated.
Method: A series of 171 BC was evaluated for SPAG5 gene copy number (using aCGH) and mRNA expression (using GEA). The expression of SPAG5 protein was evaluated in BC and OCV cell line and in 1650 primary BC. The association between SPAG5 and response to CT was investigated in three independent datasets: 350 ER- BC treated with adjuvant ATC-CT, 250 BC treated with neo-adjuvant (NEO-A)-ATC-CT, and 200 primary OVC treated with cisplatinum.
Results: 5 % of BC showed amplification of SPAG5 locus at 17q11.2. SPAG5 mRNA expression displayed a significant correlation with its copy number. In BC, SPAG5+ was associated with aggressive phenotypes ($p<0.0001$) and poor survivals ($p<0.0001$). Anthracyclin CT had a positive impact on clinical outcome of SPAG5+ BC ($p<0.0001$). SPAG5+ BC received NEO-A-ATC based CT achieved 38 % pathological complete response (pCR) and SPAG5 protien expression was confirmed as an independent predictor for pCR ($p=0.001$). Similarly, SPAG5- OVCs were resistant to platinum ($p<0.001$) and independently associated with poor survival ($p<0.001$).
Conclusion: SPAG5 is an important novel gene implicated in the survival of BC & OVC cells and its protein expression is an independent predictor for CT.

OFP-01-002

Intraoperative evaluation of breast cancer sentinel lymph node metastasis with an automated molecular detection method as an alternative to standard pathological evaluation

F. Beca*, E. Rios, P. Pontes, I. Amendoeira
*Centro Hospitalar de São João, Anatomic Pathology, Porto, Portugal

Objective: One-step nucleic acid amplification assay (OSNA) from Sysmex® is an automated system to detect sentinel lymph node (SLN) metastasis in breast cancer patients. This assay is based on the detection of cytokeratin 19 mRNA amplification by reverse-transcription loop-mediated isothermal amplification. Traditionally intraoperative evaluation of SLN is accomplished by cytology and/or frozen section, accounting for heavy workload to pathology department. The objective of this study is to compare the OSNA assay with our standard processing for intraoperative SLN evaluation.
Method: 82 SLN from 45 patients with CK19+ and invasive primary carcinomas where simultaneously evaluated by cytology and/or frozen section and by OSNA assay. Results where compared with gold-standard definitive H&E evaluation (serially sectioned at 150 μm intervals).
Results: The sensitivity and specificity of OSNA assay was 92.3 % and 98.2 %, respectively with a positive predictive value (PPV) and a negative predictive value (NPV) of 96 %. For standard intraoperative evaluation, specificity was 100 % and sensitivity was 73.0 %.

Conclusion: OSNA assay showed similar specificity and higher sensitivity than standard pathologic examination. These findings suggest it can be used as an accurate tool for intraoperative evaluation of SLNs metastasis and possibly contribute to reducing the need for re-intervention for axillary lymph node dissection.

OFP-01-003

Topoisomerase 2A expression as a predictive marker of chemotherapy efficacy in breast cancer patients

E. Bonanno*, M. Chimenti, I. Portarena, M. Roselli, O. C. Buonomo, L. G. Spagnoli

*Università di Roma Tor Vergata, Dept. of Biopathology, Italy

Objective: Antracycline-based chemotherapy represents a standard of care in breast cancer patients especially who overexpress HER-2. Topoisomerase 2A has been considered a molecular target for antracyclines and its co-amplification with HER-2 genes has been proposed. In our study we investigated if Topoisomerase 2A overexpression can be used as a molecular marker on predicting response to antracycline-based chemotherapy.

Method: Breast cancers tissues from 40 patients underwent to antracycline-based neoadiuvantchemotherapy and 267 treated with adiuvant therapy were collected into 4 Tissues microarrays, and classified according to pathological stage, ER, PR, HER-2 and TOPO2A status. The expression of topoisomerase 2A has been correlated to response to chemotherapy.

Results: Our results show that TOPO2A expression is significantly higher in neoplasms with larger size, nodal metastasis, scant ER end PR receptors, and amplification of HER-2 gene ($p<0,00$, *T*-test). Cancers in witch high level of TOPO2A has been found exhibit a better clinical response to treatment with anthracycline ($p<0,0000$, *T*-test). Therefore TOPO2A expression could be considered both as predictive and prognostic marker.

Conclusion: The employment of TOPO2A as a predictive marker in clinical practice may be useful for the medical therapy of non-endocrine-responsive patients candidate to undergo treatment based on anthracycline, that is no free from adverse effects as cardiomyopathy and leukemia.

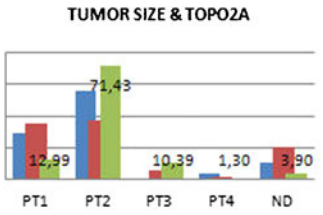

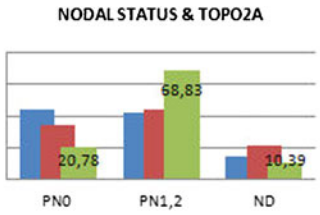

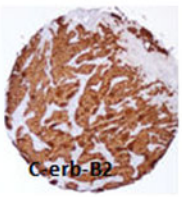

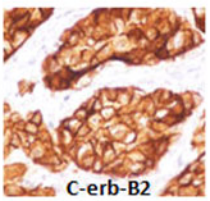

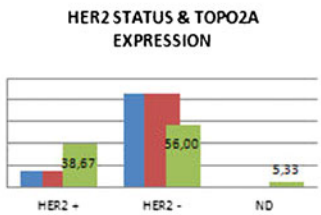

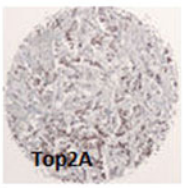

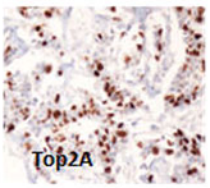

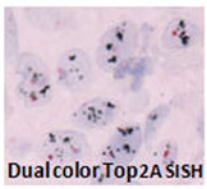

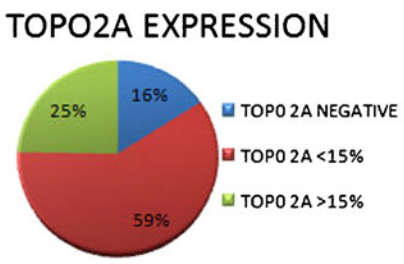

Statistical analysis T-test	Topo 2A negative vs topo2A <15%	Topo 2A <15% vs Topo 2A >15%
variabile	*P value*	*P value*
T	0,0100	0,4157
N	0,0000	0,0001
c-erbB2	0,0000	0,0001
HER2	0,0018	0,0000
Clinical response to therapy	0,0001	0,0035
Hormonal status	0,0018	0,0028

OFP-01-004

Stem cells in triple negative breast cancer and associated in situ lesions

M. Comanescu*, M. Dobre, G. Bussolati
*Institutul Victor Babes, Dept. of Pathology, Bucharest, Romania

Objective: Triple negative breast cancer (TNBC) (negative for expression of estrogen and progesterone receptors (ER, PR) and HER2/neu protein) represent a subtype of breast cancer associated with poor prognosis and highly aggresive behaviour. Genetic characterization of stem cell (CD 44,....) in this type of carcinoma might provide important data concerning origin and evolution. Data of the literature focused specifically on TNBC but, despite the interest shown to stem cells recently, there are no data concerning the genetic characterization of stem cells in the context of cell biology of TNBC as compared with associated DCIS.
Method: We investigated, through immunohistochemistry, the expression and distribution of several stem cell/related antigens, exploring the association of TNBC with DCIS and comparing the presence of stem cells in the invasive and in the in situ component.
Results: The multiplicity of parameters to be detected for characterising stem cells and of the diagnostic materials that are available would prevent a straightforward approach and a sequential combination will have to be planned.
Conclusion: Optimization of detection, identification and characterisation of tumourigenic breast cancer stem cells might permit further identification of targeted treatment.

OFP-01-005

Over- and undergrading of Breast Cancer on core biopsies in comparison to surgical specimens

T. Decker*, C. Focke, D. Gläser
*D. Bonhoeffer Medical Center, Dept. of Pathology, Neubrandenburg, Germany

Objective: To evaluate the relevance of histological grading (HG) based on core biopsies (CB) for clinical decision making in breast cancer (BC) we evaluated the concordance with HG from surgical specimen (SSP) and the reasons for under- or overgrading.
Method: CB and related SSP of 398 BCs were prospectively graded according to the Nottingham grading system (SSP: 65 G1, 162 G2 and 171 G3). CB/SSP agreement rates and positive predictive values (PPV) of CB based HG were calculated. Rates of over- and underestimation of glandular differentiation (GD), nuclear pleomorphism (NP) and mitotic activity (MA) were calculated.
Results: CB/SSP agreement rates came out with 95 % for G1, 73 % for G2, and 56 % for G3. The PPVs of CB based HG were 56 % for G1, 61 % for G2 and 100 % for G3. The overgrading and undergrading rates on CB were 1 % and 37 %, respectively. Main causes for undergrading in CB were underestimated MA (40 %) and a combination of underestimated NP and MA (32 %).
Conclusion: Whereas overgrading on CB is an exception, undergrading derives largely from underestimation of proliferation. Agreement of HG between CB and SSP ranges from almost perfect for G1, moderate for G2 to slight for G3 tumours.

OFP-01-006

Comparative histopathology of mammary alterations in women and dog

V. Deckwirth*, P. Kronqvist, M. Lintunen, A. Sukura
*University of Helsinki, Dept. of Veterinary Pathology, Finland

Objective: Companion animals such as dogs share the same environment with people. Mammary tumours are the most prevalent spontaneous neoplasia in intact bitches. More animal models are needed for human mammary tumour research. Our objective was to describe equivalent non-neoplastic and neoplastic mammary gland alterations in woman and dog.
Method: Formalin-fixed, paraffin-embedded archived human and canine mammary gland tissue samples. Epidemiological data were collected and analyzed from human (n=1935) and canine (n=161) patients for the years 2003–2005. Histological comparison was performed with HE-stained tissue sections and immunohistochemistry. Applied antibodies included CK5/6, ERα, PR, Ki67, Her2, p63, SMA, E-cadherin and calponin.
Results: Several comparable benign and malignant mammary gland alterations were identified, consisting of lobular, tubular and ductal as well as mesenchymal of origin. Most of these have not been described previously. The epidemiological results show also shared characteristics.
Conclusion: Although there are canine specific lesions there also exist equivalent entities. Our results indicate the female canine as a suitable model for translational research.

OFP-01-007

St. Gallen intrinsic subtyping of breast cancer: Influence of proliferation assessment methods

C. M. Focke*, D. Gläser, K. Finsterbusch, T. Decker
*Dietrich Bonhoeffer Klinikum, Abt. Pathologie, Neubrandenburg, Germany

Objective: The St. Gallen Conference 2011 strongly recommends intrinsic subtyping of breast cancer (BC) for therapeutic

decisions. We analyzed the influence of different proliferation assessment methods on the BC subtype distribution.
Method: Intrinsic subtyping was performed according to the St. Gallen criteria on 225 BCs. Proliferation was assessed by Mitotic Activity Index (MAI) (area: 1,59 mm², cut-off ≥10) and by several variants of Ki67-Labeling-Index counting any nuclear staining of (1) 100 tumor cells within the hot spot (Ki67-100), (2) 1020 tumor cells in 3 HPF in the tumor periphery, including the hot spot (Ki67-1020periphery), and (3) 1020 tumor cells in 3 HPF, including hot spot, cold spot and an intermediate area (Ki67-1020spectrum) using the recommended cut-off of <14 %.
Results: Of 225 carcinomas, 10 % were Triple-negative, 2 % Her2+, 6 % Luminal B Her2+, and 9 % Special Type. The rates of Luminal A vs. Luminal B-Her2neg BCs after different proliferation assessment methods were: MAI 49 % vs. 24 %; Ki67-1020spectrum: 34 % vs. 39 %, Ki67-1020 periphery: 24 % vs. 49 % and Ki67-100: 10 % vs. 63 %.
Conclusion: Subtyping of Luminal A and Luminal B Her2-neg BCs according to St. Gallen 2011 is highly influenced by the method of proliferation assessment used. Its biological relevance seems to be not unequivocal.

OFP-01-008

The utility of cytological smears allied to the OSNA method for intraoperative analysis of sentinel lymph-node metastasis in breast cancer patients

S. Foreid*, M. Martins, H. Pereira, M. Oliveira
*Loures, Portugal

Objective: One-Step-Nucleic-Acid-Amplification (OSNA) is a recently introduced PCR method to evaluate intraoperative sentinel lymph-node metastasis in breast cancer. It assesses the whole lymph-node in a 20-minutes protocol. Many studies have reported it to be more sensitive than frozen section and/or cytology. Yet, it is more expensive and takes longer to perform.
Method: Between 2010 and 2012 at CHLC, we have performed the intraoperative analysis of sentinel lymph-node using both OSNA and cytological smears in a group of patients.
Results: 35 lymph-node evaluations were done. 16 cases were OSNA positive (5 micrometastasis and 11 macrometastasis). Of those, 11 were also positive for tumor cells on cytological smears. 19 cases were negative by both methods and 5 cases were detected by OSNA but not on cytological smears. Importantly, all macrometastasis diagnosed by cytology were confirmed by OSNA. Of notice, in this series, 69 % of the positive cases detected by OSNA were also detected by cytological smears.
Conclusion: Like previously reported, OSNA showed a greater sensibility than cytology to diagnose sentinel node metastasis. However, the majority of metastasis can be detected by cytological smears alone. Our results suggest that a less expensive and faster cytological analysis should precede OSNA, and if positive, the latter method could be disregarded.

Tuesday, 11 September 2012, 17.00–19.00, Forum Hall
OFP-02 Oral Free Paper Session Breast Pathology II

OFP-02-001

Intraductal concentration of HER2-ECD and CA15-3 in early breast cancers

S. Ichihara*, S. Moritani, M. Oiwa, M. Shiraiwa, T. Endo, T. Morita, A. Kato, T. Hayashi, Y. Sato, A. Saito
*Nagoya Medical Center, Pathology, Japan

Objective: Tumor markers may be concentrated intraductally in early breast cancers.
Method: To test this hypothesis, HER2-ECD and CA15-3 of the needle washout fluid from 29 benign lesions, 26 DCIS, and 95 invasive carcinomas of the breast were measured using chemiluminescence. The measuring limit for HER2-ECD (0.5 ng/ml) and that for CA 15-3 (4 U/ml) were used as the cutoff values, respectively.
Results: The proportion of patients with any biomarker elevation was 6.9 % in cases of benign lesions, 46.2 % in DCIS, and 15.8 % in invasive carcinomas. Thus, biomarker elevation was most frequent in DCIS, followed by invasive carcinomas ($P<0.01$). HER2-ECD values over 6 ng/ml or CA 15-3 values over 25 U/ml were s een exclusively in DCIS or invasive ductal carcinomas with an extensive intraductal component, supporting the hypothesis.
Conclusion: Our approach may be useful to identify a subset of breast cancer patients who are suitable for intraductal molecular targeted therapy.

OFP-02-002

Biological significance of proliferation and HER2 over-expression in luminal/oestrogen receptor-positive breast cancer

D. Jerjees*, A. Green, A. Benhasouna, A. Alshareeda, R. Abduljabbar, F. Barros, C. Nolan, I. Ellis, E. Rakha
*University of Nottingham, Dept. of Oncology, United Kingdom

Objective: In this study, we have compared the biological significance of proliferation; assessed using Ki67 labelling index (Ki67-LI), with respect to HER2 expression in oestrogen receptor positive (ER+) breast cancer to assess the impact on growth fraction and biological characteristics of luminal breast cancer.
Method: 1562 well-characterised ER + breast cancers were assessed for expression of a large panel of biomarkers (no=30).
Results: 53 % of the cases showed high Ki67-LI (>13 %) and 12 % showed HER2 over-expression and both were positively associated with younger age, higher tumour grade, lymph node stage and shorter outcome. Both markers were associated with up-regulation of ER-coactivators (CD71, CARM1, PI3KCA&TK1), P-cadherin, p53 and with lower levels of ER expression and down-regulation of ER-related genes (PgR,

AR&GATA3) and BRCA1. Neither of the two markers was associated with expression of basal-associated cytokeratins. High Ki67-LI was associated with down-regulation of luminal enriched markers including luminal cytokeratins, MUC1, GCDFP-15, FHIT, and transcription and differentiation ER-related genes (FOXA1 and TFF3). In contrast, HER2 expression was associated with up-regulation of luminal cytokeratins, GCDFP-15, FHIT and E-cadherin.
Conclusion: Unlike high Ki67-LI, HER2 overexpression is not associated with the down-regulation of luminal enriched genes. Increased growth fraction in ER + tumours may be driven by different mechanisms in HER2+&HER2- disease.

OFP-02-003
Loss of Drosha expression is associated with poor survival in breast cancer patients
S. Khoshnaw*, T. Abdel-Fatah, C. Nolan, Z. Hodi, E. Rakha, D. Macmillan, I. Ellis, A. Green
*University of Nottingham, Breast Cancer Pathology, United Kingdom

Objective: Drosha is a protein that plays a key role in the biogenesis of microRNAs which are well known to be deranged in human breast cancer. The purpose of this study was to investigate the hypothesis that Drosha is significant in the development and progression of breast cancer and has clinical relevance as a potential predictive and prognostic target.
Method: We have examined Drosha protein expression, using microarray and immunohistochemistry, in a well-characterised series of unselected invasive breast cancer patients (n=750) with long-term follow-up and documented expression characteristics for a large range of biomarkers of known relevance in breast cancer. Furthermore, a smaller cohort of selected breast cancer cases (n=24) was also investigated for differential Drosha protein expression in distinct stages of tumour progression, including in situ (DCIS), invasive and metastatic components.
Results: Drosha cytoplasmic and nuclear expression was lost with cancer progression, and was associated with loss of BRCA1 expression. Multivariate statistical analyses showed that Drosha cytoplasmic expression was an independent predictor of breast cancer specific survival, tumour recurrence and metastases.
Conclusion: Drosha cytoplasmic expression in breast cancer is an independent predictor of patient outcome, tumour recurrence and metastasis. These observations imply that alterations in mechanisms of miRNA regulation can influence tumour behaviour.

OFP-02-004
Prognostic impact of proliferation markers Ki-67, PHH3 and mitotic count in breast carcinomas
G. Knutsvik*, I. M. Stefansson, K. Collett, L. A. Akslen
*Haukeland University Hospital, The Gade Institute, Bergen, Norway

Objective: Determination of proliferation in breast carcinomas is highly prognostic and can have treatment implications. However, there is no consensus on issues such as counting area or cut-off values. Our aim was to examine and compare Ki-67 counts in various tumor areas, the novel mitosis marker PHH3, and standard mitotic count.
Method: We examined a nested case–control series (n= 190) as part of the population-based Norwegian Breast Cancer Screening Program. Mitotic count (mitosis per mm2) was assessed on H&E-sections. The percentage of Ki-67 positive nuclei among 500 tumor cells was recorded for both hot-spots (HS; highest proliferation) and cold-spots (CS; lowest proliferation). PHH3 counts (per mm2) were evaluated by immunohistochemistry.
Results: The upper quartiles for Ki-67-HS, Ki-67-CS, PHH3 and mitotic count consistently showed the strongest associations with known unfavorable tumor features (high histologic grade, ER negativity, HER2 positivity, CK5/6+, P-cadherin+). Univariate survival analysis showed comparable prognostic strength of Ki-67-HS, PHH3 count and mitotic count. In multivariate analysis, mitotic count was the strongest prognostic factor among these.
Conclusion: By upper quartile, Ki-67-HS, PHH3 and mitotic count all showed strong associations with various tumor features. In multivariate survival analysis, mitotic count was the strongest proliferation marker.

OFP-02-005
Comparison of Ki67 labelling index of five antibodies in breast cancer and their prediction capacity of disease-free survival
J. Kulka*, A. Kovács, L. Madaras, R. Keszthelyi, Á. Meczker, A. Voigt, R. Hajós, G. Szekeres, M. Szász
*Semmelweis University, 2nd Dept. of Pathology, Budapest, Hungary

Objective: Ki67 LI is a good marker of breast cancer prognosis. We aimed at comparison of performance of 5 Ki67 antibodies.
Method: 283 breast cancer cases were retrieved. Immunohistochemical staining for 5 Ki67 clones (30-9, B56, MIB1, polyclonal, SP6) performed in TMA-s in automated immunostainer. Evaluation performed on digital slides utilizing linear 0–10 frequency score.
Results: Average scores: SP6:3.791, 30-9:3.397, poly:3.054, MIB1:2.395, B56:2.342. Antibodies correlated with the expression of MIB1 (correlation coefficients shown): B56:0.841, 30-9:0.812, SP6:0.784, poly: 0.755. Each clone was able to split prognostic subgroups at 15 % threshold (HRs and 95 % CIs shown): B56:2.750 (1.827–4.138), 30–9:2.291 (1.694–3.099), poly:2.187 (1.560–3.066), MIB1:2.160 (1.499–3.111), SP6:1.629 (1.206–2.203). Cohen's Kappa coefficient was

calculated between MIB1 and other antibodies: 30-9:0.602, B56:0.621, poly:0.665, SP6:0.485, representing moderate (30-9 and SP6) and substantial (B56 and poly) agreement.

Conclusion: Each tested Ki67 clone is suitable for predicting DFS. The clones display different staining frequencies. Grant support: TÁMOP-4.2.2/B-10/1-2010-0013. MKOT-GSK-2010

OFP-02-006

Elemental composition of breast microcalvification: Comparative study in benign and malignant lesions

M. Scimeca*, E. Bonanno, C. Pistolese, F. Dellagatta, L. G. Spagnoli

*University Tor Vergata di Roma, Dipr. di Biopathologia, Rome, Italy

Objective: Pattern and density properties of mammary calcifications are used to screen by imaging breast cancer without reference to their elemental composition.

Method: In order to characterize microcalcification composition related to pathology and mammography we utilized ultrastructural microanalysis, to analyze the elemental composition of microcalcifications in 30 mammary biopsies. Microcalcifications were taken from tissue sections and processed for the electron microscopy and microanalysis.

Results: The elemental composition of the microcalcifications of the analyzed tissues demonstrated calcium oxalate in 16 %, hydroxyapatite in 38 % and Mg-substituted hydroxyapatite (Mg-HA) in 46 % of cases. Noteworthy, hydroxyapatite resulted to be present in the 50 % of hyperplasia, in the 33 % of fibrosis and in the 17 % of carcinomas whereas Mg-HA mainly correlated with the ductal in situ carcinoma, 86 %. The density of mammographic Mg-HA is greater than hydroxyapatite and calcium oxalate one.

Conclusion: Our data suggest a strong correlation between Mg-HA and the ductal in situ carcinoma. The ability of these calcifications to sequester interstitial magnesium determines a local magnesium deficiency which could favor the carcinogenesis and/or tumor progression mechanisms. Further studies to correlate mammographic density to the Mg-HA, could improve the discrimination of calcification associated to malignant mammary lesions.

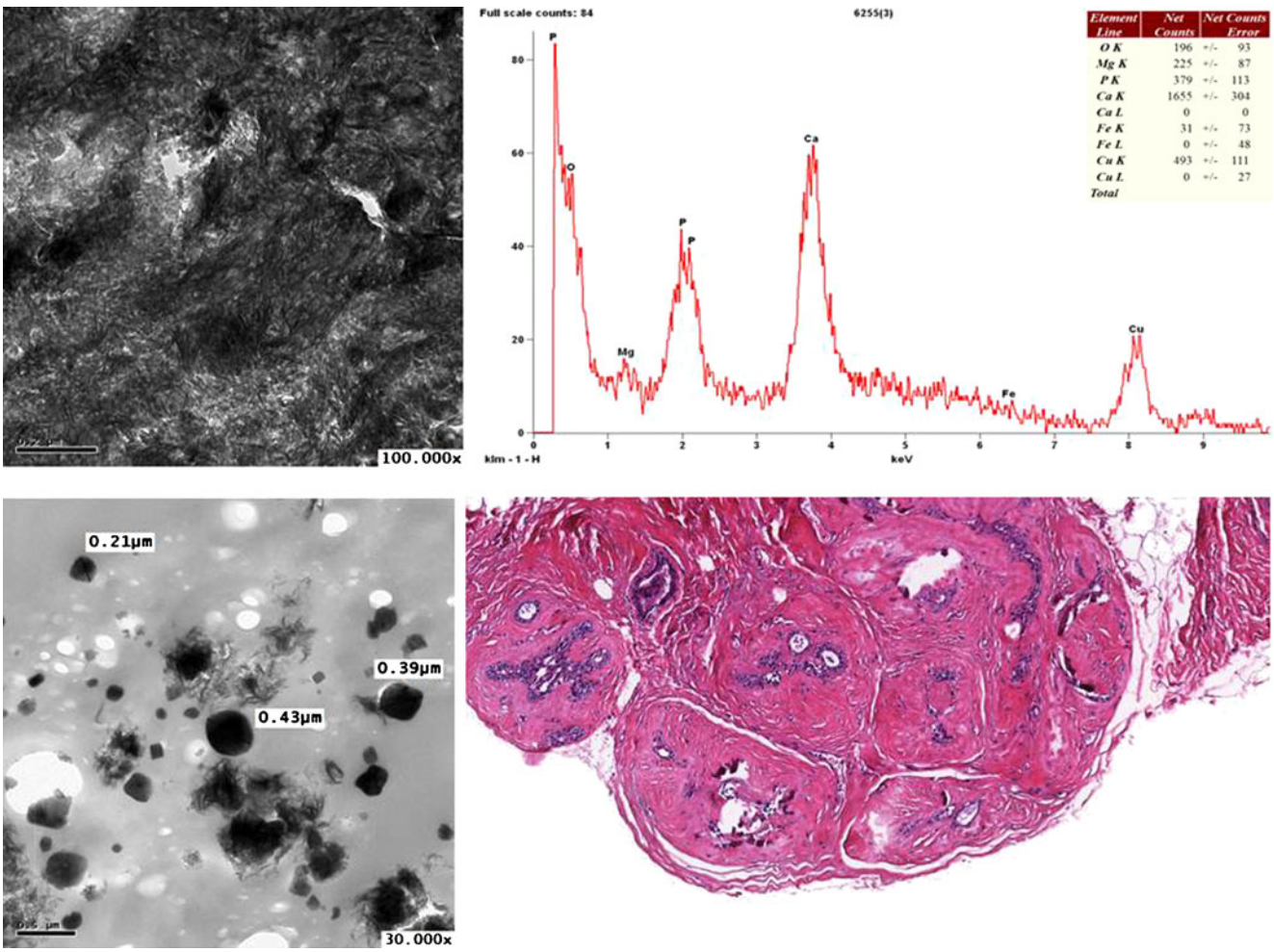

OFP-02-007

Connexin 26 and 46 expression improves prediction of neoadjuvant chemotherapy in breast cancer

I. Teleki*, T. Krenacs, A. M. Szasz, J. Kulka, C. Leo, B. Papassotiropoulos, C. Riemenschnitter, H. Moch, Z. Varga
*Semmelweis University, 1st Dept. of Pathology, Budapest, Hungary

Objective: In breast cancer, classification systems are used to assess pathological response to neoadjuvant chemotherapy. Biomarkers are still needed to better predict the efficiency of primary systemic therapy. Dysregulation of connexin (Cx) channels (gap junctions) is involved in carcinogenesis and tumor progression.
Method: We have correlated Cx expression and the pathological response in neoadjuvant treated breast cancers. Fifteen of the 21 human Cx isotypes were pre-screened. Cx26, Cx32, Cx43 and Cx46 were found widespread and tested in tissue microarrays of 96 breast cancers prior to and after neoadjuvant chemotherapy. Pathological response was characterized according to the EWGBSP, CPS-EG, Miller-Payne, Sataloff, and NSABP classification systems.
Results: Only the CPS-EG classification had prognostic relevance by score 1–2 cases presenting better overall survival (p=0.015) than those scoring 3–5. Cx43 levels pre-chemo correlated with hormone receptor status pre- and post-chemo and had inverse correlation with HER2 levels pre-chemo. Reduced Cx26 expression (<5 %) post-chemo correlated with better overall survival (p=0.011). Moderate or higher Cx46 expression (>20 %) pre-and post-chemo was also associated with better survival in the EWGBSP TR2b (ppre=0.006), Sataloff TB (ppre=0.005; ppost=0, 029) and Miller-Payne G3 (ppre=0.002; ppost=0.012) subgroups.
Conclusion: Classifications combined with testing for Cx46 and Cx26 expression can improve prediction of neoadjuvant chemotherapy in breast cancer.

OFP-02-008

Atypical vascular lesions after radiation therapy for breast cancer: A clinicopathologic study and outcomes of 24 cases

H. Gobbi*, C. Fraga-Guedes, M. Mastropasqua, M. Kneubil, E. Botteri, G. Viale
*UFMG, Dept. of Anatomic Pathology, Belo Horizonte, Brazil

Objective: We assessed clinicopathologic features and outcomes of 24 cases of atypical vascular lesions (AVL) in patients submitted to radiation therapy for breast carcinoma.
Method: Data from all patients were retrieved from the files of the European Institute of Oncology (EIO), Milan. Histopathological review of all cases was carried out.
Results: All patients were women (median age: 58 year, range: 36–81 year). Median lesion size was 0.5 cm (range: 0.3 to 1.1 cm). Median latency interval from radiation to AVL diagnosis was 49 months (range: 17 to 124 months). 62.5 % of cases presented as an erythematous unique papule confined to superficial/middermis with proliferation of thin-walled, vascular channels, lined by a single layer of bland endothelial cells. No prominent nucleoli, mitoses or blood lakes were seen. Patches of chronic inflammatory infiltrate accompanied all AVL. One patient (4.2 %) developed local recurrence, and two patients (8.3 %) developed angiosarcoma in the previous biopsy site, 19 and 89 months later. Margin involvement was associated to unfavorable outcome.
Conclusion: Our data suggest that post-radiation AVL and angiosarcoma may represent a spectrum of the same disease process. The development of local recurrence and subsequent angiosarcoma indicate that AVL must be completely excised, with free surgical margins, and patients must be accompanied by clinical exams and imaging.

Monday, 10 September 2012, 17.00–19.00, North Hall
OFP-03 Oral Free Paper Session Digestive Diseases Pathology I

OFP-03-001

Gastric dysplasia: Immunophenotypic classification and expression of CDX2 and ALDH1

H. Baldaia*, P. Valente, M. Garrido, F. Baldaque-Silva, J. Lopes, F. Carneiro
*Centro Hospitalar S. João, Pathology, Porto, Portugal

Objective: Gastric dysplasia is classified as gastric/foveolar and intestinal/adenomatous according to morphological (architectural and cytologic) features. The immunophenotypic classification of dysplasia, based on the expression of mucins and CD10, recognizes three major types: gastric (MUC5AC and/or MUC6); intestinal (MUC2 and/or CD10); hybrid (gastric and intestinal markers). CDX2 is a transcription factor responsible for early intestinal differentiation. ALDH1 is recognized as a stem cell marker in several organs.
Method: Nineteen cases of dysplasia were classified as gastric/foveolar (n=8) or intestinal/adenomatous (n=11) and graded as low-grade (n=9) and high-grade (n=10). Immunophenotypic classification showed gastric (n=5; 26 %), intestinal (n=6; 32 %) and hybrid (n=8; 42 %) phenotypes.
Results: Cases classified by morphology as gastric/foveolar-type displayed gastric (50 %) or intestinal (50 %) immunophenotype, whereas intestinal/adenomatous-type cases displayed gastric (9 %), intestinal (55 %) or hybrid (36 %) immunophenotype (p=0.023). High-grade dysplasia was identified in cases with gastric (80 %), intestinal (17 %) and hybrid (63 %) immunophenotype (p=0.085). CDX2 expression was significantly lower (p=0.044) in gastric

(60 %) than in intestinal and hybrid immunophenotypes (100 %). ALDH1 expression was displayed only in gastric (80 %) and hybrid (50 %) immunophenotypes (p=0.023).
Conclusion: Gastric dysplasia is heterogeneous and morphology is insufficient to elucidate cell differentiation. High-grade dysplasia, decreased CDX2 expression and high ALDH1 expression are associated with gastric immunophenotype.

OFP-03-002

Tumor budding in pancreatic cancer: Are we missing important prognostic information?

D. Born*, I. Zlobec, M. Montani, B. Gloor, A. Lugli, E. Karamitopoulou-Diamantis
*Universität Bern, Inst. für Pathologie, Switzerland

Objective: Tumor budding is defined as single tumor cells or small cell clusters at the invasive front of gastrointestinal (including colorectal, gastric and ampullary) carcinomas and is linked to adverse prognosis. To date it has not been reported in pancreatic ductal adenocarcinomas (PDACs). We assessed the presence and prognostic importance of tumor budding in PDAC.
Method: Whole-tissue sections of 120 PDACs with full clinico-pathological and follow-up information were stained with pancytokeratin. Tumor budding was assessed in 10 high-power fields (HPFs) by two pathologists and considered high-grade (HG) when an average of >10 buds was counted. Measurements were correlated to the patient and tumor characteristics.
Results: Inter-observer agreement was strong (ICC=0,72). HG-budding was found in 70.3 % of cases and was linked to advanced pT-stage (p=0.0463), lymphatic invasion (p=0.0192) and decreased disease-free and overall survival (p<0,0001 and p=0,0005). There was no association with pN, pM, R-stage or vascular invasion. In multivariate analysis the prognostic effect of HG-budding was independent of lymphatic invasion, pN and R-stage [p<0,0001, HR (95 % CI)=3,65(2,1-6,4)].
Conclusion: Tumor budding occurs frequently in pancreatic cancer, is an indicator of worse outcome and adds independent prognostic information. Routine use of tumor budding would help to better stratify patients into prognostic subgroups.

OFP-03-003

Epstein-Barr virus and p53 in the development of gastric cancer

V. Genitsch*, M. Cathomas, L. Terracciano, L. Tornillo, A. Lugli, A. Marx, G. Sauter, F. Carneiro, F. Hofstädter, N. Willi, G. Cathomas
*Kantonsspital Baselland, Abt. Pathologie, Liestal, Switzerland

Objective: Epstein-Barr virus (EBV) is associated with a subset of gastric cancers (GC). In this study, the prevalence of EBV and its presence in the development of GC were assessed.
Method: EBV was evaluated in GC by tissue microarrays using in situ hybridization for EBER (n=610). Non-tumorous, dysplasia, intramucosal and invasive carcinomas and metastasis of EBV positive GC were analyzed (n=22). p53 expressen was evaluated in EBV positive and a subset of 84 EBV negative GC.
Results: 4.9 % of gastric cancers were positive for EBER. All invasive cancers showed diffuse EBER positivity and only 2 lymph nodes revealed a focal loss of EBER. In 13 GC with foci of atypia/low grade dysplasia, no or only focal EBER positivity was observed. p53 was overexpressed in 24 of 84 EBV negative but not in EBV positive GC (28.6 % vs. 0 %; p=0.007).
Conclusion: EBV is diffusely expressed in invasive GC and only occasionally lost in metastasis. In low grade dysplasia, however, EBV is often focal or missing, indicating that EBV infection may be associated with progression from low grade dysplasia to invasive cancer and this progression is p53 independent.

OFP-03-004

P2X7R attenuates colitis associated carcinogenesis

P. Hofman*, T. Juhel, M. Ilie, O. Bordonne, O. Boyer, X. Hebuterne, S. Adriouch, V. Vouret-Craviari
*CHU de Nice, LPCE, France

Objective: It is now well established that patients with inflammatory bowel disease presented a higher risk to develop a colon cancer. Our previous works characterized the link that exists between bacterial infection and inflammation and highlighted the role of the microenvironment on the onset of chronic inflammation. Here, we wished to understand the role of inflammasome, a complex of proteins that is activated by microbial motifs and the purinergic receptor P2X7 and involved in the maturation of IL-1β.
Method: We treated P2X7R knockout mice to induce acute colitis (3 % DSS) or colitis associated colon cancer (AOM and DSS).
Results: We showed that P2X7R KO mice are more resistant than wild type mice to a DSS-induced colitis. Further, we demonstrated that P2X7R KO mice are highly susceptible to inflammation driven colon tumorigenesis. In addition, we showed that tumors from P2X7R KO contained more neutrophils (CD11b+/Ly6G+cells) and less macrophage (CD11b+/Ly6G–) than tumors obtained from WT mice.
Conclusion: We will present results on the characterization of the pro tumoral tumor associated neutrophils and the molecular mechanisms that are linked to the presence of such immune cells.

OFP-03-005

IEL counts and distribution in normal duodenum, non-GSE IELosis and GSE: Do we need a cut-off?

B. A. Karabork*, S. Yuksel, B. Savas, A. Ensari
*Ankara University of Medicine, Dept. of Pathology, Turkey

Objective: Intraepithelial lymphocytosis (IELosis) is a characteristic feature of gluten-sensitive enteropathy (GSE), though, the cut-off is still debatable. We aimed to evaluate the number and distribution of IELs in normal duodenum, and in non-GSE IELosis and GSE.

Method: The study group comprised of a spectrum of normal duodenal biopsies (n=31), non-GSE IELosis (n=30), Type 1 (n=22) and Type 3 (n=21) serologically diagnosed GSE cases. The number of IELs/100 enterocytes and distribution on H&E and CD3-immunostained sections, were assessed for each group. Chi square test was used for statistics.

Results: IELs increased significantly through the spectrum (15,81–21,55 in normal, 25,73–40,37 in non-GSE, 37,05–54,00 in Type 1, 67,86–85,10 in Type 3) on H&E and CD3, respectively (p<0,001). IEL counts ≥20 on H&E and ≥25 on CD3 had a sensitivity of 95,35 % and 100 %, and a spesificity of 40,98 % and 32,79 %, respectively, for GSE. IEL distribution was diffuse in Type 1 (95,5 %), Type 3 (100 %) but focal in non-GSE (80 %) (p<0,001).

Conclusion: The current cut-off for IEL counts seems to be sensitive for IELosis, though, not specific for GSE and needs to be accompanied by the diffuse distribution of IELs.

OFP-03-006

Geographic analysis of the protein expression of metastasis suppressor gene RKIP and its clinical relevance in colorectal cancer

V. Koelzer*, E. Karamitopoulou, H. Dawson, A. Lugli, I. Zlobec
*University of Bern, Inst. of Pathology, Switzerland

Objective: Loss of Raf-1 Kinase Inhibitor Protein (RKIP) expression has been implicated in disease progression in several tumor types. The aim of this study was to evaluate RKIP expression in colorectal cancer stratified by histological "zones" and to determine the zone responsible for its clinical relevance.

Method: Immunohistochemical expression of RKIP was assessed in 100 colorectal cancers using whole tissue sections. Four different areas were evaluated using 10 high-power-fields (HPFs) each: normal mucosa, tumor center, invasion front and tumor buds. The average expression for each zone was assessed for its clinical relevance.

Results: Expression of RKIP was diffuse in normal mucosa and progressively lost towards the tumor center and front (26 %, 15 % and 8 % RKIP-positivity, respectively; p<0.0001). Only 3 % of tumor buds were RKIP-positive. RKIP loss in the tumor center only corresponded to more frequent lymph node positivity (p=0.0766), distant metastases (p=0.0243), lymphatic invasion (p=0.0533) and more advanced TNM stage (p=0.0278). RKIP loss was highly prognostic (HR (95 % CI): 0.45 (0.2–0.9); p=0.0288) independently of TNM and therapy.

Conclusion: The clinical relevance of RKIP is restricted to the tumor center where it acts as an independent prognostic factor. Its absence in tumor buds provides further evidence to support their hypothesized metastatic potential.

OFP-03-007

Outcomes of neoadjuvant chemoradiation for rectal carcinoma

G. Ozgun*, F. Oz Atalay, N. Ugras, O. Yerci
*Uludag University, Dept. of Pathology, Bursa, Turkey

Neoadjuvant radiation and chemoradiation is currently the treatment of choise for patients with locally or advanced carcinoma of the rectum. Patients treated with neoadjuvant chemoradiatheraphy with good clinical response and tumor regression present a controversial management dilemma. To assess the effects of chemoradiation on tumor regression and disease free survival, consecutive series of 27 patients receiving neoadjuvant chemotheraphy or chemoradiation and a control series of 32 patients without pretreatment were studied. The overall survivals and disease free survivals were compared in terms of variables such as tumor regression grade, stromal response in tumor bed, state of lymph node metastasis, and the localization of the tumor in between patients treated with chemoradiation and the control group. Neoadjuvant treatment is one of the treatment modalities in rectal carcinomas. We want to present our experience between 2005 and 2011 in our institution. Key words: Rectal carcinoma, neoadjuvant treatment, pathologic complete response

OFP-03-008

Identification of Tissue Microvascular Invasion Biomarkers in Hepatocellular Carcinomas by MALDI Imaging Mass Spectrometry

N. Poté*, T. Alexandrov, J. Le Faouder, S. Laouirem, J. Belghiti, J. M. Camadro, V. Paradis, P. Bedossa
*Paris, France

Objective: Microvascular invasion (mVI), a major predictive factor of tumoral recurrence and mortality in patients with hepatocellular carcinoma (HCC), is only detectable on pathological examination. So far, there is no reliable tool to identify mVI prior to surgical procedures. MALDI Imaging Mass Spectrometry (IMS) represents a new analytical tool to provide the relative abundance and distribution of the whole

proteins expressed in a tissue section. The aim of this study was to compare, using MALDI IMS, the tissue proteome of HCC without and with mVI in order to identify surrogate biomarkers of mVI.
Method: A total of 56 HCC samples obtained from surgical specimens, for which frozen samples were available, were retrospectively collected. Two groups of tumors were defined (26 HCC without mVI; 30 HCC with mVI) and were analysed by MALDI IMS. A statistical comparative analysis of acquired mass spectra was then performed in order to identify protein peaks differentially expressed between the two groups.
Results: 30 protein peaks were differentially expressed between the two groups, all overexpressed in HCC with mVI. Protein characterization of some of these peaks is in progress.
Conclusion: These results highlight the potential of MALDI IMS to uncover new biomarkers in liver carcinogenesis. The identification of mVI biomarkers would be helpful in the therapeutic strategy of patients with HCC.

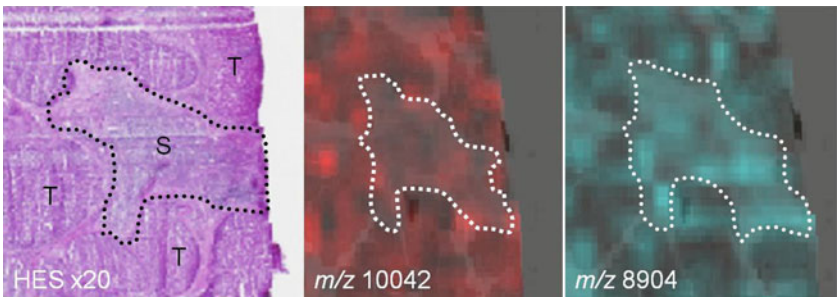

OFP-03-009
A histopathological scoring system can predict the recurrence of hepatocellular carcinoma in liver transplant patients treated with transarterial chemoembolization
F. Rosini*, F. Vasuri, D. Malvi, P. Baldin, W. F. Grigioni, A. D´Errico-Grigioni
*University of Bologna, Dept. of Anatomic Pathology, Italy

Objective: Aim of this study is to define the histopathological features predictive of hepatocellular carcinoma (HCC) recurrence in patients treated with orthotopic liver transplantation (OLT) after tumoral transarterial chemoembolization (TACE), in order to establish a predictive "score" applicable by pathologists for recipient risk stratification.
Method: We retrospectively enrolled 110 patients (276 total neoplastic or necrotic nodules) who received TACE for HCC downstaging before OLT. The following data were collected: number of neoplastic/necrotic nodules, microscopic thrombosis, the residual neoplastic tissue (RNT), and dysplastic nodules. Sizes, percentage of necrosis, Edmondson's grade, clear cell features were also collected for each nodule.
Results: Median follow-up was 1230 days: 14 (13 %) HCC recurrence cases were recorded. Statistically RNT (best cut-off 3 cm3, P=0.032), the total nodule number (best cut-off ≥ 3, P=0.001), and the neoplastic thrombosis (P=0.011) were the only variables predictive of HCC recurrence. Scoring 1+ each parameter, recipients with 0 (n=43) had 0 % recurrence rate; recipients with 1+/2+ (n=49) had 12 %; recipients with 3+ (n=18) had 44 % recurrence rate (P<0.001).
Conclusion: We were able to stratify OLT recipients with TACE-treated HCC in 3 risk groups based only on histopathological analysis.

OFP-03-010
Discovery of a new histopronostic factor in rectal adenocarcinoma treated by radiochemotherapy followed by surgical resection
A. Sannier*, J. Lefèvre, F. Bretagnol, D. Cazals-Hatem, Y. Panis, P. Bedossa, N. Guedj
*Paris, France

Objective: Neoadjuvant radiochemotherapy (RCT) followed by surgical resection became the treatment for locally advanced rectal cancer. Pathological diagnosis is important for the prediction of prognosis and adjuvant treatment. Study aim was to identify histopronostic factors in a consecutive series of patients treated by RCT and surgery.
Method: 113 patients were included, follow-up, tumor morphologic pattern and Modified Rectal Cancer Regression Grade (m-RCRG) were assessed. Univariate and multivariate analysis were used to assess predictors of disease-free survival (DFS).
Results: 5-years DFS was 58 %. In univariate analysis, ypT, budding, calcifications, circumferential margin, node involvement, invaded margin, vascular emboles and perineural involvement were pronostic factors (p<0.05). In multivariate analysis, presence of calcification in tumor bed (p=0.027) and small circumferential margin (p=0.037) were the only two independent factor of worse DFS. mRCRG was not correlated

to DFS. Among the 50 mRCRG1 tumor, DFS was significantly better in patient with ypT0 than in other ypT stages (p=0.003).
Conclusion: Presence of calcification in tumor bed is a new major histopronostic factor described for the first time in rectal cancer. Our results raised the question of whether ypT stage or histological tumor regression is more important in the prediction of patient prognosis.

Tuesday, 11 September 2012, 17.00–19.00, Club D
OFP-04 Oral Free Paper Session Digestive Diseases Pathology II

OFP-04-001
Histological grading: A prognostic factor for stage I colorectal cancer?
V. Barresi*, L. Reggiani Bonetti, G. Branca, C. Di Gregorio, M. Ponz de Leon, G. Tuccari
*University of Messina, Dept. of Human Pathology, Italy

Objective: The most widely used system for histological grading of colorectal cancer (CRC) is based on the degree of gland formation, despite significant interobserver variability and low prognostic value. Herein we analyzed the prognostic significance of a grading system based on the presence of poorly differentiated clusters in stage I CRC.
Method: Poorly differentiated cancer clusters were assessed by two independent pathologists in stage I CRC characterized or not by disease progression. Tumors with <5, 5 to 9, and >10 clusters were classified as G1, G2, and G3, respectively. The prognostic value on disease-free survival and the association with other clinicopathologic characteristics of the conventional and novel grading systems were analyzed.
Results: K statistics for inter-observer variability in the assessment of histological grade based on poorly differentiated custers was 0.728 (good). High histological grade assessed with the novel system, but not with the traditional one, represented a negative significant prognostic factor for disease-free survival and it was significantly associated with venous invasion, lymphatic invasion, budding, invasive growth and nodal micrometastases.
Conclusion: We suggest that a tumor grading system based on the number of poorly differentiated clusters has a stronger power to stratify stage I CRC patients by prognostic outcome than conventional grading.

OFP-04-003
Cytokeratin 7: A marker for BRAF mutated colorectal carcinomas?
S. Gurzu*, Z. Szentirmay, I. Jung
*University of Targu Mures, Dept. of Pathology, Romania

Objective: Cytokeratin20+/Cytokeratin7− (CK) is used as the characteristic immunophenotype of colorectal carcinomas (CRC). Some new studies suggested that aberrant pattern CK20/CK7 can be identified in colorectal cancer with microsatellite instability (MSI). Our aim was to establish which factors may determine changing in this immunophenotype.
Method: In 70 CRC, randomly selected, we performed immunohistochemical stains with CK20 and CK7 and analyzed the microsatellite status and BRAF mutations with real time PCR.
Results: From the 70 CRC, 15 were MSI and 55 MSS (microsatellite stable) cases. 90 % of MSS cases diffusely expressed CK20 without CK7 expression. From the 15 MSI cases, 6 presented BRAF mutations. In MSI cases with BRAF mutations, CK20 was focally expressed or negative and CK7 was diffusely expressed.
Conclusion: Cytokeratin7 positivity may be used to select BRAF mutated MSI colorectal carcinomas. Both CK7 and CK20 should be used for differential diagnosis of colorectal cancer.

OFP-04-004
Intratumoral budding in preoperative biopsies predicts local and distant metastasis in colorectal cancer patients
A. Lugli*, M. Hädrich, D. Inderbitzin, M. Borner, I. Zlobec
*Medizin. Universität Bern, Inst. für Pathologie, Switzerland

Objective: In 2011, the term “intratumoral budding, ITB” was used to describe the presence of tumor buds within the main tumor body and was correlated to worse clinical outcome in colorectal cancer patients. Here, we further elucidate the potential clinical role of ITB in pre-operative biopsies using pan-cytokeratin stained tissues and a quantitative scoring system.
Method: 139 pre-operative biopsies from patients with colorectal cancer underwent immunohistochemistry for pan-cytokeratin (AE1/AE3). ITB were counted in the area of densest budding (40×) and classified as high-grade when >10 buds/HPF were observed based on receiver operating characteristic (ROC) curve analysis.
Results: High-grade ITB occurred in 26.6 % of cases and was associated with right-sided tumor location (p= 0.0356), more advanced pT (p=0.0198) and pN (p< 0.0001) classifications, distant metastasis (p=0.0164), higher tumor grade (p=0.0037) and lymphatic invasion (p=0.0445). The specificity and positive predictive value for lymph node metastasis was 86.7 % and 75.6 %, respectively. Disease-free survival was significantly worse in patients with high-grade ITB (5-year survival=25 %) in comparison to patients with low-grade ITB (5-year survival= 55 %) (p=0.0157).
Conclusion: The assessment of ITB in pre-operative biopsies is predictive of local and distant metastasis in corresponding resections and should be considered in daily management of colorectal cancer patients.

OFP-04-005

Alpha-methylacyl-CoA (AMACR) in gastric cancer - Correlation with clinicopathological data and disease free survival

A. Mroz*, M. Kiedrowski, Z. Lewandowski
*CMKP, Gastroenterology and Hepatology, Warsaw, Poland

Objective: Diagnostic and prognostic significance of alpha-methylacyl-CoA (AMACR) has been established in many human cancers. Its correlation with clinical and pathological data in gastric cancer has not been fully elucidated and its impact on surveillance has not been studied thus far.
Method: We analyzed consecutive gastric cancer cases in terms of AMACR immunohistochemical expression and clinical/pathological characteristics and followed patients' postoperative history.
Results: AMACR was expressed in 94/164 gastric cancers (57.3 %). We did not find correlation between AMACR expression and gender, age, location, histological type, pTN staging, vascular and nerve sheaths invasion. Overall disease-free survival tended to be worse in AMACR positive patients (p=0.062), and in adenocarcinoma subgroup it was significantly shorter (p=0.021).
Conclusion: AMACR expression might represent promising adverse prognostic factor in gastric cancer, particularly in adenocarcinoma histological type.

OFP-04-006

Development of a rabbit monoclonal antibody for determining hENT1 status and predicting response to gemcitabine in pancreatic ductal adenocarcinoma

M. Raponi*, J. Isaacson, J. Ranger-Moore, J. Clements, B. Richardson, S. Ormanns, K. Winter, A. Allen, R. Andersson, V. Heinemann, A. P. Dicker
*Clovis Oncology, San Francisco, CA, USA

Objective: Human equilibrative nucleoside transporter 1 (hENT1) is the primary membrane channel through which gemcitabine (Gem) enters pancreatic tumor cells, and patients whose tumors have low expression of hENT1 may derive little benefit from Gem therapy.
Method: An analytically validated rabbit monoclonal antibody immunohistochemistry (IHC) in vitro diagnostic (IVD) for assessing the degree of hENT1 expression in pancreatic adenocarcinoma using an automated IHC platform has been developed.
Results: Using primary tumor samples (n=201) from a randomized controlled clinical adjuvant trial (RTOG 97-04), we developed and verified a hENT1 scoring methodology and cut-off for identifying patients least likely to benefit from Gem (hENT1-low). The distribution of hENT1 expression was similar between these samples and an independent set of 130 pancreatic adenocarcinoma specimens from the AIO-PK0104 study of which 77 were confirmed metastatic biopsies. Overall, using this cut-off, approximately two thirds of pancreatic tumors displayed low-hENT1 expression across the different data sets.
Conclusion: A robust hENT1 IHC IVD has been developed using a rabbit monoclonal antibody and identifies two thirds of primary and metastatic PDAC cases as having low expression of hENT1.

OFP-04-007

Hypoxia activates pancreatic stellate cells: Development of an organotypic culture model of thick slices of normal human pancreas

V. Rebours*, M. Albuquerque, P. Ruszniewski, P. Lévy, A. Sauvanet, V. Paradis, P. Bedossa, A. Couvelard
*Beaujon Hospital, Pancreatology Unit, Clichy, France

Objective: Pancreatic stellate cells (PSC) promote oncogenesis by modulating cell proliferation. Aim- To evaluate the early activation of PSC in case of hypoxia in normal human pancreas.
Method: An organotypic culture model of thick sections of human pancreas has been developed and validated. Slices of pancreas (300 μm) were prepared from surgical specimens and cultured in hyperoxia conditions. Half of the samples underwent an initial phase of culture in normoxia (21 % O2) to reproduce hypoxia. The total duration of culture was 72 h. Cell viability, hypoxia, apoptosis and activation were monitored.
Results: 30 sections per specimen were cultured. Analysis was performed at baseline, 24 h, 48 h and 72 h. Morphological analysis showed gradual appearance of ductal/acinar dedifferentiation. At 72 h, foci of necrosis were identified. Hypoxia was confirmed by the expression of HIF1 and CA9 at 48 h (10 % and 50 % of labeled cells). Apoptosis was limited, acinar cells expressed caspase 3 at 48 and 72 h. Analysis of proliferation using Ki67 index showed significant activation of PSC at 48 h (×5/baseline) and at 72 h (×6/baseline). Activation of PSC was confirmed by smooth muscle actin immunochemistry.
Conclusion: Organotypic culture of normal human pancreas is possible with optimized cell viability at 72 h. Hypoxia-induced activation of PSC occurs very early.

OFP-04-008

Intraductal Papillary Neoplasms of the bile duct (IPN): Stepwise progression to invasive carcinoma comprises alterations of KRAS, p53, p16, ß-catenin, HER2, EGFR and smad4

A. M. Schlitter*, D. Born, M. Bettstetter, B. Terris, Y. Zen, B. Sipos, J. Siveke, A. Perren, G. Klöppel, I. Esposito
*Technische Universität München, Inst. für Pathologie, Germany

Objective: IPN are still poorly characterized precursor lesions of bile duct adenocarcinoma. We present a multicenter study with focus on morphology, subtyping and prognosis and provide a detailed molecular analysis in the stepwise progression from low-grade to high-grade lesions and invasive carcinoma.
Method: Fourty-five patients with biliary IPN were included into the cohort, twenty-two patients with conventional adenocarcinoma of the bile duct served as control cohort. Subtyping was performed based on histomorphology and expression profile of mucins and cdx2 expression. Furthermore, low grade lesions (n=14), high-grade lesions (n=38) and invasive components (n=13) of IPN as well as conventional bile duct adenocarcinomas (n=22) were investigated individually for alterations of common oncogenic pathways using immunohistochemistry, real-time polymerase chain-reaction and direct sequencing.
Results: IPN are mainly detected at preinvasive stage (71 %), pancreato-biliary and intestinal type are the most common subtypes (36 and 29 %, respectively). Detailed molecular analysis showed that p53 overexpression, k-ras mutation, loss of heterozygosity of p16 locus and nuclear ß-catenin expression are early events and loss of smad4 and overexpression of EGFR and HER2 are later events in the tumor progression of IPN.
Conclusion: Stepwise alterations of common oncogenic pathways are required for progression of biliary IPN from non-invasive precursors to invasive carcinoma.

OFP-04-009

Influence of BRAF mutations and RAC1b/RAC1 mRNA ratio or protein expression on outcome in patients with metastatic Colorectal Cancer (mCRC) treated with first-line chemotherapy

M. Cuatrecasas*, V. Alonso-Espinaco, P. Jares, C. Horndler, A. Castells, J. J. Lozano, J. Maurel
*Hospital Clinic, Barcelona, Spain

Objective: Metastatic colorectal cancer (mCRC) patients with BRAF mutation V600E present poor overall survival (OS). RAC1b, a RAC1 spliced variant, is overexpressed in CRC and impairs apoptosis by activation of nuclear-factor-KB. We evaluated if RAC1b was an independent prognostic factor in mCRC.
Method: We examined BRAF (V600E) mutational status, RAC1b by immunohistochemistry, RAC1b/RAC1 expression ratio by mRNA RT-PCR, and mismatch repair (MRR) deficiency by microsatellite instability (MSI) analysis, in 186 mCRC patients treated in first-line therapy with FOLFOX or CAPOX from three Spanish institutions. We assessed whether these biomarkers were independently predictive of progression free survival (PFS) or OS.
Results: 7 % CRC had BRAF mutations, 5 % MSI-H, 20 % high RAC1b/RAC1 ratio, and 25 % RAC1b protein overexpression. Five of 11 CRC (46 %) with BRAF mutations had high RAC1b/RAC1 ratio/protein vs 25/144 (18 %) without BRAF mutation (p=0.036). All BRAF mutated or RAC1b/RAC1 high were MSS. Low RAC1b/RAC1 ratio and BRAF WT had higher response rate (68 % vs 43 %; p= 0.035). Multivariate regression analysis identified ECOG PS as a significant variable for PFS and LDH levels, PS and high RAC1b/RAC1 ratio for OS.
Conclusion: High RAC1b/RAC1 expression ratio or immunoexpression constitutes a marker of poor OS and a potential marker of acquired chemo-resistance in mCRC treated with oxaliplatin-based therapy.

Monday, 10 September 2012, 17.00–19.00, Terrace 1
OFP-05 Oral Free Paper Session Endocrine Pathology

OFP-05-001

Morphological and biochemical atypism of papillary thyroid cancer

T. Pavlova*, I. Pavlov, D. Kolesnicov, L. Pavlova, I. Goncharov, I. Bashuk
*Belgorod State University, Dept. of Pathology, Russia

Objective: Annually more than 120.000 new cases of papillary thyroid cancer, that is 1 % of malignant tumors, are registered all over the world.
Method: There are clinical and morphological methods: immunohistochemistry (MMP-2, MMP-9, TIMP-1, TIMP-2), light, transmission, electron, probe and scanning microscopy with the trace element analysis. It was studied 1541 cases of thyroid cancer since.
Results: At the papillary thyroid cancer progression matrix metalloprotease and specific tissue inhibitors of metalloprotease (TIMP-2) increased in the cytoplasm of tumor cells, but the concentration of TIMP-1 decreased. Tumors with low degree of ultrastructural differentiation were presented by cells with electron-dense dark cytoplasm and cells with poor cytoplasm organelles and differently formed nucleus with numerous deep invaginations. High level of some matrix metalloproteaseexpression (MMP-9) and low level of TIMP expression (TIMP-1) were observed in current cases more (45 % and 58 % respectively), than at more differential papillary thyroid cancer (23 % and 37 %). At performance of atomic force microscopy it was shown that connection between cells had become weak at the decreasing of malignancy degree. It was revealed the significant increasing of oxygen, magnium, potassium, calcium in tumor nodes.
Conclusion: Conducted comlex morpho-chemistry analysis display diagnostic patterns of papillary thyroid cancer.

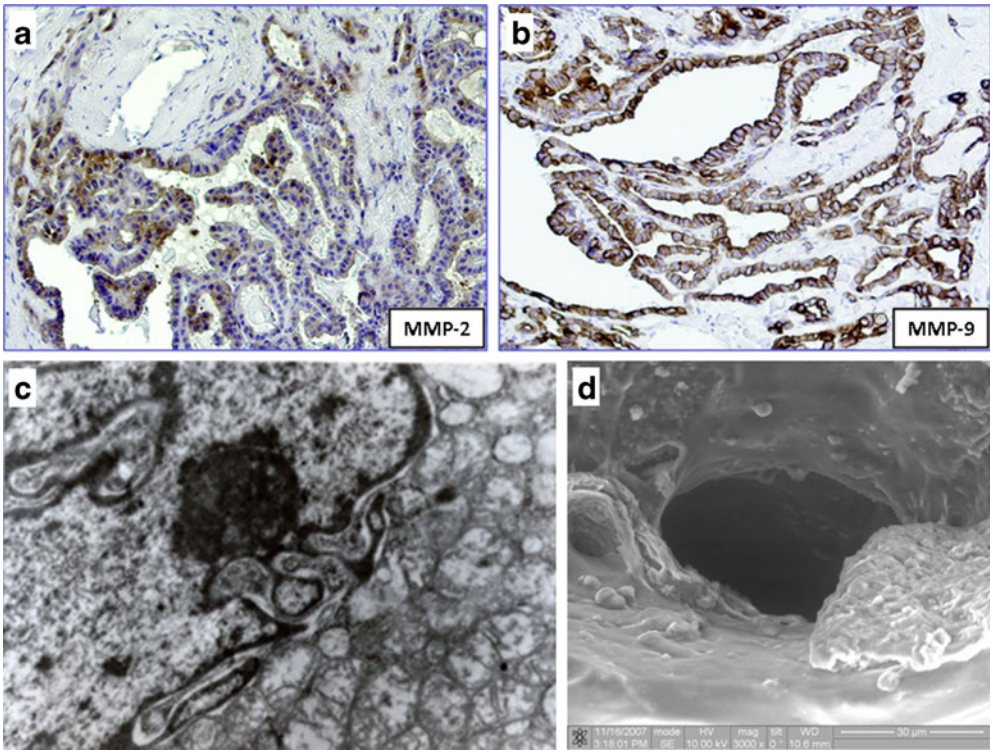

OFP-05-002

Benign Thyroid Nodules with Papillary Hyperplasia (BTN-PH): A retrospective cytological study of 48 cases with surgical follow-up

M. Pusztaszeri*, J. Krane, E. Cibas, W. Faquin
*Vandoeuvres, Switzerland

Objective: Cytological features of BTN-PH, sometimes interpreted as papillary carcinoma (PC) on fine-needle aspiration biopsies (FNAB), have not been studied extensively.
Method: Available material from 48 BTN-PH was reviewed retrospectively and compared with 15 PCs.
Results: FNAB diagnoses were: non-diagnostic (n=1), benign (n=18), AUS/FLUS (n=10), suspicious for follicular neoplasm (n=4), suspicious for malignancy (S-PC) (n=13), and malignant (P-PC) (n=2). The extent of papillary hyperplasia on histology was higher in S-PC/P-PC diagnostic categories (50 %; P=0.019; range: 5–90 %). On cytology, papillary structures, present in 53 % of BPN-PH cases, were more frequent and numerous in the S-PC/P-PC group (89 %; P= 0.0093). Focal nuclear atypia was seen in all S-PC/P-PC cases, including rare grooves (87.5 %), enlargement/crowding (75 %), chromatin clearing/rare pseudoinclusions (25 %), but were less than in PCs (P<0.0001). Nuclei were smaller in BTN-PH than in PCs (mean diameter/range (μm): 8.2/6-12 vs 14.2/7-26; P=0.0001). All BTN-PH tested (n=9) were immunonegative for HBME-1, galectin-3, and keratin-19.
Conclusion: BTN-PH diagnosed as S-PC/P-PC often show papillary structures and focal nuclear features of PC but they are significantly less than in classical PCs, stressing the need to apply strict criteria for PC diagnosis.

OFP-05-003

Genetic alterations in glucagon cell adenomatosis

T. Henopp*, M. Anlauf, S. Biskup, G. Klöppel, B. Sipos
*Medizin. Universität Tübingen, Inst. für Pathologie, Germany

Objective: Glucagon cell adenomatosis (GCA) was recently recognized by us as a multifocal neoplastic disease of the endocrine pancreas unrelated to MEN1. Multiple micro- and a few macrotumors are found on the background of a hyperplasia of glucagon cells. The disease may cause unspecific abdominal symptoms and only rarely a glucagonoma syndrome. Recently a mutation in the glucagon receptor (GCGR) gene was described in one GCA patient.
Method: The extracted DNA of five patients with GCA was sequenced and the GCGR gene analyzed for mutations.
Results: Sequencing of the GCGR gene revealed germline mutations in three out of five patients. One patient shows

two different heterozygous point mutations in the hyperplastic alpha cells as well as in the non-tumorous tissue leading to two premature stop codons. One patient harbors a homozygous stop mutation. The third patient shows two homozygous missense mutations of the GCGR gene that most likely also led to a dysfunction of the GCGR. In the two other patients no germ line mutations of the GCGR gene were detected. These variants were not identified in healthy subjects.

Conclusion: The finding of germ line and somatic "loss of function" mutations of the GCGR gene in three of five patients with GCA suggests that a change in the signalling function of the GCGR may cause glucagon cell adenomatosis via glucagon cell hyperplasia.

OFP-05-004

TIMP-1 expression and hypoxia in papillary thyroid carcinoma: Relationship to BRAFV600E mutation and clinical behavior

M. Ilie*, S. Lassalle, P. Brest, C. Bonnetaud, A. Bozec, N. Guevara, J. Haudebourg, I. Birtwisle-Peyrottes, J. Santini, P. Hofman
*CHU de Nice, LPCE, France

Objective: BRAFV600E causes up-regulation of TIMP-1, promoting cell invasion in papillary thyroid carcinoma (PTC). HIF-1α is regulated by hypoxia but also by BRAFV600Emediated signaling pathway in PTC. We assessed the impact on clinical behavior in PTC of TIMP-1, HIF-1α and the hypoxia-inducible CAIX and CAXII.

Method: The protein expression was assessed by Western blot in two cell lines, TPC-1/BRAFWT and BCPAP/BRAFV600E. TMA-immunohistochemistry analysis was used to study protein expression in 114 PTC samples. BRAF status was analyzed by pyrosequencing. Data were correlated with clinicopathological variables of patients.

Results: Higher expression of all proteins was detected in BCPAP exposed to hypoxia. TIMP-1 expression displayed 87 % sensitivity and 83 % specificity for identifying BRAF mutation ($P<0.001$), and was associated with pT-stage ($P=0.001$), pN-stage ($P=0.02$), and multifocality ($P=0.03$). HIF-1α expression was correlated to pT-stage ($P=0.05$). CAIX expression was related to pN-stage ($P=0.02$), and both CAIX ($P=0.004$) and CAXII ($P=0.05$) were highly associated with vascular invasion.

Conclusion: TIMP-1 protein expression is reliable surrogate of BRAF mutated status in PTC. TIMP-1 and hypoxia-regulated proteins have potential for future use as predictors of the malignant change in PTC, and warrant further investigation as new therapeutic targets for the treatment of highly aggressive form of PTC.

OFP-05-005

A microRNA profile signature can distinguish hereditary medullary thyroid carcinoma (HMTC) from sporadic MTC (SMTC)

S. Lassalle*, M. Ilie, E. Long, V. Hofman, C. De Micco, M. Patey, F. Tissier, G. Belléannée, H. Trouette, B. Catargi, I. Birtwisle-Peyrottes, J.-L. Sadoul, O. Bordone, C. Bonnetaud, C. Butori, N. Guevara, J. Santini, G. Lemaire, O. Blank, P. Vielh, B. Mari, P. Hofman
*Nice University Hospital, LPCE, France

Objective: MTC are usually aggressive tumours which account for 3–5 % of all thyroid carcinomas. Most of MTC are sporadic, the remaining tumours are due to hereditary forms with germline activating mutations of the RET proto-oncogene. The aim of this study was to assess the microRNA profiling expression in both sporadic and hereditary forms of MTC.

Method: A total of 40 frozen MTC from patients with well-documented clinico-pathological parameters were used for microarray analyses (14 HMTC and 26 SMTC) using Human MicroRNA Mircoarray Kit version 2 (Agilent Technologies). After identification of a set of miRNA of interest, validation was done using qPCR.

Results: When comparing HMTC harbouring germinal RET mutation with SMTC, seven miRNA were significantly deregulated (miR-96, −10a, −376c, −15a, −7–2*, −106b, −132). The most highly discriminative miRNA in tumoral samples (>3 fold change) identify miR-375, −129-3p, −136, −376c and −451. Moreover, 5 miRNA could segregate MTC with good prognosis and better clinical outcome (miR-137, −144, −224, −144 and −224).

Conclusion: A specific microRNA signature in HMTC can be identified. Moreover, detection of microRNAs in tissue samples might be of interest for improved clinical management and treatment of patients with MTC.

OFP-05-006

Focus on the follicular variant of papillary thyroid carcinoma: Combination of the immunohistochemical markers CK19, HBME1 and TPO is associated with histopathological diagnosis, better than molecular markers

F. Renaud*, V. Gnemmi, J. Salleron, S. Aubert, M. Crépin, C. DoCao, F. Pattou, B. Carnaille, P. Pigny, J.-L. Wémeau, E. Leteurtre
*CHRU Lille, Inst. of Pathology, France

Objective: The follicular variant (FVPTC) is the major variant of papillary thyroid carcinoma (PTC), ranging from 9 % to 22 % of all PTC. It remains however a problematic entity. Some consider that the encapsulated FVPTC (enFVPTC) have an excellent prognosis like follicular adenomas (FA); others showed that enFVPTCs had potential for hematogenous spread like follicular carcinoma. Its place in the spectrum

of well-differentiated thyroid follicular lesions (WDTFL) is discussed. Our objective was to assess the immunohistochemical and molecular profiles of WDTFL with a focus on FVPTC.
Method: 190 WDTFL (66 PTC, 29 FVPTC, 95 FA) were tested for CK19, HBME1 and TPO expression by immunohistochemistry. Pyrosequencing analysis of BRAF, KRAS, NRAS, HRAS mutations was performed on paraffin-embedded samples.
Results: We identified an immunohistochemical profile HBME1+ and/or CK19+/TPO + associated to FVPTC whereas FA were frequently HBME1-/CK19-/TPO + (kappa=0.73). This association was not reinforced by molecular analysis. Our highly sensitive pyrosequencing method detected NRAS mutation in 28 % FVPTC and 9 % FA. NRAS mutation was significantly associated with TPO expression by multivariate analysis (p=0.01).
Conclusion: We identify an original combination of immunohistochemical markers associated to the diagnosis of FVPTC. NRAS mutation correlates with TPO expression meaning with achieved follicular differentiation. FVPTC appears thereby as an individual entity among WDTFL.

OFP-05-007

Prognostic role of CXCR4 and BRAF V600E analysis in poorly differentiated and anaplastic thyroid carcinomas

E. Rossi*, M. Martini, P. Straccia, S. Capodimonti, M. Palumbo, L. Revelli, C. Lombardi, E. Stigliano, L. Larocca, G. Fadda
*Universita´ Cattolica di Roma, Anatomic Pathology and Histology, Italy

Objective: Poorly differentiated (PDC) and anaplastic thyroid carcinomas (ATC) represent aggressive thyroid cancers both sharing controversial pathogenesis and poor prognostic outlook. CXCR4 is a chemokine inducing cell adhesion associated with tumour progression and nodal spread in WDC. The aim of this study is to compare CXCR4 expression and BRAF mutational analysis in the groups of PDC/ATC respect to WDC.
Method: The study include the surgical specimens of 23 WDC, 23 PDC and 9 ATC on which immunohistochemistry for CXCR4 and mutational analysis for BRAF V600E were carried out.
Results: CXCR4 resulted negative in all PDC/ATC cases and positive in 79 % WDC. A BRAF wild-type was present in all PDC/ATC cases whereas WDC showed a BRAF mutation in 75 % of cases. CXCR4 and BRAF analysis show a significant correlation (p<0.001) in WDC compared with PDC/ATC. CXCR4 predicts nodal involvement (p< 0.002) in WDC, while its absence in PDC/ATC is linked with haematogenous metastases in 54 % of cases.
Conclusion: CXCR4 is important in predicting nodal metastases in WDC whereas its absence is an unfavourable prognostic marker in PDC/ATC. BRAF V600E mutation in WDC predicts a more aggressive behaviour whereas it is constantly absent in PDC/ATC.

Tuesday, 11 September 2012, 17.00–19.00, Terrace 1
OFP-06 Oral Free Paper Session Gynaecological Pathology

OFP-06-001

Human Papilloma Virus (HPV) in patients with cervical pathology compared with general population. A study of 6375 cytology samples in 3 years

A. Cuesta Diaz de Rada*, J. S. Salas Valien, M. A. Gonzalez Moran, P. Castro Val, A. Rubio de las Heras, T. Ribas Ariño
*Hospital de León, Anatomía Patológica, Spain

Objective: HPV prevalence and genotypes in correlation with cytological findings in patients with cervical pathology, compared with general population data from the Cervical Cancer screening program in Castilla y León.
Method: We compile 6375 cytological studies made in our Pathology Service, from years 2009, 2010 and 2011. Every sample was taken by liquid-based cytology and a Papanicolaou smear was performed in addition to a HPV testing with the system CLART® HPV2.
Results: We obtained 76,8 % of normal cytological studies, while in general population there are 97 %. The prevalence for high risk viruses was 25.6 %, 3.7 % for intermediate risk and 4.8 % for low risk, while in general population it is of 4 %, 1.2 % and 1.5 % respectively.
Conclusion: The most frequent cytological lesion in our compilation was LSIL (17.6 %) while in general population it is ASCUS (0.8 %). The most prevalent genotype was 16 (9.7 %) while in general population it is placed under low and intermediate risk genotypes. It is important to study women under 35 when they have symptomatology since 60 % of them are positive for HPV (being 45.7 % for high risk HPV) and 45 % have cytological abnormalities.

OFP-06-002

Histological and immunohistochemical characterization of squamous differentiation (SD) in endometrial endometrioid adenocarcinomas (EEASD)

C. Bartosch*, C. Jerónimo, J. M. Lopes
*IPO-Porto, Pathology, Portugal

Objective: SD occurs in≈20 % of endometrial endometrioid adenocarcinomas (EEA), and displays intra/extraglandular, morular (M)/squamoid (S) phenotype which raise diagnostic controversies.
Method: Evaluation of morular, squamoid, and mixed phenotype, p63, CDX2, 34βE12, ER, PR, p53

immunohistochemistry, grade (G), and FIGO stage of EEASD with >10 % SD of Centro Hospitalar S. João (2000–2011) hysterectomies.
Results: 31 EEASD (17 % of EEA) were identified, with 4.4 cm mean size, 65 years mean age, in multiparous (77 %), post-menopausal (81 %) and obese (52 %) women; 67 % EEASD were FIGO stage I, 35 % with vascular invasion (VI); G1(55 %), G2 (32 %), and G3 (13 %). SD: M (29 %), S (52 %), and mixed (19 %); M significantly associates with lower grade and S phenotype with higher grade. M significantly associates with greater extension of CDX2 expression whereas S phenotype associates with p63 extent; 34BE12 was common in well differentiated/keratinized areas of S; and ER, PR and p53 absent/scarce in SD. Overall mean survival: 97 months (CI 95 % 85.3–109.6), and 84 % 5-year survival rate. In univariate analysis: stage and VI were prognostic, but only stage in multivariate analysis.
Conclusion: SD characterization, including p63, CDX2 and 34βE12 immunohistochemistry, may assist differential diagnosis of EEASD, namely with solid patterns and other EEA, and influence treatment option decisions.

OFP-06-003
Liquid-based cytology-new possibilities in the diagnosis of cervical lesions
N. Fayzullina*, E. Kogan, T. Demura, A. Kozachenko
*Obstetrics, Gynecology and Perinatology, Moscow, Russia

Objective: The aim of this study was to analyze the correlation between p16-INK4a and Ki-67 immunoexpression in cervical cytologic samples and human papillomavirus (HPV) detection by polymerase chain reaction (PCR) from the same sample.
Method: Liquid-based cytology (LBC)- cervical cytology samples, prepared and stained by Papanicolaou method (B & D TriPath), were analyzed using Bethesda cytologic classification. A second slide, prepared from the same sample, was immunostained for p16INK4a and Ki-67 using CINtec PLUSCytology Kit (mtm laboratory, Germany). Residual material was used for 14 HR HPV DNA detection by the PCR based cobas test (Roche Molecular Systems).
Results: A total of 50 Pap tests with the following cytologic diagnoses: 6 NILM, 31 ASCUS,5 LSIL, 8 HSIL. Expression of p16INK4a and Ki-67 was detected in all smears with HSIL (8/8) and LSIL (5/5), while in ASCUS – only in 3 of 31. In contrast to HR HPV DNA detected in 7 of 8 HSIL, in 4 of 5 LSIL, in 3 of 31 ASCUS, in 3 of 6 NILM.
Conclusion: We noticed a good correlation between the expression of p16INK4a, Ki-67 and the cobas test results in liquid-based cytology with atypical cells of cervix.

OFP-06-004
Atypical epithelial inclusion in a para-aortic lymph node in a young woman with chlamydia salpingitis
K. Honma*, A. Hayashida, S. Tanaka, T. Mashiko, S. Shiraishi
*Dokkyo University Hospital, Dept. of Pathology, Mibu, Japan

Objective: Mullerian derivatives often are responsible for epithelial inclusions in the abdominal lymph nodes. It is rare, however, for the epithelial cells to present with cellular atypism.
Results: Case Report: A 24-year old diabetic woman underwent laparotomy under the presumptive diagnosis of ovarian cancer because of elevated levels of CA 125 and CA19-9 and mild FDG uptake of the bilateral uterine adnexa and para-aortic lymph nodes. No gross tumor was found at laparotomy and right salpingectomy with excisional biopsy of the para-aortic lymph node was performed. Pathologic examination revealed acute salpingitis with marked endosalpingiosis involving the peritoneum. The para-aortic lymph node bore several clusters of glandular epithelium showing cellular atypism and a few mitoses. Immunohistochemistry revealed p53 positive cells along with increased MIB-1 reactivity (13 %). The peritoneal glands involved in endosalpingiosis also exhibited p53 immunoreactivity. The patient remains free of symptoms 3 years after the operation with normalized values of the tumour markers and persistent FDG uptake in her ovaries.
Conclusion: It is possible to assume that the epithelial inclusions of the lymph node associated with atypical endosalpingiosis per se might give rise to primary abdominal and pelvic malignancies without involvement of the female genital tract proper.

OFP-06-005
Geometric relations in histologic sections predict the outcome of CIN 1 lesions
K. Metze*, R. Triglia, R. Adam, L. Andrade
*University of Campinas, Pathology, Brazil

Objective: Cervical Intraepithelial Neoplasias (CIN) are precancerous lesions, which may regress or progress to a higher grade. The analysis of the histologic architecture in neoplasms may reveal information about the pathophysiology, The aim of our study was to investigate whether an analysis of the geometric relations in CIN 1 lesions could help to predict their evolution.
Method: 74 patients with a biopsy-proven diagnosis of CIN 1 were submitted to a second biopsy during follow-up. In routine paraffin sections of the first biopsy, the hematoxylin stained nuclei were interactively marked and their geometric relations (syntactic structure) analyzed by Delaunay triangulation. The prognostic relevance was calculated with the help of Cox regressions.
Results: 19 CIN 1 lesions regressed, 29 patients maintained their diagnosis in the second biopsy and 26 women had

progressed to CIN 2 or 3. The maximum angle of the Delaunay triangels was an important prognostic factor: Cases with large values had an increased probability to progress whereas CIN 1 lesions with smaller ones were prone to regress.
Conclusion: In CIN 1 lesions discrete alterations of the tumor architecture indicate different evolutions and can be used for prognostication. Financial Support: CNPq, FAPESP.

OFP-06-007
Prognostic and Pathogenetic Relevance of Stem Cell Factors for Serous Ovarian Carcinomas
A. Staebler*, A. Fischer, D. Pham, P. Bareiss, C. Bachmann, H. Neubauer, F. Fend, S. Perner, C. Lengerke, T. Fehm
*University of Tuebingen, Inst. of Pathology, Germany

Objective: Tumor stem cells and reexpression of stem cell factors are thought to contribute to therapy resistance and recurrent disease. Therefore, we performed a comparative analysis of stem cell markers in serous ovarian carcinomas.
Method: 155 ovarian serous carcinomas (147 high-grade, 8 low-grade) were analyzed by immunohistochemistry in a tissue microarray for SOX2, Nanog and Oct4 as well as ALDH1 and proliferation marker Ki67. A double immunostaining experiment compared the percentage of Ki67-positive cells in the ALDH1-positive and -negative cell fractions case by case. The effect on overall and disease-free survival was analyzed (Kaplan-Meier).
Results: Regarding SOX2 we confirmed the association with poorly differentiated tumors and improved recurrence-free survival (median survival 27 months vs. 21 months, $p=0.041$). Oct4 or Nanog were not detected. We observed a correlation between ALDH1 and Ki67, indicating a role of ALDH1 in cell proliferation. However, double staining showed, that ALDH1 is mostly expressed in the in the non-proliferating cell fraction.
Conclusion: Stem cell factors show divergent association with tumor characteristics like poor differentiation or survival (SOX2) and resting populations in proliferating tumors (ALDH1). These findings suggest that stem cell factors in serous ovarian tumors do not reflect a unique stem cell phenotype.

OFP-06-008
Estrogen receptor a loss in endometrial carcinoma is associated with epithelial-to-mesenchymal transition and a potential for PI3Kinase inhibition
E. Wik*, M. Rader, C. Krakstad, J. Trovik, H. Erling, S. Mjos, I. Stefansson, K.-H. Kalland, L. Akslen, H. Salvesen
*University of Bergen, Dept. of Clinical Medicine, Norway

Objective: We hypothesized that ERα loss, associated with poor prognosis in endometrial carcinomas, is reflected in transcriptional signatures representing a molecular basis for tumor phenotype and targets for new therapy.
Method: Endometrial carcinoma samples were analyzed in a primary investigation cohort ($n=76$) and three independent validation cohorts ($n=155/286/111$). Biomarkers were assessed by IHC, DNA oligonucleotide microarray, qPCR, SNP array and sequencing.
Results: ERα loss was correlated to poor prognosis. Activation of genes involved in Wnt-, Sonic hedgehog- and TGF-β signaling was highly associated with loss of ERα ($p<0.001$). An association between receptor loss and activation of EMT was validated in three independent data sets. Transcription factors cross-linking with TGF-β were activated in the ERα negative tumors in an EMT promoting way. Furthermore, drug signatures for PI3Kinase- and mTOR inhibitors were highly significantly associated with the signature for ERα loss. PIK3CA amplification, a PI3K activation score and Stathmin were associated with ERα loss (all $p<0.02$).
Conclusion: ERα loss in endometrial cancer is associated with epithelial-to-mesenchymal transition. Inhibitors of the PI3Kinase-AKT- mTOR signaling pathway as well as EMT inhibitors are supported as promising drugs to be tested in clinical trials in metastatic ERα negative endometrial carcinomas.

Tuesday, 11 September 2012, 17.00–19.00, North Hall
OFP-07 Oral Free Paper Session Haematopathology

OFP-07-001
Comparison of prognostic markers in acute myeloid leukemia
K. Metze*, M. R. Mello, K. Albanez, R. Adam, I. Lorand-Metze
*University of Campinas, Pathology, Brazil

Objective: In acute myeloid leukemia (AML), several cytogenetic and molecular features are independent prognostic factors. In other malignant diseases descriptors of nuclear chromatin texture have been found to be of prognostic relevance. The aim was to analyze in AML patients the relations between molecular features, morphometric characteristics and methylation pattern in AML and survival.
Method: AML patients without cases of promyelocytic leukemia entered the study. Mutations of FLT3 and NPM1 and the methylation status of CDKN2B, > CDKN2A, CDKN1C, and ESR were recorded. MGG-stained bone marrow blasts were digitalized and studied by computerized texture analysis. The prognostic relevance of molecular and nuclear was studied by Cox regressions.
Results: We studied 87 cases of AML. Blast nuclei of AML without maturation showed higher entropy, contrast, energy and diagonal moment and lower second angular moment. In

the multivariate Cox regression the FLT3-ITD mutation (p= 0.001) was an independent poor prognostic factor, whereas the goodness-of-fit of the Minkowski fractal dimension an independent favorable prognosticator (p=0.025). The karyotype had no influence on survival.
Conclusion: FLT3-ITD and chromatin fractal characteristics were more important as prognostic factors for overall survival than karyotype and gene methylation status. Financial Support: FAPESP and CNPq.

OFP-07-002

Incidence of preclinical manifestations of mantle cell lymphoma and mantle cell lymphoma in situ in reactive lymphoid tissues

P. Adam*, A.-I. Schiefer, S. Prill, T. Henopp, L. Quintanilla-Martínez, H.-C. Bösmüller, A. C. Chott, F. Fend
*Medizin. Universität Tübingen, Inst. für Pathologie, Germany

Objective: The prevalence of Cyclin D1 (CyD1) positive B-cells with mantle cell lymphoma (MCL) phenotype in the mantle zones of reactive lymph nodes ("in situ" MCL/MCLIS). and related minimal MCL infiltrates in reactive lymphoid tissues of healthy individuals and in MCL patients are unknown.
Method: All 1.292 reactive lymph nodes from unselected consecutive surgical specimens of 131 patients without a history of lymphoma obtained over a 3 months´ period were stained for CyD1. Additionally, all morphologically reactive lymph nodes and extranodal lymphoid infiltrates of MCL patients from 2000 to 2011 were studied. Samples predating the lymphoma diagnosis for at least 2 months were available from 37/423 (8.7 %) patients.
Results: A MCLIS was not identified. However, in four MCL patients, an early manifestation of MCL with mantle zone growth pattern was detected retrospectively, antedating the lymphoma diagnosis for 3–86 months. In six MCL patients, only small groups of CyD1 positive cells in morphologically reactive extranodal infiltrates were detected more than 2 months before the diagnosis of MCL (range 3–59 months).
Conclusion: MCL "in situ" is an extremely rare phenomenon in morphologically reactive lymph nodes. In MCL patients, however, immunohistochemically detectable infiltrates of MCL cells antedating the lymphoma diagnosis were found in a significant proportion of cases (10/37=27 %).

OFP-07-003

E2F-1's relationship with tumor growth in Hodgkin's lymphoma is regulated by p53 status

E. Georgiadi*, G. Dimtsas, T. P. Vassilakopoulos, V. G. Gorgoulis, I. A. Doussis-Anagnostopoulou
*Larisa, Greece

Objective: E2F-1 is a member of the E2F family group of transcriptional factors that play a major role in cell cycle progression and arrest, as well as in apoptosis. In different tumors E2F1 can demonstrate opposing roles, acting either as an oncogene or as a tumor suppressor gene.
Method: We have previously established E2F-1's immunohistochemical expression in Hodgkin lymphoma (HL) and its correlation with p53 expression, although no relationship with either proliferation or apoptosis was demonstrated. A further investigation in a larger series of 100 cases of primary HL with the addition of new apoptotic techniques and the use of p21 expression as an indicator of p53 functional status was undertaken.
Results: Following stratification of our cases based on p53 functionality, E2F-1 was inversely correlated with the proliferation marker TopoIIa. Independently of p53, high levels of E2F-1 expression showed a linear trend with apoptosis and an inverse trend with proliferation (borderline p value in both cases).
Conclusion: Both E2F-1 and p53 activity is upregulated in HL, however it seems that p53 status is a major regulator of the relationship between E2F-1 expression and tumor growth. Alternatively, E2F-1 may use p53-independent pathways to induce apoptosis.

OFP-07-004

EBV replication in tumor samples of Post-transplant Lymphoproliferative Disorders (PTLD) is associated with aggressive clinical course

B. Gonzalez*, J. Rovira, A. Valera, D. Martinez, A. B. Larque, C. Sole, L. Colomo, E. Gine, E. Campo, A. Lopez Guillermo, A. Martinez
*Hospital Clinic Barcelona, Dept. of Pathology, Spain

Objective: PTLD represent a spectrum of usually EBV-driven lymphoplasmacytic proliferations in the settings of immunodeficiency associated with allograft. EBV infects cells in latent or lytic forms. Although viral oncogenes are expressed in latency programs, lytic EBV replication is required to develop lymphomas in mouse models. The role of intratumoral EBV replication in PTLD has never been addressed before.
Method: A series of 35 PTLD was reviewed and EBV latency genes were explored in all cases and included EBER1-2, LMP1 and EBNA2. Moreover, two early lytic genes involved in EBV replication, BZLF1/ZEBRA and EAD11 were also analyzed. All clinical and pathological data were collected.
Results: The median age was 50 years (27–77) with a male predominance (26 M: 9 F). EBV infection was observed in 28 cases (80 %). EBV replication was observed in 40 % of the cases. These were more likely to be polymorphic PTLD with latency III in the context of stem cell transplantation. Moreover these cases had atypical clinical presentations such as brain involvement or disseminated disease with aggressive behavior (OS: 11 months vs. 48 months).
Conclusion: EBV replication occurs in tumor cells of PTLD-patients associated with poor outcome and may be

used to select high-risk patients that may benefit of antiviral therapies.

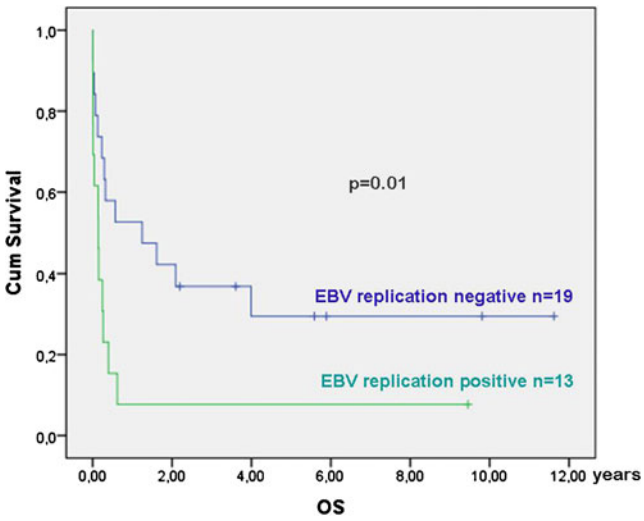

OFP-07-005

Peripheral T cell lymphoma, not otherwise specified, follicular variant with classical Hodgkin-Reed-Sternberg like cells

V. Tabanelli*, E. Sabattini, C. A. Sagramoso-Sacchetti, C. Agostinelli, P. P. Piccaloluga, F. Bacci, A. Gazzola, S. Righi, S. A. Pileri
*Bologna, Italy

Objective: We present the case of a peripheral T cell lymphoma-NOS, follicular variant (PTCL-NOS fv), morphologically resembling the "lymphocyte predominance Hodgkin's lymphoma" subvariant but with a classical Hodgkin's phenotype in the HRS-like cells, occurring in a 69-year-old man first treated as a HL with rapid relapse.
Method: Formalin-fixed paraffin-embedded tissue. Histology: H&E and Giemsa. Immunohistochemistry performed with RealDetection Kit (DAKO). In situ hybridization for EBV with PNA detection kit (DAKO); TCR/IgH/IgL genes rearrangement performed according to Biomed2 protocol.
Results: Histologically, the lymph-node architecture was substituted by vague nodules made of small/medium and few larger mononuclear lymphocytes, admixed with a minor component of HRS-like cells. The phenotype of the former component was: CD3+/CD4+/CD8−/CD2+/CD5+−/CD7−/CD20−/Pax5−/CD30−+/CD15−/PD1+/CD10+/CXCL13−+/Bcl6+/IRF4−+/ki67 60 %. The phenotype of HRS-like cells was: CD30+/CD15−/CD20−/PAX5+/IRF4+/CD4−/CD8−/CD2−/CD5−/CD7−/PD1−/CD10−/CXCL13−/Bcl6−/Ki67+; HRS-like cells were surrounded by neoplastic T cells. EBER was negative in HRS-like and neoplastic T-cells. TCR, but not IgH/Igk, was monoclonally rearranged.
Conclusion: To our knowledge cases of PTCL-NOS fv with HRS-like cells provided with classical phenotype posing the differential diagnosis between composite lymphoma or HL features in PTCL-fv has never been previously reported.

OFP-07-006

Mantle Cell Lymphoma Prognostic Index and proliferative activity are strong prognostic markers in clinical practice: A retrospective study on 235 patients of the Czech Lymphoma Study Group

L. Boudová*, P. Veselá, D. Šálek, S. Vokurka, M. Moulis, R. Kodet, Z. Velenská, J. Stritesky, Z. Vernerova, M. Trneny, M. Michal
*Charles University, Faculty of Medicine, Pilsen, Czech Republic

Objective: Prognostic factors of mantle cell lymphoma (MCL) are searched as outcome and therapy are heterogeneous and largely unsatisfactory. A new MCL prognostic index (MIPI) has a strong significance in academic studies on selected types of patients, yet it has not been tested in an unselected population. The aim is to test suitability of MIPI for clinical practice in an unselected series.
Method: 235 patients, their FFPE specimens, diagnosed as MCL between 1996 and 2008, followed-up till April 2012. Proliferative activity assessed using Ki-67 immunostaining. MIPI and biological-MIPI were calculated, Kaplan-Meier survival curves and log-rank test were used for statistical analysis.
Results: Median survival (MS) of all patients was 48 months, median progression free survival (MPFS) 22 months. With a cutoff 30 %, cases were divided according to low and high proliferation, with MS 63 and 21 months, (P<0,0001), MPFS 27 and 15 months, (P<0,0001). MIPI distinguished cases with low, intermediate, and high risk, showing MS 101, 58, 24 months, (P<0,0001); MPFS 43, 25, 16 months (P< 0,0001). Biological MIPI distinguished 2 groups, with MS 94 and 24 months (P<0,0001), MPFS 41 and 16 months, (P<0,0001).
Conclusion: This large study with a long follow-up confirms that MIPI, proliferative activity, and biological-MIPI are robust prognostic factors suitable for clinical practice.

OFP-07-007

Immunohistochemistry combined with fluorescent in situ hybridization helps to differentiate CD20+/CD5+ diffuse large B cell lymphoma from blastoid variants of mantle cell lymphoma

A. Farkasova*, T. Balharek, Z. Kviatkovska, L. Plank
*JFM CU, Dept. of Pathology, Martin, Slovakia

Objective: Diffuse large B-cell lymphoma (DLBCL) and blastoid variants of mantle cell lymphoma (bMCL) may

share common morphological and phenotypical features. In routine praxis, their differential diagnosis might represent a challenge requiring a specific work-up of immunohistochemical (IHC) and fluorescent in situ hybridization (FISH) analyses.
Method: Paraffin sections from 17 CD20+/CD5+ blastic B-NHL were examined for cyclin-D1, CD10, bcl-6 and MUM-1 IHC expression together with FISH method using probes for CCND1 rearrangement and/or IGH/CCND1 translocation. The final diagnosis was established according to the criteria of WHO classification.
Results: 11/17 cases were diagnosed as bMCL showing cyclin-D1 positivity and CCND1 rearrangement, other analysed IHC markers were negative. Five of these cases were polyploid. 6/17 cases were diagnosed as CD5+ DLBCL in spite of coexpression of cyclin-D1 in 2 of them, as they showed various CD10, bcl-6 and MUM-1 expressions and missed CCND1 gene rearrangement.
Conclusion: Cyclin-D1 positivity may appear in other than MCL lymphomas due to changes at transcriptional or post-transcriptional level. In spite of overlaping phenotypes, FISH analysis of CCND1 represents an effective tool to increase the diagnostic accuracy to distinguish CD5+ DLBCL from bMCL. Supported by VEGA grant Nr. 1/0378/12 and projects CEPRII (IMTS: 26220120036) and MDCC (IMTS: 26220220113) co-financed by EU sources.

OFP-07-008

Still's Disease associated lymphadenopathy: Report of two cases resembling malignant lymphoma with review of possible morphological findings

K. Kamarádová*, M. Nova, M. Kalinova, V. Campr
*Prague, Czech Republic

Objective: Still's disease (or systemic onset juvenile idiopathic arthritis, SOJIA) is a systemic inflammatory disorder characterized by fever, rash, and arthritis. It has a peak of incidence in early childhood with rare occurence in adulthood (adult-onset Still's disease, AODS). Several other symptoms as hepatosplenomegaly, leukocytosis and lymphadenopathy may be associated possibly mimicking malignant lymphoma.
Method: We present two cases of Still's disease associated lymphadenopathy in a child and in an adult simulating morphologically peripheral T-cell lymphoma and classical Hodgkin lymphoma respectively.
Results: Histological, immunohistochemical and molecular examination revealed non-neoplastic lymphadenopathy with atypical paracortical T-cell hyperplasia with immunoblastic reaction in the former and burnt-out histiocytic pattern in the latter, both falling into a broad spectrum of reactive lymph node changes associated with Still's disease.
Conclusion: The lymph node lesions in Still's disease can be histologically divided into four major categories: 1) simple atypical paracortical hyperplasia, 2) burnt-out histiocytic pattern, 3) exuberant immunoblastic reaction in paracortical hyperplasia and 4) follicular hyperplasia. The second and the third pattern may closely resemble malignant lymphoma. Extended and careful clinical examination with relevant laboratory findings and possible complex histochemical and molecular analysis are necesarry to rule out the suspition of lymphoma. Supported by the project (Ministry of Health, Czech Republic) for conceptual development of research organization 00064203 (University Hospital Motol, Prague, Czech Republic).

OFP-07-009

Intravascular large B-cell lymphona: A rare type of lymphona frequently undiagnosed until autopsy

S. Medina Román*, G. Tapia, I. Ojanguren, D. Naranjo, R. Gomez Bellido, L. Tria, J. L. Mate
*HUGTiP, Dept. of Pathology, Barcelona, Spain

Objective: Intravascular large B-cell lymphoma (IVLBCL) is a rare form of diffuse large B-cell lymphoma characterized by exclusive or preferential intravascular growth. IVLBCL often goes clinically unrecognized. We report three clinically unsuspected cases of classic variant IVLBCL.
Method: Cases diagnosed as IVLBCL were collected from the pathology files of Germans Trias i Pujol Hospital. The diagnosis was reviewed in agreement with WHO 2008 criteria and immunophenotypic and clinical data were gathered.
Results: A 71-year-old male and an 87 year-old-male showed neurological symptoms leading to progressive deterioration and death. A 79-year-old female presented with fever of unknown origin and died 2 days after admission. At autopsy there were no gross findings suggestive of a neoplastic process in any instance. Histologic study showed intravascular large B cells with vesicular nuclei involving predominantly the central nervous system in the first two cases and the adrenal glands, liver, and spleen in the third case.
Conclusion: The three cases of aggressive, advanced-stage lymphoma herein described illustrate how the clinical diagnosis of IVLBCL remains elusive due to its low frequency and variegated clinical presentation and how the pathologic diagnosis of IVLBCL continues to be highly dependent on autopsy examination.

OFP-07-010

Post-Transplant Lymphoproliferative Disorders (PTLD) after renal transplantation in the Republic of Ireland: A 20 year review

S. Prendeville*, J. O´Regan, C. Power, S. Deady, Y. Williams, P. O´Kelly, H. Comber, P. Conlon, M. Leader
*Beaumont Hospital, Dublin, Ireland

Objective: The World Health Organisation (WHO) currently recognises four categories of PTLD, which are lymphoid/plasmacytic proliferations occurring due to immunosuppression after organ transplantation. The aim of this study was to examine the clinicopathologic characteristics of PTLD occurring after renal transplantation in the Republic of Ireland.
Method: The National Renal Transplant Registry from 1991 to 2000 (inclusive) was cross referenced with the National Cancer Registry to identify renal transplant recipients who had developed PTLD up to the present day. Review of Pathology and chart review was conducted for each case.
Results: Of 2,441 patients (2,667 allografts), 34 cases of PTLD were identified, with pathology review possible in 33 cases. There were 26 (79 %) Monomorphic PTLD (23 Diffuse Large B Cell {DLBCL}, 1 Anaplastic Large Cell, 1 Burkitts-like, 1 Myeloma], 3 Hodgkin-type PTLD, 1 (3 %) Polymorphic PTLD and 1 (3 %) early lesion. In addition, there was 1 Mantle cell lymphoma and 1 Lymphomatoid Granulomatosis. The annual incidence of PTLD was estimated as 0.2 % (95 % CI 0.14–0.28). Median time to diagnosis was 8.7 years (Range 2 to 19.2 years).
Conclusion: Similar to other studies, Monomorphic PTLD is the most common type, with DLBCL representing the majority of cases. Of interest, early onset PTLD was very uncommon in this study.

Monday, 10 September 2012, 17.00–19.00, Forum Hall
OFP-08 Oral Free Paper Session Head and Neck Pathology

OFP-08-001

Human papilloma virus associated oropharyngeal carcinoma is strongly correlated with cancer of unknown primary

S. Ihrler*, G. Assmann, P. Zengel, M. Mollenhauer
*Medizin. Universität München, Institut für Pathologie, Germany

Objective: Human papillomavirus (HPV) associated oropharyngeal carcinoma has been identified as a distinct entity within squamous cell carcinoma of the head and neck and is preponderantly restricted to palatinal tonsils and base of tongue. These two primary locations have for long - and HPV-associated carcinomas have recently - been associated with the clinical situation of cancer of unknown primary (CUP).
Method: To investigate the relationship between HPV and CUP in detail, we studied 26 consecutive patients who initially presented as CUP and were finally diagnosed with carcinomas of these two locations.
Results: Twenty-one carcinomas (81 %) proved to be positive for high-risk HPV (p16 and polymerase chain reaction). They were frequently very small (smallest: 0.3 cm; 6 cases: ≤ 0.6 cm; on average 0.9 cm) and located in a deep, submucosal position.
Conclusion: This demonstrates an overrepresentation of HPV-associated carcinoma in patients who were initially diagnosed with CUP, supporting a strong causal relationship between HPV-association and CUP. The frequent manifestation as CUP presumably is caused by the unusual predisposition for small size and submucosal location, combined with frequent and early lymphatic metastization. In order not to miss these small, clinically occult carcinomas, consequent interdisciplinary cooperation and meticulous histological work-up is mandatory.

OFP-08-002

Methylthioadenosine phosphorylase inactivation depends on gene deletion in laryngeal squamous cell carcinoma

A. Nadal*, L. Conde, I. Vilaseca, L. Alos, M. Bernal-Sprekelsen, A. Cardesa
*Hospital Clínic Barcelona, Dept. of Pathology, Spain

Objective: Methylthioadenosine phosphorylase is an essential enzyme for the methionine and adenosine salvage pathway in normal cells, frequently inactivated in many different human cancers. The MTAP status could be important for tumor cell sensitivity to adjuvant chemotherapy. To date there are no reports on MTAP status in laryngeal carcinoma.
Method: A series of 31 laryngeal squamous cell carcinomas was investigated for MTAP mRNA expression through reverse transcription and quantitative PCR (qPCR) as well as for MTAP gene deletion and/or promoter hypermethylation through qPCR and methylation-specific PCR respectively.
Results: Low MTAP mRNA expression was found in 32 % of cases, associated with MTAP gene deletion in 70 % ($p<$ 0.001) but not to MTAP promoter hypermethylation, indicating that in this tumors gene deletion is the main mechanism of MTAP inactivation. Neither low mRNA expression nor gene deletion was associated with any of the clinicopathologic parameters investigated.
Conclusion: Given the significance of MTAP status for cell sensitivity to different chemotherapeutic regimes, our results suggest that determination of MTAP inactivation could be useful for adjuvant therapy selection in laryngeal squamous cell carcinomas.

OFP-08-003

ERCC1, p16 and ki-67 immunohistochemical expression as predictive and prognostic markers in head and neck squamous cell carcinoma treated with platin-based induction chemotherapy

H. Roussel*, M. Housset, H. Tournat, P. Ravel, S. Hans, C. Badoual
*HEGP, Dept. de Anatomie-Pathologie, Paris, France

Objective: ECC1 enzyme has been associated with resistance to platinum-based chemotherapy. The purpose of this study was to evaluate the role of ERCC1 expression with p16 and Ki-67 as predictive and prognostic markers in the response to platin-based induction chemotherapy in patients with head and neck carcinoma (HNSCC).
Method: 208 patients treated from 2000 to 2006 by an induction chemotherapy regimen for HNSCC were included retrospectively. We assessed response to treatment, progression-free survival (PFS) and overall survival (OS).
Results: 68 % and 81.5 % of HNSCC showed low expression of 8 F1 and FL297 ERCC1. No correlation was found between the two clones (p=0.1). In the 129 patients treated with cisplatin-5FU chemotherapy, a low expression of 8 F1 ERCC1 was associated with a better response (p=0.027). Over expression of p16, (34.5 % of cancers of the oropharynx) was correlated with a better OS (p=0.0007) and a better PFS (p=0.01).
Conclusion: These results suggest that ERCC1 expression might be a useful predictive marker of HNSCC in patients treated by cisplatin-based chemotherapy. The 8 F1 ERCC1 clone appears to be the best for immunohistochemistry. Our study confirms the prognostic value of the over expression of p16 in carcinoma of the oropharynx.

OFP-08-004

The prognostic value of proportion of tumor in layringeal squamous cell carcinoma

S. Sarioglu*, M. Unlu, O. Cetinayak, D. Onder, C. Ecevit, F. C. Akman, A. O. Ikiz, E. Ada, B. Karacali
*Dokuz Eylul University, Faculty of Medicine, Izmir, Turkey

Objective: Tumor-stroma ratio or proportion of tumor (PT) has been presented as a prognostic factor in colorectal and breast adenocarcinomas, but there is no information about squamous cell carcinomas (SCC) and laryngeal carcinomas in particular.
Method: Eighty-five laryngeal carcinoma cases were included in this series. Five digital images of the tumor sections were obtained (H&Ex20). Percentage of epithelial tumor component was determined by software allowing the pathologist's selection of tiny areas as carcinomatous and stromal region for statistical analysis as a prognostic marker.
Results: Median follow up was 48 months (range 3–194). The mean PT was (48,63+18,18). There was no difference for PT when tumor grade and stage were considered. Although statistically insignificant, the mean PT was the lowest (37,46+12,49) for subglottic carcinomas and cases with perinodal invasion (44,72+20,23), and highest in pN0 cases (50,05+17,34) but there was no statistical significance. The over all and disease free survival analysis did not reveal significance for PT. Only pathological stage was an independent factor for over all survival (p=0,08).
Conclusion: Although there might be an association with adverse prognostic factors and low TP, the findings in this series does not support PT as a prognostic marker in laryngeal carcinomas.

OFP-08-005

Tumoral microvasculature in ameloblastoma subtypes

C. H. Siar*, K. H. Ng
*University of Malaya, Dept of. Oral Pathology, Kuala Lumpur, Malaysia

Objective: Angiogenesis is essential for tumoral growth and progression. The ameloblastoma is a benign but locally-invasive odontogenic neoplasm with distinct behavioural characteristics of its subsets. Whether angiogenesis contributes to a more aggressive course in these variants remains unclear. The aim here was to determine and compare the tumoral microvasculature in different ameloblastoma subtypes and to speculate on their significance.
Method: Immunohistochemical staining for 4 vascular markers (CD31, CD34, CD105 and VEGF) was performed on archival tissues of 40 cases solid/multicystic (SMA), 20 unicystic (UA), 3 desmoplastic (DA) and 14 recurrent ameloblastoma (RA). Mean microvessel density (MVD) at the tumour advancing front and centres were obtained.
Results: VEGF was heterogeneously expressed in the tumoral epithelium in all ameloblastoma subtypes. Protein localization was membranous/cytoplasmic. Mean MVD was slightly higher in SMA compared to UA but the difference was not significant (P>0.05). Mean MVDs were not significantly different between primary and recurrent ameloblastoma; and between tumoral centre and advancing front of each subtype (P>0.05).
Conclusion: Although ameloblastoma subtypes are distinctive in their clinicopathologic presentations and behaviour, their tumoral microvasculature is not different. This suggests that angiogenesis is not a major factor influencing the progression of these ameloblastoma subsets.

OFP-08-006

An immunohistochemical study of E-Cadherin and snail expression in laryngeal squamous cell carcinoma

A. Tanoglidi*, M. Tsopanomichalou, C. Barbatis, C. Kostopoulos, O. Pantzartzi, V. Gorgoulis
*Hellenic Red Cross Hospital, Dept. of Pathology, Athens, Greece

Objective: Snail 1 and 2 (Slug) are zinc-finger transcription factors, repressing the E-Cadherin in epithelial tumors. Published data in Head and Neck Squamous Cell Carcinoma show either inverse relationship or unrelated co-expression, but E-Cadherin reduction/loss and Snail overexpression seem to confer an aggressive phenotype.

Method: Thirty cases of laryngeal squamous cell carcinomas (LSCCs) (gradeI: 11, gradeII: 8, gradeIII: 11) and one large cell neuroendocrine carcinoma (NEC) were studied using double staining immunohistochemical method for E-Cadherin (mAb-DAB) and SNAIL + SLUG (pAb–AP). The colocalization of both molecules was assessed and the expression was compared to the adjacent normal or dysplastic epithelium and the histological grade.
Results: Normal squamous and dysplastic epithelium show strong nuclear Snail expression and complete E-Cadherin membranous positivity. Reduction/loss of Snail with or without E-Cadherin membranous expression is observed in 14/30 (47 %) LSCCs with a tendency for inverse relationship with E-Cadherin at the invasive front. 16/30 (53 %) LSCCs strongly express nuclear SNAIL, without absolute relationship to the reduction/loss of E-Cadherin, with a tendency for SNAIL negativity in grade II (75 %). The NEC is nuclear SNAIL negative but cytoplasmic positive.
Conclusion: SNAIL and E-Cadherin may be retained, reduced or lost in LSCCs, without a definite inverse relationship. These immunophenotypic combinations need further investigation.

OFP-08-007

Non-sebaceous lymphadenoma of salivary glands: Proposed development from intraparotid lymph nodes and risk of misdiagnosis

C. Weiler*, A. Agaimy, P. Zengel, S. Ihrler
*Munich, Germany

Objective: Non-sebaceous lymphadenoma (NSLA) is a recently described, rare benign salivary tumour composed of lymphoid and epithelial components, definitionally lacking sebaceous differentiation.
Method: Nine cases of NSLA were immunohistochemically stained for CK5/6, CK7, CK14, CK18, p63, and Ki67.
Results: All tumours (6 males, 3 females, mean age 50 years) were located in the parotid gland and showed intimate intermingling of lymphoid tissue with islands of epithelium with a wide spectrum of histological differentiation. The immunohistochemical profiles mirrored the epithelial differentiation; tumours with basaloid or lymphoepithelial differentiation strongly expressed CK5/6, CK14, p63, while tumours with ductal differentiation showed strong positivity for CK18/CK7 and CK5/6/CK14/p63 in luminal and basal cell layers, respectively. A hilus structure with salivary inclusions or D2-40 (podoplanin) positive marginal sinus were identifiable in 4 and 9 of the cases, respectively, confirming origin within intra-/periparotid lymph nodes. Six cases were initially misdiagnosed as other benign (n=4) or malignant (n=2) tumours.
Conclusion: Our study provides strong evidence that NSLA belongs to the group of salivary tumours that pathogenetically develop from embryonic salivary inclusions in intra-/periparotid lymph nodes. Knowledge of the wide histological spectrum of this rare tumour is important in order to avoid misdiagnosis.

OFP-08-009

CRTC1/MAML2 fusion transcript in central mucoepidermoid carcinoma of mandible: Diagnostic/Histogenetic implications

D. Bell*
*MD Anderson Cancer Center, Dept. of Pathology, Houston, TX, USA

Objective: MEC typically arises from major/minor salivary glands. Intraosseous salivary carcinomas are extremely rare (2–3 % of all MECs reported). The t(11; 19) and its CRTC1/MAML1 fusion transcript have been identified in MEC at different sites and are associated with development of a subset of these tumors. We report 9 examples of central MEC of the mandible, including a case with a history of primary retromolar MEC.
Method: RT-PCR and DNA sequencing analyses used to study microdissected components of 9 central MEC and 1 noncentral MEC. Of the central MEC tumors, 5 arose from ectopic salivary rests; others appeared to be of glandular odontogenic origins.
Results: We identified CRTC1/MAML1 in 5 central MEC arising from ectopic salivary rests. This fusion transcript was not detected in non-central MEC or in another 4 central MEC arising from a glandular odontogenic etiology.
Conclusion: Central MEC can manifest the fusion transcript in a subset of central MEC originating from ectopic salivary rests, and may have diagnostic/histogenetic roles in the future analysis of this entity, given the absence of the fusion transcript in MEC with glandular odontogenic precursors. Since the initial clinical and radiological diagnosis in three central low-grade MECs was a benign odontogenic cyst, our findings support a future role for the fusion analysis in initial diagnostic efforts.

OFP-08-010

Salivary duct carcinoma: Morphological and immunohistochemical study of 15 cases

M. Vazmitel*, A. Dubrovskij, R. Smoljakova, S. Rjabceva
*Minsk, Belarus

Objective: An evaluation of morphological and imunohistochemical features of salivary duct carcinoma (SDC).
Method: 15 cases SDC were retrieved from tumor archives collected at Belarusian Cancer Centre from 2002 to 2011 years. Immunohistochemistry, FISH.
Results: A man to women ratio was 10:5; median age 61,5 years (average 35–85). Tumors arose in the parotid

(n=13), submandibular (n=2) glands. SDC developed from pleomorphic adenoma (n=3) or de novo (n=12), there were foci of ductal carcinoma in situ (n=4), sialodochodysplasia (n=4) and Pagetoid spread (n=1) additionally to usual features of SDC. As well, tumors demonstrated acinic cell carcinoma-like (n=2) and micropapillary growth patterns (n=1), oncocytic (n=4), clear cells (n=3), apocrine (n=1) and mucinous (n=1) changes. Immunohistochemically, tumors were characterized by AR-expression (n=9), Her2/neu overexpression (n=7), of them score 2+ in 2 cases. CK8 and S-100 positivity, STAT5 negativity was detected in one case with acinic cell carcinoma-like pattern. Foci of SDC in situ were highlighted by CK14 and calponin. Amplification of c-erb2-gene was found in 1 case, ETV6/NTRK3 gene was not identified in acinic cell carcinoma-like SDC.
Conclusion: Salivary duct carcinoma, like breast cancer, is characterized by wide variability of morphological patterns and immunohistochemical features reflecting possible molecular heterogeneity, which need further investigation.

Sunday, 9 September 2012, 17.00–19.00, Meeting Hall V
OFP-09 Oral Free Paper Session IT in Pathology

OFP-09-001
Quantification of protein expression in immunohistochemical sections using a newly launched image analysis software
M. Braun*, R. Kirsten, N. Rupp, H. Moch, G. Kristiansen, S. Perner
*Universitätsklinik Bonn, Inst. für Pathologie, Germany

Objective: Quantification of protein expression based on immunohistochemistry (IHC) is an important step for translational research and clinical routine. However, routinely used eyeballing scoring systems are time-consuming and subject to significant intra- and interobserver variability. Aim of our study was to explore, whether an image analysis software proves sufficient as an alternative tool to assess protein expression.
Method: 630 prostate cancer specimens were stained with one nucleus specific marker (i.e., ERG), one cytoplasmic specific marker (i.e., SLC45A3), and one marker expressed in both compartments (i.e., TMPRSS2). A pathologist visually quantified all stainings, applying a four-step scoring system. For digital quantification, an image analysis software (Tissue Studio v.2.1) obtained a continuous spectrum of staining intensity.
Results: For each of the three antibodies we found a strong correlation of the eyeballing protein expression score and the score of the image analysis software (correlation coefficient of 0.94, 0.92, and 0.90 for ERG, SLC45A3, and TMPRSS2, respectively, $p<0.01$).
Conclusion: Our data suggest that Tissue Studio is a powerful tool for the quantification of protein expression in IHC stainings. Further, since the digital analysis is precise, it might help to overcome intra- and interobserver variability and increase objectivity of IHC based protein assessment.

OFP-09-002
Is quality of histological and cytological slides a palatable issue?: The TASTE project
M. Comanescu*, G. Bussolati, A. Sapino, G. Butur, F. Schmitt, F. Feoli, T. Tot, E. Ovcin
*Institutul Victor Babes, Dept. of Pathology, Bucharest, Romania

Objective: The TASTE (technological platform and repository of high quality images and slides) project aims at developing a novel tele-pathology system by means of modern ICTs (Information and Communication Technology) and is addressed to technicians and doctors.
Method: Histological and cytological preparations are the basis for pathological diagnosis performed in daily practice throughout Europe in a number of several millions per year and correctness and reproducibility of such diagnosis are heavily dependent on the technical quality. Yet, quality is variable in different places and countries, related to school level, technicians' dedication, standard of apparatuses and reagents. Variation in technical quality of the preparations prevents their open circulation at European level and precludes optimal diagnosis.
Results: The TASTE project tackles these problems by building-up an ICT environment TASTE System where professionals from different countries will submit, via Web, "virtual slides" of their own preparations to a panel of internationally recognized experts who will give comments and suggestions on the quality of the preparation.
Conclusion: The present approach (unprecedented at world level) will fuel a Web-based community, aimed to a levelling and improvement of histopathological and cytopathological preparations, thus leading to an innovative training and more reproducible diagnosis, a basic requisite for disease treatment.

OFP-09-003
Hypertext Atlases of Pathology
J. Feit*, L. Hejtmánek, M. Procházka, S. Licehammer, L. Matyska
*Masaryk University, Inst. of Pathology, Brno, Czech Republic

Objective: Hypertext Atlases of Pathology are available on the web (http://atlases.muni.cz) since 1998 with 25000 of registered users. The atlases contain more than 9000 images.
Method: A new virtual microscope interface will be presented. The interface is based on jpeg2000 compression that enables fast access to stored images and reduces disk usage

of the whole atlases. Virtual microscope positions can be stored in the memory and users can navigate quickly back and forward similarly to web pages. All these features are available through any web browser without need to install any additional software.
Results: In addition to the current atlases (Dermatopathology, Fetopathology, Pathology of the Newborn and Bone Marrow), an interdisciplinary Atlas of Pathology for pregraduate students of Medicine is under development. It will contain full size annotated virtual slides. The Atlases are free of charge, but registration is required. In order to ease the access, the Atlases are connected to 15 national academic identity federations. The members of institutions connected to identity federations can use theirs home credentials without revealing them to the Atlases.
Conclusion: The atlases can serve not only to the students as a source of information, but they can be used by teachers as a source of teaching material.

OFP-09-004
Proving experiment of international virtual slide telepathology, Japan-Vietnam and Japan-China trial
I. Mori*, S. Aida, Y. Osamura
*International University of Health, Dept. of Pathology, Tokyo, Japan

Objective: The communications between Asian countries are growing. In the field of medical information and technologies, the necessity of communication is also required. In this work, as communication of pathology field, we tried to prove that international remote pathology diagnosis is possible using virtual microscopy (VS) telepathology.
Method: We put VS scanner and server to 1) our Hospital, Tokyo, Japan, 2) Cho-Rai Hospital, Ho-Chi-Minh city, Vietnam, and 3) Chinese Rehabilitation Research Center, Beijing, China. Pathologists go and look the VS through leased optical line circuit and make diagnosis. Discussion was made through teleconference system.
Results: The VS image maintained adequate quality for pathology diagnosis even looked cross-border. The diagnoses matched well between hospitals. The response of VS viewer was also good this time. When we use too much band width to the Teleconference system or we sent too many data in the background, the response deteriorate, and was not good enough for diagnosis.
Conclusion: It was confirmed that the international VS telepathology diagnosis is now reached to a stage of actual use at least when connected by leased optical line circuit.

OFP-09-005
Challenges and solutions in the setup of a findings database for a large scale tissue collection
R. Reihs*, H. Müller, S. Sauer, K. Zatloukal
*Medizin. Universität Graz, Inst. für Pathologie, Austria

Objective: Many medical centres have acquired through the last years huge data collections of great relevance for biomedical research. In order to utilize this knowledge it is necessary to analyse this records in a structured way. In our use case the starting point were approximately 1.4 million pathological findings of a non-selected patient group.
Method: We developed software tools for the classification of medical records using a phonetic a multi-level spell correction module and an ontology term extraction and decision tree text classification system. With the help of a visual editor a comprehensive decision tree (4174 nodes) was set-up by a team of bioinformaticians and medical experts.
Results: With our tool set we achieved in the ICD-10 classification a F-Score of 89,7 % (precession 83,2 % and recall 97,5 %) For the interpretation of the classification results we developed visualization tools and applied the whole software suite at several test cases, e.g. the analysis of a colon data-set with 216.000 findings over 28 years.
Conclusion: We developed an automatic classification and visualization system and applied the results in a series of research projects. The software suite is currently used in several research projects and can be easily adjusted to specific phrases used in different institutions and languages.

OFP-09-006
An image repository for decision support
O. Eichhorn*
*Aperio, Vista, USA

Objective: Pathology is a visual field, and pathologists make decisions based on visual information. An online repository of easily searched, well-categorized pathology images can be of immense use to pathologists, scientists, educators, and students.
Method: Individuals and institutions all over the world have accumulated collections with thousands of slides representing a huge variety of pathologies. Some collections are digitized and available online, while others remain libraries of glass slides, with a variety of formats for case information and other metadata. Working with collectors to publish their slides and aggregating them together can yield an amazing decision support resource.
Results: Long-term archival storage is a key issue for organizations adopting ePathology. A cloud-based repository can provide an inexpensive and scalable solution. ePathology is increasingly used for remote consultations. Cases managed by online consultation networks can be de-identified and contributed to a common repository, increasing the value of the decision support tool while providing a long-term archive.
Conclusion: This talk will present concepts for an Image Repository for Decision Support, and discuss technical and

business considerations for making it a reality, including ways to curate image metadata, organizational principles and search tools, relationships with users and contributors, access methods, and security and privacy considerations.

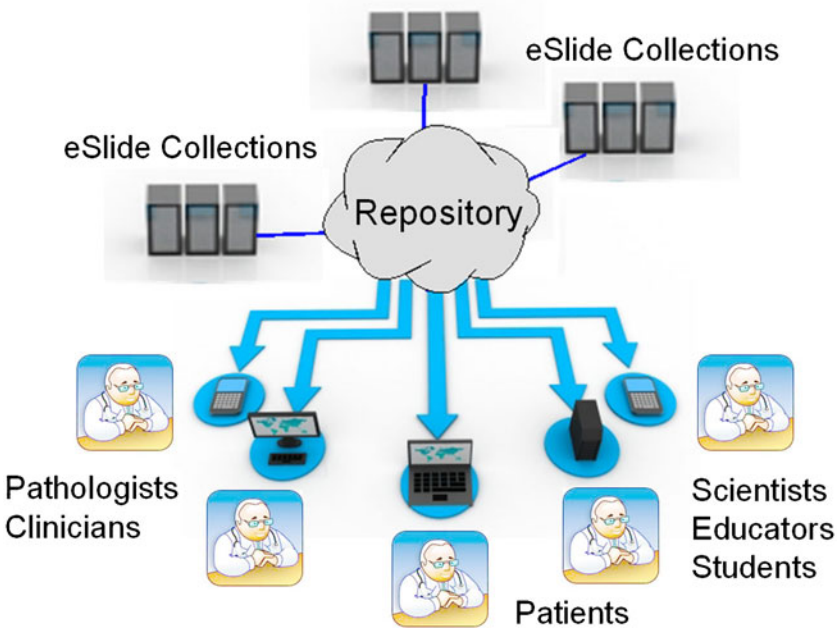

OFP-09-007

Perfect diagnostic accuracy using pathomorphological diagnosis spectra constructed with the help of whole slide imaging

K. Furuya*, T. Maeda, K. Kito

*Ehime Prefectural Central Hospital, Dept. of Pathology, Matsuyama, Japan

Objective: Pathomorphological diagnosis (PD) is important for estimation of clinical trials and new medical equipment such as elastography. However, interpretation of pathomorphological findings is often subjective, and pathology publications show only a limited number of photographs. Because pathomorphological changes occur in succession, we attempted to construct PD spectra to improve PD accuracy.

Method: PD spectra are defined as the series of pathomorphological images arranged in the order of disease progression or cell cycle procession. The images from the whole slide imaging (WSI) server were arranged in order in Power Point files at a fixed magnification, and 4 PD spectra were constructed: chronic hepatitis staging, nuclear grading of hepatocellular carcinoma, nuclear grading of breast cancer, and Ki-67 labelling index (LI). The numbering of all images in the PD spectra corresponded with that of the WSI images so that the whole slides could be viewed alongside. Next, these tools were tried out by 6 people.

Results: These tools brought on perfect accuracy with regard to staging and grading, and very high precision of Ki-67 LI for breast cancer.

Conclusion: PD spectra are valuable not only for PD but also as learning tools and have a worldwide applicability for measuring PD online.

OFP-09-008

Color correction of immunohistochemistry stained tissue section images by histogram transfer according to control tissues

S. Sarioglu*, S. Seyrek, M. Sakar

*Dokuz Eylul University, Faculty of Medicine, Izmir, Turkey

Objective: For semiquantitative and quantitative analysis, previous normalization attempts of images of tissue sections are not satisfactory. In this study we evaluated, if color correction can be achieved by histogram transfer depending upon control tissue image (CTI) differences.

Method: Images from colon and placenta sections stained by anti-CD34 were used as CTI and/or sample tissue images (STI). Thirty-four but one (standard stained slide with images sCTI and sSTI), was stained for different durations and dilutions than the standard

procedures. Digital images taken by a CCD camera connected to a light microscope without normalization was stored at a computer. Software was prepared in order to find the histogram difference between two CTIs and transfer the difference to the STI for achieving a corrected STI (corSTI). sSTI (one image) and STI and corSTI (34 images each) were semiquantitatively scored by two observers in blind fashion and the STI and corSTI scores were compared with sSTI score.

Results: The wKappa was 0,59 for two observers. The STI semiquantitative score was same as the sSTI in 23,5 % of the STI but this was 76,35 % for corSTI.

Conclusion: It seems histogram transfer depending upon CTIs may be a valuable tool for color correction of tissue section images.

Sunday, 9 September 2012, 14.15 - 16.15, Terrace 1
OFP-10 Oral Free Paper Session Molecular Pathology I

OFP-10-001

Prognostic significance of circulating melanoma cells detection using the CellSearch® System in patients with Metastatic Melanoma

D. Giacchero*, E. Long, M. Ilie, E. Selva, J.-P. Lacour, P. Hofman, P. Bahadoran
*Nice University Hospital, Dept. of Dermatology, France

Objective: There is a crucial need for identification of markers to choose the best treatment schedule and monitor the effectiveness of treatment in metastatic melanoma (MM). The detection of circulating tumor cells (CTC) correlates with prognosis in different cancer subtypes. CTC can be detected by direct and indirect methods such as cytopathological approach, RT-PCR or immunomagnetic separation using the CellSearch (CS) method.

Method: From June 2011 to December 2011, blood was drawn from 27 patients with MM and 10 controls patients and processed into 72 h by the CS method. The primary end-point was the overall survival (OS) of MM patients.

Results: Enumeration of at least 1 CMC was effective in 61.5 % of patients with MM (n=16) and in 20 % of controls patients (n=2). Nine patients (35 %) had ≥ 2CMC. None of the controls patients had more than one CMC. Mean OS time was 5.6 months among patients with MM and <2 CMC (n=8) and mean OS time was 1.7 months among patients with MM and CMC ≥2 (n=26) (p=0.002).

Conclusion: Our results demonstrate that detection of CMC correlates with OS in melanoma. Thus, CMC monitoring should be developed to ensure the best treatment follow-up for patients with MM.

OFP-10-002

Significance of Circulating Tumor Cells (CTCs) detection using the CellSearch system in patients with locally advanced Head and Neck Squamous Cell Carcinoma (HNSCC)

A. Bozec*, M. Ilie, E. Long, O. Dassonville, G. Poissonnet, J. Santini, E. Chamorey, F. Peyrade, K. Benezery, A. Sudaka, E. Selva, P. Hofman
*Centre Antoine Lacassagne, Dept. of Surgery, Nice, France

Objective: The significance of CTCs in patients with HNSCC is debated currently. We evaluated the potential detection of CTCs using the CellSearch (CS) Assay TM (Veridex, NJ, USA) in HNSCC patients and to identify the clinical factors predictive of the presence of CTCs in this population.

Method: Forty-nine patients with locally advanced HNSCC were included. The presence and number of CTCs were determined using the CS system in all patients prior to the initiation of therapy, in 21 patients 3 months after treatment, and in 10 healthy individuals.

Results: The CS system was able to detect the presence of CTCs in 8 of 49 patients (16 %) before therapy and in 4 of 21 disease-free patients (19 %) after therapy. No CTC was found in the control group. When considering the presence of CTCs before or after therapy, the presence of CTCs was statistically associated with patients' age (p=0.04; t-test) and N-stage (p=0.02; Fisher's exact test).

Conclusion: CTCs are identified in a relatively low proportion of patients with locally advanced HNSCC and correlated with initial lymph node involvement. CTC detection could be a future useful prognostic tool to adapt the treatment intensity in HNSCC patients.

OFP-10-003

The diagnostic utility in identifications of an aneuploid chromosomal (Ch.) pattern by using Urovysion™: A Fluorescence in Situ Hybridization (FISH) commercial test, to improve the efficacy of cytology in peritoneal effusions

L. Baron*, M. Postiglione, C. Trombetta, F. Quarto
*P.O.S. Leonardo, S.O.C. di Anatomia Patologica, Castellammare di Stabia, Italy

Objective: The challenge in diagnosis of effusion is in differentiation of reactive and neoplastic mesothelial or metastatic cells and identification of primary neoplasia. The difficulties in this differential diagnosis derived from the low sensitivity (~ 50 %) and specificity of effusion cytology. By identification of tumor associated aneuploidy FISH could enhance the cytodiagnostic yield in effusions.

Method: We used Urovysion™ (Abbott), a FISH commercial kit, designed for identifications of Ch. 3, 7, 17 polisomy and 9p21 loss in urothelial tumors. It has been applied to

detect chromosomal aneuploidies as a marker of malignancy in 64 effusions with or without known source primary tumors. Also was evaluated reproducibility of molecular alterations with primary tumors and any their specific aneuploidies.
Results: FISH positivity was observed in 44 (69 %) of cases, whereas 31 were positive at cytology (48 %). Overall results of cytology and FISH together rised to 75 %.
Conclusion: Urovysion™ test could be an useful tool to distinguish malignant cells in inconclusive effusions cytology but it doesn't seem to be used to provide definitive indications about primary neoplasia.

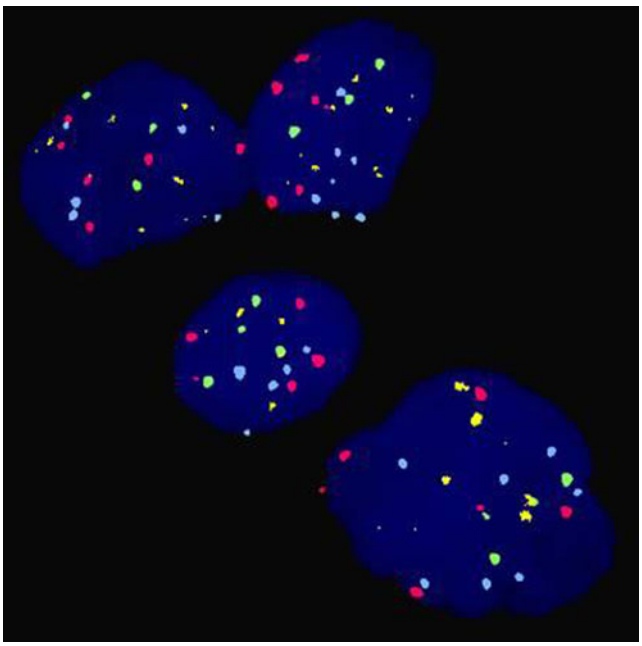

OFP-10-004
Loss of imprinting of isulin-like growth factor 2 (IGF2) in colon carcinomas leads to the cell cycle genes activation -hints to intense proliferation
D. Belharazem*, J. Kunanz, A.-K. Henne, P. Kienle, P. Ströbel
*Inst. of Pathology, University of Medicine, Mannheim, Germany

Objective: The insulin-like growth factor 2 (IGF2) gene is regulated by imprinting in normal tissues. The loss of imprinting (LOI) results in the bi-allelic expression of IGF2. Its increased activity has been associated with many cancers including colorectal cancer (CRC). To investigate the significance of IGF2 in CRC, normal tissue and tumor biopsies from 400 patients were analyzed and correlated with clinical outcome and the KRAS and PIK3 status.
Method: The IGF2 820 G/A gene polymorphism and imprinting status were examined by restriction fragment length polymorphism of DNA derived from normal tissues and tumors then of RNA from heterozygous cases. IGF2 protein analysis as well as an RNA microarray were performed.
Results: 41 % of the analysed cases were heterozygous. LOI was detectable in both normal tissues and tumors in 60 % of cases. Tumors with LOI had significantly higher IGF2 protein levels. Gene expression analysis revealed significance of cell cycle progression and mitosis genes in LOI.
Conclusion: IGF2 LOI is a common and early change in patients with CRC and in normal tissues, provides possibly a preneoplastic change. However increased IGF2 protein levels as well as a different cell cycle specific gene expression profile were detected in tumors with LOI. Future studies must be performed to find out, whether such subsets of tumors differ in their response to chemotherapy or alternative therapies.

OFP-10-005
Detection of EZH2 and CD79B mutations in B-cell Non-Hodgkin lymphomas utilizing cytological preparations for high-throughput sequencing
G. Da Cunha Santos*, M. A. Saieg, W. Geddie, S. Boerner, D. Bailey, M. Crump
*University Health Network, Laboratory Medicine Program, Toronto, Canada

Objective: Novel high-throughput technologies has revealed numerous genomic abnormalities in B-cell non-Hodgkin lymphomas (NHL). This study aimed to detect point mutations involving EZH2 and CD79B in a population of B-cell NHL by applying a multiplex mutation assay to minimal residual material from needle aspirates, and to determine the evolution of their mutational status overtime using all sorts of available samples from these patients.
Method: DNA was extracted from residual cytological material stored on FTA® Cards as well as from archived cytological and histological specimens. The presence of point mutations was investigated by a specifically developed assay utilizing MassARRAY spectrometry and confirmed by direct sequencing.
Results: All 121 samples from 80 B-cell NHL cases were successfully analyzed. Mutations in EZH2 (Y641) and CD79B (Y196) were detected in 13.2 % and 8 % of the samples, respectively. Mutational status varied in one third of the positive cases, with either gain or loss of mutations over the course of time.
Conclusion: Minimal material from lymph node fine needle biopsy is a reliable source for high-throughput multiplex analysis for the detection of point mutation involving EZH2 and CD79B. Whenever possible, the most recent sample should be tested to verify the current status of the disease.

OFP-10-006

MicroRNA expression profile identifies a distinct molecular signature between MYC translocation-positive and negative Burkitt Lymphoma cases

G. De Falco*, A. Onnis, F. Morettini, F. Fuligni, C. Bellan, E. Rogena, P. P. Piccaluga, L. Leoncini
*University of Siena, Dept. Human Pathology and Oncology, Italy

Objective: The molecular hallmark of Burkitt Lymphoma (BL) is a dysregulation of MYC oncogene, due to one of the three translocations leading to IG-MYC fusion. However, about 10 % of BL cases lack an identifiable MYC rearrangement, although no significant difference of MYC expression among cases has been observed. Additional mechanisms alternative to translocations were explored by microRNA profiling.
Method: Ten MYC translocation-positive and ten MYC translocation-negative formalin-fixed and paraffin-embedded BL specimens were used for this study. For microRNA and gene expression profile, the samples were hybridized on the miRCURY™ LNA Array and the Illumina DASL whole genome Assay, respectively.
Results: Our results identified a panel of four microRNAs which are differentially expressed between the two groups. Importantly, these microRNAs control relevant biological processes, such as the angiogenesis, apoptosis and cell proliferation, according to Gene Ontology categories. Furthermore, the impact of microRNA dysregulation on the gene expression pattern identified genes which more likely are regulated by the selected microRNA.
Conclusion: Using this approach, we showed a clear-cut microRNA and gene signature between MYC translocation-positive and negative BLs. The identification of specific altered microRNAs may represent an alternative molecular mechanism leading to MYC over-expression in the absence of genetic alteration in cancer.

OFP-10-007

Droplet Digital PCR: A highly sensitive assay for B-Raf, K-Ras and EGFR mutation detection

J. Frampton*, C. Thorne, V. Spivey, J. Goodall, C. Lowe
*Horizon Discovery, Dept. of Diagnostics, Cambridge, United Kingdom

Objective: Droplet Digital™ PCR (ddPCR™) enables the absolute quantitation of nucleic acids in a sample. Horizon Discovery's patented gene editing technology enables it to manufacture reference material that is genetically defined and validated for the allelic frequency of the mutation. These reference standards were used to test the sensitivity of Bio-Rad's QX100™ Droplet Digital™ PCR platform.
Method: A panel of defined genomic DNA allelic standards and formalin fixed paraffin embedded (FFPE) cell line samples were used in this study. This panel covered EGFR (G719S, T790M, L858R and L861Q), K-Ras (codon 12) and B-Raf (V600E and V600K) mutations containing allelic frequencies between 0.05 % and 50 %. Droplet Digital™ PCR was performed using mutation specific TaqMan custom SNP assays.
Results: There was a strong correlation between the predicted and actual allelic frequencies even down to 0.05 %. The allelic frequency called by the ddPCR™ platform was highly reproducible between experiments particularly in the 1–50 % dilution range.
Conclusion: This study has demonstrated that the Droplet Digital™ PCR QX100™ platform can detect allelic frequencies down to at least 0.05 % using genomic DNA purified from cell lines and down to at least 3.5 % using genomic DNA extracted from FFPE cell lines.

OFP-10-008

Chromothripsis and focal copy number alterations determine poor outcome in malignant melanoma

T. Gaiser*, D. Hirsch, R. Kemmerling, J. Camps, T. Ried
*Medizin. Universität Mannheim, Inst. für Pathologie, Germany

Objective: Genetic changes during tumorigenesis are usually acquired sequentially. However, a recent study showed that in 2–3 % of all cancers a single catastrophic event, termed chromothripsis, can lead to massive genomic rearrangements confined to one or a few chromosomes.
Method: In order to explore whether the degree of genomic instability and chromothripsis would influence prognosis in cancer, we applied high-resolution array comparative genomic hybridization to 20 malignant melanomas (MM) that were, despite comparable conventional clinical and pathological parameters, defined by a profoundly different clinical course.
Results: We observed a striking association between both number and structure of chromosomal aberrations and outcome. MM associated with good prognosis showed only few chromosomal imbalances (average 1.6 alterations per case), predominantly presented as whole chromosome or chromosome arm gains and losses. MM with poor prognosis harbored significantly more chromosomal aberrations (13.9 per case; $p=0.008$). These aberrations were mostly focal events, which culminated in two cases in a pattern consistent with chromothripsis.
Conclusion: Here, we describe for the first time the phenomenon of chromothripsis in primary MM and reveal a link between focal copy number alterations and chromothripsis with poor outcome in MM patients ($p=0.0002$), providing a genetic approach to predict outcome in histopathologically indistinguishable MM.

OFP-10-009

Targeting endometrial stromal sarcoma: Histone deacetylase and PI3K/Akt/mTOR signaling

P. Quan*, E. Lederer, I. Halbwedl, H. Denk, K. Zatloukal, J. Haybaeck
*Institute of Pathology, Medical University of Graz, Austria

Objective: Endometrial stromal sarcoma (ESS) is a gynecological malignancy with few therapeutic options. Up-regulated histone deacetylase (HDAC) 2 was observed in ESS patients. The HDAC inhibitor SAHA reduced ESS cell growth by inhibiting mTOR. The PI3K/Akt/mTOR signaling cascade, vital to cancer growth is a critical target in cancer therapy. This study aimed at investigating if HDACs interact with the PI3K signaling in ESS pathogenesis and thus might serve as targets for ESS therapy.
Method: Tissue microarrays were used to determine HDAC expression in ESS specimens. Western blots revealed protein expression levels of HDACs and PI3K related molecules in two independent ESS and one control cell lines (ESS-1, MES-SA and HESC).
Results: Elevated HDAC1 and 2 levels were found in ESS tissues and cell lines. Increased cell growth and Akt/mTOR cascade hyperactivation were detected in ESS cells. SAHA reduced growth of all cells, and induced cell death in ESS cells. SAHA reduced phosphorylated 4EBP1 in all cells, but only inhibited activation of Akt and p70S6k in ESS-1 cells.
Conclusion: HDACs are linked to PI3K signaling during ESS pathogenesis. SAHA reduced cell growth via inhibiting PI3K/Akt/mTOR components suggesting that a combination of SAHA with PI3K inhibitors might be effective in treating ESS.

OFP-10-010

Usefulness of linking biobanking field and animal model: High successful rate of human primary Non-small Cell Lung Carcinoma (NSCLC) xenografts in a model system separated by distance and time

M. Ilie*, L. Blot, V. Hofman, E. Long, M. Nunes, C. Butori, E. Selva, A. Merino-Trigo, N. Vénissac, J. Mouroux, P. Vrignaud, P. Hofman
*CHU de Nice, LPCE, France

Objective: With the ongoing need to improve therapy for NSCLC, there has been an increasing interest in the development of reliable preclinical models to test novel therapeutics. The aim of this study was to evaluate the rate of establishment of patient-derived NSCLC xenografts in the context of a long-distance research network.
Method: Fresh surgically resected NSCLC specimens were addressed from the human biobank hospital (Nice) to the animal facilities (Sanofi, Vitry-sur-Seine). Shipment was performed in AQIX medium at room temperature. Within 24 h post surgery, tumour fragments (~63 mm3) were subcutaneously implanted in female SCID mice. The growing tumours were passaged in new mice (≤10 passages). The xenografts were histologically checked to eliminate human or murine lymphoma.
Results: Overall, 98 NSCLC samples were implanted leading to 32 (33 %) NSCLC xenografts. The rate of tumour growth was higher in non-adenocarcinoma specimens (23/45; 51 %): 20/38 (53 %) for squamous cell carcinoma, 2/4 (50 %) for large cell carcinoma, and 1/3 (33 %) for pleomorphic carcinoma, when compared to adenocarcinoma samples (8/51; 16 %).
Conclusion: We report a high successful rate of xenotransplantation established from patient-derived NSCLC tissues. Our biobanking model system, regardless to extended time and distance, provides a stable and reliable animal model in human lung cancer research.

Monday, 10 September 2012, 14.15 - 16.15, North Hall
OFP-11 Oral Free Paper Session Molecular Pathology II

OFP-11-001

Macrophages recruitment with different roles at different stages of tumor growth

L. Maruscakova*, O. El-Hassoun, Z. Valaskova, M. Kopani, J. Jakubovsky, E. Kovacova, I. Hulin
*Comenius University, Medical School, Bratislava, Slovakia

Objective: We tried to interpret "the job" of MF in different stages of tumor growth by monitoring the dynamics of their distribution.
Method: On a rat model of experimental tumorigenesis using BP6 fibrosarcoma cells injected intraperitoneally, we performed a semiquantitative analysis of the recruitment of MF in the tumor compartment (microenvironment) as well as in peripheral blood.
Results: We observed a slow increase of MF count in the initial phase of tumor growth followed by a slow decrease in the late phase within the tumor compartment. Simultaneously peripheral blood showed constant increase throughout the experiment resulting in typical leukocytosis accompanying developed tumors.
Conclusion: Increased MF in the initial phase could reflect their enrollment to "prepare a suitable microenvironment for tumor seeding". Their decrease began after the tumor size was macroscopic, thus it was time for them to carry out a "different job". In the mean time their amount in peripheral blood started becoming significant, this is also the time when tumor - host interactions reach a systemic level. In futher experiments we will attempt to verify our assumption: When the tumor flourish in the host organism, it uses informed, transformed and recruited macrophages for growth

and building construction of the tumor, and for communication with distant organs on a regulatory level.

OFP-11-002

WWTR1 and CYR61 are early markers of Barrett's esophagus malignant progression

M. Mesquita*, J. Cardoso, A. Pereira, S. Braga, M. Bettencourt-Dias, P. Chaves, J. Pereira-Leal
*IPOLFG, Dept. of Pathology, Lisboa, Portugal

Objective: Barrett's esophagus (BE) is the major risk factor for esophageal adenocarcinoma (EA). BE has a low risk of progression to EA, being imperative to identify markers to stratify the risk. Our aim was to look for potential early biomarkers of BE malignant progression.
Method: Three available microarray datasets were analyzed with R Statistical Computing software complemented with Bioconductor. Biomarker prioritization included: 1) Expression Barcode 2.0; 2) filtering using differential expression analysis. Candidate genes were validated by qRT-PCR on RNA from paraffin embedded samples (RNA-PES) of BE patients with high-grade dysplasia/ADC diagnosed during surveillance and of their index endoscopy dysplasia-free samples. As controls, we used samples from BE patients who have not progressed.
Results: Under conservative criteria, we identified 19 up-regulated genes that distinguish EA-progressed from non-progressed BE samples. A second filter, followed by qRT-PCR validation, trimmed the candidates to 2 markers (WWTR1 and CYR61). qRT-PCR on time-series RNA-PES of EA-progressed and EA-free BE samples showed these genes are up-regulated years before the development of EA as compared to patients who did not developed EA.
Conclusion: WWTR1 and CYR61 were identified as early risk markers for BE neoplastic progression and may have a potential role in BE risk stratification.

OFP-11-003

Combined microRNA in situ hybridization and immunohistochemical detection of protein markers

B. Nielsen*, T. Møller, K. Holmstrøm
*Bioneer A/S, Dept. of Molecular Histology, Hørsholm, Denmark

Objective: MicroRNAs are small noncoding RNAs that constitute a novel group of biomarkers with exciting functions in cell differentiation, proliferation and apoptosis by mediating degradation or destabilization of target mRNAs. miR-21 is highly prevalent in malignancies. Previous reports on miR-21 in situ hybridization (ISH) in colon and breast cancer identified expression in the stromal cell population that was related to recurrence and cell proliferation (Nielsen et al., Clin Exp Metastasis 2011, 28:27; Rask et al., APMIS 2011, 119:663). Here, we present a histological assay platform that allows parallel localization of microRNAs and protein markers.
Method: Routinely processed paraffin embedded breast cancer samples were analyzed. MicroRNA ISH probes were detected with fluorescent tyramine reagents and primary antibodies with compatible immunofluorescence. The reagents were introduced on a semi-automated platform, HistoFlex, which has a precise temperature control unit and utilizes continuous liquid flow.
Results: By combination of miR-21 ISH and PDCD4 immunofluorescence we found differential expression in many but not all miR-21 positive cells. Using the HistoFlex, the double fluorescence assay was reduced from 7 to 2 h without loss of sensitivity and specificity.
Conclusion: A 3-fold faster assay platform was developed and our in vivo findings support the assumption that PDCD4 is a target of miR-21.

OFP-11-004

The TNF-superfamily members APRIL and BAFF and their receptors (BAFFR, BCMA, TACI) are differentially expressed in tumors and normal tissues and exert specific effects related to cell fate and differentiation

V. Pelekanou*, V.-I. Alexaki, G. Notas, M. Kampa, E. Stathopoulos, A. Tsapis, E. Castanas
*University of Crete, Pathology, School of Medicine, Heraklion, Greece

Objective: Classically, tumor immune-related microenvironment was synonym of inflammatory cell infiltrate. Recently, the detection of synthesis and secretion of immune mediators by tumor cells highlighted TNF-superfamily (TNFSF) members as key counterparts of cell fate-related signals. Here, we assayed the synthesis-expression-function of a subset of TNFSF ligands and receptors (BAFF, APRIL, BAFFR, BCMA, TACI) in normal epithelial tissues and tumors and resident adult mesenchymal stem cells.
Method: Tissues (breast, CNS, kidney, skin, adipose tissue) have been assayed by means of immunohistochemistry and Real-Time PCR. Cell models were used for signaling, transcriptomics and functional assays.
Results: All tumors expressed this TNF-SF subset. BAFFR is absent, while its specific ligand BAFF is ubiquitously expressed; contrairewise, APRIL, BCMA and TACI are expressed in tissue-specific manner. APRIL relays on tumor evolution/grade and is involved in tumor proliferation/differentiation/apoptosis signaling through NFκB-related, or a novel pathway, implicating JNK/FOXO3A/GADD45, triggering transcriptional events.
Conclusion: Autocrine/paracrine effects of APRIL and its receptors BCMA and TACI in normal/tumoral parenchyme and the recruitment/attraction of immune-related cells could orchestrate tissue response, regulating cell fate, differentiation,

inflammation, tissue remodeling and cancer, with potential tailored-therapy application.

OFP-11-005

Mutations of cKit and PDGFRa genes in GIST patients diagnosed within the centralized diagnostic program in Slovakia in the years 2004–2008

L. Plank*, M. Gabriel, L. Zora, S. Tomas, B. Tatiana, S. Peter, B. Veronika, P. David, S. Jozef
*Jessenius Medical Faculty, Dept. of Pathology, Martin, Slovakia

Objective: Mutation analysis of KIT and PDGFRA genes is currently used in gastrointestinal stromal tumors (GIST) as an important step in diagnostic protocol.
Method: DNA samples obtained from parafin-embedded biopsy material of 278 GIST patients diagnosed in 2004–2011 were screened for mutations in exons 9, 11, 13 and 17 of KIT and 12, 14 and 18 of PDGFRA. Results were tested for associations with clinical parameters of the tumor.
Results: Causal mutations (according to in silico analysis with PolyPhen-2 predictor) were identified in 83.8 % of patients, most frequently in KIT exon 11 (62.95 %). The KIT exon 9, PDGRFA exons 18 and 12, KIT exon 13, PDGFRA exon 14 and KIT exon 17 mutations appeared with frequencies 8.3 %, 7.6 %, 2.5 %, 1.4 %, 1.1 % and 0.0 % resp. Genotype-phenotype correlation analysis revealed statistically significant association between intestinal localization of tumors and presence of KIT exon 9 p.503-504_dup2 mutation and gastric localization of tumors and presence of PDGFRA exon 18 p. D842V mutation.
Conclusion: Centralized and standardized GIST diagnosis offers clinically and prognostically relevant informations and is necessary for the indication of appropriate targeted therapy of GIST patients. Supported by projects CEPR II (IMTS 26220120036) and MBCC (IMTS 26220220113) at CU JFM co-financed by EU and by grant Novartis Slovakia.

OFP-11-006

Frequency of mutations of the Cystic Fibrosis Transmembrane Regulator (CFTR) gene in a cohort of consecutive patients candidate for assisted reproductive techniques

M. Rongioletti*, F. Papa, M. B. Majolini, C. Vaccarella, I. Simonelli, A. Luciano, P. Pasqualetti, G. Liumbruno
*San Giovanni Calibita Hospital, Dept. of Clinical Pathology, Rome, Italy

Objective: An association between cystic fibrosis transmembrane regulator (CFTR) gene mutations and infertility may occur. This study investigated the frequency of mutations in the CFTR gene, of a group of consecutive patients candidate for assisted reproductive techniques with the aim of identify subjects carriers of the most severe ones.
Method: We screened 11208 healthy subjects (5943 females and 5265 males) for 56 CFTR gene mutations and IVS8-poliT polymorphism utilizing the CFTR INNO-LiPA Amplification kit including both general and Italian regional strips.
Results: CFTR mutations were detected in 6.2 % of the patients, a percentage similar to that reported in the general population. The most common mutation was ΔF508/N observed in 0.9 % of patients. No difference in the gender distribution was evidenced. In the large group of patients analyzed 87.7 % were wt, 11.8 % carrier of one mutation, and interestingly 0.5 % compound heterozygous.
Conclusion: Our data support the relevance of an accurate determination of mutations in the CFTR gene in order to inform the couple of their carrier risk and the possibility on having affected child. Moreover our findings highlight the potential of genetic screening as a tool to identify possible compound heterozygous subjects without CF-like symptoms.

OFP-11-007

Still room for improvement: An update of the ESP KRAS EQA scheme

S. Sterck*, M. Ligtenberg, H. van Krieken, E. Dequeker
*KU Leuven, Dept. of Public Health, Belgium

Objective: A patient's response to cancer treatment can depend on their biomarker status. Therefore it is important that laboratories perform their biomarker tests well. In 2009 an international external quality assessment scheme for KRAS mutation analysis on FFPE slides was set-up.
Method: This scheme was run for 3 years by the coordination center, a medical and technical expert and scheme organizers under the umbrella of ESP. Participants received 10 samples. Genotype results were analyzed and labs with good performance were listed on the ESP website. Written reports of 2011 were evaluated in detail.
Results: In 2011, 79 % of participants identified all samples correctly. Results seemed to improve over the years from 9.49/10 to 9.62/10. Genotype results from laboratories that participated for 3 years appeared to improve overtime, although this couldn't be statistically proven. In the reports some important elements weren't always present. For example, the patient's name was only present in 80 %, correct HGVS nomenclature in 90 % and interpretation of results in less than 40 %.
Conclusion: KRAS-EQA probably facilitates improvement of laboratory testing. The quality of reports of KRAS tests needs to be improved. A guideline for reporting molecular pathological results would be a good instrument for both participants and assessors.

OFP-11-008

Comparative analysis of MIR-155 and MIR-21 expression in MSI and MSS Colorectal cancers complicating Inflammatoty Bowel Diseases (IBS)

M. Svrcek*, N. El-Murr, K. Wanherdrick, S. Dumont, L. Beaugerie, J. Cosnes, E. Tiret, J.-F. Flejou, T. Lesuffleur, A. Duval
*AP-HP, Dept. de Anatomie Pathologique, Paris, France

Objective: Microsatellite instability (MSI) due to mismatch repair (MMR) deficiency is reported in a fraction of colorectal cancers (CRCs) (5–10 %) complicating IBDs (IBD-CRCs). Our recent findings argued for the existence of yet unknown mechanisms underlying MMR-deficiency in IBD-CRCs, different from those involved in sporadic and hereditary MSI CRCs. Here we hypothesized that over-expression of miR-155 and miR-21, two inflammation-related miRNAs that target core MMR proteins, could constitute a mechanism underlying MMR deficiency in IBD-CRCs.
Method: We compared the expression of both miRs in IBD-CRCs and non-IBD hereditary or sporadic CRCs using non-neoplastic IBD and healthy mucosa samples as controls.
Results: Overall, miR-155 and miR-21 were significantly over-expressed in both non-neoplastic and neoplastic mucosa of IBD patients as compared to healthy controls. MiR-155 alone was preferentially expressed in MSI vs. MSS IBD-CRCs. In contrast, miR-155 was poorly deregulated in non-neoplastic and neoplastic tissues of non-IBD MSI or MSS CRCs.
Conclusion: miR-155, alone or synergistically with miR-21, may favor the emergence of MSI IBD-CCRs. Since its deregulation was not limited to neoplastic tissues but extends to non-neoplastic normal mucosa as well, the hypothesis of a miR-155 field defect promoting MMR deficiency and yet MSI-driven transformation can be proposed.

OFP-11-009

PI3K, AKT and PTEN expression in enucleated Brazilian uveal melanoma cases using tissue microarray

G. Freeman*, D. Begnami, A. Damascena, J. Neves, S. Nonogaki, F. Soares
*São Paulo, Brazil

Objective: In the world literature, little has been published on the molecular pathways in primary uveal melanoma or subsequent development of metastases. The PI3K pathway has been implicated in regulation of apoptosis, cell cycle regulation, transcription and translation.
Method: We used immunohistochemistry with TMA to investigate expression of PI3K, AKT and Phos- AKT, and PT in over 200 formalin fixed paraffin embedded blocks of uveal melanoma from the A.C. Camargo Hospital, São Paulo, Brazil from 1988 to 2005. FISH was performed for PTEN copy numbers.
Results: In this study, neither immunohistochemistry nor FISH results showed a statistically significant difference between the primary tumors and the tumors which metastasized. Statistical analysis of all tumors together (TMA) revealed only one molecular marker (PTEN), which gave results close to statistical significance.
Conclusion: This is the first large study of Brazilian patients for PI3K, PTEN AKT expression by Immunohistochemistry and PTEN using FISH. Expression values for molecular markers chosen did not reach statistical significance, although PTEN values were close. Use of FISH to distinguish metastatic from non metastatic cases also came close to statistical significance. These results suggest that the expression of PTEN in uveal melanoma may be a good topic to investigate further.

Tuesday, 11 September 2012, 17.00–19.00, Panorama Hall
OFP-12 Oral Free Paper Session Nephropathology

OFP-12-001

Molecular signatures of chronic rejection of renal allografts

J. Maluskova*, P. Hribova, J. Slatinska, I. Brabcova, O. Viklicky, E. Honsova
*IKEM, Dept. of Pathology, Praha, Czech Republic

Objective: Chronic antibody-mediated (CAMR) and chronic T-cell-mediated rejection (CTCMR) represent predominant reason for late graft dysfunction. Both categories share similar morphological features. We ask the question whether there are differences between CAMR and CTCMR on the molecular level.
Method: Graft biopsies (>3 M) were performed and evaluated according to the Banff classification. Biopsy specimens with CAMR (n=13), CTCMR (n=9) and from protocol biopsies with normal histology (n=10) were stabilized in the RNA-later. Using the Taqman Low Density Array, the intrarenal expressions of 378 genes relating to immune response (B-cell activation, T-cell activation, chemokines, growth factors, immune regulators and apoptosis) were analyzed.
Results: Both categories of chronic rejection were associated with up-regulation of many genes in comparison with the control group: chemokines (CCL4, CCL5, CXCL9, CXCL10, CXCL11), growth factor TGFB1, MHC class II (HLA-DMA, HLA-DMB, HLA-DR, UBD), and in T-cell dependent mechanisms (CD3, CD86, LAG3), including cytotoxic T-cell associated transcripts (GBP1, GZMK). In hierarchical clustering, CAMR and CTCMR gene expression profiles were similar.
Conclusion: Chronic rejection very probably involves prolonged cooperation of innate immunity and allospecific

immune response. Our study showed that CTCMR and CAMR do not differ on the molecular basis.

OFP-12-002

Podocyte loss and glomerulosclerosis in inducible mouse model of podocin mutation-related Nephrotic Syndrome

I. Simic*, M. Tabatabaeifar, G. Mollet, C. Antignac, S. Weber, F. Schaefer

*Universitätskinderklinik, Nephrologisches Labor, Heidelberg, Germany

Objective: Mutations in NPHS2 gene, encoding podocyte specific protein podocin, cause hereditary nephrotic syndrome. Knock-in mice carrying the R140Q mutation, murine analogue of the most common human mutation R138Q, show developmental arrest of podocytes and renal failure at neonatal age. The aim of this study was to quantify renal histopathological changes in mice with postnatally induced R140Q hemizygosity.

Method: C57BL/6 mice with Nphs2Flox/R140Q, Cre + genotype were injected with Tamoxifen for 5 days to induce hemizygosity for R140Q-mutant podocin. Tissue samples were collected at defined intervals after induction. Renal morphology was evaluated by quantitative histology, immunohistochemistry and electron microscopy.

Results: Animals developed proteinuria within 1 week that progressed into renal failure and advanced uremia at week 12–16. The number of podocytes per glomerulus started decreasing at week 2 (42±19 vs. 98±31, $p=0.05$), whereas glomerular sclerosis index increased from week 4 (1.5±0.15 vs. 0.25±0.08, $p<0.00001$). Interstitial changes included fibrosis (up to 20 % of section area in end stage renal disease), tubular atrophy and dilatation.

Conclusion: Our results implicate that the expression of mutated podocin in induced R140Q-podocin mice leads to podocyte loss that precedes interstitial damage and glomerulosclerosis. Quantification of histological changes will enable better evaluation of the efficacy of different pharmacological approaches directed to improvement of podocyte viability and attenuation of glomerulosclerosis.

OFP-12-003

Heavy chain deposition disease in kidney biopsies

A. Vizjak*, J. Mraz, J. Lindic, D. Ferluga

*University of Ljubljana, Faculty of Medicine, Slovenia

Objective: Heavy chain deposition disease (HCDD) is a rare and not yet fully explored monoclonal immunoglobulin-related disorder.

Method: We studied the histopathology in 4 kidney biopsy cases of HCDD, representing a 0.07 % prevalence among 5481 native kidney biopsies.

Results: HCDD was diagnosed in kidney biopsies of 4 women (mean age 73.0 years). Light microscopy showed diffuse nodular glomerulosclerosis (4/4), associated with mesangial proliferation (3/4) and capillary aneurysms (4/4). Immunofluorescence showed abundant mesangial deposits and ribbon-like deposits along glomerular, capsular, tubular and vascular basement membranes, positive for heavy chain IgG3 (3/4) and IgG1 (1/4), with deleted gamma CH1 domain (4/4). Complement C3 and C1q stained positive in all cases. By electron microscopy, punctate and powdery electron-dense deposits were found on the same locations.

Conclusion: Immunofluorescence examination of kidney biopsies, including testing for immunoglobulin heavy and light chains, is crucial for diagnosis of HCDD. Our study confirmed that HCDD is peculiar among monoclonal immunoglobulin deposition diseases not only because of its rarity but also because of uniform histomorphologic pattern of nodular glomerulosclerosis with pronounced capillary aneurysms and significant proliferation due to complement activation. Deletion of the heavy chain CH1 domain and its significance in the pathogenesis has to be emphasized.

OFP-12-004

Two cases of ANCA associated vasculitis with geographical necroses in the kidney tissue

A. Bartonova*, E. Honsova, R. Rysava

*IKEM, Dept. of Pathology, Praha, Czech Republic

Objective: ANCA associated vasculitides (AAV) are rare systemic autoimmune diseases affecting small to medium-sized blood vessels. In kidney biopsy samples, AAV usually demonstrate pauci-immune necrotizing crescentic glomerulonephritis (GN).

Method: Among 198 cases of AAV evaluated at IKEM during 10 years, 2 had a very unusual pattern of renal involvement.

Results: The first patient had been treated for recurrent otitis media with unilateral hearing loss. He also suffered from artralgias and hematuria. An ultrasound study revealed a tumor-like mass in his kidney. During exploratory surgery, the lesion appeared to be infiltrative and a nephrectomy was performed. The second patient presented a granulomatous inflammation in a scar. A month later she developed multiple kidney and spleen "abscesses" with negative hemoculture, and underwent a nephrectomy with splenectomy. In both cases, the final pathological diagnosis was necrotizing granulomatous vasculitis of small and medium-sized vessels, with large geographical necroses of kidney tissue simultaneously with necrotizing crescentic GN. Tests for ANCA antibodies were positive. No microbial pathogens including mycobacteria were detected.

Conclusion: This extremely rare renal presentation of AAV can mimic other granulomatous inflammation or tumor lesions, which can be misleading and cause a diagnostic delay.

OFP-12-006

Murine IgA nephropathy induced by O-glycosylated IgA rheumatoid factor

M. Otani*, Y. Wada, S. Izui
*Centre Médical Universitaire, Dept. of Pathol. Immunology, Geneva, Switzerland

Objective: IgA nephropathy is known to be associated with structural aberrations of O-linked glycans in the IgA1 hinge region. We explored the nephritogenic potential of two different monoclonal IgA anti-IgG2a rheumatoid factors (RF) in relation to the possible presence of O-linked glycans in their hinge regions.
Method: 6–19 or 46–42 IgA hybridoma was implanted into BALB/c mice, and serum levels of RF and renal lesions were assessed. The oligosaccharide profiles of both IgA RFs were analyzed by the MALDI linear-TOF MS.
Results: In parallel to increases in serum levels of IgA RF, mice implanted with 6–19 IgA, but not 46–42 IgA, hybridoma developed acute glomerular lesions within 2–3 weeks. They were characterized by mesangial expansion with mesangial cell proliferation and IgA deposits accompanied by IgG2a and C3 deposition. The analysis of oligosaccharide structures revealed the presence of highly galactosylated O-linked glycans in the hinge region of 6–19 IgA, but not 46–42 IgA.
Conclusion: Glomerular lesions resembling human IgA nephropathy were induced by 6–19 IgA anti-IgG2a RF, which is highly O-glycosylated in its hinge region. This experimental model could provide a useful tool to better define the immunopathological mechanisms critically involved in the development of himan IgA nephropathy.

OFP-12-007

Pathology of resolving polyomavirus nephropathy

H. Hopfer*, T. Menter, M. Mayr, H. H. Hirsch, S. Schaub
*Basel, Switzerland

Objective: Polyomavirus nephropathy (PVN) is a common complication after renal transplantation. Virus control is achieved by a reduction of immunosuppression allowing an effective T cell-mediated antiviral immune response. The morphology of resolving PVN has not been investigated.
Method: 101 protocol biopsies of 34 patients with PV viremia treated by reduction of immunosuppression only were included and scored according to Banff criteria. The extent of interstitial inflammation was estimated as % of cortex. The number of tubular cross sections with SV40+ cells per mm of biopsy length was counted. Findings were grouped as pre-, increasing, decreasing, and post-viremia.
Results: During the phase of decreasing viremia, we found a significant increase in the tubulitis score, the extent of tubules with intraepithelial lymphocytes, and interstitial inflammation ($p<0.001$). These, to a lower extent, persisted after virus clearance. The number of SV40+ tubules correlated with the virus load in the serum, but SV40 immunohistochemistry was frequently negative (33/55 cases), especially if viremia was below 106 geq/ml.
Conclusion: Resolving PVN is characterized by a self-limiting acute interstitial nephritis. Our findings are important because the diagnosis of interstitial rejection depends on the same morphological criteria. Therefore, acute interstitial rejection cannot be diagnosed with certainty during PV viremia.

OFP-12-008

Neural cell adhesion molecule and fibroblast growth factor receptor positive interstitial cells increase in interstitial fibrosis in different renal diseases

J. Markovic-Lipkovski*, C. Müller, S. Cirovic, S. Tatic, D. Mitrovic, G. Müller
*University of Belgrade, Faculty of Medicine, Serbia

Objective: NCAM + cells with dendritic morphology are rarely present in normal renal interstitium. The aim of this study was to evaluate presence of NCAM + cells in kidney biopsies of different renal diseases with and without interstitial fibrosis (IF). Further immunophenotyping of NCAM + renal interstitial cells was performed.
Method: 97 kidney biopsies, after routine diagnosis, were stained applying antibodies against NCAM clone123C3.D5 or cloneEric1. For double immunofluorescence, antibodies against NCAM cloneEP2567Y and FGFR1, alpha5beta1 integrin, alphaSMA, cadherin9, cadherin11 were used. By RPCR, different NCAM isoforms (120,140,180) were detected using specific primers in 11 renal tissues with and without IF.
Results: NCAM + interstitial cells were identified in 48 cases: 69 % lupus nephritis, 64 % focal segmental glomerulosclerosis, 64 % IgA nephropathy, 55 % membranoproliferative glomerulonephritis, 50 % membranous glomerulonephritis. NCAM + cells coexpressed FGFR1 and alpha5beta1 integrin, and were increased in IF. NCAM + cells did not coexpress alphaSMA, cadherin9 and cadherin11, although they were closely colocalised. All normal renal tissues tested for RPCR showed presence of all NCAM isoforms, however NCAM180 lacked in some tissues with IF.
Conclusion: NCAM + renal interstitial cells coexpress FGFR1 and alpha5beta1 integrin and are increased in renal diseases with IF, mostly in diffuse proliferative lupus

nephritis. In contrast to normal kidneys, in renal tissue with IF NCAM180 is present in a lesser extent.

OFP-12-009

Reproducibility for C4d immunohistochemistry in renal allografts: Results from the Banff Trial

M. Mengel*, S. Chan, J. Climenhaga, P. Randhawa, H. Regele, Y. Kushner, R. Colvin

*University of Alberta, Laboratory of Medicine, Edmonton, Canada

Objective: Detection of C4d is crucial for diagnosing antibody mediated rejection, yet formal reproducibility studies are limited.

Method: We conducted an international multi-center trial to assess the reproducibility for C4d immunohistochemistry on paraffin-sections. A tissue microarray (TMA) was constructed comprising 44 kidney allograft specimens representing negative, focal, and diffuse C4d positive cases. Participants stained the TMA slides, evaluated their stains and entered their scores online. Stained slides were returned for centralized panel scoring. Weighted kappa statistics were used to determine reproducibility.

Results: Inter-institutional reproducibility, i.e. the product from variability between observers and staining methods was low (mean kappa 0.17). Inter-observer reproducibility was fair (kappa 0.39), while inter-laboratory reproducibility was moderate (kappa 0.49). Inter-observer reproducibility could be significantly improved by omitting the Banff C4d grading schema and only considering +/− calls (kappa 0.60). Scoring only C4d+/− inter-laboratory reproducibility improved considerably (kappa 0.78). Higher dilutions of the primary antibody were associated with worse reproducibility. Fixation <1 h or fixation in ethanol had significant negative impact on inter-laboratory reproducibility.

Conclusion: C4d results reported from paraffin section are highly variable between institutions. Simplification of the grading schema would improve reproducibility between observers. Technical reproducibility between laboratories is acceptable but could further be improved by standardizing protocols.

OFP-12-010

Heparanase in diabetic nephropathy: Mode of action and therapeutic implications

T. Neuman*, A. M. Rubinstein, E. Zcharia, R. Goldberg, I. Vlodavsky, M. Elkin

*Hadassah Medical Center, Dept. of Pathology, Jerusalem, Israel

Objective: Heparanase is a predominant mammalian enzyme that cleaves heparan sulfate, the key polysaccharide found in the basement membranes and at cell surface. Heparanase is overexpressed in the diabetic kidney; however, its role and mode of action in diabetic kidney disease remains largely unclear.

Method: Applying heparanase-null mice we found that deletion of the heparanase gene protects diabetic mice from diabetic nephropathy (DN). Recombinant heparanase enzyme and a specific heparanase inhibitor (SST0001) were used to explore its mode of action in several in vivo and in vitro models.

Results: There is essential involvement of heparanase in the pathogenesis of DN. Deleting the heparanase gene protects diabetic mice from DN and administration of specific heparanase inhibitor decreases the extent of albuminuria. In vitro, heparanase enhances macrophage activation by diabetic milieu components, and thus increases the kidney-damaging properties of macrophages.

Conclusion: Our results validate the role of heparanase in DN and reveal the mechanism of heparanase action emphasizing its function in coupling chronic inflammation, macrophage activation and diabetic kidney injury. These findings will help in developing effective strategies to disrupt the heparanase-driven sequence of events in diabetic kidney disease, and in designing novel therapeutic interventions in DN.

Sunday, 9 September 2012, 17.00–19.00, Terrace 1
OFP-13 Oral Free Paper Session Neuropathology

OFP-13-001

Microvascular angiogenesis occurs in a subset of only the arteriovenous types of vascular malformations and is more abundant in men than in women

L. B. Meijer-Jorna*, C. M. van der Horst, C. M. van der Loos, A. C. van der Wal

*Medical Center Alkmaar, Symbiant Pathology Center, Netherlands

Objective: Episodic volume expansion may complicate the very slow growth pattern of congenital vascular malformations. We investigated the role of microvascular angiogenesis in this process of sudden growth.

Method: 100 resection specimens of symptomatic vascular malformations were screened for presence and extent of sheets or clusters immature microvessels, interpreted as microvascular angiogenesis. Microvessel density (MVD), mast cell density (MCD) and Ki67 labelling index of endothelial cells (EC) were assessed immunohistochemically and quantified. Extent of angiogenesis was correlated with the type of vascular malformation and clinical characteristics.

Results: Of 107 cases, 71 were arteriovenous malformations (AVM), 21 were venous (VM), and 8 were lymphatic (LM). Microvascular angiogenesis was observed in 30 % of all vascular malformations, of which 94 % appeared to be AVM. MVD, MCD and Ki67 labelling indexes of EC were

significantly higher in immature vessel areas. Moreover, in affected patients these angiogenic responses were far more extensive (in terms of area involvement) in men than in women ($p<0.05$).
Conclusion: Microvascular angiogenesis appears a specific feature of the arteriovenous type of vascular malformations, and is much more extensive in men than in women. We suggest that these microvascular responses may contribute to onset of symptoms due to a mass forming effect.

OFP-13-002

The impact of ventricular assist device prior to transplantation on acute cellular rejection and antibody-mediated rejection in cardiac allografts with due consideration of seasonal behaviour: A prospective study

K. Wassilew*, E. Potapov, C. Knosalla, T. Krabatsch, M. Hummel, R. Hetzer
*Deutsches Herzzentrum Berlin, Germany

Objective: This study evaluated the impact of bridge-to-transplant ventricular assist device support on development of acute cellular (ACR) and antibody-mediated rejection (AMR) with due consideration of seasonal behaviour in cardiac allografts.
Method: We studied 263 consecutive right ventricular endomyocardial biopsies (EMB) between 01/2011 and 03/2012 prospectively. Paraffin-embedded sections were evaluated for acute cellular rejection, endothelial cell swelling and capillary deposition of C4d, C3d and IgA/M/G. The effects of VAD ($n=101$) on ACR and AMR, classified according to the ISHLT, were studied for seasonal effects and compared to results of EMB harvested from patients without VAD support ($n=162$).
Results: Our results did not reveal significant differences between the two groups in any given parameter. A positive correlation was found for endothelial cell swelling and capillary C4d deposition; the data failed to show a correlation between C4d and C3d deposition or C3d deposition and endothelial swelling. Complement and immunoglobulin depositions seemed to be more pronounced but without statistical significance in autumn and winter.
Conclusion: Our results demonstrate only statistically insignificantly more pronounced capillary complement deposition in autumn and winter. The use of VAD did not predict development of AMR or ACR. The C3d staining does not add to the pathological diagnosis of AMR.

OFP-13-003

Relevant changes of the molecular profile in the recurrence of glioblastomas with respect to the correspondent primary tumors

M. Idoate*, J. Echeveste, R. Diez Valle, M. Montanana, J. Sola, T. Labiano
*University of Navarra, Dept. of Pathology, Pamplona, Spain

Objective: In the literature, there is not enough information about changes of relevant molecular parameters in the recurrent glioblastoma.
Method: The study included a total of 11 grade IV astrocytomas (OMS) and their correspondent recurrences in a series of patients treated by 5-ALA guided surgery. All patients received similar treatment. A comparative histologic and molecular study which included LOH of PTEN region, EGFR amplification SISH, methylation of MGMT by MSP-PCR and sequencing of EGFR variant III mutation on representative tumor samples was obtained.
Results: The recurrences appeared adjacent to surgical cavity in seven cases. The mean time between the diagnosis of primary and the recurrence was 500 days (215–1670). The primary glioblastomas showed LOH10q23 in 82 % of cases, hypermethylation of MGMT in 50 %, EGFR amplification in 45 % and EGFRvIII in 37 %. In five cases (45 %) the molecular profile of the recurrences was different to the primaries and most of them (80 %) in the group of vaccines treated glioblastomas. The molecular profile change included one to several of the studied parameters. In one case all of the molecular parameters had changed.
Conclusion: The molecular profile change of the recurrences of glioblastomas in respect to the primaries is a frequent event that could be due to the selection of tumor cells due to both heterogeneity and treatment effect.

OFP-13-004

The proliferative activity of the border of glioblastoma defined in vivo by 5-aminolevulinic fluorescence is a relevant independent prognostic marker in glioblastomas

M. Idoate*, R. Diez Valle, J. Echeveste, M. Montanana, M. D. Lozano, H. Quiceno
*University of Navarra, Dept. of Pathology, Pamplona, Spain

Objective: There is not literature reference on the prognostic significance of the proliferative activity in the border of tumor. A large series of patients with glioblastomas operated by fluorescence guided surgery with uniform treatment and enough follow-up have been studied.
Method: A total of 207 samples of different fluorescence quality from 67 glioblastomas, 44 primaries and 23 recurrences, were studied. For each tumor, the maximum value of Ki-67 was determined by a semiquantitative counting by two observers and by an autoanalyzer. These values were compared with relevant oncologic parameters.
Results: The results of Ki67 according both counting methods were concordant. The Ki67max values of red (center), pink (intermediate) and blue (border) fluorescence samples obtained by quantitative analysis were 28 % 11 % and 6 %. In the Cox regression analysis for overall survival, the Ki67 value was an independent prognostic factor, stronger than

other relevant clinical parameters studied (p=0.002). In the Kaplan-Meier for a Ki67 cut-off of 5 %, the median overall survival was 25.1 months against 13.0 months (p=0.023). For the patients with recurrent glioblastomas the overall survival according to Ki67 values was also significant (p=0.017).
Conclusion: The evaluation of the proliferative activity by Ki-67 in the border of tumor defined by 5-ala fluorescence is a relevant independent prognostic marker of primary and recurrent glioblastomas.

OFP-13-005
Prognostic value of estrogen receptor expression measured by IHC in brain metastases of breast carcinoma
D. Rotin*, N. Lobanova, O. Paklina, O. Potapova, M. Stepanyan
*N.N. Burdenko Neurosurg. Institute, Dept. of Pathology, Moscow, Russia

Objective: According to the levels of estrogen receptor (ER) expression, primary breast carcinoma (BC) cases are divided into two groups: ER-positive and ER-negative (Godhirsch et al. 2011). In metastatic BC, and especially in brain metastases (BM) of BC, the role of ER expression is not clearly defined. Aim: Investigate ER expression levels in brain metastases of BC and evaluate its prognostic significance.
Method: Surgically obtained tumor specimens from sixty BC female patients (median age 52, ranges 29–73) with BM BC were stained with antibodies to ER (DAKO). IHC expression was evaluated according to the semi-quantitative method. Survival was estimated by means of Kaplan-Meyer curves. Statistical analysis was performed using STAITISTICA 8.0 software.
Results: ER expression was detected in 52 % of patients (31/60), and 48 % (29/60) were ER-negative. Median time period between primary diagnosis and BM development was significantly (p<0.05) longer in ER-positive group compared to ER-negative group (48 and 23 months, respectively). Recurrent BM developed in both groups with a similar frequency (32 % and 34 %, respectively). General survival was significantly (p=0,026) higher in ER-positive patients compared to that of ER-negative group.
Conclusion: ER expression is considered to be an important prognostic factor for development of BMBC. Nevertheless, further studies involving more patients with BMBC are required.

OFP-13-006
Dopamine and alpha synuclein interplay in neurodegeneration: A rat animal model
G. Stoica*, G. Lungu, N. Bjorklund
*Texas A&M University, Veterinary Pathobiology, College Station, USA

Objective: A spontaneous autosomal recessive rat model for neurodegeneration was developed in our laboratory. These rats demonstrate progressive increases in alpha synuclein (α-syn) in the brain mesencephalon followed by loss of dopaminergic terminals in the basal ganglia and motor impairments.
Method: Histology, immunohistochemistry, transmission electron microscopy were used for morphological analyses. For α-syn assessment real-time PCR and western blot were used. Dopamine measurements were performed by ion mobility mass spectral (IMMS).
Results: The severity of pathology is directly related to the overexpression of α-syn and parallel decrease in dopamine (DA) level in the striatum (ST) of affected rats. The neurodegeneration in this model is characterized by the presence of perikarya and neurites Lewis bodies (LB) and diffuse marked accumulation of perikaryal α-syn in the substantia nigra (SN), brain stem, and striatum along with neuronal loss. Light and ultrastructural analyses revealed that the process of neuronal degeneration is a "dying back" type. The disease process is accompanied by gliosis and release of inflammatory cytokines.
Conclusion: Decrease dopamine and overexpression of α-syn in the brain mesencephalon may provide a naturally occurring animal model for Parkinson's disease and other synucleinopathies that reproduces significant pathological, neurochemical, and behavioral features of the human disease.

Sunday, 9 September 2012, 14.15 - 16.15, Meeting Hall V
OFP-14 Oral Free Paper Session Other Topics I

OFP-14-002
Proliferation indices of PHH3/MART1 double stains are strong independent predictors of clinical outcome in primary cutaneous melanoma
T. Steiniche*, P. S. Nielsen, H. Schmidt, T. O. Jensen, R. Riber-Hansen
*Aarhus University Hospital, Dept. of Pathology, Denmark

Objective: The mitotic index in thin primary melanomas replaced Clark level in the 2009 staging system of the AJCC. However, the recommended quantification of proliferation by hot spots on HE stains is criticized. An alternative may be the immunohistochemical proliferation marker phosphohistone H3 (PHH3) visualizing all mitotic cells. And, when combined with the melanocytic marker MART1, PHH3 insures quantification of proliferating melanocytes, only.
Method: 153 primary melanomas with a median follow-up of 12 years for patients with event-free melanoma were included. PHH3/MART1 stains were performed by an indirect sequential immunoenzymatic technique. The number of

PHH3/MART1 positive cells was counted in a fixed 1-mm2 frame in the dermal area with the highest concentration of positive cells (hot spots).
Results: In multivariate analysis, PHH3 in hot spots was a strong independent prognostic marker for recurrent disease (HR=3.7, 95 % CI, 1.4 to 9.6; *P*=.008) and melanoma-specific death (HR=3.4, 95 % CI, 1.3 to 9.0; *P*=.013), when corrected for primary tumor thickness and ulceration.
Conclusion: Cellular proliferation is an independent prognostic marker in primary cutaneous melanoma. However, accurate quantification is crucial for correct clinical staging. For this purpose, proliferation indices of the novel PHH3/MART1 double stains seem very promising.

OFP-14-003
Matrix metalloproteinases underexpression in melanoma with regression
S. Zurac*, G. Negroiu, S. Petrescu, I. Tudose, R. Andrei, T. Tebeica, C. Popp, C. Solovan, M. Neagu, C. Constantin, F. Staniceanu
*Colentina University Hospital, Dept. of Pathology, Bucharest, Romania

Objective: Melanoma regression results as a complex interaction between tumor and host immune response; it has debatable prognostic significance but promising anti-cancer vaccine strategies were proposed based on immune-mediated destruction of tumor cells from regression areas. Alterations of matrix metalloproteinases (MMP) expression may be involved in tumor regression.
Method: We analyzed 35 cases of superficial spreading melanomas (22 cases with regression – 6 segmentary regression (SR), 8 partial regression (PR) and 8 segmentary&-partial regression (SPR); 13 cases with no regression ((NR); we investigated MMP1, MMP2, MMP3, MMP11 and MMP13 immunohistochemical expression in both NR cases and nonregressed&regressed component in melanoma with regression.
Results: MMP1 presented significantly lower expression in nonregressed component in both SPR and SR + SPR groups versus NR (*P*=0.041 and *P*=0.050); similar results were recorded in PRvsNR cases for MMP11 (*P*=0.037); all the other MMPs had similar expression in nonregressed component (irrespective of regression type) and NR. Nonregressed versus regressed component analysis in the same tumor identified overexpression of MMP3, MMP11 and MMP13 in nonregressed component (*P*<0.05).
Conclusion: Regression in melanoma is correlated with diminishing expression of MMP3, MMP11 and MMP13 in regressed component; certain types of regression associate MMP1 and MMP11 underexpression in nonregressed tumor. Acknowledgments: project partially supported by Postdoctoral Program POSDRU/89/1.5/S/60746

OFP-14-004
New morphological feature of Reinke's edema
S. Milenkovic*, M. Jovanovic
*Dept. of Pathology, Clinical Hospital Center Zemun, Belgrade, Serbia

Objective: Some of the more common benign vocal fold lesions are polyps, nodules and polypoid corditis (Reinke's edema). The majority of vocal fold pathology develops in the mucosal layer of the vocal fold, precisely in Reinkes space. Basic science and clinical research over past decades has led to advances in our understanding of benign laryngeal lesions. The aim of our study was compared contact telescopy findings with histological analyzes in a patients with Reinke's edema.
Method: The our study included 80 consecutive patients with clinical diagnosis of Reinke's edema. Videoassisted contact telescopy was performed in all cases under general anesthesia and mucosa was stained by methylene blue. Tissue biopsies were taken from areas exhibiting visible pathological changes and sent to routine histopathology and immunohistochemical analyses. We analyzed expression of pancytokeratin antibodies, vimentin and CD 34.
Results: In the all case of Reinke's edema, contact telescopic scans showed a change of direction or a disappearance of regular distribution and morphology of blood vessels (irregular shapes, positions, and patterns, apparently running in random directions) in vocal fold mucosa. Marked pathological changes were noted by contact telescopic scans, confirmed with histopathology analyses.
Conclusion: Contact telescopy is a useful additional diagnostic tool regarding Reinke's edema.

OFP-14-005
Volunteering in Malawi: A snapshot of surgical pathology in sub-Saharan Africa
S. Berezowska*, T. Tomoka, S. Kamiza, D. A. Milner jr., R. Langer
*Universität Bern, Institute of Pathology, Switzerland

Objective: The breadth of material found in surgical pathology services in African countries significantly differs from the common spectrum of "the West". We report our experience in the pathology departments of Blantyre and Lilongwe, Malawi.
Method: During a six-week period 405 cases were processed (378 histology, 27 cytology).
Results: The vast majority of cases showed significant pathological findings (n=369; 91.1 %): 175 (47.4 %) were non-tumoral conditions and 39 (10.6 %) benign tumors or tumor like lesions. The large group of malignancies (n=140; 37.9 %) comprised 11 pediatric tumors (e.g. rhabdomyosarcoma, small blue round cell tumors), and 129 adult tumors. Amongst women (n=76), squamous cell carcinomas (SCC) of the cervix uteri predominated (n=25; 32.9 %), followed by breast carcinomas (n=12; 15.8 %), and esophageal SCC (n=9; 11.8 %). Males (n=53) most often showed SCC of the esophagus (n=9; 17.0 %), and SCC of the urinary bladder (n=7; 13.2 %). Lymphomas (n=7) and Kaposi's sarcomas (n=6) were less frequent.
Conclusion: Providing pathology service in a low resource country may be handicapped by lack of personal, inadequate material resources, or insufficient infrastructure. Rotating volunteers offer a bridge for capacity building of both personnel and the local medical service; in addition, the volunteer's horizons are broaden professionally and personally.

OFP-14-006

Comparative analysis of antinuclear antibodies by indirect immunofluorescence and immunoblot tests

O. El-Hassoun*, J. Rajcani, M. Bencat, J. Papanova, N. Kojtalova
*Alphamedical Laboratories, Dept. of Pathological Anatomy, Martin, Slovakia

Objective: Antinuclear antibodies (ANA) are routinely tested by indirect immunofluorescence (IF) and immunoblot. In this paper we aim to retrospectively analyze results of both methods.
Method: On two cohort groups: A (a total of 5518 samples), and B (a total of 2615 samples) we performed IF on commercially obtained Hep-2 cell, and immunoblot on (strips Euroline).
Results: IF revealed at least 14 different morphological patterns of ANA staining, which we grouped into 5 easily distinguished categories: speckled nuclear fluorescence, homogenous nucleoplasmic fluorescence, multiple nuclear dots, nucleoli staining, and scattered nucleoplasmic dots. We compared these groups according to frequency, type of antibody and correlation with immunoblot resuts.
Conclusion: We summed the characteristics of each IF category, and noticed that both cohorts revealed 7.4 % and 6 %, respectively of sera, which did not show positive IF at an acceptable dilution (only by 1:10) or were fully negative in IF test, but were clearly positive in immunoblot test. This was especially alarming with anti-Scl-70 antibodies, which could be barely recognized in IF test, but were clearly present in 53 of 407 positive stained strips (cohort A) and/or 14 out of 156 positive stained strips (cohort B).

OFP-14-007

Macrophages and their subtypes in tumorigenesis and growth

O. El-Hassoun*, L. Maruscakova, Z. Valaskova, M. Kopani, J. Jakubovsky, I. Hulin
*Alphamedical Laboratories, Dept. of Pathological Anatomy, Martin, Slovakia

Objective: It has been established that Macrophages (MF) play a basic role in the tumor microenvironment. Still, the definition of the function of MF with relation to tumors is still vague, mainly when MF are observed acting occasionally as pro tumor and elsewhere as anti tumor.
Method: In this paper we attempt to sum up the accumulating observations of MF function with respect to the microenvironment and the tumor entity.
Results: Through the different stages of tumorigenesis and growth, macrophages are engaged in various signaling cascades that tame them to perform a certain function in a given microenvironment. This makes MF a multi-program cell with unique adaptivity. We assume that without the macrophages tumors cannot progress.
Conclusion: The available MF subtype analysis is still inadequate and doesn't bear into account the dynamics of tumorigenesis and growth. Our presented MF schemes provide an insight on the tumor microenvironment with respect to stage. A complex view on the signaling cascades affecting MF is needed to formulate a novel classification of MF based on their programming. This consequently can be the basis of the development of "anti-MF therapy" or on a larger scale "anti-tumor microenvironment therapy".

OFP-14-008

Needle aspiration in the diagnosis of metastatic bone disease

A. B. Larque*, X. Tomas, B. Gonzalez, A. I. Garcia, J. Pomes, P. Castillo, M. Del Amo, J. Ramirez
*Hospital Clinic Barcelona, Dept. de Anatomia Patologia, Spain

Objective: There is an increasing number of bone needle aspirations. To evaluate the accuracy of this technique in the diagnosis of metastatic carcinoma we performed this study.
Method: Retrospective series of patients with needle study of bone lesions, either by cytology (FNA) or biopsy (Core) that were diagnosed as metastatic bone disease, between 2003 and 2011.
Results: The study included 167 CT-guided needle specimens (156 patients). Bone needle aspiration biopsy showed metastatic carcinoma in 153 aspirates (92 %). In 83.76 % of FNA we made the diagnosis of Metastasis: 40.8 % without specific site of origin & 59.2 % Specific site. On the other hand, in 94.25 % of Core we made the diagnosis of Metastasis: 14.6 % without specific origin & 85.4 % with specific site. Thus, the primary tumors were identified in 115 cases (68.9 %), with the aid of Immunohistochemistry (CK7 and CK20). In 2003 there were just 4 Core within the total number of 27 aspirates, but in 2011 there were 20 Core over a total number of 26.
Conclusion: In patients with metastasis to bone, the needle biopsy is a very effective technique. The best results obtained in Core diagnosis can explain the upraising number of such procedures over the last 10 years.

OFP-14-009
Lodox X-ray is an invaluable asset in autopsy procedures
L. Liebenberg*
*University of Cape Town, Dept. of Forensic Medicine, South Africa

Objective: The field of autopsy performance has faced numerous challenges internationally. Minimal background information on the deceased, various religious and personal objections regarding cutting a deceased body as well as health hazards face the pathologist regularly. Lodox X-ray is a huge help for the pathologist.
Method: Lodox X-ray (low dose X-ray) using the Statscan has proven invaluable in busy forensic pathology laboratories in Cape Town, South Africa. The digitally captured radiology images render a wealth of clear, recognizable, easily documented and user friendly images for use in diagnosis and court evidence.
Results: The use of the Statscan has revolutionized the process of forensic autopsy procedures in Cape Town, South Africa. The radiology images obtained in an unusually user friendly and time efficient way have improved efficacy, efficiency, accuracy and pro-active occupational health safety in our forensic laboratories.
Conclusion: Lodox X-ray is a proven invaluable special investigation in forensic, and also academic, autopsy examination procedures.

Sunday, 9 September 2012, 17.00–19.00, Club D
OFP-15 Oral Free Paper Session Other Topics II

OFP-15-001
Whole exome sequencing identifies potential therapeutic targets for castration resistant prostate cancer
R. Menon*, M. Deng, D. Boehm, F. Fend, S. Biskup, S. Perner
*Universitätsklinikum Bonn, Inst. für Pathologie, Germany

Objective: Castration resistant prostate cancer (CR-PCa) is the most aggressive form of prostate cancer (PCa) posing a significant therapeutic challenge. Our aim was to perform whole exome-sequencing on 5 CR-PCa/normal paired formalin fixed paraffin embedded (FFPE) samples using the SOLiD4 next generation sequencing platform (NGS). We identified two promising genes- YWHAZ and PTK2, that could serve as novel potential therapeutic drug targets in PCa.
Method: Genomic DNA was sequenced from 5 CR-PCa/normal paired FFPE samples. A set of amplified/deleted genes were validated using fluorescence in-situ hybridization (FISH) assays using a PCa progression cohort consisting of 138 cases for localized PCa, 105 patients with primary PCa and corresponding LN metastasis, and 39 samples for CRPCa.
Results: Exome-sequencing identified regions of deletions/amplifications, including NKX3.1, PTEN, CMYC and AR genes, known to play a role in PCa. We identified several amplified genes as druggable targets such as PTK2 and YWHAZ. For YWHAZ we identified 3.5 % amplification in localized PCa, 24.2 % amplification in LN metastasis and 45.5 % amplification in CRPCa. For PTK2 we 4 % amplification for localized PCa and 34 % for both LN metastasis and CR-PCa.

Conclusion: This is the first study to use exome-sequencing approaches on FFPE CR-PCa to understand the biology of disease and its plausible treatment options.

OFP-15-002

A study of d-Np63 (p40) expression in tumours of stratified epithelium

D. Nonaka*

*The Christie Hospital, Dept. of Histopathology, Manchester, United Kingdom

Objective: p63 can be expressed by a minority of adenocarcinomas. ΔNp63 (p40), isoform of p63, has recently been reported as more specific in lung squamous cell carcinoma (SCC) than p63, and it appears to be a more reliable marker for SCC. There is no comprehensive study on p40 expression in tumours of different histotypes.
Method: 460 tumours of various hisotypes were studied, including tumours of stratified epithelium such as SCC (84 cases) of the skin, head/neck, lung, cervix, and oesophagus, urothelial carcinomas (18), cutaneous basal cell carcinomas (5), thymomas (20) and thymic carcinomas (5), adenocarcinomas (210) from multiple organs, germ cell tumours (25), brain tumours (17), lymphomas (14), and sarcomas (12). p40 immunostains were performed on tissue microarrays and staining extent was evaluated as focal (1–50 %) and diffuse (50–100 %).
Results: All but one tumours of stratified epithelium diffusely expressed p40. The negative case represents spindle cell SCC. Other tumours except for basal/squamous component of two teratomas, one breast metaplastic carcinoma, and squamous component of 5 adenosquamous carcinomas were all negative for p40.
Conclusion: p40 is specific in tumours of stratified epithelium and its sensitivity appears comparable to p63. p40 can serve as a marker for tumours of stratified epithelium.

OFP-15-003

Glyoxal fixation: 10-years' experience of formaldehyde substitute fixative for diagnostic surgical pathology

S. Simonetti*, N. Perez Muñoz, A. Elguezabal, M. A. Carrasco Garcia

*Capio Hospital General, Dept. of Surgical Pathology, Sant Cugat del Valles, Spain

Objective: Although formaldehyde is the standard fixative used in routine histopathology, it is not considered an "ideal" fixative. Formaldehyde presents carcinogenic properties, a slow fixation and produces cross-links with proteins and nucleic acids. Formaldehyde-free fixatives are commercially available.
Method: From 2002 to 2012 we used Glyo-Fixx (Thermo Scientific, US), a glyoxal-based fixative, as formaldehyde substitute, analysing 54314 surgical pathology specimens and 205 autopsies. All samples were processed and stained routinely. Moreover we performed immunohistochemistry by an automated immunostainer and special stains with standard techniques, where needed. In tumoral cases we fixed 1 cm3 sample in neutral buffered formalin and compared the results with Gyo-Fixx fixation.
Results: Glyo-Fixx fixation needed less hours than formaldehyde and not harden the tissues. On gross examination of the adipose tissue, lymph nodes were easily found, due to a more marked whitish appearance. Morphologically we have not found differences between formalin and Glyo-Fixx, except for the eosinophils degranulation. Special stains resulted similar to those with formaldehyde fixations. Almost all antibodies not required pretreatment, but needed adjusts in the standardized protocol for formaldehyde.
Conclusion: Our experience demonstrated Glyo-Fixx is a good non-toxic alternative to formaldehyde in routine pathology, capable to preserve morphology and protein integrity of the tissues.

OFP-15-004

Liposarcoma with solitary fibrous tumor-like dedifferentiated areas: Clues on differential diagnosis

M. Aizpurua*

*HUVH/ICS, Dept. of Pathology, Barcelona, Spain

Objective: Well-differentiated liposarcoma (WDLS) can undergo dedifferentiation to nonlipogenic sarcomas. Solitary fibrous tumour (SFT) characteristics have not been highlighted as a pattern of dedifferentiated liposarcoma (DLS). However, this does occur and could be the cause of diagnostic pitfalls in atypical locations or partial tumoral resections. The aim of this comparative study is to demonstrate that some DLS's may show morphologic features resembling SFT's, and furthermore to describe the clue features supporting differential diagnosis.
Method: Study comprised 11 WDLS-DLS and 12 SFT (4 malignant). Histological features were systematically reviewed, and CD34/CD99/S100/BCL2 immunostains and MDM2 FISH-analysis were evaluated in all cases.
Results: There are many overlapping characteristics between DLS and SFT (Table 1). Significant differences between both tumor types were observed in lipoblast-like cells (lpc); mature adipocitic cells within tumor (mac); stromal bands surrounding adipose tissue with atypical cells (sac); patternless (pa); keloidal-collagen (kcm) and haemangiopericytoid-pattern (hp). Diagnostic accuracy of different features is shown in table 2.

Conclusion: The dedifferentiated component in some liposarcomas may resemble SFT. In the DLS/SFT differential diagnosis, immunohistochemistry may be confusing. Presence of WDLS areas is the main diagnostic clue and MDM2 FISH amplification is successful in distinguishing DLS from SFT.

FEATURE	DLS	SFT	p
Sclerosing collagen matrix	9/11	10/12	1
Keloidal collagen matrix	6/11	11/12	0.52
Storiform-pattern	3/11	3/12	1
Hemangiopericytoid vascular pattern	4/11	10/12	0.31
Patternless	8/11	11/12	0.76
Alternating hyper/hypocellular areas	10/11	10/12	1
CD99 reactivity	10/11	10/12	1
CD34 reactivity	9/11	12/12	0.77
BCL2 reactivity	10/11	11/12	1
S100 reactivity	5/11	0/12	0.05

Table 1

%	SENSITIVITY	SPECIFICITY	PPV	NPV
LPC+MAC+SAC	100	92	92	100
PA+KCM+HP	75	91	90	77
MDM2	100	100	100	100
IHQ (CD99+CD34+BCL2)	75	33	60	50

Table 2

OFP-15-006

Osteoblastoma and diagnostics pitfalls

W. Ouahioune*

*EHS Douera, Dept. of Pathology, Algiers, Algeria

Objective: Osteoblastoma is a rare benign osteoblastic tumor with a potential for local bone destruction and aggressiveness. The most common site of osteoblastoma is the vertebral column particularly the posterior elements and the sacrum.

Method: In this study we present nine cases of osteoblastoma and the principal differential diagnosis.

Results: On a period of 10 years, nine cases of osteoblastoma had been diagnosed including seven males and two females. The age of those patients ranged from 5 to 29 year old. The tumor was localized in the spine in five of the nine cases and the other ones in the long bones. The radiological diagnosis of osteoblastoma was made in just two cases. The diagnosis was made by histology in eight cases. All our patients had been treated with curettage. On the nine patients, just one of them had developed two successive recurrences.

Conclusion: Osteoblastoma is a rare benign tumor which is rarely diagnosed by radiology alone. The pathologist should always suspect an osteoblastoma in front of a vertebral localization of any tumor.

OFP-15-007

Congenital hepatic fibrosis. Radiology – Pathology correlation

D. S. Rosero Cuesta*, E. Del Valle Sánchez, I. Quintana Martínez, J. M. Cirac Collados, A. Puertas Cantería, S. Vicente Arregui, E. Mejía Urbáez, J. Marroyo Laso, M. Alastuey Aísa

*Hospital Miguel Servet, Anatomía Patológica, Zaragoza, Spain

Objective: Congenital hepatic fibrosis (CHF) is a developmental disorder of the portobiliary system. Clinical findings usually include enlarged liver, well-preserved hepatocellular function and portal hypertension. CHF is frequently associated with hepatorenal fibrocystic disease.
Method: A 29-year-old woman was referred to our hospital for further evaluation of hepatomegaly, and portal hypertension was found. Laboratory tests were all negative. MRI identified hepatosplenomegaly with hypertrophic left medial segment, high uptake nodular areas and homogeneous boundary liver. Needle biopsy was performed.
Results: The biopsy demonstrated slight portal fibrosis and fibrous septa with proliferation of numerous biliary ducts, some of them containing inspissated bile. It was also noticeable the few number of portal vein branches. There was no inflammation or hepatocyte necrosis. Therefore, our diagnosis was congenital hepatic fibrosis. We correlated these results with radiology. Magnetic resonance cholangiopancreatography showed peripherally dilated biliary intrahepatic branches contrasting with preserved caliber of main intrahepatic branches. These findings were also diagnostic for CHF.
Conclusion: The low prevalence of CHF makes it hard to think about this entity in patients with portal hypertension and normal laboratory findings. The histological differential diagnosis must be done mainly with cirrhosis, but also with idiopathic portal hypertension and, in small biopsies, with biliary hamartoma.

OFP-15-008

Digestive lymphomas in the Central Tunisia: Epidemiological and anatomoclinical study of 97 cases

M. Nabiha*, B. Y. Yossra, W. Majdoub, S. Cyrine, M. Samira, M. T. Yacoubi, H. Sihem
*Farhet Hached Hospital, Dept. of Pathology, Sousse, Tunisia

Objective: Digestive tract lymphoma is the main extranodal type lymphoma worldwide, digestive tract counting about 35.4 % of extranodal lymphomas in the Centre of Tunisia. The aim of this study was to describe the epidemiological status and the anatomo-clinical features of digestive tract lymphomas in the Centre of Tunisia.
Method: All digestive tract lymphoma cases diagnosed in the Pathology Department, Farhet Hached Hospital, Sousse during a 15-year period were analyzed.
Results: A total of 97 cases of digestive tract lymphoma were reported (64 males, 33 females) with a sex-ratio of 2.0. The patient age ranged between 6 and 82 years with a median age of 48 years. Stomach location was the most frequent with 80 % of cases followed by intestine (15 %) and colon (5 %). Among the 97 digestive tract lymphomas, 48 % were of Marginal zone type (MALT) and 47 % were large B-cell lymphoma. According to the Ann Arbor staging system, 85 % of patients were diagnosed at stage I and II.
Conclusion: Lymphomas of the digestive tract are still frequent in the Centre of Tunisia. The Malt Type lymphoma is main reported histological type. The association with the Helicobacter pylori should be considered.

OFP-15-009

Collecting duct carcinoma in the west of ireland: A rare experience

A. Shalaby*, C. E. Connolly
*University Hospital Galway, Dept. of Histopathology, Ireland

Objective: Collecting duct carcinoma is a rare renal neoplasm arising from the epithelium of Bellini's ducts in the distal part of the nephron.
Method: We describe our experience of this entity in University Hospital Galway with a series of four cases diagnosed between 2003 and 2011.
Results: Three patients aged between 35 and 62 years presented with either lymph node or bone metastases without evident abdominal mass. In each case the biopsy from the metastatic lesion showed adenocarcinoma with an immunohistochemical profile suggestive of renal origin and a renal mass was subsequently confirmed by radiology. The fourth patient was an 81 year old male who presented with haematuria. Abdominal CT scan revealed a 5.6 cm mass in the right kidney extending into the renal vein. Biopsy of the renal mass in all cases confirmed adenocarcinoma with a tubular pattern with positive cytokeratin and Vimentin staining and CD10 negative staining. One patient was treated with nephrectomy with post-neoadjuvant chemotherapy and died 25 months after surgery. The other three patients died few months after their diagnosis.
Conclusion: Collecting duct carcinoma is a rare renal neoplasm that can be difficult to diagnose on core biopsies, however, it can be identified based on radiological findings, gross, microscopic, histochemical and immunohistochemical features.

Monday, 10 September 2012, 17.00–19.00, Panorama Hall
OFP-16 Oral Free Paper Session Perinatal and Paediatric Pathology

OFP-16-001

Tissue factor expression is upregulated in primary and metastatic tissue samples of Wilms Tumor

V. Duval da Silva*, C. Costa Moreira, N. A. Azevedo, E. Gesswein, T. Giuliani Lopes, E. O. Maciel, G. Franco Carvalhal, D. Santiago Santos, E. L. Batista jr.
*PUCRS, Dept. of Pathology, Porto Alegre, Brazil

Objective: Wilms Tumors (WT) is the most frequent renal tumor of children. Genetic alterations have been suggested

as associated factors but the exact pathogenesis of WT is not fully characterized. Tissue factor (TF) is a glycoprotein which happens to be a key receptor for factor VII/VIIa and a primary initiator of coagulation. TF has also been associated with angiogenesis. Recent evidence pointed out an important role for TF in cancer progression and metastasis.
Method: In the present investigation the differential expression of TF in WT was assessed by real-time PCR of RNA retrieved from paraffin sections using microdissection.
Results: Different histological components of WT were analysed. The results revealed that TF was upregulated in blastema and epithelial components as compared to non-neoplastic tissue (14.38 and 16.02-fold respectively, $P<0.001$). Stroma and non-neoplastic tissue presented low levels of TF expression. TF expression in WT metastatic lesions was also significantly upregulated as compared to non-metastatic WT. Microvessel density was positively correlated with TF expression ($r=0.721$).
Conclusion: As described in other tumors, TF seems to play a significant role in the behavior of WT. Further investigations are warranted to better understand the pathways by which TF exerts its effects on tumor progression and its potential as a target for therapy.

OFP-16-002

Histopathological markers as clinical indicators of early liver transplantation in biliary atresia

L. R. Longo-Santos*, W. Teodoro, A. P. Velosa, E. Mello, E. Parra, M. C. Coelho, V. Alves, V. Capelozzi, U. Tannuri
*Faculdade de Medicina da USP, Disciplina Cirurgia Pediátrica, São Paulo, Brazil

Objective: Biliary atresia (BA) is the most common neonatal cholestatic disorder and the prime indication for liver transplantation (LTx) in children. Histopathological markers in liver biopsies emerge promise as indicator of early LTx in patients with BA.
Method: Ductular proliferation, ductal plate malformations and type I, III, IV and V collagen deposition were evaluated on Kasai portoenterostomy (KPE) and liver transplantation (LTx) biopsies from 36 children with BA. Formalin fixed and paraffin embedded liver biopsies were stained with hematoxylin-eosin, picrosirius-polarization and immunofluorescence methods. There were analyzed liver histoarchitecture, biliary ductus and collagen deposition in hepatic compartments. Pathologic findings were graded according to a 5-point semi-quantitative severity-based scoring system. Impact of these markers was tested on LTx time (<2 year and >2 year).
Results: Median age of KPE was 12 weeks (range 6–20) and of LTx was 27 months (range 6–120). In KPE liver biopsies, ductular proliferation, ductal plate malformations and collagen deposition were increased but these parameters presented no association with clinical evolution for early LTx. Furthermore, collagen V prominent deposition was found along of hepatic sinusoids and type I, III and IV were more frequent in portal compartment.
Conclusion: These results suggest that histopathological parameters evaluation presented may not determine early LTx in biliary atresia.

OFP-16-003

The role of Hofbauer cells on villous vasculature in early fetal losses

E. Özer*, Y. Arman Karakaya
*Dokuz Eylul University, Dept. of Pathology, Izmir, Turkey

Objective: The aim of this retrospective study is investigate the role of Hofbauer cells in early fetal losses.
Method: The slides obtained from archieval blocks of missed abortion (MA, $n=15$) and blighted ovum (BO, $n=15$) cases and unwanted pregnancies materials (control group, $n=15$) were stained by immunuhistochemical methods using CD68 and CD31 antibody to label Hofbauer cells and endotelial cells, respectively.
Results: The mean number of vilous Hofbauer cells was found to be significantly higher in both BO and MA in contrast to the control group ($p=0.005$ and $p<<0.001$, respectively). However it was not significantly different between BO and MA ($P=0.04$). Chalkey method revealed no statisticaly significant difference in the control group in comparison with MA and BO in ($P=0.29$, $P=0.09$, respectively). Higher microvessel scorring were found in MA in contrast to BO and the control group ($p=0.003$ and $p=0.003$, respectively). However, there was no difference between the control group and BO ($p=0.54$).
Conclusion: We think that Hofbauer cells may be of biological importance in early fetal losses and play a role on defective vasculature formation in MA.

OFP-16-004

Placental VEGF and its receptors expression patterns in preeclampsia

K. Pavlov*, E. Dubova, A. Shchegolev, G. Sukhikh
*V.I. Kulakov Scientific Center, Dept. of Pathology, Moscow, Russia

Objective: Placental angiogenesis anomalies play an important role in some complications of pregnancy development, including preeclampsia (PE). VEGF and its receptors – one of the key placental angiogenic factor. Aim: to evaluate patterns of VEGF and its receptors (VEGFRs 1, 2 and 3) expression in placentas from PE complicated pregnancies.
Method: We performed complex morphological and immunohistochemical study of 9 term placentas from mild preeclampsia (mPE) cases (1st group), 6 term placentas from

severe preeclampsia (sPE) cases (2nd group) and 10 term placentas from uncomplicated pregnancies (control group).
Results: We revealed significantly increased syncitial VEGF expression levels in preeclamptic placentas terminal villi and these changes were much prominent in sPE. We also detected insignificantly increased endothelial VEGF expression levels in preeclamptic placentas terminal villi. VEGFR-1 syncitial expression levels in sPE terminal villi were significantly higher in compare to the mPE and control groups. VEGFR-2 endothelial and syncitial expression levels were significantly lower in both PE groups terminal villi and these changes were much prominent in mPE. Patterns of VEGFR-3 expression in preeclamptic and control groups were multidirectional.
Conclusion: Revealed patterns of VEGF and its receptors expression point on altered placental angiogenesis in PE and reflect different degree of such alteration in mild and severe PE.

OFP-16-005

Placental VEGF and it receptors expression in diabetic pregnancies: Clinical and morphological correlations

A. Shchegolev*, E. Dubova, K. Pavlov, R. Esayan, E. Bessmertnaya, M. Shestakova, G. Sukhikh
*V.I. Kulakov Scientific Center, Dept. of Pathology, Moscow, Russia

Objective: Chorionic villi vascularity disturbances, caused by abnormal expression of angiogenic factors could correlate with maternal and fetal complications in diabetic pregnancies.
Method: Aim: to evaluate the patterns of VEGF receptors (VEGFR1, VEGFR2 and VEGFR3) expression in placentas from gestational diabetes (GD) and type 1 diabetes (D1) pregnancies and correlation between them and some clinical parameters in newborn (placental weight (PW), newborn weight (NW), placental/newborn weight index (PNWI),1st day of life blood glucose test results (1BGTR)). 29 term placentas from D1 (n=16) and GD (n=20) and 12 term placentas from normal pregnancy (control group) were studied.
Results: In both D1 and GD group we revealed significantly higher level of VEGFR1 (p=0.0001), VEGFR2 (p=0.001) and VEGFR3 (p=0.01) endothelial expression in terminal villi. Difference in VEGFR1 expression among D1 and GD groups was also significant (p=0.0009) as difference in its expression between D1 and control group (p=0.002). Among clinical parameters we only revealed significant increase in 1BGTR in diabetic groups (p=0.03) with marked difference between D1 and control group (p= 0.002). We revealed multidirectional correlation between VEGF and VEGFR2 expression and NW in D1 and GD groups.
Conclusion: Revealed changes reflect placental angiogenesis disturbances influence on intrauterine fetal development.

OFP-16-006

Microvillus inclusion disease (MVID) is a disorder of defective intracellular trafficking and disrupted epithelial cell polarity

C. Thoeni*
*Division of Cell Biology, Medical University Innsbruck, Austria

Objective: MVID is a congenital enteropathy characterized by loss of microvilli and formation of microvillus inclusions (MI) in enterocytes. MVID is caused by mutations in the MYO5B gene, coding for the Myosin Vb (M5B) motor protein involved in intracellular transport and maintenance of epithelial cell polarity. We examined the effects of loss of M5B in enterocytes of MVID patient and in a CaCo-2 cell model.
Method: The expression and localization of cell membrane transporters (CD36, Na/K ATPase) and various cell organelle markers : endosomal Rab GTPases [Rab5,7,8,9,11]; early (EEA1) and late endosome (LAMP2), and Golgi (Giantin)) were analyzed using multilabel immunofloures-cence and confocal microscopy of a duodenal biopsy from MVID patient and in CaCo-2 cells following M5B si RNA knock-down (Hum Mut 31:1-8,2010).
Results: Depletion of M5B in both enterocytes and CaCo-2 cells resulted in disruption of epithelial cell polarity with loss of apical microvilli, formation of MI; mislocalization of transporters as well as aggregation of epitopes for different Rab GTP ases, early and late endosomes.
Conclusion: M5B plays a critical role in polarized organization of enterocytes in MVID - a disorder characterized by defective intracellular trafficking and altered endosomal sorting. CaCo-2 cells provide an excellent model to study the pathogenesis of MVID.

OFP-16-007

Beta-catenin expression and mutational analysis of CTNNB1 gene in pediatic Adrenocortical Tumors (ACT)

R. Alaggio*, P. Dall'Igna, A. Martines, E. Lalli, R. Boldrini, V. D´Onofrio, G. Esposito
*Università di Padova, Dipt. di Pathology, Italy

Objective: ACT have an unpredictable clinical behaviour, and no liable histological or molecular parameters are available to predict outcome. The activation of WNT/β-catenin pathway, involved in tumor growth and progression in adult ACT has been explored only in Brasilian pediatric ACT. The aim of this study is the investigation of the possible prognostic role of β-catenin accumulation and/or CTNNB1 (β-catenin gene) mutations also in Italian pediatric ACT.

Method: β-catenin immunostaining and mutational analysis of CTNNB1 gene at exons 3 and 5, when possible, were carried on a series of 19 ACT (7 malignant and 12 benign, according to Wieneke classification), from patients enrolled in the Italian Pediatric Rare Tumor (TREP) Study.
Results: Immunostaining for β-catenin showed membrane/cytoplasmic staining in 9 cases, 5 benign and 4 malignant, and nuclear staining in 1 malignant. No mutations of CTNNB1 gene were found in the 8 tumors analyzed.
Conclusion: CTNNB1 gene mutations do not appear to be involved in pathogenesis of pediatric ACT. The accumulation of protein might be related to different mechanisms. Its presence in the majority of malignant ACT suggests a possible role in tumor progression.

OFP-16-008

Neuroblastoma presenting like a Wilms' Tumor with thrombus in inferior vena cava: A case series

H. Sartelet*, G. Gaetan, A. Ouimet, C. Lapierre, P. Teira
*CHU Sainte Justine, Dept. of Pathology, Montreal, Canada

Objective: Neuroblastomas and Wilms' tumors are frequent pediatric solid tumors. The first is frequently detected in the adrenal gland and the second develops in the kidneys. The extension through the vena cava and the lung metastases are frequent in Wilms' tumors and are rarely in neuroblastoma. We present the cases of three children with abdominal tumors with thrombus in the inferior vena cava and pulmonary metastases were discovered yet demonstrated a stage 4 neuroblastoma.
Method: The three male patients were between 23 and 48 months old. They presented an abdominal mass, near the superior pole of the kidney. Thrombus of the vena cava was evoked on imaging studies in all cases and pulmonary metastases were always found. Catecholamine metabolites were present in the first case and negative in the two others. Two out of three patients had a radical nephrectomy.
Results: The pathological analysis always found a neuroblastoma poorly differentiated or undifferentiated without MYCN amplification and confirmed the tumoral thrombus in the second case. The evolution of the two first patients was unfavorable and the third is alive.
Conclusion: Invasion of the inferior vena cava and pulmonary metastases in children with neuroblastoma is uncommon and can modify the surgical management.

OFP-16-009

EpCAM - A marker for Tufting enteropathy (TE) and a useful tool in the differential diagnosis of congenital enteropathies

C. Thoeni*
*Division of Cell Biology, Medical University Innsbruck, Austria

Objective: Congenital enteropathies (CE) are characterized by villous atrophy and disruption of apical microvilli in duodenal enterocytes. TE is characterized by focal eptithelial tufts and mutations in the EpCAM gene, coding for epithelial cell adhesion molecule, important for cell-cell contacts. Microvillus inclusion disease (MVID), shows loss of apical microvilli and formation of intracytoplasmatic microvillus inclusions. MVID is caused by mutations in the MYO5B gene, important for intracellular transport and organization of epithelial cell polarity. In this study, we identified a new EpCAM mutation in a patient with TE and used anti-EpCAM antibody as a marker for the diagnosis of TE and distinction from MVID.
Method: We used Immunohistochemistry (IHC) with monoclonal EpCAM antibody (mouse monoclonal AB for EpCAM, NCL ESA/Leica Microsystems) on routinely processed duodenal biopsies from patients with TE, MVID and age matched controls. Immunostaining for E-Cadherin served as reference.
Results: EpCAM expression was completely absent in the biopsy from TE patient homozygous for a novel EpCAM mutation (c227 C>G, Ser 76X). E-Cadherin showed normal expression and distribution pattern in the enterocytes. In MVID, expression and distribution pattern was comparable to controls for both EpCAM and E-Cadherin.
Conclusion: Loss of EpCAM is specific and a sensitive marker for confirmation of TE. EpCAM antibody is useful in the differential diagnosis of CE.

Monday, 10 September 2012, 08.30 - 12.00, Club D
OFP-17 Oral Free Paper Session Pulmonary Pathology I

OFP-17-001

Rapid on site evaluation of bronchoscopy specimens for EGFR mutation analysis. A retrospective study of 354 consecutive bronchoscopies

W. Pokieser*, C. Andreas, M. Kneussl, S. Publig, M. Hubner
*Wilhelminenspital, Pathology, Vienna, Austria

Objective: In pulmonary adenocarcinoma EGFR mutation analysis has become an important part of the diagnostic work-up. Frequently the tissue of bronchoscopies is of limited diagnostic value. The aim of the present study was to evaluate the impact of ROSE on brochoscopy specimens with regard to EGFR mutation.
Method: ROSE was used for adequacy of the specimen and for separating adenocarcinomas and carcinomas NOS from other neoplasms in the lung. If it was not possible to retrieve material for histology, cytology and cellblock were made. If adenocarcinoma or carcinoma NOS was suspected in ROSE, further two biopsies or two cell blocks were

obtained. EGFR mutation analysis was performed by PCR (Light Cycler 480; EGFR RGQ PCR Kit; Qiagen).
Results: Malignancy was diagnosed in 93 of 354 cases by histology or on cytology with and without cell blocks. Adenocarcinomas (n=30) and carcinomas NOS (n=9), SCC (n=26), SCLC (n=13), and rare tumors (n=15) were diagnosed, respectively. Among the group of adenocarcinomas and carcinomas NOS (n=39), EGFR mutation analysis was performed in 29 (74,3 %) cases and showed mutations in 3 (10,3 %) and "wild type" in 26 (89,7 %) tumors. No material was left in 10 (25,6 %) cases.
Conclusion: ROSE supports bronchoscopic procedures to retrieve adequate specimens for tumor diagnosis and subsequent EGFR mutation analysis.

OFP-17-002
FGFR1 amplification in metastatic squamous cell carcinoma of the head and neck: A potential target for a rational therapy?
F. Göke*, A. Franzen, R. Menon, A. Schroeck, R. Kirsten, D. Boehm, W. Vogel, F. Bootz, S. Perner
*Universitätsklinik Bonn, Inst. für Pathologie, Germany

Objective: Patients with Fibroblast growth factor receptor 1 (FGFR1) amplified squamous cell lung cancers (L-SCC) are treated in phase I clinical trials using small molecule inhibitors (SMI). SCC of the lung share common molecular alterations with squamous cell head and neck cancers (HN-SCC). Aim of our study is to assess if HN-SCCs also harbor FGFR1 amplifications. Furthermore, we aim to inhibit cell proliferation of FGFR1 amplified HN-SCC cell lines using a SMI.
Method: The cohort consists of 227 patients suffering from HN-SCC, 97 of these suffering from metastatic disease. Primary tumors and metastatic tumors were assessed for FGFR1 copy number status using fluorescence in-situ hybridization (FISH). We tested cell lines for FGFR1 amplification status and inhibited these with SMIs.
Results: 16 % of primary HN-SCC displayed FGFR1 amplifications. Of interest, almost all metastatic tumor samples revealed a FGFR1 amplification if the corresponding primary tumor harbored the amplification. The cell lines HN and SCC-25 harboured FGFR1 amplifications. HN cell proliferation was inhibitable with small molecule inhibitors.
Conclusion: FGFR1 amplification frequently occurs in primary and metastatic HN-SCC and proves as a potential target for small molecule therapy. Cell growth of FGFR1 amplified cell lines is inhibitable with SMIs. Further functional studies are needed for further validation.

OFP-17-003
The antioxidant components in the pequi (Caryocar Brasiliense Camb) oil fruit diminish the oxidative stress status and the DNA damage in experimental lung cancer
N. Colombo*, E. R. Parra, C. Koppe Grisólia, D. Pens Gelain, C. E. Schnorr, E. Kolling, M. Hage, D. Frediani Barbeiro, V. L. Capelozzi
*Universidade de São Paulo, Dept. of Pathology, Brazil

Objective: The pulp of pequi has high levels of antioxidants properties.
Method: Eighteen male BALB/c mice divided: 14 animals received by gavage 0,5 μL/mg/day of pequi oil (Control + CBCoil=4) during 75 days. After 15 days, 10 of these mices received two doses of 1,5 g/kg intraperitoneal of urethane (Urethane + CBC oil=10). The other 4 animals were only submitted to two doses of 1,5 g/kg intraperitoneal of urethane (Urethane group=4). After 75 days, groups were sacrificed. Antioxidant activity was evaluated in the lung tissues by TBARS (Thiobarbituric acid-reactive substances), CAT (catalase) and SOD (superoxido dismutase) test. DNA damage was estimated by comet test.
Results: The lung parenchyma from Urethane groups without oil and with oil showed neoplasic formations induced by the chemical carcinogenesis in contrast with Control + CBC oil group. The results of TBARS test showed a significant decrease of lipid peroxidation in the Urethane + CBC oil, than Urethane group. The CAT and SOD test didn't show a significant difference. Comet assay showed a significant decrease of DNA damage in Urethane + CBC oil when compared with Urethane group.
Conclusion: The antioxidant components in the pequi oil diminish the oxidative stress status and DNA damage in chemical carcinogenesis, suggesting that this type of strategies may have a greater impact in lung cancer treatment.
Financial Support: FAPESP.

OFP-17-004
An algorithm for gene mutation analysis in lung cancer
M. Comanescu*, C. Iosif, M. Dobre, L. Buburuzan, G. Bussolati, F. Vasilescu, C. Ardeleanu
*Institutul Victor Babes, Dept. of Pathology, Bucharest, Romania

Objective: Somatic alterations of K-RAS, EGFR and ALK which are increasingly requested in order to predict response to personalized therapies in lung cancer are mutually exclusive and are represented in over 50 % of lung adenocarcinomas. The approach to be followed for planning analyses is not standardized in the literature.
Method: We have studied by molecular methods (PCR-RFLP for K-RAS, direct sequencing for EGFR and FISH

for ALK) 185 formalin fixed, paraffin embedded cases of lung adenocarcinomas of different subtypes.
Results: Based on rational, biological and economic considerations we started with K-RAS analysis by PCR-RFLP, which showed mutations in 38 cases (37 with mutation on codon 12 and one case with mutation on codon 13), The 147 residual cases were all analyzed for EGFR mutations. FISH for ALK translocation followed in EGFR- wild cases.
Conclusion: The analysis for K-RAS mutations allows to select the significant percentage (approximately 25 % of adenocarcinomas) when EGFR mutation analysis by direct sequencing can be postponed. K-RAS and EGFR wild cases will then undergo FISH analysis for ALK translocation. ACKNOWLEDGEMENTS Study conducted with the support of the following project: Project PERSOTHER - SMIS-CSNR: 549/12.024; With the support of Sectoral Operational Programme "INCREASE OF ECONOMIC COMPETITIVENESS" Priority Axis 2: Research, Technological Development and Innovation for Competitiveness.

OFP-17-005

Gene mutation analysis in adenosquamous carcinomas of the lung

M. Comanescu*, G. Bussolati, C. Ardeleanu, L. Daniele, G. Gaina, C. Luca, A. Sapino
*Institutul Victor Babes, Dept. of Pathology, Bucharest, Romania

Objective: Adenosquamous carcinomas of the lung constitute a rare and aggressive variant of lung cancers. The pressing interest in evaluating the mutational status in lung carcinomas for predicting responsiveness to targeted therapies is presently focused on adenocarcinomas (of different sub-types), which makes preliminary histological typing a crucial step in order to select cases to be genetically analyzed. Hence the interest in deciding if adenosquamous carcinomas should be included among adenocarcinomas or, viceversa, if they should be interpreted as a variant of squamous cancers and excluded from the process of gene analysis.
Method: We have thus collected, from our two Institutions a large number (45 cases) of cancers showing the histological definition of adenosquamous carcinomas according to the WHO criteria and performed gene analysis for k-RAS (codons 12, 13) and EGFR (codons 18, 19 and 21) mutations. The detection of rearrangements of the ALK gene by FISH was also performed.
Results: The results indicate that k-RAS and, specifically, EGFR mutations are detectable in a fraction of these tumors.
Conclusion: In conclusion, adenosquamous carcinomas should not be denied the chance of genetic analysis eventually leading to a targeted therapy. Acknowledgement Project PERSOTHER - SMIS-CSNR: 549/12.024 Romania.

OFP-17-006

Pathology of the lung progenitor cells and their niches in idiopathic interstitial pneumonias and lung sarcoidosis

S. Demoura*, E. Kogan, V. Tuong, O. Kichigina
*Moscow, Russia

Objective: The aim of the study was to investigate the morphological and the molecular-biological changes of the lung progenitor cells and their niches in idiopathic interstitial pneumonias (IPF) and lung sarcoidosis (LS).
Method: We performed an immunohistochemical study on open lung biopsies from 250 patients (usual IPF – 87, desqvamative interstitial pneumonia-37, nonspecific IPF – 42, Cryptogenic IPF – 20, LS – 32, control – 34 patients). Immunochemistry was done on step paraffin sections with monoclonal and polyclonal antibodies: Apo-Cas, PCNA, CK 5-7, 18, 19, TNF-α, TGF-β, PDGF, FGF, IGF II, CD 34, MMP 1, 2, 7, 9, TIMP 4, CD 68, SMA, EMA.
Results: Deep injury of Clara cells together with pneumocytes II and their nishes were found in usual IPF, SK with prominent IPF and desqvamative interstitial pneumonia. Myofibroblast proliferation, neoangiogenesis, adenomatosis and fibrosis with high production of TNF-α, TGF-β, PDGF, FGF, IGF II, CD 34, MMP 1, 2, 7, 9, TIMP 4 accompanied proliferation of these epithelial cells. While in other variants of IPF pathological changes were localized in the interstitium, vessels and basal bronchiolar epithelial cells.
Conclusion: Localization of injury and inflammation in progenitor cells niches results in pathologic reparation, sclerosis and precancer lesions.

OFP-17-007

A small immunohistochemical panel allows for accurate diagnosis of primary and metastatic lung cancer in biopsy specimens

D. Felizardo*, R. Henrique, A. L. Cunha
*Instituto de Oncologia Porto, Dept. of Pathology, Coimbra, Portugal

Objective: Precise subclassification of lung cancer, mostly performed in biopsy or fine needle-aspiration specimens, is required for appropriate therapy. Moreover, distinction between primary and metastatic carcinoma is critical. Thus, the role of immunohistochemistry (IHC) has been emphasized, although an optimal IHC diagnostic algorithm has not been firmly established. Herein, we evaluated the performance of the IHC panel used at our institution in subclassification of lung cancer and identification of metastatic carcinoma.
Method: Cases of non-neuroendocrine lung carcinoma, diagnosed from March 2011 to April 2012 were selected. IHC

was performed for CK7, CK20, TTF-1 and p63. Resection specimens were compared with the respective biopsy.
Results: Of 184 cases analysed, 73 (39.7 %) were diagnosed as lung adenocarcinoma, 59 (32.1 %) as epidermoid carcinoma, 22 (12 %) as other forms of NSCLC, and 17 (9.2 %) as metastasis. Importantly, 26 % of primary lung adenocarcinomas were initially suspected to be metastasis. In 26 cases submitted to surgical resection, 22 (84.6 %) were correctly diagnosed in the biopsy, revealing a substantial agreement (κ-value=0,757).
Conclusion: Our IHC panel allows for reliable subclassification of lung carcinomas in most cases and is decisive for appropriate diagnosis in patients suspected of lung metastasis, which is critical issue in a cancer institute.

OFP-17-008

Rationale for treatment of metastatic squamous cell carcinoma of the lung using FGFR1 Inhibitors

F. Göke*, A. Franzen, A. Schroeck, V. Scheble, R. Kirsten, R. Menon, D. Goltz, D. Boehm, W. Vogel, S. Perner
*Universitätsklinik Bonn, Inst. für Pathologie, Germany

Objective: We previously identified amplified fibroblast growth factor 1 (FGFR1) as a therapeutic target for small molecule inhibitor (SMI) therapy in squamous cell lung cancer (L-SCC), resulting in currently running clinical trials treating patients with stage III disease. As most patients present with metastatic stage of disease, we attempt to demonstrate FGFR1 amplification in lymph node metastases of amplified primary tumors. Our study aims to give a rational to include these patients in a targeted SMI therapy.
Method: We assessed 75 formalin-fixed paraffin-embedded (FFPE) primary L-SCC samples. 46 samples were primary tumours with corresponding FFPE lymph node metastasis. The biotin-labelled FGFR1 target probe (8p11.23 to 8p11.22) was used to determine the FGFR1 amplification status performing fluorescence in situ hybridization (FISH).
Results: Of 39 assessable metastatic L-SCC, 7 samples displayed FGFR1 amplification (18 %). All of these primary tumors also harbored FGFR1 amplification in their lymph node metastasis. Non-amplified tumors never displayed FGFR1 amplification in corresponding metastases.
Conclusion: We found FGFR1 amplification not only in primary L-SCC, but also in corresponding lymph node metastasis, suggesting that this genetic aberration is a clonal event in tumor genesis. Our study provides data indicating new therapeutic possibilities for patients suffering not only primary, but also metastatic FGFR1 amplified SCC lung cancer disease.

OFP-17-009

KRAS mutation spectrum in 485 primary lung adenocarcinoma from a French Caucasian population: Correlation with smoker status, histological subtypes, pathological staging and clinical behaviour

V. Hofman*, M. Ilie, E. Long, V. Lespinet, C. Bonnetaud, C.-H. Marquette, J. Mouroux, P. Hofman
*Nice University Hospital, LPCE, France

Objective: Lung cancer patients with mutant KRAS tumours fail to benefit from adjuvant chemotherapy, and their disease does not respond to EGFR inhibitors. There is a dire need for therapies specifically for patients with KRAS mutant NSCLC, which may depend on KRAS oncogene substitutions.
Method: 485 lung adenocarcinoma French Caucasian patients were tested for KRAS mutation hot spots in codons 12, 13 and 61 by pyrosequencing. PCR amplification was performed using the corresponding Therascreen® Pyro kits (KRAS Pyro® kit, Qiagen, Hilden, Germany). Spectrum of KRAS mutations were correlated with main clinico-pathological parameters.
Results: 195/485 (40 %) of tumours were KRAS mutated. KRAS mutation was a G to T transversion in 80 % of the smoker NSCLC population and a G to A transition in 98 % of the non smoker NSCLC population. Mutations were noted at codon 12 (90 %), codon 13 (8 %) and codon 61 (2 %). A KRAS mutation was a negative prognostic factor with a hazard ratio for death of 1.38 (95 % confidence interval, 1.16–1.63). A mucinous histological subtype was observed in more than 75 % of KRAS mutated tumours.
Conclusion: KRAS oncogene substitution must be accurately determined in primary lung adenocarcinoma for correlation with tumour behaviour and clinico-pathological parameters.

OFP-17-010

Plasma miR-155, miR-152, miR-20a, miR-223, miR-126 and miR-199a expression as a novel prognostic signature of resectable Non-small Cell Lung Carcinoma (NSCLC)

M. Ilie*, C. Sanfiorenzo, P. Brest, A. Belaid, F. Barlési, J. Mouroux, C.-H. Marquette, P. Hofman
*CHU de Nice, LPCE, France

Objective: There is an urgent need for diagnosis of NSCLC at its early-stages and for improving the survival rate of patients. MicroRNAs, small non-coding RNAs, are frequently deregulated in NSCLC. This study aimed to explore plasma microRNAs for diagnostic value, and evaluated the correlation between expression profiles of plasma microRNAs and disease-free survival (DFS) in NSCLC patients.
Method: We selected eighteen most frequently expressed microRNAs in NSCLC. Total plasma RNA including microRNAs was isolated and reverse-transcribed into cDNAs. The level of microRNAs was determined by quantitative real-time RT-PCR in 42 resectable NSCLC patients

and 10 matched cancer-free individuals. The correlation between the expression of microRNAs in plasma and patient DFS were examined by log-rank and Cox analysis.
Results: Expression levels of miR-320,−296,−145,−199a, −191,−223,−24,−152,−126, and let-7f in the plasma of NSCLC including stage-I patients were significantly higher compared with controls ($P<0.0001$). The combination of these microRNAs yielded 87 % sensitivity and 90 % specificity (AUC=0.934) in discriminating NSCLC patients from controls. The levels of miR-155, −152, −20a, −223, −126 and miR-199a were significantly associated with DFS ($P<0.05$).
Conclusion: Our results suggest that high expression of 6-plasma miRNAs signature would provide potential non-invasive blood-based biomarker for the prognosis of NSCLC.

Monday, 10 September 2012, 14.15 - 16.15, Terrace 1
OFP-18 Oral Free Paper Session Pulmonary Pathology II

OFP-18-001
Dynamic responses of carbonic anhydrase isoforms IX and XII during tumour reoxygenation: Contribution to an aggressive phenotype and discrimination of clinical outcome in Non-small Cell Lung Cancer (NSCLC)
M. Ilie*, V. Hofman, C. Butori, C. Bonnetaud, J. Mouroux, N. Mazure, J. Pouysségur, P. Brest, P. Hofman
*CHU de Nice, LPCE, France

Objective: Intratumoral disorganized neo-vasculature induces oxygen fluctuations which contribute to tumour growth and metastatic potential. Although the activation by hypoxia of the carbonic anhydrases CAIX and CAXII is well known, responses of these proteins under reoxygenation remain to be elucidated.
Method: In this study we evaluated the effects of hypoxia-reoxygenation on CAIX and CAXII expression and cell proliferation in A549 and H1975 lung adenocarcinoma cell lines. We further investigated by immunohistochemistry on tissue microarray the value of the combined expression of these proteins to predict outcome in 552 NSCLC patients.
Results: CAIX expression was maintained at high level after reoxygenation in contrast of the rapid CAXII down-regulation, whereas the cell proliferation rate was significantly increased. Survival analyses showed that high CAIX/low CAXII was associated with high cumulative incidence of relapse and with poor overall survival of NSCLC patients ($P<0.05$).
Conclusion: Our results provide insight into understanding dynamic responses of CAIX and CAXII expression under tumour cells reoxygenation and demonstrate a critical role for reoxygenation on CAIX and CAXII levels that may select for aggressive lung cancer phenotype. These findings suggest that CAIX and CAXII play selective roles in tumour progression and emphasize their significant prognostic and potential therapeutic value.

OFP-18-002
ALK-gene rearrangement: A comparative analysis on Circulating Tumour Cells (CTCs) and tumour tissue from lung adenocarcinoma patients
M. Ilie*, E. Long, C. Butori, V. Hofman, C. Coelle, V. Mauro, K. Zahaf, C.-H. Marquette, J. Mouroux, P. Paterlini-Bréchot, P. Hofman
*CHU de Nice, LPCE, France

Objective: Until now the ALK status in CTCs isolated from lung cancer patients has not been characterised. We assessed the ALK status in CTCs detected in lung cancer patients and correlated the results to the ALK status defined in the corresponding tumour tissue.
Method: 87 lung adenocarcinoma patients showing CTCs isolated using the Isolation by Size of Epithelial Tumour cell method were screened for their ALK status both in tumour samples and in CTCs. ALK break-apart fluorescence in situ hybridisation (FISH) and immunochemistry using an anti-ALK antibody were done on CTCs and compared with results obtained on corresponding tissue specimens.
Results: 5 patients showed ALK-gene rearrangement and strong ALK protein expression in CTCs and corresponding tumour samples. Negative results were found for 82 patients in CTCs and corresponding tumour samples.
Conclusion: We demonstrate that the ALK status can be determined in CTCs from lung cancer patients both by immunocytochemistry and FISH analysis. A strong correlation was found for the ALK status obtained from corresponding tissue specimens. These results favour non-invasive, ALK-gene status pre-screening on a routine basis on CTCs isolated form lung cancer patients and open new avenues for real-time monitoring for adapted targeted therapy.

OFP-18-003
Detection of EGFR mutations and EML4-ALK rearrangements in lung adenocarcinomas using archived cytological slides
E. Imyanitov*, N. Mitiushkina, A. Iyevleva, A. Poltoratskiy, A. Ivantsov, A. Togo, I. Polyakov, S. Orlov, D. Matsko, V. Novik
*N.N. Petrov Institute of Oncology, St. Petersburg, Russia

Objective: While the molecular analysis of EGFR and ALK in archival lung cancer tissues is relatively well established, the acceptability of genetic investigation of cytological material in clinical routine remains a subject of debate.

Method: Islets of malignant cells were visually located on the archived cytological slides, lysed in situ by the drop of SDS-containing buffer, and subjected to the standard DNA and RNA extraction. Examination of paraffin-embedded tissue blocks from the same patients was done in parallel.
Results: 75 cytological/histological lung adenocarcionoma sample pairs underwent the analysis for EGFR mutation. 2 cytological and 1 morphological samples failed to produce DNA. Concordance for the wild-type and mutation status was observed in 53/72 and 14/72 informative pairs, respectively; 1 pair was non-interpretable; 3 and 1 pairs had mutation only in the cytological or histological material, respectively. RNA extraction followed by RT-PCR analysis for the EML4-ALK translocation was done for the 51 pair; failures were observed for 3 cytological and 8 histological samples. 34/40 informative pairs were concordant for the norm, 3 contained identical translocations, and 2 were non-interpretable. 1 pair demonstrated ALK rearrangement in the tissue block but not in the histological slide.
Conclusion: Archived cytological slides appear to be well suitable both for EGFR and ALK analysis.

OFP-18-004
Accuracy and efficiency of intraoperative pathologic consultations of thoracic surgery specimens

B. Ince Alkan*, A. Sasmaz, Y. Aksogan, B. Temel, M. Aybal, E. Solakoglu, L. Tunc, S. Percinel, S. Dizbay Sak, A. Kayi Cangir, C. Ates
*Ankara University, Turkey

Objective: Intraoperative consultations are indicated to influence the type, nature and extent of surgery. The aim of the current study was to compare frozen section (FS) and final histological diagnoses (FHD) of thoracic surgery specimens and to investigate discordant diagnoses to enhance diagnostic accuracy of FS.
Method: The diagnoses obtained by FS and FHD were compared in thoracic surgery specimens between 2005 and 2011 retrospectively. Specimen sites were divided into five groups (thorax/supradiaphragm, diaphragm, subdiaphragm, resection margins and lymph nodes) according to the indications of intraoperative consultations. Sensitivity and specificity of FS were calculated.
Results: A total of 2949 (99.6 %) FS diagnoses and 2580 (87.2 %) FHD were obtained in 1612 patients. Concordance between FS diagnoses and FHD was 98 % for malignant and 97.5 % for benign categories. 15.3 % of intraoperative consultations were deferred. While 16 diagnoses were regarded as "overdiagnosis", 35 were interpreted as "underdiagnosis". Sensitivity and specificity of FS diagnosis and AUC (95 % confidence interval) were calculated to be 0.92, 0.94 and 0.9817 (0.9760–0.9861), respectively according to Binormal ROC Curve. Discordant diagnoses were mostly due to sampling errors and misinterpretation.
Conclusion: FS examination of thoracic surgery specimens is associated with a high degree of accuracy and efficiency.

OFP-18-005
Increased sirtuin expression in lung adenocarcinoma and squamous cell carcinoma

S. Isajevs*, D. Isajeva, G. Strazda, U. Kopeika, I. Ronis, M. Apsvalks, I. Silins, I. Taivans
*University of Latvia, Dept. of Pathology, Riga, Latvia

Objective: Non-small cell lung cancer (NSCLC) represents a heterogeneous group of cancers consisting mainly of squamous cell carcinoma (SCC) and adenocarcinoma (AD). Increased sirtuin (SIRT-1) expression leads to deacetylation of p53 that could be important in the pathogenesis of lung cancer. Differences of the molecular mechanisms in NSCLC subtypes may follow subtly different pathways to tumorigenesis. The aim of our study was compare SIRT-1 expression in lung adenocarcinoma, squamous cell carcinoma and control group.
Method: 25 patients with stage 2 lung cancer were enrolled in the study. 14 patients had adenocarcinoma, but 11 patients had squamous cell carcinoma. Lung tissue for control group were selected from 15 autopsy cases. Immunohistochemical and western blot methods were used to evaluate SIRT-1 expression in lung tissue.
Results: Obtained results showed that patients with lung cancer had increased SIRT-1 expression compared to control group (146±111 vs. 21±16 cells/mm2, $p<0.0001$). In addition, patients with squamous cell carcinoma had increased SIRT-1 positive cells compared to patients with adenocarcinoma (203±143 vs. 95±49 cells/mm2, $p=0.03$).
Conclusion: Lung cancer is characterized by an increased SIRT-1 expression which ir more prominent in squamous cell carcinoma. Supported by ERAF Project 2010/0202/2DP/2.1.1.2.0/10/APIA/VIAA/013.

OFP-18-006
A new experimental model of orthotopic lung transplantation: Padova experience

N. Nannini*, F. Lunardi, M. Vadori, A. Dedja, E. Cozzi, F. Rea, F. Calabrese
*University of Padova, Italy

Objective: Transplantation is the only treatment for several end-stage lung diseases but limited by chronic allograft dysfunction particularly obliterative bronchiolitis (OB) and its correlate bronchiolitis obliterans syndrome. The development of preclinical models is crucial to better identify immunological/non-immunological mechanisms leading to OB.

Method: Lung allografts from Lewis rats were orthotopically transplanted into Fisher 344 rats [21 cases]. At 30 [group A] and 90 days [group B and C] post-transplant, animals were sacrificed. In animals from group C, cyclosporine was administered at sub-optimal dose. Lung rejection was graded according to the working formulation of ISHLT and the presence of circulating donor-specific (DSA) antibodies determined by flow cytometry.
Results: In group A, acute rejection (AR) or OB occurred in 33 % and 17 % of animals, respectively. AR occurred in 33–44 % of animals in group B and C respectively. OB was detected in 33 % and in 44 % of group B and C respectively. High levels of DSA IgG were observed in cases with AR.
Conclusion: A novel model of pulmonary OB was developed in the rat. To obtain a reproducible onset of OB, short-term and sub therapeutic cyclosporin administration appears indispensable, at least in our species combination.

OFP-18-007

Epithelial dysplasia and lung cancer in end-stage idiopathic pulmonary fibrosis: Padova experience

N. Nannini*, F. Lunardi, E. Balestro, E. Rossi, M. Loy, M. Saetta, F. Rea, F. Calabrese
*University of Padova, Italy

Objective: Idiopathic pulmonary fibrosis (IPF) is associated with increased risk of lung cancer. The prevalence of high grade dysplasia/lung cancer was studied only in a small number of IPF patients. The aim of our study was to investigate the prevalence of precancerous/cancerous changes and their relationship with both metaplastic changes and clinical data.
Method: Native lungs from 66 IPF patients were studied. The degree of honeycomb changes and squamous, cuboidal and bronchial cell metaplasia were graded (score: 0–3). The presence or absence of precancerous/cancerous changes were also evaluated.
Results: Three patients showed neoplastic transformation (4 %) and nine high grade dysplasia (14 %) ("cancer" group). The "cancer" group had similar smoking history, sex, age and duration of disease than the "no cancer" group. All lungs showed metaplasia, the score of squamous (p= 0.0001), cuboidal (p=0.018) and bronchial cell (p=0.018) metaplasia was significantly higher in the "cancer" than in the "no cancer", while the honeycomb score was similar in the two groups.
Conclusion: Advanced IPF patients have a high prevalence of high grade dysplasia/lung cancer, complex epithelial metaplasia, particularly squamous type, is more frequent in "cancer" group, independently from all clinical parameters, including smoking history.

OFP-18-008

Primary pulmonary adenocarcinoma with enteric differentiation, morphologically indistinguishable from metastatic colorectal adenocarcinoma: Case report with a history of metastatic colon adenocarcinoma

S. Percinel*, P. Celepli, H. Nalbant, Y. Yuyucu Karabulut
*Ankara, Turkey

Objective: According to a computerized medline search in the English literature, the present case is thought to be the first primary pulmonary adenocarcinoma with enteric differentiation, completely resembling metastatic colorectal adenocarcinoma morphologically, with a history of metastatic colon adenocarcinoma.
Results: A 62 year old man with a history of colon adenocarcinoma which was detected in 2007 underwent radiologic evaluation. A chest computed tomography scan revealed a 7 mm solitary nodule in the left lower lobe which enlarged in 1 year. The patient underwent left lower lobe wedge resection. Macroscopically, an irregular whitish nodule of 1.5 cm in greatest diameter was detected. Microscopically, the nodule was entirely composed of glandular and papillary structures, some of which had a cribriform pattern, lined by tumor cells that were cuboidal to tall columnar with nuclear pseudostratification, eosinophilic cytoplasm, brush-border, luminal necrosis and nuclear debris. Tumor cells were diffusely positive for cytokeratin (CK)7 and negative for thyroid transcription factor-1, surfactant protein-A, CDX-2 and MUC2. Only a very few tumor cells stained for CK20.
Conclusion: Enteric morphology with consistent expression of CK7 and a scattered positivity for CK20 helped in the distinction from metastatic colon adenocarcinoma and favored the diagnosis of primary pulmonary adenocarcinoma with enteric differentiation.

OFP-18-009

Expression of CXCR4 and CXCL12 in pulmonary carcinoids

S. Seiwerth*, L. Brcic, A. Sepac, A. Zanko
*Zagreb School of Medicine, Pathology, Croatia

Objective: CXCR4 and its chemochine ligand CXCL12 seem to play an important role in the process of tumor metastasis and, possibly, homing of metastatic tumor cells. The chemochine seems to be responsible for creating micro-enviromental predispositions for survival of metastatic cells, in a similar way it is done for developing immuno-competent cells. In contrast, expression of CXCL 12 in primary tumor cells, is thought to be associated with lower metastatic potential. CXCR4 is expressed in a wide range of tumors, and is thought to be crucial for the metastatic process and tissue-specific spread firstly of breast and prostate cancer. The role of CXCR4 signaling has been poorly

evaluated in carcinoids in general and not at all in pulmonary carcinoids.
Method: Immunohistochemically we investigated the expression of CXCR4 and CXCL12 in pulmonary carcinoids.
Results: Together 60 tumors (47 typical and 13 atypical) where investigated. In 6 there was a metastatic process (in 4 typical and 2 atypical). Ligand CXCL12 expression was negative in all of the metastatic tumors and in two without known metastasis in contrast to only two non-metastatic tumors showing negative reaction. CXCR4 positivity was found in both metastatic and non-metastatic carcinoids. The other investigated parameters where present in both metastatic and non-metastatic tumors.
Conclusion: These results point on a antimetastatic role of CXCL12 expression in lung carcinoids.

Monday, 10 September 2012, 17.00–19.00, Club D
OFP-19 Oral Free Paper Session Pulmonary Pathology III

OFP-19-001
Increased decorin and type V collagen in SSc pulmonary fibrosis
W. Teodoro*, A. P. Velosa, A. Marcelino, P. Martin, S. Carrasco, C. Goldenstein-Schainberg, E. Parra, N. Yoshinari, V. Capelozzi
*Faculdade de Medicina da USP, Disciplina de Reumatologia, São Paulo, Brazil

Objective: To evaluate COL V and decorin expression in pulmonary tissue and to characterize biochemical profile of COLV from lung fibroblasts culture from SSc patients.
Method: We evaluated COL V and decorin expression and tridimensional reconstruction (3D) of 6 patients with SSc without pulmonary hypertension that underwent surgical lung biopsy and as control was obtained lung fragments from 6 normal individuals who died from trauma. COL V amount in lung sections was evaluated with immunofluorescence. To biochemical characterization of COL V from lung fibroblasts culture was used quantitative immunoblot.
Results: It was found that the structure of COL V fibers was distorted and strongly thickened in lung tissue from SSc patients compared with thin fibers pattern in the healthy controls. Decorin was distributed around COL V fibrils in the bronchovascular interstitium and vascular walls. Histomorphometric analysis of SSc lung demonstrated increased expression of both COL V and decorin when compared to the control ($p<0.01$). The semiquantitative imunoblot detected an increased high molecular weight COLV fraction in patients when compared to the control.
Conclusion: The over expression and unusual organization of COLV fibers with biochemical changes associated to increased decorin indicates that matrix signalization pathway is involved in COLV fibrillogenesis process in SSc pulmonary fibrosis.

OFP-19-002
Application of combined light microscopy and confocal laser endomicroscopy diagnostics in studying of solitary and multiple lung consolidations
F. Zabozlaev*, A. Sorokina, O. Danilevskaya, D. Sazonov, A. Averyanov, O. Kuzovlev, O. Shablovskiy
*FRCC FMBA Russia, Dept. of Pathology, Moscow, Russia

Objective: Probe-based confocal laser endomicroscopy (pCLE) is a new method used during bronchoscopy by means of special miniprobe Alveoflex and based on the visualization of intraalveolar structures which possess autofluorescence. Aim: to compare the visual signs of a healthy and pathologically changed lung tissue received at pCLE in patients with infiltrative and local lung nodules with the diagnosis, delivered by light microscopy.
Method: An autopsy and surgical material was fixed in 10 % neutral formalin solution and was analyzed by studying with a new method for visualization of structures. Histological specimens were studied at that spaces, where the pCLE was applied. We compared our results by using qualitative method.
Results: Normal lung tissue structures include alveolar septum with the high light emission and light-negative spaces - the alveolar spaces. In case of pneumonia alveolar septum were saved, but the light density of alveolar spaces was higher in compare with the normal tissue. In case of alveolar proteinosis we observed unique globules, which had the highest light emission. We found out several authentic signs, which are representative for each kind of pathological feature. Moreover, we revealed some other characteristics, which help us to distinguish some types of lung cancer.
Conclusion: pCLE can be used as an additional method of noninvasive diagnostics in vivo.

OFP-19-003
Increased copy nember of alk gene is not associated with increased immunoreactivity of alk protein in lung adenocarcinomas
T. Balharek*, A. Farkasova, Z. Kviatkovska, K. Scheerova, P. Tilandyova, Z. Hutka, L. Plank
*Comenius University, Dept. of Pathology, Martin, Slovakia

Objective: Anaplastic lymphoma kinase (ALK) gene rearrangements represent an important predictive marker and promissing therapeutic target in small subset of non-small cell lung carcinomas (NSCLC). Immunohistochemical (IHC) screening of ALK abnormalities in NSCLC was reported to have variable reliability. We analyzed

association between ALK immunoreactivity and increased number of ALK gene copies often seen in NSCLC.
Method: We examined 10 clinically selected EGFR negative lung adenocarcinomas. ALK protein expression was detected by IHC using antibody clone ALK1 (Dako). ALK gene status was assessed by fluorescent in situ hybridization using LSI ALK Dual Color Rearrangement probe (Abbott) and SPEC ALK/EML4 TriCheck probe (ZytoVision).
Results: Increased ALK gene copy number was identified in 7 cases, 3 of them showed cytoplasmic ALK positivity. In 2 of these cases we detected rearrangement of ALK locus, once represented by ALK-EML4 fusion combined with more complex cytogenetic abnormalities. Remaining third ALK + case was negative for ALK rearrangement.
Conclusion: IHC seems to be useful method for initial screening of ALK rearrangements in NSCLC. There is no clear association between ALK protein expression and number of ALK gene copies. Prognostic relevance of ALK copy gains or amplification in lung adenocarcinomas remains to be determined, together with role of ALK-inhibitors in those cases.

OFP-19-004
Expressions of EGFR, ERCC-1, ß Tubulin III, RRM-1 in advanced non-small cell lung carcinoma
N. Bassullu*, E. Namal, I. Turkmen, R. Yasar, P. Y. Korkmaz, Z. Akcali, G. Demir, G. B. Dogusoy
*Istanbul Bilim University, Dept. of Pathology, Turkey

Objective: EGFR, ERCC1, RRM1 and βTubulinIII predicts sensitivity to therapeutic agents and provide prognostic information in Nonsmall cell lung cancer (NSCLC) which is the most frequent worldwide cause of cancer death.
Method: We investigated the expressions of EGFR, ERCC1, βTubulinIII, RRM1 immunohistochemically in 42 advanced NSCLC cases and their correlations with other pathologic features.
Results: The age distribution was 30–82 with an average of 63,02. Male/female ratio was 34/8. ERCC1 protein was detected in nuclei of carcinoma cells in 38 patients (90,5 %) (H score >1). BTubulinIII expression was detected in cytoplasm of cancer cells in 41 patients (97,6 %) (score ≥ 50). ERCC1 and βTubulinIII expression were not associated with pathological factors. RRM1 was negative (score<9) in 29 (69 %) cases and negativity was significantly correlated with male gender (p<0,032). EGFR was negative (score<200) in 40 (95,2 %) cases and negativity was nearly correlated with absent necrosis (p<0,065). No significant correlations were found between EGFR, ERCC1, βTubulinIII, RRM1 and the pathological parameters.
Conclusion: In our study, as a first step, EGFR, ERCC1, βTubulinIII, RRM1 showed no significant correlation with pathologic features. We look forward to obtain further results in the next study consisting of correlations with follow ups.

OFP-19-007
Proliferative markers in idiopathic pulmonary fibrosis: Clinical, radiological and functional significance
E. Parra*, M. Cornati, V. Capelozzi
*FMUSP, Dept. of Pathology, São Paulo, Brazil

Objective: Natural course of idiopathic pulmonary fibrosis (IPF) could be predicted by proliferative markers of the fibrotic process, such as myofibroblasts and interleukins (IL)-13 and IL14. Our primary aim was to determine whether these proliferative markers influence the course of IPF course measured by a radiological/functional score.
Method: Twenty-eight patients with biopsy-proven IPF disease, who underwent pulmonary evaluation by high-resolution computed tomography (HRCT) fibrosis score and pulmonary function tests were studied. Five normal lung tissues (NLT) were included Biomarkers in lung tissues were detected by immunohistochemistry and quantified by histomorphometry for myofibroblasts alpha-smooth muscle actin (α-SMA), anti-interleukin (IL)-4 and IL-13.
Results: Myofibrobalst amount, IL-4 and IL-13 expression were higher in IPF than in NLT (p<0.01). Myofibroblast expression of α-SMA was positively correlated to IL-14 and IL-13 expression. Lung tissue from patients with high HRCT fibrosis scores expressed significantly greater α-SMA+, IL-4 and IL-13 when compared with patients with low HRCT fibrosis scores (p<0.05). Negative correlations were found between myofibroblasts α-SMA + and VC and DLCO.
Conclusion: Proliferative markers, detected by immunohistochemistry, in lung tissue allowed recognizing a dichotomous distribution of HRCT fibrosis course and influenced pulmonary function tests, suggesting that they may be promising markers of prognosis in these patients. Financial Support: FAPESP, CNPq.

OFP-19-008
Comparison of survival of patients with different histological subtypes of epithelioid pleural mesothelioma
A. Sepac*, V. Klaric, A. Zenko, L. Brcic, A. Znaor, Z. Slobodnjak, S. Smojver Jezek, S. Seiwerth
*School of Medicine Zagreb, Dept. of Pathology, Croatia

Objective: Epithelioid mesothelioma is the most common histologic type of the diffuse malignant pleural mesothelioma, also having the best prognosis. Although a great variety of histological patterns within epithelioid type has been described, a clear impact of histological subtyping on clinical outcome is unknown (Kadota et al., 2011.). Here we compared median survival of six histological subtypes of epithelioid mesothelioma.

Method: We examined hematoxylin and eosin-stained slides of 74 patients diagnosed with epithelioid mesothelioma. According to previously described predominant histological features we grouped them into six subtypes: trabecular, solid, microglandular, tubulopapillary, micropapillary and pleomorphic.
Results: The median survival of all 74 patients with epithelioid mesothelioma was 14.5 months. The best median survival was in trabecular and micropapillary subtypes (each 18 months, $n=20$ and $n=5$, respectively), followed by tubulopapillary (17 months, $n=18$), microglandular (16 months, $n=7$) and solid (11 months, $n=19$) subtypes. The worst median survival was in pleomorphic subtype (5 months, $n=5$).
Conclusion: Epithelioid type of diffuse malignant pleural mesothelioma shows a great diversity of histological patterns that likely have an impact on the clinical outcome and patient's survival. Further investigations of genetic variations among different subtypes may provide valuable information for better understanding of pathogenesis of these tumors.

Tuesday, 11 September 2012, 17.00–19.00, Meeting Hall V
OFP-20 Oral Free Paper Session Uropathology

OFP-20-001

Comprehensive characterization of ploidy and proliferation levels in prostate cancer: Progression and prediction of lymph node metastasis

M. Braun*, J. Stomper, R. Kirsten, W. Vogel, D. Boehm, Z. Shaikhibrahim, N. Wernert, G. Kristiansen, S. Perner
*Universitätsklinik Bonn, Inst. für Pathologie, Germany

Objective: Genetic instability resulting in both aneuploidy and polyploidy are discussed to be involved in prostate cancer (PCa) development and progression. Aim of this study was to comprehensively characterize the ploidy status and proliferation levels in PCa with regard to disease progression.
Method: Using FISH, we assessed 112 localized PCa, 75 PCa with 125 corresponding lymph node metastases, and 42 hormone-refractory distant metastases for losses and gains of all 24 chromosomes. The proliferation rate was assessed using pHH3 and Ki67 immunohistochemistry.
Results: We observed significant increases in aneuploidy with advancing tumor stage ($p<0.05$). Chromosomes X, 21, Y, 14, 16, and 8 were most frequently numerically altered. Increased levels of proliferation were significantly associated with the extent of aneuploidy and tumor stage ($p<0.01$). Combining aneusomy of chromosomes 4, 6, 20, and X with PHH3 immunoreactivity resulted in a prediction model for lymph node metastases with a sensitivity of 73.3 % and a specificity of 72.6 %.
Conclusion: We present evidence that genomic instability leading to aneuploidy is an important factor in PCa progression. Furthermore, we demonstrate that increased Ki-67 and PHH3 expression are potential indicators of metastatic disease. Lastly, we suggest a new approach to preoperatively determine lymph node metastasized disease in PCa.

OFP-20-002

ERG protein expression and genomic rearrangement status in primary and metastatic prostate cancer: A comparative study of two monoclonal antibodies

M. Braun*, D. Goltz, Z. Shaikhibrahim, W. Vogel, D. Boehm, A. Dobi, N. Wernert, G. Kristiansen, S. Perner
*Universitätsklinik Bonn, Inst. für Pathologie, Germany

Objective: Overexpression of the ERG protein is highly prevalent in prostate cancer (PCa) and most commonly results from gene fusions involving the ERG gene. Recently, an N-terminal epitope targeted mouse and a C-terminal epitope targeted rabbit monoclonal anti-ERG antibody have been introduced for the detection of the ERG protein. Here, we are the first to compare the mouse ERG-MAb to the rabbit ERG-MAb for their concordance on the same PCa cohort. Furthermore, we assessed if the ERG protein expression is conserved in lymph node and distant metastases.
Method: We evaluated tissue microarrays of 278 specimens containing 265 localized PCa, 29 lymph node, 30 distant metastases, and 13 normal prostatic tissues. We correlated the ERG protein expression with the ERG rearrangement status using an ERG break-apart fluorescence in-situ hybridization (FISH) assay and IHC of both ERG antibodies.
Results: ERG protein expression and ERG rearrangement status were highly concordant regardless of whether the mouse or rabbit ERG-MAb was used (97.8 % versus 98.6 %, respectively).
Conclusion: This is the first study to comprehensively compare the two ERG-MAbs. By demonstrating a broad applicability of IHC to study ERG protein expression using either antibody, this study adds an important step towards a facilitated routine clinical application.

OFP-20-003

Improved method of detecting the ERG gene rearrangement in prostate cancer using combined dual-color chromogenic and silver in-situ hybridization

M. Braun*, J. Stomper, D. Boehm, W. Vogel, N. Wernert, G. Kristiansen, S. Perner
*Universitätsklinik Bonn, Inst. für Pathologie, Germany

Objective: The recently detected ERG rearrangement revealed as a recurrent and prevalent prostate cancer (PCa) specific event. To detect this alteration, FISH is the method of choice. However, FISH harbors disadvantages for widespread adoption in clinical practice. Subsequently, the

chromogenic in-situ hybridization (CISH) and the enzymatic metallography silver in-situ hybridization (SISH) emerged as promising bright-field alternatives. We aimed to develop a combined CISH and SISH (CS-ISH) gene break-apart assay on the example of the ERG gene.
Method: We assessed and compared 178 PCa and 10 benign specimens for their ERG rearrangement status applying a dual-colour FISH and CS-ISH ERG break-apart assay on consecutive sections.
Results: We observed a highly significant concordance (97,7 %) between FISH-based and CS-ISH-based results (Pearson's correlation coefficient 0.955, $P<0.001$).
Conclusion: We demonstrate that the ERG rearrangement status can reliably be assesed by CS-ISH. Further, we confirm that the CS-ISH technique combines the accuracy and precision of FISH with the ease of bright field microscopy. We developed a tool which allows a broad spectrum of applicants to study the biological role and clinical utilization of ERG rearrangements in PCa. Moreoever, our study is the first proof-of-principle for bright-field CS-ISH gene fusion or break-apart assays.

OFP-20-004
Rearrangement of the ETS genes ETV-1, ETV-4, ETV-5 and ELK-1 is a clonal event during prostate cancer progression
M. Braun*, Z. Shaikhibrahim, W. Vogel, D. Boehm, R. Menon, N. Wernert, G. Kristiansen, S. Perner
*Universitätsklinik Bonn, Inst. für Pathologie, Germany

Objective: ETS gene rearrangements are frequently found in prostate cancer (PCa). Recently, we observed that ERG rearrangement in primary PCa transfers into lymph node metastases, suggesting it to be a clonal expansion event during PCa progression. Here, we investigated whether this also applies to the less frequent ETS genes, ETV-1, ETV-4, ETV-5 and ELK-4.
Method: Using break-apart FISH assays, we evaluated the status of above mentioned ETS gene rearrangements on a cohort comprising of primary PCa, corresponding lymph node and distant metastases.
Results: ETV-1, ETV-4, ETV-5 and ELK-4 rearrangements were found in 10 %, 6 %, 1 % and 2 % of the primary PCa, respectively, and in 8 %, 6 %, 6 %, 1 % of the corresponding lymph node metastases, respectively. Rearrangements of ETV-1 and ETV-5 were not found in any of the distant metastases cases, whereas ETV-4 and ELK-4 rearrangements were found in 4 % and 4 % of the distant metastases, respectively.
Conclusion: Our results suggest that rearrangement of the less frequent ETS genes is a clonal event during prostate cancer progression. Our findings provide insights into potential clonal expansion events during PCa progression and may have significant implications in understanding the molecular basis of the metastatic cascade of PCa.

OFP-20-005
Comparative analysis of two prostate biopsy systems: A study of 120 cases
F. E. Costa*, R. Dias, J. R. Vizcaíno
*Centro Hospitalar do Porto, Braga, Portugal

Objective: It's expectable that the higher the number of prostate biopsies the greater the probability of prostate cancer detection, presumably improving the diagnostic accuracy and treatment decision.
Method: Under this assumption, since May/2010, Santo António's Hospital implemented a prostate mapping system, increasing the number of biopsies performed from 8–12 to 16–18 and processing each core independently. We intend to establish a comparison between the traditional prostate biopsy system (TS) and the prostate mapping system (MS). For this study, all biopsy slides and corresponding surgical specimens from 60 patients subjected to MS and 60 patients subjected to TS were reviewed. Gleason score, percentage of tumor present in prostatic tissue (expressed as small $\leq$ 5 %, medium 6–19 % and large $\geq$20 %) and presence of tumor in prostate apex and base were analyzed.
Results: Comparing MS with TS, the correlation coefficient was 53,5 % and 31,9 % for Gleason score and 46,9 % and 37,4 % for the percentage of tumor present in prostatic tissue, respectively. Mapped biopsies were able to detect the tumor in the apex and base in 72 % and 80 % of cases.
Conclusion: These results suggest that prostate MS improves the diagnostic accuracy of prostate cancer and has a good ability to predict the presence of tumor in prostate apex and base.

OFP-20-006
Frequency and prognostic significance of TMPRSS2-ERG gene fusion in lymph node positive prostate cancers
A. Fleischmann*, I. Zlobec, T. Visakorpi, G. Thalmann
*Universität Bern, Inst. für Pathologie, Switzerland

Objective: TMPRSS2-ERG incidence and prognostic significance in lymph node positive prostate cancer are virtually unknown.
Method: A tissue-microarray was constructed from 119 hormone-naïve nodal positive, surgically treated prostate cancers containing samples from all Gleason patterns (GP) present in every primary tumor (PT) and corresponding lymph node metastases (MET). TMPRSS2-ERG status was determined by fluorescence in-situ hybridization and correlated with various histomorphological tumor features (Gleason score, stage, cancer volume, nodal tumor burden) and biochemical recurrence-free, cancer-specific and overall survival.
Results: TMPRSS2-ERG fusion was present in 43.5 % (homogeneous 25.2 %, heterogeneous 18.3 %) of the PT and in 29.9 % (homogeneous 28.7 %, heterogeneous 1.2 %) of the MET. Percentage of TMPRSS2-ERG in GP3/4/5 of PT and

MET were: 38 %/37 %/24 % and 23 %/30 %/39 %. Concordance in TMPRSS2-ERG status between PT and MET was poor (Kappa 0.39) showing 20.9 % and 8.1 % of cancers with gene fusion solely in the PT and MET, respectively. TMPRSS2-ERG fusion was not correlated with histopathological tumor features and predicted late biochemical recurrence independently (p=0.041) when present in PT.

Conclusion: TMPRSS2-ERG fusion in PT is more frequent and its distribution more heterogeneous compared to MET. The gene fusion in primary tumors independently predicts late biochemical recurrence.

OFP-20-007

WNT and SHH pathways activation in penile carcinoma

A. Silva*, T. Almeida, F. Soares, M. Buim
*Hospital AC Camargo, Investigative Pathology, São Paulo, Brazil

Objective: Penile carcinoma (PC) is rare in developed countries, accounting for less than 1 % of all neoplasms in men, and biological characteristics of this tumor are poorly known. WNT and SHH pathways are important for cell proliferation, differentiation and survival, and therefore, play a role in carcinogenesis of various organs. The goal of this study is to investigate the expression profile of WNT and SHH pathway proteins in PC, characterizing the expression of target proteins from WNT (Wnt-1, Wnt-2, Wnt-2 Gsk3β, β-catenin, D1 Cyclin, MMP7, C-myc, CD44) and SHH (Shh, Smo, Gli, EGFR) pathways.

Method: For that, 18 samples of PC were obtained from the files of Anatomic Pathology department from A.C. Camargo Hospital (Brazil) and submitted to immunohistochemistry.

Results: We observed that Wnt-1 and Wnt-2 were expressed in 15 and 16 cases, respectively, out of the 18 evaluated samples. Strong Shh expression was detected in 16/18 cases, whereas weak and negative expression was seen only in one case each. Smo and Gli-1 proteins were expressed in almost all cases (17/18), and also D1 Cyclin, b-catenin and EGFR were frequently expressed.

Conclusion: These preliminary results suggest that WNT and SHH pathways may be active and participating in the progression of penile cancer.

OFP-20-008

Expression of the multidrug resistance protein 4 correlates with longer PSA relapse free survival and androgen receptor and forkhead box A protein expression in prostate cancer

M. Montani*, G. Kristiansen
*Medizin. Universität Bern, Inst. für Pathologie, Switzerland

Objective: Multidrug resistance protein 4 (MRP4) a transmembranary transport protein has shown to be expressed in prostate cancer cell lines and cancer cell specimens and turned out to be among the highest upregulated genes in an array-based transcription analysis. Its expression is regulated in an androgen dependent manner, possibly modulated by forkhead box A (FoxA), an androgen receptor (AR) co-activator. Therefore, we investigated its expression in a large cohort of neoplastic and non-neoplastic prostate tissues (n=441) and evaluated its prediction of PSA relapse free survival (RFS).

Method: TMA (n=441) stained for MRP4, FoxA, AR, ER, PSA, Ki-67: radical prostatectomies (RPE) (n=332), castrate resistant prostate cancer (CRPC) (n=26), metastases (n=39) and non-neoplastic (n=187). PSA-RFS of 258 patients; mean 70 months.

Results: MRP4 expression decreases with tumor progression into castrate resistant disease, correlates with PSA, AR and FoxA expression and inversely correlates with Gleason score. Moreover, a strong MRP4 expression is significantly associated with a longer PSA RFS in RPE patients. Normal tissues from the transitional zone show a weak MRP4 expression compared to the peripheral and central zones.

Conclusion: MRP4 expression seems to predict PSA relapse free survival in prostate cancer patients. Since its expression is androgen dependent it decreases with tumor progression into CRPC.

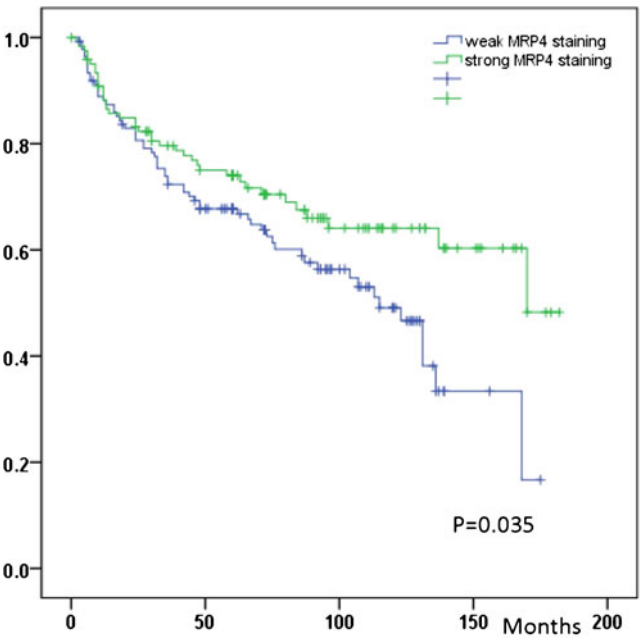

OFP-20-009

Synchronous Angiomyolipoma and renal tumors in patients without Tuberous Sclerosis: Clinico-pathological study of 18 cases

F. J. Queipo*, R. A. Carías, Án. F. Panizo, M. L. Gómez-Dorronsoro, F. J. Pardo
*Clínica Universidad de Navarra, Pathology, Pamplona, Spain

Objective: Simultaneous existence of AML and renal neoplasia is frequent in Tuberous Sclerosis (TS) patients, but uncommon in non-TS cases.
Method: A total of 18 cases of coexistent renal neoplasia and AML in non-TS patients were identified. Clinico-pathological features were studied.
Results: 18 patients: 10 M/8 F (mean age 62,77 year; range: 35–83). Mean AML size: 0,82 cm (range: 0,2–3,4). The main size of the renal neoplasms was 5,09 cm (range 1,2–15). AML morphology: 6 leiomyomatous, 4 classic-triphasic, 4 lipomatous, and 4 epithelioid. Three cases had multifocal AML. 15 cases had ipsilateral tumors associated with AML: 6 CCRCC (1 sarcomatoid), 4 ChRCC, 1 RO, 1 TFE3 RCC, 1 hybrid (RO-ChRCC) renal-cell tumor, 1 urothelial carcinoma, and 1 case had 2 tumors: MTSC-RCC and concomitant PRCC. 2 cases had contralateral tumours associated with AML: 1 ChRCC and 1 RO. One patient had bilateral tumors associated with AML: an ipsilateral RO and a contralateral CCRCC. The median follow-up was 36,85 mths (range 0,4–199,8): all patients were alive without disease.
Conclusion: The coexistence of renal tumors with AML is a rare event, usually incidental. If AML is found incidentally together with other renal tumors, it is important to exclude TS retrospectively.

OFP-20-010

Primary renal synovial sarcoma: A clinicopathologic, immunohistochemical and molecular genetic study of 16 cases

J. Schoolmeester*, J. Cheville, A. Folpe
*Mayo Clinic, Dept. of Anatomic Pathology, Rochester, MN, USA

Objective: Primary renal synovial sarcoma (R-SS) is a rare malignant neoplasm. Approximately 45 cases have been described, chiefly as case reports or as part of relatively limited small studies. We studied the clinicopathological, immunohistochemical (IHC) and molecular genetic features of 16 well-characterized R-SS.
Method: All available slides for 16 institutional and consultation cases of R-SS were reviewed. An IHC panel (TLE1, BCL2, cytokeratins, S100, CD34, INI1) was performed. RT-PCR for SS18-SSX1/2 or FISH for SS18 rearrangement was performed. Follow-up was obtained.
Results: The patients (9 M, 7 F) ranged from 17 to 78 years (mean 46). All tumors were of monophasic fibrous type. IHC results: all cases were strongly positive for TLE1 and BCL2; focally positive or negative for cytokeratins; negative for S100 and CD34; and showed retained INI1 expression. Molecular genetic results were: SS18-SSX1 (5 cases), SS18-SSX2 (10 cases), SYT rearrangement (1 case). Follow-up (5 cases): 3 dead of disease, 2 alive without disease.
Conclusion: Our data show a striking overrepresentation of the SS18-SSX2 fusion subtype among R-SS, in contrast to other SS, in which the SS18-SSX1 fusion subtype accounts for two-thirds of cases. The reasons for this difference are unclear. The prognosis for R-SS appears similar to that of SS of more common locations.

Poster Sessions

Sunday, 9 September 2012, 09.30 - 10.30, Congress Hall Foyer 3rd Floor
PS-01 Poster Session Pulmonary Pathology

PS-01-001

Histological and immunohistochemical study of lung carcinomas from the files of the Institute of Pathology of Medical Faculty of the P.J. Safarik University in Kosice (2007–2011)

A. Boor*, I. Jurkovic, K. Dudrikova, L. Babjakova, A. Mikulakova, E. Stammova, P. Kocan, J. Belak, L. Slavik, V. Zak
*Medical Faculty of UPJS, Dept. of Pathology, Kosice, Slovakia

Objective: New data related to the diagnosis and therapy of lung cancer have also affected the position of the pathologist in this area. Principal changes in its classification have appeared in relation to adenocarcinoma and partly also in the large cell type of lung cancer.
Method: Presented data represent a five-year retrospective study of a series of 546 cases of lung cancers analyzed in our Institute. Besides routine HE staining the following immunohistochemical reactions were used: antibody against TTF-1, Surfactant A, Chromogranin, Synaptophysin, CK7, AE1/AE3, p63, 34βE12, CD56 and Napsin A.
Results: Using the WHO, 2004 Classification of Lung Cancer, an unusual phenomenon of the return of squamous cell cancer (SCC) prevalence over adenocarcinoma has been documented, which in the earlier years has equated the SCC. The difference in obtaining the tissue samples, and changes in the geographical origin of certain patients of Eastern Slovakia may partly explain these differences. Though the new Travis classification (J Thorac Oncol, 2011) was not used, there prevailed mixed forms also in our series.
Conclusion: It is important to respect new information regarding the Classification of Lung Cancer, especially in the category of adenocarcinoma. The constructive collaboration of pathologists with clinicians is recommended.

PS-01-002

An exceptional coexistence of MALT lymphoma and carcinoid tumor in the lung

E. Braham*, E. Boudabbous, M. Zarrouk, A. Marghli, M. Mlika, A. Ayadi Kaddour, O. Ismail, M. Yahia, T. Kilani, F. El-Mezni
*Abderrahmen Mami Hospital, Dept. of Pathology, Ariana, Tunisia

Objective: Extranodal marginal zone lymphoma MALT lymphoma and carcinoid are neoplasms occurring most frequently in the gastrointestinal tract and respiratory system. Although each of them occurs relatively frequently and separately, the simultaneous appearance of these two neoplasms is exceptionally rare.
Method: We report an exceptional synchronous association of MALT lymphoma and typical carcinoid in the lung.
Results: A 52-year-old male with Sjögren's syndrome presented with cough and chest pain with no improvement after antibiotherapy. Bronchial fibroscopy was normal. Computed tomography showed a diffuse interstitial pneumopathy with a persistent left lower lobe nodule suspected of malignancy. A surgical resection of the nodule was achieved. Histopathologically, it measuring 1.2 cm in diameter and was composed of association of malt lymphoma and typical carcinoid tumor which were focally admixed. Immunohistochemical stains were strongly reactive to endocrine marker in carcinomatous component. Tumor cells were diffusely CD20 positive in lymphomatous component. Assessment of extent of lymphoma revealed a gastric location. The patient received chemoptherapy. He's still alive since 8 months.
Conclusion: The best of our knowledge, this is the first report of such a collision lung tumor at the same anatomical site. The aim of this study is to describe the pathogenesis and clincicopathological feartures of such exceptional association.

PS-01-003

Primary mucoepidermoid carcinoma of lung: Clinicopathological analysis of 15 cases

E. Braham*, E. Boudabbous, M. Yahia, H. Ben Rejeb, M. Mlika, A. Ayadi Kaddour, O. Ismail, T. Kilani, F. El-Mezni
*Abderrahmen Mami Hospital, Dept. of Pathology, Ariana, Tunisia

Objective: Primary mucoepidermoid carcinoma is rare comprise less than 1 % of all lung tumors. It is characterized by the presence of squamoid cells, mucin-secreting cells and intermediate type. On the basis of morphological and cytological features, it is divided into low and high-grade types.
Method: We report a retrospective study of 15 cases diagnosed during a 15-year period. Diagnosis was made by histological examination of specimen obtained from lobectomy in 13 cases and pneumonectomy in 2 cases. No patient had history of salivary mucoepidermoid carcinoma.
Results: There were 13 men and 2 women ranging in age from 10 to 76 years. Computed tomography showed a well circumscribed tumor arising in bronchus in all cases. A bronchial fibroscopy showed a main, lobar or segmental mass. Bronchial biopsy revealed a non-small-cell carcinoma in only one case. Histologically, tumors were classified into 7 low grade mucoepidermoid carcinoma and 8 high grade mucoepidermoid carcinoma. Patients with low grade carcinoma remain alive after surgery alone. Patients with high grade carcinoma received chemotherapy, four of them developed distance metastasis.
Conclusion: Mucoepidermoid carcinoma is a rare primary malignancy of the tracheobronchial tree which is difficult to diagnose by limited biopsy. The prognosis is variable and depends upon the histological grade.

PS-01-004

Primary pulmonary marginal zone B-cell lymphoma of mucosa-associated lymphoid tissue: Clinicopathological analysis of 6 cases

E. Braham*, E. Boudabbous, S. Aouadi, A. Ayadi Kaddour, M. Mlika, O. Ismail, M. Yahia, I. Drira, T. Kilani, F. El-Mezni
*Abderrahmen Mami Hospital, Dept. of Pathology, Ariana, Tunisia

Objective: Primary pulmonary MALT lymphoma is considered to originate from MALT of the bronchus secondary to autoimmune or inflammatory processes. Although, it comprises more than two-thirds of all primary non-Hodgkin's lymphoma of the lungs, it is a rare entity and accounts for less than 1 % of all lymphomas.
Method: We report a retrospective study of 6 cases of Malt pulmonary lymphomas diagnosed during an 8-year period. Diagnosis was made on surgical pulmonary biopsy in 2 cases, bronchial biopsy in 3 other cases and on lobectomy in one case.
Results: There were 4 women and 2 men ranging in age from 48 to 74 years. Two patients had a history of Sjoren's syndrome and one had a history of previous mammary carcinoma. Computed tomography revealed bilateral nodules in 3 patients, lung mass in 2 patients and an area of consolidation in one patient. Fiberoptic bronchoscopy showed bronchial stenosis in only 3 cases. Morphologically, the neoplasms had features typical of MALT lymphoma. One patient was treated with surgery alone and 5 received chemotherapy. Five patients remained alive while one patient presented with recurrence.
Conclusion: Pulmonary MALT lymphomas are characterized by an important dissociation between clinical expression and radiological pattern. Therefore, histological documentation is mandatory to ensure diagnosis.

PS-01-005

Expression of Carbonic Anhydrase IX in malignant mesothelioma

L. Capkova*, R. Kodet
*University Hospital Motol, Pathology and Molecular Med., Prague, Czech Republic

Objective: Malignant mesothelioma (MM) is an aggressive tumour with a poor prognosis. Carbonic anhydrases and their inhibitors offer an opportunity for developing novel anticancer drugs, as well as diagnostic and prognostic tools. Carbonic anhydrase IX (CAIX) is a membranous metalloenzyme involved in cell adhesion and pH homeostasis. It is a direct target of hypoxia-inducible factor and serves as a marker of hypoxia. This study was designed to assess systematically CAIX expression in MM of pleura and peritoneum, and their benign counterparts.
Method: 47 MMs of pleura (41 epithelioid, 1 biphasic, 2 sarcomatoid) and peritoneum (3 epithelioid), and 14 normal or reactive pleural samples were analyzed. CAIX expression was determined using immunohistochemistry. Membranous immunoreactivity was evaluated semiquantitatively. Specimens were divided into five subgroups according to the staining pattern and intensity.
Results: 95,7 % (45/47) of MMs expressed CAIX. All epithelioid mesotheliomas showed at least a weak focal (8,5 %, 4/47), but predominantly a strong diffuse (70,2 %, 33/47) staining with CAIX antibody, without any perinecrotic pattern. Sarcomatoid mesotheliomas were negative. Normal mesothelial cells were diffusely positive.
Conclusion: These data suggest that mechanisms of CAIX overexpression in MM are different than due to hypoxia and appear promising in prospective use of specific therapeutic CAIX targeting in advanced mesothelioma.

PS-01-006

ALK expression in pulmonary adenocarcinomas

L. Carvalho*, A. Alarcão, A. F. Ladeirinha, M. Reis Silva, M. J. d'Aguiar, T. Ferreira, V. Sousa
*Amadora, Portugal

Objective: EML4-ALK crizotinib therapy needs validation at lower cost and rapid answer in Pathology routine.
Method: Histological/WHO 2004 and CK7, TTF1, CK5.6, CD56/chromogranin and vimentin panel classifications with ALK (clone 5A4, Novocastra Laboratories Ltd, Newcastle, United Kingdom) were applied to paraffin sections of 35 bronchial-pulmonary carcinomas: 20 adenocarcinomas, 6 epidermoid carcinomas, 4 pleomorphic carcinomas (mixed type adenocarcinomas with large/giant/fusiform cells), 4 neuroendocrine carcinomas (NEC) (1 combined large cell NEC with adenocarcinoma and 2 with epidermoid carcinomas; 1 SCLC chromogranin positive combined with adenocarcinoma) and 1 adenosquamous carcinoma.
Results: The applied antibodies specified bronchial pulmonary carcinomas subtypes clearly. In 3 over 60 years old non-smoking females mixed type adenocarcinomas ALK expression was over 50 %: acinar, solid, micropapillary and microacinar patterns; one glandular mucinous pattern (mucinous BA pattern) and one BA pattern, all expressing TTF-1.
Conclusion: In this study, 3/20 adenocarcinomas of older women had ALK protein expression, only one with a mucinous pattern. As protein positivity cases comprise a lower number, FISH described by S. Lantuejoul seems to be the most appropriate method. It is now necessary to decide whether KRAS and EGFR mutations have to be determined together and/or select TTF-1 positive adenocarcinomas (from terminal respiratory unit) raised by this approach.

PS-01-007

Pet activity for bronchial-pulmonary carcinomas and adenocarcinomas subtyping

L. Carvalho*, J. A. Dias, A. F. Ladeirinha, V. Sousa, M. Reis Silva, M. J. D'Aguiar, T. Ferreira, A. Alarcão
*Amadora, Portugal

Objective: The 5 year survival of bronchial-pulmonary carcinomas remains poor, between 6 % and 14 %/men and 7 % to 18 %/women. Treatment orientation is influenced by clinical staging and morphological classification in biopsies of 70 % of the cases.
Method: This study comprised 41 surgical specimens where we compared immunohistochemistry in-between Adenocarcinomas (18), Epidermoid Carcinomas (12) and the heterogeneous groups of Large Cell Neuroendocrine Carcinoma (3), Small Cell Lung Cancer (1), Large Cell Carcinoma (2), Adenosquamous Carcinoma (2) and Pleomorphic Carcinomas (3) with Max 18 F-Fluordesoxiglucose (FDG), a clinical parameter based in PET to preview diagnosis and prognosis.
Results: We found significant differences ($p=0.028$) between TTF-1 positive and negative Adenocarcinomas where the 18 F-FDG capture was lower in TTF-1 positive cases, indicating lower metabolic activity. TTF-1 negative Adenocarcinomas have similar and higher metabolic activity as Epidermoid Carcinomas. The other histological types have FDG capture similar in between the two defined groups.
Conclusion: Immunohistochemical and 18 F-FDG analysis correlate with clinical differences between Adenocarcinomas and Epidermoid Carcinomas, where TTF-1 negative Adenocarcinomas are biologically similar to Epidermoid Carcinomas, requiring a different medical approach as well as molecular pathology particular interpretation. These results strain the classification of bronchial TTF-1 negative Adenocarcinomas because they are different from the terminal respiratory unit TTF-1 positive Adenocarcinomas.

PS-01-009

Influence of microorganisms on activation of monocytes in bacterial pneumonias

A. Dorosevich*, R. Zibirov, D. Kozlov, O. Krechikova, N. Ivanchik
*Smolensk Institute of Pathology, Russia

Objective: According to researchers pneumonias are characterized by increase number of alveolar macrophages population after increased migration of monocytes from bone marrow and blood into the alveolar space.
Method: We examined 60 observations of pneumonia with bacteriological, histological and blood monocytes examination in all cases. Bacteriological study was performed at the Institute of antimicrobial chemotherapy. Histological examination was performed in the Smolensk regional institute of pathology.
Results: In the foci of pneumonias we discovered mainly mixed gram positive and gram negative microorganisms. Ten observations were characterized by an increase in the absolute number of blood monocytes. Fifty observations did not reveal excess levels of blood monocytes. In all cases with an increase in the number of blood monocytes, gram negative bacteria were isolated. In cases with normal number of blood monocytes some of the microorganisms were gram positive.
Conclusion: Gram negative bacteria result in activation of the monocytes and their entry from the bone marrow into the blood more than gram positive bacteria.

PS-01-010

Carcinoid and schwannoma in lung: Two cases

H. Erdem*, M. Oktay, A. K. Uzunlar, L. Yilmaz Aydin, A. N. Annakaya, U. Yildirim, C. Sahiner
*Duzce University, Dept. of Pathology, Turkey

Objective: Bronchial carcinoids and schwannomas are uncommon, slowly growing, low-grade neoplasms. Carcinoid tumors are thought to arise from neuroendocrine/Kulchitsky's cells of bronchial epithelium. Schwannomas are thought to originate from schwann cells. Clinically they may be asymptomatic or present with non resolving recurrent pneumonia, hemoptysis, respiratory distress.
Conclusion: We present two cases of respiratory distress in two teenage patients.

PS-01-011

Pulmonary hamartomas mimicking metastatic carcinomas

H. Erdem*, L. Yilmaz Aydin, A. K. Uzunlat, M. Oktay, A. N. Annakaya, U. Yilderim, F. Basar
*Duzce University, Dept. of Pathology, Turkey

Pulmonary hamartomas are usually found incidentally and they mimick metastic tumours. We report a case of a 47 year-old man who admitted to Chest Disease service for cough. He had laryngectomy operation formerly and diagnosed as squamous cell carcinoma. Chest-X-ray and computed tomography revealed pulmonary nodules. It was removed but there was not metastatic carcinomas. This case was presented because it can be difficult to make diagnosis when the patient has malignancy.

PS-01-012

Collagen V is modulated by IL-17 in late stage of experimental pulmonary fibrosis: A possible new pathway of fibrosis

A. T. Fabro*, M. S. de Almeida, I. O. Minatel, E. d. Costa Prando, C. A. Rainho, W. R. Teodoro, E. R. Parra Cuentas, H. Popper, V. L. Capelozzi
*FMB - UNESP, Dpto. di Patologia, Botucatu, Brazil

Objective: Experimental models of pulmonary fibrosis (PF) has been proposed and its later phase tend to the resolution in different degrees depending on the drug/strain/inflammatory-pattern. Thus the maintenance of these mechanisms may participate in the PF-progression. Our objective was to determine the immune-fibrotic-pattern in models of pulmonary fibrosis in the late stage (21d).
Method: Distinct animal models were used, including Balb/c, C57BL/6 and IL17RA-KO-C57BL/6 mice by Bleomycin and Paraquat. We analyzed the amounts of total peribronchiolar-interstitial collagen (TPC-TIP) by picrosirius and Col3-Col5 by immunofluorescence through the morphometric evaluation. These data were validated by RT-PCR.
Results: The TPC did not differ between the treated groups. TIC was higher in the C57BL/6 strain, independent of the absence of IL-17RA. The Col5-immunoexpression was higher in control and BLM-treated IL17RA-KO-C57BL/6 than in wild-mice and lower in BLM-Balb/c mice. The Col3immunoexpression was higher in BLM-Balb/c. Likewise, the Col5 gene expression was higher in the IL17RA-KO mice and lower in the BLM-Balb/c.
Conclusion: The perpetuation of fibrosis in PF-susceptible-mice can be modulated by IL-17-dependent Col5-hiperexpression and by Col3-subexpression. This suggests that Col5 is an important component responsible for the development of PF.

PS-01-013

The prognostic role of Filamin A protein expression in patients with non-small-cell lung cancer

M. Gachechiladze*, J. Skarda
*Palacky University, Pathology, Olomouc, Czech Republic

Objective: An actin-binding protein Filamin A (FLNA) serves as a scaffold in various signaling pathways. Recently, it has been reported that FLNA interacts with BRCA1 protein and is required for efficient regulation of early stages of DNA repair processes. As DNA repair proteins are important prognostic markers for non-small-cell lung cancer (NSCLC) patients, we aimed to investigate the role of FLNA protein expression in NSCLC, as well as its correlation with BRCA1 protein expression.
Method: We performed a preliminary study of FNLA and BRCA1 protein expression in 50 NSCLC patients. Formalin-fixed paraffin-embedded tissue sections were stained by immunohistochemistry using antibodies against FLNA C-terminus (EP2405Y, LSBio), BRCA1 N-termunus (MS110) and against phosphorilated forms of BRCA1 at ser1524 and ser1423 (Abcam). Staining intensity was estimated semi-quantitatively and correlated with all available clinico-pathological factors.
Results: FLNA expression was significantly higher in cancer, compared to normal lung tissue. Positive correlation has been revealed between FLNA and BRCA1 phospho-ser1423 expression. Also, 5 year overall survival rate was higher in patients with strong FLNA expression.
Conclusion: According to our preliminary study results the prognostic role of FLNA protein expression deserves to be a subject for further studies in patients with NSCLC.

PS-01-014

Pulmonary nodular lymphoid hyperplasia ("pulmonary pseudolymphoma") – The significance of increased numbers of IgG4 positive plasma cells

D. Guinee*, A. Gerbino, S. Murakami, M. Koss
*Virginia Mason Medical Center, Pathology, Seattle, USA

Objective: Pseudolymphomas of the skin, breast, and lacrimal glands show an increase in IgG4 positive plasma cells. We hypothesized that a similar increase in IgG4 positive plasma cells occurs in pulmonary nodular lymphoid hyperplasia (PNLH).
Method: Immunohistochemical stains for IgG4 and IgG were performed in 2 cases of PNLH, 7 cases of BALT lymphoma, 8 cases of intraparenchymal lymph nodes (IPL) and 1 case of follicular bronchiolitis (FB). The mean number of IgG4- and IgG- positive plasma cells and the IgG4/IgG ratio was obtained from a manual count of three separate high power fields (hpfs) of areas of highest cellularity.
Results: The average number of IgG4 positive plasma cells and the IgG4/IgG ratio was increased in PNLH (case 1: 225/hpf, ratio: 0.39, case 2: 280/hpf, ratio: 0.59). In comparison, average IgG4 positive plasma cells per hpf were much lower in BALT lymphoma (range=0–2.3/hpf, ratio=0–0.03), IPL (range IgG4/hpf=0–102, ratio=0–0.23) and FB (1/hpf, ratio=0.03).
Conclusion: The increase in IgG4 positive plasma cells and IgG4/IgG ratio in PNLH aids in diagnosis and supports our current understanding of PNLH as a distinct form of reactive lymphoid proliferation. The relationship between PNLH and IgG4-related sclerosing disease requires further study.

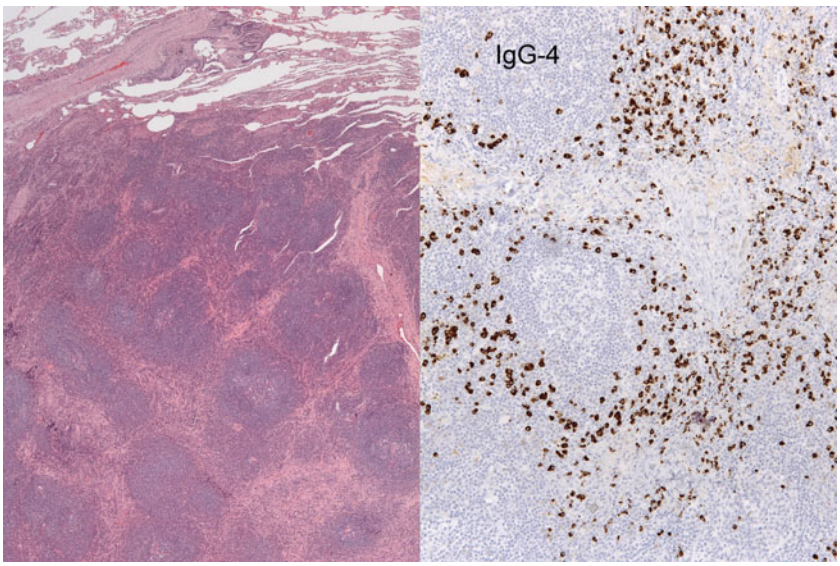

PS-01-015

Calretinin, CK5/6, TTF-1, CEA, Ber-EP4, and CD15: A useful combination of immunohistochemical markers for differentiating pleural mesothelioma from pulmonary adenocarcinoma

N. Gursan*, M. Calik, E. Demirci, S. Sipal, B. Gundogdu, C. Gundogdu
*Ataturk University, Medical Faculty, Erzurum, Turkey

Objective: The distinction between pleural epithelial mesothelioma and peripheral lung adenocarcinoma involving the pleura is still an important diagnostic problem for surgical pathologists. The aim of our study was to identify the most specific and sensitive markers for the positive identification of mesothelioma.
Method: Paraffin-embedded blocks from surgical material of 19 pleural epithelial mesotheliomas and 22 pulmonary adenocarcinomas were retrieved from the files in our department. The primary antibodies used in each case were the following: antibody anticalretinin, EMA; CEA, BerEP4, TTF-1 and CD15.
Results: Of the mesotheliomas, 100 % stained for calretinin, 63.2 % for CK5/6, 78.9 % stained for EMA and AE1/AE3. Of the lung adenocarcinomas, 9.1 % cases showed reactivity for calretinin, 27.3 % for CK5/6, 77.3 % for CD 15, all for TTF-1, 50 % for CEA, 59.1 % for Ber-EP4, 90.1 % for EMA, and all for AE1/AE3.
Conclusion: Calretinin were the highly specific positive mesothelial markers, whereas CK 5/6 showed high sensitivity but low specificity. Among negative markers, we advocate the use of TTF-1, CEA and CD15 which were the most specific in differentiating mesotheliomas from adenocarcinomas.

PS-01-016

Cyclooxygenase-2 expression in NSCLC

I. Kern*, E. Sodja, M. Rot
*University Clinic Golnik, Slovenia

Objective: Overexpression of COX-2 correlates with aggressive disease of NSCLC. Aim of our study was to determine the COX-2 expression levels by two methods.
Method: Analysis was done on 24 consecutive surgical specimens of NSCLC fixed in Paxgene tissue system. Relative quantification of COX-2 mRNA expression was performed by quantitative RT-PCR using intron-spanning primer-probe set. COX-2 protein expression was assessed by immunohistochemistry (IHC). Scoring was performed using an intensity-extent system, both parameters on the scale 0-3 and multiplied to give IHC index.
Results: There were 12 cases of adenocarcinoma, 11 cases of squamous cell carcinoma and one typical carcinoid. COX-2 mRNA expression was detectable in all specimens. The median COX-2 mRNA expression value, normalized against he internal reference gene GADPH, was 0,53 (range 0,08–12,49). We observed cytoplasmic and membranous immunohistochemical reaction patterns. Average IHC index was 3,8. There was positive correlation between mRNA and protein COX-2 expression (R2=0,31). Adenocarcinoma cases had average relative mRNA expression value 2,45 and IHC index 5,08, while squamous cell carcinoma had average relative mRNA expression value 0,67 and IHC index 2,73.
Conclusion: COX-2 is expressed in NSCLC with various IHC reaction patterns. Adenocarcinoma and squamous cell carcinoma have different COX-2 expression levels.

PS-01-017

Clinicopathological correlations of mTOR and pAkt expression in non-small cell lung cancer

H.-J. Kim*, M.-H. Oh, H.-J. Lee, S.-B. Yoo, X. Xu, J.-S. Choi, Y.-H. Kim, S.-Y. Lee, C.-T. Lee, S.-H. Jheon, J.-H. Chung
*Seoul National University Hospital, Dept. of Pathology, Republic of Korea

Objective: The Akt/mammalian target of rapamycin (mTOR) pathway is up-regulated in many human cancers, and agents targeting the mTOR pathway are in various stages of clinical development and application.
Method: Expression of pAkt and mTOR was studied by immunohistochemical analysis of 574 surgically resected non-small cell lung cancer (NSCLC) specimens on a tissue microarray (TMA).
Results: The results were correlated with clinicopathological features. Expression of mTOR showed a strong correlation with the expression of pAkt ($p<0.001$) and was significantly associated with female gender, tumor size ≤3 cm, adenocarcinoma (ADC), non-smoker status, and lower pathological stage. Expression of pAkt was correlated with older age (≥ 65), ADC, non-smoker status, and lower T stage. Univariate survival analysis revealed that the mTOR and pAkt positive group had a significantly longer cancer-specific survival than the mTOR and pAkt negative group ($p=0.038$ and $p=0.024$, respectively). Coexpression of pAkt and mTOR correlated with better prognosis than either single or double negative pAkt and mTOR groups ($p=0.016$). However, multivariate analysis proved that mTOR and pAkt expression are not independent prognostic factors for cancer-specific survival.
Conclusion: Expression of pAkt and mTOR expression is more significantly associated with ADC than squamous cell carcinoma (SCC) and expression of these proteins is associated with better prognosis.

PS-01-018

PAK 6 immunohistochemistry marker in non-small cell lung cancer (NSCLC)

A. Kucukosmanoglu*, O. D. İlara Colakkadıoglu, K. Bakir
*University of Gaziantep, Pathology, Turkey

Objective: PAK 6 is a member of P21-activated kinase family. Many human tumor express and activate this family. Because of their role in cell transformation, they become therapeutic targets. They have important roles in cell survival, cell proliferation and cell migration. They affect cell growth and tumor invasion.

Method: 175 cases with NSCLC reported in Gaziantep University Pathology Department between 2000 and 2010, reviewed retrospectively. Immunohistochemically nuclear and cytoplasmic PAK 6 stainings were considered positive and scored according to degree of staining.

Results: Our cases included 110 squamous cell carcinoma, 49 adenocarcinoma, 9 adeno squamous carcinoma and 7 large cell carcinoma. There was no significantly associated between tumor types and PAK6 staining. 38 of 175 patients showed recurrence and of 23 cases showed nuclear staining but there were no statistically significance (p:0,267). 31 cases died from the disease and in 21 of these cases nuclear stainig was very intresting, inspite of statistical results.

Conclusion: In this study PAK 6 staining patern and score were compared with tumor type, size, recurrence, mortality and lymph node involvement in NSCLC. And we found no statistically significance. 150 of 175 case with NSCLC stained with PAK 6. These results suggest that PAK 6 was expressed in lung like prostat, plasenta and breast.

PS-01-019

Pleural Fibroelastosis is a similar spectrum of Histopathology in Chronic Fibrosing Lung Disorders

L. Marcal*, E. R. Parra, L. Antonangelo, V. Capelozzi, F. Vargas, E. C. Nascimento, V. Teodoro, K. C. Silva
*Lia Junqueira Marçal, São Paulo, Brazil

Objective: Parenchymal fibroelastosis in chronic fibrosing lung disorders has been much investigated, but little attention has been directed at the visceral pleura (VP) participation in these situations. Our aim was to verify whether elastic deposition accompanies collagen deposition in the repairing process of chronic lung injury. In this work we studied the distribution of these fibrous components of VP in bullous disease type I and II, smoking-related interstitial fibrosis and usual interstitial pneumonia (UIP).

Method: We employed histochemical methods on conventional histological slides. We measured, by image analysis, the content of fibres of the collagenous and elastic systems of the visceral pleura in histological slides sampled from surgical lung biopsies and bullectomy, using the picrosirius-polarization method and Weigert's resorcin-fuchsin stain, respectively.

Results: Four groups were studied: I, 7 patients with spontaneous pneumothorax due to type I bullous disease; II, 12 patients with spontaneous pneumothorax due to type II bullous disease; III, 5 smoking-related interstitial fibrosis; and IV, 5 patients with idiopathic pulmonary fibrosis. The first two groups were used as controls. The content of fibers of the collagenous systems was similar in groups I (40.58± 15.95), II (40.71±15.86) and IV (40.99±13.99) when compared with group III (26.51±1.01).

Conclusion: A similar spectrum of histopathology was found in chronic fibrosing lung disorders.

PS-01-020

Autopsy: Undifferentiated tumor in men with type II Pneumocytes experimental transplantation

E. Mejía*, C. Hörndler Argarate, A. Puertas Cantería, D. S. Rosero Cuesta, M. Alastuey Aisa, J. Marroyo Laso
*H. Universitario Miguel Servet, Anatomía Patológica, Zaragoza, Spain

Patient diagnosed with Idiopathic pulmonary fibrosis (2009), in which experimental transplantation was performed of type II pneumocytes, ingress to the hospital for further study groundmass of the right lung. In the postmortem study a 2340 gr. mass was identified, the mass was formed by sarcomatous cells habit, undifferentiated and pleomorphic, with the presence of multiple implants and adhesions in rib cage, diaphragm, pericardial fat. IHC profile was performed: vimentin (+), EMA focally (+), WT1, CK8, TTF1, CKAE1/AE3, S100, CD34, CD31 and CD45 (−) and low proliferation index, the diagnosis undifferentiated malignant tumor. With inconclusive IHC profile, so blocks were sent to Clinic Barcelona Hospital, for study. The estimated prevalence of idiopathic pulmonary fibrosis is 20 cases per 100,000 population in men, with a mortality of 50 % at 5 years of diagnosis. Cancer rate of in transplanted patients is within the range between 4 % and 18 %. Could the appearance of this tumor be related either to transplanted pneumocytes or it is inmunosupression the main risk factor? Current treatments for idiopathic pulmonary fibrosis are not effective, which requires the study and development of new therapeutic options, using fibroblast proliferation inhibitors, as well as prospective studies, in the long term, the evolution of these patients and the development of secondary entities to it.

PS-01-021

Mediastinal hemangioma: A retrospective study about 5 cases

M. Mlika*, E. Boudabbous, A. Ayadi-Kaddour, M. Yahia, E. Braham, O. Ismail, F. El Mezni
*Abderrahman Mami Hospital, Dept. of Pathology, Tunis, Tunisia

Objective: Mediastinal hemangiomas are rare tumors accounting for 0,5 % of all mediastinal tumors. These tumors are challenging because of the lack of clinical and radiologic specific signs. Their diagnosis is mainly based on microscopic study.
Method: We report a 10-year-experience of a single institution. We describe 5 cases of mediastinal hemangioma.
Results: Our study contained 2 men and 3 women with a mean age of 60.4 years. Symptoms consisted mainly in chest pain. Neurologic signs were observed in 2 patients. Surgical treatment was performed in all patients dealing with a total resection in 4 patients. The most used surgical approach was a posterolateral thoracotomy. Video-assisted thoracic excision was tried in one patient and was converted into a median sternotomy. Microscopic examination concluded to a mediastinal hemangioma in all cases. All the patients presented no complications after a follow up periods varying from 9 months to 2 years.
Conclusion: Mediastinal hemangiomas are rare tumors whose diagnosis is based on microscopic findings. Their surgical management may be challenging because of their connection to the adjacent structures. Video-assisted thoracic excision is being more frequently used by experienced surgeons. These tumors are benign with a good behavior.

PS-01-022

Pulmonary actinomycosisa retrospective study about 6 cases

M. Mlika*, M. Yahia, A. Ayadi-Kaddour, E. Boudabbous, E. Braham, O. Ismail, F. El Mezni
*Abderrahman Mami Hospital, Dept. of Pathology, Tunis, Tunisia

Objective: Actinomycosis is an infectious disease caused by Actinomyce israeli in 85 % of the cases. It is mainly observed in alcoholic patients and affects mainly cervicofacial, abdominal and thoracic regions. Pulomnary actinomycosis accounts for 15 % of the localizations and is caused by the inhalation of septic particles causing granulomatous lesions, the extension to the adjacent organs and a cutaneous fistulae. It represents a real pitfall and mimics malignant lesions, tuberculosis or other infectious diseases.
Method: We report a retrospective study about 6 cases of pulmonary actinomycosis diagnosed over a 17-year-period.
Results: We describe the cases of 6 men aged between 35 and 46 years who presented with respiratory signs. Radiologic investigations showed in all cases parenchymal masses with irregular margins mimicking malignant processes. Positivie diagnosis was based on microscopic examination. The treatment was based on surgical excision associated to a medical treatment without complications after a follow up period ranging from 3 months to 18 months.
Conclusion: Pulmonary actinomycosis shares usually the same clinical and radiologic features as malignant lesions. Positive diagnosis is based on microscopic findings. It inducesusually surroundng organs and may affect, in some cases, the vital prognosis.

PS-01-023

Over expression of hyaluronan syntehase-2 activity has impact in the remodeling process and survival evolution in patients with idiopathic pulmonary fibrosis

E. Parra*, V. Capelozzi
*FMUSP, Dept. of Pathology, São Paulo, Brazil

Objective: The idiopathic pulmonary fibrosis (IPF) is a terminal illness characterized by unremitting extracellular matrix (ECM) deposition in the lung. In this regard, the myofibroblasts and the ECM components such as collagen and hyaluronan (HA) have an important role in the fibrosis. We analyzed the expression of HAS1 (HA synthase 1), HAS2, HAS3 and hyaluronic acid receptor (CD44) by epithelial and myofibroblasts cells in patients with IPF and we correlated with a survival.
Method: HAS-1, HAS2, HAS3 and CD44 epithelial and myofibroblast expression were evaluated in 27 surgical lung biopsies from patients with IPF in minimal and severe fibrosis by the point-counting technique. Impact of these markers was tested on pulmonary functional tests and follow-up until death from IPF.
Results: HAS2 and CD44 expression were significantly increased and directly associated with severe fibrosis. Myofibroblast HAS2 activity was indirectly associated to DLO/VA (r= −0.584; p=0.05). Kaplan Maier curves determined a higher risk of death for patient with high HA2 (>6.83 %) expression than in low expression (Log Rank p=0.05, Figure).
Conclusion: The increased HAS-2 activity in epithelial and myofibroblast cells have impact in the remodeling process and the survival evolution, suggesting that strategies aimed at preventing the effect of this ECM component may have a greater impact in patient's outcome. Financial Support: FAPESP, CNPq.

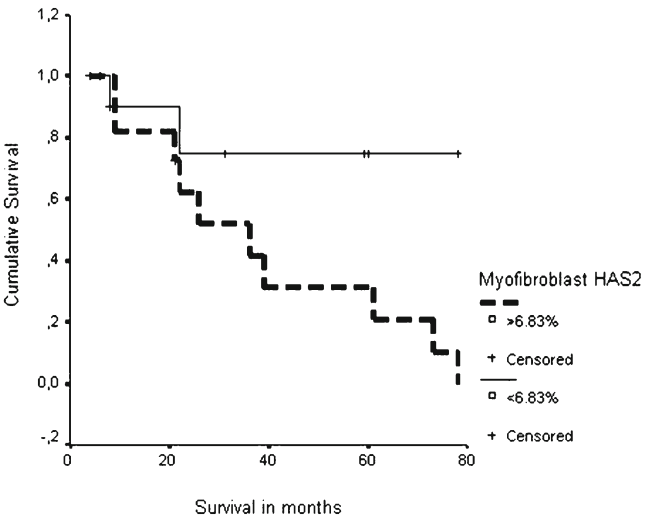

PS-01-024

Viral antigens are more frequently observed in acute interstitial pneumonia than in other types of idiopathic interstitial pneumonias

E. Parra*, G. C. dos Santos, F. Weisshaupt Stegun, C. dos Santos Cirqueira, M. I. Seixas Duarte, V. L. Capelozzi
*FMUSP, Dept. of Pathology, São Paulo, Brazil

Objective: The etiology of idiopathic interstitial pneumonias (IIPs) remains unclear. Many researches assumed that viruses can represent an important factor of aggression to the lung provoking fibrosis. In this regards, we researched the presence of virus infections in patients with IIPs.
Method: Biopsy samples from 13 patients with idiopathic interstitial pneumonia (IPF); 8 patients with nonspecific interstitial pneumonia (NSIP); 13 patients with acute interstitial pneumonia (AIP) and 4 patients with idiopathic cetrilobular fibrosis (ICLF) were used to investigate by microarray and immunohistochemistry the presence of measles virus (MV), hepatitis-C virus (HCV), adenovirus (ADV), respiratory syncytial virus (RSV), Epstein-Barr virus (EBV), herpes I and II viruses (HVI and HVII).
Results: We detected the epithelial alveolar infection by MV and CMV in 30.8 % and 15.4 % in AIP, respectively. Endothelial CMV infection was observed in 25 % of ICLF group. When we compared with the age of these patients, patients with ≤ of 43 years old had more infection by MV and CMV than the group with ≥ 72 years old. The other viruses were not detected in the different groups.
Conclusion: The viral infections observed in AIP and ICLF groups reinforce the possible viral participation in these pulmonary diseases. Financial Support: FAPESP.

PS-01-025

Abnormal up regulation of cyclooxygenase-2 is observed in idiopathic pulmonary fibrosis

E. Parra*, F. Lin, W. Teodoro, A. P. Velosa, V. L. Capelozzi
*FMUSP, Dept. of Pathology, São Paulo, Brazil

Objective: Several factors modulate fibroblast proliferation and collagen deposition in pulmonary fibrosis diseases, including cyclooxygenase (COX). The main of this study was observed the relationship between COX1 and COX2 in surgical lung biopsies from patients with idiopathic pulmonary fibrosis (IPF).
Method: Twenty four patients (64±8.9 year) were characterized with IPF. Immunohistochemistry and histomorphometry were used to evaluate the amount of COX1 and COX2 expression in lung specimens. The expression of these markers was tested with their pulmonary function tests.
Results: Significantly a higher amount of COX-2 was observed in IPF patients principally in normal and vascular areas (p=0.05) when compared with control group (Figure), contrasting with similar amounts of COX-1 in both groups. An important negative correlation was observed between total lung COX-2 expression and DCO/VA (r=0.694, p=0.01) in IPF patients.
Conclusion: Higher vascular expressions of COX2 probably mediated the inflammatory reaction in patients with IPF and have an important impact with pulmonary function tests, suggesting that a participation in the pathway of IPF. Financial Support: FAPESP.

Error barr shows the correlations between COX-2 expression in normal and vascular areas of IPF compared with control group

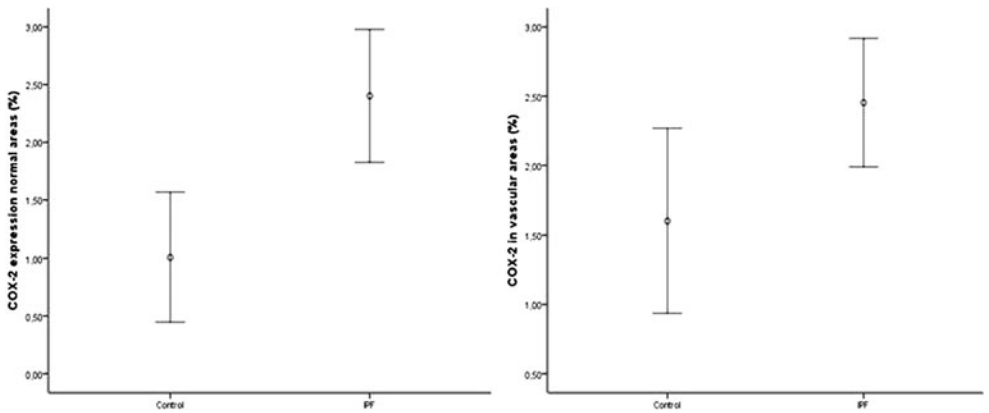

PS-01-026

Multiplex Ligation Probe-dependent Amplification (MLPA) as an ancillary method for the diagnosis of malignant pleural effusion

E. Parra*, D. Rosolen, L. Kulikowski, R. Dutra, V. l. Capelozzi, F. Vargas, M. Acencio, L. Antonangelo
*FMUSP, Dept. of Pathology, São Paulo, Brazil

Objective: A definitive diagnosis provided by the finding of malignant cells in pleural fluid (PF) can be established in around 50 % of patients with pleural malignancy. However, underdiagnosis risk in cytological suspicious cases is high, which makes the cytological diagnosis quite limited. This is an important clinical problem, especially if we consider that some patients, in bad clinical conditions, can not be submitted to a guided thoracoscopic biopsy.
Method: Using multiplex ligation probe-dependent amplification (P315-MRC-Holland) we have studied sequence variations of EGFR gene and amplifications/deletions of chromosomal regions frequently associated to tumors (ATG4B, PAHs, PROS, NSD1, and CDGIF genes).
Results: Forty-three malignant PF samples from patients with different cancers were evaluated, even in those cases with scarce pellet cells. Four benign pleural effusions were used as control. Gene sequence changes were observed in 13 (30.2 %) cases, while others copy number abnormalities were found in 19 (44.2 %).
Conclusion: The findings suggest that MLPA could be considered an alternative tool to detect molecular genetic changes in malignant pleural effusions, since this technique is relatively low expensive and not time consuming. Our next challenge is to find the best combination of probes capable to recognize malignant cells of any origin in fresh samples of PF.

PS-01-027

Multiple primary pulmonary myopericytoma: Case presentation

N. Petre*, F. Pop, D. Leonte, S. Bedereag
*Medcenter Bucharest, Dept. of Pathology, Romania

Objective: Myopericytoma is described as a perivascular myoid tumor which usually develops as a solitary mass in the subcutaneous tissues of the extremities, in adults.
Method: The chest radiography of a 52-year-old woman showed multiple, bilateral lung nodules. After the surgical excision of one of them, the histopathologic examination revealed a well circumscribed nodule, composed of fusiform or oval cells, with eosinophilic cytoplasm and ovoid nuclei, without atypia, in a concentric pattern, intimately associated with thin-walled vessels, within a myxoid stroma.
Results: The spindle cells were diffusely positive for vimentin, smooth muscle actin (SMA) and occasionally for desmin. CD31 and CD34 were positive only in endothelial cells. Ki 67 was positive in less than 4 % of neoplastic cells.
Conclusion: The histological and immuno-histochemical findings led to the diagnosis of multiple primary pulmonary myopericytoma.

PS-01-028

Five cases of lung pneumocytoma: Clinico-pathological, immunohistochemical and ultrastructural study

I. Rodriguez*, A. Panizo, B. Larrinaga, I. Amat
*C. Hospitalario de Navarra, Dept. of Pathology, Pamplona, Spain

Objective: Lung pneumocytoma (LP), also called sclerosing hemangioma, is an uncommon tumor of uncertain histogenesis.
Method: We analyzed the clinical, morphological, immunohistochemical and ultrastructural features of 5 LP.
Results: All 5 patients were women, with median age of 48 year (range: 29–73). Mean size was 26 mm (range 15–45 mm). All tumors were located within the right lung (upper-lobe: 1; middle-lobe: 2; lower-lobe: 2). All cases showed solid, papillary, sclerotic, and hemorrhagic patterns. The tumors were composed of 2 cells types: pale polygonal and surface cells. EMA, TTF1, and PR were observed in both type cells. The surface cells showed also positivity for CK7, Napsin-A, and surfactant-A, whereas the polygonal cells for vimentin. Surface cells had short microvilli and lamellar bodies in their cytoplasm. Polygonal cells contained abundant microfilaments and rough endoplasmic reticulum. All patients were alive and well without recurrence at the last follow up.
Conclusion: LP is likely to be an epithelial tumor with a differentiation toward type II pneumocytes, which exhibits various architectural patterns. The IHC profile provides useful clues for the diagnosis of this lung neoplasm when typical features are absent. All our cases had an excellent prognosis with no evidence of recurrence following surgery.

PS-01-029

Rare tracheobroncheal lesions diagnosed by small bronchoscopic biopsies

A. Sasmaz*, S. Yuksel, H. Nalbant, P. Celepli, E. Kadan, S. Percinel, S. Dizbay Sak
*Ankara, Turkey

Objective: Six different, rarely seen tracheobronchial lesions, taken by bronchoscopy as small fragments were discussed with an emphasis on morphological findings and differential diagnosis.
Results: Six patients were men and two patients were women with an age range of 50 to 70 years. Most of the lesions were symptomatic and discovered as small masses by

bronchoscopy. The tracheobronchial lesions varied from polypoid, nodular, well-demarcated, fragile masses to nodular thickenings. Microscopically, a polyp composed of a fibrovascular stroma with scattered mononuclear inflammatory cells was compatible with fibroepithelial polyp. Mature adipocyte proliferation in two cases, S-100 and CD68 positive polygonal or ovoid cells with abundant eosinophilic, granular cytoplasm having small, hyperchromatic nuclei, smooth muscle actin and desmin positive spindle cells in interlacing fascicles within a myxoid and collagenous stroma with mononuclear inflammatory cells, CD34 and CD31 positive thin-walled vascular channels, filled with red blood cells and S-100 positive spindle cells having palisading of wavy nuclei in two cases, located in the submucosa were main findings of lipoma, granular cell tumor, inflammatory myofibroblastic tumor, cavernous hemangioma and schwannoma, respectively.

Conclusion: Tracheobronchial biopsies, even with small fragments of lesions can allow to render rare specific histopathological diagnoses, some of which need to be confirmed by immunohistochemistry.

PS-01-030

Immunohistochemical expression of matrix metalloproteinases 1,2 and 9 in small cell lung carcinoma

V. Siozopoulou*, A. Batistatou, E. Lampri, D. Stefanou
*University of Ioannina, Dept. of Pathology, Greece

Objective: Small cell lung carcinomas (SCLC) are aggressive neoplasms that give very early distant metastases. Matrix metalloproteinases (MMPs) are a family of endopeptidases which degrade extracellular matrix and modulate cell adhesion, playing a crucial role in cancer cell invasion and metastasis. The aim of the present study is to investigate the immunohistochemical expression of MMP-2, MMP-9 (type IV collagenases) and MMP-1 (interstitial collagenase) in patients with SCLC.

Method: Formalin-fixed, paraffin-embedded lung biopsy specimens from 40 patients with SCLC (M:F=29:11, median age=66.7) were immunostained for MMP-1, MMP-2 and MMP-9 (anti-MMP-1 polyclonal antibody, anti-MMP-2 72 kDa Collagenase IV antibody, anti-MMP-9 92 kDa Collagenase IV antibody, Spring Bioscience).

Results: Immunohistochemical expression of MMPs was detected in the cytoplasm of neoplastic cells. Immunoreactivity was designated positive when >10 % of neoplastic cells were stained. Overall, MMPs were expressed in the majority of SCLC. Specifically, MMP-1 was positive in 90 % (36/40), MMP-2 in 87.5 % (35/40) and MMP-9 in 82.5 % (33/40) of SCLC. Non-neoplastic lung parenchyma did not stain for MMPs.

Conclusion: The majority of SCLC express immunohistochemically MMP-2, MMP-9 and MMP-1. Given the role of MMPs in cancer progression and metastasis, their expression in SCLC may contribute to their aggressive course.

PS-01-031

Diagnosis of pulmonary adenocarcinoma by immunohistochemistry

J. Stojsic*, J. Markovic, I. Jovanic
*Clinical Center of Serbia, Service of Pathology, Belgrade, Serbia

Objective: Number of pulmonary adenocarcinoma (ADC) patients incresease. Treatment of non-small cell pulmonary carcinoma depends of its histological type in era of target molecular therapy particulary of ADC: Diagnosis of ADC is established on small-sized pulmonary biopsies obtained on bronchoscopy and by transthoracic needle pulmonary biopsy. The aim of this study was to evaluate optimal panel of monoclonal antibodies in diagnosis of pulmonary ADC on small-sized biopsy pulmonary samples.

Method: Analysis of 50 small-sized biopsy pulmonary samples. Diagnosis of ADC was established on hematoxillyn-eosin stained (H&E) samples and confirmed immunohistochemicaly by Thyreoid Transcription Factor-1 (TTF-1), Napsin-A, Surfactant B and Cytokeratin7 (CK7). Descriptive statistical method (%) was used.

Results: TTF-1 specificity was 86 %(43/50), Napsin-A-82 %(41/50), SurfactantB – 56 %(28/50) and CK7-90 %(45/50) in ADCs. Two monoclonal antibodies were positive in 24 % (12/50) ADCs, one of them was necessary TTF-1 or Napsin-A. Three monoclonal antibodies were positive in 40 %(20/50) and 4 in 36 %(18/50) ADCs, respectively. There is not statistical significans in number of monoclonal antibodies for diagnosis of ADC.

Conclusion: No one monoclonalantibody is specific for one histological type of carcinoma and its origin. TTF-1, Napsin-A, SurfactantB and CK7 belong in optimal panel for diagnosis of pulmonary adenocarcinoma.

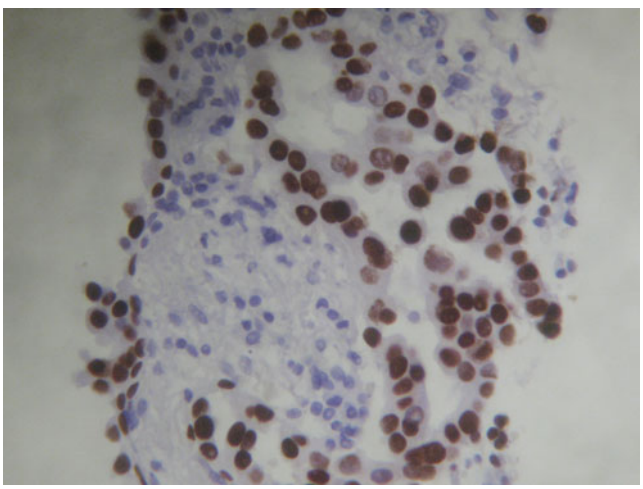

PS-01-032

Expression of CD44, E-Cadherin and Bcl-2 in lung cancer

I. Strumfa*, A. Abolins, J. Gekis, K. Pavlovs, A. Vanags, J. Grusina-Ujumaza, G. Volanska, J. Gardovskis
*Riga Stradins University, Dept. of Pathology, Latvia

Objective: Lung cancer represents major problem in oncology as the incidence and mortality is high (Parkin et al., 2005). Molecular studies could reveal additional targets for intervention or prognostic evaluation. However, the published data are controversial (Renouf et al.,2009; Leung et al.,2010; Maraz et al.,2011; Ko et al.,2011).
Method: Consecutive lung cancer cases (278) were retrieved by retrospective archive search. The diagnostics has been performed systematically in accordance with WHO classification (Travis et al.,2000). The expression of CD44, E-Cadherin and Bcl-2 was analysed by immunohistochemistry and evaluated semiquantitatively.
Results: The intensity of Bcl-2 expression was highest in small cell cancer, reaching the mean value 2.25. No or very low Bcl-2 expression was found in adenocarcinoma, carcinoid and squamous cell cancer. The membranous expression of E-Cadherin showed significantly higher mean intensity in adenocarcinoma (1.93) and carcinoid (1.90) than in small cell cancer (0.14) and squamous cell cancer (0.85). Cytoplasmic E-cadherin expression was observed in small cell cancer. CD44 expression was widespread and frequent in non-small cell lung cancer.
Conclusion: The main histological types of lung cancer show different immunophenotype. Bcl-2 expression is found in small cell cancer. The expression of E-Cadherin is characteristic in adenocarcinoma and carcinoid. CD44 is expressed in non-small cell lung cancer.

PS-01-033

Localized nodular pulmonary and thoracic cage amyloidosis

I. Strumfa*, A. Abolins, J. Gekis, K. Pavlovs, A. Vanags, B. Strumfs, G. Volanska, J. Gardovskis
*Riga Stradins University, Dept. of Pathology, Latvia

Objective: Localised amyloidosis represents a rare differential diagnosis of neoplasms. However, in some cases amyloid deposits are manifestation of tumour itself. To increase awareness about these uncommon but important differential diagnostic issues, we show here three well-characterised cases of thoracic cage or pulmonary localised nodular amyloidosis.
Method: The cases were identified by systematic retrospective archive search, 2000–2011. Congo red stain, polarisation microscopy and immunohistochemical analysis was applied.
Results: There were 2 males and 1 female among the patients diagnosed with thoracic cage or pulmonary amyloidosis. The patients were 67–84 years old and had no history of previous malignancy. Clinically, either lung cancer or sternal osteochondroma was suspected. Radiologically, 1–2 nodules measuring 1.5–9.0 cm were found in lungs (2 cases, one of these being bifocal) or sternum (1). Surgical treatment was applied in all cases. Amyloid deposits were identified by Congo red stain and polarisation microscopy. AL type of amyloid was confirmed. In case of bone lesion, the plasma cells were monoclonal justifying the diagnosis of multiple myeloma.
Conclusion: Localised amyloidosis can involve lung or sternum as tumour-like mass. The lung lesions can be single or multiple. Association with haematologic neoplasm is likely if bone is affected. Clonality analysis of plasma cells surrounding amyloid deposits is mandatory.

PS-01-034

Pleural localization of Castleman Disease: A rare entity

E. Tastekin*, F. Oz Puyan, E. Isler, U. Usta
*Trakya University, Dept. of Pathology, Edirne, Turkey

Objective: Castleman disease (CD) comprises a heterogeneous group of disease with various clinical presentations and prognosis. By definition; CD is a lymphoproliferative disorder of the mediastinal lymph nodes and extranodal tissues with follicular and interfollicular abnormalities. Pleural localization is an unusual presentation of CD.
Method: A 27-year-old man applied to the hospital because of cough. Chest x-ray and CT images showed an irregular, 35×56×67 mm sized intrapleural-extrapulmoner mass in the paramediastinal region. Surgical specimen was consisting of a 7×5×3.5 cm sized, irregular-round shaped, gray colored calcified mass. Microscopically, a lymphoid proliferation with distorted follicles and increased dendritic cells (with CD21) was detected. Lymphocyte depleted germinal centers resembling "onion skin" appearance with penetrated sclerosing hyalinized blood vessels were also seen. Interfollicular region was composed of proliferating blood vessels lined by plump endothelial cells and few lymphoplasmositer infiltration. There was heterogeneous positivity with CD3 and CD20. Expanded mantle zones showed diffuse bcl2 positivity. Ki67 proliferation index was low. The mass was diagnosed as "Castleman Disease, hyaline vascular type". Typical appearance of the follicular and interfollicular abnormalities allowed definitive differentiation from mesothelioma and solitary fibrous tumor of the pleura.
Conclusion: Pleural CD is a rare lesion but should be considered especially on young patients in the differential diagnosis of pleural masses.

PS-01-035

Collagen V-induced nasal tolerance increase FOXp3 in systemic sclerosis model

W. Teodoro*, A. P. Velosa, I. Brindo da Cruz, A. Santos Filho, S. Fernezlian, E. Parra, N. Yoshinari, V. Capelozzi
*Faculdade de Medicina da USP, Disciplina de Reumatologia, São Paulo, Brazil

Objective: To evaluate FOXp3 expression in bronchus-associated lymphoid tissue (BALT) and correlate with the inflammatory process and collagen content in the lung tissue in an experimental model of scleroderma (SSc) after type V collagen (COL V)-induced nasal tolerance.
Method: Female New Zealand rabbits (N=12) were immunized with 1 mg/ml of COL V in Freund's adjuvant (IM). After 150 days, six immunized animals were nasally tolerated with COL V (25 νg/day), during 60 days (IM-TOL). Animals (N=6) only tolerated served as control (CT). FOXP3 expression in BALT and inflammatory cells in pulmonary interstitium were evaluated by point counting method. Types I, III and V collagen gene expression were evaluated by Real-time PCR.
Results: IM-TOL when compared to IM presented decreased lymphocytes, macrophages and monocytes and types I (p=0,002) and V (p=0,009) collagen mRNA expression in pulmonary tissue. T lymphocytes FOXp3 were expressed in 100 % of IM-TOL and 33,3 % of CT (p= 0,03). Additionally, BALT was higher expressed in IM-TOL in relation to CT.
Conclusion: COL V-induced nasal tolerance in SSc model induces FOXp3 regulatory T cells in BALT which can trigger an immune regulatory mechanism resulting in decreased inflammation and collagen expression. It suggests that COL V tolerance could be a promising therapeutic for human scleroderma treatment.

PS-01-036

IgG4-related lung disease

T. Tichy*, H. Hornychova, J. Jankova, J. Skarda, B. Krajsova
*University Hospital Olomouc, Inst. of Pathology, Czech Republic

Objective: IgG4 –related lung disease is one of the manifestations of IgG4-related systemic disease. Obliterative vasculitis is considered an organ specific feature of IgG4-related disease in the lung. We report a case of a 78-year-old man with multifocal subpleural consolidations in both lungs. Histologic examination revealed IgG4-related lung disease with obliterative lymphoplasmacytic vasculitis.
Method: Histological sections from paraffin blocks were used for hematoxylin-eosin and special stains (elastica-Masson trichrome, PAS, Geimsa, Grocott), for immunohistochemistry (antibodies against kappa and lambda light chains, CD20, CD3, IgG, IgM, IgA, IgG4, LMP1) as well as for EBER in situ hybridisation and PCR.
Results: The lung tissue was irregulary fibrotic with dense lymfoplasmacytic infiltration concentrated in the walls of pulmonary arteries. Some arteries were obliterated by intimal fibrosis. Infiltrating lymphocytes were small and without atypias. The majority of lymphocytes were CD3 positive, nearly all plasmocytes showed IgG positivity. IgG4/IgG ratio was 60 %. EBER in situ hybridisation was negative and monoclonal reaarangement of T cell receptor or immunoglobulin heavy chain genes were not detected.
Conclusion: IgG4-related lung disease is rare. Obliterative vasculitis and high percentage of IgG4 positive plasmocytes are main histological features of this entity.

PS-01-037

Primary lung adenocarcinoma with heterotopic osteocartilaginous formation

H. Yaegashi*, S. Hatakeyama, N. Tomichi, H. Ono, J. Abe, H. Niikawa, H. Ooura, M. Handa
*Iwate Prefectural Central Hospital, Dept. of Pathology, Morioka, Japan

Objective: Primary lung carcinoma with heterotopic osteocartilaginous formation is exceedingly rare. To date only 38 cases have been reported in the literature and the pathogenesis is not fully investigated. We report a case of pulmonary adenocarcinoma with osteocartilaginous formation with immunohistochemical staining of bone morphogenetic proteins (BMPs).
Method: A 59-year-old man was admitted to our hospital for a lung tumor in his left upper lobe. An open lung biopsy followed a lobectomy was done. The resected tissue was fixed with 10 % formalin and embedded in paraffin. Sections, cut from paraffin blocks, were subjected to hematoxylin and eosin (HE) staining and Masson-Goldner staining, in addition to immunohistochemical staining.
Results: The tumor was poorly differentiated adenocarcinoma with heterotopic ossification. Some of the tumor cells were positive for BMP-2, 6, and 7. Some of mesenchymal cells in tumor interstitium were positive for osteoblast (OB)- cadherin or BMP receptor-IA.
Conclusion: We report a case of primary lung adenocarcinoma with heterotopic osteocartilaginous formation and reviewed previously published reports. To our best

knowledge, this was the first case that not only BMP was expressed in tumor cells but also OB-cadherin or BMP receptor in some mesenchymal cells of tumor interstitium.

PS-01-038

Expression of transforming growth factor ß1 and e-cadherin in lung adenocarcinoma

J. Yoo*, S. Y. Park
*St. Vincent's Hospital, Pathology, Suwon, Republic of Korea

Objective: There is evidence supporting the concept of tumor progression from pulmonary adenocarcinoma in situ (formerly bronchioloalveolar carcinoma, BAC) to adenocarcinoma with varying degrees of invasion. The aim of this study was to investigate the role of TGFß1in tumor invasiveness in lung adenocarcinoma, and to determine the potential relationships between its expression and immunophenotypes of cell adhesion molecules.
Method: Tumor samples (n=40) from adenocarcinoma in situ (n=13), minimally invasive adenocarcinoma (formerly BAC with ≤5 mm invasion, n=2), and lepidic predominant invasive adenocarcinoma (formerly mixed adenocarcinoma showing non-mucinous BAC features with >5 mm invasion, n=25) were examined for the expression of TGFß1, E-cadherin, N-cadherin, and H-cadherin proteins using immunohistochemistry.
Results: Twenty-five tumors (63 %) were positive for TGFß1. The frequency of immunoreactivity in patients with adenocarcinoma in situ, minimally invasive adenocarcinoma, and lepidic predominant invasive adenocarcinoma was 23 % (3/13), 50 % (1/2), and 84 % (21/25), respectively (p=0.001). Loss of E-cadherin expression was more frequently observed in invasive adenocarcinomas than in adenocarcinomas in situ (p=0.034). TGFß1 expression showed a statistically significant correlation with H-cadherin expression (p=0.040), but not with E-cadherin expression (p=0.752).
Conclusion: These results suggest that TGFß1 and E-cadherin may play an important role in invasive progression of lung adenocarcinoma through regulating epithelial-to-mesenchymal transition.

PS-01-040

LIN28A expression as prognostic indicator in lung adenocarcinomas

V. Zolota*, V. Tzelepi, G. Psiouri, I. Lilis, N. Panagopoulos, C. Sirinian, C. Scopa
*Medical School of Patras, Dept. of Pathology, Greece

Objective: LIN28A is implicated in stem cell pluripotency by blocking let-7miRNAs and Oct-4 is a transcription factor highly expressed in embryonic stem cells. The present study investigates the prognostic significance of both markers in lung adenocarcinomas.
Method: We evaluated, by immunohistochemistry, LIN28A and Oct-4A expression in formalin-fixed, paraffin-embedded tissues from 92 lung adenocarcinomas. Immunoreactivity was scored as 1+, <1 % positive tumor cells (ptc); 2+, 1–5 % ptc; 3+, 5–10 % ptc; and 4+, >10 % ptc and was compared with clinicopathologic features and overall survival.
Results: Regarding LIN28A expression 23 % of tumors were recorded as 1+, 51 % as 2+, 14 % as 3+ and 12 % as 4+. The stratification for Oct-4 expression was 19 % (1+), 50 % (2+), 23 % (3+) and 8 % (4+). LIN28A and Oct-4 expression was not significantly associated with age, gender and tumor grade or stage. LIN28A 4+ expression predicted a shorter overall survival (P<0.05) on univariate analysis. Oct-4 was not associated with patients' prognosis. Cox multivariate analysis showed that age, TNM and LIN28A 4+ expression were independent prognostic factors of survival.
Conclusion: LIN28A expression appears to be an independent predictor of poor outcome in lung adenocarcinomas. Further studies are warranted in order to investigate its role in stratifying patients at increased risk for poor outcome.

PS-01-041

Comparison of the mutation status of EGFR and KRAS on pulmonary adenocarcinoma and corresponding brain metastasis

C.-C. Huang*, H.-K. Chen, K.-M. Rau
*Chang Gung Memorial Hospital, Dept. of Pathology, Kaohsiung, Taiwan

Objective: EGFR and KRAS mutation statuses have been known associated with the sensitivity of tyrosine kinase inhibitor treatment in pulmonary adenocarcinoma. However, the mutation analyses were usually performed on the primary tumors only, due to the availability of the tumor tissue.
Method: To compare the KRAS and EGFR mutation statuses between pulmonary adenocarcinomas and corresponding metastases, we performed direct sequencing, followed by Scorpion ARMS method on wild-type cases for EGFR analysis, and allele-specific real-time PCR for KRAS analysis, on the paired samples of pulmonary adenocarcinoma.
Results: Thirty-one (63.3 %) pulmonary adenocarcinomas and 30 (61.2 %) brain metastases out of the 49 paired specimens have EGFR mutations, and 30 (61.2 %) paired specimens were concordant for the EGFR mutation status between the primary and metastasis. In addition, 17

(51.5 %) pulmonary adenocarcinomas and 17 (51.5 %) brain metastases out of the 33 paired specimens have KRAS mutations, and only 16 (48.5 %) paired specimens were concordant between the primary and the metastasis.
Conclusion: The status of EGFR mutation is relatively consistent between primary and metastasis comparing to that of KRAS mutation in pulmonary adenocarcinomas. However, discordance for the mutation statuses does happen. Accordingly, repeat analysis is recommended if tissue from metastatsis or recurrence is available.

PS-01-042
Morphologic analysis of pulmonary neuroendocrine tumors
S.-Y. Ha*, S.-S. Lee
*Gachon University Gil Hospital, Dept. of Pathology, Incheon, Republic of Korea

Objective: We tried to measure and analyze characteristics of neuroendocrine tumors in lung by image analysis and help to diagnose them.
Method: It was analysed that sixteen cases of typical carcinoid tumors, five cases of atypical carcinoid tumors, fifteen of small cell carcinomas, fifty one cases of large cell neuroendocrine carcinomas. We analyzed the nuclear area, perimeter, major axis and minor axis using i-solution image analyzer software package.
Results: The mean nuclear area was 488.00 μm2 in the typical carcinoid tumors, 499.30 μm2 in the atypical carcinoid tumors, 481.48 μm2 in the small cell carcinomas, and 684.05 μm2 in the large cell neuroendocrine carcinomas. After the statistical results, every method was effective to distinguish large cell neuroendocrine carcinoma from other tumors and the circumferences of nucleus was the most effective to distinguish among them.
Conclusion: Pulmonary neuroendocrine tumors were the nuclear morphologic differences of each tumors. Therefore, diagnosis that considers morphologic differences of pulmonary neuroendocrine tumors contributes to increase reproducibility and accuracy.

Sunday, 9 September 2012, 09.30 - 10.30, Congress Hall Foyer 3rd Floor
PS-02 Poster Session Cytopathology

PS-02-001
Cytolytic vaginosis: May cause infertility?
I. I. Akgun*, L. E. Yazici Ensari
*Mardin Maternity Hospital, Dept. of Pathology, Turkey

Objective: Vagina is covered by the flora dominated by Lactobacillus spp. durig the term from puberty to the menopause. An abundant growth of lactobacilli may result in lysis of vaginal epithelial cells, named as Cytolytic Vaginosis. This cytolytic process may cause the symptoms as seen in candidiasis. We observed Pap smears to evaluate if cytolysis has a relationship with infertility.
Method: In the Pathology department of Mardin Maternity Hospital, 2011–2012 period, we examined Pap smear cases suffering from the similar syptoms as candidiasis. Of the 4672 smears, 82 were diagnosed as "Cytolytic Vaginosis". No growth was observed in cultures.
Results: The number of the cases suffering from the infertility was 261 (%5.58) among 4672 cases. In the cytolytic vaginosis group this ratio was %32.9 (n=27). The ratio of the infertil cases of cytolytic vaginosis group over general population was significantly higher ($p<0.05$).
Conclusion: Our results are in favour of supporting the hypothesis of the relation between cytolytic vaginosis and infertility. Lactobacilli are thought to have inhibitive role in fertility by changing the vaginal ph and adhering to the epithelial cells so inhibiting the sperm penetration.

PS-02-002
Penicillium and aspergillus spp. on pap smears from the surprising origin
I. I. Akgun*, B. A. Borsa
*Mardin Maternity Hospital, Dept. of Pathology, Turkey

Objective: Fungal organisms are commonly seen on smears. Some unusual species as Aspergillus and Penicillium are so rare and generally seen via contamination. In this study, we investigated the origin of the many extraordinary fungal organisms seen on Pap smears in series in only a few months.
Method: In Pathology department of Mardin Maternity Hospital, we observed both smear and vaginal discharge materials, came from the same hospital but different clinicians, for 3 months.
Results: 149 smears came from clinician A and 335 smears from clinician B. Curious fungal organisms with huge branching hyphas and macrochonidias were seen in 15 smears among 149 smears (2 Aspergillus and 4 Penicillium species were recognized morphologically). No growth was observed in cultures. Interestingly, among all 335 smears came from clinician B, there was no abnormal funguses. The smear samples with unusual fungal components all came from the same gynecologist. This made us strongly consider the probability of contamination.
Conclusion: Penicillium and Aspergillus spp. are extremely rare in vaginal smears. In our study, these funguses are thought to be airborne passed from the thick layer of the mold spreading on the ceiling of the office.

PS-02-003

Hybrid Capture 2 and Cervista: Comparison in the determination of HPV

F. Alameda*, L. Garrote, B. Lloveras, J. Munné, L. Comerma, M. Muset, B. Bellosillo, S. Serrano
*Hospital del Mar, Dept. de Anatomia Patologica, Barcelona, Spain

Objective: Nearly all cervical cancers are related to human papillomavirus (HPV) infection. Hybrid Capture 2 - HC2 (Qiagen, Hilden, Germany) is the method to determine the presence of high risk HPV (HR HPV) in cytology samples with the best clinical sensitivity.
Method: In our study we compared the results of the HPV test in 742 ThinPrep® cervical samples using first HC2 and secondly Cervista (Hologic, Madison). Samples were divided in two groups for the statistical analysis. The first group were HSIL cases confirmed by biopsy (n=65) and the second group cytology samples reported as negative, ASC-US or LSIL (without biopsy or biopsy, not HSIL) (n=677).
Results: Overall, concordance between the two techniques was 92 % (683/742). There were 23 cases HC2+ Cervista−, and 36 cases HC2 −Cervista+. The average HC2 viral load in discordant cases was 2.83. In our series the HC2 sensitivity for ≥ CIN2 was 100 % (65/65) and the specificity was 85.4 % (578/677). Cervista results were 98.5 % (64/65) and 83.3 % (564/677), respectively. In the HSIL cases the coincidence was 98.5 % (64/65).
Conclusion: Cervista results showed good clinical sensitivity and high concordance with HC2, with a slightly lower specificity. In conclusion, according to our data the determination of HPV with Cervista is comparable with HC2.

PS-02-004

Mammary analogue secretory carcinoma of salivary glands: 2 cases including Cytology, Histology, IHC, EM, RT-PCR and FISH

P. Farrajota*, E. Tani, C. Carvalho, J. Wejde, G. Elmberger
*Centro Hospitalar do Porto, Dipt. do Anatomia Patologica, Portugal

Objective: Mammary analogue secretory carcinoma (MASC) of the salivary glands was described in 2010 by Skálová et al. in a series of 16 cases. We present 2 new molecularly confirmed cases with focus on detailed cytomorphological features and correlation with special studies.
Method: A 75 year old man and a 68 year old female presented with history of slow growing parotid and submucosal buccal tumors, respectively. Two fine needle aspiration biopsies (FNAB) were performed in each case. The surgical resection specimens were routinely processed and special studies applied on paraffin tissue section. The FNAB smears were retrospectively studied.
Results: All smears showed similar features of abundant proteinaceous background, moderate cellularity including macrophages and irregular and variable sized groups of cells with slightly enlarged round hypercromatic nuclei and abundant bluish vacuolated cytoplasm frequently containing small reddish granulations. The first FNAB reports confirmed salivary origin and the second ones alert for possible neoplastic nature, advising surgical resection. Electron microscopy performed in the parotid case caracterized the granules as mucigen. Subsquent pathologic evaluation and molecular confirmation was carried out.
Conclusion: MASC is a low grade malignant tumor capable of simulating a benign salivary gland process so it is important to know its cytological characteristics.

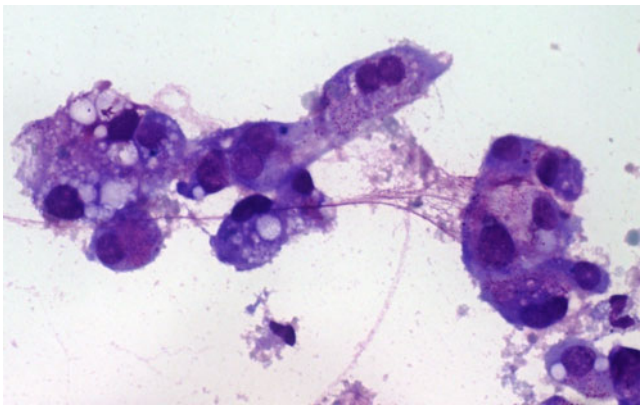

PS-02-005

Adenosquamous lung carcinoma: The importance of cyto-histologic correlation

D. Felizardo*, A. L. Cunha, R. Henrique, C. Lobo
*Instituto de Oncologia Porto, Dept. of Pathology, Coimbra, Portugal

Objective: Adenosquamous lung carcinomas (ASC) are uncommon and aggressive tumors. Identification of a squamous component within a NSCLC is critical as it excludes anti-VEGF therapy. Likewise, recognition of an adenocarcinoma component is also relevant because it prompts the search for EGFR mutations. Since 70 % of lung cancers are diagnosed in small biopsies/cytological specimens, cyto-histological correlation is crucial for correct diagnosis. Thus, we aimed at determining the relevance of combining cytologic and histologic findings in initial diagnostic work-up of ASC.
Method: We searched for cases of ASC diagnosed at our institution from March 2011 to April 2012. Cytologic and histopathologic findings were evaluated and their accuracy for diagnosing ASC was assessed.
Results: Of 184 cases of lung cancer in biopsy, 11 (6 %) corresponded to probable ASC and in 9 cases cytologic examination was also performed. In 7 cases, cytology was

not conclusive, but in 2 cases it demonstrated cytomorphological features of probable ASC. We emphasize one case in which only the squamous component was valued by histology, but cytology provided clues that prompted immunohistochemical analysis which led to the diagnosis of probable ASC.
Conclusion: Cyto-histological correlation augments the diagnostic accuracy in ASC of the lung, emphasizing the complementarity of both procedures.

PS-02-006
The impact of the Bethesda System for Reporting Thyroid Cytopathology (TBSRTC): A retrospective study of 828 aspirates with emphasis on the prior "indeterminate" category
C. Ferreira*, P. Lima, M. Mentem, J. Espósito, L. Wasserstein, A. Felipe-Silva
*Hospital Universitário da USP, Serviço de Anatomia Patológica, São Paulo, Brazil

Objective: We evaluated the impact of implementing TBSRTC in an academic community hospital.
Method: FNAs from Jan/2004 to Dec/2010 were reclassified in TBSRTC: nondiagnostic (ND), benign (B), atypia or follicular lesion of undetermined significance (AUS/FLUS), suspicious for follicular neoplasm (FN), suspicious for malignancy (S) and malignant (M). FLUS and FN were classified according to presence of Hürthle cells as HCLUS and FN-HC.
Results: A total of 828 FNAs (480 patients) were obtained: 46 ND (5.55 %), 682 B (82.4 %), 9 S (1.1 %) and 25 M (3.0 %). The 66 (8.0 %) indeterminate categories were reclassified: 1 ND (1.5 %), 8 B (12.1 %), 5 AUS (7.6 %), 34 FLUS (51.5 %), 5 HCLUS (7.6 %), 3 FN (4.5 %), 9 FN-HC (13.6 %) and 1 S (1.5 %). Thyroidectomies were performed in 125 patients (26 %): benign lesions in 83 (66.4 %), 7 (5.6 %) follicular adenoma and 2 (1.6 %) follicular carcinomas, 1 (0.8 %) medullary carcinoma, 21 (16.8 %) papillary carcinomas and 16 (12.8 %) papillary microcarcinomas (PMC). Risk of malignancy (RM) excluding PMC: B 1.4 %, AUS/FLUS/HCLUS 5 %, FN/FN-HC 11.1 %, SM 50 % and M 77.8 %.
Conclusion: TBSRTC criteria led to more specific diagnosis. FN/FN-HC category has a two-fold RM when compared to AUS/FLUS/HCLUS.

PS-02-007
FNA of thyroid lesions: A brief report
İ. E. Gürer*, S. S. Tuncer, G. A. Ocak, H. Altunbas
*Akdeniz University, Dept. of Pathology, Antalya, Turkey

Objective: The material of this study is consisted of selected FNA biopsies performed in the last 10 mounths period and followed by the Endocrinology Department.
Method: The Bethesda System of reporting thyroid cytopathology was used. Slides were stained with Papanicolaou preparations.
Results: Totally 380 cases were examined, 288 of which were female and 92 were male. Age of the patients varied between 5 and 88. 121 cases were diagnosed as nondiagnostic or nonsatisfactory. 211 cases diagnosed as consistent with a benign follicular nodule. Only 4 cases were diagnosed as a consistent with lymphocytic thyroiditis in corelation with the clinical features. Only 1 case diagnosed as a granulomatous thyroiditis. Diagnosis as "Atypia of undetermined significance or follıcular lesion of undetermined significance "was made only in 2 cases whereas "Follıcular neoplasm or suspicious for a follıcular neoplasm" was diagnosed in 1 case. "Suspicious for malignancy" diagnosed in 15 cases. 2 cases were diagnosed as malignant.
Conclusion: Although diagnostic terminology and morphologic criteria for cytologic diagnosis of thyroid lesions are well established in The Bethesda System, difficulty in categorizing the cases and underestimation or overdiagnosis are quite frequent issues. To solve this problem, retrospective studies which include surgical and cytopathologic reports, to examine slides by at least two different pathologists in different times will be helpfull.

PS-02-008
Metastatic pulmonary adenoid cystic carcinoma: Report of a case diagnosed by fine-needle aspiration cytology
P. Karabagli*, S. Ozbek
*Selcuklu Medical Faculty, Dept. of Pathology, Konya, Turkey

Objective: A rare case of adenoid cystic carcinoma of ceruminal gland with pulmonary metastasis presented with characteristic cytological and histological findings.
Method: The biopsy specimen of the patient, a 45 year-old man with painfull, growing mass in his external auditory canal was interpreted as an adenoid cystic carcinoma. He was treated surgically and received post-operative radiotherapy. After 8 years, a distant metastasis relapse was observed. Computed tomography (CT) of the chest depicted multiple spiculated masses suggestive of metastases throughout both lung fields, the diameter of the largest measuring 2 cm. CT guided percutaneous transthoracic fine needle aspiration biopsy was performed from the largest lesion.
Results: Cytological examination of the aspirates revealed large spherical hyaline globules representing basement membrane material surrounded by neoplastic cells. The cells were cohesive, closely packed, and had uniform round to oval hyperchromatic nuclei with scanty cytoplasm. These features were suggestive of an adenoid cystic carcinoma.
Conclusion: Patients with adenoid cystic carcinoma could be frequently encountered with disease recurrence confined to the lung. Fine-needle aspiration cytology provided a conclusive diagnosis of adenoid cystic carcinoma.

PS-02-009

Diagnostic usefulness of MUC1 and MUC4 for distinguishing between metastatic adenocarcinoma cells and reactive mesothelial cells in effusion cell blocks

J. S. Lee*, G.-E. Kim, J. H. Lee, C. Choi
*Chonnam National University Hwasun Hospital, Pathology, Jeollanam-Do, Republic of Korea

Objective: Differentiating metastatic adenocarcinoma cells (MAC) from reactive mesothelial cells (RMC) in effusion fluids based on cytomorphologic features alone can be very challenging. The aim of our study was to determine the value of MUC1 and MUC4 for distinguishing between MAC and RMC in effusion fluids.
Method: A total of 237 cell block specimens including 196 malignant effusions with MAC and 41 benign effusions with RMC were stained with antibodies against MUC1 and MUC4.
Results: MUC1 immunoreactivity was observed in 194 (99.0 %) of 196 cases of MAC and 20 (48.8 %) of 41 cases of RMC. MUC4 immunoreactivity was observed in 174 (88.8 %) of 196 cases of MAC and 4 (9.8 %) of 41 cases of RMC. In distinguishing MAC from RMC, the presence of MUC1 reactivity was found to be 99.0 % sensitive and 51.2 % specific. The sensitivity of MUC4 for MAC was 88.8 % and the specificity was 90.2 %. The combination of positive staining for MUC1 or MUC4 was 100 % specific for MAC, whereas a combination of negative staining for both MUC1 and MUC4 was 97.6 % specific for RMC.
Conclusion: The combination of MUC1 and MUC4 is a useful diagnostic adjunct with which to distinguish MAC from RMC in cell block preparations.

PS-02-010

Polyvinyl alcohol foam cell blocks from a needle hub residue device

F. Mayall*
*Musgrove Park Hospital, Dept. of Cellular Pathology, Taunton, United Kingdom

Objective: Often some of a fine needle aspiration (FNA) sample is left behind in the hub of the needle when the specimen is ejected on the slides (Figure 1A).
Method: We have designed a device that collects this material. It consists of a plastic adaptor that has a core of polyvinyl alcohol foam protruding from its lumen at one end (Figure 1B). The other end of the adaptor then fits on to the syringe (Figure 1 C). As the FNA is being performed the sample material flows up the lumen of the needle's shaft and emerges into the hub of the needle where it is absorbed into the tip of the foam core (Figure 1D). Smears are made by ejected the specimen from the needle onto a slide by air pressure from an attached syringe. The air passes through the foam forcing some of the sample in the foam back down the needle but some remains behind. The device is then removed and placed in a formalin specimen pot. Once fixed the core is pulled from the adaptor (Figure 1E), processed and sectioned as for routine histology specimens (Figure 1 F). On microscopic examination cells are seen in the spaces in the foam matrix (Figure 1 G). Immunohistochemistry and other molecular investigations can be performed (Figure 1 H; Cytokeratin 7) as for routine histology specimens.

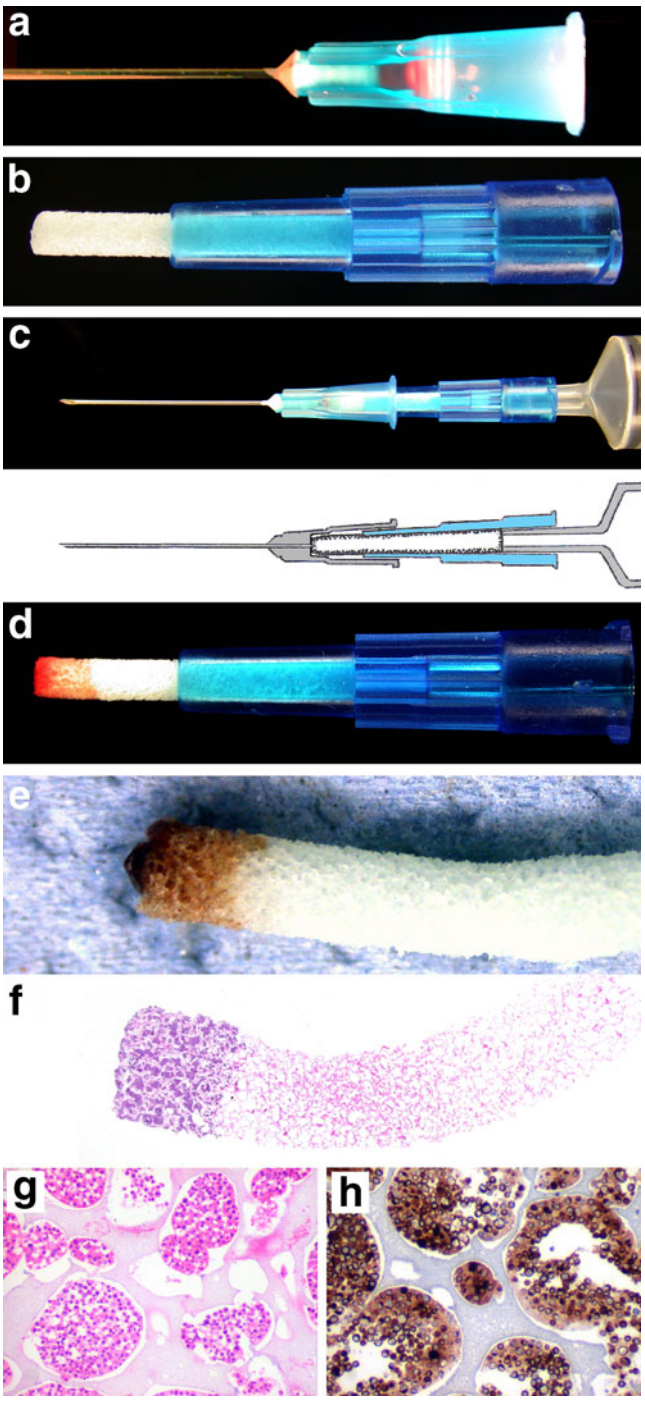

PS-02-011

Assessment of Dendritic/Langerhans Cells (DCs) in cytological specimens and corresponding histology of Papillary Thyroid Carcinoma (PTC) by immunochemistry

M. Pusztaszeri*, P. Sadow, W. Faquin
*Vandoeuvres, Switzerland

Objective: The presence of DCs has been studied histologically in PTC, but their presence and potential diagnostic value in thyroid FNAs has not been evaluated.
Method: We assessed the presence of DCs in cytological samples of histologically confirmed PTCs (n=31) and benign thyroid nodules (BTN) (n=29) using CD1a. Corresponding PTCs (n=11) and BTN (n=10) from surgical excisions were stained with both CD1a and Langerin.
Results: CD1a + DCs were identified in 30/31 PTCs on cytology (97 %). They were either isolated in the background or more typically closely associated with tumor cell clusters. The 3 PTC cases with the least DCs corresponded to the follicular variant on histology. In contrast, most BTN (69 %) lacked CD1a + DCs. When DCs were present, they were primarily isolated in the background although 5/29 cases (17 %) contained rare DCs among tumor cells. Tumor-infiltrating DCs and background DCs were both higher in PTCs than in BTN, but only the former was statistically significant (P<0.0001 and P=0.1173 respectively). Similar findings were found on histology where all PTCs contained CD1a + and Langerin + DCs while only 2/10 BTN (20 %) contained rare DCs.
Conclusion: DCs are present in FNAs of PTC, typically among tumor cell clusters, while they were absent or rare in FNAs of BTN. Thus DCs may be useful as an additional diagnostic marker for PTC.

PS-02-012

Significance of p 16 immunostaining in postmenopausal women with atypical squamous cells

A. Repse Fokter*, K. Gornik Kramberger, S. Hutter Čelik, S. Sramek Zatler
*Celje General Hospital, Dept. of Pathology and Cytology, Slovenia

Objective: The evaluation of postmenopausal Pap smears can often be challenging. Degeneration associated with atrophic vaginitis, hyperchromatic crowded groups, parabasal cells with organophilic cytoplasm or variations in nuclear size may be falsely interpreted as squamous atypia or even more severe lesion.
Method: The study included 25 postmenopausal Papanicolaou patients (26 smears) with the initial cytological diagnosis of ASC-US or ASC-H. The smears were decolorized and immunostaining for p16(Ink4a) was applied. In 21 patients (22 smears) tissue biopsy and histological examination was performed and four ASC-US cases had cytological follow up only.
Results: Among cases with histological examination positive p16 reaction was found in 17 patients (18 smears). The histological diagnoses were: CIN1 (3), CIN 1-2 (2), CIN2 (1 case), CIN3 (5 patients/6 smears), AIS (1 case) and invasive squamous carcinoma (2 patients). Two p16 positive patients with three smears and initial negative histology had CIN3 after 2 years. Among p16 negative patients there were two with CIN3 and two with normal histology. Four ASC-US patients without histological examination had normal cytological follow up.
Conclusion: P16 is a useful marker in detecting of clinically significant cervical lesions in postmenopausal women.

PS-02-013

Endoscopic-ultrasound guided fine needle aspiration cytology of intraductal papillary-mucinous neoplasms of the pancreas: Report of two cases and review of the literature

E. Tejerina González*, A. López García, C. González Lois, F. Fernández García, A. Herreros de Tejada, E. Sanz
*HU Puerta de Hierro-Majadahonda, Dept. de Anatomía Patológica, Spain

Objective: Intraductal papillary-mucinous neoplasms (IPMN) of the pancreas are mucin-producing tumors recently recognized as a distinct entity among other mucinous pancreatic tumors. Endoscopic-ultrasound guided fine needle aspiration (EUS-FNA) is a sensitive technique which can be very useful in the accurate diagnosis of these neoplasms.
Method: We present a case of a 30-year-old female with recurrent episodes of acute pancreatitis and a 49-year-old male with abdominal pain. TC showed a 26 mm-cystic tumor at the uncinated process of the pancreatic head and cystic dilatation of the main pancreatic duct, respectively. In both cases EUS-FNA was performed.
Results: Smears showed medium-to-large, cohesive groups and complex papillary clusters set in a clean, mucoid background, composed of cuboidal or columnar epithelial cells with abundant clear or mucinous cytoplasms. A honeycomb arrangement was occasionally seen. Although nuclei were predominantly medium-size and uniform, some groups showed some nuclear enlargement and pleomorphism with visible nucleoli. A diagnosis of “mucinous neoplasm with papillary pattern”

was rendered in both cases, followed by partial pancreatectomy. The histologic examination was consistent with IPMN.

Conclusion: The cytologic features of intraductal mucinous papillary neoplasms of the pancreas, evaluated by EUS-FNA, seems to be quite characteristic of these tumors and allow to suggest a correct preoperative diagnosis.

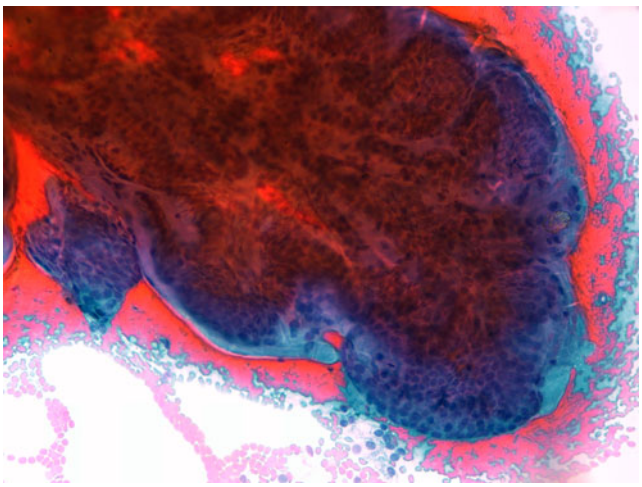

PS-02-014

IGH FISH-CISH DNA probe split signal: An additional tool in clonality assessment of lymphoproliferative processes

P. Zeppa*, L. V. Sosa Fernandez, E. Vigliar, I. Cozzolino, M. Salatiello, M. Picardi, U. Malapelle, G. Troncone, L. Palombini
*A.O.U. Salerno, Dept. of Surgical Pathology, Italy

Objective: The human IGH locus at chromosome 14q32 is frequently involved in different translocations of non Hodgkin Lymphoma (NHL), and the detection of any breakage involving the IGH locus should identify a B-cell NHL. The split signal IGH FISH-CISH DNA probe (IFCD) is a mixture of two fluorochrome-labeled DNAs that binds the telomeric and the centromeric segments, on the IGH breakpoint respectively. We tested the capability of the IFCD to detect IGH translocations and diagnose B-cell NHL on cytological samples.

Method: Fifty cytological specimens from lymphoproliferative processes were tested using the IFCD and the results compared to light chain assessment by flow cytometry (FC), IGH status by PCR, and to clinical-histological data.

Results: IFCD analysis detected 29 positive, 15 negative and 6 inadequate cases; there were 29 true positive (66 %), 9 true negative (20 %), 6 false negative (14 %) and 0 false positive cases (0 %). Comparing the sensitivity of the IFCD with FC and PCR, the highest sensitivity was obtained by FC followed by IFCD and PCR.

Conclusion: The IFCD is effective in detecting any translocation involving the IGH locus; it can be employed on different samples from different B-cell NHL whereas it is not useful to classify the specific entities.

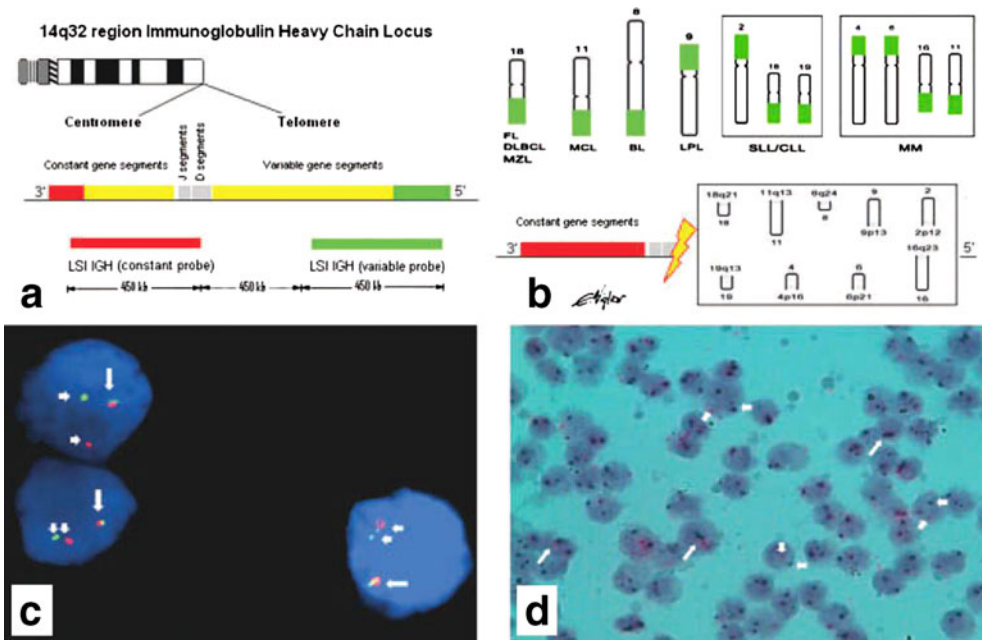

Sunday, 9 September 2012, 09.30 - 10.30, Congress Hall Foyer 3rd Floor
PS-03 Poster Session IT in Pathology

PS-03-001
Recognition of the cross-section of colon glands in histological images based on sequential algorithm as a introduction to morphometry
T. Markiewicz*, R. Koktysz, M. Muszynski, W. Kozlowski, M. Szczepkowski, A. Kobus
*Military Institute of Medicine, Dept. of Pathomorphology, Warsaw, Poland

Objective: Morphometric analysis of the glands and inflammatory cells proportions in colon mucosa may be crucial for distinction of subtle changes. The most important step is a recognition and proper segmentation of the separate glands, even branched, atrophic or distorted.
Method: New sequential algorithm has been proposed, based on mathematical morphology transformations, such as extended regional maxima, hit-or-miss, opening and closing operations. For lumen opened glands snake algorithm with closing has been applied to surrounding elements with sequential elimination of the closed contours under decreasing area criterion. Proposed method has been used to evaluate 47 cases of diversion colitis to compare specimens sampled from functional part of colon and defunctioned distal one.
Results: The appropriate results were obtained for specimens with different section planes with efficiency 89 %. In comparison of the B to A was observed decreased participation of epithelium in the glands area measured in deep region (an average 57 % instead 68 %). In addition, the area of the gland was slightly reduced from 51 % to 46 % of the mucosa.
Conclusion: The proposed method can be useful to automatic morphometry analysis of the gland shape in colon mucosa. The recognition of the opened glands improves previously designed algorithms.

PS-03-002
Various approaches of image segmentation explored in immunohistochemical histological samples with nuclei reaction
T. Markiewicz*, J. Slodkowska, M. Muszynski, W. Kozlowski
*Military Institute of Medicine, Dept. of Pathomorphology, Warsaw, Poland

Objective: Quantitative analysis of the immunohistochemical histological samples plays an important role in the diagnosis and prognosis of many cancers. The commercial and non-commercial software's to computerized image analysis of microscopic images based in several approaches.
Method: The advance segmentation scheme usually consists of preprocessing, nuclei extraction and classifier blocks. When the preprocessing step includes filtering and conversion to the most discriminative representation and the classifier can be realized by various tools, especially Support Vector Machine as a state-of-art, nuclei extraction is the most crucial part of any algorithms. We compare single thresholding methods such as Otsu, Kurita, minimum error, entropy thresholding, with the sequential thresholding approaches combined with area criteria, local threshold value or extended regional maxima. All of them are accompanied by watershed method and filtration.
Results: For Ki-67 stained meningioma specimens in the fields of view without overlapping nuclei the most advance methods are adequate. When increasing the cell number, only sequential thresholding with area criteria and extended regional maxima give acceptable results. The mean relative error is 2.6±2.2 and 5.4±6.4 % respectively.
Conclusion: The results confirm the efficiency of using sequential methods for segmentation of cell nuclei. For best results, use sequential thresholding with area criteria.

PS-03-003
NHS improvements: Enhanced IT project for histopathology
F. Mayall*
*Musgrove Park Hospital, Dept. of Cellular Pathology, Taunton, United Kingdom

Objective: Many histopathology laboratories are using antiquated software that hobbles their performance.
Method: We developed open source Filemaker Pro based histopathology reporting software with innovations based on Lean principles to enhance work flow. These include: - Colour coded visual workflow control - “One-click” extra-work requests with order tracking - User defined template reporting - Reporting of complex cases using benchmark profomas - Exportable data-sets using Open Database Connectivity - Easy local customisation and enhancement by the user.
Results: The software was used by 15 staff to report more than 7000 histopathology specimens at two histopathology laboratories. Many of these cases were complex cancer resection cases requiring key data capture. The histopathology staff using the software were surveyed on their experience of using the software.
Conclusion: The key steps in Lean IT development: - Start with a small idea - Develop software with multiple Plan, Do, Study, Act (PDSA) cycles - Ask users for more ideas for enhancements - Recruit others into the project by allowing them to use the software and experience its benefits - Standardise new reporting process by achieving agreement between users - Design a project that requires minimal financial investment This open source software is available for download from www.FreeDP.org.

Sunday, 9 September 2012, 09.30 - 10.30, Congress Hall Foyer 3rd Floor
PS-04 Poster Session Neuropathology

PS-04-001
Sacrococygeal extraspinal mass: A rare presentation of myxopapillary ependymoma
G. Aktürk*, A. Ersen, S. Men, K. Yucesoy, T. Canda
*Dokuz Eylül University Hospital, Dept. of Pathology, Izmir, Turkey

Objective: Myxopapillary ependymomas (MPE) often occur at the filum terminale but occasionally occur outside the central nervous system (CNS). Common site for these extraneural tumors is sacrococcygeal area.
Method: A cocygeal MPE with radiologic, gross and microscopic features will be presented.
Results: A 39 year old female admitted Neurosurgery Department with painful coccygeal mass. Magnetic resonance imaging revealed a coccygeal, well-demarcated, non-enhancing mass of 4×5 cm in diameter. The mass did not have any connection with the spinal cord. It was completely excised and grossly the cut surface of the encapsulated mass was soft. Microscopically the tumor was comprimised of myxoid stroma with pseudopapillary structures around hyalinized vessels. The tumoral cells showed intracytoplasmic dot-like positivity with EMA. There were no mitosis, and the Ki67 labeling index was low.
Conclusion: Extraspinal MPEs are rare and the most common location is sacrococygeal area. These masses are often preoperatively misdiagnosed as pilonidal sinus. Unlike the CNS MPEs, extraspinal MPEs have a potential to metastasize even if they do not show any anaplastic morphological feature. Long term follow-up is recommended as metastases can occur up to 20 years after initial presentation.

PS-04-002
Cerebellar liponeurocytoma: Report of two cases
L. Andres*, I. Hernandez, B. Mateos, J. I. Lopez, L. Zaldumbide, A. Perez Zabala, N. Cerda, G. Muniz
*Hospital University de Cruces, Dept. of Pathology, Barakaldo, Spain

Objective: Cerebellar liponeurocytoma (CL) is a rare neoplasm with neuronal, astrocytic and lipomatous differentiation arising in adults. The entity is considered as a grade II neoplasm in the last WHO classification of central nervous system tumours. We show two typical cases of this entity stressing the spectrum of histological changes and its differential diagnosis.
Method: Patient 1 is a 72-year-old woman with a history of headaches and instability. CT scans and MRI showed a 5 cm in diameter relatively ill-defined, poorly enhanced, round tumour mass in the left hemisphere. Patient 2 is a 56-year-old woman with a history of headaches and instability. MRI showed a 6.5 cm in diameter well-defined triangular lesion in the right hemisphere.
Results: Complete surgical resection was achieved in both cases. Both tumours showed highly cellular neoplasms composed by round to polygonal cells with scant cytoplasm and round nuclei with fine chromatin pattern. Mitoses were not seen. Well differentiated lipomatous cells grouped in irregular nests were intermingled with the predominant neuronal component.
Conclusion: Cerebellar liponeurocytomas are located in the cerebellar hemispheres and pursue a non aggressive clinical course, with local recurrences detected mainly after incomplete resections. The typical adipous tissue is the result of a lipidization process and not a true metaplasia.

PS-04-003
Giant cell tumor of the temporal bone: Report of a case
N. Arnogiannaki*, M. Sofopoulos, E. Pigadioti, N. Koufopoulos, A. Vacarciuc, A. Apostolaki
*Saint Savvas Hospital, Dept. of Pathology, Athens, Greece

Objective: Giant cell tumor of bone is an uncommon neoplasm that accounts for about 5 % of all bone tumors. It usually involves long bones and is very rarely encountered in the skull where it mostly involves the sphenoid and temporal bones. It is a benign neoplasm but can be locally aggressive.
Method: We present a case of a 32 year old woman with history of multiple sclerosis whose routine CT scan revealed a mass with corrosive features and calcification situated at the petrous portion of her left temporal bone. A biopsy was sent to our laboratory.
Results: Histopathologic examination revealed a neoplasm composed of sheets of oval mononuclear cells, with uniformly distributed nuclear chromatin, evenly intermixed with numerous giant cells that contain a variable number of nuclei with features similar to those of mononuclear cells. Cytoplasm of either cell type was eosinophilic and cell borders were indistinct. Mitoses were scarce and regular. Foamy histiocytes, hemosiderin and microscopic nodules of cartilage formation were also noted.
Conclusion: Although giant cell tumor is a benign neoplasm its' localization in this case posses a threat that should be managed surgically and by adjuvant radiotherapy if complete excision is unobtainable.

PS-04-004
Leptin and leptin receptor expression in pituitary adenomas
G. Ayranci*, T. Avsar, A. Seker, T. Kilic, S. Bozkurt
*Marmara University, Dept. of Pathology, Istanbul, Turkey

Objective: Leptin is a regulatory hormone which is mainly synthesized by adipocytes and regulates body fat mass. Leptin also has regulatory function on anterior pituitary. In

this study, we have investigated the expression levels of leptin (Ob) and its receptor (Ob-R) in various types of pituitary adenomas and normal anterior pituitaries.
Method: 50 pituitary adenoma cases between 2006 and 2011 were selected. Immunohistochemistry for leptin (Ob) was performed for each 10 cases of null cell, GH, ACTH, prolactin and FSH/LH secreting adenomas. Western blot was performed for leptin receptor (Ob-R) in 9 cases consisting of all five subtypes.
Results: Immunohistochemical staining showed greater immunoreactivity for leptin in normal pituitaries compared to adenomas. Except for ACTH-secreting pituitary adenomas, all other four subtypes showed widespread and intense staining for leptin ($P<0.0001$). Null and FSH/LH-secreting subtypes were mainly showed cytoplasmic and nuclear staining. Western blot analysis showed leptin receptor expression in all types of adenomas except null cell.
Conclusion: Leptin immunoreactivity is decreased in pituitary adenomas compared to normal pituitary. Leptin receptor is found in various types of pituitary adenomas except null cell adenoma. This finding shows regulation of leptin and leptin receptor n has role in secretory function of pituitary adenomas.

PS-04-005
Association between expression of KAI1, MMP-2, CD44v6 and malignancy of human primary brain tumors
J. Bar*, B. Paradowski, A. Halon, A. Lis-Nawara, L. Zub, M. Jelen
*Wroclaw Medical University, Dept. of Pathomorphology, Poland

Objective: Primary malignant brain tumors often present local invasive growth. The study aimed to estimate the expression of KAI1 protein, MMP-2, CD44v6 and their correlation in gliomas of different grade of malignancy.
Method: Expression of MMP-2, CD44v6 and KAI1 was evaluated on 154 formalin fixed paraffin-embedded tissue blocks divided into: pilocytic astrocytoma ($n=15$), fibrillary astrocytoma ($n=17$), anaplastic astrocytomas ($n=27$), anaplastic oligodendrogliomas ($n=27$), glioblastoma multiforme ($n=54$) and normal brain tissue ($n=14$) using immunohistrochemistry.
Results: MMP-2 and CD44v6 was observed frequently in gliomas with high grade of malignancy. KAI1 immunoreactivity was mainly observed in specimens with low degree of malignancy. MMP-2 and CD44v6 expression was significantly increased when the degree of malignancy of the gliomas increased ($p<0.05$). Whilst KAI1 expression increased when the degree of gliomas malignancy decreased ($p=0.03$). Positive correlations between MMP-2 and CD44v6 ($p=0.01$) and inverse between KAI1 and MMP-2 expression ($p=0.02$) were found in gliomas.
Conclusion: These results indicate that association between MMP-2 and CD44v6 expression may increase dissemination of tumor cells. Whereas, high expression of KAI1 protein might suppress the function of MMP-2 in gliomas.

PS-04-006
Pediatric glioblastoma: A case report
A. Barin*, S. Ekici, C. Altunkaya, S. Yilmaz, G. S. Yalcin, G. Hatipoglu, M. Caydere, H. Ustun
*Ankara Education Hospital, Dept. of Pathology, Turkey

Objective: Glioblastoma is the most common malignant tumor of central nervous system in adults which characterized by malignant pleomorphic astrocytic cells with marked nuclear atypia, mitotic activity, necrosis and/or microvascular proliferation. Glioblastoma may manifest at any age but usually affects adults especially older than 50 years. In this case, we present a pediatric glioblastoma case because it has seen rarely under 20 years and it is so important owing to its prognosis.
Method: An 11-year-old boy has had headache for 20 days. According to radiological imagings 23×20 mm in diameter infiltrating mass has seen in temporal lobe contains 15×7 mm in diameter cystic component and contrast enhancement was noted. Clinically grade 3 astrocytoma has thought primarily and he has been operated.
Results: In microscopic examination nuclear atypia, mitotic activity and microvascular proliferation has seen without necrosis.
Conclusion: This case has reported as Glioblastoma (WHO grade IV).

PS-04-007
Gliosarcoma: A study of 3 cases
A. Bdioui*, M. T. Yacoubi, S. Hmissa, N. Labaied, S. Miladi, A. Ben Abdelkhader, M. Mokni
*CHU Farhat Hached, Dept. of Pathology, Sousse, Tunisia

Objective: Gliosarcomas are biphasic neoplasms composed of a glioblastoma admixed to a sarcomatous component with different lines of differentiation. Histogenesis of these tumors is still discussed. Our objective is to specify pathological characteristics of this neoplasm its related to or not to glioblastoma.
Method: 3 cases of gliosarcomas diagnosed in our department of pathology. Clinical, radiological, therapeutic and follow-up data were reviewed. Histological features and immunohistochemical results were also established.
Results: 3 female patients with a median age of 46 years (ranging 30–69 years). intracranial hyperpressure and paralysis are main symptoms. The brain imaging showed frontal, fronto- parietal and intra ventricular expansive process, respectively. Microscopically, a biphasic pattern, with anaplastic astrocytic cells alternated with malignant mesenchymal areas,

demonstrating a fibrosarcoma pattern, in two cases and rhabdoïd pattern in one case. Immunohistochemical stain confirmed the diagnosis of gliosarcoma in each case. Patients were treated by surgical excision; One patient was lost on follow-up. One patient died by postoperative complications.
Conclusion: Clinical, radiological and follow-up features of gliosarcomas share great similarities with glioblastomas. Histopathological, histochemical and immunohistochemical studies are helpful in accurate diagnosis. Cytogenetic and molecular data support a monoclonal origin for these tumors.

PS-04-009
Synoviosarcoma of nerve: Case report
S. Costantini*, A. Tosi, G. Fraternali Orcioni, D. De Biase, Y. Ishikawa, V. Eusebi
*Bellaria Hospital, Dept. of Anatomic Pathology, Bologna, Italy

Objective: Case of biphasic synovial sarcoma of nerve in a 59 year-old female located between flexor muscles and radial diaphysis and adherent to median nerve and ulnar artery is presented.
Method: Tissue was fixed in formalin, embedded in paraffin and stained with Haematoxylin and Eosin. Periodic Acid-Schiff stain without diastase pre-digestion was obtained. Ventana antibodies were employed: TTF-1, ER, EMA, S100, CK 14, CK 7 and MNF 116. SS18-SSX fusion gene transcript was detected with conventional RT-PCR and qRT-PCR.
Results: Macroscopically nodule had smooth circumscribed borders, grey-yellowish colour and measured 3,7×3×2,5 cm. Histologically it was delimited by a dense sclero-hyaline capsule and constituted of numerous glands lined by one layer of cuboidal-columnar cells showing eosinophilic cytoplasm and round to ovoid nuclei with a single small nucleolus. They contained dense eosinophilic strongly PAS and EMA positive material. Glands were immersed within tightly packed spindle cells. Mitoses were scanty. Necrosis was absent. EMA strongly stained most of the glandular as well as scanty spindle cell elements. Chromosomal reciprocal translocation t (X; 18) with positive signal for SS18-SSX1 transcript was seen.
Conclusion: Synovial sarcoma of nerve is a rare condition that has to be distinguished from histologically similar lesions.

PS-04-010
Rabdoid meningioma: Presentation of a rare case
I. Dimitriadis*, A. Heva, I. Matzarakis, A. Sekouli, P. Sakellariou, L. Sakkas
*Hospital of Thessaloniki, Dept. of Pathology, Greece

Objective: In 1998, Keppes and later Perry suggested the term rhabdoid meningioma which was adopted into the WHO classification (grade III) in 2000.
Method: We present a rare case of a rabdoid meningioma and study the clinicopathological characteristics of the neoplasm.
Results: A 68-year-old woman was submitted in surgical excision of an endocranial tumour (d:3 cm) in our hospital. The histological examination revealed entirely rabdoid morphology. The neoplastic cells expressed the following immunohistochemical phenotype: S100+, Vimentin+, EMA+, GFAP−, PR+, HMB45−, A1/AE3+(focally), CK8/18+(focally), SMA−, Ki-67 (<1)%.
Conclusion: Rabdoid phenotype represents an indicator of malignant transformation regardless of the tumor's histogenesis. Expression of Ki-67 antigen correlates with recurrence even in meningiomas with minimal atypical features, which should prompt closer surveillance after excision. Rabdoid meningiomas behave aggressively and have bad prognosis contrary to the classic meningioma. Prognosis is influenced by it's complete excision and the expansion within the intracranial cavity. It has to be distinguished from glioma, melanoma and metastatic carcinoma. The patient after 1 year is in generally good health, and is followed up by oncologists.

PS-04-012
Atypical Extraventricular Neurocytoma (Case Report)
S. Ersöz*, U. Yazar, A. Reis, K. Kuzeyli
*Karadeniz Technical University, Pathology, Trabzon, Turkey

Objective: Central neurocytomas are rare intraventricular tumors with neuronal differentiation, typically located in the ventricles while tumors located outside the ventricles designated as "extraventricular neurocytomas" (EVN). Neurocytomas are classified as atypical if they exhibit a MIB-1 labeling index >2 % or atypical features, like focal necrosis, vascular proliferation, and increased mitotic activity. We here report a case of atypical EVN of the left frontal lobe.
Method: A 60-year-old woman patient admitted to hospital for headache. CT scan showed a large partially calcified cystic mass. MR imaging showed circumscribed, solid mural nodule within the cystic mass. The patient underwent a left frontal craniotomy. Specimens were fixed in 10 % formalin and stained with hematoxylin and eosin. For immunohistochemistry, sections were incubated with monoclonal antibodies to synaptophysin, neurofilament protein, MAP-2, NSE and GFAP. The proliferative index was assessed with MIB-1.
Results: Histopathological examination revealed a neuronal neoplasm composed of uniform cells in solid sheets. Small necrosis areas and mitotic figures were evident. Immunohistochemical examination revealed positive results for synaptophysin, neurofilament protein, MAP-2, and NSE. GFAP staining was negative. MIB-1 index was calculated as 5 %.

Conclusion: In general, central and extraventricular neurocytomas have a good prognosis. Atypical extraventricular neurocytomas are quite rare like this case with malignant histopathological properties.

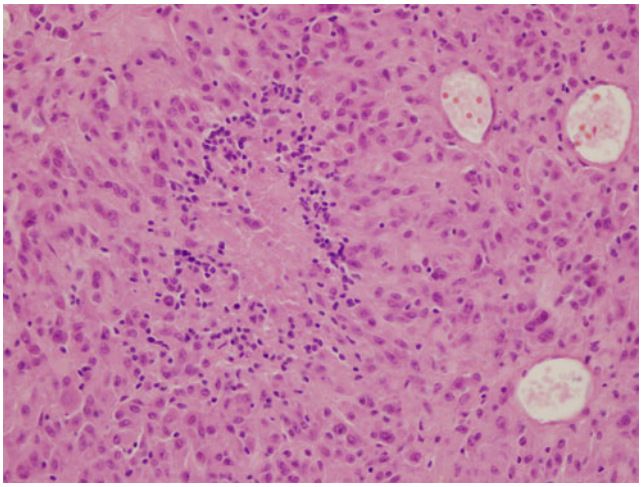

PS-04-013

Meningioma and Schwannoma associated with Neurofibromatosis Type 2: A case report of rare genetic disorder

O. E. Gürer*, R. Tuncer
*Akdeniz University, Dept. of Pathology, Antalya, Turkey

Objective: Neurofibromatosis is a group of genetic disorders referred as phakomatoses. There are two main forms called NF1 and NF2 which have different incidence, molecular characteristics, and clinical exhibitio. Both have higher risk for the development of certain rare malignant tumors that occur in the brain, nerves or spinal cord.
Method: Here, we present a rare case in which multiple meningiomas and vestibular schwannomas diagnosed in the same operation.
Results: A 23 year old woman presented with hearing loss clinically. She underwent surgical treatment for tumoral lesions in two different localization in the same session. One of them resected from pontoserebellar location was diagnosed as a schwannoma and the other one located on dura was diagnosed as a meningioma respectively.
Conclusion: NF2 is far less common than NF1 and strict diagnostic criteria have been described each of them. Since difficulty to detect genetic abnormalities and no single criteria is pathognomonic, clinical characteristics much more valuable for differentiation. Knowledge of associated clinical features will help to correct diagnosis and to predict much more devastating clinical course for NF2.

PS-04-014

Diagnostic confusion: Central neurocytoma

N. Gursan*, E. Demirci, M. Calik, F. Daloglu, C. Gundogdu
*Ataturk University, Medical Faculty, Erzurum, Turkey

Objective: Central neurocytoma is a rare intraventricular brain tumor that affects young adults and presents with increased intracranial pressure secondary to obstructive hydrocephalus. They are usually located in the supratentorial periventricular region. Because of some clinical and radiological findings CNS neurocytomas were confused with other intraventricular lesions.
Method: A 37-year-old male was admitted with chronic headache with 6 months duration on July 21, 2011, when there were no neurological deficits or physical abnormalities. Computed tomographic (CT) scans showed 51×40 mm a mixed density mass with amorphous calcification in the right lateral ventricle, which was irregularly enhanced by contrast medium. Light Microscopy showed sheets of monotonously neoplastic cells with uniform round-to-oval nuclei and inconspicuous nucleoli. The cytoplasm was clear or eosinophilic with indistinct border. Capillary networks were well developed and divided the tumor cells into groups. No nuclear pleomorphism or mitosis was seen. We present a case of intraventricular neurocytomas confirmed by immunohistochemical studies.
Conclusion: This rare tumor causing diagnostic confusion, discussed by the literature.

PS-04-015

A case of oligodendroglioma with neuronal differentiation

T. Hirose*, S. Nobusawa, Y. Nakazato, A. Sasaki
*Tokushima Pref. Center Hospital, Dept. of Diagnostic Pathology, Japan

Objective: We report a case of oligodendroglioma showing marked neuronal differentiation.
Method: A 46-year-old female visited an emergency room because of an attack of convulsion. Imaging analyses disclosed a calcified, 3.5×3 cm tumor in the right frontal lobe.
Results: The resected tumor was composed of a mixture of oligodendroglioma-like (OLG) and gangliocytoma-like (GC) areas. In the former, fried-egg appearance and more cellular nodules were recognized. In the latter, there were numerous small neuron-like cells with basophilic cytoplasm. OLG areas showed immunoreactivity for Olig2, GFAP and mutant IDH1, while GC areas were positive for synaptophysin and NeuN. Ki-67 labeling index was about 10 % in cellular nodules of OLG areas. At least one allelic loss of 1p/19q was detected in 53.4/61.2 % cells in OLG areas and 47.2/40.6 % in GC areas with FISH analyses. Furthermore, an identical mutation of IDH1 (G395A, R132H) was demonstrated in both OLG and GC areas.

Conclusion: Genetic abnormalities including 1p/19q loss and IDH1 mutation indicate that this case is an oligodendroglioma associated with prominent ganglion cell differentiation. Oligodendrogliomas with neuronal differentiation like our case may suggest a close relationship between oligodendroglial progenitor cells and neuronal cells.

PS-04-016

Gemistocytic astrocytoma with granulomatous inflammation

O. Ipci*, E. Atik Dogan, T. Ozgur, H. Gokce, N. Yilmaz, A. Yilmaz
*Mustafa Kemal University, Dept. of Pathology, Hatay, Turkey

Objective: The coexistence of granulomatous inflammation and astrocytoma is extremely rare. Hemostatic agents are used to control intraoperative bleeding in many surgical subspecialties, including neurosurgery. There are occasional reports of granulomatous reaction to biomaterials.
Method: We aimed to present a 35 year old female patient, who was operated because of the tumor at left frontoparietal region. Tumor was histopathologically reported as oligoastocytoma. However, no granulomatous inflammation was detected beside the tumor. After 6 months, patient was reoperated because of tumor recurrence, abscess and inflammatory necrotic tissue beside the tumor. Histopathologically, gemistocytic astrocytoma with granulomatous inflammation and abscess formation was reported. No micro-organism had grown in any kind of cultures. At our neurosurgery department surgicel is used after craniotomy as hemostatic agent. It's raw material is cellulose and absorbed in about 3 months.
Results: In the literature, germinoma accompanied by granulomatous inflammation have been reported. However, astrocytic tumors don't express such an association. The patient doesn't use any drugs forming granuloma reported in the literature.
Conclusion: We encountered that Surgicel causing granulomatous inflammation in very few cases in the literature. The findings might be secondary to surgicel that used in the first operation.

PS-04-017

Allelic loss and microsatellite instability in astrocytic tumors

N.-R. Kim*, Y.-S. Chae, S.-J. Cho
*Gachon University Gil Hospital, Dept. of Pathology, Incheon, Republic of Korea

Objective: Astrocytic tumors show various molecular and genetic alterations in its development and progression. Glioblastoma multiforme (GM) develops as either de novo or by progression from diffuse astrocytomas (DA) or anaplastic astrocytomas (AA) by genetic alterations.
Method: Loss of heterozygosity (LOH) and microsatellite instability (MSI) was investigated in 40 cases of astrocytic tumors (DAs [n=12], AAs [n=15] and GMs [n=13]) with 14 microsatellite markers and 5 microsatellite markers harboring p53 and PTEN, respectively. The patients' age ranged from 27 to 77 years (mean, 50 years).
Results: LOH was statistically significant in AAs and GMs, compared to that of DAs (p=0.023). LOH for 17p13 and LOH-H group for 10q23 were statistically significant in AAs and GMs (p=0.045 and p=0.001). MSI rate in DAs, AAs and GMs was detected in 16.7 %, 13.3 %, 23.1 %, but it showed no significant correlation with prognosis factors. MSI and MSI-H rates were correlated with younger (〈50 years) group (p= 0.040, p=0.011, respectively).
Conclusion: Alterations on PTEN and p53 may contribute to the development and progression of astrocytic tumors. Especially, LOH-H for 10q23 and 17p13 is considered as clinical application of discriminating the AAs and GMs from DAs. MSI might be involved in the tumorigenesis of relatively young patients.

PS-04-018

Histopathologic findings of three Charcot-Marie-Tooth patients with PMP22 mutation and Dejerine-Sottas Syndrome

H.-S. Koo*, S.-H. Kim, B.-O. Choi, J.-Y. Park
*Ewha Womans University, School of Medicine, Seoul, Republic of Korea

Objective: Charcot-Marie-Tooth disease (CMT) III or Dejerine-Sottas syndrome is a severe hereditary demyelinating motor and sensory neuropathy presenting in infancy or early childhood with delayed motor milestone and extremely slow nerve conduction velocities.
Method: Among 530 unrelated Korean CMT patients, mutational screen for well known CMT genes reveals three patients with PMP22 de novo mutation showing DSS. The histopathological findings of distal sural nerves are analyzed in all patients twice; Cases 1 and 2 with 10 years interval and Case 3 with 17 years.
Results: On semi-thin transverse sections, all the remaining axons (thinly myelinated or demyelinated) are surrounded by classic or basal lamina onion bulbs (OBs). The first biopsy of Case 1 (2 years-old) shows OBs (4,452/mm2), which consists of 2,295 (51.55 %) MFs with OBs and 2,157 (48.45 %) demyelinated axons with OBs. The second biopsy shows OBs (2,275/mm2), consisting of 425 (18.68 %) MFs with OBs, 489 (21.49 %) demyelinated axons with OBs, and 957 (42.07 %) OBs with no discernible axons.

Cases 2 and 3 show similar histopathologic findings with main differences in numbers of OBs.
Conclusion: Although the differences noted in two biopsies are probably due to age of the patients, correlations with clinical symptoms will be helpul for management of the patients.

PS-04-019
Histopathological findings of sural nerves in three patients with seipin gene mutation
H.-S. Koo*, H.-K. Jung, B.-O. Choi
*Ewha Womans University, School of Medicine, Seoul, Republic of Korea

Objective: Two mutations of the seipin gene (N88S and S90L) have been reported and known to cause neurodegenerative disorders. We performed whole exome sequencing in two Charcot-Marie-Tooth families and identified three patients with two causative heterozygous mutations (N88S and S90W) and S90W is a novel mutation.
Method: The histopathological findings of distal sural nerves are analyzed in two patients (Cases 1 and 2) with S90W novel mutation (FC305) and a patient (Case 3) with N88S mutation (FC51).
Results: Transverse semi-thin sections reveal increased numbers of myelinated fibers (MFs) (11,898/mm2; 11,429/mm2; 9,430/mm2) with increased small MFs forming regenerative axon clusters and loss of large MFs. Histogram shows unimodal distribution pattern. Cases 1 and 2 show the similar ranges and average of diameter of MFs (1.46~13.24 μm, 5.13 μm). Case 3 shows more numbers of small MFs (0.82~10.50 μm, 3.73 μm). Ultra-structural examination reveals MFs with myelin abnormalities, pseudo-onion bulb formation including single axon or axon clusters, and thick MFs.
Conclusion: The findings are consistent with axonal neuropathy with features of demyelination. Additional cases will be necessary to know the significance of differences between these cases.

PS-04-020
Immunohistochemical subtyping of primary and secondary glioblastomas
K.-S. Lee*
*Seoul National University Hospital, Republic of Korea

Objective: Glioblastomas (GBLs) may develop de novo (primary GBL; P-GBL) or through progression from low-grade or anaplastic astrocytomas (secondary GBL; S-GBL). For subtyping of GBLs, we tried immunohistochemical anaysis.
Method: We collected 150 cases of GBLs in SNUBH and SNUH. The mean age at the time of the primary surgery was 58.8 years (range 19–85). Immunohistochemical studies were performed for EGFR, p53 and IDH-1.
Results: According to clinical history, GBLs consisted of 146 primary and four secondary GBLs. However, EGFR(+)/p53(−) immunohistochemical features of P-GBL consisted 41.3 % and EGFR(−)/p53(+) immunohistochemical features of S-GBL consisted 28.6 % among 150 cases. EGFR(+)/p53(+) was noted in 20.6 % and EGFR(−)/p53(−) in 9.3 %. Immunohistochemical expression of IDH-1 was noted in 14 cases (9.7 %) out of 144 cases. Expression of IDH-1 and EGFR(−)/p53(+) showed positive correlations with young age. Characteristic features of S-GBL were noted in 3.5 % of clinically P-GBL.
Conclusion: We analyzed immunohistochemical subtypes of Korean glioblastomas. Combination of EGFR and p53 was unsatisfactory but combination of EGFR, p53 and IDH-1 can be a good tool for immunohistochemical subtyping of glioblastomas.

PS-04-021
Contribution of muscle biopsy to the diagnosis of extraocular mitochondrial myopathies: Survey of case series
D. R. Lujan Rodriguez*, M. Moreno Vadallares, E. Rivas Infante, M. Moreno Valladares
*Hospital Virgen del Rocío, Dept. de Anatomía Patológica, Sevilla, Spain

Objective: The diagnosis of mitochondrial myopathy depends on a variety of clinical findings, family history, muscle involvement features, specific laboratory abnormalities, and results of histological, biochemical and genetic analysis. Chronic progressive external opthalmoplegia (CPEO) is the most common phenotypic syndrome of the mitochondrial myopathies, characterized by slowly progressive paralysis of the extraocular muscles.
Method: Retrospective study of the utility of histochemical stains in muscle biopsy of 12 patients over 14 years old with clinical diagnosis of CPEO. Muscle sections were stained with hematoxylin and eosin (HE), Masson trichrome (MGT), oil red (OR), and enzyme histochemistry for succinic dehydrogenase (SDH) and cytochrome oxidase (COX).
Results: The mean number of abnormal muscle fibers with increased cytoplasmic granularity and basophilia on HE and Ragged Red Fibers (RRF) on MGT was 10 %; 14 % showed blue ragged on SDH; 40 % were negative on COX stain. Mild lipid droplets accumulation on OR stain were demonstrated in just a few individual muscle fibers of 7 cases of the series.
Conclusion: Histochemical stains of muscle biopsy may provide helpful clues for specific mitochondrial syndromes, despite the need for genetic analysis for accurate diagnosis. CPEO is characterized by RRF, strong SDH staining and

COX-deficient fibers on muscle biopsy, reflecting respiratory chain complex deficiency.

Fig. 1. Staining procedures showing morphological findings of extraocular mitochondrial myopathy in a patient diagnosed with CPEO: (A) abnormal granular fibers (HE, 40x); (B) characteristic RRF (MGT, 40x); (C) blue ragged fibers (SDH, 20x); (D) cytochrome C oxidase negative fibers creating a mosaic appearance (COX, 20x); (E) increased lipid droplets deposits (OR, 20x)

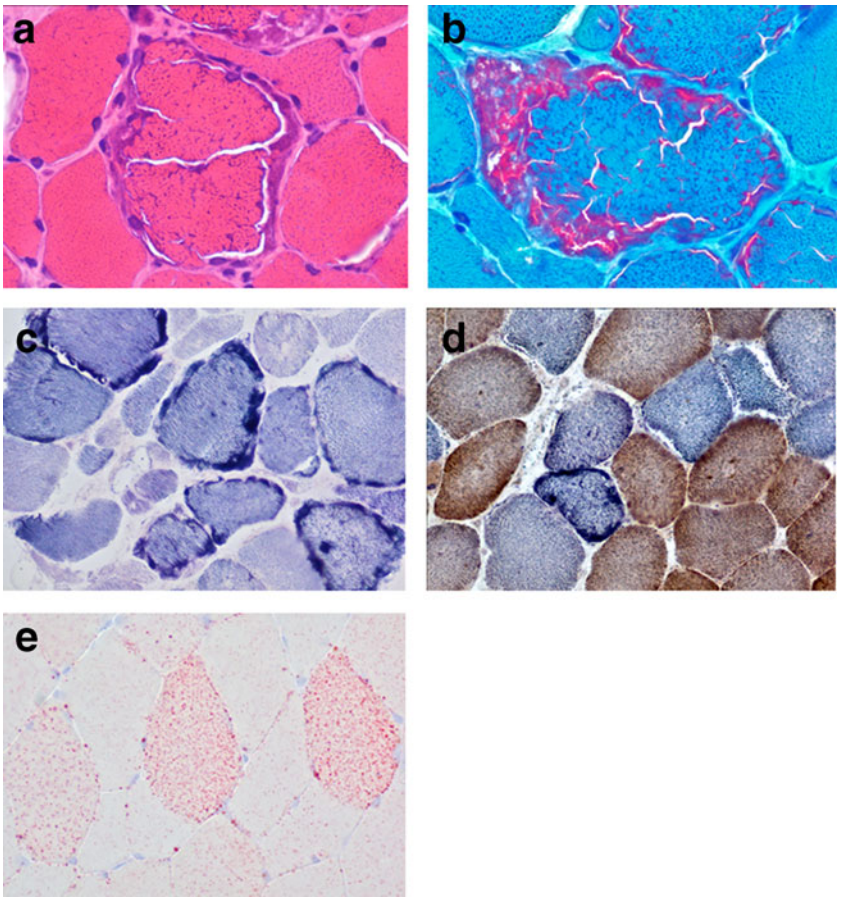

PS-04-022

An immunohistochemical study of HER2 expression in meningioma and its correlation with tumor grade

P. Mahzouni*, M. Movahedipour
*Isfahan University of Medicine, Dept. of Pathology, Esfahan, Iran

Objective: Meningiomas account for about 15–30 % of all primary intracranial tumors. According to the 2007 WHO classification, meningiomas are divided into three grades (I, II and III). Recurrence is an issue following surgical treatment of meningioma, especially in grades II and III. HER2 (also known as erbB-2) is a 185-kD transmembrane glycoprotein with tyrosine kinase activity. HER2 is expressed in some human malignancies and can be a potential target for therapeutic intervention with selective inhibitors. There are only a few studies on the relationship between meningioma and HER2 expression, and the results are different as well. The aim of this study was to determine this relationship.
Method: Seventy-two paraffin blocks of meningioma were selected randomly and immunohistochemical staining was then performed for each specimen.
Results: Thirty-one of the 72 meningiomas were HER2-positive. HER2 expression was observed in 11 (55 %) of the 20 grade II/III, and 20 (38.5 %) of the 52 grade I meningiomas.
Conclusion: Consequently, HER2 expression was detected in 43 % of meningiomas. No significant difference was seen between grade I and II/III meningiomas, primary and recurrent tumors, and males and females from the point of view of HER2 expression.

PS-04-024

Is accumulation of iron in the human brain dependent on the microenvironment in certain regions?

L. Maruscakova*, O. El-Hassoun, M. Kopani, J. Jakubovsky, I. Hulin
*Comenius University, Medical School, Bratislava, Slovakia

Objective: In our previous papers we studied accumulation of iron and proteoglycans in the brain. The aim of this analysis is to build on our previous results alongside other authors to investigate the reason for the presence of excessively accumulated iron observed in Parkinson disease (PD).
Method: Postmortem samples taken from the globus pallidus were prepared for light microscopy for iron and proteoglycans detection. Patients had neither iron metabolism disorders nor had clinical signs of neurodegeneration. The samples were analysed using electron paramagnetic resonance (EPR) to investigate the bounds between iron and proteoglycans.
Results: EPR measurements confirm the presence of complex bounds between Fe(III) and proteoglycans.
Conclusion: Previous data showed a possible dependance between accumulated iron, proteoglycans, ferrireductive alpha-synuclein and Lewy bodies. We propose a mechanism of toxic iron accumulation in the brain in PD. This cyclic process of amplification is presented by onward steps. It is completed by our own observations into one cycle. The initiator of this vicious circle is probably an impirement of the equilibrium in the presence of useful amount of iron. Understanding these relations could bring new insights to the neurodegenerative disease.

PS-04-025

Role of PDGFR overexpression in Schwannoma, and its diagnostic and therapeutic implications

T. Neuman*, Y. Fellig
*Hadassah Medical Center, Dept. of Pathology, Jerusalem, Israel

Objective: Platelet-Derived- Growth- Factor- Receptors (PDGFR) are transmembrane tyrosine kinase receptors that function as relay points for signaling pathways. They play a key role in numerous processes that affect cell proliferation, tumor genesis, cancer invasion, metastasis, and modulation of apoptosis. Recently, PDGFR has been demonstrated to be overexpressed in Schwannoma in vivo, and in a small series of acoustic neuromas. However, its phenotypic expression in different variants of Schwannoma remains largely unclear.
Method: Immunohistochemical staining was used to detect PDGFR expression in archived formalin-fixed, paraffin-embedded Schwannoma tissue samples (n=24). Clinical and pathological data including age, sex, location, histological variants and staining patterns were correlated with kinase expression.
Results: PDGFR was expressed in 22 (91.6 %) out of 24 Schwannoma samples. In two of these cases PDGFR overexpression was a key feature in the pathological diagnosis of Schwannoma.
Conclusion: Exploring PDGFR overexpression in Schwannoma, as demonstrated in our study might serve in the pathological diagnosis of challenging cases. Also, there are implications regarding the molecular targets involved in the development of this tumor and possible treatment by Gleevec (Imatinib Mesylate) was suggested.

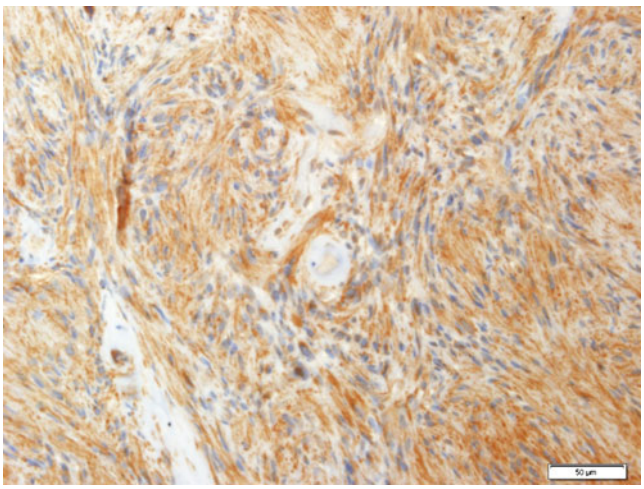

PS-04-026

Spinal Schwannomatosis: Three cases of Spinal Schwannomatosis

S.-S. Paeng*, W.-G. U, S.-H. Lee
*Wooridul Hospital, Dept. of Pathology, Seoul, Republic of Korea

Objective: Schwannomas are slow growing benign peripheral nerve tumors. Schwannomatosis is defined as an extremely rare tumors characterized by the presence of multiple schwannomas in the absence of typical signs of NF1 and NF2 syndromes, and show a distinct clinical and genetic syndrome.
Method: We reviewed 63 cases of patients with pathologically defined schwannomas and identified those with schwannomatosis. All 3 cases was retrospectively reviewed clinical-pathologic and radiologic findings.
Results: Case 1.) A 41-year-old man with a 3 months history of low back pain. MRI showed well enhanced intradural-extramedullary mass 2.9 cm at L4-L5 level, and 0.9 cm at L2-L3. Case 2.) A 55-year-old woman with low back and buttock pain. MRI presented 0.6 cm well enhancing mass at T12-L1 level, and 0.3 cm at L2-L3. Case 3.) A

68-year-old woman with a 1 month of leg pain. MRI revealed well enhanced mass 3.3 cm at T12-L2 level, and 0.5 cm at L2-L3. Follow-up ranged from 10 months to 7 years without recurrence.
Conclusion: We presented three cases of spinal schwannomatosis without recurrence or any other lesion after surgery. Schwannomatosis is a different disorder distinct from neurofibromatosis. Molecular diagnosis rules out NF2 and follow-up with careful monitoring is necessary.

PS-04-027
Spinal Meningiomas in male
S.-S. Paeng*, W.-G. U, S.-H. Lee, J.-I. Suh
*Wooridul Hospital, Dept. of Pathology, Seoul, Republic of Korea

Objective: Spinal meningiomas are relatively rare in comparison to the intracranial compartment accounting approximately 1.2 % of all meningiomas of the central nervous system. Spinal meningiomas are predominant in women. On the other hand, atypical and particulary anaplastic meningiomas show a male predominence.
Method: We reviewed 54 patients with meningiomas were surgically treated in our hospital between 2005 and 2011. Clinicopathological and radiological features were analyzed.
Results: Among 54 spinal meningiomas patients. 8 patients were male and 46 were female. All spinal meningiomas in male were located in thoracic area, and presented meningothelial subtype. Mean age was 45 (range 26–74). Follow-up range was from 1 month to 9 years. There is no evidence of recurrence. In 46 female spinal meningiomas, there were clear-cell (1 case), rhabdoid (1 case), and metaplastic subtypes (1 case).
Conclusion: Although good prognosis and same treatment in both sex groups, spinal meningiomas showed different clinicopathological findings including age, location, and subtype.

PS-04-028
Brain metastases of pancreatic ductal carcinoma as the first symptom of disease: Case and autopsy report
O. Paklina*, D. Rotin, G. Setdikova, L. Shishkina
*Burnacyan FMBC FMBA, Dept. of Pathology, Moscow, Russia

Objective: Pancreatic ductal carcinoma (PDC) has one of the worst prognoses. Up to 90 % of pancreatic cancers are diagnosed at the locally advanced or metastatic stage. However, brain metastases from pancreatic carcinoma are extremely rare since less than 20 cases have been reported in the literature since 1978.
Method: We report a case of a brain metastasis from pancreatic adenocarcinoma occurred in a 66 years old women.
Results: 62-year-old woman developed severe neurological symptoms and progressively decreased consciousness. CT revealed cystic tumor in cerebral peduncle and medulla oblongata. Stereotactic biopsy revealed metastasis of carcinoma. The patient died from of the twelfth day after STB because of recurrent hemorrhage. Autopsy revealed well-differentiated papillary adenocarcinoma in the head of pancreas and with multiple metastases in liver and two metastases in medulla oblongata and cerebral peduncle. IHC staining for cytokeratins 7, 18 and 19, mucin 1 and 5 AC types was strongly positive. Ki67 labeling index was 14 %.
Conclusion: We reported an autopsy case of brain metastases from pancreatic cancer, in which the patient initially developed symptoms of a neurologic disorder without exhibiting any symptoms of pancreatic disease.

PS-04-029
The use of Bone Morphogenetic Proteins (BMP2) with nunostrucnure Grey implant in reparation of bone tissue defect
T. Pavlova*, L. Pavlova, A. Nesterov, I. Goncharov, D. Kolesnicov
*Belgorod State University, Dept. of Pathology, Russia

Objective: The matters of materials development of scull bones defect plastic are obviously necessary this time. The experience in use of nanocostructive titans, composites, bone morphogenetic proteins was accumulated.
Method: Implant, made of nanoconstructed titan Grey, covered by 1 layer (gelatin, dextran), 2 layers (1- gelatin, dextran, 2- hydroxyapatite, collagen, dextran) and by 2 layers with use of bone morphogenetic proteins BMP-2. The experiment was conducted on 240 rat-males. In order to study the regeneration processes it were used light, fluorescence, probe and scanning microscopy with the trace element analysis.
Results: The most active changes were registered in the experimental group with use of composite from titan Grey with 2 layers of covering and BMP-2. The covering compound increase the rate of regeneration processes due to creation calcium and phosphorus ion depot and perform support function for again-formed tissue. Increase in the concentration of calcium, phosphorus, sodium, magnesium in trabeculae of bones in comparison with matrix bone at term of 12 weeks testify about active regenerative processes; the mature smooth surface with structured relief of bone trabeculae and diploic veins were detected.

Conclusion: Results can be used in neurosurgery, traumatology-orthopedics, dentistry, plastic and cosmetic surgery.

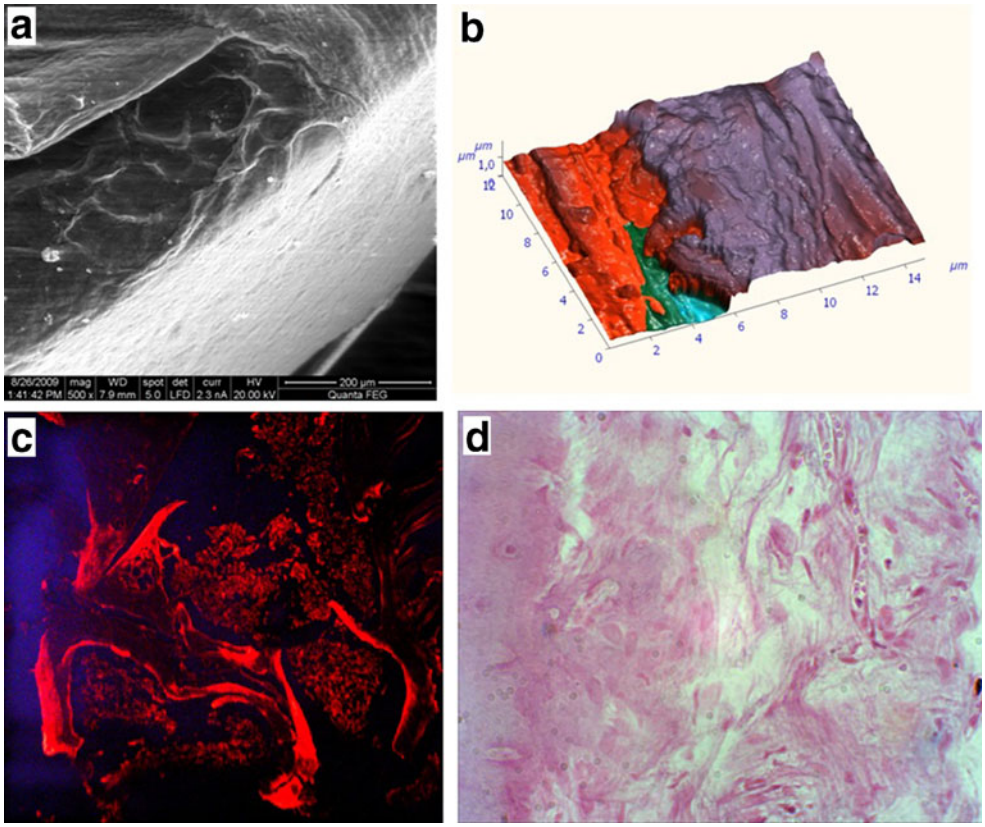

PS-04-031

Alpha-synuclein (AS) pathology of the Peripheral Autonomic Nervous System (PANS) in Parkinson Disease (PD) and other Lewy Body Diseases (LBD)

T. Ribalta*, E. Tolosa, J. Navarro Otano, E. Gelpi
*Hospital Clinic of Barcelona, Dept. of Anatomic Pathology, Spain

Objective: PD and other LBD have been associated with AS aggregates in the central nervous system (CNS). However, autonomic dysfunctions may appear at any time in the course of the disease. Our objective was to investigate the distribution of AS in the PANS in synucleinopathies.

Method: We examined PANS structures obtained at post mortem from 28 subjects (19 female, age range 69–93, mean 81) at our Brain Bank with a diagnosis of PD (10); Lewy body dementia (5); Alzheimer's disease (9); mixed dementia or other (4). A complete neuropathological study of PANS was performed, including dorsal spinal ganglia, vagus nerve, paraspinal sympathetic ganglia, mesentery, adrenals, digestive and genitourinary systems, heart, and skin. Routine and immune stains for AS and tyrosine-hydroxylase were applied. Cases were semiquantitatively assessed.

Results: 71 % of cases showed AS pathology in the CNS. Of them, AS aggregates were additionally present in the PANS in 80 %. A gradient in involvement was observed, being the paraspinal chain (particularly the stellate ganglion) the most constantly involved structure, followed by digestive system, adrenals, and GU system.

Conclusion: These findings indicate that AS aggregates are extensively found in PANS in synucleinopathies. The highest expression is found in the paraspinal ganglion chain and decreases in other PANS regions. Our results provide valuable information about potential development of new diagnostic and therapeutic strategies.

PS-04-032

Chordoid meningioma: A case report

S. Rjabceva*, M. Vozmitsel, M. Padrezenka
*Belarussian Medical Academy, Bio-Medical Research Center, Minsk, Belarus

Objective: Chordoid meningioma is an uncommon histopathological variant of meningioma.
Method: We report one case of chordoid meningioma occurring in adult patient. Paraffin embedded tissue was stained with hematoxylin–eosin. We used immunohistochemical markers such as CEA, EMA, vimentin and TLE3.
Results: A 81-year-old woman was hospitalized with clinic of an intracranial hemorrhage. Axial computed tomography (CT) of the brain revealed a 3.1*5.2*4.9 cm lesion with perilesional edema in the left temporoparietal region. Foci of intratumoral hemorrhage were also seen. Compression of the left lateral ventricle and midline shift to right side was seen. The patient underwent a left temporoparietal craniotomy for resection of the tumor and died 3 days after surgery. Histologically, sections revealed sheets, trabeculae and lobules of tumour cells scattered in a pale basophilic myxoid matrix. Some of these cells exhibited characteristic cytoplasmic vacuolization. A typical focal meningiomatous pattern was also observed. The tumor cells were diffusely positive for epithelial membrane antigen, vimentin and a strong nuclear immunoreactivity for TLE3. These cells showed negative immunostaining for CEA.
Conclusion: Chordoid meningioma should be distinguished from chordoma, chondrosarcoma, metastatic mucinous carcinoma and other variants of meningioma.

PS-04-033

Morphology of non-specified encephalopathy in cases of polymerase chain reaction proved presence of human herpesvirus-6

S. Roga*, I. Strumfa, S. Kuleznova, S. Chapenko, S. Rasa, M. Murovska
*Riga Stradins University, Teaching Department, Latvia

Objective: The morphology of non-specified encephalopathy is a complex medical problem. Human herpesvirus-6 (HHV-6) infection can be discussed as a predisposing factor. The aim of the present study was to investigate the presence of beta HHV-6 in non-specified adult encephalopathy cases.
Method: The blood, meninges and brain tissue were obtained in adult (aged 42–74 years) autopsies including 21 cases with encephalopathy and 23 cases in the control group. Tissues were submitted for routine histology including haematoxylin-eosin stain. The presence of HHV-6 genome (DNA) was analysed by nested polymerase chain reaction (nPCR), HHV-6 variants by restriction endonuclease analysis.
Results: The gross and microscopic structure did not reveal any specific changes. In the encephalopathy group, HHV-6 DNA sequence was found in meningeal tissues (16/21 cases; $p=0.0036$), in brain tissues (15/21 cases; $p=0.0007$), and both in brain and meningeal tissues (10/21 cases; $p=0.0174$). In the control group, the viral DNA was identified in meningeal tissues (7/23 cases), in brain tissues (4/23 cases), both in brain and meningeal tissues (3/23 cases). HHV-6B variant was detected in all cases.
Conclusion: On the basis of the present study it can be concluded that HHV-6 is a pathogenic factor that can predispose to encephalopathy.

PS-04-034

Pathological variants of brain metastases of breast carcinoma and their prognostic and predictive role in different age groups

D. Rotin*, O. Paklina, N. Lobanova, R. Sycheva, G. Kobyakov, O. Potapova, M. Stepanyan, E. Vetlova
*N.N. Burdenko Neurosurg. Institute, Dept. of Pathology, Moscow, Russia

Objective: Brain metastases of breast cancer (BMBC) are biologically heterogeneous group of tumors with different molecular changes and behavior. Aim: To evaluate prognostic and predictive role of pathological variants in BMBC in patients of different age groups.
Method: Sixty patients with BMBC after neurosurgery were divided into two age groups: Group I contained patients<50 years of age (43 %, 26/60), and Group II contained patients>50 years (57 %, 34/60). Tumor tissues were stained with H&E and antibodies for Ki-67, ER, PR, Her-2-neu. To clarify the Her-2-neu when its score was 2+ by IHC, FISH method was performed. For statistical analysis STATISTICA 8.0 software was used.
Results: All BMBC were divided into 5 IHC variants: luminal A, luminal B, luminal Her+(prevalent in Group II (35 %), classic Her+, and triple-negative BC (predominant in Group I (31 %). Recurrent BMBC was observed in 50 % (13/26) in Group I and in 21 % in Group II (7/34). Recurrence free-survival in Group I was significantly worse ($p=0.019$).
Conclusion: In younger patients (Group I), more BMBC patients had triple-negative BC, which had more

aggressive behavior. Recurrence-free survival in younger patients was significantly worse than that in older patients, where most frequent variant of BMBC was Luminal Her +.

PS-04-035

Meningeal hemangiopericytoma a pathological dilemma: Immunohistochemical and genetic study

T. Saoussen*, M. T. Yacoubi, D. H´Mida Ben Brahim, M. L'Adib, B. Ben Abdelkader, S. Hmissa, M. Mokni, A. Saad
*Farhat Hached Hospital, Dept. of Cytogenetics, Sousse, Tunisia

Objective: Meningeal Hemangiopericytoma (MHPC) is vascular tumor arising from pericytes. Most intracranial hemangiopericytomas apparently arise from the meninges, and often misdiagnosed as meningiomas.
Method: We report 8 cases of MHPS in comparison with 5 cases of meningiomas collected from Departement of histopathology in University Hospital of Sousse (Tunisia) in the period from 2007 to 2011. Immunohistochemistry (IHC) was performed by using EMA, Vimentine, CD99, Bcl-2, CD56, S100, Synaptophisine, P21, CD34, NSE, ACE, FVIII, Desmine, GFAP, P16 antibodies. Additionally we focused on the analysis of a large panel of genetic markers using molecular technique: Multiplex Ligation Probe Amplification (MLPA).
Results: Both MHPC and meningioma showed 100 % Vimentine positivity. The four useful IHC markers (Bcl2, EMA, CD34 and CD99) were 87 %, 37 %, 62 % and 62 % respectively in MHPC. However, the P21 antibody was seen positive in 62 % of HPC and less than 1 % in all meninigiomas.
Conclusion: Meningiomas and MHPC seems to be as spectrum of tumor that IHC can not absolutely differentiate between them because of their unspecific IHC profile. Despite of the help given by genetic investigations to characterize these two tumors, their prognosis still depends on histological grade.

PS-04-036

Intramedullary spinal cord metastases as initial presentation of lung cancer

M. Skender Gazibara*, E. Manojlovic Gacic, T. Gazibara, S. Raicevic, D. Grujicic, D. Radulovic
*University of Belgrade, Institute of Pathology, Serbia

Objective: It is extremely rare that the intramedullary spinal cord metastases (ISCM) are the first manifestation of cancer.
Method: In database of neurosurgery biopsies from 2002 to 2011 two cases of ISCM were found without preoperative signs of primary neoplasm. Surgically removed tissue was stained with hematoxylin-eosin and immunohistochemically using following markers: AE1/AE3, CK7, CK20, mammaglobin, TTF-1, GFAP, S-100 and vimentin.
Results: One patient was male aged 51 and another female aged 44. They presented with neck pain and rapidly progressive upper and lower limb weakness. Imaging analysis showed contrast-enhancing mass at the level C4-C6 in male and C2-C4 in female, reported as an ependymoma. Grossly, tumor tissue was of soft consistency and grey white color with yellowish foci of necrosis. Histopathology revealed moderately differentiated adenocarcinoma with distinct border to surrounded glial tissue. In both cases, tumor cells were immunopositive for AE1/AE3, CK7 and TTF-1 indicating primary lung origin. Postoperatively primary cancer was found in upper lobe of the left lung in both cases, without evidence of lymphadenopathy and other distant metastatic lesions in female.
Conclusion: Diagnosis of ISCM in both cases without preoperative signs of neoplasm in other organs was surprising. Immunohistochemical analysis was essential for determination of cancer origin.

PS-04-038

Meaning of alpha internexin (INA) expression related with molecular characteristics in adult glioblastoma and oligodendroglioma

J.-H. Suh*, S.-H. Park, C.-K. Park
*Seoul National University Hospital, Dept. of Pathology, Republic of Korea

Objective: Alpha-internexin (INA) is a proneuronal gene-encoding neurofilament interacting protein. INA is related to 1p/19q codeletion, and is a favorable prognostic marker. We studied INA expression in oligodendrogliomas (ODGs) and glioblastomas (GBMs) to verify its association with several molecular phenotypes, 1p/19q codeletion, and epidermal growth-factor-receptor (EGFR) amplification.
Method: A total of 230 low- and high-grade ODG and GBM cases were analyzed for INA expression by immunohistochemical staining, and 1p/19q and EGFR gene status was examined by fluorescence in-situ hybridization.
Results: INA was positive in 80.3 % of ODGs and in 34.3 % of GBMs. 1p/19q codeletion was detected in

77.0 % of ODGs and 5.5 % of GBMs. INA and 1p/19q codeletion were strongly correlated ($p<0.0001$). The specificity of INA expression for 1p/19q codeletion was 70.8 %, sensitivity was 100 % in all 228 tumors. INA expression was correlated with better progression- free survival (PFS) and overall survival (OS) [$p=0.0001$].

Conclusion: In conclusion, INA expression had high specificity and sensitivity to predict 1p/19q codeletion, and it was well correlated with PFS of both ODGs and GBMs. Therefore, INA expression could be a simple, reliable, and favorable prognostic and surrogate marker for 1p/19q codeletion.

PS-04-039

Atypical Teratoid/Rhabdoid Tumor Arising in Pleomorphic Xanthoastrocytoma: A Case Report

Y.-L. Suh*, J. Y. Jeong
*Samsung Medical Center, Pathology, Seoul, Republic of Korea

Objective: Atypical teratoid/rhabdoid tumor (AT/RT) is a rare, highly malignant, true rhabdoid tumor in the central nervous system predominantly presenting in young children. AT/RT typically shows rhabdoid cells which can be seen in other tumors also, but it is differentiated from other tumors by the specific genetic alteration involving the INI-1/hSNF5 gene. Only a few cases of AT/RT arising in low-grade glioma have been reported.

Method: A 13-year-old girl presented with headache, dizziness, nausea and vomiting. A 4.7 cm cerebellar mass was found on MRI image. The mass was totally removed.

Results: Histologically, the tumor revealed 2 distinct morphologic appearances: central areas of AT/RT containing rhabdoid cells and sarcomatous component in the background of pleomorphic xanthoastrocytoma (PXA). Immunohistochemically, PXA areas retained nuclear expression of INI-1 and low Ki-67 proliferation index, whereas AT/RT component showed loss of INI-1 nuclear expression and markedly elevated Ki-67 proliferation index. Epithelial membrane antigen (EMA), smooth muscle actin (SMA), and p53 protein were positive only in AT/RT and sarcomatous component. BRAF V600E mutation was identified in PXA by real-time polymerase chain reaction.

Conclusion: We report a rare case of AT/RT arising in PXA which is supposed to progress by inactivation of INI-1 in a pre-existing PXA.

PS-04-040

Prognostic Significance of Tetraspanin CD151 in Newly Diagnosed Glioblastomas

Y.-L. Suh*, D. Lee, T.-I. Park
*Samsung Medical Center, Pathology, Seoul, Republic of Korea

Objective: Tetraspanin CD151 is a positive effector of cancer invasion and metastasis in many tumor types.

Method: We investigated the protein expression of CD151 in 211 cases of WHO grade I to IV gliomas. Additionally, we performed O6-methylguanin-DNA methyltransferase (MGMT) methylation analysis using real-time methylation-specific PCR in 36 glioblastomas, and the prognostic significance of these biomarkers in glioblastomas was evaluated.

Results: CD151 was overexpressed in a significant proportion (55.6 %) of glioblastomas, while it was not deetected in most of grade I to III glial tumors except for rare overexpression in anaplastic astrocytoma (2/10, 20 %) and oligoastrocytomas (3/23, 13 %). CD151 overexpression was closely associated with MGMT methylation ($P=0.014$), and it was a prognostic factor for predicting worse overall survival (OS; $P=0.002$) and progression-free survival (PFS; $P=0.043$). Combination of CD151 overexpression and MGMT methylation better stratified the patients' OS ($P=0.001$) and PFS ($P=0.009$). In multivariate analysis, CD151 overexpression was an independent prognostic factor for predicting OS over MGMT methylation ($P=0.012$).

Conclusion: CD151 seems to have a critical role for high grade progression in astroglial tumors. CD151 is a good tissue marker for predicting worse prognosis in glioblastomas.

PS-04-041

Role of Hippo Pathway molecules in meningiomas

A. Theodoropoulou*, G. Klironomos, F. Aggelatou, A. Mitsacos, H. Papadaki
*Rio, Greece

Objective: Meningiomas are frequently diagnosed primary brain tumors. Most of them are benign, but 10 % exhibit malignant features. Hippo signaling pathway is a kinase cascade. Its inhibition leads to translocation of YAP and TAZ transcription co-activators into the nucleus. This result in over expression of their target genes with anti- apoptotic and proliferative function. We hypothesize that inhibition of the hippo

pathway may be correlated to the malignant behavior of meningiomas.
Method: The expression of CD44, YAP, TAZ components of the Hippo pathway was studied by immunohistochemistry in 53 cases of meningiomas (34/53 WHO I, 19/53 WHO II/III).
Results: Nuclear YAP and TAZ immunopositivity and cytoplasmic CD44 immunolocalization significantly correlated with high grade meningiomas compared with low grade tumors.
Conclusion: Our findings suggest that Hippo pathway seems to be critically implicated in high grade memingiomas pathogenesis. Further studies are needed in order to clarify its exact role in meningiomas aggressive biological behaviour.

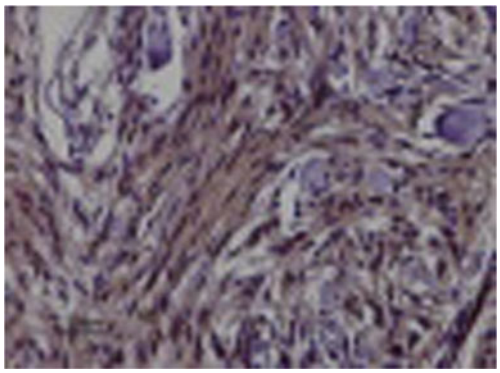

PS-04-042
Myxomas and neurothekeomas of the meninges. A single entity with two names?: Report of a case and review of the literature
E. Torres*, M. Brell Doval, J. Ibañez Dominguez, I. Amengual Antich, M. E. Couce
*Hospital Universitari Son Espa, Dept. of Pathology, Palma de Mallorca, Spain

Objective: Myxomas are benign tumors arising from cells of primitive mesenchymal origin, accounting for about half of the benign cardiac tumors. Primary intracranial myxoma is an exceedingly rare tumor with only eight cases reported in the literature.
Method: We report a case of a 30-year-old man with a 1 year history of oppressive bitemporal headaches. Neurological examination was unremarkable. Magnetic resonance imaging demonstrated a heterogeneously enhancing extra-axial mass arising from the falx cerebri, resembling a meningioma.
Results: A gross total resection of the tumor was achieved. Histological examination revealed a paucicellular tumor with lobulated architecture and abundant myxoid stroma, containing stellate or spindle cells lacking mitotic activity. Alcian blue and mucicarmin histochemical stains were diffusely and strongly positive. Immunohistochemical analysis showed diffuse reactivity for vimentin and scattered cells positive for CD34. Stains for EMA, GFAP, S100 protein, cytokeratin and smooth-muscle actin were negative.
Conclusion: Primary intracranial myxoma should be distinguished from other myxoid intracranial tumors such as myxomatous meningioma, epithelioid hemangioendothelioma or sarcoma through appropriate pathological and inmunohistochemical analysis. A metastasic cardiac myxoma should also be ruled out through cardiac evaluation including an echocardiography. The distinction between this entity and the reported neurothekeoma of the meninges needs to be re-evaluated.

PS-04-043
Holocord pylocitic astrocytoma associated to syringomyelia
J. Trillo-Tinoco*, T. Garibay-Huarte, E. Gómez-Apo, M. A. Rodríguez-Florido, L. Chávez-Macias, J. E. Olvera-Rabiela
*Hospital General de Mexico, Dept. of Surgical Pathology, Mexico City, Mexico

Objective: Spinal intramedullary tumors sometimes extend both superiorly and inferiorly along almost the entire cord, and those diagnosed as pilocytic astrocytoma are rare. The syringomyelia is an ependimary or periependimary cavitation of the spinal cord and is considered a suffering of degenerative and irreversible type, 58 % of the cases is associated with intramedullars tumors.
Method: A three-year-old girl with history of headache, progressive weakness, 3 months before, she was hospitalized for pneumonia, had impairment of neurologic functions and died of cardiac arrest. The autopsy was performed.
Results: The neuropathologic study revealed a intramedullary holocord tumor with secondary syringobulbia, cervical and lumbar syringomyelia. Histopathological examination of all specimen resulted in diagnosis of a pilocytic astrocytoma. Although no signs of atypia were present, an elevated proliferative activity of endothelial vessels was noted.
Conclusion: Gross total resection of holocord and longitudinally extensive intramedullary spinal cord tumors can be

achieved with preservation of long-term neurological function and also solved the syrinx.

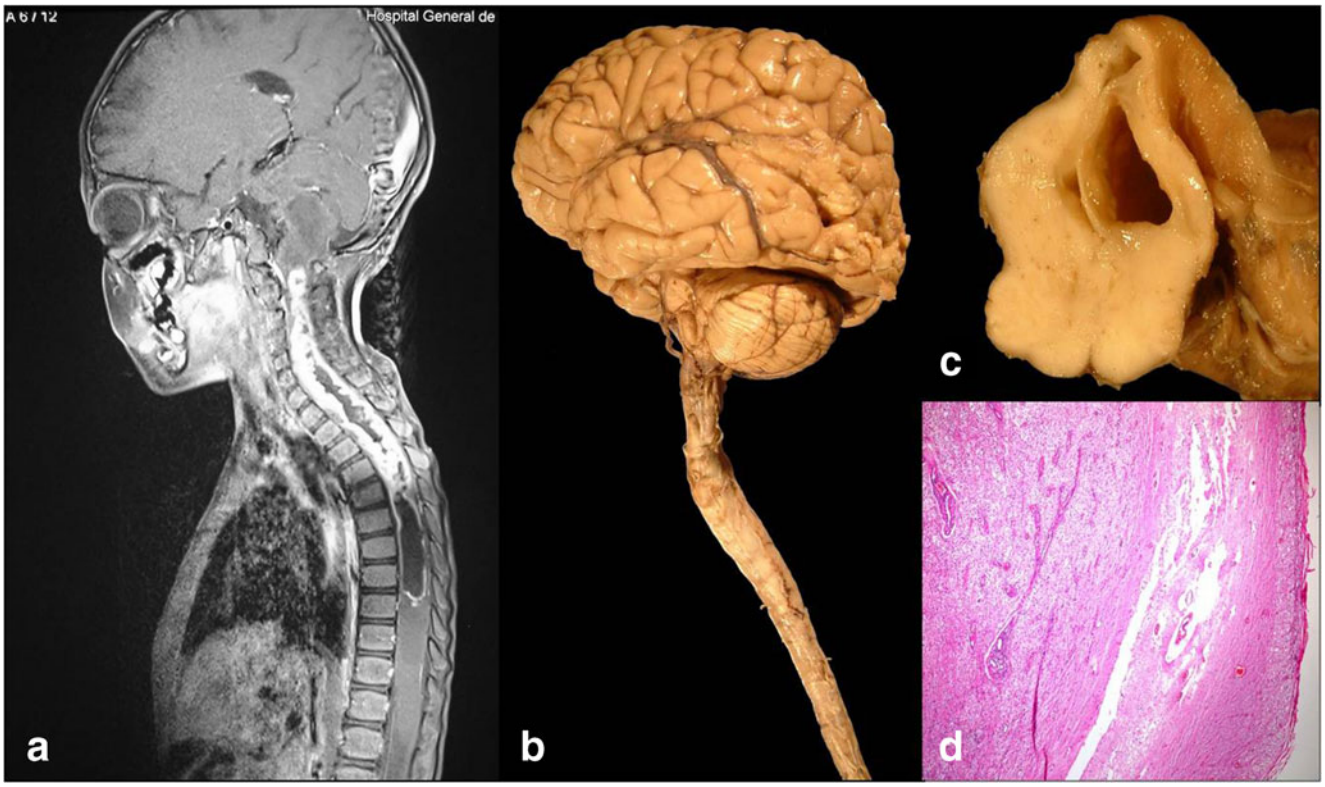

Sunday, 9 September 2012, 09.30 - 10.30, Congress Hall Foyer 3rd Floor
PS-05 Poster Session Endocrine Pathology

PS-05-001
Immunohistochemical expression of Epithelial Cellular Adhesion Molecule (Ep-CAM) in Thyroid Tumors using Ber-EP4

E. Alcaraz Mateos*, I. Aranda Lopez, E. Ortiz Ruiz, A. Chaves Benito
*Hospital Morales Meseguer, Dept. de Anatomia Patologica, Murcia, Spain

Objective: Epithelial cellular adhesion molecule (Ep-CAM) has been studied in many tissues and neoplasm, including thyroid and thyroid tumors. This is a preliminary study to assess the immunohistochemical expression of Ep-CAM in thyroid tumors using Ber-EP4.

Method: We examined the expression of Ep-CAM using the monoclonal antibody Ber-EP4 in 36 cases of thyroid tumors, including 4 adenomas, 11 papillary carcinomas, 5 follicular carcinomas, 8 medullary carcinomas, 2 poorly differentiated carcinomas, and 6 anaplastic carcinomas. We assessed the positivity as a predominantly membranous staining of the cells, and was scored according to the estimated percentage tumor cells in the total tissue section (negative: 0–10 %; positive: ≥10 %).
Results: Ber-EP4 expression was detected in normal thyroid tissue (perilessional), in all the adenomas, follicular carcinomas, and medullary carcinomas. Papillary carcinomas showed in 36 % lacking areas of expression, coinciding histopathologically one case with poorly differentiated component. All of the poorly differentiated and the anaplastic carcinomas were negative.
Conclusion: The expression of Ep-CAM, using Ber-EP4, was related to normal thyroid tissue and well differentiated neoplasms. Our study suggest that lost of expression is

associated to dedifferentiation. This results match up with the literature. In addition, clinical data and follow up are required to correlate focal areas of lost of expression of Ber-EP4 with dedifferentiated areas of the tumor.

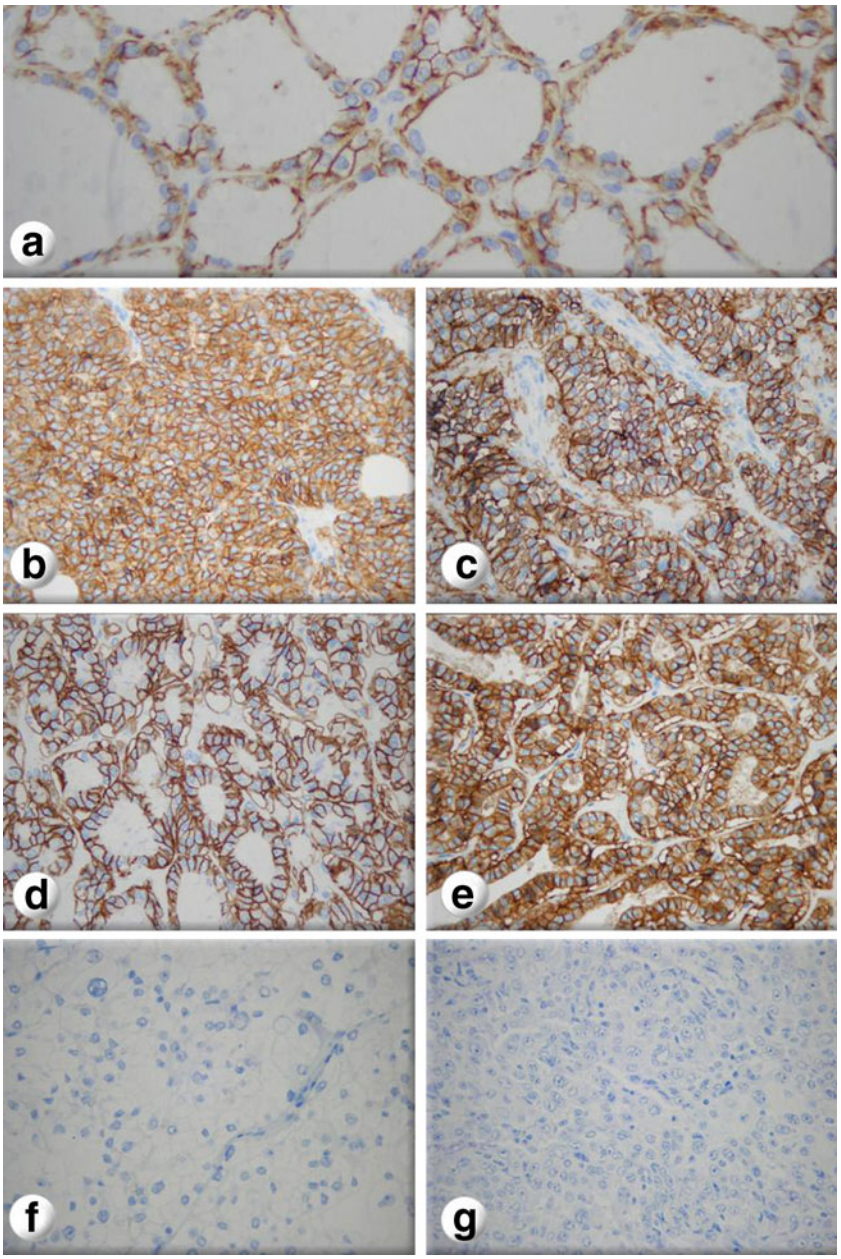

PS-05-002

The pathological effects of estradiol valerate on testis tissue: Size and weight in male rat

F. Bidhendi*, R. Ahmadi
*Imamkhomeini Hospital, Dept. of Radiology, Tehran, Iran

Objective: Studies show that estrogens can influence reproductive system differentiation. The main aim of this study was to determine pathological effects of estradiol valerate on testis histology and morphology in male rats.

Method: Adult male albino Wistar rats were divided to control and estradiol valerate (200 μg/kg/day) receiving groups. Estradiol valerate was applied subcutaneously. After 4 weeks, testes were excised and studied morphologically and histologically. Data were

statistically analyzed and compared between groups using ANOVA.
Results: Our findings revealed that estradiol valerate injection resulted in reducing of testes weight and size ($P<0.05$). Semeniferous tubules were apparently deformed in estradiol valerate receiving animals and cellular density was also reduced. Number of spermatocytes, spermatids and sperms was decreased in estradiol valerate receving rats compared with control animals ($P<0.001$).
Conclusion: Estradiol valerate has considerable pathological effects on testes morphology and histology in male rats.
Key words: Estradiol, Testes.

PS-05-003
Are tumor-dimension, Galectin-3 and CyclinD3 useful to characterize oncocytic adenomas and carcinomas?: Preliminary results
C. Cacchi*, L. Axt, H. M. Arnholdt, B. Märkl
*Klinikum Augsburg, Abt. für Pathologie, Germany

Objective: Routine histology of follicular oncocytic lesions is not always clear-cut. Therefore, we investigated the usefulness of morphometric and immunohistochemical criteria.
Method: All oncocytic follicular adenomas and carcinomas (OFA, OFC) between 2003 and 2007 have been retrieved from the archive of our institution. After a review of the histology and measuring the dimension (cm) of all tumors (nine Adenomas and eight Carcinomas, four oncocytic Metaplasia) immunohistochemistry with Galectin-3 and Cyclin D3- antibodies was performed.
Results: The mean of diameter of malignant lesion was significantly larger than that of the adenomas (3.77 ± 1.85 vs 1.77 ± 0.64 $P=0.0084$). Galectin-3 stained all but one carcinoma and two adenomas: percent of positive cells carcinoma vs adenoma (34.4 % vs 2.2 % $P=0.0029$). Cyclin D3 stained all carcinomas and six adenomas (40 % vs 13.4 % $P=0.17$). A panel using both markers has a high sensitivity (93.7) % but a low specificity (55.5 %). The positive predictive value was 65.7 % and the negative predictive value was 90.9 %.
Conclusion: These preliminary results suggest that additional criteria (dimension and immunostaining with Galectin-3 and Cyclin D3) can help distinguishing between OFA and OFC if the routine histology is doubtful.

PS-05-004
Heterogeneity in mutation status between primary tumour and metastases in papillary thyroid carcinomas
C. Cacchi*, H. Arnholdt, B. Märkl, M. Anthuber, C. Hass
*Klinikum Augsburg, Abt. für Pathologie, Germany

Objective: Papillary thyroid carcinoma (PTC) is the most common thyroid malignancy, harbouring BRAF-V600E mutations in about 45 % of cases. The first clinical manifestation of this tumour is often represented by lymphatic metastases.
Method: Twelve cases of PTC and respective lymph node metastases were retrieved from our archive from 2010 to present. Formalin fixed paraffin embedded tissue sections were stained with routine hematoxilin-eosin and representative tissue areas for both tumour and metastases were microdissected and DNA was extracted. After PCR amplification the mutational status of BRAF and RAs was determined by DNA sequencing.
Results: Seven cases of twelve (58 %) showed a BRAF-V600E mutation. Interestingly, only in three these cases (43 %) there was concordance in the mutational status between primary tumour and metastases. Moreover, all metastase of wild type carcinomas were also wyld type.
Conclusion: Even with an overall good prognosis, PTC is characterized by high incidence of lymph node metastases. As BRAF mutational status correlates well with prognosis and tumour progression, a correct molecular assessment is of paramount importance. Our data may indicate that, because the possibility of discrepancy in the mutational status between primary tumour and metastases, molecular analysis should be performed on the primary tumour.

PS-05-005
Carcinoma Showing Thymus-like Elements (CASTLE) of the thyroid: Case report with immunohistochemical and molecular study
J. Cameselle Teijeiro*, R. Celestino, A. Veiga, C. Eloy, I. Abdulkader, R. Reyes, P. Soares, M. Sobrinho Simões
*Clinical University Hospital, Dept. of Pathology, Santiago de Compostela, Spain

Objective: Carcinoma showing thymus-like elements (CASTLE) is a rare thyroid tumour thought to arise from the ectopic thymus, thymopharingeal duct or branchial pouch remnants in the thyroid gland and neck.
Method: Here we report the pathological, immunohistochemical and molecular findings in a CASTLE presented in a 36-year-old woman.
Results: The left thyroid lobectomy showed a solid, well circumscribed, slightly lobulated, gray tumor, with 34 mm of largest diameter. Microscopically, the neoplastic cells were arranged in broad anastomosing islands surrounded by desmoplastic stroma associated with lymphocytes and plasma cells. Tumour cells were squamoid with mild pleomorphism and occasional Hassal-like corpuscles. Less than 4 mitotic figures per 10 high-power fields were found. Positivity was found for keratins (CK7, CK19, CK34βE12, CKAE1/AE3), CD5, CEA, c-KIT (CD117), p63, p53, p27, cyclin D1 and Bcl-2, whereas no immuno-reactivity for CK20, TTF-1, thyroglobulin, thyroperoxidase, calcitonin,

and Epstein-Barr virus was detected. The proliferative index (Ki-67) about 20 %. No PAX8/PPARgamma rearrangements nor BRAF, N-RAS, H-RAS or K-RAS mutations were detected in the molecular analysis. There was no evidence of recurrence after a follow-up of 48 months.
Conclusion: Molecular alterations typically found in well differentiated follicular-cell derived neoplasms are lacking in CASTLE, and its phenotype suggests differentiation along a thymic/branchial line.

PS-05-006
Neurotensin and Chitosan-based dressings repair ulcers of diabetic mice
L. Carvalho*, L. Moura, A. Dias, H. Sousa, E. Carvalho
*Amadora, Portugal

Objective: Diabetes may cause chronic and non-healing diabetic foot ulcers (DFU) decreasing the welfare of patients. Some neuropeptides, Substance P and neurotensin (NT), may act as inflammatory modulators and improve wound healing. Natural biopolymers, chitosan derivatives, are receiving great attention as powerful wound dressing materials for wound healing applications due to their favorable properties. The work aim was to use 5-methyl pyrrolidinone chitosan (MPC) as a platform for the delivery of NT.
Method: Diabetes was induced by intraperitoneal injection of 200 mg/kg streptozotocin. Mice were anesthetized and two 6 mm excision wounds were created dorsally. MPC alone, NT alone, MPC loaded with NT or PBS were placed daily on wounds. Histological analysis of skin, at days 0, 3 and 10, was done through H&E and Masson´s Trichrome stainnings.
Results: In diabetic mice, the healing process was slower, showing an engulfment of acute inflammatory cells that triggered macrophage activity when compared with controls. At day 3, MPC treatment leaded to a faster healing with retraction of the wound site, NT induced a slower non-contracting healing and combined application delayed inflammatory repair with persistent neutrophils.
Conclusion: At day 10, all treatments induced a total healing however, MPC + NT reduced neutrophils infiltration compared with MPC alone.

PS-05-007
Acth producing nasal paraganglioma: Case report
J. Cassis*, A. Galzerano, M. Chorão
*Hospital Egas Moniz, Dept. of Anatomy Pathology, Lisboa, Portugal

Objective: Female patient with chronic sinusitis and hypertension presents with lipothymia, dizziness, polyuria and polydipsia. Laboratory studies showed hyperglicemia, leucocytosis, hypokalemia, hypercortisoluria and elevated serum ACTH levels. Head MRI revealed tumor in the right nasal cavity with implantation at the cribiform plate of the ethmoid bone.
Method: Microscopically the tumor had lobular architecture with big, round cells and with eosinophilic granular cytoplasm. These cells were NSE+, synaptophysin+, CD56+, CD57+ and ACTH+. Surrounding the tumor lobules were several spindle cells S-100+ (sustentacular cells).
Results: The lobular growth pattern, the presence of sustentacular cells (S-100 positive), and the ACTH producing granules favours an ACTH producing nasal paraganglioma diagnosis.
Conclusion: Head and neck paragangliomas account for 0,12 % of the tumors in this region, and are mainly located in the carotid bodies. Paragangliomas arising in the nasal cavity are rare, only 23 cases reported so far. They affect the middle or upper turbinates, and also the etmoid, maxillary and sphenoidal sinuses. We report the third case in literature of a ACTH producing paraganglioma in the nasal cavity.

PS-05-008
Sporadic aggressive silent somatotroph pituitary adenoma in the young: Report of two cases
L. Chinezu*, A. Vasiljevic, S. Achard Peyregne, G. Raverot, E. Jouanneau, J. Trouillas
*Emergency County Hospital, Pathology, Tg. Mures, Romania

Objective: Silent pituitary adenomas are infrequent tumors in adults and exceptional in young.
Method: We describe two cases of 20-year-old girls with pituitary adenoma without genetic history, revealed by visual field defects, with panhypopituitarism in one patient. In both cases, MRI showed giant pituitary adenoma, with invasion of the cavernous and sphenoidal sinuses. Hormone assays revealed normal GH, PRL and IGF1 plasma values. Surgery was incomplete in both cases.
Results: Both tumors presented a diffuse pattern. The cells exhibited large nuclei with prominent nucleoli. By immunocytochemistry, focal and low percentages of GH- and PRL-immunoreactive cells were observed respectively in both tumors (GH=1–30 % and PRL=1–5 %). CgA was positive. Cytokeratin and others antibodies against pituitary hormones were negative. Both tumors had high proliferative indexes: Ki-67>3 % (4–10 %) and elevated mitotic number (1–13 mitoses). Detection of p53 was also positive (0.5–5.7 %). The cases were diagnosed as atypical adenomas, according to the WHO classification.
Conclusion: The pathological diagnosis of these aggressive GH-PRL tumors has to be taken into account by the clinician to choose the optimal therapeutic strategies. Despite of the important side effects of the radiotherapy, this aggressive treatment might be proposed earlier, even for the young patients, to avoid the tumoral progression.

PS-05-009

Intrauterine growth retardation with high fat diet in rats markedly disturbs islet morphology characterized by peri-islet inflammation, fibrosis and haemosiderosis

J. Dahlstrom*, V. Delghingaro-Augusto, L. Madad, A. Chandra, E. Bean, C. Simeonovic, C. J. Nolan
*ACT Pathology & ANUMS, Dept. of Anatomical Pathology, Garran, Australia

Objective: Pre- and post-natal factors such as intrauterine growth retardation (IUGR) and high fat (HF) diet contribute to type 2 diabetes (T2D). Our aim was to determine if IUGR and HF diets interact in T2D pathogenesis.
Method: A surgical model of IUGR (bilateral uterine artery ligation) in Sprague–Dawley rats with sham (SH) controls was used pups were fed either HF or chow (CH) diets from weaning. Serial measures of body weight and glucose tolerance were made. At 25 weeks, rat pancreases were harvested for histological assessment.
Results: IUGR vs SH pups weights were 17 % lower. HF diet caused excess weight gain, dyslipidaemia, hyperinsulinaemia and mild glucose intolerance not further aggravated by IUGR. Markedly abnormal islet morphology was evident in 0/6 SH-CH, 5/8 SH-HF, 4/8 IUGR-CH and 9/9 IUGR-HF rats (chi-sq, $p=0.008$). Abnormal islets were characterised by larger size, irregular shape, peri-islet inflammation with CD68 positive cells and marked haemosiderosis. Overall beta-cell mass was not altered by IUGR, with a trend for it to be mildly increased in both HF-fed groups.
Conclusion: HF and IUGR independently and together contribute to islet injury. The marked islet haemosiderosis associated with IUGR and HF diets warrants further investigation as iron is toxic to β-cells.

PS-05-010

Malignant adrenocortical tumour in the setting of adreno-hepatic fusion

N. De La Ossa Merlano*, E. Mejia, C. Bartolomesanz, E. Fornas, A. Alastrue, I. Ojanguren
*I.C.S., Dept. of Pathology, Badalona, Spain

Objective: Adreno-hepatic fusion (AHF) is defined as adhesion of the liver and right adrenal gland with or without a fibrous capsule dividing both organs. We report a surgical case of AHF in which a virilising malignant adrenocortical tumour protruded into the liver mimicking a hepatic mass.
Method: A 36-years-old woman presented with mid-right abdominal pain and marked hirsutism. Computed tomography (CT) revealed an apparently intrahepatic solid tumour suggestive of a giant hepatic adenoma. The right adrenal gland was not visible on CT and the right kidney showed marked downwards displacement. A radical right adreno-hepatectomy was performed, with a satisfactory outcome.
Results: Grossly, a giant, partially encapsulated mass was seen to protrude from the right adrenal gland into the liver. Microscopically, the tumour was constituted by atypical clear cells with nuclear polymorphism, necrosis and moderate mitotic activity. Tumour cells expressed vimentin and Melan-A protein.
Conclusion: To our knowledge, this is the first description of a malignant adrenal tumour in the setting of AHF. As illustrated by this case, awareness of AHF as an entity and attention to its distinctive gross and histologic features are essential to avoid confusion between adrenal and hepatic lesions, especially when imaging studies have provided misleading findings.

PS-05-011

ACTH producing pheochromocytoma: A case report

M. Decaussin-Petrucci*, A. Vasiljevic, Y. Liu, J. Trouillas, J. L. Peix, G. Raverot
*Lyon Sud Hospital, Dept. of Pathology, Pierre Benite Cedex, France

Objective: Cushing's syndrome (CS) is a rare disease, resulting in the majority of cases from ACTH hypersecretion. 70 % is of pituitary origin, 20 % of adrenal origin, and only 10 % from ectopic ACTH production.
Method: We reported a rare cause of ectopic ACTH dependent CS, caused by a pheochromocytoma.
Results: A 54-year-old male was hospitalized for severe high blood pressure, depression and weight loss. Biological investigation revealed serious hypokaliema, severe ACTH dependent hypercortisolism with elevated urinary free cortisol secretion, loss of diurnal variation, and excess plasma ACTH level. CT-scan revealed a nodular lesion in the right adrenal gland with hyperplasia in the left one. The nodular lesion was assumed to be a pheochromocytoma based on the elevated serum and urinary catecholamine and metabolites and local uptake in right adrenal gland in 131 I-MIBG scan. Right adrenalectomy was performed. Macroscopic examination revealed a 4 cm, well-circumscribed, tan-brown tumor, associated with diffuse adrenocortical hyperplasia. Histological examination confirmed the diagnosis of pheochromocytoma, without signs of aggressiveness. The tumor cells were immunopositive for Chromogranin A, Synaptophysin and ACTH. After surgery, catecholamine secretion returned quickly to normal level. Biological and clinical CS regression was noted.
Conclusion: Despite the rare association of CS with pheochromocytoma, preoperative diagnosis is required to an appropriate therapy.

PS-05-012

A rare case: Extralobar pulmonary sequestration mimicking neuroblastoma

G. Emiroglu*, N. Özsan, S. Tiryaki, A. Çelik, Y. Ertan
*Ege University, Dept. of Pathology, Izmir, Turkey

Objective: Extralobar intraabdominal pulmonary sequestrations are rare congenital malformations which are characterized by disorganized and nonfunctioning pulmonary parenchyma. These lesions have no communication with the bronchial tree and pulmonary arteries. They receive their blood supply from the systemic circulation.
Method: We describe a 5 days old male infant admitted to the hospital with a left subdiaphragmatic, 50×40×35 mm, hiperechogenic and, solid mass that was identified during ultrasonography on the 26th week of gestation.
Results: Abdominal computerized tomography demonstrated a 48×37×33 mm, solid, vascularized, encapsulated, mostly cystic suprarenal mass with no calcification reported to be highly suspicious for neuroblastoma. The mass was completely excised. Gross pathologic examination revealed a well circumscribed spongy lesion that mimicked a lung tissue. On microscopic examination, a disorganized lung tissue that was composed of alveoli, alveolar ductus and bronchioles was seen. Normal adrenal tissue was not observed. Later, we learnt that the lesion's arterial blood supply was from the abdominal aort. Based on these findings, our diagnosis was intraabdominal extralobar pulmonary sequestration.
Conclusion: Intraabdominal extralobar pulmonary sequestrations should be kept in mind in cases of the adrenal masses as the surgical resection is the adequate treatment method for these lesions.

PS-05-013

Axillary lymph node metastasis of papillary thyroid carcinoma showing anaplastic transformation with cutaneous metastasis

S. Erkilic*, A. Ozkur, U. Elboga, F. Celenk, M. Kanlikama
*Gaziantep University, Medical Faculty, Turkey

Objective: Papillary thyroid carcinoma (PTC) rarely metastasizes to axillary lymph nodes. Although anaplastic transformation (AT) may occur in the cervical lymph node metastasis from PTC, it is rarely observed in the metastatic axillary lymph nodes. Furthermore, cutaneous metastasis from anaplastic thyroid carcinoma (ATC) is extremely rare.
Method: A 65-year-old male patient who had operated for multinodular goiter 8 years ago presented with neck swelling on the right side. Residual thyroid tissue was detected and the lesion was removed surgically in combination with a right neck dissection. Histopathologic examination was consistent with PTC and metastatic lymph nodes. The patient received radioactive iodine therapy. Afterwards, the patient presented with a right axillary mass 14 years after the first operation and underwent surgical excision.
Results: Histopathologic examination showed PTC with anaplastic transformation. Histopathologically confirmed multiple skin metastases from ATC emerged in thoracic and abdominal regions 3 months after the last operation. Patient died 3 months after the diagnosis of anaplastic carcinoma.
Conclusion: Although most PTCs show an indolent course and have a favorable prognosis, distant metastasis and anaplastic transformation of the metastatic lymph nodes may occur even more than many years after the primary treatment.

PS-05-014

Local „bystander"effect of gene therapy on human tumor cells of medullary thyroid carcinoma in vivo

L. Feketeova*, M. Poturnajová, L. Kucerová, P. Babál
*Comenius University, Inst. of Pathology, Bratislava, Slovakia

Objective: Gene therapy acts on change of prodrug into cytotoxic drug inside tumor cells transfected by foreign enzyme. It uses also "bystander" effect on surrounding tumor cells without enzyme. We used yeast Cytosine deaminase (yCD) in combination with 5- fluorocytosine (5FC) converted into 5- fluorouracil (5FU) and its metabolites. Medullary thyroid carcinoma (MTC) is a malignant tumor often with therapy resistant distant metastases. Patients with sporadic form have metastases at the time of diagnosis, mostly in bones, lungs and liver. The aim of this study was to evaluate the efficiency of yCD/5FC in MTC treatment using xenotransplants derived from model TT cell line in nude mice.
Method: Tumors were immunohistochemically stained with polyclonal antibody anti-EGFP (enhanced green fluorescence protein) and monoclonal antibodies anti-PCNA and anti-Ki67. Positivity was semiquantitatively evaluated.
Results: Diffuse positivity for PCNA was seen in untreated and treated tumors, respectively. Positivity for Ki-67 was diffuse in untreated and only sporadic in treated tumors.
Conclusion: Diffuse PCNA positivity in treated tumors suggests that the tumor cells stopped in S phase. Scattered positivity of Ki-67 after treatment document suppressed proliferation mediated by yCD/5FC gene therapy, which implies therapeutic application in patients with metastatic MTC. (ITMS 26240220052, VEGA 2/008/11, VEGA 2/0146/10).

PS-05-015

E-cadherin/ß-catenin immunoexpression in thyroid carcinomas

K. Ivanova*, E. Onal, J. Ananiev, T. Vlaikova, M. Gulubova
*Trakia University, General and Clinical Pathology, Stara Zagora, Bulgaria

Objective: The aberrant activation of Wnt signaling pathway may be a common denominator for the development of thyroid tumorigenesis. It was announced that the loss of E-cadherin rather than β-catenin mutation represents a crucial

event in determining the degree of differentiation of thyroid carcinomas. The aim of the study was to evaluate the expression of E-cadherin and β-catenin in the thyroid cancer tissue and to correlate these data with some histological and clinical parameters of the tumors.
Method: We investigated 57 patients, having thyroid tumors – papillary, follicular, anaplastic and oncocytic carcinomas immunohistochemically with antibodies against E-cadherin and β-catenin. Survival analyses were done.
Results: E-cadherin expression was focally retained in the tumor cell membranes and in the tumor cell cytoplasm of the papillary, follicular and oncocytic thyroid cancers, weather in anaplastic cancers it was almost lost (p=0.0042, and p=0.019, respectively, Fisher's Exact Test). The expression of β-catenin in tumor cytoplasm and membrane in papilary cancers was higher as compared to that in the other tumors (p=0.111, and p=0.0104, respectively).
Conclusion: Not surprisingly, the presence of aberrant expression of E-cadherin and/or β-catenin in thyroid cancer has been associated with better patients' prognosis and more well differentiated tumor histology.

PS-05-016

Correlation between Estrogen receptor and progesterone receptor with some prognostic factors in papillary thyroid carcinoma

M. Jalali Nadoushan*, R. Amirtouri, A. Davati
*Shahed University, Dept. of Pathology, Tehran, Iran

Objective: The more prevalence of papillary thyroid cancer in women shows the probability of the role of sex hormones in the cancer. The aim of this study was determination of relation between sex hormones receptors and some prognostic factors.
Method: We studied 92 patients with pathology report of papillary thyroid carcinoma after thyroidectomy between 2006 and 2009. The specimens were stained immunohistochemically for ER and PR. The other informations such as sex, age, tumor size and lymph nodes involvement obtained from the patients documents.
Results: The average age of patients was 39.32+16,93. 46.7 % t of samples were ER positive while this was 6.5 % for PR. The percentage of lymph nodes involvement was 23.9 %. The size of tumors was 3.60+2.21 cm. There was a direct relationship between female sex and positivity of ER ($p \leq 0.014$). But there was no significant relationship between ER and PR with age, tumor size and lymph nodes involvement.
Conclusion: It seems to be that ER is more prevalent in females but for showing of its role in prognosis, further studies are recommended.

PS-05-017

Mixed pituitary adenoma/craniopharyngioma: Clinical, morphologic, immunohistochemical and ultrastructural study of a case

S. La Rosa*, G. Finzi, M. Cerati, A. Marando, C. Zoia, E. Piantanida, F. Ferreli, C. Capella
*Ospedale di Circolo, Dept. of Pathology, Varese, Italy

Objective: Mixed pituitary adenoma/craniopharyngiomas are rare tumors, accounting for about 15 reported cases. Most of them are composite neoplasms and tumors showing combined features are extremely rare.
Method: We describe the clinical, morphologic, immunohistochemical and ultrastructural features of a case.
Results: A 75-year-old woman presenting with diplopia due to a sixth left nerve palsy underwent head CT scan and MR which showed a sellar mass suggestive for a pituitary macroadenoma. Endocrine testing demonstrated only a slightly increased prolactin. The patient underwent endoscopic endonasal transphenoidal approach with resection of multiple fragments. The tumor was composed by a pituitary ACTH adenoma admixed with islands of adamantinomatous craniopharyngioma representing 40 % of the lesion. Electron microscopy showed cells of a sparsely granulated ACTH adenoma admixed with craniopharyngioma component and some cells showing both patterns. The patient completely recovered the nerve palsy and the post-operative endocrine tests were normal. A 5 months post-operative head MR confirmed the complete resection of the lesion.
Conclusion: We report a rare mixed sellar tumor showing an ACTH secreting pituitary adenoma admixed with an adamatinomatous craniopharyngioma, with some hybrid cells suggestive of a common histogenesis of the two components of the neoplasm.

PS-05-018

Sitagliptin treatment delays the progression of pancreatic and renal lesions and reduces tissular oxidative stress in a type 2 diabetes animal model

C. Mega*, H. Vala, J. Oliveira, R. Fernandes, F. Mascarenhas-Melo, B. P. Parada, R. P. Pinto, F. Teixeira, F. Reis, E. Teixeira de Lemos
*Coimbra University, Medicine, Pharmacol. & Therapeutics, Portugal

Objective: Type 2 diabetes mellitus (T2DM) treatment aims to control metabolic effects, preserve pancreatic function and reduce complications, such as nephropathy. This study intends to evaluate the effects of sitagliptin, a dipeptidyl-peptidase-4 inhibitor, in pancreatic and renal lesions in Zucker Diabetic Fatty (ZDF (fa/fa)) rats, an animal model of T2DM.
Method: Male obese diabetic ZDF (fa/fa) rats, 20-weeks-old, were treated with vehicle or sitagliptin (10 mg/kgBW/

day) for 6 weeks, and compared with lean control ZDF rats (n=8 each). Biochemical parameters as well as pancreatic and renal lipid peroxidation and histopathology profile were assessed. Specimens we stained with haematoxylin-eosin and periodic acid of Schiff, and examined by light microscopy. Lesions were evaluated by a semiquantitative rating. Endocrine/exocrine pancreas and renal glomerular, tubulointerstitial and vascular lesions were assessed and scored (0 3/0-2). Results are mean ± SEM; ANOVA and Duncan's post-hoc analysis ($P \leq 0.05$ was considered as significant).
Results: Sitagliptin improved metabolic parameters, reduced lipid peroxidation ($p<0.001$) in both organs and significantly prevented major diabetic pancreatic and renal lesions in obese diabetic ZDF rats.
Conclusion: Sitagliptin seems to comply with the three main objectives of T2DM therapeutic management. Underlying molecular mechanisms deserve further elucidation, but could be related with metabolic improvement and reduction of oxidative stress.

PS-05-019

HBME-1, Cytokeratin-19, Galectin-3, CD56 and p63 expression in thyroid tumors of uncertain malignant potential

A. Nechifor-Boila*, A. Borda, G. Sassolas, Z. Hafdi-Nejjari, F. Borson-Chazot, N. Berger, M. Decaussin-Petrucci
*University of Medicine and Pharmacy, Tirgu-Mures, Romania

Objective: Thyroid tumors of uncertain malignant potential (TT-UMP) include follicular and well-differentiated tumors of UMP (FT-UMP/WDT-UMP), as it refers to the presence of questionable capsular/vascular invasion or incompletely developed papillary thyroid carcinoma (PTC)-type nuclear changes. However, a diagnosis of TT-UMP is difficult in most cases. We aimed to investigate whether immunohistochemistry (HBME-1, Cytokeratin-19, Galectin-3, CD56 and p63) provides additional information concerning such lesions.
Method: We performed an immunohistochemical analysis on 14 WDTs-UMP and 4 FTs-UMP.
Results: In the WDT-UMP group, HBME-1 was positive in 6/14 (42.9 %) cases. CD56, a marker whose expression is reduced in thyroid carcinoma, showed a "malignant" profile (no expression) in 9/14 (64.3 %) cases. 6/14 (42.9 %) cases were positive for both antibodies. One case showed the co-expression of HBME-1, CD56, Galectin-3 and Cytokeratin-19. Only one FT-UMP case was positive for HBME-1. The follow-up data revealed no distant metastases or persistent disease.
Conclusion: TT-UMP demonstrated very heterogeneous immunohistochemical profiles. WDTs-UMP revealed a certain tendency toward a PTC profile, suggesting a possible pathogenetic link between these two entities. However, immunohistochemistry is to be regarded more as a supporting factor, while morphological criteria should always prime in the diagnostic decision.

PS-05-020

CD68, TGF-ß1, Smad4, Smad7 and TGFßRII and thyroid cancer

E. Onal*, K. Ivanova, J. Ananiev, A. Zdraveski, H. Pehlivanov, H. Stoyanov, J. Gerenova, M. Gulubova
*Trakia University, General and Clinical Pathology, Stara Zagora, Bulgaria

Objective: Many growth factors such as TGFbeta promote macrophage recruitment, survival and differentiation in tumors. In many human tumors a high frequency of infiltrating tumor associated macrophages (TAMs) has been asssociated with tumor development and poor prognosis. It was shown that in poorly differentiated thyroid cancers TAMs support tumor progression. The aim of our study was to investigate the association between TAMs and the proteins of the TGFbeta signaling pathway for the progression of thyroid cancer.
Method: We investigated 57 patients, having thyroid tumors – papillary, follicular, anaplastic and oncocytic carcinomas immunohistochemically with antibodies against CD68, TGFbeta, Smad4, Smad7 and TGFbetaRII. Survival analyses were done.
Results: The higher expression of TGFbeta and TGFbetaRII in papillary and follicular cancers was associated with higher CD68 infiltration in the invasive margin (median 20.7 cells/mm2, p=0.052, median 20.7 cells/mm2, p= 0.035, respectively, Mann–Whitney U test) compared to anaplastic cancers. Similarly, the expression of Smad4 and Smad7 in papillary and follicular cancers was associated with higher CD68 infiltration in tumor stroma (median 19.7 cells/mm2, p=0.012, Mann–Whitney U test) in comparison to anaplastic cancers, with mising TGFbeta immunoexpression (median 2.4 cells/mm2).
Conclusion: Our results suggest that TAMs may facilitate tumor progression.

PS-05-021

Immunohistochemical seperation of thyroid papillary carcinoma follicular variant from follicular adenoma and RET/PTC correlation

T. Ozgur*, E. Atik, M. Guray, R. Gunesacar, T. Canda
*Mustafa Kemal University, Medical Faculty, Antakya, Turkey

Objective: The accurate diagnosis of benign and malign thyroid tumors is very important for the clinical management of patients. The distinction of thyroid papillary carcinoma follicular variant and follicular adenoma can be difficult.

Method: We applied immunohistochemical markers; CK19, HMWCK, Galectin-3, HBME-1 and Fibronectin and PCR analyses for detecting RET/PTC rearrangement. Formalin-fixed parafin embedded tissues from 46 surgically total resected thyroids, included 26 thyroid papillary carcinoma follicular variant (TPCFV), 8 Follicular Adenoma (FA), 6 Minimal invasive follicular carcinoma (MIFC) and Follicular Carcinoma (FC).

Results: There was a positive correlation between TPCFV and HMWCK, CK 19, HBME1, Galectin 3, Fibronectin ($p<0.05$), but there was no correlation with TPCFV and RET/PTC ($p>0.05$). HBME-1 and CK 19 stained strong and diffuse positive in TPCFVs but weak and focal in FAs.

Conclusion: Our study suggests that morphologic features combined with immunohistochemical panel of HMWCK, CK19, HBME-1, Galectin-3 and fibronectin can help to distinguish benign and malign thyroid neoplasms and TPCFV from follicular adenomas. RET/PTC expression has been non-specific but its detection can be a useful tool combined with immunohistochemistry for diagnosing TPCFV.

PS-05-022

Morphological features of the system mother-placenta-fetus during pregnancy on diabetes mellitus

T. Pavlova*, V. Petrukhin, E. Malutina, A. Nesterov, L. Pavlova, I. Goncharov, D. Kolesnicov

*Belgorod State University, Dept. of Pathology, Russia

Objective: Combination of diabetes mellitus and pregnancy has a special concern.

Method: It were studied 50 pregnants with diabetes mellitus type 1 and 29 pregnant with gestational diabetes mellitus (GDM). The methods were used: light, transmission, electron, probe and scanning microscopy with microelement analysis.

Results: The pregnancy at diabetes mellitus type 1 and GDM proceeds with complications: treat of pregnancy termination (64,0 % and 50,0 %), hydramnion (27,0 and 62,5 %), preterm birth (36,0 and 12,5 %). It was displayed decreasing of oxygen in mother's erythrocytes. At the diabetes mellitus in uterus of women in birth there are violations of spiral arteries as well as circulatory disorders (stasis, sludge, thrombosis and diapedetic bleedings), that is significantly expressed at gestosis. Tendency to cell form changing is observed in erythrocytes at diabetes mellitus, especially at diabetes mellitus type 1. The frequency of placental insufficiency in pregnant with diabetes mellitus type 1 were 75 %, at GDM- 50 %. The gestosis accession were resulted to birth's increasing of children with prenatal injury of central nervous system at diabetes mellitus type 1 in mother and diabetic fetopathy at GDM.

Conclusion: The clinical and morphological parallels of the system mother-placenta-fetus were presiced ad diabetes mellitus type 1 and GDM.

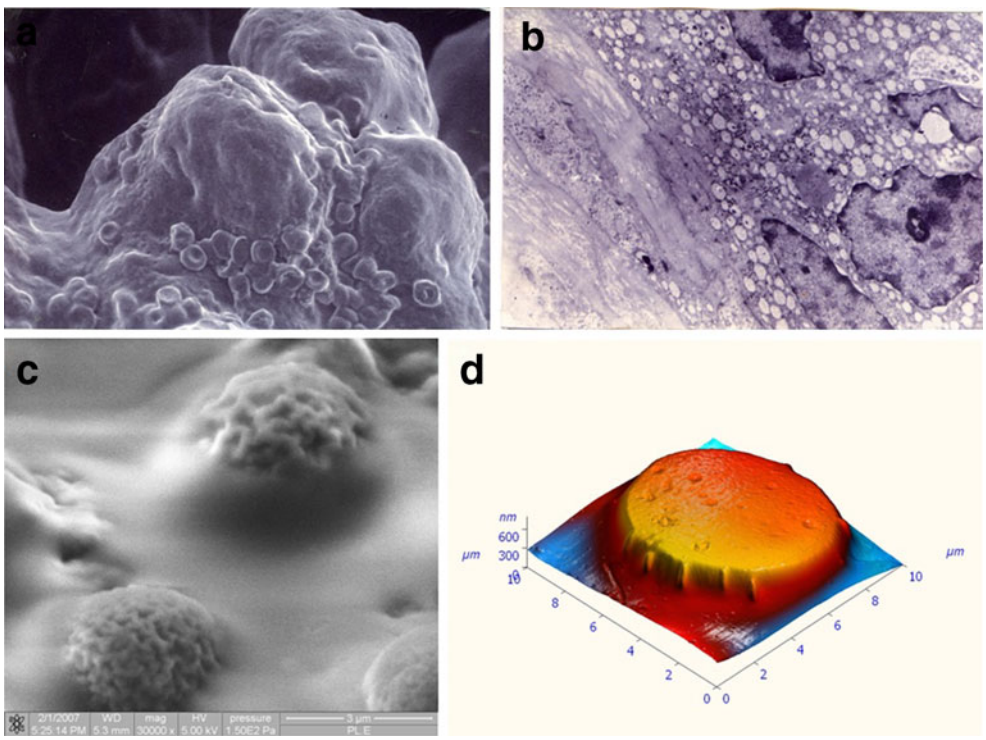

PS-05-023

Sclerosing mucoepidermoid carcinoma of the thyroid in a 13 year-old female

A. Polónia*, L. Santos, C. Eloy, R. Celestino, P. Soares, M. Jácome, C. Lobo
*IPO-Porto, Pathology, Rio Tinto, Portugal

Objective: Sclerosing mucoepidermoid carcinomas (SMECs) are low-grade malignant tumours with both squamous and mucinous differentiation representing less than 1 % of thyroid malignancies. SMECs are usually associated to Hashimoto thyroiditis and classically disclose eosinophilia.
Results: A 13 year-old female with Hashimoto thyroiditis presented a 2.5 cm nodule in the left lobe of the thyroid. The total thyroidectomy specimen disclosed a firm, well circumscribed, non-encapsulated tumour. Microscopically, the tumour was composed by anastomosing clusters of squamoid cells in a sclerotic background without eosinophils. Intra-cytoplasmatic PAS/diastase positive material was focally found. The tumour cells expressed AE1.AE3, TTF-1 and p63 whereas no expression was observed for thyroglobulin, calcitonin and CD5. The Ki-67 labeling index was 5 %. In the molecular analysis no mutations were detected in BRAF or (K-, N-, H-) RAS genes nor RET/PTC or PAX8/PPARgamma rearrangements. The remaining thyroid showed Hashimoto-type thyroiditis. A cervical lymph node metastasis was identified. The patient was treated with radioactive iodine and is alive without signs of disease after 10 months of follow-up.
Conclusion: SMECs may not disclose the classical eosinophilia and represent rare low-grade tumours that can give rise to metastases. The most frequent molecular alterations found in thyroid tumours were not detected in this case.

PS-05-024

ALK1 and BMP-9 overexpression as a cause of ossifying papillary thyroid carcinoma

J.-Y. Sung*, K.-Y. Na, S.-K. Lee, W.-W. Jung, Y.-W. Kim, Y.-K. Park
*Kyunghee University Hospital, Dept. of Pathology, Seoul, Republic of Korea

Objective: Ossification is an often encountered finding in papillary thyroid carcinoma (PTC). We hypothesized that osteogenic signaling may be related to osteogenesis of PTC. Bone morphogenic protein (BMP)-9 is the most osteogenic subtypes among BMPs. And as a cellular receptor, activin receptor-like receptor (ALK)1 has been emphasized in BMP-9 induced osteogenic signaling. We investigated the expression of ALK1 and BMP-9 and their correlation with ossification in PTC.
Method: ALK1 and BMP-9 expression were investigated by immunohistochemistry in tumors and adjacent normal follicles of 78 PTCs with bone formation and 64 PTCs without bone formation. ALK1 and BMP-9 expression were further verified by quantitative real time polymerase chain reaction in each group of 15 cases of PTCs with or without bone formation.
Results: ALK1 and BMP-9 immunoreactivity were increased in PTC with bone formation when compared to those without bone formation ($P<0.001$ and $P=0.001$). Both mean values of ALK1 and BMP-9 mRNA expression were elevated in PTCs with bone formation compared with those without bone formation ($P=0.037$ and $P<0.001$).
Conclusion: ALK1 and BMP-9 overexpression may be underlying the molecular alteration that accounts for osteogenesis in PTC.

PS-05-025

Multiple metastases of renal clear cell carcinoma within adenomatous nodule in multinodular goiter

E. Tamponi*, G. Faa, S. Soddu, G. Senes, P. G. Calò, M. L. Lai
*Anatomia Patologica, AOU Cagliari-PO S.G. Didio, Italy

Objective: Thyroid is an extremely rare site of metastases. Renal clear cell carcinoma (RCCC) is one of the most frequent primary malignancies causing thyroid metastases as a single nodule (77 %) or multiple nodules (23 %). We report the case of a 62-years-old female patient affected by multinodular goiter, who was diagnosed with RCCC, treated with nephrectomy.
Method: Due to compressive symptoms, 6 years after nephrectomy, the patient underwent thyroidectomy and the thyroid was sent for histology.
Results: Histology showed multinodular goiter. In the largest hyperplastic adenomatous nodule (left lobe, diameter mm 53), multiple solide yellow-orange areas were detected grossly. These areas were microscopically composed of sheets of large cells with clear cytoplasm and small hyperchromic nuclei, with a focally infiltrative growth pattern. At immunohistochemistry clear cells were negative for TTF1, HBME1, galectin-3 and positive for CD10.
Conclusion: This is a rare case of multiple RCCC metastases within an adenomatous nodule in goiter. Clinical diagnosis of RCCC metastases to thyroid is extremely difficult, even more if metastases grow in multinodular goiter. It

should be always suspected in patients with a clinical history of RCCC.

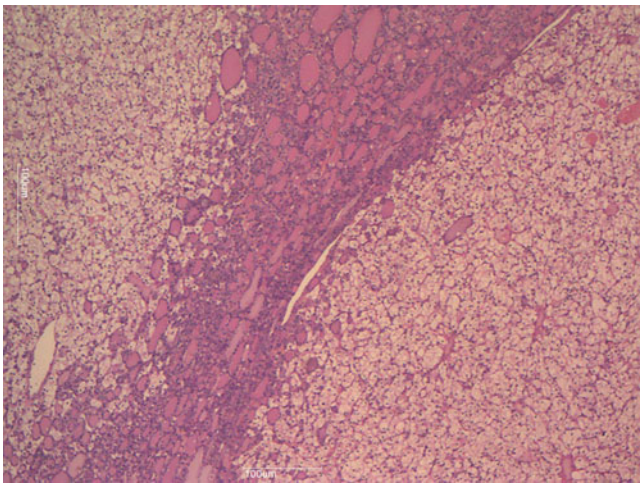

PS-05-026

A case of follicular carcinoma, oncocytic variant, misdiagnosed as medullary carcinoma by fine-needle aspiration cytology

J. Watanabe*, M. Kai, Y. Murakami, N. Murakami, H. Higuchi, H. Yoshida, H. Yano
*Yame General Hospital, Dept. of Pathology, Japan

Objective: Follicular carcinoma, oncocytic variant, is a rare type of thyroid carcinoma. We examined a case of oncocytic carcinoma misdiagnosed as medullary carcinoma on fine-needle aspiration (FNA) because it was associated with amyloid material.
Method: A 73-year-old female rheumatoid arthritis (RA) patient had a 4.0 cm mass in the right lobe of her thyroid, which showed no enhancement effect on CT scan and was diagnosed as a "cyst". FNA was performed, and she subsequently died of unrelated causes. An autopsy was performed.
Results: Cytology: Large and small round-shaped tumor cells were present with round nuclei with granular chromatin. Double- or triple-nucleated cells and amyloid material were observed. Histology: oncocytic round cells proliferated diffusely in the fibrous capsule. Extra-capsular invasion and vascular infiltration by the tumor cells were recognized. Electron microscopy: the cytoplasm of tumor cells was full of mitochondria. Therefore, we diagnosed this as follicular carcinoma, oncocytic variant. Amyloid deposition was also observed in several other organs.
Conclusion: Amyloid deposition was caused by amyloidosis secondary to RA. Narrowing of the tumor feeder artery due to amyloidosis may have prevented early enhancement on the CT image.

Sunday, 9 September 2012, 09.30 - 10.30, Congress Hall Foyer 3rd Floor
PS-06 Poster Session Digestive Diseases Pathology I: Upper Gastrointestinal Tract

PS-06-002

Immunoexpression of metaloproteinases 2 and 14 and tissue inhibitor of metaloproteinases-2 in gastric cancer

P. Almeida*, D. Gurgel, R. Vieira, J. Maia-Filho, C. Dornelas, R. Ribeiro
*Federal University of Ceará, Dept. of Pathology, Fortaleza, Brazil

Objective: Gastric cancer is the second leading cause of cancer death worldwide. Metaloproteinases 2 and 14 (MMP-2; MMP-14) and Tissue Inhibitor of Metaloproteinases-2 (TIMP-2) are involved in epithelial-mesenchymal transition and tumor progression in cancer. Aim: to evaluate their immunoexpression and correlations with clinicopathological parameters in gastric carcinomas.
Method: Samples from intestinal (n=53) and diffuse (n=30) gastric carcinomas (Lauren classification), underwent tissue microarrais and immunohistochemistry. Immunoxpression of MMP-2, MMP-14 and TIMP-2 was measured according to scores 0=negative; 1=discrete; 2=moderate; 3=strong, (all staining in >50 % of cells), modified from Buskens et al. 2003, Gut, 52:1678-83. CD68 antibody was used to characterize mononuclear cells.
Results: MMP-2 was stained more often in women (67 % & 19 %-men; p<0.005, Fisher's exact test). MMP-2 and MMP-14 were mostly expressed in mononuclear (macrophages) than in epithelial cells, in both sites, principally, lymph nodes (MMP-2: lymph node=81 % & 35 %-stomach; p<0,005). Moreover, TIMP-2 was observed mainly in neoplastic cells of primary intestinal tumours.
Conclusion: In this study, MMP-2 immunoexpression was far more prevalent in women. MMP-2 and MMP-14 predominant expression in mononuclear stromal cells in the lymph node metastases reinforces the central role of these cells in the tumor microenvironment in the progression of gastric carcinoma.

PS-06-003

The relationship between tumor infiltrating immunologic cells and the survival of gastric carcinoma patients

S. Amoueian*, A. Attaranzadeh, M. Montazer
*Imam Reza Hospital, Dept. of Pathology, Mashhad, Iran

Objective: We investigated the prognostic significance of immune cell counts in the gastric cancer stroma.
Method: This historical cohort study was conducted on50patients with non-metastatic intestinal-type adenocarcinoma who have been undergone curative gastrectomy during2004-2008in Mashhad Medical University. Immunohistochemistry staining forCD56, CD68, CD117 andCD1a was performed to detect NKCmacrophages, mast cells and Langerhans cells, respectively. The immune cells were counted. The prognostic significance of two grouping (low or high immune cell counts) was analyzed using the Kaplan Meier method and Cox proportional hazards regression modeling.
Results: 38(76 %) male and 12(24 %) female patients enrolled the study with a mean (±SD) age of 66.0(±9.2) years old. The median survival time was 15.0(95 % CI: 5.5-24.5) months. Natural killer cells, mast cells and Langerhans cells showed positive effect on survival, whereas the reverse was true for macrophages. Multivariate analysis showed that the independent prognostic factors were location of the tumor (cardia/non-cardia), stage, the presence of extra-cytoplasmic mucin, tumor associated macrophage status (low/high), and tumor associated Langerhans cell status (low/high).
Conclusion: In the studied population, gastric carcinoma proved to have a very poor prognosis. Multivariate analysis showed that the prognostic effect of natural killer and mast cells in tumoral tissue were dependent on the Langerhans cell count.

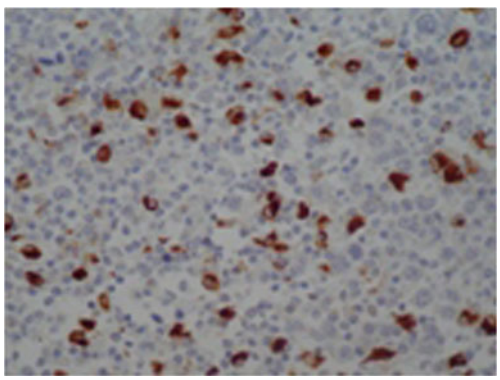

PS-06-004
Correlation of p53, HER2 and E-cadherin expression with clinicopathological parameters of gastric carcinoma
B. Andrejic*, M. Milic, S. Knezevic-Ušaj, T. Ivkovic-Kapicl, Z. Nikin, A. Lovrenski
*Medical Faculty Novi Sad, Dept. Histology and Embryology, Serbia

Objective: Gastric cancer is the second most common cancer in humans. Numerous genes are possibly involved in carcinogenesis and tumor progression of gastric cancer.
Method: Material of 45 patients diagnosed with gastric carcinoma at the Institute of Oncology, Sremska Kamenica was analyzed using antibodies to P53, HER2 and E-cadherin and correlated with following clinicopathological parameters: gender, age, endoscopic type of cancer, localization, histologic type, grade, vascular and neural invasion, depth of infiltration, distant metastasis.
Results: 78 % of patients were aged over 60 years. p53-positivity was found in 47.17 %, HER2-positivity in 6.52 % and loss of E-cadherin expression in 43 %. p53-positivity showed statistically significant relevance correlated to gender, age, histologic type, localization, vascular invasion and depth of infiltration. HER2 overexpression was statistically relevant compared to endoscopic type of cancer and vascular invasion. E-cadherin was positive in all female and 33.3 % of male subjects. Loss of E-cadherin expression didn't differ among histological types but it showed statistically significant relevance correlated with high grade, deeper infiltration and vascular invasion. Loss of E-cadherin expression was verified in 83.3 % of HER2-positive tumors ($p<0.005$).
Conclusion: P53, HER2 expression and loss of E-cadherin expression may give valuable information for predicting vascular invasion and aggressive tumor behavior.

PS-06-005
Does immune profile of gist differ up to localisation?
U. Bayol*, A. Ozguzer, N. Demirgünes, O. Turelik, Z. Yildirim
*Tepecik Training and Research Center, Izmir, Turkey

Objective: Though immune profile of gastrointestinal stromal tumor (GIST) has been documented detailly, there has been no attracting data about correlation of the immune profile and localisation.
Method: Archival data of GIST cases has been documented as regards age, localisation, tumor size, mitotic activity rate, CD117 and CD34 immunopositivity. Results have been compared.
Results: Most of the 91 GIST cases were gastric and ileal ones. Mean age and mitotic activity rates were similar, abdominal (extra gastrointestinal tract) tumors were larger than the others. CD117 expression was significantly lower in colonic tumors and CD34 expression was significantly lower in abdominal ones (attached comparison chart).
Conclusion: CD117 and CD34 expressions are significantly lower in colonic and abdominal GISTs consequently. For the diagnosis of colonic and abdominal GISTs these data should be regarded.

	Stomach	Small bowel	Colon	Abdomen	Total
91 cases	30	37	9	15	91
Mean age	60	58	58	52	58
Mean Tm size (cm)	7	7.62	7.27	17.7	9.7
Mitosis	4/50 hpf	14/50 hp	20/50 hpf	14/50 hpf	11/50 hpf
CD117 (+)	26 (86.6%)	30 (81%)	3 (33.3%)	14 (93.3%)	73 (80.2%)
CD34 (+)	28 (93.3%)	25 (67.5%)	7 (77.7%)	5 (33.3%)	65 (71.4%)

PS-06-006

Whipple's Disease: A challenge of clinical, histopathological and electronomicroscopical diagnosis. Experience of a Romanian Tertiary Center - A five-case series

G. Becheanu*, A. Pop, E. Mandache, M. Gherghiceanu
*Bucharest, Romania

Objective: Whipple's disease is an infectious disease caused by Tropheryma whipplei, an ubiquitous Gram-positive Actinobacteria. The incidence of the disease is less than 1 per 1 milion. We report five new consecutive cases, four males and one female, diagnosed in our clinic from August 2002 to January 2012.

Method: Diagnosis was reached with the help of gastroduodenal endoscopy and histopathological examination of the duodenal biopsies, by lymph node biopsy and by electron microscopy.

Results: The main symptoms were arthralgia, weight loss and diarrhea. The endoscopic aspect of the small bowel mucosa varied from congestion, granularity of the mucosa to whitish plaques. All patients showed PAS positive, diastase resistant, Ziehl-Neelsen negative macrophages in the lamina propria of the duodenal mucosa and, in one patient, suspected for lymphoma, in an abdominal lymph node. The diagnosis was confirmed by electron microscopy in all cases. Classic Whipple's disease was the diagnosis in all five cases, but one patient showed involvement of the endocardium and two patients showed lymphadenopathies.

Conclusion: Clinical evolution was favorable under long-term antibiotics (Cephtriaxone/Trimethoprim-Sulfamethoxazole) and follow-up biopsies in three patients showed a normal endoscopical mucosa and a reduced but persistent number of PAS positive macrophages in the duodenal mucosa.

PS-06-007

Neuroendocrine Neoplasms of gastrointestinal tract: Forms of presentation and histological characteristics in a series of 11 Tunisian patients

A. Ben Salem*, I. Chelly Enneifer, H. Azzouz, H. Nfoussi, K. Bellil, A. Dhaoui, R. Hamrouni, B. Chelly, S. Haouet, N. Kchir, M. Zitouna
*Charles Nicolle Hospital, Dept. of Pathology, Tunis, Tunisia

Objective: Neuroendocrine neoplasms (NENs) of the gastrointestinal tract are rare tumors with an estimated incidence of 1 to 2 per 100,000.

Method: We reviewed the cases of gastrointestinal tract's neuroendocrine neoplasms presented to our department during 1 year (2010–2011) and we assessed the occurrence, form of presentation and histological characteristics of these tumors (we used the new OMS classification of NEN proposed on 2010).

Results: Eleven cases of NEN of gastrointestinal tract were identified. They were 6 men and 5 women with a mean age of 53.09 years. The most common localization was the appendix (7 cases). The 4 other cases were localized in the small intestine, the ileo caecal valve, the fundus and the bulb. The mean tumor's size was 13.8 mm. Mitoses were absent in the majority of cases (72,7 %). All the tumors were well differentiated classified as grade 1 in 9 cases and grade 2 in 2 cases. The tumor was aggressive in 2 cases. The small intestine's NET was multifocal infiltrating the subserosa with lymph node metastasis classified pT3 N1. The ileo caecal valve's NET was also aggressive with lymph node and hepatic metastasis classified pT4N1M1. All patients underwent surgical treatment.

Conclusion: Gastrointestinal NENs are complex tumors whose incidence is rising and whose treatment requires precise classification and risk stratification.

PS-06-008

Multiple duodenal stromal tumors associated with Neurofibromatosis-1

G. Benkhedda*, Y. Lamouti
*CHU Frantz Fanon, Dept. of Pathology, Blida, Algeria

Objective: Gastrointestinal stromal tumors (GIST), most commonly occur sporadically, but there seens to be some increased tendency for these tumors to develop in patients with neurofibromatosis1(NF1). There is no histological difference between the NF1 assocaciated cases and the sporadic cases. However, tumors associated with NF1 frequently show multiplicity.

Method: A case of multiple duodenal gastrointestinal tumor arising in a 45 year old mal with NF1 is reported. The

abdominal exploration revealed multiple solid nodules in the duodenum, and the pancretecticoduodenectomy was performed.
Results: Macroscopy: the resected segment of the duodenal showed seven suberosal solid masses. The largest mass measured 3,5 cm×2 cm×3 cm, and is coupled with the bors lower pancreas but remains limited by a capsule. The cut surface was smooth and white in appearance. Microscopy: the tumors were composed of interlacing fascicles of the uniform spindle cells with elongated cytoplasm. The tumor cells lacked pleomorphism, and mitotic figures were absent. Immunohistochechemistry: the tumors cells were diffusely positive for CD117, CD34, and negative for desmin, AML and pS100.
Conclusion: GIST are rarely noted in association with neurofibromatosis-1. Duodenal GISt are most frequently diagnosed in the workup of symptoms not specific to these masses. Duodenal resection is rarely indicated except in the case of duodenal GIST and early-stage adenocarcinoma or if the tumor appeared involve the pancreatic parenchyma on preoperative imagings.

PS-06-009
Periampullary adenomyoma: A true trap diagnosis
G. Benkhedda*, Y. Lamouti
*CHU Frantz Fanon, Dept. of Pathology, Blida, Algeria

Objective: Adenomyoma is a term generally applied to nodular lesions showing proliferation of both epithelial and smooth muscle components. It is usually presented as biliary obstruction. Most cases are misdiagnosed as adenoma or carcinoma by preoperative endoscopic or radiologic. Therefore, it is frequently treated with extensive surgery.
Method: We report a case of a 28 year-old man with an adenomyoma located in the ampulla of vater diagnosed by endoscopic piecemeal resection.
Results: On histologic examination, the lesion consisted of hyperplastic glandular lobules, mainly located in the muscle layers of the vaterian system. The lobular formations consist of small glands surrounded by myofifroblastic, fibroblastic proliferation, sparse capillaries and inflammatory cells. IHC: Ki67: rare cells with a positive nuclear staining were presenting in the epithelial and mesenchymal components AML: The myofibroblastic of most spindle cells was confirmed by a strong cytoplasmic expression.
Conclusion: Real incidence of adenomyoma of the vaterian system is difficult to appreciate as different names (adenomyoma, adenomyomatosis, myoepithelial hamartome) are used to designate the same histological lesion. Adenomyoma was diagnosed only in adult patients –mean age: 63 y). The histogenesis is still a subject of controversy. The most widely accepted hypothesis is that the lesion may represent a form of incomplete heterotopic pancreas. Adenomyoma is considered as benign and slow growing, but its potential neoplastic nature cannot be excluded.

PS-06-010
So-called carcinosarcoma of the duodenum: Case report and review of the literature
L. Berdica*, T. Bushati, S. Erekul, A. Doniku, A. Orlandi
*American Hospital, Dept. of Pathology, Tirana, Albania

Objective: Carcinosarcomas are rare tumors. Duodenal carcinosarcomas of the duodenum are rare.
Method: H-E and IHC staining.
Results: We present a polypoid so-called carcinosarcoma of the duodenum in the Papilla Vater region in a patient of 59 years old. Tumor of 7 cm resected together the pancreatic tissue from the head of the pancreas. The tumor was diagnosed as Popypoid so-called carcinosarcoma of the duodenum with a wide peduncul infiltrating the Vater papilla. It contains two histologic components, one of well-differentiated adenocarcinoma that covers and infiltrates the tumor and a malignant fusiform component that serves as a stalk to the tumor.
Conclusion: Our case must be the fourth reported in the english literature. They have been reported in various forms, but most of them have been so-called carcinosarcomas. However, the histogenesis of these tumors is subject to further study. Carcinosarcoma of the digestive organs has been reported to exhibit aggressive behavior. Carcinosarcomas in digestive organs have been reportedly associated with a poor prognosis.12,13 However, some cases that have been treated with a curative operation showed long-term survival.

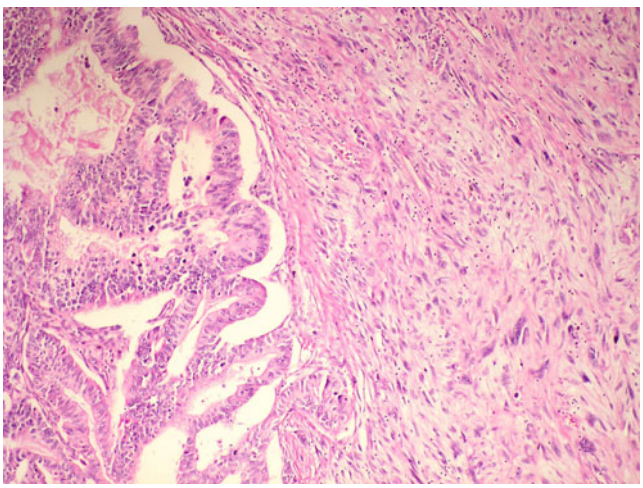

PS-06-011
Analysis of HER2 expression level in gastric carcinomas
M. Bialas*, A. Sinczak-Kuta, A. Lazar, K. Urbanczyk, K. Galazka, J. Szpor, S. Demczuk, D. Adamek
*Jagiellonian University, Dept. of Pathomorphology, Krakow, Poland

Objective: The expression of HER2 – an oncoprotein belonging to tyrosine kinase family belongs to recently evaluated prognostic and predictive factors in gastric cancer. Overexpression of HER2 is observed in about 8–27 % gastric cancers. According to many authors, overexpression and/or amplification of HER2 correlates with poor prognosis. The aim of our study was to analyze HER2 expression in gastric cancer in material routinely examined in Pathomorphology Department, JUMC.
Method: We have analyzed 50 cases of gastric cancers. The material came from 19 females and 31 males, age: 21-86. Immunohistochemical reactions were performed automatically on BenchMark BMK Classic (Ventana) using PATHWAY HER-2/neu (4B5) antibody. Scoring system for HER2 expression was ranged from 0 to 3+ where: 0 and 1+ were regarded as a negative, 2+ as equivocal and 3+ as positive.
Results: Most cases of gastric cancers were HER2-negative (45/50): including 0 score (38 patients) and 1+ (7 patients). Three cases were equivocal and two cases showed 3+ expression level.
Conclusion: The lower level of HER2 expression in the analyzed material in comparison with literature could be related to a relatively small group of cases but one cannot exclude that there exist some other factors that stand behind this and surely the investigations should be continued.

PS-06-012
MAPKAP kinase 2 overexpression influences prognosis in gastrointestinal stroma tumors, associates with copy number variations on chromosome 1, and expression of p38 MAP kinase and ETV1
P. Birner*
*Medizinische Universität Wien, Institut für Klinische Pathologie, Austria

Objective: ETV1 has been proposed to be activated by KIT-mutations in gastrointestinal stromal tumors (GISTs). Aim of the study was to evaluate the role of ETV1 and associated proteins in GIST.
Method: Expressions of ETV1, MAPKAP kinase 2 (MAPKAPK2), phosphorylated p38 MAP kinase (pp38), phosphorylated MSK1, phosphorylated RSK1, COP1 and KIT were determined immunohistochemically in 139 GISTs. Sequence analysis of KIT, PDGFRA and MAPKAPK2 and FISH of ETV1 and chromosome 1 was performed.
Results: Prominent ETV1 expression was seen in 50 % of GISTs, but no correlation with clinical outcome was found. Correlation of ETV1 expression and KIT mutation was seen in 60 % of cases. MAPKAPK2 overexpression (n=62/44.6 %) correlated with pp38 expression (p=0.021) and alterations of chromosome 1 (p=0.024). In one cases with high MAKAPK2 expression, a MAPKAPK2 gene mutation was found. All relapsing GISTs with very low/low risk showed high MAPKAPK2 and KIT expression. MAPKAPK2 overexpression was an independent prognostic factor for disease free survival (p=0.006).
Conclusion: ETV1 is not universally overexpressed in GIST and seems to be induced also by other pathways than KIT-mutation. MAPKAPK2-overexpression is associated with shorter survival in GIST. Patients with low risk GISTs overexpressing MAPKAPK2 might profit from adjuvant tyrosine kinase inhibitor therapy.

PS-06-013
Gastrointestinal stromal tumors: Comparison of two risk stratification systems in a multicenter study of 1963 Turkish cases
G. Bulbul Dogusoy*
*Gayrettepe Florence Nightingale, Dept. of Pathology, Istanbul, Turkey

Objective: A nationwide database was performed for gastrointestinal stromal tumors (GISTs) in a large series of primary GISTs surgically treated at centers all around Turkey. The aim of this multicenter study was to analyze and compare the performance of the National Institute of Health (NIH) and Armed Forces Institute of Pathology (AFIP) risk criteria to determine the ideal risk stratification system.
Method: Statistical analysis of a nationwide database is consisted of age, gender, location, risk groups, histopathologic features and the results of CD117, CD34, Desmin, SM Actin, S-100 protein, and Ki67 immunohistochemistry.
Results: In 1965 cases registered in database, male to female ratio was 1.20 and mean age was 57.64 years. Most common location was stomach (47.5 %) followed by small intestine, omentum- peritoneum, large intestine, and esophagus (30.3 %, 12.1 %, 9.1 %, 1.0 % respectively). Comparison of the two risk-stratification systems demonstrated that proposed modified AFIP seems to be better when compared with NIH system. Many histopathologic and immunohistochemical findings showed significant correlation with risk groups of AFIP, even with 'not sufficient data' group (p<0.005).
Conclusion: The results of this multicenter study demonstrates that although follow up results are not provided, AFIP risk criteria seems to be more useful in prognostication for GISTs among the two systems.

PS-06-014
HER2 and Kras in gastric cancer patients
M. L. Caruso*, M. Di Maggio, A. M. Valentini, M. Pirrelli, R. Armentano
*IRCCS S de Bellis, Dept. of Pathology, Castellana Grotte, Italy

Objective: HER 2/neu overexpression or amplification is an important biomarker for identifying patients with intestinal-

type gastric cancer who respond to therapy with Trastuzumab. Moreover, intestinal type gastric cancer shares many phenotypic and molecular genetic changes with colorectal cancer. In particular a progression from chronic gastritis to intestinal metaplasia, dysplasia, and finally malignant transformation is probably the sequence of gastric carcinogenesis. Somatic mutation of K-ras gene is common in colorectal cancer, being found in more than one-third of cases, but it seems to have, mostly in intestinal-type gastric cancer, a low incidence (7–20 %). The purpose of this study is to assess HER2 gene amplification and K-ras mutational status in a series of intestinal-type gastric carcinoma patients.
Method: Twenty paraffin embedded gastric cancer specimens were tested for HER2 amplification by chromogenic in situ hybridization (CISH) and K-ras mutational status (codon 12 e 13) by PCR-RFLP.
Results: Six (30 %) cases were HER2 amplified. Only one case (5 %) was found to have K-ras mutation (codon 12), but it was HER2 not amplified.
Conclusion: The frequency of K-ras mutation and HER2 amplification are in agreement with other studies on this topic. In our study, the two seem mutually exclusive events.

PS-06-015
IL-6-174 as a gastric carcinogenesis marker in biopsies
L. Carvalho*, A. Sampaio, S. Balseiro, A. Alarcão, M. J. D'Aguiar, D. Oliveira, T. Ferreira, M. Reis Silva
*Amadora, Portugal

Objective: Gastric carcinoma is related with cancer genetic susceptibility that can be investigated as single nucleotide polymorphisms (SNPs) and as cytokine genes are known to predispose to malignant disease, several polymorphisms of Interleukin-6 (IL-6) gene have been reported to in some may be associated with tumour progression including inhibition of malignant epithelial cells apoptosis and stimulation of angiogenesis.
Method: The aim of this study was to clarify the association between IL-6 polymorphisms and the risk of gastric cancer and chronic gastritis development or maintenance. PCR-SSP genotyping for IL-6 -174 C>G polymorphism was performed in 100 biopsies of gastric carcinoma and in 100 biopsies of chronic gastritis.
Results: There was association between IL-6 -174 C allele (p=0,0466) and -174CC, low producer, genotype (p= 0,0466) and gastric carcinoma, whereas IL-6 G allele (p= 0,0278) and IL-6GG (p<0,0001), high producer, genotype was associated with gastritis.
Conclusion: We conclude that IL-6 -174, low producer genotypes, may have an important role in gastric carcinogenesis and the polymorphism study of this molecule could be a good marker for gastric carcinoma susceptibility when high grade dysplasia is seen in biopsies.

PS-06-016
Giant Gastric Stromal Tumor in a 25-year-old man
R.-M. Closca*, S. Taban, C. Ardeleanu, A. Dema
*City Hospital, Pathology, Timisoara, Romania

Objective: Gastrointestinal stromal tumors are the most common mesenchimal tumors of the gastrointestinal tract, representing 1–3 % of all the malignant tumors.
Method: We present the case of a 25-year-old man with a giant gastrointestinal stromal tumor of the stomach. The patient was admitted in the hospital for a palpable abdominal mass and a suboclusive syndrome. CT examination revealed a giant abdominal tumor. For the immunohistochemical (IHC) study we used the following antibodies: Vimentin, CD117, PDGFR, Nestine, D2- 40, PKC, CK MNF116, CK7, Synaptophysine, S100, CD34., En Vision system, visualization with diaminobenzidine.
Results: On gross examination, the tumor of 40/27 diameter, was soft, relatively well circumscribed, brown-tan on cut section, with cyst formation. Microscopically the tumor had an epithelioid growth pattern; the tumor had a low mitotic activity. Immunohistochemical stains showed, in the tumor cells, positive reaction for Vimentin, CD117, PDGFR, Nestine, D2- 40, PKC, and lack of reactivity for panCK, CK7, Synaptophysin, S100, CD34. Based on data offered by gross examination and by usual stains in conjunction with IHC profile we established a diagnosis of gastrointestinal stromal tumor.
Conclusion: Gastrointestinal stromal tumor have always been challenging for pathologists. The particularity of our case is the patient's young age and the large size of the tumor.

PS-06-017
Analysis of microsatellite instability in gastric malt lymphoma
A. Degroote*, T. Tousseyn, M. Spaepen, G. Matthijs, G. De Hertogh, S. van der Borght, D. Owen, D. Schaeffer, K. Lambein, L. Libbrecht, X. Sagaert
*UZ Leuven, Dept. of Pathology, Belgium

Objective: In Helicobacter pylori gastritis, constant antigenic stimulation triggers a sustained B-cell proliferation. Errors made during this continuous DNA replication are corrected by the DNA mismatch repair mechanism. Failure of this mechanism has been described in HNPCC and results in a replication error phenotype. Inherent to their instability during replication, microsatellites are the best markers of this replication error phenotype. We aimed to evaluate the role of defects in the DNA mismatch repair mechanism and

microsatellite instability (MSI) in gastric mucosa-associated lymphoid tissue (MALT) lymphoma.
Method: We examined 10 microsatellite loci (BAT25, BAT26, D5S346, D17S250, D2S123, TGFB, BAT40, D18S58, D17S787 and D18S69) for instability in 28 patients with MALT lymphomas. In addition, these tumors were also immunostained for MLH1, MSH2 and MSH6, as well as screened for the presence of t(11;198)(q21;q21) by real time polymerase chain reaction (RT-PCR).
Results: We found MSI in 5/28 (18 %) lymphomas, with one tumor displaying high levels of instability. MSI occurred in both t(11;18)(q21;q21)-positive and –negative tumors.
Conclusion: Our data suggest that a MMR-defect may be involved in the development of gastric MALT lymphomas, and mutations in the MSH6 MMR gene or hypermethylation of the MSH6 promoter might be associated with MSI-driven gastric lymphomas.

PS-06-018
Mitosis-specific marker phospho-histone H3 in the diagnosis of gastrointestinal stromal tumors
A. Dolzhikov*, A. Tverskoi, K. Hizhnyakov
*Regional Pathology Hospital, Dept. of Oncomorphology, Belgorod, Russia

Objective: The assessment of proliferative activity is one of the major parameters in the proper grading of gastrointestinal stromal tumors (GISTs). In the low level of mitotic activity it is difficult to calculate dividing cells correctly. Phospho-histone H3 (PHH3) is a recently introduced immunomarker for mitotic cells.
Method: Immunohistochemical study of 46 cases of GISTs of different malignant potential, statistical analysis.
Results: The count of PHH3-immunoreactive cells demonstrates the strong correlation (Gamma 0,756; $p<0,05$) with malignant potential of GISTs detected by standard parameters. It clearly separates true mitotic cells from apoptotic and piknotic nuclei. In all cases PHH3 count was slightly higher than the mitotic index in H&E stained slides. We have found that PPH3 demonstrated the two types of staining: nucleosomal dot-like type and mitotic homogenous type. The first type, probably, reflects the fraction of cells just before the prophase, which cannot be identified in H&E slides.
Conclusion: Immunostaining of PPH3 is a useful additional marker in detection of proliferative activity in GISTs, helping to identify true dividing cells correctly.

PS-06-019
HER2 assessment in gastric carcinoma using IHC and FISH
P. Drev*, B. Gazic, J. Contreras
*Institute of Oncology, Dept. of Pathology, Ljubljana, Slovenia

Objective: HER2 in gastric cancer (GC) should be assessed following guidelines - recommended testing algorithm employs IHC as a screening tool and is followed by ISH to clarify equivocal cases. Reported incidences of HER2+ GC vary substantially and discordant results are frequent. In a series of GC HER2 was assessed by IHC and FISH to determine incidence of HER2+ GC, concordance of the methods and reevaluate the recommended algorithm.
Method: HER2 was assessed by both IHC (Pathway 4B5™) and FISH (PathVysion™) in 164 GC samples. Reactions were evaluated according to guidelines. HER2 was considered positive in case of strong protein expression (3+) and/or gene amplification (ratio ≥2.0). Frequencies of IHC and FISH scores, incidence of HER2+ GC and concordance (chi-square) of applied methods were analysed.
Results: IHC score distribution: neg(0) 63.3 %, neg(1+) 19.1 %, equiv(2+) 10.8 % and pos(3+) 10.8 %. FISH results distribution: nonampl 85.4 %, ampl 13.4 % and equiv 1.2 %. 36.5 % of IHC equiv 2+ tumors were amplified. There were no discordant cases resulting in excellent concordance ($p<0.0001$).
Conclusion: Approximately 15 % of GC are HER2+. Application of standardised tests results in excellent concordance and, consequently, the proposed testing algorithm enables detection of all HER2+ GC.

PS-06-021
Glomus tumor of the stomach: A case report
J. Ferreira*, R. Fonseca, P. Chaves
*IPO Lisboa Francisco Gentil, Serviço de Anatomia Patológica, Portugal

Objective: Gastric glomus tumors are rare neoplasms originated from modified smooth muscle cells of the glomus bodies. Such lesions present a diagnostic challenge in biopsy material. Herein, we report a case of gastric glomus tumor in a 35-year-old woman.
Method: A 35-year-old woman presented with refractory epigastralgy. A gastrointestinal stromal tumor of the gastric antrum was suspected. The diagnosis was made after ultrasound-guided endoscopic biopsy, followed by an endoscopic submucosal resection.
Results: The biopsy showed tight convolutes of capillary-sized vessels surrounded by collars of small, rounded cells set in a hyalinized, myxoid stroma. Immunohistochemically, these cells were positive for smooth muscle actin and type IV collagen (pericellular pattern), synaptophysin (focal positivity) and negative for CD34, CD117, desmin, S100 and cytokeratins. The diagnosis of gastric glomus tumor was rendered. The resection specimen revealed a submucosal well-circumscribed 2×1,5×1,5 cm nodule with identical histological features. The patient was disease-free 12 months postoperatively.

Conclusion: Visceral glomus tumors are rare neoplasms. When they arise in the gastrointestinal tract, the stomach (antrum) is the most frequent location. The differential diagnosis includes NET, epithelioid GIST and hemangiopericytomas. They usually behave in a benign fashion, although malignant cases have been reported. Surgical excision is the standard treatment.

PS-06-022

Immunohistochemical evaluation of replication Protein-A1 in gastric cancer: Clinicopathological associations

H. Gakiopoulou*, E. Fourtziala, G. Levidou, A. Stofas, N. Alexakis, P. Korkolopoulou, E. Patsouris
*University of Athens, 1st Dept. of Pathology, Greece

Objective: Replication protein A1 (RPA1) is required for stabilization of single-stranded DNA at early and later stages of DNA replication being thus critical for eukaryotic DNA replication. In this study, we investigated for the first time the immunohistochemical expression of RPA1 protein in a series of 73 gastric carcinomas in relation with clinicopathological parameters (age, sex, Lauren's histologic classification, histologic grade, lymphovascular invasion, tumor size, depth of invasion (T), lymph node metastasis (N) and stage).
Method: A standard immunohistochemical method and a semi-quantitative evaluation for the detection of RPA1 Labeling Index (LI) were applied.
Results: Nuclear RPA1 immunoreactivity was seen in all carcinomas with a mean value of 26.5 %. Statistical significant correlations emerged between: 1. RPA1 LI and low T-category (p=0.009) 2. RPA1 LI and absence of lymph node metastasis (p=0,014). RPA1 LI was higher in cases without lymphovascular invasion; however this association did not reach statistical significance.
Conclusion: The widespread expression of RPA1 in gastric carcinomas suggests that this protein is implicated in gastric cancer growth. The observed significant associations between RPA1 LI and low T as well as N0 tumors could imply that RPA1 might offer a growth advantage in the early stages of gastric cancer progression.

PS-06-024

Pigmented histiocytic "Pseudotumoral" reaction due to endoscopic tattooing of the duodenum with India Ink

R. Hadhri*, C. Souki, A. Moussa, S. Korbi, L. Njim, H. Mahmoudi, A. Zakhama
*Fattouma Bourguiba Hospital, Dept. of Pathology, Monastiir, Tunisia

Objective: India ink has been used for endoscopic tattooing to facilitate localization of a luminal abnormality at the time of surgery or repeat endoscopic examination. Recognition of this phenomenon is important to prevent misinterpretation of this _nding as other cause of black tissue deposits. Some of them can be easily excluded by microscopic examination; the others, however, necessitate special stains or, as illustrated by our observation, an adequate clinical information!
Method: A 76-year-old man was referred for enteroscopy for microcytic anemia. The procedure revealed a 2 cm flat umbilicated lesion of the duodenum. Endoscopic tattooing was performed to guide surgical excision.
Results: Histologic examination of the surgical specimen revealed a tubulovillous adenoma with low-grade dysplasia. The submucosa showed numerous aggregates of large cells containing a heavy black pigmentation. Special histologic stains were inconsistent with melanin or iron. This submucosal cellular infiltration was linked to the preoperative use of India ink when the notion of tattooing was "kindly" provided by the surgeon!
Conclusion: Despite a striking and misleading appearance, the microscopic finding of such phenomenon does not represent a pathologic state. Nevertheless, communication between enterologists, surgeons and pathologists are mandatory to assure prompt recognition and avoid unnecessary investigations.

PS-06-025

Altered gastric surface marker and mucin expression in first degree relatives of gastric cancer patients

M. Halpern*, D. Boltin, Z. Levy, A. Vilkin, S. Morgenstern, Y. Niv
*Hasharon Hospital, R.M.C., Raanana, Israel

Objective: Gastric cancer phenotypes may be classified according to mucin secretion and surface markers as intestinal, gastric type or unclassified. This is the first study to assess the surface marker and mucin phenotype in first degree relatives of gastric cancer patients.
Method: 48 patients were prospectively recruited at out institution. Sections of gastric mucosa were stained immunohistochemically for CD10, MUC1, MUC2, MUC5AC and MUC6, and scored based on stain extent and intensity.
Results: Expression of CD10 was intermediate in 8 and 5 controls (p=0.02). MUC1 in superficial glands was intermediate in 12, high in 7 (p=0.015). In the deep glands MUC1 expression was intermediate in 8 and 2 controls, and high in 32 and 6 controls (p=0.66). One case show intermediate MUC2. MUC5AC expression was high in superficial mucosa in all cases and controls, and in the deep glands was intermediate in 8 and 2 controls (p=0.67). MUC6 was absent in superficial glands of all cases and controls, but highly expressed in deep glands. H. pylori was found in 8 cases and 2 controls (p=0.67).
Conclusion: Gastric CD10 expression is reduced and MUC1 expression is increased in first degree relatives of gastric cancer patients.

PS-06-026

Primary gastric choriocarcinoma: Two case reports

S. Haraoka*, A. Iwashita, I. Iwashita
*Fukuoka University, Chikushi Hospital, Chikushino, Japan

Objective: Choriocarcinoma is a malignant neoplasm secreting β-hCG that grows rapidly and metastasizes widely. Primary gastric choriocarcinoma is very rare. We report two cases of primary gastric choriocarcinoma, one of which combined with adenocarcinoma.
Method: Two patients are 73-year-old woman and 77-year-old man. Gastroscopy revealed the protruded tumors with ulceration approximately 8.5 cm and 5 cm in size, respectively. In both cases, urine β-hCG was high. Both patients died 8 months and 1.5 months after the initial diagnosis due to distant metastasis.
Results: Histological examination confirmed the choriocarcinoma composed of intimate admixtures of cytotrophoblasts and syncytiotrophoblasts, associated with hemorrhage and necrosis. In one case, a small area of well to moderately differentiated tubular adenocarcinoma was contiguous to the choriocarcinoma component with relatively well-defined. The choriocarcinoma foci and adjacent adenocarcinomatous area showed positive immunoreactivity for β-hCG, but negative for CEA. However, adenocarcinoma component was positive for CEA, but negative for β-hCG.
Conclusion: In coexistent choriocarcinoma and adenocarcinoma of the stomach, a transitional form of tumor cells is occasionally found, so that a retrodifferentiation theory from adenocarcinoma to choriocarcinoma is supposed.

PS-06-027

Gastrointestinal stromal tumors and rare synchronous neoplasms

A. C. Iorgescu*, E. Stoica-Mustafa, C. Pechianu, V. Herlea
*Fundeni Clinical Institute, Dept. of Pathology, Bucharest, Romania

Objective: Gastrointestinal stromal tumors are mezenchimal tumors which originatte from interstitial cells of Cajal or related stem cells from the gastrointestinal wall and have a typical immunoreactivity for CD117(c-kit protein). The most frequent localization is the stomach (about 50-60 %), followed by the duodenum and small intestine (30–40 %), esophagus (about 5 %), rectum (about 5 %), colon (about 2 %). Their association with other gastrointestinal tumors has been reported rarely in literature most frequently with adenocarcinoma or lymphoma and less with neuroendocrine tumors or squamous cell carcinoma.
Method: We present two cases of synchronous tumors.
Results: First case is that of a 73 years old man who underwent surgery for gastric neuroendocrine carcinoma accompanied by a gastric stromal tumor. The second case refers to a 74 years old male with squamous cell carcinoma in the middle third of the esofagus coexisting with gastric stromal tumor with a very low risk.
Conclusion: In literature there are reported less then 30 cases of sinchronous gastrointestinal stromal tumors with neuroendocrine tumors or scuamous cell carcinoma. A multidisciplinary approach is vital for treatment succes.

PS-06-028

The number of metastatic lymph nodes in adenocarcinoma of ampulla of Vater as a prognostic factor

H.-J. Kang*, S.-H. Eo, E.-S. Yu, H. Cho, S.-M. Hong
*Asan Medical Center, Dept. of Pathology, Seoul, Republic of Korea

Objective: Although the increase of the number of lymph node (LN) metastasis indicates worse prognosis in carcinomas from other gastrointestinal tract organs, the prognostic implication of the number of metastatic LNs has not been well characterized in adenocarcinomas of ampulla of Vater (AAs).
Method: The number of metastatic LNs was evaluated with 1058 surgically resected AAs having at least 12 examined lymph nodes from the population based SEER database. A complex pattern of survival versus the metastatic LNs was captured by censored local regression. The effect of metastatic LNs on patient's survival time was investigated by the adaptive partitioning algorithm for identifying the most significant cutoff points of metastatic LNs.
Results: Two significant cutoff points (0 and 2) for the metastatic LNs were identified. These cutoff points segregated the patients into 3 groups with the statistically significant difference in median survival (no metastatic LNs, 478 cases, median survival time, 99 months; 1-2 metastatic LNs, 279 cases, 29 months; >3 metastatic LNs, 301 cases, 19 months, $p<0.01$).
Conclusion: On the basis of the present results, we propose that the nodal classification of AAs should be further classified into N0 (no metastatic LNs), N1 (1–2 metastatic LNs) and N2 (>3 metastatic LNs).

PS-06-029

Correlation of expression of yes-associated protein and phosphorylated yes-associated protein with clinicopathologic parameters in esophageal squamous cell carcinoma

K.-H. Kim*, J.-M. Kim, K.-S. Song
*Chungnam National University, Cancer Research Institute, Daejeon, Republic of Korea

Objective: Yes-associated protein (YAP) has been investigated in carcinomas as a candidate human oncogene serving as a transcription co-activator in nucleus. The phosphorylated

form of YAP (pYAP) locates to the cytoplasm, preventing cellular proliferation by spatially segregating YAP from the nucleus.

Method: Samples from 142 patients of esophageal squamous cell carcinoma (ESCC) were studied using immunohistochemistry for YAP, pYAP and Ki-67.

Results: In 142 cases of ESCC, higher nuclear expression of YAP was correlated with tumor diameter, pathologic T category (1 versus 2–4), pathologic TNM stage (I versus II–IV) and Ki-67 expression in univariate analyses. Higher nuclear expression of YAP was significantly associated with worse overall and disease-free survival from Kaplan–Meier plots. Multivariate analysis showed higher nuclear expression of YAP to be an independent prognostic marker for overall survival. The cytoplasmic expression of pYAP in ESCC was not correlated with Ki-67 expression and was higher than in the normal esophageal epithelium, whereas nuclear expression of pYAP was not different in the two tissues.

Conclusion: Our results suggest that YAP shifts from the nucleus to the cytoplasm as a consequence of phosphorylation and is inactivated in ESCC. The nuclear expression of YAP is correlated with tumor growth and is an independent predictor for a worse prognosis of ESCC.

PS-06-031

Oesophageal metastasis from ovarian serous adenocarcinoma: A case report

M.-M. Koumpanaki*, P. Xirou, E. Michalopoulou, B. Christoforidou, S. Barbanis, N. Vladika, F. Patakiouta
*Thessaloniki, Greece

Objective: Oesophagus is an uncommon site of metastases, mainly originating from lung and breast. Ovarian carcinomas usually metastasize to pelvic structures and peritoneum and only two cases of ovarian metastasis to the oesophagus have been reported in the literature. We report a rare case of metastatic ovarian serous adenocarcinoma to the esophagus.

Method: Our patient, a 67 year-old woman, was diagnosed with carcinoma of the left ovary 8 years ago. She received neoadjuvant chemotherapy and underwent total hysterectomy. After a disease free interval of 5 years she complained of progressive dysphagia. An oesophageal biopsy was taken endoscopically.

Results: Microscopic examination showed infiltration of oesophageal mucosa by a moderately to poorly differentiated papillary adenocarcinoma, immunohistochemically positive for CK8/18, CK7, CA-125 and WT-1. Morphological and immunohistochemical features of the neoplasm were consistent with metastatic ovarian serous adenocarcinoma to the esophagus. The patient received adjuvant chemotherapy and was free of symptoms for 2 years, until recently, when her condition dramatically worsened.

Conclusion: Oesophageal metastases are rare, constituting approximately 2,7 % of malignant oesophageal neoplasms, and must be differentiated from primary tumours. Metastatic neoplasms may reach the oesophagus by haematogenous or lymphatic dissemination. Chemotherapy is the treatment of choice and ultimate prognosis is poor.

PS-06-032

Lesions associated with gastric cancer with implications in gastric carcinogenesis

D. C. Lazar*, S. Taban, A. Dema, M. Cornianu, F. Baderca, D. Koukoulas, A. Goldis, I. Sporea
*University of Medicine, Pathology, Timisoara, Romania

Objective: Recently, the pathological aspects implicated in "Correa's cascade" of gastric carcinogenesis were assessed.

Method: Our batch: 61 gastric cancer patients,43 males,18 females, average age=59.34 years. Witness group: antral biopsies from 96 patients with dyspeptic syndrome. We assessed the incidence of premalignant lesions.

Results: Gastric carcinomas: intestinal type(IT)(62.3 %), diffuse type(DT)(27.9 %), and mixed type(MT)(9.8 %). IT develop on the background of atrophic chronic gastritis (ACG)(65.8 %), with intestinal metaplasia(IM). ACG: more frequent in IT vs. DT(65.8 % vs.29.4 %, $p=0.0122$). IM: significantly more frequently in IT(68.4 %) and MT (66.7 %) vs. DT(23.5 %) ($p<0.001$). Type III IM: more frequent in IT(29 %) and MT carcinomas (33.3 %) vs. benign lesions(3.1 %) ($p=0.00006$). Witness group:10 patients presented epithelial dysplasia(10.4 %). Dysplastic lesions: more frequent in carcinomas of MT(66.7 %) and IT (60.5 %) vs. DT(23.5 %) ($p=0.0011$). Incidence of bacterial colonization: greater in IT(73.7 %) and DT(64.7 %) vs. witness group(51 %) ($p=0.00729$).

Conclusion: Our observations sustain the different histogenesis of cancers divided after Lauren classification and the etiopathogenic role of H.pylori in the development of gastric carcinomas. Assessment of type III IM is useful in early diagnosis of gastric cancer.

PS-06-033

The role of endo-biopsy in evaluating inflammatory and pre-neoplastic gastric lesions

D. C. Lazar*, S. Taban, A. Dema, M. Cornianu, E. Lazar, F. Baderca, A. Goldis, I. Sporea
*University of Medicine, Pathology, Timisoara, Romania

Objective: Our aim was to assess the concordance between the endoscopic and histopathologic diagnosis of gastritis.

Method: We included 96 dyspeptic patients; according to the Sydney system, we designed a protocol for description of endoscopic lesions and taking of the biopsies.

Results: We included 96 patients (58 females;38 males), mean age 60.1 years were. More severe gastritis: gastric body vs. antrum (p=0.041). In patients with endoscopic antral gastritis, histological confirmation had: sensitivity 97.9 %, specificity 50 %, PPV 98.9 %, NPV 33.3 %. In patients with endoscopic aspect of body gastritis, histological confirmation had: sensitivity 41.3 %, specificity 100 %, PPV 100 %, NPV 6.897 %. Infection with H. pylori:51 % of antral and 37.5 % of gastric body biopsies. Most cases of erosive antral gastritis, diffuse erythematous and petechial body gastritis were H. pylori(+). In some cases the endoscopy was normal, but histopathological examination identified H.pylori. Atrophy:48 % of antral and 54.2 % of gastric body biopsies, more frequent in older patients. Intestinal metaplasia:20.8 % antral 25 % gastric body biopsies. Dysplastic lesions:10.4 % of patients, 2(2,1 %) with high-grade dysplasia, in patients with antral diffuse erythematous gastritis.
Conclusion: Histopathological exam is mandatory for the diagnosis of gastritis, identifying pre-neoplastic lesions and confirmation of H.pylori.No concordance between endoscopic and histologic diagnosis of atrophy.

PS-06-034
Coexistence of Mixed Adenocarcinoma with Neuroendocrine tumor G1 (MANEC) and Leiomyomas of the stomach
M.-A. Lianou*, C. Magkou, M.-E. Kopaka, M. Chantziara, P. Kara, E. Gioti, D. Riga, M. Konstantinou, C. Lariou
*Athens, Greece

Objective: Mixed adenocarcinoma of the stomach with a NET as the neurondocrine component of the tumor is rare, as well as intramural leiomyomas. We present a case of a combined mixed epithelial carcinoma and neuroendocrine tumor with a random finding of mesenchymal tumor.
Method: A 72 year-old male came to our hospital complaining of abdominal pain. Endoscopic biopsy revealed the presence of invasive adenocarcinoma and a total gastrectomy was performed.
Results: The histopathological report concluded the presence of MANEC. The neuroendocrine component comprised a NeuroEndocrine Tumor (NET) G 1, which showed a strong immunoreaction to Chromogranin A, Synaptophysin and CD56 and none to Gastrin, Serotonin and ACTH. Mitotic rate, Ki-67 measured 1 %. The immunohistochemical control of the exocrine component was positive for CK7, CK20. That of the incidental finding of four small leiomyomas was positive for a-SMA and Desmin and negative for CD117, DOG-1 and CD34.
Conclusion: Gastric MANEC with a NET G1 component is a rare tumor. Gastric leiomyomas are also considered a rare finding. The coexistence of the two different neoplasms is even rarer, thus making it an interesting case report.

PS-06-036
Refractory celiac disease: Clinicopathological features of 12 cases
C. Meléndez*, F. Climent, M. J. Paúles, M. Varela, J. M. Botargues, F. Rodriguez, E. Condom
*Bellvitge Hospital, Dept. of Pathology, L´Hospitalet de Llobregat, Spain

Objective: Intraepithelial lymphocytes (IEL) in celiac disease (CD) are CD3+ and CD8+ and exhibit a polyclonal profile for T-cell receptor (TCR) rearrangement. In contrast, refractory CD (RCD) may be subdivided into type I (IELs polyclonal and normal phenotype) or type II (IELs monoclonal and/or aberrant phenotype). The aim was to analyze the RCD cases in our institution.
Method: The clinical, pathological, immunophenotypical and molecular findings of 12 RCD cases were reviewed.
Results: Our series comprised 7 men and 5 women with a median age of 57 years (range: 20–76). One patient had RCDI and 11 patients had RCDII. Six patients presented with no prior clinical or biopsy evidence of gluten sensitivity. Three patients developed RCDII after a history of CD of 12, 60 and 144 months and 1 of them developed EATL. Two patients presented IEL and EATL simultaneously. Phenotype was aberrant in 8 out of 11 and TCR was monoclonal in 10 out of 10 tested cases.
Conclusion: In our series, 6 cases presented as RCDII de novo. The IEL phenotype study and the TCR rearrangement were useful for identifying cases with RCD.

PS-06-037
Gastritis cystica polyposa in an unoperated stomach treated by endoscopic polypectomy
M. Molaei*, F. Lahmi, S. R. Fatemi, M. R. Zali
*RCGLD, Shahid Beheshti University, Tehran, Iran

Objective: Gastritis cystica polyposa is a unique lesion found on occasion at the stoma of a gastrojejunal anastomosis. However, GCP is rarely found in an unoperated stomach.
Method: A 51-year-old woman with abdominal discomfort and vomiting. Physical examination, routine hematological examination and biochemical tests were within normal limits, exept mild anemia.
Results: Upper GI endoscopic examination revealed a pedanculated polyp, in the greater curvature. Endoscopic ultrasonography revealed a polypoid heteroechoic mass with cystic area and 20×22 mm diameter in posterior wall of gastric body. Polypectomy was performed without any complications. Histological examination of the protruding lesion revealed some misplaced cystic glands were entrapped in dense disorganized bundles of smooth muscle of muscularis mucosa surrounded by a rim of lamina propria. These findings were consistent with gastritis cystic polyposa.

Conclusion: GCP is a unique type of chronic gastritis represented by a sessile elevated lesion along a suture line, occurring a long time after Billroth- II surgery or simple gastrojejunal anastomosis. When these findings are considered, it may be reasonable to speculate that there are close relationships among DGR, GCP and gastric stump carcinomas.

PS-06-038

Gastrosplenic Fistula from Hodgkin‘s Lymphoma, manifesting as upper gastrointestinal bleeding

E. Nour*, B. Y. Lamia, B. Wassila, B. Nizar, B. Khedija, D. Mohamed Hedi, S. Attafi
*FSI, Gastroenterology, Tunis, Tunisia

Objective: Primary gastric Hodgkin's lymphoma is reported in only 2 % of patients with primary gastric lymphomas. Most cases are observed in the course of systemic disease.
Method: We report a case of Hodgkin's lymphoma that was complicated by gastrosplenic fistula manifesting as upper gastro-intestinal hemorrhage.
Results: We report the case of a 52 years old man with a 10 years history of untreated Hodgkin’s lymphoma. He was hospitalized for a massive upper gastrointestinal bleeding. The gastroscopy showed a large malignant ulcer of the small curve of the stomach. A gastric fistula on the posterior fundus was objectived. Histological examination of biopsies taken showed the ulcer to be benign and the edges of the orifice of the fistula to be Hodgkin lymphoma by detection of Reed Sternberg cells. A panel of immunohistochemical markers were stained for. A predominant expression of CD30 and CD15 were seen in the cells while being negative of CD3 and EMA. An abdominal CT demonstrated a cavitary splenic lesion with an air-fluid level and extravasation of gastric contrast into the hilum of the spleen, consistent with a gastrosplenic fistula. The diagnosis of gastrosplenic fistula from Hodgkin’s lymphoma was made.
Conclusion: Gastrosplenic fistula is an unusual occurrence and should be recognized as a possible complication of Hodgkin’s lymphoma with splenic or gastric involvement.

PS-06-039

An extremely rare tumor of distal duodenum: Adenosquamous carcinoma

F. Oz Atalay*, G. Ozgun, O. Yerci
*Uludag University, Dept. of Pathology, Bursa, Turkey

Objective: Tumors of the duodenum commonly arise around the ampulla of Vater, and most common tumor type is adenocarcinoma. A review of the English literature revealed a few cases of pure squamous cell carcinoma of the duodenum and only one case of adenosquamous carcinoma. Here, we reported a primary adenosquamous carcinoma of duodenum unrelated to papilla vateri.
Method: A fifty-seven years old female was admitted to our hospital with weakness, constipation and back pain after meals. The endoscopic examination revealed a duodenal tumor distal to the ampulla of vater. Computed tomography also detected a mass in the head of the pancreas. After the endoscopic biopsy of duodenum was reported as 'adenocarcinoma with squamous differentiation', Whipple procedure was performed.
Results: Macroscopically, tumoral lesion was seen in duodenum, 2 cm distal to the papilla vateri, infiltrating the adjacent pancreatic tissue. Distal stomach and papilla vateri were tumor-free. Microscopic examination revealed adenosquamous carcinoma, and immunohistochemical-histochemical studies displayed the two different component of the tumor. One peripancreatic lymph node was metastatic.
Conclusion: Adenosquamous carcinoma is an extremely rare tumor of duodenum. Only one case has been published in the literature so far. Although we assume that it may derived from the pluripotent stem cells, its exact pathogenesis is still unclear.

PS-06-040

Significance of mucin expression patterns, EGFR expression and HER2 expression/amplification in gastric carcinoma

E. E. Pala*, U. Bayol, O. Akman, A. Ozguzer, S. M. Dogan
*Tepecik Training and Research Hospital, Izmir, Turkey

Objective: The gastric carcinomas with MUC1 expression are more likely to be advanced stage. MUC5AC is expressed in diffuse type, MUC2 is expressed in mucinous carcinoma. EGFR overexpression commonly leads to radiation resistance. HER2 gene amplification has been detected in 10–20 % of gastric adenocarcinomas. Expression of these markers are important to predict clinical outcome and targeted therapy modalities.
Method: Fifty-five patients were included to clarify the relationship between histopathologic features and immunohistochemical MUC1, MUC2, MUC5AC, EGFR, HER2 expression profiles, HER2 amplification status in gastric carcinoma.
Results: Of the 46 MUC1(+) cases, 37 were T3/T4, 31 showed perineural invasion. There was a statistically significant correlation between MUC2 expression-mucinous subtype; MUC5AC expression-poorly cohesive subtype ($p<$ 0.01. HER2 expression was 0 in 78,2 %, 1+ in 9,1 %, 2+ in 5,5 % and 3+ in 7,3 % of the samples. Of the 6 HER2 amplified 4 cases were (+++) and 2 cases were (++) by IHC. HER2 overexpression showed a significant association with HER2 amplification ($p<0.001$). EGFR expression levels were 0 in 80 %, 1+ in 10,9 %, 2+ in 1,8 %, 3+ in 7,3 % of the cases. HER2 amplified 4 cases showed negative immunoreactivity with EGFR antibody.

Conclusion: Although we studied a small group, all the results were concordant with the literature data.

PS-06-041

HER2 status in gastric cancer: A comparison of two novel in situ hybridization methods (IQ FISH and dual colour SISH) and two immunohistochemistry methods (A0485 and Herceptest)

E. E. Pala*, U. Bayol, A. Ozguzer, O. Akman
*Tepecik Training and Research Hospital, Izmir, Turkey

Objective: Contrary to breast HER2 testing, optimal ISH method and antibody for gastric HER2 testing is unclear. The aim of the study was to examine HER2 status in gastric adenocarcinomas comparing rabbit polyclonal antibody A0485 and Herceptest immunohistochemistry (IHC) with dual probe HER2 IQ fluorescence in situ hybridization (FISH) and fully automated dual colour silver in situ hybridization (SISH) methods.
Method: IHC and ISH were carried out on gastrectomy specimens of 88 patients.
Results: HER2 expression was (−) in 65, (+) in 5, (++) in 6, (+++) in 12 cases by A0485 IHC. IHC (+) 3cases and (++) 3 cases were (−) by Herceptest. IHC (−) amplified one case was (++) by herceptest. All A0485 and Herceptest (+++) 12 cases were amplified and HER2 amplification was detected in 15.9 % of the cases by SISH and FISH. IHC (+) two cases showed focal heterogeneous low level amplification by SISH and IHC (++) 2 cases also showed focal amplification by FISH and SISH.
Conclusion: In focal amplified cases it's diffucult to decide if the percentage of the amplified cells meet the '10 %' cut off value. The concordance between HercepTest/A0485 IHC and ISH is perfect in (+++) cases. But (+)/(++) rates are lower and less related with amplification in HercepTest than routine IHC.

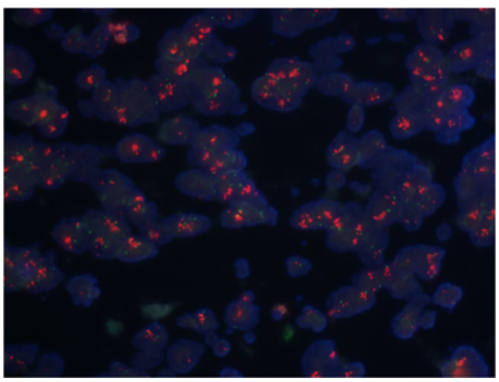

PS-06-042

The distribution and intensity of amyloid deposition in gastric biopsies

B. Pehlivanoglu*, B. Doganavsargil, M. Sezak, B. Sarsik, S. Sen
*Ege University Medical School, Dept. of Pathology, Izmir, Turkey

Objective: Amyloidosis is characterized by localized or systemic amyloid deposition. Although rectal biopsies are generally preferred for diagnosis of systemic amyloidosis, upper gastrointestinal tract is not infrequently involved. However, less is known about the presence, distribution and intensity of amyloid deposition (AD) in gastric biopsies.
Method: Hematoxylin-eosine (HE) sections of endoscopic biopsies of 77 patients with systemic amyloidosis were reevaluated and Congo-red staining was used for definitive diagnosis.
Results: AD was found in 69 (89.6 %) cases. The intensity was severe (easily visible at scanning magnification on HE) in 48.1 %, moderate (suspicious on HE and positive with Congo-Red) in 32.5 % and mild (barely visible even with Congo-red) in 9.1 % of them. AD was most frequently encountered in vasculary walls (88.2 %) followed by muscularis mucosa (62.3 %) and lamina propria (46.8 %). Fourteen patients (18 %) had only vascular and one patient (1,29 %) had only muscular deposits, Thirty cases (39 %) showed vascular, muscular and stromal AD. Stromal involvement was only seen in widely distributed cases. ADs tended to involve more than one localization as intensity increased ($p<0.0001$, chi-square).
Conclusion: Upper gastrointestinal involvement is frequently seen in systemic amyloidosis. AD can be either vascular, stromal or muscular and easily be detected by HE.

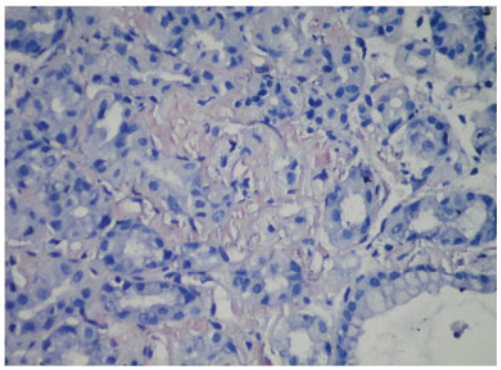

PS-06-043

Histopathological aspects of gastric neuroendocrine tumors with and without lymph nodes metastases and prognostic significance

O. B. Popescu*, E. Stoica Mustafa, C. Pechianu, M. Hortopan, C. Stroescu, S. O. Dima, T. Dumitrascu, V. Herlea
*Bucharest, Romania

Objective: Gastric NETs are uncommon tumors with increasing incidence in the latest decades. The aim of this study was the histopathological analysis of 8 cases.
Method: We present 8 cases of gastric NETs (surgical resected) diagnosed in Fundeni Clinical Institute between 2005 and 2011, reviewed according to the WHO 2010. The

mean age was 67.37 (range 53–78 years), a female to male ratio of 1:1. One of the tumors was multicentric. The average size is 6.82 (range 0.3–14 cm). Six (75 %) present metastases in lymph nodes. One (12.5 %) is pT1, four (50 %) pT3 and one (12.5 %) pT4. Immunohistochemistry for general neuroendocrine markers (synaptophysin, chromogranin A, Ki 67) was performed in all cases.
Results: According to WHO 2010 classification, one (12.5 %) was neuroendocrine neoplasm G1, four (50 %) were neuroendocrine carcinomas G2, all of these four (100 %) with lymph nodes metastases. Three (37.5 %) were neuroendocrine carcinomas G3, 2 of them (66.6 %) with lymph nodes metastases. The patients with lymph nodes metastases had a worse clinical outcome.
Conclusion: The type and stage of the gastric NETs are among the most important things for best management. With an exact diagnosis and adequate treatment has improved the prognosis.

PS-06-044
Eosinophil granulocytes: New players in gastric carcinogenesis induced by Helicobacter pylori?
C. Popp*, G. Micu, S. Zurac, A. Bastian, L. Nichita, M. Olariu, T. Tebeica, A. Birceanu, R. Mateescu, F. Staniceanu
*Colentina University Hospital, Dept. of Pathology, Bucharest, Romania

Objective: Popp and Micu are first authors in equal proportions Helicobacter Pylori (HP) induces a continuum of lesions (chronic gastritis, glandular atrophy, intestinal metaplasia and dysplasia – carcinogenetic cascade [CC]) evolving towards intestinal type gastric carcinoma, but also potentially reversible after HP eradication.
Method: Our study included 3069 gastric endoscopic biopsies diagnosed using Sydney criteria by two independent fully trained pathologists. We evaluated several histopathological parameters, correlating the degree of inflammation, atrophy, metaplasia, regenerative hyperplasia and dysplasia with the presence of HP infection.
Results: Some of our results confirmed theory of HP-triggered CC, several data suggesting the idea that there are understudied factors involved in modulating carcinogenesis. Correlations of intestinal metaplasia and activity of gastritis showed that the number of neutrophils is directly proportional with extension of intestinal metaplasia and inverse proportional with gastric atrophy (P=1.01028E-07), suggesting that the presence of neutrophils is the trigger of phenotype alterations leading to metaplasia. Simultaneous presence of numerous eosinophil granulocytes and very few neutrophils was identified associated with mild or absent intestinal metaplasia, supporting the idea that eosinophils favor regenerative changes to the detriment of intestinal metaplasia.
Conclusion: This study identifies histopathologically quantifiable factors interfering in carcinogenesis which can influence management of HP infected patients.

PS-06-045
Gastric carcinoma with osteoclast-like giant cells
C. Poulios*, T. Koletsa, G. Karagianopoulou, E. Vrettou, I. Kostopoulos
*AHEPA Hospital, Dept. of Pathology, Thessaloniki, Greece

Objective: Throughout the vast variety of gastric neoplasms, gastric carcinoma with osteoclast-like giant cells (OGCs) is one of the rarest. To the best of our knowledge only 9 other cases have been reported in the English literature. We present a case of gastric carcinoma with OGCs in an 81 year-old male patient.
Method: We received a specimen of subtotal gastrectomy and lower esophagectomy. At the gastro-esophageal junction an exophytic tumor, 2.2 cm in greatest diameter, was observed. Multiple sections from the tumor were examined histologically and immunohistochemically.
Results: Sections from the tumor showed gastric carcinoma of intestinal type, stage pT1bpN0. Diffusely among the neoplastic cells giant multinuclear cells, resembling osteoclasts, were observed. Those cells were positive for CD68, lysozyme, vimentin and negative for AE1/AE3, CK8/18, hHCG and LMP1. Moreover in a random section from the gastric fundus a spindle cell lesion was revealed, which was positive for CD117 and CD34 and was diagnosed as GIST.
Conclusion: The presence of OGCs is an extremely rare finding in gastric carcinomas. Due to the low number of reported cases its prognostic value is under discussion. Furthermore this is the first reported case of co-existence with GIST.

PS-06-046
Assessment of human papillomavirus DNA in esophageal squamous cell carcinoma
S. Saadi*, H. Piessevaux, P. Deprez, A. Jouret-Mourin
*Saint-Luc University Hospital, Dept. of Pathology, Brussels, Belgium

Objective: Human papillomavirus (HPV) infection is a known risk factor for the development of squamous cell carcinoma (SCC) of the cervix, the oropharynx and the anogenital region. The aim of our investigation was to assess the prevalence of HPV DNA in patients with esophagus cancer in the Western population.
Method: Formalin-fixed paraffin-embedded blocks from 37 consecutive patients who underwent esophageal endoscopic mucosal resection or esophagectomy for SCC were tested for the presence of HPV DNA by polymerase chain reaction using consensus primers GP5+/GP6+. Viral genotyping was determined by type-specific primers.

Results: Among the total of 37 cases, no HPV DNA was detected in 33 cases (89.2 %). 4 cases were tested HPV positive (10.8 %), of which 1 was HPV 16+, 1 was HPV 18+ and 2 were non-high-risk HPV type. The non-high-risk HPVs were detected in patients with previously treated SCC of the mouth ($n=1$) and the oropharynx ($n=1$). Patients with high-risk HPV-positive tumors had no history of oropharyngeal cancer.
Conclusion: Our study revealed the presence of oncogenic HPV genotypes in a subset of esophageal cancer. The low rates of viral infection detected suggest that HPV unlikely represents a significant etiologic factor in esophageal carcinogenesis. Further studies are needed to confirm these data in larger populations.

PS-06-047
pERK activation in esophageal carcinomas: Clinicopathological associations
A. Saetta*, K. E. Tasioudi, G. Levidou, S. Sakellariou, N. V. Michalopoulos, D. Theodorou, P. Korkolopoulou, E. Patsouris
*University of Athens, 1st Dept. of Pathology, Greece

Objective: MAPK (Mitogen-Activated Protein Kinase) pathway is considered a control regulator in various malignant tumors. In our study we examined the possible prognostic significance of MAPK pathway in Greek patients with esophageal cancer.
Method: We searched for mutations in exons 18, 19, 20, 21 of EGFR gene, codons 12 and 13 of K-RAS gene and exon 15 of B-RAF gene by High Resolution Melting Analysis (HRMA) and Pyrosequencing in 44 esophageal carcinomas. Immunohistochemistry was performed in 29 cases in order to evaluate expression levels of pERK (Extracellular - signal Regulated Kinase).
Results: A somatic K-RAS mutation at codon 12 was detected in one laser microdissected squamous cell carcinoma, whereas none of the cases displayed mutations in EGFR and B-RAF genes. Elevated nuclear as well as cytoplasmic pERK expression (100 % and 62 % of cases respectively) was observed independently of EGFR and B-RAF mutational status. Increasing pERK nuclear and cytoplasmic expression as well as the intensity of nuclear staining was found to be significantly correlated with tumor grade in univariate and multivariate statistical analysis.
Conclusion: Our findings demonstrate the presence of activated ERK despite the low frequency of upstream alterations, implicating ERK activation in the acquisition of a more aggressive phenotype in esophageal cancer.

PS-06-048
Gastroblastoma: A rare epitheliomesenchymal biphasic tumour of the stomach
R. Silva*, J. M. Lopes, F. Carneiro, C. Souto Moura
*Centro Hospitalar de São Joâo, Serviço de Anatomia Patológica, Porto, Portugal

Objective: Gastroblastoma is a recently described gastric tumour that occurs in children and young adults, displaying epitheliomesenchymal biphasic features.
Method: An 18-year-old female, asymptomatic until 4 months before admission, complained of abdominal pain. Imaging evaluation disclosed a solid and cystic tumour involving the stomach. The surgical specimen displayed a nodular, solid and cystic tumour with 10.5 cm largest dimension. Histologically, the tumour was biphasic with epithelial and predominantly mesenchymal components. The epithelial component was arranged in nests, cords and tubules; the mesenchymal component comprised short bundles of spindle cells, foci of multinucleated cells and variable myxoid/collagenous stroma. Tumour cell atypia was mild and mitotic index low. There was no evidence of lymphovascular/perineural tumour invasion. Lymph nodes were free of metastases. Immunohistochemically, epithelial cells expressed AE1/AE3, CAM5.2, CD56 and, focally, CD10; mesenchymal cells expressed vimentin, CD10 and, focally, CD56. Altogether, these features support the diagnosis of gastroblastoma.
Conclusion: Gastroblastoma is a rare tumour (only 4 cases reported so far by Miettinen et al., 2009 and Shin et al., 2010). In the differential diagnosis, synovial sarcoma, carcinosarcoma and teratoma should be considered. Gastroblastoma behavior remains unsettled, having been suggested to be a low-grade malignant tumour.

PS-06-049
Mixed adenoneuroendocrine carcinomas among gastrointestinal tract carcinomas
E. Stoica-Mustafa*, C. Pechianu, V. Herlea
*Fundeni Clinical Institute, Dept. of Pathology, Bucharest, Romania

Objective: Mixed adenoneuroendocrine carcinomas (MANECs, WHO,2010) of the gastrointestinal tract are rare neoplasms, presenting at least 30 % of each component. Aim: To increase the awareness of MANECs in gastrointestinal tract carcinomas.
Method: We present a series of four cases of gastrointestinal MANECs admitted in Fundeni Clinical Institute (2007–2010)-two of the stomach, one of the colon and one of the choledocus.
Results: All of the patients were males with the age range between 38 and 62 years. All of them underwent surgical resections. The tumors varying in size from 1 cm (choledocus) to 12 cm (stomach); all of them were infiltrative, invading the adjacent organs (except one case of the stomach). Microscopically, the tumors had two distinct components: adenocarcinoma with varied grade of differentiation (G1-G3) and neuroendocrine carcinoma, grade 2 or 3. One case had mixed lymph node metastases. The immunohistochemistry were

performed in all cases and included panCK, CK7, 19, 20-pozitive in epithelial component, Chromogranine, Synaptophysine, NSE-pozitive in neuroendocrine component and Ki67. One of the patients died in 2 days after surgery, other three were alive at the time of report.
Conclusion: Gastrointestinal MANECs constitute a diagnostic challenge because of frequent identification only of one component of the neoplasm, which leads to an incomplete diagnosis and suboptimal treatment.

PS-06-050
GIST and adenocarcinoma combination in digestive system
S. Todorov*, O. Kit
*Oncology Institute, Pathology, Rostov-On-Don, Russia

Objective: GIST and adenocarcinoma combination are rare diseases, mechanism of its development is not clear. Histogenesis and morphogenesis of these oncological pathology discuss.
Method: We have 3 cases of GIST and adenocarcinoma of the gaster, colon during 2000–2012 year. Clinico-morphological analysis was performed. Histological, imminohistochemical, histochemical techniques were used.
Results: GIST demonstrated spindle-like and epithelioid types tumours, invading wall of the gaster with secondary changes (hemorrhages, necrosis, infalammation). In 1 case we found metastasis of GIST in gastric lymphatic nodes. Sizes of tumours were more than 5 cm in diameter. Adenocarcinoma was tubular, mucous types of the colon with deep invasive character of growth all wall the colon.
Conclusion: We concider that combination of GIST of the gaster and adenocarcinoma of the colon have common pathogenesis. Cells of the GIST have multifunctional capacities. Combination of the GIST and adenocarcinoma can reflect mutations of the genes participating in its development but this position need to future investigation.

PS-06-051
Her-2/neu assessment for gastric carcinoma: Validation of scoring system
S. Tomic*, I. Mrklic, A. Bendic, N. Kunac, J. Bezic, G. Forempoher, M. Glavina Durdov, I. Karaman, I. Kuzmic Prusac, V. Pešutic Pisac, K. Vilovic
*Clinical Hospital Centre Split, Dept. of Pathology, Croatia

Objective: Gastric cancer is the second leading cause of cancer mortality in the world. Amplification of HER-2/neu oncogene has become an important biomarker for identifying patients who will respond to HER-2 targeting therapy. The rate of HER2 positivity in gastric cancer is variable, ranging from 6 % to 35 %.
Method: In our study HER-2/neu expression was assessed on 73 samples of primary gastric cancer, using immunohistochemistry. For 19 patients preoperative biopsy samples and resected specimens were available. Additionally, internal ring study was performed to estimate intraobserver variability of IHC scoring among pathologists at our Department.
Results: HER-2/neu overexpression was found in 10 (13.6 %) of the tested samples, and it was more common in intestinal (22.5 %) than the diffuse type (3.7 %). Not one of the 6 analyzed mixed type tumors showed HER-2/neu expression. For the paired samples (preoperative biopsy samples and resected specimens) the concordance rate for HER-2/neu expression was 94.7 %. Concordance rate of 95 % was established among pathologists with Fleis kappa 0.88.
Conclusion: According to high concordance rate in paired samples we consider appropriate to evaluate HER2 expression on biopsy specimens, especially in unresectable cases, and to re-evaluate it on resected specimens if available, due to high heterogeneity of a gastric cancer.

PS-06-052
Apoptosis and cytotoxic T-cells in lymphocytic oesophagitis
L. Veits*, R. Wirtz, J. Drgac, T. Schulz, M. Vieth, R. Rieker
*Klinikum Bayreuth, Institut für Pathologie, Germany

Objective: Lymphocytic oesophagitis is a poorly understood disease of unknown origin, said to be characterized by an epithelial infiltration of lymphocytes. Up to date only few and non-specific histological changes were described.
Method: We collected 37 biopsies of 32 patients with lymphocytic oesophagitis (20 men, 12 women). Grading was done according to Purdy et al. and by the number of intraepithelial lymphocytes (50/HPF as cut off value). The inflammatory cells were characterized by using the t-cell and chemokine STRATIFYER robot (STRATIFYER Molecular Pathology GmbH, Cologne, Germany).
Results: Apoptotic keratinocytes could be detected in 71,4 % of severe cases (15/21) as well as in 25 % of mild cases (4/16) and were found in all epithelial layers. High levels of cytotoxic T-cells were present in 80 % of severe cases with apoptosis (12/15) and in 5 cases without apoptosis, mostly mild cases.
Conclusion: Our data show that apoptosis is usefull in grading of lymphocytic oesophagitis, as it can be found predominantely in severe forms. Due to the presence of cytotoxic T-cells an underlying form of lichenoid inflammation can not be fully excluded in these cases. Further studies should focus on the question, whether

our findings are a hint to an autoimmunologic mechanism or not.

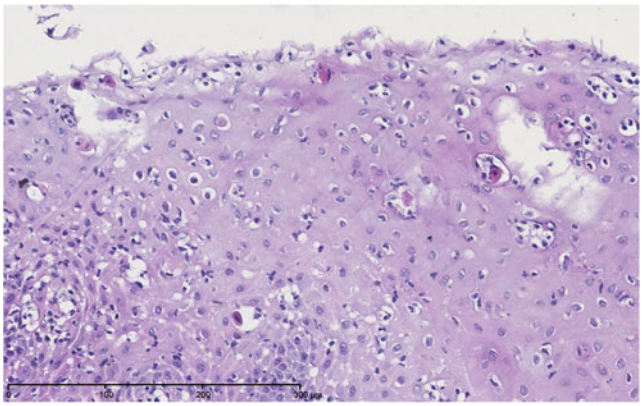

PS-06-053

CDX2 and mucins expression in gastric intestinal metaplasia

S. Vernygorodskyi*, L. Degtiariova
*VNMU, Dept. of Pathology, Vinnitsa, Ukraine

Objective: The homeobox protein CDX2 is a transcription factor involved in early intestinal differentiation and regulates the transcription of several intestinal genes, including intestinal mucin (MUC2). The genetic events responsible for the transdifferentiation that occurs in intestinal metaplasia (IM) are not well understood.
Method: In the 6 year period between 2005 and 2010 a 152 gastric biopsies were examined at the Pathology Department of VNMU. Our panel of primary monoclonal antibodies included: CDX2 (1:100; DAKO, Denmark), anti-MUC5AC (1:100; Novocastra, UK), anti-MUC2 (1:100; Novocastra, UK), anti-MUC6 (1:100; Novocastra, UK).
Results: CDX2 protein was strongly expressed in the nuclei of both goblet cells (GC) and absorptive cells (AC) in the foci of complete IM, but it was significantly decreased in the foci of incomplete. MUC5AC was expressed in the cytoplasm of both GC and AC in incomplete IM, whereas it was expressed in only a few GC but not AC in complete IM. MUC6 was expressed in several deeper glands of incomplete IM but not in complete IM.
Conclusion: CDX2 can be used as an important marker in the pathological diagnosis of early gastric IM. IM with low expression of CDX2 and MUC5AC may serve as predictive markers for gastric cancer.

PS-06-054

Gastrointestinal stromal tumor mimicking pancreatic carcinoma

T. Yalta*, F. Özyilmaz, S. Oguz, G. Kazindir, E. Tastekin, A. R. Hatipoglu, K. Kutlu
*Trakya University, Dept. of Pathology, Edirne, Turkey

Objective: Gastrointestinal stromal tumors (GISTs) are primary mesenchymal tumors that arise in the GI tract. Only 3–5 % of GISTs occur in the duodenum. Here, we report a rare case of duodenal GIST with extramural growth that mimicked a pancreatic tumor.
Method: A 57 years old male patient was admitted to our hospital for duodenal ulcer and gastrointestinal bleeding which was diagnosed in an another clinic by endoscopy. Abdominal MR of the patient showed a 5×5,5 cm necrotic mass in the uncinate process of the pancreas which was excised by whipple operation.
Results: Macroscopically, the resected specimen consisted of solid mass that was connected to the patient's duodenal wall but not to the parenchyma of the pancreas. Microscopic examination of the tumor showed spindle shaped and epithelioid cells with mild nuclear pleiomorphism. Immunohistochemistry revealed that the cells are strongly positive with CD117, with focal expression of CD34 and SMA.
Conclusion: GISTs are low-grade malignant mesenchymal tumors of the GI tract and are believed to originate from the neoplastic transformation of the Cajal cells, which are located between the longitudinal and circular layers of the muscularis propria. They most frequently arise from the second part of the duodenum where they push or infiltrate into the pancreas. In our case report, the patient's tumor exhibited extramural growth and mimicked a pancreatic tumor.

PS-06-055

Reflux oesophagitis: A delusion of endoscopist and/or pathologist?

Y. Yuyucu Karabulut*, B. Savas, A. Ensari
*University of Ankara, Medical School, Turkey

Objective: Reflux oesophagitis comprises patients diagnosed as endoscopic oesophagitis (EO) with minimal histologic abnormality and those showing "microscopic oesophagitis" (MO) with normal endoscopy. We, therefore, aimed to evaluate the discriminatory value of histologic criteria for both groups with reflux oesophagitis.
Method: The study group comprised of 416 patients (145 children and 271 adults) who underwent upper gastrointestinal endoscopy where 113 were diagnosed as EO. Histological assesment for basal cell hyperplasia (BH), papillary elongation (PE), dilatation of intercellular spaces (DIS), intraepithelial eosinophils, neutrophils and lymphocytes was performed. Chi-square test was used for statistical analysis.
Results: All morphologic parameters were more commonly observed in patients without EO. The presence of severe PE (p=0.001) and DIS (p=0,01), together with high lymphocyte and neutrophil counts (cut off values of >10 and >2,

respectively) ($p<0.001$) were the most discriminatory features for the diagnosis of MO. EO was significantly more frequently observed in children compared to adults ($p<0.005$). The presence of DIS ($p<0,001$), PE ($p=0,001$), and high neutrophil counts ($p<0.05$) was significantly more common in adults.
Conclusion: The results of our study suggest that endoscopic biopsy is necessary in all patients with or without EO for the diagnosis of reflux oesophagitis.

PS-06-056
Invasion line complexity analysis in resectable gastric cancer cases reveals differences in histoarchitectonic and invasiveness
E. Zembala-Nozynska*, J. Nozynski, D. Lange, A. Stanek-Widera, J. Wydmanski
*Sklodowska Curie Cancer Center, Tumor Pathology Dept., Zabrze, Poland

Objective: Characterization of gastric cancer invasiveness seems to be one of most important predictor of clinical outcome, dependent on a G and pT grade. Moreover, image differs along tumor invasion line. From the other side, fractal measurement seems to be appropriate for complexity analysis. Thus we attempted to characterize gastric cancer invasion line using complexity measurements, fractal parameters as fractal dimension (D and ΛD), lacunarity and image statistics.
Method: The study based on 19 resectable gastric cancer cases, 13 Laurén intestinal type gastric cancer and 6 diffuse type. Full depth gastric wall slides were stained with pan-cytokeratin. Serial digital images were collected, local pT, G, and image fractal measurements were established for each image.
Results: The presence of necrosis played an significant role in estimating complexity only in Laurèn intetstinal type (lowering ΛD and lacunarity). Histoarchitectonic elements in intestinal cancer type could be characterized by D, inflammation intensity was dependent on the length of the invasion line and ΛD. The pT showed dependence on lacunarity, budding type reflected in D. In gastric cancer diffuse type only inflammation and pT showed dependence on fractal dimensions.
Conclusion: Fractal analysis and image statistics provides a new diagnostic support in gastric cancer studies.

PS-06-057
The factors influencing on histological tumor regression grade (TRG) in gastric cancer
E. Zembala-Nozynska*, J. Nozynski, D. Lange, A. Stanek-Widera, J. Wydmanski
*Sklodowska Curie Cancer Center, Tumor Pathology Dept., Zabrze, Poland

Objective: The identification of factors influencing on the histological tumor regression grade (TRG) seems to be important in therapy planning. The aim was the assessing of histological features and other parameters influencing on the grade of TRG.
Method: The study encompassed 66 cases with gastric cancer subjected to gastrectomy, after preoperative radio-chemotherapy (years 2003–2010) in our Institute. The dependences between the TRG grade, and sex, age, tumor localization, tumor gross morphology, tumor histology, and invasion data were statistically assessed. (nonparametric methods).
Results: Patients age varied between 36 and 78 years old, (mean 58,6±9,4 years; 25 females and 50 males). Despite radio/chemotherapy histological examination showed in 12 % no response, in subsequent 30,6 % - partial response low grade, whereas in 34,7 % - partial response high grade and in 22,7 % complete therapeutic response. Analysis of cancer types in resected tissues showed in 66 % adenocarcinoma, in subsequent 30 % poorly cohesive carcinoma, 4 % specific type of gastric cancer. Only histological type of tumor, pT and N stages were correlated with TRG grade.
Conclusion: Tumor response to radio/chemiotherapy depends mainly on tumor histotype and clinical staging.

PS-06-058
Clinicopathological and prognostic significance of p53 and TGF-beta 1 in patients with gastric cancer
Y. Ananiev*
*Medical Faculty, Trakia University, Gen. and Clinical Pathology, Stara Zagora, Bulgaria

Objective: The aim of this study is to investigate p53 value and it relationship with TGF-beta1 expression, clinicopathological parameters and survival in patients with gastric cancer.
Method: In 53 patients who had undergone gastrectomy for gastric cancer, the expression levels of p53 and TGF-beta1 in gastric cancer tissues were examined immunohistochemically (IHC). p53 gene alterations were examined by fluorescence microscope after in situ hybridization performing.
Results: We found p53 expression in all of gastric cancer specimens. Also, 47.2 % of specimens were TGF-beta1 expression positive. The patients with p53 expression had worse prognosis after surgical therapy compared to those without. The median survival of p53-positive patients was 4.8 months whereas the median survival of p53-negative patients was 9.1 months ($p=0.027$; log-rank test). Also, 88.9 % from patients with p53-positive status is in T1-T2 stage vs. 37.8 % in T3-T4 ($\chi 2=7.88$, $p=0.005$). Finally we found that 56.1 % from p53 expressive tumors have TGF-beta1 expression and 16.7 % were non-expressive ($\chi 2=5.79$, $p=0.016$).

Conclusion: In conclusion our results suggest that low expression of p53 and TGF-beta1could be useful as a marker of poor prognosis and had prognostic value for gastric cancer patients.

PS-06-059

Primary gastric mantle cell lymphoma diagnosed from gastrectomy specimen: A case report

S. Ekici*, A. Barin, C. Altunkaya, S. Yilmaz, G. S. Yalcin, M. Caydere, H. Ustun
*S.B Ankara E.A.H, Pathology, Turkey

Mantle cell lymphoma (MCL) is relatively a rare subgroup of non-Hodgkin lymphoma. We have experienced an uncommon case of MCL. A 65-year-old man was admitted to emergency service for upper gastrointestinal bleeding as melena. Gastric corpus wall thickness found increased and splenomegaly determined at whole abdominal ultrasonography. Endoscopic examination revealed subsequently, 1 cm diameter polypoid lesion at corpus anterior wall and 2 cm dimensioned elevated and vascularised lesion at corpus posterior wall. Endoscopic biopsy had reported as active gastritis and mucosal reactive hyperplastic changes with ulcerative background. After than total gastrectomy and splenectomy specimens examined diffuse infiltration of monotonous medium-sized, atypical lymphoid cells with hyperchromatic nuclei. These cells were positive for CD20, CD5, CD43, bcl-2 and CD79a, but negative for CD10, CD23 and bcl-6. Atypical lymphoid cells were present even in splenic hilus and lesser curvature lymph nodes. We reported this case as Primary Gastric Mantle Cell Lyphoma according to morphologic and immunohistochemical staining features.

PS-06-060

How about gastric HER2 positivity in our institute?

E. E. Pala*, U. Bayol, O. Akman, A. Ozguzer
*Tepecik Training and Research Hospital, Izmir, Turkey

The published data of the multicenter phase III trial (ToGA study) showed that patients with tumors which overexpress HER2 as defined by immunohistochemistry (IHC) 2+ and ISH positive or IHC 3+ are eligible for the targeted therapy. The aim of this study was to find out HER2 overexpression and amplification rates in gastric cancer cases from our archives. Eighty eight formalin fixed and parafin embedded tumor tissue samples from Turkish gastric carcinoma patients were studied with (IHC) and brightfield double in situ hybridization (BDISH). The criteria defined by Hofmann et al. was uesd for IHC evaluation. HER2 expression was found (−) in 65 (73.9 %), (+) in 5(5.7 %), (++) in 6 (6.8 %), (+++) in 12 (13.6 %). BDISH showed that HER2 gene was amplifie (d in 18(20.5 %) of the patients. Of the amplified cases 12(66.6 %) was (+++), 3(16.6 %) (++), 2 (11.2 %) (+), 1(5.6 %) (−). Highly, homogenous amplified cases were neither (+++) nor (++) and correlated with protein overexpression. IHC (−)/(+) cases showed heterogeneous, low level amplification. HER2 amplification was significantly associated with HER2 overexpression, histological subtype, location, depth of invasion, size ($p<0.05$). IHC and BDISH correlation is perfect for (+++) cases. Unlike breast carcinoma, 5 % of IHC (−)/(+) gastric carcinoma cases show heterogeneous amplification.

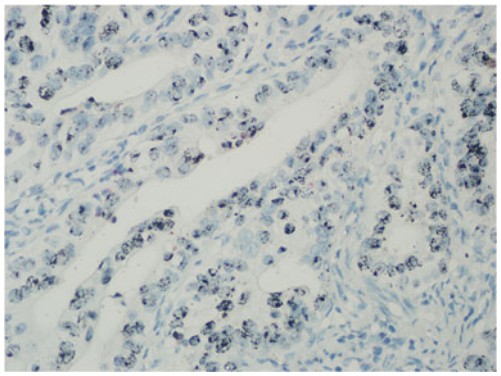

PS-06-061

Morphometric analysis in gastrointestinal stromal tumors

S. Rjabceva*, M. A. Vozmitsel, I. S. Dulinez
*Belarussian Medical Academy, Bio-Medical Research Center, Minsk, Belarus

Objective: Gastrointestinal stromal tumors (GISTs) have a spectrum from minimal indolent neoplasms to sarcomas. In this study the tumor behavior are compared with morphometric results.
Method: Morphometric cellular parameters such as mean nuclear area (MNA), mean nuclear length (MNL), mean nuclear width (MNW), mean nuclear density (MND), mean cytoplasmic area (MCA) and mean nuclear-cytoplasmic ratio (MNCR) were evaluated in hematoxylin and eosin stained slides of 36 spindle-cell GISTs (11 benign and 25 malignant) by using a computer-assisted image analysis system. Morphometric results were compared with tumor behavior.
Results: MNA, MNL, MNW and MCA are 50.57±5.63, 15.35±1.18, 4.49±0.56 and 135.72±13.85 mcm in benign GISTs, respectively. MND and MNCR are 179±13.6 and 1:2.7 also in benign group. MNA, MNL, MNW and MCA are 51.03±5.55, 14.75±0.70, 4.72±0.43 and 127.22±11.58 mcm in malignant GISTs, respectively. MND and MNCR are 193.9±16.6 and 1:2.5 also in malignant group. No correlation was found between morphometric features and gastrointestinal stromal tumor behavior ($p>0.05$).
Conclusion: This study showed that the tumor cellularity and nuclear-cytoplasmic ratio aren't the parameters to predict

aggressiveness of GISTs. These morphometric parameters may not be used in the prognosis of GISTs behavior.

PS-06-062

Signet ring cell carcinoma of stomach diagnosed with bone marrow metastasis: A case report

G. S. Yalcin*, C. Altunkaya, S. Yilmaz, A. Barin, S. Ekici, H. Ustun, T. Fen
*S.B Ankara E.A.H, Pathology, Turkey

We report a 74-year-old man who had been searched for bicytopenia (anemia and thrombocytopenia). Bone marrow examination revealed extensive bone marrow metastasis of signet ring cell carcinoma. PAS, d-PAS and mucin histochemical markers performed to bone marrow sample which were all positive. Immunohistochemical markers were positive with MUC-1, MUC-5 AC, MUC-2 (focal staining), CK7, CK20, EMA, CEA and negative with vimentin, CD10, chromogranin. According to morphologic and immunohistochemical results we thought primarily gastrointestinal system malignancy, particularly stomach carcinoma. Upper gastrointestinal endoscopy performed subsequently, hemorrhagic ulcerative lesion had seen and taken biopsies. Endoscopic biopsy results showed metastatic signet ring cells origin from stomach. We report this case because bone marrow metastasis can be found commonly in some malignant tumors but diagnosing a nonhematologic malignancy from bone marrow is an unusual event.

PS-06-063

Gastric Her2 Immunocytochemistry: Differences in methodology affecting membrane staining and interpretation. Findings of the UK NEQAS ICC & ISH external assessment service

S. Parry*, K. Miller, J. Starczynski, N. Wong, B. Jasani, I. Nagelmeier, M. Ibrahim
*UK NEQAS ICC & ISH, London, United Kingdom

Objective: Gastric cancer patients showing IHC 3+ & 2+ and ISH amplified expression benefit significantly from Trastuzumab treatment. With increasing numbers of laboratories carrying out gastric HER2 immunohistochemistry (HER2 IHC) testing, UK NEQAS ICC&ISH has developed a gastric HER2 IHC service to closely monitor staining methodologies and interpretation.
Method: Participating laboratories were sent unstained composite slides consisting of 3+,2+,1+ and negative tumours to stain using their routine method. Participants were requested to return the slide along with a stained in-house control section along with methodological details. Slides were assessed for quality of staining and interpretability by a panel of expert assessors.
Results: Data showed an 'acceptable' pass rate of 54 % (N=89); Borderline pass 17 % and unacceptable staining in 29 %. In-house slides showed an acceptable rate of 33 %, borderline pass 38 % and unacceptable rate 29 %. The Ventana 4B5 system, used by 51 % (n=45), had an overall pass rate of 76 %. The second most popular method was the 'home-brew' (15 %, n=13), with a pass rate of only 15 %.
Conclusion: Using 'home-brew' methods for gastric HER2 testing can result in misinterpretation of membrane staining. An EQA for gastric IHC testing can help ensure reliable results and rectify suboptimal performance.

Sunday, 9 September 2012, 09.30 - 10.30, Congress Hall Foyer 3rd Floor
PS-07 Poster Session Other Topics

PS-07-001

Evaluation of accuracy of frozen section in diagnosis of ovarian neoplasms by revision of the slides in Urmia, Iran

F. Abbasi*, Z. Yekta, F. Noroozinia, M. Motazakke, F. Javanmard
*Imam Khomeini Hospital, Dept. of Pathology, Urmia, Iran

Objective: Ovarian neoplasms are a heterogenous group of benign, borderline and malignant tumors of epithelial, stromal and germ cell origin. Since different therapeutic methods are used to treatment of different tumors, intraoperative diagnosis provide guidance for appropriate surgical management. Frozen section is a usual method for this purpose. This study was done to determine the accuracy of frozen section in diagnosis of ovarian neoplasms in Urmia University of Medical Sciences.
Method: In this cross sectional study the slides of all 154 frozen section samples of ovarian neoplasms in teaching hospitals of Urmia University of Medical Sciences during 2003–2009 revised by 2 pathologists separately. Then the results compared with their final permanent section diagnoses.
Results: We had 102 cases of benign, 39 cases of malignant and 13 cases of borderline ovarian tumors. The most common subtypes were teratoma (16 %), benign mucinous cyst (15 %), papillary serous carcinoma (12 %) and benign serous cyst (11 %). Accuracy, sensitivity, specificity, positive and negative predictive values of frozen section were 98 %, 94.8 %, 99 %, 97.3 %, and 98.2 % respectively.
Conclusion: The results showed that in this university, interpretation of frozen section in diagnosis of ovarian neoplasms is done with acceptable accuracy and can be performed for intraoperative diagnosis as a reliable method.

PS-07-002

The pathological effects of salvia officinalis extract on serum level of alkaline phosphatase in male rats

E. Abdollahi*, R. Ahmadi
*Tehran University, Iran

Objective: Studies show that there is association between salvia officinalis extract administration and liver or heart functions. The main aim of this study was to determine the effects of salvia officinalis extract on serum level of alkaline phosphatase in male rats.
Method: Male wistar rats were randomly divided into control, normal saline receiving and salvia officinalis extract (100, 150 or 200 mg/kg/day) receiving animals of 5 in each group. After a period of 6 weeks, blood samples were collected using cardiac puncture method. Following serum collection, serum alkaline phosphatase levels were measured by spectrophotometry method. Data were statistically analyzed and compared between groups using ANOVA.
Results: The results indicated that Serum alkaline phosphatase levels were significantly increased in salvia officinalis extract (100, 150 or 200 mg/kg/day) receiving animals compared with control rats.
Conclusion: Our findings show that salvia officinalis extract is enhancer of serum alkaline phosphatase according to which, impairing effect of the extract on certain tissues is conceivable.

PS-07-003

The pathological effects of waterpipe smoking on serum levels of CEA, alkaline phosphatase or creatine kinase in male and female rats

R. Ahmadi*, M. Mafi
*Islamic Azad University, Dept. of Physiology, Hamedan, Iran

Objective: Various studies show that smoking can influence serum levels of tumor markers such as carcino embryonic antigen (CEA) and kinase or phosphatase enzymes. The main aim of this study was to determine the pathological effects of waterpipe smoking on serum levels of CEA, alkaline phosphatase (ALP) or creatine kinase (CK) in male and female rats.
Method: Male and female Wistar rats were randomly divided into control and waterpipe smoking groups of 5 in each. After a period of 10 weeks, blood samples were collected using cardiac puncture method. Following serum collection, serum CEA, alkaline phosphatase or creatine kinase levels were measured. Intestinal tissue was also examined histologically. Data were statistically analyzed and compared between groups using ANOVA.
Results: The results indicated that serum CEA, ALP or CK levels were significantly increased in male and female waterpipe smoking animals ($P<0.01$, $P<0.01$ or $P<0.001$, respectively). There was not gender effect on serum CEA, ALP or CK levels. There were also histological changes in intestinal tissue including increased tissue plasma cells infiltration and inflammation.
Conclusion: Our findings show that waterpipe smoking is an enhancer factor of serum CEA, alkaline phosphatase or creatine kinase levels, according to which, damaging effects of waterpipe smoking on various tissues, particularly intestine should be considered seriously.

PS-07-004

The effects of acute or chronic immobilization stress on serum level of creatine kinase and alkaline phosphatase in male rats

M. Alinavaz*, R. Ahmadi, M. Mafi
*Islamic Azad University, Nutrition, Tehran, Iran

Objective: Studies show that immobilization stress has a variety of effects on serum levels of liver enzymes. The main aim of this study was to determine the effects of immobilization stress on serum level of creatine kinase and alkaline phosphatase in male rats.
Method: 50 male Wistar rats weighing 200±30 g were randomly divided into control, acutely or chronically immobilized animals of 5 in each group. Animals were immobilized for 2 h/day or 8 h/day for a period of 3 weeks or 1 week in chronically or acutely immobilized groups, respectively. Blood samples were collected using cardiac puncture method. Following serum collection, creatine kinase or alkaline phosphatase level was measured by spectrophotometery method. Data were statistically analyzed and compared between groups using ANOVA.
Results: The results indicated that serum creatine kinase level was significantly increased in rats enduring acute or chronic immobilization compared with control animals ($P<0.001$), however, there was not significant difference between serum alkaline phosphatase levels in immobilized animals compared with control rats.
Conclusion: Immobilization stress may leave pathological effects in liver or other organs leading to enhanced serum creatine kinase level.

PS-07-005

Immunoexpression of lactoferrin in bone metastases and corresponding primary carcinomas

V. Barresi*, A. Ieni, G. Giuffrè, G. Branca, G. Tuccari
*University of Messina, Dept. of Human Pathology, Italy

Objective: With reference to primary bone tumors, we previously found lactoferrin (Lf) immunoreactivity in chondroblastomas, chondromyxoid fibromas, giant cell tumours and osteoid osteomas, while no immunoexpression for this

protein was detected in chondrosarcomas and osteosarcomas. Herein we aimed to analyze Lf distribution in bone metastases from cancers of different sites.
Method: Lf immunohistochemical expression was investigated in 25 formalin-fixed and paraffin-embedded specimens of human bone metastatic lesions as well as in the primitive corresponding carcinomas. The primitive sites of carcinomas were: breast (8), prostate (4), kidney (4), lung (3), colon-rectum (2), uterus (4). A Lf intensity-distribution (ID) score was calculated for each case by multiplying the values of the area staining positivity and the intensity staining.
Results: Lf immunostaining, with variable ID scores, was encountered in 11/25 (44 %) metastatic bone lesions. Immunoreactivity for Lf was found in primary carcinomas with a percentage of neoplastic cells ranging between 50 tand 75 %, although this positivity decreased in breast carcinomas (37.5 %) and was totally absent in lung cancers.
Conclusion: The immunohistochemical concordant evidence of Lf in bone metastases and corresponding primary carcinomas strongly supports the hypothesis of an autoctone production of this protein by the neoplastic elements themselves in order to get a greater availability of iron for their increased turnover.

PS-07-006

Retroperitoneal mature teratoma simulating liposarcoma

A. Bdioui*, S. Mestiri, M. T. Yacoubi, S. Ziadi, C. Souki, A. Anjoren, W. Majdoub, M. Mokni
*CHU Farhat Hached, Dept. of Pathology, Sousse, Tunisia

Objective: Teratomas are germ cell tumors, uncommon in retroperitoneum. Their diagnosis can be difficult on biopsy material where they can be easily confused with ovarian tumors.
Method: A 26 year-old man presented with history of abdominal pain and vomiting. On computed tomography, there was a multiloculated retroperitonal cyst of 18 cm in length.
Results: A biopsy was performed, showing an adipous tissue with thick fibrous septa, there were many large cells with a clear, vacuolated cytoplasm simulating lipoblast. In front of the retroperitoneal location and cells morphology, a liposarcoma was suspected. The tumor was surgically removed. At gross, It measured18×12×8 cm, containing a combination of solid areas and multilocular cystic spaces containg sebaceous material and hair. Microscopic examination revealed a mature cystic teratoma characterized by cystic spaces lined with either a Malpighian or respiratory regular epithelium. There were areas of cartilage, bone, striated muscle and bronchial glands. Calcifications were also noticed.
Conclusion: Teratomas are uncommon in retroperitoneal area; On biopsy material, histopathological diagnosis can be difficult, simulating either benign or malignant lesions.

PS-07-007

Extracellular Microenvironment in Methotrexate (MTX): Treated rheumatoid arthritis patients

G. Butur*, C. Ardeleanu, D. Predeteanu, G. Manda, C. Ursaciuc, M. Comanescu
*Institut Victor Babes, Dept. of Pathology, Bucharest, Romania

Objective: The pathogenesis of rheumatoid arthritis (RA) is mainly produced by an imbalance between pro-anti-inflammatory factors and other molecules released by different cell types in the synovial extracellular microenvironment. Aims: Assessing Foxp3 positive lymphocytes and some molecular mediators in the joint microenvironment of patients with rheumatoid arthritis (RA) treated with MTX compared with untreated patients.
Method: Synovial fluid (SF) and synovial membrane (SM) from 24 patients with RA were analyzed for the expression of Foxp3, IL1, IL 6, IL17, TGF beta, VEGF, MMP9 by immunohistochemistry (IHC) and IL1, IL6, IL17, by flow cytometry (FC). Twenty patients were treated with MTX and five untreated patients served as control.
Results: It was observed a negative correlation between IL1/IL6 and IL17/Foxp3 concentration in the SF as measured by FC, before the treatment. In the SM, IL6 and MMP9 were strongly expressed in macrophages, fibroblasts, endothelial cells and the extracellular matrix of control cases, but reduced significantly in the treated cases ($p<$ 0, 05). Il 17 and Foxp3 positive cells remained costantly in a reduced number in the MS.
Conclusion: As the proinflammatory cytokines decreased after the therapy, we can conclude that these are more efficiently influenced than some immune cells participating in the autoimmune process.

PS-07-008

Histological evaluation of the spleen after acute bleeding followed by blood replacement with two different physiologic solutions

M. Cabral*, A. L. Ortiz, C. Venâncio, J. Mesquita, C. Vasconcelos-Nobrega, A. Silva, H. Vala, D. Ferreira
*Polytechnic Institute of Viseu, Agrarian Superior School Viseu, Portugal

Objective: The spleen is important for many hematopoietic and immunological functions, namely hemodynamic compensation during hemorrhagic shock, with a crucial role in the compensation of hypovolaemia, on restoring blood volume in situations of acute haemorrhage. Also, the administration of physiological solutions is of great importance for the correction of circulating volume, avoiding the complications of hypovolaemia. Objectives: To evaluate spleen's histopathological changes in pigs associated with volume

replacement using two different physiologic solutions, after acute bleeding.
Method: 31 Large White pigs under general anaesthesia with propofol and remifentanil. A total of 25 ml/kg of blood was passively removed during 20 min. Intravascular volume was replaced using Ringer Lactate 25 ml/kg (Group 1- thirteen pigs) and HES 130/0.4 20 ml/kg (Group 2- eleven pigs). Spleen samples were processed for routine hystologic evaluation. Congestion, inflammatory infiltrate, ellipsoids enlargement and follicular lymphoid hyperplasia were evaluated in a semi-quantitative score.
Results: Follicular lymphoid hyperplasia was exacerbated in group 1 (84.6 %; grade III), when comparing with group 2 (36.4 %; grade III). The remaining lesions did not show differences between group 1 and group 2.
Conclusion: Volume replacement with HES 130/0.4 may reduce follicular lymphoid hyperplasia when compared with volume replacement with Ringer Lactate.

PS-07-009
Project Uganda and haemopathology: St. Mary's Hospital Lacor, Gulu, Uganda
G. De Falco*, K. Schurfeld, V. Calbi, M. Ogwang, M. Mwanda, L. Leoncini
*University of Siena, Dept. Human Pathology and Oncology, Italy

Objective: Lacor Hospital is the second hospital of Uganda and serves almost 3 million inhabitants. In 2005, the figures were as follows: for the 34.498 patients admitted, 245.086 patients were treated in the out patient departments. There were available surgery, X-Rays and ultrasound, vaccinations, laboratory tests, but no pathology service was available until 2008.
Method: In 2008 the Italian NGO"Patologi oltre Frontiera" launched a project aiming at establishing a pathology laboratory at Lacor. Spaces were assigned by the hospital and equipments for specimen processing were provided thanks to the Province of Bolzano, Italy. The project aims also at ensuring the local presence of pathologists, on a voluntary base.
Results: 11 pathologists have been working at Lacor since 2008, for time periods of 1–4 months. The most frequent biopsy sites were: Soft tissue, Prostate, Skin, Uterus cervix, Lymph nodes, Liver, Breast. PAP smears were offered to women comming to the hospytal for different reasons (AIDS clinic, delivery, bleeding). At the moment no screening program is present at Lacor. Thanks to the establishment of a pathology service in loco, differential diagnosis was improved since 2008.
Conclusion: The project is still ongoing. Future steps will include the establishment of immunohistochemistry, and the presence of a local pathologist, who will be trained and assisted by volunteer pathologists.

PS-07-010
Splenic localization of the peritoneal mesothelioma: Case report
A. N. Deger*, C. Kocak
*S.B. DPU. Kec. EA Hastanesi, Patoloji Bolumu, Kutahya, Turkey

Objective: Peritoneal mesothelioma is a very rare diagnosis. It accounts for 20–30 % of all mesothelioma type cancers. We report a case of a 65-years-old woman was operated because of mass in the spleen and was performed total splenectomy.
Method: Operation specimen included spleen as well as various sizes of nodular peritoneal lesions. Sectioning of the spleen material revealed tumoral lesion ranging in size from 4×3,5×3 cm and it was located in hilus as well as it infiltrated parenchyma. On the other hands, multinodular tumoral tissues were observed and this tissues derived from periton. Tissue sections were prepared by H.E. and immunohistochemical stainings.
Results: Microscopically, tumoral tissue consisted of atypical epithelial cells with abundant eosinophilic cytoplasm and with eosinophilic nucleolus and characterized by acinar or glandlike structures. Sections of tumoral tissue included atypical mitotic figures and necrosis focuses. In immunohistochemical examination, it was shown that calretinin, mesothelioma Ab-1, vimentin, pancytokeratin was positive.So, the tumoral lesion was diagnosed as peritoneal mesothelioma based on these findings.
Conclusion: Peritoneal mesothelioma is a rare form of malignant mesothelioma, making up <30 % of diagnosed mesothelioma cases. The reported case refers to a particular localization of a peritoneal mesothelioma, the spleen, discovered only after a splenectomy.

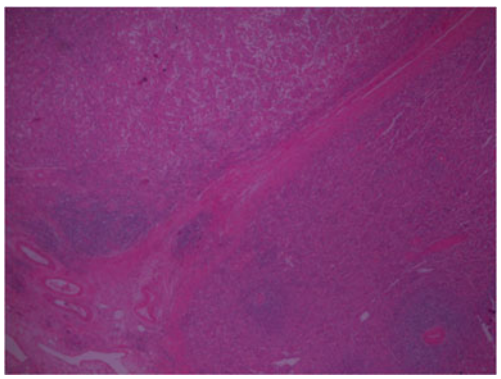

PS-07-011
Chondromyxoid fibroma, a report from the Turkish bone and soft tissue pathology study group
B. Doganavsargil*, B. Bilgic, S. Dervisoglu, R. Tanritanir, M. Sezak, U. Yalcinkaya, G. Basdemir, F. Kabukcuoglu, B. Muezzinoglu, S. Baris, G. Gonlusen, I. E. Gurer, P. Temiz, K. Kosemehmetoglu
*Ege University, School of Medicine, Izmir, Turkey

Objective: Chondromyxoid fibroma is a rare benign lesion accounting for less than 0.5 % of all primary neoplasms of bone. A study was conducted to assemble a national study group for rare entities and share the experience of different centers.
Method: The data was collected from the pathology archives of 13 referral hospitals in Turkey.
Results: Among the 61 cases enrolled in the study, 57.4 % (n=35) of them were male. Median age was 35±18 years-old (Range: 6–67). The most frequent localizations were tibia (28 %, n=17), femur (n=10, 16.4 %) and pelvic bones (n=9, 14.8 %), followed by feet bones (11.5 %), fibula (8.2 %), humerus (4.9 %), hand bones (4.9 %), cranium (3.3 %), costa (3.3 %), radius (1.6 %), scapula (1.6 %), and vertebrae (1.6 %). Although the cases with appendicular skeleton involvement was younger than the others (median age: 29.5±17.03 vs 53±11.5 respectively) no significant correlation was found between age, gender and localization.
Conclusion: Cases displayed a wide age-range with a slight male predominance. The most frequent localizations were tibia, femur and pelvic bones. Rare localizations such as temporal frontal bones, vertebrae and scapula were also observed. The study, which may serve as a preliminary work for future studies was presented to share our experience on this rare entity.

PS-07-012
Histological changes and granulocytes redistribution in adjuvant arthritis
L. Feketeova*, P. Jancová, P. Moravcová, A. Janegová, K. Bauerová, S. Poništ, D. Mihalová, P. Janega, P. Babál
*Comenius University, Inst. of Pathology, Bratislava, Slovakia

Objective: Adjuvant arthritis (AA) is an induced systemic disease primarily with inflammatory joints destruction similar to human rheumatoid arthritis (RA). Spleen and the thymus are organs of immune system involved in RA development. Polymorphonuclear leukocytes (PMN) are cells of first defence line participating at joints affection. First line therapy in RA is Methotrexate (MTX). The aim of the study was to evaluate histological changes of the spleen during AA and effect of MTX on granulocytes redistribution.
Method: Tissues of spleen, thymus and knee joints were histochemicaly stained for detection of chloracetatesterase activity, which showed granulocyte infiltration that was morphometrically evaluated.
Results: We observed significant reduction of spleen white pulp in AA and correction to normal level after MTX administration. The same was seen also in number of PMN. The opposite tendency was observed in knee joints with massive PMN infiltration in AA, which was significantly reduced after MTX administration. No significant changes were observed in the thymus.
Conclusion: Our results indicated the connection between the PMN accumulation in sites of inflammation during AA mirroring their decreased number in the spleen and effect of MTX on spleen histological changes. This observation points to the eventual mechanism of MTX effect on lowering the inflammatory reaction in vivo. (APVV 51-017905, VEGA 2/0093/08).

PS-07-013
Spectrum of histopathological changes in the livers of organ donors: Microscopic evaluation of livers unused to transplantation
A. Halon*, E. Iwaneczko, P. Donizy, R. Matkowski, D. Patrzalek
*Wroclaw Medical University, Dept. of Pathomorphology, Poland

Objective: Liver transplantation is the only chance of rescue for patients with end-stage of many diseases of this organ. The aim was the histopathological assessment of retrieved livers but not used for transplantation.
Method: Forty-four livers were analyzed. The age range of donors was between 23 and 69 years (mean 51). Microscopic preparations were stained with standard HE and van Gieson's methods.
Results: The following categories of organs were distinguished: I – liver with no microscopic changes: 7 cases; II – I° steatosis only: 4; III – II° steatosis only: 1; IV – cholestasis only: 1; V – I° and II° steatosis with cholestasis: 1; VI - G0/G1 inflammation with cholestasis: 2; VII - G0/G1 inflammation with steatosis (<35 % hepatocytes): 6; VIII – III° steatosis only: 2; IX - steatosis (<35 %), G0/G1 inflammation with cholestasis: 5; X – III° and IV0 steatosis: 2; XI – steatosis (>35 % hepatocytes) with inflammation: 1; XII – inflammation with fibrosis: 1; XIII – steatosis, inflammation with fibrosis: 8; XIV – steatosis, inflammation, fibrosis with cholestasis: 3.
Conclusion: The livers which were classified to the I-IV categories are either good or very good organs with no contraindications to transplantation. The livers qualified among the V- IX categories may be in some specific circumstances an additional and valuable pool of organs.

PS-07-014
Metal debris in inguinal lymphadenopathy after mega prosthesis for malignant fibrous histiocytoma
A. Hens*, A. Calvo, C. d. la Vega, G. Munoz, M. Garcia, Mº d. C. Munoz, Mª d. M. Pleite
*Hospital Puerto Real, UG A. Patológica Bahía de Cádiz, Spain

Objective: Surgical treatment options of malignant tumors of the knee includes reconstruction with incorporation megaprosthesis. Inguinal lymphadenopathy due to the lymphatic uptake of metal debris has been described, and may be clinically confused with tumor metastasis.
Method: We report the case of a 39-year-old woman with inguinal lymphadenopathy caused by metallic debris from a knee mega prosthesis for Malignant Fibrous Histiocytoma.
Results: The histopathological changes seen in lymph node were metal debris containing sinusoidal macrophages in a background with numerous epithelioid granulomata in the remaining lymph node.
Conclusion: The identification of regional lympadenopathy in patients with past history of malignancy usually indicates metastatic disease. Post-prosthesis lymph node histiocytosis resembling metastatic disease is described, and that is why we need resect and examine lymph nodes with the use of polarized light microscopy to identify birefringent particles of prosthetic debris for an accurate histologic diagnosis.

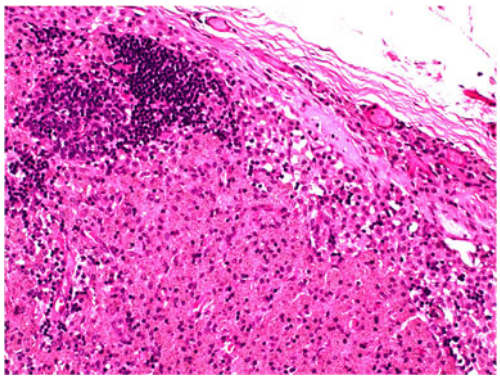

PS-07-015
Fine needle aspiration diagnosis of Rosai-Dorfman Disease in patient with multiorgan neoplastic, infectious and autoimmunity pathology
A. Hens*, M. Moreno, M. Añón, G. Muñoz, N. Navas, M. Mosteiro, F. Gómez
*Hospital Puerto Real, UG A. Patológica Bahía de Cádiz, Spain

Objective: Sinus Histocytosis with Massive Lymphadenopathy, also known as Rosai-Dorfman disease, is an idiopathic histiocytic proliferation affecting lymph nodes. the cause is still unknown, but it's related to an immune dysregulatory process. Patients publications sometimes includes autoimmune disorders and any neoplasm, being exceptional a case with multiorgan neoplastic, infectious and autoimmunity pathology as the present.
Method: A 77-years-old woman with breast cancer, tuberculosis, rheumatic heart disease, diabetes mellitus, eosinophilic gastroenteritis, intestinal angiodysplasia, chronic hepatopathy non-alcoholic and penicillin allergy among other diseases, consulting for constitutional syndrome with conglomerate inguinal lymph nodes.
Results: Fine needle aspiration cytology revealed histiocytes showing emperipolesis with mature lymphocytes and plasma cells background. Hence, diagnosis of Rosai-Dorfman disease was made.
Conclusion: The case report is a rare presentation of Rosai-Dorfman disease associated with a wide range of illness, some simultaneous. We believe that all the patient illness are related, and it could correspond with a complex disease as a immune system alteration expression.

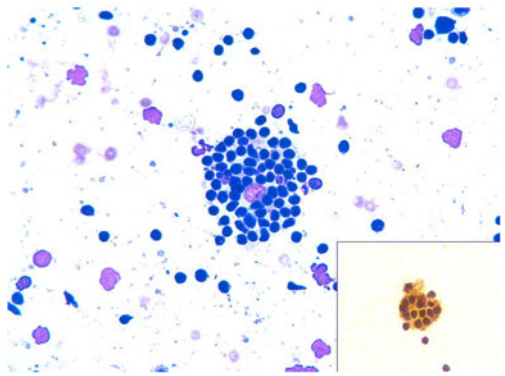

PS-07-016
Causes of death of psychiatric patients: An autopsy study
R. Jankovic*, P. Salevic, I. Savic, D. Mitrovic, J. Markovic-Lipkovski
*University of Belgrade, Faculty of Medicine, Serbia

Objective: Numerous researches documented disproportionate somatic morbidity and earlier death among people with psychiatric diseases.
Method: Causes of death of psychiatric patients was analyzed on 5 years autopsy records on Institute of Pathology, Medical Faculty, University of Belgrade. Equal number of randomly selected non-psychiatric cases (n=80) formed control group.
Results: Life longevity of psychiatric patients was approximately 10 years shorter, than in control group (57.8±14.0 vs 68.3±11.8; p<0.001) with significant predominance of males (55:25; p<0.001). Most common causes of death in decreasing order was: bronchopneumonia, pulmonary thromboembolism, COPD, hypertensive heart disease, left heart failure, acute cor pulmonale, diabetes mellitus and food aspiration. Bronchopneumonia (p< 0.01), acute cor pulmonale, diabetes mellitus and food aspiration (p<0.05) was more frequent in group of psychiatric patients. There was statistically significant high relative risk only for bronchopneumonia as cause of death in psychiatric patients (RR=1.79; 95 % CI=1.09–2.89) either they were

hospitalized in psychiatric hospital or not ($p>0.05$). Contrary, pulmonary thromboembolism was more frequent in those hospitalized in psychiatric hospitals ($p<0.05$).
Conclusion: Lung and heart diseases and diabetes mellitus are more frequent in psychiatric patients and cause earlier dying, particularly in males, than in those without psychiatric diseases.

PS-07-017
Intraarticular osteoid osteoma: Case report
E. Kimiloglu Sahan*, F. A. Ahlatci, I. Ulusoy, N. Erdogan
*Taksim´s Hospital, Dept. of Pathology, Istanbul, Turkey

Objective: Osteoid osteoma occupies %11 of all benign bone tumors.It commonly affects the extraarticular portions of the long bones in young patients.It frequently causes persistent pain that worsens at night and is relieved by NSAIDs. The typical radiographic appearance is that of a lucent nidus with surrounding dense cortical thickening.
Method: We present a case of an intraarticular osteoid osteoma in 24 year-old man.He had progressive pain in the right patella, occured 1 year before hospital application and also the pain was not relieved by NSAIDs. The patient applied to the orthopaedic clinic of our hospital in March 2012. The Magnetic Resonance (MRI) imaging results showed the lesion in the anterior epiphysis of the proximal tibia. This lesion located subcortical and the diameter of the lesion was 6 mm.
Results: Microscopically, the nidus was a well-demarcated osteoblastic mass and consisted of interlacking network of osteoid trabeculae with different levels of mineralization, rimmed by abundant short spindled or polygonal osteoblasts and numerous osteclast –like multinucleate giant cells. The diagnosis was osteoid osteoma.
Conclusion: Because intra-articular localization is rare in osteoid osteoma and the pain was not relieved by NSAIDs in our patient, we present the case here.

PS-07-018
Human frozen tissue biobank in Latvia: The first results
I. Liepniece-Karele*, J. Eglitis, M. Leja
*Riga ECUH, Dept. of Pathology, Latvia

Objective: The incidence of malignant disease in Latvia is closed to the average in Europe and still is inadequately high. The aim of project was to create a modern human tissue biobank containing samples of malignant tumours, precancer conditions as well as autoimmune diseases. The project is funded from the European Social Fund Project „Mutidisciplinary research group for early cancer detection and cancer prevention".
Method: Frozen tissue samples, blood as well as clinical information was collected from each patient. DNA samples were extracted and stored in collaboration with Latvia Genome centre. Standartized pathology reports were used. The hospital pathologist was involved in biobank work: 1) in making diagnostic decisions and 2) in rewiewing specimens.
Results: In total 1870 patients with oncological and premalignant diseases were enrolled in the research during the 2010–2012. Frozen tissue samples were obtained from 211 patients (101 breast, 80 gastric and 30 colorectal cancer cases). Tissue material were examined according to the established morphological protocols. Blood samples were taken from 699 patients (10 melanoma, 206 gastric, 250 breast, 178 prostatic, 55 colorectal cancer and premalignant diseases cases). Tissue biobank material is enrolled in scientific research both in Latvia and abroad (Lithuania, Israel).
Conclusion: We expected that our biobank will join international biobanking network and organizations.

PS-07-019
A case of paravertebral mediastinal chordoma without bone destruction
J. Matsubayashi*, T. Nagao
*Tokyo Medical University, Anatomic Pathology, Japan

Objective: Chordoma is a slow-growing malignant bone tumor that exhibits notochordal differentiation. Nearly 90 % of cases occur in the sacrococcygeal region and in the base of the skull. The remaining cases develop in the mobile spine, predominantly in the cervical and lumbar vertebrae. We report a rare case of paravertebral mediastinal chordoma without bone destruction.
Method: Case report.
Results: A 47-year-old Japanese woman was admitted to hospital after a tumor was incidentally detected on a plain chest X-ray image. The tumor was located in the paravertebral region of the mediastinum and did not show any destruction of the thoracic vertebra radiologically. The tumor was clinically diagnosed as a benign neurogenic tumor and the tumor was easily removed surgically. Microscopically, the tumor mainly consisted of tumor cells with extensively vacuolated cytoplasm, arranged in cord- and nest-like fashion in a myxoid matrix background. Immunohistochemically, the tumor cells showed diffuse positivity for pancytokeratin (AE1/AE3), vimentin. The tumor cell nuclei were positive for brachyury, which is a key transcription factor of notochordal development.

Conclusion: These results confirmed the tumor to be an extraosseous chordoma in the paravertebral mediastinal region, which is rather an extremely rare location for usual chordoma.

PS-07-020

Testicular papillary mesothelioma: A case with borderline features

S. Mavropoulou*, Z. Tatsiou, P. Nasos
*General Hospital, Laboratory of Pathology, Xanthi, Greece

Objective: Well-differentiated papillary mesothelioma occurs rarely in the paratesticular region, with only a few published case reports.
Method: We describe a case of a 37-year-old man who initially presented with discomfort in the left testis and underwent resection of a hydrocele in the left testis. A hydrocelectomy was performed, during which a pedunculated mass, 2,5 cm in greatest dimension, was found attached to the testis.
Results: Microscopically, the mass was composed of multiple branching papillary structures with fibrovascular cores covered by a single layer of low cuboidal to cuboidal cells with predominantly bland nuclear and cytologic features and rare microscopical necrosis. Immunohistochemical staining for calretinin and cytokeratines 5/6 was positive and proliferative marker Ki67 was <2 %. Accordingly the diagnosis of a well-differentiated papillary mesothelioma was made. The patient has not received additional therapy and is disease free 15 months after diagnosis.
Conclusion: In conclusion, we report a rare case of a well-differentiated papillary mesothelioma of the tunica vaginalis of the testis. The combination of benign and semimalignant characteristics can make the diagnosis of such a lesion problematic and pathologic distinction from malignant mesothelioma is crucial, although it may be difficult because of the variability of associated histologic features.

PS-07-021

Occurrence of Kimmelstiel-Wilson like lesions in the absence of diabetic nephropathy in dogs, may provide a natural model for further research in the corresponding human form

C. Mega*, J. Mesquita, C. Nóbrega, R. Cruz, F. Esteves, C. Santos, E. Teixeira de Lemos, F. Reis, H. Vala
*Coimbra University, Medicine, Pharmacol. & Therapeutics, Portugal

Objective: Nodular glomerulosclerosis occurring in non-diabetic patients is an unexplained renal condition that resembles Kimmelstiel-Wilson lesions (K-W), associated almost exclusively with diabetic nephropathy. This study aimed to assess the presence of nodular glomerulosclerosis in dogs with non-diabetic chronic kidney disease (CKD) and evaluate similarities with human condition, and thus, establish the dog as a natural disease model for further studies.
Method: Kidneys from dogs (n=27) with non-diabetic CKD were evaluated for the presence of nodular glomerulosclerosis. Samples were stained with haematoxylin-eosin and periodic acid of Schiff. Lesions were classified as absent or present, the later, classified as non- convincing and convincing K-W like lesions.
Results: Nodular glomerulosclerosis was present in 66.66 % of evaluated cases (n=18), of which, 38.88 % (n=7) were convincing K-W like lesions and the remaining 61.11 % (n=11), although similar, didn't exhibit typical microscopic characteristics and were classified as non-convincing. Fibrosis was positively associated to diagnosis of K-W lesions (OR=6; p<0.05).
Conclusion: As in man, Kimmelstiel-Wilson like lesions may also occur in dogs in the absence of diabetic nephropathy and reveal similar microscopic aspects to the description related in humans and, that some factors, others than hyperglycaemia, may be responsible for the appearance of these lesions. Thus, dogs may provide a model of natural disease for further elucidation.

PS-07-022

Modulated electro-hyperthermia induced programmed cell death in HT29 colorectal carcinoma xenograft

N. Meggyesházi*, G. Andocs, T. Krenacs
*Semmelweis University, 1st Dept. of Pathology, Budapest, Hungary

Objective: Modulated electro-hyperthermia (mEHT) is a non-invasive technique for targeted tumor treatment. The mEHT generated capacitive coupled modulated radiofrequency selectively accumulates in the tumor tissue without major effect in the surrounding normal tissues.
Method: HT29 human colorectal carcinoma cell line xenografted to both femoral region of BalbC/nu/nu mice was treated when reaching ~1.5 cm by using a single shot mEHT treatment (LabEHY, Oncotherm Ltd, Páty, Hungary) for 30 min. Sampling was made after 0, 1, 4, 8, 14, 24, 48, 72, 120, 168, 216 h in 3 mice each group by keeping 5 untreated animals. Histomorphologic, immunhistochemical and TUNEL assay results were tested in digital slides and analyzed semi-quantitatively. The apoptosis protein array results were evaluated using the ImageJ software.

Results: mEHT caused programmed cell death related destruction from the tumor centre. TRAILR2 and FAS proteins were upregulated 8 h post treatment. Cleaved caspase-3 positive cells appeared only at the tumor periphery between 4 and 14 h. AIF nuclear translocalisation at 14–24 h and massive TUNEL positivity at 24–48 h indicated DNA fragmentation. At 72–216 h myeloperoxidase positive leukocyte infiltration ring supported tumor elimination.
Conclusion: In HT29 colorectal cancer xenograft mEHT caused programmed cell death. DNA fragmentation followed rather a caspase independent and AIF dependent subroutine.

PS-07-023
Metaphyseal parosteal lipoma of the distal femur: Case report
D. Milutin*, S. Mocan, A. Ivanescu
*Emergency County Hospital, Pathology, Tirgu Mures, Romania

Objective: Lipoma of the bone is a rare benign adipocytic tumor that arises intraosseous and rarely on the cortex or on the surface of the bone (parosteal lipoma). Parosteal lipoma affects the long bones diaphysis of adults over 40 years old.
Method: We present the case of a 23 years old female with clinical diagnosis of femoral exostosis. Conventional radiographs shows the presence of a 5 cm length area of lucency on the femoral metaphyseal surface with a periostal reaction at the base of the lesion.
Results: Gross examination reveals a 5 cm osseous tumor, whitish on the surface and yellow on the section. On microscopic examination there are mature adipocytes with small foci of bone scattered throughout the adipocytes and hyaline cartilage at the perifery of the lesion. The gross and microscopic examinations correlated with conventional radiographs led us to diagnosis of parosteal lipoma.
Conclusion: This case is interesting being a rare bone tumor, the young age of the patient and the location on the surface of the bone.

PS-07-024
Application of Scanning Acoustic Microscope to evaluate lymph node lesions
K. Miura*
*Hamamatsu University, School of Medicine, Japan

Objective: A scanning acoustic microscope (SAM) is a device that uses ultrasound (frequency, >20 kHz) to image an object or tissue. Because it is known that the harder the tissue, the more the speed of ultrasound, SAM can provide data on the elasticity of cells and tissues.
Method: We compared lymph node lesions between acoustic and light microscopic images to evaluate the usefulness of SAM.
Results: SAM system discriminated lymph node components and demonstrated distinct acoustic images of the lymph nodes such as cancer metastasis, lymphomas, granulomatous diseases, and deposition diseases such as amyloidosis. Areas with desmoplastic reactions associated with cancer invasion or post-inflammatory fibrosis showed the greater speed of sound than normal lymph nodes. These results corresponded well to those obtained using the conventional microscope.
Conclusion: SAM provides the following benefits: (1) images are acquired in only few minutes without requirement for staining, (2) imaging pattern is similar to that of light microscope, and (3) speed of sound from each lesion is digital and statistical analysis is possible among diseases. Although resolution of SAM is little lower than that of light microscope, the SAM can be an ancillary tool for histological diagnosis and clinical research.

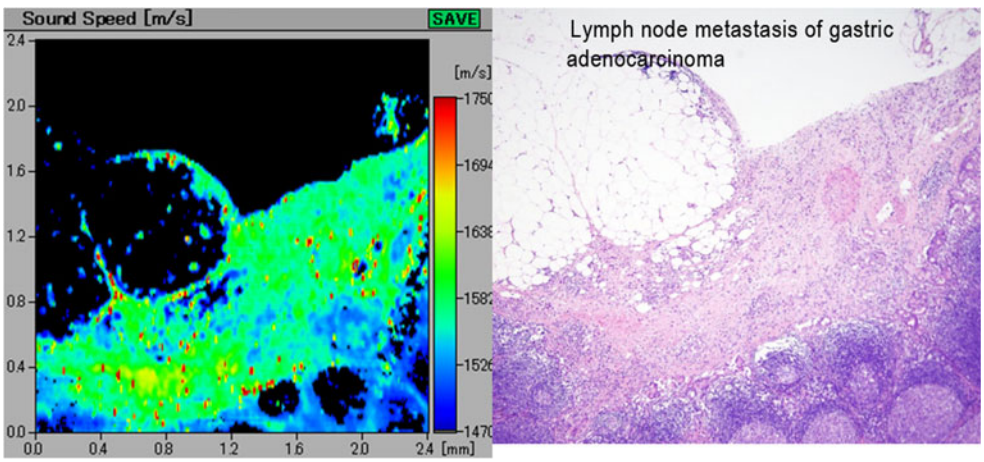

PS-07-027

Oxidative stress parameters in patients with Parkinson Disease

G. Nikolova*, V. Mancheva, Y. Karamalakova, B. Grigorov, I. Manchev, A. Zheleva, V. Gadjeva
*Trakia University, Dept. of Chemistry and Biochemistry, Stara Zagora, Bulgaria

Objective: Parkinson's disease (PD) is considered one of the major neurological disorders of the population, and there is increasing data provides enough evidences confirming the involvement of free radicals and other reactive oxygen species (ROS) in a number of physiological and pathological processes. The aim of the present study was to evaluate, the effect of therapy in patients with Parkinson disease on biomarkers of oxidative stress, such as products of lipid peroxidation by two different methods: Electron Paramagnetic Resonance and visible spectrophotometry.
Method: The study was performed in blood samples of patients with PD -with therapy, patients with PD -without therapy and healthy volunteers as controls. The products of lipid peroxidation were measured as malondialdehid (MDA), spectrophotometrically by thiobarbituric acid (TBA) method. The levels of lipid radicals were determinated ex vivo at room temperature on an X-band EMX-micro spectrometer, Bruker, Germany.
Results: By the present study we reported higher levels of oxidative stress in PD patients without therapy compared to those with therapy. These results were comfirmed by the EPR method.
Conclusion: The increase of oxidative stress, in PD patients' might be an additional reason for many secondary complications.

PS-07-028

Melanoma incidence rate in the Republic of Mordovia according to the cancer-register covering the period from 2006 to 2010

N. Plotnikova*, H. Kuzma
*Saransk, Russia

Objective: Objective – epidemiology of melanoma incidence in the Republic of Mordovia covering the period from 2006 to 2010.
Method: Based on cancer-register data.
Results: Melanoma incidence in the Republic in 2006 amounted to 7,3 0 000, in 2007 – 4,8 0 000, in 2008 – 7,2 0 000, in 2009 – 5,8 0 000, in 2010 - 6,6 0 000. The first time proven case is morphologically confirmed in 2006 – in 87,3 %, in 2007 – in 85,3 %, in 2008 – in 95,0 %, in 2009 – 97,9 %, in 2010 – in 98,1 % of cases. Detectability at early stages increased. In 2006 cases of I – II, III and IV stages amounted to 36,5 %; 27,0 %; 8,0 %, in 2007 – 51,2 %; 21,9 %; 12,2 %, in 2008 – 50,8 %; 32,7 %; 8,2 %, in 2009 – 51,0 %; 14,2 %; 14,2 %, and in 2010 – 56,3 %; 5,4 %; 7,2 %. Peak incidence at 55–60 years of age for males and at 50–55 years of age for females.
Conclusion: There is an increase in skin melanoma incidence rate in the region; increase in morphologically confirmed diagnoses and in disease detectability at early stages.

PS-07-029

Rare association between malignant phyllodes tumor of the breast and cutaneous malignant melanoma: Case report

C. Popp*, M. Petre, S. Zurac, S. Gheorghita, R. Andrei, C. Socoliuc, F. Staniceanu
*Colentina University Hospital, Dept. of Pathology, Bucharest, Romania

Objective: Popp and Petre are first authors in equal proportion Phyllodes tumors are rare (<1 %), biphasic breast tumors composed of a hypercellular mesenchimal proliferation layered by epithelial cells.
Method: We present the case of a 60 years old woman diagnosed with malignant melanoma of the right calf in Nov. 2011 and with malignant phyllodes tumor of right breast in Jan. 2012.
Results: The patient underwent resection of a tumor of the right calf which proved to be a malignant melanoma (superficial spreading type, Clark V, Breslow 4,45 mm); regional lymph node biopsy showed no metastasis (pT4apN0). During postoperative evaluation, a second tumor was discovered in her right breast. Intraoperative histological diagnosis was phyllodes tumor with unknown biological behavior. Microscopic examination on paraffin embedded sections showed a proliferation of mesenchymal elongated cells, with basophilic or clear cytoplasm and elongated, irregular nuclei in a fibrous, hyaline stroma with myxoid areas. Immunohistochemical assays were performed for establishing the biological potential of the tumor (Ki67, p53, CD10, VEGF) and the final diagnosis was malignant phyllodes tumor.
Conclusion: This is the first reported association of these two malignant tumors, in our knowledge, raising the question if is only an incidental association or there is a subsequent connection between them.

PS-07-030

X-linked lymphoprolifetative syndrome: A case of autopsy

Y. Rangel Mendoza*, M. T. Gonzalez Serrano, C. M. Villar Pastor, M. Medina, M. Santamaria Osorio
*Hospital Reina Sofia, Dept. de Anatomia Patologica, Cordoba, Spain

X-linked lymphoproliferative disease (XLP) is caused by mutations in the genes SH2D1A and XIAP. The 3 most commonly recognized phenotypes of SH2D1A related XLP are hemophagocytic lymphohistiocytosis (HLH)

associated with Epstein -Barr virus (EBV) infection (58 %), dysgammaglobulinemia (31 %), and lymphproliferative disorders (30 %). A 10 month old male with clinical history of fever and diagnosis of Infectious Mononucleosis (EBV+), presented with hepato-splenomegaly, high liver enzymes, and clinic hemophagocytic syndrome. Posteriorly he presented dyspnoea, bradycardia, seizures and death. Autopsy examination showed pleural effusion and ascites. Congestive lungs. Liver of 785 g, spleen of 130 g; both with congestive aspect, and multiple adenopathies (we send material to the hospital department of immunology). Histological examination showed on liver and spleen a prominent lymphocytic infiltrate, positive to CD4, CD8, LMP and EBER immunohistochemistry stain with hemophagocytic lymphohistiocytosis, also seen in lymphoadenopathies. There were T lymphocyte cell perivascular in brain and lung. Making an immunology and autopsy outcome of X-linked lymphoproliferative disease. The diagnosis of XLP must be considered in males with fatal or near fatal EBV infecttion, HLH resulting from EBV or other viral disease, hypogammaglobulinemia or common variable immunodeficiency, lymphoma and family history of XLP.

PS-07-031

Aneurysmal bone cysts of hands and feet: A clinical and pathological review of 10 cases out of a series of 78

Y. Rodrigues*, L. Guerra, M. Prieto, F. López-Barea, E. Bravo, M. Salcedo, D. Bernabeu
*Hospital Universitario La Paz, Anatomia Patologica, Madrid, Spain

Objective: Primary Aneurysmal Bone Cyst (ABC) is a histologically complex and mainly cystic lesion that accounts for 2 % of all primary bone tumors. Information regarding its clinical presentation and management in hands and feet remains sparse.
Method: The medical records ABC in hands or feet in Hospital La Paz Pathology Department from 1966 to 2011 were retrospectively reviewed and compared with existing data. We also propose pathological criteria for differential diagnosis between ABC and giant cell reparative granuloma (GCRG).
Results: Ten ABC in hands or feet were identified, out of 78 (12.8 %), Five tumors were in metacarpals, 4 in metatarsals and 1 in phalanx. Radiographs showed expansile lytic lesions in metadiaphyseal region, sometimes with aggressive appearance. Histologically, ABC showed a mixture of blood-filled spaces with connective tissue septae containing osteoclast giant cells and foci of osteoid. Scattered areas of so called "blue bone" were present in 5 cases (50 %). There were two solid variants. Five patients underwent resection and 5 curettage, three of which relapsed (30 %).
Conclusion: ABC should be considered in the radiologic differential diagnosis of hands and feet tumours because these lesions can even mimic malignancies. Although clinicopathologically some authors consider GCRG is related to the ABC solid variant, we believe they are different entities.

PS-07-032

Carb-3 is the superior anti-CD15 monoclonal antibody in optimized protocol settings

R. Røge*, S. Nielsen, M. Vyberg
*Inst. of Pathology, Aalborg, Denmark

Objective: Immunohistochemical detection of CD15 is important in diagnosis of Hodgkin lymphoma and may be relevant in classification of renal tumours. In four tests with 71–121 participating laboratories conducted by the NordiQC external quality assessment scheme only 50–76 % of CD15 stains were sufficient, mainly because of too diluted primary antibody concentration, insufficient HIER and less successful antibody clone. The purpose of this study was to evaluate three anti-CD15 antibodies based on vendor and in-house optimized protocols.
Method: Multitissue blocks with various malignant lymphomas, renal tumours and normal tissues (n=218) were stained with three concentrated (conc) antibodies (Carb-3, MMA and BY87) according to predetermined in-house optimized protocols on two staining platforms. Ready-to-use (RTU) solutions of Carb-3 and MMA were also examined. Extension and intensity of stains was scored using the H-score method.
Results: Carb-3conc with an in-house optimized protocol gave the highest H-scores in classical Hodgkin lymphoma, renal tumours and normal kidneys. Carb-3RTU and MMA-conc gave slightly lower scores, while MMARTU and BY87conc gave the lowest scores and a large proportion of false negative reactions. All in-house optimized protocols gave better staining results than vendor protocols.
Conclusion: The importance of antibody selection and protocol optimization in immunohistochemical laboratories is emphasized.

PS-07-034

Markers of early myocardial infarction - To increase autopsy quality

L. Szylberg*, M. Bodnar, A. Marszalek
*Collegium Medicum Bydgoszcz, Dept. of Clinical Pathomorphology, Poland

Objective: Autopsy-based morphologic diagnosis of early phase of myocardial infarction is a challenge. Therefore, specific diagnostic methods are needed to confirm the early myocardial infarction. Recent reports indicate that h-FABP and MYBPC3 protein are highly sensitive and specific markers for the early myocardial infarction. The objective of this study was to evaluate the diagnostic value of h-FABP

and MYBPC3 proteins as markers of early myocardial infarction in autopsy tissue section.
Method: 20 cases of myocardial infarction and 20 cases with suspected myocardial infarction were selected from 236 autopsy examination performed in 2006–2010 at the Department of Pathology. The control group consisted of 20 sections of normal myocardium. The immunohistochemistry was performed on formalin fixed paraffin embedded tissue sections using antibodies against h-FABP and MYBPC3.
Results: h-FABP and MYBPC3 proteins revealed various expression levels in selected groups. The control group revealed strong cytoplasmic expression of both determined proteins. The expression of h-FABP and MYBPC3 in patients with suspected or diagnosed myocardial infarction was reduced.
Conclusion: H-FABP and MYBPC3 proteins may be usefull markers in diagnosis of early myocardial infarction, especially in patients with uncertain cause of death.

PS-07-035
The Pathological Effects of Immobilization Stress on Testes Tissue and Serum Testosterone level in Rats
P. Tavakoli*, R. Ahmadi, M. Mafi
*Islamic Azad University, Dept. of Biology, Tehran, Iran

Objective: Studies show that there is association between stress and pathophysiological changes in reproductive system. The main aim of this study was to determine the pathological effects of immobilization stress on testes tissue and serum testosterone level in male rats.
Method: Wistar rats were randomly divided into control, acutely or chronically immobilized groups of 10 in each. Animals were immobilized for 2 h/day or 8 h/day for a period of 3 weeks or 1 week in chronically or acutely immobilized groups, respectively. After 6 weeks, blood samples were collected using cardiac puncture method. Following serum collection, testosterone level was measured by radioimmunoassay method. The effect of immobilization stress on testes histology was also examined. Data were statistically analyzed and compared between groups using ANOVA.
Results: Serum level of testosterone was decreased in acutely or chronically immobilized rats compared with control animals ($P<0.001$). In histological study, semeniferous tubules were significantly deformed and cellular concentration was reduced in immobilized rats compared with control animals ($P<0.05$). The number of spermatocytes, spermatids or sperms was also decreased in immobilized rats ($P<0.001$) and this pathologic change was more prominent in acutely than chronically immobilized rats.
Conclusion: Our findings show that immobilization stress can leave pathological effects in male reproductive system leading to reduced cellular concentration in semeniferous tubules and decreased serum level of testosterone.

PS-07-036
Aggressive systemic mastocytosis with Charcot-Leyden crystals-associated crystal storing histiocytosis in bone marrow
Z. Vernerova*
*3rd Faculty of Medicine, Dept. of Pathology, Prague, Czech Republic

Objective: Crystal storing histiocytosis (CSH) is a rare phenomenon characterized by cytoplasmic accumulation of crystaline material in macrophages. Several different subtypes of CHS have been described depending on etiology or according to the chemical nature of the crystals.
Method: We report a 56 -year-old man with 3 year history of systemic mastocytosis with slight splenomegaly and hepatomegaly. Laboratory investigations showed severe macrocytic anaemia (Hb85g/L; Hct 0.251 L/L; MCV 108.2 fl; MCH 36.6 pg; RDW 17.1), slight leukopenia and eosinophilia.
Results: Microscopic examination of bone marrow revealed sheets of polygonal or spindle-shaped mastocytes with no associated clonal hematological malignancy. Around mast cell infiltrates were interspersed histiocytes with abundant opaque cytoplasm containing eosinophilic crystaline inclusions (Charcot –Leyden crystals).
Conclusion: We report a case of crystal storing histiocytosis of bone marrow in a 56-year-old men with systemic mastocytosis. Around 90 % of CSH is associated with lymphoproliferative or plasma cell disorders, but not all cases are hematologically related. Only small number of non-immunological variants of CSH is reported in the literature.

PS-07-037
Do we overestimate on counting mitosis?
N. Yigit*, A. Gunal, Z. Kucukodaci, A. Ozcan, O. Onguru
*GATA, Dept. of Pathology, Ankara, Turkey

Objective: The number of mitotic figures in a particular microscopic area is an important criterion, changes the diagnosis or determines the prognosis of many tumors. These criteria are generally accepted for each case in the light of the original studies and determined by counting mitotic figures in certain number of fields. The detected number of mitotic figures is affected by the field of view. Field of view depends on the ocular diameter and magnification value. The ocular lens diameters of the old types of microscopes used in original literature were smaller than

current microscopes with a narrower field of view. The purpose of this report was to emphasize these differences in the mitotic counting.
Method: In this report, the mitotic counting criteria for pathological diagnoses were reviewed from the original literature. Whether there is a difference between original literature criteria and evaluation with current microscopes according to ocular diameter, field of view and assessed total area were investigated.
Results: Review carried out was determined certain differences between the criteria of the original literature and evaluation with current microscopes.
Conclusion: Due to wider field of view in modern microscopes used in the current, number of field counted in original criteria though to need correction.

PS-07-038
Analysis of Nestin expression in pediatric and adult cases of high-grade osteosarcoma
I. Zambo*, M. Hermanova, D. Adamkova Krakorova, P. Mudry, K. Zitterbart, M. Kyr, K. Vesely, J. Sterba, R. Veselska
*St. Anne´s University Hospital, 1st Dept. of Pathologic Anatomy, Brno, Czech Republic

Objective: Nestin, an intermediate filament protein, has been detected in different tumors. In addition, nestin expression is associated with worse prognosis in some malignancies. Our study analyzed clinical significance of nestin expression in pediatric and adult cases of high-grade osteosarcoma.
Method: Using immunohistochemistry and immunofluorescence, nestin expression was examined in osteosarcoma tissue samples taken from 45 patients [24 males, 21 females; median age 19 years (range 6–85 years)]. In both methods, the frequency of nestin + tumor cells was stratified into three categories and clinicopathological correlations were statistically analyzed.
Results: Variable frequent nestin + tumor cells were identified in all examined osteosarcoma samples. In the entire cohort of 45 patients, high levels of nestin expression detected by immunofluorescence were associated with significantly worse clinical outcomes (OS, p=0,031; EFS, $p<$ 0,001). However, only statistically nonsignificant trends for shorter survival were revealed using generally more sensitive immunohistochemistry. Analogical results were obtained when comparing groups of patients by age or gender.
Conclusion: Despite significantly shorter survival rates observed in patients with high levels of nestin expression assessed by immunofluorescence, nestin does not seem to represent a powerful prognostic marker for patients with high-grade osteosarcomas.

PS-07-039
Benign atypical intravascular CD30+ T-cell proliferation: A reactive condition mimicking intravascular lymphoma
R. M. Garcia Martin*, E. Riveiro Falkenbach, M. T. Fernández Figueras, J. L. Rodriguez Peralto
*Hospital 12 de Octubre, Dept. of Pathology, Madrid, Spain

Objective: Intravascular lymphoma (IVL) is a very aggressive disease that can involve the skin in 40 % of the patients. The majority of IVL are of B-cell lineage, although cases with a T-cell phenotype and, rarely, natural killer (NK)-cell phenotypes have been reported. Indeed, two cases of intravascular large CD30+ T-cell lymphoma were described in the literature, both with a fatal outcome.
Results: Herein, we report two patients with skin lesions showing an atypical intravascular CD30+ T-cell proliferation. The rearrangement of immunoglobulin heavy chain gene and T-cell receptor gamma gene studied by the polymerase chain reaction were polyclonal. Indeed, both patients did not present systemic disease and therefore exhibit a favorable outcome.
Conclusion: To the best of our knowledge, this is the second report of a benign intravascular CD30+ T-cell proliferation that represents an intriguing differential diagnosis for intravascular lymphoma.

Monday, 10 September 2012, 09.30 - 10.30, Congress Hall Foyer 3rd Floor
PS-08 Poster Session History of Pathology

PS-08-001
Medical research through historical resources: Talking objects at the Pathology Museum of Florence
R. Santi*, A. Franza, G. Nesi
*University of Florence, Pathological Anatomy Section, Italy

Objective: The Pathology Museum of the University of Florence is an example of an institution in which pathological specimens from the nineteenth century become talking objects. Through analysis of the original Catalogue and investigation by means of modern scientific techniques, discovering the story behind the object becomes a feasible challenge.
Method: A case of a parasitic perineal monstruosity from the Museum collection is described on the basis of the original medical records and illustrations.
Results: The surgeon Giorgio Pellizzari (1814–1894) first reported this extraordinary case of sacrococcygeal teratoma containing rudimentary arm bones and a hand. Reader of Descriptive Anatomy, Pellizzari was a well-known Anatomy Dissector and Curator of the Physiological Museum of the Regio Arcispedale di Santa Maria Nuova in Florence.

Conclusion: This report underlines the importance of studying the archive material in order to thoroughly comprehend a single museum object. This handling of matters will help to turn anatomical collections into a unique teaching tool for modern medical practice and a noteworthy documentation of scientific, artistic and historical value.

PS-08-002

The importance of Prof. Dr. Hamdi Suat Aknar in the history of pathology in Turkey

S. Seckin*
*Ankara Numune Hospital, Turkey

Objective: A system of pathology based on practice, training and research could be institutionalized in Turkey in earlier 20th. century. Until 19th. century medical education was theoretical. It is known that dissection and autopsy was allowed in 1841 and Turkish became the lecturing language in 1870 during Ottoman Empire era.
Method: It is Prof.Dr. Hamdi Suat Aknar who had founded modern and organizational pathology in Turkey. After training in pathology in Germany (1900–1904), he returned and remained as a dedicated professor until 1933. He was the first who taught pathology in systematic order. Along with his routine work and lecturing, Prof. Aknar conducted numerous researches basically on skin lesions and tumors. He published 40 articles in German and French.
Results: Through the publications and presentations at the congresses, he obtained an important standing and became a well-known pathologist in Europe. He was selected as the member of editorial board of the distinguished journal Acta Cancrologica published in Budapest. He pioneered the first organized activities against cancer in Turkey and contributed to the foundation of the Society Against Cancer.
Conclusion: Pathology, founded in Turkey under the leadership of Prof. Aknar, has further developed with the efforts of eminent scholars.

Monday, 10 September 2012, 09.30 - 10.30, Congress Hall Foyer 3rd Floor
PS-09 Poster Session Head & Neck Pathology

PS-09-001

Clear cell odontogenic carcinoma: A distinct odontogenic neoplasm with squamous differentiation

A. Afrogheh*, A. F. Bezuidenhout, N. Mohammed, J. Hille
*Cape Town, South Africa

Objective: Clear cell odontogenic carcinoma (CCOC) is a rare odontogenic neoplasm with a propensity for recurrence and distant metastasis. We report a case of CCOC of the anterior maxilla in a 53 year old male.
Method: CT scans revealed a destructive lytic expansile lesion originating from the anterior alveolar process of the maxilla. Histology disclosed a biphasic neoplasm with nests of central clear cells and peripheral polygonal hyperchromatic cells with marked cytoplasmic eosinophilia.
Results: The tumour cells were immunoreactive for MNF116, CK14, CK19, CK5 and EMA. Both cell types were negative for S100 protein, vimentin, SMA, RCC, CD10, CK7 and CK20. The proliferation index, Ki67, was low and its expression, similar to CK14, was confined to the peripheral cells. Electron microscopic examination showed desmosomes and tonofilaments confirming the squamous origin of the lesion.
Conclusion: CCOC is a distinct odontogenic neoplasm of squamous phenotype. Surgical resection with wide tumour free margins remains the mainstay of therapy. Its overall high recurrence rate even after radical surgical excision, necessitate close follow up of the patients.

PS-09-002

Extramedullary plasmocytoma of the sinonasal tract: Report of a case

I. Ágota*, S. Mocan, M. Gyorgy, E. Horvath, T. Mezei
*Emergency County Hospital, Pathology, Targu Mures, Romania

Objective: Extramedullary plasmocytoma is an uncommon plasma cell tumor localized preferentially in the upper aerodigestive tract, with no evidence of underlying multiple myeloma. It accounts for less than 1 % of head and neck tumours.
Method: We report a case of a 57-year-old male patient with reccurent left-sided epistaxis and nasal obstruction. CT-scan showed a left maxillary mass eroding the lateral wall of the nasal cavity. The tumor was surgically removed.
Results: Histologic examination showed a diffuse infiltrate of neoplastic cells in the submucosa, arranged in a scant vascularized stroma. The neoplastic cells were large to medium- sized with amphophilic cytoplasm, irregular nuclei and proeminent, eosinophilic nucleoli. Mitotic figures were frequent. Imunohistochemical stains were performed in order to make a differential diagnosis: the tumor cells were positive for CD38 and CD138 and they expressed cytoplasmic immunoglobulin with kappa light chain restriction. Most of the tumor cells were also CD56 and EMA positive.
Conclusion: Even though extramedullary plasmacytoma of the sinonasal tract is rare, it should be included in the differential diagnosis. The cooperation among the otorhinolaryngolists, pathologists and hematologists are required to manage the patients effectively in order to provide optimal treatment.

PS-09-003

Carcinosarcoma of the parotid gland featuring foci of malignant giant cell tumor

D. Athanazio*, J. C. Geraldes Filho, L. Carvalho, N. Pinheiro Junior, L. A. Rodrigues de Freitas, P. Athanazio
*Federal University of Bahia, Dept. of Pathology, Salvador, Brazil

Objective: Malignant mixed tumors of the salivary glands are uncommon. Salivary gland carcinosarcoma is a rare neoplasm in which both the stromal and epithelial components meet the microscopic criteria for malignancy. Seventy-four cases have been reported in English-language literature to date.
Method: Case report.
Results: An 81-year-old male patient with a carcinosarcoma of the parotid gland featuring foci of undifferentiated carcinoma, and sarcomatous components characteristic of chondrosarcoma, high-grade undifferentiated sarcoma and malignant giant cell tumor. Stromal areas of the tumor expressed vimentin and smooth muscle actin. Positive staining for the S-100 protein was noted in areas of chondroid differentiation. Giant cells from areas identified as malignant giant cell tumor were positive for CD68, in contrast to the bizarre/atypical giant cells of the high-grade sarcomatous component, which were CD68-negative.
Conclusion: Foci of malignant giant cell tumors in salivary gland carcinosarcomas has been described in only two previous reports. This case highlights the occurrence of a giant cell tumor component, which may be indistinguishable from its counterparts in the bone and soft tissues and may lead to the diagnosis of salivary gland osteoclast-like giant cell tumor. Extensive sampling may be crucial to correctly identify carcinosarcoma in such cases.

PS-09-004

Osteopontin expression is an independent factor for survival in oral squamous cell carcinoma

M. Avirovic*, K. Matušan, R. Cerovic, M. Juretic, N. Jonjic, K. Lucin
*University of Rijeka, Dept. of Pathology, Croatia

Objective: Ostepontin (OPN) is phosphorilated glycoprotein involved in various physiological and pathological events, including tumor progression. The aim of this study was to analyze the expression of OPN in oral squamous cell carcinoma (OSCC), and to assess its prognostic significance.
Method: The expression of OPN was immunohistochemicaly analyzed in 86 OSCC tissue microarrays and compared with clinicopathological variables such as tumor size, nodal stage, WHO clinical stage, Ki-67 proliferation index, and patients' outcome.
Results: The expression of OPN protein was observed in OSCC tumor cells (tOPN) and various stromal cells (sOPN), including granulocytes, macrophages, lymphocytes, plasma cells, and fibroblasts. OPN expression was higher in OSCC tumor cells compared to adjacent normal mucosa ($p<0.001$), and was associated with advanced nodal stage ($p=0.03$), WHO clinical stage ($p=0.045$), and poor clinical outcome ($p=0.023$). In multivariate analysis tOPN emerged as an independent factor for survival ($p=0.049$). There was no association between sOPN and clinicopathological variables, although a trend for higher sOPN toward the longer patients' survival was found ($p=0.12$).
Conclusion: OPN protein is upregulated in OSCC. While tOPN is involved in OSCC progression and can independently predict the clinical outcome, the role of sOPN is probably different and needs to be further elucidated.

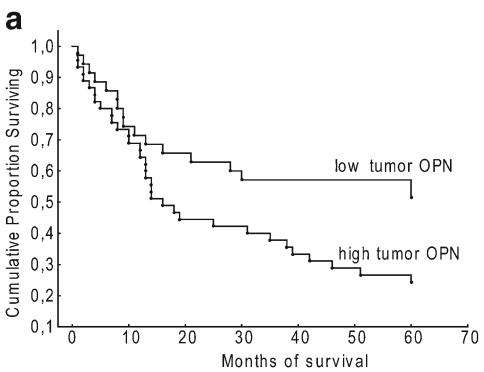

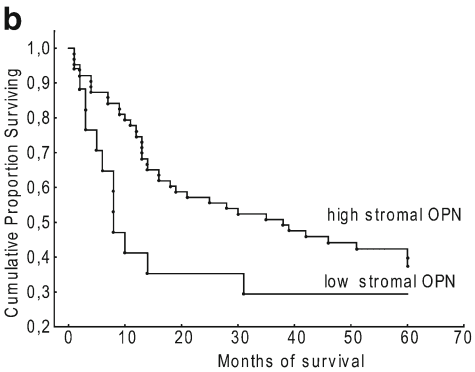

PS-09-005

Immunohistochemical evaluation of non-intestinal sinonasal adenocarcinomas

F. Baderca*, E. Lazar, M. Raica, N. Balica
*Medical University Timisoara, Dept. of Histology, Romania

Objective: Non-salivary sinonasal adenocarcinomas can be divided into intestinal and non-intestinal, both with low-grade and high-grade subtypes.
Method: We analyzed two patients, one 78-y-o female and one 79-y-o male, presenting nasal obstruction and epistaxis

for the last 18 month. Specimens were obtained by endoscopic biopsies, fixed in formalin and embedded in paraffin. Three micrometers thick sections were used for immunohistochemistry.
Results: The tumors were morphologically characterized by proliferation of glands lined by a single layer of columnar epithelium with minimal cellular and nuclear atypia. Tumor stroma contains lymphocytes, plasma cells and extravasated erythrocytes. CK 18 and 20 were intensely positive in the cytoplasm of tumor cells, but with heterogeneous distribution. The reaction for CK19 and CK7 was weakly, with cytoplasmic and granular pattern, emphasizing the brush border. CK8, 34βE12 and MUC2 were negative. The immunoreaction for S100 protein was heterogeneous, with strong positive areas alternating with negative ones and cytoplasmic pattern. Proliferation index determined by Ki-67 antibody clone MIB1 was less than 5 %.
Conclusion: Sinonasal non-intestinal type adenocarcinomas are very rare tumors, which can pose serious diagnostic problems. Immunohistochemical findings and clinical information stand out in the differentiation of adenocarcinoma's subtypes.

PS-09-006
Histological and ultrastructural features of cutaneous free flaps employed in the oral cavity
C. Baldovini*, C. M. Betts, A. Tarsitano, C. Desiderio, C. Marchetti, M. P. Foschini
*Bellaria Hospital, Dept. of Pathology, Bologna, Italy

Objective: Cutaneous free flaps (CFF) are routinely used to repair tissue defects resulting from oral surgery. The concept of "mucosalisation" has been proposed although some Authors recently have supported the preservation of the cutaneous phenotype. The aim of this study was to re-evaluate histological and ultrastructural features of skin flaps in order to make a valid contribution to the debate.
Method: Five cases of forearm free flaps were compared, by histological examination and micrometric measurement, with 1 case of forearm skin and with 12 cases of oral mucosa. Ultrastructural examination was performed on 5 cutaneous flaps, 1 case of forearm skin and mucosa.
Results: At histology the CFF showed hyperkeratosis, a variable inflammatory infiltration and the presence of atrophic adnexa. Micrometric measurements revealed that the epidermis and the mucosal epithelium had similar average thickness related to the hyperkeratosis and the hypergranulosis occurring in the transplanted skin. Electronic microscopy highlighted the presence of intraepithelial Langerhans cells (LC) lacking Birbeck granules. Immunohistochemical S-100, CD1a and Langerin positivity also confirmed LC identity.
Conclusion: Histological and ultrastructural analysis confirmed that the cutaneous phenotype was preserved in all cases of CFF.

PS-09-007
Detection of EBV and HPV-high risk viruses in lymphoepithelial carcinoma of head and neck
C. Barbatis*, C. Poullou, M. Tsopanomichalou, M. Kefala, S. Kalantzakis
*Hellenic Red Cross Hospital, Dept. of Pathology, Athens, Greece

Objective: EBV is accepted as the main virus related to lymphoepithelial-like undifferentiated carcinoma (LEC), but recent reports indicate that HPV-16 is involved in the above type of Head and Neck carcinomas (HNC).
Method: Our aim is to compare the association of the above viruses with LEC in HNCs using immunohistochemical (p16 and LMP1) and chromogenic in situ hybridization (CISH). In the BondMax autostainer, the ready to use probes (Leica) for EBER and HPV-high risk were used. 17 cases with histological features of LEC were studied: nasopharyngeal (11), oropharyngeal (1), parotid (3) and oral cavity (2). p16 positive cases were nuclear and/or cytoplasmic in >70 % of cells while LMP-1 cytoplasmic positivity was assessed. EBER and HPV detection was always nuclear.
Results: 72.7 % of cases express EBER with cytoplasmic LMP1 positivity in 21.45 %. Six out of 17 LEC strongly expressed p16 (35.3 %) with an interesting finding 3/3 positive parotid cases. Fifty per cent of p16(+) were expressing HPV. Dual infection with CISH was observed only in one case of parotid gland LEC.
Conclusion: EBV remains the predominant virus in LEC, but several cases show strong expression of p16 with HPV detection in a substantial number, evidence of HPV-High Risk involvement in LEC HNC.

PS-09-008
Prognostic relevance of CD105 and HIF-1 L in laryngeal squamous cell carcinoma
M. Bodnar*, L. Szylberg, W. Kazmierczak, A. Marszalek
*Collegium Medicum Bydgoszcz, Dept. of Clinical Pathomorphology, Poland

Objective: Neoangiogenesis is the crucial process in tumor progression and promoted by HIF-1α which is associated with endoglin (CD105) overexpressed in de novo formed endothelial cells.
Method: The immunohistochemical analysis for CD105 and HIF-1α expression was performed on 78 samples of 60 laryngeal squamous cell carcinoma (SCC) and 18 of normal mucosa. Automated morphometric methods were

used based on ImageJ software and own developed protocols. Analysis of microvessels density was performed in three hot spots, and included the area of positively stained endothelial cells (0-100), level of CD105 expression (0-255) and MDV/CD105 factor was calculated. We correlated morphometric data with clinico-pathological data (lymph nodes without [N(0)] and with metastases [N(+)]).
Results: The median value of MVD/CD105 in laryngeal SCC was 119.3163 (SD=103.42). It was higher in N(+) group (MVD/CD105 was 151 (SD=108)) than in the N(0) group (MVD/CD105 83.59 (SD=71.42)). Analysis of correlation of CD105 expression in N(0) vs N(+), demonstrated a statistically significant difference (p= 0.000007). Expression of HIF-1α in tumor and tumor stroma was found as nuclear and/or cytoplasmic. Expression of HIF-1α was higher in *N*(+) vs *N*(0) cases.
Conclusion: MVD/CD105 and HIF-1α could be an important prognostic factors in laryngeal SCC.

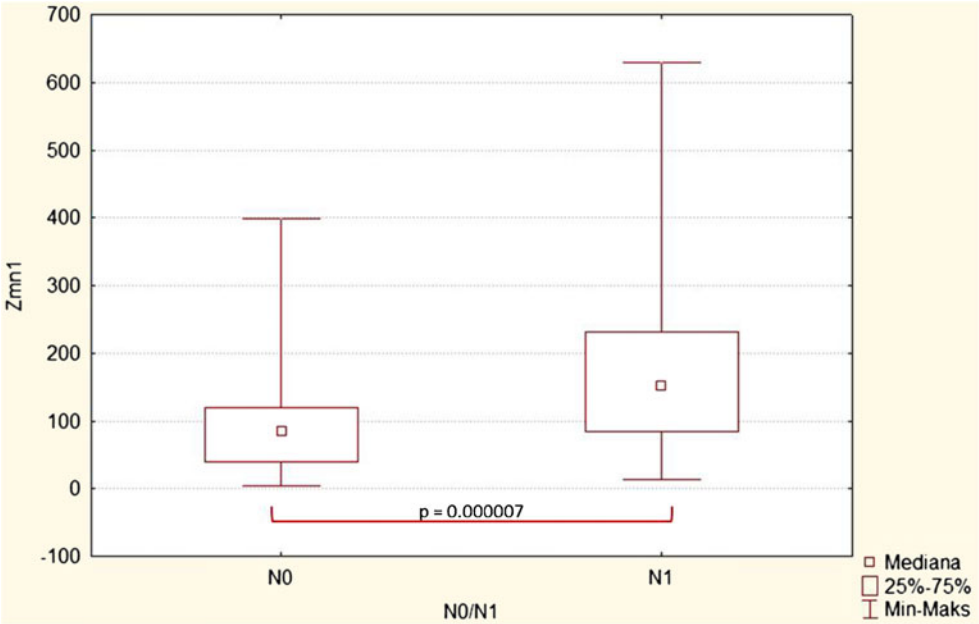

PS-09-010
Sinonasal malignant melanoma: A case report of 2 cases
S. Bozkurt*, E. Kombak, F. Yildirim, E. Cigerciogullari, D. Filinte, S. Celilov
*Marmara Universitesi Tip Fakulti, Dept. of Pathology, Istanbul, Turkey

Objective: Sinonasal malign melanoma is a rare antity, mostly arising from nasal cavity and accounting for <5 % of all sinonasal tract neoplasms.
Method: We report two patients complaining of nasal obstruction and epistaxis. Endoscopy revealed partially haemorrhagic mass obliterating nasal passage. In one patient diagnosis was done as a plasmacytoma by pathologist in an another hospital. Multiple biopsies were taken. Microscopically, the tumour was consisted of medium sized cells, which had high nuclear to cytoplasmic ratio with pleomorphic nuclei containing eosinophilic nucleoli and intranuclear cytoplasmic inclusions. The cytoplasms contained variable amount of melanin pigment. Mitoses – including atypical forms- were easily detectable. There were mild inflammatory infiltrate against the tumour and rare tumour necrosis. One was showed pseudopapillary growth pattern and lymphovascular invasion.
Results: Immunhistochemically, tumour cells showed immunreactivity for S-100, Vimentin, HMB-45 and Melan-A(MART-1). Tumour cells were negative for CD-20, CD-3, CD-138, CD-56, SMA, Pan-CK and Desmin. Submandibulary lymph node metastasis was observed in one patient. This patient has undergone chemotherapy of temozolomide and 23 cures of regional radiotherapy. For the other patient, there were no metastasis detected by PET-CT.
Conclusion: Sinonasal malign melanoma is a rare malignacy, but this entity could be kept in mind to avoid missdiagnosis with other tumors sharing similar morphology.

PS-09-011

The remodeling of the human vocal fold in muscular-lamina propria interface is age-related

A. Branco*, A. T. Fabro, A. B. Pessin, L. E. Moz, M. A. Custódio Domingues, R. H. Garcia Martins
*FMB - UNESP, Dept. de Otorrinolaringologia, Botucatu, Brazil

Objective: Significant changes in the voice occur after 50 years. Vocal quality is dependent on the vocal fold (VF) tissue biomechanics that derive from the extracellular matrix composition and organization. We studied muscular-lamina propria interface of human VF in the aging.
Method: Two authors evaluated density of vessels and the thickness of the deep and muscle layer by HE and IHC (collagenIV) with semiquantitative score. These data were validated by point-counting morphometric method.
Results: With the aging of the vocal folds we identified increased of vessels density in the muscle and deep layers, increasing the matrix density and thickness of the deep layer, and "dissection" of muscle fibers by dense connective tissue.
Conclusion: The progressive structural changes in muscle-lamina propria interface play a crucial role in the remodeling and vocal quality. The increased density of vessels and matrix in aging may contribute to the preservation of vocal function by the physiological repairing.

PS-09-012

"Lymphoepithelioma-like" thymic carcinoma in Parotid Gland

M. Bugdayci*, G. Atay, B. Sozeri, G. Guler Tezel
*Hacettepe University, Pathology, Ankara, Turkey

Objective: We report a 27-year-old woman presented with a slow growing painless mass beneath the right ear. A fine-needle aspiration revealed Whartin tumour. The patient underwent parotidectomy and histopathological examination showed thymic carcinoma with areas of thymoma.
Method: Histopathological examination was done according to conventional protocols. Immunohistochemical stainings were performed using LSAB methods. PanCK, CD3, CD20, CK5/6, CK7, Vimentin, Ki-67, CD5, Bcl-2, CD1a, S100, SMA, TdT antibodies were used.
Results: Histopathologically, a well circumscribed, nodular, hybride neoplasm finely seperated from parotid gland had two components, uniform spindle cells in basaloid form lobulated by fibrous septae and large epitheloid cells with vesicular nuclei and meganucleoli, suggesting thymoma and thymic carcinoma, respectively. Prominent lymphocytic reaction with germinal centers, high mitotic activity, small necrotic foci and microabcesses were also seen. Immunohistochemisty revealed PanCK, vimentin, CD5 and CD1a positivity. The diagnosis of "lymphoepithelioma-like" thymic carcinoma was made.
Conclusion: Thymic carcinoma is a rare tumor most commonly located in the anterior mediastinum. Thymic carcinoma which originates from ectopic rests of thymic tissue caused by defective migration of the embryonic thymus, is extremely rare. In the presented case a thymic carcinoma was found in parotid gland which is an unusual site.

PS-09-013

Evaluation of Wnt Pathway in the development of human oral tissue and Oral Squamous Cell Carcinoma

M. Buim*, A. Q. Cardoso Cardoso, A. M. Silva, S. V. Lourenço, F. A. Soares
*Hospital A. C. Camargo, Dept. of Anatomy Pathology, São Paulo, Brazil

Objective: Activation of Wnt pathway can modulate cell proliferation, survival, cell behavior, and cell fate in both embryos and adults. Its deregulation has been linked with carcinogenesis of a variety of human cancers. Oral diseases present a major and prevalent public health problem. This study investigated the role of Wnt pathway in the development of human oral mucosa and oral cancer tissue.
Method: Expression of Wnt-1, Wnt-2, Frizzled-1, β-catenin, Gsk3-β, axin, Mmp7, and c-myc was investigated in 30 human fetuses oral samples, 16 normal oral tissue from adults and 75 OSCC samples using immunohistochemistry.
Results: We observed similar and high expression, in almost all proteins analyzed in oral fetuses and OSCC tissue (Wnt-1, 89 % and 90 %; Wnt-2, 100 % and 84 %; Frizzled-1, 96 % and 93 %; β-catenin, 89 % and 89 %; Gsk3 β, 78 % and 96 %; Axin, 93 % and 100 %, Mmp7, 89 % and 97 %; c-myc, 96 % and 87 %, respectively). Additionaly, in normal oral tissue from human adults these proteins showed lower expression than in fetuses and OSCC samples (Wnt-1, 56 %; Wnt2, 67 %; Frizzled, 85 %, β-catenin, 75 %, Gsk3 β, 94 %, Axin 76 %, Mmp7, 64 % and c-myc, 76 %).
Conclusion: We suggest important roles for Wnt signaling activity in human oral development that could contribute to OSCC progression.

PS-09-014

Thyroid glands involvement in advanced Acquired Immunodeficiency Syndrome (AIDS): An autopsy-based study

M. Carvalho*, L. Liporoni, R. Gerhard, P. Saldiva, P. Vargas
*Recife, Brazil

Objective: The course of HIV infection and the AIDS can be complicated by a variety of endocrine abnormalities. The aim of this study was to assess the frequency and the major

histopathological characteristics of thyroid involvement in autopsy of patients with AIDS.
Method: The thyroid were obtained from 60 patients with AIDS that were autopsied in the Death Verification Service of the Capital, Faculty of Medicine, University of São Paulo (SVOC-FMUSP) between 1996 and 1999, from a time before the use of highly active antiretroviral regimens.
Results: The anatomopathological lesions detected in 23 glands (38.3 %) were colloid goiter (52.2 %); colloid goiter + follicular hyperplasia (8.7 %); follicular hyperplasia (4.3 %); thyroiditis lymphocytic cronic (8.7 %); papilary carcinoma (4.3 %); cryptococcosis (4.3 %); tuberculosis (8.7 %); epithelioids granulomas (8.7 %) which were negatives for Ziehl-Neelsen staining. Although thyroid disease had not been clinically diagnosed, its involvement was significant and in 3 cases (13 %) it was related to the immunodeficiency, with Mycobacterium tuberculosis being the most common opportunistic agents.
Conclusion: Thyroid lesions are not uncommon in AIDS patients, occurring over a third of the patients studied. Thus, the analysis of the thyroid from autopsies of patients with AIDS can help identify most frequent lesions and help in early diagnosis and appropriate treatment for these diseases.

PS-09-015
Imaging by confocal endomicroscopy: New insight for in vivo tissue diagnosis of head and neck cancer
O. Casiraghi*, M. Abbaci, M. Ferchiou, J. Bosq, S. Temam, C. Laplace-Builhe
*Institut Gustave Roussy, Villejuif, France

Objective: Fibered confocal endomicroscopy (CEM) is a non invasive technology which allows the achievement of in vivo "optical biopsies". A morphological correlation study was performed between CEM, confocal microscopy (CM) and optical microscopy (OM) images.
Method: Forty-seven non cancerous and cancerous tissue samples of head and neck cancer and precancerous lesions were taken from fresh surgical specimens. After topical application of two fluorochrome agents, samples were imaged with CEM and CM. A morphologic correlation study was subsequently performed on CEM images, CM images and Hematoxylin-Eosin-Safran (HES) slides. The images were randomly interpreted by three pathologists. Statistical correlation between CEM, CM and HES has being finalized.
Results: CEM and CM allowed to differentiate invasive carcinoma from normal tissue with high sensitivity and specificity. They however were less performent to distinguish intra epithelial neoplasia from normal tissue or invasive carcinoma.
Conclusion: This study demonstrated the CEM ability to provide "histological-like images" that can be interpreted by pathologists, even in case of complex images as provided by head and neck cancers. Our study conducted jointly with engineers and a surgeon has identified the conditions of transfer of confocal endomicroscopy into clinical conditions and showed that this technique could help significantly the clinician during endoscopy or surgical procedure.

PS-09-016
Tumors of the salivary glands express receptors for growth hormone - Releasing hormone: Diagnostic and therapeutic implications
I. Chatzistamou*, K. Bali, E. Farmaki, A. Schally
*University of Athens, Dental School, Greece

Objective: Recent in vitro and in vivo studies have shown that several malignant tumors express an alternatively spliced variant of the receptor of growth hormone –releasing hormone (SV1), which operates by a ligand-dependent and independent manner.
Method: Nine (9) adenocarcinomas, 11 pleomorphic adenomas and 11 Warthin tumors were studied by immunohistochemistry for SV1 expression and visualized by diaminobenzidine staining.
Results: SV1 expression was cytoplasmic and was detected in 6/8 malignant (75 %) and 11/11 (100 %) Warthin tumors. However, only 1/11 (9 %) pleomorphic adenomas expressed SV1 ($p<0.05$, $x2$-test). Immunoreactivity ranged from mild to intense in all positive specimens, with the exception of Warthin tumors at which only intense immunoreactivity was recorded.
Conclusion: Our study, for the first time reports the presence of anti-SV1 immunoreactivity in tumors of the salivary glands. Furthermore, the high association of SV1 expression with the malignant as opposed to the benign neoplasms implies a role of SV1 in the progression of the disease. A surprising finding of our study was the high positivity for SV1 exhibited by the Warthin tumors that implies biological similarities between these histopathological entities of the salivary glands. These results imply that the use of antagonistic analogs of GHRH merit further investigation.

PS-09-017
Sialadenoma Papilliferum with inverted pattern: A case report in a young patient
F. E. Costa*, R. Dias, A. Coelho, P. Farrajota, R. Sampaio, J. R. Vizcaíno
*Centro Hospitalar do Porto, Braga, Portugal

Objective: Sialadenoma papilliferum (SP) is a rare, benign neoplasm of salivary gland origin which manifests as an exophytic papillary excrescence of the mucosa. Indeed, SP is both an exophytic proliferation of papillary stratified squamous epithelium above the mucosal surface and an endophytic salivary ductal proliferation

beneath the mucosa. It arises predominantly in minor salivary glands and usually affects patients in the age range of 32–87 years, with reports in young patients being exceedingly rare.
Method: We report a case of a previously healthy 20 year-old man diagnosed with a nodular mass in the upper lip buccal mucosa. The tumour was excised and submitted for microscopic examination.
Results: Histologic examination revealed a biphasic proliferation of papillary stratified squamous and salivary ductal epithelia, both underneath the mucosal surface.
Conclusion: In this unique case, as the classical SP, the tumour has a biphasic proliferation of squamous and ductal epithelia. However, unlike the classical SP, both epithelia grow under the mucosal surface. As a result, it didn't manifest as an exophytic proliferation, but as a nodule. We excluded squamous papilloma, inverted ductal papilloma, intraductal papilloma and mucoepidermoid carcinoma, the principal entities in the differential diagnosis of SP, and concluded it to be a SP with inverted pattern.

PS-09-018
Interest of histopronostic classification in three grades in the therapeutic management of primary epithelial parotid carcinoma
V. Costes*, V. Szlaweski, M. Wassef, V. Rigau, R. Garrel
*CHU Montpellier, Anatomie et Cytologie Pathologie, France

Objective: The surgical management of primary parotid cancers (PPC), which is drove by tumor staging and histological grade, remains controversial. A two-grade histological classification is used in therapeutic recommendations. Following new information in salivary gland carcinoma outcomes we assessed the value of a three-grade histological classification.
Method: A 20-year standardized single center treatment including total parotidectomy, neck dissection and radiotherapy has been assessed retrospectively. The histological review of 155 consecutively treated parotid malignancies identified 98 suitable cases for univariate and multivariate survival analyses.
Results: Treatment involved total parotidectomy in 91.6 % of cases, partial or total facial nerve resection respectively in 16.7 % and 13.5 %, neck dissection in 83.3 % and postoperative radiotherapy in 70.8 %. Tumors were high grade in 61.5 % of cases. The 5-year overall survival, disease specific and recurrence free survival rates were 79.4 %, 83.5 % and 70.8 % respectively. Univariate analysis confirmed the classical prognostic factors, whilst multivariate analysis identified clinical stage and grade, especially when analyzing three groups, as the most important prognostic factors.
Conclusion: This study supports total parotidectomy with neck dissection for the treatment of PPC and identifies the possible prognostic significance of intermediate grade tumors.

PS-09-019
Epithelial-myoepithelial carcinoma of salivary gland with pleural metastasis: A case report
L. De Carvalho*, A. P. Baptista, D. Alves-Lima, A. Nostre Júnior, L. Da Silva, E. Pereira
*Centro Universitário Lusíada, Dept. of Pathology, Santos, Brazil

Objective: Epithelial-myoepithelial carcinoma (EMC) is a rare neoplasm occurring predominantly in the parotid gland. The histological hallmark is a biphasic cell arrangement. EMC is a low-grade malignant tumor.
Method: A 45-year-old white woman presented right chest pain for few weeks. The chest computed tomography revealed pleural effusion and thickening in the right lower lobe. There were no parenchymal nodules. Excisional biopsy was performed.
Results: Microscopic examination showed a biphasic tumor with a prominent myxoid stroma and tumor cells with clear cytoplasm involving pleural tissue. Immunohistochemistry showed tumor cells positive for keratin, S100 protein, smooth-muscle actin, p63 protein, vimentin. Histological and immunohistochemical features confirmed the diagnosis of epithelial-myoepithelial carcinoma. The patient underwent a right parotidectomy 3 years earlier for removal of 3.5 cm mass diagnosed as EMC.
Conclusion: Epithelial-myoepithelial carcinoma of salivary gland is a rare low-grade malignant neoplasm with a potential for local recurrence and metastases. Rare metastases for lungs, kidney and brain were reported. We described an additional case of pleural metastasis.

PS-09-020
Fetal parotid gland morphology complicated with growth retardation at late gestation
O. Denga*, S. Morozov, O. Reshetnikova
*Inst. of Statotology, Odessa, Ukraine

Objective: Salivary defense system recognized as an important protective factor of the child oral environment. Research data reveal that bacterial infection, dental caries and periodontal diseases have a higher incidence in cases of salivary glands dysfunction. The aim of present study was to find out the morphological peculiarities of the fetal parotid gland in cases of restrictions of its intrauterine growth (IUGR) at late gestation.

Method: Parotid gland of twenty human fetuses with IUGR from the late spontaneous abortions material were compared with fifteen fetal glands in cases of induced abortions due to psychological reasons (control group). Tissue samples were stained with hematoxylin and eosin. Stereological examination was done to find out volume fractions of parotid gland structural components.
Results: Results have shown the reduction of the area of acini, large collected ducts, striated and intercalated ducts in IUGR group. The volume fractions of vessels were also lower than on controls. The foci of immature secretory lobes in cases of growth restriction occupied wider zones within loose, poorly cellular, fibrous stroma.
Conclusion: Our study demonstrates the delay of the parotid gland structural maturation in pregnancies complicated with IUGR. Impaired growth and secretory gland's dysfunctions may cause pathological changes in oral ecosystem of a child.

PS-09-021
Carcinoma ex pleomorphic adenoma successfully treated with trastuzumab and radiotherapy
S. Di Palma*, S. Whitaker, K. Potter, L. Pitkin
*The RSCH and Division of Clinical Medicine, Guildford, United Kingdom

Objective: Carcinoma ex Pleomorphic Adenoma (CXPA) is an aggressive tumour with metastatic disease and rapid clinical course. Some CXPA harbour HER-2 gene amplification and protein overexpression suggesting potential role for Trastuzumab therapy. There are occasional reports of such treatment in salivary duct carcinoma but little is known for CXPA.
Method: A 59 year old man presented in February 2010 with T2N2 M0 CXPA treated by nerve-sparing total parotidectomy and adjuvant radiotherapy. In May 2011 he relapsed in cervical nodes (biopsy proven) along with multiple metastases to the bone, adrenals and retroperitoneum. Tumour cells showed high levels of HER2 gene amplification when tested with in silver situ hybridization (SISH).
Results: The patient received palliative radiotherapy to the spine and commenced trastuzumab, at 3 weekly intervals on 5th August 2011. He experienced resolution of symptoms and repeat CT scans after 3 cycles revealed a good partial response. He continues on maintenance trastuzumab to date.
Conclusion: This case illustrates that Trastuzumab therapy can be successfully used in CXPA. The histological features of salivary duct carcinoma may not be present in the subtype of CXPA and the tumour may still benefit of this targeted treatment. Pathologists should be performing HER2 status in presence of CXPA.

PS-09-022
Chondroid chordoma of cervical spine: A case report
I. Dimitriadis*, S. Papaemmanouil, A. Sekouli, I. Matzarakis, G. Hristos, L. Sakkas
*Hospital of Thessaloniki, Dept. of Pathology, Greece

Objective: Chondroid chordoma was described by Heffelfinger as a biphasic malignant neoplasm possessing elements of both chordoma and cartilaginous tissue.
Method: A 47-year-old man presented with a painful mass in the pharynx area. MRI revealed an ill-defined mass, arising from the body of (C4) vertebra, which extended to the around soft tissue. The diagnosis of chondroid chordoma was suspected in the material biopsy from the pharynx and the patient underwent a radical excision of the mass. The surgical specimen consisted of multiple pieces of whitish tissue measuring 0.8×1.7×2.8 cm in aggregate. The sections were examined with H + E stain and followed by immunohistochemical study.
Results: The lesion was composed of a mixture of areas that resembled typical chordoma and others low grade chondrosarcoma. Immunohistochemical study: chordoma areas, (AE1/AE3+, Ck 8/18+, Ck19+, EMA+, S-100+, Vimentin, CD34−, CD31−, SMA−), low grade chondrosarcoma's areas (Vimentin+, Ki-67:3 %). The above findings confirmed the preoperative diagnosis.
Conclusion: The extent of surgical resection, the histological subtype, and the Ki-67 index can help to predict the clinical outcome for chondroid chordoma's patients. The patient after 3 months is in generally good health, and is followed up by oncologists.

PS-09-024
Basaloid squamous cell carcinoma of the head
A. Dumitriu*, S. Dumitriu
*UMF Iasi, Dept. of Neurology, Romania

Objective: Basaloid squamous cell carcinoma is an uncommon variant of SCC and seems to have a poorer survival than classical SCC.
Method: Pathologically specimens can have nearly pure basaloid features or a mixture of basaloid and squamous features. Basaloid squamous cell carcinoma is also commonly confused histologically with poorly differentiated SCC.
Results: The presence of particular histologic features may be associated with poorer outcome survival in the basaloid squamous cell carcinoma group was less than half in the poorly differentiated squamous cell carcinoma groups. Distant metastases occured in 73 % of patients with basaloid squamous carcinoma and 10 % of patients in the poorly differentiated squamous cell carcinoma groups.

Conclusion: Considering the high distant metastatic rate of basaloid squamous carcinoma and poorer overall survival rate a more extensive survey is indicated in these patients before surgery is recommended.

PS-09-025

Clinical and pathological characteristics of polymethylmetacrylate and hialuronic acid in the rat tongue: An experimental model to evaluate the effect of dermal fillers

V. Duval da Silva*, S. Pozatti Moure, K. Fróes de Vargas, R. Loureiro Borghetti, F. Gonçalves Salum, K. Cherubini
*PUCRS, Dept. of Pathology, Porto Alegre, Brazil

Objective: Dermal fillers are injectable products commonly used in aesthetic medicine. This type of treatment, which often replaces traditional surgical procedures provides satisfactory cosmetic results. It is known, however, that there is a risk of undesired effects at the site of injection of the product or even at a distance. Literature reports numerous cases of orofacial injuries caused by dermal fillers. The aim of this study is to evaluate two of the most widely used facial dermal fillers for aesthetic purposes in an effort to identify adverse reactions they may produce.
Method: Two of the most commonly used materials for aesthetic purposes by dermatologists and plastic surgeons, polymethylmetacrylate and hialuronic Acid were injected in rat tongues: 10 % polymethylmethacrylate (n=16) and 20 mg/mL hyaluronic acid (n=18), compared to an inert solution for control (n=16). After 7, 60 and 90 days, local clinical and histological alterations were analyzed.
Results: The following factors were verified: intensity of the inflammatory response (H&E), amount of newly formed blood vessels (IHC) and macrophages and collagen fibers density (picrosirius). Results showed that both filling materials triggered local inflammatory response to a greater or lesser degree.
Conclusion: polymethylmethacrylate showed cases of foreign body reaction, while hyaluronic acid demonstrated characteristics suggesting biocompatibility.

PS-09-026

Comparison of effects of clodronate and zoledronic acid on the repair of maxilla surgical wounds: Histomorphometric, receptor activator of nuclear factor-kB ligand, osteopro-tegerin, von Willebrand factor, and caspase-3 evaluation

V. Duval da Silva*, A. C. U. Vasconcelos, S. A. Berti-Couto, A. A. Azambuja, F. G. Salum, M. A. Figueiredo, K. Cherubini
*PUCRS, Dept. of Pathology, Porto Alegre, Brazil

Objective: The aim of this study was to compare clodronate and zoledronic acid regarding their influence on the repair of surgical wounds in maxillae (soft tissue wound and tooth extraction) and their relation to osteonecrosis.
Method: Thirty-four Wistar rats were allocated into three groups according to the treat-ment received: (i) 12 animals treated with zoledronic acid, (ii) 12 animals treated with clodronate and (iii) 10 animals that were given saline solution. All animals were subjected to tooth extractions and surgically induced soft tissue injury. Histological analysis of the wound sites was per-formed by means of hematoxylin–eosin (H&E) staining and immunohistochemical staining for receptor activator of nuclear factor-kB ligand (RANKL), osteoprotegerin (OPG), von Willebrand factor, and caspase-3.
Results: The zoledronic acid group showed higher incidence of non-vital bone than did the clodronate group at the tooth extraction site. At the soft tissue wound site, there were no significant differences in non-vital bone between the test groups. RANKL, OPG, von Willebrand factor, and caspase-3 did not show significant differences between the groups for both sites of surgical procedures.
Conclusion: Both of the bisphosphonates zoledronic acid and clodronate are capable of inducing maxillary osteonecrosis. Immunohistochemical analysis suggests that the involvement of soft tissues as the initiator of osteonecrosis development is less probable than has been pointed out.

PS-09-027

Differential diagnosis of lichen planus and lupus erythematosus oral lesions using PAS and immunohistochemistry

V. Duval da Silva*, M. Fava, T. G. Lopes, F. G. Salum, M. A. Figueiredo, K. Cherubini
*PUCRS, Dept. of Pathology, Porto Alegre, Brazil

Objective: The aim of this study was to evaluate the expression of CD1a, CD4, CD8, CD20, caspase-3, tryptase and basement membrane thickness in oral lesions of lichen planus (LP) and lupus erythematosus (LE).
Method: Oral lesions of LP (n=21) and LE (n=23) were biopsied. After confirmation of diagnosis, the specimens were submitted to PAS and immunohistochemistry.
Results: CD1a expression was significantly greater in epithelium and connective tissue in LP. Epithelial CD4 and CD20 did not differ between the diseases, but were greater in connective tissue in LP. CD8 expression was greater in both epithelium and connective tissue in LP. Caspase-3 did not differ between the groups, whereas tryptase was greater in LE epithelium. Basement membrane thickness did not differ between LP and LE.
Conclusion: CD1a, CD4, CD8, CD20, caspase-3 and tryptase expression and the basement membrane thickness are

not definitive criteria for differential diagnosis of oral lichen planus and lupus erythematosus.

PS-09-028

Usefulness of p16 immunostaining in Squamous Cell Carcinomas (SCC) of the larynx and hypopharynx

M. C. Etxezarraga*, E. Fuertes, G. Cancho, M. Zufiaurre, L. Ortega, J. Velasco, J. C. Lopez, J. Bilbao, M. M. Ramirez, C. Ereño
*Hospital Universitario Basurto, Dept. de Anatomia Patologica, Bilbao, Spain

Objective: HPV status has been surrogated in routine practice by p16 immunostaining. The aim of this study is to define the histological features and overall survival of p16(+) versus p16(−) laryngeal and hypopharyngeal SCC cases.
Method: A total of 80 SCC of the larynx and hypopharynx diagnosed during the 4 years were randomly selected, their histological sections were re-evaluated and follow up was retrieved from the medical files. P16 and p53 immunostaining was performed. Viral status was analyzed by PCR and in situ hybridization. Kaplan-Meier survival curves and log rank test was performed using SPSS software.
Results: 31 % (25/80) were p16 (+)/p53 (−), and 68 %(55/80) were p16(−)/p53(+). The 92 %(23/25) of p16(+) cases were in males with an average age of 54,4 years (range 20–77). The 72 %(18/25) of p16(+) tumors were well-moderately differentiated SCCs. Viral status was obtained in 44 %(11/25) of the cases, 63 %(7/11) being HPV-16. 5-year survival was 84 % for p16(+) tumors and 56 % for p16(−)s (log rank, $p<0.05$).
Conclusion: With reliability, p16 immunostain may surrogate the determination of HPV status in SCC of the larynx and hypopharynx. Overall survival is significantly better in p16(+) cases, most being SCC well-moderately differentiated neoplasms.

PS-09-029

Screening for Human Papillomavirus (HPV) in Squamous Cell Carcinomas (SCC) of the Upper Aerodigestive Tract (UADT): A clinicopathologic study of 136 cases

M. C. Etxezarraga*, G. Cancho, M. Zufiaurre, L. Ortega, E. Fuertes, J. C. Lopez, J. Bilbao, M. M. Ramirez, C. Ereño
*Hospital Universitario Basurto, Dept. de Anatomia Patologica, Bilbao, Spain

Objective: HPV detection in UADT cancer have prognostic implications. This study try to establish the clinicopathological features and overall survival differencies between p16 (+) versus p16(−). Method:
Method: A total of 136 SCC diagnosed during 3 years were randomly selected, their histological sections were re-evaluated and follow up was retrieved. P16 and p53 immunostaining was preformed. Viral status was determined by PCR and in situ hybridation. Kaplan-Meier, log rank and Cox tests was preformed using SPSS software.
Results: 31 %(43/136) were p16(+)/p53(−) and 68 %(93/136) were p16(−)/p53(+). In 92 % (35/38) of p16(+)/p53(−) cases DNA viral was present, being the most frecuent HPV 16, 33 types, mostly located in larynx (41 %, 18/43). Significative correlations was established between HPV(+) and p16(+) cases (Spearmen). Interestingly, 10 of patients develop metachronic second primary tumor. Thirty months overall survival was 81 % for p16(+) tumors versus 53 % for p16(−), log rank $p=0{,}0089$ ns. Differences are related with existence of second primary neoplasms (Cox $p=0{,}0004$).
Conclusion: The immunostaing for p16 is a tool for identification HPV related tumors. In our material HPV(+) cases are located more in larynx than oropharynx. The overall survival differences were due to the presence of second primary tumors.

PS-09-030

Case report: An 80 year old man with odynophagia

P. Farrajota*, R. Sampaio, F. Costa, L. Ribeiro, P. Cusati, G. Falconieri, G. Elmberger
*Centro Hospitalar do Porto, Dipt. do Anatomia Patologica, Portugal

Objective: Odynophagia may be caused by inflammatory/infectious conditions and tumors arising within the oropharynx. We present an unusual case of a follicular dendritic cell sarcoma (FDCS) of the tonsil manifesting with odynophagia.
Method: An 80 year-old man presented with odynophagia refractory to medical therapy; a 0.9 cm left tonsillar mass was noted on inspection. Bilateral tonsillectomy was performed. A panel of antibodies was applied on paraffin tissue section.
Results: Grossly, the left tonsil featured a 1.2 cm well circumscribed grey lesion. Histologic examination showed a proliferation of spindle to ovoid cells arranged in fascicles with swirling qualities admixed with scattered lymphocytes. Frequent mitoses and apoptotic bodies were seen but no "tumoral" necrosis was recognized. Tumor nests were separated by thin stromal septi containing a prominent glioblastoma-like microvascular proliferation with focal formation of glomeruloid tufts. The tumor cells were immunoreactive for CD21, CD23 and vimentin.

Conclusion: FDCS'-s are rare recently described and likely under-recognized malignant tumors capable of simulating poorly differentiated carcinoma, melanoma or lymphoma. In the initial assessment, an extended panel of antibodies inclusive of FDC markers is of valuable diagnostic help.

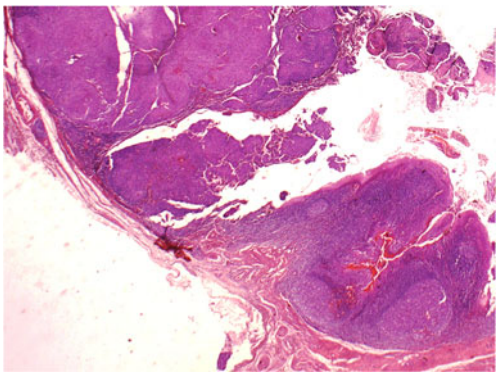

PS-09-031

Ceruminal gland derived pleomorphic adenoma with intrasialodochal and intracapsular epithelial proliferation of atypical ductal hyperplasia or low-grade ductal carcinoma in situ breast-type

P. Farrajota*, C. Dias, F. Costa, A. Olsson, G. Elmberger
*Centro Hospitalar do Porto, Dipt. do Anatomia Patologica, Portugal

Objective: Primary tumors of the external auditory canal are rare and often difficult to diagnose. We present a case of ceruminal gland derived pleomorphic adenoma with unusual features.
Method: A 55 year-old man presented with a slow growing lesion in the left external auditory canal. The resection specimen was routinely processed.
Results: The specimen consisted of a 1.8 cm sized well circumscribed yellowish nodule covered on one side by skin. The histological examination revealed a partially encapsulated tumor composed of fat and myxochondroid tissue separating biphasic epithelial-myoepithelial elements of diverse patterns and including an intraductal (intrasialodochal) epithelial proliferation of ADH or low-grade DCIS-like character. Ductal tumor cells were immunoreactive AR, ER, Mammaglobin, S-100, CK-HMW, CK5, E-cadherin and Vimentin; Ki-67 (2–4 %). Ductal structures were surrounded by intact myoepithelial layer. ETV6-NTRK3 gene rearrangement was negative. The preferred diagnosis was ceruminal gland derived pleomorphic adenoma with intrasialodochal and intracapsular atypical proliferation of ADH/LGDCIS-breast type. Our differential diagnosis also included ceruminal gland adenoma NOS, polymorphous low grade adenocarcinoma and mammary analogue secretory carcinoma.
Conclusion: Ceruminal gland pleomorphic adenoma is rare and can develop atypias along the carcinoma ex pleomorphic adenoma spectrum.

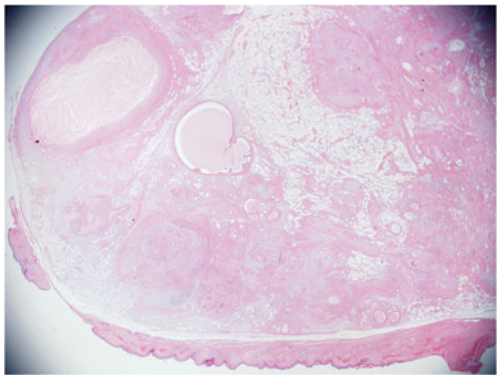

PS-09-032

Cystic lesions of the jaws

F. Flamminio*, M. Bombardi, G. Marucci, L. Gentile, M. P. Foschini
*Ospedale Bellaria, Dipt. di Anatomia Patologica, Bologna, Italy

Objective: A great variety of cystic lesions can affect the jaws, varying from epithelial or non-epithelial, odontogenic or non-odontogenic, developmental, inflammatory or neoplastic in origin. It is important to recognize and correctly diagnose these lesions.
Method: All cases of cystic jaw lesions present in the files of the Anatomic Pathology of the University of Bologna at Bellaria Hospital in the period 1-01-1992\\31-12-2011 were retrieved.
Results: The cases series consisted of 1141 cases. The most frequent types were radicular cysts (537 cases, 47.06 %), keratocystic odontogenic tumours (Keratocyst)(TcO)(199 cases, 17.44 %) and dentigerous cysts (120 cases, 10.52 %). In patients younger than 18 years of age the percentage of radicular cysts was lower (38 %) than in adults, while increased the percentage of dentigerous cysts (35 %). The percentage of TCO was 17 %, being related to the Gorlin-Goltz syndrome.
Conclusion: The present series confirms that the radicular cyst is the most common type of cystic lesion affecting the jaws. The similar neoplastic cystic lesion as TCO is the second most frequent type. Therefore attention should be taken in order to provide the correct diagnosis of cystic lesions of the jaws and to avoid misdiagnosis of neoplastic odontogenic cysts.

PS-09-033

Risk of neoplastic transformation in oral epithelial precursor lesions

F. Flamminio*, S. Peluso, A. Farnedi, E. Leonardi, L. Gentile, D. Gissi, C. Marchetti, L. Montebugnoli, M. P. Foschini

*Ospedale Bellaria, Dipt. di Anatomia Patologica, Bologna, Italy

Objective: Oral squamous cell carcinoma (OSCC) is usually preceded by epithelial precursor lesions (EPL). The aim of the present study is to assess the risk of developing OSCC in EPL, as graded according to WHO 2005 criteria. The Ljubljana classification will be followed.

Method: All oral biopsies diagnosed as EPL in the period 1992–2006 were retrieved from the files of the Section of Anatomic Pathology of the University of Bologna at Bellaria Hospital. The details Follow-up was obtained from clinical records.

Results: Follow-up varied from 12 to 216 months. OSCC arose in 2/54 cases of simple hyperplasia (3.7 %), in 2/16 cases of basal-parabasal cell hyperplasia (2.5 %), in 9/32 cases of atypical hyperplasia/carcinoma in situ. Time elapsed from the initial biopsy and OSCC appearance varied from 99.5 months (range 67–132) in simple hyperplasia; 22 months (range 19–25) in basal/parabasal hyperplasia, and 50,4 months (range 12 to 156) in cases of atypical hyperplasia or carcinoma in situ.

Conclusion: The data presented demonstrates that simple hyperplasia has a low risk (<4 %) of neoplastic transformation. The risk increases when EPL appear and is related to the degree of epithelial atypia.

PS-09-034

The prognostic value of resection margins in oral squamous cell carcinoma

F. Flamminio*, T. Beccarini, L. Gentile, E. Leonardi, A. Farnedi, D. Gissi, C. Marchetti, L. Montebugnoli, M. P. Foschini

*Ospedale Bellaria, Dipt. di Anatomia Patologica, Bologna, Italy

Objective: Resecting oral squamous cell carcinoma (OSCC) with appropriate margins of uninvolved tissue is of critical importance.

Method: 180 surgically resected OSCC with follow-up varying from 6 to 120 months (media 40 months) were histologically reviewed.

Results: Lymph-node metastases were found in 43 % of cases showing depth of invasion >5 mm and in 14.5 % of cases which showed depth of invasion <5 mm. Furthermore they were found in 53.2 % of cases with nerve invasion and in 28.3 % of cases without nerve invasion. Recurrences appeared in 39.4 % of cases with minimum distance from resection margins <5 mm, and in 23.45 % of cases with minimum distance >5 mm. The second OSCC appeared in 37.5 % of cases with high grade epithelial precursor lesions (EPL) on surgical margins and in 16.12 % of cases without EPL on surgical margins.

Conclusion: The present data confirms that accurate evaluation of histological features has a strong prognostic impact on lymph-node metastases, recurrences and appearance of second OSCC.

PS-09-035

Peripheral cemento-ossifying fibroma: A clinicopathologic and immunohistochemical study of 11 cases

R. Hadhri*, M. Njima, A. Moussa, S. Fouli, L. Njim, A. Zakhama

*Fattouma Bourguiba Hospital, Dept. of Pathology, Monastiir, Tunisia

Objective: Peripheral cemento-ossifying fibroma (PCOF) is a growth of the gingival tissues that predominantly affects women and is usually located in the maxilla anterior to the molars. Its pathogenesis remains unknown. We present a study of a series of PCOF and discuss pathogenesis, clinical, histologic and immunohistochemical features as well as differential diagnosis.

Method: This is a five-year (2006–2010) retrospective study of 11 cases of PCOF. Medical files and histologic slides of all eleven patients were reviewed.

Results: There were 3 male and 8 female patients. The mean age was 31.8 years (range 30–87). Patients presented with a polypoid gingival lesion measuring 0.7 to 2.5 cm. The definitive diagnosis was established by histological examination which showed a cellular connective tissue containing focal areas of cementum-like material or trabecular bone. The immunohistochemical study revealed that the proliferating cells showed myofibroblastic characteristics and weak focal positivity with progesterone receptors but did not express estrogen receptors.

Conclusion: Our results indicate that PCOF can be considered as a myofibroblastic proliferation with focal calcifications of odontogenic origin and a putative hormonal influence. Although, PCOF is a benign lesion, we think it deserves recognition because of its relatively high postoperative recurrence rate, up to 20 %.

PS-09-038

Myoepithelioma of tongue

H. Gokce*, O. Ipci, E. Atik, T. Ozgur, E. Akbay

*Mustafa Kemal University, Dept. of Pathology, Hatay, Turkey

Objective: Myoepitheliomas are rare benign neoplasms that may be located in various organs as salivary glands, breast, skin, lung. The most of them are usually seen in the parotid gland and the minor salivary glands of the hard palate. They consist mostly of myoepithelial cells with variable cellular morphologies including spindle, epithelioid, plasmacytoid, or clear cells. A variable stromal component can be seen in these tumors.
Method: A 25-year-old female patient who complained with a tongue swelling was admitted to the Otorhinolaryngology Service. Intraoral examination revealed a mass measuring 2.5 cm in diameter on the right side of her tongue. Excional biopsy was performed and the surgical specimen was sent for histopathological analysis.
Results: Histopathologically, the tumor was thinly encapsulated and had got oedematous/myxoid stroma. It was composed of spindled and plasmositoid cells. 1 or lower mitotic figure per 10 high power fields was seen. The positive staining for pancytokeratin, epithelial membran antigen, smooth muscle actin, S-100 protein, and glial fibrillary acidic protein were seen in tumoral cells on immunostaining. Ki-67 labelling index was 2–3 %.
Conclusion: Theoretically, a myoepithelioma in the tongue may be seen. But, to date, and in our knowledge, none of the myoepitheliomas has been reported in the tongue.

PS-09-040

Nasopharyngeal carcinoma and prognostic indicators: EGFR, P53 and LMP1

E. Kerboua*, A. Boufenara, K. Bouzid
*Pierre & Marie Curie Center, Medical Oncology, Algiers, Algeria

Objective: Nasopharyngeal Carcinoma (NPC) is the most common epithelial malignancy of the nasopharynx. Undifferentiated NPC (UCNT), the most frequent histological type, represent a distinct entity.
Method: The study involved 75 patients (pts), 50 H/25 F, an average age of 37 years. All our pts had a nasopharyngeal biopsy with overexpression of EGFR research by immunohistochemistry and 13 pts have benefited from the search for LMP1 and P53, in addition to the EGFR.
Results: Among 75 pts, 15 did not overexpress EGFR (20 %) 60 overexpress EGFR (80 %). Among the 60 positive patients, EGFR is correlated to a chemoresistance, a decrease in response time (p=0.0008), a decrease in disease-free survival (p=0.0008) and a decrease in overall survival (p=0.0001). The results on 13 pts revealed a positive immunostaining for EGFR and LMP1, negative for P53. 100 % of pts are at stage IV with a time of relapse average of 4 months, a Diesease free survival 7.2 months and overall survival of 8 months.
Conclusion: The overexpression of EGFR in UCNT is proved with a 80 % overexpression, it is a prognostic factor certain to be systematically integrated with other conventional factors. In addition to its prognostic value, EGFR positivity can be used to indicate an anti-EGFR targeted therapy in NPC.

PS-09-041

Immunohistochemical Characterization of Salivary Gland Tumors

S. Kiremitci*, S. Dizbay Sak, D. Kankaya, S. Percinel
*Ankara University Medical School, Pathology, Turkey

Objective: Salivary gland tumors reveal a broad morphology and immunohistochemistry may be helpful.
Method: We examined 12 mucoepidermoid (MEC), 8 adenoid cystic (ADC), 3 asinic cell (ACC) and 4 salivary duct carcinomas (SDC); 2 myoepitheliomas (ME), 5 basal cell (BCA), 31 pleomorphic adenomas (PA) and 18 Warthin tumors (WT) for SMA, Calponin, S100, CD10, GFAP, p63, CEA, GCDFP15, GLUT1, 34BE12, CK14, CK19, CD117 and Galectin3, using tissue microarray.
Results: Tumors expressing myoepithelial markers were ADC (SMA, Calponin), BCA (SMA, Calponin, p63), PA (SMA, Calponin, S100, CD10, GFAP, p63), ME (S100, CD10, GFAP), MEC (p63) and WT (p63); PA being the only tumor expressing all of the markers in the panel. GFAP, S100, CK14, p63, CK5/6 and Galectin3 expressions were higher in benign and CK19 was higher in malignant tumors (p<0.05). Some of our findings helping in differential diagnosis are as follows: In differentiation of PA from ADC: GFAP, CD10, GCDFP15 positivity; higher expression of S100; lower expression of CK14 and CD117 favors PA. In differentiation of PA from BCA: GFAP and CD10 positivity favors PA. In differentiation of MEC from SDC: CD10, CK14, p63 and CK5/6 positivity favors MEC.
Conclusion: We conclude that salivary gland tumors may be well characterized by using distinct markers in each differential diagnosis.

PS-09-042

Salivary immunoglobulins for assessing cariogenicity in children with intrauterine growth retardation

K. Kosenko*, O. Denga, S. Morozov, O. Reshetnikova
*Inst. of Stomatology, Odessa, Ukraine

Objective: It is known that salivary glands pathology results in oral homeostasis disturbances and increases risk of infection diseases like caries.It is known that salivary glands pathology results in oral homeostasis disturbances and increases risk of infection diseases like caries.
Method: Oral examinations were performed in 30 children aged 6 years with IUGR (group I) and 20 controls without IUGR in anamnesis (group II). Non stimulated whole saliva samples were collected. The concentration of sIgA was determined using an immunoassay kit. The salivary flow rate was determined from the volume yielded within 5 min; the pH was measured by pH-electrode. Microbiologically the level of MS in saliva was found.
Results: The results have shown the increased level of sIgA and MS in group I. It was accompanied with the lowered saliva flow rate and buffer capacity. Caries experience was also higher in group I.
Conclusion: This finding tends to support the hypothesis that structural and functional retardation of salivary glands may decrease the oral immune defense and stimulate the early childhood caries development.

PS-09-044
Urbach-wiethe disease (lipoid proteinosis); A case report
U. Kucuk*, I. G. Erdogan, U. Bayol, N. Hacioglu, I. Cukurova, C. Bicakci
*Tepecik Training Hospital, Dept. of Pathology, Izmir, Turkey

Objective: Lipoid proteinosis is a rare autosomal resessive disorder of variable severity that may involve the skin, mucous membranes of the upper respiratory tract and internal organs that may display different clinical manifestations based on the site of involvement.
Method: A 34 year old male patient was admitted to our hospital with a complaint of hoarseness present since childhood but had worsened in recent years. A dermatological examination revealed light brown papillomatous skin lesions on the dorsum of both hands and elbows present for a long duration. Endoscopic examination of the larynx revealed widespread mucosal thickening and irregularity.
Results: Microscopic examination reveales the deposition of PAS positive eosinophilic hyaline materials negative for Congo red stain in the dermis and submucosal regions. His final diagnosis was lipoid proteinosis with skin and larynx involvement.
Conclusion: The case presented here, which is a typical sample, has been reported to draw attention to the fact that lipoid proteinosis is also included in the differential diagnosis in patients presenting with hoarseness in childhood in otolaryngology.

PS-09-045
Nasal septal lobulary capillary hemangioma
A. Kurt*, A. Duman, A. Ertas, I. Erdem
*Bölge Egitim ve Arastirma Hastanesi, Dept. of Pathology, Erzurum, Turkey

Objective: Lobulary capillary hemangioma (LCH) is a benign, rapidly growing vascular lesion of the skin and mucous membrans. It may rarely present as a mass of considerable size and thus entirely fill the nasal cavity. It occasionally appears in the nasal region as a pedunculated or broad base mass. Trauma and hormonal influences are the most common presumed etiologic factors. LCH usually involves the gingiva, lips, tongue, and buccal mucosa. The most common symptoms are epistaxis and nasal obstruction.
Method: In this report; a case of 14 years old boy operated surgically of LCD of the nasal septum, which occurred post delivery was described.
Results: On examination, a red pedunculated bloody swelling 3,5*2 cm was noted arising from the posterior part of the nasal septum to nasopharinx. Histopathologically LCH has characteristics consistent with lobular prolifeation of capillaries in a fibromyxoid stroma.
Conclusion: We emphasise that rarely seen LCH must be kept in mind in the differantial diagnosis of a rapidly growing mass, who is cured surgically. Follow up 2 months later showed no recurrance. Although the head and neck is not an uncommon region, the nasal cavity is extremely rare sites for LCH in children.

PS-09-046
Large Cell Neuroendocrine Carcinoma as mucosal lesion (M-LCNEC) of the head and neck regions in Japanese patients: A new clinico-pathologic entity
K. Kusafuka*, M. Abe, Y. Iida, T. Onitsuka, T. Nakajima
*Shizuoka Cancer Center, Pathology Division, Nagaizumi, Japan

Objective: Large cell neuroendocrine carcinoma (LCNEC) is well known as a subtype of lung cancer. Our objective is to establish mucosal LCNEC (M-LCNEC) as a new entity in the head and neck regions.
Method: We re-estimated 814 surgically resected specimens of the primary mucosal carcinoma in the head and neck regions during 2002–2009. The immunostainings for neuroendocrine (NE) markers such as CD56, chromogranin-A and synaptophysin were performed. In the cases, which were positive for>two NE markers, we re-diagnosed as "M-LCNEC".
Results: Only eight cases (0.98 %) were re-diagnosed as M-LCNEC. All cases were male and their mean age was 64.6 years old. Three cases occurred in the oro-pharynx, four cases in the larynx and one case in hypopharynx. A half

of the cases showed dead of disease. Histologically, M-LCNEC showed the organoid pattern growth of large basaloid cells, in which were seen the central necrosis, rosette formation, peripheral palisading, and high mitotic figures (>15/hpf). Immunohistochemically, M-LCNEC indicated to be positive for two or three NE markers.
Conclusion: M-LCNEC, which occurs as mucosal lesion in the head and neck regions, indicated relatively poor outcome. We propose that M-LCNEC is a new clinico-pathlogical entity.

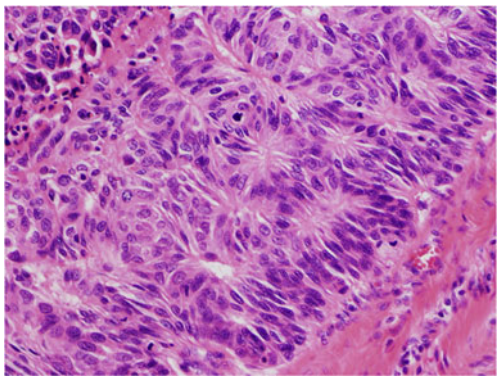

PS-09-047
Expression of claudins −1, −3, −5, −7 and −11 on the progression of squamous cell carcinoma of the lip
N. Lascane*, A. d. Moraes Carvalho, A. d. Costa Neves, C. M. Coutinho-Camillo, M. M. Simonsen Nico, S. V. Lourenço
*University of São Paulo, Dept. of Oral Pathology, Brazil

Objective: Claudins are integral transmembrane proteins of tight junctions, critical for maintenance of cell adhesion and polarity. Altered claudin expression has been detected in carcinomas and correlates with tumour progression. Actinic cheilits is a pathologic condition that affects the lower lip, caused by chronic exposure to solar radiation; it corresponds to the early phase of squamous cell carcinoma. We investigated claudin patterns in phases of actinic cheilitis, as alterations in adhesion molecules are considered important during the progression of this process.
Method: Immunohistochemistry against claudins −1, −3, −5, −7 and −11 was performed in 100 cases of actinic cheilitis/squamous cell carcinoma; results were analysed qualitatively.
Results: Actinic cheilitis (low grade intraepithelial squamous cell carcinoma), and the invasive front of superficially invasive squamous cell carcinoma and in situ squamous cell carcinoma were negative for claudins −1, −3 and −7. Claudin −5 was present on all epithelial layers in most cases evaluated. Claudin −11 was present in all epithelial layers in actinic cheilitis, but negative in cases of superficially invasive and deeply invasive squamous cell carcinoma.
Conclusion: Altered expression of claudins is present in AC from its incipient phase throughout the progression of the disease to invasive squamous cell carcinoma.

PS-09-048
Fibrous dysplasia vs ossifying fibroma of the jaw: Immunological characterization performing osteoprotegerin, RANK and RANKL proteins
N. Lascane*, C. M. Coutinho-Camillo, A. d. Moraes Carvalho, F. A. Soares, S. V. Lourenço
*University of São Paulo, Dept. of Oral Pathology, Brazil

Objective: Fibrous dysplasia of the jaws and ossifying fibroma are maxillofacial fibro-osseous lesions that should be distinguished from each other as they show distinct patterns of disease progression. However, both lesions often show similar histological and radiological features, making distinction between the two a diagnostic challenge.
Method: In this study, we performed immunological analyses of 16 ossifying fibromas and 16 cases of gnathic fibrous dysplasia with typical histological aspects. We examined the difference between fibrous dysplasia and ossifying fibroma in the expression of the OPG/RANK/RANKL markers. This cascade is a final mediator of osteoclastogenesis as well as osteoclastic development demands specific factors produced by preosteoblastic/stromal cells.
Results: Osteocytes, osteoblasts and osteoclasts showed similar expression patterns for all markers tested. Immunoreactivity for RANKL and OPG was positive in 75 % and 81,25 % of the osteoblasts, respectively in the cases of FD, however RANK was expressed in the giant cells (osteoclasts) in all cases they were present (50 %). The OFs expressed RANKL in 56,25 % and OPG in 87,5 % of the osteoblasts and RANK in 56,25 % of the cases in osteoclasts.
Conclusion: These findings suggest a mild suppression of the osteoclastogenesis in both lesions, mostly in OFs, although RANKL was expressed in the majority of the cases.

PS-09-049
Unusual tumours of the mandible? Think of metastases!
K. Lawes*, M. Danford, S. Di Palma
*Leicester Royal Infirmary, United Kingdom

Objective: Metastases to the jaw bones are uncommon and are most likely to arise from primary lung, breast, prostate or kidney tumours. Jaw bone metastases from a primary oesophageal carcinoma are especially rare, with only seven reports published in the literature.
Method: Here, we describe the case of a 69 year-old male patient where 7 years elapsed between the

diagnosis and successful treatment of a poorly differentiated, stage pT2N0 primary oesophageal adenocarcinoma and re-presentation with jaw pain due to a metastatic mandibular deposit.
Results: The morphological appearance of the metastasis and immunohistochemical positivity with CK20, CK7 and CDX2 strongly supported an adenocarcinoma of upper gastrointestinal tract origin.
Conclusion: This case is of particular interest as there is an unusually long time between the detection of the primary oesophageal adenocarcinoma and diagnosis of metastatic disease. The longest period of time we have found for this reported in the literature is 9 months, although it is known that some oral metastases may appear more than 10 years following the primary tumour diagnosis.

PS-09-050
Melanotic oncocytic metaplasia of the nasopharynx - A report of three cases and review of the literature
J. S. Lee*, J. Y. Na
*Chonnam National University, Hwasun Hospital, Pathology, Jeollanam-Do, Republic of Korea

Objective: Melanotic oncocytic metaplasia of the nasopharynx is a rare condition which is characterized by the presence of usually a small, brown to black colored pigmented lesion around the Eustachian tube opening. Although it is a benign lesion, it may be clinically misdiagnosed as malignant melanoma. Microscopically, melanotic oncocytic metaplasia is a combination of oncocytic metaplasia of the epithelium of the gland and melanin pigmentation in its cytoplasm.
Method: In our present study, we report three cases of melanotic oncocytic metaplasia of the nasopharynx.
Results: All the three cases occurred in men and were presented as multiple black pigmented lesions around the torus tubarius. Microscopically, mucous glands with diffuse oncocytic metaplasia and numerous black pigments were observed. No cellular atypia was observed. Immunohistochemically, the scattering of S-100 protein-positive, and HMB-45-negative dendritic melanocytes was evident.
Conclusion: This is the first report of cases of oncocytic metaplasia of the nasopharynx in Korea.

PS-09-051
Hemangioma in a lymph node: A case report
R. Limani*, L. Kondirolli, B. Blakaj, L. Gashi Luci
*Inst. of Pathology, Faculty of Medicine, Pristina, Republic of Kosovo

Objective: Hemangioma is a benign vascular tumor that is extremely rare in lymph nodes. Up to date, only 21 cases of lymph node hemangioma, including ours, have been reported in the literature. We report a case of a hemangioma arising in a cervical lymph node.
Results: A 42-year-old man, presented with a palpable right-sided submandibular mass. He had no significant prior medical history, or any other complaints. The ultrasound of the neck revealed a 4.8×2.7 cm hypervascular, hyperechogenic cervical node, at the level of the right common carotid artery bifurcation. It was recommended for surgical resection. On gross examination, it appeared as a well circumscribed, firm and whitish, node, with small punctuate hemorrhagic foci. Whereas, histopathological examination revealed a dense proliferation of small capillary-sized blood vessels with elastic change, that almost entirely had replaced the lymph node parenchyma. Intercapillary stroma was scant. Immunohistochemically, it was immunoreactive for CD34, confirming the diagnosis of a primary capillary hemangioma of the lymph node. There was no indication of malignancy. Fifteen months after surgery, no recurrence was seen.
Conclusion: Despite its rare occurrence lymph node hemangioma should be considered in the differential diagnosis of malignant vascular tumors. Surgical resection is curative in primary nodal hemangioma.

PS-09-052
Adhesion molecules in primary oral mucosal melanoma: Study of integrins, claudins and immunoglobulins in a series of 35 cases
S. Lourenco*, S. Bologna, C. Coutinho-Camillo, J. Fernandes, M. Sangueza, F. Soares, M. Menta
*Universidade de São Paulo, Dept. of General Pathology, Sao Paulo, Brazil

Objective: Primary oral mucosal melanoma is a rare and aggressive tumor. Recent studies have reported a correlation between increased tumor invasion and metastatic phenotype with an altered expression of adhesion molecules profiles. The present study analyzed the expression of integrins, claudins and immunoglobulins in oral mucosal melanomas and correlated results with clinical features of patients.
Method: Immunohistochemistry against these molecules was performed in thirty-five cases of primary oral mucosal melanomas organized into “tissue microarray” and the results were related to clinical and histological features of patients.
Results: Some subunits of integrins presented downregulation and this was associated with vascular invasion. Increased expression of integrin beta3 and immunoglobulin CD166 (ALCAM) was statistically associated with cases with extensive vascular invasion ($p<0,05$). Lower

expression of the immunoglobulin CD54 (ICAM) was associated with cases with extensive necrosis. Most cases with metastasis were negative for immunoglobulin CD66 (CEACAM). Several subunits of claudins showed down-regulation in the cases analyzed, and, although not statistically significant, it showed to be partially related with histological factors of poor prognosis.
Conclusion: Altered patterns of adhesion molecules, mainly integrins and immunoglobulin seem to participate in the pathogenesis and outcome of oral mucosal melanomas.

PS-09-053

A rare carcinoma of minor salivary gland

I. M´Sakni*, A. Chaabane, F. Bougrine, B. Laabidi, A. Bouziani
*Rades Meliane, Tunisia

Objective: Clear cell tumor is an uncommon subgroup of salivary neoplasia, and case with predominantly myoepithelial differentiation is extremely rare. It is important to recognize the clinicopathologic features of this unusual tumor, because of its histological similarity to several other primary and metastatic clear cell tumors and its aggressive behavior.
Method: We report a case of minor salivary gland clear cell myoepithelial carcinoma of the retromolar region.
Results: A 49-year-old man, presented with recent fall of left mandibular molars Computed tomography scan identified an osteolytic expansile mass of the horizontal branch of the mandible with definite margins. The patient underwent mass resection. Grossly, the tumor mass, measuring 4 cm on its greater diameter, was indurated, multilobulated, and whitish gray. Microscopically, the tumor was arranged in nests, trabeculae, and cords. Tumoral cells had abundant eosinophilic or clear cytoplasm, focally accompanied by spindle cells and plasmacytoid cells. Immunohistochemically, the tumor cells were positive for S100, cytokeratin (KL1) and Smooth Muscle Actin (SMA) while negative for CD10 and vimentin.
Conclusion: Clear cell myoepithelial carcinoma is an extremely rare tumor. Due to the rarity of this tumor and its histologic similarity to other neoplasms, resulted in difficult diagnosis, treatment, and prognosis estimation.

PS-09-054

Mixed Adenoneuroendocrine Carcinoma (MANEC) of the nasal cavity: Clinico-pathologic and molecular study of a case

A. Marando*, S. La Rosa, D. Furlan, M. Frattini, N. Sahnane, M. Turri-Zanoni, P. Castelnuovo, C. Capella
*University of Insubria, Dept. of Surgical, Varese, Italy

Objective: Mixed adenoneuroendocrine carcinomas (MANEC) of the nasal cavity are extremely rare and their molecular alterations are largely unknown.
Method: We describe the clinico-pathologic features, methylation profile, chromosomal gains and losses, and mutation analysis of KRAS, BRAF and p53 in such neoplasm.
Results: The tumor was composed of an intestinal-type adenocarcinoma (ITAC) and of a poorly differentiated neuroendocrine carcinoma (NEC) positive for CK20, CDX2, p53, serotonin and glicentin, and CK7 negative. Gains and losses were found at 17p13 (TP53), 14q24 (MLH3), 19q13 (KLK3), 5q21 (APC), 7q21 (CDK6), 9q34 (DAPK1), 12q13 (TNFRSF 1A, CDKN1B), 13q12 (BRCA2), 17p13.3 (HIC1), 18q21 (BCL2), and 22q12 (TIMP3). Aberrant methylation of APC and DAPK1 genes was detected only in the NEC component. No mutation of KRAS, BRAF, and p53 was found.
Conclusion: The genetic relationship between ITAC and NEC component supports the hypothesis of a monoclonal origin of the tumor from a pluripotent cell that undergoes a biphenotypic differentiation after carcinogenesis is initiated, as already proposed for MANEC of other sites. In agreement with previous molecular studies, the NEC component showed a more complex genetic profile, suggesting that the neuroendocrine differentiation is from an exocrine to an endocrine pathway.

PS-09-055

A rare case of solitary oral angiokeratoma in an adult

S. Mavropoulou*, Z. Tatsiou, S. Tsiligiris
*General Hospital, Laboratory of Pathology, Xanthi, Greece

Objective: Angiokeratoma is a rare cutaneous lesion. Mucosal involvement is occasionally found as part of a more generalized cutaneous disease. Isolated angiokeratoma in the oral mucosa is extremely rare with only a few cases reported thus far.
Method: We report the case of a 61-year-old female presented with a painless lesion on the left bucal mucosa, of 4 months duration. On clinical examination, a solitary purple lesion of approximately 4 mm in diameter was found.
Results: The lesion was excised and the histological examination revealed a tumour involving lamina propria, composed of large dilated vascular spaces, lined by normal appearing endothelium and filled with blood or with fibrin thrombi. The overlying epithelium showed variable degree of acanthosis and hyperkeratosis. Accordingly the diagnosis of angiokeratoma was made. On clinico-laboratory examination no angiokeratomas were found anywhere on the skin as well as no other malformation or metabolic disorder. The patient received no further treatment and 2 years later remains disease free.

Conclusion: In conclusion we report a case of a solitary angiokeratoma of the oral mucosa. Although rare, it should be included in the differential diagnosis when evaluating any lesion in this location and further investigations should be performed to rule out a metabolic or systemic disease.

PS-09-056

Primary nasal meningioma: A case report

S. Mocan*, B. Torok, M. Doina, F. Constantin
*Emergency County Hospital, Dept. of Pathology, Tirgu Mures, Romania

Objective: Primary extracranial meningiomas are rare neoplasms, frequently misdiagnosed, resulting in inappropriate clinical management.
Method: We present a case of 37 years old man, admitted to our hospital with complaint of nasal obstruction and nasal discharge that had arisen 1 year earlier. Rinoscopic examination revealed soft mass in right nasal cavity between the septum and the turbinates. After the computed tomography evaluation the patient underwent a nasal endoscopic surgery.
Results: The nasal lesion was composed of lobules and whorls of neoplastic epithelioid cells with indistinct borders. The nuclei were round and oval, with occasional pseudoinclusions. Psammoma bodies were identified. Immunohistochemical stains showed strong and diffuse positivity for EMA and Vimentin. Isolated tumor cells showed nuclear labelling with ki-67. The patient had a good transoperative and postoperative course. After 6 month of follow-up, the patient is asymptomatic, with normal nasal endoscopic examination and no sign of recurrence.
Conclusion: Primary ectopic meningiomas involving the nasal cavity and paranasal sinuses should be distinguished from the extracranial extension of an intracranial meningioma. This tumors require separation from other types, by both histologic and immunohistochemistry studies, because they behave as slow growing neoplasms with a good prognosis, with longest survival associated with younger age and complete resection.

PS-09-057

MicroRNA miR-203 and protein p63 in verrucous and conventional squamous cell carcinoma of the head and neck

K. Odar*, E. Boštjancic, D. Glavac, N. Gale, N. Zidar
*UKC Ljubljana, Ginekološka Klinika, Slovenia

Objective: Verrucous carcinoma (VC) is a variant of well differentiated squamous cell carcinoma (SCC). In contrast to conventional SCC, VC doesn't metastasize. Foci of SCC in VC (hybrid carcinoma) harbour metastatic potential and must be properly recognised pathohistologically. Molecular basis of morphological and clinical differences between VC and SCC is poorly understood.
Method: We compared the expression of miR-203 and protein p63 between VC and SCC, by using real-time polymerase chain reaction and immunohistochemistry. 30 cases of VC, 10 cases of hybrid carcinoma, 30 cases of well/moderately differentiated and 20 cases of poorly differentiated SCC of the head and neck were included. Control group consisted of 30 samples of normal squamous epithelium of similar localisation.
Results: In comparison to normal epithelium, miR-203 was upregulated in VC, but downregulated in poorly differentiated SCC. p63 was downregulated in VC, but upregulated in SCC. Differential expression of miR-203 in VC and SCC correlated inversely with expression of p63. Immunostaining against p63 labeled foci of SCC in VC.
Conclusion: Differential expression of miR-203 and its target p63 between VC and SCC could be associated with morphological and clinical differences between these tumours. p63 could be used as marker for pathohistological detection of hybrid carcinomas.

PS-09-058

Osteochondrolipoma of the lip: Case report

G. Orgun Sonmez*, U. Bayol, E. Usturali Keskin, I. Gokcol Erdogan, O. Ugur
*Tepecik Research and Training Hospital, Izmir, Turkey

Objective: Lipomas are common, benign, slow-growing, soft tissue neoplasms of mature adipocytes. They are uncommon in the oral region. The incidence of oral lipomas is thought to be 1 % to 4 % of all benign oral lesions and lips are the last affected region of oral cavity. Lipomas with osseous, cartilaginous metaplasia are rare histological variants and these lesions have been called chondrolipoma, osteolipoma, lipoma with chondroid and osseous metaplasia, lipoma with cartilaginous, osseous change and ossifying lipoma. In this article we report a case with a osteochondrolipoma of lower lip.
Method: Case: 60-years old male patient admitted to hospital because of swelling of his lip. Physical examination detected a tumoral mass in lower lip. The tumor was excised totally.
Results: Macroscopically there was a well circumscribed nodular tumor below the oral mucosa, it was yellow-white in color and 1,5 cm in greatest diameter. Microscopically the tumor was composed of mature adipocytes and chondrocytes. There were mature osseous tissue in focal areas. The lesion had a pushing pattern of growth and therefore had a pseudocapsule. With these features our diagnosis was osteochondrolipoma of the lip.
Conclusion: We present this case due to its unusual localisation and to remind this rare entity.

PS-09-059

A middle ear adenoma

H. E. Ozcan*, F. Bora, A. Ozbey, M. Duymus, N. Eryegen
*Kafkas University, Dept. of Pathology, Kars, Turkey

Objective: 56 year-old female patient with pain, tinnitus and hearing loss complaints is diagnosed to have a hearing loss of 73–23 dB in her left ear and left tympanic membrane was intact but abnormally thicker.
Method: Temporal CT (64 sliced) showed soft tissue densities in left external ear and mastoid antrum and tympanic cavity enclosed with ossicules. Tympanic membrane couldn't be discriminated from the soft tissue densities.
Results: Histopathologically in macroscopy, the cystic lesion was determined as a small part of tissue in white –grey color, in sizes of 0,6×0,5×0,3 cm. In microscopic evaluation, the epithelial tumor cells were formed mostly tubular, partially in solid form and broadly making pseudopapillary pattern in stromal tissue. In the luminal structures formed by tumor cells, there has been mucin as dark basophilic stained with PAS/Alcian blue (PH: 2, 5). The tumor cells are strong and have common positivity with CK7, and have negativities with CK20 (B-SA method). In the focal area that the tumor cells got the solid pattern, synaptophysin and chromogranin to evaluate the neuroendocrine differentiation wasn't determined.
Conclusion: The lesion in the medial part of the tympanic membrane of the patient was reported as colesteatom and the lesion in the middle ear was reported as middle ear adenoma.

PS-09-060

Histopathologic evaluation for Helicobacter Pylori as a possible etiopathogenic factor in chronic tonsillitis

E. Özgün*, D. Altinel, A. Albayrak, A. Tan, S. Sayhan, N. Bozlak
*Nevehir Devlet Hastanesi, Dept. of Pathology, Turkey

Objective: Helicobacter Pylori is the major gastric pathogen which has an important role in the etiopathogenesis of chronic gastritis. We investigated the presence of Helicobacter Pylori as an extragastric reservoir in the tonsillectomy specimens to display if it is an etiologic factor in the development of chronic tonsillitis.
Method: In the current study, 100 cases with chronic tonsilitis were examined in bilateral tonsillectomy specimens. The colonization of the microorganism have been evaluated with Hemotoxylin-eosin and Giemsa stains under the the light microscope.
Results: Helicobacter Pylori has been detected in 33 cases (33 %) on one side of the bilateral tonsillectomy specimens while it has been seen in 15 cases (15 %) on both sides which demonstrated positivity in 48 cases (48 %) in total. No colonization has been observed in the remaining 52 cases (52 %).
Conclusion: Due to the considerable positivity in our study, the histopathologic evaluation of tonsillary Helicobacter Pylori colonization may be instrumental in the etiologic association with chronic tonsillitis.

PS-09-061

Inverted papilloma with squamous cell carcinoma

T. Ozgur*, S. Toprak, E. Atik, H. Gokce, S. Okuyucu
*Mustafa Kemal University, Medical Faculty, Antakya, Turkey

Objective: Inverted papillomas are benign sinonasal lesions that have tendency to recur and associated with squamous cell carcinoma in approximately 5 % of patients. We present a 80 year old male patient with clinic, radiologic and pathologic findings to remind coexistance of inverted papilloma and squamous cell carcinoma in the same case.
Method: 80 year old male patient referred to our hospital Otolaryngology outpatient clinic with difficulty in breathing and persistant mass in his nose. A vegetative polypoid mass in his right nasal cavity that extended to nasopharynx has been determined in anterior rhinoscopy and computer tomography scan. The mass has been excised by endoscopic surgery and sent to pathology laboratory for examination.
Results: Grossly the polypoid mass was in 40 cc volume, grey white and easily dispersible. Histologically, there has been polipoid structures that have edematous and inflammatory stroma surrounded with squamous epithelium. We have determined carcinoma insitu and invazive focuses in the epithelium.
Conclusion: The etiology of inverted papillomas is unclear. Malignant transformation has been observed in less than 7 % of cases. Total excision is the preffered therapotic approach but recurrence rates are not uncommon.

PS-09-062

Anaplastic Large T cell lymphoma, ALK negative presented with tonsillar hypertrophy and systemic lymphadenopathy with granulomatous infiltrate

A. Padron*, G. Tapia, M. Fantova, O. Garcia, R. Muns, J. F. Casamitjana, J. Chamizo, C. Admella
*Hospital de Mataro, Dept. of Pathology, Spain

Objective: Tonsils are uncommonly affected by granulomatous inflammation, been systemic disease and infections more frequent causes than neoplasms. Regarding tonsillar lymphomas the vast majority are of B-cell origin and with intermediate to high-grade histology.

Method: We present a case of a 64 year old caucasian male, with obstructive sleep apnea syndrome, odynophagia and cervical lymphadenopathy. The physical examination showed severe right tonsillar hypertrophy and the scanners revealed generalized lymphadenopathy.
Results: The histological features of the tonsil and cervical lymph node specimens were similar, both presented a pleomorphic lymphoid infiltrate surrounded by abundant epithelioid histiocytes forming non-necrotizing granulomas. Granulomatous infection diseases were dismissed. The neoplastics cells were positive for T cell markers, MUM-1 and CD30, and negative for ALK1. The proliferative index Ki67 was 60 % of the tumor cells. The molecular study showed T-cell clonal population The morphologic and immunophenotypic features, together with the molecular results were consistent with anaplastic T cell lymphoma ALK-negative.
Conclusion: The morphology and immunophenotype features, with the molecular study report support the diagnostic of anaplastic T cell lymphoma ALK- negative, with Lennert pattern. This case illustrate how a granulomatous infiltrate can mask a lymphoproliferative disorder, mostly of T-cell type, although a careful study of the biopsy allow a correct diagnosis.

PS-09-063
Salivary duct carcinoma, oncocytic variant: Case report
E. E. Pala*, U. Bayol, O. Akman, S. Cumurcu, I. Erdogan, U. Kucuk
*Tepecik Training and Research Hospital, Izmir, Turkey

Objective: Salivary duct carcinoma (SDC) is a rare, aggressive malignancy with poor prognosis. Its histomorphology is distinctly reminiscent of the ductal carcinoma of the breast.
Method: A 48-year-old man was admitted with a mass of the right preauricular area. The mass had been enlarging steadily for the past 7 months. Computed tomography (CT) of the neck revealed 4×3×3 cm contrast enhancing solid mass with irregular borders at the right parotid region. Thorax CT, abdominal and thyroid ultrasonography were unremarkable. As the aspiration cytology was malignant right parotidectomy and right cervical lymphadenectomy was performed.
Results: Histopathological examination showed a mixture of ducts, nests and cords of cells often embedded in a desmoplastic stroma with comedonecrosis of some ductal structures. The tumor cells were polygonal with vesicular nuclei, prominent nucleoli and eosinophilic, oncocytic cytoplasm. The tumor margins were lobulated and irregular with perineural invasion. Mucin stains were negative. We noted high proliferative index and cerbB2 overexpression. The tumor was classified as a salivary duct carcinoma, oncocytic variant of parotid gland. The resection margins were negative and the lymph nodes were reactive.
Conclusion: As high proliferative index and cerbB2 overexpression are predictive factors, close clinical follow up is recommended for the risk of local recurrences and metastasis.

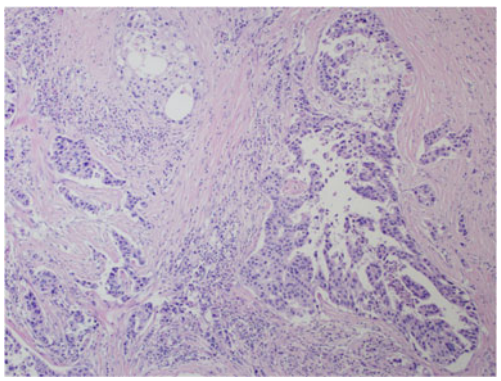

PS-09-064
Immunohistochemical expression of Bcl-2 and Ki-67 in oral lichen planus and leukoplakia with different degrees of dysplasia
F. Pigatti*, L. A. de Assis Taveira, C. T. Soares
*University of São Paulo, Oral Pathology, Brazil

Objective: The oral lichen planus (OLP) is a chronic inflammatory disease of unknown cause, and its malignant potential is a very controversial issue. Therefore, the aim was to evaluate the immunohistochemical expression of apoptosis-related proteins and cell proliferation in OLP and epithelial dysplasia in order to investigate changes related to carcinogenesis and emphasize the importance of long-term follow-up of patients with OLP.
Method: For this purpose, we selected 14 samples of OLP, 14 samples of leukoplakia with epithelial dysplasia, and 09 samples of normal oral mucosa as controls. The evaluation of the expression of Bcl-2 and Ki-67 was conducted in accordance with the immunoperoxidase technique.
Results: There was also a high expression of Blc-2 protein in inflammatory cells in OLP lesions and leukoplakia with epithelial dysplasia. The expression of Ki-67 marker was higher in all analyzed tissue levels in the lesions of OLP and leukoplakia with epithelial dysplasia when compared with the control group.

Conclusion: The highest expression of proteins Bcl-2 and Ki-67 in cases of OLP and leukoplakia with epithelial dysplasia may reveal the possible presence of molecular alterations morphologically imperceptible.

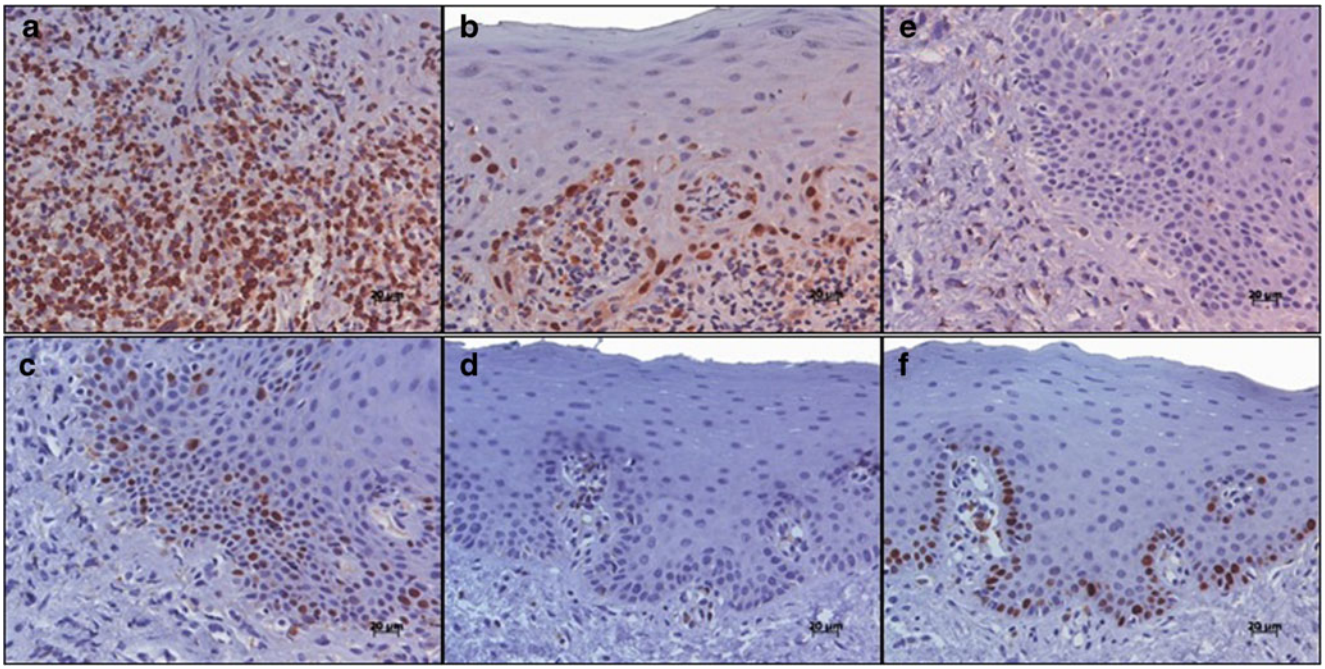

PS-09-065

Evaluation of benign and malignant tumors of the oral cavity using DNA flowcytometric analysis

A. Raafat*, H. Attia, M. Mekki
*National Cancer Institute, Pathology Dept., Cairo, Egypt

Objective: Biologic behaviour of benign and malignant tumors of the oral cavity is influenced by many factors. Proliferative activity of the tumor is one of these factors, serving to estimate prognosis and design of treatment. Flowcytometric analysis allows quantitative estimation of DNA content and measurement of cells in the S phase fraction (SPF) representing the proliferative potential of the tumor.

Method: DNA content and S-phase fraction (SPF) of oral tumors from Egyptian patients were measured by flowcytometry and related to clinicopathologic parameters.

Results: Thirty percent of malignant cases were diploid and 70 % were aneuploid. Sixty-six point seven percent of diploid cases showed low SPF and 33.3 % showed high SPF. Only 16.7 % of aneuploid cases showed low SPF, and 83.3 % showed high SPF. All benign cases were diploid with a low SPF with a statistically significant difference from malignant cases ($p<0.001$). There was a directly proportionate relationship between flow cytometric parameters and histopathologic grade. SPF correlated significantly to the presence of lymph node metastasis ($p=0.03$).

Conclusion: DNA ploidy and SPF are important prognostic factors in tumors of the oral cavity and maxillofacial region. Management decision for individual patients could make use of these parameters.

PS-09-070

DNA copy number alterations in pleomorphic adenomas and carcinoma ex-pleomorphic adenomas

B. Senguven*, E. Gultekin, A. High, C. Daly, P. Rabbitts
*Gazi University Dental Faculty, Dept. of Oral Pathology, Emek, Turkey

Objective: Pleomorphic adenoma (PA) is the most common benign salivary gland neoplasm of the major and minor salivary glands. Pleomorphic adenoma was shown sometimes to undergo malignant transformation in its natural course. Carcinoma ex pleomorphic adenoma (CPA) is a rare salivary gland malignancy that may develop from either a long-standing primary or a recurrent PA. The genetic mechanisms involved in the progression of adenoma to a carcinoma is still unclear. To identify the predictors of disease, more knowledge about their genetic profiles is necessary. This study aimed to characterize alteration in the DNA copy number of PA and CPA.

Method: We used next-generation sequencing technologies to produce genomic copy number data on three formalin-fixed paraffin-embedded CPA, three PA and one PA with carcinoma insitu areas.
Results: Aberrant chromosomal areas were detected in all tumors. The most common frequent gains in bening tumors were detected at 20p, whereas loss at 5q, 6q, and 16q. Our analysis detected DNA copy number changes in carcinomatous components of CPA, mostly gains compared to PA. The chromosomal regions including 3p, 8q and 18p, 6q abnormalities were consistently identi_ed.
Conclusion: All of the three carcinomatous components and all of the four adenomatous components showed various DNA copy number changes.

PS-09-072
Clinic-histologic aspects of twenty-five cases of minor salivary gland sialolithiasis
S. Sousa*, C. Lemos jr., F. Prosdocimi, M. T. Brazão-Silva
*University of São Paulo, Dept. of Oral Pathology, Brazil

Objective: Sialolithiasis in minor glands is rare. Presently we analyze clinical and microscopic findings as well as clinical data and also clinical diagnosis since many cases are misdiagnosed at first. Data were obtained from the Department of Oral Pathology file (2000–2011).
Method: Cases were selected among those with a final diagnosis of sialolithiasis, or others that might lead to a histological suspicion such as sialadenitis and duct ectasia. Gender, age, site, clinical diagnosis, gland and ductal alterations and aspects of sialoliths were analyzed.
Results: Twenty-five cases were retrieved. Age average was 62.5 years (26–76), mostly on 7th or 8th decades (55.0 %). Male/female ratio was 1.3:1, mostly involved upper lip (46 %) and buccal mucosa (38 %). Main clinical diagnosis were mucocele and fibroma. Clinical misdiagnosis was 88.0 %. Sialoliths were commonly superficial (66.7 %) and composed by concentric layers (70.8 %) with varied grades of mineralization. Chronic periductal and/or intraparenchymatous inflammation were frequent (64 % for each). Ducts commonly presented squamous metaplasia (58.3 %) and also ectasia, squamous and mucous metaplasia, mucous plugs and/or cellular debris.
Conclusion: In conclusion, clinical suspicion of sialolithiasis should be encouraged for upper lip and buccal mucosal lesions. Based on histomorphological diversity of sialolith and gland alterations it is possible to suppose a multifactorial cause.

PS-09-073
Expression of p27 in oral leukoplakias in smokers and nonsmokers
S. Sousa*, L. Corrêa, J. Lima
*University of São Paulo, Dept. of Oral Pathology, Brazil

Objective: Leukoplakia is an oral premalignant white lesion. Although its etiology may vary, smoking has been implicated as a possible risk factor. The p27 protein has been shown to inhibit kinases, and it is known that its expression is decreased during carcinogenesis. The reduced expression of p27 has been correlated with poor prognosis in carcinoma. In this study a role for the smoking habit in the expression of this protein was investigated.
Method: Forty cases clinically diagnosed as oral leukoplakias and that presented a mild to intense degree of epithelial dysplasia and could not be diagnosed as any other disease were selected. Twenty cases were from current smokers (more than 20 cigarettes/day for at least 1 year) and never-smokers. Thirty-six cases of leukoplakia without dysplasia were used as controls. Histological sections of each lesion were subjected to the estreptoavidin biotin immunohistochemical method for detection of p27.
Results: A semi quantitative analysis was performed and the results showed that the expression of p27 was independent of the smoking status of the patient (p=0, 5237), using Kruskal-Wallis and Mann–Whitney tests.
Conclusion: Although not statistically significant, due to the small number of cases, the results indicate that the counting of p27 in leukoplakia correlates inversely with degree of epithelial dysplasia.

PS-09-074
Low-level laser therapy may influence on the Akt/mTOR signaling pathway in oral cancer cells
F. Sperandio*, F. Giudice, L. Correa, D. Pinto jr., S. de Sousa
*University of Sao Paulo, Dept. of Oral Pathology, Brazil

Objective: Distinct cells respond differently to low-level laser therapy (LLLT), while the exact molecular mechanisms involved in cell proliferation or growth inhibition, after light stimulation remain poorly understood. Although LLLT has shown promising results in accelerating wound healing and preventing or treating oral mucositis, there is no evidence-based consensus of what this energy could cause in cancer cells. This should be highly pondered when an oral cancer patient is treated with LLLT due to oral mucositis, for example.
Method: Two tongue squamous cell carcinoma cell lines (SCC9 and SCC25) were utilized to find the effect of low-level laser irradiation on the Akt/mTOR signaling pathway. Laser irradiation (660 and 780 nm) consisted on 40 mW of power and energy densities of 2, 3 and 6 J/cm2. After a single irradiation the most significant energy densities found with MTS assay were employed to analyze Akt/mTOR signaling pathway related proteins through immunofluorescence and western blotting.
Results: Beyond modifying the growing rates of cancer cells, low-level laser irradiation was able to induce different variations in the studied pathway, however a direct correlation among the proteins was not found.

Conclusion: LLLT may act on Akt/mTOR/Cyclin D1 signaling pathway, which has a widely recognized role in head and neck cancer progression.

PS-09-076

Mucins as predictors of recurrent pleomorphic adenoma of salivary glands: An immunohistochemistry analysis of over 60 cases

T. Teshima*, R. Ianez, C. Coutinho-Camillo, S. Lourenço
*São Paulo, Brazil

Objective: Pleomorphic adenoma (PA) is the most common tumor of salivary glands and, despite its benign behavior, the recurrence after primary surgery is significant. In attempt to find a marker capable to predict the recurrence of this lesion, this study aims to analyze the expression of mucins MUC 1, 2, 4, 5 AC and 6 in 62 cases of PA, considering that mucins have been related to tumour growth of some organs.
Method: This study was performed in 62 cases in PA, which 5 of them presented recurrence after the initial surgery. All the primary tumors were histologically processed and submitted to the immunohistochemistry reaction. The antibodies for MUC 1, 2, 4, 5 AC and 6 were used and then analyzed with conventional optical microscope.
Results: MUC1 was the only mucin significantly expressed in most of all cases (88 %), being present within ductal lumen and cytoplasm. The other mucins showed a focal positivity in few cases, where MUC 2, 5 AC and 6 were cytoplasmic, while MUC4 was expressed in ductal lumen and blood vessels.
Conclusion: The most relevant expression of MUC1 could suggest a contribution of this mucin to predict the development of PA recurrences or even predict cellular dysfunctions capable to promote adenomas.

PS-09-077

CA EX pleomorphic adenoma: A clinicopathologic study of six cases

O. Tzaida*, I. Kasselaki, C. Valavanis, G. Chinari, G. Vecchini, G. Tassopoulos, P. Arapantoni-Dadioti
*Anticancer Hospital Metaxa, Peiraias, Greece

Objective: Ca ex pleomorphic adenoma (Ca ex PA) is a rare salivary neoplasm with aggressive behavior arising from a primary or recurrent pleomorphic adenoma.
Method: Six cases of Ca ex PA are presented. Three females and three men (median age of presentation 66 years) were diagnosed in our department during six last years in a total of 214 salivary neoplasms (2,8 %), comprising 10.8 % of salivary malignancies and 8.6 % of PA.
Results: Three cases were arising de novo and the rest from a PA recurring seven, twenty -seven, and thirty years after initial diagnosis. Three cases were localized to parotid and the rest to submandibular gland. Microscopically all tumors were composed of a mixture of PA and carcinoma of various type. All tumors, except one, had areas of necrosis. Four cases were encapsulated. All patients were underwent an ablative surgical procedure. Two women, both with extensively infiltrating tumors, died with recurrences and distal metastasis, within one and four years respectively, after carcinoma diagnosis, despite the application of combined radiotherapy and chemotherapy.
Conclusion: Ca ex PA, a rare salivary malignancy, occurs either as a primary involvement or as a PA late recurrence. The disease has a fatal course relating with tumor invasiveness.

PS-09-078

HPV existence, TP53 and E-Cadherin expressions and correlations between clinicopathologic variables in squamous cell carcinoma of larynx

A. Uguz*, F. Yilderim, A. Acikalin, O. Tarkan, M. Ergi
*Cukurova University, Dept. of Pathology, Adana, Turkey

Objective: In our study we purposed that to detect interactions between HPV existence and squamous cell carcinoma of larynx (SCCL), and the correlations among the clinicopathologic variables; levels of p53 and E-cadherin expressions, and surveillance.
Method: The 149 SCCL and 50 control cases are included the study. Immunohistochemically p53 and E-cadherin antibodies were performed and polyclonal HPV was analyzed with polimerase chain reaction (PCR). In positive cases, HPV types 16, 18, 31, 33 were investigated.
Results: Polyclonal HPV was detected in 149 of 9. Six cases were positive for HPV16 and one case was positive for HPV18. Remain two were negative for HPV 31 and 33. So type of these cases could not be identifiedSignificant correlations were detected between gender, survey and LN metastases and p53 and E-cadherin expressions. Also significant results were obtained between p53 positivity and grade and between E-cadherin positivity and TNM stage.
Conclusion: Contribution of HPV existence shows geographic diversities in tumorigenesis. The preoperative detection of LN metastases is crucial for patient management. LN metastases increase in tumors with high p53 positivity and low E-cadherin expressions. These features can be informative for clinicians.

PS-09-080

Gingival metastasis from prostatic adenocarcinoma: A case report and review of literature

E. Omoscharka*, K. Lankachandra
*University of Missouri, Dept. of Pathology, Kansas City, USA

Metastatic disease of the oral cavity is extremely rare. Only 1 % of oral tumors are considered to be due to metastasis. Jaw bones are affected more often than soft tissues. The

clinical presentation of metastatic lesion in the oral cavity can be deceiving and extremely challenging for the clinicians and the pathologists and can lead to misdiagnosis of either a benign process or primary tumor. Therefore, in any case of unusual clinical presentation, especially in patients with known malignancy elsewhere a diagnostic biopsy should be mandatory. We present a rare case of a 92-year-old male patient with previously diagnosed and treated prostate cancer who presented with a gingival mandibular mass and lower lip paresthesia. Only two cases of oral soft tissue metastasis from prostate have been reported in the literature.

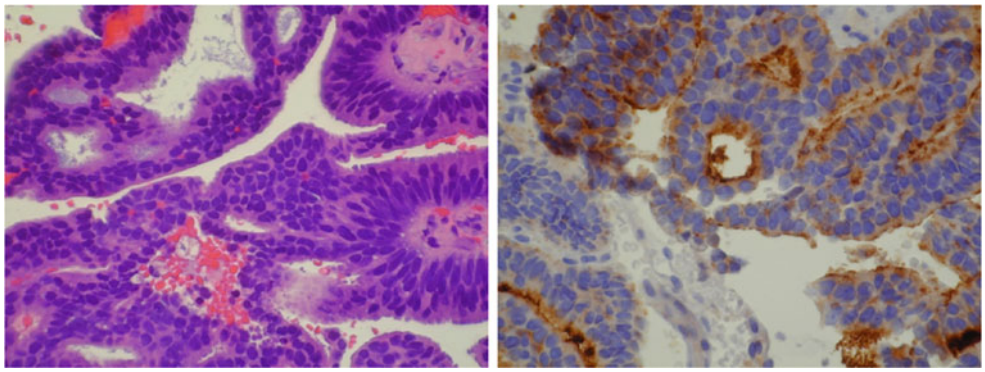

PS-09-081

Correlation between fine needle aspiration cytology and histopathology results of salivary gland masses

S. Yilmaz*, C. Altunkaya, A. Barin, S. Ekici, G. S. Yalcin, H. Ustun

*Ankara Education and Training Center, Turkey

Objective: In this study, we evaluated the diagnostic value of fine needle aspiration cytology (FNAC) in salivary gland masses retrospectively.We compared FNAC and postoperative histopathologic results of patients.

Method: Ninety-two patients (47 females, 45 males; mean age 46,6; range 15 to 78 years) having salivary gland masses who underwent FNAC and surgical treatment between January 2007 and November 2011 were included in the study. FNAC and histopathologic results were compared retrospectively. The sensitivity, specificity, positive and negative predictive values and accuracy rate of FNAC in salivary gland masses were evaluated under the light of the results.

Results: The most common benign and malignant FNAC results were pleomorphic adenoma (38 patients, %41) and mucoepidermoid carcinoma (3 patients, %3). FNAC results of six patients were nondiagnostic and this patients were excluded. According to the FNAC and histopathologic results, sensitivity has found %64, specificity %100, positive predictive value %100, negative predictive value %93 and accuracy rate of FNAC %92.

Conclusion: FNAC is a reliable method that has high specificity to distinguish between benign and malignant salivary gland lesions. Our sensitivity has found lower than expected because the samples didn't represent lesion exactly.

Monday, 10 September 2012, 09.30 - 10.30, Congress Hall Foyer 3rd Floor

PS-10 Poster Session Molecular Pathology

PS-10-001

Regulation of multidrug resistance in NSCLC by miRNAs

J. Škarda*, M. Janíková, V. Žižková

*Olomouc, Czech Republic

Objective: Drug resistance remains a major problem in the treatment of NSCLC cancer patients for both, conventional chemotherapeutic and novel biological agents. Intrinsic or acquired resistance is caused by a variety of mechanisms, including increased drug elimination, decreased drug uptake, drug inactivation and alterations of drug targets. Recent data showed that drug resistance mechanisms might also be regulated by microRNAs (miRNAs).

Method: We tested 65 lung cancer samples. The total RNA was isolated from individual specimens and then RT-PCR and pre-amplification were performed. We detected levels of miR-21, miR-23a, miR-23b, miR-126, miR-205, miR-335*, miR-3163, miR-491-3p, miR-548p, miR-548x, miR-576-5p, miR-590p, miR-655, miR-656 and miR-944 using TaqMan® MicroRNA Assays by LightCycler® 480 Real-Time PCR System. We assigned obtained results using statistical methods.

Results: Our results suggest that miR-590-5p and miR-655 are involved in apoptosis. The higher levels of miR-590-5p correlate with Bcl-2 positivity and pro-apoptotic protein BAX seems to be regulated by miR-655. The level of LRP protein responsible for drug resistance in lung cancer patients seems to be regulated by miR-255.

Conclusion: Within our cohort of NSCLC patients we did not find any correlations between the expression profiles of the abovementioned miRNAs and survival.

PS-10-004

The role of secondary mutations in the mechanisms of the drug development in the gastrointestinal stromal tumors

A. Augustinakova*, I. Hilska, M. Kalinova, L. Krskova, H. Brizova, R. Kodet

*University Hospital Motol, Dept. of Pathology and Molecular Medicin, Prague, Czech Republic

Objective: Gastrointestinal stromal tumors (GISTs) are characterized by a gain of function mutations of the KIT or PDGFRA genes. Activated KIT and PDGFRA proteins are important therapeutic targets of the therapy with imatinib mesylate (IM). Although most patients with advanced GIST benefit from IM treatment, a portion of patients develop resistance to the agent. The most common mechanism of the acquired resistance of GIST is the acquisition of secondary mutations.

Method: Mutation analysis was performed on genomic DNA extracted from formalin-fixed, paraffin-embedded or fresh frozen tumor tissues. Exons 9, 11, 13 and 17 of the KIT gene and exons 12, 14 and 18 of the PDGFRA gene were evaluated for mutation by PCR amplification and direct sequencing of the amplification products.

Results: We analyzed 95 tumor samples acquired from 82 patients treated with IM. In 11 specimens from 7 patients we detected secondary mutations. Secondary mutations were clustered in exon 13 or exon 17 of the KIT gene.

Conclusion: The acquired resistance is an important phenomenon of the targeted biological therapy failure. Molecular analysis of GISTs and detection of secondary mutations might become a clue to the design and management of second generation kinase inhibitors or alternative therapeutic strategies. Support: PCDRO (MH CZ) 00064203.

PS-10-005

Modified methacarn fixation as an excellent preservation of histology, protein immunoreactivity and RNA integrity in paraffin embedded tissue specimens

P. Babal*, R. Milcheva, P. Janega, P. Celec

*Comenius University, Dept. of Pathology, Bratislava, Slovakia

Objective: Fixation techniques preserving morphological fidelity, immunoreactivity and integrity of nucleic acids may have a high impact on both basic and applied research and diagnostic pathology.

Method: We investigated the effect of formalin, absolute ethanol and methanol; ethanol supplemented with acetic acid and modified methacarn fixative on the tissue morphology and immunoreactivity of different types of tissues and the preservation of RNA fragments of different lengths.

Results: The modified methacarn fixation provided a histomorphological quality comparable to the formalin-fixed tissue specimens. The immunoreactivity was superior in the buffered than in the untreated formalin and the preservation of protein antigenicity in normal and pathologically changed tissues tested with several antibodies was excellent with the use of alcohols with acetic acid. The acidic ethanol and the modified methacarn fixative showed the best preservation of the integrity of RNA in satisfactory quantity and quality of fragments up to 577 bp, which was reliable for relative evaluation of gene expression.

Conclusion: The presented data provide evidence that the modified methacarn fixative is an excellent alternative to formalin when tissue specimens are evaluated for tissue morphology, immunoreactivity and RNA expression profile. Supported by ITMS: 26240220052.

PS-10-006

Differential connexin expression in giant cell tumour of bone (GCTB)

P. Balla*, M. Maros, I. Teleki, M. Szendroi, Z. Sapi, L. Kopper, M. S. Benassi, P. Picci

*Semmelweis University, 1st Dept. of Pathology, Budapest, Hungary

Objective: Intercellular communication through connexin (Cx) channels is known to regulate cell homeostasis and play crucial roles in promoting signals and nutrients between osteoblasts and osteocytes. Giant cell tumour of bone (GCTB) is an aggressive osteolytic lesion, in which neoplastic stromal cells drive osteoclastogenesis. Here we tested if Cx expression correlates with GCTB progression.

Method: Tissue microarrays of 94 primary and 82 recurrent GCTB cases were immunostained for connexin isotypes and the results were scored in digital slides including image quantitation.

Results: Cx37 and Cx40 were detected only in endothelial cells and Cx23, Cx26, Cx43 and Cx46 were found primarily in mononuclear cell fraction. Double labelling revealed connexins both stromal and monocytic lineage cells. Cx23 was also seen consistently and Cx46 occasionally in giant cells. None of the Cx isotypes showed statistical preference between primary and recurrent cases, though Cx43 displayed a tendency for upregulation in recurrent cases. Concerning clinico-radiological stage, only Cx26 showed significantly elevated ($p<0.05$) expression in aggressive compared to active GCTB cases.

Conclusion: Though a wide range of connexins can be detected in GCTB, some of them have not been published in osteoblasts, stromal cells or monocytes, their expression is not statistically lined with GCTB progression/recurrence.

PS-10-007

Heterogeneity of KRAS mutational status in colorectal adenocarcinomas with a mucinous component

V. Barresi*, A. Simone, R. Scarfì, A. Ieni, G. Branca, G. Giuffrè
*University of Messina, Dept. of Human Pathology, Italy

Objective: KRAS mutations in colorectal cancer (CRC) are predictive of nonresponse to anti-epidermal growth factor receptor therapy. More than 90 % of CRCs are adenocarcinomas and some of these show mucinous areas. Only when more than 50 % of the lesion is composed of pools of extracellular mucin containing malignant epithelium the CRC is considered as a histopathological variant and it is classified as mucinous adenocarcinoma.
Method: We analyzed the mutational status of KRAS on a series of 20 formalin-fixed, paraffin-embedded, advanced CRC specimens taken from an equal number of patients. Each sample was classified as adenocarcinoma with mucinous areas (<50 %) and DNA extraction was performed by laser-microdissection with respect to the different histological types present in the same section. A reverse-hybridization-based assay was utilized in the identification of the most frequent KRAS mutations.
Results: We found a KRAS single mutations in 10/20 (50 %) patients. In particular, in 9 patients the same mutation was detected in adenocarcinomatous as well as in mucinous areas. On the contrary, in one case we found a mutation (Gly12Asp) in the adenocarcinomatous area but not in mucinous component of the same tumour.
Conclusion: Intratumoral heterogeneity of KRAS status is not frequent in adenocarcinomas with a mucinous component.

PS-10-008

cFLIP supports the maintenance of resistance to apoptosis in thymic carcinoma cell line 1889c

D. Belharazem*, P. Ströbel, J. Pfannschmidt, P. Rieker, A. Marx
*Inst. of Pathology, University of Medicine, Mannheim, Germany

Objective: cFLIP prevents the apoptosis by caspase 8 inhibition, its overexpression correlates with the progression of different tumors. Thymomas and thymic carcinomas are thymic epithelial tumors, in which the regulation of apoptosis is still unknown. We investigated the role of cFLIP in regulating the viability of thymus carcinoma cell line 1889c using an RNA Interference. The cell line HaCat was used as a control.
Method: 1889c and HaCat cell lines were transfected with an established "short Hairpin" pIRES/PURO cFLIP-shRNA expression vector. CFLIP suppression and its Effect on pro and antiapoptotic molecules were analyzed using q-PCR and western blot. Apoptosis was quantified using the flow cytometry.
Results: The 1889c-shcFlip, but not the shcFlip-HaCat, showed sensitivity to TRAIL (tumor necrosis factor-related apoptosis-inducing ligand), accompanied by an overexpression of both the pro-apoptotic protein Noxa ($p<10–4$) and the anti-apoptotic proteins BIRC2, BIRC3 and XIAP compared to the non-transfected cells ($p<10–4$).
Conclusion: cFLIP shRNA seems to induce apoptosis in the thymus carcinoma cell line. Simultaneously antiapoptotic proteins (AIPs) BIRC2, BIRC3 and XIAP were up regulated in order to protect the cell from apoptosis. Could these AIPs provide the way to escape the cell death? AIPs Selective inhibitions could represent a promising therapeutic approach for malignant thymic carcinomas.

PS-10-010

Quantitative measurement of cyclin D1 mRNA expression level helped with diagnosis in small lymphocytic lymphoma type B-CLL with aberrant protein cyclin D1 expression detected by immunohistochemistry

H. Brizova*, I. Hilska, M. Mrhalova, R. Kodet
*Charles University, 2nd Medical Faculty, Prague, Czech Republic

Objective: Cyclin D1 is a molecular marker of mantle cell lymphoma (MCL) and it may be examined by immunohistochemistry at the protein level or by PCR at the mRNA level. Despite the cyclin D1 specifity for the MCL diagnosis we discovered rare cases of small B-cell lymphocytic lymphoma of B-cell leukemia type (B-CLL/SLL) with aberrant cyclin D1 protein expression detected by immunohistochemistry.
Method: Using quantitative PCR we analyzed cyclin D1 mRNA expression level in 10 B-CLL/SLL cases with immunohistochemically positive cyclin D1 protein. Simultaneously we measured the mRNA cyclin D1 level in 289 MCLs, 67 other B-cell non-Hodgkin's lymphomas (B-NHL) and 5 reactive lymphadenopathies.
Results: The cyclin D1 mRNA level was overexpressed above the cut-off limit that we established in the MCL specimens specifically. The 10 B-CLL/SLL cases with cyclin D1 protein immunohistochemical positivity showed

the cyclin D1 mRNA level below the cut-off limit within the range of nonMCL B-NHLs and reactive lymphadenopaties.
Conclusion: A precise cyclin D1 mRNA level measurement was useful in distinguishing between the cyclin D1 overexpression that is a MCL hallmark and the aberrant expression in B-CLL/SLL, and thus helped to decrease the risk of MCL misdiagnosis in cyclin D1 immunohistochemically positive B-CLL/SLLs. Support:CZ.2.16/3.1.00/24022, 00064203.

PS-10-011

Monphasic synovial sarcoma of the pleura: A potential diagnostic challenge

C. Cacchi*, H. Jähnig, S. Raab, C. Aulmann, C. Haas, H. M. Arnholdt, B. Märkl
*Klinikum Augsburg, Abt. für Pathologie, Germany

Objective: Synovial sarcoma is a very unusual malignancy that often affects the extremities in proximity of large joints. The diagnosis of this tumour in pleura may be a challenge due to the broad spectrum of differential diagnosis.
Method: Pleural biopsy of a 35 years old female patient was performed in chest-surgery department because a relapsing pleural effusion, there is no history of trauma or asbestos exposition. Formalin fixed paraffin embedded blocks were stained with routine Haematoxylin and Eosin and two representative blocks were selected for immunohistochemistry and real-time PCR (RT-PCR).
Results: The tumour is composed of monotonous spindle cells with a high mitotic activity (18 M/10 HPF). There are neither necrosis nor epitheliod areas. The tumour stained with bcl-2 and vimentin, with only focally reaction for Epithelial Membran Antigen (EMA) and for CD99. There was no reaction for WT-1, Calretinin, Pan-Cytokeratin CD 34, desmin, smooth muscle actin and S-100. RT-PCR showed a distinct 98 bp product of the translocation t (X;18).
Conclusion: Synovial sarcoma of the pleura is very rare, with to our best knowledge only 35 cases reported in the literature. A multidisciplinary approach, based on clinical, pathological and molecular information is crucial for a correct diagnosis and therapy.

PS-10-012

Nuclear and cytoplasmic expression of nucleolin depends on accurate validity

L. Carvalho*, A. Alarcão, A. F. Ladeirinha, M. J. D'Aguiar, T. Ferreira, V. Moura, M. Lacerda, P. Figueiredo, S. Simões, J. N. Moreira
*Amadora, Portugal

Objective: Nucleolin is a multifunctional DNA-, RNA- and protein-binding protein, involved in fundamental aspects of transcription, cell proliferation and growth. It is located in the nuclei/nucleolus, cytoplasm and on the cell surface. The present study aimed at optimizing the histological identification of nucleolin.
Method: Mamary invasive ductal carcinoma 3 μm paraffin sections were pretreatead with pronase at room temperature (5–10 min) to epitope exposure. Biotinilated peptide against nucleolin was applied (1/1.5 mM dilutions), incubated at room temperature for 30 min/overnight at 4 °C; after phosphate-buffered saline, peptide binding was identified by peroxidase-conjugated streptavidin and 3,3-diaminobenzidine tetrahydrochloride applied according to manufacturer's instructions before haematoxylin counterstaining.
Results: Pretreatment for 5 min at 1.5 mM of biotinilated peptide showed only nuclear expression, as 1 mM/10 min pretreatment with overnight peptide incubation; positive cytoplasmic expression was obtained also after 30 min incubation/room temperature. At 1.5 mM concentration for 10 min epitope retrieval, cytoplasmic and nuclear positivity raised over 75 % expression, independently of peptide exposure (overnight/room temperature).
Conclusion: For optimizing peptides/antibodies, we have to be aware that nuclear/cytoplasmic expressions depend on digestion and peptide concentration. Histological morphology is also important and discordant results may be erroneously obtained.

PS-10-013

KRAS testing in clinical laboratory: Optimizing targeted therapy

L. Cheng*, L. Miravalle
*Indiana University, Dept. of Pathology, Indianapolis, USA

Objective: Activating mutations in the KRAS gene are found in more than 30 % of colorectal tumors, where they are associated with a poor response to anti-epidermal growth factor receptor therapies. Mutation testing techniques have therefore become an urgent concern. Several methods for KRAS mutation detection have been described in the literature. Most of these are laboratory developed tests and only a few commercial assays are currently available.
Method: We studied the performance characteristics of a KRAS mutation detection assay on the ABI-3130XL genetic analyzer using a new commercial mutation detection kit. Samples were analyzed in parallel by different reference laboratories using alternative methodologies. Various sample types were used including formalin-fixed paraffin-embedded tissue, fine-needle aspirates, and cyst fluid specimens.
Results: A high level of agreement (100 % correlation for formalin-fixed paraffin-embedded tissue and fine-

needle aspirate samples and 93 % correlation for cyst fluid specimens) was obtained despite the use of different methodologies.
Conclusion: Shift termination assay is a simple, robust, and sensitive method for the identification of KRAS mutations in wide variety of specimen types.

PS-10-014
DNMT over-expression based on microRNA modulation in HIV-related aggressive B-cell lymphomas
G. De Falco*, A. Luzzi, F. Morettini, A. Onnis, S. Mannucci, E. Rogena, C. Bellan, W. Mwanda, L. Leoncini
*University of Siena, Dept. Human Pathology and Oncology, Italy

Objective: Immune activation of B-cells contributes to the increased frequency of B-cell malignancies observed in HIV-infected individuals. The Tat protein may participate in B-cell abnormalities as it may be released by infected cells. Tat increases the expression of specific cellular genes, as IL6, which may upregulate the expression of DNA methyltransferase 1 (DNMT1), which epigenetically regulates gene expression. Dyregulation of DNMTs results in abnormal patterns of DNA methylation, which is frequent in cancer. HIV is reported to upregulate DNMT1 expression. We have analyzed the expression of DNMTs and their regulatory microRNAs in HIV-positive tumors and in Tat-transfected cell lines.
Method: HIV-positive and HIV-negative DLBCL and BL were tested for their expression of DNMTs by qRT-PCR and IHC. The expression of specific microRNAs was then investigated. The in vivo results were further confirmed in Tat-transfected human cell lines.
Results: DNMTs were found upregulated both in HIV-positive primary tumors and in Tat-transfected cell lines. In accordance, the expression of specific microRNAs was found downregulated. Up-regulation of DNMTs resulted in the aberrant methylation of genes, as INK4/p16, and microRNAs.
Conclusion: Dysregulation of DNA methyltransferases may result in the aberrant methylation of important tumor suppressor and cell cycle regulatory genes, eventually initiating neoplastic growth.

PS-10-015
EBV-Bart-6-3p induces cell proliferation and escape of immunosurveillance in BL cell lines and primary tumours
G. De Falco*, M. Navari, A. Onnis, L. Di Lisio, N. Martinez, E. A. Leon, S. Montes-Moreno, E. Rogena, C. Bellan, M. A. Piris, L. Leoncini
*University of Siena, Dept. Human Pathology and Oncology, Italy

Objective: Burkitt Lymphoma is an aggressive B-cell lymphoma presenting in three clinical forms: endemic, sporadic and immunodeficiency-associated. More than 90 % of eBL carry latent EBV, whereas only 20 % of sBL are associated with EBV. Recent data suggests a microRNA dysregulation in sBL and eBL cases. Furthermore, EBV itself encodes viral miRNAs, which may partecipate in BL pathogenesis. We profiled human and viral miRNA expression in eBL and sBL cases.
Method: Fresh tissues of eighteen BLs (six EBV-pos and twelve EBV-neg) were used for this study. For miRNA profiling Agilent® microRNA expression microarray technology was used.
Results: Comparison between EBV-pos and EBV-neg BL revealed that a few cellular miRNAs are differentially expressed. The profiling identified viral miRNAs expressed in EBV-pos BL cases. Target genes of differentially expressed miRNAs were searched, which were then classified in functional categories, according to the Gene Ontology. In particular, the role of EBV-BART6-3p was evaluated. Among others, Bart6-dependent dysregulation of PTEN and IL6 receptor was observed.
Conclusion: PTEN downregulation results in enhanced cell proliferation whereas gp130 downregulation determines escape of immunosurveillance. Viral miRNAs are of particular interest, as they may affect the expression of cellular genes which may represent targets for tailored therapies.

PS-10-016
Expression of MicroRNAs in pediatrics astrocytomas paraffin embedded
P. Eguía Aguilar*, M. Peréz Peña Diaz Conti, E. Benadón Darszon, F. Chico Ponce de León, S. Sadowinski Pine, F. Arenas Huertero
*Hospital Infantil de México, Dept. of Pathology, México City, Mexico

Objective: MicroRNAs (miRs) are small RNAs that modulate protein expression via post-transcriptional regulation of mRNA. They are related to malignancy in several tumors. Deregulation of miRs expression has been described in high grade astrocytomas of adult patients, however there is scarce information in pediatric patients. In this work we quantified the expression profiles of miRs in pediatrics astrocytomas.
Method: Total RNA was extracted from 59 astrocytomas and 8 normal brain (NB) tissues, formalin fixed paraffin embedded. The expression levels of miR-124, miR-128-1 and miR-221 were quantified by using miRNA-specific TaqMan miRNA assays.
Results: The miR-128-1 was more abundant in NB against to miR-124 and -221 ($p<0.05$). MiR-124 and

miR-128-1 were significantly down-regulated in all grades compared to NB ($p<0.05$) but in grade IV was more decreased: 8000- and 1200-fold, respectively. In patients with recurrent tumor, the expression of miR-221 was lower ($p<0.002$). Live patients expressed high levels of miR-128 ($p<0.02$) and miR-221 ($p<0.0026$) against deceased.

Conclusion: MicroRNAs are differentially expressed between astrocytomas and NB. The low expression of miR-128 and -221 could be a potential marker in recurrent pediatric astrocytomas, and both are associated to less survival. Embedded tissue is useful to describe and evaluate expression of molecular markers of malignancy.

PS-10-017

Gene protein detection platform: An automated technique of combined immunohistochemistry and Brightfield double in situ hybridization in the Context of HER2 protein, gene and chromosome 17-centromere evaluations for breast cancer

P. Farrajota*, A. Olsson, G. Elmberger

*Centro Hospitalar do Porto, Dipt. do Anatomia Patologica, Portugal

Objective: Human epidermal growth factor receptor 2 (HER2) immunohistochemistry (IHC) and fluorescence in situ hybridization (FISH) are semiquantitative assays for selecting breast and gastric cancer patients for HER2 antibody therapy. However, current procedures are labor intensive, require skilled technologists and pathologists trained in FISH, and FISH slides cannot be stored and reviewed. Our aim was to test a recent automated technique of combined IHC and brightfield double in situ hybridization (BDISH) – Gene Protein Detection Platform – in the context of HER2 protein, gene and chromosome 17-centromere status evaluations.

Method: The combined IHC-BDISH technique performance was evaluated in 50 consecutive invasive breast cancer cases with HER2 IHC 2/3+ scoring results. Interpretation of HER2 IHC, BDISH, FISH and Gene-protein stains were conducted by 2 pathologists using conventional brightfield and fluorescence microscopes with 60x objectives.

Results: This recent combined IHC-BDISH technique has equivalent results compared to standard separate IHC, BDISH and FISH protocols.

Conclusion: The combined IHC/BDISH technique is robust and has the advantages of being less tissue and time consuming. Most pathologists prefer the brightfield solution and stains can be stored. Furthermore, the advantage of assessing gene and protein status simultaneously on all cases may improve the performance of the integrated testing algorithm.

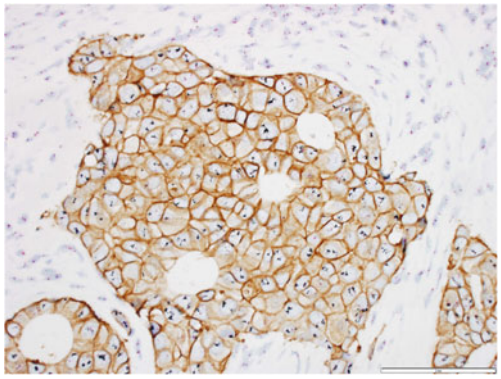

PS-10-018

Formalin Fixed Paraffin Embedded (FFPE) Reference Standards B-Raf, EGFR, K-Ras and PI3Ka Validated using Droplet Digital™ PCR

J. Frampton*, C. Thorne, V. Spivey, A. Moffatt, R. Nelson, E. Oliver, S. Dixon, J. Goodall, C. Lowe

*Horizon Discovery, Dept. of Diagnostics, Cambridge, United Kingdom

Objective: Isolation of genomic DNA from formalin fixed paraffin embedded (FFPE) tissues is a critical step for molecular diagnostic assays. Horizon Diagnostics has generated FFPE cell line reference standards containing defined mutant allelic frequencies, enabling the quality control of both assay sensitivity and DNA extraction.

Method: A panel of X-Man™ (gene-X, Mutant And Normal) cell lines were developed using our patented gene editing technology (GENESIS™) including; B-Raf V600E, V600K; EGFR ΔE746-A750, T790M, L858R, L861Q; K-Ras G12A, G12C, G12D, G12R, G12S, G12V, G13D; PI3Kα E542K, E545K, H1047R. FFPE blocks containing specific allelic frequencies including: 50 %, 33 %, 25 %, 20 % or 5 % were generated and sections cut. DNA was extracted using five different extraction methods and analysed using Droplet Digital™ PCR.

Results: Mutant alleles could be detected using Droplet Digital™ PCR at each defined allelic frequency and the reproducibility of each test was very high. The allelic frequency was consistent throughout each block. The total DNA yield from each section was consistent using the same extraction method but varied between methods.

Conclusion: This study has demonstrated Horizon Diagnostic's FFPE Reference Standards have a highly accurate defined mutation specific allelic frequency together with a consistent DNA quantity.

PS-10-019

Transcript variants and isoforms of the phosphatase subunit PPP2CA and its regulatory binding partners in haematological malignancies

G. Grech*, C. Saliba, B. Shawn, R. Avellino, P. J. M. Valk, R. Delwel
*University of Malta, Dept. of Pathology, Msida, Malta

Objective: The importance of feedback mechanisms involved in suppression of growth factor-induced signals is gaining importance both to understand molecular mechanisms of disease and also as potential therapeutic targets. Our previous studies show that erythroid differentiation can be blocked by constitutive expression of the pp2a inhibiting subunit, alpha4. The aim of this study was to identify variants and transcript isoforms of PPP2CA and the inhibiting subunits alpha4 and SET, using (1) cell lines derived from haematopoietic disease, and (2) Chronic Myeloid Leukemia (CML) and Acute Myeloid Leukemia (AML) patient material.
Method: High Resolution Melting (HRM) analysis was used to scan the cDNAs for variants and isoforms. Principle component analysis clustered the amplicons into genotypic groups. These genotypes were further analysed by direct sequencing.
Results: HRM identified mutants in SET and alpha4. Of interest the cell line, U937 has multiple mutations in the coding region of SET. PPP2CA isoforms were identified in patient material. One of the isoforms lacking exon5, is predominantly expressed in 15 % of CML (n=19) and AML (n=344) patients.
Conclusion: The presence of SET variants result in deregulated pp2a activity. The PPP2CA isoform (del.exon5) results in loss of phosphatase function, predicting sensitivity to the pp2a activator, FTY720.

PS-10-020

PAXgene® Tissue fixation technology for simultaneous preservation of morphology and biomolecules

D. Groelz*, S. Gündisch, C. Viertler, N. Dettmann, I. Blassnig, R. Wyrich, L. Rainen
*QIAGEN GmbH, DSPS, Hilden, Germany

Objective: PAXgene Tissue (PAXgene) is a new, formalin-free fixation technology. PAXgene fixed, paraffin embedded (PFPE) tissue is suitable for conventional histochemical and immunohistochemical staining as well as for extraction of high quality nucleic acids and proteins including phosphoproteins.
Method: Cases of human cancer were divided and fixed in formalin, PAXgene, or snap frozen in liquid nitrogen (LN2). FFPE and PFPE tissue were stained with H&E and IHC stains. Nucleic acids were isolated and analyzed in RT-qPCR, by agarose gel electrophoresis, long-range, and multiplex PCR. Proteins and phosphoproteins were evaluated by western blot analysis.
Results: Morphology of PFPE samples and IHC staining intensities were similar to that for FFPE tissue. High correlation of RNA and miRNA expression between PFPE and LN2 samples, but poor correlation between FFPE and LN2 was observed. DNA from LN2 and PFPE was of high molecular weight and performed well in PCR, but DNA from FFPE failed in most PCR assays. Signal intensities for phosphoproteins in western blots were comparable between LN2 and PFPE, but weaker for FFPE tissue.
Conclusion: PAXgene Tissue simultaneously preserves morphology and biomolecules for morphological and multimodal biomarker testing within one sample. For research use only. Not for use in diagnostic procedures.

PS-10-022

STAT3 plays a pivotal role in cell adhesion in mouse hepatocytes by regulating E-cadherin expression

S. Haga*, H. Inoue, A. Kano, X.-Y. Fu, K. Terui, M. Ozaki
*Hokkaido University, Dept. of Dermatology, Sapporo, Japan

Objective: Epithelial cells grow by proliferation and adhesion, which will form an organ/tissue. STAT3 is involved in cell proliferation and various cellular events. In the present study, we studied the role of STAT3 in cell adhesion in hepatocytes.
Method: STAT3 knockout cells (S3KO cells) and liver-specific STAT3KO (L-S3KO) mice were generated. Cellular adhesion was analyzed by light/electron microscopy. Expression of adhesion molecules was examined by immunohistochemistry and western blot analysis. Protein expression and cellular adhesion were also examined in the pre-/post-hepatectomy liver tissue in control and L-S3KO mice.
Results: mRNA and protein of E-cadherin were not expressed in S3KO cells. IL-6 up-regulated E-cadherin in control cells but not in S3KO cells, and induction of constitutively active mutant of STAT3 restored E-cadherin level in S3KO cells. Interestingly, membrane-bound beta-catenin expression was not affected, but released to cytosol in S3KO cells. S3-KO cells showed almost normal proliferation but did not form cell cluster due to lack of E-cadherin. Electron-micrograph confirmed lack of intercellular adhesion structures (desmosome) in S3KO cells. Also in L-S3KO mice, hepatocytes lack desmosome structure and cell adhesion.

Conclusion: STAT3 may play a pivotal role in cell adhesion by up-regulating E-cadherin expression.

PS-10-023

CXCR4 mRNA overexpression in high grade prostate tumors: Lack of association with TMPRSS2-ERG rearrangement

S. Hernández Llodrà*, S. De Muga, M. Salido, L. Agell, N. Juanpere, J. A. Lorente, S. Serrano, J. Lloreta
*Pompeu Fabra University, Dept. of Experimental and Health Sciences, Barcelona, Spain

Objective: Many prostate carcinomas (PrCa) harbor the fusion TMPRSS2-ERG, that results in ERG protein expression. Different studies have suggested an association between CXCR4 and ERG protein overexpression resulting from TMPRSS2-ERG rearrangement. The aim of this study is to investigate the relationship between CXCR4 expression, TMPRSS2-ERG fusion and Gleason grade in PrCa
Method: TMPRSS2-ERG rearrangement was investigated by FISH (n=44), ERG protein expression by IHC (n=84), and CXCR4 mRNA expression by quantitative RT-PCR (n=44) in primary PrCa (Parc de Salut MAR Biobank, Barcelona, Spain).
Results: TMPRSS2-ERG rearrangement and ERG protein overexpression were present in almost 50 % of cases, without statistical differences among Gleason groups. There was a very high concordance between FISH and IHC (Kappa= 0.954). 70 % of Gleason ³ 8 tumors overexpressed CXCR4 mRNA (p=0.009), without association between ERG protein and CXCR4 mRNA expression.
Conclusion: CXCR4 mRNA overexpression is associated with high Gleason grade, regardless of TMPRSS2-ERG status. TMPRSS2-ERG is not associated with grade. ERG IHC is very useful for TMPRSS2-ERG rearrangement detection.

PS-10-024

Oncogenic KRAS copy gain in colon carcinoma is associated with higher tumor grade

D. Hershkovitz*, E. Simon, E. Sabo, O. Ben-Izhak
*Rambam Health Care Campus, Dept. of Pathology, Haifa, Israel

Objective: Oncogene gain of function mutations in cancer are traditionally considered as heterozygous mutations, i.e., the malignant cell is expected to contain one copy of mutated gene and one copy of the wild type gene. However, recent studies have demonstrated a phenomenon of mutant allele imbalance, characterized by gaining additional copies of mutant allele. The purpose of this study was to determine the extent of this phenomenon and its clinical relevance in colon carcinoma.
Method: Based on the results of previous molecular morphometric study that quantitated the amount of wild type and mutated alleles among the tumor cells we now calculated the mutated allele gain in 42 samples of colon carcinoma harboring KRAS mutation and evaluated its association with tumors' grade and stage.
Results: Of the 42 samples 14 (33 %) showed mutant KRAS gains. The tumors with gains were associated with lower differentiation (4/21 in the well differentiated as compared to 10/21 in the moderately to poorly differentiated group, p=0.05). No association was found between copy number gains and tumor T stage or metastasis.
Conclusion: Our data indicates that oncogenic KRAS copy gain is associated with colon carcinoma grade. Further studies are needed to determine the role of this parameter in clinical practice.

PS-10-026

Molecular diagnosis of ALK positive anaplastic large cell lymphoma

M. Kalinova*, I. Hilska, M. Mrhalova, R. Kodet
*University Hospital Motol, Pathology and Molecular Med., Prague, Czech Republic

Objective: ALK positive anaplastic large cell lymphoma (ALCL) is characterized by anaplastic lymphoma kinase (ALK) expression, most commonly associated with the t (2;5)(p23;q35), fusing the ALK and nucleophosmin (NPM) genes. However, in a significant proportion of cases the ALK gene has a number of other than NPM translocation partners. The aim of the study was to detect the NPM/ALK fusion gene and the other possible fusion genes.
Method: NPM/ALK was detected by RT-PCR, NPM/ALK negative lymphomas were analyzed by ALK specific Rapid Amplification of 5´cDNA Ends (5´ RACE). We prepared Q-RT-PCR assay for quantification of 3´ ALK mRNA. Molecular findings were correlated with I-FISH.
Results: We analysed 42 ALK positive ALCL. Chromosomal breakpoints affecting the ALK locus were detected by I-FISH in all patients. The NPM/ALK was detected in 32/42 patients. 5´ RACE identified ATIC/ALK in 3, CLTC/ALK in 2 patients. Other fusion genes (TPM4/ALK, TPM3/ALK, ALO17/ALK) were found in one patient. In all specimens, overexpression of 3´ALK mRNA suitable for the minimal residual disease (MRD) detection was found.
Conclusion: Molecular diagnostics allows for detecting of various ALK gene translocation partners. Q-RT-PCR based analysis of 3´ALK mRNA is a promising and rapid approach for diagnosis and MRD monitoring in patients with ALK positive ALCL.

PS-10-027

Clonality analysis of giant cell tumor of bone and aneurysmal bone cyst

L. Krskova*, J. Hacek, P. Macokova, J. Fejfarkova, R. Kodet
*University Hospital Motol, Pathology and Molecular Med., Prague, Czech Republic

Objective: A 17 year-old girl, presented with an osteolytic epiphyseal lesion of the distal ulna. Based on histopathological examinations, the lesion was classified as giant cell tumor of bone (GCT). Four years later, the girl developed a second lesion at the same site. The histopathological examination revealed aneurysmal bone cyst (ABC) with solid spindle celled and giant celled areas which raised a question of a recurrent GCT or a primary ABC. The aim of this study was to analyze the clonality of these two processes. Determination of maternal and paternal X chromosome activation status is useful in the diagnostic analysis of nonrandom X inactivation patterns.
Method: The human androgen receptor (HUMARA) gene polymorphism assay was used to identify the clonality of these two processes.
Results: The patient was identified as heterozygous for the HUMARA allele. The GCT and ABC samples exhibited a monoclonal pattern, but one of them was with maternal and the other with paternal X chromosome origin.
Conclusion: The findings of this case report demonstrate the clonal behavior of both lesions with different clonal patterns. The above investigation proved to be helpful in distinguishing between recurrent GCT and de novo ABC in the field of previous surgical intervention.

PS-10-028

Study comparison of different methods cytogenetic vs. QRT-PCR in the diagnosis of gastric cancer for HER2/NEU

S. Libor*, P. Dundr, S. Lísová, D. Tvrdík, M. Ludvíková, C. Povýšil
*General Faculty Hospital, Inst. of Pathology, Prague, Czech Republic

Objective: In approximately 20 % of gastric adenocarcinoma was found expression of Her2 receptor which correlate with worse prognosis.
Method: For immunohistochemistry (IHC) was used certified kits (HercepTestTM, Dako) and (PATHWAY® HER2/neu (4B5) Ventana, Roche). For in situ hybridizacion (ISH) was used fluorescence in situ hybridizatiom (FISH) (PathVysion HER-2 DNA Probe Kit Abbott molecular, USA), and FISH ZytoLight® SPEC HER2/CEN 17 Dual Color Probe Gastric Cancer and robotic method SISH (HER2 Dual Colour ISH, Ventana, Roche). In all specimens gen Her2/neu was quantifed agains reference gen by qRT-PCR method (LyghtCycler® 480 II, Roche).
Results: The results of cytogenetic analysis have been showed in 40 % that didn´t corespond with the results of qRT-PCR quantification. On the contrary the results of IHC was correlated with the results of qRT-PCR in 100 %. Methods SISH vs FISH has in 25 % different of results. In regard to the quality of ISH signals the SISH is more preferable for determination Her2/neu.
Conclusion: A pilot study conducted on a group of 20 patients showed that among the methods used in the process of determining HER2/neu amplification are significant differences, even in evaluation and interpretation of test results. Regardless of the histological type of tumors (diffuse and intestinal type) as problematic for the evaluation of samples proved to be endoscopic route.

PS-10-029

The use of molecular methods in diagnosis of malignant melanoma of biopsy

S. Libor*, P. Dundr, S. Lísová, C. Povýšil
*General Faculty Hospital, Inst. of Pathology, Prague, Czech Republic

Objective: Distinction between benign and malignant melanocytic lesions commonly represents a big challenge for the pathologist. In this case it appears as a useful auxiliary method of fluorescence in situ hybridization (FISH). The aim of this study was by using fluorescently labeled probes detection of numerical changes occurring in malignant melanoma and thus supply or confirm the diagnosis.
Method: The retrospective study included 14 samples tissue with an established histological diagnosis (6x malignant melanoma, benign melanocytic lesions 8x). For detection was used probe Vysis LSI RREB1/LSI Myb/LSI CCND1/CEP6 (Abbott Molecular, USA), Olympus AX70 fluorescent microscope (immersion lens 1000x). In the area of the tumor were calculated signals of individual probes and evaluated according to the manufacturer's instructions.
Results: Evaluable results were obtained in 10/14 Cases (71 %) of the melanomas were 4 and 6 benign melanocytic lesions. In all four cases of malignant melanoma have been burdened with genetic changes, mainly in the CCND1 (in 55 %) gene amplification and PREB1 (in 40 %) and MYB (in 5 %). In contrast, for all 8 benign melanocytic been demonstrated normal findings.
Conclusion: DNA abnormalities detected by FISH occurr in the vast majority of malignant melanomas but are not seen in benign nevi. This fact make the FISH test an important extra step in the differential diagnosis melanocytic lesions with ambiguous or borderline histological findings.

PS-10-030

Gene expression analysis of MEN1 and EGFR in operated for primary lung cancer patients

D. Marinova*, D. Kachakova, G. Stancheva, Y. Slavova-Marinova, V. Maksimov, A. Mitkova, R. Kaneva, V. Mitev
*University Hospital Sofia, Dept. of Pulmonary Diseases, Bulgaria

Objective: EGFR is a receptor on the cell membrane with tyrosine-kinase activity and which is a regulator of proliferation, apoptosis, angiogenesis, tumor invasion. He is found to be overexpressed in some lung cancer histological subtypes. MEN1 is a tumor suppressor gene, with a role in cellular growth and differentiation, DNA reparation, and apoptosis.

Method: Surgically resected specimen from 99 patients (men $n=66$; women $n=33$, age 57 ± 11) with lung cancer were studied: carcinoid tumors (CT)-23, small cell lung carcinomas (SCLC)-13, large cell neuroendocrine carcinomas (LCNEC)-6, adenocarcinomas (AC)-29, and squamous cell carcinomas (SCC)-28. The histological subtype, pTNM stage, and gene expression of MEN1 and EGFR in tumor and normal lung tissue were evaluated.

Results: Overexpression of EGFR was observed in 34 %(SCC–61 %, AC–31 %, SCLC–23 %, LCNEC–17 %, CT-13 %). Decreased expression was observed in 22 %(LCNEC–66 %, SCLC–54 %, CT–22 %, AC–14 %, SCC–7 %) ($p<0.001$). Overexpresssion of MEN1 was observed in 57 % of all tumors (SCLC-69 %, CT-65 %, SCC-57 %, LCNEC-50 %, AC-48 %) ($p>0.05$). Significant correlation between overexpression of MEN1 and early stage SCC was observed ($p=0.03$).

Conclusion: EGFR is a target for therapy with monoclonal antibodies, so the tumors that overexpress EGFR can be considered for treatment with these drugs. MEN1 can eventually be a marker for good prognosis and a potential target for therapy.

PS-10-031

PROX1 overexpression alters gene expression profile in oral squamous cell carcinoma cell lines

F. Nunes*, P. Severino, M. F. Setubal D. Rodrigues
*Universidade de São Paulo, Dept. of Oral Pathology, Brazil

Objective: Homeobox genes encode transcription factors controlling cellular proliferation and differentiation. Altered expression of PROX1 homeobox gene is related to many cancers, including breast, esophagus, lymphatic and oral.

Method: After overexpression of PROX1 gene in SCC9 cell line, total RNA was extracted from three overexpressing-PROX1 clones (OC) and one control-transfection cell clone (CC). Microarray analyses were performed using the Whole Human Genome 44 K according to the manufacturer's instructions. Genes with a fold change of greater or lower than 2.0 in OC versus CC, were considered as increased or decreased, respectivelly. Gene Ontology (GO) was used to assign biological process related to significantly differentially expressed genes.

Results: Down-regulated genes MMP2, TIMP3 and NOTCH1 were further validated by qRT-PCR. Comparative gene analysis of OC and CC revealed 925 up-regulated and 789 down-regulates genes. Pathways induced upon PROX1 overexpression in GO terms included vascular development control, cellular adhesion, regulation of proliferation, among others. MMP2, TIMP3 and NOTCH1 expression by qRT-PCR showed reduced expression leves in OC. These genes are commonly overexpressed in oral squamous cell carcinoma and have been related with metastatic tumors and worse prognosis.

Conclusion: Overexpression of PROX1 alters the expression of genes involved in oral squamous cell carcinoma development. MMP2 and TIMP3 reduced expression following PROX1 overexpression suggest this gene function as a tumor suppressor.

PS-10-032

Analysis of alterations in epithelial DNA methylation as potential epigenetic biomarkers of neoplastic progression in Barrett's Esophagus

A. Puertas Cantería*, C. Hörndler, A. Lanas, E. Piazuelo, E. Chueca, D. Rosero, P. Sota, M. Strunk, G. Muñoz
*Hospital U Miguel Servet, Serv. de Anatomía Patológica, Zaragoza, Spain

Objective: Barrett´s Esophagus is the unique known precursor for esophageal adenocarcinoma (EAC), in a gradual progression to dysplasia. Our objective is to determine the correlation between the hypermethylation in CpG islands of the promoter region of p16 tumoral suppressor gen in epithelial DNA and the histopathological pattern, as possible biomarker for risk of progression.

Method: 1. A study was performed about the evolution of precursor lesions, in a group of 55 patients diagnosed following the Vienna classification. 2. p16 hypermethylation is analyzed in paraffin embedding samples, through laser microdissection, DNA extraction, PCR amplification, pyrosequencing and quantification.

Results: 1.14 of 20 cases with 2 to 5 biopsies remained as ND, ID or LGD, and 6 cases progressed to HGD and/or EAC. 2. Within the control group the methylation grade is 6.53 % and in the diagnostic groups is 12.04 % (ND), 7 % (ID), 17.05 % (LGD), 8.50 % (HGD) and 23.33 % (EAC).

Conclusion: 1. 70 % remained stable, but those reaching HGD all progressed to ACE (only in 50 % of the latter, HGD is recognized with H&E). 2. Methylation´s grade is higher in all diagnostic groups comparing to the control group, progressively increased as the dysplasia grade found with H&E, so it may be a good biomarker for neoplastic progression.

PS-10-033

Comparison of HPV OncoTec and NucliSENS Easy Q Test in preneoplastic lesions of the cervix

M. Rongioletti*, F. Papa, C. Vaccarella, M. B. Majolini, F. Neri, M. Belli, V. Mazzucchi, D. French, G. Liumbruno
*San Giovanni Calibita Hospital, Dept. of Clinical Pathology, Rome, Italy

Objective: In High Risk HPVs the expression of oncoprotein E6 is responsible for the degradation of p53, while E7 inactivates pRb and causes the progression to S phase of cell cycle, both sustaining the conversion to and the maintenance of malignancy. The aim of this study is to compare the performance in the detection of the E6 and E7 mRNA expression of HR-HPV using the NucliSENS Easy q test (bioMerieux) or HPV OncoTect (IncellDx) a test based on Flow cytometry-FISH method.
Method: We enrolled 50 patients positive for HR-HPV DNA and/or pap smears. All subjects underwent a colposcopy histological evaluation and were tested both for the NucliSENS Easy q test and HPV OncoTect.
Results: 31 out of 50 subjects resulted positive for RNA expression. The patients were divided into two cohorts based on the histological diagnosis: low grade lesions (CIN1) and high grade lesion (CIN2+). Patients with CIN1 were 26 with NucliSENS Easy q test and 13 with HPV Onco Tect, those with CIN2+ were 5 with either tests.
Conclusion: These preliminary results suggest that HPV OncoTect have a better specificity than NucliSENS Easy q test, while more samples need to assess the difference in sensitivity.

PS-10-034

Detection of PIK3CA/AKT mutations in human meningiomas

A. Saetta*, G. Tomara, I. Chatziandreou, P. Tsioli, E. El-Habr, I. Sakalidou, G. Vretakos, E. Boviatsis, P. Korkolopoulou, E. Patsouris
*University of Athens, 1st Dept. of Pathology, Greece

Objective: The PI3K/AKT pathway is a major signaling pathway frequently activated in human cancer due to PIK3CA and AKT1 gene mutations thus representing a potential therapeutic target and prognostic biomarker. In this study, we examined the mutational status of PIK3CA and AKT1 in meningiomas.

Method: 91 meningiomas were screened for activating mutations in "hot spot" exons 9, 20 of PIK3CA using Real Time PCR and High Resolution Melting Analysis. PIK3CA wild-type samples were analyzed for mutations in exon 4 of AKT1. The mutations were verified by sequencing and/or pyrosequencing
Results: Mutations were detected in 2 out of 91 samples (2 %) in exon 9 of PIK3CA and were identified as p.E547K and p.S541F. Regarding exon 20, 7 out of 91 samples (7,5 %) showed the following mutations: p.R1023Q, p.T1025T, p.H1020V, p.M1043I, p.H1047R (2 cases), p.H1046T. Finally, in exon 4 of AKT1, 8 mutant cases were detected (9 %) all identified as p.E17K. In 19 % of the patients the activation of the PI3K/AKT pathway is due to mutations in the two examined genes.
Conclusion: Aberrant activation of the PI3K/AKT pathway due to PIK3CA and AKT1 mutations is commonly observed in human meningiomas and these genes could be considered as potential targets in new therapies for cancer.

PS-10-035

Study of PI3K/AKT/mTor pathway in urothelial bladder carcinoma

A. Saetta*, N. Prekete, E. Trigka, G. Levidou, M. Karlou, P. Pavlopoulos, P. Korkolopoulou, E. Patsouris
*University of Athens, 1st Dept. of Pathology, Greece

Objective: Deregulation of the PI3 kinase-AKT/mTOR pathway is a frequent event in tumorigenesis. We examined the possible significance of the components of this pathway in bladder urothelial carcinoma (UC).
Method: 108 cases with bladder UC were screened for mutations in exons 9, 20 of PIK3CA gene and exon 4 of AKT1 by PCR-SSCP, HRMA, sequencing and/or Pyrosequencing. The expression of p-mTOR, p-4E-BP1, p-p70S6K, p-AKT, FGFR3 and p-ERK was evaluated by immunohistochemistry.
Results: 4,6 % of the cases were mutant in PIK3CA gene and 3 % in AKT1. Cases with wild type AKT1 displayed higher FGFR3 receptor expression (p=0.0521). p-4E-BP1 expression was more frequent in low grade (p=0.018) and in pTa-T1 tumors (p=0.053). Furthermore, superficial tumors presented higher levels of p-p70S6K expression (p=0.035) and lower levels of p-AKT expression (p=0.048). In multivariate survival analysis, p-4E-BP1 immunoexpression emerged as an independent prognostic factor of adverse survival (HR=9.207, p=0.0039), along with tumor grade and T-category.
Conclusion: Activation of PI3K/AKT/mTOR pathway in bladder UC is not exclusively related to the presence of AKT1 and PIK3CA mutations. Expression of p-4E-BP1 could serve as an independent prognosticator.

PS-10-036

Comparison of DNA extraction methods of formalin fixed, paraffin-embedded archival tissues

B. Senguven*, E. Baris, T. Oygur
*Gazi University Dental Faculty, Dept. of Oral Pathology, Emek, Turkey

Objective: Formalin fixed, paraffin-embedded (FFPE) archival tissues are valuable resources for many molecular studies. The goal of this study is identify the optimal method for DNA extraction from FFPE tissues.
Method: 32 human gingival tissues which has obtained from patients with gingival hyperplasia were used. Serial sections of 10 μm thickness obtained using a standard microtome. Half of the sections were deparaffinized on glass, the other half collected directly to a 1,5 ml tube. In order to identify the optimal method for DNA extraction, we compared phenol-chloroform protocol and DNA Extraction Mini Kit. The duration of proteinase K digestion were also compared. Spectrophotometric evaluation of the yield and purity of DNA was conducted. To deteminate the amplifiablity of extracted DNA, three different bp fragment of the beta-globin gene were amplified using PCR.
Results: The phenol-chloroform method had the lowest yield and purity. Deparaffinized specimens on glass, digested for 72 h and isolated using mini kit had the highest yield. Amplification of the 120 bp fragment of beta-globin gene was successful in all samples.
Conclusion: According to our results deparaffinization on glass, increasing the time of proteinase K digestion and using commercial kits for isolation seems the best method to obtain amplifiable DNA from archival specimens.

PS-10-037

MicroRNA signatures associate with Fallopian tubal implantation in humans

R. Shao*
*Gothenburg University, Physiology and Endocrinology, Sweden

Objective: MicroRNAs are small non-coding RNA molecules that regulate a large number of cellular pathways and deregulation or altered expression of miRNAs is associated with many disease states. The function of the Fallopian tubes appears to involve orchestrated spatiotemporal alterations in transcriptome profiles, the regulation of tubal gene expression and function by miRNAs may thus be of primary importance in tubal ectopic pregnancy.
Method: Both implantation sites and non-implantation sites of Fallopian tubes from women with EP and decidual biopsies from women undergoing therapeutic surgical termination of pregnancy were collected and analyzed by miRNA array. The unique miRNA profiling results were validated by TaqMan qRT-PCR, and bioinformatics' analysis was employed to further predict the miRNA targets.
Results: A total of 47 miRNAs were differentially expressed in implantation sites compared with those in non-implantation sites of Fallopian tubes after comparison of decidual miRNAs, among which 19 were up-regulated while 28 are down-regulated. The miR-424 was significantly increased, whereas let-7i, miR-149, and miR-182 were significantly decreased. Differentially expressed miRNAs were predicted to be related with several signaling pathways in normal intrauterine implantation.
Conclusion: Our findings establish an miRNA signature associated with tubal implantation and provide the experimental basis for further understanding the molecular and cellular mechanisms of initiation and development of tubal EP in humans.

PS-10-039

Does Hsp90AA1-2 and Hsp90AB1 expression in lung tissue can be a marker of increase of warming in Mexico from 1970 to 2009?

J. Trillo-Tinoco*, F. Arenas-Huertero
*Hospital General de Mexico, Dept. of Surgical Pathology, Mexico City, Mexico

Objective: In Mexico the maximum increase of the temperature from 1971 to 2009 is 7.5 °C with a mean of 1.6 °C. Lung is an organ that can sense any perturbation of the air, due to its constant interaction (long live) of the air. Our hypothesis was that lung could be an organ sensor of climatic change observed today.
Method: This preliminary study analyzed the expression of 3 isoforms of the genes of Hsp90. The cases were chosen from archive of autopsies from 1970 to 1979, with different diagnosis, and were matched in sex and age with a same number of cases chosen from 2000 to 2009. The expression was studied by RT-PCR from lung tissue embedded in paraffin, 20 samples of each decade.
Results: The expression levels of Hsp90 were normalized to β-actine. We found expression in six cases of 2000–2009: five for Hsp90AA1-2, and 1 for Hsp90AB1, one case expressed both. Their matched cases in 1970–1979 never expressed any isoform. The cause of dead in all cases doesn't fit with any pattern.
Conclusion: With these results we propose than the lung could be a sensor of global warming, and the expression of these genes could be molecular markers of this climatic change.

PS-10-040

Apoptosis associated genes and their role in predicting responses to neoadjuvant breast cancer therapy

D. Tvrdík*, H. Skálová, P. Dundr, L. Stanek, C. Povýšil, L. Petruželka
*General University Hospital, Institute of Pathology, Prague, Czech Republic

Objective: Neoadjuvant chemotherapy is used in the treatment of breast carcinoma because it substantially reduces the size of the primary tumor and lymph node metastases. This present study is aimed at the investigation of biomarkers that can predict a pathologic response to the therapy.
Method: The transcriptional profile of 84 key apoptosis genes was evaluated in both pre-therapeutically obtained tumor tissue by core needle biopsy and in specimens removed by final surgery, using a pathway-specific Real-Time PCR assay.
Results: On the basis of a hierarchical cluster analysis of 13 significantly changed genes, we divided patients into good and bad prognosis groups, which correlate well with progression-free survival. In the good prognosis group, we found a statistically significant downregulation of the expression of MCL1 and IGF1R genes after neoadjuvant treatment. We also found a statistically significant overexpression of BCL2L10, BCL2AF1, CASP8, CASP10, CASP14, CIDEB, FADD, HRK, TNFRSF25, TNFSF8 and CD70 genes. In contrast, we found upregulation of IGF1R after the treatment in the group with poor prognosis.
Conclusion: As we have shown, gene expression profiling after neoadjuvant chemotherapy is a valuable research tool for investigating molecular markers, which may better reflect tumor biology and treatment response than standard prognostic and predictive factors.

PS-10-041
Genetic changes in non-small cell lung carcinoma
M. Uvirova*, I. Urbanovska, D. Konvalinka, J. Šimova, B. Kubová, M. Jaluvkova, J. Zmolikova, D. Ziak, J. Dvorackova
*CGB Laboratoy a.s., Dept. of Genetics, Ostrava, Czech Republic

Objective: Non-Small Cell Lung Carcinoma (NSCLC) is one of the most serious cancers. Identification of genetic changes (mutations, amplifications or rearrangements) within EGFR, KRAS and ALK oncogenes, associated with NSCLC, allows choosing the patients, benefit from biological therapy with tyrosin kinase inhibitors.
Method: DNA is isolated from formalin fixed paraffin embedded specimens or cytology specimens. Mutation detection is performed by real-time PCR, fragment analysis, primer-extension analysis and mutant-enriched PCR. Wt-EGFR patients (e.g. with no mutation detected) are tested for ALK gene rearrangement and EGFR gene polysomy or amplification using the fluorescence in situ hybridization (FISH) method.
Results: Since 10/2010 till 2/2012, 238 DNA samples were analyzed. Out of these, 17 patients (7,14 %) were found to be positive for activating mutations within EGFR gene. Since 07/2011 till 2/2012, 80 patients were analyzed for ALK gene rearrangement, EGFR gene polysomy or amplification. ALK gene rearrangement has been proven in 5 (6,25 %) cases, ALK gene amplification in 2 (2,5 %) cases and EGFR gene polysomy or amplification in 35 (43,75 %) cases.
Conclusion: Determination of genetics changes in tumor can provide powerful tool for setting up strategy and therapeutic protocols in NSCLC patients.

Monday, 10 September 2012, 09.30 - 10.30, Congress Hall Foyer 3rd Floor
PS-11 Poster Session Digestive Diseases Pathology II: Lower Gastrointestinal Tract

PS-11-003
Primary peritoneal mesothelioma complicating intussusception
A. Arnaout*, E. Sarkady, J. Read
*Croydon University Hospital, Dept. of Histopathology, United Kingdom

Objective: A 61 year old gentleman, ex-smoker with a history of asbestos exposure presented to the emergency department with a 1 day attack of severe abdominal pain and bilious vomiting. History of abdominal pain, lethargy, and weight loss over the last 12 months and 4 years of recurrent pleural effusion. Pleural aspirates and a video-assisted thoracic biopsy were negative.
Method: X-ray confirmed small bowel obstruction and an emergency laparotomy performed. The terminal ileum was intussuscepted into the caecum causing proximal obstruction. A right hemi-colectomy was performed.
Results: On gross examination there was intussusception of the terminal ileum secondary to a polypoid mass at the ileo-caecal valve. Histology showed an oncocytic tumour with neuroendocrine features arising from the serosa of the small bowel. The tumour cells were positive for CK7, calretinin, and vimentin but negative for CK20, chromograninA, CD56 and TTF-1. The features were in keeping with a malignant peritoneal mesothelioma infiltrating the small bowel wall.
Conclusion: Peritoneal malignant mesothelioma is an uncommon tumour which rarely causes mechanical small bowel obstruction. To our knowledge this is the first case of localised primary peritoneal mesothelioma presenting with intussusceptions.

PS-11-004
Giant mesenteric cystic lymphangioma in adult; rare tumor, unusual location and uncommon age of occurrence: A Tunisian case report
S. Attafi*, W. Ajouli, N. Bouchiba, A. Chouchene, M. H. Balti, K. Bellil
*FSI Hospital, Dept. of Pathology, Marsa, Tunisia

Objective: Cystic lymphangioma is a rare benign neoplasm arising from the lymphatic system. It occurs as a result of congenital malformations of the lymphatics, leading to the obstruction of local lymph flow and the development of lymphangiectasia. Lymphangioma is common in pediatric patients, but it is extremely rare in adults, with only about 100 cases reported in literature. Most lymphangiomas are found in the head and neck; intraabdominal and specially mesenteric locations are very unusual. The aim of this work was to study its clinical, histological and therapeutic features and their diagnostic difficulties.
Method: We report the case of a 46 years-old woman, who presented a painful syndrome of the right iliac fossae (RIF). The physical examination found a mass of the RIF. Abdominal ultrasonography and magnetic resonance image showed a mesenteric cystic formation. At laparotomy, a large cystic tumor of the caecal mesentery, measuring 23 cm, was found. Histopathology showed a fibrous and thin walled cyst, lined by flat low lying epithelium with surrounding tissue of scattered lymphoid cells.
Results: The diagnosis of cystic lymphangioma was retained.
Conclusion: Mesenteric lymphangiomas are very rare, but they can cause acute abdomen that requires an emergent surgery. Therefore, they should be included in the differential diagnosis of cystic intra-abdominal lesions raises several possibilities, including both malignant and benign soft tissue tumours.

PS-11-005
Multiple splenic metastasis from colon cancer
F. Baderca*, I. Mates, D. Lazar, M. Raica, O. Cretu, F. Hut
*Medical University Timisoara, Dept. of Histology, Romania

Objective: The spleen metastases from colon cancer are rare conditions and usually associated with extensive disease. There are only eight reports in English-language literature of isolated splenic metastases from colorectal carcinoma, which generally metastasize to regional lymph nodes, liver and abdominal peritoneum.
Method: We report a case of multiple splenic metastases in a 60-year-old woman.
Results: In November 2009, the patient had undergone right hemicolectomy, lymphadenectomy and chemotherapy for stage III tubular adenocarcinoma of the ascendant colon with positive pericolic lymph nodes. In December 2011, she was admitted in our hospital for diffuse abdominal pain and intestinal transit disorders. Computed tomography of the abdomen revealed multiple metastases of different sizes in liver and spleen. During the surgery, which was performed with the goal of curing metastatic disease, there were found two nodular hepatic secondary tumors, and numerous spleen metastases, with diameters from 0.2 cm to 1.5 cm. The histopathological evaluation of splenectomy specimen revealed a metastatic tumor deposit, histologically similar to the primary tubular adenocarcinomas of colon.
Conclusion: This is the ninth documented case of splenic metastasis from colon cancer. Previously reported cases of this type were isolated tumor, this one being the first reported with multiple splenic metastases.

PS-11-006
The role of fatty acid synthase in Inflammatory Bowel Disease (IBS)
E. Bas Bozkurtlar*, N. Ozkan, A. E. Kedrah, C. Celikel
*Marmara University, Dept. of Pathology, Istanbul, Turkey

Objective: It was demostrated that FAS expression increases not only in mucosa involved by active colitis but also in normal mucosa of ulcerative colitis (UC) patients. Our aims were to evaluate the role of FAS expression in differential diagnosis of IBD, to search for any possible change during the progression of the disease in patients with clinical and endoscopic follow-up.
Method: Among 82 colonoscopic biopsy samples of 50 UC cases,13 samples were classified as remission,15 as resolution, and 54 as active period;35 samples of 30 Crohn Disease (CD) cases were classified as active period. Fifteen cases with normal endoscopic and morphologic findings comprised the control group.
Results: Between UC and CD active periods and control group, a significant difference was found (p=0,0001). There was a statistical correlation between FAS expression of basal crypt of normal mucosa in UC active period and the disease duration (p=0,036).
Conclusion: The increasing in FAS expression in patients with IBD can not be explained only by the inflammation. FAS expression can not aid us in the differential diagnosis of UC and CD, but it seems that it is related to the extent of inflammation in UC. The relation between the disease duration and an increase in FAS expression active UC, might have a significant role in carcinogenesis in UC.

PS-11-007
Micropneumatosis – An (un) usual finding in gastrointestinal specimen?
K. Blaue*, M. Plauth, J. Knolle
*Städtisches Klinikum Dessau, Pathology, Dessau-Roßlau, Germany

Objective: A rather rare disease, micropneumatosis describes the findings of cyst-like cavities devoid of lining epithelium in the gastrointestinal wall. Micropneumatosis is often secondary to intestinal bacterial infection or mechanical factors. This

study evaluates the incidence of micropneumatosis in our institute.
Method: We analyzed all cases of micropneumatosis obtained in our institute between 2001 and 2011. Available data were retrieved from patients' records.
Results: Out of 300.000 specimens obtained between 2001 and 2011, 71 cases (0.02 %) presented with micropneumatosis (37 female, 34 male; mean age 61 years, age range 18 to 85 years). Most common site was the colon (32 cases), followed by stomach (30), small intestine (8) and greater omentum (1).
Conclusion: Micropneumatosis represents a rare but harmless diagnosis in gastrointestinal specimen. Due to the histological picture, which may be confused with dilated lymphatic vessels, submucosal lipomas, and, to the untrained eye, even with signet ring cell carcinoma, incidence may even be higher. In unclear cases, where there seems to be a endothelial layer, immunohistochemistry may be necessary to confirm diagnosis of micropneumatosis. This study shows that micropneumatosis should be considered in differential diagnosis in every age and sex.

PS-11-008
Predicting lymph node metastasis in pT1 colorectal cancer – A meta-analysis providing rationale for therapy decisions
S. Bosch*, I. Nagtegaal
*Radboud University Nijmegen, Pathology, Netherlands

Objective: We conducted a meta-analysis of published reports on the predictive value of risk factors for lymph node metastases (LNM) in pT1 colorectal cancer in order to provide a rationale for choosing follow-up or radical surgery after local excision.
Method: Local excision is an attractive treatment option for colorectal cancer, but is only safe in the absence of LNM. Several pathological factors have been associated with LNM, however it remains unclear how to integrate these in clinical decision making.
Results: A Pubmed search revealed 17 studies totaling 3741 patients. Strong predictors of LNM were lymphatic invasion (RR 5.2 [95 % CI 4.0–6.8]), budding (RR 5.1 [95 % CI 3.6–7.3]), and high grade histology (RR 4.8 [95 % CI 3.3–6.9]). Deep submucosal invasion was also strongly associated with LNM, however in a risk stratification model this factor was of limited added value.
Conclusion: The absence of lymphatic invasion, budding and high grade histology may justify withholding radical surgery. The independent role of submucosal invasion depth is probably limited. Models for risk stratification based on these factors need to be validated.

PS-11-009
S 100 reactive protein in the intestinal wall with Crohn's Disease and in colitis ulcerosa
P. Bušíková*, D. Danis, S. Polak, S. Durdik, O. Hassoun, M. Bencat
*Cytopathos, s.r.o., Dept. of Pathology, Bratislava, Slovakia

Objective: Dendritic S100+ cells in intestines have been described in more studies. Their connection to S100+ fibres of nervous system is lesser of an object of interest.
Method: We have processed the samples of intestinal mucosa of people with Crohn's disease and colitis ulcerosa by the means of form-paraffine technique and anti S100 antibodies.
Results: In lamina propria and in submucosa at Crohn's disease were S100+ the fibres of various width and orientation. Outside of them the diffusely scattered round S100+ mononuclear cells could be seen. Contrary to colitis ulcerosa the granulation tissue at Crohn's disease contains in the area around abscesses a thick accumulation of S100+ cells and this is similar also in the formed lymphoid tissue.
Conclusion: The positive fibres can be seen in submucosa at the edge as well as in LPM between the bases of the glands. In between the plexus/ring and longitudinal muscle there are massive bands of connective tissue which contains bundles S100+ of ganglion cells and nerve fibres. The fibres are present in ring as well as in longitudinal muscle. In this area S100+ fibres can also be seen in vessel walls. Numerous bundles of granulatory tissue do not contain positively reacting substance. In the basal part lamina propria there are visible S100+ cells as well as long, smooth, positively reacting fibres.

PS-11-010
NCF1-deficient mice with impaired oxidative bursthave a more agressive progression of Dextran Sulfate Sodium (DSS) -induced colitis
L. Carvalho*, T. Rodrigues-Sousa, A. Alarcão, A. F. Ladeirinha, M. Souto-Carneiro
*Amadora, Portugal

Objective: Intestinal Inflammatory Disease (IID) as a primary immunodeficiency depends on mutations in the NADPH oxidase complex, responsible for the production ofreactive oxygen species (ROS). One of the most common clinical patterns in IID is chronic colitis. Ncf1-mutation in mice leads to deficiency in ROS, rendering them susceptible to autoimmunity. Here we studies how ROS-deficiency in Ncf1-mutant mice influenced the immune response to DSS colitis, its recovery and answer to a second induction.
Method: Colitis was induced in wild type (WT) and Ncf1-mutant (Ncf1) B10.Q mice by administration of 3.5 % DSS in the drinking water for 1 week. After 1 week recovery, DSS

was administered for another week. Mice were sacrificed at days 0, 7, 14 and 21, the colon was removed and folded into a Swiss roll. Sections of the colon were stained with HE, and monoclonal antibodies against B cells (B220), CD3+ T cells; and macrophages (Mac1/CD11b) were applied.

Results: Colitis was more severe in Ncf1 than WT mice, with epithelial dysplasia, hyperplasia of Peyer's patches and poor epithelium recovery (hyaline scars). At all time-points the amount and location of colonic B cells, T cells and CD11b + cells was distinct between groups. These results suggest that ROS are crucial for leukocyte recruitment and tissue-repair in DSS-induced colitis.

PS-11-011

Histopathological pattern of polypoid lesions of colon in Albanian population

G. Cekodhima*, A. Cekodhima, A. Beqiri, G. Andrea
*University Hospital Maria Teresa, Dept. of Pathology, Tirana, Albania

Objective: Our aim was to study histopathologic pattern of the polypoid lesions in Albania.

Method: We studied 216 lesions, 184 polypectomies and 32 colorectal surgery in 139 patients in Tirana.

Results: There were observed 216 polypoid lesions of large intestine in 122 males and 91 females.105(48.6 %) were adenomatous polyps, 31(14.35 %) were hyperplastic, 24 (11 %) were inflammatory polyps with ulcerative colitis, 10 (4.6 %) were inflammatory 6(2.77 %) were juvenile polyps, 2(0.92) non Hodgkin's lymphoma and 1 (0.46) was fibrolipoma. Tubular adenomatous polyps were the commonest polyps. They were more common 56 (25.9 %) in male population as compared to female 19(8.79 %). High grade dysplasia was present in 50 (23.14 %) and malignant change in 26 (12 %). The size of the polyps range from 0.5 to 4 cm.

Conclusion: Adenomatous polyps were the most frequently found polyps in our study; the approximately 24 % were advanced lesions.

PS-11-014

The role of cancer stem cells in biology and prognosis of colon cancers

A. F. Çiçek*, Ö. Öngürü, M. Gamsizkan, A. Günal
*Gülhane Military Medical Academy, Dept. of Pathology, Ankara, Turkey

Objective: This study was designed as a retrospective clinicopathological observation based on immunohistochemical and statistical findings to show the relationship between the disease progression and the intensity of the stem cell population within the tumor for colorectal cancers.

Method: For this purpose, we investigated 97 colorectal carcinoma cases, retrospectively. Paraffin embedded blocks was obtained from pathology archive and demographical patients' data from the patient's files of Gastroenterological Surgery Department. Immunohistochemically, we used CD133 and Musashi-1 antibody to determine the stem cells within the tumor. We noted the age of the patients, histopathological diagnose, tumor location, grade, TNM status, clinical stage, disease-free-survival and the outcome. Then we statistically compared all prognostic data with the immunohistochemical findings

Results: All of the cases were immunoreactive for both antibodies, furthermore we found a significant statistical correlation ($p=0.043$) between CD133 expression value and patient outcome. When the value of CD133 expression was high, clinical outcome was poor. In addition, there was a relation between high Musashi-1 expression and poor outcome.

Conclusion: Based on these findings we reported that overexpression of both CD133 and Musashi-1 antibodies may be a poor prognostic factor in colorectal cancers.

PS-11-015

Immunohistochemical evaluation of VEGF expression in colorectal carcinomas

D. Crisan*, M. Florea, D. Fodor
*University of Medicine and Pharmacy, Pathology, Cluj-Napoca, Romania

Objective: Vascular endothelial growth factor (VEGF) is an important angiogenic glycoprotein secreted by the tumor cells and host cells which proved to be a powerful prognostic factor in various human cancers. The aim of our study was the evaluation of VEGF expression in colorectal carcinomas using immunohistochemistry, in order to identify the relationship between the presence of the protein in the tumor cells and a series of morphological parameters.

Method: We analyzed 30 consecutive surgically removed colorectal carcinomas. Immunohistochemistry was done on formalin-fixed and paraffin embeded tissue sections, using the anti-human VEGF-A monoclonal antibody (clone VG1, Dako). The extent and intensity of staining were graded and used to calculate the immunoreactive score for each case. Statistical analysis was performed with SPSS (Statistical Package for the Social Sciences), using non-parametric tests. The level of statistical significance chosen was $p<0.05$.

Results: VEGF was expressed in all tumors, with a heterogeneous distribution. The only parameters that correlated with high VEGF positivity were the extent of the tumor necrosis and the presence of lymph node metastases ($p=0,001$).

Conclusion: High levels of the VEGF expression may be an indicator of poor prognosis in colorectal carcinomas.

PS-11-016

Collision tumour of the appendix: Mucinous cystadenoma and carcinoid - Report of a case

C. Dastamani*, A. Paraskeva, E. Carvounis, T. Theodosopoulos, A. Kondi-Pafiti
*Aretaieion Hospital, Dept. of Pathology, Athens, Greece

Objective: Appendiceal carcinoids are usually located at the tip of the appendix and occur as incidental findings. Epithelial neoplasms of the appendix are uncommon and consist of mucinous adenomas, carcinomas and neoplasms with features of both carcinoid and adenocarcinomas.
Method: A case of dual mucinous cystadenoma and carcinoid of the appendix is reported.
Results: The patient, a 57-year old- asymptomatic female presented with a cystic right iliac fossa mass. The excised specimen was appendix cystically dilated measuring up to 8,5 cm in diameter. The luminal content consisted of viscid mucin. The base of the appendix was thickened (up to 1,5 cm) and firm. Microscopically the cystic part of the specimen had features of mucinous cystadenoma with adenomatous epithelium extending as well over the thickened appendiceal wall. At that area the wall was involved by a well differentiated neuroendocrine neoplasm WHO gr I (carcinoid). The neoplastic cells infiltrated the entire thickness of the appendiceal wall, the mesoappendix and reached the serosal surface. The two neoplasms where separate and there was no transitional zone between them.
Conclusion: Dual carcinoid/epithelial neoplasia is a rare occurrence in the appendix. The prognosis appears to be no worse than for either of the two components alone.

PS-11-017

Gastrointestinal Stromal Tumor (GIST) of the anal canal: A case report

L. De Carvalho*, P. A. Teixeira, V. G. Siqueira, M. Pereira, T. Or, E. Pereira
*Centro Universitário Lusíada, Dept. of Pathology, Santos, Brazil

Objective: Gastrointestinal stromal tumors (GIST) are mesenchymal tumors derived from interstitial cells of Cajal. They are found more frequently in the stomach, small intestine while colon and rectum represent unusual sites. GIST's of the anal canal are extremely rare.
Method: 43-years-old woman who presented bleeding, pain and constipation for several months. The rectal examination revealed a well defined mass located within 10 cm of the anal verge. The magnetic resonance imaging confirmed a well-circumscribed mural mass without adenopathy. The local excision of the tumor was performed for pathological study.
Results: Gross examination showed a 4.5×3.0 cm fibrous mass. Histological examination revealed a spindle cell tumor with moderate atypia and mitotic count of 6 mitosis/50HPF. Neoplastic cells showed marked positivity for c-Kit and CD34 and negativity for muscular markers. A diagnosis of GIST with intermediate risk of aggressive behavior was made.
Conclusion: GISTs of the anal canal are extremely rare with only few cases reported in the literature. We described an additional case of GIST of the anal canal with histological and immunohistochemical study.

PS-11-018

Intestinal graft versus host disease with giant cells

B. Doganavsargil*, A. Vink, E. J. Petersen, G. J. Arnold Offerhaus
*Ege University, School of Medicine, Izmir, Turkey

Objective: Graft-versus-host disease (GVHD) is a common complication of allogeneic bone marrow transplantation in which immune cells in the transplanted marrow attack the immunocompromised host. It can occur in either an acute or in a chronic form and may affect various organs. Intestinal GVHD is particularly important because of its frequency, severity and its effects on the general condition of the patient.
Method: Here we report a 68-year-old man who developed GVHD, 8 months after receiving allogeneic non-myeloablative peripheral blood stem cell transplantation for refractory chronic lymphocytic leukemia. Colonic biopsies revealed an edematous and congested lamina propria, dilated crypts lined by flattened epithelium, increased apoptotic figures and vanishing crypts. Notably there were some giant cells in between crypts. However subsequent sections and special stains didn't show any granuloma formation or presence of an infectious agent.
Results: To our knowledge presence of giant cells in GVHD hasn't received proper attention before. Although we don't know the actual importance or clinical consequences of the entity yet, we report this case to increase awareness of this feature within the context of GVHD. We have seen more cases with giant cell GVHD afterwards; comparison with other cases of GVHD without giant cells may help clarifying their significance.

PS-11-021

Differential mutation patterns of KRAS and BRAF in adenomatous and serrated neoplastic sequences

O. Erdogan*, B. Savas, A. Ensari
*Ankara University, Faculty of Medicine, Turkey

Objective: Colorectal carcinomas develop through adenomatous or serrated neoplastic sequence. Different molecular mechanisms underly these morphologic sequences which may be translated into different therapies. We aimed to assess adenomatous and serrated neoplastic sequences in terms of KRAS and BRAF mutations.
Method: The study group comprised of adenomatous polyps (APs, n=20, 13.6 %), conventional adenocarcinomas (ConCA, n=30, 20.4 %), serrated polyps (SPs, n=67, 45.6 %) and mucinous adenocarcinoma (MucCA, n=30, 20.4 %). KRAS mutation was assessed for exon 2 and exon 3 using pyrosequencing while BRAF V600E mutation was analysed using allele specific PCR. Chi square test was used for statistics.
Results: KRAS mutations were observed in 41.5 % of carcinomas and 25.3 % of polyps. KRAS mutation rate was significantly higher (p<0.05) in ConCA (85 %) than in MucCA (50 %), and in APs (55 %) than in SPs (16.4 %). BRAF mutation was found in one MucCA (1.7 %) while all SPs were mutated. TSAs had the highest KRAS mutation rate (36.8 %) in comparison to SSA/Ps (17.6 %) (p<0.001) whereas SSA/Ps and HPs had significantly higher rates of BRAF mutation (64.7 %, 61.1 %, respectively) than TSAs (26.3 %) (p<0.001).
Conclusion: KRAS seems to take part in adenomatous sequence while BRAF, seem to play a significant role in serrated neoplastic progression of the colorectum.

PS-11-022
Characterizing quiescent ulcerative colitis: Pathologic review of 45 cases
J. Ferreira*, R. Fonseca, R. Ilgenfritz, I. Rosa, A. Nunes, A. Vieira, J. De Freitas, A. Dias Pereira, P. Borralho, P. Chaves
*IPO Lisboa Francisco Gentil, Serviço de Anatomia Patológica, Portugal

Objective: Quiescent ulcerative colitis (Q-UC) is morphologically characterized by typical architectural and cellular mucosal changes that define the process as chronic. It is not clear which of these changes are more ubiquitous in Q-UC. Our aim was to evaluate which classical histological findings of Q-UC are more prevalent in rectal samples.
Method: Rectal biopsies were collected from patients with clinical and endoscopical Q-UC. The biopsies were evaluated for mixed inflammation in the lamina propria, crypt architectural abnormalities, basal plasmacytosis, fibrosis, and Paneth cell metaplasia as well as for features of active disease (cryptitis, lamina propria neutrophils and erosion).
Results: Forty-five patients (64 % female; median age 56 years) were included. Thirteen (28,9 %) biopsies showed focal activity and four cases (8,9 %) had criteria for active disease. Epithelial distortion, chronic inflammatory infiltrate and basal plasmacytosis emerged as features present in 95, 81 and 73 % of biopsies. Overall, 4 biopsies were histologically normal (no chronic features, no active disease).
Conclusion: Rectal mucosa from patients with clinical and endoscopical Q-UC can show microscopic active disease, which illustrates that endoscopy alone may be insufficient to identify quiescent disease. In Q-UC, the most frequent changes (present in over 75 % of the biopsies) were epithelial distortion and chronic inflammatory infiltrate.

PS-11-023
Vacuum-based preservation of colorectal cancer specimens: A comparison with formalin fixation
J.-F. Fléjou*, S. El-Naderi, P. Cervera
*Hôpital Saint-Antoine, Dept. de Anatomie Pathologique, Paris, France

Objective: In Pathology, an alternative to immediate fixation in neutral buffered formalin (NBF) is vacuum sealing and cooling (VSC) ("Tissue safe" system). There have been few evaluations of VCS.
Method: We assessed MSI, KRAS, BRAF in colorectal cancers, conserved with VCS before fixation (51 cases with surgery in a hospital distant from our centre), or immediately fixed in NBF (56 cases with surgery during the same period in our hospital). DNA was extracted from paraffin embedded tissue. MSI was assessed by MLH1 and MSH2 immunohistochemistry and PCR; KRAS and BRAF were screened by multiwell-plate based real-time PCR (LightCycler® 480, Roche), confirmed by Sanger sequencing.
Results: There was no difference regarding morphological analysis. Immunohistochemistry was interpretable in all cases, with 4 negative cases in the VCS group (4 MLH1), 11 negative cases in the NBF group (10 MLH1, 1 MSH2), and a 100 % correlation between immunohistochemistry and PCR. DNA extraction was possible in all cases. KRAS and BRAF mutations were detected in 21 and 1 cases in the VCS group and 16 and 7 cases in the NBF group, respectively.
Conclusion: We show that analysis of MSI, KRAS and BRAF is feasible in surgical specimens after VCS. This procedure can be an alternative to formalin fixation.

PS-11-024
Clinical significance of CD204-positive M2 macrophage in colorectal cancer
S. Fushimi*, M. Matsumoto, S. Takahashi, T. Ogino, J. Itakura, T. Ito, A. Matsukawa
*Okayama University, Dept. of Pathology, Japan

Objective: Tumor-associated macrophages are divided into two phenotypes, termed M1/M2 macrophages. M1 macrophages promote tumoricidal responses whereas M2

macrophages assist tumor progression and metastasis. In this study, we have analyzed a clinical significance of M2 macrophages in excised sections from patients with colorectal cancer.
Method: Patients who had surgical resection for colorectal cancer between 2005 and 2006 were identified from a prospective database. Tissue sections with adenocarcinoma in pT3 category were employed in this study. The sections were stained with anti-CD204, a marker of M2 macrophages. The relation between the staining pattern and tumor budding or patient prognosis was examined.
Results: Fifty-two patients (30 male, 22 female) with a median age of 67 years (range 23–86) were studied. The tumors were classified into four subtypes according to the staining patterns of CD204-positive cells, i.e. sparse type (n=9), invading-tip type (n=6), peri-nest type (n=18), and dense diffuse type (n=19). Only a dense diffuse type was related to the high degree of tumor budding. The prognosis with a dense diffuse type demonstrated a poor prognosis as compared to the other types.
Conclusion: Even the case with comparable tumor depth, CD204-positive macrophages with dense diffuse distribution was related to the poor prognosis.

PS-11-025

Analysis of the pathological response in patients with locally advanced rectal cancer after pre-operatory treatment

J. Gordillo Chavez*, J. Moreno Casado, S. Moreno Martín, J. L. Domínguez Tristancho, L. Pozzati, A. Macayo, A. Plasencia, M. Escribano, M. Ortiz Monterrey, J. C. Melón
*Hospital de Merida, Anatomía Patológica, Merida (Badajoz), Spain

Objective: The treatment of locally advanced rectal cancer has shown a significant development over the last decade. The total mesorectal excision and the use of pre-operative radio (chemo)-therapy are leading the patients to a gradual improvement of local control of the disease. The aim of this study is to evaluate the pathological tumour response to pre-operative treatment through correlation between the clinical stage (cTNM) and the pathological stage (ypTNM).
Method: Since 2009, 35 patients with locally advanced rectal cancer, assessed by high resolution magnetic resonance imaging (HR-MRI) and TNM staging system, have been evaluated by the Colorrectal Multidisciplinary Team. Pre-operative radio (chemo)-therapy was mandatory before undertaking standard surgery. Surgical specimens were evaluated according to the Vikingo Project's protocol implemented by The Spanish Association of Surgeons.
Results: 34 patients completed the pre-operatory treatment. After evaluation of clinical and surgical study specimens, we observed variable degree of downstaging in 27 (79,5 %) patients, 5 of whom showed complete response. The 7 (20,5 %) remainig patients were assessed as stable disease. No local progression of tumours was observed.
Conclusion: In this study, approximately 80 % of patients, who were staged by HR-MRI and underwent preoperative radio (chemo)-therapy for locally advanced rectal cancer, showed some degree of downstaging. We remark the fact that nearly 15 % of patients reached complete response.

PS-11-026

The density of macrophages in colorectal cancer is inversely correlated to TGF-BETA1 expression and patients' survival

M. Gulubova*, I. Manolova, J. Ananiev
*Trakia University, General and Clinical Pathology, Stara Zagora, Bulgaria

Objective: The role of macrophages in colorectal cancer tumorogenesis is complex because they can both prevent and promote tumor development. We investigated CD68 infiltration in tumor tissue and its correlations with proteins ot TGF-beta1 signaling pathway.
Method: A nonselected panel of 206 primary tumors of colorectal origin was investigated immunohistochemically with antibodies against CD68, TGF-beta1, Smad4, Smad7, TGFRII and levels of TGF-beta1 were measured by ELISA.
Results: Lower CD68 infiltration in tumor nests was associated with expression of TGF-beta1 (chi2=9.236, p=0.002) and Smad4 (chi2=2.871, p=0.090) in tumor cells and with TGFRII expression (chi2=5.699, p=0.017) in tumor cells membranes. There was not correlation between CD68 cell numbers in tumor tissue and TGF-beta1 serum levels. We have found higher frequency of liver metastases in patients with lower infiltration with CD68 in invasive margin (chi2=11.364, p=0.001). The survival time was shorter for patients with low CD68 infiltration in tumor nests and invasive margin, compared with the survival time for patients, with higher CD68 infiltration in both tumor compartments (p<0.001).
Conclusion: The increased levels of TGF-beta1 in the tumor have an immunosuppressive effect on CD68 infiltration.

PS-11-027

Inflammatory myofibroblastic tumor of the colon: The 25th reported case

S. Gurzu*, T. Bara, I. Jung
*University of Targu Mures, Dept. of Pathology, Romania

Objective: Inflammatory myofibroblastic tumor (IMT) is a very rare tumor of the colon in which the diagnosis is

especially based on immunohistochemistry. In the colon, we report the 25th case of IMT.
Method: Case presentation
Results: We report the case of a 56-year old male who presented with symptoms suggesting colon cancer. A 20 mm protruded tumor was endoscopically described in the ascending colon. Right hemicolectomy was performed. Macroscopically the tumor was well defined, covered by normal mucosa with a central depressed area, suggesting a GIST (Gastrointestinal Stromal Tumor). Microscopically spindle cells with fascicular arrangement admixed with mononuclear leukocytes were observed. The tumor cells expressed Vimentin, SMA, Desmin and ALK and were CD34 and CD117 negative. Intense angiogenesis and CD117 expression in the endothelial cells were also observed.
Conclusion: In the IMT of the colon, clinical endoscopic and gross feature can imitate a carcinoma or a GIST. The IHC pattern of IMT can offer informations about its histogenesis. Based on the immunophenotype, we hypothesize that this tumor seems to occur from the the pluripotent stromal cells, CD34 positive which can be either differentiated in the interstitial cells of Cajal (telocytes), which are also CD34 positive or, during differentiation, can loss CD34 positivity.

PS-11-028
Development of a computerized morphometry application for assessment of tumor fraction in colon carcinoma tissue samples
D. Hershkovitz*, T. Hershkovitz, A. Shenhav, E. Sabo, O. Ben-Izhak
*Rambam Health Care Campus, Dept. of Pathology, Haifa, Israel

Objective: Determining the fraction of tumor cells in colon carcinoma samples analyzed for KRAS mutation is important for choosing the proper testing modality. However, when asked to determine tumor cell fraction in tissue samples, different pathologists give considerably different estimations, possibly leading to erroneous interpretation of KRAS mutation analysis results and poor treatment choices.
Method: We developed a free, easy to use computer program that estimates tumor cell fraction on colon carcinoma slides that are immune-stained with anti-cytokeratin antibody. Sixty samples were evaluated by the program and results were compared to actual measurement of tumor fraction.
Results: The tumor cell fraction estimated by the computer program showed highly significant correlation with the actual measurements (R=0.64, p<0.001). Additionally, we found that a short calibration step prior to beginning the computer estimation increased the accuracy of the results. In four cases (7 %) there was some discrepancy between the computer estimation and the actual measurements, however, this was attributed to lower quality immunohistochemical staining.
Conclusion: In conclusion, we believe that this program can be used for standardizing the evaluation of tumor cell fraction in colon carcinoma, and that its use might aid in making better diagnosis and treatment choices for these patients.

PS-11-029
Magnetic resonance imaging assisted tumour block selection in colorectal cancer
C. Hunter*, G. Brown, L. Temple, M. Abulafi, A. Arnaout
*Croydon University Hospital, Dept. of Colorectal Surgey, United Kingdom

Objective: Inadequate sampling may result in understaging in colorectal cancer. Fat clearance techniques and whole mount sections are time consuming and costly. We hypothesise that high resolution Magnetic Resonance Imaging (MRI) of the colorectal cancer specimen may aid histological sampling and result in upstaging.
Method: Patients undergoing resection are prospectively recruited, and randomised to "conventional histology" or "MRI assisted histology". In addition to routinely selected tumour blocks, 4 additional blocks and any additional lymph nodes are selected with the aid of specimen MRI or visual inspection and palpation according to group. T stage, depth of extramural invasion, distance to resection margin, lymph node (LN) number and involved LN are compared between the two groups.
Results: To date, 116 of 218 patients have been recruited. We present the methods and preliminary results. There is a trend towards greater T stage and LN yield. No difference in N stage, extra-mural vascular invasion or involved non-peritonealised resection margin has yet been observed.
Conclusion: Early results suggest that specimen MRI may upstage colorectal cancer specimens by aiding tumour block selection. We will complete recruitment of 218 colorectal cancer patients over the next 12 months to determine whether observed differences are significant.

PS-11-030
Diverticular disease of transverse colon is rare and perforation may occur in Crohns Disease
C. Hunter*, A. Arnaout
*Croydon University Hospital, Dept. of Colorectal Surgey, United Kingdom

Objective: Diverticular disease commonly affects the sigmoid colon in the West and the right colon in Asia. Perforation is uncommon affecting 4/100 000 per year. Perforated diverticular disease of the transverse colon is therefore very rare. We present a case of Crohns disease complicating

transverse diverticular disease that lead to perforation and unfortunate death.
Method: Radiological and histopathological features are presented with a review of the literature
Results: To the best of our knowledge, this is the first reported case of Crohns disease complicating diverticular disease of the transverse colon. We suggest that distal stricturing leading to increased intraluminal pressure or increased weakening of the colonic wall due to coincident Crohns fissure and diverticulum are possible pathogenic mechanisms.
Conclusion: Crohns disease complicating transverse diverticular disease is uncommon, but may be one pathogenesis leading to the rare event of transverse colon diverticular perforation.

PS-11-031
Analysis of acute cellular rejection in a series of 16 adult intestinal transplants of the Hospital 12 de Octubre (series 2004–2011), Madrid, Spain
C. Ibarrola*, P. López-García, G. López-Alonso, M. A. Martínez-González, M. Abradelo, A. Manrique, J. Calvo, C. Jiménez, E. Moreno-González, F. Colina
*Hospital 12 de Octubre, Pathology, Madrid, Spain

Objective: Intestinal transplantation is a therapy for irreversible intestinal failure. Acute rejection (AR) is the main cause of morbi-mortality.
Method: Review of 12 intestinal and 4 multivisceral transplants in 15 adult recipients with follow-up of 745 days (31-2019) to investigate the incidence, significance and outcome of AR.
Results: There were 12 episodes in 9 patients. They start between day 7 and 499 (178±159 days). Duration ranged from 3 to 87 days (27±22). The three moderate and the three mild AR reversed with treatment. Of the 6 severe AR, 3 caused the failure of the graft. Five episodes de AR began as moderate or severe directly. Severity in the course of each episode was fluctuating. Sixteen indeterminate rejections were seen in 9 grafts (did not reach definitive criteria). They lasted 1–31 days (mean: 5±8 days).
Conclusion: 1-Acute rejection is the most common cause of morbidity in the intestinal transplant (56 % of the grafts). 2-It can develop at any time and relapse. 3-The duration and severity of the episodes are fluctuating. 4-In our series, 75 % reversed, but severe rejection often lead to graft loss (50 %).

PS-11-032
Histopathological study of 7 intestinal grafts lost in a series of 16 adult transplants. Hospital 12 Octubre. Madrid. Spain
C. Ibarrola*, P. López-Garcia, G. López-Alonso, M. A. Martínez-González, M. Abradelo, J. Calvo, C. Jiménez-Romero, E. Moreno-Gónzalez, F. Colina
*Hospital 12 de Octubre, Pathology, Madrid, Spain

Objective: Intestinal transplantation is a therapy for irreversible intestinal failure. In 2004- 2011, 16 transplants were performed (12 isolated, 4 multivisceral) in 15 adults with a follow-up of 745 days (31-2019). Our goal is to determine the causes of intestinal graft loss (IGL).
Method: We studied 4 explants and 2 autopsy. The autopsy was not authorized in one death.
Results: Seven grafts were lost in 6 patients (3 multivisceral). Two types of failure were seen. A) local: 3 severe acute rejections (AR) (days 77, 158, 511) and 1 lymphoproliferative syndrome (LPS) in day 148; B) systemic: 3 sepsis (days 31,88,161). AR showed 3 types of morphology: ulcerative, pseudomembranous and with disappearance of the villi preserving the crypts. LPS was a high-grade B lymphoma and affected the graft and the lymph mesenteric nodes with venous thrombosis that cause ischemic necrosis. The 3 sepsis were due to acinetobacter, to adenovirus in the graft and pulmonary aspergillosis and to pseudomona aeruginosa with necrohemorrhagic pancreatitis.
Conclusion: 1- The incidence of IGL was 44 %. 2- The cause of IGL was local (AR and LPS) in 57 % and sepsis in 43 %. 3- Severe AR was the most frequent cause of failure. 4- Histological examination properly determine and document the causes of IGL.

PS-11-033
Cap polyposis: Report of two cases
R. Ivanova*, D. Kyoseva, G. Trifonov, R. Nikolov
*Hospital of Endoclinology, Laboratory of Pathology, Sofia, Bulgaria

Objective: Cap polyposis is a rare colorectal disease characterized by mucoid, bloody diarrhea associated with multiple inflammatory polyps covered by a cap of fibrinopurulent mucous. The disorder was first described in 1985 and up to date a small number of cases has been reported in the literature.
Method: We report two cases with multiple polyps of rectum and sigma, which were histologically diagnosed as cap polyposis.
Results: The cases were two males on age of 18 years and 64 years. In both cases there was a history of mucoid and bloody diarrhea. On the basis of colonoscopy findings, in the young patient there was a broad differential diagnosis including M. Crohn, inflammatory pseudopolyps and Cronkhite–Canada syndrome. In the second case the clinical diagnosis was polyps of sigma. Endoscopic biopsies and polypectomy were done. In both cases, the histology showed typical histological features of cap polyposis - polypoid lesions containing elongated, tortuous and often distended crypts covered by a cap of inflammatory granulation tissue.

Conclusion: The recognition of this rare disease is of practical significance because its clinical symptoms have some similarity with inflammatory bowel disease or irritable bowel syndrome.

PS-11-034

Histopathological findings in 496 consecutive appendectomies: A retrospective analysis

J. Jeruc*, Z. Dolenc Stražar, V. Jovic, A. Cerar, N. Zidar
*University of Ljubljana, Faculty of Medicine, Slovenia

Objective: Appendectomy is one of the most common surgical procedures. Histology usually confirms the clinical suspicion of acute inflammation, but sometimes other clinically relevant diagnoses are made. The aim of our study was to audit the appendectomies at our institution and summarise atypical pathological findings with emphasis on benign and malignant tumours.
Method: We reviewed the histopathology results of 496 consecutive appendectomies received in a 5-year period.
Results: Excluding three cases of metastatic process, appendiceal tumour was found in 21 cases (4.2 %), which is a higher rate than reported in the literature. There were four endocrine tumours, all G1, three cases of classical adenomas, 10 cases of low-grade appendiceal mucinous neoplasm (one associated with pseudomyxoma peritonei) and three cases of carcinoma (one mucinous adenocarcinomas, one intestinal type, one undifferentiated carcinoma). We also diagnosed one case of multicystic mesothelioma. Endometriosis was diagnosed in seven cases. In 18 cases appendicitis was associated with diverticula, in 6 cases changes were suggestive for Crohn's disease and in one case for cystic fibrosis. Negative appendectomy rate was 10.3 % that falls within the range reported in the literature.
Conclusion: Histopathological examination of appendectomy specimens may reveal many different conditions not previously suspected; therefore, it should be performed in all cases.

PS-11-035

CDX2 and MUC protein expression in small intestinal adenocarcinomas and their prognostic significances

S.-Y. Jun*, D.-W. Eom, Y.-K. Bae, K.-T. Jang, S.-M. Hong
*Incheon St. Mary's Hospital, Dept. of Pathology, Republic of Korea

Objective: Clinicopathological and prognostic significances of CDX2 and mucin core (MUC) proteins expression have not been comprehensively evaluated in the small intestinal adenocarcinoma (SIAC).
Method: Immunohistochemical expressions of CDX2, MUC1, MUC2, MUC5AC, and MUC6 in tissue microarrays of 189 surgically resected SIAC cases were examined and compared with clinicopathologic variables, including patients' survival.
Results: CDX2, MUC1, MUC2, MUC5AC, and MUC6 expression was observed in 39.7 % (75 cases), 35.4 % (67 cases), 27.5 % (52 cases), 28.6 % (54 cases), and 16.9 % (32 cases), respectively. While SIAC patients with CDX2 expression showed less nodal metastasis ($p=0.01$), those with MUC1 expression tended to have SIACs with nodular or infiltrative growth ($p=0.003$), poor differentiation ($p=0.005$), and more lymphatic invasion ($p=0.04$). MUC5AC expression was associated with SIACs with well differentiation ($p=0.02$) and frequent pancreatic invasion ($p=0.04$). Patients with CDX2+/MUC1- had more polypoid ($p=0.02$) and well differentiated ($p=0.006$) tumors and a significantly better survival (median, 80.8 months, $p<0.0001$) than those with other immunophenotypes (CDX2−/MUC1+, CDX2+/MUC1+, and CDX2−/MUC1−). Patients with CDX2 expression (median, 71.2 months) had a significantly better survival than those without CDX2 expression (23.0 months) by univariate and multivariate analyses ($p<0.0001$).
Conclusion: CDX2 expression is an independent good predictor of survival in surgically resected SIAC patients.

PS-11-036

Small neuroendocrine tumor of appendix with metastasis in the ileocecal lymphnode: A case report

G. Kalan*, S. Tušar, N. Zidar
*General Hospital Jesenice, Dept. of Pathology, Slovenia

Objective: Neuroendocrine tumors (NET) of appendix are believed to behave less aggressively than NETs at other sites. Separate staging criteria have therefore been proposed, and tumor size >2 cm appears to be the dominant criterion for aggressive behavior in appendiceal NETs. However, it is controversial whether radical surgery is indicated in tumors measuring >2 cm. We report a case of a 13-year-old girl with acute appendicitis in whom appendectomy and right-sided hemicolectomy were performed.
Method: Surgical specimens were sampled and processed according to standard histological and immunohistochemical (IHK) procedures.
Results: In the base of appendix, there was a tumor measuring 1.5 cm in diameter, focally invading mesoappendix, with free resection margins. Microscopically, tumor exhibited characteristic features of NET G1, with positive IHK for chromogranine and synaptophysin, and Ki67 index <2 %. IHK for podoplanin revealed focal lymphovascular invasion. In the right-sided hemicolectomy specimen, there was no residual tumor, metastasis was found in one ilecoecal lymphnode.
Conclusion: Our case shows that appendiceal NET smaller than 2 cm can metastasize to regional lymphnodes. IHK against podoplanin might be helpful in searching for lymphovascular invasion, helping to separate it from the

retraction clefts, thus providing additional information concerning risk factors for a more aggressive behavior.

PS-11-037

Lipomatosis of ileocaecal valve causing small bowel obstruction mimicking Crohn´s Disease

M. Kalman*, P. Szépe, J. Marcinek, T. Balhárek, L. Plank
*University Hospital Martin, Dept. of Pathology, Slovakia

Objective: Lipomatosis of ileocaecal valve is a rare cause of small bowel obstruction.
Method: We describe a 41-year-old male treated for Crohn´s disease and clinical and imaging presentation of chronic small bowel stenosis and obstruction.
Results: A right hemicolectomy was performed, and hypertrophy of Bauhin´s valve causing intestinal obstruction was found. Microscopical examination of the specimen revealed morphological changes consistent with lipomatosis of the ileocaecal valve. The ileum and colon were macroscopicaly unremarkable and histomorphological features of Crohn´s disease were absent.
Conclusion: Many patients with lipomatosis of the ileocaecal valve are asymptomatic, or the lipomatosis gives causes insignificant symptoms only or rarely obstruction may occur. Then, as in the presented case, the surgical resection with ileo-colic anastomosis is the only effective treatment.

PS-11-038

Overexpression of CXCR4 in tumor buds is a strong predictor of lymphatic invasion and lymph node metastasis in colorectal cancer

E. Karamitopoulou-Diamantis*, D. Kassahn, I. Zlobec, V. Koelzer, H. Dawson, A. Lugli
*Universität Bern, Inst. für Pathologie, Switzerland

Objective: CXC chemokines enhance tumor cell survival and proliferation. Especially CXCR4 promotes tumor development by stimulating angiogenesis and favoring metastasis. In contrast, CXCR3 is angiostatic and may exert an anti-tumor effect. Since tumor budding is linked to vascular/lymphatic invasion and lymph node (LN) and/or distant metastasis in colorectal cancer (CRC), here we explored the expression of CXCR3+4 in relation to tumor budding.
Method: A multiple-punch tissue microarray of 220 CRCs with full clinicopathological information including therapy underwent immunohistochemistry for CXCR3 and CXCR4. Expression was evaluated in tumor-center, -front and -buds and correlated to clinical data.
Results: CXCR3-expression was homogeneous throughout tumor-center, -front and -buds (average 40 %) and was unrelated to clinicopathological features or survival. CXCR4-expression was high in tumor-center and -front but reduced ($p<0.001$) in buds (76 %, 77 %, and 20 %, respectively). Maintenace of CXCR4-expression within buds was predictive of LN-positivity ($p<0.0001$) and lymphatic invasion ($p<0.0001$) but not of venous invasion or distant metastasis. CXCR4-positivity in buds was associated to poor outcome ($p=0.0048$) in LN-negative CRCs ($p=0.0191$).
Conclusion: Maintenance of CXCR4-expression in buds has a profound effect on tumor aggressiveness and prognosis in LN-negative CRC-patients. This would help in establishing a tumor budding "profile" especially linked to LN-metastasis in CRC.

PS-11-041

COX-2 expression in serrated polyps of the colon does not discriminate specific histological subtypes

M. Kiedrowski*, A. Mroz, A. Felisiak, A. Rembiszewska, J. Orlowska, J. Kupryjanczyk
*Oncology Center Warsaw, Dept. of Pathology, Poland

Objective: COX-2 expression was investigated in colorectal cancer and colorectal precancerous lesions. Its expression in adenomas is associated with increasing size and neoplastic potential. Little is known about COX-2 expression in subtypes of serrated colonic polyps, which constitute substantial number of colon cancer precursors. The aim of the study was to assess COX-2 expression in serrated polyps of the colon and to investigate its potential discriminative role.
Method: 175 consecutive serrated polyps were analyzed. They included: 26 traditional serrated adenomas (TSA), 36 sessile serrated polyps (SSP) and 113 hyperplastic polyps (HP). COX-2 expression was assessed semi-quantitatively (0–3). Kruskall-Wallis test was used for the comparison of COX-2 expression between serrated categories ($\alpha=0.05$).
Results: We found COX-2 positivity in 19 of 26 TSA (73.0 %), 27 of 36 SSP (75.0 %), 78 of 113 HP (69.0 %), respectively. No differences in COX-2 expression were found between serrated subgroups.
Conclusion: The results may suggest no discriminative role of COX-2 within serrated neoplasia pathway.

PS-11-042

Heterogeneous expression of Ki67 staining in tumor buds implies different prognostic outcomes in colorectal cancer

A. Lugli*, H. Dawson, V. Koelzer, E. Karamitopoulou--Diamantis, I. Zlobec
*Medizin. Universität Bern, Institut für Pathologie, Switzerland

Objective: In colorectal cancer (CRC), tumor buds represent a more aggressive tumor cell type at the invasive front

with apparently low proliferation. The aim of this study was to determine the proliferation potential of tumor buds by comparing Ki67 staining across different tumor areas and adjacent normal tissue.
Method: Whole tissue sections from 197 patients with CRC underwent immunohistochemistry for Ki67. 10 high-power-fields were evaluated for each of the following regions: normal mucosa, tumor center, tumor front and tumor buds. Ki67-positivity was correlated to patient outcome.
Results: Average Ki67-positivity was 5.2 % in normal mucosa and significantly higher in the tumor center (38.2 %; $p<0.0001$) and invasion front (34.9 %; $p<0.0001$). Strikingly, only 0.3 % of all tumor buds showed Ki67-positivity ($p<0.0001$). Although Ki67-positivity in the tumor center or front was unassociated with clinicopathological features or patient survival, the greater the number of Ki67-positive tumor buds, the worse the prognosis. This effect was also found after adjusting from TNM stage (HR (95 % CI): 2.25 (1.1–4.5); $p=0.0193$)).
Conclusion: A marked absence of Ki67 staining is found in most tumor buds, suggesting a substantially decreased proliferation rate. However, the association of Ki67-positivity with worse prognosis in 15 % of cases points towards a heterogeneous population of tumor buds.

PS-11-043
Kayexalate and intestinal necrosis: An underrecognised entity
P. Luís*, A. Alves, C. Ferreira
*Hospital de Santa Maria, Dept. de Anatomia Patológica, Lisboa, Portugal

Objective: There are only few cases of intestinal necrosis secondary to administration of kayexalate described in the literature, most of them from postoperative patients, having the largest study only 11 patients in 9 years. We report our experience in the last 4 years with a brief review of the pathophysiology and histologic aspects of the lesions induced by the kayexalate.
Method: Between 2008 and March 2012 seven patients were diagnosed with ischemic necrosis related to kayexalate administration, five in colon biopsy and two in resection specimens. They're comorbidities and clinical evolution was extracted from the medical records.
Results: The patients' age ranged between 47 and 78 years. In one case we had the clinical information of chronic renal insufficiency. In three of them, there was no previous history of renal impairment. One patient developed symptoms after one single administration of kayexalate. The clinical presentation ranged from abdominal pain, gastrointestinal bleeding and three of them had a fatal outcome.
Conclusion: The administration of kayexalate can have associated risks with different clinical impact in any patient. We must be aware of the related complications, as the histological identification of the kayexalate crystals indicates the etiology of the ischemic lesions to the clinicians and alerts them to the dangers of this therapeutic.

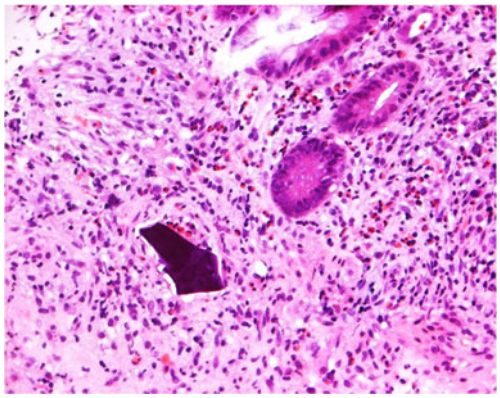

PS-11-044
Absence of K-Ras mutations in colorectal cancer is associated with EGFR overexpression
E. Melucci*, V. Dimartino, M. G. Diodoro, V. D´Alicandro, A. Di Benedetto, C. Ercolani, B. Antoniani, F. Cognetti, C. Garufi, E. Pescarmona, M. Mottolese
*Regina Elena Cancer Institute, Dept. of Pathology, Rome, Italy

Objective: EGFR plays an important role in colorectal cancer (CRC) progression and represents a natural target for molecular anticancer drugs. In this study we evaluated 800 consecutive CRC aimed to analyze K-Ras mutational status in relationship to: different clinical-pathological parameters, EGFR immunohistochemical (IHC) expression, response to cetuximab treatment.
Method: K-Ras mutations and EGFR expression were determined by direct cycle sequencing and IHC respectively in 565 surgical specimens and 235 biopsies. IHC findings were evaluated using four different score systems.
Results: The distribution of K-Ras mutations did not significantly vary between surgical or bioptic specimens or with respect to different anatomic tumor localization. In contrast, K-Ras is more frequently mutated in EGFR negative/low score tumors than in positive ones ($p<0.0001$). Focusing on the 419 surgical treated CRC patients, we found a higher percentage of K-Ras mutations in T4 CRC ($p=0.01$) and in younger patients ($p=0.002$). Finally, we observed that 6 % of primary CRC, concomitantly evaluated with their paired metastases, changed K-Ras mutational status during progression.
Conclusion: Our data showed that tumor size, patient age and EGFR IHC expression significantly influenced K-Ras

mutations. Interestingly, we observed that cetuximab treated patients, had a better clinical outcome when EGFR presented a high IHC score.

PS-11-045

Multiple Immunohistochemical investigation of signaling pathways in colorectal cancer

T. Micsik*, L. Kopper, T. Krenács, Z. Nagy, O. Horváth
*Semmelweis University Budapest, 1st Department of Pathology, Hungary

Objective: Despite the recent advances in therapeutic armamnet colorectal cancer (CRC) remains one of the leading cancer deaths worlwide. CRC has a heterogenous molecular background with known prognostic and predictive markers, but the whole picture is rather complex with many unexplored connections.
Method: We performed multiple immunohistochemical stainings on tissue microarrays (TMA) made of 95 CRC cases to study the correlations between EGFR-RAS, cell cycling, apoptosis, cell adhesion and tumor invasion pathways. We evaluated digitized slides using matrix scores considering both the frequency and positivity of cells and statistical analysis followed.
Results: We found strong linear correlation between positivity and (p-1068, p-1173) phosphorylation of the EGFR receptor and p53 positivity detected with different clones. Furthermore, phospho-NF-KB p65 positivity was strongly linked to Survivin-expression.
Conclusion: Activation of EGFR-related pathways including NF-kB is a key factor in CRC-growth. The strong link between cancer promoting EGFR signaling and the mutational lack of the p53 driven apoptosis suggests a deadly cooperation, which can be further aggravated by forced tumor survival through survivin. Correlation of these markers potentially predict poor disease outcome but can be specifically targeted by the upcoming new molecules of tailored therapy.

PS-11-047

KRAS status in colorectal carcinoma: Assessment in primary and metastatic tumors

E. Musulen*, A. M. Munoz Marmol, C. Sanz, J. Alvaro, M. Lopez Pena, V. Jerez, A. Ariza
*Hospital Germans Trias i Pujol, Dept. of Pathology, Barcelona, Spain

Objective: KRAS mutational status is important in colorectal carcinoma (CRC). It is unclear, however, which is the most informative tissue source for study in CRC cases showing more than one tumor mass. To explore this issue we determined KRAS status in a series of primary (PT) and metastatic CRCs.
Method: A total of 68 tumors belonging to 25 patients (17 males and 8 females) with ages ranging between 46 and 80 years (average, 64 years) were studied. KRAS mutation hotspots in codon 12 and 13 were analyzed by polymerase chain reaction and sequentiation. wt-KRAS cases were confirmed with the KRAS StripAssay TM.
Results: KRAS mutations were found in 11 (44 %) of the 25 PTs, 8 (73 %) in codon 12, and 3 (27 %) in codon 13. PTs and their metastases showed similar genotypes in 21 (84 %) cases. The 4 (16 %) cases with dissimilar results showed the following combinations: wt-KRAS/KRAS c.35 G>A:p. Gly12Asp (n=1); wt-KRAS/KRAS c.35 G>T:p. Gly12Val (n=1); wt-KRAS/KRAS c.50 G>T:p. Ser17Ile (n=1) and KRAS c.35 G>A:p. Gly12Asp/wt-KRAS (n=1).
Conclusion: Most primary CRCs and their metastases are genotypically very similar. Even so, if metastatic tumor tissue is available we recommend its study over that of the PT, since de novo mutations may supervene in CRC metastases.

PS-11-048

Usefulness of EPCAM expression in the algorithmic approach to Lynch Syndrome in colorectal carcinoma

E. Musulen*, C. Carrato, M. T. Fernandez Figueras, R. Marginet, I. Blanco, A. Ariza
*Hospital Germans Trias i Pujol, Dept. of Pathology, Barcelona, Spain

Objective: Lynch syndrome (LS), the most frequent form of hereditary colorectal cancer (CRC), is caused by germline mutations in the mismatch repair system genes. A recently identified mechanism involving the EPCAM gene is responsible for 6.3 % of MSH2-negative LS cases. We herein explore EPCAM protein expression in LS-associated, MSH2-negative CRCs to evaluate its potential value in the algorithmic approach to LS population screening.
Method: We studied a total of 19 MSH2-negative CRCs from 14 different patients in whom we were able to perform a complete germline analysis. Expression of both MSH2 (1:200 dilution, clone G219-1129, Pharmingen) and EPCAM (1:100 dilution, clone Ber-EP4, Dako) was evaluated by immunohistochemistry (IHC).
Results: Nine patients showed a deleterious germline mutation that involved the MSH2 gene in three instances and the EPCAM gene exon 9 in six instances. All patients harbouring the EPCAM mutation belonged to the same family. Of the19 CRCs, EPCAM expression loss was seen in only five, all of them were from patients with a germline EPCAM deletion.
Conclusion: Due to the high specificity of EPCAM protein loss for identifying LS patients with an EPCAM deletion, we recommend adding EPCAM IHC to the LS diagnostic algorithm in MSH2-negative CRC cases.

PS-11-049

BRAF mutation in colorectal carcinomas with signet ring cell component

O. Onguru*, S. Yalcin, E. Altayli, M. Ozturk, N. Ersoz
*GATA, Dept. of Pathology, Ankara, Turkey

Objective: Colorectal carcinoma with signet ring cell component (CRC-SRC) is a rare and distinct subtype with little molecular information. We investigated the frequency of BRAF mutation in 28 CRC-SRCs and its relation with clinicopathologic parameters.
Method: We categorized tumors into groups 0–9 %, 10–24 %, 25–49 % and >50 % according to signet ring cell component. Genomic DNA was isolated from parafin blocks and analyzed for BRAF V600E mutation by polymerase chain reaction - restriction fragment length polymorphism (PCR-RFLP).
Results: Eleven of cases showed BRAF mutation (39.3 %). The results were also confirmed with sequence. No statistically significant differences were found in clinicopatologic parameters between BRAF wild-type and mutant CRC-SRC. On the other hand, when we adjusted age, gender, percentage of signet ring compenent and stage, we found a statistically significant increased risk in BRAF mutant group compared to BRAF wild-type in Cox regression analysis (HR=7.68, 95 % CI=1.06–55.78, p=0,044)
Conclusion: BRAF mutation is frequent in CRC-SRCs. This finding may support its diverse molecular pathogenesis and could have important therapeutic implications for those patients. To clarify the relation of BRAF mutation with clinicopathologic parameters and prognosis in CRC-SRC, studies with multi-instutional larger series are needed.

PS-11-050

Coexisting lipomas and adenocarcinoma of the colon: Case report

G. Orgun Sonmez*, U. Bayol, O. Akman, S. Cumurcu, M. Olmez
*Tepecik Research and Training Hospital, Izmir, Turkey

Objective: Lipomas of the large bowel are rare, they are invariably submucosal and therefore may intussuscept. Infrequently lipomas may also present in the form of multiple polypoid masses in the colon. We present a 69-years old female with 3 submucosal lipomas and a coexisting adenocarcinoma of transverse colon.
Method: 69-years old female patient was admitted to hospital because of rectal bleeding for 3 months. Colonoscopic examination revealed mucosaly intact polypoid tumoral masses and an ulcerated tumoral mass in transverse colon. Biopsy of the ulcerated mass was diagnosed as adenocarcinoma. Extended right hemicolectomy was performed.
Results: Grossly, ulcerated tumor was 1,5×1×0,4 cm and there were 3 polypoid tumors in cecal area of the right colon which were 2.5–2.0–1.5 cm in their greatest dimensions. Polypoid tumors were yellow, lipomatous on cut surfaces. Microscopically ulcerated tumor was composed of adenocarcinoma morphology and the other polypoid tumors were composed of submucosal mature adipocytes with a thin capsule around them. The diagnosis was colonic adenocarcinoma (pT1N0M0) and submucosal lipomas of colon. The patient had no additional therapy and she is healthy with no evidence of recurrence.
Conclusion: This case is presented to remind that there may be multiple lipomas of colon with coexisting malignant epithelial tumors.

PS-11-051

Myxoid liposarcoma of the ileum: A case report

Y. Otsuki*, S.-I. Shimizu, Y. Egawa, H. Sugimura, H. Kobayashi
*Seirei Hamamatsu General Hospital, Dept. of Pathology, Japan

Objective: Primary liposarcoma of the small intestine is exceedingly rare. To our knowledge, only 7 cases have been reported so far. We report a case of the primary myxoid liposarcoma of the ileum.
Method: The patient was 77-year-old woman. CT and MRI revealed a 6-cm-intrapelvic mass, which was proved to be a tumor of the distal part of the ileum, and, therefore, partial ileectomy was performed.
Results: The tumor was 6.7×6.3×3.7 cm in size, relatively well circumscribed and located within the intestinal wall without invasion to the neighboring tissues. Microscopically, the tumor had mixture of cellular and myxoid areas, showing proliferation of short spindle and stellate shaped cells in a delicate capillary vasculature. Univacuolated tumor cells and a small number of lipoblast-like cells were also seen. Immunohistochemically, these proliferating cells were positive for S-100 protein. According to these pathological findings, we diagnosed the tumor as myxoid liposarcoma. FISH methods showed the tumor had chromosomal translocation t(12;16)(q13;p11).
Conclusion: The differential diagnosis of this includes other spindle cell tumors such as GIST and myogenic tumors. But we could arrive at the proper pathological diansosis following the above morphological features and the specific chromosomal

translocation. We will also discuss the clinico-pathological features of the cases including ours.

PS-11-052

Prognostic significance of selected immunohistochemical markers in colorectal cancer

E. Paltseva*, O. Samofalova, Y. Gorbacheva, P. Tsarkov
*First Moscow State Medical University, Pathology, Russia

Objective: The aim of our study was to identify a combination of markers whose expression is predictive of invasion and metastasis of colorectal carcinoma.
Method: The expression of E-cadherin, β-catenin, tenascin C, KAI-1, epidermal growth factor receptor (EGFR) and vascular endothelial growth factor (VEGF) was studied immunohistochemically and correlated clinicopathologically in 72 primary colorectal carcinoma cases (26 with metastatic lymph nodes). 17 patients (24 %) developed haematogenous metastases at median 6,5 months postoperatively (3–11).
Results: Expression of following markers significantly correlated with depth of tumour invasion: cytoplasmic accumulation of E-cadherin (p=0,035), nuclear staining for β-catenin (p=0,03), increased tenascin C expression (p=0,001), and loss of EGFR and VEGF expression (p=0,015 and 0,02, respectively). Decreased tenascin C and KAI-1 expression associated with the presence of lymph node metastases (p= 0,027 and 0,046, respectively). Weak cytoplasmic E-cadherin expression correlated with distant metastases (p=0,045).
Conclusion: Our results suggest that abnormal expression of proteins involved in cell adhesion and migration (E-cadherin, β-catenin, tenascin C, EGFR) and angiogenesis (VEGF) may be related to the invasion of colorectal carcinoma. Detecting the expression of E-cadherin, tenascin C and KAI-1 probably possesses clinical significance in evaluating lymph node and distant metastasis and predicting the prognosis of colorectal cancer.

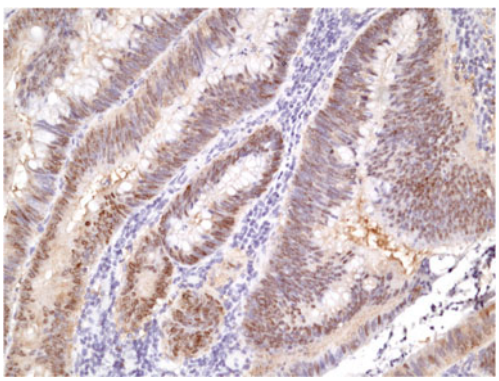

PS-11-053

p53 and PTEN immunoexpression in colon adenomas

Z. Pap*, L. Dénes, S. Mocan, K. Brînzaniuc, I. Jung, Z. Pávai
*UMF Targu Mures, Dept. of Anatomy, Romania

Objective: The PI3K signaling pathway is antagonized by phosphatase and tensin homologue (PTEN) activity. In human cells, the activation of PI3K signaling by mutations in PTEN can lead to activation of p53.
Method: We studied immunoexpression of PTEN and p53 in 59 colon adenomas and polyps (A/P): hyperplastic polyps (HP), serrated adenomas (SA), tubular adenomas (TA), tubulo-villous adenomas (TVA), and 7 in situ carcinomas (CC), using the Ultravision Labeled Polymer System method. We established frequency (p53, PTEN) and intensity of the reaction (PTEN).
Results: PTEN expression was decreased in 42 % of A/P and in 57 % of CC. PTEN expression is more frequently lower in HP, A/P with dysplasia, A/P located in the left colon and in case of young patients. A/P are mainly p53+/PTEN+, while CC are p53+/PTEN−. The majority of TA and SA are p53+/PTEN+, and HP are p53+/PTEN−.
Conclusion: p53 overexpression is associated with altered PTEN expression in colorectal carcinogenesis. Acknowledgments: This study is partially supported by the Sectoral Operational Programme Human Resources Development, financed from the European Social Fund and by the Romanian Government under the contract number POSDRU/89/1.5/S/60782.

PS-11-054

Immunohistochemical expression of mismatch repair proteins in colorectal carcinomas of the Epirus region

M. Papageorgiou*, A. Batistatou, A. Papoudou-Bai, V. Siozopoulou, D. Stefanou
*Ioannina, Greece

Objective: In colorectal adenocarcinomas (CRCs) microsatellite instability (MSI) can be documented by immunohistochemical detection of mismatch repair proteins (MMR). The aim of the present study is to identify the percentage of MSI-positive CRCs, in the Epirus region of Greece and compare it to the international data.
Method: A total of 50 cases of sporadic CRCs, 25 adenomas and 10 hyperplastic polyps, formalin-fixed paraffin-embedded, were examined immunohistochemically using standard methods (En Vision system), with the antibodies MLH1 (Clone ES05), MSH6 (Clone PU29) and PMS2 (Clone M0R4G) (Novocastra-Menarini). Immunostained sections were evaluated semi-quantitatively, taking in account the percentage of neoplastic positive cells and estimating nuclear staining intensity, compared to the internal positive controls (normal epithelium, lymphocytes).
Results: All hyperplastic polyps and adenomas expressed the examined MMR. Two out of 50 CRCs were negative for MSH6 and PMS2, while one of them was also negative for MLH1. Interestingly, one of these two CRCs had an

adjacent adenoma, which also showed negative staining for MSH6 and PMS2.

Conclusion: Immunohistochemical staining for MMR is possible in archival material. Loss of MMR varies, depending on the protein examined. In CRCs from the Epirus region the estimated loss of at least two MMR is 4 %.

PS-11-055

Gelatinases expression in 53 Tunisian sporadic colorectal cancer cases

B. Saadia*, K. Triki, D. Ounissi, M. Khiari, I. Chaar, A. Semeh, G. Lassad, B. H. Abdelmajid, M. Sabeh
*Mongi Slim Hospital la Marsa, Cytology and Pathology, Tunis, Tunisia

Objective: Matrix metalloproteinases (MMPs) are a family of zinc-dependent neutral endopeptidases collectively capable of degrading essentially all extracellular matrix (ECM) components. Genetic alterations in MMP-2 and MMP-9 have been implicated to play an important role in colorectal carcinogenesis (CRC). The aim of this study was to investigate the hypothetic correlations between the MMP-2 and 9 mRNA expression and the clinicopathologic variables of the CRC.

Method: The expression of MMP-2 and -9 mRNA was assayed by RT-PCR for 53 Tunisian sporadic colorectal adenocarcinomas.

Results: MMP-2 was highly expressed in the 53 cases. MMP-9 was not detected in 18 cases and moderately or highly expressed in 35 cases. Absence of MMP-9 mRNA expression was significantly related to an advanced tumoral invasion stage (pT3) ($p=0.003$).

Conclusion: Our study suggests that the overexpression of MMP-2 could be the result of an imbalance in the system of transcriptional regulation of MMP-2, which would involve the loss of expression or activity of its inhibitor: TIMP-2. A variable expression of transcripts of MMP-9 could be explained by the hypothesis of hypermethylation of the promoter or degradation of its transcript after protein translation.

PS-11-056

Relationship between matrix metalloproteinases 2 and 9 promoter polymorphisms and colorectal cancer risk

B. Saadia*, D. Ounissi, K. Triki, I. Chaar, M. Khiari, A. Semeh, G. Lassad, B. H. Abdelmajid, M. Sabeh
*Mongi Slim Hospital la Marsa, Cytology and Pathology, Tunis, Tunisia

Objective: The carcinogenic schema of colorectal cancer (CRC) follows a multistep process governed by mutational events that affect multiple micro-environmental factors, including matrix metalloproteinases (MMPs). This present work aims to contribute to a better understanding of MMP-2 and -9 promoter polymorphisms involvements in the genesis and progression of sporadic CRC in Tunisian population.

Method: The MMP-2 and MMP-9 promoter genotypes were determined by PCR-RFLP in 53 Tunisian patients with sporadic colorectal cancer and 69 healthy control subjects.

Results: No significant associations were found regarding MMP-2 (-1306 C/T) polymorphism and CRC susceptibility. There was a connection between the MMP-2-1306 promoter polymorphism and gender ($p=0.012$). The MMP-9 (−1562 C/T) was significantly associated with CRC (OR= 2.39 [1.023 to 5.58]). No implication of MMP-9-1562 promoter polymorphism in the clinicopathological parameters of CRC was evident.

Conclusion: Our findings suggest that the MMP-2 promoter polymorphism was not a predictive factor for the CRC occurrence while the MMP-9-1562 CT genotype was a risk factor for CRC susceptibility.

PS-11-057

Hodgkin's lymphoma in distal rectum in a patient with Crohn´ Disease treated by biologic therapy – A case report

R. Sampaio*, F. Costa, E. Diane, J. Palla Garcia, J. R. Vizcaino
*Anatomia Patológica, Valpaços, Portugal

Objective: Rare cases of Hodgkin`s lymphoma have been reported in the setting of inflammatory bowel disease.

Method: We report a case of Hodgkin`s lymphoma in a 37 years old male patient with corticosteroid-dependent Crohn´ Disease (CD) who had been medicated with azathioprine for many years. In the last 4 years he began periodical therapy with infliximab, till the time when he complained of worsening of symptoms and the appearance of asthenia, tenesmus and weight loss. Infliximab was withdrawn and replaced by adalimumab. A colonoscopy with several biopsies revealed the presence of a Hodgkin Lymphoma.

Results: The histological examination revealed granulation tissues where we identified atypical cells (Reed-Sternberg cells) with the following immunohistological staining: CD30+, CD15+, LMP1+LCA-, CD20-, CD3-, ALK-. These results in conjunction with the morphological aspects and the clinical history of CD favored the diagnosis of Hodgkin Lymphoma in a patient with preceding CD. The patient was subjected to radical colectomy. Postoperative pathological examination showed CD with involvement of the distal rectum by Hodgkin's lymphoma.

Conclusion: The present report may serve as a reminder to clinicians of the possibility of occult lymphoma in patients with colonic CD treated with biological therapy.

PS-11-058

Immunohistochemical testing of microsatellite instability in Stage II Colon Cancer: Outcome analysis of 352 cases

M. Saravia*, N. Tarazona Llavero, C. Mongort, D. Roda Perez, A. Cervantes, S. Navarro
*Hospital Clinic University Valencia, Dept. of Pathology, Spain

Objective: DNA mismatch repair (MMR) status in sporadic colonic cancers (CCs) had provided valuable prognostic and predictive information in the appropriate clinical setting; however there are no definitive guidelines for microsatellite instability (MSI) testing. We evaluated the expression of MMR proteins and correlated them with outcome in a cohort of patients with sporadic colon cancer.
Method: We reviewed 352 cases of sporadic stage II colonic cancer from Abril 27th 1995 to December 12th 2009. Clinical data including tumor grade, prognostic factors, therapy and outcome were searched for. Tissue microarrays using a manual Beecher system were constructed and stained with antibodies for MLH1, MSH2, PMS2 and MSH6.
Results: 8 % (28) of 352 CCs had loss of expression of one or more MMR proteins, including defect in 1 protein 3.7 % (13), 2 proteins 3,7 % (13) and tree proteins 0,6 %(2). The mean overall survival was 144 months with no significant differences in patients between microsatellite stable and unstable tumors.
Conclusion: We detected a fairly low prevalence of the loss of immunohistochemical expression of MMR proteins. This result might have influence our mean overall survival between microsatellite stable and unstable tumors.

PS-11-059

The pathological effects of orchidectomy on intestine tissue and serum level of carcino embryogenic antigen

S. Sattari*, R. Ahmadi
*Azad University of Iran, Science Dept., Hamedan, Iran

Objective: Carcino Embryogenic Antigen (CEA) is a well-known tumor marker influenced by carcinogenic changes in intestine tissue. The purpose of this study was to determine the effects of orchidectomy on serum level of CEA and histological changes of intestine in male rats.
Method: Male Wistar rats were randomly divided to control, sham, uni-orchidetomised and biorchidectomised groups of 5 in each. 10 weeks after operation, blood samples were collected using cardiac puncture method. Serum CEA level was measured using ELISA method. The effect of orchidectomy on intestine tissue was also histologically studied. The results were statistically analyzed using ANOVA.
Results: Serum level of CEA was significantly increased in orchidectomised rats compared with control animals ($P<0.001$). The increase in serum CEA level was more in biorchidectomised than uniorchidectomised rats ($P<0.001$). There was also an enhancement in tissue lymphocytes, plasma cells and inflammation in intestine of orchidectomised animals.
Conclusion: The results showed that orchidectomy results in pathological changes in intestine tissue leading to increased serum CEA level.

PS-11-060

The plasma cells density in pararectal lymph nodes of patients with rectal cancer after neoadjuvant therapy

M. Sezak*, N. Ozsan, B. Pehlivanoglu, S. Ozkok, T. Yoldas, B. Daganavsargil
*Ege University, Dept. of Pathology, Izmir, Turkey

Objective: Neoadjuvant chemoradiotherapy (NT) is standard procedure for locally advanced rectal cancer. In this study, we compared the morphology of lymph nodes and the amount of plasma cells in the interfollicular region of lymph nodes in rectal tumour surgical excision material, between two groups who had received and not received NT prior to surgery.
Method: Fifty cases with NT and forty cases without NT were included. The number and diameter of lymph nodes were recorded. The morphology of the lymph nodes were evaluated, and the percentages of interfollicular plasma cells were demonstrated immunohistochemically (CD138). Tumor regression grade was assessed using Mandard scoring system.
Results: Average number and diameter of lymph nodes were greater in patients without NT ($p<0,05$). Atrophy of germinal centers was noted as 54 % in NT group, versus 5 %. The amount of plasma cells in the interfollicular region was found to be higher than fifty-one percent in 54 % of NT group versus 5 % ($p<0,05$), as well. Complete response rate (Mandard's: 1) was 18 %. No significant association was found between the amount of plasma cells and tumor regression.
Conclusion: NT leads to a decrease in the volume of the lymph nodes and atrophy of germinal centers, conversely, causes stimulation of the proliferation of interfollicular plasma cells.

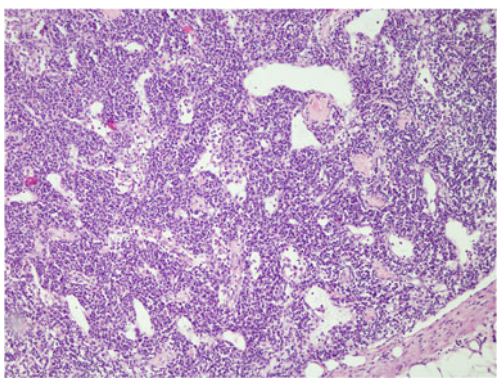

PS-11-061

Adenomyoma of the ileum: Pathohistological features with reference to pathogenesis

B. Snezana*, B. Andrejic, N. Solajic
*Clinical Center of Vojvodina, Center for Pathology, Novi Sad, Serbia

Objective: Adenomyoma is a rare benign non-neoplastic tumor-like lesion. It originates from abnormal embryonic buds but its pathogenesis has not been fully elucidated.
Method: A 63-year old man with severe pain, intussusception and ileus underwent a resection of a part of the intestine containing a tumor mass acting as a lead point. Tissue was analysed using H&E, histochemical and immunohistochemical stains.
Results: Lesion located in the mucosa, submucosa and muscularis propria consisted of glandular structures varying in size and morphology, the larger ones containing papillary projections and the smaller ones being similar to Brunner's and peribiliary glands, both of them surrounded by smooth muscle bundles. The lesion was not accompanied by ectopic pancreas, and it indicated a diagnosis of adenomyoma of the ileum. Glandular elements were CK7+ and CK20− and CDX-2−, opposite to intestinal mucosa.
Conclusion: Adenomyoma is a mass lesion rarely found distal to the duodenum, which bares close clinical and morfological resemblance to a tumor and some non-neoplastic conditions. Cytokeratin expression favors the heterotopic pancreas theory of pathogenesis, but abnormal interaction between the endoderm- and mesoderm-derived tissues can not be excluded.

PS-11-062

Smoothelin in biopsies of colorectal carcinomas as marker of muscularis propria invasion

P. Stoemmer*, P. Torres-Galea
*Gemeinschaftspraxis Pathologie, Forschungslabor, Augsburg, Germany

Objective: Staging of colorectal carcinomas is of eminent importance for prognostication and treatment; preoperative distinction between high grade dysplasia, invasion of submucosa (with permigration of the muscularis mucosae MM) and infiltration of muscularis propria (MP) is difficult in biopsies, due to similarities of smooth muscle cells in MM and MP. Smoothelin is a robust marker of the MP in normal colon, not expressed in MM.We analysed it value for distinguishing MP and MM near carcinomas.
Method: 50 colorectal carcinomas, diagnosed in biopsy particles and staged in the surgical specimens were analysed by IHC for expression of smoothelin (MoAb R4A, DCS Hamburg).
Results: Desmin and SMA were consistently expressed in the smooth muscle cells of MM and MP near and distant to carcinoma cells. Smoothelin showed little expression in MM. In MP however, the invasion by carcinoma cells caused a total or subtotal loss of Smoothelin in the cytoplasm of the smooth muscle cells.
Conclusion: Expression of Smoothelin correlates to mechanical tension in the cells. The reliable difference in the IHC-expression of Smoothelinin MM and MP in normal colon is not seen in near infiltrating carcinomas. Relying on Smoothelin in biopsies for the determination of the depth of invasion is dangerous.

PS-11-063

Anal tuberculosis: Report of a case

I. Themeli*, E. Moula, V. Theodorou, A. Giannouli, G. Panselinas, A. Nikolaidou
*Theagenion Hospital Thessaloniki, Dept. of Pathology, Greece

Objective: Tuberculosis can affect any part of the gastrointestinal tract. Anal localization, in particular, has a very low incidence (0,7 %).
Method: A 66 year-old male presented, complaining of perianal pain, constipation, weight loss of 5 kilos the last 4 months and night sweating. Physical examination was normal, except for an ulcerated lesion in the anal region. The patient was submitted to computerized tomography (CT) and incisional biopsy of the lesion.
Results: The CT of the chest revealed multiple, scattered, calcified nodules in the upper zones of both lungs and histological examination showed confluent, non-necrotizing, epithelioid granulomas with the presence of Langhans' multinucleated giant cells. Acid-fast bacilli were detected both within the anal lesion and in the sputum. Mantoux test was positive. The patient had a history of pulmonary tuberculosis 40 years ago. A diagnosis of anal tuberculosis was made and the patient was put on a four drug anti-tuberculous regimen. In 6 months the symptoms improved and the perianal lesion healed.
Conclusion: A tuberculous origin must be considered when the cause of anal and perianal lesions is unclear. Therefore histological and bacteriological confirmation is essential in order to avoid undue delay in diagnosis and treatment.

PS-11-064

The relation of BRAF V600E Mutation and microsatellite instability in colorectal carcinomas

I. Turkmen*, N. Bassüllü, B. Toptas, T. Öztürk, R. Yasar, P. Korkmaz, N. Saygili, O. Öztürk, G. Demir, G. Dogusoy
*Istanbul Bilim University, Dept. of Pathology, Istanbul, Turkey

Objective: Colorectal carcinogenesis is associated with various morphological and molecular pathways. Microsatellite instability (MSI) pathway has familial and sporadic forms.

Among CRC's %15 of the sporadic cases are associated with MSI and these have hypermethylation of the MLH1 promoter associated with BRAF V600E gene mutation. Familial forms do not show BRAF V600E mutation.
Method: We investigated the microsatellite instability (MSI) by immunohistochemical study of MLH1, PMS2, MSH2 and MSH6 together with the BRAF mutation presence and their correlation with standard histopathological parameters in 54 sporadic CRC cases.
Results: The age distribution was 25–88 with an average of 67,9. Immunohistochemical expression loss of MLH1, PMS2, MSH2 and MSH6 was seen in 18,5 %, 22,2 %, 7,4 % and 11,1 % of the total 54 cases respectively. MSI was seen in 27,8 % of the cases. The BRAF V600E gene mutation was seen in 18 cases and among these 8 cases (44,4 %) showed MSI, while MSI frequency was 19,4 in non-mutated group. And this was statistically significant ($p<0.05$). MSI was found significantly correlated with grade and lymph node number ($p<0.05$).
Conclusion: Our study confirmed that sporadic cases of CRC with MSI are associated with the BRAF V600E gene mutation. MSI is correlated with histologic grade and dissected lymph node number.

PS-11-065
Colon biopsy diagnostics may reliably be performed using virtual microscopy
R. S. van der Post*, J. A. van der Laak, B. Sturm, R. Clarijs, H. E. Schaafsma, J. H. van Krieken, M. Nap
*Radboud University Nijmegen MC, Pathology, Netherlands

Objective: Virtual microscopy using whole slide images (WSIs) is a feasible alternative to optical microscopy, offering major advantages for pathology practice. The present study aims to prove reliability of this promising technique for colon biopsy diagnostics.
Method: Colon biopsies ($n=295$) were assessed (into 7 main diagnostic groups) using both glass slides and WSIs by 4 pathologists and 2 residents. Two of the pathologists having ample experience using WSIs, scored the biopsies in a primary diagnostic setting. For each case the criterion standard diagnosis was defined based on glass slide diagnoses. Accuracy was defined as the percentage of concordance with the criterion standard. Kappa statistics were calculated as a measure of observer agreement.
Results: The overall concordance rates were 89.5 % for WSIs and 91.4 % for conventional microscopy. The intraobserver (WSIs versus glass slides) agreement was good to excellent, with kappa values ranging from 0.73 to 0.87 (mean 0.78) and was higher than the interobserver agreement for glass slides (mean 0.71). Concordance with the criterion standard varied less between WSIs and glass slides in the diagnoses of pathologists with virtual experience.
Conclusion: This study showed good diagnostic accuracy and reproducibility for WSIs, indicating this technology may be used for colon biopsy diagnostics.

PS-11-066
Intestinal occlusion due to colonic lipoma: A case report
F. Vukmirovic*
*Clinical Center of Montenegro, Dept. of Pathology, Podgorica, Montenegro

Objective: Lipomas of the digestive tract are rare benign tumor and most often found incidentally during a colonoscopy, computed tomography scan, surgery or autopsy. Lipomas of the colon were first reported by Bauer in 1757 and are most often located in the ascending colon. The incidence of this lesion is estimated between 0.2 and 4.4 % and represents 1.8 % of the colonic benign lesions. We report a case of patient with symptoms of ileus due to colonic lipoma.
Method: A 78-year-old man patient was urgently admitted with symptoms of ileus. Right hemicolectomy was performed, and clinical impression was that it was a malignant tumor.
Results: Examination of the cecum we found polypoid whitish yellow tumor, size 4×2,5 cm. On histology the tumor was composed of mature adipose tissue without cellular atypia. The tumor was located into submucosa. Larger parts of the surface mucosa was eroded. The postoperative course was uneventful and intestinal passage was quickly established.
Conclusion: Although colonic lipomas seldom cause severe symptoms in patients and are easily removed by endoscope while they are small, severe symptoms like abdominal fullness, intestinal obstruction, intestinal bleeding and intussusceptions may appear as a lipoma grows larger. In some cases lipoma may clinically mimic colonic carcinoma.

PS-11-067

Prognostic impact of lymph node ratio outperforms positive lymph nodes and lymph nodes harvested: A time-dependent analysis in mismatch repair-proficient and -deficient colorectal cancers

I. Zlobec*, E. Karamitopoulou, L. Terracciano, D. Inderbitzin, A. Lugli
*University of Berne, Inst. of Pathology, Bern, Switzerland

Objective: We compare the prognostic strength of the lymph node ratio (LNR), positive lymph nodes (+LNs) and collected lymph nodes (LNcoll) using a time-dependent analysis in colorectal cancer patients stratified by mismatch repair (MMR) status.
Method: 580 stage III-IV patients were included. Multivariable Cox regression analysis and time-dependent receiver operating characteristic (tROC) curve analysis were performed. The Area under the Curve (AUC) over time was compared for the three features. Results were validated on a second cohort of 105 stage III-IV patients.
Results: The AUC for the LNR was 0.71 and outperformed + LNs and LNcoll by 10–15 % in both MMR-proficient and –deficient cancers. LNR and + LNs were both significant ($p<0.0001$) in multivariable analysis but the effect was considerably stronger for the LNR [LNR: HR=5.18 (95 % CI: 3.5–7.6); +LNs=1.06 (95 % CI: 1.04–1.08)]. Similar results were obtained for patients with >12 LNcoll. An optimal cut-off score for LNR=0.231 was validated on the second cohort ($p<0.001$).
Conclusion: The LNR outperforms the + LNs and LNcoll even in patients with >12 LNcoll. Its clinical value is not confounded by MMR status. A cut-of score of 0.231 may best stratify patients into prognostic subgroups and could be a basis for the future prospective analysis of the LNR.

PS-11-068

Prognostic value of tumor-stroma ratio in rectal adenocarcinomas

S. Zoidze*, R. Scheer, J. Klaase, M. Elferink, A. Baidoshvili
*Laboratorium Pathologie Oost, Enschede, Netherlands

Objective: Recently, tumor-stroma ratio (TSR) has been identified as a strong predictor for survival in colorectal cancer. Despite an identical biology clinical implications are quite different for colon and rectal cancer regarding to anatomical differences.
Method: TSR was estimated on H&E stained histological sections of 154 patients who underwent resection for rectal adenocarcinoma between 1996 and 2006. None of these patients had received neoadjuvant chemo- or radiotherapy. The TSR was determined, by two independent investigators, in different layers of the rectal wall at the point of highest tumor infiltration and at the border of the tumor. TSRs were categorized into three categories: TSR-low, TSR-moderate and TSR-high.
Results: Patients with stage I and II disease (T1-4 N0) and TSR-high showed significantly better 5 year survival rates for overall survival compared to TSR-low and TSR-moderate ($p=0.010$) and a trend to a better disease specific survival ($p=0.067$) and disease free survival (0.057). In a multivariate Cox regression analysis the TSR remained an independent prognostic factor for overall survival, when adjusted for age, pT-status and grading.
Conclusion: TSR as a prognostic tumor characteristic can be used to identify patients with a good and a poor outcome in lymph node metastasis negative cases.

PS-11-069

A mixed neuroendocrine tumor loceted in appendix vermiformis: "Goblet cell carsinoid"

E. Ayhan Cinar*, B. Sarsik, M. Sezak, T. Yoldas, B. Doganavsargil
*Ege University, Pathology, Izmir, Turkey

Objective: Goblet cell carcinoid (GCC) of appendix vermiformis is a rare neoplasm that share histological features of both adenocarcinoma and carcinoid tumor. While its malignant potential remains unclear, GCC's particularly show transmural dissemination and are more aggressive than conventional carcinoids. Patients usually present with acute appendicitis. They usually lack the formation of a well-defined tumor mass; thus, it is somewhat difficult to accurately assess their size.
Method: Case Presentation: Fifty years old male patient applied to the emergency service with abdominal pain and laparatomy was performed with suspicion of acute appendicitis. Grossly, conjestion and exudation on the distal edge of appendectomy material were seen. A 1×1 cm lesion which was spreading into peripheral adipose tissue was seen on the cut surface. Microscopically, tumor was composed of goblet cell groups resembling “signet ring cells”. Tumor was infiltrated into muscularis propria and mesoappendix. Immunohistochemically, chromogranin, synaptophysin, cytokeratin 20, mCEA and p53 were stained positive. Ki67 (MIB 1) proliferation index was 18 %.
Conclusion: Adenocarcinoid of the appendix is a rare tumor, which is very difficult to diagnose preoperatively and even macroscopically, making histological examination essential. Immunohistochemical staining is required for definitive and differential diagnosis. Here, we present this rare case with literature reviewed.

PS-11-070

Normal colon tissue and colon carcinoma show no difference in heparanase promoter methylation

D. Hershkovitz*, Y. Peerless, E. Simon, E. Sabo, O. Ben-Izhak
*Rambam Health Care Campus, Dept. of Pathology, Haifa, Israel

Objective: Heparanase, the sole heparan sulfate degrading enzyme, has a role in cellular invasion. Accordingly, a large number of studies have demonstrated an association between heparanse expression and tumor stage and patients' prognosis. In colon carcinoma, heparanase shows increased expression in tumor compared to normal tissue and its expression correlates with the presence of metastasis. One of the regulatory mechanisms of heparanase expression is methylation on its promoter. In the present study we evaluated the role of heparanse promoter methylation in colon carcinoma.
Method: Analysis of heparanse promoter methylation was done on 32 samples of colon carcinoma as well as 30 sample of normal colonic mucosa. DNA was extracted from FFPE tissue and subjected to bisulfite conversion. The relative fraction of methylated and unmethylated DNA was evaluated with real-time PCR.
Results: The fraction of methylated DNA was 1 %±0.6 in the colon carcinoma group, and 2.4 %±0.6 in the normal colon group (P=0.11). Only one case in the normal group and one case in the tumor group showed more than 10 % methylation in the heparanase promoter.
Conclusion: We did not find any difference in heparanase promoter methylation between colon carcinoma and normal colonic mucosa, suggesting that heparanase overexpression in colon carcinoma is mediated by other mechanisms.

Monday, 10 September 2012, 09.30 - 10.30, Congress Hall Foyer 3rd Floor
PS-12 Poster Session Haematopathology

PS-12-001
Neural cell adhesion molecule (CD56) expression in diffuse large B cell lymphomas
B. Akkaya*, S. Yildirim, A. Timuragaoglu
*Akdeniz University, School of Medicine, Antalya, Turkey

Objective: Among B-cell non-Hodgkin's lymphomas, neural cell adhesion molecule/CD56 expression is exceptional. The aim of this study is to report unusual CD56 (neural cell adhesion molecule, NCAM) expression on diffuse large B cell lymphoma (DLBCL).
Method: The panel of antibodies included CD3, CD20, CD10, bcl-2, bcl-6, MUM-1 and CD56.
Results: A total of 50 cases of DLBCL were identified and one case was also detected positive for CD56. The subject was female, 48 years old. The patient had presented generalized lymphadenopathy. She had not documented involvement of extranodal sites. The case is alive with disease 1 year after diagnosis and chemotherapy treatment.
Conclusion: CD56 expression is an uncommon finding in B cell lymphomas. To date the literature reports a variable expression of CD56 in B cell lymphoma, ranging from 0.5 to 5.5 % of all B cell lymphomas. The presence of CD56 reported by the literature on certain DLBCL with extranodal presentation might be related to mechanisms involved in growth and expansion. Our case had not documented involvement of extranodal sites. The reason why CD56 expression is present in B cell lymphoma is not yet clear. Further studies are necessary to clarify the biological role of Cd56 in B cell lymphoma.

PS-12-002
Indolent onset of a T cell lymphoblastic lymphoma: Case report
P. Baldin*, F. Bacci, S. Carlo, M. Pizzi, S. A. Pileri, E. Sabattini
*University of Bologna, Dept. of Anatomic Pathology, Italy

Objective: A case of mediastinal T-cell lymphoblastic lymphoma with indolent clinical course in a 52-year-old man was studied by immunohistology and molecular biology.
Method: Formalin-fixed sample. Histology with Ematoxilin&Eosin and Giemsa; immunohistochemistry by APAAP method. T-cell receptor gamma rearrangement by BIOMED2 protocols.
Results: After one fainting episode the patient was found to have pericarditis caused by a XX-cm-diameter mediastinal mass. The 2 first biopsies were unsuccessful and the third diagnostic one was done 6 months later. In this time-period the patient was well without symptoms and the mass stable. After two mediastinal biopsies with unspecific features (Castleman disease?), the diagnostic one showed fibrosis, abundant small reactive lymphocytes (CD20+/CD3+) and areas with diffuse small-medium size lymphocytes positive for CD3, TdT, CD34, CD7, LMO2 and high Ki67. T-cell receptor gamma genes were monoclonally rearranged.
Conclusion: Indolent T-LBL is exceedingly rare: for this reason in our case LMO2 was a key marker for the diagnosis which was delayed for the presence of fibrosis and reactive B cells.

PS-12-003
Granulocytic sarcoma of the spinal cord: Case report
U. Bayol*, S. Unluoglu, O. Turelik, O. Yaman
*Tepecik Training and Research Center, Izmir, Turkey

Objective: Granulocytic sarcoma (GS), also termed myeloid sarcoma or chloroma, is a rare malignant solid tumor

resulting from the extramedullary proliferation of myeloblasts or immature myeloid cells. GS most frequently occurs in patients with acute myeloid leukemia, myeloproliferative neoplasms or myelodysplasia. GS rarely presents in the absence of systemic myeloid disease. GS most commonly occurs in the soft tissues of the head and neck, bone, skin and less often in the central nervous system and spinal cord.

Results: A 40 year old woman presented with 1 month history of weakness of both legs. MRI of the thoracal spine showed 4 cm diameter epidural mass compressing the dural sac in the spinal canal at the T9-10 levels. Decompressive laminectomy and tumor removal were performed resulting in neurological improvement. Histologically neoplastic cells have round nuclei with finely dispersed chromatin and scant cytoplasm proliferating in a diffuse pattern. Immunohistochemically, tumor cells were positive for MPO, CD117, CD45, CD99. Diagnosis was GS without bone marrow involvement.

Conclusion: We report the case of GS due to unusual localization and nonleukemic presentation.

PS-12-004

Hairy cell leukemia: Retrospective study of 6 cases

Y. Ben Youssef*, A. Bdioui, H. Regaieg, B. Achour, S. Hmissa, A. Khelif

*Farhet Hached Hospital, Dept. of Hematology, Sousse, Tunisia

Objective: Hairy cell leukemia (HCL) is a rare indolent B cell non Hodgkin's lymphoma with a characteristic presentation of pancytopenia, splenomegaly, and immunophenotype circulating hairy cells.

Method: Retrospective study about 6 cases of HCL diagnosed between 1993 and 2007 at the Hematology Department, Farhat Hached Hospital.

Results: There were 5 males and 1 female with a median age of 40 years (22–79 years). Physical examination shows splenomegaly in all cases and hepatomegaly in 2 cases, hematological parameters shows lymphocytosis with peripheral hairy cells in all cases. Flow cytometric immunophenotyping was done in 2 cases, and confirmed the diagnosis of HCL with CD11c, CD25+, CD103+, CD123 +, and CD5-, CD10-, and CD23-. Bone marrow biopsy was done in all cases, showing massive infiltration with villous cytoplasmic projection cells that were CD20 positive. The treatment consists of blood transfusion in all cases, associated with splenectomy in 3 cases, only 1 patient was treated with (2 CDA: cladribine) with a complete remission after a follow up of 24 months.

Conclusion: HCL has consistent cytologic histologic and immunologic features that make classification reliable and reproducible; it remains problematic because of the variety of the disorders and the differential diagnosis of splenic lymphoma of the marginal zone.

PS-12-005

Primary cerebral lymphoma: A retrospective study of 5 immunocompetents

Y. Ben Youssef*, A. Bdioui, R. Haifa, Z. Kahra, S. Hmissa, M. T. Yacoubi, K. Abderrahim

*Farhet Hached Hospital, Dept. of Hematology, Sousse, Tunisia

Objective: Primary CNS lymphomas (PCNSL) are uncommon tumors in immunocompetent patients, they represent up to 1 % of non Hodgkin lymphomas (NHL) and 3–5 % of all brain tumors. The majority of PCNSL are diffuse large B cell lymphomas, 2–5 % are T cell lymphomas, in rare instances low grade B cell lymphomas. We determine clinical characteristics, histological findings and treatment outcome of PCNSL.

Method: Five cases of PCNSL occurring between 1993 and 2007 were retrospectively reviewed.

Results: They were 4 males, 1 female, median age 50 years, range (23–74). Most common symptom was neurological deficits (4cases). MRI of the brain revealed an expansive tumor affecting the parietal bone in 3 cases, the temporal bone in 1 cases and the frontal bone in 1 case. Immunohistological finding showed large B- cell NHL in 2 cases, anaplastic lymphoma in 2 cases, and large- cell immunoblastic lymphoma in 1 case. Treatment consists on exclusive tumoral resection in 3 cases, surgery and chemotherapy (1 case), complicated by death in all these cases. Surgery followed by high dose chemotherapy and radiotherapy (1 case) with complete remission after a follow-up of 7 years.

Conclusion: Chemotherapy followed by involved field irradiation appears to be an adapted therapy.

PS-12-006

Primary cutaneous lymphoma: A retrospective study

Y. Ben Youssef*, W. Boukattaya, T. Zahmoul, H. Regaieg, B. Wafa, K. Zahra, M. T. Yacoubi, C. Belajouza, K. Abderrahim

*Farhet Hached Hospital, Dept. of Hematology, Sousse, Tunisia

Objective: Primary cutaneous non-Hodgkin's lymphoma (PCNHL) is defined as lymphoma limited to skin without extra-cutaneous involvement at presentation. We describe here epidemiological and histo-pathological aspects of PCNHL.

Method: Retrospective review of clinical data of PCNHL patients diagnosed in Hematology Department, Frahet Hached Hospital, Sousse (1993–2012).
Results: Fourty three patients with PCNHL, median age: 48 years (11–84), sex-ratio was 2.3. The site of cutaneous involvement was upper lumb in 4 cases, lower lumb in 7 cases and disseminated in 23 cases. PCNHL was small T cell lymphoma in 13 cases, large B cell lymphoma in 16 cases, anaplastic, CD4+ CD56+ hematodermic neoplasm, and follicular type in 1 case respectively. According to TNM classification 21 cases were T3bNxMx, 12 cases were T1N0M0. After first line therapy, 26 patients in CR, PR was obtained in 1 case and failure in 6 cases, 10 patients relapsed within 1 to 72 months (median 6 months), all of them were disseminated cases.
Conclusion: Our study indicate that the extend of cutaneous involvement at the time of diagnosis is a significant prognostic factor in PCNHL.

PS-12-007
Follicular lymphoma: Multicentric retrospective study
Y. Ben Youssef*, A. Naoures, S. Boukhris, H. Regaieg, E. Moez, M. T. Yacoubi, S. Hmissa, K. Abderrahim
*Farhet Hached Hospital, Dept. of Hematology, Sousse, Tunisia

Objective: Follicular lymphomas (FLs) account for one third of non Hodgkin lymphomas (NHLs) in adults. The disease is characterized by a response to initial treatment, followed by relapses, sometimes associated with histologic transformation into high grade NHL. Analyze epidemiological characteristics of patients with FL.
Method: Retrospective study of 22 of adult FLs diagnosed in Hematology Department (2000–2011).
Results: Median age was 59 years (29–77), sex-ratio: 1.7 The most frequent clinical symptom at diagnosis was lymphadenopathy in 13 cases. Involvement of the spleen in 3 cases. B symptoms were present in 10 cases. Performance status was more than 1 in 4 cases. According to the international prognostic index (FLIPI), 7 patients have low index, 5 have intermediate index, and 10 have high index. Grade 2 FL was seen in the majority of cases. Treatment modalities varied over time and according to the disponibility of drugs especially to anti CD20 monoclonal antibody. CR was obtained in 13 cases, PR in 6 cases; 3patients relapsed within 8–48 months. Histologic transformation was seen in 3 cases, we have noted 10 deaths related to the disease in 7 cases.
Conclusion: Treatment results in FL might not only be improved by more effective induction regimens but also by maintenance treatment.

PS-12-008
Primary mediastinal large B-cell lymphoma: A single center study of clinicopathologic characteristics
Y. Ben Youssef*, A. Bdioui, H. Regaieg, M. Zaier, S. Hmissa, M. T. Yacoubi, M. Mokni, K. Abderrahim
*Farhet Hached Hospital, Dept. of Hematology, Sousse, Tunisia

Objective: Primary mediastinal large B – cell lymphoma (PMLBCL) is a subset of LBCL with unique clinicopathologic features. Objective: Study clinical, biological, histogenesis and phenotype of patients with PMLBCL.
Method: Retrospective clinicopathologic analysis of 10 patients with PMLBCL from a single center from 2001 to 2009.
Results: Six were women and 4 were men, aged from, aged from 17 to 73; 3 were at stage I-II, 3 at stage III, and 4 at stage IV, all patients had bulk disease with superior vena cava syndrome,8 had contiguous infiltration, 7 had lactate dehydrogenase elevation, Bsymptoms were present in all cases Microscopic examination shows infiltration of medium-large cells surrounded by collagen fibrosis, neoplastic cells express B-cell markers, CD30+ in 1 case, CD3 negative in all cases Five patients received chemotherapy plus Rituximab and radiotherapy in 2 cases with complete remission in 4 cases, 5 patients received chemotherapy only with relapse in 3 cases.
Conclusion: The relative rarity of this type of lymphoma necessitates clinical trials in order to define the better treatment.

PS-12-009
A potantial diagnostic pitfall: Frequent CD99 and FLI-1 coexpressions in diffuse large B cell lymphoma
U. Berber*, A. Haholu, I. Yilmaz, Z. Kucukodaci
*GATA HEH, Dept. of Pathology, Istanbul, Turkey

Objective: CD99 and FLI-1 are widely used for their diagnostic utility in Ewing sarcoma/peripheral neuroectodermal tumor (ES/PNET). CD99 expression has been documented in a variety of tumors, including lymphoid malignancies of T cell origin. Also FLI-1 expression is common in different tumor types. However, few studies have investigated the CD99 and FLI-1 immunoreactivity in diffuse large B-cell lymphoma (DLBCL). We aimed to determine the frequencies of CD99 and FLI-1 immunohistochemical expressions in DLBCL which may lead to a misdiagnosis.
Method: CD99 and FLI-1 expressions are retrospectively investigated by immunoperoxidase staining in prechemoterapy primary tumors of 42 DLBCL cases.

Results: Out of 42 cases, CD99 and FLI-1 expressions were observed in 14 (33.3 %) and 7 (16.7 %) tumors, respectively. Concomittant expressions of CD99 and FLI-1 proteins were found in 5/42 (11.9 %) cases.

Conclusion: The present study revealed that CD99 and FLI-1 are frequently expressed in DLBCL, thus DLBCL should be considered in the differential diagnosis of CD99+ and FLI-1+ neoplasms.

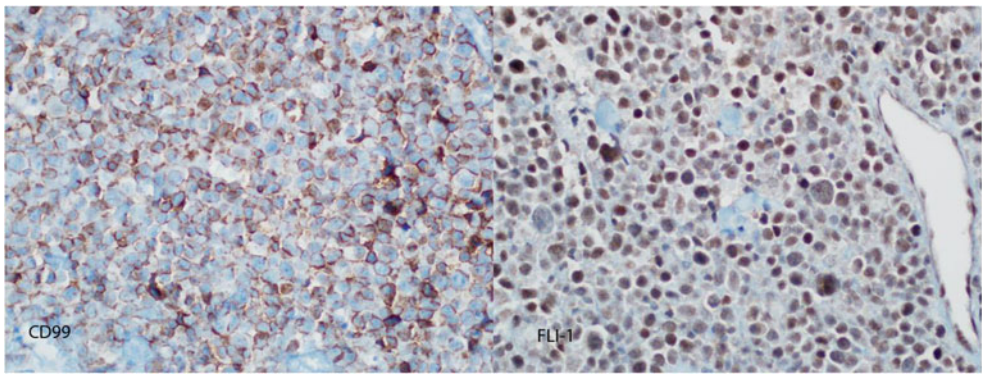

PS-12-010

Primary cutaneous marginal zone lymphoma with biclonality

E. Beretouli*, T. Koletsa, A. Bouzakis, S. Mavropoulou, G. Karkavelas, I. Kostopoulos
*AHEPA Hospital, Dept. of Pathology, Thessaloniki, Greece

Objective: Primary cutaneous marginal zone lymphoma (PCMZL) represents a B-cell lymphoma which presents with papules, plaques or nodes. The presence of a monotypical light chain B cell population supports the diagnosis of PCMZL. We describe a case of PCMZL which showed different light chain restriction in two heterochronous lesions.
Method: A 50 year-old male patient presented in 2004 with a cutaneous nodule in the anterior surface of the tibia, which was totally excised. The patient did not show other lesions since 2011, when a new cutaneous nodule located in the right ankle, was appeared. Immunohistochemical analysis was performed in both biopsies.
Results: Histological and immunohistochemical findings of both biopsies were consistent with marginal zone lymphoma of the skin with lambda light chain restriction in the biopsy of the first lesion and kappa light chain restriction in the biopsy of the second lesion. Blood laboratory studies, chest and abdominal computerized tomography scans revealed no evidence of systemic involvement by lymphoma.
Conclusion: The finding of both kappa and lamda light chain restricted B cell populations in PCMZL is unusual. The monoclonal light chain switching in PCMZL is rare and its pathogenesis is discussed.

PS-12-011

Microvascular density assessed using CD34 immunostaining does not have prognostic significance in mantle cell lymphoma: Retrospective clinicopathological analysis of 177 patients of the Czech Lymphoma Study Group

L. Boudová*, P. Veselá, Z. Tonar, D. Šálek, R. Kodet, M. Trnený, S. Vokurka, Z. Vernerova, M. Moulis, P. Kašparová, M. Michal
*Charles University, Faculty of Medicine, Pilsen, Czech Republic

Objective: Microvessel density (MVD) has prognostic significance in some malignancies. Little information exists about angiogenesis in mantle cell lymphoma (MCL), although antiangiogenic drugs are used experimentally. Prognostic factors of MCL are needed as outcome and therapy are heterogeneous and often unsatisfactory. The aim is to assess MVD in MCL and to evaluate its prognostic significance.
Method: 177 MCL specimens (FFPE) were examined by immunohistochemistry with anti-CD34 antibody. MVD was quantified using systematic uniform random sampling and unbiased counting frames. Clinical data were analyzed in Kaplan-Meier survival curves and log-rank test.
Results: Median survival (MS) of all patients was 46 months, median progression-free survival (MPFS) 22 months. Mean MVD was 172,7 microvessels/mm2, median 158,2/mm2. Dividing cases into quartiles: <117,4/mm2, <158,2/mm2, <206,6/mm2 and ≥206,6/mm2 (43, 44, 45, 45 cases), MS and MPFS did not differ statistically significantly between these groups (P=0,307; similar for therapy groups). Visible differences are only between the fourth quartile and the rest:

MS of the first three quartiles (132 cases): 56 months, of the fourth quartile (45 cases): 30 months (P=0,084); MPFS: 22 versus 18 months (P=0,069).
Conclusion: MVD assessed using CD34 immunostaining does not have prognostic significance in a large series of MCL with a long follow-up.

PS-12-012

Clinico-pathological study of 5 cases of Plasmablastic Lymphoma in HIV positive and negative patients

R. Carías*, A. Panizo Santos, C. Panizo, J. M. Martinez-Peñuela, H. Quiceno Arias, F. J. Queipo, J. Pardo
*Clinica Universidad De Navarra, Anatomical Pathology, Pamplona, Spain

Objective: Plasmablastic lymphoma (PBL) is a rare aggressive subtype of diffuse large-B-cell lymphoma which occurs primarily in the oral cavity of HIV-positive patients. It is extremely rare in immunocompetent patients.
Method: A total of 5 cases of PB were retrospectively analyzed. All cases had tissue available for immunohistochemistry and in situ hybridization.
Results: The age range of the 5 patients was 35–81 years (median 68) and all were men. Three patients were HIV negative. HIV + patients: tumors involved the oral cavity (n=1), and small intestine (n=1). HIV- patients: tumors were located in bone marrow (n=1) and lymph nodes (n=2). All tumors were composed of monomorphic plasmablastic cells. Tumors were negative for CD45 and CD20, while they showed diffuse positivity for CD138, CD38, MUM1 and EMA. By ISH, monoclonal light chain restriction was detected. EBV (EBER) was positive in all cases. The median overall survival was 21,4 months regardless of the intensity of chemotherapy. Only one patient is alive 1 month after diagnosis.
Conclusion: PBL may appear in non immunocompromised patients and other locations than oral cavity. Any patient diagnosed with PBL should be tested for HIV. Patients who had HIV-negative PBL have lower rates of oral involvement.

PS-12-013

Spinal granulocytic sarcoma preceding clinical manifestation of acute myeloid leukemia

V. Cemerikic-Martinovic*, N. Drndarevic, N. Andjelkovic, P. Djordjevic, D. Jovanovic, R. Nikolic, T. Martinovic
*Beo-lab, Dept. of Pathology, Belgrade, Serbia

Objective: Granulocytic sarcoma is a rare malignant neoplasm of primitive myeloid cell origin, most commonly found in association with acute myeloid leukemia. Granulocytic sarcomas generally occur in the soft tissues, bone, and skin.
Method: We report a case of a 55-year old man with spinal granulocytic sarcoma manifesting as rapidly progressive paraplegia preceding clinical manifestation of acute myeloid leukemia.
Results: Magnetic resonance imaging revealed a tumor in lumbal spine (L1-L3). Baseline laboratory data were normal. He underwent emergent laminectomy and the tumor was totaly resected. Histological examination of lesion demonstrated diffuse proliferation of large atypical cells with round nuclei with delicate chromatin and one or more prominent nucleoli. Immunohistochemical studies revealed positive staining for LCA, CD33, CD43, CD163, Lysozyme and CD15 while myeloperoxidase, lymphoid, neuroendocrine markers, S-100 and CD99 were negative. The final histological diagnosis was granulocitic (monoblastic) sarcoma. No chromosomal aberrations were detected by FISH. A month later, acute myelomonocytic leukemia was diagnosed upon a peripheral blood and bone marrow examination showing an increased number of abnormal monoblasts. Chemotherapy, with multiple regimens for leukemia in combination, did not affect the tumor and the patient died.
Conclusion: Granulocytic sarcoma should be considered in the differential diagnosis of spinal tumors.

PS-12-014

Survivin expression in patients with newly diagnosed nodal diffuse large B-cell lymphoma treated with immunochemotherapy

V. Cemerikic-Martinovic*, O. Markovic, D. Marisavljevic, T. Martinovic, N. Andjelkovic, P. Djurdjevic
*Beo-lab, Dept. of Pathology, Belgrade, Serbia

Objective: Survivin, a member of the inhibitor of apoptosis family might play an important role in the pathogenesis of diffuse large B cell lymphoma (DLBCL). We investigate clinical and prognostic significance of survivin expression in nodal DLBCL.
Method: Biopsy specimens obtained from 56 patients with newly diagnosed nodal DLBCL treated with immunochemotherapy (R-CHOP) were immunostained for survivin.
Results: Survivin immunoexpression (>45 % positive tumor cells) has been found in 22 (39.28 %) patients. Significant difference in immunoexpression was noticed between GCB and non-GCB subtype of DLBCL (p=0.031). There was no significant association with IPI, „bulky“disease, Ki-67 immunoexpression or other clinico-pathological parameters. Univariate analysis showed that survivin expression was unfavorable factor for therapy response and shorter survival in patients with DLBCL (p=0.048 and p=0.034, respectively). Patients with survivin overexpression experienced relapse more often that the patients without expression of this apoptotic protein (27.3 % vs. 11.8 %), but this difference did not reach statistical significance (p=0.131).

Conclusion: The results of this study showed that disregulation of survivin expression had the important role in determination of course of disease in pateints with nodal DLBCL treated with R-CHOP. Therefore, survivin represent potential therapeutic target in DLBCL.

PS-12-015

Langerhans cell histiocytosis of the jaws: A report of ten cases with an analysis of the mechanism of eosinophilic infiltration

Y.-A. Cho*, H.-J. Yoon, S.-D. Hong, J.-I. Lee, S.-P. Hong
*Seoul National University, Dept. of Oral Pathology, Republic of Korea

Objective: Langerhans cell histiocytosis (LCH) frequently presents eosinophilic infiltration. Here we report ten cases of LCH that involved the jaws and our investigation of the mechanism underlying eosinophilic infiltration in LCH.
Method: We evaluated the CCL-11/eotaxin-1 expression of LCH cells via immunohistochemical staining. Toluidine blue staining was used to inspect the densities of mast cells, with ten periapical granuloma specimens serving as a control group.
Results: Every patient was classified as having single-system LCH, even though acute lymphoblastic leukemia occurred in one patient during LCH treatment. The ratio of mandible to maxilla LCH was 5:1. The jaw lesions were the earliest manifestation in seven patients with multifocal LCH. Toluidine blue staining revealed that the number of mast cells in LCH lesions was not significantly higher than in periapical granulomas. However, upon immunohistochemical examination, most of the patients showed diffuse positivity for eotaxin-1 in LCH cells, while few eosinophils/T cells were immunoreactive.
Conclusion: We surmise that the eotaxin-1 expression of LCH cells may be relevant to eosinophilic infiltration in LCH. Further studies of the eotaxin-1 functions including its influence on the immature state of LCH cells may be needed to understand the pathogenesis of LCH as well as the role of tissue eosinophilia in LCH.

PS-12-016

Sclerosing Angiomatoid Nodular Transformation (SANT) of the spleen: The unusual entity

A. Djikic Rom*, J. Jotanovic, M. Micev, V. Jeremic
*Clinical Center of Serbia, Dept. of Histopathology, Belgrade, Serbia

Objective: Sclerosing angiomatoid nodular transformation (SANT) is an unusual and rare nonneoplastic vascular lesion of the spleen well characterized by Martel et al. in 2004.
Method: We report a case of SANT in 53 years-old man presented with abdominal discomfort and pain in a left lumbal region. Abdominal computed tomography scan revealed a massive haematoma extended from spleen to the enlarged left kidney and left retroperitoneal space. The patient also had a spontaneous rupture of right kidney 2 years ago.
Results: Macroscopically, the cut surface of spleen showed multiple well circumscribed red brown nodules. Microscopically, SANT consists of multiple well-circumscribed angiomatoid nodules showing plump endothelial cells and extravasated erythrocytes. Nodular formations are surrounded by a variable lymphoplasmacytic infiltrate, spindle cells and collagenous stroma. Immunohistochemical staining displayed endothelial phenotype that resembled splenic capillaries (CD34+/CD31+/CD8−). Expression of CD68 was also present.
Conclusion: The differential diagnosis of SANT includes splenic hamartoma, inflammatory myofibroblastic tumor, littoral cell angioma and hemangioendothelioma. It has been postulated that SANT represents a peculiar hamartomatous transformation of splenic red pulp in response to an exaggerated nonneoplastic stromal proliferation. SANT has a benign clinical course and splenectomy has been supposed as curative.

PS-12-017

Collision tumor of menningioma and non Hodgin malignant lymphoma of cerebellum

H. Erdem*, A. K. Uzunlar, U. Yildirim, A. Sav, M. Dosoglu
*Duzce University, Dept. of Pathology, Turkey

Primary central nervous system lymphoma (PCNSL) constitutes a rare group of extranodal non-Hodgkin's lymphomas (NHLs), primarily of B cell origin, whose incidence has markedly increased in the last three decades. Immunodeficiency is the main risk factor, but the large majority of patients are immunocompetent. This report presents the case of a 71-year-old woman with a collision tumor of primary malignant lymphoma and meningioma in the cerebellum. Collision tumor of primary malignant lymphoma and meningioma have not been described in the literature. The morphological aspect is interesting with regard to the problem of collision tumors.

PS-12-018

Prognostic significance of immunohistochemical expression of the angiogenic molecules VEGF-A, VEGFR-1 and VEGFR-2 in patients with Classical Hodgkin Lymphoma

E. Georgiadi*, G. Dimtsas, P. Karakitsos, T. Vassilakopoulos, I. Thymara, P. Korkolopoulou, E. Patsouris, C. Kittas, I. Doussis-Anagnostopoulou
*Larisa, Greece

Objective: Classical Hodgkin Lymphoma (cHL) is characterized by the presence of a small percentage of

malignant Hodgkin and Reed-Sternberg (HRS) cells amongst a reactive background. The role of angiogenesis in cHL is still unclear. The aim of the study was to evaluate the expression of VEGF-A, VEGFR-1 and VEGFR-2 and their correlation with clinicopathological parameters and prognosis.

Method: The immunohistochemical expression of VEGF-A (VG1, Dako), VEGFR-1 (RB-9049, Neomarkers) and VEGFR-2 (sc-6251, Santa Cruz) was studied in a large cohort of 199 patients with cHL and the results were correlated with clinical characteristics and patient outcome.

Results: The neoplastic HRS cells expressed VEGF-A, VEGFR-1 and VEGFR-2 in 90.3 %, 97.2 % and 94.1 % of the cases respectively and their expression levels were intercorrelated. Expression of VEGFR-1 and VEGFR-2 was significantly and positively correlated with early disease stage, absence of B-symptoms, WBC <15.000, Alb ≥4, IPS ≤2. VEGFR-2 was additionally positively correlated with male gender and ESR <50. All three molecules were statistically correlated with ramifications of blood vessels but not with microvessel density.

Conclusion: Based on our results, we could speculate that, in contrast to solid tumours, the process of angiogenesis is probably an early event in neoplastic progression in the context of Hodgkin's Lymphoma.

PS-12-019

P53 upregulation is associated with proliferation and is not capable of inducing apoptosis in Hodgkin's lymphoma

E. Georgiadi*, G. Dimtsas, T. P. Vassilakopoulos, V. G. Gorgoulis, I. A. Doussis-Anagnostopoulou
*Larisa, Greece

Objective: P53 is a tumor suppressor protein described as the "guardian of the genome". In a normal cell, p53 is inactivated by its negative regulator, Mdm2. Once activated, p53 induces cell cycle arrest and apoptosis by activating various cell cycle related genes, like WAF1/CIP1 encoding for p21. Although mutations that deactivate p53 are the most common genetic alteration found in cancer, they are rare in the context of Hodgkin's lymphoma (HL).

Method: P53 immunohistochemical expression was investigated in a subset of 81 cases of primary HL. The study of the p53-downstream protein p21 was used as an indirect way of analyzing its functional status. P53 expression was correlated with proliferation, apoptosis, clinicopathological data and prognosis of the patients.

Results: P53 showed a median value of 32.4 %, suggesting an upregulation of the p53 gene in HL, and a significant correlation with p21 (p=0.043) and the proliferation marker MIB1 expression (p=0.038).

Conclusion: Although p53 overexpression is a frequent finding in HL and there is indication of its functionality, this upregulation does not lead to apoptosis. It can be speculated that this is possibly due to Mdm2-p53 interactions.

PS-12-020

Simultaneous gastric adenocarcinoma and B cell lymphoma of the stomach

F. Gerin*, K. Turkoz, B. Kantarcioglu, C. Ataizi Celikel
*Marmara University, Dept. of Pathology, Istanbul, Turkey

Objective: The simultaneous association of gastric carcinoma with gastric lymphoma is a rare event.

Method: We describe a 52 years old man, who had been diagnosed as marginal zone lymphoma in a cervical lymph node biopsy 3 years previously.No endoscopic examination was evaluated then. There was no pathological appearance in the gastrointestinal system by CT scanning and patient was considered nodal marginal zone lymphoma. Patient had taken 8 cycles of chemotherapy which consisted of rituximab, cyclophosphamide, vincristine, and prednisolone.2,5 years after completion of chemotherapy, a gastric wall thickening compatible with gastric lymphoma or linitis plastica was detected on CT and gastroscopic examination was indicated. Endoscopic examination revealed an erosive, fragile, hemorrhagic, malignant-looking lesion with a diameter of 4.5 cm in the cardia. Besides, rugae of fundus and corpus were severely rough and hyperemic suggesting a diffuse malignant infiltration. Multiple biopsies were taken from cardia, fundus and corpus of the stomach.

Results: Cardiac samples showed pancytokeratin positive signet ring cells which contain neutral and acidic mucine in microscopic examination. Samples of corpus and fundus did not show similar carcinoma cells, instead, there was diffuse infiltration of atipical lymphocytic infiltration consistent with marginal cell lymphoma both morphologically and immunophenotypically.

Conclusion: Co-occurrence of carcinoma and marginal zone lymphome is a rare event and dramatically exacerbates prognosis of a patient with such an indolent lymphoma.

PS-12-021

Assessment of demographic data, staging and experesion of CD20, CD30, CD15, Bcl-2 in Reed-Sternberg cells of Hodgkin lymphoma cases in their first admission in Urmia Imam Komini Hospital

B. Ilkhanizadeh*, P. Mazlomi
*Imam Komini Hospital, Dept. of Pathology, Urmia, Iran

Objective: Immunohistochemistry plays an important role in diagnosis of Hodgkin lymphoma. Beyond diagnostic importance of Immunohistochemistry, so far many studies

have investigated the correlation between cellular markers and the prognosis of patients with Hodgkin lymphoma. Amongst other markers, CD20 is one of the most studied marker with a lot of controversy around it.
Method: Retrospectively 66 eligible patients entered the study. Clinical and laboratory Data and Immunohistochemistry findings analyzed for possible correlation between disease stage and other parameters.
Results: In our study 63.6 %, 90.9 % of cases respectively expressed cellular markers CD15 and CD30 while only 18.2 % of cases expressed CD20. Furthermore statistical analysis revealed that CD15 was inversely correlated with disease staging. (P=0.027). In contrast we didn't find any relation between CD20 or CD30 positivity with disease staging. (P=0.482, P=0.376). However in our study expression of CD20 was not related to stage or other parameters of poor prognosis which proposes that in our patients this marker possibly was not related to disease prognosis.
Conclusion: Therefore we suggest that cellular marker CD20 is not beneficial beyond IPS factors and its usage should be confined to diagnostic purposes.

PS-12-022

Primary naturall killer cell lymphoblastic leukemia/ lymphoma of central nervous system

G. Karagkounis*, T. Argyrakos, E. Ronne, E. Dimitriadis, D. Papadopoulos, G. Stranjzalis, D. Rontogianni
*Athens, Greece

Objective: A 25-year old woman with a 2-year history of a multifocal lesion occupying the cerebellum who periodically received cortisol and etoposide as it was considered tumor-forming multiple sclerosis.
Method: Two years after initial clinical diagnosis a stereotactic biopsy was performed. Immunohistochemistry and in situ hybridization were performed on the tissue sample.
Results: The perivascular (Virchow-Robin) space of microvessels was occupied by middle sized lymphocytes with blastic chromatin and scant cytoplasm. The neoplastic cells were negative for: 1. B-cell markers: CD19, CD22, CD20, CD79a, Pax-5, 2. Myelogenous differentiation antigens: MPO, CD13, CD33, 3. Plasmacytoid dendritic differentiation antigens: CD123, TCL1, 4. Blastic cells markers: CD34, CD117 5. T-cell markers: CD3, CD5 with restricted expression of CD2 and CD7 in a few cells, 6. Cytotoxic enzymes TIA-1, Granzyme-B and perforin. All cells expressed intensely CD56 and TdT and some of them CD16. In situ hybridization for EBV virus (EBERS) was negative. PCR analysis: T-cell receptor and immunoglobulin genes were in germ line. Bone marrow was negative.
Conclusion: The diagnosis of Natural Killer Lymphoblastic Leukemia/Lymphoma, leukemia of ambiguous lineage was established according to the WHO/2008 classification of lymphomas. To our knowledge this is the first case of primary CNS NK lymphoblastic lymphoma in the literature.

PS-12-023

Combined immunological, morphological and cytochemical research of cells with the usage of microarrays

N. Kiryanov*, A. Shishkin, N. Ovchinina, S. Bessmeltsev, E. Nikitin
*Izhevsk State Medical Academy, Russia

Objective: Tumor cells immunophenotyping with the usage of flow cytofluorimetry, immunoenzymometric and immunofluorescence methods is quite expensive. The new method of cell surface antigens detection with the usage of immunological microarrays was proposed.
Method: The microarray represents a solid substrate, on which the specified antibodies are immobilized in the particular places ("stains"). During the analysis the microarray is incubated with the cell suspension. The cells which possess determined cell surface antigens, specifically communicate within stains. Different cell surface antigens on various cells can be indentified through one microarray. Microarrays are manufactured on transparent and chemically-proof substrates and it allows to carry out the coloring of communicated cells for research with the help of light microscopy. The whole procedure can be performed on cells from the blood, bone marrow during 1–2 h.
Results: With the help of microarrays we conducted researches dedicated to the study of various types of normal blood cells, cells of acute and chronic leukemia, non-Hodgkin's lymphoma. The big spectrum of cell surface antigens and the histological types of cells which possess each type of defined antigens were simultaneously determined.
Conclusion: The techniques of the combined research of cells proposed by us make microarrays convenient method for solving diagnostic and research problems.

PS-12-024

Epidemiology, morphology of nodal/exstranodal lymphomas in the Ural region of Russia

N. Kiryanov*, S. Suchanov, E. Lozhkin
*Izhevsk State Medical Academy, Russia

Objective: Lymphomas constitute 33,65 cases on 100 000 inhabitants annually, its frequency grows.
Method: This work presents epidemiological, morphological analysis of nodal/exstranodal lymphomas. Analysis of data from Izhevsk cancer center during 2009–2011 was carried out.
Results: Lymphoma appeared in 2.94 % among first diagnosed malignant tumors. The panel of monoclonal antibodies was used for tumor immunophenotype identification. Nodal lymphomas presented 183 cases: 55 - Hodgkin lymphoma (HL), 128 – non-Hodgkin lymphoma (NHL). Exstranodal

lymphomas presented 111 cases, various variants of NHL were more frequent. Small lymphocyte lymphoma - 37, diffuse large B-cell lymphoma (DLBCL) - 36, follicle center lymphoma - 18, mantle cell lymphoma – 8 were frequent among nodal lymphomas. T-cellular NHL presented 16 cases (6 - peripheral T-cell lymphoma, 7 - angioimmunoblastic T-cell lymphoma). Among other organs of lymphatic system lymphomas appeared in tonsils (19), thymus (15) and spleen (9). Exstranodal NHL were registered in stomach (25), rarely in other organs - testis (7), central nervous system (3), nose (3), breast (3). As rule DLBCL was more frequent (36).
Conclusion: Results coincide with data on lymphoma's frequency and morphological characteristic in other regions.

PS-12-025
In situ mantle cell lymphoma in nasopharynx
T. Koletsa*, F. Tsiompanou, C. Poulios, G. Karkavelas, I. Kostopoulos
*AUTH, Dept. of Pathology, Thessaloniki, Greece

Objective: The nasopharynx normally contains abundant lymphoid tissue and it can be the site of both lymphoid hyperplasia and lymphomas. We present the first case of the recently described in situ mantle cell lymphoma (MCL) in nasopharynx.
Method: A 70 year-old woman presented with nasal obstruction in 2008. A mass located in nasopharynx was found. Biopsy was sent for histological examination. A new biopsy was taken 3 years later. Histological, immunohistochemical and FISH studies were performed.
Results: Histological examination of both biopsies revealed lymphoid hyperplasia, characterized by CD5 and cyclinD1 positive cells of mantle zones, findings consistent with in situ MCL. The diagnosis of in situ MCL confirmed by FISH analysis for t(11;14). The patient examined thoroughly and has remained free of an overt lymphoma to the present day.
Conclusion: Pathologists and otorhinolaryngologists should be aware that in situ MCL may be observed in nasopharynx. It may be appropriate to perform cyclinD1 immunostain, even in cases with clinical and histological findings compatible with lymphoid hyperpasia. The patients should be examined thoroughly, since in situ MCL may accompanied by an overt lymphoma in other sites or it may be a precursor of an overt MCL.

PS-12-027
Multisystem Langerhans' cell histiocytosis coexisting with metastasizing adenocarcinoma of the lung
A. Lovrenski*, M. Panjkovic, Z. Eri
*Institute for Lung Diseases, Dept. for Pathology, Sremska Kamenica, Serbia

Objective: Langerhans' cell histiocytosis (LCH) is an uncommon disease of unknown etiology characterized by uncontrolled proliferation and infiltration of various organs by Langerhans' cells. To our knowledge, this is the first case reporting an association of multisystem LCH with metastasizing adenocarcinoma of the lung.
Method: We present the case of a 54-year-old man, heavy smoker, with dispnea, cough, hemoptyses, headache and ataxia, who died shortly after admission to our hospital. On the autopsy, we found tumor in the posterior segment of the right upper pulmonary lobe as well as a right-sided occipito-parietal lesion which penetrated into the right ventricle resulting in internal and external hematocephalus. Histologically and immunohistohemically, the diagnosis of primary lung adenocarcinoma with brain metastasis was made (tumor cells showed positivity for CK 7 and TTF-1 which confirmed the diagnosis). Light microscopic examination of the other organs showed LCH involving the pituitary gland, hypothalamus, spleen, mediastinal lymph nodes, and lungs. Immunohistochemical studies revealed CD68, S-100 and CD1a immunoreactivity within the Langerhans' cells.
Conclusion: Multisystem form of LCH with extensive organ involvement was an incidental finding, while the metastatic lung adenocarcinoma to the brain, that led to hematocephalus, was the cause of death.

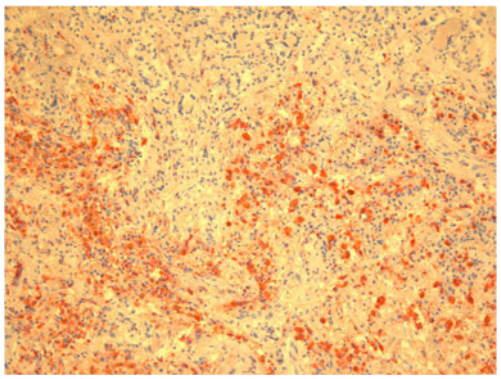

PS-12-028
Langerhans cell histiocytosis associated with extramedullary hematopoiesis in a 65-year-old male patient
L. Lungoci*, L. Elena, B. Flavia, M. Rodica
*City Hospital, Pathology, Timisoara, Romania

Objective: Langerhans cell histiocytosis is a rare disease histologically characterized by the proliferation of Langerhans cells.
Method: A 65-year-old male came to our attention presenting with erythematous-squamous lesions all over the body, axillary and inguinal adenopathies and hepatosplenomegaly. We have taken a cutaneous and an axillary lymph node biopsy.
Results: Microscopic examination of the cutaneous fragment revealed the presence of a dermal infiltrate of large cells with an eosinophilic cytoplasm and vesicular, nucleolated nuclei

with an irregular nuclear margin, raising suspicion of a cutaneous lymphoma. Immunohistochemical stains for CD45, CD20, CD79a, CD3, CD5, CD15, CD30, and Bcl-2 were negative, and the previous diagnosis was not confirmed. The microscopic examination of the axillary lymph nodes showed foci of extramedullary hematopoiesis, raising suspicion of a lymphoproliferative process, but the immunohistochemical stains and the paraclinical data didn't confirm it. Based on the intense positive reaction for CD68, S100 and Ki-67 showed by the tumoral cells from the prelevated tissues, correlated with the clinical and paraclinical findings, a diagnosis of Langerhans cell histiocytosis was established.

Conclusion: The particularity of our case consists in the presence of extramedullary hematopoiesis in the lymph nodes of a patient diagnosed with Langerhans cell histiocytosis.

PS-12-030

Unusual primary cutaneous presentation of B-cell chronic lymphocytic leukaemia

S. Mavropoulou*, Z. Tatsiou, G. Xanthopoulidis, A. Goutzouvelidis

*General Hospital, Laboratory of Pathology, Xanthi, Greece

Objective: B-cell small lymphocytic lymphoma/chronic lymphocytic leukaemia (B-CLL) is a low-grade lymphoproliferative disorder and cutaneous lesions are rarely the presenting findings.

Method: We report the case of a 62-year-old woman who presented in winter with erythematous plaque on her nose, of 3 months duration. Laboratory data showed elevated white blood cell count (40.000/mm3) with small mature lymphocytes predominance (60 %).

Results: Histopathologic examination of the skin lesion reveals infiltration of the reticular dermis and subcutis, consisting mostly of small lymphoid cells, without epidermotropism. Immunohistochemical examination revealed positivity for CD20, CD79a and CD5 in the neoplastic cells. According to the laboratory and histopathologic findings the diagnosis was consistent with B-CLL with a primary cutaneous presentation. A staging bone marrow aspiration and biopsy showed 80 % infiltration by a clonal B-cell proliferation with typical CLL immunophenotyping. CT-imaging was normal, so stage I according to Binnet classification was confirmed. The patient received 6 cycles of chemotherapy and remained in remission for 1 year, when the skin lesion recurred in winter, at the same location.

Conclusion: In conclusion we report an extremely rare case of subclinical B-CLL with cutaneous presentation. It is important to maintain a high index of suspicion for a lymphoproliferative process in skin lesions with atypical lymphocytic infiltration.

PS-12-031

Myeloid sarcoma mimicking nasal polyp

S. Mungan*, U. Cobanoglu, S. Ersoz, G. Guvendi, M. Yilmaz

*Karadeniz Technical University, Pathology, Trabzon, Turkey

Objective: A myeloid sarcoma is a tumour mass consisting of myeloid blasts with or without maturation occuring at an anatomical site other than the bone marrow. Every site of the body can be involved, skin, lymph node, gastrointestinal tract, bone, soft tissue and testis. %10 cases presents at multiple anatomical sites.

Method: The current case is 75 year old woman presenting with nasal polyp and underwent polypectomy. The polyp was 2,5 cm in diameter and had a bloody appearance. By microscopic examination there was a diffuse infiltration of neoplastic cells under the cilliated epithelium. The mitotic index was high in neoplastic lymhoid cells. Immunohistochemical study was helpful for the differential diagnosis.

Results: The immunohistochemical panel was LCA(+), Myeloperoksidase (+), CD117(+), CD34 (−), CD20 (−), CD3 (−), CD2 (−), S100 protein (−), CD56 (−), CD99 (−), CD79a (−), CD138 (−), CD30 (−), ALK (−), Desmin (−), Pancytokeratin (−), Pax5 (−), Synaptophysin (−), Myogenin (−), CD5(−). The bone marrow aspiration showed a ratio of %20 myeloblasts.

Conclusion: We report a rare case of myeloid sarcoma presenting with nasal cavity involvement. The differential diagnosis include lymphoblastic lymphoma, Burkitt lymphoma, diffuse large B-cell lymphoma, small round cell tumors.

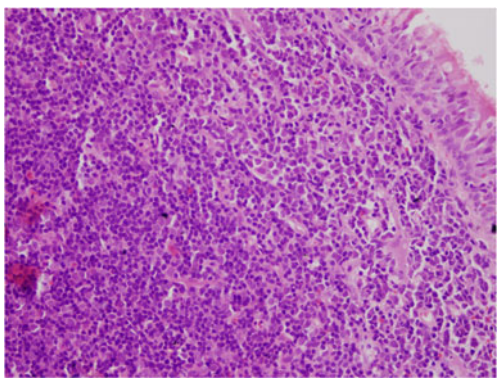

PS-12-032

Ear, nose and throat lymphomas in Central Tunisia: Epidemiological and anatomoclinical study of 34 cases

M. Nabiha*, B. Y. Yossra, B. Ahlem, S. Cyrine, A. Affisath, Y. Mohamed Tahar, H. Sihem

*Farhet Hached Hospital, Dept. of Pathology, Sousse, Tunisia

Objective: The aim of this study was to describe the epidemiology and anatomo-clinical features of the ear, nose and throat (ENT) lymphomas in the Centre of Tunisia.
Method: All ENT lymphoma cases diagnosed in the Pathology Department, Farhet Hached Hospital, Sousse during a 15-year period were analyzed.
Results: A total of 34 cases of ENT lymphoma were reported (21 males, 13 females) with a sex-ratio of 1.4. The age at diagnosis varied from 9 to 85 years with a median age of 56.5 years. The majority of ENT lymphoma cases (81 %) were of B cell type including large B-cell lymphoma (58 %) and small-cell B lymphoma (23 %). Nasopharynx and tonsils were the most involved areas with 44 % and 42 % of cases, respectively. According to the Ann Arbor staging system, these lymphomas are diagnosed in the stage II (42 %) followed by stage I (30 %).
Conclusion: The most frequent lymphoma developed in ENT region was B cell lymphoma, especially located in nasopharynx and Tonsils.

PS-12-033

Paediatric lymphomas in Central Tunisia: Epidemiological and anatomoclinical study of 44 cases

M. Nabiha*, B. Y. Yossra, M. Wiem, B. Ahlem, A. Affisath, E. Ahlem, Y. Mohamed Tahar, H. Sihem
*Farhet Hached Hospital, Dept. of Pathology, Sousse, Tunisia

Objective: Lymphomas are the most second tumour in children worldwide. In Tunisia, lymphomas are ranked second after leukaemias (25.7 %). The aim of this research was to describe the epidemiology and anatomo-clinical features of childhood lymphomas in the Centre of Tunisia.
Method: All paediatric lymphomas diagnosed in the Pathology Department, Farhet Hached Hospital, Sousse during 15-year period were analyzed.
Results: A total of 44 cases were reported (26 males, 18 females) with a sex-ratio of 1.4. The median age was 10 years (range: 3–15 years). Lymph node lymphomas were the most frequent accounting for 63.6 %, followed by ENT, mediastinum, and haematopoietic system (6.8 % each one); cutaneous and digestive location were less frequent (4.5 % each one). Among the 44 patients, 23 (52.3 %) had had Hodgkin's lymphoma and 21 (47.7 %) had had non-Hodgkin's lymphoma (NHL). Diffuse large B-cell lymphoma was the most diagnosed (57 %) followed by Burkitt lymphoma (23.8 %) and T-cell lymphoma (9.5 %). According to the Ann Arbor staging system, 29.6 % of patients were diagnosed in an advanced stage.
Conclusion: Lymphomas are the second paediatric tumour in the Centre of Tunisia. Large B-cell lymphomas are the most frequent. Third of cases are diagnosed in advanced stage.

PS-12-035

EBV positive diffuse large B-cell lymphoma in angioimmunoblastic T-cell lymphoma (a composite B and T -cell lymphoma)

I. Rodriguez*, A. Panizo, J. M. Martinez Penuela, J. Feliu, M. J. Larrayoz
*C. Hospitalario de Navarra, Dept. of Pathology, Pamplona, Spain

Objective: Angioimmunoblastic T-cell lymphoma (AILT) is a rare neoplasm with an Epstein-Barr virus (EBV)–infected B-cell population and occasional Reed-Sternberg-like cells (RS).
Method: We present a case of composite AILT and diffuse large B-cell lymphoma (DLBCL) A 45-year-old woman with multiples lymph nodes. Biopsy of inguinal node was performed. Three months later the patient had enlarged cervical node which was removed.
Results: Firstly, the inguinal lymph node was diffusely infiltrated by small-medium size lymphocytes with scanty cytoplasm. The nuclei were irregular. Several large cells were observed in a background of prominent arborizing high endothelial venules. The small cells were CD3 positive. The large cells were CD79a, CD30 positive. Theses cells showed nuclear positivity for EBER by ISH. Secondly, the cervical lymph node showed large areas of necrosis admixed with pleomorphic and medium size T lymphocytes. There were a population of neoplastic EBV + pleomorphic B lymphocytes; some of them with RS-like morphology. We performed B and T-cell clonality studies. We detected TCR-gamma T-cell and IgH B-cell gene clonal rearrangement.
Conclusion: Occasionally IgH gene rearrangement has been detected but only a few cases have demonstrated, morphologically, composite AILT and EBV-associated diffuse large B-cell lymphoma (DLBCL).

PS-12-036

Typhlitis as initial manifestation of granulocytic sarcoma of the appendix: A case report

P. Rohani Doost*, B. Ilkhanizadeh, F. Noroozinia, A. Mohammadi
*Urmia University of Medical Sciences, Iran

Objective: Myeloid sarcoma is a localized mass of myeloblasts or immature myeloid cells involving any extramedullary site. Reports in the literature documenting leukemic infiltration of appendix are uncommon and extremely rare when symptoms mimicking typhlitis.

Method: A 30-year-old man with a history of relapsed acute myelogenous leukemia (FAB classification, M2) admitted for receiving induction chemotherapy. After 10 days of chemotherapy, he presented with fever, nausea, vomiting, abdominal pain and severe neutropenia (0.026×109/L as absolute neutrophil count). This manifestation was attributed to typhlitis and he received antibiotic therapy, but he came back 50 days later with acute abdomen prompting exploratory laparotomy which revealed inflamed appendix.

Results: Histologic examination showed diffuse appendiceal wall infiltration of mononuclear cells with medium-to-large vesicular nuclei, conspicuous nucleoli and pale eosinophilic cytoplasm. Immunostains showed the diagnosis of granulocytic sarcoma with myeloperoxidase, leukocyte common antigen, CD15, CD117 and CD68 positivity and epithelial membrane antigen, keratin, CD3, CD5, CD10, CD79a and CD20 negativity.

Conclusion: Our case declares that physicians and surgeons should be aware of granulocytic sarcoma in the differential diagnosis of mild tenderness on palpation of the abdomen as a complication of acute myelogenous leukemia.

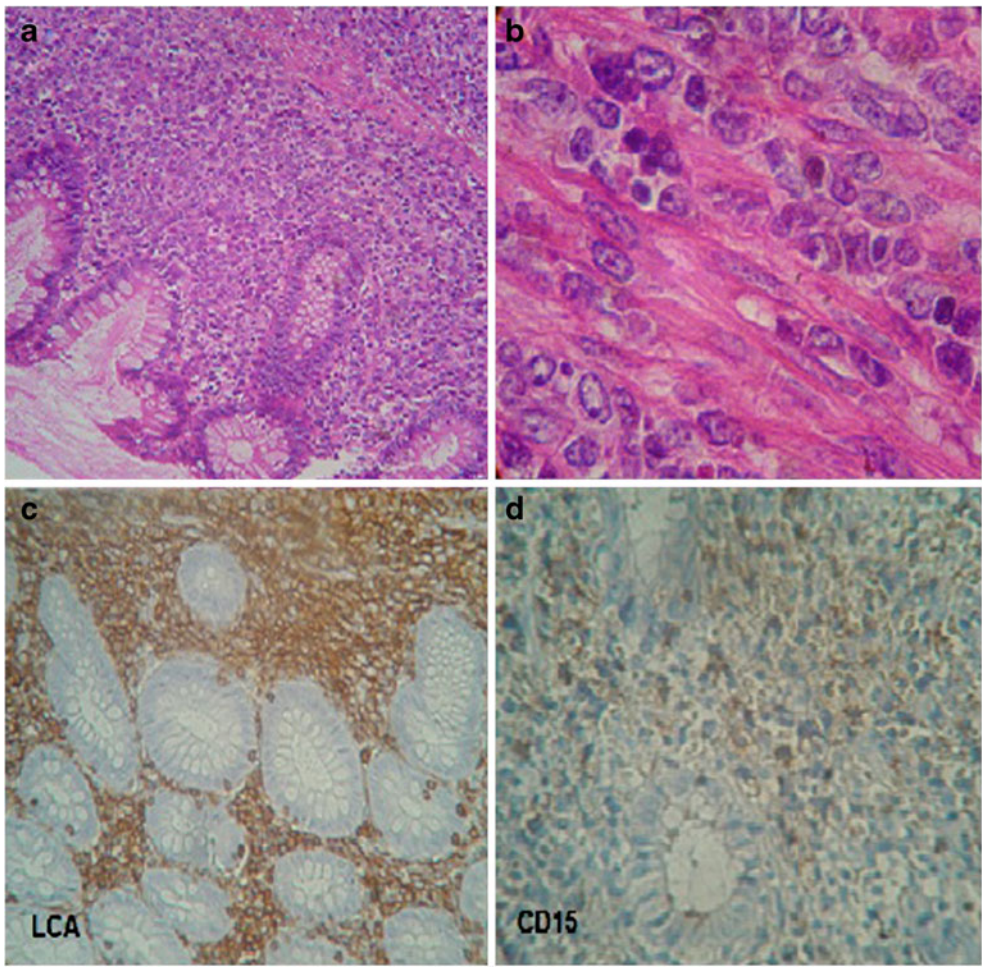

PS-12-037

Angioimmunoblastic T-cell lymphoma: A report of 3 cases

S. Miladi*, S. Mistiri, S. Ziadi, A. Afissat, N. Labaied, C. Souki, M. T. Yacoubi, M. Mokni
*University of Medicine, Dept. of Anatomic Pathology, Monastir, Tunisia

Objective: Angioimmunoblastic T-cell lymphoma (AITL), one of the most frequent entities among peripheral T-cell lymphoma, is characterized by lymphadenopathy, B-symptoms, and an aggressive behaviour.
Method: We reported 3 cases of AITL during a period of 4 years (2004–2007).
Results: The age of patients varied between 20 and 73 year-old. They hadn't any pathologic history. Two patients presented with a multiple cervical lymphadenopathy, and weight loss. The other patient had fever and sweat. Physical examination found multiple lymph nodes with hepatosplenomegaly in 2 patients. Abdominal ultrasound and CT-scan showed diffuse lymphadenopathy with features raising the possibility of lymphoma. The diagnosis of AITL was confirmed by a microscopic and an immunhistochemical study of lymph node or liver biopsy. 2 patients received a cure of chemotherapy
Conclusion: Angioimmunoblastic T-cell lymphoma (AITL) is an aggressive non-Hodgkin T-cell lymphoma. AITL is frequently associated to immunological and hematologic diseases such as autoimmune hemolytic anemia, vasculitis, rheumatoid arthritis, and autoimmune thyroid disease. Its natural history has been the subject of controversy, considered for many years to be a non-malignant disorder or a dysimmune disease, until the clonal nature of AITL was proven by molecular studies. Although patients are usually treated with corticosteroids, chemotherapy, and/or plasmapheresis, outcomes were dismal.

PS-12-038

The indolent Nodal B-cell Lymphomas (NBCL) in the Center of Tunisia: A series of 50 cases

S. Miladi*, M. T. Yacoubi, N. Zoubaida, B. Y. Yosra, A. Essakly, M. Wiem, S. Hmissa, M. Mokni
*University of Medicine, Dept. of Anatomic Pathology, Monastir, Tunisia

Objective: Low grade lymphomas (indolent) are commonly located on extranodal sites. nodal location are relatively of low incidence. Our aim is to describe the epidemiological status of NBCL and to assess their pathological features in the center of Tunisia.
Method: We report 50 cases of indolent NBCL diagnosed in the department of pathology, during a period of 10 years (2000–2009). Clinical, pathological and immunohistochemical (large panel of antibodies), treatment and outcome data are collected.
Results: The mean age was 63 year old (33 and 89 years). The sex ratio was 1.27. NBCL was 6.5 % of all N H lymphomas and 42.73 % of indolent NBCL of any sites. Nodal enlargement and hepatomegaly were the main symptoms. Small Lymphocytic lymphomas were the most frequent variant (56 %), followed by follicular lymphomas (26 %). Mantle cell lymphoma and marginal zone B cell lymphoma were rare (12 % and 6 %, respectively). They were exclusively of B cell type. 76 % of cases were in stage III-IV. 90 % of patients received chemotherapy. 2 % of recurrence and 48 % of death were found.
Conclusion: NBCL in the center of Tunisia are relatively uncommon. Small lymphocytic lymphoma is the most frequent in our population. They are still of relatively worse prognosis.

PS-12-039

Bone marrow metastasis of signet ring cell carcinoma with an unknown primary site

S. Sezgin Ramadan*, O. Yapicier, K. Berberoglu, M. Sezer, H. Onat, Z. Gulbas
*Anadolu Medical Center, Dept. of Pathology, Kocaeli, Turkey

Objective: Bone marrow metastases can be found in some malignant tumors, but diagnosing a nonhematologic malignancy from marrow is an unusual event. Herein we present a case of metastatic signet ring cell carcinoma with an unknown primary site.
Method: A 39 year-old woman admitted to the Hospital with weakness and bone pain. Positron emission tomography/computed tomography (PET/CT) revealed disseminated bone lesions showing increased metabolic activity. Bone marrow biopsy and aspiration were performed.
Results: Bone marrow biopsy revealed extensive necrosis and nearly total replacement of normal bone marrow elements by atypical tumoral cells. Tumoral cells were arranged individually or in small clusters, having hyperchromatic, eccentric located nuclei and abundant cytoplasm with signet ring cell morphology. Even after thourough investigation of all the systems, a primary site of malignancy could not be detected. She received nine cycles of chemotherapy. Craial MRI revealed multiple metastatic lesions. 9 months after the initial diagnosis, she died of disseminated metastatic lesions.
Conclusion: Even after thorough investigations, a primary site of malignancy could not be detected. In the literature, all the presented cases had very short survival varying from days to a few months. Our patient lived for 9 months with multidiciplinary approach.

PS-12-043

Most t(14;18) negative follicular lymphomas are nodal marginal zone lymphomas

M. van den Brand*, H. van Krieken, K. Hebeda
*Radboud University Nijmegen MC, Pathology, Netherlands

Objective: Approximately 20 % of follicular lymphomas (FLs) are bcl2 negative and 10–15 % of FLs lack a translocation t(14;18). Previously we have found that negative bcl2 staining in cases that do have a t(14;18) is caused by mutations in the epitope for the bcl-2 antibody, but this is never the case in bcl-2 negative, t (14;18) negative cases. Now that translocation detection is more commonly performed we noticed that many of the cases that were referred to us as translocation negative FL are actually often nodal marginal zone lymphomas (NMZLs) with extensive follicular colonization.
Method: t(14;18) negative cases that on H&E sections look like FL were analyzed by morphology and immunohistochemistry, including antibodies against CD10, bcl-2, Ki-67, and CD23.
Results: Careful observation of the bcl-2 staining pattern revealed that follicles that appeared positive at low power contained negative cells at high magnification. The amount of negative cells varied from follicle to follicle and was associated with the extent of Ki-67 positivity.
Conclusion: Based on morphology and immunohistochemistry we reclassified many cases of bcl-2 positive, t(14;18) negative FL into NMZL. Although there is presently no positive marker for NMZL, we believe that such cases are responsible for most t(14;18) negative FL.

Monday, 10 September 2012, 09.30 - 10.30, Congress Hall Foyer 3rd Floor
PS-13 Poster Session Electron Microscopy

PS-13-002

Ultrastructure of cutaneous lichen planus lesions evidenced in various types of disease correlated with tissue levels of gelatinase-B

V. Groma*, I. Legusa, I. Mikazans
*Riga Stradins University, Inst. of Anatomy, Latvia

Objective: Recent studies do not provide a definite answer on the origin and pathogenesis of lichen planus (LP). Histologic findings are the same, regardless of the area involved. Electron microscopy is useful to confirm the diagnosis in atypical cases and monitoring LP development. This study aimed an ultrastructural characterization of keratinocyte degeneration in pemphigoides, hypertrophic, and follicular LP types correlating this with levels of gelatinolytic activity caused by metalloproteinase-9 (MMP-9).
Method: Skin biopsies were processed conventionally and examined in a JEOL 1011 transmission electron microscope. MMP-9 expression was detected immunohistochemically.
Results: LP pemphigoides demonstrated intact basal keratinocyte cell membrane, and the lamina densa lining blister cavity correlating with moderate basal MMP-9 expression of weak intensity. Hypertrophic type demonstrated good preservation of keratinocytes and their junctions along with strong basal and suprabasal MMP-9 expression of moderate intensity. Both types demonstrated diffuse and strong MMP-9 immunostaining in dermal lymphohistiocytic infiltrate. A hypertrophic type revealed an increase of expression within dermal sweat glands comparing with LP pemphigoides. A diffuse and strong epidermal and follicular MMP-9 staining was noticed in follicular variant of LP.
Conclusion: Ultrastructurally keratinocyte involvement displays deviations in various types of LP, and these changes correlate with levels of gelatinolytic activity caused by MMP-9.

PS-13-004

Ultrastructural findings of myopathy induced by long-term therapy of clevudine

J.-Y. Park*, Y.-K. Chun
*KNUH Hospital, Dept. of Pathology, Daegu, Republic of Korea

Objective: Clevudine is a recently introduced anti-viral agent that shows efficacy against hepatitis B virus related chronic liver diseases. However, it has been reported that certain patients who have received long-term administration of clevudine exhibit myopathy involving mitochondrial abnormalities. To make a differential diagnosis congenital mitochondrial myopathy and drug induced mitochondrial myopathy, we investigate ultrastructural findings of drug induced myopathy.
Method: We studied histopathological features of myopathy focused on the various ultrastructural mitochondrial abnormalities found in 18 patients with long-term clevudine therapy.
Results: In every case, ragged red fibers and multinucleated fibers with eosinophilic granules were observed. Additionally, type 2 fiber atrophy was found in 6 cases. Mainly concentrated in subsarcolemmal or inter-fibrillar areas, the abnormal mitochondria were enlarged and swollen, showing a variety of morphological types. Most of the abnormal mitochondria indicated structural abnormalities in cristae, including the apparent decrease in the number, concentric lamellar pattern, and structure that is branched or lattice-like.
Conclusion: From the overall analysis, clevudine-induced myopathy is characterized by ragged fibers showing proliferation of abnormal mitochondria with various forms of inclusion bodies and abnormal cristae. Another particular feature of interest is the presence of multinucleated fibers, which, in most cases, are filled with abnormal mitochondria.

PS-13-006

Ultrastructural features of human mature oocytes subjected to cryopreservation

S. A. Nottola*
*University La Sapienza, Dipt. die Anatomia Histol., Rome, Italy

Objective: Oocyte cryopreservation protocols have not been fully optimized yet. Our aims were to evaluate and compare the ultrastructure of human mature oocytes frozen-thawed (F/T) after slow freezing and vitrification.
Method: The oocytes, fixed at sampling (fresh controls) and after freeze/thawing, were processed for light and transmission electron microscopy (LM and TEM) observations.
Results: By LM, both fresh and F/T oocytes were rounded cells surrounded by an intact zona pellucida (ZP) and containing uniformly distributed organelles. By TEM, numerous vacuoles were found in F/T oocytes after slow freezing. On the contrary, vacuoles were only occasionally detected in F/T oocytes after vitrification, and in fresh controls as well. Amount and density of cortical granules (CGs) appeared abnormally reduced in F/T oocytes, irrespective of the protocol applied.
Conclusion: In conclusion, a) cryopreservation currently ensures a good overall preservation of the oocyte; b) however, vacuolization appears as a recurrent form of cell damage during slow freezing, whereas the quasi absence of vacuoles seems the most relevant marker of quality in vitrified oocytes; c) premature CG exocytosis - and the consequent hardening of the ZP - seems a non-specific, ubiquitous phenomenon occurring during freeze/thawing, suggesting the appropriateness of the use of ICSI as the preferred insemination method after cryopreservation.

Tuesday, 11 September 2012, 09.30 - 10.30, Congress Hall Foyer 3rd Floor
PS-14 Poster Session Digestive Diseases Pathology III: Liver, Biliary and Pancreas

PS-14-001

Pancreatic mucinous cystadenocarcinoma: Study of 5 cases

A. Bdioui*, S. Hmissa, A. Essakly, N. Labaied, S. Miledi, L. Jaidaine, M. T. Yacoubi, S. Badreddine
*CHU Farhat Hached, Dept. of Pathology, Sousse, Tunisia

Objective: Mucinous cystic epithelial neoplasms of the pancreas are uncommon with 2–5 % of all exocrine pancreatic tumours. They occur exclusively in aged women. Here, we report the pathological, clinical and prognosis particularities of pancreatic mucinous cystadenocarcinoma (PMC).
Method: Retrospective study was performed on 5 cases of PMC diagnosed in the Pathology Department, Farhat Hached Hospital, Sousse.
Results: There were 3 women and 2 men with a median age of 60 (range 45–80 years). Symptoms were dominated by abdominal pain, jaundice, vomiting, and alteration of the general condition. Radiologic investigation showed multiloculated cystic mass of the pancreas, associated to splenic thrombosis and bone metastasis in one case. In gross, we received multilocular cysts of 3 to 16 cm in wall, their wall was fibrous, and thick, the internal surface showed many papillary projections and mural nodules. There was no communication with the duct system. On histologic examination, cysts had a fibrous wall lined by mucinous atypical cells showing frank anaplasia, wall's cyst was invaded by anaplastic glands; the stroma was of ovarian type in all cases.
Conclusion: PMC are uncommon neoplasia, their diagnosis is based on the histopathologic exam, their diagnosis is better than duct carcinoma and depends on the extent of tumour invasion.

PS-14-002

Heterotopic pancreas of the gallbladder associated with acute cholecystitis

O. Akman*, E. E. Pala, U. Bayol, M. Emiroglu
*Tepecik Training Research Center, Dept. of Pathology, Izmir, Turkey

Objective: Pancreatic heterotopia is a rare entity, which is commonly found in the stomach, duodenum, jejunum and Meckel's diverticulum. Heterotopic pancreas is extremely rare in the gallbladder. Despite being a congenital condition, it takes years to become symptomatic. It can be associated with cholecystitis or cholecystolithiasis.
Method: A 21-year-old female patient was admitted to emergency service with abdominal pain. On physical examination, right upper abdomen was tender without defense or rebound. Abdominal ultrasonography revealed small sized gallstones and pericholecystic fluid. Magnetic resonance cholangiography showed dilated intrahepatic and extrahepatic bile ducts. Laparoscopic cholecystectomy was performed.
Results: Cholecystectomy specimen was 75×35×30 mm. On gross examination we noted a few milimetric yellow colored stones and 12 mm yellow solid intramural nodule. The mucosa was covered with fibrinopurulent exudate. Microscopic examination revealed acute cholecystitis and aberrant pancreatic tissue consisting of acini and ductules. The phlegmonous inflammation of the gallbladder infiltrated the aberrant pancreatic tissue. The patient recovered completely after cholecystectomy.
Conclusion: We found this case worth reporting because, pancreatic heterotopia of the gallbladder is a rare, clinically

silent entity unless complicated with gallstones and acute cholecystitis.

PS-14-003

Expressions of c-erb-B2, EGFR, p27, PTEN, mTOR, PI3K in hepatocellular carcinomas and adjacent liver tissues

N. Bassullu*, I. Turkmen, M. Dayangac, P. Yagiz Korkmaz, R. Yasar, O. Yaprak, M. Akyildiz, Y. Tokat, Y. Yuzer, G. B. Dogusoy
*Istanbul Bilim University, Dept. of Pathology, Turkey

Objective: We investigated the expressions of c erb B2, EGFR, PTEN, mTOR, PI3K, p27 in Hepatocellular carcinomas (HCC) cases and their correlations with other pathologic features.
Method: Fifty HCC cases were stained immunohistochemically with these markers. Correlations between the markers and pathologic characteristics were analyzed.
Results: The cases had an average age of 56,72. Male/female ratio was 44/6. HBV is more common in advanced stages and right lobe location ($p<0.05$). Tumor size is significantly larger in patients older than 50 years ($p<0,04$). No membranous c erb B2 staining was seen while cytoplasmic positivity was present in 92 % and significant correlation was found with multiplicity ($p<0.041$) and p27 positivity ($p<0,011$). EGFR membranous positivity was present in 90 % and significantly correlated with stage ($p<0.05$). p27 was negative in 92 % and PTEN is reduced or absent in 56 %. All markers were similarly expressed in adjacent noncancerous tissue. No significant correlations were found between PTEN, mTOR, PI3K and the pathological parameters.
Conclusion: In our study, as a first step, none of the markers among c-erb-B2, EGFR, p27, PTEN, mTOR, PI3K was found significant in correlation with pathologic features. We look forward to obtain further results in the next study consisting of correlations with follow ups.

PS-14-004

The value of echo guided liver biopsy in the positive diagnosis of a rare primary liver tumor – pathological approach

G. Becheanu*, V. Herlea, V. Serban-Barbu, M. Dumbrava, S. Enache, G. Smira, C. Angelescu, A. Pop, M. Diculescu
*Bucharest, Romania

Objective: Hepatic angiomyolipomas are rare mesenchymal hepatic tumour. The most important problem about their diagnosis on biopsy specimens is to exclude a hepatocellular carcinoma.
Method: We present two cases of hepatic angiomyolipoma diagnosed in Fundeni Clinical Institute, Bucharest. Both females patients, 39 and 43 years old, were imagistically diagnosed with a 13 cm hepatic left lobe tumor in the first patient, respectively a 10.5 cm hepatic right lobe tumor in the second one. Both tumors were echo guided biopsied. The biopsy specimens measured about 8 mm, respectively 20 mm. The tumors were surgical removed. The biopsy and resection specimens were analyzed in light microscopy, including immunohistochemistry.
Results: Initial diagnosis on HE stain was cell variant hepatocellular carcinoma, in the 8 mm biopsy, respectively suspicious for angiomyolipoma in the second case. Further immunohistochemical studies showed positivity for Vimentin, HMB45, MELAN A, S100 and actin, and negativity for OCH1E5, CK7, CK8/18, CEA, CD34, Ki67 and Factor VIII in both biopsy specimens, consistent with hepatic angiomyolipoma diagnosis, confirmed on surgical specimens too.
Conclusion: Diagnosing a hepatic angiomyolipoma is not easy to do especially on a biopsy. The size of biopsy specimens plays a very important role in a correct diagnosis.

PS-14-005

Adult pancreatic hemangioma: Case report and literature review

A. Ben Salem*, N. Znaidi Sabbegh, Y. Zidi, F. Fareh, N. Kourda, I. Chelly Enneifer, S. Rammeh, R. Zermani
*Charles Nicolle Hospital, Dept. of Pathology, Tunis, Tunisia

Objective: Pancreatic vascular neoplasms are rare lesions accounting for 0.1 % of all pancreatic tumors. Adult pancreatic hemangiomas are extremely uncommon. Only 12 cases of adult pancreatic hemangiomas have been reported in literature since 1939.
Method: We report a new case with literature review.
Results: A 62-year-old woman presented with a 2-day history of nausea, fever and diffuse abdominal pain. CT scan revealed a well circumscribed small lesion of the pancreatic body. On arterial phase imaging, the mass was of low density relative to the pancreas without marked contrast enhancement. Based on these findings, the patient underwent surgical resection of this mass and a distal

spleno-pancreatectomy was performed. Microscopic examination showed a well circumscribed but non encapsulated soft tissue proliferation consisted of blood vessels lined by a single layer of uniform flattened cells, with dilated lumen filled with red blood cells and inflammatory cells. Immunohistochemical staining confirmed the vascular nature of the lesion. The diagnosis of pancreatic hemangioma was made.
Conclusion: Adult pancreatic hemangioma is an extremely rare tumor. The review of all published cases showed that this tumor often do not demonstrate the contrast-enhanced CT features typical of an hemangioma, so a poor arterial phase enhancement cannot rule out pancreatic hemangioma and the histological examination is very important in these cases.

PS-14-006
Hepatocholangiocarcinoma - Clinicopathological features: Case report
A. Ben Salem*, N. Kourda, R. Aloui, Y. Zidi, I. Chelly Enneifer, N. Znaidi Sabbegh, H. Mekki, A. Moussa, T. Najjar, R. Zermani
*Charles Nicolle Hospital, Dept. of Pathology, Tunis, Tunisia

Objective: Hepatocholangiocarcinoma (HCC-CC) is an uncommon form of primary liver cancer with features of hepatocellular and biliary epithelial differentiation. It accounts for 0.4–14.2 % of all primary liver carcinomas. Many of the demographic and clinical features of this tumor remain unclear. It was previously suggested that coexisting chronic liver diseases were rarely seen in patients with HCC-CC.
Method: We report a case of HCC-CC diagnosed in patient with cirrhosis.
Results: A 48 year-old man presented with ascites, jaundice, vomiting and symptoms of portal hypertension. On abdominal CT scan the right hepatic segment was heterogeneous, hypervascular in the late arterial phase and low-attenuated on portal venous phase. Based on a these clinicoradiological informations, diagnosis of infiltrating hepatocellular carcinoma was made and hepatic biopsy was performed. Histopathologic examination showed, in addition to features of liver cirrhosis, the presence of malignant proliferation composed of tubular structures as well as microtrabecular and compact foci. On Immunohistochemical stainings the tumor cells expressed cytokeratins 7 and 20. Cells lining the tubular structures reacted with cytokeratin 19 allowing the diagnosis of hepatocholangiocarcinoma.
Conclusion: Hepatocholangiocarcinoma is a rare primary liver cancer. Preoperative noninvasive diagnosis with conventional radiography is often difficult especially when occurring in patients with liver cirrhosis or other hepatic chronic disease. The diagnosis is frequently made only after histological and immunohistochemical examination.

PS-14-007
Morphological changes in different zones of the gallbladder in cholelithiasis
M. Bokhodir*, T. Vervekina
*Tashkent Medical Academy, Dept. of Patological Anatomy, Uzbekistan

Objective: Gallstone disease remains a serious problem of modern surgery. An important aspect of the problem is the question of the urgency of surgical intervention, depending on the condition of the gallbladder.
Method: It was carried out the analysis of 1130 case histories and excised gallbladder with different forms of cholelithiasis. 81.3 % were women in the age of 41–50 years. Acute catarrh cholecystitis was found out in 20 % cases, acute phlegmonous - in 21 % cases, acute gangrenous - in 11 % cases, chronic – in 28 % and chronic relapsing – in 21 % cases.
Results: All forms of cholecystitis characterized by a maximum thickness of the body wall, minimal at the bottom of the gallbladder. In all forms adipose tissue inflammation in the connective tissue layer was increased and it was found out the atrophy of the mucosa. In the inflammatory infiltrate in acute forms of inflammation were found neutrophilic and basophilic leukocytes: with simple acute cholecystitis - in the bottom, and with acute phlegmonous and gangrenous cholecystitis - in the area of the body of the gallbladder. In the cases with chronic cholecystitis were dominated mononuclear cells in all areas, and in the cases with chronic relapsing - neutrophilic and basophilic leukocytes in the bottom and the body, and mononuclear cells - in the neck of the gallbladder.

PS-14-008
Histological features of chronic hepatitis C in hemodialysis patients
I. Delladetsima*, A. Kokkori, V. Sypsa, M. Psichogiou, S. Sakellariou, J. Boletis
*Athens University, 1st Dept. of Pathology, Greece

Objective: Chronic hepatitis C (CHC) in hemodialysis patients has not been thoroughly investigated, despite its high frequency. The present comparative study aims to highlight the histological features of CHC and its association with putative pathogenetic parameters in this specific group of patients.
Method: Sixty-one biopsies of hemodialysis patients and 326 biopsies from the general population with CHC were comparatively evaluated for the severity and specific histological features of CHC. Results were examined in relation to age, time of dialysis, viral load and genotype.
Results: Patients on hemodialysis were older than patients of general population (p=0.031), showing a similar genotype distribution (p=0.328) and lower viral loads (p=0.001). CHC on hemodialysis was significantly milder according to stage

(p=0.033), activity and its parameters (p<0.001). Significantly reduced was also the frequency of lymphoid aggregates (p< 0.001), bile duct damage (p<0.001) and steatosis. (p=0.033). Severity of hepatits was not associated with time on hemodialysis. In multivariate analysis the differences were independent of age, which was associated with more severe disease. Steatosis was associated with hemodialysis duration and age.
Conclusion: CHC in hemodialysis patients is significantly milder than in general population. Limited necroinflammatory activity and absence of immune mediated lesions are indications of defective immune response although involvement of low viral load cannot be overlooked.

PS-14-009

Inflammatory (myofibroblastic) pseudotumor of the liver: Case report

E. Demiralay*, S. Altaner, H. Özdemir
*Baskent University, Dept. of Pathology, Istanbul, Turkey

Objective: Inflammatory pseudotumor of the liver (IPT) is a rare, benign tumor-like lesion of which etiology is not fully known. It is confused with primary and metastatic malignant tumors as it seems as an occupying mass on radiologic examinations.
Method: Thirtyeight-year-old male patient who had fatigue and dyspepsia was detected to have elevated liver enzymes and hepatomegaly. On computed tomography, two masses of which middle is mildly hypometabolic, measuring 34× 31 mm in right liver lobe and 45×39 mm in left liver lobe were detected. Biochemical tests were normal except elevated AST and ALT levels. Ultrasound-guided needle biopsy was done for two masses.
Results: On microscopic examination, a lesion composed of abundant fusiform fibroblastic cells and vascular structures among inflammatory cells composed of lymphocytes, plasmocytes, histiocytes and eosinophillic leucocytes and including sharp margins between regenerated liver tissue was observed. On immunohistochemical examination, SMA was stained focal positive in fibroblastic cells. Staining with desmin, S-100, PanCK, CD34, Ki-67 and CD117 was not seen.
Conclusion: IPT does not have a specific radiologic finding and definite diagnosis is made with pathologic examination. This case is presented as it is rarely seen, radiologically resembles to malignant tumors and for review of pathological differential diagnosis.

PS-14-010

Enhancer of Zeste Homologue 2 (EZH2) expression in malignant and benign hepatic tumors

K. Dezso*, V. Szabó, E. Bugyik, K. Schlachter, S. Paku, Z. Schaff, P. Nagy
*Semmelweis University, 1st Dept. of Pathology, Budapest, Hungary

Objective: The immunohistochemical demonstration of Enhancer of zeste homologue 2 (EZH2) proved to be a useful marker in several tumor types, including hepatocellular carcinomas.In order to recognize the diagnostic value of this protein in hepatic tumors we have investigated the presence of EZH2 in the most common liver neoplasms.
Method: The presence of EZH2 has been studied by standard immunohistochemistry in several formalin-fixed paraffin-embedded tumor samples (hepatocellular adenoma, hepatocellular carcinoma, cholangiocarcinoma, hepatoblastoma, metastatic liver tumors and primitive childhood tumors).
Results: Forty of 44 hepatocellular carcinomas, 22 of 23 cholangiocarcinomas, 29 of 31 hepatoblastomas and 14 of 17 metastatic liver tumors stained positively, but all the investigated hepatocellular adenomas (n=24) and proliferating biliary structures were negative. The other primitive childhood tumors that were examined all expressed EZH2.
Conclusion: Based on these results EZH2 is a sensitive marker of malignancy in hepatic tumors regardless of their histogenesis. In routine surgical pathology EZH2 could be helpful to diagnose hepatocellular carcinomas and it might be the first marker to distinguish transformed and reactive cholangiocytes.

PS-14-011

Nuclear ploidy as a marker of intraductal papillary-mucinous pancreatic neoplasms malignancy

E. Dubova*, O. Mishnev, A. Shchegolev
*V.I. Kulakov Scientific Center, Dept. of Pathology, Moscow, Russia

Objective: Intraductal papillary-mucynous pancreatic neoplasm (IPMN) represents 0,5 to 9.8 % of all tumors of exocrine pancreas. Our aim was to study nuclear ploidy of malignant and benign IPMNs cells.
Method: We studied 20 pancreatic surgical specimens from 5 females and 15 males. We performed histological, morphometrical and ploidy analysis of all specimens.
Results: IPMN cells nuclear perimeter and size was higher than in normal pancreatic duct cells. This parameters were higher in malignant noninvasive IPMN than in benign tumor. Nuclear size and perimeter of invasive malignant IPMN were in intermediate position between benign and malignant noninvasive tumor. Mean nuclear ploidy (MNP) of normal ductal pancreatic cells was 2.4c. MNP of benign IPMNs was 2.5c, borderline tumors – 3.0c. MNP of noninvasive malignant IPMNs was 5.1c, of invasive IPMNs – 4.5c. We also revealed that aneuploidy coefficient (AC) of benign IPMNs was 0 (there weren't aneuploid nuclei in its cells). AC of borderline IPMNs was 0.11. Maximal level of

AC was in malignant noninvasive IPMNs whereas AC of invasive IPMNs was lesser.
Conclusion: Nuclear morphometric parameters and mean nuclear ploidy level as well as aneuploidy coefficient could be used as additional criteria for determining malignant potential of IPMNs.

PS-14-012

An intraductal papillary mucinous neoplasm of the pancreas with concomitant neuroendocrine tumor: A case report

J. Garcia*, F. E. Costa, R. Sampaio, R. Dias, A. Duarte, J. Ramon Vizcaíno
*Lisbon, Portugal

Objective: Intraductal papillary mucinous neoplasms (IPMNs) are a recently classified pancreatic neoplasm with an increasing incidence. IPMN of the pancreas is a lesion consisting of mucin-producing cells with neoplasic potential, characterized by papillary intraductal growth and varying degrees of cytologic atypia. Neuroendocrine tumors of pancreas (PNET) are rare pancreatic neoplasms comprising 1–2 % of all pancreatic tumors. PNETs express neuroendocrine markers, however the true cell or cells of origin are not fully understood. PNETs are classified as functional or nonfunctional based on the presence or absence of a specific clinical syndrome associated with hormone oversecretion. Intraductal papillary mucinous neoplasm of the pancreas with concomitant Neuroendocrine tumor are a highly rare occurrence.
Method: A literature review of IPMNs and PNET was made, as well as a review of the clinical data of a patient with IPMN and concomitant PNET.
Results: A 60-years-old Caucasian female, underwent a laparoscopic distal pancreatectomy with splenectomy for IPMN. Macroscopic examination revealed discrete dilatation of pancreatic ducts and nodule in the pancreas tail. Hystologic examination revealed neoplasic lesion of intraductal papillary-mucinous in the body and tail of pancreas with moderate dysplasia (IPMN borderline) and Neuroendocrine Tumor grade 1 (WHO 2010).
Conclusion: This case reports a highly rare occurrence.

PS-14-014

Glypican 3 and agrin expression in hepatocellular carcinoma and cholangiocellular carcinoma: A immunochemistry study

N. Gursan*, H. Balta, B. Gundogdu
*Ataturk University, Medical Faculty, Erzurum, Turkey

Objective: Glypican 3 (GPC3), which plays a role cellular growth, differentiation and migration is one of members of glypican family. Although GPC3 expression in the liver, glypican upregulation of the vast majority of tumors are available. Agrin is found the surface on the cells and the extracellular matrix, the micro-vessels
Method: In this study, formalin-fixed, paraffin-embedded surgical specimens from 20 patients with hepotocellular carcinoma and 20 patients with cholangiocellular carcinoma diagnosed between 2000 and 2011 years in Ataturk University, Faculty of Medicine, Department of Pathology were studied with immunohistochemistry Agrin and GPC3.
Results: We detected agrin in around bile ducts and blood vessels within the portal areas in the normal liver. İn the malignant hepatocellular carcinoma (HCC) is seen in a dramatic increase in the quantity of agrin. GPC3 immunpositivity showed in %85 of HCC and %15 of cholengiocellular carcinoma. Agrin immunpositivity showed in %95 HCC and %50 of cholangiocellular carcinoma.
Conclusion: GPC3 and Agrin, that is useful in early diagnosis of HCC cases; cholangiocellular carcinoma, or not enough was understood to be very limited.

PS-14-015

Value of glypican 3, Hep Par and alpha fetoprotein in diagnosis of hepatocellular carcinoma

N. Gursan*, H. Balta, B. Gundogdu
*Ataturk University, Medical Faculty, Erzurum, Turkey

Objective: Glypican 3 showed high expression of the embryonic liver and intestine, is silenced in normal adult tissues. It is an oncofetal protein. İn general, oncofetal proteins, while having a critical role in tumor progression or immunotherapy is a potent tumor marker used as a target. Alpha fetoprotein, clone C3 localized, normally produced by gestational age, fetal liver and yolc salc, glycoprotein structure emerging marker for patients with HCC. Hep Par 1 antibody was developed in 1993 using fixed liver as immunogen.
Method: İn this study formalin-fixed, paraffin-embedded surgical specimens from 20 patients with hepatocellular carcinoma diagnosed between 2000 and 2011 years in Ataturk University, Faculty of Medicine Department of pathology were studied with immunohistochemistry GPC3, Heppar 1, and AFP. GPC3, Heppar 1 and AFP expression was divided into 2 categories negative (negative or weak under %5 tumor cells cytoplasmic staining) and positive (and %5 over of tumour cells) moderate or strong cytoplasmic with membranous accentuation.
Results: Immunpositivity at GPC3, Hep Par 1 and AFP were 85 %, 95 %, 75 % respectively.
Conclusion: İn this study, GPC3, AFP and Hep Par 1 may aid in the accurate diagnosis of HCC.

PS-14-016

Expressions of fibroblast growth factor receptors as an independent prognostic factor in hepatocellular carcinoma

H.-J. Kang*, H.-J. Lee, K.-M. Kim, E.-S. Yu
*Asan Medical Center, Dept. of Pathology, Seoul, Republic of Korea

Objective: Fibroblastic growth factor receptor (FGFR) family is known to be related to the development and progression of various types of cancers. The aim of this study is to determine the clinical implication of FGFR expressions in patients with hepatocellular carcinoma (HCC).
Method: Immunohistochemical analysis was done in 842 cases of HCC using tissue microarray. Diffuse cytoplasmic staining for FGFR1, 2, 3 and 4 in more than 10 % of tumor cells were designated as positive. The results were analyzed in terms of various clinicopathologic parameters.
Results: On univariate analysis, the overall survival rates of patients with FGFR2 expression (152 cases, 18.1 %) were significantly lower than those with no expression (HR 1.838, 95 % CI 1.452–2.328, $P<0.001$). However, the overall survival rates of patients with FGFR4 expression (446 cases, 59.6 %) were significantly higher than those with no expression (HR 0.636, 95 % CI 0.521–0.776, $P<0.001$). There was no statistical significance between patients' overall survival rates and expressions of FGFR1 (46 cases, 5.5 %) or FGFR3 (33cases, 4.0 %). On multivariate analysis, only FGFR2 expression is independently associated with reduced OS (FGFR2: HR 1.790, 95 % CI 1.404–2.282, $P<0.001$).
Conclusion: The FGFR2 expression can be used as an independent prognostic factor in patients with surgically resected HCC.

PS-14-018

Hurp overexpression in pancreatic adenocarcinomas correlated with worse prognosis

M. Lambropoulou*, E. Nikolakopoulou, G. Trypsianis, T.-E. Deftereou, I. Grammatikopoulou, A. Kiziridou, E. Chouridou, S. Kakolyris, N. Papadopoulos, E. Chatzaki, M. Koffa
*Democritus University of Thrace, Medical School, Alexandroupolis, Greece

Objective: HURP (hepatoma upregulated protein) is a putative oncogene, overexpressed in many human cancers, including hepatocellular carcinoma. It has also been shown recently that high HURP protein levels correlate with resistance to chemotherapeutic agents. In the present study we investigate the expression of HURP and its correlation with pancreatic adenocarcinoma, prognosis and patient survival. Pancreatic adenocarcinoma is one of the most aggressive types of cancer and represents the fourth most common cause of death, either in the male or in the female population of the United States of America.
Method: HURP immunoreactivity was assessed by immunohistochemistry in a series of 28 primary pancreatic adenocarcinomas. In parallel, HURP expression was examined in 10 normal pancreatic tissues. Statistical analysis related HURP expression levels with clinicopathological characteristics and survival.
Results: Results showed a positive correlation between HURP overexpression and grade as well as lymphovascular invasion. All non malignant biopsies were negative. Furthermore, positive expression of HURP appeared to be an important independent prognostic factor too, related with poor survival rates.
Conclusion: Our results showed that HURP overexpression is associated with poor prognosis in pancreatic adenocarcinoma and indicated a diagnostic potential of this protein. Its role in the carcinogenetic process awaits further elucidation.

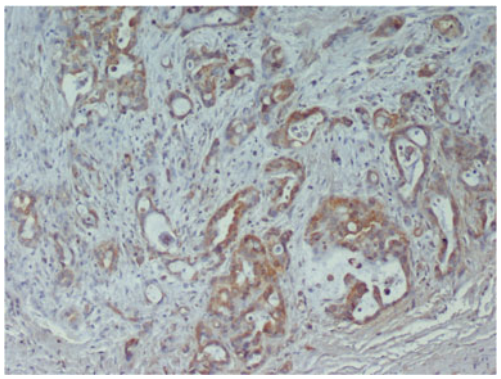

PS-14-019

Hepatocellular carcinoma in patient with hepatic porphyria: A case report

J. Marcinek*, P. Szépe, T. Balhárek, M. Kalman, L. Plank
*University Hospital Martin, Dept. of Pathology, Slovakia

Objective: Hepatocellular carcinoma (HCC) is frequently associated with liver cirrhosis or chronic hepatitis of various etiology, less often with other chronic hepatopathies, including hepatic porphyria. We present a case report of HCC diagnosed in patient with clinically unrecognized porphyria cutanea tarda (PCT).
Method: A 70-year old male was admitted to hospital complaining of a pressure below low costal margin, anamnesis of a trauma 1 year ago and clinical suspicion of a posttraumatic intrahepatic haematoma. By a surgery, a partialy necrotic and hemorrhagic tumor mass 10 cm in diameter was removed.
Results: The mass corresponded histologicaly to moderately differentiated clear cell HCC, resembling renal clear-cell carcinoma. The surrounding parenchyme showed steatohepatitis with fibrosis and distinct intracellular porphyrin crystals.
Conclusion: Development of HCC is a well documented complication of PCT, a disorder of porphyrin biosynthesis. PCT can be inherited (autosomal dominant trait), the acquired form (sporadic PCT) is more common. Known etiological factors of PCT include toxins, alcohol abuse, estrogens or chronic viral hepatitis, or association with other

hepatic diseases like iron overload (including hereditary haemochromatosis) or chronic hepatitis C, increasing the risk of malignancy. However, in the presented case none of these associations was recognized and its etiology remains obscure.

PS-14-020

Undifferentiated carcinoma with osteoclast-like giant cells – Rare variant of pancreatic cancer– Case report

D. Milutin*, S. Mocan, O. Budisca
*Emergency County Hospital, Pathology, Tirgu Mures, Romania

Objective: Undifferentiated carcinoma with osteoclast-like giant cells is a rare pancreatic tumor that could be associated with an adenocarcinoma or a mucinous cystic neoplasm of the pancreas.
Method: We present the case of a 63 years old man with clinical diagnosis of hemorrhagic retroperitoneal tumor penetrating the tail of the pancreas, spleen, inferior cava vena and posterior gastric wall.
Results: Gross examination reveals multiple whitish tumor fragments with necrosis and hemorrhage. Microscopically: round to spindle atypical cells and large non-neoplastic multinucleated giant cells infiltrating the pancreas. First impression is that it looks like a giant cell MFH infiltrating the pancreas. On closer examination we see can small areas of adenocarcinoma that have been better highlighted by citokeratin antibody. Immunohistochemically: the mononuclear tumor cells are positive for vimentin and part of them for p53 and CD68, the multinucleated giant cells are positive for CD68 and adenocarcinoma tumor cells for citokeratin.
Conclusion: The diagnosis is made by the microscopic features associated with pancreatic adenocarcinoma that sustains the pancreatic origin and exclude the giant cell MFH that, usually, arises in deep intramuscular soft tissue of the extremities.

PS-14-021

Unusual malignant tumor of the gallbladder

N. Labaied*, S. Ziadi, T. Mounir, S. Cyrine, B. Ahlem, M. Wiem, S. Badreddine
*CHU Farhat Hachad, Dept. of Pathology, Sousse, Tunisia

Objective: Signet ring cell carcinoma is an extremely rare type of gallbladder carcinoma composed overwhelmingly (90 %) of signet ring cells. Only a few cases of this histologic type have been published and detailed knowledge of this disease is not available.
Method: We report a case of signet-ring cell carcinoma of the gallbladder in a 70-year-old woman who was admitted with epigastric pain. Under the preoperative diagnosis of cholangiocarcinoma, which was based on findings of CT scan and ultrasonography. Cholecystectomy was performed.
Results: Microscopic examination revealed a signet ring cells tumor that arose from the sub epithelial layer of mucosa and involved all the layers of gallbladder. Nuclear atypia and mitoses were present. Periodic acid schiff (PAS) stain highlighted the intracellular mucin in the tumor cells. Lympho-vascular emboli were detected in the subserosal layer. The cystic duct surgical margins were invaded.
Conclusion: Gallbladder adenocarcinomas are seen frequently, but signet-ring cell carcinoma is a rare entity. Owing to the location of the gallbladder, dissemination of the tumour to the adjacent tissues is usually presented at the time of the diagnosis. It is necessary to exclude a gastric or colonic signet ring cell carcinoma secondarily involving the gallbladder.

PS-14-022

Extragastrointestinal stromal tumor of the pancreas: A case report

O. Paklina*, G. Setdikova, S. Vaskanyan
*Burnacyan FMBC FMBA, Dept. of Pathology, Moscow, Russia

Objective: Gastrointestinal stromal tumors (GISTs) are mesenchyme neoplasms of the gastrointestinal tract which express CD117. GISTs can occur in the entire length of gastrointestinal tract, but very seldom can also arise in omentum, mesentery and retroperitoneal space, kidney, urinary bladder etc. There they are located adjacent to stomach or intestine, but not originated from the latter. These tumors are designated as "extra-gastrointestinal stromal tumors" (EGISTs). There are only 14 description of the Primary EGISTs reported in the literature.
Method: We report a case of a pancreatic EGIST in a 38-year-old female patient.
Results: CT scan showed a mass in the head of pancreas. Grossly encapsulated tumor, 9 cm in diameter, was found in the head of the pancreas (Figure 1). Histologically, tumor demonstrated spindle-cell pattern consisted of distinct fascicles and bands. The number of mitoses was 1-2/50 high power fields in “hot-spot” areas. IHC revealed strong positivity for CD117, CD 34 in neoplastic cells and negative for SMA, desmin, S-100. Ki67 labeling index was 3 %.
Conclusion: We presented a rare case of pancreatic GIST. The tumor has very good prognosis.

PS-14-023

Hepatoblastoma in adult age

C. Pechianu*, E. Stoica-Mustafa, I. Popescu, V. Herlea
*Institutul Clinic Fundeni, Pathology, Bucharest, Romania

Objective: Hepatoblastoma is a rare malignant tumor of the liver and usually occurs in the first three years of life.

Hepatoblastoma is classified as epithelial (56 %) or mixed epithelial/mesenchymal (44 %). Epithelial hepatoblastoma is further divided to pure fetal (31 %), embryonal (19 %), macrotrabecular (3 %) and small cell undifferentiated (3 %).
Aim: To increase the awareness regarding possibility of hepatoblastoma in adult age.
Method: We review four cases of hepatoblastoma epithelial type diagnosed in Pathology Department of Fundeni Clinical Institute between 2009 and 2012. Immunohistochemistry was done in all cases: CEA, Vimentin, CK 8/18, CK 19, CK 20, Ki 67, TTF1, CD 10, CD 34, CD 56, MUC 5A, alpha-fetoprotein.
Results: Two of the patients were males and two females with age ranging between 17 and 27 years. The tumors varying in size from 8 to 12 cm. On microscopic examination the tumor was composed mainly of epithelial elements. The pathological diagnosis was epithelial hepatoblastoma epithelial type.
Conclusion: Hepatoblastoma is a rare tumor in adult age and epithelial type is the rarest from all type of hepatoblastoma in adult age. The pathological diagnostic is quite difficult even using immunohistochemistry because none of the markers are not specific for hepatoblastoma.

PS-14-024
Submassive hepatic necrosis with regenerative nodules: A series of cases
Y. Rodríguez-Gil*, J. Salazar, J. Delgado Sánchez, G. López Alonso, C. Ibarrola de Andrés, F. Colina Ruizdelgado
*Hospital Universitar 12 de Octubre, Dept. of Surgical Pathology, Madrid, Spain

Objective: Confluent hepatic necrosis is the morphological correlate of fulminant liver failure. A group of these livers develop a combination of areas of necrosis and regenerative macronodules (RMN).
Method: Sequential biochemical and clinical data and tissues from two groups of patients were compared. Group 1: 10 cases of submassive necrosis associated with RMN; Group 2: 19 cases with total confluent necrosis without nodular regeneration.
Results: Group 1: mean age was 33,6 years (ranged 10 months-63 years); group 2 mean age was 42,6 years (ranged 18 months-63 years) ($p>0,05$). A longer course (42,8±34,6 days vs 12,6±6,0, $p<0.05$) and higher maximum serum bilirubin levels (23,5 mg/dl ±13,08 vs 14,9 mg/dl± 10,9, $p<0.05$) were observed in group 1. Serum AST, ALT and gamma-GT were lower in group 1 ($p>0.05$). Morphologically livers from group 1 showed well defined regenerative green-yellow nodules with large regenerative hepatocytes in acinar pattern without surrounding fibrosis. The remaining parenchyma showed confluent necrosis, haemorrhage, mixed inflammatory infiltrate and ductular proliferation.
Conclusion: A special anatomoclinical form of subacute liver failure was characterized by regenerative macronodules in a background of extensive confluent liver necrosis. Illness duration was longer and had higher maximum bilirubin levels than those without RMN.

PS-14-025
Immunohistochemical study of MUC gene family in pancreatic cancer
G. Setdikova*, O. Paklina
*Moscow, Russia

Objective: Investigation of the MUC gene in pancreatic ductal adenocarcinomas (PDA).
Method: In the present study, we examined the expression of MUC1, 2 and 5 AC types by immunohistochemical analyses in PDA from 74 patients. Overall survival curves were drawn by the Kaplan-Meier method. For all analyses, $p<0.05$ was considered to be statistically significant.
Results: In our cases most of the PDA was presented as MUC1+/MUC5AC + phenotype - 42 % cases (31/74). The group with intestinal phenotype mucin, which characterized by positive expression of MUC2 and CDX2, was only 7 % (5/74). The group which characterized by positive expression only MUC5AC (gastric phenotype), was 15 % (11/74). The survival rate of patient better in group with MUC2 expression. Cumulative survival at 12 months after surgery was 1.0 and the median postoperative follow-up period was 17 months. The most aggressive behavior was PDA with expression only MUC1 ("true pancreatobilliary type"). Cumulative survival at 12 months after surgery was 0.25 and the median postoperative follow-up period was 7 months.
Conclusion: The mucin profile as a prognostic factor is important not only for intraductal pancreatic mucinous neoplasm, but and for ductal pancreatic adenocarcinoma.

PS-14-026
Hepatocellular carcinoma microvessels density depends on tumor differentiation: Radiologic-pathologic correlations
A. Shchegolev*, E. Dubova, U. Tumanova
*V.I. Kulakov Scientific Center, Dept. of Pathology, Moscow, Russia

Objective: Prognosis and recurrence level in hepatocellular carcinoma (HCC) depends on microvessels density.
Method: We performed CT and pathological correlations in 22 cases of HC (5 cases of highly (h-HCC), 11 cases of moderate (m-HCC) and 4 cases of low differentiated HCC (l-HCC)).
Results: Vessels number in w-HCC in compare to m-HCC was higher by 26.1 % ($p<0.05$). Total vessel area was higher in m-HCC and l-HCC than in w-HCC by 11.7 % and 20.4 % accordingly. We observed positive correlation between CT density of h-HCC and number and total vessel area. Correlation between h-HCC CT density and mean vessel area was negative. We also revealed modest negative correlation between m-HCC density and the number vessels in all phases of CT. Negative correlation between total and mean vessel area and m-HCC density was revealed in native and arterial CT phases in compare with venous and delayed phases where positive correlation was revealed. In all phases of CT we revealed strong negative correlation between l-HCC density and the number of vessels whereas correlation between l-HCC density and mean vessel area was strongly negative.
Conclusion: We revealed decreasing in angiogenic activity in HCCs neoplastic progression and growth. CT signs correlate with HCC histological differentiation.

PS-14-027
Primary sporadic liver schwannoma: An extremely rare diagnosis
R. Silva*, C. Eloy, J. M. Lopes
*Centro Hospitalar de São Joâo, Serviço de Anatomia Patológica, Porto, Portugal

Objective: Primary liver schwannoma (PLS) is extremely rare.
Results: Case Report: A 69-year-old female with previous history of cholecystectomy, appendectomy, arterial hypertension and diabetes mellitus was admitted due to an intrahepatic nodular lesion identified in routine ultrasound examination. She was submitted to partial hepatectomy with postoperative uneventful evolution. Macroscopically, the specimen disclosed a 2.1 cm nodular, well circumscribed, yellowish tumour. Histologically, the tumour displayed an expansive growth pattern, comprising short bundles of spindle cells with mild atypia, without mitotic figures or necrosis. Immunohistochemically, the tumor cells expressed diffusely vimentin, S-100 and GFAP, in the absence of AE1/AE3, CAM5.2, CD117, and HMB45; Ki-67 index was 2 %. Staging procedures did not disclose evidence of any other tumor. There was no personal or family evidence of neurofibromatosis. These features are consistent with sporadic PLS.
Conclusion: Schwannoma is a rare benign tumour in the gastrointestinal tract with few cases reported in the liver. The clinical presentation is usually an upper abdominal pain but they can be asymptomatic. Secondary cystic degeneration and hemorrhage are common in large tumours. Differential diagnosis by imaging evaluation includes several benign and malignant, namely metastatic, tumours. Therefore, the pathological examination is crucial for the diagnosis of primary liver schwannoma.

PS-14-028
Metastases of hepatocellular carcinoma to the costa and soft tissue: A very rare entity
E. Tastekin*, T. D. Yalta, O. Yalcin, T. Ciftci
*Trakya University, Dept. of Pathology, Edirne, Turkey

Objective: Hepatocellular carcinoma (HCC) is the most common primary tumor of the liver with a potential of metastasis primarily to the lung, abdominal lymph nodes and bone. However, metastases to the costa, soft tissue are rare.
Method: An 82-year-old man was admitted to hospital with weakness, anorexia. Chest x-ray and CT-scan demonstrated a 5×5 cm sized, intrathoracic mass on the lateral-side of the left 2.costa and also infiltrating the axillary soft tissues.A secondary mass with the identical radiological features was also detected within the C7-vertebra. Whole-body CT-scan was planned.A 2×2 cm sized nodular, hipodense mass was detected in the upper segment of the liver. Interestingly, none of these masses demonstrated a significant pathological FDG-uptake in the PET.A trucut biopsy was taken from the axillar. Microscopically, large tumoral nests were observed in connective tissues. Polygonal shaped tumoral cells were found to have granular cytoplasm, pleomorphic nuclei. Immunohistochemistry results: Positive cytoplasmic reaction with Heppar, TTF-1; canalicular staining with Polyclonal-CEA, CD10; weak cytoplasmic staining with pankeratin, B72.3; Negative reaction with Vimentin, AFP, CK7, CK20.
Results: These histomorphological, immunohistochemical findings strongly supported to the diagnosis of HCC metastasis.
Conclusion: HCC that is, in general, morphologically similar to mesenchymal and epithelial tumors, should be considered among the differential diagnosis of unknown primary tumors.

PS-14-029
Morphological justfication of using pulsed electric discharge in surgical treatment of echinococcosis
M. Tussupbekova*, D. Kaliyeva, E. Turgunov
*Medical University Karaganda, Dept. of Pathological Anatomy, Kazakhstan

Objective: Echinococcosis is characterized by lesions of internal organs, severe complications, often lead to disability and death.
Method: New method of processing of the residual cavity with impulsive electric discharge after echinococcectomy was experimentally developed and introduced into clinical practice. The effectiveness of the method is confirmed by morphological examination of operational bioptic of the liver tissue.
Results: 20 patients underwent surgical treatment with the new method (Patent of the Republic of Kazakhstan ¹ 63558). Parasitic cysts with an inner germinal layer and protoskoleks, outdoor layer - chitinous shell with a productive reaction with lymphocytes infiltration, single eosinophils, separate groups of hydatid bubbles with their invasion in the liver tissue were detected in the histological examination of material taken intraoperatively prior processing of residual cavity with electropulse discharge. Fibrinoid necrosis, destruction of germinal elements, single lymphoid infiltration, hyperemia of blood vessels, absence o inflammatory reaction were marked in the histological material after processing by impulsive electric discharge.
Conclusion: The results showed that echinococcectomy with processing of the residual cavity with impulsive electric discharge is an alternative for pericystectomy and liver resection.

Tuesday, 11 September 2012, 09.30 - 10.30, Congress Hall Foyer 3rd Floor
PS-15 Poster Session Paediatric and Perinatal Pathology

PS-15-001
Congenital peribronchial myofibroblastic tumor: Case report and review of the literature
A. Acikalin*, D. Gumurdulu, G. Gonlusen, S. Iskit, E. Bagir
*Cukurova University, Dept. of Pathology, Adana, Turkey

Objective: Congenital peribronchial myofibroblastic tumor is a rare, solid mesenchymal tumor of the fetus and neonate, usually associated with nonimmune hydrops fetalis. We report the case with clinical, radiological and pathologic findings and review the other cases in the English language literature.
Method: We present a case of CPMT, whom a right lung mass was detected in intrauterine life. 12 days after delivery by cesarean section, right lobectomy was performed.
Results: The tumor was limited to lung, and composed of spindle cells, proliferating around bronchial unit. Central necrosis and 4-5/10 hpf was present. Patient is well 15 months after surgery.
Conclusion: Congenital peribronchial myofibroblastic tumor is a rare solid pediatric tumor of lung which was named differently in the past, such as congenital fibrosarcoma, congenital leiomyosarcoma, congenital mesenchymal malformation of the lung, neonatal pulmonary hamartoma. albeit it resembles sarcoma with high cellularity, mitosis and necrosis features microscopically, no additional therapy to tumor resection is needed. So it is important to keep in mind this scary looking, but innocent tumor both in prenatal and postnatal evaluation.

PS-15-002
Morphologic alteration of metastatic neuroblastoma in bone marrow after chemotherapy
G.-E. Bae*
*Samsung Medical Center, Dept. of Pathology, Seoul, Republic of Korea

Objective: The aims of our study are to evaluate the histologic features of metastatic neuroblastoma in bone marrow (BM) in comparison with those of primary neuroblastoma, and to compare the histologic characteristics of metastatic neuroblastoma in BM before vs. after chemotherapy.
Method: Total 92 biopsies from 19 children diagnosed as stage 4 neuroblastoma with BM metastasis were examined histologically; 19 primary neoplasm biopsies, 19 BM biopsies before chemotherapy, 19 primary neoplasm excision biopsies after chemotherapy, and 35 BM biopsies after chemotherapy.
Results: 1) Primary neoplasms were classified as neuroblastoma poorly differentiated (n=10), neuroblastoma differentiating (n=5), ganglioneuroblastoma intermixed (n=1) and neuroblastoma type unclassifiable (n=3). 2) Metastatic foci in BM before chemotherapy were composed of undifferentiated and/or differentiating neuroblasts but not ganglion cells, in neuropil but not schwannian stroma. 3) Metastatic foci of BM after chemotherapy showed differentiation such as ganglion cells and schwannian stroma, which was more prominent after more cycles of chemotherapy. 4) Metastatic neuroblastomas in BM after chemotherapy were as mature as or less mature than those in primary neuroblastomas after chemotherapy.
Conclusion: Metastatic neuroblastomas in BM initially consist of more immature components than primary neuroblastomas, whereas they become differentiated as primary neuroblastomas after multi-cycle chemotherapy.

PS-15-003
Morphometric evaluation and clinical correlations in malignant small round cell tumors
C. Bansal*, A. Gupta, A. Kumar, A. Srivastava
*CSMMU, Dept. of Pathology, Lucknow, India

Objective: Nuclear size increases in malignant tumors and reflects DNA content, ploidy and proliferation index. Present study investigated; could nuclear morphometery

differentiate histomorphologically similar paediatric malignant small round cell tumors in H & E stained sections for using in a poor resource country?
Method: Morphometric analysis was done in 26 confirmed but difficult to differentiate round cell tumors histomorphologically and were analyzed by cell images from 6 different areas in each section, using Leica Q win 500 images software.
Results: Nuclear measurements were obtained for retinoblastoma (9), Hodgkin lymphoma (6), Wilms tumor (3), medulloblastoma (2), Ewing's sarcoma (2), alveolar rhabdomyosarcoma (1), malignant hemangiopericytoma (1), non-Hodgkin lymphoma (1) and neuroblastoma (1). Amongst the retinoblastomas, maximum mean nuclear area percent (24.93) was seen in cases with nerve involvement and metastasis, followed by cases with only nerve involvement (21.60) and smallest area (16.57) was in non-nerve involving, non metastatic cases. Wilms tumor cases with metastasis had higher nuclear area (21.25) than non metastatic (19.47). Non-Hodgkin lymphoma nuclear area (20.03) was more than Hodgkin's (18.60). Amongst all tumors, minimum value (14.93) was seen in malignant hemangiopericytoma.
Conclusion: Morphometric evaluation in paediatric malignant round cell tumors have generated useful data, and needs further multicentric confirmation for implementation.

PS-15-004
Immunohistochemical expression of survivin in Wilms tumor
G. Basta Jovanovic*, D. Brasanac, J. Milasin, L. Bogdanovic, S. Djuricic, S. Radojevic-Skodric
*School of Medicine, Inst. of Pathology, Belgrade, Serbia

Objective: Survivin, a bifunctional protein that regulates cell division and suppresses apoptosis, may play an important role in tumorigenesis. The aim of this study was to determine survivin expression patterns in Wilms tumor (WT) and to analyze it in relation to stage, prognostic category and histological type.
Method: Immunohistochemical expression of survivin was analysed in 59 cases of primary WT and in 10 normal kidney specimens uninvolved by the tumor.
Results: Fifty one out of 59 cases of WT (86.44 %) showed decreased cytoplasmic survivin expression compared to the expression in normal kidney tissue. Decreased cytoplasmic expression (in all components of WT) of survivin was found significantly more often in low stage compared to high stage WTs (86.7 % vs. 27.3 %; p=0.002). Tumors of intermediate risk group showed more often decreased cytoplasmic expression of survivin in comparison to high risk group, but the difference was not significant. Decreased survivin expression was found more frequent in WTs with diffuse anaplasia and in epithelial WTs compared to other histological types, but without statistically significant difference.
Conclusion: Decreased survivin cytoplasmic expression may be associated with the favorable prognosis WT.

PS-15-006
Uncommon solid hepatic tumor in a fetus
N. Ben Jamaa*, M. T. Yacoubi, A. Lahmar-Boufaroua, A. Masmoudi, S. Kacem, S. Jabnoun, S. Siala Gaiga
*Menzah, Tunisia

Objective: Hepatic tumors accounted 5 % of congenital neoplasms. Mesenchymal hamartoma of the liver is a rare benign tumor of children. We report a case of hepatic mesenchymal hamartoma in a premature male neonate.
Method: A premature neonate born at 33 gestational weeks from 34 year-old mother, G3P3 with non-consanguineous marriage; prenatal ultrasonography showed a fetal macrosomia, a highly vascularized abdominal mass occupying two-third of the abdomen and displacing the bowel loops associated with poly-hydramnios. The newborn examination showed abdominal firm lump. Ultrasound found and anterior highly vascularized mass displacing the left lobe of liver. The infant died few hours later. A complete autopsy was performed.
Results: External examination showed a male neonate anatomically of 34–35 week having an increased periombilical diameter and a macrosomia, ascitis, pulmonary hypoplasia, cardiomegaly, pleuropericardial effusion, liver tumor developed in left lobe and dilation of renal vessels. Histologically the tumor showed a mixture of normal liver tissues with blood or lymphatic vessels, bile ducts within an abundant edematous and myxoid stroma.
Conclusion: In neonate and fetus, prenatal diagnosis is possible by ultrasonography. Large tumors can affect the viability of the newborn. Adequate excision is curative in most of cases.

PS-15-007
NCAM polysialylation as potential initiator of differentiation and proliferation of renal progenitors in human fetal tissue
S. Cirovic*, J. Tadic, N. Radunovic, C. Müller, G. Müller, J. Markovic-Lipkovski
*Inst. for Pathology, Nephropathology, Belgrade, Serbia

Objective: Objective: Neural cell adhesion molecule (NCAM) is widely expressed on mesenchymal and early tubular epithelial cells during kidney development although with still undefined function. NCAM can be polysialylated and as PSA-NCAM has been shown to be involved in proliferation and migration of neuronal cells during brain

development. The aim of this study was to evaluate the presence of PSA-NCAM in nephron precursors in relation to the expression of renal progenitor and proliferation markers.
Method: Human fetal and neonatal kidneys were analyzed using double-immunofluorescence (dIF) staining and Western Blot (WB) analysis. Specific antibodies against NCAM, PSA-NCAM, EpCAM, CD24 and Ki-67 were applied.
Results: On WB only fetal tissue samples have bands with NCAM at 140 to 250 kDa which suggest that NCAM molecule is polysialylated; dIF analysis of fetal tissue show PSA-NCAM + Ki-67+ cells in all structures known as nephron precursors. While in neonatal tissue PSA-NCAM and Ki-67 were positive only on rare single cells in intersticium.
Conclusion: PSA-NCAM expression appears to characterize a very early stage of induced nephron progenitors differentiating from NCAM + EpCAM- mesenchymal cells. According to PSA-NCAM localization and coexpression with Ki-67 during development and its practically absence in neonatal tissue, suggest that PSA-NCAM present potential initiator of proliferation and differentiation of renal progenitor.

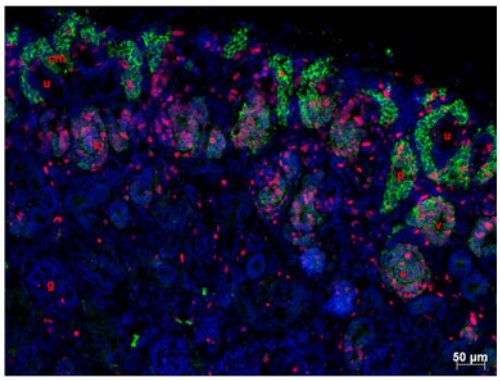

PS-15-008
Autopsy findings in fetuses with cystic hygroma colli: A perinatal survey in a Greek University Hospital
C. Dastamani*, D. Grapsa, A. Tsagkas, A. Melloy, A. Paraskeva, A. Kapsimali, A. Kondi-Pafiti
*Aretaieion Hospital, Dept. of Pathology, Athens, Greece

Objective: Cystic hygroma (CH) typically develops in utero, late in the first trimester to early in the second trimester of gestation. Many of the fetuses with CH present additional malformations commonly associated with chromosomal anomalies.
Method: A review of 548 fetal autopsies performed over a 10 year period revealed 19 cases of CH (3,4 %). The results of cytogenetic analysis and the prenatal ultrasound findings were retrieved and compared to the autopsy findings.
Results: Fetal death was due to therapeutic abortion in 9/19 cases, intrauterine death in 8/19 cases, and spontaneous abortion in 2/19 cases. Cytogenetic analysis was available in 12 cases. The results showed an abnormal karyotype in 7 cases (5 cases of Turner syndrome and 2 cases of trisomy 21). The mean size of CH was 5,4 cm. Other findings suggestive of the cause of fetal death were diagnosed in 10/19 cases (52,6 %). The most common autopsy findings were hydrops and central nervous system anomalies. The autopsy findings were in agreement with the prenatal ultrasound findings in 14/19 cases, while in 5 cases (26,3 %) additional findings were detected during autopsy.
Conclusion: Our study is confirms the strong correlation between CH and chromosomal anomalies of the fetus.

PS-15-009
Immunohistochemical expression of E-cadherin in primary and metastatic nephroblastoma cases
I. Franckevicha*, R. Kleina
*University Children´s Hospital, Dept. of Pathology, Riga, Latvia

Objective: In nephroblastoma cases association between decreased E-cadherin expression and higher stage of tumor (Safford SD, 2005) and lower expression in metastatic tumors (Alami J, 2003) was described. Some authors considered that E cadherin is not likely to play tumor suppressor role in nephroblastoma (Shulz S, 2000). Purpose of this study was to compare the expression of E-cadherin in metastatic and primary tumor cases in Latvia.
Method: 26 cases of primary tumors, 8 metastases and 1 case of relapse were analyzed immunohistochemically using visualization system EnVision. The number of E-cadherin positive structures per field was assessed (magnification× 100). Comparison between primary tumors and metastatic/relapse tumors groups was made using Mann–Whitney test.
Results: In primary tumor group the number of positive structures in the field ranged from 0 to 86, average 27.19, SD 24.13. In the metastatic tumor group, the number of positive structures varied from 0 to 40, average 9.89, SD 14.87. Comparison of expression observed in both primary and metastatic tumors groups showed the decreased E-cadherin expression in metastatic tumor group ($Z = -2.33$, $p = 0.046$).
Conclusion: Expression of E-cadherin is lower in metastatic tumor group that may suggest about negative correlation between it and higher tumor grade.

PS-15-010
Testicular fibrous hamartoma: A case report
A. Kilitci*, F. Yilmaz, S. Yanik, H. Ozturk
*Abant Izzet Baysal University, Dept. of Pathology, Bolu, Turkey

Objective: Fibrous Hamartoma (FH) of childhood is uncommon benign tumor. They are generally seen in the head

and neck region, gastrointestinal system and lung. As in the case we report, they may also occur in other unusual sites such as groin and testis. The clinical presentation is almost always a mass or swelling, however our case was admitted to our hospital because of a left testicular atrophy. We report a FH in the testis, which has a rarely location and clinical presentation.

Method: A 7-year-old male presented to department of pediatric surgery because of left testicular atrophy. Left orchiectomy was performed.

Results: In macroscopic examination, testis dimension was 1.5×1.3×0.4 cm. Its cut surface was smooth and dirty-white. In microscopic examination, the tumor showed disorganized matur tissue that composed of fibrocollagen stroma, vessels, muscular and adipose tissue. By this findings, it was diagnosed as testicular fibrous hamartoma (TFH).

Conclusion: In conclusion, TFH should be always kept in mind with testicular atrophy not only testicular mass or swelling. And knowledge of this particular type lesion is important to distinguish the FH of childhood from other situations in testis such as testicular torsion, incarcerated hernia, malign neoplasm, etc. in order to allow a correct diagnosis and avoid inadequate treatment.

PS-15-011

Placental pathologic features in diabetes and hypertension

P. Luís*, A. Costa-Silva, A. Alves
*Hospital de Santa Maria, Dept. de Anatomia Patológica, Lisboa, Portugal

Objective: The aim of this study was to evaluate the most frequent placental findings in diabetes and hypertension and their main differences.

Method: Retrospective study of 229 selected placentas from 19 to 41 weeks gestation, in a universe of 3231 placentas examined over the last 10 years (6 % associated with hypertension, 1,5 % with diabetes and 0,4 % with both diabetes and hypertension (DwH).

Results: In diabetes the most frequently found abnormalities were immature villi (35 %) and infarction (27 %). In DwH the most frequent lesions were the immature villi (29 %) and inflammatory lesions (either acute or chronic) (29 %). In the hypertension group the most frequently found lesions were infarction (54 %) and accelerated maturation of the villi (23 %). In 35 % of placentas in diabetes, 21 % in DwH and only 15 % in hypertension, no lesions were found. The incidence of fetal death was 8 % in diabetes, 0 % in DwH and 5,5 % in hypertension. When evaluating placental weight, small placentas were more frequent in the hypertension group (37 %), and large placentas were more frequent in diabetes (27 %).

Conclusion: Our findings may contribute to evaluate the consequences of diabetes and hypertension in fetal outcome. As inflammatory conditions are usually not directly attributed to diabetes or hypertension, placental examination may help in diagnosis of associated pathology like infection.

PS-15-013

Placental villi morphometry in preeclampsia

K. Pavlov*, E. Dubova, R. Shmakov, A. Shchegolev
*V.I. Kulakov Scientific Center, Dept. of Pathology, Moscow, Russia

Objective: Terminal villi structure abnormalities could play an important role in preeclampsia (PE) and its complications development. Our aim was to perform comparative morphometric study of the placentas from mild and severe PE pregnancies.

Method: Complex morphological and morphometric study of 9 term placentas from mild PE (mPE) cases (1st group), 6 term placentas from severe PE (sPE) cases (2nd group) and 10 term placentas from uncomplicated pregnancies (control group) was performed.

Results: We revealed significant decreasing in terminal villi size in both preeclamptic groups in compare to control. This decreasing was much prominent in sPE group. We also observed significant terminal villi perimeter decreasing in both PE groups without any difference between mPE and sPE groups. Morphometry of CD31 stained specimens revealed significant decreasing in mean capillary number in both PE groups. Single capillary area and perimeter were significantly lower in mPE and sPE groups and these changes were much prominent in sPE group. Total villous capillary area and perimeter were significantly lower in both PE groups with minimal values in sPE group. Degree of villous capillarisation was significantly lower in both PE groups.

Conclusion: Revealed features reflect villous structure changes in preplacental hypoxia, caused by mild and severe preeclampsia.

PS-15-014

Sudden intrauterine death: The usefulness of autopsy

F. Portelli*, E. Orlando, E. Di Stefano, E. Maresi
*University of Palermo, Section of Pathology, Italy

Objective: We investigated in 1006 autopsies of stillbirths the usefulness of autopsy even in the absence of risk factors and/or apparent anatomical/clinical causes which could explain the death.

Method: From January 1990 to December 2010 (Institute of Pathology, Paolo Giaccone- Palermo) 2643 autopsies on dead uterine foetuses were performed. 1637 cases were abortions (<25 weeks), 1006 were stillbirths (≥25 weeks). In all cases the autopsy included

a macroscopic and microscopic examination both of the foetus and the placenta. The final diagnosis of death was based on both the morphological and clinical data. Of the 1006 stillbirths, 715 cases were "risk factor pregnancies", 291 non.

Results: The stillbirth mortality was classified as follows: - Sudden Intrauterine Unexplained Death (SIUD,"-sine materia" and absence of risk factor autopsies),4 cases; - Explained Intrauterine Death ("cum materia" with or without risk factor autopsies),987 cases; - Borderline Intrauterine Death ("sine materia" and presence of risk factor autopsies),15 cases.

Conclusion: In the absence of autopsy in 715/1006 cases it was possible to establish the cause of death based on the presence of risk factors. In the absence of risk factors the autopsy showed a certain anatomical cause in 287/1006, only in 4/1006 it was "sine materia".

PS-15-015

The role of "traditional" and "tomography" autopsy in foetal Congenital Heart Disease (CHD)

F. Portelli*, F. P. Busardò, L. Gutsul, L. Averna, E. Orlando, E. Maresi

*University of Palermo, Section of Pathology, Italy

Objective: The role of systematic autopsy in foetal CHD is to identify the morphology of cardiac and possible associated extracardiac malformations (ECM) and the correlation between morphology, suspected clinical etiology and genetics. We evaluated the role of autopsy in 643 foetal CHDs with/without prenatal diagnosis.

Method: From January 1990 to December 2010 (Institute of Pathology, Paolo Giaccone – Palermo), 2371 foetal autopsies were performed. The autopsy protocol used was "tomography" for abortions, the "traditional" technique was adopted for stillbirths.

Results: In 643 cases CHDs were identified. In 196 cases CHD diagnosis was made only through autopsy, in 447 after a certain (244) or suspect (203) clinical/genetic diagnosis. The etiology of CHD associated to ECM (621) was: chromosomic type (271), syndromic/sequence type (233), association type (117). The etiology of CHD without ECM (22) was never syndromic.

Conclusion: "Traditional" and "tomography" autopsy plays a key role in the diagnosis and counselling of CHD, either when it represents the only diagnostic tool (30,48 %) or when it is preceded by a clinical/genetic study. In the latter cases, its value depends on the detection of ECM, useful to "consolidate" a suspect clinical diagnosis (31,57 %) and to

"complete" a malformative picture etiologically known thanks to a clinical/genetic analysis (37,9 %).

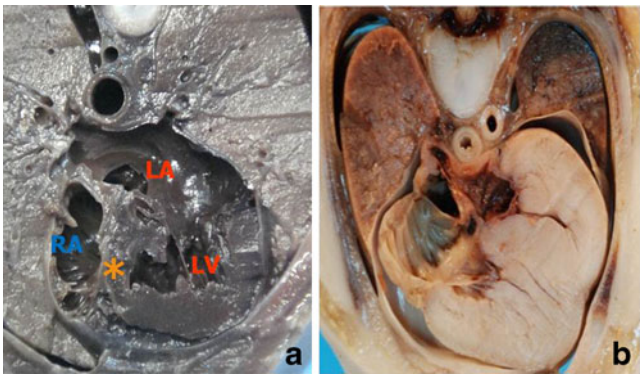

PS-15-016

Amplification of cyclin A gene in Wilms tumor

S. Radojevic-Skodric*, D. Brasanac, I. Novakovic, L. Bogdanovic, Z. Krstic, G. Basta-Jovanovic
*School of Medicine, Inst. of Pathology, Belgrade, Serbia

Objective: Deregulation of cell cycle control is a hallmark of cancer. We have examined protein expression and gene amplification of cyclin A in Wilms tumor (WT) and to analyze it in relation to tumor stage, prognostic group and histological type.
Method: Real-Time Quantitative PCR was used to detect gene amplification of cyclin A in tumor tissue from 36 patients with WT, while immunohistochemistry was applied to detect protein expression of the same cyclin.
Results: Cyclin A gene amplification was found in 4 out of the 36 (11.8 %) cases of WT. Cyclin A protein overexpression was detected in all four cases, but was also found in 84.7 % of cases without detectable gene amplification. So, there was no significant correlation between cyclin A gene amplification and protein overexpression. All cases with amplification of cyclin A were of favorable histological type, intermediate risk group and three out of four cases were low stage WTs. On the other hand, overexpression of cyclin A was found significantly more often in high stage WTs compared to low stage WTs (p=0.04).
Conclusion: Cyclin A gene amplification might be associated with the favorable prognosis of WT (low stage, intermediate risk group and non-anaplastic tumors).

PS-15-017

Alveolar capillary dysplasia with misalignment of pulmonary veins: Pathological and molecular diagnosis

N. Toran-Fuentes*, A. Navarro, Y. Castilla, I. Valenzuela, A. Moreno, M. Molina, S. Ramón y Cajal, J. C. Ferreres
*University Vall d´Hebron, Dept. of Pathology, Barcelona, Spain

Objective: Alveolar capillary dysplasia (ACD) with misalignment of pulmonary veins (MPV) is a rare cause of persistent pulmonary hypertension in newborns (PPHN). The gold standard to diagnose is lung biopsy or necropsy. Up to 40 % of cases have mutations or deletions in the gene FOXF1 (cr16q24.1) who plays a crucial role in the development of the lung vasculature.
Method: We report a case of a term newborn female affected of ACD/MPV who was diagnosed by a lung biopsy. She died at 38 days of life. Autopsy and molecular diagnosis were also performed
Results: In the biopsy and autopsy specimens a decline in the number of capillaries in the alveolar septa and detachment of the epithelial lining was observed. Secondary proximal plexiform arteriopathy, muscularization of arterioles and venous-venular dilatation and proliferation were evident. A pathogenic mutation in the gene FOXF1 (frame shift mutation in the first exon) confirmed our diagnosis.
Conclusion: ACD is defined by a decrease in capillaries with alveolar septal thickening and hypertrophy of the middle muscular layer of arterioles. MPV suggests an imbalance of angiogenesis. The FOXF1 mutation helps to prenatal diagnoses of high risk families and to give the diagnosis to patients who fail to perform biopsy or autopsy.

PS-15-018

Notch pathway activation in childhood rhabdomyosarcoma

N. Toran-Fuentes*, P. Velasco, J. Roma, A. Massià, J. C. Ferreres, M. Garrido, J. Sánchez de Toledo, S. Ramón y Cajal, S. Gallego
*University Vall d´Hebron, Dept. of Pathology, Barcelona, Spain

Objective: Prognosis of Rhabdomyosarcoma (RMS) has improved significantly over the last 20 years. Overall survival (OS) is>80 % in the majority of patients; even though, children with metastatic tumors have a dismal prognosis with an OS <30 %.
Method: We analyzed in 18 cases, the possible correlation of Notch activation with histology, presence of metastasis and outcome. Immunohistochemistry (IHC) was performed for the Notch downstream effectors Hes1 and Hey1.
Results: Hes 1 was strong or moderate in 95 % of the cases. Hey1 was positive in 50 %. 3 out of 4 alveolar RMS (aRMS) were positive for Hes1 and 1 was positive for Hey1. Both stains were negative in the fusion-negative aRMS. In embryonal RMS (eRMS), eight out the 9 were Hey1 positive and 14 of the 17 were Hes1 positive. The 2 patients whit metastases had staining for Hes1 and Hey1. 3 patients who died showed Hes1(+). 14 of the 15 patients in remission showed positivity for Hes1 and 7 for Hey1.
Conclusion: Hes1 expression was found in the majority of RMS while Hey1 was more eRMS specific. Is no correlation between pathway activation, metastasis or outcome. The blockage of the pathway with specific inhibitors could offer a new therapeutic option for this patients.

PS-15-019

A renal epithelioid angiomyolipoma in a young woman with tuberous sclerosis complex, cortical tubers by neuroimaging, facial angiofribromas and lung lymphangioleiomyomatosis

J. Trillo-Tinoco*
*Hospital General de Mexico, Dept. of Surgical Pathology, Mexico City, Mexico

Objective: Tuberous sclerosis (TS) is a genetic disorder affecting cellular differentiation and proliferation, which results in hamartoma formation in many organs like skin, brain, lung, kidney and heart.
Method: A seventeen-year-old female with history of facial angiofibromas a 10 years before, right renal tumor diagnosed a year before as theratoid-rhabdoid tumor, with chemoradiation as adjuvant treatment, cortical tubers by neuroimaging a few months before, and diagnosis of lung lymphangioleiomyomatosis recently. After last diagnostics, we reviewed again the renal tumor, new orientation of tissue, with new histological sections were performed. (Fig)
Results: At histological examination, the kidney showed an infiltrating tumor, very cellular, consisting mainly of polygonal cells with eosinophilic cytoplasm, other multinucleated similar to the ganglion cells, also small hamartomatous areas with smooth muscle, fat and blood vessels proliferation. The tumor cells expressed HMB45, MART-1, SMA, VIM and CD10, CKAE1/3 were negative. (Fig)
Conclusion: The majority of renal angiomyolipomas is sporadic and 50 to 80 % occurs as part of TS, and their partnership is more close with epithelioid variant, recently, a rare entity with aggressive behavior, difficult histological characterization and poor prognosis.

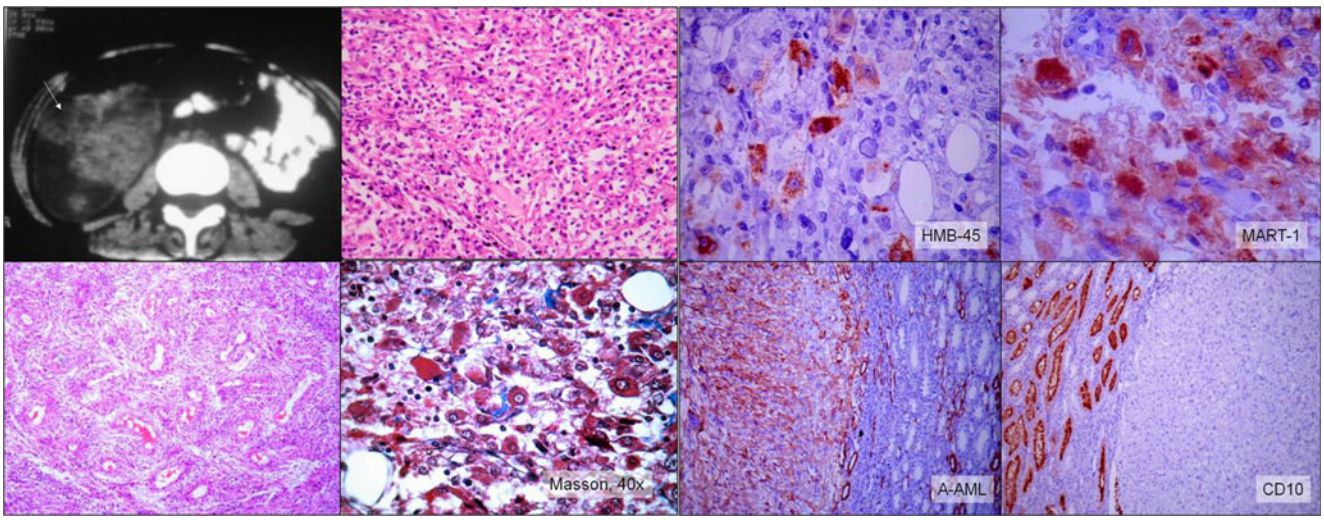

PS-15-020

Pulmonary mast cells in sudden infant death syndrome (SIDS)

C. Zaharia*, C. Loddo, P. Schmidt, R. M. Bohle
*University of Saarland, Inst. of Pathology, Homburg, Germany

Objective: Several theories of the underlying mechanisms of SIDS have been proposed, one of them is focusing on shock including anaphylaxis. Increased concentrations of mast cell tryptase in post mortem blood have been observed without increased mast cell numbers in lung tissue. The aim was to evaluate the age-related distribution of pulmonary mast cells in infants dying of sudden infant death syndrome and controls.
Method: 6 infants (up to 1 year of age) who died of SIDS and 23 controls who died of other non-pulmonary causes were examined. Peribronchial mast cells exhibiting tryptase immunoreactivity were evaluated and quantified in high power fields in lung sections.
Results: The number of mast cells in peribronchial regions amounted to 18,9 (± 6,6)/mm2 in children aged 1 month up to 13 months. Mast cells in SIDS cases were 21,2 (± 4,5)/mm2. The difference was not significant (P=0,113, Student's t test).
Conclusion: It is unlikely that increased pulmonary mast cells are indicators of SIDS. The role of mast cells in SIDS remains controversial.

PS-15-021

Trophoblast apoptosis in placentas from pregnancies complicated by preeclampsia

S. Zekic Tomas*, I. Kuzmic Prusac, D. Roje, I. Tadin
*Clinical Hospital Centre Split, Pathology, Croatia

Objective: To assess trophoblast apoptosis separately in cytotrophoblast, syncytiotrophoblast, total villous trophoblast and syncytial knots, as well as to investigate the expression of apoptotic factors Fas ligand (FasL), Bcl-2 and proliferation marker Ki-67 in trophoblast of placentas from preeclamptic patients.
Method: The study included placental samples from 25 preeclamptic and 25 normal pregnancies. For the detection of apoptosis and proliferation antibody M30 and antibody against Ki-67 antigen were used. Expression of Fas ligand and Bcl-2 was assessed using semi quantitative HSCORE method. Syncytial knots were expressed as the number of syncytial knots per individual villus and as the total number of syncytial knots in each placental sample.
Results: apoptosis in all stages of trophoblast differentiation, number of syncytial knots per individual villus and the total number of syncytial knots were significantly higher in preeclamptic placentas than in control group placentas. Fas ligand expression was significantly less, and Bcl-2 expression significantly greater in the villus trophoblast among the study subjects compared with controls. There was no difference in the trophoblast proliferation between groups.
Conclusion: our findings might suggests that increased apoptosis and syncytial knots formation combined with reduced Fas ligand expression could be involved in pathophysiological mechanisms of preeclampsia.

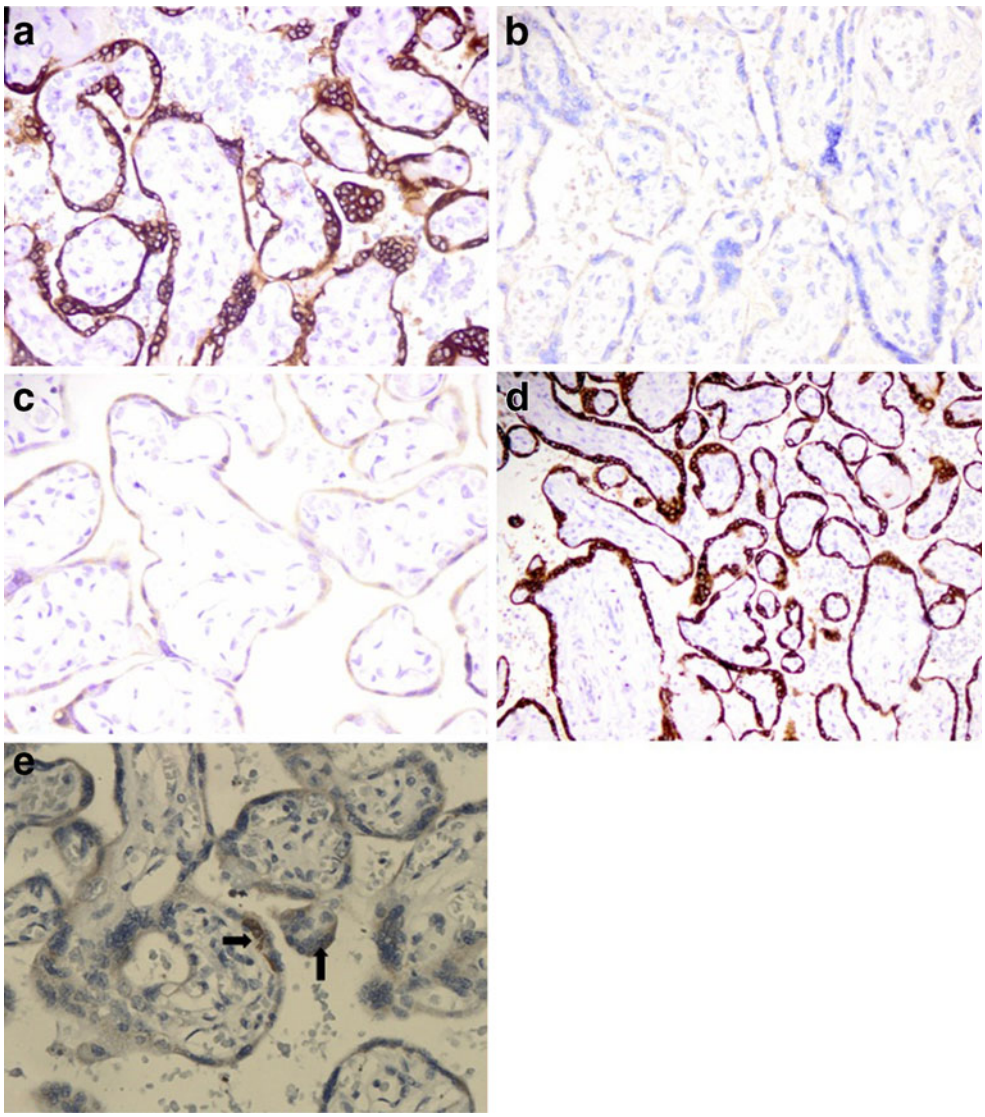

PS-15-022

Contribution of fetal autopsy for diagnosis of Meckel-Gruber Syndrome

M. Jo*, I. Guerra, G. Perez de Nanclares, P. Morales, J. J. Aguirre, Z. S. Quintero, C. Gomez, N. T. Villagra
*Hospital Txagorritxu, Pathology, Vitoria, Spain

Objective: Meckel-Gruber Syndrome (MGS) is a lethal rare autosomal recessive malformation. The six implicated genes encode proteins involved in primary cilia function. Groups of families in Finland, India and North of Africa have been identified.
Method: A fetus,46 XY, karyotype, therapeutically aborted at 21 weeks with alobar holoprosencephaly in ultrasound. Fetal autopsy was performed. Genetic counseling was proposed to the family revealing Moroccan origin and consanguinity, the parents were first cousins.
Results: A male fetus showing cyclopia, proboscis and a single opening with two rudimentary eyes was the external morphology. Histological examination confirmed holoprosencephaly and also showed bilateral corticomedullary renal multicystic and periportal hepatic fibrosis with bile duct dilatation. The main diagnosis was MGS although other ciliophaties and non-ciliopathies conditions were considered, such as Bardet-Bield, Joubert, Smith-Lemli-Opitz syndrome and trisomy 13. However, the pathological characterization, parent's consanguinity and their North African origin makes MGS the likely diagnosis.A genetic study on paraffin-embedded material was requested, the poor quality of DNA stopped definitive genetic diagnosis.
Conclusion: The pathologist may encounter atypical cases that require morphologic diagnosis to determine the type of underlying mutation and provide genetic counseling to parents.A meticulous autopsy is necessary to establish the diagnosis of MGS. Fresh material would have to be frozen in order to make current diagnostic techniques of molecular pathology.

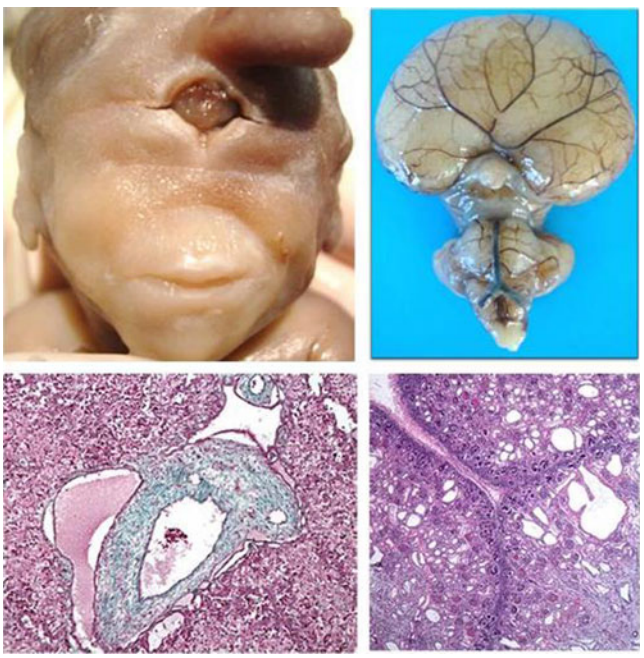

PS-15-023

Mesenteric cysts in the pediatric age group

R. Jankovic*, J. Sopta, M. Stojanovic, B. Lekic, B. Jovanovic, Z. Stojsic
*University of Belgrade, Faculty of Medicine, Serbia

Objective: Mesenteric cysts are extremely rare lesions arising with an incidence of 1/20,000 admissions in children. Clinically, mesenteric cysts are generally comprehended as a unique diagnostic entity, although they exhibit histological diversity. The objective of this study was to determine the incidence and the histology of the mesenteric cysts in the pediatric age.
Method: All cases of mesenteric cysts operated at the University Children's Hospital Belgrade over the 10-year period of 2002 to 2011 were reviewed using pathology reports from the files of the Institute of Pathology. Histological slides were re-examined and immunohistochemistry was applied, when necessary.
Results: A total of 27 cases of mesenteric cysts were identified. Cysts of lymphatic origin (cystic lymphangiomas) were recorded in 12 patients (44 %), cysts of enteric origin - in 14 patients (52 %): 13 duplication cysts and one isolated enteric cyst of the mesenterium. Only one example of the cyst of mesothelial origin, i.e. benign cystic mesothelioma was diagnosed (4 %). The most frequent site was mesenterium and mesocolon (86 %), followed by omentum (7 %) and the retroperitoneum (7 %).
Conclusion: Cysts of enteric origin are easily recognized. It is important to differentiate between cystic lymphangioma and cystic mesothelioma due to their different natural history.

Tuesday, 11 September 2012, 09.30 - 10.30, Congress Hall Foyer 3rd Floor
PS-16 Poster Session Soft Tissue Pathology

PS-16-001

Myxoid liposarcoma of the breast

B. Andrejic*, S. Božanic, N. Šolajic, J. Ilic
*Medical Faculty Novi Sad, Dept. of Histology and Embryology, Serbia

Objective: Myxoid liposarcoma belongs to the group of soft tissue sarcomas with lipomatous differentiation. Breast is a rarely affected (only 0.3 % of breast sarcomas), and often misdiagnosed.
Method: A 67-years old woman presented with a painful timorous lump of the left breast. Mammography showed oval, lobulated lesion between medial quadrants, while ultrasonography revealed hipoechogenic, inhomogeneous nodule. Patient underwent core biopsy which was histologicaly inconclusive and followed by quadrantectomy with excision of both medial quadrants.

Results: A lump (6 cm) was visible on the skin surface. Serial sectioning revealed solid gray–white tumor with cystic and prominent necrotic areas. The tumor was located in the deep mammary tissue an it infiltrated the overlying dermis without involving the epidermis. It consisted of atypical stelate and spindle cells with infrequent mitoses and low Ki-67 proliferative index. On the periphery mature adipocytes and lipoblasts were present. Stroma was abundant, myxoid with plexiform capillary pattern. The myxoid substance stained slightly Alcian-blue positive and tumor cells showed cytoplasmic immunopositivity for S100. Phyllodes tumor was excluded because of absence of epithelial component.
Conclusion: Myxoid liposarcoma has a distinct morphology, rarely confused with other soft tissue tumors, although on cytological smears or biopsy samples it may be unrecognized.

PS-16-002
INI-1 and TLE-1 expression in five synovial sarcomas diagnosed by fluorscent in situ hybridization
T. Argyrakos*, M. Kopaka, G. Karagkounis, M. Lianou, E. Ronne, C. Lariou, D. Rontogianni
*Evaggelismos Hospital, Dept. of Pathology, Athens, Greece

Objective: Synovial sarcoma poses a difficult diagnostic challenge since it can be confused with other benign or malignant entities.
Method: Four biphasic and one monophasic synovial sarcomas were studied. We used the break apart/split signal kit (VYSIS) to detect the t(X;18) translocation and we performed immunohistochemistry for TLE-1, INI-1, D2-40, CD56, CD99, bcl-2, EMA, CK7, CD34, S-100, Desmin and Claudin-1.
Results: Immunohistochemically we observed: TLE-1+(5/5), INI-1 (4/5) with reduced nuclear and (1/5) with no expression, D2-40+(1/5), CD56+(5/5), CD99+(5/5), bcl-2+(5/5), EMA focal expression (5/5), CK7−(5/5), CD34−(5/5), S-100−(5/5), Desmin−(5/5), Claudin-1+(5/5). FISH revealed the split signal between the centromeric and telomeric end of the SYT gene.
Conclusion: t(X;18) translocation remains the diagnostic hallmark of synovial sarcoma. INI-1 which is typically negative in atypical teratoid/rhabdoid tumor, epithelioid sarcoma and myoepithelial carcinoma seems to be reduced or even negative in synovial sarcomas. The focal expression of D2-40 must be considered when the differential diagnosis includes mesothelioma. Finally TLE-1 is a very sensitive marker for synovial sarcoma.

PS-16-004
"Mixed aneurysmal bone cyst" and "simple bone cyst", represent a different group of cystic lesion
E. Ayhan Cinar*, B. Doganavsargil, M. Sezak, F. Oztop
*EGE University, Pathology, Izmir, Turkey

Objective: There are some mixed cysts (MC) with overlapping histological features of aneurysmal bone cyst (ABC) and simple bone cysts (SBC).
Method: We reviewed 69 pure ABC, 40 SBC and 23 "Mixed Cysts (MC)", and compared them by nonparametric tests.
Results: MCs, mainly showed two paterns as "Type 1: SBC with secondary ABC foci (n=18)"and "Type 2: Cysts with fully developed SBC and ABC areas (n=5)". The median age for ABC, SBC, and MC were 16±18.2 (range: 3–53), 21±13.7 (range: 3–54) and 9±11.47 years old (range: 3–50) respectively. MCs were more frequent in males than ABC and SBC (p=0.017) and the most frequently involved bones were humerus-femur-pelvic bones in descending order (p= 0,021). "Type 1 MC" showed more frequent cementum-like amorph material (p<0.001), ectatic venules (p=0.040), calcifications (p=0.044), less cholesterol deposition, necrosis and no different fracture and osteoid matrix when compared with Type 2 MCs and SBCs.
Conclusion: Cysts with overlapping features of ABC and SBC are not uncommon. Though they usually represent "SBCs with secondary ABC component", they have dissimilarites with ordinary SBCs which needs to be further clarified with larger series.

PS-16-005
Pitfalls in evaluating neoadjuvant chemotherapy response in bone resection specimens
U. Aykutlu*, B. Doganavsargil, M. Argin, M. Sezak, D. Sabah, F. Oztop
*Ege University, Faculty of Medicine, Pathology, Izmir, Turkey

Objective: Percent of tumor necrosis after neoadjuvant chemotherapy, determined by detailed specimen mapping, has a high prognostic value. However both the mapping and grading systems has some practical problems.
Method: 128 cases were reviewed for potential pitfalls in handling and reporting processes and correlated with radiological findings by nonparametric-tests.
Results: Most of the tumors were osteosarcoma (74.2 %) and Ewing Sarcoma (16.4 %), located in femur (53 %), tibia (22,7 %) and humerus (10.2 %). Cortex, soft tissue and joint invasion was observed in 94 %, 77.6 % and 30.3 % of the cases, respectively. A median of 27.5 tumor blocks (9–74± 14,64) were submitted for histology. Tumors were totally necrotic in 30 cases (24 %) (Huvos Grade-HG-IV), HG III in 20.3 %, HG II in 28.1 % and HG I in 24.2 % of the cases. Overall good (HG III-IV) and poor responders (HG I-II) correlated well with radiological findings (p<0.001). Discrepant cases showed extensive oedema and congestion enhancing contrast medium, patchy necrosis unabling accurate histologic evalation, or failure to prove tibiofibuler joint involvement because of sagittal sectioning (p<0.05).

Conclusion: Evaluating chemotherapy responce is a laborious work. Radiologic orientation prior to grossing and applying morphometric technics may enhance more accurate evaluation.

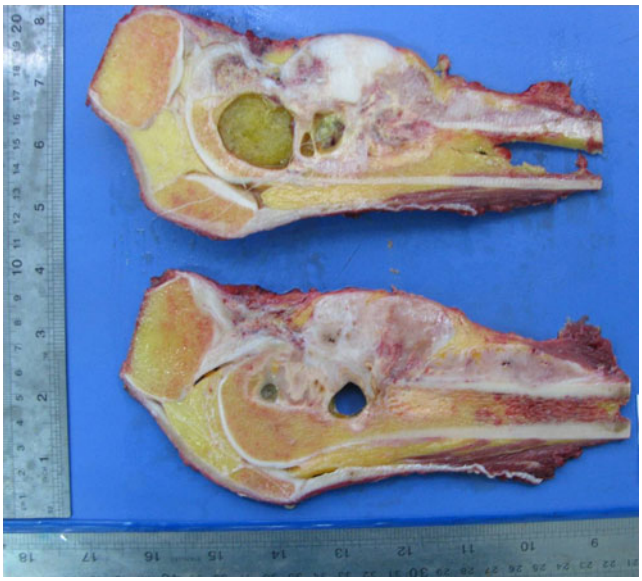

PS-16-006

Atypical Ewing sarcoma/Primitive neuroectodermal tumor with unusual melanocytic differentiation – A case report

P. Buzrla*, J. Dvorackova, I. Urbanovska, H. Bielnikova
*Inst. of Pathology, Ostrava-Marianske Hory, Czech Republic

Objective: Atypical Ewing sarcoma/primitive neuroectodermal tumor with the melanocytic differentiation is a very rare, malignant tumor which occurs in infants and adolescents. It is localized mainly in soft tissues. Its biological behavior is aggressive, but its response to the chemotherapy is prognostically good.
Method: A 4-month old male is presented with the 17×11 cm tumor of the soft tissue, localized in the right front over the cranial margin of the orbit. The tumor was surgically exstirpated and then sent to the histological investigation with the additional immunohistochemistry and the FISH.
Results: Microscopically, the tumor is hypercelullar and consisted of oval to polygonal cells with the vesicular nuclei, the prominent nuclei and the amphophilic cytoplasm. In other parts of the tumor, there are smaller neoplastic cells with hyperchromatic nuclei. Some neoplastic cells contain the melanin pigment in the cytoplasm, which was positive in Fontana-Masson method. The immunohistochemical stains for vimentin, AE1/3, CK7, CD99, HMB-45, FLI-1 were positive. The FISH investigation demonstrated the translocations (t 11;22, q24;q12) in 95 % of neoplastic cells and (t 21;22, q12;12) of 5 % ones.
Conclusion: In literature, the Ewing sarcoma/PNET showing the myogennic differentiation is usual, but the melanocytic differentiation is rare and can be confirmed not only immunohistochemically, but also by FISH investigation.

PS-16-007

Expresion of poly(ADP-ribose) polymerase-1 protein in neoplasms and its importance in their biological behavior

Z. Cierna*, M. Mego, D. Svetlovska, D. Macak, K. Machalekova, V. Miskovska, M. Chovanec, V. Usakova, P. Babal, J. Mardiak
*Faculty of Medicine, Pathological Anatomy, Bratislava, Slovakia

Objective: Poly(ADP-ribose) polymerase-1 (PARP-1) is a nuclear enzyme involved in the repair of DNA single-strand breaks. PARP-1 inhibitors may be efficient in therapy of malignancies. This report evaluates the expression of PARP-1 in primary testicular germ cell tumors and correlates expression patterns with histological subtypes and patient/tumor characteristics.
Method: Group of 124 patients with testicular germ cell tumors were investigated for PARP-1 expression by immunohistochemistry, scored by the multiplicative quickscore (QS) method and compared to PARP-1 expression in normal testis.
Results: We observed higher expression of PARP1 in testicular tumors compared to normal testis (mean QS=10.04 vs. 3.60, $p<$ 0.0000001). The PARP-1 overexpression (QS>9) was most often detected in intratubular germ cell neoplasia ITGCN (100 % of specimen with PARP-1 overexpression), compared to 1.9 % of normal testicular tissue specimen. There was no association between PARP-1 expression and clinical variables.
Conclusion: PARP-1 expression is higher in tumor tissue than in normal testis. PARP-1 could represent a novel treatment target in TGCTs and the assessment of PARP-1 expression in tumor samples may lead to the consideration of TGCTs patients for PARP inhibitor therapy. Supported by 2007/30-NOU-01, VEGA 1/0724/11 and ITMS: 26240220052 cofinanced by European Regional Development Fund.

PS-16-008

Gardner fibroma - implications of a diagnosis

N. Coimbra*, M. Caldas, F. Menezes, L. Leça, M. Bom Sucesso, C. Pinto, J. Vieira, M. Teixeira, R. Henrique, M. Afonso
*IPO Porto, Anatomia Patológica, Vila Nova de Gaia, Portugal

Objective: Gardner fibroma (GAF), a rare lesion, typically occurs in infants, children and young adults, with predilection for the trunk (particularly paraspinal region) and no gender predominance. GAF is an ill-defined plaque-like

mass, with rubbery consistence, usually asymptomatic, ranging from 0.3 to 12 cm. Although benign, 70–90 % of the cases may be associated with APC mutations, familial adenomatous polyposis (FAP) and/or Gardner Syndrome (GS). We report 2 cases of GAF, which allowed the identification of 2 families with GS.
Results: CASE 1: 7-month-old boy, with 2 nodules in the left paraspinal region, the largest with 2.5 cm. CASE 2: 5-month-old boy, presenting a 1.5 cm ill-defined deep right scapular mass. Both lesions were infiltrative, paucicelular densely collagenized proliferations of bland spindle cells. A GAF diagnosis was made and clinical/genetic investigation advised. APC gene sequentiation revealed, in both cases, a frameshift germline mutation in exon 15. Additionally, case 1 presented a del(5)(q11q35). Heredogram showed typical manifestations of GS: CASE 1: Mandibular osteomas, epidermoid cysts, "soft-tissue tumours", colo-rectal carcinoma. CASE 2: Hepatoblastoma, colo-rectal carcinoma.
Conclusion: Given the high association with GS and the fact that it can be its first manifestation, GAF is considered a sentinel lesion for this syndrome. Therefore, an accurate diagnosis is of the utmost importance.

PS-16-009

Prognostic significance of bcl-2, c-myc and survivin in synovial sarcoma

D. Demir*, B. Yaman, Y. Anacak, B. Keçeci, G. Kandiloğlu, T. Akalın
*Ege University, Pathology, Izmir, Turkey

Objective: In this study, we evaluated 81 synovial sarcoma cases, who had been referred to our tertiary tumor center during the last 20 years. We applied bcl-2, c-myc and survivin as immunohistochemical markers and evaluated the relation with conventional prognostic findings and prognosis for those 64 patients who have follow-up.
Method: In this study; ten-year tumor free survival rate was 38 % reflecting the agressive behaviour of synovial sarcoma. Tumor grade was the most valuable prognostic input. Progression free survival (PFS) was 159 months for gradeII cases (40 cases) and 36 months for gradeIII cases (24 cases) (p=0,000).
Results: Immunohistochemically, there was weak relation between bcl-2 staining intensity with prognosis. Overall survival was 211 months for weak or negative cases (9cases), 132 months for focally intense cases (21cases) and 101 months for diffuse and intense cases (34 cases) (p= 0,042). There was also weak relation with c-myc staining pattern with prognosis. Overall survival was 193 months for c-myc negative cases (25cases), 114 months for cytoplasmic positive cases (23cases) and 68 months for nuclear positive cases (16 cases) (p=0,043). There was no relation between survivin and prognosis.
Conclusion: In conclusion; tumor grade is the most valuable prognostic parameter in synovial sarcomas. Immunohistochemically c-myc and bcl-2 staining have weak relation with synovial sarcoma prognosis.

PS-16-011

Immunohistichemical profile of primary and recurrent desmoids

E. Dubova*, T. Sidorenko, A. Shchegolev, A. Adamyan
*V.I. Kulakov Scientific Center, Dept. of Pathology, Moscow, Russia

Objective: Desmoids is a locally recurrent and invasive but not metastatic tumor. Our aim was to study immunohistochemical profile of primary and recurrent desmoids.
Method: Complex morphological study of 16 abdominal desmoids. All the tumors were divided into 3 groups: primary, first recurrent and second and more recurrent cases. We used antibodies against β-cathenin, COX-2, APC, survivin and Ki-67 for immunohistochemical study.
Results: Nuclear and cytoplasmic β-cathenin expression levels were significantly higher in recurrent than in primary desmoids. APC cytoplasmic expression level was also significantly higher in recurrent tumors. We revealed only cytoplasmic COX-2 expression in desmoids, and its level was significantly higher in recurrent tumors with the activity increasing accordingly to the number of recurrences. Survivin expressed both in nuclei and cytoplasm of the tumor cells and its expression levels were significantly lower in recurrent desmoids.
Conclusion: Revealed immunohistochemical properties of primary and recurrent desmoids reflect tumor transformation and progression and could be used as additional prognostic markers in this disease.

PS-16-012

Chemokine expression in a xenograft model of human sarcomas

F. Giner*, E. Mayordomo, I. Machado, J. A. López Guerrero, A. Llombart Bosch
*University of Valencia, Dept. of Pathology, Spain

Objective: Many bone and soft tissue sarcomas (BSTS) are aggressive tumors with fatal prognosis. The importance of angiogenesis for the growth and progression of solid BSTS is now well recognized. A variety of chemokines have been described that either promote (angiogenic) or inhibit (angiostatic) angiogenesis. The aim of this study is to characterize the expression profile of some chemokines in a series of xenotransplanted human BSTS.
Method: One Ewing sarcoma (ES), 1 grade 3 chondrosarcoma (Chs), 1 osteosarcoma (Os), 1 synovial sarcoma (SS), 1 fibrosarcoma and 1 gastrointestinal stromal tumor (GIST)

were xenotransplanted into the backs of nude mice (athymic Balb-c nude mice). When the tumor size reached the 3 cm, animals were sacrificed and tumors analyzed for the expression of CXCL1/2/3, CXCL9 and CXCL10, using two-color staining fluorescence on each slide under a confocal microscope (Olympus FV1000).
Results: We observed that angiostatic chemokines (CXCL9 and CXCL10) presented higher expression than angiogenic (CXCL1/2/3) chemokines in ES, grade 3 Chs, Os and GIST whereas fibrosarcoma and SS were more positive for angiogenic chemokines.
Conclusion: The expression profile of angiostatic and angiogenic chemokines depends on the type of BSTS and could be related to their different biological behaviour. Other elements such as angiogenic or pro-inflammatory markers should also be considered.

PS-16-013
Predictive diagnostics of rhabdomyosarcomas
P. Janega*, L. Feketeova, A. Janegova, M. Leitnerova, E. Klincova, D. Sejnova, D. Ilencikova, H. Gergisakova, Z. Cierna, P. Babal
*Faculty of Medicine, Comenius, Dept. of Pathology, Bratislava, Slovakia

Objective: The wide range of differential diagnostic possibilities of rhabdomyosarcomas (RMS) shows the need for more specific and sensitive markers. Low survival rates of high risk RMS patients require new prospective therapeutic targets.
Method: Archival material FFPE samples of 15 RMS (12 embryonal -eRMS, 3 alveolar -aRMS) and non-RMS soft tissue tumors were evaluated by immunohistochemistry for myogenin, MyoD1, EGFR, VEGF, COX-2, p-Akt and p-mTOR expression. The presence of PAX3/7-FKHR forming translocations, myogenin, MyoD1, gamma subunit of fetal acetylcholine receptor (AChR) and K-RAS mutational state were determined by RT-PCR.
Results: 10/12 eRMS and 3/3 aRMS showed expression of myogenin, MyoD1 and gamma AChR. Non-RMS tumors were negative. Translocations were only found in aRMS. EGFR expression was characteristic for eRMS, without the presence of activating K-RAS mutation. Strong expression of VEGF was detected in all samples. p-AKT and p-mTOR showed overlapping expressions in 86,7 % RMS. In most of the samples weak COX-2 positivity was demonstrated.
Conclusion: Myogenin, MyoD1 and the fetal AChR are specific and sensitive diagnostic markers of RMS. RMS subtypes are identifiable by PAX3/7-FKHR detection and probably EGFR expression. The results indicate VEGF, EGFR, COX-2 and Akt-mTOR pathway directed therapy to be considered in RMS. Supported by ITMS 26240220052.

PS-16-014
Immunohistochemical analysis of potential targets in desmoid tumor therapy
A. Janegova*, Z. Hlavata, P. Babal, P. Janega
*Comenius University, Dept. of Pathology, Bratislava, Slovakia

Objective: Desmoid tumors (DTs) are clonal fibroblastic/myofibroblastic proliferations. Although histologically benign, desmoids are locally invasive and often have an unpredictable clinical course. DTs are infrequent lesions, but they have a high incidence in patients with familial adenomatous polyposis (FAP). The treatment of DTs needs to be individualized.
Method: To explore the molecular bases of potential pharmacologic targets in DTs we evaluated the immunohistochemical expression of steroid hormone receptors (ERa, ERb, PR) and COX-2 protein in sporadic (n=6) and FAP-associated desmoid tumors (n=9) together with GI adenomas of FAP patients (n=5).
Results: Nuclear ERb expression was found in 14/15 DTs. All adenoma samples showed nuclear ERb positivity, which was weaker than in the surrounding normal epithelial cell. ERa and PR expression were lacking in all samples. COX-2 was found in 14/15 DTs. Adenomatous polyps showed intense COX-2 expression compared to surrounding normal mucosa.
Conclusion: High incidence of ERb positivity in DTs supports the usage of hormonal therapy in these lesions. Open question is the effect of anti-estrogen therapy in DT patients with adenomatous polyps, as in adenomas estrogen seems to have preventive potential. COX-2 expression suggests the benefit of anti-inflammatory treatment in DTs adenomatous polyps. Supported by ITMS: 26240220052.

PS-16-015
Retroperitoneal sarcomas: Clinicopathological features in a series of 68 cases
E. Kairi-Vasilatou*, A. Tsagkas, A. Melloy, A. Paraskeva, A. Kondi-Pafiti
*Aretaieio Nosokomeio University, Dept. of Histopathology, Athens, Greece

Objective: Retroperitoneum is the less common site of origin accounting for approximately 10 % of soft tissue sarcomas.
Method: Between January 1990 and December 2010, our hospital's records of 68 patients with retroperitoneal sarcomas were retrospectively studied.

Results: The patient median age was 57 years and there was no sex predominance. Median tumor size was 18.5 cm (ranging from 6 to 55 cm) with 60 % of them being larger than 10 cm. The most common histological type was liposarcoma (36/68–52,9 %), followed by leiomyosarcoma (16/68–23,5 %) and undifferentiated soft tissue sarcoma (7/68–10,2 %). The remaining 9 tumors (13,2 %) included 2 chondrosarcomas, 2 well-differentiated fibrosarcomas, 1 PEComa, 1 hemangiopericytoma, 1 Ewing sarcoma and 1 malignant peripheral nerve sheath tumor. 44 of the sarcomas were high grade (65 %) and 24 (35 %) low grade. 1-year recurrence rate was 34,3 %. The 3- and 5-year overall survival rates were 56,2 % and 53,1 % respectively. Seven patients received adjuvant chemotherapy.
Conclusion: The most commonly encountered histologic subtypes are liposarcoma and leiomyosarcoma, which are consistent with the results of the present study. Complete tumor resection at first operation is the only treatment factor that consistently predicts improved survival.

PS-16-016
Abdominal desmoid tumor
Y. Lorenzo Mahia*, M. San Martin Alonso, B. Iglesias Rodriguez
*Hospital Maixoeiro, Anatomia Patologica, Vigo, Spain

Objective: Abdominal desmoid tumours are rare benign neoplasms. They are commonly found in the mesentery, while they are rarely found in the intestinal wall. Most cases are sporadic, although there is a link with colonic polyposis, trauma, and oestrogen. They predominate in 25–35 year-old women. This present case is notable due to its location in the jejunal wall, possible relation with previous surgery, and the age and sex of the patient.
Method: We present a 51-year-old male patient previously operated for umbilical hernia years before. He came to the consultation on noticing an abdominal mass. Since the initial suspicion was of jejunal wall GIST tumour, surgery was performed.
Results: The histopathological and immunohistochemical findings, support the diagnosis of desmoid tumour.
Conclusion: Desmoid tumours consist of fibroblastic monoclonal proliferation developed from aponeurotic muscle structures. Some authors consider them non-neoplastic processes given their limited aggressiveness while others classify them within distinct low-grade sarcomas. Their origin is not well established, although there are known factors involved such as mutations in the APC gene or beta-catenin and trisomy 20 and 8. The originating cell, the myofibroblast, is involved in post-traumatic cellular regeneration. This explains why we find these tumours associated with previous surgery.

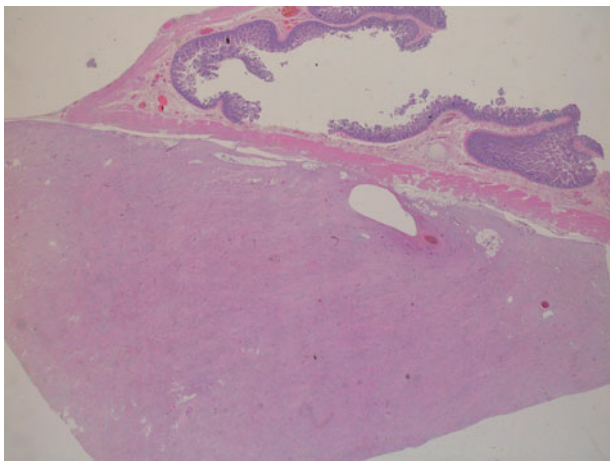

PS-16-017
Treatment of advanced dermatofibrosarcoma protuberans with imatinib mesylate with or without surgical resection
W. Michej*
*Cancer Centre Institute of Warsaw, Dept. of Pathology, Poland

Objective: Dermatofibrosarcoma protuberans (DFSP) is a rare soft tissue sarcoma of the skin characterized by the presence of specific COL1A1-PDGFB fusion protein, which appears as a consequence of the t(17;22) (q22;q13) translocation.
Method: The aim of the study was to perform an analysis of patients with advanced DFSP treated with imatinib, with or without surgery. We examined 15 patients (6 male, 9 female; median age 56 years) with locally advanced/initially inoperable and/or metastatic DFSP treated with imatinib 400–800 mg daily between 12/2004 and 06/2009. All diagnoses were ascertained cytogenetically (fluorescent in situ hybridization). Median follow-up time was 16 months (range: 4–81).
Results: Metastases were present in 8 cases (two lungs, two soft tissue, two lymph nodes). Fibrosarcomatous transformation was confirmed in 7 patients. After treatment with imatinib overall responses were: 10 partial responses, 2 stable diseases (13 %) and 3 progressive diseases (20 %). Seven patients (47 %) after resection had residual disease confirmed by pathologic examination and remained free of disease.
Conclusion: We proved that anti-tumour effect of imatinib in DFSP with presence t(17;22) had in most cases good responses. Imatinib therapy may in some cases leads to tumour resection because of lesser size.

PS-16-018

Clinicopathologic features of osteosarcoma in Turkish population: A 10 year report of 745 cases

B. Muezzinoglu*, S. Dervisoglu, B. Bilgic, B. Doganavsargil, F. Kabukcuoglu, I.. Gurer, S. Baris, R. Tanritainir, G. Basdemir, P. Demireli, M. Sezak
*Kocaeli University, Dept. of Pathology, Turkey

Objective: At an estimated incidence of 2 cases per million per year, osteosarcoma is the most common malignant primary bone tumor.
Method: We conducted a retrospective study to identify the osteosarcoma cases diagnosed at major tertiary care hospitals in Turkey.
Results: Our study group was made up of 745 cases: 440 men, 305 women, aged 3–82 years (mean 23.7 year). All patients had been diagnosed with skeletal osteosarcoma between 2001 and 2011 at one of the 10 tertiary care referral center. Tumor was most frequently located in femur (50.4 %) followed by tibia. Apart from the long bones, pelvic and gnatic bones were the next in location, 4.4 % and 1.6 % respectively. There were 16 (2.1 %) secondary osteosarcomas, related to previous irradiation and various underlying diseases. For the histological types conventional osteblastic intramedullary tumors were most prevalent, making 71.8.% of the cases. Chondroblastic and telengiectatic osteosarcoma are the next common histologic types. Surface tumors were detected in 51 (6.8 %) cases. Rare histological types like small cell, epitheloid, chondroblastoma like and fibrous dysplasia like were also reported.
Conclusion: This study is conducted as a preliminary work to form the basis of a pathologic database for the osteosarcoma cases diagnosed in our country.

PS-16-019

Kaposi's sarcomas in Central Tunisia: Epidemiological and anatomoclinical study of 71 cases

M. Nabiha*, B. Y. Yossra, M. Wiem, B. Ahlem, L. Nizar, E. Ahlem, Y. Mohamed Tahar, H. Sihem
*Farhet Hached Hospital, Dept. of Pathology, Sousse, Tunisia

Objective: Kaposi's sarcoma is a rare disease likely associated with human herpes virus 8 infection, and occurs predominantly in Jewish, Mediterranean and middle eastern men. Since there is a paucity of reports on the pattern of its occurrence in Tunisia, we here analysed the epidemiological pattern and anatomoclinical features.
Method: We retrospectively studied 71 consecutive cases of Kaposi's sarcoma diagnosed in the Pathology Department, Farhet Hached Hospital, Sousse during a 15-year period.
Results: Kaposi's sarcoma represented 21 % of soft tissue sarcomas. There were 23 (32.4 %) females and 48 (67.6 %) males (male-to-female ratio: 2.1:1). Median age at diagnosis was 69 (range: 10–98 years). The age distribution showed that elderly (≥60 years) were the most affected patients with a frequency of 66.2 %, followed by patients aged 31–59 years (25.3 %), and patients under 30 years (8.4 %). The most common location was the lower limbs, particularly the distal lower extremity (73.3 %), followed by contiguous location (7 %), and soft tissue, NOS (7 %).
Conclusion: Kaposi's sarcomas were more frequently diagnosed in elderly. The distal lower extremities were more involved.

PS-16-020

Rhabdomyosarcomas in Central Tunisia: Epidemiological and anatomoclinical study of 47 cases

M. Nabiha*, B. Y. Yossra, M. Wiem, B. Ahlem, L. Nizar, B. A. Atef, M. Samira, J. Lilia, Y. Mohamed Tahar, H. Sihem
*Farhet Hached Hospital, Dept. of Pathology, Sousse, Tunisia

Objective: Rhabdomyosarcoma is the most common soft tissue sarcoma in the first two decades of life. In this study, we analysed the epidemiological pattern and antomoclinical features of rhabdomyosarcoma in Central Tunisia.
Method: We retrospectively studied all cases of rhabdomyosarcoma diagnosed in the Pathology Department, Farhet Hached Hospital, Sousse during a 15-year period.
Results: There were 15 (31.9 %) females and 32 (68.1 %) males (male-to-female ratio: 2.1:1). Median age at diagnosis was 9 (range: 0–85 years). Rhabdomyosarcoma was more frequently diagnosed in childhood (63 %) than in adults (37 %). In children, the tumour size was higher than 5 cm in 73 % of cases, the embryonal subtype was the most frequent (60 %) and the two most common sites of disease were the head and neck (50 %) and genito-urinary tract (23.3 %). In adults, the tumour size was higher than 5 cm in 90 % of cases, the pleomorphic subtype was the most diagnosed (41 %), and limbs were the most involved sites (41 %).
Conclusion: Rhabdomyosarcomas is more frequently diagnosed in children than in adult. Head and neck locations were the most involved and embryologic type was the most diagnosed. In adults, rhabdomyosarcomas were more frequently localized in limbs and diagnosed as pleomorphic type.

PS-16-021

Microarray-based DNA methylation study in Ewing sarcoma of bone

H.-R. Park*, Y.-K. Park
*Hallym University, Sacred Heart Hospital, Anyang, Republic of Korea

Objective: Alterations in the DNA methylation pattern are a hallmark of malignancy and also of Ewing sarcomas. However, most epigenetic studies in Ewing sarcoma have focused on the analysis of few candidate genes and comprehensive studies are required.
Method: Here, we report for the first time a microarray-based DNA methylation study of 1505 CpG sites of cancer-related 807 genes in 69 Ewing sarcomas. We used Illumina's GoldenGate Methylation Cancer Panel I microarray.
Results: Using appropriate controls (n=14), we identified a total of 104 CpG sites hypermethylated in Ewing sarcoma. Most of hypermethylated genes are related with cell adhesion, cell regulation, development, and signal transduction. We compared the methylation mean of each tumor according to the survival data. The methylation mean was significantly higher in the alive patient group (0.25±0.03) compared to the dead patient group (0.22±0.05) (p=0.0322). However, the methylation mean was not significantly correlated with age, sex, or tumor location. We selected the most popular hypermethylated genes, GDF10, OSM, APC, and HOXA11, but, their methylation levels were not significantly correlated with the survival data.
Conclusion: We have characterized the DNA methylation profile of Ewing sarcomas and detected 104 CpG sites that were significantly hypermethylated in Ewing sarcomas. These might therefore play an important role in the development of Ewing sarcomas.

PS-16-022

Pleomorphic and dedifferentiated leiomyosarcoma associated with Lynch syndrome: A case report

H. Quiceno*, F. J. Queipo, R. Carías, J. J. Sola, F. J. Pardo
*Clinic University of Navarra, Anatomical Pathology Lab, Pamplona, Spain

Objective: The Lynch syndrome or hereditary non-polyposis colorectal cancer (HNPCC) is a hereditary syndrome that predisposes to different types of colonic and extracolonic cancer, mainly in endometrium, stomach, ovary, and hepatobiliary and urinary tract. Occasional sarcomas have been reported in HNPCC patients.
Method: We describe a pleomorphic and dedifferentiated leiomyosarcoma of the gluteus in a patient with Lynch syndrome. We study her clinical, pathology, immunochemistry and molecular alterations.
Results: We present a 71 year old woman with previous colorectal, endometrium and breast cancers in a Lynch syndrome with mutations in exons 1 and 2 of MLH2, which appeared with a right gluteus mass. Grossly, it was encapsulated, whitish-yellowish with necrotic areas and measured 7,2 cm. Microscopically, the tumor was composed by a diffuse and polymorph spindle cells with fascicular pattern, focally myxoid and zones of necrosis and large hyalinization. The cells had large nuclei, sometimes giant multinucleated, with a brisk atypical mitosis activity. There was IHQ variability: positivity to desmine, MSA, calponin and negative to caldesmon and SM. There was loss of MSH2 and MSH6 repair proteins.
Conclusion: We must suspect a Lynch Syndrome relational sarcomas if we found one in a patient with HNPCC in order to test to mismatch repair proteins.

PS-16-023

Immunohistochemical review of 42 synovial sarcomas, including expression of TLE1: A "new" marker, with molecular confirmation in 21 cases

B. Rekhi*, R. Basak, S. Desai, N. Jambhekar
*Tata Memorial Hospital, Dept. of Pathology, Mumbai, India

Objective: Synovial sarcoma displays a wide clinicopathological spectrum and a specific translocation t(X; 18)(SYT-SSX)(p11.2; q11.2). Cost constraints limit molecular confirmation in every case. Lately, TLE1 has been recognized as a useful IHC marker. Herein, we present IHC review of 42 synovial sarcomas, including TLE1 expression.
Method: Forty-two synovial sarcomas included monophasic spindle-cell type (26) (61.9 %), biphasic 13 (30.9 %), calcifying (2) (4.7 %) and poorly-differentiated type (1) (2.3 %). 21 tumors were confirmed with molecular analysis. TLE1 immunostaining was graded from 0, 1+, 2+, 3+, with 2+ or 3+ grades interpreted as positive staining.
Results: On IHC, various synovial sarcomas were positive for EMA (26/34)(76.4 %), CK7 (6/10) (60 %), CK/MNF116 (6/21)(28.6 %), BCL2 (36/37)(97.3 %), MIC2 (23/31)(74.1 %) and TLE1 (40/42)(95.2 %), while negative for CD34 (0/21). Among 70 other tumors, TLE1 was positive in schwannomas (5/5) (100 %), neurofibromas (2/2)(100 %), MPNSTs (2/12)(17 %) and PNETs (4/10)(40 %). Sensitivity and specificity of TLE1 for synovial sarcoma was 95.2 % and 72 %.

Conclusion: Although molecular confirmation remains its diagnostic gold standard, TLE1, EMA, BCL-2, MIC2, CKs and CD34 constitute an optimal for synovial sarcoma. Awareness of TLE1 expression in other tumors and its correct interpretation are necessary.

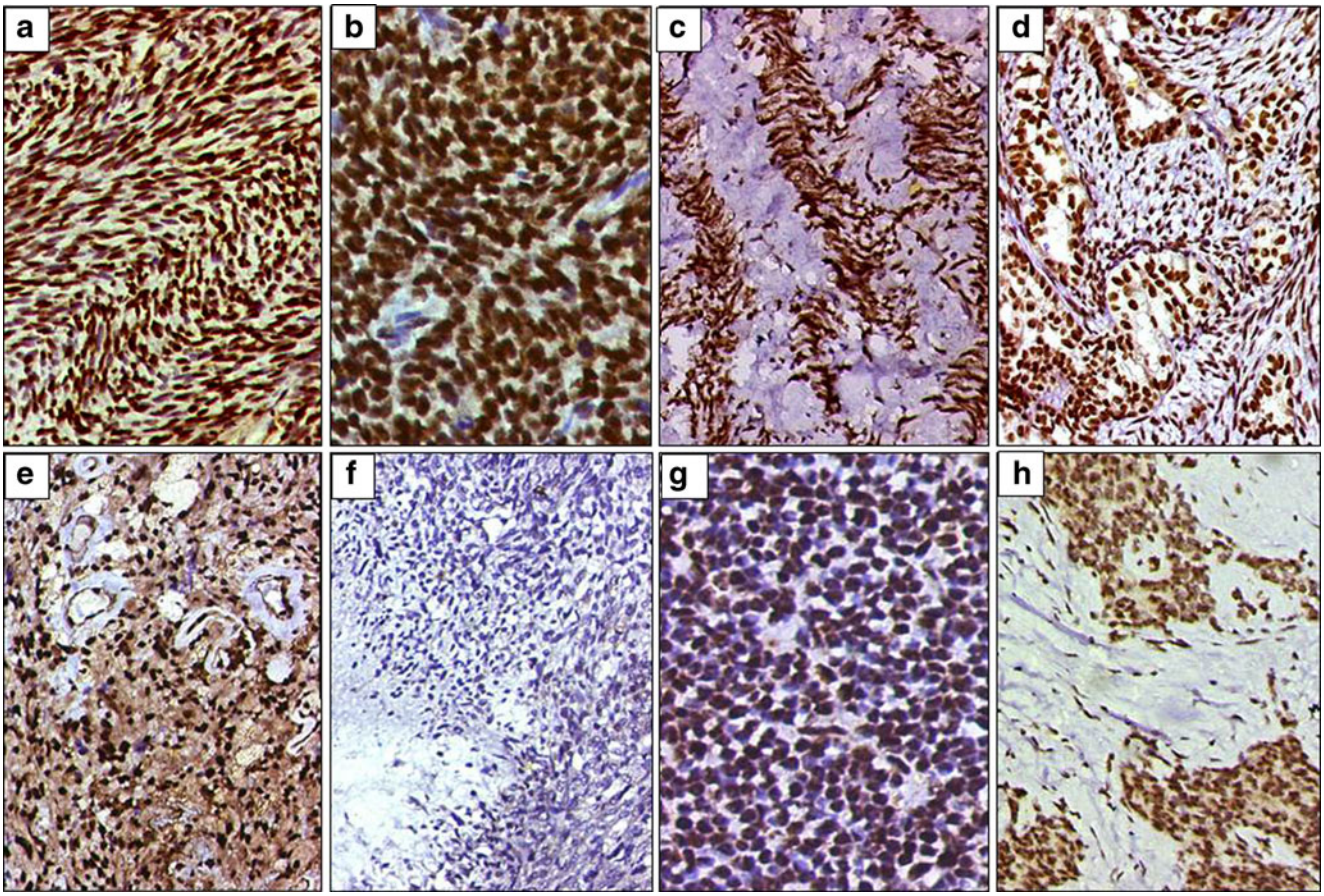

PS-16-024

HER3 (ErbB3) overexpression in Peripheral Nerve Sheath Tumors (PNST)

C. Romagosa*, C. Teixidó, A. Garcia, S. Simonetti, T. Moliné, J. Hernandez Losa, S. Ramon y Cajal

*Hospital Vall d´Hebron, Dept. of Pathology, Barcelona, Spain

Objective: Malignant peripheral nerve sheath tumors (MPNST) comprise 5–10 % of sarcomas. Prognosis is poor and the search for new treatments is ongoing. HER3 is a crucial receptor for neuregulin signalling in Schwann cells but to date, has not been studied in sarcomas. Our aim was to determine the prevalence of HER3 receptor expression in soft tissue tumors, including MPNST.

Method: HER3 expression was evaluated by immunohistochemistry in a total of 50 benign and 71 malignant mesenchymal tumors, including 16 neurofibromas, 16 schwanomas, 14 MPNST and 75 other lesion (uterine and non-uterine leiomiomas and leiomiosarcomas, synovial sarcomas, undifferentiated pleomorphic sarcomas (UPS)).

Results: HER3 overexpression was found in 31 % of cases. Significantly, HER3 positivity was present in

50 % of PNST (75 % of schwanomas, 50 % of MPNST and 25 % of neurofibromas). In contrast, HER3 positivity was observed in 20 % of other mesenchymal tumors (28 % uterine and 9 % non-uterine leiomiomas, 18 % uterine and 25 % non-uterine leiomiosarcomas, 29 % UPS).
Conclusion: HER3 overexpression is frequently found in PNST, including 50 % of MPNST. Due to the crucial role of HER3 receptor in cell signalling as a main activator of the PI3K pathway, these results support the rationale of developing new therapeutic approaches in MPNST.

PS-16-025
Giant cell tumor of tendon sheath with t(1;2)(p13;q37) translocation: A case report
J. Rys*, M. Iliszko, A. Ambicka, M. Vogelgesang, K. Knapczyk, A. Kruczak, J. Limon
*Center of Oncology, Dept. of Tumor Pathology, Kraków, Poland

Objective: Tendosynovial giant cell tumor (TGCT) is a common neoplasm of synovium and tendon sheath. However, clonal chromosome aberrations characteristic for TGCT have been reported in no more than 30 cases. The aim of the study is a presentation of solitary TGCT with morphological, ultrastructural and cytogenetic analysis of tumour.
Method: A 44 year-old male was operated on because of a nodule, localized in soft tissue of medial ankle region and attached to the tendon of flexor muscle of toes. Small fragments of fresh tumour tissue were taken for ultrastructural, flow cytometric and cytogenetic studies. Paraffin-embedded material was examined histologically and immunohistochemically.
Results: Histologically, the tumor was built of ovoid and epithelioid mononuclear cells which present a moderate amount of cytoplasm and round nuclei with a single prominent nucleolus. Together with mononuclear cells, there was a moderate number of osteoclast-like multinucleated giant cells, foam cells and siderophages. Both the mononuclear and multinucleated cells stained with CD68, whereas only giant cells were positive for CD45. At the ultrastructural level, mononuclear cells displayed features of both histiocyte-like and fibroblast-like cells. Cytogenetic studies detected a clonal translocation: 46, XY, t(1;2)(p13;q37)[5]/46, XY[6].
Conclusion: The clonal genetic aberrations support the concept of neoplastic nature of the TGCT.

PS-16-026
Nonneural granular cell tumour of the breast: A case report
J. Rys*, A. Ambicka, A. Harazin-Lechowska, A. Kruczak
*Center of Oncology, Dept. of Tumor Pathology, Kraków, Poland

Objective: Nonneural granular cell tumour (NNGCT) is a rare neoplasm described in 1991 by Leboit et al. Till now, no more than 35 cases have been presented in the literature, nearly all were limited to the skin. We report the first NNGCT of the breast and present its morphological and immunohistochemical characteristics.
Method: A 39 year-old female underwent lumpectomy because of tumour of the breast. After routine histological examination, the immunohistochemical studies were performed using commercially available antibodies against cytokeratins (AE1/AE3), CD68, CD1A, S100, CD34, smooth muscle actin, desmin, miogenin, inhibin, and Ki67 antigen (MiB1).
Results: Microscopically, the tumour was composed of ovoid and polygonal cells with abundant granular, eosinophilic cytoplasm. The cells presented mild or moderate polymorphism and trace mitotic activity. They were arranged in diffuse sheets with no evidence of nesting or fasciculation. The histological texture of the tumour resembled that of classical granular cell tumour of Abrikosoff. However, the tumour cells were strongly immunoreactive for CD68 and inhibin, whereas the reactions against S100 protein as well as other antigens studied gave negative results. The value of Ki67 index did not exceed 2–3 %.
Conclusion: The differential diagnosis of granular cell myoblastoma (Abrikossoff tumour) should include the nonneural granular cell tumour.

PS-16-027
Low grade fibromyxoid sarcoma: A study of 10 cases
K. Shelekhova*, A. Konstantinova
*Petrov´s Research Institute for Oncology, St. Petersburg, Russia

Objective: Low grade fibromyxoid sarcoma (LGFMS) is a specific type of fibrosarcoma with deceptively banal appearance and malignant behavior.
Method: A 5 year retrospective study revealed 10 LGFMS cases. Morphological and immunohistochemical analysis was performed. Follow-up information was obtained for 5 cases.
Results: All tumors occurred in adults (mean 40 year). They developed in neck (1), extremities (6) and trunk (3). Beside classical morphology of LGFMS following features were observed: necrosis (3), rosettes (3), areas of increased cellularity (5), foci of epithelioid cells (5), marked nuclear pleomorphism (1), prominent myxoid change (3), invasive border (6), bone formation (1), focal retiform pattern (1) and sclerosing epithelioid fibrosarcoma-like areas (1). Immunoprofile was the follow: vimentin (100 %), EMA (30 %), CD34 (10 % focally), S100 (0), SMA(0), desmin (0), AE1/AE3 (0). Two patients were without evidence of disease, one developed lung metastasis after 1 year. Two patients developed secondary tumours in 6 and 12 years after initial diagnosis. There were differences in the location and histologic features compared with primary ones. Secondary

tumors were less cellular, without necrosis or epithelioid cells. Behavior of secondary tumors did not fit to the classical concept of tumor progression that implies increase of malignancy.
Conclusion: LGFMS is a distinctive but unusual type of soft tissue sarcoma demonstrating a wide histologic spectrum and behavioral range.

PS-16-031
Immunohistochemical and mutational study of synovial sarcomas
K. Specht*, M. Bettstetter, G. Keller, H. Rechl, R. von Eisenhart-Rothe, H. Höfler, M. Straub
*Technische Universität München, Inst. für Pathologie, Germany

Objective: Synovial sarcomas are mesenchymal tumors of unknown histogenesis. Their molecular signature is a specific t(X; 18)(p11.2;q11.2) translocation. No effective targeted therapies are currently available. The aim of this study was to evaluate the expression and mutational status of potential molecular therapeutic targets.
Method: 38 molecularly confirmed cases of synovial sarcomas were included in this study. Immunohistochemical stainings of the EGF-R family (EGF-R, HER2/neu, HER3), and signaling molecules implicated in the mTOR pathway (AKT, mTOR, PTEN), as well as E-Cadherin and snail was performed. In addition, cases were screend for mutations in the EGFR, PIK3C, B-RAF, K-RAS, and N-RAS genes.
Results: EGF-receptor family members as well as E-Cadherin and snail are important for defining the tumor phenotype by determining epithelial-mesenchymal transition of synovial sarcomas. Activation oft the mTOR pathway is seen in a significant number of cases. Mutations of the genes studied are an overall rare event in synovial sarcomas and other types of sarcomas studied.
Conclusion: EGF-R expression is found in many synovial sarcomas, however, mutations of EGFR or downstream molecules appear to be rare. Activation of mTOR pathway is frequently seen in synovial sarcomas. The benefit of targeted therapy against these genes in synovial sarcomas remains to be determined.

PS-16-032
Collagen V induces differentiation of rabbit adipose tissue-derived stem cells in chondrocyte-like phenotype
W. Teodoro*, I. Brindo da Cruz, A. P. Velosa, S. Carrasco, C. Goldenstein-Schainberg, R. Fuller, E. Parra, V. Capelozzi
*Faculdade de Medicina da USP, Disciplina de Reumatologia, São Paulo, Brazil

Objective: Stimulated mesenchymal stem cells (MSCs) have capacity of differentiation in many cell types. It is being used in degenerative diseases treatment protocols. We evaluated the collagen V (COL V) and collagen XI (COL XI) influence in the differentiation of rabbits adipose tissue-derived MSCs in a chondrocyte-like cell phenotype.
Method: MSCs isolated of New Zealand rabbits adipose-tissue were maintained in culture by 4 weeks. COLV, COLXI and COLV/XI (10 μg/ml) were added to culture during 72 h. The cells aggregates were stained with Toluidine blue, Alcian blue and Picrosirius. Chondrocyte-like phenotype was confirmed by immunofluorescence to CD34, vimentin and collagens I, II and III.
Results: MSCs stimulated with COLV expressed proteoglicans and collagen, when compared with COLXI and COLV/XI and control. In the presence of COLV, MSCs was capable to increase collagen II expression confirming its chondrocyte-like cell phenotype. In contrast, MSCs cultured with COLXI and COLV/XI express collagen I and III.
Conclusion: The data suggest that COLV may facilitate the differentiation of rabbit adipose tissue-derived stem cells into a chondrocyte-like phenotype. Further studies are urged in order to evaluate the influence of COLV in the ability of chondrocytes to remodel osteoarthritic joint surface at ultra structural and molecular levels.

Tuesday, 11 September 2012, 09.30 - 10.30, Congress Hall Foyer 3rd Floor
PS-17 Poster Session Breast Pathology

PS-17-001
Targeting XRCC1 (X-ray Repair Cross-complementing Gene 1) deficiency in human cancer for personalized cancer therapy
T. Abdel-Fatah*, R. Sultana, R. Abbotts, I. Seyer, A. Green, S. Chan, I. Ellis, S. Madhusudan
*Nottingham City Hospital, Dept. of Clinical Oncology, United Kingdom

Objective: XRCC1 is essential for DNA base excision repair, single strand break repair and nucleotide excision repair.
Method: We evaluated XRCC1 immunohistochemically in early stage breast (n=2046), ovarian (n=157), gastric (n=140), colorectal (n=250) and pancreaticobiliary cancers (n=240). Pre-clinically, we evaluated a panel of XRCC1 deficient and proficient Chinese hamster ovary and human cancer cell lines. Double strand break repair (DSB) inhibitors targeting ATM (KU55933), DNA-PKcs (NU7441) and ATR (NU6027) were evaluated for synthetic lethality and cisplatin alone or in combination with DSB inhibitors for chemopotentiation.
Results: In breast cancer, XRCC1 loss (16 %) was associated with a 2-fold increase in risk of death and metastasis (p< 0.0001). In ovarian cancer, XRCC1 positive tumours (44 %) were more resistant to platinum chemotherapy (p=0.0001). XRCC1 positivity conferred a 2 fold increase of risk of death

(p=0.002) and independently associated with poor survival (p= 0.002). Pre-clinically, KU55933, NU7441 and NU6027 were synthetically lethal in XRCC1 deficient compared to proficient cells as evidenced by DSB accumulation, G2/M cell cycle arrest and apoptosis. XRCC1 deficient cells were hypersensitive to cisplatin which was enhanced by DSB repair inhibitors compared to in proficient cells.
Conclusion: Conclusions: XRCC1 deficiency in human tumours may be suitable for synthetic lethality application and exploited for cisplatin chemotherapy potentiation.

PS-17-004
Analysis of BCL2 oncoprotein expressing breast cancer by molecular subtype
A. Abolins*, I. Strumfa, Z. Simtniece, A. Vanags, G. Trofimovics, J. Gardovskis
*Riga Stradinš University, Inst. of Oncology, Latvia

Objective: Breast cancer is the most common malignancy in Western women. Despite the progress in morphological investigation, active research is devoted to potentially important targets for prognosis and intervention. BCL2 oncoprotein represents such factor.
Method: Consecutive breast cancer cases were examined by routine protocol approach. The BCL2 oncoprotein expression was detected immunohistochemically. Expression was considered positive if it was in more than 25 % of tumour cells. The molecular subtype (Luminal A(LA), Luminal B(LB), HER2 positive(HER2) or triple negative(TN)) was determined as well.
Results: Among 159 invasive breast cancer cases, positive expression of BCL2 was detected in 66.7 %. The BCL2 positive group included: LA 86.8 % [95 % confidence interval 79.0–92.0], LB 4.7 % [2.0–10.6], HER2 0.9 % [0.2–5.2] and TN 7.6 % [3.9–14.2]. The BCL2 negative group consisted of LA 34 % [22.7–47.4], LB 3.7 % [1.0–12.8], HER2 26.4 % [16.4–39.6] and TN 35.8 % [24.3–49.3].
Conclusion: 1. BCL2 positive breast cancer possesses mostly Luminal A molecular subtype. Among BCL2 negative tumours, there is significantly higher fraction of HER2-positive and triple negative subtypes. 2.In breast cancer, BCL2 expression is associated with favourable prognostic indicators and should be analysed in complex with other parameters.

PS-17-005
Extramammary tumour metastasis in the breast
A. Abolins*, I. Strumfa, G. Volanska, A. Vanags, B. Strumfs, J. Gardovskis
*Riga Stradinš University, Inst. of Oncology, Latvia

Objective: Breast cancer is the most common malignant tumour of Latvian women (www.csb.lv). Correct diagnosis, including identification of tumour histogenesis, is the prerequisite for appropriate treatment.
Method: Consecutive breast tumour cases were selected by systematic retrospective archive search and were examined by breast cancer panel. If expression of oestrogen and progesterone receptors and HER2 protein was negative, mammaglobin, cytokeratin AE1/AE3, vimentin, CD45, CDX2, cytokeratin 20, TTF-1 and melanosome protein HMB-45 were detected.
Results: Five patients (0.89 %, 95 % CI=0.38–2.10 %) with secondary breast tumours were identified among 559 cases. Breast was affected by metastatic small cell lung cancer (1), malignant neuroendocrine tumour of small intestine (1) as well as by epithelioid melanoma metastasis in breast tissues (2) or intramammary lymph node (1). Analysing medical records, multiple synchronous and/or metachronous metastasis, involving brain, kidneys and ovaries, were found in all patients with haematogenous tumour metastases in the breast. In contrast, the lymphogenic tumour spread was isolated.
Conclusion: 1. Lymphogenic or haematogenous metastasis rarely (0.89 % of malignant breast tumours by morphology) can develop in breast tissues. It should be taking into account when planning the differential diagnostic approach, especially immunohistochemistry. 2. Haematogenous metastases in breast are associated with a wide synchronous or metachronous extramammary tumour spread.

PS-17-006
The prognostic significance of tumor-associated stroma in invasive breast carcinoma
S.-M. Ahn*, J.-H. Cho, J.-Y. Sung, E.-Y. Cho
*Samsung Medical Center, Dept. of Pathology, Seoul, Republic of Korea

Objective: Fibroblasts in the stromal component of a tumor may influence tumor progression in various organs. The prognostic significance of tumor-infiltrating lymphocytes is also frequently reported. However, the prognostic significance of the stromal component in breast cancers, particularly those of high grade, has not been established.
Method: In this study, we analyzed surgically resected specimens from 545 patients with breast carcinoma, including 193 high grade tumors, for tumor-stroma ratio, dominant stroma type (collagen (C), fibroblast (F) or lymphocyte (L) dominant type), and central fibrosis on hematoxylin-eosin stained histological sections. We correlated these features with clinical prognosis.
Results: Among the 533 specimens examined, 127 (23.3 %) were of C type, 292 (53.6 %) of F type, and 114 (20.9 %) of L type. Central fibrosis was found in 99 tumors (18 %). The dominant stroma type was a significant prognostic factor on univariate and multivariate analyses, together with T classification, nodal status and Bloom-Richardson grade. Tumor-stroma ratio and central fibrosis did not predict survival on multivariate analysis. Even in high-grade tumors, relapse-

free intervals differed significantly according to dominant stroma type.
Conclusion: Conventional hematoxylin-eosin stained tumor slides may contain more prognostic information than previously thought; in particular, the dominant stroma type in invasive breast cancer may potentially be used to predict outcome.

PS-17-007
Pathology in breast implants substitution
L. Alfaro*, J. Serra, J. M. Ibañez
*Valencia, Spain

Objective: Health alert concerning breast implants brand PIP led to a review of patients harboring these prosthesis and in many cases replacement by new ones. Anaplastic lymphoma described in these patients has been an additional problem to be faced by plastic-surgeons and pathologists.
Method: Ninety two cases of women with breast implants were studied. Most of them had PIP implants (although no information of prosthesis type was available in all cases). Eighty of them presented with ruptures of different size. After implant replacement, histopathologic analysis of fibrous capsules and liquid from seromas in periprosthetic cavities was carry out. Following FDA recommendations, immunohistochemical studies to rule out lymphoma was performed in 85 cases.
Results: Fibrous capsules showed synovial metaplasia in all cases. Morphology was practically identical that in real articular synovial cells, and occasionally intracavitary nodules were seen detached from the surface in a process similar to synovial chondromatosis. No cases of lymphoma were seen and no expression of CD30 or ALK markers occurred. A case of pericapsular ductal invasive carcinoma was discovered.
Conclusion: Synovial metaplasia seems to be very common in capsules around breast implants. Development of conventional breast carcinoma is probably much more frequent than lymphomas independently of the possible implant influence.

PS-17-009
Post-radiation angiosarcoma of the breast: Report of a case
A. Apostolaki*, M. Sofopoulos, S. Tsitsiou, E. Pigadioti, N. Mylona, N. Arnogiannaki
*Agios Savvas Hospital, Dept. of Anatomical Pathology, Athens, Greece

Objective: Post-irradiation angiosarcoma generally occurs after breast conservation and radiation therapy. It affects the dermis of the breast within the radiation field. The incidence of post-radiational angiosarcoma is about 0.14 %.
Method: An 82-year-old woman who had undergone conservative surgery and radiotherapy for breast cancer 10 years ago presented with multiple red-purplish papules on the skin of her right breast. Excisional biopsy followed by simple mastectomy was performed.
Results: Excisional biopsy revealed a neoplasm composed of highly pleomorphic cells with prominent nucleoli forming solid areas and neoplastic slit-like vascular channels. Many mitotic figures and some individual apoptotic cells were also present. The tumor cells were positive for endotelial cell markers (factor VIII, CD31, CD34) and negative for CK7. The gross inspection of the mastectomy specimen showed multiple reddish-purple papule-like lesions on the skin, spreaded in an area of 12×10 cm. Sectioning showed numerous homogenous slightly hemorrhagic white nodules measuring from 2 to 12 mm located in the dermis. Histopatology and immunohistochemistry findings were consistent to those of the excisional biopsy. Infiltration of the subdermis was noted.
Conclusion: Diagnosis was high grade post-irradiation angiosarcoma. Simple mastectomy is the treatment of choice. Adjuvant chemotherapy should be considered in high grade neoplasms like this one.

PS-17-010
Prognostic factors in invasive lobular carcinoma of the breast
G. Askan*, G. Ayranci, N. Özkan, H. Kaya, U. Ugurlu
*Marmara University, Dept. of Pathology, Istanbul, Turkey

Objective: Determination of molecular features in breast carcinomas, such as hormone receptor expression, can guide clinicians to the optimal choice of therapy. In this study, the relationship between the histologic grade, pathologic stage and the prognosis of invasive lobular carcinoma of the breast, and the tissue expression levels of ER, PR, HER-2/neu, p53, bcl-2, Ki-67 and E-cadherin was investigated.
Method: 31 cases of invasive lobular carcinoma of the breast, from 2003 to 2011, were included in this study. A single best representative paraffin block was selected for each case and H&E staining and immunohistochemistry procedures were performed. Ki-kare test was used for statistical method.
Results: 24 of 31 cases had classical lobular carcinoma, 7 cases had tubulolobular, pleomorphic, signet ring cell, or apocrine features. The median age of patients was 54 years. ER and PR were positive in 28 cases. All cases were negative for E-cadherin. Ki-67 was greater than %15 in 2 cases with pleomorphic lobular carcinoma. p53 positivity increased with grade. In 14 cases p53 was negative and bcl-2 was positive. Bcl-2 and p53 were positive in 29 and 17 cases respectively.

Conclusion: In contrast to the literature, there was no correlation between bcl-2 status and other molecular markers, including p53.

PS-17-012

Rapid immunohistochemistry in intraoperative sentinel axillary lymph node evaluation

P. Baldin*, M. C. Cucchi, Y. Ishikawa, V. Eusebi, M. P. Foschini
*University of Bologna, Dept. of Anatomic Pathology, Italy

Objective: Sentinel lymph node (SN) examination is the current procedure to establish the status of axillary lymph nodes in breast cancer. To avoid a two step delayed surgical procedure, a reliable and quick method of SN evaluation is advocated. Rapid immunohistochemical technique (UICH) for keratin has been only recently proposed. Aim of this study is to apply keratin UICH in frozen sections (FSs) of SNs.
Method: A consecutive series of 231(Series A) SN cases was studied at FS level followed by two sections stained with keratin UIHC. All procedure requires 23 min. For comparison 131 consecutive cases (series B) of SN were studied with FS only. All residual tissue from both series was paraffin embedded (PS).
Results: Series A: SNs showed tumour involvement in 41 cases (17.7 %). In only 8 cases (3.75 %), PS sections evidenced additional neoplastic cells (micometastases) not seen with keratin UIHC, that led to a delayed axillary dissection. Series B: PS sections revealed metastatic deposits (micrometastases) not seen in FS in 6.1 % of cases.
Conclusion: FS coupled with keratin UHIC of all the entire lymph node accurately evidences carcinoma cells in SNs.

PS-17-013

High concordance of 6 HER2 in situ hybridization methods with Abbott FISH

J. Boers*, L. Krol, C. Netjes, H. Meeuwissen, C. Prinsen, C. van Krimpen, E. van der Logt, J. Bart, E. Schuuring
*Isala Klinieken, Dept. of Pathlogy, Zwolle, Netherlands

Objective: We conducted a comprehensive concordance study of 6 ISH methods with Abbott FISH in a large series of breast carcinomas.
Method: Tissue Micro Arrays (TMA) were constructed by taking 3 tissue-cores from praffin blocks of 402 primary breast carcinomas. Up to 384 cases were analyzable in 7 ISH assays. Scoring was performed by two independent observers without knowledge of the other ISH data according the ASCO-guidelines for HER2-testing. Cases were considered positive when the ratio was ≥2.0. Discordant cases were reviewed and scores were reassigned on consensus of opinion. Concordance and Cohen's kappa score were calculated in relation to FISH, Abbott.
Results: In 372 cases analyzable with Abbott HER2 FISH, 12.1 % were HER2-positive. Concordances (kappa-scores) of the 6 other assays were: DAKO FISH 98.1 % (0.90), DAKO duoCISH 97.2 % (10.4 %), Zytovision FISH 99.1 % (0.96), Zytovision duoCISH 99.1 % (0.96), single probe SISH Ventana 98.9 % (0.95), dual probe SISH Ventana 99.4 % (0.97).
Conclusion: Conclusion: Concordance of 6 HER2 ISH assays with Abbott FISH were shown to be 97.2 % or higher. In this study, DAKO assays had a lower kappa score with Abbott FISH than Ventana or Zytovision assays.

PS-17-014

Which is the best method to measure multiple breast cancer?

M. Boros*, C. Marian, O. Pop, S. Stolnicu
*UMPh Targu Mures, Pathology, Romania

The size of the breast tumor is relevant in a patient s management also affecting the prognosis. For unifocal lesions, tumor staging depends on the maximum diameter of the tumor, whereas in multiple lesions, this issue is not standardized. The aim of this paper is to study which is the best method in the assessment of the tumor size in multiple invazive carcinomas (multifocal and multicentric) in correlation with the lymph node metastases developement. Two different assessments of the tumor size (diameter of the largest focus=LD, and combined, aggregate diameter of all the foci=AD) were used in 418 primary invasive breast lesions (91 multiple, 327 unifocal) and compared with the nodal status (CHI- test). The use of combined tumor focus upstaged 23 (25.27 %) patients with multiple tumors (16 upstaged from pT1 to pT2 and 7 from pT2 to pT3). There was no difference in nodal positivity based on pT status between LD and AD. We observed a statistically significant difference in the mean diameter of the largest focus between the unifocal and multifocal group (31,47 vs 39,67 mm) (p=0,0013). Aggregate diameter in multiple breast cancer is not correlated with an increase of axillary metasases and should not be used for staging.

PS-17-015

Central nervous system metastases in women with invasive breast carcinoma, not otherwise specified, are associated with estrogen receptor status

E. Cambruzzi*, A. G. Reginatto, C. G. Zettler, K. L. Pêgas, V. Grings, J. M. Venites, C. A. Coelho
*ULBRA and UFRGS, Dept. of Pathology, Porto Alegre, Brazil

Objective: Central nervous system metastases (CNSM) from breast cancer (BC) are relatively common and can

present as the first site of disease progression. Lymph node status and tumor size are regarded as important prognostic indicators for disease-free and overall survival in BC. The aim of this study was to investigate prognostic/predictive pathological data in BC that could define a high-risk group to develop CNSM.
Method: The authors evaluated 97 female patients with invasive breast carcinoma, not otherwise specified, previously submitted to setorectomy/mastectomy, in order to determine lymph node status, tumor size, histologic grade, estrogen receptor status (ER) and immunoexpression of HER2/neu. Of these cases, 10 patients developed CNSM.
Results: The patients who developed CNSM were younger (median age 54.7±8.152 years/p=0.251) and more likely to have T2N2 disease than patients with no CNSM. The presence of encephalic disease was associated with ER (p=0.031). Lymph node status (p=0.84), tumor size (p=0.339), histologic grade (p=0.933), and HER2/neu expression (p=0.31) were not significant risk factors.
Conclusion: Although the literature data discriminate that HER2/neu overexpression in BC is related with CNSM, the authors suggests that these lesions can be related to ER too. Efforts to determine other risk factor for development of CNSM may be warranted.

PS-17-018

Androgen receptors and sex hormone serum levels in breast carcinoma: Study of the ORDET cohort

L. Cimetti*, S. Sieri, A. M. Chiaravalli, N. Sahnane, F. Sessa, C. Riva, C. Capella
*University of Insubria and Ospedale di Circolo, Varese, Italy

Objective: Androgens and androgen receptors (AR) are involved in breast cancer (BC) pathogenesis. High testosterone serum levels increase the risk of developing mainly ER + BC, especially after menopause, although androgen role in tumor progression is not clearly elucidated.
Method: Correlations between serum sex hormones and clinico-pathological features of 131 BC arisen among 10,786 women previously recruited for ORDET study were investigated. Prediagnostic estradiol, testosterone (free/total) and SHBG serum levels were available. Immunohistochemistry for AR was evaluated along with ER, PR, HER-2 and MIB-1.
Results: AR + was found in 90.8 % of BC. Higher estradiol (p=0.0001), free testosterone (p=0.02) and SHBG (p=0.02) were seen in premenopausal patients. In dead patients higher free testosterone was observed (p=0.0003). No correlation was found for hormone levels vs stage, histotype and grade. Higher SHBG was seen in PR-rich tumours (p=0.02). HER-2+/ER- cases showed a trend for a higher total testosterone (p=0.18) and SHBG (p=0.2). Testosterone, estradiol and SHBG were similar in AR + and AR- tumors. Among triple negative, AR + tumours showed higher free testosterone (p=0.04). BC with few AR + cells showed higher total testosterone (p=0.0004) and a worse outcome (p=0.29).
Conclusion: Our results confirm the role of AR in BC and suggest the androgen involvement in tumour progression.

PS-17-019

Mitotic count in metastatic breast carcinoma to lymph nodes: Preoperative study

A. Córdoba*, L. Gomez, F. Vicente, I. Amat, C. Llanos, D. Guerrero
*Hospital Navarra, AP, Pamplona, Spain

Objective: Axillary lymph node metastasis (ALNM) is one of the most important prognostic factors in breast cancer. The reasons why tumours are capable to result in axillary metastasis remain unclear. The evaluation risk of ALNM would improve the treatment planning. We study the metastatic breast carcinoma to the lymph node to obtain information about the metastatic risk.
Method: We study 65 patients with metastatic breast carcinoma to the lymph node diagnosed preoperatively by needle biopsy. We study the mitotic average (×10 HPF), metastasis size, positive lymph nodes, total lymph node studied, lymph node ratio (nº of positive node/total nodes nº), primary tumour size and grade.
Results: All the cases with high mitotic count were associated with macrometastasis. We didn't find any relation between the mitotic rate or the metastatic size with the number of lymph node affected, and the lymph node ratio. Breast carcinomas G1, T1, <6 mitosis/HPF lymph nodes showed 25–50 % of positive lymph nodes.
Conclusion: We tried to obtain information from the metastatic breast carcinoma to the lymph node to predict the axillary status. In our cases we couldn't predict the lymph node involvement based in the tumour size, grade, metastatic size, and metastatic mitotic rate. The preoperative study of a breast tumour and their lymph node metastasis don't allow predicting the lymph node status in our series.

PS-17-020

RASSF1A hypermethylation is associated to the presence of tumoral cells detected by One-step Nucleic Acid Amplification (OSNA)

A. Córdoba*, F. Vicente, N. Perez Janices, J. Perez Vizcaino, E. Gochi, N. Torrea, D. Guerrero
*Hospital Navarra, AP, Pamplona, Spain

Objective: One-step nucleic acid amplification (OSNA) is used in routine clinical use for sentinel lymph node biopsy (SLNB). It consists of the molecular quantitation of a

tumoral marker (cytokeratin-CK 19 mRNA). Gene hypermethylation is one of the most common mechanisms of inactivation of suppressor genes. RASSF1A gene, is a region frequently hypermethylated in breast cancer.
Method: 51 patients with breast cancer were included in the study, and a total of 87 lymph nodes were analysed.
Results: 41 %, 33.3 % and 21.6 % of the tumours were of low, intermediate and high-grade, respectively. In 40.8 % of the cases there are not tumoral cells, in contrast to 12.2 %, 4.1 %, 14.3 %, 28.6 % that showed low number of cells/ITC (<250 copies/sample), Micro- (<5000 copies/sample) and Macro-Mtx, respectively. There is a very clear association between RASSF1A hypermethylation and the presence of tumoral cells (p= 0.004), being more frequent in Macro-mtx compared to the rest of groups (P=0.007). RASSF1A hypermethylation is also correlated to unfavorable histologic grade in the tumour (P=0.025) and lymph node involvement at the diagnosis (0.001).
Conclusion: The analysis of RASSF1A hypermethylation could provide additional information to OSNA to detect tumoral cells in lymph nodes. The spare tissue material derived from OSNA could be good material to consider new molecular studies.

PS-17-021
Breast Cancer profile in young Romanian women
M. Cristina*, M. Boros, M. D. Podeanu, S. Stolnicu
*University Emergency County Hospital, Dept. of Pathology, Targu Mures, Romania

Objective: A variety of previous studies have shown a higher prevalence of prognostic parameters associated with poor survival in young women with breast cancer. The aim of this study is to reveal the morphologic aspects and hormonal status in patients with breast cancer under 35 from the Pathology Department of Targu Mures.
Method: 949 patients with breast cancer have been diagnosed in 5 years (2006–2011), 17 being under 35 years old (1,79 %).
Results: Of these, 15 patients (88,23 %) had palpable tumor at presentation, 12 (70,58 %) with palpable axillary adenopathy. In 10 cases (58,82 %) the tumor diameter was over 2 cm at the time of diagnosis. In 15 cases (88,23 %) the histological type was infiltrative ductal carcinoma, with 13 cases having high grade. Most of the tumors expressed ER and PR and were Her-2 negative (none was triple negative). However, in 11 cases (64,70 %) the ki-67 index was more than 50 %.
Conclusion: Young women with breast cancer have been shown to have a poorer prognosis because of the high grade and hormonal status. Our study shows some similar aspects, but the hormonal status is totally different from the dates in the literature, revealing a possible better response to hormonal treatment and a better survival.

PS-17-022
Immunohistochemical predictive markers for trastuzumab resistence
A. Cuesta Diaz de Rada*, E. Honrado Franco, M. Baltasar Moreira, F. M. Izquierdo Garcia
*Hospital de León, Anatomía Patológica, Spain

Objective: HER2 positivity defines a clinically challenging subgroup of patients with breast cancer with variable prognosis and response to therapy. The main aim of this study is to identify immunohistochemical markers to predict trastuzumab resistence.
Method: Tumours from 57 patients with Invasive Ductal Carcinoma, who were previously treated with trastuzumab, were included in a tissue microarray and stained for ER, Ki67, p53, cyclin D1, p16 and for HER2 and SISH (silver in situ hybridization).
Results: After 5 years of follow up, 80 % of patients with p53 negative tumours were disease free (p 0.029) and 90 % were alive (p 0,014) and the patients cyclin D1 positive, 90 % were alive (p 0.031) and 84 % were disease free (p 0.005). Among HER2 3+, 10 % did not amplify (polysomy 17). Moreover, 12 % of treated patients were HER2 0−2+ and did not amplify by SISH.
Conclusion: The best immunohistochemical markers to predict a good response to trastuzumab treatment were P53 negative and/or cyclin D1 positive. All HER2 positive 3+ tumours should be confirmed by hybridization, since polysomy 17 is found in 10 %, and these tumours should not be treated with trastuzumab. Variations in the immunostaining techniques could induce trastuzumab treatment to patients with HER2 non amplified tumours.

PS-17-023
CD99 expression in breast carcinoma
P. Czapiewski*, J. Szade, A. Zaczek, M. Welnicka-Jaskiewicz, W. Biernat
*Medical University of Gdansk, Dept. of Pathology, Poland

Objective: CD99 is a membraneous protein that is expressed widely among various soft tissue tumors. There is growing evidence that its expression in some carcinomas correlates with epithelial to mesenchymal transition (EMT) and is a poor prognostic factor. Its importance in the breast carcinoma remains unsettled.
Method: The analysis was performed on breast cancer samples from 122 patients. Tumors were graded histologically according to the Nottingham system. CD99 expression was scored by grading system used for HER-2. Only cases showing grade (3+) were regarded as positive. Additionally,

expression of estrogen (ER) and progesterone receptor (PR), HER-2, E-cadherin, Vimentin, Twist, Ki-67, c-myc, cyclin D1 and Topoisomerase 2alfa was performed. Expression of the CD99 was correlated with all these markers and with clinical outcome.
Results: Expression of CD99 was observed in 11 patients and correlated significantly with negative PR status (p=0,01), higher histological grade (p=0,05), positive Twist (p=0,04) and Topoisomerase2alfa expression (p=0,04). There was also a trend toward higher frequency of cyclin D1 positivity (p= 0.09). No impact on prognosis for CD99 expression was found.
Conclusion: Expression of CD99 correlates with high histological grade, negative progesterone receptor status and expression of certain EMT and proliferation markers, but it does not influence prognosis in breast carcinoma.

PS-17-024

Primary plasmacytoma of the breast: A case report

L. De Carvalho*, G. G. Monteiro, L. Casagrande, T. Ricci, T. Lebrão, V. Tarricone, P. Dinamarco
*Centro Universitário Lusíada, Dept. of Pathology, Santos, Brazil

Objective: extramedullary plasmacytomas of the breast are extremely rare, especially those that are not associated with multiple myeloma and they can mimic mammary carcinoma.
Method: case report:69-year-old woman presented a palpable mass in the left breast previously diagnosed as a lobular carcinoma by core biopsy performed in other service. In our institution a conservative surgery with lymph node dissection was proposed.
Results: Frozen section was required and the gross examination showed a 4.0×4.0×3.0 cm firm-elastic nodule with surgical margins free of tumor and the microscopic examination showed tumor cells with abundant cytoplasm with hyaline appearance. The paraffin sections showed a proliferation of plasma cells with moderate atypia. The immunohistochemical study confirmed the diagnosis of plasmacytoma. There was no axillary lymph node involvement. There were no bone lesions in the additional investigation.
Conclusion: primary plasmacytomas of the breast are extremely rare and have to be included in the differential diagnosis with breast carcinomas especially in material of core biopsy.

PS-17-025

Sentinel lymph node in breast cancer: Form morphology to molecular examination

L. Di Tommaso*, B. Fernandes, B. Fiamengo, C. Navligu, P. Spaggiari, S. Manara, C. A. Garcia Etienne, G. Masci, A. Testori, C. Tinterri, M. Roncalli
*IRCCS Istituto Clinico Humanitas, Dept. of Pathology, Rozzano, Italy

Objective: Sentinel lymph node (SLN) examination is a standard in breast cancer treatment. It can be performed on formalin-fixed paraffin-embedded material (FFPE) or on frozen sections (FS). FFPE or FS suffer two drawbacks: 1) partial examination; 2) operator's dependence. To avoid these limitations, a molecular technique (OSNA) targeted to quantify a tumoral fingerprint (CK19), has been introduced. Our aim is to compare the performance of FFPE, FS and OSNA.
Method: We evaluated the clinical-pathological features of three series of SLN-patients from a single Institution. The series consists of 540 FFPE (2000–2005), 390 FS (2009) and 198 OSNA (from October-2011 to march-2012) patients.
Results: Positive SLN were disclosed in 162/540 (30 %) FFPE, 87/390 (22 %) FS and 55/198 (28 %) OSNA and represented by metastases-micrometastases [FFPE: 61–38 %, FS: 74–26 %, OSNA: 71–29 %]. After axillary dissection, additional metastasis were observed in 53/162 (33 %) FFPE, 27/87 (31 %) FS and 16/53 (30 %) OSNA patients, with further involvement more frequent with metastasis (FFPE 43 %, FS 36 %, OSNA 36 %) rather than micrometastasis (FFPE 16 %, FS 17 %, OSNA 14 %).
Conclusion: OSNA provides results overlapping to those of FFPE and FS, thus representing a valid and objective alternative for intraoperative SLN examination in breast cancer.

PS-17-026

HER2 assessment in invasive breast cancer using IHC and FISH: Results from 7479 consecutive cases

P. Drev*, B. Gazic, J. Contreras
*Inst. of Oncology, Dept. of Pathology, Ljubljana, Slovenia

Objective: HER2 in invasive breast cancer (IBC) should be assessed according to recommended algorithms employing IHC as screening tool and ISH only in equivocal cases. Therefore there is little data on possible missdiagnosis in discordant cases.
Method: HER2 was assessed by both IHC and FISH in 7479 consecutive IBC. Distribution of IHC and FISH scores, incidence of HER2+ IBC, concordance and level of amplification in discordant cases were analysed.
Results: IHC distribution: neg(0) 49.6 %, neg(1+) 27.0 %, equivocal(2+) 11.3 %, pos(3+) 12.1 %. FISH distribution: nonamplified 84.6 %, amplified 13.6 %, equivocal 1.8 % of which in 42.1 % ratio was ≥2.0. 15.0 % IBC were HER2+ and 0.7 % were double-equivocal. 14.4 % of equivocal(2+) were amplified. Discordance was infrequent (1.2 %) (p< 0.0001): among neg(0) and neg(1+) 0,3 % and 1,6 % were amplified, while among pos(3+) 4.7 % were nonamplified. 64 IHC negative tumors, representing 5.7 % of all HER2+, were amplified, however in 89.1 % ratio was ≤4.0.

Conclusion: 15 % IBC are HER2+. Application of two standardised methods results in excellent concordance and enables detection of all HER2+ IBC, while recommended algorithms lead to missdiagnosis in 6 % of HER2+ IBC, but in these amplification is low-level.

PS-17-027

Case report: Unusual breast cystic lesion in a 46-year-old female

P. Farrajota*, P. Cusati, D. Esteves, C. Dias, C. Carvalho, G. Falconieri
*Centro Hospitalar do Porto, Dipt. do Anatomia Patologica, Portugal

Objective: Papillary carcinoma of the female breast may exhibit a broad phenotype. We present an unusual case of a pseudoencapsulated invasive papillary carcinoma featuring transitional cell features.
Method: A specimen of internal right female breast biquadrantectomy was routinely processed and a panel of antibodies applied on paraffin tissue section.
Results: Grossly, the specimen showed a 12.5 cm cystic lesion with fibrino-hematic material and multiple pinkish-grey papillary structures, the largest measuring 4 cm. The histological examination revealed a malignant epithelial papillary proliferation reminiscent of transitional cell carcinoma, with high nuclear grade, frequent mitotic figures, multiple areas of invasion and rare necrotic foci. Tumor cells were immunoreactive for p63, 34βE12 and Ki-67 (90 %) and negative for other stains including HER2/neu, estrogen and progesterone receptors. Our differential diagnosis included a metastasis from a primary urothelial carcinoma, an intraductal papillary lesion, a metaplastic carcinoma and a papillary adnexal neoplasm, all reasonably excluded after careful clinico-pathologic evaluation.
Conclusion: Metastatic involvement of the breast is uncommon but it should be considered if tumor phenotype is inconsistent within usual or "special type" breast carcinoma. Yet, some rare primary misleading lesions are difficult to recognize.

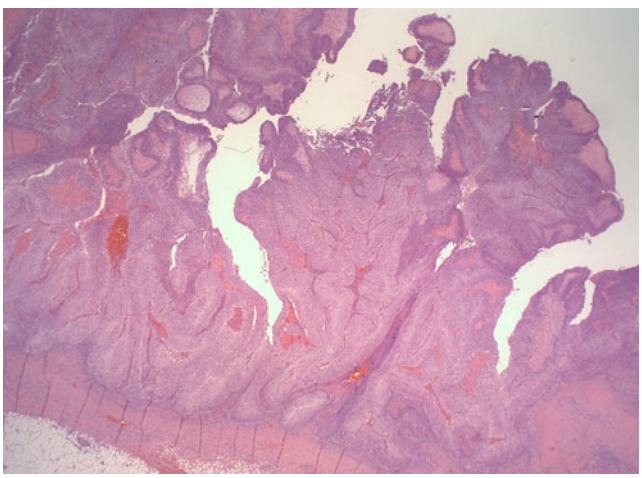

PS-17-028

Volume measurement of female Sprague–Dawley mammary tumors induced by N-methyl-N-nitrosourea: Comparing ultrasonography and caliper

A. Faustino-Rocha*, C. Teixeira-Guedes, J. Pinho-Oliveira, R. Soares-Maia, R. Arantes-Rodrigues, B. Colaço, R. Ferreira, P. Oliveira, M. Ginja
*UTAD, Dept. of Veterinary Sciences, Vila Real, Portugal

Objective: N-methyl-N-nitrosourea (MNU) is a chemical carcinogen frequently used to induce mammary tumors in female rats, which experimental evaluation requires the monitoring of tumor's volume. For this purpose several methods are described, namely: caliper and ultrasonography measurement. The aim of this work was to compare data obtained by caliper and ultrasonography.
Method: Twelve female Sprague–Dawley rats with 187.7± 14.3 g body weight were intraperitoneally injected with MNU (50 mg/Kg) at 50 days of age. Thirty-six weeks after MNU administration forty-one tumors volume was determined by caliper (Vito®) and ultrasonography (LOGIQP6®, General Electric Healthcare) measurement. The tumor volume (V) was calculated according to the following formula $V=\pi$. ⟦S_1^2⟧ ^ .S_2⁄12, being S_(1) and S_2 the tumor diameters (S_(1)<S_(2)).
Results: The means tumor caliper and ultrasonography measures were 4.116±5.801 cm3 and 2.578±4.302 cm3, respectively. The ICC for scoring reproducibility was 0.75 (95 % Confidence Interval, 0.57 to 0.86) and Paired-Sample *T*-Test was significant ($p<0.01$).
Conclusion: Usually mammary tumors in rat are measured by caliper. However, our results showed that there are volume differences between both methods studied. Ultrasonographic method is more accurate and more precise than caliper. Therefore, we recommend the use of ultrasonography to rat tumor evaluation.

PS-17-029

Involvement of PI3K/Akt pathway alterations in breast cancer treated with trastuzumab

M. Fernández García*, I. Centeno Ramos, L. Suárez Fernández, N. Fuentes, B. Vivanco Allende, C. García Pravia, M. Balbín Felechosa, M. F. Fresno Forcelledo
*Oviedo, Spain

Objective: There is a significant percentage of patients with breast cancer and HER2 receptor overexpression that do not respond to trastuzumab-directed therapy. The aim of this paper is to study the alterations of one of the HER2 signalling pathways related to trastuzumab response in breast cancer.
Method: The study comprised 127 cases of breast carcinoma in different stages of evolution with HER2

overexpression (HercepTest 3+) or gene amplification (FISH). All patients were treated with trastuzumab. The assessment of PTEN and pAkt expression was based on staining intensity and percentage of stained cells. We also determined the molecular alterations in PIK3CA.
Results: Our series showed a statistically significant association between a positive expression of PTEN and the absence of PIK3CA mutations with better overall survival from treatment onset with trastuzumab (p=0.022 and p= 0.003, respectively). The association with the expression of pAkt was statistically significant if survival is evaluated from the pathological diagnosis of the tumor (p=0.043), pAkt positive tumors had worse survival.
Conclusion: PTEN expression and PIK3CA mutations could be considered prognostic biomarkers in trastuzumab-treated breast cancer. The relationship with pAkt expression depends on other factors, not just the mechanism of action of trastuzumab.

PS-17-030
Mammaglobin expression in primary breast cancer and corresponding metastases
J. Ferrer Lozano*, O. Burgués, J. Furriol, M. J. Nicolau, J.-A. Pérez Fidalgo, P. Eroles, A. Bosch, B. Bermejo, A. Lluch
*Hospital Clínic - INCLIVA, Dept. of Pathology, Valencia, Spain

Objective: Expression of mammaglobin A (MG-A) in breast cancer has been reported to be of prognostic value and to be associated to hormone receptor-positivity. MG-A is also useful in the diagnosis of metastatic breast cancer. The present study evaluates the differential MG-A expression in two subsets of primary breast cancer (metastasizing vs. non-metastasizing) and in their correspondent metastases.
Method: Immunohistochemical analysis of MG-A (clone 304-1A5) was performed in 55 non-metastasizing primary breast tumors and 19 paired primary and metastatic breast cancers. A percentage of 1 % of stained tumor cells was considered positive. The expression of MG-A in the different groups, together with other clinicopathologic factors (grade, size, hormone receptors, HER2, etc.) was analyzed by t-test.
Results: Expression of MG-A was significantly higher in estrogen receptor-positive (ER+) tumors (p<0.003). A trend was noted for ER + metastasizing primary breast cancers to show a higher expression of MG-A, compared to those non-metastasizing (p=0.064). No significant differences were noted in the expression of MG-A between metastasizing primary tumors and their correspondent metastases, with a good correlation (p=0.033).
Conclusion: These results suggest that MG-A might be of prognostic value in determining a subset of ER + breast cancers prone to progression. Larger series are needed to confirm these observations.

PS-17-031
Concordance of St. Gallen intrinsic subtypes in core biopsies and related surgical specimens of breast cancer
C. M. Focke*, T. Decker
*Dietrich Bonhoeffer Klinikum, Abt. Pathologie, Neubrandenburg, Germany

Objective: To evaluate the relevance of intrinsic breast cancer subtyping (IBCS) on core biopsies (CB).
Method: IBCST was performed on CB and related surgical specimen (SSP) of 398 breast cancers according to the clinicopathological criteria of the St. Gallen Consensus 2011. To discriminate Luminal A and Luminal B Her2 negative tumors we used the Mitotic Activity Index with a cut-off of ≥10 for high proliferation (WHO 2003, Baak 2008). Agreement rates of CB and SSP and positive predictive values (PPV) of CB based IBCS were calculated.
Results: IBCS of SSP came out with 52 % Luminal A, 22 % Luminal B Her2neg, 6 % Luminal B Her2+, 2 % Her2+, 11 % Triple-negative, and 8 % Special Type. The CB/SSP-agreement rate of IBCS was complete with exception of Luminal B with only 33 %. Accordingly, the PPV of CB based Luminal A was 78 % whereas IBCS for all other types was 100 %. Both exceptions are due to underestimation of proliferation in CB.
Conclusion: Agreement of IBCS in CB and SSP and the PPVs of CB based IBCS are generally high. This means that IBCS on CB specimen can be used for preoperative decision making in the vast majority of cases.

PS-17-032
HER2 testing in Russia: The results of the 10 years of experience. ASCO/CAP recommended score system
G. Frank*, L. E. Zavalishina, J. J. Andreeva, A. E. Matsionis, S. V. Sazonov, I. J. Vinogradov, S. V. Petrov, E. E. Leenman, S. B. Glatko, M. Z. Gorelik
*Research Oncology Institute, Dept. of Pathomorphology, Moscow, Russia

Objective: We analyzed using of score system criteria for HER2 testing in breast cancer.
Method: In 2001–2011 176028 new invasive breast cancer cases were investigated in Russia. IHC testing was made using HER2 antibody (A0485, Dako and Confirm HER2 Ventana) in 79 regional laboratories, samples were retested in 8 reference centers with HerceptTest (Dako). Equivocal results IHC (2+) were retested using ISH: FISH (Dako), BDISH (Ventana). Scoring criteria was 10 % of tumor cells (till 2009) and 30 % of tumor cells according to the ASCO/CAP recommendations (2010).

Results: 39384 samples were tested in 2009. Score 0 was found in 45.43 % cases, 1+ in 28.86 %, 2+ in 12.97 %, 3+ in 14.73 %. The amplification was revealed in 32.12 % of 2+ cases, 15.82 % tumors were 3+/FISH+. 43485 cases were tested in 2011: score 0 −38.42 %, 1+ 30.61 %, 2+ 15.65 %, 3+ 15.32 %. The amplification was seen in 28.17 % 2+ cases and 18.68 % tumors became 3+/FISH+. There was no significant distinction using 10 % and 30 % cells score system for 3+ tumors, whereas for groups 1+ and 2+ it was.
Conclusion: ASCO/CAP scoring criteria developed in 2007 have no effect on HER2-positive tumors detection but increases number of cases with equivocal result, what require retesting with ISH.

PS-17-033
Microvessel density in triple-negative breast cancer: Characteristics and prognostic implications
H. Gobbi*, M. De Brot, R. Rocha, F. Soares
*UFMG, Dept. of Anatomic Pathology, Belo Horizonte, Brazil

Objective: We assessed topography and characteristics of blood vessels in triple-negative breast cancer (TNC) and examined their association(s) with clinicopathological features, basal-like phenotype and influence on patient prognosis.
Method: Blood vessels were assessed in tissue sections from 133 TNCs stained for CD34. Slides were scanned using ScanScope® XT and analysed with Aperio ImageScopeTM, Microvascular Density v1 algorithm. Microvessel density (MVD) was assessed in three areas: intratumoural (IT), peripheral tumoural (PP) and peritumoural (PT), and correlated with clinicopathological features and prognosis.
Results: The majority of blood vessels were located largely at the peripheral tumoural and peritumoural areas. Tumours with higher total MVD and PT-MVD were significantly associated with the presence of recurrence (p=0.05; 0.01), distant metastasis (p=0.01; 0.005), hematogenous metastasis (p=0.006; 0.01); and shorter overall survival (OS; p=0.006; 0.01) and disease free interval (DFI; p=0.04; 0.09). High PT-MVD correlated with a higher stage at diagnosis (III and IV; p=0.02), lymph node (LN) metastasis (p=0.04), basal-like phenotype (p=0.01), high histologic grade (p=0.05), presence of distant metastasis (p=0.02), and shorter OS (p=0.01).
Conclusion: Blood vessels are mainly located at the peritumoural and peripheral areas in triple negative breast cancers and seem to have a major role in tumour progression by representing means for disease dissemination.

PS-17-034
Expression of CD44 and CD24 in primary ductal invasive carcinoma of breast and metastatic lymph nodes
M. Gudadze*, K. Kankava, T. Javakhishvili, M. Sarishvili, G. Burkadze
*Central University Clinic, Dept. of Pathological Anatomy, Tbilisi, Georgian, Republic of Georgia

Objective: Cancer stem cells are believed to have certain role in progression, metastatic potential and outcome of ductal invasive carcinoma of breast.
Method: The archived materials of 2008–2012 years from the Department of Pathological Anatomy, N. Kipshidze Central University Clinic were used for the research. 196 cases of ductal invasive carcinoma were chosen for the study. The CD44, CD24 immunohistochemistry (Biocare Medical) was used for staining. Evaluation was performed using SPSS software.
Results: The results showed: 68.5 % of grade II cases and 90.5 % of grade III cases were lymph node positive. CD24 positivity in grade II tumors was seen in 29.6 % of primary site and 45.9 % of metastasis; in grade III tumors-50 % of primary site and 55.2 % of metastasis. CD44 positive cases in grade II-48.1 % for primary tumor and 27 % in metastasis, for grade III- 73.8 % for primary tumor and 39.4 % for metastasis.
Conclusion: The results show that CD44 positivity is significantly less frequently seen in metastasis than in primary tumor; CD24 positivity is more frequently seen in metastasis for grade II cases. This indicates, that cells with stem cell phenotype decrease in metastasis reflecting heterogeneity between primary and metastatic sites, which should be taken into consideration for assessing progression and treatment.

PS-17-035
Solid neuroendocrine breast carcinoma: Three case reports
B. Ince Alkan*, S. Yuksel, E. Kadan, S. Percinel, S. Dizbay Sak
*Ankara University, Turkey

Objective: It seems that neuroendocrine breast carcinoma (NEBC) is underrecognized in routine practice. 2003 World Health Organization classification of tumors of the breast defined NEBC as a subtype of invasive mammary carcinoma in which >50 % of the tumor cells express neuroendocrine markers. Three cases compatible with solid NEBC are discussed with an emphasis on identifying features useful in recognition of this tumor type.
Results: The patients were 35, 55 and 57 years old women. All patients presented with a palpable mass, two in the right and one in the left breast. Microscopically, infiltrating, solid cohesive nesting pattern with delicate sinusoidal vasculature

or peliosis and papillary pattern were observed. The tumor cells were round or polygonal with abundant granular, eosinophilic cytoplasm. The nuclei had hyperchromatic/vesicular or "salt and pepper" chromatin. Two cases had ductal carcinoma in situ component. All cases were positive for synaptophysin and chromogranin A in >50 % of tumor cells. While a positive status for estrogen receptor was detected in all cases, progesterone receptor was observed in two cases. None of the tumors displayed HER2 overexpression.
Conclusion: Morphological clues suggestive of NEBC must be recognized for immunohistochemical confirmation for appropriate classification of this clinically distinct subtype of invasive breast carcinoma.

PS-17-036
Comparison of automated and manual FISH for evaluation of HER2 gene status on breast carcinoma core biopsies
W. Jochum*, C. Öehlschlegel, D. Kradolfer, M. Hell
*Kantonsspital St. Gallen, St. Gallen, Switzerland

Objective: Automation of HER2 FISH may improve HER2 gene testing. The aim of our study was to evaluate an automated HER2 FISH assay for assessing the HER2 genomic status.
Method: Core biopsies of 100 invasive breast carcinomas were analysed in parallel using the manual PathVysion™ HER-2 DNA Probe Kit and the automated Leica HER2 FISH System for the BOND™ instrument. To assess inter-method agreement, concordance analysis was performed for various numerical and categorical parameters.
Results: Carcinomas with all HER2 immunohistochemical scores were included (0+: 20; 1+: 20; 2+: 30; 3+: 30). Using either HER2/CEP 17 ratio >2.2 or ≥2.0 as criterion for HER2 amplification, high levels of concordance were observed between automated and manual FISH (concordance rate 96 %, K coefficient 0.92). High levels of inter-method agreement were also found for HER2 copy number, CEP17 copy number, HER2/CEP17 ratio, the percentage of carcinoma cells with HER2/CEP17 ratio >2.2, and the presence of HER2 genetic heterogeneity, HER2 clusters and CEP17 polyploidy.
Conclusion: HER2 testing using automated FISH is feasible on breast carcinoma core biopsies. Automated HER2 FISH using the Leica HER2 FISH System for BOND is an alternative to manual HER2 FISH in evaluating the HER2 status of primary invasive breast carcinomas.

PS-17-037
Myofibroblastoma of the breast: Presentation of three cases
E. Kairi-Vasilatou*, C. Dastamani, A. Tsagkas, A. Paraskeva, A. Kondi-Pafiti
*Aretaieio Nosokomeio University, Dept. of Histopathology, Athens, Greece

Objective: Myofibroblastoma is a rare, usually solitary, benign spindle cell tumour composed of myofibroblasts. It affects both genders equally.
Method: Three cases diagnosed in our laboratory are presented.
Results: Two patients were postmenopausal females (53 and 75 years old) and one was male (55 years old). The tumour was 1,6 cm in greatest diameter in the first case, 7 cm in the second and 2 cm in the third. Microscopically, all neoplasms were circumscribed and consisted of uniform, bland spindle cells separated by broad bands of hyalinized collagen. The neoplasmatic cells had abundant eosinophilic cytoplasm, oval nuclei and were arranged in fascicles. Cellular atypia was found only in one case and mitoses were scarce. Immunohistochemically, all neoplasms were strongly positive for vimentin, CD34 and Bcl-2, while the expression of desmin and SMA varied. S-100 protein was negative. The neoplasms of the female patients were strongly positive for ER and negative for PgR. The stains for estrogen and androgen receptors were not carried out in the case of the male patient.
Conclusion: Differential diagnosis can be complex. Fibromatosis of the breast, nodular fasciitis, myoepithelioma, myofibrosarcoma, solitary fibrous tumor, inflammatory myofibroblastic tumour should be excluded based on the histological and immunohistochemical findings.

PS-17-038
Morphological analysis of stromal population of mast cells in breast cancer
L. Kakturskiy*, M. Mnikhovich
*Institute of Human Morphology, Central Laboratory of Pathology, Moscow, Russia

Objective: Mast cells in breast cancer are not studied enough.
Method: Using light- and transmission electron microscopy fragments of mammary gland tumors, received intraoperative, from 58 patients 26–82 years with infiltrative ductal breast cancer were studied.
Results: Most of the mast cells were localized in the areas of infiltrative growth, at a background of lymphohistiocyte infiltration and in peripheral part of the tumor. Intratumourous mast cells were totally degranulated. The mast cells with intact structure at a background of cells and tissue destruction were also in mammary gland. In destructive mast cells the nucleus with electron-dense circle and chain of granules were observed. On transmission electron microscopy their deformations and the decrease of density were revealed. The mast cells were of elongated of rounded shape with large nucleus and invaginations of karyolemma. The nucleus occupies almost completely the cell's area. It has a ring of large but pale granules. Small protuberances were observed

on the surface of the cell membrane. Their number decreased in direct proportion to the size of must cells and their remoteness from microvessels. Such protuberances are necessary for mast cells in moving. Destructively changed cells with the signs of swelling, vacuolization and clasmatosis were frequent in breast cancer.

PS-17-039

Study of the effect of concurrent mutations of HER-2 and TP53 on angiogenesis of invasive ductal carcinoma and other tissue prognostic factors

E. Keyhani*, A. Muhammadnejad, F. Behjati, F. Aghakhani Moghaddam, E. Darabi, R. Pazhoomand
*University of Social Welfare, Genetics Research Center, Tehran, Iran

Objective: Determination of eligibility of breast cancer patients for treatment with anti-angiogenic drugs has been always considered as a challenge for oncologists. Each mutation in the genes of proliferation phase enhances the angiogenesis of tumor. We aimed to determine the effect of concurrent mutations of HER-2 and TP53 on angiogenesis.
Method: 32 Women affected by invasive ductal carcinoma (IDC) sporadic breast cancer were included. Immunohistochemical study was performed with HER-2, TP53, Ki-67 and AnnexinV markers. Angiogenesis index was semi-quantitatively calculated by MVD-CD34 technique. Statistical associations between parameters were evaluated.
Results: Prevalence of HER-2 positive and TP53 positive cases were 21.4 % and 20.0 %, respectively. 6.5 % of patients showed concurrent mutation of these genes. Concurrent mutation led to significant increases in both angiogenesis and proliferation and a significant decrease in apoptosis. There was no statistically significant association between concurrent mutation and tumor grade.
Conclusion: This study demonstrates that most of the tissue prognostic factors are poor in concurrent mutation of both genes. Also, our study illustrates that the concurrent mutation correlates with a higher angiogenesis and thus an increased risk of recurrence. We can conclude that in priority setting for administration of anti-angiogenic agents, patients with concurrent mutations are more eligible.

PS-17-040

Adenoid cystic carcinoma in male breast: A case report

E. Kimiloglu Sahan*, U. Karinoglu, A. Akyildiz Igdem, N. Erdogan
*Taksim´s Hospital, Dept. of Pathology, Istanbul, Turkey

Objective: Adenoid cystic carcinoma of the breast is a rare variant of breast cancer that accounts for 0.1 % of all breast carcinomas and occurs commonly in women between the ages of 25 to 80. In the literature, only a few examples have been reported in men. It is well-differentiated tumour with favorable prognosis and generally presents as a painful breast mass.
Method: Here, we are presenting a 60 years old male patient with a 13×8 mm diameter solid mass on left breast retroareolar region. On fine needle aspiration biopsy, there were 'atipical proliferating ductal epitelial groups'. Then, hookwire localization and excision have been performed. Microscopically, there were tubulary and cribriform islands composed of basaloid type cells with eosinophilic cytoplasm and myxoid material in the cribriform spaces at the center of the islands. We used immunohistochemical markers such as P 63, S 100, CK 7, CD 117, CK 14 and Smooth Muscle Actin for differential diagnosis.
Results: The diagnosis was 'Adenoid Cystic Carcinoma'. The margins of the tumor were positive, so radical mastectomy was performed for treatment.
Conclusion: Because adenoid cystic carcinoma of the breast in male is a very rare example, we present our case here.

PS-17-041

Comparison between the Bond Oracle HER2 immunohistochemical system, the polyclonal HER2 Dako antibody and Chromogenic In Situ Hybridization in breast carcinoma

H. Kourea*, V. TzelepiI, I. Nikolatou, P. Ravazoula, V. Zolota
*University of Patras, Dept. of Pathology, Greece

Objective: The sensitivity and specificity of immunohistochemical (IHC) methods for HER2 testing are very important given the therapeutic implications. This study compares the concordance between Oracle and the HER2 Dako polyclonal antibody (HER2), in breast carcinomas (BCs) that were equivocal (2+ or not evaluable/NE), by HER2 staining, considering as gold standard the chromogenic in situ hybridization (CISH).
Method: BCs (n=34), problematic by HER2 staining (1−2/2+ or NE), and studied by CISH in our institution, and 24 additional consecutive BCs were stained with HER2 and Oracle, and scored separately by three pathologists. Consensus scoring for each IHC method and CISH results were recorded. Descriptive statistics and measurement of the Cohen's Kappa coefficient were performed.
Results: The overall agreement between the 2 tests in a 3×3 analysis shows a concordance in 62 % of cases (κ=0.405). Among the cases studied by CISH, equivocal were 26 and 11 cases, for HER2 and Oracle, respectively. Seventeen HER2 equivocal cases were negative with Oracle and CISH. In problematic cases, using CISH as gold standard, the sensitivity, specificity, positive and negative predictive values for HER2 and Oracle were 100, 20.7, 17.9, 100 and 100, 72.4, 38.5, 100, respectively.

Conclusion: In problematic cases, Oracle testing shows higher specificity and positive predictive value.

PS-17-042

Stromal P53 and Ki67 expressions of the mammary phyllodes tumors: Are they the clues in determination of tumor grade?

U. Kucuk*, U. Bayol, E. E. Pala, S. Cumurcu
*Tepecik Training Hospital, Dept. of Pathology, Izmir, Turkey

Objective: Conventionally growth pattern, stromal overgrowth, stromal cellularity, stromal mitotic activity are the main parameters in grading of phyllodes tumors. Recent studies revealed that P53 and Ki67 expressions are both correlated with grade of phyllodes tumors of the breast.
Method: We searched for p53 and Ki67 expression rates of benign and malignant phyllodes tumors in our archival data and correlated them with conventional parameters such as stromal cellularity and mitotic activity rates. 17 benign, 9 malignant phyllodes tumors were reevaluated as regards stromal cellularity (low/moderate and high), mitotic activity (low and high), p53 expression (low, moderate, high), Ki67 expression (low and high) rates. Statistical correlation amongst the whole parameters were searched with Chi-Square test.
Results: Stromal cellularity, mitotic rate, p53 and Ki67 expression rates were all closely correlated (p=0.000–0.001) for benign and malignant histologic subgroups. Ki67 expression was significantly correlated with histologic subgroups, stromal cellularity and mitotic rate (p=0.000–0.001). Similarly P53 expression was correlated with histologic subgroups, stromal cellularity and mitotic rate (p=0.000–0.002).
Conclusion: Both Ki67 and p53 expression rates are statistically significantly correlated with grade of mammary phyllodes tumors, so they can be used in determination of tumor grade, especially for differential diagnosis of benign and malignant ones.

PS-17-043

Quantitative measure proliferative markers by image analysis of invasive ductal carcinoma

A. Kudaybergenova*, S. Kalantarli
*RSCRCT, Dept. of Immunohistochemistry, St. Petersburg, Russia

Objective: We analyzed a total number of tumor cells) in invasive ductal breast carcinoma, proliferative activity (% Ki67-positive cells) and mitotic index (% phh3 – positive cells) to establish absolute quantity tumor cells per sq.mm of histological slide and relations this measure with proliferation and mitosis.
Method: The study included 46 patients diagnosed with breast carcinoma from Baku Oncology Hospital during the 2001–05. After whole slide scanning by Mirax scanner (3DHistech, Budapest) of HE, Ki67 and phh3 stained slides we juxtaposed all three slides in one screen to the found area with maximal ki67 level in tumor and the corresponding area in other slides. Morphometric analysis was performed using the Pannoramic Viewer software (3DHistech, Budapest). For each case we analyzed a total number of tumor cells in1 mm2, number of Ki67 and phh3 positive cells.
Results: Mean tumor cells in 1 mm2 of histology slide was 4180+\\−251 cells, median – 3976 cells, 1185+\\−166 (31 %) were positive for Ki67 and 124+\\−23 (3 %) were in mitosis. There was moderate correlation between cell density and Ki67 r=0,44 (p=0,0032) and phh3 r=0,42 (p=0,0018).
Conclusion: By analysis of breast cancer, was established a total tumor cell per mm2 and main proliferative characteristics for invasive ductal carcinoma.

PS-17-044

Malignant adenomyoepithelioma of the breast

S. Y. Kwon*, Y. N. Kang, M. Choe, H. R. Jung, I. Hwang, J. Y. Park
*Dongsan Medical Center, Pathology, Daegu, Republic of Korea

Objective: Adenomyoepithelioma of the breast is a very rare benign tumor with biphasic proliferations of epithelial and myoepithelial elements. It is morphologically and immunohistochemically identical to epithelial-myoepithelial cell carcinoma of the salivary gland. The histologic criteria of malignant AME is not well-established because of the rarity of AME. We report a case of malignant adenomyoepithelioma in a 65-year-old woman.
Method: On ultrasonography, a well-marginated and lobulated solid mass was found at LIQ of the right breast.. An ultrasono-guided core biopsy was performed. The diagnosis of core biopsy was myoepithelial lesion. She subsequently underwent a wide local excision of the lesion.
Results: Microscopically the tumor mass was composed of biphasic patterns which showed formation of tubules lined by an inner layer of ductal epithelial cells surrounded by proliferation of myoepithelial cells that also formed solid nests. But this tumor had foci of infiltrating margins and proliferation of spindle cell components. Also noted are numerous mitotic figures and increased mylepithelial Ki-67 positivity (10–15 % of tumor cells).
Conclusion: Breast lesions which have predominently myoepithelial cells can be divided into myoepithelial hyperplasia, adenomyoepithelioma and malignant adenomyoepithelioma. Tavassoli divied AME into tubular, papillary, and solid subtypes. The criteria of malignant AME is not well-established but some criterias can apply to make a diagnosis of malignant AME.

PS-17-045

Association among residual cancer burden, molecular subtype, and chemosensitivity-related protein expression in breast carcinoma treated with neoadjuvant chemotherapy

H.-C. Lee*, H.-S. Ko, H.-S. Seol, D.-Y. Noh, T.-Y. Kim, S.-A. Im, I.-A. Park
*Chungbuk National University, College of Medicine, Cheongju, Republic of Korea

Objective: Neoadjuvant chemotherapy (NACT) is available for patients with breast carcinoma. However, resistance to chemotherapy is still a main cause of mortality.
Method: Differentially expressed genes were identified from previously published studies that examined chemoresistant and chemoresponsive cell lines or patients with breast carcinoma. The expression of 14 selected gene products was assessed in tissue microarray slides comprising 75 post-NACT resection specimens from breast carcinoma patients using immunohistochemistry, and analyzed according to the molecular subtype and Residual Cancer Burden (RCB) grade.
Results: Most cases were positive for ABCB1 (97.7 %) and MYC (96.0 %), but negative for TOP2A (100 %). RCB-II cases expressed much higher levels of MUC1 (p=0.011) and CLU (p=0.021) than RCB-III cases. Positive expression for CALR (p=0.002) and LGALS3 (p=0.018) was observed more often in triple negative types than in luminal types, and cytoplasmic CDKN1B expression was observed more often in luminal types (p=0.014).
Conclusion: Positive expression of ABCB1 and MYC and negative expression of TOP2A in the residual carcinoma after NACT implies general resistance to NACT. Expression of CALR, LGLAS3 and cytoplasmic CDKN1B may be associated with resistance depending on the subtype. Expression of MUC1 and CLU can be used to predict the RCB grade or response to NACT.

PS-17-046

Primary and metastatic melanoma of the breast-review of 4 cases

I. Liepniece-Karele*, L. Osipova, M. Sperga, S. Isajevs, A. Grjunbergs, J. Eglitis
*Riga ECUH, Dept. of Pathology, Latvia

Objective: Primary breast melanoma is a very rare tumour accounting for <5 % of all malignant melanomas. The malignant melanoma can be with different manifestation in the breast (primary breast tissue or primary breast skin melanoma as well as metastatic melanoma).
Method: In this study 4 cases of breast melanoma were identified from our records of the past 3 years (0.41 % of all breast cancer cases). A histological and an immunohistochemical (IHC) study was performed using antibodies against CKAE1/3, HMB-45 and Melan-A on both the biopsy and operation material.
Results: Obtained results showed that in 3 cases pigmented, epitheloid and spindle cell melanoma, but in one case epitheloid cell amelanotic melanoma was found. By IHC the melanoma cells expressed HMB45 in three cases, melan-A and S100 in all cases. No expression of CKAE1/3 was observed.
Conclusion: Careful histological and immunohistochemical examination of malignant tumour is essential for adequate diagnosis, follow-up and treatment of breast melanoma.

Age,year	The manifestation of melanoma in the breast	Location	Treatment	Follow-up status
48	Melanoma metastasis to the breast 5 years after primary surgery	Left and right breast, multiple	INF2α	Died after 14 months with distant metastasis
49	Melanoma metastasis to the breast from unknown primary site	Right breast, 1.8 cm diameter	Mastectomy+ ALND	Alive for 2 years with distant metastasis
59	Melanoma metastasis to the breast from unknown primary site	Left breast	Biopsy, INF2α	Disease free for 11 months
71	Primary melanoma of the breast skin	Left breast with ulcerated tumour, 12.0 cm diameter	Mastectomy+ ALND	Disease free for 15 months

PS-17-047

Stem cell expansion in ductal carcinoma in situ of breast

C. Lopes*, A. Paula, O. Marques, A. Rosa, A. Rema, F. Carvalho
*ICBAS, Dept. of Pathology, Porto, Portugal

Objective: The aim is to study the ability of a cell marker panel - ALDH1, CD44 and Ki67 – to identify breast stem cells in no malignant and ductal carcinoma in situ.
Method: Double-color triple-immunohistochemistry - to ALDH1, CD44 and Ki 67 - was done in 169 paraffin

embedded tissue specimens from 111 patients arrayed in tissue microarray blocks. Statistical was done using Chi-square probability test: differences were considered significant when $p<0.05$.

Results: Significantly higher immunoreactivity was seen in DCIS than in benign lesions of breast ($p<0.01$) with used markers. In a total of 169 specimens, CD44+/ALDH1+/Ki67- cells were identied in 110 cases. The distribution was as follows: DCIS (79/57); fibroadenoma (45/29), Atypical hyperplasia (23/13); other benign lesions (22/11) Individually, expression of ALDH1 was: DCIS - 72/79; FAD - 45/45; ADH - 23/23; OBL - 21/22. For CD44: DCIS - 77/79; FAD - 44/45; ADH - 22/23; OBL - 21/22. For Ki67: DCIS - 67/79; FAD - 43/45; ADH - 22/23; OBL - 21/22. The expression values of ALDH1 and Ki-67 were significantly higher in DCIS than in benign lesions ($p=0.028$ and $p<0.01$).

Conclusion: Stem cell expansion is higher in DCIS than in non malignant, supporting their participation in the carcinogenesis of the breast.

PS-17-048

Expression of Calcium Sensing Receptor (CaSR) in patients with disseminated breast cancer

H. Majewska*, P. Winczura, K. Mielcarek, B. Pieczynska, J. Lakomy, A. Badzio, J. Jassem, W. Biernat
*Medical University of Gdansk, Dept. of Pathology, Poland

Objective: Data from in vitro and clinical studies suggest that CaSR expression can be associated with the development of bone metastases. Most probably CaSR stimulates production and secretion of PTHRP via EGFR pathway. The aim of our study was to assess expression of CaSR in the primary breast cancer and correlate it with the risk of bone metastases.

Method: We have analysed 170 patients with the breast cancer. Bone metastases were diagnosed in 102 cases, 68 patients died without skeletal involvement (control group). CaSR expression was assessed in primary tumors using tissue microarray (TMA) and immunohistochemical technique (polyclonal antibody Pierce Bio. PA1-37213). To evaluate cytoplasmatic CaSR expression we have used 0–1 point scale in which 1 was defined as uniformly strong or medium staining in more than 50 % of tumor cells.

Results: Strong or medium staining in more than 50 % was identified in most studied cases, however it was more predominant in patients diagnosed with bone metastases than in the control group (93,14 % vs 83,82 %), $p=0,053$.

Conclusion: Expression of CaSR is common in primary tumors of patients with disseminated breast cancer irrespectively of the metastatic site. However, the patients with bone involvement have higher rate of expression, that is borderline significant statistically. As a result, a group of patients with very high risk of bone dissemination might be separated.

PS-17-049

Bcl2 expression is associated with centromere 17 alterations in luminal B breast cancer

A. Matsionis*, I. Pavlenko, A. Petrov
*Rostov Refional Institute, Dept. of Experimental Pathology, Rostov Regional Institute

Objective: Bcl2 is an important established prognostic parameter in human breast cancer (BC) and chromosome 17 centromere (CEP17) copy number is proposed to be the same too. We evaluated Bcl2 expression in different BC's molecular subtypes in relation to increased CEP17 level (CEP17>3 per nucleus).

Method: Immunohistochemistry for Bcl2 assessment and fluorescence in situ hybridization for detection of CEP17 alterations were used. Statistical analysis was performed with Fisher's exact test.

Results: A total of 226 cases of female invasive BC's were analyzed (2010–2011). The tumour subtypes were as follows: luminal A (ER/PR+, Her2/neu-, Ki67<14 %) – 118; luminal B (ER/PR+, Her2/neu-, Ki67>14 % or ER/PR+, Her2/neu+) – 62; Her2/neu+(ER/PR-, Her2/neu+) – 24; triple-negative - 20. In our study group, Bcl2- cases were preferentially ER- in agreement with previous reports. However, 20,5 % tumours of luminal B subtype were Bcl2- too and all of them had increased CEP17 copy number ($p=$ 0,0011, $r\varphi=0,57$). We therefore hypothesized that not only ER had influenced Bcl2 in luminal B BC but CEP17 alterations also.

Conclusion: Centromere 17 alterations are associated to bcl2 downregulation in luminal B BC's. The mechanisms responsible for that remain to be established but the underlying cause could be promoter methylation or transcriptional repression.

PS-17-050

Outcome of excision of radial scar diagnosed on core biopsy: A single centre analysis

F. Menezes*, M. Caldas, N. Coimbra, C. Leal
*IPO Porto, Dept. de Anatomia Patologica, Portugal

Objective: Radial scar (RS) is a sclerosing lesion of the breast which may be associated with a spectrum of epithelial proliferative lesions and carcinoma. It is frequently subject to biopsy when presenting as a mammographic abnormality. The need to excise RS diagnosed on core biopsy (CB) remains controversial. The aim of our study is to determine the frequency of upgrade in diagnosis after excision of RS.

Method: A retrospective study of RS diagnosed on CB in our department between 01/01/2000 and 31/12/2011 was performed.

Results: 117 cases were retrieved, all women, with a median age of 53 years. Of these, 101 pairs of CB/resection specimens were obtained. CB diagnosis was RS without atypia in 79 cases, RS with atypia in 19 cases and RS with in situ carcinoma in 3 cases. After excision, 21/79 (26,6 %) cases diagnosed as RS without atypia were upgraded: 17 to atypia, 3 to in situ carcinoma and 1 to invasive carcinoma. Of those cases diagnosed on CB as RS with atypia, 9/19 (47,4 %) were upgraded: 8 to in situ carcinoma and 1 to invasive carcinoma.
Conclusion: Our results support the excision of all lesions diagnosed on biopsy as RS. *FM and MC are joint first authors.

PS-17-051
Outcome of excision of papillary lesions diagnosed on core biopsy: A single centre analysis
F. Menezes*, M. Caldas, N. Coimbra, C. Leal
*IPO Porto, Dept. de Anatomia Patologica, Portugal

Objective: Papillary lesions of the breast (PLB) comprehend a spectrum of entities with different morphologies and malignancy risk, which present a diagnosis challenge on core biopsy (CB). Although diagnostic accuracy has improved with immunohistochemistry, the need to excise benign PLB remains controversial. The aim of our study is to determine CB diagnosis accuracy in PLB, and subsequent need to excise all lesions.
Method: A retrospective study of PLB diagnosed by CB in our department between 01/01/2000 and 31/12/2011 was performed.
Results: 96 cases were identified, with a median age of 59 years. CB diagnosis was benign in 66 cases, some kind of atypia found in 10, and malignant lesions ('in situ' and encysted/invasive types of carcinoma) in 20. Surgical excision was performed on 70 cases, including all cases with carcinoma. Following excision, 6/42 and 4/42 benign CB results were respectively upgraded to atypical and malignant; 3/8 with atypia were upgraded to malignant. Overall, 14 % (7/50) of benign and atypical PLB CB diagnosis therefore missed malignancy.
Conclusion: Our results show that, despite good correlation between CB and excision diagnosis, some cases of carcinoma are missed on CB, so the excision of all PLB remains advisable. *FM and MC are joint first authors.

PS-17-052
Myoepithelial carcinoma of the breast: A case report
I. Michalopoulou Manoloutsiou*, B. Christoforidou, P. Xirou, V. Bostani, E. Goupou, I. Themeli, F. Patakiouta
*Theagenion Hospital Thessaloniki, Dept. of Pathology, Greece

Objective: Myoepithelial carcinoma of the breast is an extremely rare tumor, composed purely of myoepithelial cells, predominantly spindle, with identifiable mitotic activity.
Method: We report a case of a 50 year-old female patient with a palpable, well demarcated lump in her left breast, measuring 3,5 cm in its maximal diameter. Surgical excision and axillary lymph node dissection were performed.
Results: Histologically, the tumor displayed an infiltrating growth pattern and consisted of spindle cells, that appear to emanate from myoepithelial cells of ductules entrapped in the center of the lesion. Mitotic activity did not exceed 5 mitotic figures/10 HPF. Immunohistochemically, the tumor cells revealed positivity for p63, cytokeratin 5/6, cytokeratin 34βE12, smooth muscle actin, CD10 and S100 protein, whereas they were negative for desmin, cytokeratin 7, CD34, HMB45, estrogen, progesterone receptors and Her-2 oncoprotein. Approximatelly 25 % of tumor cells showed nuclear positivity for MIB-1/Ki-67. All axillary lymph nodes were free of metastases.
Conclusion: Myoepithelial carcinoma of the breast is a potentially highly aggressive neoplasm and its differential diagnosis is fairly broad, including metaplastic spindle cell carcinoma and a variety of myofibroblastic lesions.

PS-17-055
Differential expression of biomarkers in stromal and epithelial cells from invasive primary ductal breast carcinomas and paired lymph node metastasis
F. Mundim*, F. Pasini, S. Nonogaki, F. Soares, M. Brentani, A. Logullo
*UNIVAS, Dept. of Pathology, Pouso Alegre, Brazil

Objective: We investigated the differential expression of several biological markers between primary invasive breast carcinomas and their paired lymph node metastasis analyzing separately epithelial and stromal components.
Method: Representative samples of 42 IDC and paired compromised lymph nodes were arrayed in a TMA and 15 selected markers: hormonal receptors, HER-1, HER-2, proliferation (p53, c-myc, pAKT, pmTOR, TGFβ1), motility (CD9 and CXCR) and basal markers (CK5, CK14, c-kit) were evaluated by IC.
Results: In the primary tumor, p53, MIB-1, TGFβ1, CD9 and CXCR4 were more expressed in epithelial cells ($p<0.05$), while pAKT, pmTOR, c-myc and c-kit showed a similar frequency in both components. Hormone receptors, HER-1/HER-2 and cytokeratins were not expressed in stromal cells. The proliferative biomarkers were concordant in the epithelial component. CD9 frequency was similar but cytoplasmic CXCR4 as opposite to nuclear was predominantly expressed in lymph nodes ($p=0.008$). Stromal cells from lymph node showed a reduced frequency of CD9 ($p=$

0.029) and c-myc (p=0.003) when compared to the stromal component of primary tumors.
Conclusion: Epithelial CXCR4 expression may facilitate lymph node metastasis whereas the low frequency of c-myc and CD9 in the lymph node stromal component indicated decreased proliferation enhanced motility of stromal cells in this site.

PS-17-056
Expression of hypoxia-inducible factor-1a and associations with vascular endothelial growth factor expression, high microvessel density and features of aggressive tumors in African breast cancer
H. Nalwoga*, J. B. Arnes, H. Wabinga, L. A. Akslen
*University of Bergen, The Gade Institute, Norway

Objective: Breast cancer in Africans is reported to have poor clinical outcome. Whereas hypoxia-inducible factor-1α (HIF-1α) expression has been linked to treatment failure and poor prognosis in breast cancer, there is a lack of reports about HIF-1α expression in Africans. The aim of this study was to evaluate HIF-1α expression in relation to vascular endothelial growth factor (VEGF) expression, angiogenesis, and other tumor characteristics in an African population.
Method: In total, we analyzed 192 breast cancers by immunohistochemical staining. We determined microvessel density (MVD), proliferating microvessel density (pMVD), and vascular proliferation index (VPI) in the most vascularized areas as well as expression of HIF-1α and other biomarkers using tissue microarrays.
Results: Expression of HIF-1α (in 128/182 tumors; 70 %) was associated with VEGF expression (p<0.0005), MVD (p=0.037), high tumor grade (p=0.001), high Ki-67 proliferative rate (p<0.0005), and p53 expression (p=0.032).
Conclusion: There is a high expression of HIF-1α in this series of breast cancer which is strongly associated with VEGF expression and increased MVD. More studies are required to assess the therapeutic implications of HIF-1α expression in this population.

PS-17-057
Breast metastasis: An unusual manifestation of a primary occult appendiceal goblet cell carcinoid
A. Nasfi*, R. Doghri, R. Sellami-Dhouib, L. Charfi, I. Abbes, S. Sassi, M. Driss, K. Mrad, D. Kacem, K. Ben Romdhane
*Salah Azaiez Institute, Dept. of Pathology, Tunis, Tunisia

Objective: Breast metastases from nonmammary malignant neoplasms are uncommon, accounting for approximately 2 % of breast tumors. Primary appendiceal goblet cell carcinoid (GCC) metastasizing to the breast have only sporadically been reported in the literature.
Method: A 47-year-old woman presented with a lump in her left breast.
Results: Clinical examination revealed a firm suspect mass in the breast. The Mammography revealed an irregular mass of 38×25 mm in the upper inner quadrant of the left breast. The patient underwent lumpectomy. The gross specimen had a tan grey firm nodule of 25×15×15 mm. Histological examination revealed a proliferation made of signet ring cell and glandular structures, with islands of goblet cells. Immunohistochemistry revealed strong positive staining with CK7 and CK20, and a sparse positive staining with synaptophysin and chromogranin.ER, PR and HER2 were negative. The patient underwent appendicectomy with a final diagnosis of breast localization of a primary occult appendiceal GCC.
Conclusion: The differential diagnosis between primary carcinoid tumor of the breast and signet ring cell carcinoma metastatic to the breast is often controversial in surgical pathology. Diagnoses need to be made correlating clinical and histological examination in difficult cases in which there is not a diagnosis of carcinoid tumor elsewhere. Their histological appearance may mimic ductal adenocarcinoma of the breast. The distinction is important due to differences in management and prognosis.

PS-17-058
Determination of HER2 gene amplification by chromogenic in situ hybridization (CISH) in breast carcinoma
M. Neagu*, C. Ardeleanu, G. Butur, A. Florin
*National Institute of Pathology, Bucharest, Romania

Objective: Detection of Her2neu amplification is an integral part of breast carcinoma diagnostics to decide therapy.
Method: We study 55 cases of breast carcinoma embended paraffin tissues, both CISH and FISH were performed on each case using (SPoT-Light HER2) for CISH and both Her-2 and chromosome 17 probes for FISH (Vysis). Sixty tumor cells were evaluated in each case. The scoring system and interpretation of CISH – INVITROGEN.
Results: Concordance between CISH and FISH was found in 94,8 % cases, considering FISH as gold standard, sensitivity of CISH was 97.5 % and specificity 94 %. CISH is more practical alternative due to lower cost, no requirement of fluorescence microscope, use of existing bright-field microscopy and techniques it s similar to IHC, archivable and quantitative results, it s easy to observe both the tissue morphology and the gene amplification evaluation Of the 55 cases analyzed, 53 showed similar results for both methods. Two cases were discordant. In these cases, low-level amplification was suggested by CISH but nonamplification by FISH.
Conclusion: our results, suggest that CISH is a useful technique to determine Her-2/neu oncogene status, in breast

carcinoma for paraffin embendded tissues, is a highly accurate, reproducible and practical technique, with a high sensitivity.

PS-17-060

Usual ductal hyperplasia with central necrosis, microcalcifications and multiple foci of pseudoinvasion arising in a radial scar: A potential diagnostic pitfall

A. Nechifor-Boila*, S. Stolnicu
*University of Medicine and Pharmacy, Tirgu-Mures, Romania

Objective: The diagnosis of radial scar (RS) is often difficult, especially when associated with proliferative changes, pseudoinvasion and necrosis.
Method: A 41-year-old woman was referred to the Surgery Department for a palpable mass in her left breast, regarded as a possible fibroadenoma on ultrasonography.
Results: Lumpectomy was performed and the macroscopy revealed a tan-white 11 mm diameter lesion, with irregular margins and firm consistency. On light microscopy, a sclerosing lesion, with a stellate arrangement of ducts surrounding a central fibro-collagenous zone was identified. Haphazardly arranged, distorted ducts associated with massive intraductal proliferation, highly suspicious of infiltrative were also present in the center of the lesion. The proliferating ducts showed slit-like, irregular, secondary lumens, several containing central necrosis and a heterogenous cell population. The presence of central necrosis and pseudoinvasion were, however, worrisome. Immunohistochemistry for p63 demonstrated the presence of myoepithelial cells surrounding all the areas with pseudoinfiltrating features, while CK 5/6 displayed a heterogenous, mosaic-like positivity, characteristic for usual ductal hyperplasia (UDH).
Conclusion: Because pseudoinvasion in benign RS can easily be misinterpreted as invasive carcinoma, immunohistochemistry is mandatory to establish the presence of myoepithelial cells. Although rare, central necrosis may occur in UDH and should not be used as a single diagnostic criterion of malignancy.

PS-17-061

Phenotypical and morphological heterogenity of breast cancer: Our experience

J. Nieslanik*, J. Dvorácková, M. Uvírová, Š. Laciok, R. Ondruššek, D. Žiak
*CGB Laboratory A.S., Dept. of Pathology, Ostrava, Czech Republic

Objective: Breast cancer is the most frequent malignant tumor in women with a rising incidence. About 4 500 new cases are diagnosed in Czeck republic every year, up to 43 % die on it´s account.
Method: In CGB laboratory are investigated 500 of malignant breast tumors every year. We evaluate the morphology, grade of differentiation and phenotype properties- hormone receptors expression, overexpression and amplification of HER-2/neu gene. 2 % of carcinomas posses significantly morphologically and phenotypically heterogenic tumor population in one and the same tumor leasion.
Results: The most often sign of phenotype heterogenity found is hormone receptors expression or overexpression of HER-2/neu gene. Often we see two morphologically different tumor populations coexisting. The most interesting cases from our practice are on the poster.
Conclusion: As for now, studies about the origin of heterogenity inside the same leasions, did not find a single theory to resolve it. A possible answer gives the theory of tumor stem cells and the model of clonal evolution. Our observations demonstrate and may explain the practical reason of different phenotype properties found in core cut biopsy where one population may be held, against the heterogenic properties of the tumor shown when resected as a whole.

PS-17-062

High grade infiltrating carcinoma with squamous features - A case report

D. R. Novac*, C. Ardeleanu, S. Taban, F. Cadariu, A. Dema
*Municipal Clinical Hospital, Anatomical Pathology, Timisoara, Romania

Objective: Apocrine carcinoma is a rare and histologically distinct type of invasive breast carcinoma.
Method: The patient, a 73 years-old woman was admitted to the hospital for a tumor mass in the upper internal quadrant of the left breast. Tissue fragments from the quadrantectomy specimen were routinely processed by paraffin embedding. For the immunohistochemical (IHC) study we used the following antibodies: CK7, androgen receptors (AR), estrogen receptors (ER), progesterone receptors (PR), high molecular weight cytokeratin (HMWCK), p63, gross cystic disease fluid protein-15 (GCDFP-15), En Vision system, visualization with diaminobenzidine.
Results: The gross examination revealed a nodular, well delineated mass of 2,5/2,7/3 cm, firm, gray-beige with areas of necrosis on cut section. Microscopically, the tumor had a predominantly solid, partially cystic and less tubular growth pattern. The tumor cells had abundant eosinophilic granular cytoplasm and pleomorphic high-grade nuclei. A small tumor contingent presented squamoid features. IHC stains showed the following profile: CK7+, AR+, GCDFP-15+, ER-, PR-, p63/HMWCK + (focal/zonal). A diagnosis of high-grade infiltrating apocrine carcinoma with squamous differentiation was established.
Conclusion: There are only a few cases of apocrine carcinoma on record and our case is even more special because of his peculiar aspect, the squamous differentiation.

PS-17-063

The effects of treadmill exercise in the number and weight of mammary tumors chemically induced in female Sprague–Dawley rats: Preliminary results

J. Oliveira*, C. Teixeira-Guedes, A. Faustino-Rocha, R. Soares-Maia, R. Arantes-Rodrigues, M. J. Pires, M. Ginja, P. Oliveira, R. Ferreira
*UTAD, Dept. of Veterinary Sciences, Vila Real, Portugal

Objective: We hypothesized that moderate exercise in Treadmill may affect the mammary tumor development. N-methyl-N-nitrosourea (MNU) is a commonly used carcinogen to induce mammary carcinomas. The aim of this study was to evaluate the influence of Treadmill exercise in the development (number and weight) of female rat mammary tumors.
Method: In this experimental protocol were used 21 female Sprague–Dawley rats. MNU was intraperitoneally administered at 50 days of age in a dose of 50 mg/Kg. Animals were randomly divided in two groups: sedentary (n=11) and exercised (n=10). The exercise program was started after carcinogen administration. Animals were exercised in a Treadmill Control LE8710® after an initial period of familiarization. Thirty-six weeks after MNU administration animals were sacrificed and tumors were counted and weighted.
Results: Sedentary and exercised group presented 25 and 20 tumors, respectively. Pearson Chi-Square value was not significant (p>0.05). The mean tumors weight of sedentary group (5.34±10.58 g) was lower than exercised group (8.64 ±13.01 g). The difference between groups was not significant (p>0.05).
Conclusion: We observed that exercised group showed minor number of tumors, however the lesions presented higher volume. Future morphological and biochemical analysis of tumors will allow a better understanding of the relation between mammary cancer and physical exercise.

PS-17-064

Multifocal malignant lymphoma of the breast

E. Özgün*, D. Altinel, A. Albayrak, S. Sayhan, A. Tan, N. Bozlak
*Nevehir Devlet Hastanesi, Dept. of Pathology, Turkey

Objective: Primary non-Hodgkin's lymphomas is an uncommon disease representing approximately 0.15 % of all reported malignant mammary neoplasms. Clinically they are mainly observed as solitary lesions but may also be seen as multiple foci. Herein, we present a very rare case with the diagnosis of multifocal malignant lymphoma of the breast with a detailed clinicopathologic evaluation.
Method: A 56-year-old-female patient with a right palpable breast lump admitted to the hospital. Mammography and ultrasonography findings showed 2 different foci of hypoechoic solid mass forming lesion in the right breast. Excisional biopsy has been performed.
Results: In the histopathological evaluation, both lesions demonstrated diffuse infiltration of mammarian tissue with foci of necrosis; mitotically active tumor cells with large nucleus and prominent nucleoli. The immunohistochemical analysis revealed diffuse and strong LCA, CD20, CD43, focal CD68 positivity while pancytokeratin, EMA, CD34, SMA were negative. The case was diagnosed as Diffuse Large B-cell Lymphoma.
Conclusion: Breast is an uncommon site for primary malignant lymphomas. We report a very rare case with a diagnosis of multifocal primary non-Hodgkin's lymphoma of the breast.

PS-17-065

Cytological, histopathological and clinical correlation at differential diagnosis of granulomatous mastitis-malignancy

T. Ozgur*, E. Atik, S. Toprak, H. Gokce, N. Sengul, M. Temiz
*Mustafa Kemal University, Medical Faculty, Antakya, Turkey

Objective: Idiopathic Granulomatous Mastitis (IGM) is a rare disease that is difficult to diagnose by only radiological methods and clinical findings.
Method: First case; a 30 years old woman with a well circumscribed mass of 5 cm diameter at right breast applied to our hospital general surgery outpatient clinic. In the examination of fine needle aspiration biopsy (FNAB), palisaded epitheloid histiocytes and scattered atypical cells have been seen on a bloody and inflammatory background. We suggested excisional biopsy. Second case; a 39 years old woman applied to our hospital general surgery outpatient clinic with a sore mass in her left breast. The mass has been excised for malignancy suspect. Foci of abscesses, active chronical inflammation, areas of hemorrhage and numerous granulomas containing epitheloid histiocytes are observed microscopically.
Results: In microscobic evaluation of the excisional biopsy of the first case prediagnosed as granulomatous mastitis invasive ductal carcinoma has been our diagnosis. In the second case there have been numerous granulomas containing epitheloid histiocytes, microscopically. Our diagnosis was Granulomatous mastitis in this patient prediagnosed as malignancy.
Conclusion: Especially FNAB findings are easy to confuse with malignancy. We wanted to emphasize to clinician and pathologist to be more alert on distinction of granulomatous mastitis and malignancy.

PS-17-066

Immunohistochemical characteristics of triple negative breast cancer

E. E. Pala*, U. Bayol, S. Cumurcu, E. Usturali Keskin
*Tepecik Training and Research Hospital, Izmir, Turkey

Objective: Triple-negative-breast-cancer (TNBC) that accounts for 10–20 % of all breast carcinomas is defined by the lack of estrogen receptor, progesterone receptor, HER2 expression with agressive clinical behavior. TNBC is categorized into basal like subtype which is characterized by the expression of basal cell markers and normal breast subtypes.
Method: We studied on 41 immunohistochemically TNBC patients to determine EGFR, Cytokeratine5/6 (CK5/6), p53, Ki67, GCDFP15 expression patterns by immunohistochemistry, HER2/Chromosome 17 gene status by FISH.
Results: Most of the tumors (90,2 %) were invasive ductal carcinomas. p53, Ki67, GCDFP15 mean positivity rates were 55,6 %; 51,7 %; 3,2 % respectively. GCDFP15 positivity was noted in 8 cases of which 6 were CK5/6(−). The cut-off value for CK5/6 positivity was 5 %. EGFR immunoreactivity was grouped into 0, 1+ as negative; 2+, 3+ as positive categories. CK5/6 was positive in 56,1 %, EGFR was positive in 51,2 % of the patients. The relation between CK5/6 and EGFR expression was statistically significant ($p < 0.01$). HER2 FISH was negative in all cases.
Conclusion: As a result GCDFP15 alone is not a useful marker to detect the metastasis of basaloid type breast cancers. CK5/6 and EGFR coexpression can be used to diagnose basaloid tumors with 5 % cut-off value.

PS-17-067

The clinical significance and incidence of lobular neoplasia: Multicenter study

J.-Y. Park*, S.-Y. Kwon, H.-R. Jung, M.-J. Gu, Y.-K. Bae, H.-K. Oh
*KNUH Hospital, Dept. of Pathology, Daegu, Republic of Korea

Objective: Lobular neoplasia (LNs) of the breast include atypical lobular hyperplasia (ALH) and lobular carcinoma in situ (LCIS). Because LNs do not present typical clinical or radiologic findings, the diagnosis is incidental. Many reports suggest that LN is not only a risk factor of invasive lobular carcinoma but also is as a precursor. It is important to know about the incidence of LNs and associated disease in Korea.
Method: A total 1551 cases of breast biopsy or excision from five major hospitals in Daegu were reviewed independently by 5 pathologists of the Daegu Breast Pathology Study Group. The incidence of ALH and LCIS, associated disease, the presence of microcalcification and necrosis were reviewed. All suspected cases of LNs were confirmed on E-cadherin immunohistochemical staining.
Results: Only 46 cases out of 1551 cases (2.9 %) revealed LNs. Associated disease were 17cases of invasive ductal carcinoma, 10cases of in situ ductal carcinoma, 6 cases of invasive lobular carcinoma, 5 cases o f other benign disease, and 3 cases of florid ductal hyperplasia or columnar cell change.
Conclusion: The incidence of LNs was similar to western women. Incidental LNs were frequently associated with invasive ductal carcinoma and further excision is suggested if it was present on the needle biopsy specimen.

PS-17-068

Silver-enhanced in Situ Hybridization (SISH) detection assay for HER2 gene status determination in breast carcinoma: A four year experience in our laboratory

F. Patakiouta*, G. C. Balis, V. Theodorou, E. Triantafillidou, C. Fotiou, I. Boukovinas, C. Andreadis, G. Sibilidis
*"Theagenion" Cancer Hospital, Dept. of Pathology, Thessaloniki, Greece

Objective: Assessment of HER2 status in breast cancer is important in the clinical management of patients and can be identified by a number of methods. In this study we present the results of the SISH technique used in our laboratory in the last 4 years.
Method: We analyzed 398 cases of invasive breast carcinoma, including 41 core biopsies, which were previously characterized immunohistochemically (CB11) as equivocal on a protein level (HER2 2+). All cases were evaluated by bright-field SISH using the automated Ventana Benchmark XT machine. Evaluation was independently performed by two pathologists (FP, GB) based upon the algorithms of the manufacturers and ASCO/CAP guidelines.
Results: Out of 398 cases the HER2 gene was amplified in 82 cases (20.6 %), while in 302 cases (75.9 %) there was no gene amplification. Fourteen of the cases (3.5 %) were characterized as equivocal. The concordance between the two pathologists was high (97.6 %).
Conclusion: The SISH method is new, fully automated and very rapid. Furthermore the bright-field SISH signal does not decay and can be visualized by any standard bright-field microscope even after long periods of time, making it particularly suitable for routine application in surgical pathology.

PS-17-069

Breast fibromatosis: A clinicopathological study of 5 cases

L. Pérez Casanova*, M. T. Soler, C. Meléndez, A. Petit, F. Climent, I. Català, G. Priego, M. J. Pla, M. Varela, E. Condom
*Bellvitge Hospital, Dept. of Pathology, Hospitalet de Llobregat, Spain

Objective: Breast fibromatosis (BF) represents 0.2 % of breast tumours that simulate carcinoma. The aim of this study is to characterize the cases of BF diagnosed in our institution.
Method: BF cases diagnosed from 1999 to 2009 were evaluated with clinicopathological and immunohistochemical parameters. We also studied mutations in exon 3 of the gene for β-catenin in 4 cases. Ultrastructural study (US) was performed in 1 case.
Results: There were 5 women between 33 and 69 years old. Radiologically they showed deeply located hypoechoic irregular lesions. Size ranged between 1 and 23 cm. Histologically they were characterized by an ill-defined spindle cell proliferation without epithelial elements or atypia. Immunohistochemical study was negative for AE1/AE3, CK5/6, P63, CD34 and BCL2. Actin was diffusely positive in 4/5, and S100 and Desmin focally positive in 4/5. β-catenin showed cytoplasmic(5/5) and nuclear(1/5) expression. The US showed double smooth muscle and myofibroblastic differentiation. Three patients showed mutations in exon 3 of the β-catenin gene (2 with substitution at codon 41 (T41A) and 1 deletion of 33 base pairs (A43_E65del)).
Conclusion: Focal desmin expression and US suggest smooth muscle differentiation in some BF. All cases showed cytoplasmatic positivity for β-catenin but nuclear expression was seen in only 20 % of cases. 75 % of the valuable cases showed genetic alterations of β-catenin.

PS-17-070

Do BRAF and KRAS mutations exist in triple negative breast carcinomas?

H. E. Pestereli*, M. Ozcan, G. Erdogan, F. S. Karaveli
*Akdeniz University, School of Medicine, Antalya, Turkey

Objective: Breast cancer is a heterogenous disease consisting of distinct entities characterized by different gene expression patterns. Gene expression profiling of breast cancer revealed 4 major subtypes, including hormone receptor (HR) positive luminal A and B, HER-2 positive and basal-like breast cancer. Most of the basal-like carcinomas are triple negative (HR and HER-2 negative). As most triple negative breast cancers express EGFR, mutations in the signal transducing cascade of RAS/RAF/MAP kinase might play a role in tumor progression. The aim of this study was to determine the incidence of KRAS and BRAF V600 mutations in triple negative breast carcinomas.
Method: Total genomic DNA was obtained from 37 formalin-fixed, paraffin embedded, triple negative breast tumors. KRAS was analyzed by pyrosequencing of codon 12, 13, 61. BRAF (exon 15, V600) mutations were analyzed with AutoGenomics INFINITI BRAF assay on the Autogenomics INFINITI analyzer.
Results: We found KRAS mutation in only one case (2.7 %), apocrine carcinoma which was Gly12Asp (GGT> GAT) mutation. The BRAF V600 mutations were not detected in all analyzed tumors.
Conclusion: We concluded that KRAS mutation was rare in triple negative breast carcinomas and high frequency of EGFR overexpression in this subtype might be related to other pathways in EGFR signaling.

PS-17-071

The pre-lymphatic system and the lymphatic network of the breast in menstruating and in menopausal women: A comparative study

S. Popovska*, I. Ivanov, T. Betova, T. Dineva, Z. Ivanova
*Medical University Hospital, Dept. of Clinical Pathology, Pleven, Bulgaria

Objective: The pre-lymphatic system was initially described in the 1960s by Casley-Smith and Florey. It consists of CD34 positive fibroblasts lined stromal spaces communicating with the lymphatic capillaries. The aim of the following investigation was to compare the lympho-vascular density and pre-lymphatic network density of breast tissues in the context of the menstrual status of the patients.
Method: Formalin-fixed, paraffin embedded tissue specimens from 105 patients with primary breast cancer were studied. Tumor-free tissue materials were selected. Tissue processing and immunohistochemical staining with D2-40 and CD34 antibody was performed in accordance to standard laboratory protocols. Quantitative evaluation of the lymphatic and pre-lymphatic system was performed. The Kruskal – Wallies test was used to compare differences between the median values of the studied variables. Statistical significance of the differences was considered if $p<0.05$.
Results: The pre-lymphatic network was found to be significantly more dense in menstruating, compared to menopausal women K-W=61.04; $p<0.0001$ $n=105$. Lymphatic vascular density was higher in menstruating compared to menopausal women K-W=7.60882; $p=0.006$; $n=105$.
Conclusion: Involution changes in the pre-lymphatic and lymphatic system of the breast were found to appear in postmenopausal women. This may be the explanation for the slow local progression of breast cancer observed often in elder patients.

PS-17-072

Comperative study of Herceptest and fluorescence in situ hybridization results in breast carcinoma: Indeterminate (2+) group must not be a wide range uncertainty category

Y. Saglican*, U. Ince
*Acibadem Maslak Hospital, Dept. of Pathology, Istanbul, Turkey

Objective: HercepTest is an exclusively used immunohistochemistry method for testing Her2/neu overexpression in breast carcinomas. The purpose of this study is to select the proper patients candidate to in situ hybridization, with an indeterminate Her2 score.
Method: A retrospective analysis of 163 cases with invasive breast carcinoma were evaluated for Her2 status using immunohistochemistry and fluorescence in situ hybridization. İmmunohistochemistry of cases that had been previously evaluated by nine different pathologists in our department, were reviewed by two experienced pathologists. Interpretation of the immunohistochemistry results was made without knowing the first results.
Results: Compared to the first evaluation; cases with score 0, 1+ and 3+correlated with the review of immunhistochemistry and none of score 0 and 1+ tumors were positive with in situ hybridization. Gene amplification was detected in 43 cases; 23 of them with 2+score. Three of 3+ tumors and 106 of 2+ cases were negative with in situ hybridization. Discordance was detected in 21 cases in 2+ score; 17 of them were reclassified as negative and 4 were technically unsatisfactory.
Conclusion: Using a different cut-off value for indeterminate Her2 results and training of pathologists to minimaze the interpretational differences, will maximize the accuracy, while not submitting to unnecessary molecular tests.

PS-17-073

Clinicopathological significance of excision repair cross-complementation 1 (ERCC1) enzyme status in breast cancer patients

F. Schmitt*, A. S. Carvalho, M. Gomes, A. Albergaria, R. Gerhard
*IPATIMUP, Dept. of Pathology, Porto, Portugal

Objective: The excision repair cross-complementation 1 (ERCC1) enzyme plays an essential role in the nucleotide excision repair pathway and is associated with resistance to platinum-based chemotherapy in different types of cancer. The aim of the present study was to evaluate the clinicopathological significance of ERCC1 expression in breast cancer patients.
Method: We used immunohistochemical to analyze ERCC1 expression in a tissue microarray from 135 breast carcinomas. ERCC1 expression analysis was available for 109 cases and was correlated with clinicopathologic factors and outcome data.
Results: ERCC1-positive was observed in 58 (53.2 %) cases and was correlated with smaller tumor size (P= 0.007) and with positivity for estrogen receptor (P=0.040). ERCC1 expression did not correlate with overall and disease-free survival rates. The majority (72.7 %) of special histological types of invasive breast carcinomas was positive for ERCC1 compared to invasive ductal carcinomas (ERCC1-positive in 51.1 % of the cases). Similarly, triple negative breast cancers (TNBC) were more frequently negative for ERCC1 (61.5 % of the cases) compared to the non-TNBC (41.5 %).
Conclusion: ERCC1 expression correlated significantly with favorable prognostic factors, such as smaller tumor size and ER-positivity, suggesting a possible role for ERCC1 as a predictive and/or prognostic marker in breast cancer.

PS-17-074

A study of CD10 positive basal/myoepithelial cells in a consecutive series of in situ lobular neoplasia of the breast

S. Shousha*, G. Forbes
*Charing Cross Hospital, Dept. of Histopathology, London, United Kingdom

Objective: We have previously reported a few sporadic cases of in situ lobular neoplasia (ILN) associated with marked proliferation of CD10 positive basal/myoepithelial cells.
Method: Twenty consecutive cases of pure ILN and 9 DCIS were studied. New sections were cut and stained for E-Cadherin and CD10.
Results: One out of the 20 cases showed foci of invasive lobular carcinoma in the new cut sections. All 20 ILN cases showed increased proliferation of CD10 positive basal cells, varying from a focal mild increase to a marked proliferation surrounding or mingling with the lobular cells. CD10 positive cell proliferation was least observed in a case of ILN with central necrosis and in foci of ILN seen adjacent to the invasive carcinoma. The invasive tumour cells were CD10 negative. All cases of DCIS had a thin layer of CD10 positive myoepithelial cells, that was incomplete or absent in some foci.
Conclusion: Our findings confirm the presence of a unique relationship between excess proliferation of CD10 positive basal cells and ILN; an association which is not seen in DCIS or invasive carcinoma. This is particularly interesting as recent evidence indicates that CD10 is involved in the regulation of mammary stem and 'sphere forming' cells.

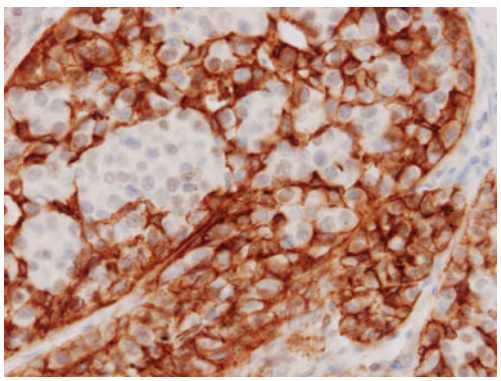

PS-17-075

Breast cancer in young Czech women: An institutional review

F. Sobande*, A. Ryška
*Dept. of Pathology, Hradec Kralove, Czech Republic

Objective: Breast cancer in young women poses unique diagnostic and management challenges however, very few large studies investigating clinico-pathologic and immunophenotypic characteristics within this group exist and varied, arbitrary age-limits are used to define 'young'.
Method: An institutional archive search was performed for breast cancer diagnosed in women <50 in 2006–2007. Age at diagnosis, tumor histological type and grade, estrogen and progesterone receptor (ER and PR), HER2/neu, Ki-67 and p53 status as well as clinical course during the follow-up period were recorded. Patients were sub-classified into age-groups of 5-year intervals for statistical analysis.
Results: Ninety of 516 carcinomas were diagnosed in women <50. They frequently displayed aggressive morphology, high proliferative activity, increased expression of p53 and high incidence of lymph node metastasis. We found a statistically significant decrease in HER2/neu over-expression with increasing age using 40 as the cut-off (<40: 42 %, ≥40: 11 %; $p=0.0032$, chi-square test). No significant age-related differences in ER or PR expression were observed within the group of women <50.
Conclusion: We show that 40 should be used as the cut-off for defining young women; in whom breast cancer is most likely to over-express HER2/neu. The mechanisms behind this finding and its significance are yet to be elucidated.

PS-17-076

Expression of cytokeratin-19 in breast carcinoma and its implication in the study of lymph node by OSNA method: An analysis of 345 cases

M. T. Soler Monsó*, A. Petit, M. Varela, L. Perez Casanova, C.-C. Loayza, F. Climent, M. T. Bajen, M. J. Pla, I. Catala
*Hospital of Bellvitge, Dept. of Pathology, L´Hospitalet de Llobregat, Spain

Objective: OSNA is a molecular assay for lymph node in breast carcinoma (BC) based on m-RNA detection of CK19. The aim of this study is to evaluate the rate of negative o heterogeneous immunohistochemical expression of CK19 in BC.
Method: CK19 was assessed in 345 consecutive samples. Cases were categorized as positive, negative and heterogeneous. Other parameters recorded where histological type and grade (Nottingham) and molecular subtype (St. Gallen2011).
Results: 319 cases (92.4 %) were CK19+. Ten (2.8 %) were CK19- and 16(4,6 %) were heterogeneous. There were 2 intraductal carcinomas, 1 heterogeneous and 1Ck19-. Among 24 invasive carcinomas, there were 9CK19-: 6 ductal, 2 papillary and 1 metaplastic. Three cases corresponded to G1, 4 G2, 1 G3 and 1T1mi not available. Five cases were Luminal A(LA), 1 Luminal B/HER2-(LB-), 1 HER2+ and 2 triple negative (TN). Among 15 heterogeneous cases, 13 were ductal, 1 metaplastic, and 1 atypical medullary carcinoma. Eleven were G3, and 4 G2. Four were LB- and 11 cases were TN.
Conclusion: All lobular carcinomas expressed CK19 CK19 was negative in 2.8 % and heterogeneous in 4.6 % of BC. They represent a heterogeneous group but half of these cases are either G3 or TN. 74 % of heterogeneous cases were TN and 26 % LB- with no LA cases in this subgroup.

PS-17-077

Case report of an extremely rare tumor of the breast: Mucoepidermoid carcinoma

F. Staniceanu*, C. Socoliuc, A. Birceanu, E. Gramada, L. Nichita, R. Andrei, A. Croitoru
*Colentina University Hospital, Dept. of Pathology, Bucharest, Romania

Objective: Staniceanu and Socoliuc are first authors in equal proportions Mucoepidermoid breast carcinoma, classified in category of purely epithelial metaplastic carcinomas, is rarely encountered with only a few female cases described in literature. It is composed by mucous, intermediate and epidermoid cells, similar to its salivary gland counterpart.
Method: We present the case of a 67 years old man with a 2,2/1,6 cm breast tumor located under the nipple, poorly circumscribed, with increased consistency and central cystic area containing serous fluid. Tissue samples were preserved using 10 % formalin. All sides were stained using hematoxylin-eosin. Immunohistochemistry was performed using labeled streptavidin-biotin method.
Results: Microscopic examination reveals islands and sheets of polygonal cell with clear/pale cytoplasm, "signet cells" figures, areas of squamous metaplasia and centrally located hyperchromatic nuclei, some with visible nucleoli and rare mitoses. Tumoral parenchyma contains ducts and cysts of varying sizes, with pale eosinophilic luminal accumulation PAS, D-Pas and Alcian Blue positive (mucin). Immunohistochemical tests were performed. Differential diagnosis was made among several benign and malignant lesions, the final diagnostic being mucoepidermoid carcinoma, low grade.
Conclusion: Mucoepidermoid carcinoma of the breast is an extremely rare entity; however its specific morphologic and prognostic features (similar to its salivary gland counterpart) allow proper diagnostic.

PS-17-078

Malignant transformation of adenomyoepithelioma of the breast by monophasic population with triple negative and bilinear immunophenotype: Report of 2 cases

S. Stolnicu*, C. Marian, C. Dobos, A. Boila, D. Soanca, M. Boros, M. Malau, M. D. Podeanu, E. Resetkova
*University of Medicine, Dept. of Pathology, Targu Mures, Romania

Objective: Malignant adenomyoepitheliomas are rare tumours of the breast and 34 cases have been so far reported in the English literature of which only 16 cases with spindle morphology.
Method: Two cases of adenomyoepithelioma of the breast with malignant transformation by monophasic spindle population of cells are presented in a 56 and 41 year old patient respectivelly.
Results: The underlying benign adenomyoepithelioma with typical biphasic architectural pattern was identified and represented at least 30 % of the tumor volume in each case. In both cases, malignant portion of tumor was composed of relatively uniform monophasic population of highly atypical cells. The malignant component in case 1 was positive for pan-cytokeratin, myoepithelial markers, and basal-type cytokeratins and also focally positive for luminal-type of cytokeratins; but negative for hormone receptors (estrogen and progesterone) and HER-2/neu protein overexpression. The malignant component in case 2 was positive for spectrum of myoepithelial markers but negative for luminal cytokeratins and hormone receptors and HER-2/neu protein overexpression.
Conclusion: The bilinear immunophenotype in the case 1 suggests that the malignant tumor may have developed from precursor multipotent stem cells that can differentiate into both luminal epithelial and myoepithelial cells, while malignant component in case 2 appears to be the of pure myoepithelial phenotype.

PS-17-079

Primary neuroendocrine carcinoma of the breast: Can it be suspected on histomorphologic grounds?

E. Tejerina González*, A. Ortiz Otero, D. García Fresnadillo, C. Salas Antón, C. Corbacho Cuevas, C. Bellas Menéndez
*HU Puerta de Hierro-Majadahonda, Dept. de Anatomía Patológica, Spain

Objective: Primary neuroendocrine carcinomas (NEC) of the breast are defined by the WHO classification as a group of neoplasms that express neuroendocrine markers in more than 50 % of the cells. These tumors can exhibit different morphologic appearances including solid, nested or alveolar pattern, papillary or mucinous differentiation or conventional ductal structures. The aim of this study is to identify histomorphological features useful in the recognition of this tumors.
Method: 160 invasive breast carcinomas were reviewed, none of them previously typified as NEC. 154 were ductal carcinomas (26 grade I, 61 grade II and 66 grade III) and 6 lobullilar carcinomas. In all cases immunohistochemical staining for the neuroendocrine marker synaptophysin was performed.
Results: Eight of the 160 cases showed intense immunoreactivity for synaptophysin. All of them were predominantly composed of solid, confluent nests and cords of cells with medium-to high grade nuclear atypia. Two cases showed intense desmoplastic or sclerotic stromal response. A colloid component was identified in another two cases.
Conclusion: Due to its morphologic variability, mammary NEC is frequently underrecognized. A predominantly solid pattern of confluent nests and trabeculae associated with a prominent sclerotic stromal response or colloid differentiation should prompt to perform additional immunohistochemical staining in order to exclude neuroendocrine differentiation.

PS-17-080

Expression of Aurora kinase A and Gamma-tubulin in breast carcinomas of patients undergoing neoadjuvant chemotherapy

A.-M. Tokes*, L. Moskovszky, A. M. Szasz, I. Kenessey, A. Kollar, Z. Bansaghi, D. Magdolna, J. Kulka
*Semmelweis University, 2nd Dept. of Pathology, Budapest, Hungary

Objective: Association between centrosome abnormalities and response to chemotherapy has not been fully elucidated in breast carcinomas (BC). Here we analysed the association between Aurora kinase A (AURKA) and Gamma-tubulin (GT) and response to neoadjuvant chemotherapy (PST) in patients treated with BC.
Method: The immunohistochemical expression of AURKA and GT was analysed in 44 core biopsies of BCs taken before administration of PST. AURKA expression was analysed using a modified Allred-like scoring system (intensity and percentage of staining combined). Cells containing one or two centrosomes as determined by GT were considered negative, whereas cells containing more than two centrosomes were regarded as positive. Centrosome amplification was graded in each specimen as follows: negative (0–2 % of cells); weak (2–10 %); moderate (11–20 %); and strong (21 %<). Pathological response rates were assessed using Chevallier's classification.
Results: Centrosome amplification was significantly higher in patients achieving complete response when compared with the cases where partial remission or no response was

defined (p=0.03), whereas we found no significant correlation between the expression of AURKA protein and response rate to neoadjuvant chemotherapy (p=0.24).
Conclusion: BCs showing centrosomal amplification as determined by GT present higher response rates to neoadjuvant chemotherapy, but need further validation.

PS-17-081

Breast granulocytic sarcoma with aleukemic presentation: A case report

O. Tzaida*, P. Giagkazogloy, P. Repousis, M. Kotsopoulou, I. Kasselaki, C. Valavanis, I. Iacovidou
*Anticancer Hospital Metaxa, Peiraias, Greece

Objective: Granulocytic Sarcoma (GS), a rare solid tumor of immature myeloid cells in exrtamedullary sites, usually occurs during the natural course of acute myelogenic leukemia (AML). Rarely is presented without overt hematological disease. The breast is an uncommon site of localization.
Method: We report a case of breast GS with aleukemic presentation, condition that is extremely rare and requires a high index of suspicion for diagnosis. A 46 year old woman, presented with a solitary, non-tender, palpable left breast mass. A lumpectomy was done.
Results: Histopathology revealed breast parenchyma diffuse infiltration, in a targetoid pattern, by immature small cells intermingled with eosinophils. Lobular carcinoma and lymphoma were considered in differential diagnosis. The myeloid origin of the neoplasm was established by immunohistochemical analysis that revealed LCA, MPO, CD34, HLADR, CD68 (Kp1) positivity. There was no evidence of leukemia in the peripheral blood and bone marrow. The patient was treated as AML with systemic chemotherapy and 5 months after the diagnosis she is without evidence of disease.
Conclusion: Breast GS is a challenging situation both for pathologists and hematologists. Available evidence strongly favors the application of systemic chemotherapy despite the appeared localized nature of the disease.

PS-17-082

Molecular subtypes of breast cancer according to expression of surrogate immunohistochemical markers: Study of 152 cases

M. Vazmitel*, A. Dubrovskij, S. Rjabceva
*Minsk, Belarus

Objective: To classify breast cancer into molecular subtypes based on immunohistochemical profile: luminal A (ER + and/or PR+; HER-2-), luminal B (ER + and/or PR+; HER-2+), HER-2-positive (ER-; PR-; HER2+), basal (ER-; PR-; HER2-; at least one of three basal markers positive), 5-negative (ER-; PR-; HER2-; CK5/6-; CK17-; EGFR-).
Method: Paraffin blocks of tumor tissue of 152 breast cancer cases collected at our Cancer Centre for 3 years. The immunohistochemical study was performed by standard techniques using following antibodies (Dako): ER, PR, HER-2, EGFR, CK5/6, CK17, Ki67.
Results: All cases were classified into the 5 subtypes: luminal A (n=91; 59.8 %); luminal B (n=13; 8.6 %); HER-2-positive (n=19; 12.5 %); basal (n=19; 12.5 %); 5-negative (n=10; 6.6 %).
Conclusion: Luminal breast cancer phenotype predominates in our collection, predictive/prognostic value of molecular genetic subtypes is planned to be investigated. We recognized statistically significant differences (P<0,001) in five-year survival rates between tumors of luminal (A, B) and basal subtypes.

PS-17-083

Proliferating trichilemmal cyst with atypical cytological features

R. G. Wright*, C. Gallivan, T. Molden-Hauer, R. Liang
*Gold Coast Hospital, Pathology Queensland, Australia

Objective: Proliferating trichilemmal cysts are relatively common occurring within the scalp of elderly women. Proliferating trichilemmal cysts of the breast, however, are rare. These cysts are benign with very few demonstrating malignant transformation.
Method: We report a case of proliferating trichilemmal cyst of the breast with atypical cytology which prompted excisional biopsy. Cytological assessment was useful in this case as it indicated excisional biopsy rather than a more extensive excision.
Results: Smears produced from the FNA showed sheets of atypical epithelial cells with foamy histiocytes, multinucleate cells and fibrotic material with evidence suggestive of fat necrosis. A cell block was acellular. A specific diagnosis was not made. An excision specimen was advised and a proliferating trichilemmal cyst was demonstrated.
Conclusion: The cytological features in this case are in keeping with previous cases reported in scalp lesions. These benign cysts can uncommonly undergo malignant transformation. While rare, proliferating trichilemmal cysts of the breast do occur and complete surgical excision is required. Cytological features are thus important to recognise. No previous cytological diagnoses of this rare breast lesion have been reported.

PS-17-084

Morphological and molecular biological features of breast cancer in patients till 35 years of age

L. Zakhartseva*, O. Lobanova, V. Cheshuk, N. Gorovenko, S. Podolskaya, I. Shchepotin
*Kiev City Oncology Center, Pathology, Kyiv, Ukraine

Objective: A large clinical value has determination of molecular subtype of breast cancer (BC). To clarify morphological and molecular biological similarities and differences between BC depending on age, we compared features between tumors of younger and older women.
Method: 573 patients with BC are included in research: from 18 till 86 years, among them 254 patients were till 35 years. ER, PR, Her-2/neu, p53, p63, Ki67, CK5/14, p21, Bag1, Mcl1, pS2, VEGFR, Her-1 were analyzed in all cases by immunohistochemistry.
Results: The younger patients with BC had higher expression of p53, p63, p21, Bag1, Mcl1, Ki-67, VEGFR, HER-1 ($p<0,001$) than older patients. There was a basal-like molecular subtype of BC 3-fold more frequent compared with older patients (21,6 % versus 7,2 %; $p<0,0001$). Three-years overall survival in patients till 35 years was by 11,5 % and a five-year overall survival was by 15,5 % lower than in patients over 35 years ($p<0,001$).
Conclusion: Aggressive clinical course of breast cancer in patients till 35 years is related to the molecular biological features of tumor.

PS-17-086
Breast HER2 Insitu Hybridization (HER2 ISH): Acceptable and unacceptable staining criteria impacting on interpretation
S. Parry*, K. Miller, M. Ibrahim
*UK NEQAS ICC & ISH, London, United Kingdom

Objective: Breast HER2 ISH relies on correct enumeration of HER2/CEP 17 signal. However, as with immunohistochemistry, there are technical pitfalls which may render ISH difficult/unreliable to interpret. The UK NEQAS has established a 'technical' ISH module to provide feedback to laboratories using both chromogen and fluorescence based tehcniques.
Method: Unstained slides consisting of 4 breast cancer cell lines were distributed. Laboratories were asked to demonstrate HER2 gene amplification using their routine assay, and then return the slides for assessment. Chromogen based methods were assessed around a multi-header microscope with 4 assessors scoring each slides, whilst the fluorescent ISH method was assessed by a single individual. Assessors scored the 'readability' of each slide, without counting the probes, and provided feedback where the hybridisation technique could hinder interpretation.
Results: CISH based methods showed acceptable staining in 50 % ($N=32$) of cases. Staining problems ranged from loss/poor HER2/CEP17 signal, non-specific staining and morphological damage. The FISH pilot assessment showed an acceptable rate of 32 % ($n=21$), with the low pass rate being attributed to poor preservation/quenching of fluorescence signal.
Conclusion: Greater emphasis needs to be placed on the 'readability' of an ISH slide, prior to carrying out the process of enumeration.

Tuesday, 11 September 2012, 09.30 - 10.30, Congress Hall Foyer 3rd Floor
PS-18 Poster Session Cardiovascular Pathology

PS-18-001
A rare tumor in the right atrium
A. Alves*, M. Ferreira, P. Luis, A. Costa-Silva
*Hospital Santa Maria, Servico de Anatomia Patologica, Lisboa, Portugal

Objective: Intravenous leiomyomatosis is a very rare growth pattern variant of leiomyoma in which nodular masses of tumor grow within venous channels. Occasionally the tumor can extend to vena cava and the right heart.
Method: We present a case of a 45-year-old woman, who was admitted in the emergency room with rapidly evolving exertional dyspnea. Cardiac ultrasonography revealed a "big mass in the right chambers". She was submitted to a right atriotomy with resection of part of the tumor, which was sent for intraoperative consultation.
Results: Grossly, the tumor was polypoid, firm, with a smooth surface. The frozen section showed a lesion composed of tortuous vessels and in some areas a fibrillar eosinophil extracellular matrix and others with spindle cells. No significant atypic or pleomorphic cells, mitosis or necrosis were observed. The diagnosis was deferred for definitive paraffin sections. In the definitive H&E and with immunohistochemical stains, the case was diagnosed as an intravenous leiomyomatosis, and the diagnosis was confirmed in the hysterectomy specimen.
Conclusion: Intravenous leiomyomatosis with cardiac involvement is an extremely rare condition. Clinical information is essential for the correct diagnosis in frozen section.

PS-18-003

Characterization of a specific mechanism for late loss of cardiac allograft: The antibody mediated rejection (AMR) as a major factor of cardiac allograft vasculopathy (CAV)

P. Bruneval*, C. Toquet, A. Loupy, P. Pouvier, A. Cazes, J.-P. Duong van Huyen
*France

Objective: The rational of this study was to investigate explanted failing grafts in the light of new concepts in rejection mechanisms, namely AMR.
Method: This retrospective multicentric study collected 31 explanted cardiac grafts failing ≥1 year posttransplantation. The vasculature of the grafts was assessed from epicardial coronary arteries to myocardial microcirculation. Immunohistochemistry was performed for C4d complement fraction deposition and CD68-positive macrophages in the explanted grafts and previous endomyocardial biopsies. Donor specific antibodies (DSA) were retrospectively assessed using Luminex SA technique.
Results: A pure classical coronary atherosclerosis pattern was observed in 6/31 (19 %). A pure pattern of CAV was present in 12/31 (39 %) and a mixed pattern associating CAV and atherosclerosis features in 9/31 (29 %). Interestingly the CAV pure and mixed patterns were associated with vascular inflammation within the arteries and/or the microcirculation with C4d deposits and macrophages (15/21) in the explanted grafts versus nil (0/6) in pure atherosclerosis pattern ($p<0.002$). Furthermore they were associated with previous AMR episodes on endomyocardial biopsies (11/21) and by positive DSA (10/14) versus nil in pure atherosclerosis pattern ($p<0.05$ and $p=0.05$, respectively).
Conclusion: In failing cardiac grafts CAV lesions are associated with makers of AMR. CAV should be the consequence in coronary arteries of an ongoing AMR process.

PS-18-004

Age related histopathological changes in cardiac conducting system in Turkish population: Evaluation of 202 autopsy cases

N. Comunoglu*, C. Comunoglu, B. Eren, N. Turkmen, U. N. Gundogmus, F. Eren, O. Tanriover
*Haydarpasa Numune Hospital, Dept. of Pathology, Istanbul, Turkey

Objective: Histopathological features of cardiac conducting system (CCS) in Turkish population have not been investigated previously.
Method: We examined CCS of 202 autopsy heart specimen dissected between the years 2004 and 2005 in Bursa Forensic Medicine Institution. Of the 202 cases from all age groups, 154 were male and 48 were female.
Results: In our cases increase in fibrous and adipose tissue concordant with age, indicating an age related nature, were detected. Fibrous and fatty tissue infiltration appeared at the age of 35. Fatty infiltration started at the age between 20 and 34 at sinoatrial node. In 4 cases calcification and in 19 cases inflammation was observed. Amyloid accumulation was not present. In 7 cases myocardial infarction not involving CCS was seen. In 1 case fibroelastoma was detected.
Conclusion: In Turkish population age related fibrosis and fatty infiltration in CCS appeared at the age of 35 and increased with age. Fatty infiltration in sinoatrial node started at a younger age than that of reported in the literature. In cases whom the cause of death could not be determined we could not detect lethal pathologic features. However we think that examination of the CCS will improve the quality of autopsy diagnosis.

PS-18-005

Periadventitial adipose tissue in human coronary atherosclerosis: A neurotrophin study

P. Ghenev*, P. Panayotov, G. Chaldakov, L. Aloe
*Medical University Varna, Dept. of Pathology, Bulgaria

Objective: Recent evidence demonstrates that epicardial adipose tissue, including coronary periadventitial adipose tissue (tunica adiposa), are paracrine sources of bioactive mediators (adipokines, NO, H2S) which may be involved in coronary atherogenesis. Because of the increasing interest for extra-neuronal effects (inflammation, wound healing, lipid and glucose metabolism) of the neurotrophins nerve growth factor (NGF) and brain-derived neurotrophic factor (BDNF), including in human coronary atherosclerosis in autopsy samples, the aim of the present study is to evaluate the expression of NGF and BDNF and their receptors (TrkA and TrkB, respectively) in cardiosurgery biopsy samples of pericoronary adipose tissue.
Method: Immunohistochemistry of NGF, BDNF and their Trk receptors.
Results: NGF, BDNF, Trk A and TrkB expression was lower in periadventitial adipose tissue of atherosclerotic coronary arteries as compared to non-affected coronaries.
Conclusion: We provide the first evidence for a possible role of neurotrophins in the molecular remodeling of tunica adiposa in human coronary atherosclerosis. This study is dedicated to 103rd Anniversary of Rita Levi-Montalcini, the Nobel laureate for the discovery of NGF.

PS-18-006

Apoptosis in dilated cardiomyopathy and myocarditis

S. Glumac*, R. Jankovic, M. Lazic, J. Markovic, I. Ranisavljevic-Katuca, A. Batistatou, J. D. Vasiljevic
*School of Medicine, Inst. of Pathology, Belgrade, Serbia

Objective: In normal myocardium, apoptotic myocytes are usually absent, or if affected, with most of 28 positive cells per million.
Method: The apoptosis was measured by the TUNEL method in 60 patients with dilated cardiomyopathy (DCM) and myocarditis (MC), and expresed by apoptotic index (AI) in 30 patients within both groups, and to correlated with ejection fraction (EF) and with different morphological stages of these entities. Statistical analisys was performed, and p values ≤ 0.05 were considered statistically significant.
Results: AI in MC cases was 4,23+12,16, and in DCM cases the value was significantly higher 5,41+9,33 ($p=0.005$). In the group MC patients, we didn't found statistically significant correlation between AI and different values of EF ($p=0.701$). The analysis of the value of AI between patients with different morphological stages of MC didn't show statistically significant correlation ($p=0.535$), as well as in DCM ($p=0.312$).
Conclusion: Apoptosis play a significant role in DCM and MC but its significance in the progression to heart failure has still to be established.

PS-18-007

"Contusio Cordis": A concealed cause of unexpected death

R. Henriques de Gouveia*, F. Costa Santos, C. Oliveira, J. Fonte Santa, B. Simões Silva, F. Corte Real, J. Costa Santos, D. N. Vieira
*Instituto Nacional Med. Legal, Forensic Pathology, Coimbra, Portugal

Objective: Cardiac lesions following blunt chest trauma are multiple and of various degrees of severity. "Cardiac Contusion" is a difficult diagnosis, especially antemortem and if signs of thoracic trauma are not evident on external habitus and on the underlying internal plans of cardiac area. Is the contusion a cause of death per se?
Method: The authors present two cases of road accident male victims, aged 43 and 50 year-old, submited to complete postmortem examination with ancillary diagnostic methods.
Results: No traumatic lesions or underlying pathology was found at the autopsy. Epicardial and myocardial hæmorrhagic foci were histologicaly documented. Toxicology was negative.
Conclusion: Cardiac Contusions are caused by one of the following mechanisms: 1) heart compression between bone structures, 2) sudden acceleration-deceleration movements and 3) sudden thoracic/abdominal pressure increase. They may be asymptomatic or lead to rhythm disturbances responsible for unexpected death (10 %). They seem to be underdiagnosed, thus suspecting the entity "Contusio Cordis" is crucial, not only antemortem for correct surveillance and treatment, but also postmortem to adequately establish causality nexus in cases of post-thoracic trauma deaths.

PS-18-008

The influence of bone marrow-derived multipotent stromal cells on myocardial scar healing in experimental myocardial infarction

L. Kakturskiy*, T. Fatkhudinov
*Institute of Human Morphology, Central Laboratory of Pathology, Moscow, Russia

Objective: Previous studies have shown the benefits of intracoronary infusion of bone marrow-derived multipotent stromal cells (BM-MSCs) in heart disease. Our aim was to study engraftment, differentiation of BM-MSCs and its role in myocardial reparation.
Method: Acute myocardial ischemia was produced by transient occlusion (total of 20 min) of the proximal left anterior descending coronary artery and followed by reperfusion. BM-MSCs were isolated, expanded by standard and labeled with PKH26 (Sigma). Cells were CD90 and CD105 positive. 30 days after occlusion during cross-clamping of aorta the cells were administered into the cavity of the left ventricle at the concentration 5×106 in saline solution. In 1 day, 2, 4 and 6 weeks after transplantation the labeled cells were detected in the cryosections and heart morphometry was performed.
Results: BM-MSCs were detected only in the scar tissue and had a fibroblast-like phenotype. They neither differentiated into cardiomyocytes nor into the cells of blood vessels. In 4 weeks after transplantation the scar thickness was higher in the group with cell transplantation ($p<0.001$).
Conclusion: Engrafted BM-MSCs promote myocardial fibrosis only in the scar, but not in the perifocal myocardium, provided strengthening of the scar, remodelling of outflow tract, and improvements the myocardial function.

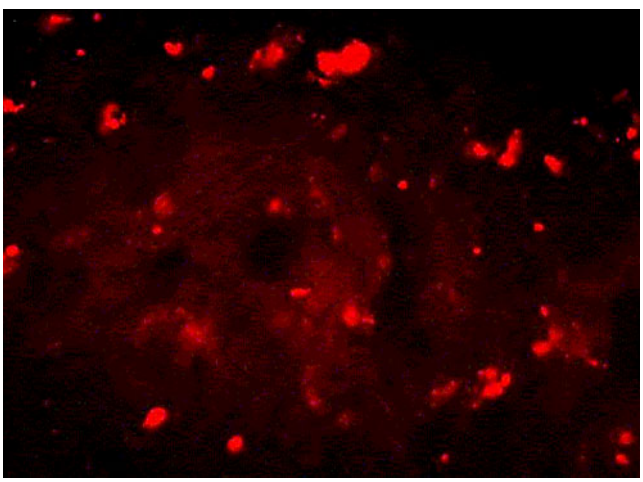

PS-18-009

Endomyocardial biopsy value in differential diagnosis of hypertrophic cardiomyopathy

J. Markovic*, I. Ranisavljevic Katuca, S. Glumac, R. Jankovic, J. D. Vasiljevic
*Clinical Center of Serbia, Dept. of Pathology, Belgrade, Serbia

Objective: Endomyocardial biopsy (EMB) may be used to diagnose different types of cardiomyopathies, to monitor transplant rejection, evaluation of myocarditis, heart failure of unknown origin, arrhythmias, drug toxicity and heart neoplasmas. The aim of this case is to show how non-invasive cardiac investigations are sometimes not sufficiently conclusive for distinguishing between hypertrophic obstructive cardiomyopathy (HOCM) and the other cardiac diseases.
Method: Thirty-one representative left ventricle biopsies were obtained following suspected HOCM. Samples underwent routine standard and special staining procedures. Five histologic parameters were used for assesment (disarray and hypertrophy of myofibers, myocardial short runs, perinuclear halo and bizarre nuclei and fibrosis) and graded from 0 to 3, presenting in summary Histological HOCM Index (HHI- ranging from 0 to 15).
Results: The histological findings in EMB of thirty-one patients, in 8 (25,8 %) patients HOCM diagnosis was confirmed, in 6 (19,35 %) patients HHI was under or equal to 50 % (8) so HOCM diagnosis couldn't be confirmed, amyloidosis in one (3,22 %) patient, myocarditis in 4 (12,9 %) patients, dilatative CMP in 6 (19,35 %) patients and unspecific cardiac changes in 6 (19,35 %) patients.
Conclusion: A definitive diagnosis can be obtained by means of a multidisciplinary approach including EMB findings.

PS-18-010

Morphometric study of structural changes in the heart of people who abused alcohol for more than 5 years

L. Mitrofanova*, E. Naumova
*Almazov Federal Heart, Blood and Cardiomorphology, St. Petersburg, Russia

Objective: The information about structural changes in the heart of people abused alcohol (PAA) is very contradictory.
Method: We studied 22 hearts of PAA (>100 g per day), 10 hearts of patients with ischemic heart disease (IHD) and 10 hearts of healthy persons. At the morphometric study of heart we measured the mean cardiomyocyte diameter (MCD), the relative areas of fatty infiltration (FI), fibrosis, cardiomyocytes. Immunohistochemistry was performed using antibodies against CD3-antigens to count the number of antigen-positive cells per 1 mm².
Results: The average heart weight, the MCD of the PAA were not significantly different compared to the ones of the control group. The average relative area of FI of RV for the group of PAA was 21±15 % and was significantly different compared to the one of both the control group and the group with IHD. The relative area of RV fibrosis in the group of PAA was 9.9±6.5 % and was not significantly different compared to the ones of the other two groups. The mean number of CD3+ lymphocytes/mm² of 23 % of PAA was more than 14.
Conclusion: The PAA did not have myocardial hypertrophy. 23 % of them had chronic myocarditis. Marked FI in PAA was significantly higher than the other two groups.

PS-18-011

Expression of angiotensin-converting enzyme 2 in ischemic myocardium

D. Pangonyte*, V. Buneviciene, I. Balnyte, L. Utkiene, D. Kazlauskaite, L. Peciulyte, J. Palubinskiene, D. Baltusnikas
*Lithuanian University of Health, Dept. of Pathology, Kaunas, Lithuania

Objective: The aim of the study was to evaluate the expression of angiotensin-converting enzyme 2 (ACE-2) in left ventricular myocardium in the presence of chronic myocardial ischemia.
Method: Heart specimens with persistent ischemia (n=43, pre-infarction ischemic heart disease (IHD) group) and post-infarction scar (n=32, post-infarction IHD group) from dissected males and heart explants (n=15, end-stage ischemic heart failure group) were studied. Heart specimens (n=29) selected at autopsy from individuals who died from accidents were used as controls. The slides of myocardium were incubated with polyclonal antibody against the ACE-2 (1:1000, ab15348, Abcam).
Results: ACE-2 expression in cardiomyocytes of the pre-infaction IHD and post-infarction IHD groups did not differ from the controls and was increased only in the end-stage ischemic heart failure group (p<0.05). ACE-2 expression in vascular endothelial cells, smoth muscle cells and macropages of the pre-infarction IHD group did not differ from the controls; but the number of ACE-2 expressing cells in the post-infarction IHD and in the end-stage ischemic heart failure groups was greater, as compared with the pre-infarcion IHD group and the controls (p<0.05).
Conclusion: Expression of ACE-2 is increasing in progression of ischemia-induced myocardial dysfunction.

PS-18-012

Thrombotic occlusion of the peripheral pulmonary arteries: Anatomical "trigger" of the massive pulmonary thromboembolism (PTE)

F. Portelli*, F. P. Busardò, L. Gutsul, P. Fleres, P. Pugnetti, E. Orlando, E. Maresi
*University of Palermo, Section of Pathology, Italy

Objective: From January 2000 to December 2009 (Institute of Pathology and Legal Medicine, Paolo Giaccone – Palermo) 57 autopsies were performed on 37 males and 20 females who died of a massive PTE.
Method: Systematic autopsy.
Results: Saddle pulmonary thrombosis in 33 cases, in 24 isolated in both the main pulmonary arteries. In all cases the transverse heart diameter was 1,5–2 cm superior to the longitudinal one, the interventricular septum became rectilinear with a right ventricular dilation. The coronary artery anatomy was: critical stenosis through fibroatheromatous plaque of the dominant right coronary artery (RCA, 2), non dominant left coronary artery (LCA, 3); non critical stenosis of RCA (14), LCA (8); absence of stenosis (30). Histological ventricular examination showed hypoxic-ischaemic and/or reperfusion and overload lesions. In all cases, the lungs showed plurifocal occlusive thrombosis of intramural pulmonary arterial (IPA) vessels associated with adjacent infarctual necrosis (49); acute partially haemorrhagic basal oedema (35) and desquamative macrophagic alveolitis (28).
Conclusion: In all cases of massive PTE the thrombosis of IPA vessels associated with an adjacent infarction (86 %) is constant. This suggests that death is nearly always preceded or triggered by one or more episodes (clinically silent or with non specific symptoms) of thromboembolism of IPA vessels.

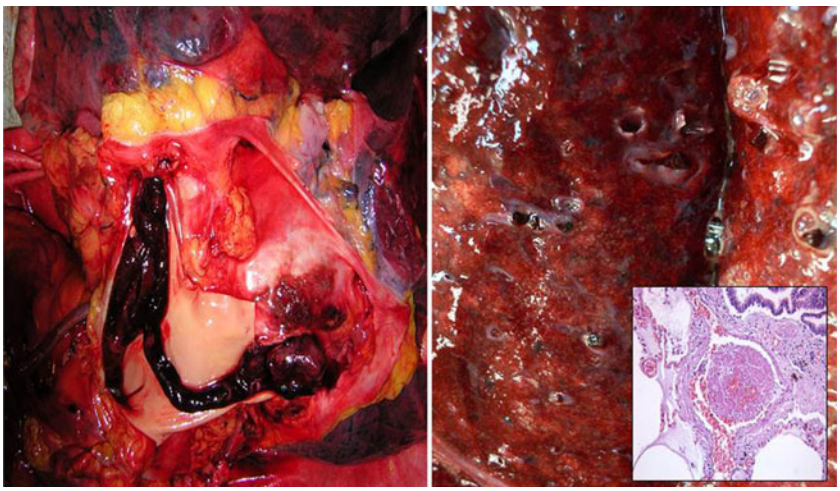

PS-18-013
Cardiac findings in routine fetal autopsies: More than it meets the eye?
E. Rios*, C. Bartosch, C. Ramalho, J. Monterroso, O. Brandão
*Centro Hospitalar S João, Pathology, Porto, Portugal

Objective: Congenital heart disease (CHD) is the most common malformation in newborns. Our aim was to evaluate the spectrum of CHD in consecutively performed fetal autopsies and to correlate prenatal and postmortem diagnoses.
Method: A retrospective study of 726 fetal autopsies was performed in a tertiary referral hospital. CHD was classified in seven categories: left ventricular outflow tract obstruction-LVOTO, right ventricular outflow tract obstruction-RVOTO, septal defects, connection anomalies, conotruncal anomalies, complex anomalies and others. Cardiac defects were also classified as isolated or associated with others anomalies.
Results: CHD was identified in 99 (13.6 %) fetuses. Most common categories were septal defects and complex anomalies. Associated anomalies were found in 67 fetuses (67.7 %). In this group, septal defects were the most common CHD, frequency being significantly higher than in the group of isolated cardiac anomalies (p=0.012). Comparison of prenatal and postmortem diagnoses (50 cases) showed complete or partial agreement in 36 and 10 cases (72 % and 20 %, respectively) and complete disagreement in 4 cases (8 %). In the latter group, prenatal diagnosis had not been done by a pediatric cardiologist.
Conclusion: The high prevalence of CHD in lost pregnancies highlights the importance of systematic fetal autopsy performed by a specialized pediatric pathologist.

PS-18-014
Morphogenetic biomineralization aspects in the human heart valve affected by atherosclerosis
A. Romanuk*, R. Moskalenko, S. Danilchenko, O. Romanyuk, J. Moskalenko, S. Romanyuk
*Sumy State University, Dept. of Pathology, Ukraine

Objective: The appearance of pathological calcification, which leads to significant changes of vascular wall, which underlie the development of atherosclerotic complications, has a great importance in the morphology of atherosclerosis development. Purpose of the work is the study of pathological biomineralization in heart valves affected by atherosclerosis.
Method: The study was conducted on sectional material of mitral and aortic valves obtained during autopsy. The tissue of heart valves was studied by methods of histology, electron microscopy, X-ray diffraction, infrared spectroscopy.
Results: Macroscopically mitral and aortic valves are thickened, opaque, dull whitish, sometimes with deformity and ulceration. Histology observed the formation of atherosclerotic plaques, fibrous changes, and inflammatory infiltration. According to X-ray phase analysis biominerals in heart valves are represented by apatite crystalline phase. Sizes of crystals have distinct age dependence. The results of infrared spectroscopy revealed absorption bands of carbonate apatite replacement; in all instances they correspond to the type of substitution B (CO3 2– replaces PO4 3–).
Conclusion: The study of pathological mineral formations on human heart valves by the range of morphological and physicochemical methods show that they are aggregates of interacting organic and mineral components, their ratio changes with "maturation": the organic component decreases and the mineral component, represented by carbonate containing hydroxyapatite doped with chlorine grows while improving, so the process is dynamic.

PS-18-015

Relationship between myocardial injury, oxidative stress mechanism and sepsis/septic shock in infants submitted to surgery for congenital heart defects

M. Silva de Oliveira*, E. Medeiros Floriano, P. Henrique Manso, R. Nilsson Sgabieri, J. Guilherme Klamt, E. Zangiacomi Martinez, W. Vilella de Andrade Vicente, S. Gusmão Ramos
*University of São Paulo, Dept. of Pathology, Ribeirão Preto, Brazil

Objective: A progressive ventricular dysfunction caused by ischemic myocardial injuries remains one of the leading causes of death during the postoperative course in congenital heart disease (CHD). The aim of this study was to investigate the role of oxidative stress in these myocardial injuries.
Method: Myocardial injuries and oxidative stress mechanisms were assessed by histopathology and immunohistochemistry and quantified by morphometrical analyses.
Results: Myocardial injury was observed in pediatric patients submitted to surgery for CHD with cardiopulmonary bypass, followed by lethal exit. Oxidative stress mechanisms were directly related to these particular types of myocardial injuries. Importantly, 4- hydroxynonenal (4-HNE), a marker of lipid peroxidation, is strongly expressed, especially in irreversible myocardial lesions. Although morphologically similar, myocardial injuries observed in patients who evolved with sepsis in the peri-operatory period exhibited a completely different set of oxidative stress mechanisms. Increased concentrations of nitrotyrosine protein adducts were observed in these patients, suggesting that peroxynitrite-mediated protein nitration may be the predominant oxidative stress mechanism found in these situations.
Conclusion: The underlying mechanisms of these lesions seem to be related to the development of ischemia or ischemia/reperfusion followed by oxidative stress mechanisms that vary depending on whether sepsis was present. While the exact mechanism is not fully understood, it has been suggested that endogenous catecholamine release could have a role in this process.

PS-18-018

Increase of ABCG2/BCRP + side population stem cells in the myocardium after ventricular unloading

J. Wohlschlaeger*, B. Levkau, J. Stypmann, C. Schmid, H. Milting, K. W. Schmid, H. A. Baba
*Universitätsklinik Essen, Inst. für Pathologie, Germany

Objective: A significant decrease of the mean cardiomyocyte DNA content and increased numbers of diploid cardiomyocytes after ventricular unloading was demonstrated, suggesting a numerical increase of cardiomyocytes. The heart harbours several stem cells populations including c-kit (CD 117) + cells and side population cells (SPC), that might proliferate after unloading and generate diploid cardiomyocytes. It was tested, whether there is an increase of ABCG2+ SPC and CD117+ cells after unloading.
Method: In paired myocardial samples (before and after LVAD), the number of cells with immunoexpression of ABCG-2, c-kit/CD 117 and MEF-2 was assessed by immunohistochemistry and morphometrically determined.
Results: A significant increase of SPC and cells with coexpression of c-kit and MEF-2 after unloading was observed (p=0.001). A significant positive correlation between both SPC and cells with coexpression of c-kit and MEF-2 expression was observed (p=0.007 and 0.01). No correlation was found between the number of SPC and the mean cardiomyocyte DNA content.
Conclusion: SPC are significantly increased in the myocardium after ventricular unloading, suggesting a role of stem cell proliferation during “reverse cardiac remodelling”. These cells might proliferate and commit to different cell lineages such as cardiomyocytes or endothelium, and thus ameliorate cardiac function.

PS-18-019

Role of elastin gene polymorphism in ascending aorta aneurysm development in patients with essential hypertension

V. Zakharova*, V. Dosenko, M. Kostiv, E. Rudenko
*Cardiovascular Surgery Institute, Pathology, Kiyv, Ukraine

Objective: There is supposition about genetic propensity in the ascending aorta aneurysm (AAA) development. Aim: to investigate role of elastin gene polymorphism (rs2071307) in AAA development in essential hypertension (EH).
Method: DNA samples from persons with AAA and EH (1 group), with EH only (2 group) and healthy subjects (3 group) were examined. Polymorphism rs2071307 was studied with real-time PCR. Histological examination of AAA walls was performed in 1 group.
Results: Distribution on genotypes A/A, A/G, G/G was the following: 1 group - 42.1 %, 42.1 %, 15.8 %; 2 group - 68 %, 24 %, 8 %; 3 group - 18.5 %, 45.6 %, 35.9 %. Fragmentation of elastic membranes and media collagen component strengthening were revealed in persons with A/A, A/G, G/G genotypes in 54.2 %, 70.8 %, 11.1 % respectively. Persons with G/G genotype have more frequently (66.6 %) than others (A/A – 16.6 %, AG – 12.5 %) signs of inflammation, which promote AAA development parallel to EH.
Conclusion: We obtained evidence that elastin gene polymorphism (rs2071307) plays important role in EH and AAA development. In persons with allele A in rs2071307 risk of EH and AAA development is higher than in G/G genotype. Mostly allele A in rs2071307 is accompanied with elastic membranes fragmentation and their substitution by collagen that decreases arterial wall elasticity.

Tuesday, 11 September 2012, 09.30 - 10.30, Congress Hall Foyer 3rd Floor
PS-19 Poster Session Ophthalmic Pathology

PS-19-001

Conjunctival reticulohistiocytoma

L. Alfaro*, F. Pastor
*Valencia, Spain

Objective: Reticulohisticytoma is an uncommon lesion of non Langerhans histiocytes with a solitary form and a multicentric variant associated with other pathologies including malignancies. It is related to juvenile xanthogranuloma, but presents a peculiar giant cell type with occasional prominent nucleoli.
Method: A 83 years old man presented with a solitary conjuctival lesion clinically suspicious of CIN or squamous cell carcinoma. Previously patient reported surgery for a pituitary adenoma. Conjunctival lesion was completely removed and histological and immunohistochemical study was performed.
Results: The lesion appeared composed mainly by giant cells with wide granular cytoplasm and one or several nuclei, intermingled with lymphocytes. Macrophage cell markers were positive (CD68 and CD163). S-100, CD1a, CD21 and CD23 were negative.
Conclusion: Reticulohistiocytoma is a benign disease but clear distinction from systemic reticulohistiocytosis is important. Other similar non Langerhans histiocytosis share the risk of developing a systemic disease with much worse prognosis.

PS-19-002

Tumors metastatic to the orbit: Presentation of two cases

C. F. Costea*, O. Dobirceanu, A. Irimia, D. Radulescu
*University of Medicine Iasi, Dept. of Ophthalmology, Romania

Objective: Our aim is to inform on the frequency, clinical aspects, and histopathological features of the tumor metastatic to the orbit. In adults, the most common tumor metastatic to the orbit are carcinomas, breast carcinoma the most frequent. Less common are the metastases from gastrointestinal tract, kidneys, and prostate. Cutaneous malignant melanoma is the most common nonepithelial tumor metastatic to the orbit.
Method: Orbital metastatic tumors may occur at any age, but most often between 40 and 70 years of age. Most reported statistics reveal a slight predominance of women, accounted for by the fact that breast carcinoma is causing metastases most frequently. A frequent finding in the cases of metastatic carcinoma is enophthalmos that is associated with scirrhous carcinomas. We present two cases of orbital metastatic tumors in which the primary tumors were a basal cell carcinoma and a cutaneous malignant melanoma.
Results: As to the metastasis from a basal cell carcinoma, the primary tumor was located in the external angle of the eyeball and metastasized the external 1/3 of the orbit. In the case of malignant melanoma, the primary tumor was located in the upper lid and invaded the orbital floor and fat. In both patients eyeball enucleation was performed.
Conclusion: We chose to present these cases given the differential diagnostic challenge and rarity of their location.

PS-19-003

Uveal melanoma

A. Dumitriu*, S. Dumitriu
*UMF Iasi, Dept. of Neurology, Romania

Objective: Uveal melanoma which arises from melanocytes residing in the stroma is the most common primary intraocular cancer in adults.

Method: We report a case of uveal melanoma presenting as complicated cataract in a 65 years-old male.
Results: The right eye was blind for 6 months. The patient underwent extended enucleation and histopathology was consistent with uveal melanoma.
Conclusion: We present this case in order to provide the medical community a basic reference that would help to make further progress in this rare disease, which remains difficult to treat.

PS-19-004
Is uveal malignant melanoma different in Brazilian patients?
G. Freeman*, A. Damascena, D. Begnami, M. Chojniak, F. Soares
*São Paulo, Brazil

Objective: Background: Information on uveal melanoma is derived chiefly from European and USA studies, with little data from the rest of the world, including Brazil.
Method: This was a retrospective chart review of 285 enucleated cases of uveal malignant melanoma from the AC Camargo Hospital in São Paulo, Brazil, from January 1988 until December 2005. Epidemiologic characteristics were studied in relation to histological findings.
Results: There were more women than men (52 % versus 48 %). Metastases developed in 39 % (total group mean follow up of 7.14 year). Mixed tumors were most common overall (43.5 %): for non metastasizing tumors there were 41.1 % mixed, 36.1 % fusiform and 17.2 % epithelioid types. For metastatic tumors there were 46.7 % mixed, 21.5 % epithelioid and 21.5 % fusiform types. The difference between cell type and metastatic development was significant in all but epithelioid compared with mixed tumors. Epithelioid type had a relative risk of mortality of 3.51 and mixed had 2.18 compared to fusiform cell type.
Conclusion: Our patients were younger, with larger tumors and different histological proportions from those of the Collaborative Ocular Melanoma Study. Five year survival times were similar to those for Europe.

PS-19-005
Uveal melanoma between preserving vision and prolonging survival. Pathological contributions to a better clinical management
M. Mera*, L. Blaga
*UMF Cluj-Napoca, Anatomic Pathology, Romania

Objective: Uveal melanoma has a high metastatic potential which is invariably fatal. There is an ongoing debate on the impact of ocular treatment on metastatic disease and survival. Improved prognostication is needed to identify cases that could avoid unnecessary loss of vision while avoiding unethical care. Our study is aimed at contributing to the developing of reliable tools to assess the metastatic risk.
Method: An accurate prediction should include both clinical features and histologic parameters as biopsy techniques continuously advance. 120 cases of uveal melanoma, either reviewed or prospectively managed in our Pathology Department, were included in a Log-logistic multivariate survival model that we have considered would best accomodate our data. The performance of the model was assessed by bootstrap re-sampling.
Results: Extravascular matrix patterns, optic nerve invasion, tumorinfiltrating lymphocytes, tumor cytomorphology, nucleolar size and the mitotic count together with initial visual acuity have been found to be the most important predictors, ahead of the traditional TNM stage. The results are provisional but encouraging.
Conclusion: There is still need for multidisciplinary approach and multicenter collaboration in an effort to elucidate the uncertainty related to the best management of one of the most traumatising types of cancer.

PS-19-006
Orbital hemangiopericytoma: A case report
E. Omoscharka*, K. Lankachandra
*University of Missouri, Dept. of Pathology, Kansas City, USA

Objective: Hemangiopericytomas are rare vascular tumors arising from Zimmerman's pericytes, which ubiquitously surround blood capillaries and post-capillary venules. They rarely occur in the orbit, accounting for only 1 % of all orbital neoplasms. In most cases the primary presentation is progressive proptosis.
Method: A 26-year-old female was first seen for the evaluation of a right orbital mass which has been causing proptosis. Associated symptoms included peripheral vision loss in the right eye, persistent headache with occasional balance problems. A palpable, 3.2× 2.5 cm well circumscribed mass with a smooth surface, resting on the inferior orbital wall was completely removed through right anterior orbitotomy. H&E stained histologic sections were studied. In addition, tissue sections were subjected to immunohistochemical stains for CD34, CD99, BCL2, SMA, desmin, EMA and S-100.
Results: The mass was composed of spindle cells with very low mitotic activity. Staghorn vascular channels were evident, and in several areas the tumor cells invaded the pseudocapsule. The tumor cells were positive for CD34, CD99 and bcl-2 supporting the histopathologic diagnosis of benign hemangiopericytoma.

Conclusion: Orbital hemangiopericytoma is a slow growing tumor with a potentially malignant behavior, and a high local recurrence rate if incompletely excised. Complete, intact removal prevents tumor recurrence and provides a good outcome.

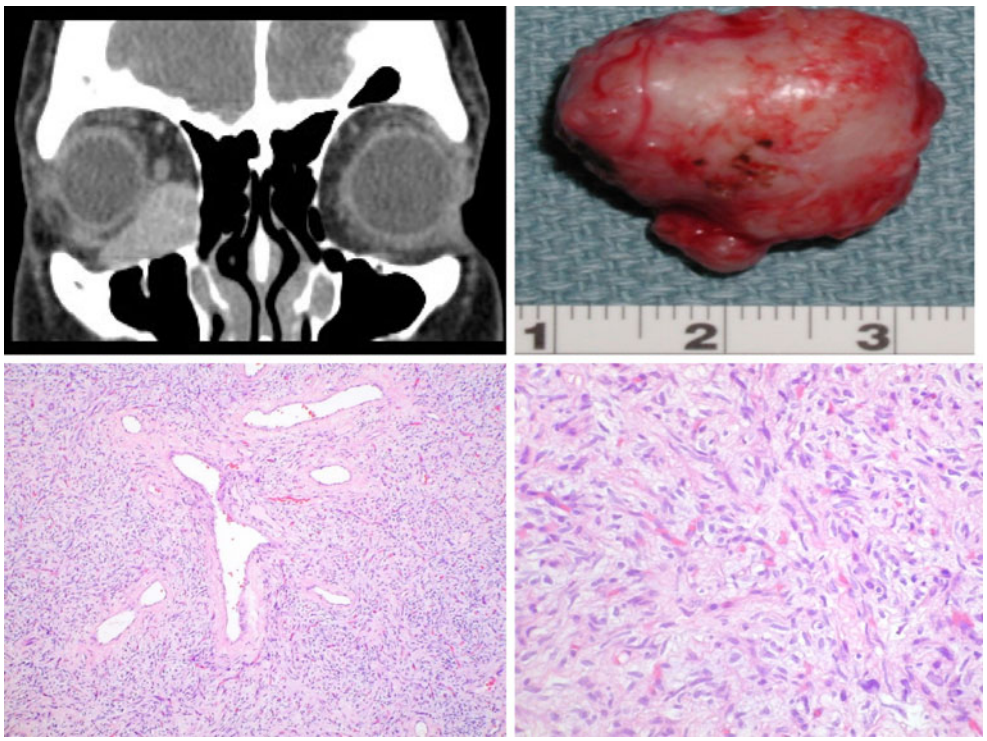

PS-19-007

Expression of SOD family in rat lacrimal gland after intermittent light exposure

C. L. Zamfir*, F. E. Zugun, E. Cojocaru, R. O. Temneanu, R. Folescu, M. Spataru
*University of Medicine Iasi, Dept. of Histology, Romania

Objective: Any disturbance of chronobiological rhytms represents a potential stressor, acting like a strong oxidant trigger. SOD family (CuZn-SOD, Mn-SOD and EC-SOD), is one of the most significant enzymatic complexes involved in antioxidant defense. Monitoring local SOD distribution in lacrimal gland after intermittent light exposure can be able to provide insights into the distinct links of antioxidant adaptative mechanisms.So long as lacrimal gland morphology and functions are dependent to a normal light exposure, mobilisation of its own antioxidant resources, especially SOD, is an usefull starting point in antioxidant ophtalmic therapy.
Method: Immunohistochemistry was performed in microscopic analysis of glandular fragments prelevated from 30 male Wistar rats, randomized in control/intermittent light exposed groups for 45 days. There have been used specific antibodies for each enzymatic member of SOD family. Blood samples were prelevated to control SOD levels. The study respected all imposed ethical criteria.
Results: Lacrimal glandular tissue exhibits a strong CuZn-SOD immunoreactivity, a moderate one for Mn-SOD and only a small EC-SOD reactivity, while the level of sanguin SOD is high, as a marker of oxidative aggression.
Conclusion: Oxidative stress may be engagged in a deep alteration of lacrimal gland. Mobilisation of SOD, depending on their specific glandular location and tissular receptivity, should be regarded as a promising alternative for antioxidant therapy.

Tuesday, 11 September 2012, 09.30 - 10.30, Congress Hall Foyer 3rd Floor
PS-20 Poster Session Thymic and Mediastinal Pathology

PS-20-001

Mediastinal liposarcomas: Clincicopathological study of 4 cases

E. Braham*, M. Yahia, M. Zarrouk, O. Ismail, M. Mlika, A. Ayadi Kaddour, E. Boudabous, T. Kilani, F. El Mezni
*Abderrahmen Mami Hospital, Dept. of Pathology, Ariana, Tunisia

Objective: Liposarcoma is the most commonly diagnosed soft tissue sarcoma in adults and occurs predominantly in the lower limbs and retroperitoneum. Primary mediastinal liposarcomas are rare accounting for less than 1 % of all mediastinal tumors.
Method: We report a retrospective study of 4 cases of mediastinal liposarcoma during an 8-year period. Diagnosis was made on mediastinal biopsy in 2 cases and on resected specimen in the 2 other cases.
Results: There were 3 men and a women ranging in age from 28 to 81 years, explored for respiratory symptoms. Radiological findings showed an anterior inhomogeneous mediastinal mass in all cases with extension to left hemithorax in one case. A surgical resection was achieved in only 2 cases but was incomplete. Histopathologically, tumors were classified into 2 well differentiated lipoma-like liposarcoma, one myxoid liposarcoma and one mixed liposarcoma (sclerosing liposarcoma with myxoid liposarcoma). All patients received adjuvant radio or chemotherapy. One of them presented lung metastasis during the follow up and another died from respiratory failure. The two other are still alive.
Conclusion: Mediastinal liposarcomas include a heterogeneous group of bulky tumours, the progression of which depends on the histological type. Histopathologic examination is always necessary as much for diagnosis as prognosis.

PS-20-002

Mediastinal epithelioid hemangioendothelioma with a high-grade clinical course

A. Konstantinova*, K. Shelekhova, V. F. Klimashevsky
*St. Petersburg State University, Russia

Objective: Epithelioid hemangioendothelioma (EH) is a rare neoplasm usually presenting in soft tissues. About twenty cases of EH have been reported in the mediastinum. Most of these mediastinal EH exhibited an indolent course.
Results: A 21-year-old woman presented with focally encapsulated mass, 5.5×4 cm in size, in the anterior mediastinum. The tumour of bone density was adhered to the lung tissue and occluded left subclavian vein. Microscopically, the tumor consisted of foci of so-called blister cells typical for EH, anastomosing cords of small epithelioid cells embedded in myxohyaline matrix with haphazardly distributed metaplastic bone and hemorrhagic cellular stroma. Spindling of the tumor cells was prominent. The tumor cells demonstrated moderate atypia, but mitotic figures were not found. Immunohistochemically, cells of primary tumor were positive for Fli1, vimentin, CD31 and CD34. Focal staining with EMA was observed. Multiple metastases were subsequently found in the liver and lungs. Metastatic deposits had the same morphology as a primary tumor.
Conclusion: We present the case of rare mediastinum epithelioid hemangioendothelioma with peculiar histological features such as prominent spindling of neoplastic cells and abundant metaplastic bone formation in aggregate with aggressive clinical behavior that exhibited a profound metastatic poteintial.

PS-20-004

Immunohistological characterization of thymic dendritic cells

A. Papoudou-Bai*, M. Bai, M. Doukas, K. Stefanaki, V. Galani, A. Goussia, A. Batistatou, P. Kanavaros
*Ioannina, Greece

Objective: Dendritic cells play key roles in the thymic histophysiology and histopathology. Therefore, we analyzed the immunotopographical distribution of cells expressing markers of dendritic cells and macrophages in thymus.
Method: In paraffin sections of postnatal thymuses were performed immunostainings for S-100, CD1a, CD207 (langerin), CD11c, CD123, CD68 and CD163. The Streptavidin-Biotin Peroxidase labeled (LSAB) and the double LSAB/Alkaline Phosphatase/anti- Alkaline Phosphatase (APAAP) immunohistochemical procedures were used.
Results: S100, CD1a, CD207, CD11c and CD123 positive cells, many of them with morphology of dendritic cells, were detected in the cortex and mainly in the medulla. These markers, except CD123, were also detected in cells of juvenile and immature Hassall Bodies (HB). CD68 and CD163 positive cells were detected in the cortex and the medulla but not in HB.
Conclusion: The immunohistological detection of S100, CD1a, CD207 and CD11c positive dendritic cells in juvenile and immature HB may reflect an important role of HB in the cooperation of epithelial and dendritic cells in the process of T-cell differentiation.

PS-20-005

Primary thymic carcinoma: Report of three cases

P. Xirou*, M. Koumpanaki, G. Balis, S. Barbanis, N. Barbetakis, N. Vladika, B. Christoforidou, F. Patakiouta
*Theagenion Cancer Hospital, Thessaloniki, Greece

Objective: Thymic carcinomas comprise rare malignant epithelial neoplasms, which exhibit a disproportionately large variety of growth patterns. We present three cases of primary thymic carcinomas, including two squamous cell carcinomas and one papillary adenocarcinoma.
Method: All three patients were males, aged 51, 61 and 77 years, and presented with mediastinal masses measuring 17 cm, 6.5 cm, 3.7 cm in maximal diameter respectively.
Results: Microscopically the first two tumors were poorly differentiated squamous cell carcinomas, immunohistochemically positive for CD5 and CD117, whereas the third

tumor was a papillary adenocarcinoma, positive for CD5 and negative for CD117 and TTF-1. Immunohistochemical features of the tumors were supportive of thymic derivation.
Conclusion: Primary thymic carcinomas are rare malignant tumors with clear-cut atypia, largely lack of organotypic features and a very diverse differentiation. Squamous cell carcinoma is the most frequent subtype. They are often a diagnosis of exclusion, since metastases to thymus and anterior mediastinum, mainly from the lung, are far more common. Immunoreactivity to CD5, CD70 and CD117 may support the thymic origin of neoplastic squamous cells. Treatment options include surgical excision, radiation and/or chemotherapy depending on tumor stage and patient's condition. The prognosis is generally poor with squamous cell carcinomas having a slightly more favorable outcome.

Wednesday, 12 September 2012, 09.30 - 10.30, Congress Hall Foyer 3rd Floor
PS-21 Poster Session Nephropathology

PS-21-002
Histopathological assessment of renal lesions after volume replacement with HES 130/0.4 or Ringer solution, following acute bleeding
R. Cruz Paiva*, A. Ortiz, C. Venâncio, J. Mesquita, A. C. Mega, A. Silva, H. Vala, D. Ferreira
*Instituto Politécnico de Viseu, Veterinary Sciences, Portugal

Objective: Surgical blood loss can lead to ineffective tissue perfusion of vital organs. Physiologic solution chosen for blood volume replacement may be determinant for preserving renal integrity. Our aim is to study kidney histopathological changes in a hemorrhagic model, followed by intravascular volume replacement with Ringer's lactate or Hydroxyethylstarch (HES) 130/0.4 solutions.
Method: Thirty one pigs under general anaesthesia with propofol and remifentanil underwent haemorrhage at a volume of 30 ml kg-1, over 20 min. After a waiting period of 20 min, intravascular volume was replaced using HES 130/0.4 (G1) and Ringer's lactate (G2). One hour after, pigs were euthanized with IV potassium chloride and sixty two renal samples were taken for histopathological examination, using PAS staining. Renal damage was assessed for glomerular, tubulointerstitial and vascular lesions.
Results: Mean arterial pressure reached 40 mmHg after bleeding, and recovered for values above 60 mmHg in both groups after volume replacement. Histopathological lesions observed in G2 were more frequent than those in G1.
Conclusion: HES 130/0.4 may reduce the incidence of histopathological lesions secondary to renal hypoperfusion after severe bleeding when compared with Ringer Lactate. Results suggest that the reestablishment of intravascular volume with HES 130/0.4 may preserve renal integrity secondary to blood loss.

PS-21-003
Expression of AEG-1, P53 and its clinicopathological significances in the malignant lesions of renal cell carcinomas
H. Erdem*, M. Oktay, U. Yildirim, A. K. Uzunlar, M. A. Kayikci
*Duzce University, Dept. of Pathology, Turkey

Objective: Astrocyte elevated gene-1 (AEG-1 also known as Metadherin) is associated with various aspects of tumor malignancy. The aim of this study was to investigate P53 relationship between AEG-1 and prognostic parameters.
Method: This study was made 50 paraffin blocks (tumoral samples), which were histopathologically diagnosed at department of pathology from 2005 to 2011. Subtypes of the cases were 24 (48 %) clear cell renal cell carcinomas (RCC) and 26 (52 %), non-clear RCC respectively. By immunohistochemical analysis, we investigated AEG-1, P53 expression in carcinomas of kidney and we determined its relationship with clinicopathological parameters.
Results: There were significant relationship between increased AEG staining score and tumor capsule (P=0.01), lymphovascular invasion (p=0.015) and significant relationship between the increased diameter with the increase of p53 (p=0.028). There were significant correlation between increased diameter of tumor and degree of increase the Fuhrman (p=0.02).
Conclusion: High AEG-1, P53 expression correlates with prognostic parameters in the RCC. In addition, AEG-1, P53 expression in RCC may be associated with tumor progression.

PS-21-004
Relationship of CD95, COX-2 and P53 in renal cell carcinomas with survival and other prognostic parameters: A tissue microarray study
H. Erdem*, U. Yildirim, A. K. Uzunlar, M. A. Kayikci
*Duzce University, Dept. of Pathology, Turkey

Objective: Renal cell carcinomas (RCC) is the seventh most common human malignancy. RCC is now recognized to be a complex neoplasm consisting of several different tumor subtypes, each with distinct genetic and clinical features. The aim of this study was to investigate the expressions of cyclooxygenase-2 (COX-2), P53 and CD95 in RCC that has different clinicopathologic characteristics.
Method: This study was conducted on a total of 49 paraffin embedded kidney samples (tumoral samples), which were histopathologically diagnosed at department of pathology

from 2005 to 2011. IHC stains for COX-2, P53 and CD95 were performed on tissue microarray using standard procedures.
Results: There were significant correlations between COX-2 and subtype (p=0,044), COX-2 and diameter (p=0,026). Significant relationships were found between p53 and age (p=0,050), P53 and diameter (p=0.050). Besides, there were significant correlations between CD95 and furhman grade (p=0,050).
Conclusion: CD95, COX-2, P53 expression correlates with prognostic parameters in the RCC patients. In addition, COX-2, P53, CD95 expression in RCC may be associated with tumor progression.

PS-21-005
Soft-tissue tumors and Ebstein Barr Virus (EBV) in kidney grafted patients
J. C. Goldberg*, M. d. Carmen Rial, J. Petroni, L. Leon, M. Amante, G. Hillchenbach, D. Casadei
*Buenos Aires, Argentina

Objective: EBV related malignancies (skin cancers, lymphomas, Kaposi sarcomas) complicates organ transplantation EBV-associated smooth-muscle tumors are rare.
Method: Among 1500 kidney grafted patients, three developed EBV-SMT. Case 1. Female 51 y, with EBV-SMT (Generalized) Case 2. Female 46 y, breast phylodes sarcoma, reviewed diagnosis: EBV-SMT. Case 3. Male 23 year, severe abdominal pain, 2 gut tumor-like nodules were excised suspection of TBC. EBV-SMT was microscopic diagnosis.
Results: Progressive weight-loss all 3patients, chronic cough in patient 1, chest X ray multiple pulmonary lesions, on CT-scan paravertebral lesions. Transthoracic biopsy: spindle cells proliferation with mixed cellularity eosinophilic cells intermingled fascicles resembling smooth muscle, mononuclear inflamatory cells and capillarie evoqued myofibroblastic tumor. No mitosis, mild nuclear atypia. Negative immunohistochemestry: CD21, CD34, CD99, EMA, cytokeratin, S100, CD117. Alpha-smooth muscle actin diffusely positive, EVB-LMP negative. In situ hybridization : EBV + nuclei. EBV-SMT was established.
Conclusion: SMT in immunocompromised are EBV associated. Primary target of EBV are B lymphocytes, may infect smooth-muscle through receptor for EBV CD21 Mechanisms of EBV related-tumor genesis is integration of EBV-DNA within ALK locus in tumor cells. ALKgene rearrangement and expression; associated with inflammatory myofibroblastic tumors, anaplastic large-cell lymphomas etc. Clonally of multifocal EBV-SMT using southern blot showed, multiple tumors constitute independent primary lesions.

PS-21-006
Glomerulosclerosis is a major contributor for chronic renal allograft dysfunction in IgA nephropathy developing after transplantation
H.-J. Jeong*, B.-J. Lim, D.-J. Joo, M.-S. Kim, Y.-S. Kim, S.-I. Kim, M.-J. Koh
*Yonsei University, Dept. of Pathology, Seoul, Republic of Korea

Objective: To explore the significance of glomerulosclerosis and glomerular injury in posttransplant immunoglobulin A nephpropathy (IgAN), we reviewed 131 renal allograft biopsies diagnosed with IgAN after transplantation.
Method: The degree of glomerulosclerosis was scored into 0–3, mesangial proliferation was scored into 0 (absent) and 1 (present), and the degree of crescents was scored into 0–2. Glomerular injury score (GIS) was obtained by adding the above 3 scores and grouped into 3 categories (group 1, score 0–1; group 2, 2–4; group 3, 5–7).
Results: Serum creatinine level was significantly increased (1.3±0.4, 1.8±0.9, 2.2±0.8 mg/dL, p=0.007), estimated glomerular filtration rate (eGFR) was significantly decreased (68.5±17.6, 52.1±22.5, 40.9±20.4 mL/min, p=0.001) and proteinuria was significantly increased as GIS increased (1.3±2.7, 1.9±1.6, 4.6±7.1 g/24 h, p=0.030). Interstitial fibrosis of more than 25 % of cortical area increased as GIS increased (2.3, 26.0, and 57.1 %, p<0.001). When a multivarate analysis was done, GIS group 3 was the most important predictive factor of eGFR (p=0.009) and proteinuria (p=0.014).
Conclusion: In conclusion, glomerular injury is a dominant feature of posttransplant IgAN and a simple surrogate marker for chronic graft dysfunction.

PS-21-007
Causes of early graft impairment after deceased donor kidney transplantation
N. Karadeniz*, M. N. Turan, B. Sarsik, E. Tatar, H. Toz, T. O. Sezer, C. Hoscoskun, S. Sen, K. Nisar
*Ege University, School of Medicine, Izmir, Turkey

Objective: The aim of the study is to evaluate the histopathological finding and the C4d staining patterns of the patients who were biopsied due to graft dysfunction (GD) after initial well-function within 1 month of deceased donor kidney transplantation (DDKT).
Method: Histological analysis and C4d immunostaining were performed 34 on needle core biopsies.
Results: Thirty-four patients (mean age: 37±8 years, male: 59 %) were included. Histological analysis revealed acute rejection (AR) (n:7), acute tubular injury (ATI) (n:8), allograft infection (n:1), borderline changes (n:8), normal morphology (n:3), and donor-related changes (n:7). C4d

staining was detected in 44 % (15 of 34) biopsies; staining patterns were diffuse (n:5), focal (n:5) and minimal (n:5). Diffuse (n:3) and focal (n:1) C4d positivity accompanied 4 of 7 cases of AR. In remaining 27 patients having non-AR histological picture, diffuse or focal C4d positivity were detected in 2 and 4 cases, respectively. Peritubular capillaritis was detected in 41.1 % (14/34) of biopsies, of which four had C4d diffuse, one had C4d focal positive.
Conclusion: Beyond cold ischemia time-induced ATI, immunological causes including antibody mediated process may play an important role in early impairment of graft function after DDKT.

PS-21-008
Immunohistochemical analysis of the renal interstitial fibroblasts
S. Kostadinova-Kunovska*, R. Jovanovic, M. Bogdanovska, V. Janevska, L. Grchevska, G. Petrushevska
*Faculty of Medicine, Inst. of Pathology, Skopje, Macedonia

Objective: Renal fibrogenesis is a process common to all progressive kidney diseases. The main executive cell of this process is the fibroblast, by secreting and remodeling the extracellular matrix. The number of fibroblasts is minor in healthy kidney interstitium, but it increases during the process of fibrosis. Their morphology and immunophenotype vary due to different intrinsic and extrinsic factors, thus making their identification and visualization, as well as determination of their origin, very difficult.
Method: We performed morphological and immunohistochemical analyses on kidney biopsies with primary glomerulopathy and interstitial fibrosis, using the following antibodies: Vimentin, α-SMA, S100A4, Cadherin 9 and CD34.
Results: Interstitial fibrosis with focal, rather than diffuse distribution, was present in all analyzed cases. The total interstitial fibroblast population was positive for Vimentin, majority of the cells were positive for S100A4, and a smaller proportion of cells were positive for α-SMA, Cadherin 9 and CD34. Furthermore, different cells in the fibroblastic population showed positivity for different markers.
Conclusion: The above stated observations contribute to the theory that different subpopulations of fibroblasts, with different origin, take part in the renal fibrogenesis.

PS-21-009
Soluble epoxide hydrolase inhibition reduce blood pressure and organ damage independently of Nitric Oxide (NO) in mice with Goldblatt two kidney, one clip model (2K1C)
P. Kujal*, L. Kopkan, L. Cervenka, Z. Vernerova
*Charles University, Third Faculty of Medicine, Prague, Czech Republic

Objective: Investigate the role of NO in the blood pressure (BP)-lowering effects of soluble epoxide hydrolase (sEH) inhibition in 2K1C model.
Method: The endothelial NO synthase gene knockout mice and their wild-type controls were used. Renal concentrations of epoxyeicosatrienoic acids (EETs) and dihydroxyeicosatrienoic acids (DHETs) were measured in nonclipped kidney. Renal NO synthase activity was determined by measuring the rate of formation of L-[14 C]citruline.
Results: Treatment with the sEH inhibitor caused the same BP decrease that was associated with increase in daily sodium excretion in both types of mice. The ratio of EETs/DHETEs in the nonclipped kidney was increased and did not alter renal NOS activity. sEH inhibition reduced significantly glomerular and tubulointestitial injury.
Conclusion: BP-lowering effects of chronic sEH inhibition in 2K1C mice are associated with normalization of the reduced availability of biologically active EETs in the nonclipped kidney and their direct natriuretic actions.

PS-21-010
Total inflammation in 6-month surveillance renal transplant biopsies is associated with decreased renal function and de novo class 2 donor specific antibody
Z. Laszik*, S. Chandran, F. Vincenti
*UCSF, Dept. of Pathology, San Francisco, USA

Objective: The goal was to correlate inflammation and acute rejection (AR) with renal function and antibody status in 6-month renal transplant surveillance biopsies.
Method: Relative risks of inflammation and AR in 380 6-month biopsies was calculated by Multivariable Poisson regression.
Results: AR was seen in 7.3 % (n=28), borderline change in 19.7 % (n=75), and C4d positivity in 2.1 % (n=8) of all biopsies. Total cortical inflammation (ti), present in 32.6 % (n=124) cases, was associated with 7 ml/min/1.73 m2 lower eGFR at 6 months (95 % CI= −10.8, −3.2). De novo HLA Class 1 was identified in 17.4 % (n=44) and Class 2 DSA in 26.1 % (n=66), with most having MFI values <1000. Increased risk of AR was seen with higher levels of de novo Class 1 (RR 1.49, 95 % CI=1.08, 2.0) or Class 2 DSA (RR 1.34, 95 % CI=1.04, 1.72). Class 2 (but not class 1) DSA was associated with a higher risk of ti (RR 1.40 for ti-score ≥1, 95 % CI=1.13, 1.72) at 6 months.
Conclusion: Both ti and AR in 6-month surveillance kidney transplant biopsies are strongly associated with de novo HLA Class 2 DSA. Total inflammation at 6 months correlates with decreased kidney function.

PS-21-012

Acute renal failure in a HIV patient with Fanconi syndrome, nephrogenic diabetes and hypokalemia: Report of a case and correlation between clinical symptoms and histology, showing tenofovir toxicity

C. L. Menendez*, M. A. de la Torre, A. Torres, D. Rodríguez Villar, V. Venta, M. Poch, N. Fdez Martinez, B. Corrales, A. Astudillo
*Gijon, Spain

Objective: Tenofovir disoproxil fumarate has been used in the treatment of HIV patients producing occasional renal dysfunction and Fanconi Syndrome.
Method: A 38-year-old patient was referred with severe acute renal failure and important metabolic acidosis and glycosuria with normoglycemia in urine analysis, altogether with urinary alkaline pH and proteinuria with a protein/creatinine ratio of 4. He was HIV and B positive diagnosed 17 years earlier. His medication regimen consisted of lopinavir, ritonavir, tenofovir and lamivudine. The patient had a history of nausea, vomiting and some diarrhea with low fluid intake for a week. Besides slight dehydration, the physical examination was unremarkable. Renal ultrasound showed normal kidneys. With adequate fluid restoration, the renal function improved but other metabolic alterations like nephrogenic diabetes remained.
Results: Renal biopsy revealed toxic acute tubular necrosis predominantly involving proximal tubules with prominent eosinophilic inclusions within proximal tubular cell cytoplasm, which represented giant, abnormal mitochondria, consistent with tenofovir toxicity. Some histochemichal studies (COX and SDH) were performed.
Conclusion: Although prospective clinical trials have demonstrated a low incidence of renal toxicity with tenofovir, there are several such reports in the literature. Current recommendations suggest close monitoring of renal function after initiation of therapy with tenofovir, specially at the beginning and when used in combination with certain antiretroviral agents.

PS-21-013

Nutcracker syndrome (NS): A case report

C. L. Menendez*, M. A. de la Torre, D. Rodríguez Villar, S. Fernández Pello, A. Torres, V. Venta, M. Poch, C. Miguel Ruiz, C. Murias, B. Corrales
*Gijon, Spain

Objective: Nutcracker syndrome (NS) is caused by compression of the left renal vein between the aorta and superior mesenteric artery. The main presenting symptom of this rare entity is haematuria, with various degrees of proteinuria. The diagnosis of NS syndrome is primarily by imaging and can sometimes be challenging.
Method: A 21-year-old male was referred to nephrology with a 3 months history of intermittent gross haematuria. All blood test including blood cell count, biochemistry, immunoglobulin electrophoresis, antinuclear antibody were normal. Urinary analysis revealed numerous red blood cells and a protein/creatinine ratio of 0.3. A previous cystoscopic examination was normal. Renal ultrasound revealed a diffuse increased echogenicity.
Results: Renal biopsy showed a normal histology with no immunofluorescence deposits. CT scan revealed dilatation of the distal left renal vein with narrowing between the superior mesenteric artery and the aorta.
Conclusion: NS is a rare entity causing haematuria. There are few reported cases with histology, although it usually shows no abnormalities. The proposed mechanism for the haematuria is an abnormal communication between the submucosal venous plexus and the calyceal system presumably induced by renal venous hypertension.

PS-21-014

Banff Initiative for Quality Assurance in Transplantation (BIFQUIT): Reproducibility for BKV immunohistochemistry in renal allografts

M. Mengel*, S. Chan, J. Climenhaga, H. Regele, B. Colvin, P. Randhawa
*University of Alberta, Laboratory of Medicine, Edmonton, Canada

Objective: Detection of BK virus associated large T-antigen is crucial for the diagnosis of polyomavirus nephropathy.
Method: In an international multi-centre trial we assessed the inter-observer and inter-laboratory variability for BK immunohistochemistry. A tissue microarray was constructed comprising 23 specimens representative of the whole analytical spectrum from negative over mild to strong SV40 positive cases. 81 participants at 60 centers stained the TMA slides using local protocols. Participants evaluated their slides following a provisional Banff grading schema. Details regarding local staining protocols and evaluation scores were collected online. Stained slides were returned for centralized panel re-evaluation. Weighted kappa statistics were used to determine the variability.
Results: The BK inter-observer reproducibility was substantial (mean kappa 0.64), but inter-laboratory reproducibility was below chance (kappa −0.22). Separating components of BK evaluation schema into stain intensity and stain percentage showed no significant improvements in reproducibility. However, collapsing the proposed BK scoring schema into a simple positive/negative call improved BK inter-laboratory variability to 0.77.
Conclusion: These results indicate a significant variability between laboratories for detecting the SV40 large-T antigen by immunohistochemistry in paraffin sections. Any

proposed grading schema for BK nephropathy, which is dependent on percentage and intensity of nuclear staining, will essentially not be reproducible between laboratories.

PS-21-015

Diagnostic significance of myelin figures in renal biopsies

M. J. Mihatsch*, H. Hopfer, D. Ferluga
*Universitätsspital Basel, Inst. für Pathologie, Switzerland

Objective: Myelin figures (MF) in podocytes is the major finding in Fabrys`s disease. MF are also found in metabolic disorders and following application of cationic amphiphilic drugs. We posed the question: Can M. Fabry and metabolic and/or drug induced MF be differentiated by LM and EM?
Method: Case reports of 7966 renal biopsies containing the terms myelin, phospholipid or Fabry were selected, then we noted sex, biopsy indications, drug therapy and pathological diagnosis. EM pictures were screened for frequency and distribution of myelin figures and curvilinear bodies (CLB).
Results: MF were rare (n=42), mainly found in podocytes (31/42), less frequently in endothelial/mesangial cells (each 8/32) or proximal tubules (6/42). CLB were seen only once in podocytes. In most cases, usually, only few cells had single MF. CLB and foam cells were absent. The etiology was usually unknown. In one case, CLB were found with MF, alongside moderate numbers of MF in moderate numbers of podocytes. Foam cells were not seen. The patient had received chloroquine.
Conclusion: In all cases with podocytic foam cells (12/31) and/or numerous MF in many podocytes and other renal cells, without detectable CLB, M. Fabry was present. Foam cells together with many MF are suspicious of M. Fabry, MF and CLB are indicative of chloroquine therapy.

PS-21-016

Simultaneous transplant glomerulopathy and recurrent glomerulonephritis in kidney allograft

J. M. Mosquera Reboredo*, E. Vazquez Martul, L. Chinchilla, R. Giocomodonato, J. A. Vázquez Bueno, A. Alonso Hernandez, C. Fernandez Rivera
*Complexo Hospitalario Universitario, Dept. of Pathology, La Coruña, Spain

Objective: We present three cases of simultaneous Transplant Glomerulopathy (TG) and recurrent glomerulonephritis in kidney allografts.
Results: CASE 1:56 year old man with Chronic Renal Failure (CRF) secondary to IgA Nephropathy who recived a kidney transplant. Five years later the patient present asthenia, deterioration of renal function, proteinuria and hypertension. Allograft biopsy showed on light and electron microscopy characteristic features of TG, but also recurrent IgA Nephropathy with mesangial staining of IgA and mesangial electrodense deposits in the glomeruli. CASE 2:43 years old man. CRF secondary to Membranous Glomerulonephritis Kidney transplant on July 2000 with decrease renal funtion and proteinuria 9 years later. Allogratf biopsy showed again characteristic features of TG and granular IgG and C3 inmunostaining in glomerular basement membranes. Ultraestructural studies confirm the TG and the subepithelial deposits. CASE 3:52 year old woman CRF secundary to membranoprolipherative glomerulonephritis type 2(DDD). Third kidney transplant on August 2006. Renal function deterioration on March 2010. Allogratf biopsy showed characteristic features of TG on light and electron microscopy but also features of DDD with C3 deposition on inmunofluorescence and ribbon-like highly electrodense intramenbranosous deposits.
Conclusion: We must consider the possibility of simultaneous transplant glomerulopathy and other recurrent or de novo glomerulonephritis in the graft biopsy. Prognosis when both entities develop in the allograft is disastrous.

PS-21-017

Cryopyrin-associated periodic syndrome with secondary amyloidosis

J. M. Mosquera Reboredo*, L. Bolaños, M. Cao, T. Hermida Romero, C. Delgado Sotorrio, T. Ferreiro, R. Hernandez Cancela, B. Veleiro, E. Vázquez Martul
*Complexo Hospitalario Universitario, Dept. of Pathology, La Coruña, Spain

Objective: Cryopyrin-Associated Periodic Syndrome (CAPS) is a rare hereditary inflammatory disorder with three differents phenotypes: familial cold autoinflamatory syndrome, Muckle-Wells syndrome and neonatal-onset multisysten inflamtory disease CAPS results from a mutation of the NLRP3 gene (1q44) coding for cryopyrin, which forms intracellular protein complexes (inflammasomes).
Results: Case report: 41 year old women with chronic renal disease stage 3 (creatinin 2,2 mg/dl and proteinuria 180 mg/24 h) who developed urticarial episodies since 6 months old related to cold exposure. After 11 years old patient describe associated to these episodios bilateral arthritis (knes, ankles and elbows), conjunctival inflammation, shivers, and asthenia, more frequently in winter and precipitated by cold exposure, air conditioning, stress and menstruatión. Aditionaly the patient developed in last years bilateral hypoacusis A kidney biopsy showed a amorphous, acellular and acidophilic material Congo red positive deposits at interstition, arteries and arterioles and less frequent at glomeruli. This material displays apple green birefringence by polarizad light microscopy. Diagnosis: SECONDARY RENAL AMYLOIDOSIS

Conclusion: The clinico-Pathologial findings of this case are compatible with Muckle-Wells syndrome. Secondary amyloidosis is a severe complication which occurs in 25 % of Muckle-Wells cases. Amyloidosis is cause by increase of C-protein and A amyloid during the episodies before described and deposition of the A amyloid in differents tissues.

PS-21-018

Glomerulocystic disease associated with thrombotic microangiopathy in two kidney allografts

J. M. Mosquera Reboredo*, E. Vazquez Martul
*Complexo Hospitalario Universitario, Dept. of Pathology, La Coruña, Spain

Objective: Glomerulocystic kidney disease (GCKD) is a rare condition usually congenital and reported in infants and young children. Only few cases of adquired GCKD had been reported often following Hemolytic Uremic Syndrome (HUS).
Method: Histological study of two kidney graft explants.
Results: We present two cases of kidney transplant who developed HUS in allografts. Both cases showed at the histological examination typical vascular and glomerular changes of Thrombotic Microangyopathy (TMA). A cystic transformation with increase of urinary space and retraction of glomerular tuft was frequently observed. Chronic transplant vasculopathy was found in the two cases. Humoral active rejection was also demonstrate in one case with moderate peritubular capillaritis and glomerulitis and diffuse C4d deposition at peritubular capillaries.
Conclusion: In a few cases GCKD appear to develop after another kidney disease includes single case reports of GCKD associated with mesangial glomerulonephritis, Wegener's granulomatosis, progressive systemic sclerosis, after HUS (include some case in adult patient). Our two cases represent a initial stage of adquired GCKD. The ethiopathogenetic relationship is not clear but some authors propous that cystic dilatation of the Bowman's capsule associated to TMA/HUS may be secondary to ischemic mechanism.

PS-21-019

Case report: Cytomegalovirus gastritis in renal transplanted man

F. Noroozinia*, K. Makhdoomi, A. Esmaeili, A. Saffarifard
*Emam Khomeini Hospital, Dept. of Pathology, Urmia, Iran

Objective: CMV is an important pathogen in immunocompromised hosts, including patients with AIDS, neonates and transplant recipients. This infection develops in 70–90 % of transplant patients. Upper GI symptoms in solid organ recipient are common (20 %) and clinical signs are more serious in 10 % of cases.
Method: We report a 30 year old man with end stage renal disease underwent kidney transplantation from a CMV negative donor on June 2011. After 1.5 months he admitted with fever, generalized body pain, oral aphtous ulcers and epigastric pain accompanied by malaise. Endoscopic examination revealed multiple antral erosions with surrounding erythema. Clinicopathological investigations revealed CMV viremia with a Ig-M antibody titer and CMV gastritis confirmed by histopathological examination.
Results: The patient was started on intravenous (IV) ganciclovir 5 mg/kg per day every 12 h initially for 3 weeks, afterwards the fever decreased; cell blood counts throwback to normal ranges and general condition of the patients improved.
Conclusion: CMV infection develops in 70–90 % of the transplant patients. The colon and stomach are the most common sites of gastrointestinal infection. Though the rate of GI affliction by CMV is high, localization to the gastric antrum is not common.

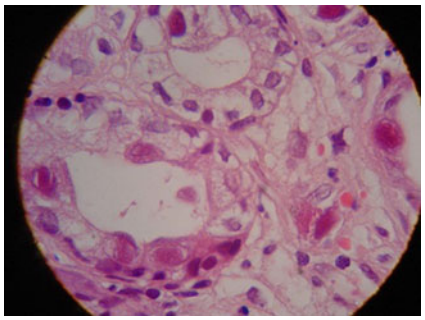

PS-21-020

Immunohistochemistry study of C-Kit expression in renal cell carcinoma

F. Noroozinia*, F. Abbasi, Z. Yekta, F. Meisami, A. Saffarifard
*Emam Khomeini Hospital, Dept. of Pathology, Urmia, Iran

Objective: Renal Cell Carcinomas include about 2–3 % of adults neoplasms and 90–95 % of all renal tumors. In many cases, it is possible to distinguish. RCC subtypes on the basis of hematoxylin-eosin staining alone. However, overlapping morphologic features pose some difficulties in making a proper diagnosis. To render an accurate diagnosis, additional methods like immunohistochemichal staining against C-Kit have been recommended.
Method: We reviewed 65 cases of RCC diagnosed during 9 years. Formalin fixed, paraffin embedded specimens was available in 65 cases. The expression of C-kit was evaluated using immunohitochemistry.
Results: Six cases of 39 clear cell type (15.4 %), 8 of 13 papillary type (61.5 %), and 11 of 11 chromophobe type (100 %) were positive for C-kit that considering Chi-Square test there is significant relevation between RCC's subtypes

and C-Kit expression (P: 0.001). From 8 cases with renal vein invasion, 3 showed positive expression of C-Kit (37.5 %) and in 55 cases with no venous invasion, C-kit expression was detected in 22 (38.6), so no significant relation was found between renal vein invasion and C-kit expression.
Conclusion: The expression of C-Kit in RCC may have diagnostic significance.

PS-21-022
Tubulointerstitial Nephritis (TIN) in IgG4-Related Systemic Disease (IgG4-RSD) with lung and lymph node involvement
J. F. Perez Ochoa*, D. Lopez, L. Serrano, V. Garcia, A. Fernandez Vasalo, P. Parrales, J. L. Mate, A. Ariza
*Hospital Germans Trias i Pujol, Dept. de Anatomia Patologica, Barcelona, Spain

Objective: IgG4-RSD shows abundant IgG4-positive plasma cells, diffuse fibrosis, and increased serum IgG4 levels. Although IgG4-RSD typically results in autoimmune pancreatitis (AIP), any organ may be involved. Thus, IgG4-RSD TIN often goes unrecognized in the absence of AIP. This is an IgG4-RSD TIN case with mediastinal lymph node and pulmonary involvement.
Method: A 73-year-old male presented with rapidly progressive renal failure, hypergammaglobulinemia, hypocomplementemia, and enlarged mediastinal lymph nodes and bilateral pulmonary nodules on CT. Renal and mediastinal lymph node biopsies were performed and IgG4 IHC was done on both after standard techniques.
Results: The renal cortex and medulla showed diffuse interstitial fibrosis with tubular atrophy and abundant plasma cells (25 IgG4-positive cells/HPF), numerous lymphocytes and some eosinophils. IF showed IgG, C3, kappa, and lambda granular deposits in tubular basal membranes and Bowmann capsules. Lymph node follicular and paracortical hyperplasia with abundance of mostly IgG4-positive plasma cells was seen. An IgG4-RSD diagnosis was rendered and high serum IgG4 levels were demonstrated. Steroid therapy resulted in lymph node and lung nodule reduction.
Conclusion: TIN with abundant plasma cells and diffuse interstitial fibrosis, especially if accompanied by hypergammaglobulinemia, hypocomplementemia, or extrarenal involvement, should suggest IgG4-RSD and prompt serum IgG4 level determination and renal IgG4 IHC.

PS-21-023
An unusual case of osmotic nephrosis
M. Rabant*, M. L. Figuere, J. Beaume, V. Vuiblet, M. Herody, G. Touchard, L.-H. Noel
*Hopital Necker, Paris, France

Objective: A 39-year-old woman was admitted for chronic renal failure. Clinical examination was normal. Biological explorations showed creatinin clearance around 55 ml/min, tubular proteinuria with Bence Jones κ protein. Serum immunoelectrophoresis identified abnormal monoclonal immunoglobulin G and κ-light chains (LC). Bone marrow histology was normal.
Method: Kidney biopsy revealed diffuse intracytoplasmic vacuoles in the proximal tubules resembling osmotic nephrosis. Distal tubules, glomeruli, vessels and interstitial compartment were normal. Immunofluorescence (including anti-κ and -λ staining) was negative. Electronic microscopy (EM) revealed intracytoplasmic immunoglobulinic crystals containing κ LC inside the vacuoles, leading to the diagnosis of Light Chain Proximal Tubulopathy (LCPT).
Results: LCPT is a rare complication of dysglobulinemia. It may be associated with crystals within the cytoplasm of proximal, less frequently distal, tubular cells, consisting more frequently in κ LC. Rarely, diffuse tubular vacuolization is present, often indistinguishable from osmotic nephrosis. In our case, there was no proximal tubular dysfunction and immunofluorescence was negative. The first evocated diagnosis by light microscopy was "osmotic nephrosis". However, we failed to identify any causal factor. Finally, the diagnosis was performed by immunoEM.
Conclusion: In conclusion, before a picture of osmotic nephrosis without obvious cause, EM and immunoEM may be helpful for the diagnosis of LCPT, often revealing a dysglobulinemia.

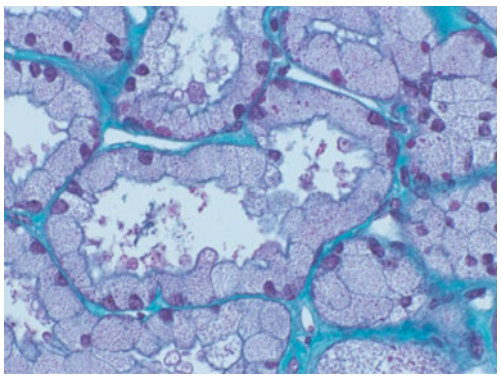

PS-21-024
Opportunistic infections in renal transplantation – A case series
R. Sampaio*, R. Dias, P. Farrajota, A. Coelho, T. Almeida, A. Duarte, J. R. Vizcaino
*Anatomia Patológica, Valpaços, Portugal

Objective: Oporto's Hospital Centre is one of the portuguese hospitals with more renal transplantation activity (performed since 1982). Although increasingly rare, opportunistic infections (OI) in transplanted patients remain a

major diagnostic challenge and are associated with high mortality rate.
Method: In order to evaluate the incidence of OI in renal transplant patients and to identify the location of infection, the respective techniques of diagnosis used and the survival time after infection, we conducted a retrospective study using the Nephrology Department's database on renal transplants. We consulted the registries from 2004 to 2012.
Results: We investigated 2041 cases and found 82 cases of OI caused by Herpes virus (n=7), Cytomegalovirus (n=27), Polyomavirus (n=16), Aspergillosis (n=4), Alternaria (n=2), Mucormycosis (n=1), Candidiasis (n=12), Tuberculosis (n=9), Cryptococcus (n=2) and Pneumocystis (n=2). The lung and urogenital system were the most affected systems. Kidneys were affected in 3 cases respectively by mucormycosis, tuberculosis and cryptococcus. Of all the cases of OI, 39 were diagnosed by the Department of Anatomic Pathology (21 by biopsy; 16 by cytology; 2 by biopsy and cytology).
Conclusion: In many cases the diagnosis could only be performed through histologic/cytologic examination. Prompt diagnosis and treatment are necessary to avoid life threatening complications and may greatly improve prognosis.

PS-21-025

Papillary renal cell carcinoma with osseous metaplasia and bone marrow elements: A case report

L. L. Santos*, A. Polónia, R. Henrique, C. Lobo
*IPO Porto, Dept. of Pathology, Viana do Castelo, Portugal

Objective: Renal cell carcinomas might display foci of calcification and even ossification. This rare event has been reported mostly in the clear cell variant. Herein, we present the case of a 69 year-old man, previously diagnosed with colon cancer, incidentally found to have a calcified mass in the kidney, which was interpreted as non-characteristic for renal cell origin.
Results: Radical nephrectomy was performed. A 5.5×5.0×4.0 cm tumor was found, with a heterogeneous brown cut surface, containing areas of necrotic tissue and extensive calcifications. Histopathologic examination disclosed papillary structures covered by small cells with scant cytoplasm, dispersed among mature bone tissue enclosing marrow elements. Epithelial tumor cells were imunorreactive for cytokeratins, CD10 and PAX2, and negative with HMB-45. Hale`s colloidal iron was negative. Trisomy of 3p, 7p and 17p was detected by FISH. A diagnosis of PRCC type 1, Fuhrman grade 2, with extensive osseous metaplasia was rendered.
Conclusion: Ossification of renal cell tumors is rare, occurring mostly in clear cell type and the underlying mechanism is unclear. These tumors show atypical radiological features and might be confused with non-renal cell tumors. To the best of our knowledge, this is the first report of PRCC with osseous metaplasia and bone marrow elements.

PS-21-026

The effect of doxycycline on glomerulosclerosis in 5/6 renal ablation

S. Sarioglu*, D. Sonmez, A. Celik, F. Saglam, O. Yilmaz, E. Koraltan, Z. Cavdar, G. Oktay
*Dokuz Eylul University, Faculty of Medicine, Izmir, Turkey

Objective: The effect of matrix metalloproteinase (MMP) inhibitors in segmental sclerosis is unknown. The aim of this study is to investigate the effect of a MMP inhibitor, doxycycline, on glomerulosclerosis (GS) in renal ablation nephropathy.
Method: Fourteen of the 32 female Wistar albinos were 5/6 nephrectomised. Doxycyline was given to half of each group (40 mg/kg/day total 28 days). After sacrification, the GS, MMP-2, MMP-9, TIMP-2 expressions were analyzed histopathologically. Pro and active MMP-2 and -9 were analyzed by gelatin zymography. TIMP-1 and TIMP-2 were measured with ELISA assay.
Results: Doxycycline administration to the 5/6 nephrectomy group improved GS, but did not inhibit glomerular MMP-9 or cortical pro- and active-MMP-2 and pro-MMP9 but increased TIMP-1 and TIMP-2 expression in all groups in cortical tissue. MMP-9 expression and GS were increased in all groups receiving doxycycline.
Conclusion: We have demonstrated improved GS in renal ablation model by doxycycline administration but also doxycycline has an unexpected adverse effect. The effect of doxycycline on the expression of MMP-2 and -9 cannot explain the improvement in GS, but increased cortical TIPM-1 and -2 may be an important contributing factor for inhibition of MMPs.

PS-21-027

Digitally reinforced hematoxylin-eosine polarization in diagnosis of renal amyloidosis

S. Sen*, B. Sarsik
*Ege University, Faculty of Medicine, Izmir, Turkey

Objective: Systemic amyloidosis is a rare disorder, characterized by extracellular accumulation of Congo-red (CR) positive fibrillar amyloid protein deposits. The kidney is the most commonly affected organ by systemic amyloidosis. CR staining which increases the positive birefringence of the weakly birefringent unstained amyloid. In this study we investigated potential power of digitally reinforced birefringence of routine Hematoxylin-eosine (HE) slides on the renal biopsies.

Method: We reviewed 130 HE stained slides for polarization. Sixty five amyloidosis cases were diagnosed by renal biopsy from 2008 to 2012 at our laboratory. All biopsies were evaluated by light and immunofluorescence microscopy. Slides were reevaluated blindly using a microscope (Olympus BX51) attached polarization filter and connected to a digital camera (Olympus DP21, SAL). Depositions which show green birefringence on HE with digitalized microscopy were considered as positive and results were confirmed using CR.

Results: Of the 65 CR confirmed amyloid positive biopsies, 61 showed green birefringence with HE. Of the 65 CR confirmed amyloid negative biopsies, two were considered as false positive. The sensitivity, specificity, positive and negative predictive values were estimated as 94 %, 97 %, 97 % and 94 %, respectively.

Conclusion: We concluded digitally polarized HE sections can be used as a fast and first step diagnostic method for renal amyloidosis.

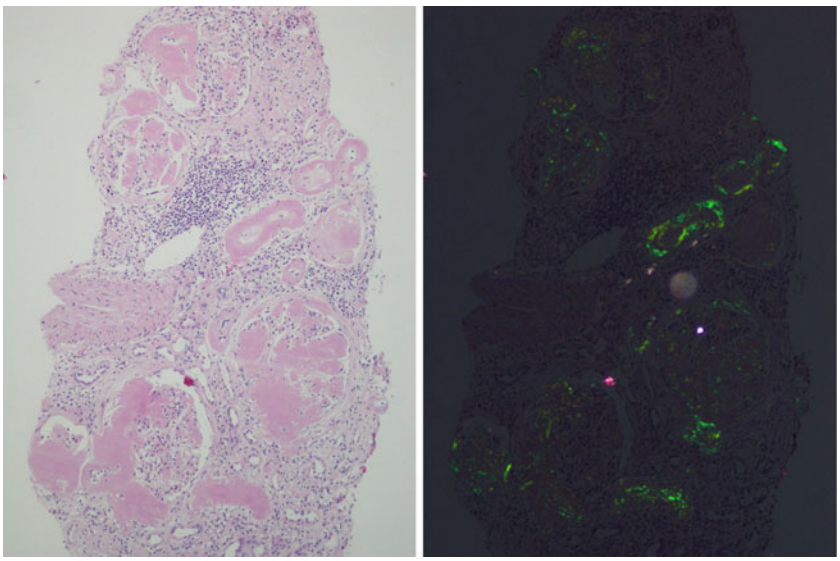

PS-21-028

Sirolimus ameliorates cyclosporin-induced nephrotoxicity in a rat model – focus on renal lesions, oxidative stress, inflammation, proliferation and angiogenesis

J. Sereno*, A. M. Romão, M. Teixeira, B. Parada, C. Mega, H. Vala, E. T. lemos, F. Teixeir, F. Reis

*IBILI, Medicine Faculty, Laboratory of Pharmacology and Experimental Therapeutics, Coimbra, Portugal

Objective: Sirolimus (SRL) have been pointed as a feasible option for minimize the use of Cyclosporin A (CsA), especially because of putatively less nephrotoxicity. This study aimed to characterize the histological lesions and the molecular pathways implicated in CsA-induced nephropathy and prevention when converted to SRL.

Method: The following 4 groups ($n=6$) were tested during 9 weeks: Vehicle, CsA, SRL and Conversion (CsA 3 weeks + SRL 6 weeks). BP and HR were monitored. Blood was collected and kidney gene expression of markers of inflammation, proliferation, angiogenesis and oxidative stress were assessed. Histology: H&E, PAS and Gordon & Sweets staining. Statistics: ANOVA and Post´hoc tests ($p<0.05$).

Results: After 9 week of CsA treatment, there was important kidney lesions, including glomerular, tubulointerstitial and vascular: mesangial expansion, atrophy, bowman capsule enlargement, hyaline cylinders formation, tubular calcification and vascular congestion, as well as arteriolar vacuolization and arteriolosclerosis. Conversion to SRL, HT and tachycardia were reduced, accompanied by amelioration of kidney dysfunction and lesions (glomerulosclerosis and tubulointerstitial fibrosis), together with reduction of oxidative stress, proliferation and angiogenesis.

Conclusion: In conclusion, SRL ameliorates CsA-induced nephrotoxicity in a rat model, which might be due to protection against oxidative stress, proliferation and angiogenesis, but these mechanisms deserve better exploitation.

Acknowledgements: FCT(SFRH/BD/63962/2009).

PS-21-029

Non-lupus "full-house" nephropathy in Serbian population in last six years

J. Vjestica*, S. Cirovic, S. Tatic, R. Naumovic, S. Simic-Ogrizovic, J. Markovic-Lipkovski

*Inst. for Pathology, Medical Faculty, Belgrade, Serbia

Diffuse glomerular and sometimes focal mesangial staining of immune complex depositas (IgA, IgG, IgM, C3, and C1q), also known as "full-house" pattern commonly indicates lupus nephritis. However, some non-lupus nephropathy also can be present with a "full-house" immunofluorescence pattern, mimicking lupus nephritis. The aim of this study was to define the clinicopathological spectrum of originally non-lupus "full-house" nephropathy. Biopsies from January 2005 till December 2011 were analyzed in order to identify all renal biopsies cases showing "full-house" pattern. The study included 192 "full-house" renal biopsy diagnosiss. From all analyzed cases 117 (60 %) had lupus nephritis expressing "full-house" pattern and 75 (40 %) cases had non-lupus "full-house" nephropathy. In the absence of clinical and/or serological evidence of systemic lupus erythematosus (SLE), at the time of renal biopsy, in 36 cases diagnose was membranous glomerulonephritis (GN), than 11 mesangioproliferative GN, 9 membranoproliferative GN, 7 IgA nephropathy, 6 rapidly-progressive GN and 6 membranous/membranoproliferative GN cases. Non-lupus "full-house" nephropathy is present in broad spectrum of different types of GN, predominantly in cases of membranous GN. The possibility of "full-house" nephropathy preceding the emergence of overt SLE remained to be clarified.

PS-21-031

A prostacyclin analogue inhibits the mitochondria-dependent endothelial apoptosis in the kidney of glomerulonephritis rats

Y. Goto*, S. Yamaguchi, M. Tamura, H. Mochizuki, H. Kurumatani, K. Okano, M. Miyamoto
*Toray Industries, Inc., Pharmaceutical Research, Kanagawa, Japan

Objective: Although the renoprotective effects of prostacyclin have been demonstrated in many studies, the protection mechanisms of prostacyclin in chronic kidney disease, especially at the terminal stage, are still remained unclear. In the present study, we performed pathological and pathphysiological analyses of prostacyclin renoprotective effects using a stable prostacyclin analogue, beraprost sodium, in the disease kidney of anti-GBM glomerulonephritis (GN) rats.
Method: Beraprost was administrated from 2 weeks after induction of GN. The condition of renal microvascular network and localization of apoptotic cells were examined using renal vascular corrosion casts, immunostainings and TUNEL-staining. The intracellular apoptotic signaling pathway was analyzed by Western blot and qPCR.
Results: In the kidney of beraprost-treated rat, significantly high density of renal microvascular network was maintained, and apoptosis of vascular endothelial cells was suppressed even at the terminal stage of anti-GBM GN. Pathophysiological analyses revealed that transcriptional and post-translational modifications of Bcl2 and XIAP, which were anti-apoptotic proteins in mitochondria dependent apoptotic pathway, were occurred in the kidney of beraprost-treated rat.
Conclusion: These results suggested that prostacyclin protects renal vascular network by inhibiting mitochondria dependent endothelial apoptosis, and it play an important role for preservation of renal function in the chronic kidney disease.

Wednesday, 12 September 2012, 09.30 - 10.30, Congress Hall Foyer 3rd Floor
PS-22 Poster Session Uropathology

PS-22-001

Villous adenoma of the urinary bladder

B. Akkaya*, G. Tasova-Yilmaz, M. F. Usta
*Akdeniz University, School of Medicine, Antalya, Turkey

Objective: Although villous adenomas commonly occur in the gastrointestinal tract villous adenomas of the urinary tract, including the bladder, are infrequently encountered.
Method: We report a case of urinary bladder villous adenoma in a 72-year-old man. The patient was undergone cystoprostatectomy because of diagnosis infiltrative urothelial carcinoma in the transurethral resection of bladder.
Results: Histopathological examination of cystoprostatectomy specimen there was no urothelial carcinoma. A 2,5 cm polypoid mass was seen at the dome of the urinary bladder. Histopathology confirmed that this tumor was a villous adenoma with a polypoid growth of the glandular epithelium consisting of small tubular glands, dilated cystic glands or papillary fronds lined by a columnar epithelium. The glandular epithelial cells displayed mild nuclear atypia and nuclear pseudostratification with some mucus cells admixed. The patient was diagnosed with a rare case of villous adenoma of the bladder. Over the past 5 months of follow up, the patient is alive and no metastasis.
Conclusion: Patients with isolated villous adenomas in the urinary bladder have an excellent prognosis and surgical resection is curative. However, it is uncertain whether an untreated lesion might eventually develop into an adenocarcinoma. Therefore, close follow up is recommended because of the possibility that this condition might be premalignant.

PS-22-002

Caprin 1 overexpression in urothelial carcinomas of bladder

B. Akkaya*, Z. Cetin, S. Berker-Karauzum, M. Baykara
*Akdeniz University, School of Medicine, Antalya, Turkey

Objective: Caprin1 encoded by Cytoplasmic Activation/ Protein-1 gene located in 11p13 chromosome region. It

has been reported that Caprin 1 is associated with cell proliferation in various types of cell lineages.
Method: We researched whether Caprin 1 might be overexpressed or not in urothelial carcinoma of bladder and its overexpression could be correlated with clinicopathologic parameter (age, sex, invasion). Fifty urothelial carcinoma of bladder (29 infiltrative; 21 non-infiltrative) were stained by immunohistochemically in tissue microarrays.
Results: The expression of Caprin 1 was observed in 24infiltrative urotelial carcinoma cases (%82) and 18 non-invasive urothelial carcinoma cases (%85). Age range was 32–85. Eight patients were female, 42patients were male.
Conclusion: In the literature Caprin 1 overexpression was reported in different types of tumors including esophageal, stomach, prostate, lung, liver. Caprin 1 overexpression might be correlated with the cellular proliferation potential. To determine of importance of Caprin -1 overexpression new studies are necessary.

PS-22-003
Pseudohyperplastic squamous cell carcinoma of the penis: A lichen sclerosus related tumor
L. Alfaro*, J. M. Castillo, Mª. J. Roca, F. Sevilla, M. Hernandez
*Valencia, Spain

Objective: Pseudohyperplastic squamous cell carcinoma of the penis (PSCC) is a low grade tumor with specific clinical and pathological features. This very uncommon tumor occurs in association with lichen sclerosus, the main location is foreskin, and the high degree of differentiation may difficult its discrimination with pseudoepitheliomatous hyperplasia.
Method: A 66-year-old male presented a penis lesion involving glans and foreskin, clinically suspicious of malignancy. Size was 1,6×1,4 cm and a conservative resection was done. Pathological study was performed, and HPV detection with a commercially available kit: PCR amplification and reverse hybridization with probes to 35 HPV types.
Results: The lesion showed a non-verrucous well differentiated squamous cell tumor. Upper layers lacked any atypia but infiltrative growth was evident in basal layers, with atypical cells and mitosis. Lichen slerosus changes were evident bordering the tumor. HPV was negative for all types studied. No further treatment was employed and after a 18 months follow-up no recurrence has been observed.
Conclusion: PSCC should be taken in mind when handling penis tumors. A correct differentiation from benign lesions and a knowledge of its low grade to avoid overtreatment will benefit patients. Lichen sclerosus and not HPV seems to play a precancerous role.

PS-22-004
Evaluation of sunitinib malate and meloxicam as single agents or in combination in bladder cancer cell lines
R. Arantes*, R. Pinto-Leite, C. Lopes, L. Santos, A. Colaço, P. Oliveira
*UTAD, Dept. of Veterinary Sciences, Vila Real, Portugal

Objective: Currently accepted for the treatment of advanced renal cancer, sunitinib malate is a small molecule inhibitor of the VEGFR family, with ability to regulate tumor growth, progression, angiogenesis and metastasis. Several reports have suggested that encouraging effects can be achieved by combining COX-2 inhibitors with anticancer agents. The goal of this work was to evaluate the effects of sunitinib malate and meloxicam isolated and combined on three human bladder cancer cell lines.
Method: T24, 5637 and HT1376 cells were treated with several concentrations of sunitinib malate and meloxicam, as single agents or in combined schedule. Their influence on cell proliferation was determined by MTT method after 72 h of treatment. Control samples were processed in the same way as treated samples but in drug-free medium. Absorbance values of each well were read at 492 nm using an ELISA plate reader.
Results: A reduction in cell proliferation rate was observed when all cell lines were treated either with sunitinib malate or meloxicam isolated. Simultaneous exposure to both agents enhances the inhibition of cell proliferation. Statistical significances were obtained when treatment groups were compared with control group.
Conclusion: These results suggest a potential clinical application of sunitinib malate in combination with meloxicam on bladder cancer.

PS-22-005
Bcl-2 expression in prostate carcinomas
B. Balinisteanu*, A. Dema, S. Taban, C. Lazureanu, D. Herman, S. Ursoniu, A. Loghin, A. Vaduva
*Municipal Hospital, Pathology, Timisoara, Romania

Objective: The disturbance of apoptosis represents an important event in the genesis of tumors with different localization. The study of anti-apoptotic protein Bcl-2 expression from the perspectives of the prognostic and predictive value in prostate cancer has led to inconsistent results, even contradictory.
Method: Expression of Bcl-2 was analyzed in 3 groups of prostatic carcinoma: localized, locally advanced and with distant metastases. For histological grading of carcinomas we used Gleason score. Classification of the tumors into prognostic subgroups was made according to NCCN Guidelines. For the immunohistochemical study we used anti-Bcl-2 antibody (clone 174), EnVision system, visualization with

diaminobenzidine. The results of immunohistochemical reaction were assessed by evaluating the extent and intensity of immunostaining. Statistical analysis was performed using STATA 9.2.
Results: 17 of the 59 analyzed cases of prostate carcinomas showed Bcl-2 over-expression: 5,9 % localized carcinomas, 23,5 % locally advanced carcinomas and 70,6 % carcinomas with distant metastases ($p<0.001$). Although most of the Bcl-2 positive tumors were poorly and moderately differentiated, the correlation between Bcl-2 over-expression and tumor grade did not show statistical significance ($p=0,085$).
Conclusion: Bcl-2 overexpression in advanced prostate carcinomas suggests involvement of this marker in the progression of tumors in this location.

PS-22-006
Urothelial carcinoma of the bladder: A clinicopathologic study of 92 cases
G. Benkhedda*, S. Khalifa, Y. Lamouti
*CHU Frantz Fanon, Dept. of Pathology, Blida, Algeria

Objective: Urothélial carcinoma (UC) accounts for nearly 90 % of urinary bladder tumors.A variety of histological variant of UC have been recently recognosed. Some variants have prognostic and therapeutic implications. The aim to this study is to assess the pathological features from our series and to compare our results that of the literature.
Method: We retrospectively studied 92 patients who were diagnosed histopthologically with urothelial carcinoma using the WHO classification system.
Results: The mean age of patients at diagnosis was 60(range, 30–70 years). 86,67 % were male (80 H/12 F). All tumors were classified as urothelial carcinomas: 2,1 % urothelial neoplasm with squamous differentiation,2,1 % with glandular differentiation,2,1 % urothelial tumors nested and 1 % sarcomatoid. In this study most tumors were grade 2 (67 cases) and stage pT1.
Conclusion: Adult urothelium has the capacity to undergo several pathways of phenotypic cellular and structural differentiation as a result of the embryological origin of the bladder from the multipotent tissues of the cloacal endoderm and the mesodermal wolffian ducts. The clinical course of bladder cancer varies depending on the histological type of neoplasm, grade and stage of the tumor. Hight-grade muscle-invasive urothelial cancers and tumors schowing variant microscopic morphology have in general hight mortality and poor prognosis.

PS-22-007
Comparison of insignificant cancer detection rates in prostatectomies performed following 6 and 12-core biopsy schemes
U. Berber*, A. Haholu, I. Yilmaz, Z. Kucukodaci, D. Demirel
*GATA HEH, Dept. of Pathology, Istanbul, Turkey

Objective: Widespread use of extended biopsy protocols have increased the prostate cancer detection rates. Besides this improvement, whether detection of clinically insignificant cancer detection rates are increased by extended biopsy protocols is not well documented. In the study, we aimed to compare the rates of insignificant cancers found in prostatectomy specimens performed following 6 and 12-core biopsy protocols.
Method: Retrospectively, we investigated the low volume/low grade (LV/LG) prostate cancers in 160 prostatectomy specimens. Tumors volumes were calculated digitally as multiplying total tumor areas by 3 mm for average block thickness, and corrected for tissue shrinkage by multiplying a factor of 1.25.
Results: Of the 160 prostatectomies, 54 were performed following sextant technique, and 106 were performed after 12-core protocol. Review of the H&E stained sections revealed 21 insignificant cancers. Number of LV/LG tumors found in 6 and 12-core groups were 3(5.6 %) and 18 (16.9 %), respectively.
Conclusion: When compared to sextant technique, detection of LV/LG tumors were significantly raised in prostatectomies performed following 12-core protocol, and this increase points out the need for new approaches in patient management to avoid overtreatment after extended biopsy protocols.

PS-22-008
Impact of total core length for cancer detection in a lateral zone targetted 12-core prostate biopsy scheme
U. Berber*, A. Haholu, Z. Kucukodaci, I. Yilmaz, D. Demirel
*GATA HEH, Dept. of Pathology, Istanbul, Turkey

Objective: A widely accepted adequacy criteria for histopathologic evaluation of prostate core biopsy protocols has not been defined yet. Selection of patients for repeat biopsies after a negative initial biopsy result is also a matter of debate. We aimed to evaluate the impact of total core length for detecting prostate cancer in a 12-core transrectal ultrasound guided biopsy scheme.
Method: Retrospectively, we investigated the core lengths of 768 patients underwent initial prostate biopsy by a lateral zone targetted 12-core protocol between 2006 and 2011.
Results: Cancer was identified in 292 (38.0 %) patients. Mean total core length for positive and negative patients were 15.3 cm and 14.6 cm, respectively. Cancer detection rates in groups for total core length <12 cm, 12–15 cm, and >15 cm were 30.9 % (55/178), 40.6 % (96/236), and 39.8 % (141/354), respectively. When a threshold of 10 cm was selected for total core length, overall cancer detection rates for <10 cm and ≥10 cm groups were 23.9 % (17/71) and 39.5 % (275/697), respectively.

Conclusion: Total core length is significantly associated with cancer detection rates and may be used as a reliable adjunctive tool in deciding repeat biopsies for patients with negative biopsy result.

PS-22-009

Primitive neuroectodermal tumor of the kidney in an adult: A case report

G. Berdan*, A. N. Petrescu, D. Radavoi, O. Codreanu, D. Badescu, C. Ardeleanu, V. Jinga
*Prof Dr.Th. Burghele Hospital, Dept. of Pathology, Bucharest, Romania

Objective: Primitive neuroectodermal tumors (PNETs) are highly malignant tumors of neuroectodermal origin. We report a case of renal PNET in a 52-year-old male with a 6-month history of intermittent hematuria.. He underwent a right radical nephrectomy. Macroscopically, the inferior pole was replaced by a multinodular, grey, glistening tumour measuring 8.7/7/6 cm, with foci of necrosis and hemorrhage.
Method: Serial histological sections have been assessed using hematoxylin-eosin and Van Gieson stain and the indirect immunohistochemical analysis for antibodies: MNF 116, VIM, CD56, NSE, MIC2/CD99.
Results: Histological examination revealed a uniform population of undifferentiated, small-to medium-sized tumor cells, arranged in alveolar-insular patterns, with round to oval nuclei, small nucleoli, numerous signs of mitosis and scattered apoptosis, geographic zones of necrosis. Dispersed cells showed cytoplasmic vimentin positivity favouring the diagnosis of PNET. Few tumoral cells appeared positive for MNF116. Expression of CD56 was positive in a large number of tumoral cells and an area of the tumour exhibit a milder reaction of positive NSE. MIC2 was positive with moderate staining in almost all tumoral cells.
Conclusion: Diagnosis is based on histology and immunohistochemistry but pathological evaluation can be challenging because of the differential diagnosis with other small round cell tumors.

PS-22-010

Nonamyloid fibrillary glomerulonephritis: Presentation of two cases

E. Beretouli*, G. Dimas, G. Karayannopoulou, T. Koletsa, D. Grekas, G. Karkavelas
*AHEPA Hospital, Dept. of Pathology, Thessaloniki, Greece

Objective: Fibrillary glomerulonephritis (FGN) is a rare disease, characterized by fibrillar deposits in the mesangium and the glomerular capillary loops. These deposits do not have an amyloid – like cross-β structure and are readily distinguishable from amyloid by the larger thickness of fibrils and lack of Congo red staining.
Method: We report two cases of a 52- and 64-year-old women, who presented with severe nephrotic syndrome, rapidly progressive chronic kidney disease and lymphoproliferative disorders. Glomerular crescents were present in about 30 % of both renal biopsy specimens (18 of 54 and 9 of 27 glomeruli, respectively). Immunohistochemical analysis, immunofluorescence and an electron microscopy (EM) studies were performed.
Results: Renal biopsy showed a deposition of an amyloid-like extraneous substance in the mesangium, as well as within the glomerular basement membranes. Congo red staining was negative. The EM examination revealed FGN.
Conclusion: FGN must be included in the differential diagnosis of rapidly progressive chronic renal disease. EM confirm the diagnosis of FGN, which suggests a poor outcome.

PS-22-011

Urachal adenocarcinoma: A report of 3 cases

M. Bergmann*, J.-C. Tille, G. J. Wirth, C. Iselin, M.-F. Pelte
*University Hospital of Geneva, Clinical Pathology, Geneva, Switzerland

Objective: Urachal carcinomas represent less than 1 % of bladder-related cancers. Most are adenocarcinomas, but urothelial, squamous and small cell carcinomas may occur. There are pathological criteria for assessing an urachal origin. A specific staging system is lacking for these tumors.
Method: A mass of the bladder dome was found in two 56 and 58 year-old men. A 76 year-old woman presented an urachal cyst. CT-scan revealed no other tumors and partial cystecomy was performed. Pathological examination showed partially cystic adenocarcinomas, one enteric type G2, and two mucinous type G1. Two tumors extended into the bladder mucosa and one was limited to the urachal cyst. Surgical margins were negative. Immunostainings were positive for CK7, CK20, CDX2, cytoplasmic beta-catenin, and negative for p63.
Results: With a follow-up of 1, 6 months and 6 years, all patients are free of disease.
Conclusion: No TNM classification exists for urachal carcinomas. Specific staging systems have been proposed by Sheldon, and more recently by the Mayo Clinic. Two cases are Sheldon IIIA/Mayo Clinic II, and one Sheldon II/Mayo Clinic I. Since stage, grade and surgical margins are the main prognostic factors, a clear and relevant staging system is needed for these rare carcinomas.

PS-22-014

Renal cell carcinoma with papillary and chromophobe features: An example of hybrid tumor

V. Caamaño*, M. Gonzalez, A. Perez, N. Cerda, A. Corominas, G. Muñiz, A. Gaafar, J. I. López
*Hospital Universitario Cruces, Dept. de Anatomia Patologica, Barakaldo, Spain

Objective: Renal cell carcinoma (RCC) with two different histologies must be included in the unclassified group (WHO classification). Whether these cases should be included in this histological subgroup or be considered hybrid RCC is a matter of debate. We report one of such cases in which papillary and chromophobe phenotypes meet.
Method: A 5 cm in diameter asymptomatic left renal mass was discovered incidentally in the radiological follow-up of a breast carcinoma diagnosed 12 years before in a 62 year-old woman. Follow-up showed right adrenal gland metastasis. Patient died 12 months later.
Results: Grossly, tumor well circumscribed, tan-yellow, with haemorrhagic and necrotic areas. The neoplasm showed two different histologies clearly defined: One showed solid nests of polyhedral cells, with eosinofilic cytoplasm, central and hyperchromatic nuclei, occasional mitosis recapitulating chromophobe RCC. The other component presented a well defined tubulopapillary growth pattern typical of papillary RCC. Focally sarcomatoid transformation, with tumor necrosis and chronic inflammation. By immunohistochemistry, chromophobe and papillary areas retained their specific phenotypes.
Conclusion: Hybrid renal carcinomas do exist, but they are most probably hidden in the unclassified group of renal tumors. However, the exact histological context for which a renal neoplasm deserves the name "hybrid" remains to be defined.

PS-22-015
Thyroid-like follicular renal cell carcinoma of the kidney
V. Caamaño*, A. Perez, M. Gonzalez, N. Cerda, A. Corominas, G. Muñiz, L. Mosteiro, J. I. Lopez
*Hospital Universitario Cruces, Dept. de Anatomia Patologica, Barakaldo, Spain

Objective: Renal cell carcinoma with thyroid-like follicular pattern is a rare histological subtype of renal carcinomas that has been very recently described.
Method: A 3.3 cm in diameter asymptomatic left renal tumor was discovered during the study of a macroscopic hematuria in a 32 years old man. The lesion was organ-confined.
Results: Grossly, the tumor was a well circumscribed, solid, brown and homogenous intraparenchymatous nodule. Proliferating cells were arranged in a microfollicular pattern with colloid-like material resembling thyroid adenoma. Cells displayed low grade nuclear features and had eosinophilic cytoplasm. Some areas showed a solid pattern of growth resembling an oncocytoid neoplasm. By inmunohistochemistry, the tumor was negative for thyroglobulin and TTF1, and positive for EMA, CK7, AE1/AE3, and e-cadherin.
Conclusion: Renal cell carcinoma with microfollicular thyroid-like features has been very recently identified in the literature. There is no agreement on the exact nature of this neoplasm so far, and the 2004 WHO classification of renal tumors still does not consider this phenotype as a distinct histological subtype. Anyway, the tumor must be distinguished from metastatic thryroid carcinoma, another quite unusual condition.

PS-22-016
Evidence for clonal fibroblast proliferation and autoimmune process in idiopathic retroperitoneal fibrosis
L. Cheng*, J. Clevenger, A. Lopez-Beltran
*Indiana University, Dept. of Pathology, Indianapolis, USA

Objective: We sought to determine if idiopathic retroperitoneal fibrosis is clonal process and if it is an autoimmune, or IgG4-driven, process.
Method: Thirty cases of idiopathic retroperitoneal fibrosis, in whom known causes of retroperitoneal fibrosis were excluded and those for which paraffin blocks were available, were included in this study. We performed clonality analysis in 16 female patients. Genomic DNA samples were prepared from formalin-fixed, paraffin-embedded tissue sections using laser capture microdissection.
Results: Eight of 15 information cases (53 %) showed nonrandom X-chromosome inactivation, or a clonal process. Of the 26 patients for which IgG4 analysis was performed, 14 (54 %) were positive for IgG4-positive plasma cells and all were negative for ALK. Of the 12 patients, for which both clonality analysis and IgG4 analysis were performed, 4 were clonal and IgG4 negative (33 %), 2 were clonal and IgG4 positive (17 %), 2 were nonclonal and IgG4 positive (17 %), and 4 were nonclonal and IgG4 negative (33 %).
Conclusion: Our data indicate that a significant proportion (53 %) of idiopathic retroperitoneal fibrosis cases in females is associated with a clonal expansion of fibroblasts. In addition, a subset of idiopathic retroperitoneal fibrosis cases could be classified in the IgG4-related sclerosing disease spectrum.

PS-22-017
Histopathology and clinical features of urethral caruncle
L. Cheng*, S. Williamson, M. Conces, R. Montironi, A. Lopez-Beltran, M. Scarpelli
*Indiana University, Dept. of Pathology, Indianapolis, USA

Objective: Urethral caruncle is a benign polypoid mass of the urethral meatus in primarily postmenopausal women. Although a conclusive association with malignancy, urologic disorder, or systemic disease has not been established, often the lesion carries a challenging clinical differential diagnosis that includes malignancy.

Method: We examined clinical and histopathologic characteristics in 41 patients. Medical records were assessed for presentation, clinical diagnosis, associated urothelial carcinoma, radiation treatment, tobacco use, immunologic/urologic disorder, and treatment strategy/outcome.
Results: The mean age was 68 (range 28–87 years). Presenting symptoms were: pain (37 %), hematuria (27 %), and dysuria (20 %), in contrast to asymptomatic (32 %). Clinical diagnosis favored malignancy in 10 % of cases. Concurrent or subsequent urothelial carcinoma was present for five patients (12 %), though none developed urethral carcinoma. Histologic features included mixed hyperplastic urothelial and squamous lining, overlying a variably fibrotic, edematous, inflamed, and vascular stroma. Invaginations of urothelium extending into the stroma were common (68 %), showing rounded nests with cystic or glandular luminal spaces, similar to urethritis cystica/glandularis, without intestinal metaplasia. Two lesions included an organizing thrombus, one with intravascular papillary endothelial hyperplasia. Twenty patients were treated with topical medications without resolution. Three lesions recurred (7 %) after excision.
Conclusion: Urethral caruncle is an uncommon lesion that may clinically mimic benign and malignant conditions, making tissue diagnosis critically important.

PS-22-018

Human Papillomavirus (HPV) is not involved in urothelial tumorigenesis

L. Cheng*, R. Alexander, A. Lopez-Beltran
*Indiana University, Dept. of Pathology, Indianapolis, USA

Objective: The purposes of this study were to investigate the possible role of human papillomavirus in the development of squamous cell carcinoma of the urinary bladder and to determine if p16 expression could serve as a surrogate marker for human papillomavirus in this malignancy.
Method: Forty-two cases of squamous cell carcinoma of the urinary bladder and 27 cases of urothelial carcinoma with squamous differentiation were investigated. HPV infection was analyzed by both in situ hybridization at the DNA level and immunohistochemistry at the protein level. p16 protein expression was analyzed by immunohistochemistry.
Results: Human papillomavirus DNA and protein were not detected in 42 cases of squamous cell carcinoma (0 %, 0/42) or 27 cases of urothelial carcinoma with squamous differentiation (0 %, 0/15). p16 expression was detected in ten cases (31 %, 13/42) of squamous cell carcinoma and nine cases (33 %, 9/27) of urothelial carcinoma with squamous differentiation. There was no correlation between p16 expression and the presence of human papillomavirus infection in squamous cell carcinoma of the bladder or urothelial carcinoma with squamous differentiation.
Conclusion: Human papillomavirus does not play a role in the development of squamous cell carcinoma of the urinary bladder and urothelial carcinoma with squamous differentiation. p16 expression should not be used as a surrogate marker for evidence of human papillomavirus infection in urinary bladder cancer.

PS-22-019

PAX8 is expressed in the majority of renal epithelial neoplasms: A study of 223 cases using a tissue microarray-based immunohistochemical approach

L. Cheng*, Y. Hu, A. Hartmann, C. Stoehr, D. Tacha, R. Montironi, A. Lopez-Beltran
*Indiana University, Dept. of Pathology, Indianapolis, USA

Objective: PAX8 is a cell lineage-specific transcription factor and plays a crucial role in organogenesis of the kidney, thyroid, and Müllerian duct. Previous study showed that PAX8 is a specific and sensitive marker for both renal and ovarian carcinomas. The purpose of this study is to investigate PAX8 expression using a new monoclonal PAX8 antibody in a larger number of renal epithelial neoplasms including clear cell renal cell carcinoma, papillary renal cell carcinoma, chromophobe renal cell carcinoma, and renal oncocytoma.
Method: PAX8 immunohistochemical staining was performed on tissue microarrays containing 84 cases of clear cell renal cell carcinoma, 66 cases of chromophobe renal cell carcinoma, 57 cases of papillary renal cell carcinoma, and 16 cases of renal oncocytoma.
Results: PAX8 expression was detected in 93 % (78/84) of cases of clear cell renal cell carcinoma, 80 % (53/66) of cases of chromophobe renal cell carcinoma, 95 % (54/57) of cases of papillary renal cell carcinoma, and 94 % (15/16) of cases of renal oncocytoma.
Conclusion: PAX8 is expressed in the majority of renal epithelial neoplasms including renal cell carcinomas and oncocytomas and this monoclonal PAX8 antibody is more sensitive than polyclonal antibody to detect chromophobe renal cell carcinoma. These results showed that PAX8 is a valuable marker for nephric neoplasms.

PS-22-020

Prostatitis as the presenting sign in Wegener granulomatosis: A case report

M. Chorti*, N. Maounis, A. Kalogirou, A. Birbakou, A. Emmanouilidou, M. Demonakou, S. Legaki
*Sismanoglion General Hospital, Dept. of Pathology, Athens, Greece

Objective: Wegener's granulomatosis (WG) is a systemic disease that is usually limited to the respiratory tract and kidneys. Prostate involvement is demonstrated histologically in 2–7 % of the patients.
Method: A 41 years old male was hospitalized with symptoms of acute urinary retention due to acute prostatitis, was treated with antibiotics and demonstrated clinical improvement. He underwent transurethral prostatic biopsy and the diagnosis of acute necrotic prostatitis was rendered. A month later, he was admitted to our hospital with features of sepsis. Abdomen CT revealed prostate abscesses and thoracic cavity CT showed bilateral pleural effusion with single peripheral nodule on the left lobe. Bronchoscopy revealed nodules on the main right bronchus. Bronchial biopsy demonstrated candida inflammation. Red cell casts in urinalysis and C-ANCA seropositivity was demonstrated. Prostatic biopsy slides were reevaluated and showed histological features of acute necrotic prostatitis associated with vasculitis and scattered multinucleated giant cells.
Results: Based on the combination of clinical, histological, biochemical and immunological features the diagnosis of WG was established. He received immunosuppressive therapy and showered significant clinical improvement.
Conclusion: Prostate involvement can rarely be the presenting clinical manifestation of WG. Early diagnosis is important expediting aggressive immunosuppressive therapy which may limit a more severe systemic disease progression.

PS-22-021

Transitional cell carcinoma arising within the renal pelvis of a patient with autosomal dominant polycystic kidney disease: A case report

A. Coelho*, R. Dias, R. Sampaio, F. E. Costa, J. Palla Garcia, A. Duarte, J. R. Vizcaíno
*Coimbra, Portugal

Objective: Cancer risk for Autosomal Dominant Polycystic Kidney Disease (ADPKD) is still unknown, but reports of Papillary and Clear Cell types of Renal Cell Carcinoma (RCC) are frequent. Transitional Cell Carcinoma (TCC) in patients with ADPKD are less frequent, with only four cases reported.
Method: A review of clinical data from an ADPKD patient with TCC admitted in our hospital and a review of current literature regarding ADPKD and TCC were made.
Results: The patient is a 77 year-old woman with chronic renal failure due to ADPKD, on hemodialysis for 2 years. She was admitted with left lumbar pain, hematuria and fever. Radiological exams revealed various complex cysts with dense material that did not enhance with contrast, compatible with hematic cysts in the context of ADPKD. The whole clinical findings suggested cystic infection complicated with sepsis, so nefrectomy was performed. Macroscopic examination of the ressected kidney revealed a white granulous nodular formation with 4.5 cm diameter in the renal pelvis. Histological examination confirmed a high-grade papillary TCC with parenchymal infiltration (pT3) and extense scamous differentiation.
Conclusion: The present case illustrates that TCC can occur in ADPKD, despite its rarity. It can be difficult to successfully diagnose TCC on ADPKD based on clinical-radiological findings.

PS-22-022

Clear cell renal cell carcinoma with syncytial-type multinucleated giant cells: Report of 4 cases of a rare variant of renal cell carcinoma

A. Corominas*, A. Perez, G. Muñiz, N. Cerda, M. González, V. Caamaño, V. Filipovski, J. I. López
*Hospital Universitario Cruces, Dept. de Anatomia Patológica, Barakaldo, Spain

Objective: Renal Cell Carcinoma (RCC) with Syncytial-type cells (SGC) is a rare variant of renal carcinoma, with few cases reported. Our aim is to define the morphologic and immunohistochemical findings of 4 new cases.
Method: Four cases of RCC with SGC have been identified in our files from 1990 to 2011. Histological slides were reviewed in all cases and inmunohistochemistry (CK7, AE1/AE3, CD10, RCC-Ma, EMA, CD117, AMACR, CAIX) performed in 3 cases.
Results: Main clinicopathological data appear in the Table. All tumors were classic clear cell RCC with SGCs distributed along the tumor. SGCs showed emperipolesis and eosinophilic hyaline globules. SGCs immunostaining was similar to conventional clear cells (CD10, EMA, AE1/AE3, RCC-Ma, CAIX positive). Two cases showed extrarrenal extension.

Conclusion: SGCs is a rare finding in clear cell RCC. The immunostaining of syncytial cells is similar to that observed in the adjacent clear cell RCC. This histologic variant seems to be more aggressive than conventional clear cell RCC; additional series are needed to delineate with certainty its clinical behaviour.

Case	1	2	3	4
Sex	M	M	F	F
Age	65	73	61	71
Size	5.5	6	4	5
Laterality	L	L	R	R
Stage	pT1b	pT3a	pT4	
Fuhrman-Grade	III	IV	III	
Direct-Extension	No	Perirrenal fatty-tissue	Adrenal gland	

PS-22-023

Primary renal carcinoid tumor: Report of 2 cases

A. Corominas*, G. Muñiz, A. Perez, N. Cerda, M. González, V. Caamaño, J. Alvarez, J. I. López

*Hospital Universitario Cruces, Dept. de Anatomia Patológica, Barakaldo, Spain

Objective: Carcinoid tumor is a very uncommon neoplasm in the kidney. We report the histopathologic and immunohistochemical (IHQ) study of two new cases.

Method: Case 1: 48 year-old female with a 4 cm asymptomatic ¨cystic¨ mass discovered in a routine exam. The patient underwent tumorectomy. Case 2: 77 year-old female with a 3 cm renal mass who underwent left nephrectomy. Two months later a needle biopsy confirmed carcinoid tumor metastasis in the liver. Both patients currently free of disease.

Results: Both tumors showed similar histologic features. Neoplastic cells were grouped in nests, ribbons, and pseudoglands with rosette-like appearance and showed eosinophilic granular cytoplasm and chromatic nuclei. Low mitotic index. IHC: diffuse/intense cytoplasmic staining for CD56, CD57, AE1/AE3, chromogranin and synaptophysin.

Conclusion: Primary renal carcinoid tumor is rare in the clinical practice. The histological findings correspond to a well differentiated neoplasm and are similar to carcinoid tumors in other locations, which makes the diagnosis feasible even without previous personal experience. IHC confirms the diagnosis. It usually behaves as a low grade neoplasm, but recurrences and metastases do occur. Only single cases and short series have been published so far. There is no accumulated experience to establish long term prognosis.

PS-22-024

Prostatic adenocarcinoma occurring simultaneously with large cell neuroendocrine carcinoma of the urinary bladder: An extraordinary collision tumor

P. Czapiewski*, M. Sieczkowski, M. Matuszewski, K. Krajka, W. Biernat

*Medical University of Gdansk, Dept. of Pathology, Poland

Objective: Radical cystoprostatectomy is a standard surgical procedure for male patients with muscle-invasive urinary bladder (UB) carcinoma. Vast majority of these tumors are urothelial carcinomas, while large cell neuroendocrine carcinoma (LCNEC) is a very uncommon tumor with less than 20 reported cases. Invasive prostate carcinoma is incidentally detected in up to 20 % of cystoprostatectomy specimens. It is usually well differentiated and shows low propensity for dissemination and local recurrence.

Method: Clinical and pathological description of an extremely rare collision tumor composed of LCNEC of

the urinary bladder and a high grade acinar prostate carcinoma.
Results: A 79-year-old male patient was admitted to the urology department due to severe gross haematuria. Cystoscopy revealed large tumor of the posterior-inferior wall of the UB with involvement of the left uretheral orifice. In the radical cystoprostatectomy specimen LCNEC of the UB, involving bilaterally prostate and spermatic vesicle (pT4a), was diagnosed. Additionally both lobes of the prostate were involved by the acinar prostatic carcinoma (pT2c, Gleason score 5+4=9).
Conclusion: High-grade prostate carcinoma may rarely co-exist with UB tumors of uncommon histology.

PS-22-025
Expression of androgen receptors in prostate carcinomas
A. Dema*, S. Taban, A. Borda, C. Lazureanu, D. Anderco, A. Muresan, A. Loghin, S. Ursoniu, R. Bardan, R. Cornea
*University of Medicine and Pharmacy, Pathology, Timisoara, Romania

Objective: Despite of numerous researches in the field, data regarding immunohistochemical (IHC) expression of androgen receptor (AR) in prostate carcinomas, in terms of prognosis and therapy, are quite controversial.
Method: The IHC expression of AR was analyzed on 3 groups, each of 20 primary diagnosed prostate carcinomas: localized, locally advanced and distant metastasized. The anti-AR antibody (clone AR441) was used. For each tumor was determined the percentage of AR-positive nuclei, assigning a staining score (0 to 4). A value of 64 % was considered to be discriminatory between tumors with high and low AR expression.
Results: All the analyzed carcinomas showed AR. 54.2 % of tumors had high AR expression and 45.8 % showed low AR expression. 7/19 localized tumors (one tumor vanished during processing), 15/20 locally advanced and 10/20 distant metastasized tumors showed high AR expression (p=0.051). 5/18 well-differentiated, 16 of 23 moderately differentiated and 11/18 poorly differentiated tumors showed high expression of AR (p=0.022).
Conclusion: Although not reaching statistical significance, the AR expression tended to correlate with the stage of disease and with the degree of differentiation in terms of an increased expression of AR in advanced, moderately and poorly differentiated tumors.

PS-22-026
Prostate tumors with atypia in the stromal compartment
A. Dema*, D. Herman, S. Taban, C. Lazureanu, D. Anderco, A. Borda, A. Cumpanas, L. Daminescu, D. Sirbu, M. Cornianu
*University of Medicine and Pharmacy, Pathology, Timisoara, Romania

Objective: Prostate lesions with atypical stromal component are rare and poorly characterized in terms of evolution and prognosis.
Method: We retrospectively analyzed 3 cases of unusual prostate tumors diagnosed on prostate needle biopsy. The biopsies were performed due to an elevated serum PSA and/or phenomena of bladder outlet obstruction. For the immunohistochemical (IHC) diagnosis there were used the following antibodies: CK AE1/AE3, PSA, PSMA, vimentin, SMA, ER, Desmin, PgR, CD34.
Results: Two of the three patients, one 68 and the other 66 years-old, with serum PSA level of 34 ng/ml and 14.58 ng/ml respectively, were diagnosed with sarcomatoid carcinoma, the former presenting with liver metastases at diagnosis. In evolution, the death of the first patient occurred 3 months after the diagnosis and the second patient refused surgery. The third patient, 75 years-old, with a nodular prostatic mass of 3.3 cm, was clinically suspected to have an unusual malignant prostatic tumor considering that, despite his 7 ng/ml of serum PSA, he presented multiple bone metastases. The histopathological diagnosis was Stromal Tumor of Uncertain Malignant Potential.
Conclusion: The prostate lesions with atypical mesenchymal component are rarities in urologic pathology. An accurate diagnosis relies on meticulous pathological examination techniques and supplemented, for rare cases, with other clinical and laboratory data.

PS-22-027
Immunohistochemistery study in a case of nephrogenic bladder adenoma
M. R. Farzaneh*, A. Safaei, A. Amin Shareefi
*Shiraz, Iran

Objective: Nephrogenic adenoma is a rare benign lesion of bladder that may be confused with malignant lesions. There is strong relation with urinary tract irritation and intravesicl instrumentations. Nephrogenic adenoma was initially thought to originate from urothelial metaplasia however no solid proof is available.

Method: We present this 55 years old lady with urinary problem. Cystocopic examination show a sessile mass and biopsy show circumscribed proliferation of tubules, cysts, and papillae lined by cells with low cuboidal to columnar epithelial cell. Nephrogenic adenoma can be a significant diagnostic pitfall as certain histological features, such as the presence of enlarged nuclei with prominent nucleoli

Results: Immunohistochemistery study showed strong reactivity to CK7, P504S, CD10, and EMA but negative for CK20, PSA, and P63.

Conclusion: We recommend that any lesion in cystoscopic examination should be followed and immunohistochmistery examination some times is mandatory to differentiate them from malignant tumors.

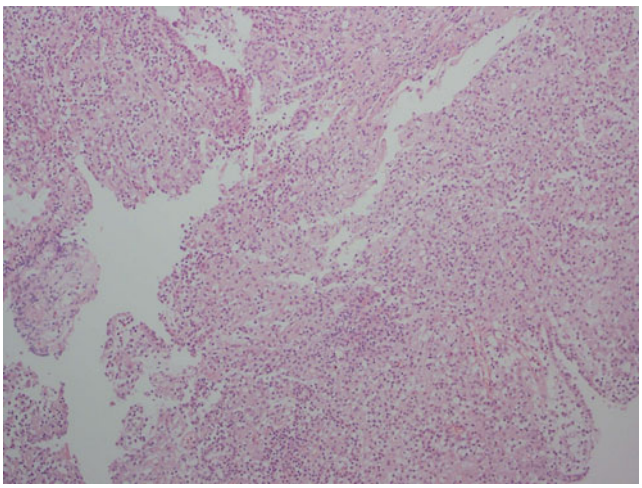

PS-22-028

Regulators of apoptosis and the cell cycle are overexpressed in bladder cancer metastases and may predict survival

A. Fleischmann*, R. Seiler, A. Perren, T. George
*Universität Bern, Institut für Pathologie, Switzerland

Objective: Expression of biomarkers and their prognostic relevance may differ between primary tumours (PT) and its metastases (MET). There is little information about this phenomenon concerning apoptosis and cell-cycle associated biomarkers in urothelial bladder cancer (UCB).

Method: Nodal positive patients (n=152) with UCB underwent cystectomy and lymphadenectomy. Immunohistochemical expression of bcl-2, bcl-6, MDM-2, p53 and CyclinD1 was quantified in tissue microarrays constructed from PT and corresponding nodal MET.

Results: Frequency of MDM-2 positivity increased from PT (17 %) to MET (37 %, p<0.001). This trend was not significant for bcl-2 (PT: 7 %; MET: 10 %, p=0.4) and bcl-6 (PT: 8 %; MET: 12 %, p=0.08). Median percentage of p53 and CyclinD1 immunostained cells increased significantly (p<0.05) from PT (15 %/30 %) to MET (40 %/50 %). MDM-2 and CyclinD1 expression were positively correlated in PT (p<0.004) and MET (p<0.002). p53 and MDM-2 positivity were inversely correlated in PT (p<0.03). Only high CyclinD1 expression in the metastases predicted early death significantly and independently (p=0.017).

Conclusion: Biomarkers of apoptosis and cell-cycle associated are up-regulated in the metastases indicating differences in survival and proliferation of cancer cell compared to primary tumours. Both tumor components may harbor different prognostic information and are not necessarily surrogates for each other.

PS-22-029

Evaluation of histopathologic and histomorphometric changes of testicular tissue and gonadotropins levels following consumption of Methylphenidate in male mice

Z. Ghahri Saremi*, S. Fazelipour, Z. Tootian, M. Shafii
*Tehran, Iran

Objective: One of the most common psychiatric disorders in children is ADHD (Attention Deficit Hyperactivity Disorder), which is treated extensively by Methylphenidate. This study investigates the assessment of the effects of methylfenidate on Histopathologic and Histomorphometric changes of testes and serum level of gonadotropin in adulthood which produces gametes and has Importance for future generations.

Method: In this study 36 adult male mice (Balb/C) were used. After determining the body weight, the animals were divided randomly into two experimental groups of and one control group. The Experimental groups received Ritalin via gavage as follow: The group 1 received 2 mg/kg/day and the group 2 received 10 mg/kg/day for a period of 40 days. After evaluation of body weight, general anesthesia was used for taking blood samples from the heart in order to measure gonadothropins levels in serum. Then for the purpose of body weighing and measuring of diameter of germinal epithelium the testes were removed and the possibility of any pathologic changes was considered.

Results: The results showed that Methylphenidate with different doses could decrease germinal epithelium and also body weight significantly. Besides some significant changes in serum gonadotropins, without any pathological changes were observed.

Conclusion: Our findings demonstrated that Methylphenidate administration in adulthood due to Influence of

gonadotropin hormones on testis function may affect on spermatogenesis.

PS-22-030

A rare bladder cancer: Report of two cases

E. Goupou*, A. Nikolaidou, C. Panagiotidis, K. Panagiotopoulou, V. Gourvas, G. Zoupoudi, R. Kotakidou
*Theagenion Hospital, Pathology, Thessaloniki, Greece

Objective: Small cell urothelial carcinoma (SCUC) comprises less than 1 % of bladder malignancies. It is characterized by an aggressive clinical course, early metastatic spread and high mortality rate. The histogenesis remains controversial and there are no well-defined protocols for therapy.
Method: We report two cases of SCUC. Both of them refer to 50 year-old males, smokers. They presented with gross hematuria. Transurethral resection bladder tumor (TURBT) specimens showed SCUC, followed by cystoprostatectomy and pelvic lymphadenectomy, confirming the initial diagnosis. Immunohistochemistry was used on paraffin embedded tissue.
Results: Microscopically, the tumor cells show a diffuse architectural pattern with occasional nesting, are small, uniform, with scant cytoplasm, nuclear crowding, nuclear molding, inconspicuous nucleoli and finely stippled chromatin. Numerous mitoses, Azzopardi phenomenon and foci of necrosis are present, as well as areas of urothelial carcinoma. Tumor cells are strongly (+) with Ker AE1/AE3, Cam 5.2 (dot-like perinuclear pattern), CD56 (the most consistent neuroendocrine marker), p53, ki-67(60 %), focally (+) with Synaptophysin and (−) with Chromogranin, Ker34βE12, Ker7, Ker 20, TTF-1, LCA.
Conclusion: Pathologic and immunohistochemical data identify SCUC. Differential diagnosis includes metastasis of a small cell carcinoma from another site, poorly differentiated urothelial carcinoma, malignant lymphoma, lymphoepithelioma like carcinoma, plasmacytoid carcinoma, and primitive neuroectodermal tumor.

PS-22-031

Rare variant: Primary renal malignant fibrous histiocytoma

N. Gursan*, E. Demirci, M. Calik, F. Daloglu, O. Ceylan
*Ataturk University, Medical Faculty, Erzurum, Turkey

Objective: Malignant Fibrous Histiocytoma is the most common subtype of soft-tissue sarcoma in adults Typical sites are the extremities followed by the retroperitoneum. Primary MFH of the kidney is extremely rare.
Method: A 77-year-old man presented with left-flank pain and fever of 1 month duration. Clinical examination revealed left renal mass, which on contrast enhanced computed tomography and magnetic resonance imaging was characterized as 8×8×7 cm sized well-demarcated left renal middle- superior polar mass with central necrosis and cystic changes. The contralateral kidney was normal. He underwent left radical nephrectomy by thoracoabdominal approach. Gross examination of the specimen revealed yellowish white 9×9×7 cm sized mass, with multifocal necrozis and cystic changes. Histopathology of these resection specimens; scattered spindle cells and foam cells, fine vascular network and necrosis. Immunohistochemistry revealed CD68-positive xanthoma cells. The tumor also stained positive for vimentin, CD34, but negative for cytokeratin, EMA, desmin, SMA and myoD1. A diagnosis of MFH was made.
Conclusion: MFH is a primitive mesenchymal tumor with some histiosytic and fibroblastic differentiation Primary renal MFH is an extremely rare lesion. Because this malign mesenchymal tumor is indistinguishable clinically and radiologically from renal cell carcinoma diagnosis and histopathology of this rare lesion are discussed.

PS-22-032

Hyaline ring granulomas in the urinary bladder: A case report

N. Hammer*, N. Gatt, J. De Gaetano
*Swatar, Malta

Objective: Hyaline ring granulomas, or pulse granulomas, are rare inflammatory responses to vegetable matter, characterised by aggregates of hyaline rings and other inflammatory components around vegetable matter. The vast majority occur in the oral cavity and only a few specific extra-oral cases have been reported. We present a case of pulse granulomas in the wall of the urinary bladder, occurring in a 50 year-old gentleman with a concurrent history of diverticulitis and colo-vesical fistula. Pulse granulomas were recently described in the bladder in association with interstitial cystitis, in mesocolonic fat and mesocolonic lymph nodes in association with inflammatory bowel disease and in enterocutaneous and recto-salpingeal fistulas in association with diverticulitis. To our knowledge this is the first case reporting the direct association of the occurrence of bladder pulse granulomas in relation to diverticulitis.
Method: The tissue sections were fixed with 10 % buffered formalin and stained with H&E.
Results: Histopathological examination revealed several hyaline ring granulomas within the outer muscle layer and serosa of the urinary bladder, together with hyaline ring

granulomata within the outer wall of the sigmoid colon associated with diverticula.

Conclusion: It is important to differentiate pulse granulomas from parasites, hyaline ring vasculopathy, granulomatous inflammatory disorders and even malignancy.

PS-22-033

Micropapillary urothelial carcinoma of the bladder: A clinicopathologic comparison with urothelial carcinoma with and without divergent differentiation

J. Hou*, J. Saab, D. Holder, M. Mansukhani, J. McKiernan, G. DeCastro, L. Harik

*Columbia Presbyterian Hospital, Pathology, New York, USA

Objective: Micropapillary carcinoma (MPC) is associated with poor prognosis, and may lead to immediate cystectomy irrespective of stage. We study MPC, with "classical" histologic features, to "stage-matched urothelial carcinoma (UCa), not otherwise specified (NOS)", and other UCa with divergent differentiation to compare outcome.

Method: 89 cases from 80 patients with MPC, UCa with squamous (SQ) or glandular (GL) differentiation, small cell carcinoma (SmCa), and nested variant (NeCa) variant of UCa were identified. Histologic and clinical data including stage and outcome were collected.

Results: All groups show male predominance and similar age range. MPC showed the highest rate of nodal metastases (Table 1). Patients with MPC tumor volume of >50 % showed the highest rate of nodal metastases of all other subgroups. The majority of patients with MPC died, a large percentage from unknown causes. Compared to MPC, SQ showed similar presentation at higher stages and similar survival, but a lower propensity for nodal metastases. In our cohort, GL presented at lower stages, showed slightly better survival, and a lower rate of nodal metastases, when compared to MPC. Our cohort included fewer cases of SmCa and NeCa. However, both patients with NeCa died of disease.

Conclusion: MPC, particularly when it represents >50 % of tumor volume, shows higher rate of nodal metastases than remaining subgroups, and is associated with a larger percentage of patient deaths.

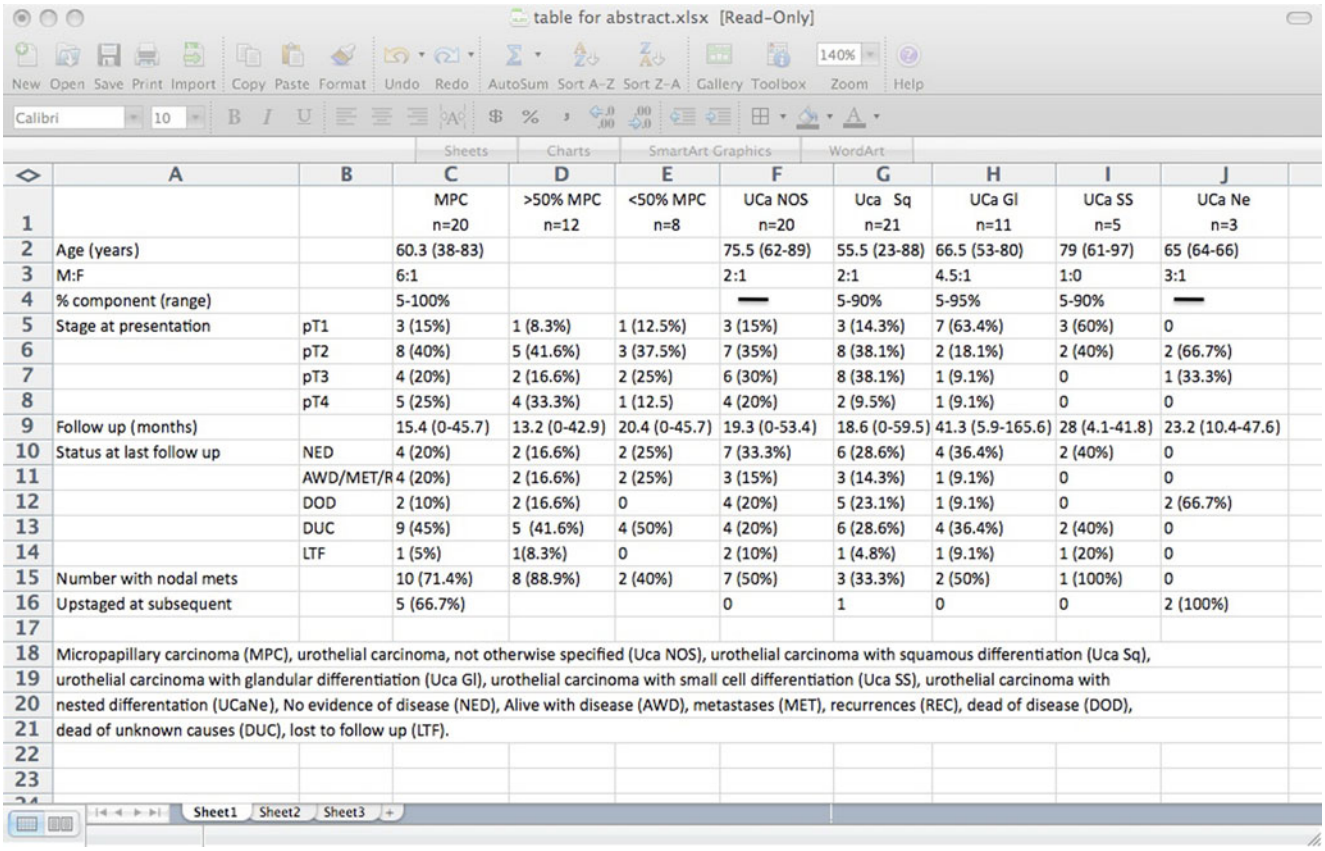

	A	B	C	D	E	F	G	H	I	J
1			MPC n=20	>50% MPC n=12	<50% MPC n=8	UCa NOS n=20	Uca Sq n=21	UCa Gl n=11	UCa SS n=5	UCa Ne n=3
2	Age (years)		60.3 (38-83)			75.5 (62-89)	55.5 (23-88)	66.5 (53-80)	79 (61-97)	65 (64-66)
3	M:F		6:1			2:1	2:1	4.5:1	1:0	3:1
4	% component (range)		5-100%			—	5-90%	5-95%	5-90%	—
5	Stage at presentation	pT1	3 (15%)	1 (8.3%)	1 (12.5%)	3 (15%)	3 (14.3%)	7 (63.4%)	3 (60%)	0
6		pT2	8 (40%)	5 (41.6%)	3 (37.5%)	7 (35%)	8 (38.1%)	2 (18.1%)	2 (40%)	2 (66.7%)
7		pT3	4 (20%)	2 (16.6%)	2 (25%)	6 (30%)	8 (38.1%)	1 (9.1%)	0	1 (33.3%)
8		pT4	5 (25%)	4 (33.3%)	1 (12.5)	4 (20%)	2 (9.5%)	1 (9.1%)	0	0
9	Follow up (months)		15.4 (0-45.7)	13.2 (0-42.9)	20.4 (0-45.7)	19.3 (0-53.4)	18.6 (0-59.5)	41.3 (5.9-165.6)	28 (4.1-41.8)	23.2 (10.4-47.6)
10	Status at last follow up	NED	4 (20%)	2 (16.6%)	2 (25%)	7 (33.3%)	6 (28.6%)	4 (36.4%)	2 (40%)	0
11		AWD/MET/R	4 (20%)	2 (16.6%)	2 (25%)	3 (15%)	3 (14.3%)	1 (9.1%)	0	0
12		DOD	2 (10%)	2 (16.6%)	0	4 (20%)	5 (23.1%)	1 (9.1%)	0	2 (66.7%)
13		DUC	9 (45%)	5 (41.6%)	4 (50%)	4 (20%)	6 (28.6%)	4 (36.4%)	2 (40%)	0
14		LTF	1 (5%)	1(8.3%)	0	2 (10%)	1 (4.8%)	1 (9.1%)	1 (20%)	0
15	Number with nodal mets		10 (71.4%)	8 (88.9%)	2 (40%)	7 (50%)	3 (33.3%)	2 (50%)	1 (100%)	0
16	Upstaged at subsequent		5 (66.7%)			0	1	0	0	2 (100%)
17										
18	Micropapillary carcinoma (MPC), urothelial carcinoma, not otherwise specified (Uca NOS), urothelial carcinoma with squamous differentiation (Uca Sq),									
19	urothelial carcinoma with glandular differentiation (Uca Gl), urothelial carcinoma with small cell differentiation (Uca SS), urothelial carcinoma with									
20	nested differentation (UCaNe), No evidence of disease (NED), Alive with disease (AWD), metastases (MET), recurrences (REC), dead of disease (DOD),									
21	dead of unknown causes (DUC), lost to follow up (LTF).									
22										
23										

PS-22-034

Expression of estrogen and progesterone receptors and Wilms tumor 1 in kidneys with chronic obstructive pathology

N. Juanpere*, J. A. Merino, T. Baró, V. Alba, Y. Zboromyrskyy, O. Bielsa, S. Serrano, J. Lloreta
*Hospital del Mar, Dept. of Pathology, Barcelona, Spain

Objective: Müllerian-like stroma with ER/PR expression is typical of renal mixed epithelial and stromal tumor and has been described in kidneys with obstructive pathology. WT1 overexpression is not reported in this setting.
Method: Immunohistochemical study for ER, PR and WT1 in autosomal dominant polycystic kidney disease (ADPKD) (n=5), acquired cystic kidney disease (ACKD) (n=5), xanthogranulomatous pyelonephritis (XP) (n=5), and renal lithiasis (RL) (n=5). Controls: fetal (<24 w, n=4; >24 w, n=4) and adult autopsy kidneys (n=5).
Results: Stromal ER was found in 100 % of ADPKD, ACKD, XP and RL; PR expression in 100 % of ADPKD, ACKD and RL and 80 % of XP, and nuclear WT1 in 20 % of XP and RL. ER were negative in 100 % of controls. We found PR expression in 100 % of fetal controls of second trimester. WT1 was negative in the stroma of adult controls (100 %). 80 % of fetal controls showed WT1 expression in the peripheral cortex.
Conclusion: ER and PR expression is frequent in kidneys with chronic obstructive and inflammatory pathology. WT1 is expressed occasionally. More studies are needed to determine whether these findings are a consequence of renal obstruction or they are involved in its pathogenesis, as well as their potential therapeutic implications.

PS-22-036

Telomerase expression in urothelial carcinomas of the urinary bladder: Does it make sense for carcinogenesis or prognosis?

D. Kankaya*, S. Kiremitci, K. Zengin, C. Tuygun, A. Sertcelik
*Ankara University Medical School, Dept. of Pathology, Turkey

Objective: Human telomerase reverse transcriptase (hTERT) has been reported as poor prognostic marker in several cancers. In the present study, we examined hTERT expression in urothelial carcinoma (UC) to investigate whether it has a role on the carcinogenesis or prognosis.
Method: Immunohistochemistry was performed to detect hTERT protein expression in tisse microarray blocks consisting of cores of papillary UC (n=63) and infiltrating UC (n=13) cases. Nucleolar staining was considered and staining scores (intensity × distribution) were determined. Tumors were grouped as low or high in terms of histological grade, and as early (Ta, T1), or late stage (T2- T4) in terms of pathological stage.
Results: hTERT expression was significantly higher in the papillary UC group (p=0.028). Tumors in late stage were more likely to show low staining scores of hTERT (p=0.013). No correlation was found with tumor grade and recurrence rate. No effect on survival.was detected.
Conclusion: These findings indicated an association of hTERT protein with early stage UCs as its expression significantly decreased with muscularis propria invasion.

PS-22-037

Incidental multifocal renal cell carcinoma in graft nephrectomy with cellular rejection findings: Concurrence of papillary renal cell carcinoma and renal carcinoma associated with Xp11.2 translocation

D. Kankaya*, S. Kiremitci, A. Ensari, A. Sertcelik
*Ankara University Medical School, Dept. of Pathology, Turkey

Objective: Malignancy represents the second main cause of death in renal transplant patients and increase markedly by 20 years after transplantation.
Method: A 41 year old male who has been on hemodialysis for 8 months for chronic renal failure, underwent living kidney transplantation from his brother. He received immunosupressive therapy of siclosporin and prednisolon. Twelve years later, due to the impairment of renal functions hemodialysis was started again and ultrasonography revealed chronic renal parenchymal disease. Graft nephrectomy was performed with the pre-diagnosis of chronic rejection.
Results: Macroscopic examination revealed two well-circumscribed tumor nodules with 12 mm and 6 mm in largest diameter. Microscopically, both tumor nodules showed tubulopapillary organization. Larger tumor consisted of clear cells with TFE3 positivity, whereas the small one showed eosinophilic cells with diffuse cytokeratin7 and AMACR positivity, without any TFE3 expression. Concurrence of papillary renal cell carcinoma and renal cell carcinoma associated with Xp11.2 translocation was reported. Non-tumoral renal paranchyme revealed interstitial inflammation, tubulitis and transmural arteritis with fibrinoid necrosis compatible with type III cellular rejection.
Conclusion: As far as we know this is the first case in the English literature demonstrating concurrence of papillary renal cell carcinoma and renal cell carcinoma associated with Xp11.2 translocation in a graft nephrectomy.

PS-22-038

The effect of postoperative intravesical BCG and Mitomycin C therapy on recurrence in superficial bladder cancer

D. Kankaya*, K. Zengin, A. Sertcelik, C. Tuygun, N. Sertcelik
*Ankara University Medical School, Dept. of Pathology, Turkey

Objective: To evaluate the efficacy of two mostly used intravesical agent, BCG and mitomycin c, in case of tumor recurrence.
Method: Between 2002 and 2008, we performed TUR-BT to 127 patients whom pathology results were superficial bladder cancer. 41 patients were treated with intravesical BCG once for week 6 weeks then monthly up to one year beginning from 14. day postoperatively. 26 patients were treated with intravesical mitomycin c, beginning from first 6 h postoperatively and once a week for 8 weeks. 60 patients didn't get any further treatment, and excluded from study.
Results: For BCG group, expected disease free interval was 58.1 months, and 34.6 months for mitomycin c group. When two groups compared for expected disease free interval, statistically significant difference observed (p=0.017). For BCG and mitomycin c group, recurrence was seen in 13 and 9 patients, respectively. For patients treated with BCG, 1 and 3 years disease free survival rate was %92.7 and %75.7, respectively. In mitomycin c group 1 and 3 years disease free survival rate was %76.9 and %62.9.
Conclusion: Intravesical adjuvant BCG maintenance therapy is more effective for tumor reccurence than intravesical mitomycin c therapy.

PS-22-039

Papillary cystadenomas of the epididymis: Case presentation

P. Katafygiotis*, L. Abou-Asabeh, A. Nomikos, S. Chranioti
*Hospital of Voula, Dept. of Pathology, Athens, Greece

Objective: Papillary cystadenomas of the epididymis are rare, first described by Sherrick in 1956. They are considered hamartomatous lesions rather than neoplastic and may be seen as intrascrotal swellings in a wide age range. We report here the case of a 32-year-old male who presented with a swelling of the right testis over the past year. His past medical history was otherwise unremarkable.
Method: Ultrasonography revealed the presence of an epididymal cyst. Grossly the cyst had a 2 cm diameter with a cyst wall of 0.2 cm thick attached to a part of epididymis measuring 2×1 cm filled with clear fluid.
Results: Histologically the cyst showed pseudopapillary structures lined by monotonous clear cells. There was mild nuclear pleomorphism, no mitotic activity and no necrosis. Immunostaining for AE1/AE3, EMA, were positive, as well as focally for CK5/6 whereas calretinin and CEA was negative. Similar pattern of staining was seen in the epididymal parenchyma.
Conclusion: Papillary cystadenomas are benign neoplasms and there have been no reports of recurrence or metastasis in the recent literature. Bilateral disease is often associated with von Hippel-Lindau syndrome. Our patient received no further treatment and remains asymptomatic and well 10 months after the intervention.

PS-22-040

Effect of neoadjuvant sorafenib treatment on histology of clear cell renal cell carcinoma and occurrence of circulating tumor fragments

G. Kats-Ugurlu*
*UMC St. Radboud, Dept. of Pathologie, Nijmegen, Netherlands

Objective: Clear cell renal cell carcinoma (ccRCC) generally presents with a micronodular phenotype (MP) due to high expression levels of vascular endothelial growth factor (VEGF-A). Earlier we have shown that MP is associated with shedding of multicellular tumor fragments (MTF) into the circulation and pulmonary metastasis. We hypothesized that VEGF inhibition will destroy MP resulting in less MTF.
Method: 8 ccRCC patients were treated for 4 weeks by daily administration of Sorafenib (400 mg bid). Three days after therapy, nephrectomy was performed and kidneys were perfused via the arteria renalis. Venous perfundate was filtered and processed to AgarCytoblocks for MTF. Treatment effects were studied using immunohistochemistry.
Results: All tumors were ccRCC as demonstrated by high VEGF-A expression. None of the tumors showed MP after Sorafenib treatment. Tumors showed large areas of necrosis and fibrinoid necrosis of the blood vessels, concomitant with profound perivascular inflammation. 6/8 ccRCC patients (75 %) had MFT vs 33 % in a control group (p= 0.03 Fisher's exact test). Individual tumor cells in the MTFs showed increased mitotic activity.
Conclusion: Sorafenib destroys MP in ccRCC, attacks tumor vasculature, causes extensive necrosis and inflammation. Post-treatment MTF are increased in venous perfundate. Care should therefore be taken with neo-adjuvant sorafenib treatment of ccRCC.

PS-22-041

Differential expression of Claudin-1, Claudin-3 and Claudin-4 in bladder lesions

T. D. Kokenek-Unal*, I. Coban, A. S. Oguz-Erdogan, M. Alper
*YB Research and Training Hospital, Dept. of Pathology, Ankara, Turkey

Objective: Claudins are major transmembrane proteins of tight junctions. As the disruption of their function have important impact on tumorogenesis, invasion and metastasis. Claudins became a focus of interest for targeting therapies. Although their expression profiles have been studied in many organs, researches on Claudin expression in bladder are in limited number. The aim of this study is to present the differential expression of Claudins in invasive urothelial cell carcinoma (IUCC), noninvasive papillary urothelial carcinoma (NPUC), carcinoma in-situ (CIS), papillary urothelial neoplasm of low malignant potentiall (PUNLMP) and control group (CG).
Results: 83 cases (31 IUCC -further divided into:15 muscle invasive UCC, 16 UCC with lamina propria invasion-, 17 NPUC, 13 PUNLMP, 7 CIS and 15 CG) were evaluated with Claudin-1, 3, 4. Interestingly, high Claudin-1 and -3 score in CG (100 %, 80 %), decreased significantly in all non-invasive lesions (mean 18 %, 22 %). Claudin-4 expression appeared to decrease in IUCC vs. Others (%52 vs mean %82).
Conclusion: Higher expression of Claudin-4 in low-grade and non-invasive lesions may be used as a diagnostic tool. In terms of Claudin-1 and -3, their decreased expression in non-invasive lesions when compared to CG and their trend to show more increased expression in IUCC needs to be studied further in larger studies.

PS-22-042

Can we rely on alternative sampling method of radical prostatectomy specimens?

T. D. Kokenek-Unal*, A. S. Oguz-Erdogan, M. Alper
*YB Research and Training Hospital, Dept. of Pathology, Ankara, Turkey

Objective: Prostatic adenocarcinoma is the most common cancer and second leading cause of cancer death in men. The incidence of prostate cancer has been increasing because of efficiency of modern cancer scanning programs and residual awareness of the patients. For that reason, there is a considerable increase in the number of prostatectomy specimens in the university and research hospitals.It is costly and time-consuming procedure and causes in turn increased workload. The aim of this study is to compare the results of total and alternative sampling methods and to delineate the differences if there are any.
Method: Totally embedded 50 radical prostatectomy specimens were randomly selected and evaluated for key pathologic parameters. These cases then were reevaluated with limited sampling. The limited sampling method was built to include similarly embedded apical margins, bladder neck margins and seminal vesicles. In addition to that new slices were selected by skipping every other slice as differently from totally sampling protocol.
Results: The %37 reduction was achieved in number of blocks. The concordance rates between two sampling methods were %40, %50.4, %70.3, and %60 respectively for Gleason scores, perineural invasion, extraprostatic extension and pathologic stages.
Conclusion: Although the limited sampling protocol provides statistically significant results, because of critical role of pathological assessment in treatment of prostatic adenocarcinoma, they can be found unsatisfactory for many pathologists.

PS-22-043

Expression of nestin in Leydig cell tumors and hyperplasia

J. Kozlowska*, G. Wirth, J.-C. Tille, C. Iselin, M.-F. Pelte
*Geneve, Switzerland

Objective: Initially described in embryonic neuroepithelium, nestin is an intermediate filament involved in cell differentiation and transiently related to vimentin, keratin and glial fibrillary acidic protein (GFAP). In tumoral and vascular proliferation, nestin is recognized in stem/progenitor cells. The octamer-binding transcription factor 4 (OCT-4) is a biomarker of this lineage. Since there are few data concerning the presence of nestin in Leydig cells and testicular tumors, our aim was to investigate a series of Leydig cell hyperplasia and tumors.
Method: 31 cases (13 hyperplasia, 14 adenomas, 2 malignant Leydig cell tumors and 2 lymph node metastases) and controls were immunostained with anti-nestin, vimentin, keratin, GFAP and OCT-4 antibodies.
Results: Twenty-six (84 %) cases (tumors and hyperplasia) were nestin positive with mostly weak, finely granular cytoplasmic staining. Four (13 %) were negative, 1 (3 %) not interpretable. Vimentin was expressed in twenty-seven (87 %) cases. Seventeen (55 %) were focally keratin positive. Only three (10 %) showed OCT-4 positivity. All were GAFP negative.
Conclusion: In Leydig cell hyperplasia, adenomas and malignant tumors nestin and vimentin are expressed frequently, sometimes with keratin. This would be a sign of epithelial-mesenchymal transition. Further investigations are needed to understand the relationship with the malignant potential of these tumors.

PS-22-044

Morphological changes of testis in atherosclerosis

N. Krupnov*, A. Astrakhantsev
*Bureau of Forensic Medical Exp., Ryazan, Russia

Objective: Up to now in the field of morphology of reproductive system of men the problems of testis involution and morphogenesis at atherosclerosis haven't been thoroughly investigated.

Method: We have investigated histologically testis of 63 died patients aged 36–89 with general atherosclerosis and testis of 38 men aged 36–89 with minimal manifestations of atherosclerosis died in an accident.
Results: The absolute volume rete testis of patients being ill with atherosclerosis decreases by 65–80 %. Absolute volume of convoluted seminiferous tubules and interstitial tissue decrease by 24–27 %. In testis there are zones of focal sclerosis of seminiferous tubules, whose area goes as far as 12.7 % of shear section area. It was revealed that on the periphery of sclerosis zones there is a reduction of transaction area of seminiferous tubules by 20–33 % with Sertolli cells quantity reduction by 17–24 %. It has been stated the downward changes in index of spermatogenesis in convoluted seminiferous tubules by 63–65.6 %, accounted for the quantity reduction of all kinds of cells.
Conclusion: Morphological changes of testis at general atherosclerosis characterize atherosclerotic testiculopatie, caused by chronic ischemia of testis.

PS-22-046

A Leydig-cell tumor in a cryptorchid testis: Report of a case

E. Lambropoulou*, A. Datsis, P. Morfaki, G. Charalambopoulou
*General Hospital of Messologhi, Dept. of Pathology, Greece

Objective: Leydig cell tumor is a rare form of testicular neoplasm, representing only 1–3 % of all testicular tumors. According to accepted medical knowledge, this type of tumor isn't linked to cryptorchidism, unlike germ cell tumors of the testicles. Herein, a case of Leydig cell tumor in a cryptorchid testis is described.
Method: A 59-year-old, unmarried man was admitted for surgical repair of inguinal hernia. His past medical history included untreated bilateral cryptorchidism first noted in childhood, as well as poliomyelitis that presented at age two. The past surgical history and review of systems were noncontributory. A CT scan of the abdomen and pelvis revealed two 3×3 cm testicles at the level of the inguinal canal. He underwent bilateral inguinal orchiectomy combined with surgical repair of his inguinal hernia.
Results: The right testis contained a solid, well-circumscribed, round, tan-colored tumor 1.5 cm in diameter. The histological appearance was that of a Leydig cell tumor exhibiting no mitotic figure. There was no clinical or radiological evidence of metastatic spread.
Conclusion: Although cryptorchidism is considered to be a risk factor for developing germ cell tumors, there have been a few reported cases of Leydig cell tumors with a history of cryptorchidism. Our case adds to the evidence that there may be a link between the two conditions.

PS-22-047

The role of CD44, E-cadherin, and ß-catenin in lesions of the prostate gland

P. Lazari*, H. Poulias, O. Pantzartzi, H. Gakiopoulou, G.-E. Thomopoulou, C. Barbatis, A. C. Lazaris
*Hellenic Red Cross Hospital, Dept. of Pathology, Athens, Greece

Objective: CD44, E-cadherin, β-catenin are "cell adhesion molecules" and appear to influence development, inflammation, cancer invasion and metastasis. We studied the expression of these CAMs in prostatic adenocarcinoma (PCa), high grade prostatic intraepithelial neoplasia (HGPIN) and nodular adenomatous hyperplasia (NH).
Method: 135 specimens of radical prostatectomies were assessed. These CAMs were determined by immunohistochemistry. All sections included PCa, HGPIN, and NH. The expression of these markers was evaluated with three scores. The correlation of immunopositivity with Gleason score and TNM stage was investigated.
Results: CD44 was strongly expressed in 41.5 %, 46.7 % and 37.8 % of NH, HGPIN and PCa, respectively. E-cadherin immunostaining was higly detected in 71.1 %, 78.5 % and 63.0 % of NH, HGPIN and PCa areas while β-catenin immunostaining was exclusively membranous in 80.7 % of NH and nuclear/cytoplasmic in 70.4 % and 48.9 % of HGPIN and PCa areas. All markers were unrelated to Gleason score (p=0.352). CD44 and E-cadherin immunopositivities were inversely associated with TNM stage (p=0.021 and p=0.042 respectively); such an association was not observed in β-catenin (p=0.556).
Conclusion: CD44 and E-cadherin decreased expression is probably associated with invasive potential of prostate cancer. β-catenin staining pattern in neoplastic lesions differs from that in non-neoplastic prostate lesions.

PS-22-048

Expression of E-cadherin in non-neoplastic mucosa, superficial and central portion of the tumor and the tumor invasive front and vimentin in tumor cells in the phenomenon of epithelial-mesenchyme transition in penile carcinoma

M. J. Leonardo*, F. Soares
*Hospital of Cancer - São Paulo, Pathology, Brazil

Objective: To analyse the e-cadherin (ECAD) and vimentin expressions in the epithelial-mesenchymal transition (EMT), and their correlation with clinical prognostic factors of patients with penile carcinoma.
Method: 91 cases without neoplasia and 151 cases presenting penile carcinoma were applied to immunohistochemical analysis of ECAD at the non-neoplastic mucosa (NNM), Tumor Superficial and Central Portion (TSCP), Tumor

Invasion Front (TIF) and vimentin expression at the cytoplasmatic portion of tumor cells.
Results: The loss of ECAD expression was significantly higher at the TIF when comparing with TSCP and NNM. The loss of ECAD was correlated with histological grade, infiltrative pattern, lymph node metastasis, perineural and vascular invasion. The vimentin expression showed association with histological grade, infiltrative pattern, T stage, lymph node metastasis, perineural and vascular invasion.
Conclusion: The loss of ECAD and the gain of vimentin expressions occur more frequently at the tumor invasion front and are associated with classic factors of poor prognosis and low survival rates.

PS-22-050
Prognostic value of immunohistochemical markers in bladder cancer
I. M´Sakni*, A. Chaabane, F. Bougrine, B. Laabidi, A. Bouziani
*Rades Meliane, Tunisia

Objective: The tumor stage and grade of bladder tumors are the major elements to define the prognosis. However, it is sometimes difficult to identify an infiltration of chorion or detrusor muscle. Moreover, the evaluation of tumor grade is subjective and not reproducible.
Method: Our objective is to study the prognostic value of the expression of proliferating cell nuclear antigen (PCNA), Ki67 antigen, the tumor suppressor gene p53, the proto-oncogene c-erb B2, the receptor for Epidermal Growth Factor (EGF-R), the apoptosis suppressor gene bcl2, carcinoembryonic antigen (CEA) and Epithelial Membrane Antigen (EMA).
Results: The study showed that the PCNA expression was significantly associated with the early recurrence ($p=0.010$) and the tumor stage ($p=0.003$). The Mib1 expression was correlated to the early recurrence ($p=0.010$), and tumor progression in stage and/or grade ($p=0.007$). The c-erbB2 expression showed significant association with the tumor grade ($p=0.007$). The prognostic value of other markers has not been proven.
Conclusion: These findings may be useful providing better classification of bladder tumors thus the better management of patients. The c-erbB2 expression contributes to refine the tumor grading. PCNA and Mib1 can predict the early tumor recurrence; they could be relevant for the determination of endoscopic controls rhythms of patients.

PS-22-051
Primary urinary bladder neuroendocrine carcinoma: A report of five cases
W. Majdoub*, S. Hmissa, A. Ben Abdelkader, S. Miladi, A. Bdoui, S. Mestiri, M. Mokni, M. T. Yacoubi
*Farhat Hached Hospital, Pathology, Sousse, Tunisia

Objective: Primary urinary bladder neuroendocrine carcinoma (PUBNEC) is a rare tumor characterised by an aggressive behaviour and poor prognosis.
Method: We report five cases of PUBNEC diagnosed in the departement pathology of Farhat Hached Hospital between 1990 and 2011.
Results: Our population is composed by four mens and a woman. All patient are heavy smokers. The most common presenting symptom is hematuria and dysuria in all cases. One patient presented a complete urinary retention. A cystoscopic examination with transurethral resection was performed in all cases. The pathological examination with use of immunohistochemical markers of neuroendocrine differentiation were consistent with a large cell neuroendocrine carcinoma in four cases and a small cell neuroendocrine carcinoma in a case. A cystoprostatectomy was made in two cases followed by chemotherapy.
Conclusion: The clinical presentation of PUBNEC is similar to other bladder cancers and is characterized by advanced stage at diagnosis and rapidly progressive disease. The diagnosis of poses several problems: a vesical metastasis has to be excluded and such lesions have to be differentiated from transitional cell carcinoma, lymphoma, paraganglioma and peripheral nerve neuroblastoma. There is no gold standard for the management of patients affected due to low disease frequency

PS-22-052
IgG4-associated Inflammatory Pseudo-tumor (IPT) of the ureter: A case report
A. Marando*, G. D´Ambrosio, F. Catanzaro, F. Sessa
*University of Insubria, Dept. of Surgical, Varese, Italy

Objective: IgG4-associated inflammatory pseudo-tumor (IPT) is a novel clinico-pathologic entity characterized by intensive infiltration of IgG4-positive plasma cells, associated with systemic IgG4-related sclerosing disease. Many reports described IgG4-related IPT in various locations such as pancreas, salivary glands, liver, breast, lung and recently also ureter.
Method: It is described a case of ureteral IPT with pathologic and immunohistochemical features of IgG4-related IPT, fibrohistiocytic type.
Results: The study case is a 82-year-old female with severe stenosis of the left ureter and hydronephrosis, who underwent to nephroureterectomy and endoscopic resection of multiple lesions in the bladder. The histological examination showed transmural fibrosing inflammatory lesion of the affected ureteral wall, with abundant plasma cells intermixed with many histiocytes, lymphocytes, fibroblasts and scattered eosinophils. The majority of infiltrating plasma cells were positive for IgG4. Bladder lesions showed similar histological

features. The diagnosis was IgG4-related IPT, fibrohistiocytic type.
Conclusion: IgG4-related IPT of ureter is extremely rare, with only few cases reported in literature. Recognition of this entity is clinically relevant because this type of IPT can be treated with steroid therapy and may be associated with sclerosing autoimmune disease in other organs.

PS-22-053
A rare case of malignant fibrous histiocytoma of the urinary bladder
S. Mavropoulou*, Z. Tatsiou, I. Amplianitis, P. Nasos
*General Hospital, Laboratory of Pathology, Xanthi, Greece

Objective: Malignant fibrous histiocytoma (MFH) is an extremely rare malignant mesenchymal neoplasm of the urinary bladder with only a few well-documented cases reported in the English literature.
Method: We report the case of an 88-year-old man who was brought to our hospital due to sudden massive haematuria. Catheterization failed to obtain haemostasis so, a suprapubic incision and direct exploration of the bladder was performed. A large solid tumor was found with a shaggy haemorrhagic surface and biopsies were taken.
Results: Histological examination revealed an infiltrating malignant neoplasm composed of variably pleomorphic ovoid neoplastic cells with eosinophilic cytoplasm, bizarre tumor giant cells and prominent stromal osteoclastic giant cell reaction. Immunohistochemical examination was negative for cytokeratin, desmin, smooth muscle actin, PSAP, NSE, S100protein and HMB45 whereas it was positive for CD68 in a large number of tumor cells. Accordingly, the diagnosis of undifferentiated pleomorphic sarcoma with histological features compatible with giant cell MFH of the urinary bladder was made. The patient died 4 days after the diagnosis.
Conclusion: In conclusion, MFH of the bladder should be kept in mind when facing with an undifferentiated malignant tumor. Despite the poor prognosis, early diagnosis and aggressive salvage therapy might offer the chance of long-term survival in selected cases.

PS-22-054
Partial nephrectomy experience at a single tertiary-care oncology centre: A clinicopathologic study of 60 cases
S. Menon*, G. Bakshi, H. Tongaonkar, V. Noronha, A. Joshi, K. Prabhash, S. Desai
*Tata Memorial Hospital, Dept. of Pathology, Mumbai, India

Objective: Partial nephrectomy (PN) is replacing radical surgery as a gold standard in the treatment of small renal masses. Intra-operative frozen consultation for margin status is aimed at achieving a disease free state in order to reduce chances of recurrence.
Method: A retrospective clinicopathologic analysis of consecutive PNs performed at our institute from 2004 to 2011 was undertaken.
Results: Sixty cases of PN were analysed. Male to female ratio was 1.8:1. Median age was 51 years. Six cases were benign: oncocytomas (3), angiomyolipoma (3); while 54 cases were malignant: renal cell carcinoma (RCC) - conventional (43), papillary (8), chromophobe (1), mucinous tubular spindle cell carcinoma (1) and one case of primitive neuroectodermal tumour. In 4 patients, the renal tumour was a second malignancy. Median tumour size was 3.5 cm with 42 cases of stage pT1. Intra-operative margin was positive in 16 cases. Mean margin for all cases was 2.3 mm. Median follow-up was of 24 months. None of the tumours recurred or metastasized during follow-up.
Conclusion: Conventional RCC is the commonest histology in PN cases. Frozen section analysis has a definite role in achieving margin free status. PN is not associated with increased risk of local recurrence in small renal tumours.

PS-22-057
Clear cell tubulopapillary renal cell carcinoma: A clinicopathologic study of two cases
G. Muñiz*, A. Corominas, N. Cerda, A. Perez, V. Caamaño, M. Gonzalez, L. Etxegarai, J. I. López
*Hospital Universitario Cruces, Dept. de Anatomía Patológica, Barakaldo, Spain

Objective: Cleal cell tubulopapillary renal cell carcinoma has been recently identified as a low grade renal cell tumor with distinct histological features.
Method: Patient 1: 65 year old female with a history of fibromyalgia and persistent loin pain. A right renal mass, 2.8 cm in diameter, was discovered in the rheumatologist's follow up. Right nephrectomy was performed and the patient is free of disease 7 months later. Patient 2; 55 year-old female with a history of diabetes mellitus type 2, hypertension and renal failure grade 3 with a 2.5 cm in diameter renal tumor in the routine studies. She underwent tumorectomy.
Results: Grossly, both were cystic tumors with gelatinous fluid and white-yellowish solid areas. Tumors showed a tubular and papillary architecture. Proliferating cells displayed clear cell cytoplasm and hyperchromatic nuclei placed in the luminal side. IHC showed positive staining with e-cadherin, EMA and CK7. Conversely, CD10, CD117 and AMACR were negative.
Conclusion: Clear cell tubulopapillary renal cell carcinoma should be considered a distinct subtype of renal cell carcinoma according to its unique morphologic and inmunohistochemical features. The few cases reported so far behave in an indolent course.

PS-22-058

Tubulocystic renal cell carcinoma: Clinicopathologic study of two cases

G. Muñiz*, A. Corominas, A. Perez, N. Cerda, M. Gonzalez, V. Caamaño, L. Andres, J. I. López
*Hospital Universitario Cruces, Dept. de Anatomía Patológica, Barakaldo, Spain

Objective: Tubulocystic carcinoma of the kidney (TCRCC) is a rare variant of renal tumor showing unique gross and microscopic features. Several recent studies favour its inclusion within the papillary renal cell carcinoma (PRCC) group.
Method: Patient 1 was a 55 year-old man with a left asymptomatic renal mass incidentally discovered by sonography. Patient 2 was a 72 year-old man with aortic estenosis and coronary disease. A right renal mass was discovered in the work up for aortic valve replacement and coronary bypass.
Results: Both tumors were well circumscribed masses with "sponge-like" appearance. On light microscopy, the tumors were composed of ectatic tubules and cysts of variable size, lined by a single layer of tumor cells with eoshinophilic cytoplasm, apocrine appearance, rounded nucleus sometimes overlapping, and prominent nucleoli. IHC showed positive staining with CK7, e-cadherin, CD10, and AMACR.
Conclusion: TCRCC has been recently recognized as a distinct subtype of PRCC by some authors. In fact, some few cases reported have histological transition between tubulocystic and papillary phenotypes on routine histological sections. Additionally, TCRCC shows trisomies of chromosomes 7 and 17. The exact location of this tumor within the 2004 WHO classification is a matter of debate.

PS-22-062

HER2 protein expression in urothelial carcinoma of the bladder

A. Nikolaidou*, G. C. Balis, G. Moustakas, E. Michalopoulou, I. Themeli, G. Demertzidis, N. Dimasis
*Theagenio Hospital, Dept. of Pathologoanatomy, Athens, Greece

Objective: Our purpose is to evaluate HER2 protein expression in urothelial carcinoma of the bladder. HER2/neu is a tyrosine kinase receptor (family of human epidermal receptors), showing overexpression in a large variety of tumor cells.
Method: 30 bladder biopsy and cystectomy specimens were included in this study. The age of the patients ranged from 25 to 86 (mean 71). Among them 25 (83.33 %) were male and 5 (16.67 %) female. All cases were reevaluated histopathologically according to WHO 2004 grading system. HER2 protein expression was detected by immunohistochemistry (CB11) using the same criteria as for breast cancer.
Results: All 30 bladder neoplasms were low- or high-grade urothelial carcinomas. HER2 protein overexpression was observed in 10 (33.33 %) cases (2+: 5 cases and 3+: 5 cases), while 20 (66.67 %) cases were negative (0: 3 cases and +1: 17 cases). Among HER2 positive cases 9 (90 %) were high-grade carcinomas, while 1 (10 %) was low-grade carcinoma. Among negative cases 14 (70 %) were low-grade carcinomas, while 6 (30 %) were high-grade carcinomas.
Conclusion: These findings indicate that HER2 protein overexpression is predominately correlated with high tumor grade in urothelial carcinoma of the bladder and patients with these characteristics could be potential candidates for targeted therapy.

PS-22-063

Mucinous adenocarcinoma of the renal pelvis: A case report and review of the literature

M. Otani*, T. Tsukamoto, H. Serizawa
*Tokyo Medical University, Division of Diagnostic Pathology, Japan

Objective: Primary mucinous adenocarcinoma of the renal pelvis is extremely rare and about 50 cases have been reported to date. We present a case of mucinous adenocarcinoma followed by renal cysts.
Method: The patient is a 52-year-old male. A renal cyst in the right upper region was found incidentally. He had no symptom at that time. After 4 years, he came to the hospital because of hematuria and back pain. The examination revealed that the renal cyst was enlarged accompanied with solid lesion. The high serum level of CEA indicated malignancy and tumorectomy was performed.
Results: Macroscopically, a renal cyst (15×10 mm) in the right upper portion was adjacent to a solid mass (22×17 mm). The tumor showed papillary growth (20×15 mm) in renal pelvis. Microscopically, the tumor was consisted of adenocarcinoma with tubular or papillary structure, spreading from cyst wall to pelvis. The tumor cells contained mucin and some showed signet-ring cell-like feature.
Conclusion: Clinically, high serum level of CEA is a marker of mucinous adenocarcinoma originated from renal pelvis. In our case, the tumor has already from pelvis to cyst wall. We thought it originated form renal pelvis, however, the renal cyst is also a candidate for its origin.

PS-22-064

Survivin expression in renal epithelial tumors: Its usage in the differential diagnosis of eosinophilic renal epithelial tumors

A. Ozcan*, N. Yigit, O. Onguru, B. A. Firat, S. Ozaydin
*Gulhane Military Medical Academy, Dept. of Pathology, Ankara, Turkey

Objective: The differential diagnosis of renal tumors can be problematic due to overlapping morphologic features. The purpose of this study was to assess the potential contribution of survivin expression in the differential diagnosis and determination of therapy modalities of these tumors.
Method: This study consisted of 15 chromophobe (ChRCC), 15 clear cell (CCRCC) and 9 papillary (PRCC) renal cell carcinomas, and 13 oncocytomas. Sections were stained against survivin antibody.
Results: PRCCs and CCRCCs showed diffuse and strong survivin expression. Survivin expression was strikingly prominent in type1 PRCCs and cystic CCRCCs. In CCRCCs, survivin expression was more pronounced in low grade areas than high grade and sarcomatoid areas. In ChRCC, survivin expression was more limited and weaker than that of oncocytomas and other malignant renal tumors. In non-neoplastic renal tissue, survivin expression was more pronounced in podocytes and atrophic tubules than other nephron parts.
Conclusion: Our findings suggest that survivin may contribute to the differential diagnosis of renal tumors because of the partially unique staining patterns. It was purposed that knockdown of survivin reduced growth, induce apoptosis and enhance in vitro radiosensitivity of RCC cells. Taken together, to be known different survivin expression patterns in renal tumors may help to determine new therapeutic strategies for RCCs.

PS-22-065

Adenomatous hyperplasia of the rete testis: Not a true hyperplasia, just proliferation!

T. Ozgur*, M. M. Akin, H. Gokce, M. Davarci
*Mustafa Kemal University, Medical Faculty, Antakya, Turkey

Objective: There are several tumor-like lesions and miscellaneous neoplasms of rete testis. We present a case with adenomatous hyperplasia of rete testis (AHRT).
Method: The patient was 24 years old with undescended testis and referred to our hospital. There was no clinical or endocrin abnormalities. Cryptoorchidism was unilateral and the other testis was normal. Right orciectomy was performed and sent to pathology labarotory for examination.
Results: There was no tumoral lesion in gross examination but in microscobic examination there was gland like tubular structures. Some of these were back to back position with little intervening stroma and mild to moderate atypia. EMA and pancytokeratin immunohistochemistry findings with morphology confirmed the diagnosis of AHRT in this case.
Conclusion: AHRT is a rare proliferatif lesion and can be confused with malignancy. It is incidentally realised in microscobic investigation. It may present as a very small lesion detected in microscobic examination or solid-cystic mass lesion which is macroscobically evident. Clinic history, localization, histologic features and immunohistochemistry are criterias for differentiating these lesions.We present this case for both surgeons and pathologists with its importance to be confused with malignancy.

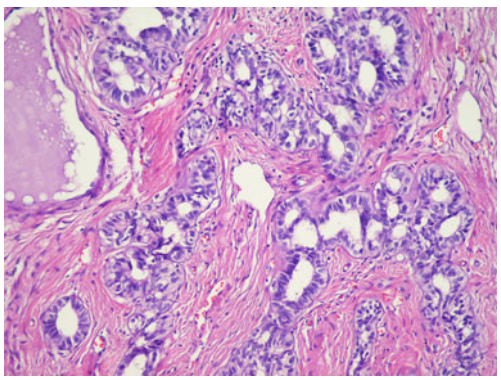

PS-22-066

AMACR and iNOS expressions in prostate adenocarcinomas

T. Ozgur*, E. Atik, S. Hakverdi, M. Yaldiz
*Mustafa Kemal University, Medical Faculty, Antakya, Turkey

Objective: Prostate cancer is the second leading cause of death in men. The localized disease often responds to conventional therapies like androgen ablation via castration and/or administration of chemical inhibitors but advanced disease resistant to any curative therapies is still challenge for investigators. There are increasing efforts to enhance the possibility of finding positive and sensitive immune markers for diagnosing and treating prostate cancer.
Method: We applied immunohistochemical markers; AMACR and iNOS. Formalin-fixed parafin embedded tissues of 64 prostate needle biopsy specimens diagnosed as prostate adenocarcinoma between 2005 and 2010 years were enrolled in the study.
Results: AMACR expression has been found in 58 (90.6 %) and iNOS expression in 54 (84.4 %) of 64 prostate adenocarcinomas.No significant relationship of AMACR and iNOS has been obtained ($p>0.05$). There was no significant

correlation of histopathologic grade of the tumors with AMACR and iNOS expression ($p>0.05$).
Conclusion: The expression of AMACR and iNOS might be important diagnostic immune markers for prostate adenocarcinomas especially in needle biopsies when the quantity and quality of tissue are limited.

PS-22-067

A tissue microarray study of Napsin-A expression in renal tumors

A. Panizo*, F. J. Queipo, J. J. Sola, J. Pardo
*Hospital de Navarra, Anatomia Patologica, Pamplona, Spain

Objective: Napsin-A is an aspartic protease present lung, renal, and thyroid cells. There are few studies evaluating Napsin-A in renal neoplasms. Therefore, we studied IHC expression of Napsin-A in a wide spectrum of renal tumors.
Method: IHC for Napsin-A (rabbit polyclonal antibody) was performed in a series of 334 cases of primary and metastatic renal tumors on TMA. Cytoplasmic immunoreactivity was scored: intensity (0–3+) and extent (% of tumor cells: 0–3). The 2 scores were added: positive case: combined IHC score>2; negative if combined score of 2 or less.
Results: Napsin-A expression was observed in 79 cases (23,7 %). Diagnosis # Napsin-A positive (%) Conventional-RCC: 30/117 (20,4) Papillary-RCC (PRCC): 27/42 (64,3) Papillary adenoma (PA): 10/10 (100) Clear-cell-papillary-RCC (CCP-RCC): 2/2 (100) Mucinous tubular spindle-RCC (MTS-RCC): 3/4 (75) Chromophobe-RCC: 2/74 (2,7) Oncocytoma: 0/34 (0) Bellini-RCC: 0/4 (0) Translocation-RCC: 1/2 (50) Unclassified-RCC: 4/7 (57,1) Urothelial carcinoma: 0/8 (0)
Conclusion: Napsin-A has distinct expression in renal tumors originated from proximal or distal nephron. Napsin-A is frequently expressed in PA, PRCC, CCP-RCC, and MTS-RCC. Napsin-A could be useful in an IHC panel for the identification of PRCC.

PS-22-068

Utility of alpha-methylacyl-CoA racemase and P63 cocktail in the diagnosis of prostatic carcinoma

A. N. Petrescu*, G. Berdan, O. Codreanu, C. Ardeleanu, V. Jinga
*Bucharest, Romania

Objective: The diagnosis of prostatic carcinoma can be challenging on needle core biopsies. The aim of this study was to assess the utility of alpha-methylacyl-CoA racemase (AMACR/P63) antibody cocktail for prostate cancer diagnosis. A prospective analysis of 50 consecutive radical prostatectomy specimens and 50 prostate needle biopsy semples was performed to select histological sections showing foci of minimal prostatic carcinoma, high grade prostatic intraepithelial neoplasia (HGPIN) and benign mimickers of prostatic carcinoma (atrophy, adenosis).
Method: Serial histological sections were stained with hematoxylin and eosin, Van Gieson and immunomarkers: AMACR and P63 using a prediluted antibody cocktail.
Results: The cocktail was very useful in highlighting prostatic carcinoma associated with HGPIN (flat or cribriform) and distorted foci of minimal carcinoma. AMACR was positive with moderate and strong staining in almost all cases for which the immunohistochemical result converted the atypical diagnosis to a final cancer diagnosis. The cases whose diagnosis was changed from "atypical" to cancer were all highly suspicious for cancer based on HE histology and negative basal cell markers.
Conclusion: This cocktail would be of diagnosis utility when limited tissue is available for histopathological evaluation of small diagnostically difficult foci (prostate needle biopsy and surgical specimens).

PS-22-069

Overexpression of Cytokeratin 20, Ki-67 and Topoisomerase-II-a can significantly stratify the recurrence risk in patients with bladder cancer after transurethral resection

S. Petrov*, K. Malkhasyan, R. Khasanov
*Kazan Cancer Center, Dept. of Pathology, Russia

Objective: The current predictive models based on main clinical tumor features are not accurate for the biggest bladder cancer patient group, who underwent the transurethral resection (TUR).
Method: Overall 103 patients with primary urocarcinoma after TUR were included in this retrospective study. The follow up plan in all cases included cystoscopy and biopsy every 3 months in the first 2 years. The recurrence criteria were cystoscopical and pathological confirmation of the tumor growth. In all cases using TMA technique (TMA Master, 3DHistech) there was done the IHC expression study of p53, p63, CK20, E-cadherine, B-catenin, CD44v6, Ki-67 (10 % cut-off), Topo-II-a (10 % cut-off) and Her2, as well c-erb-B2 amplification study (CISH).
Results: There were no association found between the Her2 expression and c-erb-B2 amplification in urocarcinoma patients. In multivariate regression analysis only CK20, Ki-67 and Topo-II-a showed the significant prognostic power in recurrence prediction. These markers were used to develop the powerful predictive index for bladder cancer patients after TUR.
Conclusion: Although the Her2 overexpression is relatively common event in bladder cancer, c-erb-B2 gene amplification isn't main mechanism of its realization. The CK20, Ki-67 and Topo-II-a are promising prognostic markers for

recurrence and should be validated in further prospective study.

PS-22-070

Solitary fibrous tumor of the urinary bladder associated with a high-grade urothelial invasive carcinoma. A case report

A. Pitino*, S. Squillaci, C. Spairani, M. Ferrari, M. F. Cosimi, W. Fusco, C. Rossi, F. Montefiore, G. L. Bigatti, V. La Paglia
*San Giacomo Hospital, Division of Anatomic Pathology, Novi Ligure, Italy

Objective: Solitary fibrous tumor (SFT) is an unusual spindle cell neoplasm, which can exceptionally occur in the urinary bladder.
Method: We present a case of urinary bladder SFT in a 60 year-old man who complained of pelvic pain. Cystoscopy revealed a large protruding, fleshy mass at the anterior wall of the bladder. A biopsy was first misclassified as inflammatory myofibroblastic tumor (IMT). Subsequent complete transurethral resection was performed.
Results: Macroscopically, a 9×7×5 cm greyish lobulated firm polypoid tumor was seen. Microscopically, it consisted of uniform spindle cells with elongated tapered ends nuclei forming a patternless growth in a collagenous background. Mitotic figures were rare. Immunohistochemically, the neoplastic cells were positive for CD34 and bcl-2, and negative for α-SMA, desmin, CK AE1/AE3 and Alk-1. The bladder urothelium showed foci of high-grade transitional carcinoma with lamina propria invasion.
Conclusion: Initially, SFTs were thought to be of mesothelial origin. Then, these tumors have also been observed in extrapleural and extraserosal sites, which suggests a mesenchymal cell origin. The differential diagnosis should always include other spindle cells lesions such as sarcomatoid carcinoma, leiomyosarcoma and IMT. To date, this is the first reported case of association of urinary bladder SFT and high-grade urothelial invasive carcinoma.

PS-22-072

Renal oncocytomas with unusual features: Clinicopathological study of 9 cases

F. J. Queipo*, H. D. Quiceno, F. J. Pardo, Án. F. Panizo, M. L. Gómez-Dorronsoro, G. Aisa, F. J. Monzón, E. Mejía, C. Del Agua, J. Alfaro
*Clínica Universidad de Navarra, Pathology, Pamplona, Spain

Objective: Oncocytoma (RO) is a benign renal neoplasm, with a wide morphologic spectrum and excellent prognosis. Recently, it has been described worrisome morphological features.
Method: RO treated in our centres were reviewed, and we focused on identifying the worrisome and the atypical features.
Results: We identified 9 RO with at least one of the worrisome feature. Patients: 5 M/4 F (mean age 72,89 year; range: 63–88). Mean tumor size: 4,24 cm (range: 1,6–11,5 cm); right kidney: 5, and left: 4 cases. Invasion into the perinephric or renal sinus fat was the most frequent worrisome feature: 7 tumors (77,8 %) and focal chromophobe carcinoma-like areas in 3 cases (33,3 %). Lymphovascular invasion, entrapped renal tubules-glomeruli, necrosis and mitosis were found in 2 (22,2 %) respectively. All but two ROs had at least 2 worrisome features. Follow-up was available for all cases (median 11 months; range 3–108): all patients were alive without recurrence or metastasis.
Conclusion: RO is a tumor which often can show worrisome and atypical morphology. It is necessary to know and recognize the worrisome features to prevent diagnostic errors, if otherwise typical oncocytoma morphology is present. Despite these atypical morphological data, the prognosis is excellent.

PS-22-073

Ki67 and p53 expression in urothelial carcinomas and clinicopathologic correlation

A. Ribeiro*
*CHLC, EPE, Serviço de Anatomia Patológica, Lisboa, Portugal

Objective: The most important predictive parameter for the biological behaviour of urothelial carcinoma is histological grade, except for depth of invasion. The aim of this study was to investigate the expression of p53 oncoprotein and Ki67 antigen in a series of transitional cell bladder carcinoma with papillary morphology (pTa – papillary carcinoma and pT1) with histological grade and recurrence.
Method: This study included 59 cases diagnosed with urothelial carcinoma with papillary morphology (pTa, pT1). Immunohistochemical expression of Ki67 and p53 were examined in each case, and were graded accordingly to the percentage of cells stained, in low, moderate and high-expression groups.
Results: As described previously in other publications the expression of p53 and Ki67 has a relationship with histological grade. We also noted that of the 13 recurrences, 11 were associated with moderate to high expression of either p53 or Ki67, or both.
Conclusion: We concluded that p53 and Ki67 expression combined with histological grade and pathological stage may be helpful in assessing more accurately the biological behaviour of urothelial carcinoma. And the overexpression of p53 and Ki67 are related with an unfavourable prognosis.

PS-22-074

Prostatic glandular and stromal hyperplasia with stromal cell atypia: A follow-up study of 1 case

Y. Rogov*, T. Liatkouskaya, N. Kornev, E. Parhovchenko, A. Krilov, N. Zhardzetskaya
*Belarusian Medical Academy, Dept. of Pathology, Minsk, Belarus

Objective: Prostatic stromal hyperplasia with atypia is a rare lesion with fewer than 200 cases reported worldwide. It can be mistaken for sarcoma because of the presence of atypical, bizarre cells. Its malignant potential is uncertain. The follow up study of every case is important.
Method: A 71-year-old man with previously diagnosed atypical prostatic adenostromal hyperplasia with atypia of stromal cells was hospitalized with urinary obstruction after transurethral resection of prostate made 6 years ago. Repeat TURP was performed and tissue specimens were investigated and compared with the initial biopsy.
Results: The second biopsy showed the benign hyperplastic prostatic glands with atypical, bizarre, frequently multinucleated giant stromal cells between them. They displayed intense immunoreactivity for actin, vimentin and androgen receptors. The microscopical picture was identical to that seen in the first specimens. The nuclear abnormalities looked like in an atypical symplastic leiomyoma of myometrium. No evidence of sarcomatous or carcinomatous transformation, mitotic index evaluation was noted.
Conclusion: This case maintains the viewpoint that the prostatic adenostromal hyperplasia with stromal cell atypia is a benign lesion. But it can recur and requires the repeat TURP or radical surgery.

PS-22-075

Cancer risk in patients with precancerous lesions of the prostate

Y. Rogov*, V. Zakharava, T. Liatkouskaya, E. Cherstvoy
*Belarusian Medical Academy, Dept. of Pathology, Minsk, Belarus

Objective: Prostatic intraepitelial neoplasia (PIN) and atypical small acinar proliferation (ASAP) has a high predictive value as markers for prostate cancer (PCa).
Method: PCa-risk in patients with precancerous lesions has been assessed on biopsy material in 172 patients having morphological suspicious to PCa. Suspicious foci were estimated with use of cocktail AMACR + HWC + p63.
Results: According to our results revealing of precancerous lesions in biopsy specimens has been associated with PCa identification in re-biopsies (F=0,04). Within the first-5-years the overall incidence of PCa in re-biopsies made 27 % in the group of precancerous lesions and 36 % – in the ASAP group. Life-time-without-PCa median made up 5-years with no reliable difference between PIN and ASAP groups (WW=2,35; p=0,06). Thus, the cumulative share of patients without PCa in the ASAP group formed 86 %-82 %-82 %-73 %-60 % at the end of the first-second-third-fourth-fifth year of supervision respectively.
Conclusion: Within the first 5 years PCa risk makes 27 % in the general group of precancerous lesions of the prostate and 36 % in ASAP group with no difference between ASAP and PIN groups. Cumulative share of patients without PCa in re-biopsy specimens decreased from 86 % to 60 % during these 5 years.

PS-22-076

Benign prostatic hyperplasia and prostate carcinogenesis after the Chernobyl accident in Ukraine

A. Romanenko*, A. Chekalova, A. Yurakh, P. Harkonen, S. Vozianov
*Institute of Urology, Kiev, Ukraine

Objective: The prevalence as well as immunohistochemical (IHC) study of latent, incidentally found prostate cancer (LPC) as well as precancer lesions, in patients, who underwent surgery for BPH were studied.
Method: BPH samples were obtained by prostatectomy from 120 Ukrainian patients consisting of 30 patients from areas without radio-contamination (control group 1) and of 90 patients living in 137Cs contaminated areas of Ukraine (group 2). Ki-67, p53, p27Kip-1, p63 and Bcl-2 proteins were IHC investigated in BPH from all patients.
Results: The incidences of LPC (Gleason score 4), chronic prostatitis, PIA and PIN were 16.67, 53.34, 20, and 26.67 % in group 1; 12.23, 64.45, 43.45 and 36.67 % in group 2, respectively. Greatly elevated levels of p53, Ki-67, Bcl-2 associated with decreased levels of p27Kip-1and p63 in areas of PIA and less LPC and PIN in group 2 to compare with group 1 patients were obtained with statistically significant differences.
Conclusion: Our study suggests that chronic long-term low-dose radiation exposure might result in the increase of chronic inflammation and it is now found to be associated with increased incidences of PIA and PIN in BPH accompanied by p53, p27KIP-1 and Bcl-2 alteration which in turn could lead to prostate carcinogenesis.

PS-22-077

Eosinophilic globules in rete testis mimicking yolk sac tumor in a testicle with seminoma

E. Ronne*, T. Argyrakos, D. Rontogianni
*Evangelismos Hospital, Dept. of Pathology, Athens, Greece

Objective: The recognition of a non-seminomatous component in an otherwise typical testicular seminoma changes the choice of adjuvant chemotherapy.

Method: A 37-year old male underwent orchiectomy for a testicular mass. Serum tumor markers levels (β-hCG/AFP/LDH) were normal.
Results: Macroscopical examination revealed a 2.1 cm white–yellow tumor. The tumor was composed of the characteristic for seminoma homogenous, clear cells arranged in nests and islands separated by septa and infiltrated by lymphocytes. Immunohistochemically the tumor cells were positive for PLAP, OCT3/4, CD117 and D2-40 and negative for CD30 and CK8.18. There was also a regular pattern of tubular structures infiltrated by the seminoma cells while retaining a low columnar type epithelium. The presence of sphaerical eosinophilic globules (PAS+/dPAS+/AFP−) within the tubular lumina was strongly reminiscent of the hyaline globules of yolk sac tumor. The tubular structures were positive for CK8.18 and negative for AFP, glypican-3 and OCT3/4.
Conclusion: The presence of tubular structures with sphaerical eosinophilic globules creates a suspicion for a yolk sac tumor component. The absence of AFP and glypican-3 expression, the regular pattern of the tubular structures and their continuity with rete testis excluded this suspicion. Hyaline eosinophilic globules in rete testis should not be confused with the globules produced by yolk sac tumors.

PS-22-078

Beta- catenin expression and CTNNB1 mutations in a series of Wilms tumours

R. Santi*, P. Pinzani, F. Salvianti, G. Baroni, M. Pepi, G. Nesi
*University of Florence, Pathological Anatomy Section, Italy

Objective: CTNNB1 mutations have been found in 15–30 % of Wilms tumour (WT) cases. Nuclear beta-catenin protein has been detected by immunohistochemistry in a higher proportion of WTs, thus suggesting alternative genetic pathways leading to beta-catenin activation in these neoplasms.
Method: Sixteen renal WTs and 7 secondary WT localizations were retrospectively investigated. The series included 17 paediatric patients, 10 females and 7 males, with a mean age of 4.5 years and a 34 year-old female patient. Immunohistochemical analysis of beta-catenin was performed and findings were reported for each neoplastic component (i.e. epithelium, stroma and blastema). Tumour DNA was extracted for direct sequencing analysis.
Results: The majority of WTs showed moderate to strong membranous staining for beta-catenin in the epithelial (76.5 %) and the blastemal (60 %) components. Nuclear beta-catenin expression was observed in combination with cytoplasmic staining in the mesenchyma and/or the blastema of two primary renal tumours. In these cases the deletion of codon 45 p.S45del and the missense substitution p.T41A were detected.
Conclusion: Preliminary results of this ongoing study highlight beta-catenin cytoplasmic and membranous expression in the tumour cells of primary and metastatic WTs, with few cases demonstrating nuclear expression. In our series, beta-catenin nuclear expression was invariably associated to CTNNB1 mutation.

PS-22-079

A preliminary study on O6-methylguanine-DNA methyltransferase and Type 2 transglutaminase expression profile of renal cell carcinomas

B. Sarsik*, B. Pehlivanoglu, D. Tunali, A. Simsir, E. Gokmen, S. Sen
*Ege University, Faculty of Medicine, Izmir, Turkey

Objective: O6-methylguanine-DNA methyltransferase (MGMT) repairs O6-methylguanine in DNA, therefore provides a tumor supressor effect. Type 2 transglutaminase (TGase–2) is a multifunctional enzyme involved in many biological processes. Few data are available in the literature on their expression in kidney cancers. In this preliminary study, we evaluated immunohistochemical expression of MGMT and TGase–2 in renal carcinoma cases.
Method: Forty cases of renal carcinoma including ten clear cell, ten chromophobe cell, ten papillary and ten urothelial carcinoma were randomly selected. Thirty-one patients were male and average age was 61,5. Staining intensity and percentage of staining tumor cells were scored. Total score was categorized as weak, moderate and strong.
Results: Strong MGMT positivity was demonstrated in 15 cases (38 %). Eight cases (20 %) showed strong TGase-2 expression. Fifty percent of clear cell carcinomas strongly expressed MGMT and TGase–2. No correlation was found between MGMT and/or TGase–2 expression, tumor size and grade. Eighty percent of urothelial carcinomas strongly expressed MGMT.
Conclusion: The prognostic value of MGMT and TGase–2 as well as their potential role in treatment response have been investigated recently. MGMT and TGase–2 may be prognostic factors in renal carcinomas. Further investigation is required to verify our findings.

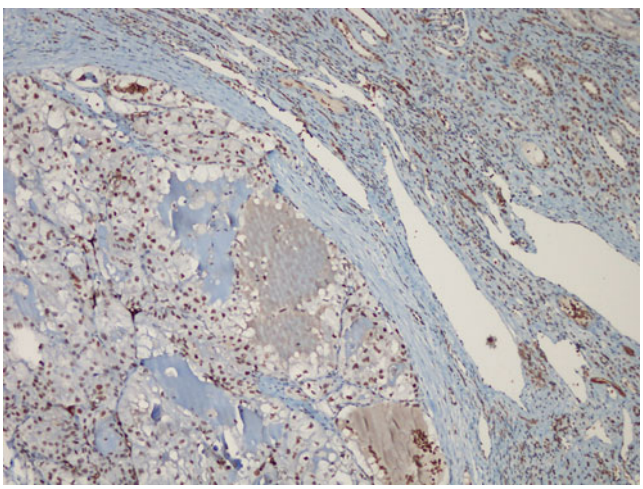

PS-22-080

Three dimensional topographic analysis of 904 cases of radical prostatectomy

A. N. Seo*, K. S. Lee, G. Choe
*Seoul National Univ. Bundang, Pathology, Seongnam-Si, Republic of Korea

Objective: Prostate cancer is typically mutifocal, and there has been no report about the exact number of prostatic carcinomas in each case. We have performed topographic analysis using three dimensional mapping technique.
Method: We established data base including 904 cases of radical prostatectomy consisting of 2717 individual adenocarcinomas, and performed comprehensive pathologic analysis.
Results: 728 cases (80.53 %) out of 904 revealed multifocal carcinomas. The mean number of multifocal carcinoma was 3.05 and the maximal number was 11. 88.27 % of carcinomas were noted in both lobes. Among 904 cases, peripheral zone was involved in 95.80 %, transitional zone in 63.83 %, central zone in 22.35 %, and anterior fibromuscular stroma in 44.03 %. Representative Gleason score consisted of 6 (17.70 %), 7 (68.92 %), 8 (2.54 %) and 9 (10.84 %). Regarding individual carcinomas, Gleason score consisted of 6 (51.99 %), 7 (41.16 %), 8 (1.73 %) and 9 (3.94 %). The mean volume of individual carcinoma was 1.68 ml (range: 0.01–93.55). 904 cases consisted of pT2a (8.76 %), pT2b (0.11 %), pT2c (53.10 %), pT3a (26.50 %), pT3b (9.76 %) and pT4 (1.77 %). High grade PIN was present in 90.04 %, and perineural invasion in 76.11 %.
Conclusion: We report comprehensive pathologic features of Korean prostate cancers, including the number and size of individual carcinomas.

PS-22-081

ERG immunohistochemistry and clinicopathologic characteristics in Korean prostate adenocarcinoma patients

J.-H. Suh*, K.-C. Moon
*Seoul National University Hospital, Dept. of Pathology, Republic of Korea

Objective: TMPRSS2-ERG gene fusion is the most common genetic alternation in prostate cancer. It is associated with the expression of oncogene ERG protein. Recently, the immunohistochemical staining method that using anti-ERG antibody was verified strong correlation with ERG protein which is the product of genetic alteration. Aim of this study is to declare that the relationship between ERG expression and clinicopathological factor.
Method: otal 307 cases of radical prostatectomy specimen were assessed. All cases were constructed tissue microarray and immunohistochemical staining was performed.
Results: ERG-positive rate was 24.1 % (74/307) and significantly higher expression of ERG expression was observed in the subgroup that has lower Gleason score. ($p<0.05$) Analysis with the histologic pattern of prostate adenocarcinoma, tumors with discrete glandular unit (Gleason pattern 3) is shown higher frequency of ERG expression ($p=0.007$).
Conclusion: ERG-positive case was smaller than that of western population (about 50 %) and other factors including age, tumor volume, initial PSA level, pathological stage and margin status were not significantly related with ERG expression. In conclusion, positive rate of ERG immunohistochemical staining is meaningful higher in the tumors with well-formed gland that is represented by lower Gleason score.

PS-22-082

Solitary fibrous tumour of the kidney mimicking renal cystic neoplasm

T. Tichy*, J. Skarda
*University Hospital Olomouc, Institute of Pathology, Czech Republic

Objective: Solitary fibrous tumour (SFT) can develop at any anatomic site, but in the kidney is described rarely. In general, SFT forms an unencapsulated solid mass. We report a case of a 57-year old woman with benign SFT of the left kidney. The tumour showed extensive pseudocystic change and mimicked renal cystic neoplasm.
Method: A nephrectomy specimen showed cystic tumour beneath renal capsule and in peripelvic adipose tisssue. Histological sections were used for hematoxylin-eosin and for immunohistochemistry (antibodies against vimentin, smooth muscle actin, desmin, S-100 protein, CD117, CD99, bcl-2, CD34, CK18, AE1-AE3, EMA).
Results: Microscopically the tumour showed uniform spindle cell proliferation with expansive tumour margins, without necrosis or hemorrhagies. Mitotic activity was 1 per 10 high power fields. Cystic spaces without epithelial lining contained eosinophilic proteinaceous fluid. Imunohistochemically tumour showed difuse positivity for CD34, CD99, bcl-2, vimentin and stained negatively for S-100 protein, cytokeratins, EMA, smooth muscle actin, desmin and CD117.
Conclusion: SFT of the kidney is infrequent. Some renal SFT can undergo pseudocystic transformation and mimic renal cystic neoplasm both clinically and macroscopically.

PS-22-083

Epitheloid renal angiomyolipoma with atypia

C. S. Topal*, M. H. Karabulut, M. S. Yilmaz, F. Gürsoy, D. Celik, G. Kir
*Umraniye Resarch and Education Center, Istanbul, Turkey

Objective: Renal angiomyolipomas are mesenchymal tumors that comprised of adipose tissue, smooth muscle like cells and

abnormal thick walled blood vessels admixed in various proportions. Epithelial renal angiomyolipomas are rare variants and may exhibit atypia. In the literature epithelioid renal angiomyolipomas with atypia are reported to have malignant potential.
Method: Left radical nephrectomy was performed due to renal mass with flank pain and hematuria.
Results: In gross examination; 6.5×3.5×3 cm gray white mass with occasionally necrotic areas at the middle portion of left kidney renal sinus and perinephritic fatty tissue, macroscopically. Microscopic eveluation reveals; tumoral lesion comprised of adipose tissue, smooth muscle and blood vessels, showing areas of epitheloid morphology and moderate to severe degree of nuclear atypia. In addition to histomorphology positivity HMB-45 immunohistocemistry elaborated to the diagnosis of "epitheloid renal angiomyolipoma with atypia".
Conclusion: This case has been presented due to its infrequent occurrence and malignancy potential.

PS-22-084
Correlation of minute focus of prostate adenocarcinoma on random multifocal needle biopsy with radical prostatectomy specimen
A. Urbanskiy*
*Russian Research Centre for Ra, Pathology, St. Petersburg, Russia

Objective: This work attempts to determine the importance of small foci of prostatic cancer in random multifocal needle biopsy specimens.
Method: 64 patients with a microscopic focus confined to a single core specimen (which defined as tumor less than 1 mm with a Gleason score of 6 or less) were identified from a retrospective review of 1206 needle biopsies of the prostate. Twelve of these 64 subsequently under went radical retropubic prostatectomy at our centre. Clinically significant tumors were defined as those with volume greater than 0.5 cc.
Results: Average tumor volume was 0,9±0,6 cc (range 0,068–2,9 cc). In 41,66 % (5) of the cases was less 0,5 cc (range 0,068–0,458 cc, mean volume – 0,22±0,15 cc). There was 1 (8,4 %) of patient with extraprostatic extension.
Conclusion: Our data have shown high frequency of revealing insignificant tumours (mean 42±28 %; P=0,95). However, about 60 % of patients had clinically significant tumors warranting definitive therapy. The smallest focus of cancer on needle biopsy is not a guarantee of a clinically insignificant tumor.

PS-22-085
E-cadherin in mice: Expression in normal urothelium, pre-neoplastic and neoplastic urothelial lesions
C. Vasconcelos Nóbrega*, C. Costa, R. Arantes-Rodrigues, A. Henriques, H. Vala, A. Colaço, L. Santos, C. Lopes, P. Oliveira
*Escola Sup. Agrária Viseu, DZERV, Portugal

Objective: E-cadherin is an adhesion molecule that promotes the integrity and stability of the urothelium. A decrease in its expression is associated with more aggressive tumour phenotypes, with the ability to invade and metastasize. Our aim was to describe the expression of E-cadherin in normal urothelium and in urothelium with pre-neoplastic and neoplastic lesions of ICR male mice.
Method: Urothelial lesions were chemically induced by N-butyl-N-(4-hydroxybutyl) nitrosamine in ICR mice, and evaluated by immunohistochemistry in order to determine the staining pattern of E-cadherin.
Results: In normal urothelium, 87.5 % of E-cadherin expression was at the cellular membrane level. In simple hyperplasia, the same pattern was observed in 66.67 % of lesions. Nodular hyperplasia exhibited a mixed pattern (50 % membrane and 50 % cytoplasmic pattern). In 86.67 % of dysplasia, a cytoplasmic pattern was seen. On invasive carcinoma the majority of invasive urothelial cells exhibited a pattern of membrane and cytoplasmic staining. On squamous metaplasia it was observed a membrane pattern on basal and intermediate layers, and a loss of immunoreactivity in the most superficial ones.
Conclusion: E-cadherin is a valuable tool for investigating the cellular adhesion status of the urothelium in mice. Neoplastic lesions exhibited an abnormal, heterogeneous staining pattern.

PS-22-088
New potential prognostic and predictive factors in conventional clear cell renal carcinoma
P. Latalova*, P. Flodr
*FMD PU and FH Olomouc, Dept. of Clinical and Molecular Pathology, Czech Republic

Objective: Biological behavior of conventional clear cell renal carcinoma (CCRC) is associated with tumour stage and grade. Cancer progression with metastasis is part of a process epithelial-mesenchymal transition (EMT) and is joined with invasiveness due to adhesion and cytoskeleton change. The central role of the EMT mechanism is attributed to Snail factor. The intermediate filament expression is changed through the progression of many types of neoplasms. These changes are organ or tissue specific and depend also on the degree of malignant transformation (genome instability acceleration). The expression changes of cytokeratin 18 (CK18) are signs of aggressive biological behaviour in some tumour types - e.g. colorectal and breast carcinoma (downregulation of expression) or CCRC (upregulation of expression). The expression of Snail and CK18 molecules and mRNA CK18 levels correlate to stage and grade of CCRC (according Messai et al. 2010). Objective: Study was based on the expression of

immunohistochemical markers (CK18, CK7, vimentin, Snail, CD10) in 15 cases with evaluation of the primary tumour and its metastasis.
Results: The difference and similarity of intensity and percentage of positive neoplastic population between the primary and the secondary carcinoma will be presented.
Conclusion: Snail and CK18 seem to be potential tumour progression factors and may be included in so called personalised medicine.

PS-22-089
Sarcomatoid carcinoma of the prostate: A case report
S. Attafi*, W. Ajouli, N. Bouchiba, A. Chouchene, M. H. Balti, K. Bellil
*FSI Hospital, Dept. of Pathology, Marsa, Tunisia

Objective: Sarcomatoid carcinoma (SC) of the prostate is a rare variant of prostatic cancer representing less than 1 % of prostate tumors. Tumors are most commonly composed of an admixture of both malignant glandular and spindle cell elements. The sarcomatoid component can vary from 5 % to 99 %.
Method: We report the case of a 63-years-old patient with an invasive tumor of the prostate for which he had a radical prostatectomy. Histopathological examination showed that the tumor was responding to an undifferentiated proliferation made of beaches and clusters of pleomorphic cells usually spindle-shaped, with eosinophilic cytoplasm, and elongated or oval nuclei, which are very irregular, sometimes monstrous, multinucleated, basophils with numerous mitotic figures. In some places, there were areas of glandular differentiation and foci of comedocarcinoma. Immunohistochemical study showed immunoreactivity of spindle and pleomorphic cells with cytokeratin and vimentin.
Results: The diagnosis of sarcomatoid carcinoma of the prostate-grade Gleason 5+5 was confirmed.
Conclusion: SC of the prostate is an exceedingly rare tumor. Retrospective analyses render prostate SC as one of the most aggressive prostate malignancies. The prognosis is dismal regardless of other histologic or clinical findings.

PS-22-091
Primary leiomyosarcoma of the kidney: Three cases
B. Akkaya*, S. S. Tuncer, I. E. Gurer, M. Baykara
*Akdeniz University, School of Medicine, Antalya, Turkey

Objective: Renal sarcomas constitute only %1–2 of malignant renal tumors in adulthood. Leiomyosarcoma is the most common histologic type of renal sarcoma (%50–60).
Method: We present three renal leiomyosarcomas. The tumors diameters were variable between 5 and 9,5 cm. The age range of the patients was 36–81 years. All of them were female.
Results: In the macroscopic examination, the tumors were seen originating from renal capsule, a well-circumscribed, gray-white, swirl cut surface. Renal pelvic and ureteral dilatation was seen in the first case because of the mass effect. Microscopically the alternating spindle tumor cells were detected which were positive with actin, desmin, caldesmon and negative with S100, Pan- CK, CD34 and CD 117.
Conclusion: Sarcoma of the kidney are extremely rare and of varied cell types. These neoplasms exhibit an aggressive biological behavior and an unfavorable prognosis and are, thus, more lethal than sarcomas of any other genitourinary sites. In the literature renal leiomyosarcomas have been reported frequently in female patients as seen as our cases. The renal leiomyosarcomas and other sarcomas should be kept in mind among the reasons of hydroureteronephrosis.

Wednesday, 12 September 2012, 09.30 - 10.30, Congress Hall Foyer 3rd Floor
PS-23 Poster Session Gynaecological Pathology

PS-23-001
Histopathological features and prognostic factors in uterine leiomyosarcoma (U-LMS): Results from two Portuguese tertiary centers
A. M. Abreu Aguiar Galaghar*, M. Guimarães, A. S. Luís, C. Bartosch, M. Afonso, J. M. Lopes
*IPO - Porto, Valongo, Portugal

Objective: Although rare, U-LMS is the most frequent malignant gynaecological mesenchymal tumor, usually disclosing unfavorable prognosis. U-LMS diagnosis may be controversial. In this study we evaluated clinical-pathological features/prognostic factors of U-LMS.
Method: All consecutive U-LMS diagnosed (1987–2012) at CHSJ and IPO-Porto and with available material were re-evaluated. The clinical files were reviewed, including demographic, clinical, imaging, surgical, staging, and follow-up parameters. The pathology features, including immunohistochemistry evaluation, were re-evaluated and the tumors staged according to most recent consensus criteria.
Results: The mean age at diagnosis of the 38 cases was 57 years (39–83); 68 % were multiparous and 60 % postmenopausal women. The majority (82 %) had symptoms at diagnosis, mostly abnormal bleeding. Histological classification displayed: 63 % spindle, 13 % epithelioid, 3 % myxoid, 10.5 % pleomorphic, and 10.5 % mixed U-LMS. Treatment included surgery (97 %), radiotherapy (67 %), and chemotherapy (63 %). Overall median survival was 49 months (CI 95 % 8.3–89.6), and 48 % 5-year survival rate. In univariate analysis only epithelioid subtype and

extra-uterine extension (FIGO stage II- IV) were significant parameters of poor prognosis. No multivariate analyses were performed due series limitation.
Conclusion: Detailed pathology evaluation, including histological subtype, and FIGO stage are essential in the adequate management decision/prognosis evaluation of U-LMS.

PS-23-002
Two cases of endometrial cancer with unusual presentation
F. Alameda*, J. Munne Collado, M. Garcia Garcia, L. Comerma Blesa, R. Murillo Garcia, M. V. Alba Amarillo, Y. Zboromyrskyy, S. Martinez Diaz, J. Genoves Gonzalez, L. Garrigos Cubells, S. Serrano Figueras
*Hospital del Mar, Dept. de Anatomia Patologica, Barcelona, Spain

Objective: Over 90 % of women with endometrial cancer show signs of uterine bleeding, so most cases are diagnosed at an initial stage. This study covers two patients who presented the first signs of this disease in an exceptional manner.
Method: Case-1 A 71-year-old woman was afflicted with a six-month toxic syndrome. An omentum tumor was identified in the x-ray. Eleven days after the excision, she demonstrated oliguria, dysuria, and scant uterine bleeding. The pelvic ultrasound revealed a uterine mass. Case-2 A 56-year-old woman demonstrated disabling right inguinal pain. After an x-ray examination of her pelvis, a metastasis was suspected. A biopsy confirmed it. The immunochemistry pointed to a gynecologic, pancreatic or intestinal tumor. The computer tomography scan revealed a uterine mass.
Results: The first case only suggested an estromal gastrointestinal tumor or a mesothelioma, misdiagnosing and missing the endometrial carcinoma. The second case was uncommon as bone metastasis is found with solid tumors but seldom occurs with endometrial cancer and even less so as a first sign.
Conclusion: We must consider endometrial cancer at signs of uterine bleeding, however, further investigation is required in order to consider the 10 % who do not show the common signs.

PS-23-003
Extrapelvic endometriosis presenting as a retroperitoneal tumor
A. Alves*, P. Luís, A. Ribeiro, M. Ferreira
*Hospital Santa Maria, Servico de Anatomia Patologica, Lisboa, Portugal

Objective: Endometriosis is a benign disease characterized by the presence of functional endometrial tissue in ectopic locations. Retroperitoneal, liver or kidney involvement are extremely rare.
Method: We present a case of a 52-year-old woman, which was referred to surgical consultation because of a retroperitoneal mass that was found on a routine abdominal ultrasonography (US). A subsequent CT scan showed a 12 cm tumor involving the liver, right kidney and adrenal gland. The gynecological US revealed ovaries with normal size and two probable uterine leiomyomas. She was submitted to a tumorectomy with segmental hepatectomy and nephrectomy.
Results: Grossly, the tumor was 12×8×6 cm, invaded the kidney, the liver and a segment of diaphragm. It was white, fasciculate and with hemorrhagic focus. Histologically the tumor was composed of a biphasic proliferation of endometrial glands and endometrial stroma, both without atypia. The case was diagnosed as deep infiltrating extrapelvic endometriosis. With a 5 years follow-up, the patient is doing well and without evidence of disease.
Conclusion: Despite being an extremely rare presentation, endometriosis can involve retroperitoneal organs and simulate a malignant neoplasm, even without a previous history of pelvic involvement.

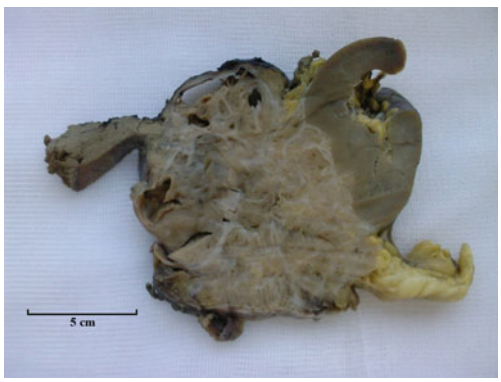

PS-23-004
Primary melanoma of the female genital tract: A report of 10 cases and review of the literature
L. Andres*, J. Diez Garcia, J. J. Burgos, G. Peiró, J. I. Aranda, L. Etxegarai, A. Corominas, M. Gonzalez Vadillo, V. Camaño, A. Gaafar
*Hospital University de Cruces, Dept. of Pathology, Barakaldo, Spain

Objective: Malignant melanoma of the female genital tract is a multifocal disease resulting from a disorder of melanocytes

within the mucosa. We report a retrospective clinicopathological analysis of 10 malignant melanomas of the female genital tract.

Method: A total of 10 patients with malignant melanomas arising in the female genital tract have been treated in our institutions in a 20 year period. Clinical data and follow-up were retrieved from the medical histories and histological slides were reviewed.

Results: The series included 6 vulvar and 4 vaginal melanomas. Average age of patients was 69. Four patients had more than one focus of melanoma. Nodular melanomas were detected in two patients. Melanoma in situ was found in an otherwise normal mucosa in two patients and vaginal melanosis in another two of them. All patients were treated by radical local excisions with or without lymph node dissection. Two patients with local recurrences within the genital tract required new surgical excisions. On follow up, 5 patients died of disease, 3 of them with metastatic disease.

Conclusion: Primary malignant melanomas are exceedingly rare in the female genital tract (2–3 %). It is suggested that melanoma of the genital tract is the result of a multifocal disorder of the melanocytes within the mucosa. The increased local recurrence rate reflects an inherent abnormality of melanocytes.

PS-23-006

Distant metastasis (DM) in uterine leiomyosarcoma (U-LMS): Study of a series and review of the literature

C. Bartosch*, A. Luís, A. Galaghar, M. Guimarães, M. Afonso, J. M. Lopes
*IPO-Porto, Pathology, Portugal

Objective: U-LMS is the most frequent malignant gynaecological mesenchymal tumor, disclosing DM; several case reports describe DM, but so far the metastatic patterns remains to be clarified. We aim to evaluate sites and timing to U-LMS metastasis in our series and reported cases.

Method: Consecutive CHSJ&IPO-Porto U-LMS (1987–2012) of patients with DM. Review of the literature (1995–2012) using PUBMED and query: uterine and leiomyosarcoma and (metastases OR metastasis).

Results: Our series: 35 (39.8 %) with metastasis; literature: 65 with metastasis. Global mean age at diagnosis: 52 years (28–74); Initial treatment: hysterectomy (96 %), radiotherapy (28 %), and chemotherapy (40 %). Metastatic site: lung (59 %), intracranial (22 %), skin/soft tissues (13 %), bone (10 %), liver (6 %), others including thyroid, pancreas, vulva/vagina, salivary gland, oral cavity, heart, mediastinum, adrenal, and breast; 38 % with metastatic related symptoms. Overall median time to first metastasis: 21 months (CI 95 % 15.5–26.5). Pancreas, heart and mediastinum were the earlier metastatic sites. Metastatic treatment: metastasectomy (55 %), radiotherapy (24 %), and chemotherapy (37 %). Overall median survival: 13 months (CI 95 % 8.5–17.4), and 8 % 5-year survival.

Conclusion: U-LMS disclose wide range DM sites and time to first metastasis, which highlights the need of long-term follow-up, high level of suspicion, and histological confirmation.

PS-23-008

Microglandular adenocarcinoma of the endometrium: Immunohistochemical characteristics and prevalence of human papillomavirus infection

Y.-Y. Chun*, H.-S. Kim, S.-R. Hong, H.-S. Jeong, J.-Y. Park
*Cheil General Hospital, Dept. of Pathology, Seoul, Republic of Korea

Objective: Microglandular adenocarcinoma (MGA) of the endometrium, a rare subtype of endometrial mucinous adenocarcinoma, has histologic similarities to the microglandular hyperplasia (MGH) of the cervix. It should not be misdiagnosed as cervical MGH especially in a small endometrial biopsy specimen.

Method: Eight cases of MGA of the endometrium and 5 cases of control MGH of the cervix were immunostained for Ki-67, CD34, p16, p53, p63, vimentin, estrogen receptor (ER), progesterone receptor (PR) and PTEN. HPV DNA analysis was performed using paraffin-embedded MGA tissue by polymerase chain reaction amplification.

Results: P16 was positive in 7 of 8 MGAs and negative in all MGHs. PTEN loss was observed in 4 MGAs, but not in MGHs. ER and PR were positive and p53 was negative in all MGAs and MGHs. Ki-67, p63, and vimentin did not show remarkable differences. There were no signals for HPV DNA in MGAs.

Conclusion: Immunohistochemical staining for p16 and PTEN can be useful in distinguishing endometrial MGA from cervical MGH. Similar to other subtypes of endometrial carcinoma, MGA of the endometrium is related to p16 positivity and PTEN loss and is not associated with HPV infection.

PS-23-009

Cotyledonoid dissecting leiomyoma

A. Cuesta Diaz de Rada*, J. Lomas García, A. M. Rubio de las Heras, A. de la Hera Magallanes, J. Santos Salas Valién, M. Asunción González Morán, E. Honrado Franco, F. Izquierdo Garcia
*Hospital de León, Anatomía Patológica, Spain

Cotyledonoid dissecting leiomyoma is a benign smooth muscle tumor which can mimic a malignant lesion due to its alarming aspect. There are some variant forms of leiomyomas with an unusual infiltrative growth pattern. Due to its worrying appearance of the gross specimen, it is often mistaken for malignant lesion and it is important to be aware of this entity not to over treat this benign smooth-muscle neoplasm. We report a case of a 55 years old woman who underwent hysterectomy because of the suspect of a tumor growing from the right lateral uterine wall. On gross study the tumor measured 10 mm in diameter and was nodular, brown in color and irregular on cut section. Histological examination showed a nodular tumor composed of smooth muscle cells with a storiform pattern which dissects the uterine wall. The tumor was highly vascularized, included a myxoid component and showed some areas with invasion of vascular components. Cellular atypia, mitosis and necrosis were absent. The patient has had a good clinical course, without relapses until the date, what supports the fact that these tumors have a benign clinical behavior, even though they may have a malignant appearance.

PS-23-010

Uterine leiomyoma with lymphoid infiltration

A. N. Deger*, C. Kocak

*S.B. DPU. Kec. EA Hastanesi, Patoloji Bolumu, Kutahya, Turkey

Objective: Although leimyomas of the uterus are common, lymphoid infiltration of leimyomas is a rare occurrence. We presented a case of a 45-year-old woman whose leiomyoma was diffusely infiltrated by lymphocytes. Lymphoid infiltration was analyzed with immunohistochemical methods and infiltration was found to be polyclonal type.

Method: A 45-year-old woman with abnormal uterine bleeding was prediagnosed uterine leiomyoma and she was applied total abdominal hysterectomy and bilateral salphingo-oopherectomy. The analysis of the sample sent to pathology lab showed two leiomyomas. Hematoxylin eosin –stained slides were prepared after sampling. ımmunohistochemical stains were applied.

Results: Microscopic examination of leiomyoma in greater diameter revealed a lesion with well-circumscribed borders composed of interlacing fascicles of bland monomorphic spindle cells diffusely infiltrated by lymphoid cells. The infiltrate not extended into the surrounding myometrium. Immunohistochemical analysis showed positive staining with CD 20, CD3, CD68. It was seen that inflammatory infiltration was polyclonal and involved T cells, B cells and histiocytes. Leiomyoma with lymphoid infiltration was diagnosed. The postoperative course was uneventful within a 6 month follow up period.

Conclusion: Leiomyoma with lymphoid infiltration first described in 1989 by Ferry et all. From that date on, the literature involves few cases. Because it is rare and differential diagnose with malignant lymphoma is crucial, we presented the case and reviewed the literature.

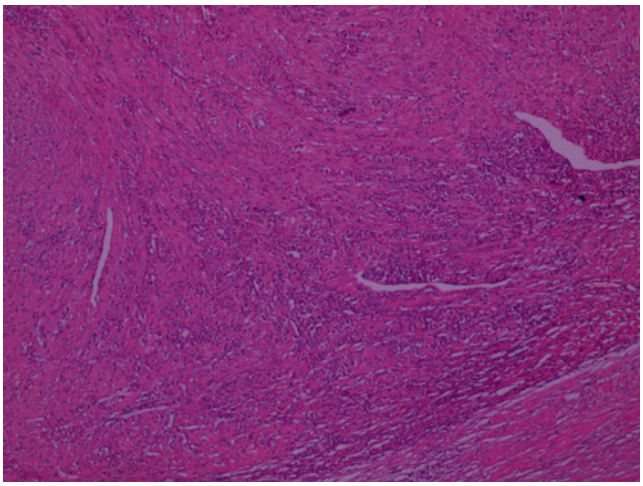

PS-23-011

Differentiated vulvar intraepithelial neoplasia: Relationship with malignant and benign vulvar lesions and immunohistochemical features

E. Demiralay*, A. N. Haberal Reyhan, Ö. Özen, B. Kisa, A. Ayhan

*Baskent University, Dept. of Pathology, Istanbul, Turkey

Objective: Vulvar intraepithelial neoplasia is divided into two groups: usual type and differentiated type. The differentiated vulvar intraepithelial neoplasia, which is frequently seen with invasive squamous cell carcinoma, can be confused with some benign lesions. The aim of this study is to analyse p16, p53, and Ki-67 expression characteristics of different histological types of vulvar intraepithelial neoplasia, invasive squamous cell carcinoma, and benign lesions of the vulva.

Method: In this study, immunohistochemical analysis of 18 vulvectomy cases with p16, p53, and Ki-67 was performed.

Results: Of 18 patients who underwent vulvectomy, nine had invasive squamous cell carcinoma and nine had vulvar intraepithelial neoplasia. Four additional vulvar intraepithelial neoplasia lesions were found accompanying the invasive squamous cell carcinomas. Nine benign lesions were found accompanying the invasive squamous cell carcinomas and

vulvar intraepithelial neoplasia. Mean Ki-67 proliferation index was 32.3 % in the usual type of vulvar intraepithelial neoplasia cases and 26.4 % in the differentiated vulvar intraepithelial neoplasia cases. No p53 expression was present in benign lesions.
Conclusion: Ki-67 PI does not recognize the usual type or differentiated type of vulvar intraepithelial neoplasia. p53 positivity can be of value in distinguishing differentiated type vulvar intraepithelial neoplasia from benign lesions.

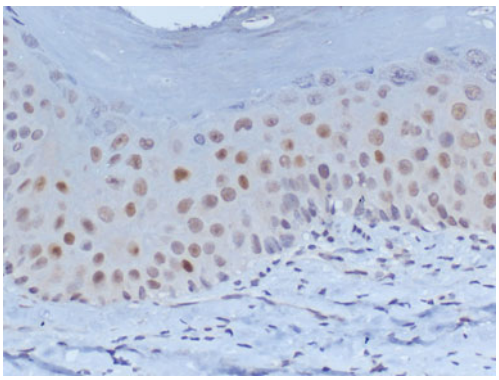

PS-23-012
An audit of surgical pathology reports of endometrial carcinoma: Experience from a referral centre in India
K. Deodhar*, B. Rekhi, S. Menon, B. Ganesh
*Tata Memorial Hospital, Dept. of Pathology, Mumbai, India

Objective: The aim was to see, compliance to minimum data information in carcinoma endometrium reports, in a team of 13 pathologists; and also to analyze these parameters e.g. tumor size, type, grade, depth of myometrial invasion, lymph node yield, pTNM stage etc.
Method: During the period of 2008–2010, from the files of Pathology department of our hospital, reports of operated 114 carcinoma endometrium cases were retrieved and analyzed for various, above mentioned, parameters.
Results: The median age was 58.04 years and median tumor size was 4 cm. Endometrioid adenocarcinoma was the commonest type (82.5 %); followed by MMMT (6.1 %) and Serous carcinoma (3.5 %). Grade 2 was the commonest tumor grade (42.1 %). Less than half of myometrial invasion was seen in 50 % of the cases, =/> half myometrial invasion was seen in 46.5 % of cases. (Information- not available in 4 cases). Parametrial involvement was seen in 5.3 % cases. The pTNM stage was not mentioned in 71.9 % reports. The median lymph node yield was 15.
Conclusion: The compliance to adhere to minimum data information in carcinoma endometrium reports is generally good. Lymph node yield is reasonable. Parametrial involvement and mentioning of pTNM staging is to be done more meticulously. Use of proformas/checklists is recommended.

PS-23-013
Extraovarian granulosa cell tumor: A case report
I. Efstratiou*, S. Pervana, E. Pazarli, D. Alataki
*Papageorgiou Hospital, Dept. of Pathology, Thessaloniki, Greece

Objective: Extraovarian granulosa cell tumor is a very rare neoplasm. We report a case of a tumor located in mesocolon.
Method: A 58-years-old woman presented with abdominal pain and fever. Abdomen CT showed a mesocolic mass adherent to the left kidney and the spleen. She underwent resection of a 22 cm long segment of the left colon with a circumscribed mesocolic tumor measuring 7×10 cm. The tumor was infiltrating the subserosa of the large intestine. Intraoperatively normal ovaries have been identified.
Results: Histologically the tumor is composed by monomorphous cells in solid nests developing cavities which contain serous or hemmorhagic fluid. The tumor cells have scanty cytoplasm and often grooved nuclei. Mitoses are very rare. The tumor cells were immunoreactive for vimentin, inhibin and progesterone receptors. The postoperative course was uncomplicated and the patient is free of disease 18 months later.
Conclusion: Light microscopic and immunohistochemical features of the tumor are similar to those of ovarian granulosa cell tumors (GCT). Since the tumor was resected in toto and the mitotic activity of the cells is very low, we expect a favorable prognosis. Extraovarian GCT are very rare and only 7 cases have been published during the last 50 years. Probably these tumors arise from residual tissue of the genital ridge (so-called secondary mullerian system).

PS-23-014
Detection of amplification of TERC and TERT genes in cytology samples from cervical neoplasias by fluorescent in situ hybridization
A. Farkasova*, E. Kudela, T. Balharek, P. Zubor, J. Danko, L. Plank
*JFM CU, Dept. of Pathology, Martin, Slovakia

Objective: Increased telomerase activity represents an early event in cervical carcinogenesis allowing cell immortality by recovering chromosomal telomeres. Thus, detection of TERC and TERT gene amplification might represent a diagnostic and valuable prognostic biomarker of cervical neoplasias.
Method: Cervical smears from 13 patients classified according to Bethesda as NILM (n=3), ASC-US (n=2), L-

SIL (n=2), H-SIL (n=4) and SCC (n=2) were analysed for TERC (3q26) and TERT (5p15) gene amplification by fluorescent in situ hybridization (FISH) in 100 cells per slide using a four-color FISH probe (FHACT™).
Results: The numbers of TERC and TERT copies, average ratio of gene copies and average number of cells with ≥4 TERC gene copies were highest in SCC, followed by H-SIL, L-SIL, ASC-US and NILM cases. Correlation between TERC/TERT amplification intensity and oncocytological findings was statistically significant (p<0.0001).
Conclusion: FISH analysis of TERC and TERT genes could be effective tool for the diagnosis of cervical neoplastic lesions. Using together with cytology and HPV DNA testing it can achieve higher sensitivity and specificity to discriminate H-SIL and invasive carcinomas from L-SIL lesions. Supported by projects CEPVII (IMTS:26220120036) and Molecular Diagnosis of Cervical Cancer (IMTS:26220220113) co-financed by EU sources and grant UK303/2011.

PS-23-016

Ovarian stromal hyperplasia and endometrioid endometrial carcinoma in an obese and premenopausal woman

M. T. Gonzalez Serrano*, D. M. Benito López, M. E. Fuentes Vaamonde, M. Medina Perez, J. Salas Molina
*Hospital Reina Sofia, Dept. of Pathology, Córdoba, Spain

Objective: Ovarian stromal hyperplasia (OSH) is characterised by non-neoplastic overgrowth of the ovarian cortical. Mild hyperplasia of the cortical and medullary stroma is found in the ovaries of about one-third of perimenopausal and postmenopausal women. It is nearly always diffusely bilateral. We report a case of OSH associated with endometrial carcinoma (EC).
Method: A 40-years-old caucasian woman, obese, smoker, with fatty liver, Gilbert´s syndrome and cholelithiasis. She had endometrial curettage biopsy for dysfunctional uterine bleeding for 5 month, which was diagnosed of complex atypical endometrial hiperplasia. A total abdominal hysterectomy whith bilateral salpingo-oophorectomy were performed.
Results: The diagnosis was Well differentiated endometrioid EC and bilateral OSH with focal stromal hypertecosis.
Conclusion: OSH of moderate to severe degree may be found in women with disorders associated with androgenic and estrogenic manifestations including EC, obesity, hypertension, and glucose intolerance, but these findings are less frequent and less obtrusive than in stromal hyperthecosis. Obese woman are at risk for developing endometrioid EC as a result of the increased capacity in adipose tissue to convert androstenedione to oestrone, and testosterone to oestradiol. A relationship in the origin of hormone-dependent endometrial pathology may exist between OSH, blood androgen levels and EC.

PS-23-017

Detection of micrometastases in para-aortic lymph nodes in patients with carcinoma of the uterine cervix after negative frozen section analysis

L.-C. Horn*, C. Kellner, R. Scherling, M. Höckel, J. Einenkel
*Medizin. Universität Leipzig, Institut für Pathologie, Germany

Objective: Previous studies considered the presence of micrometastases (MM) in pelvic lymph nodes as clinically relevant prognostic indicator.
Method: Frozen section analysis was performed in all cases. After FS-examination nodes were examined by one H&E-stained slide. All nodes without metastatic disease after frozen section and permanent section examination were subject of the present study. 43 patients and 418 PAN were enrolled and immunohistochemical staining using two cytokeratin-cocktail antibodies (AE 1/AE 3 and KL-) was performed.
Results: In one case, one single node showed micrometastasis, representing an incidence of 2.3 % of the studied cases and 0.23 % of the examined lymph nodes. In three cases benign endosalpingiosis was seen. The patient with MM is alive without evidence of disease 96 months after surgery. ITC were not observed.
Conclusion: The frequency of MM in PAN is very low. There are only limited data regarding their prognostic impact within the literature. After careful examination of all removed PAN using H&E-staining (and step sectioning), immunohistochmeical ultrastaging cannot be recommend for routine use.

PS-23-018

Serous tubal in situ carcinoma (STIC) in tubal and primary peritoneal carcinomas

L.-C. Horn*, K. Leonhardt, S. Kafkova, J. Einenkel
*Medizin. Universität Leipzig, Institut für Pathologie, Germany

Objective: Serous tubal in situ carcinoma (STIC) has been defined as one important precursor of pelvic serous cancer. Morphologically, STIC is defined by are cytologic atypia, high proliferative index and strong staining for p53.
Method: The present study evaluates the presence of STIC and p53-signature in consecutive cases of 12 prophylactic salpingo-oophorectomy in women with BRCA-1-mutaion (BSO), 11 macroscopically inconspicuous tubes of patients with primary tubal cancer (TC) and 9 cases of primary peritoneal cancer (PPC) using immunohistochemistry against Ki-67 and p53 (clone DO-7).
Results: The frequency of p53-signature and STIC was 8 % and 0 % in cases of prophylactic surgery, 9 % and 18 % in TC and 0 % and 33 % in PPC.

Conclusion: STIC and p53-signature as precursor lesions of pelvic serous cancer is seen in macroscopically inconspicuous Fallopian tubes in unilateral TC in patients with elective BSO and patients affected by PPC. We propose that the sectioning and extensively examining the fimbria protocol be applied to all cases with PPC, TC and in women with prophylactic BSO.

PS-23-021

Primary intestinal-type adenocarcinoma of the vulva

M. Jimeno*, P. Regueiro, M. Pujol, M. Castellarnau, M. Alejo
*Hospital Gral l´Hospitalet-CSI, Pathology, L´hospitalet de Ll., Barcelona, Spain

Objective: Primary adenocarcinoma of the vulva is rare, and enteric differentiation is excepcional. Only a few cases of neoplasms of pure intestinal-type in the low genital tract have been reported. They are considered to arise from cloacal remants or from intestinal heterotopia.
Method: We present the case of a 54 year-old woman, with a histerectomy performed 10 years before. On clinical examination a polipoid lesion in the vulvar vestibule was noticed. Biopsy revealed a tubular adenoma of intestinal type with a focus of adenocarcinoma. The first histologic interpretation was a metastatic intestinal tumor. Clinical examination, recto-colonoscopy and magnetic resonance imaging of the abdomen excluded this possibility.
Results: The immunohistochemical study showed reactivity with citokeratin 20 but didn't with citokeratin 7. All this led to conclude that it was a primary intestinal-type adenocarcinoma of the vulva arisen from an adenoma.
Conclusion: On our knowledge there are less than 100 reported cases of intestinal adenoma in the genital tract. They have been described also in the vagina and cervix but only a few developed an adenocarcinoma. It is important to be aware of this tumor type and to distinguish it from metastatic colorectal adenocarcinoma in order to plan appropriate treatment.

PS-23-023

Ligneous cervicovaginitis and endometritis: Case report

M. Koyuncuoglu*, E. Dogan
*Dokuz Eylul University, Dept. of Pathology, Izmir, Turkey

Objective: Ligneous (wood-like) disease is a rare chronic pseudomembraneous inflammation of the mucous membranes which may also affect genital tract. The underlying pathogenesis is still unclear and an effective method of treatment has not yet emerged.
Method: Here we present a 32 years old female patient presented to our clinic with 7 years of unexplained infertility. Her diagnostic infertility work-up revealed no abnormality. However, at gynecologic examination there was a thick and hard granulation tissue at the cervix extending to the posterior vaginal wall. Transvaginal ultrasound was unremarkable except for increased endometrial thickness.
Results: Cervicovaginal and endometrial biopsy with diagnostic hysteroscopy was performed which demonstrated ligneous inflammation of both cervix and vagina. Endometrial biopsy was reported as chronic non-specific endometritis with dense fibrin deposition.
Conclusion:. The disease may also affect other organs including oral cavity and eyes. This unusual condition is difficult to treat and lack of awareness makes the diagnosis also problematic.

PS-23-024

Benign (LM) and borderline uterine smooth muscle tumors (STUMP) harboring necrosis

A. Luís*, A. Galaghar, C. Bartosch, J. M. Lopes
*IPO-Porto, Anatomia Patológica, Portugal

Objective: Differential diagnosis LM vs STUMP may be controversial, especially regarding necrosis evaluation; few studies address the relation between different treatments and their morphological effects. We aim to characterize a series LMs and putative STUMPs harboring necrosis.
Method: Consecutive putative STUMPs (1995–2012) and a series of LMs with necrosis diagnosed at CHSJ & IPOP-Porto. Clinical files, particularly previous hormonal treatment (HT), gross specimen and histology features.
Results: 18 putative STUMPs and 35 LMs with necrosis. LMs mean age at diagnosis: 43 years; mean size: 9.0 cm (2.3–18); 45 % with other LMs; treatment: myomectomy (49 %) and hysterectomy (51 %); 23 % peri-partum, 8.5 % post-uterine artery embolization; 17 (49 %) previous HT: progestin (17 %), oral contraceptive-OC (20 %), hormonal-IUD (8.6 %), and medical assisted reproduction (8.6 %). STUMPs mean age at diagnosis: 45 years; mean size: 10 cm (2.0–20); 44 % with other LMs; low mitotic index-MI (mean 3.16; median 1/10HPF); slight cell atypia; variable ischemic/tumor-type necrosis. Treatment: myomectomy (22 %), hysterectomy (83 %) and radiotherapy (11 %); 12 (67 %) previous HT: progestin (22 %), OC (39 %), hormonal-IUD (11 %); no recurrence in remaining cases (n=6): median follow-up: 97.5 months.
Conclusion: LMs with necrosis and STUMP may display overlapping features. Diagnosis of STUMP should consider previous HT, detailed morphology (necrosis type/atypia/MI), to prevent overdiagnosis of STUMP.

PS-23-025

Malignant deciduoid mesothelioma mimicking a gynecological tumor

C. B. Marta*, R. Guarch, A. Yagüe, X. Tejada, F. Garcia, Y. Laplaza, J. Sola, C. Guarch
*Hospital Virgen del Camino, Dept. de Anatomia Patologica, Pamplona, Spain

Objective: Malignant deciduoid mesothelioma (MDM) is a variant of epithelioid mesothelioma that might be associated with asbestos exposure and poor prognosis. Described by Nascimento et al. in 1994, frequently mistaken with florid mesothelial hyperplasia or peritoneal deciduosis, 44 cases are reported in the literature.
Method: A 76 year-old woman, without asbestos exposure, discovered vaginal lateral wall tumour, CT: mass in right adnexa/parametrium. RMN: tumour with imprecise boundaries in Douglas cavity. Tumour markers negative. Exploratory laparoscopy with intraoperative biopsy diagnosed a MDM. Consequently; total mass excision was performed including uterus, both annexed, vaginal dome, sigma and rectum.
Results: An 8 cm tumour was revealed in Douglas cavity, histologically, deciduoid morphology was predominant with abundant atypical mitoses and massive neutrophyls infiltration. Immunohistochemical positivity: calretinin, cytokeratin5-6, CAM5.2, cytokeratinAE1AE3, E-cadherin, vimentin, HMBE1, CA125 and negativity: CD99, CD1a, melan-a, MyoD1, Wt-1, CD10, HMB45, actin, thrombomodulin, desmin, alpha-fetoprotein, Moc31, CERB-2, estrogen and progesterone. Normal DNA-repair proteins expression.
Conclusion: MDM is highly aggressive neoplasm, differential diagnosis includes: squamous carcinoma, GIST, deciduosis pseudotumoral, anaplasic large cell lymphoma, trophoblastic tumour, oxyphilic variant of ovarian clear cell carcinoma. This case represent a rare variant of mesothelioma, in which, was possible a complete resection with a probably better pronostic unlike most of these cases.

PS-23-026

Quality assessment of the registration of vulvar and vaginal premalignant lesions at the Cancer Registry of Norway

E. Enerly*, F. Bray, C. Mellem, B. T. Hansen, G. Kjølberg, T. Dahl, T. B. Johannesen, M. Nygård
*Oslo University Hospital, Cancer Registry of Norway, Norway

Objective: A crucial factor concerning the utility of Cancer Registries is the data quality with respect to comparability, completeness, validity and timeliness. However, the data quality of the registration of premalignant lesions has rarely been addressed. This necessitated evaluation of the quality of registration of VIN and VaIN at the Cancer Registry of Norway (CRN).
Method: We re-collected all notifications with high grade VIN and VaIN diagnoses during 2002–2007 from pathology laboratories, and compared these to the data in the CRN database.
Results: Over the period 2002–2007 we estimated the completeness of the 1556 VIN and 297 VaIN notifications to be 95.0 % and 92.9 %, respectively. The original and reabstracted topography codes showed major discrepancies for 12 of 642 (1.9 %) VIN and 7 of 128 (5.5 %) VaIN notifications. The morphology codes were identical for 724 out of 814 notifications. For the period 2002–2007 the median time elapsed between date of diagnosis and registration was 436 and 441 days for VIN and VaIN cases respectively.
Conclusion: Based on the present analysis of the comparability, completeness, validity and timeliness of premalignant lesions of the vulva and vagina, we conclude that the CRN is able to monitor these premalignant lesions satisfactorily.

PS-23-028

Immunohistochemical properties of the gonad in adult patient with testicular feminization syndrome (TFS). A case report

M. Mrcela*, J. Rajc, M. Erman Vlahovic, Z. Topolovec
*KBC Osijek, Dept. of Pathology, Croatia

Objective: We evaluated morphological features of male gonad in an adult patient with TFS with an accent on its immunohistochemical properties.
Method: Our 47 years old patient had a primary amenorrhea. External genitals were female, without pubic and axillary hair. US confirmed cystic formation of the left gonad and lack of uterus. Tumor markers were normal but testosterone was high. Cystic formation of the left gonad was surgically removed, initially specified as a left ovary, as well as the other gonad. Pathohistological examination and karyotyping was done.
Results: Immunohistochemical analyzes of the gonad sample reveal that Sertoli cells showed positivity for Inhibin α, Vimentin, CD99, CKAE1/AE3 and Calretinin and Leydig cells showed positivity for Inhibin α, Vimentin, CD99, CKAE1/AE3 and Calretinin, and weak positivity for S-100, Synaptophysin i NSE. Immunoreactivity for CD99 in hyperplastic areas of Leydig cells showed the most intensive

positivity. PLAP and Chromogranin were negative. Ki-67 nuclear positivity was found in less than 1 % of Sertoli cells and in about 1 % of Leydig cells in hyperplastic areas. Karyotype was 46xy.
Conclusion: Although, surgical pathologists encounter TFS rare in a clinical practice, they should be aware of this condition, especially in lack of relevant clinical data, when it could be interpreted as a tumor.

PS-23-029
Mucinous tumors of the ovary: Diagnostic challenges at frozen section and clinical implications
A. Nasfi*, L. Charfi, R. Sellami-Dhouib, K. Mrad, S. Sassi, I. Abbes, M. Driss, R. Doghri, S. Nechi, N. Ben Hamida, K. Ben Romdhane
*Salah Azaiez Institute, Dept. of Pathology, Tunis, Tunisia

Objective: Frozen section (FS) diagnosis of ovarian mucinous tumors can be difficult due to the size of these tumors, heterogeneity and potential risk of metastasis from gastrointestinal (GI) neoplasms.
Method: We reported 79 ovarian mucinous tumors submitted for (FS) evaluation between January 2007 and Avril 2012 was conducted.
Results: FS and final pathology results were collected. The average tumor size was 22,1 cm (1–55 cm). The FS and final pathology diagnosis were concordant in 84,8 % (67/79) of the cases. Of the 12(15,1 %) discordant cases, one (1,2 %) was downgraded and 8 cases (13,9 %) were upgraded. Of the 30 tumors interpreted as borderline mucinous tumors (BMT) on FS, 8(26,6 %) were malignant at final diagnosis (4 ovarian, 4 GI), 21 (70 %) remain as BMT and 1 (3,3 %) was benign. Of the 18 benign tumors on FS, 3 cases (17, 6 %) were upgraded to BMT at final diagnosis. Tumors with a malignant diagnosis on FS (30 cases) were 100 % concordant with final diagnosis.
Conclusion: Our study showed a 15,1 % rate of discordance between FS and final diagnosis. Given that GI origin is a possible finding, intraoperative assessment of the appendix should be performed in all mucinous ovarian tumors.

PS-23-030
Uterine müllerian adenosarcoma: A clinicopathologic study of 31 cases
A. Nasfi*, L. Charfi, K. Mrad, S. Sassi, R. Sellami-Dhouib, R. Doghri, M. Driss, I. Abbes, S. Nechi, W. Jomaa, K. Ben Romdhane
*Salah Azaiez Institute, Dept. of Pathology, Tunis, Tunisia

Objective: Müllerian adenosarcoma (MA) is a distinctive type of uterine tumor, traditionally regarded as a low-grade variant of mixed müllerian tumors.
Method: Thirty one cases of adenosarcoma were examined during a period of 19 years (May 1993–February 2012).
Results: Thirty tumors were of the uterine corpus and one of the cervix. The mean patient age was 54,2 years (range: 16 to 73 year). The main clinical manifestations were vaginal bleeding and pelvic pain. Physical examination showed cervical/vaginal mass or pelvic mass. Treatment was known in 25 cases: Patients underwent hysterectomy with bilateral salpingo-oophorectomy in 17 cases and lymphadenectomy in 6 cases. Tumor size ranged from 2,5 to 12 cm (mean: 7.1 cm). Microscopically, sarcomatous overgrowth was found in 4 cases (13 %), heterologous elements in 5 (16 %). Eleven cases (35 %) had myometrial invasion involving the internal half of the myometrial thickness in 9 cases, and more than 50 % in 3 cases (9 %). The cervical tumor presented as an endocervical polyp without invasion of the cervical wall.
Conclusion: Uterine MA are low-grade neoplasms capable of local recurrence and much less commonly distant metastasis. Surgical excision is the main treatment strategy with a good prognosis in the early stage disease. The 2 most important adverse prognostic factors are deep myometrial invasion and sarcomatous overgrowth.

PS-23-032
Spectrum of epithelium changes in adenomyosis
N. Nizyaeva*, E. Kogan, T. Demura
*Scientific Center of Obstetric, Dept. of Pathology, Moscow, Russia

Objective: Adenomyosis (AM) is a very common gynecological disorder. Despite high incidence of the disease epithelial changes precise developmental events leading to the condition remain controversial. The aim of the study was to investigate and compare epithelium morphologicaly and markers expression of proliferation, apoptosis, invasion and neoangigogenesis in AM foci.
Method: This study was done on biopsy samples of uterus taken from 70 women with adenomyosis. Immunohistochemical staining of tissues was performed with antibodies to ApoCas, Ki-67, MMP-2, TIMP-1, claudins 3, 5 (CL3,5), E-cadherin, COX-2, EGFR, VEGF.
Results: Four variants of epithelium changes were found in AM foci such as proliferative type, hyperplastic type with and without atypia, and atrophic type.

Hyperplastic tipe with and without atypia in AM foci was characterized by increase ApoCas, Ki-67, EGFR, COX-2, VEGF, MMP-2, decrease E-cadherin, TIMP-1. CL-3,5 were revealed in cytoplasm of cells. The level of expression of these markers in the epithelium of AM foci with hyperplasia with atypia was very close to endometrial carcinoma of the uteri body ($p<0.05$).
Conclusion: Atypical epithelium in AM foci may be the source of carcinoma of the uterine body.

PS-23-033
Clinicopathologic and molecular profile in endometrial carcinoma: An immunohistochemical analysis of 95 cases
O.-L. Pinzon*, I. Costa, J. Montesinos, J. Antoni, N. Combalia, L. Palacio, M. Rey
*Hospital Tauli, Patologia, Barcelona, Spain

Objective: Endometrial carcinoma (EC) displays variable outcomes.
Method: Immunohistochemistry for p53, Ki67, EGFR, HER-2 (%positive), PTEN, estrogen and progesterone receptors (ER/PR), pERK, pJNK (H-score) in TMA from 95 EC: 26 endometrioid (ADE) grade(G) 1, 28 ADEG2, 16 ADEG3, 18 serous(ADS), 4 clear cell (ADCC), 2 carcinosarcomas and 1 undifferentiated carcinoma. Survival and disease status data.
Results: ADE: ER/PR mean H-score from 70/190 to 11/110, from G1 to G3, 34 for PTEN, 13 and 67 for pERK and pJNK, two ADEG3 >75 % p53 and one 20 % Ki67. ADS: 55 % >75 % p53 and 42 % >10 % Ki67, 14/61 for ER/PR, 79 for PTEN, 18 and 116 for pERK and pJNK. ADCC: none ER/PR; 90, 144 and 73 for pERK, pJNK and PTEN, and 50 % >75 % p53 and none >5 % Ki67. HER-2 expression >50 % in one ADS and one ADEG3; EGFR >50 % in one ADEG1 and 25–50 % in one ADEG1, 3 ADEG2 and 1 ADS. 20 patients died of disease (DOD): 9 ADS and 6 ADEG3; 66 were alive without disease: 49 ADEG1 and ADEG2. ADE poor outcome correlated with low ER/PR (16/71G2 and 20/106G3) and PTEN (1G2, 3G3); pERK showed low expression in ADS DOD.
Conclusion: Histologic types of EC show molecular profiles with probable prognostic and pathogenic significance.

PS-23-034
MicroRNA expression in uterine smooth muscle tumors
M. Pusztaszeri*, T. McKee, M. Berczy, C. Delucinge-Vivier, E. Oliva
*Vandoeuvres, Switzerland

Objective: miRNA expression profiling may provide new insights for diagnostic and therapeutic purposes in uterine smooth muscle tumors.
Method: Expression profiling of 654 miRNAs was studied in 10 leiomyosarcomas (uLMS),4 leiomyomas (uLM), myometrium (3), and 6 non-uLMS, using NanoString nCounter™ Assay System. ANOVA was used to identify statistically significant differential miRNAs expression (fold-change>2 and $P<.05$).
Results: 51, 35 and 13 miRNAs were deregulated in uLMS compared to uLM, myometrium, and non-uLMS, respectively. 16 were deregulated in uLM compared to myometrium. 7 identical miRNAs (21/29a/126/139-5p/140-3p/193a-5p/1247) were deregulated in all tumor groups while uLMS and non-uLMS shared 19 deregulated miRNAs (15b/106b/130b/155/494/708/1246/1308 upregulated; 30c/92b/125a-5p/125b/197/199/216a/328/455-5p/873/let-7c down-regulated) compared to uLM and myometrium, several known to be involved in cell-cycle and/or apoptosis pathways (p53, RB, E2F, cyclin-D1/E) and/or metastasis.
Conclusion: Albeit some overlap, miRNA expression profile of uLMS is different from uLM but relatively similar to non-uLMS. uLMS and non-uLMS share deregulation of several miRNAs that may be linked to specific cell-cycle/apoptosis pathways, not dysregulated in uLM. These miRNAs may deserve further study for potential diagnostic, prognostic and/or therapeutic utility.

PS-23-035
Clinicopathological spectrum of 18 adenosarcomas reviewed at a tertiary cancer referral centre
B. Rekhi*, K. Deodhar, S. Menon, A. Maheshwari, R. Kerkar, J. Bajpai, J. Ghosh, R. Engineer, S. Shrivastava
*Tata Memorial Hospital, Dept. of Pathology, Mumbai, India

Objective: Adenosarcomas of female genital tract are uncommon.
Method: Over a 7-year period, 18 adenosarcomas were critically reviewed.
Results: Eighteen adenosarcomas occurred within age-range 21–65 years (mean, 42.9), involving uterus (8), cervix (2), uterus + cervix (5) and ovary (2), with size 3–15 cm (mean, 7.4). Histopathologically, tumors were low-grade (10) (55.5 %) and high-grade (8) (44.4 %), latter with sarcomatous overgrowth (SO) (6/8). De-differentiation (9, 50 %) included rhabdomyoblastic (5), cartilaginous (2), adipocytic (1) & sex-cord-type (1). Four cases had leiomyomas; 2 developed on endometriosis; 1 in treated cervix carcinoma and 1 displayed decidualization. Immunohistochemically,

tumors focally expressed CD10 (4/5), SMA (3/8), vimentin (4/4, diffuse) and desmin (9/10), latter mostly in rhabdomyoblasts. MIB1 (5 cases) varied 5–20 %. All 15 cases underwent surgery, mostly TAHBSO (9) (50 %) and 4 high-grade cases received adjuvant treatment. Five tumors recurred (4 high-grade tumors with SO) and 1 metastasized. Among 10 cases, 5 were alive-with-disease (mean, 29.4 months) and 5 free-of-disease (mean, 15 months).

Conclusion: Adenosarcomas are uncommon, with a wide clinicopathological spectrum. Whereas the commoner low-grade adenosarcomas are less-aggressive, high-grade tumors with SO recur more. Surgery is treatment-mainstay. Adjuvant treatment is considered in high-grade subtypes.

A. Polypoid glands with sarcatomatous stroma (phylloides-like pattern). B. Periglandular condensation. C. Sarcomatous overgrowth. D. Decidualization. E. Cartilagenous dedifferentiation. F. Rhabdomyoblastic dedifferentiation (**Inset**). G. Vimentin positivity. H. Desmin in rhabdomyoblasts. I. ER positive glands.

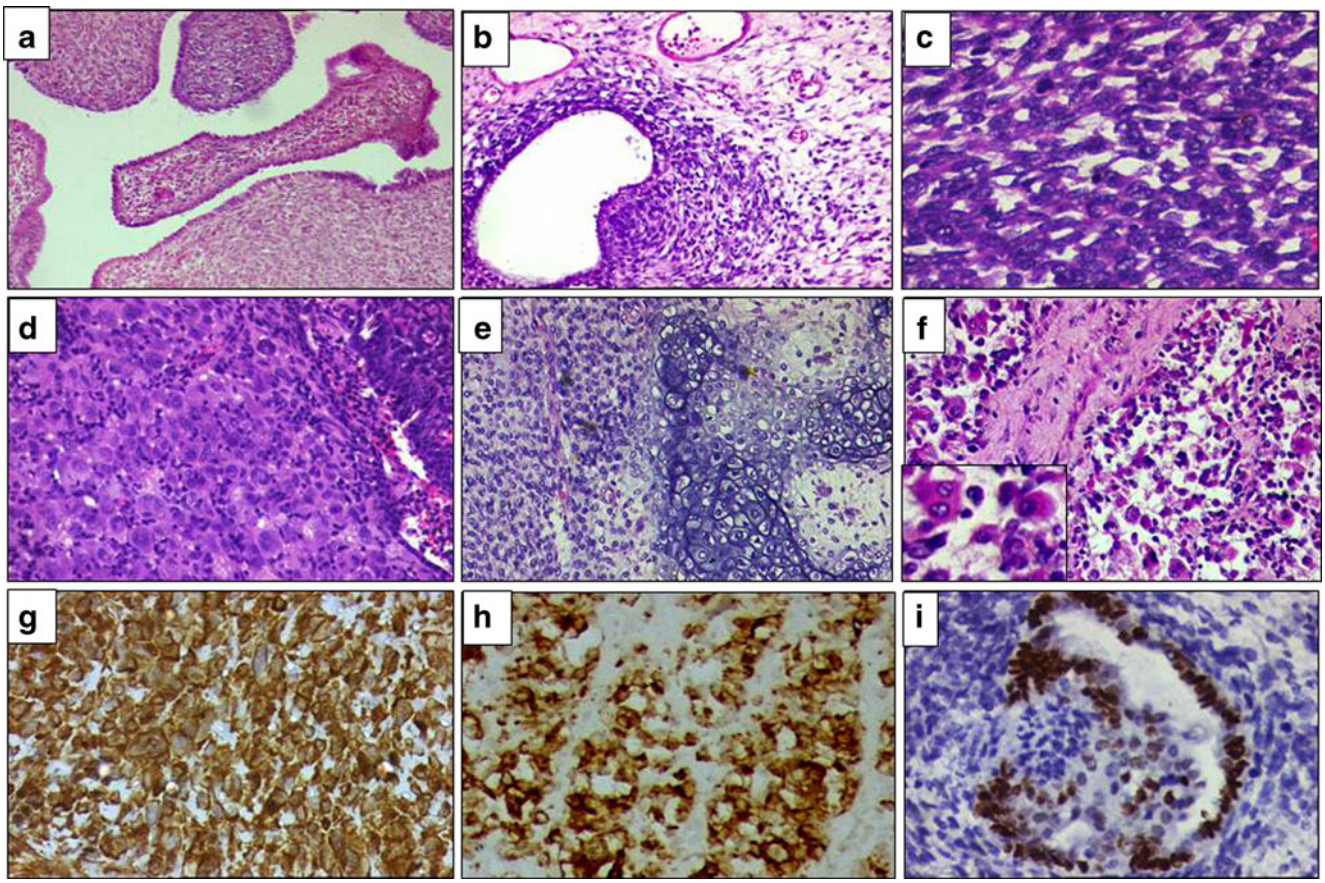

PS-23-036

Morphological changes of complex endometrial hyperplasia with intraepithelial neoplasia during conservative treatment: A report of 3 cases

Y. Rogov*, M. Metelskaya, E. Parhovchenko

*Belarusian Medical Academy, Dept. of Pathology, Minsk, Belarus

Objective: Endometrial endometrioid carcinoma is the most common malignant tumor of the uterine corpus usually developing in postmenopausal women. More seldom it occurs in young reproductive age and sometimes develops from an endometrial intraepithelial neoplasia (EIN). The EIN diagnosis and treatment in such patients have some difficulties.

Method: We have studied curettage tissue specimens from three women with ages 27, 33 and 35, with abnormal uterine bleeding and obesity. The severe complex endometrial hyperplasia with low grade intraepithelial neoplasia was revealed in all cases. These biopsies were repeated some

times during 3 years and investigated using routine light microscopy and immunohistochemistry (IHC) to control the treatment response.
Results: In the course of progestin treatment the complex endometrial hyperplasia with intraepithelial neoplasia became histologically less complicated and than normal. IHC profiles and Ki-67 expression had the same dynamics. In the youngest patient the unusual gland cell atypia with focal calcification was observed one time and hysterectomy was considered.
Conclusion: The study confirms that the repeated curettages with conservative treatment and histological studying can be successfully used in some cases of complex endometrial hyperplasia with intraepithelial neoplasia.

PS-23-037
Value of Ki67, P16 and CK17 markers in differentiating cervical intraepithelial neoplasia and benign lesions
A. Safaei*, M. Pourjabali, F. Sari Aslani, M. Momtahan
*Shiraz University of Medical Sciences, Iran

Objective: The cervical cancer is one of the most common cancers among women worldwide. Diagnosis of CIN affected by high rates of discordance among pathologists. Therefore, we need to other adjunct methods for accurate diagnosis of CIN versus benign lesions in equivocal cases. The aim of this study was evaluation of Ki-67 (MIB-1), CK17 and P16 INK 4a (P16) markers by immunohistochemical method in differentiating CIN from benign cervical lesions.
Method: Seventy-seven cervical biopsies that originally diagnosed as non-CIN (n=31) and CIN (n=46), were reviewed by three pathologists and re-classified as non-CIN (n=54) and CIN (n=23), based on agreement between at least two of three, to obtain a consensus diagnosis. Consensus diagnosis was defined as the "Gold Standard". Then immunostaining for Ki67, P16 and CK17 was performed on all cases and their results were compared with original and consensus diagnosis.
Results: The overall agreement between original and consensus diagnosis was 67.5 % (Kappa=0.39, P-value< 0.001). The sensitivity and specificity of Ki67 immunostaining were 95.6 % and 85.1 % and for P16 were 91.3 and 98.1 %, respectively. The sensitivity and specificity of CK17 negative staining for CIN detection were 39.1 % and 40.7 % respectively.
Conclusion: We recommended using Ki67 and P16 markers as complementary tests for differentiation between dysplastic and non-dysplastic lesions.

PS-23-038
WT1 expression in ovarian borderline and malignant surface epithelial tumors
M. Tahamtan*, F. Sari Aslani, A. Safaee
*Shiraz, Iran

Objective: Wilms tumor gene product, a tumor suppressor gene, now is considered to have oncogenic functions. There seems to be differences in WT1 expression among surface epithelial ovarian tumor subtypes.
Method: Immunohistochemistry for WT1 was done on 35 serous & 3 mucinous cystadenocarcinomas, 9 borderline serous & 10 borderline mucinous tumors, 7 endometrioid ovarian carcinomas, 3 clear cell carcinomas, 1 malignant Brenner tumor, 2 metastatic adenocarcinomas and 6 endometrial adenocarcinomas. A tumor was considered negative if<1 % of tumor cells were stained. Positive reactions were graded :1+,1–24 %; 2+,25–49 %; 3+,50–74 %; 4+,75–100 %.
Results: Of serous cystadenocarcinomaes, 30(85.7 %) were positive,4 showed reactivity of<50 % of the tumor cells and one were negative. All borderline serous tumors were positive. All mucinous tumors, endometrioid carcinomas, clear cell carcinomas, metastatic adenocarcinomas and primary endometrial carcinomas were negative. The single malignant Brenner tumor were positive for WT1.
Conclusion: WT1 is a good marker to distinguish primary ovarian serous carcinomas from other surface epithelial tumors (especially endometrioid subtype) and metastatic carcinomas (especially endometrial serous carcinoma), other than malignant mesothelioma. Degree of expression is not an indicator to separate high grade borderline serous tumors from low grade ones.

PS-23-039
Female adnexal tumor of probable Wolffian origin (FATWO): A case report
V. Theodorou*, N. Vladika, A. Baliaka, E. Michalopoulou, I. Themeli, A. Giannouli, E. Goupou, G.-C. Balis, F. Patakiouta
*Theagenion Hospital, Dept. of Pathology, Katerini, Greece

Objective: FATWO is a rare neoplasm originating from the mesonephric duct remnants that occurs predominantly in the broad ligament but also in the ovary. It is considered a low-malignant potential tumor. However local recurrences and metastases have been reported.
Method: A 45 year-old female, on routine gynecological physical examination, followed by pelvic ultrasonography and computer tomography was diagnosed with a mass at the right ovary. A salpingo-oopherectomy was performed. On gross examination a well-circumscribed, solid and focally

cystic tumor measuring 10,5×7×5,5 cm arose in the ovarian hilus.
Results: Microscopically the tumor consisted of medium-sized, ovoid to polygonal cells arranged in a solid, tubular and sieve-like pattern. Some cystic spaces were lined by low-cuboidal cells and contained amorphous, eosinophilic material. Cellular atypia and mitoses were rare. The tumor cells were positive for Vimentin, Inhibin-a (focally), CD10, cytokeratins 8/18, 19 and 7 (focally) and negative for cytokeratin 20, epithelial membrane antigen, carcinoembryonic antigen and a-fetoprotein.
Conclusion: Histopathological and imunohistochemical findings consistent with an ovarian FATWO. Differential diagnosis includes endometrioid carcinoma, clear-cell carcinoma, Sertoli-Leydig cell tumors (retiform variant) and rete ovarii adenoma. Surgical excision is the optimal treatment. Radiation therapy, chemotherapy or even targeting molecular therapy is questionable.

PS-23-040
Müllerian adenosarcoma family: Report of two sisters uterine tumors
S. Vicente Arregui*, M. J. Ríos, A. Puertas, E. Mejía, D. S. Rosero, M. Alastuey, J. Marroyo, M. I. Valero, E. Gimeno
*Hospital Miguel Servet, Anatomía Patológica, Zaragoza, Spain

Müllerian adenosarcoma is a rare mixed tumor of low malignant potential. Usually presented as a large endometrial polyp in postmenopausal women. They are associated with tamoxifen or radiation therapy. Microscopy shows a mixture of benign glandular epithelium and low-grade endometrial sarcoma is typically concentrated around the glands. The differential diagnosis is made with the adenofibroma, but now is doubted the existence of this tumor and is considered more of a distinct adenosarcoma. The treatment is total hysterectomy. Sisters of 24 and 16 years with a history of dysmenorrhea. Hysteroscopy was performed to the eldest one, in which multiple polyps are observed and partially resected. The pathological diagnosis was Mixed Mullerian tumor, adenofibroma/adenosarcoma. Total abdominal hysterectomy was performed. Histological examination showed a mixed tumor with glandular component and a low-grade sarcomatous, scarce mitosis, mild atypia and no necrosis. The diagnosis was: mullerian adenosarcoma. A year later, a hysteroscopy and endometrial biopsy was performed to the youngest sister, that showed endometrial polyps with stromal predominance, and no significant atypia. With the diagnosis of mullerian adenosarcoma, and taking into account family history, total hysterectomy was performed. Adenosarcoma is a rare tumor whose family presentation is not described in the literature.

PS-23-041
Gliomatosis peritonei is associated with frequent relapse but not affects overall survival in patients with ovarian immature teratoma
N.-R. Yoon*
*Samsung Medical Center, Dept. of Pathology, Seoul, Republic of Korea

Objective: Gliomatosis peritonei (GP) associated with ovarian teratoma has known to have no adverse prognostic effect. We investigated the clinicopathological features of ovarian teratoma associated with GP, and compared immature teratomas (ITs) with GP to ITs without GP.
Method: We investigated 16 patients with ovarian teratoma with GP and 27 patients with IT without GP, who were diagnosed at Samsung Medical Center (seoul) from January 1995 to August 2010.
Results: Six patients with IT with GP (37.5 % of 16 patients) had recurrence. When IT with GP (n=15) was compared to IT without GP (n=27), patient of IT with GP showed larger tumor size (median, 19 cm vs. median 13 cm) (P<0.001), more frequent relapse (40 %, 6/15 vs. 3.7 %, 1/27) (P=0.005), and frequently elevated pre-operative CA125 level (100 %, 12/12 vs. 50 %, 10/20) (P=0.004). Survival curves showed significantly shorter relapse-free survival in patients of IT with GP (P=0.002). Two-year relapse-free survival rates were 59.3 % and 96.3 % in IT with GP and IT without GP, respectively. However, all patients except one case of IT with GP alive.
Conclusion: Ovarian IT with GP was characterized by larger tumor size and frequent elevation of preoperative CA125 level, and GP was associated with frequent relapse in patients with ovarian IT.

PS-23-042
Corelation between histopathologic diagnosis with p16 and Ki67 immunostaining, cytologic features in cervical neoplasia
C. Altunkaya*, S. Yilmaz, A. Barin, S. Ekici, G. S. Yalcin, M. Caydere, H. Ustun
*S.B Ankara E.A.H, Pathology, Turkey

Objective: Frequency of cervical carcinoma decreases nowadays since cytologic screening methods have been using extensively. The incidance of cervical intraepithelial neoplasia increases. Cytologic diagnosis og these lesions are substantially important. So we aim to identify the role of p16 and Ki67 immunostainings for predictive factors of cervical neoplasia.
Method: The study was conducted January 2007 to January 2012. Ninety-three cases (mean age 43,9; range 22–71 years) diagnosed as squamous intraepithelial lesions were included,

which were examined histopathologically, and in terms of cytologic features, p16 and Ki67 immunoexpression.
Results: Cervical smear samples from 93 patients were diagnosed as 6 AGUS, 9 ASCUS, 12 ASC-H, 19 HGSIL, 47 LGSIL cases. 28 of 93 patients (%30,1) were HGSIL and 65 cases (%69,9) were LGSIL in cervical biopsy. 14 of 28(%50) HGSIL cases were diagnosed as HGSIL and 38 of 65(%58,5) LGSIL patients were diagnosed as LGSIL in cervical cytology. All HGSIL cases were positive with p16 and Ki67. 54 of 65(%83,1) LGSIL cases were positive with p16 and 61 of 65(%93,9) LGSIL cases were positive with Ki67. p16 and Ki67 overexpression are independent variables for diagnosing HGSIL and LGSIL (p<0,005).
Conclusion: These immunostaining results have been proven useful for accurately assessing of cervical lesions that hardly diagnosed.

PS-23-043
Cavernous lymphangioma of the uterine cervix
A. Kilitci*, F. Yilmaz, B. Duran
*Abant Izzet Baysal University, Dept. of Pathology, Bolu, Turkey

Objective: Lymphangiomas are rare benign proliferations of the lymphatic system. Three types are generally acknowledged: circumscriptum (or capillary), cavernous, and cystic. We present a case of cavernous lymphangioma of the cervix in a 54-years-old female.
Method: Case Report: A 54-years-old woman presented to the department of obstetrics and gynecology at our hospital. For uterin myoma, she underwent total abdominal histerectomy and bilateral salpingo-oophorectomy. Operation material was sent to pathology department. Macroscopic evaluation revealed, cut surface of cervix was blackish and had many cavities. Microscopic examination showed cavernous lymphangioma; composed of cavernous lymphatic spaces which contain lymphatic fluid. Immunhistochemically, factor VIII, CD 34, SMA were positive in lymphatic endotelium.
Conclusion: Cavernous lymphangioma is a rare lesion in the uterin cervix. To our knowledge this is one of the few cases documented in English literature. As our case, vascular lesions of cervix or another site of female genital tract can be detected coincidentally at histerectomy materials.

Wednesday, 12 September 2012, 09.30 - 10.30, Congress Hall Foyer 3rd Floor
PS-24 Poster Session Dermatopathology

PS-24-002
Spitz nevus, Atypical Spitz Tumor or Spitzoid Melanoma: Which morphological criteria ensure the diagnosis?
S. Arslankoz*, Ö. Gököz
*Pathology, Ankara, Turkey

Objective: Spitzoid lesions continue to be a devastating problem in dermatopathology. Diagnoses as Spitz nevus (SN), atypical Spitz tumor (AST) and Spitzoid melanoma (SM) is an adjunctive classification based on several morphological criteria and survival results.
Method: Thirty-one Spitzoid lesions were reviewed by a scoring system based on seven selected criteria reported previously appreciating characteristics of Spitzoid lesions. As a prevailing criteria, presence of deep mitoses had a score of 2; ulceration, asymmetry, epidermal consumption, solid growth pattern, loss of maturation, pigment heterogeneity were scored as 1 for each. Final diagnosis was SM for scores 4-8, AST for 1-3, SN for 0.
Results: The most frequently seen criteria, loss of maturation was present in 12 SM (n=12), 7 AST (n=16) and epidermal consumption in 8 SM, 3 AST. Deep mitoses were present in only 7 SM. Ulceration was present in 4 SM and 1 AST. Asymmetry, solid growth pattern and pigment heterogeneity were nearly equally seen in SM and AST. First diagnoses of 16 SN switched to AST, 8 to SM, and of 2 AST to SM.
Conclusion: Presence of deep mitoses is the single criteria present only in SM. Loss of maturation, epidermal consumption and ulceration can be used to differentiate AST from SM.

PS-24-003
CD10 and P53 expression in basal cell carcinoma and benign adnexial neoplasm of hair follicle apparatus
C. I. Bassorgun*, O. Ozkan, M. A. Ciftcioglu
*Akdeniz University, Dept. of Pathology, Antalya, Turkey

Objective: Basal cell carcinoma (BCC) of the skin is the most common form of human cancer. Sometimes the histological appearances of benign adnexial neoplasm of hair follicle apparatus tumors (trichoepithelioma, trichoblastoma) are diffucult to distinguish from BCC. The aim of this study is to investigate the usefulness of CD10 and p53 in distinguishing BCC and benign adnexial neoplasm of hair follicle apparatus tumor.
Method: This study included 237 BCC and 27 benign adnexial neoplasm of hair follicle apparatus tumor. We used immunohistochemical stains for p53 and CD10 in all cases.
Results: In BCC cases the expression of CD10 was noted in tumor cells in 222 cases. In 20 benign adnexial neoplasm of hair follicle apparatus tumor cells were negative stain with CD10. Only 7 benign adnexial neoplasm of hair follicle apparatus tumor were positive CD10. The rates of p53 immunostaining of BCC and benign adnexial neoplasm of hair follicle apparatus tumor were 91 % and 25,9 %. Chi-square test revealed a significant correlation that P53 and CD10 expression in BCC and benign adnexial neoplasm of hair follicle apparatus tumor were significantly different (p<0,0001).

Conclusion: We conclude that CD10 and P53 expression may be a useful adjunct marker in distinguishing BCC and benign adnexial neoplasm of hair follicle apparatus tumor.

PS-24-004

Pigmented purpuric dermatosis: Study of a series of six patients

A. Ben Mna*, I. Chelly, A. Souissi, H. Azzouz, M. Mokni, S. Haouet, N. Kchir, M. Zitouna
*La Rabta Hospital, Dept. of Anatomopathology, Grombalia, Tunisia

Objective: Pigmented purpuric dermatosis (PPD) comprises a group of vascular disorders of unknown etiology. Histologically, it is characterized by lymphocytic capillaritis in the papillary dermis.
Method: A retrospective and monocentric study concerning the cases of PPD diagnosed in the department of anatomopathology La Rabta over 6 years (from 2006 to 2011). These cases were studied clinically and histopathologically. Hepatitis C and B profile was carried out to evaluate a possible relation.
Results: 6 cases of PPD have been diagnosed; 2 men and 4 women, aged from 20 to 80 years. Only one patient tested positive for hepatitis C with an elevated viral load. she had a profuse eruption involving the trunk and the limbs of 4 years duration, contrary to the other patients in whom only the lower limbs were affected. she has been treated by alpha interferon and ribavirin with a disappearance of the eruption within 3 months. In the five other patients, the lesions resolved spontaneously within a period of 2 to 9 months.
Conclusion: Hepatitis C may play a role in the pathogenesis of PPD especially when the lesions are profuse and long-standing. In our patient, the disappearance of lesions 3 months after the onset of interferon alpha therapy with a significative decrease of viral load is an argument supporting our hypothesis.

PS-24-005

Fibrolipomatous hamartoma of nerve

M. Costache*, M. Sajin, O. Simionescu, A. M. Oproiu, D. Costache, A. M. Catrina, M. Radasan
*INCDVB, Dept. of Pathology, Bucharest, Romania

Objective: Fibrolipomatous hamartoma of nerve is a benign lesion, very rare in medical practice, occurring in children or young adults. Case report: A 44 year old woman, G. N., presented with a slowly growing plantar mass in the right foot that had been present for 7 years. Neither the patient nor members of her family had a history of neurofibromatosis or other soft tissue tumors. She had no pain at rest, but she had shooting pain while running or walking. Physical examination revealed a mobile, tender mass located in the plantar soft tissue.
Method: After surgical excision, the lesion was well circumscribed, 20/10/8 mm, white colour with yellow areas. Tissues specimens were fixed in 10 % buffered formalin, routinely processed and embedded in paraffin, sectioned at 3 μm, then stained routinely by Hematoxylin – Eosin, than examined by light microscopy.
Results: The lession is characterized by proliferation of mature fatty and fibrous tissue within the epineurium of the nerve accompanied by prominent concentric perineurial fibrosis. The histopathological diagnosis was fibrolipomatous hamartoma of nerve.
Conclusion: The tumour usually affects nerves of the upper extremities, most commonly the median nerve. Involvement of other nerves is rare. The lesion is benign and the recommended treatment is surgical excision.

PS-24-006

Chymase + and tryptase + mast cells and endoglin expression in melanocytic skin lesions

G. Dyduch*, E. Pescarini, M. Bialas, J. Szpor, S. Demczuk, K. Okon
*Jagiellonian University, Dept. of Pathomorphology, Krakow, Poland

Objective: Mast cells are known to participate in cancer formation. The aim of the study was to evaluate number of tryptase and chymase positive mast cells and their relationship with neoangiogenesis in pigmented nevi and melanoma.
Method: Material consisted of 24 pigmented nevi (PN), 19 dysplastic nevi (DN) and 18 melanomas (MM). Chymase and tryptase positive cells and CD105 postive vessels were counted inside the lesion and at the interface with the stroma.
Results: The mean intralesional tryptase + cell count was 15.75 for PN, 21.78 for DN, and 8.07 for MM. The chymase + intralesional count was 14.89 for PN, 21.88 for DN, and 11.34 for MM. The tryptase + cell perilesional count was 16.89 for PN, 15.93 for DN, and 15.71 for MM. The chymase + perilesional count was 16.52 for PN, 16.16 for DN, and 14.77 for MM. The mean perilesional CD105 + vessel density was 2. 71 for PN, 4.49 for DN and 33,93 for MM. The vessel density was correlated with intralesional tryptase + mast cells. Perilesional CD105+ vessels were correlated with mitotic activity of melanomas.
Conclusion: The mast cells may participate in angiogenic switch of melanocytic skin lesions.

PS-24-007

HER-3 expression may influence progression of cutaneous malignant melanoma

G. Dyduch*, J. Szpor, M. Bialas, M. Zrebiec, K. Okon, S. Demczuk
*Jagiellonian University, Dept. of Pathomorphology, Krakow, Poland

Objective: There are several prognostic factors in melanoma. It was suggested that HER-3 expression may influence the tumor behavior. The aim of the study was to investigate the relationship of HER-3 expression with various prognostic factors.
Method: HER-3 expression was evaluated in 52 melanomas, 26 without metastases and 19 with lymph node and 7 with distant metastases. Membranous, cytoplasmic and nuclear HER-3 expression was separately analysed. The staining intensity and percentage of positive tumor cells were evaluated.
Results: The cytoplasmic staininig was seen in all cases, with average intensity of 2 and percentage of positive cells ranging from 5 % to 90 % (mean 48.8 %). The percentage of cytoplasmic HER-3 positive cells was inversely correlated with Clark and Breslow stage ($R=-0.29$ and $R=-0.43$). Cytoplasmic HER-3 reaction was significantly stronger in cases with lymph node metastases (2.3 vs. 1.8 $p<0.03$). In 22 cases a dot-like cytoplasmic reaction was seen. Membranous positivity was seen in 28 cases (54 %).
Conclusion: HER-3 may play a role in melanoma progression. It may be involved in lymphatic dissemination. Further studies of prognostic significance of HER-expression in melanoma are needed.

PS-24-008
Hypopigmented mycosis fungoides with unusual vitiligo-like presentation in child
H. Erdem*, N. Buyukbabani, H. Turan
*Duzce University, Dept. of Pathology, Turkey

Objective: Mycosis fungoides (MF) is the cutaneous T cell lymphoma. Classical, clinical and histopathological findings of MF are detected in most of the patients. However, some of the patients have defined atypical MF. hypopigmented MF (HMF) is one of the atypical forms. HMF could be misdiagnosed with clinical and histopathological examination. HMF is considered mistakenly vitiligo. Therefore, it should be considered differential diagnosis. MF is usually seen in the middle aged and elderly. The occurrence of mycosis fungoides in children is very rare.
Method: An 7-year-old girl child attended dermatology clinic with complaints of pruritus and hipopigmented patches. Lesions was performed punch biopsy and reported HMF.
Conclusion: Herein, this case presented because it was considered vitiligo as clinically and diagnosed HMFas histopathologically.

PS-24-009
Reducing block sampling in wide local excisions for melanoma
C. Fives*, C.C.B.B. Heffron
*Cork University Hospital, Dept. of Histopathology, Ireland

Objective: It is established practice that wide local excision (WLE) is undertaken for the further management of cutaneous melanoma, however, definitive guidelines for macroscopic sampling have not been established. Our aim was to determine whether our sampling of WLE specimens was adequate, inadequate or excessive and to establish guidelines for these specimens.
Method: 128 cases which underwent initial biopsy and subsequent WLE in 2010 were identified. We recorded the specimen size, macroscopic appearance, number of blocks sampled and margins of the original biopsy.
Results: There was wide variation in the number of blocks sampled (range 1–27). Residual melanoma was identified in 7 of the cases (9.4 %) which had clear margins on the original biopsy. Of these, 4 had evidence of a pigmented lesion on macroscopic examination. The remaining 3 cases had margins of 1 mm or less on the original excision. No subsequent surgery was performed on these cases.
Conclusion: Our study has shown that in WLE specimens with no evidence of a macroscopic lesion and in which margins of the original biopsy were clear by greater than 1 mm, little is to be gained from extensive sampling. Reduced sampling would result in saving laboratory resources with a predicted 49 % block reduction in our laboratory alone.

PS-24-010
Functioning oxyphil adenoma of parathyroid gland: A case report
M. Genadieva - Yordanova*, S. Hristova, A. Vlahova, G. Todorov, B. Miserliovska, S. Yordanov
*Alexandrovska Hospital, Dept. of Pathology, Sofia, Bulgaria

Objective: The most frequent cause of primary hyperparathyroidism are adenomas of the parathyroid gland, the majority of which are composed of chief cells. Oxyphil adenomas are uncommon and account for 3 % of functioning parathyroid adenomas. Up until 1978 year they have been considered non-functional.
Method: Laboratory findings revealed calcium levels of 2.86 prior to operation. The serum parathyroid hormone level was 151.40 pg/ml. A CT scan of the neck showed normal size thyroid lobes with heterodense structure with an oval hypodense lesion in the lower right pole of the thyroid.
Results: At surgery a mahagony-brown mass measuring 10 mm in diameter was removed and reported as oxyphil adenoma on frozen section. Histopathological examination revealed encapsulated adenoma composed of oxyphil cells with abundant, granular pink cytoplasm and a rim of normal parathyroid tissue. Mitotic figures were absent. Postoperatively, a decrease of the serum

calcium down to 2.31 mmol/l was declared. The follow-up period was unremarkable.
Conclusion: There appear to be a growing evidence that a big part of oxyphil adenomas of parathyroid gland can produce parathyroid hormone and contribute to the cases of primary hyperthyroidism.

PS-24-011
Effectiveness of UVB phototherapy on mycosis fungoides using histologic guitart criteria in Iranian patients
A. Ghanadan*, A.-H. Ehsani, H. Seirafi, M. Khiabani
*Tehran University, Razi Hospital, Iran

Objective: Mycosis fungoides (MF) is the most common primary cutaneous lymphoma. Mycosis fungoides often develops slowly over many years, presenting with a generalized erythroderma, skin patches or plaques. The diagnosis of MF requires the integration of clinical and histopathologic findings. Narrowband UVB (NBUVB) is widely used to treat MF. To evaluate the effectiveness of therapy the histopathologic findings before and after NBUVB reviewed using GUITART criteria.
Method: We enrolled 20 patients (12 women, 8 men; age range, 10–80 years; mean age, 45.5 years) with clinically and histologically proven MF. The patients received NBUVB phototherapy three times a week. A biopsy was performed 3 months after onset of the treatment and GUITART criteria used to scoring MF before and after therapy.
Results: Phototherapy was reduced the primary intraepidermal atypical lymphocytes (P value=0.008), dermal atypical lymphocytes (*P* value=0.008), epidermotropism (*P* value=0.001), density of infiltration (*P* Value=0.002) and lymphocytic infiltrate without inflammatory features (*P* Value=0.046) in all patient. But the relationship between the reticular fibroplasia of papillary dermis and phototherapy was not proved (*P* value=0.18). Overall score of patients was significantly lower after phototherapy (*P* value=0.000).
Conclusion: Our data suggest that NBUVB therapy is reduces histiologic score of MF and is effective for the treatment of Iranian patients.

PS-24-012
Nodular colloid degeneration of the skin: Report of three cases
A. Ghanadan*, K. Kamyab-Hesari, M. Daneshpajouh, K. Balighi, M. Khosravi
*Tehran University, Razi Hospital, Iran

Objective: Nodular colloid degeneration (NCD) is a rare dermatological disorder and also a rare type of colloid milium. The degeneration may be related to sun exposure.
Method: Three cases of NCD were enrolled from the archive of dermatopathology department of Razi hospital during 2009–2011.
Results: In this report, three cases, all presented with multiple plaques and nodules in the nose and the face, are depicted. Histologically, these nodular masses were homogeneous, with eosinophilic clefted materials expanding the papillary dermis and extending into the deep dermis. Histochemical review showed the reactivity of the colloid materials via the PAS, crystal violet and methyl violet staining. All the three cases were finally diagnosed as nodular colloid degeneration.
Conclusion: NCD is a rare disease but it should be considered in any cases with a history of long exposure to the light. We suggest the long term exposure to the sun as an etiologic factor thus, sun protection would be the most preventive and available treatment.

PS-24-013
Glypican-3 protein expression in melanoma: A immunocytochemistry study
N. Gursan*, H. Balta, B. Gundogdu
*Ataturk University, Medical Faculty, Erzurum, Turkey

Objective: Glypican-3 (GPC3) is a cell surface heparan sulfate proteoglycan. Serum GPC3 was shown to be expressed in 40 % of melanomas (Ms) but GPC3 expression in Melanoma tissues had not been investigated.In this study, immunohistochemical analysis of GPC3 protein expression was investigated in histologic sections from Melanoma tissues.
Method: 60 melanoma patients, twenty patients with insitu melanoma, twenty patients stage 0 and stage I melanoma, twenty patients stage II and stage III melanoma. All cases were stained with anti-GPC3 antibody. GPC3 expression was divided into 2 categories: negative (negative or weak cytoplasmic staining) and positive (moderate or strong cytoplasmic with membranous accentuation).
Results: GPC3 immunopositivity. showed in 40,3 % of melanomas. GPC3 expression at stage 0, I, II, III were 44.4 %, 40.0 %, 41.6 %, 35 % respectively.

Conclusion: GPC3 is apparently a novel tumor marker useful for the diagnosis of melanoma, especially in early stages of the disorder.

PS-24-014

Cutaneous leishmania in Eastern Anatolia: 6 case reports

N. Gursan*, A. N. Yilmaz, H. Bilen, N. Akdeniz, M. Atasoy
*Ataturk University, Medical Faculty, Erzurum, Turkey

Objective: Leishmaniasis refers to the spectrum of diseases caused by Leishmania species, which are Protozoa of order Kinetoplastida. Clinically leishmaniasis is divided into visceral (kala-azar), cutaneous, mucosal, and mucocutaneous syndromes. The final diagnosis of the disease, lesions of the parasites, as well as shown smear'lerde factor confirmed by histopathological and clinical evaluation.
Method: In our study, 6 patients with the diagnosis of Leishmania cutaneous between 2006 and 2012 in Department of Pathology, Ataturk University Faculty of Medicine were presented.
Results: Four (66.6 %) cases were females and 2(33.3 %) were males. Age ranging of cases was found from 0 to 60 years and median age 31.85±12.15 years. The lesions were found on the face in patients. Facial skin biopsy specimens were taken in all cases. Giemsa-stained touch preparation of the skin biopsy revealed amastigotes inside macrophages, consistent with leishmaniasis. Lesions of 2 patients who have long been different from the rest of them were those who migrated to the Cukurova region.
Conclusion: Leishmaniasis is public health problem in Southeastern Anatolia region of Turkey, especially in Sanliurfa and Çukurova region.

PS-24-015

Autoimmune blistering skin diseases in East Anatolia

N. Gursan*, O. Ceylan, H. Bilen, N. Akdeniz, M. Atasoy
*Ataturk University, Medical Faculty, Erzurum, Turkey

Objective: Autoimmune blistering skin diseases can be divided into pemphigus diseases and subepidermal bullous diseases. In pemphigus, the autoantibodies are directed against intercellular contact structures; in the pemphigoid diseases, the autoantibodies are directed against adhesion molecules of the basal membrane zone.
Method: A retrospective study of 102 cases of autoimmune blistering skin diseases obtained over a period of 7 years from 1st October 2005 to 31st December 2011 in the Department of Pathology, Medical Faculty of Ataturk University was designed.
Results: In the present study, the mean age was 52 years and male: female ratio was 0,7. The most commonly affected sites were the buccal mucosa and the palate. %18 of cases, the oral cavity was the primary site of involvement. In histopathological examination we showed intraepithelial vesicle formation, subcorneal separation with acantholysis, and the presence of Tzanck cells in biopsy specimens.
Conclusion: The incidence of autoimmune blistering skin diseases in our department increased in the past 7 years. Pemphigus vulgaris is the most common of these diseases. %70 of autoimmune blistering skin diseases was pemphigus diseases.

PS-24-016

Prevalence of vasculitis in Sweet syndrome

R. Hadhri*, I. Ghali, L. Njim, J. Belhouane, H. Belhajali, A. Moussa, J. Zili, A. Zakhama
*Fattouma Bourguiba Hospital, Dept. of Pathology, Monastiir, Tunisia

Objective: Acute febrile neutrophilic dermatosis (Sweet syndrome) is the most common neutrophilic dermatosis. A dense dermal neutrophilic infiltrate is the usual histological findings. The absence of histological image of vasculitis has been considered a characteristic of the disease and a distinctive feature of the other neutrophilic dermatoses. However, recent reports suggest that vasculitis should not exclude the diagnosis.
Method: This retrospective study examines 32 cases collected over a period of 14 years (1996–2009). We studied its clinical and histological characteristics. Skin biopsy specimens were reviewed to determine the prevalence of vasculitis.
Results: Sweet syndrome is significantly more common in women than in men (sex-ratio=1/15). The patient's mean age was 51 years. Disease developed most often in autumn. Atypical presentation was noted in 18 patients. Skin biopsy revealed a sweet syndrome pattern in all cases. The prevalence of vasculitis (vessel wall damage with fibrinoid necrosis) was 28 % (9 of the 32 patients).
Conclusion: Our series of patients is particular by the frequency of atypical clinical presentation and the presence of vasculitis in histologic examination, a feature that shouldn't exclude the diagnosis. It was suggested that vasculitis in Sweet syndrome represents an epiphenomenon rather than a primary immune-mediated process.

PS-24-017

Dermal lymphangitic carcinomatosis as a primary manifestation of lung carcinoma: Report of an unusual case

C. Hadjileontis*, E. Angelidou, A. Kafanas
*Serres General Hospital, Dept. of Pathology, Greece

Objective: Although dermal lymphangitic metastases are reported to range between 1 and 4,5 % of all visceral carcinomas, their presence as a primary manifestation of the tumor is rather unusual.

Method: We report the case of a 77 year old man presenting with an erythematous plaque of the right hemithorax.
Results: Macroscopically the lesion had irregular borders and was mildly infiltrative with a violet hue. Microscopic examination revealed tumor cells within lymphatic spaces, without infiltration of the adjacent stroma. The histologic and immunophenotypic characteristics of these cells were compatible with a carcinoma of lung origin. CT scan revealed a lung mass as well as multiple liver and chest wall metastases.
Conclusion: Malignancies originating from the breasts, lungs and large bowl are the most common to involve the lymphatic net of the skin. Melanoma on the other hand is more frequently presenting with lymphangitic invasion, whereas inflammatory carcinomas may also affect lymphatic vessels and may be confused with erysipelas. The revelation of the primary origin is not always easy and differential diagnosis should also include gynecological malignancies, kidney and urinary bladder carcinomas. In our patient the diagnosis was established on the grounds of histology and immunohistochemistry, and was supported by the clinical and radiological findings.

PS-24-018
Inverted follicular keratosis
R. Hamrouni*, I. Chelly, H. Kamoun Azouz, H. Nfoussi, B. Chelly, A. Ben Salem, A. Dhaoui, N. Kchir, S. Haouet
*Pathology, Ariana, Tunisia

Objective: Inverted follicular keratosis (IFK) is almost always a solitary lesion occuring mainly in adult life. Men are affected twice as often as women. Pathologically, They can be confused with a variety of lesions, both benign and malignant. Squamous carcinoma is the most serious differential diagnosis.
Method: We decribe a retrospective study about 7 cases of IFK diagnosed over a 18-year-period (1994–2012).
Results: We collected 7 lesions, all treated by surgical excision. Haemalum eosin sections were studied in all cases. All lesions were single. Five, of them, were situated on the face and two on the scalp. All the patients were adults with a mean age of 34 years, average between 19 and 66 years. They presented mostly as asymptomatic papules and all were small lesions. The different sections of the lesion showed skin well delineated endophytic epithelial proliferations with inverted papillomatous and acanthotic components containing several circumscribed squamous eddies. They was no atypia, mitotic activity necrosis or stromal invasion.
Conclusion: IFK pose very real diagnostic problems unless one is aware of this entity. In fact, they may mimic malignant lesions especially squamous cell carcinoma, both clinically and pathologically.

PS-24-019
Primary cutaneous follicular lymphoma with prominent spindle cell areas. So called spindle cell follicular lymphoma. Case report
G. Ivády -Szabó*, T. Strausz, E. Tóth
*National Institute of Oncology, Dept. of Surgical Oncology, Budapest, Hungary

Objective: Spindle cell type variant of cutaneous follicular lymphoma is a rare histologic variant of primary cutaneous follicular lymphomas. It is caracterised by the presence of spindle and bizarr cells. We present a case of a 25 years old man who had a nodule on his scalp and two smaller nodules on his frontal region. We examined an excisional biopsy specimen of the forehead.
Method: HE, Stains all and Immunohistochemical stains were used.
Results: Histology revealed dense lymphoid infiltrate showing nodular pattern in the dermis and in the subcutis. The lymphoid infiltrate predominantly composed of large centrocytes. There were areas where the neoplastic cells show spindle cell morphology with bizarre nuclei and in these areas the stroma were myxoid, mucinous. With immunohistocemical stains the neoplastic cells were positive for CD20, Bcl-6, and negative for CD5, CD10, vimentin, CD34, S100, actin, desmin, AE1/AE3. CD21 showed residual network of follicular dendritic cells in the background.
Conclusion: Spindle cell lymphoma is a very rare variant of cutaneous follicle centre cell lymphoma and the presence of the spindled bizarre cells can cause differential diagnostic problems. The main differential diagnostic entities are primary or metastatic spindle cell sarcoma and spindle cell melanoma. Careful morphological and immunohistochemical analysis are required to the correct diagnosis.

PS-24-020
The histopathologic and immunohistochemical features of mycosis fungoides
B. A. Karabork*, A. Okcu Heper, S. Yuksel, I. Kuzu
*Ankara University of Medicine, Dept. of Pathology, Turkey

Objective: The histopathologic diagnosis of early mycosis fungoides (MF) is often difficult. The lesions can mimic a variety of inflamatory dermatitis. We aimed to establish and draw attention to the most frequent histopathologic and immunohistochemical features of MF.
Method: We reviewed 115 skin biopsies of clinicopathologically diagnosed MF cases at Medical University of Ankara. We looked for a) epidermotropism, atypical lymphocytes, morphologic features in the epidermis, dermoepidermal junction and dermis b) immunohistochemical

staining ratios of CD3, CD4, CD8, CD20, CD30 and expression loss of CD5, CD7.
Results: Atypical lymphocytes) (96 %), dermal fibrosis (90 %), epidermotropism (86 % single cells, 44 % linear arrangement, 15 % Pautrier's microabscesses, 83 % 'haloed' lymphocytes), epidermal acantosis (72 %), basal vacuolar degeneration (focally 43 %, marked 15 %) and a perivascular lymphocytic infiltrate were the most common and important features. Dermal edema (46 %) extravasated erythrocytes (34 %), spongiosis (27 %), eosinophils (17 %) and necrotic keratinocytes (14 %) were the less seen and non-specific ones. Immunohistochemical results correlated with a ratio of 78 % CD4, 22 % CD8 positive MF. Expression loss of CD7 was seen in 73 %, CD5 in 31 % of cases.
Conclusion: Diagnosis of early MF requires the correlation of morphologic, immunohistochemical and clinical features. Also due to the disease's heterogenity, biopsies from different locations and rebiopsies will enhance the diagnosis.

PS-24-021
Connexins of cutaneous melanocytic tumours
G. Kiszner*, Z. Buday, I. Teleki, E. Varga, I. B. Nemeth, I. Korom, T. Krenacs
*Semmelweis University, 1st Dept. of Pathology, Budapest, Hungary

Objective: Connexins (Cx) form transmembrane channels that can transport ions and small regulatory molecules between adjacent cells. They also function as hemichannels and through protein interactions and are involved in the control of cell replication and maintenance of multicellular homeostasis.
Method: We have tested the expression of connexins in melanocytic tumours using immunohistochemistry in tissue microarrays of 21 common and 73 dysplastic nevi, and 61 primary and 23 metastatic malignant melanomas.
Results: Cx23 was not found in melanocytic tumours despite expressed in the basal epidermis. Cx30.3 reaction showed punctate cell membrane staining in 71 % of naevi in their superficial regions including atypical nests, and displayed cytoplasmic staining in 28 % of melanomas. Low levels of Cx32 were revealed in the cytoplasm of >80 % of naevi and melanomas but only 23 % and 8 % showed membranous positivity, respectively. Cx36 perinuclear/cytoplasmic immunostaining was observed in 57 % of naevi and 24 % of melanomas and as cell membrane reaction in 24 % and 12 %, respectively. Punctate Cx43 reaction was detected in vertical tumour nests in 69 % of naevi, while only 11 % of melanomas proved positive and showed cytoplasmic Cx43 delocalization.
Conclusion: Therefore, most tested connexins were significantly down-regulated in malignant vs. benign melanocytic tumours that possibly contribute to their malignant phenotype.

PS-24-022
Quantitative follow up study of CD 1a, CD 8 and CD 68 positive cells in multiple basal cell carcinoma cases after combined treatment
R. Kleina*, I. Truksane, J. Kisis, I. Franckevica
*Riga Stradins University, Dept. of Pathology, Latvia

Objective: In last years appear more cases with multiple basal cell carcinomas (BCC). Skin immune system reaction is especially important in nonsurgically treated cases. Aim of study is to evaluate the dynamics of CD 1a, CD 68, CD8 marked cells in BCC and in skin adjacent to tumour (5 and 10 mm) before and after the treatment with cryotherapy and imiquimodum.
Method: From 68 BCC cases with multiple tumours investigated immunohistochemically, in dynamics we have characterized 8 patients. Antibodies for CD1a, CD8, CD68+ cells in derma and epidermis were used. They were evaluated in 3 fields of vision (400×) before and after treatment. 5 % imiquimod cream and double freezing was used. Control group: three normal skin samples. Statistical analyses of results were done.
Results: After treatment were erythema, then crust and exfoliation. Microscopically expressed fibrosis instead BCC was found. Amount of immune cells before and after treatment were: CD8 25±3,1/34±4,8 (also in epidermis), Langerhans cells 7±2,3/14±3,4, CD 68 19±3,8/10±2,9.
Conclusion: All immune cells of skin react to the combined treatment of BCC in radius of 5 mm. There is significant statistical difference between the numbers of Langerhans cells in normal epidermis and in BCC cases treated with cryomethod and imiquimodum.

PS-24-023
Regulatory T-cells in invasive and in situ squamous cell carcinoma of the skin and actinic keratosis
H. Kourea*, A. Stravodimou, V. Tzelepi, H. Papaioannou, H. Papadaki, C. Scopa
*University of Patras, Dept. of Pathology, Greece

Objective: Regulatory T-cells (Tregs) participate in tumor tolerance and facilitate tumor growth and Foxp3 transcription factor is necessary and sufficient for their development and function. We investigated the presence of T-regs in invasive (IN) and in situ (IS) squamous cell carcinoma (SCC) of the skin and actinic keratosis (AK).
Method: Tregs were identified using immunohistochemistry for Foxp3 and recorded using image analysis in 55 cases of INSCC (and their adjacent IS, AK or benign tissue (BN), when present), in 18 cases of IS and 46 cases of AK (and

their adjacent BN tissue). Statistical analysis was performed using the paired *T*-test. *p*-values <0.05 were considered statistically significant.

Results: In INSCC cases, Tregs in the tumor were more numerous than the adjacent BN (n=46) (mean 155 vs. 79, p <0,001). Additionally, adjacent IS had more Tregs than adjacent AK (n=6) (160 vs. 86, p=0,045). Significant differences between INSCC, and IS or AK were not observed. In IS and AK cases, Tregs were more numerous than the adjacent BN (206 vs. 42, p<0,001 and 148 vs. 47, p< 0,001), respectively.

Conclusion: Treg infiltration of the skin increases early from the precancerous AK, indicating early involvement of Tregs in the development of SCC.

PS-24-024

Cutaneous mastocytosis: Report of 6 cases

C. Kouvidou*, C. Vourlakou, M. A. Lianou, M. E. Kopaka, P. Kara, D. Violidaki, G. Anastasiadis, D. Rontogianni
*Athens, Greece

Objective: Mastocytosis is a rare disorder and its true incidence is unknown. Skin is most commonly involved, followed by the bones and the gastrointestinal tract.

Method: Five men presented with many brown lesions in the trunk and one woman with multiple redish brown non-pruritic macules in the extremities. We used immunohistochemistry for c-kit and tryptase for the definite diagnosis. The expression of CD25 and CD2 were also evaluated.

Results: Histology showed five cases of urticaria pigmentosa with severe diffuse infiltration of the papillary dermis by mast cells and one case of telangiectasia macularis eruptiva perstans (TMEP) with scattered mast cells around dilated capillaries and venules of the papillary dermis. The mast cells were positive to c-kit and tryptase and only in one case there was a coexpression of CD25 and CD2 >50 % of the mast cells. In that case involvement of bone marrow was observed and the diagnosis of indolent systemic mastocytosis was established according to WHO 2008 criteria.

Conclusion: Urticaria pigmentosa is the most common form seen in adults while TMEP is an uncommon form that occurs exclusively in adults. The skin involvement in indolent systemic mastocytosis is a part of the spectrum of the disease.

PS-24-025

Subvisual nuclear characteristics are different between keratoacanthoma and keratoacanthoma-like squamous cell carcinoma

K. Metze*, M. Tabai, R. Adam, I. Watanabe, A. de Moraes, M. Cintra
*University of Campinas, Pathology, Brazil

Objective: The differential diagnosis between keratoacanthorna and keratoacantoma-like squamous cell carcinoma may be extremely diffcult. Our objective was to study whether computerized image analysis could be helpful.

Method: In 34 patients biopsies of keratoacantoma-like lesions were taken at admission. One month later surgical excision was performed in growing lesions, whereas regressing lesions were left untreated. A final diagnosis was established combining clinical and histological evaluation, Digitalized images from KI-67 immunostained and hematoxylin counterstained sections of first biopsies were obtained. Tumor nuclei were marked interactively. An inhouse computer program analyzed the geometric relations between the nuclei. Nuclear gray values and their histogram entropy were calculated.

Results: 27 keratoacnthomas and 7 keratoacantomalike squamous cell carcinomas entered this investigation. Basic variables of the geometric analysis did not differ between the two entities regardless whether all nuclei or only the Ki67 positive ones had been examined. Chromatin gray values were significantly lower and their histogram entropy higher in the keratoacantoma-like squamous cell carcinomas.

Conclusion: Basic geometric variables do not seem to be different beteen both lesions, but a shift in the gray value histogram to lower values with increased entropy in carcinomas indicated important differences of the chromatin structure, Supported by FAPESP and CNPq.

PS-24-026

Non-infectious erythematous papular and squamous lesions of the skin in our institute, with clinicopathologic correlation

T. Ozgur*, A. C. Dogramaci, E. Atik, S. Hakverdi, M. Yaldiz, Z. A. Tas
*Mustafa Kemal University, Medical Faculty, Antakya, Turkey

Objective: Non-infectious erythematous, papular and squamous lesions of the skin are basic lesions that pathologists differentiate in routine laboratory examinations. Our aim has been to analyse these lesions by pathologic and clinical findings in our institute with determining clinicopathologic correlation.

Method: In our study 420 cases prediagnosed as erythematous, papular and squamous lesion by dermatologists and evaluated in pathology laboratory between 2004 and 2010 have been reviewed.

Results: The lesions comprised %14.3 of the total load of surgical pathology and 9.1 % of total number of skin biopsies. The highest percentage was in the 41–50 year age group (39.1 %) with a female predominance of 51.2 %. The limbs were most frequently involved (36.9 %). Psoriatic

lesions were the commonest (50.7 %), classic generalized plaque variant psoriasis (89 %) being the most frequent. Correlation with the histopathologic diagnosis was positive in 75.3 % cases and negative in 24.7 % cases.

Conclusion: The contribution of histopathology to the final diagnosis was significant. It confirmed the diagnosis in 75.3 % cases and gave the diagnosis in 7.3 % cases.

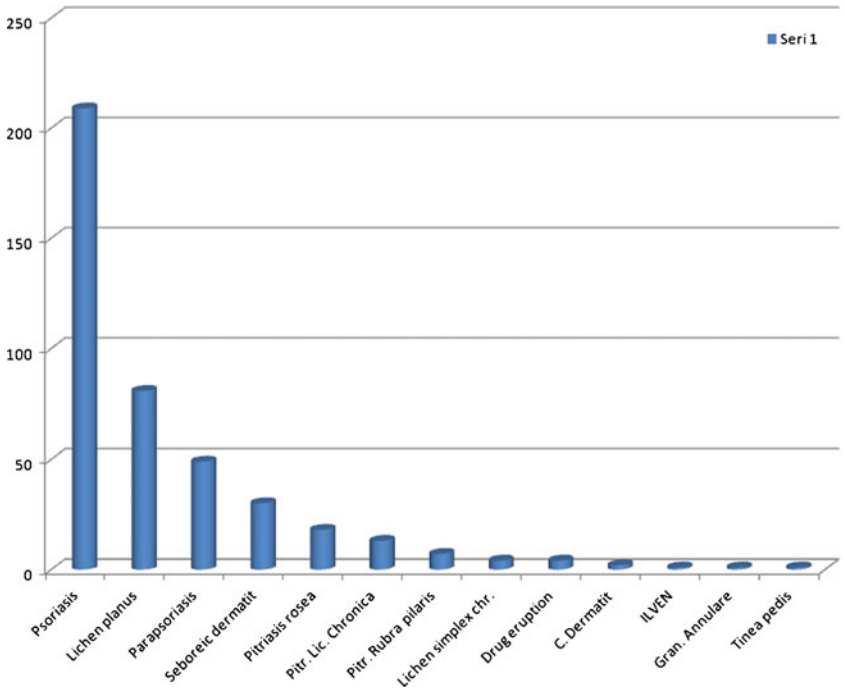

PS-24-027

Vulvar lichen sclerosus: A misnomer for an entity with decreased fibrillar components and increased amorphous components in extracellular matrix remodeling

E. Parra*, C. A. Pires de Godoy, V. L. Correia Feitosa, W. Teodoro, A. P. Velosa, V. L. Capelozzi
*FMUSP, Dept. of Pathology, São Paulo, Brazil

Objective: The hyalinization of subepidermal skin is one of the histopathological characteristics of the vulvar lichen sclerosus (VLS). It was found that patients with VLS present autoantibodies against the extracellular matrix protein 1 (ECM-1) and the deficiency of this protein is responsible for the development of a different disease, the Lipoid Proteinosis. This disease shows a similar histology with VLS and has better characterized morphology.
Method: We analyzed 20 VLS patients biopsies and the control group was composed by 20 vulva samples from authopsy. The biopsies and control samples were analysed by immunofluorescence for collagen I, III and V and th total collagen fibers by Picrosirius staining. The elastic fibers were stained with Verhoeff and the proteoglycans and glycosaminoglycans with Periodic Acid-Schiff and Alcian Blue. Collagen quantification was performed through image analysis.
Results: It was observed a significant reduction in all studied collagens as well as in the elastic fibers. On the other hand, the proteoglycans were increased in the VLS biopsies.
Conclusion: This study did not found an increase in collagen sclerosis that would justify the term used for the LS. It was observed a predominance of the edema area probably caused by the increase of glycoproteins as in lipoid proteinosis.

PS-24-028

Combined high-grade basosquamous carcinoma and malignant melanoma of the scalp (malignant basomelanocytic tumor) metastasizing to the breast. A case report

A. Pitino*, S. Squillaci, C. Spairani, F. Ottelli Zoletti, M. F. Cosimi, M. Ferrari, A. Tropiano, P. C. Rassu, F. Tuo, P. Maiocchi
*San Giacomo Hospital, Division of Anatomic Pathology, Novi Ligure, Italy

Objective: Background. Basal cell carcinoma (BCC) is a very low grade, usually not metastasizing skin malignancy, which needs to be radically excised.
Method: Methods. An 80 year-old woman was treated for a 3×2,2 cm multinodular mass in the scalp. One month later

an ultrasonography of the left breast showed a 5,5 cm mass which was excised with clean margins. Axillary lymph nodes were free of metastasis.
Results: Results. The dermal tumor presented well demarcated basaloid epithelial nests with squamous differentiation focally connected with the epidermis. They showed peripheral palisading and high nuclear grade with pleomorphism, brisk mitotic activity and multiple prominent nucleoli. Atypical cells, arranged as strips, nests or isolated elements, were observed at the tumor edge, separated by a grey-zone from the overlying malpighian epithelium. Immunostains were positive for cytokeratins, melanocytic (S-100/HMB-45/MART-1) and neuroendocrine (CD56/NSE/Cromogranin) markers. The 4,8 cm breast tumor corresponded to a high grade metastatic BCC with reactivity for epithelial markers, S-100 and CD56.
Conclusion: Conclusions. The literature reported 32 cases of combined tumors composed of BCC and malignant melanoma (MM) with 5 patients showing local recurrences. The term << malignant basomelanocytic tumor >> describes these biphasic tumors. The knowledge of this entity expands the differential diagnosis of skin tumors with melanocytic component.

PS-24-029
Superficial granulomatous pyoderma: Three cases of this rare variant
I. Rodriguez*, A. Cordoba, M. C. Llanos, A. M. Valcayo, C. Ros
*C. Hospitalario de Navarra, Dept. of Pathology, Pamplona, Spain

Objective: Pyoderma gangrenosum (PG) was described at first by Brocq and named by Brunsting et al. in 1930. Superficial granulomatous pyoderma (SGP) was described as a variant of PG in 1988. We present three cases of this rare variant.
Method: There were two women and one man with age ranging from 40 to 78 years. All of them had a long history of a slowly enlarging, eritematous and ulcerative plaque in different areas including leg and breast skin. A biopsy was performed in all cases.
Results: The superficial dermis showed neutrophilic inflammation with an admixture of granulomatous inflammation and sinus formation. There wasn't vasculitis and fat tissue was not affected.
Conclusion: SGP is a rare variant of PG. Diagnosis of this entity generally is made on the basis of skin biopsy results with all features mentioned previously and a typical clinical appearance. Most of times, these lesions are diagnosed as granulomatous dermatitis, thinking in infectious pathology. This is the most important differential diagnosis, because SGP is responsive to corticosteroids. The pathogenesis of PG is unknown, though is now believed to altered neutrophil chemotaxis and some authors suggest that SGP may be a delayed-type hypersensitivity to an unknown antigen. Pathergy is the inciting factor in several patients.

PS-24-030
High concordance in BRAF status between native-BRAF malignant melanoma and matched lymph node metastases
A. Santos Briz*, E. Godoy, L. Arango, P. Antúnez, M. Yuste, C. Roman, E. Fernández, M. D. Ludena
*Hospital Universitario Salamanca, Dept. de Anatomía Patológica, Spain

Objective: The discovery of selective v-raf murine sarcoma viral oncogene homolog B1 (BRAF) V600 mutation as an oncogenic mutation in cutaneous malignant melanoma (MM) has changed the treatment paradigm for melanoma. Selective BRAF inhibitors have demonstrated response rates far higher than standard chemotherapeutic options. BRAF mutation analysis is usually performed on primary tumour tissue; however, no conclusive data are available on the concordance of test results between primary tumours and corresponding metastases. We assessed the concordance of BRAF mutation status in a study of 16 primary BRAF-native tumours and their corresponding lymph node metastases.
Method: 16 patients with histologically confirmed non-mutated BRAF MM who underwent surgical resection of the primary tumour and positive selective lymph node biopsy or lymphadenectomy were included. Mutation status was determined by means of a realtime PCR assay (Cobas 4800 BRAF V600 Mutation Test, Roche Molecular Systems).
Results: There was a 100 % concordance of the BRAF results in primary tumor and corresponding metastases in 16 analyzed pairs.
Conclusion: Our findings show total concordance in BRAF status between primary BRAF native tumors and their paired metastases, and suggest that acquisition of BRAF V600 mutation in metastases from primary native tumors is a rare event.

PS-24-031
Dermatoscopic and histologic score correlation in atypical Spitz/Reed nevi
M. Saravia*, Z. Pellicer, J. M. Martin, C. Monteagudo
*Hospital Clinic University Valencia, Dept. of Pathology, Spain

Objective: Different dermatoscopic scores of pigmented skin lesions have provided a valuable tool in daily routine practice to differentiate malignant from benign lesions.

However, these semiquatitative methods have a high rate of false positives in Spitz/Reed nevi. We have compared semiquantitative histopathologic and dermatoscopic findings in a series of Spitz/Reed nevi.
Method: We collected 19 cases (15 female and 4 men) of atypical Spitz and/or Reed nevi. All cases were microscopically confirmed. A histologic index (HI) was constructed scoring the following findings: symmetry, sharp demarcation, architectural dysplasia, melanocytic atipia and nest size, and compared with validated dermatoscopic scores (ABCD score, 7-point checklist and Menzies score). Distributions of these scores for the different dermatoscopic patterns were also analyzed.
Results: Median age at presentation was 15 years (range 1 to 36). The HI varied from 0 to 5 points. We found a strong positive correlation between the HI and Menzies score (r=0,539, p=0,01). In addition, HI values differed significantly when the multicomponent dermatoscopic pattern group was compared with the other patterns (U=22, 5 Z=−2,25, p=0.01).
Conclusion: Menzies is the only dermatoscopic score which strongly correlates with histologic findings in Spitz/Reed nevi and may be useful in the diagnosis of atypical lesions.

PS-24-033
Correlation of nonmolecular and molecular subtyping of inherited epidermolysis bullosa
K. Veselý*, H. Bucková, L. Fajkusová, M. Veselá, B. Jerábková
*St. Anne's Hospital, Dept. of Pathology, Brno, Czech Republic

Objective: Inherited epidermolysis bullosa (EB) is a heterogeneous group of hereditary mechanobullous diseases with skin blister formation of variable severity and numerous extracutaneous manifestations. EB comprises three main groups and many subtypes and their recognition is important for prognosis and genetic counselling.
Method: We examined skin biopsy samples of 42 patients with EB using transmission electron microscopy, immunofluorescence antingen mapping (AM) and their peripheral blood samples by mutational analysis.
Results: In the total number of 42 cases, concordant results of molecular and nonmolecular methods were found in 35 cases (83 %). In 7 patients (17 %) mutational analysis did not confirm the results of ultrastructural and AM analysis.
Conclusion: Strong correlation in the results obtained by different methods was observed. Using combination of nonmolecular and molecular diagnostics methods high diagnostic accuracy can be achieved.

PS-24-034
Granulomatous Slack Skin (GSS): A case report with evidence of T cell clonality
I. Yilmaz*, H. Baloglu, U. Berber, Z. Kucukodaci, M. Arcila
*GATA HEH, Dept. of Pathology, Istanbul, Turkey

Objective: GSS is a very rare variant of MF. We describe an additional case of this rare disorder in a 42 yo female that has been approved by TCRB&G Tcell Clonality Assay.
Method: A 42 yo female with a single bulky skin lesion in the inguinal fold which had first appeared 6 y before and enlarged up to 20 cm, referred to plastic surgery for esthetics. H&E section of the deep skin biopsy of lesion showed a granulomatous infiltrate in the dermis. Nuclear atypia and epidermotropism is not significant. But there is numerous multinucleated histiocytic giant cells. Elastophagocytosis are present. TCRB&GT cell Clonality Assay showed a clonal rearrangement in TCR gamma gene. She was referred to dermatology for treatment and now she is getting UVA1 phototherapy.
Results: The diagnosis of GSS is difficult in early stages of the disease. Clonal rearrangement of TCR genes can be a useful diagnostic tool in early stages of the disease.
Conclusion: 20–50 % of patients with GSS carry a risk for the development of a second malignancy. GSS may be associated with lymphoproliferative disorders. Therefore, follow up of the patient is important. This case report supports that GSS is an indolent variant of MF due to clinical, histological and T-cell gene rearrangement results.

PS-24-035
Unusual occurrence of multicentric reticulohistiocytosis with systemic involvement in childhood
S. Zurac*, C. Dobrea, A. Diaconeasa, A. Colita, C. Solovan, C. Arion, F. Staniceanu
*Colentina University Hospital, Dept. of Pathology, Bucharest, Romania

Objective: Multicentric reticulohistiocytosis (MR) with systemic involvement is an extremely rare disease afflicting mainly adults.
Method: We report a case of SR arising in a 3 year 7 month old boy with concomitant celiac disease.
Results: Since 6–7 months, he developed several brown to dark-red skin nodules (up to 0.8 cm) located mainly on face and arms; current episode include hemorrhagic syndrome, severe pancytopenia and massive hepato-splenomegaly. Bone marrow aspirate ruled out acute leukemia and tezaurismoses; bone marrow biopsy and skin biopsy showed important infiltration with numerous large cells with abundant fine granular/ground glass eosinophilic cytoplasms in a

reactive inflammatory stroma (lymphocytes, few plasma cells and few eosinophils); bone marrow cells were mononucleated, cutaneous cells were both mono&multinucleated; tumor cells immunophenotype was consistent with histiocytes (CD68+, S-100 protein + (faint), CD1a-, langerin-) both in bone marrow and skin biopsies; no hemophagocytosis was seen. MR with systemic involvement of skin, bone marrow, liver and spleen was diagnosed. Cyclophosphamide therapy was instituted with initial diminishing of splenomegaly; latter on, despite adding cyclosporine and etoposide, no further impact on pancytopenia and hepatosplenomegaly was recorded.

Conclusion: Complete hematologic examination is mandatory for patients diagnosed with cutaneous reticulohistiocitosis, irrespective of their age, in order to identify MR and institute proper treatment.

PS-24-036

Primary cutaneous follicle centre lymphoma: A case report and review of literature

K. Diamantopoulou*, C. Zorzos, C. Eftychiadis, I. Famellos, G. Piagkos, G. Karamanis, I. Babalis, S. Binder, H. Mahera
*General Hospital Kat, Pathology, Athens, Greece

Objective: Primary cutaneous follicle centre lymphoma (PCFCL) is an indolent, primary cutaneous B-lymphoma with an excellent prognosis but a high incidence of reccurence. Apart from standard surgery and local radiotherapy, targeted strategies with anti-CD20 (rituximab) has introduced new treatment modalities.

Method: Woman, aged 82, with solitary skin lesion on her face. After surgical excision, histo- and immunohistochemistry with the ABC system on paraffin embedded tissue was performed.

Results: Microscopically, a non-epidermotropic perivascular and periadnexal neoplastic infiltrate with a follicular growth pattern was observed. The lesion consisted of predominantly medium-sized centrocytes and several centroblasts enmeshed in a network of CD23(+) dendritic cells. Immunohistochemically, the neoplastic lymphoid cells were CD20, CD79a, BCL2 and BCL6 positive. CD30, MUM1 and Ig were all negative. The patient received one cycle of rituximab and 6 months later is free of disease.

Conclusion: Primary cutaneous B-cell lymphomas (CBCL) account for 25 % of cutaneous lymphomas. PCFCL is one of the three major categories of CBCL, recently classified by WHO, (the other two: PCMZL and PCDLBCL, leg-type). BCL-2, except for systemic follicular lymphoma, it can also occur in PCFCL, as in our case. PCFCL, usually locally treated with surgery and radiotherapy, could possibly offer a candidate for anti-CD20 targeted therapy, especially in multifocal lesions.

PS-24-037

Concurrent CD8 and CD30 positivity: Pityriasis lichenoides et varioliformis acuta (PLEVA) or lymphomatoid papulosis?

O. Kurtulan*, M. Bugdayci, Ç. Aydin, Z. Yusifli, S. Ersoy Evans, A. Okçu Heper, Ö. Gököz
*Hacettepe University, Pathology, Ankara, Turkey

Objective: Thirteen and ten years old male patients admitted with 4 months interval, having diffuse hemorrhagic papules on extremities and trunk. The first has not responded to methorexate previously. The second had varicella infection 3 months before and, his rushes spreaded out recently.

Method: Multiple punch biopsies of the first patient revealed epidermal necrosis, basal vacuolisation and subepidermal diffuse infiltrate composed of CD3 and mostly CD8 positive T cells showing a striking angiocentric distribution. There were CD30 positive large cells with vesicular nuclei both in epidermis and dermis. Some of the vessels exhibited lymphocytic vasculitis with fibrinoid necrosis. Punch biopsy of the second patient revealed subcorneal pustule, dyskeratosis and basal vacuolisation, papillary dermal edema, erythrocyte extravasation and severe lymphocyte-rich cellular reaction infiltrating the interface. Lymphocytes were CD3 and mostly CD8 positive. In between, there were large cells with vesicular nuclei exhibiting CD30 positivity.

Results: Diagnoses were PLEVA based on the vascular and interface changes in accordance with clinical findings. Both patients responded to oral antibiotics.

Conclusion: PLEVA is among the reactive conditions that can simulate CD30 positive lymphoproliferative diseases. Although CD8 positive lymphomatoid papulosis is defined in pediatric patients, no response was seen to oral antibiotics.

PS-24-038

Are HMB-45 and MIB1 results reliable for safe diagnosis of nevi?

Z. Yusifli*, O. Kurtulan, Ç. Aydin, M. Bugdayci, Ö. Gököz
*Hacettepe University, Pathology, Ankara, Turkey

Objective: Melanocytic lesions having subtle features suspicious for malignancy create considerable difficulty in decision-making.process. Lack of deep HMB-45 positivity and low dermal MIB-1 index can be reliable tools in association with morphology.

Method: Twenty-seven acquired melanocytic lesions in which HMB-45 and MIB-1 have been performed are reviewed to determine the importance of these markers in routine diagnostic practice. Asymmetry, focal loss of maturation, presence of mitoses, epidermal consumption and lymphocytic inflammation were the morphological features that have created difficulty especially when seen alone in a bland appearing nevus.

Results: All cases with epidermal consumption and/or mitoses and nearly half of cases with inflammation, asymmetry and focal loss of maturation was associated with.focal deep dermal HMB-45 positivity. Thirteen cases had an MIB-1 index of ≤1 %. Two of 3 cases with MIB-1 index of >1 % had also HMB-45 positivity and/or inflammation. The case with a MIB-1 index of 8 % was an acral nevus bearing 4 of the evaluated morphological features.
Conclusion: Focal deep dermal HMB-45 positivity goes parallel with epidermal consumption and dermal mitoses, mostly used prevailing criteria of malignancy in melanocytic lesions but it's expression is not adequate for diagnosis of melanoma. Low MIB1 index can be a reliable marker of benignity.

Wednesday, 12 September 2012, 09.30 - 10.30, Congress Hall Foyer 3rd Floor
PS-25 Poster Session Infectious Diseases Pathology

PS-25-001
Ionic imbalance, renal pathology and lack of effect of adjuvant treatment with methylene blue in the hamster model of leptospirosis
D. Athanazio*, C. Santos, E. C. Azevedo, L. M. Soares, M. O. Seixas Carvalho, A. D. Chagas-Junior, C. L. da Silva, U. M. Russo Chagas, E. Reis, M. Reis
*Federal University of Bahia, Dept. of Pathology, Salvador, Brazil

Objective: Leptospirosis in humans usually courses with hypokalemia and hypomagnesemia, and the putative mechanism may be related to nitric oxide production. Methylene blue is a known inhibitor of inducible nitric oxide synthase, and have beneficial effects on clinical and experimental sepsis.
Method: Serum creatinine and ionic changes were evaluated at various time points (4, 8, 16 and 28 days) in hamsters. We also determined the effect of methylene-blue treatment when used as adjuvant therapy combined with a late start of standard antibiotic (ampicillin) treatment.
Results: Rather than K and Mg depletion, hyperkalemia and hypermagnesemia were observed during acute infection. These findings are probably associated with an accelerated progression to renal failure, since this model is not feasible to mirror the supportive therapy (including fluid expansion) that retards progression to the oliguric/hyperkalemic state. Infected hamsters at day 8 presented diffuse tubular cell swelling with mild or no nephritis. At days 16 and 28 they showed variable degrees of acute tubular changes, regeneration of tubular epithelia and nephritis. Survival and renal pathology did not differ among different treatment groups.
Conclusion: Adjuvant methylene blue had no effect on the survival, renal pathology or Mg and K serum levels during acute-phase leptospirosis in hamsters.

PS-25-002
Occupation of the striated muscle fibre by Trichinella spiralis is associated with increased intracellular sialylation
P. Babal*, R. Milcheva, D. Ivanov, S. Petkova
*Comenius University, Dept. of Pathology, Bratislava, Slovakia

Objective: The knowledge about glycoproteome in skeletal muscle is limited and most of the information come from studies on aberrant glycosylation in inherited muscle diseases. This work describes the intracellular changes in sialylation of skeletal muscle fiber during the process of its transformation into a nurse cell after occupation by the nematode Trichinella spiralis.
Results: The study was performed at defined time points post infection. Lectin histochemistry with TML, MAL and SNA detected increased production of sialylated glycoproteins within the affected fibers, and it was evaluated by acidic ninhydrin reaction in muscle homogenates. Increase of total sialyltransferase activity was estimated by measurement of incorporated CMP-N-[14 C]-acetylneuraminic acid, and immunohistochemistry showed higher expression of α-2,3-sialyltransferases II and IV within the affected fibers. SNA lectin affino-blots showed at least four protein bands with approximate molecular weight between 126 and 159 kDa, which were more reactive to SNA compared to their counterparts from the control samples.
Conclusion: It is evident that skeletal muscle injury induced by Trichinella activates biosynthesis of glycoproteins bearing sialic acids, which are not present in the normal muscle fiber. However, the protein identity, function and the biological significance of these sialoglycoproteins remain to be elucidated. BG051PO001-3.3.04/46, 28.08.2009; ITMS: 26240120023.

PS-25-003
Cerebral amebic abscess in immunocompetent patients: Two case report
A. Ben Salem*, H. Azzouz, B. Kilani, I. Chelly Enneifer, H. Nfoussi, N. Kchir, S. Haouet, M. Zitouna
*Charles Nicolle Hospital, Dept. of Pathology, Tunis, Tunisia

Objective: Protozoal and helminthic infestations of the central nervous system (CNS) are rare and their incidence is less than 1 %. They are more common among children, the elderly and immunocompromised individuals and tend to follow a fatal course.
Method: We report 2 cases of cerebral amebic abscess occurring in 2 immunocompetent men.
Results: They were 2 men aged of 43 and 18 years old. Headache; altered mental status and fever were common presenting symptoms. In the 2 cases the diagnosis of cerebral abscess was suspected on cerebral CT scan. Histopathologic analysis revealed extensive areas of necrosis and hemorrhage with granulomatous lymphoplasmacytic inflammatory infiltrate.

Different structures (isolated or forming small clusters) with the morphological characteristics of amoeba trophozoites were identified in the areas of necrosis with and without an inflammatory reaction. The diagnosis of cerebral amebic abscess was then made. The 2 patients received antibiotic treatment.
Conclusion: Cerebral amebic abscess is rare but has poor prognosis. It should be considered as a diagnosis for any patient with subacute and/or chronic meningoencephalitis without evident bacterial etiology. More effective antibiotic drugs can be chosen for post-surgical treatment; furthermore, better survival may be achieved by diagnosing the disease in early stages.

PS-25-004
Morphometric characteries of women placenta which can be different forms of syphilis
M. Bokhodir*, G. Raimnazarova, Z. Parpiev
*Tashkent Medical Academy, Dept. of Patological Anatomy, Uzbekistan

Objective: Many literary information give us about getting down coefficient of fertitity -placenta at women which suffer from pregnancy with syphilis.
Method: Verified data analysis about morphometric placentae and it's comparison with newly- born child at 50 women which suffer from different forms of syphilis.
Results: Research placenta with syphilis show us the area of placenta surface is decreased, it was formed primary syphilis −297,+−42,1 sm, secondary −316,8±28.8sm and with latent form of syphilis 319,7±28.8(at control 331.4±234,8sm2 $p>$ O.l), at that time as a mass, placentary cell was been bigger and it formed (at primary- 589.1±32.7gr and at secondary- 568,2±25,5gr and at latent form of syphilis 582.8±20.7gr, then in control (555,0±35,7) but all this different were been statistically unreliable ($p>0,05$). Comporision mass of placenta and mass newly born- child show us corfficient of fertitity-placenta is make up (5,86±0,21) and actually it is not different at control fact group.
Conclusion: The change coefficient of fertitity -placenta was typifying for until penicillin era, that time. When actual condition, treatment syphilis with antibiotic to bring on development phathomorphism placentae with out different coefficient of fertitity -placenta.

PS-25-005
Influenza B virus-associated pneumonia: Report of one fatal case associated with sickle-cell trait
L. De Carvalho*, L. Avila, H. Camargo, C. Torriso, R. Penny, A. Sementilli
*Centro Universitário Lusíada, Dept. of Pathology, Santos, Brazil

Objective: Influenza virus pneumonia complicated with acute respiratory distress syndrome is rare and has a high mortality rate. Patients with sickle cell trait are asymptomatic, however, complications with increased risk of thromboembolism can occur.
Method: Case report: A 30-year-old woman with no preexisting medical conditions presented nonproductive cough and fever for 4 days. For the next 3 days, developed acute respiratory failure. She was treated for septic shock and acute respiratory distress syndrome without success with death. Expectoration and blood cultures were negative and the real-time polymerase (RT-PCR) of the thracheal swab was positive for influenza B virus.
Results: The autopsy showed a diffuse necrotizing alveolitis and intra-alveolar hemorrhage with pulmonary infarction. There was no histological evidence of bacterial pneumonia. An evident blood cell sickling was observed associated with sickle cell trait. RT-PCR was also positive for influenza B virus in pulmonary tissue and the immunohistochemistry was negative for influenza A virus.
Conclusion: Severe hypoxemia caused by the acute respiratory distress syndrome was a possible cause of the blood cell sickling and thrombotic events.

PS-25-006
Report of three lupus vulgaris cases
H. Erdem*, H. Turan, M. Oktay, A. K. Uzunlar, L. Yilmaz Aydin, D. Ozcelik, C. Aliagaoglu, U. Yilderim, C. Sahiner, F. Basar
*Duzce University, Dept. of Pathology, Turkey

Objective: Lupus vulgaris (also known as "Tuberculosis luposa") are painful cutaneous tuberculosis skin lesions with nodular appearance, most often on the face around ears nose, eyelids and lips, cheeks. ıt is still a major health problem in developing countries. Cutaneous tuberculosis is a rare form of extrapulmonary tuberculosis. Lupus Vulgaris (LV) is the most common form of cutaneous tuberculosis. LV should make differential diagnosis other granulomatous disease. All three cases of old female patient.
Conclusion: Herein, three cases were presented which they treatment with correlation clinical and histopathological examination.

PS-25-007
Actinomycosis: A retrospective study of 56 cases
R. Hamrouni*, H. Kamoun Azouz, H. Nfoussi, I. Chelly, A. Dhaoui, A. Ben Salem, B. Chelly, S. Haouet, M. N. Kchir, S. Attafi
*Pathology, Ariana, Tunisia

Objective: Actinomycosis is a rare, chronic, and slowly progressive granulomatous disease caused by filamentous Gram positive anaerobic bacteria from the Actinomycetaceae family. It is often misdiagnosed because it can mimic

other conditions such as malignancy and tuberculosis. It occurs normally in the mouth and tonsils, however, it can sometimes occur in the chest, abdomen, pelvis or other areas of the body.

Method: We describe a retrospective study about 56 cases of actinomycosis diagnosed over a 21-year-period (1990–2011).

Results: The 56 cases were divided in 20 cervicofacial actinomycosis, 18 genito-urinary tract actinomycosis, 8 cutaneous actinomycosis, 7 abdominal actinomycosis and 3 cases occur in central nervous system. All patients were symptomatic. The most frequent symptom consisted in fever. The diagnosis was based on histologic study in all cases. Tissue histologic studies show suppurative and granulomatous inflammatory changes, connective proliferation, in which bacteria form typical granular colonies composed of radiating gram positive filaments.

Conclusion: Diagnosis of actinomycosis is usually made retrospectively by means of histologic examination of surgically obtained specimens, but rarely preoperatively. It is generally treated with long term antibiotics.

PS-25-008

Expression of angiogenesis factors in placentas with intrauterine transmission of HIV

A. Kolobov*, E. Musatova, V. Karev, V. Zinserling, D. Niauri
*St. Petersburg, Russia

Objective: Placenta plays an important role in the prevention of the mother-to-child transmission of HIV during pregnancy. The purpose of this investigation was to study expression CD31, bFGF and TGFβ in human placentas in cases of intrauterine HIV infection.

Method: Group A - 11 placentas from women and children with HIV infection. In control – Group B, were 16 placentas from women without HIV infection. On paraffin slices expression of CD31, bFGF, TGFβ and p24 was evaluated. We counted the area of positive cells related to the square of the slice.

Results: In all placentas with HIV infection p24 has been found in placental macrophages and villi's vessels. In group A expression of CD31 in endothelial cells was 4,22±0,85 % of the slice's square (in control - 3,69± 0,53 %) ($p>0,05$). Expression of bFGF in villi's stroma was 5,49±1,48 % (in control - 4,01±0,6 %) ($p>0,05$). Expression of TGFβ in villi's vessels was 11,2±3,6 % (in control - 2,71±0,63 %) ($p<0,05$).

Conclusion: Thus, placentas in cases with intrauterine transmission of HIV are characterized by increased expression of TGFβ the significance of this fact is still to be evaluated.

PS-25-009

1709 unilocular cystic echinococcosis in Erzurum during last 30 years

A. Kurt*
*Bölge Egitim ve Arastirma Hastanesi, Dept. of Pathology, Erzurum, Turkey

Objective: Unilocular cystic echinococcosis which Echinococcus granulosis causes is seen frequently in the animal husbandry practised underdeveloped countries.

Method: The 1709 unilocular cystic echinococcosis cases which were seen in the eastern part of Turkey, in 30 years between 01.01.1981 and 01.01.2010, except Faculty of Medicine of Atatürk University are presented.

Results: Organ distribution: Female: Liver 557 (SD:15.614), lung 259 (SD 15.928), spleen 42 (SD 13.108), abdomen 25 (SD 11.55), kidney 21 (SD 11.92); Male: Liver 331(SD 15.406), lung 233 (SD 18.027), spleen 25 (SD 10.12), brain 23 (SD 11.55), soft tissue 15 (SD 14.197).

Conclusion: The frequently seen organs in both gender are liver and lung. The rarely seen organs were spleen 67, brain 40, abdomen 39, kidney 36, vertebrae 29, soft tissue 27, pleura 26, bone 25, breast22. The others were very rare: eye 4, gallbladder 4, thyroid 4, neck 4, ovary 1, testis 1.

PS-25-010

Relation of the length of appendix and parasitosis: Preliminary report

A. Kurt*, S. A. Özmen, I. Erdem
*Bölge Egitim ve Arastirma Hastanesi, Dept. of Pathology, Erzurum, Turkey

Objective: Is there an effect of the length of appendix vermiformis on the settlement of the bowel parasites? We have decided to research.

Method: It was studied retrospectively for not to be under the influence. Randomly chosen from the archives, 65 parasitic appendix (41 women + 24 men) and 65 appendix vermiformis (41 women and 24 men) lengths were compared. The last 65 appendix materials of the appendixes which include parasites (56 E.vermicularis, 8 A.lumbricoides,1 T.saginata) and operated any causes were examined. Placeholder conditions such as fibrous obliteration and tumour were excluded. The premeasured length of the appendix in the series (65+65=130) were listed with the gender.

Results: Appendix length in the control series: The length of appendix in men:7.15 The length of appendix in women:6.85 The length of appendix in both gender:6.95 cm. The length of parasitic appendix: The length of appendix in men:7.30 The length of appendix in women:6.76 The length of appendix in both gender:6.94.

Conclusion: The mean length of appendix in both series was about 6.95 cm. There were no important difference of the length of either parasitic appendixes or all cause appendectomy materials. In this study, it is concluded that there isn't an effect of the length of appendix on the settlement of bowel parasites.

PS-25-011

About a rare and challenging disease: Multiple thoracic hydatidosis

M. Mlika*, E. Boudabbous, A. Ayadi-Kaddour, M. Yahia, E. Braham, O. Ismail, F. El Mezni
*Abderrahman Mami Hospital, Dept. of Pathology, Tunis, Tunisia

Objective: Cystic hydatid disease (CHD) is an infection produced by larvae of the parasite platyhelminth Echinococcus granulosus. Living in a rural area is an important risk factor for this disease. It is still an endemic disease in some regions of the world, particularly in many Mediterranean countries. The organs most commonly affected are the liver and the lungs.
Method: We present a new case of multiple thoracic hydatidosis.
Results: We present the case of a 37-year-old Caucasian man who presented chest pain and dyspnea. Chest-x-ray showed a well limited cardiac opacity of the upper lobe and of the right lung. Chest-CT-scan showed a mediastinal cyst evoking a hydatid cyst in the left ventricle associated to a right pleural effusion. The patient underwent surgery that consisted in the drainage of multiple pericardial cysts, cystectomy of a left ventricle cyst and right pleural cystectomy. Microscopic examination showed a pleura-pulmonary and cardio-pericardial hydatidosis. The patient was treated with albendazole and did not present complications or recurrences after 1 year of follow up.
Conclusion: Multiple thoracic hydatidosis is rare. Cardiac location is the most challenging because it is difficult to manage and is life threatening. Treatment modalities are mainly based on surgery. Preventive measures are necessary to avoid disease recurrence.

PS-25-012

Role of peripheral lymph node biopsy in patients with HIV infection

F. Staniceanu*, L. Nichita, S. Zurac, A. E. Bastian, G. Micu, R. T. Andrei, T. Tebeica, M. Petre, A. L. Birceanu Corobea, M. Ivan
*Colentina University Hospital, Dept. of Pathology, Bucharest, Romania

Objective: Lymphadenopathy is frequently present in HIV positive patients, especially in those with severe immune deficiency and consequently elevated risc of opportunistic infections and neoplasms. Considering the large spectrum of possible differential diagnosis a thorough lymph node analyses should be performed.
Method: We examinated 30 peripheral lymph nodes from 27 patients from latero-cervical, axilar, inguinal and supraclavicular regions; 10 nodes (33,3 %) had diameter less then 1 cm.
Results: Histopathological findings indicated mycobacterial infection in 15 patients (55,5 %), reactive hyperplasia in 7 patients (25,9 %), lymphoma in 3 patients, metastasis from Kaposi sarcoma in 2 and supurative inflamation in 1. Clinically suspected lymphoma was microscopically infirmed in all 4 cases. 4 cases of tuberculosis, 1 of lymphoma and 1 of Kaposi sarcoma metastasis were identified, all of them without prior clinical suspicion We identified tuberculosis, lymphoma and metastasis in 33,3 % of nodes smaller then 1 cm.
Conclusion: In 74 % of cases lymph node biopsy identified tuberculosis or malignancy, and established a reliable diagnosis in various clinical suspicions. We consequently emphasize the importance of lymph node examination in the evaluation of lymphadenopathy in HIV positive patients, even is not prominent. Stăniceanu and Nichita are first authors in equal contribution.

PS-25-013

The importance of autopsy in HIV infected patients

F. Staniceanu*, L. Nichita, S. Zurac, E. Gramada, C. G. Socoliuc, L. Sticlaru, S. S. Gheorghita, R. Chirculescu, M. Olariu, A. Streinu-Cercel
*Colentina University Hospital, Dept. of Pathology, Bucharest, Romania

Objective: Nowadays possibilities of medical investigations offer miriads of accumulating data regarding HIV infected patients status. Correlation and/or validation of these informations with pathological findings is mandatory to establish in order to ensure appropiate management of HIV infection.
Method: We performed a comparative study between clinical/paraclinical and autopsy findings in some of the most frequent afected organs in HIV infection; we studied in 31 HIV positive patients autopsied between 2000 and 2011; all patients had no or incipient (up to 1 year) antiretroviral treatment.
Results: 26 patients presented lung pathology, clinico-pathological correlations revealing 13 discrepancies, 13 total concordances and 5 partial concordances. Most of these inconsistencies referred to opportunistic infections, clinically suspected and pathological refuted in 9 cases and clinically unsuspected and pathological identified in 7 cases. Clinically suspected neurological alterations were microscopically infirmed in 33,3 % of cases, while 3 cases presented unsuspected lesions. Opportunistic infections were

detected in 38,8 % of liver examinations and in 38,0 % of lymph nodes, all of them clinically unsuspected.
Conclusion: Autopsy evaluation allows proper selection of relevant biological/clinical/paraclinical data in order to establish a better understanding of this complex disease. Stăniceanu and Nichita are first authors in equal contribution.

PS-25-014

Morphological features of erythropoietin and mesenchymal stem cells application in experimental sepsis in rats

F. Zabozlaev*, A. Sorokina, A. Averyanov, A. Konoplyannikov, D. Akulshin, O. Kuzovlev
*FRCC FMBA Russia, Dept. of Pathology, Moscow, Russia

Objective: On the basis of recently detected receptors for erythropoietin on the surface of MSCs we hypothesized that introduction of EPO together with MSCs may enhance their effect and improve the results of sepsis treatment.
Method: 50 Wistar male rats were randomized into 5 groups with 10 animals in each: Group1 - the healthy controls, 2–5 Groups were intraperitoneally introduced bacterial LPS 20 mg/kg. Group3–4 got×105 allogeneic MSCs, Group4 - 8.5 μg of recombinant EPO-beta, Group 5 - MSCs and EPO in the same doses. The morphological study of liver, spleen, thymus, lung and kidney was performed. Histological specimens were evaluated by qualitative, semi-quantitative and quantitative methods.
Results: In lung tissue the thickness of alveolar septums progressivly reduced from Group 3 to 5.In kidney and liver tissue the dystrophy of hepatocytes and nefrocytes and a blood vessel's dilatation in studied groups also reduced.In lien tissue we observed hyperplasia of white pulp in groups 4 and 5. Structural features of thymus were connected with patterns of T-lymphocyte proliferation and differentiation.
Conclusion: Combined treatment with EPO and MSCs can reduce acute lung injury and kidney damage, cause hyperplasia of lymphoid tissue and enhance the immune response more than separate treatment in an experimental model of sepsis in rats.

PS-25-015

Mycobacterial spindle cell pseudotumor of the liver

A. Alves*, A. Costa, A. Fernandes, G. do Carmo, I. Tavora
*Hospital Santa Maria, Servico de Anatomia Patologica, Lisboa, Portugal

Objective: Spindle cell pseudotumors are rare manifestations of mycobacterial infections. We describe a case in the liver in an immunocompromised patient with tuberculosis.
Method: A 28-year-old man, with active substance dependency, HIV-1 infection known for 7 years and acquired immunodeficiency syndrome for 3 years, was receiving tuberculostatic medication for disseminated tuberculosis and investigated for persistent fever. A liver ultrasonography confirmed a moderate hepatomegaly and showed multiple dispersed nodules in both lobes, with 1 to 3 cm of greater diameter.
Results: A needle biopsy from one of the nodules showed a proliferation of spindle cells without atypia, grouped in intersecting bundles, with immunoreactivity to vimentin, CD68 and lysozyme and negative for CD34, pS100, SMA and desmin; a Ziehl-Neelsen stain revealed several acid fast bacilli in the spindle cells. They were PAS negative.
Conclusion: Pseudotumoral lesions in hepatic tuberculosis usually correspond to granulomatous inflammation. A spindle cell proliferation, like that seen in other organs are more frequently associated with non tuberculous mycobacteria, is very rare. We found only another case in the literature of liver spindle cell pseudotumor associated with tuberculosis. This lesion must be differentiated from mesenchymal neoplasms.

PS-25-016

Sixteen months follow-up in a treated case of Whipple Disease (WD)

C. Popp*, M. Petre, G. Micu, A. Bastian, R. Chirculescu, R. Mateescu, F. Staniceanu
*Colentina University Hospital, Dept. of Pathology, Bucharest, Romania

Objective: WD is a rare, multi-systemic infection caused by a ubiquitous environmental bacteria -Tropheryma whipplei - that affects the duodenum and small intestine but also the brain, endocardium, skin, lungs and joints.
Method: We are presenting a 49 years old man with a 2 years history of diarrhea, malabsorption and weight lost (about 30 kg). Endoscopical examination revealed an unspecific, yet unusual pattern of lesions: small, yellow, multiple, slightly elevated patches involving duodenum and jejunum. Histological examination revealed numerous foamy macrophages in lamina propria with PAS (+), Ziehl-Neelsen (−) material in cytoplasm.
Results: Treatment with trimethoprim/sulfamethoxazole was initiated with a spectacular response: after 2 days of therapy the patient had normal stool and in 6 months he already gained back 20 kg. After 1 year of treatment the biopsy confirmed a partial remission with fewer macrophages persisting in lamina propria of duodenum. After 16 months of treatment (March 2012), very few macrophages with PAS (+) material are still identified on duodenal biopsy.
Conclusion: WD is a potentially fatal disease with unspecific clinical and endoscopical signs that can be diagnosed on duodenal biopsies. Histological follow-up is a useful tool of managing the treatment and histopathological confirmation of the absence of foamy macrophages is mandatory in discontinuing therapy.